International Solvent Extraction Conference

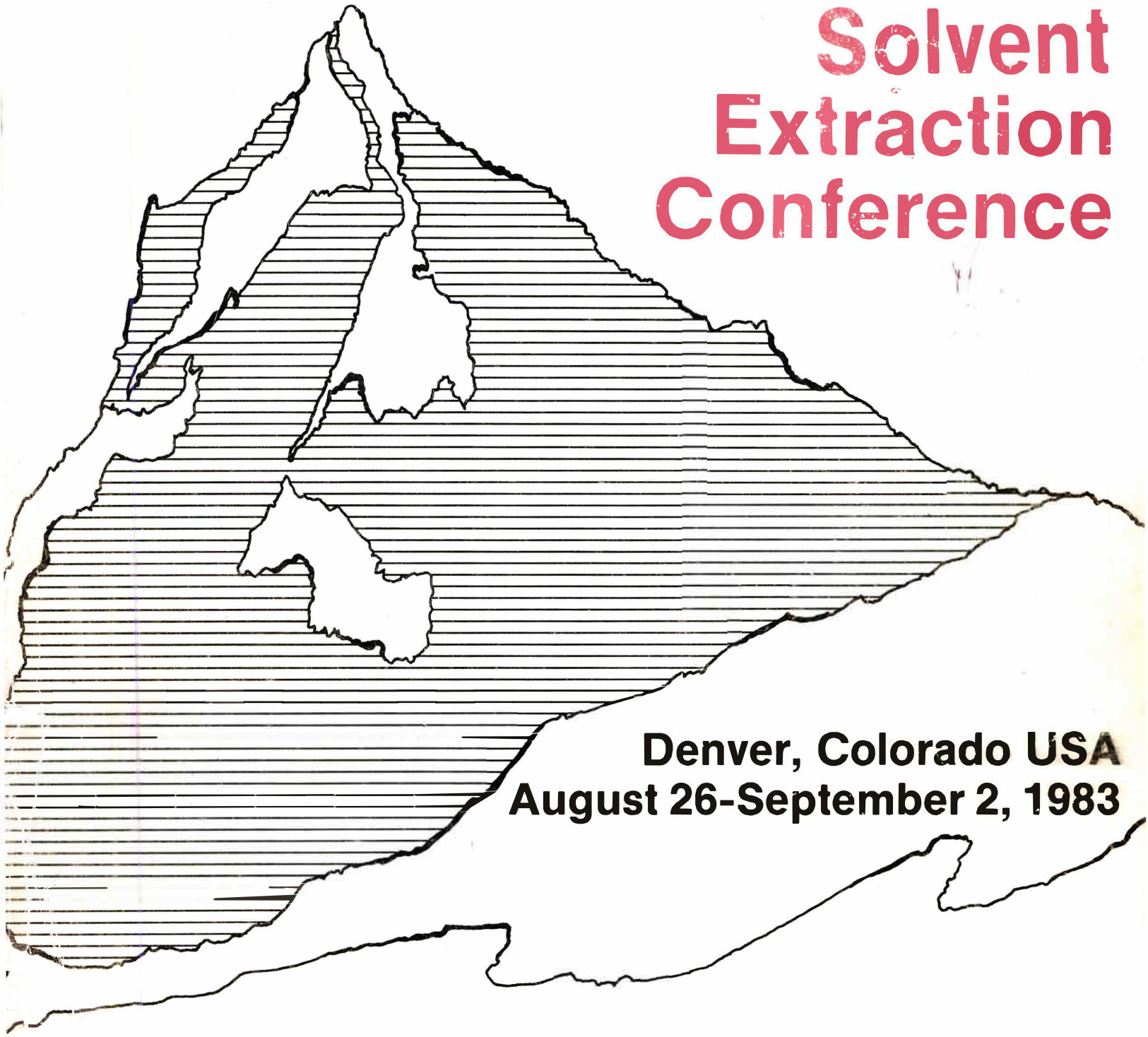

Denver, Colorado USA
August 26-September 2, 1983

ISEC '83

INTERNATIONAL SOLVENT EXTRACTION CONFERENCE

Denver, Colorado USA

August 26-September 2, 1983

Presented by:

The International Committee
for Solvent Extraction Chemistry
and Technology

Sponsored by:

American Institute of Chemical Engineers

Cosponsored by:

Division of Industrial & Engineering Chemistry
American Chemical Society

And

The Metallurgical Society of American Institute
of Mining, Metallurgical and Petroleum Engineers Inc.

COPYRIGHT FOR ISEC

Library of Congress Cataloging in Publication Data
International Solvent Extraction Conference (1983 : Denver, Colo.)
Proceedings : Denver, Colorado, August 26—September 2, 1983.

1. Solvent extraction—Congresses. I. American Institute of Chemical Engineers. II. Title.
TP156.E81518 1983 660.2'84248 83-17144
ISBN 0-8169-0254-2

PREFACE TO PROCEEDINGS OF ISEC '83

The ISEC Conferences are now a well-established feature of the calendar for all concerned with separation processes. Their origin can be traced back nearly thirty years. While the early events were very much limited to the chemistry of metals extraction relevant to the nuclear industry, no such limitation has been involved since the mid-1960s and the Conferences have truly covered both the science and technology of solvent extraction as applied in all sections of industry. This tradition is continued in ISEC '83, which also looks at techniques such as liquid membranes which are evolving from basic concepts developed for solvent extraction.

The successful application of solvent extraction on an industrial scale is essentially an inter-disciplinary operation, demanding close co-operation and communication between chemist and chemical engineer. This has always been emphasized in the ISEC Conferences, which have provided a regular and recognized meeting place for all those concerned with development of the subject, hopefully helping to minimize resistance to information transfer across disciplinary boundaries. The same applies to the interface between academic and industrial workers. The importance of bringing together these diverse groupings, all of whom are individually making important contributions to our knowledge of solvent extraction, cannot be over-emphasized. The result is one of the unique features of the ISEC Conferences.

A second feature is their international character. They have known no geographic or political boundaries and have brought together scientists from countries in all parts of the world. Many lasting friendships have been established and the Conferences have always been characterized by their atmosphere of collaboration and goodwill: truly a meeting of friends. This is a precious heritage which we must seek to maintain.

Finally, reference should be made to arrangements for the organization and continuity of the ISEC Conferences. The early events arose spontaneously and successors came by some person or group offering at one meeting to organize the next. However, as they grew in size and scope, with attendant increase in financial commitment, it became necessary to look for sponsorship from learned societies. At the same time, there was a clearly-seen wish to avoid the Conferences becoming the monopoly of any particular society but for them to remain independent and international. This led, at ISEC '74, to the establishment of the International Committee for Solvent Extraction Science and Technology. This is an informal body with an international membership of workers concerned for the future of solvent extraction. Its role is one of co-ordination, with the aim of maintaining an orderly continuation of the ISEC Conferences with appropriate timing and location in the best interests of development of the subject throughout the world. Each individual meeting is then sponsored by a scientific or professional society in the host country, detailed organization being entirely in the hands of a local committee. This devolved method of organization gives each meeting its own particular character and style, providing variety which should add to the pleasure and value of attendance.

ISEC '83 has been sponsored by the American Institute of Chemical Engineers in association with the Division of Industrial & Engineering Chemistry of the American Chemical Society and The Metallurgical Society of the American Institute of Mining, Metallurgical and Petroleum Engineers Inc. On behalf of the international community, I would like to record our thanks to all these bodies for their support, without which the meeting could not have taken place. However, the real work of organization has lain with individuals. An event of this size requires an enormous amount of preparation and the members of the Organizing Committees have given unstintingly of their time over the three years which have been involved. While it may seem invidious to select individuals for special mention when the organization has been very much a team effort, I feel I must make separate reference to the contributions of Mr. Robert B. Akell, who has shouldered the heavy responsibilities involved with Chairmanship of the Executive and Organizing Committees, and Professor C. Judson King, who accepted the onerous task of chairing the technical Program Committee and thus became the focal point for communications with contributors. Then there are those hidden people whose names are not recorded in any program but who have played a vital part working in offices throughout the USA to support the committee members. To all of them, I offer sincere thanks on behalf of the International Committee for Solvent Extraction Chemistry and Technology and all those who will attend or otherwise benefit from ISEC '83

Carl Hanson
Secretary General
International Committee for Solvents
Extraction Chemistry and Technology

A MESSAGE FROM THE ISEC '83 CHAIRMAN

I would have preferred to write these words after the meeting so that I could, I hope, have said with honest conviction: It was a good meeting. Because these Proceedings are printed before the meeting, I shall paraphrase the words my wife often uses when she serves a dish made from a new recipe: "It ought to be good; I used good ingredients." ISEC '83 ought to be good - we used good ingredients!

There are many people who supplied those "good ingredients." I should like to avail myself of this opportunity to record my appreciation for their efforts. I am sure that delegates to the meeting will share in this expression.

The International Committee for Solvent Extraction Chemistry and Technology, with Dr. Carl Hanson as its Secretary General, undertook the responsibility of setting the avenue for the triennial ISEC meetings. The relatively informal meetings begun about two decades ago have grown with their help to become important meetings in this field.

The American Institute of Chemical Engineers enthusiastically agreed to sponsor the meeting providing guidance, staff, and funds. We thank the Officers and Council of AIChE for their support. Special praise goes to J. Charles Forman, Secretary and Executive Director; Gerard F. Chiffriller, Director of Professional Services, and members of his staff: Don Nowak, Beth van Dijk, and Marie Stewart; and Larry Resen, Director of Publications and Technical Services.

Cosponsors of the meeting, Division of Industrial and Engineering Chemistry, American Chemical Society, and the Metallurgical Society of American Institute of Mining, Metallurgical and Petroleum Engineers, Inc., provided program liaison and use of their mailing lists.

Many individuals worked diligently to bring ISEC '83 into being. To each of them, and their employers who permitted them to spend time and money, we give our words of appreciation. Their names can be found in the Program and the Proceedings; space limitations do not permit me to name them all here. However, the Executive Committee has been working for, in some cases, four or five years on this meeting. They deserve special praise:

James L. Baird, Vice Chairman and Secretary, supervised preparation of the Program, Proceedings, mailing lists, and performed many other tasks as my "right-hand man."

James Y. Oldshue as Treasurer managed the meetings finances.

C. Judson King and his Program Committee are responsible for the many fine technical presentations in the plenary lectures, oral sessions, and poster sessions.

Allan L. Turner and his committee put together the excellent trips and social events.

David B. Todd was responsible for the equipment exhibit.

Looking back on what I have just written, I can only repeat: ISEC '83 should be good; it had good ingredients.

Robert B. Akell

FOREWORD FROM THE TECHNICAL PROGRAM CHAIRMAN

The International Solvent Extraction Conference for 1983 is by far the largest ever held. In fact, the number of papers has grown to the point where we have made basic changes in the format of the Conference. Over two-thirds of the papers have been presented in poster sessions, making ISEC '83 one of the first large international scientific conferences to use this medium of presentation so heavily.

Even though the Proceedings from ISEC '83 are imposing in size, it has also been necessary to make format and policy changes for them. Except for speakers in plenary sessions, authors have been limited to eight conventional typewritten pages, converted to two pages of the Proceedings upon reduction. For many of the papers it has therefore not been possible to present more than an Extended Summary. Consequently authors have been permitted to publish their paper in full elsewhere, should they desire.

The growth in size of ISEC '83 reflects the increasing breadth of solvent extraction and its applications. A perusal of these Proceedings will show much more concern with specific processing applications than for earlier ISEC's. There have been a number of new applications in recent years, spurred on by new processing needs, newly discovered extraction chemistry, environmental problems, and needs to reduce energy consumption in large-scale separations. In addition to the well established uses of solvent extraction in the hydrometallurgical, nuclear, inorganic, and petrochemical areas, there are growing applications in processing of pharmaceuticals, synthesis of chemicals from biomass, and production of new chemicals. Extraction with supercritical and near-critical fluids is a field of burgeoning interest, and there has also been much recent research on novel implementations of extraction in the form of emulsion- and solid-supported liquid membranes.

To support the development of these new applications, and to further the knowledge needed for design and analysis of solvent extraction systems, there has been continuing research in underlying areas of engineering science, such as mass transfer, fluid dynamics, emulsification and coalescence, axial dispersion, and modelling techniques. Research in solvent-extraction chemistry has continued apace as well, led by needs for better understanding of complexation mechanisms, the hope of improving extraction equilibrium, and the rapid growth of high-pressure liquid chromatography as a routine analytical technique.

Special thanks go to the members of the Technical Program Committee and to the Co-Chairmen of the various sessions—all listed elsewhere—for their willing and constructive efforts in building the largest and hopefully the most stimulating of the International Solvent Extraction Conferences. It is our hope that the Proceedings of ISEC '83 will serve as an important reference volume for years to come.

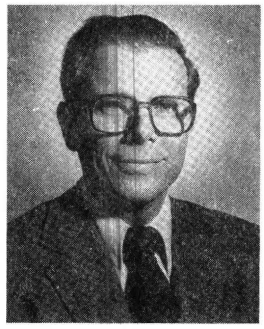

C. Judson King
University of California
Technical Program Chairman, ISEC '83

INTERNATIONAL COMMITTEE FOR SOLVENT EXTRACTION CHEMISTRY & TECHNOLOGY

Prof. C. Hanson, Secretary General
University of Bradford
Bradford, United Kingdom

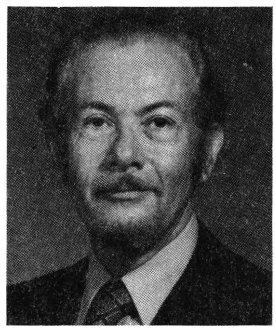

Prof. H. Freiser
University of Arizona
Tucson, Arizona USA

Mr. R. B. Akell
E.I. DuPont de Nemours & Co.
(Retired)
Wilmington, Delaware, USA

Prof. G. A. Yagodin
Mendeleev Institute of Chemical Technology
Moscow, USSR

Dr. H. W. Brandt
Bayer AG
Leverkusen, West Germany

Dr. D. S. Flett
Dept. of Industry
Stevenage, Herts, United Kingdom

Prof. A. S. Kertes
The Hebrew University of Jerusalem
Jerusalem, Israel

Dr. P. J. Lloyd
Chamber of Mines of South Africa
Johannesburg, South Africa

Dr. T. Misek
Research Institute of Chemical Equipment
Prague, Czechoslovakia

Prof. H. R. C. Pratt
University of Melbourne
Melbourne, Victoria, Australia

Mr. G. M. Ritcey
Dept. of Energy, Mines Branch
Ottawa, Ontario, Canada

Prof. J. Rydberg
Chalmers University of Technology
Goteborg, Sweden

Prof. T. Sato
Shizuoka University
Hamamatsu, Japan

Dr. M. Zifferero
Comm. Nazional per l'Energia Nucleare
Rome, Italy

Prof. F. J. Zuiderweg
Tech. Hogeschool Delft
Delft, The Netherlands

ISEC '83 EXECUTIVE COMMITTEE

CHAIRMAN
Mr. R. B. Akell
E.I. DuPont de Nemours & Co.
(Retired)
Wilmington, Delaware, 19898

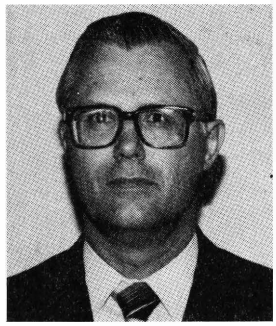

SPECIAL FUNCTIONS
Mr. A. L. Turner
Stearns-Roger Engineering Corp.
Denver, Colorado 80217

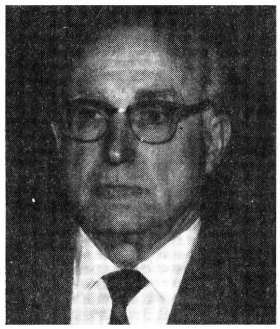

VICE CHAIRMAN & SECRETARY
Mr J. L. Baird
Artisan Industries Inc.
Waltham, Massachusetts 02154

EXHIBITS
Dr. D. B. Todd
Baker Perkins, Inc.
Saginaw, Michigan 48601

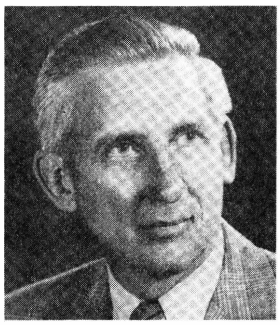

TREASURER
Dr. J. Y. Oldshue
Mixing Equipment Co., Inc.
Rochester, New York 14611

ARRANGEMENTS
Mr. G. F. Chiffriller
American Institute of Chemical
Engineers
New York, New York 10017

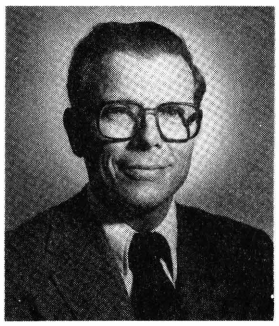

TECHNICAL PROGRAM
Prof. C. Judson King
University of California
Berkeley, California 94720

EUROPEAN LIAISON
Prof. C. Hanson
University of Bradford
Bradford, United Kingdom

ISEC '83 ORGANIZING COMMITTEE

Mr. R. B. Akell
E.I. DuPont de Nemours & Co.
(Retired)
Wilmington, Delaware, USA

Mr J. L. Baird
Artisan Industries Inc.
Waltham, Massachusetts USA

Prof. H. Freiser
Dept. of Chemistry
University of Arizona
Tucson, AZ USA

Prof. C. Hanson
University of Bradford
Bradford, United Kingdom

Prof. A. S. Kertes
The Hebrew University of Jerusalem
Jerusalem, Israel

Prof. C. Judson King
University of California
Berkeley, California USA

Dr. T. C. Lo
Hoffman-LaRoche, Inc.
Nutley, New Jersey USA

Dr. J. Y. Oldshue
Mixing Equipment Co., Inc.
Rochester, New York USA

Dr. D. B. Todd
Baker Perkins, Inc.
Saginaw, Michigan USA

Mr. A. L. Turner
Stearns-Roger Engineering Corp.
Denver, Colorado USA

ISEC '83 DENVER ORGANIZING COMMITTEE

John E. Litz
Hazen Research Inc.

Sylvia Navratil
Author

James D. Navratil
Rockwell International

Judy L. Turner
Educator

Allan L. Turner
Stearns-Roger Engineering Corp.

Sandy Zbranek
Shattuck Chemical Company

Vladimir Zbranek
Stearns-Roger Engineering Corp.

TECHNICAL PROGRAM COMMITTEE
ISEC '83

	Liaison with Session
Prof. C. Judson King, *Chairman* Dean, College of Chemistry, and Dept. of Chemical Engineering University of California Berkeley, CA USA	1, 11, 14, 17, 18, 25 29, 36, 37, 38, 42
Prof. H. Freiser University of Arizona Tucson, Arizona USA	3, 22, 32, 34, 41
Mr. Joe E. House Vice President, Minerals Industries Henkel Corporation Minneapolis, MN USA	4, 5, 6, 12 16, 23, 31
Dr. Kenneth D. MacKay (ACS) Liaison Director, Research Henkel Corporation Minneapolis, MN USA	9, 15, 21, 28, 30, 33
Dr. W. Jack McDowell Chemical Technology Division Oak Ridge National Laboratory Oak Ridge, TN USA	20, 24, 27, 35, 40
Prof. Kwadwo Osseo-Asare (TMS-AIME Liaison) Dept. of Materials Science & Engineering Pennsylvania State University University Park, PA USA	19, 26, 39
Prof. Raymond C. Waggoner (AIChE Liaison) Dept. of Chemical Engineering University of Missouri Rolla, MO USA	2, 7, 8, 10, 13

American Institute of Chemical Engineers

Officers

R. H. Marshall ..... *President*
J. H. Sanders ..... *Vice-President*
J. C. Forman ..... *Secretary*
J. Y. Oldshue ..... *Treasurer*
R. R. Hughes ..... *Past-President*

Division of Industrial & Engineering Chemistry American Chemical Society

Officers

K. C. Taylor ..... *Chairman*
B. L. Crynes ..... *Chairman-Elect*
W. N. Smith ..... *Secretary*
L. A. Casper ..... *Treasurer*
R. A. Stowe ..... *Past-Chairman*

The Metallurgical Society of American Institute of Mining, Metallurgical and Petroleum Engineers Inc.

Officers

M. E. Wadsworth ..... *President*
E. D. Verink, Jr. ..... *President-Elect*
A. Lawley ..... *Past-President*
G. S. Ansell ..... *Treasurer*

TABLE OF CONTENTS

PREFACE TO PROCEEDINGS OF ISEC '83 I
A MESSAGE FROM THE ISEC '83 CHAIRMAN II
FOREWORD FROM THE TECHNICAL PROGRAM CHAIRMAN III

Chemical Reactions in Liquid-Liquid Extraction Systems

THE RELATIVE IMPORTANCE OF DIFFUSION AND CHEMICAL REACTIONS IN LIQUID-LIQUID EXTRACTION KINETICS, Pier Roberto Danesi 1-3
THE ROLE OF THE INTERFACE IN THE EXTRACTION OF METAL CHELATES, Henry Freiser 4-5

Nuclear Extraction Processes - I (Chemistry)

PROGRESS IN TRIVALENT ACTINIDE LANTHANIDE GROUP SEPARATIONS, C. Musikas, P. Vitorge, D. Pattee 6-8
AN EXTRACTANT (TRPO) FOR THE REMOVAL AND RECOVERY OF ACTINIDES FROM HIGH LEVEL RADIOACTIVE LIQUID WASTE, Zhu Yongjun, Jiao Rongzhou, Wang Shouzhong, Fan Shiguo Liu Bingren Zheng Hualing, Zhou Shunli, Chen Shuming 9-10
POLY-(DIPHENYLPHOSPHINYLMETHYL)ARENES - NEW PHOSPHOR-ORGANIC EXTRACTANTS OF TRANSPLUTONIUM ELEMENTS, B. F. Myasoedov, G. V. Bodrin, M. K. Chmutova, N. E. Kochetkova T. Ya. Medved' Yu. M. Polikarpov, M.I. Kabachnik 11
IMPURITY REJECTION IN THE REFINING OF URANIUM WITH TRIBUTYL PHOSPHATE, D. G. Garratt and R. K. Badiani .. 12-13

Interfacial Kinetics - I

A GENERAL MODEL TO ACCOUNT FOR THE LIQUID-LIQUID KINETICS OF EXTRACTION OF METALS BY ORGANIC ACIDS, M. A. Hughes and V. Rod 14-15
LASER LIGHT SCATTERING STUDIES OF THE INTERFACIAL CHEMISTRY IN SOLVENT EXTRACTION SYSTEMS, Ronald D. Neuman and Anilkumar G. Gaonkar 16-17
KINETICS AND MECHANISM IN METAL SOLVENT EXTRACTION BY SOME ORGANOPHOSPHOROUS EXTRACTANTS, C. Cianettti and P. R. Danesi 18-19
REACTION IN VOLUME AND REACTION AT INTERFACE. CALCULATION OF THEIR CONTRIBUTIONS TO OVERALL EXTRACTION RATE, G. Yagodin, V. Tarasov, A. Pichugin 20-21
KINETICS AND MECHANISM OF COPPER EXTRACTION WITH 8-DODECYLBENZENESULFONAMI DOQUINOLINE, Fumiyuki Nakashio, Kazuo Kondo, Michiaki Matsumoto and Kazuharu Yoshizuka 22-23

Solvent Extraction Equipment and Equipment Design - I

STUDY OF AGITATOR TYPE IN MIXER-SETTLERS, Z. J. Shen and Q. Y. Zhang, B. Y. Sun, J. Li and Y. F. Su 24-25
MASS TRANSFER CHARACTERISTICS OF THE IMI TURBINE PUMP-MIX, G. Harel, M. Kogan, D. Meyer and R. Semiat 26-27
AXIAL MIXING CHARACTERISTICS OF INDUSTRIAL AND PILOT SCALE KUHNI COLUMNS, U. Bühlmann, J. C. Godfrey J. Breysse 28-29
DEVELOPMENT OF THE CASCADE WEIR TRAY FOR EXTRACTION, R. J. Fiocco 30-31
NEW EXTRACTION EQUIPMENT FOR NUCLEAR FUEL REPROCESSING APPLICATIONS, S. B. Koganti, R. Natarajan G. R. Balasubramanian 32-33

Plenary Lecture

METALLURGY TODAY - PROBLEMS AND OPPORTUNITIES, Wayne C. Hazen 34-35

Performance of Commercial Solvent Extraction Processes - I

INDUSTRIAL EXPERIENCE WITH PULSE COLUMNS IN URANIUM ORE PROCESSING, L. Clappier P. Michel, C. Duchamp and E. Henry 36-37
SOLVING THE HIGH ORGANIC ENTRAINMENT PROBLEM: THE EFFECT ON CATHODE COPPER CRYSTALLIZATION UNDER SPECIFIC OPERATING CONDITIONS, Gabriel E. Larrondo 38-39

Nuclear Extraction Processes - II (Engineering)

RECOVERY OF URANIUM FROM CHLORIDE SOLUTIONS RESULTING FROM HCI LEACHING OF ORES AND CONCENTRATES, G. M. Ritcey, E.W. Wong and K.T. Price 40-41
INTERFACIAL PHENOMENA IN URANIUM EXTRACTION FROM WET PROCESS PHOSPHORIC ACID, Armand Davister and Andre Dubreucq 42-43
IMPROVED DIALKYL PHOSPHORIC ACID, PHOSPHINE OXIDE, SYNERGISTIC SYSTEMS FOR URANIUM RECOVERY FROM PHOSPHORIC ACID LIQUORS, C. Ginisty 44-45
SOLVENT EXTRACTION PROCESS AND EQUIPMENT FOR A LMFBR FUEL REPROCESSING PILOT PLANT, G. Koch H. J. Bleyl, G. Boehme, H. Goldacker, H.O. Haug, W. Ochsenfeld, H. Schmieder 46-47
RECOVERY OF RHODIUM FROM SPENT NUCLEAR FUEL, The Extraction of Rhodium from Aqueous Nitric Acid Media, by Dinonylnaphthalene Sulphonic Acid, N. M. Patel, J. R. Thornback and J.H. Miles 48-49

Fluid Mechanics Phase Separation, and Interfacial Phenomena - I

ELECTRIC FIELD AND CAPILLARY EFFECTS ON DROP CIRCULATION AND MASS TRANSFER, Loto S. Chang and John C. Berg 50-51
DROP-SIZE, SPECIFIC AGITATION-POWER AND ENERGY-DISSIPATION FOR COUNTERCURRENT EXTRACTION COLUMNS, G. Husung, W. Gaubinger, R. Marr 52-53
COALESCENCE OF DROPS IN IMMISCIBLE LIQUIDS AT INCLINED PLATES, Eckhart Blass, Dieter Rautenberg 54-55
CONTINUOUS DROP FORMATION AT AN ORIFICE, A. Bright, C. Hanson, G. S. Virdee 56-57

Emulsion Liquid Membranes - I

EXTRACTION OF RARE EARTH BY LIQUID SURFACTANT MEMBRANES, Zhu Yongjun, Jiang Changyin, Wang Shizhu Liu Zaoqi and Yu Jianhan 58-59
A LIQUID MEMBRANE SEPARATION OF IONIC SPECIES USING A REDOX REACTION AS A DRIVING POTENTIAL, Makoto Takagi, Akira Ohki and Keihei Ueno 60-61
MEMBRANE EXTRACTION IN PRECONCENTRATION OF SOME URANIUM FISSION PRODUCTS, F. Macášek, P. Rajec R. Kopunec, V. Mikulaj, J. Mišianik 62-63
SELECTIVE EXTRACTION OF ZINC IN A COUNTERCURRENT KÜHNI EXRACTOR USING LIQUID SURFACTANT MEMBRANE EMULSIONS, D. Melzner, A. Mohrmann, W. Halwachs and K. Schügerl 64-65
DEVELOPMENT OF A CONTINUOUS PROCESS FOR METAL ION RECOVERY BY LIQUID MEMBRANE PERMEATION, M. Prótsch, R. Marr 66-67

Nuclear Extraction Processes - III

SIMULATION OF THE EXTRACTANT RADIO-DECOMPOSITION IN EMULSIONS, F. Macášek, R. Čech, L. Mátel 68-69
USE OF TETRACYCLINE AS EXTRACTING AGENT FOR SOME FISSION PRODUCTS, Ieda I. L. Cunha and M. J. C. Nastasi 70-71
SYNERGISTIC EXTRACTION OF PLUTONIUM AND AMERICIUM BY BIFUNCTIONAL ORGANOPHOSPHORIC REAGENTS, Anthony C. Muscatello, James D. Navratil and Milton E. Killion 72-73
EXTRACTION OF FISSION PRODUCTS WITH AMINES, Manfred Beer, Brunhilde Gorski 74-75
SOME REDOX REACTIONS OF URANIUM AND PLUTONIUM IN A SYSTEM INVOLVING TRIBUTYL PHOSPHATE (TBP) IN DODECANE AND AN AQUEOUS NITRATE SOLUTION, S. Tachimori and Z. Kolarik 76-77
PHYSICAL AND CHEMICAL ASPECTS OF URANIUM EXTRACTION FROM H_2SO_4 LEACH SOLUTIONS AND STRIPPING WITH AMMONIUM SULFATE, W. Howell, G. M. Ritcey, J.A. Golding 78-79
CONSOLIDATED FUEL REPROCESSING PROGRAM SOLVENT SCRUBBING KINETICS OF URANIUM - AND ZIRCONIUM-DIBUTYL PHOSPHATE COMPLEXES, J. C. Mailen, D. E. Horner S. M. Robinson, S. E. Dorris 80-81
EXTRACTION OF BERKELIUM (IV) BY NEUTRAL PHOSPHORORGANIC COMPOUNDS AND MULTIMOLECULAR AMINES, B. F. Myasoedov, M.S. Milyukova, D. A. Malikov 82-83
COMPARISON OF PUREX-PROCESS METHODS TO SEPARATE URANIUM AND PLUTONIUM, G. Petrich and H. Schmeider 84-85
EXPERIMENTS ON A MODIFIED THOREX FLOWSHEET FOR Th-Pu FUEL, G.R. Grant, R.E. Hollies, J.J. Hawton and Y.-K. Sze 86-87
INFLUENCE OF CATIONS ON CRUD FORMATION IN URANIUM CIRCUITS, G. M. Ritcey and E. W. Wong 88-89
CONSOLIDATED FUEL REPROCESSING PROGRAM ALTERNATE EXTRACTANTS TO TRIBUTYL PHOSPHATE FOR REACTOR FUEL REPROCESSING, D. J. Crouse, Fuel Recycle Division, W. D. Arnold and F. J. Hurst 90-91
REMOVAL OF TRIBUTYL PHOSPHATE AND ITS DEGRADATION PRODUCTS FROM AQUEOUS SOLUTIONS IN THE PUREX EXTRACTION PROCESS, W. Ochsenfeld, J. Schön 92-93
THE EFFECT OF TRIBUTYL PHOSPHATE DEGRADATION PRODUCTS UPON IMPURITY TRANSPORT IN THE REFINING OF URANIUM, D. G. Garratt 94-95
URANIUM CONCENTRATION PROFILE ALONG THE PULSED COLUMN, ITS DETERMINATION AND IMPORTANCE WITH REGARD TO SOLUTE'S ACCOUNTABILITY, Anthony F. Cermak 96-97

Modelling and Axial Dispersion - I

AXIAL MIXING OF CONTINUOUS PHASE IN A ROTATING-DISK EXTRACTION COLUMN, Li-zhu Lu, Zheng Fan and Chia-yung Chen 98-99
BACKMIXING INVESTIGATION IN A KUHNI EXTRACTION COLUMN, Gyula Vatai and Aleksandar Tolić 100-101
AXIAL DISPERSION STUDIES IN A RECIPROCATING PLATE COLUMN, N. V. Rama Rao, N. S. Srinivas and Y. B. G. Varma 102-103
A STUDY OF AXIAL MIXING IN PULSED, SIEVE PLATE EXTRACTION COLUMN, Shen Zhong-Yao, Dai You-Yan Zhu Shen-Lin and Wang Jia-Ding 104-105
LIQUID-LIQUID EXTRACTION COLUMN MASS TRANSFER PARAMETERS FROM CONCENTRATION PROFILES, Dr. W. J. Korchinsky, R. Al-Husseini and C. H. Young 106-107
MASS TRANSFER IN A CONTINUOUS FLOW STIRRED TANK REACTOR, P. M. Bapat and L. L. Tavlarides 108-109
HYDRAULIC AND MASS TRANSFER MODEL FOR HIGH CAPACITY LIQUID-LIQUID EXTRACTORS FILLED WITH STACKED PACKINGS, Prof. Dr.-Ing. Reinhard Billet, Dr.-Ing. Jerzy Mackowiak 110-112

SOLVENT EXTRACTION RELATED TO OPERATING PARAMETERS THROUGH ABSOLUTE STAGE EFFICIENCY, Ertan Yuzak and Raymond C. Waggoner 113-114
A REVIEW OF THE EXTRACTION FACTOR METHOD, W. R. Clingan 115-116
STAGE ADDITIVITY METHOD AND ITS APPLICATION TO CALCULATION OF COUNTER-CURRENT EXTRACTORS WITH BACKMIXING, Aleksandar S, Tolić 117-118
IMPROVED MATHEMATICAL MODELS IN SOLVENT EXTRACTION SYSTEM INVOLVING Pu-U-Th-HNO_3-TBP, R. Natarajan K. Rajamoorthy and G. R. Balasubramanian 119-120
RISK EVALUATION IN EXTRACTION EQUIPMENT DESIGN BASED ON TWO-STAGE LABORATORY EXPERIMENTS, Marin R. Mehandjiev 121
DESIGN AND EVALUATION OF AIR PULSERS FOR PULSE COLUMN CONTACTORS IN SOLVENT EXTRACTION, Arlin L. Olson and Professor C. A. Rhodes 122-123
STUDY OF THE MATHEMATICAL SIMULATION OF RARE EARTH EXTRACTION, Yun-yu Shen, Wei-juan Ying, Wen-hou Ya, De-xiang Ma 124-125
A KINETIC MODEL FOR THE SIMULATION OF INDUSTRIAL COPPER SOLVENT EXTRACTION PLANTS, C. M. Meier and J. D. Miller 126-127
INVESTIGATION OF LONGITUDINAL MIXING IN A 300mm PULSED EXTRACTION COLUMN FOR THE PUREX PROCESS, R. Britsch and K. Ebert 128-129
AXIAL DISPERSION, WITH AND WITHOUT MASS TRANSFER IN BOTH PHASES OF A RECIPROCATING PLATE EXTRACTION COLUMN, A. Bensalem, L. Steiner and S. Hartland 130-131

Solvent Extraction Equipment and Equipment Design - II

THE DEVELOPMENT OF MIXER-SETTLERS WITH DOUBLE MIXERS IN EACH STAGE, Li-Min Su and Guo-Peng Li 132-133
OPTIMAL DESIGN OF AN AIR PULSED MIXER SETTLER, M. Venkataraman, R. Natarajan and G. R. Balasubramanian . . . 134-135
PERFORMANCE OF THE KREBS SOLVENT EXTRACTION SYSTEM, D. Goodman & A. Sonntag 136-137
A PHASE RECIRCULATION IN A CENTRIFUGAL EXTRACTOR, G. I. Kuznetsov, A. V. Kosogorov, A. A. Pushkov, L. I. Shklyar 138
GAS DISPERSION IN LIQUID-LIQUID EXTRACTION, Ron Priestly and S. Suppiah 139-140
THE STUDY OF PERFORMANCE OF MASS TRANSFER IN SIEVE PLATE EXTRACTION COLUMN WITH SWIRL FLOW AND TRAPEZOIDAL PULSE, Dai Wiezhi, Tai Derong, Hu Xien, Wan Chunrong, Yang Lichun, Qi Xiaotian Duan Shihao and Fan Shuru 141-142
A MODIFIED ROTATING DISK CONTACTOR WITH WIRE MESH COALESCERS, F. G. Zhu, X. D. Ni and Y. F. Su 143-144
SULZER STATIC MIXERS AS A PACKING IN LIQUID/LIQUID EXTRACTION, S. J. Jancic, F. J. Zuiderweg, F. Streiff 145-146
PERFORMANCE OF KENICS IN-LINE MIXER IN SOLVENT EXTRACTION, Yi-yuan Li and Chenming Wang 147-148
COMPARISON OF SOLVENT EXTRACTION EQUIPMENT FOR A MODIFIED PUREX PROCESS, Barbara J. Smith Peter E. Bain, Larry L. Martella and James D. Navratil 149-150
AMPLIFICATION OF THE SCALE - UP PROCEDURE FOR THE RECIPROCATING PLATE EXTRACTION COLUMN, Andrew E. Karr 151-152
PERFORMANCE OF A LIQUID-LIQUID EXTRACTION COLUMN WITH ENHANCED COALESCENCE LATTICE PLATES, L. Steiner, E. V. Fischer and S. Hartland 153-154
CENTRIFUGAL EXTRACTION WITH AXIAL COUNTERCURRENT FLOW OF THE LIQUID PHASES, L. Steiner, K. Gebauer and S. Hartland 155-156

Fluid Mechanics, Phase Separations, and Interfacial Phenomena - II

STEADY-STATE DROPLET SIZE DISTRIBUTION, IN A PULSED PLATE EXTRACTION COLUMN, M. O. Garg and H. R. C. Pratt, ... 157-158
INFLUENCIAL PARAMETERS OF SIZE DISTRIBUTION IN VARIOUS DISPERSION PROCESSES, Jacques Dollfus 159-160
DEVELOPMENT OF A NOVEL PHOTOGRAPHIC DESIGN FOR DROP SIZE MEASUREMENT IN AGITATED VESSELS, H. Topuz 161-163
HOLDUP, DROP SIZE AND AXIAL MIXING OF PULSED EXTRACTION COLUMNS, Hans Schmidt 164-165
THE DYNAMICS OF PULSED PLATE EXTRACTION COLUMNS PART I: DISPERSED PHASE HOLDUP, DROPLET SIZE AND FLOODING RATES, IN A 3 in. DIAMETER PULSED PLATE COLUMN, W. Batey, T. Arthur, P. J. Thompson and J. D. Thornton 166-167
THE HYDRODYNAMIC BEHAVIOUR OF A PULSED PERFORATED-PLATE COLUMN, G. Vassallo, J. D. Thornton, and H. Dworschak 168-169
HOLDUP MEASUREMENT IN A ROTARY-AGITATED EXTRACTION COLUMN, Siu-Ming Yih, Ray-Kuo Pan and Yau-Ming Wu 170-171
DROP FORMATION AT ROTATING ORIFICES IN A CENTRIFUGAL FIELD, Reinhold Schilp and Eckhart Blass 172-173
A NEW LOOK AT THE HYDRODYNAMIC BEHAVIOR OF ROTATING DISC CONTACTORS, W.-Y. Fei and M. J. Slater . . . 174-175
PHASE INVERSION AND ENTRAINMENT CHARACTERISTICS OF LIX64N IN ESCAID AND WATER, J. C. Godfrey and J. Gledhill 176-177
ENERGY UTILIZATION IN LIQUID-LIQUID MIXING IN EJECTORS, D. Mukherjee, M. N. Biswas and A. K. Mitra 178-179
THE APPLICATION OF ELECTRIC FIELDS TO PHASE SEPARATION IN A SOLVENT EXTRACTION SYSTEM, P. J. Bailes and S. K. L. Larkai 180-181

DISPERSED PHASE BEHAVIOUR IN CONTINUOUS LIQUID EXTRACTION COLUMNS, G. Casamatta, C. Gourdon G. Muratet 182-183

Plenary Lecture

DEVELOPING SOLVENT EXTRACTION PROCESSES, AN INTEGRATED INTERDISCIPLINARY ACTIVITY, Ruth Blumberg 184-188

Novel Extractants - I

NOVEL SOLVENT EXTRACTANTS FOR CHLORIDE LEACH SYSTEMS, Raymond F. Dalton, Raymond Price and Peter M. Quan 189-190
THE LIX®860 SERIES: UNMODIFIED COPPER EXTRACTION REAGENTS, Gary A. Kordosky, J. Michael Sierakoski and Joe E. House 191-192
SOME NEW LIQUID EXTRACTION SYSTEMS FOR SEPARATION OF COBALT FROM NICKEL AND MATHEMATICAL MODELING OF THESE EXTRACTION PROCESSES, Chuei Biing-yi, Yu Jing-fen, Zhang Liang-ping 193-194
COBALT-NICKEL SEPARATION BY SOLVENT EXTRACTION WITH A DIALKYLPHOSPHINIC ACID, W. A. Rickelton D. S. Flett and D. W. West 195-196

Inorganic Extraction Processes - I

EXTRACTION OF CADMIUM FROM PHOSPHORIC ACID SOLUTIONS, S. Stenström and G. Aly 197-198
EXTRACTION OF RHODIUM FROM HNO_3 SOLUTIONS WITH ORGANIC SULPHIDES, Erich Fritsch, Brunhilde Gorski Manfred Beer 199-200
SOLVENT EXTRACTION OF LITHIUM, H. J. Bart and R. Marr 201-202

Modelling and Axial Dispersion - II

THE DESIGN OF LIQUID-LIQUID CONTACTORS: PAST, PRESENT AND FUTURE, H. R. Clive Pratt 203-204
EFFICIENT USE OF THERMODYNAMIC PROPERTIES FOR PHASE-EQUILIBRIUM CALCULATIONS IN SOLVENT EXTRACTION, P. F. Bryan and E. A. Grens II 205-206
MASS TRANSFER TO NON-UNIFORM DISPERSIONS IN COUNTER-CURRENT FLOW LIQUID-LIQUID EXTRACTION COLUMNS, J. J. C. Cruz Pinto, W. J. Korchinsky and R. Al-Husseini 207-208
DYNAMIC SIMULATION OF PULSED PACKED COLUMNS, A. J. F. Simons and C. Nap 209-210

Fuel and Chemical Extraction Processes - I

SOLVENTS FOR BULK REMOVAL OF ORGANICS FROM COAL-CONVERSION CONDENSATE WATERS, Donald H. Mohr and C. Judson King 211-212
SHALE OIL UPGRADING PROCESS BASED ON NITROGEN REMOVAL FROM CRUDE SHALE OIL BY LIQUID EXTRACTION, Ajay M. Madgavkar 213-214
LIGHT AROMATICS EXTRACTION FROM PETROLEUM FRACTIONS WITH ALKYLSULFONAMIDES, Roben Loutaty and Charles Yacono 215-216
SOLVENT EXTRACTION OF AROMATICS BY ALKYLENE CARBONATES, M. Cristina Annesini and Luigi Marrelli Robert De Santis, and Ireneo Kikic 217-218
ACID EXTRACTION BY AMINES, M. Siebenhofer, R. Marr 219-220

Metallurgical Extraction Processes - I

EXTRACTION OF COPPER FROM SULPHATE AQUEOUS SOLUTION BY OXIME TYPE EXTRAGENSES, A. Kostić-Pulek 221
EXTRACTION OF ANTIMONY AND ARSENIC FROM COPPER REFINING ELECTROLYTE, Jeffrey M. Cohen 222-223
COPPER-NICKEL SEPARATION FROM AMMONIACAL SOLUTIONS USING HYDROXYOXIMES REAGENTS, Corneille S. Ek 224-225
ZINC SEPARATION FROM COMPLEX SULPHATE-PHOSPHATE SOLUTIONS BY SOLVENT EXTRACTION PROCESS, A. Lupu and B. Flicstein 226-227
EXTRACTION AND SEPARATION OF COBALT AND MANGANESE FROM CHLORIDE SOLUTIONS WITH A TIOA-PERCHLORO-ETHYLENE SOLVENT MIXTURE IN A COLUMN EXTRACTOR, M. Verhaege, F. Leysen A. Van Peteghem 228-229
A SELECTIVE METALLURGICAL EXTRACTANT SYSTEM TO RECOVER NICKEL AND COBALT FROM ACID SOLUTIONS, Robert R. Ginstead and Annel L. Tsang 230-231
SOLVENT EXTRACTION OF COBALT AND NICKEL BY A PHOSPHONIC ACID ESTER, D. S. Flett, J. Melling and E. Itoh 232-233
EXTRACTION OF TUNGSTEN AND MOLYBDENUM BY SULFOXIDES, Dai Ge-Sheng, Xian Bao-Yuan and Su Yuan-Fu . . 234-235
SOLVENT EXTRACTION SEPARATION OF MOLYBDENUM AND TUNGSTEN USING DI(2-ETHYL HEXYL) PHOSPHORIC ACID (HDEHP) AS AN EXTRACTANT, N. R. Das, B. Nandi and S. N. Bhattacharyya 236-237
RECOVERY OF MOLYBDENUM AND RHENIUM BY SOLVENT EXTRACTION, Chen Tingzhang, Yuan Chusheng, Zhou Zhonghua and Ma Rongjun 238-239

THE EFFECT OF BENZENE AS DILUENT IN THE EXTRACTION OF CHLOROMETALLIC ACIDS BY DIISOPROPYL ETHER, Darko Maljković, Alojzija Paulin and Dubravka Maljković 240-241
MUTUAL INFLUENCE OF IRON (III) AND GALLIUM (III) AS, MACROCONSTITUENTS IN THE EXTRACTION BY A MIXTURE OF DIISOPROPYL ETHER AND n-PENTYL ALCOHOL, Dubravka Maljković, Darko Maljković and Alojzija Paulin 242-243
THE EXTRACTION OF SOME METALS FROM ALKALINE SOLUTIONS BY ALKYLATED HYDROXYQUINOLINE, Taichi Sato, Takato Nakamura and Hiroyuki Oishi 244-245
KINETICS OF HYDROLYTIC STRIPPING OF IRON FROM VERSATIC ACID SOLUTIONS, Luiz A. C. Teixeira and A. John Monhemius 246-247
SOLVENT EXTRACTION OF IRON FROM LIQUID WASTES OF METALLURGICAL PROCESSES, Iginio Colussi Ireneo Kikic, Ugo Preti, Antonio Cocco 248-249
SOLVENT EXTRACTION OF ALUMINUM, IRON AND TITANIUM CHLORIDES, G. Z. Sheng and M. J. Murtha and G. Burnet 250-251
EXTRACTION OF ZINC AND CADMIUM BY HIGH MOLECULAR WEIGHT AMINES, Anil K. De, Uday S. Roy and Narahari Parhi 252
MERCURY ISOLATION BY SOLVENT EXTRACTION AND NON-ELECTROLYTIC METHOD FROM LOW CONCENTRATION CINNABAR ORES, Victor Arenas, Hernán Lizama, Ricardo Schrebler, Ignacio Gardiazabal 253-254
SOLVENT EXTRACTION OF URANIUM IMPURITY TO PRODUCE NUCLEAR-GRADE ZIRCONIUM, D. J. MacDonald H. G. Henry, and D. J. Bauer 255-256

Physical Chemistry (General)

A DATA BASE FOR SOLVENT EXTRACTION CHEMISTRY, W. J. McDowell, D. C. Michelson, B. A. Moyer, C. F. Coleman 257-258
IMPROVED AKUFVE SYSTEM FOR FAST AND ACCURATE SOLVENT EXTRACTION STUDIES, J. Rydberg J. O. Liljenzin and Y. Albinsson 259-261
THE POSSIBILITY OF HYDROXONIUM ION EXISTENCE UNEQUILIBRIUM EXTRACTS, A. Chekmarev, G. Yagodin S. Dmitriev 262-263
SOME OBSERVATIONS ON THE EXTRACTABILITIES OF UNIVALENT CATIONS WITH CROWN-ETHERS (2), Yuko Hasegawa 264-265
PHYSICAL CHEMISTRY OF N,N-DIBUTYL-2-ETHYL-HEXYLAMIDE AS EXTRACTANT FOR URANIUM, Miroslav M. Kopečni and Djordje M. Petković 266-267
INTERFACIAL PROPERTIES AND METAL EXTRACTION CHEMISTRY OF THE ORGANOPHOSPHORUS ACIDS: $(RO)_2PO(OH)$; $(RO)RPO(OH)$; $R_2PO(OH)$, Michael Cox, Maria Elizalde and Jose Castresana 268-269
ADVANCES IN THE EXTRACTION CHEMISTRY OF AROMATIC HYDROXYOXIMES, Yuan Chengye, Xiang Caili, Li Shusen Jiang Xiqi, Wang Jiao, Pan Boxi & Cao Chiming 270-271
SOME NEW ASPECTS IN THE STRUCTURE-REACTIVITY STUDIES OF ORGANIC EXTRACTANTS, Yuen Chengye (C. Y. Yuan) 272-273
DETERMINATION OF THE HEAT CHANGE IN SOLVENT EXTRACTION OF METALS—THE EXTRACTION OF ZINC(II) FROM HYDROCHLORIC ACID SOLUTIONS BY HIGH MOLECULAR WEIGHT AMINES IN VARIOUS ORGANIC SOLVENTS, Taichi Sato, Takato Nakamura and Masami Kuwahara 274-275
MONOLAYER STUDIES OF SOLVENT EXTRACTION REAGENTS, D. J. Chaiko and K. Osseo-Asare, ... 276-277
ELECTROPHORETIC MOBILITY STUDIES IN LIQUID-LIQUID EXTRACTION SYSTEMS, K. L. Lin and K. Osseo-Asare .. 278-279
THE THEORETICAL AND EXPERIMENTAL INVESTIGATION OF THE SEPARATION OF RARE EARTH ELEMENTS BY ALKYLAMMONIUM SALTS, A. A. Kopyrin, V. V. Proyaev 280-281

Emulsion Liquid Membranes - II

SCALE-UP OF LIQUID MEMBRANE PERMEATION PLANTS, J. Draxler, R. Marr, A. Bouvier, A. Kriechbaumer, M. Prötsch 282-283
METAL EXTRACTION WITH 4-ACYLPYRAZOL-5-ONES: SYNERGISTIC EFFECTS WITH LIPOPHILIC AMMONIUM SALTS; APPLICATION TO LIQUID MEMBRANE TRANSPORT, J. P. Brunette, Z. Lakkis, M. Lakkis and M. J. F. Leroy 284-285
EXTRACTION KINETICS OF COPPER WITH LIQUID SURFACTANT, MEMBRANES CONTAINING HYDROXYOXIME IN A STIRRED TRANSFER CELL, Kazuo Kondo, Fumiyuki Nakashio and Keisuke Funatsu 286-287
ANALYTICAL AND EXPERIMENTAL STUDIES OF MASS TRANSPORT THROUGH LIQUID MEMBRANES, H. S. Park J. H. Yoo, I. S. Suh, P. S. Han, W. K. Kang, M. Burgard and M. J. F. Leroy 288-289
THE USE OF NEW EXTRACTANTS IN LIQUID SURFACTANT MEMBRANES, Mamoun Muhammed and Manuel Valiente 290

Interfacial Kinetics - II

USE OF IMAGE INTENSIFICATION FOR SIMULTANEOUS MASS AND HEAT TRANSFER STUDIES IN LIQUID-LIQUID SYSTEMS, F. J. Aguirre, G. E. Klinzing, S. H. Chiang 291-292
A FLOW-THROUGH CONSTANT INTERFACE CELL TO STUDY THE KINETICS OF EXTRACTION IN THE Cu/LIX 64N SYSTEM, M. Bhaduri, C. Hanson, M. A. Hughes, R. J. Whewell 293-294
THE INFLUENCE OF LIX63 ON COPPER EXTRACTION INTO LIX65N, E. Y. O. Paatero, and J. A. Golding 295-296

INTERFACIAL TENSION AND MASS TRANSFER RATE MEASUREMENTS FOR COPPER EXTRACTION WITH A HYDROXYOXIME EXTRACTANT, Jorge M. R. de Carvalho and Michael J. Slater 297-298
INTERFACIAL PHENOMENA IN COPPER EXTRACTION, V. Tarasov, G. Yagodin, A. Pichugin, S. Ivakhno 299-300
EXTRACTION RATES OF COPPER WITH SME529, MECHANISM AND EFFECTS OF SURFACTANTS, Yoshikazu Miyake Yoichiro Takenoshita and Masaaki Teramoto 301-302
EXTRACTION KINETICS AND MECHANISM OF NICKEL WITH SME529, Katsutoshi Inoue, Hiroki Tsunomachi, Shin-ichi Tomita and Takeshi Maruuchi 303-304
THE KINETICS OF THE EXTRACTION OF V(IV) FROM ACID SULPHATE MEDIA BY DI-2-ETHYLHEXYLPHOSPHORIC ACID, M. A. Hughes and K. Ipinmoroti 305-306
EXTRACTION MECHANISM FROM THE KINETIC STUDY OF INTERFACIAL MASS TRANSFER OF TERBIUM IN DI(2-ETHYL HEXYL) PHOSPHORIC ACID IN CYCLOHEXANE-NITRIC ACID SYSTEM, S. Sarker K. M. Ganguly and S. N. Bhattacharyya 307-308
EXTRACTION KINETICS OF POTASSIUM WITH CROWN ETHERS, Masaki Yoshio, Hideyuki Noguchi and Katsutoshi Inoue 309-310
EXTRACTION RATES OF ACETIC ACID WITH LONG-CHAIN ALKYLAMINES IN HORIZONTAL RECTANGULAR CHANNEL, Yoshinobu Kawano, Kazuhito Kusano 311-312
MASS TRANSFER IN CATALYTIC SYSTEMS: MICELLES, LIQUID MEMBRANES AND SINGLE DROPS, K. Osseo-Asare K. L. Lin and D. J. Chaiko 313-314
USE OF MICROEMULSIONS AS ORGANIC PHASE FOR FASTER KINETICS, D. Bauer, and J. Komornicki 315-316
PREDICTION OF INTERFACIAL REACTIONS, Sümer M. Peker 317-318
TOLUENE AND BENZENE SULPHONATION UNDER LAMINAR CONDITIONS, Morteza Sohrabi 319-320

Performance of Commercial Solvent Extraction Processes - II

DISPOSITION AND CONTROL OF IMPURITIES IN NICKEL AND COBALT SOLVENT EXTRACTION CIRCUITS IN THE PROCESSING OF LATERITE-DERIVED AMMONIACAL LEACH LIQUORS, D. N. Nilsen, R. E. Siemens 323-324
TEST OF AN AMINE PROCESS FOR REPROCESSING NATURAL URANIUM FUEL AT THE EUREX PILOT PLANT, G. R. Grant, D. G. Boase and D. R. McLean, F. Pozzi, A. Hall, V. Pagliai and G. Alonzo 325-326
STUDIES ON REPROCESSING FBR FUEL, H.-J. Bleyl, K. H. Ebert, D. Ertel, W. Ochsenfeld 327-328
PLUTONIUM RE-EXTRACTION BY ELECTRO-REDUCTION IN A PULSED COLUMN, H. Goldacker, U. Galla, M. Kluth R. Schlenker, H. Schmieder, H. Evers 329-330

Characterization of Organic Species in Solvent Extraction Processes - I

ELECTRON SPIN RESONANCE SPECTROSCOPY. A TECHNIQUE ALLOWING DIRECT DETERMINATION OF SPECIATION OF METAL COMPLEXES FORMED BY COMMERCIAL SOLVENT EXTRACTION REAGENTS, P. O'Brien and J. R. Thornback 331-332
EXTRACTION OF SULPHURIC ACID AND URANYL SULPHATE WITH BENZENE SOLUTION OF PRIMARY AMINE PRIMENE JM-T, Miroslav Mrnka, Prokop Nekovář, Vladislav Bizek, Daria Schrötterová and Alexander Mikhailovich Chekmarev Alexander Vasilevich Ochkin, Svetlana Vladimirovna Chizevska 333-334
FTIR AND NMR STUDIES OF THE STRUCTURE OF ORGANIC PHASE OF SOME SAPONIFIED ACID EXTRACTANT-OCTYL ALCOHOL-KEROSINE MICROEMULSION SYSTEMS, Wu Jinguang, Gao Hongcheng, Shi Nai, Chen Dian, Jin Tianzhu Xu Zhenhwa, Weng Shifu and Xu Guangxian 335-336
THE EFFECT OF SUBSTITUENTS ON THE STRENGTH OF O-HYDROXYARYLOXIME COPPER EXTRACTANTS, Raymond F. Dalton and Raymond Price 337-338
SOLVENT EXTRACTION OF TUNGSTEN AND MOLYBDENUM FROM HYDROCHLORIC ACID, BY 1-PHENYL, 3-METHYL, 4-BENZOYLPRAZOLONE(5), Gu Yidong, Song Yuan and Su Yaodang 339-340
FAR INFRARED SPECTRA OF SOME RARE EARTH EXTRACTANTS AND EXTRACTED COMPLEXES, Wu Jinguang, Shi Nai Jin Tianzhu, Chen Dian, Gao Hongcheng, Guo Hai, Weng Shifu and Xu Guangxian 341-342
EXTRACTION OF SALTS BY TBP CHARACTERIZATION OF THE EXTRACTED SPECIES, Jacques Ly, Claude M. Poitrenaud 343-344
CHARACTERIZATION AND REACTIVITY OF HYDROXY OXIME COMPLEXES OF COPPER AND NICKEL, M. E. Keeney and K. Osseo-Asare 345-346
SOLVENT EXTRACTION OF METAL PERCHLORATES WITH TRIOCTYLPHOSPHINE OXIDE, Satoshi Kusakabe and Tatsuya Sekine 347-348
INFLUENCE OF ELECTRONIC STRUCTURE OF NEUTRAL NITROGEN-CARBONYL-CONTAINING COMPOUNDS ON THEIR REACTIVITY IN EXTRACTION PROCESSES, B. N. Lascorin, G. M. Chumakova, L. I. Rusin, V. S. Uljanov 349-350

Plenary Lecture

ION-PAIR DISTRIBUTION OF ORGANIC COMPOUNDS IN SOLVENT EXTRACTION AND HIGH-PERFORMANCE LIQUID CHROMATOGRAPHY, Göran Schill 351-356

Metallurgical Extraction Processes - II (Process Chemistry)

NON-CHELATING OXIMES IN THE SOLVENT EXTRACTION OF BASE METALS, John S. Preston 357-358

THE DETERIORATION OF NICKEL EXTRACTANT LIX64N AND ITS REGENERATION, Mitsuo Takahashi, Takashi Ogata, Hiroshi Okino and Yoshibumi Abe 359-360
REMOVAL OF COPPER AND IRON FROM NICKEL AND COBALT SULFATE SOLUTION CONTAINING CHLORIDE ION BY EXTRACTION WITH QUATERNARY AMMONIUM CHLORIDE, Xue-xi Zhou, Quan ling Suo Tun Zhu and Shu-lan Huang 361-362

Characterization of Organic-Phase Species in Solvent Extraction Systems - II

X-RAY DIFFRACTION STUDIES OF THE STRUCTURES OF ORGANIC-PHASE SOLVENT-EXTRACTION COMPLEXES, John H. Burns 363-364
COEXTRACTION OF URANIUM AND TECHNETIUM IN TBP-SYSTEMS, T. N. Jassim, J. O. Liljenzin, R. Lundqvist G. Persson 365-366
SYNERGISM IN THE EXTRACTION OF ZINC(II) AND, CADMIUM(II) WITH LOWER FATTY ACIDS IN THE PRESENCE OF NITROGEN CONTAINING ORGANIC BASES, S. K. Gogia, D. Singh, O. V. Singh and S. N. Tandon 367-368
SOLVENT EXTRACTION OF METAL IONS BY IONIZABLE CROWN ETHERS, Richard A. Bartsch, Witold A. Charewicz and Sang Ihn Kang 369-370
THE APPLICATION OF LANTHANIDE INDUCED SHIFTS IN SOLUTION NMR STUDIES OF COORDINATED EXTRACTANTS, Dale G. Kalina and E. P. Horwitz 371-372

Solid-Supported Liquid Membranes - I

URANIUM RECOVERY WITH COUPLED-TRANSPORT MEMBRANES, Walter C. Babcock, Donald J. Kelly Dwayne T. Friesen 373
MODELING OF FACILITATED TRANSPORT IN HOLLOW FIBER TUBES, Richard D. Noble 374-375
ENRICHMENT AND SEPARATION OF METALS BY LIQUID MEMBRANE WITH TRI-n-OCTYLAMINE, Makoto Harada, Fumio Yamazaki, Motonari Adachi and Wataru Eguchi 376-377
PERMEATION RATE OF METAL SPECIES THROUGH SUPPORTED LIQUID MEMBRANES: DIFFUSIONAL AND CHEMICAL RESISTANCES WITH CATIONIC AND ANIONIC CARRIERS, P. R. Danesi, E. P. Horwitz and P. G. Rickert 378-380

Pharmaceutical and Biological Extraction Processes - I

USING GELS AS SIZE-SELECTIVE EXTRACTION SOLVENTS, E. L. Cussler and Marcus Stokar 381-382
THE EFFECT OF AQUEOUS ORGANIC ALCOHOL/AMINE SOLVENTS IN THE DELIGNIFICATION OF WOODY BIOMASS, Ramkrishna G. Nayak, Gary C. April, John K. McGee, Perry L. Daley, Jamal Meraab 383-384
EXTRACTION OF CHOLESTEROL FROM BLOOD USING LIQUID MEMBRANES, G. Yagodin, Yu Lopukhin, E. Yurtov T. Guseva, V. Sergienko 385-386
HIGHER YIELDS IN FURFURAL PRODUCTION BY USING SOLVENT EXTRACTION, G. Aly, R. Wennersten and G. Zacchi 387-388
PREPARATION OF L-AMINO ACIDS BY MEANS OF CONTINUOUS ENZYME-CATALYZED D,L-AMINO ACID, ESTER HYDROLYSIS INSIDE LIQUID SURFACTANT MEMBRANES, T. Scheper, W. Halwachs, K. Schügerl 389-390

Solid-Supported Liquid Membranes - II

MASS TRANSFER IN THREE-LIQUID-PHASE SYSTEMS, L. Boyadzhiev, Z. Lazarova, E. Bezenshek 391-392
MASS TRANSFER RATE THROUGH SOLID SUPPORTED LIQUID MEMBRANES. USE OF A TERTIARY AMINE SALT AS CARRIER OF METAL SPECIES FROM CHLORIDE MEDIA (1), R. Chiarizia, A. Castagnola 393-394
THE RECOVERY OF PLUTONIUM BY MEANS OF SOLID SUPPORTED LIQUID MEMBRANES, Giulio M. Gasparini Giuseppe Grossi, Maurizio Casarci and Armando D'Andrea 395-396
COUPLED TRANSPORT IN URANIUM EXTRACTION, T. J. Hardwick 397-398
LIQUID MEMBRANE STUDIES: TRANSPORT AGAINST THE CONCENTRATION GRADIENT OF $AuCl_4^-$, M. Burgard P. Elisoamiadana and M. J. F. Leroy and H. S. Park 399-400

Inorganic Extraction Processes - II

THE EXTRACTION OF IRON (III) FROM ALUMINIUM NITRATE SOLUTIONS WITH VERSATIC ACID, M. I. Stefanakis and A. J. Monhemius 401-402
SOLVENT EXTRACTION SEPARATION STUDY OF Fe(III) AND, Zn(II) FROM AQUEOUS SOLUTION WITH D2EHPA AND D2EHPA MIXED WITH TBP IN HYDROCARBON DILUENTS, Ying-Chu Hoh, Jin-Pang Wang and Tieh Ma 403-404
PROCESS DEVELOPMENT FOR THE COMPREHENSIVE UTILIZATION OF LUDWIGITE, Yu Da-Yue, Yang Xiao-Dong and Zhu Pin-Hua 405-406
STUDY OF SOLVENT-EXTRACTION OF PHOSPHORIC ACID WITH DBSO, Zhou Jian-Zhong, Jian Yu-Ming and Li Dao-Chun 407-408
MECHANISM OF SYNERGISTIC EXTRACTION OF RHENIUM(VII) BY PRIMARY AMINE & NEUTRAL PHOSPHORUS ESTER, Shu-chiou Yu and Chia-yung Chen 409-410
RECOVERY OF ACIDS AND REACTIONS IN CONCENTRATED AQUEOUS SOLUTIONS MEDIATED BY ACID-BASE SOLVENTS, Aharon M. Eyal, Klara Hajdu, Charles Appelbaum, Avraham M. Baniel 411-412

USE OF CONCENTRATED BRINE TO IMPROVE PHOSPHORIC ACID EXTRACTION, E. Ben-Yoseph, D. Kellerman D. Meyer, S. Wahrmann 413-414
THE LINEAR RULE OF INDIVIDUAL RARE EARTHS EXTRACTION, Li Han 415-416
MATHEMATICAL SIMULATION OF MIXED RARE EARTHS EXTRACTED WITH HEH (EHP), Li Han, Wan Xiong, Lin Suxian and Meng Shulan 417-418
SEPARATION AND PREPARATION OF GADOLIUM OF HIGH PURITY (99.99%) BY SYNERGIC EXTRACTION WITH QUARTERNARY AMMONIUM SALT AND TBP OR DI(1-METHYL-HEPTYL)METHYL PHOSPHONATE MIXED EXTRACTANTS, Chen Dian, Li Sengchung and Zhang Roufei 419-420
A PROCESS FOR THE DEPHOSPHORIZATION OF IRON ORES, I. Grenthe, M. Muhammed and Y. Zhang 421
PILOT-PLANT INVESTIGATION ON H_2SO_4 EXTRACTION BY ALCOHOLS FROM SPENT ELECTROLYTES, Dante Buttinelli, Carlo Giavarini, Andrea Mercanti 422-423

Analytical Chemistry - I

1-PHENYL-3-METHYL-4-ACYLOXIMEPYRAZOL-5-ONES AS CHELATING EXTRACTANTS, Amrit N. Patel 424-425
SOLVENT EXTRACTION OF METALS WITH SOME SCHIFF BASE LIGANDS, G. N. Rao and A. Varadarajulu 426-427
ON THE MECHANISM OF THE MUTUAL INFLUENCE OF METALS IN THEIR EXTRACTION WITH GAS NITRATES, Yu A. Zolotov, V. V. Bagreev and S. O. Popov 428-429
1-(2′-THIAZOLYLAZO)-2-NAPHTHOL AS EXTRACTIVE SPECTRO-PHOTOMETRIC REAGENT FOR SOME TRANSITION ELEMENTS, M. C. Eshwar, U. G. Gaokar and J. Krishnamacharyulu 430-431
SOLVENT EXTRACTION AT NEAR-NEUTRAL pH, Nandani Rajapakse and Harmon L. Finston 432-433
EXTRACTION AND BACK-EXTRACTION OF METALS WITH ORGANIC REAGENTS IN CHELATE EXTRACTION AND THE ION-ASSOCIATION EXTRACTION SYSTEMS, Honjo Takaharu 434
EXTRACTION CHROMATOGRAPHIC SEPARATION OF VANADIUM, MOLYBDENUM, GOLD AND GERMANIUM WITH TRIBUTYL PHOSPHATE, S. N. Bhosale and S. M. Khopkar 435-436
EXTRACTION SPECTROPHOTOMETRIC DETERMINATION OF PALLADIUM AS RESACETOPHENONEOXIMATE, G. R. Reddy and K. Saraswathi and S. Brahmaji Rao 437-438

Novel Extractants - II

SYNTHESIS OF SULFOXIDES AND THEIR STRUCTURE - REACTIVITY STUDIES ON THE LANTHANIDE EXTRACTION, Yuan Chengye, Long Haiyan, Ma Enxin, Chen Wuhua and Yan Xiamin 439-440
EXTRACTION OF U(VI) FROM NITRIC ACID BY DI(2-ETHYLHEXYL) SULFOXIDE, A PROMISING NEW BRANCHED-CHAIN EXTRACTANT, Bruce Moyer, W. J. McDowell and G. N. Case 441-442
N-NITROSO-N-CYCLOHEXYLHYDROXYLAMINE AS A REAGENT FOR THE GROUP SOLVENT METAL EXTRACTION, O. Petruchin and N. Kolycheva 443-444
NN′ DIALKYL ALIPHATIC AMIDES AS ALTERNATIVE EXTRACTANTS FOR ACTINIDES: FURTHER STUDIES ON THE INFLUENCE OF THE CHEMICAL STRUCTURE ON THE EXTRACTIVE BEHAVIOR, Giuseppe Grossi, Giulio M. Gasparini, Maurizio Casarci 445-446
DOAA—AN EXCELLENT NOVEL EXTRACTANT, Yuan Chengye, Tu Tongyan, Ma Enxin and Li Shusen 447-448
NEW BIDENTATE EXTRACTANTS FOR ACTINIDES(III) AND LANTHANIDES(III) SEPARATIONS FROM CONCENTRATED NITRIC ACID, C. Musikas, H. Hubert 449-450
OCTYL(PHENYL)-N,N-DIISOBUTYLCARBAMOYLMETHYLPHOSPHINE OXIDE AS AN EXTRACTANT FOR ACTINIDES FROM NITRIC ACID WASTE, E. P. Horwitz, H. Diamond, D. G. Kalina, L. Kaplan and G. W. Mason 451-452
CHEMISTRY OF CROWNETHER COMPLEXES OF ACTINIDES: INVESTIGATION ON THE EXTRACTION OF U(IV) AND U(VI) WITH CYCLOPOLYETHERS, Zhu Lin, Chen Shaojin, Feng Yijuin, Liu Zongquin, Chen Wenjuin 453-454
FURTHER STUDIES OF MACROCYCLIC COMPOUNDS AS SIZE-SELECTIVE SYNERGISTS IN SOLVENT EXTRACTION SYSTEMS, W. J. McDowell, G. N. Case, D. W. Aldrup 455-456

Analytical Chemistry - II

SEPARATION OF URANIUM ON POLYURETHANE FOAM IMPREGNATED WITH TRI-OCTYLPHOSPHINE OXIDE, J. Korkisch and I. Steffan 457
LIQUID ANION EXCHANGE EXTRACTION AND SEPARATION OF LANTHANIDES, V. M. Shinde 458-459
SULFOXIDES AS POTENTIAL EXTRACTANTS FOR ACTINIDES, J. P. Shukla, M. S. Nagar and M. S. Subramanian 460-461
EXTRACTION OF CHROMIUM(III) AND CHROMIUM(VI) INTO ORGANOPHOSPHORUS COMPOUNDS AND AMINE SYSTEMS, V. M. Rao and M. N. Sastri 462-463
EXTRACTION OF Sr AND Ba BY THE NITROBENZENE SOLUTION OF COBALT DICARBOLIDE IN THE PRESENCE OF ETHYLENOXIDE COMPOUNDS, E. Makrlik, P. Selucký, P. Vanura, J. Rais, M. Kyrš and I. Podzimek 464-465

Thermodynamics of Phase Equilibria in Solvent Extraction Systems - I

CORRELATION OF PHASE EQUILIBRIA IN THE WET-PROCESS PHOSPHORIC ACID/SULFURIC ACID/ISOBUTANOL SYSTEM, Steven J. Dougherty 466-467
LIQUID-LIQUID EQUILIBRIUM DATA FOR SYSTEMS CONTAINING HEAVY SOLVENTS, P. O. Ferreira, A. G. Medina 468-469
THE EXTRACTION OF IRON(III) FROM 6M HCl BY LONG CHAIN AMINES DISSOLVED IN CHLOROFORM, Robert W. Cattrall and Mirna Z. Ilic 470-471

THE EFFECT OF DILUENT FOR THE SEPARATION OF Zn(II) AND Pb(II) HALIDE COMPLEXES IN AMINE EXTRACTION SYSTEMS, Carlo Abbruzzese 472-473
THE PECULIARITIES OF ZIRCONIUM SULPHATE EXTRACTION BY PRIMARY AMINES, G. Yagodin, M. Mrnka, A. Chekmarev 474-475
THE CAUSE OF ZIRCONIUM (HAFNIUM) EFFECT ON HDEDHP EXTRALIABILITY, A. Afanasiev, O. Sinegribova, G. Yagodin 476-477
PERIODIC VARIATIONS OF LANTHANIDES SYNERGIC EXTRACTION BY THENOYLTRIFLUOROACETONE AND TRIPHENYLPHOSPHINE OXIDE MIXTURE, H. F. Aly, S. M. Khalifa and Nadia Zakareia 478-480
THE DETERMINATION OF THE ACTIVITY COEFFICIENTS OF TBP AND EXTRACTION COMPLEX $UO_2(NO_3)_2 2TBP$ IN VARIOUS SOLVENTS, Gao Hong-Cheng, Pen Qi-Ziu, Pen Li-E, Wang Wen-Qing and Hsu Kwang-Hsien 481-482
SYNERGISTIC EXTRACTION OF ABB AND ABC TYPES EXTRACTION MECHANISM OF URANIUM(VI) WITH TERNARY SYSTEM PMBP + TBP + ϕ_2SO AND PMBP + TBP + ϕ_4AsCl, Wang Wenqing, Yi Min, Chen Dinfong, Mou Xiru 483-484
EFFECT OF NONELECTROLYTES ON THE SOLVENT EXTRACTION OF URANYL AND NITRIC ACID BY TBP, J. Ortega and J. A. Suárez 485-486
DISTRIBUTION OF U(IV), U(VI), Pu(III), Pu(IV), AND NITRACID BETWEEN TRIBUTYL PHOSPHATE (TBP) IN, DODECANE AND AQUEOUS NITRATE SOLUTIONS, S. Tachimori and Z. Kolarik 487-488
EXTRACTION OF CHROMIUM (VI) BY TRI-n-DODECILAMONIUM CHLORIDE AND TRI-n-DODECILAMONIUM HYDROGENSULPHATE DISSOLVED IN BENZENE, A. Sastre, N. Miralles, M. Aguilar and M. Elizalde 489-490
ON THE AGGREGATION OF 5,8-DIETHYL-7-HYDROXYDODECAN-6-OXIME IN TOLUENE, M. Aguilar and M. P. Elizalde and J. M. Castresana 491-492
EXTRACTION OF Ni(II) BY 5,8-DIETHYL-7-HYDROXYDODECAN-6-OXIME IN MIXTURES WITH OTHER EXTRACTANTS AND TOLUENE, M. Aguilar and M. P. Elizalde and J. M. Castresana 493-494
EXTRACTION OF Co(II) - AND Zn(II) - THIOCYANATE COMPLEXES BY TRILAURILAMMONIUM NITRATE DISSOLVED IN BENZENE, J. M. Madariaga, R. M. Jiménez, M. D. Ruiz and M. Aguilar 495-496
EXTRACTION OF CADIUM(II) - CHLORIDE BY TRI-n-DODECYLAMMONIUM CHLORIDE DISSOLVED IN BENZENE, J. de Pablo and M. Aguilar and M. Valiente 497-498
CONCISE QUANTITATIVE DESCRIPTION AND PREDICTION OF LARGE FILES OF ANION-EXCHANGE EXTRACTION CONSTANTS FOR VARIOUS ANIONS BY MEANS OF LINEAR FREE ENERGY EQUATIONS, V. S. Shmidt, E. A. Mezhov K. A. Rybakov 499
PREDICTION OF DILUENT NATURE INFLUENCE ON PHYSICAL PARTITION BY MEANS OF BP*-PARAMETERS, V. S. Shmidt K. A. Rybakov 500
THE THERMODYNAMICS OF THE EXTRACTION OF Eu(III) AND Am(III) WITH SYNERGISTIC MIXTURES OF THENOYLTRIFLUOROACETONE AND A LINEAR POLYETHER, D. D. Ensor and A. H. Shah 501-502
QUANTITATIVE TREATMENTS OF DISTRIBUTION EQUILIBRIA IN EXTRACTION METAL SALTS BY ALCOHOL, G. Yagodin B. Sergievsky, O. Kunelskaya 503-504

Pharmaceutical and Biological Extraction Processes - II

EXTRACTIVE BIOCONVERSIONS, Hydrolysis of starch in an aqueous two phase system, Ronald Wennersten, Folke Tjerneld, Mats Larsson and Bo Mattiasson 505-506
INVESTIGATION OF ETHANOL EXTRACTION FROM FERMENTATION LIQUORS, G. Zacchi, G. Aly and R. Wennersten 507-508
FACTORS INFLUENCING SOLVENT SELECTION FOR EXTRACTION OF ETHANOL FROM AQUEOUS SOLUTION, Curtis L. Munson and C. Judson King 509-510
EXTRACTION OF ETHANOL FROM WATER WITH LIQUID PROPYLENE, John G. Victor 511-512
LIQUID-LIQUID EXTRACTION: A PROCESS FOR RECOVERY OF ORGANONITROGEN COMPOUNDS AND POLLUTION CONTROL, Teh C. Lo 513-514
THE APPLICATION OF DUAL-SOLVENT EXTRACTION TO THE REFINING OF A COMPLEX NATURAL SYSTEM, J. J. Warner and I. J. Harris 515-516
STUDY ON EXTRACTION OF CITRIC ACID, Jian Yu-Ming, Li Dao-Chen and Su Yuan-Fu 517-518

Extraction with Supercritical and Near-Critical Solvents - I

PLANTS AND PROCESS ENGINEERING FOR HIGH-PRESSURE EXTRACTION OF NATURAL PRODUCTS, E. Lack, G. Bunzenberger, R. Marr 519-520
MASS TRANSFER FROM SOLID MATERIAL IN GAS EXTRACTION, G. Brunner 521
RESIDUUM OIL/PROPANE-PHASE EQUILIBRIUM UNDER SUPERCRITICAL CONDITIONS, H. H. Oelert, U. Lutz 522

Fuel and Chemical Extraction Processes - II

SELECTIVE SOLUBILIZATION IN AQUEOUS MICELLAR SOLUTIONS, E. Ruckenstein and R. Nagarajan 523-524
SIMULTANEOUS STRIPPING AND EXTRACTION FOR RECOVERY OF AMMONIA FROM SOUR WATER, Patricia D. Mackenzie and C. Judson King 525-526

INVESTIGATION OF PARAMETERS AFFECTING ATMOSPHERIC EXTRACTION YIELDS AND EXTRACT QUALITIES OF TWO TURKISH LIGNITES, Türker Gürkan and Sedat Gürer 527-528
ALTERNATIVE METHOD FOR POLYAMINE SALTS SYNTHESIS, K. Y. Lee 529

Metallurgical Extraction Processes - III (Process Development)

THE SOLVENT EXTRACTION OF GOLD FROM AUROCYANIDE SOLUTIONS, Michael B. Mooiman, Jan D. Miller and Maribel M. Mena 530-531
RECUPERATION AND SEPARATION OF COPPER AND ZINC FROM CYANIDE ELECTROPLATING EFFLUENTS BY SOLVENT EXTRACTION, P. Van Acker, M. Verhaege, A. Van Peteghem, L. Gyselinck 532-533
PROCESS FOR RECOVERY OF COPPER FROM AMMONIACAL ETCH LIQUOR USING A MIXED EXTRACTANT, G. M. Ritcey and E. W. Wong 534-535
EXTRACTION OF CUPRIC CHLORIDE FROM IRON CHLORIDE LEACH LIQUORS, T. Danielssen, G. H. Bøe, P. M. Finne 536

Thermodynamics of Phase Equilibria in Solvent Extraction Systems

PHASE EQUILIBRIA IN MULTICOMPONENT SOLVENT EXTRACTION SYSTEMS, J. E. Alter and R. Blumberg 537
PHASE EQUILIBRIA IN SOLVENT EXTRACTION - THERMODYNAMIC DESCRIPTION, Alexander Apelblat 538-539
REVIEW OF THE THERMODYNAMICS OF SYNERGISM, Gregory R. Choppin 540-541
THERMODYNAMICS OF THE EXTRACTION OF Hf(IV) WITH ACETYLACETONE, Robert F. D. Lundqvist 542-543
PREDICTION OF TERNARY LIQUID-LIQUID EQUILIBRIA, Ireneo Kikic, Paolo Alessi, Romano Lapasin, Maurizio Fermeglia 544-545
PREDICTION OF TWO-PHASE EQUILIBRIUM DATA AND DETERMINATION OF ACTIVITY COEFFICIENTS IN SOLVENT EXTRACTION OF METALS BY AN IMPROVED SCATCHARD-HILDEBRAND MODEL, Teng Teng Li Yi-gui, Han Jin-wen, Ding Hong-bing 546-547

Analytical Chemistry - III

EXTRACTION OF TRIVALENT ACTINIDES WITH 1-PHENYL-3-METHYL-4-(3:5-DINITROBENZOYL) PYRAZOLONE-5 AND ITS SYNERGISTIC MIXTURES WITH NEUTRAL DONORS, P. K. Khopkar and J. N. Mathur 548-549
COLUMN EXTRACTION CHROMATOGRAPHY: A USEFUL TOOL FOR THE SEPARATION AND DETERMINATION OF RADIONUCLIDES IN ENVIRONMENTAL AND BIOLOGICAL SAMPLES, Corrado Testa 550-551
EXTRACTION AND COMPLEX FORMATION OF PLUTONIUM (IV) WITH 1-PHENYL-2-METHYL-3-HYDROXY-4-PYRIDONE (PMHP), M. J. Herak and Z. Kolarik 552-553
EXTRACTION COLORIMETRIC AND FLUORIMETRIC DETERMINATION OF ALKALI AND ALKALINE EARTH METAL IONS USING CROWN ETHER-BASED ORGANIC REAGENTS, Makoto Takagi, Hiroshi Nakamura and Keihei Ueno 554-555

Extraction with Supercritical and Near-Critical Solvents

SOME EXTRACTIONS AND SEPARATIONS WITH CARBON DIOXIDE AT NEAR-CRITICAL CONDITIONS, T. R. Bott M. B. King and D. M. Kassim 556-557
SELECTION OF SOLVENTS FOR SUPERCRITICAL EXTRACTION, Gerd Brunner and Siegfried Peter 558-559

THE RELATIVE IMPORTANCE OF DIFFUSION AND CHEMICAL REACTIONS IN LIQUID-LIQUID EXTRACTION KINETICS

Pier Roberto Danesi

Chemistry, Division, Argonne National Laboratory
Argonne, Illinois 60439 USA

INTRODUCTION

The kinetics of solvent extraction of metal species is in general a function of both the kinetics of the chemical reactions occurring in the system and the rates of diffusion of the species present in the two phases. In fact, since the final products of the extraction process are in a chemical state different from that of the starting materials, it follows that rupture and formation of chemical bonds occur during the extraction. As a consequence whenever one or more reaction steps of the overall reaction mechanism, either occurring in the bulk phases (homogeneous reaction) or at the liquid-liquid interface (heterogeneous reaction) are slow enough, their slowness will reflect in the overall rate of extraction. In addition, since chemical species are transferred from one phase into another, the transport of material from the bulk of the phases to and from the interface is another very important factor to be taken into consideration. This means that diffusion processes can be also rate determining. However, since in most of the extraction processes having some practical interest the two phases are more or less efficiently stirred, the diffusion processes are generally limited to a zone located in the immediate proximity of the interface. Two stationary liquid layers, one on the aqueous side and the other on the organic side of the interface (Figure 1) then control the diffusional processes. The thickness of these two stationary layers, also called diffusion films, is of course a function of the hydrodynamic conditions inside the apparatus where the extraction takes place. Only when the hydrodynamics is such that this thickness can be assumed equal to zero, does the diffusional contribution to the rate of extraction completely disappear. It is worth mentioning that many physicochemical properties of the region very close to the interface, such as viscosity, dielectric constant, density, etc., can be appreciably different from those of the bulk phases. Unfortunately very little is known about these properties. Nevertheless, some information on the interface can be obtained from interfacial viscosity, interfacial potential, interfacial polarity and interfacial tension measurements. However, with the exception of the interfacial tension, such measurements are difficult to perform and the interpretation of the results obtained is still open to discussion. Interfacial tension studies are in this respect an exception and they are particularly important since they can provide useful information about the interfacial concentration of the extracting reagent. In fact, as a general rule, extracting reagents are good surfactants because of their simultaneous hydrophilic-hydrophobic nature. It follows that, as a result of their surface-active nature, the interfacial concentrations of the extracting reagents can be remarkably high. This fact is of particular relevance since it can favor the occurrence of interfacial reactions. In turn when these reactions are sufficiently slow, they show up as an interfacial resistance. If on the other hand, the chemical reactions, irrespective of their locale, are sufficiently fast, the extraction process is rate determined only by the diffusion processes occurring in the two diffusion films. In this case the extraction process is said to occur in a "diffusional regime." At the other extreme, when the diffusional processes can be considered practically instantaneous with respect to the chemical reactions, the extraction process is considered entirely chemically controlled and to occur in a so-called "kinetic regime." In this case to describe the extraction kinetics information is needed about the rates at which the various chemical species react. Only in this instance the solvent extraction kinetics can be treated entirely in terms of chemical kinetics. Unfortunately, in practical experimental work it is often difficult to draw a sharp line between these two limiting cases. In fact, although criteria that can help to distinguish between kinetically-controlled and diffusion-controlled processes have been reported (1,4), they are often difficult to apply and do not always lead to a completely unambiguous picture. It follows that in many experimental studies the simultaneous presence of mixed diffusional-kinetic regimes cannot be excluded. In this case to fully describe the extraction kinetics it is necessary to solve simultaneously the differential equations which describe the diffusion and the chemical kinetics (4). The "mixed regime" can then be described as a case of mass transfer with slow chemical reactions. Here the rates of diffusion and of the chemical reactions can never be neglected with respect to each other. Finally it has to be mentioned that it is generally very difficult to draw conclusions on the nature of the extraction regime only on the basis of the experimentally observed laws which correlate the rate of extraction with the chemical composition or the concentration variations with time. In fact these laws are often the same even when very simple diffusional or kinetic processes are involved.

In the present paper the main criteria which have been generally used to evaluate the relative importance of diffusion and chemical reactions in liquid liquid extraction kinetics are briefly reviewed.

CRITERIA USED TO IDENTIFY THE EXTRACTION REGIME

The criteria which have been used to distinguish between a diffusional regime and a kinetic regime are (1,4):

1) dependency of the rate of extraction on the rate of stirring of the two phases,

2) comparison between the heat transfer coefficient and the mass transfer coefficient,

3) evaluation of the activation energy.

*Work performed under the auspices of the Office of Basic Energy Sciences, Division of Chemical Sciences, U. S. Department of Energy under Contract W-31-109-ENG-38.

Criteria 2) and 3) are difficult to apply and have been only occasionally used to evaluate the extraction regime. According to 2), when the same dependence of the heat transfer coefficient and mass transfer coefficient on the stirring rate of the phases is observed the conclusion can be reached that the extraction occurs in a diffusional regime. Apart from the several experimental difficulties associated with the measure of the heat transfer coefficient, this criterion seems to suffer from the main drawback that in a multicomponent system, undergoing chemical reactions, the "true" heat transfer coefficient of the extracted species is often hard to separate from the heat transfer coefficient of other chemical species. As far as criterion 3) is concerned, the same criticism holds. Furthermore there are many cases where the chemical changes associated with liquid-liquid extraction processes are characterized by the same values of the activation energies as diffusional processes. Criterion 1) seems by far the simplest one to use and this is proved by the large number of investigators who have used it. In general a process occurring in a diffusional regime is characterized by an increase of the rate of extraction as long as the stirring rate of the two phases is increased (Figure 2, Zone A). When on the other hand the rate of extraction is independent of the stirring rate (Figure 2, Zone B) it is sometimes possible to assume that the extraction process occurs in a kinetic regime. The rationale behind this criterion is that an increase in stirring rate produces a decrease in thickness of the diffusion films (Figure 1). Consequently the rate of extraction increases as long as a process is diffusion controlled. When eventually the thickness of the diffusion films is reduced to zero only chemical reactions can be rate controlling and the rate of extraction becomes independent of the stirring rate. This kind of reasoning has been applied both to vigorously stirred reactors, where the two phases are highly interdispersed, and to constant interfacial area stirred cells. However in both cases the criterion can lead to erroneous conclusions. In the case of constant interfacial area stirred cells, while Zone A is certainly an indication that the process is occurring in presence of diffusional contribution, the opposite is not true for Zone B. In fact it may occur that in spite of the increased stirring rate the thickness of the stagnant diffusion films does not further decrease. This "slip effect" can therefore simulate a kinetic regime.

As far as vigorously stirred reactors are concerned strong ambiguities are also present when applying criterion 3). In fact, unless the overall interfacial area is known and taken into consideration when evaluating the rate of extraction, an increase in the rate of extraction with the stirring rate can take place when the system is in a kinetic regime determined by an interfacial chemical reaction. The increase observed in Zone A in this case indicates an increase in the number of droplets of the dispersed phase and not a decrease in the thickness of the diffusion film. Moreoever, the plateau region of Zone B does not necessarily prove that the extraction occurs in a kinetic regime. In fact, although at high stirring rates eventually the number of droplets of the dispersed phase becomes constant, since the rate of formation equals the rate of coalescence, lack of internal circulation and poor mixing can occur inside the droplets of the dispersed phase. This is particularly true with small droplets and in the presence of extractants which are strong surfactants. It follows then that also in this case a plateau region can simulate a diffusional regime.

SIMULATION OF INTERFACIAL REACTIONS BY DIFFUSION

A further ambiguity on the kind of regime which controls the rate of extraction is obtained when one tries to derive conclusions on the basis of the observed dependency of the rate of extraction on the concentration of the species involved in the extraction process. As a typical example of this ambiguity we will describe the case of diffusion mimicing an interfacial two-step chemical reaction (3). This latter mechanism basically consists of the following steps:

a) formation of an interfacial complex between the interfacially adsorbed molecules of the extractant and the extractable metal species,

b) transfer of the interfacial complex from the interface to the bulk organic phase and simultaneous replacement of the interfacial vacancy with bulk organic molecules of the extractant.

The mechanism is described by the following equations:

$$A^+ + (BH)_i \underset{k_{-1}}{\overset{k_1}{\rightleftharpoons}} (AB)_i + H^+ \tag{1}$$

$$(AB)_i + \overline{BH} \underset{k_{-2}}{\overset{k_2}{\rightleftharpoons}} (BH)_i + \overline{AB} \tag{2}$$

$$r_i^o = \frac{k_1'[A^+][\overline{BH}]}{[H^+](k_{-2}/k_2) + [\overline{BH}]} \left(\frac{Q}{V}\right) \tag{3}$$

$$k_1' = k_1[(BH)_i] \tag{5}$$

A^+ represent the extractable metal cation, BH the extracting reagent, sub-

script i indicates interfacially adsorbed species, the bar indicates organic species, r_i^o is the initial rate of extraction and (Q/V) is the ratio between the interfacial area and the volume of the aqueous phase. With most of the strong surface-active extractants used in practice k_i' is a constant when the bulk concentration exceeds 10^{-3} M.

The dependence of the interfacial flux $J_o = r_i^o \times (V/Q)$ on $[\overline{BH}]$ and $[H^+]$ is shown in Figure 3. This kind of dependency has been observed in many extraction kinetics studies performed with constant interfacial area stirred cells (4).

When the extractant is at least in part solubilized in the aqueous phase the alternative mechanism can occur:

a) fast partitioning of the reagent between the organic and aqueous phase,

b) slow formation of an aqueous phase complex between the metal and the reagent,

c) fast partitioning of the metal complex between the aqueous and the organic phase.

In this case the mechanism is described in the following equations:

$$A^+ + BH \underset{k^*_{-1}}{\overset{k^*_1}{\rightleftharpoons}} AB + H^+ \tag{4}$$

$$K_p = [\overline{BH}]/[BH] \tag{5}$$

$$r_a^o = \frac{k_1^*}{K_p}[A^+][\overline{BH}] \tag{6}$$

r_i^o and r_a^o have the same dependency on $[\overline{BH}]$ and $[H^+]$ at low extractant and high acid concentration. Nevertheless, a distinction between the two kinetic regimes can be made by operating in a wide range of concentrations and by studying the influence of Q/V on the extraction rate. On the other hand, a real ambiguity about the mechanism exists if the stirring of the system is not sufficient to substantially reduce the thickness of the diffusion film and an aqueous phase reaction, such as (4), is occurring on the aqueous side of the interface. In this case the diffusional contribution can give rise to a rate equation identical to (3). The equation describing the extraction rate, derived in reference (3), is:

$$r_d^o = \left(\frac{D}{\delta}\right)\left(\frac{Q}{V}\right)\frac{[A]\,[\overline{BH}]}{[H^+]\,K_e^{-1} + [\overline{BH}]} \tag{7}$$

where (D/δ) is an average diffusional parameter equal to the ratio between the diffusion coefficient and the thickness of the diffusion film, and

$$K_e = \frac{k_F}{k_R} = \frac{k_1^*\,K_p(BH)}{k_{-1}^*\,K_p(AB)} \tag{8}$$

$$K_p(BH) = [\overline{BH}]/[BH],\ K_p(AB) = [\overline{AB}]/[AB] \tag{9}$$

A comparison between equations (7) and (3) shows that the extraction rates have exactly the same kind of dependency on [BH], $[H^+]$ and (Q/V). It follows that, because of insufficient mixing of the two phases, a diffusional contribution coupled to a one-step chemical reaction occurring on the aqueous phase of the interface can mimic an interfacial two-step reaction.

The above reported discussion seems to lead to rather pessimistic conclusions about the possibility of definitely identifying the extraction regime. However, the situation improves when more than only a single criterion is used. Moreover, the knowledge of the chemical properties of the system can be sometimes of great help in understanding whether the extraction process is occurring in a diffusional or kinetic regime. In general, extractants reacting through a chelation mechanism, which implies the dehydration of the metal cation, and extractable metals exhibiting very low rates of water exchange (Cr^{+3}, Al^{+3}, Fe^{+3}, etc.) favor kinetic regimes, providing suitable hydrodynamic conditions are present. In fact in these cases the Eigen-Wilkins mechanism (5), consisting of the rapid formation of an outer-sphere association complex followed by the slow substitution of a water molecule of the primary coordination sphere with the ligand, generally holds. This I_d mechanism (dissociative interchange mechanism) leads to slow rates of complex formation with metal ions characterized by low rate constants of water exchange. Moreover, if the extractant exhibits high interfacial concentrations and very low aqueous solubilities, the kinetic regime can be determined by interfacial reactions. In this case the same direct proportionality between the (Q/V) ratio and the extraction rate, as observed with diffusion controlled process, must be experimentally measured.

AN EXAMPLE OF A METAL EXTRACTION PROCESS OCCURRING IN A KINETIC REGIME

As an example of a system where the extraction of a metal species is very likely to take place in a kinetic regime we can quote the extraction of Fe^{+3} from aqueous nitrate solutions by toluene solutions of tri-n-butylaceto hydroxamic acid (6) (hereafter HX). In this case the extraction kinetics were studied in a highly stirred tank at 2,150 rpm, where the two phases were completely dispersed. Furthermore, the extracting reagents bind to the metal forming a hexacoordinated chelated species. In this chelation process the six water coordination molecules of Fe(III) are replaced with three C=O and three N-O$^-$ groups. This ligand exchange reaction was shown to occur very slowly also with water soluble hydroxamic acids. The slow chemical reaction is caused by the low value of the rate constant of water exchange (1.5×10^2 sec^{-1}) of Fe^{+3}. Furthermore, HX shows appreciable interfacial activity (Figure 4) and an organic/water partition coefficient $K_p = 40$. It follows that a kinetic regime characterized by slow chemical reactions is very likely to occur under vigorous mixing conditions. The type of rate of extraction vs extractant concentration dependencies that we can expect in the case of a kinetic regime when, for the sake of simplicity, the contribution of the $FeOH^{2+}$ species (enough acid to suppress hydrolysis is present) and of the backreaction (the rates are extrapolated to time zero), are not considered are the following.

A. Aqueous phase kinetic regime. In this instance the equations which describe the system are

$$Fe^{+3} + HX(water) \xrightarrow{k_a} FeX^{+2} + H^+ \tag{10}$$

$$r_a^o = \frac{k_a}{K_p}[Fe^{+3}][\overline{HX}] \tag{11}$$

$$K_p = [\overline{HX}]/[HX] = 40 \tag{12}$$

The expected dependency of r_a^o on $[\overline{HX}]$ is shown in Figure 5A.

B. Interfacial kinetic regime. The equations which describe the system are:

$$Fe^{+3} + HX_{(interfacial)} \xrightarrow{k_i} FeX^{+2}_{(interfacial)} + H^+ \tag{13}$$

$$r_i^o = k_i\left(\frac{Q}{V}\right)[Fe^{+3}][(HX)_i] = k_i'\left(\frac{Q}{V}\right)[Fe^{+3}] \tag{14}$$

$$k_i' = k_i[(HX)_i] \tag{15}$$

The data of Figure 4 indicate that $[(HX)_i]$, the interfacial concentration of HX, becomes constant when $[HX] > 10^{-3}$ M. Before saturation of the interface the interfacial concentration is instead given by

$$[(HX)_i] = \frac{[\overline{HX}]\,\theta}{1 + [\overline{HX}]\,\theta} \tag{16}$$

where θ is a Langmuir adsorption constant. The expected dependency of r_i^o on [HX] is shown in Figure 5B.

C. Aqueous phase-interfacial kinetic regime. In this case the overall rate of extraction will be simply the sum of r_a^o and r_i^o, i.e.:

$$r^o_{total} = r_a^o + r_i^o = [Fe^{+3}]\left(\frac{k_a}{K_p}[\overline{HX}] + k_i'\frac{Q}{V}\right) \tag{17}$$

The expected dependency of r^o_{total} on $[\overline{HX}]$ is shown in Figure 5C. The experimental dependency of the initial extraction rate, divided by the initial Fe(III) concentration, on the organic HX monomer concentration is shown in Figure 6. The plot clearly indicates that the overall rate data fall on a straight line not going through the origin of the axes and supports a mixed contribution of a slow aqueous phase and interfacial chemical reaction. The slope of the straight line and k_p allow one to evaluate $k_a = 11$ ($M^{-1}\cdot sec^{-1}$). This value is in very good agreement with the literature values (7) of the rate constants of many Fe(III) ligand substitution reactions. This result gives further support to the proposed mechanism which assumes that the extraction process is entirely occurring in a kinetic regime.

REFERENCES

1. C. Hanson, Recent Advances in Liquid-Liquid Extraction, C. Hanson, Ed., Pergamon Press, Oxford, 1971, Chap. 12.
2. D. A. Frank-Kamenetskii, Diffusion and Heat Transfer in Chemical Kinetics, Plenum Press, New York (1969).
3. P. R. Danesi, G. F. Vandegrift, E. P. Horwitz, and R. Chiarizia, J. Phys. Chem. 84, 3582 (1980).
4. P. R. Danesi and R. Chiarizia, The Kinetics of Metal Solvent Extraction, CRC Critical Reviews in Analytical Chemistry, CRC Press, Vol. 10 No. 1 (1980).
5. M. Eigen and R. W. Wilkins, Mechanism of Inorganic Reactions, Advances in Chemistry Series, No. 49, Am. Chem. Soc., Washington, D. C. (1965).
6. R. Chiarizia, P. R. Danesi, and S. Fornarini, J. inorg. Nucl. Chem. 41, 1465 (1979).
7. A. E. Martell, Editor, Coordination Chemistry, Vol. 2, ACS Monograph 174, Washington, D. C. (1978).

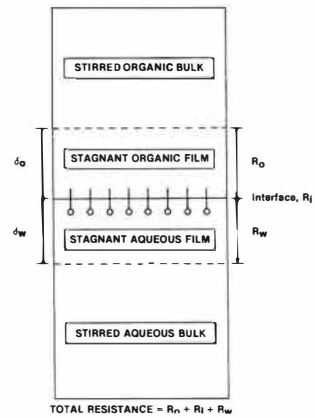

FIGURE 1. SCHEMATIC DESCRIPTION OF A TWO-PHASE LIQUID SYSTEM. DIFFUSIONAL FILMS AND INTERFACIALLY ADSORBED EXTRACTANT MOLECULES ARE SHOWN.

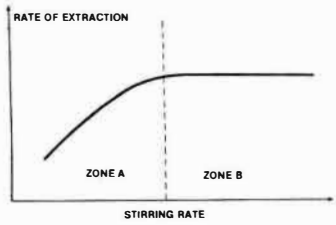

FIGURE 2. TYPICAL RATE OF EXTRACTION VS STIRRING RATE CURVE.

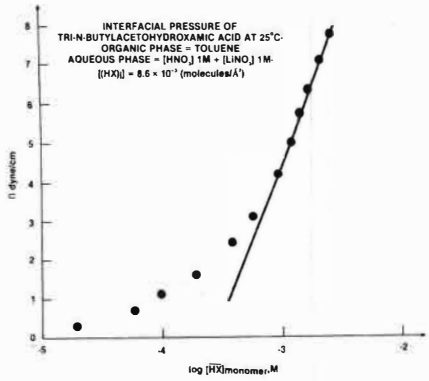

FIGURE 4. INTERFACIAL PRESSURE VS EXTRACTANT CONCENTRATION.

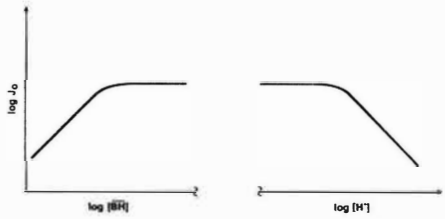

FIGURE 3. INITIAL INTERFACIAL FLUX VS CONCENTRATION FOR INTERFACIAL TWO-STEP REACTIONS.

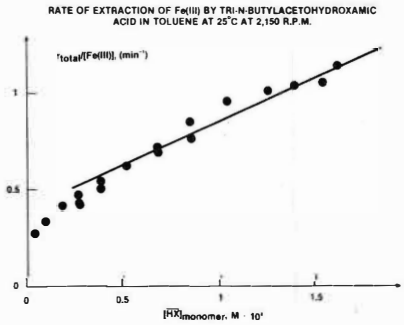

FIGURE 5. RATE OF EXTRACTION VS EXTRACTANT CONCENTRATION FOR AQUEOUS AND INTERFACIAL REACTIONS.

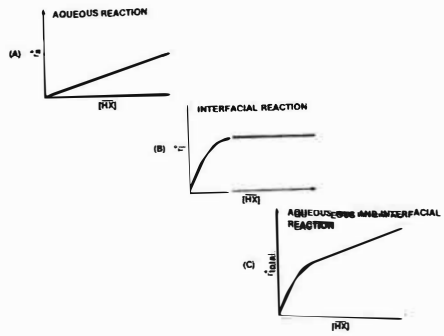

FIGURE 6. RATE OF EXTRACTION OVER Fe(III) CONCENTRATION VS EXTRACTANT CONCENTRATION.

THE ROLE OF THE INTERFACE IN THE EXTRACTION OF METAL CHELATES

Henry Freiser

The University of Arizona
Tucson, Arizona 85721 USA

Our study of the kinetic aspects of metal chelate extractions has addressed itself to resolution of questions of both fundamental and practical interest. Some of the questions include: How are extraction rates affected by structural changes in the extractant? How large is the effect of ligand structure on reaction rates of metal chelate formation and dissociation? Does the nature of the rate-limiting step, i.e. the mechanism, change as the molecular weight and, therefore, the hydrophobicity of the extractant increases? When, if ever, does the liquid-liquid interface become significant? In this report, our efforts to determine the role of the interface in metal chelate extraction will be described.

Since its introduction in 1962 (1),the method of determining the kinetics of inherently rapid reactions via solvent extraction has not attracted many users. Aside from Zangen who used this approach to determine the kinetics of the formation of Hg(II) bromide complexes(2), Haraguchi, in the determination of the kinetics and mechanism of Ni complexes of 8-quinolinol(3), 2-(2-thiazolylazo)-4 methylphenol, and 1-(2-thiazolylazo)-2-naphthol (4),and two kinetic studies of organic reactions,rapid hydrolysis of esters (5),and carbonium ion reactions (6), we remain essentially the sole practitioners of this method. For this reason,some attention here to the methodology and its evolution would seem to be in order.

Simply expressed, under conditions of vigorous shaking(1,7) or high speed stirring (8,9), mass transfer rates in metal chelate solvent extraction processes are much faster than chemical reaction rates, particularly when, by means of favorable distribution characteristics, the concentration of one of the reactants is very low. It is axiomatic that in any multistep process, the overall kinetics of the process gives information about the slowest,i.e.,the rate-determining step(rds). We have employed this approach using the classical Morton flask assembly(10) with stirring speeds of up to 20,000 rpm. Our apparatus (8) is always operated on the plateau of extraction rate vs. stirring speed where further stirring energy does not reduce drop size of the dispersed phase but simply contributes to the overall convective movement in the reaction flask. The data we obtain are highly reproducible and almost always result in simple experimental rate expressions having very nearly integral reaction orders.

In contrast, others interested in mass transfer kinetics in liquid-liquid distribution systems almost invariably start by considering diffusion as the primary source of 'resistance' and then modify this concept to include slow chemical reaction kinetics as added 'resistances', usually without attempting to account quantitatively for the reaction rate constants. These workers tend to favor experiments in which the interfacial area is fixed. Fixed interfacial area designs (11-16) are rooted in the assumption that the reaction is either diffusion or interfacially controlled. Inasmuch as rate constraints of such reactions must be expressed in terms of unit interfacial area, fixed interface experiments permit this measurement to be made. This has not been considered to be possible with high dispersion experiments because the interfacial contact area is unknown. Most fixed interface experiments have been performed with either a single drop in a continuous phase or a Lewis cell. In the single drop method a droplet of one phase is allowed to rise (or fall) through a column containing the second phase. This approach has been criticized for not overcoming diffusion effects in the droplet. The Lewis cell is designed so that both phases stand in contact with each other while each phase is stirred separately. Stirring supposedly overcomes diffusion problems by replenishing the interface with reactant from each bulk phase. Nevertheless, since the vigor of the stirring must be severely limited to avoid vortex formation, mass transfer effects are certainly not eliminated.

Extraction kinetics studies involving high dispersion is achieved by vigorous shaking or stirring of the two phases(1,7,8,9,23). These experiments are capable of attaining the fastest extraction rates. From the point of view of a mechanism in which a homogeneous chemical reaction is the rds, a high dispersion is needed to reduce the time required for mass transfer processes so that diffusion effects are not involved in the observed reaction velocity and rate equations. In the case of an interfacial mech- anism, a high dispersion maximizes the interfacial surface area, leading to a faster rate. Recently, Tavlarides (17) has critically reviewed most of the previous high dispersion and fixed interface experimental techniques and concluded each of them was seriously compromised.

One unequivocal way in which to resolve these controversies or at least to validate our own experimental approach to extraction kinetics, would be to compare the values of the chemical reaction rate constants derived from our experiments with those obtained elsewhere in the chemical literature. Yet another mode of resolution of these problems, particularly that designed to clarify the role of the interface, would be to develop an experimental configuration in which results obtained with little or no interfacial region, could be compared with those obtained with a large (and reasonably constant) interfacial region. Recently, we have developed just such a measurement system which is based on the use of a selective Teflon phase separator which permits the sampling of the organic phase while it is still intimately mixed with the aqueous phase under high-speed stirring conditions (18). With the help of this automated extraction apparatus, we have studied the pH dependence of the equilibrium distribution of dithizone and a series of alkyl derivatives as will be described in greater detail below. We are able by these means to distinguish between those systems in which surface active components are present and those which are not. When they are present, quantitative evaluation of the role of the interface can be made.

Recently, we conducted a detailed study of the kinetics of extraction of Cu(II) with aromatic and aliphatic hydroxyoximes, which were introduced in the 1960's by General Mills for the large scale extraction of copper. Our earlier work suggests that with extractants of higher molecular weight and hence of larger K_{DR} values, the observed rates of inherently faster metal substitution reactions, e.g. those of Cu^{2+} will become slow enough to be accessible to the solvent extraction technique. Furthermore, the kinetics of copper-LIX extractions are of great practical importance and have already been the subject of some study. Our interest in these systems was further enhanced by the wide spread claim that the mechanism of such systems, unlike those we studied, involve a slow interfacial reaction.

Most of the theoretical studies have been performed with 2-hydroxy-5-nonylbenzophenone oxime (LIX65N) and 5,8-diethyl-7-hydroxydodecan-6-one oxime (LIX63). Previous workers, pointing to the low aqueous solubility of the LIX reagents, almost invariably discard the possibility of chelate formation in the aqueous phase and propose that interfacial reaction kinetics, rather than homogeneous chemically controlled rates, are dominant. Thus, in a review of the kinetics and mechanisms of Cu(II) by the LIX reagents, Flett(19) simply asserted that because these reagents are "so hydrophobic", their aqueous phase solubility could be ignored. This, without any attempt to measure phase distribution constants! Adopting this stance, when chemical parameters appeared in the extraction rate expressions, these investigators naturally invoked an "interfacial reaction" as the rds in developing a mechanism.

We first determined the distribution equilibrium of LIX65N between chloroform and water to be $10^{4.6\pm0.3}$ (9) which is significantly less than that of dithizone, an extractant whose kinetic behavior has been accepted as proceeding through an aqueous phase mechanism. On the basis of our kinetic data the rate expression for the extraction of copper by LIX65N can be quantitatively described by the following expression:

$$-\frac{d[Cu^{2+}]}{dt} = k' \frac{[Cu^{2+}][HL]_o^2}{[H^+]} \qquad (6)$$

where HL represents LIX65N.
It is noteworthy that all of the experimentally observed orders are integers.

From this experimental rate expressions the following mechanism may be deduced:

$$HL(o) \underset{}{\overset{K_{DR}^{-1}}{\rightleftharpoons}} HL \qquad \text{fast} \qquad (7)$$

$$Cu^{2+} + HL \overset{\beta_1 K_a}{\rightleftharpoons} CuL^+ + H^+ \qquad \text{fast} \qquad (8)$$

$$CuL^+ + HL \overset{k_1}{\rightleftharpoons} CuL_2 + H^+ \qquad \text{slow} \qquad (9)$$

$$CuL_2 \overset{K_{DC}}{\rightleftharpoons} CuL_2(o) \qquad \text{fast} \qquad (10)$$

where K_{DR} and K_{DC} represent the distribution constants of ligand and chelate, K_a the acid dissociation constant of LIX65 and β_1 the equilibrium formation constant of CuL^+ from Cu^{2+} and L^{-1}. The overall extraction rate, under conditions where extraction is essentially complete at equilbrium, would be determined by the rate of the slow (eq.9):

$$-\frac{d[Cu^{2+}]}{dt} = k_1 [CuL^+][HL] \qquad (11)$$

By substituting appropriate equilibrium expressions from (7) and (8) into (11), one obtains

(12)

in which the observed dependence on metal ion, ligand and pH are explained. Further, the observed reaction rate constant, k', is seen to be

$$k' = \frac{k_1 \beta_1 K_a}{K_{DR}^2} \qquad (13)$$

Although, unfortunately, the formation equilibria of Cu^{2+} LIX65N have not been studied, a reasonable approximately of $\beta_1 K_a$ (to within about one order of magnitude) can be estimated from values obtained with salicylaldoxime, a closely related ligand. In fact, inasmuch as within a given ligand family changes in β_1 tend to be compensated by counter changes in K_a, the product tends to remain relatively constant (with a noticeable but small increase with increasing K_a). Hence, from the measurement of $\beta_2 K_a$ of salicylaldoxime and Cu^{2+} of $10^{4.2}$ (20), we may take $\beta_1 K_a$ as $10^{2.0}$. Together with the value of K_{DR} as $10^{4.6}$ and log k' of 1.37, k_1 is $2.2 \times 10^7 M^{-1} s^{-1}$, a value that is quite similar to typical substitution reactions of Cu^{2+} (the corresponding rate constant for Cu and phenanthroline is only three times larger (20).

This agreement with generally oberved rate constant for copper substitution reactions in aqueous media represents strong evidence for the mechanism of the Cu-LIX65N extraction developed here. If chemical reactions at the interface were significant, far larger apparent rate constants would be calculated as a result of the incorporation of the bulk organic phase ligand concentration of the ligand concentration, in the rate expression instead of the significantly larger concentration of the ligand, as a surface active material, at the interface.

Even more convincing proof of the mechanism described above can be obtained by testing the validity of eq.13, using a series of organic solvents in parallel rate studies. Thus, Akiba (21) found the observed rate of extraction of copper with LIX 65N, k',to vary by three orders of magnitude when seven organic solvents ranging from trichloromethane to n-heptane were used. The variation of log k' with log K_{DR} was linear and had a slope of two, as required by eq.13. Similarly, in the case of the extraction kinetics of nickel with LIX 65N (found to be first order in ligand), the plot of k' vs. K_{DR} is linear, in keeping with the mechanism having as the rds, the formation of NiL^+ in the aqueous bulk phase (21). The exact correspondence of variation of the observed rates to inverse first (with Ni) and second(with Cu) orders of the ligand distribution constants with the same set of solvents rules out any possible influence of interfacial effects in these systems.

This is not to be taken to mean that interfacial influence on extraction kinetics conducted under under high speed stirring conditions will never occur. Indeed, we set about to search for systems in which just such effects could occur by preparing and studying a series of symmetrically dialkylated dithizones, from methyl to hexyl. It seemed appropriate to start with derivatives of the extractant having the highest K_{DR} of all of the extractants studies to date. Using the automated extraction apparatus cited above (18), at high pH values, a drop in the alkylated dithizone concentration in chloroform was observed which varied with stirring speed up to a plateau region. The extent of the decrease in concentration varied with pH at stirring speeds in the plateau region in a manner parallel to the non-stirring experiment permitting us to obtain a $pH_{1/2}$ value. The difference in $pH_{1/2}$ values (stirring vs. no stirring) increased from 0.16, 0.66, 3.0, and 5.0 as the alkyl group varied from methyl, to ethyl, to butyl, to hexyl, while no such change was observed with dithizone itself. These changes are indicative of the dramatic effect on the heterogeneous acid-base equilibrium that occurs because the anionic alkyldithizonati (but not the neutral ligand) is surface active and is adsorbed into the interfacial region (22).

The extraction kinetics of nickel and zinc with the alkyldithizonates (23) closely resembled that with dithizone and its analogs studied earlier (7) in that the rate was first order each in metal and ligand and inverse first order in hydrogen ion. The bidg difference appeared when we assumed that the mechanism remained the same, i.e. that the rds was the formation of the 1:1 complex from metal and ligand anion in the aqueous phase. This assumption led to increases in the second order reaction rate constant with increasing size of alkyl group until, with the hexyldithizone, the values for both Ni and Zn exceeded the diffusion limited rate constant for bimolecular reaction!

Upon recognizing that the locus for the formation of the 1:1 complex is the interfacial region and calculating the correct value of the ligand anion concentration in the interface from the observed differences in $pH_{1/2}$ values (v.s.), we obtained values for rate constants that were eminently reasonable, i.e. essentially constant for all the alkylated dithizones and of values consistent with those obtained for these metals in a broad corss-section of ligand substitution reactions. Our results further show that the interfacial region is essentially aqueous in character in the systems studied.

Literature Cited

1. Honaker,C.B.,Freiser,H., J. Phys. Chem. 66, 127 (1962).
2. Zangen,M.,Israel J.Chem., 2, 91 (1964).
3. Yamada,K.,Nakagawa,K.,Haraguchi,K.,Ito,S.,Nippon Kagaku Kaishi,1975, 1431.
4. Ito,S., Haraguchi,K., Nakagawa,K., Yamada,K., Nippon Kagaku Kaishi,1973,948.
5. Nanda,K.,Sharma,R.,Chem. Eng. Sci., 22,769(1967)
6. Hoogeveen,G., Chem. Commun.,1967,634
7. McClellan,B.E., Freiser,H., Anal.Chem., 36, 2262 (1964).
8. Carter, S.P., Freiser, H., Anal.Chem. 51, 1100 (1979).
9. Carter, S.P., Freiser, H., Anal.Chem. 52, 511 (1980).
10. Morton,A.A., Fallwell,J., J.Am.Chem.Soc. 60, 1429 (1938).
11. Farber, L., McKay, H.A.C., Wain, A.G., Proc. Intl. Solvent Extraction Conf., Lyon, France (1974).
12. Whewell, R.J., Hanson, C., Hughes, M.A., J. Inorg. Nucl. Chem. 37, 2303 (1975).
13. Atwood, R.L., Thatcher, D.N., Miller, J.D., Metall. Trans. B.6, 465 (1975).
14. Fleming, C.A., N.I.M. Report No. 1793, Johannesburg, S. Africa, 1976.
15. Lewis, J.B. Chem. Eng. Sci. 3, 284 (1954).
16. Pratt, H.R.C., Ind. Chem., 63 (1955).
17. Tavlarides, L.L., Chem. Eng. Commun., 8, 133 (1981).
18. Watarai, H., Cunningham L., and Freiser, H., Anal. Chem., 2390-2392, 1982.
19. Flett, D.S.,Accounts Chem. Res., 10,99(1977)
20. Sillen, L.G., Martell,A.E., ed.,STABILITY CONSTANTS, Chem. Soc.(London), Spec. Publ. No. 17(1964)
21. Akiba, K., and Freiser, H., Anal.Chim.Acta., 329-337, 1982.
22. Watarai, H., and Freiser, H., J.Amer.Chem.Soc., 1983.
23. Watarai, H., and Freiser, H., J.Amer.Chem.Soc., 1983.

PROGRESS IN TRIVALENT ACTINIDE LANTHANIDE GROUP SEPARATIONS

C. Musikas, P. Vitorge, D. Pattee

Centre d'Etudes nucléaires de Fontenay-aux-Roses
DGR-SEP-SCPR BP n° 6 - FONTENAY-AUX-ROSES - France

I. INTRODUCTION

The separation of the long half lives α emitters from the shorter half lives β emitters contained in highly radioactive wastes is suitable to improve nuclear wastes storage safety. This separation is complicate, mostly because no satisfactory trivalent actinide lanthanide group separation is known. The presently known processes have many defects, one particulary important is to generate large amounts of radioactive wastes. Their main features are :

- TRAMEX (1) : this process is based on the selective extraction of trivalent actinides into tertiary amine chloride (alamine 336-HCl) from 10 to 11 M aqueous LiCl solutions with acidities in the range 0.02 to 0.25 M. In addition to the wastes produced by the aqueous solutions, the process is difficult to handle because of pH buffering difficulties due mainly to radiolysis.

- TALSPEAK (2) : this process is based on the selective extraction of trivalent lanthanides by di2ethylhexylphosphoric acid (HDEHP) into diisopropylbenzene from aqueous solutions of carboxylic acids and diethylenetriaminopenta acetic acid (DTPA). The waste problems is less important than in the TRAMEX process but the major component of the mixtures (lanthanide) is extracted. pH buffering problems and low kinetics do not yield, in counter current separations, the separation factors expected from the values of batch distribution ratios. THIOCYANATE process (3) in which trivalent actinide are selectively fixed on anion exchange resin from rather concentrated NH_4 NCS, produced large amounts of wastes and has its specific inconvenients, one of which, is the decomposition of NH_4NCS by radiolysis into elemental sulfur. All these reasons urge on search for actinide lanthanide group separations new extractants with the following requirements.

- The aqueous phases must have no inorganic salts and must be self buffered (low pH).
- The trivalent actinides must be preferentially extracted.
- The kinetics of extraction and back extraction must be rapid.

Additionnal basic chemistry was necessary to find out which ligands have higher affinity for the 5f trivalent ions than for the 4f. In order to compare several kinds of ligands we used the S_F number (separation factor) which is equal to $2(\Delta G_{Ac(III)} - \Delta G_{Ln(III)}) / \Delta G_{Ac(III)} - \Delta G_{Ln(III)}$ where the ΔG are the free enthalpy of homologuous complexes formation for an actinide (III) - lanthanide (III) pair. Some Am(III) - Eu(III) S_F values are given table I.

Table I : S_F value for selected ligands (Am(III) - Eu(III)).

ligand	Complex	S_F	Donor atom electro-negativity
F^-	MF^{2+}	- 0.084	4.0
$CH_3CO_2^-$	$M(CH_3CO_2)^{2+}$	0.03	3.5
N_3^-	$M(N_3)^{2+}$	0.93	3.0
phen	$M(phen)^{3+}$	0.69	"
TPTZ	$M(TPTZ)^{3+}$	0.38	"

If can be seen that the ligands of which donor atoms have the lower Pauling's electronegativity yield the highest S_F factors. Nitrogen and sulfur donors are better ligands than oxygen donors for actinide-lanthanide group separations also we pursued these investigations by testing extractants containing N or S donor atoms.

II. NITROGEN DONORS

Among the various nitrogen ligands which complexe preferentialy trivalent actinides (4) (5) (6) we selected the aromatic polyimines because of the possibility to make them lipophilic by adding aliphatic radicals to the basic squeleton which contain the active donor group. The most promessing results were obtained with 2,4,6 tri (2 pyridyl) 1,3,5 triazine (TPTZ) commercially available (figure 1) :

TPTZ is a dibasic ligand with $pka_1 = 3.8$ and $pka_2 = 2.7$. Its rather low solubility into low polarity diluents make necessary the addition of lipophilic acidic extractants for a) increasing its solubility b) formation of lipophilic metallic neutral complexes.

Two acidic reagents were tested α bromocapric acid and dinonylnaphtalensulfonic acid (figure 1).

II.1. Extraction of trivalent 5f and 4f ions into α bromocapric - TPTZ solutions.

Carboxylic acids extract trivalent lanthanides, with distribution ratios which are not very dependant of Z contrary to others acidic extractants like di 2 ethylhexyl phosphoric acid (HDEHP) or 2 thenoyltrifluoroacetone (HTTA). Consequently carboxylic acids seem convenient as acidic extractant in synergistic mixtures for 4f - 5f group separations. α bromocapric acid (HA) was selected because of its rather low pka (≈ 3.0) when compaired with carboxylic acid (pka (≈ 4.5), this extraction might take place at lower pH.

The increasing solubility of TPTZ in decanol by addition of HA indicated that an adduct $(HA)_2$ TPTZ is obtained. The low value of its formation constant (K = 50) suggests that HA and TPTZ are linked by hydrogen bonds. Am(III) and Eu(III) distribution ratios as a function of pH, C_{HA} and C_{TPTZ} are shown figure 2 to 4. The whole data can be interpreted by the extraction mechanisms

$$M(III) + \overline{TPTZ} + 3\ HA \rightleftharpoons 3\ H^+ + \overline{MA_3\ TPTZ}$$

$$M(III) + \overline{2(HA)_2.TPTZ} \rightleftharpoons 3\ H^+ + \overline{MA_3TPTZ} + \overline{HA} + \overline{TPTZ}$$

The Am(III) - Eu(III) separations factors are lower than the aqueous TPTZ complexes β_{11} ratios probably because the replacement of water molecules by α bromocaprate ions increases the metal - TPTZ nitrogen distances.

The mixtures α bromocapric acid - TPTZ in decanol are however effective for 5f - 4f trivalent ions group separation since Am(III) and Cm(III) distribution coefficients are very close to each other when Ln(III) distribution coefficients are in a narrow values range and always inferior to the actinides (III) values (by a factor of 8).

II.2. Extraction of trivalent actinide and lanthanide into HDNNS - TPTZ mixtures.

α bromocapric acid - TPTZ mixtures did not yield to sufficiently high Am(III) - Eu(III) separation coefficients at low pH. HDNNS was tested as acidic extractant in place of the carboxylic acids. t-butylbenzene was used as a diluent. From the extraction data slope analysis and from TPTZ - HDNNS association investigations it can be concluded that we are dealing mostly with the mechanisms :

$$2\ \overline{(HDNNS)_q} + q\ \overline{TPTZ} \rightleftharpoons m\ \overline{\left[(HDNNS)_2\ TPTZ\right]_{q/m}}$$

$$2\ Am^{3+} + 2\ \overline{\left[(HDNNS)_2TPTZ\right]_{q/m}} \rightleftharpoons 2\ \overline{\left[Am(DNNS)_3TPTZ\,[(HDNNS)_2TPTZ]^{2q-3m}\right]_{2m}} + 4H^+ + TPTZ\ H_2^{2+}$$

The double overheadings indicate the micellar nature of the species and we supposed that Am^{3+} was extracted into $\overline{\left[(HDNNS)_2\ TPTZ\right]_{q/m}}$ micelles without changing its size, hypothesis probably correct only at low Am concentrations. Similarly to the HA - TPTZ synergistic system the HDNNS-TPTZ mixtures are suitable for 5f - 4f group separations, (table II), but the increasing separations factors and the lower pH at which extractions were carried out constitute a very interesting improvement.

Table II : Distribution ratios of various trivalent 5f and 4f ions between HDNNS 0.01 M, TPTZ 0.01 M in t-butylbenzene and nitricacid.

Aqueous phase	D_{Am}	D_{Cm}	D_{Ce}	D_{Eu}	D_{Gd}	D_{Tb}	D_{Yb}
HNO_3 0.12	1.35	1.4	0.158	0.199	0.178	0.14	0.22
HNO_3 0.08	6.3		0.4	0.5	0.45	0.38	0.55

* All ionic strengths were I = 1 M (KNO_3 added)

III. EXTRACTION OF Am(III) and Eu(III) BY THE DIALKYLDITHIOPHOSPHORIC ACIDS

Am(III) and Eu(III) distribution ratios into dodecanic solutions of di2ethylhexyldithiophosphoric acid (HDEHDTP) as a function of aqueous pH are shown figure 5. Extraction at low pH is due to the presence of small amounts of impurities (monothio, and phosphoric acid) which are stronger extractants of trivalent ions than HDEHDTP.

The Am(III) - Eu(III) separation factors are low, but the addition of TBP yields higher separation factors and strong Am(III) synergistic effect (figure 6). Drastic changes in Eu(III) charge transfer spectra are observed, upon the TBP addition (figure 7) and can be interpreted as a shortening of the Eu-S distance. As it was pointed out that trivalent actinide - lanthanide separations stem out from higher covalent interactions of actinide with the soft donor ligands, figure 5 to 7 illustrate fairly well the grounds of the hypothesis, the shorter Eu - S distance (presence of TBP) is the best conditions for covalent bonding and Am-Eu separation factors increase (figure 6).

IV. CONCLUSION

Rather soft nitrogen and sulfur donor extractants used in synergistic mixtures are promessing for trivalent actinide lanthanide group separations from low pH nitric acid solutions.

The effect of the second extractant is more important than expected because the covalent interactions with the 5f ions which allow the separations are very sensitive to metal ligand distances.

REFERENCES

1 - K.E. LEUZE, M.H. LLOYD, Prog. Nucl. En. Process Chemistry, 4, 549 (1970)

2 - B. WEAVER, F.A. KAPPELMANN, J. Inorg. Nucl. Chem. 30, 263, (1968)

3 - J.S. COLEMAN, L.B. ASPREY, R.C. CHISHOLM, J. Inorg. Nucl. Chem. 31, 1167 (1969)

4 - C. MUSIKAS, C. CUILLERDIER, J. LIVET, A. FORCHIONI, C. CHACHATY, Inorg. Chem. (in press).

5 - C. MUSIKAS, G. LE MAROIS, J. RACINOUX, Thermodynamics of nuclear materials, Vol II, IAEA SM 236/78, 105 (1980)

6 - C. CUILLERDIER, CEA-R-5140 (1981)

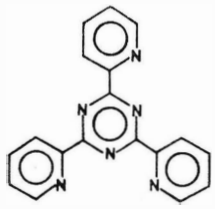

TPTZ

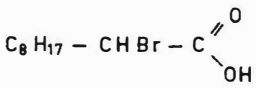

HA

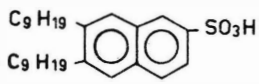

HDNNS

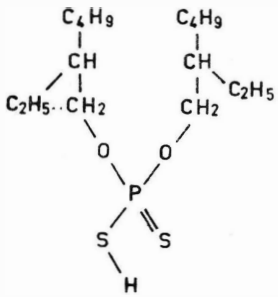

HDEHDTP

FIG. 1._EXTRACTANTS USED IN THE PRESENT INVESTIGATION

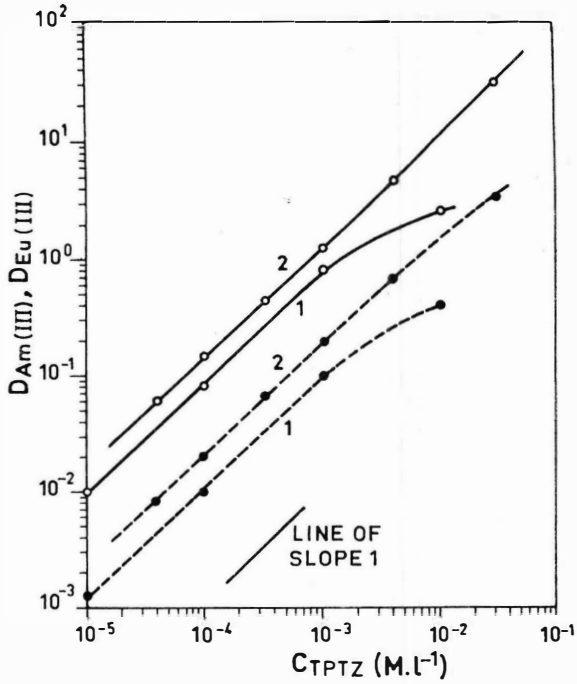

FIG. 2._ Am (III) ● Eu (III) ○ DISTRIBUTION AS A FUNCTION OF C_{TPTZ}

ORGANIC PHASES : 1 - α BROMOCAPRIC ACID 0.1 M IN DECANOL
2 - α BROMOCAPRIC ACID 1 M IN DECANOL

AQUEOUS PHASES : 1 - 1 M KNO_3, pH 3.25
2 - 1 M KNO_3, pH 2.8

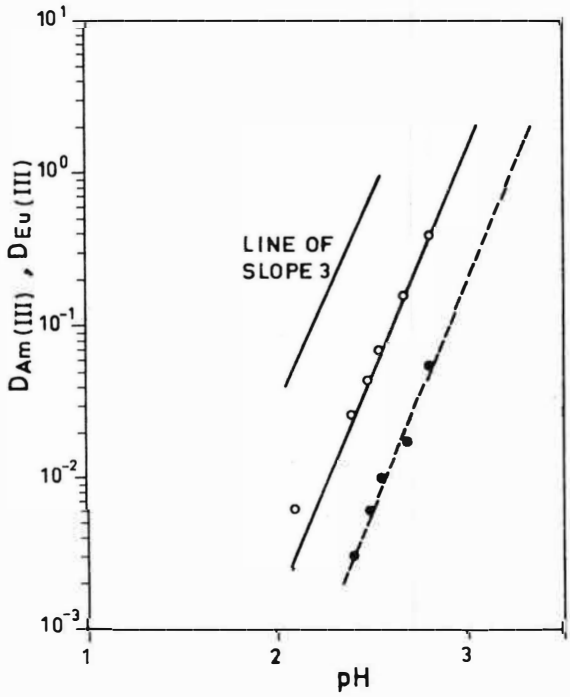

FIG. 3._ Am (III) ● Eu (III) ○ DISTRIBUTION AS A FUNCTION OF pH (1 M KNO_3)

ORGANIC PHASE : HA 0.1 M, TPTZ 0.01 M IN DECANOL

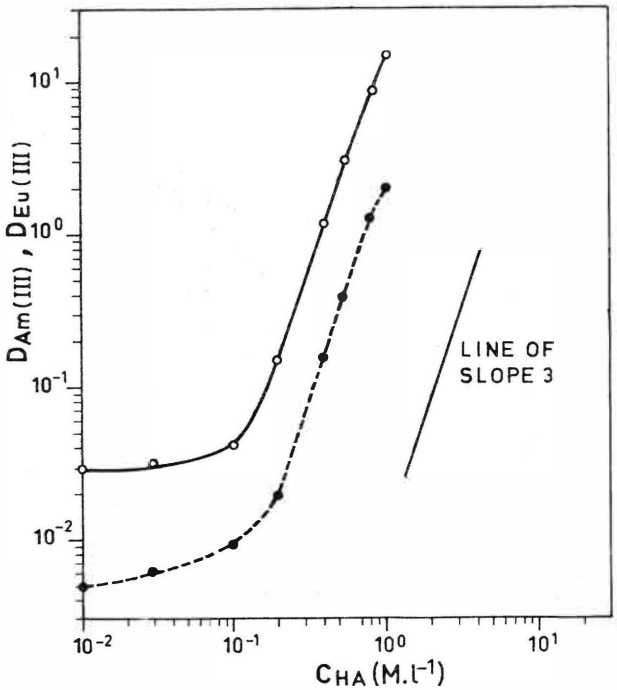

FIG. 4._Am (III) • Eu (III). DISTRIBUTION RATIOS AS A FUNCTION OF α BROMOCAPRIC ACID CONCENTRATION (HA)

ORGANIC PHASE : TPTZ 0.01 M IN DECANOL
AQUEOUS PHASE : KNO_3 1 M, pH 2.8

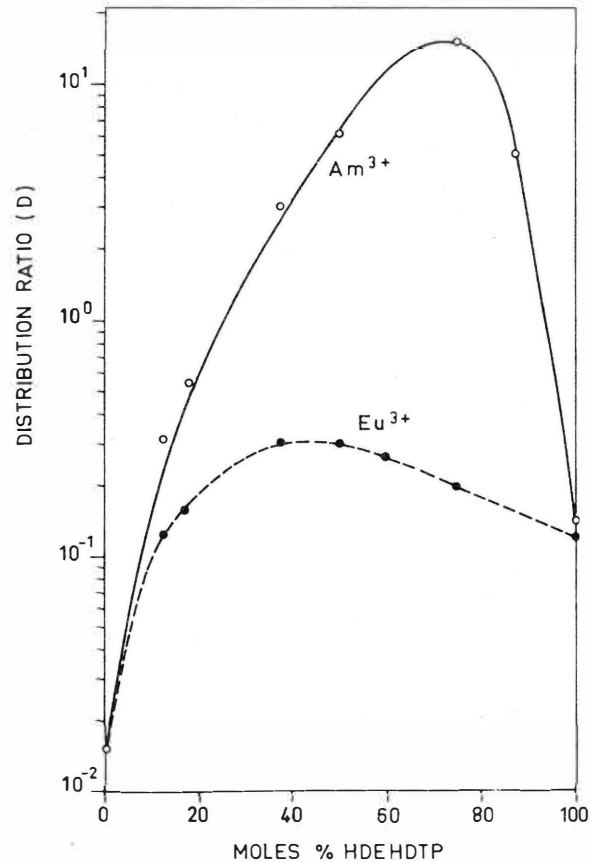

FIG. 6._ Am^{3+}-Eu^{3+} DISTRIBUTION BETWEEN 0.05 M HNO_3 AND 1 M HDEHDTP + TBP IN DODECANE.

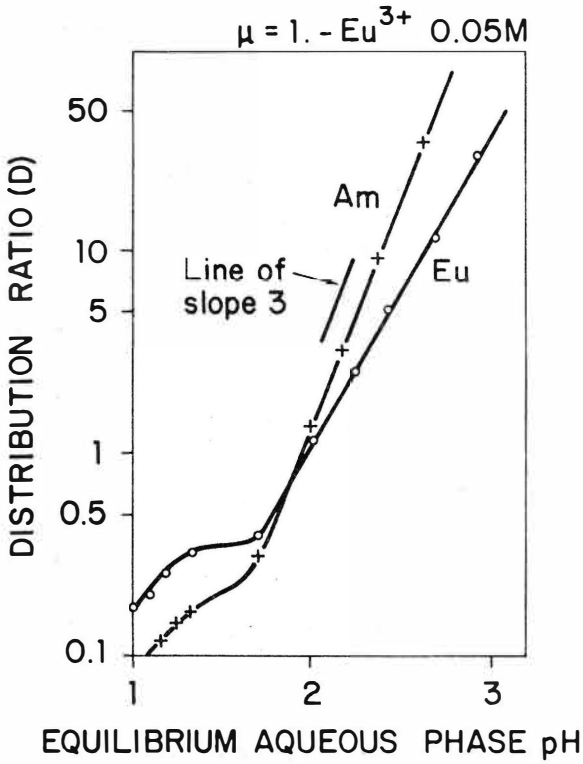

FIG. 5._ DISTRIBUTION OF Am-Eu BETWEEN 1M HDEHDTP AND AQUEOUS NITRATE SOLUTIONS.

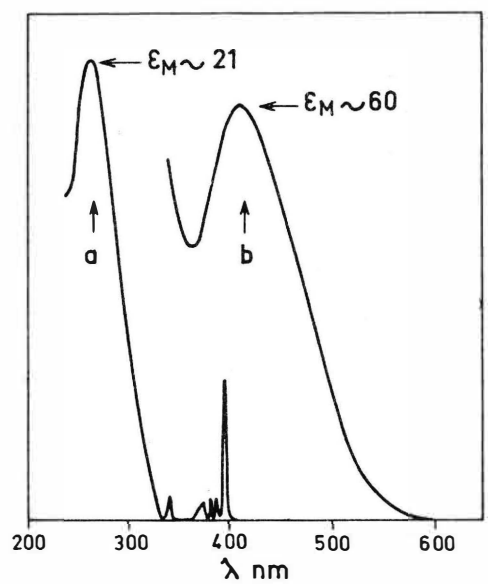

FIG. 7._ UV SPECTRUM OF $Eu(DEHDTP)_3 \times H_2O$ (a) AND $Eu(DEHDTP)_3 \cdot TBP$ (b)

AN EXTRACTANT (TRPO) FOR THE REMOVAL AND RECOVERY OF ACTINIDES FROM HIGH LEVEL RADIOACTIVE LIQUID WASTE

Zhu Yongjun, Jiao Rongzhou, Wang Shouzhong, Fan Shiguo
Liu Bingren, Zheng Hualing, Zhou Shunli, Chen Shuming
Tsinghua University
Beijing, China

The removal of long-lived α-emitting actinides from high radioactive waste (HAW) is a problem commonly concerned with. Solvent extraction is an effective method and several flowsheets based on different extractants, such as D2EHPA, DHDECMP, DBBP and TBP have been developed (1-4). TRPO, a new extractant, has been proved to be a competitive extractant and may have some advantages.

THE EXTRACTANT

TRPO is a specific alkyl phosphorous compound. It is a liquid at room temperature and is miscible with kerosene diluent in all proportions. It's density is ~0.9 g/cm^3 and its solubility in water is ~0.1 g/l at room temperature.

Composition and structure of TRPO were studied by infra-red spectrometry. Results show that polymer peak exist in infra-red spectra of concentrated TRPO-kerosene solution, that means TRPO molecules are linked together by hydrogen bond, but when the solution becomes dilute, depolymerization occurs and in 5 vol% kerosene solution TRPO mainly exists as monomolecules.

EXTRACTION AND SEPARATION OF HAW CONSTITUENTS BY TRPO

The extraction behavior of TRPO for HAW constituents (metallic ions and nitric acid) and different influence factors (diluent, TRPO concentration, temperature, salting agent etc.)have been studied.

Kerosene (No. 240, hydrogenated), n-dodecane, cyclo-hexane, m-xylene, carbon tetrachloride and chloroform were tested as diluent and their effect on the distribution behavior of TRPO were observed. The distribution ratios of trivalent actinides and lanthanides decreases as the dielectric constant of diluent increases. Nitric acid is also extracted by TRPO. When aqueous phase HNO_3 concentration is higher than 7-8 M., a second organic phase appears as kerosene and n-dodecane are used as diluent. Such high HNO_3 concentration doesn't occur in HAW treatment, so kerosene is the best choise.

Effect of TRPO concentration in kerosene on extration was tested and the dependence of distribution ratio of trivalent europium (D_{Eu}) on TRPO concentration (C_{TRPO}) and aqueous phase nitric acid concentration (C_{HNO_3}) can be expressed as follows:

TRPO concentration in kerosene, vol%	empirical formulas
5 -10	$D_{Eu} = 466 C_{TRPO}^{2.03} C_{HNO_3}^{1.68}$
10-30	$D_{Eu} = 111 C_{TRPO}^{1.58} C_{HNO_3}^{1.52}$
30-55	$D_{Eu} = 348 C_{TRPO}^{1.41} C_{HNO_3}^{1.12}$

The increase of distribution ratio of europium with TRPO concentration slows down along with the increase of TRPO concentration, because the fraction of polymerized TRPO molecules increases. In the light of distribution ratio , extraction capacity, viscosity and density of organic phase, 30 vol% of TRPO in kerosene is appropriate.

The variation of apparent extraction equilibrium constant $\tilde{K}$ of Eu with temperature (organic phase: 30 vol% TRPO in kerosene) can be expressed as follows:

$$\ln \tilde{K} = 2332\ 1/T + 2.107$$

Distribution ratio decreases slightly as temperature becomes higher and extraction is practical at temperature between 15 to 30 °C.

In the case of micro amount of Eu^{3+}, the existence of macro amount of $NaNO_3$ increases D_{Eu} strongly. As the concentration of HNO_3 in aqueous phase increases, the effect of $NaNO_3$ on D_{Eu} is weakened due to the competition of HNO_3 extraction. When aqueous phase HNO_3 concentration is equal to or higher than 0.5 M., the increase of nitrate ion concentration has little effect on D_{Eu}. When the HNO_3 concentration of equilibrated aqueous phase is 0.2 M., the addition of 0.48 M. $NaNO_3$ into aqueous phase will change D_{Eu} from 60 to larger than 120.

The distribution ratios of HAW constituents between 30 vol% TRPO in kerosene and aqueous nitric acid are shown in Figure 1 and 2. Results show that TRPO is a good extractant for actinide ions. At equilibrated aqueous phase nitric acid concentration 0.3 M., distribution ratios of 4+, 6+ actinide ions are very high and distribution ratio of Am^{3+} is high than 60. In the absence of 5+ valence state, 98% of actinides can be removed from the aqueous phase in one extraction stage. When aqueous phase nitric acid concentration is adjusted between 0.15 to 1.0 M., more than 90% of the actinides in HAW can be removed in one extraction stage. The distribution ratios of trivalent lanthanides are similar to that of Am^{3+} and distribution ratios of ruthenium, strontium and cesium are low. So, under certain conditions, constituents of HAW can be separated into several groups.

The extraction reaction of cation M^{n+} with TRPO in nitrate media may be expressed as follows:

$$M^{n+} + n\ NO_3^- + q\ TRPO = M(NO_3)_n \cdot qTRPO$$

n is the charge of the cation
q is the solvation number of the solvate extracted

and the apparent equilibrium constant $\tilde{K}$ is expressed as:

$$\tilde{K} = \frac{[M(NO_3)_n \cdot qTRPO]_o}{[M^{n+}]_a [NO_3]_a^n [TRPO]_o^q} = \frac{D}{[NO_3^-]_a^n [TRPO]_o^q}$$

D is the distribution ratio
[ ] is the concentration of species in aqueous (a) or organic (o) phase

The variation of distribution ratios of nitric acid and some lanthanide and actinide ions with TRPO concentration at definite aqueous nitric acid concentration and ionic strength was determined and the value of q and $\tilde{K}$ derived are given in the following table:

Table Solvation number and apparent equilibrium constant in TRPO extraction (25±1°C)

M^{n+}	acidity (M)	q	log $\tilde{K}$	$\tilde{K}$	solvate
H^+	0.5	1.28	0.995	9.02	$HNO_3 \cdot TRPO$
Pm^{3+}	0.28	2.96	3.37	2.3×10^3	$Pm(NO_3)_3 \cdot 3TRPO$
Eu^{3+}	0.20 (+6M. $NaNO_3$)	2.66	5.48	3.0×10^5	$Eu(NO_3)_3 \cdot 3TRPO$

Table (continued)

M^{n+}	acidity (M)	q	log $\tilde{K}$	$\tilde{K}$	solvate
UO_2^{2+}	0.16	1.93	4.48	3.0×10^4	$UO_2(NO_3)_2 \cdot 2TRPO$
Np^{4+}	0.9	1.75	5.01	1.0×10^5	$Np(NO_3)_4 \cdot 2TRPO$
Pu^{4+}	7.0	1.71	5.15	1.4×10^5	$Pu(NO_3)_4 \cdot 2TRPO$
Am^{3+}	0.3	2.88	3.05	1.13×10^3	$Am(NO_3)_3 \cdot 3TRPO$

The stripping of actinides and lanthanides from loaded TRPO can be conducted effectively with mixed solution of amino-polycarboxylic acid (TTHA or DTPA) and hydroxycarboxylic acid at different pH values. The composition of stripping solutions may be as follows:

a. 1M. R(OH)COOH - 0.01 M. TTHA (or DTPA) - pH 2.7 for the stripping of Pu^{4+}

b. 1-1.5M. R(OH)COOH - 0.05-0.2M. TTHA(or DTPA) - pH 2.8-3.5 for the stripping of Am^{3+}

c. 1M. R(OH)COOH - 0.05M. TTHA (or DTPA) - pH 4.5 for the stripping of lanthanides

RADIATION STABILITY OF TRPO

Radiation stability of TRPO has been tested. Pure TRPO-kerosene solution and TRPO-kerosene containing nitric acid were irradiated to 10^6 -10^7 rad and studied by infra-red spectrometry. Their physical data and extraction properties were also determined. Results show that the composition and behavior of TRPO changed not seriously until 10^7 rad.

Based on these experimental results, two flowsheets for the treatment of HAW by TRPO extraction have been suggested. The first one is an actinides partitioning process and the second one is an actinides and lanthanides partitioning and recovery process. These two processes are going to test in bench scale multistage micro annular centrifugal extractors.

REFERENCES

1. G. Koch, Z. Kolarik, H. Haug, W. Hild, and S. Drobnik, Recovery of Transplutonium Elements from Fuel Reprocessing High-Level Waste Solutions, in Symposium on the Management of Radioactive Wastes from Fuel Reprocessing, Paris France, November 27-December 1. 1972 (CONF-721107, 99 1081-1110)
2. W. W. Schulz, Bidenate Organophosphorus Extraction of Americium and Plutonium from Hanford Plutonium Reclamation Facility Waste, USAEC Report ARH-SA-203 (1974)
3. G. L. Richardson, Americium Recovery by DBBP Solvent Extraction Pilot Plant Demonstration, USAEC Report BNWL-CC-1503 (1968)
4. J. M. Mckibben, H. P. Holcomb, D. A. Orth, W. E. Prout, and W. C. Scotten, Partitioning of Light Lanthanides from Actinides by Solvent Extraction with TBP USAEC Report DP-1361 (1974)

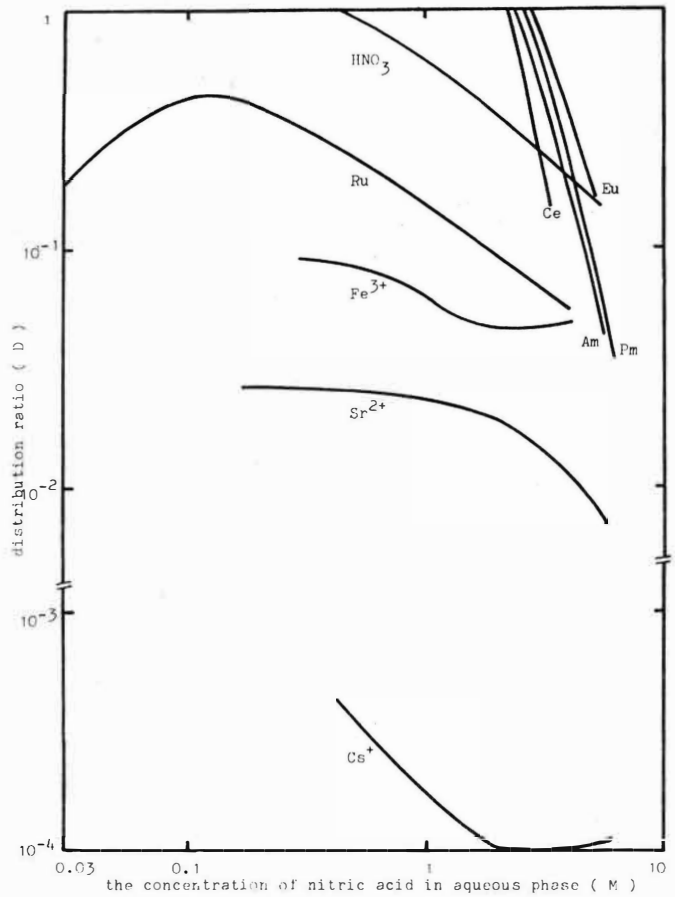

Figure 1 and 2. The distribution ratio of HAW constituents between 30 vol% TRPO- kerosene and HNO_3 solution

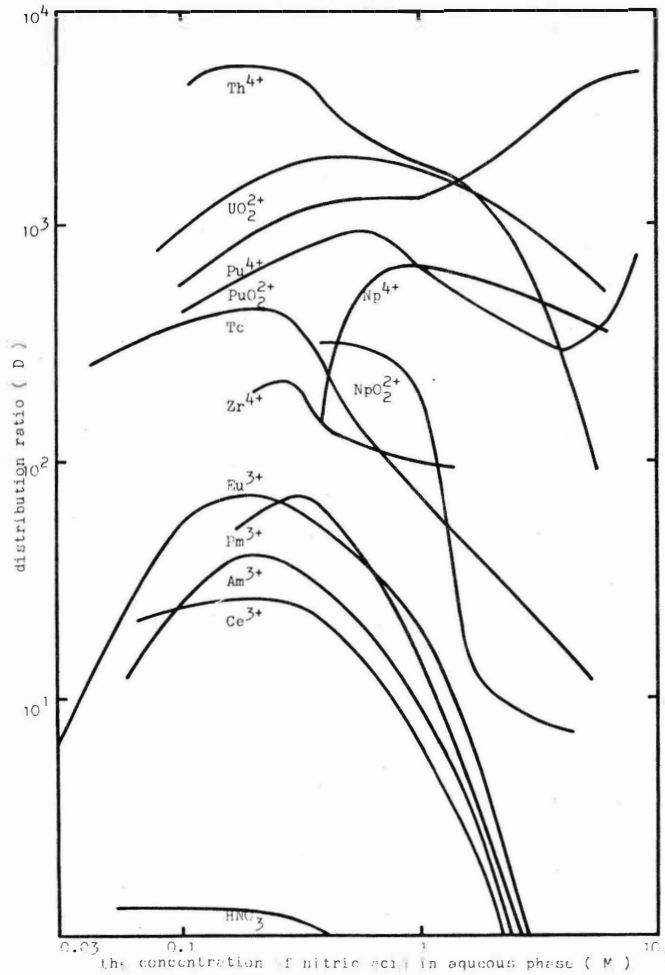

POLY-(DIPHENYLPHOSPHINYLMETHYL)ARENES - NEW PHOSPHOR - ORGANIC EXTRACTANTS OF TRANSPLUTONIUM ELEMENTS

B. F. Myasoedov, G. V. Bodrin, M. K. Chmutova, N. E. Kochetkova
T. Ya. Medved', Yu. M. Polikarpov, M.I. Kabachnik

Vernadsky Institute of Geochemistry and Analytical Chemistry
USSR Academy of Sciences
Moscow, USSR

It is well-known that certain bidentate neutral organophosphorus compounds are efficient extractants of actinides from highly acidic solutions.

We have studied extraction capacity of the large group of tetraphenylalkylene (vinylene) diphosphine dioxides and diphenyl [dialkylcarbamoylmethyl] phosphine oxides and have found reagents for quantitative actinide concentrating from highly acidic media (1,2).

However the reagents are non-selective and may be used only for group extraction of elements.

The problem we were interested in was synthesis of selective extractants.

It is established that selectivity of polydentate ligands depends on the conformational mobility of these ligands. If P=O groups are bounded by the bridge giving conformational hardness to the molecule of a reagent the selectivity of the reagent is raised.

In the present work we have considered the extraction properties of reagents in which the fragments of different methylsubstituted aromatic compounds serve as hard bridges connecting the P=O functional groups (table).

We have investigated the extraction of trivalent transplutonium elements (TPE), trivalent rare earth elements (REE), uranium (VI), plutonium (IV) by chloroform solutions of these reagents as a function of HNO_3 and ligands concentration. The table illustrates factors of separation of some elements.

The table shows the reagents studied may be divided into two groups:

- the first one includes reagents in which the substituents of the aromatic ring are situated only in o-positions with respect to each other;
- the second one includes reagents in which at least two substituents are situated in meta-positions with respect to each other.

Reagent XI is poorly soluble in $CHCl_3$ and it is non-selective with respect to the elements studied.

Reagents of the first group are characterized by high factors of U(VI)/Am(III), Pu(IV)/Am(III) separation and small factors of Eu(III)/Am(III) separation.

Reagents of the second group are characterized by small factors of U(VI)/Am(III), Pu(IV)/Am(III) separation as well as by the irregular increase in TPE and REE distribution coefficients with the growth of the ordinal number. They are also characterized by the same factors of intragroup separation of TPE and REE and by the same composition of the complexes extracted.

Inside each group reagents don't differ much in their extraction capacity.

The selectivity of reagents was found to depend only on mutual arrangement of P=O groups in the bridge regardless of their number.

Conformational analysis of the reagents described have been used to establish their structure and the cause of their selectivity with respect to one or another element.

Table

The separation factors for some elements in the extraction from nitric acid by 0.025 M solutions of reagents in $CHCl_3$

Reagent	The separation factors				
	U(VI)/Am(III)	Pu(IV)/Am(III)	Eu(III)/Am(III)		
	3M HNO_3	3M HNO_3	3M HNO_3	7M HNO_3	9M HNO_3
I	3.10^4	$1.5\cdot10^4$	-	-	-
II	$1.2\cdot10^3$	$2.8\cdot10^3$	1.0	1.0	1.0
III	$2.5\cdot10^3$	1.10^3	1.0	1.0	-
IV	2.10^4	1.10^4	2.0	2.0	-
V	$6.2\cdot10^3$	1.10^4	0.6	0.41	-
VI	5.10^2	2.10^4	-	-	-
VII	42.0	100	4.0	7.0	8.1
VIII	21.8	40.0	4.0	5.6	8.0
IX	24.0	56.2	6.0	8.0	8.5
X	60.0	60.0	5.0	6.6	12.0
XI	18.2	12.0	-	-	-

Reagents

(The group-CH_2-P(O)-Ph_2 is designed by ⋀)

I	
II	
III	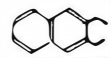
IV	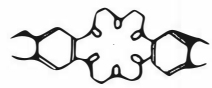
V	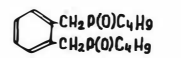
VI	
VII	
VIII	
IX	
X	
XI	

References

1. M.K.Chmutova, N.E.Kochetkova, B.F.Myasoedov, Radiokhimiya 20, N 5, 713 (1978).
2. M.K.Chmutova, N.P.Nesterova, N.E.Kochetkova, O.E.Koiro, B.F.Myasoedov, Radiokhimiya 24, N 1, 31 (1982).

IMPURITY REJECTION IN THE REFINING OF URANIUM WITH TRIBUTYL PHOSPHATE

D. G. Garratt and R. K. Badiani

Eldorado Resources Limited
Research and Development Division
Ottawa, Ontario, Canada

The potentiality of tri-n-butyl phosphate, TBP as an extractant for uranium has been known for many years. Indeed the uses of TBP in solvent extraction systems for the lanthanides and actinides have been the subject of considerable experimental investigation for more than thirty years. This paper reports the results of recent studies carried out at Eldorado Resources Limited, R&D Laboratories related to difficulties encountered in our Refinery in processing high molybdenum uranium concentrates.

EXPERIMENTAL APPROACH

Bench scale tests involving 3-stage counter-current simulations of extraction were carried out using an aqueous feed, 2.0 N in 'free' HNO_3, at a temperature of 50°C, with an O/A ratio of 4/1. The organic phase was 25 vol % TBP in Isopar M or regenerated plant solvent. The aqueous feed was prepared from a calcined ammonium diuranate concentrate which analyzed 82% U, 0.39% Mo and 0.078% Fe.

Of particular interest was the possible effect of the addition of iron (III) nitrate to the feed, since earlier studies had indicated that the presence of high ferric iron concentrations in the feed slurries might improve the discrimination between uranium and molybdenum.

As shown in Figure 1 uranium loadings are not affected by the presence of added iron (III) nitrate, but the selectivity for uranium over molybdenum is increased by such additions by a factor of approximately 50% near saturation loadings with respect to uranium. The presence of ortho-phosphoric acid in the feed, nominally to control thorium, at concentrations similar to those used in our Refinery decreases the selectivity for uranium over molybdenum, but does not decrease the effectiveness of high iron (III) levels as is demonstrated by Figures 2 and 3.

In general better discrimination between uranium and molybdenum was found for freshly prepared solvent than for regenerated plant solvent: indicating that the normal Na_2CO_3 wash used in regeneration was not as efficient as would be desired in the removal of degradation products which effectively complex with molybdenum. For example, it was possible using fresh solvent to achieve molybdenum loadings in the organic in the range of 0.32-0.52 mg/L, whereas for plant solvent under equivalent conditions the molybdenum concentrations were much greater, in the range of 8.5-17.8 mg/L. A substantial improvement in decreasing molybdenum loadings is, however, possible if the plant solvent is preacidified prior to use in extraction to a 'free acidity' of 0.21-0.32 N HNO_3 compared to the value of 0.02 N HNO_3 normally utilized.

In model studies using ammonium molybdate, molybdenum trioxide, and dodeca-molybdo-phosphoric acid as sources of molybdenum in 2.0 N HNO_3 solutions/slurries it was shown that molybdenum loading in the absence of uranium is of approximately the same level or slightly higher than that found in the presence of uranium (1-3 mg/L). In agreement with the initial studies, the addition of iron (III) nitrate to the synthetic molybdenum feeds lowers the concentration of loaded molybdenum by 40 to 60%. Of greater impact, however, is the observation that the addition of ortho-phosphoric acid to the synthetic feeds increases the concentration of loaded molybdenum by a factor of 40 to 200 depending upon the 'age' of the feed solution, and that the effectiveness of iron (III) nitrate decreases as the 'age' of the feed increases. For example, if a preformed molybdenum-phosphoric acid complex is used as a synthetic feed or if such a complex is allowed to form prior to the addition of iron (III) nitrate, the level of molybdenum loading increases dramatically: 2,780 mg/L versus 2.8 mg/L in the organic phase. Quite clearly the loading of molybdenum is determined to a greater extent through the formation of an organic soluble complex with phosphoric acid than it is by complexation with TBP.

Further studies showed that the effectiveness of added iron (III) nitrate in decreasing molybdenum loading where a stable "molybdenum-phosphoric acid complex" has not formed is about twice that found relative to the case where a stable complex is formed.

High levels of iron (i.e. Fe:Mo greater than 6 on a mass basis) do not significantly improve molybdenum rejection; however, in these cases the presence of ortho-phosphoric acid is no longer detrimental, as shown in Figure 4, and on specification uranyl nitrate (with respect to molybdenum) is achievable after 3 stages of extraction. Furthermore, it may be shown that the source of ferric iron is not important. The presence of high levels of iron in the commercial uranium concentrates is equally as effective in decreasing molybdenum loadings.

CONCLUSIONS

In conclusion this investigation demonstrated:

a) that molybdenum loading during uranium extraction is effectively minimized by the preacidification of the organic feed with nitric acid to 0.2-0.3 N;

b) that ferric iron causes a small improvement in decreasing molybdenum loading in the absence of ortho-phosphoric acid;

c) that molybdenum loading is increased by the presence of ortho-phosphoric acid; and

d) that ferric iron complexes with ortho-phosphoric acid more effectively than molybdenum, and thus decreases indirectly the extraction of molybdenum.

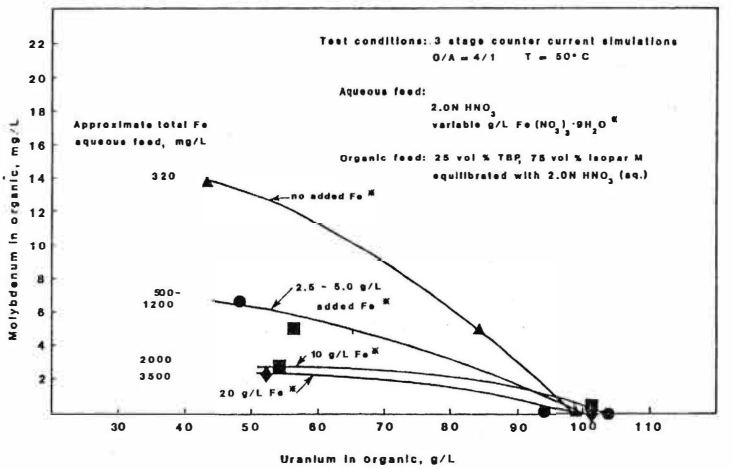

Figure 1. Effect of added $Fe(NO_3)_3 \cdot 9H_2O$ on molybdenum rejection.

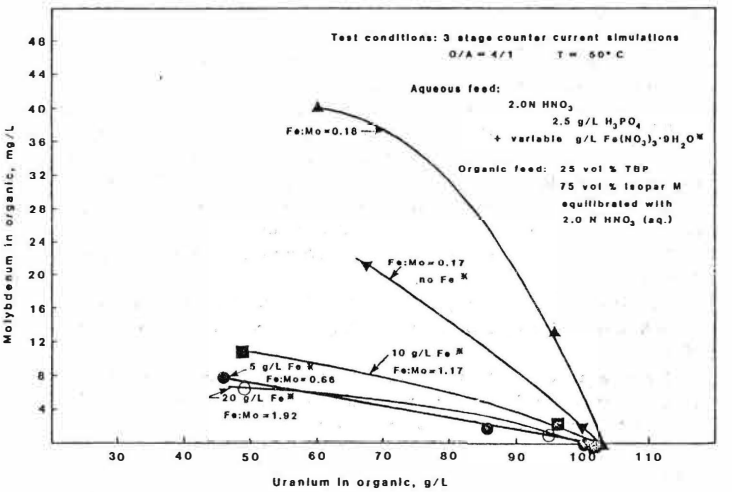

Figure 2. Effect of added $Fe(NO_3)_3 \cdot 9H_2O$ on molybdenum rejection in the presence of H_3PO_4.

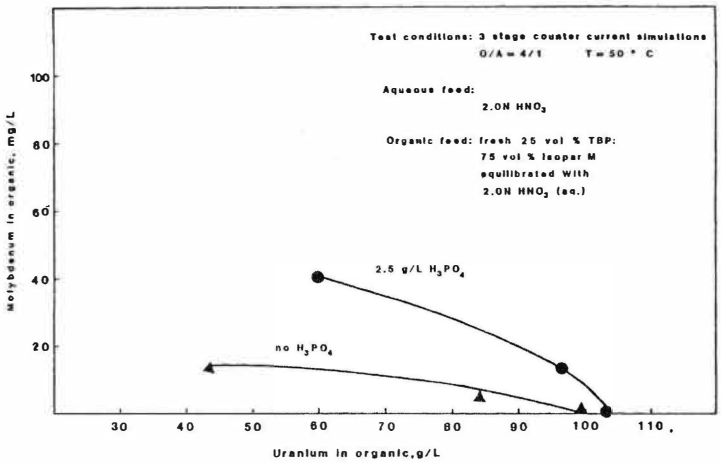

Figure 3. Effect of H_3PO_4 on molybdenum rejection.

Figure 4. Effect of iron concentration upon molybdenum rejection in the presence and absence of H_3PO_4.

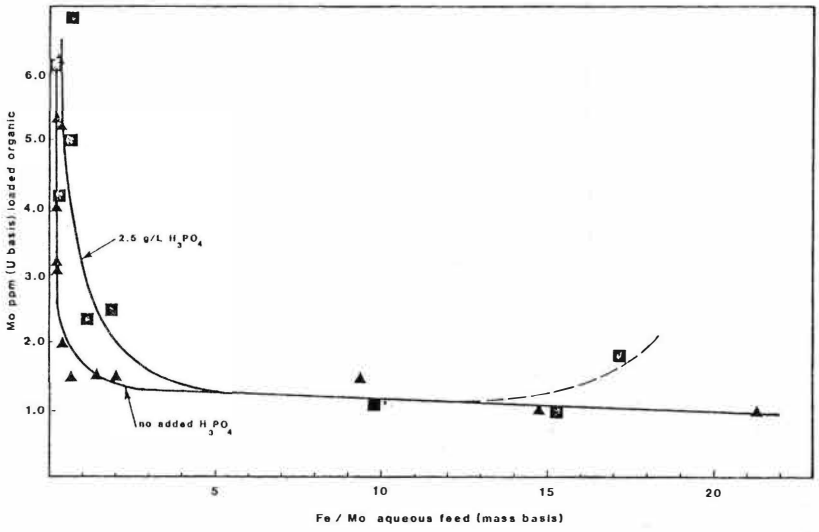

A GENERAL MODEL TO ACCOUNT FOR THE LIQUID-LIQUID KINETICS OF EXTRACTION OF METALS BY ORGANIC ACIDS

M. A. Hughes and V. Rod

Schools of Chemical Engineering
University of Bradford
Bradford, U.K.

Institute of Chemical Process Fundamentals
Czechoslovak Academy of Science
Prague, Czechoslovakia

Danesi (1) has shown how a combination of experimental technique with concentration can result in one particular set of controlling features for the rate of metal extraction with the organic acid HR. Either true chemical kinetic control or true mass transfer control holds but many systems will probably exhibit mixed control. Further discussion concerns the site of the chemical reaction which can be in the bulk aqueous continuous phase, in an aqueous film adjacent to the interface or at the interface proper. This general model accommodates these possibilities.

Rod and co-workers (2) suggest a model for mass transfer with a fast reversible reaction and product extraction in a metal system, this is examined further.

THE MODEL

The concentration profiles for this model are shown in Figure 1. It is taken that reaction must be at the interface and/or extending out into the aqueous diffusion film. It should be noted that as $P_{HR} \to \infty$ and $P_{MR_2} \to \infty$ (the partition coefficients of the extractant and complex respectively expressed as their equilibrium concentration in the organic phase divided by their equilibrium concentration in the aqueous phase) then the profile for c_{HR} and c_{MR_2}, in the aqueous phase, are coincident at zero. Also, under these conditions, the c_H and c_M profiles in the aqueous phase become linear as shown by the dotted lines; λ_d is the diffusion film thickness and λ_r is the reaction zone thickness. For a divalent metal M^{2+}:

(1) $H^+ + R^- \rightleftharpoons HR \qquad K_{HR} = \dfrac{c_{HR}}{c_{H^+} \cdot c_{R^-}}$

(2) $M^{2+} + R^- \overset{k_R}{\rightleftharpoons} MR^+ \qquad K_{MR} = \dfrac{c_{MR^+}}{c_{M^{2+}} \cdot c_{R^-}}$

(3) $MR^+ + R^- \overset{k^1_R}{\rightleftharpoons} MR_2 \qquad K_{MR2} = \dfrac{c_{MR2}}{c_{MR^+} \cdot c_{R^-}}$

(4) $M^{2+} + 2HR \rightleftharpoons MR_2 + 2H^+ \qquad K_{EX} = \dfrac{\bar{c}_{MR2} \cdot c^2_{H^+}}{c_{M^{2+}} \cdot \bar{c}^2_{HR}}$

Reactions (2) or (3) may be rate controlling. Superscript bar will indicate the organic phase, subscript i will denote an interface condition and N will denote a flux. The film coefficients are k_o for organic and k_{aq} for water. D is a diffusivity within the films.

If reaction (2) is rate determining then:

A for the organic phase (involving, in part, Astarita's method):

(5) $$N_{HR} = \sqrt{\frac{k_R D_{HR}}{P^2_{HR} K_{HR}} \cdot \frac{c_{M,i}}{c_{H,i}} \left(1 - \frac{c^2_{Hi} \cdot \bar{c}_{MR2,i}}{K_{EX} \bar{c}^2_{HR,i} c_{Mi}} \right) \left(\bar{c}^2_{HR,i} - P^2_{HR} c^2_{HR} \right)}$$

(6) $\bar{c}_{HR,i} = \bar{c}_{HR} - N_{HR}/k_{NR,o}$

(7) $\bar{c}_{MR2,i} = \bar{c}_{MR2} + N_{HR}/2k_{MR2,o}$

B for the aqueous phase:

(8) $$c_{HR} = \frac{1}{P_{HR}} \left\{ \frac{-P_{MR2} D_{HR} c^2_H}{4P^2_{HR} K_{HR} K_{EX} c_M} + \sqrt{\left(\frac{P_{MR2} D_{HR} c^2_H}{4P^2_{HR} K_{HR} K_{EX} c_M} \right)^2 + \frac{c_H}{K_{EX} c_M} \left(\bar{c}_{MR2,i} + \frac{D_{HR} P_{MR2} \cdot \bar{c}_{HR,i}}{2D_{MR2} \cdot P_{HR}} \right)} \right\}$$

(9) $c_{MR2} = K_{EX} (c^2_{HR} c_M / c^2_H) \; (P^2_{HR}/P_{MR2})$

(10) $c_{M,i} = c_M - N_{HR}/k_{M,aq} + (D_{HR}/D_H P_{HR}) \; (\bar{c}_{HR,i} - c_{HR} P_{HR})$

(11) $c_{H,i} = c_H + 0.5 \, N_{HR}/k_{H,aq} - (0.5 \, D_{HR}/(D_H P_{HR})) \; (\bar{c}_{HR,i} - c_{HR} P_{HR})$

Special cases may be noted which are summarised in Table 1.

TABLE 1

Special Cases of the General Model

PARTICULAR CASE	VALUES OF KEY PARAMETERS		
	k_R	P_{HR}	$\theta_1 = \dfrac{k_R D_{HR}}{P^2_{HR} \cdot K_{HR}}$
Reaction in the film	finite	finite	finite
Equilibrium reaction in the film	∞	finite	∞
Reaction at the interface	∞	∞	finite
Instantaneous reaction at the interface (Chapman's model) (3)	∞	∞	∞

site of reaction

Note that if reaction (3) is rate determining then Equation (5) becomes:

(12) $$N_{HR} = \sqrt{\frac{k^1_R D_{HR} K_{MR}}{P^3_{HR} K^2_{HR}} \frac{c_{M,i}}{c_{H,i}} \left(1 - \frac{1}{K_{EX}} \frac{c^2_{H,i} \bar{c}_{MR2}}{c_{Mi} \bar{c}^2_{HR}} \right) \left(\bar{c}^3_{HRi} - P^3_{HR} c^3_{HR} \right)}$$

But the other equations remain as before.

Chapman's model is of particular interest but is only one special case for under his assumed conditions then $k_R \to \infty$, $\theta_1 = \dfrac{k_R D_{HR}}{P^2_{HR} K_{HR}} \to \infty$, $P_{HR} \to \infty$, K_{EX} is finite.

Thus in the case of Chapman, Equation (5) transforms to:

(13) $$\left(\frac{c^2_{H,i} \bar{c}_{MR2,i}}{K_{EX} \bar{c}^2_{HR,i} c_{M,i}} - 1 \right) = 0$$

Equation (6) remains as $\bar{c}_{HR,i} = \bar{c}_{HR} - N_{HR}/k_{HR,o}$

Equation (7) remains as $\bar{c}_{MR2,i} = \bar{c}_{MR2} + N_{HR}/(2k_{MR2,o})$

(14) Equation (8) transforms to $c_{HR} = 0$

(15) Equation (9) transforms to $c_{MR2} = 0$

(16) Equation (10) transforms to $c_{M,i} = c_M - N_{HR}/k_{M,aq}$

(17) Equation (11) transforms to $c_{H,i} = c_H + 0.5 \, N_{HR}/k_{H,aq}$

IMPORTANT PARAMETERS OF THE MODEL

The two most sensitive parameters in the model are:

$$\theta_1 = \frac{k_R D_{HR}}{P^2_{HR} K_{HR}} \text{ (Equation (5))} \quad \text{OR} \quad \theta^1_1 = \frac{k^1_R D_{HR} K_{MR}}{P^3_{HR} K^2_{HR}} \text{ (Equation (12))}$$

together with P_{HR}. Their values decide the location of the reaction and characteristics of the transfer process; Table 2 illustrates this in a general way.

TABLE 2

P_{HR}	θ_1 OR θ_1^1	PARTICULAR CASE	DESCRIPTION OF PROCESS
finite	finite	Reaction in the film	Diffusion coupled with kinetics of reaction in the film
finite	$\to \infty$	Equilibrium reaction in the film	Diffusion coupled with Equilibrium in the film
$\to \infty$	finite	Reaction at the interface	Diffusion and reaction kinetics at the surface
$\to \infty$	$\to \infty$	Instantaneous reaction at the interface	Diffusion and equilibrium at the surface

THE POSSIBILITY OF BULK PHASE REACTION

In order to consider the possibility of reaction in a bulk aqueous phase, the thickness of the reaction zone ζ must be considered. Since:

$$(18)\quad \zeta = \frac{\lambda r}{\lambda d} \approx \frac{3}{P_{HR}} \left(\frac{k_{HR}\bar{c}_{HR}}{N_{HR,i}} - \frac{k_{HR,aq}}{k_{HR,o}} \right)$$

only if ζ >1 can reaction occur in the bulk phase.

MATHEMATICAL TREATMENT OF THE SIMULTANEOUS EQUATIONS (5) TO (11)

The implicit function for N_{HR} may be written:

$$(19)\quad F\,(N_{HR},\ cj,\ (K_{EX},\ K_{HR},\ P_{MR_2},\ k_R,\ Dj),\ (k_{aq}, k_o)) = 0$$

The physical parameters are regrouped to give: $\left(K_{EX},\ \theta_1,\ \theta_2, \frac{D_j}{D_{HR}}\right)$

in which $\theta_1 = \frac{k_R D_{HR}}{\partial^2 K_{HR}}$, $\theta_2 = \frac{D_{HR} P_{MR_2}}{D_{MR_2} P_{HR}}$. The ratio $\frac{D_j}{D_{HR}}$ refers to a transferring species j with diffusivity D_j and this ratio is relatively easy to obtain from generalized correlations and in any case the flux N_{HR} is not very sensitive to this ratio. Thus in any problem K_{EX}, θ_2 and $\frac{D_j}{D_{HR}}$ are known or may be estimated for a given system and the data from the experimental technique may be fitted by the model optimising the best value of θ_1, k_{aq} and k_o by a computer program. It is k_{aq} and k_o, the hydrodynamic parameters, which change from one technique to another.

THE SENSITIVITY OF THE MODEL TO THE PARAMETERS.

The sensitivity of the model to the parameters depends on whether the rate is measured near to equilibrium or far away from equilibrium together with the bulk concentration conditions; the most important parameters for the varying conditions are high lighted in each case in Table 3. The behaviour of the model will be demonstrated in the lecture.

TABLE 3

The Most Important Parameters of F (Equation 19) Dictated by Position of Rate and Bulk Concentration

Regions of Rate	$\bar{c}_{HR} >> c_{M^{2+}}$	$\bar{c}_{HR} \approx c_{M^{2+}}$	$c_{HR} < c_{M^{2+}}$
Far from equilibrium e.g. initial rates	k_{aq}	θ_1	k_o
Near to equilibrium e.g. in real contactors	K_{EX}, k_{aq}	K_{EX}, θ_1	K_{EX}

APPLICATION OF THE MODEL TO DATA FOR THE LIX64N/$CuSO_4$/H_2SO_4 SYSTEM

We have tested this model on the LIX64N/$CuSO_4$/H_2SO_4 system using data from two entirely different techniques (4,5) of contacting the two phases but using bulk concentration in both phases which are of commercial interest. In particular the pH range is commercially more realistic than that adopted by Albery and Fisk (6) in a rotating diffusion cell with the oxime P5000. The parameters are reported in Table 4.

TABLE 4

Parameter Estimates for Copper Extraction Systems

Data	θ_1 $(m/s)^2$	k_o μms^{-1}	k_{aq} μms^{-1}	θ_2 -
Cu/LIX64N Gauze Cell	$7.0.10^{-12}$	6.7	3.3	11.0
Cu/LIX64N Rising Drops	$7.0.10^{-12}$	150	100	11.0
Cu/P5000 Diffusion Cell (6)	$6.8.10^{-9}$	10.4	21.8	1.0

The value of θ_1 is 6.9×10^{-12} if it is determined independently for the drop data alone. The model appears successful especially since it accounts for rates measured both at initial times and near to equilibrium as demonstrated in the lecture.

REFERENCES

1. P.R. Danesi and R. Chiarizia, Critical Reviews in Anal. Chem., ed.B. Campbell CRC Press, Chapter 10, p 1., 1980.
2. V. Rod, L. Strhadová, V. Hančil, Z. Šír, Chem. Eng. J. 21, 187, 1981.
3. W. Chapman, R. Caban and M. Tunison, A.I. ChE Symp. Ser., 71, 151, 1975.
4. R.J. Whewell, M.A. Hughes and C. Hanson, J.I.N.C., 87, 2323, 1975.
5. M. Bhaduri, C. Hanson, M.A. Hughes, R.J. Whewell, Paper No. 22c, ISEC'83, Denver, 1983.
6. W.J. Albery and P.R. Fisk, Hydrometallurgy 81, paper 5/3, Procs. Soc. Chem. Ind. Symposium, Manchester, 1981, publ. Soc.of Chem. Ind., 1981.

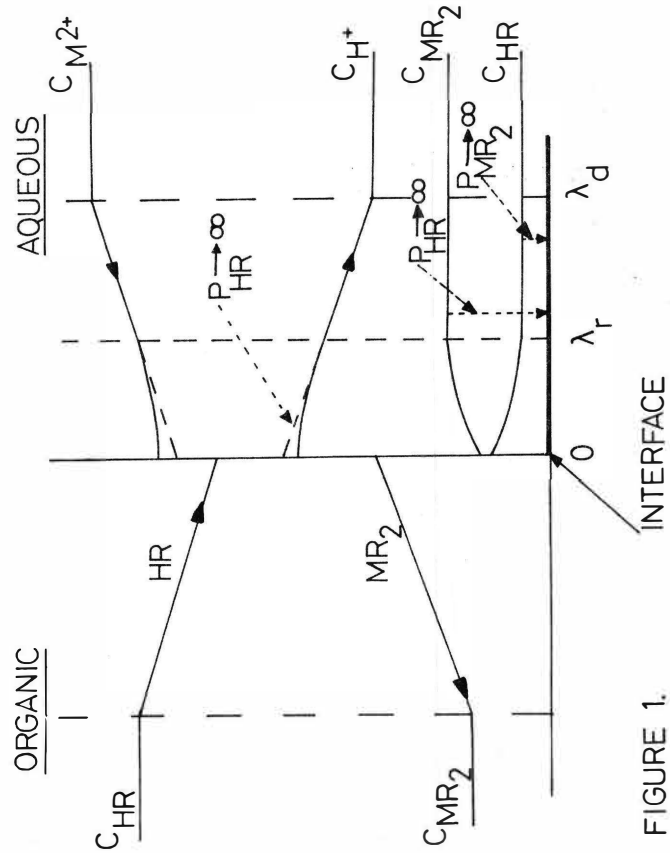

FIGURE 1.

LASER LIGHT SCATTERING STUDIES OF THE INTERFACIAL CHEMISTRY IN SOLVENT EXTRACTION SYSTEMS

Ronald D. Neuman and Anilkumar G. Gaonkar

University of Minnesota
St. Paul, Minnesota 55108 USA

It is now recognized that the liquid/liquid interface plays a key role in the solvent extraction of metal ions from an aqueous phase to a nonpolar organic phase. The interfacial chemistry, however, is still not fully understood. A unique experimental approach to furthering our understanding of this complex chemistry involves investigating the interfacial behavior of extractant molecules and their interactions with metal ions using recently developed laser light scattering techniques.

The laser light scattering technique has several advantages compared with classical surface-chemical approaches and methods. The main advantage is that the interface is essentially undisturbed during the measurements. There are no mechanical probes (du Noüy ring or Wilhelmy plate) in the interface, thus the large errors often involved when measuring the interfacial tension of surfactant solutions due to contact angle changes and non-equilibrium effects can be avoided. The laser light scattering technique also has been employed to quantitatively determine the viscoelastic parameters, namely, the film dilational elasticity and film dilational viscosity, of monomolecular films at the air/water interface (1). Recently this laser technique has been used to measure liquid/liquid interfacial tensions (2). For some systems, it now seems possible to obtain new information on the viscoelastic properties of extractant films at liquid/liquid interfaces. Interfacial viscoelastic properties not only have a significant influence on the rate of mass transfer (3) but they also can significantly influence the rate of droplet coalescence in emulsion systems (4).

The purpose of this paper is to show that (a) laser light scattering techniques can be extended to interfacial systems of importance to solvent extraction and that (b) it should be possible to obtain information on the viscoelastic properties of adsorbed or spread monolayers at liquid/liquid interfaces using this novel technique. It also is to be emphasized that new information on the HDEHP/n-hexane/aqueous system was obtained when stringent surface-chemical techniques and purification procedures were employed.

LASER LIGHT SCATTERING

If a light beam is incident on a fluid/fluid interface, most of the light is reflected or refracted. A very small part of it, however, is scattered in all directions by thermally excited capillary waves, i.e., ripplons. In the present work, an argon ion laser (Lexel Model 95-2) operating at 488 nm and about 100 mW illuminates the liquid/liquid interface. The scattered light is mixed coherently on the photocathode of the detector with a much stronger reference beam generated by a transmission diffraction grating. The projected grating technique greatly facilitates heterodyne detection since the intensity of the reference beam can be adjusted using a variable neutral density filter (1). The light scattered by capillary waves of a given wavevector, k, defined as $2\pi/a$ where a is the wavelength of the capillary waves, coincides with a particular order of the diffraction spots in the detector plane. An aperture is used to select a single diffraction spot and, hence, capillary waves of some particular k for study. The photodetector current is then readily analyzed in the time domain by a Langley-Ford 128-channel correlator. The photocurrent autocorrelation function reflects the autocorrelation function of the capillary waves.

The autocorrelation function, $G(\tau)$, of the capillary waves is approximately an exponentially damped cosine function,

$$G(\tau) \simeq A \cdot e^{-\Gamma\tau} \cdot \cos \omega_0 \tau + B, \tag{1}$$

which is the form of the function used by the Terak microcomputer (64k RAM) for fitting to the measured data. Thus, ω_0, the resonance frequency, and Γ, the measured damping, of the capillary waves are determined. The measured damping is corrected for instrumental effects to yield the "true" damping coefficient, α, of the capillary waves using the procedures described by Hård and Neuman (1).

The values of the frequency, ω_0, and temporal damping coefficient, α, of the capillary waves found in this way are interpreted using an appropriate hydrodynamic theory of capillary waves. The theoretical dispersion relation (5) used to compute values of interfacial tension or interfacial viscoelastic parameters is as follows:

$$[\eta'(k + m') + \eta''(k + m'') - \frac{\varepsilon^* k^2}{i\omega}][\eta' \cdot \frac{m'}{k}(k + m') + \eta'' \cdot \frac{m''}{k}(k + m'') - \frac{\gamma k^2}{i\omega}] = [\eta'(k - m') - \eta''(k - m'')]^2, \tag{2}$$

where $\omega = \omega_0 - i\alpha$, ω_0 = frequency of capillary waves k, α = temporal damping coefficient of capillary waves k, η' = shear viscosity of lower phase, ρ' = density of lower phase, η'' = shear viscosity of upper phase, ρ'' = density of upper phase, γ = interfacial tension, $\varepsilon^* = \varepsilon - i\omega\kappa$, ε = interfacial dilational elasticity, κ = interfacial dilational viscosity, $m' = [k^2 - (i\omega\rho'/\eta')]^{1/2}$, $m'' = [k^2 - (i\omega\rho''/\eta'')]^{1/2}$, and Re $[m', m''] > 0$.

Laser light sources have noise characteristics that usually are of little concern for light scattering measurements of capillary wave motion at air/water interfaces. However, at liquid/liquid interfaces, e.g., the n-decane/water interface, the scattered light is more than 10 times weaker than that scattered from the air/water interface and the resonance frequency is lower for the same wavevector. For many systems, the autocorrelation function is then recorded over that part of the frequency band which also includes strong noise components (<1200 Hz). With decreasing interfacial tension, the laser noise becomes even more of a problem. The interfering laser noise, fortunately, can be suppressed by a differential or compensational technique. A schematic diagram of the laser heterodyne light scattering apparatus, using the differential technique, is shown in Figure 1.

The differential technique permits more precise measurements on liquid/liquid interfaces. Figure 2 illustrates how the measured autocorrelation function changes when a long-chain alkyl phosphate is spread at the n-decane/water interface at 20°C. The resonance frequency is observed to decrease when an interfacial film is present. Furthermore, after spreading, the autocorrelation function continues to slowly change due to desorption of the film molecules from the interface. Thus, desorption kinetics at liquid/liquid interfaces can be conveniently monitored by the laser light scattering technique. The desorption behavior of extraction reagents can provide valuable information on the structure and dynamics of extractant molecules.

We have been further developing the light scattering technique in an attempt to measure the interfacial viscoelastic properties of adsorbed or spread films at liquid/liquid interfaces. Figure 3 illustrates the range of values of interfacial dilational viscosity accessible by the light scattering technique. The relationship between the temporal damping coefficient, α, and the interfacial viscosity, κ, for a typical interfacial film at the n-hexane/water interface was calculated for three wavevectors of 10,000, 60,000, and 200,000 m^{-1} using the dispersion relation presented earlier. The interfacial viscosity affects the autocorrelation function of the capillary waves at this interface more so than at many other liquid/liquid interfaces including n-decane/water, CCl_4/water, and toluene/water interfaces. A solvent extraction system, thus, where the interfacial viscosity appears amenable to study is the n-hexane/aqueous system. Although the changes in the damping coefficient amount to only about 20%, compared to 300% in the case of air/water systems, it should be possible to extract information on the viscoelastic parameters if high resolution measurements are made.

INTERFACIAL TENSION MEASUREMENTS

The determination of interfacial viscoelastic properties by the light scattering technique requires simultaneous and accurate measurements of the interfacial tension. The prerequisite apparatus and techniques required to obtain accurate and reproducible interfacial tension measurements on HDEHP/n-hexane/aqueous systems have been developed. Di(2-ethylhexyl) phosphoric acid (HDEHP) was selected for study because of its technological relevance to solvent extraction (6).

An interfacial tensiometer was constructed to measure the interfacial tension of liquid/liquid solvent extraction systems. It consisted mainly of a thermostatted cabinet and thermostatted Pyrex cell, Cahn Model 2000 electrobalance, Bailey TH-6D digital thermometer, and precision motorized vertical translator. The interfacial tension was determined by measuring the maximum pull on a Wilhelmy plate. The best results consistently were obtained when sandblasted glass plates were used. Furthermore, the du Noüy ring method was found to give erroneous results. The interfacial properties are very sensitive to trace contaminants. Thus, it is essential to generate interfaces free of interfering surface-active impurities. The stringent precautions and purification procedures employed for HDEHP, n-alkanes, inorganic acids, and water are fully described elsewhere (7).

The effects of HDEHP concentration, various inorganic acids, acidity, and calcium ions on the interfacial tension of HDEHP/n-hexane/water systems were studied at 20°C. The effect of HCl, HNO_3, H_2SO_4 and $HClO_4$ on the interfacial tension was investigated. There is no effect of substituting one acid for another at constant normality when extraneous surface-active contaminants are absent. Literature values for comparison with the interfacial tension of HDEHP/n-hexane/aqueous systems are not available. Therefore, in order to ascertain the purity of our HDEHP/n-alkane/aqueous systems, n-dodecane was substituted for n-hexane. Our interfacial tension values for purified HDEHP/n-dodecane/0.001N HCl systems were found to be as much as 1 to 9 mN/m higher than those reported by others (8,9), thus demonstrating that significant extraneous surface-active impurities were present in earlier studies.

There are discrepancies between our results and those of earlier studies. In the γ-log [HDEHP] curves reported by other investigators, an inflection or plateau appears to occur near the onset of the linear portion (8), and it tends to become much more pronounced at lower acid concentrations (9). This behavior, however, was not observed in our highly purified systems even when n-dodecane was substituted for n-hexane. Possible explanations for these discrepancies include (a) changes in the wettability of the platinum-iridium ring used in these studies due to adsorption of HDEHP and (b) equilibrium measurements not being obtained with the du Noüy method. In addition, significant surface-active contaminants were present in these earlier studies and their role in interfacial tension behavior is not fully understood. These findings are discussed in greater detail elsewhere (7).

A preliminary study of the interfacial tension behavior of HDEHP/n-hexane/aqueous systems when the aqueous phase contained multivalent metal ions was also undertaken as part of our investigation into solvent extraction mechanisms. The addition of Ca^{2+} to the aqueous phase at very low pH values has no effect on the γ-log [HDEHP] curve. Figure 4, however, shows the significant interfacial tension lowering and abrupt change in the slope of the γ-log [HDEHP] curve which occurs when Ca^{2+} is present at pH $\geq$ 3. This appears to be due to the ionization of HDEHP and the subsequent formation of the calcium salt of HDEHP. Structural

changes very likely are occurring in the HDEHP/n-hexane/Ca^{2+}/HNO_3/H_2O system although the nature of any changes in the bulk phase or liquid/liquid interface remains for future research. Our results, nevertheless, indicate that HDEHP cannot be totally unionized at pH 3 as others have assumed in the past (10).

Spontaneous interfacial turbulence can strongly affect the rate of mass transfer (11,12). Preliminary experiments have demonstrated under what conditions the extraction of Ca^{2+} from aqueous solutions to n-alkane solutions containing HDEHP should be enhanced by interfacial turbulence. Talc particles were used as tracers to determine whether violent agitation or disturbances could be observed at the liquid/liquid interface. The pH of the aqueous phase and the concentrations of both HDEHP and Ca^{2+} are important factors governing interfacial turbulence. At pH < 3, interfacial turbulence could not be seen even at very high concentrations of Ca^{2+} and HDEHP. On the other hand, at high pH values (pH > 10), no interfacial turbulence could be observed at very low concentrations of Ca^{2+} and HDEHP. Presumably very little interfacial complexes form under these conditions so that there is no significant transfer of Ca^{2+} to the organic phase. Referring to Figure 4, interfacial turbulence was observed only at HDEHP concentrations above the break in the interfacial tension curve. Thus, it appears we have discovered a correlation between interfacial turbulence and interfacial properties which may be very important to solvent extraction processes. Work is in progress studying the rate of mass transfer in these systems.

CONCLUSIONS

Recently developed laser light scattering techniques represent a novel approach for examining the interfacial properties of solvent extraction systems. Mass transfer, interfacial turbulence, and coalescence studies also should be performed on one common, relatively simple, but well-characterized extractant system. Such an investigation correlating interfacial properties with the results of mass transfer and coalescence studies would make a significant contribution to the science and technology of solvent extraction.

ACKNOWLEDGMENTS

Financial support from the Division of Chemical Sciences in the Department of Energy is gratefully acknowledged.

REFERENCES

1. S. Hård and R. D. Neuman, J. Colloid Interface Sci., 83, 315 (1981).
2. H. Löfgren, R. D. Neuman, L. E. Scriven, and H. T. Davis, to be communicated.
3. J. T. Davies and E. K. Rideal, Interfacial Phenomena, Academic Press, New York, 1963.
4. Th. F. Tadros, Colloids Surfaces, 1, 3 (1980).
5. L. Kramer, J. Chem. Phys., 55, 2097 (1971).
6. C. F. Coleman and J. W. Roddy, Solvent Extraction Revs., 1, 63 (1971).
7. A. G. Gaonkar and R. D. Neuman, to be communicated.
8. G. F. Vandegrift and E. P. Horwitz, J. Inorg. Nucl. Chem., 39, 1425 (1977).
9. R. M. Machado, Interfacial Properties of Bis(2-ethylhexyl) Phosphoric Acid at the Dodecane-Hydrochloric Acid Interface, ANL, Argonne, IL, 1979.
10. G. F. Vandegrift and E. P. Horwitz, J. Inorg. Nucl. Chem., 42, 119 (1980).
11. C. V. Sternling and L. E. Scriven, AIChE J., 5, 514 (1959).
12. P. R. Danesi and R. Chiarizia, CRC Crit. Rev. Anal. Chem., 10, 1 (1980).

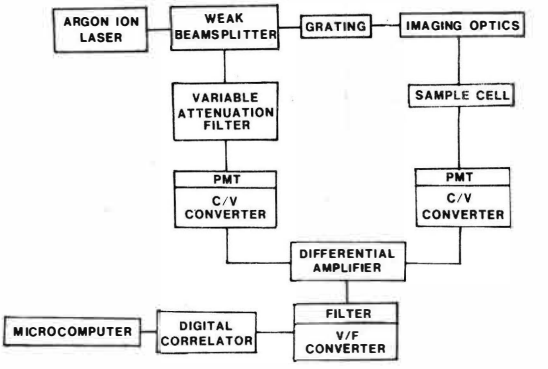

FIGURE 1. SCHEMATIC DIAGRAM OF LASER LIGHT SCATTERING APPARATUS

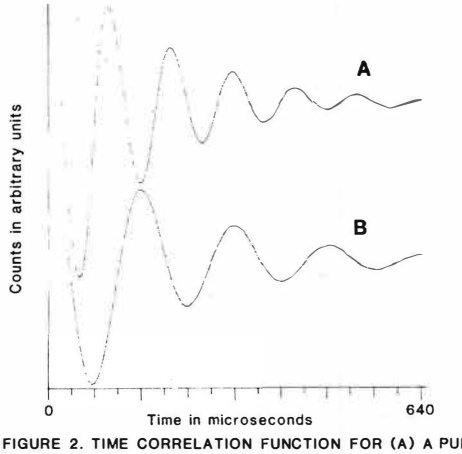

FIGURE 2. TIME CORRELATION FUNCTION FOR (A) A PURE n-DECANE-WATER INTERFACE AND (B) AFTER SPREADING A MONOTETRADECYL PHOSPHATE FILM

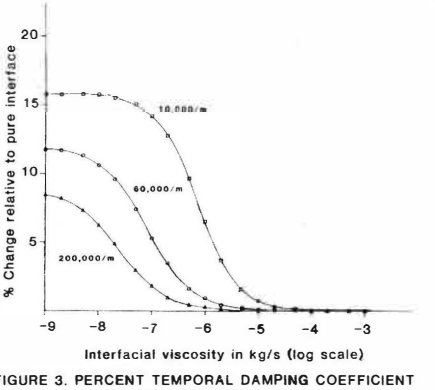

FIGURE 3. PERCENT TEMPORAL DAMPING COEFFICIENT CHANGE CALCULATED FOR THREE WAVE VECTORS

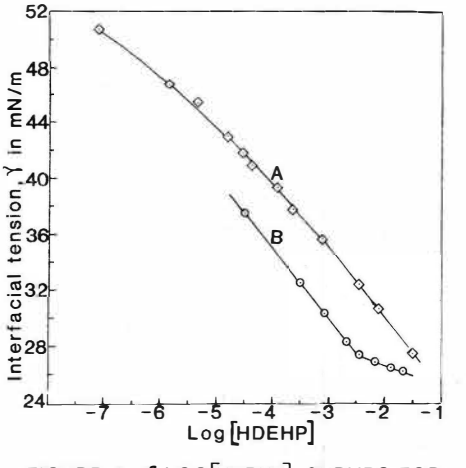

FIGURE 4. γ-LOG[HDEHP] CURVES FOR n-HEXANE-0.001M HNO_3 INTERFACE IN (A) ABSENCE AND (B) PRESENCE OF 0.01M $CaCl_2$

KINETICS AND MECHANISM IN METAL SOLVENT EXTRACTION BY SOME ORGANOPHOSPHOROUS EXTRACTANTS

C. Cianettti and P. R. Danesi

Chemistry Division
Argonne National Laboratory
Argonne, Illinois 60439 USA

INTRODUCTION

The liquid-liquid extraction kinetics of metal species can be determined by interfacial diffusional processes and by the rate of the chemical reactions occurring in the biphasic system. When the two phases are efficiently mixed, the extractant is strongly adsorbed at the liquid-liquid interface and exhibits negligible solubility in the aqueous phase, the possibility exists that interfacial chemical reactions can show up as rate determining processes. When this is the case the values of the rate constants must somehow reflect the physico-chemical properties of the environment where the reactions take place, i.e., the interface. In this paper, some recent work performed in our laboratory on the extraction kinetics of metal ions by HDEHP and some bifunctional organophosphorous extractant is briefly reviewed. In addition to the traditional interpretation of the rate data, based on rate determining macroscopic film diffusion processes (mass transport), an alternative explanation is herein presented where interfacial chemical reactions are assumed to be rate controlling.

EXPERIMENTAL PROCEDURE

The liquid-liquid extraction kinetics data have been obtained using a highly stirred constant interfacial area cell, ARMOLLEX (1). This apparatus allows one to continuously monitor the concentration variations and keep the interface quiescent, while stirring the two phases (water-dodecane) up to 750 rpm. All the kinetic experiments described here were carried out at stirring speeds of the two phases where the rate of mass transfer was independent from rpm. In the plateau region of the mass transfer rate vs stirring speed it is possible to assume that the extraction process is controlled by chemical reactions, providing slipping effects are not present. Further, since in the investigated systems the extraction rate was proportional to the ratio between the interfacial area and the volume of the phases, we also assumed that the extraction rate was controlled by interfacial chemical reactions.

INVESTIGATED SYSTEMS

Tables I and II report the results of the kinetic measurements expressed as pseudo first order rate constants of the interfacial reaction, k_1,

$$(1) \qquad M^{+z} + nE_{interfacial} \xrightarrow{k_1} \text{interfacial complex}$$

where E is HDEHP or the carbamoylphosphoryl extractant. If a diffusion model is alternatively assumed to explain the results, k_1 stands instead for the aqueous to organic mass transfer coefficient. The data of Table I for Fe^{+3} and Be^{+2} were not obtained in our laboratory, nevertheless they are here reported for comparison since they were obtained in experimental conditions very similar to ours. $km\text{-}H_2O$ is the rate constant of the water exchange process for the hydrated non-complexed ions.

The description of the carbamoylmethylphosphoryl extractants is shown in Table II. Table II also shows two parameters which correlate with the basicity of the phosphoryl group of the bifunctionl extractants, i.e., the infrared stretching frequency of P=O, $\nu_{P=O}$ (7,8), and the concentration of HNO_3 extracted by the bifunctional extractant after four equilibrations of a 0.5 M solution in o-xylene with 3 M aqueous HNO_3 (9). As expected, the basicity varies in the order:

DHDECMPO > HHDECMP > DHDECMP

DISCUSSION

The results presented in Tables I and II can be interpreted in terms of diffusional processes. In this case the rate controlling step of the extraction kinetics is assumed to be the macroscopic diffusion of each species to and from the interface through stagnant organic and aqueous diffusion films. In this instance k_1 represents the mass transfer coefficient and identical results should be obtained for identical hydrodynamic conditions irrespective of the different chemistry of the systems. However the data for Eu^{+3} with lactate and HEDTA and the ones for Fe^{+3} with acetate and citrate seem to contradict this hypothesis. An alternative explanation, which reconciles:

- the observed differences in the presence and absence of aqueous complexing agents,
- the trend observed for the bifunctional extractants

can be instead formulated when rate determining interfacial chemical reactions are assumed. Interfacial chemical reactions have been frequently suggested both in organic reactions (10) and in the solvent extraction of metal species (11). If they are rate determining, the overall rate constant of the interfacial chemical rection, k_1, must reflect both the reaction mechanism of the extraction process and the physico-chemical properties of the interfacial environment. Since our extractants are all surface active agents, which are interfacially adsorbed with the polar groups (P=O or $P\overset{O}{<}_{OH}$) facing the aqueous side of the interface, it follows that the interface can be schematically viewed as a surface carrying an excess of negative charges (Figure 1). As a consequence the water molecules adjacent to the interface will tend to orient their dipoles in such a way to form a sort of ice-like structure. The presence of interfacial structured water in proximity to flat solid surfaces has been recognized since long ago (12). More recently Drost-Hansen (13) concluded from conductivity measurements that a structure of "modified water," having a thickness of 0.05 to 0.2 μm, exists at glass-water interfaces. The properties of this "vicinal water" were reported to be different from those of ordinary water. In particular a higher viscosity characterizes these layers of interfacial water. By measuring the depression of the infrared continuum and the diffusion coefficient of the excess proton interfacial structured water, having a minimum thickness of 45 Å, was again confirmed at solid-liquid interfaces (14,15). More recently, the presence of viscous ice-like structured water was recognized also at aqueous-organic interfaces by measuring the interfacial ice-nucleation temperature (16,17). From what is reported above it follows that interfacial reactions (1) are likely to be influenced by the more viscous micro-environment where they occur. A probable mechanism for the ligand substitution reactions occurring at the interface is then a mixed associative-dissociative interchange mechanism, i.e.,

$$(2) \qquad M(H_2O)_n^{+z} + L_i \underset{\text{slow}}{\overset{\text{Step 1}}{\rightleftharpoons}} \underbrace{[M(H_2O)_n^{+z}\ldots L]_i}_{\text{outer-sphere}} \underset{\text{slow}}{\overset{\text{Step 2}}{\rightleftharpoons}} \underbrace{[LM(H_2O)_{n-1}^{+z}]_i}_{\text{inner-sphere}} + H_2O$$

The subscript i represents interfacial species. According to mechanism (2) the Eigen-Wilkins mechanism, which applies to many aqueous phase ligand-exchange reactions, is here modified by the presence of a preceding slow associative step (Step 1). The formation of the outer-sphere complex, which is controlled by the diffusion of the metal ion through the viscous layers of interfacial water, is now slow because of the inverse proportionality existing between the rate constant of the diffusion controlled step and the viscosity of the medium. Step 2 is, on the other hand, still controlled by the rate of the water exchange process. If the metal is complexed in the aqueous phase by a ligand A the overall mechanism can be described by:

$$(3) \qquad AM(H_2O)_{n-1}^{+z} + L_i \underset{\text{Step 1}}{\rightleftharpoons} [AM(H_2O)_{n-1}^{+z}\ldots L]_i \underset{\text{Step 2}}{\rightleftharpoons} [LM(H_2O)_{n-1}^{+z}]_i + A$$

When the reaction takes place in the aqueous bulk (Step 1 is fast) step 2 of equation (3) is known to be faster than Step 2 of equation (2), since the replacement of some water molecules with a labile ligand, such as carboxylate anions, increases the rate of exchange of the remaining ones. When on the other hand, the ligand is a multidentate anion, forming strong chelating bonds, which replaces most of the solvating water molecule, such as polyaminocarboxylic acids, the opposite takes place, The data of Table I seem to indicate that the same effect holds for ligand exchange reactions occurring with our extractants. In fact the presence of acetate, lactate, or citrate anions seems to accelerate the otherwise slow Step 2's of Fe^{+3}, Co^{+2}, Ni^{+2}, and Eu-HEDTA. When the rate constant of the water substitution reaction is not as slow as for Fe^{+3} or Eu-HEDTA, the overall rate constants seem to be determined only by the rate of diffusion (Step 1). The rate of Step 1 is then determined only by the rate of diffusion of the hydrated-complexed ion through the viscous interfacial water.

The influence of the different extent of water orientation can be evidenced when extractants, having similar structure but different electronic densities on the hydrophilic group, are used. In the frame of the proposed model the extent of water structuring, and consequential water viscosity, should parallel the extractant basicity, i.e.,

DHDECMPO > HHDECMP > DHDECMP.

The decrease of k_1 with $\nu_{P=O}$ and its increase with $[\overline{HNO_3}]$, shown in Table II, is in agreement with the proposed model.

REFERENCES

1. P. R. Danesi,C. Cianetti, E. P. Horwitz, and H. Diamond, Sep. Sci. Tech. 17, 962 (1982).
2. P. R. Danesi and G. F. Vandegrift, J. Phys. Chem. 85, 3646 (1981).
3. P. R. Danesi and C. Cianetti, Sep. Sci. Tech. 17, 969 (1982).
4. C. Cianetti and P. R. Danesi, Solvent Extraction and Ion Exchange 1, 1 (1983).
5. J. W. Roddy, C. F. Coleman, and S. Asari, J. inorg. Nucl. Chem. 33, 1099 (1960).
6. C. F. Coleman and J. W. Roddy, Solvent Extraction Reviews, Y. Marcus, Ed., Marcel Dekker, Inc., New York (1971), pp. 61-90.
7. E. P. Horwitz, A. C. Muscatello, D. G. Kalina, and L. Kaplan, Sep. Sci. Tech. 16, 417 (1981).
8. D. G. Kalina, E. P. Horwitz, L. Kaplan, and A. C. Muscatello, Sep. Sci. Tech. 16, 1127 (1981).

*Work performed under the auspices of the Office of Basic Energy Sciences, Division of Chemical Sciences, U. S. Department of Energy under Contract W-31-109-ENG-38.

9. E. P. Horwitz, D. G. Kalina, L. Kaplan, G. W. Mason, and H. Diamond, Sep. Sci. Techn. 17, 1261 (1982).

10. F. Menger, Chem. Soc. Rev. 1, 229 (1972).

11. P. R. Danesi and R. Chiarizia, CRC Critical Reviews in Analytical Chemsitry, Vol. 10, No. 1 (1980).

12. R. E. Grim, Clay Mineralogy, McGraw-Hill (1953), pp. 162-164, and references therein.

13. J. A. Schufle, C. T. Huang, and W. Drost-Hansen, J. Coll. Int. Sci. 54, 184 (1976).

14. N. K. Roberts and G. Zundel, J. Phys. Chem. 84, 3655 (1980).

15. N. K. Roberts, J. Phys. Chem. 85, 2706 (1981).

16. J. Rosinski, J. Phys. Chem. 84, 1829 (1980).

17. J. Rosinski and A. Lecinski, J. Phys. Chem. 85, 2939 (1981).

Table I. Kinetic Data for the Extraction of Some Metal Ions by HDEHP in n-Dodecane at 25°C.

Ion	Aqueous Accelerating Agent	Aqueous Retarding Agent	k_1 (cm/sec)	Ref.	k_{m-H_2O} (sec^{-1})
Zn^{2+}	-	-	1.4×10^{-3}	(4)	5×10^7
Am^{3+}	-	-	1×10^{-3}	(2)	10^8 (?)
Co^{2+}	Acetate	-	3.6×10^{-3}	(4)	5×10^6
Ni^{2+}	Acetate	-	4.6×10^{-3}	(4)	5×10^4
Eu^{3+}	-	-	1×10^{-3}	(2)	10^8
Eu^{3+}	Lactate	-	1×10^{-3}	(3)	10^8
Eu^{3+}	-	HEDTA	2×10^{-5}	(3)	10^8
Eu^{3+}	Lactate	HEDTA	1.4×10^{-4}	(3)	10^8
Fe^{3+}	-	-	$\sim 1 \times 10^{-5}$	(5)	10^2
Fe^{3+}	Acetate	-	$\sim 2 \times 10^{-4}$	(5)	10^2
Fe^{3+}	Citrate	-	$\sim 2 \times 10^{-4}$	(5)	10^2
Be^{2+}	-	-	$\sim 1 \times 10^{-4}$	(6)	10^2

Table II. Kinetic Data for the Extraction of Am(III) by Carbamoylmethylphosphoryl Extractants in Diethylbenzene at 25°C

Extractant	k_1 (cm/sec).10^3	$\nu_{P=O}$	$[\overline{HNO_3}]$, M
DHDECMP (phosphonate)	2.55	1255	0.53
HHDECMP (phosphinate)	2.16	1222	0.61
DHDECMPO (phosphine oxide)	2.07	1167	0.65

DHDECMP: dihexyl-N,N-diethylcarbamoylmethylphosphonate $(C_6H_{13}O)_2POCH_2CON(C_2H_5)_2$

HHDECMP: hexyl,hexyl-N,N-diethylcarbamoylmethylphosphinate

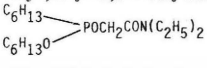

DHDECMPO: dihexyl-N,N-diethylcarbamoylmethylphosphine oxide $(C_6H_{13})_2POCH_2CON(C_2H_5)_2$

SIMPLIFIED PICTURE OF THE INTERFACIAL STRUCTURING EFFECT OF AN ORGANIC SOLUBLE EXTRACTANT

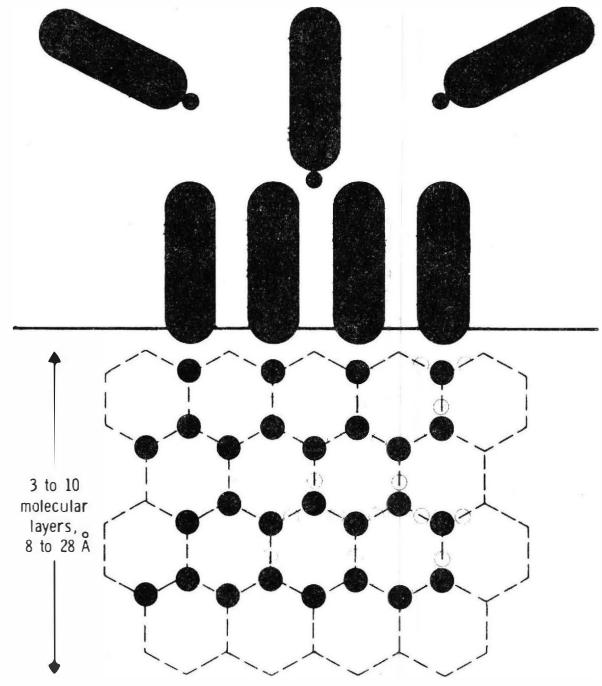

REACTION IN VOLUME AND REACTION AT INTERFACE. CALCULATION OF THEIR CONTRIBUTIONS TO OVERALL EXTRACTION RATE

G. Yagodin, V. Tarasov, A. Pichugin

Mendeleev Institute of Chemical Technology
A-47, Miusskaya sq., 9.
Moscow, USSR

The reactions in liquid-liquid systems are widely spread phenomena. In particular, the extraction of inorganic substances realizes practically as a result of chemical interactions, completing the formation of extracted substances, with their subsequent dissolving in organic phase. The reverse process (stripping) necessary is to involve the decay of the extracted complexes. In many cases, chemical reactions limit overall extraction rate.

From the point of view of the reaction mechanism studies and the development of the methods controlling reaction rate, it is necessary to distinguish the reactions in volume (RV) and reactions at interface (RI). In the first case the adsorption properties of reagents and other components are not essential. In the second case - the extraction rate depends to a significant extent on the adsorption conditions at the interface, and therefore, on the presence of a small quantity of the surfactant in the solutions.

In the case of the real extraction process the situation becomes more complicated, because of the RV and RI take place parallelly and simultaneously. Therefore, important practical and theoretical task is the calculation of the contributions of RS and RV to the formation of finite product. This task has not been solved yet. One can see that short-time phase contact method (STCM) presented in the paper (1,2) helped us to solve this task.

Let's consider the situation, when in the system consisting of two mutually unsoluble, homogeneous, isotropic, one - dimensional and half-infinite phase, the substance A is transported from phase 1 into phase 2 and undergoes chemical reactions $A \xrightarrow{kv} B$ (RV) and $A \xrightarrow{ki} B$ (RI). Mass transport substances A and B realize by means of unstationary molecular diffusion in accordance with the Fick's equations. We describe the given task with such equations:

$$\begin{cases} D_{A1}\dfrac{\partial^2 C_{A1}}{\partial x^2} = \dfrac{\partial C_{A1}}{\partial t} \\ D_{A2}\dfrac{\partial^2 C_{A2}}{\partial x^2} = \dfrac{\partial C_{A2}}{\partial t} + K_v C_{A2} \\ D_{B2}\dfrac{\partial^2 C_{B2}}{\partial x^2} = \dfrac{\partial C_{B2}}{\partial t} - K_v C_{A2} \end{cases}$$

initional conditions: $C_{A1}(x,0) = C$; $C_{A2}(x,0) = 0$; $C_{B2}(x,0) = 0$
boundary conditions: $C_{A1}(-\infty,t) = C$; $C_{A2}(+\infty,t) = 0$; $C_{B2}(+\infty,t) = 0$

$$C_{A1}(0,t) = \alpha C_{A2}(0,t); \quad D_{B2}\frac{\partial C_{B2}}{\partial x}\bigg|_{x=0} = K_s C_{A1}\bigg|_{x=0};$$

$$D_{A2}\frac{\partial C_{A2}}{\partial x}\bigg|_{x=0} + K_s C_{A1}\bigg|_{x=0} = D_{A1}\frac{\partial C_{A1}}{\partial x}\bigg|_{x=0}$$

The solution of this task leads to the following expressions for the quantity of substance B in phase 2 formated by RI(q_{RI}), RV(q_{RV}) and both reactions (q_{RI+RV}), when $t \to \infty$

$$q_{RI} = g\varphi(\varphi+1)^{-1}\cdot t^{1/2} - \varphi(\varphi+1)^{-2}\cdot h \qquad (1)$$

$$q_{RV} = g(\varphi+1)^{-1}\cdot t^{1/2} - (\varphi+1)^{-2}\cdot h \qquad (2)$$

$$q_{RI+RV} = g t^{1/2} - (\varphi+1)^{-1}\cdot h \qquad (3)$$

Where $g = 2C(D_{A1}/\pi)^{1/2}$, $h = \alpha C D_{A1}(K_v D_{A2})^{-1/2}$ $\varphi = \alpha K_i (K_v D_{A2})^{-1/2}$. The contribution of RI(Pi) is equal q_{RI}/q_{RI+RV}, and of RV(Pv) is equal q_{RV}/q_{RI+RV}. If $t \to 0$, the rate of RI reaches the value KsC, and the rate of RV tends to zero. Consequently, in initial period of contacting extraction take place by RI. During to time the contribution of RI decreases from 1 to $\varphi(\varphi+1)^{-1}$. On the contrary, the contribution of RV increases from zero to $(\varphi+1)^{-1}$. The contribution are the finite and constant values, because in the periods of $t \to \infty$ the rates of increasing of quantity of substance B for both RI and RV decreases according to identical low: $\exp(\lambda^2 t)\,\mathrm{erfc}(\lambda t^{1/2})$.

The analysis of (1-3) points out that if $\varphi \gg 1$, then RI prevails and its contribution tends to 1 for any times of contacting. If $\varphi \ll 1$, then prevails RV. As at the first moment the rate of RI is a finite quantity and unequal zero, while the rate of RV equals zero, we can destribute and calculate the contribution of each reaction. The relationship $4r_0 m(\pi g)^{-1}$ (where $r_0 = K_s C = dq/dt|_{t\to 0}$; $m = \varphi\pi D_{A1}[2K_s(\varphi+1)]^{-1}$ is calculated the contribution of RI. Parameters r_0, m we can calculate from diagrams q = f(t) and q = f(t½), resulted by means of STCM.

Ourself method of contributions calculation was tested on the kinetic extraction data in system $UO_2(NO_3)_2$ - H_2O - TOPO - Toluen (Table 1). It became clear that in the wide concentration range the RI is prevail. This statement is conformed conclusion on process mechanism (3).

It is known that interfacial chemical reactions are limited copper extraction rate by oxyoximes. Kinetic and mechanism of this reactions recently have been the subject of intensive studies. At the same time the essential question as to the localization of chemical reactions limiting the extraction rate remains unsettled.

In this paper has shown that contributions of RI and of RV depend on time of contacting. Probably, for reactions, whose order more than 1, contributions will depend on concentration of reagents.

Using the copper extractions (stripping) kinetic data to the calculation of RI and RV contributions. We have shown that values of RI and RV contributions are comparable in the wide concentration range. With the decrease of extractant concentration (in case of extration) the reaction at the interface became dominating.

Table 1. Stripping kinetics in system: $UO_2(NO_3)_2$-H_2O-TOPO-toluen

C^o_{Cu} $\frac{kmol}{m^3}\cdot 10^3$	$Ks\cdot 10^6$ $\frac{m}{c}$	$4g/m^2 C^o_{Cu}\cdot 10^6$ $\frac{m}{c}$	Pi	Pv
3,6	6,3	6,4	0,98	0,02
7.2	12.8	13.3	0.86	0.04
14.4	13.0	13.8	0.94	0.06
28.8	10.0	11.2	0.89	0.11
43.2	5.2	5.9	0.88	0.12
57.5	3.2	3.4	0.94	0.06
73.0	2.1	2.3	0.91	0.09

Table 2. Copper extraction (stripping) kinetics in system: $CuSO_4$ - H_2O - 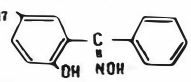 - toluen

Extraction: $pH_o=3.0$; $C^{H_2O}_{Cu}=0.02\frac{kmol}{m^3}$ Stripping: $pH_o=2.4$

C^o_{ex} $\frac{kmol}{m^3}$	Pi	Pv	$C^o_{Cu}\frac{kmol}{m^3}$	Pi	Pv
0.22	0.31	0.69	0.031	0.37	0.63
0.11	0.31	0.69	0.018	0.39	0.61
0.08	0.41	0.59	0.010	0.38	0.62
0.06	0.74	0.26	0.008	0.40	0.60
0.0028	0.86	0.14	0.003	0.42	0.58

C^o_{ex} - extractant concentration in toluen

C^o_{Cu} - copper concentration in organic phase.

REFERENCES

1. V. Tarasov, G. Yagodin, A. Ivanon, N. Krutchinina. Izv. Vish. Shk. Khim. i khim. Technol., 1977, t. 20, N 4, p. 530-532.
2. Osnovy zidkostnoj ekstraksii. Red. G. Yagodin, Moskwa, "Khimija", 1981.
3. G. Yagodin, V. Tarasov, A. Ivanov, N. Krutchinina. Dokl. Acad. Nauk SSSR, 1979, t. 246, N 6, p. 1431-1434.

KINETICS AND MECHANISM OF COPPER EXTRACTION WITH 8-DODECYLBENZENESULFONAMI DOQUINOLINE

Fumiyuki Nakashio,* Kazuo Kondo, Michiaki Matsumoto and Kazuharu Yoshizuka
Kyushu University
Fukuoka, Japan

*(F. Nakashio is Member of AIChE)

As the selective extractant of copper from diluted acidic liquors, LIX 34 was recently introduced by General Mills Inc.(1). Several studies concerning LIX 34 were carried out by Virnig (2) and Hoh et al (3,4,5) on the solvent extraction equilibrium and kinetics for several metals. In order to clarify the extraction mechanism, however, it might be required to investigate on the extraction kinetics by using the pure active component of the commercial extractant LIX 34, because the rate of metal extraction is influenced by a small quantities of surface active species such as dodecylbenzenesulfonylacid which is a by-product in the synthesis of 8-dodecylbenzenesulfonamidoquinoline, the active component of LIX 34.

In this work, 8-dodecylbenzenesulfonamidoquinoline (henceforth DBSAQ, abbreviated as HR) purified was used to clarify the extraction mechanism by measuring the extraction rate of copper with DBSAQ in a stirred transfer cell, along with the measurements of the extraction equilibrium and the interfacial adsorption equilibrium.

EXPERIMENTAL

Reagents: DBSAQ was prepared with 8-aminoquinoline dissolved in pyridine and adding in small portions p-dodecylbenzenesulfonylchloride in benzene(6,7). After purification by chromatography over silicagel column with benzene, the white solid product was obtained, having the structure shown in Figure 1. The complex of DBSAQ-Cu(II) prepared by usual procedure (8) is a brownish black solid. All the reagents used in the synthesis was commercial G.R. grade. Toluene of commercial G.R. grade was used as organic solvent without further purification. Other inorganic reagents used was commercial G.R. grade, such as copper nitrate, sodium acetate, acetic acid and hydrochloric acid.

Measurements of extraction equilibrium: The organic solution was prepared by dissolving DBSAQ in toluene. The aqueous solution was prepared by dissolving copper nitrate in deionized water and adjusting pH with adding 0.1 mol/l sodium acetate-acetic acid buffer solution and/or 0.1 mol/l nitric acid.

Extraction equilibrium was measured at 30°C. The concentration of copper in aqueous solution was determined by atomic absorption spectrophotometer (Shimadzu AA-646). Copper complex in organic solution was stripped by about 2 mol/l hydrochloric acid to determine the concentration by atomic absorption spectrophotometer.

Interfacial adsorption equilibrium: Interfacial tension in the solvent extraction system was measured at 30°C by the drop weight method to examine interfacial adsorption equilibria of DBSAQ and the copper complex.

Measurement of extraction rate of copper by DBSAQ: The stirred transfer cell, so-called Lewis type cell, was used to measure the rate of copper extraction by DBSAQ at 30°C. The cell consists of two compartments, that is, the upper compartment for the organic solution and the lower compartment for the aqueous solution. The volume of each compartment was about 110 cm^3 and the interfacial area of both solutions was 12.42 cm^2. Both solutions in the cell were stirred in opposite direction by two flat-blade stirrers at 150 rpm. Experimental appratus and procedure were described in detail previously (9,10).

RESULTS

Extraction equilibrium: Apparent molecular weight of DBSAQ in toluene was measured by vapor-phase osmometry to obtain the mean aggregation number of DBSAQ. The result suggested that DBSAQ in toluene is in monomer state.

As shown in Figure 2, the distribution constant of copper, D, defined by Eq. (1), was proportional to the square of the concentration ratio of extractant to hydrogen ion, that is, C_{HR}/C_H.

(1) $D = [Cu]_{org} / [Cu]_{aq}$

where $[Cu]_{org}$ and $[Cu]_{aq}$ were total concentration of copper in organic and aqueous solution, respectively. The result suggested that extraction equilibrium of copper with DBSAQ can be expressed as follows;

(2) $Cu^{2+}_{aq} + 2HR_{org} \rightleftharpoons CuR_{2\,org} + 2H^+_{aq}$ $\quad K_{ex}$

where K_{ex} is the extraction equilibrium constant. Since $[Cu]_{org}$ and $[Cu]_{aq}$ are respectively the concentration of $CuR_{2\,org}$ and Cu^{2+}_{aq} under this experimental condition, the relation between K_{ex} and D can be written as follows;

(3) $\log D = \log K_{ex} + 2 \log C_{HR}/C_H$

It was found from Figure 2 and Eq.(3) that K_{ex}= 3.29 for DBSAQ and K_{ex}= 0.92 for OSAQ (octanesulfonamidoquinoline).

Interfacial adsorption equilibrium: The relations between interfacial tension and the concentration of DBSAQ and of DBSAQ-Cu(II) complex are shown in Figures 3 and 4, respectively. The results suggested that the copper complex does not adsorb at the interface, but DBSAQ adsorbs at the interface, that is, the adsorption equilibrium of DBSAQ is expressed as follows;

(4) $HR_{org} \rightleftharpoons HR_{ad}$ $\quad K_{HR}$

where K_{HR} is the adsorption equilibrium constant. According to Gibbs adsorption isotherm, the interfacial tension is derived as a function of C_{HR}, as follows (11);

(5) $\gamma = \gamma_0 - (RT/S_{HR}) \ln(1 + K_{HR} S_{HR} C_{HR})$

where γ_0 is the interfacial tension between toluene and water and S_{HR} is the interfacial area occupied by unit mole of DBSAQ. The values of K_{HR} and S_{HR} are obtained from the experimental results of γ and Eq.(5) by non linear regression using modified Marquardt's method, as shown in Table 1. A solid curve in Figure 3 is calculated by Eq.(5).

Extraction rate of copper by DBSAQ: The initial extraction rate, R_0, was obtained under various experimental conditions.

The effect of copper concentration on R_0 is shown in Figure 5. R_0 was pro-

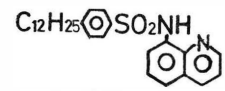

FIGURE 1. STRUCTURE OF DBSAQ

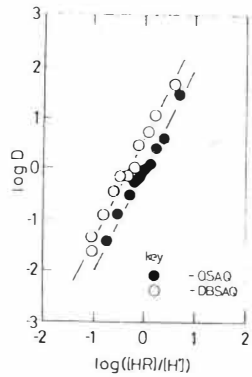

FIGURE 2. EXTRACTION EQUILIBRIA OF COPPER WITH SULFONAMIDOQUINOLINE

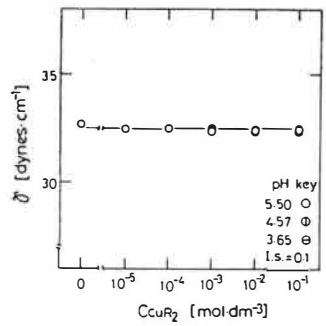

FIGURE 4. INTERFACIAL TENSION OF METAL COMPLEX IN TOLUENE

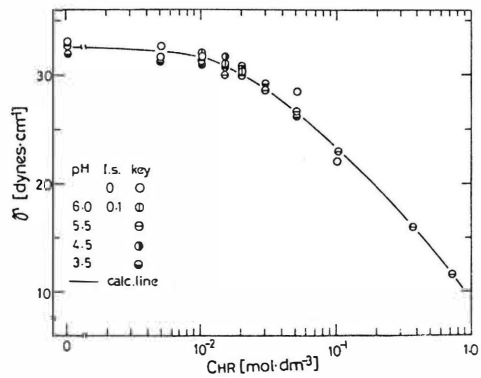

FIGURE 3. INTERFACIAL TENSION OF DBSAQ IN TOLUENE

portional to the initial copper concentration, C_{Cu0}, in the range of higher pH and lower C_{Cu0}, but in the range of lower pH and higher C_{Cu0} the slope of $\log R_0$ vs. $\log C_{Cu0}$ was slightly smaller than 1.0.

The effect of DBSAQ concentration on R_0 is shown in Figure 6. In the range of lower initial concentration of DBSAQ, C_{HR0}, the slopes of $\log R_0$ vs. $\log C_{HR0}$ are about 1.5, but in the range of higher C_{HR0}, the slopes approach to zero.

The effect of pH on R_0 is shown in Figure 7. In the range of lower pH, the slopes of $\log R_0$ vs. pH are 1.0, but in the range of higher pH the slopes approach to zero.

From the above results, it could be considered that the extraction mechanism in the higher pH range is different from that in the lower one.

DISCUSSION

Interfacial Reaction Model: As mentioned above, DBSAQ adsorbs at the interface between the aqueous and organic solutions, but the complex of DBSAQ-Cu(II) does not. Furthermore, the distribution constant of DBSAQ, D_{HR}, defined by $D_{HR} = C_{HRaq}/C_{HRorg}$, equals to 2.2×10^{-6} at 30°C and the reaction rate constant between copper and chelating reagent in aqueous solution might be expected to be rather large. On these premises, it could be considered that the reaction between copper and DBSAQ occurs at the interface as follows;

(6) $Cu^{2+}_{i} + HR_{ad} \rightleftharpoons CuR^{+}_{ad} + H^{+}_{i}$ K_1

(7) $CuR^{+}_{ad} + HR_{ad} \rightleftharpoons CuR_{2i} + H^{+}_{i}$ K_2

where K_1 and K_2 are equilibrium constant of each reaction, the subscript "ad" denotes the adsorption state at the interface and the subscript "i" denotes the aqueous phase or the organic phase adjacent to the interface. Since the species of CuR^{+} could be expected to have the interfacial adsorption constant as much as DBSAQ, the reaction step shown by Eq.(7) can be considered as the rate controlling step in the interfacial reaction process, expressed by Eqs.(4),(6) and (7). Using the Langmuir's adsorption isotherm and assuming that the interfacial area occupied by unit mole of CuR^{+} equals to S_{HR}, the interfacial reaction rate, R, is derived as follows;

$$(8)\quad R = \frac{k_f K_{HR}^2 K_1 \left(C_{Cui} C_{HRi}^2/C_{Hi} - C_{CuR_2 i} C_{Hi}/K_{ex} \right)}{\{1 + K_{HR} S_{HR} C_{HRi} + K_{HR} S_{HR} K_1 C_{Cui} C_{HRi}/C_{Hi}\}^2}$$

where k_f is the reaction rate constant of the reaction step shown by Eq.(7), and $K_{ex} = K_1 K_2 K_{HR}$. The concentration of each species adjacent to the interface is obtained by assuming the pseudo steady state conditions in the vicinity of the interface, that is, the interfacial reaction rate equals to the mass transfer rate of each species, as follows;

$$(9)\quad R = k_{Cu}(C_{Cu} - C_{Cui}) = (k_{HR}/2)(C_{HR} - C_{HRi}) = k_{CuR_2}(C_{CuR_2 i} - C_{CuR_2})$$

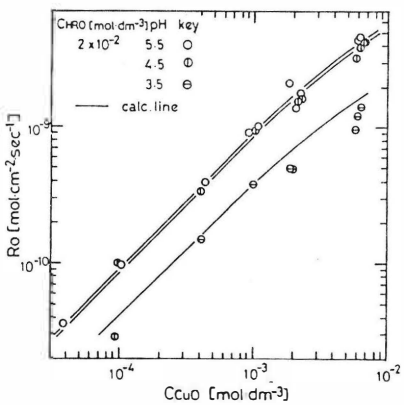

FIGURE 5. EFFECT OF COPPER CONCENTRATION ON THE INITIAL EXTRACTION RATE

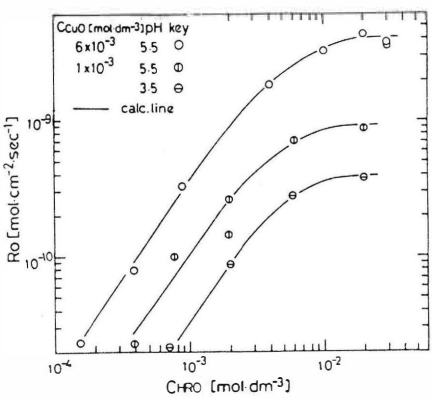

FIGURE 6. EFFECT OF DBSAQ CONCENTRATION ON THE INITIAL EXTRACTION RATE

where k_j and C_j are the mass transfer coefficient and bulk concentration of species j (j=Cu,HR and CuR_2), respectively. The concentration of hydrogen ion adjacent to the interface C_{Hi} could be considered to equal to the bulk concentration C_H, because buffer solution is used.

Analysis of the initial extraction rate: The initial extraction rate R_0 is calculated from Eqs (8) and (9) by giving the initial condition and the values of k_f, k_{Cu}, k_{HR}, K_{CuR_2}, K_1, K_{HR}, S_{HR} and K_{ex}. Among of them, K_{HR}, S_{HR} and K_{ex} are already given from the extraction and adsorption equilibrium. From the experimental results of R_0 and Eqs (8) and (9), the values of k_f, k_{Cu}, k_{HR} and K_1 were evaluated with the non-linear regression as mentioned above, assuming the reverse reaction term of Eq (8) is neglegible. The solid curves shown in Figures 5,6 and 7 are calculated by using Eqs (8) and (9) and the values shown in Table 1.

Simulation of Extent of copper extracted: Simulation of the experimental results in the range of high extent of copper extracted was carried out to confirm the availability of the interfacial reaction model. The concentrations of the species in the aqueous and organic solution in the cell are expressed as follows.

$$(10)\quad -V_{aq}\frac{dC_{Cu}}{dt} = -2V_{org}\frac{dC_{HR}}{dt} = V_{org}\frac{dC_{CuR_2}}{dt} = A\,R$$

where $V_{aq} = V_{org} = 110\ cm^3$, $A = 12.42\ cm^2$ and t is the extraction time. Eqs. (8), (9) and (10) are simultaneously solved by Runge-Kutta-Gill method to obtain the extent of copper extracted, E_{calc}. The value of k_{CuR_2} used is also shown in Table 1, which is obtained from the rate of stripping. The calculated results are compared with the observed results E_{obs} in Figure 8.

CONCLUSION

Along with the extraction equilibrium and the interfacial adsorption equilibrium, the extraction rate of copper with DBSAQ was measured in the stirred transfer cell to clarify the extraction mechanism. The experimental results suggested the abailability of the interfacial reaction model which includes the interfacial reactions and the diffusions of copper, DBSAQ and the metal complex.

REFERENCES

1. G.A.Kordosky, K.D.Macky and M.I.Virning, paper presented at 105th A I M E Annual Meeting, Feb. (1976)
2. M.J.Virnig, Proc. of I S E C 77, Vol. 2, 535 (1977)
3. Y.C.Hoh and W.K.Wang, J. Chem. Tech. and Biotech., 31, 345 (1981)
4. Y.C.Hoh, N.P.Chow and W.K.Wang, I & EC Proc. Des. & Dev., 21, 12 (1982)
5. C.H.Wang and Y.C.Hoh, Hydrometallurgy, 8, 161 (1982)
6. M.Takagi, T.Omori, S.Matsuo, K.Ueno and S.Ide, Chem. lett., 387 (1980)
7. M.Matsumoto, K.Yoshizuka, K.Kondo and F.Nakashio, Submitted to J.Chem.Eng.Japan
8. G.B.Joshi, G.S.Patel and V.M.Thakor, J.Indian Chem. Soc., 52, 1207 (1975)
9. K.Kondo, S.Takahashi, T.Tsuneyuki and F.Nakashio, J. Chem. Eng. Japan, 11, 193 (1978)
10. K.Kondo, T.Tsuneyuki and F.Nakashio, Proc. I S E C '80, Vol. 3, 80-211 (1980)

TABLE 1. ANALYTICAL RESULTS OF EXTRACTION RATE OF COPPER WITH DBSAQ

$k_f K_{HR}^2 K_1$	1.13 ± 0.13	$[cm^4.mol^{-1}.s^{-1}]$
K_{HR}	(6.22 ± 0.79) x 10^{-6}	$[cm^3.cm^{-2}]$
S_{HR}	(3.18 ± 0.23) x 10^9	$[cm^2 mol^{-1}]$ 53 Å²/mol
K_1	(1.69 ± 0.25) x 10^{-2}	[-]
k_f	(1.73 ± 0.47) x 10^{12}	$[cm^2.mol^{-1}.s^{-1}]$
k_{Cu}	(9.52 ± 0.64) x 10^{-4}	$[cm.s^{-1}]$
k_{HR}	(9.19 ± 0.48) x 10^{-4}	$[cm.s^{-1}]$
K_{ex}	3.29 ± 0.26	[-]

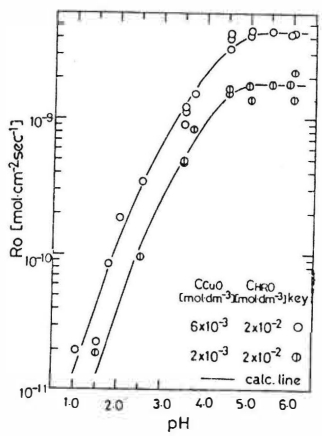

FIGURE 7. EFFECT OF pH ON THE INITIAL EXTRACTION RATE

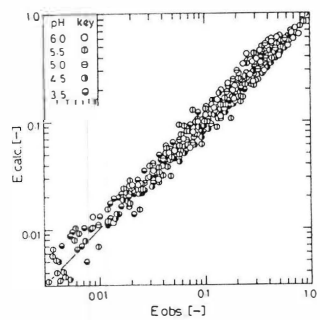

FIGURE 8. COMPARISON OF Eobs. AND Ecalc.

STUDY OF AGITATOR TYPE IN MIXER-SETTLERS

Z. J. Shen
Department of Chemical Engineering
McMaster University
Hamilton, Ontario, Canada

and

Q. Y. Zhang, B. Y. Sun, J. Li and Y. F. Su

East China Institute of Chemical Technology
Shanghai, China

INTRODUCTION

Mixer-settlers are widely used as liquid-liquid contacting apparatus both in the laboratory and in industry. With a view to improving the stage efficiency and reducing the power consumption, many new designs have been introduced of late (1,2,3,4). The present investigation chiefly concerns the power consumptions in mixer-settlers using four different types of impellers and design configurations, with three different systems. These impellers act as pumping-mixing devices in a laboratory box-type mixer-settler operating in steady state of the flow rates and uniformly dispersed conditions.

APPARATUS

The apparatus employed is a single stage box type mixer-settler and the 4 types of impeller selected for comparison are large delta, medium delta, flat paddle and Rushton turbine. Figure 1 shows the schematic configuration diagram of the mixer-settler with a delta type impeller and Figure 2 shows the 4 types of impellers used in the present investigation. All the impellers have both a pumping action which expedites the flow of the two phases into the mixer through the draft opening on the base, and a mixing action which disperses one phase into another. The experimental apparatus diagram for stage (n) shown in Figure 3 indicates that the heavy liquid phase enters into mixer from an adjacent (n-1) stage through the interface controller 10, while the light liquid phase overflows from stage (n+1) through the light phase overflow tube 11 then entering the mixer. The plexiglass mixer-settler has a mixing chamber volume V_m = B x B x 1.2 B = 4.05 liter (B is the width of square cross-section) and the volume of settler is V_s = 10.13 liter adjoining the mixer (not shown in Figure 3). The agitator is driven by a variable speed D.C. motor 5 which is connected with a silicon speed controller 7, voltmeter 8 and ammeter 9. The actual rotating speed is shown digitally on the rota-speed detector 6.

The diameter of the liquid inlet d and the position of the agitator in the mixer (indicated as the clearance h between the top of the liquid draft opening and the bottom of the agitator, see Figure 3) can be adjusted as required.

EXPERIMENTAL METHODS

In the absence of mass transfer and under constant operating conditions (throughput 0.022 l/s each phase, phase ratio O/A = 1, contacting time 91 sec.), three systems, i.e. mutually saturated water/n-butanol, water/kerosene and water/n-heptane were used. The properties of the systems are as follows:

Systems		viscosity μ (kg/ms) (16°C)	density ρ(kg/m^3)	conductivity λ(μω/cm)	interfacial tension γ(N/m)
1	water	1.147×10^{-3}	990.5	4.6×10^{2}	2.6×10^{-3}
	n-butanol	3.667×10^{-3}	849.3	0.82	
2	water	1.128×10^{-3}	1001	6.7×10^{2}	35.6×10^{-3}
	kerosene	1.671×10^{-3}	800.7	0.33	
3	water	1.128×10^{-3}	1001	6.7×10^{2}	51×10^{-3}
	n-heptane	0.49×10^{-3}	689.2	0.25	

Experiments were carried out to measure the minimum net power consumption P_n (watt) in each case to achieve uniformity of mixing and the constancy of the throughput of both phases. The measuring methods of above experiments were described in reference (5). The parameters changed were the 3 systems, 4 types of agitators, the diameter d of the liquid draft opening and the clearance h as shown in Figure 3. The values of variables d and h studied are as follows:

d	B/5		B/3.75		B/3	B/2.5
h	B/25	B/12	B/7.9	B/6	B/4.75	B/3

After the hydrodynamic optimum operating parameters (rotation speed n, d, h) for each agitator and system adopted had been obtained in the absence of mass transfer, an aqueous solution with a fixed concentration of n-butyric acid was used as feed in a comparative study of the single stage mass transfer efficiency. Four types of agitators and the three organic phases indicated previously, running at their respective hydrodynamic optimum operating conditions, were employed and comparisons were made with the same feeds equilibrated in a separatory funnel.

POWER CONSUMPTION AND CORRELATIONS

The minimum power consumption data under the hydrodynamic optimum operating conditions were obtained for each of the four agitators with the three systems. The relationships between the minimum net power consumption per unit volume $P_n \cdot V_m^{-1}$ and the system properties (interfacial tension γ, density difference $\Delta\rho$) for the different agitators can be correlated in the form of Equation (1). Figure 4 shows the comparison of experimental and calculated $P_n \cdot V_m^{-1}$.

$$P_n \cdot V_m^{-1} = k\,\gamma^{b}\,\Delta\rho^{c} \qquad (1)$$

the values of the constant k and the exponents b and c are listed as follows:

Agitator	▲	✱	□	△
k	0.016	0.98	2.44×10^{-3}	1.2
b	0.24	0.58	0.305	0.6
c	0.5	0.17	1.0	0.1

The power number N_p for each agitator was determined by dimensional analysis. Since both the square shape of the mixing chamber and the perforated top baffle serve to prevent vortexing, the gravitational effect is negligible (6), then:

$$N_p = \frac{P_n}{\bar{\rho}\, n^3 D_5} = k_r\,(N_{RE})_M^{x}\,(N_{WE})_M^{y} \qquad (2)$$

where $(N_{RE})_M$, $(N_{WE})_M$ are the Reynolds number for mixing and Weber number for mixing respectively, k_r is an overall dimensionless shape factor, and P_n, $\bar{\rho}$, n and D are respectively the total net power consumption, average density of the system, rotational speed and diameter of the agitator. The values of k_r and exponents x and y are listed as follows:

Agitator	▲	✱	□	△
k_r	0.18	0.48	0.36	0.26
x	0.14	0.24	0.06	0.095
y	0.04	0.012	0.017	0.004

The power numbers calculated from Equation (2) for each agitator are plotted versus Reynolds number in Figure 5. It should be mentioned that the Reynolds numbers here were calculated only from the optimum operating conditions in three systems used.

DISCUSSIONS AND CONCLUSIONS

As indicated, the mixing of liquids in a vesssel depends on the type of the agitator as well as the configuration of the mixing chamber. If several agitator types provide uniformity of mixing in addition to the steadiness of flow of the continuous countercurrent fluids, the type with higher mass transfer efficiency and lower power consumption is chosen by the designer.

In the present work, a liquid inlet diameter d in a range of B/5 to B/3.75 has been found to be suitable (5). If d is too small, the flow resistances are increased and the agitator cannot effectively disperse the concentrated fluid stream; thus, more energy will be dissipated. However, in the case of larger d, due to the non-uniform distribution of the suction head, back-mixing of the mixed phase can occur.

The most suitable agitator position in the mixer was found to be a clearance h varying between B/8 to B/4.5 depending on the different system properties and agitator type used (5). A higher agitator position provides more uniform mixing but the suction head of the rotating agitator will be reduced.

For low γ and $\Delta\rho$ systems such as system 1, which are easier to disperse and slower to coalesce, less energy is needed to maintain a uniform dispersion, so that the minimum power consumptions per unit volume under the optimum operating conditions for each of 4 agitators are not much different as shown in Figure 4. However, when the γ and $\Delta\rho$ are increased, greatly different values of the optimum power consumption for different agitators are found. The flat paddle, the Rushton turbine and the medium delta impeller consume more power for the systems tested, but the large delta impeller in the present investigation always consumes the lowest power.

The lower power requirements of the larger impellers may be explained in terms of the relationship between the agitator's area and the drop size distribution. In mixing vessels, conditions in the region of intense turbulent shear around the agitator edges or tips moving at the tip speed primarily determine the local turbulent intensity and hence the drop size. The agitator area determines the flow of liquid through the agitator and thus most of the energy transferred by the agitator to the flow of liquid (7). If it is considered as a combination of several gradually shortened flat paddles, the large delta impeller can be seen to be more efficient in transporting larger scale turbulence to a main flow stream and thus in creating more local turbulence and circulation throughout the mixer. As a consequence, since uniform distribution of the drop size has been obtained, there is no necessity for consuming more energy.

The Rushton turbine is a smaller area multi-bladed agitator, which creates less circulation with more fine droplets locally around the agitator edges or tips. Obviously, much more power must be consumed to form a dispersion in fluid remote from the agitator, so that a non-uniform drop size distribution is an unavoidable result. This disadvantageous factor was

confirmed in settling operations. When mixing was done with the Rushton turbine, the thickness of dispersion band in the settler was increased significantly with serious entrainment especially in the low γ case, and the settling was slow with a tendency to flooding. Even in the high γ system, the thickness of dispersion band was always higher than the height of the organic phase layer in the settler.

Another explanation may come from the impeller's pumping characteristics, although no experimental data are available for comparison. From the viewpoint of the fraction of swept area, the paddle type agitators have diameter D of 0.73 B, much greater than the 0.33 B of the turbine type; thus the paddle agitator provides 4.89 times as much fraction swept area as the Rushton turbine, so that the more uniform suction head from the paddle type agitator plus an appropriate diameter of liquid inlet opening makes it possible to pump the flow stream between stages with a much lower power consumption. The plotting of power number N_p versus $(N_{RE})_M$ supports the above explanation. Figure 5 shows that the N_p values of 3 paddle-type agitators are very similar while that of the Rushton turbine is higher.

In the present work, the power consumption correlation includes both the uniformity of mixing and the steadiness of throughput. The concept of a large delta shaped impeller is shown to meet the mixer-settler operational necessity of more suction from beneath the impeller, to eliminate the head drop between stages, and provide slightly reduced (but still needed) circulation effect at the top edge to maintain the volume circulation of dispersion.

The above comparison between large delta impeller and Rushton turbine was also confirmed visually by the high speed cine pictures.

The experimental single stage mass transfer efficiencies η with corresponding specific power consumptions $P_n \cdot V_m^{-1}$ are listed as follows:

Agitator		▲	✳	□	△
water/	η(%)	99.7	97.8	97.2	99.6
n-butanol	$P_n \cdot V_m^{-1}$ (W/ℓ)	0.0464	0.0715	0.0557	0.0552
water/	η(%)	97	97	98	97
kerosene	$P_n \cdot V_m^{-1}$ (W/ℓ)	0.101	0.353	0.178	0.291
water/	η(%)	94.4	94.4	92.1	91.9
n-heptane	$P_n \cdot V_m^{-1}$ (W/ℓ)	0.145	0.382	0.306	0.322

Though the mean drop size measured from the motion pictures for the case of large delta impeller in water/kerosene system is larger (1.5 - 2.0 mm) than that given by the Rushton turbine and the optimum power consumption is lower than for any other agitators in all systems, the mass transfer efficiencies η are same or a little bit higher. This could be due to the fact that although small drops offer a larger specific area than do large ones, internal circulation and external oscillation of the large drops can result in a much larger mass transfer coefficient. The present investigation confirms that the new developed large delta impeller is the most suitable as an agitator both for mixing and settling in mixer-settler operation.

For a given system, total throughput and contacting time, two correlation equations in the present investigation make it possible to estimate the total net power consumption P_n and the optimum agitation speed n for a selected agitator type.

ACKNOWLEDGEMENTS

The authors are grateful to Dr. M.H.I. Baird, Chairman of the Dept. of Chemical Engineering, McMaster University, for his valuable discussions and suggestions and support to Z.J. Shen for attending the ISEC'83.

REFERENCES

1. T.C. Lo, M.H.I. Baird, C. Hanson, (eds.) Handbook of Solvent Extraction, Chapt. 9, John Wiley (1983).
2. R.E. Treybal, Liquid Extraction, McGraw-Hill, (1963).
3. P.J. Bailes; C. Hanson; M.A. Hughes, Chem. Eng. (N.Y.) 83(2), 86 (1976).
4. J.B. Scuffham, CMS: A Davy McKee Concept, The Chem. Engr., July (1981).
5. Z.J. Shen, B.Y. Sun, J. Li, J. Bachelart, A Study on Selection Agitator Type and Power Consumption of Mixer-Settler, Journal of East China Institute of Chem. Tech. (in Chinese) (1), 47, (1982).
6. F.A. Holland, Fluid Flow, Edward Arnold Ltd., (1973).
7. V.W. Uhl, J.B. Grey, Mixing Theory and Practice, II Academic Press (N.Y.), (1967).

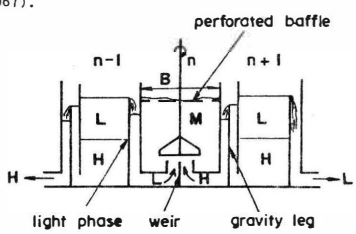

Figure 1 SCHEMATIC CONFIGURATION OF MIXER-SETTLER IN PRESENT WORK.

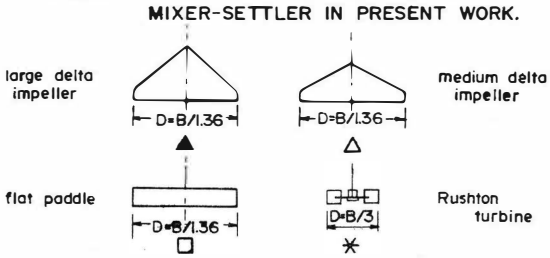

Figure 2 AGITATORS USED AND THEIR SYMBOLS

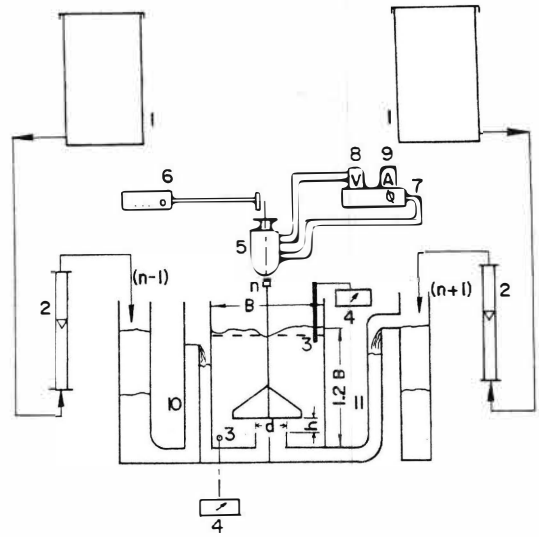

Figure 3 SCHEMATIC DIAGRAM OF EXPERIMENTAL APPARATUS.

1. head tank
2. rotameter
3. probe
4. conductivity meter
5. motor
6. rota-speed detector
7. silicon controlled speed adjuster
8. voltmeter
9. ammeter
10. interface controller
11. light phase overflow

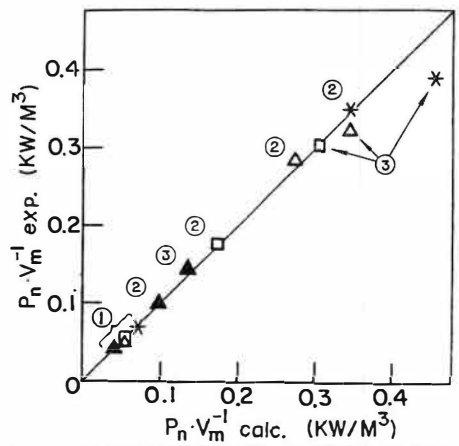

Figure 4 COMPARISON OF EXPERIMENTAL AND CALCULATED POWER CONSUMPTION

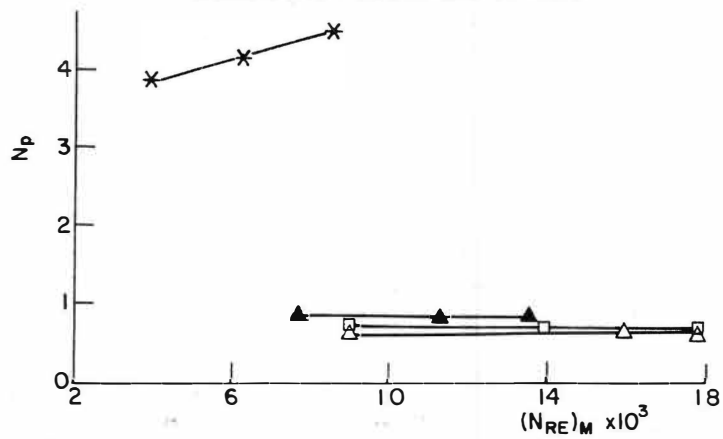

Figure 5 POWER NUMBER VERSUS REYNOLDS NUMBER IN OPTIMUM OPERATING CONDITIONS.

MASS TRANSFER CHARACTERISTICS OF THE IMI TURBINE PUMP-MIX

G. Harel, M. Kogan, D. Meyer and R. Semiat

IMI (Tami) Institute of Research and Development Ltd.
P.O. Box 313
Haifa 31002, Israel

Introduction

The IMI Turbine Pump-Mix was originally conceived to obviate some of the problems encountered in applying conventional mixing technology to liquid-liquid systems having "difficult" phase separation characteristics. The physical embodiment of the concept has been described previously[1,2,3,4]; briefly, it consists of a turbine of large turbine/tank diameter ratio, revolving fairly slowly, with forced recirculation in the mixing compartment to ensure full utilization of the energy absorbed for both pumping and mass transfer. It was quickly recognized that the configuration chosen had advantages for systems of relatively slow mass transfer, requiring relatively long residence times, and the first industrial implementation of the unit was for such a case.

Potentially, the Turbine Pump-Mix also has benefits for systems of "fast" mass transfer, where a reduction in the mean residence time requirement in the mixer, while keeping the energy delivered to the system almost constant, may yield a significant payoff in terms of accelerated separation. This aspect is the subject of the investigation which follows.

Conceptual Approach

The Turbine Pump-Mix has two functions, namely to deliver a dispersion at the required hydrostatic head and to promote mass transfer with minimum effect on phase separation. An analysis of the efficiency with which both functions are performed is possible if the mass transfer behaviour can be correlated with the relationship between the net throughput and the recirculation flow. Pumping performance is usually expressed by the H-Q characteristic at various speeds, which can be reduced to a single design curve by plotting dimensionless head against net throughput, i.e. gH/N^2D^2 against Q/ND^3[2]. The energy delivered to the system in transporting the dispersion at a given head is proportional to ρQgH, while the energy delivered in the total flow through the impeller is proportional to ρN^3D^5. The ratio between these groups is a dimensionless group which expresses the relationship between net throughput and the sum of throughput and recirculation. The energy delivered to the system is proportional to $\rho N^3D^5\tau$. Therefore comparing mass transfer efficiency with mean residence time, the relation between throughput and recirculation, and the absorbed energy will permit full analysis and optimization of pump-mix design.

Experimental

The chemical system selected for the initial investigations of mass transfer described herein was the system diesel oil - water - acetic acid. The operation investigated was the stripping of acetic acid from loaded diesel oil by water. Phase compositions were determined by potentiometric titrations. Residence time distribution was investigated by the injection of Methylene Blue dye into the system and colorimetric analysis.

The experiments were done in a pilot model of the Turbine Pump-Mix, 0.45m in diameter and having an active volume of $0.045m^3$.

The separate phases were fed by centrifugal pumps, and measured by calibrated rotameters. The turbine motor was equipped with an electronic speed variator. Heating/cooling systems were provided to ensure isothermal operation. The dispersion was delivered to a settler, which returned the separated phases to the pump suction tanks. The acetic acid for mass transfer tests was injected into the organic stream in the pump suction line.

The two phases were equilibrated by operation in closed cycle. The solute was injected, and the samples of feed and dispersion were taken after one mean residence time. Samples for analysis were taken as soon as sufficient clear liquid had separated. Equilibrium mass transfer was determined by recontacting the separated phases for an adequate period.

Residence time distribution was obtained by the analysis of the tracer concentration in a series of the outlet stream samples taken by a fractional collector at measured time intervals.

Results and Discussion

The operating characteristics of the Turbine Pump-Mix are shown in Figs. 1 and 2.

The experimental data of the hydrostatic head developed in relation to the throughput at various rotational speeds are given in Fig. 1. The "flatness" of the characteristics demonstrates the flexibility of the unit as a pump, i.e. the head developed changes very little for considerable throughput variations. In addition, the data are linear over the entire range of measurement, indicating that the design can be readily and simply extrapolated. The experimental data are reduced to a single function by expressing them as dimensionless functions of flow, head, rotational speed and turbine diameter in Fig. 2. The consistency of the pump performance is well illustrated by the conformity of the experimental data. Most of the experimental points fall within ± 10% of the best fitting line.

The efficiency of mass tranfer $\eta = (C_i-C_o)/C_i-C^*)$ is plotted against mean residence time τ in Fig. 3, τ being calculated as the ratio of pumping chamber volume to volumetric throughput. The results are as anticipated, increasing rotational speeds and residence times giving closer approaches to equilibrium mass transfer. Here again, the consistency of the data is remarkable, and indicates the extent to which the performance of the unit as a mass transfer tool can be predicted. This conclusion receives support from the study of residence time distribution. Fig. 4 shows the residence time distributions for a single liquid as a function of rotational speed, and also (insert) for transfer of the tracer from one phase to another. The graph shows that as the rotational speed is increased, the behaviour of the turbine tends towards that of a fully back-mixed reactor, in which the mass transfer efficiency would tend to unity.

The distribution curve for the dispersion shows similar behaviour, with a small displacement in time due to the transfer of tracer from one phase to the other. As explained previously, the Turbine Pump-Mix relies for its working on a combination of forced recirculation flow and pumping. This quantity is plotted against the efficiency of mass transfer in Fig. 5. This shows that, as can be expected, mass transfer efficiency tends towards a value of unity as zero throughput is approached; on the other hand, as recirculation is reduced, mass transfer efficiency drops and tends to a low value of 0.6. The relation of the energy delivered to the system to the efficiency of mass transfer is illustrated by Fig. 6. It is quite apparent that there is a region beyond which an increase in the quantum of energy delivered to the system gives no further benefit in terms of mass transfer.

The efficiency of a mixer-settler is a combination of the opposing requirements of mass transfer and phase separation. The relation of the quantum of energy absorbed by the system to the mass transfer characteristic on the one hand, and the phase separation characteristic on the other, makes possible a quantitative approach to mixer-settler design.

List of References

1. J. Mizrahi, E. Barnea and D. Meyer, Efficient Design of Mixer-Settlers. Proc. Int. Solv. Extr. Conf ISEC 74, Lyon, 8-14 Sept. 1974.
2. E. Barnea, D. Meyer and S. Wahrmann. Logical Design of Mixers. Proc. Int. Solv. Extr. Conf ISEC 80, Liege, 6-12 Sept. 1980.

3. E. Barnea, D. Meyer. Chapter: IMI Mixer-Settlers. Handbook of Solvent Extraction. T.C.Lo, M.H.I. Baird, C. Hanson (Eds) John Wiley & Sons (in Publication).

4. U.S. Pat. 3,973,759 August 10, 1976.

List of Symbols

- C : dimensionless concentration = $\tau C_i / \Sigma \Delta t$
- C_i : initial solute concentration
- C_o : final solute concentration
- C^* : equilibrium solute concentration
- D : impeller diameter
- g : gravitational constant
- H : developed hydrostatic head
- Q : volumetric flow
- t : time
- η : mass transfer efficiency
- θ : dimensionless residence time = t/τ
- ρ : dispersion density
- τ : mean residence time

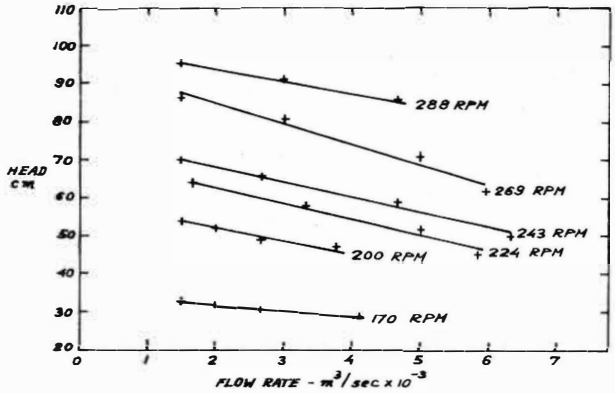

FIG 1 : HEAD-FLOW CHARACTERISTIC

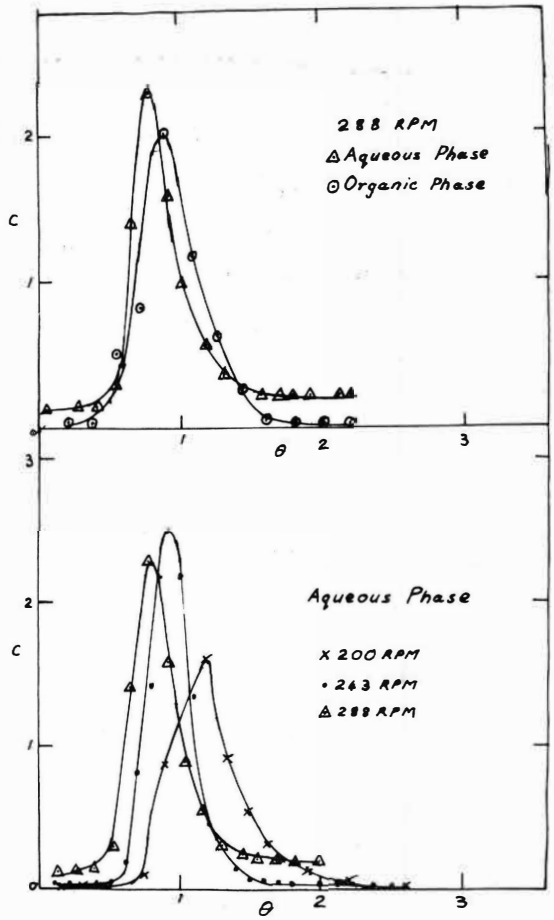

FIG 4 : RESIDENCE TIME DISTRIBUTION

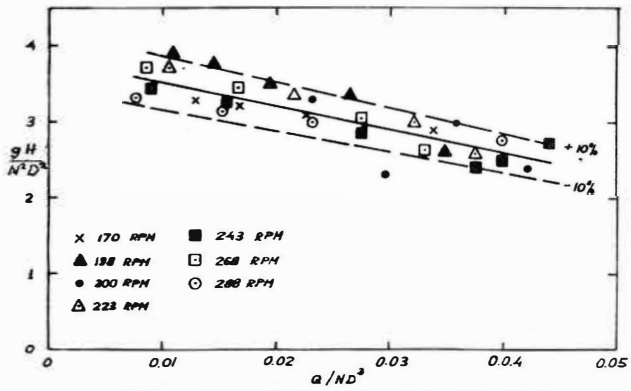

FIG 2 : DIMENSIONLESS HEAD - FLOW CHARACTERISTIC

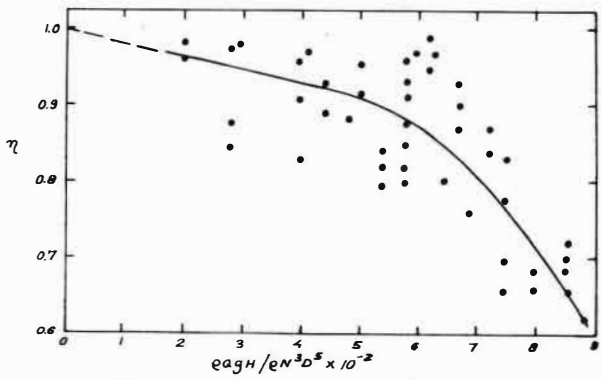

FIG. 5 : MASS TRANSFER EFFICIENCY vs RATIO OF NET THROUGHPUT TO RECIRCULATION

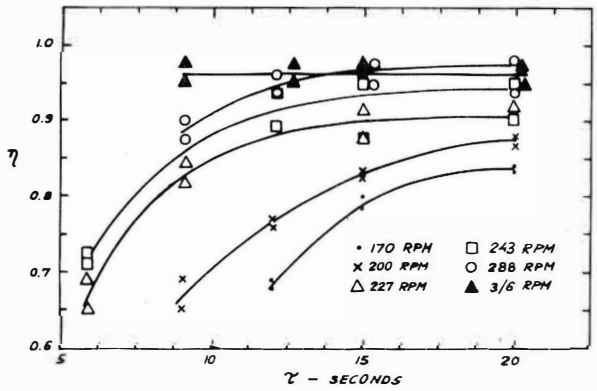

FIG. 3 : MASS TRANSFER EFFICIENCY vs MEAN RESIDENCE TIME

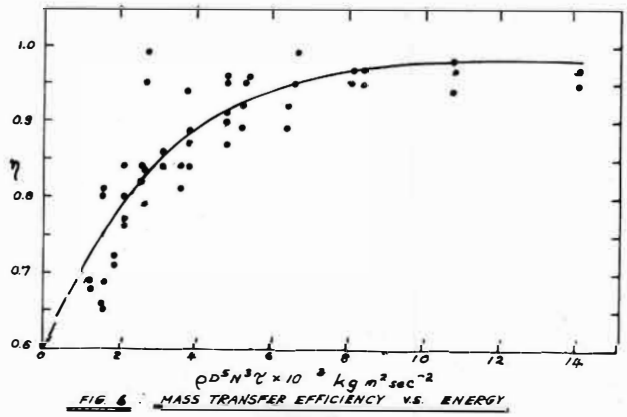

FIG 6 : MASS TRANSFER EFFICIENCY V.S. ENERGY DELIVERED

AXIAL MIXING CHARACTERISTICS OF INDUSTRIAL AND PILOT SCALE KUHNI COLUMNS

U. Bühlmann
Kühni Ltd.
Allschwil, Switzerland

J. C. Godfrey
University of Bradford
West Yorkshire, U.K.

J. Breysse
Rhone - Poulenc Ind.
69150 Decines, France

INTRODUCTION

The Kuhni column is a mechanically agitated, multi-compartment, liquid-liquid contactor. The compartments are defined by stator plates with large holes and agitated by a turbine type impeller. The present study is part of an extensive programme on column performance using Kuhni, rotating disc, pulsed and packed contactors. The paper describes single phase axial mixing characteristics determined at three locations: Bradford University, Rhone-Poulec St. Fons, Ciba-Geigy Huningue. A combination of simple techniques for measurement, modelling and correlation was used.

AXIAL MIXING

Simple design procedures for mass transfer in extraction columns include mass transfer coefficients, hold up and drop size but the plug flow assumption leads to an unrealistically low value of HTU. The use of axial mixing coefficients to describe more realistic flow characteristics gives a better basis for design. The coefficients are functions of operating conditions, column design and scale but because of the limited accuracy of mass transfer and drop size data and the greater dependence of performance on these terms simple models and correlations are adequate for axial mixing data.

The simple backflow and dispersed plug flow models have been widely used. More sophisticated models have been developed but the increased number of model parameters present disadvantages. Backflow is described by a velocity term, αv, relating to a forward velocity of $(1+\alpha)v$ for a contactor of n well mixed stages. This model is the basis of most design procedures but the dispersed plugflow model, described by a single axial dispersion coefficient (E) is more widely used to interpret experimental data. For many purposes, particularly when there are a large number of stages, the parameters of the two models can be directly related. The correlation of axial mixing with operating conditions, column geometry and scale is usually presented in terms of an axial dispersion coefficient or a compartment Peclet number incorporating the coefficient. The R.D.C. has recently been described by(1):

(1) $E/h_c v_c = 0.5 + 0.028\ (nd_i/v_c)G$

and the Kuhni column by a similar relationship between $E/h_c v_c$ and nd_i/v_c(2). When experimental data is to be examined this form of correlation can give a misleading graphical presentation. The relationship can be written as:

(2) $E = c_1 nd_i h_c G + C_2 h_c v_c$

and has been studied as the combination of independent impeller speed and flow terms. If this is realistic it should be possible to study the impeller speed term in a no-flow test.

EXPERIMENTAL

The techniques used for the three columns differed with regard to choice of tracer, measuring procedure, etc. and are not described in detail here because of lack of space. Stationary phase experiments were conducted in the absence of flow by injecting a tracer pulse at the centre of the column and monitoring the concentration of tracer at the ends of the working section. For precise data analysis it is desirable that the column is 'closed'. This is achieved by the air/water interface at the top of the column and an immiscible heavy liquid in the non-active section at the bottom of the column. The measured response is very close to the form predicted from the dispersed plug flow model and the scatter is very small. The axial coefficient can be determined directly from the half life of the response (3)

(3) $E = 0.14z^2/t_{½}$

This procedure has been demonstrated for the R.D.C. but the relationship to other measuring techniques has not been much explored.

Back mixing experiments were conducted by measuring the steady state concentration gradient developed against the direction of flow by a continuously injected tracer. Axial dispersion coefficients were determined directly from the concentration gradient:

(4) $E = v_c z\ /\ \ln(C_z/C_o)$

This experiment can produce good date but the concentration gradient and the calculated coefficients show more scatter than the stationary phase data.

In the pulse injection procedure the tracer was introduced into the inlet stream and pulse broadening was monitored at two points downstream to minimize the influence of inlet pulse shape on data processing. The technique used for data processing is more complicated than for the two previous techniques and a convolution method was chosen to minimize problems caused by the experimental method. The scatter in the calculated coefficients is similar to that for the back mixing data.

RESULTS

The relationship between the coefficients determined by the stationary phase technique and impeller speed was linear for all three columns with larger coefficients being obtained from the larger columns. With three columns only it is not possible to examine the influence of column diameter, compartment height and free area in detail but the results (Figure 1) are well correlated by equation 2 for $v_c = 0$:

(5) $E = 0.046\ nd_i h_c \varepsilon$

The coefficients determined from the back mixing experiments are consistent with the values obtained for the stationary phase measurements with respect to the influence of impeller speed and the geometrical parameters of equation 5. This is particularly so for the data for the 150mm diameter column. The data for the two larger columns is more scattered but it is possible to correlate all of the back mixing data using equation 2 with $C_1 = 0.046$ and $C_2 = 0.14$. A comparison of the experimental data and equation 2 is shown in Figure 2 and for most of the data the agreement is within ±15% or better. Also shown in Figure 2 is the data obtained from the stationary phase experiment.

The form of equation 2 is very similar to that used by Venkatarama et. al. for the rotating disk contactor where the geometric term (G) corresponds to the free area term (ε) used here. Venkatarama has no stationary phase data but was able to correlate back mixing and axial dispersion data with equation 1. It is usually assumed that similar values of E can be obtained from the two experiments at high impeller speeds where back mixing effects predominate; at lower impeller speeds the values of E obtained are usually expected to be larger for the axial dispersion measurement. This difference may be obscured by the traditional plot of Pe^{-1} and nd_i/v_c which includes v_c^{-1} on both axes and disguises the influence of v_c.

It is more difficult to assess the quality of axial dispersion data than is the case for stationary phase or back mixing. However it was found that the coefficients obtained were always larger than the back mixing values for both the 150mm and 600mm columns. As this difference is greatest at high values of v_c it would not be obvious on the Pe^{-1} and nd_i/v_c plot. The effect of impeller speed is consistent with both the stationary phase and back mixing techniques and the difference between axial dispersion and back mixing measurements is associated with the influence of flow rate as described by the second term of equation 2. This could be used to describe both stationary phase and axial dispersion data but would require a larger value of C_2 than used for back mixing data. Some of the differences between back mixing and axial dispersion can be explained if more sophisticated models are used and study is continuing on this topic.

CONCLUSIONS

(i) The influence of column size on axial mixing can be described by existing correlating procedures in terms of compartment height, impeller diameter and stator free area.

(ii) The influence of impeller speed can be assessed by any of the three techniques used with stationary phase data giving the best accuracy. In the study of scale up this technique also provides a simple and accurate procedure for the investigation of the influence of column geometry.

(iii) The simple correlation used describes the influence of both impeller speed and liquid velocity and there is no detectable interaction between the two variables.

(iv) The axial dispersion experiment gave consistently larger coefficients than obtained from back mixing for all test conditions. The difference is not important in column design at the present state of the technology but is important in the understanding of the axial mixing process.

(v) Mass transfer, concentration profile and two phase axial mixing experiments are in progress and will allow the application of single phase data in column design and scale up to be examined.

ACKNOWLEDGEMENTS

The authors would like to acknowledge the cooperation and assistance of the groups supporting these research programmes: Separation Processes Service, Rhone Poulene, Kühni AG, Ciba - Geigy, They would also like to acknowledge the contributions made by many colleagues in the supporting groups.

NOMENCLATURE

C_1	constant, agitation term of equation (2)	
C_2	constant, flow term of equation (2)	
C_o	concentration at tracer inlet	kg/m^3
C_z	conventration distance z from tracer inlet	kg/m^3
d	column diameter	m
d_i	impeller diameter	m
E	axial dispersion coefficient	m^2/s
L_c	compartment height	m
G	geometric parameter in equation (1)	
n	rotational speed	r.p.s.
$t_{½}$	Half life of stationary phase experiment	s
z	distance between sample points	m
ε	free area if stator plates	

REFERENCES

1. Venkatarama, J., Degaleesan, T.E. and Laddha, G.S., Can. J. Chem. Eng., 1980, 58, 206

2. Mögli, A. and Bühlmann, U. in Handbook of Solvent Extraction, eds Baird, M., Lo,T., and Hanson, C.; Wiley - Interscience, 1983

3. Misek, T., Coll. Czech. Chem. Commun., 1975, 40, 1686

d (m)	di (m)	hc (m)	ε (-)	n (r.p.m.)
.150	.085	.070	.30	50-250
.600	.30	.170	.30	16-64
.800	.40	.185	.20	20-75

Table 1 : Column dimensions

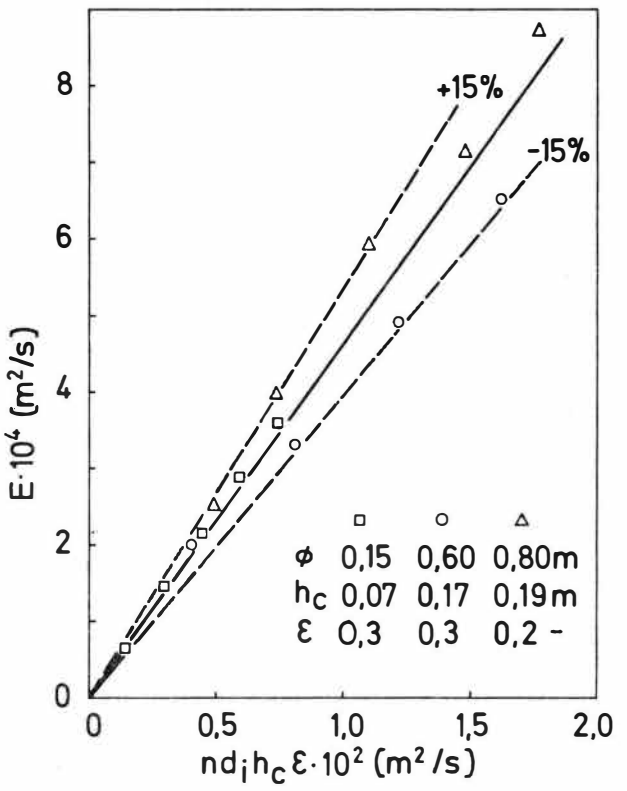

fig1: correlated stationary phase results

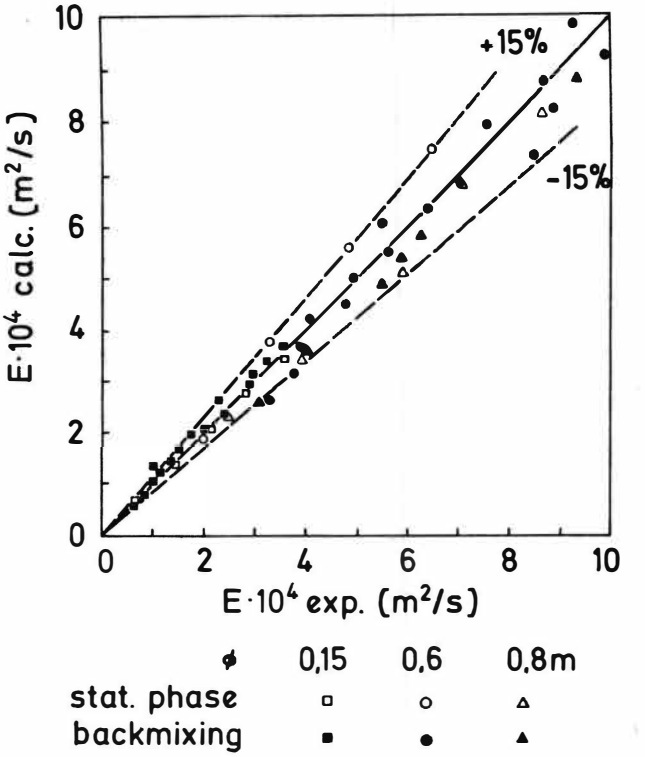

fig 2: calculated versus experimental dispersion coefficients

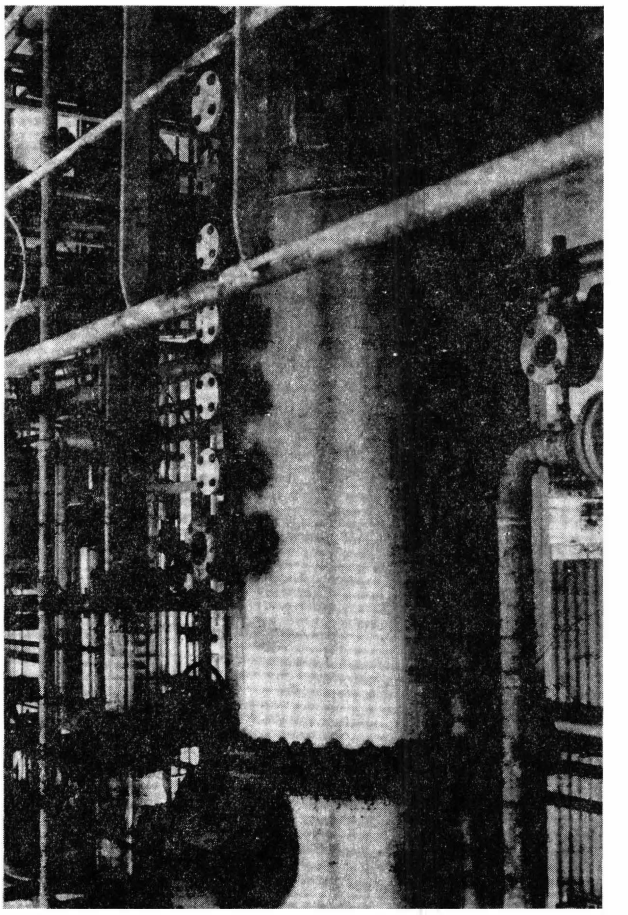

FIGURE 3: Industrial Scale (800 mm) and Pilot Scale (150 mm) Kühni Columns

DEVELOPMENT OF THE CASCADE WEIR TRAY FOR EXTRACTION

R. J. Fiocco

Exxon Research & Engineering Company
Florham Park, New Jersey USA

A long-term effort, dating back to the late 40's, led to the development of a high-performance tray currently used for solvent treating of lube oil feedstocks in Exxon's EXOL N process. As will be discussed in this paper, this service presents a particularly difficult design problem, and the tray development history has several interesting aspects. In view of the paucity of literature on the design of industrial liquid-liquid extraction equipment, this development can provide insight into the area, particularly for engineering students and academic researchers.

BACKGROUND

EXOL N extraction is the name given to Exxon's lube extraction process using N-methyl-2-pyrrolidone (NMP) as the selective solvent to remove aromatics and other undesirable compounds from lube feedstocks. The extraction step is carried out in a tower containing specially designed trays, named cascade weir trays, to achieve the desired extraction. Figure 1 shows a schematic of a lube extraction process. Various high-boiling fractions of crude oil from a pipestill or a deasphalting unit are used as feedstocks in blocked operation, each stock running for a few days at a time.

To achieve staging in the extractor, the oil feed is dispersed, separated, and redispersed several times as it moves up the tower countercurrent to the solvent. Interfacial tension between the liquids is low (e.g., less than a few dynes per centimeter), thus making it easy to disperse the oil as small droplets. However, since the difference in density of the phases can also be quite low (e.g., less than a tenth of a gram per cubic centimeter), separation, rather than dispersion, is normally the limiting step in the design of the extractor. An added complication results from the blocked operation. With different feedstocks, the physical properties and feed and solvent rates vary, and the relative flow rates of the two phases vary throughout the tower. Therefore, the extraction tower internals must be flexible enough to handle a wide range of flow rates for both phases, as well as to accommodate varying viscosity and density differentials. An additional practical requirement is that the tower must continue to perform after introduction of dirt, sludge and corrosion products over a long period of operation.

EARLY TRAY DESIGNS

Exxon's development work on extraction tray designs began in the late 1940's, with an emphasis on general applicability and high efficiency. The concept of a two-zone tray evolved, with one zone designed to meet dispersion requirements and the other zone to meet separation requirements, thus giving a configuration similar to a series of stacked mixer-settlers.

One of the early designs, called an "inverted step" tray, is shown in Figure 2A. Oil phase is dispersed upward through sieve holes at one end of the tray into a mixing zone. At the top of the mixing zone, solvent phase jets downward through opposing sieve holes to create an intense mixing action. The rest of the tray is devoted to separation of the phases before they are finally redispersed. This tray was commercially tested in a 12 foot diameter tower, with tray efficiencies reported to be greater than 50%. However, because of the fixed area for flow of each phase, it became clear that the tray did not have adequate flexibility to handle the wide range of feed stocks and flow rates encountered in lubes processing.

A short time afterward, another design called a "variable dispersion area" tray was developed. This tray, which allowed onstream adjustments to the dispersion area of each tray, is shown in Figure 2B. The dispersion area for oil phase consists of a fixed orifice plate with an identical overlaying orifice plate which can be adjusted from outside the tower. A simple open downcomer is used for heavy solvent phase. The variable dispersion area feature allows a wide range of flow rates to be processed with optimum mixing energy as set by the orifice open area and the head of oil under each tray. However, to make effective use of this concept, reliable interface detection devices are needed under the trays, and adjustments are required for each feed stock change. Difficulties were encountered in a commercial trial as the sliding plates began to bind and could not be easily adjusted.

In the mid-1950's, "underflow weir" trays were developed and applied to several commercial installations. The principal feature of this tray, shown in Figure 3, is the use of V-notched weir boxes to gently disperse oil phase into continuous solvent phase in the mixing zone. The notched weirs at the base of the open boxes present, in effect, a variable area to accommodate a wide range of oil flow rates. In the settling zone, final separation of the droplets takes place and the oil phase is readied for redispersion into the next mixing zone. An important aspect of the hydraulic performance of this design is the "lift" effect shown on the figure. This hydraulic lift is caused by the lower density of the two-phase mixture in the mixing zone, relative to the two-phase mixture in the settling zone and downcomer. Because of this lift effect, dimensions in the area of the seal box and weir box are critical to avoid excessive oil holdup in the mixing zone. Scaleup criteria developed for this tray served well for towers up to about 12 feet in diameter. However, as towers above this diameter began to come onstream in the 1960's, unexpected capacity and efficiency limitations were encountered, particularly with some of the heavy feedstocks.

EXTENSIVE R&D PROGRAM UNDERTAKEN

An extensive laboratory program was undertaken in the late 1960's to investigate the problem with the underflow weir tray and subsequently to develop the improved tray design now used in EXOL N treater towers. To provide a realistic simulation of hydraulic behavior in commercial size towers, a large two-dimensional extractor slice was constructed. The unit measures approximately 10 feet across by 13 feet tall by 7 inches deep, and is much larger than the unit used in earlier tray development work. It has glass panels on the front and back faces for viewing purposes, and is surrounded by a transparent enclosure for personnel protection. The unit accommodates several trays, so that tray interactions can be observed with tray spacing representative of commercial towers. Tray designs or dimensions can be changed in a few days, to determine their effects on performance.

To simulate properly the liquid-liquid system properties, phenol, which was the solvent used commercially at the time, was used as the solvent phase and low viscosity industrial oil stock was used as feed. Tests carried out with easier-to-handle aqueous systems were inadequate, even when surfactants were used to decrease interfacial tension.

Studies in this unit revealed an inherent hydraulic instability with underflow weir trays having dimensions representative of the larger towers. This instability is due to the enhanced lift which arises at startup, when oil first spills under the weirs into the mixing zone. The excessive oil flow results in a cyclic dumping of the oil in the seal box, particularly for feeds which would have a high steady-state lift. This, in turn, causes excessive mixing energy, and forms fine droplets which are more difficult to separate. These oil droplets ultimately are entrained in the solvent phase leaving the tower, thereby reducing oil yields.

CASCADE WEIR TRAY DEVELOPED

Attention then focused on developing a stable tray for large diameter towers, with capability to handle wide ranges of feedstock and flow rates at high efficiency. After testing various designs, the "cascade weir" tray shown in Figure 4 was developed. In this patented design, a seal box is provided for the oil phase, to prevent the solvent phase from bypassing the tray. To give controlled droplet formation and avoid the lift effect, sieve holes are used in place of notched weirs for oil dispersion. Weirs are used to segregate rows of sieve holes so that the optimum number of holes are used for each flow rate, and the head of oil under the trays is relatively constant. Thus, a wide range of flow rates can be accommodated. For example, if flow rate increases, oil spills under the next weir and utilizes the next set of holes. The elevated seal box also performs a secondary function. It segregates the rather turbulent mixing zone from the more quiescent settling zone.

Critical design and scaleup criteria developed in the laboratory studies were initially used to engineer replacement trays for underflow weir trays in existing phenol extraction towers. Capacity increases up to 50%, yield increases up to 33%, and corresponding operating cost savings were realized when the new trays were installed in a 19 foot diameter tower. The new cascade weir trays were also scaled up for use in what is probably the world's largest lube extraction tower, 25 feet in diameter in the main section.

APPLICATION TO THE EXOL N PROCESS

These cascade weir trays were subsequently applied to NMP solvent systems in the EXOL N process. Bench scale characterizations showed that this new, selective solvent system was superior to phenol and generally separated faster. Consequently, it was determined that phenol solvent could be simply replaced with NMP in existing treaters, without need for any tray modifications, and that capacity as well as yield increases would result. These factors were valuable in allowing quick conversion of several existing phenol extraction units to use NMP solvent without extensive downtime to modify the trays.

To sum up, extensive studies have been carried out on the engineering of the tower internals for the extraction of difficult-to-process lube oil systems. Large scale laboratory tests with liquid phases which properly simulate operating conditions were invaluable in identifying scaleup problems and developing an improved design. Feedback on the actual performance of several commercial units has confirmed and sharpened the engineering design methods.

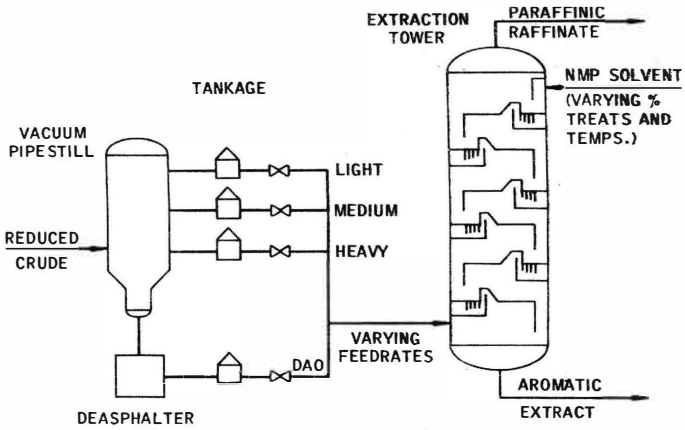

Figure 1. LUBE EXTRACTION TOWER MUST BE FLEXIBLE

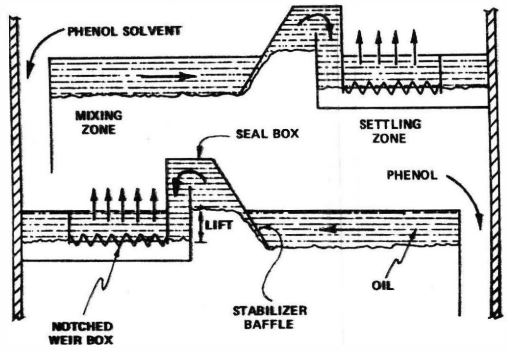

Figure 3. UNDERFLOW WEIR TRAYS DEVELOPED IN MID-1950'S

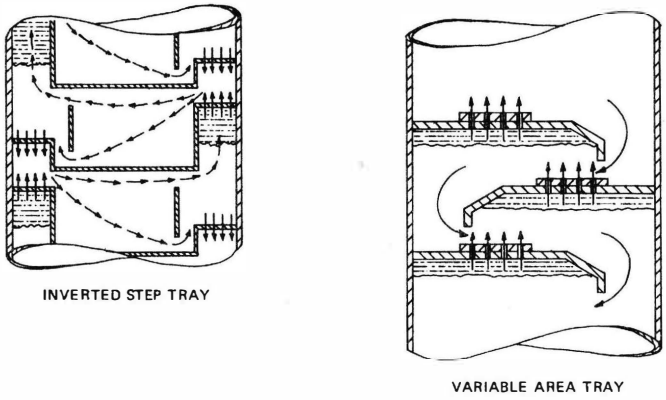

Figure 2. TWO EARLY EXTRACTION TRAY DESIGNS DEVELOPED FOR LUBES TREATING

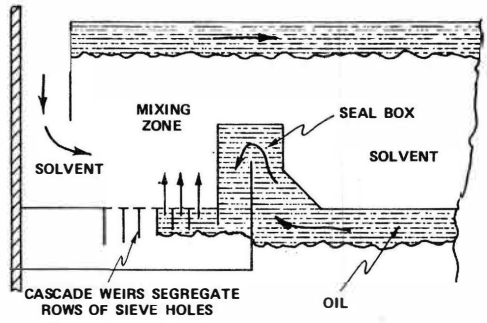

Figure 4. CASCADE WEIR TRAY PROVIDES STABLE OPERATION

NEW EXTRACTION EQUIPMENT FOR NUCLEAR FUEL REPROCESSING APPLICATIONS

S. B. Koganti, R. Natarajan, G. R. Balasubramanian

Reactor Research Center
Kalpakkam, India

To cater to the specific solvent extraction requirements of the nuclear fuel reprocessing industry, two new types of extractors, one a horizontal baffled contactor (HBC) and another, a vertical mixer column(VMC), have been conceived and developed at our laboratory. Salient features of these contactors and operating performance are discussed in this paper.

HORIZONTAL BAFFLED CONTACTOR

The schematic of the equipment which is shown in Figure 1 an extension of Morris contactor(1) with four mixing and three transfer sections separated by alternate weirs and baffles. Heavy phase flows out through jackleg and light phase overflows through a weir.

PULSING MECHANISM

The schematic of the pulsing mechanism is shown in Figures 2A and 2B. Each mixing section consists of two probes connected alternately to vacuum and air pressure sources through two, 2 way-3 port solenoids. The vacuum and pressure are so adjusted to keep the liquid level inside the probes oscillate well above the liquid level in the equipment thus avoiding air sparging into the equipment. An electronic timer operates the solenoids in such a way that the pulsing in the probes is 180° out of phase so arranged to avoid air sparging as well as to ensure that the holes are submerged in liquid. The liquid jets issuing out of the holes in the probes cause dispersion.

VERTICAL MIXER COLUMN

This equipment is a modified version of the sieve plate pulsed column wherein instead of pulsing the bulk of the liquid column, localised pulsing between alternate sieve plates is done which drastically reduces the back mixing. Figure 3 gives the details of the column. A modified version of this is being fabricated and is shown in Figure 4. Pulsing mechanism is same as for HBC.

VOLUMETRIC CAPACITIES

In our study no attempt was made to optimise the contector internals. The effect of agitation was studied by varying only the pulsing frequency, keeping the amplitude constant at 24-25cms. Flooding rates are determined by increasing the dispersed phase flow rates, keeping the continuous phase flow rate and other conditions constant. Flooding capacities are determined with 30% TBP in Shell Sol T as the organic phase and HNO_3 as the aqueous phase with or without Uranyl Nitrate at approximately 10gpl concentration, under reduced mass transfer conditions by suitably equilibrating the two phases.

Figure 5 indicates the throughput variations as a function of aqueous to organic flow ratio for the HBC without Uranium in aqueous phase and Figure 6 gives the variations for VMC.

MASS TRANSFER RUNS

With HNO_3 as the transferring solute from aqueous to organic (aqueous as the continuous phase) in the HBC, it may be seen in figure 7, (NTU)oy, (Number of transfer units based on organic solute concentration) increases with frequency initially and decreases at higher frequencies. This is probably due to increased back mixing. Since contactor effectiveness (CE), defined as the ratio of number of stages to the total residence time, is a better index for comparing different types of contactors, a plot is made with CE versus aqueous to organic phase flow ratio for both the contactors at different frequencies with Uranyl Nitrate as the transferring solute. It is shown in Figure 8. The plot indicates that the VMC is atleast 3 to 4 times more effective than the baffled contactor.

DISCUSSIONS

CE, which is a function of throughputs and stage residence times of the two phases, is distinctly high for the contactors under discussion compared to the conventional mixer settlers and pulsed columns, typical values being $12hr^{-1}$ for mixer settler $20hr^{-1}$ for pulsed column, $22hr^{-1}$ for HBC and $35hr^{-1}$ for VMC. Our previous studies(2)have showed that for reprocessing plants having less than 5TPD capacity mixer settler will be economical whereas above 5TPD, pulsed column may score over others. Our present study shows that HBC and VMC are potential candidates for Fast Reactor fuel reprocessing applications. The possibility that part of the HBC can be operated under phase inversion conditions(3) which increases CE and the presence of a single interphase in the equipment which reduces the control problem make this equipment attractive. This also facilitates the removal of interfacial crud which normally builds up during the solvent extraction of fast reactor fuel reprocessing. Thus HBC has distinct advantages over mixer settler. More elaborate studies are being planned with stainless steel units of the above models.

REFERENCES

1. J.MORRIS, British patent 885503 and 974829
2. R.Natarajan et al, Symposium on solvent extraction of metals, Bombay, (1979)
3. D.R.Arnold, Proceedings of the International Solvent Extraction Conference, 1619, (1974)

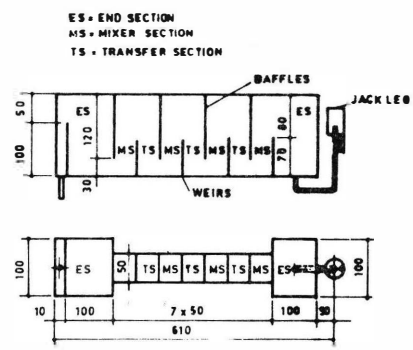

FIG.1 HORIZONTAL BAFFLED CONTACTOR

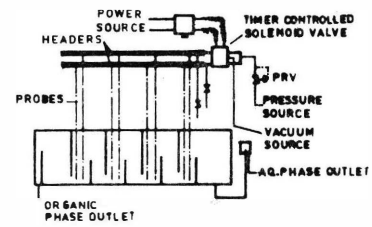

FIG.2A PULSING MECHANISM

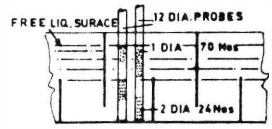

FIG.2B PROBE DETAILS

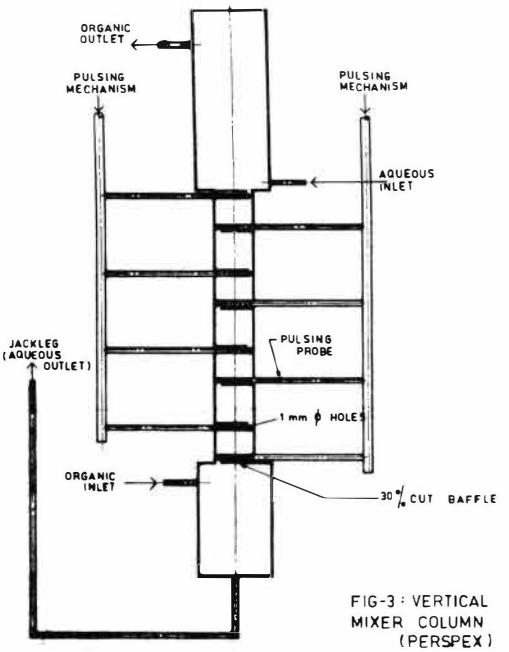

FIG-3 : VERTICAL MIXER COLUMN (PERSPEX)

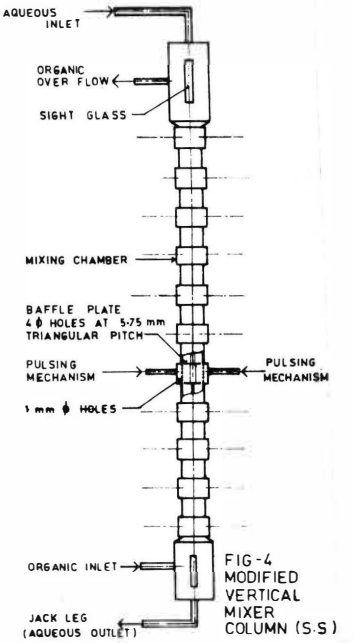

FIG-4 MODIFIED VERTICAL MIXER COLUMN (S.S)

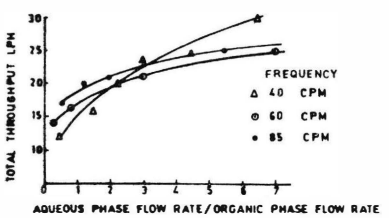

FIG. 5: THROUGHPUT CHARACTERISTICS OF HBC

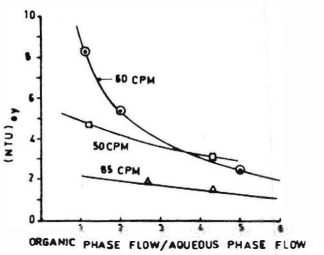

FIG. 7 : MASS TRANSFER CHARACTERISTICS OF HBC

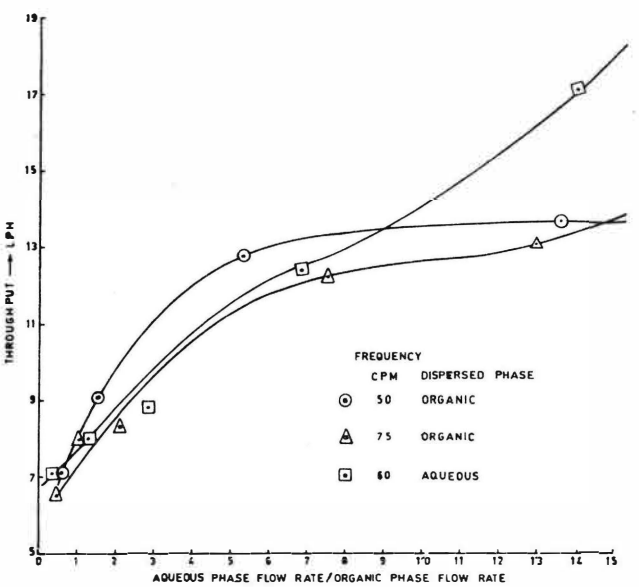

FIG. 6: THROUGHPUT CHARACTERISTICS OF VERTICAL MIXER COLUMN

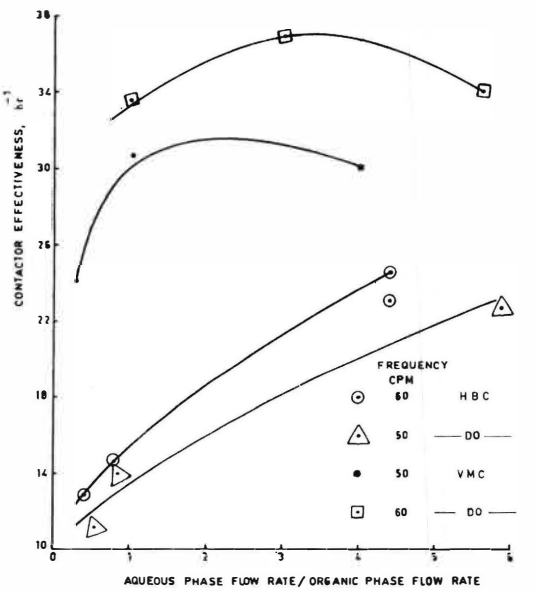

FIG. 8 : COMPARISON OF MASS TRANSFER CHARACTERISTICS BETWEEN HBC & VMC

METALLURGY TODAY - PROBLEMS AND OPPORTUNITIES

Wayne C. Hazen

Hazen Research, Inc.
Golden, Colorado USA

There are many excellent technical papers which review the professional aspects of hydrometallurgy and metallurgy in general. This morning I do not intend to be concerned with individual processes, types of solvents, or grades and recoveries attainable by any particular process. This review will not be concerned with technical metallurgy. Rather, I would like to spend the time to talk about what I believe are significant underlying changes taking place in our society and in the industry we serve. These changes represent a threat to the future viability of mining in the United States and at the same time represent an opportunity for redirection and growth.

It is surely no news to anyone in this audience that the profession of metallurgy has been traveling a difficult road for the past few years.

During a period when the mining industry is in a depression and each company's efforts are directed toward survival, it is difficult enough to keep one's job, let alone to suggest to management some program of improvement in processing which might require any kind of capital outlay or a diversion of the efforts from the single minded goal of staying alive. Thus it is not surprising that there have not been many substantially new developments in plant metallurgy which can have the same major impact on the industry that solvent extraction has had. That is not to ignore the improvements which are being implemented such as the char-in-pulp circuits for gold recovery and in the multitude of research activities still going on. These innovations, however, are at low ebb compared with the myriad of new metallurgical processes under active development up to 1980 — a natural outcome of the bad times.

As if this problem by itself were not enough trouble to keep the profession from any bustling vitality, our industry has been undergoing major management restructuring also. About eight to ten years ago developments in the oil business led that industry to conclude that natural resources other than oil might be a worthwhile investment. With that decision, there was a heavy investment by oil companies in some of the old-time mining companies which had arrived at a position where an infusion of new capital was required. One does not have to detail the changes which have taken place in the operations of Anaconda Copper, for example, to recognize that the acquisition of Anaconda by Atlantic Richfield has made changes in that company's mining activities. Other changes such as the acquisition of Cyprus by Amoco, and Kennecott by Sohio come to mind.

If this new infusion of capital had restored the vitality and health of the mining companies, it would have been a significant association. Unfortunately, even though both industries, mining and oil, have elements in common — exploration geology, drilling, etc. — there are nevertheless significant differences in style and philosophy.

Oil company management has somewhat different views of capital investments and return on investment than have been customary for mining industries. As an example, the costs for exploration and drilling in the oil industry are high, as is the risk; however, if a discovery is made and an oil reserve is developed, the oil is saleable in its raw form. In the mineral industry the discovery, drilling, and delineation of a large ore body is only the beginning of the time, effort, and capital investments required before a saleable product can be produced. This gives management of mining companies and management of oil companies a somewhat different time perspective and a different view of the swiftness with which invested money can be returned. With high interest rates and concerns about continued inflation, it has been impossible for financial people to go along with supplying the money that is required to bring a new large mining property into production. Under present circumstances and reasonable projections of the price of copper, for example, it is doubtful if a big porphyry copper deposit has much chance for development in the coming five years, largely because of the staggering capital investment. This is an area where we metallurgists can seek major opportunities to improve matters by innovative technology.

To make matters worse, as bad times came to the oil producers in the past few years as well as to the mines, the oil companies began to divest themselves of of their new mining assets. There are examples such as Occidental Petroleum's disbanding of their OXY Minerals group, the sale of the Cities Service copper and milling activities in Arizona to Newmont, the sale of the Getchell gold property by Conoco, the apparent diminished interest in mining on the part of Exxon, and others to make this point. A broad picture of the mining industry in the United States in the past decade thus reveals the entrance of strong companies with a different management philosophy. Now this new management group is backing away from the previous investment before really having had an opportunity to see its policies go into effect. It leaves the question, "Who is going to be running mining activities in the United States?" I don't think that this morning we are going to find an answer to that question but it does serve to pinpoint one of the serious impacts on the development and vitality of metallurgical activities. With this kind of uncertainty, it is not likely that one is apt to find an atmosphere which fosters continued development of better technologies for mineral recovery.

In addition to the problems having to do with the broad change of management philosophy, as times have worsened, various organizations have found it necessary to disband their technical establishments in order to diminish the cash drain for salaries and facilities. It takes a long time to assemble a good metallurgical team that is capable of producing the sort of information, plant assistance, and process improvement required for continued profitability of a mining company. Once such a group is disbanded, the assembly process must start all over again when the industry begins to recover. This has a long-term crippling effect on metallurgical progress.

Along this line, in the summer of 1982, Metals Week published a list of major production cutbacks in North America. They listed 180 operations which have had some kind of postponement, closure, or cutback in the past three years. When you contrast this with the excitement and multiple new activities that were going on about five years before with a copper price of a dollar per pound and a uranium price of thirty dollars per pound, the negative impact is perfectly clear. The fact is that many metal prices are cyclic and the metal markets are cyclic, but this particular cycle has been close to disastrous. The cutback in these mining activities has been accompanied by a parallel cutback in technical staff which has wounded the industry's capability for recovery, even though it has been necessary for survival.

Thus we have seen many changes taking place at the same time: substantial changes in senior management style and, because of the depression in metals and minerals, a serious weakening of our technical establishment.

As if this were not enough in the way of difficult problems to beset a particular industry and a particular profession, it is also clear that there are profound changes taking place from a social point of view. We are all familiar with the problems that have been raised by new environmental constraints, by government regulations, and by what appears to be a hostile public attitude toward business operations, mining in particular.

While we are talking about these social change, I would like to comment on the historical amnesia which seems to afflict those environmentalists who have as their theme "conservation," particularly energy conservation. This is not as exciting a subject as it was before the OPEC cartel ran into difficulties in price fixing, but we should remember that the energy resources which the human race used in all history before 1800 were dependent upon horses, oxen, human backs, and the warmth of sunlight. There are those who claim that the "hard technologies" which are energy intensive have spoiled our lives and the world is becoming less and less safe because of the pollution of our air and water by these technologies. These proponents of energy conservation should remember that 100% of what the world now means by energy would not have existed if it had not been for technological innovations.

There are indeed environmental problems that we must resolve, and swiftly, but I am not sure that the smog problem created by automobile exhausts in Philadelphia is more difficult to cope with than the problem created by the 50 tons a day of horse manure that was ground into the Philadelphia streets and dispersed as fine dust on hot summer days before the invention of the automobile. I certainly am not trying to say that pollution is good for you, but I am saying that throttling technological advance is not a good way to solve the environmental problems. The solution to the problems of pollution will depend on technology also, not upon turning our backs upon the use of energy. We should not lose sight of the fact that the environmental movement flourishes only in affluent nations and only among groups of people whose basic subsistence and security needs have been satisfied by the network of institutions which have been established to improve the quality of our lives.

This is not the time to debate the environmental issue but it is clear that a major metallurgical problem is the development and adoption of technological systems for mineral treatment and metal recovery which minimize the impact on our surroundings. This is a tough challenge, and I am not commenting as to whether the environmental restrictions and constraints that have been placed on the mining industry are apropriate or not. I am only calling to your attention the fact that this is a problem for the metallurgical profession which so far we are not meeting very well — or at least not meeting as well as the regulatory bodies wish we would.

But it has not just been the changes in social attitudes, it also seems as though there has been a change in the ability of our profession to mount a viable technical change and develop a new process in which the first plant can begin operations in any successful fashion. In the past decade or so there have been an alarming number of new plants that exceeded their cost estimates by a factor of two or more, and that had long, difficult startups and struggled for years before, if ever, they reached the anticipated tonnage, recovery, and operating cost. It is not particularly helpful or popular to list disasters and discuss them in detail because they are seldom a matter of pride to the people involved. It has been suggested that the metallurgical societies should form a committee to document the real reasons for major metallurgical bloopers. It might be called "Failures Anonymous" and would add immeasurably to our knowledge of how to keep out of trouble when building a new venture. We have much to learn, however, from pondering the questions as to why there should seem to be such an apparent rash of failures in the development of new mining enterprises.

These difficulties have not necessarily been confined to starting up hitherto untried new processes. In the last decade there have been clear examples where terrible operating troubles were encountered in new enterprises in iron ore, uranium, and nickel, even though the technology for these particular commodities has been well established. It is thought provoking to ponder possible reasons why these ventures have been so ill fated. Part of it is due to the different philosophy which permeated thinking about some of the mining enterprises during the '70's. There was an increasing tendency to make engineering decisions on financial grounds. It is entirely understandable for a management faced with a cost overrun during the construction period to require the engineering companies and designers to cut down on costs. This results in financial

judgment of such items as removing surge tanks between parts of a process because they are not used to capacity all the time. The result on operating continuity usually is very detrimental.

This is linked to a change in the viewpoint of management of mining companies occasioned by the unusual and difficult financial environment in which they found themselves. A plant engineered by the accounting department will have a difficult startup. Of course, if the engineering is carried to the point of bankruptcy, the enterprise will not prosper either. But there is more to the story than that.

There is a Rand study concerning the apparent reasons for massive failures of major enterprises during attempts to get their projects on stream. Surprisingly, they found that the majority of the big project overruns and capacity shortfalls which occurred in the mid-1970's were not due to an unexpected inflation factor. The commonest reasons were related to changes of scope part way through the project, inadequate process development and demonstration, or the overlapping of the process development with actual plant design.

Also involved in this question is the problem generated by setting time schedules for reasons other than the requirements of the engineering, equipment, and process design. For example, if the time schedule is rushed by the necessity to meet a particular market circumstance, this results in inadequate detail in the engineering design and construction.

In any event, it is true that the metallurgical profession has participated in some pretty dramatic fiascoes. I believe that the deepest cause for these fiascoes has to do with the adequacy of the technical preparation. This must include items such as the problems of scaleup, materials handling, stability of control, etc. — all part of the metallurgical engineer's broad responsibility.

We have enumerated some of today's problems in metallurgy as being nontechnical. They are problems of management change, scattering of substantial technical support structure, social pressures of fact and fancy, declining prices with the accompanying general panic for fear of going broke, and it seems that we have added to these problems in some plant enterprises by insufficient care in execution of our professional talents.

As far as the United States mining industry is concerned, we have the additional problem that our competition in some of the less developed countries is going to keep on producing whether they make any money or not for reasons that include the need for foreign currency, the requirement of continued employment for political as well as economic reasons, etc. This means that most of the production curtailment has fallen on the North American producers who have to cut back when the market falls. When you add changes in social viewpoint as has happened in Canada, the impact on our profession and our industry is nearly catastrophic.

It is important for us to recognize the changes which are taking place in our social and political systems because they have such a direct impact on our profession. We have borne the brunt of a great deal of the criticism leveled against the industry, and I feel that we have received more than our fair share of abuse. It is not enough, however, to merely remind people that a society's standard of living can be perhaps equated pretty directly to the health of its mineral and metal producing sector. We should attempt to understand what is happening in a little deeper way. Here I think it is useful to recall that we as a nation really have three systems in one even though we may call it a democracy or capitalism or whatever. The three systems are an economic system, a political system, and a cultural system. If it turns out that any one of these is seriously injured, then the others will be wounded also. Historically, the economic system, by being reasonably unfettered and free of regulations or restraints, was able to produce an unparalleled wealth for society as a whole. The economic system, from the standpoint of just economics indeed produced tremendously. Along with the flood of goods came some of the social problems we have mentioned.

The political system, which is charged by society with the responsibility for making the laws and regulations to keep us reasonably restrained, observed the vast wealth that was created by the economic system and decided that it would be useful to redistribute this wealth to alleviate what were conceived to be social evils. In so doing, they appropriated the capital and income that is required for the operation of the economic system and distributed it to a broad spectrum of the population. By so doing, they sapped the vitality of the economic system.

It turns out that if you make things tough enough for the business community to operate because of lack of investment capital, then business is unable to function in a way which will continue to produce the wealth to be distributed. A point is reached where the political system has wrecked the economic system and accuses it of having failed the country. We are in the beginning stages of recognizing that if political systems have made it impossible for an economic system to prosper, then cultural values are going to be equally damaged. We, as a nation, are searching for some kind of a balance that will permit us to restore the vitality of the industry base upon which so much of our present standard of living is built.

I do not believe that a political system which imposes business restraints of the seriousness that we have at present will permit accumulation of capital for new enterprises in high technology industries either, let alone the mining industry. There needs to be a rethinking of the relation between the three aspects of society: the economic, political, and cultural.

Since we are trying to identify the broad principles which have brought pressure upon the metallurgical profession and which, in my view, have resulted in a diminution of its vitality, there is one factor which results from the others but which will perhaps be more difficult to correct. That is the view of our profession held by those who are considering what kind of career to enter when the begin their major studies. This is not an entirely new problem. Twelve years ago the National Academy of Sciences wrote a report called, "Mineral Science and Technology: Needs, Challenges, and Opportunities." Their opening paragraph says: "Despite the key role of minerals in our society and the vastly increasing worldwide demand for mineral products, mineral technology in the United States is in a declining state and serious trouble lies ahead for the nation unless corrective actions are taken promptly."

Well, corrective actions were not taken at that time and, certainly, mineral technology of late has been in a declining state. That report pinpointed one of the major causes of the serious trouble, and it concerned trained technical manpower. Remember — this was written twelve years ago, before the energy crisis or before any of the other troubles of an environmental or financial nature had become as serious as they have become in the past decade. One finding of that report was that there are not enough people entering the profession to carry out the required improvement of metallurgical technology to keep the industry vital. It has not been an attractive business for young people to enter. I really don't know why this should be so because I find it very attractive and have enjoyed it for many years. Maybe it is because it didn't have as many problems when I entered the profession. Nevertheless, the following table listing the number of people who graduated as metallurgical engineers in the last ten years is illustrative of the problem. There appears to have been a gradually declining interest in the metallurgical engineering degree.

Year	Metallurgical Engineer	Year	Metallurgical Engineer
56-57	577	68-69	717
57-58	670	69-70	748
58-59	724	70-71	623
59-60	682	71-72	579
60-61	720	72-73	558
61-62	679	73-74	458
62-63	721	74-75	393
63-64	686	75-76	351
64-65	851	76-77	
65-66	781	77-78	420
66-67		78-79	420
67-68		79-80	585

With all of these various pressures coming upon us at the same time, it makes one wonder where there is cause for optimism. Well, it is precisely because there are so many things changing that there are opportunities. Without available mineral technology and resources, industrial activities cannot meet the demands of a modern society. The multiple pressures that have resulted in such problems for the mining industry and the metallurgists who serve it will force the adoption of new methods, new thoughts, and will bring new opportunities.

The major factors leading toward improvement in metallurgical technology are:

1. Striving to improve cost.
2. Social pressures, i.e., environmental controls, working conditions, et al.
3. New knowledge or progress in some other area which can be transferred to metallurgy.
4. New requirements by other industries, i.e., silicon for solar energy, europium for television screens, germanium for LED's, etc.

An example of how these create opportunities is shown clearly by the development of solvent extraction. Knowledge developed by a chemical company and transferred to the mining industry made this development possible.

New devices such as the plasma arc furnace, high vacuum technology, ultra high pressure, etc., can open up new vistas for the imaginative metallurgist. The list is endless of the possibilities for application of micro-processor technology. New chemistry, including chloride technology, can be expected to make big changes in our views of lead, copper, and zinc processing.

All of us must learn to view our metallurgical problems and development from the perspective of various kinds of broad changes that I have been discussing. It will be important that we consider the treatment of any ore in any ore body from an overall point of view and stop fussing about whether hydrometallurgy is better than pyrometallurgy or electrolysis better than hydrogen reduction, or sweeping statements that wet methods are less polluting than dry, etc. We must adopt the viewpoint that there are dozens of technical ways of treating any particular mineral-related problem, and that for the flexible, small production plants which will be required in the future, we must use the most intelligent mixture of all the ways we know. For any given ore body, there will be a certain set of constraints concerning not only its mineralogy and grade but also location, the specifics of social questions, markets, energy choices, etc. The good metallurgist is going to be a complete generalist using knowledge from all the sciences and many of the humanities.

The major opportunity presented by the upheaval in our industry now is the chance to make changes. Joe House, President of Henkel, in his 1981 Gaudin lecture on the development of his company's LIX reagents, described the entrenched resistance on the part of much of the metallurgical profession to acceptance of the novelty of solvent extraction. But that was twenty-five years ago and I contend that today is a different ball game.

We must be innovative and flexible, using whatever ideas are available from other industries and adapt them to our problems. Having at our disposal instant capital and operating cost estimates via microprocessing equipment is another tool which we can use for faster decisions and better project guidance.

Above all, this is the time to review the training of students for our profession. As pointed out in the report by the National Academy of Sciences, there are not enough people entering the profession and being trained to carry out the required improvement of metallurgical technology to keep the industry vital in the long run.

I would propose that the present efforts on the part of the professional metallurgical societies and some universities to collaborate on curricula and teaching methods should be intensified. Specifically, we should encourage substantial trading between operating managers and college professors. It has been stated by some schools that they are training engineers for industry. Some industrial and operating engineers feel that the purpose of some academic members is to train students to become professors. It is no longer enough to be well grounded in theory, as important as that is. The skill needed for transferring theory to practice is vitally needed today.

A new understanding of business management methods is coming about and we hear more of the search for excellence, of quality circles in production, and of long-term objectives besides the bottom line.

So, even though the present moment is difficult for our profession, I expect this decade to be one of unprecedented opportunity and achievement for the metallurgy profession if we understand what is happening and react forcefully and intelligently to the challenges we face.

INDUSTRIAL EXPERIENCE WITH PULSE COLUMNS IN URANIUM ORE PROCESSING

L. Clappier and P. Michel

Sté industrielle des minerais de l'ouest - VELIZY - FRANCE

C. Duchamp

Cie miniére de Dong-Trieu - JOUAC - FRANCE

E. Henry

C.E.A. - ERIES-MARCOULE - FRANCE

Pulse columns have been used for more than 20 years in the reprocessing plants of the Commissariat à l'Energie Atomique (CEA) now owned and operated by COGEMA.

Their performances achieved being good, non nuclear applications have been sought. The field of non-ferrous metal hydrometallurgy has appeared as very favourable for such an application. However the size of the columns used in the reprocessing plants was rather low (diam. $\leqslant$ 0.4 m) and it could be feared that the manufacturing of the columns would be difficult and their performances poor when scaling up them.

A joint venture called ERIES has been established in 1974 with the C.E.A. and the Robatel-SLPI Company which could use the means of investigation of the C.E.A. and the industrial means of Robatel-SLPI to develop and manufacture extraction equipment.

1) Characteristics of the pulse columns (Reminder)

A pulse column is a continuous contactor (Fig.1) which consists of:

- A vertical cylinder containing a packing, generally consisting of fixed plates (perforated or baffle).
- Two larger part at the top and at the bottom to allow phases disengagement.
- A pulsatory device which periodically shakes the phases inside the column.

In liquid-liquid extraction, one phase is continuous, the other one is dispersed. The flows in the column vary with the nature and the physical properties of the phases, such as viscosity, specific gravity, interface, tension ; with the pulsation characteristics, i.e amplitude and frequency ; with the ratio of the flowrate of each phase. If the maximum possible flowrate is exceeded, the column is flooded and the phases go out of the column on the wrong end (2,3).

A continuous phase is chosen a priori, generally the receiving phase. An interesting characteristics of the pulse columns is that they accept a dispersed phase without any recycling, the flowrate of which is ten or fifteen times higher than the continuous phase flowrate.

On normal running, the heavy phase is fed at the top and drawn off at the bottom and the light phase is fed at the bottom and overflows at the top.

The dispersion, characterized by the dispersed phase rate, is achieved by pulsation.

2) Development of the pulse columns

The pulse columns used in the reprocessing plants had the main following features :

- small diameter
- packing : perforated plates

The scaling up of these columns of larger diameter (2 meters for instance) lead to a lower efficiency as it can be seen on the table 1. Moreover the cost of large size perforated plates was very high. Finally it could be hazardous to use them with liquors containing suspended solids and/or precipitable compounds.

Investigations have been carried out in the C.E.A. to use pulse columns for solid-liquid extraction. They lead to the design of baffle plates as shown on the figure 2. They are called "plate" and "ring" hereafter.

Use of this plate type for liquid-liquid extraction has given very interesting results : the efficiency does not vary too much when the diameter is increased (H.E.T.S. = 0.75 to 1 meter for all diameters between 0.1 and 1 meter).

The specific flowrate varies with the system solvent-solution used. For the mixture 30 % T.B.P -dodecane and uranium nitric solutions a specific flowrate of 4 $l.h^{-1}.cm^{-2}$ can be achieved in the extraction section.

With the system Alamine 336 - kerosene-uranyl sulfate solutions a specific flowrate of 3 $l.h^{-1}cm.^{-2}$ can be achieved. It means that 50 to 70 $m^3.h^{-1}$ can be processed in a 1.8 meter diameter column.

All these tests have been carried out in a C.E.A service in Marcoule.

3) Industrial application

3.1. Compagnie Minière de Dong-Trieu (MINATOM) - Jouac Plant

The extraction equipment of that plant only includes pulse columns provided by ERIES. The three columns of the extraction section have the features reported in the table 2.

The columns have been operated under the conditions reported in the table 3. The solvent is stripped using a sodium chloride brine.

As it can be seen in the table 3, the uranium recovery is high taking into account the high uranium and chloride content of the stripped solvent.

3.2. Société Industrielle des Minerais de l'Ouest

(COGEMA Group), Bessines Plant.

A column has been put in operation in Bessines to increase the capacity of the solvent extraction unit which include 2 lines of mixers-settlers for extraction and one line for stripping.

The loaded solvent is stripped using a solution of ammonia and ammonium sulfate.

The features of the column are shown in the table 2 and the operating results in the table 3.

The column efficiency is favourably compared to the one of a line of 4 mixers-settlers.

3.3. Results common to both plants

The operation of the column is stabilized by controlling the flowrate of the raffinate using the measurement of the interphase level in the lower settler. In the SIMO Plant the interphase is measured with a gamma densimeter which is very efficient and not sensitive to cruds.

Cruds are drawn off periodically through valves placed on the settler. That way cruds do not disturb the column operation.

The solvent losses (entrainment) are lower than the losses achieved with the mixers-settlers and are always less than 0.3 $l.m^{-3}$(300 ppm).

4) Conclusion

Pulse columns fitted with baffle plates are efficient and easy to operate. The performance achieved can be favourably compared to the mixers-settlers performances.

Their capital cost, solvent inventory and space required are lower. In the present status of art their use may be recommended for :

- Plants of which the volume of influent to be processed is less than 85 $m.^3 h^{-1}$.
- Modular increasing of the capacity of a solvent unit.

If the maximum diameter is 2 meters, it is needed one column for every 85 $m^3.h^{-1}$. The present investigations allow to forecast to manufacture large diameter columns with mechanical pulsing device. A 2.5 meter diameter column could process 135 $m^3.h^{-1}$ and a 3 meter diameter column almost 200 $m^3.h^{-1}$.

References

1) H. ROUYER, J. LEBOUHELLEC, E. HENRY and P. MICHEL, Proceedings of I.S.E.C 74, Paper 256 p.2339 (1974)

2) G. SEGE and F.W WOODFIELD, Chem.Eng.Prog. 50, 396 (1954)

3) D.H. LOGSDAIL and J.D THORNTON, Trans.Inst.Chem.Eng.35, 316 (1957)

Table 1

Pulse columns with perforated plates. Influence of diameter on H.E.T.S.

Column diameter in meters	0.3	0.6	1
HETS in meters	0.7 - 0.8	1 - 1.2	2

Table 2

Technical features of pulse columns

	D 310	D 311	D 320	SIMO
Effective height (m)	8	8	12	6
Overall height (m)	12.4	14.2	16.4	12.2
Diameter (m)	1.3	1.8	1.3	1.8
Pulsation	Periodic with compressed air			
Packing	Plates 28 Rings 26	16 14	26 26	17 16
Free area (%)	25	25	25	25

Table 3

Operating features of pulse columns

	D 310	D 311	D 320	SIMO
Operation type	Extraction	Extraction	Stripping	Extraction
Dispersed phase	Aqueous	Aqueous	Organic	Aqueous
Dispersed phase hold-up (%)	14.1-17.7	27.7-34.2	16.2-20.5	25-45
Feed U $g.l^{-1}$	2-2.9	1.4-2.7	-	0.3-0.8
Solvent U $g.l^{-1}$	0.25-0.6	0.25-0.5	-	<0.03
Loaded solvent U$g.l^{-1}$	5.7-7	5.6-7.4	-	3-4
Raffinate U$mg.l^{-1}$	3.6-11	2.9-5.1	-	⩽ 2
Extraction efficiency %	99.6-99.9	99.8-99.9	-	99.6-99.9
Stripping solution U $g.l^{-1}$	-	-	19-32	-
Specific flowrate $l.cm^{-2}h^{-1}$	2.7-3.9	1.4-2.1	0.65-1.3	2.2-2.8

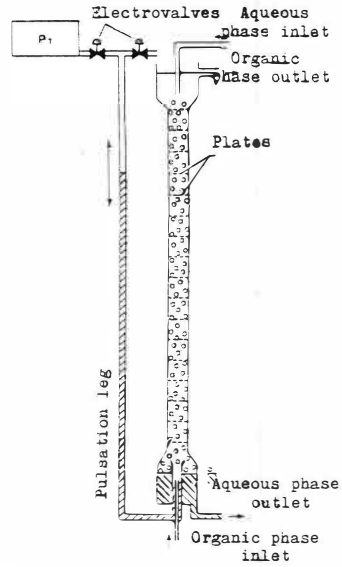

Figure 1: Simplified sketch of a pulse column

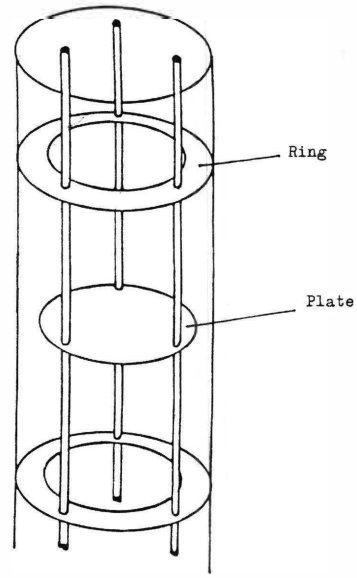

Figure 2: Assembly of baffle plates

SOLVING THE HIGH ORGANIC ENTRAINMENT PROBLEM: THE EFFECT ON CATHODE COPPER CRYSTALLIZATION UNDER SPECIFIC OPERATING CONDITIONS

Gabriel E. Larrondo

Chief Metallurgist
Sociedad Minera Pudahuel
Santiago, Chile

1.- FOREWORD : DESCRIPTION OF THE PLANT

SMP is a chilean private company that owns the Lo Aguirre Copper Mine, located approximately 30 Km west of Santiago, on the highway to Valparaíso, the main chilean port.

The metallurgical plant processes the ore of the Lo Aguirre copper deposit which is an open pit facility having ore reserves of 11 million MT. The copper tenor in the ore ranges from 2.0% oxidic to 2.0% sulfidic species The oxidic copper tenor varies as the mining works become deeper ultimately reaching sulfidic ores.

The metallurgical plant includes the following process units : (See Fig. N° 1)

- Thin layer leaching

  2.900 MTD of ore are counter currently leached for 18 days in two cycles after a curing step with strong sulfuric acid which is partially supplied by bleed of electrolyte from EW. Process water is also used to agglomerate the ore.

- Solvent Extraction

  One train of 4 low profile mixer settlers, having two extraction and two stripping stages, transfers the copper content of the 2.000 GPM stream of 6 gpl Cu pregnant liquor (PS), to 450 GPM of 50 gpl electrolyte.

- Electrowinning

  72 EW cells, including 8 starter cells, plate 45 MTPD of copper cathodes having 99,98% Cu, < 10 ppm sulphur, < 5 ppm Fe and < 3 ppm Pb. Copper cathodes have been mainly sold at premiun prices to european companies for continuous rod production.

2.- RISE OF METALLURGICAL PROBLEMS

2.1 DESIGN :

The design criteria for the Lo Aguirre Plant stated :

i) 80 ppm organic entrainment during the first six months of operation and 60 ppm from then on. The organic in present use is 30% Lix 64N LS and 70% Escaid 100 (18.4% Lix 64 NHS and 81.6% Escaid 100)

ii) Pregnant Solution
Specific gravity : 1.1 gr/cc
Viscosity : 2.0 cp

2.2 OPERATING EXPERIENCE : ORGANIC ENTRAINMENT

Organic entrainment since start up was at least twice the figure considered in plant design.

As can be seen in Fig. N° 2, until Nov. 81, the first year of operation, the entrainment was between 150 and 180 ppm based on inventory figures.

Research was undertaken and small design changes were made for both decreasing plant entrainment levels and recovering entrainment organic. The following is a summary of the efforts made to reduce entrainment losses, which were evaluated at about U$ 700 per ppm per month.

- The introduction of air in the mixing chambers of the mixer settlers was reduced by :
  - i) eliminating the cascading of incoming emulsion
  - ii) operating with organic and aqueous boxes at higher liquid levels and
  - iii) installing a floating plate in the mixing chambers to avoid vortexing
- Mixing time was decreased and settling time increased by using just one of the auxiliary mixers in each settler, while not jeopardizing the chemical transfer.
- A thicker phase band was established in E 2 by setting a baffle midway between the picket fence and the organic weir.
- Organic was recovered from the electrolyte surge tank by a floatation machine prior to the CE NATCO OFX filter.
- Organic was recovered from the raffinate tank by setting up baffles and returning skimmed organic back to E 2 .

Besides the cost of replacement, the high entrained organic was highly deleterious in leaching, causing impermeability of ore beds. Organic coated zones of the pad did not allow liquors to percolate, lowering recoveries up to ten points.

From Nov. 81 to June 82, organic entrainment increased to 350 ppm at it's worst.

Because the specific gravity of PS reached 1.27 gr/cc at a viscosity of 5 cp (abnormal according to design), new attempts were made to control entrainment via PS dilution. Positive results were obtained by adding 500 lpm of water to the E 2 mixing chamber during a one day trial. Nevertheless, the water balance did not allow for extra water to be added to the system, especially in winter time, so this could not be adopted as a normal operating procedure.

A very unusual heavy rain period began and both specific gravity and viscosity decreased along with organic entrainment. (See Fig. N° 2).

Very shortly after this, some very unusual facts began to appear :

- Abnormal crystal growth in copper cathodes was observed characterised by sharp edges and lustrous appearance. Individual crystal could be seen. As a direct consequence of this abnormal crystallization pattern, electrolyte was occluded, strongly increasing sulphur content in cathodes. It reached 85 ppm in the worst moment. (Sep. - Oct. 82)
- It was possible to wash out from the organic a yellow

water soluble unknown contaminant (YC) highly solu - ble in PH 9 amoniacal water.

- A green sludge appeared floating in the electrolyte surge tank after filtration, prior to the tank house.

2.3 CATHODE QUALITY

By compiling the observations it was possible to plot an historic graph of the following data :

- Organic entrainment
- YC in organic
- Sulphur in copper cathodes (an indirect way of measuring electrolytic deposit quality)
- Viscosity and sp. gr. of pregnant liquor

The following facts emerged from the analysis of graphed data. (See Fig. N° 2)

i) YC increased in the organic, since start up, going from a relative colorimetric value of 0.3 to a maximum of 1.2, after one year of operation.

ii) YC content began decreasing with the advent of winter rains. Being water soluble, YC was trans - ferred from the organic to the aqueous phase. YC contamination in the electrolyte ultimately spoil ed copper cathode quality. The YC which finally reported to the raffinate, recontaminated the or ganic in extraction since the raffinate is used on the leach pads. The only contaminant bleed in the SX - leaching system was that contaminant lost in tailings moisture.

iii) The viscosity of leach solution in a reasonable range, is a relevant factor, but only directly related to organic entrainment in the prescence of highly contamined organic. Entrainment de - creased at the same rate as viscosity did, but, since less contaminant was present in organic , entrainment values kept decreasing when viscosity levels were naturally maintained or ever increa - sed. In the summer of 83 viscosity reached its highest values and entrainment remained as low as 100 to 150 ppm, because of low contaminant levels.

With the previous facts in mind, it was decided to per form a series of tests in a bench scale EW plant unit , including filtering. The conclusions reached from the testworks were :

a) YC causes abnormal crystal growth in cathodes by behaving as a polar molecule at the copper-electro lyte interface.

b) It was absolutely necessary to clean out the YC from the organic, through amonia washing, to obtain lower YC levels.

This operation is very difficult, due to the slow and incomplete phase disengagement of the stable third phase emulsion formed with the YC contaminant. This emulsion allowed the organic to keep a highly concentrated YC aqueous entrainment that eventually reached the tankhouse.

c) A 55 ppm chlorine addition to the electrolyte was found to be the optimum for proper crystal growth in the presence of YC in electrolyte.

d) It was found that filtering tankhouse solution in the CE NATCO DFX seperator caused the YC to report to the electrolyte.

The effect of YC by itself in the electrolyte is more deleterious to cathode quality than when present with organic. For this reason the filter was taken off line, and organic contamination was controlled through aeroflotation and hand skimming.

2.4 FINAL ANSWER

A balance of YC in the plant taking into acount all of the possible ways of its building up, leads us to the conclusion that its generation takes place in the curing step previous to leaching, where the entrainment organic, from the bleed of electrolyte, is degraded by the shock of contact with concentrated sulfuric acid. The practi ce of adding electrolyte bleed in curing was abandoned in Dec. 82 and YC content in organic is decreasing slowly to the original figures.

The chlorine addition to the electrolyte has been slowly decreased as the YC content in the organic is decreasing.

It has been determined (Feb. 83) that the YC is mainly 2 Hydroxy - 3 Nitro Benzophenone, an organic degrada - tion product generated in the curing process.

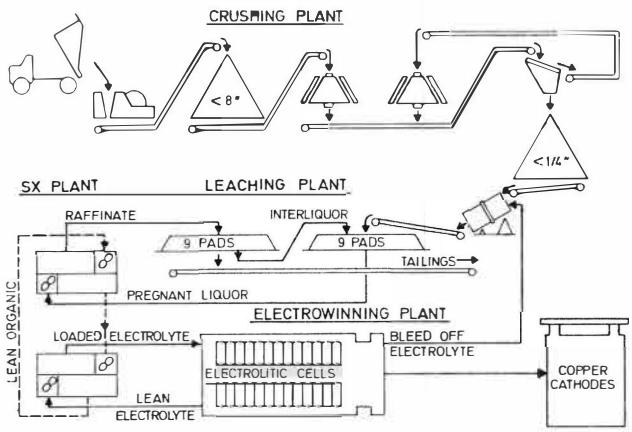

FIGURE N°1
LO AGUIRRE PLANT FLOW DIAGRAM

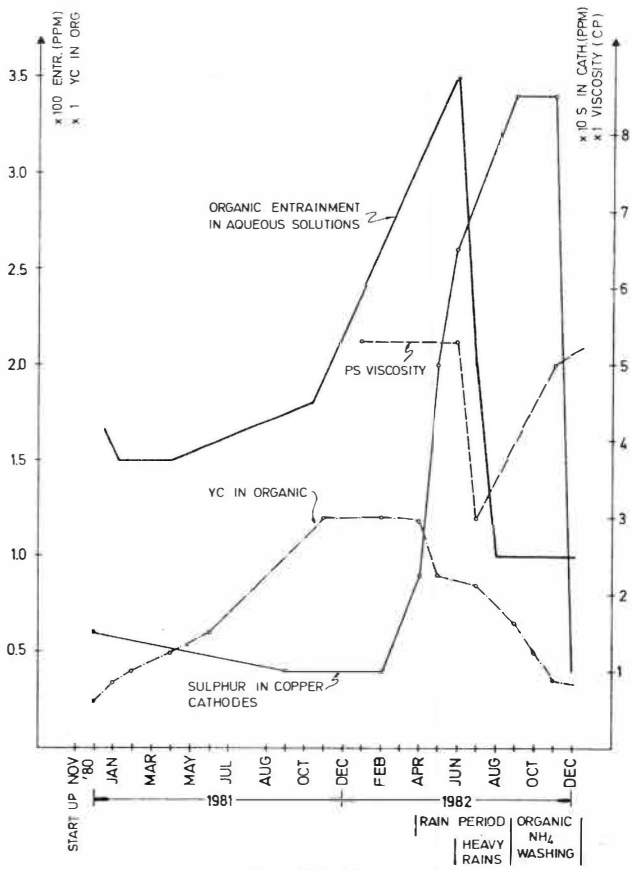

FIGURE N°2

RECOVERY OF URANIUM FROM CHLORIDE SOLUTIONS RESULTING FROM HCl LEACHING OF ORES AND CONCENTRATES

G. M. Ritcey, E.W. Wong and K.T. Price

CANMET
Energy, Mines and Resources Canada
555 Booth Street
Ottawa, Ontario
Canada K1A OG1

INTRODUCTION

At present, most of the uranium extraction in Canada is by a sulphuric acid leaching of the ore, followed by purification by either solvent extraction or ion exchange and subsequent precipitation of the uranium. Though commercially successful, this process leaves nearly all the radionuclides (Ra^{226}, Pb^{210}, Th^{232}, etc.) in the tailings.

Thus, primarily for environmental concern but with economic reasons in mind, research is on-going at the Canada Centre for Mineral and Energy Technology (CANMET) to develop an alternate process for uranium extraction that would solubilize radionuclides to enable their isolation in the mill.

Tests using hydrochloric acid and chlorine-assisted leaching on various ores have indicated good extraction (11).

This paper describes the development of a process for solvent extraction of uranium from chloride leach liquors and the subsequent testing of this process in a small continuous circuit.

RESULTS

Extraction

The result of screening tests on selected extractants indicated that TOPO (Tri-octyl-phosphine-oxide) was the most promising. Table 1 shows the analyses of the chloride leach liquor resulting from HCl leaching Elliot Lake ore.

Table 1 - Analysis of Feed from Elliot Lake Ore Leaching

Element	Concentration (g/L)
U	0.65
Th	0.20
Fe^{T}	3.09
Fe^{+2}	2.33
Ra	3720 (pCi/L)
Si	.075
Free HCl	14.4

The feed was treated with 30 ppm of a flocculent reagent - Polyox - to remove silica.

In Tables 2 and 3 are shown data for U, Th and Fe extraction using 5% and 2.5% TOPO in Shell 140. Comparative isotherms are shown in Figure 1.

Table 2 - Extraction by 5 w/o TOPO in Shell 140

A/O	% Extraction		
	U	Th	Fe
20/1	55.23	0.225	0.437
15/1	58.89	0.5	0.734
10/1	76.51	1.20	1.26
5/1	81.82	4.10	2.91
3/1	85.86	8.33	4.64
1/3	99.74	66.00	18.45
1/5	99.73	75.00	21.04

While 5% TOPO gave better U and Th extraction, 2.5% TOPO was chosen because at the proposed A/O ratio for the pilot plant - 3/1 - its performance was slightly better. Also, the overall increase in extraction by 5% TOPO was not enough to make a doubling of concentration economically worthwhile. Finally 2.5% TOPO loaded less iron as an impurity as well as less Th. The McCabe Thiele diagram is shown in Figure 2.

Stripping

Extensive screening tests were performed on twenty different stripping agents, for TOPO proved to be a difficult solvent from which to strip uranium.

Table 3 - Extraction by 2.5 w/o TOPO in Shell 140

A/O	% Extraction		
	U	Th	Fe
20/1	24.77	0.1	0.097
15/1	17.03	0.367	0.177
10/1	45.76	0.350	0.236
5/1	67.78	1.1	0.602
3/1	90.40	2.83	1.29
1/3	100.	39.00	11.65
1/5	75.76	52.50	15.05

The best stripping solution was a combination of H_2SO_4 + H_2O_2 which also gave excellent separation time (~10 sec), and no emulsion. There was no significant difference between 5% H_2SO_4 + 5% H_2O_2 and 10% H_2SO_4 + 5% H_2O_2. For economic reasons, the lower concentration was used. A stripping isotherm using 5% H_2SO_4 + 5% H_2O_2 is shown in Figure 3. Table 4 shows the relative effectiveness of the stripping agent on the organic for different elements. Although Fe stripping percentage was high, it should be noted that the actual Fe concentration in the organic was low to start with (.007 g/L Fe).

Scrubbing

A solution of 15 g/L U in Cl^- solution at pH 0.5 was recommended for scrubbing purification before stripping of uranium.

Table 4 - Stripping with 5% H_2SO_4 + 5% H_2O_2

O/A Ratio	% Stripped		
	U	Th	Fe
7/1	24.68	95.23	48.99
5/1	31.14	63.33	88.57
3/1	44.49	61.11	80.95
1/1	69.44	66.67	100.00
1/3	99.79	100.00	100.00
1/5	85.24	83.33	100.00

The problem with stripping in a sulphate medium was that sulphate loaded onto the organic, which was undesirable for two reasons. It occupied sites on the organic, which would decrease the extracting efficiency of the TOPO as it was recycled. The sulphate would also allow Ra^{2+} to form $RaSO_4$ precipitate when recycling the chloride raffinate. Screening of scrubbing agents indicated that several contacts with 2M NaCl would scrub the majority of the sulphate off the TOPO.

CONTINUOUS TESTING

The circuit used 2.5% TOPO in Shell 140, and the leach feed analysed, in g/L: U = 0.70; Th = 0.25; Fe = 2.09 and Ra = 23,300 pCi/L. The extraction isotherm (Fig. 2) suggested that 5 stages would be needed to bring the raffinate to a U concentration of .005 g/L. The circuit, with 5 stages, was started at an A/O ratio of 3.2/1 (192 mLs/60 mLs per minute as flowrates).

The first 4 hours run showed higher than 99% extraction, with raffinate at less than 0.0002 g/L U. Extraction remained high throughout, with the final raffinate showing no higher than 0.0002 g/L U as the ratio was increased to A/O 4.5/1 after 8 hours. The composite organic contained 2.77 g/L U, 0.071 g/L Fe and .0006 g/L Th.

There were 2 stages of scrubbing with 15 g/L U at pH 0.5 at O/A = 2/1, followed by 7 stages of stripping with 5% H_2SO_4 + 5% H_2O_2. Stripping was at O/A = 3/1. Initially one stage of sulphate scrub with 2M NaCl at O/A = 2/1 was placed at the end of the circuit. However, to ensure sufficient scrubbing, the organic was run through another 5 scrub stages.

The strip raffinate sent for U precipitation contained 10.4 g/L U, .023 g/L Th, and .005 g/L Fe. After final scrubbing, the organic contained 0.88 g/L U, <.001 g/L Th and .0006 g/L Fe.

A schematic of the overall flowsheet is shown in Figure 4.

REFERENCES

1. Haque, K.E., Lucas, B.H. and Ritcey, G.M. "Hydrochloric acid leaching of an Elliot Lake uranium ore"; CIM Bulletin 73:819:141-147; 1980.

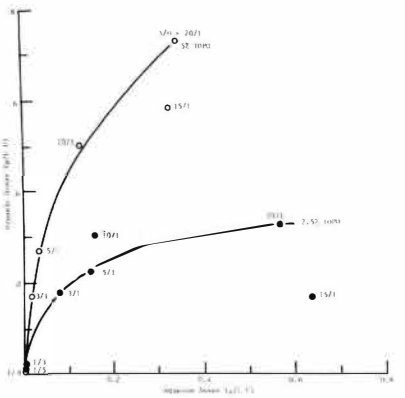

Figure 1. Extraction of Uranium with TOPO in Shell 140.

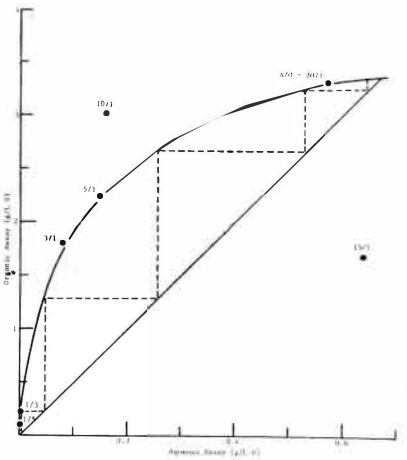

Figure 2. McCabe-Thiele diagram for uranium loading - 2.5% TOPO in Shell 140.

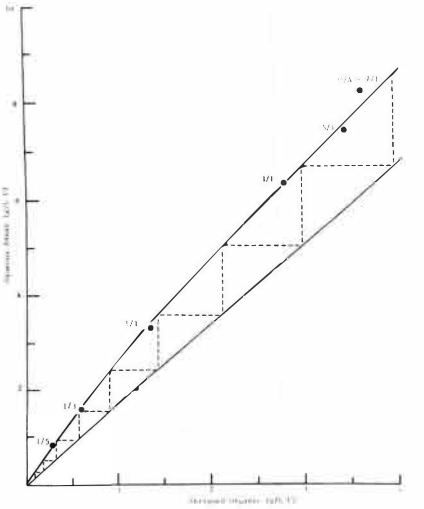

Figure 3. McCabe-Thiele plot of uranium stripping - 5% H_2SO_4 + 5% H_2O_4.

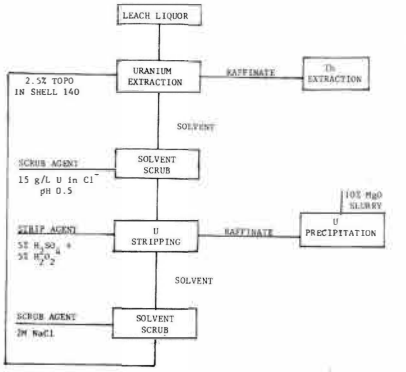

Figure 4. Schematic flowsheet.

INTERFACIAL PHENOMENA IN URANIUM EXTRACTION FROM WET PROCESS PHOSPHORIC ACID

Armand Davister and Andre Dubreucq

Société Chimique PRAYON-RUPEL S.A.
Engis, Belgium

INTRODUCTION

Cruds formation is a problem common to most solvent extraction operations and uranium extraction from phosphoric acid is no exception. In fact, one of the producers reported (1) a generation of 2 tons/day of "dry" cruds (after washing and filtration), which is roughly equivalent to 4 kilos of dry cruds per kilo of U308 recovered. This figure was achieved despite pre-treatment of the phosphoric acid fed to the extraction and it is roughtly estimated (2) that, without pre-treatment, cruds would be generated at a rate of about 50 liters per kilo of U308 recovered.

Cruds represent a serious problem because, if left untreated, they will accumulate in the whole plant up to the point where operation of the various extraction equipments will no longer be possible. Moreover, they represent an expensive loss of the costly organic and a disposal problem since they contain both flammable material and slightly radioactive contaminants.

Our approach, when considering our uranium extraction plant, has been to design the acid pre-treatment operation so that cruds formation is avoided or, at least, strictly minimized.

ACID PRE-TREATMENT OBJECTIVES

It is very well known, in uranium extraction from phosphoric acid, that cruds are due to the presence of solids particles and "humic" acids in the phosphoric acid feed. Very little is known about cruds exact composition except that they are constituted by a mixture, in varying proportions, of aqueous, solids, and organic. In the mixer-settlers, two types of cruds appear : "floating cruds" that concentrate at the upper part of the organic layer, and "interfacial cruds" that accumulate in the interphase area. Generally speaking, but this is not an absolute rule, floating cruds contain more solids while interfacial cruds originate merely from humates present in the acid.
During the pilot scale tests, various acid pre-treatment techniques were tried with the aim of avoiding cruds formation. Acid coming out of these tests was contacted, in a laboratory mixer-settler with organic (D2EHPA-TOPO in a kerosene-type diluent) which was continuously recirculated. It was soon obvious that, if cruds formation was to be avoided, the phosphoric acid should behave like a water-like liquid. For anyone familiar with wet-process phosphoric acid manufacture, this represents and unheard-of challenge since raw phosphoric acid is very impure, contains humic acids and a lot of impurities in a super saturated state. This last characteristic causes scaling of the pipes and equipments and is the main reason for "post-precipitation" : if the acid is aged, each impurity will tend to reach its solubility equilibrium, thus the super saturation will decrease by precipitation of the amount of impurities in excess of the solubility limit. This processus usually takes several days, or even weeks in some extreme cases, and starts again every time the temperature or the P205 concentration of the acid is changed since the solubility of the major impurities is temperature and P205 concentration dependant.

Objectives assigned to pre-treatment of the acid were thus :

- to remove all the insoluble mineral and organic impurities.
- to remove enough organic soluble impurities.
- to desaturate the acid so that post-precipitation will not occur during extraction.

Extensive pilot scale tests allowed to establish a flow-sheet which has been incorporated in the final design of our industrial plant.

This plant was started-up in may 1980. The nominal capacity is 130.000 T P205/Y (or 45 m^3/h of 30 % P205 acid), based on acid from MOROCCO phosphate which contains about 140 ppm U308. The pre-treatment section was designed to process acid from MOROCCO rock, however the system had to be flexible enough to accomodate acids made from other phosphates and this has been successfully demonstrated during subsequent industrial scale trials.

ACID PRE-TREATMENT PROCESS DESCRIPTION

1. Cooling

The first operation is to cool the acid coming from the phosphoric acid plant, from 55 to 60°C down to 30°C. This lowers the solubility limit of most of the impurities and is beneficial for the extraction since the extraction coefficient is improved by a lower temperature.

Due to the scaling properties of fresh raw acid and the precipitation of impurities due to cooling, choice and design of the cooling equipment is critical. We use a two-stages vacuum cooler in which cooling is achieved by flash evaporation of water from phosphoric acid under low absolute pressure (25 m bar). This type of equipment is well suited for this purpose since the acid retention time is very low (thus scaling has a very short time to develop), it is easy to control, may be operated under scaled conditions and easy access is provided for cleaning.

2. Desaturation

Cooled acid is dynamically desaturated for 24 hours in an agitated tank in which most of the super saturated impurities precipitate. Some gypsum crystals from the phosphoric plant attack tank, are added for seeding purpose.

A specially designed agitator provides a very high flow inside the tank so that conditions are kept homogeneous and the seeds are well distributed inside the whole volume.

3. Clay addition

Activated clay is added at this point to adsorb most of the long chain organic material present in the acid. A commercially available activated clay is used for this purpose.

4. Floc addition

A high molecular weight flocculant is added in view of the subsequent solids separation. This floc coalesces all the small particles together, and, to some extend, also coagulates some of the organic material. Non-ionic or anionic long chain polymer flocculant, typical in phosphoric acid industry, is used.

5. Solids separation

Solids resulting from desaturation and from gypsum and clay additions are separated on a Pannevis-type filter. As solids from desaturation show very poor filtration characteristics, gypsum added in the desaturation tank acts as a kind of precoat to trap the fine particles and protect the filter cloth from clogging. Typical solids content of the filtered acid is lower than 50 ppm W/W.

6. Activated carbon treatment

Filtered acid is passed through activated carbon adsorption columns for removing the short chain humates. After saturation, the carbon is chemically regenerated by caustic soda. This way of operation is very economical since the carbon may be regenerated a great number of times before its looses its adsorption characteristics.
Based on our present experience, the carbon life is expected to exceed five years so that the actual cost of carbon treatment is minimal.

7. Reheating

Acid out of the carbon colums is reheated by a few degrees prior to extraction so that the latter takes place at a temperature higher than the desaturation temperature and thus post-precipitations is avoided.

RESULTS OF PRE-TREATMENT

Phosphoric acid out of pre-treatment has the following characteristics :

- solids content : less than 50 ppm W/W.
- desaturation : after 48 hours under agitation, solids content is still lower than 50 ppm W/W.
- humic acid content : this characteristic is measured by spectrophotometry at 408 nanometers.

For reference purpose, water has a "colour" taken as zero. Raw acid has a colour varying between 0,8 and 1,5 while pre-treated acid has a colour of 0,15.

BENEFICIAL EFFECTS OF PRE-TREATMENT

- When the plant is operated under normal conditions, there is no cruds formation during extraction.
- Scaling and post-precipitation do not take place during extraction. In fact, during more than three years of operation, the acid lines between pre-treatment and extraction, and the extraction section have never been cleaned. It will be appreciated that in most phosphoric acid plants, all the acid lines have to be cleaned during at least one shift par week, or in some processes, during one or two hours every day.
- Due to the absence of scaling, flow control equipment is reliable and this results in perfect extraction control thus higher than average extraction efficiency.
- For the same reason, there is no downtime for vessels and equipment washing. This contributes to high efficiency, to an excellent on-stream time and reduces organic losses as well as organic effluents pollution and fire risk.
- After uranium extraction, the acid is returned to the phosphoric acid plant as a high quality product. This is a definite advantage for down-stream usages.

CRUDS TREATMENT

As mentioned above, under normal operating conditions, cruds do not appear. However, some cruds develop from time to time due to misoperation in the pre-treatment section or due to changes in the phosphate rock composition. The latter requires a change of the pre-treatment operating parameters and sometimes, the pre-treated acid is not on specification during the adaptation period. Approximately 5 to 8 cubic meters of cruds per year have been generated by this way.

Several tests have been conduted in order to give the operators a possibility

to remove this small amount of cruds before it becomes a problem.
Final choice was made on a small disc "desludger" centrifuge. This machine has a capacity of about 1 cubic meter per hour and mechanically breaks the cruds by applying to them a centrifugal acceleration of about 7.000 g.

Typically, when treating cruds through this machine, 95 to 98 % of the solvent is recovered as a clear solution containing less than 0,02 % V/V of solids. This clear organic phase may thus be recycled directly to the extraction while the "compacted cruds" which represent only about 1/30 of the original volume contain 40 to 45 % V/V of solids and are practically free of organic since the accompanying liquid is phosphoric acid.

CONCLUSION

If not seriously addressed to, cruds formation during uranium extraction from phosphoric acid represents a serious problem leading to operation disturbances, expansive organic losses, pollution and fire risk.

Our industrial experience shows that the best way to solve this problem is through an extensive pre-treatment of the phosphoric acid aimed at removing the solids, the humic acids and stabilizing the acid. This pre-treatment operation gives also additional benefits with regards to extraction efficiency, on-stream time and quality of the phosphoric acid returned to the phosphoric acid plant.

Cruds produced by accidental misoperation may be efficiently treated by centrifugation.

References

1. L. ELIKAN, R.R. STANA and R.W. YORK, AICHE 74th Annual Meeting, New Orleans, LA. (1981).

2. W.W. BERRY, A. DUBREUCQ, ISEC'80, 80-235, Liège, Belgium (1980).

IMPROVED DIALKYL PHOSPHORIC ACID, PHOSPHINE OXIDE SYNERGISTIC SYSTEMS FOR URANIUM RECOVERY FROM PHOSPHORIC ACID LIQUORS

C. Ginisty

Centre d'Etudes Nucléaires de FONTENAY-AUX-ROSES, France

Uranium contained in phosphoric acid liquors can be recovered by solvent extraction. Various processes are available, including one using the synergistic mixture HD_2EHP/TOPO (1), but their efficiency is limited. Their performance can be improved by the new extractants synthetized by IRCHA (Institut de recherche chimique appliquée BP n°1 91710 VERT-LE-PETIT, FRANCE).

RESEARCH ON PHOSPHINE OXYDES.

A study of different synergistic systems led us to investigate a large number of phosphine oxides. To modify the molecular structure we introduced one or more complementary functions, including ether oxide, amide, sulfine, or even phosphine oxide.

Other structural modifications can be used to lengthen or shorten the alkyl radicals or to branch these radicals.

The results of these experiments (2) showed that the introduction of an ether function is the essential modification required to increase uranium extraction. For example, octoxymethyl radicals can be substituded for octyl radicals in the TOPO formula to yield compounds 2,3 and 4 in Table I. Figure 1 compares the extractive power of these new extractants in relation to TOPO.

The best results are obtained with only one octoxymethyl radical in the molecular structure. The poor results obtained with compound 4 can be explained by the decreasing basicity with an increasing number of octoxymethyl radicals.

A general formula can be expressed :

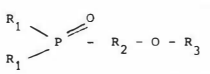

with R_2 limited to CH_2 because of the synthesis difficulties.

For R_1 the best results are obtained with alkyl radicals with 6 to 8 carbon atoms, and for R_3, the best results are obtained with C_8H_{17} which can be linear or branched.

The phosphine oxide selected was the compound 5 in Table I : DinHMOPO. Compared to TOPO, this compound improves extraction by a factor of 1.5 (3). It is a liquid and totally miscible with the organic phase, facilitating its industrial use.

RESEARCH ON ORGANOPHOSPHORIC ACIDS.

Similary, various organophosphoric acids were tested with TOPO in synergistic systems. It soon appeared that the best results were obtained with acids whose radicals contained an ether function. Oxygen in the radicals increases the acidity by an inductive effect.

The result of this study shows that the closer the oxygen is to the phosphoryl group the stronger the inductive effect, with improved uranium extraction. Two alternatives are essentialy available for the molecular structure. If the synthesis is performed with a primary or secondary alcohol, the compound obtained resembles compound 7 or 8 in the Table II respectively. Figure 2 shows increased uranium extraction with longer alkoxyalkyl radicals.

This effect is important for the two structures with primary or secondary alcohol, but two oxygens per radical are intoduced with a secondary alcohol, both near the phosphoryl group, explaining the good results obtained with this compound.

Problems are encountered (third phase formation) when light compounds are employed when uranium is stripped with a carbonate aqueous phase, this can be avoided by increasing radical length.

Hence some specifications can be retained for the organophosphoric acid struture :

- For primary alcohol esters :

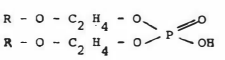

where R is C_nH_{2n+1} and n is at least equal to 8.

- For secondary alcohol esters :

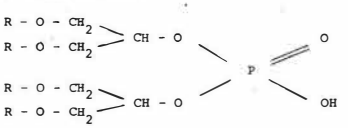

where R is C_nH_{2n+1} and n is at least equal to 4.

For an industrial application, we selected the acidic compound 8 (HBiDiBOPP = Hydrogéno Bis DiButOxy 1,3 Propyl 2 Phosphate) in table II on account of its easy synthesis and low cost (4).

BEHAVIOR OF THE HBiDiBOPP/DinHMOPO MIXTURE.

Figure 3 shows the synergism with a maximum in uranium extraction versus the mole ratio of the extractants. The HBiDiBOPP/DinHMOPO mixture gave similar variations to the HD_2EHP/TOPO mixture when the H_3PO_4 concentration or temperature was increased. HBiDiBOPP/DinHMOPO system contacted with a 8,3 M H_3PO_4 aqueous phase gave identical uranium extraction coefficients than the HD_2EHP/TOPO system contacted with a 6 M H_3PO_4 aqueous phase. With HBiDiBOPP/DinHMOPO mixture, extraction performed at a temperature of 60°C gave uranium extraction coefficients twice better than with HD_2EHP/TOPO mixture contacted at a temperature of 40°C.

Comparative experiments were conducted with an industrial phosphoric acid (27% P_2O_5, U = 130 $mg.l^{-1}$, Fe = 1.72 $g.l^{-1}$) and with different extractant mixtures. One volume of organic phase was contacted 8 times with one volume of new aqueous phase at each contact.

Figure 4 very clearly shows the superiority of the HBiDiBOPP/DinHMOPO mixture.

Uranium extraction coefficients and concentration factors are reported below :

Synergistic mixture	$E_a°$	Concentration factor
HD_2EHP / TOPO	5,6	2,6
HD_2EHP / DinHMOPO	7,8	3,0
HBiDiBOPP / TOPO	10,6	4,1
HBiDiBOPP / DinHMOPO	16,0	6,1

Concentration factors are calculated for a 99% uranium recovery with 5 extraction stages.

A process (5) has been tested successfully by COGEMA (Compagnie Générale des Matières Nucléaires) and flowsheet is shown in figure 5. The test was performed with a 4 $l.h^{-1}$ phosphoric acid flowrate and also with a 60 $l.h^{-1}$ phosphoric acid flowrate in a larger installation.

This one cycle process is based upon the selective stripping which allows iron-uranium separation. Iron is precipitated as hydroxide and uranium remained in solution as carbonate complex. In the extraction, scrubbing and reacidification sections, phase disengagements are excellent. Reacidification was a difficult operation with the HD_2EHP/TOPO mixture.

Recovered uranium has the required purity for commercial use.

CONCLUSION.

This work has demonstrated the efficiency of new industrial extractants in the laboratory and on a pilot scale. The HBiDiBOPP/DinHMOPO mixture extracts uranium three times better than the standard HD_2EHP/TOPO mixture with the same neutral and acidic reagent concentrations.

Both extractants are liquid and totaly miscible in the organic phase, facilitating their industrial use. The pilot scale experiments showed the good hydrodynamic behavior of these compounds as compared to the standard HD_2EHP/TOPO mixture.

At laboratory scale, the best results are obtained with the acidic compound 9 in table II (HBiDiHOPP).

The HBiDiBOPP/DinHMOPO mixture offers an extraction yield five times better than HD_2EHP/TOPO, but HBiDiHOPP purification has not yet reached the industrial stage.

To sum up, we have developped a more effective process than previous ones to recover uranium in phosphoric liquors.

A significant improvement can be achieved by substituting HBiDiHOPP to HBiDiBOPP.

REFERENCES

1 - F.J. HURST, D.J. CROUSE, US Patent 3 711 591 (1973)

2 - C. GINISTY, A. BATHELLIER, DGRST Report 76-7-0008 (1977)

3 - A. BATHELLIER, C. GINISTY, FRENCH Patent 78-33543 (1978)
79-15397 (1979)

4 - C. GINISTY, A. BATHELLIER, DGRST Report 80-D-0705 (1982)

5 - C. GINISTY, M. MARTEAU, B. MAUBORGNE, FRENCH Patent 80-24253 (1980)

N°	R (R_3PO)	ABBREVIATION	FORMULA
1	Tri-n-octyl	TOPO	$(C_8H_{17})_3$ PO
2	Di-n-octyl octoxymethyl	DinO MOPO	$(C_8H_{17})_2PO(CH_2-O-C_8H_{17})$
3	n-octyl Dioctoxymethyl	nODi MOPO	$C_8H_{17}PO(CH_2-O-C_8H_{17})_2$
4	Tri-octoxymethyl	Tri MOPO	$(C_8H_{17}-O-CH_2)_3$ PO
5	Din hexyl octoxymethyl	DinH MOPO	$(C_6H_{13})_2PO(CH_2-O-C_8H_{17})$

TABLE I

N°	R $\left(\begin{matrix}R-O\\R-O\end{matrix}\!>P\!\!\begin{matrix}=O\\OH\end{matrix}\right)$	ABBREVIATION	R FORMULA
6	Ethyl 2 hexyl	HD_2 EHP	$C_4H_9-\underset{C_2H_5}{CH}-CH_2-$
7	Ethyl 2 hexoxyethyl	HD_2EH OEP	$C_4H_9-\underset{C_2H_5}{CH}-CH_2-O-C_2H_4-$
8	Dibutoxy 1,3 propyl 2	H Bi Di BOPP	$(C_4H_9-O-CH_2-)_2$ CH -
9	Dihexoxy 1,3 propyl 2	H Bi Di HOPP	$(C_6H_{13}-O-CH_2-)_2$ CH -

TABLE II

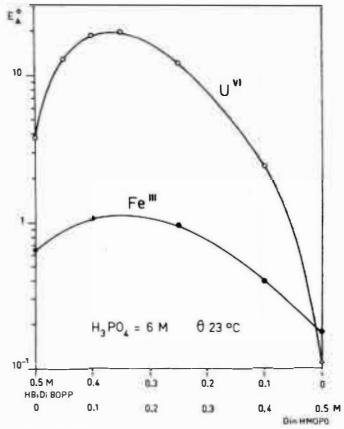

FIG. 3.- SYNERGISTIC EFFECT OF HBiDiBOPP/DinHMOPO ON URANIUM AND IRON EXTRACTION. [HBiDiBOPP] + [DinHMOPO] = 0.5 M

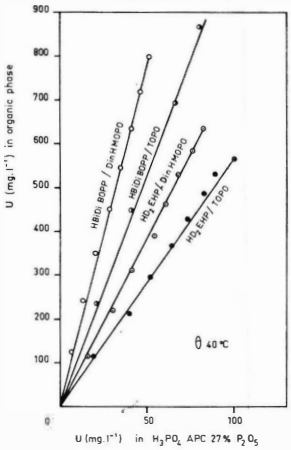

FIG. 4.- URANIUM EXTRACTION WITH DIFFERENT ORGANIC SYNERGISTIC SYSTEMS.

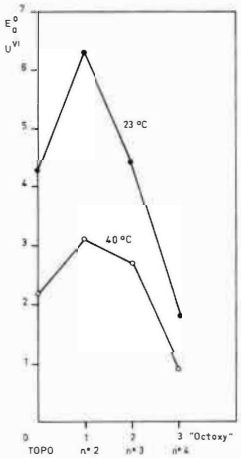

FIG. 1.- PHOSPHINE OXIDES: INFLUENCE OF THE NUMBER OF ETHER OXIDE FUNCTIONS. HD_2EHP = 0.5 M ; PHOSPHINE OXIDE = 0.125 M ; H_3PO_4 = 6 M ; U (VI) = 1 g l^{-1}

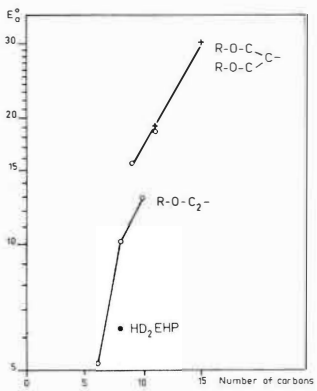

FIG. 2.- ORGANOPHOSPHORIC ACIDS : INFLUENCE OF THE NATURE AND LENGTH OF ALKOXY-ALKYL RADICALS.

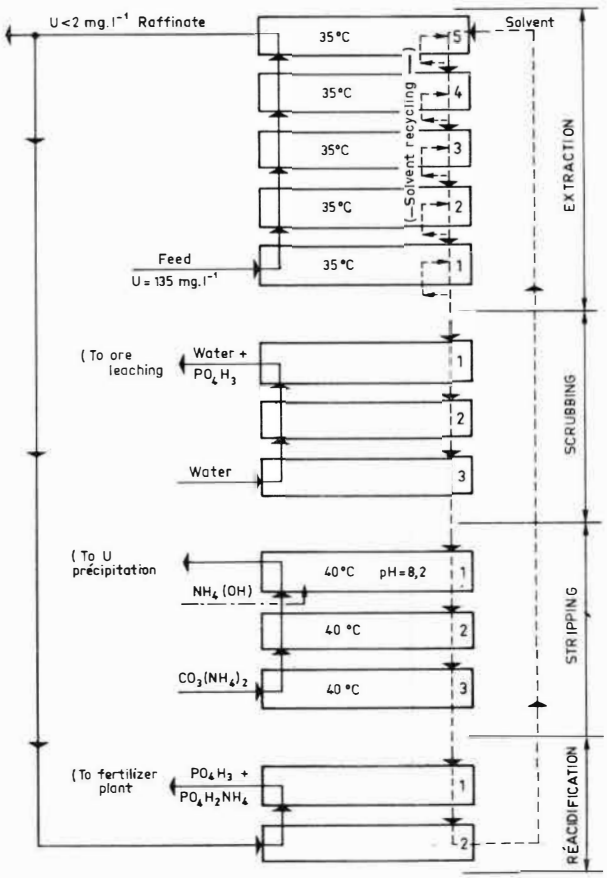

FIG. 5.- URANIUM RECOVERY FROM PHOSPHORIC ACID. FLOWSHEET

SOLVENT EXTRACTION PROCESS AND EQUIPMENT FOR A LMFBR FUEL REPROCESSING PILOT PLANT

G. Koch, H. J. Bleyl, G. Boehme, H. Goldacker, H.O. Haug, W. Ochsenfeld, H. Schmieder

Kernforschungszentrum Karlsruhe
Karlsruhe, Federal Republic of Germany

A conceptual study of a LMFBR fuel reprocessing pilot plant, internally nicknamed "MILLI-II", has been carried out at KfK (1). The plant is primarily designed to process spent fuel elements from the German sodium-cooled fast-reactor power stations KNK-II (Karlsruhe, 20 MWe) and SNR-300 (Kalkar, 300 MWe); in addition the design provides for potential pilot-scale processing of other types of LMFBR fuel elements, and mixed-oxide fuel elements from advanced light-water reactors.

The design throughput of MILLI-II has been fixed at 50 kg of uranium and plutonium per day, and the minimum fuel cooling time at 180 days. The fundamental process applied to recover highly decontaminated plutonium and uranium products consists of mechanical disassembly of the fuel element, shearing of the fuel pins, leaching with nitric acid, and PUREX-type solvent extraction with tributyl phosphate.

SOLVENT EXTRACTION PROCESS

Basic flow scheme. A schematic flow diagram of the standard solvent extraction process, including the acid recovery and waste systems, is given in Figure 1. Uranium and plutonium are decontaminated by a PUREX co-decontamination cycle (HA-HS-HC extractors), followed by a partitioning cycle (1A-1BX-1BS-1C extractors), and the separated products are each purified through a final cycle of TBP solvent extraction (2A-2AS-2BX/2BS-2C for Pu, 2D-2E for U). For better illustration, a very much simplified equipment scheme of the co-decontamination and partitioning cycles is shown in Figure 2, and a similar scheme of the final purification cycles in Figure 3, symbolizing extraction columns as the extraction equipment. Interconnection between solvent extraction equipment will be provided such that partitioning can alternately be carried out in the first extraction cycle; in this case, the sequence of extractors is HA-HS-1BX-1BS-HC as the first cycle, the uranium product emerging from the HC extractor is purified in the 1A-1C and 2D-2E cyles, and the plutonium product emerging from the 1BS extractor is purified in the 2A-2AS-2BX/2BS-2C cycle. The standard solvent specified is 30 vol.-% TBP in a kerosene-type n-alkane diluent but different solvent compositions may be applied for experimental purposes. A wide range of flowsheet conditions can thus be tested under pilot plant conditions, and a high flexibility of the plant is expected to result. Intercycle evaporation is provided after the co-decontamination cycle but not after the partitioning cycle; both the uranium and plutonium final products are concentrated by evaporation. Specific features of the process are outlined in the paragraphs below.

Feed pretreatment. The fuel is dissolved under conditions where most of the fission product iodine is expelled from the fuel solution into the off-gas from where it is removed by a caustic soda scrub (2). The fuel solution is transferred into a reaction tank where residual radio-iodine, when still present, can be removed into the off-gas by additional chemical treatment. After clarification by a centrifuge, the fuel solution is made up to extraction feed conditions.

Co-decontamination. The standard chemical flowsheet is a conventional high-acidity PUREX cycle applying an aqueous nitric acid concentration of approximately 3 moles per liter in the extraction (HA) and lower scrub (HS1) sections and a low-acidity scrub (1.5 m/l nitric acid) in the upper scrub (HS2) section. The HSS2 scrub stream is a "freshwater" scrub, i.e. it is made up from tritium-free acid and water; tritiated water is thus confined to the high-activity part of the plant. The metal loading of the organic phase at the organic outlet of the HS column (HSP) is 75,6 g U/l and 8.4 g Pu/l, or approximately 65% of the maximum theoretical loading.

Electro-redox procedures. The concept makes extensive use of the in-line electro-redox procedures developed by KfK (3). Both the plutonium/uranium partitioning in the the 1BX column and the final-cycle plutonium backwash in the 2BX column are performed by in-line electro-reduction (ELKE process), while intercycle re-oxidation of the plutonium is carried out by electro-oxidation (ROXI process). ROXI-type electro-oxidation cells are in addition used to decompose hydrazonium ion present in the aqueous solvent-wash streams of the process (see below).

The R column. The aqueous raffinates from the partitioning and purification cycles (1AW, 2AW and 2DW streams) which are essentially "salt-free" are routed into a medium-active acid recovery system consisting of a two-stage evaporator and rectification unit (designated 2WI - 2WII - AFII in Fig. 2). Entrained organic solvent phase is removed by an internal steam strip in the 2WI evaporator. The highly decontaminated acid and water fractions from the AFII fractionator are recycled into the process via the low-active Make-up II unit. The 2WI evaporator concentrate is routed into the Rework or R column where Pu and U are extracted by a small stream of 30% TBP which is recycled into the HA column while fission products and neptunium are rejected into the aqueous raffinate. The latter is combined with the high-active aqueous raffinate from the HA column (HAW), and is fed into the high-active acid recovery system consisting of a two-stage evaporator plus rectification unit (1WI - 1WII - AFI). The HAW is concentrated by a factor of approximately 4, and the high-active waste concentrate (1WW) is intermediately stored for final solidification. The acid fraction from the AFI fractionator is recycled into the head-end stage via the medium-active Make-up I unit while excess water is treated as low-active aqueous waste (LAW).

Solvent Cleanup. The concept provides for three independent solvent recovery systems (designated SR in Figs. 2 and 3), i.e. SR I for spent solvent from the co-decontamination cycle, SR II for that from the partitioning and Pu purification cycles, and SR III for that from the U purification cycle. Hydrazine carbonate is used as the aqueous solvent-wash solution in all three systems to remove metal traces and acidic solvent decomposition products (3), and the purified solvent is recycled into the process. The spent aqueous wash streams are routed through a ROXI-type electro-oxidation cell to decompose the hydrazine. The resulting solution which is essentially salt-free is fed into a multi-purpose evaporator, concentrated to a small volume, and the evaporator concentrate is routed into the high-level waste evaporator (1WI). (For better legibility, both the aqueous wash streams and the ROXI/multi-pupose evaporator system have been omitted from Figs. 2 and 3).

The benefit from the procedures described in the last three paragraphs is that no medium-active aqueous waste (MAW) will be produced during routine operation of the plant. Instead, the process raffinate liquors are split into a small volume of high-active waste, and into acid and water fractions which, apart from excess water, are recycled into the plant. Evidently this statement is not applicable for non-routine waste liquors resulting from plant decontamination operations.

Product wash. Organic solvent phase entrained or dissolved in aqueous U and/or Pu bearing product streams is removed before entering into an evaporator by sorption on a fixed bed of a LEWAPOL-type polystyrene-based organic resin (LEWAPOL is a trademark of Bayer AG, Leverkusen). Experience with this process is reported elsewhere in this conference (4).

SOLVENT EXTRACTION EQUIPMENT

Conventional pulsed columns are applied as the solvent extraction equipment, except for the solvent-wash contactors which are Holley-Mott-type mixer-settlers because of the long residence time of the aqueous wash solution and the very high organic: aqueous phase ratio. In-line electro-reduction is carried out using diaphragma-free electro-columns (ELKE). ROXI-type electro-oxidation cells are of the flat-cell design (3). Recent experience with this type of electro-equipment is reported elsewhere in this conference (5).

For criticality control, geometric limitation of equipment dimensions is applied as the primary measure. In addition, heterogeneous poisoning by hafnium metal absorber structures will be applied when necessary. E.g., a ROXI-type electro-oxidation cell with casing manufactured from hafnium has been successfully tested (5).

INSTALLATION AND MAINTENANCE

The plant concept is based on remote maintenance of equipment. To this effect the high-activity plant complex is subdivided into three separate areas, see Figure 4: (a) The mechanical head-end hot-cell complex where all mechanical treatment of fuel elements is done, (b) a single, highly shielded process cell where all chemical treatment from fuel dissolution down to product purification is carried out, and (c) a hot repair area where failed equipment can be disassembled and either repaired or disposed of.

The chemical process cell which houses all the solvent extraction equipment is designed as a tunnel-like complex of approximately 30 m internal length, 9 m i.width, and 17 m internal hight. It is subdivided by a lock into a highly shielded high-activity process area and a lower-shielded medium-acitivity area. The lock is locked under normal operation conditions to provide radiation shielding but the two areas are serviced by one and the same remotely operated, TV-controlled bridge-crane system assisted by a remote electro-manipulator system. Process equipment is mounted in "racks" which are suspended from the side walls of the cell. As an example, Figure 5 shows the two racks housing the first (co-decontamintion) extraction cycle, with the HA, HS, and HC columns plus auxiliary equipment mounted in one rack, and the feed adjustment and supply tanks in the second one. As can be seen from this figure, the cell is widened up in its top region by approximately 1,5 m on each side. Piping from and to process racks is mounted on the "balcony" so formed, and is connected to the rack piping by remotely operated multiconnector flanges. Furthermore, auxiliary equipment like sampling stations etc. is installed on this "balcony". Remote operation of the cell top region is carried out by conventional master-slave manipulators and direct viewing through shielding windows, in addition to the bridge-crane system mentioned earlier.

REFERENCES

1. G. Koch, H.J. Bleyl, G. Böhme, H. Goldacker, H.O. Haug, E. Henrich, W. Köhler, H. Iahr, W. Ochsenfeld, H. Schmieder, Atomwirtschaft Atomtechnik 27, 445 (1982).

2. E. Henrich, R. Hüfner, F. Weirich, Fast Reactor Fuel Cycles, London 1981, p.369.

3. H. Schmieder, H. Goldacker, M. Heilgeist, G. Petrich, Fast Reactor Fuel Cycles, London 1981, p.361.

4. W. Ochsenfeld, J. Schön, ISEC, Denver 1983, paper No. 10r.

5. H. Goldacker, U. Galla, M. Heilgeist, M. Kluth, R. Schlenker, H. Schmieder, H. Evers, ISEC, Denver 1983, paper No. 23d.

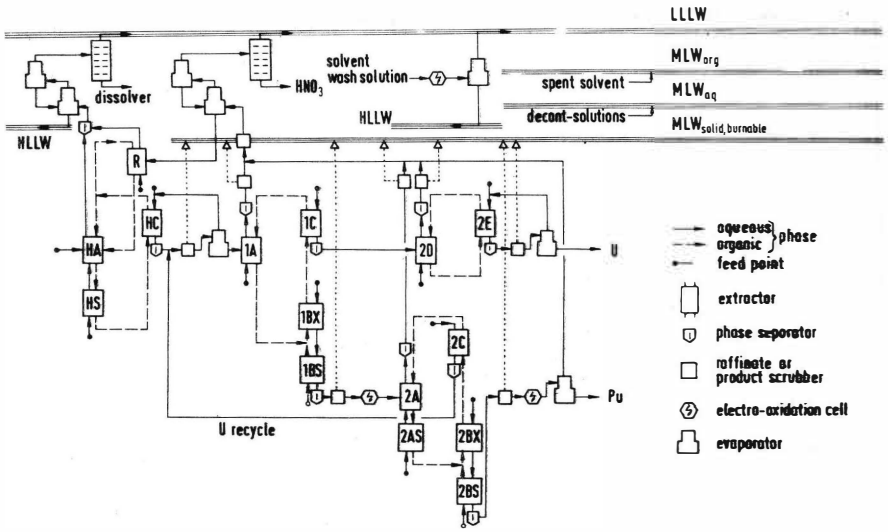

FIGURE 1. SOLVENT EXTRACTION, BASIC FLOWSHEET

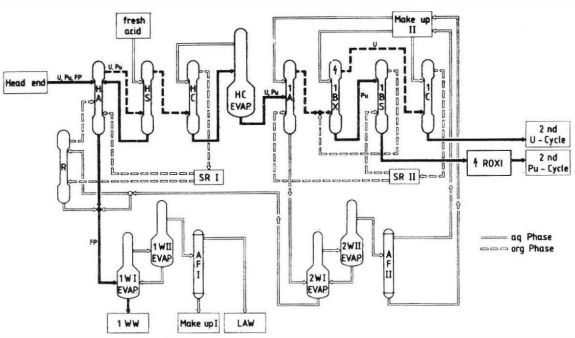

FIGURE 2. FLOW DIAGRAM, CODEKONTAMINATION/PARTITIONING

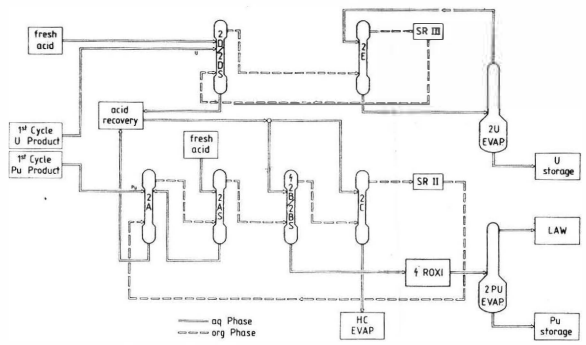

FIGURE 3. FLOW DIAGRAM, FINAL PURIFICATION

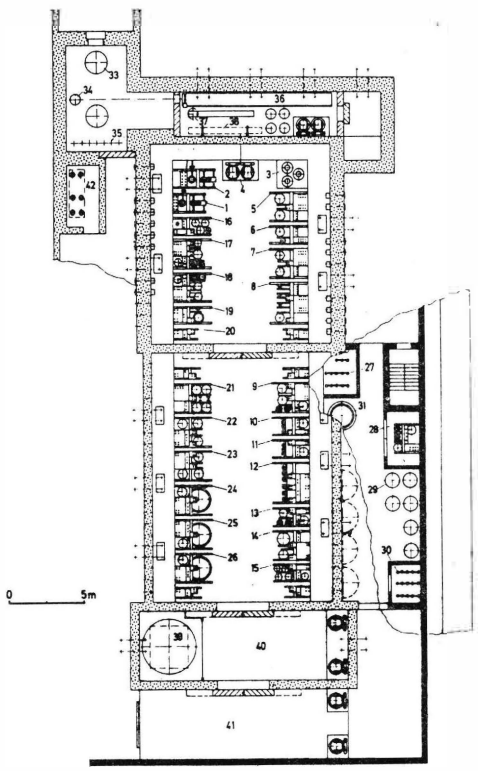

FIGURE 4. HOT-CELL GROUND PLAN

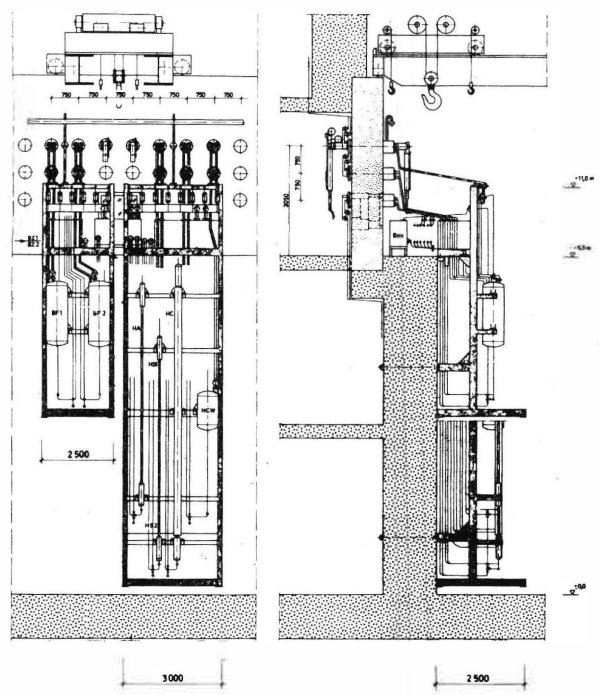

FIGURE 5. EQUIPMENT RACKS, 1ST EXTRACTION CYCLE

RECOVERY OF RHODIUM FROM SPENT NUCLEAR FUEL

The Extraction of Rhodium from Aqueous Nitric Acid Media by Dinonylnaphthalene Sulphonic Acid

N. M. Patel, J. R. Thornback and J.H. Miles*

Nuclear Chemistry Department
Loughborough University of Science and Technology
Loughborough, Leicestershire, United Kingdom

*United Kingdom Atomic Energy Authority
Harwell, Didcot, Oxon, United Kingdom

INTRODUCTION

The world resources of the platinum metals are limited, the abundance of these metals being only 10^{-7} - 10^{-6}% of the earth's crust. Nevertheless, they are exceedingly important in modern industry owing to their good catalytic properties, chemical inertness over a wide temperature range and their high melting points (1).

There is, however, another potential source of rhodium which, at present is not exploited: that produced by fission in nuclear reactors. A commercial nuclear station produces 19 kg of rhodium per GW(e)y and so in 1979 in the UK, about 60 kg of rhodium were produced, which will be stored with other fission products in the highly active waste tanks at Windscale. At the 1979 price, 60 kg of rhodium has a sale value of about $1.5M.

The rhodium is present mainly as the stable isotope ^{103}Rh. It also contains small amounts of ^{102}Rh (3μCi/g; half-life of 2.9y), but after 20 years this will have decayed to a harmless level and so will allow fission product rhodium to be used in place of natural rhodium for many of its applications.

It is therefore important to understand the behaviour of rhodium in the highly active waste solutions and to devise a process which could allow it to be separated for sale.

CHEMICAL STATE OF RHODIUM

The chemistry of rhodium in nitric acid is poorly understood but at low levels of nitrate ion the $Rh(H_2O)_6^{3+}$ species predominates but increasing nitrate ion results in substitution of 1 or more of the water molecules. These various species may be shown by ^{103}Rh nuclear magnetic resonance spectroscopy.

EXTRACTION OF RHODIUM

There are no previous reports of the liquid-liquid extraction of rhodium from nitric acid. We have investigated a wide range of reagents of different types as possible extractants for rhodium. The results are shown in Table 1. On the basis of these tests dinonylnaphthalene sulphonic acid (HD) was chosen for intensive study. The $SnCl_2$/MIBK process was rejected since chloride ion is corrosive and not favoured by the nuclear industry. HD has been proposed as an agent for rhodium, iridium separation from chloride media (2) but not followed up commercially.

Experimental

Rhodium hydroxide was precipitated by the slow addition of 1M NaOH to an aqueous solution of rhodium chloride (Johnson Matthey) until precipitation was complete. After thorough washing in water the precipitate was dissolved in 10 mls of concentrated nitric acid and the solution evaporated on a hot plate to near dryness. The residue was dissolved in various concentrations of nitric acid to give solutions approximately 0.02 M in rhodium.

Standard rhodium solutions for colorimetric analysis by the tin(II) chloride method (3) were prepared from ammonium chlorohodate (Johnson Matthey specpure) and standardised by a gravimetric procedure (4).

HD was donated by K & K - Greeff Chemicals Ltd. It was diluted with odourless Kerosine to give a stock 0.2 F solution. The stock solution was standardised by potentiometric titration with standard t-butyl ammonium hydroxide in a 1:1 toluene-methanol mixture.

Distribution isotherms were determined by equilibrating aliquots of the stock rhodium and HD solutions in either 20 ml glass vials or 100 ml conical flasks for 15 mins. in a thermostated water bath. Phase separation was achieved by centrifuging the samples at 2000 rpm for 5 minutes. Aliquots of the aqueous phase were then taken for analysis.

The hydrogen ion dependecy and HD dependency were determined by a similar procedure using rhodium solutions approximately 0.004 M.

Results

HD is a liquid cation exchanger analogous to cation exchange resins such as the Dowex 50 series. The extractant forms inverted micelles in organic media which alter markedly the extraction equations which was found to be the following:

$$Rh(H_2O)_6^{3+} + (HD)_x \rightleftharpoons Rh(H_{x-3}D_x) + 3H^+ + 6H_2O$$

The graph of log D against log H^+ has a slope of - 2.95 but the dependence on the formal concentration of $(HD)_x$ is unity where $(HD)_x$ is determined by titration. At low concentrations of HD polymerisation is less marked and the slope of the graph increases (5). At ligand concentrations of use commercially however, the concentration of monomer is probably small.

Increasing nitric acid concentrations result in a decrease in the distribution coefficient while increasing temperature enhances the extraction markedly (Figures 3 and 4). The former effect is due to increasing nitrate substitution on the rhodium atom and the pKa of the ligand while the latter is related to the enthalpy of the ion exchange reaction and that of the polymerisation reaction of the ligand.

Stripping of the organic phase is readily accomplished using 2M HNO_3 (Figure 5). Equilibria are rapidly attained (< 2 min. shaking) and so this process for rhodium is suitable for multi-contactor apparatus.

The effects of addition of other elements present in radioactive waste and the separation factors from rhodium containing mixture will also be reported and the overall usefulness of this process to radioactive waste discussed.

References

1. R.J. Downing, Metals and Materials 1980 (July), 32.
2. M. Ali Khan, D.F.C. Morris, J.Less Common Metals, 13, 53 (1967).
3. G.M. Ayres, B.L. Tuffley and J.S. Forrester, Anal.Chem., 27, 1742 (1955).
4. J.E. Currah, W.A.E. McBryde, A.J. Cruickshank and F.E. Beamish, Ind.Eng. Chem.Anal.Ed., 18, 120 (1946).
5. P.R. Danesi, R. Chiarizia, M.A. Raieh and G. Scribona, J.Inorg.Nucl.Chem., 37, 1489 (1975).

TABLE 1

SHAKE-OUT TESTS

Rh = 0.001 M Equilibration Time = 1 hr.
Temperature = 20°C A/O = 1:1

	Aqueous Phase	Organic Phase	% Extraction
1)	0.1 - 4M HNO_3	MIBK	<1
2)	1 - 5M HNO_3	20% TBP/OK	<1
3)	0.1 - 8M HNO_3	Butyl ether	<1
4)	2M HNO_3	1% mercaptobenzothiazole in MIBK	<3
5)	2M HNO_3, 0.5M Sodium Tartrate	30% TBP/Ethyl Ether	<1
6)	0.1 - 1.5M HNO_3	10% D2EHPA/OK	<1
7)	0.01 - 3M HNO_3	20% D2EHDTPA/OK	~70 Extraction at 0.01M HNO_3 <1% at 1 & 3M HNO_3
8)	0.1 - 5M HNO_3/2M HCl + $SnCl_2$	MIBK	~30
9)	0.1 - 1M HNO_3	10% HD/OK	86 - 20

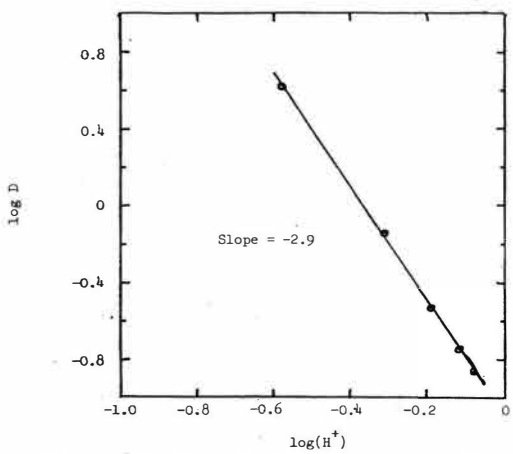

Figure 1 — Dependence of the hydrogen ion concentration on the extraction of rhodium into odourless kerosine from aqueous HNO_3 (HD) = 0.206 F.

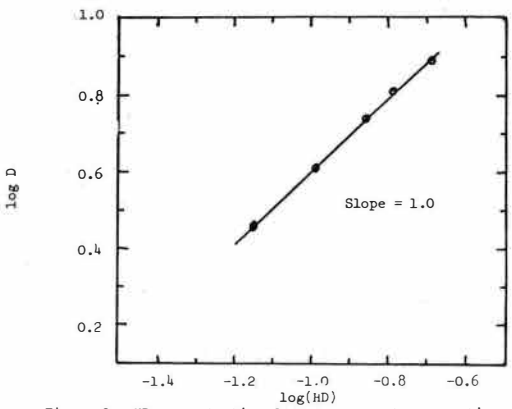

Figure 2 — HD concentration dependency on the extraction of rhodium from 0.102 M HNO_3.

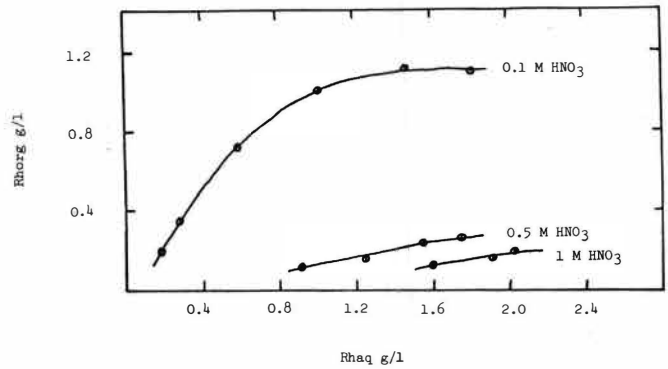

Figure 3 — Equilibrium curves for the extraction of rhodium into odourless kerosine at various concentrations of HNO_3.. (HD) = 0.1 F.

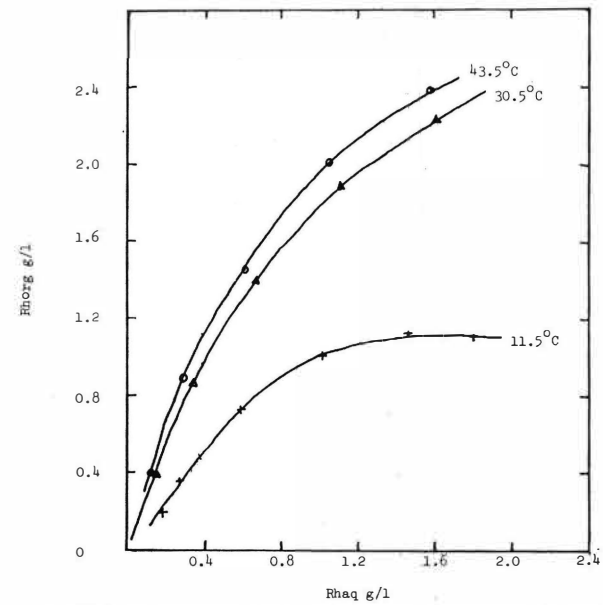

Figure 4 — Distribution of rhodium at various temperatures. HNO_3 = 0.102 M, (HD) = 0.1 F

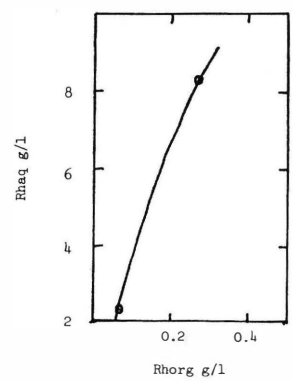

Figure 5 — Stripping equilibrium curve. HNO_3 = 2 M.

ELECTRIC FIELD AND CAPILLARY EFFECTS ON DROP CIRCULATION AND MASS TRANSFER

Loto S. Chang and John C. Berg

Department of Chemical Engineering BF-10
University of Washington
Seattle, Washington 98195 USA

The literature contains experimental evidence to suggest that electric fields might be used to enhance mass transfer performance in dropwise liquid extraction (1, 2) and gas absorption (3), but no substantial attempt has been made to develop theory to explain these effects. Decreases in drop size, increases in drop velocity, alterations in drop trajectory, increases in drop shape oscillation, and induced internal circulation all may play a role, but published experimental studies do not provide sufficient information to sort out or isolate these effects. The present work seeks to examine one of these effects in some detail, viz., the electrical inducement of circulation in single drop systems undergoing mass exchange with surroundings, and to assess the influence of such circulation on the rate of mass transfer.

G. I. Taylor in 1966 (4) was first to show that circulation may indeed result when an electric field is imposed upon a drop of a weakly conducting fluid suspended in another such fluid, and to provide the description of such flow shown in Figure 1. A double torus is established in which, depending on the electrical properties of the fluids, the surface flow may be either from the equator toward the poles or vice versa. The circulation is caused by the tangential stresses generated by the charge density distribution along the drop interface. Morrison (5) later provided computations to assess the convective heat or mass transfer due to Taylor circulation. The hybrid circulation which must result when drops undergoing the Taylor effect are rising or falling by gravity, and the influence of solute adsorption during mass transfer (and the resulting interfacial tension variations) have not yet been described, however, nor has the net influence of the electric field in such systems been assessed. The present work examines these factors and reassesses the promise of mass transfer augmentation through the use of electric fields.

ANALYSIS

We first consider the transient and quasi-steady state heat or mass exchange between a moving drop and its surroundings in a uniform electric field for the case of low Reynolds number and high Peclet numbers. The steady creeping flow in both phases is described by the axisymmetric Stokes stream functions obtained by the superposition of the Hadamard-Rybczynski and the Taylor EHD stream functions

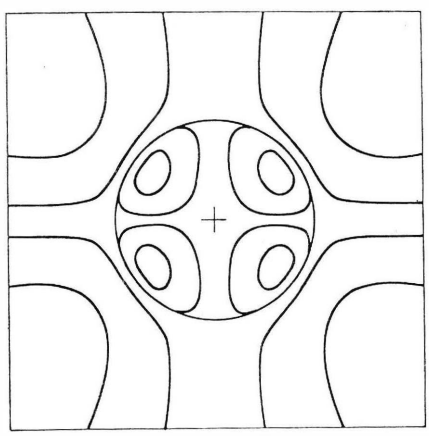

FIGURE 1. TAYLOR EHD FLOW PATTERN FOR A STATIONARY DROP IN A UNIFORM ELECTRIC FIELD

assuming a spherical droplet (6). Similarity transformation and finite difference schemes are then employed to solve the energy or diffusion equation. A parameter W, which characterizes the relative importance of electrical and gravitational effects, emerges, viz.,

$$W = \frac{4V(1 + X)}{|U|} \tag{1}$$

where V is a characteristic velocity generated by the electric field (4, 6), U is the terminal velocity of the drop falling or rising in a medium of infinite extent, and X is the viscosity ratio (disperse phase/continuous phase). It is found that only when the absolute value of W is larger than unity is the rate of transport enhanced by the imposed electrical field through the EHD effect.

The above analysis is extended to the case of intermediate Reynolds numbers since a range of 10-100 is more typical of extraction units in practice. Approximate solutions for fluid motion are obtained using the Galerkin method. Continuous-phase mass transfer rates are evaluated for various values of Reynolds number and viscosity ratio and are shown in Figure 2. The creeping flow result for the case of continuous-phase-controlling is also shown for comparison. It is shown that the threshold value of W at unity still holds (7). Thus once the threshold is passed the rate of mass transfer can be significantly enhanced before the breakage of the drop.

Some order-of-magnitude calculations of the value of W for a few practical extraction systems are shown in Table I. It is seen that in many systems, W is too small to suggest that significant enhancements are likely. Systems can be found, however, which do yield high values of W. These are principally systems in which the ratio of the resistivity of one phase to that of the other is small. Thus we speculate that, by adding suitable species to the organic phase, the resistivities of the two phases can be drawn sufficiently close to one another that a favorable value of W can be produced.

The added conducting species may well be surface-active. Thus the effect of surface tension gradients on the drop interface, which may result from mass transfer or from added surfactant contamination, is also investigated. Stream functions are derived and show that the terminal velocity is affected by both the surface tension gradient and the electric field. The convective-diffusion equation for the case in which the disperse phase is an air bubble and a trace of surfactant is present in the continuous phase is solved by using an orthogonal collocation on finite elements scheme. The interfacial velocity is shown to be retarded due to the presence of the surfactant, as depicted in Figure 3, where the ratio of u_{i_0} to u_{i_E} reflects the effect of the surface tension gradient upon interfacial velocity at a certain electric field strength. It is seen that the surface tension gradient effect significantly reducess the surface mobility at the rear portion of the drop if the absolute value of W is less than one. We may use the following expression for the mass transfer (8):

$$Sh = \left(\frac{2}{\pi}\right)^{1/2} \left[\int_0^{\pi} u_i \sin^2\theta d\theta\right]^{1/2} Pe^{1/2} \tag{2}$$

which is valid for the steady-state mass transfer from the bubble, since the Peclet number in the continuous phase is large. The results show that the Sherwood number ratio between the electrified case and the free-rising case is always very close to unity if the absolute value of W is less than one. In other words, the threshold value of W still exists even in the presence of the surface tension gradient.

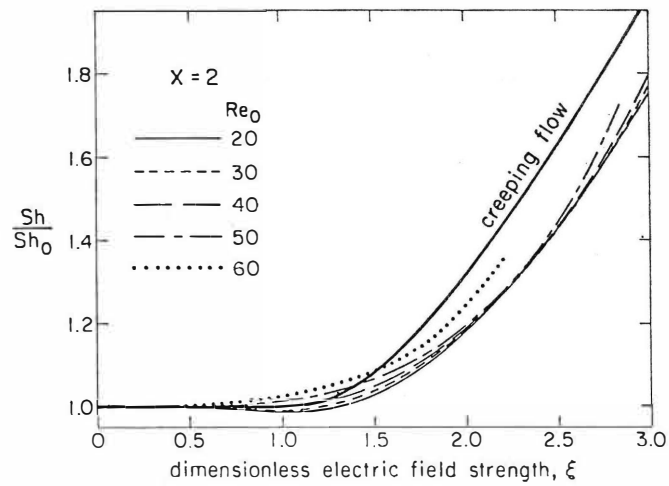

FIGURE 2. RATIO OF CONTINUOUS-PHASE SHERWOOD NUMBER FOR A DROP IN BOTH GRAVITATIONAL AND ELECTRIC FIELDS TO THE CORRESPONDING VALUE FOR A DROP TRANSLATING BY GRAVITY ALONE AS A FUNCTION OF DIMENSIONLESS ELECTRIC FIELD STRENGTH, ξ, FOR VARIOUS REYNOLDS NUMBERS AT A VISCOSITY RATIO OF X = 2.

Other interesting phenomena occur in such contaminated systems. If W has an absolute value greater than unity, the flow separates either at the rear or in front of the droplet. The retardation in the interfacial velocity for positive W systems then happens primarily near the equator, whereas for negative systems it appears in the vicinity of both the rear and the front of the droplet. This is a consequence of the surface concentrations of the surfactant, as shown in Figures 4 and 5. These retardations will lead to a stagnant "belt" or two stagnant "caps" if rates of surfactant transfer are very low.

It is important to note that we have considered only the case of an eleectric field parallel to translation, which is the usual configuration for the application of a DC field. A field perpendicular to translation results in a far more complex (non-axisymmetric) situation, and has not been considered in the present work. The criterion for EHD mass transfer enhancement in terms of the parameter W is still expected to hold qualitatively, however.

CONCLUSIONS

Mass transfer rates in both pure and contaminated systems are evaluated. The results for various cases show that the rate of transport is enhanced significantly by the electrohydrodynamic effect as long as the value of the

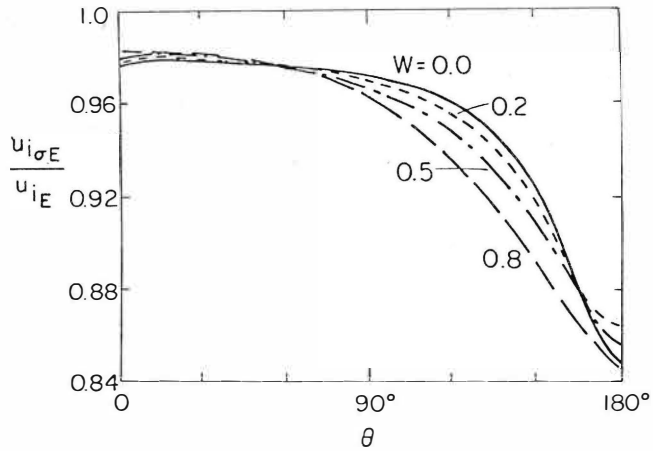

FIGURE 3. RATIO OF INTERFACIAL VELOCITIES SHOWING THE EFFECT OF THE SURFACE TENSION GRADIENT AT A FIXED ELECTRIC FIELD STRENGTH.

parameter W passes the threshold value of unity.

For certain pure systems, and by addition of conducting species to many other systems, it is possible to achieve favorable values of W for producing significant heat or mass transfer enhancements by the EHD flows.

Finally, in the systems contaminated by surfactants or containing added conducting species, we predict the existence of a stagnant belt or two stagnant caps formed by the surface-active agents along the droplet interface. This has also been verified by experiments. Such behavior may later be found important not only in liquid extraction or gas absorption, but also in such electrified processes as electrical emulsification and coalescence.

REFERENCES

1. P. J. Bailes and J. D. Thornton, Proc. Int. Solvent Extr. Conf. 2, 1431 (1971).
2. P. J. Bailes, Ind. Eng. Chem. Process Des. Dev. 20, 564 (1981).
3. T. W. Gault, M.S. Thesis, University of Washington (1978).
4. G. I. Taylor, Proc. Roy. Soc. 291A, 159 (1966).
5. F. A. Morrison, J. Heat Transfer, ASME Series C 99, 269 (1977).
6. L. S. Chang, T. E. Carleson and J. C. Berg, Int. J. Heat Mass Transfer 25, 1023 (1982).
7. L. S. Chang and J. C. Berg, Int. J. Heat Mass Transfer (in press).
8. A. C. Lochiel and P. H. Calderbank, Chem. Eng. Sci. 19, 471 (1964).

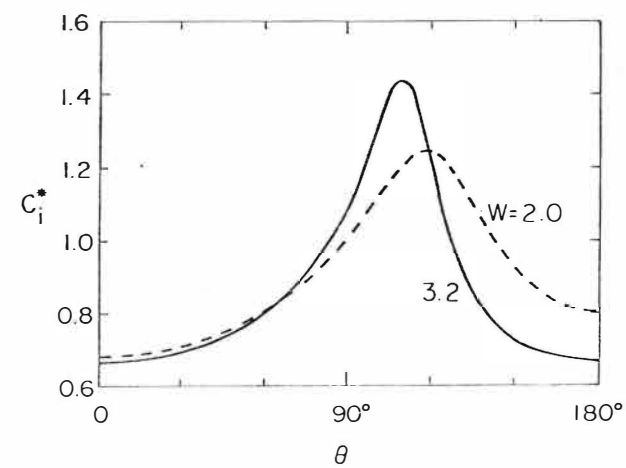

FIGURE 4. SURFACE CONCENTRATION OF SURFACTANT FOR TWO SYSTEMS WITH CIRCULATION FROM POLES TO EQUATOR AS A FUNCTION OF THE POLAR ANGLE MEASURED FROM THE FORWARD STAGNATION POINT.

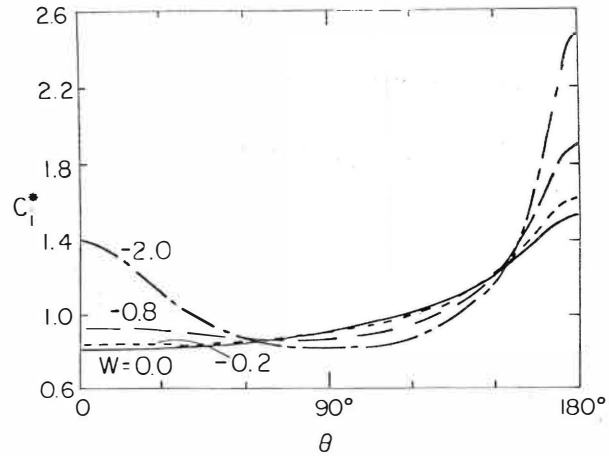

FIGURE 5. SURFACE CONCENTRATION OF SURFACTANT FOR SEVERAL SYSTEMS WITH CIRCULATION FROM EQUATOR TO POLES AS A FUNCTION OF THE POLAR ANGLE MEASURED FROM THE FORWARD STAGNATION POINT.

TABLE I. Approximate W-Values for Several Liquid-Liquid Systems

Calculations Based Upon a Drop 2-mm in Diameter Under an Electric Field Strength of 0.1 MV/m

Continuous Phase	Disperse Phase	W
n-heptane	water	-10^{-9}
n-heptane	furfural	-10^{-8}
ethyl acetate.	water	-10^{-2}
glycerol	carbon tetrachloride	0.1 - 1
benzene	glycerol	1 - 10
benzene	water	1 - 10
aniline	water	1 - 10
MIBK	water	1 - 10
chloroform	water	1 - 10
phenol	water	1 - 10
benzonitrile	water	10 - 100

DROP-SIZE, SPECIFIC AGITATION-POWER AND ENERGY-DISSIPATION FOR COUNTERCURRENT EXTRACTION COLUMNS

G. Husung, W. Gaubinger, R. Marr

Institut of Chemical Engineering
Technical University Graz
Graz, Austria

The following paper shows a way to optimize the geometric relations and the design of internals used in agitated extraction columns. Up to now there are only a few methods based on empiric dates. Scaling up extraction columns these ways of design are very difficult and require a great deal of effort, especially when HTU-values determined in laboratory columns with the use of international testing systems are applied.
These expenditures can be reduced when mass transfer area, drop-size and axial mixing parameters are measured. Such investigations can be done with low effort when calculating apparatus with well known geometric relations.

The optimisation of internals is much more difficult. Without results determined in industrial columns the only way seems to be the investigation and determination of the flow conditions in the dispersion cells of the columns. Herein the parameters of the turbulent flow seem to be most important, as those have essential influence on dispersion, mass-transfer and axial mixing. The dispersion is discribable by the size of the drops and their distribution, which is one of the main parameters with equal order for all countercurrent extraction columns working in gravity and with mechanical agitation.
Therefore first investigations should lead to relations between the drop-size and the parameters of the turbulent flow.
Fig.1 shows the design of internals of a rotating-disc-contactor, the left hand side picture with geometric relations used in laboratory columns. Hereby two torus-flows occure.

At the rim of the torus-flow the energy dissipation shows a maximum value.
Scaling up all lengths with the same scale in the range of D_k= 200 - 300 mm several problems occure. Instabilities of the shown flow lead to a complete destruction of the torus-flow. Voluminous eddies are built up and cause low frequency disturbances that move along the whole length of the column. Normaly those currents are caused by the effects of axial mixing. It must be noticed that at constant specific throughput the Reynolds-number of the axial flow increases proportional to the scaled-up diameter.

These problems are solved by lowering the relations H_c/D_k (Fig.1 - right hand side). At very low relations of H_c/D_k no torus-flow is built but irregular eddies can be seen. No rotary symmetrie is observed anymore. Hydrodynamically you get two complete different apparatus.
Fig.2 shows the dependence of the Newton-number on the Reynolds-number for these two cases. The experiments were performed in a 200 mm column with a swing drive motor /1/. The Newton-number is related to one cell.
In case of H_c/D_k= 0.36 the torus flow becomes turbulent at Re= 10^4. Full turbulence is reached at Re= 1.5 10^5, the influence of viscosity and therefore the stabilizing influence of the column wall disappear. A practicable performance in the field of full turbulence might not be found and, based on main physical properties of the system (testing system) it may only be expected at diameters greater than 300 mm.
The lowered height of the cell leads to lower numbers of revolution the range of total turbulence is only reached at extreme high speed of the agitator.
As there is no kink in this function Ne= f(Re) you may say that torus-flow is not built up in this case.
From the Newton-number you can calculate the torque. Then the energy input for one cell is

$$(1) \quad P_c = M \cdot \omega$$

The specific agitation power becomes

$$(2) \quad \varepsilon_w = \frac{P_c}{m_{fl,c}}$$

A further type of column which was investigated is called SHE /2/ (Fig.3). The dispersion and the formation of the drops occurs in the free stream flow area of the agitator where you can find the maximum of the local dissipation-energy.
As the formation of the drops takes place in this area, investigations of the turbulences are concentrated to this locality.
As measuring equipment a hot film probe and a constant temperature anemometer were used. The main direct current as well as the effective value of the superposed alternativ current are determined. These signals are proportional to the local speed when using the time dependence as a basis. High and low pass filters permit the investigation of special frequency ranges.
The determined signals can be represented by an energy-distribution shown in Fig.4.

One distribution was determined without dispersed phase, the other one (dashed line) with the presence of dispersed toluene. The other parameters were held constant.
It can be observed, that for the second experiment the distribution is shifting to higher frequency. This phenomenon is caused by the splitting of the drops when crashing against the probe.
By use of the theories of Kolmogoroff /3/ and Heisenberg /4/ several parameters can be determined from these energy distributions.
In a first step the energy distribution is standardized.

$$(3) \quad \gamma(f) = \frac{E_u}{\bar{u}^2}$$

By this the micro scale

$$(4) \quad \left(\frac{\bar{u}}{2\pi\lambda}\right)^2 = \int_0^\infty f^2 \gamma(f)\, df$$

is determined and as a result the local energy dissipation is

$$(5) \quad \varepsilon = 15\, \nu \frac{\bar{u}'}{\lambda^2}$$

As the deviations of the velocities throughout the measured range don't show a dependence on the direction it is possible to use the described theory.
Fig.5 shows the dependence of the deviation-velocities on the number of revolutions of the agitator. With increasing Reynolds-numbers the two lines get closer and at about Re = 1.5 10^5 they become equal.
The evaluation (Fig.6) shows constant local dissipation-energy for a constant drop-size. The specific power however decreases for increasing column diameters.
A correlation of this specific power in connection with the drop-size is hardly possible. For the dissipation-energy this can be done independent of type and size of the apparatus (Fig.7).
With the results of this investigations it is possible to do hydrodynamic experiments without the presence of dispersed phase. This gives the great advantage in scaling-up extraction columns, as for to get a drop-size distribution in the scaled up plant identical to that of the testing column you only have to reach the same turbulent flow conditions. These conditions can be ascertained by the described method.

Nomenclature

d_s	drop diameter /mm/	Λ	macro scale
D_R	diameter of agitator /m/	γ	standardized energy distribution
D_k	diameter of column /m/	ε_w	specific agitation power
E_u	energy /V^2/Hz/	ε	energy-dissipation
f	frequency /Hz/	λ	micro scale
H_c	height of one cell /m/	ν	viscosity /m^2/s/
m_{fl}	fluid volume /m^3/	ρ	density /kg/m^3/
M	torque /Nm/		
n	number of revolutions /rps/		
P_c	energy input /W/	Re	Reynolds-number
$\bar{U}$	mean a.c. /V/	Ne	Newton-number
$\bar{u}$	mean velocity /m/s/		
$\bar{u}'$	mean deviation velocity		

References

/1/ G, Husung, Theses, Technical University Graz, 1976

/2/ G. Husung, R.Marr, B, Wolschner, G. Gaubinger:"2nd World Congress of Chemical Engineering" 1981, Montreal, Paper Vol.IV 439

/4/ Sammelband zur Statistischen Theorie der Turbulenzen, Akademieverlag Berlin 1958

/5/ J.O. Hinze: Turbulence, Mc Graw-Hill, New York 1959

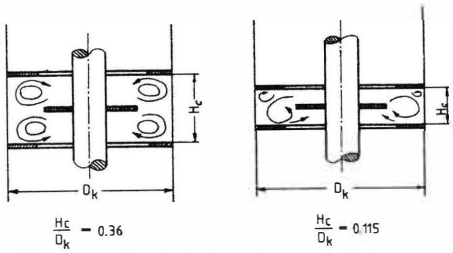

Fig.1: Geometry of the stirring cell in an RDC

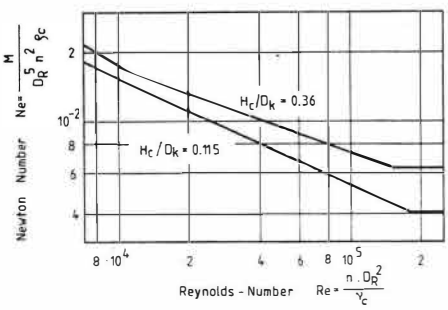

Fig.2: Ne versus Re for different geometric relations

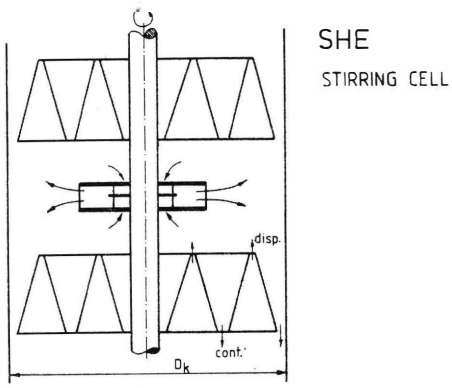

Fig.3: Internals of the SHE

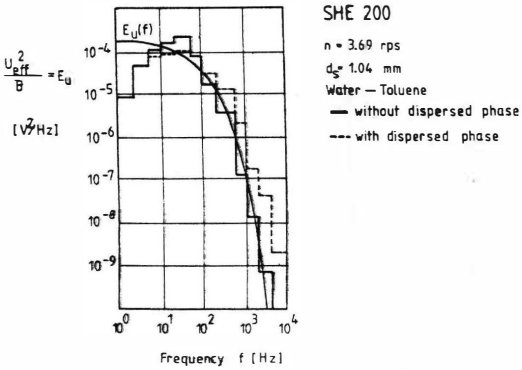

Fig.4: Energy-distribution in an SHE 200

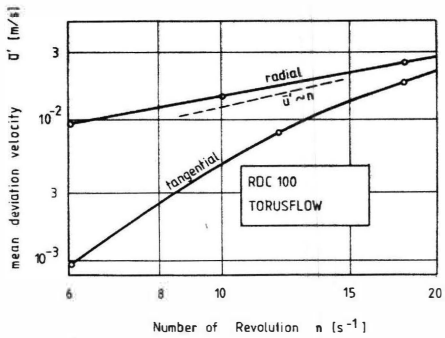

Fig.5: Deviation-velocity depending on agitation speed

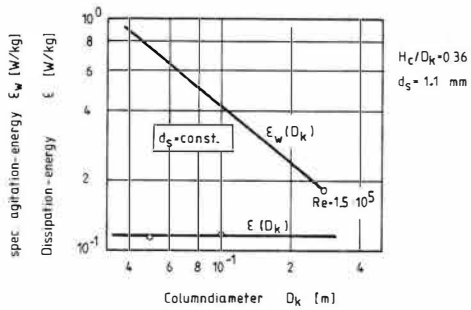

Fig.6: Dissipation energy and agitation energy in scale-up

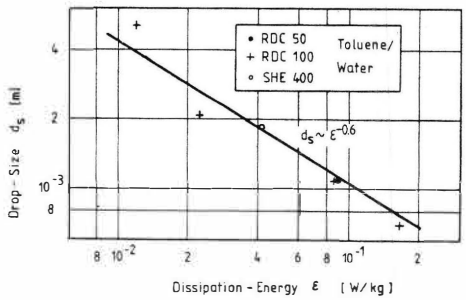

Fig.7: Dissipation energy depending on the drop-size for different columns

COALESCENCE OF DROPS IN IMMISCIBLE LIQUIDS AT INCLINED PLATES

Eckhart Blass, Dieter Rautenberg

Technische Universität München
Munich, Federal Republic of Germany

INTRODUCTION

Separation process of immiscible liquid-liquid dispersions in mixer-settlers or in extraction columns is accomplished in several consecutive steps: the approach of the drops to the horizontal interface where a thin film of continuous phase is trapped between the drops and the liquid-liquid interface, film drainage, and finally rupture of the thin liquid film till the drops enter their homophase. Most of time required for coalescence process of a drop is the drainage of the film. During this time the drop is resting on the thin film which slowly drains away. However, the coalescence time cannot be calculated so far because of the inevitable enrichment of surface-active agents in technical liquid-liquid interfaces.

To avoid this we replaced the horizontal liquid-liquid interface by an inclined plate which is wetted by the dispersed phase quite well. One end of this plate is reaching the plane, principle interface. At this tilted plate, the coalescing drops produce a falling film carrying the tensides permanently away from the real coalescence point to the horizontal interface.

For the first time we could establish the efficiency of this concept measuring the coalescence times of dispersed liquid-liquid systems used in extraction. Fig.1 shows that after a short operating time a plane interface already produces a broad cumulative distribution and large values of coalescence times. To the contrary, at the inclined plate we could determine very close cumulative distributions and very short values of coalescence times for droplets greater than 1 mm. These measured values had been up to one hundred times smaller than at plane interfaces.

The use of plates as mechanical settling aid low inclined to the horizontal enables us to model the coalescence process as an absolutely fluiddynamic one without influence of Marangoni effects. Till now, we only investigated coalescence of single droplets at an inclined but foreign generated falling film of dispersed phase /1/. But already this relatively simple special case of droplet coalescence led to results useful for practical settler design.

MATHEMATICAL MODELLING OF SINGLE DROP COALESCENCE AND EXPERIMENTAL RESULTS

Princen /2/ calculated the deformation of drops resting on plane interfaces in dependence on Bond number. That means: in dependence on density difference of continuous and dispersed phase $\Delta\rho$ surface tension between the two liquids σ, and the radius of the rigid sphere of equal volume r_p.

$$Bo = \frac{\Delta\rho\, g}{\sigma}\, r_p^2 \qquad (1)$$

where g is the acceleration due to gravity. However, in our model the coalescence of drops takes place at a falling film inclined less than 10 degrees to the horizontal. In this case, we can assume that the forces acting on the drop are almost equal to those acting on a drop coalescing at a plane interface.

We also could calculate the critical film thickness of thin liquid films at which spontaneous rupture occurs. Vrij and Overbeek /3/ derive an equation down to what critical film thickness a drop must approach the interface till the draining film ruptures.

$$h_c = 0.267 \left(\frac{H_{c,d}^2 \; r_f^2}{6\, \sigma\, \Delta\rho} \right)^{1/7} \qquad (2)$$

where r_f is the radius of the draining film which is trapped between the drop and its homophase. It will be computed from the shape of the drop /2/. By means of equation (2) we have calculated the critical film thickness for a density difference of 150 kg/m^3 and a Hamaker coefficient of 10^{-20} J as can be seen from fig. 2. Very important is the knowledge that the critical thickness of the draining film is not constant like elsewhere being supposed. It depends on physical properties, drop diameter and Hamaker coefficent. If the uncertainty of the bibliography on the Hamaker coefficient is still relatively great, so equation (2) shows, that the critical film thickness in proportional to the fourth root of the Hamaker coefficient.

Next we have analysed theoretically and experimentally the hydrodynamics of the falling film at a tilted plate for liquid-liquid flow. The surface of the laminar flowing liquid film has been always smooth. With regard to the obtained coalescence times of the drops, this is a conservative condition. Regarding two phase flow we must take into account momentum transport to the second liquid phase. We already reported about this in Liege in the year 1980 /4/. Since that time we have been able to calculate the thickness and the velocity profiles of the two liquid films between two inclined parallel plates in dependence on distance of the plates, angle of inclination, flow rate of the falling film, and physical properties. For computation of coalescence time the relative velocity between the coalescing drop and the surface of the falling film is more decisive than the absolute value of the actual drop velocity. However, it is nearly impossible to pre-calculate theoretically the absolute velocity of particles floating along an inclined rigid plane. For that reason we analysed experimentally steady-state motion of droplets at tilted plates as well as at inclined falling films. The results then have been evaluated by means of a dimensional analysis. Accordingly we can calculate the absolute velocity of the moving droplets by the following equations:

$$Re_p = 1{,}641\, Re_F^{0.333}\, Ga_p^{0.193}\, We_p^{0.314} \quad \text{for } Ga < 1000 \qquad (3)$$

and

$$Re_p = 3.264\, Re_F^{0.333}\, Ga_p^{0.224}\, We_p^{0.257} \quad \text{for } Ga > 1000 \qquad (4)$$

The dimensionless groups are defined as follows:

Reynolds number of the particle: $Re_p = d_p\, v_p\, \rho_c/\eta_c$

Reynolds number of the falling film: $Re_F = \dot{V}_F\, \rho_d/(\eta_d\, b)$

Galileo number of the particle: $Ga_p = d_p^3 \rho_c\, \Delta\rho\, g\, \sin\alpha/\eta_c^2$

Weber number of the particle: $We_p = d_p\, v_p^2\, \rho_c/\sigma$

where d_p is the diameter and v_p the absolute velocity of the particle, $\dot{V}_F$ the volume flow rate of the falling film, b the depth of the tilted plate, α the angle of inclination to the horizontal, $\rho_{c,d}$ and $\eta_{c,d}$ the densities and dynamic viscosities of the continuous and dispersed phase, respectively.

Finally balancing the forces between the drops and the draining liquid film, we could derive the following equation for the coalescence time of a single drop at an inclined falling film

$$t = \frac{r_f}{2\,v_r} \ln\left(\frac{\dfrac{h_1^2}{\dfrac{v_r}{r_f} + \dfrac{\sigma\, h_1^2}{3\, R\, \eta_c\, r_f^2}}}{\dfrac{h_c^2}{\dfrac{v_r}{r_f} + \dfrac{\sigma\, h_c^2}{3\, R\, \eta_c\, r_f^2}}}\right) \qquad (5)$$

where v_r is in the relative velocity between the coalescing drop and the boundary velocity of the falling film, h_1 the initial thickness of the draining film and R the overall radius of curvature of the deformed drop contacting the falling film. For a simple mathematical handling of this problem it was necessary to assume an infinitely rigid cylinder instead of a rigid sphere. This assumption must cause a longer coalescence time. Generally the trapped thin liquid film is draining away in all directions and the surface of the drop will may be mobile, too. The initial film thickness h_1 is without significance for the calculation of the coalescence time. It is about two to three decades greater than the critical film thickness h_c. All the other variables necessary for computing equation (5) have been derived above.

INTERPRETATION OF THE MATHEMATICAL MODEL

As it had been expected by equation (5) the calculated coalescence times are up to 50% greater than the measured values. But the fundamental trend of the coalescence times at the tilted plate in depence on the volumetric flow rate of the falling film is quite well. With decreasing difference between the drop velocity and the boundary velocity of the falling film the coalescence times suddenly increase steeply. So it is possible by means of equation (5) to determine a reasonable flow rate using a tilted plate as a mechanical settling aid. Furthermore as it can be seen by fig.3 this model allows the following statements:

- Little drops cause long coalescence times because of the minor forces acting on the draining film and because of the lower relative velocity between the drop and the boundary velocity of the falling film.
- Great drops cause increasing coalscence times because of increasing deformation of drop shape, which retards drainage of the trapped thin film.
- Decreasing surface tension and increasing density difference shift the right branch of the curve to minor droplet diameters. We can interprete this as an increasing retard of film drainage. Through that the range of short coalescence times becomes smaller.
- Increasing volume flow rate of the falling film and increasing dynamic viscosity of the continuous phase cause increasing coalescence times because of decreasing relative velocity of the drops.
- Increasing of the angle of inclination of the tilted plate causes the absolute velocity of the particle to increase more than the boundary velocity of the falling film. Thus the coalescence times decrease because of the greater relative velocity of the drops.

ACKNOWLEDGEMENT

The authors wish to thank the Deutsche Forschungsgemeinschaft of the Federal Republic Germany for their financial support during the course of this work.

REFERENCES

1. D. Rautenberg. Koaleszenz von Einzeltropfen an geneigten Platten in Flüssigkeiten
   Dissertation, Technical University of Munich, 1983
2. H.M. Princen. Surface and Colloid Science, vol 2, p 1-84, J. Wiley 1969
3. A. Vrij, J. Th. G. Overbeek. J. Americ.Chem.Soc.90 No 12, 3074 (1968)
4. E. Blass, D. Rautenberg. ISEC 1980 No 80-40

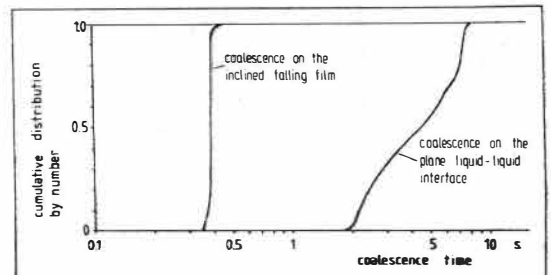

Figure 1 Comparison of cumulative distribution of coalescence times from toluene-drops (d_p = 6.8 mm) on an inclined falling film of dispersed phase with those on a plane liquid-liquid interface

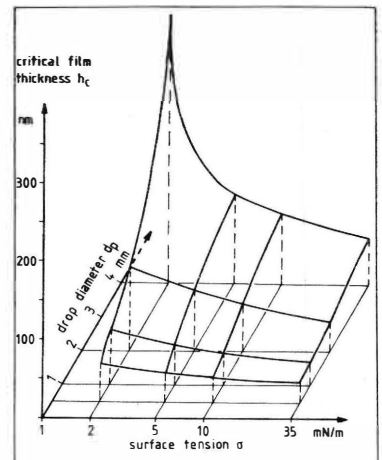

Figure 2 Critical film thickness h_c depending on surface tension σ and drop diameter d_p

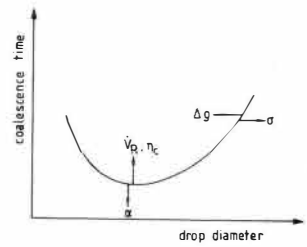

Figure 3 Principle dependence of coalescence time and drop diameter, influence of density difference Δg, surface tension σ, volume flowrate of falling film $\dot{V}_R$, slope angle α and viscosity of continuous phase η_c

CONTINUOUS DROP FORMATION AT AN ORIFICE

A. Bright

Open University, Milton Keynes, U.K.

C. Hanson

University of Bradford, U.K.

G. S. Virdee

Teesside Polytechnic, Middlesbrough, U.K.

A knowledge of drop size and of drop size distribution is of fundamental importance for an understanding of the performance of liquid extraction contactors. In certain designs of column contactor, noteably sieve tray and pulsed perforated plate columns, the drops are formed from an orifice. At reasonably high flow rates, a jet of dispersed phase emerges from each orifice and subsequently breaks into a series of drops. The object of the work described was to obtain a better understanding of drop sizes formed from a single orifice in this so-called "jetting" regime.

In the jetting regime of drop formation from an orifice, drop size is governed by jet stability. Linearised stability analysis predicts a minimum drop volume when the jet is split by a single wavelength of the fastest growing capillary wave. Experimental measurements of drop formation times for decane jets in water show that 'families' of drops are formed during breakup in the jetting regime. The drops in the families have discrete volumes which are integer multiples of the minimum drop volume. The composition of drops in each family is determined by the interaction of the fundamental wave with lower frequency harmonics.

Drop size predictions.

Kumar and Hartland (1) have summarised the main empirical correlations for predicting the mean drop size from jet breakup. The jetting regime extends approximately over the range $2 < We < 8.6$. The minimum value corresponds to the transition from drops forming at the orifice tip to drops formed from a jet. The maximum value corresponds to the maximum length of jet before the mechanism of drop formation changes from symmetric to asymmetric wave growth. This latter condition is characterised by the formation of drops of the minimum size.

Skelland and Johnson (2) suggested the use of the maximum jetting condition in the correlation of mean drop size as a function of nozzle velocity. This predicts a rapid decrease in mean drop size with increase in jet velocity. Horvath et al (3) have proposed an empirical equation to describe this trend. The predictions of this equation for the range of conditions studied in our work are shown as a dashed curve in Figure 1. Such a curve can be used for predicting drop size in the jetting regime provided an estimate can be made of the minimum drop size d_m. Linear stability analysis gives:

$$(1) \qquad \frac{d_m}{d_o} = \left[\frac{1.5\pi}{(ka)_m}\right]^{1/3}$$

Burkholder and Berg (4) have solved the general linear instability equations for the breakup of laminar liquid jets in liquids, which reduces to the formulation of Meister (5) when there is no mass transfer occurring. For liquid-liquid systems with a low viscosity jet issuing into low viscosity surroundings, the critical wavenumber $(ka)_m$ depends only on the density ratio of continuous to dispersed phases.

In practice the theoretical values of d_m are lower than those measured experimentally. In addition there is no single value of minimum drop size as expected from equation (1) but a range of values. Christiansen and Hixson (6 reported experimental results with $1.76 < d_m/d_o < 2.36$.

Drop formation times

N-decane (GPR grade) was injected through a series of hypodermic needles into a 100 mm square sided column containing distilled water. The phases were mutually saturated and the temperature was controlled at 20°C. Eight needles were used with diameters ranging from 0.22 - 1.19 mm covering a jet velocity range from 0.3 - 1.2 m/s. Drop formation times were measured by recording the highest frequency at which a stroboscope (Crompton Type 721) could freeze the breakup pattern of the jet.

Our experimental data are shown as points in Figure 1, showing a departure from the Horvath et al correlation as reported by others. The jet breaks up into distinctive families of drops at different points in the jetting regime. Figure 2 shows two such families corresponding to the data points A and B in Figure 1. The measured formation time for a family group τ_g was found to be an exact integer multiple of the minimum time to freeze the growing wave on the jet τ_f. This latter time determines the fundamental wave frequency $\omega_f = 2\pi/\tau_f$, and the minimum drop volume $V_f = \dot{Q}\tau_f$. For example for the two families of Figure 2: in A, $\tau_g = 5\tau_f$ corresponding to a family of two $2V_f$ drops and one V_f drop; in B, $\tau_g = 3\tau_f$ with a family of one $2V_f$ drop and one V_f drop. Such regular family groupings occurred for all the needles studied and considerably simplifies the task of calculating the mean drop size, i.e.

$$(2) \qquad d_m = \left[\frac{6V_f}{\pi}\right]^{1/3}$$

$$(3) \qquad \frac{d_{sv}}{d_m} = \frac{n_1 + 2n_2 + 3n_3 + \ldots}{n_1 + 2^{2/3}n_2 + 3^{2/3}n_3 + \ldots}$$

Harmonic ratio

The formation of distinctly related drops in family groups suggests that the fundamental wave of frequency ω_f interacts with various harmonics of frequency ω_h. This interaction gives rise to a beat frequency which can be identified with the frequency of formation of the family group, i.e. $\omega_g = \omega_f - \omega_h$. Thus a family group is characterised by a particular 'harmonic ratio', given by

$$(4) \qquad \frac{\omega_h}{\omega_f} = \frac{\text{number of drops in family}}{\text{number of fund. volumes in family}} = \frac{n_1 + n_2 + n_3 + \ldots}{n_1 + 2n_2 + 3n_3 + \ldots}$$

For example, the family group A in Figure 2 has a harmonic ratio of $3 \div (2 + 2 + 1) = 0.6$, produced by the interaction of the fundamental ω_f with the harmonic $\frac{3\omega_f}{5}$ - the minor sixth in musical terminology.

This approach suggests that the harmonic ratio will be a more appropriate correlating factor to describe drop formation in the jetting region than those proposed previously. This is substantiated by the data in Figure 3 which show a simple proportionality between the square root of the harmonic ratio and the jet velocity ratio.

Minimum drop size

For a cylindrical jet moving with velocity U in a stationary medium it can be shown that the phase velocity of a wave on the jet is given by

$$(5) \qquad \frac{\omega}{k} = \frac{U}{(1 + sK^*/I^*)}$$

Figure 4 summarises the results of 71 experimental runs with the eight needles. All the results are in the range

$$0.51 < \frac{(ka)_m}{(1 + sK^*/I^*)} < 0.68$$

This corresponds to $0.64 < (ka)_m < 0.94$ or $1.71 < d_m/d_o < 2.25$, which agrees with previously reported results.

Conclusions

Drop sizes in the jetting regime of drop formation are closely interrelated. Drop volumes are integer multiples of the minimum drop volume deduced from stability analysis. Mean drop size can be correlated with jet velocity through the calculation of the harmonic ratio which characterises the regular breakup of the jet into families of drops.

Nomenclature

a	jet radius
d_m	minimum drop diameter
d_o	orifice diameter
d_{sv}	volume/surface diameter of drops
I_o	Modified Bessel function of the first kind of order zero
I_1	Modified Bessel function of the first kind of order one
I^*	ratio I_o/I_1
k	wave number
K_o	Modified Bessel function of the second kind of order zero
K_1	Modified Bessel function of the second kind of order one
K^*	ratio K_o/K_1
n_1, n_2, etc.	number of drops of volume V_f, $2V_f$ etc. in family
$\dot{Q}$	volumetric jet flowrate
s	density ratio (continuous/dispersed phases)
U	jet velocity
U_m	maximum jetting velocity
V_f	minimum drop volume
We	jet Weber number, $U^2 d_o \rho/\sigma$
σ	interfacial tension
τ	formation time
ω	frequency of formation, $2\pi/\tau$

References

1. A. Kumar and S. Hartland, Trans I.Chem E, 60, 35 (1982)
2. A.H.R. Skelland and K.R. Johnson, Can J Chem Eng, 52, 732 (1974)
3. M. Horvath, L. Steiner and S. Hartland, Can J Chem Eng, 56, 9 (1978)
4. H.C. Burkholder and J.C. Berg, AIChEJ, 20, 872 (1974)
5. B.J. Meister, PhD Thesis, Cornell University (1966)
6. R.M. Christiansen and A.N. Hixson, Ind.Eng.Chem.49, 1017 (1957)

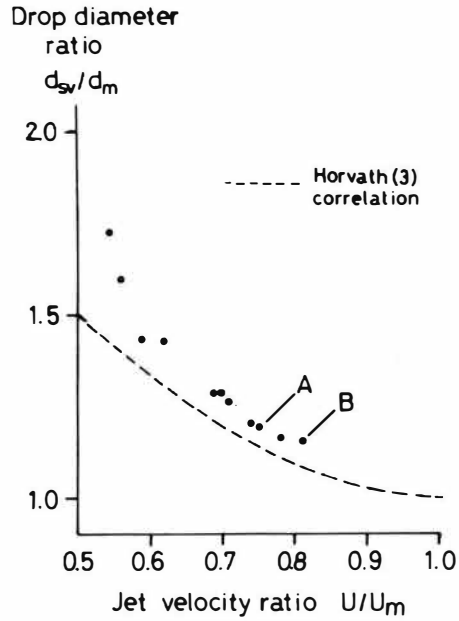

Figure 1 Mean drop size for decane jets in water $d_o = 0.35$ mm; $d_m = 0.71$ mm; $U_m = 1.04$ m/s

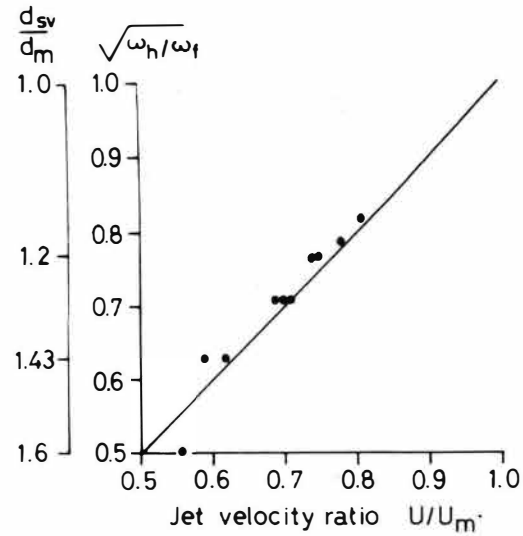

Figure 3 Relation between harmonic ratio and jet velocity ratio. Data points from Figure 1.

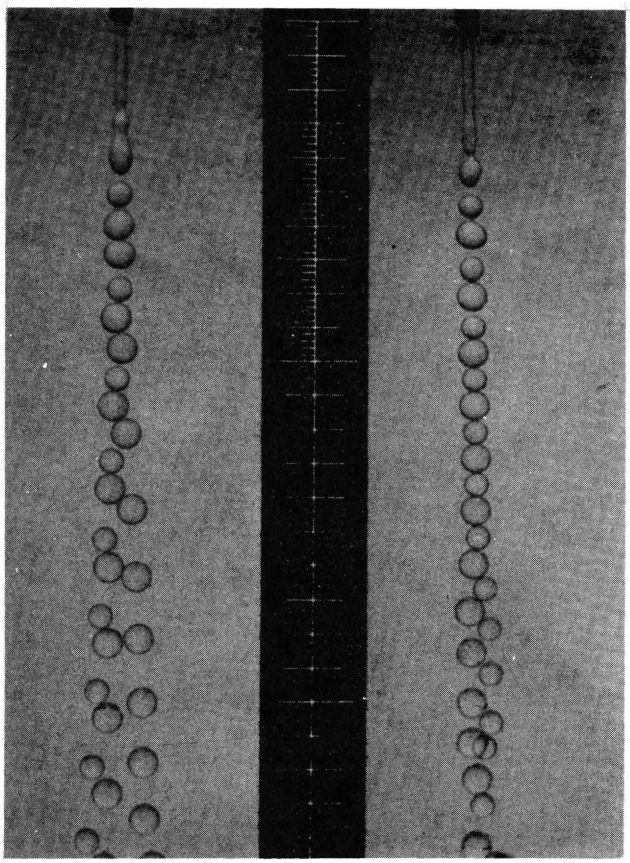

Figure 2 Drop families from 0.35 mm needle
Family A: U = 0.77 m/s Family B: U = 0.85 m/s

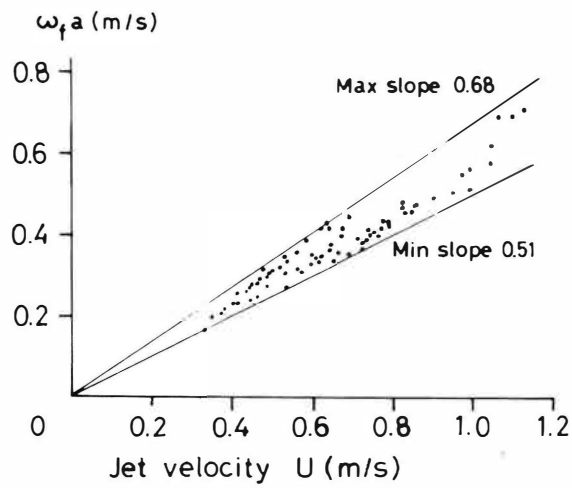

Figure 4 Variation of fundamental frequency with jet velocity. $0.22 < d_o < 1.19$ mm

EXTRACTION OF RARE EARTH BY LIQUID SURFACTANT MEMBRANES

Zhu Yongjun, Jiang Changyin, Wang Shizhu, Liu Zaoqi and Yu Jianhan

Qinghua University
Beijing, China

INTRODUCTION

In this paper, the preliminary results of the study of extraction of lanthanides by liquid membrane from the sodium chloride leaching solution of ion absorption type rare earth sand is presented. In the NaCl leaching solution, the concentration of the mixed rare earth is about 7.1×10^{-3} M and NaCl concentration is 1.2 M. A synthetic solution of lanthanum chloride and sodium chloride is used in the experiments as the external phase. The liquid membrane is composed of di-2-ethyl-hexyl phosphoric acid (carrier), surfactant and kerosene, and the internal phase is aqueous hydrochloric acid. Lanthanum ion and hydrogen ion counter transfer through the membrane phase by carrier-mediated transport. Owing to the hydrogen ion concentration of internal phase is much higher than that of the external phase, lanthanum can be effectively extracted from NaCl solution and highly concentrated in the internal phase. Both batch extraction and continuous countercurrent extraction have been studied.

BATCH EXTRACTION

Theoretical It has been shown that the transport process in many liquid membrane systems can be described by an "Advancing Front Model"(1-4). In this model, it is assumed that: (1) in view of the presence of surfactant in the membrane phase, no internal circuration exists within the emulsion globules, (2) the controlling resistance in the transport process is the diffusion of the component through the membrane phase, (3) the component extracted reacts instantaneously with the internal reagent of the emulsion at a reaction interface that advances into the globules as the reagent is consumed.

Ho, Hatton, Lightfort and Li (1) developed a diffusion controlled model to described the transfer mechanism of the LM process and a regular perturbation solution is obtained. In some practical systems, the distribution ratio of the component reacted between the external phase and membrane phase is varied during mass transfer. For example, in the DEHPA carrier-mediated transport of lanthanum, the distribution ratio of lanthanum reduces as the pH value of the external phase is lowered due to the exchange of the lanthanum ion and hydrogen ion. When the distribution ratio changes with time, the solution of Ho's equation is complicated. We have obtained simplified mathematical equation for the LM systems with variable distribution ratio as follows:

$$(1) \qquad -V_e \frac{dC}{dt} = \frac{3DH}{R_e}(V_m+V_i)\left(\frac{R_f}{R_e-R_f}\right)C$$

C is the concentration of component transferred in the external phase at time t (mole/l).
D is the diffusivity in the emulsion phase (cm^2/s).
H is the distribution ratio of component transferred between the membrane phase and the external phase.
R_e is the average diameter of emulsion globules (cm).
R_f is the average diameter of the reaction front in emulsion globules (cm).
V_e is the total volume of the external phase (cm^3).
V_i is the total volume of the internal phase (cm^3).
V_m is the total volume of the membrane pfase (cm^3).
t is the contact time (s).

When the concentration of the lanthanum ion in the membrane phase is ignorred, equation (2) can be obtained by mass balance:

$$(2) \qquad G(C_o-C) = 1-\left(\frac{R_f}{R_e}\right)^3, \quad G = \frac{GV_e}{V_i C_i}$$

C_o is the concentration of component transferred in the external phase at t = 0 (mol/l).
C_i is the concentration of internal reagent in the internal phase at t = 0 (mol/l).
G is the number of moles of the internal reagent reacted with one mole of the component.

By approximating, we get

$$(3) \qquad 1-\left(\frac{R_f}{R_e}\right)^3 = \left(\frac{3.0-2.31GC_o}{1-0.77GC_o X^{0.5}}\right)\left(\frac{R_e-R_f}{R_f}\right), \quad X = \frac{C}{C_o}$$

When $0<GC_o<0.8$, the error between equation (3) and (2) is lower than 5%. Substituting equation (3) into (1), and assuming H constant, equation (4) can be obtained as follows:

$$(4) \qquad \ln X^{-1} - (1-X) - 1.54GC_o(1-X^{0.5}) + 0.513GC_o(1-X^{1.5})$$
$$= \frac{3DHt}{R_e^2}\left(\frac{V_m+V_i}{V_e}\right)\left(\frac{3-2.31GC_o}{GC_o}\right)$$

Equation (4) is an approximation of Ho's equation. When H is a function of C, substituting this function and equation (3) into equation (1), the equation can be solved rather easily. For instance, when

$$(5) \qquad H = \frac{C_c}{3C_o}X^{-\frac{1}{3}} \qquad (0.03<X<1)$$

the equation (6) can be obtained:

$$(6) \qquad 3(1-X^{1/3}) - 0.924GC_o(1-X^{5/6}) - 0.75(1-X^{4/3}) + 0.42GC_o(1-X^{11/6})$$
$$= \frac{DtC_c}{R_e^2 C_o}\left(\frac{V_m+V_i}{V_e}\right)\left(\frac{3-2.31GC_o}{GC_o}\right)$$

C_c is the concentration of the carrier in the membrane phase (mol/l).

Experimental Polyamine S-205 (produced by Shanghai Petroleum Refinery) was used as surfacctant. A commercial kerosene having a specific gravity of 0.75 g/cm^3 and a viscosity of 1.6 cp at 25°C was used as the solvent of the membrane phase. Hydrochloric acid solution of different concentration was used as internal phase. The membrane phase was mixed with the internal phase at a stirring speed of 4000 rpm for 20 min. The volume ratio of membrane phase and internal phase was 1:1 or 2:1. The internal phase droplets diameter was $1\text{-}5\times10^{-4}$cm. The external phase was a mixed solution of $LaCl_3$(7.1×10^{-3}M) and NaCl(1.2 M) having a pH of 3.5. Extraction runs were conducted at a mixing rate of 200 rpm and room temperature. Experimental conditions of five extraction runs are given in Table 1 and results are shown in Figure 1. It is shown that the mass transfer rates and the percent extraction values of lanthanum increase when the value of pH in the external phase, the concentration of carrier in membrane phase and the initialconcentration of internal phase reagent increase. When the volume ratio of membrane phase and internal phase (V_m/V_i) changed from 2:1 to 1:1, the mass transfer rate of lanthanum increases.

Table 1 The conditions of batch extraction

Run	C_c(M)	C_i(M)	V_m/V_i	pH adjustment
a	3×10^{-2}	1	2:1	no
b	3×10^{-2}	1	1:1	no
c	6×10^{-2}	1	2:1	no
d	6×10^{-2}	2	2:1	no
e	3×10^{-2}	1	2:1	3.5

C_o is 7.1×10^{-3} M, $(V_m+V_i)/V_e$ is 1:10, the initial pH of external phase is about 3.5.

In experimental runs a,b and c the distribution ratio H varied with time. In runs a and b H determined are approximately equal to $C_c/3C_o$. The H value of run c can be expressed approximately by equation (5), and its mass transfer process can be expressed by equation (6). The experimental results in terms of C/C_o vs. Dt/R_e^2 are compared with the value calculated by equation (4) and (6) in Figure 2. The diffusivity D of trivalent lanthanum complex in emulsion phase is 1×10^{-6} cm^2/s (4). The emulsion glo-

bule sizes R_e were determined and expressed in term of average diameter. The differences between the calculated and experimental results may be due to errors in the estimation of D and R_e and the breaking leakage of the liquid membranes.

CONTINUOUS EXTRACTION

The continuous extraction was conducted in an Oldshoe-Rudston column. The column is made of plexiglass, diameter 10 cm, effective height 70 cm, distance between plates 10 cm, and the diameter of central hole of the plates 3.0 cm. The external phase (continuous phase) entered the column at the upper end and flowed downward, the emulsion entered the column at the lower end and flowed upward. The two streams contacted countercurrently in the column. When steady state was reached, samples of the external phase were taken at different positions of the column, and the lanthanum concentration and pH value were determined. The influence of several parameters, including pH of external phase, acidity of internal phase, treat ratio $(V_m+V_i)/V_e$, concentration of carrier etc. to extraction of lanthanum were tested. The variation of lanthanum concentration of the external phase along the column is shown in Figure 3. The experimental conditions are given in Table 2. The curve a shows that the extraction of lanthanum is not effective, if the pH of external phase is not adjusted along the column, but when alkaline solution is added to the external phase in the middle of the column, as shown by curve d, the extraction of lanthanum is much more improved. When the initial concentration of lanthanum in the external phase is about 3.5×10^{-3} M (curve e), the extraction efficiency is ideal too. So a two column system with an intermediated adjustment of pH is suggested.

The results of batch and continuous extraction of lanthanum by LM are compared in Figure 4. The time for continuous extraction is the average residence time of the external phase in the column. The experimental conditions of curve c and d are the same as that of curve a and b respectively, which are given in runs b and c of Tab. 2. It is clear that the continuous countercurrent extraction of lanthanum by liquid membranes is more efficient than the batch extraction. The mathematical model for the continuous countercurrent extraction of lanthanum by liquid membranes based on the diffusion resistances of the external aqueous phase and oil membrane phase has been obtained.

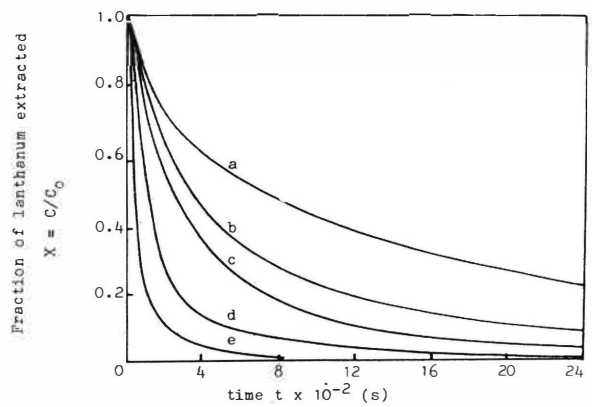

Fig. 1 The extraction of lanthanum in batch extraction

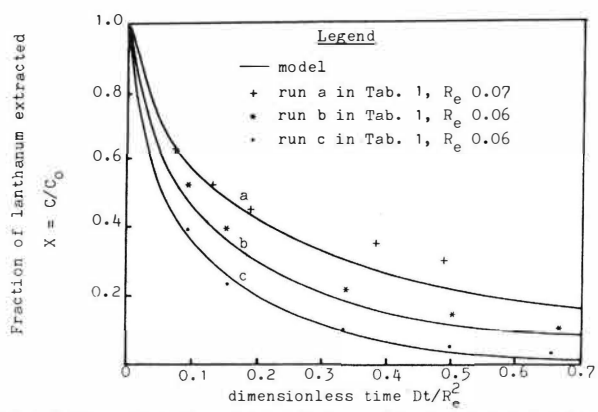

Fig. 2 Comparison of model prediction with experimental data

Table 2 The coditions of continuous extraction

Run	C_o (M)	C_i (M)	$(V_m+V_i)/V_e$	pH adjustment
a	7.1×10^{-3}	1	1:20	no
b	7.1×10^{-3}	2	1:40	no
c	7.1×10^{-3}	2	1:20	no
d	7.1×10^{-3}	1	1:20	yes
e	3.5×10^{-3}	1	1:40	no

V_e is 5.55 ml/s, C_c is 7.5×10^{-2} M, V_m/V_i is 1:1.

References

1. W.S.Ho, et al., AIChE, 28(4), 662(1982).
2. R.E.Terry, et al., J.Membr.Sci., 10, 305(1982).
3. R.Marr, et al., J.Ber.Bunsenges.Phys.Chem., 83, 1097(1979).
4. Jiang Changyin, et al., J.Chem. Ind.Eng.(China), No.3, pp 225 (1982).
5. Yu Jianhan, et al., Membr.Sep.Tech.(China), No.2, pp 1(1982).

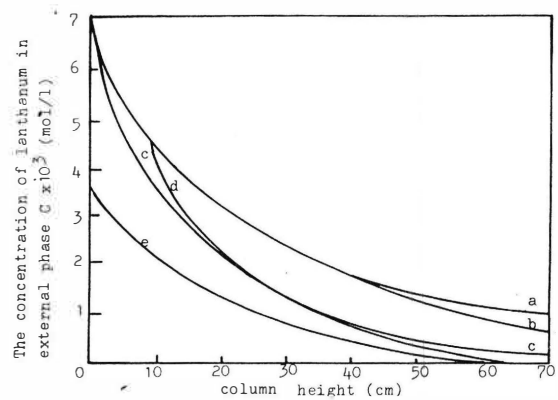

Fig. 3 The extraction of lanthanum in continuous extraction

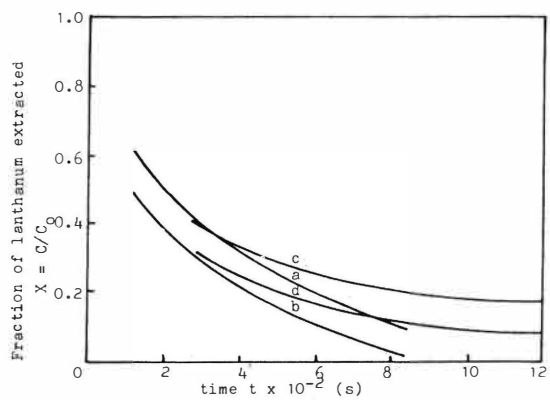

Fig. 4 The comparison of the continuous extraction and the batch extraction

A LIQUID MEMBRANE SEPARATION OF IONIC SPECIES USING A REDOX REACTION AS A DRIVING POTENTIAL

Makoto Takagi, Akira Ohki and Keihei Ueno

Department of Organic Synthesis, Faculty of Engineering
Kyushu University, Higashi-ku, Fukuoka, 812 Japan

Separation using liquid membrane is supposed to be one of the promissing techniques for industrial metal recovery (1,2). The driving energy for the separation is usually supplied by a pH gradient between two aquous solutions separated by an organic liquid membrane, but any chemical potential may be applied to drive the separation process.

We attempted to use a redox reaction for the separation of ionic species with particular emphasis to transition metals. Several metal ions were selectively transported against their own concentration gradient (active transport) through a polymer-supported liquid membrane as well as through a liquid surfactant membrane, taking advantage of the variation in their valence states. The reactions were based on the extractability difference between different valence states of metal ions. The separation system was extended to include the use of photo-induced redox reaction which led to a light-driven metal transport.

TETRATHIOETHER-MEDIATED COPPER TRANSPORT THROUGH LIQUID MEMBRANES

Polymer-Supported Liquid Membrane. In our previous works (3,4), a redox potential- or light-driven copper transport through a liquid membrane was achieved by using Bathocuproine as a carrier. A subsequent study indicated that a tetrathioether, compound 1 or 2, could also be used for the same purpose. Figure 1 illustrates the transport mechanism. Copper(II) is reduced to copper(I) in the presence of the thioether and a reducing agent, and the resultant cationic complex $[Cu^{I}L]^{+}$ is readily extracted to organic solvents forming a lipophilic ion-pair $[Cu^{I}L]^{+}\cdot X^{-}$ with an appropriate anion X^{-}. On contact with an oxidizing agent, the complex in organic solution is decomposed to liberate copper(II) and the pairing anion in aqueous solution, leaving L in organic solution. The overall reaction is the transport of one mole each of copper(II), anion X^{-}, and electron from the W_{red} to W_{ox} phase.

Figure 2 shows the apparatus used. The cell was consisted of two compartments, W_{red} and W_{ox}, each 150 mL capacity, which were separated by a plastic-film supported liquid membrane of effective area 28 cm^2. A micro-porous polypropylene film, Duragard 2500 (Polyplastics Ltd.) was used as a support, on which a diphenyl ether solution (ca. 0.04 ml) containing a carrier compound was applied. The W_{red} phase (reducing aqueous phase) contained a reducing agent or a photo-sensitizer system, while the W_{ox} phase (oxidizing aqueous phase) contained an oxidizing agent. The aqueous solutions were stirred at 30°C, and the aliquots of the solutions were taken periodically and analyzed.

The results were illustrated in Figure 3, showing that when a redox agent was eliminated (without $(NH_3OH)_2SO_4$ in the W_{red} phase or without $Ce(SO_4)_2$ in the W_{ox} phase), the transport rate of copper ion was markedly decreased in comparison with that in the complete system. These results support the transport mechanism shown in Figure 1. A blank experiment (without $Ce(SO_4)_2$) indicated that the oxygen dissolved in the W_{ox} phase could act as oxidizing agent though not as effectively as cerium(IV) salt.

As for the pairing anion X^{-} (forming $[CuL]^{+}\cdot X^{-}$ in the membrane phase), the transport rate decreased in the order, $PF_6^{-} > ClO_4^{-} > Cl^{-} \approx NO_3^{-}$, and was considerably affected by their concentration in the W_{red} phase. These results suggest that the anion concentration potential is also essential to the transport process as well as redox potentials. The transport process was completely selective to copper, and hence the coexisting zinc and cadmium ions were not transported at all.

The use of photo-sensitizer system (TiO_2 - glucose - hν, Figure 4) (5) instead of a reducing agent in the W_{red} phase resulted in a light-driven transport of copper ion; irradiation was provided by a 500 W xenon lamp without filter.

Liquid Surfactant Membrane. The copper transport reaction in the above section was extended to a water-in-oil-in-water (w/o/w) type liquid surfactant membrane sysytem (Figure 5). The W_{out} (outer aqueous phase) and W_{in} (inner aqueous phase) notations in Figure 5 correspond to the W_{red} and W_{ox} phases in Figure 1, respectively. A toluene solution (membrane solution) containing a surfactant (Span 80, 2 wt%) and a carrier was emulsified with a W_{in} solution, and the resultant water-in-oil emulsion was then dispersed in a W_{out} solution under mechanical stirring (240 rpm, 25 °C), giving the desired w/o/w emulsion; the volumes of each phase were 200 mL (W_{out}), 33 mL (membrane), and 17 mL (W_{in}), respectively.

The change in the copper concentration in the W_{out} phase with an elapse of time was determined. The results are shown in Figure 6 (under ordinary redox conditions) and in Figure 7 (under photo-sensitized conditions). The presence of either a reducing agent (ascorbic acid) or a photo-system (TiO_2 - glucose) under illumination in the W_{out} phase drove the transport reaction illustrated in Figure 5 to work effectively. Under optimum conditions, the copper concentration in the W_{in} phase went up to 45-fold of that in the W_{out} phase after 45 minutes reaction.

TRANSPORT OF OTHER METAL IONS USING LIPOPHILIC AMMONIUM SALT AS A CARRIER

A lipophilic cation such as trioctylmethylammonium ion (Capriquat, Dojindo Ltd.) is able to extract some anionic metal complexes (MX_n^{-}; M^{n+}, metal ion) to organic solutions (6). The extractability of the complexes may be controlled on each side of the membrane by changing the valence state of metal ions, and this will give an efficient metal transport system through a liquid membrane.

Figure 8 shows an example. At the W_{ox}/membrane interface, $Fe^{III}Cl_4^{-}$ complex generated in the W_{ox} phase is extracted to the membrane phase forming an ion pair $Q^{+}\cdot FeCl_4^{-}$ with Capriquat (Q^{+}). On contact with a reducing agent at the other side of the membrane (W_{red}/membrane interface), iron(III) is reduced to iron(II) and liberated into aqueous solution, since the chloro-complexes of iron(II) are too hydrophilic to be extracted.

Polymer-supported liquid membrane experiments were performed in the manner analogous to that previously mentioned. The membrane phase was diphenyl ether solution containing Capriquat carrier. Figure 9 shows typycal results of active transport of iron ion. As for a reducing agent, molecular hydrogen with platinum asbestos catalyst was superior to ascorbic acid. This is explained by the fact that ascorbic acid in the W_{red} phase partially permeated through the membrane into the W_{ox} phase, reducing iron(III) to iron(II) which cannot form extractable complexes. When cobalt, nickel, or copper ion coexisted with iron in aqueous solutions, the transport of iron was almost selective, and the rate of transport was scarcely affected by the coexisting metals.

The iron transport could also be carried out in the liquid surfactant membrane. However, the transport was not efficient, so that the amount of iron transported after 90 minutes reaction was about half of that initially added in the W_{out} phase. This is also ascribed to the leakage of ascorbic acid to the W_{out} phase.

The addition of an oxidizing agent, cerium(IV) sulfate, in the W_{out} phase did not improve the transport reaction.

Further, Capriquat is able to extract some metal complexes of such aminopolycarboxylic acid as EDTA and NTA (7). A cobalt-NTA complex could be transported through a supported liquid membrane containing Capriquat carrier under redox conditions in a similar manner to that shown in Figure 8.

Extraction experiments confirmed the following observation; by using the extraction agent, Capriquat, cobalt(II) ion in the aqueous solution containing NTA and an oxidizing agent (hydrogen peroxide) was readily extracted into organic solutions, but in the presence of a reducing agent (ascorbic acid), the metal was not extracted at all. The transport reaction through a liquid membrane was just as expected from the extraction behavior; cobalt ion was transported from the W_{ox} to W_{red} phase (Figure 10). The photo-system, TiO_2 - glucose - hν, could be coupled with the transport.

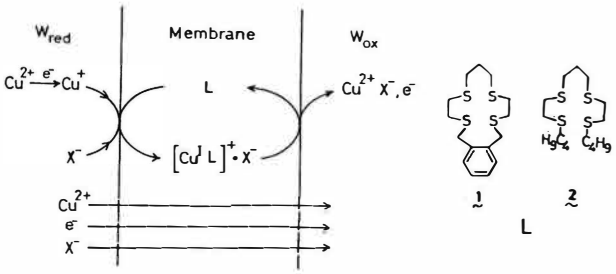

Fig. 1. Thioether-mediated copper transport through liquid membrane.

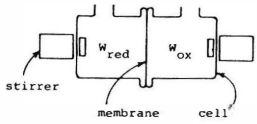

Fig. 2. Schematic view of the apparatus.

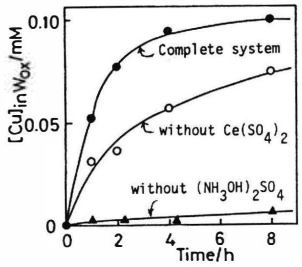

Fig. 3. Thioether-mediated copper transport.

W_{red} : 0.1 mM $Cu(NO_3)_2$, 10 mM $(NH_3OH)_2SO_4$, 10 mM $NaPF_6$, 0.1 M $CH_3CO_2NH_4$ (pH 5.8)
W_{ox} : 4 mM $Ce(SO_4)_2$, 3 % H_2SO_4 (pH<1)
Membrane : 100 mM Thioether 1

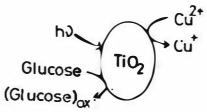

Fig. 4. Photo-sensitized copper reduction.

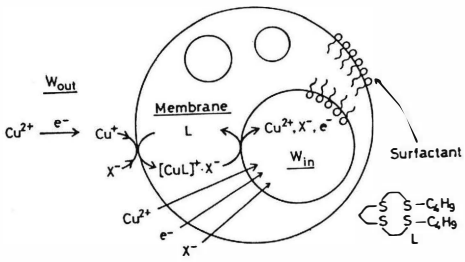

Fig. 5. Thioether-mediated copper transport through liquid surfactant membrane.

CONCLUSIONS

Redox potential- or light-driven transport of several metal ions were studied in the supported liquid membrane as well as in the liquid surfactant membrane. Thioether 1 or 2 could serve as a carrier for copper ion, and a lipophilic ammonium ion, Capriquat, was able to transport several metal ions which formed extractable anionic complexes with appropriate ligands (Cl^-, NTA). It is hoped that the idea of redox potential- or light-driven ion transport leads to a practical separation and concentration of metal ions and the effective utilization of solar energy in the future.

REFERENCES

(1) H. Halwachs and K. Schügerl, Chem. Ing. Tech., 50, 767 (1978).
(2) R. Marr and A. Kopp, Chem. Ing. Tech., 52, 399 (1980).
(3) A. Ohki, S. Matsuno, T. Takeda, M. Takagi, and K. Ueno, Sep. Sci Technol , 17 1237 (1982).
(4) A. Ohki, T. Takeda, M. Takagi, and K. Ueno, Chem. Lett., 1529 (1982).
(5) T. Kawai and T. Sakata, Nature, 286, 474 (1980).
(6) M. Okazaki, T. Horiguchi, and K. Watanabe, Nippon. Kagaku Zasshi, 84, 917 (1963).
(7) H. M. N. H. Irving and R. H. Al-Jarrah, Anal. Chim. Acta., 63, 79 (1973).

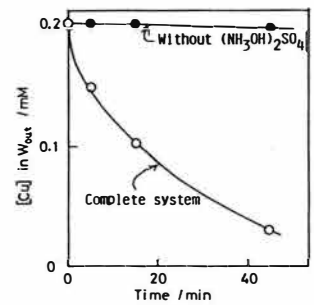

Fig. 6. Copper transport through liquid surfactant membrane.

W_{out} : 0.2 mM $Cu(NO_3)_2$, 10 mM $(NH_3OH)_2SO_4$, 0.1 M $NaClO_4$, 0.1 M $CH_3CO_2NH_4$
W_{in} : 3 % H_2SO_4
Membrane : 0.1 mM Thioether 2

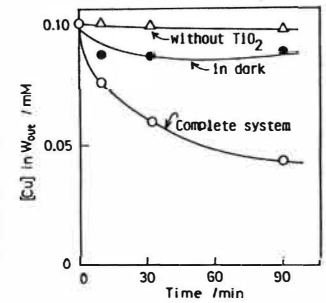

Fig. 7. Light-driven copper transport through liquid surfactant membrane.

W_{out} : 10 mM Glucose, 100 mg TiO_2, 0.1 mM $Cu(NO_3)_2$, 0.1 M $NaClO_4$, 0.1 M $CH_3CO_2NH_4$; Xe lamp
W_{in} : 3 % H_2SO_4
Membrane : 0.1 mM Thioether 2

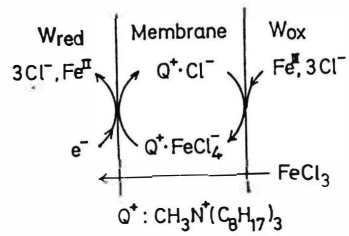

Fig. 8. Capriquat-mediated iron transport through liquid membrane.

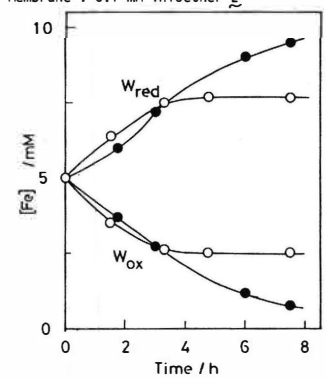

Fig. 9. Capriquat-mediated iron transport.

W_{red} : 5 mM $FeCl_3$, 1 M HCl (pH<1),
○ : 15 mM Ascorbic acid
● : H_2 on Pt asbestos
W_{ox} : 5 mM $FeCl_3$, 1 M HCl (pH<1)
Membrane : 0.5 M Capriquat

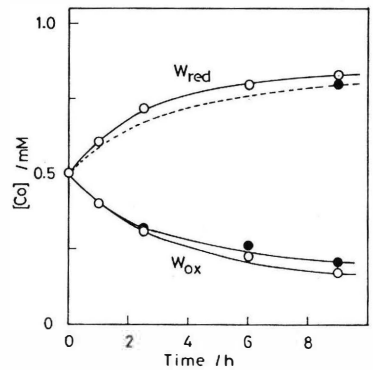

W_{red} : 0.5 mM $Co(NO_3)_2$, 0.5 mM NTA, 10 mM KCl, Bicine-NaOH buffer (pH 7.9)
○ : 15 mM Ascorbic acid
● : 15 mM Glucose, 100 mg TiO_2; Xe lamp
W_{ox} : 0.5 mM $Co(NO_3)_2$, 0.5 mM NTA, 10 mM KCl, 0.01 % H_2O_2, Bicine-NaOH buffer (pH 7.9)
Membrane : 0.2 M Capriquat

Fig. 10. Capriquat-mediated cobalt transport.

MEMBRANE EXTRACTION IN PRECONCENTRATION OF SOME URANIUM FISSION PRODUCTS

F. Macášek, P. Rajec, R. Kopunec, V. Mikulaj, J. Mišianik

Department of Nuclear Chemistry, Comenius University
842 15, Bratislava, Czechoslovakia

Since N.N.Li introduced the multiple emulsion principle in separation science (1) and E.L.Cussler demonstrated the high efficiency of metal transport activated by complex compound formation (2) a number of papers dealing with various aspects of liquid membrane extraction (MX) have appeared (3). The aim of the present work was to find how far the conventional principles of solvent extraction (SX) can be transferred to the field of MX and applied practically to laboratory preconcentration of radionuclides, uranium and its fission products, in particular (4,5).

THEORETICAL

If the transport of a solute from volume V_I through a liquid membrane into volume V_{II} obeys a Fickanian law (6) then, for a flat membrane of an average thickness δ and area S

$$(1) \quad -\frac{dn_I}{dt} = \frac{P\,S}{\delta}(\bar{c}_I - \bar{c}_{II})$$

where n_I is the number of moles transferred from solution I,

P is permeation coefficient,

$\bar{c}_I$ and $\bar{c}_{II}$ are the concentrations of solute at membrane boundaries with solution I and II, respectively.

The latter are connected with concentrations in the outer (I) and the internal (II) solutions through distribution ratios $D_I=\bar{c}_I/c_I$ and $D_{II}=\bar{c}_{II}/c_{II}$. In equilibrium the fraction of solute recovered from solution I is

$$(2) \quad R_{MX} = \frac{p\,D_I\,r_I}{1 + p\,D_I\,r_I}$$

where

$$(3) \quad p = 1 + 1/D_{II}r_{II}$$

is an enhancement factor for pertraction into a stripping solution and $r_I=V_M/V_I$ and $r_{II}=V_M/V_{II}$ are the volume ratios to the membrane volume (V_M). The recovery fraction for conventional SX at the condition of interface I equilibrium is $R_{SX} = D_I r_I/(1+D_I r_I)$.

The factor $p > 20/D_I r_I$ is sufficient to reach high yield R_{MX}. This is important for absolute preconcentration but in case of several solutes the selectivity (relative preconcentration) expressed in terms of enrichment factors, may be lost in the region where all R's are close to unity.

A value N which corresponds to the number of repeated SX operations leading to the same recovery of solute as achieved in a single MX step,

$$(4) \quad N = \frac{\log(1-R_{max})}{\log(1-R_{SX})}$$

is a further parameter suitable for characterization of MX. The N necessary to compensate for the effort needed for the emulsion preparation or to achieve a substantial economy of extractant, say $N > 4$, is to be expected, if $p \leq 1000$, only at $R_{SX} \leq 0.9$, i.e. at a sufficiently low ratio r_I (or distribution D_I).

Due to the thermodynamic instability (7) and the dynamics of membrane breakage (8) the reachable R in membrane extraction is always less than the value given by Equation (2) - Figure 1 .Ideal kinetics ensuing from Equations (1) and (2), at a linear concentration gradient in membrane, will be as follows :

$$(5) \quad -\log(1-R/R_{MX}) = k\,t$$

where

$$(6) \quad k = \frac{2\,P\,S\,D_I}{\delta\,V_T\,\ln 10}\;\frac{p}{R_{MX}(2p-1)}$$

In this oversimplification, the k is of the same order as in SX, unless the emulgator affects the process (9). Because the second term of Equation (6) varies between $1/R_{SX}$ (when p=1) and $1/R_{MX}$ (when $p \gg 1$), D_{II} is of minor use as a controlling factor but the regulation by D_I can be considered for non-equilibrium separation. The geometrical components of the effective rate constant k , however, are not constants and the reaction rate (10) or diffusional resistances and convection cannot be neglected. Hence, even for simplified globules (6) Equation (5) provides only a rough approximation of pseudo-steady-state kinetics curve while many other peculiarities remain to be solved by numerical simulation. Namely, for such a solution the program METRICO for HP 9825A computer is developed (11).

EXPERIMENTAL

A turbine-type impeller of our own construction (12) was used for preparation of the liquid membranes with volume ratio $r_{II}=1$ and at mixing rate 4000-6000 rpm for 3-5 min. The emulsions were considered to be usable when the percentage of their rupture was less than 2 % after 1 hr standing, but some emulsions remained stable for days and even weeks. When an immediate breakdown of the emulsions was desired, higher ketones or alcohols (metyl isobutyl ketone, n-octanol etc.) were added. The extraction in multiple W/O/W emulsions was performed in a glass vessel by stirring with a magnetic rod (50x10 mm) stirrer at 300-600 rpm, usually with 20-50 ml of outer (feed) solution. Radionuclides Sr-85, Tc-99m, Cs-137 and Ce-144 were used as tracers for metals at concentrations about 0.1 mmol/l. The extraction was followed by sample taking (0.2-0.5 ml) from the outer solution and measuring gamma activity on MODUMATIC III (Packard) automatic counting device which was connected on-line with HP 9825A (Hewlett-Packerd) computer (4). Uranium concentration was determined by Arsenazo III method.

RESULTS AND DISCUSSION

The parameters of typical systems investigated are listed in Table 1 and demonstrated by Figures 2-5. The apparent rate constants k given in Table 1 are of no theoretical significance as given by Equation (6) but used only for characterization of a particular experimental run. According to the criteria introduced in the theoretical part of this work, primarily the systems using DEHPA as chelating carrier for Sr and U are highly suitable for preconcentration. Strontium is quantitatively extracted, with impressive high equivalence number N, in the presence of calcium, which is rather important for radiochemical analysis of biological samples. Uranium is also well extractable with oxine and KELEX 100 in membrane. The systems with inner solutions of higher hydrogen and sulfate ionic activities seem to be perspective for large scale applications (13), while the pertraction of uranium into Arsenazo solution is suitable for selective extraction-photometric analysis (14). The transfer of cobaltous ions through the LIX 64N/toluene membrane exhibits very good kinetics, too, and no complications arise from the cobalt oxidation.

Neutral and basic carriers are obviously less convenient in the membranes under study. However, the complexing agents emulgated in TOPO/cyclohexane solutions increase their efficiency for 5-8 times in cerium(III) extraction. Transfer of acids, especially with tri-n-octylamine membranes, appeared to be dangerous in systems without a buffering capacity. Surprisingly, the systems working on ion-exchange mechanism (dipicrylamine - DPA, 8,8'-dibromo-bis(1,2-dicarbollyl)cobalt(III) anion - Br_2DCC, Aliquat 336) were found to yield much smaller R_{max} than expected according to calculated R_{MX} values and sometimes even smaller than R_{SX}. It seems probable that charging of the membrane interface or neutral detergent layer influences the overall transport mechanism.

CONCLUSION

The most perspective emulsion membrane systems for metal preconcentration, the uranium fission products and other radionuclides in particular, are those with chelating agents, especially at low concentrations (substoichiometric amounts), low volume ratios r_I and high competing ion concentrations when high enhancement coefficients for pertraction can be achieved.

ACKNOWLEDGEMENTS

The authors would like to acknowledge the financial support from the International Atomic Energy Agency (Contract 2662/RB).

The authors are grateful to Ms.E.Ronecová, Ms.A.Čechová, Mr.J.Rezbárik and Mr.V.Řeháček for their experimental assistance and also to Dr.Ľ.Mátel for provision of dibromo-bis(1,2-dicarbollyl)cobalt(III) salt and Atlas Chemical Industries N.V. and Oleofina S.A. for samples of commercial emulsifiers.

REFERENCES

1. N.N.Li, AICHE Journal 17, 459 (1971).
2. E.L.Cussler, AICHE Journal.17, 1300 (1971).
3. J.Mišianik, M.Koreňovská and F.Macášek, Chem.Listy 77, 136 (1983).
4. F.Macášek, R.Kopunec, V.Mikulaj, P.Rajec and A.Švec, Membrane extraction in radiochemical analysis, Report I.A.E.A. Contract 2662/RB, Chemical Institute Comenius University, Bratislava 1981.
5. F.Macášek, R.Kopunec, V.Mikulaj, J.Mišianik and P.Rajec, Membrane extraction of some fission products, 10th Radiochem. Conf., Mariánske Lázne, Czechoslovakia 26.-30.4.1982.
6. V.J.Kremesec, Sep.Purif.Meth. 10, 117 (1981).
7. G.A.Yagodin, S.I.Ivakhno, V.I.Gusev and A.V.Levkin, Dokl. AN SSSR 266, 1198 (1982).

8. S.Schlosser and E.Kossaczký, Pertraction through liquid membranes, Report A-1980-158/b, Slovak Technical University, Bratislava 1980.

9. J.Breysse and E.S.Pérez de Ortiz, Paper G 2.6, 7th Int.Congr. Chem.Engineering CHISA'81, Praha, Czechoslovakia, 31.8.- - 4.9.1981.

10. P.R.Danesi, E.P.Horwitz, G.F.Vandegrift and R.Chiarizia. Sep.Sci.Tech. 16, 201 (1981).

11. F.Macášek, The modelling of transport of ions and complex compounds through membranes, 38th Annual Meeting of Czechoslovak Chemical Society, Praha, Czechoslovakia, 6.-9.7.1982.

12. A.Švec and P.Rajec, Chem.Listy 77, 206 (1983)

13. F.Macášek, P.Rajec and V.Řeháček, Czechosl.Pat.Appl., PV 6704-82, 17.9.1982.

14. F.Macášek and R.Kopunec, Radiochem.Radioanal.Lett., to be published.

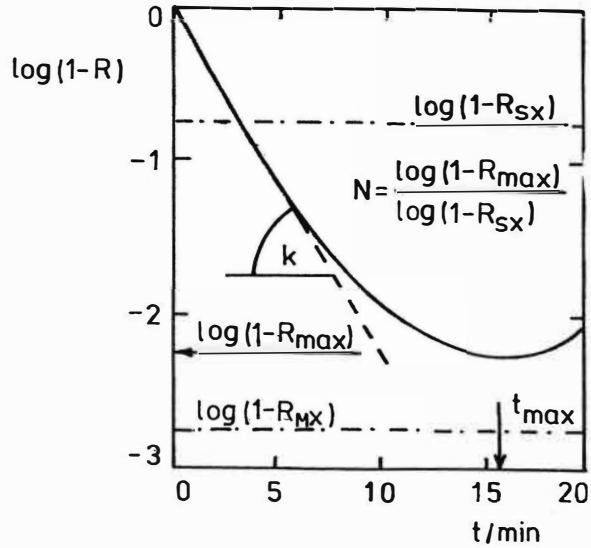

FIGURE 1. The coordinates and values used in Table 1 and Figures 2-5.

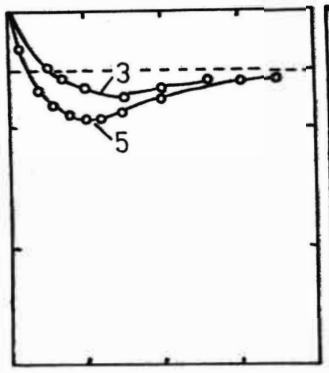

FIGURE 2. Cesium extraction -system No 3 and 5 (Table 1).

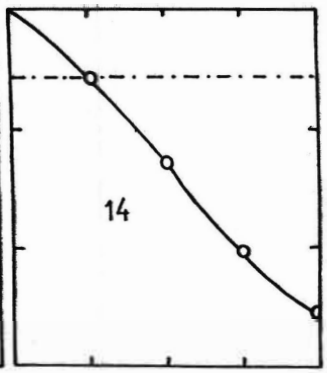

FIGURE 4. Uranium extraction -system No 14 (Table 1).

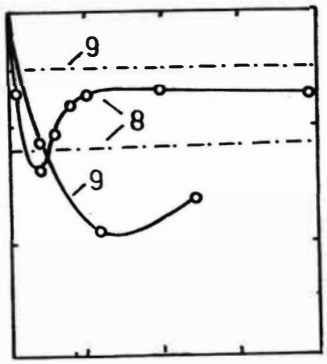

FIGURE 3. Strontium extraction - system No 8 and 9 (Table 1).

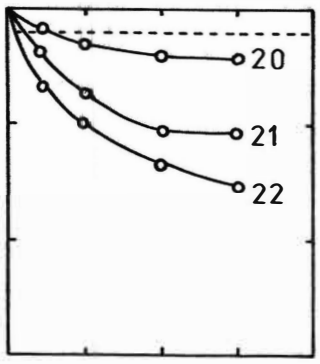

FIGURE 5. Cerium(III) extraction - systems 20-22, Table 1.

TABLE 1 Data on typical systems investigated (r_{II}=1.0)

No	Ion	Solution composition: outer (feeding)	Solution composition: membrane	Solution composition: internal (stripping)	r_I	10^3 k (s^{-1})	R_{max}	t_{max} (min)	N	Note
1	Cs^+	0.01 M HNO_3	0.1 M DPA, 4% RADIASURF 7155/7355, NB	0.2 M HNO_3	0.100	4.0	0.46	5	1.7	
2	"	"	" " "	1 M KNO_3	"	12	0.70	3	3.2	
3	"	"	0.01 M Br_2DCC, 4% SPAN 80/85, NB	0.1 M KNO_3	"	11	0.80	6	1.4	Figure 2
4	"		" " "	1 M KNO_3	"	15	0.92	4	2.3	
5	"	"	" " "	1 M HNO_3	"	15	0.87	5	1.8	Figure 2
6	Sr^{2+}	0.01 M HCl, 0.02 M $CaCl_2$	0.01 M Br_2DCC, 0.5% PEG300, 5% SPAN80, NB	0.05 M sodium citrate	"	7.1	0.80	3	1.3	
7	"	0.01 M HCl	1.5 mM Br_2DCC, 0.7% PEG300, 3% SPAN80, NB/H	0.05 M EDTA, pH 7.1	"	9.9	0.996	3	0.99	
8	"	0.01 M HCl, 0.15 M LiCl	4.5 mM Br_2DCC, 0.3% PEG300, 3% SPAN80, NB/H	" "	"	10	0.95	3	1.1	Figure 3
9	"	acetate buffer, pH 5.5	13 mM HDEHP, 2.5% RADIASURF 7155, HX	0.1 M HNO_3	"	10	0.988	6	3.8	Figure 2
10	"	" , pH 5, 0.01 M $CaCl_2$	" " "	1.0 M HNO_3	"	-	0.990	16	4600	
11	"	" , " , 0.025 M $CaCl_2$	" " , dodekane	1.0 M HNO_3	"	-	0.990	4	1900	
12	UO_2^{2+}	0.1 M Na_2SO_4, pH 2.0	0.05 M TOPO, 4% SPAN80, CHX	0.2 M sodium citrate	"	0.4	0.59	80	0.33	
13	"	" , "	" , 3% RADIASURF 7155, CHX	0.05 M EDTA, pH 11.2	"	0.2	0.68	80	0.55	
14	"	" , "	0.075 M HDEHP, 1% SPAN 80, CHX	1.3 M H_2SO_4	0.125	2.0	0.997	20	4.7	Figure 4
15	"	" , pH 5.3	5% KELEX 100, 1.5% SPAN 80, CHX	0.01 M H_2SO_4	0.125	-	0.46	25	10	
16	"	0.01 M DCTA, pH 7.5	0.02 M oxine, 1.5 % SPAN 80, CHX	0.05% Arsenazo III, pH 4.0	0.040	-	0.99	5	-	
17	Co^{2+}	borate buffer, pH 7.95	0.35% LIX 54N, 2.1% ARLACEL 80, toluene	0.1 M DTPA, pH 5.0	0.100	8.0	0.98	12	31	
18	"	" , $5x10^{-3}$ M Co	" " "	" "	"	3.5	0.97	30	100	
19	"	" , $1x10^{-2}$ M Co	" " "	" "	"	1.5	0.85	60	120	
20	Ce^{3+}	0.1 M HNO_3, 6 M $NaNO_3$	0.1 M TOPO, 3% SPAN 80/20, CHX	1 M HNO_3	0.167	5.5	0.63	15	2.1	Figure 5
21	"	" "	" " "	0.01 M EDTA, pH 6.0	"	3.0	0.915	10	5.0	Figure 5
22	"	" "	" " "	0.05 M sodium citrate, pH8	"	10	0.985	20	8.7	Figure 5
23	"	0.1 M HNO_3	0.1 M HDEHP, 2% SPAN 80/20, CHX	1 M HNO_3	"	0.2	0.258	25	5.2	
24	"	"	0.4 M HDEHP, " "	"	"	3.6	0.89	10	2.5	
25	TcO_4^-	0.1 M HNO_3	5% TOA, 3% SPAN 80, CHX	0.5 M NH_4OH	0.500	2.2	0.79	5	0.6	
26	"	"	" " "	0.1 M HNO_3, 1 M KNO_3	"	2.1	0.980	25	1.4	
27	"	"	0.5% ALIQUAT 336, 3% SPAN 80, CHX	0.5 M NH_4OH	0.100	1.3	0.51	5	0.6	
28	"	"	" " "	0.1 M HNO_3, 1 M $NaNO_3$	"	1.3	0.49	10	0.6	
29	"	"	" " "	0.1 M N_2H_2, 0.1 M NaOH	"	2.7	0.63	5	0.9	
30	"	"	" " "	1 M $NaClO_4$	"	3.3	0.916	5	2.4	

NB - nitrobenzene
HX - hexane
CHX- cyclohexane
PEG - polyethyleneglycol
DPA - dipicrylamine
Br_2DCC - dibromo-bis(1,2-dicarbollyl)cobalt(II
DCTA - diaminocyclohexanetetraacetic acid
DTPA - diethylenetriaminepentaacetic acid

SELECTIVE EXTRACTION OF ZINC IN A COUNTERCURRENT KÜHNI EXTRACTOR USING LIQUID SURFACTANT MEMBRANE EMULSIONS

D. Melzner, A. Mohrmann, W. Halwachs, K. Schügerl

Institut fúr Technische Chemie Der Universität Hannover
Callinstr. 3, 3000 Hannover 1, Federal Republic of Germany

The extraction of metal ions by means of liquid surfactant membrane emulsions leads to high enrichment factors in the inner aqueous phase. Therefore, at low metal concentrations, the liquid membrane technique is a very interesting alternative to conventional solvent extraction.

We are working on separating Zn from Co, Cu and Ni by means of liquid membrane emulsions with several carriers, especially Di-2-ethyl-hexyl phosphoric acid (D2EHP).

The extractions were carried out at low pH values in a continuously operated multistage column. During start-up and steady-state operations of the reactor the longitudinal concentration profiles of the solutes were measured as functions of time at different flow rates of both phases and at different stirrer speeds.

Based on these investigations and holdup and droplet size distribution measurements a mathematical model was developed to simulate the reactive extraction process in the multistage column reactor.

EXPERIMENTAL

For the continuous extraction by means of liquid surfactant membrane emulsions we used a Kühni extractor which seems to be suitable for this purpose. This extractor allows to vary the residence times and flows in a wide range. Furthermore, a good dispersion of the emulsion is important because of its high viscosity.

In order to produce the liquid membrane emulsion sulfuric acid was emulsified in the organic phase using an Ultra Turrax 4TS stirrer.

As an organic phase we used Kerosine containing the carrier (10 %) and a tenside (5 %) to stabilize the emulsion. It is important to standardize the production of the emulsion in order to get reproducible results.

The metal concentration was analyzed by an atom-absorption spectrophotometer, the data were stored and processed by a PdP 11 computer with hard discs. All programs are written in FORTRAN.

In our experiments we separated zinc from cobalt and copper by means of the carrier D2EHP. The initial conditions were:
- temperature: 25 °C
- metal concentration: 100 ppm
- phase ratio org./strip: 1/2

The following parameters were varied:
- stirrer speed,
- dispersed phase flow,
- continuous phase flow.

The axial concentration profile of the continuous phase was measured and compared with the concentration profiles which were computed according to the cell model and the dispersion model (1-5). The dispersion model was used to compute the mass transfer coefficients of the extraction.

With a Fortran program the mass transfer coefficient in a nonlinear differential equation of the second order was varied until the resulting concentration profile corresponded to the marginal conditions.

Figures 1 and 2 show a plot of the dispersion coefficient and the number of cells vs. the flow rate of the continuous phase. The dispersion coefficient is independent of the flow rate of the continuous phase, the computed number of vessels increased from 4 at a flow rate of 50 l/h to 9 at 120 l/h.

HOLDUP OF THE EXTRACTION

The rate of extraction is mainly given by the specific interfacial area of the two phases which can be calculated from the droplet size distribution and the holdup. The holdup is a function of the stirrer speed, the medium droplet size and the physical characteristics of the system.

Fig. 3 shows the holdup as a function of the continuous flow. The dispersed flow (5 l/h) and the stirrer speed (100 rpm) were kept constant.

The holdup rises until phase inversion is reached at 150 l/h. We have no real flooding point of the column, phase inversion begins with a strong increase in the holdup near the inlet of the column.

RESULTS OF CONTINUOUS ZINC EXTRACTION

We studied the effects of the flow rates of the two phases and the stirrer speed on the extraction rate and the selectivity. The experimental conditions are listed above. In all cases the axial concentration profile was measured at steady state operation.

The concentrations at the outlet of the column were measured every 15 minutes in order to control the steady state of the column

Fig. 6 shows the extraction rate as a function of the continuous phase flow rate (dispersed flow rate = 5 l/h, stirrer speed = 100 rpm) The extraction rate decreases from 60 % at a flow rate of 70 l/h to 35 % at 100 l/h. Within the range of 100 l/h to 150 l/h it remains nearly constant.

Fig. 7 shows an increasing extraction rate with an increase in the dispersed phase flow rate due to the higher holdup. A higher stirrer speed effects a strong increase in the extraction rate as well (Fig. 8) the reason being a smaller average droplet size and a higher interfacial area.

Fig. 9 shows the concentration profiles in the Kühni extractor as a function of the stirrer speed. The computed and experimental data show good agreement. The computed mass transfer coefficients are in the range of 2.5 to $3.3 \cdot 10^{5}$ cm/sec.

The concentration profiles in the Kühni extractor as functions of the continuous and the dispersed flow are shown in Figures 10 and 11.

CONCLUSIONS

The results of the continuous experiments with liquid membrane emulsions show that the Kühni extractor is suited for this technique. There were no difficulties, such as adherence of the emulsion in the column.

We attained an extraction rate of 80 % at a flow rate of the continuous phase of 100 l/h, a dispersed flow rate of 5 l/h and a stirrer speed of 100 rpm. We did not try to attain the maximum extraction rate because an increasing number of stages of the column will cause an increasing rate of extraction.

The modelling of the continuous extraction is possible with mass transfer coefficients which were obtained from stirred cells experiments.

A comparison of the concentration profiles resulting from the dispersion model and the cell model shows:

- The dispersion model shows a very good fit between the computed and the experimental data.
- The cell model is less suited to compute real concentration profiles, especially at low vessel numbers.

REFERENCES

1. Levenspiel, O. The Chemical Reactor Omnibook, OSU Book Stores, Corvallis, OR

2. Sarkar, S., Mumford, C.J., Phillips, C.R. Liquid-liquid Extraction with Interphase Chemical Reaction in Agitated Columns. 1. Mathematical Models. Ind. Eng. Process Des. Dev. 19, 665 (1980)

3. Mecklenburgh, I.C. The Theory of Backmixing. Wiley & Sons, London, 1975

4. Halwachs, W. Habilitation Thesis, Hannover 1981

5. Ricker, N.L., Nakashito, F., King, C.J. An Efficient, General Method for Computation of Countercurrent Separation Processes with Axial Dispersion. AIChE Journal 27 277 (1981)

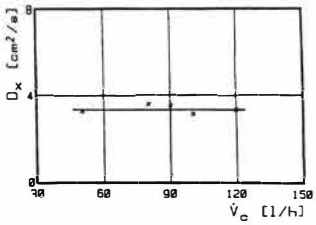

Fig. 1: Dispersion coefficient vs. continuous flow

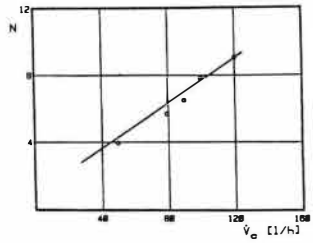

Fig. 2: Number of vessels vs. continuous flow

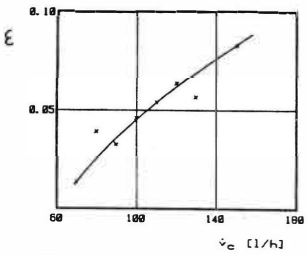

Fig. 3: Holdup vs. continuous flow

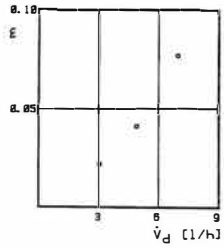

Fig. 4: Holdup vs. disperse flow

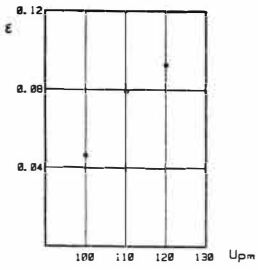

Fig. 5: Holdup vs. stirrer speed

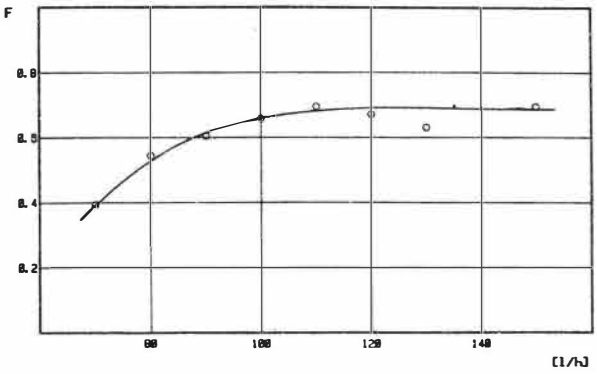

Fig 6: Zinc extraction vs. continuous flow

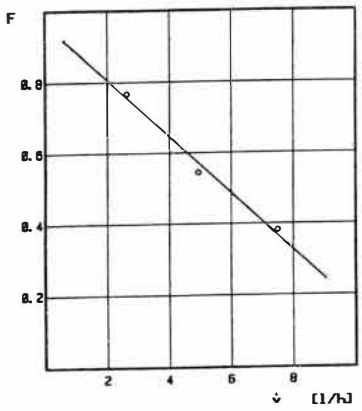

FIGURE 7. Zinc extraction vs. dispersed flow

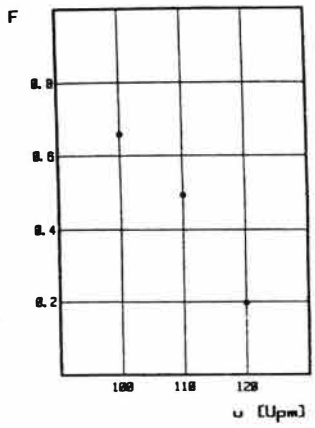

FIGURE 8. Zinc extraction vs. stirrer speed

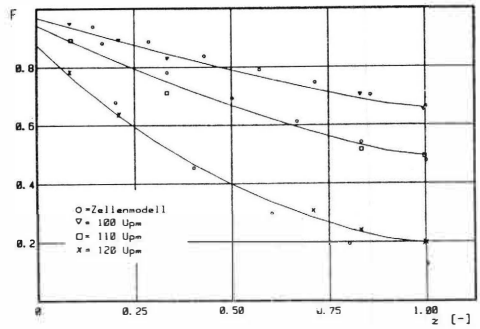

FIGURE 9. Comparison of computed axial concentration profiles with experimental data as a function of the stirrer speed

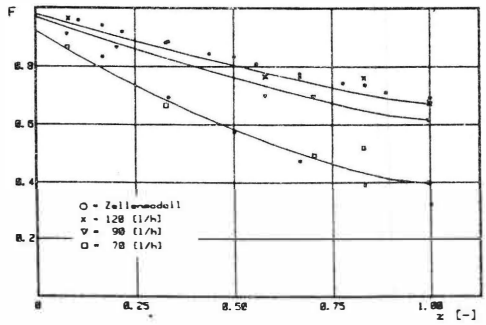

FIGURE 10. Comparison of computed axial concentration profiles with experimental data as a function of the continuous flow

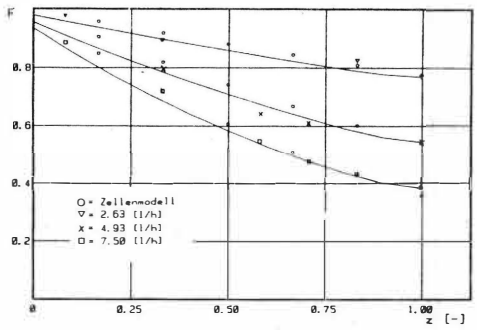

FIGURE 11. Comparison of computed axial concentration profiles with experimental data as a function of the dispersed flow

DEVELOPMENT OF A CONTINUOUS PROCESS FOR METAL ION RECOVERY BY LIQUID MEMBRANE PERMEATION

M. Prótsch
Chemiefaser Lenzing AG
Lenzing, Austria

R. Marr
Institute of Chemical Engineering
Technical University Graz
Graz, Austria

INTRODUCTION

Within the last years growing interest is in recycling due to an increasing environmental consideration and rising prices of natural sources. An approach to this may be the development of the liquid membrane permeation technique (LMP) by N.N.Li "(1)". This new technic allows to treat very dilute liquors. With a 'carrier-facilitated' transport it is possible to get highly enriched stripping phases.

Within the closed cyclus of the carrier (Figure 1) is a certain part of unloaded carrier (extractant) molecules, which enhance equilibrium and kinetics. This is an advantage, especially for diluted wastes and process effluents.

The LMP unit operation can be classified into four steps (Figure 2):

- emulsification of stripping phase with carrier phase
- permeation; contact of emulsion with effluents at required time
- settling of this multiple system
- splitting of the emulsion

The most difficult and vital step with this technique is the splitting of the emulsions "(2,3,4)". Since there wasn't much work in literature we did especially work on this field.

Splitting can be done with thermal, chemical,ultrasonical, centrifugal and electrostatical devices. The latter one offers high advantages since splitting is without degradiation of the organic phase at a very low energy input.

From an analogy to solvent extraction one can use columns or mixer-settlers to perform LMP. As far as diluted and high volume materials are concerned and there is no exaggerated slow mass transfer, columns should be prefered.

CONTINUOUS EXPERIMENTS IN A SMALL SCALE COLUMN

Apparatus

This apparatus consists of a continuous homogenizer (IKA - Ultra-Turrax), a permeation cloumn and a device for an electrostatic splitting of the emulsion. The counter-current column with a height of 1,4 m and a diameter of 50 mm can work as a RDC, drop column and stirred column with more than 95% free space.

Experiments with RDC. These experiments showed satisfying mass transfer but also an adherence of the emulsion drops in the dead zones of the cells. These drops have an enhanced residence time which leads to more osmosis and cause a diminuation of the cross-sectional area and of the volume of the column. Together with more break-up and entrainment these appearences lead to dramatic deterioration of the efficiency of the permeation.

Drop columns. There is too little residence time for a sufficient mass transfer.

Stirred counter- current column. This column was used to avoid the disadvantageous characteristics of a RDC and nevertheless obtain a good mass transfer.

All these columns were equipped with an installation of an electrostatic splitting. These instalations were similar to those used for the drainage of mineral oils, and were adapted for the special use in permeation.

RESULTS FOR THE CONTINUOUS SEPARATION FROM SYNTHETIC WATERS

Table 1 shows some results of an experimental series for the separation of following metals:

Zinc: $Zn^{2+} + 2\,\overline{HDEHP} \rightleftharpoons \overline{Zn(DEHP)_2} + 2\,H^+$

Tungsten: $HW_6O_{21}^{5-} + 5\,H^+ + 5\,\overline{R_3N} \rightleftharpoons \overline{(R_3NH)_5HW_6O_{21}}$

Copper: $Cu^{2+} + 2\,\overline{HX} \rightleftharpoons \overline{CuX_2} + 2\,H^+$

Vanadium: $V_3O_9^{3-} + 3\,\overline{R_4N^+} \rightleftharpoons \overline{(R_4N)_3V_3O_9}$

In all these experiments the concentration of the surfactant, the carrier and the stripping agent was constant, so the different velocity of the mass transfer at different stirring speed is proportional to the interface area, but one must also consider the different diffusion velocity of the metal-carrier complex through the membrane phase.

SEPARATION OF ZINC OUT OF A VICOSE WASTE WATER

The target was to separate zinc selectively from calcium out of a very polluted waste water in the viscose industry. After having obtained good results in batch experiments, continuous experiments were made with following data:

The zincconcentration could be reduced from 180 ppm to 45 (32) ppm by dispersing an emulsion, which consisted of a 30% sulfuric acid as inner water phase and a solution of 2,5% surfactant and 5% HDEHP in Shellsol T as membrane phase, in a waste water stream of 30 l/h at nearly constant zinc concentrations. The throughputs of the inner water phase and the membrane phase were: 0,25 + 1 and 0,5 + 2 l/h resp. (Figure 3 and Table 1). After leaving the column the emulsion was split within 2 (4) minutes at a voltage of 0,5 kV/cm and a surface of electrodes of 30 cm^2. The membrane phase was reused for the preparation ofthe emulsion, the concentration in the inner water phase is shown in table 1.

LAY-OUT OF THE ZINC- LMP- PILOT PLANT

Scale up of a factor 10 was done after small scale continuous and batch laboratory experiments. Main parameters for the pilot plant were specific throughput and mean residence time in the permeator and electric field when splitting the emulsion. An additionally condition was: cleaning of the feed liquor from 150 to 200 ppm zinc and enrichment to about 15 g/l. With a throughput of 500 l/h waste water the column diameter is 150 mm and active column height is 6,75 m (Figure 4)

RESULTS

Crude formation. As expected no influence of suspended solids and humic materials on mass transfer was seen. However, when emulsion droplets coalesce, there is some occlusion of these materials within the organic phase. In comparison with solvent extraction a 3 to 5 times higher value was observed. Entrained crude tends to disintegrate emulsions, but addition of surfactant stops this effect. The problem is not important, since there is no further accumulation. Also splitting of emulsion is constant at 1,5 to 2,5 Wh/l emulsion, which is considered to be very low. Entrainment of dispersed organic in the raffinate is similar to solvent extraction.

Stability of extractant. Within our pilot experiments hydrolytic decomposition of the extractant, Bis-(2-ethylhexyl-)phosphoric acid (HDEHP) was observed. After some experimental work it was evident, that a combination of HDEHP, SPAN 80, and humi effluentliquors cause this effect. Therefore a test series with new extractants (phosphonic and phosphinic acids) and other surfactants is currently done. "(6)"

Mass transfer. The lay-out of the process is difficult since there are enormous differences in the entering zinc concentration. High flexibility of the plant is vital. Under constant permeation conditions you always will permeate a constant zinc quantity, regardless of the entering zinc concentration (Figure 5a, 5b). Flexibility can be reached via alteration of phase ratios and rotation speed of the impeller in the column (Figure 5). Scale-up from batch experiments to columns can be directly performed. The maximum enrichment factor of 100 in the batch experiments was exceeded in the pilot plant. For example: with a 200 (170) ppm zinc in the

entering liquor an enrichment to 45600 (37500) ppm in the resulting strip phase was achieved within one stage.

ECONOMICS

With the experiences of this pilot-plant LMP is evidently more economic than solvent extraction. This is because low level input streams can be treated with extreme phase ratios. As an example , the ratio of the waste water phase to the organic phase is about 10 to 100 and waste water phase to stripping phase is at about 50 to 500. Apparatus size and investment costs can be drastically reduced. However, this is only true at the ppm-range. So a comparison with ion exchange is more appropriate than with solvent extraction.

CONCLUSIONS

Results from labor experiments showed, that LMP is ready for an industrial use, which was confirmed by a pilot plant. In this pilot plant zinc was successfully separated from a viscose waste water stream. For this problem a column with a throughput of 1000 m^3/h is to be built in the next few years.

REFERENCES

1. Li N.N. , US Patent 3779907, 1973
2. Bouvier A., Draxler J., Marr R., Prötsch M., Proceedings 2nd world congress of chem. engin., Montreal 1981. IV, 205
3. Marr R., Kopp A., Chem. Ing. Techn. 52 (1980) 5, 399
4. Bouvier A. Thesis TU Graz 1982
5. Marr R., Prötsch M. Austrian Patent A 2170 182
6. Marr R., Draxler J., Kriechbaumer A., Chem.Ing.Techn. (in press

V_{III}/V_{II}	20	20	10	13,5
V_{III}/V_{I}	165	165	100	150
rpm	60	60	60	70
run	a	b	c	d

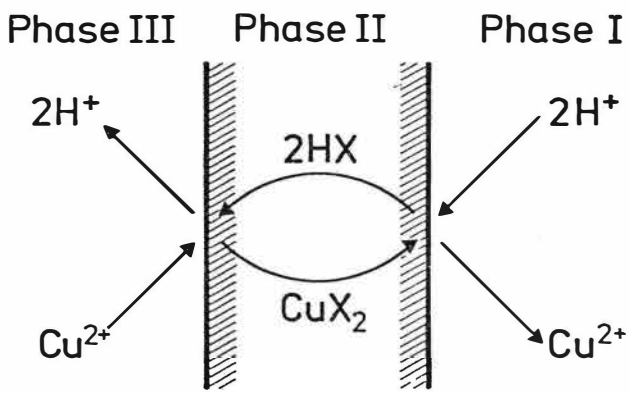

FIGURE 1. COPPER TRANSPORT MECHANISM

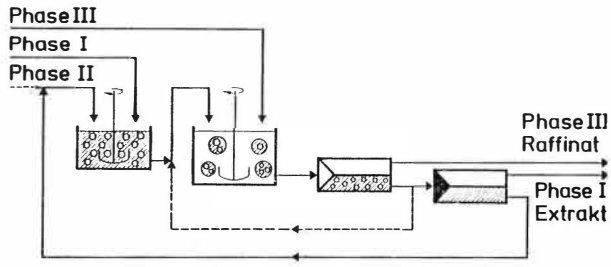

FIGURE 2. PROCESS STEPS OF A PERMEATION PLANT

Tab.1 Permeation data from continuos runs

Throughput (l/h)				feed ppm		raff. ppm		PH	
phase	I	II	III	I	II	I	II	III_{in}	III_{out}
zinc	o,25	1	30	-	180	15000	45	4	2,6
zinc	o,5	2	30	-	180	8300	32	4	2,6
zinc	o,33	o,67	30	-	1260		770	4	
tungsten	o33	o,67	30	-	284		26	4	
copper	o,33	o,67	30	-	219		186	4	
vanadium	o,33	o,67	30	-	150		53	8	

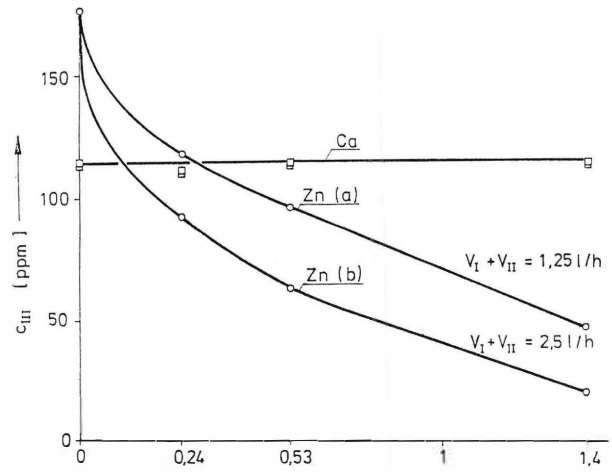

FIGURE 3. ZINC SELECTIVITY OVER CALCIUM

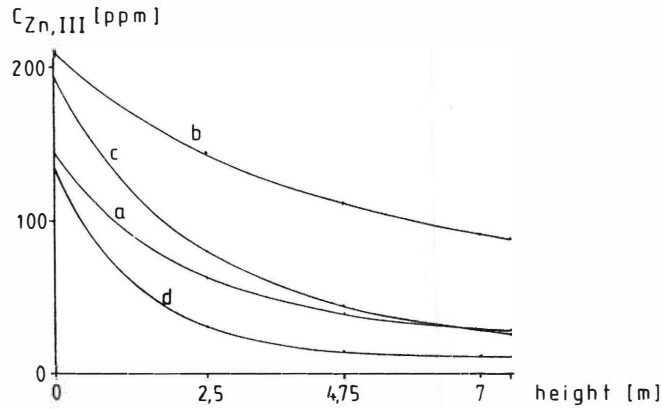

Fig.4 Variation of parameters in the pilot plant

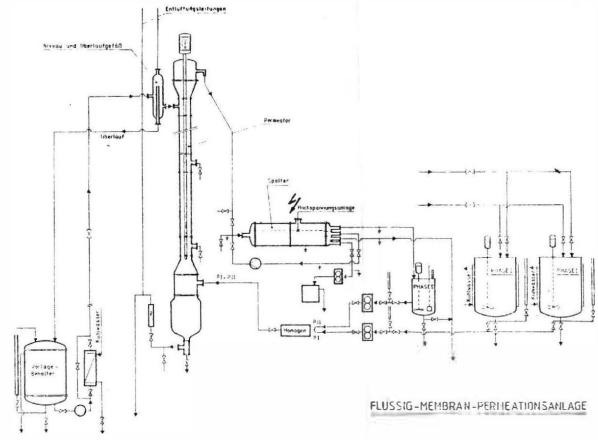

FIGURE 5. FLOW SHEET OF PILOT PLANT

SIMULATION OF THE EXTRACTANT RADIO-DECOMPOSITION IN EMULSIONS

F. Macášek, R. Čech, Ľ. Mátel

Department of Nuclear Chemistry
Comenius University
842 15, Bratislava, Czechoslovakia

CHARACTERISTIC OF LIQUID-LIQUID SYSTEMS RADIOLYSIS

The typical half-lives of radical species, except of peroxo-radicals, in solution are from the interval 10^{-7} - 10^{-5} s and their corresponding diffusion path about 10^{-6} - 10^{-5} cm (1). Therefore, very fast interfacial reactions of radicals are of great interest in the microheterogeneous systems ; biological vesicles being typical examples (2). On the other hand, for the solvent extraction systems, such extremaly developed interfacial areas are not typical and it is the mass transfer of substrates (solutes and solvents) which may become a controlling factor of radiolysis (3,4). This means that if a substrate S is attacked by radical R which is generated by irradiation from a precursor P, i.e.

(1) $P \rightsquigarrow R$

(2) $S + R \longrightarrow$ products

the reaction (2) rate is controlled

(i) by diffusion of organic substrate S to a water phase where the R is produced, or

(ii) by diffusion of hydrophilic precursor P to the organic phase.

The same substance which is a precursor in one phase can be a substrate in the second one, and vice versa. However, one phase is always acting as a "reactive" one (where both reactions (1) and (2) proceed) and the second phase merely serves as a buffer reservoir of "reactants" P and S.

The following products in reaction (2) can be considered of interest :

(a) Remarkable formation of surface-active products, at relatively low doses of the order 10^5 Gy, if they are from the class of higher carboxylic acids.

(b) The by-extractant (i.e. an extractant for impurities) formation, in a wide dose interval 10^6-10^8 Gy, where the critical (unity) distribution ratio of impurities by chelating reactions in acid medium (a_H about 1) is to be expected.

(c) Appreciable destruction (loss of 10-20 % of extraction capacity) of an extractant E, at the dose about $D=5\times10^5\ \bar{c}_E\ /G(-E)$, where G(-E) stands for the radiation yield of the destruction (molecules per 100 eV).

In any case, irradiation of components of extraction systems should be carried out both in the regime of mutual saturation and at relatively high radiation doses to obtain the expected effect as a result of extractant decomposition. Hence, it is necessary

(i) to establish the reactive phase (or the reactivity proportion of both phases), and

(ii) to consider a diffusional regime of radiolysis in the case when the phases are not sufficiently agitated.

It was demonstrated (3) that radiolysis in the presence of competing substrates can be successfully approximated in diffusion equations by a fraction-order reaction rate

(3) $r = - k_m c_S^m$

where m=1 (pseudo-first-order) for minor substrates (e.g. with a low solubility in reactive phase) and m=0 (pseudo-zero-order) for the substrates which are principal radical scavengers.

RADIOLYSIS IN EMULSIONS

In conditions of efficient phase contact the existing equilibrium is practically not disturbed by irradiation and homogeneity of reaction can be assumed (see the next part).

The gross yield ($_TG$) of substrate S radiodecomposition in such two-liquid systems (reactive phase I and buffer/reactive phase II) is as follows.

Experimentally it can be established, as substantiated in our paper (4), in the form :

(4) $_TG = 9.62\times10^9\ n/\dot{D}\ t\ V_T$ molecules/100 eV

where n is the number of moles of the product, $\dot{D}$ is the dose rate (Gy s^{-1}) for water (Fricke dosimeter), t is the time of irradiation (s) and V_T is the total volume (cm^3) of phases. Then

(5) $_TG = w\ G + z\ _{II}G\ w_{II}$

where G and $_{II}G$ = partial yields in phase I and phase II (subscripts I are omitted),

w and w_{II} = volume fractions of the phases, and

$z = \dot{D}_{II}\ \rho_{II}\ /\ \dot{D}\ \rho$ is the ratio of dose rates and densities of the phases.

The relation (5) is isomorphous with the additivity rule for radiation yields in homogeneous binary mixtures. However, in this case the ratio can differ not only due to various electrone densities of the phases but also because of various specific activities (alfa and beta) by autoradiolysis of real extraction systems. In the kinetical regime the partial yield in reactive phase is is connected with reaction rate (3) as

(6) $G = - r\ /\ f\ \dot{D}\ \rho$ molecules/100 eV

where $f=1.04\times10^{-7}$ mol eV J^{-1}.

RADIOLYSIS IN LAYERED PHASES

For reasons of experimental simplicity, the unmixed two-phase systems are often used for simulation of extraction emulsion irradiation. Such a radiolysis regime can also be closer to the one in settler parts of extraction equipment.

The diffusional flux of substrate transported from the buffer to reactive phase can be precisely calculated only by numerical methods, using the concept of pseudo-steady concentration of radicals (3). However, at a pseudo-m-th-order rate, given by Equation (3), the steady state substrate flux j into a quasi-semi-infinite layer of reactive phase can be calculated by Frank-Kamenetskii relationship (1) :

(7) $j = 10^{-3} \sqrt{2\ D_{eff}\ k_m\ \bar{c}_S^{\,m+1}\ /\ (m+1)}$ mol cm^{-2} s^{-1}

where D_{eff} = effective diffusivity of substrate S in the reactive phase, cm^2 s^{-1},

$\bar{c}_S$ = concentration of substrate at interface with buffer phase, mol dm^{-3}.

For the fraction-order kinetics, according to Zeldovich theory (1), the reactive phase layer can be considered as semi-infinite when its thickness δ reaches a critical value L , and in the case investigated it is

(8) $L \cong \sqrt{c_S\ D_{eff}\ /\ k\ f\ G\ \dot{D}}$ cm

where c_S is the concentration of a major substrate and k is a ratio of the substrate rate constants in reaction (2) to rate constant of a competing substrate (probably, k = 1). Therefore, the radiolysis will often proceed in the diffusional regime even in relatively thin unmixed layers, e.g. in typical values $D_{eff} = 10^{-5}$ $cm^2 s^{-1}$, G=1, $\dot{D}$= 1 Gy s^{-1} and $c_S=10^{-3}$ mol dm^{-3} it is at δ = 0.3 cm. Hence, the steady state which is characterized

by the exhausting of substrate in the depth of reactive phase and reached within a characteristic time $\tau = t\, D_{eff} / L^2 = 1$ (about t=2.5 hr for the previous example) will cause a remarkable decrease of G-values, obtained in the experiments with unmixed phases, down to a steady state value

$$(9) \qquad G_{st} = \frac{1}{\delta f \dot{D} \varrho} \sqrt{2\, D_{eff}\, k_m\, c_S^{*\, m+1} / (m+1)}$$

where δ = thickness of the reactive column (cm).

PHENOMENOLOGICAL COMPARISON

If the yield of a product observed is not identical with the yield of substrate decomposition, i.e.

$$(10) \qquad G(\text{product}) = \alpha\, G(-\text{substrate})$$

and $\alpha \neq 1$, then the G-values in Equations (6) and (9) will be divided by the coefficient α (to avoid a substantial correction for α, a major product should be chosen for the comparison). Now, combining Equations (6) and (9), the relation which enables a comparison of radiation yields, occured in kinetical regime (in emulsions) and steady-state regime (with unmixed phases and semi-infinite reactive column) of irradiation, is obtained (4) :

$$(11) \qquad G = \frac{f(m+1)}{2\alpha} \frac{\dot{D}\, \varrho}{D_{eff}\, c_S} (\delta\, G_{st})^2$$

For its application, knowledge of reaction rate constant is unnecessary, the m=1 or m=0 can be chosen for substrates with a low and high concentration, respectively.

The numerical proof of formula (11), obtained by computer simulation of radiolysis in various regimes (4), demonstrated that great differences between G-values obtained under various geometrical conditions could be diminished.

EXPERIMENTAL

Carbon tetrachloride (analytical grade) contacted with 0.4 M H_2SO_4 water solution in sealed glass ampules (ø 12 mm), nitrogen atmosphere, was irradiated with ^{60}Co gamma-rays at the dose rate 0.925 Gy s^{-1} and the temperature 32±2 °C. Mixing of phases was performed by rotation turning of ampules at 50 rpm. After irradiation, the ampules were cooled, opened and chloride anions were estimated by the potentiometric (argentometric) titration. The gross yield of chlorides was calculated according to formula (4).

RADIOLYSIS OF CARBON TETRACHLORIDE IN PRESENCE OF WATER

Emulsions

The overall radiation yields are given in Table 1. The partial yields were calculated from pairs of experiments at various phase ratios v and appeared to be rather close. Because the mechanism of chlorides formation at radiolysis of water solution of CCl_4 and carbon tetrachloride solution of H_2O can be quite different, the similarity seems to be accidental. The gross yields depend upon the phase ratio, as follows

$$(12) \qquad {}_TG = a - b\, w$$

where the empirical constants for different doses D are

D	a	b
3 kGy	20	12
12 kGy	11	5.9

Layered phases

The yields of Cl^- formation in unmixed, layered systems decrease markedly with the dose applied (Table 2). Because both phases are reactive and the process is limited by diffusion of water to carbon tetrachloridě and vice versa, and also the dose dependence of yields is not linear in mutually saturated phases, the interpretation of data is not easy. Inspite of it, the results of the experiments with a column of CCl_4 overlayered by a thin layer of water phase (No 4-7, Table 2) can be treated according to formula (11), supposing that ${}_TG_{st} \cong z\, {}_{II}G_{st}$ (w=0.024). Diffusion coefficients were calculated by means of Einstein-Stokes equation, approximating $r = (4\pi N_A \varrho / 3M_r)^{1/3}$, so that for H_2O in CCl_4 $D_{eff} = 1.6 \times 10^{-5}$ $cm^2\, s^{-1}$ (and for CCl_4 in H_2O $D = 7.5 \times 10^{-6}$ $cm^2 s^{-1}$). Solubility of H_2O in CCl_4 was taken to be $c_S = 8 \times 10^{-3}$ M. It was believed that the reaction order was close to zero (m=0) and each decomposition of H_2O molecules led to the formation of two molecules of HCl (α =2). Then we get

$$(13) \qquad {}_{II}G = \frac{1.04 \times 10^{-7}}{2 \times 2} \frac{(0.925)(1.59)(3.2)^2}{(1.6 \times 10^{-5})(8 \times 10^{-3})} ({}_{II}G_{st})^2 = 3.06\, ({}_{II}G_{st})^2$$

The results from a short irradiation time within the errors of estimation are the same as the ones for mixed systems. For higher doses the decrease of G-values is more pronounced. Taking the value $z\, {}_{II}G_{st} = 1.1$ (${}_{II}G_{st}$=0.53) from the experiment No 7, Table 2, we obtain ${}_{II}G$=0.86 from relation (13). If the value ${}_TG_{st}$ is corrected for the chlorides accumulated in the kinetical stage of radiolysis (within the first hour), value ${}_{II}G$=0.6 is obtained.

Despite the fact that further experiments are necessary to elucidate the α ratio and dose dependence of G-values in emulsions, the G-values received according to (13) are certainly closer to those expected in mixed systems at high doses. This confirms the idea (3) of diffusion as having a potential limiting role at the radiolysis of systems with two-liquid partitioning of substrates and being an important factor of radiation yield decrease in unmixed systems at higher doses and low solubility of substrates.

REFERENCES

1. D.A.Frank-Kamenetskii, Diffuziya i teploperedacha v khimicheskoi kinetike, 2nd ed., Nauka, Moscow 1967.
2. J.H.Fendler, J.Phys.Chem. 84, 1485 (1980).
3. F.Macášek and R.Čech, Radiat.Phys.Chem., in press.
4. F.Macášek, Radiat.Phys.Chem., in press.

TABLE 1

The gross (${}_TG$) and partial (${}_IG$ and ${}_{II}G$) radiation yields (G molecules per 100 eV) of chlorides in carbon tetrachloride emulsions, nitrogen atmosphere, T = 305 K.

Phase I : 0.4 M H_2SO_4

Phase II: CCl_4

$\dot{D}$ = 0.925 Gy s^{-1} ; z = 2.06

No	$V_I:V_{II}$	t (hr)	D (Gy)	${}_TG$	w	${}_IG$	${}_{II}G$
1	1:5	1.0	3.30×10^3	18.0±1.6	0.167	8.4	9.7
2	5:1			12.4±1.0	0.833		
3	1:5	4.0	1.30×10^4	10.2±1.6	0.167	5.3	5.5
4	5:1			7.7±0.7	0.833		

TABLE 2

Radiolysis of carbon tetrachloride in unmixed systems (as given in Table 1)

No	$V_I:V_{II}$	δ_I (cm)	δ_{II} (cm)	t (hr)	${}_TG$
1	1.0	2.0	2.0	4	10.5
2	"	"	"	96	5.5
3	"	"	"	192	4.1
4	0.025	0.08	3.2	1	23.6
5	"	"	"	4	15.4
6	"	"	"	48	2.1
7	"	"	"	96	1.1

USE OF TETRACYCLINE AS EXTRACTING AGENT FOR SOME FISSION PRODUCTS

Ieda I. L. Cunha and M. J. C. Nastasi

Radiochemistry Division
Instituto de Pesquisas Energéticas e Nucleares
Comissao Nacional de Energia Nuclear
Caixa Postal 11049 - Pinheiros
Sao Paulo - Brasil

ABSTRACT

The behavior of tetracycline as extracting agent of some fission products (^{131}I, ^{140}Ba, ^{99}Mo, ^{99m}Tc, ^{95}Zr, ^{95}Nb, ^{137}Cs, ^{103}Ru, ^{132}Te, ^{144}Ce, ^{140}La), ^{239}Np and uranium is presented.

The influence of pH of the aqueous phase upon the extraction behavior of the radioisotopes mentioned was studied.

As a practical application, the possibility of using tetracycline-benzyl alcohol system for the separation of the fission products present in their mixture, as well as for their separation from uranium, was tested.

INTRODUCTION

The antibiotic tetracycline(TC) has been used as complexing agent for several elements(1-3). One of the first applications of TC for an analytical separation was a solvent extraction procedure presented by Masters(4) for the determination of ^{90}Sr in environmental grass samples. In a further study Masters(5) verified the feasibility of application of TC to the extraction of other metallic elements.

Studies have been carried out in our laboratories concerning the behavior of TC as complexing agent for the lanthanide and actinide elements(6-13). This paper presents the studies on the use of tetracycline-benzyl alcohol system for the isolation of some fission products by means of the solvent extraction technique.

EXPERIMENTAL

U_3O_8 (2.6g) was irradiated for 100 hours in a thermal neutron flux of about $10^{12}n/s\ cm^2$ and cooled for 2 months. The irradiated U_3O_8 was dissolved with nitric acid solution and uranyl nitrate solution containing the fission products was used for the extraction experiments. The gamma-rays emitting radioisotopes present in the mixture, after 2 months cooling were ^{137}Cs, ^{140}Ba, ^{140}La, ^{144}Ce, ^{103}Ru, ^{95}Zr and ^{95}Nb.

Tetracycline hydrochloride was dissolved with benzyl-alcohol previously washed with distilled water. The extraction system was made up of tetracycline-benzyl alcohol solution and of uranyl nitrate solution. The uranium concentration was $2x10^{-3}M$ and the fission products were carrier-free. The concentration of tetracycline in benzyl alcohol was $2x10^{-2}M$.

For the determination of the extraction curves of the radioisotopes mentioned $NaNO_3$, at a concentration equal to 0.1M, was used as electrolyte in the aqueous phases. The acidity of the aqueous phases varied from 10M to $10^{-10}M$. The phases were mechanically shaked for 30 minutes at a temperature of 25.0 ± 0.5°C. The phases were separated, centrifuged and the pH's of the aqueous phases were measured. Activities of the radioisotopes were measured in a Ge-Li detector coupled to 4096-channel analyser. Concentration of uranium in both phases was determined by using the epithermal neutron activation analysis method(14). In this case use was made of a 7.5 x 7.5cm NaI(Tl) well type scintillation detector coupled to a 400-channel analyser.

For the study of the behavior of tetracycline as extracting agent of ^{99m}Tc, ^{99}Mo, ^{239}Np, ^{131}I and ^{132}Te, U_3O_8 (0.25g) was irradiated for 4 hours in a thermal neutron flux of about $10^{12}n/s\ cm^2$ and cooled for 5 days. The extraction experiments were made as mentioned before.

RESULTS AND DISCUSSION

In order to determine if benzyl alcohol would extract the ions of the elements studied by itself, extraction experiments were carried out by agitating benzyl alcohol without TC with aqueous solutions of radioactive tracers of the elements under study. These experiments showed that technetium as pertechnetate ions as well as molybdenum and iodine ions are extracted into benzyl alcohol, the extraction depending on the acidity of the aqueous phase as well as on the nature of the electrolyte present. For the other elements studied namely, zirconium, niobium, ruthenium, barium, tellurium, cerium, lanthanum, neptunium, cesium and uranium no radioactivity was detected in the organic phase, showing that benzyl alcohol alone does not extract these ions. Extraction experiments carried out in presence and in absence of TC showed that its addition into benzyl alcohol enhances molybdenum extraction in the acidity range from 10M to $10^{-9}M$; nevertheless in the case of technetium extraction the addition of TC makes difference only when the acidity of the aqueous phases is bellow 2.0M. These experiments showed also that the extraction of iodine is due only to the presence of benzyl alcohol.

Figure 1 shows the extraction curves for long lived fission products and uranium obtained for the extraction system TC-benzyl alcohol. Cesium ions are not extracted into the organic phase under the experimental conditions employed. The extraction curves presented in Figure 1 show that the separation of uranium from cesium, barium, cerium and lanthanum is feasible provided the extraction operation is carried out at a convenient pH value. The extraction of uranium in pH = 1.8 is practically complete, while barium, cesium, lanthanum and cerium are not extracted into the organic phase at this pH value. In this same pH value it is possible to separate uranium from ruthenium, since under these experimental conditions only 5% of ruthenium are extracted into the organic phase. The separation of uranium from zirconium is possible when the acidity of the aqueous phase is 2.0M. In this case 55% of zirconium are extracted into the organic phase while uranium remains in the aqueous phase. In order to obtain this separation multiple extraction operation has to be used. The same curves presented in Figure 1 show that for isolating uranium from niobium more than one extraction operation will be necessary to obtain a complete separation. In the case of separation of fission products it is simple to obtain separation of barium from zirconium, niobium, cerium, lanthanum, ruthenium and cesium by a proper choice of the pH value at which the extraction operation is to be carried out. From Figure 1 it can be seen that barium can be isolated from ruthenium and cesium if the extraction operation is carried out at pH 9.0. Barium is quantitatively extracted into the organic phase while at this pH value ruthenium and cesium remain in the aqueous phase. For the separation of barium from the other fission products the extraction operation is carried out at pH 4.5. At this pH value extraction of cerium, zirconium, niobium and lanthanum into TC-benzyl alcohol is practically complete while barium is not extracted into the organic phase. From the extraction curves of Figure 1 it can be seen that separation of cerium and lanthanum from zirconium and niobium, can be achieved provided the extraction operation is carried out at a pH 1.7. In this case cerium and lanthanum remain in the aqueous phase while 90% of zirconium and 65% of niobium are extracted into the organic phase. The extraction curves of Figure 1 show also that a single extraction operation is not enough to separate cerium from lanthanum neither zirconium from niobium. In order to obtain these separations multiple countercurrent extraction procedures have to be used. Separation of ruthenium from cerium and lanthanum is performed when the pH of the aqueous phase is 9.0. Cerium and lanthanum are quantitatively extracted into the organic phase while ruthenium remains in the aqueous phase. For the separation of ruthenium from zirconium and niobium the pH of the aqueous phase must be kept at 1.8. Zirconium and niobium are extracted into the organic phase while only 5% of ruthenium are extracted under the experimental conditions employed.

Figure 2 shows the extraction curves for short-lived fission products and uranium obtained for the extraction system TC-benzyl alcohol. Tellurium ions are not extracted into TC-benzyl alcohol solutions. Figure 2 shows that the fission

products ^{99}Mo and ^{99m}Tc can be separated from uranium. Within the acidity range from 2.0 to 8.0M, the extraction of these radioisotopes is of about 60% while uranium is not extracted. In this same experimental condition it is possible to separate uranium from iodine since iodine is quantitatively extracted into the organic phase. The extraction curves presented in Figure 2 show that the separation of uranium from tellurium and neptunium is possible. At pH 1.7 the extraction of uranium is nearly complete while tellurium and neptunium are not extracted. The separation of neptunium from tellurium is possible when the pH of the aqueous phase is kept within the range from 4.0 to 6.0, since the extraction of neptunium is higher than 80% while tellurium is not extracted. For the separation of neptunium from technetium, molybdenum and iodine, the acidity of the aqueous phase must be kept above 10^{-1}M. Neptunium remains in the aqueous phase while the other radioisotopes are extracted into the organic phase. It can be seen in Figure 2 that separation of technetium and molybdenum from iodine would only be possible by use of a multi-stage extraction procedure. The extraction curves for technetium and molybdenum are too close one to the other to allow the separation of both elements using the system TC-benzyl alcohol.

Based on all information obtained from extraction experiments it is seen that the tetracycline-benzyl alcohol system can be used for isolating fission products present in their mixture, as well as for the separation of uranium from some fission products.

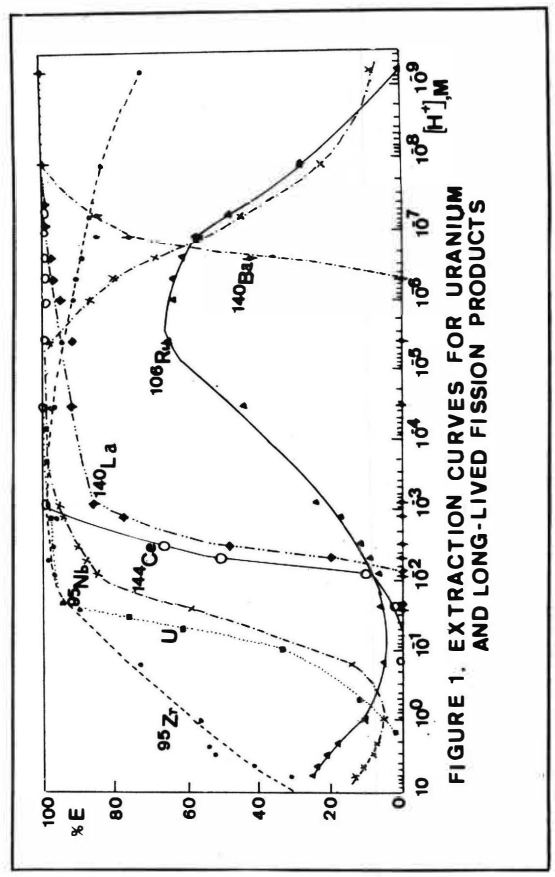

FIGURE 1. EXTRACTION CURVES FOR URANIUM AND LONG-LIVED FISSION PRODUCTS

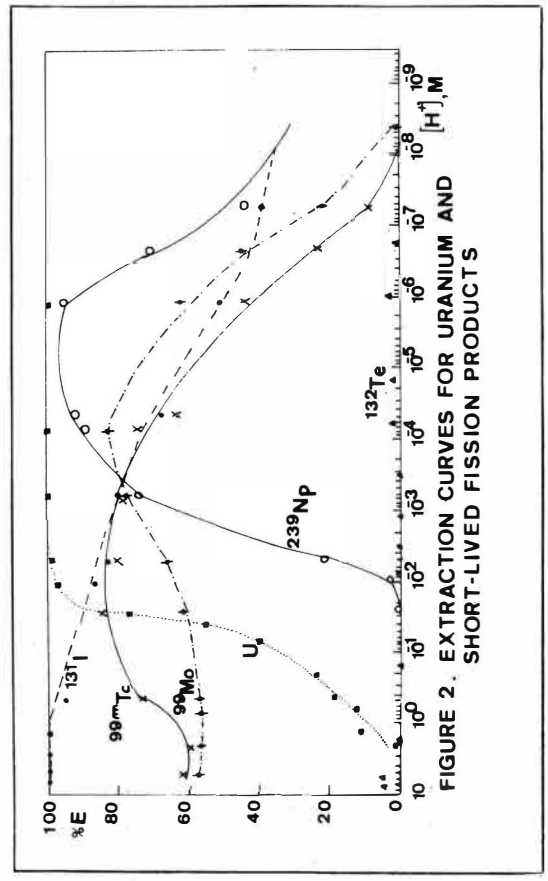

FIGURE 2. EXTRACTION CURVES FOR URANIUM AND SHORT-LIVED FISSION PRODUCTS

REFERENCES

1. A.Albert, C.W.Rees. Nature 177, 433 (1956).
2. J.T.Doluisio, A.N.Martin. J.Med.Chem.6, 16 (1963).
3. D.C.Maxwell, J.A.Wilford. Nature 198, 577 (1963).
4. L.W.Masters. Washington, D.C., American University (1968) (M.Sc.Thesis).
5. L.W.Masters. In: La Fleur, P.D. ed. NBS technical note 508. Washington, D.C. NBS (1970) p. 115 (Activation Analysis section).
6. M.J.C.Nastasi, F.W.Lima. Radiochem.Radioanal.Lett. 29, 61 (1977)
7. M.Saiki, F.W.Lima. Radiochem. Radioanal. Lett. 29, 67 (1977).
8. M.Saiki, F.W.Lima. Radiochem. Radioanal. Lett. 30, 1 (1977).
9. M.Saiki, F.W.Lima. J.Radioanal.Chem. 36, 435 (1977).
10. M.Saiki, F.W.Lima. Radiochem. Radioanal. Lett. 35, 53 (1978).
11. M.Saiki, F.W.Lima. Radiochem. Radioanal. Lett. 35, 63 (1978).
12. M.Saiki, F.W.Lima. J.Radioanal. Chem. 50, 77 (1979).
13. M.Saiki, M.J.C.Nastasi, F.W.Lima. J.Radioanal.Chem. 64, 87 (1981).
14. L.T.Atalla, F.W.Lima. J.Radioanal.Chem. 20, 507 (1974).

ACKNOWLEDGEMENT

The authors are grateful to the Brazilian Comission of Nuclear Energy who partly sponsored the present work.

SYNERGISTIC EXTRACTION OF PLUTONIUM AND AMERICIUM BY BIFUNCTIONAL ORGANOPHOSPHORIC REAGENTS

Anthony C. Muscatello, James D. Navratil and Milton E. Killion

Rockwell International Rocky Flats Plant
P.O. Box 464
Golden, Colorado 80402-0464 USA

INTRODUCTION

The extraction chemistry of bifunctional organophosphorus compounds is currently under investigation at the Rocky Flats Plant in support of actinide recovery process development and americium purification processes(1-3). Previous reports from this laboratory have described the extraction behavior of americium and plutonium with DBDECMP (dibutyl-N,N-diethylcarbamoylmethylphosphonate) plus TBP (tri-n-butyl phosphate)(4), and americium with DBDECMP and DBDECP (dibutyl-N,N-diethylcarbamoylphosphonate) plus TBP(5). Addition of TBP to DBDECMP increased the distribution ratio of both plutonium and americium and a small but significant synergistic effect was observed. This paper further describes the results of experiments using concentration dependencies to determine the extraction mechanism for a variety of mixed extraction systems: DBDECP, DHDECMP (dihexyl-N,N-diethylcarbamoylmethylphosphonate) and OØD(IB)CMPO (octylphenyl-N,N-diisobutylcarbamoylmethylphosphine oxide) in combination with one or more of TBP, TOPO (trioctylphosphine oxide), DB[BP] (dibutylbutylphosphonate) and DBP (dibutylphosphate).

EXPERIMENTAL

Reagents and procedures were described previously(4,5) with the following exceptions. TOPO (reagent grade) was supplied by Eastman Kodak Co. DB[BP] was 95 percent pure material from K & K Laboratories. DBP was a 50-50 mixture with the monobutyl ester from K & K Laboratories (technical grade). DHDECMP was 84 percent pure material free from acidic compounds obtained from Bray Oil Co. OØD(IB)CMPO was synthesized and kindly supplied as a 95 percent pure liquid by E. P. Horwitz of the Argonne National Laboratory.

D values were calculated by dividing the americium or plutonium concentration in the organic phase by the corresponding actinide concentration in the aqueous phase. Material balances were better than 95 percent. Average deviation in D values of duplicate experiments was 10 percent.

RESULTS AND DISCUSSION

Extraction of Americium (III). The results of the extraction of americium (III) by DBDECP as a function of the concentration of TBP, TOPO, DB[BP] and DBP are shown in Figure 1. The log-log plots all have the same general shape, gradually increasing with added extractant concentration except for TOPO. Other experiments show the dependency on DBDECP concentration is third power either with or without added extractants. However, the distribution coefficients are greater than D_0, the distribution coefficient in the absence of added extractant, only at the highest concentrations of TBP, DBP, and DB[BP] studied. D-values for TOPO are greater than D_0 at all concentrations from 7M HNO_3. However, extraction by TOPO alone is not negligible. After correction, the net extraction of americium is also less than D_0.

A possible explanation for the antagonistic behavior of TBP, DBP, TOPO, and DB[BP] is that DBDECP is bidentate and the three DBDECP molecules and the three nitrate ions completely fill the americium coordination sphere, leaving no room to add the monofunctional extractant.

Figure 2 shows the effect of TBP on the extraction of americium (III) by OØD(IB)CMPO. The dependency on OØD(IB)CMPO concentration is approximately third power from 7M HNO_3, slightly less (~2.5) from 0.35M HNO_3 at a constant concentration of TBP (0.3M). The dependence on TBP concentration at constant [OØD(IB)CMPO] at 0.35M HNO_3 is small with little enhancement in extraction. At 7M HNO_3, the dependence approaches first power, with a large enhancement above D_0. The indicated formula for the extracted complex is $Am(NO_3)_3(OØD(IB)CMPO)_3(TBP)$.

Table I shows the results of some extractions of Am(III) with DHDECMP plus TBP and DB[BP]. The largest synergistic enhancement for TBP is found at the highest ratio of TBP to DHDECMP, similar to the results given above and to previously studied systems (4,5). For the single combination of DHDECMP and DB[BP] studied, a synergistic enhancement similar to that for TBP occurs.

TABLE I

DISTRIBUTION RATIO DATA FOR AMERICIUM AND PLUTONIUM WITH DHDECMP, TBP, DB[BP], DHDECMP + TBP, and DHDECMP + DB[BP] IN DIISOPROPYLBENZENE

AQUEOUS PHASE	CONC. DH-TBP	D^{DH}_{Am}	D^{TBP}_{Am}	D^{DH+TBP}_{Am}	SYNERGISTIC FACTOR
7M HNO_3+ 0.01g/ℓ Am	0 - 1.00M		0.0006		
	0.25-0.75	0.286±0.001	-	0.667±0.056	2.3
	0.50-0.50	2.82±0.16	-	4.38±0.38	1.6
	0.75-0.25	8.57±0.15	-	10.5±0.4	1.2
	1.00-0	25.1±6.3			
0.2M HNO_3+ 0.01g/ℓ Am	0 - 1.00M		0.00225		
	0.25-0.75	0.0123±0.0007	0.0009	0.0349±0.0004	2.6
	0.50-0.50	0.101±0.003	-	0.132±0.008	1.3
	0.75-0.25	0.260±0.008	-	0.306±0.010	1.2
	1.00-0.0	0.569±0.017	-		

TABLE I (cont)

AQUEOUS PHASE	CONC. DH-DB[BP]	D^{DH}_{Am}	$D^{DB[BP]}_{Am}$	$D^{DH+DB[BP]}_{Am}$	SYNERGISTIC FACTOR
7M HNO_3+ 0.01g/ℓ Am	0.50-0.50M	2.41±0.05	<0.007	3.60±0.30	1.5
0.35M HNO_3+ 0.01g/ℓ Am	0.50-0.50M	0.0355±0.0004	<0.006	0.103±0.003	2.9

AQUEOUS PHASE	CONC. DH-DB[BP]	D^{DH}_{Pu}	$D^{DB[BP]}_{Pu}$	$D^{DH+DB[BP]}_{Pu}$	SYNERGISTIC FACTOR
7M HNO_3+ 0.10g/ℓ Pu	0.50-0.50M	111±6	194±2	39.6±2.5	0.13
0.35M HNO_3+ 0.10g/ℓ Pu	0.50-0.50M	14.2±0.8	46.9±6.0	17.0±1.2	0.28

In our previous study(5), shifts in infrared absorption of the phosphoryl bond indicated that TBP was bound directly to the americium ion in the extracted mixed complexes with DBDECMP. The similarity in the distribution data given here indicates that a similar mechanism would hold for the OØD(IB)CMPO and the DHDECMP mixed systems.

Extraction of Plutonium (IV). Figure 3 summarizes the results of the extraction of plutonium with DBDECP as a function of the concentration of added extractant. All the curves show a small dependence of extraction on the concentration of the monofunctional extractant with D-values somewhat greater than D_0. However, after subtracting the contributions to the extraction by the DBDECP and by the monofunctional compound, the results are very different, except for TBP, where the net extraction is a factor of 8 to 9 greater than the sum of two extractants independently. For added DB[BP], TOPO, and DBP the extraction of plutonium is greater than the sum of that by the mixed extractants alone, only from 7M HNO_3 and at the lower concentrations of DB[BP], TOPO, and DBP.

A possible explanation for this antagonistic behavior is that complexes form between the DBDECP and the added extractants, lowering the effective concentrations of both components. This is consistent with the results given above for americium where lower than expected extraction is observed also.

Figure 4 illustrates that similar results are found for the extraction of plutonium by OØD(IB)CMPO plus TBP. Here too, subtraction of the contributions of the individual extractants results in negative net extraction. Table 1 shows that a similar decrease in extraction of plutonium occurs when DHDECMP is combined with DB[BP]. Apparently, complexes between OØD(IB)CMPO and TBP form, but in this case, the complexes do not interfere with the extraction of americium.

Third Phase Formation. Mixing DHDECMP or similar compounds in n-dodecane and nitric acid usually results in the formation of third (organic) phases. However, a solution of 40 vol % TBP with 20 vol % DHDECMP in n-dodecane maintains a two-phase system when contacted with 5M HNO_3. The 30-40 vol % TBP appears to be critical since 5M HNO_3 contacts of solutions with 10 or 20 vol % TBP plus 20, 30, or 40 vol % DHDECMP did produce third phases.

SUMMARY

We have studied the extraction chemistry of plutonium (IV) and americium (III) from 0.35M and 7M nitric acid using the bifunctional organophosphorus compounds DBDECP and OØD(IB)CMPO, each in combination with one or more of TBP, DB[BP], TOPO, and DBP. Synergistic enhancement of extraction of both plutonium and americium occurs as well as antagonistic decrease of extraction under some conditions. Concentration dependencies suggest a simple adduct formation for the extraction mechanism.

The DHDECMP+TBP and OØD(IB)CMPO systems will be evaluated for actinide recovery and americium purification processes at the Rocky Flats Plant. The use of mixed extractants permits lower solvent inventory of the expensive bifunctional extractants. Furthermore, aliphatic diluents such as kerosene and n-dodecane can be used without the formation of third-phases.

REFERENCES

1. J. D. Navratil and G. H. Thompson, Nucl. Technol. 43, 136 (1979).
2. J. D. Navratil, L. L. Martella, and G. H. Thompson, in Actinide Separations, J. D. Navratil and W. W. Schulz, Eds., American Chemical Society, Washington, D. C., 1980, p. 455.
3. W. I. Yamada, L. L. Martella, and J. D. Navratil, J. Less Common Metals 86, 211 (1982).
4. J. D. Navratil and L. L. Martella, Sep. Sci. Technol. 16, 1147 (1981).
5. A. C. Muscatello, J. D. Navratil, and M. E. Killion, Solv. Extn. Ion Exch., in press.

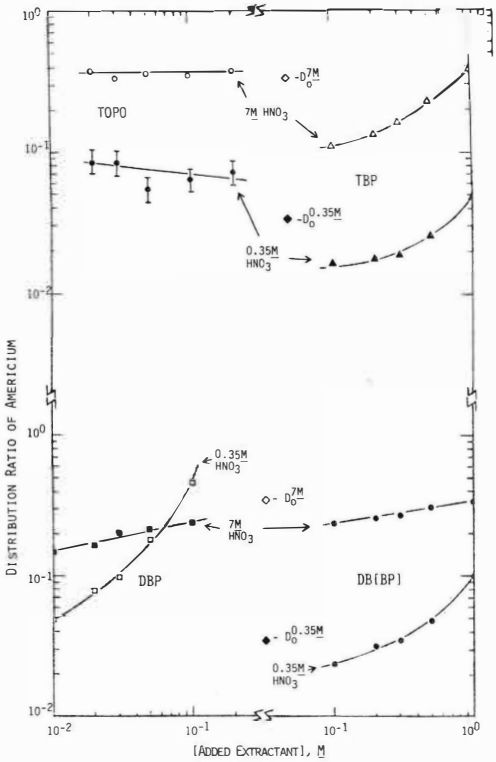

FIGURE 1. EXTRACTION OF AMERICIUM WITH 0.315M DBDECP IN CCl_4

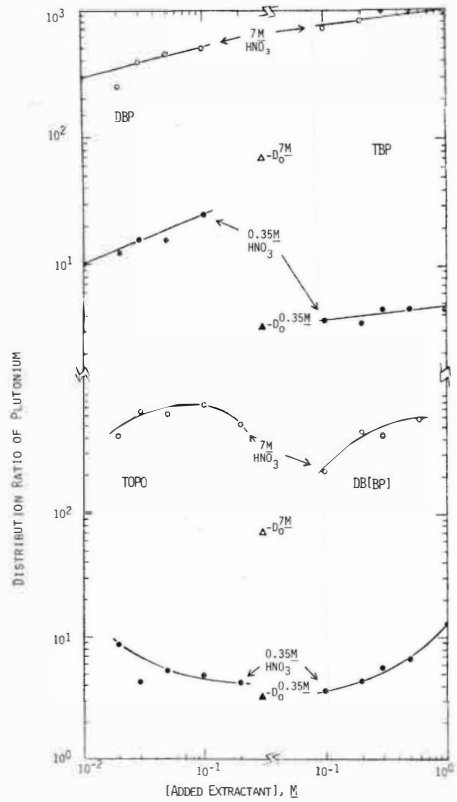

FIGURE 3. EXTRACTION OF PLUTONIUM WITH 0.315M DBDECP IN CCl_4

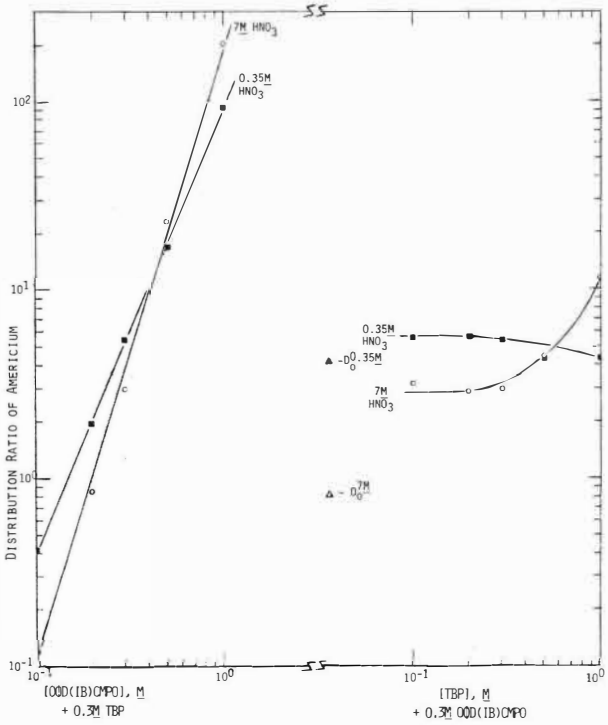

FIGURE 2. EXTRACTION OF AMERICIUM WITH OOD(IB)CMPO PLUS TBP IN CCl_4

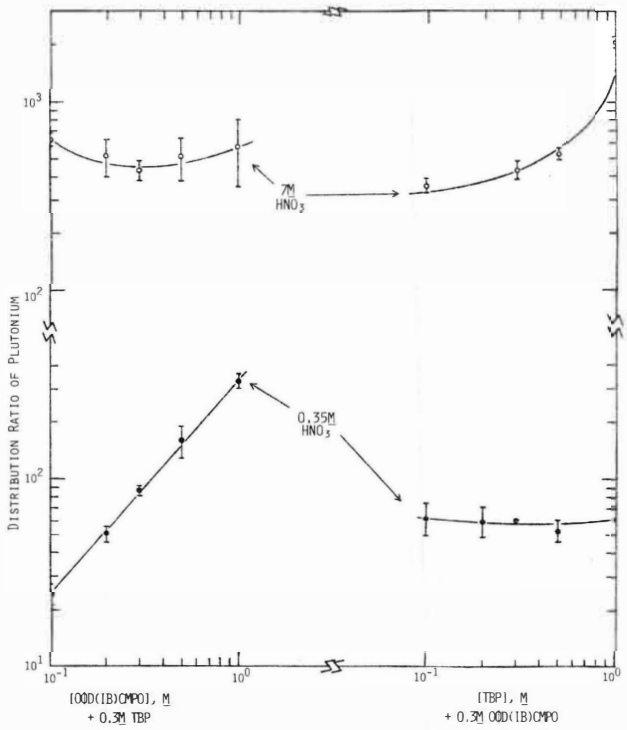

FIGURE 4. EXTRACTION OF PLUTONIUM WITH OOD(IB)CMPO PLUS TBP IN CCl_4

EXTRACTION OF FISSION PRODUCTS WITH AMINES

Manfred Beer, Brunhilde Gorski

Academy of Sciences
Central Institute for Isotope and Radiation Research
Leipzig; GDR

For the separation of Pd, Tc, and Rh from nitric acid solutions of fission products and noble metal wastes tertiary amines seem to be suitable extractants. Basic research with trioctylamine (TOA) leads to suggestions of processes, parts of which have been tested successfully in laboratory scale (1,2).

Elaborating practicable processes we ought to use only low-priced amines (3). Their selection requires assurence of equivalent or better properties in reference to extraction, solubility, and phase separation besides availability from possibly alternative sources.

The commercially available cheapest intermediates and by-products of detergent synthesis

A	$R\text{-}NH_2$	with	1	$R = C_6/C_9$ -
B	$R_2N.H$	or	2	$R = C_{10}/C_{14}$ -
C	$R\,N(CH_3)_2$	or	3	$R = C_{16}/C_{18}$ -

are not practicable because of low solubility of their nitrates in commercial aliphatic and aromatic diluents. Another dimethylamino-paraffin product, the dimethylamino group of which is distributed statistically at the carbon atoms of the paraffin, shows sufficient solubility. But it reduces Pd to the metal even after careful distillation or washing procedures (olefines).

In the row of the conceivable resultant product amines which can be synthesized from the chemicals upper cited the methyl-di-alkylamines $R_2N\text{-}CH_3$ (MDAA) deserve particulary interest because

- methylation of $R_2N\text{-}H$ leads to tertiary amines with good solubility and relatively low viscosity.
- methylation causes only low increase of molecular weight and keeps high concentration of N, i.e. high capacity per mass unit of amine.
- methylation is the mostly simple industrially used alkylation process.

The first MDAA we sythesized by reaction of the amine B 2 with dimethylsulfate (DMS). The determination of Pd extraction (Pd we have used as an indicator causing the most problems and having the smallest distribution coefficient D_{Pd} in the interesting system) showed remarkable higher extraction power than TOA. At first we supposed that to be a structural effect of the methyl group in constellation with two long-chained alkyl groups.

But comparsion of solutions of analytical pure freshly distilled in vacuo TOA and MDOA (methyl-dioctylamine) did not verify this assumption (Figure 1a,b). Both pure amines in 0,1... 0,5 M solutions show almost equal dependence of D_{Pd} from HNO_3 and Pd concentrations. Only at very low Pd concentrations TOA gives an increase of D_{Pd} which is difficult to explain. On the contrary the synthesized mixture of MDAA even at 0,1 M concentration shows D_{Pd} values which in the whole investigation interval are more than 10 times greater than those of TOA and MDOA in 0,5 M solution.

The next assumption was that we took too much or too less of DMS for methylation in consequence of wrong analyses of primary and secondary amine content of the industrial product and therefore got a mixture containing secondary amines respectively quarternary ammonium salts or hydroxids (QAS) besides the tertiary amines.

Although the QAS are known to be not distillable we tried to exclude quarternisation and synthesized the methyl product by means of the reductive alkylation (LEUCKART-WALLACH-reaction, LW). We got a product with the same range of boiling points and the same average molecular weight. It did show lower D_{Pd} values than the DMS product but, nevertheless, with 0,1 M solution they were throughout nearly as high as with 0,5 M TOA or MDOA solutions. The shape of the curve of the dependence from Pd concentration also differed from them.

The same increasing effect of MDAA mixtures we could observe at methylation products of longer and shorter chained secondary amines B1 and B3. (But that of B3 shows insufficient solubility). The extremely high effect in case of DMS methylation seems to occur only in case of excess of DMS. In all other cases we did find only little differences between DMS and LW methylation (MDAA IV in Figure 2).

The shape of the curves of D_{Pd} over Pd concentration of the several MDAA points out the influence of different amounts of a substance besides the MDAA which either acts synergistic or has a significant higher D_{Pd} than the tertiary amine in question. Synergistic effects with amine mixtures have been cited (3).

We compared the effect of partially substitution of a LW product by its secondary amine and couldn't find any change of D_{Pd} at $[Pd] = 10^{-3}$ M up to 30 % substitution. However partial methylation (10 %) of the same LW product with DMS and transferring to the NO_3^-- form increased D_{Pd} more than 5 times.

Comparing with Pd the Tc extraction shows the same effect (Figure 2b). The extraction of Rh from nitrate solutions containing nitrite (4) is not altering essentially if we change from pure to commercial amines.

In opposite to our knowledge thus far we must consider that high molecular tertiary amines, even after correct distillative purification contain little amounts of QAS which can cause serious changes in extraction dates of several elements. This also seems to be the case with amines which are not produced by direct methylation (e.g. TOA). Commercial, in industrial scale produced amines which are synthesized from starting materials with broader interval of boiling points contain not only traces of QAS (e.g. Alamine). This effect can get dominating influence on extraction behaviour of an element and must be considered before development of practicable processes.

Literature

(1) F. MACASEK, P. RAJEC, V. MICULEJ, R. KOPUNEC, P. CECH Proc. IV Symposium of SEV in Karlovy Vary, Prague 1977, Vol. II, 188

(2) B. GORSKI, M. BEER, M. RICHTER, M. HENNRICH, K. ZIEGER Proc. V Symposium of SEV in Marianske Lazne, Prague 1981, Vol. III, 304-23

(3) V.S. SCHMIDT Ekstrakzija Aminami, Atomisdat, Moskva 1980

(4) M. BEER, B. GORSKI, L. RUSS Paper at XXXIII. Berg- und Hüttenmännischer Tag, Freiberg 1982

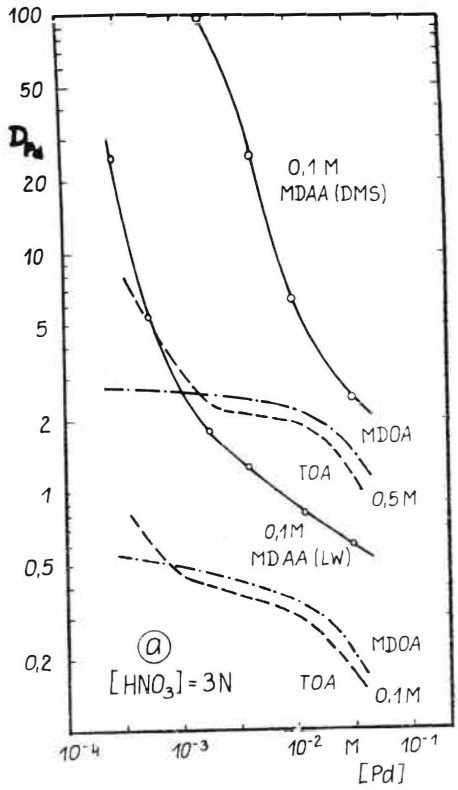

Fig. 1a D_{Pd} = f [Pd] with TOA, MDOA and MDAA in toluen

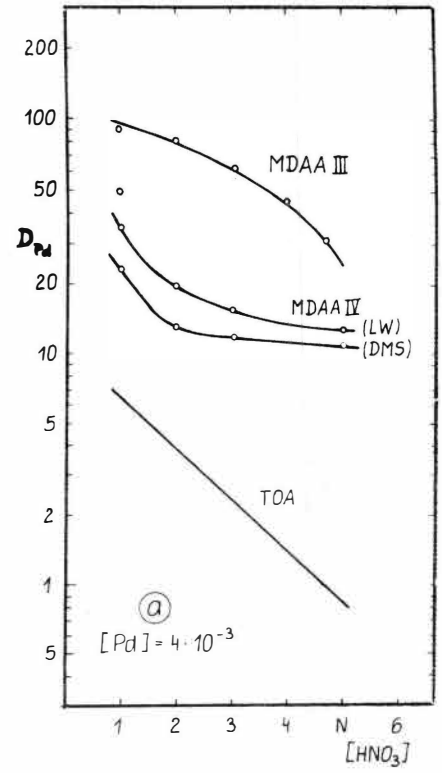

Fig. 2a D_{Pd} = f [HNO_3] with 0,5 M amines (in toluen, alkyl- = C_6/C_9)

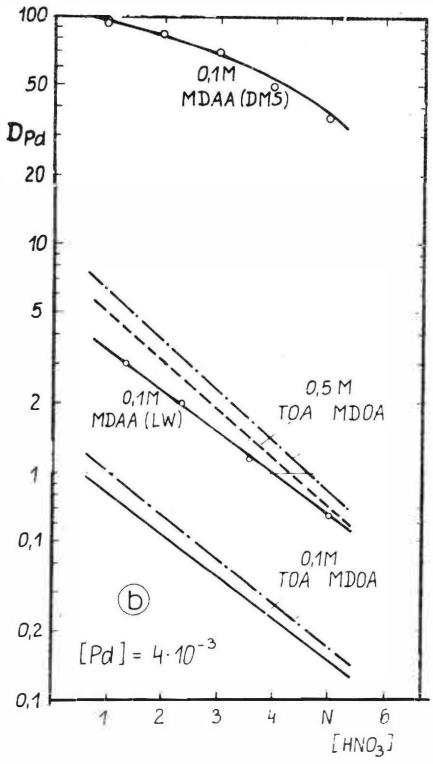

Fig. 1b D_{Pd} = f [HNO_3] with amines (like in 1a) (alkyl- = C_{10}/C_{14})

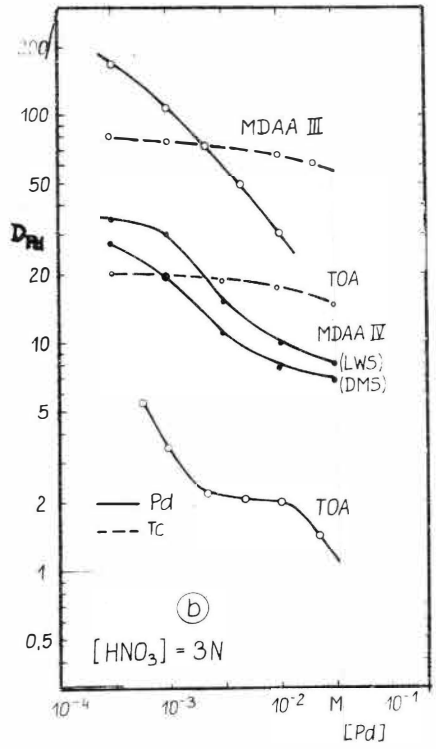

Fig. 2b D_{Pd} = f [Pd] resp. [Tc] with 0,5 M amines (diluent and alkyl- like 2a)

SOME REDOX REACTIONS OF URANIUM AND PLUTONIUM IN A SYSTEM INVOLVING TRIBUTYL PHOSPHATE (TBP) IN DODECANE AND AN AQUEOUS NITRATE SOLUTION

S. Tachimori and Z. Kolarik

Institute of Hot Chemistry, Nuclear Research Centre
Karlsruhe, Federal Republic of Germany

Uranium(IV) nitrate is used as a reducing agent for plutonium(IV) in the separation of Pu from U in the Purex process. Knowledge of oxidation kinetics of U(IV) in extraction systems involving TBP is useful, if conditions are sought under which a good separation efficiency is attained. We studied the oxidation of U(IV) in liquid-liquid dispersions and in a separate loaded organic phase.

OXIDATION OF U(IV) BY AIR OXYGEN IN LIQUID-LIQUID DISPERSIONS

The organic phase was a 30 vol.% solution of TBP in dodecane, loaded to <20% of its capacity with U(IV) nitrate and also containing nitric acid. The aqueous phase contained U(IV) nitrate, nitric acid, hydrazine nitrate, and in some cases also Pu(III) or V(IV) nitrates. All experiments were performed at 25.0°C without light access. As shown in (1), the oxidation of U(IV) in the absence of air is extremely slow (there is almost no change of the U(IV) concentration during 7 h) but air, sparged through the dispersion, oxidizes U(IV) at a moderate, well measurable velocity.

Oxidation in the absence of foreign metal nitrates. To check the reproducibility of results reported in (1), we first repeated some of the experiments described therein. For the repetition we took two new stock solutions of U(IV) nitrate. The oxidation of U(IV) in the repeated experiments obeyed the same rate equation as the results reported previously (1), namely

$$(1) \qquad C^{*}_{U4,init} - C^{*}_{U4,t} = kt \quad \text{with } k = a(C_H^b + cC_H^d)^{-1},$$

where $C^{*}_{U4,init}$ = the sum of the equilibrium molar concentrations of U(IV) in the organic and aqueous phases at zero reaction time,

$C^{*}_{U4,t}$ = the same sum of concentrations at a reaction time t (given in hours), and

a, b, c and d = parameters.

However, if one of the two stock solutions of U(IV) nitrate (solution A) was taken for the experiments, the oxidation of U(IV) was much faster than observed previously (1). This is documented by the comparison of the corresponding dependences of log k on log C_H in Figure 1 (curves 1 and 3). With the other stock solution of U(IV) nitrate (solution B) used in the repeated experiments, a comparable oxidation kinetics was found as in (1): compare curves 2 and 3 in Figure 1. The solution of U(IV) nitrate used in the previous work (1) and the solutions A and B used in this work differed in details of the progress of their preparation. All of them were prepared by electrolytic reduction of U(VI) in a solution containing uranyl nitrate, nitric acid and hydrazine nitrate. Hydrazine nitrate was almost completely destroyed during the preparation of the solution A, nitric acid was destroyed during the preparation of the solution used in (1), and none of these components was destroyed to a large extent during the preparation of the solution B. The solution A, although stable during several weeks if kept in a refrigerator without access of air and light, probably contained as far unspecified components formed during the electrolytic reduction of U(VI) and destabilizing U(IV).

Oxidation in the presence of Pu(III) nitrate. Pu(III) has been shown to suppress the rate of the oxidation of U(IV) by air (1). In this work we extended the study for investigating the effect of the Pu(III) concentration. The stock solution B was used as a source of U(IV). The decelerating action of Pu(III) was confirmed but, surprisingly, found to be independent of the Pu(III) concentration in the range 0.001 - 0.01M. The kinetics of the oxidation of U(IV) can again be described by equation (1), in agreement with previous results (1), but a somewhat faster reaction was observed in this work than in (1): compare the corresponding dependences of log k on log C_H obtained with and without Pu(III) present (curves 2, 2a, 3 and 3a in Figure 1).

Oxidation in the presence of V(IV) nitrate. Vanadium(IV) decelerates the oxidation of U(IV) by air more strongly than Pu(III). At initially 0.016 - 0.08M U(IV), 0.04 - 0.2M nitric acid, and 0.001M V(IV) in the auqeous phase, the oxidation rate can approximately be described as

$$(2) \qquad dC^{*}_{U4}/dt = 0.0056(C^{*}_{u4})^{2.4}/C_H^{2.0}$$

Variation of the V(IV) concentration from 5×10^{-4} to 0.005M indicated the reaction order to be -1 with respect to V(IV).

OXIDATION OF U(IV) IN SEPARATE ORGANIC PHASE

All experiments were performed in an initially 30 vol.% solution of TBP in dodecane, without access of air and light, and at 25°C. Without any foreign metals present or without any addition of nitrous acid, U(IV) is stable in the separate organic phase: its concentration remains unchanged for several hours and an autocatalytic oxidation starts as late as after 10 h (1). In the presence of Pu(III) nitrate the induction time is significantly or even completely suppressed and the autocatalytic reaction is accelerated. V(IV) nitrate has no effect on the stability of U(IV) in the separate organic phase.

Oxidation of U(IV) by nitrous acid in the absence of Pu(III). Independent portions of the organic phase were loaded with the reaction components, one of them with U(IV) nitrate and nitric acid and the other with nitrous acid, by contacting with aqueous solutions. After the separation from the aqueous phase the portions were mixed (reaction time zero) and the concentrations of U(IV) and both acids were measured as functions of the reaction time. Contrary to data reported in (2), at <0.6M nitric acid and 0.03 - 0.12M nitrous acid the oxidation of U(IV) was slow, with a half-time of ≥10 h and with little tendency to an autocatalytic acceleration. The reaction order with respect to U(IV) was one. Reaction orders with respect to nitric and nitrous acids could not be determined, because the reproducibility of the results was rather poor and none of the acids seemed to influence significantly the oxidation kinetics.

Oxidation of U(IV) in the presence of Pu(III). The organic phase was loaded with U(IV) nitrate, nitric acid, and a small amount of Pu(III) nitrate by contacting with an aqueous solution of an appropriate composition, also containing hydrazine nitrate. The end of disperging the phases was taken as the zero reaction time for the oxidation of U(IV). Nitrous acid was not added. After discharging the aqueous phase, the U(IV) concentration was measured as a function of the time. The analytical concentration of Pu was determined after complete oxidation of U(IV) and the concentration of nitric acid was determined once to three times during the oxidation or only after the oxidation. The initial concentration of U(IV) was 0.03 - 0.08M.

Examples of the time dependence of the U(IV) concentration are given in Figures 2 and 3. They illustrate the effect of the

concentrations of nitric acid and Pu(III) on the course of the oxidation. An increase of the concentration of one of these components suppresses the induction period and accelerates the autocatalytic reaction, but does not necessarily enhance the oxidation rate after the induction period and the autocatalytic acceleration. At >0.001M Pu(III) the induction period is almost eliminated and the oxidation kinetics is little influenced by variations of the concentrations of Pu(III) and nitric acid. Such an insignificant influence of the initial acid concentration on the oxidation kinetics of U(IV) has already been observed in the reaction of U(IV) with air oxygen in a separate organic phase (1). After the induction period and after the autocatalytic acceleration, the oxidation approaches a reaction order of 1 with respect to U(IV). The reciprocal of the total time (i.e. also including the induction period) needed for the oxidation of 50% of the initial U(IV) amount is a linear function of the concentrations of Pu(III) and nitric acid, indeed at <0.0015M Pu(III) only.

CONCLUSIONS

The oxidation of U(IV) in the liquid-liquid dispersion and the separate organic phase differ in such important aspect as the reaction order, the influence exhibited by Pu(III) on their velocity, and the tendency to have an autocatalytic character. The autocatalytic character is ascribed to the absence of the virtually unextractable hydrazine nitrate in the separate organic phase, where nitrous acid is not prevented to accumulate. In the dispersion, any small amount of nitrous acid formed during the oxidation of U(IV) is immediately decomposed by excess hydrazine nitrate present in the auqoeus phase. A mathematical treatment of the oxidation kinetics of U(IV) is attempted.

REFERENCES

1. Z. Kolarik, J. Inorg. Nucl. Chem. 43, 1633 (1981).

2. A. L. Slade, Report DP-554 (1961).

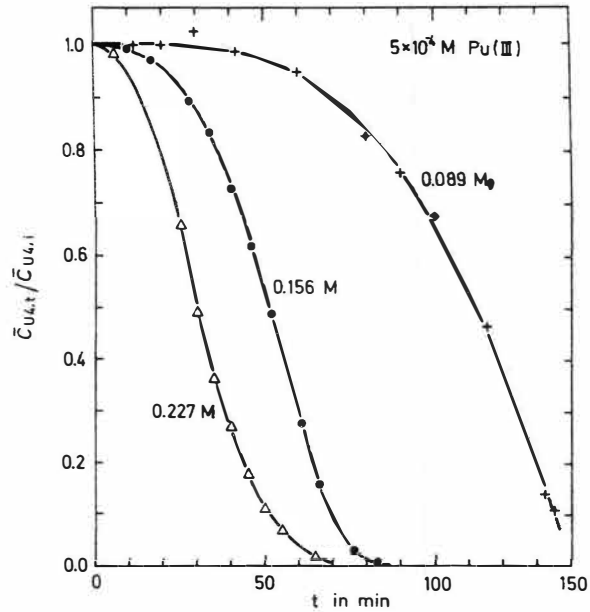

FIGURE 2. OXIDATION OF U(IV) IN A SEPARATE ORGANIC PHASE AT 25°C: DEPENDENCE OF THE RELATIVE CONCENTRATION OF U(IV) ON THE REACTION TIME AT A CONSTANT INITIAL CONCENTRATION OF Pu(III) AND DIFFERENT INITIAL CONCENTRATIONS OF NITRIC ACID

Subscripts t and i denote concentrations at reaction times t and zero respectively

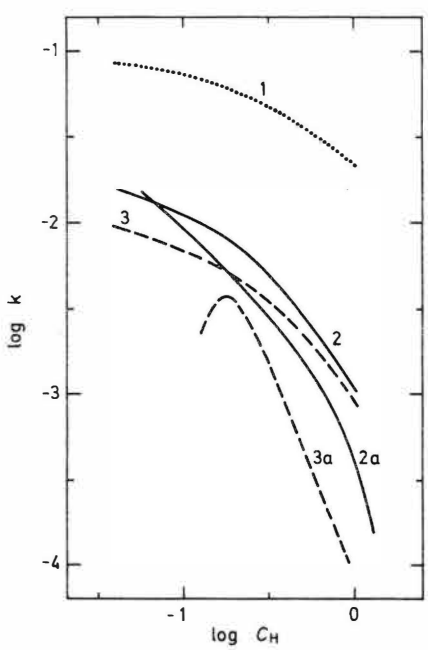

FIGURE 1. OXIDATION OF U(IV) BY AIR OXYGEN IN LIQUID-LIQUID DISPERSIONS: LOGARITHMIC DEPENDENCE OF THE ZERO ORDER RATE CONSTANT ON THE CONCENTRATION OF NITRIC ACID IN THE AQUEOUS PHASE

Curves 1 to 3 - oxidation in the absence of Pu(III): 1 - with U(IV) solution A, this work; 2 - with U(IV) solution B, this work; 3 - taken from (1)

Curves 2a and 3a - oxidation in the presence of Pu(III): 2a - at initially 0.0015 - 0.015M Pu(III) in the aqueous phase, with U(IV) solution B, this work; 3a - at initially 0.001M Pu(III) in the aqueous phase, taken from (1)

Initially 0.02 - 0.08M U(IV) in the aqueous phase, 25°C

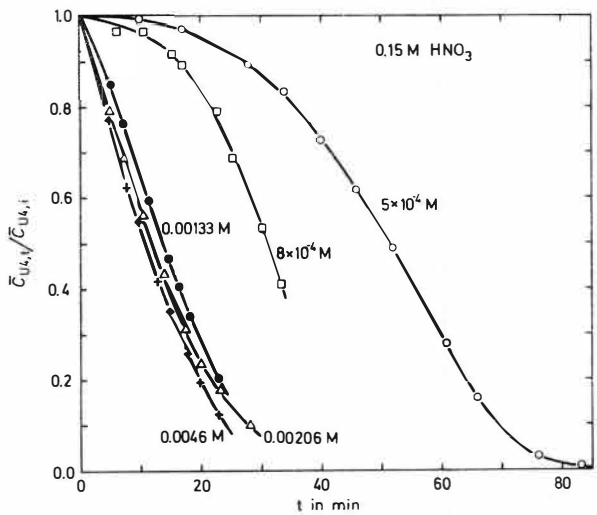

FIGURE 3. OXIDATION OF U(IV) IN A SEPARATE ORGANIC PHASE AT 25°C: DEPENDENCE OF THE RELATIVE CONCENTRATION OF U(IV) ON THE REACTION TIME AT A CONSTANT INITIAL CONCENTRATION OF NITRIC ACID AND DIFFERENT INITIAL CONCENTRATIONS OF Pu(III)

Subscripts t and i denote concentrations at reaction times t and zero respectively

PHYSICAL AND CHEMICAL ASPECTS OF URANIUM EXTRACTION FROM H_2SO_4 LEACH SOLUTIONS AND STRIPPING WITH AMMONIUM SULFATE

W. Howell, G. M. Ritcey[1], J.A. Golding[2]

Department of Chemical Engineering
University of Ottawa
Ottawa, Ontario, Canada

(1) Canmet, Lebreton St., Ottawa, Canada.
(2) Person to whom correspondence should be addressed.

INTRODUCTION

Liquid-liquid extraction is one of the methods employed for the recovery of uranium from leach liquors during the manufacture of yellow cake. The most widely used of these extraction processes is the "Amex" process (1) where uranium is first extracted from the leach liquors using an amine extractant followed by ammonium sulfate stripping to recover the uranium from the organic phase. Mixer settlers are used in these industrial operations see (2). The work reported here is part of an overall project studying the mass transfer and hydrodynamic characteristics of solvent extraction equipment. The work involved an investigation of mass transfer, dispersion, settling as well as crud formation (3) a process that may occur simultaneously in a mixer settler unit used for uranium mill processing.

EQUIPMENT

In this investigation a one stage mixer settler was used. This is shown schematically in Figure 1. The mixing cell was fully baffled (4 baffles of width one tenth of the mixer diameter) and was fitted with a window for taking photographs of the dispersion, together with a phase sampler for each phase. The phase samplers consisted of phase preferential filter paper supported on a porous teflon disc and were installed flush in the upper half of the wall of the mixing cell. The overflow from the mixer was fed into the middle of the settler dispersion via a rectangular channel. The settler area, and therefore its capacity, could be varied by changing the position of a partition. A microscope/35mm camera combination was used for photomicrography of the droplets passing through the viewing window. Lighting was provided by a flash unit.

PHASE PREPARATION, COMPOSITION, AND PHYSICAL PROPERTIES

Synthetic solutions resembling industrial process streams were prepared for the experiments. Tap water and technical grade chemicals were used in the preparations. Equipment was cleaned by scrubbing and washing with warm water. The phase compositions, densities, and viscosities are given in Table I. Interfacial tension for both extraction and stripping was between 10 and 13 dynes/cm at room temperature (20-25°C). There were indications of an increase in interfacial tension at higher uranium concentrations in the organic phase.

ONE STAGE MIXER SETTLER RUNS

Variables and conditions: The chosen conditions and variables for this project are summarized in Table II. Both extraction and stripping runs were carried out.

Procedure: The equipment was operated for 10 residence times (from 3 to 10 minutes) to approach steady state. (True steady state operation would require much longer run times, especially with regard to coalescence and crud formation in the settler). Phase sampling directly form the mixer was started, and photographs were taken of the dispersion. Samples were also taken from the phases at the settler outlets. The dispersion band thickness was noted and attempts were made to describe phase entrainment. The total run time was about 20 residence times. Uranium concentrations were determined by X-ray fluorescence while drops were measured with the aid of an image analysis tablet.

RESULTS

Drop sizes in the mixer: Figure 2 shows typical drop size distributions as photographed in the mixer "window". The form of the distributions included bimodal distributions, skewed distributions with a long tail of smaller drop sizes, and approximately gaussian distributions. There are limitations to the accuracy of the distributions obtained as larger drops would stick to the "window" and there was considerable difficulty in distinguishing small drops in the highly agitated dispersions. The Sauter mean drop diameter was calculated for selected runs based on the standard formula;

$$d_{32} = \Sigma d_i^3/\Sigma d_i^2 \quad (1)$$

The apparent mean drop diameters are plotted against impeller rpm in Figure 3. Because of the likely errors some caution should be used in their interpretation. There is an important effect of impeller speed on drop sizes. Whether extraction or stripping was occuring, and the presence of solids appears to have some influence on drop sizes, especially at low impeller speed. The effect of mass transfer is not clear form these results. Also shown in Figure 3 are two curves resulting from correlations of Bouyatiotis and Thronton (4), who worked with aqueous continuous dispersions in the absence of mass transfer. Their predictions are for drop sizes close to the bottom of the wall of the mixing vessel (geometrically similar to ours), and not opposite the impeller as in our case.

Dispersion band height in the settler: The dispersion band height in the settler varied markedly depending on throughput, mass transfer, the presence of solids, and whether extraction or stripping was taking place. Figure 4 is intended to give only a relative idea of the variation of the dispersion band height. A "normalized" height is shown as a function of impeller speed. This attempts to correct for differences in settling area and throughputs so as to present results on a comparable basis. The following relationship was used to correct the data (5);

$$\Delta H = C(Q/A)^q \quad C,q \text{ - constants} \quad (2)$$

A constant exponent q = 2.5 was calculated based on data for runs without mass transfer, and was assumed to apply to the other runs as well. A standard Q/A of 9.1 $cm^3/cm^2 \cdot min$ was chosen for normalization. A similar procedure was used to compare results of the effect of adding solids to the feed in Figure 5.

The settler dispersion band showed both sensitive (dispersion band height increasing) and insensitive (dispersion band height constant or nearly so) behaviour with respect to the impeller speed. Extraction runs with little or no mass transfer were insensitive, while stripping runs and extraction runs with high mass transfer and solids were sensitive. Note that with the sensitive system there appears to be some point at which further increases in impeller speed have little or no effect on the dispersion band. It is also interesting to note that the presence of crud at the interface did not result in a thicker dispersion band, but in fact the solids added resulted in a very thin dispersion band.

Crud formation: Table III is a summary of observed crud formation after adding solids to the aqueous feed.

TRANSFER OF URANIUM BETWEEN THE PHASES

Primarily due to the lack of precise control of flowrates, calculated mass balances for uranium were badly scattered. The method of phase sampling for the mixer cannot therefore be fully evaluated, but there were fairly consistent differences in the analysis of uranium for the mixer as opposed to the analysis of samples taken from the settler. Figures 5 and 6 show the trend with impeller speed of the extraction efficiency of uranium between the phases, based only on the aqueous phase analysis in the mixer for a few select runs.

It is to be noted that the transfer of uranium in the mixer went to at least 80% completion for all runs of extraction and stripping, independantly of the flowrates or impeller speeds used. Stripping runs were more difficult to control so as to obtain constant equilibrium pH and consistent results. Similar high extration efficiencies have been reported (6) previously.

CONCLUSIONS

The equipment used in this experiment can potentially be used for studying in depth a number of the processes occurring simultaneously in a one state, continuous mixer settler operation. In particular, the procedure for continuously bleeding off a stream of dispersion from the mixer allows the use of conventional microscopes and lighting arrangements to obtain an indication of trends in drop sizes within the mixer as compared to previous techniques used (7)(8). The results of experimentation thus far serve to indicate the range of drop sized, uranium transfer, settler dispersion band heights, and crud formation to be expected in future experiments. Results of particular note are the varying sensitivity of the dispersion band height to the impeller speed, the great variations of dispersion band heights depending on the nature of the feed phases, and the rapidity of the transfer of uranium between the two phases. The effect of solids on both the dispersion band and crud formation was also notable. See reference (9) for a full description of this work.

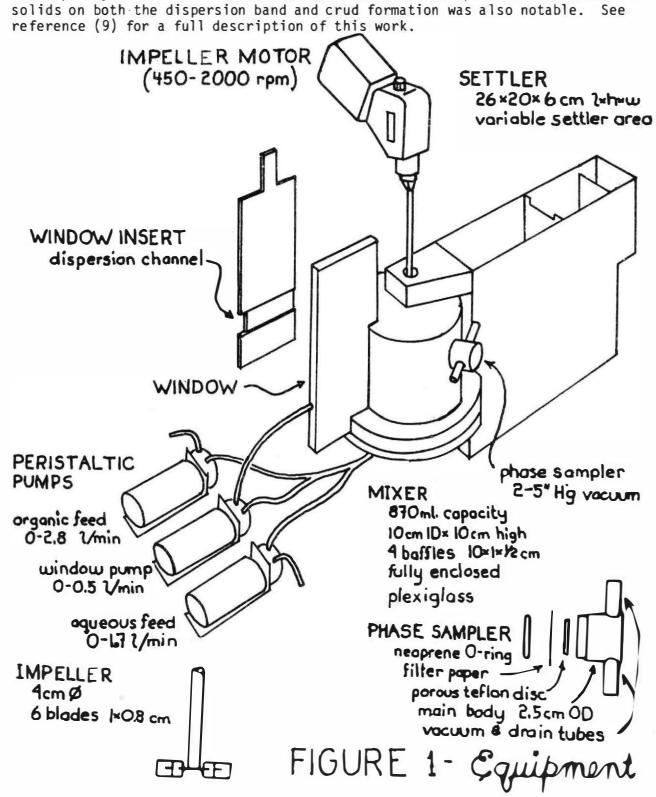

FIGURE 1- Equipment

TABLE I - PHASE COMPOSITIONS AND PHYSICAL PROPERTIES

PHASE	COMPONENT	CONCENTRATION g/l	BULK DENSITY g/cm^3	BULK VISCOSITY cp
Aqueous Leach	Uranium	1.4-5.1	1.03	1.1
	NA_2SO_4	16.8		
	H_2SO_4	7.0		
Aqueous Strip	$(NH_4)_2SO_4$	120	1.07	1.2
	NH_4OH	1.7		
Organic Phase	Adogen 364	3.5%	0.80	1.6
	Isodecanol	3.5%		
	Shell 140	93.0% - aliphatic kerosene		

Solid particles for curd formation runs were taken from a uranium ore from Rabbit Lake, Canada, 80% minus 100 mesh.

TABLE II - EXPERIMENTAL VARIABLES AND OPERATING CONDITIONS

DEPENDENT VARIABLES	INDEPENDENT VARIABLES	FIXED CONDITIONS
Uranium transfer	Impeller RPM (450-2000 RPM)	Temperature (20-25 C)
Settler Dispersion Band Height	Residence time (20-60 secs.)	Geometry: Mixer, settler, impeller
Mixer drop size distribution	Solids content (0-500 PPM)	Initial phase compositions
Crud formation		Feed O/A ratio (1.5:1) Equilibirum pH; Extraction 1.6 stripping 4.0

TABLE III - OBSERVED CRUD FORMATION IN THE SETTLER

Solid in feed ppm	0	50	100	500	100	100
Impeller rpm	870	870	870	870	450	1490
Thickness of crud, mm	0	1-2	1-2	F	F	3
% of interface covered	0	5-10	30-40	100	20	60

F - fingers of crud extended into the aqueous phase

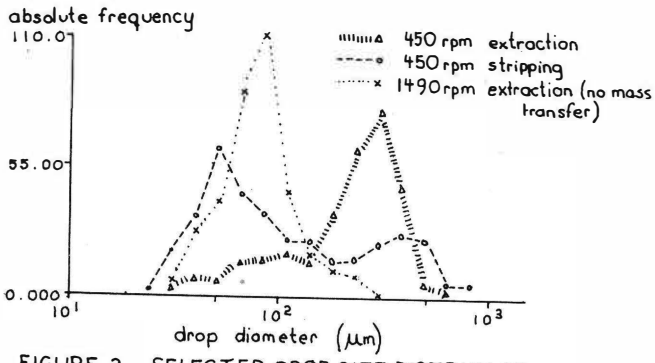

FIGURE 2 SELECTED DROP SIZE DISTRIBUTIONS

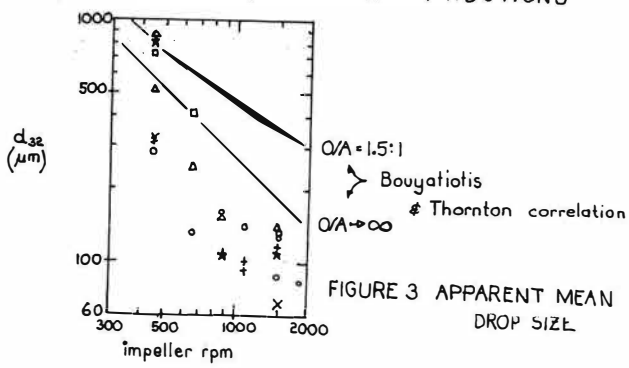

FIGURE 3 APPARENT MEAN DROP SIZE

NOMENCLATURE

A	Settler area; (cm^2)
d	Drop diameter; (μm)
ΔH*	Settler dispersion band height normalized according to equation (2); (cm)
Q/A	Total volumetric flowrate; (cm^3/s)
q	Constant exponent in equation (2)

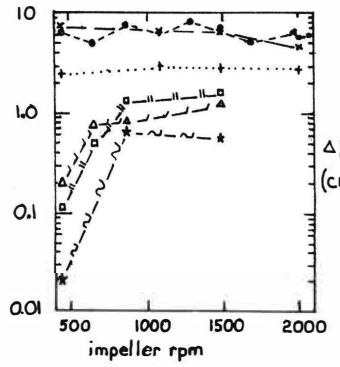

FIGURE 4 THE EFFECT OF IMPELLER SPEED ON THE SETTLER DISPERSION

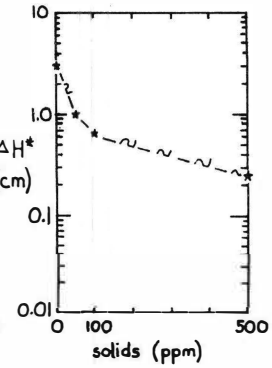

FIGURE 5 THE EFFECT OF THE SOLIDS ADDED ON THE SETTLER DISPERSION (@ 870 rpm)

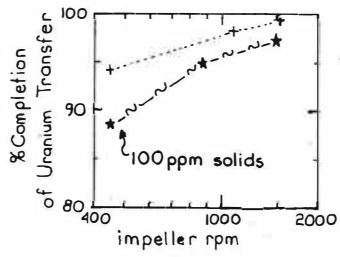

FIGURE 6 THE DEGREE OF COMPLETION OF URANIUM TRANSFER WITHIN THE MIXER (EXTRACTION)

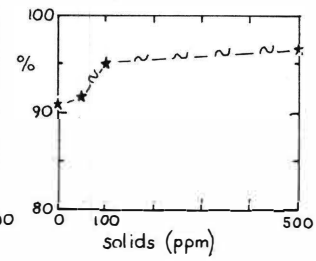

FIGURE 7 URANIUM TRANSFER IN THE PRESENCE OF SOLIDS (EXTRACTION, 870 rpm)

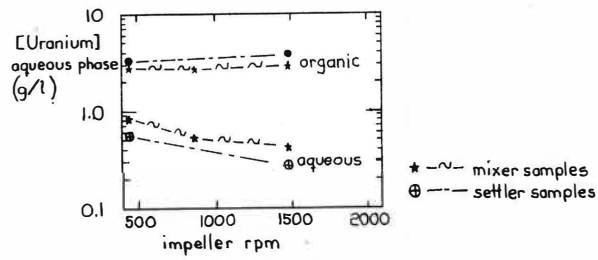

FIGURE 8 COMPARISON OF MIXER AND SETTLER ANALYSIS

KEY TO THE RUNS

	residence time	initial uranium	special conditions
— — — ∘ extraction	1 min.	none	preacidified organic
····· + extraction	1 min	1.4 g/l	"
— — × extraction	½min	"	"
— — — Δ stripping	1 min	4.4 g/l	
—"— □ stripping	⅓min	"	
—~— ★ extraction	1 min	4.9 g/l	non preacidified organic solids present

REFERENCES

1. G.M. Ritcey and A.W. Ashbrook, "Solvent Extraction - Principles & Applications to Process Metallurgy Part II -- Elsevier (1979).
2. D. Glasser, D.R. Arnold, A.W. Bryson, A.M.S. Vieler, Mineral Sci. Engng. 8, No. 1, 23 (1976).
3. G.M. Ritcey, Proc. 14th Int. Mineral Process Conf. Toronto, (1982).
4. B.A. Bouyatiotis, J.R. Thornton, I. Chem. E. Symposium Series No. 26,
5. E. Barnea, J. Mizrahi, Trans. Instn. Chem. Engnrs. 53, 61 (1975).
6. A.D. Ryon, F.L. Daley, R.S. Lawrie, Chem. Engng. Prog. 55, No. 10, 71 (1959).
7. R. Shinnar, J.M. Church, Ind. & Engng. Chem. 52, No. 3, 256 (1960).
8. Z. Kolarik, N. Pipkin, Int. J. Hydromet. 9, No. 3, 256 (1983).
9. B. Howell, MSC Thesis, Dept. Chem. Eng., Univ. of Ottawa (1983).

CONSOLIDATED FUEL REPROCESSING PROGRAM SOLVENT SCRUBBING KINETICS OF URANIUM - AND ZIRCONIUM-DIBUTYL PHOSPHATE COMPLEXES

J. C. Mailen, D. E. Horner S. M. Robinson, S. E. Dorris

Chemical Technology Division
Oak Ridge National Laboratory*
Oak Ridge, Tennessee 37830 USA

*Operated by Union Carbide Corporation for the U.S. Department of Energy.

INTRODUCTION:

Tributyl phosphate (TBP), which is diluted with a normal paraffin hydrocarbon (NPH) for use in solvent-extraction processing of spent reactor fuel elements is partially degraded by exposure to nitric acid and radiation. Some of the degradation products, particularly dibutyl phosphoric acid (HDBP) and monobutyl phosphoric acid (HMBP), form strong complexes with uranium, plutonium, and certain fission products such as zirconium which are retained to some extent in the organic phases and are not easily stripped out with dilute acid. These complexes must be removed from the spent solvent prior to its recycle. Ordinarily, a sodium carbonate solution is used for this purpose, but this reagent introduces sodium ion into the waste solution and consequently limits waste volume reduction. Alternative scrubbing agents such as hydrazine carbonate (1) and hydrazine oxalate (2), which can be decomposed to water and gases, have been proposed for this purpose.

Operating experience has shown that zirconium is not completely removed in sodium carbonate scrubbers (3,4), presumably due to slow interphase transfer kinetics. The purpose of the present study is to obtain data on the transfer kinetics for solvent scrubbing in systems using sodium carbonate, hydrazine carbonate, and hydrazine oxalate which will aid in the design of solvent scrubbing contactors and will help to identify any slow processes in the removal of the metal-ion complexes.

EXPERIMENTAL:

The simulated degraded organic phases contained 30% TBP-0.02 M DBP-0.02 M UO_2^{2+} (balance dodecane) or 30% TBP-0.02 M DBP-0.02 M Zr (balance dodecane). Kinetics determinations used the standard falling-rising drop (5,6) and Lewis cell techniques (5-7).

MATHEMATICAL RELATIONS:

The differential rate equation describing mass transfer is

$$\frac{dc'}{dt} = \frac{kac}{V'} - \frac{k'ac'}{V'} , \quad (1)$$

where c' is the concentration in the aqueous phase, c is the concentration in the organic phase, a is the interfacial area, V' is the aqueous phase volume, k is the organic-to-aqueous transfer rate constant, k' is the aqueous-to-organic transfer rate constant, and t is time. In solvent scrubbing the equilibrium greatly favors the aqueous phase; thus, the second term in Equation (1), defining transfer from the aqueous phase to the organic phase, can be neglected. Near initial time, as in most experiments to be reported, the concentration in the organic phase is nearly constant ($c = C_0$). Then the integrated form of Equation (1) for both the Lewis cell and drop tests is

$$k = \frac{c'V'}{aC_0t} , \quad (2)$$

where C_0 is the initial organic-phase concentration of the species being considered.

ANALYTICAL METHODS:

Analyses for uranium and zirconium were by x-ray fluorescence. Analyses for HDBP and DBP were by ion chromatographic methods (8) modified by J. M. Keller of the ORNL Analytical Chemistry Division to allow their application to the solutions used in these studies.

RESULTS AND DISCUSSION:

The interphase transfer kinetics for the scrubbing of an organic phase containing the U-DBP complex by sodium carbonate and mixed sodium carbonate-sodium nitrate solutions were measured by the Lewis cell and falling-drop techniques. The results of these tests are presented in Figure 1 and are summarized below:

a. The Lewis cell and drop test are generally in agreement.
b. Examination of the data at 0.3 M Na_2CO_3 shows no significant nitrate effect on the uranium scrubbing transfer rate constants.
c. The scrubbing transfer rate constant increases with about the second power of the carbonate concentration.

Scrubbing transfer rate data were obtained in Lewis cell experiments for HDBP, U (for U-DBP complex), DBP (for U-DBP complex), DBP (for Zr-DBP complex), and Zr (for Zr-DBP complex) when using hydrazine oxalate, hydrazine carbonate, sodium carbonate, and sodium carbonate-sodium hydroxide solutions (Table 1). A summary of the experimental results follows:

a. In all cases the scrubbing transfer rate constants for Zr-DBP are significantly lower than those for U-DBP. This confirms the operating experience (3,4) that zirconium removal is a relatively slow step. The scrubbing rate is not so slow, however, as to cause severe problems in a solvent cleanup system.
b. The scrubbing transfer rate constants obtained using hydrazine oxalate are comparable to those using sodium carbonate with the exception of a lower rate constant for U scrubbing from the U-DBP complex. The rate constants obtained using hydrazine carbonate for U-DBP scrubbing were lower than those for either hydrazine oxalate or sodium carbonate.
c. The DBP is scrubbed from the U-DBP solution faster than the uranium with both the hydrazine salts. These are the only cases where the cation and the DBP were not removed at the same rates.

This last observation led us to perform a special test. An organic phase containing the U-DBP complex was mixed with a 0.23 M aqueous hydrazine oxalate solution, pH 8, with the mixer speed controlled to leave a small, clear aqueous phase. Samples of the aqueous phase were taken as a function of time and analyzed for both uranium and DBP. The transfers of uranium and DBP can be described by the differential equations:

$$\frac{dC_U}{dt} = -\frac{k_U C_U a}{V} , \quad (3)$$

and

$$\frac{dC_{DBP}}{dt} = -\frac{k_{DBP} C_{DBP} a}{V} , \quad (4)$$

where C is the indicated concentration in the organic phase, k is the transfer rate constant from the organic phase to the aqueous phase, a is the interfacial area, V is the organic phase volume, and t is time. The integrated equations are

$$\ln(C_U/C_{U,0}) = -k_U \frac{a}{V} t , \quad (5)$$

and

$$\ln(C_{DBP}/C_{DBP,0}) = -k_{DBP} \frac{a}{V} t , \quad (6)$$

where $C_{U,0}$ and $C_{DBP,0}$ are initial concentrations in the organic phase. Dividing the equations gives

$$\frac{\ln(C_{DBP}/C_{DBP,0})}{\ln(C_U/C_{U,0})} = \frac{k_{DBP}}{k_U} . \quad (7)$$

Table 2 gives the values of C_U, C_{DBP}, and calculated ratios of k_{DBP} to k_U. This experiment indicates that the rate constant for DBP removal is about three times that for uranium removal. This value compares to an average ratio of k_{DBP}/k_U from all the hydrazine carbonate and hydrazine oxalate rate constants determinations of 3.8. The chemical interpretation of this difference in rates is not obvious, but may involve complexing of the DBP by hydrazine followed (slower step) by complexing of uranyl by carbonate or oxalate.

CONCLUSIONS:

The scrubbing rate constants for uranium from U-DBP with hydrazine carbonate and hydrazine oxalate solutions are slightly lower than those obtained using sodium carbonate solutions; however, the rates are adequate for process uses. The transfer rate constant for scrubbing DBP was about three times greater than that for uranium when scrubbing U-DBP with either hydrazine salt. The significance, if any, of this observation in process use is unknown. The transfer rate constants for the removal of zirconium from the Zr-DBP complex are about the same for all the scrubbing solutions. The scrubbing rate constants determined in this work are smaller than the few values in the literature (1). Our value for HDBP scrubbing by 0.5 M Na_2CO_3 is 4×10^{-3} cm/s compared to 1.9×10^{-2} cm/s for 0.45 M Na_2CO_3. The literature data indicate that the scrubbing of Zr-DBP by sodium carbonate is about a factor of 5 slower than for HDBP; our data indicate the Zr-DBP removal is slower by a factor of about 10 compared with HDBP. These differences cannot be explained.

The rate-controlling step for the removal of HDBP and the metal ion complexes could involve diffusion of the HDBP or the complex to the interface, reactions at the interface, diffusion of the products of the interfacial reaction into the bulk aqueous phase, or combinations of these steps. In earlier studies (9) of solvent extraction in the Purex and Thorex processes it was concluded that the rate of reaction is controlled by the interfacial reaction. The evidence is not as conclusive in solvent scrubbing, but the bulk of the data supports the chemical reaction at the interface as the rate-controlling step. The evidence includes:

a. The rate constants for Lewis cell and drop tests are about the same although the surface-to-volume ratios and degrees of mixing are significantly different.
b. Chemical variables in the aqueous phase affected the scrubbing rate. Since these changes would not affect the viscosity of either phase significantly, they are not likely to influence a diffusion-controlled reaction.
c. The different rate constants for uranium and DBP in the scrubbing of U-DBP by hydrazine salts must surely result from differing chemical reaction rates. If diffusion were the rate-controlling step, both components of a complex must diffuse as a unit at the same rate.

If the rate-controlling step is the rate of the chemical reaction at the interface, the overall reaction rate in process equipment can be calculated from the kinetic constants presented here plus knowledge of the interfacial area created by mixing in the equipment under study.

REFERENCES:

1. H. Goldacker, H. Schmieder, and F. Stieglitz, Kerntechnik 18, 426 (1979).
2. O. K. Tallent and J. C. Mailen, Nucl. Tech. 59, 51 (1982).
3. D. A. Orth and T. W. Olcott, Nucl. Sci. Eng. 17, 593 (1963).
4. A. J. Haggard and B. F. Warner, Nucl. Sci. Eng. 17, 638 (1963).
5. D. E Horner, J. C. Mailen, S. W. Thiel, T. C. Scott, and R. G. Yates, Ind. Eng. Chem. Fundam. 19, 103 (1980).
6. D. E. Horner, J. C. Mailen, J. R. Coggins, Jr., S. W. Thiel, T. C. Scott, N. Pih, and R. G. Yates, Ind. Eng. Chem. Fundam. 19, 287 (1980).
7. J. C. Mailen, D. E. Horner, S. E. Dorris, N. Pih, S. M. Robinson, and R. G. Yates, Sep. Sci. and Tech. 15(4), 959 (1980).
8. R. P. Lash and C. J. Hill, J. Liq. Chromatogr. 2(3), 417 (1979).
9. J. C. Mailen, Sep. Sci. and Tech. 16(19), 1373 (1981).

Table 1. Interphase transfer kinetics of HDB, U-DBP and Zr-DBP in solvent scrubbing using hydrazine oxalate, hydrazine carbonate and sodium carbonate-sodium hydroxide solutions[a]

Solution	Transfer rate constant (cm/s)				
	HDBP	U-DBP		Zr-DBP	
		U	DBP	Zr	DBP
Hydrazine oxalate					
0.25 N, pH 7	1×10^{-2}	1.5×10^{-3}	4×10^{-3}	5.8×10^{-4}	4.8×10^{-4}
0.23 N, pH 8	9.3×10^{-3}	1.1×10^{-3}	7×10^{-3}	3.5×10^{-4}	6.4×10^{-4}
0.45 N, pH 7	9.5×10^{-3}	1.1×10^{-3}	5×10^{-3}	8.2×10^{-4}	6.7×10^{-4}
Hydrazine carbonate					
0.25 N, pH 7	1.7×10^{-3}	4.6×10^{-4}	1.8×10^{-3}	4.7×10^{-4}	3.9×10^{-4}
0.25 N, pH 8	2.9×10^{-3}	9.7×10^{-4}	2.5×10^{-3}	4.5×10^{-4}	3.1×10^{-4}
0.5 N, pH 7	4.6×10^{-3}	7.2×10^{-4}	2.2×10^{-3}	4.6×10^{-4}	N.D.[b]
Na_2CO_3-NaOH					
0.1 M, $NaCO_3$	4×10^{-3}	2.7×10^{-3}	2×10^{-3}	1×10^{-4}	5.9×10^{-4}
0.5 M, Na_2CO_3	4×10^{-3}	4.6×10^{-3}	6.5×10^{-3}	9×10^{-4}	3.7×10^{-4}
0.1 M, Na_2CO_3 +0.8 M, NaOH	5.4×10^{-3}	7×10^{-3}	9.5×10^{-3}	N.D.[b]	N.D.[b]

[a]Lewis cell experiments.
[b]Not determined.

Table 2. Results of mixer test examining removal of uranium and DBP from the U-DBP complex

t (s)	Aqueous phase		Organic phase, calculated		
	DBP (μmol/mℓ)	U (μmol/mℓ)	DBP (μmol/mℓ)	U (μmol/mℓ)	k_{DBP}/k_U
0	0	0	17.0	18.9	N.D.[a]
15	0.46	0.14	16.2	18.7	4.5
30	0.69	0.35	15.8	18.3	2.3
45	1.1	0.57	15.2	18.0	2.3
60	2.0	1.08	14.0	17.3	2.2
75	4.6	1.74	10.7	16.5	3.4
				Average ratio	2.9

[a]Not determined.

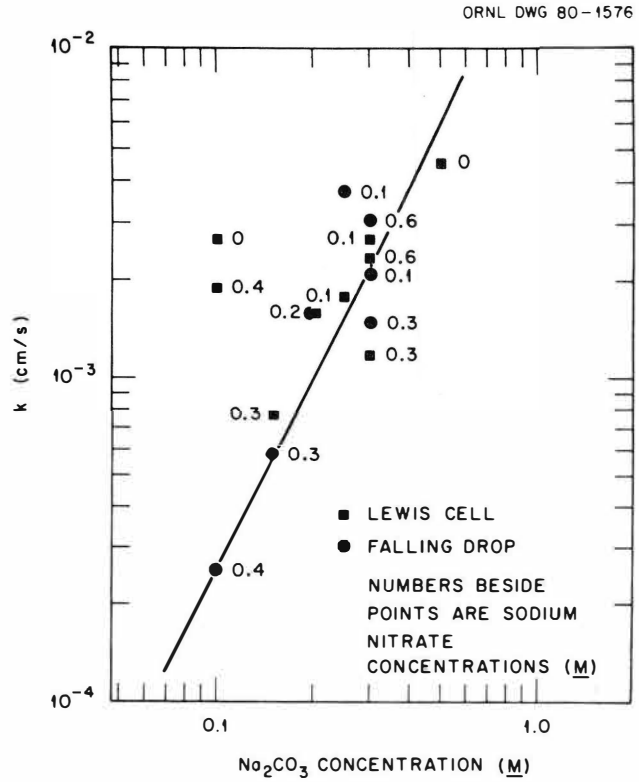

Figure 1. Rate constants for scrubbing of U (U-DBP complex) by Na_2CO_3-$NaNO_3$ mixtures

EXTRACTION OF BERKELIUM (IV) BY NEUTRAL PHOSPHORORGANIC COMPOUNDS AND MULTIMOLECULAR AMINES

B. F. Myasoedov, M.S. Milyukova, D. A. Malikov

Vernadsky Institute of Geochemistry and Analytical Chemistry
USSR Academy of Sciences, Moscow, USSR

The presentation deals with the extraction of berkelium (IV) by trialkylphosphate, trialkylphosphine oxides and multimolecular amines from the mineral acid solutions depending on the nature and concentration of acid, extractant, organic solvent and oxidant.

Tributylphosphate (TBP), trioctylphosphine oxide (TOPO) and triphenylphosphine oxide (TPPO) have been found to extract berkelium (IV) quantitatively from nitric acid solutions containing potassium bromate as an oxidant. The efficiency of berkelium (IV) extraction increases with the increasing of nitric acid concentration and achieves in the definite range of acid concentrations maximum and constant value. Tributylphosphate solutions in the organic solvents quantitatively extract berkelium (IV) from 10-12 M nitric acid and trioctylphosphine oxide solutions in dichloroethane and cyclohexane do it from 3-12 M and 1-14 M nitric acid respectively.

Distribution coefficients of berkelium (IV) have been shown to vary proportionally to the fourth degree of an acid concentration witnessing the extraction of berkelium (IV) as a neutral tetranitrate complex.

The efficiency of berkelium (IV) extraction by neutral phosphororganic compounds also considerably depends on the nature of organic solvent. TBP extracts berkelium (IV) quantitatively with heptane, dichloroethane and carbon tetrachloride as solvents. All the examined organic solvents (heptane, dichloroethane, carbon tetrachloride, cyclohexane, chloroform) apart from kerosene and aromatic hydrocarbons are suitable for quantitative berkelium (IV) extraction by the solutions of TOPO. The range of nitric acid concentrations where berkelium (IV) is extracted quantitatively by TOPO solutions is wider than in the case of TBP. TOPO solutions in heptane or cyclohexane extract berkelium (IV) quantitatively from 1-10 M and 1-14 M nitric acid respectively. TPPO extracts berkelium (IV) quantitatively only with dichloroethane and chloroform as the solvents.

The data obtained for the dependence of the completeness of berkelium (IV) extraction on TBP, TOPO and TPPO concentration show that two molecules of an extractant are solvated with one extracted berkelium complex. Hence bekelium (IV) is extracted in organic phase by neutral phosphororganic extractants as disolvate of berkelium tetranitrate $BK(NO_3)_4 \cdot 2S$ and equation of the extraction may be written as

$$2S + BK^{4+} + 4NO_3^- = BK(NO_3)_4 \cdot 2S,$$

where S=TBP, TOPO, TPPO.
Earlier (1-4) thorium, tetravalent plutonium and neptunium and other elements have been shown to be extracted from nitric acid solutions also as analogous compounds i.e. as disolvates of tetranitrate.

Berkelium (IV) has been found to be extracted from hydrochloric and sulphuric acids by TOPO alone, the efficiency of berkelium (IV) extraction from these acids being considerably lower than from nitric acid. The distribution coefficients of some elements and the separation factors BK/Me during extraction by 0.7 M TBP and 0.1 M TOPO solutions in heptane from 10 M nitric acid are listed in Table 1. As seen from the table the use of TOPO and TBP as extractants permits to separate berkelium from trivalent americium and curium, rare earths and several fission products rather effectively.

Tetravalent berkelium can be extracted from mineral acid solutions by multimolecular amines. However the efficiency of berkelium (IV) extraction depends on the nature and concentration of an oxidant, extractant and organic solvent. Berkelium (IV) is extracted by tertiary amines (0.4 M TOA in carbon tetrachloride) quantitatively from 10 M nitric acid containing potassium bichromate as an oxidant. The increasing of amine alkyl chain over C_8 was found to lead to decrease of tetravalent berkelium distribution coefficients. It seems to be due to steric hindrance. Tetravalent berkelium is not practically extracted after oxidation with bromate ions.

The use of silver nitrate and ammonium persulphate mixture as an oxidant permits to separate berkelium from cerium during the extraction by TOA in carbon tetrachloride. In these conditions berkelium (IV) is reduced to trivalent state and remains in aqueous phase.

Extraction of tetravalent berkelium by quaternary ammonium salt (Aliquate 336-S) depends on the initial nitric acid concentration in aqueous phase. The completeness of extraction increases with the increasing of solution acidity. In the presence of potassium bichromate tetravalent berkelium is extracted quantitatively from 10-12 M nitric acid. The quantitative extraction of berkelium oxidized by bichromate ions in 10-12 M nitric acid was found to occur when 30% aliquate solution in carbon tetrachloride or dichloroethane was used.

We have obtained interesting results during the extraction of berkelium (IV) by multimolecular amines from nitric and sulphuric acid solutions in the presence of heteropolyanions. Berkelium oxidized by bromate ions in the presence of heteropolyanions was found to be quantitatively extracted by the primary, secondary and tertiary amines and quaternary ammonium base salts. The degree of tetravalent berkelium extraction in the presence of heteropolyanions depends on the nature of amine and nitric acid concentration in aqueous phase. Decylamine extracts berkelium (IV) quantitatively in more wide range of nitric acid concentrations (0.5-6 M HNO_3) than dioctyl- and trioctylamine (0.5-1 M HNO_3) and Aliquate 336-S-NO_3 (0.1-2 M HNO_3). Lower amine concentrations are demanded for the maximum berkelium (IV) extraction (TOA- 1%, Aliquate 336-S-NO_3 - 0.5-1%) than that during the extraction from nitric acid solutions containing bichromate ions in the absence of heteropolyanions.

It is important to underline that berkelium (III) is not extracted in the presence of heteropolyanions by multimolecular amines in these conditions.

It has been established that heteropolyanions not only stabilize tetravalent berkelium but enter in the composition of extracted ions as well.

The stoichiometry of berkelium (IV) extraction has been studied and the composition of the extracted compounds have been determined. The distribution coefficients of some elements and separation factors BK/Me during the extraction by 3% decylamine solution in chloroform are given in the Table 2.

The data obtained have made it possible to work out the extraction methods of separation and purification of berkelium from TPE, rare earths and several fission products with the use of neutral phosphororganic compounds and multimolecular amines as extractants.

References

1. E.Hesford, H.A.C.McKay, D.Scargill. J. Inorg. Nucl. Chem., 4, 321 (1957).
2. V.V.Sergievsky, L.V.Evdokimova, G.A.Yagodin. Radiochim.,23, 512 (1981).
3. J.R.Ferraro. J. Inorg. Nucl. Chem.,10, 319 (1959).
4. T.V.Healy, H.A.C.McKay. Trans. Faraday Soc.,52, 633 (1956).

Table 1

Distribution coefficients (D) and separation factors (S) of berkelium (IV) and several metals during the extraction by TOPO and TBP solutions in heptane from 10 M nitric acid, containing 0.5 M $KBrO_3$

Extractant		Me								
		^{249}Bk	^{144}Ce	^{241}Am	^{243}Cm	$^{95}Zr+^{95}Nb$	^{90}Sr	^{137}Cs	$^{104-106}Ru$	$^{152-154}Eu$
0.1 M TOPO in heptane	D	155.8	8.2	0.007	0.003	2.77	0.035	0.020	0.017	0.018
	S		19.0	$2.4\cdot10^4$	$4.6\cdot10^4$	56.2	$4.5.10^3$	$7.8\cdot10^3$	$9.2\cdot10^3$	$8.7\cdot10^3$
0.7 M TBP in heptane	D	51.7	3.0	0.012	0.013	0.946	0.105	0.006	0.009	0.033
	S		17.2	$4.3\cdot10^3$	$4.0\cdot10^3$	54.7	$4.9\cdot10^2$	$8.8\cdot10^3$	$5.9\cdot10^3$	$1.6\cdot10^3$

Table 2

Distribution coefficients (D) and separation factors (S) of berkelium (IV) and several metals during the extraction by 3% decylamine solution in chloroform from 6 M nitric acid containing 4.10^{-5} M $K_{10}P_2W_{17}O_{61}$

Me	^{249}BK	^{241}Am	^{243}Cm	^{144}Ce	$^{152-154}Eu$	^{137}Cs	^{106}Ru	^{90}Sr
D	99	0.014	0.017	49	0.006	0.007	0.055	0.018
S		$7.1\cdot10^3$	$5.8\cdot10^3$	2.02	$16.5\cdot10^3$	$14.1\cdot10^3$	$1.8\cdot10^3$	$5.5\cdot10^3$

COMPARISON OF PUREX-PROCESS METHODS TO SEPARATE URANIUM AND PLUTONIUM

G. Petrich and H. Schmeider

Kernforschungszentrum Karlsruhe
Institut für Heiße Chemie
D-7500 Karlsruhe, Federal Republic of Germany

Four U/Pu separation processes were developed to technical maturity:

- Ferrosulfamate process e.g.[1]
- Uranium(IV) process e.g.[2, 3]
- Hydroxylamine nitrate (HAN) process e.g.[4, 5]
- Electro reduction process e.g.[6]

Process technology and process chemistry are principally known for fuel with low Pu content (different flowsheet variations experimentally investigated and published). Very little is known, however, for high Pu content fuel. The purpose of this paper is therefore to quantitatively compare the processes by numerical simulation (e.g.[7]) using a model FBR-fuel with a model flowsheet and to discuss the general advantages and disadvantages of the processes.

CHEMICAL REACTION KINETICS

The basics of the model (distribution equilibria, mass transfer kinetics, mixer-settler model) was previously described, e.g.[7]. In addition the following redox equations were used for the calculations. Material balances were calculated from the reaction stoichiometries. K_P and K_U are hydrolysis and dissociation constants for Pu and U resp. The reaction constants k are given for 30°C. Ω_c and Ω_a are the specific cathode and anode areas of the electro-process in 1/cm.

*Reduction of Pu(IV) by U(IV), BIDDLE et al. [8]:

$$d[Pu(IV)]/dt = -k\cdot[Pu(IV)]\cdot[U(IV)]/\{([HNO_3]+K_P)\cdot([HNO_3]+K_U)\}$$

$k(aqu)=15200$ mol/min, $E_A=104$ kJ/mol (NEWTON [9])

The organic reaction is not well known. It was assumed to be a factor 100 slower than the aqueous reaction [10].

*Reduction of Pu(IV) by hydroxylamine nitrate, BARNEY [11]:

$$d[Pu(IV)]/dt = -k\cdot[Pu(IV)]^2\cdot[NH_3OH^+]^2/\{[Pu(III)]^2\cdot[HNO_3]^4\cdot([NO_3^-]+K_P)^2\}$$

$k=1.74$ mol^5/min, $E_A=130$ kJ/mol

*Reduction of Pu(IV) by hydrazine, KOLTUNOV [12]:

$$d[Pu(IV)]/dt = -k\cdot[Pu(IV)]\cdot[N_2H_5^+]/([HNO_3]+K_P)$$

$k=0.038$/min, $E_A=93$ kJ/mol, k(Pt-catalyzed)=k+0.22•Ω_c (HEILGEIST [13])

*Cathodic reduction of Pu(IV), SCHMIEDER et al. [14]:

$d[Pu(IV)]/dt = -k\cdot\Omega_c\cdot[Pu(IV)]$, k(35°C, Ti-cathode, stirred)=0.23 cm/min

*Cathodic reduction of U(IV) [14]:

$d[U(VI)]/dt = -k\cdot\Omega_c\cdot[U(VI)]$, k=0.008 cm/min

*Anodic reoxidation of Pu(III) [14]:

$d[Pu(III)]/dt = -k\cdot\Omega_a\cdot[Pu(III)]$, k(35°C, Pt-anode, stirred)=0.25 cm/min

*Oxidation of Pu(III) by HNO_2 (aqueous phase), DUKES [15], modified:

$$d[Pu(III)]/dt = -k\cdot[Pu(III)]\cdot[HNO_2]\cdot([HNO_3]-0.4)\cdot[NO_3^-] = -2\cdot d[HNO_2]/dt$$

$k=144/(\text{mol}^3\cdot\text{min})$, $E_A=59$ kJ/mol

*Oxidation of Pu(III) by HNO_2 (organic phase), BIDDLE et al. [10] modified:

$$d[Pu(III)]/dt = -\exp\{5.28\cdot([HNO_3]+0.8)\cdot[Pu(III)]\cdot[HNO_2] = -2\cdot d[HNO_2]/dt$$

*Reaction of HNO_2 with hydrazine, BIDDLE et al. [16]:

$$d[HNO_2]/dt = d[N_2H_5^+] = -60000\cdot[HNO_2]\cdot[N_2H_5^+]\cdot[HNO_3]^2$$

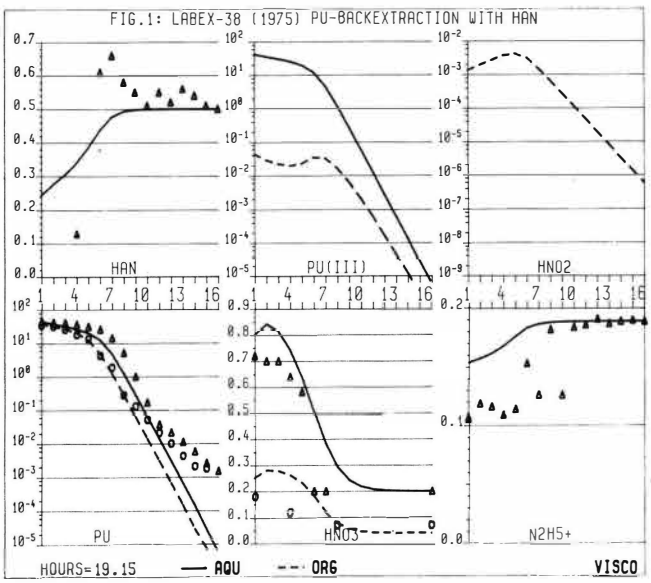

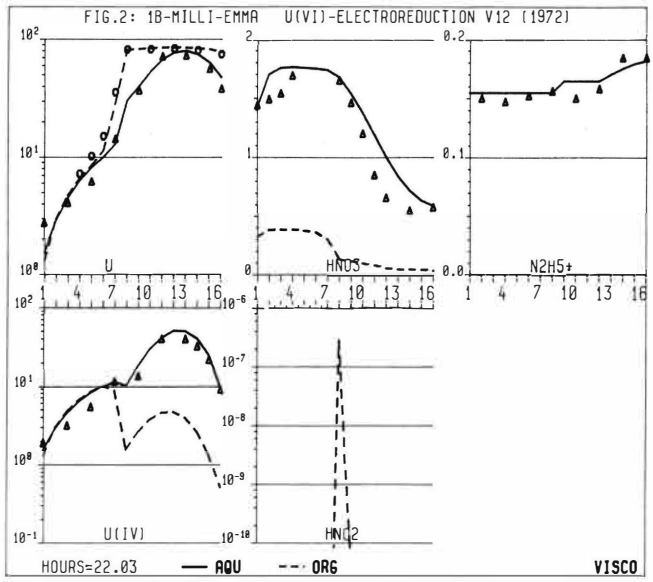

*Reaction of HNO_2 with hydroxylamine nitrate, BARNEY [17]:

$$d[HNO_2]/dt = d[NH_3OH^+]/dt = -k\cdot[HNO_2]\cdot[NH_3OH^+]\cdot[HNO_3]$$

$k=600/(\text{mol}^2\cdot\text{min})$, $E_A=48$ kJ/mol

COMPARISON OF EXPERIMENTAL PROFILES WITH NUMERICAL SIMULATION

The quality of the model has been frequently proven with good results especially for low Pu content fuel. Three typical examples are given in figs.1-3. Molar concentrations and metal concentrations in g/l are plotted for the individual species vs. stage number. Organic (o) and aqueous (Δ) measurements are given where available.

Fig.1: Pu backextraction with HAN at 50°C [18]. Small parameter variations show the extreme sensitivity of this process to organic reoxidation. The tailing of the Pu profile is probably due to the formation of Pu-HDBP complexes which are not yet accounted for by the model.

Fig.2 demonstrates in-situ electro-reduction of U(VI) in the absence of Pu.

Fig.3 is an example of the electro-reduction process. Since calculations of the U(IV)-process employ the same model without electro-redox equations, this figure serves as a demonstration of the numerical capabilities for this process as well.

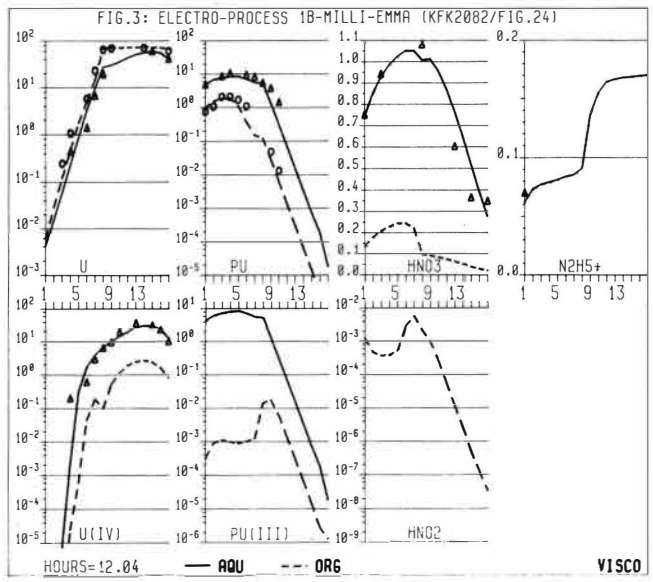

MODEL FUEL AND FLOWSHEETS FOR THE PROCESS COMPARISON

For all processes a 4-stage scrub (for U) and a 6-stage extraction (for Pu) mixer settler is employed, operating at 80% stage efficiency. The organic scrub flow BSX is 20l/h, 30%TBP. Organic feed HSP is 100 l/h, 0.2 M HNO_3, 75.7 gU/l, 9.3 gPu/l, 0.001 M HNO_2, 30%TBP. Strip solutions BXS1 and reductant and/or stabilizer feed BXS2 (close to HSP-feed) are as follows:

HAN-------BXS1: 37 l/h, 0.20 M HNO_3, 0.53 M HAN, 0.15 M $N_2H_5^+$

BXS2: 3 l/h, 0.05 M HNO_3, 0.30 M $N_2H_5^+$

U(IV)-----BXS1: 30 l/h, 0.20 M HNO_3, 12gU(IV)/l, 0.16 M $N_2H_5^+$

BXS2: 10 l/h, 2.00 M HNO_3, 232gU(IV)/l, 0.15 M $N_2H_5^+$

Electro---BXS1: 40 l/h, 0.20 M HNO_3, 0.16 M $N_2H_5^+$

BXS2: -----

NUMERICAL RESULTS OF THE MODEL PROCESS CALCULATIONS

PROCESS	°C	Pu Concentr. Factor CF	Reductant Excess: Reductant / Pu(Feed)	Hydrazine Supply: N_2H_5 / Pu(Feed)	Hydrazine Consume: ΔN_2H_5 / Pu(Feed)	Pu Deco Factor	U Deco Factor
HAN	40	2.5	5	1.65	0.06	250	500
	50	2.5	5	1.65	0.07	1000	220
	50	2.5	5	----	----	1440	100
	50	3.33	5	1.65	0.11	43	1250
U(IV)-Feed	30	2.5 (*)	5	1.65	0.88	30	5
	30	2.5	5	1.65	0.97	17150	5
	30	3.33	5	1.65	1.2	17100	11
	30	4.0	5	1.65	1.5	16000	16
	30	4.0	5	1.50	1.50	4	6
	30	5.0	5	3.30	1.4	5750	16
Electro-Reduction	35	2.5	1.5	1.65	0.56	13550	13
	35	2.5	1.5	----	----	1230	6
	35	3.33	1.5	1.65	0.67	13100	75
	35	4.0	3 (**)	1.65	0.68	11350	130
	35	5.0	5 (**)	1.65	0.75	1260	350

(*) Without U(IV) in BXS1. (**) Increased cathode area.

FERROSULFAMATE-PROCESS

This process is well-proven with regard to separation efficiency and reliability in different plants. Unfortunately, the oxidation product of the reductant cannot be recycled, however, and may cause corrosion problems. Furthermore huge excess amounts of reductant are necessary (20 to 40 fold). Waste costs are therefore intolerably high for fuel with large Pu concentrations.

HYDROXYLAMINE NITRATE-PROCESS

Principal advantages of this process are the possibility of complete decomposition of the reductant to inert gases and the large reduction rate. This rate is drastically reduced, however, with the square of the Pu(III) concentration and the fourth power of the nitric acid concentration which are reaction products. Therefore, for a technical process acceptable rates will only be achieved at elevated temperatures and large reductant excess. Furthermore Pu complexed by dibutylphosphate can only be inc mpletely stripped with this reductant [19], in contrast to U(IV) as reductant. Maximum Pu concentration factors are 2.5-3. Not well understood is the role of hydrazine which is usually additionally fed close to the organic feed point. Market availability of concentrated HAN solutions is limited.

URANIUM(IV)-PROCESS

The extractable reductant U(IV) should be ideally suited for a high separation efficiency. In practice, however, separation is deteriorated at least in mixer-setllers due to the autocatalytic oxidation reaction of Pu(III) with nitrous acid and the combined oxidation of U(IV) in the organic phase. For reasonably good separation a large excess of U(IV) is required therefore (4 to 6 fold stoichiometry) and at least two U(IV) feed-points are necessary. This reduces also the danger of a local depletion of stabilizer and reductant which was occasionally observed as a spontaneous malfunction in several plants. Along with the U(IV) production cell (fed with about 30-60% of recycled product uranium for FBR-fuel) this means significant additional equipment. Figs.4-7 show as an example the initial phases of a malfunction. Starting profile fig.4 is the steady state result for the case CF = 4, hzdrazine/Pu = 1.65 of the table. Malfunction occurs by reducing hydrazine/Pu to 1.5.

ELECTRO-REDUCTION-PROCESS

This process shows all the advantages of the U(IV)-process but avoids its drawbacks. Neither product-U recycle nor additional U(IV) feeds are necessary. Local depletion of stabilizer and reductant has never been observed up to now (the reductant is homogeneously produced within the extractor from process inherent U). From the above calculations there seems to be even the chance to completely avoid the stabilizer hydrazine which is also plausible from thermodynamic considerations. Laboratory tests of electrode corrosion (Ti, Pt) show a very high stability of these materials. The long term tests of the technical equipment has been started with the installation of a mixer-settler in the Wiederaufarbeitungsanlage Karlsruhe in 1980.

REFERENCES

[1] R.L.Walser, USAEC Report ARH-SA-69 (1970)
[2] E.N.Jenkins, R.J.W.Streeton, AERE-R3158 (1959)
[3] C.S.Schlea, M.R.Caverly, H.E.Henry, W.J.Jenkins, USAEC Report DP808 (1963)
[4] D.A.Orth, J.M.McKibben, W.C.Scotten, Proc. ISEC71, London (1971)
[5] P.Patigny, J.Regnier, P.Miquel, D.Taillard, Proc. ISEC74, Lyon (1974)
[6] F.Baumgärtner, H.Schmieder, Radiochimica Acta 25,191 (1978)
[7] G.Petrich, Proc. IASTED Symp. on Modelling, Identification and Control, Davos, March 2-5, 1982, p.49.
[8] P.Biddle, J.H.Miles, M.J.Waterman, J.Inorg.Nucl.Chem. 28, 1736 (1966)
[9] T.W.Newton, J.Phys.Chem. 63, 1493 (1959)
[10] P.Biddle, H.A.C.McKay, J.H.Miles, "Solvent Extraction Chemistry of Metals", Harwell, 27.-30. Sept. 1965
[11] G.S.Barney, J.Inorg.Nucl.Chem. 38, 1677 (1976)
[12] V.S.Koltunov, G.I.Zhuravleva, Radiokhimiya 16, 84(1974)
[13] M.Heilgeist, Dissertation Universitaet Heidelberg (1983)
[14] H.Schmieder, H.Goldacker, M.Heilgeist, M.Kluth, H.Hausberger, L.Finsterwalder, KfK-2957 (1980)
[15] E.K.Dukes, J.Am.Chem.Soc. 82, 9 (1960)
[16] P.Biddle, J.H.Miles, J.Inorg.Nucl.Chem. 30, 1291 (1968)
[17] G.S.Barney, ARH-SA-97 (1971)
[18] W. Ochsenfeld, private communication.
[19] L.Stieglitz, W.Ochsenfeld, H.Schmieder, KfK-691 (1968)

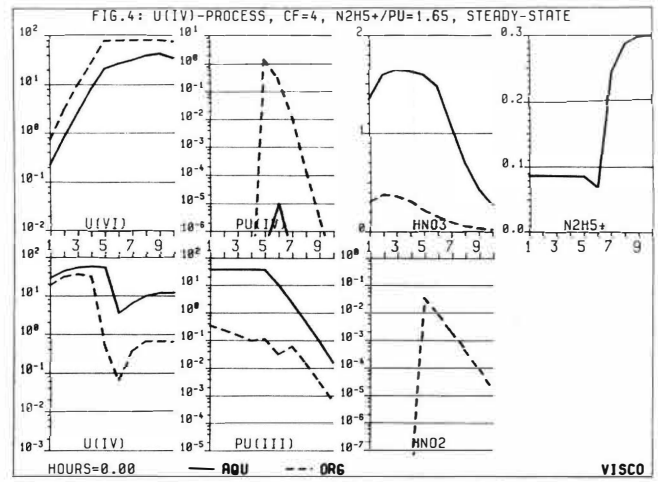

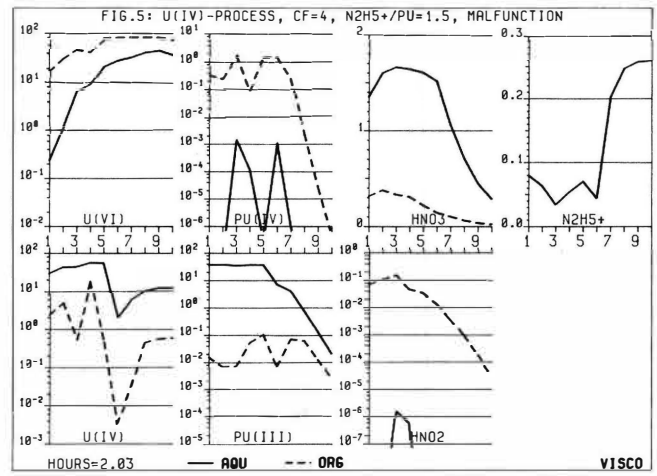

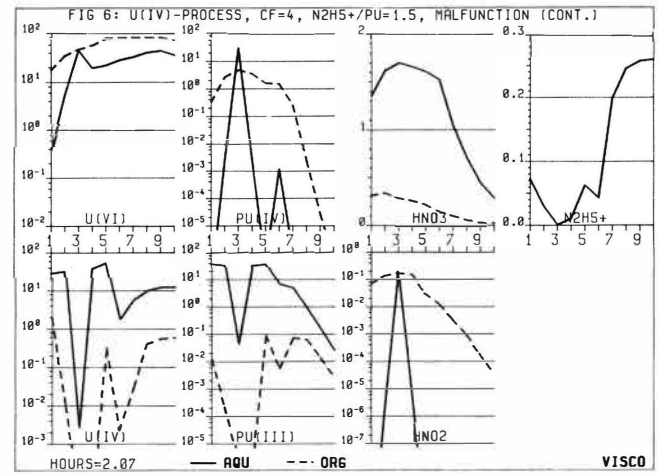

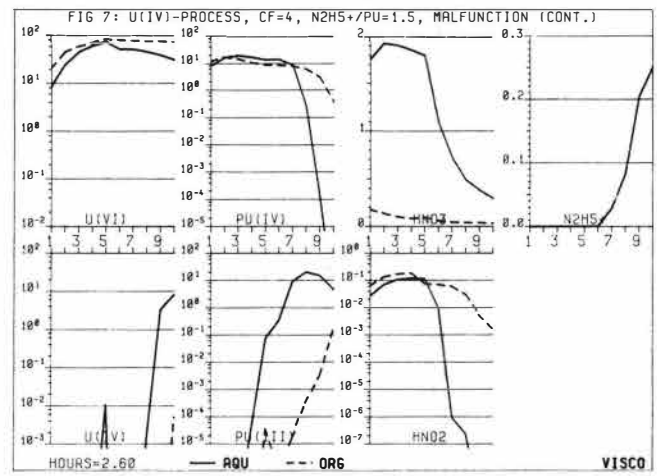

EXPERIMENTS ON A MODIFIED THOREX FLOWSHEET FOR Th-Pu FUEL

G.R. Grant, R.E. Hollies, J.J. Hawton and Y.-K. Sze

Atomic Energy of Canada Limited
Whiteshell Nuclear Research Establishment
Pinawa, Manitoba, Canada ROE 1LO

INTRODUCTION

Improved use of uranium resources is promised through the introduction of advanced fuel cycles to nuclear power programs. In the Canadian context, this is not likely to be needed until the next century, but we are currently doing the research and development necessary to pursue this option when the need arises.

To initiate thorium fuel cycles in Canadian CANDU reactor systems, the plutonium derived from irradiated, natural uranium fuels could be used as the initial fissile material. Following irradiation, the thorium fuel would be reprocessed to remove fission products and to recover the thorium, the unconsumed plutonium, and the uranium-233 produced.

FLOWSHEET DEVELOPMENT

Based on distribution data obtained in our laboratories, the flowsheet shown in Figure 1 was devised to accomplish the above separations. It is similar to the acid THOREX flowsheet (1), but modified in some respects because of the presence of plutonium in the process. The extractant is 30% tributyl phosphate (TBP) in a kerosene diluent, modified by the addition of an aromatic (10% diethylbenzene) to prevent third-phase formation.

The first two solvent-extraction contactors comprise a single co-decontamination cycle, which rejects most of the fission products to the aqueous waste from the first contactor. The three actinides are stripped to the aqueous phase in the second contactor. Following evaporation and plutonium valency adjustment, the solution is fed to the primary separation section of the flowsheet, where conditions are adjusted in Contractors 3, 4 and 5 to recover Pu(III), thorium, and uranium, respectively.

The success of the flowsheet was established "inactively" (i.e. in the absence of fission products) in the laboratory using small 12- or 16-stage mixer-settlers (2).

To test the performance of the flowsheet under "active" conditions, a small experimental facility, called the Thorium Fuel Reprocessing Experiment (TFRE), was assembled in the Hot Cells at the Whiteshell Nuclear Research Establishment (WNRE). The experimental program was designed to obtain information on

(1) thoria fuel dissolution characteristics,
(2) effects of insolubles,
(3) fission-product decontamination factors,
(4) product losses,
(5) product separation factors, and
(6) waste characteristics.

THE TFRE FACILITY

The facility was assembled in modules outside the Hot Cells for inactive commissioning. The modules were then moved and re-assembled in the Hot Cells for additional commissioning prior to starting the experimental program. Four cells and an adjacent shielded glove box are dedicated to this experiment. One cell is used for head-end operations such as dissolution, acid adjustment, clarification, and accountability. A second cell and the shielded glove box are used for solvent-extraction operations, solvent recovery, and concentrating products and wastes. Calcination and vitrification of the high-level wastes are done in a third cell, and a fourth cell is used for chemical analyses.

OPERATION OF THE TFRE FACILITY

Fuel for each experiment was disassembled and chopped, one element at a time. In experiments conducted to date, the zirconium alloy sheaths were manually separated from the powdered fuel, which was weighed into batch sizes of about 3 kg each. These were transferred to the dissolver and THOREX dissolver solution (HNO_3 = 13 mol/L, F^- = 0.05 mol/L and Al^{3+} = 0.1 mol/L) was added. Dissolution was complete after refluxing for about eight hours. Excess acid was distilled, and the fuel solution was diluted to the desired conditions for solvent-extraction operations (i.e. Th ≈ 200 g/L and HNO_3 = 3 mol/L). The dissolver solution was filtered to remove undissolved solids and transferred to an accountability tank where final adjustments were made. The feed stream (1AF) was transferred to the first mixer-settler using a constant-volume feeder (rotating buckets) at a rate of about 1 mL/min, giving the facility a throughput of about 300 g(Th) per day. In each experiment, the facility was operated continuously for five or more days with two 12-h shifts per day. Each process stream was sampled and analyzed two or three times per day to obtain flowsheet data.

One disadvantage of the low throughput of the facility is that steady state is approached slowly and the length of time at steady state is limited by batch size. Obtaining good steady-state data over several consecutive days for flowsheet evaluation is, therefore, hampered to some extent.

Following exhaustion of the feed solution, the facility was flushed using a dummy feed solution of 3 mol/L HNO_3, to minimize radiation damage to the equipment and solvent and to prevent blockages due to crystallization in lines over extended shut-down periods.

During a run, the solvent was continuously circulated through a solvent-recovery facility in the shielded glove box, where it was washed first with 0.05 mol/L KOH solution, then with 0.01 mol/L HNO_3.

EXPERIMENTAL DATA AND DISCUSSION

Table 1 gives data on the fuels used to date to test the flowsheet under active conditions. Burnups have been between 300 and 400 MWh/kg of initial heavy element, and cooling times have varied from 1 to 10 years. Since irradiated ThO_2 fuel, containing plutonium as the initial fissile material, was not yet available in Canada, $Pu(NO_3)_4$ solution was added to the dissolver following dissolution of the fuel in one of the experiments, to test the flowsheet as fully as possible. (Some ThO_2 - PuO_2 fuel is currently undergoing qualification testing in the WR-1 Reactor at WNRE, but it will not be available for a few years.)

TABLE 1

FUELS PROCESSED IN THE TFRE

Fuel Type	ThO_2-$^{235}UO_2$ Fast Neutron Fuel	Expt'l ThO_2-$^{235}UO_2$ Fuel	Expt'l ThO_2-$^{235}UO_2$ Fuel*
Reactor	NRU	WR-1	WR-1
Burnup (MWh/kg)	305	410	391
(MWd/Mg)	12 700	17 080	16 290
Cooling Time (a)	10	3.3	1.1

* $Pu(NO_3)_4$ solution added to dissolver

Plutonium Valency Adjustment. Before extraction in the first contactor, plutonium was adjusted to the Pu(IV) state by adding NO_2^- to the feed solution. We have used two different procedures for this:

(1) an excess of $NaNO_2$ solution was added to the feed, or
(2) a 4:1 mixture of NO and O_2 was bubbled through the fuel solution, producing the NO_2^- in situ (3).

The latter procedure was considered preferable since it eliminated the introduction of sodium (which has an important impact on waste management), and some improvement in decontamination from ruthenium was anticipated because formation of the less extractable nitrito-nitroso ruthenium complexes should have been favoured over the corresponding nitrato complexes (3).

Plutonium valency adjustment was also required before, or in, the third contactor where plutonium was to be reduced to Pu(III), to prevent its extraction and allow its separation from thorium and uranium.

Several different reductants (and holding reductants) were tested in our "inactive" development work. These are listed in Table 2 together with comments on how successful they have been.

TABLE 2

REDUCTANTS TESTED FOR Pu(III) SEPARATION FROM THORIUM AND URANIUM

Reagents	Concentrations in 3AS(mol/L)	Comments
Ferrous sulfamate Sulfamic acid	0.05 0.05	Successful separation*
Hydroxylamine nitrate (HAN) Hydrazine nitrate (HYD)	0.3 0.1	Unacceptable Pu losses to solvent**
Ferrous nitrate HAN HYD	0.05 0.3 0.1	Successful separation**
2,5 di-tert-amylhydroquinone	0.03	Unacceptable Pu losses**
Acetaldoxime HAN	0.6‡ 0.1	Successful separation

* Same reagents and concentrations used in feed solution (3AF) to pre-reduce Pu to Pu(III).
** HYD-stabilized HAN used in 3AF to pre-reduce Pu to Pu(III).
‡ Acetaldoxime added only to 3AF (not 3AS). HAN also used to pre-reduce Pu to Pu(III).

Although ferrous sulfamate (FeSA) was very successful, its disadvantages (major contribution to wastes and corrosion due to H_2SO_4) are well known, and efforts continue to find more acceptable reducing agents.

One of the more promising reagent combinations for plutonium separation from uranium is hydrazine-stabilized hydroxylamine nitrate (HYD-HAN) where, e.g. in the PUREX process, successful separations have been obtained (4). However, for THOREX flowsheets, conditions required for extraction of thorium (as opposed to uranium), i.e. higher acidity and higher solvent-to-feed flow ratio, combined with the salting effect of $Th(NO_3)_4$ on plutonium, all conspire to decrease the effectiveness of HAN. In all of our THOREX flowsheet work with HYD-HAN, unacceptable plutonium losses to the solvent stream were observed.

Barney (5) and McKibbon and Bercaw (6) have reported a catalytic effect of iron on the rate of reduction of plutonium to Pu(III) when using HAN. We have also tested this combination of reagents in our modified THOREX flowsheet and have obtained very satisfactory separations of Pu(III) from thorium and uranium. The scrub stream (3AS) was prepared from ferric nitrate solution to which

HYD-HAN was added to reduce Fe(III) to Fe(II). The success of these reagents is attributed to the fast reduction kinetics for the Fe(II) + Pu(IV) reaction, coupled with the relatively fast reaction of HAN + Fe(III) to produce Fe(II), to maintain an adequate reducing potential in the contactor.

Of the reducing reagents listed in Table 2, the only one tested "actively" in the TFRE facility has been the Fe(II)-HAN-HYD combination. In all of these experiments, plutonium was adjusted to the Pu(III) state in the 3AF feed solution before it was added to the solvent-extraction contactor. In most of the "inactive" experiments, this pre-reduction was performed with HYD-HAN. However, to ensure reduction to Pu(III) in the continuously operating TFRE facility, where faster kinetics were thought to be necessary, Fe(II)-HYD-HAN was used.

The plutonium losses observed when using HYD-HAN were probably due to an autocatalytic oxidation of Pu(III) to Pu(IV) in the solvent phase, combined with the relatively slow reduction of Pu(IV) by the HAN, which acts only in the aqueous phase (7). Both the substituted hydroquinone and acetaldoxime (see Table 2) are soluble to some extent and are, therefore, capable of reacting with other species in the solvent phase. Hydroquinone is an effective Pu(IV) reductant, but in our THOREX tests, it was not completely successful, and plutonium losses were again observed. We suspect that partition failure was due to the relatively high acidity and high solvent-to-feed flow ratio (i.e. the same reasons that led to the failure with HYD-HAN). Acetaldoxime, on the other hand, is an excellent scavenger of nitrous acid, which appears to be responsible for the autocatalytic oxidation of Pu(III). Although most of the acetaldoxime added with the feed stream remains in the aqueous phase, enough of it does extract to prevent initiation of the autocatalytic oxidation of Pu(III) and good plutonium separation is achieved. Tests have indicated that the acetaldoxime remaining with the plutonium product is easily destroyed by evaporation of the solution and, therefore, its use should not present problems in product conversions or fuel refabrication.

Flowsheet evaluation. Flowsheet data from the "active" experiments reported here continue to show the viability of our modified THOREX flowsheet. Table 3 lists data for the products. Losses to the various waste streams (i.e. to the 1AW stream from Contactor 1 and to the solvent) were at, or below, the limits of detection and represented a maximum of 1.5% of the uranium, 0.2% of the thorium and ~ 1% of the plutonium. Separation of the three products from each other was good, especially the removal of thorium from the uranium and plutonium products, where decontamination factors of 5000 or more were obtained in a single cycle. The separations of uranium and plutonium from the thorium product do not appear to be as good, simply because analytical detection limits were approached readily due to the low initial concentrations.

Fission-product decontamination data are shown in Table 4. The decontamination factor (DF) for ^{144}Ce was $> 10^4$ and for ^{137}Cs $> 10^5$. These were obtained for the first solvent-extraction cycle only. Additional decontamination is expected in the second cycle, but it could not be quantified because activity levels were already at the detection limits.

The decontamination factor of ~ 200 for ^{106}Ru is that obtained for both the thorium and uranium products, i.e. over two solvent-extraction cycles. This DF is somewhat lower than desired, but not unexpected. Higher DF values from ruthenium have been reported in the literature (8,9), also shown in Table 4, but these higher DF values were achieved only when the feed solution was made acid deficient. The lower DF values quoted were obtained with acidic feed solutions. We chose not to use acid-deficient solutions in our flowsheet because of the possibility of plutonium polymerization under such conditions.

TABLE 3

SUMMARY OF PRODUCT DATA

Product	Loss to Wastes (%)	Impurity Content (g/g (product))		
		Th	U	Pu
Uranium	< 1.5	< 0.01	–	$< 5\times10^{-4}$
Thorium	< 0.2	–	$< 2\times10^{-4}$	$< 5\times10^{-4}$
Plutonium	< 1	~ 0.01	$\sim 1\times10^{-3}$	–

TABLE 4

FISSION PRODUCT DECONTAMINATION FACTORS*

Nuclide	Decontamination Factors	
	This Work	Literature Data
^{144}Ce	$> 1\times10^4$	3×10^4 - 5×10^6 (Julich**)
^{137}Cs	$> 1\times10^5$	
^{106}Ru	2×10^2	1×10^2 (Hanford+) 20 - 2×10^4 (Julich**)
$^{95}Zr/Nb$	N/A‡	1×10^2 - 1×10^6 (Julich**)

* For thorium and uranium products.
** From reference 8.
\+ From reference 9.
‡ N/A = not available.

Only very preliminary data are available for the behaviour of $^{95}Zr/Nb$ in the one experiment using short-cooled fuel. Indications are that DF values for zirconium may not be any higher than those measured for ^{106}Ru. The relatively low DF values for both ^{106}Ru and ^{95}Zr are, however, still considered acceptable, because the activity of these fission products is less than that due to ^{232}U and ^{228}Th and their daughters in the products themselves.

SUMMARY AND CONCLUSIONS

Experience gained in design, fabrication and operation of the Thorium Fuel Reprocessing Experiment in the WNRE Hot Cells has made a useful contribution to AECL's Advanced Fuel Cycle Program.

Our modified THOREX flowsheet has been tested successfully using irradiated-fuel solutions. Separation of thorium, uranium and plutonium from each other has been good, and product losses have been low. High decontamination factors have been obtained for rare earths and for cesium. Lower decontamination factors have been obtained for ruthenium and for zirconium, but they are considered acceptable.

Reductive stripping of Pu(III) and its separation from thorium and uranium have been demonstrated, but this has proven to be a more difficult task than the comparable separation of plutonium from uranium in the PUREX process.

Acetaldoxime has been shown to be a promising Pu(III) stabilizer in mixer-settler operations, and further work is planned to determine its viability in an "active" experiment.

ACKNOWLEDGEMENTS

The support provided by the Design and Project Engineering Branch, the Maintenance and Construction Branch, and the Analytical Science Branch at WNRE is gratefully acknowledged.

REFERENCES

1. R.H. Rainey and J.G. Moore, Nucl. Sci. Eng. 10, 367 (1961).
2. G.R. Grant, W.W. Morgan, K.K. Mehta and F.P. Sargent, ACS Symposium Series 117, 351 (1980).
3. D. Scargill, R.J.W. Streeton and C.E. Lyon, AERE-R-4786 (1965).
4. G.L. Richardson and J.L. Swanson, HEDL-TME-75-31 (1975).
5. G.S. Barney, ARH-1920 (1971).
6. J.M. McKibben and J.E. Bercaw, DPSPU 69-30-16 (1969).
7. Y.-K. Sze, L.J. Clegg, A.F. Gerwing and G.R. Grant, Nucl. Technol. 56, 527 (1982).
8. L. Küchler, L. Schäfer and B. Wojtech, Kerntechnik 12, 327 (1970).
9. R.L. Walser and R.R. Jackson, eds., ARH-2127 (1977).

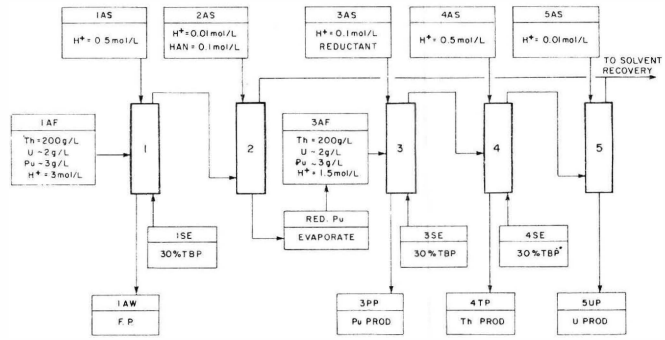

FIGURE 1: MODIFIED THOREX FLOWSHEET FOR Th-Pu-U FUEL

INFLUENCE OF CATIONS ON CRUD FORMATION IN URANIUM CIRCUITS

G. M. Ritcey and E. W. Wong

CANMET, Energy, Mines and Resources Canada
555 Booth Street
Ottawa, Ontario, Canada K1A OG1

INTRODUCTION

Solvent losses in processing by solvent extraction can be attributed to entrainment, solubility, evaporation, degradation, adsorption on solids, formation of stable emulsions and cruds, spillage and sampling. These solvent losses, and particularly those losses attributed to emulsion and crud formation, can in part be related to nature of feed, reagent choice, continuous phase, equipment selection and method of operation, such as the droplet size, excessive turbulence, etc.

Common to all or most solvent extraction operations in the mining industry is the problem of stable emulsions and the eventual formation of cruds. The crud can constitute a major solvent loss to a circuit and therefore adversely affect the operating costs. Because there can be many causes of crud formation, each plant may have a crud problem unique to that operation. Factors such as ore type, solution composition, solvent composition, presence of other organic constituents, design and type of agitation, etc. can adversely affect the chemical and physical operation of the solvent extraction circuit, and result in crud formation.

Crud is defined as the material resulting from agitation of an organic phase, an aqueous phase, and fine solid particles, that form a stable mixture. Crud usually collects at the interface between the organic and aqueous phases. Other names that have been used for the phenomena are grungies, mung, gunk and sludge.

In an earlier paper by the author, a review was made of the causes of crud and possible treatment methods (1).

The present paper is concerned with the crud generated in uranium solvent extraction circuits, its analyses and identification, and possible treatment methods, together with the results of laboratory tests carried out to generate crud, using the ore leach solution from a Canadian uranium mill as well as tests on synthetic solutions.

FEED MATERIALS AND PROCEDURE

The tests were performed on both synthetic leach liquors as well as actual leach soltuions. Because crud generation is a relatively slow process involving contacting large volumes of liquor to obtain sufficient material for analyses, the tests were conducted in a continuous mixer settler unit. The leach feed solution for the work was prepared by duplicating the leaching conditions for a Canadian uranium ore as well as the liquid-solids separation procedure. A typical analyses of the leach liquor is shown in Table 1.

Table 1 - Typical Analyses of Leach Feed Solution

	g/L
U	1.87
Th	0.003
Mo	0.0008
Fe_T	1.84
Al	2.11
Si	0.44
Ca	0.30
Mg	9.89
Zn	0.015
V	0.006
Ti	0.004
pH	1.6

Unclarified pregnant solution ≈100 ppm suspended solids, 73 g/L total solids.
Clarified pregnant solution <50 ppm suspended solids.

The tests on the synthetic feed solution, containing 1.6 g U/L at pH 1.6, contained Fe Al Ca Mg Si which were varied in content in a factorial designed set of tests. The solvent composition used for the investigation consisted of 3.5% Adogen 364 plus 5% isodecanol in Shell 140 diluent. The tests were carried out in a Bell Solvent Extraction Unit, incorporating 4 stages of extraction (A/O 1.5/1), 3 stages of stripping (O/A 2/1) using 130 g/L $(NH_4)_2SO_4$ or 50 g/L Na_2CO_3 and one stage of acid equilibration with 5% H_2SO_4 (O/A 2/1). Each continuous run was for a duration of 2.5-6.0 hours, depending upon the crud formation and thus the necessity for shut-down. The agitation used in the pump-mix design of the mixers was in the range of 800-1200 rpm. All tests resulted in the extraction of 99.99% of the uranium from the feed solution.

RESULTS

Characterization of Crud and Analyses

The initial work by CANMET on crud from uranium circuits (2) was performed on samples of crud obtained from three operating mills located in New Mexico and Wyoming in the U.S.A. and in Saskatchewan, Canada. Chemical analyses were performed on the crud and tests were performed to break the crud. When sufficient information had been obtained on crud characterization, the subsequent research involved the generation of crud in the laboratory. This was to verify whether a crud could be produced that was similar to that generated at the uranium mill site.

The data indicated a reasonably close relationship between the major metal constituents in the cruds from the extraction circuits. The major elements are Si, Al, Fe, Ca, Mg, C and U. The crud analysis from the strip circuit is somewhat parallel to the extraction circuits, but lower in metal content except for uranium. Also, Zr could be a major cause contributing to crud, if present in the circuit. Silica was still present. The total organic in all three cruds was approximately of equal content (as indicated by analyses for total C). There was also a relationship between the feed analysis and the crud analysis, for extraction and stripping circuits for two separate mills, indicating a good parallel between the metals content of the solvent extraction feed and the crud, whether in the extraction or stripping circuits. Si is noticeably concentrated in the extraction crud. In the stripping circuit crud, the analysis showed a reasonable indication that impurities from the feed solution are getting through to the stripping circuit to constitute the crud. These are mainly Si, Al and Fe with lesser amounts of Mo, Ca, Zr and Mg.

The analyses of crud material from both the extraction and strip circuits of the plant operation are given in Table 2. The high metal losses in the stripping circuit can possibly be attributed to the localized precipitation of uranium when stripping with $(NH_4)_2SO_4$.

Effect of Humic Acid, Isodecanoic Acid and Phenol in Crud Generation

The effect of organic acids on crud formation was investigated, using humic acid and phenol. Also, because it was thought that isodecanol could be degraded in the solvent extraction process to isodecanoic acid, that acid was also studied. Both clarified and unclarified pregnant solutions were used, in contact with the plant organic solvent mixture. Agitation was at 1600 rpm for two minutes at A/O 1.5/1. The qualitative results of these tests indicated that the organic acids, if present in sufficient amount, can cause crud formation, and that crud is more readily formed in the unclarified pregnant solution.

The results also showed that freshly prepared organic solvent showed no crud tendency. This may indicate that in the recycled plant solvent, if a break-down of isodecanol to isodecanoic acid has occurred this decay product may be the cause of the crud formation. Addition of humic acid to the freshly prepared solvent produced a white precipitate. Addition of humic acid to the plant solvent produced additional precipitate.

Table 2 - Analyses of Crud in Extraction and Stripping Circuits

	Extraction (%)	Stripping (%)
U	11.3	12.1
Mg	2.49	4.49
Si	13.1	7.45
Fe	5.4	8.0
Mo	0.11	0.72
Cd	0.10	0.01
Mn	0.05	0.009
Al	3.96	.077
Cu	0.08	0.01
Ag	0.009	0.001
Na	0.09	<0.001
Sn	0.008	<0.001

Effect of Cations on Crud Formation

The results of the factorial designed tests on a synthetic leach liquor containing varying amounts of Fe Al Si Ca Mg are summarized in Table 3, in which the tests were carried out with the aqueous feed being the continuous phase. The strip reagent was a solution of 50 g/L Na_2CO_3. The tests indicated that, in all but a few of the solution compositions tested, precipitates and/or crud were produced early in the extraction circuit, which were then carried over into the stripping circuit. In some tests the crud that was produced became very voluminous resulting in early shut-down of the circuit. A preliminary mathematical analysis of the work indicated iron and silica to be the major elements in initiating the generation of crud and this occurred in solutions containing 1.75 g Fe/L or greater. Aluminum, calcium and magnesium had essentially no effect due to compositions in the feed.

Although the crud was generally produced in the extraction circuit, nevertheless it also formed in the stripping circuit. This was probably due to there being no scrub stage between extraction and stripping. Also, the silica in the synthetic was added as sodium silicate, and so the crud tendency would be much less than would be encountered in leach solutions already containing colloidal silica.

As to the cause of the crud in the extraction circuit, when only a clear aqueous feed solution containing a few metals are present, it can possibly be attributed to the high shear and pressure exerted upon a droplet by the pump-agitator. Precipitation of metals from solution is enhanced by pressure, parricularly those that tend to hydrolyse or those that may be unstable. High concentration of iron in solution, perhaps in combination with Si, or Al and Mg appear to have adverse affects. Also a combination of high Al and high Mg (Test F4) appears to enhance crud formation. The Si Fe Mg tend to hydrolyse first, during extraction, while carry over and formation of crud in the stripping circuit occurs due to Al and Ca as well as Fe, Mg, Si (Test F15). Although only one test (at the time of writing) was performed with the organic being the continuous phase, it appears that crud is more easily formed from the aqueous continuous system (Test 14B).

Table 3 - Cation Concentration and Crud

Test No.	Feed Analyses (g/L)					Strip Crud Analyses (%)							Ext. Crud Analyses (%)			
	Fe	Al	Si	Ca	Mg	Fe	Al	Si	Ca	Mg	U	Fe	Al	Si	Ca	Mg
F13	0.50	2.8	0.40	0.45	8.5	NO		CRUD		FORMED						
F8	0.70	3.0	0.35	0.27	4.1	NO		CRUD		FORMED						
F4	0.70	12.0	0.33	0.27	16.0	1.3	17.4	0.38	0.32	2.7	6.4					
F12	0.88	3.2	1.4	0.52	8.9	NO		CRUD		FORMED						
F7	0.89	12.0	1.2	0.40	3.6	NO		CRUD		FORMED						
F15	1.6	3.2	0.25	0.51	8.2	8.4	10.4	2.4	1.1	3.3	ND	12.9	2.4	10.2	.20	.15
F9	1.3	5.3	0.57	0.48	9.7	3.3	10.5	5.3	1.1	1.0	5.0					
F10	1.4	5.2	0.53	0.46	7.8	2.8	9.8	1.9	1.1	3.8	ND					
F17	1.6	3.0	0.57	0.51	6.6	7.5	16.3	2.7	1.8	0.87	3.5					
F11	2.3	3.4	0.30	0.51	7.7	CRUD		NOT		ANALYSED						
F1	2.7	11.8	1.2	0.26	16.4	4.9	16.4	2.5	0.52	4.0	2.1					
F2	3.0	12.0	0.32	0.55	2.6	4.0	22.6	0.59	3.85	0.60	1.7					
F3	2.7	2.7	1.1	0.25	3.8	15.2	8.2	6.3	1.0	1.9						
F14A	3.1	2.8	0.56	0.46	7.5	8.4	7.7	3.1	0.51	2.1	3.2					
*F14B	3.8	4.6	0.83	0.47	1.1	NO		CRUD		FORMED						

ND - not determined
* - organic continuous

Effect of Solids Content, Scrubbing and Stripping Agent

Actual pregnant leach solution had 30 ppm slimes added to it before being contacted with freshly prepared solvent consisting of 3.5% Adogen 364 plus 3.5% isodecanol in Shell 140. Four stages of extraction were followed by four stages of stripping with 130 g/L $(NH_4)_2SO_4$ controlled at pH 4.0-4.2 with NH_4OH. The flows, O/A, in extraction were 180/120; in the strip circuit 120/60 and acid equilibration was 120/60. The running time was 4 hours. Because of the iron carry-over into the stripping circuit, another similar run was made where a single water scrub stage was employed. The run was similar in crud and emulsion characteristics as the previous run. Phenol was also detected in the crud material.

These results indicated that considerable iron was carried through the system when there was no scrub stage following the 4 stages of extraction. Also, the major uranium precipitation occurring during stripping was due to the difficulty in maintaining good pH control.

Because of the apparent difficulty in controlling the $(NH_4)_2SO_4$ stripping, bench tests were performed with 5% and 10% Na_2CO_3, and as a result of phase disengagement rates the 5% Na_2CO_3 was selected as the better medium. A similar continuous run was made on feed containing 30 ppm solids, using 4 stages extraction (O/A 1.5/1), two stages water scrubbing (O/A 1.5/1), three stages stripping with 5% Na_2CO_3 (O/A 1.5/1), and a single stage of acid equilibration. The entire run of 5 hours duration was satisfactory, with no stable emulsions or crud formed. A repeat test with a single H_2O scrub stage resulted in crud in the stripping circuit, as a result of carry-over from extraction. Therefore, it appears that two stages of scrubbing are necessary.

With a feed containing 60 ppm solids, and in a similar extraction-scrubbing-stripping sequence, emulsion and crud build-up started in the No. 4 settler of the extraction circuit (where the feed aqueous enters). The crud carried-over into the water scrub stages and then into stripping. Analyses of the accumulated crud in the stripping circuit crud are given in Table 4. The results appear to indicate that 60 ppm of solids are more than a pump mix design of mixer settler can handle without forming crud.

Table 4 - Effect of Suspended Solids, Scrubbing and Stripping Agent on the Strip Circuit Crud

ppm solids in feed:	30		30	60
Strip:	$(NH_4)_2SO_4$		Na_2CO_3	Na_2CO_3
Scrub:	None	Single	Two	Two
U	50.0	23.7		7.24
Fe	11.46	6.7	No	3.98
Si	2.43	9.6	Crud	0.13
Mg	0.02	0.02		11.7
Al	1.08	5.9		6.21
Ca		0.03		0.13
Mo		0.02		0.04
Zr				0.30
Phenol	0.01			

Investigation of Other Contactors

The data obtained from the pump-mix design mixer settlers showed that if the feed solution contained about 30 ppm solids and if two water scrub stages were used, followed by Na_2SO_3 as the stripping agent, then no crud resulted. However, the mixer settler design exhibits a high shear performance, producing much finer droplets than actually required for mass transfer, because of the necessity for pumping. Two alternative types of contactors were therefore examined, both possessing good mass transfer characteristics without the disadvantage of the excessive turbulence which we believe is partly the cause of the stable emulsion in a pump-mix mixer settler. The two contactors selected for the tests were the Kenics in-line mixer and the RTL contactor (formerly Graesser "raining bucket" contactor).

Kenics In-Line Mixer

Contact of a leach solution containing 60 ppm solids with the solvent was co-current in a 330 cm long x 1.27 cm diameter column. The retention time was 1.6 minutes. Following extraction, the loaded solvent was stripped with 50 g/L Na_2CO_3. Both extraction and stripping performed well, with no crud or precipitates formed.

RTL Contactor

Similar tests were run in a 101.6 cm long x 15.2 cm diameter RTL contactor. The solvent was fed countercurrent to the feed solution. Again the physical operation was good, and solutions containing up to 100 ppm solids were successfully treated.

CONCLUSIONS

The conclusions that can be drawn from these crud studies are summarized as follows:

a) there is a relationship between the composition of the feed to solvent extraction and the analysis of the crud. Although much of the crud is due to fines carry-over from insufficiently clarified feed solution, crud can also be produced from clear aqueous solutions.

b) the major constituents of crud are Si Al Fe Mg Ca, together with U.

c) strip cruds contain large amounts of uranium, due to possibly poor pH control in the NH_4-$(NH_4)_2SO_4$ stripping, resulting in localized precipitation of uranium and consequently heavy crud formation.

d) Fe, Si, Ca, Mg, Al appear to be carried through the extraction circuit and report in the strip circuit crud. Tests indicate the requirement for 1-2 scrub stages between extraction and stripping to remove such impurities which could aggravate emulsions and crud formation.

e) other organics in the system (humic acid, phenol, lignin, and carboxylic acids) may constitute a cause for crud formation. Unclarified feed is more susceptible to crud formation in the presence of the organics than is clarified feed.

f) the continuous phase may play an important part in the crud that may be generated.

g) a Na_2CO_3 strip solution, instead of $(NH_4)_2SO_4$, appeared to be more suitable for stripping to minimize crud formation.

h) the pump-mix design for agitation may tolerate in the range of 30-60 ppm suspended solids, but with the high shear of such a design crud prevention above these levels is difficult.

i) use of other types of contactors, where high shear is eliminated during the mass transfer, should be considered.

ACKNOWLEDGEMENTS

The authors gratefully acknowledge the assistance of Mr. R.F. Pilgrim for the design of the experiments and the mathematical interpretation of the results; also to the Chemical Laboratory for the numerous analyses.

REFERENCES

1. Ritcey, G.M. "Crud in Solvent Extraction Processing - A Review of Causes and Treatment"; Hydrometallurgy, 5, 1980, 97-107.

2. Ritcey, G.M. "Crud in Uranium Solvent Extraction"; Presented at the 14th International Mineral Processing Congress, Toronto, October 1982.

CONSOLIDATED FUEL REPROCESSING PROGRAM ALTERNATE EXTRACTANTS TO TRIBUTYL PHOSPHATE FOR REACTOR FUEL REPROCESSING

D. J. Crouse, Fuel Recycle Division
W. D. Arnold and F. J. Hurst, Chemistry Division

P.O. Box X
Oak Ridge National Laboratory*
Oak Ridge, Tennessee 37830 USA

*Operated by Union Carbide Corporation for the U.S. Department of Energy.

INTRODUCTION:

Because of its many favorable properties, tributyl phosphate (TBP) is the chosen extractant throughout the world for the reprocessing of power reactor fuels (Purex process). These properties include (1) adequate extraction power for uranium and plutonium, (2) good selectivity for these elements relative to elements in the fission product spectrum, (3) amenability to stripping with dilute nitric acid, and (4) good phase separation.

Despite the overall success of TBP, it has some weaknesses which result in process problems. Most of its process disadvantages derive from the fact that it is subject to chemical and radiation degradation to form principally dibutyl phosphoric acid (HDBP) and monobutyl phosphoric acid (H_2MBP). These products decrease the fission product decontamination efficiency and can prevent complete uranium and plutonium stripping, resulting in their losses to the solvent wash wastes. In addition, certain metal (Th, Zr, Pu) complexes of the HDBP and H_2MBP have low solubilities in the aqueous and organic phases and sometimes precipitate and interfere with system operation. A further complication is the significant solubility of TBP in the aqueous phase. Any process solution that has been contacted with TBP will contain about a quarter of a gram of TBP per liter. If this solution is allowed to stand for an extended period or is sent to an evaporator, the TBP degrades, and the resulting HDBP tends to cause precipitation of plutonium or fission products. The presence of TBP has also been blamed for an explosion that occurred during denitration of a uranyl nitrate solution. For these reasons, it is standard practice to steam strip uranium and plutonium product solutions or scrub them with a diluent to remove dissolved TBP prior to evaporation.

Our studies of alternate extractants, which are presently inactive, had the objective of retaining the many advantages of TBP while eliminating or mitigating its disadvantages. Thus, the studies were limited to compounds of the same class as TBP, that is, trialkyl phosphates, but with longer alkyl chains. Increasing the molecular weight lowers the aqueous solubility of the extractant to a negligible value (<0.001 g/L) and increases the organic phase solubility of the metal complexes of both the primary extractant and its degradation products. In addition, Russian studies with tributyl phosphate isomers have shown that it is an advantage to introduce branching of the alkyl chain at the second carbon from the phosphorus since this increases the resistance to acid hydrolysis (1).

Table 1 shows four compounds that were considered attractive for evaluation studies, but only two of these, tri(n-hexyl) phosphate (THP) and tri(2-ethylhexyl) phosphate (TEHP), have been tested. Most of the studies were with TEHP because it is available commercially at high purity.

The tests confirmed that both TEHP and THP have some important process advantages over TBP, although also some disadvantages; further study of these and other similar alternate extractants appear warranted.

EXTRACTION BEHAVIOR:

Most of the tests were made with 1.09 M solutions of the extractants in n-dodecane (NDD) or normal paraffin hydrocarbon (NPH) diluents. This corresponds to 30 vol % concentration for TBP, 41 vol % for THP, and 52 vol % for TEHP.

Isotherms for extraction of uranium show the extraction power to be in the order TEHP>THP>TBP (Figure 1). At low solvent loadings, the extraction coefficients with TEHP are about 1.6 and 2, respectively, times those of THP and TBP. This is consistent with earlier studies by Siddall (2,3) which showed that the uranium extraction power increases with increase in the molecular weight of trialkyl phosphates. All three extractants reached a maximum uranium loading of about 125 g/L, equivalent to about 0.5 mole of uranium per mole of extractant. Study of the effect of varying the extractant concentration on the uranium extraction coefficient showed about a 1.4 power dependence for TBP and THP and a 1.6 dependence for TEHP in the concentration range of 0.3 to 1 M.

The Pu(IV) extraction power is also in the order of TEHP>THP>TBP. In this case, the extraction coefficients showed about a 1.4 power dependence on extractant concentration for all three extractants. Figure 2 shows the effect of temperature on plutonium extraction.

The extraction of thorium follows a different pattern, with THP being the strongest and TEHP the weakest extractant. A third phase formed at thorium solvent loadings of >40 g/L with TBP, but THP and TEHP were loaded to >60 g/L without formation of a third phase.

Fission Products. The behavior of the more important fission products, zirconium and ruthenium, was examined in batch extraction tests and in batch extraction-scrubbing-stripping tests that simulated a process cycle. Extraction of zirconium was about equivalent for all three extractants. Ruthenium extraction coefficients, on the other hand, were about equivalent for TBP and THP but about four times those for TEHP in the HNO_3 concentration range of 0.2 to 4 M (Figure 3). In the simulated process cycle tests, overall decontamination factors from ruthenium were highest with TEHP and lowest with TBP. Zirconium decontamination factors were 1200 for TBP and THP and 2600 for TEHP when the contact times were 2 to 5 min. For long contact times (15 min), TBP gave the best results.

Because of the complex behavior of ruthenium and zirconium, tests of this type, made in the absence of uranium, give only a rough indication of the comparative results that can be expected in process operations, but they indicate that decontamination efficiencies with THP and TEHP should be a least as good as those obtained with TBP; in the case of TEHP, the efficiencies may be appreciably better. Also, it should be mentioned that the higher uranium and plutonium extraction power of THP and TEHP compared to TBP offer opportunity for operation of the extraction-scrubbing system at higher solvent metal loadings. It is well known that this has a beneficial effect on decontamination efficiencies.

Mass Transfer Rates. Studies of U(VI) transfer rates for various trialkyl phosphates in a Lewis cell by J. C. Mailen, D. E. Horner, and J. K. Storey of the Oak Ridge National Laboratory (ORNL) showed that the uranium transfer rates in both the extraction and stripping modes decreased as the alkyl chain length and branching increased. The decrease was in the order TBP>THP>TEHP. Although uranium transfer was a factor of 5 to 10 slower with TEHP than with TBP, transfer was still very rapid. The significance of these lower transfer rates for THP and TEHP solvents needs to be evaluated in typical solvent extraction contactors.

EXTRACTANT STABILITY:

The stabilities of the TBP, THP, and TEHP were compared by contacting them with 1 M HNO_3, both in and out of a radiation field, and measuring the in-growth of the respective dialkyl phosphate degradation product. The three extractants showed essentially equivalent radiation stability up to a solvent dose of 4 W·h/L, and results were unaffected when uranium was added to the system.

The rates of chemical degradation (acid hydrolysis) of TBP and THP were about equivalent and at least five times the TEHP rate (Figure 4). The presence of uranium appreciably increased the degradation rates. The degradation was slow under the test conditions but would be considerably faster at the higher temperatures and acidities typical of process operations. Also, it has been found (4) that the hydrolysis is catalyzed much more strongly by tetravalent metals such as zirconium, uranium (IV), and thorium than by uranium (VI); a single ORNL test also showed a large effect of Pu(IV). Radiolytic degradation has usually been considered the more important contributor to the total solvent degradation, but these findings indicate that chemical degradation can be of equal or greater importance, particularly if the system is operated at elevated temperatures and centrifugal contactors are used in the extraction step.

Precipitation. The zirconium and thorium complexes of DBP and MBP tend to precipitate from the solvent especially at the lower acidities typical of the stripping system. This has been a serious problem in treating thorium fuels (Thorex process). In comparative batch extraction-stripping tests, THP and particularly TEHP showed a much lower tendency toward such precipitation than did TBP, indicating that less trouble from interfacial solids could be expected with the alternate extractants.

PHASE SEPARATION:

The phase separation of TEHP was decidedly poorer than that of TBP when the extractants were compared on an equimolar basis (30 vol % TBP versus 52 vol % TEHP). However, the phase separation rates in contact with HNO_3 of 30 vol % TEHP (~0.6 M) and 30 vol % TBP were essentially the same with organic-continuous mixing conditions; with aqueous-continuous mixing, TBP separations were somewhat faster. This was true also in the solvent wash system (0.3 M Na_2CO_3 at 40°C) except that equivalent separation was obtained with aqueous-continuous mixing; organic-continuous mixing resulted in poor phase separation with both extractants.

Because of phase separation considerations, use of TEHP at a molar concentration of 0.6 M, or lower, is recommended.

SOLVENT WASHING:

For effective solvent washing with sodium carbonate, conditions must be changed from those ordinarily used for intercycle removal of the dialkylphosphate (HDBP) degradation product from TBP since the sodium salt of di(2-ethylhexyl) phosphoric acid (Na-DEHP) distributes much less favorably to the aqueous phase compared to Na-DBP. Very efficient removal of Na-DEHP was obtained, however, with a two-stage crosscurrent washing treatment using 0.3 M Na_2CO_3 in the first stage and 0.01 M Na_2CO_3 in the second. Washing of the TEHP as received from the manufacturer

gave considerable trouble since it contains an emulsion-forming impurity. This was removed in initial contacts, resulting in greatly improved separation in subsequent contacts.

Continuous Countercurrent Tests. Flowsheet tests of TEHP as a reprocessing extractant were made at ORNL in mixer-settler tests with simulated fast breeder fuel solutions (U and Pu only) in glove boxes and with irradiated light-water reactor fuel solutions in a hot cell with favorable results.

The hydraulic performance of 0.6 M TEHP solutions (normal paraffin hydrocarbon diluent) in the mixer-settlers was good. Recoveries of uranium and plutonium were high and separations from fission products were efficient with both the TEHP and TBP solvents. Decontamination from ^{95}Zr was better with TBP than TEHP, but ^{106}Ru and ^{95}Nb decontaminations were poorer. Accumulation of interfacial solids appeared less with TEHP.

CONCLUSIONS:

Both THP and TEHP have some important potential process advantages over TBP for reactor fuel reprocessing. These include negligible aqueous phase solubility and less tendency toward third phase and crud formation. The alkyl chain branching of TEHP makes it much more stable to chemical degradation than TBP and probably also accounts for its much weaker ruthenium extraction. The higher uranium and plutonium extraction power of THP and TEHP allows higher solvent loadings in extraction but makes them somewhat more difficult to strip.

The phase separation properties of 1.09 M solutions of THP and TEHP are inferior to those of 1.09 M TBP (30 vol %) but are favorable at lower concentrations. Use of more dilute THP and TEHP solutions is recommended for this reason and to obtain a better balance of extraction power in the extraction versus stripping steps.

ACKNOWLEDGMENTS:

The authors are indebted to M. H. Lloyd and S. E. North of ORNL for plutonium extraction tests with the alternate extractants and to E. D. Collins, D. E. Benker, and B. A. Hannaford of ORNL for mixer-settler tests.

REFERENCES:

1. V. V. Yakshin et al, Radiokhimiya 19, 775 (1977).
2. T. H. Siddall, Ind. Eng. Chem. 51(1), 41 (1959).
3. T. H. Siddall, J. Inorg. Nucl. Chem. 13, 151 (1960).
4. R. G. Wilbourn and G. E. Benedict (GA Technologies, Inc.), "Study of the Effects of Thorium, Uranium, and Zirconium on the Tributyl Phosphate Hydrolysis Rate," personal communication to D. J. Crouse (Oak Ridge National Laboratory) January 1980.

Table 1. Trialkyl phosphate extractants

Structure	Extractant	Molecular Weight
$(C-C-C-C-O-)_3P=O$	TBP	266
$(C-C-C-C-C-C-O-)_3P=O$	THP	350
$(C-C-C-C-C-C-O-)_3P=O$ C C	TEHP	434
$(C-C-C-C-O-)_3P=O$ C	TMBP	308
$(C-C-C-C-O-)_3P=O$ C C	TEBP	350

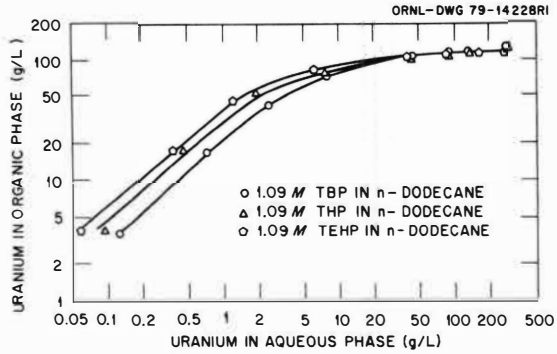

FIGURE 1. ISOTHERMS FOR EXTRACTION OF URANIUM FROM 3 M HNO_3 at 23°C.

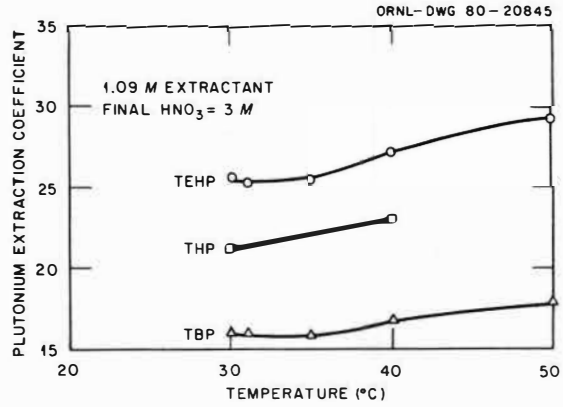

FIGURE 2. EFFECT OF TEMPERATURE ON PLUTONIUM EXTRACTION.

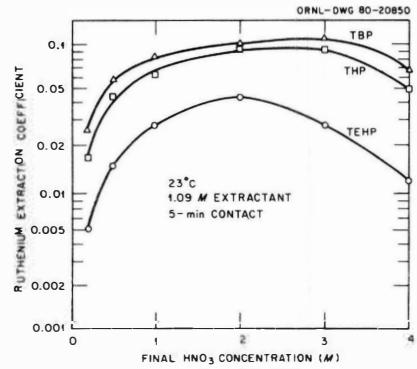

FIGURE 3. EFFECT OF NITRIC ACID CONCENTRATION ON RUTHENIUM EXTRACTION.

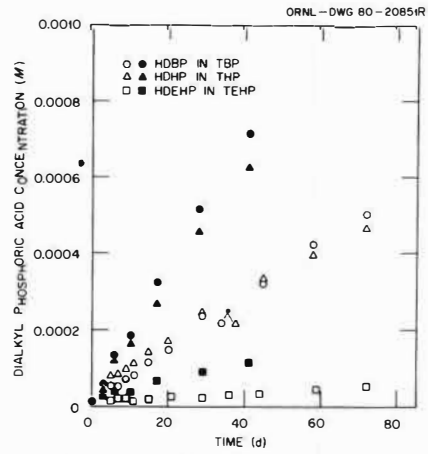

FIGURE 4. HYDROLYTIC DEGRADATION OF 1.09 M TRIALKYL PHOSPHATE SOLUTIONS IN CONTACT WITH 1 M HNO_3 AT 23°C. THE DARKENED POINTS ARE FOR TESTS WITH URANIUM PRESENT (20 g/L IN ORGANIC PHASE).

REMOVAL OF TRIBUTYL PHOSPHATE AND ITS DEGRADATION PRODUCTS FROM AQUEOUS SOLUTIONS IN THE PUREX EXTRACTION PROCESS

W. Ochsenfeld, J. Schön

Kernforschungszentrum Karlsruhe
Institut für Heisse Chemie
D-7500 Karlsruhe, Federal Republic of Germany

Tributylphosphate (TBP) diluted by kerosene is today used as extractant in the PUREX-process for reprocessing irradiated reactor fuel. TBP is only slightly soluble in aqueous solutions, but soluble enough to give rise to disturbances in further operations, especially at high temperatures at evaporation. Therefore TBP and its degradation products have to be removed as far and as soon as possible following the extraction. The methods used so far, steam stripping and kerosene washing are not optimal with regard to purification efficiency and to waste minimization. A new procedure for removal of TBP and its degradation products from aqueous solutions by sorption on macroporous polystyrene divinylbenzene resins was studied in our institute. This procedure is used since 1975 in the highly shielded facility MILLI and also actually in the extraction cycle of the testing facility PUTE.

THE PURIFICATION REQUIRED

Dissolved or entrained solvent in operations following the extraction can give rise to formation of heavy organic phases and precipitates, so called "cruds". Heavy phases are formed if the solubility of some metal-TBP complexes is exceeded.

Precipitations in the PUREX-process are mainly formed by the degradation products di(DBP)- and mono(MBP)-butylphosphate in the extraction and the degradation of the incompletely removed TBP from aqueous solutions. Ideal would be a procedure which would allow the removal of the degradation products beside TBP. This can not be achieved by kerosene washing or steam-stripping. To avoid precipitation of Pu(IV)-DBP, the least soluble compound in the system, concentrations of less than 2 mg/L DBP and TBP respectively in the feed to the evaporator are required.

These requirements can be achieved by sorption of the organics on columns filled with macroporous resins.

BASIC DATA

Sorption of TBP from aqueous solutions by different resins was investigated. The highest capacity for TBP was found with the commercial resins Amberlite XAD-4 of Roehm & Haas and Lewatit OC 1031 of Bayer AG and the research resins of Bayer AG, C and M (1).

Data of the commercial resins are given in Table 1. Both show a very similar behaviour regarding the sorption of organics relevant to the PUREX-Process.

Table 1 Resin data

Resin	Lewatit OC 1031	Amberlite XAD-4
Surface m^2/g	400	750
Pore size A	30-35	50
Porosity %	25	51
Density g/cm^3	1.02	1.02

Distribution data of TBP on different resins are compared with those of TBP with dodecane (2) in Figure 1. Distribution coefficients of 1000 to 5000 were achieved on resins. They are by a factor of about 10 higher than the distribution coefficients with dodecane. The distribution on resins are even better at low TBP concentrations. Loadings of 300 g TBP/L resin are reached at usual TBP concentrations of 300 mg TBP/L in the aqueous feed solution.

Distributions of TBP, DBP, butanol, butyric acid and alkane were measured on different resins. Equilibrium data with Lewatit OC 1031 are shown in Figure 2.

Sorption of TBP on the resin is not influenced by nitric acid concentrations between 0 and 3 M. DBP-sorption, about tenfold lower than that of TBP, is slightly increased with acid concentration from 0.1 to 3M HNO_3. Sorption from pure aqueous solutions is about 2 to 10 fold lower (1,3).

Sorption of butanol and butyric acid is slightly decreased from 0 to 5M HNO_3 aqueous solutions. No mutual influence was observed in case of simultaneous sorption of TBP and butanol or butyric acid. The sorption of alkane from aqueous solutions is favoured by the presence of TBP.

The kinetics of the TBP sorption on the commercial resins Amberlite XAD-4 and Lewatit OC 1031 was investigated. The equilibrium of TBP sorption was reached in statical experiments in about 20 minutes. Sorption is quicker on Amberlite XAD-4 than on Lewatit OC 1031, due to the larger surface and porosity of XAD-4. At beginning, in the time interval until 5 minutes, a halftime of 2 minutes was measured on XAD-4 and about 3 minutes on OC 1031.

Dynamic experiments in columns were done with flowrates of 2-24 ml/cm^2 min, corresponding to contact times of 1.4 to 0.2 minutes. Loadings of 200 g TBP/L resin were measured with feed solutions about 300 mg TBP/L at 50% break-through (4). In these experiments HTS of 1 to 3 cm were found, the larger HTS values corresponding to the higher flowrates.

The high distribution coefficients of TBP and the low hights of theoretical stages allow an excellent removal of TBP, and a simultaneous DBP-sorption as shown in Table 2.

Table 2 Data of TBP and DBP breakthrough

Feed: 418 mg TBP/L, 18 mg HDBP/L, 0.5 M HNO_3

Flowrate: 20 ml/cm^2 min.
Resin bed: 5 x 41 cm, 800 ml, Lewatit DC 1031

Throughput bed volumes [BV]	Effluent mg TBP/L	Effluent mg DBP/L	% Sorption TBP	% Sorption DBP
390	<2	<3	>99.5	>83.2
450	<2	5	>99.5	82.2
540	<2	9	>99.5	76.9
600	21	18	99.3	72.1

As shown in Figure 3 these values are even better than those achieved on 10 ml laboratory scale columns. Beside sorption of organics sorption of the fission products Zr/Nb and Ru and of uranium and plutonium was observed from original PUREX solutions(4). From 0.1 to 1.2 M HNO_3 solutions distribution coefficients of 0.5 to 1,5 for Ru 106 and 1 to 6 for Zr 95 were found. These fission products can be removed by washing the resins with <0.5 M oxalic acid. 95% of Zr and 30-35% of Ru sorbed were removed.

The sorbed actinides can be washed out by reducing 0.1 M HNO_3 solutions to a rest of less than 0.1% of the total throughput. In Table 3 some characteristic data are presented for different product streams of the PUREX-process. The variation of the losses is due to the different conditions of washing.

Beta, gamma radiation up to 20 Mrad showed no influence on the sorption of resins, so that purification of all PUREX-type solutions can be achieved, except the highly activ waste solutions (HAW).

Table 3 Losses on resins

Process-solution	Throughput kg	Losses %
1 CU	13,91 U	0,002-0,09
2 EU	23,73 U	0,001-0,02
1 BP, 2 BP	1,03 Pu	0,001-0,09
1 CP	0,20 Pu	0,07
	0,78 U	0,12

Used resins can be either reused after removal of organics by methanol or treated as waste after intense wash, specially of Pu. The resin can than be stored directly or after volume reduction by wet incineration.

In our experiments 2340 L uranium solutions containing 110 kg U and 530 L plutonium solutions with 5.7 kg Pu were effectively purified from TBP and DBP by sorption on resin beds. One part of these solutions originated from reprocessing highly burned up nuclear fuel in the facility MILLI (5,6).

References

(1) H. Eschrich, W. Ochsenfeld, Sep. Sc. Technol. 15, 697 (1980)
(2) P. Michel, T. Kikindai, CEA-N-816, 173 (1967)
(3) J. Schön, E. Tullius, W. Ochsenfeld, Proceedings Jahrestagung Kerntechnik, 319 (1981)
(4) J. Schön, W. Ochsenfeld, KfK-Nachrichten 11, 30 (1979)
(5) J. Schön, W. Ochsenfeld, KfK-Nachrichten 14, 148 (1982)
(6) W. Ochsenfeld, W. Diefenbacher, H.C. Leichsenring KfK-2364 (1977).

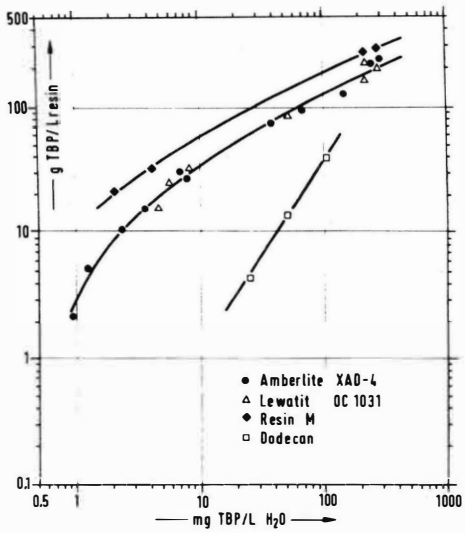

Fig.1 Distribution data of TBP with different resins

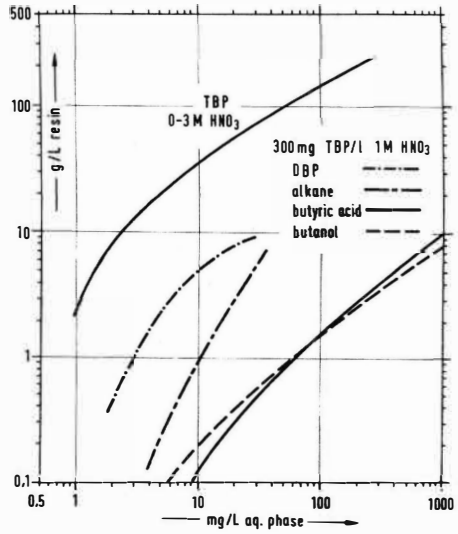

Fig. 2 Equilibrium data on Lewatit OC 1031

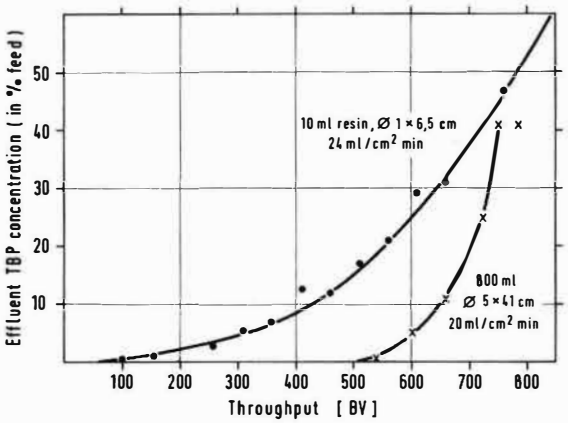

Fig.3 Breakthrough curves of TBP on Lewatit OC 1031

THE EFFECT OF TRIBUTYL PHOSPHATE DEGRADATION PRODUCTS UPON IMPURITY TRANSPORT IN THE REFINING OF URANIUM

D. G. Garratt

Eldorado Resources Limited
Research and Development Division
Ottawa, Ontario, Canada

In the refining of uranium using the $UO_2(NO_3)_2$ - H_2O - HNO_3 - TBP extraction system, the main difficulties introduced by the chemical reactivity of tri-n-butyl phosphate, TBP, are those associated with its' acid catalyzed hydrolysis to form dibutyl phosphoric acid, HDBP, monobutyl phosphoric acid, H_2MBP, and ortho-phosphoric acid, H_3PO_4. Since each of these species may itself form complexes with uranium and the various metals present as impurities in the uranium concentrates, the ability of any solvent extraction circuit to effectively and efficiently discriminate amongst the plethora of ions may be greatly reduced once the primary extractant, in this case TBP, has begun to degrade.

The purpose of this summary is to briefly describe a series of investigations carried out in the R & D laboratories of Eldorado Resources Limited to delineate the effect of these degradation products upon the ability of the solvent to selectively extract uranium in the presence of the high levels of molybdenum found in some uranium concentrates. This study was prompted in part by the necessity to be able to process high molybdenum uranium concentrates and the suggestion that molybdenum may have a marked catalytic effect on the hydrolysis rates of TBP, HDBP, and H_2MBP.

EXPERIMENTAL APPROACH

Bench scale 3-stage counter current simulations of extraction were carried out using an aqueous slurry prepared from a calcined ammonium diuranate concentrate. The uranium concentrate utilized in this study assayed at 82% U, 0.39% Mo, 0.078% Fe, and 0.09% V. The extractions were carried out at 50°C with an O/A ratio of 4/1. Selected solvent mixtures containing TBP, HDBP, H_2MBP, and Isopar M (a kerosene-like diluent) were prepared and equilibrated with 2N HNO_3 prior to use in extraction. Testwork was divided into four subsets. The first utilized a 2 to 2.4 N HNO_3 slurry containing 350 to 390 g/L dissolved uranium. The second set was the same as the first, except for the addition of 2.5 g/L ortho-phosphoric acid. This is the concentration of phosphoric acid normally present in our refinery aqueous feeds to solvent extraction for the control of thorium. The third and fourth sets were identical to the first and second, respectively, except for the presence of 20 g/L iron (III) nitrate monahydrate, $Fe(NO_3)_3 \cdot 9H_2O$, which was added to these slurries to give ferric iron concentrations similar to those found in typical feed blends, while maintaining the levels of other impurities essentially constant.

In general it was observed that the extraction of molybdenum increases with increasing levels of HDBP and H_2MBP as demonstrated by Figures 1-4. As per earlier studies (see paper no. 2d this symposium) the presence of ortho-phosphoric acid increases molybdenum loading, whereas ferric iron decreases the extraction of molybdenum. For example, in the absence of either added ferric iron or H_3PO_4 the volume percentage incremental increase in HDBP and H_2MBP of 0.5, 1.0, 1.5, 2.0, and 2.5 lead to molybdenum loadings on a uranium basis of 11.1, 57.1, 116, 243 and 250 ppM, respectively, versus a baseline value of 3.2 ppM in the absence of the hydrolysis products. The corresponding values for a feed containing 2.5 g/L H_3PO_4 are: 14.5, 90.1, 87.9, 174, and 293 ppM versus a baseline value of 4.0 ppM. When the aqueous feed contains 20 g/L $Fe(NO_3)_3 \cdot 9H_2O$ but no H_3PO_4 the corresponding values are: 8.7, 55.7, 124, 126, and 139 ppM versus a baseline value of 1.8 ppM. Repeating the last series of experiments but with the addition of 2.5 g/L H_3PO_4 gives values of: 12.3, 32.7*, 12.8*, 224, and 85.3*ppM respectively, versus a baseline value of 2.5 ppM molybdenum on a uranium basis. The three concentrations marked with an asterisk, *, arose from experimental runs which utilized an aqueous feed containing a nominal excess of nitric acid in the range 1.3 to 1.5 N versus the 2.0 to 2.2 N normally used. These data thus suggest that discrimination between uranium and molybdenum may be improved by carrying out the extractions at a lower 'free acidity'.

It is useful to observe that uranium loadings were not adversely affected by the presence of the high levels of HDBP and H_2MBP although the co-extraction of molybdenum would definitely yield a final product which is off-specification with respect to molybdenum. It should however be borne in mind that the affects of scrubbing and stripping stages were not evaluated in this report, and thus no comment may be made as to effective yields of uranium. The most important observation is that molybdenum forms organic soluble complexes with HDBP and H_2MBP just as it does with H_3PO_4. This is significant since the presence of one or all three of these species will increase the extraction of molybdenum and may thus lead to a uranyl nitrate product which is off-specification with respect to molybdenum. This observation also demonstrates a rather novel aspect of molybdenum chemistry since the complexes of most transition metals, lanthanides, and actinides with H_3PO_4, H_2MBP and to a lesser extent HDBP show a higher affinity (higher solubility) for the aqueous phase than for the organic phase.

The ability of ferric iron to decrease the extractability of molybdenum would appear to be the result of the propensity of ferric iron to form more stable complexes with phosphate derivates than molybdenum. The observation that the effectiveness of ferric iron to compete with molybdenum appears to vary with changes in the relative concentrations of TBP, HDBP, and H_2MBP may be explained by the presence of multiple speciation on the part of molybdenum. Indeed previous studies have indicated that molybdenum forms a series of complexes with HDBP of the following stoiciometries: $MoO(DBP)_4 \cdot 4$ HDBP, $MoO(DBP)_4$, $MoO_2(DBP)_2 \cdot 2$ HDBP, and $MoO_2(DBP)_2$; the speciation being determined by the relative concentrations of molybdenum, HDBP, pH, and temperature.

Figure 2. Effect of TBP Degradation Products (HDBP and H_2MBP) Upon Extraction of Uranium and Molybdenum from Uranium Concentration Slurries Containing 2.5 g/L H_3PO_4.

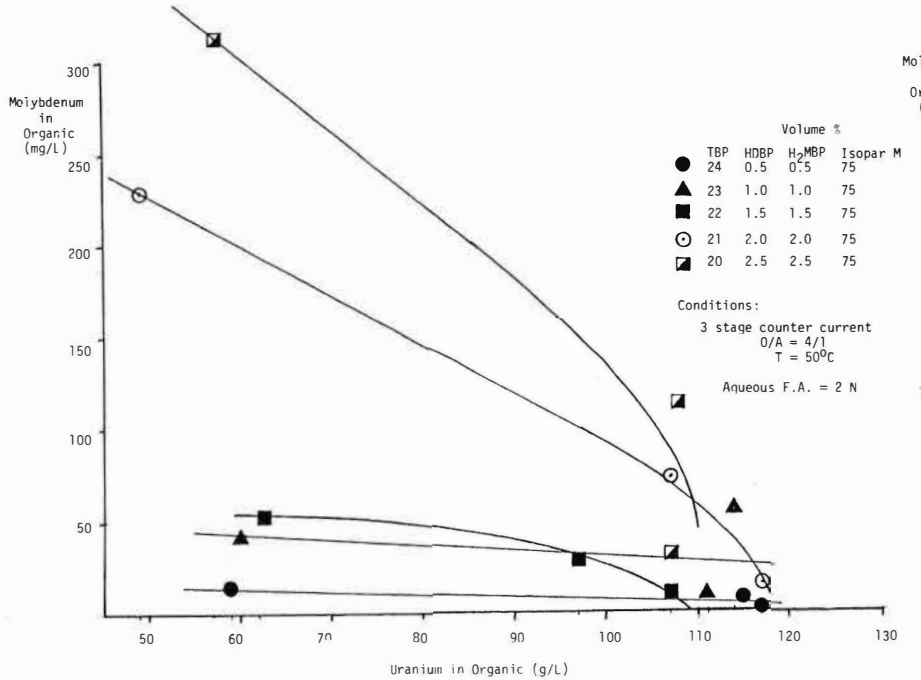

Figure 1. Effect of TBP Degradation Products (HDBP and H_2MBP) upon Extraction of Uranium and Molybdenum from Uranium Concentrate Slurries.

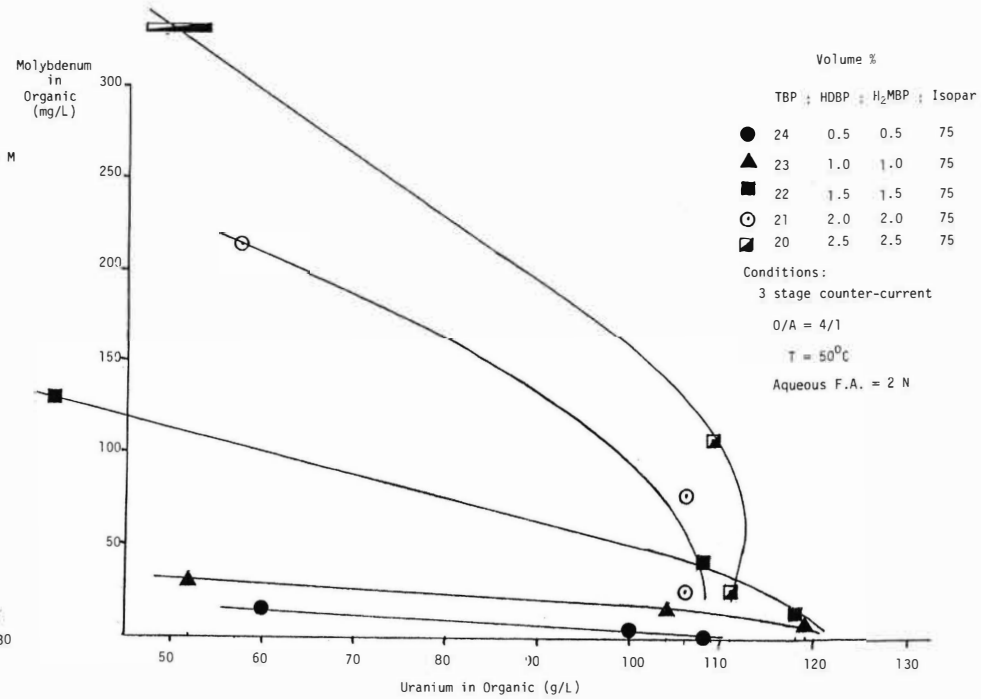

Figure 4. Effect of TBP Degradation Products (HDBP and H_2MBP) upon Extraction of Uranium and Molybdenum from Uranium Concentrate Slurries containing 2.5 g/L H_3PO_4 and 20 g/L $Fe(NO_3)_3 \cdot 9H_2O$.

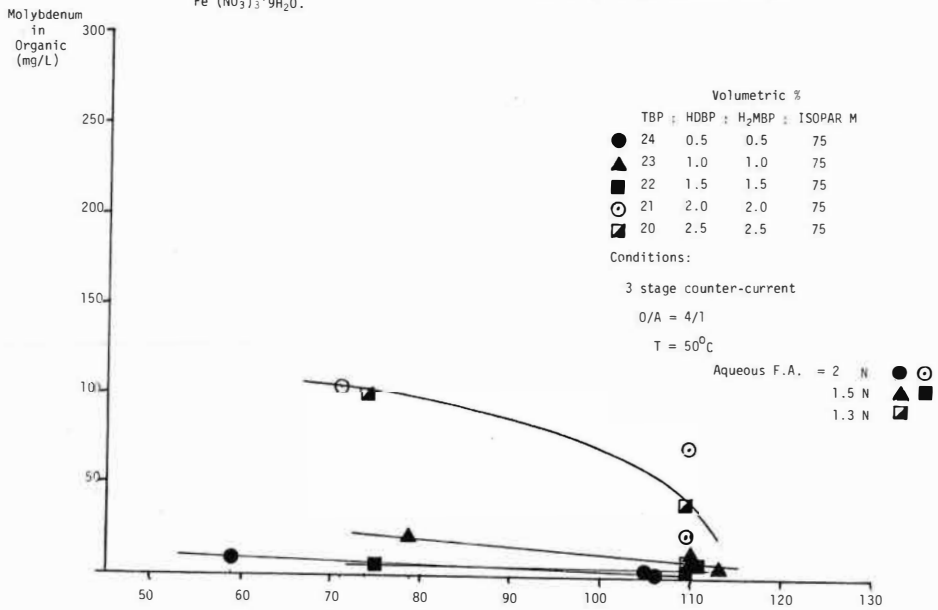

Figure 3. Effect of TBP Degradation Products (HDBP and H_2MBP) upon Extraction of Uranium and Molybdenum from Uranium Concentrate Slurries Containing 20 g/L $Fe(NO_3)_3 \cdot 9H_2O$.

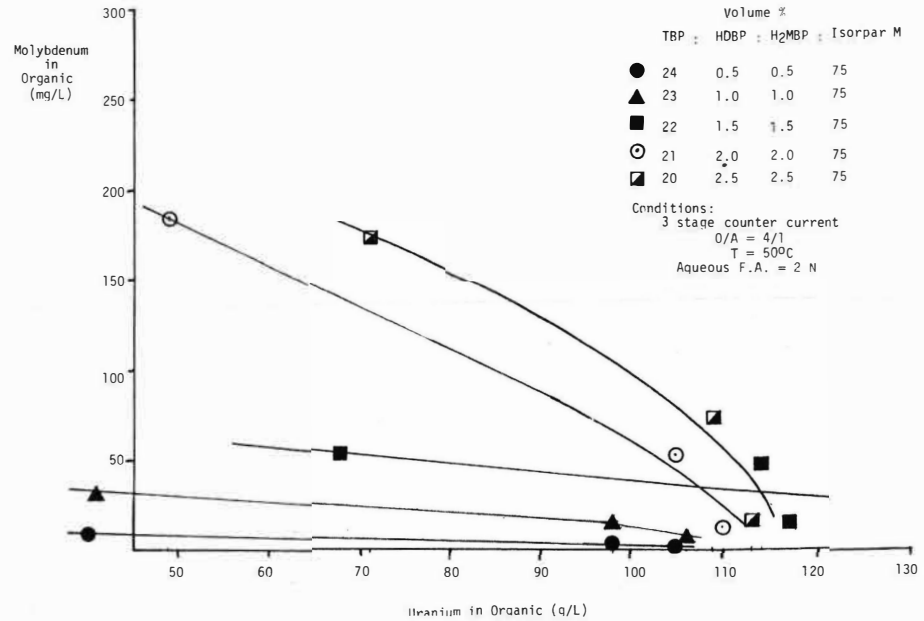

URANIUM CONCENTRATION PROFILE ALONG THE PULSED COLUMN, ITS DETERMINATION AND IMPORTANCE WITH REGARD TO SOLUTE'S ACCOUNTABILITY

Dr. Anthony F. Cermak

Allied-General Nuclear Services
Post Office Box 847
Barnwell, South Carolina 29812 USA

Considerable interest has been shown in recent years in developing reliable nuclear materials accounting systems for enriched uranium and plutonium in nuclear fuel reprocessing plants. This paper discusses a method which utilizes the experimental (or computed) solute concentration profiles and dispersed phase holdup values within the contactor. The method was developed using uranium inventory data from Barnwell Nuclear Fuel Plant (BNFP) pilot-scale pulsed columns.

Mass transfer tests using uranium were performed in the pilot-plant equipment to simulate actual flowsheet conditions used in the first uranium-plutonium cycle, second uranium cycle, and second and third plutonium cycles. In all runs, samples were taken along the length of the column under steady state conditions and analyzed for solutes content. Analytical data were evaluated and the actual concentrations of uranium and nitric acid were determined for each sampling point. Usually, the continuous phase sample (I) contained only traces of the dispersed phase, whereas the dispersed phase sample (II) contained both phases in a measurable quantity. The solute's actual concentration in the dispersed phase was calculated from the mass-balance equation

1 $$C_d = C_{ds} + \frac{V_c}{V_d} \cdot (C_{cs} - C_c)$$

In some cases, when both samples (I and II) contained the continuous as well as dispersed phase in a measurable amount, the solute's actual concentration was determined from equations (1)

2 $$C_c = \frac{\left[C_{ds} + (Vc/Vd).C_{cs}\right]_I - \left[C_{ds} + (Vc/Vd).C_{cs}\right]_{II}}{(Vc/Vd)_I - (Vc/Vd)_{II}}$$

and

3 $$C_d = \left[C_{ds} + (Vc/Vd).C_{cs}\right]_I - (Vc/Vd)_I.C_c$$

or

4 $$\left[C_d = C_{ds} + (Vc/Vd).C_{cs}\right]_{II} - (Vc/Vd)_{II}.C_c$$

Using sample analyses and the above equations, the solute's concentration profiles were calculated (2). The pilot-plant 2D and 2E columns concentration profiles for uranium are shown in Figures 1 and 2 as examples of the results.

By determining the solute average concentration in each section of the column, as shown in Figures 3 and 4, and the dispersed phase holdup (X_d) from the empirical equation (3):

5 $$X_d \approx 0.2\ U_d^{0.11} \cdot (2fA_o + \Delta U_{d-c})^{2.8}$$

the solute inventory (M_s) in the column can be evaluated using the following equations:

For a dual process, bottom interface column in Figure 3: (2D column)

6 $$\begin{aligned} M_s = {} & V_1.\bar{C}_{(A)1} \\ & + V_2 \cdot \left[\bar{C}_{(O)2} + X_{d(E)} \cdot \left(\frac{D_c}{D_s}\right)^2 \cdot \left(\bar{C}_{(A)2} - \bar{C}_{(O)2}\right)\right] \\ & + V_3 \cdot \left[\bar{C}_{(O)3} + X_{d(E)} \cdot \left(\bar{C}_{(A)3} - \bar{C}_{(O)3}\right)\right] \\ & + V_4 \cdot \left[\bar{C}_{(O)4} + X_{d(S)} \cdot \left(\bar{C}_{(A)4} - \bar{C}_{(O)4}\right)\right] \\ & + V_5 \cdot \bar{C}_{(O)5} \end{aligned}$$

For a single process, top interface column in Figure 4: (2E column)

7 $$\begin{aligned} M_2 = {} & V_1 \cdot \bar{C}_{(O)1} \\ & + V_2 \cdot \left[\bar{C}_{(A)2} + X_d \cdot \left(\frac{D_c}{D_s}\right)^2 \cdot \left(\bar{C}_{(O)2} - \bar{C}_{(A)2}\right)\right] \\ & + V_3 \cdot \left[\bar{C}_{(A)3} + X_d \cdot \bar{C}_{(O)3} - \left(\bar{C}_{(A)3}\right)\right] \\ & + V_4 \cdot \bar{C}_{(A)4} \end{aligned}$$

Similar equations, applicable to the dual process column with the top interface and single process column with the bottom interface, can be obtained by reversing indexes (O) and (A) in equations 6 and 7, respectively.

Using this concentration profile-holdup method, the inventory of uranium and nitric acid was calculated in each tested column. It correlated well with the inventory determined from the volume and concentration measurements of each phase after draining the column. For illustration, a comparison summary of experimental uranium and nitric acid inventory data is presented in Table 1. A computer method for determining concentration profiles (4)(5)(6) will preclude the need for extensive sampling and will permit the determination of dynamic inventories of full-scale pulse columns using the concentration-profile method.

NOTATIONS:

C_c	solute's actual concentration in the continuous phase (g/ℓ), (M)
C_d	solute's actual concentration in the dispersed phase (g/ℓ), (M)
C_{cs}	solute's concentration in the continuous phase of the sample (g/ℓ), (M)
C_{ds}	solute's concentration in the dispersed phase of the sample (g/ℓ), (M)
V_c/V_d	ratio of the continuous to the dispersed phase volume in the sample
X_d	dispersed phase holdup
U_d	dispersed phase superficial velocity (cm/sec)
U_c	continuous phase superficial velocity (cm/sec)
f	pulse frequency (1/sec)
A_o	pulse amplitude (cm)
M_s	solute's column inventory (g), (mols)
V_1 to V_5	volume of the column section (ℓ)
$\bar{C}_{(A)}$	solute's average concentration in the heavy aqueous phase (g/ℓ), (M)
$\bar{C}_{(O)}$	solute's average concentration in the light organic phase (g/ℓ), (M)
D_c	column diameter (cm)
D_s	disengaging section diameter (cm)
E	extraction
S	scrubbing

REFERENCES

1. A. F. Cermak, J. C. Neace, and R. G. Spaunburgh; "Coprocessing Tests with Uranium on the Electropulse Column, and Pilot-Scale Pulse Columns Simulating the Second and Third Plutonium Process Cycles," AGNS-35900-4.1-20 (1979).

2. A. F. Cermak, "Pilot-Scale Pulsed Columns, Column Profile, and Holdup Studies," AGNS-35900-3.1-111 (1980).

3. A. F. Cermak, "Pilot-Scale Pulsed Columns, Aqueous Continuous Dual Process and Holdup Studies," AGNS-35900-2.5-124 (1981).

4. E. A. Hakkila, et al; "Material Management in an Internationally Safeguarded Fuels Reprocessing Plant," Los Alamos Scientific Laboratory, Report LA-8042 (1980).

5. D. D. Cobb and C. A. Ostenak, "Dynamic Materials Accounting for Solvent Extraction Systems," Los Alamos Scientific Laboratory, Report LA-UR-79-3221 (1979).

6. L. Burkhart, "A Survey of Simulation Methods for Modeling Pulsed Sieve-Plate Extraction Columns," AMES Laboratory, Iowa State University, Report UCRL-15101 (1979).

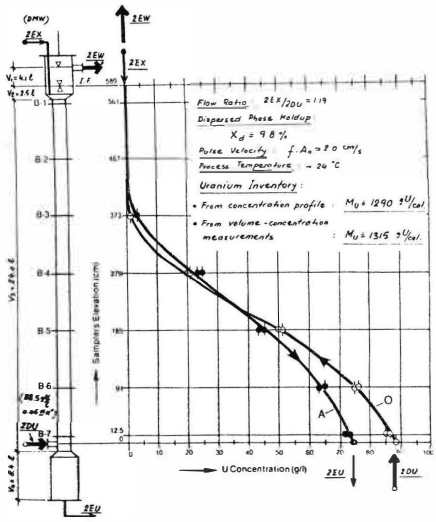

FIGURE 1. THE 2D COLUMN EXPERIMENTAL CONCENTRATION PROFILES FOR RUN 2D-2 (30 V/O TBP)

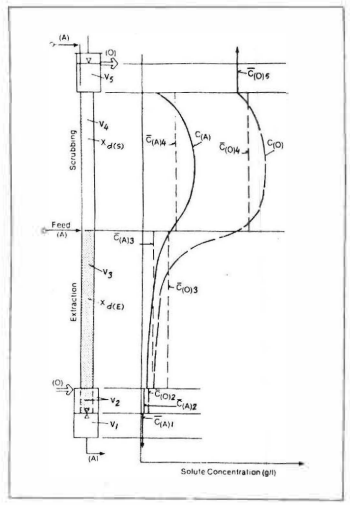

FIGURE 3. SOLUTE CONCENTRATION ALONG THE DUAL PROCESS (EXTRACTION-SCRUBBING) COLUMN

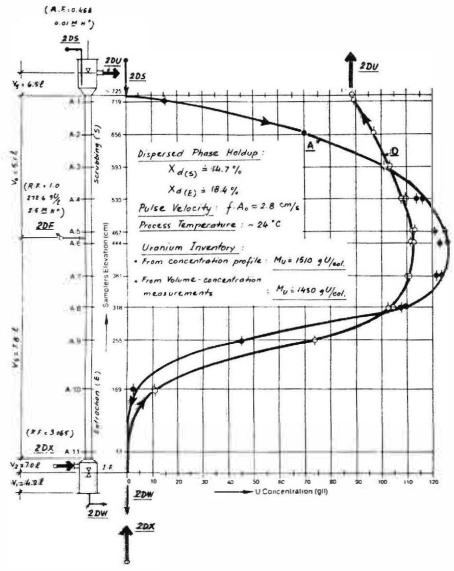

FIGURE 2. THE 2E COLUMN EXPERIMENTAL CONCENTRATION PROFILES FOR RUN 2D-2

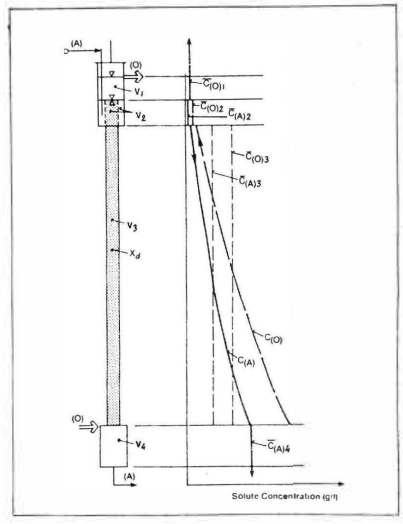

FIGURE 4. SOLUTE CONCENTRATION ALONG THE SINGLE PROCESS (STRIPPING) COLUMN

TABLE 1. SUMMARY OF EXPERIMENTAL COLUMN INVENTORIES

Experimental Run:	Dual Process Column Bottom Interface (Extraction & Scrubbing)				Single Process Column Top Interface (Stripping)			
	U Inventory: (g U/col.)		HNO_3 Inventory: (g HNO_3/col.)		U Inventory: (g U/col.)		HNO_3 Inventory (g HNO_3/col.)	
	From Concentration Profile and Holdup Data:	From Volume and Concentration Measurements:	From Concentration Profile and Holdup Data:	From Volume and Concentration Measurements:	From Concentration Profile and Holdup Data:	From Volume and Concentration Measurements:	From Concentration Profile and Holdup Data:	From Volume and Concentration Measurements:
HS - 5 (1st Cycle)	~1190	1140	1510	1547	1150	1203	140	153
2D - 2 (2nd U Cycle)	1510	1430	920	856	1290	1315	40	44
2A - 2 (2nd Pu Cycle)	1310	1260	1425	1344	870	940	605	557
3A - 2 (3rd Pu Cycle)	1370	1320	1390	1415	760	715	335	363

AXIAL MIXING OF CONTINUOUS PHASE IN A ROTATING-DISK EXTRACTION COLUMN

Li-zhu Lu, Zheng Fan and Chia-yung Chen

Institute of Chemical Metallurgy
Academia Sinica
Beijing, China

ABSTRACT

The effect of axial mixing on the design and performance of a rotating-disk extraction column(RDC) is very important. The residence time distribution of continuous phase in a rotating-disk column has been studied with or without the flow of disperse phase at the same time. Equations were developed to predict the effect of disperse phase flow on the axial mixing of continuous phase. Physical model developed and experimental results indicate the axial mixing of continuous phase could be enhanced or diminished by disperse flow under different operating conditions.

ANALYSIS

The effect of axial mixing on the design and performance of a RDC has attracted many people's attention so that a number of papers(1-7) have been published before. The purpose of the present work is to study the axial mixing of continuous phase from the pattern of fluid flow in the column. The effect of flow of dispersed phase on the axial mixing of continuous phase was also studied.

The RDC is formed into compartments by horizontal annular baffles. There is a horizontal rotating-disk centrally located in each compartment. For single phase flow, the overall axial mixing is contributed by eddy diffusion and also by channeling phenomenon. The fluid flow in the column can be characterized by the flow Reynolds number ($Re_f = U_c D \rho_c / \mu_c$) and rotation Reynolds number of disks($Re = ND_r^2 \rho_c / \mu_c$). When the fluid flow through the column, the presence of disks and stator rings makes part of the fluid moving faster than the rest in the axial direction to give channeling phenomenon. The larger the Re_f, the more serious the channeling effect becomes. However, the rotation of disks has the effect of mixing the fluid of different speed within each compartment to reduce the channeling effect or the axial mixing coefficient is reduced with the increasing of Re_n. The axial mixing due to channeling effect could be correlated by a dimensionless group (Re_f/Re_n). On the other hand, the rotation of disks enhances the eddy diffusion. By increasing of Re_n to infinity, the whole column would behave like a perfect mixer. However, this tendency is diminished by the fluid flow in the axial direction. The axial mixing due to eddy diffusion could be correlated by the ratio of Re_n to Re_f. Therefore, the axial mixing of continuous phase in the RDC could be represented by the following equation:

$$(1) \qquad E_s/U_cH = K_1 + K_2(Re_n/Re_f) + K_3(1/(Re_n/Re_f))$$

Where E_s is the axial mixing coefficient for single phase flow,
U_c is the superficial velocity of continuous phase,
H is the height of a compartment.

or

$$(2) \qquad E_s/U_cH = K_1 + K_2(ND_r/U_c) + K_3/(ND_r/U_c)$$

Where N is the rotation speed of the disks.

For two-phase counterflow in the column, the energy which breaks the disperse phase into drops and maintains it in droplet form arises from the otation of the disks. Assumption is made that the energy from the rotation of disks is even distributed to the fluid in the compartment. Then the energy dissipation rate per unit mass of fluid could be calculated by

$$(3) \qquad \hat{\epsilon} = 0.154\, \nu^{1/2} \omega^{7/2} D_r^4/(D_t^2 H)$$

Chen and his coworkers[8] have suggested that the turbulent flow field may be characterized by an energy spectrum function $E(\alpha)$. The following equation was given by Hinze[9] for $E(\alpha)$:

$$(4) \qquad E(\alpha) = K_\alpha \epsilon^{2/3} \alpha^{-5/3}$$

A droplet with diameter D is stabilized by its surface energy $\pi D^2 \sigma$ and it could be deformed and broken in turbulent field due to turbulent fluctuation energy. Thus the probability P(D) for the droplet to exist in an equilibrium size D is a function of the ratio of turbulent fluctuation energy to the surface energy. Hence

$$(5) \qquad P(D) = \Phi\left[\frac{\rho_c D}{\sigma} \int_{1/D}^{\infty} E(\alpha)\, d\alpha\right]$$

Equation(6) can be derived from Equations (3-5) as

$$(6) \qquad P(D) = \Phi(We\, Re_n^{-1/3} \quad (D/D_t)^{5/3})$$

or

$$(7) \qquad \bar{D}/D_t = K_4 \cdot We^{-3/5} \cdot Re_n^{1/5}$$

Where We is Weber number ($\rho_c N^2 D^3/\sigma$) and $\bar{D}$ is mean drop diameter. From Equation 7, the mean drop diameter $\bar{D}$ of dispersed phase in a column is a function of Weber number We and rotation Reynolds number Re_n.

As the drops move in a continuous liquid medium, the wakes of continuous phase develop behind the drops. In strong turbulent flow field, the wake is unstable. However, there is a "quiet zone" between two neighboring rotating disks in RDC, where the wake of droplet is stable and can be fully developed

Suppose that the thickness of the "quiet zone" is 2δ and the time for a droplet to pass through the "quiet zone" is Δt. The motion of wake with drops produces the backmixing of continuous phase. Based on momentum balance, the following equation could be obtained:

$$(8) \qquad (v_d \rho_d \Delta U/\Delta t) + (v_w \rho_c (U_o - U_c + U_c)/\Delta t) = (1/6)\pi D^3 \Delta\rho g$$

Assuming that the velocity of droplets in axial direction is constant ($\Delta U = 0$), Equation(8) could be rearranged into:

$$(9) \qquad V_w = 1/6\pi D^3 g(\Delta\rho/\rho_c)(\Delta t/U_o)$$

The stability of the wake of drops depends on the difference of the velocities at both ends of the wake in the turbulent field. According to Kolmogoroff's theory[5], the following equations could be obtained:

$$(10) \qquad \delta = 1/K_5 Re_n^{2.5}$$

$$(11) \qquad \Delta t = 1/(K_5' \cdot Re_n^{2.5} \cdot (U_o - U_c))$$

Uc is small in comparison with Uo and could be neglected from Equation (11). The volume of wake (V_w) carried by a drop of diameter D can be calculated by

$$(12) \qquad V_w = K_5'' D/Re_n^{2.5}$$

By using the mean drop diameter to represent the diameter of the non-uniform drops and neglecting the effect of interactions among the drops, the total wake volume carried by a swarm of drops can be considered as algebraic sum of the volume of wakes carried by all the drops, thus

$$(13) \qquad \Sigma V_w = K_6\, U_d/(Re_n^{2.9} We^{-1.2})$$

The backmixing ratio F_w due to wake movement can be represented by

$$(14) \qquad F_w = K_6(U_d/U_c)/(Re_n^{2.9} We^{-1.2})$$

Actually there are interactions and coalescence among the drops, Equation (14) is modified to the form of Equation (15) to account for these unknown effects:

$$(15) \qquad F_w = K_6((U_d/U_c)/(Re_n^{2.9} We^{-1.2}))^{K_7}$$

The movement of a swarm of drops in a continuous phase will reduce the channeling phenomenon of continuous phase. Suppose that in a single phase flow there is a channeling flow with velocity Ug. With dispersed phase present, the velocity of the channeling flow will be U. The decrease in the momentum of fast moving channeling fluid is directly proportional to the additional number of drops encountered by the channeling fluid, the projective area of each droplet and the square of slipping velocity of the drops. Therefore the momentum balance equation can be represented as follows:

$$(16) \qquad U_g \Delta S \rho_c (U_g - U) = 3K_8' x \Delta S(U_g - U_c)\pi \bar{D}^2 \rho_d U_s^2/(2\pi \bar{D}^3)$$

Where ΔS is the area of cross section of the channeling flow,
X is the hold up of dispersed phase,
U_s is the slipping velocity of drops,

It has been reported in the literature[10-12] that the slipping velocity of the drops is an exponential function of their diameters. So from Equation (16)

$$(17) \qquad U_g - u = K_8'' \cdot x(\rho_d/\rho_c)(U_g - U_c/U_g)\bar{D}^{-K_9}$$

The decrease in the ratio of forward mixing ΔW is

$$(18) \qquad \Delta W = (U_g - U) \cdot \Delta S/U_c A$$
$$= K_8'' x(\rho_d/\rho_c)(1/U_c - 1/U_g)\bar{D}^{-K_9} \cdot (\Delta S/A)$$

Where A is the area of cross section of the column.

In Equation (18) there are two unknown variables, i.e. ΔS and U_g. It could be supposed that ΔS is only dependent on geometric arrangements of the column and U_g depends on the operating conditions only and could be expressed as

$$(19) \qquad U_g = K_{10} U_c / N D_r^2$$

From this analysis, it can be shown that the axial mixing of continuous phase due to channeling phenomenon is reduced by the movement of droplets as

$$(20) \qquad W = K_8 x (\mu_c / U_c D_t \rho_d)(1 - K_{10} N D_r^2 \rho_c / \mu_c)(We^{-0.6} Re_n^{0.2}) K_9$$

The contribution of disperse phase to the axial mixing of continuous phase is given by $(F_w - \Delta W)$. So the axial mixing of continuous phase in countercurrent flow with disperse phase can be represented by the following Equation:

$$(21) \qquad E_c/U_cH = E_s/U_cH + F_w - \Delta W$$

The first term on the right hand side should be modified with disperse phase hold-up x as:

$$(22) \qquad E_s/U_cH = K_1 + K_2 N D_r (1-x)/U_c + K_3/(N D_r (1-x)/U_c)$$

EXPERIMENTAL RESULTS

The RDC used in this experiment is made of polymethyl methacrylate. It is 120 cm high with internal diameter of 14.3 cm. The diameter of the metal rotating disks is 7.0 cm. There are 34 compartments in the column with compartment height of 2.12 cm each.

In the experiment, water was used as continuous phase and kerosene as disperse phase. The operating temperature was always kept at 22°C.

Anilinc black was injected into the column as tracer. A tiny optical fiber head was used to measure the optical density of tracer in continuous phase. The tracer used is kerosene insoluble and the amount injected is not enough to change the physical properties of the water phase. The pulse input tracer was injected into the ninth compartment from the top of the column and its concentration response was measured at the twenty-first compartment. The residence time distribution was calculated by the first and second moments of response curves.

The results for the inverse of Peclet number $(E_s/(U_cH))$ for continuous phase flow only are shown in Figure 1 and Equation 2 used for data correlation can be represented as

$$(23) \qquad E_s/U_cH = 0.5 + 0.004(N D_r/U_c) + 5.616(N D_r/U_c)^{-1}$$

It can be shown from the above equation that when ND_r/U_c is either very small or very large, $E_s/(U_cH)$ is large. It seems that this is the first equation, as understand, to represent the experimental fact that E_s/U_cH increases at low ND_r/U_c due to serious channeling phenomenon.

For two-phase counterflow, Figure 2 represents E_s/U_cH as a function of N, U_c and U_d. Equation 15 and Equation 20 can be represented as follows respectively:

$$(24) \qquad F_w = 5.07 \times 10^4 (U_d/U_c We^{-1.2} Re_n^{2.9})^{0.52}$$

$$(25) \qquad \Delta W = 1.898 (x \mu_c / U_c D_t \rho_c)(1 - 2.076 \times 10^{-5} N D_r^2 \rho_c / \mu_c)(We^{-0.6} Re_n^{0.2})^{-0.86}$$

Figure 3 shows the opposite effects of F_w and ΔW on axial mixing of continuous phase with the counterflow of disperse phase. One interesting point indicated in Fig.3 is that under some operating conditions, the combined effect of F_w and ΔW on axial mixing of continuous phase is negative. The movement of droplets decreases the channeling flow of continuous phase and the effect of wake of droplets on backmixing of continuous phase is comparatively small in these cases. The comparison of experimental data with the values calculated from Equations (21), (24) and (25) is shown in Fig.4.

CONCLUSIONS

The axial mixing coefficients of continuous phase in RDC with or without counterflow of disperse phase were measured and correlated. Effect of flow rate and rotation speed on axial mixing coefficient has been correlated by dimensionless groups. With counterflow of disperse phase, the axial mixing coefficient of continuous phase will be either increased or decreased under different operating conditions. Problem is analysed based on the flow of fluid and droplets. Work has been done so far using one column with fixed dimensions of baffles and disks and with only one liquid system. More work is planned to substantiate the present results.

NOTATION

D_r	= diameter of rotating disks	L
D_t	= diameter of column	L
E_c	= two-phase counterflow axial mixing coefficient of continuous phase	L^2/T
E_s	= single phase flow axial mixing coefficient	L^2/T
U_o	= final velocity of drops in continuous phase	L/T
U_c	= superficial velocity of continuous phase	L/T
U_d	= superficial velocity of disperse phase	L/T
V_d	= volume of a droplet	L^3
x	= hold-up of disperse phase	
ν	= kinematic viscosity	L^2/T
μ_c	= coefficient of viscosity of continuous phase	G/LT
ρ_c	= density of continuous phase	G/L^3
ρ_d	= density of disperse phase	G/L^3
σ	= surface tension	G/T^2
ω	= angular speed of rotating disks	Rad/T

LITERATURE CITED

(1) Strand, C. P. et al., AIChE. J., 8 252 (1962)

(2) Westerterp, K. R. et al., Chem. Eng. Sci., 17, 363 (1962)

(3) Teruratsu, M. et al. AIChE. J., 12, 508 (1966)

(4) Misek, T., Coll Czeck. Chem. Comm. 40 1686 (1975)

(5) Bruin, S., Trans. Instn. Chem. Eng. 51 355 (1973)

(6) " Axial mixing and effect of side flow on axial mixing in a RDC " Institute of Chem. Metall., Academia Sinica (1981)

(7) Blagez, L., Chem. Zvesti 32 328, 341, 356 (1979)

(8) Chen Hsiao-tsung, et al., AIChE. J., 13 989, (1967)

(9) Hinze, J. O., "Turbulence", McGraw-Hill Co. N. Y. (1959)

(10) Shengen, H. et al., AIChE. J., 1 42 (1955)

(11) Edge, R. M., et al., Chem. Eng. Sci., 26 1001 (1971)

(12) Roger, E. B. et al., AIChE. J., 12 473 (1966)

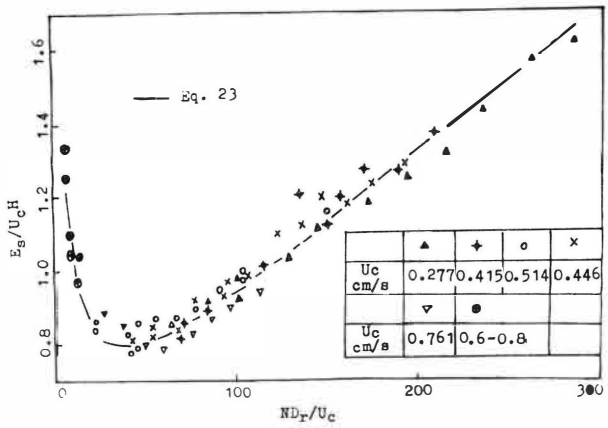

FIGURE 1. AXIAL MIXING OF CONTINUOUS PHASE FLOW IN RDC.

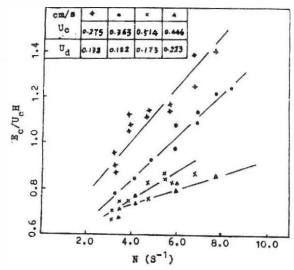

FIGURE 2. E_c FOR TWO-PHASE COUNTERFLOW IN RDC.

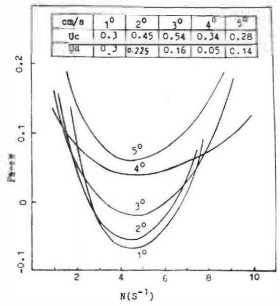

FIGURE 3. RELATIONSHIP BETWEEN $(F_w - \Delta W)$ AND N.

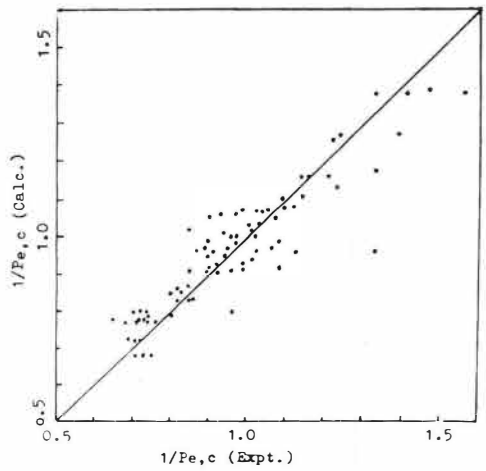

FIGURE 4. COMPARISON OF EXPERIMENTAL PECLET NUMBERS OF CONTINUOUS PHASE WITH CALCULATED VALUES (TWO-PHASE FLOW).

BACKMIXING INVESTIGATION IN A KUHNI EXTRACTION COLUMN

Gyula Vatai and Aleksandar Tolić

University of Novi Sad
Novi Sad

and

University of Belgrade
Belgrade, Yugoslavia

The investigations of axial diffusion in Kühni extraction column published in the papers (1,2,3) have determined the dependence of axial diffusion and set the basic correlation terms for the case of mass transfer absence. In order to give a broader approach to hydrodynamic investigations of Kühni column, we have started our work which represents only the first step in such endeavourings. This paper deals only with the determination of backmixing in a single phase-water flow and two phase flow systems, water - kerosene and water - trichloroethylene. Water - kerosene system has been chosen due to its simplicity and attractivity from the aspect of physical characteristics significant for any investigations of extractor hydrodynamics without mass transfer. In choosing the second mentioned system the requirement was to have a system with different physical characteristics in comparison with those of the first one.

EXPERIMENTAL

Pilot - plant for experimental determinations consists of Kühni type extractor diameter (D) of 100 mm, pumps, tanks, flow meters, compensation vessels and the control system for the interphase level and the other auxiliary equipments.

Working part of the column with the height (H_c) of 1080 mm, is divided into 18 compartments by means of perforated plates whereas the height (H) of each compartment is 60 mm. Free surface of the perforated stator plates for an axial flow amounts to 20 % of the total surface of the column cross-section. Each section is equipped with a turbine impeller whose diameter (R) is 68 mm, with impeller rings interspace of 10 mm each. Starting from the second compartment each third compartment has an opening for sample taking or for the measuring elements.

Evaluation of axial diffusion coefficients (E_c) in the Kühni column, has been done on the base of one-dimensional diffusion model. The degree of backmixing in the column was measured using the steady state tracer injection technique, described many times in the literature (4,5,6). Tracer for an aqueous phase in these determinations has been kalium chromate that satisfies the basic requirements established for the labelled substance in an aqueous phase, i.e. it neither dissolves in an organic phase nor reacts with it. The average fractional hold-up of dispersed phase (X) in the investigations of two-phase systems has been determined by shut off method.

During the investigations of backmixing for a single-phase flow, direction of aqueous phase was from the top toward the bottom of the column, as the case was for the water - kerosene system, while for the water - trichloroethylene system, water was the lighter phase and it flowed from the bottom toward the top of the column. In both systems water has been taken as a continuous phase.

Investigations of backmixing in acontinuous phase for both systems, as well as for the single-phase flow have been carried out for various mixing speeds, continuous phase flowrates and various flowrates of dispersed phase.

According to the experimental results we have plotted the dependences of the coefficients of axial diffusion in a continuous phase on the superficial velocity of continuous phase (U_c), at constant velocities of dispersed phase (U_d) and rotor speed (N). Considering these relations given in Table 1 one may conclude that the coefficient of axial diffusion in continuous phase increases with an increase in superficial velocity of continuous phase in the water - kerosene system, as well as with an increase of water flowrate in the course of sinle-phase flow investigations, while in the water - trichloroethylene system it decreases with an increase in superficial velocity of continuous phase. As it is seen from Table 1 and illustration shown in Figure 1, these dependences can be given by the following linear equation :

$$E_c = a\,U_c + b \qquad (1)$$

where the values of slope (a) and intercept (b) for all investigated conditions and systems, are given in Table 1.

Coefficient of axial diffusion increases in all cases linearly with an increase in the mixing speed, i.e. rotor speed, as it seen from Table 2 and is evident from illustration shown in Figure 2, whereas this straight-line relation can be given by the expression :

$$E_c = a'N + b' \qquad (2)$$

where the value of slope (a') and the intercept (b') for all investigated conditions and systems, are given in Table 2.

Starting from the correlations for the coefficient of axial diffusion applied for extraction columns with stirrer (7) for a single-phase flow :

$$\frac{E_c}{U_c\,H} = p\,\frac{R\,N}{U_c} + q \qquad (3)$$

and for a two-phase flow :

$$\frac{E_c}{U_c\,H} = p\,(1 - X)\,\frac{R\,N}{U_c} + q \qquad (4)$$

TABLE 1. Dependence of axial diffusion coefficient on superficial velocity of continuous phase ($E_c = aU_c + b$)

System	$U_d \cdot 10^3$ (m/s)	N (s^{-1})	Slope, a (m)	Intercept, $b \cdot 10^4$ (m^2/s)
Single phase flow (water)		0.95	0.033	0.350
		1.95	0.070	0.625
		2.80	0.095	0.925
		3.90	0.121	1.150
		4.75	0.149	1.575
Two phase flow:				
Water - kerosene	0.43	0.95	0.014	0.525
		1.95	0.033	0.850
		2.80	0.047	1.175
		3.90	0.060	1.550
		4.75	0.108	1.825
	0.64	1.95	0.030	0.700
		2.80	0.040	0.730
		3.90	0.121	0.740
	0.85	1.95	0.024	0.690
		2.80	0.030	0.765
		3.90	0.039	0.850
Water - trichloro-ethylene	0.85	0.95	- 0.004	1.075
		1.95	- 0.004	1.500
		2.80	- 0.043	2.300
		3.90	- 0.095	3.200
		4.75	- 0.144	3.975

we have evaluated parameters for the equations (3) and (4) according to the obtained experimental data, applying the least squares method. Values of the real parameters as well as the correlation coefficients for the two-phase and single-phase systems are given in Table 3. In all three cases values of the correlation coefficient indicate that the correlation line fits satisfactorily the experimental values.

Besides the correlations known from literature (1,4,5,6,7), experimental values for the coefficients of axial diffusion in a

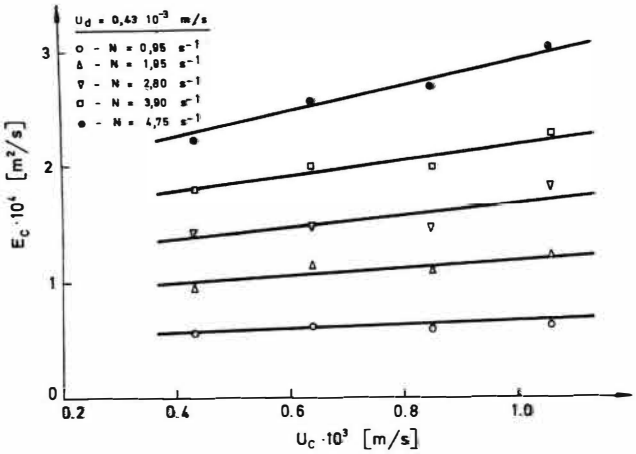

Figure 1. Two phase backmixing: effect of continuous phase superficial velocity on axial mixing in system water - kerosene

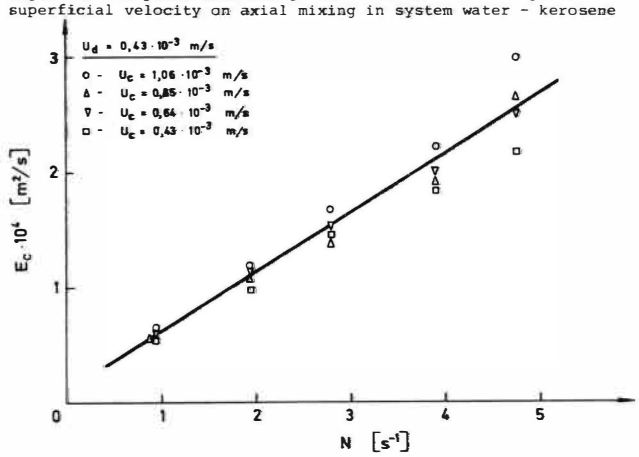

Figure 2. Two phase backmixing: effect of roto speed on axial diffusion coefficiet in system water - kerosene

TABLE 2. Dependence of axial diffusion coefficient on rotor speed ($E_c = a'N + b'$)

S y s t e m	$U_d \cdot 10^3$ (m/s)	Slope, $a' \cdot 10^4$ (m^2)	Intercept, $b' \cdot 10^4$ (m^2/s)
Single phase flow (water)	-	0.562	-
Two phase flow :			
Water - kerosene	0.43	0.512	0.100
	0.64	0.297	0.310
	0.85	0.200	0.420
Water - trichloro-ethylene	0.85	0.494	0.562

TABLE 3. Parameters in equations (3) and (4)

S y s t e m	Slope, p (1)	Intercept, q (1)	Corr. coef. (1)
Single phase	0.0123	0.275	0.983
Water - kerosene	0.0100	0.382	0.844
Water - trichloro-ethylene	0.0167	0.399	0.970

continuous phase have been correlated with the correlation obtained by dimensional analysis. Physico-chemical characteristics of the fluids, operating conditions in the column and the dimension of this column have been taken as independent variables for developing this correlation. According to the experimental values obtained for two-phases systems, and by means of the least squares method, the following equation has been obtained for Bodenstein ´s number :

$$(5)\quad \frac{E_c}{U_c H} = 1{,}54 \cdot 10^{-3} \left(\frac{\mu_d}{\mu_c}\right)^{-3{,}6} \left(\frac{\Delta\rho}{\rho_c}\right)^{-1{,}65} \left(\frac{U_d}{U_c}\right)^{-0{,}2} \left(\frac{RN}{U_c}\right)^{1{,}02} \cdot Re_N^{0{,}073}\, We_N^{-0{,}17}$$

where: μ_d, μ_c - viscosity of dispersed and continuous phase, ρ_c - density of continuous phase, $\Delta\rho$ - density difference of continuous and dispersed phase, Re - Reynolds number, We - Weber number.

Figure 3 illustrates the comparison of the experimental and calculated values of Bodenstein´s number. According to this diagram and based on the correlation coefficient (0,913) it may be expected that the obtained equation predicts satisfactorily the values for the coefficients of axial diffusion in continuous phase.

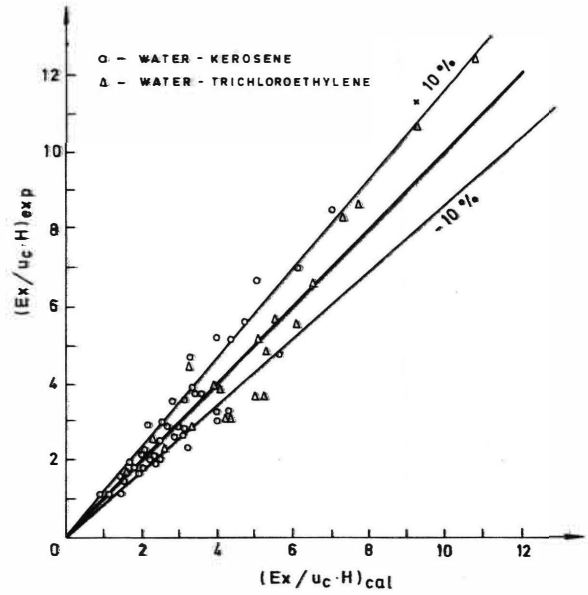

Figure 3. Comparison of the experimental and calculated values of Bodenstein´s number

CONCLUSION

Investigating the behaviour of axial diffusion coefficients in Kühni clumn it has been found that the coefficient increases linearly with an increase in the superficial velocity in continuous phase of the water - kerosene system and with an increase in water flow for a single-phase flow, while in a continuous phase of the water - trichloroethylene system it decreases with an increase in superficial velocity in continuous phase. It was also concluded that the coefficient of axial diffusion increases linearly with an increase in the mixing speed for all investigated systems.

The obtained correlations can be succesfully used for the calculation of the coefficient of axial diffusion in Kühni column for the investigated systems. They can be also applied to similar systems but with smaller accuracy.

REFERENCES

1. J.Ingham, R.J.Bourne, A.Mögli, Proceedings ISEC 74, 1299, (1974)
2. A.Fischer, Chem.Rundschau, 26, 1, (1973)
3. D.Hody, Chem.Rundschau, 28, 9, (1975)
4. F.P.Stainthorp, N.Sudall, Inst.Chem.Eng., 42, T 198, (1968)
5. K.R.Westerterp, W.H.Keyberg, Chem.Eng.Sci., 17, 373, (1962)
6. S.Stemerding, E.C.Lumb, J.Lips, Chem.Ing.Tech., 35, 844, (1963)
7. K.R.Westerterp, P.Landsman, Chem.Eng.Sci., 17, 363, (1962)

AXIAL DISPERSION STUDIES IN A RECIPROCATING PLATE COLUMN

N. V. Rama Rao

Corresponding author, Dept. of Chem. Eng.
McMaster Univ
Hamilton, Ontario, Canada L8S 4L7
and
N. S. Srinivas and Y. B. G. Varma

Department of Chemical Engineering
Indian Institute of Technology
Madras, Tamil Nadu, India 600 036

INTRODUCTION

Reciprocating plate columns (RPC), especially the column developed by Karr (1) with large hole diameter and free flow area, are increasing in importance. Recently, Ioannou et al. (2) reported that RPC with low plate free area consume less power compared to RPC with large free area, to do a given job. Baird and co-workers (3,4,5) and Prochazka and co-workers (6,7) have done considerable work on the axial dispersion of the RPC of varying plate free area. In the present study, axial dispersion coefficients in the continuous phase have been measured in an RPC with low plate free area.

EXPERIMENTAL

The glass shell of the reciprocating plate column, as shown in Figure 1 was 15.3 cm inside diameter and 100 cm in height. The perforated plates of identical plate geometry were mounted on a central rod in a stack of height 90 cm. The stroke of the reciprocating motion, A, was taken as the distance travelled by the plate from its minimum to maximum position. The frequency, f, was recorded using a tachometer. The flow of the phases was countercurrent with the continuous (water) and the dispersed (kerosene) phases fed at the top and bottom of the column respectively. The control valves on the outlet line of the continuous phase served to maintain the constant interface level at the top of the column. Under steady state conditions, the residence time distribution of the continuous phase (RTD) was measured by injecting a pulse of sodium chloride solution at the top of the column and following the response at the exit of the column, using a conductivity meter.

RTD CURVES AND MEASUREMENT OF DISPERSION COEFFICIENT, E

Good agreement was found with 5% standard deviation between the mean residence time, $\Sigma\, c_i t_i / \Sigma\, c_i$, calculated from the known concentration-time, curve and the mean holding time, $\bar{t}$ (continuous phase volume/flow rate). The concentration c and time t were made dimensionless as

(1) $C(\theta) = c/(Q/\bar{t})$

(2) $\theta = t/\bar{t}$

and

(3) $F(\theta) = \int C(\theta)\, d\theta$

where Q is the area under c-t curve.

Typical curves for variation in RTD with continuous phase velocity, u_c and with dispersed phase velocity, u_d are given in Figure 2. The experimental data were compared with the diffusional mixing model due to Morris et al. (8) which was given as

(4) $$F(\theta) = \frac{1}{2}\left\{\left[1 - \mathrm{erf}\left(\frac{1-\theta}{2\sqrt{\theta/Pe}}\right)\right] + e^{Pe}\left[1 - \mathrm{erf}\left(\frac{1+\theta}{2\sqrt{\theta/Pe}}\right)\right]\right\}$$

where the Peclet number, $Pe = LU_c/E$ and L = test section length.

The first term in the equation is identical to the solution of the diffusion equation of Danckwerts (9) and the second term is small for large L or small E. The direct search method due to Rosenbrock and Storey (10) was used to minimise the root mean square deviation in comparison of the model with the experimental data. The agreement was very good, showing the applicability of the dispersion model.

CORRELATION OF THE DATA

The dispersion coefficient, E was correlated to the system variables, using linear least square technique as

(5) $$E = 4.0\, A^{0.5} \cdot f^{0.33} \cdot U_c^{0.6} \cdot d^{0.2} \cdot S^{-0.6} \cdot H^{-0.69}$$

with E varying from 1.75 to 6.0 cm^2/sec

where A = stroke (1.4 - 3.8 cm)
f = frequency (0.75 - 3.0 Hz)
U_c = continuous phase superficial velocity (0.1785 - 0.4689 cm/sec)
d = hole diameter (0.3 - 0.8 cm)
S = free flow area (0.092 - 0.189)
H = plate spacing (2.0 - 5.0 cm)

Equation (5) is empirical and employs the units given for the above quantities; it is valid between the above limits. The dispersion coefficient, E obtained from the fitted curve according to equation (4) was found in good agreement (with 10% standard deviation) with the E_c, as calculated from equation (5); this is shown in Figure 3.

COMPARISON WITH OTHER WORKERS' DATA

(a) The RTD is influenced by A and f to a different extent, as shown in equation (5). This is in contrast to the dispersed phase holdup, where the effects of A and f can be combined as a product variable, Af, as found by Kim and Baird (4). The dispersion coefficient in the RPC of the present study, as shown in Figure 4 is less than that in an RPC with large plate free area, an observation in agreement with that of Hafez et al. (5). Hence Karr and Lo (11) have suggested the use of baffle plates to reduce axial dispersion in RPC with large free area.

(b) The RTD of the continuous phase depends on u_d, in agreement with the observations of Prochazka et al. (6). No significant effect of u_d, the dispersed phase velocity (varied from 0.027 - 0.22 cm/sec) was found in this work, whereas Kim and Baird (4) observed, a slight increase in E with increase in u_d at low Af and a decrease in E at high Af, with E being constant at intermediate values of Af. Prochazka et al. (6) reported a slight decrease in E with increase in u_d, while Nemecek and Prochazka (7) observed no apparent effect of u_d on E in the mixer-settler and dispersion regions.

(c) The RTD is influenced by d, S and H, in agreement with the observations of Kim and Baird (3). Kim and Baird (4) reported an increase in E to the 1.8 power of d, as against a power of only 0.2 in the present study. The inverse dependence of S is in agreement with that reported by Nemecek and Prochazka (7). Decrease in E with increase in H was also noticed by Prochazka et al. (6), Kim and Baird (3) and Hafez et al. (5).

CONCLUSIONS

The RPC of the present study has a lower free area and hole diameter than that of the Karr column and exhibits lower axial dispersion coefficients. Thus, it could be advantageously used for treating poisonous/expensive gases and for liquid-liquid systems in pharmaceutical industry, where high efficiency (low height of transfer unit) is desired. On the other hand, the lower plate open area will be expected to reduce the throughput obtainable due to flooding restrictions.

ACKNOWLEDGEMENTS

One of the authors, Dr. N.V. Rama Rao, is grateful to Dr. M.H.I. Baird for many valuable suggestions.

References

1 Karr, A.E.; A I Ch E J., 5, 446 (1959).

2 Ioannou, J., M.M. Hafez, and S. Hartland; Ind. Eng. Chem. Proc. Des. Dev., 15(3), 469 (1976).

3 Kim, S.D. and M.H.I. Baird; Can. J. Chem. Eng., 54, 81 (1976).

4 Kim, S.D. and M.H.I. Baird; Can. J. Chem. Eng., 54, 235 (1976).

5 Hafez, M.M., M.H.I. Baird and I. Nirdosh; Can. J. Chem. Eng., 57, 150 (1979).

6 Prochazka, J., J. Landau, J. Souhrada, and A. Heyberger; Brit. Chem. Eng., 16, 42 (1971).

7 Nemecek, M. and J. Prochazka; Can. J. Chem. Eng., 52, 739 (1974).

8 Morris, D.R., K.E. Gubbins, and S.B. Watkins; Trans. Inst. Chem. Engrs., 42, T323 (1964).

9 Danckwerts, P.V.; Chem. Eng. Sci., 2, 1 (1953).

10 Rosenbrock, H.H. and C. Storey; Computational Techniques for Chemical Engineers, Pergamon Press, New York (1966).

11 Karr, A.E. and T.C. Lo; Proceedings of Intl. Solvent Extn. Conf., The Hague, p. 299, 1971 (Soc. Chem. Ind., London, 1, (1971)).

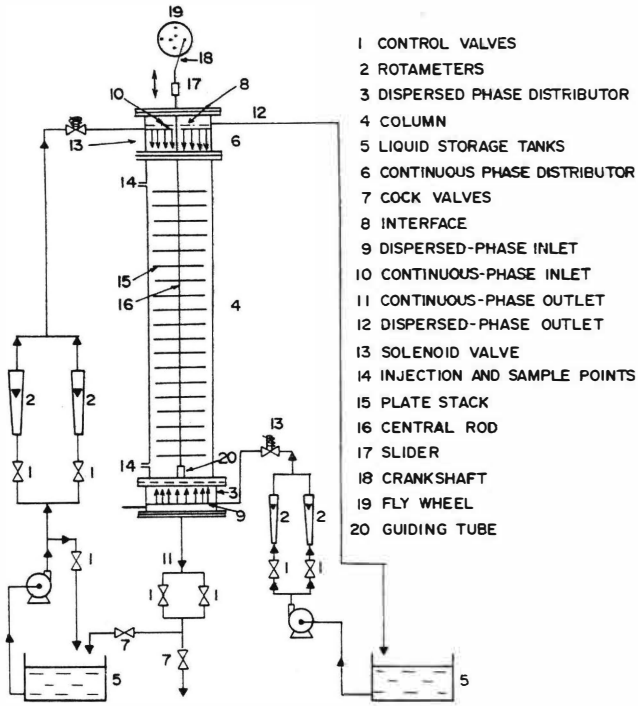

FIGURE 1 SCHEMATIC DIAGRAM OF THE EXPERIMENTAL SET-UP FOR LIQUID-LIQUID SYSTEM

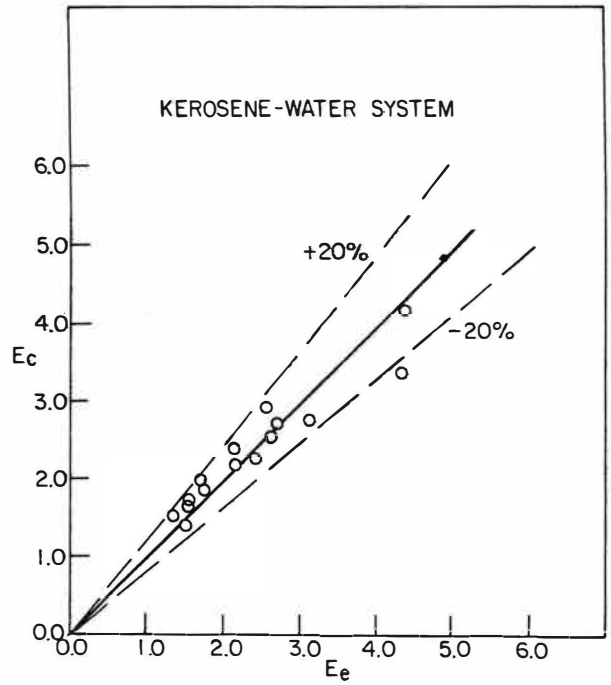

FIGURE 3 COMPARISON OF EXPERIMENTAL AND CALCULATED AXIAL DISPERSION COEFFICIENT

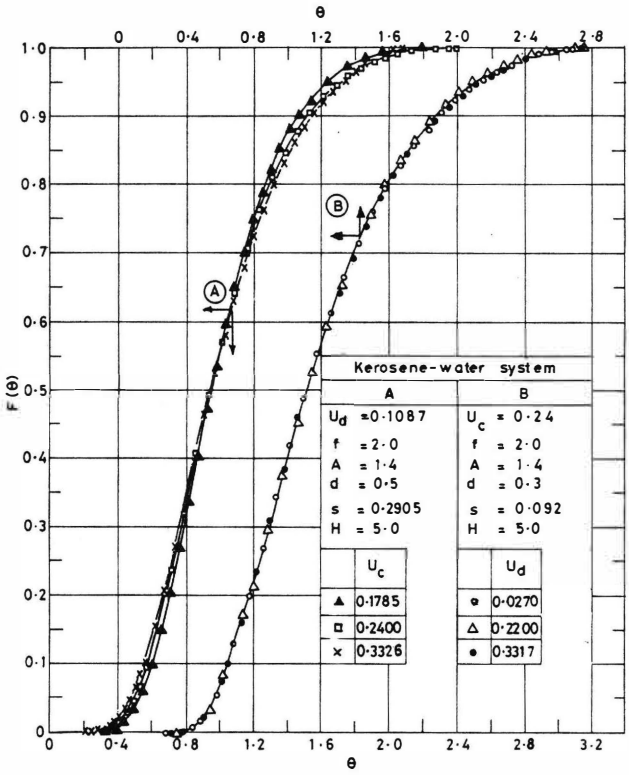

FIGURE 2 VARIATION IN RTD WITH CONTINUOUS PHASE VELOCITY AND WITH DISPERSED PHASE VELOCITY.

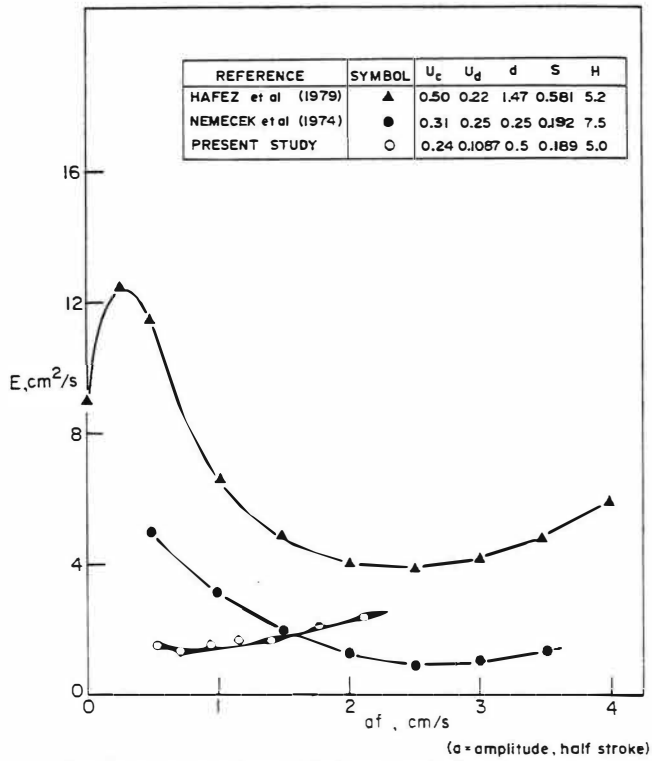

FIGURE 4 EFFECT OF AGITATION ON AXIAL DISPERSION COEFFICIENT

A STUDY OF AXIAL MIXING IN PULSED SIEVE PLATE EXTRACTION COLUMN

Shen Zhong-Yao, Dai You-Yan, Zhu Shen-Lin and Wang Jia-Ding

Tsinghua University
Beijing, China

OBJECTIVE:

Axial mixing characteristics of continuous phase is studied by stimulus-response technique in a pulsed column equipped with "dispersion-coalescence" type sieve-plate cartridge. In a previous study (1) on extraction of HNO_3(aq) into 30% TBP (in kerosene) in column equipped with this type of cartridge has shown a 20% reduction of apparent HTU, (H_{oxp}) in comparison to the conventional "standard" cartridge, and this reduction is resulted from less degree of axial mixing as indicated by the simultaneously determined Peclet number and "true" HTU, (H_{ox}), from measured concentration profiles under steady state. Study of flooding with this type of cartridge (six systems without mass-transfer were tested) has also shown a 100% increase in throughput over the "standard" type (1). In the present work axial mixing in the conventional "standard" sieve-plate column has also studied for comparison under corresponding operation conditions.

This work, as a starting, is aiming to the development of a suitable scale-up procedure for this type of column internal.

EXPERIMENT AND DATA PROCESSING:

Experiments were carried out in a glass column of 4 cm in diameter. The organic-phase wettable louver plates (Fig.1) were made of plexiglass (polymethyl-methacrylate) and each of this plate were arranged in between sections of three sieve plates to form the "dispersion-coalescence" cartridge having effective height of 110 cm with 2.5 cm of plate spacing. The geometric factors of the standard sieve-plate cartridge are as follows:

Diameter of holes	0.3 cm
Free area	23%
Thickness of plate	0.1 cm
Spacing of plates	5.0 cm

Material: Stainless steel

Kerosene was dispersed into water which flowed at a constant velocity of V_c= 0.6 cm/sec (superficial velocity) data were taken at various superficial velocity of dispersed phase:

V_d = 0.0, 0.088, 0.275, 0.39 cm/sec

Air pulse was used with amplitude, (A) varied from 1.0 to 1.6 cm and frequency, (f) from 1.5 to 2.5 sec^{-1}. Operation conditions throughout the test were thus kept in the emulsion regime.

Stimulus-response technique was used in this investigation with imperfect pulse injection of KCl as tracer. Water samples (free from organic phase) were drawn continuously at two levels down stream of the flow. The measured conductance signals were amplified and collected in a digital computer and processed. The least-square fitting method in the time domain was used for data processing. The superiority of this method of data collecting and processing for the study of axial mixing in extraction column has been discussed elsewhere (2).

Hold-up of dispersed phase (x) were also measured at all runs of experiment in this work.

SUMMARY OF RESULTS:

Results of the present work are summurized as shown in Fig.2 and Fig.3. The axial mixing coefficient of continuous phase (E_c) for two-phase flow in pulsed-sieve-column with both types of cartridge increases with increase of pulse intensity (Af). At given pulse condition, E_c decreases with increase of superficial velocity of dispersed phase (V_d) while the superficial velocity of water phase is kept constant (V_c= 0.6 cm/sec). Each point in the figures represents an average value of 5-6 parallel experimental results. These results have the same trend as those obtained by T. Miyauchi (3) and summarized by M.H.I. Baird (4)(5).

It can be seen from Fig.3 that under the same operation condition, E_c in column with "dispersion-coalescence" cartridge is obiously lower than that with conventional "standard" type cartridge. These results are consistent with those obtained in the previous work (1) while mass transfer being present.

Curves in Fig.3 also indicate that for "standard" cartridge, E_c under each set of pulse condition decreases linearly with increase of superficial velocity of dispersed phase (V_d), but that for "dispersion-coalescence" cartridge drops sharply from the initial value of V_d= 0 (i.e. E_c of single phase) and then it flattens at rather low value of V_d (0.088 is the lowest value in the present work). A plot (not presented in this abstract) of E_c versus the slip-velocity V_s (= $V_c/1-x + V_d/x$) has shown that for "standard" cartridge, E_c decreases linearly with decrease of V_s, while on the contrary, for "dispersion-coalescence" cartridge E_c decreases with increase of V_s. This could be explained from the flow characteristics of dispersed phase in pulsed-sieve-column equipped with the two different types of cartridges. For "standard" type cartridge, the slip-velocity V_s= $V_o(1-x)^n$ (where n equals practically 2 for kerosene dispersed in water)(6)(7), thus, V_s always decreases with increase the fractional hold-up (x) of dispersed phase. For "dispersion-coalescence" type cartridge V_s increases with increase of hold-up, x has been reported in Ref. (1) as the result of coalescence of droplets induced by the organic-phase wettable louver plates. Based on the experimental results and the above analysis, a relation:

$$E_c \propto Af(1-x)^n$$

is suggested for correlation of data obtained. By regression with

n =2 for "standard" cartridge

n =1 for "dispersion-coalescence" cartridge

gives straight line in either case as shown in Fig.4 and Fig.5. All points (each point represent the average value of 5-6 parallel experimental results) fall in the region of ±10% deviation. Noting that the values of E_c of single phase for "standard" type cartridge are included in the correlation while those for the "dispersion-coalescence" type are excluded because of the obvious change of performance resulted from the induced coalescence of droplets even at very small V_d.

CONCLUSION:

Determination of axial mixing coefficient by stimulus-response technique in the present work gives consistent results to those obtained by simultaneous determination of Peclet number and "true" H.T.U. from measured concentration profiles. Results indicate that

axial mixing of continuous phase are obviously retarded while coalescence louver plates are introduced into pulsed-sieve-plate column.

The relationship of $E_c \propto Af(1-x)^n$ is valid only for emulsion regime under operation of the present work. Further work should be done to study its applicability to wider range of operation conditions (e.g. pulse intensity and flow-rate range of both phases).

As the pulsed-sieve-plate column with "dispersion-coalescence" cartridge has shown its superiority both in throughput and efficiency in liquid-liquid extraction, extensive works are worthwhile to be carried out for its scale-up. Under the assumption that H_{ox} is independent of column diameter (this might be more true while the louver plates also serve as redistributors of dispersed phase), scale-up procedure might be established by correlation of axial mixing coefficient with column diameter and flow characteristics under conditions without mass transfer.

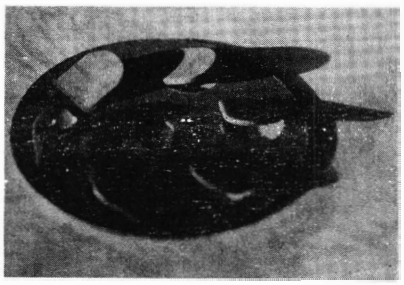

Fig.1 Photograph of Louver Plate

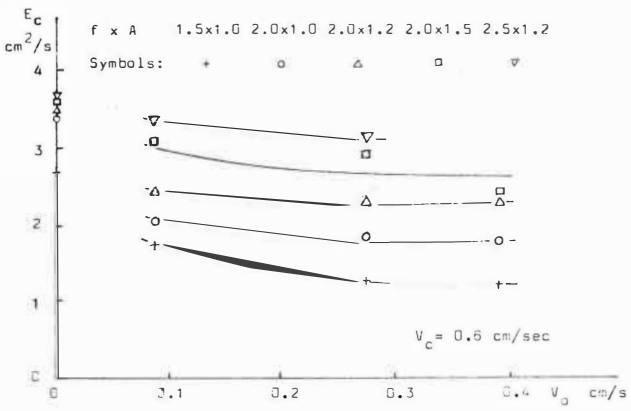

Fig.2 Effect of V_d to E_c for "D-C" cartridge

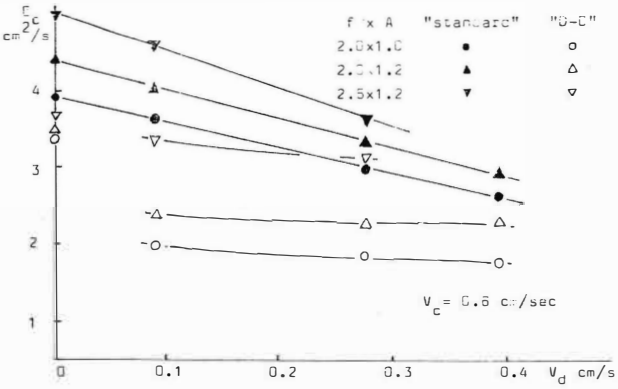

Fig.3 Comparison of E_c for "standard" & "D-C" cartridge

NOTATION:

A	= Amplitude	cm
E	= Axial mixing coefficient	cm^2/sec
f	= Frequency	sec^{-1}
V	= Superficial velocity	cm/sec
V_s	= Slip-velocity	cm/sec
x	= Fraction, hold-up of dispersed phase	

Subscript:

c = continuous phase

d = dispersed phase

REFERENCES:

1. X. Lei, Y.Y. Dai, Z.Y. Shen, J.D.Wang, Proc. CIESC/AIChE Joint Meeting of Chem. Eng. Vol.II, 538 (1982).
2. J.C. Yang, W.Y. Fei, Z.Y. Shen, J.D. Wang, J. Chem. Ind. & Eng. (China) No.2, 173 (1982).
3. T. Miyauchi, K. Oya, AIChE J. 11, 395 (1965).
4. M.H.I. Baird, Can. J. Chem. Eng. 52, 750 (1974).
5. M.Y. Hafez, M.H.I. Baird, I. Mirdosh, Can. J. Chem. Eng. 57, 150 (1979).
6. J.D. Wang, Z.Y. Shen, C.F. Wang, J. Chem. Ind. & Eng. (China), No.4, 215 (1985).
7. S.L. Zhu, B.Q. Zhang, Z.Y. Shen, J.D. Wang, J. Chem. Ind. & Eng. (China), No. 1, 1 (1982).

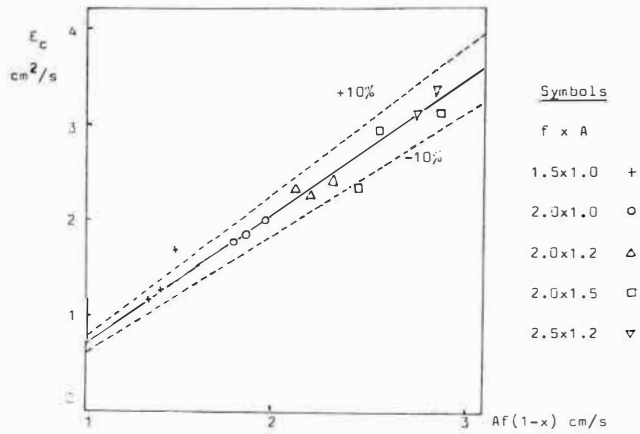

Fig.4 E_c vs $Af(1-x)$ for "D-C" cartridge

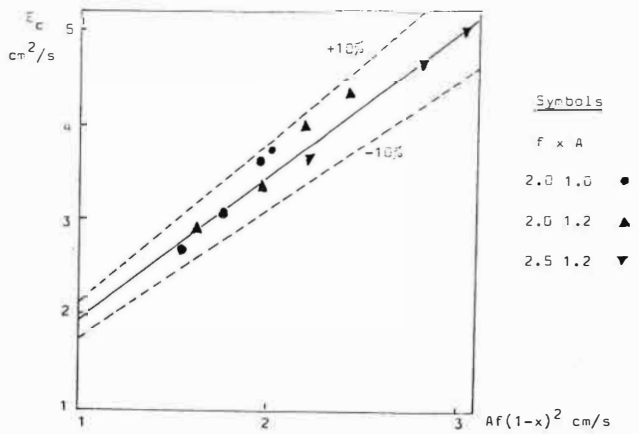

Fig.5 E_c vs $Af(1-x)^2$ for "standard" cartridge

LIQUID-LIQUID EXTRACTION COLUMN MASS TRANSFER PARAMETERS FROM CONCENTRATION PROFILES

Dr. W. J. Korchinsky, R. Al-Husseini and C. H. Young

Department of Chemical Engineering
University of Manchester Institute of Science and Technology
Manchester, England

INTRODUCTION

Previous attempts to determine extraction column model parameters have not been successful. These have been based largely on the axial dispersion model, which fails to adequately describe the dispersed phase behaviour (1,2). The forward mixing model, which takes into account the influence of drop size and residence time variations (1-4), more accurately reflects this behaviour. Calculation techniques for performance prediction, including more accurate drop mass transfer rate prediction (5,6) have been published (2,5,6,7) but the use of this model has not been extended to the prediction of model parameters from experimental data. This was the objective of this work. Young (8) developed the computational procedures required to utilise the theory to generate parameter values. Al-Husseini (9) obtained the experimental data and used Young's technique to generate parameter values from the data.

THEORY

Mass transfer performance in an extraction column may be predicted (6) by model equations in which the following are assumed:

1. The dispersed phase consists of spherical drops of different sizes travelling at different velocities through the column.
2. Continuous phase flows through the column countercurrently to the dispersed phase, with plug flow modified by an axial diffusional process.

The drop side mass transfer process has been modelled by several (10-13) models, depending on assumed drop mobility. Previous calculations have shown (5, 14, 15) that the Handlos-Baron turbulent circulating model (12) provides close predictions of experimental data. Parameter estimation procedures therefore were based on the assumption that the Handlos-Baron model predicted the drop-side mass transfer process. The continuous phase mass transfer, and the axial dispersion, coefficients were the parameters determined from the measured solute concentration profiles.

The equations utilized were the following:

Drop Side Mass Transfer - Handlos-Baron (10)

$$(1)\quad \frac{\partial y}{\partial z} = \frac{V_s}{128 d V_d (1+\mu_D/\mu_C)\,(1-\xi')}\,\frac{\partial}{\partial \xi'}\left(1-5\xi'+10\xi'^2-6\xi'^3\right)\frac{\partial y}{\partial \xi'}$$

Column Mass Transfer

$$(2)\quad \frac{d^2x}{dz^2} + \frac{Q_c}{SE_c}\frac{dx}{dz} = \frac{\rho_D Q_D}{SE_c\rho_c}\sum_{i=1}^{N} g_i \frac{dy_i}{dz}$$

$$(3)\quad \frac{dy_i}{dz} = \frac{6\,K_{OD,i}\,(y^*-y_i)}{d_i\,V_{d,i}}$$

There are varying degrees of accuracy to which these equations may be solved (6), depending on the boundary conditions assumed at the drop surface and whether variations with height are taken into account. The most accurate solution requires the numerical solution of the drop-side and column model equations simultaneously. Though this has been done, to use this numerical solution in a parameter estimation routine would have involved the use of excessive computation time. To avoid this the influence of the variation in continuous phase concentration with height, on the drop-side mass transfer rates, was neglected. The number of plug flow transfer units thus predicted will differ from the 'exact' by about 2% (6).

For each drop size, therefore, the overall mass transfer coefficient, dispersed phase basis, was calculated as follows:

$$(4)\quad K_{OD,i} = -\frac{d_i V_{di}}{6Z}\ln\left[2\sum_{n=1}^{\infty} B_n^2 \exp\left[-\lambda_n \frac{V_{s,i} Z}{128\, d_i V_{d,i}(1+\mu_D/\mu_C)}\right]\right]$$

where λ_n are eigenvalues of the Sturm-Liouville equation,

$$(5)\quad \frac{d}{d\xi'}\left[(1-5\xi'+10\xi'^2-6\xi'^3)\frac{\partial y}{\partial \xi'}\right] + \lambda_n\,(1-\xi')y=0$$

The eigenvalues and coefficients were accurately calculated using the techniques developed by Cruz-Pinto (5,6). Further details of the method of solution of these equations to determine both phase concentration profiles may be obtained from Ref. 5 and 6.

These equations were therefore used to predict continuous phase concentration profiles, which were then compared with experimental profiles. The continuous phase mass transfer coefficient, k_c, and axial dispersion coefficient, E_c, were varied to obtain a minimum 'least-squares error' between predicted and experimental values using the technique of Young's (8). For initial values, correlations of Misek (16) for E_c, and of Calderbank and Moo-Young (17) for k_c, were utilised.

EXPERIMENTAL

A rotating disc contactor with a diameter of 21.9 cm and a total height of 147 cm was used in this study (8). Other column dimensions: disc diameter - 11.0 cm, stator ring inside diameter - 13.2 cm, compartment height - 7.2 cm.

Experimental measurements were made, during mass transfer runs, with the toluene(dispersed) - acetone - water (continuous) system, of the following -

- drop size distributions at several levels in the column
- dispersed phase hold-up fraction
- extraction efficiencies
- continuous phase profile concentrations

Now as the model equations have certain limitations, great care was taken in the experimental programme to keep within these limitations. Low acetone concentrations were used to maintain constant flow conditions. More importantly, drop size variation with column height was kept to a minimum with the use of perforated plate distributors to introduce the dispersed phase at a controlled drop size. There were slight reductions in drop size due to drop break-up, but with the low dispersed phase hold-up levels, and particular conditions used in these test runs, coalescence was avoided. Mass transfer direction was limited to that from the continuous into the dispersed phase, also to avoid coalescence.

RESULTS

Over 50 runs have been made with three dispersed phase distributors and with varied flow rates and rotating disc speeds. Typical of the data obtained are those tabulated in Table 1, where data for 8 runs at constant flows are summarised. Drop size variation with column height for these runs is illustrated in Fig. 1. Experimental concentration profiles for two of the runs are plotted in Fig. 2 and 3.

With change in inlet distributor to increase the inlet drop size, column performance deteriorated as extraction efficiencies, and the related plug-flow numbers of transfer units, decreased. From the result of all the runs it was found that in going from Dist. I to Dist. III, at constant disc speed, an average increase in drop size of 55% led to an average reduction in interfacial area of 50% and in number of transfer units of 40%.

Increases in disc speed caused slight reductions in drop size, but much greater increases in the dispersed phase hold-up values, which resulted in increases in extraction efficiencies and numbers of transfer units.

Experimental concentration profiles, illustrated in Fig. 2 and 3, are typical in showing the concentration jump at the continuous phase inlet due to axial mixing.

The appropriate data, including drop size distributions and the concentration profiles, were used in a computer programme to generate values of the continuous phase mass transfer coefficients, k_c, and axial dispersion coefficients, E_c. These are tabulated, for the eight runs, in Table 1. The theoretical profiles which result are illustrated for two of the runs, in Fig. 2 and 3. As expected, k_c and E_c increase with disc speed. The influence of flow rates and of the distributor, or of drop size independent of disc speed, is less obvious. The values of k_c generated for all runs indicate that there is no significant variation between Distributors or with flow rates, and that k_c depends only on disc speed - as illustrated in Fig. 4. The variability in E_c is greater but in addition to the significant increases with disc speed, there is evidence to indicate that E_c values also increase with total flow of both phases, and with inlet drop size (or Distributor) independent of disc speed (see Fig. 5).

SUMMARY

With care, experimental measurements obtained during mass transfer runs may be used to generate parameter values for the assumed model, in this case, taking into account axial dispersion in the continuous phase and drop size and residence time variation. With some exceptions, to experimental error, the generated values of the continuous phase mass transfer coefficient, k_c and axial dispersion coefficient, E_c, followed identifiable trends.

An important discovery was that k_c was independent of drop size at a given disc speed. This would confirm that the increase in the overall mass transfer coefficient with drop size predicted by the Handlos-Baron model is correct. Though it must be added that the k_c values are somewhat low, and that it is entirely possible that the Handlos-Baron model predicts the correct trend, but that the drop size mass transfer rates predicted may be too high, requiring the low k_c values to give the "correct" overall K_{OD}.

The evidence is strongly against the application of either the rigid drop or Kronig-Brink mass transfer model because both predict a decrease in dropsize mass transfer coefficient with increase in drop size.

The experimental evidence again strongly supports the conclusion that drop size must be closely controlled to obtain the best column performance. It follows that predictable performance, from generated model parameters, will only be possible if drop size is accurately controlled.

REFERENCES

1. Chartres, R.H., Ph.D. Thesis, The Victoria University of Manchester, 1975
2. Chartres, R.H. and Korchinsky, W.J., Trans. Inst. Chem. Engrs., 1975, 53 247
3. Rod V., Br. Ch. Eng., 1966, 11 483
4. Olney, R.B., A.I.Ch.E.J., 1964, 10(6), 827
5. Cruz-Pinto, J.J.C., Ph.D. Thesis, the Victoria University of Manchester, 1979
6. Korchinsky, W.J. and Cruz-Pinto, J.J.C., Chem. Eng. Sci., 1979, 34, 551
7. Korchinsky, W.J. and Azimzadeh-Khatayloo, S., Chem. Eng. Sci., 1976, 31, 871
8. Young, C.H., M.Sc. Dissertation, the Victoria University of Manchester, 1979
9. Al-Husseini, R., Ph.D. Thesis, The Victoria University of Manchester, 1983
10. Newman, A.B., Trans. A.I.Ch.E. 1931, 27, 310
11. Kronig, R. and Brink, J.C., Appl. Sci. Res., 1950, A-2 142
12. Handlos, A.E. and Baron, T., A.I.Ch.E.J., 1957, 3, 127
13. Rose, P.M. and Kintner, R.C. A.I.Ch.E.J., 1966, 12, 530
14. Korchinsky, W.J. and Cruz-Pinto, J.J.C., Proc. International Solvent Extraction Conference, Liege, Belgium, Sept. 1980.
15. Korchinsky, W.J., Loke, C.T., and Cruz-Pinto, J.J.C., Chem. Eng. Sci, 1982, 37, 781
16. Misek, T., Coll. Czech, Chem. Comm., 1975, 40, 1686
17. Calderbank, P.M. and Moo-Young, M.B., Chem. Engng. Sci., 1961, 16, 39

NOTATION

B_n	proportionality constants
d_i	drop diameter, i^{th} fraction
d_{32}	Sauter-mean drop diameter ($\sum_i n_i d_i^3 / \sum_i n_i d_i^2$)
E_C	axial dispersion coefficient, continuous phase
E_{OD}	extraction efficiency, dispersed phase basis
g_i	volume fraction of dispersed phase, drop diameter d_i, kinetic basis
k_c	mass transfer coefficient, continuous phase
$K_{OD,i}$	overall mass transfer coefficient i^{th} fraction, dispersed phase basis
m	solute distribution coefficient, y^*/x
n	RDC disc speed
N_{ODP}	plug flow number of transfer units, dispersed phase basis
Q_C, Q_D	volumetric flow rates, continuous and dispersed phases
r	radial co-ordinate
S	column cross-sectional area for flow
$V_{d,i}$	drop vertical velocity, i^{th} fraction
$V_{s,i}$	drop slip velocity i^{th} fraction
x	weight fraction solute, continuous phase
y_i	dispersed phase solute weight fraction, i^{th} fraction
y	weight fraction solute, variable within drop
y^*	weight fraction solute, equilibrium with continuous phase
z	column vertical height.

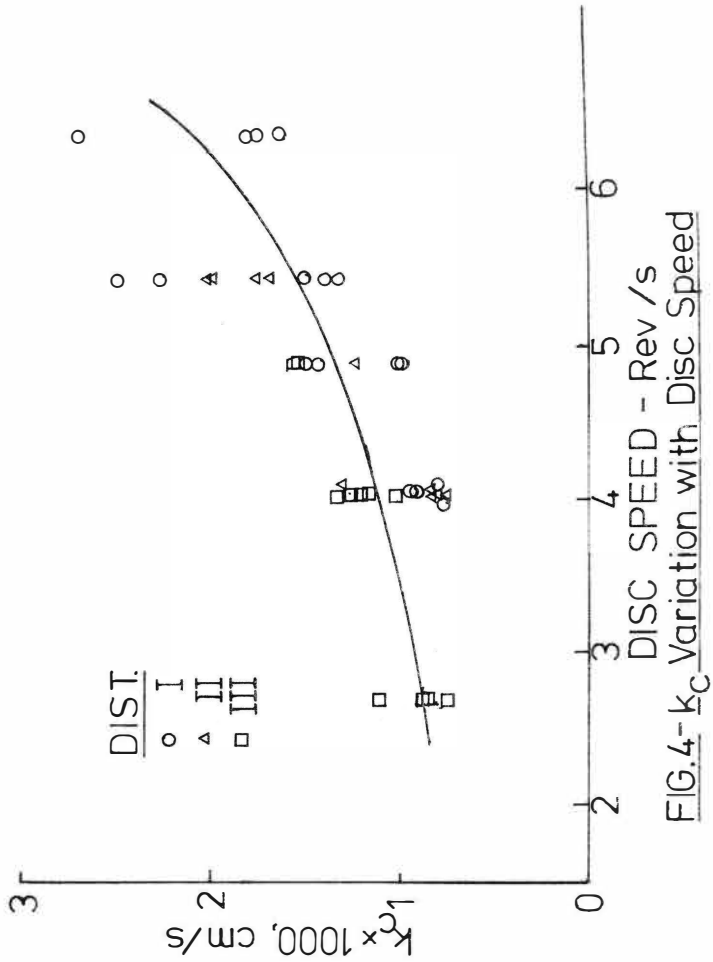

FIG.4- k_c Variation with Disc Speed

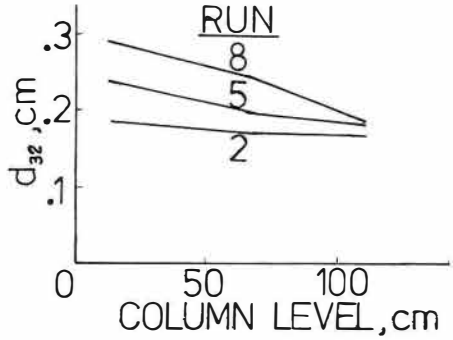

FIG.1 Column Drop Size Profiles

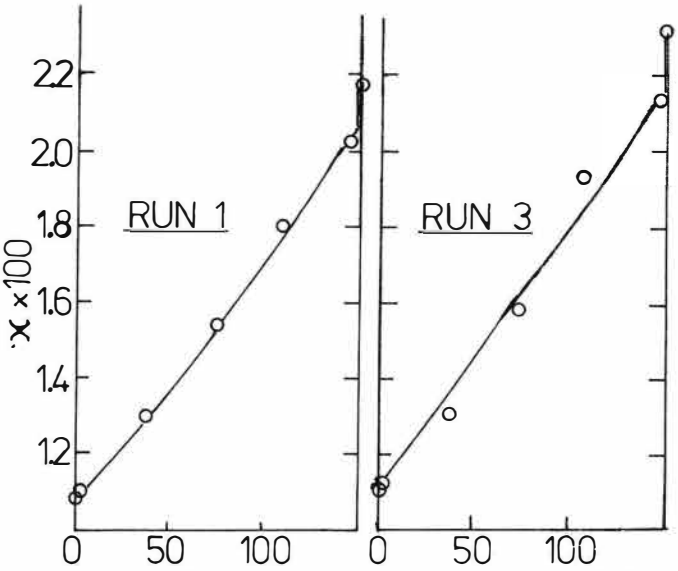

FIG. 2-Concentration Profiles -FIG.3

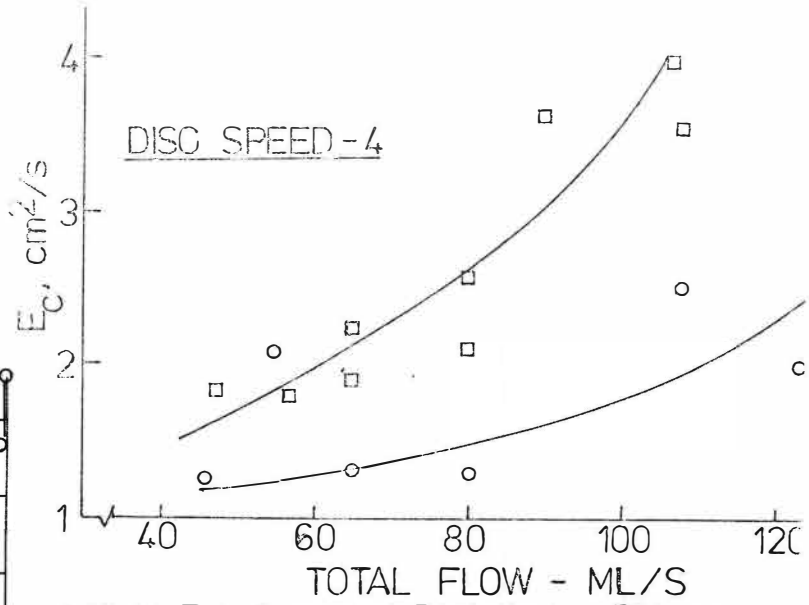

FIG. 5-E_C: Flow and Distributor Effects

TABLE 1 - RESULTS, FLOWS - Q_C = 48.2 cm³/s, Q_D = 60.4 cm³/s

Run No.	Dist. No.	Disc Speed rev/s	d_{32} cm	ϕ	E_{OD}	N_{ODP}	Optimum Values 1000 k_c cm/s	E_c cm²/s
1	I	4.00	0.180	0.0543	0.654	1.66	0.95	2.50
2	I	4.88	0.168	0.0718	0.724	2.05	1.49	2.90
3	I	5.43	0.147	0.0808	0.786	2.79	2.48	4.05
4	II	4.00	0.219	0.0545	0.576	1.18	0.94	3.95
5	II	4.88	0.204	0.0704	0.679	1.72	1.23	4.16
6	II	5.43	0.184	0.0766	0.720	1.99	1.74	6.13
7	III	4.00	0.289	0.0462	0.509	0.97	1.14	3.94
8	III	4.88	0.241	0.0524	0.582	1.16	1.49	4.56

MASS TRANSFER IN A CONTINUOUS FLOW STIRRED TANK REACTOR

P. M. Bapat and L. L. Tavlarides

Department of Chemical Engineering and
Materials Science, Syracuse University
Syracuse, New York USA

The investigations dealing with the two phase phenomena are generally directed to characterize the spread of the dispersed phase particulate properties. The state of the dispersed phase can be formally obtained as the solution to the population balance equation (1-4). However, the multidimensionality of the distribution of the dispersion, such as the one in which mass transfer and/or reaction are occurring, renders the the numerical solution to the population balance equation increasingly unwieldy. Monte Carlo simulation offers an attractive alternative for obtaining the dispersion state by obviating the need for solving the involved multidimensional integrodifferential equations. An event oriented simulation technique based on the method of interval of quiescence is developed in this work to evaluate the performance of the CFSTR as a liquid extractor by predicting the dispersed phase drop size distribution and mass transfer efficiency at steady state. The validity of the algorithm is provided by the agreement of the predictions with the experimental results.

SIMULATION MODEL

A collection of droplets representing the entire drop population in the reactor is monitored as it reaches the final steady state from its initial state. The evolution of the sample is marked by the successive droplet events separated from each other by an interval of quiescence. The drop events considered are: 1. entry (feed), 2. exit, 3. breakage and 4. coalescence. Except for the first activity which is considered to occur deterministically at a fixed frequency, all the remaining activities are treated stochastically. The drop event frequencies used in this work are enumerated below.

1. Feed Frequency:

(1) $$f_f=(V_d/\tau)/v_f$$

2. Exit Frequency:

(2) $$f_e=N/\tau$$

The above formulation is based on the assumption that the CFSTR is perfectly mixed. The following frequencies are postulated for homogeneous isotropic dispersions (4).

3. Breakage Frequency:

(3) $$f_b = \sum^{N}(C_1\,\epsilon^{1/3}/[(1+\phi)a_i^{2/3}]).\exp[-C_2\rho(1+\phi)^2/(\rho_d\,\epsilon^{2/3}a_i^{5/3})]$$

The daughter droplet probability volume distribution of the binary breakage is given by the β-distribution.

(4) $$\beta(a_i,a_j) = 30\,(a_i^3/a_j^3)^2(1 - a_i^3/a_j^3)^2$$

4. Coalescence Frequency:

(5) $$f_c= [\,0.5\,C_3\,\epsilon^{1/3}/(1+\phi)]\sum_{i}^{N}\sum_{j\neq i}^{N}(a_i+a_j)^2(a_i^{2/3}+a_j^{2/3})^{1/2}$$
$$.\exp[-\{C_4\mu_c\rho_c\epsilon/(\sigma^2(1+\phi)^3)\}\{a_ia_j/(a_i+a_j)\}^4]$$

The interarrival time for the randomly occurring events is computed by the Poisson arrival pattern analysis (5) as follows:

(6) $$t_{IQ} = -(\ln x)/(f_b+f_c+f_e)$$

Mass Transfer. Apart from the drop interactions, the dispersion is also subjected to isothermal interphase mass transfer of a single solute. With the mass transfer resistance localized to the continuous phase, the quasi steady state analysis provides the amount of solute transferred from the drop of diameter a_i in time t_{IQ} as

(7) $$m_i = (\pi/6)\,a_i^3\,(C^*_{d,i} - KC_c)\,[1 - \exp[-6\,Sh_i\,D_c t_{IQ}/(Ka_i^2)]]$$

The mass transfer efficiency is given by

(8) $$E = (C_c - C_{c,f})/(C_{c,e} - C_{c,f})$$

where C_c is obtained by a simple discretized solute balance over the continuous phase.

The assumptions of the quasisteady state ($K\,Pe^{0.5} \gg 1$) and the localization of mass transfer resistance to the continuous phase ($K(D_d/D_c)\,Pe^{-1/2} \gg 4 \times 10^{-2}$) hold true if K has a sufficiently high value (6).

The Sherwood number in this work has been calculated according to the semiempirical correlation proposed by Levins and Glastonbury (7).

(9) $$Sh_i = 2 + 0.47\,(a_i^{4/3}\,\epsilon^{1/3}/\nu)^{0.62}\,(d_T/D_T)^{0.17}\,Sc^{0.36}$$

EXPERIMENTAL WORK

To assure the dispersion homogeneity, cyclohexane/carbontetrachloride(d)-[iodine]-water(c) system was studied in a 1 liter CFSTR. The flow diagram is given in Figure 1. The drop size distribution was obtained by in situ photomicrography while the mass transfer efficiency was obtained by the spectrophotometric measurement of the solute concentrations in the dispersion phases separated by a specially developed in situ filtration technique.

RESULTS

Figure 2 shows the simulated and the experimental volume density function for a batch experiment. The constants indicated in the figure are used throughout the subsequent simulations.

The influence of the dispersed phase fraction on CFSTR performance is shown in the Figure 3. The results indicate that both the sauter mean diameter and the extraction efficiency increase with increasing phase fraction. The increase in drop size is attributed to the turbulence damping while that in the efficiency is attributed to the greater drop interaction.

Figure 4 depicts the extractor performance as a function of residence time. The mass transfer efficiency increases with the residence time. The decrease in the sauter mean diameter with the residence time indicates that the drop interaction dynamics is breakage dominated.

The comparison of the experimental results for dispersions without mass transfer and with transfer from the dispersed organic to the continuous aqueous phase indicates that the average drop size increases as a result of iodine transfer. The expected suppression in coalescence when iodine is transported in the opposite direction is negligible. This absence of quantitative influence is attributed to the low surface activity of iodine. For future work investigating the effect of mass transfer direction on coalescence, it is suggested that a solute capable of significantly altering the interfacial tension between the two immiscible phases of the dispersion should be used.

The simulated sauter mean diameters are within ±5.0% of the experimental results. The predicted mass transfer efficiencies are accurate to within ±3.4%. This close agreement validates the drop rate models and the simulation algorithm used in this work.

ACKNOWLEDGMENT. This research was financed by the National Science Foundation Grant CPE-80-21039.

NOTATION

a = drop diameter, m
$A_v(a)$ = probability volume density function of a drop of diameter a, m^{-1}
C = solute concentration, M
C_1, C_2 = constants in the breakage frequency function, eq. (3)
C_3, C_4 = constants in the coalescence frequency function, eq. (5)
d_I = stirrer diameter, m
D_I = tank diameter, m
D = solute molecular diffusivity, m^2/s
E = reactor mass transfer efficiency
f_b = sample breakage frequency, s^{-1}
f_c = sample coalescence frequency, s^{-1}
f_e = sample exit frequency, s^{-1}
f_f = sample feed frequency, s^{-1}
$g(a)$ = breakage frequency of a drop of diameter a, s^{-1}
m_i = solute exchanged by the ith drop in time t_{IQ}, mole
N = total number of drops in the sample
Pe = Peclet number
Re = Reynolds number
Sc = Schmidt number
Sh = Sherwood number
t_{IQ} = interval of quiescence, s
v_f = average volume of the feed drops, m^3
V = sample phase volume, m^3
x = uniform random number between 0 and 1

Greek Symbols

$\beta(a_i,a_j)$ = probability density function of a drop of diameter a_i when a drop of diameter a_j breaks
ϵ = power dissipation per unit mass, m^2/s^3
K = solute equilibrium distribution constant
μ = dynamic viscosity, kg/(m.s)
ν = kinematic viscosity, m^2/s
ϕ = dispersed phase holdup fraction
ρ = density, kg/m^3
σ = interfacial tension, N/m
τ = residence time, s

Subscripts/Superscripts

c = continuous phase
d = dispersed phase
e = equilibrium
f = feed
* = initial

REFERENCES

1. Valentas, K. J. and Amundson, N. R. Ind. Eng. Chem. Fund. 5 533 (1966).
2. Bayens, C. A. and Laurence, R. L. Ind. Eng. Chem. Fund. 8 71 (1969).
3. Bajpai, R. K., Ramkrishna, D. and Prokop, A. Chem. Eng. Sci. 31 913 (1976).
4. Coulaloglou, C. A. and Tavlarides, L. L. Chem. Eng. Sci. 32 1289 (1977).
5. Graybeal, W. J. and Pooch, U. W. Simulation: Principles and Methods Winthrop Publishers, Inc. Cambridge, Massachusetts, 1980.
6. Dang, V., Ruckenstein, E. and Gill, W. N. The Chemical Engineer no. 241 248 (1970).
7. Levins, D. M.and Glastonbury, J. R. Trans. Inst. Chem. Engr. 50 132 (1972).

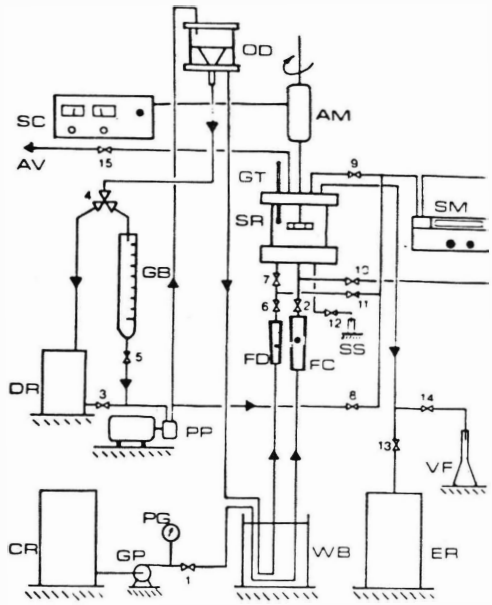

Figure 1. Experimental flow system. (AM: stirrer motor; AV: vacuum line; CR: continuous phase feed reservoir; DR: dispersed phase feed reservoir; ER: effluent reservoir; FC: continuous phase flowmeter; FD: dispersed phase flowmeter; GB: graduated buret for dispersed phase flow measurement; GP: continuous phase feed gear pump; GT: mercury-in-glass thermometer; OD: overhead overflow device; PG: pressure gage; PP: peristaltic pump for dispersed phase feed; SC: stirrer speed controller; SK: sink line; SM: spectrophotometer; SR: continuous flow stirred tank reactor; SS: sampling station; VF: volumetric flask for dispersion flow rate; WB: water bath.)

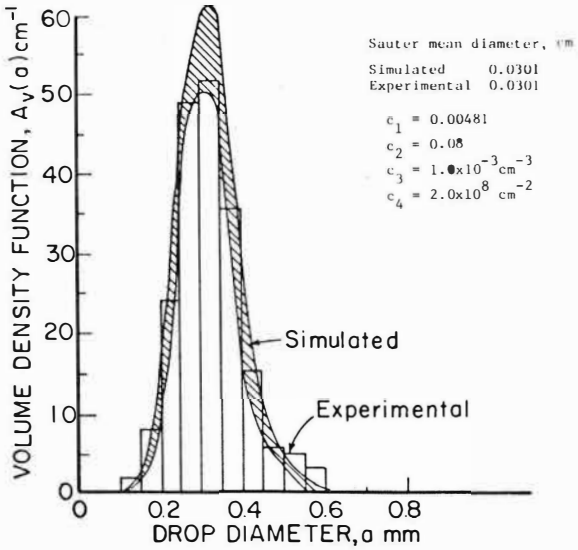

Figure 2. Experimental and simulated drop size distribution for physical dispersion. (Bath operation; R.P.M. 400; ; = 0.10.)

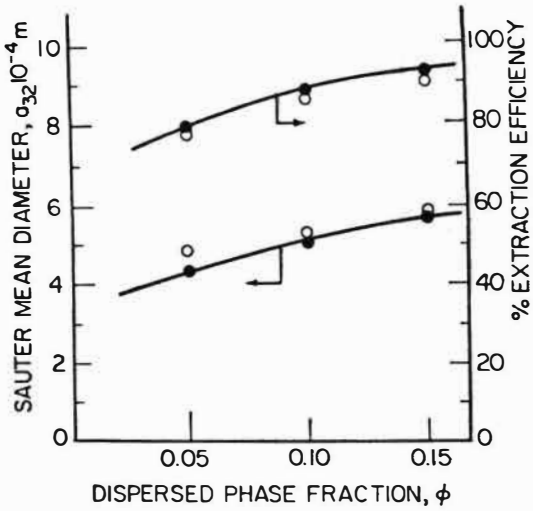

Figure 3. Influence of dispersed phase fraction on CFSTR performance. R.P.M. 350; τ = 60 s; $C_{d,f}$ = 1x10^{-3}M; $C_{c,f}$ = 0. (●: experimental; o: simulated)

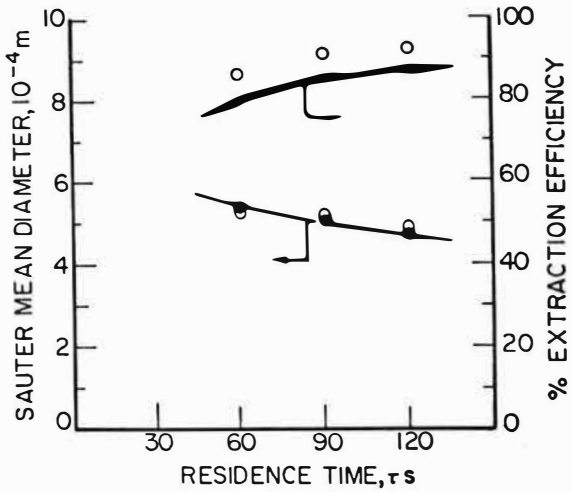

Figure 4. Drop size and efficiency versus residence time. (R.P.M. 350; ϕ = 0.10; $C_{d,f}$ = 1x10 M; $C_{c,f}$ = 0.) (●: experimental; o: simulated)

HYDRAULIC AND MASS TRANSFER MODEL FOR HIGH CAPACITY LIQUID-LIQUID EXTRACTORS FILLED WITH STACKED PACKINGS

Prof. Dr.-Ing. Reinhard Billet, Dr.-Ing. Jerzy Mackowiak

Ruhr-Universität Bochum
Department of Thermal Separation Processes
D-4630 Bochum - Universitätsstrasse 150 - Geb. IB 5/151

1. INTRODUCTION

According to latest findings the application of metallic Bialeckirings employed as packing elements in so-called Tube Columns, Fig. 1 a, or employed as a packing, Fig. 1 b, results in a significant increase in the maximum throughput of both phases as well as in a reduction of the mixing effects due to uniform distribution of the droplets and of the continuous phase over the entire column cross-sectional area (1-6).

A characteristic hydraulic feature of these extractors is the fact that up to a loading of about 65% the liquid hold-up x of the dispersed phase is essentially independent of the superficial velocity u_C of the continuous phase and has proven in this regime to be merely a linear function of the superficial velocity u_D of the dispersed phase. However the liquid hold-up x of the dispersed phase was not predictable by calculation and required test work for the system in question.

In this study a model will be presented from which a generally valid method can be derived by which the liquid hold-up x can be calculated for any system. The equation developed for the liquid hold-up x of the dispersed phase is employed to determine the separation effect of the extractors shown in Fig. 1 in analogy to the theory of the non-stationary diffusion. The equations presented pertain to the cases for which mass transfer resistance is exclusively controlled by the droplets. The mathematical models presented are compared and discussed with data obtained in extensive experiments comprising columns with diameters of 25 to 225 mm and packing height of 0,5 to 3,2 meters employing 5 different test systems.

2. LIQUID HOLD-UP OF THE DISPERSED PHASE

The generation of droplets is the consequence of the kinetic energy E_K with which the phase impacts the internals. Droplets such formed are stable only when a certain relation between their kinetic energy E_K and the interfacial energy E_σ is satisfied (7,8)

(1) $$\frac{E_\sigma}{E_K} = C_0 \quad , \text{ with } C_0 \gg 1 \text{ for } E_\sigma > E_K \, .$$

This pertains furthermore to the regime in which the relation of liquid hold-up x and the specific throughput u_D of the dispersed phase behaves linearly

(2) $$x = C_1 \cdot u_D \qquad [m^3/m^3] \, . \quad \text{for } u_C \leq 0.65 \cdot u_{C,Fl}$$

In consideration that in this regime the absolute droplet velocity $\bar{u}_D$ can be equated with the relative droplet velocity u_R as expressed by

(3) $$u_R = \bar{u}_D = \frac{u_D}{\varepsilon \cdot x} \qquad [m^3/m^2 \cdot s] \quad \text{for } \bar{u}_D \gg \bar{u}_C = \frac{u_C}{(1-x)\varepsilon}$$

and since the droplet diameter d_{VS} can be calculated according to Sauter by

(4) $$d_{VS} = C_2 \cdot \sqrt{\frac{\sigma}{\Delta\rho \cdot g}} \qquad [m] \, ,$$

one can derive, consistant with expression (1), an equation for determining the liquid hold-up x of the dispersed phase (7)

(5) $$x = \frac{C_3}{\varepsilon} \cdot We^{0.5} \qquad [m^3/m^3]$$

with

(6) $$C_3 = \sqrt{\frac{C_2}{12} \cdot C_0} \, ,$$

or

(7) $$C_0 = 12 \cdot \frac{C_3^2}{C_2}$$

and

(8) $$We = \frac{\rho_D \cdot u_D^2}{(\Delta\rho \cdot g \cdot \sigma)^{0.5}}$$

As an example the function

(9) $$x \cdot \varepsilon \cdot \frac{(\Delta\rho \cdot g \cdot \sigma)^{0.25}}{\rho_D^{0.5}} = f(u_D)$$

was shown in Fig. 2, which is valid for the column packed as shown in Fig. 1 b with 25 mm Bialeckirings, the slope of which is the constant C_3. For rising droplets, according to Fig. 2, a numerical value for C_3, which is system independent, was derived to be for falling droplets

(10) $$C_3 = 1.62 \quad \text{for } \rho_D < \rho_C \, .$$

Based on experimental work with the system dichlorethane (D)/water and tetrachlor carbon (CCl_4) (D)/water the C_3-value was determined to be

(11) $$C_2 = 1.2 \quad \text{for } \rho_D > \rho_C \, .$$

With C_3 being known one can now derive the constant C_0 by means of equation (7)

(12) $$C_0 = 3.15 \gg 1 \quad \text{for } \rho_D < \rho_C$$

and

(13) $$C_0 = 21.7 \gg 1 \quad \text{for } \rho_D > \rho_C \, ,$$

the numerical values of which confirm the original assumption according to equation (1).

The constants presented apply to the 25 mm and 50 mm Tube Column according to Fig. 1 a as well as to the metallic packing with 25 mm Bialeckrings according to Fig. 16.

3. MASS TRANSFER, D → C

Based on extended mass transfer tests D → C with systems toluene (D) acetic acid/water, CCl_4 (D) - acetic acid/water, for which the total mass transfer resistance is practically entirely controlled by the droplets, it could be shown that the theory of non-stationary diffusion is applicable for extractors shown in Fig. 1 a and 1 b (5,6,7).

For the volumetric mass transfer coefficient $\beta_D \cdot a$, which holds for the entire separation effect, the relation was established (7)

(14) $$\beta_D \cdot a = \frac{12}{C_2} \cdot \sqrt{\frac{C_3}{\pi \cdot l}} \cdot \frac{(\Delta\rho \cdot g)^{0.375} \cdot \rho_D^{0.25} \cdot D_D^{0.5}}{\sigma^{0.625}} \cdot u_{D\,[1/s]} \, ,$$

while for the hight of a mass transfer unit (HTU_D) the following equation was derived (7)

(15) $$HTU_D = \frac{C_2}{12} \sqrt{\frac{\pi \cdot l}{C_3}} \cdot \frac{\sigma^{0.625}}{(\Delta\rho \cdot g)^{0.375} \cdot \rho^{0.25} \cdot D_D^{0.5}} \, [m] \, .$$

According to this model the mass transfer D → C in an extractor, filled with orderly arranged packing elements, is dependent on the physical properties of the components of the system to be separeted, by the diffusion coefficient of the extracted component in the dispersed phase as well as by the design of the extractor.

According to equation (14) respectively (15) the separation effect of the extrator increases with decreasing contact length l, which, based on theoretic considerations possesses the following values (5,6)

for the 25 mm tube column

(16 a) $l = 0.0188$ m

for the 50 mm tube column

(16 b) $l = 0.0375$ m

for the orderly packed column filled with non-aligned 25 mm Bialeckirings

(16 c) $l = 0.050$ m.

A comparision between the experimental and calculated $\beta_D \cdot a$ values by equation (14) is shown in Fig. 3 for the system CCl_4 (D)-acetic acid/water and in Fig. 4 for the system toluene (D)-acetic acid/water.

The maximum deviations between the experimentally determined $\beta_D \cdot a$ values and those, which were calculated according to the model by equation (14), are not greater than 12 % although the column diameter varied between 25 and 225 mm and the height of the packing between 0,5 and 3,2 m. These results suggest that for the experimental extractor which is filled with Bialeckirings, of which each layer is shifted by 25 mm, no significant scale-up problems are to be expected provided that the total mass transfer resistance is controlled by the droplets. This observation is of particular significance when establishing design parameters for extractors for which the main mass transfer resistance is controlled by the continuous phase.

The particular advantage of equation (14) respectively (15) is the fact that for design calculations physical data such as τ, $\Delta\rho$, ρ_D, of the pure substances can be employed.

NOMENCLATUR

C_0, C_1, C_2, C_3		constants or parameters
D_D	$[m^2/s]$	diffusion coefficent of the disolved components in the dispersed phase
E_K, E_σ		kinetic energy and interfacial energy of droplets
d	[m]	diameter of a packing element
d_s	[m]	column diameter
d_{VS}	[m]	droplet diameter according to Sauter $d_{VS} = \Sigma n d_i^3 / \Sigma n d_i^2$
g	$[m^2/s]$	gravitational acceleration
h	[m]	height of a packing element
H	[m]	height of a layer of packing elements
HTU_D	[m]	height of a mass transfer unit referring to the dispersed phase
l	[m]	contact lenght
u_C, u_D	$[m^3/m^2 \cdot s]$	superficial velocity of the continuous or dispersed phase resp.
u_R	$[m^3/m^2 \cdot s]$	relative droplet velocity
x	$[m^3/m^3]$	liquid hold-up of the dispersed phase relating to the empty column volume
$\beta_D \cdot a$	[1/s]	volumetric transfer coefficient from the droplet into the continuous phase
σ	[N/m]	interfacial tension
ε	$[m3/m3]$	gap volume
λ		phase throughput ratio, $\lambda = u_D/u_C$
$\Delta\rho$	$[kg/m^3]$	density difference between the two not mixable liquids
τ	[s]	contact period
$We = \frac{\rho_D \cdot u_D^2}{(\Delta\rho \cdot g \cdot \sigma)^{0,5}}$		Weber number

ABBREVIATIONS

e.g. 25 BR	Bialeckirings 25 mm in diameter
M	metal
Rk	tube column with lined up rings
Fk	orderly packed column filled with non-aligned rings

REFERENCES

1. R. Billet, G. Husung, J. Mačkowiak, Chemie Technik (Heidelberg) 8 No. 1, 25/29 (1979)

2. R. Billet, J. Mačkowiak, Chem.-Ing.-Techn. 52 No. 2, 170/171 (1980)

3. R. Billet, J. Mačkowiak, Germ.-Chem.-Eng. 3 No. 4, 234/240 (1980)

4. R. Billet, J. Mačkowiak, Indian Chem. Eng. World (CEW) 15 No. 10, 29/45 (1980)

5. R. Billet, J. Mačkowiak, Proceedings Chempor 81, 3rd Int. Chem. Eng. Conference, Povoa de Varzim, 20 - 24 April 81, Portugal, Vol 1, 1.32/1.56 (1981)

6. R. Billet, J. Mačkowiak, vt "verfahrenstechnik" 15 No. 12, 898/904 (1981)

7. J. Mačkowiak, Theorie der nichtstationären Diffusion zur Bestimmung der Wirksamkeit von Extraktionskolonnen mit regelmäßig angeordneten Füllkörpern, tutorial lecture at Institute for Thermo- and Fluiddynamic at Ruhr-University Bochum 18.02. (1982)

8. N. Bohr, I.A. Whealer, Phys. Dev. 56, 426 (1939), cit. by M. Stölting, Chemie Technik 9 No. 2, 77/81 (1980)

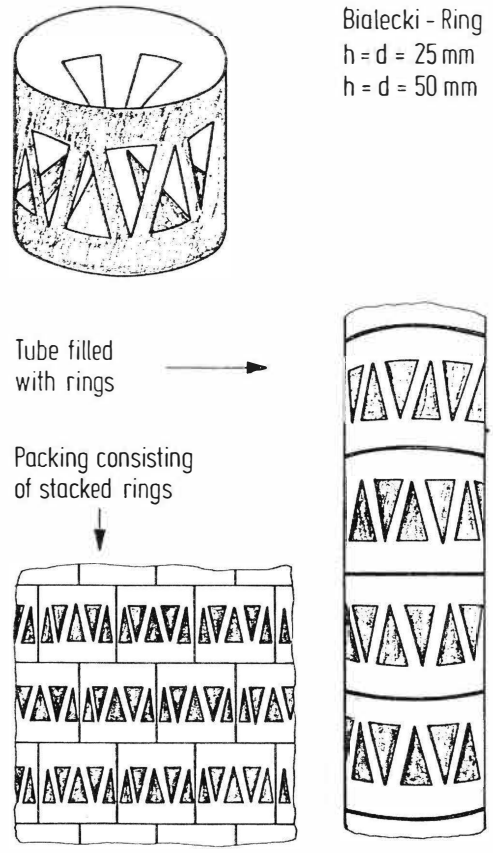

Fig. 1 Presentation of Bialeckirings

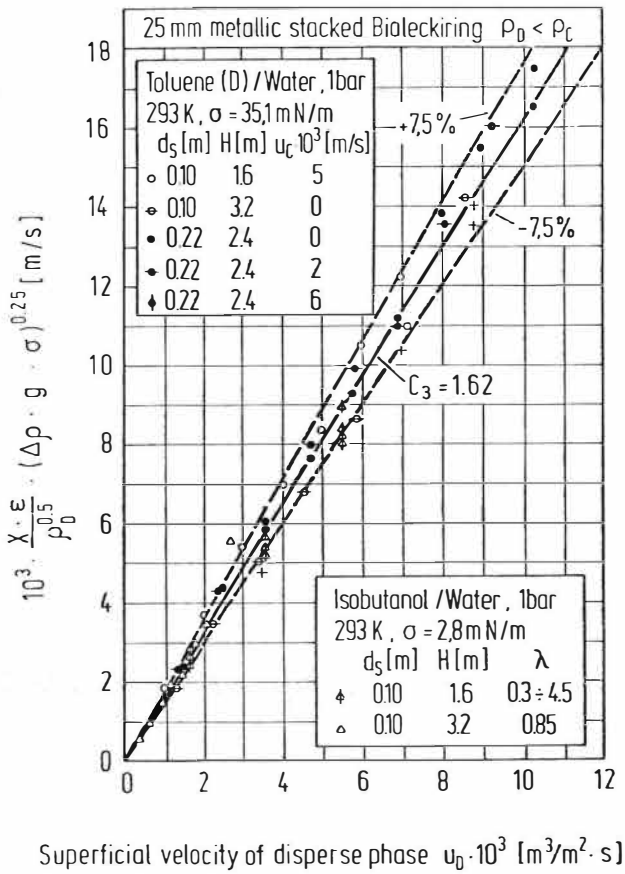

Fig. 2 Determination of the constant C_3 for equation (5) demonstrated on the metallic packing with Bialeckirings shifted by 25 mm

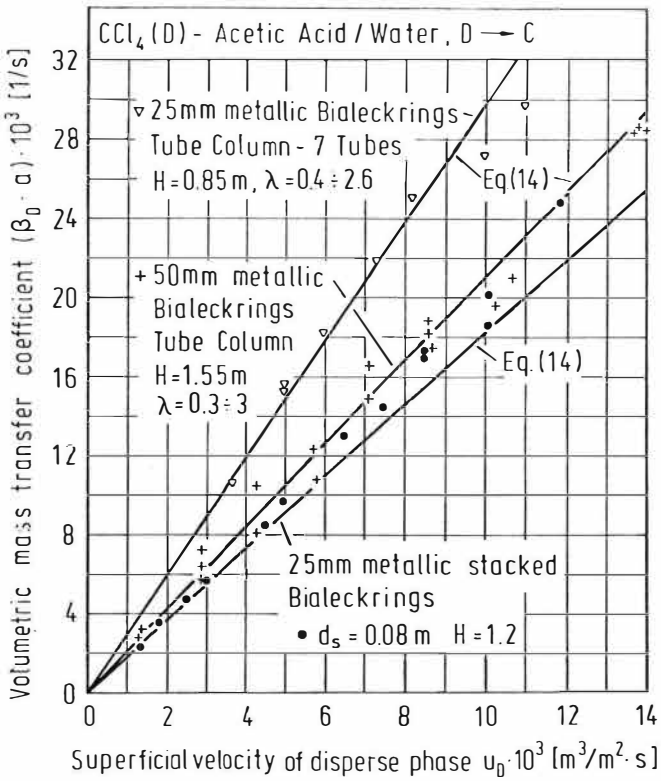

Fig. 3 Comparison of the measured volumetric mass transfer coefficients $\beta_D \cdot a$ with those calculated according to equation (14) (steady lines), valid for the system CCl_4(D)-acetic acid/water, D → C, $\rho_D > \rho_C$

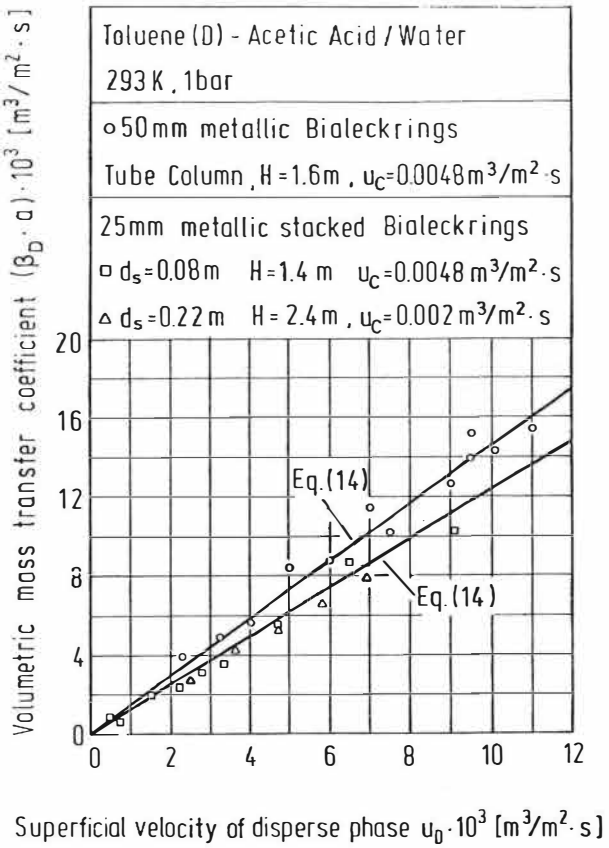

Fig. 4 Comparison of the measured volumetric mass transfer coefficients with those calculated according to equation (14) (steady lines), valid for the system toluene (D)-acetic acid/water, D→C, $\rho_D > \rho_C$

SOLVENT EXTRACTION RELATED TO OPERATING PARAMETERS THROUGH ABSOLUTE STAGE EFFICIENCY

Ertan Yuzak and Raymond C. Waggoner

University of Missouri-Rolla
Rolla, Missouri 65401 USA

Overall mass transfer coefficients for solvent extraction are related to operational parameters through a model imbedded in a multi-stage, multi-component rating simulation. Mass transfer rates are related to inlet concentration differences to improve correlation results. An absolute stage efficiency is defined to describe deviation from equilibrium stage operation.

INTRODUCTION

Various procedures have been developed (Smith (1), Eubanks and Lowe (2), Hanson, Duffin, and Somerville (3), Holland (4), Cohen, et. al., (5), Tierney and Bruno (6), Roche (7), Jelinek and Hlavacek (8)) to calculate the ideal concentration profiles for equilibrium stages. However the streams leaving one of the stages of a multistage extractor may not be equilibrium because of non-uniform mixing or insufficient contact time for mass transfer. For non-equilibrium operations, single-phase component material balances may be replaced by two-phase component material balances which utilize explicit descriptions of mass transfer between phases. Simultaneous solution of the compositions in both phases and on all stages must be obtained. The quin-diagonal algorithm, reported by Waggoner and Eye (9) may be applied to solve these balance equations. If the overall mass transfer coefficients can be estimated, the actual concentration profiles can be obtained without iteration. An iterative search matching the computational balance solutions to experimental data may be used to estimate overall mass transfer coefficients.

OVERALL MASS TRANSFER COEFFICIENTS RELATED TO OPERATING PARAMETERS

The following derivation is developed to describe the transfer of a low concentration solute from phase V to phase L in a multistage mixer-settler system. The rate of this transfer may be represented by the following differential equation.

$$(1)\quad -\frac{dw_{DEA,V}}{dt} = K^{\circ}_{y} a V_M \Phi_V \rho_V (y-Kx)$$

If the mass of V-phase material, W_V, does not change, the flux may be described in terms of concentration, y.

$$(2)\quad -\frac{dy}{dt} = K^{\circ}_{y} a \frac{V_M \Phi_V \rho}{W_V} (y-Kx)$$

or

$$(3)\quad -\frac{dy_e}{dt} = K^{\circ}_{y} a (y-Kx)$$

When mass transfer in the mixer is complete, equilibrium composition, y_e, is obtained and $y_e = K_e$. Therefore,

$$(4)\quad -\frac{dy_e}{dt} = K^{\circ}_{y} a (Y_e - Kx_e)$$

When composition is expressed as deviation from equilibrium, the following equation is obtained:

$$(5)\quad -\frac{d(y-y_e)}{dt} = K^{\circ}_{y} a \left(1+\frac{KV}{L}\right)(y-y_e)$$

If $K^{\circ}_{y}a$ and K are not functions of composition, Equation (5) may be integrated across a stage to obtain the following,

$$(6)\quad \ln \frac{y_o-y_e}{y_{in}-y_e} = K^{\circ}_{y} a \left(1+\frac{KV}{L}\right) \frac{V_M \Phi_V \rho_V}{V}$$

The limits on time make up the mean residence time, i.e.

$$(7)\quad \theta = \frac{V_M \Phi_V \rho_V}{V}$$

Absolute efficiency, η, is defined as a measure of mass transfer accomplished compared to that theoretically possible.

$$(8)\quad \eta = \frac{y_{in}-y_o}{y_{in}-y_e}$$

Absolute efficiency may be related to mass transfer through Equation (6)

$$(9)\quad 1-\eta = e^{-K^{\circ}_{y} a \left(1 \frac{KV}{L}\right) \theta}$$

Absolute efficiency would also be found useful in those cases in which mass transfer is accompanied by chemical reaction since η takes into account the theoretically possible concentrations and not the relative values of the concentrations in two phases.

When the mass transfer coefficient is based on the inlet concentration difference, the absolute stage efficiency η may be related to a mass transfer coefficient based on the inlet concentration difference. This mass transfer coefficient, designated $K_{yF}a$, may be calculated as follows:

$$(10)\quad (y_{in}-y_o)\, V = K_{yF} a\, \rho_V\, \phi_V\, V_M\, (y_{in} - Kx_{in})$$

Equation 10 may be written as the defining equation for $K_{yF}a$,

$$(11)\quad \frac{y_{in}-y_o}{y_{in}-Kx_{in}} = K_{yF} a \frac{\rho_V \Phi_V V_m}{V}$$

The term on the left hand side may be related to composition. When the equilibrium relation, $K=y_e/x_e$, is inserted into the component material balance around the stage and the resulting expression is rearranged, the following expression is obtained:

$$(12)\quad y_e = \frac{y_{in} + \frac{L}{V} x_{in}}{1 + \frac{L}{VK}}$$

By subtracting both sides of Equation 12 from y_{in} and rearranging,

$$(13)\quad y_{in}-y_e = \frac{\frac{L}{V}(y_{in}/K - x_{in})}{1 + \frac{L}{VK}}$$

Combining Equation (13) with the definition of η, Equation (8), the following expression may be obtained.

$$(14)\quad y_o = \frac{y_{in} + \frac{L}{V} x_{in}}{1 + \frac{L}{VK}} + \eta \frac{L}{V} \frac{(y_{in}-Kx_{in})}{(K + L/V)}$$

An expression for the composition change across a stage may be written

$$(15)\quad y_o - y_{in} = \frac{y_{in} + \frac{L}{V} x_{in}}{1 + \frac{L}{VK}} - \frac{y_{in}\left(1 + \frac{L}{VK}\right)}{1 + \frac{L}{VK}} + \eta \frac{L}{V} \frac{(y_{in} - Kx_{in})}{(K + L/V)}$$

Composition changes may be related to absolute efficiency by rearranging Equation 15.

$$(16)\quad \frac{y_{in} - y_o}{y_{in} - Kx_{in}} = \frac{L}{V} \frac{(1-\eta)}{(K + L/V)}$$

Equation (11) may be substituted to obtain the following relation between absolute efficiency and the cross-stage mass transfer coefficient.

$$(17)\quad K_{yF} a = \frac{L}{\phi_V \rho_V V_m} \frac{(1-\eta)}{(K + L/V)}$$

Equation (9) implies that the absolute efficiency, η, depends on the flow parameters only, except the slight dependence of the equilibrium coefficient concentration. Equation (17), however, is completely independent of the model assumed in deriving Equation (9). As long as a good estimate of the absolute efficiency is available, Equation (17) provides a reasonably accurate estimate of the mass transfer coefficient when based on the inlet compositions driving force.

TWO-PHASE COMPONENT MATERIAL BALANCES FOR USE WITH K_{yF}

When it is desired to use K_{yF} instead of $K_y a$ to describe interphase mass transfer, two-phase component material balances cannot be solved directly by the quin-diagonal algorithm. The coefficient matrix is expanded when bi-directional backmixing takes place. Three, rather than two, upper and lower codiagonals have non-zero elements. A preliminary row operation may be developed to enable the solution to be obtained from the quin-diagonal algorithm.

The terms of the coefficient matrix are developed as the essential first stop of the sequence. The streams entering the leaving stage j of a multi-stage extraction column are shown in Figure 1. There may be two feed and two withdrawal streams, one for each phase as well as the backmixing streams. If the amount of V stream entrained in L phase is given by $o_j L_j$, this amount of V moves oppositely to the normal direction, i.e., instead of going to stage j-1, it goes to stage j+1. An amount of L stream, given by $e_j V_j$, may backmix similarly. There would be at least two feed streams L_{F_1} and $V_{F_{NS}}$ for a multistage unit of NS stages.

The amount of component i transferred from one phase to the other in stage j is

$$(18)\quad K_{yF} a_{ji} \rho_V \Phi_V V_M (z_{y_{ji}} - K_{ji} z_{x_{ji}})$$

where $z_{y_{zii}}$ and $a_{x_{ji}}$ are the overall V and L phase concentrations of all streams entering stage j. The variables, $z_{y_{ji}}$ and $z_{x_{ji}}$, are given by Equations (19) and (20) respectively.

$$(19)\quad z_{x_j} = \frac{(L_{j-1}-W_{L_{j-1}})x_{j-1}+F_{L_j}+e_{j+1}(V_{j+1}-W_{V_{j+1}})x_{j+1}}{(L_{j-1}-W_{L_{j-1}})+F_{L_j}+(V_{j+1}-W_{V_{j+1}})e_{j+1}}$$

$$(20)\quad z_{y_j} = \frac{(V_{j+1}-W_{V_{j+1}})+F_{V_j}\,x_{FV_j}+o_{j-1}(L_{j-1}-W_{L_{j-1}})y_{j-1}}{(V_{j+1}-W_{V_{j+1}})+F_{V_j}+(L_{j-1}-W_{L_{j-1}})o_{j-1}}$$

The following two-phase component material balances can be written for component i at stage j:

$$(21)\quad (L_{j-1}-W_{L_{j+1}})x_{j-1} + L_{F_j}x_{FL_j} + e_{j-1}\,(V_{j+1}-W_{V_{j+1}})\,x_{j+1}$$

$$+ K_{yF}a_j\,\Phi_V\rho_V V_M(z_{y_j} - K_j z_{x_j}) = L_j x_j + e_j V_j x_j$$

$$(22)\quad (V_{j+1} - W_{V_{j+1}})\,Y_{j+1} + V_{F_j}x_{FV_j} + o_{j-1}(L_{j-1} - W_{L_{j-1}})\,Y_{j-1}$$

$$= K_{yF}a_j\Phi_j\rho_V V_M(z_{y_j} + V_j y_j) + o_j L_j y_j$$

The set of Equations (22) and (23) contains 2NS linear equations in 2NS unknowns, the unknowns being x_{ji} and y_{jj} on each stage. This system of equations is shown in Figure 2 as a matrix equation. The values of the non-zero elements inthe coefficient matrix are given by Yuzak (10).

AN EXPRESSION TO RELATE ABSOLUTE EFFICIENCY TO OPERATING PARAMETERS

A semi-empirical expression, which relates the absolute stage efficiency to the concentration and the fraction of the mixer occupied by the organic phase, was developed:

$$(24)\quad \eta_j = e^{-\alpha(1-\Phi_V)}\left[\beta + \frac{y_{FV}-y_j}{y_{FV}}\right]$$

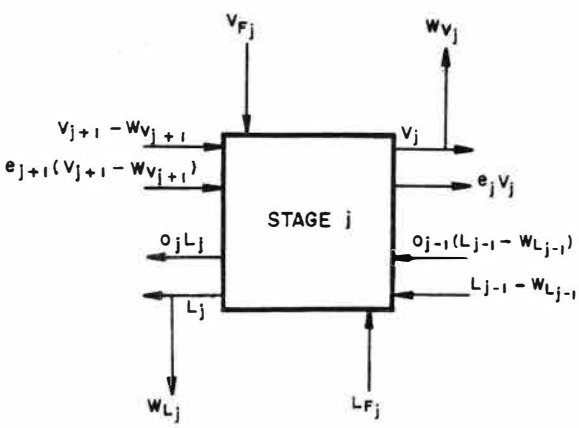

FIGURE 1. STAGE J OF A MULTISTAGE EXTRACTOR

where j represents any of the NS stages. α and β are parameters obtained numerically and y_{FV} is the outlet concentration of the intermediate stage j.In Figure 2 the values of η predicted by Equation (23) are plotted against the experimental values. α and β were calculated by using procedure NLIN, a nonlinear regression procedure of Statistical Analysis System (Helwig, et. al., (11), α and β were calculated to be 10.6 and 0.0901 respectively for the distribution of diethylamine between methyl-isobutyl ketone and water.

CONCLUSION

Non-equilibrium operation of multi-stage liquid extractors may be related to the operational parameters of the separation. This relationship is established through use of the described "absolute efficiency", Equation (11), and a cross-stage driving force to represent interphase mass transfer. Initially, absolute efficiency would be determined from recorded concentration profiles. The cross-stage mass transfer coefficient is then obtained from this value, Equation (24), and used in two-phase component-material balance equations. These material balance equations are then solved by conventional methods (9).

REFERENCES

(1) Smith, B.D., Design of Equilibrium Stage Processes, McGraw-Hill, New York, N.Y., 1963.
(2) Eubanks, J.D. and J.T. Lowe, Ind. Eng. Chem., Process Des. Dev., 7, 172, 1968.
(3) Hanson, D.N., J.H. Duffin, and G.F. Somerville, Computation of Multistage Separation Processes, Reinhold, New York, N.Y., 1962.
(4) Holland, C.D., Fundamentals of Modeling of Separation Processes, Prentice-Hall, Englewood Cliffs, N.J., 1975.
(5) Cohen, G., et. al., Chem. Eng. Sci., 26, 2051 (1971).
(6) Tierney, J.W. and J.A. Bruno, AIChE J., 13, 556 (1971).
(7) Roche, E.C., Brit. Chem. Eng., 14, 1393 (1969).
(8) Jelinek, J. and V. Hlavacek, Inc. Eng. Chem., Process Des. Dev., 15, 481, 1976.
(9) Waggoner, R.C. and J.M. Eye, Computers and Chemical Engineering 6, 265 (1982).
(10) Yuzak, E., Determination of Concentration Profiles in Multistage Extraction, Dissertation, University of Missouri-Rolla, 1981.
(11) Helwig, J.T., et. al., (ed.), SAS User's Guide, SAS Institute, Raleigh, N.C., 1979.

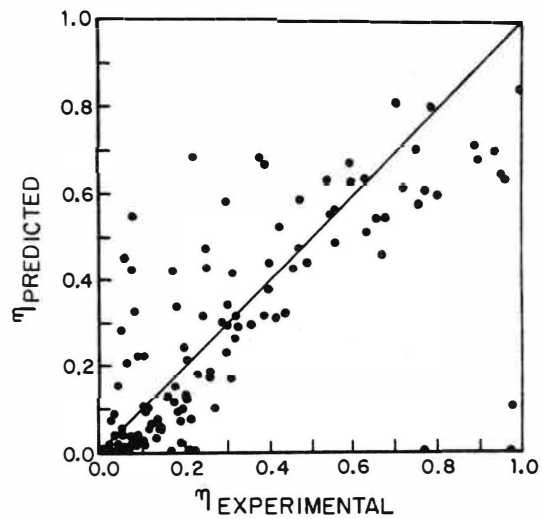

FIGURE 2. ABSOLUTE STAGE EFFICIENCY

A REVIEW OF THE EXTRACTION FACTOR METHOD

W. R. Clingan

Mallinkrodt, Inc.
St. Louis, Missouri USA

INTRODUCTION

When an engineer practicing in the chemical industry endeavors to solve a liquid-liquid extraction problem, an enormous volume of literature is available. It provides several alternative methods for the solution of such problems. The customary treatment of methods of solution first introduces the reader to triangular phase diagrams for ternary systems, followed by rectangular diagrams using solvent-free coordinates. In some instances, the use of the extraction factor method is noted under limited conditions.

Multicomponent systems include virtually all processes of industrial significance. For such systems, the graphical methods are not rigorous or convenient. In contrast, the extraction factor method is well suited to treat multiple components, one at a time.

It is an objective of this paper to provide a partial classification of this literature to increase its accessibility to industrial practitioners.

The scope is limited to simple forward extraction (a single unit section) with a constant extraction factor. The convention used here is that of Hartland (1), that is designation of the raffinate phase as liquid and the extract phase as gas.

APPLICATION OF THE EXTRACTION FACTOR METHOD

The extraction factor method is not necessarily straightforward in application. The extraction factor has been denoted by many symbols in the literature, including C, D, E, ε, J, R and U, as well as groupings such as mG/L, etc. Another source of confusion is the prevalence of two definitions for the extraction factor. Some authors invoke $y_E=mx$ and some $y_E=mx+b$ as necessary conditions for application of the extraction factor method, and in Sherwood and Pigford (2), each is used in a different chapter. Similarly, the symbols used for the compositions and flows of the extract and raffinate phases vary widely. A matter of still greater concern is ensuring the correctness of the formula used. As Hartland (1) points out, many of the published equations of the extraction factor method are not consistent.

The success of the extraction factor naturally depends on the quality of the data used in its application. In order to provide meaningful data, multicomponent, countercurrent extractions generally require simulation of the desired contacting pattern. This is accomplished by the laboratory procedures described by Alders (3) and Treybal (4). Hunter and Nash (5) report that these procedures, called "pseudo countercurrent extraction", were originally devised by Watanabe and Morikawa (6). However, it can readily be seen that there is a close resemblance to the older "Shanks System" for batch countercurrent solids washing (7).

It is commonly known that simulation by these procedures provides valuable data on the equilibrium lines for the various components prevailing for the desired conditions. Although noted by Treybal (4), it is much less well known that similar information is generated on the operating lines for the countercurrent cascade.

A plot of the interstage extract vs. raffinate concentrations represents the operating points graphically. A comparison of the operating line slopes thus obtained with the solvent ratio can indicate whether an assumed model or mechanism for the extraction is realistic.

The order of calculation for a system with a large number of components is a matter of some concern. Behavior such as association, dissociation, ion aggregation and solvation may produce synergistic or antagonistic effects.

In describing a trial and error graphical procedure for a uranium purification extraction scheme, Codding, Haas, and Heumann (8) presented an appropriate calculation order for such a system:

(1) Salting or complexing agent, (2) "Macro" components, (3) "Tracer" components

Modern electronic equipment permits a hybrid analytical/graphical method in which calculations are performed analytically, but displayed graphically as in the older graphical methods. A significantly improved accuracy is obtained by this technique.

CLASSIFICATION OF LITERATURE

Much of the valuable work on the equations of the extraction factor method was performed in the allied unit operations of gas absorption and stripping, liquid-solid extraction, and distillation. As a result, some of this work does not appear in the literature of liquid-liquid extraction.

In order to increase its accessibility, there are many possible criteria by which the literature of the extraction factor method might be classified. A number of these are:

1. Order of historical development
   a. Overall
   b. Within each field
2. Type of unit operation of application
3. Limits of applicability imposed by assumptions
   a. Distribution coefficient unity, $D = 1$, $\varepsilon = R$
   b. Solvent pure, $Y_{in} = 0$
   c. Extraction factor constant
      (1) For $\varepsilon \equiv DR$, $y_E = Dx$
      (2) For $\varepsilon \equiv mR$, $y_E = mx + B$
   d. Two values for extraction factor
      (1) For $\varepsilon_E \neq \varepsilon$
      (2) For $\varepsilon_S \neq \varepsilon$
   e. General rigorous equation for variable extraction factor $\varepsilon_1 \neq \varepsilon_2 \neq \ldots \neq \varepsilon_n$
4. Configuration and complexity of process
   a. Number of unit sections/number of feed streams
      (1) Simple extraction (1 unit section)
         (a) Forward extraction
         (b) Back extraction
      (2) Compound extraction (2 unit sections)
         (a) Fractional extraction
         (b) Multiple feed extraction
      (3) Compound extraction (3 unit sections)
         - Multiple feed, fractional extraction
   b. Use of reflux

This review attempts to classify the literature by the first three of these categories.

HISTORICAL DEVELOPMENT

The historical and conceptual development of the extraction factor method is presented in Table I.

The equations of the extraction factor method are usually credited to Kremser [Eq. 3] (9) and Souders and Brown [Eq. 4-7] (10). According to Klinkenberg (11), however, Sorel (12) first derived the equations of the extraction factor method for distillation in 1895. In 1917, Hawley [Eq. 1] (13) derived the equation of Kremser for solids washing with pure solvent within the final step of expressing the geometric series in closed form. In 1928, Silberstein (14) published complicated expressions for solids washing with pure solvent for three-, four-, and five-stage systems, which can be simplified to one of the extraction factor equations. Thormann (15) published Silberstein's equations in German in 1929. In response to Silberstein's article, Turner [Eq. 2] (16) published the form of the Kremser equation for solids washing with a pure solvent in 1929. Colburn (17) reports that other published work preceding Kremser included that of Iredell (18) in 1928 for liquid-solid extraction and that of Thormann (19) in 1928 for distillation.

The first publication describing the use of an extraction factor equation was by Hunter and Nash [Eq. 8] (20) in 1932. The equations presented included a sign error in the denominator. In 1934, Underwood (21) published the first correct extraction factor equations. His equations included a dimensional form explicit in x_{out} and implicit in x_{in}, y_{in}, E, and N [Eq. 9], a dimensionless form explicit in the fraction of the feed not extracted (the raffinate yield) and implicit in E, N and a dimensionless parameter U not considered in the prior literature [Eq. 10], and the reduced form of the Kremser equation for pure solvent [Eq. 11].

In 1934, Silver (22) published two new forms of the extraction factor equations, for gas absorption. The first of these [Eq. 12] had the familiar "Kremser function" $\frac{A-1}{A^N-1}$ on the right-hand side, with the left-hand side rearranged to include the effect of an impure solvent. Scheibel later presented this equation [Eq. 16] in inverted form, as defined by Hartland (1), for extraction (23) and leaching (24) operations. This form is suggested by King (25) as most convenient when equilibrium is closely approached. Silver's second equation [Eq. 13] is the reduced form of the first for the indeterminate case of $A=\varepsilon=1$. Colburn (17) published new forms of these equations [Eq. 14-15], explicit in N, in 1941. The cases of both forward and back extraction were treated, and the analogy drawn with the allied processes of gas absorption, stripping and distillation.

Smith [Eq. 17] (26) presented an equation for the fraction of the total input of a component which exits with the raffinate phase. It was simplified from the general equation of Smith and Brinkley (27) for a fractional extraction cascade with extract and raffinate reflux. It can be reduced to Underwood's equation.

Hartland (1) enumerated the possible separation factors from the various ratios of the differences of y_{in}, y_{out}, $y_E(x_{in})$ and $y_E(x_{out})$, and derived the extraction factor equation for each independent combination. Apart from Eq. 18 and 19, the remaining forms presented by Hartland duplicate those of Souders and Brown and Scheibel.

Several of these involved $y_E(x_{out})$ -- including those recommended for use use by Hartland. This makes them less desirable for use in industry than many of the earlier forms of Kremser, Souders and Brown, and Underwood.

THE DEFINITION OF THE EXTRACTION FACTOR

The most fundamental definition of the extraction factor, ε, is given by Alders (3) and Treybal (4). This is the ratio, $\frac{y_E}{x}$, of the quantity of a component in the two liquid phases (extract/raffinate) prevailing at equilibrium. By this definition, the extraction factor is equal to the product of the equilibrium distribution coefficient D, and the phase ratio, R.

An alternate definition for the extraction factor is fairly common in gas absorption (2, 25, 28) but less so in extraction (1). This is the ratio of the slopes of the equilibrium and operating lines. The phase ratio, R, (quantity of added phase to quantity of phase to be separated) is the reciprocal of the slope of the operating line on a distribution (y vs. x) diagram of the extraction process. For the case of a straight equilibrium curve passing through the origin, the equilibrium distribution coefficient is equal to the slope of the equilibrium line.

In extraction, however, straight equilibrium curves are the exception rather than the rule. For any equilibrium curve not straight with zero y-intercept, the distribution coefficient is represented geometrically by the slope of the chord between the point on the equilibrium curve and the origin, not the slope of the tangent to the equilibrium curve itself.

These are the assumptions made by a majority of early workers in deriving the equations of the extraction factor method. However, it is only necessary to assume constancy of the extraction factor to derive these equations. The distribution coefficient and phase ratio could vary, provided that their product, the extraction factor, remains constant.

The use of this equilibrium relation was reportedly (17) first suggested by Thormann (19) in 1928. It was noted by Underwood (29) in 1932 and by Colburn (17) in 1941. It was put to use by Sherwood and Pigford (2) in 1952, and by McCabe and Smith (28) in 1956. This equation was later used by Hartland (1) in 1970 and by King (25) in 1971.

If the "ratio of slopes" is taken as the definition for the extraction factor, the equations of the extraction factor method applies equally well to a straight equilibrium line of the form $y = mx + B$.

This definition, by itself, is fairly limited in utility, except possibly in the case of reactions leading to non-extractable species. However, several such lines can be fitted together to yield a good approximation to a curved equilibrium line (1) to extend the applicability of the extraction factor method.

TABLE I - EXTRACTION FACTOR EQUATIONS

REFERENCE	EQUATION	ASSUMPTIONS	AUTHOR
1	$Z_N = \dfrac{1}{1 + R + R^2 + R^3 + \ldots + R^N}$	D = 1, U = 0	Hawley
2	$Z_N = \dfrac{1 - R}{1 - R^{N+1}}$	D = 1, U = 0	Turner
3	$y_{out} = \dfrac{(A-1)}{A^{N+1} - 1}\, y_{in} + \dfrac{A\,(A^N - 1)}{A^{N+1} - 1}\, Dx_{in}$	$y_E = Dx$	Kremser
4	$x_{out} = x_{in}\left(\dfrac{\varepsilon - 1}{\varepsilon^{N+1} - 1}\right) + \dfrac{y_{in}}{D}\left(\dfrac{\varepsilon^{N+1} - \varepsilon}{\varepsilon^{N+1} - 1}\right)$	$y_E = Dx$	Souders & Brown
5	$\dfrac{y_{in} - y_{out}}{y_{in} - Dx_{in}} = \dfrac{A^{N+1} - A}{A^{N+1} - 1}$	$y_E = Dx$	Souders & Brown
6	$\dfrac{x_{in} - x_{out}}{x_{in} - \dfrac{y_{in}}{D}} = \dfrac{\varepsilon^{N+1} - \varepsilon}{\varepsilon^{N+1} - 1}$	$y_E = Dx$	Souders & Brown
7	$\dfrac{x_{out} - x_{in}}{x_{in}} = \left[1 - Z_N\right] = \dfrac{\varepsilon^{N+1} - \varepsilon}{\varepsilon^{N+1} - 1}$	$y_{in} = U = 0$	Souders & Brown
8	$x_{out} = \dfrac{y_{in}\,\varepsilon^{-1}\left(\dfrac{1}{\varepsilon^{-N}} - 1\right) + x_{in}\,\varepsilon^{-N}\left(\varepsilon^{-1} - 1\right)}{\left(\varepsilon^{-1} - 1\right)\varepsilon^{-1} + \left(\varepsilon^{-N} - 1\right)}$	$y_E = Dx$, NOTE: This equation not valid due to sign error.	Hunter & Nash

REFERENCE	EQUATION	ASSUMPTIONS	AUTHOR
9	$x_{out} = \dfrac{x_{in}\left(\varepsilon - 1\right) + y_{in}\left(\varepsilon^N - 1\right)}{\left(\varepsilon^{N+1} - 1\right)}$	$y_E = Dx$	Underwood
10	$Z_N = \dfrac{\left(\varepsilon - 1\right) + U\left(\varepsilon^N - 1\right)}{\left(\varepsilon^{N+1} - 1\right)}$	$y_E = Dx$	Underwood
11	$Z_N = \dfrac{\varepsilon - 1}{\varepsilon^{N+1} - 1}$	$y_E = Dx$, $y_{in} = 0$	Underwood
12	$\dfrac{y_{in} Z_N - x_{in} D}{y_{in} - x_{in} D} = \dfrac{y_{out} - x_{in} D}{y_{in} - x_{in} D} = \dfrac{A - 1}{A^{N+1} - 1}$	$y_E = Dx$	Silver
13	$\dfrac{y_{in} Z_N - x_{in} D}{y_{in} - x_{in} D} = \dfrac{y_{out} - x_{in} D}{y_{in} - x_{in} D} = \dfrac{1}{N + 1}$	$E = A = 1$	Silver
14	$N = \dfrac{\log\left[\left(1 - \varepsilon\right)\left(\dfrac{x_{in} - y_{in}/D}{x_{out} - y_{in}/D}\right) + \varepsilon\right]}{\log \varepsilon}$	$y_E = Dx$	Colburn
15	$N = \dfrac{\log\left[\left(1 - \varepsilon^{-1}\right)\left(\dfrac{y_{in} - Dx_{in}}{y_{out} - Dx_{in}}\right) + \varepsilon^{-1}\right]}{\log \varepsilon}$	$y_E = Dx$	Colburn
16	$\dfrac{x_{out} - y_{in}/D}{x_{in} - y_{in}/D} = \dfrac{\varepsilon - 1}{\varepsilon^{N+1} - 1}$	$y_E = Dx$	Scheibal
17	$f = \dfrac{1 - A^N + \left(\dfrac{1}{1 + V}\right)\left(A^N - A\right)}{1 - A^{N+1}}$	$y_E = Dx$	Smith
18	$\dfrac{x_{in} - x_E\left(y_{out}\right)}{x_{out} - x_E\left(y_{in}\right)} = \varepsilon^{-N}$	$Y_e = mx + B$	Hartland
19	$\dfrac{y_{in} - y_E\left(x_{out}\right)}{y_{out} - y_E\left(x_{in}\right)} = \varepsilon^{N}$	$y_E = mx + B$	Hartland

NOMENCLATURE

A = Absorption Factor = I/E.

D = Equilibrium Distribution Coefficient or Ratio = y/x.

E = Extraction Factor or Ratio of Quantity of Component of Interest in Two Phases = DR.

f = Fraction of Total Quantity of Component Entering the System Which Leaves with the Extract Phase $= \dfrac{X_{out}}{X_{in} + Y_{in}} = \dfrac{Z_N}{1 + U}$.

G = Flow Rate of Extract Phase.

L = Flow Rate of Raffinate Phase.

m = Slope of the Equilibrium Curve $= \dfrac{dy_E}{dx}$.

N = Number of Theoretical Stages in the Process.

R = Phase Ratio (Extract/Raffinate) $= \dfrac{G}{L}$.

U = Ratio of Quantity of Component in Solvent to Quantity in Feed $= \dfrac{Y_{in}}{X_{in}} = \dfrac{Y_{in}}{x_{in}}\dfrac{G}{L}$

x = Concentration of Component of Interest in Raffinate Phase $= \dfrac{X}{L}$.

X = Flow Rate of Component of Interest in Raffinate Phase = xL.

y = Concentration of Component of Interest in Extract Phase $= \dfrac{Y}{G}$.

Y = Flow Rate of Component of Interest in Extract Phase $= yG$.

Z = Fraction of Quantity of Component of Interest Remaining in Raffinate Phase after Extraction; Raffinate Yield $= \dfrac{X_{out}}{X_{in}}$.

SUBSCRIPTS

E....In Equilibrium with (Determined by Equilibrium Curve).

N....Obtained from a Countercurrent Cascade of N Stages.

in...Refers to Input Stream.

out..Refers to Output Stream.

REFERENCES

1. S. Hartland, Countercurrent Extraction, (1970).
2. T. K. Sherwood and R. L. Pigford, Absorption and Extraction, 2nd Ed., (1952).
3. L. Alders, Liquid-Liquid Extraction: Theory and Laboratory Practice, 2nd Ed. (1959).
4. R. E. Treybal, Liquid Extraction, 2nd Ed. (1963) (1930).
5. T. G. Hunter and A. W. Nash, Ind. Eng. Chem., 27, No. 7, 836 (1935).
6. Watanabe and Morikawa, J. Soc. Chem. Ind. (Japan), 36, 585B (1933).
7. R. E. Treybal, Mass Transfer Operations, 1st Ed., 590 (1955).
8. J. W. Codding, W. O. Haas and F. K. Heumann, Ind. Eng. Chem., 50, No. 2, 145 (1958).
9. A. Kremser, Natl. Petroleum News, 22, No. 21, 43 (1930) Proc. Calif. Natural Gasoline Assoc., 5, No. 2 (1930).
10. M. Souders and G. G. Brown, Ind. Eng. Chem. 24, No. 5, 519 (1932).
11. I. A. Klinkenberg, Plenary Paper, Proc. 1971, Soc. Chem. Ind. (London), 1455 (1971).
12. E. Sorel, La Distillation, 175 (1895).
13. L. F. Hawley, Ind. Eng. Chem. 9, No. 9, 866 (1917).
14. L. Silberstein, "Quantitative Relations of the Countercurrent Washing Process", Ind. Eng. Chem. 20, No. 9, 899 (1928).
15. K. Thormann, Chemische Apparatur, 16, 185, 209 (1929).
16. S. D. Turner, Ind. Eng. Chem., 21, 190 (1929).
17. A. P. Colburn, Ind. Eng. Chem. 33, No. 4, 459 (1941).
18. Iredell, Chem. & Met. Eng., 35, 685 (1928).
19. K. Thormann, Destillieren Und Rektifizieren, (1928).
20. T. G. Hunter and A. W. Nash, Soc. Chem. Ind. 51, 285T (1932).
21. A. J. V. Underwood, Ind. Chemist, 10, 128 (1934).
22. L. Silver, Trans. Inst. Chem. Engrs. (London), 12, 64 (1934).
23. E. G. Scheibel, Ind. Eng. Chem., 46, No. 1, (1954).
24. E. G. Scheibel, Chem. Eng. Progr., 49, No. 7, 354 (1953).
25. C. J. King, Separation Processes, 1st Ed., (1971).
26. B. D. Smith, The Design of Equilibrium Stage Processes, (1963).
27. B. D. Smith and W. K. Brinkley, A.I.Ch.E. J., 6, 446 (1960).
28. W. L. McCabe and J. C. Smith, Unit Operations of Chemical Engineering, 1st Ed., 604-608 (1956).
29. A.J.V. Underwood, "The Theory and Testing of Stills", Trans. Inst. Chem. Engrs. (London), 10, 110 (1932).

STAGE ADDITIVITY METHOD AND ITS APPLICATION TO CALCULATION OF COUNTER-CURRENT EXTRACTORS WITH BACKMIXING

Aleksandar Š. Tolić

University of Belgrade
Belgrade, Yugoslavia

There are several approaches to the modelling of mass transfer in counter-current extractors, but the most studied one is based on backmixing (1 - 3), while the recent one in the case of polydispersed nature of the dispersed phase take into account the effect of a drop size and its distribution (2, 4). Two models based on backmixing are basical, the so-called differential backmixing model and stagewise backmixing model.

Analytical solutions for both models are restricted to the linear case of solute distribution (1, 2), while for the general case of equilibrium distribution different and very complex numerical procedures are used for numerical solutions (2, 3). For a rapid calculation of counter-current extractors based on the two backmixing models, numerous approximate methods have been proposed (2, 3, 5-8), but application of the majority of the methods is restricted primarily to the linear case of equilibrium distribution, or to the scale of backmixing in both phases.

In this paper the recently developed approximate method - the so-called "Stage Additivity Method" and its application to the calculation of counter-current extractors with backmixing is considered (5-7).

STAGE ADDITIVITY METHOD

The stage additivity method based on stagewise backmixing model is described by the following equation quantitatively (5-7):

$$N = N_M + (N_D - N_T) + \Delta N \tag{1}$$

in which: N - is the total number of stages in extractor: N_T - is the number of stages when mass transfer is infinitelly great ($1/t = o$) and backmixing does not exist ($f = s = o$), i.e. the number of theoretical stages, N_M - is the number of stages when backmixing is absent in both phases ($f = s = o$); N_D - number of stages when mass transfer is infinitelly great ($1/t = o$) and backmixing present ($f \neq o$ and/or $s \neq o$), i.e. the number of equilibrium stages; and ΔN - correction term including nonadditivity effects, i.e. correction number of stages. Due to simplicity N_M, N_T and N_D are named the fictive number of stages denoting it with N_i, where i = M,T.D. The following expression for correction number of stages was obtained (5, 6):

$$\Delta N = \frac{1 - (C + C_1 F)\ (N_T - 1)\ \ln F}{1 + t\ (1 + Ft)}\ f + \frac{1 + (C + C_1/F)\ (N_T - 1)\ \ln F}{1 + t\ (s + F)}\ s \tag{2}$$

in which: F - is extraction factor; f and s - are backmixing coefficient in phase (x) and (y); t - true number of transfer unit in a stage. The constants C and C_1 were evaluated (5) by minimising the relative deviations between the number of stages obtained from Eg. (1) and the number of stages calculated from the exact expressions for the linear case (1). For this purpose, the number of stages for all combinations of wide selected extraction parameters was calculated and all results for which $N_T \geqslant 1.5$ and $\Psi_N \leqslant 0.990$ were used for evaluating the constants. The obtained values of constants: C = 0.79 and C_1 = 0.14, give mean square deviation of $\pm$ 1.2% in the number of stages and the corresponding extreme deviation of - 4.5% (5).

In order to calculate correction number of stages for the general case of distribution the equation for calculating the mean value of F was derived in the implicit form (6):

$$\ln F = \frac{N_M}{N_T} \ln \frac{1 + Ft}{1 + t} \tag{3}$$

By testing the stage additivity method for a wide range of combinations of selected extraction parameters and characteristic types of equilibrium lines for general case of the equilibrium distribution, the obtained results of comparing the number of stages calculated by the stage additivity method with the exact values of N show (5) that average least square deviation is $\pm$ 2.3%, and the corresponding extreme deviations are within $\pm$ 5.5%.

ANALYTICAL PROCEDURE FOR A LINEAR CASE OF EQUILIBRIUM DISTRIBUTION

In the case of a linear equilibrium distribution and constant extraction parameters the stage additivity method enables straightforward analytical procedure for calculating N, while iteration procedure is needed for solving Ψ_N or t (5, 7).

The proposed analytical procedure for determination of N by means of Eg. (1), for a given Ψ_N,F,s,f and t, consists of calculating fictive number of stages: N_T, N_M and N_D, by analytical expressions presented in Table 1, and evaluation of ΔN based on Eq. (2).

NUMERICAL PROCEDURE FOR A GENERAL CASE OF EQUILIBRIUM DISTRIBUTION

The proposed numerical procedure for calculating N by Eg. (1),for a given value of f, s, t, flow rate-Q, inlet and autlet concentration in (x) and (y) phase- $x_{in}, y_{in}, x_{out}, y_{out}$, and for a general case of equilibrium distribution: $x_n^* = x_n\ (y_n)$, was simply obtained by applying derived numerical procedures for calculating the fictive number of stages and the correction number of stages (6, 7). The procedure for the calculation of N_i is of general validity and is based on succesive solutions of the system of material balance equations for steady state for (x) phase around n-th stage - Eq. (4) and for both phases for the first n stages - Eg. (5), and equilibrium equation - Eq. (6), introducing the corresponding conditions for the definition of N_T, N_M and N_D (6). The procedure for the calculation of correction number of stages is based on Eq. (2) using Eq. (3) for calculation of F.

$$(1 + f)x_{n-1} - (1 + 2f)\ x_n + fx_{n-1} - t(x_n - x_n^*) = 0 \tag{4}$$

$$x_o + f\ x_{n+1} - (1 + f)\ x_n - (1/Q)y_1 - (s\ /Q)y_n + (1/Q)\ (1 + s)\ y_{n+1} = 0 \tag{5}$$

$$x_n^* = x_n(y_n) \tag{6}$$

The program for digital computer CDC 3600 has been developed (7) so to enable either the calculation of the total number of stages in the extractors or the calculation of the number of mass transfer units in the stage from the experimental data for a general case of equilibrium distribution.

GRAPHICAL PROCEDURE FOR A GENERAL CASE OF EQUILIBRIUM DISTRIBUTION

The proposed graphical procedure for the calculation of N for a given value of f, s, Q, x_{in}, y_{in}, x_{out}, y_{out} and $x_n^* = x_n\ (y_n)$ by Eg. (1), consists of graphical calculation of N_T and N_M by wellknown methods (9, 10) and N_D by recently developed method (8),

Table 1. Analytical expressions for calculating the fictive number of stages (N_T, N_M and N_D) for a linear case of equilibrium distribution

a) $F \neq 1$

$$N_T = \frac{\ln \dfrac{1 - \Psi_N}{1 - \Psi_N F}}{\ln F}$$

$$N_M = \frac{\ln \dfrac{1 - \Psi_N}{1 - \Psi_N F}}{\ln \dfrac{1 + Ft}{1 + t}}$$

$$N_D = \frac{\ln \dfrac{F + s + Ff}{1 + s + Ff} \; \dfrac{1 - \Psi_N}{F(1 - \Psi_N F)}}{\ln \dfrac{F + s + Ff}{1 + s + Ff}}$$

b) $F = 1$

$$N_T = \frac{\Psi_N}{1 - \Psi_N}$$

$$N_M = \frac{\Psi_N \, (1 + 1/t)}{1 - \Psi_N}$$

$$N_D = \frac{\Psi_N \, (1 + 2f + 2s) - (s + f)}{1 - \Psi_N}$$

while ΔN is calculated from Eqs. (2) and (3). In order to simplify the calculation of the average value of extraction factor in a general case of equilibrium distribution, graphical plots for determination of F were done (7).

The graphical procedure is very simple and rapid and can be applied without difficulties to any form of equilibrium line. The procedure can be extended to the case of mutually soluble solvents and variable flows.

APPLICATION OF THE STAGE ADDITIVITY METHOD TO MULTICOMPONENT EXTRACTION

In principle none obstacles for the application of the stage additivity method to multicomponent extraction have been caused by the method. But general dilemmas in multicomponent extraction with respect to adequate definitions and determinations of extraction parameters exist and could of course, cause some difficulties and/or limitations for the application of the stage additivity method. In connection with this graphical procedure based on the proposed method for the calculation of compound counter-current extractors with backmixing for the case of two interdependent solutes has been developed (11). The graphical prodedure for the determination of N for the solute by means of Eq. (1) for the given extraction data: consists of graphical calculation of the fictive number of stages, and evaluations of ΔN by Eg. (2). Calculation principle of N_D and N_T and N_M, respectively, is based on the graphical procedure for the calculation of the number of equilibrium stages for general case of equilibrium distribution of two interdependent solutes (8). Since in some cases the graphical procedure could be time consuming we are developing numerical appreach using a digital computer.

In order to apply the stage additivity method to the general case of multicomponent extraction, we are considering the possibility of extending the approaches used by the general methods of calculation of multicomponent extraction (12-13).

REFERENCES

1. Hartland, S., Mecklenburgh, J.C., Chem. Eng. Sci., 21, 1209 (1966)
2. Mišek, T., Rod, V., in Hanson, C. (Ed.), Recent Advances in Liquid-Liquid Extraction, Chapter 7, Pergamon Press, London, 1971
3. Mecklenburgh, J.C., Hartland, C., The Theory of Backmixing, John Wiley and Sons, London, 1975
4. Korchinsky, W.J., Cruz-Pinto, J.J.C., Proc. Intern. Solv. Extr. Conf., The Liege, 1, 1980, Paper 80-176
5. Tolić, A., Rod, V., Jevtović, V., Bull. Soc. chim, Beograd, 38, 571 (1973)
6. Ibid., Idem, 38, 581 (1973)
7. Ibid., Idem, 38, 591 (1973)
8. Tolić, A., Miyauchi, T., J.Chem. Eng. Japan, 6, 242 (1973)
9. McCabe, W.L., Thiele, E.W., Ind. Eng. Chem., 17, 605 (1925)
10. Murphree, E.V., Ibid, 17, 747 (1925)
11. Tolić, A., Kocić, S., The 6. International Congress of Chemical Engineering, Chemical Equipment Design adn Automation, CHISA'78, Prague, Czechoslovakia, Paper H3.2
12. Rod, V., Vrba, J., Chem. Prim., 24, 438 (1974)
13. Vrba, J., Collection Czech. Chem. Commun., 42, 1786 (1977)

IMPROVED MATHEMATICAL MODELS IN SOLVENT EXTRACTION SYSTEM INVOLVING Pu-U-Th-HNO_3-TBP

R. Natarajan, K. Rajamoorthy and G. R. Balasubramanian

Reactor Research Center
Kalpakkam, India

It is proposed to use modified purex and thorex processes for reprocessing of Fast Reactor fuels and blankets respectively using solvent extraction system as a main tool for separation of fission products and heavy elements. As per our programme, the systems involved will be having nitrates of Th, U, Pu and HNO_3 in aqueous solution in various combinations and tributyl phosphate in kerosene type diluent, as solvent. In order that, flow sheets are formulated and optimised, an equilibrium model is developed using the data available in the literature.

EXTRACTION EQUILIBRIUM

It is well known that Tri-n-butyl phosphate (TBP) forms stable complexes with nitrates of actinides(M^{n+}) according to the following equation:

$$(1) \quad (M^{n+})_{aq} + n(NO_3^-)_{aq} + K(TBP)_{org} \rightleftharpoons (M(NO_3)_n \cdot KTBP)_{org}$$

From this equation, the equilibrium constant, E can be inferred as,

$$(2) \quad E = \frac{(M(NO_3)_n \cdot K\ TBP)_{org}}{(M^{n+})_{aq}\ (NO_3^-)^n_{aq}\ (TBP)^K_{org}}$$

where the brackets represent activities. If the activities are converted into concentrations, the equation(2)becomes

$$(3) \quad G = \frac{[M(NO_3)_n \cdot K\ TBP]_{org}}{[M^{n+}]_{aq}\ [NO_3^-]^n_{aq}\ [TBP]^K_{org}}$$

The terms inside the brackets are concentrations. The equlibrium behaviour of the actinide ion can be determined from the concentrations, if G is known. Since the activity coefficients change with salting strengths, G is a function of salting strengths, and once this function is evaluated from experimental results, prediction of the equilibrium concentrations becomes possible. Salting strengths are determined from the concentrations of the interacting solutes(2). Mole ratio of TBP to the nitrate salt, K in the organic complex have been established(1).

MODEL DEVELOPMENT

Solute free concentrations:Since there is volume change in the solutions (because of their non-ideal behaviour), the concentrations (normally expressed in moles of the solute/ unit volume of the solution) should be corrected to exclude the effect of solutes. Fort(2) has shown the effects of nitrates of U, Pu and HNO_3 in aqueous and TBP solutions. The effect of $Th(NO_3)_4$ is determined from the data of Kumar(3).

Choice of model for U-Pu-HNO_3-TBP-H_2O system: Three semi-empirical models of Katoh et al(4), Rozen et al(5), Groenier(6), are chosen for evaluations of the 1981 purex data bank of Petrich(7). Over 1000 data points from different authors are chosen from this data bank. The model of Katoh has given intolerably large errors. The Groenier model shown in Appendix-2 has given a mean error of 21% and a standard deviation(SD) of 38% for U and -6% mean with 90% SD for Pu. Corresponding values for Rozen model are 7.1% and 23% for U and 69% and 180% for Pu. The Groenier model is chosen since it gives better prediction for Pu, though the U results ere comparable.

Model for Thorium extraction:The data as well as mathematical models for thorium equilibrium ere very limited. The model for thorium equilibrium is determined from the available data of Srinivasan et al(8) and Blanchard(9). This involves evaluation of the value G of Th, GTH in equation(4) or (5) as a function of salting strength. This is done using least square fit.

Unified model for U-Pu-Th-HNO_3-TBP system: The above two models are combined and a unified model is given as an algorithm in Appendix-3. This model is used for verifying U-Pu-Th-HNO_3-TBP data of Chitnis(11). The results are shown in Figures 1&2.

CONCLUSIONS

The effect of diluent in evaluating the concentration on solute free basis should be verified and if needed modified in the model. This accounts for roughly 10-15% variation in the predicted concentration. The 5% TBP data shows a scatter compared to 30% TBP data. But on the whole, the proposed model gives reasonably good prediction.

REFERENCES

1. J.F.Flagg, Chemical processing of reactor fuels, pub. Academic Press, 228(1961)
2. L.A.Fort, ARH-CD-510, Dec(1975)
3. S.V.Kumar et al, BARC - 933(1977)
4. N.Katoh et al, Journal of Nucl. Science and Technology 11, No.7, 293(1974)
5. A.M.Rozen et al, Atomnaya Energia, 37, No.3, 187(1974)
6. W.S.Groenier, ORNL-4746, 25(1972)
7. G.Petrich et al KFK 3080 (1981)
8. N.Srinivasan et al, BARC 681, (1973)
9. J.C.Blanchard et al, SCCI-117, (1968)
10. G.R.Balasubramanian et al, BARC-940(1977)
11. R.T.Chitnis, FRD, BARC, Bombay, private communication.

APPENDIX-1

$$(4) \quad GTH = EXP(3.623-3.761*SS+1.01*SS^2-0.122*SS^3+0.0054*SS^4) \quad \text{for } SS \leqslant 8$$

$$(5) \quad GTH = 0.09235 \text{ for } SS>8$$

$$(6) \quad XU1/XU = XH1/XH = XPU1/XPU = XTH1/XTH = 1-0.0724XU-0.0309XH+0.0174XTH-0.13XPU$$

$$(7) \quad YU1/YU = YH1/YH = YPU1/YPU = YTH1/YTH \doteq 1-0.097YU-0.046YH+0.18YTH-0.139YPU-0.0174H_2O$$

$$(8) \quad XU/XU1 = XH/XH1 = XPU/XPU1 = XTH/XTH1 = 1+0.0724XU1+0.0309XH1-0.0174XTH1+0.13XPU1$$

$$(9) \quad YU/YU1 = YH/YH1 = YPU/YPU1 = YTH/YTH1 = 1+0.097YU1+0.046YH1-0.18YTH1+0.139YPU1+0.0174H_2O$$

$$(10) \quad H_2O = (4.2-0.015T)\left(1-\frac{2YU}{TBPM}-\frac{3(YTH+YPU)}{TBPM}-\frac{0.6YH}{TBPM}\right)TBP^{1.69}$$

$$(11) \quad 3.66TBP - X - 2(GU(I)*XU1+GPU(I)*XPU1*TNT^2)TNT^2X^2 - GH(I)*X-2.3GTH*XTH1*TNT^4X^{2.3} = 0$$

WHERE,

XU, XPU, XH, XTH	- Aqueous Molar Concentrations of U, PU, HNO_3 and Thorium, Moles/Lit
XU1, XPU1,XH1,XTH1	- Aqueous solute free concentrations of U, PU, HNO_3 and Thorium, Moles/Lit
YU, YPU, YH, YTH	- Organic Molar concentrations of U, PU, HNO_3 and Thorium, Moles/Lit
YU1,YPU1,YH1,YTH1	- Organic solute free concentrations of U, PU, HNO_3 and Thorium, Moles/Lit
H_2O	- Corrections for water in water-saturated-TBP
T	- Temperature, °C
TBP	- Volume fraction of TBP in Organic
TBPM	- 3.66 TBP

APPENDIX . 2

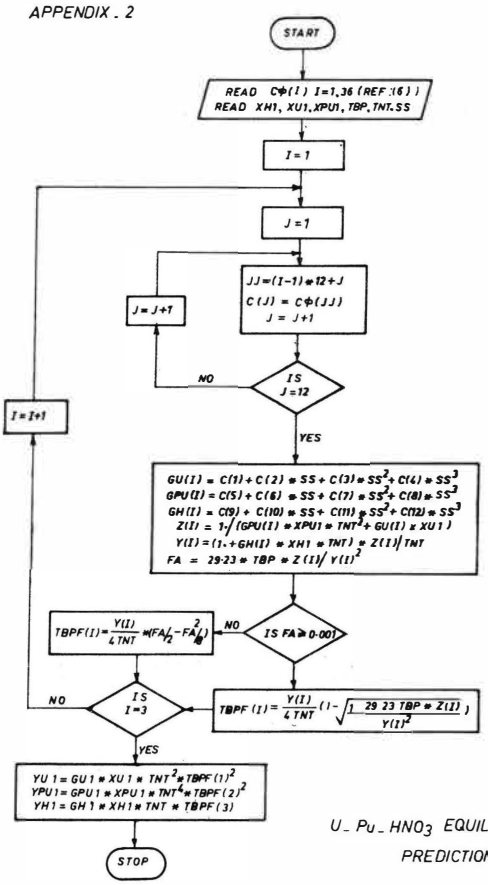

U_Pu_HNO_3 EQUILIBRIUM PREDICTION

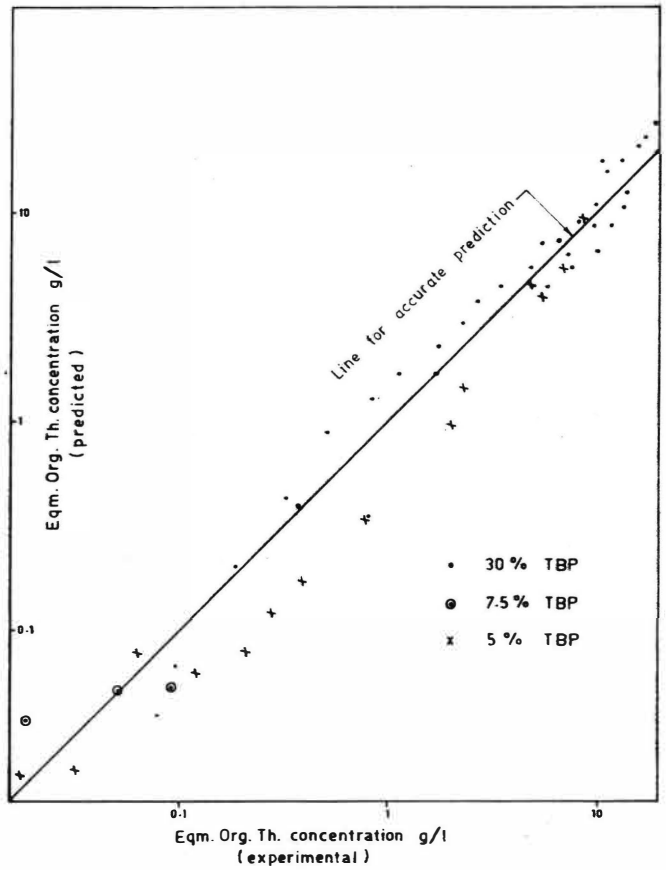

FIG. 1: PREDICTION OF $Th(NO_3)_4$ EQUILIBRIUM

APPENDIX . 3

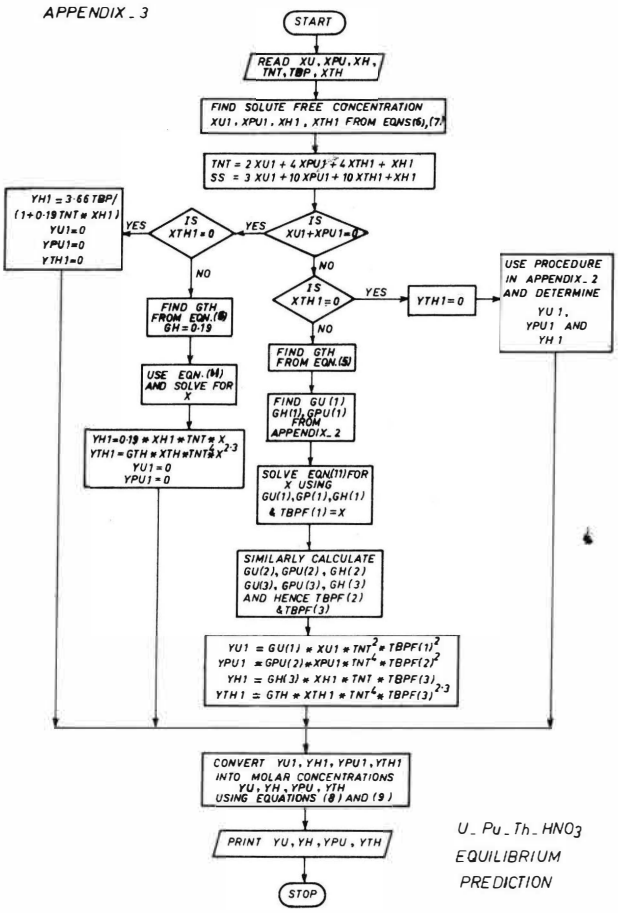

U_Pu_Th_HNO_3 EQUILIBRIUM PREDICTION

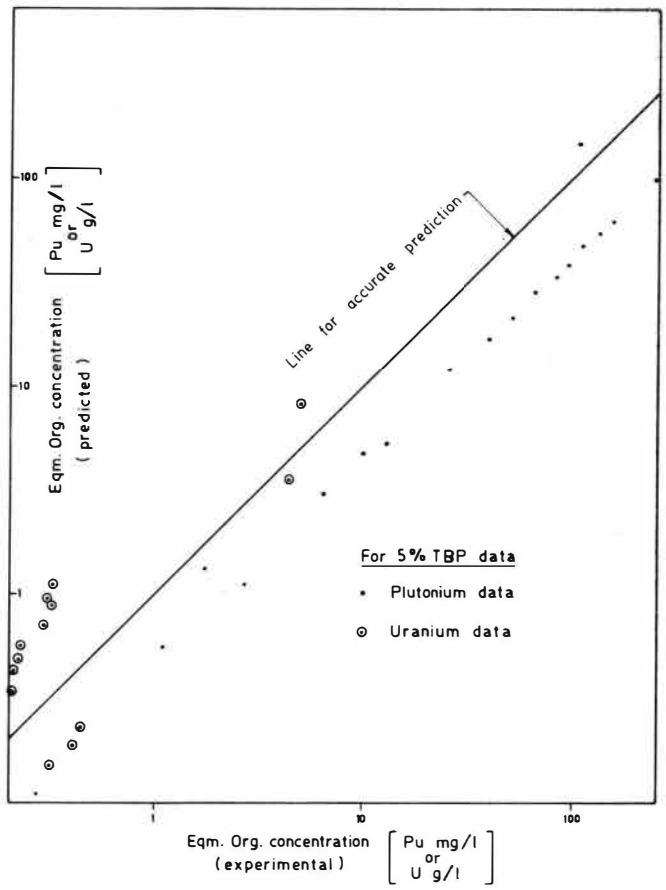

FIG. 2: PREDICTION OF $Pu(NO_3)_4$ & $UO_2(NO_3)_2$ EQUILIBRIUM

RISK EVALUATION IN EXTRACTION EQUIPMENT DESIGN BASED ON TWO-STAGE LABORATORY EXPERIMENTS

Marin R. Mehandjiev

SEO "Chimcomplect"
Sofia, Bulgaria

Research phases of capital projects in chemical industry consist of consecutive or parallel experimental stages, carried out with definite installations. A full equipment set for research phase could include (1): 1/ laboratory - bench scale - equipment, destined for investigation on the optimum masses' and phases' ratios; granularities and concentrations of raw materials, final and waste products, as well as for determination of process kinetic factor values; 2/ enlarged laboratory equipment - for studying of basic dynamic factors of the process, as well as for an approximate estimation of process economics; 3/ pilot plant - for checking of some optimum and extreme values of dynamic, kinetic or economic factors, obtained in laboratory studies; 4/ prototype devices - prototype industrial equipment - full scale-made single devices for demonstrative or check performance of basic process stages; they should be constructed in default of similar appliances; 5/ experimental production plants - complete production units, including all technological stages, designed with a capacity, sufficient for economic effectiveness of the production; 6/ prototype plants - industrial plants, erected with all ofsite facilities and based on designs, allowing extension of capacity by increase of the number of production lines. The first two equipment kinds correspond to the initial research stages, most often designated as "laboratory study". It is assumed as a rule that, uncertainty and risk in design based on experimental results only, could be little, if the design phase follows a study including laboratory and pilot plant experiments and could be negligible after studies employing the full set of experimental equipment listed above.

The uncertainty in design would be, undoubtedly, minimum when the foregoing research covers the whole set of experimental installations including prototype plants, but the unpracticality of such approach is obvious in wastewater treatment process studies. On the other hand, researches associated with environment protection must be finished at accelerated rates. Furthermore, in spite of the study performance using statistical experiment design technique, or applicating the methodology with simultaneous - technological and economic - optimization of factor values (2,3), the design risk reduction by pilot plant tests could not be proved especially in the design of basic extraction equipments for wastewaters purification - e.g. in an extractive treatment process for wastewater discharged from phenol-formaldehyde resins producing plant - on account of the lack of criteria for pilot plant capacity choice, as well as through the difficulty in extraction column modelling. Since the pilot plants are expensive non-profitable installations, most often with one-time use, and since the demand of research time shortage cannot be neglected, a new procedure has been suggested for those research cases. It includes two-stage laboratory study as well as a methodology for design risk assessment; the pilot plant tests are dropped in the procedure. The two-stage laboratory study consists in consecutive performance of similar kinetic and dynamic tests at optimum technological factor values, using in each stage similar equipments of different, although laboratory scale. The ratio between chosen dimensions of the devices, used in consecutive stages, must be not less than 20.

In the evaluation of risk in the design based on research stages' results, one must compare two alternatives, acceptable as "strategies": Strategy No.1 - Design, based on two-stage laboratory study and Strategy No.2 - Design, based on laboratory stage and on additional research, e.g. on additional pilot plant study results. The design risk, associated with each strategy is defined by:

- Profits /losses/ expected in strategy realization, determined using: A/ All known or planned research expences; pilot plant equipment costs; project delay and other available data; B/ Losses, caused by the impossibility of research results' reproduction in industrial scale devices;
- Degrees of confidences: F_A /part of unity/ in the realization of profits /losses/ and F_B /part of unity/ in the impossibility of reproduction of the results, obtained in experimental study.

F_A for Strategy No.1 i.e. F_A/No.1/, as well as F_A/No.2/ can be assumed with equal value of 0.8 - 0.9 . There are no criteria for preliminary assessment of F_B/No.2/-value; according to our experience, that value could be not bigger than 0.7 in the considered research cases. In the methodology here interpreted, the evaluation of F_B/No.1/ is based on the criterial equations of similarity, which associate a chosen response factor Y, simbatic to the production costs, with a product of similarity criteria or simplexes X_i, raised to powers with exponents: a,b,...,z :

$$Y = W.X_1^a.X_2^b.....X_n^z$$

where a,b,....,z are experimentally determined in the consecutive two laboratory stages. Indexing by "1" and "2" the factor values, observed or calculated in the first and second stage respectively, and since the values of similarity criteria or simplexes are specially maintained approximately equal in the two experimental stages: $X_{11} = X_{12}$; $X_{21} = X_{22}$; ... ; $X_{n1} = X_{n2}$, Y_1 and W_1 can be made equal to Y_2 and W_2 respectively by recalculation of exponent values. Thus, F_B/No.1/ can be determined by following expression:

$$F_B/\text{No.1/} = \frac{a_1' + b_1' + \ldots\ldots + z_1'}{a_2 + b_2 + \ldots\ldots + z_2} \leqslant 1 ,$$

where a_1' , b_1' , ... , z_1' are the recalculated exponent values, which ensure the equalities: $Y_1 = Y_2$; $W_1 = W_2$. For an extractive wastewater treatment process, the value of F_B/No.1/ has been bigger than 0.7 . In such cases we should give preference to Strategy No.1. When F_B/No.1/ $< F_B$/No.2/ = 0.7 , the calculation of losses can determine the preferable strategy, or can point out that, a prototype device construction is inevitable. The procedure described above can be applicated to each two consecutive research stages.

REFERENCES

1. M.R.Mehandjiev. Paper No.K5.3 of 7th CHISA-Congress, Praha, Czechoslovakia 1981 .
2. M.R.Mehandjiev. Paper of 9th IMP-Congress, Praha, Czechoslovakia 1970 , Proceed., p.271.
3. M.R.Mehandjiev. Methodical experiment planning and organigrammes in chemical technological researches. Edit. of HFEI, Svishtov 1983 /Bulg/.

DESIGN AND EVALUATION OF AIR PULSERS FOR PULSE COLUMN CONTACTORS IN SOLVENT EXTRACTION

Arlin L. Olson and Professor C. A. Rhodes

Allied-General Nuclear Services
P.O. Box 847
Barnwell, South Carolina 29812 USA

Uiniversity of South Carolina
Columbia, South Carolina 29202 USA

Pulsers which employ air pressure rather than reciprocating pistons have been developed and used in the spent nuclear fuel reprocessing field for many years. Their use has been reported by Weech and Knight (1).

The air pulser system can be described mathematically by sets of differential equations which govern the air and liquid components of the system. Essentially, three equations are required to characterize the system; the air behavior during the inlet cycle, the air behavior during the exhaust cycle, and the liquid behavior in the pulse leg and column under the effects of the air pressure. The system is shown in Figure 1.

AIR SYSTEM*

First, a simple mass balance around the reservoir can describe the air accumulator.

(1) $$\rho v_1 A_1 - \rho v_2 A_2 = Vr \frac{d\rho}{dt}$$

By assuming that the density of air at low pressures can be replaced by $\frac{PM}{RT}$,

Substituting into equation (1), and simplifying gives

(2) $$\frac{d}{dt} Pr = \frac{P_1 v_1 A_1 - P_2 v_2 A_2}{Vr}$$

*Note nomenclature at end of article.

The behavior of a compressible fluid flowing in a conduit can be described by the following equation:

(3) $$\frac{\rho L}{g}\frac{dv}{dt} + \frac{2fL\ \rho\ v}{gD} + \Delta P = 0$$

Where f is the fanning friction factor and has the value (2);

$f = 16/Re$ for $Re < 2100$

$f = 0.0001\ Re^{0.575}$ for $2100 < Re < 3500$

$f = 0.0035 + 0.264\ Re^{-0.42}$ for $Re > 3500$

Substituting for ρ in equation (3) and rearranging gives the following expression for air flowing to the accumulator:

(4) $$\frac{dv_1}{dt} = \frac{P_1 - P_r - \frac{2f\ LF1\ P_r M v_1^2}{g\ D_1 RT}}{\frac{L_1}{g}\frac{PrM}{RT}}$$

Using equation (3) and modifying it to separate the design parameters into a more convenient form gives an expression for air flow from the reservoir to the pulse leg.

(5) $$\frac{dv_2}{dt} = \frac{Pr - P_2 - \frac{2f\ LF\ P_2 M\ v_2^2}{DgRT}}{\frac{M}{gRT}(PrLc + P_2 L_2)}$$

A means for solving for the variable pressure is now required. A force balance around the air inlet to the pulse leg gives:

(6) $$P_2 - Pt = \frac{K\ \rho\ v_2^2}{2g}$$

A mass balance around the same point gives;

(7) $$\rho v_2 A_2 = \frac{d}{dt}\rho V$$

Now, the variable volume occupied by air in the pulse leg can be defined as:

(8) $$\frac{dV}{dt} = -A_3 \frac{dX}{dt}$$

By substituting and rearranging equations (6), (7), and (8), the following design equation is arrived at:

(9) $$\frac{dP_2}{dt} = \frac{\left[\frac{P_2 v_2 A_2 + P_2\left(1 - \frac{KMv_2^2}{2\ RT}\right)A_3 \frac{dX}{dt}}{A_3(LL-X)}\right] - \left(\frac{P_2 KMv_2}{g\ RT}\right)\frac{dv_2}{dt}}{\left(1 - \frac{KMv_2^2}{2g\ RT}\right)}$$

The equations for the air exhaust cycle are very similar to those for the inlet cycle and are derived in the same manner.

(10) $$\frac{dv_2}{dt} = \frac{P_A - P_2 - \frac{2F\ LF\ P_2 Mv_2^2}{Dg\ RT}}{\frac{M}{gRT}(P_2 L_2 + P_A L_3)}$$

(11) $$\frac{dP_2}{dt} = \frac{\left[\frac{P_2\left(1 + \frac{KeMv_2^2}{2gRT}\right)A_3 \frac{dX}{dt} - P_2 v_2 A_2}{A_3(LL-X)}\right] - \frac{(P_2 KeMv_2)}{g\ RT}\frac{dv_2}{dt}}{1 + \left(\frac{KeMv_2^2}{2gRT}\right)}$$

LIQUID SYSTEM

The equation for the liquid system is simpler and is as follows:

(12) $$\left[\left(\frac{\rho mH}{g}\right)\left(\frac{L}{AC}\right) + \frac{\rho LX}{g}\right]\frac{d^2X}{dt^2} + \left[\rho m\left(\frac{AL}{Ao}\right)^2 \frac{N}{2gC^2} + 2f\rho L\frac{(Xe + X)}{g\ D_L}\right]\left(\frac{dX}{dt}\right)^2 + \rho LX - \rho mH - Pa = -PT$$

We now have five unknowns (Pr, v_1, v_2, P_2 and X) and five equations [(2), (4), (5), (9), and (12)] which must be solved simultaneously in order to describe the system. Two of those equations, (5) and (9), must be replaced by equations (10) and (11) during the exhaust portion of the pulse cycle.

CONCLUSIONS

These equations can be solved quite easily with a digital computer and using an IBM computer code called the Continuous System Modelling Program (CSMP-III). A small Fortran data set which includes constants and the equations is all that is required.

Figure 2 indicates a pressure-time relationship resulting from a sample pulser installation. These type of calculations can be utilized to develop or evaluate piping networks for the air system.

The column amplitude-accumulator pressure relationship shown in Figure 3 may also be generated. The pulse column amplitude-frequency product is a major parameter in determining flooding within the column and its efficiency during normal operation. It should also be noted that the column static weight has a significant effect on the amplitude produced by a particular accumulator pressure.

NOMENCLATURE

A_1, A_2, A_3, A_L, A_o, A_c	= Area of air-inlet pipe to the reservoir, area of air-inlet pipe to pulse leg, $A_3 = A_L$ - Area of pulse leg, free area of pulse column plates, area of column in the plate section, square feet.
C	= Orifice coefficient of holes through the pulse plates, dimensionless.
D_1, D, D_L	= Diameter of air-inlet pipe to accumulator, diameter of air-inlet pipe to pulse leg, diameter of pulse leg, feet.
f	= Fanning friction factor, dimensionless.
g	= Gravitational constant, ft-lb/lb-sec2.
H	= Height of fluid in column from pulse leg entrance to column overflow, feet.
K, Ke	= Hydraulic enlargement coefficient, hydraulic contraction coefficient, dimensionless.
L_1, L_2, L_3	= Line length from PCV to accumulator on air inlet line, line length from inlet poppet valve to pulse leg, line length from poppet valve to vent, feet.
L_c, L_L,	= Line length from air accumulator to inlet poppet valve, total height of pulse leg from column inlet to air inlet, feet.
LF_1, LF	= Total line length plus all fittings, bends, that contribute to friction loss for line to accumulator and from accumulator to pulse leg, feet.
M	= Molecular weight of air, lb/lb mole.
N	= Number of plates in pulse column.

P_1, P_R, P_2, P_T, P_A = Air pressure at the PCV, pressure in accumulator, pressure in air-inlet line to pulse leg, pressure above liquid in pulse leg, pressure in vent, lb/sq ft.

R, Re = Universal gas constant, ft-lb/mole °R, Reynolds Number, Dimensionless.

T = Temperature, °R.

t = Time, sec.

V, V_R = Volume in pulse leg above liquid level, volume of accumulator, cubic feet.

X, Xe = Variable height of liquid in pulse leg from inlet point of leg into column, equivalent length of fittings in leg connections to the column, feet.

ρ_L, ρ_M = Density of liquid in pulse leg, density of pulse column contents, lb/cu ft.

μ, μ_L = Viscosity of air, viscosity of liquid in pulse leg, lb/ft sec.

v_1, v_2 = Velocity of air in air-inlet line to accumulator velocity of air in air-inlet line to pulse leg, ft/sec.

REFERENCES

1. M. E. Weech and B. E. Knight, I & EC Process Design and Development, 6, 480 (1967).

2. J. M. Meyer, Chemical Engineering, March 10, 1980, p 139.

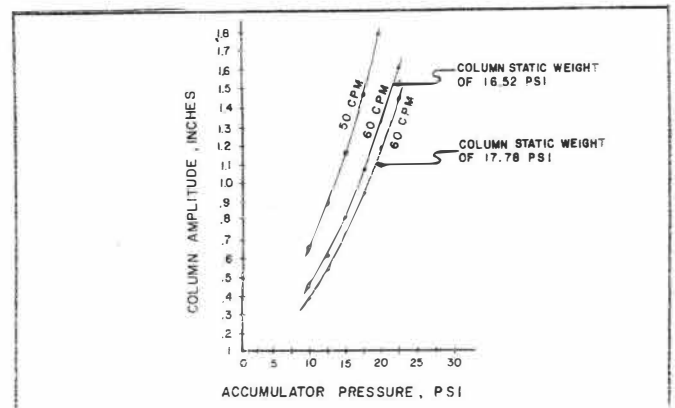

FIGURE 3 COLUMN AMPLITUDE VS. ACCUMULATOR PRESSURE FOR DIFFERENT FREQUENCIES AND STATIC WEIGHTS

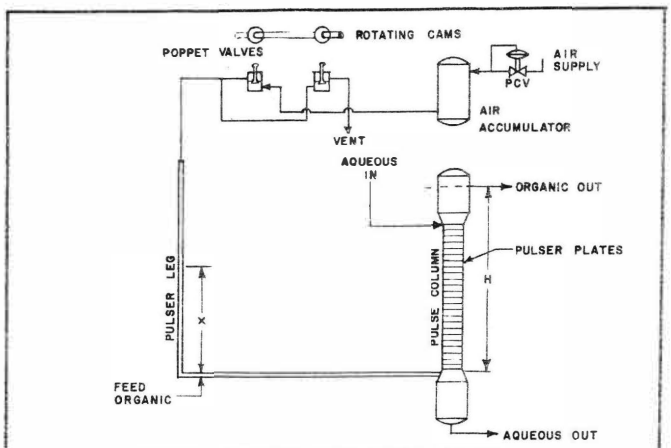

FIGURE 1 SCHEMATIC OF AIR PULSER SYSTEM

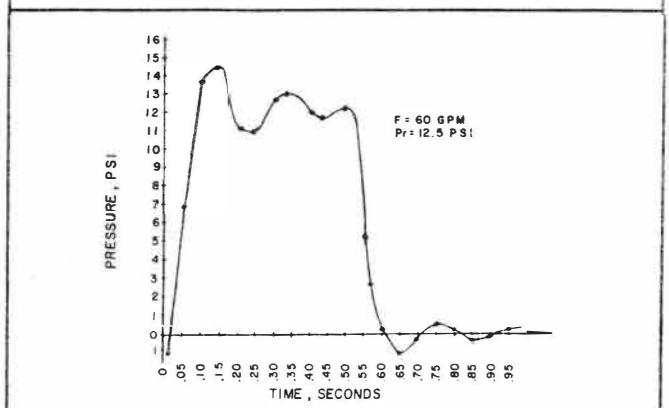

FIGURE 2 PULSE LEG AIR PRESSURE VS. TIME FOR ONE CYCLE

STUDY OF THE MATHEMATICAL SIMULATION OF RARE EARTH EXTRACTION

Yun-yu Shen, Wei-juan Ying, Wen-hou Ya, De-xiang Ma

General Res. Inst. Nonferrous Metals, MMI.
Beijing, China

This work studied the mathematical simulation of steady state of fractional counter current extraction. An extraction equilibrium model has been established for this purpose. By this simulation, we have studied some regularities of the fractional extraction, designed the separation process of Tb from Dy, selected the optimization process. The result of the mathematical simulation was compared with that of the experiment, and these are in good agreement.

THE EXTRACTION EQUILIBRIUM MODEL

The extraction equilibrium of the system $TbCl_3$-$DyCl_3$-HCl-H_2O-1M HDEHP (kerosene solution) has been studied. The total rare earth concentration in the organic phase Y(1) is a function of X(1),X(3),X(5), where the total rare earth concentration, X(1)=0.05-0.96m, the mole fraction of $TbCl_3$, X(3)=0.1-0.92, the acidity, X(5)=1.1-3.4m, in the equilibrium aqueous phase. An empirical model has been established.

$$Y(1)=\sum_{i=0}^{M}\sum_{j=0}^{N}\sum_{k=0}^{P} A_{ijk}\,(X(1))^i\,(X(3))^j\,(X(5))^k$$

where M,N,P are integers. The coefficient A_{ijk} of the term $(X(1))^i(X(3))^j(X(5))^k$ of the polynomail can be determined by the least square method. The program has been written in ALGOL, and was calculated in DJS-6 digit computor. When M=N=P=2,27 coefficients are obtained, and the model had the best accuracy of approximation. The correlation coefficient is 0.9957. The average relative error of the model is 3.24%, and that of the predictive value is 3.01%.

The concentrations of Tb and Dy in organic phase may be calculated from Y(1) by the separation factor, β Dy/Tb, which is 2.69±0.056 within the experimental ranges.

THE MATHEMATICAL SIMULATION OF THE STEADY STATE EXTRACTION PROCESS

The mathematical simulation of the steady state of fractional extraction gives the distribution of solutes in two phases in different stages under given conditions.

Computor calculation

Fig. 1 is the schematic diagram for fractional extraction.

In Fig. 1, if the solute concentrations in the raffinate are known, i.e. set the arbitrary values to X(N,J). Since Y(N+1,J) are zero in most cases, by using the extraction equilibrium model and the material balance alternatively, the solute concentrations can be calculated stage by stage from right to left to obtain the values of X(0,J). Thus X(0,J)=f'(N,F,L,L1,V,V5,X(N,J)). Under given conditions of N,F,L,L1,V,V5, for different values of X(N,J), the corresponding X(0,J) values are obtained. These are meaningless in extraction process. In extraction process, X(0,J) must be equal to V(J). Let W be the allowable error in calculation, thus

$$X(0,J) - V(J) = R(J)$$
$$|R(J)| < W$$

therefore R(J)=f"(N,F,L,L1,V,V5,X(N,J)) is the solution required. The computor calculation use iteration method[1]. As $|R(J)| > W$, X(N,J) increase or decrease a steplength, new values of X(N,J) are obtained. As the signs of R(J) change, the steplength decreases by half. This is continued until it is in convergence.

A BASIC program has been written and was calculated in DJS 131 digit computor.

Studies of some regularities of steady state extraction process by mathematical simulation

Some regularities of steady state has been studied by the mathematical simulation:

Factors influence the purities and recoveries The composition of the feed solution used contains Tb and Dy 50% each, and the solution has the concentrations of $ReCl_3$ 0.5m, acidity 0.8m. The scrub, HCl, is 3.0m. Fig. 2 and 3 are the influences of extraction stage and solvent flow rate respectively.

It can be seen from these figures, the increase of extraction stages or solvent flow rates increase the purities of Tb and recoveries of Dy. The difference is increasing extraction stages has only very little or no influence in Tb recoveries and Dy purities, but increasing solvent flow rates will decrease these obviously. The influences of the wash stages and scrub flow rates have the same effects.

The position of feed stage The change of the position of feed stage in an extraction system means the increase of stages in one section (extraction section, for example), and decrease of stages in other section (wash section), it will influence the purities and recoveries of the two products.

If the aqueous stream entering the feed stage has the same composition as the feed, the most effective separation can be obtained. The following is the example.

The feed used contains Tb,Dy 50% each with concentrations of $ReCl_3$ 0.5m, (H^+) 0.8m. N=9, L1:L=0.5:0.5.

Table 1 The position of feed stage

F	V	Tb Purity %	Tb Recovery %	Dy Purity %	Dy Recovery %	Stage with aqueous stream in same composition as feed
6	3.5	90.03	90.00	88.94	88.10	4
5	3.26	90.91	91.00	90.87	91.91	4

When the feed stage changes from 6 to 5, the solvent used is decreased, the purities and recorveries of Tb and Dy are increased.

The position of feed stage can be found by mathematical simulation.

SELECTION OF OPTIMIZATION PROCESS

Optimization techniques are applied to various regions with the development of computor. It was also used to design the rare earth extraction plant[2].

Realization of optimization process depends upon an accurate mathematical model; a technical economical index, the objective function, for measuring the design quality; and the method for seeking the optimization process by computor.

From the previous work, we have established the mathematical simulation mathod that is necessary for selecting the optimization process.

An optimization process with product in certain purity and recovery requires the lowest cost. This is rather a complicate problem. For simplicity, we used T to represent the objective function, and is expressed as following

$$T = \frac{N \times V}{(N,2)\times(L1+L)}$$

where N, the total stages, denotes the degree of difficuties in separation, V, solvent flow, represents the quantity of solvent used. Since solvent is the most expensive material, it is used to express the cost. The denomination represents the quantity of product per unit time. Thus, T means the quantity of solvent used per Kg. product. The smallest T means the optimization process.

The computor selected the optimization process by direct seeking method. The program has been written in BASIC, and was calculated in digit computor DJS 131.

The feed used contains Tb 30% by weight with concentrations of $ReCl_3$ 0.5m, and $[H^+]$ 0.8m. The product Tb requires the purity and recovery 80% each in order to have the values within the ranges of the model. The computor calculated 81 sets of conditions with 95 mins. In these calculations T drops from the initial value 432 to the smallest value 292.

THE EXPERIMENT

The mathematical simulation has been compared with an experiment in order to test the precision of the predictive value. Accorcing to the selected optimization process, the experiment has been done in 100 ml. Separatory funnels to simulate the fractional counter current extraction. The same conditions were used both in the mathematical and the experimental simulations. The feed used contains Tb 30.33%, Dy 69.67% with concentrations of $ReCl_3$ 0.5023m, $[H^+]$ 0.8042m. The scrub, HCl, is 2.1892m. N=8, F=3, flow rates L1:L:V=7.94:9.68:43.82 ml. The two phases were mixed for 30 mins., and allowed to separate for 15 mins. at the temperature 25±0.20C. The results are compared in table 2 and Fig.4 and 5.

Table 2 Comparison of solute concentrations in different stages in the two simulations

Stage NO.	Total Rare Earth Calc.	Total Rare Earth Exp.	Tb,m Calc.	Tb,m Exp.	Dy,m Calc.	Dy,m Exp.	$[H^+]$,m Calc.	$[H^+]$,m Exp.
A1	0.1619	0.1579	0.03299	0.03567	0.1289	0.1222	1.6973	1.7783
A2	0.2735	------	0.07351	-------	0.1999	------	1.3625	------
A3	0.3708	0.3796	0.1247	0.1318	0.2461	0.2479	1.1410	1.1863
A4	0.3333	0.3470	0.1346	0.1438	0.1987	0.2034	1.2534	1.2468
A5	0.2868	0.2975	0.1430	0.1540	0.1438	0.1434	1.3931	1.3877
A6	0.2315	0.2377	0.1421	0.1494	0.08941	0.08829	1.5588	1.5707
A7	0.1658	0.1650	0.1210	0.1206	0.04479	0.04445	1.7559	1.8159
A8	0.0801	0.0788	0.06625	0.06491	0.01390	0.01382	2.0129	2.0945
O1	0.0789	0.0782	0.00685	0.00774	0.07200	0.07043		
O2	0.1080	------	0.01299	-------	0.09506	-------		
O3	0.1283	0.1241	0.02033	0.01996	0.1079	0.1042		
O4	0.1168	0.1168	0.02350	0.02498	0.09334	0.09186		
O5	0.1018	0.1048	0.02747	0.03085	0.07431	0.07398		
O6	0.0831	0.0865	0.03085	0.03439	0.0532	0.05210		
O7	0.0608	0.0625	0.03049	0.03265	0.03036	0.02981		
O8	0.0344	0.0309	0.02201	0.02005	0.01242	0.01080		

From Table 2 and Fig. 4 and 5, it can be seen that the values obtained from the two simulation methods are in good agreement. The relative error of Tb,Dy purities are less than 1.6%, and of recoveries are less than 4.5%. The concentrations of Tb in organic phase have the larger erorrs because the values are closed to the boundry value of the model, and these are too small so that the experimental errors are larger.

The comparison of the results obtained indicated that the mathematical simulation is accurate and reliable.

CONCLUSIONS

1. A polynomail empirical model has been extablished. It can be used to predict the extraction equilibrium relationships.

2. A BASIC program has been written to simulate the fractional counter current extraction. It can be used to study the regularities of the steady state feature and to design different extraction processes.

3. With an establishing objective function, a BASIC program has been written to select the optimization process by direct seeking method. The separation of Tb from Dy has been simulated. The results were compared with the experimental simulation. They are in good agreement.

4. Through this study, a complete mathematical simulation method, i.e. the modelling of the extraction equilibriums, the simulation of the fractional counter current extraction, and the selection of optimization process, is established. the technique is accurate and reliable.

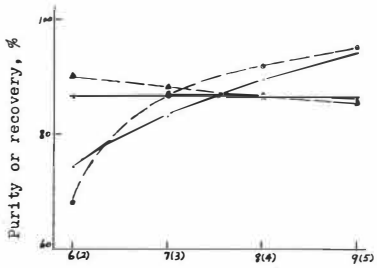

Total No. of stage (extraction stage)

Fig. 2 Effect of No. of extraction stage

L1:L:V = 0.5:0.5:3.5

--•--Tb purity--▲--Tb recovery

--x--Dy purity--⊙--Dy recovery

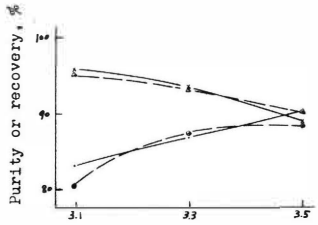

Solvent flow rate

Fig. 3 Effect of solvent flow rate

N = 9; F = 6; L1:1 = 0.5:0.5

--•--Tb purity--▲--Tb recovery

--x--Dy purity--⊙--Dy recovery

5. This method can be used to simulate the separation of any binary metals, and may be used for any other acid phosphate extractants.

SYMBOLS

N	Total No. of stage
F	Stage where the feed enters
L	Flow rate of feed, Kg sol./unit time
L1	Flow rate of scrub, Kg sol./unit time
V	Flow rate of solvent, kg sol./unit time
X(J)	Solute concentration in aqueous phase,m
X(F,J)	Solute concentration in feed,m
X(N,J)	Solute concentration in raffinate,m
X(O,J)	Solute concentration in scrub,m,calculated
V(J)	Solute concentration in scrub,m
Y(J)	Solute concentration in organic phase,m
Y(I,J)	Solute concentration in extract in I stage,m
G(J)	Recovery of solutes,%
P	Percentage extracted
T	Objective function
J=1	Total rare earth
J=2	Tb
J=3	M.F.of Tb in aqueous phase, M.F.of Dy in organic phase
J=4	Dy
J=5	HCl

REFERENCES

1. Totaro Goto ISEC 1971,1011

2. Roger F. Sebenik, Martin Smutz I.E.C. process des. and dev. 8(2), 225,1969

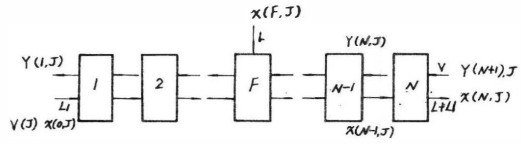

Fig.1 Schematic diagram for fractional counter current extraction

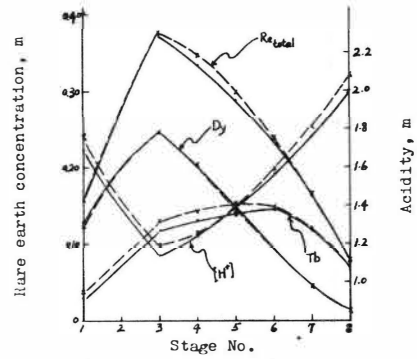

Fig. 4 Solute concentrations in aqueous phase in different stages

--•--Mathematical simulation

--x--Experimental simulation

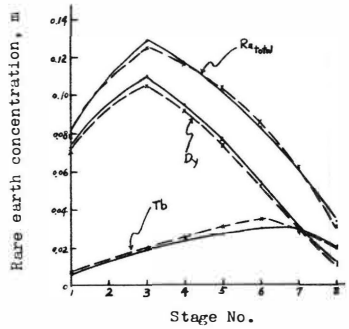

Fig. 5 Solute concentrations in organic phase in different stages

--•--Mathematical simulation

--x--Experimental Simulation

A KINETIC MODEL FOR THE SIMULATION OF INDUSTRIAL COPPER SOLVENT EXTRACTION PLANTS

C. M. Meier and J. D. Miller

Department of Metallurgy and Metallurgical Engineering
University of Utah
Salt Lake City, Utah 84112 USA

Due to the growing importance of solvent extraction as an industrial unit process, considerable research effort has been concentrated on the characterization of the extraction kinetics and the behavior of the dispersed phase mixer. It seems that sufficient knowledge may be available to predict the performance of an industrial solvent extraction plant from fundamental kinetic details, and research effort is in progress to develop a kinetic model for solvent extraction plants. An extension and modification of a previous model is described for multistage extraction with perfect phase disengagement using the intrinsic extraction kinetics for the copper/LIX 64N system.

DEGREE OF SEGREGATION

A prerequisite for the development of an accurate comprehensive simulator is the assessment of the correct degree of segregation of the dispersed phase. Until now, little attention has been paid to the homogeneity of the dispersed phase, i.e. do drops coalesce so fast that they have identical concentrations or is coalescence so slow that substantial concentration differences exist between individual drops? This knowledge is essential for an accurate prediction of extraction in a dispersed phase mixer because drop interactions affect the reaction kinetics.

Concentration differences between individual drops may arise either due to age or size. In solvent extraction mixers, drops are fairly large as they enter the mixer. The extraction proceeds while the feed drops of organic phase are gradually broken into smaller drops. On the average, therefore, larger organic drops should have a lower copper concentration because they are younger and have a lower specific area. Significant coalescence leads to more uniform concentration between drop sizes. The degree of segregation can, therefore, qualitatively be assessed from any size/concentration measurement.

A continuous experimental technique was designed whereby a steady-state sample was taken from the dispersion (organic dispersed) and the organic drops were subsequently separated by size while preventing any concentration or size changes. The apparatus is shown in Figure 1 and consists of a 4" mixer, 3, which is connected through a 3" ball valve, 2, to a rising drop column, 1. The organic phase is dispersed and the mixer is operated continuously (CSTR) until steady state is obtained. At this point, the impeller is stopped, and, simultaneously, a sample is taken from the dispersed phase through the valve. Being less dense, the organic drops rise through the column and separate by size due to the difference in rising velocity. The drops are collected by size intervals, 9, at the top of the column and analyzed for copper content.

The concentration versus drop size measurements are presented in Figure 2. The steep slope indicates that under all circumstances investigated in this study, large size/concentration differences were measured in the dispersed phase. The degree of segregation may qualitatively be determined from the concentration plateau reached at smaller dorp sizes. See Figure 2. This plateau may result either due to the coalescence of smaller droplets or due to the fact that these drops are approaching equilibrium. The two cases can easily be distinguished as illusterated in Figure 3. Increasing coalescence between large and small drops decreases the average concentration of fine drops below the equilibrium value. The difference between the plateau and the equilibrium concentration hence provides a very conclusive indication on the extent and significance of coalescence. The deviation from equilibrium concentration measured in these experiments is so small (~2%) that it may be concluded that the dispersed phase behaves almost perfectly segregated. Furthermore, this implies that for systems of interest with retention times of less than several minutes, coalescence in the mixer is a minor event as compared to breakage.

MATHEMATICAL MODEL--SOLVEX

In a segregated-flow reactor, the concentration of the various species in the dispersed phase may be calculated from the batch extraction and the residence time distribution by,

$$A_i = A_i^{in} - \int_0^{\infty} \alpha_i^B(t) \cdot E(t)dt \tag{1}$$

where A_i is the average dispersed phase concentration, $\alpha_i^B(t)$ the batch extraction of component i, and E(t) the residence time distribution. The batch extraction is in turn determined by the intrinsic reaction kinetics and the interfacial area of the dispersion,

$$\alpha_i^B(t) = \int_0^t A(t) \left(\frac{dn_i}{dt}\right)dt \tag{2}$$

A(t) is the interfacial area and $\frac{dn_i}{dt}$ the reaction rate of component i.

Interfacial Area. The interfacial area depends on the drop size distribution of the dispersion,

$$A(t) = \int_0^{\infty} \frac{\psi(d,t)d(t)}{d} \tag{3}$$

This distribution $\psi(d,t)$ may be obtained using the population balance model. For the batch dispersion under consideration, the equation states that the evolution of the drop size distribution is governed by the occurrence of drop breakage. As indicated above, coalescence is a minor event and can as a first approximation be omitted from the model. The overall equation reduces to,

$$\frac{\partial\psi(d,t)}{\partial t} = -\psi(d,t)\cdot S(d) + \int_d^{d_{max}} \psi(d',t)\cdot B(d,d')\cdot S(d')\cdot d(d') \tag{4}$$

$\psi(d,t)$ is the population density function. The first right-hand term takes into account the disappearance of drops of size d due to breakage. The proportionality function S(d) is the so-called selection function and gives the relative breakage chance for drops of size d. The second term provides the generation of drops of size d due to the breakage of larger drops, d'. B(d,d') gives the fraction of drops of size d' that break to a drop of size d. The selection function for this model was from Coulaloglou and Tavlarides; the breakage function was taken to be normal around the half-volume of the parent drop.

$$S(d) = C_1\cdot d^{-2/3} \cdot D_I^{2/3} \cdot \frac{N}{1+\phi} \exp\left\{\frac{-C_2\sigma(1+\phi)^2}{\rho_d d^{5/3} D_I^{4/3} N^2}\right\} \tag{5}$$

$$B(d,d') = \frac{7.2d^2}{d'^3} \cdot \exp\left\{-4.5\left(2\left(\frac{d}{d'}\right)^3 - 1\right)^2\right\} \tag{6}$$

The resulting differential equation is size discretized into a set of n simultaneous linear differential equations, which may be represented more conveniently by a matrix equation,

$$\frac{d\underline{\psi}(t)}{dt} = -\{\underline{I} - \underline{B}\} \cdot \underline{S}\, \underline{\psi}(t) \tag{7}$$

The equations are decoupled and solved analytically.

Intrinsic Reaction Kinetics. The chemistry and kinetics for the industrial copper extractant, LIX 64N, have been the subject of numerous investigations. A review of the work published on the kinetics indicates that in the region of interest, the extraction is chemically rate-limited and that the most appropriate rate expression is,

$$\frac{dn_{Cu}}{dt} = k_f \frac{Cu\cdot\overline{R}}{H} - k_r\overline{Cu}\cdot H \tag{8}$$

The back reaction must be included because all industrial circuits are operated close to equilibrium. The equilibrium surface of the system may be calculated using Hughes' polynomial model.

Little information is available on the coextraction of iron by LIX 64N. In view of the saturation of the interface by LIX 64N (13,14) and assuming a reaction mechanism similar to the copper system, equation (9) is used to describe the iron extraction kinetics,

$$\frac{dn_{Fe}}{dt} = k_f \frac{Fe\cdot\overline{R}}{H} - k_r\overline{Fe}\cdot H \tag{9}$$

Equations (8) and (9) constitute a set of highly non-linear differential equations which can't be solved analytically. Therefore, a fourth-order Runge Kutta procedure with Adams' predictor corrector was selected for integration.

Overall Model. Upon combination with the appropriate mass balances, equations (1-10) suffice to model a single solvent extraction stage. Extension to a multi-stage countercurrent circuit requires only extra mass balances and a multivariable Newton Raphson rootfinder method. The resulting program, SOLVEX, is capable of describing the steady-state behavior of an industrial Copper/LIX 64N solvent extraction plant. The program can be applied towards a variety of plant configurations including optional recycles on each stage. Residence time distributions can be selected according to the tanks-in-series model. The program can simulate the simultaneous extraction level of each component, the stage efficiency, and the overall process selectivity.

SIMULATIONS

A number of typical simulations were conducted for a copper-only and a copper-iron circuit. The copper-only runs are designed to investigate the influence of major operating variables on the copper recovery and stage efficiency. The copper-iron calculations provide valuable information on how process variables influence the selectivity of the extraction. Some of the more interesting simulations are presented here to illustrate the capabilities of the SOLVEX program.

Phase Continuity. As illustrated by the experiments described above, the dispersed phase is assumed perfectly segregated. The continuous phase, however, is homogeneous throughout. Therefore, it may be expected that the kinetic behavior of the system will be slightly different, depending upon which phase is continuous. A simulation was performed to compare the extraction stage efficiency for organic continuous to the extraction stage efficiency for aqueous continuous under identical operating conditions. As illustrated in Figure 4, the organic continuous system gives significantly faster extraction rates than the aqueous continuous. This effect has been observed and reported by Rowden et al., although no explanation was given. Under identical operating conditions, Rowden et al. report a 91% state efficiency for the organic conti-

nuous stage as compared to 84% for aqueous continuous. These results coincide remarkably well with the simulation results. From a kinetic point of view, it would hence be preferable to perform extraction in organic continuous circuits. This practice is limited by entrainment considerations; most industrial operations run the first stage aqueous continuous to prevent the entrainment of iron-rich liquor in the loaded organic.

Selectivity. It is generally accepted that the intrinsic selectivity of copper over iron in the LIX 64N system is thermodynamic in nature, as contrasted to another commercial extractant, KELEX 100, where selectivity seems to be a result of kinetic factors. However, due to the faster intrinsic kinetics for the copper extraction, it is possible to realize higher selectivities over iron at intermediate reaction times. A simulation of the extraction for a typical three-stage circuit indicates that under the conditions of the investigation, maximum selectivity is obtained when the copper stage efficiency approaches 85 to 90%. See Figure 5. This coincides fairly well with the actual working conditions in industry; at the Chingola and Bluebird operations, stage efficiencies on the order of 85% have been reported.

Aqueous Recycle. In industry, the first extraction stage is normally operated aqueous continuous to prevent the entrainment of iron-rich liquor in the organic. This continuity of the aqueous phase may be realized using aqueous recycle. It is instructive to simulate what happens to the process selectivity if more aqueous is recycled than the minimum amount required to guarantee phase continuity. In such a situation, the high phase ratio may result in partial depletion of the extractant and create conditions which favor high selectivity. Due to the high phase ratio, large amounts of copper may be extracted without a significant drop in the copper driving force. The increase in copper extraction reduces the available extractant and puts the iron in competition with the copper. The gain in selectivity for a typical three-stage operation is shown in Figure 6. Unfortunately, if the aqueous to organic ratio becomes too high, the entrainment level increases, and the gain in selectivity is outbalanced by increase in physical carryover of iron.

CONCLUSION

In this study, the degree of segregation in a dispersed phase mixer for the Copper/LIX 64N extraction was investigated using a novel experimental set-up consisting of the mixer and a rising drop column. The experimental results clearly demonstrate for retention times of interest (less than 3 minutes) that the level of coalescence in the mixer is low compared to the rate of breakage and that the dispersed phase behaves almost perfectly segregated.

A mathematical model was developed for the simulation of copper extraction by LIX 64N for industrial multistage operations. The model is based on reversible reaction kinetics, a shifting equilibrium, and a segregated dispersed phase. The interfacial area is characterized using a simplified population model. The resulting program, SOLVEX, is capable of simulating the simultaneous extraction of copper and iron in an industrial multistage operation.

The simulation results coincide with the reported behavior of copper solvent extraction plants and confirm various statements concerning the influence of the operating variables on extraction efficiency and selectivity. The SOLVEX program may, therefore, be used for the simulation of existing or future plants and the optimization of such countercurrent circuits. Adaptation to other SX systems may be possible if the intrinsic reaction kinetics are known and other conditions specified in the model are satisfied.

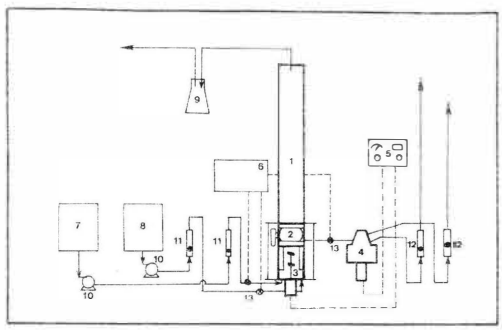

Figure 1. Schematic representation of the experimental set-up.

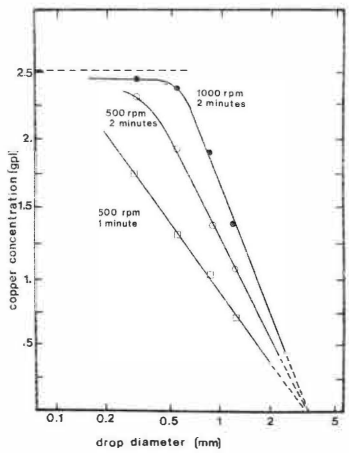

Figure 2. Concentration dependency on drop size in a continuous flow mixer. Aqueous Phase: 3.65 gpl Cu, pH 1.8; Organic Phase: 10% LIX 64N, Diluent--Escaid 200; $Q_{aqueous}$: 4.44 ml/sec; $Q_{organic}$: 2.22 ml/sec; Res. Time: 2 min.

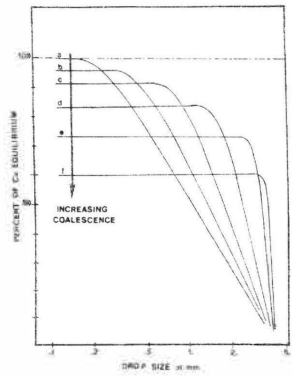

Figure 3. Schematic representation of the influence of coalescence on the concentration-drop size dependency.

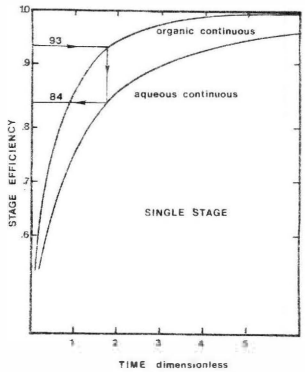

Figure 4. Effect of phase continuity on copper extraction for a standard single-stage system. Phase ratio: 1.0, Res. time: 2.0 min.

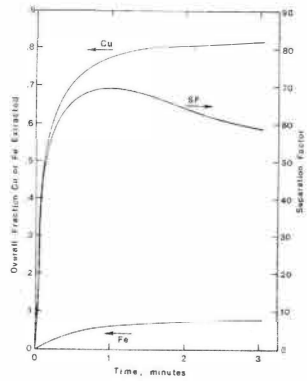

Figure 5. Influence of residence time on the process selectivity in a typical three-stage system.

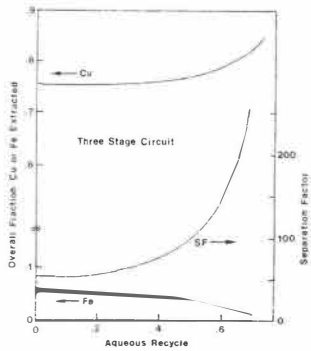

Figure 6. Effect of aqueous recycle on the process selectivity in a typical three-stage system.

INVESTIGATION OF LONGITUDINAL MIXING IN A 300 m m PULSED EXTRACTION COLUMN FOR THE PUREX PROCESS

R. Britsch and K. Ebert

Institut für Heisse Chemie
Kernforschungszentrum
7500 Karlsruhe
Federal Republic of Germany

Investigations of longitudinal mixing in a 300mm glass-column of 5m height are carried out to enable the design of an accordingly large scale column of titanium with electroreduction of U(VI) and Pu(IV).
Sieve plates with 3.5mm holes, 22.4% free area and 50mm distance are used to achieve dispersion. The disperse organic phase is 30% TBP in kerosene the continuous aquous phase 1.5m nitric acid. Electrolytically formed gas will be simulated at future measurements, by air entering through special nozzles. Flow ratios (org./aq.) between 1:1 and 20:1 were applied, mostly working at about 80-90% of flooding.

Measuring Technique

For backmixing studies a method using radioactive tracers and the non-steady--state-technique was developed. For aquous phase studies ^{61}Cu [$^{59}Co(\alpha,2n)^{61}Cu$] having a low distribution coefficient org./aq. can be used. Organic phase investigations need a tracer with a high distribution coefficient, therefore 1-^{128}J-dodecane is suitable [$^{127}J(n,\gamma)^{128}J$]. Both isotopes are γ-ray-emmitters with a half-life-time short enough to allow new measurements after 1-2days. The tracer is injected through a syringe (see fig. 1) which is moved pneumatically and controlled by a computer. Counts are collected by scintillation detectors located in lead housings along the axis of the column (see fig. 2). A 100x10mm slot at the front side of the housing serves as an inlet for the γ-rays.
After a time interval, depending on flow conditions, the detected rates are transferred to a computer. Then the counters are reset and restarted. Data are normalized to unity and stored on disc.

Calculation Technique

The dispersion model for endless reactors, open at both ends, is used for calculations. The time dependant solution (1) in the form of equation 1 is integrated numerically, using the data points of detector 2 as an entrance function. By varition of the constants D and v, the calculated exit function at the position of detector 1 or 3 is fitted to the measured data points by the least square method.

$$(1) \qquad c_3(t)=\frac{1}{2}\cdot\sqrt{\frac{L^2}{\pi D}}\cdot\int_0^t \frac{c_2(\tau)}{(t-\tau)^{3/2}}\cdot\exp\left\{-\frac{v^2}{4D(t-\tau)}\left[\frac{L}{v}-(t-\tau)\right]^2\right\}d\tau$$

Conclusions

Organic phase investigations show no dependance of backmixing coefficients from volume flow ratio or absolute flow of organic and aquous phase. Linear velocity is only determined by the difference in density and by pulse amplitude i.e. drop size distribution. Visual impression shows fewer but big drops at amplitudes up to 1cm and more but small drops at amplitudes of 1.5cm and higher. Backmixing increases according to that visual impression. Increasing pulse frequency also results in higher axial mixing.
In the continuous aquous phase a different picture is obtained. Up to flow ratios of 8:1(org./aq.) there is a maximum of mixing at a pulse of 1.0cm (some kind of resonance effect). Beside that there is no big difference between the dispersion coefficients at all pulse amplitudes at these flow ratios. Backmixing only increases according to decreasing linear velocity (i.e. higher residence time) of the aquous phase. Higher flow ratios also show higher dispersion coefficients with increasing pulse amplitude, which might mean that the stirring effect of the organic drops over a longer time gain influence.

Table of Symbols

A = pulse amplitude [cm]
$c_1(\tau)$ = rel. concentration at detector 1 at the time τ
$c_2(\tau)$ = rel. concentration at detector 2 at the time τ
$c_3(t)$ = rel. concentration at detector 3 at the time t
D = dispersion coefficient [cm^2/min]
L = distance of detector 2 and 3 [cm]
Pe = peclet number [cm^{-1}]
v = linear velocity [cm/min] of phase in the column calculated by diffusion model

References

(1) Bauer R. Chemische Rundschau 26(1975) page 5

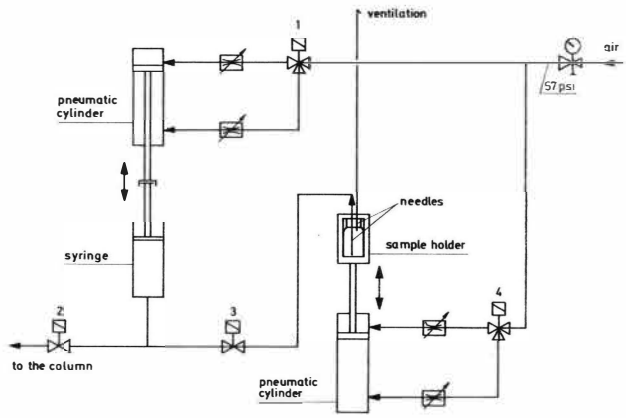

FIGURE 1: TRACER INJECTION

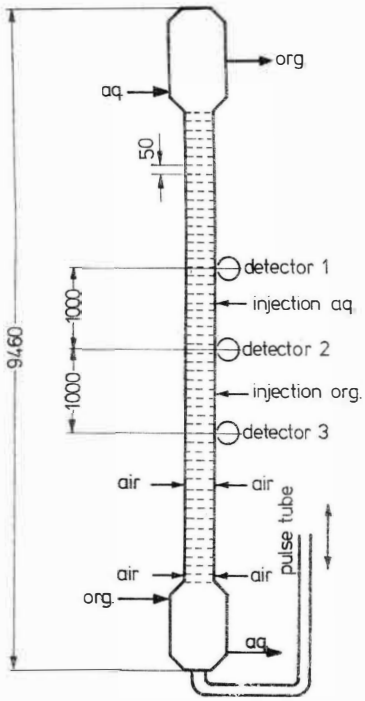

Figure 2: 300mm column

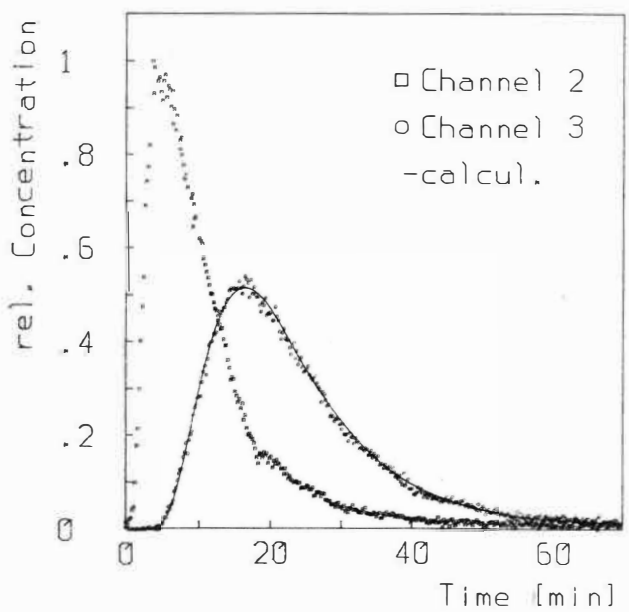

Figure 3: Example of experimental and calculated data

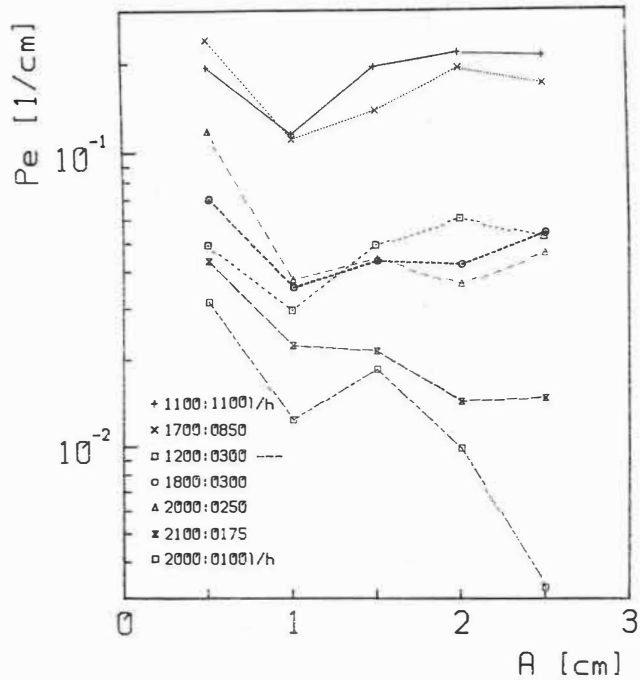

Figure 4: Peclet numbers of aqueous phase

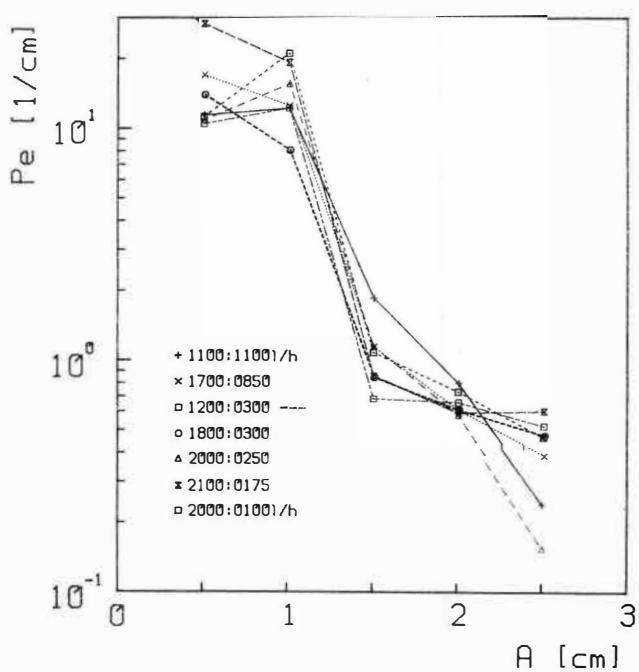

Figure 5: Peclet numbers of organic phase

AXIAL DISPERSION, WITH AND WITHOUT MASS TRANSFER, IN BOTH PHASES OF A RECIPROCATING PLATE EXTRACTION COLUMN

A. Bensalem, L. Steiner and S. Hartland

Swiss Federal Institute of Technology
Department of Industrial and Engineering Chemistry
Universitätstrasse 6, CH-8092 Zurich, Switzerland

INTRODUCTION

Efficient scale-up of extraction columns from laboratory experiments is difficult because of the lack of sufficient data on axial dispersion in both phases under real operating conditions. This is particulary true for reciprocating plate extraction columns (RPEC) where there is no published data on backmixing in both phases, even without mass transfer (1,2).

The present study is concerned with the measurement and correlation of the axial dispersion in both phases of an RPEC-column with and without mass transfer.The one-dimensional dispersion model is used for describing and correlating the longitudinal mixing in both phases (3).The least-squares method in the time or frequency domains is employed for reducing the response curves for both phases, rather than the easier but inaccurate method of moments or the method of the maxima which have been discussed eleswhere (3,4,5).

In our previous study, we found that the dispersion flow model successfully described and correlated the longitudinal mixing in the continuous phase, and fairly well in the dispersed phase (3).

EXPERIMENTAL

Apparatus

The RPEC-column , was constructed from two flanged glass sections with a nominal internal diameter of 76 mm, with an overall height of 2650 mm and a reciprocating plate stack of 1900 mm. The dimensions of the column are given in Table-1. Further details for this column are available in a previous publication (3).

Table 1. Column dimensions :

.Diameter	76 mm
.Total number of plates (including 6 baffle-plates)	55
.Plate spacing (average)	32.2mm
.Plate free area	60 %
.Hole diameter	16 mm
.Active height	1900 mm

Further details for the design of RPEC-columns may be found eleswhere (6).

Operating procedure

In this study we have used one of the test systems suggested by the European Federation of Chemical Engineering, Toluene-Acetone-Water (7).The deionized water phase was discarded after each run , and the organic phase was distilled after about every five runs ; crud which formed at the interface, during mass transfer experiments, was removed at this stage.Figure 1 shows the experimental arrangement.The outlet concentration of the aqueous phase was monitored using an automatic density-meter ; it was found that the steady-state was only reached after the contents of the column had been replaced at least five to six times (not three times as previously reported (6)).

Measurement techniques

Axial mixing in the continuous phase was measured by use of the conventional pulse injection of a salt tracer solution with the response measured by two conductivity-cells located downstream from the injection point ,as shown in Figure 1.

A similar technique was used for measuring the axial mixing in the dispersed phase, in which a soluble organic dye was injected into the organic phase.A novel technique was employed for detecting the response to the pulse injection. Two probes, each consisting of a photo-cell facing a light emitting diode located downstream of the organic tracer injection point , measured the dye concentration in the colored drops. The location of the injection and measuring points for both phases are shown in Figure 1.

The recorded responses for both phases were reduced using the one-dimensional dispersion model and the least-squares method in the frequency domain (3).

RESULTS AND DISCUSSIONS

In the results described below the mean residence times computed from the hold-up measurements of the dispersed phase and from the residence time distribution curves are compared.Only those runs are retained in which agreement between the computed mean residence times was within ±20% for the continuous phase, and ±30% for the dispersed phase.

No mass transfer

.Axial mixing in the continuous phase

The axial dispersion coefficients in the continuous phase, E_c , shown in figure 2, tend to be highest at low agitation due to circulation effects, and decrease as the agitation increases. E_c apparently increases wuth increase in the amplitude of reciprocation, A, and the dispersed phase flow, Q_{Tol}. (due to increase in the hold-up of the dispersed phase).Previous evidence for two-phase flow conditions (1), is scanty but supports the present results.

.Axial mixing in the dispersed phase

The axial dispersion coefficients in the dispersed phase, E_d, are much higher than those in the continuous phase, E_c, and E_d decreases rapidly with higher agitation, as shown in Figure 3. This could be due to the wide drop size distribution at low agitation which leads to a large variation in drop rise velocities. E_d increases for lower flow rates of the dispersed phase, because the drops are easily entrained by the continuous phase.

With mass transfer

.Axial mixing in the continuous phase

E_c,shown in Figure 4, are higher when mass transfer occurs from the dispersed to the continuous phase (when rapid coalescence occurs) than when mass transfer is in the opposite direction. Little coalescence then occurs between the drops and the value of E_c is close to that with no mass transfer.A possible explanation is that the large rise velocities of coalesced drops increase the circulation in the continuous phase.

.Axial mixing in the dispersed phase

For the axial dispersion in the dispersed phase, shown in Figure 5, the values of E_d are higher when mass transfer occurs from the continuous to the dispersed phase (leading to retarded coalescence and smaller drops) than when mass transfer is in the opposite direction (which enhances coalescence).At high agitation the value of E_d, when mass transfer occurs from the dispersed to the continuous phase, is similar to that with no mass transfer.This could be explained by the fact that the smaller drops are easily entrained by the flow of the continuous phase.

Effects of throughputs

Figure 6 clearly shows that the values of E_d (dotted curves) are greater than E_c (solid curves) and that the direction of mass transfer has a large effect on E_d, which is higher when mass transfer is from the continuous to the dispersed phase and further more increases rapidly with total throughputs.The axial dispersion coefficients in both phases tend to become equal at high

agitation rates close to the flooding point, as observed by Kagan in other agitated columns (8).

References

1) Hafez M.M. et al, Can.J.Chem.Eng. 57, 150 (1979).

2) Kim S.D. et al, Can.J.Chem.Eng. 54, 235 (1976).

3) Bensalem A., Can.J.Chem.Eng. 60, 603 (1982).

4) Clements, W. C., Chem.Eng.Sci. 24, 957 (1969).

5) Clements, W.C. et al, Chem.Eng.Sci. 27, 2311 (1972).

6) Karr, A.E., AIChE J. 5, 446 (1959).

7) Misek T. (editor), Recommended systems for liquid extraction studies, European Federation of Chemical Engineering, Inst. of Chemical Engineers, London (1978).

8) Kagan, S.Z. et al, Zhurnal Prikladnoi Khimii, 39, 88 (1966).

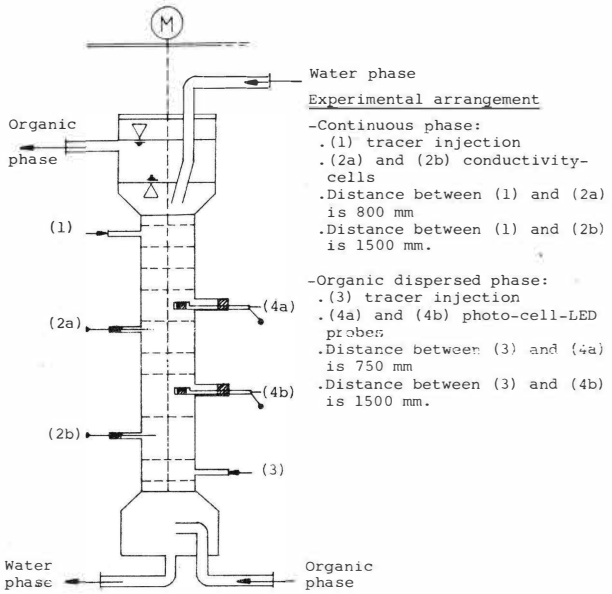

Figure 1. Experimental arrangement

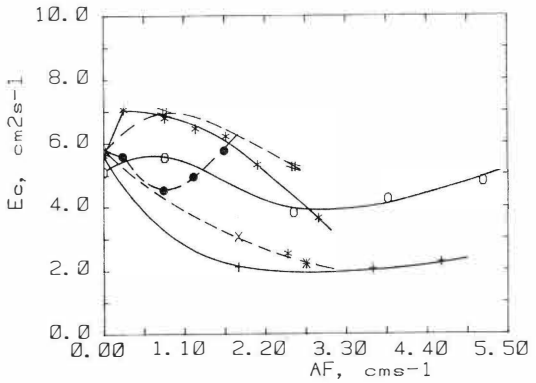

Figure 2. Effects of agitation on axial dispersion coefficients in the continuous phase, without mass transfer.
· Q_{H_2O}= 100 l/hr, Q_{Tol}= 25 l/hr } —— , 0: A= 1.60 mm , +: A= 1.10 mm ,and *: A= 0.50 mm.
· Q_{H_2O}= 100 l/hr, Q_{Tol}= 100 l/hr } ---- , ≠: A= 1.60 mm , x: A= 1.10 mm, and ●: A= 0.50 mm.

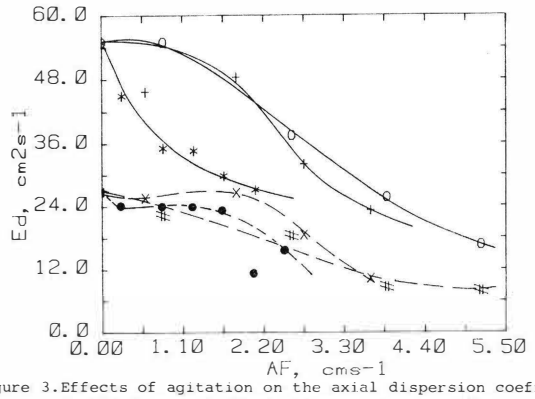

Figure 3. Effects of agitation on the axial dispersion coefficients in the dispersed phase, without mass transfer. (Same symbols as figure 2).

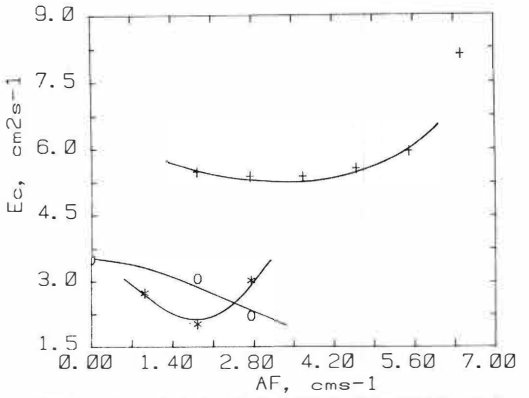

Figure 4. Effect of agitation on the axial dispersion coefficients in the continuous phase, with and without the presence of the solute.
Q_{H_2O}= 100 l/hr, Q_{Tol}= 100 l/hr, and A= 1.10 mm.
0: without mass transfer , +: mass transfer from dispersed to continuous phase, *: m.t. from continuous to dispersed phase.

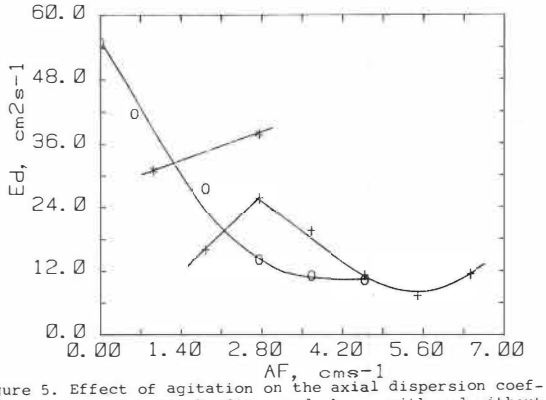

Figure 5. Effect of agitation on the axial dispersion coefficients in the dispersed phase, with and without mass transfer. (Same symbols as in figure 4).

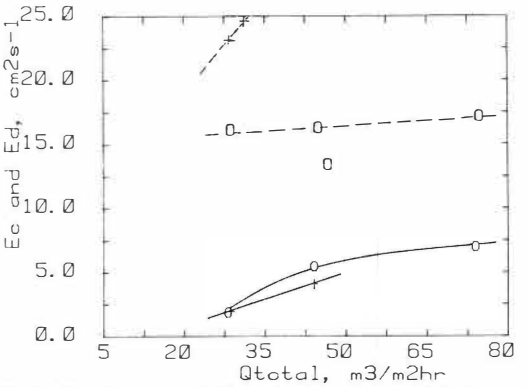

Figure 6. Effect of total throughputs on the axial dispersion coefficients in the continuous phase, E_c, and in the dispersed phase, E_d.
A= 1.10 mm, F= 100 min^{-1} , and Vol. phase ration d/c is 1.6 .
0: mass transfer from the dispersed to the continuous phase.
+: mass transfer from the continuous to the dispersed phase.
E_c : solid curves (——) , and E_d: dotted curves (----).

THE DEVELOPMENT OF MIXER-SETTLERS WITH DOUBLE MIXERS IN EACH STAGE

Li-Min Su and Guo-Peng Li

Institute of Chemical Metallurgy
Academia Sinica, Beijing, China

Mixer-settlers, widely used equipment for solvent extraction processes, have been modified and improved successfully since the seventies. The increase of stage efficiency and capacity of solutions treated and the reduction of entrainment of the organic phase in aqueous solution are the chief achievements of the commercial size mixer-settlers during the last decade (1-6).

In order to simplify the construction and improve the performance of mixer-settlers, the present work has been concentrated on the development of double mixer type mixer-settlers (DMMS) and of the proper type of impeller used in the mixers since the end of 1979.

CHARACTERISTICS OF THE DMMS DESIGNED

(1) The mixer is approaching to the condition of hydraulically independent to the settler so that both short cut and back-mixing phenomena in the equipment are decreased.

(2) The height of the interfacial surface between the two phases in the settler can be adjusted. The dispersed phase flows into the settler along the interface and the two phases flow out from the settler through their own overflow weirs separately, so turbulence, back flow of the two phases, dead zone and short cut of flow in the settler are reduced.

(3) With two mixers in series in each stage, the residence time distribution of fluid approaches plug flow. The construction of the DMMS is simple with the using of two equal size mixers.

(4) Smaller agitator is used in the second mixer to decrease the intensity of stirring, thus the difficulties encountered in phase separation and extraction are reduced.

(5) As the two mixers in series in each stage are on the same level, the energy consumption for pumping and the cost support of shallow settlers are decreased.

(6) A newly designed half open flat blade turbine (HOFBT) type agitators were used in mixers. This agitator has simple construction and develops high pumping capacity and also high intensity of agitation.

EXTRACTOR DIMENSIONS AND EXTRACTION SYSTEMS USED IN TEST WORK

The rough sketch of a DMMS is shown in Fig. 1. The size of DMMS used in laboratory is 56 x 56 x 56 mm for the mixer and 46 x 72 x 150 mm for the settler with total effective volume of 0.001m^3 for each stage. Fig. 2 shows the sketch of a HOFBT agitator. The agitators used in laboratory have the diameters of 28, 35, 40 and 50 mm respectively. The extraction systems used for experiments are given in Table 1.

Extraction Systems Tested — Table 1

No.	Aqueous Phase (gpl)	Organic Phase (% vol.)	No.	Aqueous Phase (gpl)	Organic Phase (% vol.)
1.	pure $CuSO_4$ soln. Cu 5.84	D_2EHPA-Na 12 TBP 1.4	5.	$NiSO_4$ Raffinate Ni 30	P507-Na 25
2.	sulphate soln. Co 10.35 Ni 60.7	Aliquat 336 thiocyanate 36 D_2EH al. 10	6.	sulphate soln. Co 22 Ni 50	P507-Ni 25
3.	$NiSO_4$ Raffinate Ni 60.4	D_2EHPA 32.1	7.	scrubbing liq. HCl 1.2N	P507-Co 25
4.	Na_3VO_4 leaching liq. V 8.5	primary amine N-1923 10 mixed al. 3	8.	stripping liq. HCl 2.5N	P507-Co 25

Note: 1. Kerosene was used as organic phase diluent.
2. Expt. No.4 to 8 are pilot plant test.

LABORATORY CONTINUOUS FLOW TEST RESULTS

Comparison of Results of Extraction between DMMS and SMMS

Experimental results are compared with DMMS and SMMS (single mixer mixer-settler) of the same mixer size used as extraction equipment respectively as shown in Fig. 3 & 4. Baffles were installed in settlers of both DMMS and SMMS for tests and results of experiments are listed in Table 2.

Results indicate that the stage efficiency of a DMMS approaches 100% and is higher than that of a SMMS and both the entrainment of organic phase and the depth of dispersion band are much less for experiments with DMMS. Using DMMS, satisfactory extraction can also be achieved with lower agitation intensity and less mixing time.

Fraction of Mass Transfer Occurred in the First Mixer From the point of putting just enough agitation intensity to the two mixers in each stage of DMMS to give high stage efficiency, contribution to mass transfer by the first mixer was determined. Results indicate about 95% of mass transfer was occurred in the first mixer and very high stage efficiency can be obtained with only two mixers in each stage as shown in Table 3.

Comparison of Phase Sepn. Effect between DMMS and SMMS — Table 2

Mixer-Settler	DMMS				SMMS			
Type of baffle in Settler	I	II	III	IV	I	II	III	IV
Volume of Dispn. Band (ml.)	68	166.9	86.8	47.6	183.4	192.4	129.5	56
Entrainment of Org. Phase(ppm)		7.5	8.3	6.0	13.1	13.8	9.8	8.9

Note: 1. Agitation intensity N^3D^2 is 58.4 and 44.9 ft^2/s^3 for 1st and 2nd mixer, respectively.
2. Mixing time 1.98 min.
3. Test system; $D_2EHPA/NiSO_4$ solution.

Characteristics of HOFBT Agitator Developed and the Combination Effect of Turbine Diameter D and Speed of Revolution N Pumping efficiencies of agitators with the types of HOFBT, OFBT (open flat blade turbine) and DSBVT (double shrouds with spoiler blades and back swept vane turbine) respectively are shown in Fig. 5. Combination effect of turbine diameter and speed of revolution of these three types of turbines on phase separation is shown in Figs. 6 & 7 respectively.

Conclusions can be drawn that HOFBT agitator developed in the present work is an effective agitator from the point of pumping capacity, phase separation and simplicity in construction. For a given N^3D^2 value, the combination of small D with large N is more suitable under the conditions of experiment investigated.

Fraction of Mass Transfer taken Place in the First Mixer — Table 3

Agitation intensity N^3D^2(ft^2/s^3)	Mixing time (min)	Stage efficiency (%)	Entrainment of org. phase (ppm)	Mass transfer in 1st mixer (%)	Test system
27.3(19.8)	3	97.5	~ 0	86.8	R_4NSCN/Co, $NiSO_4$
27.3(17.5)	5.6	99.5	≦ 10	95.2	P507-Na/$NiSO_4$
27.3(17.5)	5.2	96.4	≦ 4	95.6	P507-Ni/$NiSO_4$
27.3(17.5)	7.7	99.0	≦ 2	94.5	P507-Co/HCl
27.3(17.5)	7.0	98.6	~ 0	95.0	P507-Co/HCl 1.2N / 2.5N

RESULTS OF PILOT PLANT STUDIES

Single Stage DMMS Tests Tests were carried out on the production of vanadium pentoxide from impure leaching solutions. Primary amine N-1923 was used as extraction agent for vanadium. Mixer size used was 450 x 450 x 450 mm while settler size 600 x 1000 x 700 mm with the total effective volume of 0.6 m^3. The scale up factor based on the laboratory size is 560 as far as the volume of the mixers is concerned. Diameters of HOFBT agitators of the first and second mixers were 220 mm and 180 mm respectively. The speed of revolution used was 220 rpm. Experimental results are listed in Table 4.

Pilot Plant Data of Vanadium Extn. by Primary Amine N-1923 in a Single Stage DMMS — Table 4

Aq. feed (gpl) V	Cr	Mixing time (min)	Agitation intensity N^3D^2(ft^2/s^3)	Extn. efficiency V (%)	Entrain. of org. phase (ppm)	Specific settling rate (m^3/m^{2}hr)	Conc. in Raffinate (ppm) V	Cr
7.95	0.55	7	25.8(17.3)	99.93	~0	2.56	12.6	1.9
9.85	0.30	5	25.8(17.3)	99.97	~0	3.70	3.4	6.6
7.95	0.27	5	25.8(17.3)	99.84	~0	3.70	12.6	7.8
Laboratory Flow Test Results								
10.31	0.51	3.5	27.3(19.8)	99.84		1.88	3.0	

The pilot plant tests gave the same results as those obtained in the laboratory. For single stage vanadium extraction, the percent of vanadium extracted is over 99% and the total amount of vanadium and chromium in the raffinate was less than 20 ppm. Entrainment of organic phase in aqueous phase approached zero while

the specific settling flow rate was 3.7 m^3/m^2hr.

Multi-Stage DMMS Tests Tests were carried out on the production of cobalt oxide and pure nickel sulfate solution from cobalt containing residue. This residue was obtained from purification of nickel electrolyze. P-507 (2-ethyl-hexyl-phosphonic acid mono-2-ethylhexyl ester) was used for separation of Co and Ni and a number of stages of DMMS in series were used. Four steps are involved in the separation, i.e. formation of nickel soap, exchange extraction of cobalt, scrubbing of nickel in organic phase and stripping of cobalt from the organic phase. The flow ratios (organic to aqueous ratio) in the four steps were 2.2, 1.7, 14.9 and 5.6 respectively. Instead of using the original 20 stages of mixer-settlers of old design (OMS), 12 stages of DMMS were used. Effective size of the mixer was 150 x 150 x 150 mm, the settler 150 x 380 x 280 mm with the effective volume of 0.023 m^3 per stage. Diameters of the HOFBT agitators of the first and second mixers were 75 and 60 mm respectively while the speed of revolution of the agitators was 460 rpm. Results are shown in Table 5.

Results of Multi-Stage Test of DMMS in Ni/Co Separation in Comparison with OMS Table 5

Extractor	Stage used	Stage efficiency(%)	Flow throughput(m^3/D)	Average N^3D^2(ft^2/s^3)
DMMS	12	95-99	1.84	22.4
OMS	20	50-70	1.44	30.7
	Specific settling rate (m^3/m^2.hr)	Entrain. of org. phase (ppm)	Purity of Co product (Co/Ni)	Purity of Ni product (Ni/Co)
DMMS	1.33	≤ 10	≥ 3000	7000
OMS	0.67		3000	7000
	Direct recovery of Co in P-507 circuit(%)	Fraction of the best quality CoO product (%)	P507 consumption (t/t Co)	Kerosene consumption (t/t Co)
DMMS	99.25	77.37	0.059	0.317
OMS	99.24	37.92	0.065	0.413

The purity of the products obtained in the process by using DMMS was just about the same as the old design mixer-settlers were used. However, DMMS are preferred to use as:

(1) The process requires about 40% less number of stages as an average increase of stage efficiency of 40% achieved.

(2) Processing capacity increases about 30%.

(3) The operating cost is decreased and the environmental protection is improved.

CONCLUSIONS

(1) The newly developed DMMS is simple in construction and gives stage efficiency up to 98% with entrainment of organic phase in aqueous phase less than 10 ppm.

(2) The DMMS developed is versatile to various extraction systems tested such as the high viscous organic phase (RANSON for Co and Ni separation with viscosity of 26.95 cp. at 20°C) and the high flow ratio (O/A= 14.9) for Ni scrubbing from P-507 organic phase.

(3) The newly developed HOFBT agitator can meet both the pumping efficiency and agitation intensity required for solvent extraction.

(4) For a given value of N^3D^2, combination of small D with large N is preferable in solvent extraction based on the results of present study.

(5) A scale-up factor of 560 based on the mixer volume has been made in the present study. The scale-up of power needed for the agitators was based on the constancy of N^3D^2. As the mass transfer occurs dominately in the first mixer, low agitation intensity should be put into the second mixer.

ACKNOWLEDGEMENT -- The authors wish to thank Professor Jiayong, Chen who warmly guided this work.

REFERENCES

1. J. R. Orjans, et al., ISEC 1977, Equipment, p340.
2. E. Barnea, ISEC 1977, Equipment, p347.
3. A. D. Kennedy, et al., ISEC 1977, Equipment, p333.
4. I. E. Lewis, ISEC 1977, Equipment, p325.
5. J. Mizrahi, et al., ISEC 1974, Vol.1. p141.
6. J. B. Scuffham, Chem. Eng.(Engl.) 370, 328 (1981).

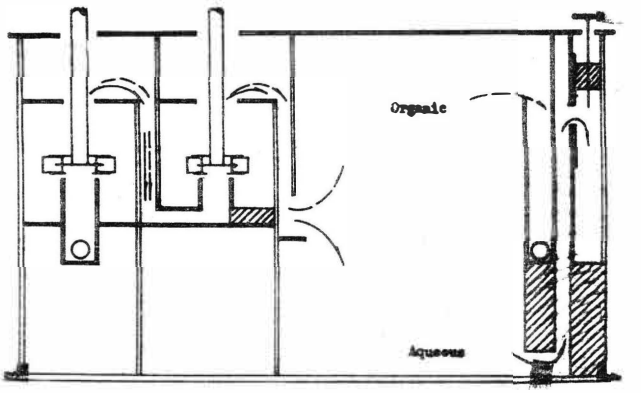

Figure 1. Sketch of a DMMS

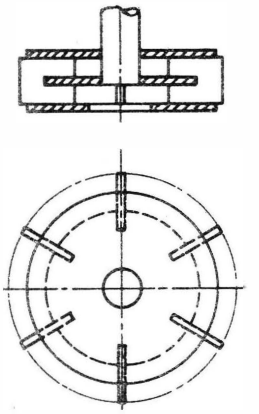

Figure 2. Sketch of a HOFBT Agitator

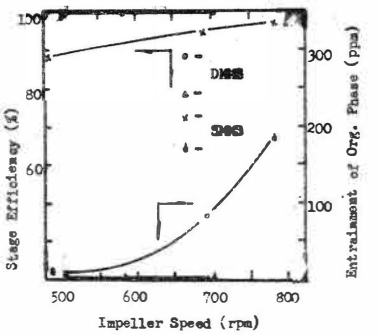

Figure 3. Effect of Number of Mixers in Series and Impeller Speed on Performance of MS

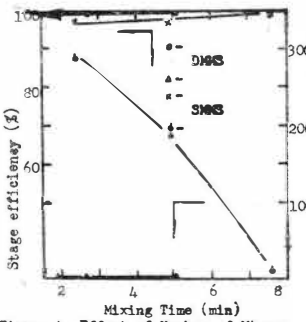

Figure 4. Effect of Number of Mixers in Series and Mixing Time on Performance of MS

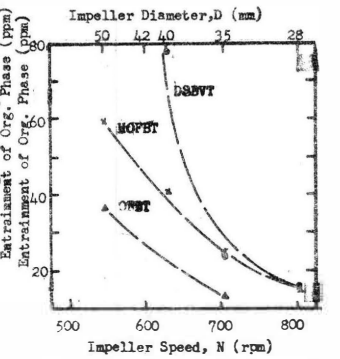

Figure 6. Effect of Different Type of Impellers and Combination of D and N on Entrainment of Org. Phase

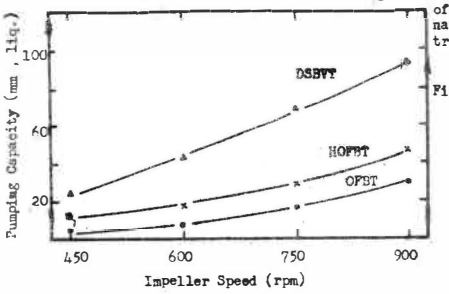

Figure 5. Pumping capacity of Different Types of Impellers

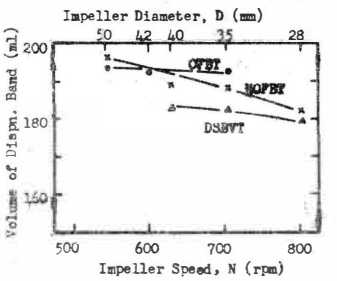

Figure 7. Effect of Types of Impellers and Combination of D and N on Volume of Dispersion Band

OPTIMAL DESIGN OF AN AIR PULSED MIXER SETTLER

M. Venkataraman, R. Natarajan and G. R. Balasubramanian

Reprocessing Development Laboratory
Reactor Research Centre
Kalpakkam, India

Air pulsed mixer settler is chosen as candidate contactor for application in reprocessing of ThO_2 blankets of experimental fast reactor at Kalpakkam, because of its adaptability for reasonably maintenance free remote operation. The development work undertaken, to arrive at a satisfactory design is described in this paper.

EQUIPMENT FEATURES

The scope of the work is to develop a contactor with the following salient features:

a) Mixing by air pulsing with probes designed for maximum mixing efficiency.

b) Pulsing system suitable for continuous operation.

c) Critically safe geometry.

d) Interstage pumping without using moving parts.

e) Ability to control interface levels in settlers remotely.

f) Facility for sampling remotely.

The details of contactor so developed, are given in Annexure 1 and Figures 1 to 4.

PULSING SYSTEM DESIGN

Pulsing Valve Design: The pulsing system consists of a pair of probes in each mixer, branching from two headers, connected alternately to pressure and vacuum sources by a four way five port multi directional valve. This is operated by a timer controlled solenoid. The pulsing is 180° out of phase in the headers to avoid level change in the mixer.

The conventional system of using single four way five port solenoid valve is unreliable for prolonged period of operation because of amplitude fluctustions. Hence, each header is independently pulsed with pressure and vacuum sources through a two way three port solenoid valve and the amplitude adjusted by bleeding. This is better than the first one as complimentary affects (unequal amplitude in a pair of probes) were eliminated.

In a third system, a cam operated multi-directional valve is used. The speed of the cam is controlled by a stepper motor thereby controlling the frequency of pulsing. This system is found to be more reliable as it replaces the solenoid completely and fluctuations in amplitude, cyclic effects are eliminated. The change over from vacuum to pressure or vice versa is found to be smooth.

Probe design: The primary objects of the probe development are to provide homogenous bulk mixing, ensuring intimate contact of the phases and creating large interfacial area for mass transfer. Experiments are conducted ensuring complete mixing through out the mixer without air purging. The jets should reach the sides as well as the bottom of the mixer. Efficient dispersion, without affecting settling adversely is also ensured. The following criteria shall be satisfied while designing the probes.

A, the area of opening in the probes in cm^2, is given by the relationship

$$(1)\quad \frac{1}{A} \geq \left[\frac{Di}{\sqrt{2}} - do\right] \left[1 + \frac{(Di^2 - do^2)h}{di^2\ Am}\right] \left[\frac{2}{\pi di^2\ Am}\right]$$

while the minimum frequency at which mixing will be good is expressed in

$$(2)\quad (\pi\, di^2\ Am\ \ f/4A) \Big/ \left[1 + \frac{(Di^2 - do^2)}{di^2\ Am}\right] \geq 100\ Vs$$

where Vs is the settling velocity of the drops, cm/sec.

Some of the probes with which the runs are carried out are shown in Figure 5 and the combination I and J was found to be satisfactory.

AIRLIFT DESIGN

Since air is supplied to air lifts from a single header, design of airlifts is critical to have uniform distribution. This is more so since the air flow required for pumping is very low, in the range of a few litres/hr. Suitable resistances are introduced in the branches to have proper air distribution without entrainment, keeping in mind the choking problem of small orifices. They are so chosen, that even if 50% of the air lifts are vented others will continue to pump. Details of these are provided in Annexure-2.

SAFETY MEASURES

The safety measures are included to prevent the liquid from entering the pulsing system in case of power failure or equipment failure. The headers are vented to the exhaust by suitably sized power-to-open type solenoid valves. These valves operating on standby power, will act even when the vacuum produced is not within the set limits. Traps are incorporated in the headers to act as secondary safety devices.

CONCLUSION

The contactor functions satisfactorily in the extraction system of Uranium and Thorium using TBP as solvent with good separation efficiency and hydraulic characteristics. Work on the scaled up model is in progress.

ANNEXURE 1 : DESIGN DETAILS

	Diameter (cm)	Height (cm)	Volume (cc)
Mixer	(Di) 4.10	(h) 20	190
Settler	5.25	20	300
Probes	(di) 1.25	11.8	
	(do) 1.60		

Pulse amplitude, Am	30 cm;
Pulse frequency, f	90-120 c/min
Residence time	3 mt/stage
Capacity	10 lph

ANNEXURE 2 : DESIGN OF AIRLIFT

Pressure in the header = Submergence + Allowable build up in the settler + Drop across the orifice.

$$\text{Drop across the orifice} \propto \frac{\text{Length of the orifice, } L}{(\text{Dia of the orifice}, D)^4} \times \text{Air flow rate, } Q_G.$$

Q_G is assumed to be 4 to 5 times the liquid flow rate Q_L. In our unit, for Q_L of 75 ml/min, Q_G is taken as 350 ml/min. Selection of L/D^4 depends on a judgement of the problems of choking of small diameter and the inconvenience of lengthy orifice. An orifice of 10 mm length and 0.5 mm dia has been operating satisfactorily in each of the airlifts.

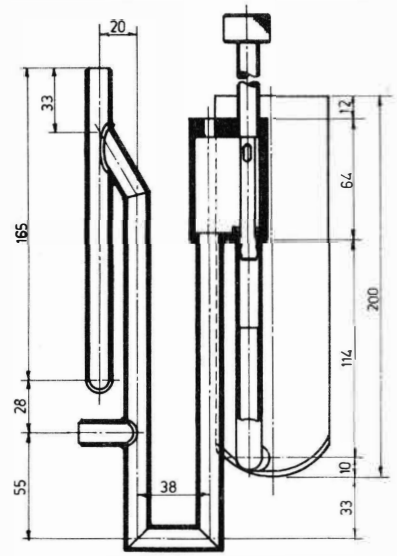

FIGURE 2
AQUEOUS OUTLET, WEIR, AIR LIFT (Section A-A)

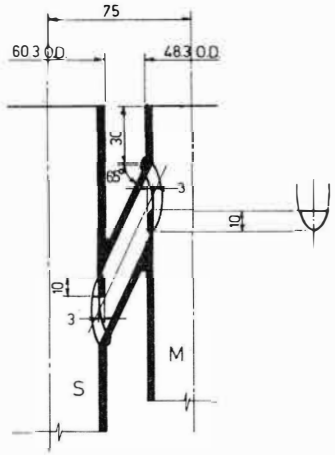

FIGURE 3
MIXER AND SETTLER CONNECTION
(Section B-B)

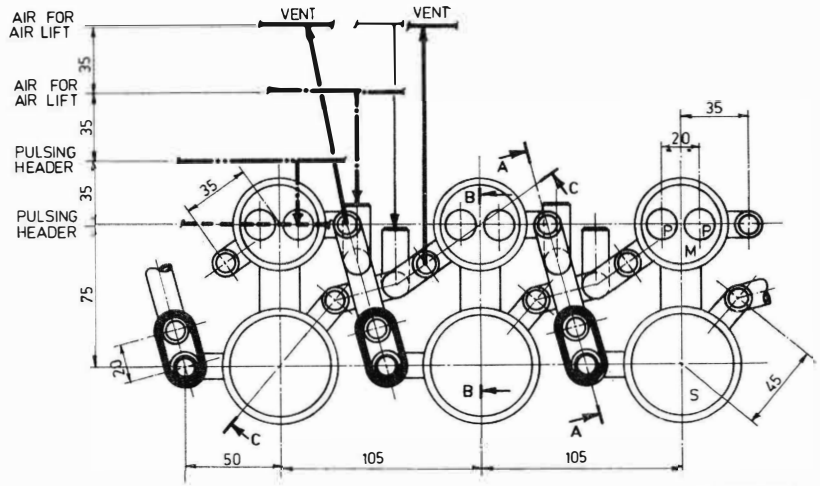

FIGURE 1. AIR PULSED MIXER SETTLER
(Plan of assembly)

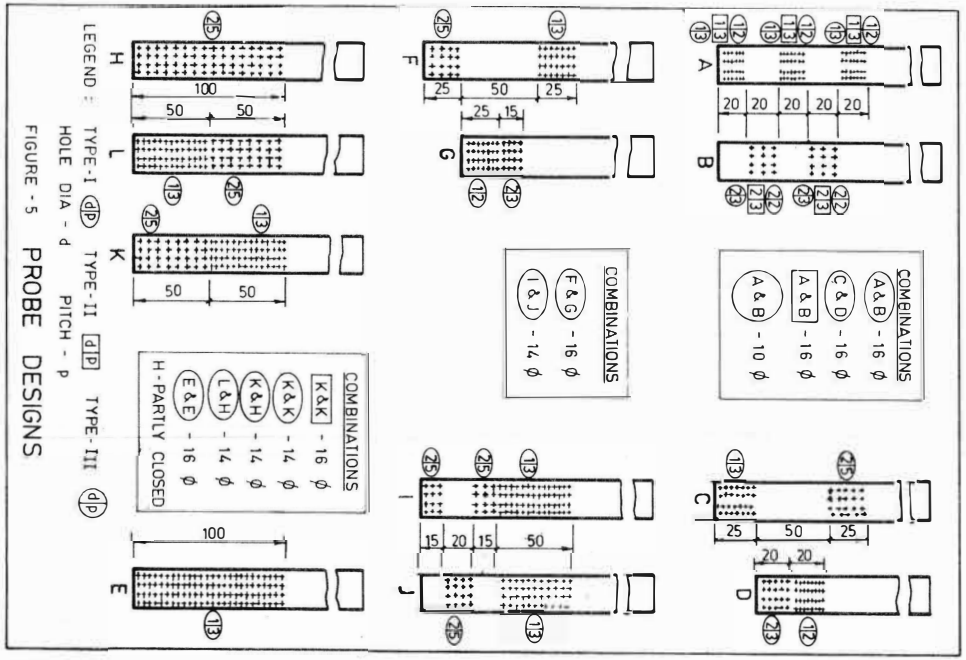

FIGURE - 5 PROBE DESIGNS

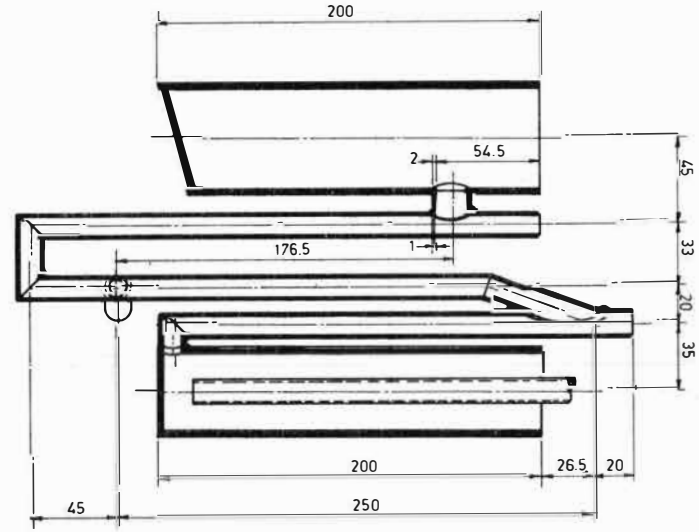

FIGURE 4. ORGANIC AIR LIFT (Section C-C)

PERFORMANCE OF THE KREBS SOLVENT EXTRACTION SYSTEM

Alain A. Sonntag and David A. Goodman

KREBS & Cie. S.A.
Bois D'Arcy, France

INTRODUCTION

The KREBS SOLVENT EXTRACTION SYSTEM utilises a unique mixer-settler design having a very high capacity per unit area and great flexibility.

The advantages of the system have been proven over a wide range of applications.

PRINCIPLES OF OPERATION

The KREBS MIXER SETTLER includes the following features, as shown in Figure 1 :

A MIXER contains the heart of the system : a low speed conical pump which provides liquid transfer from the mixing chamber to the settler through a launder. The mixer impeller (agitator) is independant of the pump and selected to best satisfy dispersion requirements.

A SUPERPOSED LAUNDER initiates phase separation and makes it possible to simplify the equipment layout.

A SETTLER of simple design has a short angled plate distributor which directs the phases into the main part of the settler without turbulence and contributes to phase disengagement. The settler itself is free of internals and provided with removable inspection covers for easy maintenance and cleaning.

An INTERFACE REGULATOR adjusts the height of the interface and maintains the level of the liquid in the settler in case of a plant shutdown or by-pass of a particular unit.

ADVANTAGES OF THE KREBS SX SYSTEM

The combination of these design features presents the following advantages :

1. Reduction in equipment size and hence plant size.
2. Independence of agitation from pumping allowing optimum conditions of mixing.
3. Simplified layout due to the "head to head" arrangement of the mixer-settler units and hence easier operation and maintenance.
4. Reduction in piping and instrumentation and easy by-passing of any mixer-settler.
5. Flexibility of the mixing and pumping unit and hence easier operation.
6. Lower capital requirements (including inventory) and lower operating costs.

Full scale plants using the KREBS SOLVENT EXTRACTION SYSTEM have now been in operation for over eight years.

Figure 2 gives a general arrangement of KREBS MIXER SETTLERS in the KREBS SOLVENT EXTRACTION SYSTEM.

APPLICATIONS OF THE KREBS SOLVENT EXTRACTION SYSTEM

The KREBS MIXER SETTLER has been studied and developed over a period of 13 years starting from a small bench scale conical pump model.

Now the KREBS SOLVENT EXTRACTION SYSTEM has found application in many fields of the hydrometallurgy industry.

The first solvent extraction plant designed and built by KREBS was part of a nickel refiney where nickel chloride solution was purified from iron and cobalt by solvent extraction of these two metals. The SX plant consists of forty one (41) mixer settlers of various sizes.

Later KREBS designed several SX plants for uranium recovery from sulfuric acid leach solution of ores.

Since 1977 four uranium solvent extraction plants have been designed and built.

1976 - 1977 = Conceptual design, engineering, construction and start up of the uranium solvent extraction plant of the MOUNANA mill (GABON - AFRICA), a COMUF property. The plant consists of four extraction, four strip, one wash and two regeneration/wash mixer settlers.

1977 = Engineering, construction and start up of the extraction unit of the SX plant at LANGOGNE plant (FRANCE) a CFMU property, consisting of four mixer settlers. The existing strip mixer settlers were converted to the KREBS system in 1982 in order to increase both product quality and plant through put.

1980-1981 = Engineering and construction of the VAAL REEFS - AFRIKANDER LEASE PROJECT uranium solvent extraction plant (REP. SOUTH AFRICA) an ANGLO-AMERICAN CORP property. The plant consists of three extraction, four scrub, three strip and one regeneration mixer settlers.

1981-1982 = Engineering and construction of the uranium SX plant of the KEY LAKE project (SASKATCHEWAN - CANADA). The plant will be commissionned in 1983. It will contain four extraction, three scrub, four strip, one ammonia scrub and one regeneration mixer settlers.

The uranium SX plant of the CLUFF LAKE project (SASKATCHEWAN - CANADA) is presently under design and engineering.

Another industrial plant was built and put on line in 1981-1982. It treats and purifies vanadium sulfate solutions in a battery of eight mixer settlers. The plant is located in BARTLESVILLE (OKLAHOMA, U.S.A.) and is a SOMEX LTD property.

During the same period extensive test work has been carried out with the KREBS MIXER SETTLER pilot unit in order to size industrial plants and to determine the behavior of the system with various solutions and solvents.

These tests have included :

- Uranium extraction from phosphoric acid.
- Niobium extraction from sulfate solution.
- Rare earth separations.
- Rhenium - molybdenum separation.
- Tantalum/niobium extraction from hydrofluoric acid solution.
- Uranium/thorium extraction from sulfate solution.
- Manganese extraction from nickel/cobalt chloride solution.
- Cu + Zn, Fe, Co extraction from chloride solution.
- Copper extraction from sulfate solution.

The copper extraction has been tested on different solutions and solvents with two sizes of KREBS MIXER SETTLER pilot units. These tests were carried out in two copper mines in the USA and three copper mines in CHILE.

Unfortunately due to the present depressed metal market many projects have been postponed preventing KREBS from installing even more industrial plants.

PERFORMANCE OF THE KREBS SOLVENT EXTRACTION SYSTEM

Performance obtained on industrial and pilot equipments have proven the advantages of the system.

For the various extractions examined, the specific flowrates experienced have been between 2 and 4 times higher than conventional equipment.

Stage efficiencies of operating industrial plants have been checked and verified over various periods of operation, as well as during test series whenever possible.

The same dispersions have been obtained at lower shear rates than in the conventional system resulting in lower organic losses for the KREBS system.

Table 1 gives the results obtained from operation and experimentation.

KREBS wide experience in the field of operation has resulted in an excellent knowledge of materials of construction to deal with the strong attack of many aqueous solutions (chlorides, fluorides, acids, etc...) and solvents (aromatic diluants, TBP, etc...)

INDUSTRIAL PLANTS

Three pictures show two uranium solvent extraction plants built by KREBS, using KREBS MIXER SETTLERS.

Figure 3 : VAAL REEFS (R.S.A.) Solvent Extraction Plant : General View. Extraction Mixer Settlers are in the foreground.

Figure 4 : VAAL REEFS (R.S.A.) Solvent Extraction Plant : Stripping Mixer Settlers.

Figure 5 : MOUNANA (GABON) Solvent Extraction Plant : General View.

TABLE 1

KREBS SOLVENT EXTRACTION SYSTEM PERFORMANCE

EXTRACTION OF VARIOUS METALS

METAL	SPECIFIC FLOW RATES: TOTAL FLOW $m^3/h.\ m^2$	TOTAL FLOW GPM/FT^2	INCREASE v/s CONV.	STAGE EFFICIENCY %	ORGANIC LOSSES ppm
Uranium industrial operation - average	11.0	4.5	3	98-99	50-100
- range	8.0-15.0	3.3-6.1	2.2-4	95-100	30-200
Uranium/H_3PO_4	7.9	3.2	2.3	NA	100-150
Copper					
1	8.8	3.65	2.5	85	10
2	8.5	3.5	2	90-95	20
3 (a)	14.1	5.8	NA	NA	NA
Vanadium	8.1-12	3.3-4.9	NA	94-96	60-80
Niobium	9.6	3.6	NA	NA	NA
Niobium + tantalum	13.4	5.5	1.8	99	NA
Rhenium/molybdenum	10.2/13.2	4.2/5.4	1.5/3.4	NA	NA
Rare earths					
1	11	4.5	3	83-95	NA
2	9.3-13	3.8-5.3	ND	ND	ND
Copper + zinc/nickel	13.3	5.4	NA	NA	50
Cobalt/nickel					
1	8.4	3.4	NA	NA	NA
2	3.3	1.35	NA	99	-200
Iron/nickel	3.4	1.4	NA	99	-200
Manganese/cobalt + nickel	4.5	1.8	NA	NA	NA

NA = Not available.
ND = Not disclosed.

All results are for organic continuous operation, unless otherwise specified.
(a) Aqueous continuous operation.

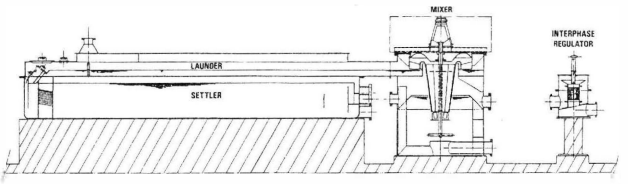

FIGURE 1
KREBS MIXER-SETTLER . CROSS SECTIONNAL VIEW

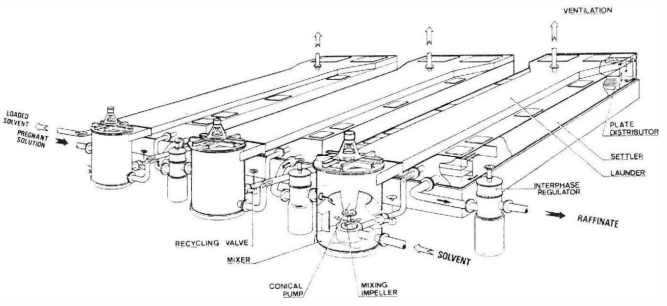

FIGURE 2
KREBS MIXER-SETTLER SYSTEM . TYPICAL ARRANGEMENT

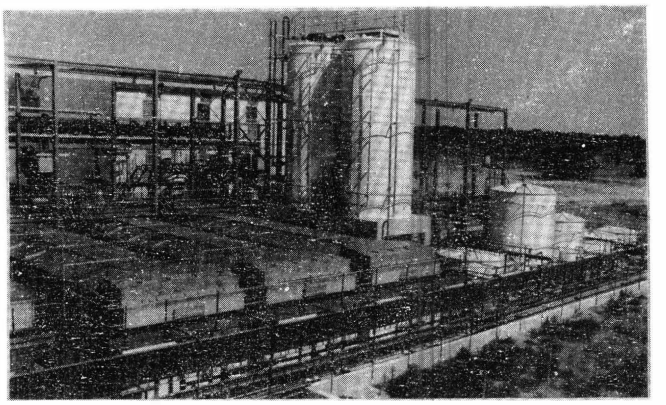

FIGURE 3
VAAL REEFS – GENERAL VIEW

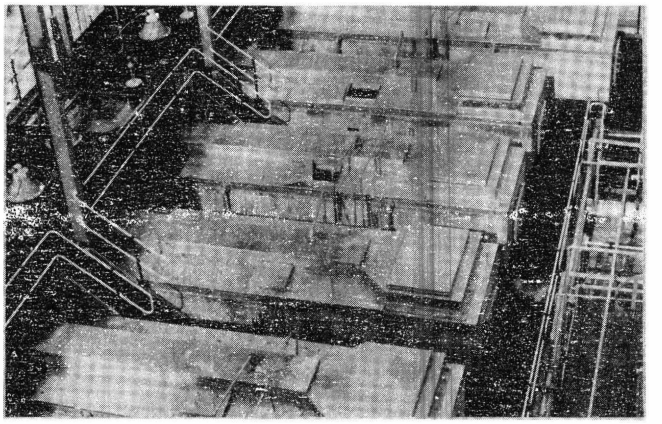

FIGURE 4
VAAL REEFS – STRIPPING MIXER SETTLERS

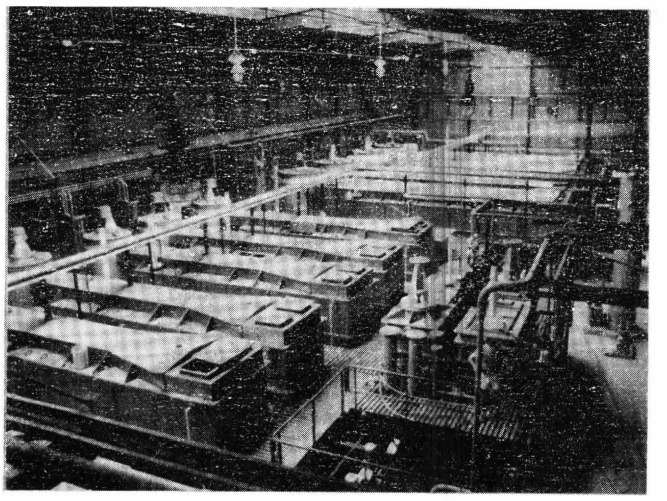

FIGURE 5
MOUNANA – GENERAL VIEW

A PHASE RECIRCULATION IN A CENTRIFUGAL EXTRACTOR

G. I. Kuznetsov, A. V. Kosogorov, A. A. Pushkov, L. I. Shklyar

State Committee for Atomic Energy
Moscow, USSR

Centrifugal extractor with a phase recirculation (1) has been devised on the basis of the onestage extractor (2), fig. 1. Feed organic and aqueous solutions are fed into the mixing chamber 1 and mixed up by the stirrer 3. Then emulsion is transferred by the blade-screw transport device 4 into the separating chamber 5 where it is separated in interplate spaces 6 under the action of centrifugal forces. Separated liquids are transferred in annular collectors for light liquid 7 and heavy liquid 8, then both liquides are driven out of the extractor.

In order to carry out the recirculation f.e. light liquid the part of collector 7 is separated by partitions 9 and connected 10 with mixing chamber.

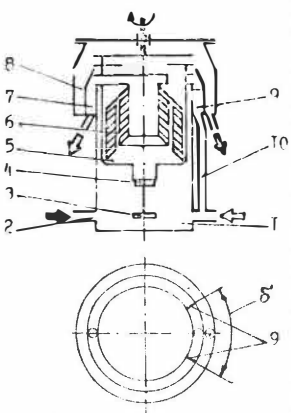

Fig. 1. Centrifugal extractor with phase recirculation.

The needed value of the recirculation $r = Q_r/Q_f$ (Q_r-recirculation flow rate, Q_f-feed flow rate) is provided with the fixation of the partitions under the definite angle: $\delta = 360\ r/1+r$ The flow rate ratio of light and heavy liquids $\alpha = Q_l/Q_h$, recirculation value (r) and the phase volume ratio in the emulsion formed in mixing chamber $\alpha_m = V_l/V_h$ are interconnected by the following dependance: when heavy liquids are recirculated: $\alpha_{mh} = /1+r$ and when light liquids are recirculated: $\alpha_{ml} = (1+r)$. The validity of these relations has been experimentally confirmed.

The recirculation of the dispersed phase increases interface surface and consequently effiency of mass transfer, if process is carried out in non-equilibrium conditions.

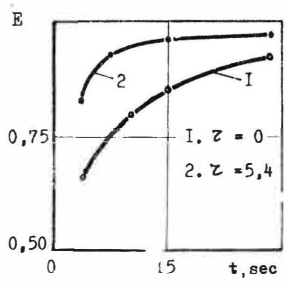

Fig. 2. The dependance of mass transfer efficiency on the time of phase contact, $\alpha = 6,4$.

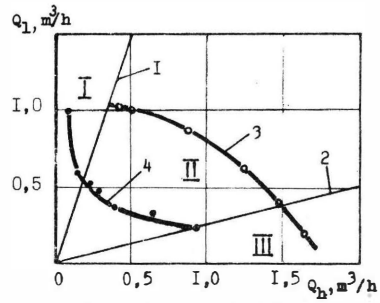

Fig. 3. Variation of Q_l with Q_h; heavy phase entrainment in light phase is constant - 0,05%.

In the system 0,1 M HDEHP in aliphatic hydrocarbons -0,05 MUO_2SO_4 in 0,5 MH_2SO_4 recirculation of the aqueous dispersed phase increased the efficiency from 0,75 up to 0,94 (fig.2) under contact time 7,5sec.

The recirculation can also change the type of emulsion in the mixing chamber and in its turn influences the throughput capacity (fig.3). Depending on the flow rate ratio Q_l/Q_h value different type of emulsions are formed: in zone I - only h/l type, in zone III - only l/h type, in zone II - the formation of both type emulsions is possible. The extractor throughput capacity at constant value of entrainment of heavy phase in light phase (0,05%) is 1,5-2 times as large as in the case of l/h type emulsion (curve 3) than in the case of h/l type emulsion (curve 4).

Thus, correct employment of the phase recirculation in a number of cases can increase throughput capacity and improve mass transfer efficiency especially for the processes with slow kinetics, which depends on interface surface.

REFERENCES:

1. L.I. Shklyar, G.I. Kuznetsov, S.M. Belyakov, A.P. Rosthin, V.A. Elin, V.A. Komarov. USSR Sertificate of Authorship No. 528100.
2. G.I. Kuznetsov, S.M. Belyakov, L.I. Shklyar, A.A. Pushkov. ISEC-80, 1, 207.

GAS DISPERSION IN LIQUID-LIQUID EXTRACTION

Ron Priestly and S. Suppiah

University of Birmingham
Birmingham, England

The mass transfer rates in a countercurrent liquid-liquid extraction column are increased considerably by the addition of a gas to the base of the column. In a gas agitated column (1), the gas bubbles rising through the continuous phase enhance the contacting efficiency because of greater turbulence. Hayakawa and Shigeta (2) studied the performance of a gas dispersed spray column where the gas was injected into liquid droplets through the inside of a double tube spray nozzle. The increase in efficiency was explained by the increase in interfacial area per unit volume of the two phase droplets and the increase in mass transfer rate generated by the higher velocity of the droplets.

A Scheibel extrator has been described (3) where the coalescing sections are knitted pads of high and low surface energy materials (stainless steel and polypropylene). It was claimed that the problems associated with phase inversion are avoided by the use of this material.

A study has been made of the performance of an extraction column where the gas injected into the column is dispersed in the organic disperse phase and the column is provided with spaced pads of knitted composite material

THE EXTRACTION COLUMN

The 15 cm diameter column was 270 cm high and fitted with 30 cm diameter settling sections similar to those recommended by Blanding and Elgin (4). The disperse phase distribution was an inverted cone with a face diameter of 15 cm in which were 41 perforations of 4.76 cm diameter. Air was injected into the column via three sintered discs with a pore size in the range 90-150 microns. These discs were equally spaced on a 10 cm diameter circle and located 8 cm above the face of the dispense phase distributor at the centre of the column.

Packing. The column was packed with 10 pads of composite knitted stainless steel/polypropylene spaced on 25 cm centres. Each pad was 10 cm deep and had a voidage of 98.7% and was self supporting on the column wall.

The top settling section was fitted with a coalescing pad of the same material and depth as the packing.

System. The system investigated was kerosine-water-benzoic acid maintained at 25°C by means of a thermostatically controlled heater in the feed storage tanks. The water was untreated (soft) tap water. The kerosine was Esso Blue with the properties as set out in Table 1. The mass transfer measurements were made with the extraction of benzoic acid from the kerosine phase into the water phase. The initial concentration of benzoic acid was maintained at approximately 5 gm/l of kerosine.

Table 1

Relative density at 60°F	0.783
Distillation	
% volume recovered at 160°C	1
% volume recovered at 200°C	12
% volume recovered at 240°C	87
Final boiling point °C	260

OPERATION OF THE COLUMN

The column was operated with a range of water and kerosine flow rates with and without the injection of air.

Observations. Without the injection of air the kerosine droplets formed at the distributor were quickly coalesced as they entered the first pad of the composite knitted material. At kerosine flow rates above ∿10 l/m the kerosine left the packed sections mainly as jets to a length of ∿5 cm before dispersing into discrete droplets. A smaller fraction of the kerosine flow emerged directly from the packed element as discrete droplets. The flooded condition was deemed to have been reached when a stable layer of kerosine formed beneath one of the packing elements.

When air was injected into the column the air bubbles and kerosine droplets ascended separately to the first packed section where the air bubbles very quickly dispersed as much smaller bubbles (< 1 mm diameter) in the kerosine rivulets rising through the packed section. The rivulets emerged from the top surface of the packed section in streams which quickly broke up to form droplets. Most of these droplets retained the small bubbles of dispersed air and rose rapidly to the next packed section. A small fraction of kerosine droplets contained no disperse air and these rose less rapidly to the next packed section. In the range of air flows that was studied, no air bubbles were observed in the continuous aqueous phase. The sketch below illustrates the formation of the two phase droplets at the upper surface of the packing element.

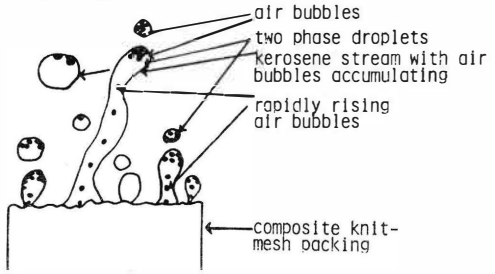

COLUMN CAPACITY

At flow rates approaching the flood point with no air flow the disperse phase droplets coalesced beneath the packed section to form a continuous layer. As the flood point was reached with increasing flow rates, the depth of this continuous layer increased rapidly. In conditions where air was injected into the column, the form of the flooding was identical to that existing with no air flow. Those disperse phase droplets containing dispersed air passed quickly into the packed section, while those droplets containing no dispersed air began to coalesce to form pools of liquid beneath the packed sections.

Effects of ageing. The flooding capacity of the column was measured before and after the column was operated to establish the mass transfer rates. The decrease in the flooding velocities with the ageing of the packing is illustrated in Figure 1. The reasons for this change in the capacity of the packing are not entirely clear. It is possible that the superficial density within a new packed section is variable with more open channels within the bed than would exist after some hours operation. A second reason may be that the surface properties of the packing material have changed with absorption of kerosine in the polypropylene fibres. It is unlikely that the accumulation of solid material in the packed section is responsible for the reduced capacity. The errosive action of the dispersed gas is remarkably effective in maintaining a clean surface.

MASS TRANSFER RATES

The effect of an injection on the rates of mass transfer is illustrated in Figure 2. The Height of a Transfer Unit (H.T.U.) with no air flow falls considerably with increasing disperse phase flow rate. With increasing air flow rates, the mass-transfer rates increase and the H.T.U. is less dependent upon disperse phase flow rates. There are three factors in the improvement in performance of the gas dispersed column:

(a) Increased velocity of the disperse phase. Because there is no air in the continuous phase, the average specific density difference ($\Delta\rho$) between the continuous phase and the disperse phase will be

$$\Delta\rho = \rho_w - \frac{\rho_k}{1 + \beta}$$

where ρ_w = sp. density of continuous phase
ρ_k = sp. density of solvent
β = ratio of air hold up/solvent hold up

Measurements of the air and solvent hold ups showed that the density difference increased to up to ∿0.6 at the lower solvent flow rates.

(b) Increased interfacial area. With air injection the jets of solvent emerging from the packed sections generated a smaller droplet size than was formed without the injection of air. The interfacial area is also increased because of the lower density of the gas dispersed droplet.

(c) Increased internal circulation. It is probable that the gas bubbles rising through the streams and droplets of the solvent increase the circulation of solvent within the streams and droplets.

CORRELATION OF MASS TRANSFER RATES

A Colburn plot (5) of the Overall Height of a Transfer Unit $(H.T.U.)_{ow}$ vs. $\frac{U_w}{U_k m}$ is shown in Figure 3 where:

U_w = water phase velocity
U_k = kerosine phase velocity

$$m = \frac{dC_w}{dC^x_k}$$

COMPARISON OF PERFORMANCE OF GAS AGITATED AND GAS DISPERSED COLUMNS

Mass transfer rates were measured with and without gas agitation in a spray column and a ceramic saddle packed column. These columns were operated with a stable dispersion of kerosine. In both columns the Height of a Transfer Unit is reduced by gas agitation, but there is a reduction in the capacity.

The performance of the gas dispersed column is consistently higher than the gas agitated columns as shown in Figure 4.

CONCLUSIONS

A gas dispersed liquid-liquid extraction column is capable of accommodating relatively high throughputs and high extraction rates over a wide range of flow rates in the water-kerosine-benzoic acid system.

It is not expected that scale-up will be a difficult problem, but other systems capable of generating a disperse phase in a bed of knitted composite material have not been investigated.

REFERENCES

1. J.B. Fernandez and M.M. Sharma. Chem.Eng.Sci. 23, 9 (1968).

2. T. Hayakawa and M. Shigeta. J.Chem.Eng. Japan. 6(6), 545 (1973.

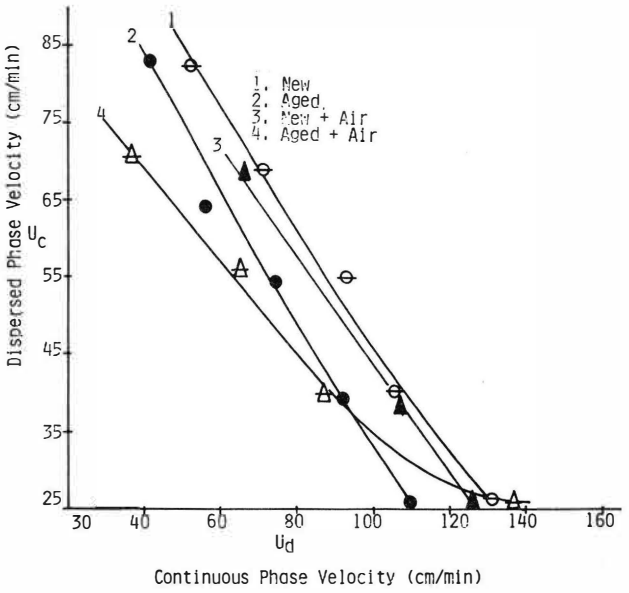

FIGURE 1

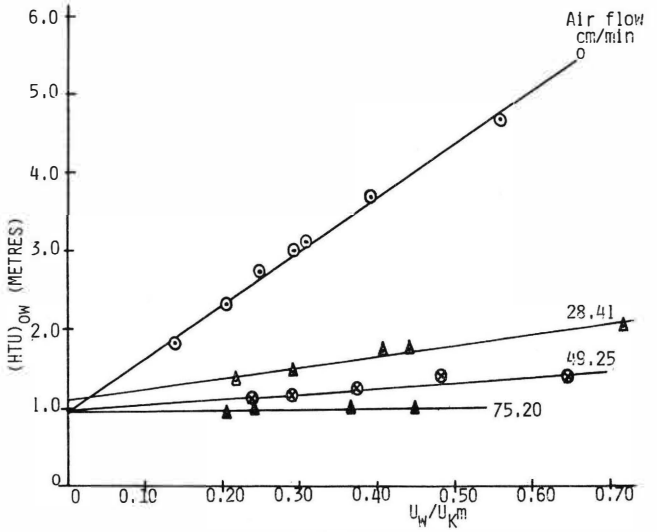

FIGURE 3

3. G.A. Davies, G.V. Jeffreys and M. Azfal. Brit.Chem.Eng. and Process.Tech. 17(9), 709 (1972).

4. F.H. Blanding and J.C. Elgin. Trans.Am.Inst.Chem.Eng. 38, 305 (1942).

5. A.P. Colburn. Trans.Am.Inst.Chem.Eng. 38, 179 (1939).

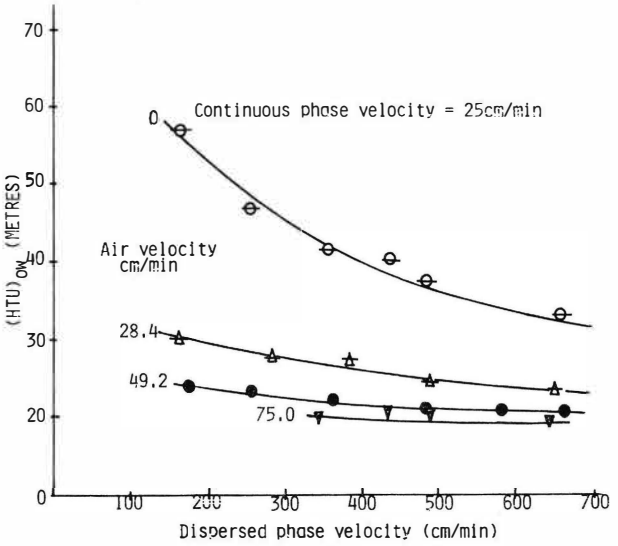

FIGURE 2

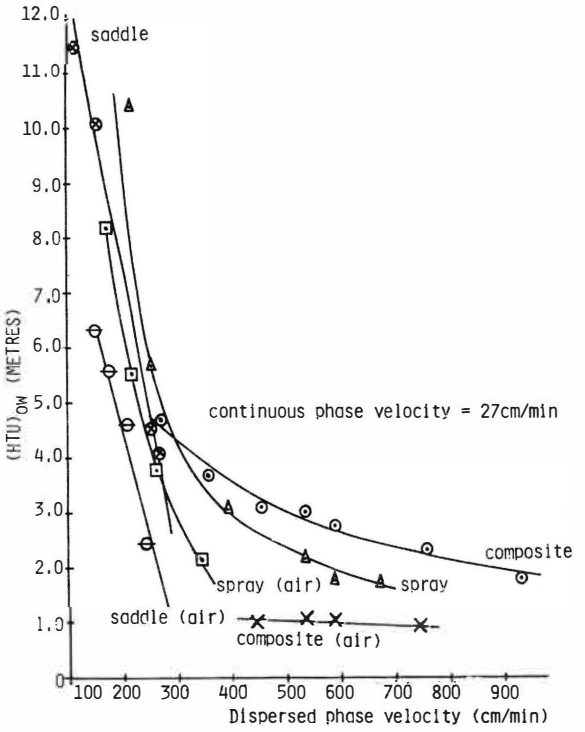

FIGURE 4

THE STUDY OF PERFORMANCE OF MASS TRANSFER IN SIEVE PLATE EXTRACTION COLUMN WITH SWIRL FLOW AND TRAPEZOIDAL PULSE

Dai Wiezhi, Tai Derong, Hu Xien, Wan Chunrong
Yang Lichun, Qi Xiaotian, Duan Shihao and Fan Shuru

Tsinghua University
Beijing, China

INTRODUCTION

Efficiency of mass transfer in pulsed column can be increased when the sine pulse was replaced by trapezoidal pulse(1), because it strengthens dispersion and coalescence of drops and decreases the axial mixing in the column. In order to improve the performance of the column Hafez(2) put a special "fan plate" between the sieve plates.

This work synthesizes the advantages of trapezoidal pulse and fan swirl flow plate. The apparent height of a transfer unit (HTU) is about 20 cm. The maximum total flow rates of two phases is about 500 $l/dm^2 \cdot hr$.

DESCRIPTION OF EXPERIMENT

Extraction column is made of glass. Its inside diameter is 50 mm. Effective height is 80 cm. The holes of sieve plates are nozzle. It is made of stainless steel. Parameters of plates are as follows:

Type of plate	diameter of hole (mm)	free area (%)
a	3.0	23.0
b	2.0	22.1
c	1.7	16.0
d	2.0	10.4

The swirl flow plates were produced by bending the blades of a radially cut disc made of 1 mm thick stainless steel plate, and it can generate a rotary flow when pulse acted.

The operation system is 30% TBP(kerosene)-HNO_3-water. Operation temperature is 25°C.

The trapesoidal pulse is produced by producer of trapezoidal wave. Value of HTU is calculated from the concentrations of nitric acid in the top and bottom of the column. Swirl flow plates are aranged between every two sieve plates. It's distance from the lower sieve plate is described by "D".

EXPERIMENTAL RESULTS

The value of HTU was determined under different conditions such as type of plate, flow ratio, amplitude and frequency of pulsation etc. Data are given in the pages that follow.

The distribution of nitric acid between 30% TBP(kerosene)-water is determined at 25°C. When the concentration of nitric acid is from 0.8N to 2.0N the distribution can be expressed as follows:

$$y^* = 0.2445x^* - 0.0253$$

where y^* is concentration of nitric acid of organic phase in equilibrium (N)

x^* is concentration of nitric acid of aqueous phase in equilibrium (N)

The experimental results are as follows:

1. Effect of swirl flow plate on HTU

The tests were made withfour different kinds of plates. Results show that the value of HTU decreases about 10-20% when plate type b,c,d with swirl flow plates were used.

2. Effect of position of swirl flow plates on HTU

These tests of changing distance of swirl flow plates (value D) were carried out with plate type d. Results show that the efficiency of mass transfer is higher when "D" is 2 cm.

3. Effect of angle θ of swirl flow plate on HTU

Effect of four different angles θ was determined with plate type d. Results show that value of θ effects the value of HTU obviously.

4. Effect of spacing of plates (ht) on HTU

The value of HTU were determined with plate type d in different ht. Results show that spacing of plates ht has little effect on the value of HTU.

5. Effect of amplitude and frequency

Results show that the effect of amplitude and frequency of pulsation on the value HTU is negligible.

6. Effect of total flow rate on HTU

The value of HTU changes a little when the total flow rates change at constant flow ratio (R = O/A = const.). The results show that pulsed column with trapezoidal wave has good operation behavior and its stability is better than that of pulsed column operated with sine pulse.

7. Effect of swirl flow plate on throughput

When the swirl flow plates are put in the column, the throughput of the column increases. The total flow rates of two phases can attain to 500 $l/dm^2 \cdot hr$. Thus, it means that stable operation range of column is extended and operation performance is improved.

CONCLUSION

1. Pulsed sieve plate column with trapezoidal wave can be operated in mixing-settling region. The efficiency of mass transfer increases in such column and the value of HTU will attain to 20 cm.
2. After puting swirl flow plates, swirl flow is produced and coalescence of droplets is strengthened and axial mixing decreases in the column. So the value of HTU will reduce about 10-20%.
3. The throughput of pulsed sieve plate column with trapezoidal wave and swirl flow increases. The operation stability of the column is improved.
4. Trapezoidal pulsed column may be operated at low pulse frequency and the energy cosumption is reduced.

REFERENCES

1. 村田・芳治, 化学工学, 31, 261, 1967.
2. Hafez M.M, Baird M.H.I, and Nirdosh I.,"Can. J. Chem. Eng." 57, 150, 1979.

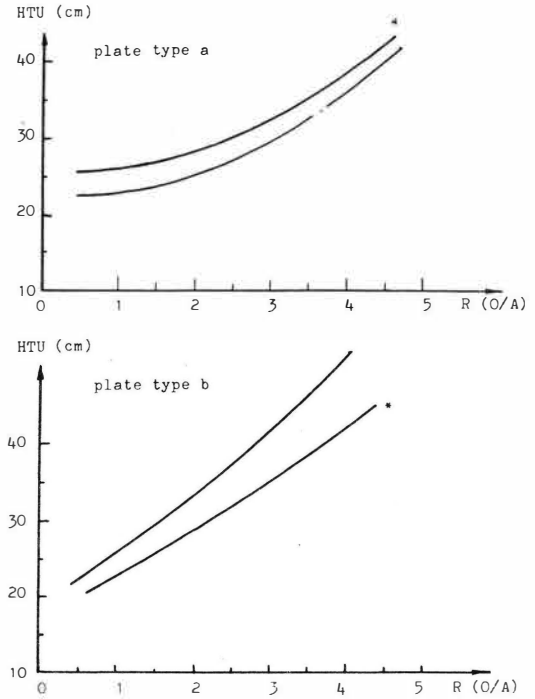

Fig. 1 Effect of swirl flow plate on HTU for plate types a and b.
* with swirl flow plates

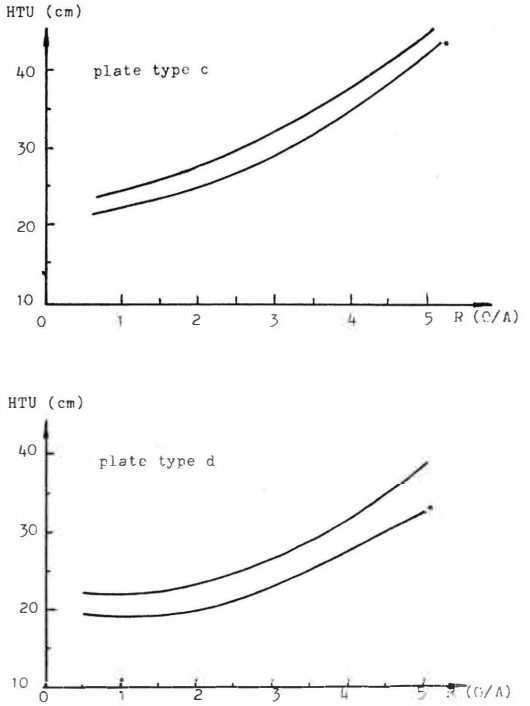

Fig. 2 Effect of swirl flow plate on HTU for plate type c and d.
* with swirl flow plates

A MODIFIED ROTATING DISK CONTACTOR WITH WIRE MESH COALESCERS

F. G. Zhu, X. D. Ni and Y. F. Su

East China Institute of Chemical Technology
Shanghai, China

A modified rotating disk contactor (MRDC) has been installed simply by inserting "rings" made of wire mesh in alternate compartments of a conventional rotating disk contactor (RDC) of 100mm diameter and 1.8 metre total height. Each ring is placed closely against the wall of the column and on a level with the rotating disk plane in order that the wire mesh may promote frequent coalescences and surface renewals when the dispersed droplets formed travel a certain distance and impinge onto it. A section of MRDC is shown in Fig. 1.

Due to the difficulty of making reliable measurements in the dispersed phase axial mixing experiments, a drop phase collector and tracer measuring devices have been designed to permit continual sampling and recording.

HYDRODYNAMICS

The result of hydrodynamic study reveals that only above certain rotating intensity, MRDC behaves quite differently from RDC and shows its unique properties as follows:

Hold-up As shown in Fig. 2, at low rotating speeds, no perceptible difference of dispersed phase hold-up x between two contactors is detected. But as rotating speed increases, the separations of the curves for MRDC from those for RDC are observed to begin at certain points which depend upon the cases whether any solute is present or in which direction the solute is transferring. At still higher rotating speeds the pair of the curves for each case diverge, i.e., the difference of dispersed phase hold-up x between two contactor increases continuously.

Average drop size Sauter mean drop diameter at any rotating condition is always larger in MRDC than in RDC due to the coalescence between droplets, when they impinge against, trap in and squeeze through the wire mesh rings before leaving it. Fig. 3 shows the case as n-butyric acid is transferring from dispersed kerosene phase to aqueous phase. The factor of increase in d_{32} may reach 1.3-1.4 at high rotor speeds.

Total throughput At low rotor speeds, the flow characteristics in MRDC do not differ from those in RDC, and the total throughput of the former is lower than the latter due to the reduction of a certain portion of the column volume occupied by the solid wire mesh. Whereas at high rotor speeds, the wire mesh coalescing rings begin to play an active role and become ever more important, and then the case is reversed as shown in Fig. 4.

Characteristic velocity Due to the coalescing and perhaps also hindering effect of wire mesh rings on the flow in MRDC, the characteristic velocity U_o is somewhat smaller than in RDC under similar conditions. The relationship between phase flow rates (U_d and U_c) and dispersed phase hold-up (x) has been found no longer to follow the correlation of Thornton et al. (1) but can be described by a similar expression proposed by Misek (2):

$$U_d/x + U_c/(1 - x) = U_o(1 - x)\exp(zx) \tag{1}$$

where z is a "coalescence index" and equals 1.8. This means the characteristic velocity is lowered by a factor of $e^{1.8x}$ in comparison with RDC.

Correlations for evaluating drop characteristic velocities with and without mass transfer in MRDC are similar to those given by Laddha et al. for RDC (3). However, a transition region has also been observed to exist as reported by Zhang et al. (4).

In the high rotor speed region, where the wire mesh rings play an important role, the unique properties of MRDC become predominant. The following correlation and Table 1 are proposed to calculate the characteristic velocity U_o in this region:

$$\frac{U_o}{\left(\sigma\Delta\rho g/\rho_c^2\right)^{0.25} G_f} = C_1 Fr^{C_2} \cdot \psi^{C_3} \tag{2}$$

where σ - interfacial tension, N/m.
ρ_c - density of continuous phase, Kg/m^3.
$\Delta\rho$ - density difference between phases, Kg/m^3.
μ_c - viscosity of continuous phase, NS/m^2.
G_f - taken to be the same as that of RDC, and equal to $(H/D_R)^{0.95}(D_S/D_R)^{2.1}(D_R/D_T)^{2.4}$
F_r - $D_R N^2/g$.
ψ - $(\sigma^3\rho_c/\mu_c^4 g)^{0.25}(\Delta\rho/\rho_c)^{0.6}$
H - height of compartment, m.
D_R, D_S, D_T - diameters of rotor, stator openning and column respectively, m.
C_1, C_2, C_3 - constants, see Table 1.

Table 1 Constants in Eq. (2)

C_1	C_2	C_3	$Fr^{-1}\psi^{0.5}$	direction of transfer
0.128	-0.88	1	≤ 13	d → c
0.0061	-0.91	2	≤ 16	no transfer
0.059	-1.04	1	≤ 21	c → d

AXIAL MIXING

Data on axial mixing of both phases have been treated by backflow model and the backflow ratios, f and s, have been correlated according to Murakami et al. for continuous phase (5).

Continuous phase axial mixing **An empirical equatinon for** the backflow ratio f of the continuous phase **in** MRDC was obtained by correlating 104 experimental points using optimization method and has been shown to have a similar form to that of Murakami:

$$f = 0.144\,(D_R N/U_c)^{0.71}(U_d/U_c)^{0.48}(H/D_T)^{-0.6}(D_R/D_T)^{2.5}\left[(D_s^2 - D_R^2)/D_T^2\right]^{0.6} \tag{3}$$

In comparison with the calculated values from the model for RDC given by Murakami, all experimental points of the present investigation only have values from 40 to 50% of the former. The decrease of axial mixing in continuous phase seems to be due to that the wire mesh rings act as small baffles.

Dispersed phase axial mixing By using highly sensitive automatic device, smooth E(t) curves for dispersed phase were obtained. Experimental values were treated in similar manner to that used in continuous phase axial mixing and the backflow ratio s may be expressed as

$$S = 0.134\,(xD_R N/U_d)^{1.13}(D_R/D_T)^2\,(D_S^2 - D_R^2)/D_T^2 \tag{4}$$

Because of scarcity of reliable data of dispersed phase axial mixing, the data from MRDC can only be compared with those obtained from parallel runs in RDC and the line given by Strand et al. (6). The present data for MRDC lie slightly below those for RDC in parallel runs but much higher than the line of Strand et al. It is interesting to note that the plot of experimental data give some clue of segregation of experimental points according to cases with and without mass transfer and the direction.

COLUMN EFFICIENCY

Experiments were carried out for water-kerosene system with butyric acid as transferring solute. The column efficiency was expressed as number of theoretical stages per metre by **calculating from measured concentrations at inlet and outlet of both phases.**

In comparison with RDC, the enhancement of column efficiency of MRDC is strongly dependent upon the direction of transfer, namely, with kerosene as dispersed phase, about 10% increase for the transfer of butyric acid from kerosene to water and as high as 100-150% increase for transfer in the opposite direction as shown in Fig. 5. The greater enhancement in column performance in one direction than in the opposite may be explained by Marangoni effect. When interfacial tension decreases with increasing solute concentration and the solute is transferring from the drop phase to the continuous, the natural coalescence between adjacent drops may occur and the use of coalescer is of **limited** help. On the other hand, if the same solute is transferring in the reversed direction, adjacent drops will tend to separate from each other, only by the aid of coalescer, such as wire mesh ring as we used, their coalescence is greatly promoted. In spite of the appreciable enhancements in column performance of MRDC, the measured power consumptions under corresponding operating conditions are practically the same in both contactors.

MASS TRANSFER COEFFICIENT

From the volumetric coefficient $K_{od}a$ calculated from flow rates and backflow ratios by the method suggested by Hartland and co-worker (7) and total interfacial area aV obtained from Sauter mean drop diameter, "true" mass transfer coefficients have been evaluated and compared with theoretical predictions in Fig. 6, in which the ratio $K_{od}/K_{od,s}$ is plotted as a function of Peclet number, $d_{32}U_s/D_d$.

An empirical correlation was obtained by using least squared polynomial regression analysis to be

$$K_{od}/K_{od,s} = 0.257 \times 10^{-14}Pe^3 - 0.920 \times 10^{-9}Pe^2 + 0.156 \times 10^{-3}Pe - 0.277 \tag{5}$$

$$R = 0.965$$

where K_{od} - overall mass transfer coefficient based on dispersed phase, m/s.
$K_{od,s}$ - overall mass transfer coefficient based on dispersed phase calculated from stagnant drop model, m/s.
Pe - drop Peclet number, $d_{32}U_s/D_d$.
d_{32} - Sauter mean diameter, m.
U_s - slip velocity, m/s.
D_d - solute diffusivity in dispersed phase, m^2/s.
a - interfacial area of contact between two phases, m^2/m^3.
V - effective column volume, m^3.

Fig. 6 and Eq. 5 indicate that the present experimental points lie on a smooth and continuous curve between theoretical predicted line representing fully turbulent drop model of Handlos-Baron (8) and experimental line obtained by Zhang et al. (4) from RDC. The experimental values are much higher than those of RDC under corresponding drop Peclet numbers and are as high as 70% of those calculated from Handlos-Baron model.

REFERENCES

(1) J.D. Thornton and H.R.C. Pratt, Trans. Inst. Chem. Engrs., 31, 289 (1953).

(2) T. Misek, Coll. Czech. Chem. Comm., 28, 426 (1963); T. Misek and J. Marek, Brit. Chem. Eng., 15, 202 (1970).

(3) G.S. Laddha, T.E. Degaleesan and R. Kannappan, Can. J. Chem. Eng., 56, 137 (1978).

(4) S.H. Zhang, X.D. Ni and Y.F. Su, Can. J. Chem. Eng., 59, 573 (1981).

(5) A. Murakami and A. Misonou, Int. Chem. Eng., 18, 16 (1978).

(6) C.P. Strand, B.R. Olney and H.G. Ackerman, AIChE. J., 8, 252 (1962).

(7) S. Hartland and J.C. Macklenburgh, Chem. Eng. Sci., 21, 1209 (1966).

(8) A.E. Handlos and T. Baron, AIChE. J., 3, 127 (1957).

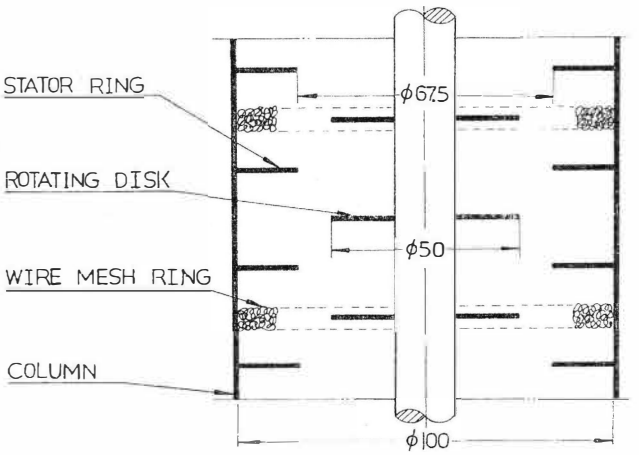

FIG. 1 MODIFIED ROTATING DISK CONTACTOR

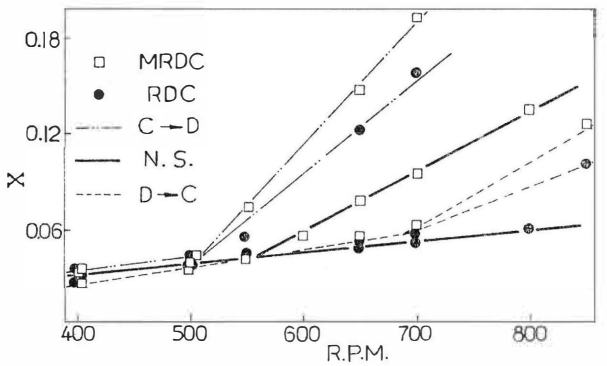

FIG. 2 COMPARISON OF HOLD-UP

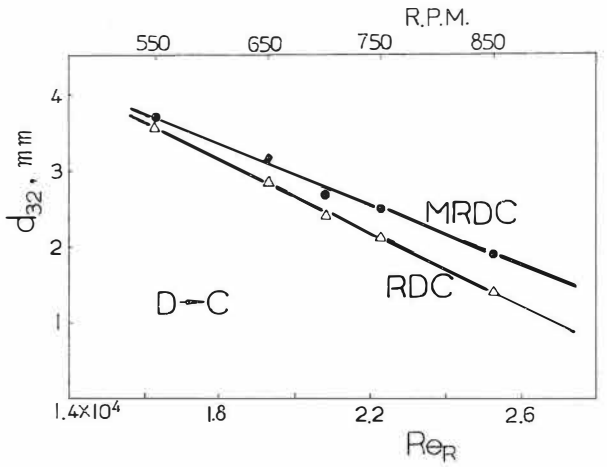

FIG. 3 COMPARISON OF MEAN DROP DIAMETER

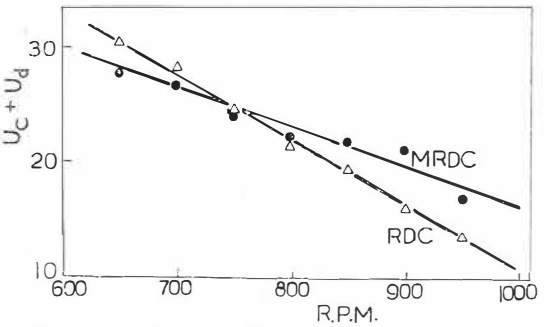

FIG. 4 COMPARISON OF FLOODING LINE

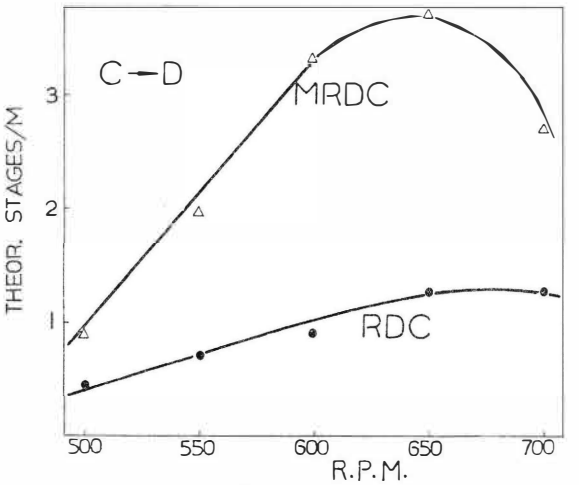

FIG. 5 COMPARISON OF COLUMN EFFICIENCY

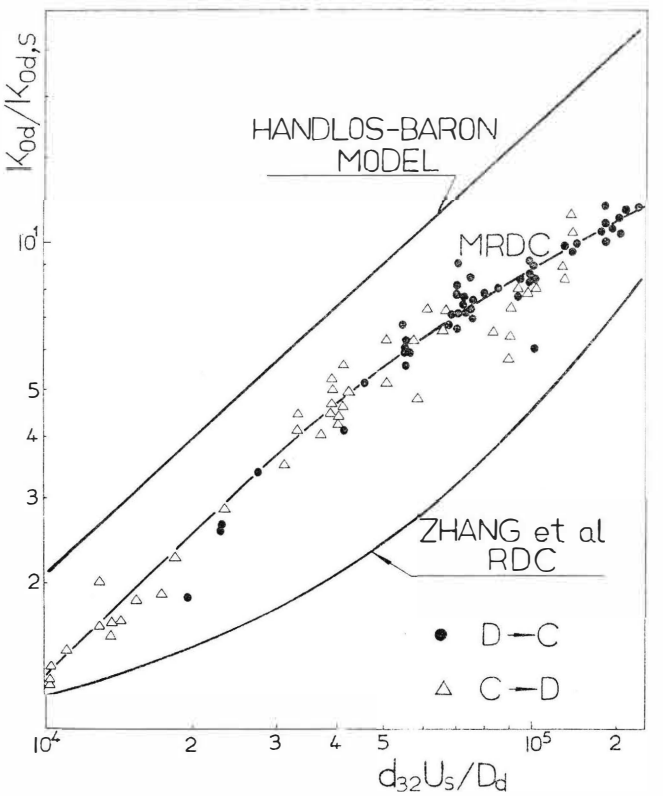

FIG. 6 CORRELATION OF MASS TRANSFER COEFFICIENT

SULZER STATIC MIXERS AS A PACKING IN LIQUID/LIQUID EXTRACTION

S. J. Jancic, F. J. Zuiderweg and F. Streiff

Laboratory for Process Equipment
Delft University of Technology
Leeghwaterstraat 44, 2628 CA Delft
The Netherlands

Sulzer Brothers
Mixing Processes VK/0634
CH-8401 Winterthur, Switzerland

INTRODUCTION

It is generally accepted that Sulzer static mixers promote radial mixing and that this leads to nearly plug flow characteristics in single phase mixing applications. This fact alone implies that the mixer is potentially suitable as a packing in countercurrent contacting and it's modified form found already application in low pressure distillation. The object of this study is to asses the applicability of Sulzer static mixers as a packing in liquid/liquid extraction. The favourable radial mixing properties of the packing are expected to contribute to a more uniform profile of countercurrent two phase flow across the column diameter. This in turn leads to a reduction of dead space and channelling and this should hold even in columns featuring large diameter. This property simplifies procedures involved with scale-up and makes it possible to evaluate the column height from small scale experiments. Such procedures should then be almost independent of column diameter and this feature is almost invariably extraneous to most large scale design configurations for liquid/liquid extraction. Due to the absence of any moving parts the packing is potentially suitable for large scale extraction duties involving high temperatures and pressures as well as process media undergoing pronounced changes in physical properties, especially in interfacial tension.

Results of preliminary studies have shown that Sulzer static mixers are suitable for liquid/liquid contacting and that the throughput capacity of the packing is sufficiently high to cope with large scale production duties. This justified further research in this direction with objective to derive design criteria with reference to packing capacity, axial mixing and mass transfer.

EXPERIMENTAL

The experimental work in this study has been performed in a 0.1 m diameter, 10 m long column with a packed height of 6 m. The column has been packed with Sulzer static mixers of the standard SMV geometry. The column was made of glass and stainless steel was used as packing material. The two phases were fed to the column by two gear pumps fitted with variable speed motors. Both phases were first pumped through filters in order to remove mechanical impurities and then were allowed to pass through plate heat exchangers in order to maintain the test temperature constant. The drop phase coalesces to be withdrawn first to the settling tank and then to the storage tank.

The column ancillaries have been designed to ensure trouble-free liquid/liquid contacting both with and without mass transfer. For this purpose two 2 m^3 feed and two 2 m^3 storage tanks have been built. The column featured facilities to operate either with light phase dispersed or with heavy phase dispersed. The column control system ensured that the two phases after leaving the column reach their respective storage tanks for either mode of operation.

The experiments have been performed in and without the presence of mass transfer, for both directions of transfer and for light phase both dispersed and continuous. During experimental work the temperature was kept constant at 20°C and the phase ratio, the extraction factor and the level of driving force were varied. The four test systems used in this study are listed in the Table of Figure 1 together with main physical properties.

PACKING CAPACITY

The relative velocity, U_r, is a simple and reliable measure of the throughput rate in the column and it's dependence on superficial continuous phase velocity, V_c, dispersed phase velocity, V_d, and dispersed phase hold-up is given by:

$$(1) \qquad \frac{V_c}{1-h} + \frac{V_d}{h} = \varepsilon U_r$$

The hold-up and flooding characteristics have been determined by "stop and measure" method and the results for four test systems used in this study are shown in Figure 1 for conditions where the light phase is dispersed. The Table in Figure 1 shows main physical properties of test system together with observed values of the mean drop diameter. Total capacities at flooding for the same conditions are plotted in Figure 2 against the phase ratio. As expected, n-butanol/water system exhibits lowest throughput capacity of all four systems (40 m^3/m^2h) due to low interfacial tension and consequently smallest drop diameter. Systems toluene/water and kerosene/water feature comparable interfacial tension and drop size buth somewhat differing density difference. For this reason the capacities for the two systems are somewhat different but still considerably higher (100 to 120 m^3/m^2h) than that obtained with low interfacial tension system. The highest capacity of all four systems was obtained with carbontetrachloride/water system (180 m^3/m^2h) due to large density difference. This latter gave rise to high relative velocities which in turn resulted in shear forces acting upon the drops and reducing drop size. Indeed, the Table presented in Figure 1 shows that low density difference and high interfacial tension in case of toluene/water and kerosene/water result in considerably larger drops than the high density and high interfacial tension carbontetrachloride system. Although these latter considerations are correct in qualitative terms, the quantitative assessment remains subject to considerable uncertainties. In order to illustrate this the relative velocity plots shown in Figure 1 are extrapolated to zero hold-up and these values are compared in Table 2 with free falling velocities based upon the observed drop size and the assumption of rigid drops. The results show that the concept of a rigid drop is only usefull in predicting falling velocities of small drops (e.g. n-butanol/water) due to the little hinder they experience in the packing. This approach is demonstrably not valid for larger drops, in which case the concept of a deformable drop undergoing hinder during countercurrent contacting in the packing should be used. In this case, the relative velocity should be formulated as a function of terminal free falling velocity, U_o, dispersed phase hold-up, h, and a parameter accounting for the influence of drop/packing interactions:

$$(2) \qquad U_r = (U_o, h, C1)$$

The terminal free falling velocity, U_o, of a drop having diameter d_p and falling under gravity, g, and density difference, $\Delta\rho$, in a continuum of density, ρ_c, follows from a balance of forces:

$$(3) \qquad U_o = \frac{4}{3}\left[\frac{d_p \, \Delta\rho \, g}{C_D \, \rho_c}\right]^{0.5}$$

where the value for the drag coefficient, C_D, should account for drop deformation.

The drop size can be obtained from previously published (2) correlation for dispersions generated in Sulzer SMV static mixers:

$$(4) \qquad d_p = C_2 \, d_h \, We^{-0.5} \, Re^{0.15}$$

where Weber and Reynolds number are based upon relative velocity, U_r, and hydraulic diameter, d_h. The constant C_2 is different from previously published (2) value for cocurrent flow and should account for the influence of drop/drop interactions, drop/packing interactions and mass transfer on drop coalescence.

Combining equations 2, 3 and 4, and relying upon parameter evaluation from experimental data, yields predictions of hindered falling velocity and these are shown in column 3 of Table 2. The good agreement with experimental values suggests that predicted hindered falling velocities for zero hold-up can be used to predict hold-up and flooding behaviour. Indeed hold-up correlation of Reman (3) and flooding criterion of Thornton (4) gave very successful predictions for the four test systems used in this work (e.g. see Figure 2). Although the agreement with experimentally obtained values is very satisfactory, it may be at least to some extent fortuitious due to limited amount of observations and due to complexity of hydrodynamics involved in liquid/liquid extraction. In view of this, experiment involving industrial liquids undergoing mass transfer of direction and intensity likely to be encountered in practice, remains a prerequisite of successful design procedure.

TABLE 2

test system	terminal velocity (1) for rigid single drops (m/s)	experimental velocity at zero hold-up	prediction for deformable drops undergoing hinder in the packing
n-butanol/water	0.034	0.031	0.035
toluene/water	0.130	0.049	0.056
kerosene/water	0.125	0.096	0.098
carbontetrachloride/ water	0.339	0.138	0.141

AXIAL MIXING

Measurements aimed at determining the level of axial mixing relied upon tracer injection and two point measurement of the tracer concentration as a function of time (5). The axial mixing coefficients were derived from the differences in variance of the concentration-time curves obtained at each point of tracer detection. Because conductivity principle was used the axial mixing in the continuous phase has been derived with organic phase dispersed and the axial mixing in the dispersed phase has been derived with organic phase continuous. The experimental values of continuous and dispersed phase Bodenstein numbers are shown in Figure 3 for the case of n-butanol/water system. The results for continuous phase indicate that the mere presence of the dispersed phase leads to considerably higher degrees of axial mixing than in the case of single phase flow and that there is a negligible further decrease for hold-up values higher than about 0.3. The dispersed phase axial mixing decreases however with increasing dispersed phase hold-up. The results indicate that most practical situations will feature a total mixing height of about 0.2 m.

MASS TRANSFER

The effect of mass transfer on column capacity is shown in Figure 4 for n-butanol/succinic acid/water system. The heights of a transfer unit are plotted in Figure 5 against total capacity for both directions of transfer. The results indicate that mass transfer from drops gives rise to higher throughput rates (about 40%) and to somewhat reduced separation effect (about 30%). This is due to Marangoni effect induced coalescence, which in turn increases drop size and capacity but reduces hold-up and specific surface area. The increase in throughput rates was significantly affected by extraction factor through the influence of initial difference of solute concentration upon interfacial turbulence.

REFERENCES

1. P.N. Rowe, Trans.Inst.Chem.Engrs., No. 39, 175, (1961)
2. F. Streiff, Sulzer Technical Review, No. 3, 108, (1977)
3. C.H. Reman, de Ingenieur, No. 45, 128, (1957)
4. J.D. Thornton, Trans.Inst.Chem.Engrs., No. 35, 316, (1957)
5. R. Aris, Chem.Eng.Sci., No. 9, 266, (1959)

		σ [N/m]	dp [m]	$\Delta\rho$ [kg/m^3]
○	Carbon tetrachloride/water	27×10^{-3}	2.5×10^{-3}	600
●	Kerosene/water	35×10^{-3}	4.5×10^{-3}	192
□	Toluene/water	35×10^{-3}	5.5×10^{-3}	133
■	n-butanol/water	1×10^{-3}	1.5×10^{-3}	129

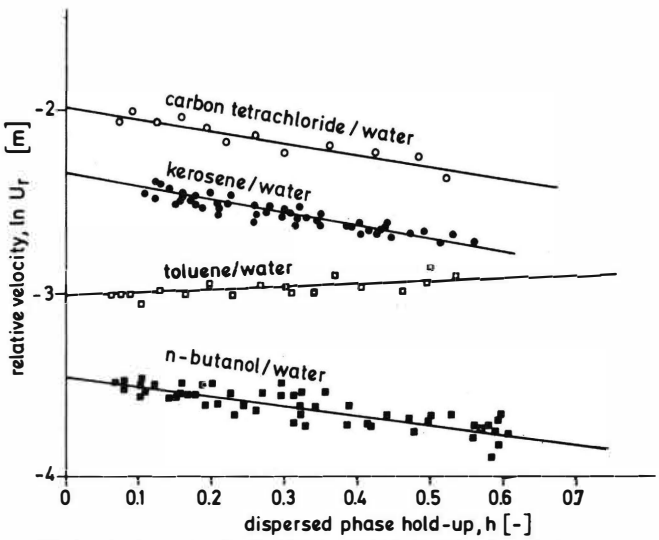

FIGURE 1. RELATIVE VELOCITY AS A FUNCTION OF DISPERSED PHASE HOLD-UP.

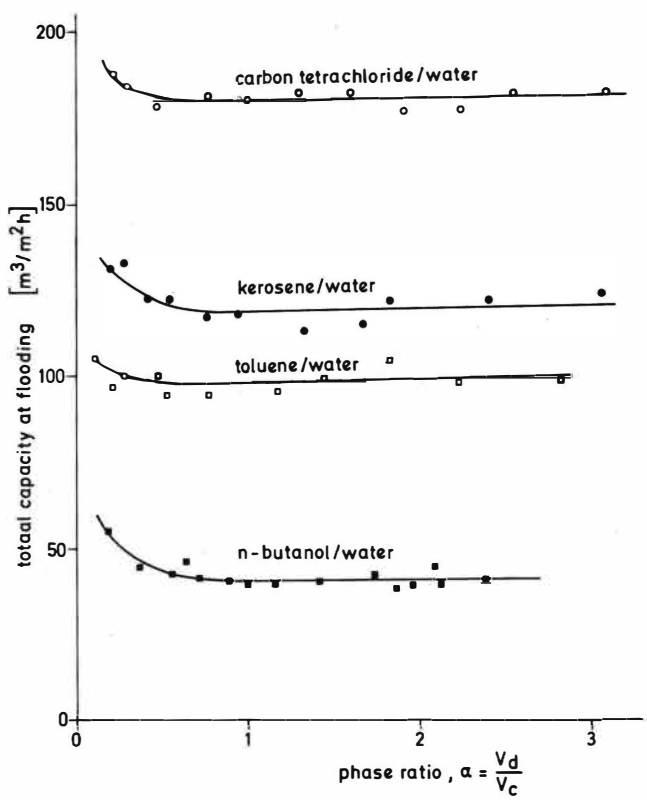

FIGURE 2. TOTAL CAPACITY AT FLOODING AS A FUNCTION OF PHASE RATIO

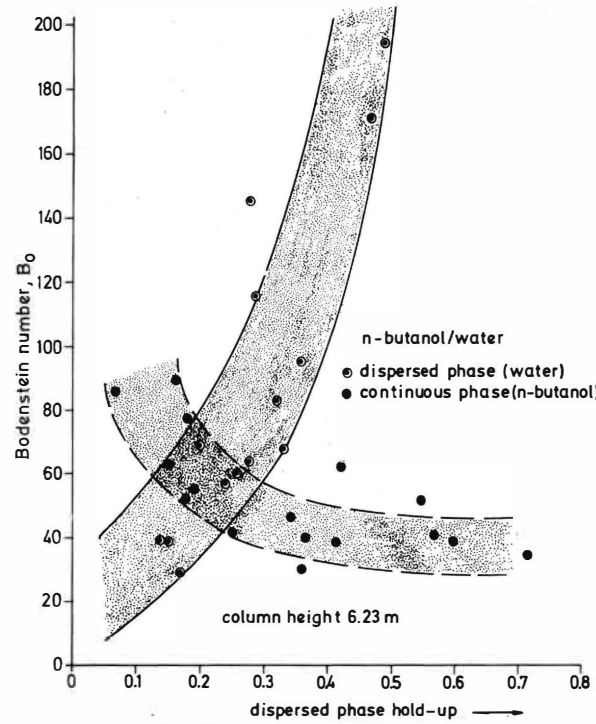

FIGURE 3. DISPERSED AND CONTINUOUS PHASE BODENSTEIN NUMBER AS A FUNCTION OF DISPERSED PHASE HOLD-UP.

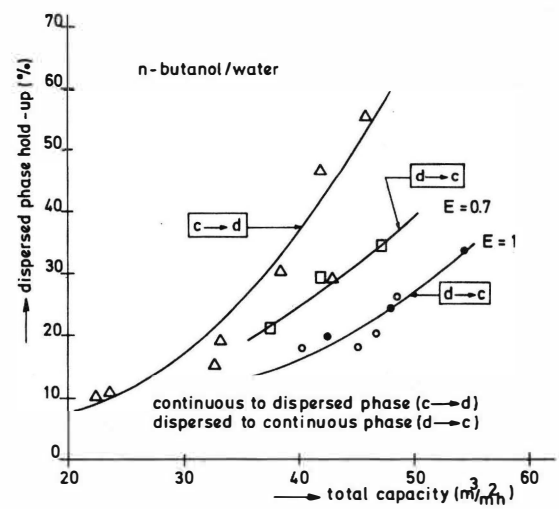

FIGURE 4. EFFECT OF MASS TRANSFER ON COLUMN CAPACITY

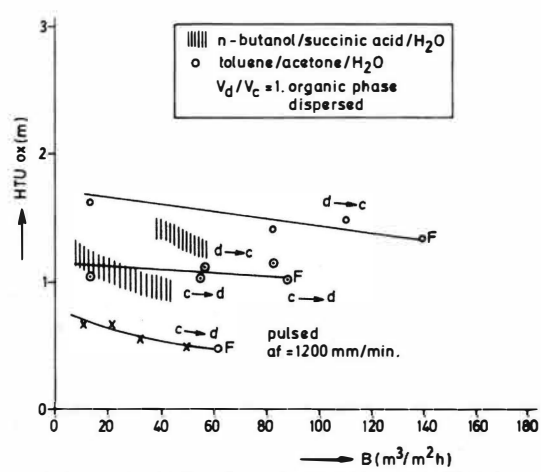

FIGURE 5. EXPERIMENTAL VALUES OF THE HEIGHT OF A TRANSFER UNIT.

PERFORMANCE OF KENICS IN-LINE MIXER IN SOLVENT EXTRACTION

Yi-yuan Li and Chenming Wang

East China Institute of Chemical Technology
Box 312
Shanghai 201107, China

In recent years static mixers have attracted much interest in the field of process equipment and their applications in solvent extraction have been investigated by several authors (1-5). Publications have dealt with Kenics design on hydraulic resistance (5-8), drop size distribution (7, 9, 10), heat and mass transfer (11-17), and mixing of solid and viscous materials (18-20). Of these, Merchuk et. al. (3, 4) compared extraction efficiency of Koch mixer with tubes packed with Intalox saddles made of ceramics and polypropylene, while paying some attention to Kenics mixer and agitated vessel.

In the present study we are trying to attack the problems of pressure drop, extraction efficiency and phase inversion phenomenon in the Kenics mixer.

EXPERIMENTAL

Hand-made copper Kenics elements, 1 mm thick, 21 mm long and 14 mm wide, are set in a 14.4 mm i. d. plexiglas pipe. The same elements coated with polymethyl methacrylate, approximately 0.1 mm thick, are also used. Most of the packed lengths used are 0.90 m long (43 elements). The settling tank is also made of plexiglas. Because of limited working space, an empty return pipe (3.60 m long) of the same diameter has to be set between the outlet of the packed tube and the entrance to the settling tank. Three taps are respectively located at packed lengths of 0.63 m (30 elements) and of 0.90 m (43 elements) and at the entrance to the settling tank. Suitable arrangement has been provided for taking photos of the dispersions. Phase continuity is detected by means of an electric conductometer. Distribution data have been determined for the kerosene-n-butyric acid-water system used for mass transfer.

Pressure Drops are measured under the following conditions:

(1) water flowing through packed length of 16 copper elements;

(2) water flowing through packed length of 43 copper elements;

(3) water-kerosene mixture of volume ratio 1:1 flowing through packed length of 43 copper elements, water continuous;

(4) water-kerosene mixture of volume ratio 1:1 flowing through packed length of 43 organic-coated elements, organic continuous.

All results are represented in Fig. 1.

Phase Inversions are investigated with packed length of 43 organic-coated elements under three conditions:

(1) water-kerosene mixtures without mass transfer;

(2) water-kerosene mixtures, mass transfer organic to water;

(3) water-kerosene mixtures, mass transfer water to organic.

Inversion points away from water-continuous are plotted in Fig. 2.

Mass Transfer is studied with packed length of 43 elements under the following conditions:

(1) from aqueous to organic, copper elements;

(2) from organic to aqueous, copper elements;

(3) from aqueous to organic, organic-coated elements;

(4) from organic to aqueous, organic-coated elements;

(5) from aqueous to organic, copper elements, samples taken at the three taps given above.

Results of (1) and (3) are given in Fig. 3 and those of (2) and (4) in Fig. 4. Pressure drops of (1) and (3) are given in Fig. 5 and those of (2) and (4) in Fig. 6. Results of (5) are discussed only.

RESULTS AND DISCUSSIONS

Pressure Drop. Pressure drop in the empty pipe, ΔP_{ST}, is calculated with the following equation:

$$\Delta P_{ST} = f \frac{L}{d} \frac{\gamma u^2}{2g}$$

where L = pipe length, d = inside diameter of pipe, u = linear flow velocity, γ = specific weight, g = gravity acceleration and f = friction factor.

For Reynolds number Re < 2000, $f = \frac{64}{Re}$

Re > 3000, $f = 0.184\ Re^{-0.2}$

The measured pressure drops in the packed pipe, ΔP_{KM}, are correclated with those in an empty pipe through a factor, K,

$$K = \frac{\Delta P_{KM}}{\Delta P_{ST}}$$

K values are calculated and plotted vs Re, Fig. 1. Fig. 1 also shows K values calculated by the method given by Chen (8), drawn into solid lines. Our K values of 53 to 59 for Re of 2000 to 4000 all agree well with Chen's. Our procedure seems working well, but its feasibility is pending further tests.

All data of pressure drop obtained with water-kerosene mixtures have been grouped according to phase continuity and plotted into two curves (not shown) with pressure drop vs total flowrate. It has been found that these two curves have nearly same curvatures and the one for organic-continuous lies slightly higher than that for water-continuous. This may be due to the wettability between the organic coating and the organic phase and a drag film may exist on the coating.

Phase Inversion. That in static mixers phase inversion is related to material of construction of packings has been mentioned in references (3, 4). The difficulty of getting organic continuous has also been pointed by Tunison (2). Fig. 2 gives three lines of the phase inversion from aqueous to organic, respectively for the conditions: no mass transfer, mass transfer from organic to water and that from water to organic. It can be seen that when mass transfer from organic to water, there is a higher tendency for the organic to be continuous than it is in the reverse direction. This phenomenon coincides with that in Figs.3 and 4, where organic is continuous only when mass transfer is from organic to water and organic-coated packings are used, while in all other cases aqueous phase remains continuous. Thus there seems doubtless that in static mixers there is more tendency for the aqueous to be continuous and the material of construction of packings has some effect on phase continuity. Also from these figures, the effect of the the direction of mass transfer on continuity is worth to be noted.

Since in static mixers high throughput means high turbulence so much as high agitator speed does in agitated vessels, our data in Fig. 2 have been replotted as volume fraction of organic vs total flowrate (not shown). Then it can be found that the aqueous continuous region is enlarged when there is mass transfer. This result agrees with those for xylene-acetone-water and xylene-propionic acid-water systems reported by Sawistowski and co-workers (21, 22).

In view of the general opinion that in solvent extraction operation it is preferred to have the organic continuous in order to diminish entrainment loss and to maintain a low O/A ratio in order to reduce investment and that in static mixers higher flowrate is good for high extraction efficiency, further investigation on phase inversion seems worthwhile to be conducted in order to satisfy these requirements.

Mass Transfer. Figs.3 and 4, representing plots of extraction efficiency vs total flowrate, show that the efficiency increases with flowrate. For these runs, pressure drops are also measured and plotted against the efficiency, Figs. 5 and 6. These figures confirm that both flowrate and pressure drop mean turbulence which promotes mass transfer.

These four series of runs also show that organic-coated packings yield higher extraction efficiency, no matter whichever phase is dispersed and no matter whatever the direction of mass transfer is. It has been pointed in discussion on phase Inversion that even with organic-coated packings there is more tendency for the aqueous to be continuous. It may be that when organic-coated packings are used, more opportunity is provided for surface renewal of the dispersed organic to yield higher efficiency because of wettability.

A series of runs has been done to find whether there is any end effect in static mixers as in packed towers. With aqueous-to-organic mass transfer and copper elements, when the total flowrate varies from 2.90 l/min to 5.90 l/min, the extraction efficiencies at 30 elements are 45.4 to 60.6%, those at 43 elements are 51.4 to 74.1% and 54.8 to 80% at the entrance to the settling tank. Thus it is evident that most of the extraction is accomplished in the section near the entrance and an empty tube can achieve only a little.

Drop Size Distribution. Photos have been taken for the dispersions with high speed camera at 10 μsec exposure. Due to the high volume fractions of the dispersed phase drops are

too crowded for accurate counting and measurement. But the narrow range of drop sizes is obvious.

CONCLUSIONS

Pressure drop in Kenics mixers can be correlated with that in an empty pipe through a parameter which is a function of Reynolds number. A simplified procedure is suggested.

In Kenics mixers the aqueous phase has higher tendency to be continuous at wide range of phase ratio and total flowrates. Material of construction of packings is important both to mass transfer and to phase continuity. Phase inversion is a problem worthwhile for further investigation.

Major portion of mass transfer is achieved at that portion of the packed length more close to the entrance, i.e., the end effect may exist.

REFERENCES

1. G. M. Ritcey and B. H. Lucas, IChemE (London) Symp. Series 42 Paper 12 (1975)
2. M. E. Tunison, Ph. D. Thesis. The University of Wisconsin, (1976)
3. J. C. Merchuk, R. Shai and D. Wolf, Ind. Eng. Chem. Process Des. Develop. 19 91 (1980)
4. J. C. Merchuk, D. Wolf, R. Shai and D. H. White, ibid. 19 522 (1980)
5. W. C. Hazen, Can. Patent 967331 (1975)
6. S. J. Chen, Chem. Eng. Prog. 71 No. 8 80 (1975)
7. S. J. Chen, Proceedings First European Conf. Mixing and Separation Paper D-2
8. S. J. Chen, Kenics Corp. Bulletin KTEK-2 (1978)
9. S. J. Chen, ibid. KTEK-5 (1978)
10. S. Middleman, Ind. Eng. Chem Process Des. Develop. 13 78 (1974)
11. S. J. Chen, Kenics Corp. Bulletin KTEK-3 (1979)
12. W. D. Morris and P. Misson, Ind. Eng. Chem. Process Des. Develop. 13 270 (1974)
13. W. D. Morris and R. Proctor, ibid. 16 406 (1977)
14. C. D. Grace, Chem. and Process Eng. July 57 (1971)
15. Huang Gong-hao, Third Inter-College Symp. Chem. Eng. China Paper C-1-6 (1981)
16. W. D. Morris and J. Benyon, Ind. Eng. Chem. Process Des. Develop. 15 338 (1976)
17. S. J. Chen, Kenics Corp. Bulletin KTEK-6 (1978)
18. S. J. Chen, ibid. KTEK-7 (1972)
19. S. J. Chen, L. T. Fan and C. A. Watson, Ind. Eng. Chem. Process Des. Develop. 12 42 (1973)
20. S. J. Chen, Chem. Eng. March 19 105 (1973)
21. R. W. Luhning and H. Sawistowski, Proceedings International Solvent Extraction Conference 1971 873 (1971)
22. S. I. Clark and H. Sawistowski, Trans. IChemE (London) 56 50 (1978)

Enquiries in connection with this work should be addressed to Professor Chenming Wang at the address on the title page.

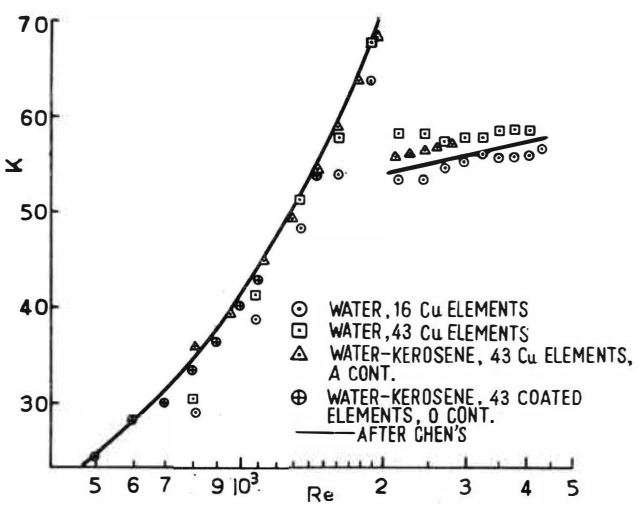

FIG. 1 K AS FUNCTION OF Re

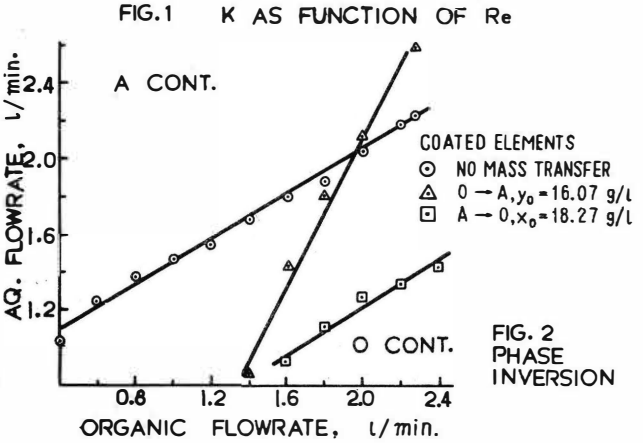

FIG. 2 PHASE INVERSION

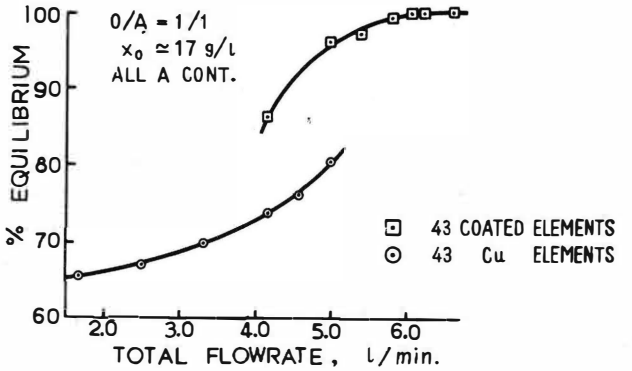

FIG. 3 EXTRACTION EFFICIENCY A → O

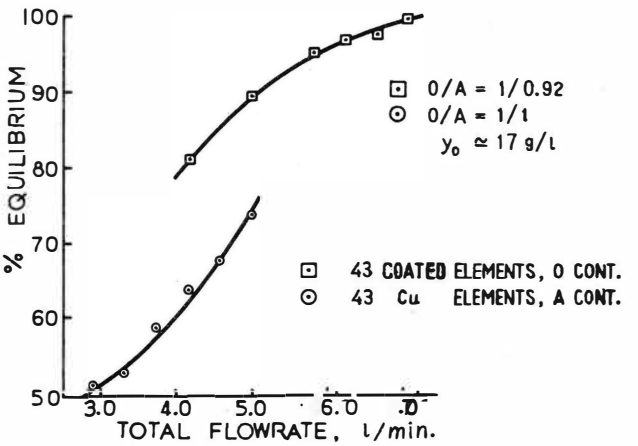

FIG. 4 EXTRACTION EFFICIENCY O → A

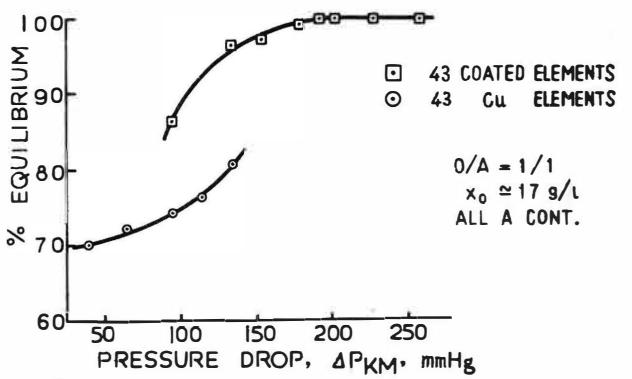

FIG. 5
PRESSURE DROP AND MASS TRANSFER, A → O

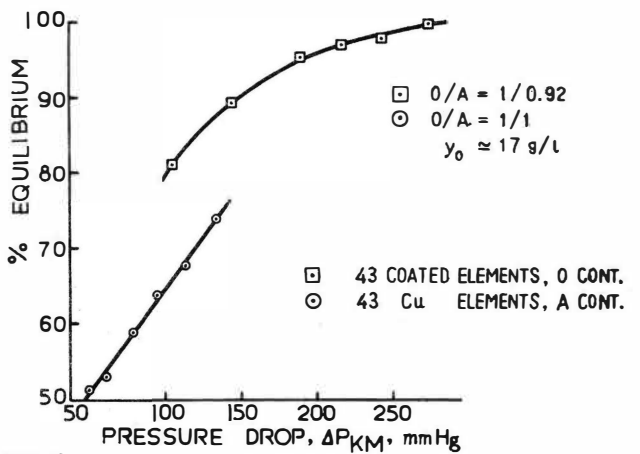

FIG. 6
PRESSURE DROP AND MASS TRANSFER, O → A

COMPARISON OF SOLVENT EXTRACTION EQUIPMENT FOR A MODIFIED PUREX PROCESS

Barbara J. Smith, Peter E. Bain, Larry L. Martella and James D. Navratil

Rockwell International
Rocky Flats Plant, P.O. Box 464
Golden, Colorado 80402-0464 USA

INTRODUCTION

Mixed plutonium and uranium residues are separated and purified at the Rocky Flats Plant (RFP) using a modified PUREX process developed by Navratil and Leebl (1). The process uses a mixer-settler operation and 30 vol % tri-n-butyl phosphate (TBP) in n-dodecane to extract uranium from 5M HNO_3-plutonium III-uranium VI feed solutions. This paper presents the results of column studies comparing the operation of York agitated versus disk extraction columns for the modified PUREX process. They were compared for the number of ideal stages, efficiency, and for aqueous entrainment in the organic continuous column.

EXPERIMENTAL

The agitated column with baffles (or paddle column-PC), and the rotating disc column (RDC) were 4 in. in diameter by 4 ft high. Figure 1 is a schematic showing the mixing and settling chambers for the two column models. Each column was run in the aqueous continuous and organic continuous modes. The test variables were shaft rotational speed, total throughput (aqueous plus organic flow rates), and aqueous-to-organic flow ratio (A/O) (2).

The experimental process equipment for the RDC and PC consisted of a partition and a strip column and four tanks. (See Figure 2.) Fluids were transferred by a fluid metering pump or by gravity. The flow rate was measured by a Brooks rotameter. A Drexelbrook probe was used as a transmitter in a proportional, integral, and derivative controller loop to control the aqueous-organic interface in both columns. The feed solution consisted of 16 g/l uranium-238 in 5M nitric acid and the strip solution was 0.01M nitric acid. The solutions were made up with deionized water and reagent grade chemicals.

The experiments lasted 2 to 6 hours, depending on total throughput. After three column volumes the uranium concentrations were within 90 percent of steady-state condition, as stated by York (3). Uranium in the aqueous and organic phases was analyzed by direct plasma emission and alpha pulse height analysis, respectively. Entrainment of water in the organic phase was determined using Karl Fisher titration.

RESULTS AND DISCUSSION

Using a subroutine from SEPHIS (4), distribution ratio correlations for uranium and plutonium IV at various nitric acid concentrations were written into a computer code for a Hewlett-Packard 85 computer. The number of theoretical stages in a column were calculated by the program using the McCabe-Thiele technique (5). The number of ideal stages for the columns operated in the organic continuous mode and for the aqueous continuous mode are listed in Tables I and II. These Tables also demonstrate how the number of ideal stages vary with rotational speed, A/O ratio, and total throughput for the RDC and PC.

Organic Continuous Mode. In the organic continuous mode the RDC has a maximum of about 3.7 stages and the PC a maximum of about 2.7 stages. The PC maximum is between 2.5 and 2.7 stages, giving an efficiency of 7.5 percent for 36 actual stages. The RDC maximum is between 3.3 and 3.7 stages and has a maximum efficiency of about 21 percent for 18 stages. At the maximum values the height of an ideal stage for the PC is 1.5 ft, and for the RDC it is 1.08 ft. With the PC the maximum occurs between A/O ratios of 0.6 to 1.2. With the RDC the maximum is shifted to higher a/o ratios between 0.8 to 1.3.

Column efficiency in the organic continuous mode increased with increasing rotational speed and decreasing throughput. At higher rotational speeds, entrainment and the risk of forming stable emulsions increased. Another consideration is how the number of ideal stages becomes constant at high A/O ratios, indicating that the percent of uranium extracted decreases as the A/O ratio increases. In Table III the PC shows this decrease, with percent uranium going from 99.93 to 99.43 percent.

Aqueous Continuous Mode. Table II shows that the number of ideal stages increases with increasing rotation speed. The data indicated that the number of stages increased slightly with increasing throughput. For the PC the maximum number of ideal stages occurs at 1.9 stages, and for the RDC the maximum was at 1.75 stages. The difference between the RDC and PC was not as significant as in the organic continuous mode. When operating the PC at maximum efficiency it was extremely easy to switch from steady-state extraction to a dispersed phase hold-up condition. When this happened a foam-like phase traveled down the column starting from the interface. With such an increase in surface area the efficiency increases, and so does the volume of the dispersed phase. Stable emulsions were easier to form in the PC than they were in the RDC.

Entrainment in the Organic. Excessive entrainment in the modified PUREX process will result in more plutonium appearing in the uranium product, or plutonium settling out and filling the surge tanks. In the RDC, entrainment varied from 0.21 to 0.22 vol % water. In the PC it ranged from 0.102 to 0.133 vol % water. The reference value of 0.102 vol % water was used as the equilibrium amount of aqueous in the organic phase. This value was determined by analysis of the organic in Tank 3. The higher rotational speeds used in the RDC experiments resulted in an increase in entrainment.

CONCLUSIONS

The overall comparison shows that for the organic continuous mode the height of an ideal stage is higher for the RDC than for the PC, or the agitated column with packing (1). Entrainment in the organic is minor and the excess water will settle out in the surge tanks before being transferred to the next column. In the aqueous continuous mode there were no significant differences between the two types of columns. Overall the RDC is the best column tested for use with the modified PUREX process for both the aqueous continuous and organic continuous modes.

REFERENCES

1. J. D. Navratil and R. G. Leebl, U.S. DOE Report, RFP-2675, Rockwell International, Golden, CO, (1978).
2. G. H. Reman and R. B. Olney, Chem. Eng. Prog., 51,141, (1955).
3. York Equipment Company, Instruction Manual, Fairfield, NJ.
4. A. D. Mitchell, U.S. DOE Report, ORNL 5471, Oak Ridge Nat. Lab., Oak Ridge, TN, (1979).
5. Treybal, Mass Transfer Operations, 3rd ed. McGraw Hill, NY, 377, (1980).

TABLE I

NUMBER OF IDEAL STAGES FOR THE RDC AND PC ORGANIC CONTINUOUS COLUMNS USING 4 TO 5M HNO_3 AND 11 TO 16 g/l URANIUM

Column	RPM	A/O Ratio	Total Throughput (GPH)	Number of Ideal Stages
RDC	800	0.22	3.0	1.02
		0.40	2.1	0.88
		0.66	2.0	1.21
		0.26	8.3	0.46
		0.46	8.2	0.62
		0.63	8.3	0.79
	1000	0.32	2.5	1.10
		0.38	2.8	1.15
		0.51	3.0	1.17
		0.55	2.1	0.99
		0.84	1.8	3.13
		1.35	2.4	3.70
		1.59	2.2	3.73
PC	250-300	0.46	2.6	1.33
		0.61	1.9	2.31
		0.44	5.6	2.07
		0.57	4.7	2.07
	500	0.40	2.8	2.14
		0.50	2.4	2.14
		0.70	2.0	2.15
		1.00	2.1	1.59
		1.43	2.6	2.04
		1.90	2.9	2.32
		0.66	5.3	2.62

TABLE II

NUMBER OF IDEAL STAGES IN THE STRIPPING SECTION FOR THE RDC AND PC AQUEOUS CONTINUOUS COLUMNS USING 0.01M NITRIC ACID

Column	RPM	A/O Ratio	Total Throughput (GPH)	Number of Ideal Stages
RDC	800	2.50	2.0	0.66
		7.50	3.0	0.94
		3.12	7.0	0.67
		2.12	7.8	0.92
		2.39	7.8	0.89
		3.90	7.8	0.97
		4.00	8.0	0.96
	1100	0.71	1.5	1.91
		0.81	1.7	0.87
		0.95	2.1	1.83
		1.27	2.5	1.99
		1.33	2.5	1.97
		1.00	4.0	1.49
		2.00	7.8	1.00
		2.84	6.8	1.00

TABLE II (cont)

Column	RPM	A/O Ratio	Total Throughput (GPH)	Number of Ideal Stages
		4.13	7.7	0.99
PC	250-300	1.10	3.8	1.00
		3.05	4.3	1.00
		0.98	8.1	1.89
		1.82	9.6	1.12
	500	1.00	4.0	0.81
		2.73	4.4	1.00
		1.00	8.0	1.90
		2.00	9.6	1.40

TABLE III

PERCENT URANIUM EXTRACTED IN 20 VOL % TBP AND n-DODECANE BY THE COLUMNS OPERATED IN THE ORGANIC CONTINUOUS MODE

Column	Throughput GPH	Throughput RPM	Uranium Extracted % A/O < 0.7	Uranium Extracted % A/O > 0.7
RDC	3	800	98.60	---
RDC	3	1000	99.54	99.98
RDC	8	800	96.40	---
PC	3	250	99.97	---
PC	3	500	99.93	99.43

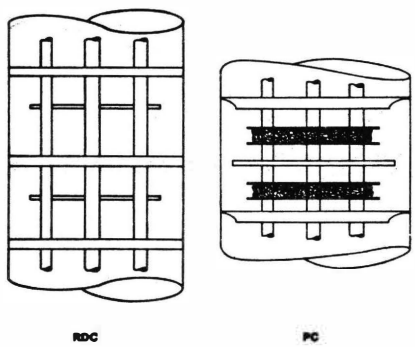

FIGURE 1: Schematic of RDC and PC mixing and settling stages.

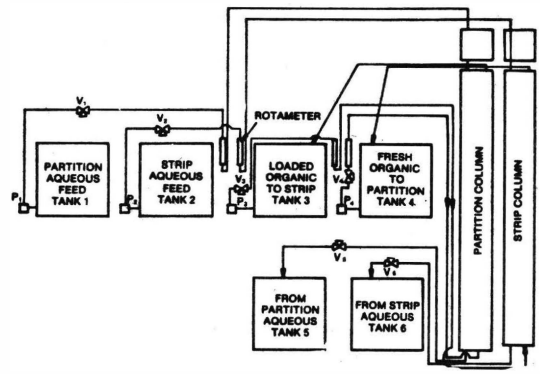

FIGURE 2: Schematic of experimental process equipment.

AMPLIFICATION OF THE SCALE - UP PROCEDURE FOR THE RECIPROCATING PLATE EXTRACTION COLUMN

Andrew E. Karr

Chem-Pro Corporation
Fairfield, New Jersey USA

Designing an extraction column from basic principles without test work is very risky. Some of the main reasons are:

a. The degree of coalescence of droplets in commercial systems cannot be predicted accurately. A rapid coalescence rate increases drop size which, in turn, necessitates high energy inputs to produce satisfactory area for mass transfer. On the other hand, if droplets have little tendency to coalesce the energy inputs have to be minimized. Mass transfer rates may be low and entrainment tends to be high.

b. Physical properties and flow rates may vary throughout the length of the column and the holdup and drop size will vary throughout the length of the column (1) unless some means are taken to overcome these variations. For example, for the reciprocating plate extraction column the plate spacing in the column can be calculated as a function of physical properties and flow rate in order to make the tendency to flood the same everywhere in the column (2). However, the procedure does not take coalescence into account.

c. Most commercial systems are contaminated. The degree and type of contamination can have a marked effect on mass transfer rates (3).

d. Axial mixing data for the dispersed and continuous phases in large diameter columns are not usually available.

Therefore, in general, it is necessary to do test work in a pilot scale column in order to categorize the system. Once the system is categorized and the test column has been optimized with respect to volumetric efficiency (and plate spacing in a reciprocating plate extraction column) the scale-up can proceed (2).

Data on the mass transfer performance characteristics of the reciprocating plate extraction column have been published (2), (4), (5), (6), (7), (8). These papers show that in small diameter columns, 50 to 150 mm, the lowest value of HETS occurs close to the flood point for low interfacial tension systems. For high interfacial tension systems there may be shallow minima in the HETS vs. f curves. As the diameter of the column is increased the minimum in the HETS vs. f curve gets steeper because of increased axial mixing. By employing baffle plates periodically in the plate stack performance is improved because the axial mixing is reduced (5), (6), but the minimum in the HETS vs. f curve persists. The objective of the scale-up procedure (2) is to predict the location of the minimum in the HETS vs. f curve. For convenience the scale-up procedure is given below.

SCALE-UP PROCEDURE

The scale-up procedure for the reciprocating plate extraction column is based on performance data obtained in 25, 76, 305 and 914 mm diameter columns (8), (4), (5), (6).

a. Data are obtained in a 25, 50 or 75 mm diameter column. The diameter selected is frequently determined by the availability of material. Many successful scale-ups have been done directly from the 25 mm column. The 50 and 75 mm pilot plant columns may be used for scale-up development where the production column is in excess of 700 mm in diameter.

b. The optimum performance of the pilot column is determined. The criteria for optimum performance is maximum volumetric efficiency in a column having optimum plate spacing (2).

c. When scaling up from the pilot data the following parameters are held constant: plate spacing, stroke length, and throughput per unit cross-sectional area.

d. The expected minimum HETS in the large diameter column is calculated from the following equation:

$$\frac{(HETS)_2}{(HETS)_1} = \left(\frac{D_2}{D_1}\right)^{0.38} = \frac{H_2}{H_1} \qquad (1)$$

The 0.38 exponent was determined for a high interfacial tension system. Somewhat lower exponents were determined for a low interfacial tension test system and lower exponents were also confirmed by various case histories. The 0.38 exponent is used for reasons of conservatism. This is discussed further below.

e. The corresponding reciprocating speed required is calculated from equation (2).

$$\left(\frac{f_2}{f_1}\right) = \left(\frac{D_1}{D_2}\right)^{0.14} \qquad (2)$$

f. Suitable baffle plates in design and spacing are provided.

The above procedure has been used to scale-up about 60 production columns, all successfully. The largest columns in operation are slightly over 1 meter in diameter.

DISCUSSION

As indicated, the optimum agitator speed corresponding to the minimum in the HETS vs. f curve decreases because of increased axial mixing as the diameter increases. A reduced agitator speed also results in a reduced mass transfer coefficient, holdup and area. However, the reduced mass transfer coefficient, holdup and area would be expected to be the same as the mass transfer coefficient holdup and area in the small diameter test column operating at the same reduced agitator speed because the agitation is relatively uniform and the same over the cross-sectional area of both columns. The difference in actual performance is due to the additional degree of axial mixing in the large diameter column. This is illustrated in Figure 1. As shown, the optimum performance of the production column is at f_2 where HETS is greater than the HETS for the test column.

From the mass transfer performance data in large and small diameter columns one can deduce the increases in the axial mixing coefficients provided an assumption is made regarding the relative values of the axial mixing coefficients for the dispersed and continuous phases. This may be the subject of a future paper. In the meantime it is instructive to examine the present scale-up procedure in more detail.

Power Consumption - The energy consumed is proportional to the cube of the frequency of reciprocation, f (9).

Therefore, from equation (2)

$$\frac{P_2}{P_1} = \frac{P_2/V_2}{P_1/V_1} = \left(\frac{D_1}{D_2}\right)^{0.42} \qquad (3)$$

Introducing equation (1),

$$\frac{P_2/A_2}{P_1/A_1} = \frac{P_2H_2/V_2}{P_1H_1/V_1} = \left(\frac{D_1}{D_2}\right)^{0.42} \cdot \left(\frac{D_2}{D_1}\right)^{0.38} = \left(\frac{D_1}{D_2}\right)^{0.04} \simeq 1 \qquad (4)$$

$$\frac{P_2}{A_2} \simeq \frac{P_1}{A_1} \qquad (5)$$

Thus the power consumption per unit of cross-sectional area is approximately the same for the test column and the production column. Similarly, the power consumption per unit of throughput is approximately the same for the test and production columns. However, the power to the production column is consumed over a greater height of column because the frequency of reciprocation is lower.

Relationship Among Variables - Energy costs have escalated rapidly. Therefore, frequently it is desirable to minimize solvent usage to reduce energy cost. To do this requires the largest number of stages consistent with good overall economics. A 50 mm diameter test column having 3 meters of plate stack will exhibit a large or small number of transfer units or stages depending on the system. Heights of a theoretical stage can vary from less than 15 cm to more than 1.5 meters in relatively rare cases depending on the system and flow rates. As of now, these wide differences are not predictable from the physical properties of the system alone. That is why it is so important to categorize the system by test work (2). For now we shall assume that the 50 mm by 3 meter plate stack will provide an optimum number of stages for most applications. The largest production column that

will be designed and guaranteed at this time is about 2 meters in diameter. The height of the production column plate stack scaled-up from the test column will be

$$\left(\frac{2000}{50}\right)^{0.38} \times 3 = 12.2 \text{ meters.}$$

Figure 2 shows plots of $\frac{H_2}{H_1}$ vs. $\frac{D_2}{D_1}$ and $\frac{f_2}{f_1}$ vs. $\frac{D_2}{D_1}$ up to ratios of $\frac{D_2}{D_1}$ of 40.

As shown above and in Figure 2, for a 40 fold increase in diameter or a 1600 fold increase in throughput, the plate stack height will increase by a factor of about 4. For a 10 fold increase in diameter or a 100 fold increase in throughput the plate stack height will increase by a factor of about 2.4. Similarly, the optimum frequency of reciprocation in the production unit will be 72.4% of that in the test unit for a 10 fold increase in diameter and 59.7% for a 40 fold increase in diameter.

Cost Implications - Let's examine the effect of some conservatism in the scale-up procedure on cost, keeping in mind that some conservatism in process design is usually justified. Based on our cost experience to date, increasing the height of the plate stack and shell of a column of fixed diameter will increase the cost of the column and drive to about the 0.4 power of plate stack height. Thus if the plate stack height is increased by 25% the cost will increase about 9.3%.

NOMENCLATURE

A = Cross-sectional area of column
D = Diameter of column
f = Frequency of reciprocation
H = Height of plate stack
HETS = Height of equivalent theoretical stage
P = Power consumed
p = P/V, power consumed per unit volume
V = Volume of column

Subscripts:
1 - test column
2 - production column

REFERENCES

1. V. Jiricny and J. Prochazka, Chemicky Prumysl 30 (2) 53 (1980)
2. A. E. Karr, Separation Science and Technology, 15 (4) 877 (1980)
3. A. H. P. Skelland and C. L. Caenepeel, AIChE Journal, 18 (6) 1154 (1972)
4. A. E. Karr, AIChE Journal 5 (4) 446 (1959)
5. A. E. Karr and T. C. Lo, "Proc. Int'l. Solvent Extraction Conf.", Society of Chemical Industry (London) 1 299 (1971)
6. A. E. Karr and T. C. Lo, Chemical Engineering Progress 72, 68 (1976)
7. R. N. Sharma and M. H. I. Baird, Canadian Journal of Chemical Engineering 56, 310 (1978)
8. T. C. Lo and A. E. Karr, Ind. Eng. Chem. Process Des. Develop. 11 (4) 495 (1972)
9. M. M. Hafez and M. H. I. Baird, Trans. I. Chem. E. 56, 229 (1978)

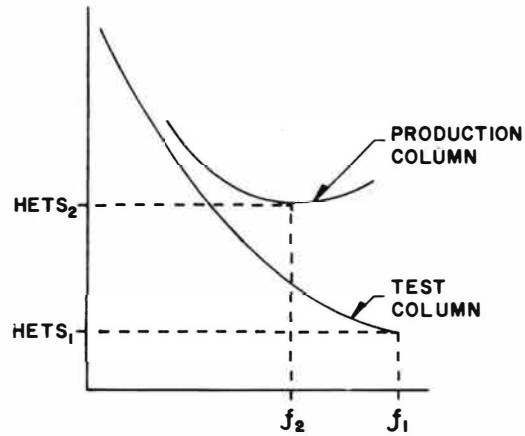

FIGURE 1
EFFECT OF COLUMN SIZE ON OPTIMUM HETS AND f

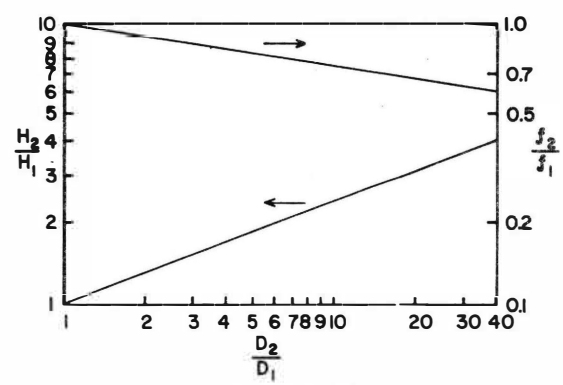

FIGURE 2
VARIATION OF $\frac{H_2}{H_1}$ AND $\frac{f_2}{f_1}$ WITH $\frac{D_2}{D_1}$

PERFORMANCE OF A LIQUID-LIQUID EXTRACTION COLUMN WITH ENHANCED COALESCENCE LATTICE PLATES

L. Steiner, E. V. Fischer and S. Hartland

Swiss Federal Institute of Technology
Department of Industrial and Engineering Chemistry
CH-8092 Zürich, Switzerland

To improve the operating characteristics of existing stirred liquid/liquid extraction columns the agitators of our column were separated by newly developed lattice plates, wetted by the dispersed phase (ISEC 1980). As shown in Figure 1, each element in the lattice is taller than its width and in some cases, the total free area of the plates is more than 90%. The dispersed phase from one agitated stage coalesces with some of the elements and is released again from the other side of the lattice into the next agitated stage. The continuous phase flows countercurrently through the remaining elements (which are not blocked by the coalesced disperse phase) so that plates with variable free area which adjust themselves to different hydrodynamic conditions are obtained. The plates are thus extremely flexible and efficient operation is possible over a wide region of throughputs and phase ratios. A comprehensive investigation into the behaviour of a pilot plant column, using these plates is presented here. This includes the optimization of the agitators and plates as well as the measurement of all relevant parameters such as hold-up,drop size distribution, backmixing in both phases and concentration profiles.

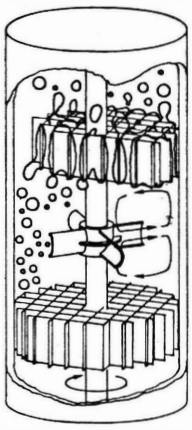

Fig. 1:
Principle of operation of the lattice EC (for Enhanced Coalescence) plates.

Plate Construction:

In a model column containing 3 stages different plate constructions were tested. It was found that the material from which the plates are made must be wetted by one of the phases and the wettability must not change with time. Fluorohydrocarbons (Teflon) were found to be the most suitable when working with dispersed organic phases and ceramics when the water phase was dispersed. The performance of the plates is not controlled by their free area (which changes with the load and phase ratio for each of the individual phases) but rather by the hydraulic diameter of the channels. As the aim of the investigation was to develop a column capable of handling large throughputs, the selected hydraulic diameter of the plates used in the final version of the column was rather high (9 mm). Most of the work was performed with plates made from corrugated, 20 mm wide stainless steel strips, point-welded and teflonized. The coating was stable and survived a two-year period of investigation without signs of deterioration.

To disperse the water phase plates were cut from a commercially available ceramic packing used normally in distillation columns. Good results were obtained with "Kerapack", produced by Sulzer of Switzerland. To improve the rigidity the plates were framed in stainless steel rings.

The Pilot Plant Column:

The column had a diameter of 80 mm and a height of 2.5 m. It contained 33 20mm high plates spaced 40 mm apart. Specially developed agitators with four round blades were placed centrally between each pair of plates and driven with a shaft connected to a motor with variable gear box.The rotational speed varied between 50 and 500 rpm. The column was equipped with the measuring devices shown in Figure 2, enabling simultaneous measurement of all the necessary parameters to be made. The system used was toluene, acetone and water.

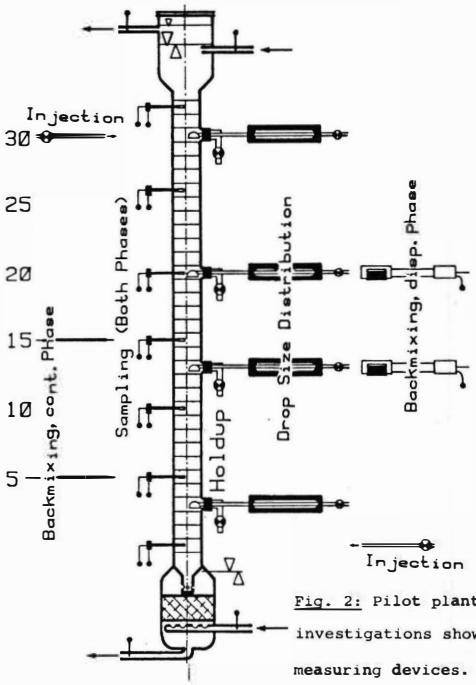

Fig. 2: Pilot plant column used in our investigations showing positions of measuring devices. Stage numbers are given on the left hand side of the figure.

To be able to use the full capacity of the column the bottom part had to be specially constructed. It was found that with very high loadings small droplets accumulated under the lowest lattice plate where the column extends into the lower settler. The droplets coalesced slowly into large ones and eventually flooded the column at this point, even when the extraction section still worked well. The design shown in Figure 3 eliminated these problems. The column ended with a funnel which accelerated the entrained droplets so that they could not accumulate in this section. The droplets were then coalesced on a special packing and reintroduced into the column with the incoming dispersed phase. "Mellpack" organized packing (Sulzer) was found to be particularly suitable for this purpose and also served to produce a uniform dispersion of the incoming lighter phase.

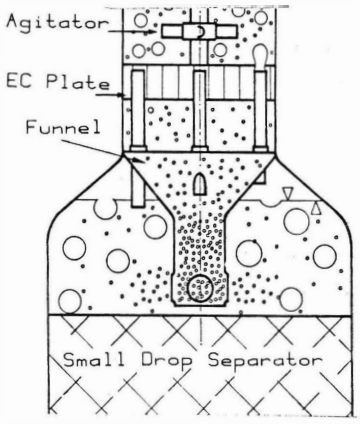

Fig. 3: Construction of the lower settler and the base of the column. The funnel channels the small droplets safely into the settler without flooding the first stage. The dispersed phase rises through the tubes shown in the upper part of the funnel.

Mass Transfer Results:

For each loading and phase ratio the separation efficiency was best at one particular agitation speed. With low speeds the phases were not in sufficiently good contact and the drops were large. Increasing the speed improved the contact, increased the hold-up and made the drops smaller, so the efficiency increased and eventually reached a maximum. A further increase in agitation prevented sufficient coalescence within the plates, increased the axial mixing and the efficiency started to decline. With very high loads flooding occurred before the maximum could be reached. Figure 4 shows the separation efficiency in terms of the total throughput and the direction of mass transfer when the phase ratio of toluene to water was 1.5. The mass transfer direction has a considerable influence on both the separation efficiency and the maximum throughput. When acetone was transferred from toluene to water the maximum efficiency was lower than for the opposite direction of mass transfer but the maximum throughput was higher.

The variation in maximum throughput with phase ratios is shown in Figure 5. With an excess of water the maximum loading was close to 50 m^3/m^2h, but when the organic flow rate was twenty times that of water the column did not flood, even when the total throughput was 160 m^3/m^2h (which was the uppermost limit of the supply system). Similar results were found with ceramic plates when water was dispersed. In this case the performance improved considerably with the excess water phase so that efficient extractants with high selectivity could well be used.

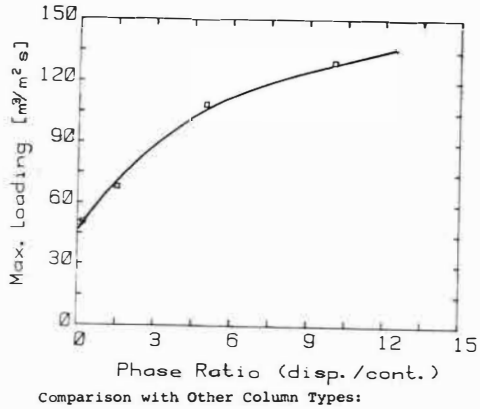

Fig. 5: Dependence of maximum achievable loading on phase ratio. System as in Fig.4 No mass transfer.

Comparison with Other Column Types:

Comparison with other types of equipment is difficult as no standard plate or column exists and the results depend strongly on the internal geometry such as free area, hole diameter or packing. The comparison shown in Figure 6 uses the diagram published by Stichlmair (Chem.Ing.Tech. 1980, 52, 253) for different types of column using the same system as used in our investigation. The working area corresponding to the lattice plate column is superimposed on to the original diagram, showing that its separation ability is similar to that of the more efficient types of agitated column which, however, operate with loadings close to 10 m^3/m^2h. The maximum efficiency of the attice EC plates was obtained with loads between 20 and 30 m^3/m^2h. The main advantage is clearly the large range of loadings in which the separation remains high, so that the same column can be used for different processes and also when the loading varies with time.

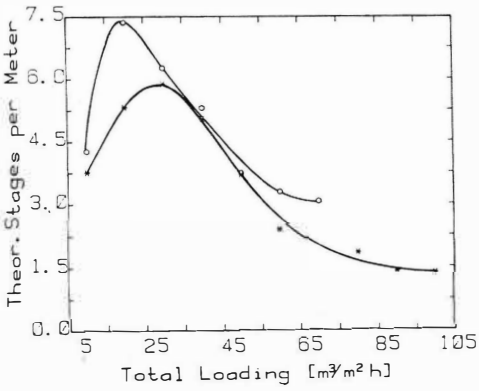

Fig. 4: Dependence of the maximum achievable separation on total loading. System: toluene-acetone-water. (o) transfer from water to toluene (*) from toluene to water. Phase ratio toluene to water was 1.5

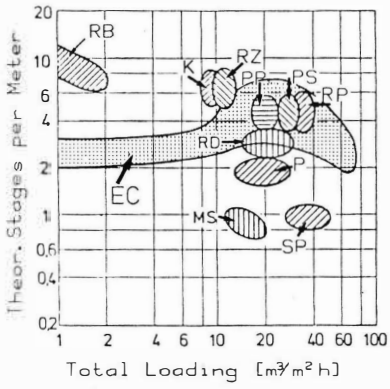

Fig. 6: Comparison of performance of different types of pilot-plant columns with typical geometry.

RB - Raining Bucket
K - Agitated column (Kühni)
RZ - Agitated column (ØVF)
PP - Pulsed Packed column
PS - Pulsed Sieve-plate column
RP - Reciprocating Plate
RD - Rotating Disc
P - Packed column
SP - Sieve Plate
MS - Mixer-Settler
EC - Enhanced Coalescence lattice plates.

CENTRIFUGAL EXTRACTION WITH AXIAL COUNTERCURRENT FLOW OF THE LIQUID PHASES

L. Steiner, K. Gebauer and S. Hartland

Swiss Federal Institute of Technology
Department of Industrial and Engineering Chemistry
CH-8092 Zürich, Switzerland

Centrifugal extractors are frequently employed for liquid systems of low density difference, high viscosity and low interfacial tension. They are particularly useful in cases where a short contact time of the liquids is essential.

Most of the existing centrifugal extractors involve radial countercurrent flow of the liquid phases, the lighter phase moving inwards from the periphery and the heavy one outwards from the centre which restricts the liquid path inside the apparatus. In addition, the centrifugal acceleration, and hence the degree of phase dispersion and coalescence, is a function of the radius. As a result, the number of theoretical stages in a typical centrifugal extractor is usually low. The aim of the present work was to develop a centrifugal extractor for separations requiring many theoretical stages. Axially countercurrent flow was found to be particularly suitable for this purpose as conditions then remain constant and the extractor length can be chosen to suit the degree of extraction required.

PRINCIPLE OF OPERATION

The extractor is essentially a tubular centrifuge with its length much longer than its diameter. The liquid phases are injected at opposite ends and form cylindrical layers covering the rotating wall. A small difference in height drives the phases countercurrently so the thickness of the liquid layers vary slightly along the extractor. In the remaining empty space along the extractor axis a centrally placed shaft with agitators is provided. When the central shaft runs slower than the column the agitators disperse the heavy phase; when faster the light phase is dispersed. The principle of phase contacting is shown in Figure 1. As shown in Figure 2, the mixing zones are separated by coalescence sections with inlays connected to the column wall where the liquids are accelerated or decelerated back to the speed of the column and the drops are coalesced.

The liquids are injected into the column tangentially at high velocity and accelerated to the column velocity before they enter the extracting section. Before leaving the column the liquids flow over circular weirs and are removed from special chambers by stationary scoops. The scoop for the heavy phase can be moved radially and is used to control the level of the interface which determines the separation efficiency and throughput. Impellers with four arms and rounded blades were found to perform efficiently and were simple to manufacture. The coalescence sections were fabricated from thin corrugated metal sheet to provide a large number of narrow channels parallel to the column axis; the free area was kept as high as possible (greater than 80%). Conical channels were somtimes used to improve transport of the phases.

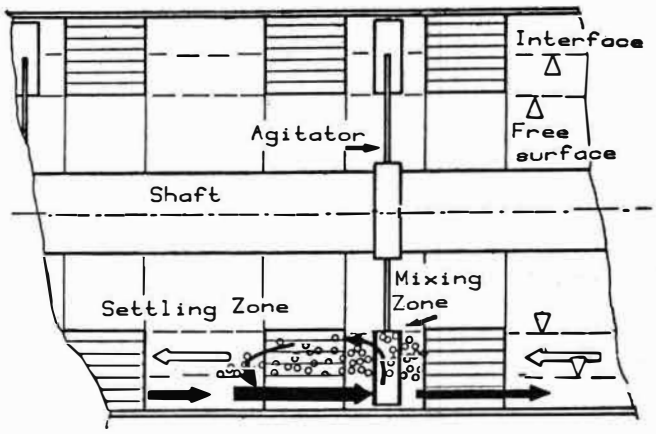

Fig. 1: Principle of mixing and settling of the phases in an axial centrifugal extractor.

SEPARATION EFFICIENCY AND THROUGHPUT

Figures 3 and 4 show the variation in stage efficiency with specific throughput. The mass transfer occurring in the phase injection ports was subtracted from the total transfer so that only the mass transfer taking place in the active length was considered. The additional mass transfer accounts for between 0.7 and 1.2 theoretical stages and can be determined by running the central shaft at the same speed as the column wall so that no agitation occurs.

The specific throughput is based on the total cross-sectional area of the column, despite the fact that only 60% is occupied by the liquids. Figure 3, obtained with the test system toluene/acetone/water, shows that stage efficiencies between 60 and 80% were achieved, depending on the direction of mass transfer. Above throughputs of 100 m^3/m^2h the liquids leaving the column were milky in appearance due to entrainment of the other phase. However this can be removed by providing larger settling zones at the column ends. Further tests were performed with the tributylphosphate (TBP)/ethylalcohol/water system for which the density difference between the two solvents is only about 20 kg/m^3 and the interfacial tension $2.5 \cdot 10^{-3}$ kg/s^2. Water and TBP form a stable emulsion when slightly shaken in a test tube. As shown in Figure 4, the extraction efficiency is about the same as with the previous system and troughputs up to 18 m^3/m^2h were achieved, demonstrating that even this system can be used in the centrifugal extractor.

The total power consumption was relatively low, being about 850 Watt at the maximum throughput of 0.63 m^3h and a separation

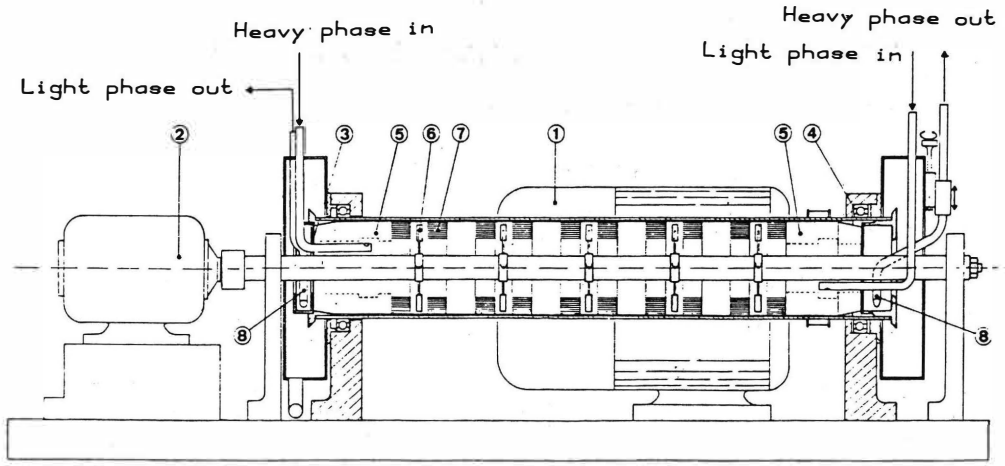

Fig. 2: Construction of the pilot-plant column.
1 - Drive (column)
2 - Drive (Agitators)
3 - Weir, light phase
4 - Weir, heavy phase
5 - Phase accelerator
6 - Agitator
7 - Stage separation
8 - Scoop

efficiency of 3.5 theoretical stages). Of this power 65% was needed to drive the empty centrifuge and 12% to drive the agitators, 10% being required for accelerating and dispersing the liquids. The remainder could in priciple be recovered by using the agitator shaft to drive a generator, if the agitators move slower than the column.

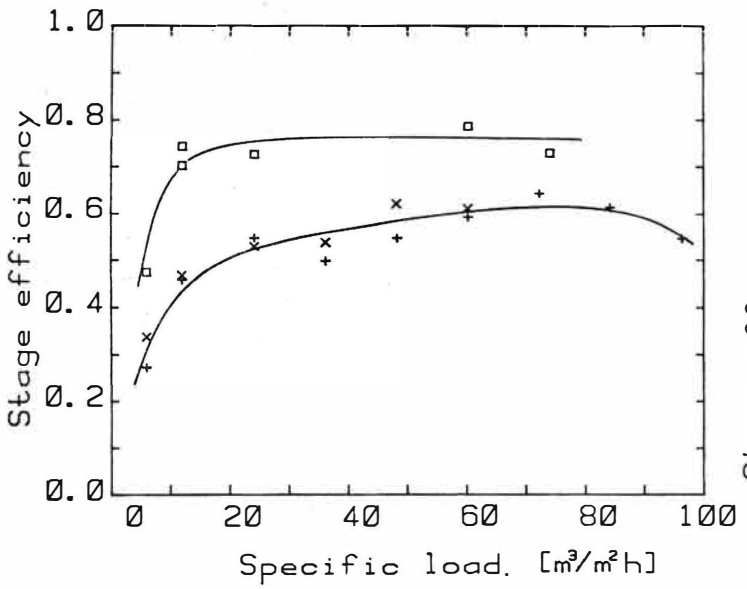

Fig. 3: Dependence of stage efficiency on specific load.
System Toluene/Acetone/Water.
(+) Mass transfer from toluene to water, phase ratio 1:1
(×) toluene to water, 1:1.5
(□) water to toluene, 1:1.5

CONCLUSIONS

The experiments have demonstrated that it is possible to operate a centrifugal extractor with axial countercurrent flow of two liquid phases. Good mass transfer at high throughput can be obtained by repeatedly mixing and separating the liquids; any desired separation can be achieved by increasing the length of the extractor.

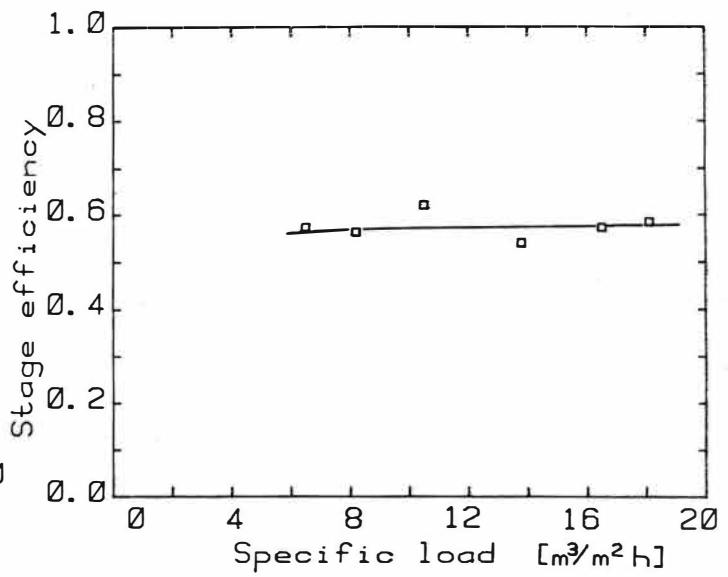

Fig. 4: Dependence of stage efficiency on specific load.
System Tri-n-butyl phosphate(TBP)/Ethanol/Water
Phase ratio 1:1.2, Mass transfer from water to TBP.

STEADY-STATE DROPLET SIZE DISTRIBUTION IN A PULSED PLATE EXTRACTION COLUMN

M. O. Garg and H. R. C. Pratt

Research & Development Dept.
Engineers India Ltd.
New Delhi, India

University of Melbourne
Parkville
Victoria, Australia

Droplet size and its distribution play a key role in the design of liquid-liquid extraction equipment. Ideally, the prediction of these should be done from first principles, based upon the modeling of droplet coalescence and breakage processes. This requires, a priori, estimates of coalescence and breakage rate constants which, at present, are available only for one system and for two column types (1,2). In the absence of such data, it becomes necessary to use suitable model distribution functions which fit the experimental data best. In the present work, four model distribution functions have been examined, using maximum likelihood principle, for their ability to represent experimental data obtained in a pulsed column.

EXPERIMENTAL WORK

Equipment details. The pulsed column consisted 24 sieve plates of stainless steel fitted closely in a 76 mm diameter QVF tube, 1.5 m in length. The plates, 1.575 mm thick, were spaced 50 mm apart and were drilled with 113 holes of 3.2 mm dia to give a free area of 21.7%. The dispersed phase was introduced through a distributor plate which carried eleven nozzles of 2.65 mm i.d. The pulsing unit on which the column rests comprised of a piston connected by a crank arm to a variable eccentric drive head. To facilitate precise measurement of droplet size, a rectangular photographic cell comprising of 220 mm x 180 parallel sides, 28 mm apart, was provided above the 24th plate. Complete detail of the equipment is given by Garg and Pratt(2).

Materials and Procedure. Distilled water and commercial grade methyl isobutyl ketone (MIBK), both mutually saturated, were used as continuous and dispersed phase respectively. The interfacial tension measured by du Nouy ring was 10.1 dynes/cm at 20°C.

The pulsed column was operated in the mixer-settler region, transition and emulsion region at the pulse frequencies of 60, 90 and 120 cycles/min respectively with a fixed pulsed amplitude of 14 mm; for each frequency total throughput rates of 10, 15 and 30 cm^3/sec were used with MIBK/water flow ratio of unity. In addition, a total throughput rate of 45 cm^3/sec was used at the two higher frequencies. At all operating conditions the droplets were found to attain a steady state size distribution after their travel through 16 plates.

In each run, 4 to 5 photographs of the photographic cell were taken on a ASA 160 slide film. The camera used had a 50 mm F 1.8 standard lens mounted on a 25 mm extension tube and was fitted with two close up lens of 40 cm focal length. The exposure time was 0.001 sec with a 500 W tungsten lamp illuminating the cell from behind.

On projecting the slides on a white screen, a magnification of 40 times the actual size was obtained and around 1000 droplets were measured for their major and minor axes at each set of operating condition. From the data, effective diameters of $de = (d_1^2 d_2)^{1/3}$ were calculated, where d_1 and d_2 are the major and minor axes respectively, and the resultant size distributions were found to be unimodal as shown in Figure 1. The complete data are given by Garg(3).

MODEL DISTRIBUTION FUNCTIONS

Various statistical distributions have been proposed in the past to represent droplet size data in an extractor. After an initial screening, four distributions were selected as the most probable candidates to represent the experimental size data; these are log-normal, Gamma, Weibull and Mugele-Evans distributions. The fitting of these functions to the experimental data involves the estimation of two parameters which define these functions, except for the Mugele-Evans, where three parameters are required to be estimated.

ESTIMATION TECHNIQUES

The size distribution function can be denoted by $P(d;\underline{\theta})$, where $\underline{\theta}$ is the vector of model parameters to be estimated from m observations of droplet size d. Three methods of estimation, namely, maximum likelihood, method of moments and method of least squares have commonly been used. Out of these, the maximum likelihood method is preferred since it yields an estimate with desirable properties such as consistency and asymptotic normality.

In the maximum likelihood method, a likelihood function of $\underline{\theta}$, $L(\underline{\theta})$ is defined as the product of the probabilities of all measured droplet diameters, i.e.

$$(1) \quad L(\underline{\theta}) = P(d_1;\underline{\theta})\, P(d_2;\underline{\theta}) \text{ ---------- } P(dm;\underline{\theta})$$

and the estimate of $\underline{\theta}$ is obtained by maximizing $L(\underline{\theta})$ or more preferably, $\ln[L(\underline{\theta})]$. Thus the M.L. estimate of $\underline{\theta}$ is obtained by solving the following equations

$$(2) \quad \frac{\partial \ln[L(\underline{\theta})]}{\partial \underline{\theta}_i} = 0 \; ; \quad i = 1, 2, \ldots\ldots, np$$

In cases such as Mugele-Evans, where the system of equations(2) is difficult to solve, the other two methods are used.

COMPARISON OF SELECTED MODEL DISTRIBUTIONS

The results of fitting the four model distributions to the experimental data are presented in Table 1. For all models, the maximum likelihood method was used except the Mugele-Evans, where the method of least squares was used. The Chi squared statistic X^2 compared in this table was obtained by dividing the sample into suitable intervals as follows :

$$(3) \quad X^2 = \sum_i^M \frac{(n_i - n_i^*)^2}{n_i^*}$$

It may be noted that due to the large sample size, the X^2 values are greatly in excess of the corresponding critical values at the 5% level of significance and hence the model which yields the lowest value of X^2 can be selected as the best fitting model.

It is apparent from Table 1 that the Weibull distribution yields the lowest X^2 values for almost all cases, and moreover, the Sauter mean diameters d_{32} predicted by this model are closest to the experimental values. Thus, it can be concluded that the Weibull distribution represents experimental data for pulsed column better than other models, an opinion also endorsed by Khemangkorn et al (4) for CCl_4 - Water System.

The close fit of Weibull distribution is also illustrated by the good linear trend of the experimental cumulative droplet size distribution plotted on the Weibull paper in Figure 2.

WEIBULL PARAMETERS

The Weibull function

$$(4) \quad P(d) = bcd^{(c-1)} \quad \exp(-bd^c)$$

TABLE 1 : Comparison of Closeness of Fit of Distribution Models

f	V_t	Exptl. d_{32}	Log-normal d_{32}	Log-normal X^2	Gamma d_{32}	Gamma X^2	Mugele-Evans d_{32}	Weibull d_{32}	Weibull X^2
60	10	1.2697	1.4440	786	1.3272	584	1.1767	1.2696	456
	15	1.3016	1.4376	627	1.3309	465	1.1948	1.2973	325
	30	1.4902	1.6756	494	1.5002	340	1.3557	1.4614	211
90	10	0.9711	1.0067	669	0.9701	550	0.8972	0.9720	353
	15	0.9257	0.9710	636	0.9363	558	0.8726	0.9248	673
	30	1.2373	1.2677	381	1.2057	245	1.1223	1.2147	133
	45	1.1741	1.2295	467	1.1588	322	1.0518	1.1573	171
120	10	0.7765	0.7967	868	0.7820	822	0.7201	0.7783	991
	15	0.7771	0.8017	846	0.7841	774	0.7241	0.7788	796
	30	0.8743	0.9068	648	0.8805	553	0.8202	0.8752	445
	45	0.9453	0.9685	648	0.9404	598	0.8737	0.9443	502

is characterized by two parameters b and c. The scale parameter b is an inverse function of the mean droplet diameter while the shape parameter c is inversely proportional to the spread of the distribution. Table 2 gives the values of the two parameters at all operating conditions.

The dependance of the Weibull parameters on column operating conditions was found to be satisfactorily represented by the following equation:

$$(5) \qquad b \text{ or } c = b_1 (f)^{b_2} (V_t)^{b_3}$$

where b_1, b_2 and b_3 for the parameter b are 2.874×10^{-4}, 2.129 and -0.390 respectively, and similarly for the parameter c are 0.776, 0.427 and -0.164. These constants along with equations (4) and (5) can be used to predict the steady state droplet size distribution for the MIBK/Water system in pulsed columns.

TABLE 2 : Weibull Parameters at Various Operating Conditions

f	V_t	Scale Parameter, b	Shape Parameter, c
60	10.0	0.6215	3.1912
	15.0	0.6366	2.9814
	30.0	0.5682	2.5869
90	10.0	1.4444	3.2579
	15.0	1.6681	3.4411
	30.0	0.8647	2.7059
	45.0	0.9702	2.7665
120	10.0	3.2781	4.1311
	15.0	3.2272	4.0341
	30.0	2.0216	3.6189
	45.0	1.5956	3.3162

CONCLUSIONS

The droplet size distribution in pulsed columns is best represented by the Weibull distribution. Thus, subject to a satisfactory correlation of the Weibull parameters with column operating variables and system physical properties, this model should form the best generalised correlation equation for droplet size when data become available for other systems.

NOTATION

b	=	scale parameter in Weibull distribution (mm units)
c	=	shape parameter in Weibull distribution
d	=	droplet diameter (mm)
d_{32}	=	Sauter mean droplet diameter (mm)
f	=	pulse frequency, cycles/min
M	=	number of size intervals
m	=	sample size
n_i	=	exptl. number of droplets in the ith interval
n_i^*	=	number of droplets in the ith interval determined from model
np	=	number of parameters in the model function
$P(d;\underline{\theta})$	=	probability density function of droplet diameter d
V_t	=	total throughput rate (continuous + dispersed) cm^3/sec.
χ^2	=	chi squared statistic
$\underline{\theta}$	=	vector of model parameters

REFERENCES

1. J.A. Hamilton and H.R.C. Pratt, AICHE Journal to appear, (1983).
2. M.O. Garg and H.R.C. Pratt, AICHE Journal to appear, (1983).
3. M.O. Garg, "Measurement and modelling of droplet coalescence and breakage in a pulsed plate liquid extraction column", Ph.D. Thesis, University of Melbourne (1982).
4. V. Khemangkorn, G. Muratet, H. Angelino, Proc. ISEC'77, Vol.1, 429, (1977).

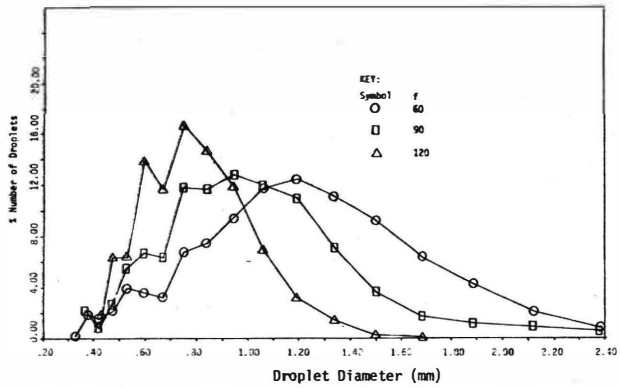

FIGURE 1 : Experimental Droplet Size Distributions at Total Throughput Rate of 30 cm^3/sec.

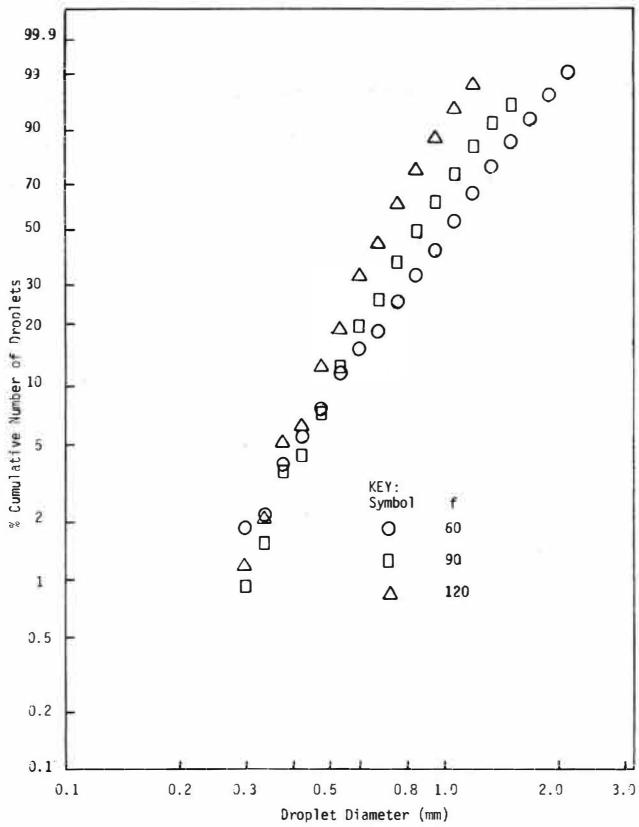

FIGURE 2 : Weibull Plots of Experimental Droplet Size Distributions at total throughput rate of 30 cm3/sec.

INFLUENCIAL PARAMETERS OF SIZE DISTRIBUTION IN VARIOUS DISPERSION PROCESSES

Jacques Dollfus

Societe Generale Pour Les Techniques Nouvelles
78184 Saint Quentin en Yvelines Cedex - France

IN ANY TWO LIQUID PHASES DISPERSION EQUIPEMENT, THE SIZE OF DROPLETS OF THE DISPERSED PHASE IS OBTAINED BY SEVERAL DIFFERENT WAYS OF ACTION. THE RELATIVE INFLUENCE OF THEM, DEPENDING ON THE PROCESSES, WILL LEAD TO DIFFERENT SIZE DISTRIBUTION DIAGRAMS.

ACCORDING TO THE FINAL PURPOSE OF THE CONCERNED TREATMENT, IT IS INTERESTING FOR THE PROCESS INGENEER, TO HAVE AN IDEA ABOUT THE POSSIBLE TYPES OF DIAGRAMS HE WILL OBTAINED AND, SO, A CONSIDERABLE HELP IN THE CHOICE OF THE EQUIPEMENT.

LIST OF INVOLVED PARAMETERS : THEY ARE OF THREE MAIN TYPES

1) PHYSICAL PROPERTIES :

- DENSITY OF EACH LIQUID PHASE
- VISCOSITY OF EACH LIQUID PHASE
- INTERFACIAL TENSION SENSIBILITY TO OTHER FACTORS AS TEMPERATURE
- WETTING ABILITY OF SOLID MATERIALS IN FRONT OF BOTH PHASES.

2) PHYSICO - CHEMICAL FACTORS :

- CONCENTRATION OF MAIN SOLUTES AND EQUILIBRIUM DIFFERENCES
- CONCENTRATION OF EVENTUEL TENSIOACTIVE SECONDARY SOLUTES
- RELATIVE SOLUBILITY OF EACH PHASE IN THE OTHER ONE.

3) MECHANICAL AND HYDRODYNAMICAL ACTIONS :

- SHEARING AND SPLITTING EFFECTS LEVEL
- GENERAL TURBULENCE LEVEL
- MEAN SIZE OF TURBULENCE LOOPS
- TURBULENCE HOMOGENEITY DISTORSIONS.

FOR A GIVEN PROCESS, SOME OF THE PHYSICAL OR PHYSICO-CHEMICAL FACTORS CANNOT BE EASILY CHANGED - NEVERTHELESS, SOME VERY FEW OTHER ONES CAN BE DIRECTED BY A PHYSICO-CHEMICAL INTERVENTION, SUCH AS :

- TEMPERATURE CHANGE
- AUXILIARY TENSIOACTIVE COMPONENT INTRODUCTION

BUT, THE MAIN POSSIBLE ACTION IS MADE BY RELATIVE USE OF MECHANICAL AND HYDRODYNAMICAL PARAMETERS IN THE DISPERSION EQUIPEMENT.

IN MOST CASES, IT IS PREFERABLE TO OBTAIN A DISPERSION SIZE DISTRIBUTION AS UNIFORM AS POSSIBLE, AND, SO, TO FIRMLY CONTROL THE SPRAYING OF SHEARING AND TURBULENCE EFFECTS WHICH GOVERN THE BREAK-UP AND THE COALESCENCE RATES.

SIZE DISTRIBUTIONS :

FOR DISCRETISED SIZE CLASSES AND A UNITY VOLUME OF LIQUID, WE HAVE :

- INTERFACIAL SURFACE

$$\Delta A_J = \pi \cdot N_J \cdot D_J^2$$

- DISPERSED PHASE VOLUME

$$\Delta V_J = \frac{\pi}{6} \cdot N_J \cdot D_J^3$$

- SPECIFIC INTERFACIAL SURFACE

$$A_S = \pi \sum (N_J \cdot D_J^2)$$

- DISPERSED PHASE CONCENTRATION

$$C_D = \frac{\pi}{6} \sum (N_J \cdot D_J^3)$$

N_J IS THE NUMBER OF DROPLETS OF THE CLASS FROM D_J TO D_{J+1}. AT THE LIMIT, EACH CLASS CONCERNS DROPLETS OF DIAMETERS BETWENN D AND $D + \delta D$ AND THE PROBABILITIES OF THESE DROPLETS ARE :

$$p(D) \cdot \delta D = p(A) \cdot \delta A = p(V) \cdot \delta V$$

THE MEAN VOLUME OF DROPLET IS

$$\overline{V} = \int_0^\infty V \cdot p(V) \cdot \delta V$$

AND THE "VARIANCE" ON THE DROPLET VOLUME :

$$S_V^2 = \int_0^\infty V^2 \cdot p(V) \cdot \delta V - \overline{V}^2$$

IN ACCORDANCE WITH A GIVEN DIAGRAM OF ONE OF THOSE PROBABILITIES $p(V)$, $p(A)$, $p(D)$, THE SIZE DISTRIBUTION IS PERFECTLY KNOWN.

FREQUENT DISTRIBUTION TYPES :

ACCORDING MANY EXPERIENCES AND MEASUREMENTS IN LIQUID - LIQUID MIXING MOST PRATICAL OBSERVED DISTRIBUTIONS TYPES ARE OF THE FOLLOWING :

- NORMAL (GAUSSIAN)
- LOG-NORMAL (OR LOG. GAUSSIAN)
- RRS (ROSIN -RAMMLER - SPERLING)
- ERLANG (OR GAMMA)

IN REAL EQUIPEMENTS, ACCORDING TO THE PROPORTION BETWEEN MECHANICAL AND HYDRODYNAMICAL FACTORS, THE DISTRIBUTION MAY BE MORE OR LESS SPRAID AROUND THE MEAN DIAMETER.

CONCLUSIONS :

ROUGHLY, SOME FOUND RESULTS ARE GIVEN IN THE FOLLOWING TABLE AND SOME EXEMPLES OF DIAGRAMS ARE MENTIONNED IN FIGURES.

IN EVERY CASES, THE MEAN SIZE DEPENDS ON THE SPECIFIC ENERGY OF AGITATION. IN THE ANNEXED DIAGRAMS THE MEAN DIAMETER IS CONSIDERED AS 1.

TABLE OF EXPERIMENTAL RESULTS

IN LINE STATIC MIXERS	RRS (ROSIN-RAMMLER)
PULVERIZER	QUASI UNIFORM
PERFORATED PLATES	LOG - NORMAL (NARROW)
BAFFLES	LOG - NORMAL (EXTENDED)
PACKING	QUASI UNIFORM (MAIN CLASS) BUT 2 POSSIBLE EXTRA SIZES
ROTATIVE AGITATOR	LOG - NORMAL (MORE OR LESS EXTENDED)
CENTRIFUGAL EXTRACTOR	LOG - NORMAL (NARROW)
PACKING WITH ALTERNATIVE PULSION	LOG - NORMAL (EXTENDED)

REFERENCES :

1. J.T. DAVIES — TURBULENCE PHENOMENA
2. SHINZI NAGATA — MIXING
3. A LE LAN — CARACTÉRISTIQUES HYDRODYNAMIQUES (INFO CHIMIE N° 210)
4. KLEMANGKORN, MURATET — STUDEY OF DISPERSION (ISEC 77)

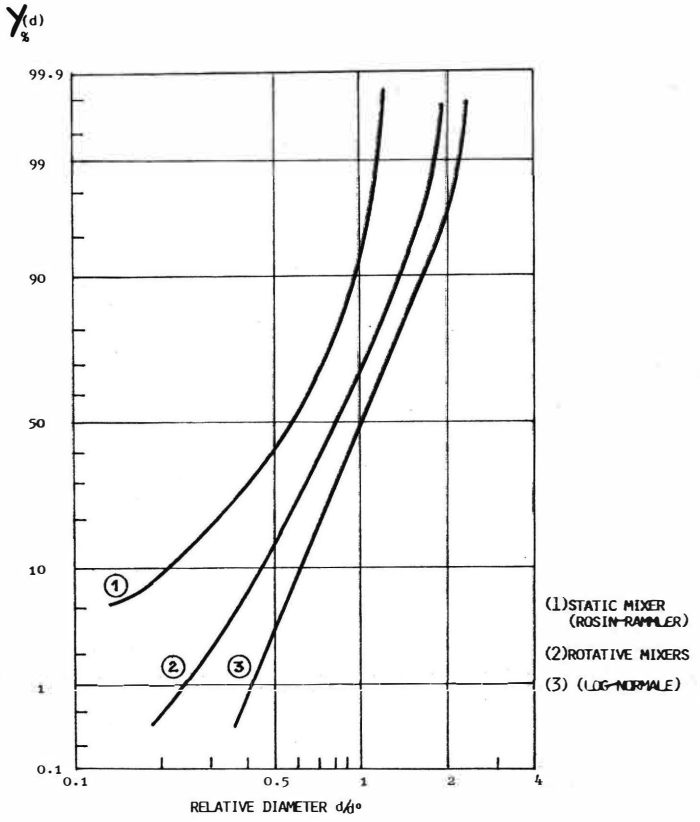

FIG. 1 - EXAMPLES OF SIZE DISTRIBUTION CUMULATED DENSITY OF PROBABILITY

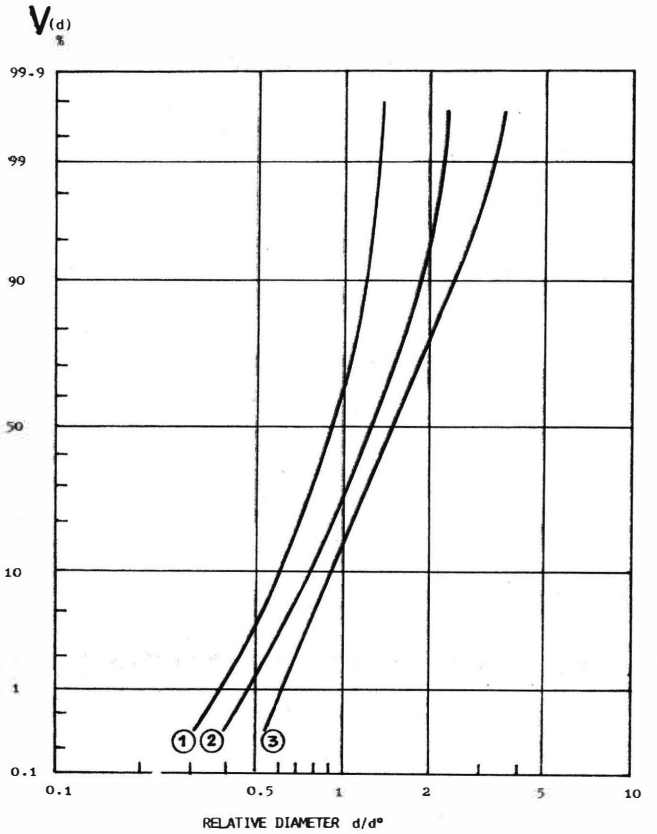

FIG. 2 CUMULATED VOLUMES OF DISPERSED PHASE

DEVELOPMENT OF A NOVEL PHOTOGRAPHIC DESIGN FOR DROP SIZE MEASUREMENT IN AGITATED VESSELS

H. Topuz

Middle East Technical University
Gaziantep, Turkey

INTRODUCTION

Dispersions are widely encountered in many branches of the process industries, particularly those concerned with solvent extraction processes. Vessels agitated by mechanically in most applications are generally operated under batch conditions, and open to the air, more commonly with a rotating impeller mounted on a vertically positioned shaft. Liquids agitated may be partially or completly miscible. Under these considerations if the vessels are not equipped with baffles then the formation of a vortex is inevitable at all, but lowest agitator speeds.

One of the aims in producing such dispertions in agitated vessels is to predict the interfacial area which has got a direct influence on the heat and mass transfer operations, and in heterogenous reactions. The equipment employed to produce these dispersions is very varied. They range from mixer-settler to spray towers. The design of these devices is rather empirical due mainly to insufficient studies on dispersion behaviour under varying conditions. For instance, althoug the design of large scale mixer-settler for the metal purifications, e.g. Uranium purification, usually carried out by simply scaling-up the existing dimensions of a smaller unit the basis for the design is still not understood well inspite of many years of operating experiences.

*H.Topuz is presently with Middle East Technical Univ.Gaziantep/TURKEY.

A fairly extensive information available in the literature in regarding to the average droplet size resulted in dispersions. Rietma (1) made a discussion of control of reaction rate in stirred tanks by means of drop size, and interfacial area. Hinze (2) says that drops are broken up by the pressure caused by the turbulent flow in the vicinity of drop surface. He said that coalescence may occur when drops collide each other. Vermeulen et al. (3) measured interfacial areas in liquid-liquid, and gas-liquid dispersions produced in baffled cylindrical tanks by use of light transmission. He correlated his data in the following form

$$\bar{D}_{32} / L_{\emptyset} = C_1 \, We^{-0.60}$$

Rodger et al. (4) did measure average drop size in liquid-liquid dispersion of equal volums of both liquids. He represented a correlation as

$$\bar{D}_{32} / L_{\emptyset} = C_2 \, We^{-0.38} \, (L/T)^{-k}$$

Here, k varies from 0.75 to 1.4 and C_2 was found to be depend upon the vessel size, T.

Caldernabk (5) made a correlation of his data derived from nearly 0 to 20 % dispersion phase presence. He correlated his findings as in the form of

$$D_{32} / L_{\emptyset} = C_3 \, f_H \, We^{-0.60}$$

where $f_H = 1 + 9.0\,\Theta$.a deviation of ± 10 % was inevitable. This is similar to Vermeulen's correlation. Shinnar and Church (6) predicted average drop size by means of Kolmogoroff's (7) theory of universal equilibrium.

Weinstein and Treybal (8), Chen and Middleman (9), Tavlarides and Coulaloglou (10), Park (11), Sprow (12) and more recently Hanson and Grilc (13) studied drop sizes by means of various methods of direct photography in agitated vessels for batch process.

Bouyatiotis and Thornton (14), Mack and Kroll (15), Schindler et al. (16), Ross and Curl (17) made extensive studies of drop size distribation in flow systems.

The primary aim of this work was carried out because it became clear from the coalescence studies that droplet size had a marked effect on settling behaviour. It would therefore be of interest to be able to predict droplet size distribution from the agitation conditions in a mixer-settler and then to study the coalescence of the resulting dispersions of immiscible liquids at various dispersed phase hold-ups. In this it would be possible to relate the design of the mixer-settler with its associated conditions.

Drop size distribution measurements in the circulation and impeller region for different dispersed phase hold-ups were made under turbulent conditions. The dispersions of methyl-iso-butyl-ketone in water, cyclohexanol in water, and 20/80 by volume tri-butyl-phosphate/odourless kerosene in 0.05 M nitric acid dispersions were produced in 6-9 inches in diameter fully baffled cylindrical, and 20 cm. a side square vessels.

Differences observed in the size distributions between the regions were markedly smaller than would be expected. This may be attributed to the lower coalescence frequency. Their sizes in the vessels were observed to moderatly dependent upon the impeller speed. The droplet size measurements indicated that little is known about the processes of drop coalescence and drop break up in agitated vessels.

The relationship determined similar to other investigators by means of Kolmogoroff's theory of local isotropy, and on the basis of the Weber Number predicted that drop sizes were controlled by the droplet coalescence and not by the drop break up. Cumulative volume frequency used against drop diameter on normal probability paper resulted a family of straight lines.

The agitator speed dependency on drop diameter markedly differend from system except that the cyclohexanol/water system seemed to close to -1.2 as predicted for the drop breakage controlled process on the basis of critical Weber Number. ($d \propto N^{-1.2}$).

The correlation derived for fully baffled cylindrical vessels under batch conditions may be represented by the following equation :

$$d_{vs} / L_{\emptyset} = 0.022 \, (1 + 3.40\,\Theta)(We)^{-0.40}$$

and for the continuous flow it is given by

$$d_{vs} / L_{\emptyset} = 0.011 \, (1 + 1.09\,\Theta)(We)^{-0.46}$$

A variation in the equation parameter to those available in literature for batch and continuous may be a result of the difference in the vessel operating and vessel contents. Bigger mean drop size obtained in continuous flow as compared with the values for batch operation may chiefly be attributed to the flow effects.

A new photographic method by use of fiber optic developed appears to well suit experimental technique for droplet size measurement purposes. It does not disturb the hydrodynamic conditions had established during processing. The range of operating conditions undertaken were dispersed phase hold-up fractions varied from 10 % to 20 %, impeller speed changed from 300 to 500 r.p.m.

The method may be useful for determination of dispersed phase coalescence frequencies in models put forward by previous investigators Miller (22), Tavlarides and Coulaloglou (10).

EXPERIMENTAL

Photographic System

Throughout for the determination of drop size distribution direct photography was used. The optic system was designed in such a way as to be able one to photograph the dispersions at different locations within the vessel with a minimum of interference to the flow regime under both batch and continuous flow conditions.

It consisted of mainly two fibre optic units, namely a light quide and a photographic probe commercially known as image conduit. With the application of heat as pressure exerted, they can be given any shape as required . See Figure 1.

LIQUIDS USED

In order to study a wide range of impeller Reynolds Number for various types of two-phase liquid systems with different density, and viscosities were used. They were selected on the basis of forming strongly, moderately and slowly coalescing systems respectively in an agitated vessel. In two systems the distilled water was used as the second phase which is the major phase, and in the third system the continous phase was made up from 0.05 M nitric acid used against 20 % tri-butylphosphate, hereby referred as T.B.P., with odourless kerosene by volume.

The three two-phase liquids systems are as follows :

(i) Methyl-iso-butyl-ketone (M.I.B.K.) with distilled water,
(ii) 20 % T.B.P. with odourless kerosene (v/v) with 0.05 M HNO_3,
(iii) Cyclohexanol with ditilled water.

All liquids used were of technical grade. They were mutually saturated before they were used for the purpose of drop size measurement studies. See Table : 1 for the physical properties of the liquids.

PROCEDURE FOR THE MEASUREMENTS

The following procedure was adopted to obtain data for the drop size determinations under batch and continous flow conditions.

(a) for batch process :

The photographic probe and the light guide were located in the vessel facing each other. Agitation was then started at the selected impeller speed. The position of the two probes were adjusted so that pictures could be taken at the location demanded without any interference with the hydrodynamic equilibrium which had been established. During the picture taking process adjustment could easily be made due to the design as shown in Figure 2. The intensity of the light guide was controlled by a switch gear attached on the light box. Before any picture taken time intervals varying from 10 to 30 minutes was allowed for the dynamic equilibrium to be attained. A minimum of 10 and a maximum of 25 exposures were taken in succession to give a drop population of 300 which is recommended to determine the sauter-mean drop diameter calculations.

(b) for continuous process :

The procedure used in the continuous flow experiments was basically the same as for the batch case, except for a few alterations as follows :

(i) more time allowed for the system to reach equilibrium.
(ii) the flows of both phases corresponding to batch process hold-up fractions were adjusted to give the same hold-up.
(iii) more exposure time was allowed as to get a population of 300 well-defined drops on negatives.

The rest was exactly the same as in the batch processing.

RANGE OF EXPERIMENTAL VARIABLES

A tabulation of the liquid-liquid systems used appears in Table 1. Distilled water used as continuous phase for cyclohexanol (dispersed) and M.I.B.K. (dispersed).

Table 1 : Physical Properties of Liquids Used at 20°C

Liquid	ρ(g/cc)	μ(cp)	σ(dyne/cm)
20 % TBP/OK	0.82	3.00	14
0.05 M HNO_3*	1.03	1.02	-
Cyclohexanol	0.96	68[1]	4.500
Distilled Water	1.00	1.00	-
M.I.B.K.[2]	0.800	0.57	10.50

(1) -- Hand book of Chemistry , 1976
(2) -- Taken from I.C.T.
* --- Interfacial tension against aqueous phase (0.05 M HNO_3)

RESULTS AND DISCUSSION

The drop size measurements were classified into size groups of 20 μ intervals, depending upon the range of sizes resulting from each particular run. The sauter-mean diameter was used in this study.

The sauter-mean is the most versatile for the prediction of the interfacial area per unit volume, may be determined by $a = 6\ \Theta/d_{vs}$. measurements were plotted on the normal probability paper in terms of cumulative frequency percentage against d_i, the drop size. This method was chosen as to show the variation in between drop size distribution on this type of plot. Drop sizes for continuous operations show a substantial variation in size fromthose for corresponding batch operating conditions. A plot of d_{vs} determined from batch and continuous conditions is given in Figure 3. A linear relationship was obtained and also the ratio of d_{vs} for continuous to the d_{vs} for batch finding seem to be in agreement with the observation of Rushton (18) Further more, the power dissipated in the systems undertaken is virtually independent of the ratio of (L/T) in the range of Reynolds Numbers that were reached.

DROPLET SIZE DISTRIBUTION

The photographs were used to obtain cumulative drop size distributions in order that the effects of the agitator speed, the dispersed phase hold-up, total flow rate, and the phase ratio of solvent-to-aqueous could be determined. Present work did not conform the log-normal distribution. The distributions gave approximately straight lines on normal probability paper, which indicate that the data are distributed normally. No significant effects of (L/T) was found on the drop size, but, moderately influenced by the agitator speeds and dispersed phase hold-ups.

Measurements of drop size were made under both batch and continuous flow conditions by use of a novel probe whichemployed fiber optics and photography in agitated vessels.

The photographs produced were used to obtain cumulative drop size distributions in order that the effects of the agitator speed, the dispersed phase hold-up, the total flow rate and the phase ratio of solvent to aqueous could be determined. The distribution studied in the present work did not conform to the log-normal distribution. They gave approximately straight lines on normal probability paper which indicates that the data are distributed normally. That as the dispersed phase fraction increased so does the drop size over a range of agitator. By this, the combined effects of hold-up of the dispersed phase and the coalescing properties among the systems studied could be understood. The effects of the hold-up on the drop size variations are not the same at different speeds for all the systems studied. These different effects may be justified on the basis of coalescence and drop break up processes. Both processes take place in the impeller region, i.e., break up in the stream emerging from the agitator and to lesser mean in the rest of the bulk flow. Although drop coalescence is going on, it can have little effect on the local drop diameter, since if it results in a bigger drop size predicted on the basis of the critical Weber Number it will be instantly followed by break up. Coulaloglou and Tavlarides (10), Mlynek and Resnick (19) reported that if the rate of coalescence is very low only a limited number of collisions are said to be effective, therefore the effect of coalescence is negligible.

The fact that the volumetric hold-up has a different effect on droplet size at different agitator speeds can be better explained by the relative values of the droplet breakage forces and the coalescing forces.

Shinnar (20), reported that in a system where drop break up is controlling the mean drop size, d_{vs} is proportional to $N^{-1.2}$ and in one in which the drop size is controlled by coalescence, the mean droplet diameter is proportional to $N^{-0.75}$.

Therefore it is expected that a change in the ratio of the two forces controlling these mechanisms as the agitator speed is varied. If is to be expected that the drop break up forces have a greater effect compared with the effects of coalescence as the agitator speed is increased.

Tavlarides and Coulaloglou (10) reported drop size proportional to $N^{-1.0}$. They stated that the drop size dependency upon the agitator speed was moderate while the coalescence frequency was a strong function of the agitator speed.

The drop size measured in the present study seemed to be moderately dependent upon the agitator speed. The drop became larger as the impeller speed decreased as expected. For the continuous process the d_{vs} found proportional to the impeller speed, $N^{-0.30}$ Wilkinson and Topuz (21).

The reason for the lower exponent may be explained by the fact that the coalescence frequency is more dependent on the impeller speed than is the drop break up process.

REFERENCES

1. K. Rietema, Segregation in Liquid-Liquid Dispersions and its Effect on Chemical Reaction, in Adv.Chem.Eng. 5,237 (1964).
2. J.O. Hinze, Fundamentals of the Hydrodynamic Mechanism of Splitting up in Dispersion Processes AIChE J., 1, 289 (1955).
3. T. Vermenlen, G.M. Williams, G.E. Langlois., Interfacial area in Liquid-Liquid and Gas-Liquid Agitation, Chem.Eng.Progr. 51, 85F (1955).
4. W.A. Rodger, V.G. Trice, and J.H. Rushton, Chem.Eng.Progr., 52,515 (1956).
5. P.H. Calderbank, Physical Rate Processes in Industrial Fermentation. Part I : The Interfacial area in gas-liquid contacting with Mechanical Agitation, Trans.Inst.Chem.Eng., 36, 43(1958).
6. R.Shinnar, and J.M. Church, Ind.Eng.Chem. 52, 233 (1960).
7. A.N. Kolmogoroff, On the Disintegration of Drops in Turbulent Flow, Doklady Akad.Nauk. U.S.S.R., 66, 825 (1949), IBID 30, 301 (1961).
8. R.E. Treybal, and B. Weistein, Liquid-Liquid Contacting in unbaffled Agitated Vessels, AIChE J., 19 304 (1973).
9. H.T. Chen, and S. Middleman, Drop Size Distribution in Agitated Liquid-Liquid Systems, AIChE J., 13 No. 5 989 (1967).
10. C.A. Coulaloglou, and L.L. Tavlarides, Drop Distributions and Coalescence Frequencies of Liquid-Liquid Dispersions in Flow Vessels. AIChE J., 22, No. 2 (1976).
11. J.Y. Park, and L.M. Blair, The Effect of Coalescence on Drop Size Distribution in an Agitated Liquid-Liquid Dispersions. Chem. Eng Sci., 30, 1057 (1975).
12. F.B. Sprow, Distribution of Drop Size Produced in Turbulent Liquid-Liquid Dispersion. Chem.Eng.Sci., 22, 435 (1967) and AIChE J., 13, 995 (1967).
13. V.Grilc, Ph.D. Thesis, University of Bradford (1976).
14. B.S. Bouyatiotis, and J.D. Thornton, Liquid-Liquid Extraction Studies in Stirred Tanks. Park I. Droplet Size and Hold-up. Inst Chem.Eng.Symp. Series (London), 26.43 (1967).
15. D.E. Mack, and E.Kroll, Chem.Eng.Prog., 44, 3 (1948).
16. H.D. Schindler, and R.E. Treybal, Continuous Phase Mass Transfer Coefficients for Liquid Extraction in Agitated Vessels. AIChE J., No.5. 790 (1968).
17. S.L. Ross, and R.D. Curl, Paper 29b presented at the fourth joint Chem Eng. Conference, Van Conver, Canada, (Sept., 9-12.1973).
18. J.H. Rushton, E.W. Costich, and H.J. Everett, Power Characteristics of Mixing Impellers Chem.Eng.Progr., 46,395 (1950).

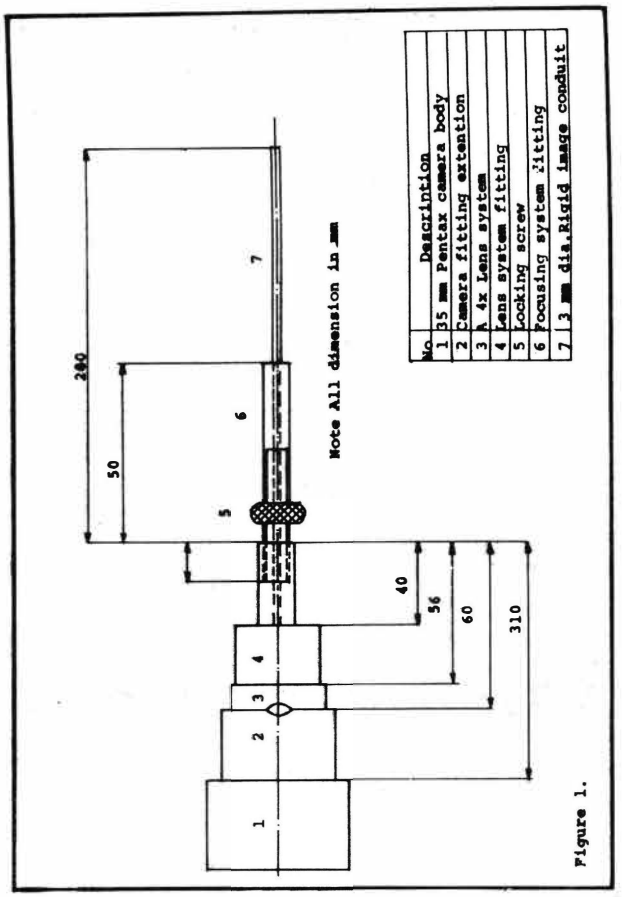

Figure 1.

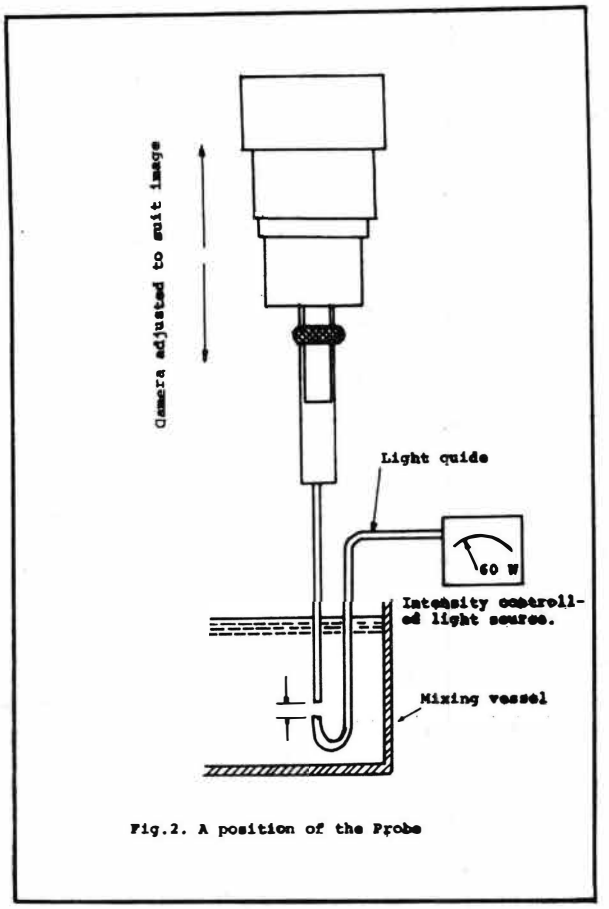

Fig.2. A position of the Probe

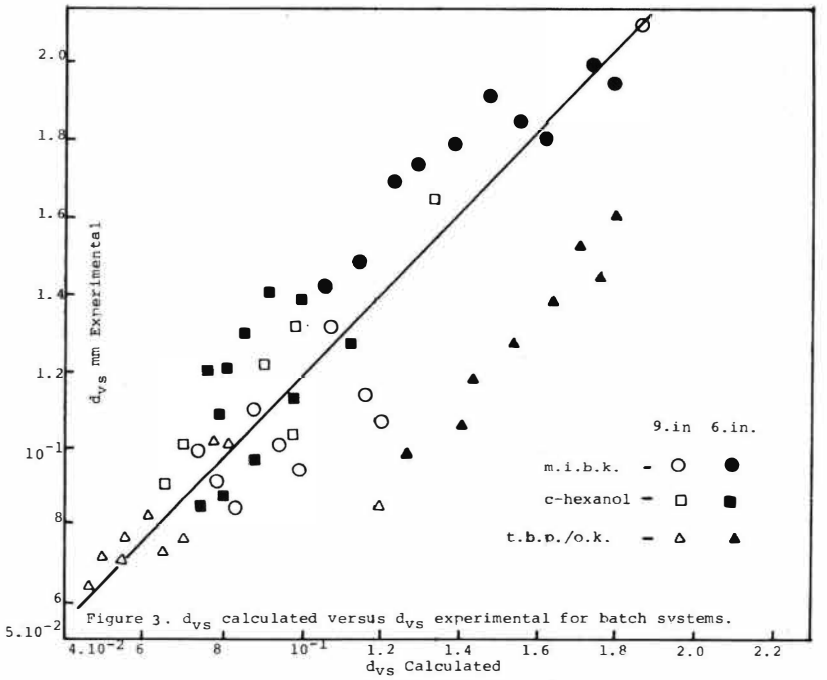

Figure 3. d_{vs} calculated versus d_{vs} experimental for batch systems.

HOLDUP, DROP SIZE AND AXIAL MIXING OF PULSED EXTRACTION COLUMNS

Hans Schmidt

Kernforschungszentrum Karlsruhe
Karlsruhe, Federal Republic of Germany

On account of the tubular vertical configuration pulsed extraction columns can be considered as one-dimensional equipment in a first approximation (Fig. 1). At the head of the column, the heavy aqueous phase enters whilst the light organic phase is supplied at the foot of the column. Both phases move in a countercurrent flow through the column equipped with equidistantly spaced perforated plates. The pulsation supplied from below causes the two liquids to rise and fall. By the pulsation and the perforated plates one of the two phases is dispersed into drops so that the transfer area necessary for extraction is provided

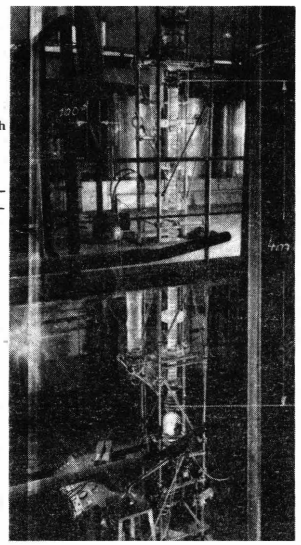

Fig. 1 Experimental Set-up

The Problem

In Fig. 2 a material balance is shown for a small section of the column. The differential mode of consideration refers to the continuous phase. Besides the convective mass flows $v_c c_c$ and the mass flow $k_c a (c_c - c_{cg})$ passing over into the other phase, longitudinal mixing by so-called dispersion flows $- E_c \delta c/\delta h$ - is taken into account in analogy with transport by diffusion. The coefficient E_c describes the mixing effects resulting from flow patterns.

$$\frac{\delta c_c}{\delta t} = E_c \frac{\delta^2 c_c}{\delta h^2} - v_c \frac{\delta c_c}{\delta h} - \frac{k_c a}{1-\varepsilon} (c_c - c_{cg}) \quad (1$$

fraction of dispersion — fraction of convection — mass transfer

Thus, to dimension a column one needs, besides the overall mass transfer coefficient k, the dispersion coefficient E, the holdup ε, and the interfacial area a. This paper reports about the fluid-dynamic variables which are important for calculating the length of the column, whereby the external and internal parameters are subjected to variations.

Publications usually are based on the previous industrial application of the extraction column which is characterized by a 1:1 to 5:1 ratio of dispersed and continuous volumetric flows. In nuclear fuel reprocessing the reduction in volume of wastes is considered to be an especially significant step in the development of a satisfactory waste management concept /1/. For instance, when scrubbing tritium from the organic product stream, one aims at achieving a very small volumetric flow rate of the aqueous scrubbing phase in order to keep low the amount of tritiated liquid effluents. In this way, one leaves behind the usual application of pulsed plate columns, and experimental work in the PUREX-specific material system (HNO_3-30 vol. % TBP) becomes necessary. Major parameters are the ratio of volumetric flows between organic drop phase and aqueous continuous phase which varies between 3 and 99, and the geometry of the holes in the column plates (Fig. 3). Further parameters include the operating temperature, the pulse frequency and the amplitude. The total volumetric flows, has been kept constant at 200 l/h, and likewise the sinusoidal pulse shape. Besides, the operating mode is varied from the aqueous continuous into the organic continuous mode in the case of the nozzle plate cartridge. Experimental details and a detailed description of the knowledge gathered so far have been published in /2/ and /3/.

Holdup

The holdup is measured by sampling and phase separation at seven points of measurement equidistantly spaced along the column. The holdup is an extremely sensitive variable and it undergoes variations with the physical properties of the two fluids, the geometric variables and the variables of operation. Moreover, it responds sensitively to changes in the coalescence behavior of the droplets and in the wetting behavior of the plates.

An increase in the dispersed volumetric flow rate leads to an increase in the drop phase in the column. Sinusoidal pulsation accelerates and decelerates the droplets. A mean velocity is established which is nearly independent of the abundance of droplets. An increase in dispersed volumetric flow is consequently expressed by a greater abundance of droplets; the holdup increases. By contrast, an enhancement of the column temperature leads to a reduction in holdup. The increase in operating temperature diminishes the viscosity while the interfacial tension rises. This reduces the shear forces in the pulsed flow field while, at the same time, raising the interfacial energy, and results in a dispersed volumetric flow consisting mainly of large-volume drops. These drops pass the column faster which causes holdup to decrease.

In Fig. 4 the holdup has been plotted versus the pulsation frequency; the pulse stroke has been kept constant at 15 mm. A continuous rise in holdup with increasing pulse frequency is observed. At constant volumetric flows the higher pulsation more and more hinders the droplets from keeping to the flow direction prescribed by the difference in densities. This results in a gradual extension of the residence time of the droplet phase and the holdup increases. Finally, a limit value is attained when the dispersed phase accumulates at its inlet of the column and is discharged together with the continuous phase. The state of flooding is attained. It is marked in Fig. 4 by cross bars at the ends of the respective solid plots of measured values.

The correlation proposed by Thornton /4/ is suited to describe the measurements. The relation found by dimensional analysis and originally established to calculate flooding is based on a characteristic velocity developed by Gayler et al./5/. Eq. 2 is the Thornton relation describing the characteristic velocity u_o whose constant C = 0.172 has been modified as a result of sieve plate studies. This velocity is calculated essentially from material properties, the geometry and pulsation are contained in the pressure loss coefficient ψ.

$$\frac{u_o \mu_c}{\sigma} = 0{,}172 \left(\frac{\psi \mu_c^5}{\rho_c \sigma^4}\right)^{-0{,}24} \left(\frac{d_o \rho_c \sigma}{\mu_c^2}\right)^{0{,}9} \left(\frac{\mu_c^4 g}{\Delta\rho \sigma^3}\right)^{1{,}01} \left(\frac{\Delta\rho}{\rho_c}\right)^{1{,}8} \left(\frac{\mu_d}{\mu_c}\right)^{0{,}3} \quad (2)$$

The holdup can be calculated using the following equation 3 by establishing a correlation between the characteristic velocity u_o and the superficial velocities derived from the volumetric flow rates for the dispersed (u_d) and continuous (u_c) phases.

$$\frac{u_d}{\varepsilon} + \frac{u_c}{1-\varepsilon} = u_o \, (1-\varepsilon) \quad (3)$$

When the expressions are derived, coalescence of droplets is ruled out. So, the relation for holdup strictly speaking applies only to the dispersion zone. In this zone the developments of holdups measured in the parameter field investigated are correctly described as regards their tendency.

Drop Size

The distributions of drop sizes encountered in the column are obtained by evaluation of photographs. The drop spectrum ranges from 0.1 - 3 mm Ø, with the maximum of abundance occurring at approx. 0.5 mm Ø. The Sauter diameter calculated from the spectrum implies considerable weighting of the large drops so that the mean drop size is greater by approximately the factor 3 than the maximum of abundance.

The drop size is largely independent of the volumetric flow rates but clearly influenced by pulsation and the system temperature. In Fig. 5 the Sauter diameter has been plotted versus the pulsation frequency at 21 °C operating temperature. The tendency can be observed that the drop diameter continuously decreases with increasing pulsation frequency. It is surprising that a large diameter of the holes and a high fraction of free area of the plates imply smaller drop diameters.

The broken line represents the development of a relation according to Kagan et al. /6/.

$$d_{32} = 1{,}7 \frac{\sigma^{0.5} \mu_c^{0.1}}{\rho_c^{0.6} g^{0.4}} (A \cdot f)^{-0{,}3} N^{-0{,}11} \quad (4)$$

The constant C = 1.7 was re-evaluated on the basis of test results with the cartridge of d_o = 4 mm. A geometry was chosen similar to that in the tests performed by Kagan et al.

Axial Mixing, Continuous Phase

Mixing is determined by the steady-state tracer method. The dye tracer entering the column at a constant rate at a fixed location remains exclusively in the continuous phase so that the term for mass transfer in Eq. (1) can be abandoned. Since a steady-state measuring technique is applied, also the time term can be abandoned, and by appropriate normalization and upon integration one obtains the simple expression

$$\ln \frac{c_o}{c} = Pe_c \cdot z \; ; \quad Pe_c = \frac{v_c H_c}{E_c} \quad (5)$$

Consequently, the mixing parameter Pe_c is determined by the logarithmic ratio of the tracer concentration as a function of the measurement location along the column.

Fig. 6 is a systematic representation of the experimental findings on a double logarithmic scale. The mixing parameter Pe_c and the transport coefficient E_c have been plotted versus the mean flow velocity of the continuous phase. The low values entered on the abscissa, i. e. the extremely small flow velocities of $< 10^{-2}$ cm/s, must be attributed to an aqueous volumetric flow rate of 2 l/h and a flow ratio, respectively, of 198/2 = 99. The measured Pe_c numbers are small which means that there has been considerable mixing. The increase in continuous volumetric flow rate to 4, 8, 20 and 50 l/h results in an increase in flow velocity of the continuous phase and causes a rise of Pe_c numbers, i.e., less mixing.

In Fig. 6 a distinction has been made between four conditions. As shown by the measurements, mixing in the absence of a drop phase, i.e., mixing caused by pulsation and cartridges in the continuous phase, is approximately three times less than in the presence of a drop phase. Thus, mixing can be conceived to be composed of two portions: pulsation and cartridges, on the one hand, and countercurrent flow of drops carrying the double weight.

The major result common to all measurements is the clear increase in mixing when the continuous volumetric flow rate decreases.

Axial Mixing, Dispersed Phase

The non-steady-state dye tracer method is used to record mixing in the drop phase. A cloud of dyed droplets is generated in the column whose residence time is measured on two successive planes along the column. A specifically de-

veloped fiber glass probe is used in this measurement which permits inline photometry by laser light with a high spatial resolution. Since the solution of the time-dependent differential equation according to the dispersion model (Eq.1) cannot be indicated explicitly, the model parameters are determined by non-linear regression comparing the complete courses of measured and calculated initial signals /7, 8/.

The mixing parameter Pe_d and the mean residence time τ characterize the behavior of the droplets within the transfer section fixed by two planes of measurement. The Pe_d numbers so determined have been plotted in Fig. 7 versus the ratio of volumetric flows.

It can be noticed that at constant pulsation and constant total volumetric flow rates mixing is not influenced significantly by the flux ratio. By contrast, the geometry of the bottom exerts a great influence. The sieve plate of 4 mm hole diameter implies great Pe_d numbers, i.e., low mixing, and this gives small mixing coefficients E_d.

As in the continuous phase, the nozzle plate and, to a higher extent, the great diameter of the hole gives the higher mixing values also in the dispersed phase. The explanation lies in the different velocities of the droplets. Low mixing is established if the content of the drop phase is moved through the column batchwise within the reaction space limited by two plates each. By contrast, the increase in pulse frequency or in the total volumetric flow rate not shown here, in other words of the parameters serving the purpose of reducing the mean droplet velocities or, in case of great hole diameters, increasing the droplet velocities, lead to a higher degree of mixing. This is an indication of a correlation existing between the plate geometry, the pulsation and the plate spacing which needs further elucidation.

Conclusions

The general aim of this work consists in demonstrating the applicability of pulsed plate columns in case there are great differences between dispersed and continuous volumetric flows, in obtaining design data for this type of column and in scaling them up to make them suitable for use in an industrial reprocessing plant. It is reported here about the first step required in this direction, i.e., fluiddynamic experiments to be performed in a column of 4 m cylinder length and 10 cm internal diameter.

The tendencies in the development of holdup measured in the HNO_3/TBP system can be described partly satisfactorily by correlation equations. The observed deviations in the holdup values are due to the fact that the influences of geometry cannot be correctly expressed at the time being by the mathematical relation (Fig. 4).

The average drop diameter is correctly reflected in its tendency as being dependent on the pulsation frequency in the mathematical relation indicated; however, no distinction can be made between the deviations observed for the plate types investigated (Fig. 5). Such influences of geometry are contained in one constant so far.

The specific transfer area formed by holdup and droplet diameter can be calculated rather statisfactorily within the frequency range of 0.6 - 1.4 s^{-1} for the plate geometry d_o = 4 mm, ε_p = 29 %. However, the correlations are not satisfactory for large hole diameters and a great fraction of free area of plates (d_o = 5 mm, ε_p = 46 %).

Axial mixing in the continuous phase greatly depends on the ratio of volumetric flows (Fig. 6). By contrast, little dependence is observed for the dispersed phase. The reason is that the velocity of the droplets is determined by pulsation whilst it is largely independent of the drop abundance. Thus, the mean drop velocity remains independent of the volumetric flow rate with the pulsation unchanged, which leads to practically constant Péclet numbers and dispersion coefficients (Fig. 7). It can be stated in general that a reduction of obstructions in the column plates by large holes and a great fraction of free area does not favorably influence the fluid dynamic behavior and promotes destabilization.

Literature

/1/ Bericht der OECD-Kernenergieagentur, Information des BMFT, Sept. 1977

/2/ H. Schmidt, H. Miller, KfK-Nachrichten (1982) Vol. 3

/3/ H. Schmidt, Ch. Rodthongkom, R. Müller, Chem.Ing.Techn. (1982) Vol.54, No.12

/4/ J.D. Thornton, Trans. Instn. Chem. Engrs. (1957), Vol. 35

/5/ R. Gayler, N.W. Roberts, H.R.C. Pratt, Trans.Instn.Chem.Engrs. (1953) Vol.31

/6/ S.J. Kagen, M.E. Aerow, V. Lonik, T.S. Volkova, Intern.Chem.Engineering (1965) Vol. 5, No. 4

/7/ R. Bauer, Diss. ETH 5741 (1976)

/8/ F. Leitner, Diplomarbiet (1978), Inst.f.Grundlagen d.Verfahrenstechnik,TU Graz

Formelzeichen

A mm	pulse amplitude, entire pulse stoke
D=100 mm	diameter of column
E cm^2/s	mixing coefficient
H mm	hight of column
H_c mm	hight of cartridge
N	number of plates
$\dot{V}$ l/h	volume flow rate
$a=\frac{6\varepsilon}{d_{32}}$ cm^{-1}	specific interfacial area
c g/cm^3	concentration
$d_{32}=\frac{\Sigma n_i d_i^3}{\Sigma n_i d_i^2}$ mm	Sauter mean diameter
d_o	diameter of holes
f s^{-1}	pulse frequency
g cm/s^2	gravitational acceleration
h cm	hight
u cm/s	superficial velocity
v cm/s	velocity
u_o cm/s	characteristic droplet velocity
z	dimensionless hight
ε %	dispersed phase holdup
ε_B %	fractional free area of plates
μ g/cm s	viscosity
ρ g/cm^3	density
σ g/s^2	interfacial tension
τ s	residence time
Φ cm^2/s^3	frictional power absorbed in the perforations of plates

Indices

a	aqueous phase
c	continuous phase
d	dispersed phase
o	organic phase

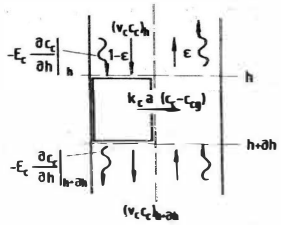

Fig. 2 Material Balance

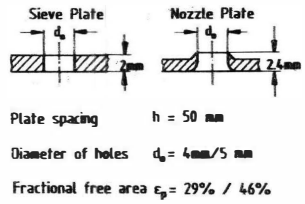

Fig. 3 Geometry of Plates

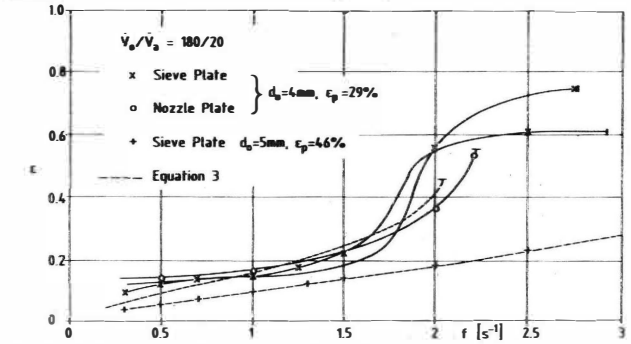

Fig. 4 Holdup versus Frequency of Pulsation

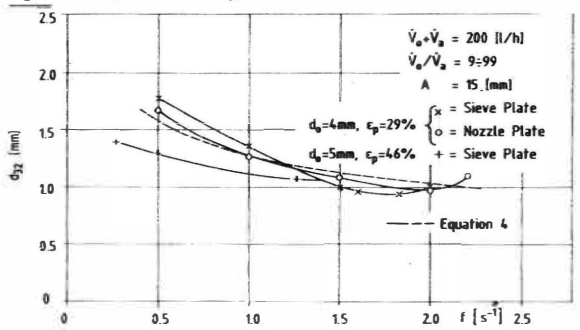

Fig. 5 Sauter Mean Diameter versus Frequency of Pulsation

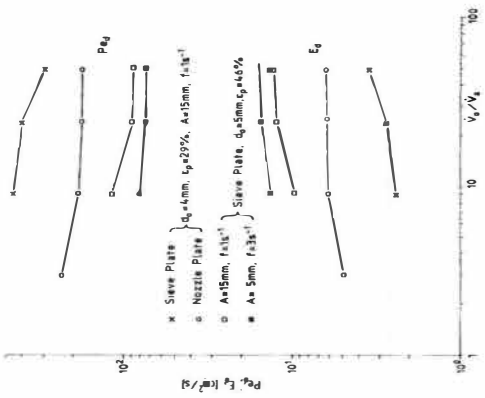

Fig. 7 Axial Mixing, Dispersed Phase

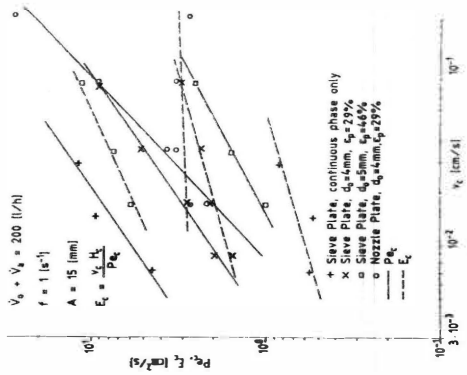

Fig. 6 Axial Mixing, Continuous Phase

THE DYNAMICS OF PULSED PLATE EXTRACTION COLUMNS PART I: DISPERSED PHASE HOLDUP, DROPLET SIZE AND FLOODING RATES IN A 3 in. DIAMETER PULSED PLATE COLUMN

W. Batey, T. Arthur, P. J. Thompson and J. D. Thornton

UKAEA
Thurso, Caithness, Scotland

University of Newcastle
Newcastle-upon-Tyne, England

SCOPE

This paper forms the first part of a series of publications from the Dounreay Nuclear Power Development Establishment aimed at developing a closer understanding of the characteristics and behaviour of pulsed sieve plate columns for the reprocessing of fast reactor irradiated fuels. The present work forms part of a comprehensive programme of liquid extraction studies and is concerned with holdup, droplet size and flooding rate measurements in the absence of any mass transfer.

The extraction system employed was 3 M aqueous nitric acid with 20% TBP/OK as the dispersed phase. The two phases were equilibrated before use.

EQUIPMENT

The column consisted of three 3 ft. sections of 3 in. diameter precision bore borosilicate glass pipeline fitted with 3 ft. settling sections at each end. The sieve plates were spaced at 2 in. intervals in each of the three main column sections and were manufactured from 1/8 in. stainless steel sheet; each plate was drilled with 1/8 in. holes on a triangular pitch to give a free area of 25%.

The column was air-pulsed in the usual way by applying a fluctuating air pressure to a 1 in. diameter leg connected to the bottom of the column. The pulse waveform was monitored over a range of frequencies and amplitudes by means of an electrical conductivity probe located in the top liquid-liquid interface. The pressure drop across the pulse leg was adjusted until the waveforms were sinusoidal.

DROPLET SIZE MEASUREMENTS

Droplet sizes were recorded photographically for a range of flowrates, pulse frequencies and amplitudes both below and at the flooding-point. Several hundred droplets were measured during each run and the mean volume-surface diameter, d_{vs}, computed. In all instances, the droplet size distribution approximated closely to a Gaussian form Figure 1.

The mean droplet size was governed by two parameters; the dispersed phase holdup (x) and the pulse velocity (fA). The latter quantity uniquely described the waveform characteristics since the pulse was sinusoidal. The data indicate that:

(a) At mean pulse velocities less than 4 cm/s (corresponding to a mean orifice velocity of 16 cm/s) the droplet sizes exhibit no trend with increasing holdup. At low mean pulse velocities (and hence low orifice velocities) the droplet size range is large but the spread in droplet sizes decreases with increasing orifice velocity. This behaviour is analogous to that observed by other workers in the case of droplets forming at submerged orifices which are wetted by the dispersed phase (2). It is likely therefore that the present behaviour arises from the fact that the sieve plates tend to be wetted on the downstream side by the solvent phase at low orifice velocities but that this tendency diminishes with increasing nozzle (orifice) velocities. Eventually at a mean orifice velocity of 16 cm/s, the droplet formation mechanism changes and the droplets begin to form in a controllable manner at the perimeters of the plate orifices instead of forming from a pool of solvent on the downstream side of the wetted plate. If this hypothesis is subsequently confirmed, it is apparent that the characteristics of a given sieve plate will depend upon the pulse and hence the orifice velocity as well as the contact angle between the plate and the dispersed phase. A given plate may thus function as a "wet" or a "dry" plate depending upon the mean orifice velocity Figure 2.

(b) At mean pulse velocities in excess of 4 cm/s, the droplets formed controllably around the plate orifices; the size range was small and the mean droplet size d_{vs} showed a slow linear increase with dispersed phase holdup due to progressive droplet coalescence. The mean droplet size at zero holdup, d_{vs}^{o}, varied inversely with the pulse velocity Figure 3.

(c) The mean d_{vs} values over the holdup range 0 to 0.50 ($\bar{d}_{vs}$) varied inversely as $(fA)^{-0.56}$ Figure 4.

DISPERSED PHASE HOLDUP

Holdup measurements below the flooding point were well correlated with the phase flowrates by the equation:

$$V_d + \frac{x}{1-x} V_c = \bar{V}_o \, x(1-x) \quad \ldots \quad \ldots \quad (1)$$

where the term $\bar{V}_o$ is the droplet characteristic velocity, i.e. the mean droplet velocity relative to the continuous phase when $V_c = o$ and $V_d \rightarrow o$. Furthermore $\bar{V}_o$ was dependent only upon the pulse velocity and varied as $(fA)^{-4/3}$. The data for the present system were therefore well correlated by the relationship:

$$\left[V_d + \frac{x}{1-x} V_c\right] \left[fA\right]^{4/3} = \text{Const. } x(1-x) \quad \ldots \quad (2)$$

as shown in Figure 5.

Since the mean droplet size $\bar{d}_{vs} \propto (fA)^{-0.56}$, the present result implies that $\bar{V}_o \propto (\bar{d}_{vs})^{2.3}$, compared with the Stokes' law dependency of $(\bar{d}_{vs})^{2.0}$.

FLOODING RATES

Differentiation of equation (1) with respect to x, treating $\bar{V}_o$ as constant and imposing the floodpoint criteria $(dV_d/dx) = o$, $(dV_c/dx) = o$, leads to the floodpoint equation (1):

$$V_{d_f} = 2\bar{V}_o \, x_f^2 \, (1 - x_f) \quad \ldots \quad \ldots \quad (3)$$

$$V_{c_f} = \bar{V}_o \, (1 - x_f)^2 \, (1 - 2x_f) \quad \ldots \quad \ldots \quad (4)$$

These imply that the limiting values of the floodpoint curve are $V_{d_f} \rightarrow (\bar{V}_o/4)$ when $V_{c_f} \rightarrow o$ and $V_{c_f} \rightarrow \bar{V}_o$ when $V_{d_f} \rightarrow o$.

The present floodpoint data were plotted in accordance with equation (1); the corresponding values of $\bar{V}_o$ were then determined directly from the slopes of the lines passing through the origins. These values were used to compute the limiting values of the floodpoint curves as indicated by equations (3) and (4). The resultant curves are shown in Figure 6.

The characteristic velocity values ($\bar{V}_o$) associated with these data varied with pulse velocity as $(fA)^{-0.52}$ which implies that at the floodpoint $\bar{V}_o \propto (\bar{d}_{vs})^{0.93}$. This compares with a dependency of $(\bar{d}_{vs})^{1.14}$ for the intermediate settling law and is the result of the somewhat larger droplet sizes associated with the higher holdup values at the flooding point.

NOMENCLATURE

A	Pulse amplitude (total excursion in the column). (cm unless otherwise stated).
d_{vs}	Mean volume-surface droplet diameter /(mm)
$\bar{d}_{vs}$	Mean volume-surface droplet diameter at x = 0.25 /(mm)
d_{vs}^{o}	Mean volume-surface droplet diameter when $x \rightarrow o$ /(mm)
f	Pulse frequency (s^{-1})
V_d	Dispersed phase superficial velocity (ft. h^{-1})
V_c	Continuous phase superficial velocity (ft. h^{-1})
$\bar{V}_o$	Droplet characteristic velocity i.e. mean droplet velocity relative to the continuous phase when $V_c = o$ and $V_d \rightarrow o$ (ft. h^{-1})
x	Fractional holdup of the dispersed phase

REFERENCES

(1) J. D. Thornton, Trans. Instn. Chem. Engrs., 1957, 35 316 (cf also J. D. Thornton, Chem. Eng. Sci. 1956, 5 201)

(2) R. E. Treybal, Liquid Extraction (2nd Edn), p 466, (McGraw-Hill, 1963)

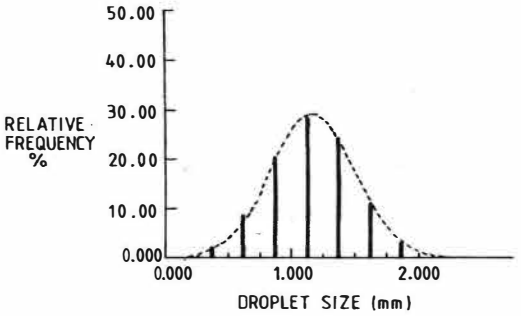

FIG. 1. TYPICAL DROPLET SIZE DISTRIBUTION

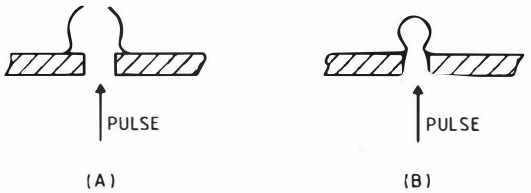

FIG. 2. (A) DROPLET FORMING AT A WETTED PLATE AT LOW ORIFICE VELOCITIES.

(B) DROPLET FORMING AT PLATE ORIFICE AT HIGHER ORIFICE VELOCITIES.

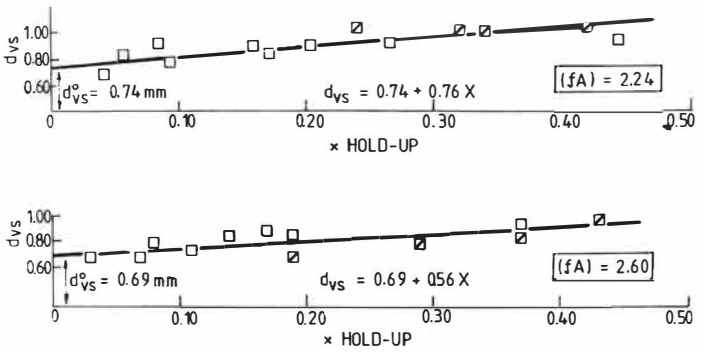

FIG. 3. VARIATION OF DROPLET SIZE WITH HOLD-UP (shaded symbols represent data at the flooding point)

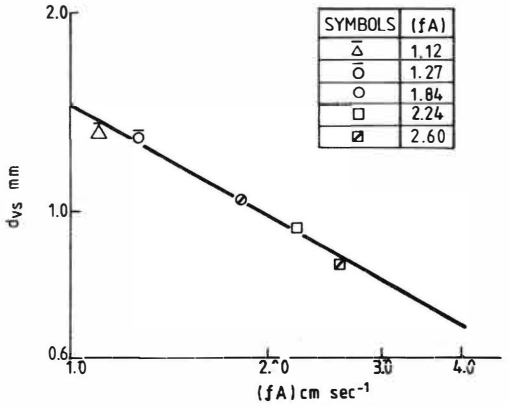

FIG. 4. LOGARITHMIC PLOT OF MEAN DROPLET SIZE VERSUS (fA)

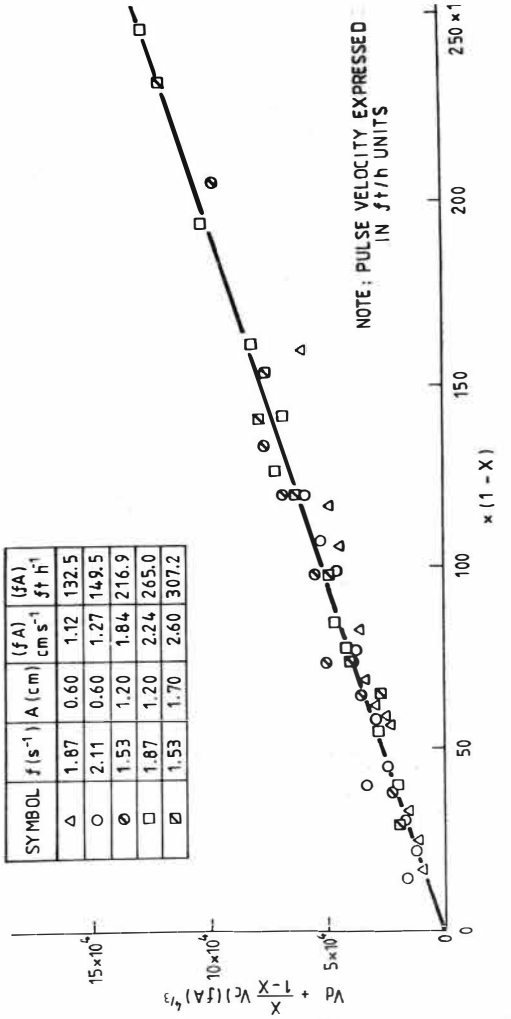

FIG. 5. PLOT OF HOLD-UP DATA FOR VARIOUS (fA) VALUES.

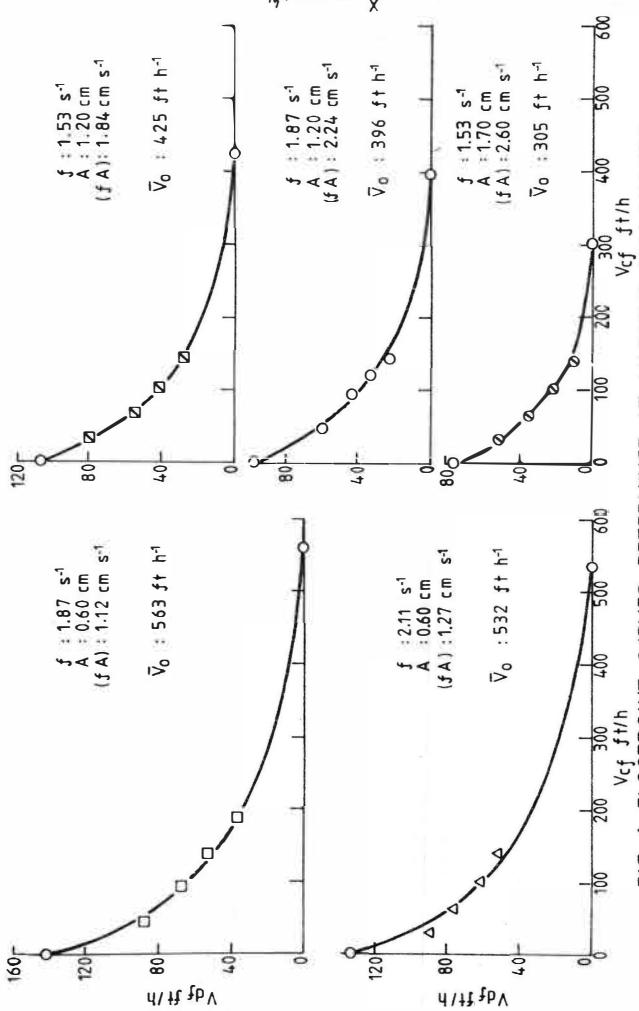

FIG. 6. FLOODPOINT CURVES DETERMINED AT VARIOUS (fA) VALUES. (limiting values of the phase flowrates are indicated on the axis).

THE HYDRODYNAMIC BEHAVIOUR OF A PULSED PERFORATED-PLATE COLUMN

G. Vassallo, J. D. Thornton and H. Dworschak

University of Newcastle
Newcastle-upon-Tyne, England

C. C. R. - Euratom
Ispra, Italy

Dispersed-phase holdup and droplet size measurements were made in a 72 mm i.d. pulsed perforated-plate column. The contactor was fitted with three cartridges each comprising of 21 stainless steel plates (perforation-size 3.2 mm, triangular pitch, free area 23 %) resulting in an effective length of approximately 3.2 m. The chemical system employed was 30 vol.% TBP/OK dispersed in 2M HNO_3. The phases were mutually saturated prior to any experiment in order to eliminate interfacial effects. Four parameters, namely pulse amplitude, frequency and both phase flowrates, were varied over a wide range of values. Nevertheless, the column was maintained predominantly in a continuous dispersion type regime throughout the experiments.

Dispersed-phase holdup measurements, both total and zonal, were obtained using a series of shutter-plates (1). The column was shut down during steady state operation, usually assumed to be attained after at least five changes in column holdup. The top disengagement section was quickly drained and the four shutter plates, situated at regular intervals along the packed section, closed. The movement of either phase across the plates was substantially reduced although a perfect hydrodynamic seal was impossible to achieve.

Holdup appeared to pass through a minimum at a constant pulse velocity corresponding to the onset of continuous dispersion type operation. The value of this minimum varied linearly with the dispersed-phase flowrate. However, various expressions based on this finding proved unsuccessful ; they were generally inaccurate and unstable.

A relationship was developed between holdup and the above operating parameters based on the slip velocity concept (2), i.e. the average velocity of the droplets relative to the continuous-phase. It was shown that the general equation lacked a term allowing for droplet coalescence which is known to increase with holdup. Misek (3) has utilized an exponential to define the ratio of velocities of coalesced and uncoalesced droplets at a finite holdup . However, the exponential is rather complex, being a function of the system, holdup and degree of turbulence. Such an intricate correction term was considered unwarrented for the present application. Instead, the term was assumed to be a power function of the group (1-x), thereby keeping the form of the general slip velocity equation intact. The data were correlated using a bounded least-squares minimization technique which resulted in the following expression :

$$(1) \qquad \frac{V_c}{1-x} + \frac{V_d}{x} = 6.19 \times 10^{-4} [af]^{-0.87} [1-x]^{0.64}$$

V_c	: superficial velocity of continuous-phase	(m/s)
V_d	: superficial velocity of dispersed-phase	(m/s)
x	: fractional holdup of dispersed-phase in effective section of column	(-)
a	: pulse amplitude in column	(m)
f	: pulse frequency	(Hz)

From this expression, it is possible to derive values of holdup and phase flowrates at flooding (4) :

$$(2) \qquad V_{d,f} = 1.64 \bar{V}_r x_f^2 [1 - x_f]^{0.64}$$

$$(3) \qquad V_{c,f} = \bar{V}_r [1 - 1.64 x_f] [1 - x_f]^{1.64}$$

$$(4) \qquad x_f = \frac{[0.41 R_f^2 + 6.56 R_f]^{0.5} - 2.64 R_f}{3.28 [1 - R_f]}$$

$\bar{V}_r$	: mean velocity of droplets relative to continuous-phase	(m/s)
R_f	: ratio of dispersed-phase flowrate to continuous-phase flowrate at flooding	(-)

subscript f : value of flooding

In the usual range of flowrates, Equation (4) can be replaced by the following expression with little loss in accuracy :

$$(5) \qquad x_f = 0.2 \log R_f + 0.38 \qquad 0.1 < R_f < 5.0$$

Droplet data were obtained by photographing the organic dispersion in the column. Two types of photographic cell were utilized : droplet distortion was minimized in both by either designing the photographic window as an integral part of the column shell or by filling the space between the window and outside of the shell with water. The negatives, which were analysed using a magnetic pen system, clearly displayed the hydrodynamic disturbances caused by the discontinuity of the column cross-section in the first cell type. The results were not reproducible and, due to the recirculation of small droplets, differed markedly from those of the second type of which three were employed.

The data were correlated in terms of the Sauter-mean droplet size. This size, at substantially zero holdup, was shown to be a function of only the energy dissipation in the column. However, attempts at incorporating this knowledge into an expression with the coalescence correction term, failed, the final correlation giving biased results.

For any liquid-liquid system, the relative droplet velocity varies with the droplet size. Values of the experimental characteristic droplet velocity were then compared with the predicted values of single droplets using the correlation of Hu and Kintner (5). It was shown, Equation (6), that the ratio of the velocities in a pulsed perforated-plate column to that of a single droplet is a function of the pulse velocity and holdup, Figure 1 :

$$(6) \qquad R_v = \frac{\bar{V}_r^{\circ}}{\bar{V}_r^{*}} = 0.483 [af]^{-0.08} x^{-0.12}$$

$\bar{V}_r^{\circ}$	: value of $\bar{V}_r$ at zero continuous-phase flowrate and essentially at zero dispersed phase flowrate	(m/s)
$\bar{V}_r^{*}$	: value of $\bar{V}_r$ for a single droplet	(m/s)

The pulsed velocity makes allowance for the resistance offered by the plates, while the holdup term takes into account the interaction of the dispersed-phase droplets. A droplet size expression based on the correlation of Hu and Kintner also failed. This suggested, however, that the range of Reynolds number observed in the column (10-40) was beyond the limits of the two theories so far employed. This supposition led to a third expression which correlated the droplet size data with negligible error :

$$(7) \qquad d_{32} = 8.36 \times 10^{-5} [[af]^{-0.87} [1 - x]^{-0.36}]^{-0.60}$$

d_{32}	: Sauter-mean droplet diameter	(m)

Equation (7) implies that $\bar{V}_r$ is proportional to d_{32} raised to the power 1.7. This is in contrast to the value of 2 for Stokes law and approximately 1.2 for the correlation of Hu and Kintner in the above range of Reynolds number. Furthermore, it was demonstrated that values of the characteristic droplet velocity based on Equations (6) and (7) and the correlation of Hu and Kintner (5) were comparable to those derived from the modified slip velocity expression, Equation (1), Figure (2).

Droplet size distributions were shown to be approximately log-normal at low pulse velocities and normal at high velocities with a mode in the region of 0.6 mm. Little axial variation occurred in either the distributions or Sauter-mean droplet size except near the dispersed-phase inlet. This is confirmed by the consistency of the holdup measurements, Figure (3). However, the geometry of the dispersed-phase distributor has a significant effect on holdup in that region of the column. This is to be expected as it is unlikely that the range of droplets leaving the distributor is comparable to the steady state droplet distribution in the column. A re-adjustment probably dominated by droplet breakup, occurs as the droplets enter the column packing. The time and therefore the length of packing required for this modification will depend on the initial dissimilarity between the distributions leaving the dispersed-phase inlet and in the column, and on the rate of droplet breakup. The significance of the dispersed-phase entry section thus becomes progressively more important as the column moves from a mixer-settler to fully dispersed regime.

REFERENCES

1. BELL R.L., Ph.D. Thesis, University of Washington (1964).
2. GAYLER R. et al., Trans. Inst. Chem. Engrs. 31 (1953), 57.
3. MISEK T., Colln. Czech. Chem. Commun. 28 (1963), 1631.
4. THORNTON J.D., Chem. Eng. Sci. 5 (1956), 201.
5. HU S., KINTNER R.C., A.I. Ch. E.J. 1 (1955), 2.

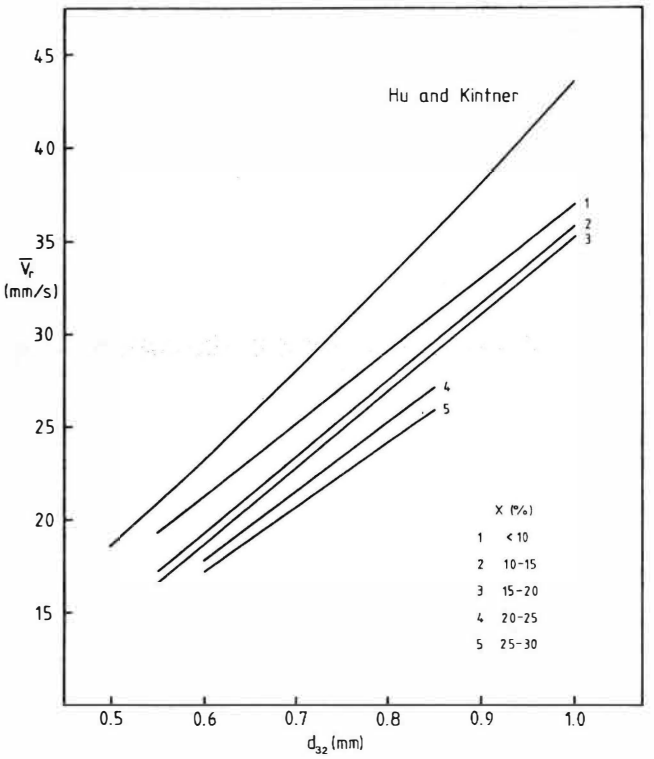

FIGURE 1. VARIATION OF $\overline{V}_r$ WITH d_{32}

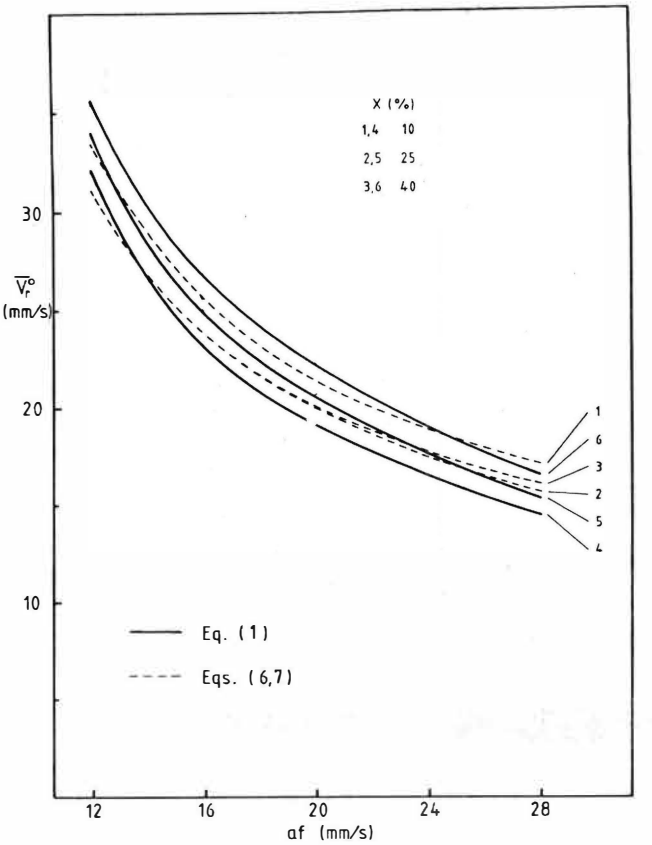

FIGURE 2. CHARACTERISTIC DROPLET VELOCITY AS A FUNCTION OF PULSE VELOCITY AND HOLDUP

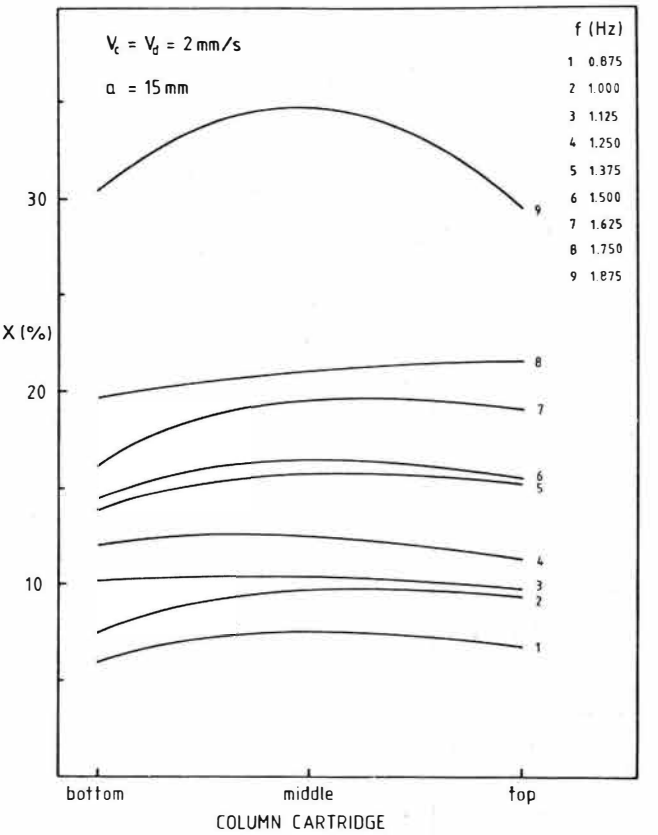

FIGURE 3. AXIAL VARIATION OF HOLDUP

HOLDUP MEASUREMENT IN A ROTARY-AGITATED EXTRACTION COLUMN

Siu-Ming Yih, Ray-Kuo Pan and Yau-Ming Wu

Department of Chemical Enigineering
Chung Yuan University
Chung Li, Taiwan ROC

ABSTRACT

The total holdup of a dispersed organic phase in a rotary-agitated Scheibel liquid-liquid extraction column is studied experimentally. The column is 2 inches in diameter and contains 11 stages with a 4-inch height packed section and a 1-inch height mixing section. The packed section is made of stainless steel wire mesh packing with a 93.74% free area and acts as a settler for the coalescence of droplets. Benzene and methyl isobutyl ketone (MIBK), which have a large difference in interfacial tension, are used respectively as the dispersed phase with water as the continuous phase. The effects of different phase flow rates and rotation speeds (450-600 rpm) on the dispersed phase holdup are studied. For benzene, the holdup is large at low rotation speeds and decreases with increasing rotation speed until a minimun holdup is reached, after this transition point, the holdup increases with increasing rotation speed. This phenomena is analogous to that found in a pulse column. For MIBK, the holdup always increases with rotation speed in our experimental range and the transition point is not observed as in benzene.

INTRODUCTION

A knowledge of dispersed phase holdup in a liquid-liquid extraction column is necessary for the evaluation of flooding data, longitudinal mixing data, and residence time distributions in the analysis of interphase mass transfer rates. If the extraction is accompanied by a chemical reaction, the rate of chemical reaction will also be dependent on the holdup of both phases. Determination of holdup in an extraction column is also essential for calculating product inventory in a separation plant. The present research investigates the dispersed phase holdup in a rotary-agitated Scheibel column as a function of column operating variables and system physical properties. These data apparently have not yet been reported in the literature.

EXPERIMENTAL

The apparatus, originally designed by E. G. Scheibel (1), is shown schematically in Figure 1. The column geometrical data are shown in Table 1 and is a type of "standard geometry". Water is selected as the continuous phase while benzene and MIBK are the two separate discontinuous phase. Both organic liquids have a specific gravity less than 1. Their specific gravity and viscosity do not differ much from each other but they have a large difference in interfacial tension. Their physical properties are shown in Table 2. The specific gravity is measured with a hydrometer. The viscosity is measured with a Brookfield Synchro-lectric viscometer and the interfacial tension by a Du-Nuoy type ring tensiometer. The measured values compared well with the values reported by Schmel and Babb (2).

TABLE 1. COLUMN GEOMETRY

Number of stages	11
Feed stage location	6th from the top
Column size, I.D., inches	2
Packing section height, inches	4
Mixing section height, inches	1
Free area of packing, %	93.74

TABLE 2. PHYSICAL PROPERTIES OF ORGANIC LIQUIDS USED

	Benzene	MIBK
Specific gravity	0.89	0.81
Viscosity, c.p.	0.80	0.72
Interfacial tension, dyne/cm	30	11.5

APPARATUS

The whole apparatus consist of (3):

1. One Pyrex glass column with (a) two inlet nozzles, center feed, and two outlet nozzles, (b) stainless steel flanges, stuffing box and vent, (c) stainless steel center shaft, agitators, and wire mesh packing sections.
2. Two 5-gallon Pyrex feed bottles and calibrated funnel for center feed.
3. Three stainless steel needle valves for feed flow control.
4. One stainless steel drain valve.
5. Three rotameters
6. One variable speed drive with 1/4 H.P. explosion-proof class I, Group D motor.
7. One overflow arrangement for interface level control.
8. All necessary connecting stainless steel and Teflon tubing.
9. One steel mounting frame approximately 24" wide and 7'6" high, with foot and wall brackets, and feed bottle shelf. Headroom requirement for complete assembly is 10 feet.

All parts of the column exposed to the process streams are type 316 stainless steel, rotameters contain Pyrex and stainless floats, and interconnections are of Teflon tubing.

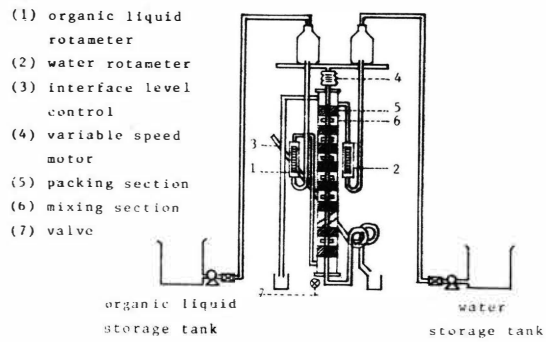

FIGURE 1. SCHEMATIC DIAGRAM OF A ROTARY-AGITATED SCHEIBEL COLUMN

TABLE 3. FLOW RATES USED FOR HOLDUP EXPERIMENTS

Water (c.c./min)	Organic liquid (c.c./min)
Benzene-water System	
92	140
143	140
173	140
143	90
143	168
92	90
173	168
MIBK-water System	
21	44
45	44
63	44
63	25
63	66
21	25

PROCEDURE

Holdup in this study is defined as the average per cent of the total volume between all stages occupied by the dispersed organic phase at steady-state operation. The organic liquid is fed from the bottom of the column while water is fed from the top of the column. The column contents are agitated with a desired rotation speed which is measured with a tachometer. A holdup measurement is initiated by closing the water and organic liquid inlet valves after the two phases have reached steady-state and equal input and output flow rates. Since some organic droplets will rise through the stages after the motor has stopped, stage-to-stage holdup cannot be measured by this technique. Accordingly, the column contents are agitated for a while and the motor is stopped, then wait until all the organic droplets rise to form a continuous layer. The organic liquid and water are drained out from the column and their volume are measured respectively so that the fractional total holdup in the column contacting section can be readily measured.

RESULTS AND DISCUSSION

Organic holdup data are obtained at several different continuous-dispersed flow rates as shown in Table 3 and a range of mixer rotation speeds (450-600 rpm). Representative results of holdup are shown in Figures 2 to 4 for benzene-water system and Figures 5 to 7 for MIBK-water system.

Effect of Phase Flow Rate. The results shown in Figure 2 for benzene-water system show that holdup is virtually independent of the water phase flow rate for the range of water flow rates investigated. However, organic holdup increases signifigcantly with dispersed phase flow rate as shown in Figure 3. This is because when the dispersed phase flow rate increases, the amount of droplet population increases and an effect of

hindered rising occurs which makes the residence time of the droplets in the column longer. In Figure 4, the use of approximately equal flow rates of both phases show the same trend as in Figure 3. This is because holdup is practically independent of continuous phase flow rate. As in the benzene-water system, there is also practically no effect of continuous phase flow rate on the holdup for the MIBK-water system as shown in Figure 5. Also, as shown in Figures 6 and 7, the holdup increases significantly with an increase in the dispersed phase flow rate.

Effect of Rotation Speed. For the benzene-water system, as shown in Figures 2 to 4, usually the holdup is large at low rotation speeds and decreases with increasing rotation speed until a minimum holdup is reached at about 550 rpm. After this transition point, the holdup increases with increasing rotation speed. This phenomena is very similar to that found in a pulse column. In analogy to a pulse column, the region below the transition point with low rotation speeds can be considered as a "mixer-settler" region, while the region above the transition point with large rotation speeds can be considered as an "emulsion" region. By visual observation, the droplets are larger and fewer in the "mixer-settler" region and coalescence of droplets occur rapidly in the wire mesh packing. On contrary, the droplets in the "emulsion" region are smaller and the droplet population density increases so rapidly that the column becomes cloudy in appearance. In this region, the holdup increases with an increase in rotation speed, possibly due to the increased circulation of droplets in the radial direction and hindered rising effect of the droplets which as a result retain the droplets longer in the column.

For the MIBK-water system, as shown in Figures 5 to 7, the holdup always increases with increasing rotation speed in the range of 450-600 rpm. Visual observation shows that at 450 rpm, the column already becomes cloudy in appearance which indicates that the operation is already in the "emulsion" region. Due to a limitation in the lower setting of the motor, the lowest rpm that can be attained in this experiment is 450 rpm. We expect that, if a still lower rpm can be operated, the transition point between "mixer-settler" and "emulsion" region can also be found.

Effect of Physical Properties. Benzene and MIBK do not differ greatly in viscosity and density but they differ significantly in their interfacial tension by almost 3 times as shown in Table 2. The miscibility of MIBK and water is larger than benzene and water. As can be seen from the above Figures, the transition point of "mixer-settler" and "emulsion" region occurs at a higher rotation speed for benzene-water than MIBK-water. This means that a higher power input to the motor is necessary to disperse benzene effectively in water than MIBK in water.

REFERENCES

1. E.G. Scheibel. Chem. Eng. Progress, 44, 681 (1948).
2. G.A. Sehmel and A.L. Babb. I.& E.C. Process Design and Development, 2, 38 (1963).
3. "XA-2-York Scheibel liquid-liquid extraction unit", York Process Equipment Corporation Manual.

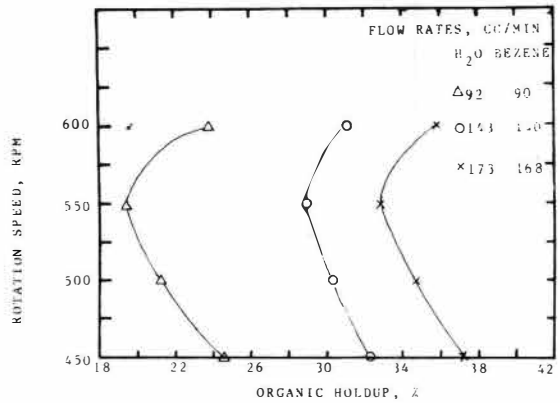

FIGURE 4. EFFECT OF EQUAL PHASE FLOW RATES ON HOLDUP FOR BENZENE-WATER SYSTEM

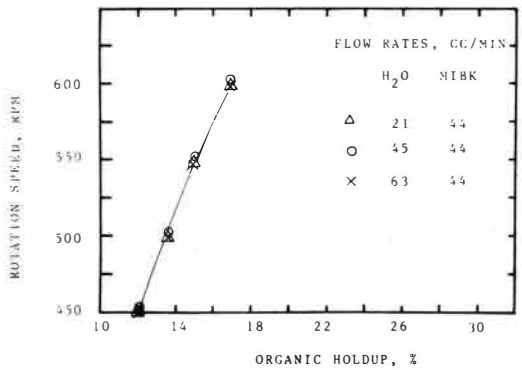

FIGURE 5. EFFECT OF CONTINUOUS PHASE FLOW RATE ON HOLDUP FOR MIBK-WATER SYSTEM

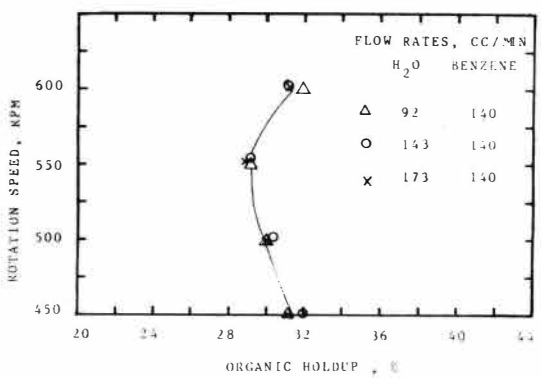

FIGURE 2. EFFECT OF CONTINUOUS PHASE FLOW RATE ON HOLDUP FOR BENZENE-WATER SYSTEM

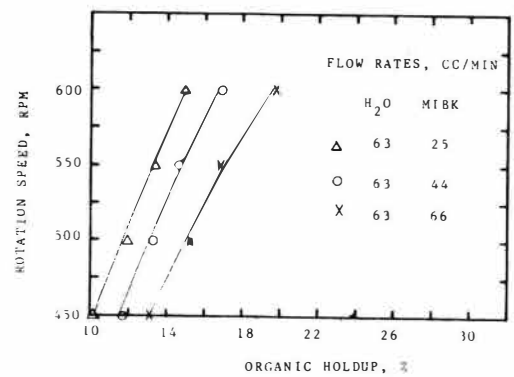

FIGURE 6. EFFECT OF DISPERSED PHASE FLOW RATE ON HOLDUP FOR MIBK-WATER SYSTEM

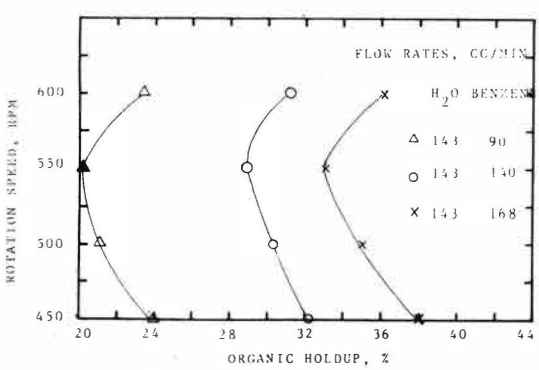

FIGURE 3. EFFECT OF DISPERSED PHASE FLOW RATE ON HOLDUP FOR BENZENE-WATER SYSTEM

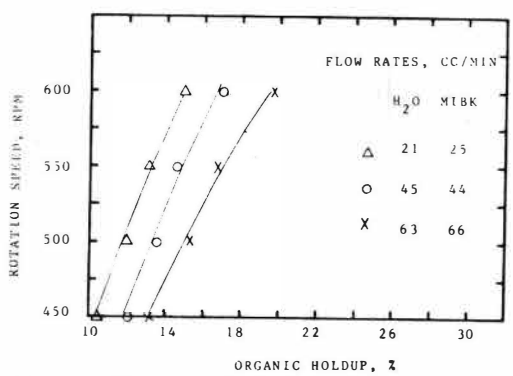

FIGURE 7. EFFECT OF EQUAL PHASE FLOW RATES ON HOLDUP FOR MIBK-WATER SYSTEM

DROP FORMATION AT ROTATING ORIFICES IN A CENTRIFUGAL FIELD

Reinhold Schilp and Eckhart Blass

Technische Universität München
Munich, Federal Republic of Germany

High centrifugal field intensities are extremely useful during extraction for the acceleration of the mixing and separating processes. This is of particular interest when one is dealing with mass systems of very small density differences, or when short contact times are necessary /1/. The calculation for centrifugal extractors is based mainly on the contact surfaces of the phases and this on the average drop size of the drop swarms. Just as important in deciding the dimensions required are the contact times, which are closely related to the settling velocities in the centrifugal field /2/. We therefore examined the fluid-dynamic processes on rotating cylindrical perforated sheets under centrifugal field intensities commonly used in industry.

For this purpose a model centrifuge was built which was resistent to the high loads produced by rotation and hydrostatic pressure, which allowed high liquid throughputs and which enabled us to observe the flow mechanism of the coloured dispersed phase and film with a high speed camera. Fig.1 shoes the model centrifuge in cross-section. The speed regulated motor is coupled at the bottom of a casing, with the centrifugal rotor, which is transparent on top, fixed to its shift. Both fluids are fed in at the middle, the dense phase being introduced inside the perforated sheets, while the light phase is brought in at the rotor periphery. both phases flow radially through the rotor in opposite direction and are then discharged into the casing.

1. DISTANCE OF THE DROP FORMATION AREA

In a rotating liquid-liquid system, with single jet and multi-jets emerging from holes a considerable orientation of the jet against the direction of rotation is shown immediately after emerging from the dispersing orifices (Fig.2). The radial interval of this disintegration point into drops, measured from the hole, is an important criterion for the smallest possible distance between the perforated sheets in the centrifuge. In centrifugal extractors the radial intervals between the perforated sheets are kept very small in order to achieve a large number of separation stages with equipment of a small size. If, however, the distances are too small no drops will be formed, for the liquid jets enter the next stationary layer with no drops dispersion. The contact surface of the phases decreases as a result to approximately 10% and the mass transfer performance is considerably reduced. The maximum interval of the curved jet Δr_{max} can be calculated with good accuracy for high field intensities with the aid of a derived equation /3/.

$$\Delta r_{max} = \sqrt{\frac{r_N\, d_N\, (\rho_d - \rho_c)}{\zeta_{Zyl}\, \rho_c}} + 0{,}3\, \frac{w_N}{\omega} \qquad (1)$$

r_N radius of perforated sheet, d_N diameter of orifice in perforated sheet, w_N hole velocity, ω angular velocity, ζ_{Zyl} drag coefficient of jet in transverse flow, $\rho_{d,c}$ density of the liquids.

Fig. 2 presents a plot of the maximum radial jet distance Δr_{max} against the angular centrifugal velocity. The plotted points represent the jet distances, measured at fifferent angular velocities under constant operating conditions, with the continuous line corresponding to Eq. (1) for these given constant operating conditions. The radial depth of penetration sinks with increasing rotational speed, on account of the stronger jet reorientation. It rises, however, with increasing geometrical dimensions and increasing hole outled velocities.

2. DROP SIZE

After the jet has left the orifice it is dispersed into primary drop-sizes. By measuring the drop-formation frequency, we can calculate the primary drop-sizes near the perforated sheet, but these are not particulary important, since at high centrifugal field intensities they immediately disintegrate further into smaller secondary drops. The larger drops are considerably deformed in the centrifugal field. With increasing drop velocities a critical deformation of the drops is reached and they disperse into smaller drops. Thus a certain drop size, which despite drop deformation remains just about stable, corresponds to a particular field intensity. From an energy analysis of the drop-disintegrationprocess a relationship can be derived which permits us to calculate the average drop-diameter according to Sauter, d_{32}, of the drop swarms as a function of its physical characteristics and the centrifugal field intensity.

$$d_{32} = 3{,}85 \sqrt{\frac{\sigma \cdot \rho_c \cdot (K_L)^{0{,}03}}{(\rho_d - \rho_c) \cdot \rho_d \cdot r\omega^2}} \qquad (2)$$

K_L liquid number, σ interfacial tension, r radius in centrifuge

Fig. 3 presents the Sauter mean diameters d_{32} measured for water dispersed in paraffin, plotted against the centrifugal field intensity. At a constant centrifugal field intensity the average drop size of the drop swarm is particulary independent of the exit velocity from the dispersing hole. At higher centrifugal field intensities the secondary drop size formed is independent of hole-diameter, of hole pitch and of the hole shape.

The contiuous line represents Eq. (2) for the secondary drop disintegration. At lower centrifugal field intensities relatively large drops would be stable while settling, but small holes only produce primary drops, which are already smaller than drops stable at the corresponding field intensity. The primary drops formed, do not disintegrate further when they continue to settle. The dot-dash lines represent the average primary drop sizes d_{32N} near the perforated sheet, calculated according to Eq. (3).

$$d_{32N} = 1{,}3 \frac{(w_N \cdot d_N^2)^{1/3}}{(r_N \cdot \omega^2)^{1/4}} \qquad (3)$$

The cause for the smaller drop diameter at lower centrifugal intensities in Fig.3 is the smaller diameter of the primary drops from small orifices in the perforated sheet.

3. SETTLING VELOCITY OF DEFORMED DROPS IN THE CENTRIFUGAL FIELD

With increasing field intensity the settling drops do not only become smaller, but also more heavily deformed. The globular shapes turn into spheroids and sperical caps. As a result of the change in the geometrical shape of the drop, the drag coefficients rise rapidly. The wake volume of the continuous phase, which the drop transports behind itself, similary corresponds closely to the extent of deformation. The wake volume influences both, the inertia of the drops at accelerated motion and the backmixing of the continuous phase. The resistance during acceleration of the contiuous phase must be taken into account when calculating the accelerated settling motion of the drops. A system of differential equations was derived for the non-stationary motion of deformed drops in the centrifugal field intensity. In this system we took into account the intertial forces consisting of the drop-mass, the wake-volume, and the virtual mass, as well as the efficient centrifugal- and lift forces, the Magnus-forces resulting from the unsymmetrically circulation around the particles and the flow resistance of the deformed drops. The results showed that the pronounced increase of velocity of the drops during the first acceleration phase may be ignored when building a model of the settling motion. After starting, the drops reach their final settling velocity within a distance of a few millimeters, a velocity which continues to rise only slowly corresponding to the

increase in field intensity. Both, the theoretical calculations and the measurements proved that the settling velocity of deformed drops is proportional to the rotational speed and increases with the square root of the radius of the centrifuge.

Fig.4 presents the local settling velocities of the average drop diameters of the drop swarms measured against the corresponding centrifugal field intensity. The settling velocities of the drops, which have the size of the Sauter mean diameter of the drop swarm, increases with the square root of the centrifugal field intensity. When looking for easy-to-handle bases for calculation it is interesting to note that the average diameter of deformed drops according to Sauter, d_{32}, multiplied by the settling velocity measured for this drop size, w_{32}, gives a constant value for all centrifugal field intensities. This value is only dependent on the physical characteristics of the liquids and can be expressed by the Reynolds number. Re_{32}. The connection between Re_{32} and the physical characteristics can be calculated from Eq. (4)

$$Re_{32} = 1{,}8\ (K_L)^{0{,}265} \tag{4}$$

Fig.5 shows the Re_{32}-number which were measured plotted against the centrifugal field intensity. In addition to the experimental Re_{32}-values, the Re_{32}-numbers calculated theoretically with Eq.(4) have been plotted as a source for comparison, for the two liquid systems examined. By means of the simple Eq.(4) it is possible to sum up the complex processes involved in drop formation and in the motion of deformed drops in the drop swarm. This then allows us, in effect, to predict by purely theoretical means the actual settling velocity w_{32} of the drop swarm for any radius in the centrifuge rotor and for any rotational speed, on the basis of the average drop size d_{32}, which can be precisely calculated by using Eq.(2) and of the Re_{32}-number, which can be determined from Eq.(4).
The settling velocity of the drop swarm in centrifugal field can be expressed by:

$$w_{32} = 0{,}47 \cdot \sqrt[4]{\frac{\sigma \cdot \Delta\rho \cdot \rho_d^2}{g \cdot \rho_c^4}} \cdot \sqrt{r\omega^2} \tag{5}$$

$\Delta\rho$ difference of densities, g gravity, r radius in centrifuge.

4. SUMMARY

It is thus possible to calculate the interfacial areas and the contact times for the drop phases in the individual radius stages of the centrifuge. Both are of fundamental importance to fluid dynamics for the calculation of mass transfer.

The authors gratefully acknowledge the financial support of the Deutsche Forschungsgemeinschaft at the work presented above.

5. REFERENCES

/1/ Blass E., et al.: Chem.-Ing.-Tech. 47 No.5 169 (1975)

/2/ Stölting M.: Dissertation, TU München (1979)

/3/ Schilp R., Blass E. : Ger.Chem.Eng. 5 No.6 364 (1982)

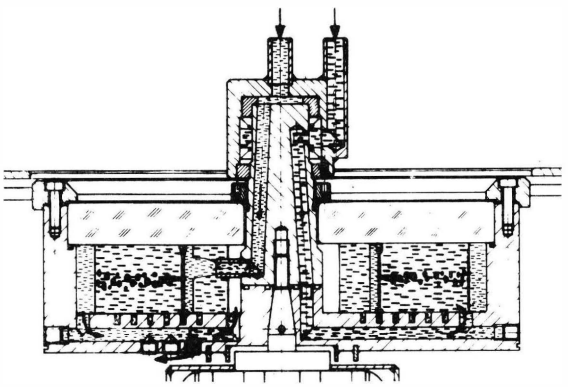

Fig.1: Sectional view of the centrifuge model

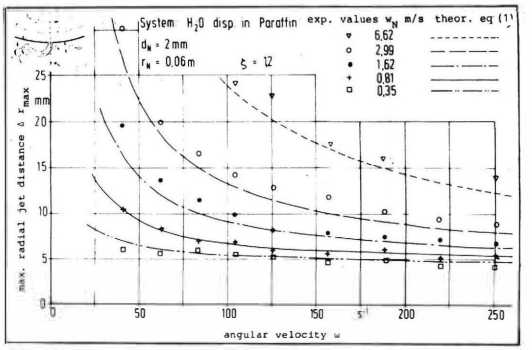

Fig.2: Radial depths of jet penetration as a function of rotational speed

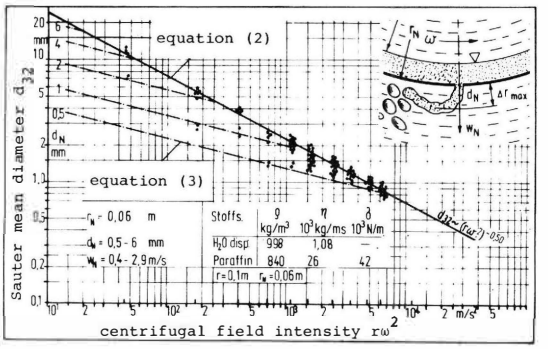

Fig.3: Drop size as a function of centrifugal field intensity

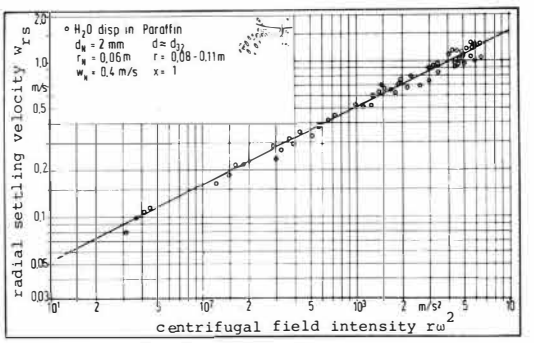

Fig.4: Settling velocities of the drop swarms in the centrifugal field

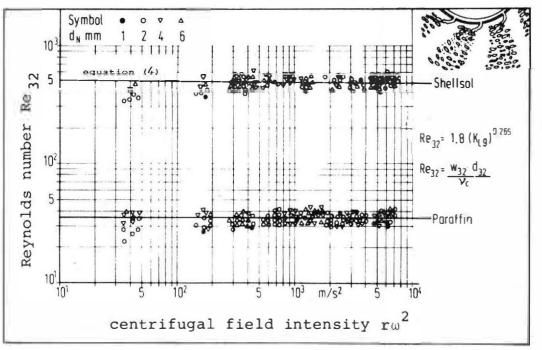

Fig.5: Connection between drop formation and drop motion in the centrifugal field.

A NEW LOOK AT THE HYDRODYNAMIC BEHAVIOR OF ROTATING DISC CONTACTORS

W.-Y. Fei

Quinghua University
Beijing, China

and

M. J. Slater
University of Bradford
Bradford, U.K.

The rotating disc contactor has been used and studied intensively for many years. In this paper we propose a better equation for calculating throughput than the usual simple equations for correlating dispersed phase hold-up with dispersed phase and continuous phase superficial velocities,(1,2).

(1) $V_{slip} = V_O (1 - x)$

(2) $V_{slip} = V_c/(1 - x) + V_d/x$

Originally, and still commonly, equation (1) is tested by plotting xV_{slip} (or $V_d + V_c x/(1 - x)$) against $x(1 - x)$ to give a line through the origin, of slope V_O. This method disguises the large scatter often observed when plotting V_{slip} directly against $(1 - x)$ and tends to hide the fact that equation (1) is only approximate.

Other equations have been used to correlate hold-up data, for example:

(3) $V_{slip} = V_K (1 - x) \exp(- ax)$ (Ref. 3)

(4) $V_{slip} = V_K \exp(- bx)$ (Ref. 4)

(5) $V_{slip} = V_K (1 - x)^m (1 + cx)$ (Ref. 5)

(6) $V_{slip} = V_K (1 - x)^m$ (Ref. 6-9)

In this work we have adopted equation (6); by examination of work on spray columns and fluidized systems in general (10 - 17) it may be shown that relatively complex relationships derived with theoretical support give very similar results to equation (6) if drop size is unchanging as hold-up changes.

A good description of the behaviour of systems at very low hold-up of dispersed phase is important if extrapolation to zero hold-up is proposed to obtain a characteristic velocity V_K in baffled and agitated columns. The work of Barnea (16) indicates that extrapolation is valid for fluidized systems of particles over a wide range of Reynolds number when equation (6) is used.

Data from the literature were analysed (all in the absence of mass transfer) for column diameters 90 to 250 mm. The statistical best fit technique was used to find m and V_K for hold-up less than 0.3 (to ensure that coalescence was unimportant). In some cases the range of hold-up measured was too small and data too scattered to obtain V_K or m with confidence. In other cases although an adequate range of hold-up was covered (0 to 0.2 for example) the standard deviations on V_K and m were unacceptable (18,19). The following data were used in this work: Kung and Beckmann, toluene/water (20), Misek, toluene/water (21), Magiera and Zadlo, CCl_4/water and CCl_4/water-Tween 80 (22), our own work on n-butanol/water and cumene/water, (23). All these data show that equation (6) is better than equation (1), with the index m varying from a maximum of about 4 falling as agitation increases (Fig. 1).

For relatively low agitation conditions (typically below the critical rotor speed given by Laddha (24)) m can be negative but increases as agitation increases. It is suggested that this type of behaviour could be due to rapid drop coalescence. Misek's data fitted by equation (3) appear to be in this region. At agitation rates above the critical rotor speed it appears that m passes through a maximum value, falls to zero as agitation increases and does not become significantly negative. Similar behaviour has been observed by us for the Kuhni column (well agitated, multistage) (25), the pulsed packed and the pulsed sieve plate column.

Drop sizes. Drop sizes are known in our own experimental work. Other authors (26 - 31) have developed equations to correlate their own drop size data (Fig. 2). The Kagan, Magiera and Jeffreys equations incorporate a change with stage number. We propose a modification to the Strand equation assuming that the Sauter mean drop size is approximately 0.4 times the maximum drop size according to the work of Misek and Marek (32). The constant C_1 used by Strand is taken here as 0.5. No drop size distribution equation can be valid for all circumstances and the constants will change according to physical properties, agitation and direction of mass transfer. Strand's equation and those of others extrapolate to unrealistically large drop sizes at low agitation so it is suggested that an upper limit be estimated using the equation (1,33),

(7) $d_{32} = 0.92 \; (\gamma/ g\Delta\rho)^{0.5}$

Correlation of characteristic velocity. It is assumed that V_K is closely related to an average terminal velocity of a swarm of drops with a distribution of sizes. We have for the present used the equations proposed by Grace (35) to calculate the terminal velocities of Sauter mean drop sizes obtained from the modified Strand equation. The terminal velocity equations are for mildly contaminated drops with partial circulation: for n-butanol drops measured terminal velocities are about 15% lower than predicted and for cumene about 10% higher.

We have plotted the ratio $V_K/V_T C_R$ against $Fr^{1.5} P^{-0.50}$ tentatively bearing in mind the inadequacies of the data, prediction of drop sizes and assumptions made (Fig. 3). C_R is the constriction factor as defined by Strand (26). The standard deviation on $V_K/V_T C_R$ is about 0.06.

Strand (26) proposed that the constriction factor C_R, when multiplied by the average terminal velocity gave the characteristic velocity. It appears from present work that only when $P^{-0.5} Fr^{-1.5}$ is greater than about 10^{-6} does V_K/V_T tend to the value of C_R.

In the work assessed C_R ranges from 0.57 to 0.36. As $P^{-0.50} Fr^{1.50}$ approaches zero (at low rotor speed for example), then V_K tends to a value slightly less than V_T, probably dependent on geometry alone. More data are required to examine this point.

A source of difficulty is the assumption of an average terminal velocity for the volume/area drop size mean (Sauter mean, d_{32}). However, work on ion exchange resins with a similar size distribution to drops suggests that this assumption is satisfactory (36).

Correlation of exponent m. An empirical correlation only can be expected because of complex flow patterns and the possible influence of coalescence. Only the well-agitated region for which m falls from a maximum value towards zero as agitation increases was considered here. Values of m for a Kuhni column (25) are not strongly dependent on dispersed phase properties (water phase continuous). It has been possible to plot m versus $P^{0.19} P_v^{-0.37}$ with success, (Fig. 4). Equations for P_v are given by Misek (32,33). The ~~standard deviation~~ on m is about $\pm$ 0.4 which is reasonable considering that the experimental data are sparse. Other correlating equations based on Fr, P and the critical rotor speed were not found acceptable.

DISCUSSION

In the range of hold-up of practical interest equation (6) fits the RDC data better than equation (1) in the absence of coalescence effects, that is, for $x < 0.3$ and adequate agitator speeds.

The characteristic velocity V_K can exceed $V_T C_R$ (the value suggested by Strand) and approaches V_T as agitation decreases. The uncertainty of prediction of drop size, size distribution and terminal velocities means that precise correlation is not yet possible. However, measured drop sizes and terminal velocities for the n-butanol and cumene systems indicate that such an approach is useful. Work in progress on single drops passing through a short RDC to determine the relationship between V_K, V_T and geometrical factors has given data in agreement with Fig. 3.

The exponent m varied in a consistent manner. The correlation proposed (for water continuous), Fig. 4, is best used to determine if operation is in a satisfactory region, with $0 < m < 3$ and low values of $P_v^{-0.37} P^{0.19}$ being avoided.

It should be noted that Fr and P_v cannot both be maintained constant on scale-up of diameter. Scale-up assuming constant P_v could change the value of $V_K/V_T C_R$ markedly for example.

CONCLUSIONS

A rational framework for understanding the hydrodynamic performance of the RDC is proposed. Despite the lack of data of high quality a coherent approach based on drop sizes, terminal velocities and geometrical factors can be established which gives confidence in applying the method to other chemical systems.

ACKNOWLEDGEMENTS

W-Y. Fei is Lecturer in Chemical Engineering, Qinghua University, which supported him at the Schools of Chemical Engineering, University of Bradford. The data on n-butanol and cumene were obtained in a programme funded by Separation Processes Service, UKAERE, Harwell, UK.

NOMENCLATURE

a,b,c	constants	
C_R	constriction factor	
D	rotor diameter	m
d_{32}	volume/surface mean drop diameter	m
Fr	Froude number $N^2 D/g$	
g	gravitational acceleration	m^2/s
m	exponent	
N	rotor speed	s^{-1}
P	physical property group $(\rho_c^2 \gamma^3/\Delta\rho g \mu_c^4)$	
P_v	power/unit volume (per stage)	W/m^3
V_{slip}	slip velocity	m/s
V_O	characteristic velocity (Pratt)	m/s
V_K	" "	m/s
V_c	continuous phase superficial velocity	m/s
V_d	dispersed " " "	m/s
V_T	terminal velocity for d_{32}	m/s
x	fraction dispersed phase hold-up	

ρ_c	continuous phase density	kg/m^3
$\Delta\rho$	density difference	kg/m^3
μ_c	continuous phase viscosity	kg/m s
γ	interfacial tension	N/m

REFERENCES

1. Gayler, R., Pratt, H.R.C., Trans. Inst. Chem. Engrs., 1953, 31, 69
2. Thornton, J.D., Chem. Eng. Sci., 1956, 5, 201
3. Misek, T., Coll. Czech. Chem. Commun., 1964, 29, 1755
4. Letan, R., Kehat, E., Am. Inst. Chem. Eng., J., 1964, 11, 804
5. Slater, M.J., Chemie Ing. Technik, 1974, 46, (15), 663
6. Beyaert, B.O., Lapidus, L., Elgin, J.C., Am. Inst. Chem. Eng. J.,1961,7,(1),46
7. Zhu, S., Zhang, B., Shen, Z., Wang, J., J.Chem.Ind.and Eng.(China),1982,(1),1
8. Godfrey, J.C., Hanson, C., Slater, M.J., Chem.Ind., 1977, 17, 713
9. Niebuhr, D., Vogelpohl, A., Chem. Eng. Conf., Montreal, 1980
10. Kwauk, M., Scientia Sinica, 1963, 12, 587
11. Richardson, J.F., Zaki, W.N., Chem. Eng. Sci., 1954, 3, 77
12. Weaver, R.E.C., Lapidus, L., Elgin, J.C., Am. Inst.Chem.Eng.J.,1959,5,(4),533
13. Lapidus, L., Elgin, J.C.,Am.Inst. Chem. Eng. J., 1957, 3, 63
14. Andersson, K.E.B., Chem. Eng. Sci., 1961, 15, 276
15. Germak, J., Klicka, V., Verfahrenstechnik, 1971, 5, (8), 320
16. Barnea, E., Mizrahi, J., The Chem. Eng. J., 1973, 5, 171
17. Maude, A.D., Whitmore, R.L., Brit. J., Appl. Phys., 1958, 9, 477
18. Kamath,M.S.,Ph.D.Thesis, Dept.of Chem.Eng.,Univ.of Mysore, India (1978)
19. Logsdail,D.H.,Thornton,J.D.,Pratt,H.R.C.,Trans.Inst.Chem.Engrs.,1957,35, 301
20. Kung,E.Y.,Beckmann,R.B.,A.I.Ch.E.J.,1961, 7, 319
21. Misek, T.,Czech.Chem.Commun., 1963, 28, 1631
22. Magiera, J.,Zadlo,J.,Inz.Chem., 1977, 7, 113
23. Bailes,P.J.,Gledhill, J.,Godfrey,J.C.,Slater,M.J.,Trans.Inst.Chem.Engrs., to be published
24. Laddha,G.S.,Degaleesan,T.E.,Kannappan,R.,Can.J.of Chem.Eng.,1978,56, 137
25. Bailes,P.J., Gledhill,J., Godfrey, J.C., Slater, M.J., Verfahrenstechnik, to be published.
26. Strand,C.P., Olney,R.B., Ackerman, G.H., Am. Inst.Chem.Eng.J.,1962, 8, 252
27. Magiera, J., Zadlo,J., Inz. Chem., 1977, 7, 127
28. Misek, T., Coll.Czech. Chem. Commun., 1963, 28, 570
29. Marr, R., Chem. Ing. Tech., 1978, 50, 337
30. Jeffreys, G.V., Al. Aswad, K.K.M., Mumford, C.J., Separation Science & Tech., 1981, 16, 1217
31. Kagan, S.Z., Aerov, M.E., Zh. Prikl. Chim., 1964, 37, 58
32. Misek, T., Marek, J., Br. Chem. Eng., 1970, 15, 202
33. Misek, T., Chapter 13.2 in Handbook of Solvent Extraction, eds. Baird,M., Lo, T., and Hanson, C.,Pub.Wiley,1983
34. Clift, R., Grace, J.R., Weber, M.E., 'Bubbles,Drops and Particles', Pub. Academic Press, New York, 1978
35. Grace, J.R., Wairegi, T., Nguyen, T.H., Trans. Inst. Chem. Engrs., 1976, 54, (3), 167
36. Slater, M.J., Ph.D. Thesis, Univ. of Bradford, 1971

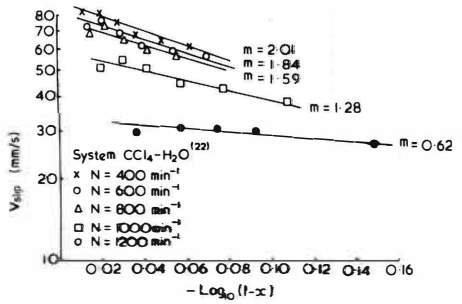

Fig. 1. Hold-up data

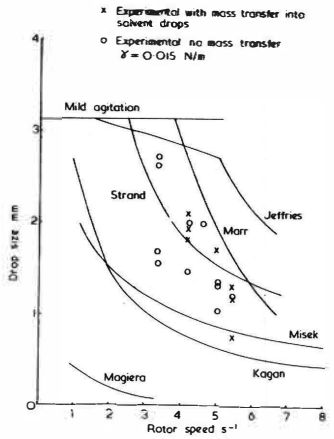

Fig. 2. Drop size correlations for cumene drops

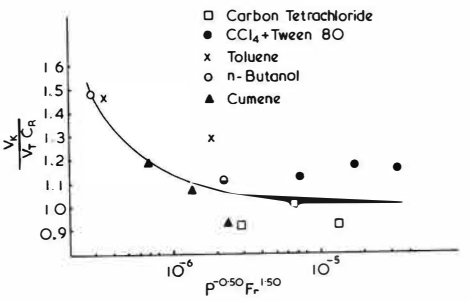

Fig. 3. Correlation of characteristic velocity V_K

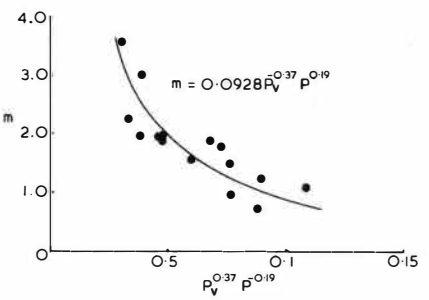

Fig. 4. Correlation of exponent m

PHASE INVERSION AND ENTRAINMENT CHARACTERISTICS OF LIX64N IN ESCAID AND WATER

J. C. Godfrey and J. Gledhill

University of Bradford
West Yorkshire, U.K.

UKAEA
Culcheth, Chesire, U.K.

INTRODUCTION

Commercial mixer-settler plant for metals extraction is often required to accommodate very large throughputs and the large plant items used can present difficulties in design and scale-up. The operating problems experienced in large plant may be related to plant deisgn or could arise from the characteristics of the liquid-liquid system. The topics of phase inversion and entrainment are often linked in the consideration of the performance of plant mixers. One of the disadvantages of uncontrolled phase inversion is that the process is frequently accompanied or followed by a considerable increase in entrainment levels. At present there is no evidence as to whether the phenomena of phase inversion and entrainment are linked in any way. Neither phenomenon has attracted extensive study but an appreciation of the principal variables has been established. The study of phase inversion and entrainment to be described here was conducted in a laboratory mixer designed to minimize the influence of design on system behaviour. To avoid problems regarding the relative contributions to pumping and mixing of the pump-mix impeller a (Rushton) six blad turbine was used and the flow of the test liquids was generated and monitored by pumps and rotameters.

Phase inversion. A number of batch laboratory studies have been conducted on topics related to phase inversion. In earlier works considerable attention was paid to the study of the preferential dispersion of one immiscible liquid as drops in another. As a wide range of experimental techniques has been used it is difficult to compare the results of one work with another. Studies have been made of the influence of equipment design, degree of agitation and physical properties on the relationship between volume fraction and preferentially dispersed phase. The principal variables emerging from this work are viscosity ratio and experimental technique. For practical purposes it is usually possible to establish the desired continuous phase by making this the majority phase at start up and by locating the impeller in that phase. Alternatively, agitation is commenced with the continuous phase only and the dispersal phase slowly added to produce a dispersion. A modification of this latter technique is often used in the study of phase inversion as distinct from preferential dispersed phase. When a dispersion has been established by one of these techniques the addition of dispersed phase can be continued until phase inversion takes place. When it is desired to conduct the study at constant volume dispersion can be removed as dispersed phase is added. Both organic drop and aqueous drop dispersions have been studied and have included the influence of viscosity ratio (1), interfacial tension (2, 3) and the study and equal density systems (4). There are examples of stable dispersions of large volume fractions (0.9) of the dispersed phase, both for aqueous (4, 5) and organic drops (5, 6). In most cases the ambivalence range, i.e. the difference between the aqueous and organic volume fraction limits, is not very wide. A variety of impeller systems have been used, often quite complicated multi-impeller designs (1, 4). There is only one study of a continuous flow mixer (5), this using a pump-mixer impeller. The influence of impeller speed was examined but not impeller size, flow rate or quality of mixing.

Entrainment. Many mechanisms have been discussed with respect to the generation of entrainment but relatively few of the studies made are directly relevant to mixer performace. It has been demonstrated that the entrainment characteristics of batch and continuous systems are very different ( ) and that the major influences are impeller speed and to a lesser degree impeller size. Some study has been conducted on the entrainment characteristics of a pump mix impeller (5) for both aqueous and organic drop dispersions and including the influence of phase ratio and impeller speed.

EXPERIMENTAL

Most of the existing data on phase inversion has been generated for pure chemicals under batch conditions. Because of the frequent problems of poor stability in plant equipment the present study has been conducted with a continuous flow mixer and with a liquid-liquid system similar to those found in operating plant. Another shortcoming of some existing data is that the quality of mixing is indeterminate with low impeller speeds and large drop sizes (6). In the present work the bulk of the investigation has been condcted under well mixed conditions but as it is possible that plant problems arise from conditions of inadequate mixing some study has also been made of this problem.

A turbine agitated tank (Perspex) of square cross section (15cm x 15cm x 15cm) was used to study phase inversion and entrainment characteristics for an organic phase of 20% LIX 64N in Escaid 100 diluent and an aqueous phase containing 2gm/ℓ sulphuric acid. A square cross-section tank was chosen for the study because of the extensive use of this geometry in industry. Two vertical baffles were used - located centrally on opposite faces - as this gave better mixing at lower impeller speeds. The tank was closed to suppress vortex formation.

A study of the effectiveness of mixing at various impeller speeds was conducted at a flow ratio A/O = 1. For a 51mm diameter turbine the minimum rotational speed necessary to prevent the formation of visible dead spaces was 600rpm. This corresponds quite well with the minimum agitation to equate mixer hold-up and flow ratio (7). Changes in flow rate did not affect performance. The mixer could be operated and give a stable dispersion at lower impeller speeds, approaching 250 rpm, but extensive dead spaces were visible and phase inversion was easily triggered by small changes in flow ratio.

Phase inversion. Both organic and aqueous drop dispersions were very stable, inversion not being observed at flow ratios of drop phase/continuous phase less than 10. In the region of inversion drop deformation and coalescence was very obvious and localized dead spaces could be seen. These dead spaces were stable and did not expand to initiate phase inversion. In all cases there was a small decrease in stability with increasing impeller speed, contrary to some earlier observations.

As aqueous drop dispersions are often preferred because of the low levels of entrainment generated this dispersion was studied in more detail. Because of the conflict with previous observations of the influence of impeller speed a further examination was made of inversion by changing speed at fixed flow ratios. This technique reproduced the combinations of impeller speed and phase ratio already noted. The influence of throughput was also studied but not effect was formed in the range 63 - 110 ℓ/hr at 900 rpm. At impeller speeds below 600 rpm aqueous drop dispersions were particularly unstable, organic drop dispersions less so. Large dead spaces could be seen with only small volumes of dispersion existing separately. At inversion the phase ratio in these small volumes was similar to that measured for inversion under well mixed conditions. However, because of the non uniformity existing in the tank phase inversion occurs at a much lower flow ratio than in a well mixed system with a dispersed/continuous ratio of approximately two at 300 rpm. Another aspect of agitation examined was the relative performance of impellers of different size. It was found that, for the same tip speed, a 76mm impeller gave a marginally more stable dispersion ($A_d/O_c \sim 15$) than the 51mm impeller ($A_d/O_c \sim 10$)

Entrainment. Previous studies (5,8) under well mixed conditions have shown that the entrainment levels for a continuous flow laboratory mixer producing aqueous drop dispersions can be very low. In the present work entrainment was examined as a function of flow ratio. There was a gradual increase of organic in aqueous entrainment with flow ratio until, as inversion was approached, a very rapid increase was observed. This marked increase in entrainment preceeds the inversion process and is a function also of impeller speed. At low flow ratios, $A_d/O_c<1$, the levels of organic in aqeous entrainment were very low. A study of aqueous in organic entrainment was made in the same flow regime, i.e. $A_d/O_c<1$, and considerable increases were observed as the ratio A_d/O_c fell. For flow ratios greater than one the entrainment of aqueous in organic was very small.

DISCUSSION

Phase inversion. Under well mixed conditions both aqueous and organic drop dispersion were found to be very stable in a continuously operated mixer. It appears that there is no particular reason why phase inversion problems should be related to either continuously operated mixers or liquid-liquid systems involving the use of LIX64N, dilutent kerosene or acid. However if the level of agitation is sufficiently low to allow segregation to develop within the tank the tolerance of the system to phase inversion is much reduced. As the widely used mixer scale up criterion of constant tip speed involves a substantial reduction in power per unit volume on scale up it is possible that the problem of inversion on large plant is associated with low mixing power.

It is interesting to note that in this particular work the stability charcteristics of the two types of dispersion are virtually equal with respect to the volume fraction of dispersed phase at inversion and the influence of impeller speed. These volume fractions are greater than observed in previous works, as is the width of the ambivalence region. It is possible that these two characteristics are more representative of the phenomena of phase inversion than those presented in previous works and that the difference is related to the greater effectiveness of agitation in the present work. When two impeller sizes were compared the larger impeller gave better mixing characteristics and greater stability for a specialised tip speed.

The greater stability and minimal dependence on impeller speed observed here is contrast with the existing theories based on earlier experimental work. The subject of phase inversion is very complex and it is not surprising to find that little progress has been made theoretically or in correlation. The theoretical work of Araschmid and Jeffreys (6) leads only to a simple correlation requiring an arbitrary constant and which has no predictive capability. The correlation of Luhning and Sawistowski (2) allows a prediction of the ambivalence range for the present liquid-liquid system. However, the range predicted, 0.52 volume fraction, is much less than the measured value of 0.85. The correlation also predicts an impeller speed dependent ambivalence range while the measured range is virtually constant.

Entrainment. The influence of phase ratio on entrainment was examined under well mixed conditions for both aqueous drop and organic drop dispersions. For aqueous drop dispersions the entrainment levels of organic in aqueous are low at all flow ratios except as phase inversion is approached when the level rises dramatically. For the same dispersion aqueous in organic entrainment increases markedly for flow ratios less than one ($A_d/O_c<1$), above this value the level was undetectable.

Organic drop dispersions produced high levels of organic in aqueous entrainment for a flow ratio of one. It is interesting to note that

this level fell as inversion was approached. It was noticeable that the entrained droplets were much larger than those observed in other experiments and that much of the entrainment would clear if samples were left to stand.

ACKNOWLEDGEMENTS

The authors would like to acknowledge the financial support of Nchanga Consolidated Copper Mines, Zambia, for this research programme.

NOMENCLATURE

A	aqueous phase flow rate	ℓ/min
O	organic phase flow rate	ℓ/min

Subscripts

c	continuous phase
d	dispersed phase

REFERENCES

1. Selker, A.M. and Sleicher, C.A., Can.J.Chem.Eng., 1965, 43, 298
2. Luhning, R.W. and Sawistowski, H. Proceedings ISEC, 1971, 2, 873
3. Clarke, S.I. and Sawistowski, H. Trans. I. Chem.E., 1978, 56, 50
4. McClarey, M.J. and Ali Mansoori, G. A.I.Ch.E. Symposium Series 1978, 74, (173) 134
5. Rowden, G.A., Scuffham, J.B., Warwick, G.C.I. and Davies, G.A. I.Chem.E. Symposium Series No. 42, 1975, 17.1
6. Arashmid, M. and Jeffreys, G.V. A.I.Ch.E. J., 1980, 26, (1) 51.
7. Godfrey, J.C. and Grilc, V. 3rd European Conference on Mixing, BHRA 1979, 189
8. Godfrey, J.C., Hanson, C., Slater, M.J. and Tharmalingham, S. A.I.Chem.E. Symposium Series 1978, 74 (177) 127

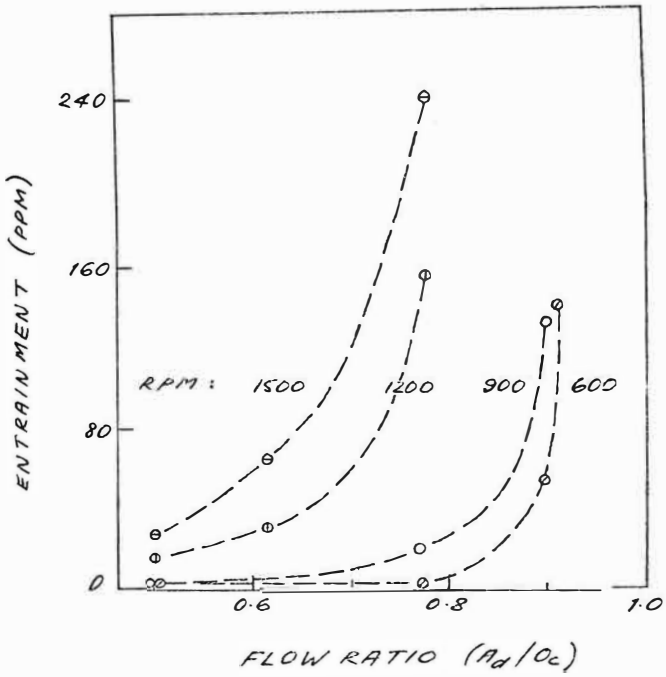

FIGURE 2 PHASE INVERSION AND ENTRAINMENT

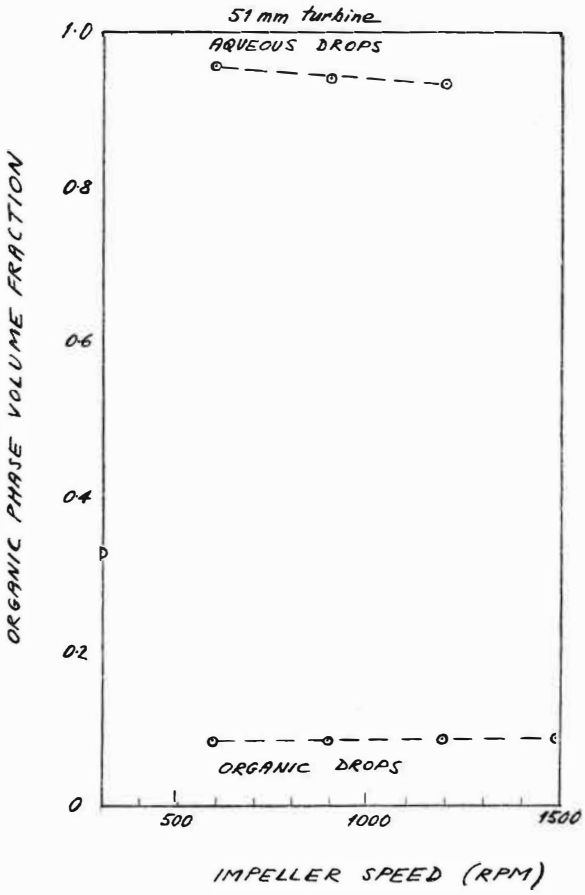

FIGURE 1 PHASE INVERSION

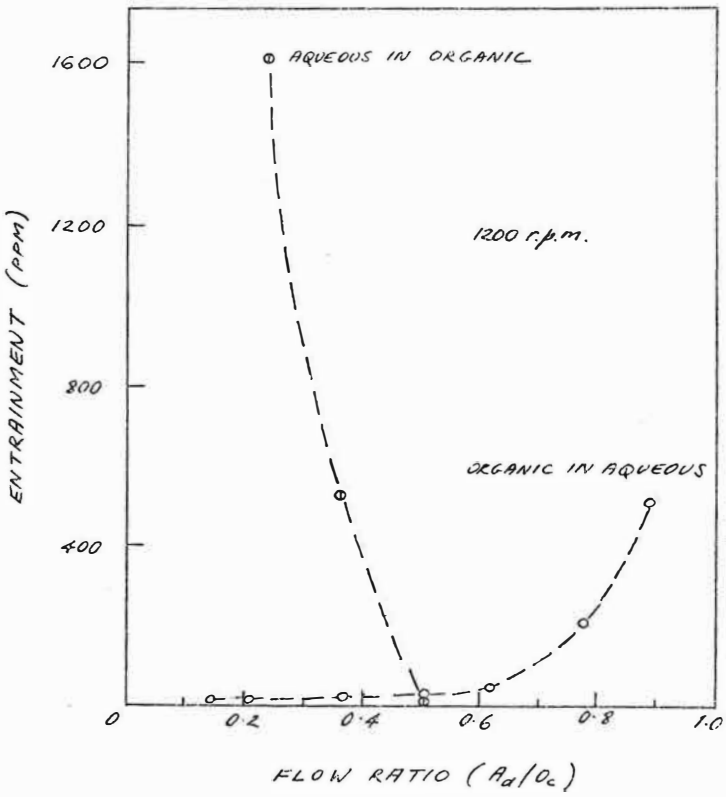

FIGURE 3 ENTRAINMENT

ENERGY UTILIZATION IN LIQUID-LIQUID MIXING IN EJECTORS

D. Mukherjee, M. N. Biswas and A. K. Mitra

Indian Institute of Technology
Kharagpur 721302, India

Efficient mixing of immiscible liquids in liquid-liquid extraction and other operations is an important problem in Chemical Engineering practice. Various different types of equipments have been developed and they have their own limitations. In recent years, concept of ejector has been enriched and amplified and its practical applications have proliferated enormously. Ejectors for liquid-liquid mixing can provide an attractive alternative because it gives high interfacial area with low energy dissipation, has low capital and maintenance cost and can easily handle corrosive or toxic systems. Further since the operation in an ejector is cocurrent in nature, it can handle high flow rates without flooding, equal density immiscible liquids and gives low pressure drop.

A review of literature shows that as compared to gas-liquid mixing very meagre studies have been reported on liquid-liquid mixing in ejectors. Only one study on liquid-liquid extraction in binary and ternary systems has been reported by Acharjee et. al.(1, 2). The present study has been undertaken to study the energy dissipation in liquid-liquid mixing in an ejector.

THEORETICAL CONSIDERATIONS :

In an ejector system the energy dissipation takes place in liquid-liquid mixing and overcoming friction in the mixing throat and in graining pressure energy in the diffuser.

An energy balance between the mixing throat inlet, 0 and outlet, t (Figure 1) gives the energy loss per unit mass flow, ε as

$$(1)\quad \varepsilon = \frac{H}{\rho_1 A_R^2}\left[\frac{K_{th}\{(1-\alpha_2)+\rho_R\,\alpha_2\}(1+\varphi_R)^3}{(1+\rho_R\,\varphi_R)} + \frac{A_R^2}{(1+\rho_R\varphi_R)} + (1+\varphi_R)^2 - \frac{2A_R(1+\varphi_R)}{(1+\rho_R\varphi_R)} + \frac{\rho_R\,\varphi_R^2\,A_R}{(1+\rho_R\varphi_R)A_{Rs}}\left\{\varphi_R\frac{A_R}{A_{Rs}} - 2(1+\varphi_R)\right\}\right]$$

where

A_R = area ratio of the throat to the nozzle

A_{Rs} = area ratio of the throat to the secondary inlet

H = nozzle velocity head, $\rho_1 V_{1n}^2/2$

K_{th} = two phase friction coefficient in throat

Q_1, Q_2 = flow rate of primary and secondary liquid respectively

V_{1n} = velocity of primary liquid through the nozzle

α_2 = holdup fraction of secondary liquid

ρ_1, ρ_2 = density of primary and secondary liquid respectively

ρ_R = density ratio of secondary to primary liquid, ρ_2/ρ_1

and φ_R = flow ratio of secondary to primary liquid, Q_2/Q_1

The ε, given by equation (1) consists of both ε_{th} and ε_m The term connected with K_{th} is ε_{th} and is given by

$$(2)\quad \varepsilon_{th} = \frac{K_{th}\cdot H\cdot(1+\varphi_R)^3}{\rho_1 A_R^2(1+\rho_R\,\varphi_R)}\left[(1-\alpha_2)+\rho_R\,\alpha_2\right]$$

The rest of the terms in equation (1) is ε_m, that is

$$(3)\quad \varepsilon_m = \frac{H}{\rho_1 A_R^2}\left[\frac{A_R^2}{(1+\rho_R\varphi_R)} + (1+\varphi_R)^2 - \frac{2A_R(1+\varphi_R)}{(1+\rho_R\varphi_R)} + \frac{\rho_R\,\varphi_R^2\,A_R}{(1+\rho_R\varphi_R)A_{Rs}}\left\{\frac{\varphi_R\,A_R}{A_{Rs}} - 2(1+\varphi_R)\right\}\right]$$

where ε_{th} = frictional energy loss in the mixing throat per unit total mass flow

and ε_m = mixing energy loss in the mixing throat per unit total mass flow.

In order to evaluate, ε_{th}, from equation 2, a knowledge of K_{th}, along with other terms is essential. Since K_{th} is the frictional loss, a momentum balance in the throat gives the following equation for K_{th}.

$$(4)\quad K_{th} = \frac{(A_R^2/H)(P_o - P_t - \rho_3 g L_t) + 2A_R - 2(1+\rho_R\varphi_R)(1+\varphi_R) + 2\rho_R\varphi_R^2 A_R/A_{Rs}}{[(1-\alpha_2)+\rho_R\alpha_2](1+\varphi_R)^2}$$

where g = acceleration due to gravity

L_t = length of the throat

P_o = pressure at the throat entry, o

P_t = pressure at the throat exit and diffuser entry, t

ρ_3 = density of the mixed liquid

Hence, it is evident that K_{th} and in turn ε_{th} can be evaluated with the knowledge of P_o, P_t, α_2 and other geometrical and physical properties of the system.

The energy dissipated due to mixing of two immiscible liquids, ε_m (given in equation 3) have been found to be a function of H, ρ_R, A_R and φ_R. In the absence of secondary flow i.e. at $\varphi_R = 0$, this loss, ε_{mo}, becomes

$$(5)\quad \varepsilon_{mo} = \frac{H}{\rho_1}\left(1 - \frac{1}{A_R}\right)^2,$$

which is analogus to the loss due to sudden jet expansion. With secondary flow, the dissipation due to jet expansion reduces and is being utilized in mixing.

In the divergent diffuser there is no further mixing but the mixed liquid gains pressure energy. Hence there is only frictional energy loss and no mixing energy dissipation. The frictional energy loss in the diffuser per unit total mass flow ε_{di}, is obtained by an energy balance between the diffuser inlet t, and exit, d (Figure 1), as

$$(6)\quad \varepsilon_{di} = \frac{(P_t - P_d - \rho_3 g L_d)}{[(1-\alpha_2)+\rho_R\,\alpha_2]} + \frac{H}{A_R^2}\left(1 - \frac{1}{A_d^2}\right)(1+\varphi_R)^2$$

where A_d = area ratio of the diffuser outlet to throat

L_d = length of the diffuser

and P_d = pressure at the diffuser outlet, d

EXPERIMENTAL :

The experimental apparatus consists of an optimum designed ejector assembly having a suction chamber, a primary nozzle, a constant area mixing throat of diameter 16.9 mm and length 184 mm and a divergent diffuser with an angle of 7° and length 204 mm. The ejector assembly was connected to a vertical column of 51.6 mm internal diameter and 2.03 m length, in order to increase the time of contact of the two liquids. Five nozzles having area ratios, A_R in the range of 1 - 50 were used. The experiments were carried out with water as the primary and kerosene/paraffin as the secondary liquid and vice-versa i.e. kerosene/paraffin as the primary and water as the secondary liquid. For the present range of experimental work, water was

found to be the continuous phase irrespective of which liquid was primary.

RESULTS AND DISCUSSIONS :

From the experimental data on P_o, P_t, α_2 for a particular primary flow and φ_R, K_{th} was evaluated through equation 5 and was used for calculating ε_{th} by equation 2. ε_{th} has been found to be a function of various different parameters like Re_{1n}, Re_{2s}, A_R, Su_{2s}, Np_1 and was generalized by least square methods. The equation obtained is

$$(7)\quad \varepsilon_{th} = 0.0004\, Re_{1n}^{0.2091}\, Re_{2s}^{1.0722}\, A_R^{-0.0198}\, Np_1^{-0.0150}\, Su_{2s}^{-0.3163}$$

where Np_1 = liquid property group for primary liquid, $g\mu_1^4/\rho_1\sigma_1^3$

Re_{1n} = Reynolds number of primary liquid based on nozzle diameter

Re_{2s} = Reynolds number of secondary liquid based on secondary inlet diameter

Su_{2s} = Suratman number of secondary liquid based on entry diameter, $\sigma_2\rho_2 ds/\mu_2^2$

μ_1, μ_2 = viscosity of primary and secondary liquid respectively

σ_1, σ_2 = surface tension of primary and secondary liquid respectively

The statistical analysis showed that the correlation is highly significant.

Typical plots of ε_m, against φ_R, for a constant H, $_R$ and A_R are shown in Figures 2 and 3 for A_R=1 and A_R>1 respectively. It may be noted from the plot of A_R = 1, that the magnitude of ε_{mo} is zero at φ_R=0 and increases with increase in φ_R for the same primary flow. For all the other cases of A_R>1, the magnitude of ε_{mo} is greater than zero and with the increase in φ_R, ε_m first decreases, reaches a minima and then increases. The initial fall in ε_m may be attributed to two reasons. Firstly starting with $\varepsilon_m = \varepsilon_{mo}$ at φ_R = 0, as soon as the secondary liquid is introduced into the system, a part of the energy available due to jet expansion is utilized in mixing and interdispersion. Secondly, as the secondary liquid is slowly increased from zero, the secondary liquid velocity increases and approaches the primary liquid velocity, thereby reducing the velocity difference between the two liquid streams. The minimum ε_m in the ε_m versus φ_R graphs correspond to the point where the kinetic energy for both the liquid streams become almost equal. Beyond this point, the kinetic energy of the secondary liquid becomes predominant and ε_m increases with further increase in φ_R. The minima points in the ε_m versus φ_R graphs may, therefore, be considered to be very significant and the flow ratio, φ_R at this point gives the best utilization of the energy input for a particular nozzle. The minima points have been determined graphically as well as by differentiating ε_m with φ_R (equation 3) and equating the differential to zero. To confirm the minima, $d^2\varepsilon_m/d\varphi_R^2$ at the minima points were calculated and were found to be positive. The optimum values of φ_R obtained by differentiating ε_m show excellent correspondence with the graphical results.

The experimental data have been used to calculate ε_{di} by equation 6. It has been found that ε_{di} has a very low value and for all practical purposes it may be neglected.

In order to make an estimate of the approach to homogeneity, a term called degree of mixing, D_m was defined as the ratio of the insitu holdup fraction, α_d and the homogeneous holdup fraction, α_{dh}.

where α_{dh} = ratio of the dispersed phase flow rate to the total flow rate.

A plot of D_m versus ε_m, in log-log scale as shown in Figure 4 gives clearly two regimes. In the region $\varepsilon_m > 10$, homogeneity or near homogeneity is achieved in the mixing process i.e. degree of mixing approaches the value of 1. Values of $\varepsilon_m < 10$ gives the idea how far it is from homogeneity. This graph gives an estimate of the ε_m at any desired level of dispersion which will be useful for optimum design of such systems.

CONCLUSIONS :

A good interdispersion between two immiscible liquids has been achieved with the help of liquid-liquid ejector system. Energy analysis in the mixing throat indicates two types of energy losses - one due to mixing and the other due to friction. The energy loss due to friction has been correlated with the different physical and system variables. The energy loss due to mixing has been quantified and the optimum point established which will give the best utilization of the energy input for a particular nozzle.

REFERENCES :

1. Acharjee, D. K., Mitra, A. K. and Roy, A. N., Can. J. Chem. Eng., 56, 37 (1978).

2. Acharjee, D. K., Mitra, A. K. and Roy, A. N., Ind. J. Tech., 16, 262 (1978).

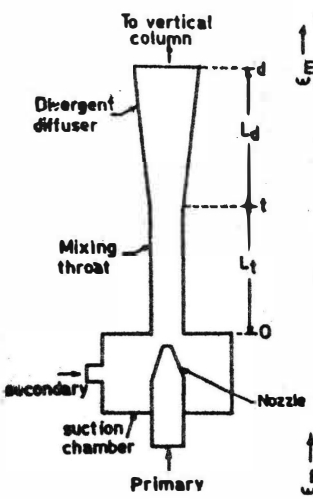

Fig.1. Schematic diagram for momentum and energy analysis.

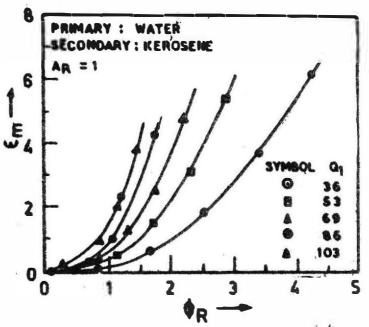

Fig.2. Variation of ε_m with ϕ_R at A_R = 1

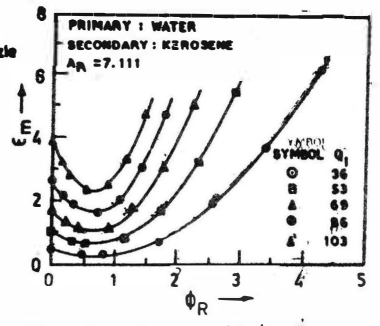

Fig.3. Variation ε_m with ϕ_R at A_R >1

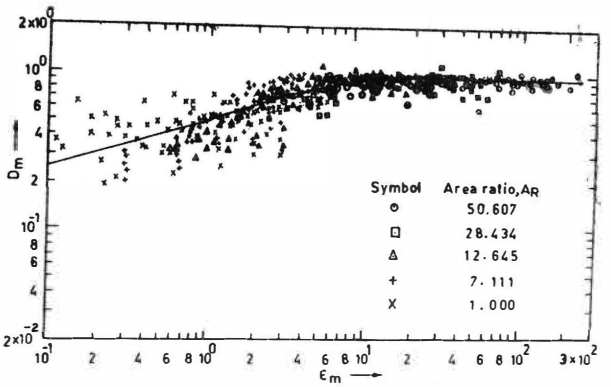

Fig. 4. Variation of degree of mixing with energy loss

THE APPLICATION OF ELECTRIC FIELDS TO PHASE SEPARATION IN A SOLVENT EXTRACTION SYSTEM

P. J. Bailes and S. K. L. Larkai

University of Bradford
Bradford, West Yorkshire, U.K.

One method of achieving process intensification in Solvent Extraction is to use electrostatic fields as a means of improving disengagement in the phase separation equipment. The principle of electrically augmented coalescence can be applied to many liquid-liquid contactors but it is most relevant to stagewise equipment, such as mixer-settlers, where phase separation is a frequent process required after each mixing operation. It offers the prospect of very compact settlers particularly for those dispersions which are slow to separate and therefore require large gravity settlers to give the necessary holding time.

Successful application of the technology should result in savings in the cost of solvent inventory which in a large hydrometallurgical plant is a significant feature in the overall economics as is the volume of the feed in a precious metals extraction. Alternatively, in the Nuclear industry solvent degradation is heavily dependent on residence time in contact with highly active fission products and here again efficient phase separation has an influence on the choice of equipment. In addition to these features, compact settlers would allow fast response for control purposes; they would minimise the space requirement and improve the likelihood of total enclosure or vertical stacking of settlers; reduce civil engineering and capital costs; and have a significant effect on evaporative, entrainment and degradation losses. The ability to adjust the electrical conditions on a settler or coalescer gives a means of countering turn-downs in throughput otherwise necessary to cope with reduced settling performance due to seasonal or diurnal variations in temperature.

ELECTRICALLY AUGMENTED COALESCENCE

An essential characteristic of solvent extraction systems is that one liquid phase is non-polar or insulating relative to the other more conducting, polar phase. There is an important distinction in liquid-liquid dispersions, however, depending on whether they are of the 'oil in water' or 'water in oil' type. The difference is that the latter type have a continuous phase of an insulating character (e.g. kerosene) and therefore will sustain a high voltage field and the polar liquid drops will retain any electrical charge which they may acquire. This is a prerequisite for all electrical coalescence equipment and thus restricts their usage to 'water in oil' type dispersions/emulsions.

Practical evidence obtained over the past seventy years with crude oil/water separations has shown that almost any type of high voltage field will promote to some extent the separation of 'water in oil' emulsions. The mechanisms whereby this can occur are not clearly understood except that the electrical forces cause very small drops to grow by coalescence with each other to a point where they fall out of the insulating phase under the action of gravity. The problem with translating this experience to solvent extraction operations is that power consumption and the risk of short circuiting increase with the percentage water content. In the Oil industry the proportion of water which can be tolerated is strictly limited, less than 10% being quite normal, whereas process considerations in solvent extraction generally prescribe dispersions containing nearer 50% of the polar phase. Recently, a novel investigation on a solvent extraction system containing a large volume fraction of dispersed aqueous phase has resulted in the discovery that pulsed dc fields applied through electrodes which are insulated can be tuned to cause excellent phase separation (1).

EXPERIMENTAL SYSTEM

The apparatus which was used consisted of a flow mixer for creating the dispersion at a fixed impeller speed of 900 rpm; an electrostatic coalescer, where the dispersion from the mixer was subjected to the electric field; and a gravity settler for measuring coalescence performance. The liquids from the electrostatic coalescer passed to the gravity settler where they formed a dispersion band, the depth of which was influenced by the field applied to the electrostatic coalescer. The percentage reduction in dispersion band depth relative to that recorded in the absence of an applied field was termed the coalescence parameter, P. The system chosen for the tests was dilute sulphuric acid - 20% LIX64N in kerosene (Escaid 100) and the phases were presaturated with one another. In the work reported here, this electric field was applied to dispersion flowing at a total rate of 1.0 ℓmin^{-1} containing equal volumes of both phases, with the aqueous phase dispersed. The dispersion completely filled the electrostatic coalescer which was a horizontal, shallow. perspex (plexiglass) duct, approximate internal dimensions in mm 180 x 180 x 25, with entry and exit lines but otherwise enclosed. A metal plate covering the top of the duct served as the energised electrode while the coalesced aqueous phase, suitably earthed, served as the other electrode. The HV electrode was thus insulated from contact with the dispersion by the intervening perspex of the duct top. This part of the duct was removable and during the series of experiments perspex sheets of 1,3,6 and 13 mm were used to separate the HV electrode from the dispersion.

A standard HV generator (Brandenburg model 2707R) was chosen as the source of steady dc with output between 0V to 15 kV at 2 mA. The voltage pulses were formed by switching on and off the steady dc by means of a purpose built modulator unit driven by a low voltage function generator (2). The shape of the high voltage pulses and their time-on in relation to time-off, that is mark/space ratio, was controlled by the low voltage waveform from the function generator.

EXPERIMENTAL RESULTS

The first important finding is that pulsed dc fields have much more effect on phase separation than constant dc fields. This is apparent from Figure 1 which shows the effect of pulsed and unpulsed dc fields of increasing magnitude on phase separation quantified in terms of the coalescence parameter. The peak electric field strength, E_{max}, is the maximum voltage gradient measured between two probes 10 mm apart inserted into the contents of the electrostatic coalescer. The insulation on the electrode tends to blur the pulse configurations applied to the electrode, so it is not surprising that phase separation is relatively unaffected by a change in pulse form of nominally square to half-wave.

Frequency of pulsation has a pronounced effect on coalescence performance. In Figure 2 it is seen that this is most marked at low values of applied voltage. There exists a single frequency, 8 Hz in this case, at which coalescence is maximised and even at applied voltage of only 200 V a substantial amount of coalescence occurs. This optimum frequency is less critical at higher voltages. The correct combination of voltage and frequency has a remarkable effect; it allows total phase separation with the 'LIX' system to be achieved and then sustained for as long as the field is applied.

A record of the current drawn shows that complete phase separation is possible with virtually negligible power consumption. An examination of Table 1 reveals that for a given applied voltage amplitude the current peaks at about the same frequency as that for which coalescence is best. This suggests that the coalescence mechanism involves the formation of chains of drops prior to coalescence since this would account for the conduction current. Chain formation is a phenomenon known to happen in both ac and dc fields (3). The repeated formation and disruption of chains which would be expected in a pulsed dc field is likely to promote drop contact and therefore coalescence. This behaviour would explain the optimum frequency in that at high frequencies insufficient time is available for a mechanical response to occur and chains are difficult to form whereas at low frequencies chains form quite readily but the frequency of formation and break up is too slow for adequate coalescence. It seems probable that the stability of chains at low frequencies does not give rise to the high currents observed with constant dc fields (2) because the chains don't grow long enough to bridge the electrodes. However, there are good reasons to suspect that several additional factors must be included in any final explanation of the coalescence process. For example coalescence may occur because the liquid between adjacent drops in a chain has been squeezed out by oscillations of the drops or the opposite poles of adjacent drops being attracted like the plates of a condenser. Alternatively, since local surface charge densities would cause a reduction in apparent interfacial tension on the surfaces of proximate drops this could promote coalescence through the Marangoni effect. This view is supported by the instantaneous nature of the observed coalescence.

The influence of electrode coating thickness is shown in Table 2. Best coalescence is obtained by using only a thin coating, because of the substantial reduction in effective field strength at a given applied voltage which results from excessive electrode insulation. The interfacial relaxation time between the electrode coating and the layer of continuous phase in the electrostatic coalescer diminishes with increased coating thickness. A more detailed study (4) has shown that the optimum frequency occurs when the angular frequency of the applied electric field is equal to the reciprocal interfacial relaxation time. This is probably the reason why the optimum frequency increased with the thickness of electrode coating in Table 2.

All the results given so far have been obtained under conditions where each voltage pulse has been followed by an equivalent time at zero potential before the next pulse. This corresponds to a mark/space ratio of unity. It is interesting to speculate whether this is the best proportionation of "on" and "off" times within the given period. Figure 3 shows the results from experiments with three different periods, as per 1.0Hz, 5.0Hz and 50Hz frequencies. The mark/space ratio within each of the three periods has been varied widely and it is apparent that the best condition is where the "time-on" equals the "time-off". This appears to be true irrespective of the frequency. The optimum frequency in this case was 5.0 Hz. If it is accepted that chain formation and disruption is the underlying mechanism of coalescence the inference which must be drawn from the mark/space data is that the rate of chain formation and the rate of chain disruption must be of similar magnitude for a given frequency and voltage condition.

Batch separation tests have shown that a great variety of electrode configurations are capable of giving excellent results with pulsed dc fields. These findings indicate that electrical factors are not going to dominate the geometry or construction of any large scale coalescer. Indeed it would be quite feasible to modify existing equipment to accommodate the desired high voltage region. Continuous flow tests with the 'LIX' system have shown bulk phase separation rates equivalent to 900 $\ell min^{-1} m^{-2}$.

CONCLUSIONS

There is sufficient evidence now available to show that liquid phase separation by electrical means is quite feasible. Many systems of the type used in solvent extraction have electrical properties which match exactly those which must be satisfied before coalescence can be accelerated by high voltage fields. The conductance problem posed by the high proportion of polar phase which is present in most solvent extraction dispersions has been solved by a novel electrostatic coalescence system. The essential features of which are that it uses a uni-directional field which is pulsed and that it uses electrodes coated with a layer of insulating material.

REFERENCES

1. Bailes, P.J. and Larkai, S.K.L., October 1981, European Patent Application No. 81305155.

2. Bailes, P.J. and Larkai, S.K.L., 1981, Trans. I. Chem. E., 59, (4), 229.

3. Pearce, C.A.R., 1954, Brit. J. Appl. Phys., 5, 136.

4. Bailes, P.J. and Larkai, S.K.L., Forthcoming publication.

Table 1. Mean Conduction currents under different field conditions.

Frequency (Hz)	Conduction current I_{mean} (μA) V_{max}=2kV(E_{max}= 300 V/cm)	V_{max}= 4kV(E_{max}= 550 V/cm)
0.5	0.0062	0.0178
1.0	0.0075	0.0253
1.5	0.0091	0.0255
2.0	0.0120	0.0306
4.0	0.0115	0.0328
6.0	0.0138	0.0370
8.0	0.0146	0.0400
10.0	0.0140	0.0361
20.0	0.0107	0.0354
30.0	0.0064	0.0366
40.0	0.0047	0.0209
50.0	0.0045	0.0151
60.0	0.0040	0.0103

Table 2. Effect of electrode coating thickness on optimum frequency at V_{max} = 0.8kV.

Frequency Hz	Coalescence Parameter P (%) t = 1 mm	t = 3 mm	t = 13 mm
0.5	87.06	68.02	8.51
1.0	90.98	77.53	12.77
1.5	93.37		
2.0	95.29	90.69	27.87
2.5	95.69 *		
3.0	94.90		
4.0	94.51	91.48	32.55
4.5		91.91	
5.0		92.71 *	
5.5		90.18	
6.0		89.88	34.26
8.0	90.20	89.58	35.11
10.0	86.28	80.77	35.20
12.0			36.94
13.5			37.35 *
15.0			29.08
20.0	82.35	62.35	27.04
30.0	79.61	34.01	14.29
40.0	75.69	25.60	10.20
50.0	71.37	21.05	8.16
60.0	68.63	19.84	6.94

* Optimum frequency t Electrode coating thickness
V_{max} Applied voltage amplitude

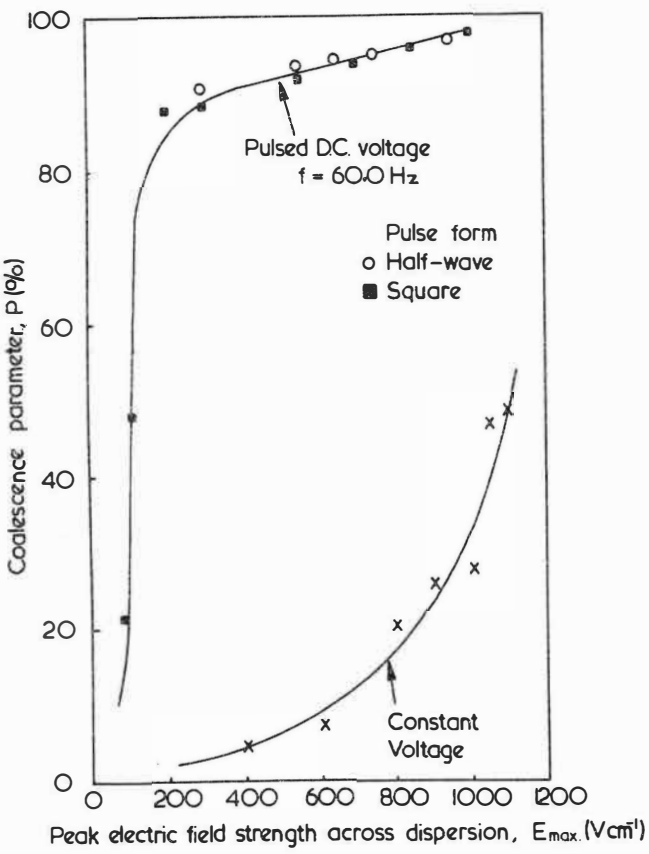

FIGURE 1: COMPARISON OF UNIDIRECTIONAL PULSED DC VOLTAGE AND CONSTANT VOLTAGE (ELECTRODE COATING THICKNESS 6mm)

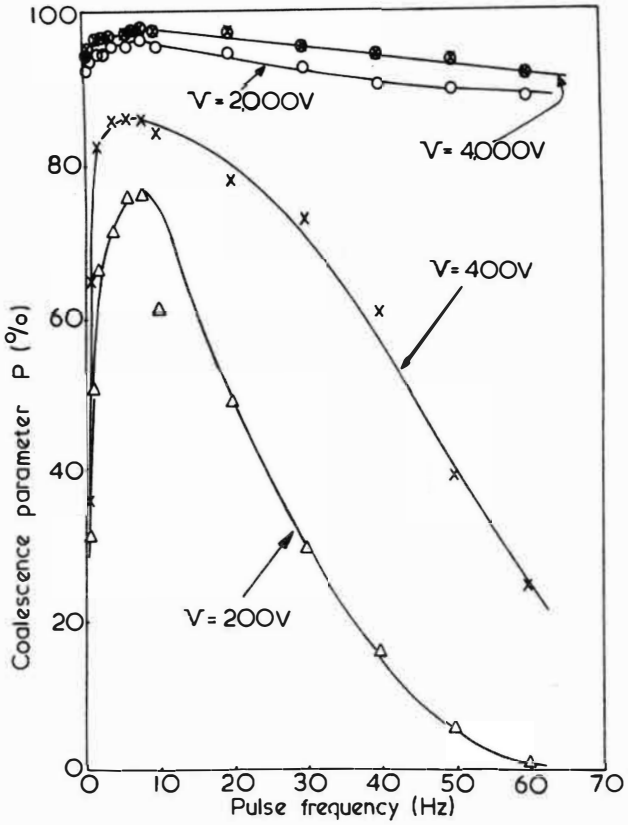

FIGURE 2: EFFECT OF PULSATION FREQUENCY ON COALESCENCE. (ELECTRODE COATING THICKNESS 6 mm)

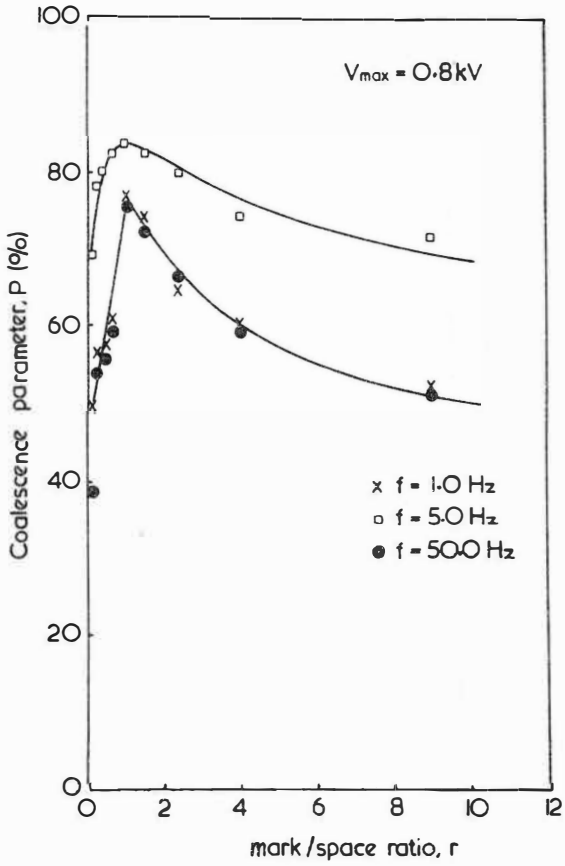

FIGURE 3: DEPENDENCE OF COALESCENCE ON MARK/SPACE RATIO (ELECTRODE COATING THICKNESS 3mm)

DISPERSED PHASE BEHAVIOUR IN CONTINUOUS LIQUID EXTRACTION COLUMNS

G. Casamatta, C. Gourdon, G. Muratet

Institut du Génie Chimique
L. A. CNRS 192
Chemin de la Loge
31078 Toulouse, France

INTRODUCTION

A constant source of difficulties in the design, and in the operation of a liquid-liquid extraction column is related to the behaviour of the dispersed phase. It has been shown (1-5), that drop size distribution (DSD) is an important factor in the efficiency of a column.

We have carried out a dynamic modelization of the physical mechanisms involved in forward mixing, and, on this basis, we show a comprehensive and general study of a column behaviour.

The continuous phase flow is described by the piston diffusion model. It is assumed that each drop of the dispersed phase undergoes the same backmixing as the continuous phase and showes a relative velocity towards the continuous phase.

Drop size distributions are described by a volume distribution and related to breakage and coalescence ; simple models for transport, rupture and coalescence have been used, and much attention has been paid to the precise description of the end sections of a column.

KINDS OF COLUMNS CONCERNED

One phase is dispersed as drops which travel under gravity with regard to the continuous counter-currently flowing phase.

The stagewise model describes a column from the level of continuous phase outlet, up to the interface which is assumed to have a constant level, as shown in Figure 1.

Even in the case of mechanically agitated columns drop breakage is neglected in the non-packed parts.

DISPERSED PHASE HOLD UP

At each level of the column, steady state solutions are given by the intersection of the curve $Z = \phi\,(1-\phi)^2$ and the straight line $Y = A\,\phi + B$ (Figure 2)

A and B depend on the flowrates, the cross area of the column and a well defined mean drop velocity FP, B is also a function of the product of the local hold up gradient $\partial\phi / \partial H$ and of backmixing intensity $\mathcal{D}$.

LOCAL FLOODING POINT

LFP is obtained when the Z-curve and the Y-straight line show a tangent point (ϕE). This corresponds to a maximal value of A, namelly A_{Max}.

N.B. : If $\mathcal{D} \cdot \frac{\partial \phi}{\partial H}$ is assumed to be negligible, and if dispersed phase entrainment can be neglected up to the flooding conditions, then our model reduces to the classical THORNTON's analysis (6).

ENTRAINMENT OF DISPERSED PHASE WITHOUT (BREAKAGE & COALESCENCE)

Monodispersed drop population. If the feed DSD is reduced to its mean value, and if the axial mixing term $\mathcal{D} \cdot \partial\phi / \partial h$ is neglected, we can calculate the maximal dispersed phase flow rate before flooding (6). On the Figure 3, this flowrate (double line) appears to be nearly equal to 18 l/h.

Under the same operating conditions but taking into account the axial mixing term (continuous line), it is shown that the dispersed phase entrainment (Q_{DE}) remains negligible up to $Q_D \sim 27$ l/h. Axial mixing leads to a complementary transport mechanism of the dispersed phase. Therefore, it can be emphasized that axial mixing delaies flooding of the column.

Distributed drop size. If we consider the true DSD (dotted line) we can see that entrainment increases regularly with Q_D and that no obvious flooding condition can be pointed out.

INFLUENCE OF COALESCENCE

With respect to the formerly defined LFP, $|A-A_{MAX}|$ is a measurement of the distance between the actual operating point and the flooding condition.

When coalescence is active (Figure 4), it is pointed out that there is a LFP for $Q_D^{\circ} = 37$ l/h, but entrainment remains negligible up to $Q_D^{*} = 45$ l/h. Above Q_D^{*}, entrainment grows up quickly, so that it is easy to define a practical criterion for flooding.

A fine scrutiny of the stage located just below the dispersed phase feed inlet (stage 7 on the Figure 1) has shown that this behaviour is due to the formation of densly packed bed of droplets on this plate, where coalescence is very strong.

HOLD UP PROFILES AND LOCAL FLOODING POINTS INFLUENCE OF FEED FLOWRATES

On the Figure 5, continuous lines are effective hold up profiles all along the column ; dotted lines are representative of local flooding points in the column : each point of these dotted lines gives the hold-up that would locally exist if the considered point of the column was flooded.

When the feed flowrates are weak, hold-up profiles are nearly flat and each value of ϕ is far from the value corresponding to a LFP, namely ϕ_E.

When increasing flowrates (for instance Q_C being fixed, by increasing Q_D), hold up profiles steepen and $\phi \rightarrow \phi_E$ (see $Q_D = 25$ l/h). For greatest values of Q_D (see $Q_D = 30$ l/h), S - type hold up profile is shown, in some parts of the column, values of ϕ higher than ϕ_E are pointed out.

CONCLUSION

Simulations have been carried out by adjusting transport and breakage laws to the case of a sieved plate pulsated column, but obtained results might be generalized.

We propose new flooding definitions, that reveal themselves as generalizing THORNTON's analysis. We distinguish the concept of local flooding point in the column and effective entrainment of the dispersed phase.

We emphasize the particular role by coalescence which leads to the concept of maximum effective load and we claim a practical interest of this working condition. We have demonstrated that backmixing contributes to the transport of the dispersed phase and delaies flooding apparition.

Lastly, we show that flooding does not afford an upper maximum value for local hold ups. In the same column, one can find higher or lower values of the hold up, with regard to the hold up at flooding.

REFERENCES

1. S.H. CHANDES, W.J. KORCHINSKY, Trans. Instn. Chem. Engrs., 53, 247 (1975).
2. R.B. OLNEY, A.I.Ch.E. Jl, 10, 827 (1964).
3. V. ROD, Br.Chem.Engng., 11, 483 (1966).
4. F. MISEK, J. MAREK, Br. Chem. Engng., 12, 202 (1970).
5. Y. PROKASKA, Summer School of Varna, 1979.
6. J.D. THORTON, Chem. Engng. Progr. Symp. Series, 50, (13), 137 (1954).

CODES FOR SIMULATED CONDITIONS

Q_C L/H \ Q_D L/H	5	10	15	20	25	30	35	40	45	50	55	60
40	Q1	Q2	Q3	Q4	Q5	Q6	Q7	Q8	Q9	Q10	Q11	Q12
60	S1	S2	S3	S4	S5	S6	S7	S8	S9	S10	S11	S12

	NO COALESCENCE	MODERATE COALESCENCE	STRONG COALESCENCE
NO BREAKAGE	A		
BREAKAGE	B	C	D

M^2/s $\mathcal{D}$ \ FEED :	DISTRIBUTION, D_0 MONODISPERSED	DISTRIBUTION, D_1	DISTRIBUTION, D_2
1 2.10^{-3}	1	2	4
2 2.10^{-4}		3	

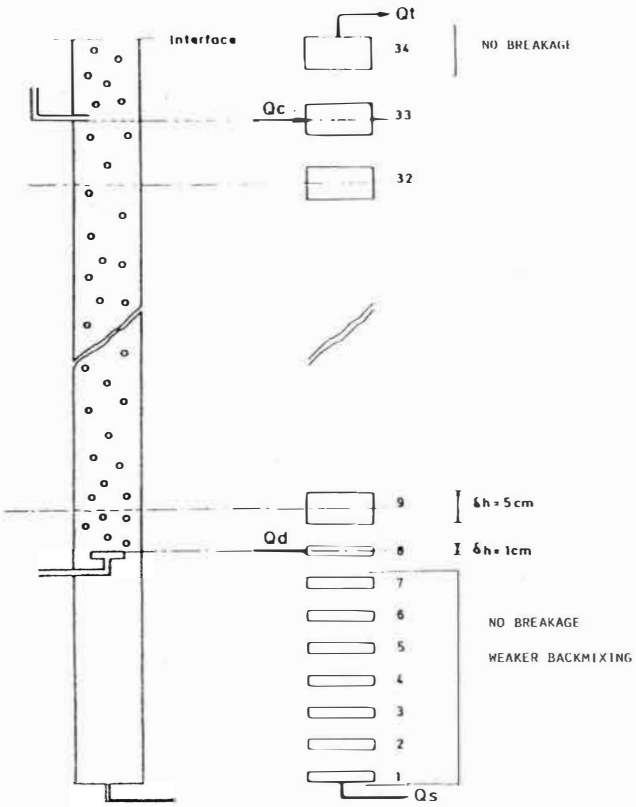

FIGURE 1 DESCRIPTION OF THE COLUMN

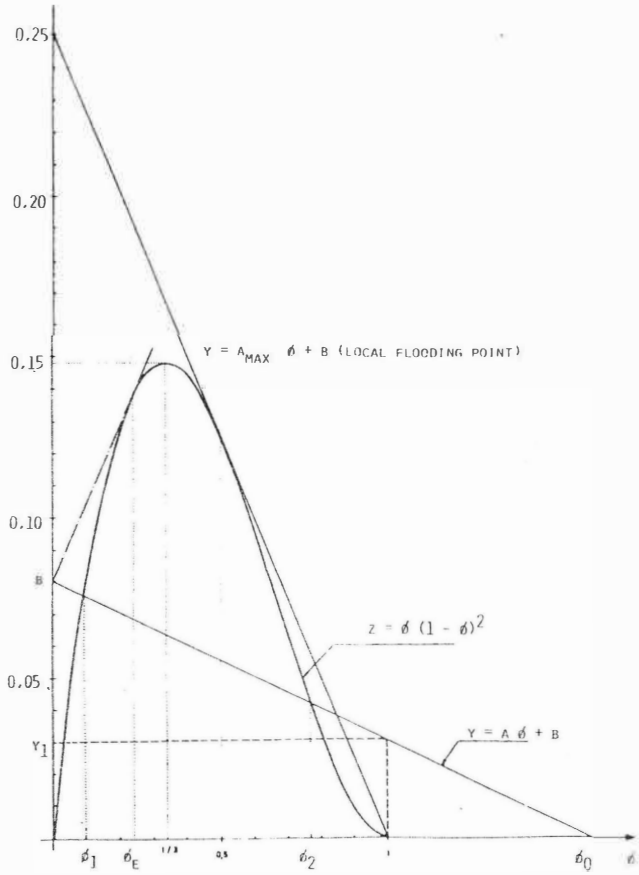

FIGURE 2 LOCAL FLOODING POINT

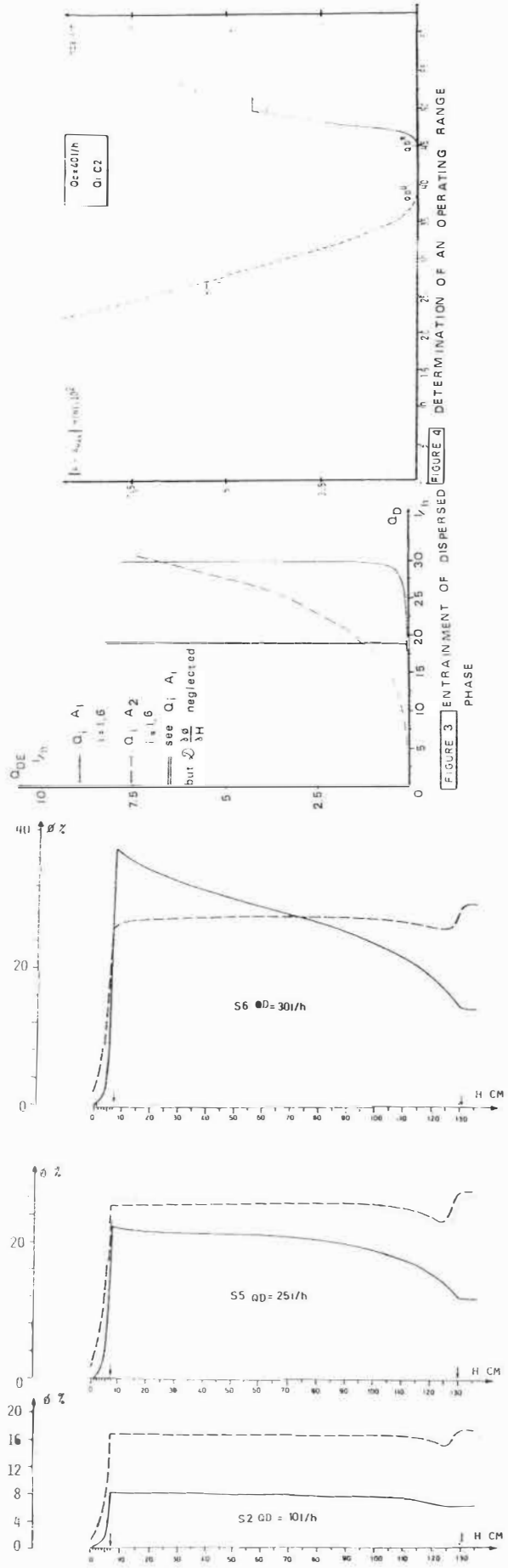

FIGURE 5 HOLD UP PROFILES

DEVELOPING SOLVENT EXTRACTION PROCESSES

AN INTEGRATED, INTERDISCIPLINARY ACTIVITY

Ruth Blumberg

Haifa, Israel
and
Miles Laboratories, Inc.
Elkhart, Indiana, USA

1. INTRODUCTORY

If one were to take the attendance list at this ISEC conference and to check the discipline in which each participant received his/her first degree, as well as that in which graduate studies were completed, one would certainly find a very wide spectrum of areas covered. Yet all have come here to ISEC expecting to participate and to benefit from the gathering together of these varied backgrounds and disciplines. Can the reason for this be other than that solvent extraction (SX), the theme of this conference, is broad enough to cater to a wide variety of interests?

The Webster Dictionary defines Discipline as a subject that is taught, or a field of study; the word derives from the Latin Disciplina which means teaching, learning; Discipulus means pupil.

Process development (PD) in its literal sense, namely the development of processes, is a discipline or field of study that is not taught formally, in the framework of the normal curricula of technological institutes. Yet it needs to be learned like any other discipline. Possibly the problem about PD is that its interdisciplinary character can hardly be encompassed in the courses offered in any single faculty; interdisciplinary faculties are rare, although some schools do try to cross the lines of faculties by having joint projects and possibly joint courses.

At present, the only way to learn PD is by working at it. It seems, therefore, to be a specialisation which starts after the "pupil" has completed a basic course of study in some field which would normally define the discipline of specialisation of the "pupil". Good process developers will result from good "in house" training, hence it is important that there be such trainees actively working on integrated projects at all stages of development. For the training to be effective the work must be directed by high caliber process developers with wide background and experience. The aim of the direction will be to supervise and train, while progressing with the project at the required rate, and to impart enthusiasm and professional appreciation of PD to all those involved.

PD is interdisciplinary, hence it requires that responsible charge or management be vested in someone who is a specialist in the field and who can span the main disciplines involved. Desirable basic capabilities of such a project manager are listed in Table I.

Developing solvent extraction (SX) processes is no different from developing other chemical processes, hence generalised statements made here can be regarded also as specific for solvent extraction. General definitions for PD are given in Table II. The difference in accent and certainty of the definition of "feasibility" in the two cases should be noted.

Novelty is not the prerogative of class or status. While it may derive from interactive thinking, in its essence it is not an interdisciplinary activity. Proving the chemical feasibility of a novel chemical idea, too, need not rely on disciplinary interaction or integration; however the development of a process from this novel idea must rely on such interaction. Due to the circumscribed studies of basic training of individuals both in science and technology, it follows that PD must be a group activity. While some individuals are able themselves to encompass a broad band of disciplines, still it is unlikely that full independence from others can be attained by any single worker in modern chemical processing. Indeed there is no reason to strive for such self-sufficiency once one has accepted the fact that PD can best be done in an interactive environment.

A chemical process has been defined as entailing some change in a bulk property of a material; the technology which brings about the change is the area of chemical engineering. Process development is the study of the means of effecting the desired change in a novel, practical, economic manner to permit industrial exploitation of the process. Aspects that fall outside this broad definition of PD are the initial definition of the transformation desired and proof in principle of its chemical feasibility, as well as eventual engineering design, fabrication and erection of plant. Process development does, however, include all the studies required in order to permit these latter stages to proceed.

Solvent extraction implies transfer of solute from one liquid phase across a boundary to another liquid phase. This transfer has two aspects, the one is "basic", relating to the mode of transfer, the other is "applied", relating to the means whereby the transfer is achieved. In the simplest context the former can be defined as chemistry, the latter as chemical engineering. No solvent extraction separation or transfer can be developed to the stage of technical feasibility, let alone process implementation, without the active interplay of these primary disciplines, hence by definition SX must be interdisciplinary. The development of a SX process should run along the rails of these disciplines in parallel, with branch lines connecting them or leading through other side disciplines back to the main lines.

In solvent extraction the separation is "system" controlled, hence a variety of systems can probably be conceived even for the separation of a specific component. Such systems will be as similar to one another, or as dissimilar, as one may wish. Not all, however, will be equally desirable nor equally feasible, so an acceptable choice must be positively made, if implementation is eventually to be attained.

2. PROCESS DEVELOPMENT FOR SX PROCESSES

2.1. Solvent extraction has been applied in a variety of fields for all sorts of purposes. The scope of the technology and its growth through the past decade can be seen from Table III, where the session titles are listed for ISEC '71 and for the current ISEC '83. Most striking is the increase in the number of sessions devoted to SX processes. If now at the present ISEC, the performance of a variety of commercial processes are being reviewed, this must mean that in the past decade considerable process development was done in the SX field.

The decision, in principle, to incorporate process development in a specific research framework is a policy decision at management level. Once decision has been reached to go ahead with PD, subsequent decisions will be mainly technological or combinations of technology and management. Success will depend on close contact and understanding between the two, and on appropriate planning and organisation.

Irrespective of the field or the technology, the development of chemical processes must go through a succession of stages. The individual stages may vary in significance according to the process involved; the order of the stages is not rigid but all must be covered in some way, if the relevant information is to be obtained which together will constitute the process. The aims of process development must be firstly to reach the point where a well based economic evaluation can be made, secondly to define the degree of uncertainty, as far as this is possible a priori, so as to enable management decision to be reached in regard to implementation, thirdly to furnish the required guide lines for basic engineering and design, and lastly to provide liaison between development and implementation.

Since it is our thesis that PD for SX processes is no different in essence from other PD cases, the relevant stages can be listed in a general way for a comprehensive PD program. This has been done in Table IV assuming a process of average complexity. In practice, SX processes may show varying degrees of complexity according to the system and the type of separation desired. The complexity usually derives from the number of transfers that are required in order to attain the separation, and from the nature of

Taking Tables V and VI together, it is clear that process and operating control have now come to the fore, hence expertise in these areas is essential, both for designing a reliable experimental system and for interpreting phenomena seen in the bench or pilot unit, in so far as these may reflect on process and operating control.

2.5. The main aim of Process Development as shown in Table IV is the preparation of a Process Package. Specifications of the Process and the Guide Lines for Basic Engineering are the culmination of the PD effort, as summarised in Table VII. Almost all the data needed will have been collected excepting for data relating to selection and sizing of equipment. This requires a special study program, and may involve disciplines not previously called upon in the PD work.

Before any work relating to equipment is started it is necessary for a decision to be taken as to the extent to which "in house" design is being planned. A study of equipment sizing and selection requires a good understanding of the properties of the system as these interact with aspects which control equipment capacity and efficiency.

In solvent extraction processes there are essentially three basic equipment types, namely mixer-settlers, columns and centrifugals. Every solvent extraction operation entails liquid-liquid contacting and liquid-liquid separation. The three types of equipment differ from one another as regards these two crucial steps and each may also be evaluated differently according to whether one is looking at the dispersion or the coalescence characteristics of the system and which one is overriding. Furthermore there may be a strong interaction of the process on the equipment selection and of the liquid system on equipment behavior.

Another aspect which needs careful study relates to materials of construction, this of course being a discipline in its own right. So we have the two way interaction of system on material and material on system. Constraints of product quality, operating conditions, and costs, all need to be taken into account in this specialised field of equipment selection,

2.6. Process development responsibility does not cease at the moment that the Process Package has been prepared. During basic engineering and later process implementation, questions will come up which were not, or could not have been foreseen earlier. The project manager of the process development program must continue to be involved by maintaining close liaison with the engineering group, and must be ready to reopen the PD studies so as to provide acceptable solutions to questions as they come up. Table VIII summarises aspects falling within the scope of PD liaison.

3. PERIPHERAL ASPECTS.

A SX process development will not be complete without due regard to a number of peripheral aspects. It is perhaps to be expected that these aspects are the very ones that require background in disciplines often far removed from the SX process itself. We have already referred to equipment selection and to materials of construction. Both of these may be regarded as peripheral, since they do not reflect directly on the separation process which is the primary aim of SX. Nevertheless they are very important and the process implementation may stand or fall depending on how knowledgeably they are handled.

Solvent losses and waste disposal are two peripheral aspects of far-reaching importance. In both cases expertise outside the normal SX steps may have to be called in. Solvent losses in waste streams may be unacceptable both economically and ecologically. A study of how and why solvent or solvent derivatives report to waste streams will need a very careful chemical and engineering analysis based on the specialised approaches of both disciplines. The questions to be answered are how to prevent solvent losses, and how to prevent waste streams or the air from being polluted by solvent. Usually the concentration levels of solvent being considered in the two cases, economic and environmental, will be significantly different. Permitted pollution levels may be orders of magnitude lower than the solubility or entrainment levels that can be accepted costwise. We may be talking, for example, of parts per billion, versus parts per million or even hundredths of a percent. Without analytical methods nothing much can be known and less can be done. Fortunately GC and HPLC procedures are ideally suited to these purposes. This means, of course, that a SX process cannot be developed without the expert services of those versed in these analytical techniques.

Prevention of environmental contamination and control of solvent losses both require a critical evaluation of the causes, a logical approach to prevention and expert practical expression in design. One need not belabour the point by listing the various disciplines that will be involved in this task.

Another peripheral aspect of any SX process will be product quality since this is the "acid test" for the separation attained. The limits of product quality may differ widely from case to case, and stress may have to be laid on entirely different aspects, depending on the process steps that follow the SX separation and recovery, and on the use of the end product. Thus SX processes have enabled wet process phosphoric acid of fertiliser quality to be upgraded for detergent purposes, for metal polishing and other technical applications, and ultimately for food grade uses. Intuitively, even without seeing the specifications, one anticipates that the quality problems will be widely different in these cases, also that phase separation and carry over of solvent may need to be considered in a very different manner in the three cases, and that the expertise involved in evaluating the level of problems likely to be encountered in production for the various grades will not necessarily coincide.

Another peripheral aspect which is specific to SX processes is solvent quality. Solvent quality may deteriorate during use for two main reasons, one being a slow accumulation in the solvent of minor components from the extraction system, the other deriving from slow degradation of solvent components by reaction in the environment of the SX process. Here, too, careful interaction of the required expertise is necessary, firstly to try to anticipate how solvent quality is likely to be impaired, then to elucidate the actual pathways and so to prescribe preventive measures and/or post-treatment. Normally positive solvent clean-up will be an integral part of any solvent extraction process, but these standard procedures, which usually rely on distillation and/or scrubbing, may not take care of the problem in all its aspects. Process changes may even be necessary in certain cases to obviate the problem in the first place. Furthermore, equipment specification may be influenced by this peripheral aspect of solvent quality; the earlier this is realised the better it will be.

Finally, for those with even the minimum experience of SX facilities, one need not stress the problems that derive from the presence of fine solids which are preferentially wetted and so caused to accumulate at the liquid-liquid interface, or, for that matter, the problem from any material which is too viscous to flow freely with the main liquid streams. It seems that notwithstanding the widely different fields of application of the SX technology, ranging from mineral processing through to biotechnology, from antibiotics to petrochemicals, and notwithstanding the variety of basic disciplines which have undoubtedly followed this problem, still it has not been satisfactorily generalised, hence solutions still remain ad hoc and specific.

4. STRATEGY AND CONSTRAINTS OF PROCESS DEVELOPMENT.

In PD the strategy is to approach the aim on as broad a front as is compatible with the external constraints. Options should be kept open for as long as practicable, provided doing so does not hinder project continuity. Definitive decisions on variable aspects must be taken as soon as the return on additional work becomes marginal, and/or in compliance with imposed technological and managerial constraints.

Often the primary managerial constraint imposed on a development project will be the timing; however, investment, scale, necessary integration with an existing facility, overall development plans, all will have bearing on the process development strategy to be employed. Early in PD it will be desirable to bring in those versed in patent matters and in commercial development, marketing and planning, since critical business aspects may thus be identified.

In order to summarise what has already been discussed, let us assume it were necessary to set up a group to develop a novel proven idea for separating and recovering some marketable value from the environment in which it is produced, through all the stages of process development and ultimately to process implementation. Initially the accent will be on chemistry, involving chemists with a variety of backgrounds and expertise. The broader the experience of these chemists in process development projects the better, and this does not mean SX processes only. As the project proceeds more accent begins to be laid on chemical engineering. Such aspects as fluid flow, mixing of liquids, separation of liquids, mass transfer, heat transfer, rates of transfer, process control, all should be considered as early as possible. Good understanding of multi-stage operation, steady state, equilibrium, accumulation, build-up, kinetics, will all help the PD stage to advance. This is particularly important if limited equipment testing must be done to enable equipment to be selected.

In preparation for implementation, the accent will be more on efficiency, yields, quality, losses, environment, waste disposal and so on. This brings in a list of disciplines not always involved prior to this

recycle streams within the overall system. The number of theoretical stages within a transfer operation does not contribute to process complexity, unless there are a multiciplicity of streams entering and exiting. Operating complexity is not necessarily the same as process complexity, so operating control problems need to be viewed separately from the PD proper.

There may not be a concensus as to the delineation of the stages of the PD program and the aim of each stage, but this is relatively secondary; the important aspect for concensus is that as one proceeds from stage to stage, one should be laying the building blocks for the flowscheme and eventually for the process as a whole.

Although as shown in Table IV, process identification falls essentially outside the defined area of PD, still it is worthwhile to spend a little time considering the aims and constraints of process identification. The separation desired needs to be specified since this will help to describe the process being aimed at. Even in an extreme case where applicability of new reagents or solvent types is the motivation, evaluation is always according to what can be achieved. The separation desired and the SX transfer need not be identical. Thus in a two solute system in which A is the value to be recovered and B is the accompanying valueless component, it may be equally valid to transfer A away from B, as B away from A.

The selection of the mode of transfer is of considerable significance for PD. Extraction systems have been classified as follows (1):

a. Distribution of simple molecules.
b. Extraction by compound formation.
c. Extraction by solvation.
d. Ion-pair formation.

Once one knows what is to be transferred one can select modes of transfer which are possible, and then the one which seems preferable. Choice of solvent type follows directly from this (2) leading then to the test of chemical feasibility. In some cases chemical feasibility may be demonstrated in a most simple manner. Let us exemplify this by a metathetic reaction:

$$MA + HB \rightleftharpoons MB + HA.$$

If, from a stoichiometric mixture of MA and HB, the solvent extracts H^+ preferentially over M^+, and extracts some A^-, then irrespective of how much B^- is extracted, the reaction has in fact been demonstrated as going from left to right.

As regards the nature of the work involved in this first stage, it can be assumed that process identification need not be an interdisciplinary activity although it may well be a group effort. This holds even when a single individual has sufficient familiarity with the chemical aspects involved in all the steps of the process identification to be capable of handling it alone.

2.2. When PD starts one assumes that one has a selected system to work with, and that this system does what one has set out to do, but the limiting framework has not been defined. Specification of limits is the first stage of process development -- here called Process Research. According to the nature of the process, the accent will be placed on different aspects; generally however, during this stage, one should derive sufficient distribution data to be able to define limits of extraction. One should have made comparisons within the family of solvents or reagents to see what aspects are favored by which members, so as to make a reasonable, more specific selection. Also one should be able to calculate separation factors hence one can define the transfer steps involved, thus going over naturally from the process research to the process study stage.

In the framework of process research, already, various disciplines may begin to enter the picture. Probably it will still remain within the scope of chemistry, though it may cover various disciplines within chemistry itself, such as inorganic, organic, physical, analytical, synthetic organic, depending on what is in fact being separated.

2.3. The Process Study is probably the heart of process development, conceptually certainly, even though not as regards effort and expenditure. The aim of the process study is to define the process by laying out the flowscheme, fixing format and working parameters. The more complex the scheme needed for eventually attaining the desired separation, the more the process study will depend on the necessary input from those with background in relevant disciplines. This is also the point at which originality in manipulating solvent extraction concepts can be displayed, hence it is the most challenging. The imprint of those who do the process study will follow the process throughout, as it is they who say: "this is how this process will look". Since this is so, it is all the more important that decisions not be taken in ignorance of constraints imposed by other disciplines. This means also that some level of process costing must be initiated as early as possible. Almost as soon as the basic flowscheme can be visualised and the primary material balance prepared, an order of magnitude economic evaluation should be made, so as to identify areas for study and development. A process study is bad, if in the next stage it turns out that the flowscheme cannot be implemented in the current "state of the art", or that it is unlikely to be economically viable.

Let us consider a process study for the metathetic reaction referred to above; let us assume that the process research has shown that the highest extraction of A^- will take place when the aqueous phase is essentially saturated with MA and when H^+ is high, which must imply B^- being high too. This finding naturally leads to the need for understanding the phase diagrams-

$$/M^+ /A^- /H^+ /B^- /H_2O / \quad \text{and} \quad /M^+ /A^- / H^+ /B^- /H_2O / \text{Solvent}/$$

as a function, say of temperature.

In this process study, the phase diagram together with distribution coefficients and separation factors, are the basis upon which the flowscheme will be built (3). A physical chemist well versed in phase diagrams, and an organic chemist with background in solvent interactions, must be active at this stage, but so must a chemical engineer who understands the kinds of problems which are likely to be encountered in the steps entailing dissolving, precipitating, contacting, separating. Analytical and process control should start at this point too; questions such as how accurately the H^+ level need be controlled, whether an acidity swing can be permitted and how this is to be controlled, will all need answering.

Let us take another case, separation of enzymes in biphase systems (4). Since it is known that such separations can be made, one can assume that a variety of systems will permit a specific separation to take place. However, an enzyme chemist and/or a protein chemist must be consulted to save the SX chemist from doing things which are not permitted for enzyme or protein processing.

As long as we stay within the framework of separation by SX there are only a limited number of possible steps. Their selection and arrangement will be based essentially on relative concentrations and separation factors, on solvent modification possibilities, within the framework of solvent compounding, and on the extent to which temperature and/or pressure are transfer variables (2). Heat effects must be carefully tested. Small scale testing cannot show up such effects. Calorimetric measurements must accordingly be made and primary heat balances calculated.

The wider the scope of the chemical input in all its aspects, the more likely that the flowscheme will be simple, elegant, original and useful; this of course, is always the ultimate aim of creativity and development.

2.4. The aim of the Bench and/or Pilot Study is to check out the selected flowscheme, as far as possible under continuous operation and to define the parameters for technological design and for a well based economic evaluation. It is at this point that the chemical engineering aspects begin to gain weight and to take over the control. It is also at this point that project management becomes a matter for consideration. Economic aspects such as benefits from successful development and timing considerations begin to be very important.

This is also the stage at which company mangement must be brought in, since from now on decisions will in many cases be business and marketing decisions, not straight scientific or technological ones.

The scale on which this study is to be performed is open, the choice depending on many factors, and relating to many aspects. There are aspects which can be studied equally well on laboratory scale by using multi-stage counter-current simulation, but there are questions that can be answered only in true continuous operation. In Table V typical aspects have been listed for laboratory simulation and for continuous operation. This, however, still does not answer the question of scale. One of the problems of bench scale operation is the difficulty of keeping steady state in small units. Also there is the danger of being misled due to the incidental character of operation in the unit selected for the test. Rarely will one expect a small unit to be a scaled down version of the full industrial plant. Even the equipment type in the small unit need not represent the final selection; at best a small continuous unit will indicate the direction to be followed in making such selection.

The true purpose of the bench or pilot study is to define the parameters for the technological design so as to be able to specify the process. In Table VI a summary list is presented of what this stage is expected to contribute to the process development, and what it will not provide.

TABLE IV

TYPICAL STAGES IN A SOLVENT EXTRACTION PROCESS DEVELOPMENT PROGRAM.

Process Identification		- Specification of separation desired. - Identification of SX transfer required. - Selection of mode of transfer. - Choice of solvent type - Test of chemical feasibility.
Process Development	Process Research	- Specification of limits.
	Process Study	- Definition of flowsheet - Format & parameters.
	Bench or Pilot Study.	- Parameters for technological design.
	Process Package	- Specifications of process. - Guidelines for basic engineering.
	Liaison	- Contact during basic engineering and process implementation.

TABLE V

ACHIEVEMENT IN LABORATORY SIMULATION VERSUS CONTINUOUS OPERATION.

Multistage Laboratory Simulation.

- Full stage efficiency
- Profile of conjugate phase compositions.
- Basic compositions for steady state operation.
- Primary material balance.
- Good indication of trends and preferences.
- Physical observations, but no estimate of physical problems.

Continuous Operation.

- Importance of procedures for filling and starting.
- Possibility of working with recycles.
- Check of material balance.
- Possibility of seeing accumulations.
- Possibility of adjusting dispersion type for good separation.
- Primary entrainment aspects.
- Checking effects of feed variability on operation.
- A basis for defining process and operating control.

TABLE VI

CONTRIBUTION OF PILOTING TO PROCESS DEVELOPMENT.

Positive

- Verification of flowscheme.
- Confirmation of material balance.
- Security as regards unexpected operating phenomena, but not necessarily so for all eventualities.
- Good indications for plant operation, process control, process sensitivity etc.
- A good model for starting up a plant, first filling, shutting down etc.
- Information necessary for preparing guidelines for basic engineering of the process.

Negative

- No data for heat balance; calorimetric measurements must be made specifically.
- Usually no design data for equipment, these must be acquired in a separate study, with or without vendor participation.
- In the normal scope of the study, the continuous small scale unit will not provide sufficient product for marketing studies.

TABLE VII

GUIDE LINES FOR BASIC ENGINEERING.

- Full process description.
- Basic flowsheet, stream compositions.
- Material balance, heat balance.
- Physico-chemical data for all steps.
- Guidelines for filling, start-up, shut-down.
- Guidelines for process control, analytical procedures.
- Guidelines for operating control
- Guidelines for materials of construction.
- Guidelines for selection and sizing of equipment.

TABLE VIII

PROCESS DEVELOPMENT LIAISON.

With basic engineering, regarding:

- Equipment selection.
- Materials of construction, selecting and testing.
- Surge and tankage.
- Control, process and operating.
- Filling, start-up, shut-down.

With service groups, regarding:

- Analytical.
- Quality assurance.
- Waste disposal, environment.
- Maintenance.
- Costing.
- Safety.
- Purchasing, solvent supplies.

With plant management and personnel, regarding:

- Operations upstream and downstream of SX.
- Training for SX.
- Trouble shooting.
- Process changes; improvements.
- Standard operating procedures.

point, as not being mandatory for the basic stages of process development. However, it should be clear that aspects which may eventually influence the implementation should be taken into account as early as possible. Hence the relevant disciplines should be brought in early, so as to avoid finding bottle-necks in implementation which could have been anticipated and dealt with earlier in the program.

Project management must not be forgotten. It is not essential that the initial project manager continue in this capacity throughout the program. As a project proceeds along the line, the accent and priorities will change, hence the choice of project manager may depend on different criteria, also on company preferences and policy, and not least on who is available at the time.

Continuing now with the same approach of setting up the group so that the necessary disciplines will be available when they are needed, it is desirable to be conversant with the many aspects of SX under study in academic circles and research institutes, so as to ensure that background in these areas will be available to the group if necessary. Basically these aspects relate to understanding what goes on in SX, since with understanding it is easier to manipulate. A few aspects stand out currently, when questions being asked are: what is the mechanism of transfer, what are the species present in the "non-aqueous" phase, what can be done to change the species? Much work is being initiated in regard to the liquid-liquid interface, what happens there, how is matter transferred, what are the kinetics of transfer? Here again feed-back from these fundamental studies to the PD group can be very valuable, as it will lay the stress on aspects which are not necessarily obvious, but once recognised may lead to interesting manipulations.

There are several areas which are contiguous to SX but with which the SX chemist will rarely come into direct contact, hence will not be able to draw analogies from them. Such contiguous areas should be identified and expertise sought there, if this can lead to a better understanding of the SX system. Examples are non-aqueous solution chemistry, the study of structure in multi-component liquids, micro-emulsions, meta-stable phases, interfacial interactions, phase transfer catalysis, liquid membranes.

Generalisations and analogies are essential for progress in any field, so too in SX and PD, which we designate by definition as being interdisciplinary.

ACKNOWLEDGEMENTS

Thanks are extended to the Technical Program Committee - ISEC '83, for inviting me to present this plenary lecture, and to the management of Miles Laboratories, Inc, for agreeing to my accepting the invitation.

Chemical process development in general, and solvent extraction in particular, have been the fields of my professional activity. The presentation made here is the culmination of over two decades of active contact with many colleagues of varying backgrounds and interests; though too numerous to list, they are all duly acknowledged.

Two however, I do thank by name:

Avram Baniel, with whom I learned that processes conceived with originality, must be developed with vision and ingenuity,
and,
"Toby" O.G. Wegrich, who showed how implementation of a novel process is approached with enthusiasm, tolerance and courage.

REFERENCES

1. Y. Marcus and A.S. Kertes, "Ion Exchange and Solvent Extraction of Metal Complexes". Wiley-Interscience, New York, (1969).
2. R. Blumberg, "Design of Solvent Extraction Systems" Separation and Purification Methods 8 (1), 45 (1979).
3. R. Blumberg, "Multi-component / Multi-phase Systems" Proceedings ISEC '77, CIM Special Volume 21 (1), 134 (1979).
4. Per-Ake Albertsson, "Partition of Cell Particles and Macromolecules", Wiley-Interscience, New York, 2nd. ed. (1971).

TABLE I.

CAPABILITIES OF A PROCESS DEVELOPMENT PROJECT MANAGER.

- To envisage the process from its earliest stages and work accordingly.
- To know when, where and from whom to seek aid for specialist aspects.
- Ability to proceed along a broad front throughout the project.
- The courage to decide that enough has been done, even though the optimum has not been attained.
- The professional standing to make others accept the reasoning.

TABLE II.

DEFINITIONS FOR PROCESS DEVELOPMENT.

- Chemical Process Development can be defined as the development of a novel idea, of proven chemical feasibility, to the point of presenting a process of proven technological feasibility.
- Chemical Feasibility, in the framework of SX, means definitive proof that the desired separation can be achieved, and that the desired product can be recovered.
- Technological Feasibility implies the likelihood of technical and economic viability.

TABLE III

ISEC SESSION TITLES.

ISEC '71	ISEC '83
Physical Chemistry of Extraction I, II.	Physical Chemistry Thermodynamics of Phase Equilibria in SX Systems I(P), II. Characterisation of Organic Species in SX processes, I, II. Novel Extractants I, II(P). Extraction with Supercritical Solvents I(P), II. Emulsion Liquid Membranes I, II. Solid-supported Liquid Membranes, I, II(P). Analytical Chemistry, I(P), II(P), III.
Nuclear Applications, I, II, III.	Nuclear Extraction Processes, I, II, III.
Chemistry of Metal Extraction I, II, III, IV. Process Development I Metal Extraction II Extraction of Non-metals Extraction of Lanthanides Application to Petroleum Industry	Metallurgical Extraction Processes I, II, III. Inorganic Extraction Processes, I, II(P). Pharmaceutical & Biological Extraction Processes, I, II(P). Performance of Commercial Solvent Extraction Processes, I, II. Fuel & Chemical Extraction Processes, I, II(P).
Transport & Interfacial Phenomena Drops & Dispersions Coalescence	Interfacial Kinetics, I, II. Fluid Mechanics, Phase separation & Interfacial Phenomena, I, II(P).
Extraction Equipment, I, II, III.	Extraction Equipment & Design, I, II(P).
Mathematical Models & Control	Modelling & Axial Dispersion, I, II.
Plenary Session - Case Histories of Industrial Applications	Plenary Session - Chemical Reactions in Liquid-Liquid Systems.
Plenary Lectures Nuclear Petroleum	Plenary Lectures Hydrometallurgy Process Development Ion-pair Distribution.

THE LIX®860 SERIES: UNMODIFIED COPPER EXTRACTION REAGENTS

Gary A. Kordosky, J. Michael Sierakoski

Henkel Corporation
Tucson, Arizona USA

and

Joe E. House
Henkel Corporation
Minneapolis, Minnesota USA

Only two classes of compounds have gained commercial acceptance as reagents to be used in the solvent extraction of copper from typical acid leach solutions: the ketoximes, for example, LIX®64N and SME®529; and the salicylaldoximes, for example, LIX 622 and ACORGA®P-5100. These two classes of compounds differ significantly in copper extractive strength. In fact, the salicylaldoximes are such strong extractants that an extraction-stripping equilibrium modifier, such as nonylphenol or tridecanol, must be used in the organic system so that adequate copper transfer can be achieved when stripping with a typical copper electrowinning liquor (1).

The use of equilibrium modifiers is not without problems. Nonylphenol is known to accelerate oxime degradation (2) as well as having deleterious effects on certain materials of construction. In addition, leach solutions containing dissolved silica frequently tend to form emulsions when contacted with metal extractant solutions, and the problem of sensitivity of copper extractants to silica during aqueous continuous operation is intensified by the presence of nonylphenol (3).

This work examines the properties of mixtures of ketoximes with salicylaldoximes as they relate to copper extraction and circuit behavior. This work also introduces the LIX 860 series of copper extractants and its three main members: LIX 860, LIX 864, and LIX 865. The composition of these reagents as well as other reagents used in this study is given in Table 1.

STRIPPING AND EXTRACTION

A solution containing ~20 v/v% HS-LIX 65N in Kermac 500T was mixed in increments of 10 v/v% with a solution containing ~20 v/v% LIX 860 also in Kermac 500T. The respective starting solutions and mixtures thereof were equilibrated with an aqueous solution containing 170 g/l H_2SO_4 and 30 g/l Cu by using one three-minute agitated contact. The respective stripped organics were then filtered and a portion of each was retained for analysis. The remainder was equilibrated with an aqueous copper solution containing 5.45 g/l Cu and 1.3 g/l Fe^{3+} at a pH of 1.90 using a vigorous five-minute contact at an O/A of 1/1. The organic and aqueous phases resulting from this contact were then sampled for analysis. The stripped organic and aqueous raffinate results are shown in Figures 1 and 2.

Similar results were obtained using mixtures of either HS-LIX 64N, SME 530 (active extractant 2-hydroxy-5-nonylacetophenone oxime), or Acorga P-17 (active extractant 2-hydroxy-5- nonylphenyl benzyl ketone oxime) as the ketoxime component; and either 5-octyl, 5-nonyl, or 5-dodecylsalicylaldoxime as the alkylated salicylaldoxime. The presence of modifiers alters the system in such a way that the deviation from straight line behavior is much less dramatic, and in fact, if enough modifier is present there is no deviation from straight line behavior(1).

The most surprising feature of the mixtures in these tests is the lower-than-expected stripped organic values. This, combined with the fact that the loading of the mixtures is additive, results in a greater-than-expected net copper transfer. In fact, this mixture of approximately equal amounts of strong and weak extractants retains virtually the same extractive strength as the modified aldoxime strong extractants such as LIX 622 or P-5100, provided the total concentration of the oximes is equal. Figure 3 shows two equilibrium isotherms generated using 20 v/v% LIX 622 and 20 v/v% LIX 864 respectively, with a synthetic copper feed solution containing 5.51 g/l Cu at a pH of 2.0. The LIX 864 isotherm is not quite as sharply bowed as the isotherm for LIX 622; however, the stripped organic for LIX 864 is 2.16 g/l Cu, ~1.17 g/l Cu less than that for LIX 622. As a result, the LIX 864 mixture retains virtually the same copper recovery in a two-stage or a three-stage extraction circuit with the feed under discussion as a similar circuit utilizing LIX 622.

KINETICS

Copper extraction kinetics of the mixtures is greater than would be predicted for a straight-line interpolation of the kinetics of the individual components. The data in Table 2 serves as one example. The presence of a kinetic additive such as LIX 63 enhances the copper extraction kinetics of both the ketoxime and the mixture. Mixtures without a kinetic additive, such as LIX 65N with LIX 860, show a more dramatic increase in copper extraction kinetics over the predicted value.

This enhancement of copper extraction kinetics is not changed by the presence of nonylphenol, a result in apparent conflict with previously reported work (1). Although the kinetics of ketoxime-aldoxime mixtures are not quite as fast as the kinetics of the aldoxime by itself, they are more than adequate to result in high mixer efficiencies utilizing the size and type of mixers normally used in the industry.

PHYSICAL BEHAVIOR

A series of circuits was run in order to compare the phase disengagement, entrainment, and crud formation properties of LIX 864, with those of HS-LIX 64N, LIX 6022, and ACORGA PT-5050. The studies were conducted at a commercial plant site operation in Arizona with all-glass phase separation cells utilizing plant leach liquor and strip electrolyte.

The testing was divided into three phases. In Phase I, two independent one-extraction plus one-strip circuits, identical in every way except for the copper extraction reagent, were run. In this phase of testing, LIX 864 was compared to LIX 6022 and then to PT-5050. The circuits were operated for six to eight hours per day and readings taken every half hour. Data on the following were recorded: phase bands, mixer continuity, temperature, aqueous entrainment in the loaded organic and stripped organic phases, and organic entrainment in the raffinate and pregnant electrolyte phases. Several important observations were made: 1) Organic entrainment in the raffinate stream was significantly lower for LIX 864 than for either LIX 6022 or PT-5050; 2) Phase continuity can have a dramatic effect on some entrainment values; 3) Phase bands were very small, running from 1/4 to 3/4 inches in extraction and 0 to 1 1/4 inches in strip, and did not appear to be reagent related; and 4) Much less crud seemed to be generated in the LIX 864 circuit than in either the LIX 6022 or PT-5050 circuits.

Phase II testing was designed to quantify the amount of crud generated when comparing LIX 864 with HS-LIX 64N and ACORGA PT-5050. Three single stage circuits were run side by side where loaded organic was continually contacted with fresh aqueous leach solution from a common source. Double phasing was a major problem with all reagents in this test. After 16 hours of operation the circuits were shut down and each settler carefully emptied into a large separatory funnel. The crud layer for each circuit was isolated, transferred to a Goetz tube and centrifuged at 2000 rpm for ten minutes. The volume of the compacted crud is shown in Table 3. The amount of crud generated by the PT5050 circuit was four times greater than the amount generated by the LIX 64N circuit and three times greater than the amount generated in the LIX 864 circuit. Whereas the absolute amount of compacted crud which was generated may not seem like very much, the volume occupied by the non-compacted crud in the circuit was 5-10 times greater.

To determine if the addition of the modifiers nonylphenol (NP) and tridecanol (TDA) to unmodified reagents would accelerate crud formation, the following tests were run. Two circuits were set up, each consisting of one extraction and one strip stage in a manner similar to Phase I testing. Each test was run for a total of 10 hours, 5 hours with leach solution at ambient temperature (29-32°C) and 5 hours with the leach solution cooled (16-18°C). At the end of a given circuit run, the crud layers were isolated and centrifuged as previously described. The results are shown in Table 4. Note that the amount of compacted crud formed in the presence of added modifier is twice the amount formed when no modifier is added. Furthermore, the crud generated in the presence of modifiers had a much greater tendency to float in the organic phase, resulting in easier crud movement to the strip stage in the circuit. Other observations worth mentioning are: 1) The circuits operating with unmodified reagents always showed lower organic entrainment in the exiting raffinate stream than the circuits operating with added modifier; 2) There were no formal phase bands in stripping, but rather one inch haze bands; 3) Phase bands were between 1/4 and 1/2 inch in extraction; and 4) There was no observable interaction between the reagent, modifier, or temperature on either the phase bands or haze bands.

CONCLUSIONS

The properties of the ketoxime-aldoxime mixtures reflect the the most desirable characteristics of the components: the extractive strength, fast kinetics, and good selectivity of the aldoximes combined with the proven, good physical performance of LIX 64N or LIX 65N. The good physical performance can be a very important feature when dealing with leach solutions that are known to be sensitive to modifiers. Examples would be agitation leach solutions which contain some solids or residual flocculant and leach solutions which contain colloidal silica.

®LIX is a Registered Trademark of Henkel Corporation
®SME is a Registered Trademark of Shell Chemicals, U.K. Ltd.
®Acorga is a Registered Trademark of Acorga Ltd.

REFERENCES

1) Tumilty, J.A., Massam, J.P., and Dalton, R.F., "The Acorga P-5000 Series: A Novel Range of Solvent Extraction Reagents for Copper", Advances in Extractive Metallurgy, 3rd International Symposium, London, 1977, pp. 123-131.

2) Acorga Mining Chemicals Technical Information MC 1.80, "Acorga P-5100 and Acorga P-5300: Long Term Laboratory Evaluation of Hydrolysis".

3) Menacho L., J., CIMM, Santiago, Chile, Private Communication, October, 1980.

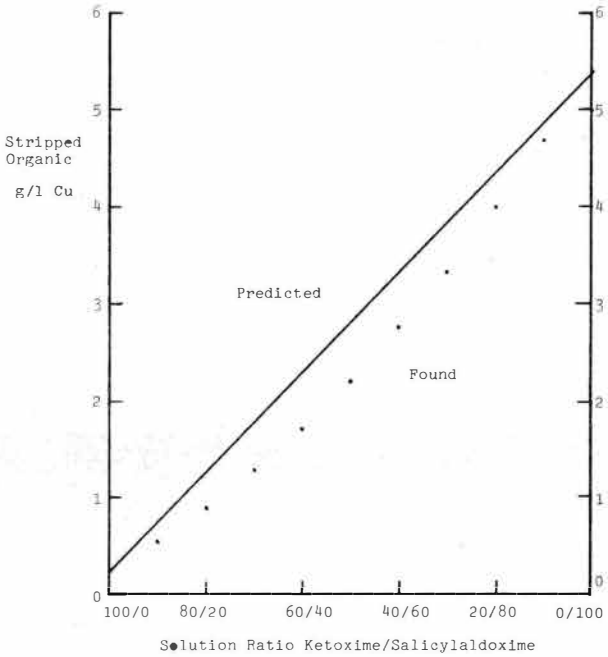

Figure 1. Stripped Organic Values as a Function of the Ketoxime/Salicylaldoxime Ratio.

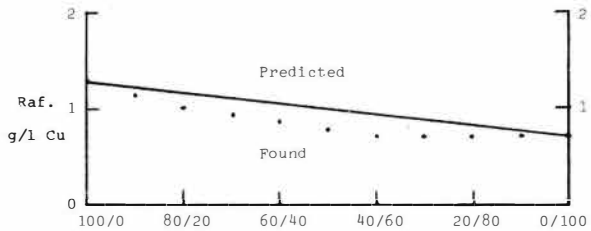

Figure 2. Raffinates from an O/A = 1/1 Contact of a 5.45 g/l Copper Feed at pH 1.9 with the Stripped Organics Corresponding to the Ketoxime/Salicylaldoxime Ratios Shown.

Table 1. Composition of Some Commercially Available Copper Extractants

Extractant	Composition
HS-LIX 64N	A mixture of 2-hydroxy-5-nonylbenzophenone-oxime, and 5,8-diethyl-7-hydroxydodecan-6-oxime in kerosene.
HS-LIX 65N	2-hydroxy-5-nonylbenzophenone oxime in kerosene.
LIX 860	5-dodecylsalicylaldoxime in kerosene.
LIX 864	A mixture of HS-LIX 64N with LIX 860.
LIX 865	A mixture of HS-LIX 65N with LIX 860.
Acorga PT-5050	A mixture of 5-nonylsalicylaldoxime and tridecanol in kerosene.
LIX 6022	A mixture of 5-dodecylsalicylaldoxime, and tridecanol in kerosene, the relative level of tridecanol being higher than in PT-5050.
LIX 622	A mixture of 5-dodecylsalicylaldoxime and tridecanol in kerosene, the relative level of tridecanol being lower than in PT-5050

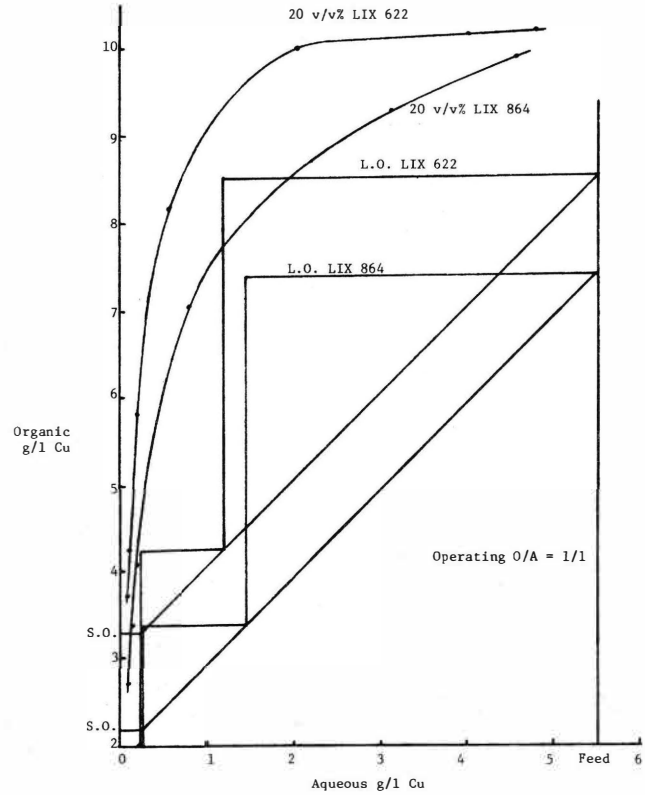

Figure 3. Comparative Extraction Isotherms Utilizing 20 v/v% LIX 622 and 20 v/v% LIX 864 with a Common Feed.

Table 2. Kinetics of Copper Extraction with HS-LIX 64N, LIX 860, and a 50/50 Mixture of Both

	10 v/v% HS-LIX 64N		50/50 Mixture		10 v/v% LIX 860	
Time	g/l Cu	% Equil.	g/l Cu	% Equil.*	g/l Cu	% Equil.
0	0.15		1.15		2.57	
30	2.68	82.4	3.71	91.8	4.64	94.5
60	2.92	90.2	3.90	98.6	4.72	98.2
300	3.22		3.94		4.76	

*Expected % equilibrium values for the 50/50 mixture at 30 and 60 seconds are 88.4 and 94.2, respectively, based on straight-line behavior.

Table 3. Volume of Compacted Crud Generated in a Series of One-Extraction Stage Circuits Over a 16-Hour Period

Organic	Milliliters of Compacted Crud
9.5 v/v% PT5050 in Kermac 500T	30-33
9.5 v/v% LIX 864 in Kermac 500T	10-11
10.5 v/v% HS-LIX 64N in Kermac 500T	7-8

Table 4. Volume of Compacted Crud Isolated as a Function of Modifier

Reagent	Circuit Hours	Compacted Crud (ml)
10.5 v/v% HS-LIX 64N	9.5	5
10.5 v/v% HS-LIX 64N + 2.5 v/v% TDA	9.5	10
8.5 v/v% LIX 864	8.0	10
8.5 v/v% LIX 864 + 2.5 v/v% TDA	8.0	20
8.5 v/v% LIX 864	10.0	7
8.5 v/v% LIX 864 + 3.0 v/v% NP	10.0	14

SOME NEW LIQUID EXTRACTION SYSTEMS FOR SEPARA COBALT FROM NICKEL AND MATHEMATICAL MODELING OF THESE EXTRACTION PROCESSES

Chuei Biing-yi, Yu Jing-fen, Zhang Liang-ping

Department of Chemistry and Chemical Engineering
Tsinghua University
Peking, China

INTRODUCTION

Sulphate and mixed sulphate-chloride solutions are conventional aqueous media for separation of cobalt from nickel with solvent extraction process. The typical feed materials are acid leached solution of matte and nickel electrolyte. Trialkyl amine type extractant (R_3N) has been successfully employed to Co/Ni separation, but it can only be used for high chloride concentration medium. D2EHPA solvent extraction process has been developed by Ritcey et al(1) for Co/Ni separation in sulphate medium. But the separation factor between cobalt and nickel is rather low in D2EHPA system and the extraction process has to be carried out under higher temperature and with many stages. This process is only suitable for aqueous feed of high Co/Ni ratio. Recently, a new acidic phosphorus-based reagent HEHEHP(2-ethylhexyl phosphonic acid mono-2-ethylhexyl ester) has been developed and commercialised in Japan for Co/Ni separation in sulphate medium(2). HEHEHP solvent extraction process has also been studied in China for Co/Ni separation in sulphate feed solution with Co/Ni ratio around 1/3.5, and has been demonstrated successfully on pilot plant scale. However, the price of HEHEHP is much higher than that of D2EHPA, and the extraction performance of HEHEHP for some impurity elements, such as Fe(III) and Ca(II), is not satisfactory. Stripping of Fe(III) from HEHEHP organic phase is very difficult. In order to develop new solvent extraction systems of better technological and economical performance, a series of new acidic phosphorus-based extractants and alkyl amine type extractants* were studied and evaluated in our laboratory. Two of them(with chinese trademark 5709 and 7407 respectively) exhibit excellent extraction performance even under ambient temperature and can be used to aqueous feed with very low Co/Ni ratio, say, 1/150 - 1/600.

EXPERIMENTAL STUDIES

The extraction performance for Co(II), Ni(II) and some impurity elements with HEHEHP, D2EHPA, 5709 and 7407 as extractants has been studied experimentally. The structures, some physical properties and relative prices of these extractants are compared in Table 1.

Table 1.

Extractant	Structure	Properties	Relative price (in China)
D2EHPA			1.0
HEHEHP	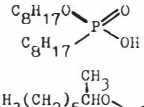	viscosity 58.5cp density 0.9560g/cm^3	5.5
5709	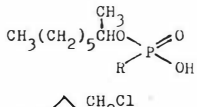	viscosity 30cp density 0.9460g/cm^3	2-2.5
7407	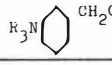	nitrogen content 2.49%	0.7

Co/Ni Separation. In contrasted with D2EHPA, extractants 5709 and 7407 can separate Co(II) from Ni(II) efficiently even under room temperature. The equilibrium distribution coefficients and separation factors for nickel electrolyte feed (sulphate-chloride media with Co/Ni ratio around 1/300) are compared in Table 2(3-7).

Table 2.

System	Conc. of extractant	Temperature	pH	D_{Co}	D_{Ni}	$\beta_{Co/Ni}$
D2EHPA	0.29M	30°C	4.5	0.25	0.113	2.2
HEHEHP	0.10M	30°C	5.0	7.316	0.0169	432.9
5709	0.10M	30°C	5.0	8.529	0.0196	435.4
7407	0.70M	30°C	2.0	2.88	0.0002	14400

It can be seen that, extractants 5709 and 7407 show much higher extraction ability for Co(II) than D2EHPA, whereas their prices are much lower than that of HEHEHP. In addition, the selectivity of extractant 7407 is excellent, it actually does not extract Ni(II) at all.

For sulphuric acid leached feed of raw cobalt material (Co/Ni ratio of 1/6), the comparison of extraction performance is given in Table 3. The dependency of extraction ability on structure of extractant is obvious and extractant 5709 seems to be the best choice.(8)

Table 3.

System	Conditions	D_{Co}	D_{Ni}	$\beta_{Co/Ni}$
D2EHPA	0.3M extractant 30°C pH = 5.0	~~12.46~~ 1.246	0.088	130
HEHEHP	aqueous phase:	20.25	0.0045	4500
5709	58.79 gNi/l 10.43 gCo/l	41.28	0.0026	16000

Extraction Behavior of Impurity Elements. Extraction behavior of some impurity elements in company with nickel and cobalt is extremely important for developing a feasible solvent extraction flowsheet. For example, Fe(III) and Ca(II) are two of the elements which effect the organisation of the process. It was noticed from experimental results that Ca(II) and Fe(III) show different behavior in HEHEHP and 5709 systems. HEHEHP extracts Ca(II) more easily than it extracts Co(II). If sulphuric acid is used as stripping reagent for Co(II), calcium sulphate will precipitate during stripping. So that Ca(II) must be removed from aqueous solution before Co(II) extraction. However, extractant 5709 extracts Co(II) preferentially, hence the stripping process for Co(II) extracted by 5709 is very simple.

Extraction rate of Fe(III) strongly depends on the structure of acidic phosphorus-based reagents.(9) Experimental results show that the extraction kinetics of Fe(III) varies with different extraction systems. Fe(III) extraction rate for 5709 system is much higher than that for D2EHPA, HEHEHP or other acidic organophosphorus-based reagents. It is found that equilibrium can be reached within 3 minutes for 5709 system. However, with D2EHPA or HEHEHP as extractant, several hours are required under the same condition. The comparison of the rate of Fe(III) extraction is given in Table 4.

Quaternary ammonium extractant 7407 exhibits excellent extraction ability for Fe(III), and stripping of Fe from organic phase is also quite easy. Because 7407 extracts Cu(II), Pb(II), Zn(II) from mixed sulphate-chloride solution simultaneously

* These extractants were synthesized by Beijing Research Institute of Uranium Ore Processing.

System	Conditions	Rate constant, sec^{-1}
D2EHPA	0.1M extractant in kerosene 25°C	$4.7x10^{-4}$
HEHEHP	aqueous phase: ionic strength = 2.0	$1.6x10^{-4}$
5709	0.4gFe(III)/l 0.5N H_2SO_4	$2.6x10^{-2}$

while leaving Ca(II) and Mg(II) in aqueous phase, it is particularly suitable for removal of impurity elements from nickel electrolyte.(6,7)

MODELING, SIMULATION AND OPTIMIZATION OF THE PROCESS

After experimental studies, process flowsheeting was conducted for 5709 and 7407 systems. In order to evaluate different process variants and to determine proper technological parameters, computer simulation is regularly carried out in this laboratory. Some results are to be described here.

Modeling of Extraction Equilibrium. For each extraction system, the experimental distribution data measured under various combination of parameters were correlated. The coefficients in the proposed formulas were computed with non-linear least-squares algorithm. Extraction equilibrium distribution models for some systems and their applicable ranges are listed in Table 5.(4-7,10) The average deviations of the calculated values from experimental ones are 3-5%.

Simulation and Optimization. A general computer program for simulation and optimization of metal solvent extraction process was set up by the authors a few years ago and has been used to various cases since then.(3-7) The output of the computation is several sets of near-optimum flowsheet parameters and corresponding values of the objective function. The final decision should then be made by the executives based on other considerations.

Table 5.

System	Models	Applicable range
Co-5709-SO_4^{-2}	$D=0.0438(R^o)^{2.806}e^{0.04t}/(H^+)^{.579}$	R^o=0.15-0.5M t= 20-50°C pH= 4-6
Ni-5709-SO_4^{-2}	$D=0.009(R^o)^{5.098}e^{-0.0244}/(H^+)^{.694}$	
Co-7407-SO_4^{-2}-Cl^-	$D'=1.01x10^{-9}(R^o)^{1.943}e^{0.01075t}$ $D=(Cl-2.802)^{4.727}D'$	R^o=0.3-0.9M t =20-50°C Cl=60-120g/l

Note: D=distribution coefficient
(R^o)=initial concentration of extractant in organic phase, M
Cl =chloride concentration in aqueous feed, g/l
t =temperature
(H^+)=concentration of H^+ in equilibrated aqueous phase,M

Table 6 illustrates the comparison of the optimized technological parameters for nickel electrolyte purification with different extractants.(3,5-7) It can be seen that both 7407 and HEHEHP are much better than D2EHPA, as they can work under lower temperature and with much less extraction stages.

Although 7407 has to be used at higher concentration, its price is much lower. So that the investment for extractant will be nearly the same. Since 7407 can extract cobalt at pH 1-2, which is the acidity of the feed electrolyte, the acidity adjustment step of the feed can be omitted, resulting significant saving of chemical consumption.

Table 6. Optimized parameters for purification of Ni-electrolyte

System	(R^o),M	t°C	Cl^-,g/l	pH	V_o/V_a	N_{stage}	Ni-loss %	Co in raff. mg/l
D2EHPA	0.29	50	(70)	4.0	1.5	29	2.5	3
HEHEHP	0.1	25	(110)	4.27	0.44	9	0.4	1.07
7407	0.7	34	110	(2)	0.55	7	0.01	1.2

Note: The figures in ( ) are not adjusted in optimization.

In addition, the separation of Co from Ni is much better for 7407 than that for HEHEHP, and the experiments show that trace impurity (Fe,Pb,Zn,Cu etc) can be extracted simultaneously with cobalt,making the separation flowsheet very simple.

After computer evaluation of flowsheets, the optimal process conditions were verified with laboratory extraction cascade experiments. Table 7 shows the comparison between calculated optimized performance and experimentally measured result. Good agreement can easily be seen.(6,7)

Economical evaluation computation for Co/Ni separation in sulphuric acid leached feed of matte has also been carried out. The results of computation show that the capital costs for 5709 and HEHEHP systems are close to each other, but the operational cost of 5709 system is only about 40% that of HEHEHP.

Table 7. Cascade verification of calculated optimal parameters for 7407-Ni-Co-SO_4^{-2}-Cl^- system

Performance	Calculated values in optimization	Values obtained in cascade experiments
Co in raffinate, mg/l	1.2	1.6
loss of Ni , %	0.01	0.01
removal of Cu,Fe, %	99.99+	99.99+

Note: The optimal parameters used:
(R^o)=0.7M; t=34°C; Cl^-=110g/l; N=7 stages; V_o=0.55V_a
Composition of aqueous feed:
70gNi/l; 300mgCo/l; 800mgCu/l; 800mgFe/l; 110gCl^-/l; SO_4^{-2}= 60g/l

CONCLUSIONS

1. For Co/Ni separation in sulphate media, new extractant 5709 exhibits the best extraction performance and economically favorable. Both 5709 and HEHEHP can extract cobalt selectively under ambient temperature, but 5709 can remove impurities more easily than HEHEHP. The price of 5709 is much lower than HEHEHP, so that 5709 is expected to be used in hydrometallurgical industry in near future.

2. For Co/Ni separation in mixed sulphate-chloride media, quaternary ammonium extractant 7407 may be the favorite choice. It can extract cobalt selectively at room temperature, little nickel is extracted simultaneously. The raw material for preparing 7407 is plentiful in China and the synthesis process has been well mastered. Its low price as well as better impurity extraction property makes it a prospective extractant for purification of nickel electrolyte.

3. It is fruitful to use computer simulation and optimization approach to study solvent extraction process. Favorite system with optimized parameters can be determined and then be verified through a small amount of experimental work.

REFERENCES

1. G.M.Ritcey, A.W.Ashbrook, B.H.Lucas, CIM Bulletin, January, p111-123(1975)
2. D.S.Flett, The Chemical Engineer, July, p321-324(1981)
3. Chuei Biing-yi, Yu Jing-fen, Zhang Liang-ping et al, Proceedings of Jingchuan annual metallurgical meeting(1980)
4. Yu Jing-fen, Zhang Liang-ping, Fu Xiu-fen, Uranium Mining and Metallurgy (in chinese), Vol. 1(3), p65-66(1982)
5. Chyu De-lin, Yu Jing-fen et al, Proceedings of Jingchuan annual metallurgical meeting(1982) (in China)
6. Chuei Biing-yi, Yu Jing-fen, Zhang Liang-ping et al, ibid
7. Sun Mei-lin, Chuei Biing-yi et al, Scientific Thesis of Tsinghua University(in chinese) (1982)
8. Yu Jing-fen, Fu Xiu-fen, ibid(1982)
9. Yu Jing-fen, Houh Yan-xue et al, ibid(1982)
10. Chyu De-lin, Yu Jing-fen, Teng Teng, ibid(1982)

COBALT-NICKEL SEPARATION BY SOLVENT EXTRACTION WITH A DIALKYLPHOSPHINIC ACID

W. A. Rickelton
Cyanamid Canada

D. S. Flett and D. W. West

Warren Spring Laboratory
Stevenage Herts, U.K.

INTRODUCTION

Historically, the SX separation of cobalt from nickeliferous sulphate solutions has been difficult because of the poor selectivity of available reagents e.g. D2EHPA. Although D2EHPA can and is being used successfully in cobalt solvex processes (1,2,3), its application has been limited to feed streams which have favourable cobalt:nickel ratios. Preconcentration is often required to produce suitable solvex feeds e.g. Matthey Rustenburg utilise the Outokumpu Oy process to concentrate a solution from 250 gpl Ni, 2-4 gpl Co to 30 gpl Co, 15 gpl Ni before a solvent extraction separation is attempted with D2EHPA(3).

This paper will describe cobalt-nickel separation using a new, highly selective cobalt extractant; CYANEX* 272. The properties of this reagent are such that solutions having high nickel and low cobalt tenors may be treated directly for cobalt recovery. Preconcentration is unnecessary.

SELECTIVITY

CYANEX 272 is a dialkylphosphinic acid extractant; specifically di(2,4,4 - trimethylpentyl)phosphinic acid. It is a member of one of three groups of organophosphorous compounds which have been examined for Co-Ni separation. The groups consist of phosphoric, phosphonic and phosphinic acid derivatives. They have the following structures:-

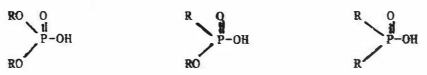

Phosphoric	Phosphonic(4)	Phosphinic(5,6)
e.g. D2EHPA	e.g. PC 88A	e.g. CYANEX 272

* Trademark of American Cyanamid Company.

Cobalt-nickel selectivity increases in the order phosphoric, phosphonic, phosphinic. This is evidenced by the cobalt-nickel separation factors shown below.

Extractant	Co/Ni Separation Factor
D2EHPA	14
PC 88A	280
CYANEX 272	7000

Conditions : 0.1 M Extractant in MSB 210.
Metal ion concentration 2.5 X 10^{-2}M
Temperature = 25°C
pH = 4
A/O = 1

pH isotherms comparing CYANEX 272 to D2EHPA are shown in Fig. 1. The isotherms were generated using an aqueous solution containing 100 gpl Ni and 2 gpl Co. The superior extractant performance of CYANEX 272 is evident.

Although the cobalt-nickel selectivity characteristics of the reagent are of primary concern, its behaviour toward other metals is also important. Calcium, in particular, can cause problems in solvex circuits due to the formation of calcium sulphate (gypsum) cruds. CYANEX 272 is a weaker calcium extractant than, for example, D2EHPA and this property helps to prevent calcium sulphate precipitation and the associated solvent losses.

Data comparing CYANEX 272 to D2EHPA as calcium extractants from single metal sulphate solutions are given in Figure 2. Similar pH isotherms for a number of other metals are shown in Table 1.

CONTINUOUS TESTING

Continuous counter-current tests were conducted using an aqueous sulphate solution containing 100 gpl Ni and 2 gpl Co. The tests were carried out with two objectives: -

- Reduce cobalt in the raffinate to <10 ug/ml
- Produce a scrubbed solvent with a cobalt/nickel ratio >1000

Test conditions were as follows:

Solvent (v/o) : 20% Extractant (CYANEX 272 - NH_4 salt), 10% p-nonylphenol in MSB 210

Aqueous Feed : 2 gpl Co, 100 gpl Ni as sulphates; 20 gpl $(NH_4)_2SO_4$, pH=5

Scrub Feed : 40 gpl Co as sulphate; pH =3

Temperature : 50°C

Table 1

Extraction from Single Metal Sulphate Solutions Using CYANEX 272 Extractant

SOLVENT : 0.6M CYANEX 272, 10 v/o nonylphenol in Kermac** 470B.

AQUEOUS : 0.015M metal as sulphate

TEMPERATURE : 50°C

pH CONTROL : NH_4OH or H_2SO_4 as appropriate

CONTACT TIME : 5 minutes

Metal	% Extracted	Equilibrium pH
Fe^{3+}	8.8	0.25
	23.6	0.85
	61.2	1.33
	88.1	1.75
	98.7	2.31
Zn^{2+}	14.6	0.90
	24.2	1.42
	53.3	1.88
	87.7	2.40
	99.4	3.08
Cu^{2+}	6.4	1.73
	17.7	2.64
	21.7	2.90
	73.9	3.56
	85.7	3.84
	94.8	4.08
Co^{2+}	9.2	1.78
	19.0	3.34
	70.8	4.11
	99.8	5.98
Ca^{2+}	3.4	4.15
	20.4	4.53
	81.7	5.38
	99.6	6.52
Ni^{2+}	27.6	6.33
	36.0	6.59
	52.3	6.72
	84.0	7.22
	92.8	7.47
Mg^{2+}	14.5	3.00
	29.7	4.20
	67.1	4.76
	82.0	4.99
	97.4	5.81
Al^{3+}	23.9	1.11
	41.9	2.50
	87.5	2.92
	97.2	3.14
Mn^{2+}	42.3	3.40
	86.1	3.96
	99.8	5.66
V^{4+}	7.9	1.11
	21.1	1.34
	46.5	1.44
	85.1	1.81

** Product of Kerr-McGee

Phase Ratios : Extraction A/O = 2

Scrubbing O/A = 32

Mixer Residence Time : 3.5 - 4 mins (Based upon total liquid flow)

The effectiveness of sulphuric and hydrochloric acids as stripping reagents were demonstrated in batch tests and, for the sake of simplicity, stripping was not included in continuous testing.

The test results are summarised in Figure 3. Both objectives were met; indicating the ability of the CYANEX 272 extractant to produce high purity cobalt from concentrated nickeliferous solutions.

REFERENCES

1. Flett D.S. and West D.W. Improved Solvent Extraction Process for Cobalt-Nickel Separation in Sulphate Solution by Use of Di(2-ethylhexyl)Phosphoric Acid. Complex Metallurgy. London. IMM. 1978 pp. 49-58.

2. Ritcey, G.M. Ashbrook A.W. and Lucas B.H. Development of a Solvent Extraction Process For the Separation of Cobalt from Nickel CIMM Bulletin 68 No. 753 January 1975 pp. 111-123

3. Clemente D. DeJ, Dewar B.I. and Hill J. MRR's Cobalt Refining Operation - South Africa's First CIMM 10th Annual Hydrometallurgical Meeting. Edmonton. October 1980. Paper #7

4. U.S. Patent 4,246,240

5. European Patent 0 046 933

6. European Patent 0 046 940

Solvent : 0.4 M Extractant in Aromatic 100

Aqueous : 100 gpl Ni, 2 gpl Co as sulphates

A/O : 1

Temp : 50°C

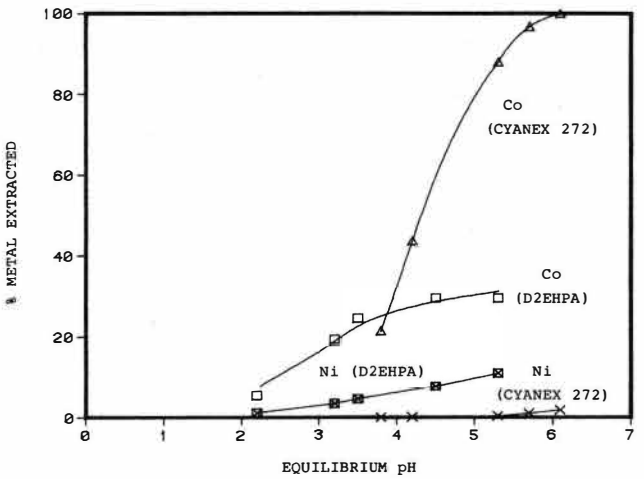

FIG. 1

Co-Ni SEPARATION WITH CYANEX 272 AND D2EHPA EXTRACTANTS

Solvent : 0.6 M Extractant 10 v/o nonylphenol in Kermac 470B.

Aqueous : 0.015 M metal as sulphate

Temp : 50°C

A/O : 1

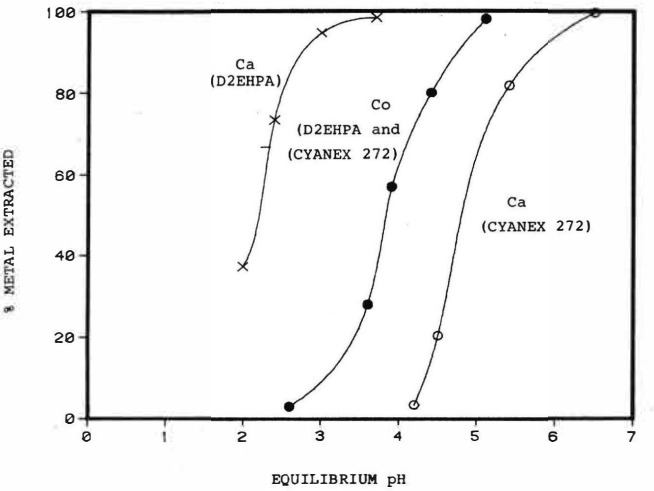

FIG. 2

Co & Ca EXTRACTION WITH CYANEX 272 AND D2EHPA EXTRACTANTS

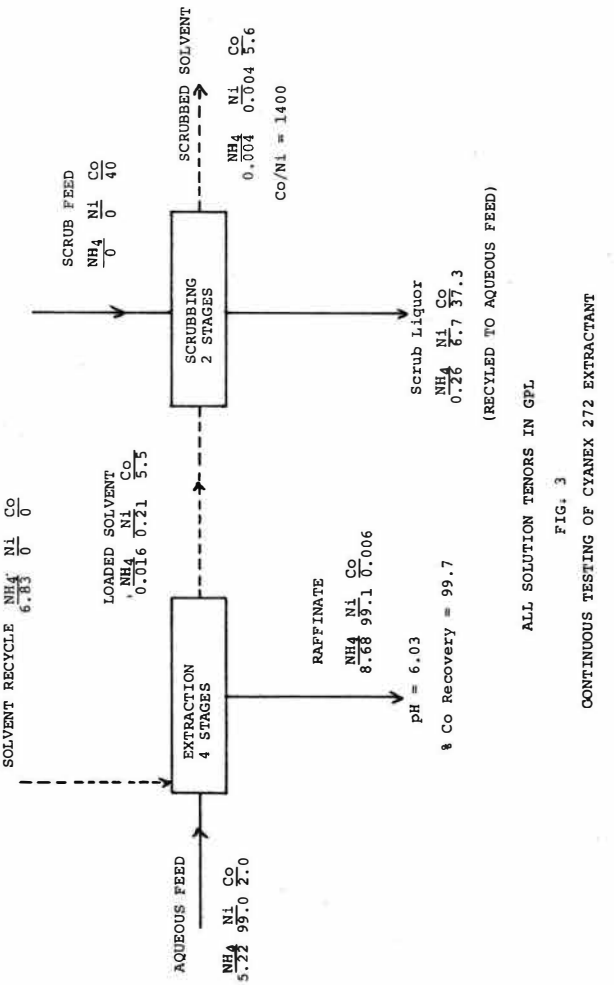

ALL SOLUTION TENORS IN GPL

FIG. 3

CONTINUOUS TESTING OF CYANEX 272 EXTRACTANT

EXTRACTION OF CADMIUM FROM PHOSPHORIC ACID SOLUTIONS

S. Stenström and G. Aly

Lund Institute of Technology
Dept. of Chemical Engineering
P.O. Box 740
S-220 07 Lund, Sweden

INTRODUCTION

In the last few years the extent of Cd pollution in Sweden was debated. The toxicity of cadmium to humans is well established (1). Cadmium generally enters the environment through the accumulator industry, metal finishing, paint, plastics, fertilizers and zinc smelting industries. More stringent environmental protection legislation has depressed the industrial use of cadmium and accelerated some scientific research activity designed to develop a pollution abatement strategy for the above mentioned industries.

Phosphoric acid is used in the manufacture of phosphate fertilizers. The concentration of cadmium in raw phosphate rocks normally varies from 5 to 20 ppm. Potential separation methods for removal of cadmium from phosphoric acid solution are sulphide precipitation, adsorption, electrolysis and solvent extraction. Few reported investigations indicate that the first three methods will be difficult to apply because of the complex nature of raw phosphoric acids. On the other hand, solvent extraction is becoming increasingly important in processes designed for the recovery or removal of heavy metals, both for production and pollution abatement purposes. For instance, about half the domestic phosphoric acid production capacity in USA is now committed to uranium recovery using solvent extraction.

One of the main objectives for this study is to investigate the technical feasibility of solvent extraction to remove cadmium from wet-process phosphoric acid. Another objective is to investigate thoroughly the various process parameters which determine the optimum extraction efficiency.

SOLVENT SELECTION

A comprehensive literature survey (2-6) revealed that cadmium can be extracted from analytical phosphoric acid solution by using zinc bis - (diethyldithiocarbamate) and various amines.

Most of the reagents used in this work are displayed in Table 1. The reagents were applied without further purification. Both wet-process and analytical phosphoric acid solutions were used as feed stocks. The analytical solution was diluted to 30% P_2O_5 corresponding to a concentration of 5.35 M H_3PO_4. A cadmium concentration of 10 ppm was obtained using a standard solution, containing 1000 ppm Cd, prepared by dissolving cadmium metal in analytical phosphoric acid.

A number of organic diluents were tested. Thus, xylene, and 10 different grades of kerosene were screened to determine the optimum diluent. This screening revealed that Shellsol-A (aromatic content of 99% v/v, $\rho_{15°C}$=0.875 g/cm^3, flame point = 50°C) fulfills most of the requirements.

The distribution coefficient of a substance is defined as the ratio of its equilibrium concentrations in the organic and aqueous phases. Equal volumes (25 ml) of the organic phase and phosphoric acid phase were shaken for 5 minutes in 100 ml separatory funnels at room temperature (22°C). The phases were then allowed to separate by decantation under 5 minutes. Three identical extractions were performed for each experiment and an averaged value of the distribution coefficient D_{Cd} was calculated. Cadmium concentrations in the aqueous phase was analysed, after repeated dilution, using an IL Model 251 Atomic Absorption Spectrophotometric unit. The distribution coefficient was calculated using material balances. To analyze for cadmium in the organic phase, the sample was stripped with an excess amount of deionized water, diluted and analysed by the AAS-unit. Mass balances were 100±10% while the relative error in analysing for cadmium was less than 10% in the concentration interval 5-20 ppm and about 15% for lower concentrations.

Table 1 displays the distribution coefficients for cadmium in both analytical and wet-process phosphoric acid. As can be seen, only DDDC was capable of extracting Cd from analytical H_3PO_4. Third phase formation was obtained with Aliquat 336 and a high concentration of HDNNS was required to obtain a D_{Cd}-value of 0.57. For the wet-process phosphoric acid, both DDDC and tertiary amines turned out to be potential reagents for cadmium extraction.

Chemical stability, commercial availability and price are obstacles for using DDDC on an industrial scale. A stability test showed that the half-time for the decomposition of DDDC/kerosene in contact with phosphoric acid is of the order of hours. This confirm the results of Bajo and Wyttenbach(7). About 99% of the extracted cadmium was easily stripped from the organic phase by using either 1 M HCl or 6.5 M H_2SO_4 solutions.

Table 1 identifies the amine extractants examined in this study. As can be seen, five commercial amines were tested together with four laboratory-quality amines. Based on their selectivity characteristics and commercial availability, high molecular weight tertiary amines (formula $(C_nH_{2n+1})_3N$) are the reagents of choice. Alamine 336, a blend of tertiary amines containing 8- and 10-carbon straight alkyl chains is the most known member of this group. Amines of this structure are not completely compatible with aliphatic kerosenes in that their salts tend to separate out of homogeneous solution as a heavy, viscous third phase in acidic solvent extraction system. Use of aromatic kerosenes together with alcohol diluent modifier eliminates this shortcoming and secondarily serves to decrease interfacial crud formation.

The effect of amine concentration was investigated and the optimum value of 2% (v/v) was chosen for the commercial amines. For stripping, 75% of the cadmium extracted can be stripped by deionized water at a phase ratio (organic/aqueous) of 10, and 82% at a phase ratio of 6.

It is noteworthy that TOPO, D2EHPA, TBP, Versatic 9113, LIX 64 N and LIX 70 all gave negative results. The synergetic mixture of 0.125 M TOPO + 0.5 M D2EHPA, specific for uranium extraction from wet-process phosphoric acid also failed in extracting cadmium.

EFFECT OF AQUEOUS PHASE COMPOSITION

Wet-process phosporic acid is a complex mixture of phosphoric acid and impurities that can vary widely in concentrations. A factorial design experiment (8) was performed to determine the effects of four components of wet-process phosphoric acid on cadmium extraction with Alamine 336. Each component was tested at a high and low concentration, as shown in Table 2. Solutions were prepared from reagent grade chemicals with all possible combinations of the aqueous phase components at the two concentraton levels. The organic phase, 2% (v/v) Alamine 336 in Shellsol-A, was equilibrated with equal volumes of 1 M HCl and scrubbed twice with deionized water. Non-equilibrated organic phase was also used for comparison. The initial concentration of Cd was 10 ppm. The test conditions and complete results are shown in Table 3 and Figure 1.

The range of cadmium distribution coefficients was from <0.05 with all aqueous phase components investigated at the low level to 15 with HCl and H_2SiF_6 at the high level. The concentrations of HCl had the largest effects on cadmium extraction followed by the concentration of H_2SiF_6. Averaged over the entire test, the cadmium distribution coefficient increased from 0.18 to 5.8 when the HCl concentration was increased from 0.0 M to 0.02 M.

CONCLUSIONS

DDDC and Alamine 336, dissolved in an aromatic diluent, were found to be the most promising reagents for the removal of cadmium from wet-process phosphoric acid. Chemical stability and commercial availability would strongly prohibit the use of DDDC on an industrial scale. A 2% (v/v) Alamine 336 solution in an aromatic kerosene is therefore recommended. For stripping, it was shown that water was capable of stripping more than 80% of extracted cadmium in one stage at a phase ratio of 6.

The effect of aqueous phase composition was studied in a factorial design test by varying the concentrations of the components individually over a range typical of their concentrations in wet-process phosphoric acid. Using pre-equilibrated organic phase, cadmium extraction was increased by increasing the concentrations of hydrochloric acid or fluorosilicic acid, and decreased by increasing the concentrations of sulphuric acid or hydrofluoric acid.

REFERENCES

1. J. Giddings and M. Monroe, Our Chemical Environment, Canfield, San Fransisco (1972).
2. S. Bajo and A. Wyttenbach, Analytical Chemistry, 49, 158 (1977)
3. N.M. Rice and M.R. Smith, J. appl. Chem. Biotechnol., 25, 379 (1975)
4. A. Alian et. al., J. Radioanalytical Chemistry, 27, 411 (1975)
5. A. Alian et. al., ibid, 27, 383 (1975)
6. A. Alian et. al., ibid, 57, 373 (1980)
7. S. Bajo and A. Wyttenbach, Analytical Chemistry, 51, 376 (1979)
8. W.D. Arnold et. al., Ind. Eng. Chem. Process Des. Dev., 21, 301 (1982)

Table 1: DISTRIBUTION COEFFICIENTS FOR CADMIUM IN ANALYTICAL AND WET PROCESS PHOSPHORIC ACID

Extractant[1]	Equilibriation	Conc.	Anal. H_3PO_4 (10.0 ppm Cd)	Wet process phosphoric acid (6.5 ppm Cd)
TOPO		0.1 M	<0.05	0.05
		0.5 M	<0.05	0.10
TOPO +		0.125 M	<0.05	<0.05
D2EHPA		0.5 M		
DDDC[2]		0.4 % (w/v)	<0.05	<0.05
		1 % (w/v)	>20	4.9
HDNNS[3]		5 % (v/v)	0.10	<0.05
		25 % (v/v)	0.57	0.14
Tri-n-hexylamine		0.1 M	<0.05[5]	0.38[5]
	pre-equilibrated[4]	0.1 M	0.44[5]	16[5]
Tri-n-octylamine		0.04 M	<0.05[5]	1.4
	pre-equilibrated[4]	0.04 M	0.06[5]	11
Tri-n-dodecylamine		0.04 M	<0.05	1.6
	pre-equilibrated[4]	0.04 M	<0.05	10
Tribenzylamine		0.1 M	<0.05	-[6]
Primene JM-T		2 % (v/v)	-[7]	<0.05
	pre-equilibrated[4]	2 % (v/v)	-[7]	<0.05
Amberlithe LA-2		2 % (v/v)	<0.05[5]	<0.05
	pre-equilibrated[4]	2 % (v/v)	<0.05	1.8
Alamine 336		2 % (v/v)	<0.05	1.2
	pre-equilibrated[4]	2 % (v/v)	<0.05	6.4
Alamine 304		2 % (v/v)	<0.05	1.0
	pre-equilibrated[4]	2 % (v/v)	<0.05	3.3
Aliquat 336		2 % (v/v)	0.72[5]	9.5

[1] dissolved in an aromatic kerosene (Shellsol-A)
[2] diethylammoniumdiethyldithiocarbamate
[3] dinonylnaphthalene sulphonic acid
[4] pre-equilibrated 5 min with 1 M HCl and scrubbed 2×5 min with de-ionized water
[5] third phase formation after phase separation
[6] reaction between extractant, diluent, phosphoric acid
[7] emulsion formation

Table 2. CONCENTRATION OF COMPONENTS

COMPONENT	CONCENTRATION	
H_3PO_4	5.5 M	
Cd	10 ppm (mg/kg)	
	low level	high level
H_2SO_4	0.0 M	0.3 M
HCl	0.0 M	0.02 M
HF	0.0 M	1.0 M
H_2SiF_6	0.0 M	0.15 M

Table 3. FACTORIAL TEST RESULTS

H_2SO_4	HCl	HF	H_2SiF_6	D_{Cd} without pre-equilibration	D_{Cd} with pre-equilibration
-	-	-	-	<0.05	<0.05
+	-	-	-	<0.05	0.11
-	+	-	-	0.36	5.4
+	+	-	-	0.95	7.2
-	-	+	-	0.19	0.34
+	-	+	-	0.14	0.25
-	+	+	-	0.68	3.2
+	+	+	-	0.55	2.3
-	-	-	+	<0.05	0.26
+	-	-	+	0.07	0.24
-	+	-	+	2.1	15
+	+	-	+	1.3	8.0
-	-	+	+	<0.05	<0.05
+	-	+	+	<0.05	0.13
-	+	+	+	0.40	3.0
+	+	+	+	0.42	2.4
- 0.0 M	- 0.0 M	- 0.0 M	- 0.0 M		
+ 0.3 M	+ 0.02 M	+ 1.0 M	+ 0.15 M		

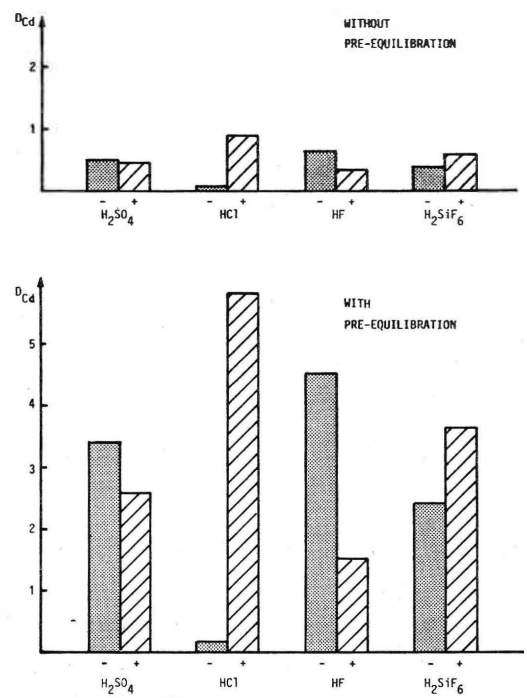

Figure 1 FACTORIAL TEST RESULTS, AVERAGE EFFECT OF SINGLE COMPONENTS ON CADMIUM EXTRACTION

EXTRACTION OF RHODIUM FROM HNO_3 SOLUTIONS WITH ORGANIC SULPHIDES

Erich Fritsch, Brunhilde Gorski, Manfred Beer

Academy of Sciences
Central Institute for Isotope and
Radiation Research
Leipzig, GDR

The noble metals, especially Au III, AgI, PdII (HgII), are extractable from hydrochloric acid and also from nitric acid solutions with organic sulphides. The extraction of the inert $Rh(H_2O)_6{}^{3+}$-complex, existing in nitric acid solutions, is not possible hitherto from nitric acid medium. But because of the good rhodium complexing properties of organic sulphur compounds (1) it was obvious to test organic sulphides as extractants.

Prelimenary tests

No remarkable extraction of rhodium was found at normal partition conditions with di-n-butylsulphide (1) and di-n-octylsulphide (2). But with increasing temperature up to the range from 40°C to 65°C slow but quite good transition of rhodium occured into the organic phase (Figure 1). However, only waterinsoluble alcohols with sufficiently high boiling point (> 100°C) are suitable as diluents. In other solvents the oxidation of the sulphides to sulphoxides is favoured. Furthermore the nitric acid concentration of the aqueous phase should be between 3N and 5N (Figure 2). High excess of extractant causes both improvement and acceleration of rhodium extraction. This effect can also be reached and strengthened by adding dimethylsulphoxide (DMSO).

Structural influences

The coordination of Rh and Pd with organic sulphides as ligands is known (2,3) like also the influence of the structural parameters for the extraction properties of the sulphides with Pd (4). For evaluation of the influences of basicity of the sulphur atom and of the chain length of alkyl groups on the extraction power we investigated the extraction ability of: Di-n-butylsulphide (1), di-n-heptylsulphide (2), di-n-octylsulphide (3), di-n-decylsulphide (4), dibenzylsulphide (5) and diphenylsulphide (6) for RhIII extraction from nitric acid solutions (conditions mentioned as above).
There are no remarkable differences to be found with the sulphides containing 4 to 10 carbon atoms in their n-alkyl groups. In opposite to their fairly good extraction diphenylsulphide, which is much less basic, is not suitable for rhodium extraction (Figure 3).
Basicity differences of the coumpounds (1) - (5) are masked by the dominating influence of temperature and HNO_3 concentration. By-products, arising from co-reactions during the extraction process seem to influence the extraction process.

Extraction mechanism

To explain the present results it is necessary to know the real mechanism of the extraction process.
The idea, that sulphoxides or carbolic acids produced by oxidation of the sulphides or alcohols, are the real effective extractants, has been disproved experimentally. Even at longer equilibration times we found $D_{Rh} < 10^{-1}$ for the pure diluent and for dioctylsulphoxide. The formation of organic intermediate or finale products by nitrosation or nitration of the diluent and/or the extractant as well as a reaction between diluent and extractant are imagineable but considering the reaction conditions they must be excluded. On the other hand a reaction of nitrous gases (evolving during mixing of HNO_3 and solvent) with the $[Rh(H_2O)_6]^{3+}$-complex, existing in aquous nitric acid solutions is possible.
Formally conceiveable are Rh-NO, Rh-$(NO)^+$ and Rh-(NO_2^-)-complexes. The last one has been proved by us for Rh-extraction from nitrate solutions with amines (5).
Therefore we used solutions of the $Na_3[Rh(NO_2)_6]$-complex (7) instead of $RhIII/NO_3^-$-solutions for the extraction of rhodium with sulphides and achieved fast and good extraction already at 23°C (Figure 3).
The extraction of the complex, which also increases with HNO_3 concentration, temperature and DMSO-addition, attains comparable D_{Rh}-values already after shorter times and at lower temperatures. The effect decreases with the age (hydrolysis) of the nitrite-complex solution. We assume that NO/NO_2, formed slowly as a result of sulphide oxidations, reacts with the $[Rh(H_2O)_6]^{3+}$-complex in the aqueous phase, forming a mixed ligand complex $[Rh(H_2O)_{6-x}(NO_2)_x]^{(3-x)}$. This complex is able to undergo faster ligand exchange with sulphide than $[Rh(H_2O)_6]^{3+}$. In the first step of the reaction "status nascendi forms" must play an important role, since experiments to realise the ligand exchange by adding NO_2^- or injecting NO or NO_2 gases have failed.
The effect of DMSO we assume as intermediary of solubility.

Selectivity

To test the selectivity of the sulphides we investigated RhIII extraction from two model solutions (Table 1), containing elements in concentrations corresponding to that in fission product solutions and solutions from noble metal wastes.

Table 1: composition of the model solutions

model solutions										
I	Me	Rh	Pd	Zr	Ce	Fe	Rb	Ru	HNO_3
	mg/ml	0,1	0,3	0,7	2,1	0,15	0,07	0,5	3,1 N
II	Me	Rh	Pd	Ag	Zn	Fe	Pb	Cu	HNO_3
	mg/ml	1,0	2,0	5,0	10	10	10	150	0,3 N

Concentrations of metals in aqueous and organic phase were determined radiometrically (6). Pb was determined by means of X-ray fluorescence analysis. From the fission-product-like solution also Pd and Ru are extracted (Figure 4). The distribution values of Tc are due to ^{99m}Tc tracer only (carrier-free).
From solution II Rh is extracted with good separation effect from Zn, Cu, Fe, Pb ($D < 10^{-2}$). PdII and AgI, which are extracted too, can be separated before RhIII extraction at lower temperatures and shorter mixing times (7). Using this method it is also possible to separate PdII and Ru from Rh in solution I.

References

(1) J.E. Fergusson; J.D. Karran; S. Seevaratnam J.Chem.Soc. 1965 2627
(2) P.A. Lewis; D.F.C. Morris; E.L. Short; D.N. Waters J.Less-Commmon Met. 45, 173 (1976)
(3) W.J. Sokol; M.A. Porai-Koshic Koord.Khim.1, No.3, 577 (1975)
(4) W.A. Pronin; M.V. Usoltseva; N.K. Gusarova; G.G. Efremova; S.V. Amonosova; V.A. Trofimov Zh.Neorg.Khim.18,3037, 1973
(5) B.Gorski; M.Beer, L.Ruß Paper 9.16, XXXIIIrd BHT, Freiberg (GDR), 1982
(6) E.Fritsch; M. Beer; B.Gorski ZfI-Mitt., (to be published)
(7) E.Fritsch; B.Gorski; M. Beer GDR Patent WP B 01-D/240 989

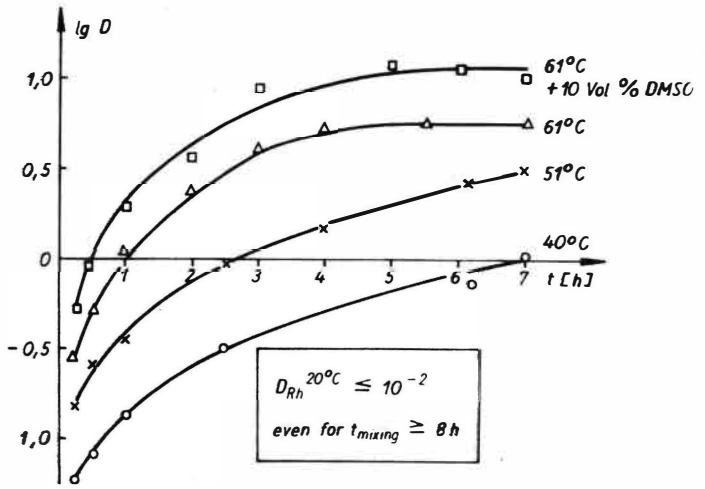

FIGURE 1. EXTRACTION OF RH III WITH DI-n-BUTYLSULPHIDE
c_{Rh}= 6·10^{-4}M; c_{HNO_3}= 3,5N; c_{DBS}= 1M in n-hexanole

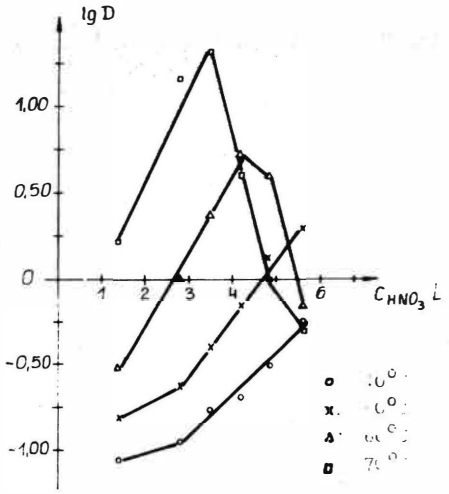

FIGURE 2. EXTRACTION OF RH III IN DEPENDENCE FROM NITRIC ACID CONCENTRATION AND TEMPERATURE
c_{Rh}= 2,6·10^{-4}M; c_{DOS}= 1M in n-hexanole
t_{mix}= 18o min.

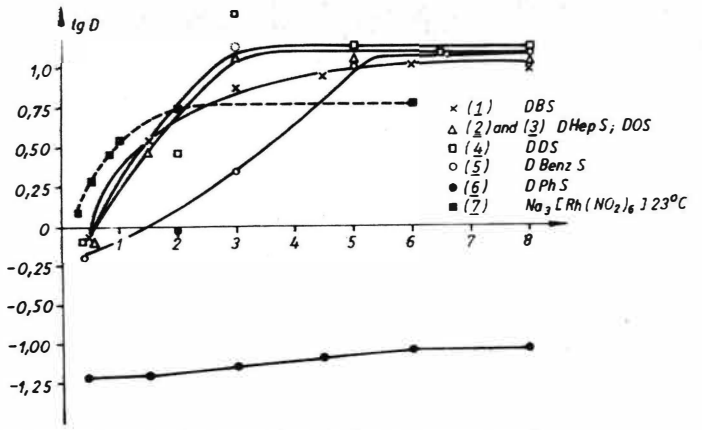

FIGURE 3. STRUCTURAL INFLUENCE OF THE SULPHIDES ON THE EXTRACTION OF RH III
c_{Rh}= 8·10^{-4}M; c_{HNO_3}= 3,5N; 10 Vol% DMSO; t= 70°C
$c_{sulphides}$= 1M in n-hexanole

■: $Na_3[Rh(NO_2)_6]$; 23°C; without DMSO; c_{Rh}= 5·10^{-3}M

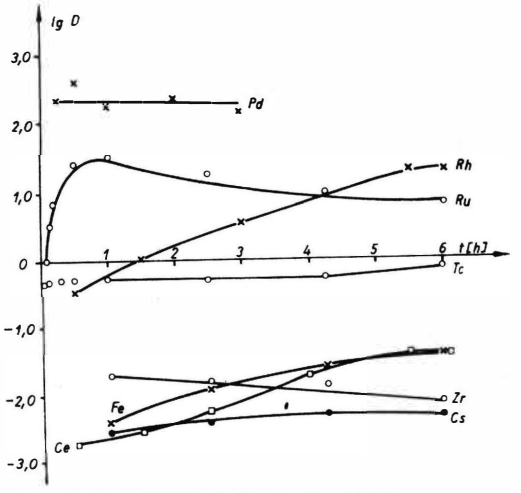

FIGURE 4. SELECTIVITY OF DI-n-OCTYLSULPHIDE EXTRACTION FROM SOLUTION 1
c_{HNO_3}= 3,1N; t= 65°C; c_{DMSO}= 2Vol%
c_{DOS}: 1M in n-hexanole

SOLVENT EXTRACTION OF LITHIUM

H. J. Bart and R. Marr

Institut für Verfahrenstechnik
Technical University
Graz, Austria

INTRODUCTION

Extraction of alkali and alkaline earth metals is a subject of considerable activity over the last decades. With positive demand prognoses also low level lithium resources are taken into consideration for recovery. However, oilfield smackover brines may be an alternative source to natural brines and bitterns /1/.

In Austria we have oilfield waters with about 90 ppm lithium. The obvious problem is to separate lithium from sodium, since sodium is the main component (Tab.1). The intention is to do this process without a solar evaporation step. That is why oilfield water is again pumped back in order to leave the oil water horizon at a constant level. Additionally, too low sun input and large area consumption make this process difficult.

Different methods can be applied for lithium extraction. The use of cation exchangers, eg. Versatic acid (V911) or bis-(2-ethylhexyl) phosphoric acid (HDEHP) is prohibitive due to their heigh regeneration costs. An economic approach to the field of processing high volume and low cost materials can only be in the use of neutral extraction systems.

They can be classified in:

- alcohols, ketons
- crown ethers /3,4/
- mixed ionic extractants /5/.

In the first case cheap extractants (MIBK, 2 ethylhexanol) offer the possibility to extract lithium from concentrated solutions /6/. However organic losses may limit application but plants are in operation /7/.

The second topic concerns size selective crown dompounds. Their use for alkali and alkaline earth metals extraction has been extensively investigated /8-12/. Markus and coworkers /13/ used DB18C6 in polar solvents for potassium extraction on a continuous scale. Lithium extraction is preferably done with small sized crown compounds having four donor atoms /14/. In practice there are many problems due to their high losses and limited solubility in the organic phase. In order to improve extraction a simultaneous transfer of the aqueous anion can be neglected if an organic counterion is present. This can be done by addition of HDEHP to the crown ether /15/ or with crown ether carboxylic acids /16/. An advantage is an obvious synergismus compared with systems of crown ethers and acid alone. The disadvantage is again in regenerating costs of the acid.

The last system deals with so-called mixed extractants. They are a stoichiometric mixture of an amine and an organic acid. According to Grinstead /7/ the reaction may be presented as

$$Mg^{2+} + 2Cl^- + \overline{2RNH_3^+\ RCOO^-} \rightleftharpoons \overline{2RNH_3Cl} + \overline{Mg(RCOO)_2} \quad (1)$$

in the case of magnesium extraction with a primary amine and a carboxylic acid. For this system the order of extraction of cations is: Ca > Mg > Li > Na > K and of anions: NO_3 > Cl > SO_4. The effectiveness of amine components is in the order: quarternary > primary > secondary > tertiary and of acid: carboxylic > alkylphosphoric > arylsulfonic. Hernandez et.al. /8/ investigated the extraction of lithium with a mixture of Primene JM-T and naphtenic acid and confirmed this trends. So our intention was, to investigate different types of P=O containing acids, since they gave a better distribution for lithium as compared with carboxylic acids.

EXPERIMENTIAL SECTION

Materials: The extractants used are bis-2-ethylhexyl phosphoric acid (HDEHP) and its analoguous phosphonic acid (HOEF 3239), both from Hoechst AG. Furthermore, a phosphinc acid with equivalent chain length (CYANEX 272) from cyanamid and a carboxylic acid, Versatic 911 (V911), from Shell Int. Primene JM-T, a primary amine from Rohm and Haas and Aliquat 336, a quarternary amine, from Henkel. Modifier was isodecanol from Hoechst. Crown ethers were from PCR and Merck, respectively, of self-synthesized. In the latter case purity was confirmed by NMR. All other reagents were Merck analar grade. Mixed ionic extractants were prepared as elsewhere /5/.

Procedure: Equal volumes of organic and aqueous solutions were stirred magnetically in a 50 ml thermostated beaker at required temperatur (20 °C) during ten minutes. This time was considered to be long enough due to kinetic experiments. PH-control, adjustment and titration of extractants was done with a autotitrator (Methrom Titroprocessor 636). Samples of a few microliters were taken from both phases via a programmable syringe (Hamilton). Most chemical analyses were performed by atomic absorption spectrophotometry. Sodium partially was measured r adiochemically. Organic samples were direct analyzed by atomic absorption spectrophotometry after due dilution in MIBK. Organic lithium standards were dayly prepared. In mixed alkaline systems internal standards according to interferences were preferred /19/.

RESULTS AND DISCUSSION

In this work we used extraction systems as abouve mentioned. At first we extracted lithium for comparison with HDEHP and V911 /20/ (Tab.2). HDEHP is the better extractant. However, we did some experiments with smackover brines. The distribution coefficient for lithium is about unity but loading in the organic phase is very low. Additionally, we did some experiments with crown ethers in order to increase the organic lithium content. Small sized compounds should be effective. We tested them under conditions similar to that of smackover brines, but no dedectable organic lithium could be seen. Also a combination of crown ethers with HDEHP gave no synergismus (Tab.3). Finally, we tried to solve our problem with mixed ionic extractants. As mentioned above, HDEHP gave better extraction results than carboxylic acids. From this view, we tested as phosphoric acid HDEHP, as phosphonic acid, HOEF 3239, and as phosphinic acid CYANEX 272. As expected extraction is in the order Mg > Li > Na. Fig.1 confirms the statement, that Aliquat 336 shows higher efficiency than Primene JM-T. The tendency within the various phosphor containing acids is not so clear. Lithium extraction (with Primene JM-T) gives the order: phosphonic > phosphinic ~ phosphoric ≫ carboxylic. In the case of sodium extraction the order is: phosphonic > phosphoric > phosphinic ≫ carboxylic. So it is evident, that different selctivities can be obtained. Thereby, selectivity of an ion M_1^+ in relation to M_2^+ is defined as followed:

$$S^{M_1}_{M_2} = \frac{\overline{M_1^+}}{M_1^+} \times \frac{M_2^+}{\overline{M_2^+}} \quad (2)$$

For instance, selectivity values of lithium in relation to sodium are shown in Fig.2. It may be observed, that lithium over sodium selectivity is better at lower concentrations with phosphinic acid at higher concentrations with carboxylic acid, respectively. However, to compare this two extractants for a speical use also their different loading ability must be taken into consideration. The same is with Aliquat 336 and Primene JM-T. Aliquat 336 offers higher loading in the organic phase but selectivity is better with Primene JM-T.

Finally, Tab.4 shows us the results of mixed ionic extractants with samckover brines. As expected, the loading of the organic phase is small. Nevertheless, a good separation resulted. From an initial molar ratio of sodium to lithium at about 100 in the aqueous phase a ratio at about unity has established in the org. phase.

CONCLUSIONS

From our present view it is evident, that crown compounds used alone, suffer on low loadings in the case of lithium. However, mixed ionic extractant systems seem to offer the possibility for lithium recovery. There is no chance to win lithium without prior concentrating via solar evaporation, as far as very dilute oilfield smackover brines are concerned. An approach to these low concentraded liquors is only promising with very selective and possibly synergistic systems. Maybe, there is some advantage by addition of crown ethers to mixed ionic systems. But with better extraction efficienty also viscosity and emulsification tendency will increase

The composition of the mixed extractant system will mainly depend on the selectivities needed. Evidentially this is a function of the final brine concentration. With this, it seems to be still a broad field to do some work on this subject.

Symbols

CYANEC 272	2-ethylhexyl phosphinic acid
HOEF3239	2-ethylhexyl phosphonic acid
HDEHP	Bis-2-ethylhexyl phosphoric acid
MC12C4, MC13C4....,	Monocyclohexyl 12 crown 4,.....,
——	bar indicates organic phase components

Literature

/1/ Collins, A.G., Geol. Survey Prof., Paper 1005, U.S. Gov. Print. Office, Washington, 1976, 116-123

/2/ Ullmanns Encyklopädie der technischen Chemie, Vol.16, 266 Ed. E. Bartholome et.al., Verlag Chemie, Weinheim 1981

/3/ Asher, L.E., and Marcus, Proceed. ISEC 77, CIM Vo.21. Toronto, 1979, 130-134

/4/ McDowell, W.J., and Shoun, R.R., ibid, 95-99

/5/ Grinstead, R.R., and Davis, J.C., U.S. Off. of Saline Water, Res. and Devel. Rept. 320 (1968)

/6/ Epstein, J.A., Feist, E.M., and Zmora, J, and Marcus Y., Hydrometallurgy, 6 (1981) 269-275

/7/ Daniel, A, and Blumberg, R., Israel Pat. 23760 (1968)

/8/ Danesi, P.R., Meider-Gorican, H., Chiarizia, R., Capuano V., and Scribona, G., Proceed. ISEC 74, Vol.II, 1761-1774, Publ. Soc.Chem.Ind., London, 1974

/9/ Pedersen, C.J., J. Amer.Chem.Soc. 1967, 89, 2495

/10/ Frensdorff, H.K., ibid, 1971, 93, 600

/11/ Dale, J., and Kane, J., J.C.S. Chem.Comm., 1972, 1012

/12/ Weber, E., and Vögtle, E., Chem.Ber., 1976, 109, 1803

/13/ Marcus, Y., Asher, L.E., Hormadaly, J., and Pross, E., Hydrometallurgy, 7, 1981, 27-39

/14/ Olsher, U., and Jagur-Grodzinski, J., J.C.S.Dalton, 1981, 501-505

/15/ McDowell, W.J., Kinard, W.F., and Shoun, R.R., Proceed. ISEC 80, Paper 80-6, Ed.Assoc.d.Ing. Sorties l'Univ. Liege, Liege, 1980

/16/ Strezelbicki, J., and Bartsch, R.A., Anal.Chem., 53, 1981, 2251-2253

/17/ Grinstead, R.R., Davis, J.C. Lynn, J., Carlesworth, R.K., Ind. Eng. Chem. Prod. Res. Dev., 1969, 8, 218-227

/18/ Hernandez, R.A., and Martinez, J.M., ibid, 1981, 20, 698-704

/19/ Hanson, C., and Hughes, M.A., and Murthy, S.L.N., J. Inorg. nucl. Chem., 37, 1975, 191-198

/20/ Bart, H.J., Thesis, 1982, Technical University, Graz

Tab.1 Lithium resources from brines /1,2/

	%	Li	Na	K	Mg	Ca	SO_4	Cl	Br
Clayton Valley (Nevada)		0,03	7,5	1.0	0,06	0,05	0.75	11.7	0
Salar de Atacama (Chile)		0,147	7,6	1,93	0,86	0,023	1,48	16,31	0
Salar de Uyoni (Bolivien)		0,024	9,24	0,51	0,44	0,05	0,72	15,9	0
Dead Sea (Israel, Jordania)		0,002	3,0	0,6	4,0	0,3	0,05	16,0	0,4
Great Salt Lake (Utah)		0,006	7,0	0,4	0,8	0,03	1,5	14,0	0
Boneville (Utah)		0,007	9,4	0,6	0,4	0,12	0,5	16,0	0
Seawater		0,000017	1,8	0,04	0,13	0,04	0,27	1,94	0
Smackover brines (Ø US)		0.014	5,6	0,25	0,25	0,28	0,04	14,2	0,25
Smackover brines (Ø Austria)		0,009	1,8	0,07	0,005	0,07	0,005	2,9	0,004

Tab.2 Comparison of HDEHP and Versatic911 for lithium (0,5m acid in Shellsol T, 6% isodecanol, 20°C, A/O=1)

initial mol/l Li aqu.	0,25	0,50	1,00	2,00
HDEHP: mol/l Li org	0,23	0,38	0,51	0,60
V 911: mol/l Li org.	0,0002	0,0022	0,0004	0,0004

Tab.3 Influence of crown compounds on lithium extraction (20°C, A/O=1) aqu.phase: 0,01 m LiCl, 1 m NaCl; (§: 0,01 m picric acid, add.)

organic phase composition	lithium org.
0,25 m MC12C4, toluene, (§)	not dedectable
0,25 m MC13C4, toluene, (§)	n.d.
0,25 m MC15C5, toluene, (§)	n.d.
0,25 m MC18C6, toluene, (§)	n.d.
0,75 m NaDEHP, ShellsolT, 6% isodecanol	30 ppm
0,75 m NaDEHP, ShellsolT, 6% isodecanol, 0,25 m MC12C4	31 ppm

Tab.4 Lithium recovery with mixed ionic extractants from Austrian oilfield smackover brines (20°C, O/A=1, diluent: ShellsolAB)

ppm org.	Li	Na	Mg
0,5m Primene JMT, 0,5mV911	0	13	3
0,5m Primene JMT, 0,5mHDEHP	4	196	45
0,5m Primene JMT, 0,5mHoef3239	5	239	67
0,5m Primene JMT, 0,5mCyanex272	2	93	61
0,5m Aliquat 336, 0,5mCyanex272	14	1630	80

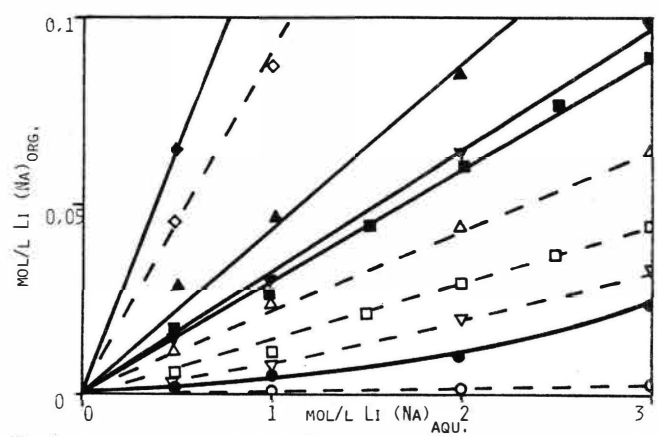

FIG.1 DISTRIBUTION OF LICL(NACL) BETWEEN WATER AND PRIMENE JM-T AND VERSATIC911 ●, HDEHP ■, HOEF3239 ▲, CYANEX272 ▼ AND ALIQUAT336/CYANEX272 ◆, WITH 0.5M AMINE/0.5M ACID, SHELSOLAB (UNFILLED SYMBOLS AND DASHED LINES ARE FOR NA).

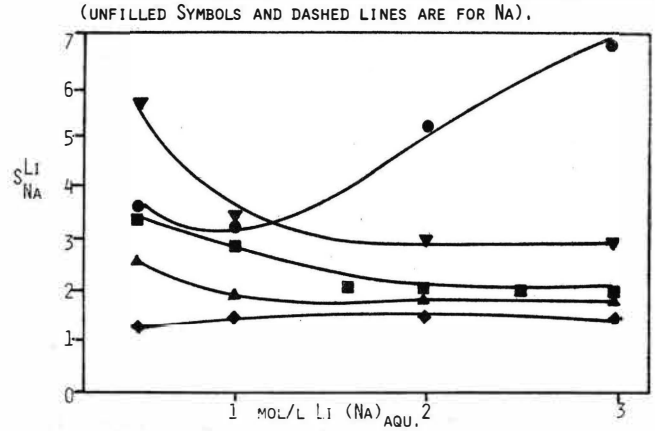

FIG.2 SELECTIVITY OF LI IN RELATION TO NA (SYMBOLS AS ABOVE)

THE DESIGN OF LIQUID-LIQUID CONTACTORS: PAST, PRESENT AND FUTURE

H. R. Clive Pratt

Department of Chemical Engineering
University of Melbourne
Parkville, Victoria 3052, Australia

INTRODUCTION

Although liquid extraction has been used in the laboratory for a considerable period and found limited industrial application early in this century, it was not until the 1920's that a fundamental appreciation of its mechanism began to emerge. Development continued at an accelerating rate due to outstanding work by Hunter and Nash, Fenske, Colburn and others, but the methods, using the transfer unit and theoretical stage concepts, were quite inadequate for design and scale-up purposes.

The great interest shown in nuclear energy from the 1940's onwards led to the successful development of liquid extraction processes for uranium purification and reprocessing of spent fuel. This stimulated work on the extraction of other metals, and at the same time new applications were found in the petrochemical field. During this period a number of atomic energy laboratories and university departments embarked on fundamental studies of extraction. Treybal's book (1), published in 1963, gave a good account of the state-of-the-art at that time; however, design and scale-up methods were still primitive.

Around 1960, a major advance was made with the recognition that departures from plug flow in column-type extractors play an important part in controlling extractor performance. Such departures, termed *axial dispersion* or *backmixing*, have been incorporated into two types of model which provide a much more realistic basis for scale-up.

MECHANICS OF TWO-PHASE FLOW

Axial Dispersion. It is now recognised that the major cause of this is the dissipation of the potential energy of the droplets as they rise (or fall), converting this into kinetic energy of adjacent continuous phase; a circulation pattern is thereby set up, in the direction of flow of the droplets in the centre with a return flow at the wall (2,3). This flow, shown in Fig.1 for a spray column, is analogous to that induced by the bubbles in an air-lift. A secondary effect is a result of the flow profile occurring with single phase flow in a channel where, to an observer moving with the flow, elements of fluid near the wall appear to be moving backwards. A third possible mechanism results from the circulatory flow patterns induced by mechanical agitation; this is the main cause of backmixing in the dispersed phase.

Two types of tracer experiment are used to measure backmixing coefficients in the continuous phase, the first involving continuous injection with upstream monitoring, and the second pulse or step injection with downstream monitoring. The first gives a direct measure of true backmixing, whereas the second, transient method determines the residence time distribution, which is "force fitted" to an appropriate backmixing model. Such models are of two types, a *diffusion* model, in which eddy back-diffusion occurs along the concentration gradient, and a *backflow* model, applicable to compartment-type columns, in which the perfectly mixed phases are contacted for a given time, after which part of one or both phases passes back to the previous stage and the remainder passes on.

Analytical solutions of the models are available for the case of a linear equilibrium (4), but are complex. However, simplified solutions of adequate accuracy, soluble by programmable calculators, which give the height or number of stages directly are available and been extended to cover non-linear equilibria (5).

Droplet Mechanics. Holdup and flooding in columns can generally be interpreted in terms of the well known slip velocity equation:

$$(1) \qquad V_d/x + V_c/(1-x) = \bar{V}_o(1-x)$$

where V_c and V_d are the continuous and dispersed phase flows and x the holdup; the (1-x) on the R.H.S. corrects the density difference to that between *dispersion* and droplets. By setting $dV_c/dx = dV_d/dx = 0$, relations are obtained for the flood point in terms of the maximum holdup, x_f, which is a function of V_d/V_c. Both holdup and flood point can therefore be correlated in terms of $\bar{V}_o$, the *characteristic droplet velocity*, which in turn is a function of physical properties and column variables.

The holdup also controls the interfacial area, via the relation

$$(2) \qquad a = 6x/d_{32}$$

where d_{32} is the Sauter mean droplet diameter. Extensive data on the latter for the packed column, obtained photographically, have been correlated (6); resulting values of a were in good agreement with those obtained directly by a chemical reaction method (7). Although droplet size data are available for some types of mechanically agitated column, unfortunately these mostly relate to single solvent systems only.

Much work has been devoted to droplet coalescence rates at interfaces, but although it is clear that these are related to the drainage times of the trapped film of continuous phase, the results do not permit of reliable prediction for design. Inter-droplet coalescence rates, thought to have an important effect on performance, have received much less attention. However, recent studies using a novel colorimetric method have enabled droplet coalescence and breakage rate coefficients (2nd and 1st order respectively) to be derived as functions of droplet size and holdup (8,9) for a packed and a pulsed plate column. Calculated droplet size distributions using these values were in good agreement with experiment. The effect on mass transfer in the extraction of acetic acid was also computed, using a Monte Carlo method, and found to reduce column height by some 4% for the packed column, and to be surprisingly small for the pulsed column.

Interfacial instability. Although the dramatic effect of interfacial tension gradients in causing liquid motion (Marangoni effect) was noted as early as 1855 by Thomson, its importance in liquid extraction has only been recognised relatively recently. Thus, its effect is particularly marked in the transfer of organic solutes from solvent into water phase, leading to droplet oscillation and growth. This in turn results in a reduced holdup and interfacial area, an increased flood-point and very often a reduced rate of mass transfer. These effects are concentration-dependent and difficult to predict; some workers have attempted to relate the interfacial instability to a critical value of the *Marangoni number* defined as

$$(3) \qquad Ma = \frac{d\gamma}{dc}\,\frac{(c_i - c)\delta}{\mu D}$$

where δ is the penetration depth, γ the interfacial tension, c the concentration, μ the viscosity and D the diffusion coefficient.

MASS TRANSFER

Rate Coefficients. Various workers have obtained mass tranfer coefficient data for isolated droplets in "single file" columns, both for the droplet phase itself and for the surrounding continuous phase. Theoretical expressions are also available, those for the droplet phase covering both rigid and circulating drops. However, the discrepancies between theory and experiment, and between the experimental results of different workers, is surprisingly large. There is therefore an urgent need for further studies, both theoretical and experimental, to clear up these differences.

However, the validity of applying data for isolated droplets to the droplet "swarms" present in extractors must also be called into question. Thus, it is not known whether the droplet surfaces are uniformly available for mass transfer under these conditions; also, in contrast to the single droplet case, the mean droplet velocity is considerably below the terminal velocity, and frequent distortion, coalescence and breakage occur.

Effects of Chemical Reaction. Chemical reaction in extraction can take two forms, viz. homogeneous and heterogeneous, the effects of which are quite different. Thus in the former, the solute reacts with a reagent in the extractant phase, and the resistance to mass transfer in that phase is thereby reduced. The theory of this process is similar to that proposed in 1930 for gas absorption by Hatta, and has been well summarized in a recent book (10).

Heterogeneous reaction presents a quite different situation in that it occurs at the interface itself and thus provides an additional resistance to mass transfer. Typical examples are the extraction of carboxylic acids into non-polar solvents in which they are dimerised; extraction of uranyl nitrate into a solvent, forming a solvated complex; and the extraction of copper by chelating solvents. It is curious that there has been a reluctance to accept the concept of an interfacial reaction; however, the electrical analogy in Fig.2 shows how the overall resistance to transfer is always increased by heterogeneous, and reduced by homogeneous reaction.

PROCESS DESIGN

The design of extraction equipment involves the prediction of two parameters, viz.(i) the permissible throughput, and hence the cross-section, and (ii), the height or number of stages required to achieve the desired performance.

Mixer-Settlers. Throughput in these is controlled by the coalescence rate in the settlers, and performance by the stage efficiency. At present, both must be determined by scale-up from pilot plant data, preferably supported by experiments with a single full-scale stage.

Columns. In the absence of Marangoni effects, the column diameter can be based on a specified proportion of the flooding rate (e.g. 50%), or a specified holdup, e.g., 15 - 20%, depending upon the flow ratio. These can be predicted from correlations of characteristic velocity, when available.

Although the principles governing the prediction of height are now undersood, in practice this must be determined by scale-up

from pilot data. Thus, the performance data together with the backmixing parameters for the pilot unit are substituted into the appropriate backflow model equations, which are solved iteratively for H_{ox}, the "true" HTU, or N_{ox}^{1}, the NTU per compartment. This is assumed to remain constant with diameter and is used, together with the backmixing parameters for the full scale column, to solve for height or number of stages (11).

Dual-Solvent Fractional Extraction. This important process which employs a centre-fed column to separate two or more solutes by fractional distribution between two immiscible solvents, is considerably more complex theoretically than simple extraction. The earliest design method, for binary separations, was graphical (12) and was followed by an analytical method for ideal systems (13). An important advance was made by Prochazka and Jiricny (14) who defined the range of flow ratios which permit of a solution, and described an iterative method of computing the number of non-ideal plug flow stages required.

The important case of multicomponent separations, i.e. of three or more solutes, has received little attention although Warner (15) has recently described a method involving the solution of a block tridiagonal matrix equation to calculate the stage requirements for the separation of a 4-component mixture simulating wool wax. Similar matrix methods, taking backmixing into account, have been developed for simple multicomponent extraction (16, 17) and are presumably capable of extension to dual-solvent operation.

MECHANICAL DESIGN

Mixer-Settlers. The range of mechanical variants of these is large, but performances do not differ greatly. The main need is for a reduction in settler size, by the use of improved coalescence devices, to reduce solvent inventory in large units. An interesting recent development is the "combined mixer-settler" (18), comprising a single vessel with mixing zone in the middle and separation zones above and below; it is claimed that the phase ratio within the mixing zone can be controlled independently of the external value by a simple hydraulic balance.

Columns. These exist in many forms ranging from simple packed, baffle plate and "bubble plate" types to those in which agitation is produced by rotating impellers or by a reciprocating motion of liquid or of perforated plates. Horizontal types are also available, e.g., with rotating discs or buckets.

The non-mechanical types are quite effective, although packed columns tend to be restricted to smaller diameters due to high packing cost. Mechanical types generally suffer from a decreasing performance with increasing diameter due to increased backmixing, requiring greater height. Rotary types have the added disadvantage that the compartment height must be increased more or less in proportion to diameter to maintain approximate geometric similarity. Considerable scope therefore exists for improvement.

Centrifugal Types. These are of two forms, mixer-settler (e.g., Luwesta) and differential (e.g. Podbielniak). They find particular application in handling unstable materials, and for emulsifiable systems, but are also being considered for radioactive processing. Their use is however restricted by mechanical complexity and consequent high maintenance costs.

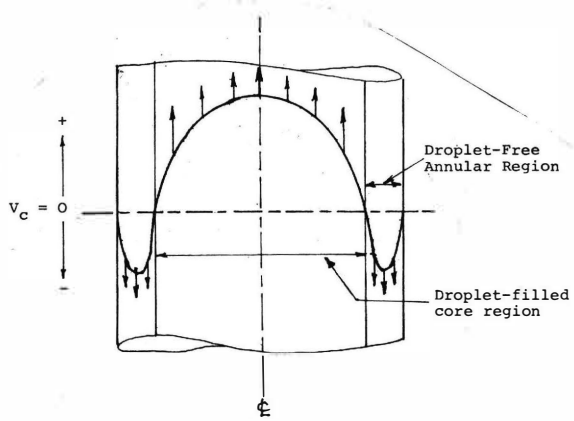

FIGURE 1. CONTINUOUS PHASE FLOW PROFILE IN SPRAY COLUMNS.

REFERENCES

1. R. Treybal, Liquid Extraction, 2nd edn., 1963(McGraw-Hill)
2. J.-B. Wijffels and K. Rietema, Trans.I.Chem.E.50,224 (1972)
3. W.J. Anderson and H.R.C. Pratt, Chem.Eng.Sci.33, 995 (1978)
4. C.A. Sleicher, A.I.Ch.E.Jnl.5, 145 (1959); 6, 529 (1960)
5. H.R.C. Pratt, I.E.C. Proc.Des.Develop.14, 47 (1975); 15,34, 544 (1976)
6. J.B. Lewis, I. Jones and H.R.C. Pratt, Trans.Inst.Chem. Eng.29, 126 (1951)
7. S.A. Puranik and M.M. Sharma, Chem.Eng.Sci.25, 257 (1970)
8. J.A. Hamilton and H.R.C. Pratt, A.I.Ch.E.Jnl. (accepted for publication)
9. M.O. Garg and H.R.C. Pratt, A.I.Ch.E.Jnl. (accepted for publication)
10. P.V. Danckwerts, Gas-Liquid Reactions, 1970 (McGraw-Hill)
11. H.R.C. Pratt and M.O. Garg, I.E.C.Proc.Des.Develop.20, 489 (1981)
12. E.G. Scheibel, Chem.Eng.Prog.44, 681, 771 (1948).
13. A. Klinkenberg et al. Chem.Eng.Sci.1, 86, 93, (1951)
14. J. Prochazka and V. Jiricny, Chem.Eng.Sci.31, 179 (1976)
15. J.J. Warner, University of Melbourne Ph.D. thesis (1982); J.J. Warner, and I.J. Harris, Proc.ISEC'83, paper no.36F (1983)
16. N.L. Ricker, F. Nakashio and C.J. King, A.I.Ch.E.Jnl.27, 277 (1981)
17. J.L. Spencer, L. Steiner and S. Hartland, A.I.Ch.E.Jnl.27, 1008 (1981)
18. J.B. Scuffham, The Chemical Engineer, No. 370,328 (July 1981)

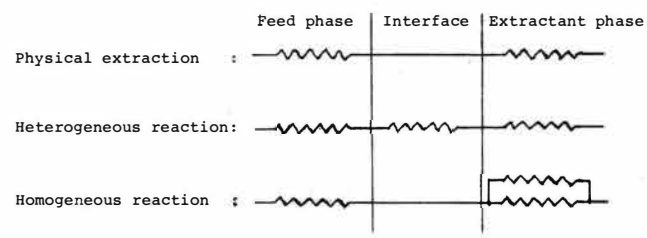

FIGURE 2. MASS TRANSFER RESISTANCES WITH CHEMICAL REACTION.

EFFICIENT USE OF THERMODYNAMIC PROPERTIES FOR PHASE-EQUILIBRIUM CALCULATIONS IN SOLVENT EXTRACTION

P. F. Bryan and E. A. Grens II

Department of Chemical Engineering
University of California
Berkeley, California 94720 USA

The design or analysis of solvent extraction systems must be based on calculations for compositions of liquid phases in equilibrium with each other. Such immiscible liquid phases will only exist for strongly non-ideal systems, which require relatively complex molecular-thermodynamic (MT) models to describe their equilibrium behavior (1). The non-idealities give rise to strongly non-linear equation systems representing the equilibrium separations, which require iterative, and frequently slowly convergent, solution procedures (2). Thus many uses of the MT models are needed, and, with the complex models that are appropriate, each involves extensive calculations; this creates a considerable computational burden. In fact, for realistic MT models, an equilibrium calculation will expend a large fraction of its computational effort in references to the MT model. For multistage, multicomponent extraction calculations, this effort can become prohibitively great. It is, therefore, necessary to devise new computational approaches that require fewer references to the MT models without sacrificing the accuracy of the results. The approach we have taken is to use a local approximation to the MT model to replace the model for most of its uses in the iterative calculation procedure, particularly those requiring derivative information. The local approximation is a simple analytic function, fitted to the MT model over a limited range of composition space and periodically revised to provide the best fit in the region of interest. This approach has worked very well in initial applications to single liquid-liquid equilibrium calculations, reducing references required to the MT model by over a factor of two.

LIQUID-LIQUID PHASE-EQUILIBRIUM CALCULATIONS

The equilibrium condition between two liquid phases in contact, for a given overall composition z_i of the system, is represented by the compositions x_i^* and y_i^* of the equilibrium phases and the fraction of the system α in the "y" phase. This condition is governed by the equality of activities in the two phases for each component

$$(1) \qquad \gamma_i^x \; x_i = \gamma_i^y \; y_i \; ,$$

by material balances for each component

$$(2) \qquad z_i = \alpha y_i + (1-\alpha)\, x_i \; ,$$

and by constitutive requirements

$$(3) \qquad \sum_{i=1}^{N} x_i = \sum_{i=1}^{N} y_i = 1 \; ,$$

where x_i and y_i are mole numbers, which at convergence are equal to mole fractions (x_i^* and y_i^*), γ_i^x and γ_i^y are the activity coefficients of component i in the two phases, and N is the number of components. The constitutive requirement may be recast to avoid certain spurious solutions (3) as

$$(4) \qquad \sum_{i=1}^{N} (y_i - x_i) = 0 \; .$$

Substitution of equations (1) and (2) reduces this to

$$(5) \qquad \sum_{i=1}^{N} \frac{z_i (K_i - 1)}{\alpha (K_i - 1) + 1} = 0 \; ,$$

where $K_i \equiv \gamma_i^x / \gamma_i^y$.

Equation (5) also applies to isothermal vapor-liquid equilibrium calculations (with appropriate redefinition of K_i). In that application the K_i are usually determined for estimates, or most recent iterates, of x_i and y_i. Equation (5) is then solved for α by Newton-Raphson (NR) iteration, and new values of x_i and y_i are found from equations (2) and (1). The procedure is repeated until the new K_i satisfy equation (5) with the previously determined α value to within some acceptable tolerance. This approach is sometimes called a "drag-along" method, since the K_i are simply found from the last available (dragged-along) compositions x_i and y_i. In this method, the composition dependence of the K_i is not taken into account in the NR solution to equation (5). For many vapor-liquid calculations, deviations from ideality in the phases are small, and the K_i depend much more on temperature and pressure than on composition; then the drag-along method works quite well. However, for liquid-liquid equilibrium calculations at least some of the K_i must depend strongly on composition, and the drag-along method can be excruciatingly slow to converge. Although certain acceleration techniques can improve the performance somewhat (4), achievement of high (second order) convergence rates requires that the composition effects on γ_i^x and γ_i^y be accounted for in the iterative solution process.

These effects are taken into account in a full multivariate NR technique applied to the system of 2N+1 equations comprising (1), (2), and (4), in the 2N+1 variables x_i, y_i, and α . The equations can be represented by a vector function $\underline{F}$:

$$(6) \qquad \underline{F}(\underline{x}) = \begin{bmatrix} \gamma_1^x x_1 - \gamma_1^y y_1 \\ \vdots \\ \gamma_N^x x_N - \gamma_N^y y_N \\ z_1 - \alpha y_1 - (1-\alpha)\, x_1 \\ \vdots \\ z_N - y_N - (1-\alpha)\, x_N \\ \sum_{i=1}^{N} (y_i - x_i) \end{bmatrix} = \underline{0}$$

$$\underline{x}^T = (x_1, \ldots, x_N, y_1, \ldots, y_N, \alpha)$$

The NR procedure applied to this system is:

$$(7) \qquad \underline{x}^{(r+1)} = \underline{x}^{(r)} - \underline{J}^{-1} \underline{F}(\underline{x}^{(r)})$$

where $\underline{J}$ is the Jacobian matrix of $\underline{F}$ given by:

$$(8) \qquad [\underline{J}]_{ij} = \frac{\partial \underline{F}_i}{\partial \underline{x}_j}$$

and $\underline{x}^{(r+1)}$ is the new iterate of $\underline{x}$ derived from $\underline{x}^{(r)}$ (Note: sometimes step-limiting is desirable with this procedure, see (5)). As might be expected, the multivariate Newton-Raphson method converges in many fewer iterations than the drag-along method for liquid-liquid equilibrium calculations. Unfortunately, each iteration for the NR method not only requires that the activity coefficients be evaluated, but also their composition derivatives, in order to generate the Jacobian matrix. In principle, each partial derivative $(\partial \gamma_i / \partial x_j)$ evaluation requires about the same computational effort as an evaluation of γ_i; it can always be computed by perturbation, which requires one additional activity coefficient evaluation for each composition derivative.

The relative efficiencies of these two approaches can be compared for a representative equilibrium calculation, for example the quaternary isooctane, cyclohexane, benzene, furfural system described in Table 1. For the purpose of these calculations the MT model used to represent this system was the NRTL model (1) with the required parameters obtained from Renon (6). The results of the drag-along and NR calculations, in terms of required MT model evaluations (one γ_i or $\partial \gamma_i / \partial x_j$) are shown in lines 1 and 2 of the table.

Table 1 Example Problem: Liquid-Liquid Equilibrium at 293 K, 1 atm

Conditions:			
Component	Overall Mole Fraction, z_i	Equilibrium Phase Compositions x_i	y_i
(1) Isooctane	0.400	0.060	0.456
(2) Cyclohexane	0.200	0.051	0.225
(3) Benzene	0.200	0.167	0.206
(4) Furfural	0.200	0.722	0.113
Fraction in "y"-phase (α) = 0.858			

Calculation Requirements:				
Method	Iterations to Converge	Number of References to MT model for γ_i	$\partial\gamma_i/\partial x_j$	Total
1. Drag-Along	25	200	0	200
2. NR	4	32	128	160
3. LA	5	88	0	88

It can be seen, then, that while the NR method converges in many fewer iterations than the drag-along method, it requires so many MT evaluations at each iteration that the computational effort is about the same for the two methods. It would be desirable to retain the convergence properties of the NR procedure while reducing its use of the MT model. One approach to accomplishing this is the use of local approximations to the MT model as described for vapor-liquid equilibria by Leesley and Heyen (7), Barrett and Walsh (8), Rebeyrote (9), and Stell (10).

THE LOCAL APPROXIMATION APPROACH

The MT models used for multicomponent systems are complicated, in part, because they must represent equilibrium over a wide range of temperature and over the complete range of composition for all components. Much simpler functions should give satisfactory approximation to this behavior over a restricted range of compositions (here at isothermal conditions). Moreover, as is very important in NR-type iterations, they can be chosen to have easily evaluated analytic derivatives. The local approximation (LA) approach uses such simple local functions, fitted to the MT model in the region of interest in composition $(\underline{x},\underline{y})$ space and with the parameters evaluated by references to the MT model. These local models are updated during the course of the NR iterative procedure to keep them appropriate to the current estimates of phase compositions.

In the use of LA methods there are a number of important factors to be considered. Among these are:

a. The form of the local approximation function.

b. The use of the MT model to evaluate parameters of the LA function.

c. The criteria and procedure for updating local models.

d. The determination of convergence to a solution compatible with the MT model.

Form of Local Approximation. The local model should be mathematically simple and contain few (2 or 3 per component) parameters, but must be consistent with the laws of thermodynamics, in particular the pure-component limits and the Gibbs-Duhem equation. The model presently being used in this work is based on representation of the multicomponent mixture by a pseudoternary system, composed of the component of interest, i, and two hypothetical solvents, B and C, which represent the latest estimates of the two phases less component i. For this pseudoternary, a two-suffix Margules representation is used for each component in each phase (i):

$$(9) \qquad \sigma^2 RT \ln\gamma_i = P_i x_B^2 + Q_i x_C^2 + R_i x_B x_C$$

where σ is the sum of the mole numbers (x_i, x_B, x_C), and P_i, Q_i, and R_i are local model parameters for component i in the phase of interest. The necessary derivatives with respect to x_i, x_B, x_C, can be calculated from Equation (9).

Parameter Fitting. The parameters P_i, Q_i and R_i for each component i in each local composition region are evaluated by standard (least squares) estimation techniques from values of γ_i found with the MT model at selected compositions. Since there are three parameters, their values could be fixed by a minimum of three such data points. However, the work of Stell (10) and this investigation have shown that this is not effective. When the parameters are determined from three data points, the region of applicability of the local model is very restricted, and the composition derivatives are unreliable, sometimes having the wrong sign. This is unacceptable in a convergence scheme such as the NR method, which makes use of these derivatives to determine the magnitude and direction of corrections to the phase compositions. Of course, it is advantageous to keep the number of data points small, since these points require reference to the MT model. One way to limit the number of points needed without sacrificing accuracy is by judicious choice of the location of the data points. The points must be located so that the data will reflect all aspects of the composition dependence of the activity coefficients. The best arrangement has used five data points. The first (central) point is chosen at the current NR estimate of the composition of the phase of interest. Two more points are generated by perturbing the mole number of the "major" (high mole fraction) pseudo-solvent by ±0.05 while holding the other components in constant proportion. A fourth point is generated by perturbing the composition of component i by -0.05 mole number, again holding all other components in constant proportion. The fifth point is found by perturbing the "minor" (low mole fraction) pseudo-solvent mole number by -0.05, holding all other components in constant proportion. The directions of the perturbations used to find the fourth and fifth points are chosen to reduce the possibility of placing a point significantly within the two-phase region for the system, where derivative behavior is inaccurate.

Updating. A given local approximation cannot be expected to apply to all the compositions encountered for a phase on the path to convergence, unless the initial estimates of the phase compositions are very close to the converged solution. The local model must therefore be updated as the composition estimates move from the region for which the local model is satisfactory. It is undesirable to do this more often than necessary, since updating calls for references to the MT model. The criterion used here to decide when to update is the distance, in composition space, from the central point around which the local model parameters were evaluated to the current estimate of the phase composition. Since the range of data points used to establish the parameters spanned ±0.05 in mole number, the local model has been updated whenever this distance exceeds 0.05. However, further investigation is necessary, and larger distances permitting fewer updates may prove advantageous.

Convergence. Convergence of the LA method occurs when the magnitude of the discrepancy vector, $\underline{F}$, is below the tolerance limit, just as with the NR method. However, to assure that the results are not influenced by the approximation used, it is necessary to evaluate $\underline{F}$ at the last iteration using the MT model to provide γ_i values. In all iterations the local models can provide the derivatives required, since these do not affect the evaluation of $\underline{F}$.

Performance of the LA method. The resulting phase compositions calculated with the LA method are the same as those for the NR method using the MT model to within the convergence tolerance. However, the number of MT model references required to achieve these results is reduced by about 50% as shown by line 3 in Table 1. Figure 1 compares the convergence behavior for compositions in one phase for the LA method with that of the NR and drag-along methods for the example described in Table 1. The success of the LA method appears to rest on the good approximations to γ_i values provided by the local models, in combination with moderately accurate derivative values (and the relative insensitivity of the multivariate NR iteration to exact values of derivatives, as long as signs and orders of magnitude are correct). This is illustrated in Table 2 where activity coefficients and their derivatives from the local model are compared to those that would be found from the MT model at the same conditions for several iterations of the example calculation.

Table 2 Comparison of γ_i and $\partial\gamma_i/\partial x_j$ used by LA method with MT values for Isooctane, Cyclohexane, Benzene, Furfural system at 273 K, 1 atm

	Local Approximation					MT Model				
	γ_i	$\partial\gamma_i/\partial x_j$				γ_i	$\partial\gamma_i/\partial x_j$			
i \ j	---	1	2	3	4	---	1	2	3	4
	First Iteration									
1	13.0	−45.7	−24.1	−24.1	9.92	12.8	−63.8	−44.5	−15.3	10.4
2	6.95	−15.7	−20.9	−15.7	5.79	7.01	−25.3	−21.5	−7.27	4.62
3	1.73	−2.22	−2.22	−1.50	0.62	1.82	−2.44	−2.05	−1.36	0.59
4	1.06	1.15	0.53	0.53	−0.23	1.05	1.16	0.90	0.41	−0.22
	Third Iteration									
1	9.94	−39.9	−21.0	−21.0	9.60	9.27	−55.0	−38.2	−12.8	10.0
2	5.89	−14.1	−18.7	−14.1	5.72	5.28	−22.2	−18.9	−6.24	4.53
3	1.60	−2.01	−2.01	−1.37	0.62	1.55	−2.19	−1.84	−1.25	0.59
4	1.11	1.24	0.57	0.57	−0.27	1.13	1.25	0.97	0.43	−0.27
	Fifth Iteration									
1	9.05	−39.4	−20.9	−20.9	9.57	9.00	−54.2	−37.7	−12.9	9.97
2	5.48	−13.9	−18.5	−13.9	5.70	5.35	−21.9	−18.7	−6.17	4.52
3	1.55	−2.00	−2.00	−1.36	0.62	1.55	−2.16	−1.82	−1.24	0.59
4	1.13	1.25	0.57	0.57	−0.28	1.13	1.25	0.97	0.43	−0.27

CONCLUSIONS

The local approximation method has achieved a savings of about 50% in references to the MT model, in comparison to the standard "drag-along" or NR methods for four-component liquid-liquid equilibrium calculations. It is expected that greater efficiencies can be achieved by further investigation of the LA approach, particularly with respect to placement of the data points used to evaluate local model parameters and to criteria for updating local models. Application to staged extractor calculations, which require repeated (during iteration over extractor profiles) equilibrium calculations, and where a given lcoal model can be used for several adjacent stages, should yield far greater advantages relative to established techniques (11). Experiences with azeotropic and extractive distillation calculations (10) indicate that reduction in references to the MT model by a factor of ten may well be expected.

REFERENCES

1. J. M. Prausnitz, "Molecular Thermodynamics of Fluid-Phase Equilibria," Prentice-Hall, Englewood Cliffs, N.J. (1969).
2. C. J. King, "Separation Processes," 2nd ed., McGraw-Hill, New York, N.Y. (1980).
3. H. H. Rachford, Jr. and J.D. Rice, J. Petrol. Tech., 4(10) (1952).
4. J. M. Prausnitz et al., "Computer Calculations for Multicomponent Vapor-Liquid and Liquid-Liquid Equilibria," Prentice-Hall, Englewood Cliffs, N.J. (1980).
5. E. Kehat and B. Ghitis, Computers & Chem. Eng., 5 (1981).
6. H. Renon et al., "Calcul sur ordinateur des équilibres liquide-vapeur et liquide-liquide," Editions Technip, Paris (1971).
7. M. E. Leesley and G. Heyen, Computers & Chem. Eng., 1 (1978).
8. A. Barrett and J. J. Walsh, Computers & Chem. Eng., 3 (1979).
9. G. Rebeyrote, "Use of Local Approximations for Thermodynamic Properties in Staged Separator Calculations," MS Thesis, University of California, Berkeley (1980).
10. M. F. Stell, "Efficient Application of Local Approximations for Thermodynamic Properties in Multicomponent Distillation Calculations," MS Thesis, University of California, Berkeley (1981).
11. J. W. Tierney et al., "Solution of Equilibrium Stage Models for Solvent Extraction Processes," ISEC Proc. (1971).

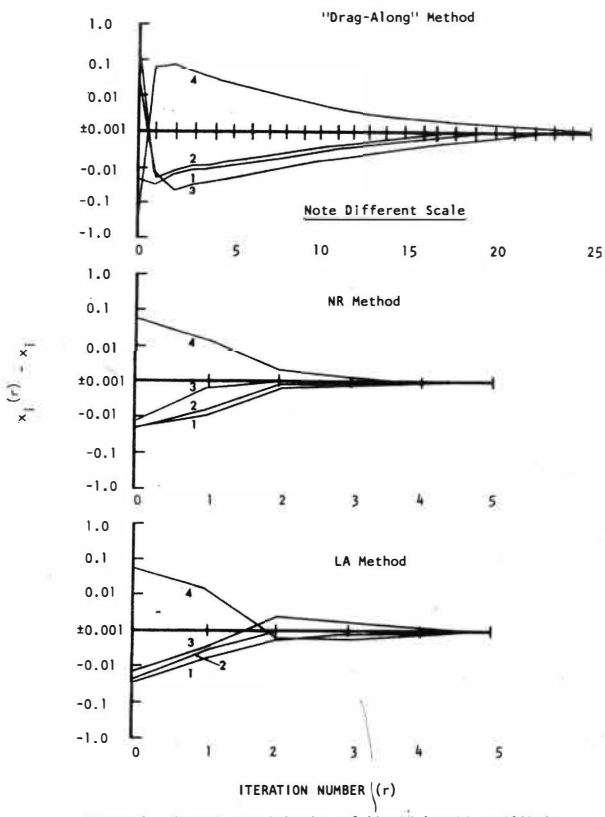

Figure 1. Convergence behavior of liquid-liquid equilibrium calculation for isooctane-cyclohexane-benzene-furfural system at 293 K, 1 atm. Given in terms of "x"-phase compositions, curves labeled with component number.

MASS TRANSFER TO NON-UNIFORM DISPERSIONS IN COUNTER-CURRENT FLOW LIQUID-LIQUID EXTRACTION COLUMNS

J. J. C. Cruz Pinto

Universidade do Minho
Centro de Quimica Pura e Aplicada (I.N.I.C.)
Braga, Portugal

and

W. J. Korchinsky and R. Al-Husseini

University of Manchester
Institute of Science and Technology
Manchester, England

INTRODUCTION

Recent theoretical and experimental work(1-6) on countercurrent flow liquid--liquid extraction resulted in the development of models and calculation techniques which more accurately predict the behaviour of the dispersed phase in extraction columns. The main feature of this behaviour is that, due to the existence of a distribution of drop sizes, each size fraction has its own residence time and mass transfer rate, and thus has a different contribution to the column overall mass transfer efficiency. However, it has so far been assumed that all drop sizes transfer solute by one and the same type of mechanism - either the Newman (7), rigid, or the Handlos-Baron (8), turbulent-circulating, mechanism.

The objectives of this work were:

1. To explore the possibility of predicting, in real dispersions, a range of drop mass transfer activity from the rigid, small drop, behaviour, to the turbulent--circulating or oscillating, large drop, behaviour.
2. To develop a realistic oscillating drop mass transfer model, applicable to real agitated dispersions.

THEORY

Predicting a Range of Drop Mass Transfer Activity

In this work, it is assumed that drops below a given size are rigid (7) and that larger drops are turbulent-circulating (8). The corresponding drop mass transfer equations are:

- rigid

$$\frac{\partial^2 y}{\partial r'^2} + \frac{2}{r'}\frac{\partial y}{\partial r'} - \frac{d^2 V_d}{4D_{AD}}\frac{\partial y}{\partial z} = 0 \qquad (1)$$

- turbulent-circulating

$$\frac{\partial y}{\partial z} = \frac{V_s}{128\, d\, V_d (1+\mu_D/\mu_C)} \cdot \frac{1}{\xi}\frac{\partial}{\partial \xi}\left[(6\xi^3 - 8\xi^2 + 3\xi)\frac{\partial y}{\partial \xi}\right] \qquad (2)$$

These partial differential equations - one for each drop size fraction- must be combined with the equation describing the concentration changes in the continuous phase,

$$\frac{d^2x}{dz^2} + \frac{Q_C}{SE_C}\frac{dx}{dz} = \frac{\rho_D Q_D}{S E_C \rho_C}\left(\sum_{rigid} g_i \frac{d\bar{y}_i}{dz} + \sum_{turb.-cir.} g_i \frac{d\bar{y}_i}{dz}\right), \qquad (3)$$

where E_C is the continuous phase axial dispersion coefficient, and the summations are over all rigid and turbulent-circulating drop size fractions present in the dispersion. A hydrodynamic model of the extraction column is also necessary to predict V_d, V_s and g_i as functions of drop diameter, details of which may be found in Reference 4.

The above equations were solved with the appropriate boundary conditions, using calculation algorithms developed by the authors (4,6). Due account was taken of the continuous phase mass transfer resistance. This procedure was combined with Young's optimization technique (9) to determine the values of E_C, k_C (continuous phase mass transfer coefficient) and f_{rig}(volume fraction of rigid drops in the dispersion) that accurately predict the continuous phase concentration profile.

A Mass Transfer Model of Truly Oscillating Drops

The Handlos-Baron model (8) of single-drop mass transfer was developed to account for the effects of higly turbulent circulation patterns within the drop and vibration of the drop. However, although the model seems to approximately predict the behaviour of large, truly oscillating, single drops, the calculations involved are complicated (eigenvalue problem), and the model is based on some physically unrealistic assumptions (4). Alternative mass transfer models (10, 11) of truly oscillating single drops have been developed in the past but, as they do not correlate the oscillation frequency directly with the intensity of agitation, they are not applicable to agitated dispersions.

A reasonable and simple way to relate the oscillation frequency of each drop to the prevailing agitation conditions is to assume that the oscillation frequency, ν, is proportional to the agitation power input per unit drop surface energy, i.e., for a drop of diameter d,

$$\nu = C_k^2 \frac{\rho_C \varepsilon}{6\sigma} d \qquad (4)$$

where ε is the power input per unit mass, and C_k is a proportionality constant. The solute mass fraction, y', within a drop surface element may then be calculated according to the penetration theory (12), by integrating the equation

$$\frac{\partial y'}{\partial \theta} = D_{AD}\frac{\partial^2 y'}{\partial z'^2} \qquad (5)$$

with the boundary conditions

(5.a) $\theta = 0$, all z'; $y' = y'_o$

(5.b) $\theta > 0$, $z' = 0$; $-D_{AD}\rho_D m \frac{\partial y'}{\partial z'} = k_C \rho_C (mx - y')$

(5.c) all θ, $z' = \infty$; $y' = y'_o$

The solution of these equations is easily obtained (13), from which an average mass tranfer flux, $\bar{\phi}_o$, and an overall dispersed phase mass transfer coefficient, K_{OD}, may be calculated by

$$\bar{\phi}_o = -\frac{1}{\theta}\int_0^\theta D_{AD}\rho_D \frac{\partial y'}{\partial z'}\, d\theta = K_{OD}\rho_D (y^* - y'_o). \qquad (6)$$

The final result for K_{OD} is

$$K_{OD} = \frac{\nu}{h}\left[e^{h^2 D_{AD}/\nu}\ \mathrm{erfc}(h\sqrt{D_{AD}/\nu}) - 1\right] + 2\sqrt{\frac{D_{AD}\,\nu}{\pi}} \qquad (7)$$

where $h = k_C \rho_C / m D_{AD} \rho_D$, and ν stands for $1/\theta$ and is given by Equation 4. It may be checked that as $k_C \to \infty$, K_{OD} tends to $2\sqrt{\frac{D_{AD}\nu}{\pi}}$, and as $\nu \to \infty$, K_{OD} tends to $k_C \rho_C / m \rho_D$.

According to the surface renewal theory (14), a distribution of contact times may alternatively be assumed, yielding an overall coefficient, K_{OD}, given by

$$K_{OD} = \frac{D_{AD}\, h\, s\,(h\sqrt{D_{AD}/s} - 1}{h^2 D_{AD} - s}, \qquad (8)$$

where s (rate of surface renewal) is proportional to the oscillation frequency, i.e. $s = C_s^2 \rho_C \varepsilon d / 6\sigma$. It may be checked that, as $h \to \infty$ or $s \to \infty$, K_{OD} tends to $\sqrt{D_{AD} s}$ or to $k_C \rho_C / m \rho_D$, respectively.

So, for truly oscillating drops, either Equation 7 or Equation 8 is used to predict K_{OD} as a function of drop size, which is then combined with the following modification of Equation 3,

$$\frac{d^2x}{dz^2} + \frac{Q_C}{SE_C}\frac{dx}{dz} = \frac{\rho_D Q_D}{S E_C \rho_C}\sum_i g_i \frac{6K_{OD,i}(y^* - y_i)}{d_i V_{d,i}}, \qquad (9)$$

to predict the changes in the continuous phase concentration. Any combination of rigid and truly oscillating drops may also be considered, as before.

EXPERIMENTAL

A rotating disc contactor with a diameter of 21.9 cm and a total height of 147 cm was used in this study (4). Mass transfer runs were conducted with the system toluene (dispersed) - acetone (solute) - water (continuous), with the solute transferring from the continuous to the dispersed phase. Through the use of distributors to produce the dispersed phase at the column inlet, and of low flows and agitation rates, uniform drop size distributions and negligible drop interaction rates were achieved. In the experiments, measurements were made (4, 15, 16) of drop size distributions (at several levels in the column), dispersed phase holdup fractions, extraction efficiencies and continuous phase concentration profiles.

RESULTS

Although the simultaneous accurate numerical integration of all drop and column differential equations has proved to be very lengthy, our attempts to predict a range of drop mass transfer behaviour (rigid to turbulent-circulating) have so far been successful, particularly where very small, and likely rigid, drops are present in the dispersion. Volume fractions of rigid drops of up to 61% have been predicted. The agreement of the predicted with the experimental continuous phase concentration profile (see Figure 1) was the criterion used in the optimization of the parameter (k_C, E_C and f_{rig}) values. Improvement of the solutions is underway,

by balancing the speed against the accuracy of the calculations.

The new oscillating drop model, when applied to real agitated dispersions in column conditions, yielded overall dispersed phase-based mass transfer coefficients, K_{OD}, like those plotted in Figure 2. The model predicts K_{OD} values which increase with drop size, although this variation is less pronounced than for Handlos--Baron (8), turbulent-circulating, drops.

When this model was used in combination with the parameter optimization procedure (9), the calculations were much faster than when directly integrating the drop diffusion equations, as expected. When only oscillating drops were assumed, optimum predicted C_k values were of the order of 6.0, meaning that a 1 mm toluene drop in water would oscillate 1.8 times per second for a typical agitation rate of 240 r.p.m..

REFERENCES

1. R.H.Chartres, Ph.D.Thesis, The Victoria University of Manchester (1975).
2. R.H.Chartres and W.J.Korchinsky, Trans.Inst.Chem.Engrs., 53, 247 (1975).
3. W.J.Korchinsky and S.Azimzadeh-Khatayloo, Chem.Eng.Sci.,31, 871 (1976).
4. J.J.C.Cruz-Pinto, Ph.D.Thesis, The Victoria University of Manchester (1979).
5. W.J.Korchinsky and J.J.Cruz-Pinto, Chem.Eng.Sci.,34, 551 (1979).
6. J.J.Cruz-Pinto and W.J.Korchinsky, Comp.& Chem.Eng.,7, 19 (1983).
7. A.B.Newman, Trans.A.I.Ch.E.,27,310 (1931).
8. A.E.Handlos and T.Baron, A.I.Ch.E.J.,3, 127 (1957)
9. C.H.Young, M.Sc.Dissertation, The Victoria University of Manchester (1979).
10. P.M.Rose and R.C.Kintner, A.I.Ch.E.J.,12, 530 (1966).
11. J.B.Angelo, E.N.Lightfoot and D.W.Howard, A.I.Ch.E.J.,12, 751 (1966)
12. R.Higbie, Trans.A.I.Ch.E.31, 365 (1935).
13. H.S.Carslaw and J.C.Jaeger, Conduction of Heat in Solids, Oxford, 71 (1959)
14. P.V.Danckwerts, A.I.Ch.E.J.,1, 456 (1955).
15. W.J.Korchinsky, R.Al-Husseini and C.H.Young, Paper 11e, ISEC'83, Denver (1983).
16. R.Al-Husseini, Ph.D.Thesis, The Victoria University of Manchester (1983).

NOTATION

d, d_i	drop diameter
D_{AD}	solute diffusivity, dispersed phase
E_C	axial dispersion coefficient, continuous phase
f_{rig}	volume fraction of rigid drops in the dispersion
g_i	volume fraction of dispersed phase, drop diameter d_i, kinetic basis
k_C	mass transfer coefficient, continuous phase
$K_{OD}, K_{OD,i}$	overall mass transfer coefficient, dispersed phase basis
m	solute distribution coefficient
Q_C, Q_D	volumetric flow rates, continuous and dispersed phases
r'	reduced drop radial coordinate
s	rate of drop surface renewal
S	column cross-sectional area
$V_d, V_{d,i}$	drop vertical velocity
V_s	drop slip velocity
x	solute weight fraction, continuous phase
y, y'	solute weight fraction, variable within drop
y_i	dispersed phase solute weight fraction, ith fraction
y^*	solute weight fraction, equilibrium with continuous phase
z	column vertical height
ε	agitation power input per unit mass
μ_C, μ_D	viscosities, continuous and dispersed phases
ν	drop oscillation frequency
ξ	dimensionless toroidal coordinate, turbulent-circulating drop
ρ_C, ρ_D	densities, continuous and dispersed phases
σ	interfacial tension

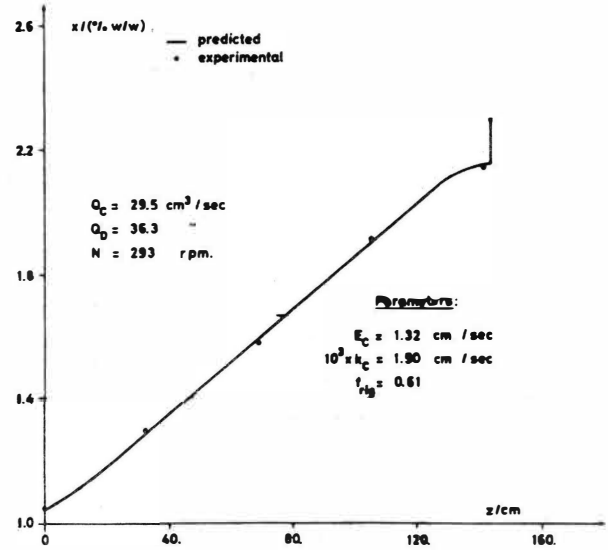

Figure 1 – Concentration Profile

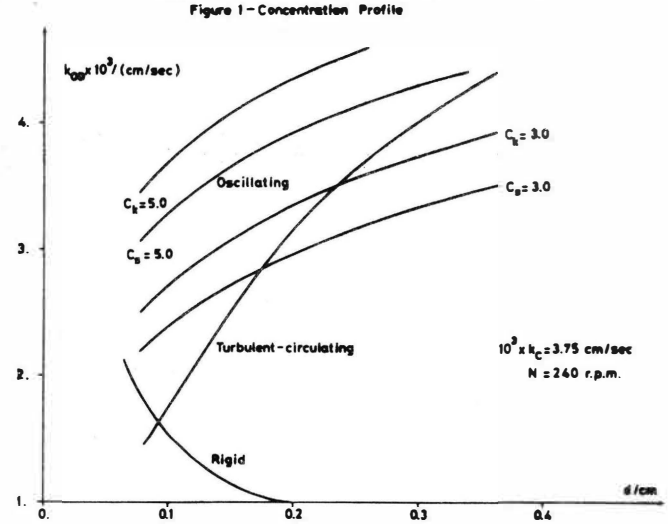

Figure 2 – Drop Mass Transfer Coefficients

DYNAMIC SIMULATION OF PULSED PACKED COLUMNS

A. J. F. Simons and C. Nap

DSM, Central Laboratories
Geleen, Netherlands

DSM and its subsidiary Stamicarbon apply Pulsed Packed Columns (PPC's) in several processes (ref. 1). An obvious advantage of the PPC is that the column length needed for achieving a given extraction efficiency is independent of the diameter. Even if the extraction process is combined with a chemical reaction, the PPC can be correctly scaled up on the basis of results of experiments in smaller diameter columns.
Although the highest throughput and mass transfer are realized near to the flooding point, it is common practice to operate the column substantially below flooding velocities to give a safety margin. Application of computer control makes it possible to safely operate the column nearer to the flooding conditions.
It is known that extraction processes are slow (ref. 2); for industrial columns this means that reaching a steady state condition can take hours. Hence the control of fluctuations in both the flow rates and feed concentrations as well as realization of new plant conditions require an understanding of the start-up and response characteristics of these columns. The analysis of the dynamic behaviour of the PPC gives as a result on the one hand an optimum process operation and on the other hand indications for optimum design.
In the literature (ref. 3) several mathematical models describing the transient behaviour of countercurrent columns have been suggested. It is striking that some of these models have not been verified experimentally. This may be due to the experimentally difficult and expensive procedures.
The mathematical model, with which the chemical-physical behaviour of actual systems is compared, must be based on a description of the elementary mass transfer process between the phases. The closer the process engineering model approaches physical reality, the more accurate the process can be controlled. Modern computer techniques allow the model to be rather complex.
This paper describes an experimental investigation of the response characteristics of PPC's combined with mass transfer of acetone from a continuous aqueous phase into a dispersed toluene phase. The model has been based on the simple stage model with which steady-state conditions of PPC's can be described reasonably well (ref. 1).
The transient behaviour is simulated with ACSL (ref. 4) and the resulting response curves are compared with the experimental column behaviour.

PROCESS ENGINEERING MODEL

Figure 1 shows the relation between the concentration of the transferring component in the flows to and from several stages. It is assumed that in each stage the phases are perfectly mixed. No consideration is given to the question as to whether or not physical equilibrium is reached in the stages.
If a column has N stages, the height ℓ of one mixing stage equals:

$$\ell = \frac{H}{N}.$$

The main objection to this model is that no distinction is made between longitudinal mixing in the raffinate and longitudinal mixing in the extract or solvent phase. In a PPC longitudinal mixing in the dispersed phase is practically always less than in the continuous phase and often negligible.
The following component balances can be arranged around th n-th stage:

- The acetone balance in the toluene phase:

$$\frac{\partial Ac_n^*}{\partial t} = M_T \cdot (Ac_{n+1}^* - Ac_n^*) + \rho_T \cdot (K_T)_n \cdot F \cdot S_n \cdot \ell \, (m_{Ac,n} \cdot Ac_n - Ac_n^*)$$

- The acetone balance in the aqueous phase:

$$\frac{\partial Ac_n}{\partial t} = M_W \cdot (Ac_{n-1} - An_n) - \rho_T \cdot (K_T)_n \cdot F \cdot S_n \cdot \ell \, (m_{Ac,n} \cdot Ac_n - Ac_n^*)$$

The boundary conditions are:

$$Ac_o = Ac_F \qquad Ac_1^* = Ac_E^*$$

$$Ac_N = Ac_R \qquad Ac_{N+1}^* = Ac_F^* = \text{zero}$$

The following equations are also valid:

$$S_n = \frac{6 \cdot \varepsilon \cdot \alpha_n}{d_{vs,n}}$$

and

$$\frac{1}{\rho_T \cdot K_{T,n}} = \frac{1}{\rho_T \cdot k_{T,n}} + \frac{m_{Ac,n}}{\rho_W \cdot k_{w,n}}$$

In arranging the component balances around the stages the following assumptions have been made:
1. the solute free mass flow rates remain constant throughout the column;
2. at the interface the system is in physical equilibrium; the equilibrium constant is defined by $m_{Ac} = Ac_i^*/Ac_i$;
3. the volume fraction of the dispersed phase in each stage is not influenced by changes in solute concentrations;
4. fluctuations in the volumetric flow rates are reflected in a new hydrodynamic steady state with a negligible time lag.

To fit the stage model to the real equipment suitable values have to be chosen for ℓ. The usual way of finding such values is by equating the respective variances of residence time distribution (σ_r^2) of the model and the equipment.
In the case of high values for N and for Pe ($\frac{v \cdot H}{E}$ = Pe > 10) it can be shown that: $\sigma_r^2 = \frac{1}{N} = \frac{2}{Pe}$.
In industrial PPC's we normally have: Pe > 50, meaning that the PPC operates virtually under piston flow conditions.

EXPERIMENTAL PROCEDURE AND RESULTS

Experiments have been carried out with PPC's with diameters of 0.05 m and 0.10 m. Both columns were filled with high-voidage packing, i.e. the 0.05 m column over 4.6 m with 15 mm SS Raschig rings ($\varepsilon \sim 0.92$) and the 0.10 m column over 8.6 m with 25 mm SS Raschig rings ($\varepsilon \sim 0.94$). Hydrodynamic steady states were estabilished at different pulsation velocities and different loads with the toluene (dispersed) - water system. At a certain point in time (t = 0) the aqueous feed was replaced by an aqueous acetone feed. Samples were taken of the aqeous phase along the column height as well as of the issueing extract phase at several time intervals.
Both the drop diameter and the dispersed phase hold-up were measured. From the steady state concentration profiles true mass transfer coefficients for use in the dynamic simulation may be calculated with the aid of the process engineering model for the PPC (ref. 5).
The drop diameter, d_{vs}, and the hold-up, α, both vary with column height and there upon the specific interfacial area S (Examples are shown in Figure 2). The corresponding overall true mass transfer coefficients consequently vary also. In Figure 3 examples have been given of experimental response curves at different column heights for both a constant load and a constant pulsation velocity. These and other response curves will be compared with model predictions.

REFERENCES

1. A.J.F. Simons, in B.H. Lucas et al, Proc. Int. Solv. Extr. Conf. 1977, vol. 2, CIM Special Volume 21, 1979, p. 677.
2. K. Tettamanti et al., Chem. Techn., vol. 20 (6), 1968.
3. C. Hanson, ed., Recent Advances in Liquid-Liquid Extraction, Perg. Press Ltd. 1971.
4. ACSL (Advanced Continuous Simulation Language), Reference Manual, Mitchell and Gauthier, Associates 1975.
5. N.M. Spaay et al. in J.G. Gregory et al. eds., Proc. Int. Solv. Extr. Conf. 1971, vol. 1, Society of Chemical Industry 1971.

LIST OF SYMBOLS

Ac	Concentration of acetone in aqueous phase	wt.%
Ac*	Concentration of acetone in toluene phase	wt.%
D_c	Column diameter	m
d_{vs}	Average drop diameter acc. to Sauter	m
E	Longitudinal mixing coefficient	$m^2.s^{-1}$
F	Cross-sectional area	m^2
f	frequency	s^{-1}
H	Height of packed column section	m
K	Overall mass transfer coefficient	$m.s^{-1}$
k	Partial mass transfer coefficient	$m.s^{-1}$
ℓ	Height of a mixing stage	m
m_{Ac}	Distribution of acetone between toluene and water, with $m_{Ac} = Ac_i^*/Ac_i$	
M	Mass flow	$kg.s^{-1}$
N	Number of mixing stages	
n	Stage number	
Pe	Peclet number: $Pe = \frac{v \cdot H}{E}$	
S	Specific interfacial area: $S = \frac{6 \cdot \varepsilon \cdot \alpha}{d_{vs}}$	m^{-1}
s	Pulse amplitude: total stroke length	m
t	Time	s
v	Superficial velocity	
α	Hold-up of dispersed phase	
ε	Bed porosity	
ρ	Liquid density	$kg.m^{-3}$
σ_r^2	Variance of residence time distribution	

Indices

E	extract phase
F	feed phase
i	interfase
N	last mixer
N+1	imaginary mixer after the N-th one (for the toluene feed phase only)
n	stage number
o	imaginary mixer preceding the first one (for the aqueous feed phase only)
R	raffinate phase
T	toluene phase
w	aqueous phase
1	first mixer

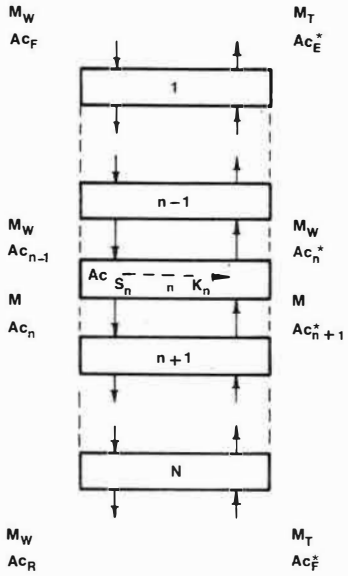

Fig. 1 Stage model

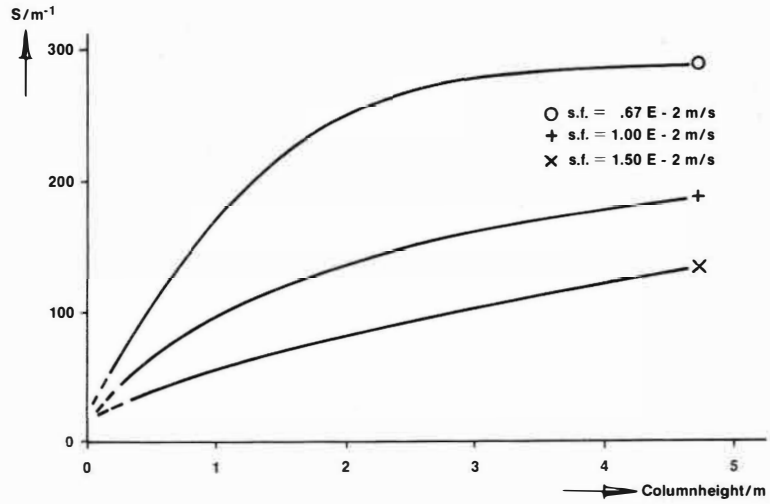

Fig. 2 S v.s. Columnheight

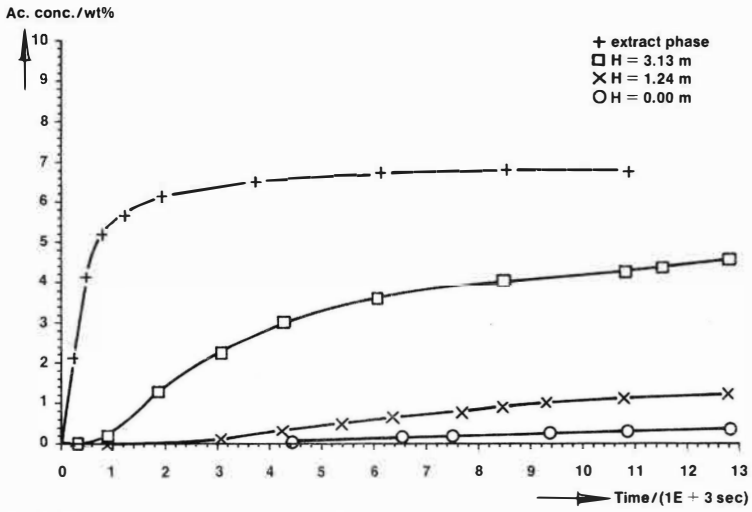

Fig. 3 Acetoneconc. v.s. time (s * f = .67 m/s)

SOLVENTS FOR BULK REMOVAL OF ORGANICS FROM COAL-CONVERSION CONDENSATE WATERS

Donald H. Mohr and C. Judson King

Department of Chemical Engineering

and

Lawrence Berkeley Laboratory
University of California
Berkeley, California 94720 USA

INTRODUCTION

When the product gases from a coal gasification reactor are cooled, the excess steam condenses and forms a condensate water. This stream is highly buffered with ammonia and carbon dioxide to a pH of about 8.5 and contains many organic compounds. A commercial scale Lurgi gasification plant with a capacity of $3x10^5$ standard m^3/h would produce an estimated $5x10^5$ kg/h of condensate water (1). The management of this water is important for both environmental and economic reasons (2). Release of potential pollutants must be controlled, and reuse of the water is important because many coal deposits are located in arid regions. In this work chemical analyses and experimental tests of extraction solvents are discussed for condensate waters from a coal gasification pilot plant.

COMPOSITION OF CONDENSATE WATERS

Condensate water samples were obtained from a slagging fixed-bed gasifier which was operated by the U.S. Dept. of Energy at the Grand Forks Energy Technology Center (GFETC) in Grand Forks ND, U.S.A. The samples were protected from oxidation and were analyzed as rapidly as possible. Reversed-phase, gradient-elution, high performance liquid chromatography (HPLC) with variable-wavelength UV absorbance detection was employed to resolve and detect the compounds in the condensate water.

The identities of the compounds eluted from the HPLC were determined by either or both HPLC co-chromatography and gas chromatography-mass spectrometry (GC-MS). For GC-MS analysis, individual fractions were collected as they eluted from the HPLC. A batch azeotropic distillation with isopropanol concentrated the solute and removed water from the sample (3). Then the sample was analyzed by GC-MS (Finnigan model 4000), and the spectrum of an unknown solute was compared to a computerized library of known spectra. The advantage of this novel sample preparation technique is that it recovers very polar compounds which are not recovered by the methylene chloride extraction step in the standard GC-MS analytical technique (denoted MC/GC-MS). However, these compounds must be less volatile than isopropanol.

Table 1 shows the analysis of one GFETC condensate water. The compounds are arranged in three groups. The first group is the hydroxybenzenes or simple phenols. These compounds are moderately polar and are easily detected by the standard MC/GC-MS technique. However, the precision of ±5% in Table 1 is an improvement over the MC/GC-MS technique because there are no losses associated with a preliminary solvent extraction step.

The second group of compounds is the dihydroxybenzenes which are more polar and much less volatile than phenol. It is important to have precise quantitative information about these compounds because they have lower distribution coefficients into many solvents (4). Since they are more difficult to extract, they have much lower recoveries in the standard MC/GC-MS technique.

The third group of compounds is the hydantoins. The major component is 5,5-dimethyl hydantoin:

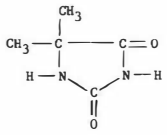

The identification of this compound was confirmed by both co-chromatography and the isopropanol/GC-MS technique. This was the first report of hydantoins in condensate waters. These compounds are still more polar than dihydroxybenzenes. Hydantoins have very low distribution coefficients into methylene chloride, and therefore should be difficult or impossible to detect by the standard MC/GC-MS analytical technique.

Table 2 shows the analyses of four GFETC condensate water samples. Concentrations, expressed as fractions of the chemical oxygen demand (COD), are reported for the three groups of compounds described in Table 1. The results in Table 2 show significant differences in the proportion of simple phenols to COD for the four samples. There are also large differences in the proportions of dihydroxybenzenes and hydantoins to COD or simple phenols. Some increase in the concentration of dimethylhydantoin was observed as the samples aged, but this was not large enough to explain the composition differences among the samples (3). Samples were stored at 4°C in the dark. The sample-to-sample variability in Table 2 is probably due to changes in operating conditions for the gasifier despite the fact that the feed coal, steam/oxygen ratio, operating pressure, and oxygen rate were nearly constant. Changes in condensate-water composition introduce a large uncertainty into any general conclusions drawn from laboratory tests of a small number of condensate-water samples.

Finally, 23 to 31% of the COD remains unidentified in these four samples. Most analyses of condensate waters using the MC/GC-MS technique fail to identify an even greater fraction of the COD--see, e.g., (3).

SOLVENT EXTRACTION OF CONDENSATE WATERS

Distribution Coefficients: Table 3 shows the distribution coefficients of phenol and the three dihydroxybenzenes into three solvents. Diisopropyl ether (DIPE) and methyl isobutyl ketone (MIBK) have been proposed as solvents for commercial-scale treatment of condensate waters (4). Comparison of K_D values for these two solvents shows that MIBK has a significant advantage over DIPE, particularly for the dihydroxybenzenes. The third solvent in Table 3 is a mixture of 25% w/w trioctyl phosphine oxide in diisobutyl ketone (TOPO/DIBK). TOPO is non-volatile and as an extractant is a strong Lewis base. This solvent mixture provides very high K_D values, even for the dihydroxybenzenes.

Dimethyl hydantoin is a very polar compound and is therefore difficult to extract from water. Tributyl phosphate (TBP) gives the highest value of K_D among the solvents listed in Table 4. Several of these solvents exhibit very low K_D values for this compound, including methylene chloride which is used in the MC/GC-MS analytical technique.

Removal of Chemical Oxygen Demand by Solvent Extraction: In Table 5 a condensate water sample from GFETC run No. 120 was contacted in batch equilibrations with several solvents at solvent-to-water ratios of 1:1 by volume. The COD of the raffinate was measured after residual dissolved solvent had been removed. MIBK was removed from the raffinates by stripping with 1.5 mole N_2/mole H_2O at 25 °C. The MIBK was purified before extraction by washing with 0.1 N NaOH and 0.1 N H_2SO_4 to remove impurities which would otherwise contribute to the COD.

A single extraction with MIBK removed nearly 90% of the COD and essentially all of the phenols and dihydroxybenzenes. A second extraction removed only a small increment of the remaining COD, indicating that most of the residual components have low values of K_D into MIBK. Lowering the pH of the condensate water from 8.5 to 3 did not significantly increase the removal of COD by MIBK. This indicates that ionizing weak acids do not compose a substantial fraction of the residual COD. As the age of the sample increased, MIBK extraction removed less of the COD; however, concentrations of all of the compounds identified in Table 2 remained essentially constant over this time interval. This indicates the importance of conducting experimental tests of treatment processes on fresh condensate water samples.

As is also shown in Table 5, TBP removed a slightly greater fraction of the COD than did MIBK. The TOPO/MIBK mixture removed about the same fraction as did MIBK alone.

Table 6 shows the removal of COD and organic nitrogen from the same condensate water at a sample age of 190 days. Organic nitrogen is defined as the difference between Kjeldahl and ammonia nitrogen, both of which were measured after nitrogen stripping to remove most of the NH_3 (3). Comparison of the fourth and fifth extractions shows that 10% of the COD in this mixture has a vanishingly small K_D into MIBK. Also, the organic nitrogen has a low value of K_D into MIBK. Since the ratio of COD to organic N can be as high as 20 for a typical nitrogen-containing compound, these compounds could account for most of the unextracted COD. Since no increase in removal of the nitrogen compounds was observed at high pH with MIBK or with a Lewis-acid solvent (methylene chloride), these compounds are not simple organic bases. Other experiments with an MIBK raffinate showed that about half of the remaining COD was more volatile than water, all of the remaining nitrogen was non-volatile with respect to water, and all of the remaining COD had a molecular weight of less than 1000 as determined by ultrafiltration.

Capabilities of Solvent Extraction: There are two important questions in the design of a condensate water solvent extraction process. The first is whether a given solvent can remove enough of the organic solutes under any conditions to meet the treatment requirements. The second consideration is the reliability and economics of a particular process.

The data discussed above raise serious questions about the ability of current solvent extraction technology to remove organics from condensate waters to an acceptable level without further treatment. The COD of these condensate waters is so high that a 90% removal still leaves a highly contaminated raffinate. Some level of organics may be acceptable in a cooling-tower make-up stream, provided that the compounds are not volatile and do not excessively foul the heat exchange surfaces through biological growth. Then a small volume of cooling-tower blowdown could be treated by other techniques.

If the residual polar and hydrophilic compounds could be identified, then it might be possible to select chemically specific solvents to remove these compounds.

A number of additional factors are important in the selection of an economically viable solvent. A volatile solvent such as DIPE or MIBK must be regenerated as a distillate, and this requires a large amount of heat to vaporize the solvent. For a non-volatile solvent, such as TBP or TOPO in a non-volatile diluent, all of the solutes must be taken overhead. In a complex mixture such as these condensate waters, it is likely that non-volatile solutes would accumulate and possibly degrade the performance of the solvent. Acidic solutes could be removed from a solvent by extraction with aqueous base, but this could require an expensive consumption of chemicals. TOPO in an appropriate diluent provides high values of K_D for phenols and dihydroxybenzenes. This allows a low solvent flow rate, and therefore a regeneration process which is expensive per unit of solvent treated may still

be economically reasonable per unit of treated water.

A second factor which is important in the economics of a solvent extraction process is the amount of solvent which is lost in the raffinate. DIPE and MIBK are volatile solvents which can be removed to low levels by stripping the raffinate. Vacuum steam stripping is particularly attractive for removal of MIBK (4). Less polar solvents such as TOPO in isobutyl heptyl ketone have a sufficiently low equilibrium solubility in water that a solvent-recovery process may not be necessary. However, it is still necessary to account for losses by emulsification, micellarization, complexation into water-soluble forms, and losses due to irregular operation of the process, particulary for the more expensive solvents.

CONCLUSIONS

MIBK provides much higher distribution coefficients than DIPE for phenol and dihydroxybenzenes. About 90% of the COD from one condensate water sample had a sufficiently high K_D into MIBK that it could be removed by this solvent in a counter-current extraction process at an economically reasonable solvent-to-water ratio. TOPO in a suitable diluent has high equilibrium distribution coefficients for phenols and dihydroxybenzenes, and therefore has the potential to remove these compounds at lower solvent-to-water ratios. However, this solvent may be difficult to regenerate in a continuous condensate-water extraction process.

Analytical techniques were discussed that provide higher recoveries for phenols and dihydroxybenzenes as compared to the standard MC/GC-MS technique. Hydantoins have been identified in four condensate water samples. About 20-30% of the COD remains unidentified in these four condensate water samples. Some of these unidentified compounds have very low values of K_D for extraction into MIBK. More information is required about these unidentified solutes before reliable solvent extraction processes can be designed.

ACKNOWLEDGEMENTS

This work was supported by the Assistant Secretary for the Environment, Office of Environmental Compliance and Overview, Division of Environmental and Safety Engineering, Environmental Control Technology Branch, U.S. Department of Energy and by the Fossil Energy Division through the Morgantown Energy Technology Center, under Contract No. DE-AC03-76SF00098.

REFERENCES

1. R. F. Probstein and H. Gold "Water in Synthetic Fuel Production: The Technology and Alternatives," MIT Press, Cambridge, MA, 1978.
2. C. J. King, S. Lynn, D. N. Hanson and D. H. Mohr, Eds. "Processing Needs and Methodology for Wastewaters from the Conversion of Coal, Oil Shale, and Biomass to Synfuels," Report No. DOE/EV-0081, U.S. Dept. of Energy, May 1980.
3. D. H. Mohr and C. J. King, Report No. LBL-15869; Lawrence Berkeley Laboratory, Berkeley, CA, July 1983.
4. D. C. Greminger, G. P. Burns, S. Lynn, D. N. Hanson and C. J. King Ind. Eng. Chem., Process Des. Develop., 21, 51 (1982).
5. J. D. MacGlashan and C. J. King, Report No. LBL-13963; Lawrence Berkeley Laboratory, Berkeley, CA, March 1982.

Table 1: Analysis of Condensate Water #RA-78 from the GFETC Slagging Fixed-Bed Gasifier

Compound	Conc. (mg/l)
Hydroxybenzenes:	
1. phenol	4,750
2. C_1-phenols	2,855
3. C_2-phenols*	450
4. o-methoxy phenol*	260
5. p-hydroxy acetophenone*	50
Dihydroxybenzenes:	
6. catechol	990
7. 4-methyl catechol	615
8. resorcinol	60
9. hydroquinone	35
Hydantoins:	
10. 5,5-dimethyl hydantoin	1,725
11. 5-methyl hydantoic acid	95
12. 5-methyl hydantoin	135

* These compounds were identified by the isopropanol/GC-MS technique. All of the compounds were identified by HPLC co-chromatography.

Table 2: Analyses of GFETC Condensate Waters Expressed as a Fraction of the COD

GFETC Run No.:	RA-78	RA-97	RA-106	RA-120
Hydroxybenzenes:	0.586	0.642	0.663	0.764
Dihydroxybenzenes:	0.095	0.059	0.006	0.0002
Hydantoins:	0.082	0.014	0.019	0.007
Total Fraction of COD Identified:	0.763	0.697	0.688	0.771
COD (mg/l):	34,870	46,670	22,920	23,390

Table 3: Distribution Coefficients (K_D) of Phenol and Dihydroxybenzenes

Solvent:	DIPE	MIBK	TOPO/DIBK*
Reference:	(4)	(4)	(5)
Phenol	36.5	100.	462.
Catechol	4.86	18.7	203.
Resorcinol	2.06	17.9	98.
Hydroquinone	1.03	9.9	35.

Solvents: DIPE: diisopropyl ether, MIBK: methyl isobutyl ketone, TOPO/DIBK: 25% w/w trioctyl phosphine oxide in diisobutyl ketone.

* The values reported here are for 2.5 moles TOPO/mole solute in the combined organic and aqueous phases. The value of K_D depends on this ratio (5).

Table 4: Equilibrium Distribution Coefficients for Dimethyl Hydantoin

Solvent	K_D
Methylene chloride	<0.05
Methyl isobutyl ketone (MIBK)	0.25
25% w/w trioctyl phosphine oxide in MIBK	1.2
25% w/w Adogen 363 (R_3N, Sherex Chemical Co.) in kerosene	<0.05
25% w/w di(2-ethyl hexyl) phosphoric acid in kerosene	<0.05
Tricresyl phosphate (TCP)	0.11
Tributyl phosphate (TBP)	2.6

Table 5: Fraction of COD Removed by Solvent Extraction from GFETC Run No. 120

Solvent	Number of Successive Batch Extractions	Sample Age (Days) 0.7	15	190
MIBK	1	0.897	0.883	0.856
MIBK	2	0.927	0.911	0.878
MIBK	1 and 1 @ pH 3	0.923	0.913	-
TBP	1	-	0.915	-
TBP	2	-	0.938	-
TBP	1 and 1 @ pH 3	-	0.945	-
25% w/w TOPO in MIBK	1	-	0.88	-
Same	1 and 1 @ pH 3	-	0.92	-

Table 6: Fraction of COD and Organic Nitrogen Removed by Extraction with MIBK. GFETC Run No. 120

COD = 23,390 mg/l
Organic Nitrogen = 220 mg/l

No. of MIBK Extractions	Fraction of COD Removed (±0.005)	Fraction of Organic N Removed (±0.10)
1	0.856	0.28
2	0.878	0.28
3	0.890	0.35
4	0.900	0.35
5	0.902	0.41
1 and 1 @ pH 12	0.878	0.23
1 and 1 with CH_2Cl_2 @ pH 12	0.880	0.10

SHALE OIL UPGRADING PROCESS BASED ON NITROGEN REMOVAL FROM CRUDE SHALE OIL BY LIQUID EXTRACTION

Ajay M. Madgavkar

Occidental Research Corporation
Irvine, California USA

A novel shale oil upgrading process is discussed which is based on removal of a substantial portion of nitrogen compounds by liquid extraction followed by mild hydrotreating of the raffinate fraction. Results of laboratory extraction experiments are presented including the effects of key process variables on nitrogen removal and oil recovery (raffinate yield). Also discussed are the results of solvent recovery/recycle studies, phase separation studies and a summary of hydrotreating studies. About 70% of feed nitrogen was removed in a single stage extraction conducted in a mixer/settler unit with oil recoveries of 80 to 85% of feed shale oil. No phase separation difficulties were encountered and efficient solvent recovery and recycle was demonstrated. A raffinate obtained from extraction of whole shale oil was hydrotreated under mild severity conditions to produce a satisfactory, high quality synthetic crude. Substantial savings in hydrogen consumption were achieved in this process as compared to whole shale oil hydrotreating.

INTRODUCTION

High nitrogen content of shale oil is its most serious drawback and a property which significantly reduces its value as synthetic crude oil. Raw shale oil contains between 1.3 to 2.5% nitrogen as compared to 0.3% or less for a typical petroleum crude. Most refining operations that utilize catalysts cannot function at such high nitrogen levels since these catalysts are readily poisoned by nitrogen compounds. Other problems caused by high amounts of nitrogen in shale oil are product instability and limited storage life, contamination during transportation in common crude oil pipelines, mutagenic properties and excessive NO_x production during combustion. These objections add up to a strong argument in support of removal of nitrogen from crude shale oil.

A lot of work has been done in the past and is currently being done in the industry on this problem as part of an overall effort in shale oil upgrading. Most of the approaches are based on high severity catalytic hydrotreating that is necessary due to excessive nitrogen in shale oils (1,2,3). Though these processes represent state-of-the-art technology in terms of technical demonstration and confidence, they require large capital and subsequently are very expensive. Upgrading costs in excess of $10/Bbl (1981) are estimated to convert whole shale oil into a low sulfur, low nitrogen, arsenic-free syncrude. Realizing this cost penalty of the approach based on hydrotreating alone, attempts have been made to devise processes that utilize mild hydrotreating of whole shale oil followed by a physical separation step such as liquid extraction to remove some portion of the nitrogen compounds from the hydrotreated oil (4,5). Though sound in principle, these processes remove only 25-30% of the total feed nitrogen in the extraction step and consequently the reduction in overall hydrogen consumption and upgrading cost is, at best, marginal.

ORC'S PROCESS

It is well known that a majority of the nitrogen containing compounds in shale oil are heterocyclic basic chemical compounds (6,7). For OXY's MIS process roughly 60 to 75% of the nitrogen compounds fall in this category (8). These basic compounds (pyridine, quinoline types) severely poison hydrotreating catalysts which are typically acidic in nature. To overcome the reduced catalyst activity therefore, high severity conditions are required in whole shale oil hydrotreating. Unfortunately, this also leads to undesirable hydrocracking side reactions which consume excessive hydrogen (beyond that required by stoichiometry) in the process. Furthermore, it is generally accepted that nitrogen removal from these aromatic compounds takes place via an initial saturation of the ring before the scission of carbon-nitrogen bond occurs (9-12). This exacerbates the non-selective and inefficient utilization of hydrogen and consequently increases shale oil upgrading costs.

ORC's approach to shale oil upgrading attempts to overcome the major problems discussed above by selectively and efficiently removing the majority of feed nitrogen (60 to 75%) from whole shale oil by a specially designed liquid extraction process. More important, the solvent selectively extracts most of the basic nitrogen compounds which are most difficult to hydrotreat and are strong catalyst poisons. The main objective of ORC's process is to upgrade the low nitrogen raffinate fraction of shale oil in a conventional low severity hydrotreating operation, preferably in an existing refinery. It is assessed that this process results in a substantial reduction in the overall shale oil upgrading costs.

This paper focuses mainly on the liquid extraction process. A separate paper will discuss the detailed results of hydrotreating the extracted shale oil (raffinate fraction) as well as the whole shale oil (13).

RESULTS AND DISCUSSION

Process Variables Study. The most important parameter affecting nitrogen extraction was found to be the solvent composition. The effect of increasing acid concentration on % nitrogen removal is illustrated by the results shown in Table I for the formic acid-water solvent system. It can be seen that at a constant solvent-to-oil weight ratio of 1.0, as the acid concentration was changed from 50 to 70 weight % in the solvent the % nitrogen removed increased from around 45 to 59%. A further increase to 89% formic acid in the solvent resulted in a nitrogen removal of about 74%. Under these conditions a shale oil raffinate fraction with only 0.4% nitrogen was obtained in a single stage extraction experiment. The raffinate yield or weight % oil recovery of around 83% was achieved in the process. It should be mentioned that the oil recovery values reported here were obtained by actual distillation of the extract phase rather than based on chemical analyses.

TABLE I

EFFECT OF SOLVENT COMPOSITION AND SOLVENT-TO-OIL RATIO FOR FORMIC ACID-WATER SOLVENT SYSTEM

Feed: OXY's MIS Shale Oil (1.53 wt% N)
Temperature: 140°F

Solvent Acid Wt.%	Solvent To Oil Ratio	Wt.%N Removal	Wt.% Oil Recovery	Extract (Oil/N)	Selectivity Ratio
89	0.5	70.09	83.85	14.98	4.24
	1.0	74.10	83.38	14.77	4.46
70	0.5	57.50	90.26	11.80	5.90
	1.0	58.77	88.09	13.13	4.93
50	0.5	40.68	94.21	10.38	7.03
	1.0	44.76	93.68	10.20	7.08

Solvent-to-oil weight ratio also affected the nitrogen removal. This was indicated by the results in Tables I but a more detailed illustration is shown in Figure 1 with additional data. A wide range of ratios (0.25 to 2) was covered in these experiments carried out at 140°F and 60 minutes settling time. The nitrogen extracted was found to be a function of the ratio up to a value of 1 or so. Beyond a solvent-to-oil ratio of 1 the increase was rather marginal as the % nitrogen removal approached the equilibrium value. This was also confirmed by conducting a few runs at ratios of around 4 for the above solvents. These results suggest that there is no advantage in operating at very high solvent-to-oil-ratios.

Solvent Recovery and Recycle Studies. Due to the large differences in the boiling points of solvent and shale oil components, separation by simple distillation was rather straightforward and efficient. By proper design and operation, complete removal of formic acid was possible from both the extract and the raffinate phases. Thus a major effort was made to characterize the recycle solvent with respect to its activity.

In this study a total of 40 sets of successive extractions/distillations were conducted. The fresh solvent was 80 weight % formic acid and the first 20 recycle runs did not include the addition of any make-up formic acid. In other words, the acid strength was intentionally allowed to progressively decline and impurities allowed to accumulate. After separating the two phases each was separately distilled to recover the solvent which was combined and used for the next extraction run with fresh shale oil. The solvent losses were mainly due to the nature of these batch distillations and the fact that the distillation scheme, though efficient, was not an ideal system resulting in a few incomplete distillations. In the last 20 sets of experiments required amounts of fresh formic acid were added to the combined recycle solvent to maintain a constant composition of 80% formic acid. In this manner a more rigorous test of solvent recyclability was obtained.

Results from the first 21 sets of runs such as % nitrogen removal, % oil recovery and raffinate nitrogen concentration are shown in Figure 2 as functions of recycle number. The solvent losses averaged a little less than 1 wt. % acid per recycle run but should be significantly less under a continuous operating system which is properly designed for solvent recovery. Corresponding nitrogen removal also declined during these 20 recycles from 68% for fresh solvent to about 50% in the 20th recycle run. This drop was, however, directly attributed to the drop in acid concentration in the recycle solvent. In other words, fresh formic acid solvent of the same concentration gave identical % nitrogen removal values. An encouraging piece of information was the fact that recycle acid contained rather low amounts of nitrogen (around 100 ppm) and this level did not rise in 21 experiments, although there was no purging attempted.

The formic acid concentration in the solvent had declined to around 60 wt. % at the end of recycle run No. 20. Therefore a significant amount of fresh acid was necessary to raise the concentration to 80 wt. % for the recycle run No. 21. After that, however, only about 3% average make-up acid was needed for the subsequent runs. An average of 97% of the formic acid was recovered in distillation of both phases in each recycle run. A remarkably constant performance in nitrogen removal and oil recovery was demonstrated in all of these twenty runs as shown in Figure 2. This proves that no detectable solvent degradation (physical or chemical) was observed in these runs. Thus from this total of 40 recovery/recycle sets of studies it is concluded that in a closed loop, steady-state extraction process solvent reuse should be technically feasible with a minimum of make-up solvent.

Phase Separation Studies. It was important to achieve efficient phase separation in the process and to quantify the disengagement characteristics of the two phase system. A simple but effective method was devised which permitted estimation of separation time by comparing solvent composition in the extract phase with its equilibrium value. Using this method it was observed that solvent composition strongly affected phase disengagement rates. For example, a 70% formic acid gave an efficient separation in about 5 minutes versus 12 to 14 minutes for a 90% formic acid solvent. Similar results were obtained with acetic acid-water system and a 90% acetic acid solvent gave an efficient separation in about 10 to 12 minutes.

A few experiments were also conducted in the mixer/settler unit to study the effect of mixing energy on phase separation. The mixer was equipped with a low shear impeller which resulted in lower mixing energy. Thus a mixture of 90% formic acid and shale oil was agitated at 250 rpm for 5 minutes at 140°F and samples were taken near the interface. The results showed a dramatic effect on the time needed for an efficient separation which was only 5 to 7 minutes versus 12 to 14 for the separatory funnel experiment, a roughly 50% reduction. These preliminary results show that for a properly designed extraction process there should not be any unusual phase separation problems.

Hydrotreating Studies. The main objectives of these studies were:

(1) Identify the hydrotreating severity conditions needed to achieve the desired product nitrogen level (500 to 1500 ppm) for a typical raffinate feed and,

(2) Estimate savings in H_2 consumption as compared to hydrotreating a whole shale oil to similar product quality.

A cooperative program was established between ORC and Armak Company, Pasadena, Texas to achieve the above objectives which were most vital for verification of the basis for ORC's extraction based shale oil upgrading process. The raffinate was obtained by extracting whole shale oil with 90% formic acid at a solvent-to-oil ratio = 1 and 140°F. This raffinate and a batch of the whole shale oil were separately hydrotreated under identical conditions. A summary of results obtained for the raffinate is shown in Table II.

TABLE II

RESULTS OF SOLVENT EXTRACTED SHALE OIL HYDROTREATING

Catalyst: $Ni\text{-}Mo/Al_2O_3$ Run Time: 1 day each

Feed: Shale Oil Raffinate (0.47 Wt. % N, 0.94 Wt. % S)

H_2: Oil (SCF/BBL) = 5500

P (PSIG)	T (°F)	LHSV (Hr^{-1})	Product N(Wt.%)	Product S(Wt.%)	H_2 Cons. (SCF/BBL)
1200	650	1	0.12	0.03	350
1200	675	1	0.05	0.02	450
1200	675	2	0.14	0.05	500

The raffinate was hydrotreated into a high quality syncrude under moderate conditions of 1200 psig, 650°F and LHSV = 1 hr^{-1}. On the other hand, the shale oil gave a product containing 0.55 weight % nitrogen (which was higher than the raffinate feed concentration itself) under identical conditions. Secondly, the chemical hydrogen consumption for raffinate hydrotreating was around 350 to 500 scf/Bbl only. Though this was only a preliminary estimate based on chemical analyses of feed and products, it must be realized that substantially higher hydrogen consumption would be required to achieve similar high quality products from whole shale oil. In fact, for shale oil hydrotreating even after 400 to 700 scf/Bbl hydrogen consumption the products still contained 0.36 to 0.64 weight % nitrogen which is unacceptably high. Therefore, it can be concluded that there will be substantial savings in hydrogen consumption in hydrotreating solvent extracted shale oil under mild conditions as compared to whole shale oil hydrotreating.

CONCLUSIONS

Preliminary technical feasibility of a shale oil upgrading process based on nitrogen removal by liquid extraction was demonstrated by key experimental results. A majority of nitrogen compounds was removed from whole shale oils at high raffinate yields while achieving efficient phase separation. Solvent composition and solvent-to-oil ratio were the major variables in the extraction process. Efficient solvent recovery was achieved and no chemical or physical degradation of the solvent was detected in recycle studies. A shale oil raffinate was hydrotreated under mild severity conditions at substantially lower H_2 consumptions over hydrotreating whole shale oils.

REFERENCES

1. R.E. Hildebrand, and B.M. Harney, ACS Meeting, Houston, Texas (1978).
2. R.F. Sullivan, B.E. Stangeland, and H.A. Frunkin, IGT Symposium, Atlanta, Georgia (1979)
3. R.F. Sullivan, B.E. Stangeland, D.C. Green, C.E. Rudy, and H.A. Frunkin, D.O.E. Report No. FE-2315-25 (1978).
4. R.P. Long, H.F. Moore, W.A. Sutton, and F.H. Turrill, 3rd Jet Fuel From Shale Oil Technology Review, Miamisburgh, Ohio (1981)
5. H.E. Reif, J.P. Schwedock, and A. Schneider, 3rd Jet Fuel From Shale Oil Technology Review, Miamisburgh, Ohio (1981)
6. G.U. Dinneen, G.L. Cook, and H.B. Jensen, Anal. Chem., 30, 2026 (1958).
7. S.A. Holmes, and L.F. Thompson, 14th Oil Shale Symposium (1981).
8. A.M. Madgavkar, Unpublished Results (1981).
9. H.G. McIlvried, Ind. Eng. Chem., Process Des. Dev., 10, 125 (1971).
10. J. Sonnemans, W.J. Neyens, and P. Mars, J. Catal., 34, 230 (1974).
11. J.R. Katzer, and R. Sivasubramanian, Catal. Rev.-Sci. Eng., 20 (2) 155 (1979).
12. S.S. Shih, J.R. Katzer, H. Kwart, and A.B. Stiles, Am. Chem. Soc., Div. Pet. Chem., Prepr., 22 (3), 919 (1977).
13. P.H. Desai, M.Y. Asim, and A.M. Madgavkar, to be presented at AIChE Meeting Denver, Colorado (1983).

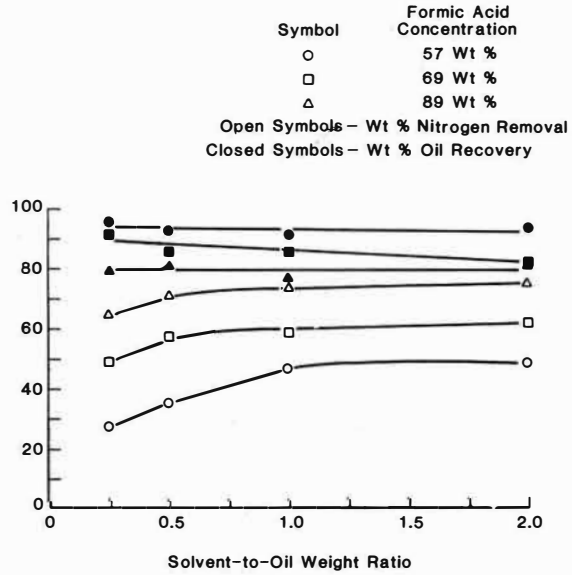

Figure 1

EFFECT OF SOLVENT-TO-OIL RATIO AND ACID STRENGTH ON NITROGEN REMOVAL AND OIL RECOVERY

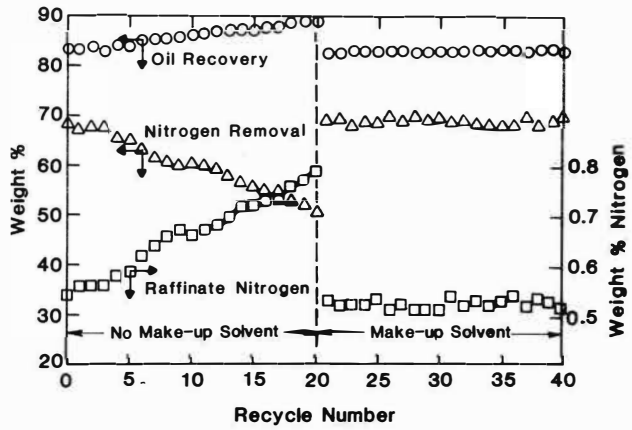

Figure 2

RESULTS OF SOLVENT RECYCLE STUDIES

LIGHT AROMATICS EXTRACTION FROM PETROLEUM FRACTIONS WITH ALKYLSULFONAMIDES

Roben Loutaty and Charles Yacono

Total-Compagnie Française de Raffinage
Centre De Recherches
B.P.27 - 76700 Harfleur, France

INTRODUCTION.

Petroleum refineries constitute the largest suppliers of light aromatics to the chemical industry. A major portion of the production comes from solvent extraction units fed with catalytic reformates mainly composed of hexanes, heptanes, benzene and toluene. Alkylsulfonamides are being considered as potential substitutes to the most common commercial solvents.

SYNTHESIS.

The fifteen compounds listed in the table below were chosen according to the two main criteria of small molecular volume and strong dipole moment.

Synthesis was carried out by action of amines on sulfonic acid chlorides. Details of the reaction (1) differed with the four groups of mono alkyls (a), symetric dialkyls (b), non symetric dialkyls (c) and sultames (d) :

$$R^1SO_2Cl + H_2NR^2 \xrightarrow{BOH} R^1SO_2NHR^2 + B\,Cl \qquad (a)$$

$$R^1SO_2Cl + HNR_2^2 \xrightarrow{BOH} R^1SO_2N\,R_2^2 + B\,Cl \qquad (b)$$

$$R^1SO_2Cl + H_2NR^2 + R^3X \xrightarrow{BOH} R^1SO_2N\begin{smallmatrix}R^2\\R^3\end{smallmatrix} + B\,Cl + BX \qquad (c)$$

$$Cl\!\left(CH_2\right)_n\!\!\diagdown SO_2Cl + H_2NR \rightarrow \left(\left(CH_2\right)_n\right)N - SO_2 \;\; (R) \qquad (d)$$

with : B = Na or K,
X = F, Cl or Br
and : n = 3 or 4.

PHYSICAL PROPERTIES.

Sulfonamides meet the necessary requirements of high boiling point, high density and relatively low "working temperature", the "working temperature" corresponding to a viscosity of 2 cP as evaluated by RENON et al.(2) from a literature survey of commercial liquid-liquid extraction processes.

All the sulfonamides tested exhibit a sufficiently high thermal stability. They become colored, from pale yellow to dark brown, after long periods of heating at 150°C but without any noticeable change of their infrared spectra.

Corrosivity seems very low. Ordinary steel can be used with DMESA even in aqueous solutions as long as the pH remains above 9.

TOXICITY.

Toxicity is small, between those of the most frequent solvents diethylene glycol and sulfolane.

EXTRACTIVE PROPERTIES.

The two relevant extractive properties, solvent power for aromatics and selectivity for the aromatics-paraffins separation, were estimated from experimental determinations of activity coefficients at infinite dilution and liquid-liquid equilibria. Continuous extraction runs were made on a laboratory scale packed column with two selected sulfonamides. Sulfolane (3,4), the often used commercial solvent, was used as reference.

Activity coefficients at infinite dilution. Activity coefficients at infinite dilution were obtained with an inert gas stripping techniques derived from that proposed by LEROI et al.(5).

(a) Monoalkyls (b) Symetric dialkyls (c) Non symetric dialkyls (d) Sultames		Ebullition temp(°C/ mmHg)	Density (20°C)	Viscosity (cSt, 50°C)	Temp(°C)at viscosity 2 cP
N-methyl methane sulfonamide	MMSA (a)	~100/0.1	1.257	4.01	75
N-methyl ethane sulfonamide	MESA (a)	"	1.201	4.34	80
N-ethyl methane sulfonamide	EMSA (a)	"	1.196	3.83	75
N-ethyl ethane sulfonamide	EESA (a)	"	1.150	5.49	85
N-propyl methane sulfonamide	PMSA (a)	"	1.144	6.16	90
NN-diethyl methane sulfonamide	DEMSA(b)	125/20	1.145	2.36	60
NN-dimethyl ethane sulfonamide	DMESA(b)	80/1	1.141	2.20	60
NN-diethyl ethane sulfonamide	DEESA(b)	85/1.4	1.073	2.18	60
N-ethane sulfonyl pyrrolidine	ESPY (b)	90/0.3	1.178	3.55	100
NN-dialkyl methane sulfonamide	DAMSA(b)	80/0.01	1.093	2.67	65
NN-methylallyl methane sulfonamide	MAMSA(c)	68/0.01	1.128	1.98	55
NN-methyl ethyl methane sulfonamide	MEMSA(c)	73/0.65	1.141	2.44	55
N-ethyl propane sultame	EPS (d)	88/0.1	1.214	3.57	80
N-methyl butane sultame	MBS (d)	90/0.2	1.248	10.77	90
N-ethyl butane sultame	EBS (d)	105/0.3	1.185	6.18	75-80

List of sulfonamides with their physical properties

Figure 1 shows the relationship at 50°C between selectivity and solvent power respectively measured by the ratio of the activity coefficient ($\gamma\infty$) of dimethyl 24 pentane (D24P) to that of benzene (BZ) and the reciprocal of the benzene activity coefficient. As for other solvents selectivity decreases with an increase in solvent power (3). Sulfolane occupies a position of high selectivity and average solvent power.

Sulfonamides rating was pursued at the previously mentioned practical viscosity of 2 cP. The transformation of the selectivity-solvent power diagram from 50°C to 2 cP resulted from a study of the variations of $\gamma\infty$ as a function of temperature. As demonstrated on Figure 2 for DMESA these variations are correctly described by simple thermodynamics formula :

$$\ln \gamma\infty = A + \frac{L^\infty}{R.T}$$

where : A = constant,
L^∞ = molar heat of solution of the given hydrocarbon at infinite dilution in the solvent,
R = gas constant,
T = absolute temperature.

Figure 3 illustrates the correlation between L^∞ and $\gamma\infty$ at 50°C established with data on the hydrocarbons-n-heptane, dimethyl 24 pentane, n-hexane, cyclohexane, toluene and benzene at infinite dilution in sulfolane, DMESA and DEMSA. The correlation led to the classification of Figure 4. In this new classification selectivities become smaller and solvent powers larger. Selectivity changes are the most pronounced with solvents having a "working temperature" greater than 90°C such as PMSA, ESPY, MBS and sulfolane (120°C).

Sulfonamides cover a very wide range of extractive properties from MMS with high selectivity but low solvent power to the group DEMSA/EBS/DAMSA with low selectivity and high solvent power. The most attractive sulfonamides are MEMSA, EPS and DMESA.

Liquid-liquid equilibria. The classification according to liquid-liquid equilibria agrees with that deduced from activity coefficients at infinite dilution. Figures 5 and 6 compare as examples the distribution curves and the selectivity diagrams of DMESA at 35°C (3.2 cP) to those published by De FRE and VERHOEYE (6) on sulfolane at 100°C (2.5 cP). As expected the distribution coefficients are greater and the selectivity diagrams maxima smaller with DMESA than with sulfolane.

Extraction runs on a laboratory scale packed column. Counter current extractions at 35°C on a 2 cm diameter glass column packed with 0.5 cm RASCHIG rings demonstrated the characteristics of DEMSA and DMESA by comparison with sulfolane. Figure 7 shows that DEMSA and DMESA need much smaller solvent to feed ratios to minimize the concentration of aromatics in the raffinate. Figure 8 confirms that the excellent capacity for aromatics is partly counterbalanced by a lower selectivity.

PROCESS DESIGN.

A liquid-liquid extraction column fed with DMESA was simulated (7) with a 16-parameter NRTL thermodynamic equation (8). The simulation was included (9) in a flowsheeting computer model of a process similar to the one used for sulfolane (4) where the extract is treated in an extractive distillation column to reject the saturates recycled as reflux into the extractor. Economics considerations (9) suggest that such a scheme could be replaced by another where the solvent is purified by extraction with a counter-solvent.

CONCLUSIONS.

Alkylsulfonamides seem an attractive solvent family for light aromatics extraction from petroleum fractions. The most promising are MEMSA, EPS and DMESA.

REFERENCES.

1. "Etude des sulfonamides utilisées comme solvants d'extraction des aromatiques", Compte rendu de fin d'études.Aide DGRST n° 78-7-0862 (Oct.1979).
2. H.RENON, C.RAIMBAULT, P.JEANJEAN and J.C.ROSADO, 8th World Petroleum Congress, PD(13)(2)(1975).
3. C.H.DEAL and E.L.DERR, I & E.C-P.D.D 3,n°4,394 (1964).
4. H.VOETTER and W.C.G.KOSTERS, 6th World Petroleum Congress, Frankfurt am Main Section III, paper 11 (1963).
5. J.C.LEROI, J.C.MASSON, H.RENON, J.F.FABRIES and H.SANNIER, I & E.C.-P.D.D, 16, n° 1,139 (1977).
6. R.M.De FRE and L.A.VERHOEYE, J.Appl.Chem.Biotechnol.,26,469 (1976).
7. R.LOUTATY, C.YACONO, M.ATLANI and C.WAKSELMAN , 3rd Int.Congress Computer and Chemical Engineering, Paris, paper 38 (1983).
8. H.RENON, L.ASSELINEAU, G.COHEN et C.RAIMBAULT, "Calcul sur ordinateur des équilibres liquide-vapeur et liquide-liquide",TECHNIP (1971).
9. Y.GERMAIN,"Contribution à l'étude de l'extraction des aromatiques des reformats par le N,N diméthyl éthane sulfonamide,Thèse CNAM,Le Havre, 1982.

ACKNOWLEDGMENTS.

The authors are grateful to Mr.COUDERC, Directeur de TOTAL TECHNIQUE, for permission to publish this paper. They wish to thank Mr.ATLANI and Mr.WAKSELMAN, Laboratoires du CNRS-CERCOA, who contributed to this research by synthesizing the alkylsulfonamides.

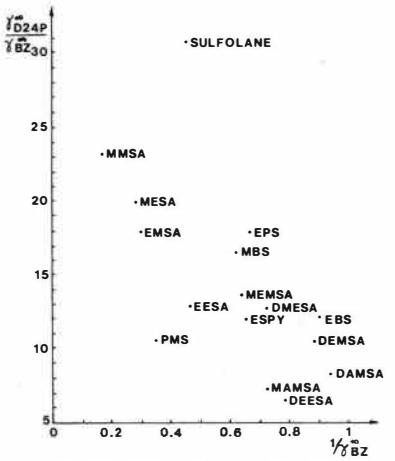

FIGURE 1. SELECTIVITY VS. SOLVENT POWER AT A TEMPERATURE OF 50°C FOR ALL SOLVENTS

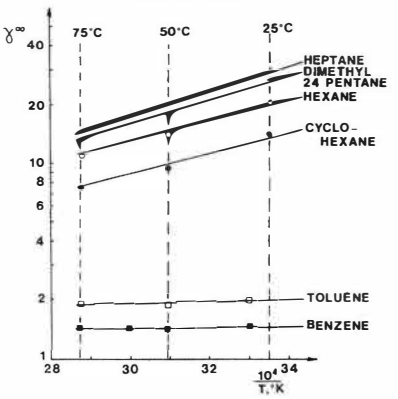

FIGURE 2. ACTIVITY COEFFICIENTS IN DMESA AS A FUNCTION OF TEMPERATURE

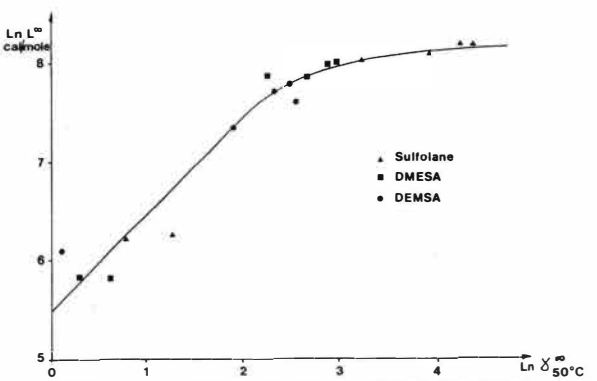

FIGURE 3 MOLAR HEAT OF SOLUTION VS. ACTIVITY COEFFICIENT

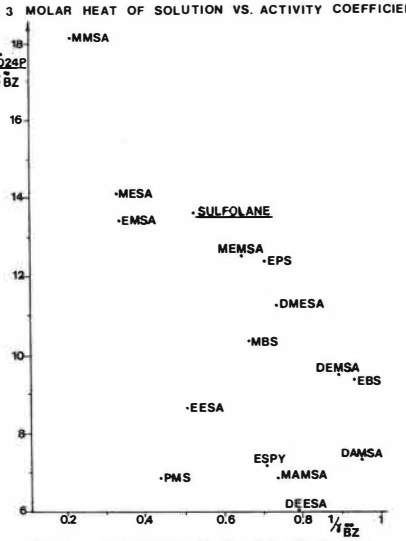

FIGURE 4. SELECTIVITY VS. SOLVENT POWER AT A VISCOSITY OF 2cP FOR ALL SOLVENTS

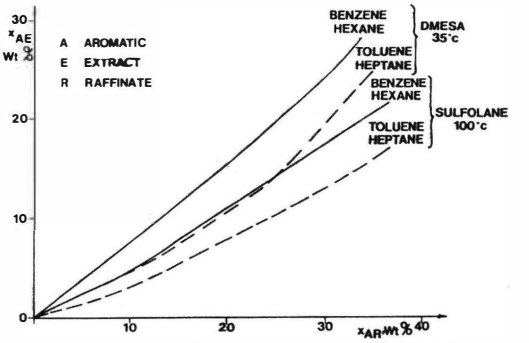

FIGURE 5. DISTRIBUTION CURVES OF BENZENE AND TOLUENE WITH SULFOLANE AND DMESA

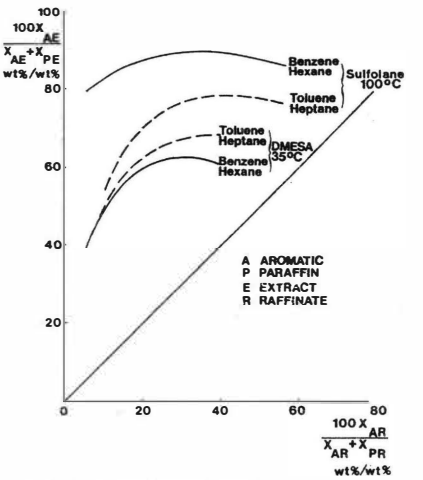

FIGURE 6. SELECTIVITY DIAGRAMS OF BENZENE AND TOLUENE WITH SULFOLANE AND DMESA

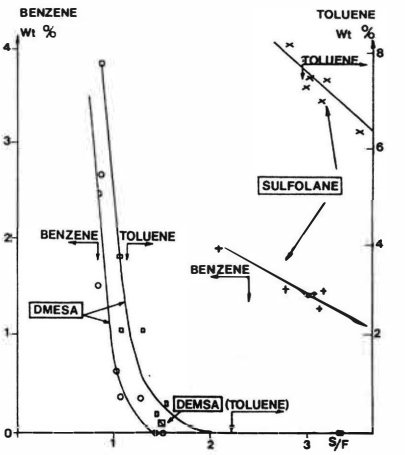

FIGURE 7. AROMATICS IN RAFFINATE VS. SOLVENT TO FEED WEIGHT RATIO

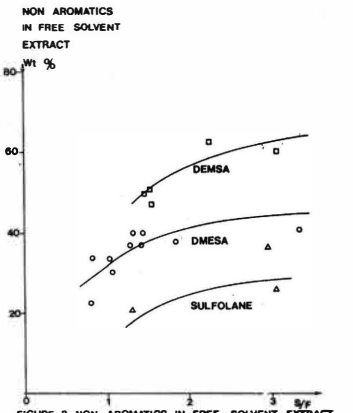

FIGURE 8. NON AROMATICS IN FREE SOLVENT EXTRACT VS. SOLVENT TO FEED WEIGHT RATIO

SOLVENT EXTRACTION OF AROMATICS BY ALKYLENE CARBONATES

M. Cristina Annesini and Luigi Marrelli
Cattedra di Principi di Ingegneria Chimica
Università di Roma, Italia

Robert De Santis
Istituto di Chimica Applicata e Metallurgia
Università di Cagliari, Italia

Ireneo Kikic
Istituto di Chimica Applicata
Università di Trieste, Italia

Alkylene carbonates (AC) are indicated in several patents as good solvents for a variety of industrial separations(1), but published phase equilibrium data are scarce.

This communication is concerned with the results obtained in the experimental determination of equilibrium properties for liquid systems containing hydrocarbons and AC. Our scope is to evaluate the solvent properties of AC in the extraction of aromatic compounds from hydrocarbon mixtures.

The solvents considered are propylene carbonate and chloropropylene carbonate. The latter one, which is not commercially available, was obtained in our laboratory from carbon dioxide and epichloridrine on ion-exchange resins. The hydrocarbons are those of the paraffinic, aromatic, olefinic and naphtenic series with 6-8 carbon atoms.

EXPERIMENTAL DETERMINATIONS

A first set of data includes the infinite-dilution activity coefficients of several hydrocarbons in AC measured at various temperatures by the gaschromatografic method (2). These data are useful to obtain some preliminary information about the separability of aromatics from other hydrocarbons.

A deeper analysis was carried out by determining liquid-liquid equilibria at 20°C of ternary aromatic-paraffin-AC systems.

In order to predict or correlate this ternary equilibria it is important to get information on the excess free energy of the mixture's constituent binaries. To this end vapor-liquid equilibria of aromatic-AC mixtures (3) and liquid-liquid equilibria of paraffin-AC systems were also measured.

Data reduction of vapor liquid equilibria gives the activity coefficients at temperatures higher than those (20° - 30°C) concerning the ternary equilibria and the infinite-dilution activity coefficients. Therefore excess enthalpies of the binaries aromatic-AC were measured to study the temperature dependence of the excess free energy (3).

SOME COMMENTS ABOUT DATA

A complete report of the results and the correlation of data will be given in the oral presentation. In this summary we make some preliminary comments, mainly based on the infinite-dilution activity coefficients. These considerations reflect only the point of view of the equilibrium, whereas an analysis of the effectiveness of AC as solvents must take into account other physical and chemical properties and economic parameters; but these aspects are beyond the scope of our work.

Some values of γ^{∞} in the solvents considered here are reported in the plots of Figures 1 and 2.

Table 1 reports some values of the selectivity $\beta_{i,B}$ with respect to benzene and of the solvency x_B^c (mol fraction solubility of benzene). These parameters are defined and calculated as follows:

$$\beta_{i,B} = \frac{x_i^H/x_B^H}{x_i^c/x_B^c} \simeq \gamma_B^{c,\infty}/\gamma_i^{c,\infty}$$

$$x_B^c \simeq 1/\gamma_B^{c,\infty}$$

Table 1. Solvency and selectivity with respect to benzene at 25°C.

	propylene carbonate	chloropropylene carbonate
Solvency	0.26	0.22
Selectivity		
- hexane	13.4	21.6
- hexene	6.0	10.4
- cyclohexane	7.3	10.7

The table shows excellent values of $\beta_{i,B}$ for the chloropropylene carbonate and a fairly good value of the solvency for the propylene carbonate. We choose propylene carbonate, which is commercially available, as solvent in the measurements of ternary liquid-liquid equilibrium.

Table 2 reports a comparison between the values of $\beta_{i,B}$ and x_B of AC and those of the most common solvents (4).

Table 2. Selectivity hexane-benzene and solubility of benzene in several solvents at 25°C.

	$\beta_{H,B}$	x_B
Sulfolane	30.5	0.42
Dimethylsulfoxide	22.0	0.29
N-Methylpyrrolidone	12.5	1.00
Dimethylformamide	12.5	0.71
Acetonitrile	9.4	0.37
Triethylene glycol	13.0	0.21
Furfural	10.9	0.38
Propylene carbonate	13.4	0.26
Chloropropylene carbonate	21.6	0.22

An exhaustive comparison of solvent properties of AC with those of other solvents can be made on the basis of ternary liquid-liquid equilibria for the solvent-paraffin-aromatic systems.

These data can be used to evaluate the composition dependence of the selectivity and of the solvency as well as to calculate the extraction operation.

To this purpose we measured several liquid-liquid equilibria of the ternary systems. Figure 3 shows the case of the propylene carbonate-toluene-heptane system. The binodal solubility curve is calculated by correlating with the NRTL equation (5) the ternary activity coefficients. The values of parameters are:

$\alpha = 0.3$

$(g_{AB}-g_{AA})/R = 1128$ K $\qquad (g_{AB}-g_{BB})/R = 2133$ K

$(g_{BC}-g_{CC})/R = 8$ K $\qquad (g_{BC}-g_{BB})/R = 523$ K

$(g_{AC}-g_{AA})/R = 417$ K $\qquad (g_{AC}-g_{CC})/R = -316$ K

These binary constants were calculated, as adjustable parameters, from ternary data, in order to obtain a good accuracy in evaluating selectivity and solvency.

However we also followed the procedure to predict the ternary equilibrium with parameters calculated from binary data. Figure 4 shows results obtained in the reduction of our vapor-liquid equilibrium data for the propylene carbonate-toluene system. In this case the values of adjustable parameters are:

$(g_{BC}-g_{CC})/R = 11$ K $\qquad (g_{BC}-g_{BB})/R = 600$ K

REFERENCES

1. M.C.Annesini, R.De Santis, L.Marrelli, I.Kikic, paper presented at the Congress "Ottenimento ed elaborazione dei dati per la progettazione di impianti chimici", Palermo, Italy, 26-28 sept. 1979.
2. D.H.Desty, W.T.Swanton, J. Phys. Chem., 65, 776 (1961).
3. M.C.Annesini, R.De Santis, I.Kikic, L.Marrelli, submitted for publication to J. Chem. Eng. Data.
4. C.H.Deal and E.L.Derr, Ind. Eng. Chem. Proc. Des. Dev., 3, 394, (1964).
5. H.Renon and J.M.Prausnitz, AIChE Journal, 14, 135 (1968).

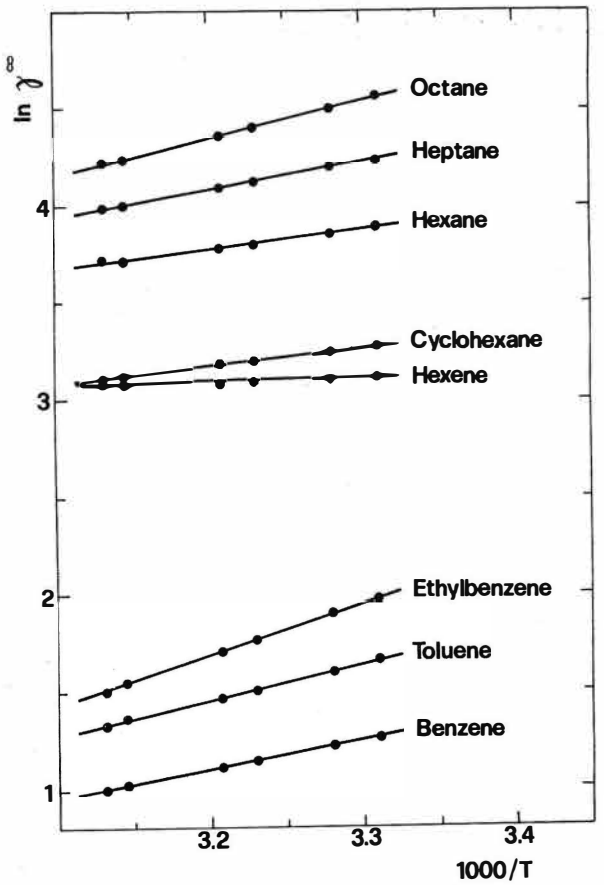

FIGURE 1. INFINITE-DILUTION ACTIVITY COEFFICIENTS IN PROPYLENE CARBONATE.

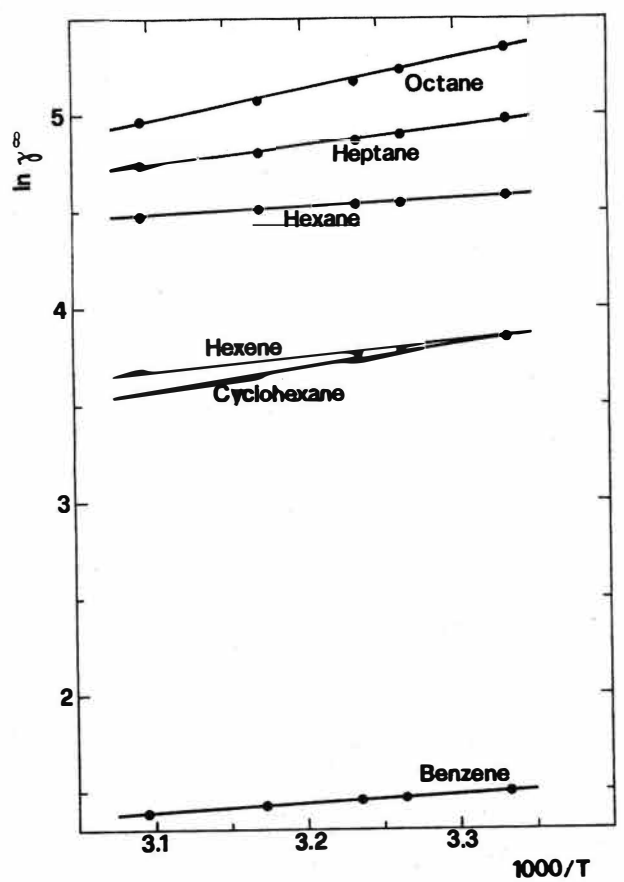

FIGURE 2. INFINITE-DILUTION ACTIVITY COEFFICIENTS IN CHLOROPROPYLENE CARBONATE.

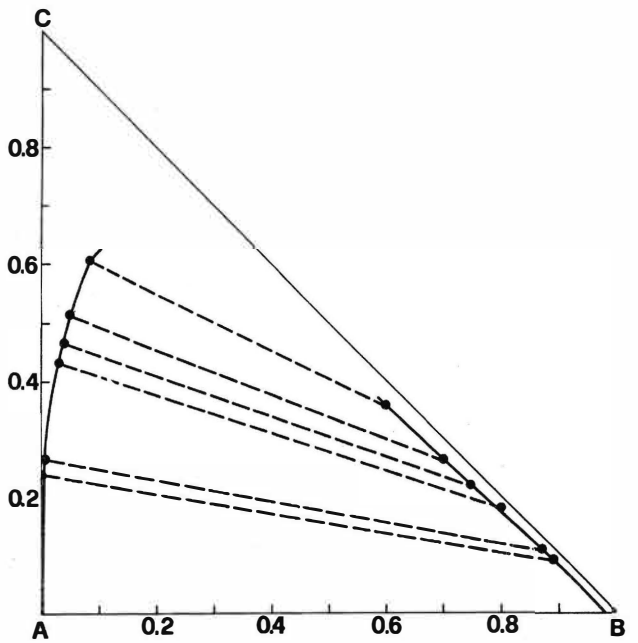

FIGURE 3. LIQUID-LIQUID EQUILIBRIUM FOR THE SYSTEM HEPTANE (A)- PROPYLENE CARBONATE (B) - TOLUENE (C) AT 20 C.

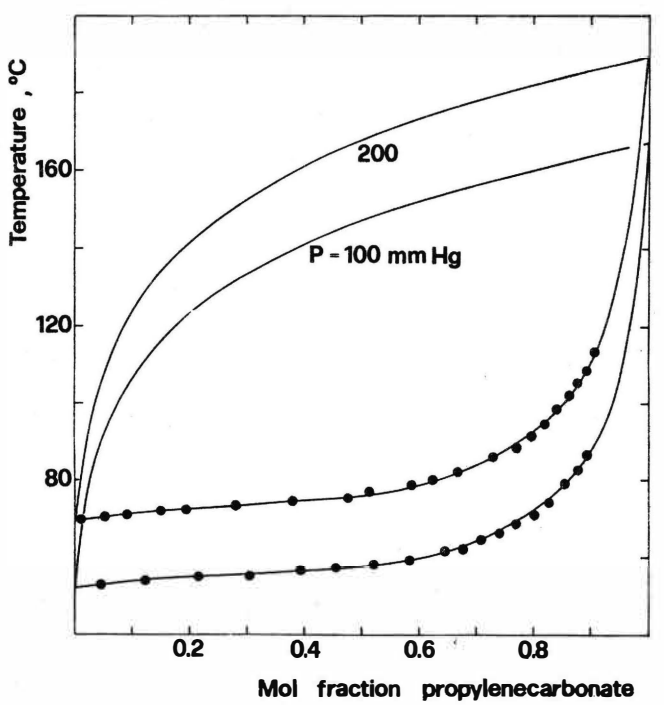

FIGURE 4. VAPOR-LIQUID EQUILIBRIUM FOR THE SYSTEM PROPYLENE CARBONATE-TOLUENE.

ACID EXTRACTION BY AMINES

M. Siebenhofer, R. Marr

Institute of Chemical Engineering
Technical University Graz
Graz, Austria

The recovery of carboxylic acids from aqueous waste by extraction-processes with chemical reaction shows an increasing technological importance. Opposite to the use of conventional solvents the mass transfer determining component, an amine, can't be used as a pure substance, as this would cause hydrodynamic troubles. Therefore you have to solute the amine in a diluent. Further the addition of modifier is necessary.
About the choice of the amine to be used as reactive component of the solvent a lot of data is reported (1,2,3,1). For given ratios of various diluent to amine contents of the solvent the influence on the distribution ratio is reported too.
Although the chemical reaction of the mass transfer can be formulated and the process can be described by the Law of Mass Action (5), there is no analytical relation known with which the liquid-liquid-distribution would be formulated by an equation. But for to compare the quantitative influence of the components of the solvent on the mass transfer behavior, it is necessary to find a mathematical description of the whole equilibrium curve.
As the distribution coefficient of a liquid-liquid-equilibrium for an extraction process with chemical reaction variies, the common way of description by the Nernst distribution law, won't be a good instrument for the comparison of the influence of the components on mass transfer.
The extraction of an acid by an amine occurs as follows:

$$1)\quad nH^+ + nA' + R_3N \rightleftharpoons R_3N(HA)_n$$

According to the law of Mass Action the equilibrium constant is defined as follows:

$$2)\quad K = \frac{(R_3N(HA)_n)_{org}}{(H^+)^n \cdot (A')^n \cdot (R_3N)_{org}}$$

With

$$3)\quad (R_3N(HA)_n)_{org} = (HA)_{org}/n$$

and

$$4)\quad R_3N_{org} = (R_3N)_{org,0} - (HA)_{org}/n$$

equation 1 becomes

$$5)\quad K = \frac{(HA)_{org}}{n.(H^+)^n.(A')^n.((R_3N)_{org,0} - (HA)_{org}/n)}$$. With

$$6)\quad \frac{(H^+)\ .\ (A')}{(HA)} = K_{DISS}$$

equation 5 can be transformed into

$$7)\quad K = \frac{(HA)_{org}}{n.(K_{DISS}.(HA))^n.((R_3N)_{org,0} - (HA)_{org}/n)}$$

Solving equation 7 by expressing the equilibrium concentration of the extracted acid as a function of the other parameters you get with the simplification

$$8)\quad (HA)_{org} = c_{org}$$

and

$$9)\quad (HA)_{aqu} = c_{aqu}$$

$$10)\quad c_{org} = \frac{n.(R_3N)_{org,0}.K.K^n_{DISS}.c^n_{aqu}}{1 + K.K^n_{DISS}.c^n_{aqu}}$$

By substituting $K.K^n_{DISS} = d$ the final equation becomes

$$11)\quad c_{org} = \frac{n.d.(R_3N)_{org,0}.c^n_{aqu}}{1 + d.c^n_{aqu}}$$

Equation 11 is similiar to the description of adsorption equilibria by Langmuir isothermes. With equation 11 it is possible to describe the equilibrium curve, although the dissociation as well as the activity coefficients of the acid in the aqueous phase are not considered.
The transformation of the component-dependend parameters into the association constant n and the defined extraction constant d enables the research worker to quantify the influence of the various components of the solvent on mass transfer.
Based on these fundamentals experimental investigations on acid extraction by amines were done.

As will be described later, the first representatives of the carboxylic acids, formic acid, acetic acid, propionic acid and butyric acid have been investigated.
The experiments were carried out with tertiary amines of technical grade as active component, isodecanol as modifier and Shellsol T as diluent.
The experiments were carried out in 100 ml shaking funnels. The quantitative determination of the investigated acids was made by titration with sodiumhydroxid at a Titroprocessor of the Metrohm AG, type E 636/100.

As shown in Fig.1 the distribution coefficients of the carboxylic acids when being extracted with pure triisooctylamine don't show a single trend of increasing or decreasing behavior with acetic acid showing the greatest deviation at lower aqueous equilibrium concentrations. This phenomenon, already observed by J.Bullock (6) contradicts the qualitative trend of the homologous series. A possible explanation for this deviation might be given by considering the distribution behaviour of multicomponent extraction with chemical reaction (7). Then the mechanism of extraction at lower aqueous feed concentration would differ from the mechanism at higher feed concentration.
Actually this distribution behavior won't be a good premise for the construction of a complete extraction process. But as can be seen from Fig.2 this deviation can be completely suppressed, when modifier is added to the solvent. For the considered extraction problem isodecanol, manufactured by Hoechst AG, was used as modifier. Although the addition of modifier to the active component of the solvent (the amine) is not necessary for to correct the hydrodynamic behavior of the solvent mixture or for to prohibit the formation of a second organic phase layer, it is an economical condition cause of its influence on the equilibrium at low acid feed concentration.

A further problem, which has to be considered, is the decision, what amine to use. As discussed above, tertiary amines with branched alkylsubstituents can be a possible choice. According to the relation between the chemical structure of the alkylsubstituents and the base strength, one would expect, to make a good choice, when using tertiary amines with linear alkylsubstituents.
As shown in Table I the extraction coefficient d is higher, when tri-n-decyl/n-octylamine (Hostarex A 327, manufactured by Hoechst AG) is used as mass transfer-determining component of the solvent, while the association constant n is higher for the branched product triisooctylamine (Hostarex A 324, manufactured by Hoechst AG).
Considering the influence of the constants n and d on the phase

equilibrium, as expressed by equation 11, it is an economical advantage to use solvents which cause a higher association constant n than extraction constant d, if the extracted acid is separated from the solvent by distillation or thermal reextraction on general.

For a succesful construction of the best solvent composition two experimental facilities are given.

On the one hand, the liquid-liquid-equilibria of the pure substances of the solvent can be worked out. After having calculated the equation constants n and d based on the solution of equation 11, the wanted content of the reactive component of the solvent can be determined.

Although this method causes a lower experimental expense, you won't get good results for the description of the equilibrium curve as equation 11 does not consider the influence of the modifier and the diluent. Experimental results show, that the association constant only slightly depends on the concentration of the amine, while the extraction constant d is a nonlinear function of the concentration of all the added components. Furthermore this method does not consider the synergetic effect of the additives on the equilibrium behavior.

Therefore it is better to use a differential method for the construction of the solvent by investigating the altering of the equilibrium curve, when having added a small amount of one of the solvent components to an investigated mixture.

Several investigations of acid extraction problems showed, that the optimum solvent composition will be given by adding a maximum content of modifier and amine to the solvent mixture. But the content of both the compounds is limited by hydrodynamic conditions such as the coalescence time. For the investigated amines and the modifier isodecanol the upper concentration limit of each of the compounds is about 30 vol%.

Based on these informations, extraction processes for the recovery of formic acid and acetic acid were performed. Pilot plant experiments with both the acids gave promising results for an extractive recovery of carboxylic acids from aqueous solutions.

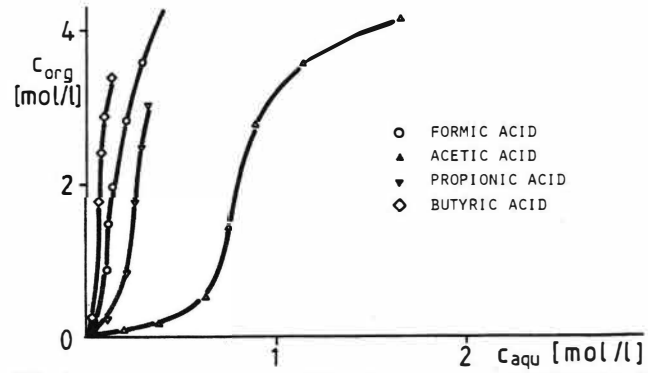

FIG. 1: LIQUID-LIQUID-EQUILIBRIUM FOR THE SYSTEM H_2O/HOSTAREX A 324/ CARBOXYLIC ACID; T = 20°C

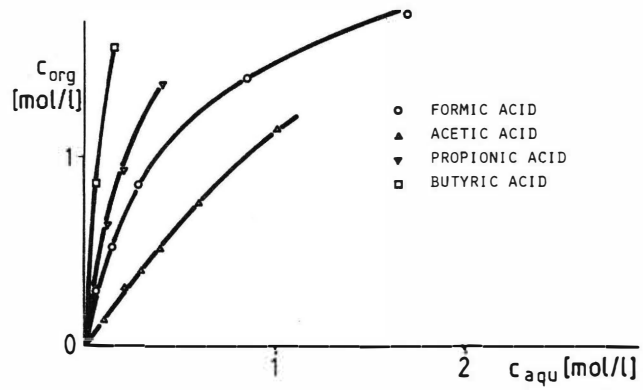

FIG. 2: LIQUID-LIQUID-EQUILIBRIUM FOR THE SYSTEM H_2O/SOLVENT/ CARBOXYLIC ACID; SOLVENT: 30 VOL% HOSTAREX A 324, 30 VOL% ISODECANOL, 40 VOL% SHELLSOL T; T = 20°C

NOMENCLATURE

A' ..... anion
c ..... concentration (mol/l)
d ..... extraction constant
H^+ ..... proton
HA .... acid
K ..... equilibrium constant
n ..... association constant
R_3N ... tertiary amine

INDICES

A 324 ..... Hostarex A 324 (triisooctylamine)
A 327 ..... Hostarex A 327 (tri-n-decyl/n-octylamine)
aqu ..... aqueous
DISS ..... dissociation
n ..... stoichiometric coefficient
O ..... feed

REFERENCES

1. J.M. Wardell, C.J. King, J. Chem. Eng. Data, 23(2),144 (1978)
2. N. L. Ricker, J. N. Michaels, C. J. King, J. Separ. Proc. Technol., 1(1), 36 (1979)
3. N.L. Ricker, E.F. Pittman, C.J. King, J. Separ. Proc. Technol., 1(2), 23 (1980)
4. C.J. King, ISEC 80, Liege, paper 80-66
5. V.S. Shmidt, Amine Extraction, Israel Program for Scientific Translations, Jerusalem, 1971
6. J. Bullock, J. Phys. Chem., 68, 2687 (1964)
7. W. Rueckl, Thesis, TU Graz (in edition)

Table I: Comparison of n and d for the reactive components Hostarex A 324 and Hostarex A 327

acid	n_{A324}	n_{A327}	d_{A324}	d_{A327}
formic	3.25	3.18	2.93	7.51
acetic	3.16	0.73	0.81	10.84
propionic	2.79	0.62	4.25	34.15

EXTRACTION OF COPPER FROM SULPHATE AQUEOUS SOLUTION BY OXIME TYPE EXTRAGENSES

A. Kostić-Pulek

Faculty of Mining and Geology
Belgrade, Yugoslavia

The extraction process of copper from sulphate solutions with two chelate extragenses of the oxime class has been investigated. The used extragenses were produced by the Acorga Company(England) and their trademarks are P-5100 and P-5300.Both these reagents contain the same active molecules,2 hydroksi,5nonylsalicilaldoxime in the admixture with 4-nonyl phenol.In the case of P-5100 extragens the mix ratio of oxime to nonyl phenol is 1:1(by weight) and for P-5300extragens the ratio is 1:3(by weight).

The method of continuous variation and slope analysis were used(L1)to determinethe stoichiometry of complex formed and the both confirmed 2:1 ratio(ligand:metal).

Experiments were performed at.293,303 and 323 K and they ilustrated negligable influence of temperature on the extraction process in that temperature range.

The selectivity of these extragenses over metals other than copper(Co^{2+},Ni^{2+},Fe^{3+} and Zn^{2+})was investigated.The obtained results confirms the satisfaid selectivity at the pH of real copper leach solution.

From extraction isotherms the thermodynamic equilibrium constants were calculated.(L2).In these experiments the aqueous phase was made from $CuSO_4$ and H_2SO_4in such a way to obtain constant ionic strenght of 0,0125M.Calculated thermodynamic equilibrium constant are compared with thermodynamic equilibrium constant for pure extragens ,without addition of 4-nonyl phenol(trademark P-1).It's constant was determined at the same conditions and by the same method(L3).

organic phase	
0,025M P-1 in CCl_4	K^o=91,30
0,025M P-5100 in CCl_4	K^o=82,10
0,025M P-5300 in CCl_4	K^o=76,13

According to the obtained results it seems that the effect of presence of 4-nonyl phenol cause some weakening of extractive power of reagent and lowering the thermodynamic equilibrium constant K^o for the reaction of extraction.It seems that the 4-nonyl phenol has an effect on the chemical activities of some species involved in the extraction reaction.

1.Y.Marcus and A.Kertes,Ion exchange and solvent extraction of metal complexes,John Wiley and Sons Ltd.London(1969)
2.Dj.Petković and A.Ruvarac,A new method for the determination of thermodynamic equilibrium constants in separatipn process,J. Radioanalitical Chem.,21,31(1:74)
3.Z.Maksimović and A.Ruvarac and A.Kostić-Pulek,Extraction of copper from sulphate aqueous solution by oxime type extragenses, Proceeding of October's meeting,Bor,2,416(1978)

EXTRACTION OF ANTIMONY AND ARSENIC FROM COPPER REFINING ELECTROLYTE

Jeffrey M. Cohen

Merck, Sharp and Dohme Research Laboratories
Rahway, New Jersey USA

INTRODUCTION

Due to more stringent rules on the capture of particulate matter in copper smelters and the processing of increasing amounts of complex ores, more arsenic and antimony is finding its way downstream into electrolytic copper refineries. Much of this greater input manifests itself in higher concentrations of these elements in copper refining electrolyte.

Solvent extraction has been investigated as a means of removing antimony and arsenic from the electrolyte itself. The extraction systems have involved organophosphorous compounds diluted with of dissolved in aliphatic organic solvents such as kerosine. Schulze and Reinhold (1) found that various acidic phosphate esters could be effective in removing antimony from copper electrolyte, but would not extract arsenic. Giganov et al (2) determined that arsenic could be extracted from copper electrolyte by tri-n-butyl phosphate, but that antimony would not be removed. Reagents have been found that can be used to extract either arsenic or antimony, this paper deals with a reagent that can remove both elements simultaneously from copper electrolyte and from which arsenic and antimony can be stripped separately.

Aliquat 336, a quaternary amine chloride, has been most notably applied as a phase transfer catalyst. There is also a considerable body of work on Aliquat 336 as a liquid ionexchange reagent, primarily in the extraction of Fe, Zn, Cd, Co and Cu from aqueous chloride solution. In this work, it will be shown how Aliquat 336 can be used to extract arsenic and antimony from copper refining electrolyte.

PROCEDURE

A stock solution of 'simulated' copper electrolyte was made up to contain:

Cu	40 g/l
Ni	12 g/l
As	12 g/l
Sb	0.4 g/l
H_2SO_4	125 g/l

and stored at 60°C. Reagent grade chemicals were used for all constituents. Arsenic and antimony were dissolved as their trioxides.

The extractant was Aliquat 336, obtained fron Henkel Corp., as a 40% (by volume) solution with 2-wthyl-Hexanol.

The extractions were performed by vigorously shaking measured amounts of organic and aqueous phases together in a separatory funnel for 5 minutes. The phases were then allowed to disengage. The aqueous phase was separated and analyzed for the several cationic constitutent.

RESULTS

Two series of experiments were run, the first set to obtain extraction isotherms for antimony and arsenic and the second to obtain antimony and arsenic balances over ten load-strip cycles.

Figures 1 and 2 give the extraction isotherms for antimony and arsenic respectively, between the aqueous copper electrolyte and Aliquat 336 dissolved in 2-ethyl hexanol.

Figure 3 shows the distribution of arsenic between the loaded Aliquat 336 phase and 0.5N H_2SO_4. Antimony is not stripped from Aliquat by dilute sulfuric acid, but is subsequently recovered by contacting the organic phase with 5% by weight aqueous NH_4OH. Thus, arsenic and antimony are simultaneously extracted from the electrolyte by Aliquat 336 qnd separated by stripping the organic phase first with dilute H_2SO_4 followed by dilute aqueous ammonia. Since aqueous ammonia will strip arsenic as well as antimony from Aliquat 336, it is necessary to perform the acid stripping before the ammonia stripping in order to achieve this separation.

Table 1 shows the results of 10 load strip cycles.

DISCUSSION

The separation of arsenic from antimony in the stripping operation brings up the possibility of recovering the arsenic as a potentially salable product, tetracupric arsenate, and for the recovery of antimony as a solid product.

Figure 4 is a block flow diagram of a process using Aliquat 336 to remove antimony and arsenic from copper refining electrolyte and the subsequent recovery of arsenic and antimony. The arsenic bearing acid from stripping has $CuSO_4$ added to it prior to neutralization with ammonia and air oxidation, precipitating tetracupric arsenate. The antimony bearing base is neutralized, precipitating Sb_2O_3. Soluable ammonium salts can be recovered by evaporative crystallization.

Beyond the inherent potential of Aliquat 336 as the basis of a new copper electrolyte purification process, there is contained within this data implications on the ionic forms of arsenic and antimony which point to some further applications of quaternary amine chlorides in hydrometallurgy.

There exists a considerable body of data on the extraction of various metal ions from acid chloride solutions using quaternary amine chlorides. The metals studied form anionic chloride complexes in these solutions, thus it would appear that in extraction from acid chloride solution, the quaternary amine chloride acts as a liquid anion exchanger. Support for this point of veiw may be found in Brinkmann et al (3) who studied the ultraviolet spectra of the metal-organic complexes formed in extracting metals from acidic chloride solutions by quaternary amine chlorides. They determined that the extracted species for Zn (II), Cd (II), Co (II) and Cu (II) was of the form MCl_4^{-2}.

Since Aliquat 336 has anion exchange properties, the ion species it will extract will be anions, which implies that, in the simulated copper refining electrolyte used in this study, arsenic and antimony are in the form of anionic complexes. Antimony is known to form anionic complexes in strong H_2SO_4 solutions (4). Trivalent antimony forms the oxoanion $SbOSO_4^-$ in 1 to 18 molar sulfuric acid and pentavalent antimony forms $Sb_3O_9^{-3}$ in the same range of sulfuric acid concentration. However, there is no similar form known for arsenic.

CONCLUSIONS

Quaternary amine chlorides show good activity in extraction of antimony and arsenic from copper refining electrolyte. Since these compounds act as anion exchangers, copper is not extracted from the electrolyte. The arsenic and antimony can be recovered separately by stripping the extractant first with acid then with base.

REFERENCES

1. J.Schulze and G. Reinhold, German Patent No. 2,515,862
2. G.P. Giganov et al, Tsvetne Metally (8), 27-29, 1978
3. U.A.Brinkmann, G. De Vries and E. Van Dalen. Z. Anorg. Allgemeine Chemie, 351, 73-80, 1967
4. F.A. Cotton and G. Wilkinson, " Advanced Inorganic Chemistry ", J. Wiley and Sons, New York, 4th Ed. (1980) pp470 471

Figure 1. Extraction Isotherm for Antimony
System Aliquat 336 in 2-Ethylhexanol-Copper Electrolyte

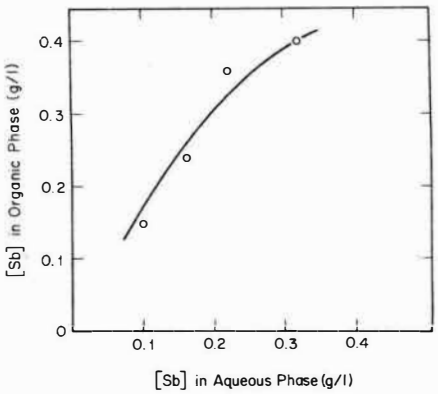

Figure 2. Extraction Isotherm for Arsenic
System Aliquat 336 in 2-Ethylhexanol-Copper Electrolyte

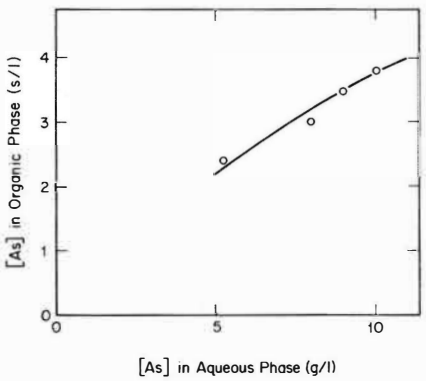

Figure 3. Stripping Isotherm for Arsenic
System Aliquat 336 in 2-Ethylhexanol-0.5 NH_2SO_4

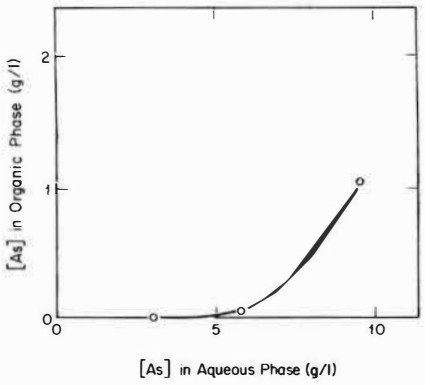

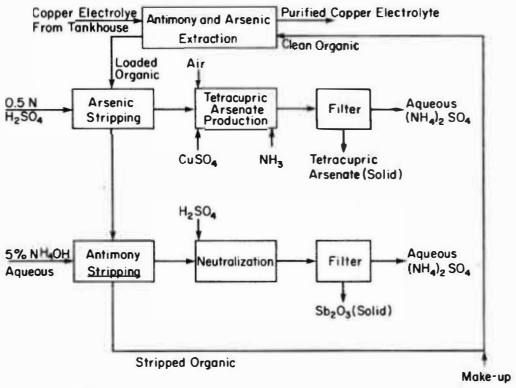

Figure 4. Process for Recovery of Antimony and Arsenic from Copper Electrolyte via Extraction with Aliquat 336

Table 1
Antimony and Arsenic Balances
Basis: 250 ml simulated Cu electrolyte feed to each cycle
all organic:aqueous ratios 1:1

Cycle	Input (g)		Raffinate (g)		NH_4OH Strip (g)	H_2SO_4 Strip (g)
	As	Sb	As	Sb	Sb	As
1	3	0.1	2.3	.044	.045	.68
2	3	0.1	2.2	.047	.048	.75
3	3	0.1	2.1	.044	.055	.65
4	3	0.1	2.1	.045	.055	.7
5	3	0.1	2.1	.047	.05	.8
6	3	0.1	2.1	.045	.06	1.0
7	3	0.1	2.2	.035	.055	.85
8	3	0.1	2.3	.044	.045	.65
9	3	0.1	2.2	.048	.055	.78
10	3	0.1	2.2	.045	.058	.8
Total	30	1.0	21.85	.444	.526	7.66

COPPER-NICKEL SEPARATION FROM AMMONIACAL SOLUTIONS USING HYDROXYOXIMES REAGENTS

Corneille S. Ek

University of Liege
Liege, Belgium

INTRODUCTION

When concentrating copper-nickel ores by flotation, occurences can exist where one of the products is a low grade sulfide concentrate unsuitable for economic smelting and recovery of both metals.

Hydrometallurgy in ammoniacal solutions, possibly by oxidative leaching under Sherritt-Gordon or Arbiter conditions, can be an answer if the metals can be easily separated and recovered from dilute solutions.

In view of selecting the proper reagents for further studies, a preliminary screening has been made with different hydroxyoxime-type reagents, when varying factors such as initial copper concentration in aqueous solution, initial pH, ammonium sulfate content and nickel additions to the ammoniacal copper solution.

Several papers have already been published on this subject (1)(2)(3)(4)(5) but the present contribution tends to survey a greater number of extractants.

EXPERIMENTAL

Results have been obtained by shake-out tests at room temperature, using organic/aqueous ratio of 1/1 throughout; solvents were 10 v/v % solutions in kerosene (with 10 % nonylphenol added for KELEX 100).

Analysis of the aqueous phase was carried out by atomic absorption, and organic metal concentrations were obtained by difference.

INITIAL COPPER CONCENTRATION

First series of tests concerned LIX 65 N, SHELL 529 and KELEX 100. Extraction in the organic phase has been complete in the following conditions, when initial copper aqueous concentration has been 0,5, 1, 2, 4, 6, 8 and 12 g/l :

LIX 65 N : Cu > 2 g/l
SHELL 529 : Cu > 4 g/l
KELEX 100 : Cu > 8 g/l

The second series of tests have been made at 5 g/l Cu_{aq}, with the following solvents : LIX 64 N, LIX 70, LIX 71, LIX 73.

INITIAL pH

Initial pH, varying between 7,5 and 9,1, has practically no influence on the copper recovery factor; final pH has always a higher value than initial pH, but the difference is smaller and smaller when initial pH is higher; this is probably due to the buffering effect of the couple NH_3/NH_4^+.

TABLE 1

Influence of ammonium sulfate additions on copper recovery factor

Reagent	$(NH_4)_2SO_4$ g/l	Cu_{aq}, g/l				
		4	5	6	8	12
KELEX-100	50					82,2
	100					82,2
	200					82,1
SHELL-529	50			77,1	59,0	
	100			75,2	54,9	
	200			74,9	54,7	
LIX 65 N	50	79,4		52,9	43,1	
	100	76,6		49,5	40,3	
	200	75,4		49,1	39,0	
LIX 64 N	50		78,5			
	100		74,2			
	200		72,5			
LIX 70	50		73,4			
	100		69,2			
	200		68,6			
LIX 71	50		72,7			
	100		70,9			
	200		68,4			
LIX 73	50		75,6			
	100		72,9			
	200		68,9			

AMMONIUM SULFATE CONTENT

Ammonium sulfate content has been set up initially at 50, 100 and 200 g/l; the copper recovery factor varies slightly with ammonium sulfate, as shown on Table 1 : the R value always decreases when ammonium sulfate content increases.

Averaging these values, the above results can be plotted in Figure 1; it is shown that, for an aqueous copper content of 5 g/l, the extractants effectiveness appears to follow the decreasing order : KELEX 100, SHELL 529, LIX 64 N, LIX 73, LIX 71, LIX 70 and LIX 65 N.

DISTRIBUTION ISOTHERMS

The distribution isotherms for the different extractants, determined after a 10 min shaking-out, are plotted in Figure 2, which shows that loading capacities follow the same order as recovery factors, but KELEX 100 is significantly better than the 6 other extractants.

INFLUENCE OF NICKEL ADDITIONS

Figure 3 shows how the copper-nickel separation factors vary according to the organic/aqueous ratio.

Nickel is not extracted in the following conditions :

1/3 < O/A < 1/2 : LIX 71, LIX 70

1/2 < O/A < 1 : LIX 64 N, LIX 73

It can be concluded that nickel is extracted only where solvent solution is not saturated with copper.

SCRUBBING

Ahead of copper stripping, the organic extract containing a small amount of nickel can be scrubbed, either with a sulfuric acid solution at appropriate pH, either with a solution containing a high amount of copper sulfate (30 g/l) and ammonium sulfate (200 g/l)

After two stages of scrubbing, using a 10 min agitation time and an O/A ratio of 1, it remains 0,01 and 0,00 g/l Ni in the solvent extract, for LIX 64 N and LIX 73, respectively. Results are less favourable for LIX 70 and LIX 71.

STRIPPING

After the two-stage scrubbing, the organic extracts have been stripped with a 150 g/l sulfuric acid solution used at an O/A of 5/1.

The results are excellent for the LIX 64 N and LIX 73 extractants, but copper content is less and nickel content is higher in aqueous extracts when using LIX 70 and LIX 71.

CONCLUSIONS

From the preliminary experimental study, it can be concluded that results are better for solvent extraction of copper compared to nickel with LIX 64 N and LIX 73 extractants; however, loading capacity of the former is slightly better and LIX 64 N can be recommended for further work.

REFERENCES

1. G.M. Ritcey and B.H. Lucas, CIM Bulletin, 65, N° 721, 46 (1972)
2. A. Warshawsky, Miner. Sc. Eng., 5, N° 1, 36 (1973)
3. G.M. Ritcey and B.H. Lucas, CIM Bulletin, 68, N° 754, 105 (1975)
4. N.M. Rice, M. Nedved, G.M. Ritcey, Hydrometallurgy, 3, N° 1, 35 (1978)
5. D.N. Nilsen, R.E. Siemens, S.C. Rhoads, U.S.B.M. Report, N° 8605 (1982)

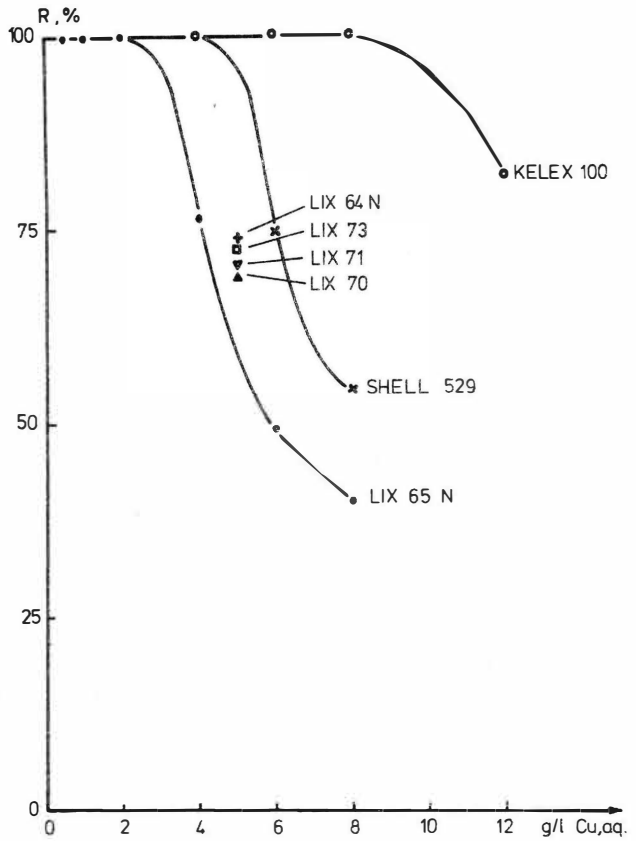

FIGURE 1. COPPER RECOVERY FACTORS

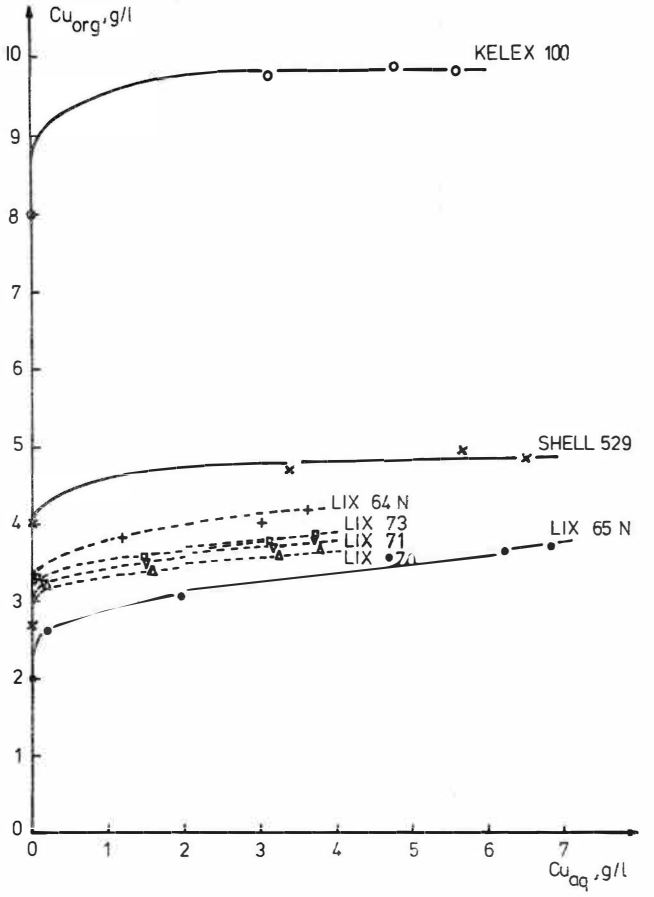

FIGURE 2. DISTRIBUTION ISOTHERMS

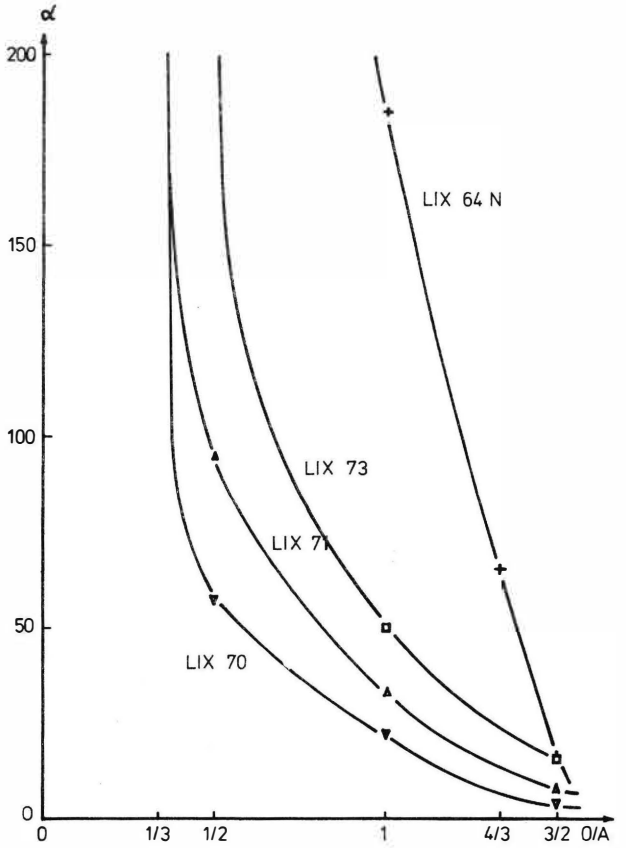

FIGURE 3. COPPER - NICKEL SEPARATION FACTORS

ZINC SEPARATION FROM COMPLEX SULPHATE-PHOSPHATE SOLUTIONS BY SOLVENT EXTRACTION PROCESS

A. Lupu and B. Flicstein

Technion-Israel Institute of Technology
Mineral Engineering Department
Haifa, Israel

The copper or copper-zinc ores are some times associated with high quantities of manganese and phosphate minerals. By the sulphuric leaching process the separation, purification and beneficiation of the components present some difficulties in the classical hydro and pyrometallurgical methods.

In the copper cementation process by zinc the beneficiation of zinc, manganese and phosphorous is very important and therefore varios methods have been studied(1-2).

Solvent extraction has been applied succesfully for recovering of metals from dilute liquors and from industrial wastes(3) and several workers have reported that carboxylic acids can be used for the solvent extraction of metals from aqueous solutions(4-8). Fletcher and wilson(6) showed that naphthenic acid are particularly suitable reagents for this type of metal extraction.

The objective of the research reported herein was the study of zinc and manganese solvent extraction from a phosphate-sulphate solution by naphthenic acid.

MATERIALS

-Aqueous phases were prepared by mixing stock solutions of the A.R.salts(B.D.H.Chemicals). The concentration of zinc, manganese and phosphorous were as in the copper cementation solutions(7g pl Zn, 0.5gpl Mn and 22gpl P.

-The naphthenic acid(Fluka S.G.), used in kerosene mixture, were characterized by an acid number of 230 and a density of 0.969g/cc.

I EXTRACTION EXPERIMENTS

Extractions were carried out by stirring the phases together at room temperature under the various conditions indicated below. The solid phase was separated by means of vacuum filtering and by D.T.A.(Standata 5-50), T.G.A.(0.1 mg precision), and X-ray analysed. After the two liquid phases separation, the organic phase was stripped with a 5% H_2SO_4 solution and twice backwased. The three phases were analysed for zinc, manganese and phosphorous. Zinc was determined by complexometric titration and manganese and phosphorous colourimetrically.

The following conditions were used throughout:

-organic/aqueous (O/A) ratio 1/1

-stirring time ..... 30 min.

-volume of each phase .....100 cc.

-naphthenic acid concentration in the organic phase was 1M.

-pH was adjusted to its final value by addition of ammonia or sodium carbonate(Metrom Herisau E 350 B pH-meter).

The experiments were carried out in the following systems:

1. $Zn_3(PO_4)_2$ - $(HR)_2$ - NH_3 ..... no extraction detected.
2. $Zn_3(PO_4)_2$ - $(HR)_2$ - Na_2CO_3..... no extraction detected.
3. $Mn_3(PO_4)_2$ - $(HR)_2$ - NH_3 ..... no extraction detected.
4. $Mn_3(PO_4)_2$ - $(HR)_2$ - Na_2CO_3 ..... no extraction detected.
5. $ZnSO_4$ - $(HR)_2$ - NH_3 ..... Figure 1
6. $ZnSO_4$ - $(HR)_2$ - Na_2CO_3 ..... Figure 2
7. $MnSO_4$ - $(HR)_2$ - NH_3 ..... Figure 1
8. $MnSO_4$ - $(HR)_2$ - Na_2CO_3 ..... Figure 2

$(HR)_2$ - naphthenic acid.

The results of this experiments lead to the following conclusions:

1) Zinc and manganese can not be extracted into a 1M solution of naphthenic acid in kerosene, when they are precipitated as phosphates(systems 1-4).

2) On the contrary, precipitated as hydroxides(systems 5-7) or carbonates(systems 6,8), are completely extracted in the organic phase. These results are in good agreement with Fletcher results(6).

3) The zinc is extracted from solutions containing free ammonia in the pH range 5-10(system 5). In the presence of ammonia the resulted ammino-zinc species(pH 7.5) are non extractable. Similar explanation were atribuated by Ashbrook for cobalt extraction and by Haffenden(10) for copper, cobalt and nickel extraction from ammonia solutions.

4) $pH_{0.5}(Zn)$ $pH_{0.5}(Mn)$, wher $pH_{0.5}$ = pH of 50% extraction. In other words, the order of extractibility of metal ions by naphthenic acid follows the lyotropic series, i.e. the basicity of the metals determines its position in the selectivity series with respect to the solution pH.

II PRECIPITATION EXPERIMENTS:

Further experiments, with cementation solutions, compare ammonia and sodium carbonate as precipitants for zinc, manganese and phosphorous. The solid phase was investigated by D.T.A., T.G.A., and X-ray analysis. The following results were obtained:

-by neutralizing with NH_4OH solutions the zinc precipitate at pH 3.5-9.5 as $Zn_3(PO_4)_2$ and the manganese as $Mn(OH)_2$ at pH 5.5-8.7, and as $Mn_3(PO_4)_2$ at pH 8.7-9.5 .

-by neutralizing with Na_2CO_3 solution(10%) the zinc precipitate at pH 3- 4.5 as $Zn_3(PO_4)_2$ and $Zn(OH)_2$. At pH 6-7 it precipitates only as $Zn_3(PO_4)_2$, and at pH 7-9.5 as $Zn_3(PO_4)_2$ and $ZnCO_3$. The manganese was precipitated as $Mn(OH)_2$ at pH 3-7 and as $Mn_3(PO_4)_2$ at pH 7.5-9.5.

III SOLVENT EXTRACTION AND PRECIPITATION EXPERIMENTS

The final set of experiments dealt with the solvent extraction of zinc, manganese and phosphorous from cementation solutions by 1M naphthenic acid solution in kerosene. Again ammonia and sodium carbonate were used as neutalizing agents, and the solid phase was analyzed by the same methods. The results appear in Figures 5-8.

DISSCUSION.

Contrary to the preliminary experiments, the order of extractibility of zinc and manganese with respect to the pH does not fellow the basicity series i.e.: $pH_{0.5}(Mn) < pH_{0.5}(Zn)$

Moreover, the form and the relative places of the curves representing zinc and manganese extraction are different when ammonia or sodium carbonate are used as neutralizing agents. The reason of this deviation is the presence of PO_4^{3-} ions, which leads to the precipitation of $Zn_3(PO_4)_2$ and $Mn_3(PO_4)_2$ in certain pH ranges and this may be explained as follows:

1. When ammonia is used as neutralizing agent:

- Zinc mainly precipitates (90%) as $Zn_3(PO_4)_2$ in the pH range 3-7; the rest of zinc is extracted in the organic phase. In the pH range 7-9.5, $Zn_3(PO_4)_2$ begins to dissolve in excess of ammonia (at pH 9.5 only 15% of zinc is precipitated as $Zn_3(PO_4)_2$ and 80% passes in the organic phase). At pH 9.5, the free ammonia forms non-extractable ammino-zinc species $Zn(NH_3)_i^{2+}$, i= 1-4, (system 5).
- Manganese extraction starts at ph 5.5 and it reaches its maximum value (75%) at pH 7.5 (in this pH range manganese is precipitated as $Mn(OH)_2$ which is extractable by the naphthenic acid -system7 -). At pH $>$ 7.5, manganese starts to precipitate as non-extractable $Mn_3(PO_4)_2$ -system 3 - .

2. When sodium carbonate is used as neutralizing agent:

- Zinc is mainly precipitated as non-extractable $Zn_3(PO_4)_2$ at pH lower than 7. At pH 7-8, the principal precipitation form of zinc is $ZnCO_3$ which is completely extracted into the organic phase. At higher pH values zinc is not extracted (probably because the anion formation -$Zn(OH)_4^{2-}$ -)
- Manganese, in the range 7-8, is present in the solution as $Mn(OH)_2$ and consequently it is extracted in the organic phase (95% at pH 8). At higher pH values the manganese begins to precipitates as the non-extractable phosphate -$Mn_3(PO_4)_2$ - .

CONCLUSIONS

The zinc and manganese extraction from a sulphate-phosphate solution by naphthenic acid in 1M solution in kerosene was found to be different as compared to zinc and manganese extraction from a sulphate solution.

The difference was explained by the presence of the PO_4^{3-} ions which produces zinc and manganese precipitation as non-extractable $Zn_3(PO_4)_2$ and $Mn_3(PO_4)_3$ in certain pH ranges and it was correlated to the nature of the neutralizing agent used.

REFERENCES

1. A. Lupu. Timna copper cementation. Technion Inst. of Research and Development. 1970
2. A. Lupu. Copper cementation by zinc and zinc beneficiation. 1972 Conf. of Mineral Technology MERC, Technion City, Haifa. Israel.
3. A.W. Fletcher. Chem. Ind. 9.414(1973)
4. A.W. Ashbrook. Min. Sci. Engng. 5.196(1973)
5. D.J. Bauer and R.E. Lindstrom. Bu. of Mines, R.I. 6396(1964)
6. A.W. Fletcher and J.C. Wilson. Trans. Inst. of Mining and Metallurgy .LXX(1960-1961)
7. L.M. Gindin. Russ. J. of Inorg. Chem. 6.1412(1961)
8. M. Olteanu. Rev. Chem. Buckarest. 14.318(1963)
9. A.W. Ashbrook. J. Inorg. Nucl. Chem. 34.1721(1972)
10. W.J. Haffenden and G.J. Lawson. Proceedings Symp. of Inst. of Min. and Metallurgy. 678(1967)

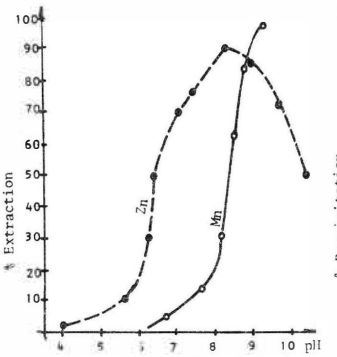

FIGURE 1. Zn AND Mn EXTRACTION FROM AQUEOUS SOLUTION BY NAPHTHENIC ACID IN THE PRESENCE OF NH_4OH.

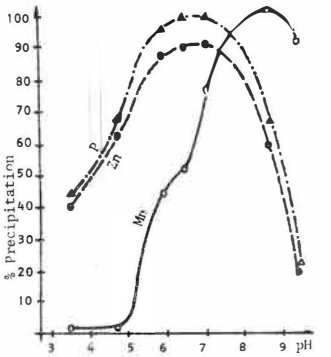

FIGURE 3. Zn, Mn AND P PRECIPITATION FROM CEMENTATION SOLUTION IN THE PRESENCE OF NH_4OH

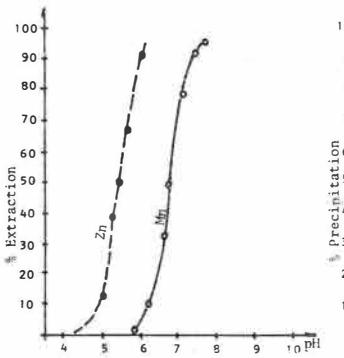

FIGURE 2. Zn AND Mn EXTRACTION FROM AQUEOUS SOLUTION BY NAPHTHENIC ACID IN THE PRESENCE OF Na_2CO_3

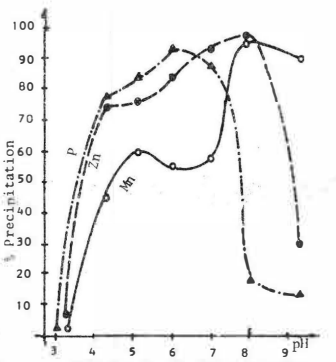

FIGURE 4. Zn, Mn AND P PRECIPITATION FROM CEMENTATION SOLUTION IN THE PRESENCE OF Na_2CO_3

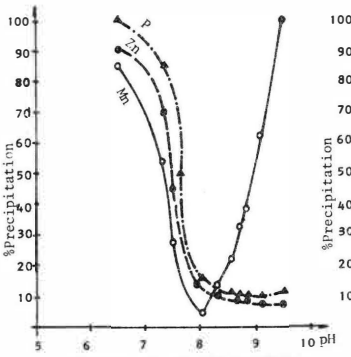

FIGURE 5. Zn, Mn AND P PRECIPITATION DURING THEIR EXTRACTION BY NAPHTHENIC ACID IN THE PRESENCE OF NH_3

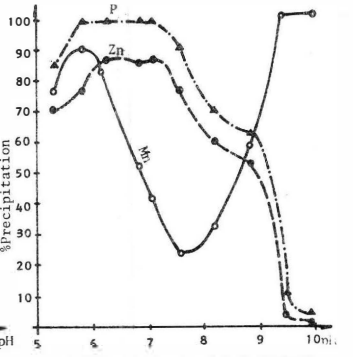

FIGURE 7. Zn, Mn AND P PRECIPITATION DURING THEIR EXTRACTION BY NAPHTHEMIC ACID IN THE PRESENCE OF Na_2CO_3

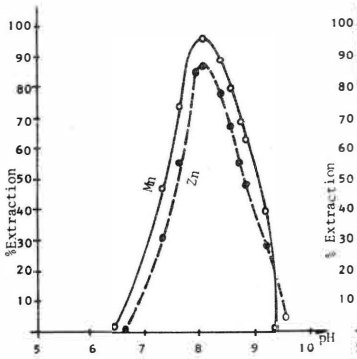

FIGURE 6. Zn AND Mn EXTRACTION BY NAPHTHENIC ACID IN THE PRESENCE OF NH_3

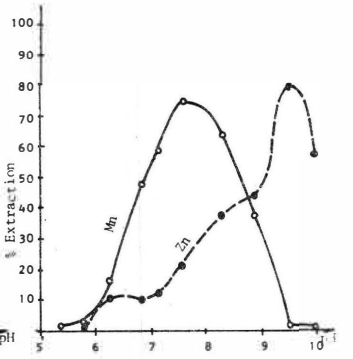

FIGURE 8. Zn AND Mn EXTRACTION BY NAPHTHENIC ACID IN THE PRESENCE OF Na_2CO_3

EXTRACTION AND SEPARATION OF COBALT AND MANGANESE FROM CHLORIDE SOLUTIONS WITH A TIOA-PERCHLORO-ETHYLENE SOLVENT MIXTURE IN A COLUMN EXTRACTOR

M. Verhaege, F. Leysen, A. Van Peteghem

University of Ghent
Ghent, Belgium

INTRODUCTION.

As cobalt and manganese frequently occur together in hydrometallurgical processtreams, we decided to look for a solvent extraction route to separate both metals. Special attention was paid to their separation from chloride solutions. The extraction of cobalt from chloride liquors using tertiary amines solved in aromatic or aliphatic diluents is well documented "(1-5)". Concerning the extraction of manganese however, only a few data are available '(6-7)". Furthermore, some authors suggested the use of chlorinated high density hydrocarbons as diluent or as additive to more common diluents in solvent extraction "(8-9)".

Extended data for the extraction and scrubbing of cobalt and manganese with this type of extractant solved in various diluents have been collected in our laboratory. Some of them have been published recently "(10-11)". The next step to be taken was to test the separative extraction of both metals in a countercurrent extraction device.

The results published here are those obtained from a laboratory scale unit consisting of one or more countercurrent extraction columns.

The feed was a synthetic cobalt-manganesechloride solution and the solvent was a TIOA-perchloroethylene mixture.

EXPERIMENTAL SET-UP.

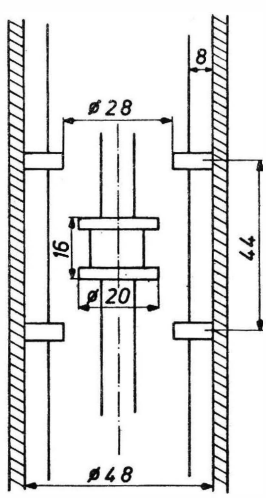

Figure 1 : Extractor design (mm)

A section of the laboratory size extractor is schematically given in figure 1.

The column body and upper and lower settling chambers are made of glass. The total length of the extractor is 1450 mm. The inner structure of the column (horizontal statorrings, vertical baffles, impellors and impellorshaft) are constructed of PERSPEX ® : The mixing turbulence is obtained by fourblade impellors mounted on the central shaft.

FEED AND SOLVENT MAKE-UP.

The solvent used was a 20 vol.% triisoöctylamine solution in perchloroethylene. The use of this high density chlorinated hydrocarbon is rather uncommon. However it has been shown by former experiments "(9-10)" that this diluent has some advantages as compared to more commonly used aliphatic or aromatic diluents. Faster kinetics and shorter settling times are indeed obtained with this solvent.

Before being fed into the system, the solvent was precontacted with an aqueous HCl solution. In this way, the extractant was converted to R_3NHCl.

The aqueous feed solutions contained various amounts of cobalt and manganese brought into solution by solving suitable quantities of cobalt- and manganesechloride. The ionic medium was a NaCl-HCl solution.

Figure 2 indeed clearly shows that the addition of sodiumchloride has a positive effect on the separation of both metals.

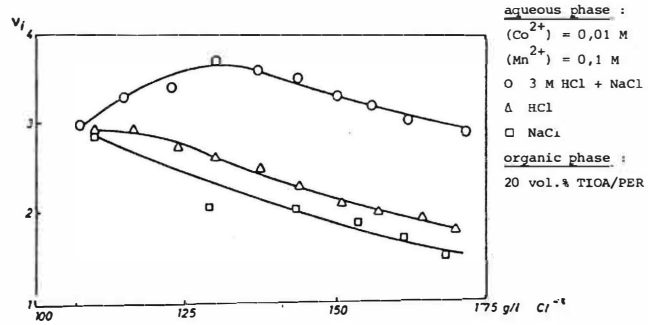

Figure 2
"Integral separation" factor as a function of Cl^- concentration

The ionic medium chosen for the extraction tests was 110 g/l Cl^- ex HCl and 25 g/l Cl^- ex NaCl.

EXTRACTION RESULTS.

Table I shows the results obtained with a feed containing 0,775 g/l cobalt and 6,79 g/l manganese.

Table I.

Dispersed phase	Solvent				
Stirrer speed	± 1100 rpm				
Flowrate aq. phase l/h (F)	0,61	0,72	0,93	0,67	0,64
Flowrate org.phase l/h (S)	1,32	1,79	3,39	3,35	4,01
F/S	0,46	0,40	0,27	0,20	0,16
$(Co)_{feed}$ mg/l	755	755	755	755	755
$(Co)_{raff.}$ mg/l	42	32	15	15	12
$(Mn)_{feed}$ g/l	6,79	6,79	6,79	6,79	6,79
$(Mn)_{raff.}$ g/l	3,46	3,62	3,24	2,63	2,61
% E Co	94,4	95,8	98	98	98,4
% E Mn	49,1	46,8	52,3	61,4	61,6

From this table, it is obvious that decreasing the ratio of F to S seriously increases manganese extraction while no complete extraction of cobalt can be obtained.

High extraction rates of cobalt combined with moderate extraction of manganese at lower F to S ratios were obtained when two similar extraction columns were coupled countercurrently. A schematic view of this experimental set-up is given in figure 3 and one of the results obtained can be seen in table II. The solvent was the dispersed phase in both columns.

The flowrate of the aqueous- and organic feed was 1,1 and 2,25 l/h respectively.

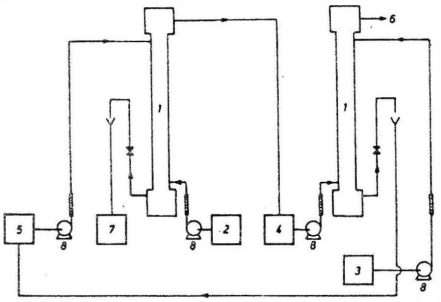

1. extr. column
2. aqueous feed
3. solvent feed
4. raff. col. I
5. extr. col. II
6. raff. col. II
7. extr. col. I
8. pump device

Figure 3

Table II

	F/S	$(Co)_{feed}$	$(Mn)_{feed}$	$(Co)_{raff.}$	$(Mn)_{raff.}$	% E_{Co}	% E_{Mn}
column I	0,49	629 ppm	5,77 g/l			87,9	18,4
column II		76 ppm	4,71 g/l	4,4 ppm	2,57 g/l	94,2	45,4

The overall percentage extraction of cobalt and manganese is 99,3 and 55,5 % respectively.

SCRUBBING TESTS.

The results of the extraction tests show that high cobalt recovery in the extractor can be achieved, but severe coëxtraction of manganese occurs under the described conditions. One of the scrubsolutions tested was a 6 M HCl solution. Table III shows the results of some of the scrubtests. In this series of experiments, an extract containing 0,214 g/l Co and 1,29 g/l Mn is fed into a column (identical with the one used in the extraction tests) and the influence of the F to S ratio on the back extraction of both metals was investigated.

Table III

Flowrate aq. feed (F)	Flowrate org. feed (S)	F/S	(Co) ppm	(Mn) g/l	% S Co	% S Mn
2,26 l/h	1,36 l/h	1,74	210	0,72	1,87	44,19
2,48 l/h	0,68 l/h	3,65	207	0,41	3,27	68,2
3,69 l/h	0,62 l/h	5,95	194	0,32	9,35	75,2

The results show that the scrubbed extract still contains considerable amounts of manganese. With the type of extractor and scrubsolution used, several possibilities can be considered to scrub more manganese without high loss of cobalt. One of the possibilities tested was a crosscurrent coupling of several scrubbers. This showed to produce better results than countercurrent coupling with the same overall F to S ratio. Figure 4 shows a scheme of the experimental set-up.

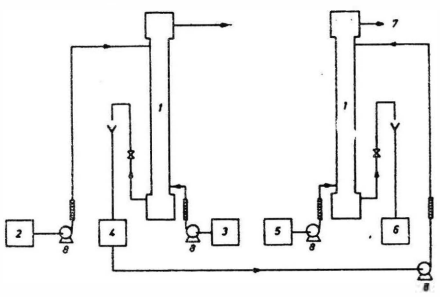

1. scrubbing column
2. extract feed
3. 5. 6 M HCl solution
4. 6. scrubbed extract
7. aq. scrub out
8. pump

Figure 4

The results obtained with a solvent loaded with 0,214 g/l and 1,29 g/l manganese can be seen in table IV.

Table IV

	Column I	Column II
Flowrate aq. feed	2,6 l/h	2,42 l/h
Flowrate org. feed	0,62 l/h	0,73 l/h
F/S	4,19	3,32
$(Co)_{org.}$ feed	214 ppm	204 ppm
$(Mn)_{org.}$ feed	1290 ppm	442 ppm
$(Co)_{org.}$ out	204 ppm	198 ppm
$(Mn)_{org.}$ out	442 ppm	153 ppm
% scurb Co	4,7 %	2,9 %
% scrub Mn	65,7 %	65,4 %

The overall percentage of cobalt and manganese scrubbed was 7,48 % and 88,14 % respectively at an overall F to S ratio of 3,72.

CONCLUSION.

From the results obtained it was calculated that starting with a feed containing 0,59 g/l Co and 5,5 g/l manganese, a scrubbed extract containing 0,244 g/l Co and 0,003 g/l Mn could be obtained with 2 extractors coupled countercurrently operating at an F to S ratio of 0,5 and up to 6 contactors coupled crosscurrently (each operating at an F to S ratio of 3,5) in the scrub section. This shows that with the contact device and solvent and aqueous scrub-solution used, a separation is possible but many practical- and economic objections can be formulated. To reduce the impact of scrubbing on the process, an extract with higher ratios of cobalt to manganese should be obtained. This goal may be reached by working closer to the maximal loading or refluxing the extract to the extraction section.

REFERENCES.

(1) E.Wigstol and K.Froyland
Proc. Int. Symp. Antwerp, May 4-5, 1972

(2) P.Brooks, G.Potter, D.Martin
U.S. Bureau of mines, Rep. Invest. RI 74-2, 1970

(3) P.Brooks, G.Potter. D.Martin
U.S. Bureau of mines, Rep. Invest. RI 7316, 1969

(4) A.Aue, L.Skjutare, G.Bjorling, H.Reinhardt, J.Rydberg
Proc. ISEC 1971, p.447-450

5) A.Van Peteghem, M.Willekens, B.Tougarinoff
Symp. Nikkel Wiesbaden 1970, p.147

(6) F.Seeley, D.Crouse
J.Chem. and Eng. data , vol. 11, 3, july 1966

(7) G.Kauwenberghs
Thesis H.I.K. , 1968

(8) M.Verhaege, G.Claus, A.Van Peteghem
Bulll. Soc. Chim. Belge, vol.91, 10, 1982

(9) M.Verhaege, G.Claus, A.Van Peteghem, P.Van Acker
Paper presented at the 111th A.I.M.E. meeting, Dallas, 1982

(10) M.Verhaege, G.Claus, F.Leysen, A.Van Peteghem
Proc. Oslo Symp. on ion exchange and solvent extraction, II.36-II.42,1982

A SELECTIVE METALLURGICAL EXTRACTANT SYSTEM TO RECOVER NICKEL AND COBALT FROM ACID SOLUTIONS

Robert R. Ginstead and Annel L. Tsang

Dow Chemical U.S.A.
Walnut Creek, California USA

Nickel and cobalt are currently obtained primarily from high grade sulfide ores which can be processed by pyrometallurgical methods (1,2). Reserves of these metals, however, exist primarily in tropical laterites, which are oxide and silicate type materials, and often require hydrometallurgical processing.

For ores without high levels of acid-consuming constituents sulfuric acid is an effective means of solubilizing nickel and cobalt. The conventional treatment of these leach solutions is precipitation of the nickel and cobalt with hydrogen sulfide (3,4) followed by redissolving the sulfide precipitate, separating and refining the metals by a complex series of processing steps (4). Until recently no simple separation system has appeared on the scene, such as the liquid-liquid extraction systems which are now so commonplace in the copper industry.

Dow Chemical U.S.A. has recently placed in the market two chelating ion exchange resins which can selectively remove nickel and cobalt from acid sulfate solutions, and which are beginning to find a place in the nickel/cobalt industry (5,6). In some situations, however, the methods of solvent extraction may be preferable, and this paper will describe an extraction system which can also selectively remove nickel and cobalt from acid solutions typical of those obtained from laterite ores.

We reported on a similar system at the preceding ISEC Conference held in Liege in 1980, but as we indicated then that system was somewhat unstable toward hydrolysis, and probably of limited use (7). The current system does not appear to possess this limitation.

NATURE OF THE SYSTEM

The extractant system consists of a solution of an N-alkylated bis-picolylamine, which we shall designate as L, and dinonylnaphthalenesulfonic acid (DNNS) dissolved in a hydrocarbon diluent.

The ratio of these two compounds is variable, but as we shall see a mole ratio (amine:DNNS) of about 1:2 seems to be optimum for nickel and cobalt extraction. In this case the amine will accept two protons from the two DNNS molecules and the extraction reaction can be represented as

$$\overline{H_2L^{++}\cdot 2DNNS^-} + M^{++} \longrightarrow \overline{ML^{++}\cdot 2DNNS^-} + 2H^+ \qquad (1)$$

where bars denote species in the organic phase.

The diluent used in the data reported here was an alkylated aromatic hydrocarbon, although preliminary tests with an aliphatic hydrocarbon on the current system suggest that diluent is not a critical factor.

EFFECT OF PROCESS VARIABLES ON THE EXTRACTION

Amine: DNNS Mole Ratio. In Figure 1 is shown the effect of varying this ratio on extraction of nickel, cobalt and iron(III). Except for one series of tests where cobalt was studied alone the data represent tests where all three metal ions were present initially at a concentration of 1 g/l, and the aqueous/organic phase ratio was three. Under these conditions complete extraction of nickel (which occurs in a few cases) results in only about 50% saturation of the organic phase. The nickel is most strongly extracted, the optimum extractant mole ratio, R, being about 0.5 (one amine: two DNNS).

The coextraction of cobalt is also greatest in the vicinity of R = 0.5, although it is not as strongly dependent on the value of R. In order to observe cobalt behavior without the interference of the extracted nickel a separate series of tests was run, and shows that, as might be expected, cobalt is extracted more extensively in the absence of nickel. The influence of R, however, remains qualitatively the same.

A rather interesting observation is that for R ~ 0.7 extraction of these two ions is quite comparable, so that depending upon whether coextraction or separation of the two is desired the flexibility to adjust the system to accomplish this may be available. This possibility has not been followed up, and most of the work in this system has been done with systems for which R was about 0.5.

Extraction of ferric iron is quite low for R > 0.5, but increases substantially at lower R values. Thus the optimum region for good nickel and cobalt extraction with low iron extraction is in the region R = 0.5-0.6.

Effect of pH. Using the same type of test as in the preceding section the extraction of the same three ions was determined for R = 0.5 over a range of pH, and the data are shown in Figure 2. In this series the aqueous phase contained 0.25 M magnesium sulfate as a background constituent, since this is much more nearly the situation encountered in laterite ore leaches. We have also included in the organic phase a proprietary diluent modifier which has the function of increasing the kinetics of extraction without significantly influencing the equilibria. We have also adopted 35°C as a somewhat more practical temperature, because of the better kinetics obtained.

Nickel extraction is quite good at any pH above about 1.5 and is significant even as low as pH 1. Cobalt, although much less strongly extracted, can be removed fairly well in the pH range 2-2.5, where iron(III) is only weakly extracted. The critical aspect of this separation is the need to maintain a pH low enough to retain iron in solution, while still extracting cobalt.

Distribution Curves. Extension of the data in Figure 2 in the form of distribution curves for nickel and cobalt is shown in Figure 3. For nickel the curve represents the equilibria at pH 2.0; for cobalt the pH is 2.65. It is clear that for both ions the organic phase concentration approaches a value of about 0.1 M (5.9 g/l) at high aqueous levels, indicating that one mole of amine extractant reacts with one mole of metal ion.

Stripping of Metals from the Organic Phase. As the data in Figure 2 suggest removal of nickel and cobalt from the organic phase can be done relatively easily with dilute mineral acid. Figure 4 presents distribution data for some HCl solutions, where the indicated HCl concentration is the actual concentration of free HCl in the equilibrium aqueous phase. Remembering that loaded organic phases of 2-5 g/l of these ions are readily obtained it can be seen that production of final aqueous strip solutions of 20-40 g/l of metal ion should be a relatively straightforward task. Sulfuric acid is also quite effective if a sulfate concentrate is preferred.

Performance With a Mixed Solution. Performance of this extraction system on a solution representative of laterite leach was observed in two tests. In the first a contact was made at pH 2.0, about where nickel extraction is maximum. The organic was stripped with 3 N sulfuric acid to determine the levels of extracted ions. A second contact was made with the same aqueous feed except that no nickel was present. The pH was 2.6, where good cobalt extraction was anticipated. This organic was stripped with 1 N HCl. Data are shown in Table I.

Extraction of nickel is quite good, with very little coextraction of other species, even including cobalt. Selectivity over cobalt (ratio of distribution coefficients) is about 17, and of the total metal ion content of the strip less than one percent are metal ions other than nickel and cobalt.

The cobalt test showed quite good extraction of cobalt at pH 2.6, in fact somewhat better than was predicted from Figure 3. Of the metal ions in the strip, about 20% were species other than cobalt.

TABLE I. EXTRACTION OF TYPICAL LATERITE LEACH.
Organic: 0.10 M amine/0.20 M DNNS/0.50 M modifier/Cyclosol 63
Extraction Phase ratio (O:A) = 1:3, Temp. 50°C, Strip Phase ratio = 1:1.

	pH	Concentrations, g/l (Sulfates)					
		Ni	Co	Mn	Mg	Al	Fe(III)
Nickel Present							
Feed		2.64	0.25	3.6	7.7	1.94	1.79
Raffinate	2.0	1.42	0.27	3.6	7.8	1.97	1.82
Strip (3N H_2SO_4)		4.17	0.046	0.010	0.014	0.003	0.022
DÅ		2.9	0.17	0.0027	0.0018	0.0015	0.012
Nickel Absent							
Feed			1.17	3.8	8.0	2.03	1.92
Raffinate	2.6	--	0.46	3.7	8.0	2.01	1.85
Strip (1 N HCl)			2.01	0.19	0.16	0.032	0.17
DÅ			4.4	0.052	0.020	0.016	0.093

CONCLUSIONS

The purpose of this study was to demonstrate that an alkyl bis-picolylamine/DNNS system can be effectively used to recover nickel and cobalt from acidic sulfate leaches of the type anticipated in laterite processing. Although considerably more work will be required to optimize this type of system the performance on a simulated leach clearly shows its capabilities. It can readily be shown that an extraction train of relatively few stages could recover essentially all of these two metals, providing the pH can be maintained in the vicinity of about 2.6. By use of separate strip stages the nickel and cobalt could also be obtained as relatively pure fractions in quite concentrated solutions.

REFERENCES

1. J. L. Blanco and B. M. Holliday, J. Metals 33 No. 4, 50 (1981).
2. H. J. Roorda and J.M.A. Hermans, Erzmetall 34 No. 2, 82 (1981).
3. M. C. Jha, G. A. Meyer and G. R. Wicker, J. Metals 33 No. 11, (1981).
4. J. H. Canterford, Rev. Pure & Appl. Chem. 22, 13 (1972).
5. R. R. Grinstead, W. A. Nasutavicus, R. M. Wheaton and K. C. Jones, in Extractive Metallurgy of Copper, Am. Inst. of Min. Met. & Petr. Engineers, (1976), vol. 2, 1009.
6. R. R. Grinstead, J Metals 31 No. 3, 13 (1979).
7. R. R. Grinstead, ISEC Proceedings, Liege, Belgium, (1980), vol. 3, Paper 80-170.

SOLVENT EXTRACTION OF COBALT AND NICKEL BY A PHOSPHONIC ACID ESTER

D. S. Flett, J. Melling

Warren Spring Laboratory
Stevenage, Hertfordshire, U.K.

and

E. Itoh

Nippon Mining Co. Ltd.
Tokyo, Japan

The extraction behaviour of a phosphonic acid ester has been examined as part of a cooperative project on Solvent Extraction Technology for the Mineral Industry Research Organisation. The influence of several factors: pH, temperature, diluent and modifier, on the separation of cobalt from nickel from sulphate solution has been determined. Comparative results have been obtained using di-2-ethylhexyl phosphoric acid (DEHPA).

INTRODUCTION

Metal cations can be extracted from aqueous solutions by solvents containing a variety of organic acids including phosphoric acid esters, phosphonic acid esters and phosphinic acids. Considerable interest has been shown in the application of these extractants to the separation of cobalt from nickel in sulphate solutions. The commercial use of DEHPA and a phosphonic acid ester has been described in a recent review (1).

Di-2-ethylhexyl phosphoric acid (DEHPA) is, of all extractants, probably used for the widest variety of applications in hydrometallurgy including the separation of cobalt from nickel. The extraction and process chemistry have been the subject of a large number of laboratory studies.

The behaviour of a series of phosphonic acid esters as metal extractants has been examined by the Daihachi Chemical Industry Co and the separation of cobalt from nickel (2), of rare earths (3,4) and the extraction of several metals (5) including aluminium has been described in the patent literature. The preferred extractant appears to be 2-ethylhexyl phosphonic acid mono 2-ethylhexyl ester which shows a higher Co/Ni separation factor than DEHPA under the same conditions. This extractant which is marketed under the trade name PC88A has replaced DEHPA for Co/Ni separation in the refinery operated by Nippon Mining Co Ltd at Hitachi, Japan (6). Nippon Mining Co Ltd hold several patents relating to this separation (7-10). Until recently an ester with the same formula was available from Shell Chemical Co under the code RD 577 and later SME 418. A process using the Shell extractant for the recovery of pure cobalt from secondary sources has been developed and tested on a laboratory scale at Warren Spring Laboratory (11).

Since completion of the experimental work reported here, the results of studies of the extraction of several metals including cobalt and nickel have been presented by Dreisinger and Cooper (12) and a comparative study by Preston (13) of cobalt and nickel extraction with DEHPA, SME 418 and the phosphinic acid Cyanex CNX has been published.

EXPERIMENTAL

The extractants SME 418 (Koninklijke Shell Labortarium, Amsterdam, Holland) and DEHPA (BDH Ltd); the diluents MSB 210 (Shell Chemical Co), heptane (East Anglia Chemicals) and xylene (Hopkin and Williams, GPR); and the modifiers isodecanol (ICI Ltd) and TBP (BDH Ltd) were used as received. SME 418 is a colourless liquid with a density, at room temperature, of 0.945 g ml^{-1} and an acidity of 3.14M determined by non-aqueous titration against standard alkali. MSB 210 is a commercial diluent containing typically 69% paraffins, 29% napththenes and 2% aromatics. Aqueous solutions were prepared from AR grade reagents. Equal volumes of solvent and aqueous solutions were contacted at 25°C for 30 min in a stirred baffled beaker. After contact the phases were separated and aliquots of the loaded solvent stripped with sulphuric acid. The raffinates and strip solutions were analysed by atomic absorption spectrophotometry and mass balances obtained.

Separation of Cobalt and Nickel

Effect of pH. The separation of cobalt and nickel from sulphate solutions containing initially 0.025M of both metals has been examined in a series of tests at 25°C over a range of equilibrium pH values using organic phases containing either 0.1M SME 418 or DEHPA in MSB 210. Separation factors $\left(\beta^{Co}_{Ni}\right)$ for both extractants at particular pH values have been interpolated from graphical plots of the data and are shown as a function of pH in Fig. 1. For SME 418, the separation factor is apparently dependent on pH and is some 10 to 100 times greater than the pH independent value for DEHPA. Independence of β on pH for both extractants is predicted from the results on single metal solutions wherein the plots of log D versus pH for cobalt and nickel are parallel. The reason for this unexpected behaviour of SME 418 is not clear but may be due to analytical error as the nickel concentrations in the strip solutions were very low indeed and aqueous phase entrainment and/or organic interference in the atomic absorption analyses cannot be ruled out.

However, Dreissinger and Cooper (12) also observed an effect of pH on separation factor although at greater concentrations of SME 418, Co and Ni than in the present study. Below 50°C they found that the separation factor increased with pH in the range 3.5-5.5 but at 50°C and 60°C a maximum was found at about pH 5.

Effect of Temperature. The dramatic influence of temperature on the cobalt/nickel separation factor with DEHPA as extractant is well known (14,15). This is due to changes in the solvent phase coordination of cobalt. Thus, whilst the nickel complex retains octahedral coordination over the temperature range from ambient to 70°C or so, the cobalt complex is present as both tetrahedral and octahedral complexes with a reduction in the proportion of the octahedral form over this temperature range. To determine the effect of temperature on separation factor for extraction with SME 418, tests under the conditions used at 25°C were carried out over the temperature range 0-75°C. Separation factors at pH 4.0, interpolated from graphical plots, are shown in Fig. 2 together with comparative values for DEHPA. Both extractants show a similar effect of temperature on separation factor, and indeed the Nippon Mining Co refinery (6) operates with the phosphonic acid extractant at a temperature of about 50°C which obviously improves the separation factor compared with ambient temperature. It is known that at this temperature the flow properties of the cobalt-loaded solvent and solubility of the cobalt complex in the solvent are also considerably improved. This effect of temperature was also found in the studies of Dreisinger and Cooper (12) and Prestion (13). The latter author also demonstrated a similar effect for the phosphinic acid, Cyanex CNX.

Effect of diluent aromaticity. The effect of diluent aromaticity on the cobalt/nickel separation factor was investigated in a series of tests using 0.5M SME 418 dissolved in a mixture of heptane and xylene and an aqueous solution containing 0.025M Co and Ni initially. Interpolated separation factors at pH 4.0 are shown in Fig. 3. There is a significant increase in separation factor with increase in aromaticity but at the expense of reduced cobalt loading. This effect was also found by Preston (13).

Effect of modifier. The addition of organic phase modifiers to DEHPA-containing solvents is known to reduce the cobalt/nickel separation factor (15, 16,17). This results from the increased tendency of the cobalt to form octahedral complexes in the presence of polar molecules such as long chain alcohols and to the depolymerising effect of such compounds. Both modifiers reduce the separation factor, isodecanol by a greater amount than TBP as was also found by Preston (13).

The effect of isodecanol was further investigated in a series of tests using modifier concentrations from 1 to 20 v/o. The results are shown in Fig. 4. It is of considerable interest to note that the extraction of the octahedral hydrated nickel complex is considerably enhanced by just about an order of magnitude by increasing the IDA content of the organic phase to 20 v/o while predictably the cobalt distribution falls but by a much smaller amount.

CONCLUSIONS

With SME 418, the cobalt/nickel separation factor apparently increases with increase in pH and increases with both increase in temperature and diluent aromaticity. The separation factor is reduced by the addition of organic phase modifiers, addition of isodecanol causing a greater reduction than addition of TBP at the same concentration. These effects on cobalt/nickel separation factor with SME 418 parallel the effects found with DEHPA in this and earlier studies. The effects of aromaticity, temperature and diluent modifiers for both DEHPA and SME 418 can be correlated by the degree of formation of the tetrahedral form of the cobalt complex in the organic phase. This is shown in a composite plot of separation factor against percentage of cobalt in the tetrahedral form in the organic phase in Fig. 5. The per cent of cobalt in the tetrahedral form was determined spectrophotometrically as previously described (15). The points all fall on a smooth curve showing an increase in separation factor as the concentration of tetrahedral cobalt relative to octahedral cobalt increases.

ACKNOWLEDGEMENT

This work was carried out as part of a repayment programme for the Mineral Industry Research Organisation (MIRO) and the authors thank MIRO for permission to publish.

REFERENCES

1. Flett, D.S. The Chemical Engineer, 1981, (370), 321-324.
2. Fujimoto, A., Miura, I. and Noguchi, K. Belg. 871,963/1979.
3. Fujimoto, A. and Miura, I. Jpn. Kokai Tokkyo Koho 79 93,672/1979.
4. Daihachi Chemical Industry Co Ltd. Fr. Demande 2 460 275/1981.
5. Fujimoto, A. and Miura, I. Jpn. Kokai Tokkyo Koho 79 38,273/1979.
6. Kasai, T., Nakayama, H., Motoba, K. and Itoh, E. Paper presented at Joint AIME/MMIJ Meeting, Tokyo, Japan, 8th Nov. 1980.
7. Ogata, T. Jpn. Kokai Tokkyo Koho 80 06,460/1980.
8. Ogata, T., Namihisa, S. and Tsumoru, F. Jpn. Kokai Tokkyo Koho 80 18,547/1980.
9. Namihisa, S. and Kondo, A. Jpn. Kokkai Tokkyo Koho 80 41,937/1980.
10. Ogata, T., Fujii, T. and Namihisa, Y. Jpn. Kokai Tokkyo Koho 80 41,938/1980.
11. Pearson, D. Proceedings of International Conference on Cobalt: Metallurgy and Uses, 10-13 November 1981, Brussels: Benelux Metallurgie, Vol. 1, 139-148.
12. Dreisinger, D.B. and Cooper, W.C. Paper presented at the CIM 12th Ann. Hydrometallurgical Mtg, Toronto, 29 Aug-1 Sept 1982.
13. Preston, J.S. Hydrometallurgy, 1982, 9, 115-133.

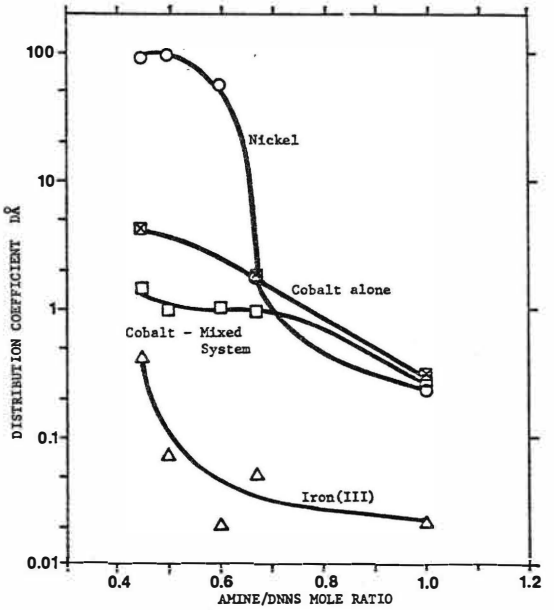

FIGURE 1. EFFECT OF AMINE/DNNS RATIO ON METAL ION EXTRACTION. Organic: 0.10 M amine, DNNS as indicated. Aqueous: mixed metal sulfates, initial concentration, 1 g/l each ion. Rm. Temp., pH 1.75, phase ratio (O:A) = 1:3.

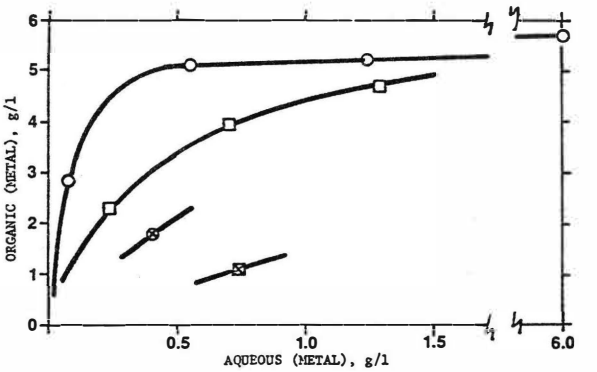

FIGURE 3. EXTRACTION EQUILIBRIA FOR NICKEL AND COBALT. Organic: 0.10 M amine/0.20 M DNNS, 0.5M modifier. Aqueous, 0.25 M $MgSO_4$. Temp., 35°C. Nickel points: ○ pH 2.0, ⊗ pH 1.35; cobalt points: □ pH 2.65, ⊠ pH 2.15.

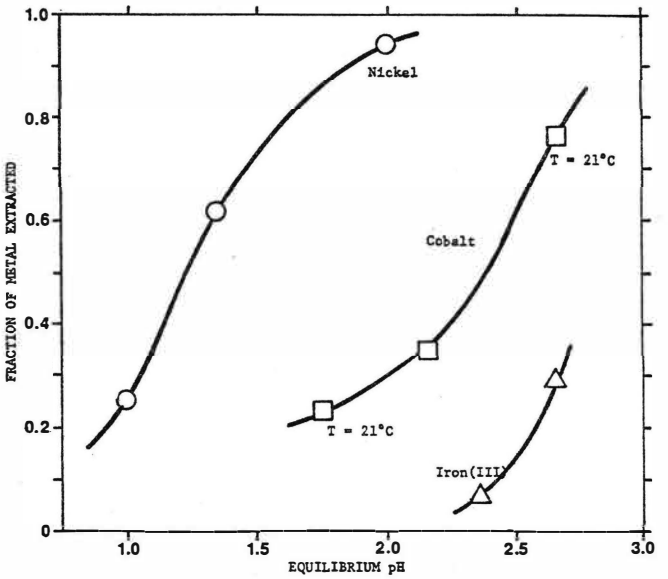

FIGURE 2. pH PROFILE OF EXTRACTION EQUILIBRIA. Organic: 0.10 M amine/0.20 M DNNS, 0.5M modifier. Aqueous, 0.25 M $MgSO_4$, initial metal ion concentration, 1 g/l. Phase ratio (O:A) = 1:3, Temp., 35°C., except as noted.

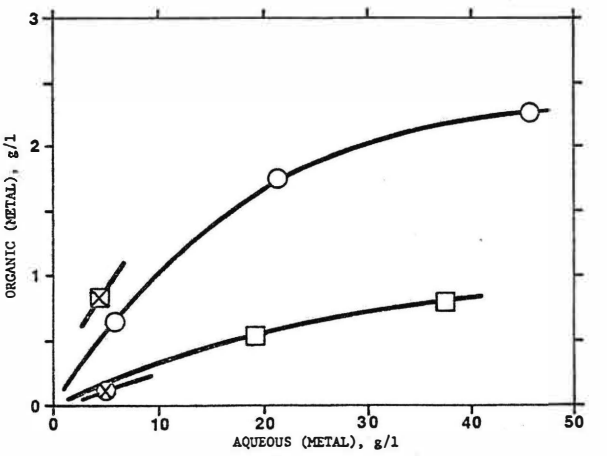

FIGURE 4. NICKEL AND COBALT STRIPPING EQUILIBRIA. Organic: 0.10 M amine/0.20 M DNNS, 0.5M modifier. Temp., 35°C. Nickel points: ○ 0.81 M HCl, ⊗ 3.0 M HCl; cobalt points: ⊠ 0.071 M HCl, □ 0.21 M HCl.

14. Barnes, J., Setchfield, J. and Williams, G.O.R. J. inorg. nucl. Chem., 1976, 38, 1065-7.

15. Flett, D.S. and West, D.W. Complex Metallurgy, London: Institution of Mining and Metallurgy, 1978, 49-58.

16. Bouboulis, C.J. Proceedings of International Solvent Extraction Conference ISEC 77, Montreal: CIMM, CIM Special Volume 21, 1979, 32-39.

17. Grimm, R. and Kolarik, Z. J. inorg. nucl. Chem., 1976, 38, 1493-1500.

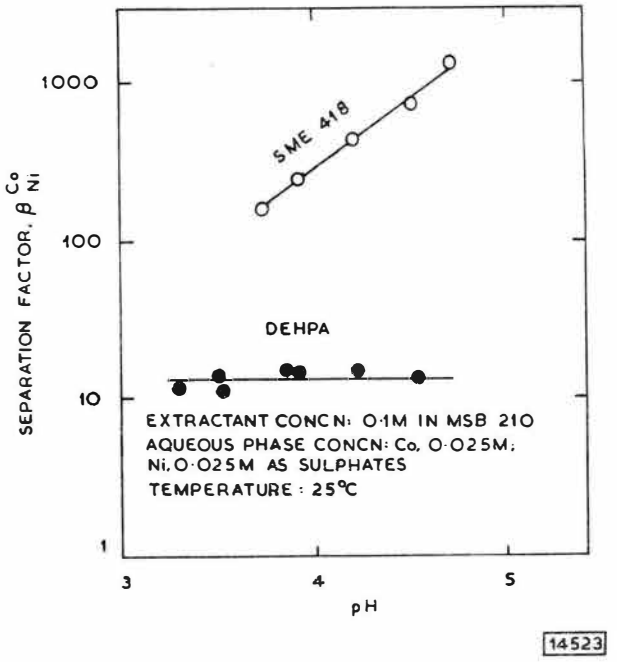

FIG.1 EFFECT OF pH ON THE Co/Ni SELECTIVITY OF SME 418 AND DEHPA

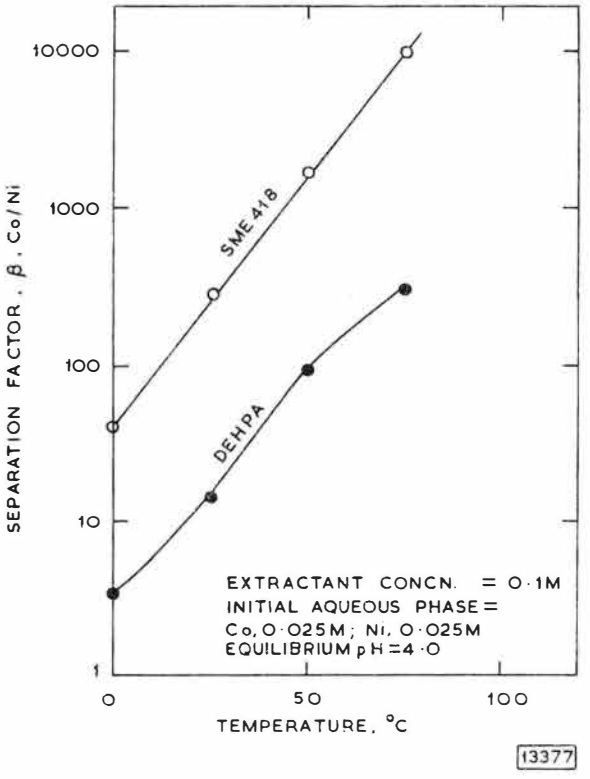

FIG.2 EFFECT OF TEMPERATURE ON THE Co/Ni SELECTIVITY OF DEHPA AND SME 418 FROM SULPHATE SOLUTION

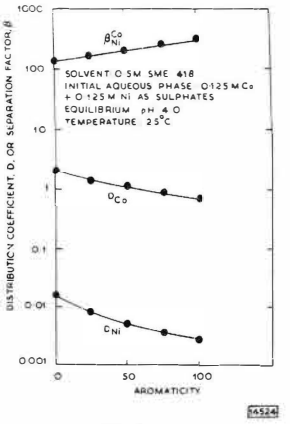

FIG 3 EFFECT OF DILUENT AROMATICITY ON THE SEPARATION OF COBALT AND NICKEL WITH SME 418

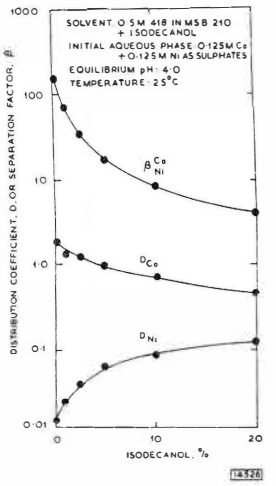

FIG.4 EFFECT OF MODIFIER (ISODECANOL) CONCENTRATION ON THE SEPARATION OF COBALT AND NICKEL WITH SME 418

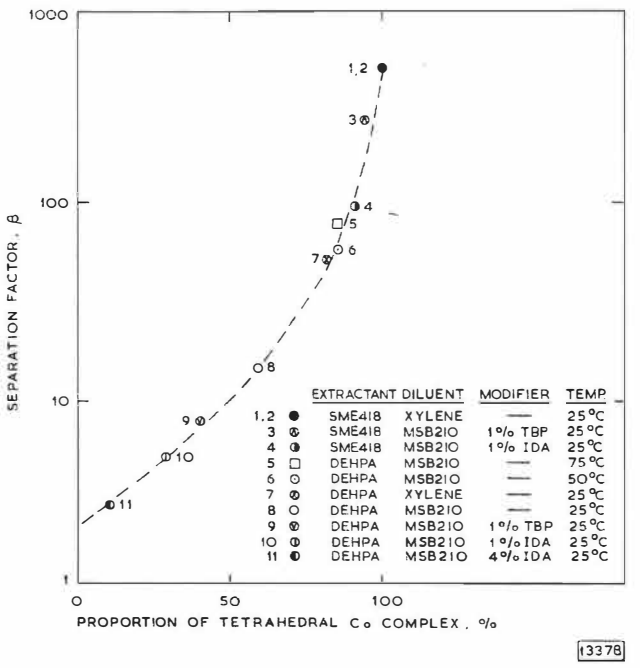

FIG 5 Co/Ni SELECTIVITY FOR DEHPA AND SME418 VERSUS PROPORTION OF TETRAHEDRAL Co II COMPLEX IN ORGANIC PHASE

EXTRACTION OF TUNGSTEN AND MOLYBDENUM BY SULFOXIDES

Dai Ge-Sheng, Xian Bao-Yuan and Su Yuan-Fu

East China Institute of Chemical Technology
Shanghai, China

The solvent extraction technique has become increasingly important in the hydrometallurgy of tungsten and molybdenum. Many research workers have engaged in finding effective extractants and developing new processes to produce tungsten and molybdenum compounds by solvent extraction. Among various extractants such as Alamine 336, MIBK, D2EHPA, TBP (1) being used in the recovery and separation of tungsten and molybdenum, the tertiary amines have been studied most extensively. The mechanism of extracting tungsten by amine from sulphuric acid medium has been put forward by Zelikman (2) and Similar studies have been made by Chen Jia-yong et al.(3). However, the separation of tungsten from molybdenum by using amines as extractants is difficult because of the similar behaviors of these two elements and their compounds. In the Proceedings of ISEC'74, Esnault (4) proposed a new process for separating tungsten from molybdenum by using D2EHPA as extractant, by which the molybdenum is first preferentially extracted and subsequently tungsten is extracted by amines. Large amounts of tungsten ($>40g/l, WO_3$) present in solution will seriously affect the extraction of molybdenum, so the application of this process is limited. Another method of processing revealed by U.S. Patent (5) in 1976 is using TBP as extractant for separating tungsten from molybdeum. In order to increase the selectivity of molybdenum the solution has to be pretreated with hydrogen peroxide. Up to now, the problem of finding a more efficient extractant and a better process for separating these two metals is still considered to be solved and worth further investigation.

The present authors have suggested the use of sulfoxides as extractant to separate tungsten from molybdenum in dilute hydrochloric acid. The experimental work were done in laboratory and the best separating conditions were found.

EXTRACTION OF TUNGSTEN AND MOLYBDENUM

Temperature of extraction Preliminary tests indicated that with dibutylsulfoxide (DBSO) the extraction of both metals favors a low temperature. But as the melting points of pure DBSO and DOSO (dioctylsulfoxide) are 32.6° and 71° respectively, all the experiments using these extractants were carried out at temperatures several degrees above their melting points in order to avoid the possibility of separation of any solid.

Time of equilibration An all glass apparatus was designed to facilitate accurate measurement of the volume changes of both phases, to maintain a proper temperature and to keep away from any moisture in air. As the mixing was done by magnetic stirrer and hence the agitation was not vigorous, the time required to attain phase equilibrium was found to be less than a quarter of an hour. Therefore, 30 minutes of equilibration were used to obtain all the experimental data.

Acidity of aqueous solution The extraction of either tungsten or molybdenum alone by pure dibutylsulfoxide depends strongly upon the acidity of the aqueous solution and the pH value always rises as the extraction proceeds. The change of distribution coefficient of individual metal with pH value of the aqueous solution at equilibrium are shown in Fig.1. From the figure it is apparent that molybdenum may be easily extracted at pH values between 4.6 and 6, whereas tungsten can be extracted appreciably only at pH below 4. It gives a clue to a great possibility of separation of these two metals under certain favorable conditions.

EXTRACTION ISOTHERMS

The equilibrium distributions of the two metals between sulfoxide and aqueous phases were determined and the results obtained for tungsten and molybdenum alone are shown in Figs. 2 and 3. The curves show that at appropriate pH conditions the pure dibutylsulfoxide can extract tungsten and molybdenum from dilute hydrochloric acid solution efficiently and the distribution coefficients have been found to be increased with decreasing concentrations of both metals. From this fact one may anticipate the possibility of high recovery of metal value even at low concentrations. The results also reveal that the loading capacity of organic phase is high, and consequently the concentration of tungsten or molybdenum in stripping liquor can be also high. This is desirable in view of energy comsumption if it is necessary to evaporate the solution for the recovery of the metal value in form of salts. From the form of extraction isotherms only a few theoretical stages are required to attain a high percentage of recovery.

SEPARATION OF TUNGSTEN FROM MOLYBDENUM

Synthetic solution When the feed solution was made of mixed pure tungstate and molybdate only, the separation factor vs equilibrum aqueous pH value is shown in Fig.4 (upper curve). Between pH values 3 and 5, the separation factors are fairly high and the curve indicates a maximum at pH=4.

The effect of even large ratios (WO_3/MoO_3) in the feed solution on the distribution coefficients and hence the separation factors was also examined, and the experimental results are illustrated by following examples:

	WO_3 in feed, g/l	WO_3/MoO_3(wt/wt)	D_{Mo}	(D_{Mo}/D_{WO_3})
(1)	61.6	30	5.63	10
(2)	93.2	150	6.35	35.7

In contrast to the result obtained by Esnault (4) employing D2EHPA as extractant, the use of DBSO enables the separation of the two metals even if the feed solution bears a high WO_3/MoO_3 ratio. The largest separation factor situates in the vicinity of pH = 4.

Solution from scheelite Extraction behavior of a solution from decomposition of scheelite by hydrochloric acid is also studied. The solution usually contains 50-100g/l WO_3 and 1-5g/lMoO_3. The distribution coefficients of both metals between DBSO and aqueous phases at different pH values were determined, and the resulting separation factor vs. equilibrium aqueous pH is also shown (lower curve of Fig. 4). Although the curve is slightly lower than that of the synthetic solution, yet the maximum separation factor is still about 12 which locates at the same pH as the latter. The slight lowering of separation factor curve may be explained by the influence of other impurities originally present in scheelite.

EFFECT OF DILUENTS

The addition of any small amount of water-immiscible organic diluent will seriously impair the extraction of both metals by DBSO as shown in Fig. 5 and Table 1.

However, in case of the added diluent which is partial miscible with water, the reduction of percentage extraction of the metals will be less. This fact leads us to suspect that the species extracted into the solvent may carry water molecules in solvated form. A preliminary test was done and the results obtained are illustrated also in Table 1. This may give a clue to induce further study in order to gain a clear insight into the mechanism of the extraction of both metals.

TABLE 1 EFFECT OF DILUENT

Extractant	Diluent	Temp. °C	Miscibility (%) Solvent in water	Miscibility (%) Water in solvent	Extractibility W	Extractibility Mo
DBSO	NO	40	7.41	30.9	strong	
1M DBSO	BuOH	13	8	16	medium	
	Bu_2O	25	0.5	3	weak	
DOSO	NO	80	1	1	medium	
1M DOSO	Xylene	25	0.013	0.04	nil	
	Bu_2O	25	insol.	0.06	nil	
	BuOH	25	0.6	10	nil	
	BuOH + EtOH	25	1	20	weak	

EXTRACTION MECHANISM

In weak acid solutions the species of both tungsten and molybdenum are very complex and their ionic states have been studied by many researchers. Based on the data presented by Tytko (6), under the present extracting conditions the tungsten may be considered to exist mainly as para-tungstate and meta-tungstate, and the molybdenum as heptamolybdate. The main ionic equilibrium and extraction equations may be as follows:

(1) $$nH^+ + mMeO_4^{2-} \rightleftharpoons Me_mO_yHp^{q-} + wH_2O$$

(1-a) $$\beta_{n,m} = \frac{(Me_mO_yHp^{q-})}{(H^+)^n(MeO_4^{2-})^m}$$

(2) $$Me_mO_yHp^{q-} + qH^+ + eR_2SO \rightleftharpoons Me_mO_yH_{p+q}\cdot(R_2SO)_e$$

Combining Eqs. 1 and 2 gives

(3) $$h_mH^+ + mMeO_4^{2-} + e(R_2SO) \rightleftharpoons Me_mO_yH_z(R_2SO)_e + wH_2O$$

(3-a) $$K_{ex,m,e} = \frac{(Me_mO_yH_z\ (R_2SO)_e)}{(H^+)^{h_m}\ (MeO_4^{2-})^m\ (R_2SO)^e}$$

where Me — tungsten or molybdenum
R_2SO — di-alkylsulfoxide

Based on above equations the expression of distribution coefficient for metals is as follows:

(4) $$D = \frac{\sum_m (H^+)^{h_m} K_{ex,m,e}\ (MeO_4^{2-})^{m-1}\ (R_2SO)^e}{1 + \sum_m (MeO_4^{2-})^{m-1} \sum_n \beta_{n,m}\ (H^+)^n}$$

According to the expression derived from the assumptive mechanism, D depends on pH, concentrations of R_2SO and metallic ions. The change of experimental values of D with these parameters agrees with the prediction.

In order to determine the value e in Eq. 4, the slope analysis was used and the data were plotted in Fig. 5. From the experimental straight line fitted by least square the molecular ratios of the extracted complexes were estimated. The slope of the line for tungsten is 2.09 and that for molybdenum is 1.96.

THE HEAT EFFECT OF EXTRACTION

The extracting equilibrium process involves solution, complex reaction and phase equilibration and is very complicated. By making some reasonable assumptions and considering all above processes as a pseudo-macroscopic process, the relation between distribution coefficient and temperature may be written as follows:

$$\ln D = \ln D^{0} + \frac{\Delta H_p}{R}\left(\frac{1}{T}\right) \qquad (5)$$

where T — temperature
ΔH_p — total extraction heat
R — the gas constant

ΔH_p for extracting tungsten and molybdenum from diluted hydrochloric acid solution were estimated from experimental data to be

$$\Delta H_{p,W} = -4.5 \text{ Kcal/mol}$$

$$\Delta H_{p,Mo} = -3.5 \text{ Kcal/mol}$$

REFERENCES

(1) A.K.De, S.M.Khopkar, and R.A.Chalmers, "Solvent Extraction of Metals" MNP Company, London 1970.

(2) A.N.Zelikman, G.M.Vol'dman, N.N.Rakova, T.P.Stepyushkina, Tsvet. Metal, 45, 38,(1972).

(3) Shuqiu Yu, Jiayong Chen, Acta Metallurgica Sinica, 18, 180, (1982).

(4) F.Benault, M.Rohaylia, J.M.Latard, J.M.Demarthe, Proceedings ISEC'74, vol. 3, 2265, (1974).

(5) A.N.Zelikman, G.M.Vol'dman, V.K.Sumyantsev, G.N.Ziberov and V.S.Kagermanian, U.S. Patent 3,960,478 (1976).

(6) Karl-Heinz Tytko and Oskar Glemser in H.J.Emeleus and A.G.Sharpe (Editors) "Advances in Inorganic Chemistry and Radiochemistry" vol. 19, Academic Press, New York, 1976, pp. 221-285.

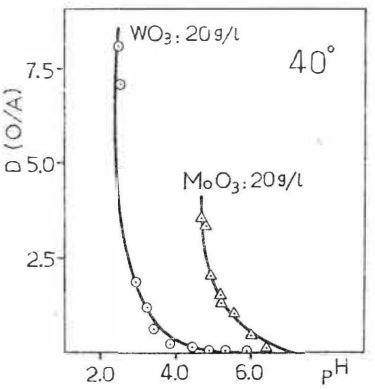

FIG. 1
EFFECT OF pH
ON
D(W) AND D(Mo)

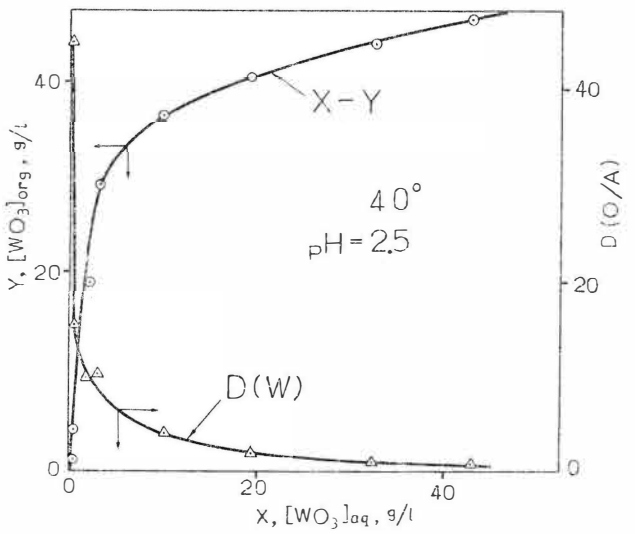

FIG.2 D(W) AND EXTRACTION ISOTHERM

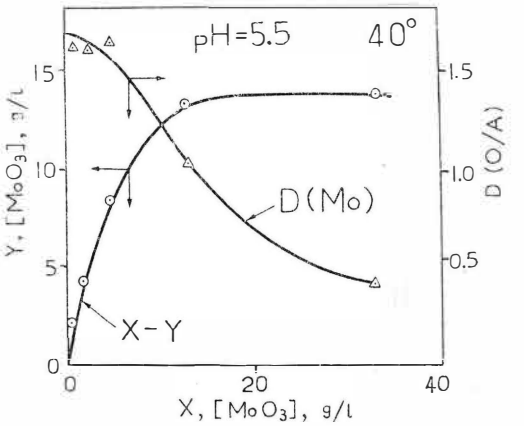

FIG. 3 D(Mo) AND EXTRACTION ISOTHERM

FIG. 4
EFFECT OF
pH ON β
⊙ SOLUTION CONTAINS W AND Mo ONLY
△ SOLUTION OBTAINED FROM SCHEELITE

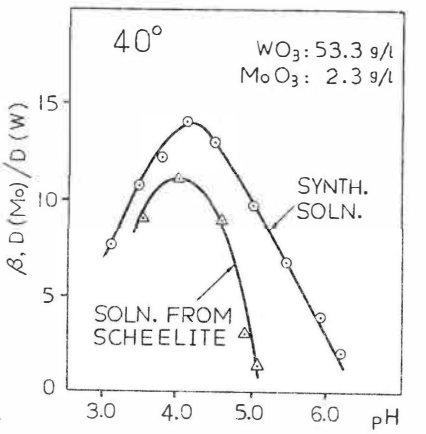

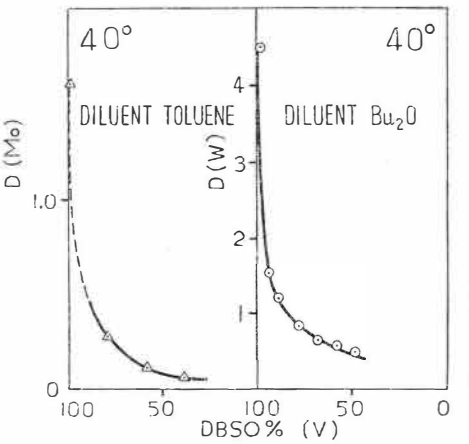

FIG. 5
EFFECT
OF
DILUENT

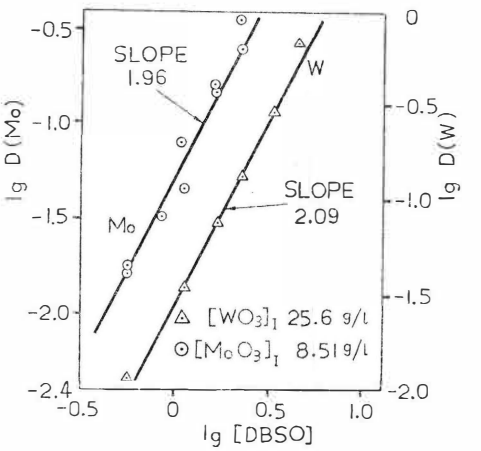

FIG. 6
SLOPE
ANALYSIS

SOLVENT EXTRACTION SEPARATION OF MOLYBDENUM AND TUNGSTEN USING DI(2-ETHYL HEXYL) PHOSPHORIC ACID (HDEHP) AS AN EXTRACTANT

N. R. Das, B. Nandi and S. N. Bhattacharyya
Nuclear Chemistry Division
Saha Institute of Nuclear Physics
92, Acharya Prafulla Chandra Road
Calcutta-700009, West Bengal, India

ABSTRACT

A possible use of di(2-ethylhexyl) phosphoric acid (HDEHP) as an effective extractant for solvent extraction separation of molybdenum and tungsten, both in tracer and macro-scales from aqueous orthophosphoric acid medium, has been probed. Structure and composition of the extracted species are also ascertained by means of IR spectrophotometric studies.

INTRODUCTION

The elements molybdenum and tungsten form one of the critical element pairs, which have very close chemical similarities and therefore there separation from each other always constitutes an important problem to the analytical chemists. One of the most efficient methods used in general for effecting their separation is solvent extraction. In our attempt to apply the reagent, di(2-ethylhexyl) phosphoric acid (HDEHP) as an extractant for the separation of various congeneric pairs of elements from each other (1,2), the separation of molybdenum and tungsten with its aid has been studied here. Studies on the extraction behaviour of molybdenum and tungsten from various acidic media using HDEHP indicate that the distribution ratios of molybdenum are always higher than those of tungsten and the trend of decrease in the distribution ratios with the increase of acidity is found to be very much pronounced in case of tungsten when orthophosphoric acid happens to be the aqueous medium. Hence, the present investigation deals mainly with the study of extraction of molybdenum and tungsten by HDEHP from orthophosphoric acid medium.

EXPERIMENTAL

Reagents. The solvents and other chemicals used were of analytical grade. The reagent, di(2-ethylhexyl) phosphoric acid, a product of ICN Pharmaceuticals, Plainview, N. Y., was used as the extractant. The radiotracers, Mo-99 in molybdate and W-187 in tungstate forms were procured from BARC, Trombay, India.

Procedure. Extraction of metal ions with the reagent, HDEHP, was carried out by equilibrating equal volumes of aqueous orthophoric acid solution containing the metal ions at different concentrations with HDEHP solutions also of varied concentrations in different diluents, namely, carbontetrachloride, n-heptane, etc. Measurements of activities in different phases were made by G. M. counters.

RESULTS AND DISCUSSION

Extraction behaviour of the metal ions at tracer levels from orthophosphoric acid medium by HDEHP solution in n-heptane over a wide pH range is shown in Figure 1. Distribution ratio of molybdenum increases linearly as the pH increases to 3 and then decreases (Figure 1, curve A). At this pH range, molybdenum mainly exists in cationic forms (3) such as MoO_2^{+2}, $MoO(OH)_2^{+2}$, etc, which can exchange with HDEHP in the following way

$$(1) \qquad MoO_2^{+2} + 2\ HDEHP \rightleftharpoons MoO_2(DEHP)_2 + 2H^+$$

The observed straight line in the pH range 0.8 - 3.0 has a slope 2 which agrees well with that required by equation (1). In the pH range ~ 3.5-7, the decrease in the distribution ratio of molybdenum can be corroborated with the fact that molybdenum gradually aggregates to heteropoly anion of the type $H_3PMo_{12}O_{40}$. In the alkaline solution, in fact, molybdenum (VI) exists as MoO_4^{-2} which does not exchange with HDEHP.

For tungsten also the extraction behaviour, as shown in Figure 1 follows a similar trend but with much lower degree of extraction. But the ranges in which the extractable species, WO_3^{+2} (upto pH 1.4) and the aggregated heteropoly tungstate species, $H_3PW_{12}O_{40}{\cdot}xH_2O$, (pH 1.4 - 4.0) exist differ to a considerable extent from that in case of molybdenum. Thus, molybdenum in the tracer scale gets extracted almost free of tungsten at pH 3.0-3.5 from orthophosphoric acid medium with 0.1M HDEHP in n-heptane. The decontamination factor was found to be more than 500 in this pH range.

Quantitave separation of the radioactive tracers, Mo-99 and W-187, in respective phases were verified further through γ-ray spectrometry. The absence of any photopeak characteristics of Mo-99 in aqueous and W-187 in organic phases respectively after separation indicates the selectivity of the extractant for molybdenum under the specific conditions. The fact that aqueous phosphorous does not exchange with that in the organic phase has been tested radiometrically using the radioactive tracer, P-32.

For macroscale extraction of the two elements it has been observed that the distribution ratios decrease with increase in the concentration of the metal ions throughout the pH range studied (Figure 2). The lowering in the distribution ratios may be due to the fact that both molybdenum and tungsten form hydrolysed polymeric species or ion clusters, the nature of which again changes from higher to lower pH. It is of interest to note that at macro concentrations the point at which distribution ratio is maximum, shifts towards the lower pH region with the increase in metal ion concentration in the aqueous solution (Figure 1 and 2).

This observed shift towards the lower pH can be explained from the consideration of the chemistry of formation of hydrolytic polymeric species of molybdenum (4) where more and more hydrogen ions are needed for the formation of MoO_2^{+2} species so that extaction by HDEHP may be effected.

In case of tungsten, however, the formation of WO_2^{+2} ion is reported (5) to occur at acid concentration lower than pH 1. Extraction of tungsten from aqueous solution at pH 1-2.5 can be thought of as due to the formation of hydrated tungstic oxides, $WO_3 \cdot H_2O$ and $WO_3 \cdot 2H_2O$ (6) and not due to WO_2^{+2} as in the tracer scale. When the pH is increased beyond 2.5, the aggregation of polyanion is pronounced and hence extraction decreases. The efficiency of separation in the macro-scale, was determined by ascertaining the extent of coextration of one in the presence of the other and the contamination due to tungsten in the separation of molybdenum does not exceed ~ 1%.

Studies on the effect of extractant concentration on the extractibility of the metal ions show that the distribution ratio of molybdenum ions increases with the increase in HDEHP concentration starting from 0.01M upto 0.2M HDEHP in n-heptane after which the rates of increase of distribution ratio values decrease. However, the extraction of tungsten, which starts from a higher concentration of HDEHP i.e., 0.1M HDEHP in n-heptane, steadily increases with increase in the concentration of HDEHP. The lowering of extration efficiency of HDEHP at higher concentration in general, could be due to larger aggregation of HDEHP molecules (7). This aggregation of the extractant molecules depends mainly upon some factors such as HDEHP concentration, nature of the metallic species and the type of the nonpolar diluents employed. In fact, the distribution ratio values are found to decrease with increase in the dielectric constant of the diluents used.

The site of the metal ion attachment as well as the structure of the extracted species were studied by taking recourse to IR spectroscopy. IR spectrum of extracted 0.02M Mo(VI) from aqueous orthophosphoric acid solution in 0.1M HDEHP in carbontetrachloride was measured in the region 700-4000 cm^{-1} and was compared with that of free HDEHP in carbontetrachloride in the same region (Figure 3). From a consideration of the changes in characteristic spectral properties such as shifting of positions of the absorption maxima, splitting of the bands, lowering of intensity of adsorption, etc., of the IR spectra of pure HDEHP and that of metal loaded HDEHP, it is suggested that the metal HDEHP complex has a close-ring structure similar to that suggested earlier by Kolarik (8).

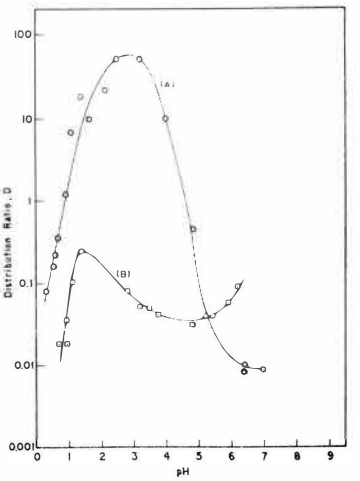

FIGURE 1. TRACER SCALE EXTRACTION OF Mo (A) AND W (B) IN H_3PO_4 BY HDEHP IN n-HEPTAN.

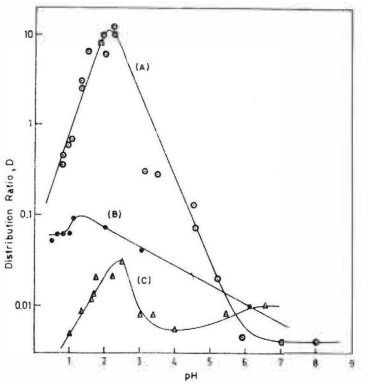

FIGURE 2. EXTRACTION OF 2.5×10^{-3} M Mo (A), 2.0×10^{-2}M Mo (B) AND 1.4×10^{-3}M W (C) IN H_3PO_4 BY HDEHP IN n-HEPTANE

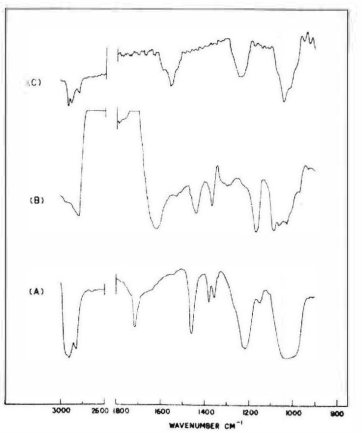

FIGURE 3. IR-SPECTRA OF HDEHP (A), Mo-HDEHP COMPLEX (B) AND DEUTERATED HDEHP (C)

REFERENCES

1. N. R. Das, B. Nandi and S. N. Bhattacharyya, Int. J. Appl. Radiat. & Isot., 32, 205 (1981)
2. Ibid, Radioanal. Chem., 62, 53 (1981)
3. S. J. Lippard, Progress in Inorganic Chemistry, 22, 35 (1979)
4. M. L. Freedman, J. Inorg. Nucl. Chem., 25, 575 (1963)
5. H. J. Emele'us and J. S. Anderson, Modern Aspects of Inorganic Chemistry, 2nd Ed., Chapt. 2, 212 (1952)
6. J. C. Bailar, H. J. Emele'us, R. Nyholm and A. F. Trotman-Dickenson, Comprehensive Inorganic Chemistry, 1st Ed. Chapt. 51, 637 (1973)
7. V. I. Spiryakov, P. G. Kurtikov, V. M. Barinov, A. S. Solovkin and G. N. Yakovlev, Radiokhimiya, 14, 574 (1972)
8. Z. Kolarik, J. Inorg. Nucl. Chem., 35, 2025 (1973)

RECOVERY OF MOLYBDENUM AND RHENIUM BY SOLVENT EXTRACTION

Chen Tingzhang, Yuan Chusheng, Zhou Zhonghua and Ma Rongjun

Changsha Research Institute of
Mining and Metallurgy

Changsha, Hunan, China

ABSTRACT

There are some methods for recovery of Mo and Re from molybdenite Among them the treatment of concentrate by pressure leaching and consequent solvent extraction to obtain Mo and Re from leach liquor shows merits of simple flowsheet, high recovery of metal and low cost. In this paper are given the results of investigation of solvent extraction of Mo and Re with one and the same solvent N235, a mixed trialkyl amine, but of different concentrations, i.e. extracting Re primarily with low concentration solvent and then Mo with high concentration solvent, then the loaded phases are stripped separately with ammonia. Ammonium perrhenate and molybdate are crystallized from stripping solutions by common way.

INTRODUCTION

The traditional process for production of Mo and Re compounds consisting of oxidizing roasting of molybdenite and recovering Re from washes of flue gases shows defects in low recovery of metals, high cost, and atmosphere pollution by SO_2. A new method should be developed to overcome these defects and more economically and effectively recover Mo and Re. The digestion of molybdenite under pressure gave ideal decomposition of raw materials. The problem remained was effective extraction of Mo and Re. Solvent extraction was thought to be the most attractive solution. So the systematic study had been proceeded on these lines.

THE CHOICE OF SOLVENT

In strongly acidic leach liquor Re and Mo occur as anions. Their separation by solvent extraction may be carried out according to such ways as (a) primary extraction of Mo and then Re (1), i.e. extraction of Mo from weakly acidic solution with 28% DEHPA, then extraction of Re with 7-8% TOA; (b) extraction of Re before that of Mo (2,3), i.e. extraction of Re with 25% DBBP - cyclosol and subsequent extraction of Mo from the raffinate with 5% DEHPA - 2% Alamine 304 - 5% TBP - kerosene, or extraction of Re from strongly acidic solution (4N H^+) with extractant A 101, leaving Mo in aqueous phase; and (c) Coextraction of Mo and Re, then separation of them in stripping solution, (4-6) i.e. extraction of Mo and Re with 5% Alamine 336, then reextraction of Re from stripping solution with 5% Aliquat 336 and recovering Mo from raffinate; or coextraction with 10% Adogen 383, neutralization of stripping solution to PH 2.5-3.5 to crystallize molybdate and extraction of Re from mother liquor of crystallization; or coextraction of Mo and Re with about 4% TOA + 1.5% Aliquat and selective stripping these metals.

From this brief review it was clear that there were a lot solvents promising for extraction of Mo and Re and the most suitable one for extraction from strongly acidic leach liquor should be selected by experimental comparison.

EXPERIMENTAL

The analysis of leach liquor of molybdenite from metallurgical plant is shown in table 1

Table 1 The analysis (g/l) of leach liquor

Mo	Re	SiO_2	Fe	Al_2O_3	Cu	CaO	MgO	NO_3	Total acidity(N)
8.7	0.19	0.45	5.5	2.5	0.5	0.45	1.3	5.25	4.5

All sovents, diluent and other reagants used were commercial products. Extractions were proceeded in mixer - setter (but screening tests - in separating funnels) at ambient temperature. The contact time was generally five minutes. Re was analysed by polarographic and tetraphenyl arsonic chloride methods, Mo was analysed by special polarographic and gravimetric methods. Impurities in products were determined by quantitative spectrometry.

RESULTS

Screening tests.

The extraction tests from leach liquors were accompanied by emulsification in all cases. The emulsion thus formed could not be broken by setting for days. The addition of fluoride or coagulant to leach liquor might break emulsion. Fluorides made higher silicates depolymerized and simple silicates did not enhance emulicfication. Additives HF and NaF had little effect on extraction of Mo and Re (see table 2).

Table 2 The effect of HF and NaF on the extraction of Mo and Re

Composition of organic phase	Quantities of added fluorides	E_{Re} %	E_{Mo} %
1.2% N235-10% aliphatic alcohol-kerosene	HF(40%) 10 ml/l	69.9	2.7
1.5% N235-10% aliphatic alcohol-kerosene	NaF 5 g/l	66	4.2

Phase ratio : O/a = 1/5

The added coagulant to leach liquor bridged silicates together to form precipitate. Table 3 and 4 show the effect of added coagulants on the precipitation of silicates and on the extraction.

Table 3 The effect of coagulant on precipitation of silicates

kind of coagulant	added quantities of coagulant (PPm)	precipitation of silicates (%)	precipitation of Mo (%)	precipitation of Re (%)
A	50	57.6	0.37	0.22
A	100	90.2	0.31	0.18
B	50	69.3	0.13	0.08

Table 4 The effect of coagulant on extraction of Mo and Re

kind of coagulant	Quantities of added coagulant (PPm) 50		100		150		200	
	ERe%	EMo%	ERe%	EMo%	ERe%	EMo%	ERe%	EMo%
A	97.3	6.7	97.2	5.2	97.1	6.1	97.1	6.9
B	97.3	1.7	97.2	5.2	97.1	6.2	97.1	6.9
C	97.0	7.6	-	-	-	-	-	-

phase ratio : O/A = 1/5 . organic phase : 2.5% N235 - 10% aliphafic alcohol - kerosene

It is found from table 3 and 4, the addition of 100 ppm Coagulant A could collect and precipitate the majority of silicates, losses of both Re and Mo were less than 0.5% and there was little effect on extraction of Mo and Re. There appeared a little increase in Mo extraction with the quantity of added coagulant B the precipitation of silicates without consequant filtration or direct addetion of coagulant to organic phase did arouse emulsification during extraction. Fluorides were more expensive and might cause secondary pollution. The addition of coagulant, therefore was prefered.

Solvents promising sepation of Mo and Re in leach liquor were widely examined. The results are shown in table 5.

TABLE 5 The extraction and separation of Mo and Re with different solvents

Solvent	ERe %	EMo %	β^{Re}_{Mo}	Notes
MIBK	13.8	6.5	2.3	
Isoamyl alcohol	63.9	4.7	37	
TBP	91.7	16.3	56	
50% TBP	86.8	7.5	44.1	
25%N235-10%aliphatic alcohol-kerosene	96.6	85.3	4.7	N235-a mixture of tertiary amines with average mol. wt. near that o TOA
1.2%N235-10% aliphatic alcohol-kerosene	69.9	2.7	83.5	
30%N503 -kerosene	63.7	3.6	47	
30% A101- kerosene	62.9	3.3	48.2	
30% mixed Secondary amine - kerosene	62.4	3.1	51.9	
10% lauryl amine- 10% TBP - kerosene	47.0	52.1	0.81	the organic phase formed emulsion
0.8 MDEHPA- kerosene	4.4	36.9	0.078	

Table 5 shows that basic solvents could not preferentially extract Mo; DEHPA extracted Mo only at PH 2 - 3 as the precipitation happened, so preferential extraction of Mo was inappopriate. The coextraction of Mo and Re with high concentration N235 followed by the reextraction of Re with quartenary ammonium salt and crystallization of molybdate from stripping solution appeared to be feasible. But the difficulty of stripping Re from quartenary ammonium salt hindered its adoption. The prior extraction of Re with low concentration N235, mixed secondary amines or acetamine was found to be possible, but only low concentration N235 was selected due to its low amount needed in use, low evaporation loss and high degree of concentrating Re. From table 5 it may also be found, that Mo might be fairly extracted with high concentration N235. We can therefore, recovery Mo and Re from pressure leaching liquors with one and the same solvent N235.

Factors affecting the extraction of Re.

Figures 1,2 and 3 give the effects of concentration of N235, the phase ratio and the acidity of aqueous phase on the extraction and separation of Mo and Re. The extraction of Mo and Re increased with the rise of solvent concentration and phase ratio. With the increase of acidity of leach liquors the extraction of Re increased and that of Mo decreased. Thus the separation factor of Re from Mo enlarged. This was in agreement with the extraction mechanism of Re and also owing to the competition of HSO_4^- ion that decreased the extraction of Mo. The third phase would appear during extraction without addition of dissolvent. The aliphatic alcohol could deminish the third phase and slightly improve the separation of Re from Mo, see Fig. 4. Because HNO_3 was added at pressure leaching of molybdenite as catalyst , the effect of this acid on extraction process had been studied. The results are shown in Fig. 5.

The extraction of Re increased and that of Mo slightly decreased with the rise of HNO_3 concentration. This phenomenum differed from the extraction of Re from HNO_3 media by TOA (7) . In the former case HNO_3 in H_2SO_4 media behaviored probably, as salting - out agent.

The extraction of Re increased for 5% as the temperature lowered from 40°C

to 5°C. Therefore, the extraction of Re at ambient temperature is reasonable. The equilibrium of Re extraction might be attained in half minute, and this fact indicated that the phase cantact appeared to be the controlling step of extraction reaction. The stripping of Re and Mo contamination were easily acomplished with 5 N ammonia at phase ratio o/a = 10/1. The loaded as well as stripped organic phases needed not scrubbing in circulation. The stripping solution of Re was evaporated to crystallize perrhanate.

Factors affecting the extraction of Mo

The plots of N235 concentration and phase ratio us Mo extraction are shown in Fig. 6 and 7. Table 6 gives the effect of aqueous acidity on extraction of Mo.

TABLE 6 The effect of acidity of raffinate after Re extraction on Mo extraction

acidity of raffinate, (N)	3.88	3.70	3.66	3.51	3.13	2.83
E_{Mo} %	71.7	70.9	71.2	73.4	72.1	78

Aqueous phase : the same in Fig. 6 , but with different additions of ammonia

Organic phase : the same in Fig. 7

phase ratio : o/a = 1/5

The extraction of Mo increased with the increase of N235 concentration and phase ratio and with the decrease of aqueous acidity. The last effect was thought to be due to HSO_4^- ion competition.

Fig. 8 shows the effect of aliphatic alcohol on Mo extraction.

Aliphatic alcohol helped dissolve the third phase, but reacted with N235 and thus lowered its Mo extraction Capacity.

In this process Fe and Cu were not extracted even in presence of chloride ions. So the separation of Mo and Fe was satisfactory. The organic phase loaded by Mo needed scrubbing with 1.6 - 1.8 N ammonia to pH about 4.5 at o/a = 5-6/1, and then contacted with 9-10 N ammonia to complete stripping.

THE PROCESS FLOWSHEET

A procedure scheme for recovery of metals was proposed and tested in counter-current way by means of laboratory mixer-settler. The results obtained are shown in table 7-10.

TABLE 7. stagenise analysis of Re at equilibrium

Extraction (gl^{-1})									stripping(gl^{-1})
1	2	3	4	5	6	7	8	9	
0.045	0.015	0.005	0.0025	0.0019	0.001	0.0004	0.0003	0.0003	0.0087 0.0024

TABLE 8. stagenise analysis of Mo at equilibrium

Extraction (gl^{-1})							Stripping (gl^{-1})	
1	2	3	4	5	6	7	1	2
5.19	2.33	1.16	0.78	0.58	0.44	0.39	0.47	0.087

TABLE 9 Technical date and Re content in the intermediate products

E_{Re} %	Raffinate gl^{-1}	Re-loaded solvent gl^{-1}	Re stripping %	stripping solution gl^{-1}	pH
99.78	0.0003	1.10	99.78	10.2	~9

TABLE 10 Technical date and Mo content in the intermediate products

E_{Mo} %	Raffinate gl^{-1}	Mo-loaded solvent gl^{-1}	Mo stripping %	stripping solution gl^{-1}	pH
95.94	0.4	26.61	99.66	160.5	9~10

With six extraction stages the Re yield achieved higher than 99%, Re content in raffinate was less than 1 mg/l and the separation factor of Re and Mo was over 9000. Six stages could extract more than 95% of Mo and its content in raffinate was less than 0.5 g/l. Both Re and Mo might be stripped to more than 99.5% with two stages. The chemical properties and technological performance of solvent was atable inprolonged operation. The unit consumption of solvent was 2.5 l/m^3 feed solution for Re and 0.64 l/m^3 feed solution for Mo. The purity of perrhenate and molybdate prepared from each stripping solution by ordinary methods is obvious from table 11 and 12. These compounds meet satisty the demands of industrial application and are in large scale production.

TABLE 11 The analysis of ammonium perrhenate product(%)

NH_4ReO_4	Cd	Be	Mn	Ti	Co	Cu	Mg	Fe	Ba	Mo	Pb	Sn	Sb	Ca	K	Na
99.99	each $< 2 \times 10^{-5}$					each $< 5 \times 10^{-5}$			Ni Pt each $< 4 \times 10^{-5}$				each $< 1 \times 10^{-4}$		$< 2 \times 10^{-4}$	$< 2.5 \times 10^{-5}$

TABLE 12 The analysis of ammonium paramolybdate product (%)

Mo	P	Pb	Cd	Bi	S	Fe	Si	Al	Sb	Co Ni Cu	Mn	Mg	Ti	V	W	HB
55.15	<0.0005	each<0.0001				each<0.0006			<0.001	each<0.0003			<0.0015		0.1	1.04

P.S. This work was done with the participation of technical staff of the metallurgical plant. Zhou Taili and Zhong Xiang had joined in doing part of this work.

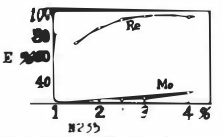

Fig. 1 The effect of concenction of N235

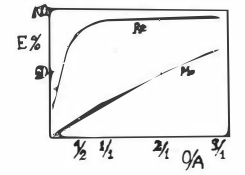

Fig.2 The effect of phase ratio

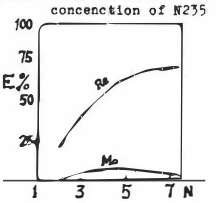

Fig.3 The effect of acidity

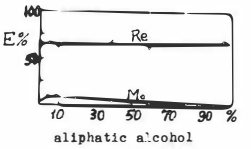

Fig.4 The effect of concenction of sliphatie alcohol

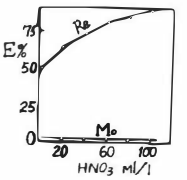

Fig.5 The effect of HNO_3 on extraction
Aqueous: Simulated, containing Re 122-134 mg/l, Mo 28.3g/l, H^+ 3.5N
Organic: 1.5% N235-3% aliphactie alcohol-kerosene o/a = 1/5

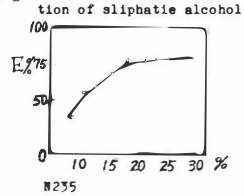

Fig.6 The effect of N235 concetration on Mo extraction
Aqueous phase: leach liquor after removing silicates and extraction of Re
Organic phase: N235-10% aliphatic alcohol-kerosene
phase ratio: o/a = 1/5

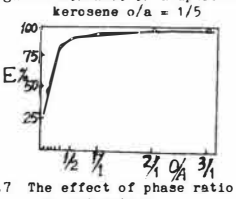

Fig.7 The effect of phase ratio on Mo extraction
Aqueous phase: the same in Fig.6
Organic phase: 15% N235-10% aliphatic alcohol-kerosene

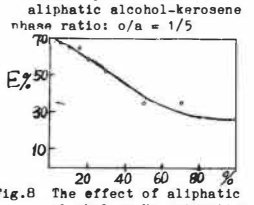

Fig.8 The effect of aliphatic alcohol on Mo extraction
Aqueous phase: the same in Fig.6
Organic phase: 15% N235-aliphatic alcohol-herosene

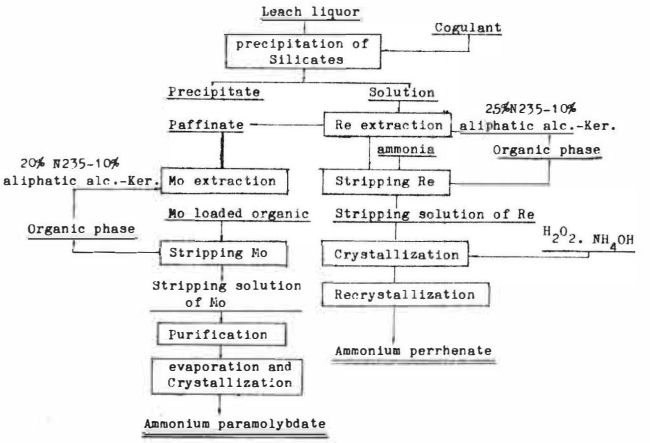

Fig. 9 The flowsheet of extraction of Mo and Re from pressure leaching liquor

REFERENCES
1. А.Н.Зеликман Извет. Вус. Учебных Заведений: Цветн. Металл
2. Piterson. H. D, U.S. Patent 3751555 8 (1973)
3. L. Karagiozov and C. Vasilev, Hydrometallurgy 4(1979) 51-55
4. Ellsworth. W. et al, U.S. Patent 3739057 8(1973)
5. 特許公報 昭 50-6405 3(1975)
6. Taili,Z., et al, Hydrometallurgy 8(1982) 379-388
7. Л.В.Борисова и др. Рений (1974)

THE EFFECT OF BENZENE AS DILUENT IN THE EXTRACTION OF CHLOROMETALLIC ACIDS BY DIISOPROPYL ETHER

Darko Maljković, Alojzija Paulin and Dubravka Maljković

Department of Chemistry and Non-Ferrous Metallurgy
Faculty of Metallurgy, University of Zagreb
Sisak, Yugoslavia

Previous investigations of the extraction of chlorometallic acids by a mixture of diisopropyl ether (IPE) and benzene gave very interesting results (1). In the systems: $FeCl_3$-HCl-H_2O-IPE-C_6H_6 (*a*) and $AuCl_3$-HCl-H_2O-IPE-C_6H_6 (*b*) under given conditions the third liquid phase or the heavy organic phase was observed in a wide concentration range. Three-phase systems containing IPE are characterised by high metal concentration in the heavy organic phase and a high distribution ratio between the heavy organic phase and the aqueous phase. This makes them very promising for separation purposes. A number of phases, phase volumes and distribution ratios were found to depend on the initial IPE concentration. In system *a* under given conditions the partial distribution ratio between the heavy organic phase and the light organic phase, $(D_c)^h_l$, of iron(III) had a minimum value at 4-5 M initial IPE concentration. In system *b* under given conditions the gold(III) extraction was enhanced, i.e. the total distribution ratio, $(D_c)_{tot}$ (definition is given later) attained a maximum at 3 M initial IPE concentration (the nearest $(D_c)_{tot}$ values were determined at 1.8 and 4.1 M initial IPE concentration). Also, it was found that the extraction behavior of system *a* considerably differs from system *b*. The third phase formation was observed also in the analogous system $GaCl_3$-HCl-H_2O-IPE-C_6H_6 (*c*) (2).

EXPERIMENTAL

IPE was purified and distilled. Other chemicals and solvents used were of analytical reagent grade. Separations were made by conventional technique (1) in separation funnels having a calibrated stem or in graduated cuvettes. The total initial volume of the systems was 12-40 mL. Equilibration of the systems was performed in a thermostat at 20.0 ± 0.05 °C during one hour. The initial phase volume ratio, r^i, was always 1.0.

The concentration of metals in the aqueous phase and in pretreated samples of the organic phase was determined by UV absorption spectrometry and complexometric titration (for larger quantities of iron(III) and gallium(III)) or by gravimetry (for larger quantities of gold(III)). Chlorides were determined by potentiometric titration. In the aqueous phase the chloride was determined directly and in the organic phase after reextraction, except in the presence of gold. In the case of samples which contained gold it was necessary to remove the gold by precipitation before titration. The water in the organic phase was analysed by Fischer's titration method modified by Laurene (3) in the presence of iron.

RESULTS AND DISCUSSION

Investigation of system *a*, stimulated by earlier results (1), on different levels of the initial concentration of iron(III) or hydrochloric acid confirmed the dependence of distribution on the initial IPE concentration. Higher partial distribution ratios $(D_c)^h_{aq}$ in three-phase systems were found, but the existence of the function maximum depended on the initial acid concentration. By additional investigation of system *b* in the same conditions as earlier (1) i.e. 0.09 M initial concentration of gold(III) and 11.8 M initial concentration of acid, the maximum value of distribution ratios D_c, $(D_c)_{tot}$ and of the average distribution ratio $(D_c)_{av}$ (definition is given later) was found at 3.6 M initial IPE concentration (Figure 1). At a lower initial acid concentration (8.0 M) the function maximum was not obtained. In system *c* the effect of initial IPE concentration on the metal concentration in the equilibrate phases was observed. Contrary to systems *a* and *b* in system *c* the maximum partial distribution ratio $(D_c)^h_{aq}$ was obtained at all investigated levels of initial gallium or acid concentration. At 8.0 M initial acid concentration and 0.17 M initial metal concentration $(D_c)^h_{aq}$ value passed through a maximum at an initial IPE concentration of about 2.6 M (Figure 2).

The appearance of three liquid phases was observed in an extended range of initial concentration of constituents in systems *a*, *b* and *c*. The volume and number of equilibrated phases in system *c* similarly to systems *a* and *b* depend on initial IPE concentration. The phase volume ratio of the heavy organic phase to the light organic phase, r^h_l, in system *c* strongly changes at a higher initial gallium concentration.

The results obtained by analyses of the heavy organic phase in systems *a* and *c* showed that the chloride/metal ratio varies slightly (3.4-3.8 and 3.6-4.1 respectively) with the initial IPE concentration increase under given conditions compared to those in system *b* (3.1-7.1, with a minimum value at 3 M initial IPE concentration) as shown in Figure 3. The difference between systems *b* and *a* is also confirmed by the results obtained for the water/metal ratio (1.7-34.0 and 3.3-5.4 respectively) as shown in Figure 4.

Equations and descriptions used in three-phase systems. The results of extraction in three-phase systems can be presented by means of the total distribution ratio, average distribution ratio or some of the partial distribution ratios. The partial distribution ratio is the ratio of the total analytical concentration of a substance in one of the two organic phases to its total analytical concentration in the other organic or aqueous phase. There are the partial distribution ratio between the heavy organic phase and the aqueous phase, $(D_c)^h_{aq}$, the partial distribution ratio between the light organic phase and the aqueous phase, $(D_c)^l_{aq}$, and the partial distribution ratio between the heavy organic phase and the light organic phase, $(D_c)^l_h$. The total distribution ratio, $(D_c)_{tot}$, is defined as a sum of partial distribution ratios $(D_c)^h_{aq}$ and $(D_c)^l_{aq}$; it is a quasi distribution ratio. The average distribution ratio, $(D_c)_{av}$, is defined as the ratio of the average analytical concentration of a substance in both organic phases to its analytical concentration in the aqueous phase. The following relations are valid:

$$(D_c)_{tot} = (D_c)^h_{aq} + (D_c)^l_{aq}; \quad (D_c)_{av} = (D_c)^l_{aq}\frac{V_l}{V_o} + (D_c)^h_{aq}\frac{V_h}{V_o},$$

where V_l, V_h and V_o are volumes of respective phases, and $V_o = V_l + V_h$. Relations between terms as applied in a real situation are presented graphically in Figure 1. Due to very strong volume changes of the equilibrate phases in the systems containing IPE, particularly in the three-phase systems, it is very interesting to compare the distribution ratios with respective extraction factors, D_m. In the presentation of results by means of D_m the circumstances are better. From the definition of D_m (the ratio of the total mass of a solute in the organic phase to that in the aqueous phase) it follows that the total and average extraction factors are equal. There are also partial extraction factors between the respective phases: $(D_m)^l_{aq}$, $(D_m)^h_{aq}$ and $(D_m)^h_l$. The following relations are valid:

$$(D_m)_{tot} = (D_m)_{av} = (D_m)^h_{aq} + (D_m)^l_{aq} = (D_c)^h_{aq}\frac{V_h}{V_{aq}} + (D_c)^l_{aq}\frac{V_l}{V_{aq}}$$

(Subscripts and superscripts used: l - of the light organic phase, h - of the heavy organic phase, aq - of the aqueous phase and o - of the total organic phase.)

REFERENCES

1. Da. Maljković and M. Branica, CIM Spec. Vol. 21, 173 (1979).
2. A. Paulin, M.Sc. Thesis, Univ. of Zagreb, Zagreb, 1981.(Croat.)
3. H.A. Laurene, Anal. Chem. 24, 1496 (1952).

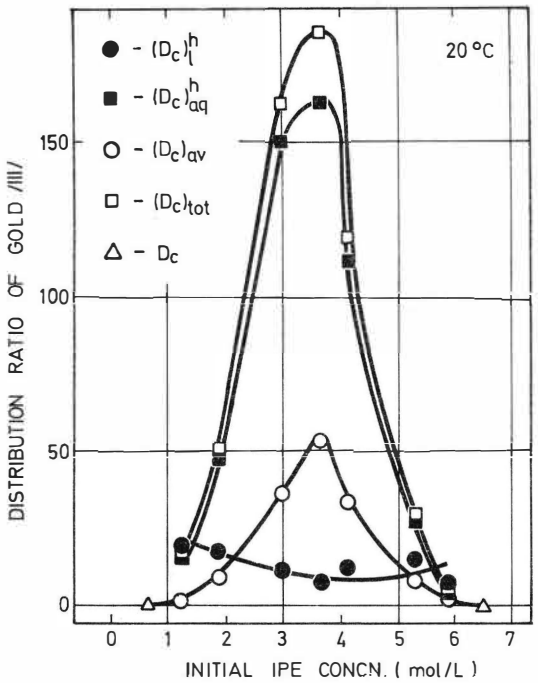

FIGURE 1. PARTIAL DISTRIBUTION RATIOS $(D_c)^h_{aq}$ AND $(D_c)^h_l$, AND DISTRIBUTION RATIOS D_c, $(D_c)_{av}$ AND $(D_c)_{tot}$ OF GOLD(III) VS. THE INITIAL IPE MOLARITY. SYSTEM: $AuCl_3$ - HCl - H_2O - IPE - C_6H_6. INITIAL CONCENTRATION OF COMPONENTS: c^i_{HCl} = 11.8 M AND c^i_{Au} = 0.09 M.

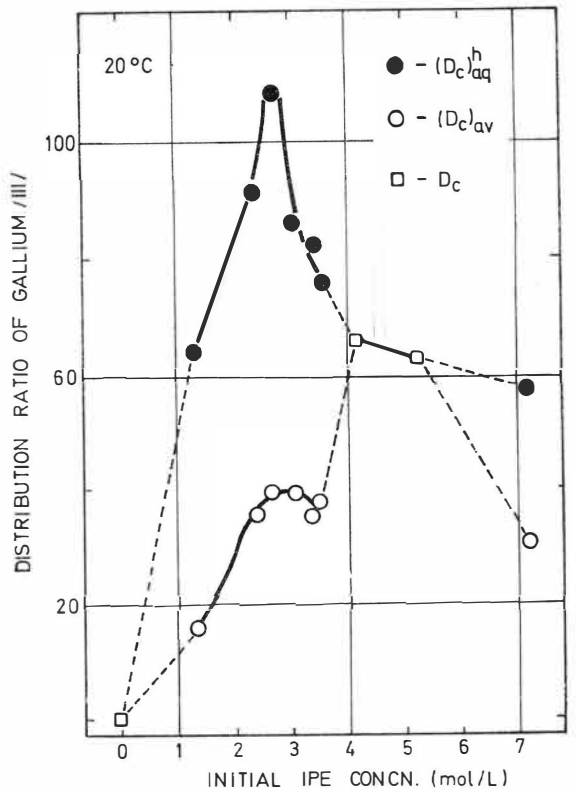

FIGURE 2. PARTIAL DISTRIBUTION RATIO $(D_c)^h_{aq}$ AND DISTRIBUTION RATIOS D_c AND $(D_c)_{av}$ OF GALLIUM(III) VS. THE INITIAL IPE MOLARITY. SYSTEM: $GaCl_3$ - HCl - H_2O - IPE - C_6H_6. INITIAL CONCENTRATION OF COMPONENTS: c^i_{HCl} = 8.0 M AND c^i_{Ga} = 0.17 M.

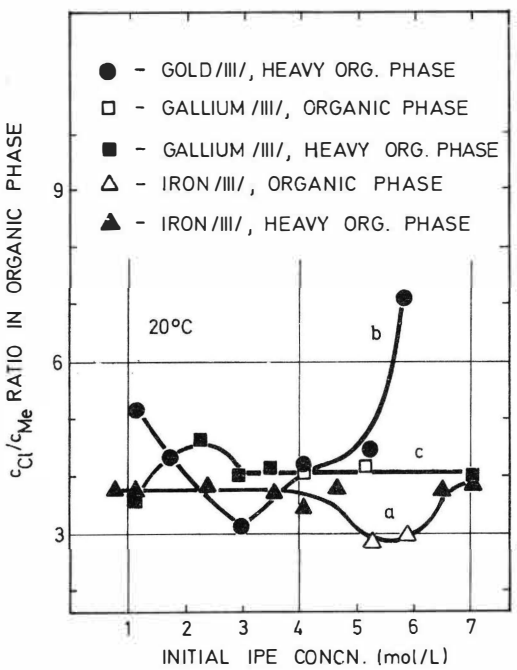

FIGURE 3. RATIO BETWEEN CHLORIDE AND METAL MOLARITIES IN THE HEAVY ORGANIC PHASE VS. THE INITIAL IPE MOLARITY IN THE SYSTEMS *a* (c^i_{Fe} = 0.28 M AND c^i_{HCl} = 7.6 M), *b* (c^i_{Au} = 0.09 M AND c^i_{HCl} = 11.1 M) AND *c* (c^i_{Ga} = 0.17 M AND c^i_{HCl} = 8.0 M).

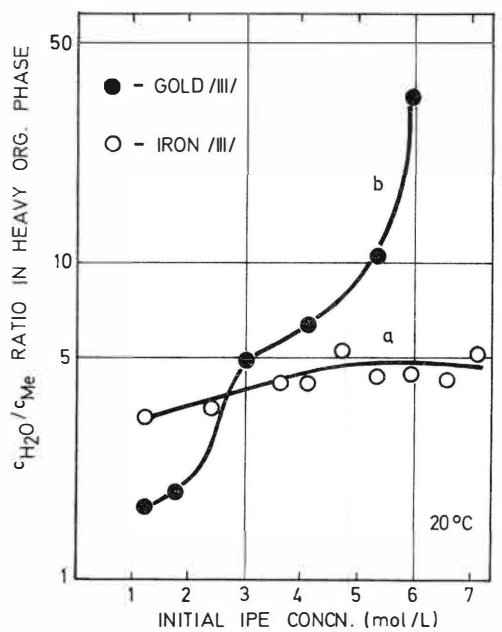

FIGURE 4. RATIO BETWEEN WATER AND METAL MOLARITIES IN THE HEAVY ORGANIC PHASE VS. THE INITIAL IPE MOLARITY IN THE SYSTEMS *a* (c^i_{Fe} = 0.28 M AND c^i_{HCl} = 8.0 M) AND *b* (c^i_{Au} = 0.09 M AND c^i_{HCl} = 11.8 M).

MUTUAL INFLUENCE OF IRON (III) AND GALLIUM (III) AS MACROCONSTITUENTS IN THE EXTRACTION BY A MIXTURE OF DIISOPROPYL ETHER AND n-PENTYL ALCOHOL

Dubravka Maljković, Darko Maljković and Alojzija Paulin

Department of Chemistry and Non-Ferrous Metallurgy
Faculty of Metallurgy, University of Zagreb
Sisak, Yugoslavia

In the course of a study of the extraction of chlorometallic acids in the systems containing diisopropyl ether (IPE) it appeared advisable to undertake investigations of the system: $FeCl_3$-$GaCl_3$-HCl-H_2O-IPE-$CH_3(CH_2)_4OH$. In such systems the coextraction effect and enhanced extraction (synergistic effect) colud be expected. In similar systems: $FeCl_3$-$AuCl_3$-HCl-H_2O-IPE and $FeCl_3$-$AuCl_3$-HCl-H_2O-C_6H_6, under certain conditions, the coextraction effect was found (1). There are numerous data in the literature about the influence of macroelements on microelements as well as about mutual influence of microelements, but there are only a few data about mutual influence of macroelements. In previous investigations of iron(III) extraction in the system: $FeCl_3$-HCl-H_2O-IPE-$CH_3(CH_2)_4OH$ it was observed that the addition of n-pentyl alcohol under particular conditions enhanced the iron(III) extraction (2, 3). Similar results were obtained for gallium(III) extraction in the analogous system: $GaCl_3$-HCl-H_2O-IPE-$CH_3(CH_2)_4OH$ (4). The extraction of hydrochloric acid in the system: HCl-H_2O-IPE-$CH_3(CH_2)_4OH$, under well-defined experimental conditions was also enhanced (5). The synergistic enhancement produced by combination of two neutral extractants as are ether and alcohol is known, but little experimental material is available on such extraction systems.

EXPERIMENTAL

IPE was purified and distilled. Other chemicals and solvents used were of analytical reagent grade.

Investigation was made by conventional technique (1) in graduated cuvettes. The total initial volume of the systems was 12 mL. Equilibration of the system was performed in a thermostat at 20.0 ± 0.05 °C during one hour.

The concentration of metals in the aqueous phase and in pretreated samples of the organic phase was determined by UV absorption spectrometry or complexometric titration (for larger quantities of metal).

In comparable extraction systems (containing single metals) $FeCl_3$-HCl-H_2O-IPE-$CH_3(CH_2)_4OH$ (*a*) and $GaCl_3$-HCl-H_2O-IPE-$CH_3(CH_2)_4OH$ (*b*) as well in system $FeCl_3$-$GaCl_3$-HCl-H_2O-IPE-$CH_3(CH_2)_4OH$ (*c*) volumes of equilibrated phases and concentration of metals in equilibrated phases were determined under the same initial conditions as follows. The initial phase volume ratio, r^i, was always 1.0. The initial concentration of hydrochloric acid, c^i_{HCl}, was always 5.0 M. The initial concentrations of metals, c^i_{Fe} and c^i_{Ga}, were 0.03 M or 0.15 M. In system *c* the initial molar ratio of iron(III) to gallium(III) was 1 or 5. The initial composition of mixed solvent was varied in the whole concentration range (10-99 % v of n-pentyl alcohol).

RESULTS AND DISCUSSION

On the basis of previous investigations of iron(III) extraction from concentrated aqueous hydrochloric acid solutions by a mixture of IPE and n-alcohol (C_1-C_5) n-pentyl alcohol as a component of mixed solvent was chosen (4). By changing initial concentration of acid it was found that the mixed solvent IPE - n-pentyl alcohol at 5 M initial acid concentration gives better results of extraction than pure IPE which on the other hand gives better results at a higher initial acid concentration (7-9 M) (2).

In systems *a* and *b* under given experimental conditions the phase volume changes are not so pronounced as in the case of a higher initial acid concentration (6). By increase of initial concentration of alcohol in mixed solvent, the volume of the aqueous phase decreases and the volume of the organic phase increases. In system *c* such symmetry was somewhat disturbed.

The concentration of metal in the organic phase in systems *a* and *b* was nearly constant, contrary to the concentration of metal in the aqueous phase which passed through a minimum value when initial concentration of alcohol in mixed solvent changed (Figure 1). As a result, maximum values of distribution ratios appeared. Figure 2 shows the influence of initial alcohol concentration on the distribution ratio of iron(III). The magnitude of synergistic enhancement of extraction ΔD (7) at 0.03 M and 0.15 M initial iron(III) concentration is 238 and 62 respectively.

In system *c*, as has been expected, a mutual influence of iron(III) and gallium(III) was found. The maxima of the distribution ratio values of gallium(III) and iron(III) in system *c* (Figure 3) appear at nearly the same initial alcohol concentrations as obtained in systems *a* and *b*, but with reduced distribution ratio of gallium(III).

Acknowledgement. Grateful acknowledgement is made to the Self Management Council for Scientific Research of S.R. Croatia for support of this work.

REFERENCES

1. Da. Maljković, Du. Maljković and M. Branica, Sep. Sci. Technol. 16 315 (1981).
2. Da. Maljković, Du. Maljković and M. Branica, Proceedings of the Advances in Separation Science Conference, Trieste, 1978, p. 99
3. Du. Maljković, "Extraction of Iron(III) with Diisopropyl Ether and Mixed Solvent Diisopropyl Ether - n-Alcohol", Ph.D. Thesis, University of Zagreb, 1978. (In Croatian).
4. Da. Maljković, Du. Maljković and A. Paulin, Euroanalysis - IV Conference, Helsinki/Espoo, 1981; to be published.
5. Du. Maljković and Da. Maljković, 7th ICNAS Conference, Nantes, 1982; to be published.
6. Da. Maljković, Du. Maljković and M. Branica, Croat. Chem. Acta, 52 191 (1979).
7. Y. Marcus and A.S. Kertes, Ion Exchange and Solvent Extraction of Metal Complexes, Wiley-Interscience, New York, 1969.

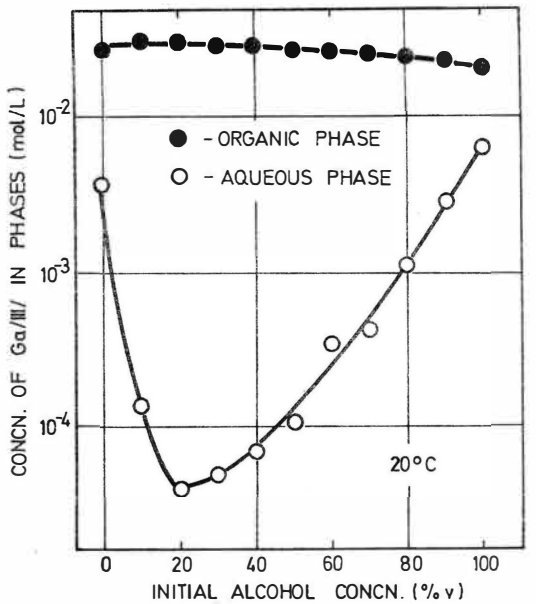

FIGURE 1. GALLIUM(III) CONCENTRATION IN THE EQUILIBRATED PHASES VS. THE INITIAL CONCENTRATION OF n-PENTYL ALCOHOL IN MIXED SOLVENT. SYSTEM: $GaCl_3$ - HCl - - H_2O - IPE - $CH_3(CH_2)_4OH$. INITIAL CONCENTRATION OF COMPONENTS: c^i_{HCl} = 5.0 M, c^i_{Ga} = 0.03 M.

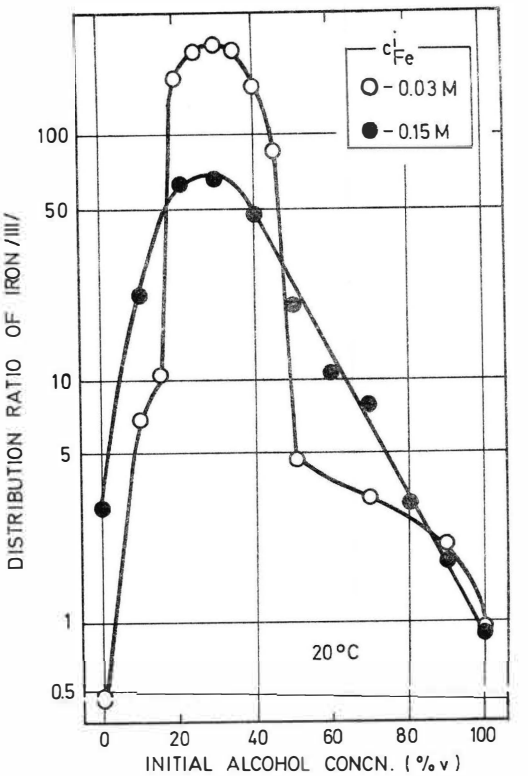

FIGURE 2. INFLUENCE OF INITIAL CONCENTRATION OF n-PENTYL ALCOHOL IN MIXED SOLVENT ON DISTRIBUTION RATIO OF IRON(III). SYSTEM: $FeCl_3$ - HCl - H_2O - IPE - - $CH_3(CH_2)_4OH$. INITIAL CONCENTRATION OF COMPONENT: c^i_{HCl} = 5.0 M.

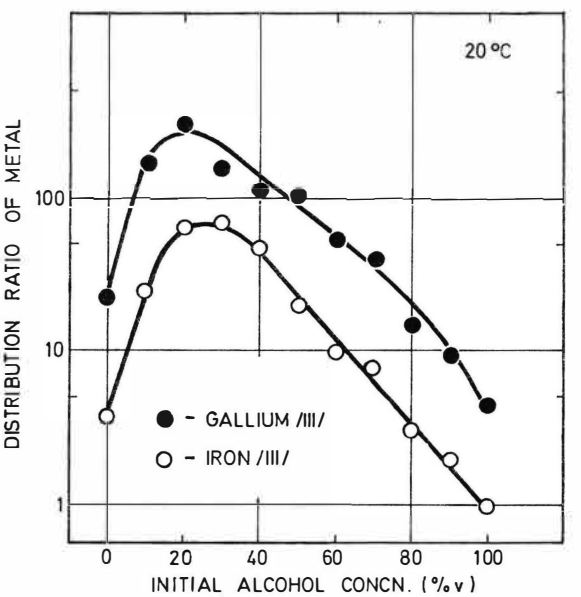

FIGURE 3. INFLUENCE OF INITIAL CONCENTRATION OF n-PENTYL ALCOHOL IN MIXED SOLVENT ON DISTRIBUTION RATIO OF METALS IN SIMULTANEOUS EXTRACTION OF IRON(III) AND GALLIUM(III). SYSTEM: $FeCl_3$ - $GaCl_3$ - HCl - H_2O - - IPE - $CH_3(CH_2)_4OH$. INITIAL CONCENTRATION OF COMPONENTS: c^i_{Ga} = 0.03 M, c^i_{Fe} = 0.15 M, c^i_{HCl} = 5.0 M.

THE EXTRACTION OF SOME METALS FROM ALKALINE SOLUTIONS BY ALKYLATED HYDROXYQUINOLINE

Taichi Sato, Takato Nakamura and Hiroyuki Oishi

Department of Applied Chemistry
Faculty of Engineering, Shizuoka University
Hamamatsu, Japan

In recent years there has been an increased interest in the metal extraction from alkaline solutions. Hydroxyoximes (1), alkylated hydroxyquinolines (2-4), alkylphenols (5,6) and quaternary ammonium salts (7,8) have been usually used as extractant for them. Hydroxioximes are in particular effective for the extraction of copper(II) and nickel(II) from ammoniacal solutions (1). Alkylated hydroxyquinolines such as 7-(5,5,7,7-tetramethyl-1-octen-3-yl)-8-hydroxyquinoline (KELEX 100, HQ) (2,4) and alkylphenols such as 2-(α-methylbenzyl)-4-*sec*-butylphenol and 4-(α,α-dioctylethyl)pyrocatechol (6) take up metal cations from their hydroxyl anions through cation exchange, while quaternary ammonium bases such as tricapryl-methylammonium hydroxide (7,8) extract oxometal anions through anion exchange. We have also assured the fact that KELEX 100 is capable of extracting gallium (III) from strong alkaline solutions and behaves as a cation exchanger (2). Thus it seems that the extraction of M^{m+} by KELEX 100 is represented by the cation-exchange reaction.

$$(1)\quad M(OH)_n^{(n-m)-}(a) + pHQ(o) \rightleftharpoons MQ_m(HQ)_{p-m}(o) + (n-m)OH^-(a) + pH_2O(a)$$

where (a) and (o) denote aqueous and organic phases, respectively. In further study, however, we have found the fact that KELEX 100 has an ability to extract zinc(II) and lead(II) from concentrated sodium hydroxide solutions. Therefore the present paper reports the results for the distribution of zinc(II), lead(II) and gallium(III) between sodium hydroxide solutions and the solutions of KELEX 100 in kerosene.

EXPERIMENTAL

Reagents. KELEX 100 (Schering AG) was distilled twice under a reduced pressure of 0.025 mmHg at 147-159 °C in order to remove 8-hydroxyquinoline. The purified KELEX 100 being pale yellow liquid was diluted kerosene or hexane. The concentration of KELEX 100 was determined by the copper loading experiment on the basis of the literature (9). Aqueous alkaline solutions of zinc(II) and lead(II) were prepared by dissolving their oxides in sodium hydroxide solution of selected concentration. Aqueous alkaline gallium solution was prepared as follows: Gallium metal (99.9999 %, Swiss Aluminium Ltd., Switzerland) was dissolved in concentrated hydrochloric acid; gallium hydroxide gel was obtained by adding sodium hydroxide dropwise to the chloride solution, centrifugalized, washed with deionized water until as free as possible from sodium and chloride ions (10), and then dissolved in sodium hydroxide solution of selected concentration. Othe chemicals were of analytical reagent grade.

Extraction and Analytical Procedures. Equal volume (15 ml each) of organic and aqueous phases placed in 50 ml stoppered centrifugal glass tube, were shaken for a certain period in a room kept at the required temperature. Initial concentrations of zinc(II), lead(II) and gallium(III) in aqueous phases were adjusted to 0.01, 0.01 and 0.0083 M, respectively, except loading experiments. Preliminary experiments showed that equilibria were complete in 10, 10 and 480 min for zinc, lead and gallium, respectively. The mixture was centrifugalized and separated, and then the portions of both phases were pipetted to determine the distribution coefficient (the ratio of equilibrium concentration of metal in organic phase to that in aqueous phase, E_d^o). Zinc and gallium in the organic phases were stripped with 2 M HCl on addition of 2-ethylhexylalcohol to get better phase separation, and lead in the organic phase with 2 M HNO_3. The concentration of metal in the aqueous solution was determined by EDTA titration using Xylenol Orange (XO) as indicator (11,12). The concentration of sodium extracted into organic phase was assayed by atomic absorption spectrophotometry using Hitachi Ltd. Model 170-50-A after stripping it into aqueous phase with 2 M HCl or 2 M HNO_3.

Infrared Spectral Measurement. Infrared (IR) spectra of the sample prepared by evaporation of the organic diluent, hexane, were recorded on a Japan Spectroscopic Co., Ltd. Model IRA-1 and IR-F infrared spectrophotometers, grating types for measurement at 4000-650 and 700-200 cm^{-1}, respectively, using capillary film between thallium plates or polyethylene films.

RESULTS AND DISCUSSION

Extraction of Sodium. Preliminarily the distribution of sodium between sodium hydroxide solutions and the solutions of KELEX 100 in kerosene at 30 °C was examined in the absence of metals. The concentration of sodium in the equilibrated organic phase *vs.* that in the initial aqueous phase is plotted in Figure 1. The distribution isotherm indicates that at the concentration of aqueous sodium hydroxide below 5 M, 0.05 M KELEX 100 in kerosene extracts less than 7×10^{-3} M of sodium, which gives the molar ratio [KELEX 100]/$[Na]_{org} > 70$, suggesting that KELEX 100 exists as HQ in the organic phase. This means that the effect of sodium is negligible for the extraction of metals. It is seen, however, that a drastic up-take of sodium occurs at the concentration of aqueous sodium hydroxide above 5 M owing to the formation of the species NaQ.

Zinc(II). The distribution of zinc(II) between sodium hydroxide solutions and the solutions of KELEX 100 in kerosene at 30 °C is illustrated in Figure 2. At the concentration of sodium hydroxide in aqueous phase below ~4 M, the distribution coefficient decreases with increasing the concentration in accord with the expectation for cation-exchange reaction represented by equation (1). Log-log plots of the distribution coefficient *vs.* the concentration of aqueous sodium hydroxide give a slope of -2. It is evident that the decrease in the distribution coefficient arises from the increase of hydroxide anion in aqueous phase. Because the distribution coefficient is little affected up to the total aqueous sodium concentration in 4 M when sodium perchlorate is added to aqueous solution containing sodium hydroxide of 0.17 or 1 M (Figure 2). From this it is deduced that the value of $n - m = 2$ holds in equation (1), corresponding to the fact that tetrahydroxozincate anion, $Zn(OH)_4^{2-}$, is predominant in sodium hydroxide solution as demonstrated by Lippincott *et al.* (13).

Assuming $p = 2$, log-log plots of the distribution coefficient *vs.* the equilibrated KELEX 100 concentration at constant sodium hydroxide concentrations in 0.17-3 M yield the straight lines with slopes of ~2. Hence it is inferred that the extraction of zinc(II) is dominated by the equilibrium

$$(2)\quad Zn(OH)_4^{2-}(a) + 2HQ(o) \rightleftharpoons ZnQ_2(o) + 2OH^-(a) + 2H_2O(a).$$

This is also supported by the continuous variation method at a constant concentration of sodium hydroxide of 0.6 M: at a fixed total concentration of initial aqueous gallium and KELEX 100 in 0.05 M, gallium concentration of organic phase shows a maximum at a molar fraction of $[Zn]_{init\ aq}/([Zn]_{init\ aq} + [HQ]_{init}) = 0.33$, implying the formation of species ZnQ_2.

At the concentration of sodium hydroxide above 4 M, on the other hand, it is noticed that there is an anomalous change in the distribution coefficient. As seen in Figure 2, the distribution isotherm of zinc(II) has a maximum at 6 M NaOH. Also the extraction from sodium perchlorate solutions in the presence of a constant concentration of sodium hydroxide at 1 M indicates an increase in the distribution coefficient with increasing total aqueous sodium ion concentration above 4 M. One can easily be conceivable that the rise is due to either the change in the distribution of hydroxozincate anions in the aqueous phase or the up-take of zinc(II) accompanied by sodium ion. As the formation of other species except tetrahydroxozincate anion in strong alkaline solutions has not been reported in any literatures (14), the former is undesirable as the cause of anomalous increase in the distribution coefficient.

The concentrations of zinc and sodium extracted into the organic phase with loading of zinc(II) were examined at 6 M NaOH. In comparison with the concentration of sodium (1.3×10^{-3} M) extracted with 0.05 M KELEX 100 in kerosene in the absence of zinc, it is apparent that the organic solutions from the extraction of zinc contain definitely higher concentration of sodium than that in the absence of zinc. When KELEX 100 is present in excess, the molar ratio $[Na]_{org,n}/[Zn]_{org}$ shows nearly unity, in which $[Na]_{org,n}$ is the net concentration increased by assuming the bond of two molecules of KELEX 100 to zinc cation:

$$(3)\quad [Na]_{org,n} = [Na]_{org} - (1.3 \times 10^{-3}/[HQ]_{init})([HQ]_{init} - 2[Zn]_{org})$$

At higher loading of zinc, however, the ratio becomes less than unity, although the net concentration of sodium in the organic phase still continues to increase.

IR spectra of the organic extracts obtained from the hexane solutions similar to those of the loading experiments were examined in order to get further information of the species formed in the organic phase. They indicate that metal saturated-organic extract contains more than one species: The spectrum exhibits the bands at 630, 590, 575, 510, 480, 460, 440 and 395 cm^{-1} in the frequency range of 700-200 cm^{-1}. It is found that some of them correspond to those in the spectra of the organic extracts from 2 M NaOH, implying that the species ZnQ_2 coexists in the organic phase at higher loading of zinc even if the concentration of aqueous sodium hydroxide is kept in 6 M. Thus anomalous extraction is regarded as being due to a reaction which takes up sodium with zinc one. A log-log plot of the distribution coefficient *vs.* KELEX 100 concentration, however, gives the lines with the same slope of 2 that for the extraction from aqueous solutions containing sodium hydroxide below 2 M.

If this speculation is accepted, the following equation can be postulated:

$$(4)\quad Zn(OH)_4^{2-}(a) + Na^+(a) + 2HQ(o) \rightleftharpoons ZnQ_2 \cdot NaOH(o) + OH^-(a) + 2H_2O(a)$$

and/or

$$(5)\quad Zn(OH)_4^{2-}(a) + 2Na(a) + 2HQ(o) \rightleftharpoons ZnQ_2 \cdot 2NaOH(o) + 2H_2O(a)$$

Lead(II). The distribution of lead(II) between sodium hydroxide solutions and solutions of KELEX 100 in kerosene at 30 °C is presented in Figure 3. The distribution behaviour at low concentrations of sodium hydroxide in aqueous phase, which shows nearly inverse first-power dependence of the distribution coefficient on the sodium hydroxide concentration, is typical for the extraction through cation exchange. This suggests the values of $n - m = 1$ identical to the charge of the species $Pb(OH)_3^-$ (15) which predominantly exists in alkali solution. Since log-log plots of the distribution coefficient *vs.* KELEX 100 concentration at constant sodium hydroxide concentrations of 0.1 - 3 M yield the straight lines with a slope of 2, it is considered that the extraction of lead(II) from aqueous solutions containing lower concentration of sodium hydroxide by KELEX 100 is expressed as

$$(6)\quad Pb(OH)_3^-(a) + 2HQ(o) \rightleftharpoons PbQ_2(a) + OH^-(a) + 2H_2O(a).$$

The continuous variation method and loading test at a constant concentration of sodium hydroxide in 1 M confirm that the species PbQ_2 is formed in the organic phase.

It is interesting that the distribution of lead(II) at higher concentration of sodium hydroxide is similar to that of zinc(II). In contrast, the distribution coefficient is little influenced by an increase of sodium concentration in aqueous phase when sodium perchlorate is added to aqueous sodium hydroxide solution at constant concentration in 0.2 or 3 M. An increase of sodium concentration somewhat acts negative to the distribution of lead(II) in the concentration range above 4 M Na(OH, ClO_4) (Figure 3). This result agrees with the fact that the concentration of sodium extracted into the organic phase is kept constant for the loading of lead(II). It is thus evident that the extraction of lead(II) at higher concentration of sodium hydroxide does not take up sodium ion. This is also proved that the difference in the IR spectra is little for the organic extracts at 1 and 6 M sodium hydroxides with 0.05 M KELEX 100. Hence it is probable that slight increase of the distribution coefficient in the sodium hydroxide concentration of 4 - 8 M is due to the change in the distribution of hydroxo species in aqueous solutions, although there is no literature about it.

At the concentration of sodium hydroxide above 8 M, moreover, analytical data suggest that the extraction of lead(II) is suppressed owing to the formation of sodium salt of KELEX 100.

Gallium(III). The distribution of gallium(III) between sodium hydroxide solutions and the solutions of KELEX 100 in kerosene at 30 °C is demonstrated in Figure 4. The distribution coefficient of gallium(III) decreases with increasing the aqueous concentration of sodium hydroxide in the concentration range of sodium hydroxide studied, and the slope of the distribution isotherms in Figure 4 is nearly unity. Taking into account the fact that gallium exists in the tetrahydroxo species, $Ga(OH)_4^-$ (16), in sodium hydroxide solution, it is expected that the extraction of gallium(III) proceeds entirely through cation exchange.

Assuming $p = 3$, log-log plots of the distribution coefficient *vs.* free concentration of KELEX 100 at constant concentration of sodium hydroxide give the straight lines with a slope of ~ 3. Accordingly the extraction of gallium(III) from sodium hydroxide solutions by KELEX 100 is governed by the equilibrium

$$(7) \qquad Ga(OH)_4^-(a) + 3HQ(o) \rightleftharpoons GaQ_3(o) + OH^-(a) + 3H_2O(a),$$

coincide with the equation proposed for the extraction of gallium(II) in sodium aluminate solutions from Bayer process by KELEX 100 in the mixture of kerosene and decanol (3).

Effect of Temperature. The extraction of zinc(II), lead(II) and gallium (III) from sodium hydroxide solutions with KELEX 100 in kerosene between 10 and 50 °C gave the results in Table 1. With increasing temperature, the distribution coefficient decreases for all of the systems studied. The values of the respective heat of reactions ($-\Delta H$, kJ mol^{-1}) are estimated to be 42, 64 and 104 for zinc(II), lead(II) and gallium(III). These values point out that the extraction of these metals from sodium hydroxide solutions by KELEX 100 at low temperature has an advantage over that at higher one.

ACKNOWLEDGEMENTS

We are grateful to the Research and Development Laboratory, Swiss Aluminium Ltd., Neuhausen, Switzerland, for a gift of gallium metal, and to Mr. Y. Kaida, National Industrial Research Institute, Kyushu, for his cooperation in analysis of sodium by atomic absorption spectrophtometry.

REFERENCES

1) D.S.Flett and J.Melling, Hydrometallurgy,4,135(1979) and the literatures cited therein.
2) T.Sato, T.Nakamura, M.Yabuta and H.Oishi, Chem.Lett.,591(1982).
3) A.Leveque and J.Helgorsky, "Proc. Int. Solvent Extraction Conf., 1977, Toronto", Vol.2, 439(1977).
4) J.Helgorsky and A.Leveque, German Patent 2,530,880(1976); French Patent 2,307,047(1976); German Patent 2.743,475(1978); French Patent 2,397,464 (1979).
5) B.F.Myasedov, Z.K.Karalova and V.V.Nekrasova, J.Anal.Chem.USSR,34,1424 (1979).
6) B.F.Myasedov, Z.K.Karalova, V.V.Nekrasova and L.M.Radionova, J.Inorg.Nucl. Chem.,42,1495(1980).
7) E.S.Pal'skin, V.V.Nekrasova, L.A.Ivanova, Z.K.Karalova and B.F.Myasedov, J.Anal.Chem.USSR,33,682(1978).
8) G.M.Ritcey and B.H.Lucas, CIM Spec. Vol.21,521(1979).
9) D.S.Flett, J.Inorg.Nucl.Chem.,37,1967(1975).
10) T.Sato and T.Nakamura, J.Chem.Tech.Biotechnol.,32,469(1982).
11) J.Körble and R.Pribil, Chemist-Analyst,45,102(1956).
12) J.Kinnunen and B.Wennerstrand, Chemist-Analyst,46,92(1957).
13) E.R.Lippincott, J.A.Psellos and M.C.Tobin, J.Chem.Phys.,20,536(1952); G. Schorsch, Bull.Soc.Chim.France,1456(1964).
14) C.F.Baes,Jr. and R.Mesmer, "The Hydrolysis of Cations", p.287, Wiley-Interscience, New York (1976).
15) G.Schorsch and N.Ingri, Acta.Chem.Scand.,21,2721(1967).
16) B.Daniel, Rev.Chim.Miner.,6,499(1969).

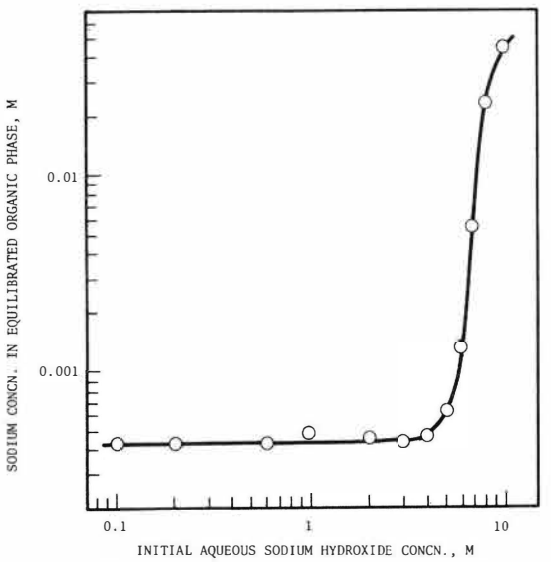

FIGURE 1. EXTRACTION OF SODIUM FROM SODIUM HYDROXIDE SOLUTIONS WITH 0.05 M KELEX 100 IN KEROSENE AT 30 °C.

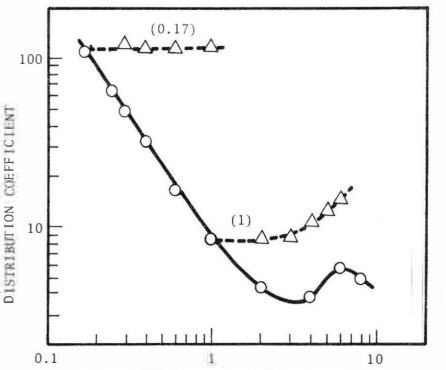

FIGURE 2. EXTRACTION OF Zn(II) FROM NaOH SOLNS. (O) OR MIXED SOLNS. OF NaOH AND $NaClO_4$ (Δ) BY 0.025 M KELEX 100 IN KEROSENE AT 30 °C (NUMERALS IN PARENTHESES ARE NaOH CONCNS., M).

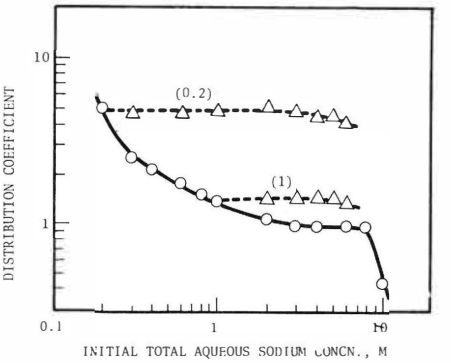

FIGURE 3. EXTRACTION OF Pb(II) FROM NaOH SOLNS. (O) OR MIXED SOLNS. OF NaOH AND $NaClO_4$ (Δ) BY 0.025 M KELEX 100 IN KEROSENE AT 30 °C (NUMERALS IN PARENTHESES ARE NaOH CONCNS. M).

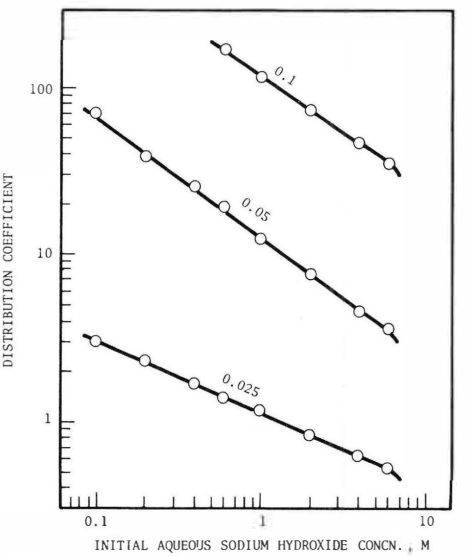

FIGURE 4. EXTRACTION OF Ga(III) FROM NaOH SOLNS. BY KELEX 100 IN KEROSENE AT 30 °C (NUMERALS ON CURVES ARE KELEX 100 CONCNS., M)

TABLE 1. TEMPERATURE-DEPENDENCE OF DISTRIBUTION COEFFICIENT ON THE EXTRACTION OF ZINC(II), LEAD(II) AND GALLIUM(III) FROM SODIUM HYDROXIDE SOLUTIONS BY KELEX 100 IN KEROSENE

METAL	$[NaOH]_{aq}$, M	[KELEX 100], M	DISTRIBUTION COEFFICIENT				
			10°C*	20°C*	30°C*	40°C	50°C*
Zn	0.4	0.03	390	190	130	73	—
Pb	1	0.025	50.2	25.1	13.2	7.00	—
Ga	2	0.05	—	16.8	6.86	2.83	1.39

* EXTRACTION TEMPERATURE.

KINETICS OF HYDROLYTIC STRIPPING OF IRON FROM VERSATIC ACID SOLUTIONS

Luiz A. C. Teixeira and A. John Monhemius

Department of Materials Science and Metallurgy
Catholic University of Rio de Janeiro (PUC/RJ)
P.O. Box 38008 - R. J. - Brazil

Department of Metallurgy and Materials Science
Royal School of Mines
Imperial College of Science and Technology
London SW7 2BP, U.K.

INTRODUCTION

Hydrolytic stripping is the name given to the method by which metal oxides or hydroxides are directly precipitated from metal-loaded carboxylic extractant solutions by reaction with water at elevated temperatures (1-4). In the case of Versatic* acid loaded with iron, hematite is produced by reaction with water at temperatures above about 130°C. The reaction may be represented in simplified form as follows:

$$2FeV_{3\,(org)} + 3H_2O \rightarrow Fe_2O_3\downarrow + 6HV_{(org)}$$

The carboxylic acid is regenerated during the hydrolysis reaction and may be recycled to a solvent extraction stage for reloading with iron.

The process offers an alternative method for the removal of iron from hydrometallurgical process liquors. Its major advantage over conventional iron-removal processes, such as jarosite or goethite precipitation, in which iron is precipitated from aqueous solutions, is that the solvent extraction of iron by carboxylic acids can be made very selective, so that the organic phase is free from other inorganic impurities. A pure hematite is thus produced by hydrolytic stripping, which should be suitable for further use in, for example, iron-making processes.

(* Tertiary C_{10} carboxylic acid - Shell trade mark)

The paper examines the kinetics and mechanism of the preciptiation of hematite by hydrolytic stripping of iron-loaded Versatic acid solutions.

EXPERIMENTAL

The organic phases comprised solutions of Versatic 10 in Escaid 110 diluent. These were loaded with iron by exchange extraction with the calcium salt of Versatic acid.

The reactions were carried out in a 300 ml stainless steel stirred autoclave, equipped with a heated reservoir. The required volume of iron-loaded organic phase was heated to the reaction temperature in the autoclave and the reaction was started by injecting a known volume of pre-heated water into the autoclave from the reservoir. The rates of precipitation were followed by sampling the organic phase from the autoclave and measuring the iron concentrations in the samples by spectrophotometry.

RESULTS

The main variables studied were:- temperature (135 - 145°C); Versatic 10 concentration (20 - 50% by volume in Escaid 110); iron concentration (7 - 20 g/l Fe^{3+}); and the effect of seeding with hematite powder (0 - 200% seed). Preliminary experiments established that the reaction rate was unaffected by the organic to water volume ratio (20 : 1 was the standard condition used) or by the agitation speed (1000 rpm standard).

A series of kinetic experiments was carried out in accordance with a sequence of factorial designs. The effects of the variables: temperature (T), [Versatic] (V), [iron] (Fe), and [seed] (S_A), on the kinetics of the precipitation, were found to be significant, as well as the factor interactions VFe and VS_A.

It was found that in solutions highly loaded with iron ($(Fe/V)_{molar} \simeq 0.19$), the reaction started via a process of homogeneous self-nucleation. Under these conditions the rates of precipitation were rapid and were unaffected by additions of seed. In solutions loaded to a lesser extent ($(Fe/V)_{molar} \leq 0.14$) the reaction could only be initiated by adding Fe_2O_3 seed material, and it proceeded at comparatively slower rates. A shift from the heterogeneous to the homogeneous mode of precipitation was seen to be favoured by increasing temperature. The apparent activation energies of these modes of precipitation were: $E_a \simeq 91$ kJ/mole (homogeneous), and $E_a \simeq 124$ kJ/mole (heterogeneous). These high values indicate that in both cases the process is rate-controlled by chemical reaction steps.

The two distinct modes of precipitation were examined separately at 140°C, as this was the temperature at which the widest range of solution composition was covered. The models found to represent the kinetics adequately at this temperature were then tested with the data obtained at 135°C and 145°C.

High-temperature infra-red spectroscopy was used to measure free (i.e. unbound) Versatic acid concentrations in the iron-loaded organic phases and the dimerization constant of the acid was obtained from these data.

HOMOGENEOUS PRECIPITATION

The homogeneous mode of precipitation was observed in only two of the seven different solution compositions examined in the programme of kinetic experiments, at 140°C. This limitation on the number of kinetic data consequently allowed only the examination of simple rate equations. A purely empirical model of the form: $r = k\,[Fe]^n$ was tried, and it was found that for n = 2 an acceptable fitting could be obtained (Figure 1 shows measured rates versus predicted rates). This model was interpreted as corresponding to a bi-molecular reaction step involving two iron-Versatic complexes of a type which occurs in appreciable quantities in highly loaded iron-Versatic solutions.

HETEROGENEOUS PRECIPITATION

The search for a mechanistic model for the heterogeneous mode of precipitation consisted of the examination of all the possible forms that the following general rate equation could take.

$$r = d\,[Fe]/dt = \frac{k_1\, S_A\, [Fe]^m}{(1 + k_2\,[Fe]^a + k_3\,[HV]^b + k_4\,[(HV)_2]^c\,)^n}$$

with: m = 0, 1/2, 1 and 2
a, b, c = 1/2 and 1
n = 1, 2 and 3

This type of equation represents the kinetics of a set of Langmuir-Hinshelwood mechanisms. The rate-controlling step can be either the adsorption of a reactant, the surface reaction, or the desorption of a product, depending on what particular values the exponents a, b, c, m, n take. In these mechanisms, adsorption-desorption steps are represented by Langmuir isotherms.

For the particular case of the hydrolytic stripping reaction it was assumed that: (i) The surface reaction step was irreversible; (ii) The surface concentration of H_2O was constant; (iii) The range of iron complexes which can engage in heterogeneous precipitation can be represented by a single average reacting complex whose concentration is proportional to the total [Fe]; and (iv) The adsorption of the inert saturated hydrocarbons of the diluent Escaid 110 is considered to be negligible.

Each form of the heterogeneous rate equation was linearized and tried on the kinetic data. Quality of fitting was judged by a sequence of statistical tests.

Five models were found to satisfy the statistical tests

in the temperature range 135 - 145°C, though four of them showed some lack of fit at 135°C.

The best model is presented below:

$$r = \frac{k_1 S_A [Fe]}{(1 + k_2 [Fe] + k_4 [(HV)_2])^3}$$

Plots of measured rates versus predicted rates at 135°C and 140°C are presented in Figure 2 (having three parameters, this equation could not be tested at 145°C).

This model was interpreted as corresponding to a surface hydrolysis reaction involving an iron-Versatic complex adsorbed on one active site and a water molecule adsorbed and dissociated on two sites.

Although this model has the inherent advantages of a mechanistic model, it suffers from two drawbacks in that it incorporates a term on free [HV] which is not a convenient operational variable and it does not contain an explicit term on the effect of temperature.

Thus, an empirical model which incorporated the effects of T, $[V]_{total}$, [Fe] and S_A was derived from the factorial designs:

$$r = k \; S_A \exp(E_a/RT) \, [Fe]^{0.78} / [V]^{1.55}$$

This model, despite its lack of mechanistic meaning, is regarded as a potentially useful design tool for the heterogeneous mode of precipitation, giving predicted initial rates of reaction within ± 25% of the measured values over the extended temperature range 135 - 160°C. A plot of measured rates versus predicted rates is presented in Figure 3.

ACKNOWLEDGEMENT

One of us (LACT) wishes to acknowledge the financial support received by him from the Brazilian National Research Council (CNPq).

REFERENCES

1. Thorsen G. and Monhemius A. J. "Precipitation of Metal Oxides from Loaded Carboxylic Acid Extractants by Hydrolytic Stripping" 108th AIME Annual Meeting, New Orleans, TMS Paper Selection No A-79-12 (1979)

2. Monhemius A. J. and Thorsen G. "The Application of Hydrolytic Stripping to the Iron Problem in Hydrometallurgy" ISEC 80 Proceedings, Liege, 3 Paper 80-113 (1980).

3. Thorsen G. and Monhemius A. J. "Precipitation of Metal Values from Organic Media" US Patent 4,282,189. Aug. 4 (1981)

4. Monhemius A. J., Teixeira L. A. C. and Thorsen G. "The Precipitation of Hematite from Iron-Loaded Versatic Acid Solutions by Hydrolytic Stripping" Proceedings of the NATO Advanced Research Institute on Hydrometallurgical Process Fundamentals, Cambridge, U. K., July (1982)

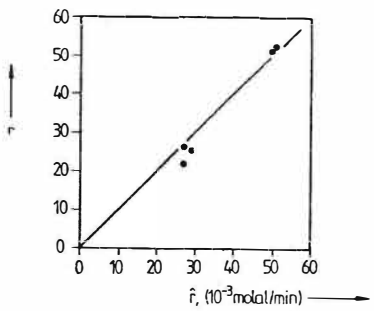

FIGURE 1 : Correlation between predicted and measured rates of homogeneous precipitation at 140°C

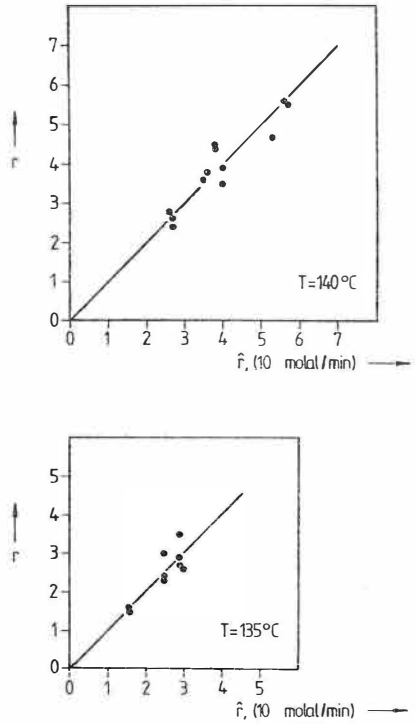

FIGURE 2 Measured rates versus predicted rates

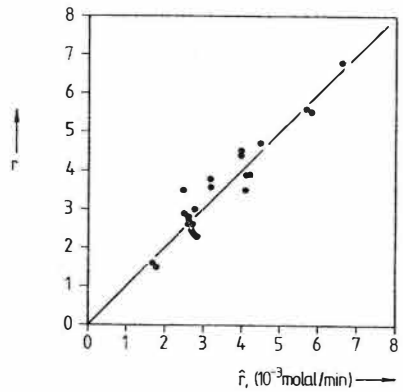

FIGURE 3 Measured rates versus predicted rates Empirical model

SOLVENT EXTRACTION OF IRON FROM LIQUID WASTES OF METALLURGICAL PROCESSES

Iginio Colussi, Ireneo Kikic, Ugo Preti, Antonio Cocco

Istituto di Chimica Applicata e Industriale
Universitá di Trieste
Trieste, Italy

Solvent extraction of iron from liquid wastes of metallurgical processes is a very interesting technique because, in many practical cases, the presence of iron hinders the recovery of other metal values.

Different organic extractants have been used to separate iron from aqueous hydrochloric solutions, but little is known about the use of these solvents in different conditions.

In the present paper, tri-n-butyl phosphate was taken into consideration as extractant of iron from hydrochloric aqueous solutions. Synthetically prepared solutions were used for the basic investigations. In particular, the study of the separation of iron from concentrated hydrochloric solutions of aluminium salts was performed; for this reason, the synthetic solutions had iron and aluminium contents like those obtained by the mineral acidic leaching processes of alumino-silicate ores.

MODEL DEVELOPMENT

Iron is extracted by TBP as an acid complex $HFeCl_4$, provided that the chloride ion concentration is sufficiently large to form $FeCl_4^-$.

Lewin et al. (1) proposed this reaction in order to represent the extraction of Fe(III) into TBP:

$$(1) \qquad H^+_{(w)} + FeCl^-_{4(w)} + 2\ TBP_{(o)} \rightleftharpoons (HFeCl_4 \cdot 2\ TBP)_{(o)}$$

The formation of the tetrachloroferrate complex is favoured by a high aluminium chloride concentration and causes a strong salting out effect.

On the other hand, it has been demonstrated (2)(3) that the extraction of aluminium into TBP is very small and decreases when the organic phase is loaded with iron (III), resulting quite insignificant when iron (III) concentration is greater than 0.1 M.

Many authors have studied the extraction of HCl into TBP (4)(5)(6)(7). The species extracted from the aqueous phase at high hydrochloric acid concentration is represented by the complex $(HCl \cdot TBP)_{(o)}$ with some water molecules: one molecule of TBP combines with one molecule of HCl.

Combining these effects, the extraction of iron (III) in the system water-hydrochloric acid - TBP - Fe(III) can be represented by the following equation:

$$(2) \qquad 2H^+_{(w)} + Cl^-_{(w)} + FeCl^-_{4(w)} + 3TBP_{(o)} \rightleftharpoons HFeCl_4 \cdot 2TBP_{(o)} + HCl \cdot TBP_{(o)}$$

The equilibrium constant, k_e, is expressed by:

$$(3) \qquad k_e = \frac{[HFeCl_4 \cdot 2TBP]_{(o)} \cdot [HCl \cdot TBP]_{(o)}}{[H^+]^2_{(w)} \cdot [Cl^-]_{(w)} \cdot [FeCl^-_4]_{(w)} \cdot [TBP]^3_{(o)}}$$

where the brackets represent the activities and the subscripts (o) and (w) denote the organic and aqueous phases respectively.

By using activity coefficients, equation (2) can be written:

$$(4) \qquad k_e = \frac{(HFeCl_4 \cdot 2TBP)_{(o)} \cdot (HCl \cdot TBP)_{(o)}}{(H^+)^2_{(w)} \cdot (Cl^-)_{(w)} \cdot (FeCl^-_4)_{(w)} \cdot (TBP)^3_{(o)}} \cdot \frac{\gamma^{(o)}_{HFeCl_4 \cdot 2TBP}\ \gamma^{(o)}_{HCl \cdot TBP}}{\gamma^2_{H^+}\ \gamma_{Cl^-}\ \gamma_{FeCl^-_4}\ \gamma^{(o)\,3}_{TBP}}$$

where the paretheses are the concentrations and γ and $\gamma^{(o)}$ are the activity coefficients in the aqueous and organic phase respectively.

The total metal ion concentration in the organic phase is expressed by the equation:

$$(5) \qquad (Fe^{+3})_{(o)} = k_e \cdot \frac{(H^+)^2_{(w)} \cdot (Cl^-)_{(w)} \cdot (FeCl^-_4)_{(w)} \cdot (TBP)^3_{(o)}}{(HCl \cdot TBP)_{(o)}} \cdot \frac{\gamma^2_{H^+}\ \gamma_{Cl^-}\ \gamma_{FeCl^-_4}\ \gamma^{(o)\,3}_{TBP}}{\gamma^{(o)}_{HCl \cdot TBP}\ \gamma^{(o)}_{HFeCl_4 \cdot 2TBP}}$$

The total metal ion concentration in the aqueous phase is expressed by the equation:

$$(6) \qquad (Fe^{+3})_{(w)} = \frac{(HFeCl_4 \cdot 2TBP)_{(o)} \cdot (HCl \cdot TBP)_{(o)}}{k_e \cdot (H^+)^2_{(w)} \cdot (Cl^-)_{(w)} \cdot (TBP)^3_{(o)}} \cdot \frac{\gamma^{(o)}_{HFeCl_4 \cdot 2TBP}\ \gamma^{(o)}_{HCl \cdot TBP}}{\gamma^2_{H^+}\ \gamma_{Cl^-}\ \gamma_{FeCl^-_4}\ \gamma^{(o)\,3}_{TBP}}$$

The distribution coefficient for Fe(III), k_d, is defined as:

$$(7) \qquad k_d = \frac{(Fe^{+3})_{(o)}}{(Fe^{+3})_{(w)}}$$

$$(8) \qquad k_d = k_e \cdot \frac{(H^+)^2_{(w)} \cdot (Cl^-)_{(w)} \cdot (TBP)^3_{(o)}}{(HCl \cdot TBP)_{(o)}} \cdot \left(\frac{\gamma^2_{H^+}\ \gamma_{Cl^-}\ \gamma_{FeCl^-_4}\ \gamma^{(o)\,3}_{TBP}}{\gamma^{(o)}_{HCl \cdot TBP}\ \gamma^{(o)}_{HFeCl_4 \cdot 2TBP}} \right)^2$$

As the aqueous phase consists of ionic species, ideality is not approached even in dilute solutions. But, with the assumption that the ratio of the activity coefficients of the species which compare in eq. (8) varies slightly with concentration, the distribution coefficient can be expressed by:

$$(9) \qquad k_d = k_1 \cdot \frac{(H^+)^2_{(w)} \cdot (Cl^-)_{(w)} \cdot (TBP)^3_{(o)}}{(HCl \cdot TBP)_{(o)}}$$

where $k_1 = k_e \cdot k^2_\gamma$

and $$k_\gamma = \frac{\gamma^2_{H^+}\ \gamma_{Cl^-}\ \gamma_{FeCl^-_4}\ \gamma^{(o)\,3}_{TBP}}{\gamma^{(o)}_{HCl \cdot TBP}\ \gamma^{(o)}_{HFeCl_4 \cdot 2TBP}}$$

Should the assumption hold, k_γ has a constant value, so that k_1 also is a constant. In addition, hydrochloric acid is considered to be completely dissociated in aqueous solution.

EXPERIMENTAL

Extractant used: tri-n-butyl phosphate reagent grade.
Diluent used: commercially available "Solvesso 100".
Aqueous hydrochloric acid solutions were 4.57 M HCl, and contained $AlCl_3$ 0.037 M.

The experiments were carried out varying the $FeCl_3$ concentration, the solvent/diluent volume ratios in the organic phase, the aqueous phase/organic phase volume ratios.

$FeCl_3$ concentrations were fixed as listed in Table I.
The solvent/diluent volume ratios had the following values: 1/1 - 1/5 - 5/1
The aqueous phase/organic phase volume ratios were: 1/1 - 5/1 - 10/1.

Experiments were performed at 25°C; organic and aqueous phases were added into 100ml glass-stoppered conical flasks and shaken for 30 seconds. After shaking, the phases were allowed to separate. The analyses were performed by common analytical methods; details can be obtained directly from authors.

RESULTS AND DISCUSSION

The distribution coefficients obtained in each test are shown in Table I.
The concentration values in the equilibrated phases for the species which appear in the proposed model for k_d (eq. (9)) are listed in Table I.

The equilibrium concentrations of $(HCl)_{(o)}$ and $(HCl)_{(w)}$ resulted in good agreement with the data obtained by Nishimura et al.(7), considering the extractant TBP as undiluted.

The proposed model gives a good prediction of the distribution coefficients for the tests in which the extractant/diluent volume ratio in the organic phase was at a minimum (1/5); in this case, k_1 assumes a quite constant value, about 23. This fact is true for all the different iron concentrations examined.

When the extractant/diluent volume ratio of the organic phase is higher,

the model is not applicable; probably, this is due to the fact that the quantity k_γ can no longer be considered a constant, but the activity coefficients of the various species must be taken into account.

TABLE 1

N°	Fe(III) total (M/l)$_{(w)}$	TBP/Diluent (volume)	Aqueous/organic (volume)	k_d	$(H^+)_{(w)}$	$(Cl^-)_{(w)}$	$(TBP)_{(o)}$	$(HCl \cdot TBP)_{(o)}$	k_1
1	0.1612	1/5	1/1	14.0	4.225	6.370	0.102	0.194	22.40
2	0.1612	1/5	5/1	1.6	4.487	6.965	0.046	0.216	24.90
3	0.1612	1/5	10/1	2.2	4.519	7.029	0.052	0.218	23.73
4	0.0698	1/5	1/1	259.7	4.300	6.420	0.270	0.200	22.39
5	0.0698	1/5	5/1	4.7	4.492	6.719	0.068	0.216	24.04
6	0.0698	1/5	10/1	2.6	4.534	6.819	0.055	0.220	23.84
7	0.0172	1/5	5/1	186.9	4.509	6.626	0.231	0.218	24.71
8	0.0172	1/5	10/1	28.4	4.535	6.664	0.126	0.220	22.77
9	0.1791	1/1	1/1	7685.8	3.891	5.950	0.979	0.500	45.50
10	0.0727	1/1	10/1	32.8	4.450	6.612	0.073	0.639	419.7
11	0.1970	5/1	5/1	683.8	4.183	6.193	0.133	0.954	255.0
12	0.0788	5/1	10/1	3793.3	4.387	6.480	0.431	1.038	916.1

CONCLUSIONS

A chemically-based thermodynamic model to predict the distribution coefficients for the solvent extraction of Fe(III) into TBP has been developed by assuming that the ratio of the activity coefficients, k_γ, varies slightly with the concentration. The model is applicable at low extractant/diluent volume ratios in the organic phase.

Further investigations have been planned with the aim to extend the validity of the model and to verify the bench-scale results by tests carried out on a pilot plant.

ACKNOWLEDGEMENT

This work was carried out with the support of "Progetto Finalizzato Metallurgia C.N.R." (Rome).

REFERENCES

1. V.I. Levin, I.V. Meshcherova, U.K. Samrov, Radiochimija, 3, 417 (1961).
2. P. Mühl, K. Gloe, C. Fischer, Hydrometallurgy, 5, 161 (1980).
3. A. Cocco, I. Colussi, I. Kikic, S. Meriani, ISEC Proc., Sect. 3, 80-186, Liegi (1980).
4. E. Hesford, H.A.C. McKay, J. Inorg. Nucl. Chem., 13, 156 (1960).
5. W.H. Baldwin, C.E. Higgins, B.A. Soldano, J. Phys. Chem., 63, 118 (1959).
6. W.H. Baldwin, C.E. Higgins, B.A. Soldano, J. Phys. Chem., 63, 113 (1959).
7. S. Nishimura, I. Tokura, Y. Kondo, Mem. Fac. Eng. Kyoto Univ., 27(2), 202 (1965).

SOLVENT EXTRACTION OF ALUMINUM, IRON AND TITANIUM CHLORIDES

G. Z. Sheng and M. J. Murtha and G. Burnet

Southwest Reactor Engineering Research and Design Center
Chengdu, Peoples Republic of China

Ames Laboratory, USDOE and Department of Chemical Engineering
Iowa State University
Ames, Iowa 50011 USA

A mixture of aluminum, iron, and titanium chlorides results from processes under development in which the metal oxides in coal conversion solid wastes are subjected to a high temperature chlorination in the presence of carbon or another suitable reductant. An essential step in these carbochlorination processes is the separation in pure form of the metal chlorides in the product mixture. Both anhydrous and aqueous schemes have been investigated.

A flow sheet for an aqueous separation process developed in this work is shown in Figure 1. Two cycles of solvent extraction and a single stage crystallization are involved. A mixed HCl solution is first contacted with Alamine 336, a ternary amine organic solvent, to extract the Fe(III) ions. This is followed by precipitation of the aluminum as $AlCl_3 \cdot 6H_2O$ and extraction of titanium from the mother liquor using tributyl phosphate.

The process is based upon a typical mixed chloride feed solution containing 2M $AlCl_3$, 0.45M $FeCl_3$, 0.07M $TiCl_4$ and 1M HCL (1). An HCl concentration greater than 1M is required to prevent $TiCl_4$ from hydrolyzing and forming a precipitate.

SOLVENT EXTRACTION OF FE(III):

The extraction of Fe(III) from an HCl solution can be accomplished using various solvents. Alamine 336, which was used here, has been shown to be effective in previous work (2, 3, 4) and to give a good separation from Al(III) and Ti(IV).

Extraction isotherms showed that there was almost no difference between the use of xylene or kerosine plus decanol as diluents for the Alamine 336. However, the use of kerosine plus decanol significantly improved Fe(III) stripping from the loaded organic phase. For this reason, plus lower cost and reduced flammability, kerosine plus decanol was used in this work.

Distribution coefficients for Fe(III) were determined as functions of feed composition and of acid, chloride ion, and extractant concentration. Fe(III) extraction and stripping isotherms (Figure 2) were also prepared. Iron extraction was found to improve markedly as chloride ion concentration was increased. Equivalent extraction at a given chloride concentration was found to be independent of whether hydrogen or aluminum was the predominant cation. Aluminum chloride is not extracted and will enhance the extraction of Fe(III) by its action as a salting-out agent. Keeping the $AlCl_3$ concentration in the aqueous phase high is beneficial both for the Fe(III) extraction and for minimizing the amount of feed solution to be processed.

To illustrate the removal of Fe(III) from the feed solution described above, let it be assumed that 20% (v/v) Alamine 336 plus 10% (v/v) 1-decanol in kerosine is used (Figure 3). Only two theoretical countercurrent stages are required to remove more than 99.9% of the iron (i.e. 1.05 mg/l Fe(III) in the raffinate) from the aqueous phase when a 1.2:1 organic-aqueous phase ratio is chosen. Similarly, when the organic/aqueous phase ratio is 1:1 for stripping with 0.03M HCl, six theoretical stages are needed to remove the iron from the organic phase, leaving it suitable for reuse.

RECOVERY OF ALUMINUM BY PRECIPITATION:

Precipitation of $AlCl_3 \cdot 6H_2O$ from the raffinate by introduction of anhydrous HCl relies on a method that has been thoroughly investigated by others (5). In this work, the sparging was continued until a desired HCl concentration was reached. After aging, the precipitate was filtered and washed with 12M reagent-grade HCl to reduce the titanium content to an acceptable level. The resulting crystals were then calcined at 700°C for two hours to produce alumina. As much as 91 percent of the aluminum in the raffinate was recovered in a single stage sparge-crystallization when the HCl concentration was brought to 9-11M.

RECOVERY OF TITANIUM BY TBP SOLVENT EXTRACTION:

An extractant consisting of 30% (v/v) TBP plus 8% (v/v) decanol in kerosine was found to be suitable for recovery of the titanium from the sparge-crystallization mother liquor (filtrate). The decanol served as a modifier to improve the titanium distribution coefficients.

Ti(IV) extraction from HCl solution with TBP is known to be strongly dependent upon the HCl concentration in the aqueous phase (6, 7). The effect of HCl concentration on Ti(IV) extraction is shown in Figure 4. When the HCl concentration in the feed was less than 6M, there was virtually no extraction of Ti(IV). Higher HCl concentrations reduced the number of theoretical stages required to carry out a given recovery. Ti(IV) was found to be easily stripped from the loaded organic phase with 1-2M HCl solutions.

CONCLUSIONS:

A relatively straightforward and efficient process has been developed for the separation and recovery of constitutents from an aqueous HCl solution of metal halides such as would be produced from the carbochlorination of coal conversion solid wastes. The process has been demonstrated on a laboratory scale. Economic feasibility will require the effective recycle of HCl and a minimization of organic phase losses in the extraction and stripping cycles.

REFERENCES:

1. D. J. Adelman and G. Burnet, Proc. IA Acad. Sci. 87, No. 4, 129 (1980).
2. F. G. Seeley, J. Chem. Eng. Data 11 No. 3, 424 (1966).
3. J. A. Eisele, L. E. Schultze, J. A. Berinati, and D. J. Bauer, U.S. Bur. of Mines RI 8188, 10 (1976).
4. R. T. Sorensen, E. B. Amey III, and D. L. Sawyer, U.S. Bur. of Mines RI 8590, 28 (1981).
5. R. R. Brown, G. E. Daut, R. V. Mrazek, and N.A. Gokcen, U.S. Bur. of Mines RI 8379, 17 (1979).
6. V. N. Startsev, E. I. Krylov, and Yu. A. Kozmin, Russ. J. Inorg. Chem 11, No. 3, 1239 (1966).
7. B. Z. I. Sevast'yanov, A.N. Nesmeyanov, and V. G. Vinogradova, Radiokhimiya 12, No. 1, 33 (1970).

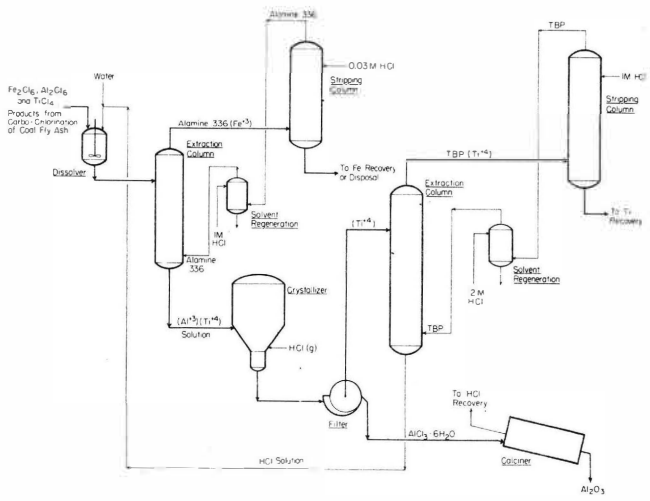

FIGURE 1. FLOWSHEET FOR THE SEPARATION OF CARBOCHLORINATION PROCESS PRODUCTS

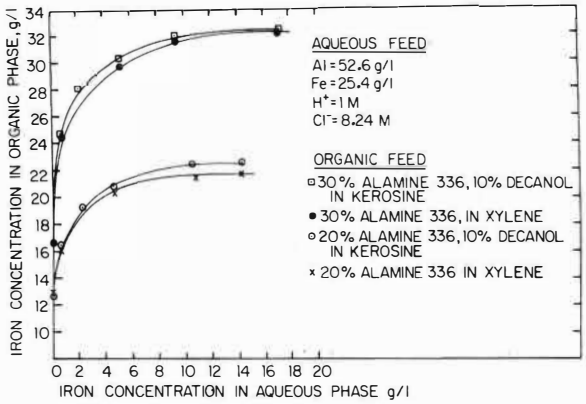

FIGURE 2. ISOTHERMS FOR THE STRIPPING OF FE(III) FROM LOADED ALAMINE 336 USING WATER

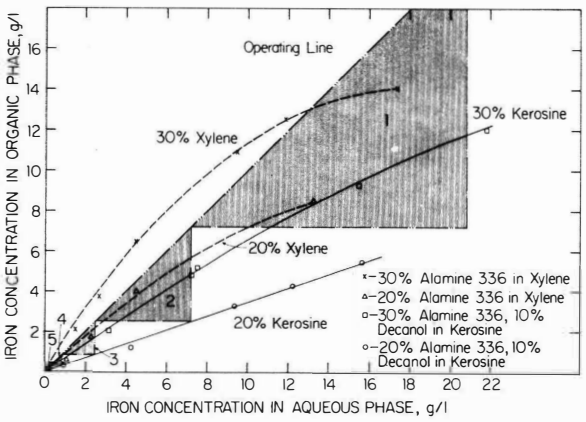

FIGURE 3. ISOTHERMS FOR THE EXTRACTION OF FE(III)

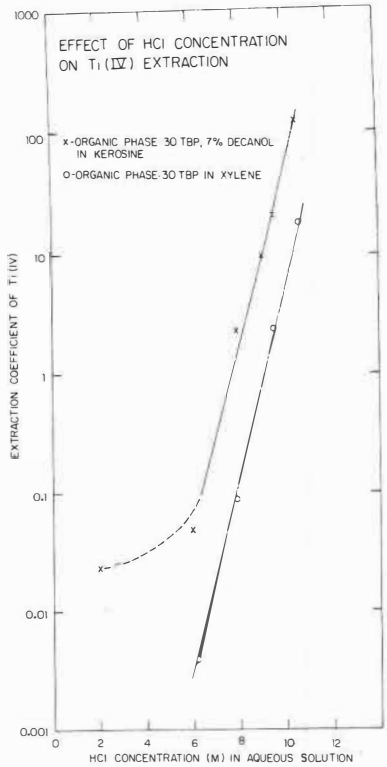

FIGURE 4. EXTRACTION COEFFICIENT FOR Ti(IV) AS A FUNCTION OF HCL CONCENTRATION IN THE AQUEOUS PHASE

EXTRACTION OF ZINC AND CADMIUM BY HIGH MOLECULAR WEIGHT AMINES

Anil K. De, Uday S. Roy and Narahari Parhi

Department of Chemistry
Visva-Bharati University
Santiniketan 731235
West Bengal, India

In recent years solvent extraction technique has found important application in pollution abatement programmes particularly for removal of toxic metals such as Zinc, Cadmium and mercury from industrial waste effluents. A rapid and selective method has been developed for extraction of Zinc and Cadmium from hydrochloric acid by high molecular weight amines in nitrobenzene.

The amines extract anionic metal complexes from aqueous solution due to their unique anion exchange ability. Amberlite LA-1, the high molecular weight Secondary amine (R_2NH), on pretreatment with hydrocholoric acid, extracts anionic chlorocomplexes of Zinc and Cadmium from hydrochloric acid medium. The extraction mechanism is shown :

$$M^{2+} + 4HCl \rightleftharpoons (MCl_4)^{2-} + 4H^+$$

$$2\,(R_2NH.HCl)_{(o)} + (MCl_4)^{2-}_{(a)} \rightleftharpoons [(R_2NH_2^+)_2(MCl_4)^{2-}]_{(o)} + 2Cl_{(a)}$$

where $M^{2+} = Zn^{2+}$ or Cd^{2+}

(o) = organic phase

(a) = aqueous phase

and R_2NH = Amberlite LA-1

The Secondary amine and its salt with anionic chlorocomplexes of Zinc and Cadmium are insoluble in aqueous solutions but are highly soluble in organic solvents. The present paper reports on the comparative solvent extraction behaviour of Zinc and Cadmium, as Chlorocomplex, with Amberlite LA-1. No such work is reported in the literature (1 - 8).

GENERAL EXTRACTION PROCEDURE

A solution containing 1-15 mg. of Zinc/Cadmium was taken in a separatory funnel (100 ml). The aqueous phase was adjusted to the optimum HCl concentration (= 2M for Zn^{2+} and = 0.5 M for Cd^{2+}) and made up to 10 ml. It was equilibrated with 10 ml of 5% V/V Amberlite LA-1 in nitrobenzene (amine: nitrobenzene = 1:20 by volume) for 5 minutes. The experiments were carried out at 27 ± 1°C. The two layers were allowed to settle for 10-15 minutes. The organic phase was separated carefully and transferred to another separatory funnel.

The residual aqueous phase was collected, excess acid neutralised by ammonia and Zinc/Cadmium estimated Complexometrically with EDTA.

The extracted organic phase was stripped with 10 ml. of 2 M HNO_3 (Zn)/ 1 M HNO_3 (Cd) for 5 minutes. The organic phase was separated carefully and the residual aqueous phase again estimated as before complexometrically after neutralisation by ammonia.

EXTRACTION PARAMETERS

Hydrochloric acid concentration -

The extraction of Zinc and cadmium increase with increased HCl concentration and become quantitative at =2M (Zn) and = 0.5 M (Cd.). The distribution ratios (D) were calculated from the eq :

$$D = \frac{V}{V'}\left(\frac{100}{100-x} - 1\right)$$

where V and V' are the volumes of aqueous and organic phases and x = percentage of metal extracted (9). Plot of log D - log [Cl] in both cases gives straight lines with slope 2.0 which indicates the formation of $(ZnCl_4)^{2-}$ / $(CdCl_4)^{2-}$ in the aqueous phase.

Amberlite LA-1 concentration

At constant metal ion and optimum HCl Concentrations, the extractions of Zinc and Cadmium become quantitative at amine : metal ratio ≥ 2. Log D - log [Amine] plots give a slope of 2.0 so that the extracted species is $[(R_2NH_2^+)_2\ (MCl_4)^{2-}]$ where M = Zn^{2+}/ Cd^{2+}.

Diluents

Several diluents were examined : n-hexane, carbon tetrachloride, benzene, xylene, toluene, chloroform, butanol and nitrobenzene. Among these nitrobenzene gave the best result. However there is no clear cut relation between dielectric constant and percentage extraction for the systems studied.

Loading Experiments

At constant amine and hydrochloric acid concentration loading experiments for metal ions were carried out. Optimum extraction was observed for 0.065 to 1.30 g/l of Zinc and 0.12 to 2.36 g/l of Cadmium. Extraction isotherms reveal metal : amine ratio = 1 : 2 in the organic phase in both the cases. This supports the proposed extracted species as

$$[(R_2NH_2^+)_2(MCl_4)^{2-}]_o$$

Extractive Separations

From experiments on the effect of diverse ions on the extraction systems it has been possible to work out several separations of Zinc and Cadmium from some ternary and quaternary mixtures.

REFERENCES

1. A Pusparaja and M. Sudersanan, Indian J.Chem. 19(A), 925 (1980)
2. H.A.Mahlman, G.W.Leddicotte and F.L.Moore, Anal.Chem.26, 1939 (1954)
3. O.V.Singh and S.N.Tandon, J.Inorg. Nucl.Chem.36, 2083 (1977) ; 37, 609 (1975)
4. L.E.Scroggie and J.A.Dean, Anal.Chem. Acta, 21, 282(1969)
5. G.Nagakawa, Nippon Kagaku Zasshi 81, 1533 (1960)
6. F.L.Moore, Environ.Letter 10, 37 (1975)
7. D. Hayati and R.W.Cattrall, J. Inorg. Nucl.Chem. 43, 599 (1981)
8. A. K. De, U.S.Roy and N. Parhi, J. Indian Chem. Soc. (in press).
9. A.K.De, R.A.Chalmers and S.M.Khopkar, Solvent Extraction in Analytical Chemistry, Van Nostrand, London(1970)

MERCURY ISOLATION BY SOLVENT EXTRACTION AND NON-ELECTROLYTIC METHOD FROM LOW CONCENTRATION CINNABAR ORES

Victor Arenas, Hernán Lizama, Ricardo Schrebler, Ignacio Gardiazabal

Universidad Católica de Valparaiso
Valparaiso, Chile

The lixiviation of a mineral with a little law in cinnabar (0,2% Hg) was carried out employing a 0,6v/v sodium hypochlorite aqueous solution of pH 6 containing NaCl. The concentrated lixiviated solutions were obtained using LIX 34 (1% in Solvesso 150) as extractant. The best conditions for Hg(II) stripping were reached with a 0,1 M HCl/1M NaCl solution which concentrates the initial mercury solution by a factor 20. From the concentrated solution it was possible to get metallic mercury by electroless at room temperature in presence of brass alloys of different compositions.

Theoretical Limitations,

From the thermodynamic point of view, cinnabar and mercury are easily dissolved by hypochlorite as can be seen in the ΔG values for this reaction (ΔG=-216 Kcal/mol HgS). By this reason, only diluted solutions are needed (1,2). The corresponding equations are :

$$HgS_{(s)} + 4\ ClO^-_{(aq)} \rightleftharpoons HgCl_{2(aq)} + 2Cl^-_{(aq)} + SO_4^{2-}{}_{(aq)}$$

$$Hg_{(s)} + Cl^-_{aq} + ClO^-_{aq} + H_2O \rightleftharpoons HgCl_{2(aq)} + 2\ OH^-_{(aq)}$$

However, in order to avoid losses of chloride, a rigorous control of pH is required. As can be seen in Figure 1, below pH 3 the HClO is reduced with evolution of gaseous chlorine (3) according to reactions :

$$2\ HClO + 2\ H^+ + 2\ \bar{e} \rightleftharpoons Cl_{2(g)} + H_2O$$

$$Cl^- + ClO^- + 2H^+ \rightleftharpoons Cl_{2(g)} + H_2O$$

Thus, the occurrence of these reactions at pH lower than 3, diminishes the yield of the extraction process. By the other hand, the existence of Hg(0) makes necessary aqueous solutions with a relatively high concentration of chloride due to the participation in the process of the redox systems :

(1) Hg^{+2}/Hg^o E = 0,79 (N. H. E.)

(2) Hg^{+2}/Hg_2^{+2} E = 0,91 (N. H. E.)

and the equilibria :

(3) $Hg_2Cl_2 \rightleftharpoons Hg_2^{+2} + 2\ Cl^-$ Ksp = 10^{-18}

(4) $HgCl_4^{2-} \rightleftharpoons Hg^{+2} + 4\ Cl^-$ $K_c = 10^{-15}$

Considering eq(3), the redox systems (1) can be put as follow :

$$E = 0,79 + \frac{0,058}{2} \log \frac{10^{-18}}{[Cl^-]^2} \quad \text{or}$$

(5) $E = 0,25 - 0,058 \log [Cl-]$

Accordingly, taking in account eq.(4) the redox system (2) can be written as :

$$E = 0,91 + \frac{0,058}{2} \log [Hg^{+2}]^2 \frac{[Cl^-]^2}{10^{-18}} \quad \text{or}$$

(6) $E = 0,55 - 0,058 \log Hg[II] - 0,18 \log [Cl^-]$

The graphic representation of equations (5) and (6) are shown in Figure 2. It can be inferred from these graphs that :

a) The specie Hg_2Cl_2 prevails in the whole range of low chloride concentration and thus, the system that participates Hg^{+2}/Hg_2Cl_2.

b) In order to get the redox system (1) without the presence of the insoluble specie Hg_2Cl_2, the chloride concentration must be higher than 3M.

EXPERIMENTAL RESULTS.

Tast polarographic technique was employed to determine Hg^{+2} in aqueous solutions in a conventional cell with three electrodes, Figure 3. The electrolyte was deareated with Argon during 3 hours and then increasing amounts of aqueous solutions of $HgCl_2$ were added. The regression straight line was obtained with a 95% confidence limit.

The microscopic analysis of the samples employed showed that the prevailing mineral species were silicates and quartz with little amounts of metallic components, mainly pyrite and cinnabar. The Atomic Absorption Analysis appears in table I.

The process of continuous lixiviation of the mineral was considered studying its yield in function of : lixiviation time, NaOCl concentration and per cent of solid matter dispersed in solution. Figures 4 and 5, show the results obtained. The best yield was reached when the mineral was lixiviated for 3 hours with 0,6% NaOCl containing NaCl and 4% of solid matter dispersed.

TABLE I

Element	Abundance	% Error
Fe	5,1%	1%
Cu	0,33%	1%
Mn	0,36%	1%
Sb	0,30%	5%
Co	0,0035%	2%
Ni	0,006%	2%
Pb	0,005%	2%

Total Mercury: 0,2%

The enrichment of the lixiviated electrolyte was made employing a continuous countercurrent extraction process with LIX 34 (RH). As the lixiviation gives an anionic complex it was necessary to convert it to the cathionic form. Furthermore, taking in account that the chloride complex is less stable than the ammonium one (K_c=2.10^{-7} and 1,6.10^{-9} respectively), the lixiviated electrolytes were treated with an aqueous solution of NH_3/NH_4^+ giving rise the formation of Hg $(NH_3)_4^{+2}$ according to reaction.

$$HgCl_4^{-2} + 4NH_3 \rightleftharpoons Hg(NH_3)_4^{+2} + 4\ Cl^-$$

As a matter of fact, the extraction of the complex ion with LIX 34 origins the liberation of protons and the alkaline media in which mercury is complexed favours the extractive process:

$$2\ RH + Hg(NH_3)_4^{+2} \rightleftharpoons HgR_2 + 2NH_3 + 2\ NH_4^+$$

For the same reason, the stripping of Hg(II) from the organic phase is favoured by contact with aqueous acid phases.

Batch studies allowed to establish that saturation of organic phase was reached with five consecutive extraction steps using a 1%v/v LIX 34 solution in Solvesso 150, Figure 6. The stripping of mercury was attained with a solution containing HCl and NaCl in order to get mercury in the complexed form. The results obtained with a continuous system of two extraction stage and two stripping stage are summarized in Table II.

TABLE II

Molar concentration of Mercury (II).

	Organic Phase	Aqueous Phase	Stage
Extraction	$1.53 \cdot 10^{-4}$	$3,53 \cdot 10^{-5}$	1
	$1.43 \cdot 10^{-5}$	0,0	2
Stripping	$8,13 \cdot 10^{-6}$	$1,33 \cdot 10^{-2}$	1
	0,0	0,0	2

The conversion of Hg (II) to Hg (0) from a 1.10^{-3} solution was made by means of an electroless process ussing brasses of variable composition. This last process is characterized by the apparition of gross metallic mercury drops because of the dealloying of the brass in strongly agressive media such as the one in the stripping step. The reaction can be put as follow :

$$Cu + Zn \longrightarrow Cu^{+2} + Zn^{+2} + 4\bar{e}$$

$$2HgCl_4^{2-} + 4\bar{e} \longrightarrow 2\ Hg^{o} + 8\ Cl^{-}$$

CONCLUSIONS.

The present results allow us to conclude that with the choice of the proper experimental conditions, it is possible to dispose of a suitable alternative for working low law mercury minerals ($<$ 1%). The solvent extraction technique allow to concentrate Hg(II) from lixiviated solutions which can be easily reduced to metallic mercury by applying an electroless process employing brasses of different compositions.

REFERENCES.

1.- G. W. Hack and J. B. Hamilton, U.S. Patent. 3.701.651 (1972).

2.- G. A. Parks and N.A. Fittinghoff, Engineering Minning Journal., 171(6), 107 - 9 (1970).

3.- B. J. Scheiner and R.E. Lindstrom, Bureau of Mines Metallurgy. Technical Progress Report. (1970).

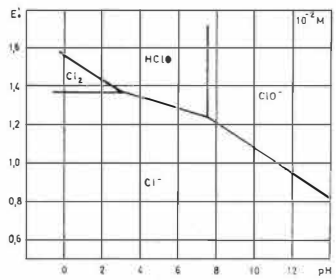

Figure 1.- POTENTIAL/pH DIAGRAMME FOR CHLORINE SPECIES.

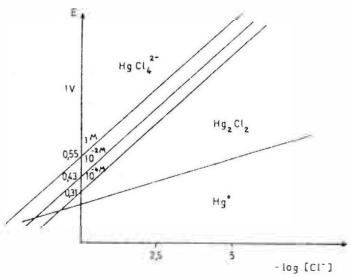

Figure 2.- VARIATION OF APPARENT NORMAL POTENTIAL OF Hg(II) SPECIES WITH CHLORIDE CONCENTRATION.

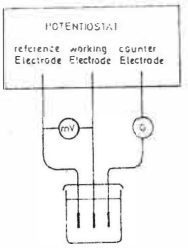

- SCHEMATIC REPRESENTATION OF THE EQUIPMENT USED FOR Hg(II) DETERMINATION.

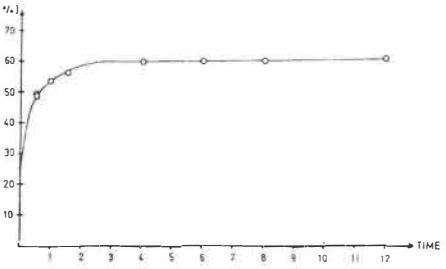

Figure 4.- LIXIVIATION YIELD V/S TIME.

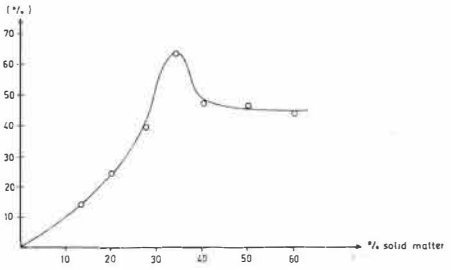

Figure 5.- LIXIVIATION YIELD V/S PERCENT OF DISPERSED SOLID MATTER.

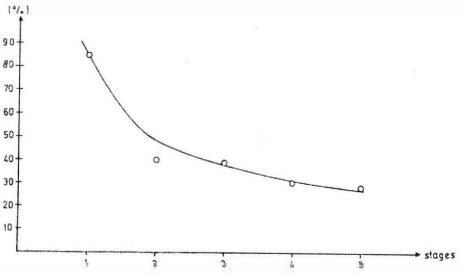

Figure 6.- LIXIVIATION YIELD V/S NUMBER OF STAGES.

SOLVENT EXTRACTION OF URANIUM IMPURITY TO PRODUCE NUCLEAR-GRADE ZIRCONIUM

D. J. MacDonald, H. G. Henry, and D. J. Bauer

Reno Research Center
Bureau of Mines
Reno, Nevada USA

ABSTRACT

In a method investigated by the Bureau of Mines for improved production of nuclear-grade ZrO_2 from zircon sand, trioctyl amine in kerosine was used to countercurrently extract zirconium from an aqueous H_2SO_4 solution. The solvent rejected hafnium and other impurities derived from zircon sand, but not traces of uranium. For example, a representative organic-phase extract contained 3.8 g zirconium and 0.002 g uranium per liter. Selective countercurrent stripping of the extract separated zirconium from uranium when high chloride-ion activity was maintained. A lean organic solvent stream was preloaded with chloride by contact with an aqueous solution of 0.5M HCl in 4.0M NaCl. The chloride-loaded solvent was used to back-extract uranium from a zirconium-laden strip liquor. The aqueous chloride solution from the chloride preloading of the organic solvent was used to strip zirconium from an organic stream formed by combining the above-mentioned zirconium-free uranium-bearing solvent and the zirconium- and uranium-bearing organic-phase extract. The resulting organic stream, bearing uranium but depleted of zirconium, was purged of uranium and readied for recycle by contact with Na_2CO_3 solution. The zirconium-bearing strip liquor resulting from these operations contained 14 g zirconium and 0.00003 g uranium per liter and yielded precipitated ZrO_2 suitable for making nuclear-grade zirconium.

BACKGROUND

In the course of investigations on separating zirconium from hafnium, Bureau of Mines research showed that a tertiary amine solvent extraction system capable of eliminating hafnium impurity was not effective in removing uranium. The specification for nuclear-grade zirconium requires a uranium content no greater than 3 ppm. The benefit of the amine extraction system could not be realized unless a procedure for removing uranium could be found. The uranium originates with zircon sand, the raw material from which zirconium is made. Zircon sand contains about 200 ppm uranium, and in the amine extraction about two thirds of it reports to the organic-phase extract with the zirconium.

An approach to the problem was suggested by the known behavior of uranium with anion exchange resin (1), as shown in table 1. Higher concentrations of HCl shift greater proportions of uranium into the resin phase. The ion exchange resin was Dowex AG1[1], which has quaternary ammonium functional groups. When a tertiary amine organic solution loaded with zirconium is contacted with an aqueous chloride solution, the zirconium is stripped. Moreover, the degree of stripping becomes more complete at higher chloride concentrations. Therefore, if the chloride activity could be kept high enough, the uranium impurity could be retained in the organic phase while zirconium is stripped.

TABLE 1. - Distribution coefficients for uranium(VI) on strong base anion exchange resin as a function of aqueous-phase HCl concentration, according to Strelow and Van der Walt (1)

HCl, mol/l	Distribution coefficient for uranium(VI)
0.1	1.0
2.0	10.4
4.0	96.0
6.0	416.0

A more detailed description of the overall process is given in Bureau of Mines Reports of Investigation (2), and a patent has been applied for (3). A generalized flowsheet is shown in Figure 1.

PROCEDURE AND RESULTS

Preliminary experiments, in which a zirconium-laden organic extract was subjected to countercurrent stripping with NaCl solutions, showed that the desired effect might be achieved, but only if the chloride activity could be made higher. The countercurrent flow sequence is shown in Figure 2. The loaded organic solvent entering the flow sequence contained 3.8 g zirconium per liter and 1.56 mg uranium per liter. Mixer-settlers, each of which had a total volume of 580 ml, were operated at an organic-to-aqueous phase ratio of 3.6. Table 2 shows that higher chloride concentrations in stripping agent solution used in the preliminary experiments resulted in smaller proportions of total uranium passing into the strip liquor. Complete stripping of zirconium occurred. The best strip liquor produced in these preliminary experiments contained 14 g zirconium per liter and 0.33 mg uranium per liter, for a uranium-zirconium ratio of 24×10^{-6}. Since nuclear-grade zirconium must contain less than 3 ppm uranium, higher chloride-ion activity was needed, but using more NaCl was ruled out by its limited solubility in the presence of HCl, and using much more HCl was unsatisfactory because of third-phase formation.

TABLE 2. - Proportion of uranium remaining in stripped organic solvent as a function of stripping agent solution chloride concentration

Stripping agent solution, mol/l		Proportion of uranium, pct	
NaCl	HCl	Strip liquor	Stripped organic solvent
2.0	0.0	79	21
2.5	.0	73	27
3.0	.0	53	47
3.5	.0	42	58
4.0	.0	34	66
4.0	.1	24	76
4.0	.5	7	93

[1]Reference to specific brand names is made for identification purposes only and does not imply endorsement by the U.S. Bureau of Mines.

To get higher chloride-ion activity in both phases simultaneously, a flow sequence designed to preload the organic phase with chloride was used. Figure 3 shows how it was arranged. Two organic streams entered, one lean and neutralized, the other carrying zirconium and uranium. The aqueous stream, called stripping agent solution, contained sodium chloride and hydrochloric acid and was used to load the lean organic stream with chloride and subsequently for zirconium stripping. In the zirconium-stripping stages all the zirconium and part of the uranium was transferred to the aqueous phase. In the uranium-back-extraction stages, uranium in the aqueous phase was transferred back into the high-chloride organic phase.

Two compositions of stripping solution, one containing 0.25M HCl in 4.0M NaCl and the other containing 0.5M HCl in 4.0M NaCl, were tested. Results are shown in table 3. The most significant results are the uranium concentrations in stage UX1. When the stripping agent solution contained 0.25M HCl, the strip liquor contained 0.19 mg uranium per liter for a uranium-zirconium ratio of 14×10^{-6}, which is still not acceptable. When the stripping solution was made 0.50M in HCl, the resulting strip liquor contained only 0.03 mg uranium per liter, for a uranium-zirconium ratio of 2×10^{-6}. The nuclear-grade specification was satisfied.

TABLE 3. - Aqueous-phase zirconium and uranium concentrations from contacting operations with the flow scheme of figure 2

Stage (aqueous phase)	0.25M HCl in 4.0M NaCl		0.50M HCl in 4.0M NaCl	
	Zr, g/l	U, mg/l	Zr, g/l	U, mg/l
First uranium-back-extraction stage (UX1)	14	0.19	14	0.03
Second uranium-back-extraction stage (UX2)	NA	0.41	NA	1.3
First stripping stage (ST1)	14	1.3	NA	1.0
Second stripping stage (ST2)	1.7	0.09	NA	.05

NA - Not available

The uranium and chloride remaining in the stripped organic phase were removed by contacting with soda ash solution, which neutralized the organic stream and made it acceptable for recycle. Zirconium contained in strip liquor was recovered as reactor-grade ZrO_2 whose purity was verified by emission spectrographic analysis performed by a commercial zirconium producer.

SUMMARY

Countercurrent scrubbing of a zirconium-bearing strip liquor with tertiary amine organic solvent preloaded with chloride was effective in removing uranium. The resulting zirconium-laden strip liquor was suitable for producing nuclear-grade zirconium.

REFERENCES

1. Strelow, F. W. E., and T. N. Van der Walt. Method to Avoid Losses of Uranium at the Interface Between Different Eluting Agents During Anion Exchange Chromatography. Anal. Chem., v. 50, No. 1, 1978, pp. 44-47.

2. MacDonald, D. J., R. A. Guidotti, and H. G. Henry. Method for Producing Zirconyl Sulfate Solution From Zircon Sand. BuMines RI 8718, 1982, 13 pp

3. MacDonald, D. J., and H. G. Henry. Separation of Zirconium and Uranium. Patent Application, Serial No. 363,367, filed March 30, 1982.

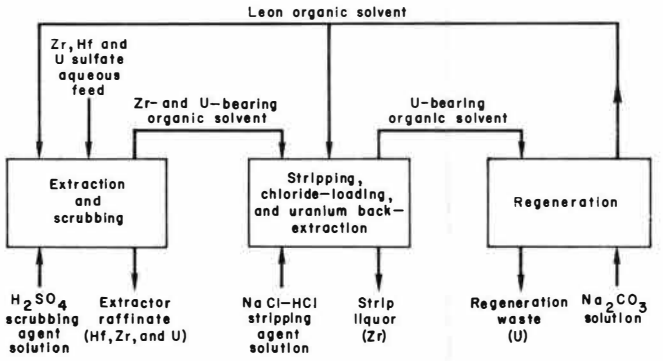

Figure 1. - Flowsheet for solvent extraction of hafnium and uranium from zirconium.

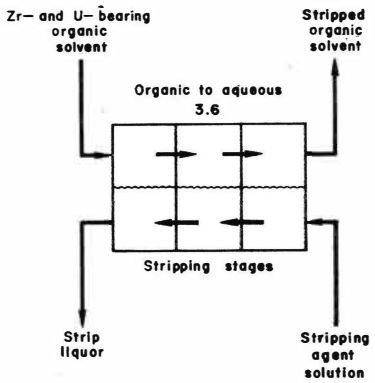

Figure 2. - Flow sequence for countercurrent stripping.

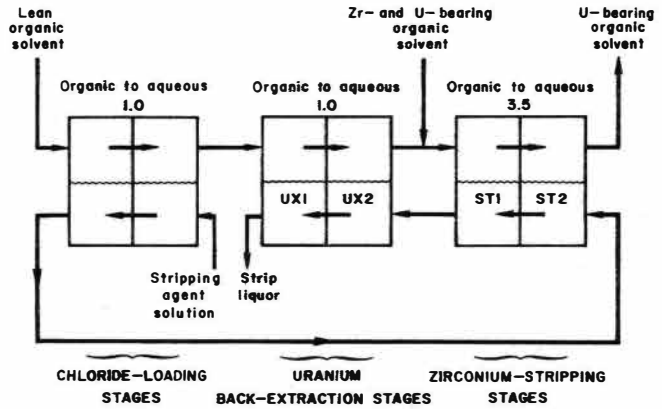

Figure 3. - Flow sequence for countercurrent chloride-loading, uranium-back-extraction, and zirconium-stripping operations.

A DATA BASE FOR SOLVENT EXTRACTION CHEMISTRY*

W. J. McDowell, D. C. Michelson, B. A. Moyer, C. F. Coleman

Chemical Technology Division
Oak Ridge National Laboratory
Oak Ridge, Tennessee 37830 USA

*Research sponsored by the Division of Chemical Sciences, U.S. Department of Energy under contract W-7405-eng-26 with the Union Carbide Corporation.

The rapid proliferation of scientific and science-related literature has made information retrieval a real problem in most scientific desciplines, but in many respects the problem is more serious in separations science than in other areas. This arises from the fact that extraction, ion exchange, and chromatographic separations are used in many different disciplines, and the same operations have acquired different names in these different disciplines. Also, different operations are sometimes referred to by the same name. As an example of the first, "liquid-liquid extraction" is called "solvent extraction" in hydrometallurgy and "phase-transfer" in biochemistry and organic chemistry. An example of the second case is "extraction," which means removing a metal from an ore body to metallurgists and removal of an essence from an herb to an organic or pharmaceutical chemist. These and similar nomenclature problems have made indexing and retrieving of separations information particularly difficult. In addition to these differences in nomenclature (including index terms and keywords), publications are in journals of various disciplines. Thus, searches with most indexes are usually both incomplete and too extensive (retrieve unwanted material) at the same time. It was found that existing indexing systems either located many references, 90% of which were of no interest, or, if the search was restricted to solve that problem, needed material was lost. Further, much of the original literature in hydrometallurgical separations is poorly indexed. Reports of many government laboratories in the period 1945 to 1967 are poorly indexed and are now difficult or impossible to find. These reports are being included in the data base described here.

In an effort to alleviate many of the above-mentioned problems, we are attempting to assemble a computer-searchable data base, called "Separations Science Data Base," that is designed specifically for retrieval of information needed in chemical separations problems. The initial aim of this data base is to emphasize solvent extraction and ion exchange literature, although the indexing is structured so as to include other separations methods such as distillation, precipitation, or flotation, for example. The data base is supported by the Oak Ridge National Laboratory computer system by a data management and retrieval system called RECON (REmote CONsole), and the reference material can be retrieved in an interactive manner not only in terms of author, title, source, and date of publication entries but also in terms of the substance separated (both those recovered and those rejected), the separation agent used, the matrix from which the separation is made, and the type of information contained in the reference.

The highly selective retrieval ability of the data base derives from a unique feature. The index terms or keywords that are usually all lumped together as a subject index are separated into five categories. These are: Separation System, Separation Agent, Separated Substance, Matrix (from which the separation is made) and Type of Information (in the source). In addition, the terms in the separated substance category can be flagged to indicate whether the substance is retained in the separation, is rejected, or cannot be separated. This categorization of index terms allows a much more selective search than is possible with conventional data bases. For example, questions of the sort "How do I separate substance A from substance B out of matrix M?" are easily answered by the retrieval of specific references. Also, the field can be further narrowed by specifying the type of reagent desired and the type of information desired. In short, searches can be extremely specific with little danger of failing to retrieve desired references. A copy of the first-page introductory material describing these fields that is obtained when one first accesses the data base on RECON is shown in Figure 1. The RECON system will display portions of any of the indexes adjacent to any term on request. Four such index segments are shown in Figure 2. Sets of references from selected terms may be combined using "and" logic to give sets of very specific references. A portion of such a search is shown in Figure 3.

An additional feature of the Separations Systems Data Base is the manner in which multi-subject reports are handled. Such reports often cause trouble because of false cross-coupling of index terms for separate subjects in such a way as to retrieve a document when, in fact, it contains no information of the type sought. This problem has been largely solved by indexing each subject of such multi-subject reports as a separate input item. Together with all of the bibliographic data, one of the subjects is indexed in a normal or "parent" reference; then each additional subject is indexed in a "split" input form that contains only the index-term lists and a cross reference to the parent reference. False retrieval from cross-coupling is thus effectively eliminated.

The process of indexing for the Separations Science Data Base has been made relatively painless by the use of input forms that contain spaces for all the pertinent bibliographic input information plus a complete thesaurus for the index terms. The indexer has only to chooose and circle or highlight the appropriate word or words in each index field (Figure 4). Space for an abstract is also provided. Single-subject papers for which an abstract is available usually require about 15 minutes each. An abstractor's manual is available. ["Separations Science Data Base: An Abstractor's Manual," J. W. Roddy, W. J. McDowell, and D. C. Michelson, ORNL/TM-7805 (July 1981)]. Authors are urged to help by indexing their own publications.

The data base is stored on the computer system at the Oak Ridge National Laboratory and is searchable through the United States Department of Energy RECON data management system. Anyone having access to the DOE/RECON system may search it directly, or searches can be made through the Western Regional Information Service Center, Lawrence Berkeley Laboratory, Building 50, Room 103, Berkeley, California 94720, phone (415) 486-6307. Printed lists of the selected references complete with abstracts may be obtained.

Although the data base is far from complete (4000 records presently, perhaps 20% of the available solvent extraction references), it has definite advantages for the separations scientist. It is a specific subject data base, and thus indexing can be much more specific because of the narrower scope and the opportunity for a more complete keyword list. The problem of non-standard and conflicting nomenclature has been eliminated because of a standardized keyword list applied by persons knowledgeable in the subject matter.

Additional information on the Separations Science Data Base can be obtained from any of the authors.

```
SEPARATIONS SCIENCE DATA BASE
(3,978 RECORDS RELOADED ON 02/07/83)
    This data base is designed specifically for the storage and retrieval of
information needed in chemical separation problems. Initial entries are
concerned primarily with solvent extraction, ion exchange and related
fields. Available indexes are:
          AU=AUTHOR                SS=SEP. SYSTEM
          TL=TITLE                 IT=SEPARATED SUBST.
          YR=DATE                  SA=SEPARATION AGENT
          LT=LITERATURE TYPE       MA=MATRIX
                                   TI=TYPE OF INFO.
Each of the indexes in the right-hand column contains index terms describing
information within that index name. By selective use of combinations of
indexes and index terms, information on specific separations under specific
conditions can be retrieved.
    SEPARATIONS SCIENCE DATA BASE Page 2
In SEPARATED SUBST. index, substance name is followed by notations giving
additional information about the separation. Name only indicates substance
is extracted (or retained on column or filter) or that specific information
on a separation is not given.
         Name -  = substance rejected
         Name ,- = subst. optionally collected or rejected
         Name +- = substance splits
         Name?   = info. in doubt
Roman numerals indicate oxidation state. Text search available on title
and abstract.
    For further information contact:
         Separations Science Data Base
         Bldg. 4500S, Mail Stop C-256
         Oak Ridge National Laboratory
         P.O. Box X
         Oak Ridge, TN 37830
         (615) 574-6714, FTS 624-6714
```

FIGURE 1. INTRODUCTORY/EXPLANATORY MATERIAL DISPLAYED BY RECON WHEN THE DATA BASE IS ACCESSED

(A)

```
EXPAND  IT=URANIUM
 REF  DESCRIPTOR                CIT
 E01  IT=TUNGSTEN ,-_____        2
 E02  IT=TUNGSTEN(V)_____        1
 E03  IT=TUNGSTEN(VI)____       10
 E04  IT=TUNGSTEN(VI)-___        8
-E05  IT=URANIUM_________      465
 E06  IT=URANIUM -_______       60
 E07  IT=URANIUM ,-______       41
 E08  IT=URANIUM(III)____        1
 E09  IT=URANIUM(IV)_____       43
 E10  IT=URANIUM(IV)-____        2
 E11  IT=URANIUM(IV),-___        5
 E12  IT=URANIUM(VI)_____      214
 E13  IT=URANIUM(VI)-____       18
 E14  IT=URANIUM(VI),-___       38
 E15  IT=VANADIUM________       59
 E16  IT=VANADIUM +-_____        3
 E17  IT=VANADIUM -______       19
 E18  IT=VANADIUM ,-_____        8
 E19  IT=VANADIUM(II)____        1
 E20  IT=VANADIUM(II)+-__        2
ENTER:                        -MORE-
```

(B)

```
EXPAND  SA=TBP
 REF  DESCRIPTOR                CIT
 E01  SA=SULFONATE_______       14
 E02  SA=SULFONE_________       5
 E03  SA=SULFONIC ACID___       71
 E04  SA=SULFOXIDE_______       62
 E05  SA=SULFUR
       COMPOUND-ORG______      167
-E06  SA=TBP____________      605
 E07  SA=TERTIARY AMINE__      447
 E08  SA=THIOPHOSPHATE-OR
       G_________________       13
 E09  SA=THIOPHOSPHORIC
       ACID-ORG__________       14
 E10  SA=TIN COMPOUND-ORG        4
 E11  SA=TOPO____________      158
 E12  SA=TOPS____________        3
 E13  SA=TRIALKYL
       PHOSPHATE_________       1
 E14  SA=TRIALKYLPHOSPHAT
       E_________________      185
ENTER:                        -MORE-
```

(C)

```
EXPAND  MA=NITRATE
 REF  DESCRIPTOR                CIT
 E01  MA=MOLTEN SALT_____       40
 E02  MA=NEUTRAL_________       88
-E03  MA=NITRATE_________    1100
 E04  MA=NITRITE_________      10
 E05  MA=ORE_____________     117
 E06  MA=ORGANIC_________     100
 E07  MA=ORGANIC ANION___      57
 E08  MA=OXALATE_________      73
 E09  MA=OXIDANT_________      31
 E10  MA=OXIDE___________      21
 E11  MA=PERCHLORATE_____     292
 E12  MA=PEROXIDE________       3
 E13  MA=PHOSPHATE_______     125
 E14  MA=PLASTIC_________       2
 E15  MA=REDUCTANT_______      59
 E16  MA=RESIDUALS_______      76
 E17  MA=RESIN___________       7
 E18  MA=SALT____________     851
 E19  MA=SILICATE________      15
 E20  MA=SULFATE_________     743
ENTER:                        -MORE-
```

(D)

```
EXPAND  AU=BROWN
 REF  DESCRIPTOR                CIT
-E01  AU=BROWN___________       1
 E02  AU=BROWN, A.E.P.___       3
 E03  AU=BROWN, K.B._____      84
 E04  AU=BROWN, P.R._____       1
 E05  AU=BROWN, W.B._____       2
 E06  AU=BRUCHLE, W._____       1
 E07  AU=BRUIN, S._______       1
 E08  AU=BRUN'KO, T.G.___       1
 E09  AU=BRUNETTE, J.P.__       3
 E10  AU=BRUNINX, E._____       1
 E11  AU=BRUNISHOLZ, G.__       1
 E12  AU=BRUSSET, H._____       1
 E13  AU=BRUTOVSKY, M.___       1
 E14  AU=BRYAN, S.E._____       1
 E15  AU=BUCHANAN, J.M.__       1
 E16  AU=BUCHANAN, J.R.__       3
 E17  AU=BUCHER, J.J.____       2
 E18  AU=BUCHIKHIN, E.P._       4
 E19  AU=BUDANOV, A.G.___       1
 E20  AU=BUDESINSKY, B.__       1
ENTER:                        -MORE-
```

FIGURE 2. PORTIONS OF THE INDEXES, (A) SEPARATED SUBSTANCE, (B) SEPARATION AGENT, (C) MATRIX, AND (D) AUTHOR, DISPLAYED BY RECON ON REQUEST

```
ENTER:SELECT URANIUM
>PROCESSING<
   1     433 IT=URANIUM
ENTER:SELECT IRON -
>PROCESSING<
   2     100 IT=IRON -
ENTER:SELECT MA=AQUEOUS
>PROCESSING<
   3    1918 MA=AQUEOUS
ENTER:SELECT MA=ACID
>PROCESSING<
   4    2117 MA=ACID
ENTER:SELECT MA=SULFATE
>PROCESSING<
   5     743 MA=SULFATE
ENTER:SELECT SA=AMINE
>PROCESSING<
   6     511 SA=AMINE
ENTER:SELECT SS=EXTRACTION
>PROCESSING<
   7    3101 SS=EXTRACTION
ENTER:COMBINE 1 AND 2 AND 3 AND 4 AND 5 AND 6 AND 7
>PROCESSING<
   8       8 1 AND 2 AND 3 AND 4 AND 5 AND 6 AND 7
ENTER:DISPLAY 8/6/1-8
>PROCESSING<
<ACCESSION NO.> 82*000254_     *******1
<AUTHOR> Babcock, W.C.; Baker, R.W.; Kelly, D.J.; LaChapelle, E.D.
<TITLE> Coupled Transport Membranes for Uranium Recovery
<ACCESSION NO.> 05Z0004086     *******2
<PARENT REF.> See accession No. 00P0004081
<ACCESSION NO.> 05Z0003955     *******3
<PARENT REF.> See accession No. 00P0003950
<ACCESSION NO.> 01Z0003702     *******4
<PARENT REF.> See accession No. 00P0003701
<ACCESSION NO.> 00P0003743     *******5
<AUTHOR> Ryon, A.D.; Johnsson, K.O.; Bauman, H.F
<TITLE> Progress Report of Process Test Section for October 1956
<ACCESSION NO.> 00P0003696     *******6
<AUTHOR> Bauman, H.F.; Buchanan, J.R.; DeCarlo, V.A.; Guymon, R.H.; Klima, B.
  McLeod, H.M.,Jr.; Manneschmidt, J.F.; Ryon, A.D.; Wiethaup, R.R.
<TITLE> Progress Report of Engineering Section Raw Materials Process Testing:
  April 1955
<ACCESSION NO.> 00U0003582     *******7
<AUTHOR> Ryon, A.D.; Daley, F.L.
<TITLE> Solvent Extraction of Uranium from Reduction Slag Slurry
<ACCESSION NO.> 00P0003423     *******8
<AUTHOR> Brown, K.B.; Coleman, C.F.; Crouse, D.J.; Ryon, A.D.
<TITLE> Progress Report on Raw Materials for November 1957
ENTER:=STOP
```

FIGURE 3. AN EXAMPLE OF A SEARCH IN WHICH THE QUESTION, "HOW DO I SEPARATE URANIUM FROM IRON OUT OF SULFATE MEDIUM USING AN AMINE EXTRACTANT?" IS ASKED. NOTE THE SPLIT RECORDS THAT ARE CROSS-REFERENCED TO PARENT REFERENCES, PROBABLY MULTI-SUBJECT REPORTS.

CAREFULLY CIRCLE OR HIGHLIGHT THE APPROPRIATE TERM OR TERMS FROM EACH TABLE

<SEP SYS>

(Sep. System)

1 Adsorption	8 Electrolysis	27 Gradient	21 Sedimentation
2 Centrifugation	9 Electrophoresis	15 Ion Exchange	22 Solid-Gas
3 Chromatography	10 Electrostatic Ppt.	16 Liquid-Liquid	23 Solid-Liquid
4 Crystallization	11 Extraction	17 Magnetism	24 Solid-Solid
5 Diffusion	12 Filtration	18 Osmosis	25 Sublimation
6 Distillation	13 Flotation	19 Photolysis	26 Zone Refining
7 Electrodeposition	14 Gas-Liquid	20 Precipitation	

<INFOTYPE>

(Type of Info.)

1 Acidity effect	10 Decontamination factor	19 Matrix concn. effect	29 Synergism
2 Agent compn. effect	11 Device	20 Mechanism	30 Temp. effect
3 Agent concn. effect	12 Diluent compn. effect	21 pH effect	31 Thermodynamics
37 Agent stability	38 Flow rate effect	22 Pres. effect	32 Theory
4 Analytical method	13 Flowsheet	23 Process	33 Transferred sub. interaction use TSI
5 Antagonism	14 Intensive properties	39 Reagent loss	34 Valenceeffect
6 At. no. effect	36 Interfacial phenomena	24 Review	
35 Bibliography	15 Isotherm	25 Sepn. degree	
7 Capacity	16 Kinetics	26 Sep. sub. concn. effect	
8 Coefficient	17 Mathematical modeling	27 Solubility	
9 Constant	18 Matrix compn. effect	28 Stoichiometry	

<SEPAGENT>

(Separation Agent)

1 Acetylacetone	28 Hydrocarbon	97 Precipitant
2 Adsorbent	29 Hydroxamic acid	58 Primary amine
3 Alcohol	30 Hydroxyoxime	59 Pyrazoline
4 Aliphatic solvent	31 Inorganic acid	106 Pyrazolone
< Alumina	32 Inorganic base	60 Pyridine
[illegible]ide	91 Inorganiccompound	61 Pyrophosphate-org
	92 Inorganic ion exchanger	62 Pyrophosphoric acid-org
	33 Isopr[illegible]bolone	63 Pyrrolidinecomp[illegible]
		64 Quat. am[illegible]
		98 Re[illegible]
		6[illegible]

FIGURE 4. A PORTION OF THE THESAURUS/INDEX FORM

IMPROVED AKUFVE SYSTEM FOR FAST AND ACCURATE SOLVENT EXTRACTION STUDIES

J. Rydberg, J. O. Liljenzin and Y. Albinsson

Department of Nuclear Chemistry
Chalmers University of Technology
S-412 96 Göteborg, Sweden

AKUFVE is a Swedish acronym for "apparatus for continuous measurement of distribution factors in liquid-liquid extraction". The system was developed during the period 1962-1967 (1-6) in order to improve accuracy and rapidity in measurements of solvent extraction data. The AKUFVE is now used in more than 50 laboratories around the world for solvent extraction studies of metals, organic acids, etc., for analytical purposes, for small scale separations, etc. A survey of the system and its applications have been given in 1973 (7) and 1982 (8).

The AKUFVE requires some peripheral hardware for efficient use: thermostats, on-line detectors, data collection and presentation equipment. This paper describes the recent replacement of the equipment, which was originally installed more than 15 years ago. The goal of the modernization has been:

1) a thermostat system of higher capacity and more constant temperature that can be used by more than one AKUFVE-unit at the same time;
2) radiometric on-line measurements which are less affected by sorption, especially at pH's where metals begins to hydrolyze;
3) use of a dataprocessor, which on-line (i) controles the extraction cycle and data collection in a programable manner, and (ii) presents the measured data and calculated functions continuously during the experiment.

This paper briefly describes the results of the present modernization.

THE AKUFVE LIQUID FLOW SYSTEM

The liquid-flow system, see Figure 1, consists of a mixing chamber connected to a continuous-flow liquid-liquid centrifugal separator (the "H-centrifuge"), from which the separated phases are returned to the mixing vessel, thus forming a closed liquid-flow system with two connected loops. Changes in the composition of the system, through addition of reagents to the mixing vessel, or through temperature change, is reflected in changes in distribution ratios, observed by the on-line detectors at the centrifuge outlets.

The heart of the system is the H-centrifuge (2,5,9), which is especially designed for short hold-up times (0.3-3s), while at the same time providing very efficient phase separation, usually with <0.1% entrainment of the "other phase" in each outgoing separated phase (9-11). High phase separation efficiency and on-line detectors are fundamental to the AKUFVE-principles of rapidity and accuracy.

Typically, a "normal run" with >30 points of D versus e.g. pH, is made in an hour, excluding time for preparation and restoring. Various modes of AKUFVE uses have been described earlier (e.g. 12-17).

A NEW TYPE OF TEMPERATURE CONTROL

Heat is developed during acceleration and retardation of the liquids in the centrifuge. This heat must be removed in order to make runs at constant temperature. Larger heat exchangers were installed to permit more rapid change in system temperature. Temperature control of the AKUFVE is complicated by the lag-time due to the existence of two liquid loops. This lag-time depends on flow rate, organic/aqueous phase volume ratio and total liquid volume, and tends to induce oscillations in a temperature control loop.

To overcome most of these difficulties and also permit independent operation of more than one AKUFVE-unit, a new thermostat system was developed, see Figure 2. This system consists of two thermostats operated at different temperatures, typically -10 and 85°C, which delivers cold and hot liquid as demanded by the temperature controllers on each AKUFVE-unit. Hot and cold liquids are mixed to obtain the desired temperature on the primary side of the AKUFVE heat exchangers. This mixing is controlled by a standard temperature controller. The set-point of that controller is given by a second temperature controller which reacts on the difference in temperature between the liquid in the AKUFVE mixing chamber and the temperature set-point prescribed by digital/analog converter connected via the IEE-488 bus to the computer. A temperature change of 10°C is typically made in 10-15 minutes, 45-60 minutes with the old system. The system permits operation of the AKUFVE from about 5°C to about 70°C. After 15 minutes the temperature is constant to within ±0.1°C and after a longer time to about ±0.06°C, somewhat depending also on the temperature selected. Generally a better temperature constancy is obtained in the middle of the available temperature range than at the extreme ends.

NEW RADIOMETRIC FLOW CELLS

Several types of liquid-flow cells have been designed, where the detector is physically (e.g. through some wall) separated from the radioactive solution (e.g. 18-20), the simplest being a piece of flexible tubing wound around a solid scintillation crystal. All these cells have an invariant deficiency: radionuclide sorbed on the cell walls interfere with the true measurement of the radioactivity in the solution. There are two ways to correct for this problem:

a) to accept adsorption, and measure and correct for it, or
b) to adjust chemical conditions so that adsorption does not interfere.

We are developing both lines.

For case (a) we use a cell, separated from the detector, with a variable volume to surface ratio, which allows separating volume activity from surface activity. This technique is applicable for γ, and strong β emitters. For case (b) we continually withdraw a small fraction of the test solution, chemically reduce sorption and measure the radioactivity in the solution through liquid-scintillation counting technique. This technique is the useful for radionuclides emitting α and soft β (21).

Cells for γ measurements. Suppose the true radioactivity in the solution is $S = R_v/V$, where R_v is the measured radioactivity from cell volume V. Also suppose that the cell is surface contaminated by the radioactivity R_s and that the detector background countrate is R_o. If cell volume can be varied from V' to V", without changing surface area or geometry, then

(1) $$S = R'_v/V' = R''_v/V''$$

(2) $$R'_{tot} = S\,V' + R_s + R_o; \quad R''_{tot} = S\,V'' + R_s + R_o$$

Thus

(3) $$S = (R'_{tot} - R''_{tot})/(V' - V'')$$

R_{tot} is the total measured radioactivity; the values of the cell volumes, V' and V", are fixed and given by the design so that V' >> V".

Figure 3 shows a cell designed according to this principle. The present cell has a liquid volume of 35 ml, but almost any size down to 1 ml can be designed. Results of runs under varying surface sorption conditions will be presented later. This type of cell has by design a very small effect on the counter pressure on the outgoing flow from the H-centrifuge at constant cell volume. However, during the volume change operation it leads to pressure transients due to the temporary increase or decrease in liquid flow rate between the cell and the mixing chamber. The operation of the H-centrifuge is also somewhat dependent on the inlet pressure. The inlet pressure will change with cell volume as the emptying or filling of the cells changes the liquid level in the mixing chamber. It has therefore been necessary to make minor changes in the centrifuge to compensate for these effects. Smaller cells would decrease these effects, but would also require a higher specific activity of the solutions used.

An alternative design is to make a cell with fixed volume but with variable surface area. Such cells are presently being designed, and will be compared with those above. Such a cell will probably also not affect the centrifuge counter pressure and could have less pressure transients.

Cells for α and β liquid scintillation counting. Cells of the type described above are unsuitable for α and soft β emitters. Since many actinides, and the biochemically important ^3T and ^{14}C, belong to this group, it is highly desirable to develop flow cells for such radionuclides. We have chosen to apply the technique of liquid-scintillation counting to meet our AKUFVE needs.

The liquid volume of the smallest AKUFVE system is 100 ml (H-10 version; Ref. 11). We have designed a flow cell according to Figure 4 for a withdrawal of 10 ul/min, or 5 ml/8 hours. This hardly affects the liquid conditions in the AKUFVE. The arrangement contains 3 pumps: (1) for feeding surface sorption depressing reagents like strong acid (e.g. 1 M HCl) and/or complex formers (e.g. EDTA), (2) for mixing and transport, (3) for feeding liquid scintillator into sample. The detector cell is of the plug-flow type and has a volume of 200 µl, and a hold-up time of 1 min. Under these conditions a suitable measuring cycle takes about 4 minutes: a 2 minute counting, beginning every 4th minute.

The scintillation flow cell is connected via a light trap to two scintillation detectors (D_1 and D_2) in a cell housing. The signals from the detectors are fed to the scaler/single channel analysers, where individual detector signals and coincidences are recorded for treatment in any desired way (see later section). Each cell housing also contains a calibration source, which is also used for obtaining quenching coefficients.

The small withdrawal requires substantial activities in a solvent extraction experiment, usually of the order of 50 µCi (~2 M Bq). E.g. for ^{239}Pu ($t_{½}$ 24.400y) this corresponds to ~1 mg in 100 ml (i.e. ~4×10^{-5} M ^{239}Pu). We are presently experimenting with various cell-types and flow mixtures to find optimal conditions. Results of runs on various α-active solutions will later be presented.

DATA PROCESSOR CONTROL

All instruments and controls on the AKUFVE unit are designed to operate on the IEE-488 bus, thus making them fairly independent of the computer used in the system. The original shake-down of the system was made using a Commodore CBM-3016 computer but this is being replaced by a Sirius-1 system. Figure 5 shows the general layout of the new data collection and control system. The radioactivity measuring system consists of two 2"x2" NaI(Tl) equipped scintillation detectors connected via amplifiers and single channel analyzers to a triple scaler-timer with IEE-488 interface. The third scaler is also connected to an amplifier/single channel analyser and used for special tasks, e.g. density measurements via gamma-absorption cells. Analog signals are measured by a four and a half digit millivolt meter with IEE-488 interface. The voltmeter input is switched to any one of four input lines by reed relays operated from a controller connected to the IEE-488 bus. One of the input lines is permanently connected to a bridge for measuring of the mixing chamber temperature using a Pt-100 resistance thermometer. The same controller also operates five reed relays for control of equipment, e.g. the volume of the measuring cells. Another controller on the bus reads the status of eight input lines which makes it possible to check operation of equipment and AKUFVE. The set-point of the primary temperature controller is given by a digital/analog converter with 8 bit resolution also connected to the IEE-488 bus via a separate controller.

REFERENCES

1. J. Rydberg, Acta Chem. Scand.23(1969)647.

2. H. Reinhardt and J. Rydberg, Acta Chem. Scand. 23(1969)2773.
3. C. Andersson, C. Andersson, J.O. Liljenzin, H. Reinhardt and J. Rydberg, Acta Chem. Scand. 23(1969)2781.
4. H. Johansson and J. Rydberg, Acta Chem. Scand. 23(1969)2797.
5. J. Rydberg and H. Reinhardt, U.S.Pat. 3.442.445 (1969).
6. J. Rydberg and H. Reinhardt, U.S.Pat. 3.615.227 (1969).
7. J. Rydberg, H. Reinhardt and J.O. Liljenzin, Ion Exchange and Solvent Extraction 3(1973)111.
8. H. Reinhardt and J. Rydberg, Handbook of Solvent Extraction (Eds. T.C. Lo, M.H.I. Baird and C. Hansson), J. Wiley, New York 1982.
9. H. Reinhardt, Dissertation. Chalmers Univ. of Techn., Gothenburg 1973.
10. H. Reinhardt and J. Rydberg, Het Ingenieursbald 41(1972)453.
11. J. Rydberg, H. Persson, P.O. Aronsson, A. Selme and G. Skarnemark, Hydrometallurgi 5(1980)273.
12. D.E. Horner, J.C. Mailen, T.C. Scott, S.W. Thiel and R.G. Yates, ORNL/TM -6786, Oak Ridge Natl. Lab. 1979.
13. P.O. Aronsson, B.E. Johansson, J. Rydberg and G. Skarnemark, J. Inorg. Nucl. Chem. 36(1974)2397.
14. J.O. Liljenzin, in Rheinstoffprobleme Band V, Akademie-Verlag Berlin 1977.
15. M. Cox and D.S. Flett, p. 204 in Proc. Int. Solvent Extraction Conf., Hague 1971.
16. S.S. Davies, G. Elson, E. Tomlinson, G. Harrison and J.C. Dearden, Chemistry and Industry (1976)677.
17. P.O. Aronsson, Dissertation. Chalmers Univ. of Techn., Gothenburg, 1974.
18. J. Krugers, Instrumentation in Applied Nuclear Chemistry, Plenum Press 1973.
19. R.A. Faires and B.H. Parks, Radioisotope Laboratory Techniques, Butterworths, London 1973.
20. G.R. Choppin and J. Rydberg, Nuclear Chemistry, Pergamon Press, Oxford 1980.
21. D.L. Horrocks, Application of Liquid Scintillation Counting, Plenum Press 1974.

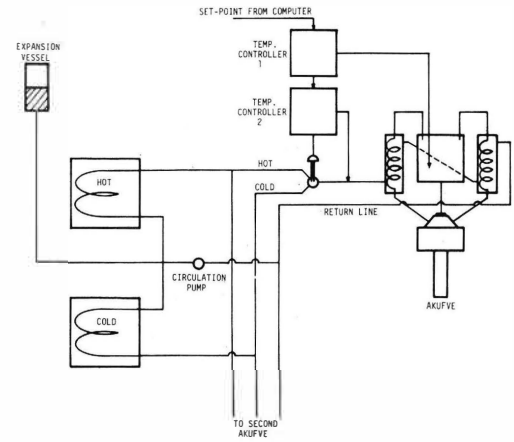

Figure 2. The principle of the new temperature control system.

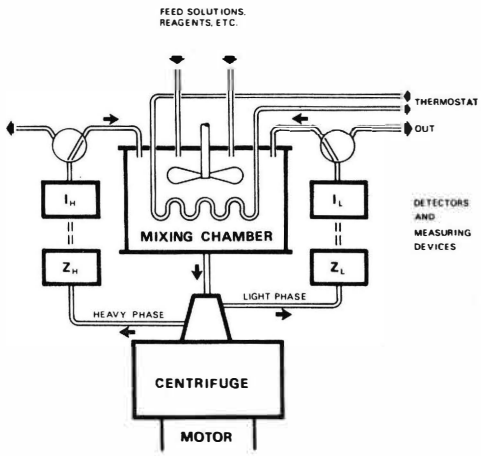

Figure 1. Schematic arrangement of the AKUFVE.

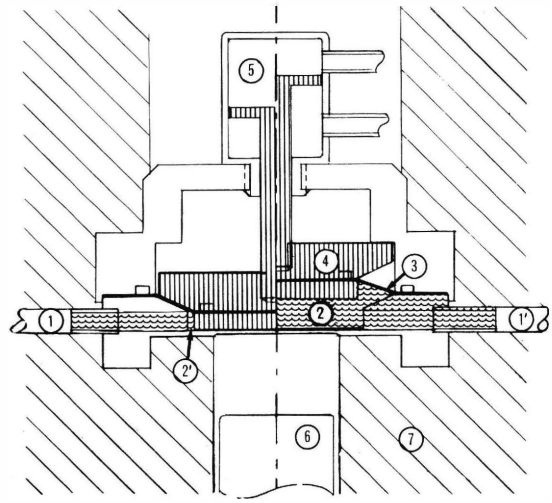

Figure 3. Liquid flow cell for variable volume/surface area ratio. 1-1' liquid in and out-flow, 2 and 2' liquid volume in cell in open and closed condition, respectively, 3 teflon membrane, 4 movable plunge operated through valve 5, 6 scintillator face, 7 lead shielding, 8 liquid bypass in closed position.

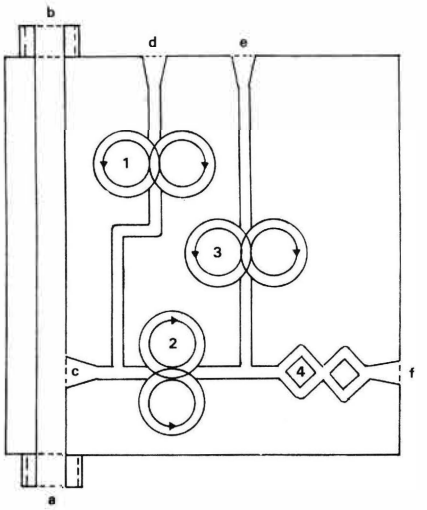

Figure 4. Flow cell for liquid scintillation counting. a-b liquid flow from centrifuge, d feed of acid and/or complexing agent, e feed of liquid scintillation cocktail; 1, 2 and 3 are cog-wheel pumps; 4 mixer; f outflow to light-trap and detector system.

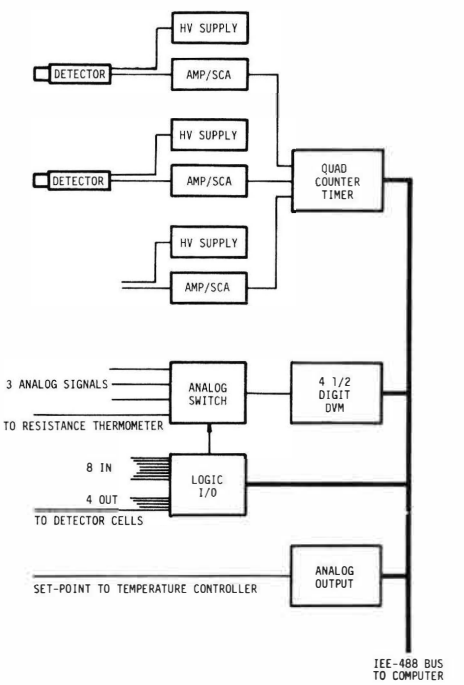

Figure 5. Diagram of the new measurement and control system.

THE POSSIBILITY OF HYDROXONIUM ION EXISTENCE UNEQUILIBRIUM EXTRACTS

A. Chekmarev, G. Yagodin, S. Dmitriev

Mendeleev Institute of Chemical Technology

A-47, Miusskaya sq., 9
Moscow, USSR

For the first time the anomalous effect of organic phase saturation in extraction of zirconium from aqueous solution of $Zr(SO_4)_2 \cdot 4H_2O$ by tri-n-octylamine (TOA) was described in [1]. It is realized in transition in organic phase at the first stage of extraction (under conditions of interphase contact limitation) such amount of metal, which exceeds considerably the equilibrium concentration. The deviation of maximum concentration from equilibrium depends on the metal concentration in the initial aqueous solution. The curves of zirconium concentration dependence in organic phase on phase contact time for different initial concentrations of $Zr(SO_4)_2 \cdot 4H_2O$ in aqueous phase in given in Figure 1. Phase contact was carried out in the Lewis cell with fixed interphase area (mixer speed was 250 rev./min.). As an extractant we used 5% benzene solution of TOA sulphate. Initial water phase ($Zr(SO_4)_2 \cdot 4H_2O$ water solution of fixed concentration) was prepared by diluting 1,85 M $Zr(SO_4)_2 \cdot 4H_2O$ water solution (keept before using at least for a month) immediately before an experiment. Equilibrium concentrations of zirconium in organic phase are shown in Figure 1 by triangles (the figures near the triangles indicate the number of the curves). For equilibration two phases were carefully mixed (emulgation) for half an hour.

The dependence of maximum concentration deviation from equilibrium concentration in organic phase against water consentration of $Zr(SO_4)_2 \cdot 4H_2O$ is shown in Figure 2. In the separate experiment we established that in the case of 0,02 M $Zr(SO_4)_2 \cdot 4H_2O$ solution there was no anomalous saturation ($\Delta = 0$).

The maximum Δ is observed for initial Zr concentration near 0,3 M (Figure 2). In the following experiments we used this very solution.

Earlier we have shown that in aqueous solutions of average concentration (near 0,3 M $Zr(SO_4)_2 \cdot 4H_2O$) there exist fragments of solid $Zr(SO_4)_2 \cdot 4H_2O$ structure [2,3]. It is just with the presence of such fragments that the effect of anomalous saturation in connected.

It is known that in dissolving solid $Zr(SO_4)_2 \cdot 4H_2O$ and in diluting its concentrated solution the salt structure is destroyed by hydrolysis of sulphate bridges between zirconium atoms [3]. In this process coordinatively unsaturated with acid ligands monomers are formed: $Zr(OH)_2(SO_4H)_2$. It is evident that analogous process can take place in extracting zirconium sulphate from water solution containing 0,3 M Zr. It is logical to suppose that in this case the first stage of extraction must be the addition reaction of amine sulphate and unsaturated monomer:

(1). $Zr(OH)_2(SO_4H)_2 + (NR_3H)_2SO_4 \rightleftarrows Zr(OH)_2SO_4(SO_4H)_2(NR_3H)_2$

Transition to organic phase coordinatively unsaturated complexes must be accompaneyd with coextraction of significant ammount of water. In Figure 3 the curve of water content in organic phase against the time of phase contact is shown.

In 20-30 minutes after the beginning of contacting in the Lewis cell dimness of organic phase was registered because of sweating (water is secriting). This phenomenon is connected with the decrease (diminution) of zirconium hydrolysis degree as a result of intermolecular reaction:

(2). $Zr(OH)_2SO_4(SO_4H)_2(NR_3H)_2 \rightarrow Zr(SO_4)_3(NR_3H)_2 + 2H_2O$.

Organic phase turns turbid in the case of phase separation in 15 minutes after the beginning of contacting (before sweating) and holding it in a closed vessel. In this case determination of H_2O content before and after dimness (without emultion separation) allowed to establish that total H_2O content increases in the process of emultion secretion.

In this case the second stage of extracion process is correctly represented by the equation (2), further stage must be analogous with the last stage of nonhydrolized sulphate complexe extraction [4]:

(3) $Zr(SO_4)_3(NR_3H)_2 + (NR_3H)_2SO_4 \rightleftarrows Zr(SO_4)_4(NR_3H)_4$

Actually, in the condition of equilibrium the ratio TOA : Zr rushes to 4 : 1 as for nonhydrolized complexes.

For confirmation of the supposed extraction mechanism IR- and PMR spectra were recorded for the intermediate and equilibrium extracts. 10% solution TOA in CCl_4 was used. Contacting was performed in the Lewis cell. The spectra were recorded immediately after phase separation.

IR spectra are shown in Figure 4: N1 - 20 min.; N2 - 90 min. (the maximum of anomalous loading); N3 - 5hrs. (the descending twig of the curve); N4 - 7hrs (near the equilibrium) - the time from the beginning of contacting; N5 - the equilibrium extract (30 min. of phases emulgation); N6 - the extract of nonhydrolyzed zirconium sulphate; N7 - 10% sulphate TOA in CCl_4.

The shape of the successive extract spectra changes gradually approach the spectra MN5 and 6, which are indistiguishable. In the region of deformation water band manifestation ($\sim 1600 cm^{-1}$) in the spectra N1 and N4 band with frequency 1660 cm^{-1} has a shoulder near 1700 cm^{-1}; in the spectrum N2 the band 1600 cm^{-1} is absent and absorption is observed only near 1700 cm^{-1}; there are

two resolute bands at 1700 cm^{-1} and 1660 cm^{-1} in the spectrum N3. In the IR - spectra N5 and N6 the band near 1700 cm^{-1} is absent.

The absorption near 1700 cm^{-1} can be assigned to the inner deformation vibration of hydroxonium ion H_3O^+ or $H_5O_2^+$. This supposition can be confirmed by the fact that for the extacts with absorbtion near 1700 cm^{-1} the absorbtion is fixed near 2000-240 cm^{-1} [5,6], whereas for equilibrium extracts absorbtion ν(OH) + ν(NH) begins only at 2400 cm^{-1}.

The PMR spectra are presented in Figure 6. (the same indication as in Figure 5). The spectra NN 5,6,7 are practically identical, only in the spectrum N5 the signal of water hydrogen shifts slightly down field. In these spectra the peaks for the N-H (amine salt) and H_2O are resolved. In the non-equilibrium extract spectra (1-4) the situation is quite different which is in good agreement with data of IR-spectroscopy. Thus, in IR-spectrum N2 there is only one band near 1700 cm^{-1} (δH_3O), in the appropriate PMR - spectrum single proton exchange signal of NH - groups and H_2O molecules. In IR-spectrum N3 two bands are well resoluted ($\sim$1600 cm^{-1} and 1700 cm^{-1}), in PMR-spectrum the proton signal of H_2O moleculs is resoluted, but besides there is proton exchange signal of NH-groups and some H_2O molecules. The increasing of contacting time (approaching the equilibrium) leads to ceasing of exchange indicating H_3O^+-ions disappearance.

Thus, IR and PMR data support the mechanism of extracts anomalous loading. It is possible to make a conclusion that at the first stage of extraction the anomalous loading effect is accompanied by H_3O^+-ion formation due to high water content of unequilibrium extracts. Under these conditions the equilibrium $R_3NH^+ + H_2O \rightleftarrows R_3NH_3O^+$, usually shifted almost completely to the left, shifts to the H_3O^+-ion formation. The decreased water content approaching the equilibrium leads to H_3O^+ destruction.

In conclusion it is possible to note that PMR-spectra of equilibrium extracts containing hydrolized sulphate zirconium complexes and higher amount of water also are characterized by the presence of single exchange signal NH^+ - H_2O.

REFERENCES.

1. G. Yagodin, A. Chekmarev, L. Vladimirova J. Inorg. Chem. (Russ.), v.14, N6, 1969, p. 1603.
2. A. Chekmarev, L. Molokanova, G. Yagodin et al. J. Inorg. Chem. (Russ.), v.23, N10, p. 2663.
3. Clearfiedl A. Rev. Pure Appl. Chem., v.14, 1964, p. 91.
4. A. Chekmarev, G. Yagodin Proceedings of Moscow Mendeleev Chem. Techn. Inst., N84, 1975, p. 29.
5. L. Chuchalin, Z. Grankina, S. Hranenko et al. J. Inorg. Chem. (Russ.), v.15, 1970, p. 170.
6. L. Chuchalin, Z. Grankina, S. Hranenko et al. J. Phys. Chem. (Russ.) v.44, 1970, p. 1455.

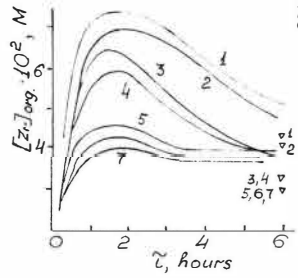

Figure 1.

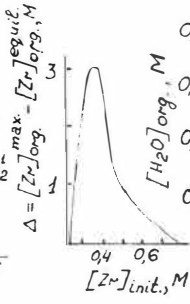

Figure 2.

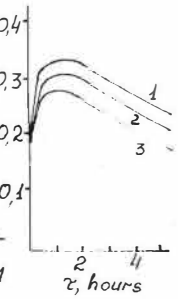

Figure 3.

Figure.1. Dependence of the organic phase loading on the initial concentration of $Zr(SO_4)_2 \cdot 4H_2O$ and on the time of phase contact in the Lewis cell (hrs.). ▽ - equilibrium Zr concentration in organic phase. Initial aqueous concentration $Zr(SO_4)_2$, M: 1 - 0,20; 2 - 0,25; 3 - 0,33; 4 - 0,40; 5 - 0,50; 6 - 0,56; 7 - 0,71.

Figure 2. Dependence of the deviation $\Delta = Zr_{org.}^{max.} - Zr_{org.}^{equil.}$ on the initial aqueous concentration of $Zr(SO_4)_2$.

Figure 3. Dependence of the org. phase water concentration on the time of phase contact in the Lewis cell. Initial water phase cons. of $Zr(SO_4)_2$, M: 1 - 0,2; 2 - 0,3; 3 - 0,4.

Figure 4. IR - spectra of the extracts obtained by contacting of 10% sulphate TOA sol. in CCl_4 with 0,3 M aqueous $Zr(SO_4)_2$ sol. Time of contacting: 1-20 min; 2 - 1,5hrs; 3 - 5,0hrs; 4 - 7,0hrs; 5 - equilibrium extract; 6 - org. phase loading with nonhydrolized zirconium sulphate; 7 - initial org. sol. 10% sluphate TOA in CCl_4. The bands assigned to the inner deformation vibration of H_2O and H_3O^+ ion are marked with asterisks.

Figure 5. PMR - spectra of the extracts (the same symbols as in Figure 4).

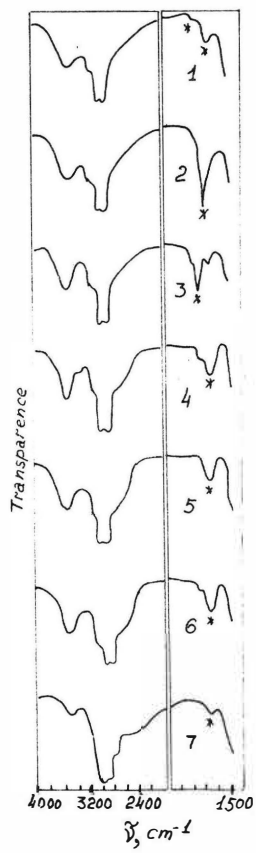

Figure 4.

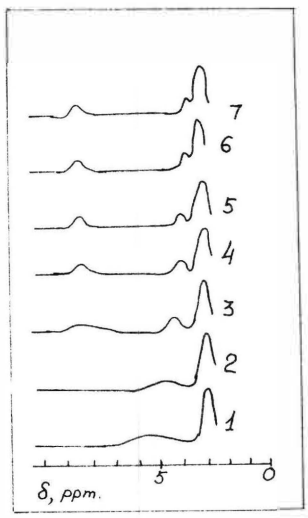

Figure 5.

SOME OBSERVATIONS ON THE EXTRACTABILITIES OF UNIVALENT CATIONS WITH CROWN-ETHERS (2)

Yuko Hasegawa

Science University of Tokyo
Tokyo, Japan

The factors affecting the extraction of the ion-pair between a metal ion complexed with a crown-ether and an anion have been studied (1). The extraction may be mainly affected by the stability of the metal-crown ether complexes in aqueous solutions. The extractability of the cationic complex should be affected by i) the interaction of the ion-pair with organic solvents and ii) nature of aqueous solutions as well as iii) the hydrophobic tendency of the complex and iv) the counter ion. The present paper will mainly describe the influence of i) and ii).

EXPERIMENTAL

The experiments were carried out at 25°C. As crown-ethers, 15-crown-5 (15C5), benzo-15-crown-5 (B15C5), 18-crown-6 (18C6) and dibenzo-18-crown-6 (DB18C6) were employed. Benzo-15-crown-5 and DB18C6 were recrystallized from heptane and benzene three times, respectively. Other reagents were used without further purification.

Two phases were placed in a stoppered glass tube and agitated vigorously. The silver(I) concentration was measured by atomic absorption method. The concentration of crown-ethers distributed to two phases was measured by spectrometry, that is, the concentration of DB18C6 and B15C5 was determined by measuring the absorption of benzene ring at 275 nm, and those of 15C5 and 18C6 were determined by measuring the absorption of DPA (dipicrylaminate) anion extracted with the crown-ether complexed with sodium(I) (for 15C5) and with potassium(I) (for 18C6).

Distribution ratio was defined as the total concentration ratio between two phases.

RESULTS AND DISCUSSION

(A) Interaction of Ag(I)-crown ether complex with TOPO.

The extraction of Ag(I) with crown-ethers and/or TOPO and picrate ion into chloroform is summarized as follows.

i) It was confirmed elsewhere (2) that Ag(I) is extractable with crown-ethers and picrate ion as the ion-pair of 1:1:1, AgE^+A^-, where E and A^- denote crown-ether and picrate ion, respectively. Then the extraction constants are:

$$Ag^+ + E_{(o)} + A^- \rightleftarrows AgE^+A^-_{(o)}$$

$$Kex_{1,0} = [AgE^+A^-]_o/[Ag^+][E]_o[A^-] \quad (1)$$

ii) Silver(I) is also extracted as the picrate, Ag^+A^-, into chloroform in the absence of crown-ether and TOPO, although the extraction is very poor.

iii) In the presence of TOPO but no crown-ether, Ag(I) is extractable as the ion-pair of 1:1:1 and 1:2:1, i.e., AgT^+A^- and $AgT_2{}^+A^-$ where T is TOPO (3).

iv) When the distribution ratio of Ag(I) was plotted against TOPO concentration at constant concentration of crown-ethers and picrate ion, the higher ratio was obtained at the higher concentration of TOPO. The enhancement is partly due to an extraction of Ag^+ ion as picrate with TOPO but it is also due to extractions of mixed species of Ag(I) containing both crown-ethers and TOPO as picrates. Then, the gross distribution ratio and the adduct formation constants can be written as,

$$D = \frac{[Ag^+A^-]_o + [AgE^+A^-]_o + \Sigma[AgT_m{}^+A^-]_o + \Sigma[AgET_n{}^+A^-]_o}{[Ag^+]} \quad (2)$$

$$AgE^+A^-_{(o)} + T_{(o)} \rightleftarrows AgET^+A^-_{(o)}$$

$$\bar{\beta}_1 = [AgET^+A^-]_o/[AgE^+A^-]_o[T]_o \quad (3)$$

$$AgE^+A^-_{(o)} + 2T_{(o)} \rightleftarrows AgET_2{}^+A^-_{(o)}$$

$$\bar{\beta}_2 = [AgET_2{}^+A^-]_o/[AgE^+A^-]_o[T]_o{}^2 \quad (4)$$

.....

The net distribution ratio with the crown-ether and TOPO can be described as,

$$D - D_0 = \Sigma[AgE^+T_nA^-]_o/[Ag^+] = Kex_{1,0}\,[E]_o[A^-](1+\Sigma\bar{\beta}_1[T]_o) \quad (5)$$

where D_0 is the distribution ratio obtained without the crown-ether otherwise identical and is calculated by introducing the equilibrium constants obtained in separate experiments into Eq.(2).

Figure 1 gives the log $(D - D_0)$ vs. log $[T]_o$ plot. The data were analyzed by the curve-fitting method. The solid lines in Fig. 1 are calculated by these constants.

(B) Effects of lithium salts on the distribution of crown ethers.

It was reported (4) that presence of lithium chloride enhances the extraction of 18C6 into dichloromethane, e.g., the distribution ratio between water and dichloromethane was 4.50 and that between 0.4M LiCl and the organic solvent enhanced to 7.4. Salt-effects on the distribution of crown-ethers have been studied more in detail. Figure 2 shows the change in the distribution ratio of DB18C6, B15C5, 15C5 and 18C6 between chloroform and lithium nitrate aqueous solution as a function of the salt concentration. The distribution ratio of 15C5 having smaller cavity than 18C6 seems to be more influenced by the salt. The distribution ratio of crown-ethers having more rigid structure with benzene ring, B15C5 compared to 15C5 or DB18C6 to 18C6, does not seem to be influenced more remarkably. The impairment of the distribution ratio may be due to the formation of the lithium complex with the crown-ether in the aqueous phase. If the assumption is correct, the extraction of crown-ethers can be improved by using more hydrophobic anion as a counter-ion. Figure 3 shows the ratio of the distribution ratio of 15C5 or 18C6 in the presence to that in the absence of lithium salt as a function of the salt concentrations. The presence of perchlorate ion leads to poorer extraction than nitrate ion, in spite of the more hydrophobic character. Moreover, the addition of lithium chloride seems to enhance the extraction of 18C6,

nevertheless chloride ion is the smallest among these three anions. The degree of impairment of the extraction is in the sequence of $ClO_4^- > NO_3^- > Cl^-$. The order agrees with the order destroying water structure by salt anion which was reported on the basis of IR measurement of various aqueous solutions (5).

CONCLUSIONS

It has been reported that a central metal ion in the comlex with crown-ethers would be still possible to form adducts with basic neutral ligands, although it has been assumed that metal ions trapped in the crown-ether ring were not hydrated or that they were hydrated similarly(6). The extraction of crown-ethers into chloroform is salted in by lithium nitrate and perchlorate. Crown-ethers are affected by electrolytes as similarly as most nonelectrolytes (7).

REFERENCES

1. Y. Hasegawa and T. Sekine, ISEC '80 Proceedings 80-3 (Liege)
2. Y. Hasegawa, N. Iizima and T. Sekine, J. inorg. nucl. Chem. 43, 633 (1981)
3. Y. Hasegawa, K. Suzuki and T. Sekine, Chem. Lett. 1075 (1981)
4. I. M. Kolthoff, Can. J. Chem., 59, 1548 (1981)
5. G. R. Choppin and K. Buijs, J. Chem. Phys., 39, 2042 (1963)
6. P. R. Danesi, H. Meider-Gorican, R. Chiarizia, V. Capuasno and G. Scibona, Proc. Int. Solvent Extraction Conf., 1974 Soc. Chem. Ind. London (1974), p.1764, J. inorg. nucl. Chem. 37, 1479 (1975)

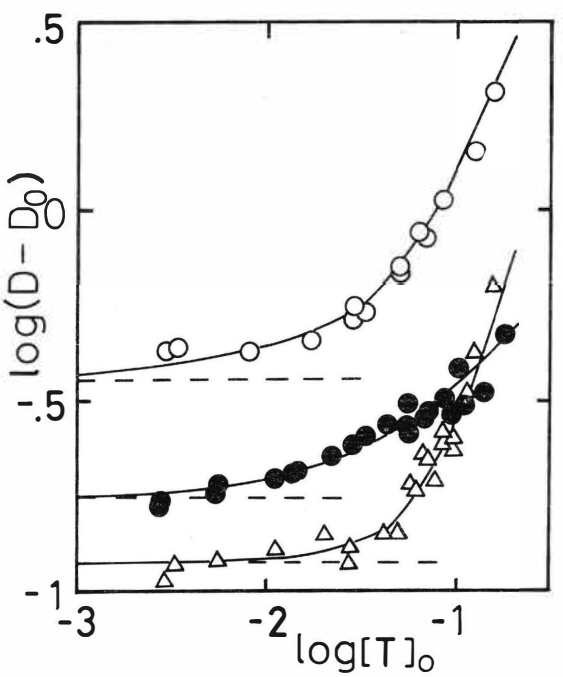

Fig. 1. The synergistic effect of 15C5 (○), B15C5 (●) or DB18C6 (△) and TOPO on the extraction of Ag(I)-picrate.

aq. phase : 7×10^{-3}M lithium picrate

org. phase : $CHCl_3$ containing 2×10^{-3}M 15C5, 7×10^{-3}M B15C5 or 8×10^{-3}M DB18C6.

$Y = \log 10^{4.5}[E]_0[A^-](1 + 10^{1.3}[T]_\bullet + 10^{1.9}[T]_0^2)$ for ○

$Y = \log 10^{3.5}[E]_0[A^-](1 + 10[T]_0)$ for ●

$= \log 10^{3.5}[E]_0[A^-](1 + 10^{2.1}[T]_\bullet^2)$ for △

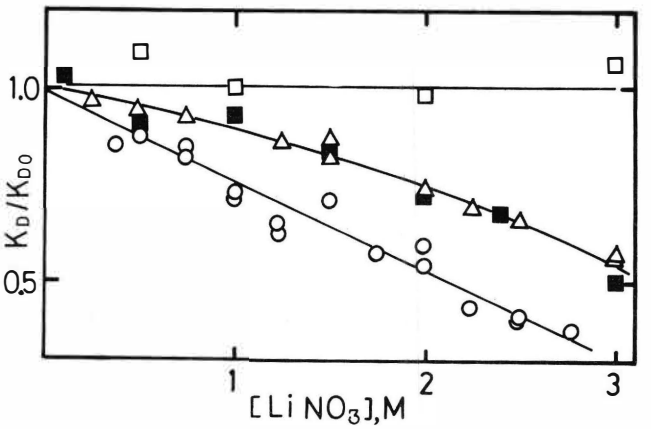

Fig. 2. The change in the distribution of DB18C6 (□), 18C6 (○), B15C5 (■) and 15C5 (△) between $CHCl_3$ and $LiNO_3$ aqueous solution as a function of the salt concentration. The value of log K_{D0} is 0.8 for 18C6, 2.4 for B15C5, and 0.9 for 15C5, where K_{D0} is the distribution ratio between water and $CHCl_3$. The solid lines are drawn arbitrarily.

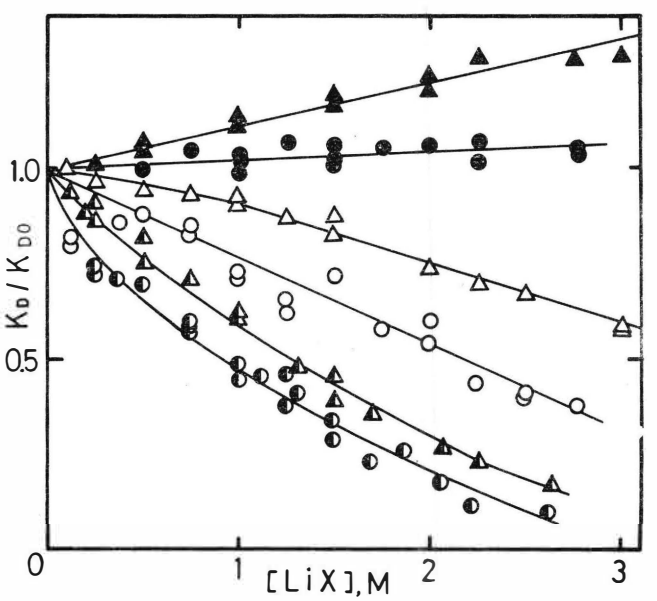

Fig. 3. The influence of lithium salts on the distribution of 15C5 (circles) or 18C6 (triangles) between LiCl (closed symbols), $LiNO_3$ (open symbols) or $LiClO_4$ (semiclosed symbols) aqueous solution and $CHCl_3$. The solid lines are drawn arbitrarily.

PHYSICAL CHEMISTRY OF N,N-DIBUTYL-2-ETHYL-HEXYLAMIDE AS EXTRACTANT FOR URANIUM

Miroslav M. Kopečni and Djordje M. Petković

Chemical Dynamics Laboratory
The Boris Kidrič Institute of Nuclear Sciences
P.O. Box 522
11001 Belgrade, Yugoslavia

A systematic investigation of the use of N,N-di-n-butyl-2-ethylhexylamide (DBEHA) as an extractant for the extraction and separation of actinides in a Purex-type flowsheet, has been studied by Gasparini and Grossi (1). They have shown that DBEHA is applicable to operating solvent extraction systems since its synthetizing is cheap, it exhibits a similar behavior as tri-n-butyl phosphate (TBP), but it has better decontamination of uranium from some fission products, uranium-thorium separation, stability and undergoes to less-deleterious degradation products than TBP.

A proper understanding of extraction technology and experience can be reached provided that there is enough information on the nature of the DBEHA extraction process and the behavior of the reagent under different conditions encountered in practice. It is therefore of great importance that good physical chemical data on chemical equilibria are available and relate to plant needs. This is the object of the present work.

DIPOLE MOMENT DETERMINATION

The dipole moment of DBEHA has been determined in n-hexane (3.67 D), cyclohexane (3.67 D), benzene (3.69 D), and tetrachloride (3.75 D). The numbers in parenthesis refer to the dipole moment values expressed in Debye units. The experimentally obtained dipole moment values have been plotted as a function of dielectric constants of diluents and extrapolated to the unity value of the dielectric constant. In such a way a 3.62 D value has been approximated as the dipole moment of DBEHA in the vapour state.

INFRA-RED SPECTRA

The infra-red spectra of DBEHA and its solutions in n-hexane and chloroform are shown in Figure 1. The peak of the DBEHA amide group is shifted towards low energies with the substitution of n-hexane with chloroform, while in pure DBEHA the spectrum shows a peak and a small shoulder situated between the peaks in n-hexane and chloroform. This can be explained as the existance of DBEHA monomer predominantly in n-hexane, appearing of the self-association of DBEHA molecules in the pure DBEHA and dissapearing of the split of the pure amide peak in the interaction of DBEHA with chloroform. These spectra show the definite influence of DBEHA molecules themselves and chloroform on the frequency of the amide group in DBEHA. The high absorptivity of the amide group made the infra-red spectra of DBEHA difficult for a quantitative treatment.

INTERACTION OF DBEHA WITH DILUENT

The self-association of DBEHA and its intermolecular association with diluents have been studied by dielectric constant measurements, gas-liquid chromatography and nuclear magnetic resonance spectroscopy (2). However, dielectric constant measurement offers a number of advantages over GLC and spectroscopy (3) techniques. By means of dielectric constant measurements on the mixtures of DBEHA with inert n-hexane and according to procedure (4), that was employed previously in studies of dimerization of TBP, the dimerization constant of DBEHA has been determined as 0.2 at room temperature. The interaction of DBEHA with chloroform, considering it as the formation of a monosolvate, $DBEHA \cdot CHCl_3$, studied by spectroscopic techniques and dielectric constant measurements, has led to the values of complex formation constant of over an order of magnitude (5). The average value of the constant based on the use of dielectric constant data, has been given as $K = 1.13\ dm^3 mol^{-1}$. In the case of carbon tetrachloride and benzene, the solvation constant values are 0.1 and 0.02, respectively, which indicates that there is little measurable interaction between DBEHA and these diluents other than that due to random collisional events.

EXTRACTION OF NITRIC ACID

DBEHA does not extract sulphuric and hydrochloric acid, even at very high concentrations of the acids in the aqueous phase. It also does not extract water as it has been proved by Karl Fisher titration of the organic layer.

In the extraction experiments n-hexane has been employed. The third phase formation has been noticed only at high loading of the organic phase and great acid content in the aqueous phase. These systems have been missed out in further considerations.

The extraction of the nitric acid can be described by the following equations.

$$H^+ + NO_3^- + S_{(org)} \rightleftharpoons HNO_3 \cdot S_{(org)} \quad (1)$$

$$K = \frac{a_{HNS(org)}}{a_H a_N a_{S(org)}} \quad (2)$$

where S stands for DBEHA, K is the thermodynamic equilibrium constant, and a denotes chemical activities of different cpecies distinguished by the corresponding easily recognized subscripts. The subscript org describes the species in the organic phase, while for the species in the aqueous phase a subscript is omitted. The standard state of all the species involved is their infinite dilution either in the aqueous or in the organic phase. The concentrations of the species are expressed in mol dm^{-3}.

The slope analysis, performed by plotting of nitric acid distribution data (Figure 2) as $\log C_{HN(org)}/C_{HN} = f\left[C_{S(org)}\right]$ for the constant concentration of nitric acid in the aqueous phase and different total concentrations of DBEHA, has confirmed the predominant formation of 1 : 1 (nitric acid : DBEHA) solvate. The thermodynamic equilibrium constant, defined by eq. (2), has been evaluated by $K = \lim \left[C_{HNS(org)} \rightarrow 0,\ C_{S(org)} \rightarrow 0\right] C_{HNS(org)} / a_{\pm}^2 C_{S(org)}$, as $\log K = -1.3$. Here $a_{\pm}$ denotes the mean nitric acid ion activities taken from literature (6).

EXTRACTION OF URANYL NITRATE

The formation of the third phase has been more pronounced in the uranyl nitrate extraction with DBEHA. Due to that undesirable effect, benzene and toluene have been chosen as diluents instead of n-hexane. The extraction of uranyl nitrate is somewhat poorer when toluene is replaced with benzene. It may be ascribed to the slight difference of the solvation of DBEHA with benzene or toluene. The extraction isotherms (Figure 3) show a maximum loading of the organic phase at about one half of the DBEHA concentration. It suggests the next equilibrium:

$$UO_2^{++} + 2NO_3^- + 2S_{(org)} \rightleftharpoons UO_2(NO_3)_2 \cdot 2S_{(org)} \quad (3)$$

with corresponding equilibrium constant expression

INTERFACIAL PROPERTIES AND METAL EXTRACTION CHEMISTRY OF THE ORGANOPHOSPHORUS ACIDS: $(RO)_2PO(OH)$; $(RO)RPO(OH)$; $R_2PO(OH)$

Michael Cox
Hatfield Polytechnic
Hatfield, Hertfordshire, U.K.

Maria Elizalde and Jose Castresana
Universidad del Pais Vasco
Bilbao, Spain

Nuria Miralles
ESTIIB. Barcelona, Spain

Recently interest has been reawakened in the use of phosphonic and phosphinic acids as metal extractants following the commercial introduction of derivatives of these acids by the Daihachi Chemical Industry Company and the American Cyanamid Company respectively. Most of the published work on these reagents has centered around the separation of cobalt and nickel (1) although earlier studies had compared the extraction of lanthanides and actinides (2). In a general survey of extraction by the three types of organophosphorus acidic extractants typified by di-2-ethylhexylphosphoric acid , HDEHP; 2-ethylhexyl-2-ethylhexylphosphonic acid, HEH[EHP] and di-n-octylphosphinic acid, HDOP, we have observed some interesting trends in the extraction behaviour of other metals. In particular it has been noticed that the pH_{50} values of calcium are very dependant on the type of extractant. This has possible commercial interest in that the widely used extractant for zinc, HDEHP, does tend to co-extract calcium.

REAGENTS AND EXPERIMENTAL PROCEDURE

The extractants HDEHP (British Drug Houses Ltd) and HEH[EHP] (Shell Chemical Co. SME 418) were commercial samples and were not further purified. The phosphinic acids were commercial samples, American Cyanamid Co. Cyanex 272, or synthesised from the alkene and hypophosphorous acid (2). Metal distribution studies were carried out using aqueous solutions of the metal nitrates in 1.00 mol dm^{-3} ammonium nitrate with pH adjustment by ammonia or dilute nitric acid. Toluene solutions were made up using the formula weight of the reagent. Interfacial tension data were obtained on toluene or heptane solutions after equilibration with the appropriate aqueous phases using a glass Wilhemy plate. All experiments were carried out at a temperature of 25°C.

RESULTS AND DISCUSSION

Reagents. All the published data indicate that these acids are dimeric in the organic diluents normally used in extraction and this has been confirmed for the new reagents used in this work. The pK_a values of the replacable proton vary with molecular structure in the order: $(RO)_2PO(OH) < (RO)RPO(OH) < R_2PO(OH)$, Table 1

	pK_a (75% aqueous/ethanol)
HDEHP	3.57
HEH[EHP] (SME418)	4.10
Cyanex 272	5.05
HDOP	4.96
HDCyP (a)	5.05
HDDcP (b)	4.85

Table 1 pK_a values in 75% aqueous ethanol

Interfacial Tension Studies. The dependency of the interfacial tension between organic - aqueous phases on equilibrium pH, reagent concentration, diluent and presence of extractable metal ions were investigated. Variation of the pH, Figure 1, shows that, as the pH rises, the activity of HDEHP increases following its dissociation. The other two reagents illustrated show little variation with pH, which is rather surprising in view of their pK_a values. A similar study (3) showed that increasing the acidity beyond pH 2 also caused an increase in activity probably by protonation of the phosphoryl oxygen.

(a) HDCyP dicyclohexylphosphinic acid
(b) HDDcP didecylphosphinic acid

Varying the bulk phase concentration of the reagent causes an abrupt change in the interfacial tension as the interface becomes saturated with reagent molecules. Using a simplified form of the Gibbs Isotherm it is possible to calculate the value of the concentration at which the interface initially reaches saturation (C) and the interfacial excess of reagent (Γ). Values for selected reagents are given in Table 2 and are largely in agreement with other work (3). Changing the diluent from aliphatic to aromatic varies C indicating the increased solvency of the aromatic diluent. HDOP is the most interfacially active species, $C < 10^{-5}$ mol dm^{-3}, in heptane, however its low solubility in this solvent precludes its use for metal extraction.

	Diluent	pH	C (mol dm^{-3})	Γ (molecule nm^{-2})
HDEHP	heptane	2.0	6×10^{-3}	0.74
	toluene	-	not saturated -	
HEH[EHP]	heptane	2.0	6×10^{-3}	0.99
	toluene	2.0	6×10^{-3}	0.81
HDOP	heptane	2.0	$< 10^{-5}$	0.71
	toluene	2.0	10^{-3}	0.44

Table 2 Interfacial saturation data derived from Gibbs Isotherm

Finally as expected the presence of extractable metal ions tends to reduce the reagent interfacial activity as the reagent molecules are replaced by less active metal complexes in solution.

Metal Distribution Studies. The extraction of a divalent ion by a dimerised organophosphorus acid can be represented by:

$$(1) \qquad M^{2+} + n\overline{(H_2A_2)} = \overline{M(AHA)_2(H_2A_2)_{n-2}} + 2H^+$$

which leads to the following expression for the distribution coefficient (D) in terms of the extraction constant (K):

$$(2) \qquad \log D = \log K + 2pH + n\log [\overline{H_2A_2}]$$

where $[\overline{H_2A_2}]$ represents the free reagent concentration in the organic phase.

This equation shows that a plot of log D against pH at constant reagent concentration should have a slope of 2. Equation 2 can be rearranged to:

$$(3) \qquad \log D - 2pH \quad \log K + n\log [\overline{H_2A_2}]$$

and thus a plot of (log D - 2pH) against log $[\overline{H_2A_2}]$ should give a straight line of slope n.

Results obtained in this study for calcium, magnesium, and zinc with phosphinic acids have confirmed the above equation with n = 2. Thus the extraction equation for these systems is:

$$(4) \qquad M^{2+} + 2\overline{(HDOP)}_2 = \overline{M[(DOP)(HDOP)]}_2 + 2H^+$$

and the phosphinic acids behave in a similar way to the phosphonic and phosphoric acids.

The extraction power of these reagents can be compared by examining the pH at which 50% of the metal ion is extracted (pH_{50}), and the value of the extraction constant (K), Table 3. The results show that the pH_{50} values of the metals follow the order HDEHP < HEH[EHP] < HDOP in accordance with the decreasing pK_a of the extractants, however the variation shown by calcium is far greater than the others. This is emphasised by calculation of the respective separation factors, Table 4. In the only similar comparative study with these reagents Peppard et al (2) found different trends for the trivalent metals, promethium and curium

$$K = \frac{a_{UNS(org)}}{a_U a_N^2 a_{S(org)}^2} \quad (4)$$

The notation has been explained when the nitric acid extraction with DBEHA was dealt with. The slope analysis of uranyl nitrate distribution data, via $\log C_{UN(org)}/C_{UN} = f\left[C_{S(org)}\right]$ for $C_{UN} = 0.4$ $mol \cdot dm^{-3}$ and different total concentrations of DBEHA has confirmed the stoichiometry given by eq. (3). The thermodynamic equilibrium constant, defined by eq. (4), has been determined by $\log K = \lim \left[C_{UNS(org)} \to 0,\ C_{S(org)} \to 0\right]\ C_{UNS(org)}/a_{\pm}^3 C_{S(org)}^2$ as $\log K = 0.8$. Here $a_{\pm}$ denotes mean uranyl nitrate ion activities taken from literature (7).

The increase of uranyl nitrate extraction with DBEHA, with the increasing aqueous phase acidity, is a consequence of the influence of nitrate ions from nitric acid on the equilibrium shown in eq. (3). It has been concluded by rearranging eq. (4) into the following form.

$$\log \frac{C_{UNS(org)}}{a_U C_{S(org)}^2} = z = \log K \frac{y_S^2}{y_{UNS}} + 2\log a_N \quad (5)$$

and plotting experimental data as $z = f(\log a_N)$. Here y represents activity coefficients of the species denoted by a corresponding subscript. The value of a_N has been approximated with the mean ion activity of nitric acid present in the aqueous phase, while a_U has been replaced by the mean ion activity of uranyl nitrate. The activities of uranyl nitrate ions in the presence of nitric acid have been corrected according to Guggenheim (8). The slope of the linear graph obtained is very close to two, while the intercept value, that is $\log Ky_S^2/y_{UNS} = 1.0$, is slightly different from $\log K = 0.8$ determined previously, due to the activity coefficient ratio involved.

A further proof of the value of equilibrium constant of the uranyl nitrate extraction with DBEHA has been offered applying the method developed in this Laboratory (9). It is based on plotting of distribution data by means of $-\log a_{\pm}^3 = f\left[C_{U(org)}\right]$ derived from eq. (4). Here $a_{\pm}$ denotes the mean ion activity of uranyl nitrate. The value of the quotient, $a_{S(org)}^2/a_{UNS(org)}$ is calculated by the total concentrations of uranyl nitrate and extractant at the inflexion point obtained (Figure 4). The ordinate value of the inflexion point and the value of the quotient has led to $\log K = 0.84 \pm 0.06$, what is in very good agreement with the value obtained previously. The advantage of our method is the possibility to determine K from a single isotherm and to avoid uncertanties encountered by the extrapolation of the apparent equilibrium constant values to infinite dilution.

REFERENCES

1. G. M. Gasparini and G. Grossi, Separation Science and Technology, 15, 825 (1980).
2. M. M. Kopečni, Doctor thesis, University of Belgrade, Belgrade, 1981, Yugoslavia.
3. M. M. Kopečni, R. J. Laub and Dj. M. Petković, J. Phys. Chem., 85, 1595 (1981).
4. Dj. M. Petković, in "Solvent Extraction Research" edited by A. S. Kertes and Y. Marcus, Wiley-Interscience, New York, 1969, p. 93.
5. M. M. Kopečni, R. J. Laub, Dj. M. Petković and C. A. Smith, J. Phys. Chem., 86, 1008 (1982).
6. W. Davis, Jr. and J. H. de Bruin, J. Inorg. Nucl. Chem., 26, 1069 (1964).
7. W. Davis, Jr. P. S. Lawson, J. H. de Bruin and J. Mrochek, J. Phys. Chem., 69, 1904 (1965).
8. E. Glückauf, Nature, 163, 414 (1949).
9. Dj. M. Petković, J. Chem. Soc. Dalton Trans., (in press)

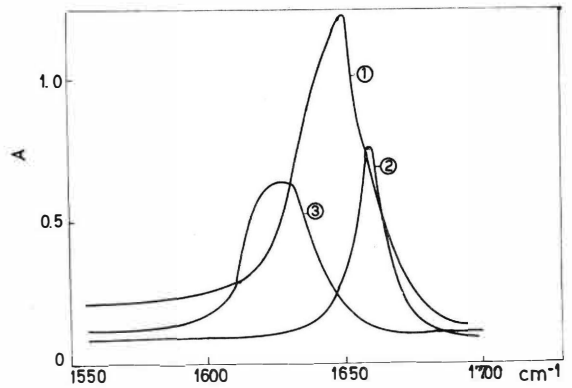

Figure 1. Infra-red spectra of pure DBEHA (1) and of DBEHA in n-hexane (2) and chloroform (3).

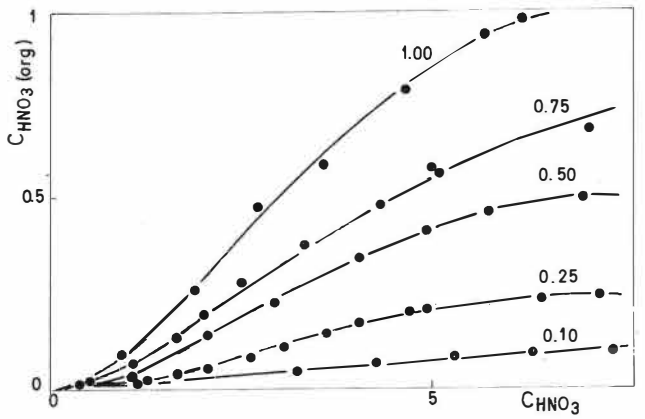

Figure 2. Distribution of nitric acid for different DBEHA concentrations (numbers in $mol \cdot dm^{-3}$) in n-hexane at 298 K.

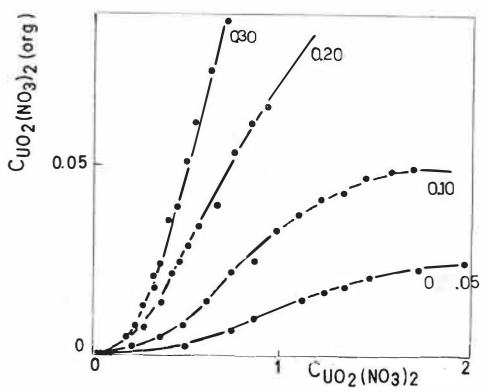

Figure 3. Distribution of uranyl nitrate for different DBEHA concentrations (numbers in $mol \cdot dm^{-3}$) in toluene at 298 K.

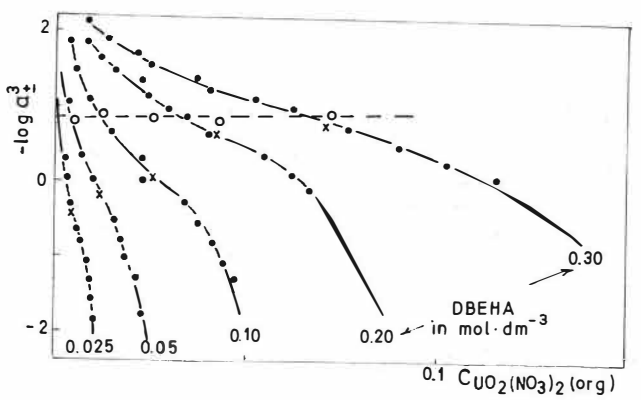

Figure 4. Crosses refer to the positions of inflexion points and circles show corresponding values of log K calculated

	HDEHP*		HEH[EHP]*		HDOP	
	pH_{50}	K	pH_{50}	K	pH_{50}	K
zinc	1.64	0.21	1.94	0.05	2.15	0.02
calcium	2.23	0.014	3.72	1.4×10^{-5}	4.80	1×10^{-7}
magnesium	3.36	7.6×10^{-5}	4.71	1×10^{-7}	5.30	1×10^{-8}

Table 3 Metal extraction data for organophosphorus acids (0.05 mol dm^{-3} H_2A_2)

from that of the divalent uranium(VI) ion. The uranium species followed the same type of extraction behaviour to the metals studied here so the findings should be comparable, Table 5. The results show that zinc, calcium and magnesium do not follow the trand of uranium(VI) with increasing extraction constant as the number of C-P bonds increases in the extractant, but are more similar to the trivalent metals. Further comparisons of other metals are required before any conclusions can be made. However the anomalous position of calcium implies that there is a significant decrease in the interaction between the metal ion and the phosphinic acid extractants. This is being further investigated by infra-red and ^{31}P nuclear magnetic resonance spectroscopy.

ACKNOWLEDGEMENTS

The authors would like to thank the British Council for some financial support for this work.

REFERENCES

1. J.S.Preston, Hydrometallurgy, 9, 115, (1982)
2. D.F.Peppard, G.W.Mason, S.Lewey, J. inorg. nucl. Chem. 27, 2065, (1965)
3. G.F.Vandegrift and E.P.Horwitz, J. inorg. nucl. Chem. 42, 119, (1980)

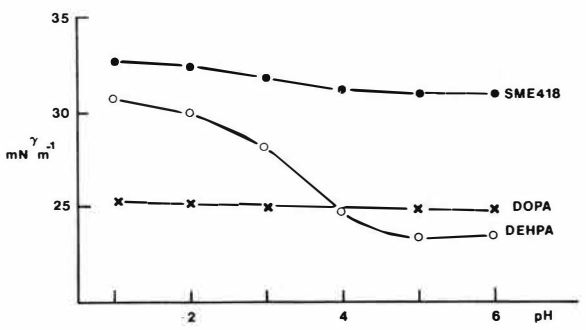

Organophosphorous acids, 0·01 mol dm^{-3} in n-heptane solution

Figure 1

	HDEHP	HEH(EHP)	HDOP
β^{Zn}_{Ca}	18	3.6×10^3	2.3×10^5
β^{Zn}_{Mg}	2.8×10^3	3.5×10^5	2.1×10^6
β^{Ca}_{Mg}	158	97	9

Table 4 Separation factors (β) using 0.05 mol dm^{-3} (H_2A_2)

	$K_{HEH(EHP)}/K_{HDEHP}$	K_{HDOP}/K_{HDEHP}
zinc	0.25	0.10
calcium	1×10^{-3}	0.7×10^{-5}
magnesium	1.3×10^{-3}	1.3×10^{-4}
uranium(VI) (ref 2)	1.8	9.9
promethium(III) (2)	0.024	0.030
curium(III) (2)	0.010	0.012

Table 5 Comparative extraction constants (K) for organophosphorus acid extractants.

* Warren Spring Laboratory unpublished results.

ADVANCES IN THE EXTRACTION CHEMISTRY OF AROMATIC HYDROXYOXIMES

Yuan Chengye, Xiang Caili, Li Shusen, Jiang Xiqi, Wang Jiao, Pan Boxi & Cao Chiming

Shanghai Institute of Organic Chemistry
Academia Sinica
Shanghai, China

INTRODUCTION

The industrial application of LIX 64N in hydrometallurgy of copper has prompted considerable development work on new extractants. An intensive studies of correlation between chemical structure and extraction beaviours of various types of aromatic hydroxyoximes have been reported for this purpose(1-4). These investigations are, however, limited by using hydroxyoximes with insufficient purity both structurally and consititutionaly as they exist in syn- and anti-forms as geometric isomers, in the meantime the structure and property parameters usually adopted in the literature are hot rigorously enough in order to get a strict and comprehensive conclusion.

In this paper we described the method of synthesis of series of aromatic hydroxyoximes with high purity, characterized by thin-layer chromatography, elemental analysies, IR, UV and 'H NMR. As structure parameter, beside pKa value, the charge density of phenolic oxygen, oximido-oxygen and nitrogen as well as energy of molecular orbital were taken based on HMO calculation. Both distribution ratio and reaction constant in copper extraction served as parameters representing extraction capability. On these bases the relationship between chemical structure and extraction properties of aromatic hydroxyoximes in copper extraction was derived.

EXPERIMENTAL

Reagents, Instruments and Methods of Estimation Aromatic hydroxyoximes were synthesized in the usual manner and identified by thin-layer chromatography, showing uniformly no impurities and followed by elemental analyses, UV, IR as well as 'H NMR.

The UV spectra were recorded using a 751 spectrophotometer. The IR spectra were recorded with a specord 75 — IR spectrometer. The 'H NMR were taken from a 60 MHZ varian EM-360L spectrometer.

The pKa values of aromatic hydroxyoximes were estimated by the method described on (5) using a pHS-2 pH meter. Ethanol was utilized as solvent with constant ionic strength by M $NaClO_4$ at 25±2°C.

The amount of anti-form of aromatic hydroxyoxime was determined in tertiary butanol by isopropanolic tetramethylammonium hydroxide potentiometrically.

Determination of Distribution Ratio and Reaction Constant in Extraction Equal volume (5ml each) of hydroxyoxime (0.05M) in toluene and aqueous solution of $CuSO_4$ (0.01M) with 0.5M$[(Na_2,H_2)SO_4]$were shaken in separatory funnel for 1 hr. at 25°C. After phase separation the copper concentration in both phases was estimated based on the EDTA Titration of the aqueous solution. The extraction reaction constant was determined by equation Kex=D $[H^+]^2/[HL]^2$ using the least squares method, on the basis of distribution ratio of copper in variation of hydrogen ion concentration in aqueous phase and ligand concentration in organic phase

HMO calculation The HMO calculation was worked out on electronic computer TQ-16. The parameters for hetero-atoms were taken from (6). $\alpha_O=\alpha_C+2\beta$, $\beta_{C-O}=0.8$; $\alpha_N=\alpha_C+0.5\beta$, $\beta_{C-N}=0.8$; $\alpha_{Cl}=\alpha_C+2\beta$, $\beta_{C-Cl}=0.4$; $\alpha_{CH_3O}=\alpha_C+1.9\beta$, $\beta_{C-OCH_3}=0.8$; $\alpha_{CH_3}=\alpha_C+2\beta$, $\beta_{C-CH_3}=0.7$; $\alpha_{N(O_2)}=\alpha_C+0.8\beta$, $\beta_{O-N(O_2)}=0.8$; $\alpha_{O_2(N)}=\alpha_C+1.2\beta$, $\beta_{O_2-N}=1.2$.

RESULTS AND DISCUSSIONS

1. Synthesis of Aromatic Hydroxyoximes

For the study of the electronic effect of substituents on the extraction behaviour of hydroxyoximes a series of compounds with general formula 2-HO-X-C_6H_3-C(Y)=NOH have been synthesized, where X represents alkyl, alkoxyl as well as electron-donating and electron-withdrawing group, Y stands as alkyl group or benzene ring with or without substituents. The physico-chemical properties of these compounds are listed on Table 1 and 2. Another series of aromatic hydroxyoxime with various alkyl group have also been prepared for the kinetic study in copper extraction which will be reported elsewhere.

Table 1 Structure of Aromatic Hydroxyoximes 2-HO-X-C_6H_3-C(Y)=NOH

NO.	X	Y	MW	UV max(nm).
1	H	C_6H_5	213	315 (3.78X10^3)
2	5-s$C_8H_{17}O$	C_6H_5	325	332.5 (3.44X10^3)
3	5-s$C_8H_{17}O$	C_6H_5	341	300 (6.95X10^3)
4	4-s$C_8H_{17}O$	C_6H_5	341	357.5 (3.46X10^3)
5	3-NO_2,5-tC_8H_{17}	C_6H_5	370	355 (3.16X10^3)
6	3-Cl, 5-sC_8H_{17}	C_6H_5	359	307.5 (4.02X10^3)
7	H	4'-$C_{12}H_{25}C_6H_4$	381	317 (3.72X10^3)
8	5-sC_8H_{17}	2'-Cl-C_6H_4	359	313 (3.94X10^3)
9	5-sC_8H_{17}	4'-$CH_3OC_6H_4$	355	300 (6.65X10^3)
10	4-s$C_8H_{17}O$	CH_3	279	285 (7.41X10^3)
11	4-s$C_8H_{17}O$	C_7H_{15}	363	327.5 (3.90X10^3)
12	5-s$C_8H_{17}O$	CH_3	279	302.5 (1.14X10^3)
13	4-s$C_8H_{17}O$	C_7H_7	307	302.5 (1.14X10^4)
14	4-s$C_8H_{17}O$	C_5H_{11}	335	298.5 (6.58X10^3)
15	4-s$C_8H_{17}O$	CH_3	279	298.5 (6.58X10^3)

Table 2 IR and NMR of Hydroxyoximes

NO.	IR ν (cm^{-1})			'H NMR (δ,ppm)		
	OH	CN	OR	P-O-H	C=N-OH	ph-H
1	3170-3470	1630	—			
2	3100-3700	1620	—	10.89	8.67	6.4-7.3
3	3100-3580	1620	1010	11.10	8.87	6.3-7.43
4	3100-3580	1610	1000	11.34	8.5	6.6-7.4
5	3100-3750	1620	—	10.50	8.16	6.7-7.3
6				11.57	8.34	6.3-7.2
7	3110-3600	1600	—	11.03	8.74	6.2-7.3
8	3050-3500	1700	—	11.8	(8.9)	6.3-7.3
9	3240-3540	1600	1038	11.27		6.3-7.2
10	3200-3700	1610	1030	11.20		6.4-7.5
11	3100-3450	1610	1050	11.33	9.17	6.7
12	3120-3580	1620	1030			
13	3100-3580	1600	1030			
14	3100-3600	1610	1050			
15	3100-3550	1620	1040			

2. Extraction Performance and Estimation of Equilibrium constants.

The extraction equilibrium was performed between equeous 0.01M Cu, 0.5M$[(Na_2H_2)SO_4]$solution and 0.05M hydroxyoxime in toluene. The distribution ratio of copper correlates linearly with various acidity (pH) of the equilibrated aqueous phase as shown on Figures 1-9

Extraction of copper by hydroxyoxime is considered to be proceeded by ion-exchange mechanism. As far as aromatic hydroxyoxime (HL) is concerned

$$Cu^{2+} + 2HL = CuL_2 + 2H^+$$

The thermodynamic equilibrium constant K is defined as

$$K = \frac{[CuL_2][H^+]^2}{[Cu^{2+}][HL]^2} \cdot \frac{\gamma_{CuL_2}\cdot\gamma^2_{H^+}}{\gamma_{Cu^{2+}}\cdot\gamma_{HL}}$$

In the course of experiment, the ionic strength of aqueous solution was kept constant and the activity coefficient product may thus be regarded as constant. Therefore the equilibrium (concentration) constant of extraction may be expressed by the following equation appoximately

$$Kex = \frac{[CuL_2]\ [H^+]^2}{[Cu^{2+}]\ [HL]^2}$$

The distribution ratio D defined as $[CuL_2]/[Cu^{2+}]$ was introduced to above equation, then we gain

$$Kex = D[H^+]^2/[HL]^2$$

Plotting log $D/[HL]^2$ versus pH of equilibrated aqueous phase in copper extraction by various hydroxyoximes gives straight line in all cases. Equilibrium constant Kex and slope of straight lines m may thus be estimated by least square method. The equation has average r = 0.9985. In Table 3 pKa of ligand and extraction parameters $pH_{\frac{1}{2}}$, Kex as well as m were given.

Table 3 Structure-reactivity studies of copper Extraction by Hydroxyoximes

Extractant	pKa	$PH_{\frac{1}{2}}$	Kex	m
2	11.12	1.93	0.1333	1.9012
3	11.48	2.05	0.0701	1.9445
4	10.99	1.45	1.6450	1.8092
5	7.70	1.93	59.4977	0.5535
7	11.29	1.72	0.4324	1.8591
8	11.08	1.94	0.1858	1.8514
9	11.08	1.93	0.1080	1.9713
10	10.56	1.44	2.5328	1.6513
11	10.68	>3	0.9363	0.8465
12	10.83	1.92	0.2091	1.8033
15	10.02	1.39	1.5700	1.8422

As indicated in Table 3, the extraction capacity of hydroxyoxime is apparently influenced by the acidity of the ligand. The lower the pKa is, the higher the Kex will be.

3. Correlation Between Structural Papameters and Extraction Behaviour of Hydroxyoximes

Some structural parameters related to extraction of hydroxyoximes have been estimated by HMO calculation. The charge densities of phenolic and oximido-hydroxyl oxygen (q^{ph}_{OH}),(q^{OXM}_{OH}) and oximido nitrogen atom. as well as the charge density of frontal orbital of nitrogen ($q_{N,H}$) and the lower occupied molecular orbital of nitroge ($q_{N,L}$) were calculated. EL represents the lower occupied molecular orbital and 4HL is the difference of E HOMO and E LOMO. As previous report (7) the pKa value of hydroxyoxime under investigation measured potentiometrically are corrected to qOH of that compound obtained by HMO calculation.

The $\Delta\delta OH$, as the parameter for strength of intermolecular hydrogen bonding, is the difference of δOH taken from ^1H NMR and qoH from HMO calculation. (Table 4)

Table 4 Structural Parameters of Aromatic Hydroxyoximes

NO.	q_{OH}^{Ph}	q_N	q_{OH}^{cam}	$q_{N,H}$	$q_{N,L}$	E_L	ΔE_{HL}	ΔpKa	$\Delta\delta OH$ (ppm)
1	1.9347	1.9293	1.9372	0.7550	0.5305	-0.45807	1.11189		
2	1.9369	1.3294	1.9372	0.6908	0.5305	-0.45807	1.10182	1.65	7.38
3	1.9376	1.3294	1.9372	0.5918	0.5305	-0.45806	1.09227	1.93	7.85
4	1.9347	1.3452	1.9396	0.7067	0.5177	-0.47739	1.08996	1.79	7.48
5	1.9311	1.3298	1.9372	0.6117	0.4172	-0.43121	1.06617	-1.05	5.95
6	1.9377	1.3294	1.9372	0.6850	0.5315	-0.45908	1.10272		
7	1.9347	1.3409	1.9390	0.7296	0.5231	-0.47425	1.10175	2.09	7.73
8	1.9369	1.3337	1.9378	0.7056	0.5263	-0.46242	1.10256	1.61	7.61
9	1.9369	1.3444	1.9395	0.7132	0.5208	-0.47887	1.09350	1.61	7.40
10	1.9342	1.3934	1.9508	0.6709	0.4518	-0.65236	1.28216	1.44	7.22
12	1.9371	1.3781	1.9467	0.4367	0.4509	-0.61442	1.26088	1.35	7.90

The figures described in Table 4 indicate that both ΔpKa and $\Delta\delta OH$ are the function of qN,H of aromatic hydroxyoximes under investigation except compound NO. 12 (Fig. 10). Meanwhile, log Kex for copper extraction correlate either with q_{OH}^{Ph} or with pKa as expected. (Fig. 11-12) The introduction of an electron withdrawing group like NO_2 in benzene lead to the decrease of the q_{OH}^{Ph} (1,9311) and pKa (7,70) and therefore to the evidently enhancement of extraction capability (Kex=59.50). These facts persuasibly indicate the important contribution of phenolic hydroxyl group in extraction reaction of copper by hydroxyoximes.

No apparent influence was found between charge density of oximido-nitrogen atom (qN) and electronic state of phenolic hydroxyl oxygen as represented by ΔpKa or $\Delta\delta OH$. The qN of O-hydroxybenzobenzone is, however, considerable lower than that of O-hydroxyacetophenone due to the conjugation effect of the aromatic ring. The position of alkyloxyl group in benzene ring plays an important role in copper extraction. The 2-hydroxy-4-alkoxylbenzophenone oximine is superror than corresponding 5-substituted compound. It may be rationalized that the 4-alkoxyl substituent locating at meta position to phenolic hydroxyl group possesses -I effect (σm 0.12) which offers lower pKa, in the meantime, the 4-substituted aromatic hydroxyoxime usually provides higher qN value.

As shown from data of Table 3, the $pH/\frac{1}{2}$ for compounds 4,10 and 15 lay on 1.4, where the $pH\frac{1}{2}$ value of other hydroxyoximes stand generally around 1.9, It is reasonable to concluded that the 4-alkoxyl substituted derrvative provides better extraction performance than corressponding 5-substituted analogues. The compound 11 gives the highest $pH\frac{1}{2}$ (>3) among the hydroxyoximes studies in this paper as the result of the presence of long chain aliphatic radical near oximido-group. It is therefore interesting to examine the extraction behaviours of 4-alkoxyl derivatives of O-hydroxyl benzophenone or acetophenone.

REFERENCES

1. Department of Extraction Chemistry, Shanghai Institute of Organic Chemistry, Academia Sinica. Unpublished Technical Report (1972)
2. B.H. Laskorin, V.V. Yaksin, V.S. Ul'yanov, A.M. Mirokhin. Proceedings ISEC 1974, P.1775
3. P. Muhl and K.Gloe Proceedings ISEC 1980, Paper NO. 80-236, 80-212
4. D. Stepniak-Biniakiewicz and J.Szymanowski Proceedings ISEC 1980, Paper NO. 80-75
5. В.В.Перекалин, З.С.Сегалина ЖОХ 24 683 (1954)
6. J.P. Lowe Quantum Chemistry, New York 1978, p. 246
7. Li Shusen et al. Acta Chimica Sinica 40 577 (1982)

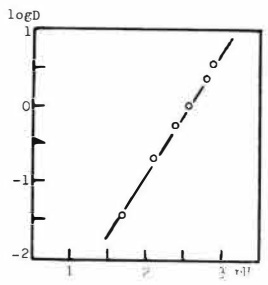

Figure 1
Plot of log D vs. pH in Copper Extraction by 2-Hydroxy-5-s.octyloxyl benzophenone Oxime

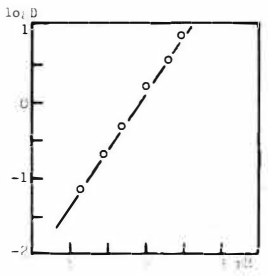

Figure 2
Plot of log D vs. pH in Copper Extraction by 2-Hydroxy-4-s.octyloxyl benzophenone Oxime

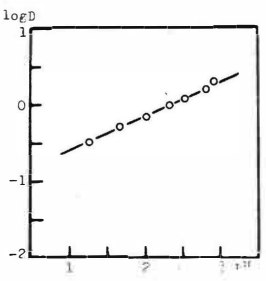

Figure 3
Plot of log D vs. pH in Copper Extraction by 2-Hydroxy-3-nitro-5-t.octyl benzophenone Oxime

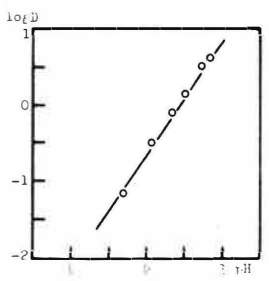

Figure 4
Plot of log D vs. pH in Copper Extraction by 2-Hydroxy-5-s.octyl benzo-2'-chlorophenone Oxime

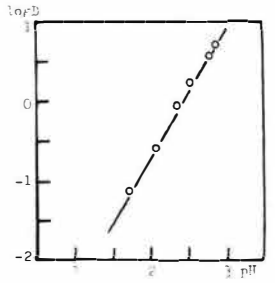

Figure 5
Plot of log D vs. pH in Copper Extraction by 2-Hydroxy-5-s.octyl benzo-4'-methoxyphenone Oxime

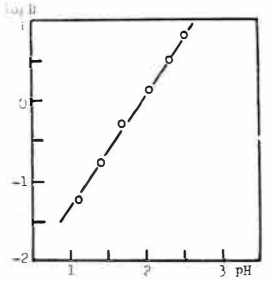

Figure 6
Plot of log D vs. pH in Copper Extraction by 2-Hydroxy-4-s.octyl-oxyl acetophenone Oxime

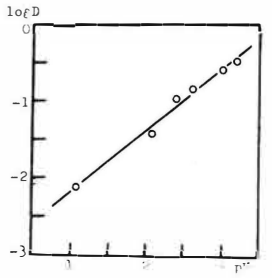

Figure 7
Plot of log D vs. pH in Copper Extraction by 2-Hydroxy-4-s.octyl-oxyl heptophenone Oxime

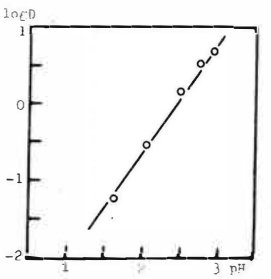

Figure 8
Plot of log D vs. pH in Copper Extraction by 2-Hydroxy-5-s.octyl acetophenone Oxime

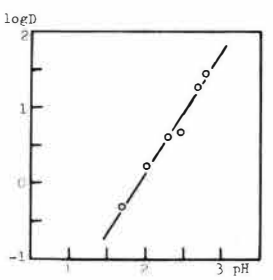

Figure 9
Plot of log D vs. pH in Copper Extraction by 2-Hydroxy-4-i.octyl acetophenone Oxime

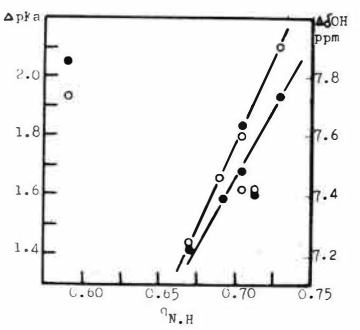

Figure 10
Dependence of qN,H on ΔpKa and $\Delta\delta OH$ of Aromatic Hydroxyoxime

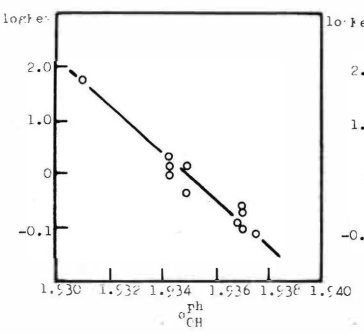

Figure 11
log Kex as the function of q_{OH}^{Ph}

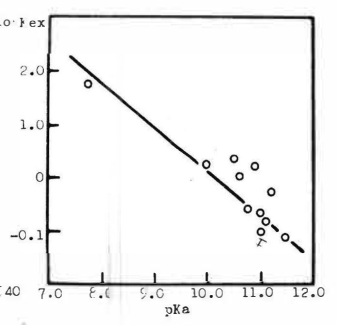

Figure 12
log Kex as the function of pKa

SOME NEW ASPECTS IN THE STRUCTURE-REACTIVITY STUDIES OF ORGANIC EXTRACTANTS

Yuen Chengye (C.Y. Yuan)

Shanghai Institute of Organic Chemistry
Academia Sinica
Shanghai, China

The study on the relationship between chemical structure and extraction behaviour of organic extractants is considered as the basis for the quantitative molecular design of effective extractants and recognized as a component part of extraction chemistry (1-3). Previous reports on this subject were, however, limited to qualitative study. The present paper deseribes some new aspects in the structure-reactivity studies of organic extractants carried on in author's Laboratory since ISEC'80 in Liege-Belgium.

STERIC EFFECT OF LIGAND IN EXTRACTION

Solvent extraction of metal ions may be regarded as a multicomponental coordinative chemical reaction between two immiscible phases. This thermodynamic process is evidently influenced by the spatial configuration of both ligand and metal ion to be extracted. The steric feature consisting of shielding, conformational and spatial effects are, however, determined by the composition, structure and configuration of the coordination compounds. Steric effects play an important role in the investigation of organic extractants with higher selectivity. In the methematical modle of the molecular design of extractants the steric constant is one of the most important terms. (4)

Steric hindrance in extraction of metals are observed in those ligands which hold a bulky side chain around coordinating atoms. In the meantime, the degree of such steric effect is largely depended on the structural feature of the extractants. There are two geometric isomers, Z (syn) and E (anti), available for hydroxyoxime or dioxime extractant depending on the location of the oxime group relating to another function radical. Only the E isomers have a configuration suited to formation of a chetaled complex with transition metals such as copper by loss of a proton from the phenolic hydroxyl group forming O-M-N coordinate bond.

Different degree of steric effect are reported by us for extraction metals with various atomic radius. This effect is evidently enhanced in extraction metal ions with various composition of extracted complex even with similar size of atomic radius. Emphasis should be placed upon the dependence of steric effect on the configuration of the coordinated compounds. For example the steric requirments for complex with square planar (i.e. Ni^{2+}, Cu^{2+}) is quite different from those with tetrahedron (Co^{2+}) or octahedron (Ln^{3+}) configuration.

The extraction behaviour of dialkyl isopropylphosphonate for rare earths was influenced, though not so strong, by the spatial configuration of the ester alkyl group of the extractants. The steric effect of there organophosphorus ligands may be represented by thermodynamic functions, especially ΔS value in extraction reaction (5).

The structure-reactivity studies of various types of acidic organophosphorus compounds in extraction of neodymium, samarium, ytterbium and ytterium as representatives of light, medium and heavy rare earths, demonstrated that both di(2-ethylhexyl) phosphinic acid and di-n-octylphosphinic acids are isomeric compounds with almost the same pKa values, but the difference in their Kex for Nd, Sm, Y and Yb extraction is in four orders of magnitude (6). This is attributed to the apparent steric hindrance arised from two branched alkyl radicals directyl linked to the coordinating group. In the former molecuis, there are two octyl groups with substitution on the β-position, which inhibit the coordination of the extractants with metal ions. The steric effect in extraction of rare earth was weakened as the increasing in atomic number while the atomic radius was decreased due to the lanthanide contraction. Analogous structure effects have been found in the extraction behaviour of dioctyl aralkylphosphonates for rare earths (7). The steric effect of acidic organophosphorus ligands on lanthanide extraction is well demonstracted by the fact that as Kex value, the ΔS calculated in the extraction reaction of rare earths by 2-ethylhexylphosphonic acid mono-2-ethylhexyl ester increases with the increase of the atomic number and reveals the "tetrad effect". (8) (FIGURE 1)

In the structure-reactivity studies of extraction reaction of cobalt, nickel and rare earth by organophosphorus acids, we found that the strength of intermolecular hydrogen bonding as represented by $\Delta\delta$OH in NMR of various bypes of monobasic organophosphorus acid is directly proportional to the charge density of the phosphoryl oxygen estimated by CNDO/2 calculation. In comparison with the $\Delta\delta$OH, the situation of phosphorus-bonded oxygen bearing ionizable hydrogen, as represented by pKa value, make greater contribution to the extraction. (9) (Table 1)

Table 1
The Strength of Intermolecular H-bonding and Charge Density of Oxygen Calculated by CNDO/2

Extractants	$\Delta\delta$OH (ppm)	qP=O	pKa	qP-OH	K^{Nd}_{ex}	Dco	$\log K^{Nd}$	$\log D^{co}$
$(iC_8H_{17}O)_2P(O)OH$	15.83	6.4667	2.74	6.3372	6.8×10^{-3}	5.67	6.05	6.23
$iC_8H_{17}O(iC_8H_{17})P(O)OH$	15.95	6.4633	4.10	6.3389	8.4×10^{-5}	2.39	8.19	8.58
$iC_8H_{17}O(sC_8H_{17})P(O)OH$	16.52	-	4.26	-	-	0.89	-	8.47
$C_6H_5O(iC_8H_{17})P(O)OH$	15.92	-	2.99	-		-	9.31	-
$C_6H_5O(sC_8H_{17})P(O)OH$	16.06	-	2.98	-		-	8.26	-
$(iC_8H_{17})_2P(O)OH$	16.65	6.4707	5.45	6.3407	4×10^{-8}	1.53	<8.95	11.08

A quantitative relationship between pKa and logK or logD has been established for a series of extraction systems, in which the steric factor is less important.

$$\log D^{co}_{com} = 1.7124pKa+1.56188, \quad r=0.9800$$
$$\log K^{Nd}_{ex,com} = 2.3766pKa-0.28967, \quad r=0.9974$$
$$\log K^{Nd}_{ex,com} = 2.3419pKa+1.03142, \quad r=0.9453$$
$$\log K^{Y}_{ex,com} = 2.5047pKa+2.51476, \quad r=0.9982$$
$$\log K^{Yb}_{ex,com} = 2.4945Pka+3.37607, \quad r=0.9974$$

Owing to the different configuration of coordination compounds in bobalt and nickel extraction by organophosphorus acids, the steric effect must be taken in full account. On the basis of experimental data the steric constant Es of various alkyl and alkoxyl group in mono-basic phosphorous acid in extraction was estimated and correlated to extraction reactions.

$$\log D^{co}_{com} = 1.7124pKa+1.56188-\Sigma Es^{co}$$
$$\log D^{Ni}_{com} = 1.7124pKa+1.02188-\Sigma Es^{co}$$

Plots of log Co/Ni versus $\Sigma\Delta$Es give straight line. (Figure 2).

It demonstrated that steric effect of ligands plays an extreme important role in the extractive sepration of such elements.

MOLECULAR ORBITAL METHODS IN STRUCTURE - RACTIVITY STUDIES OF EXTRACTANTS

As shown in our previous paper that Hücked molecular orbital (HMO) method has been successfully used in structure-reactivity studies of hydroxyoxime extractants. (3) The HMO method may also be applied for other types of extractants including neutral and acid organophosphorus compounds, β-diketones as well as hydroxy ketones. (10) The molecule of these extractants may be considered as conjugated ststem containing heteroatoms. In such cases, the Coulomb & resonance integrals may be altered by expressions $\alpha_x=\alpha_c+h_x\beta_{c-c}$ and $\beta_{c-x}=h_{c-x}\beta_{c-c}$ in the HMO calculation. The high degree secular equation in HMO calculation was solved by the standard programme of Jacobi method, by which the characteristic root and factor of real symmetric matrix were solved. The calculation was worked out on electronic computer CJ 719. The structure parameters, such as charge density (q_x), bond order ($P_{c=x}$), π bond energy (E^{π}_{c-x}), energy of MO ($\Sigma\lambda_i$) as well as superdelocalizability for nucleophilic reaction (S^N_r), thus calculated was discussed with the extraction behaviours of various extractaants towarding uranium, thorium, rare earths, copper and lithium.

The extraction ability of neutral organophosphorus compounds closely relates to the charge density of phosphoryl oxygen (q_o) and phosphorus stoms (qp). It was found that the distribution ratio of cerium enhanced as the q_o and q_p values was increased, meanwhile a linear free-energy relationship exists between the $\Sigma\lambda_i$values and the Kabachnik constant ($\Sigma\sigma^*_p$) of substituents. As estimated by least squares method, an empirical equation $\Sigma\sigma^*_p=-3.84+0.168\Sigma\lambda_i$ was deduced.(Figure 3)

The extraction constants(Kex) of neodymium, samarium, ytterbium of various acidic organophosphorus compounds are governed chiefly by the charge density of hydroxyl oxygen atom (HOMO) in grouping >P(O)OH. The plot of Kex of rare earths versus q_o (HOMO) values of these compounds gives straight line as anticipated, owing to the direct influence of q_{OH} value on the pKa of ligands. A quantitative relationship also exists between the $\Sigma\lambda_i$and $\Sigma\sigma^*_p$ values of acidic organophosphorus extractants, (Figure 4,5) i.e.

$$\Sigma\sigma^*_p = -4.12+0.166\Sigma\lambda_i$$

The extraction behaviours of β-diketone are directly infulenced by the superdelocalizability and the bond order of carbonyl group (Table 2)

Table 2
Structure-Reactivity Relationship in Lithium Extraction by β-Diketones

β-diketones	q_{OH} HOMO	q_{OH} Total value	S^N_O	$P_{c=o}$	pKa	% of Li extraction
$CH_3COCH_2COCH_3$	0.1476	1.8971	-0.5761	0.6725	8.9	18
$C_6H_5COCH_2COCH_3$	0.1634	1.8961	-0.7586	0.6713	8.7	97
$C_6H_5COCH_2COC_6H_5$	0.0607	1.9065	-0.9280	0.6253	9.35	100

There are no evidence for the relationship between the extraction property and the charge density of enolic oxygen. As indicated by IR spectra a linear free energy relationship exists only between the carbonyl stretching frequency ($\nu_{c=o}$) and bond order of carbonyl group corrected by intramolecular hydrogen bonding (Pc=o cor.). (Table 3) The strength of intramolecular hydrogen bond is closely related to the difference of values before and after dissociation with hydrogen. The larger the $|\Delta P_{c=o}|$ value is, the stronger the hydrogen bonding will be.

PATTERN RECOGNITION PROCESSING

The previous studies on the relationship between chemical structure and extraction properties of organic extractants were limited to certain individual structural effect, so it is difficult to evaluate the overall characeteristic

of the whole molecule structure. In recent years, pattern recognition, an efficient computational method for the analysis of multivariate data, was developed. A nonparametric, Linear Mapping method by using Karhunen-Loeve transformation has been introduced by us for the structure-reactivity studies of phosphorus-based extractants.(3) In this paper another nonparametric method - K - nearest Neighbor method (KNN) is reported. (11) The program for KNN method were written in basic language and operated on the DJS-131 minicomputer. The weight of every feature and classified results were output by the printer and X-Y plotter. The listed weights showed the contribution of various characteristics of molecular structure to classification.

Table 3

Correlation of $P_{C=O}$ and $_{C=O}$ of Aromatic Hydroxyketone(aldehyde)

Aromatic hydroxy-ketone (aldehyde)	$P_{C=O}$	$P_{C=O}$ (Corr)	$\Delta P_{C=O}$	$\nu_{C=O}$	$\Delta\nu_{C=O}$
2-OH-C_6H_4CHO	0.6720	0.7242	0.0522	1665	38
2-OH-$C_6H_4COCH_3$	0.7749	0.6964	0.0785	1645	43
2-OH-$C_6H_4COC_6H_5$	0.6860	0.6446	0.0414	1620	33
2-OH-4-CH_3O-$C_6H_3COC_6H_5$	0.6762	0.6353	0.0409	1600	
2-OH-4-C_6H_5O-$C_6H_3COC_6H_5$	0.6759	0.6352	0.0407	1600	

The program KNBP is applied to the classification of distribution coefficient of uranium in extraction by eight-two organophosphorus compounds which belong to eleven structures (the number of each kind of compounds is in parenthesis):R_3PO(4), $R_2P(O)OR'$(3), $RP(O)(OR')_2$(7), $(RO)_3PO$(4), G-$\phi P(O)(OR)_2$ (14),$R_2N(CH_2)_nP(O)(OR')_2$(15), $R_2N(CH_2)_nP(O)OR(OH)$(14), $R_2P(O)OH$(1), G-$\phi P(O)OR(OH)$(5), G-ϕ-$(CH_2)_nP(O)OR(OH)$(4), G-$\phi CH_2P(O)(OR)_2$(11),where R is alkyl, G is p-substituents in benzene ring including X (electron-withdrawing group) and Y (electron-donating group). Seventeen features are selected. (Table 4)

For environment descriptors, the phosphorus atom is taken as center and then the nearest atoms or bonds are considered. For bond environment (BD): single bond=1; double bond=2; triple bond=3; aromatic bond=4; C-H bond is neglected. For atom environment (AD): atoms are assigned according to the following order C, 2; N, 3; S, 4; F, 5; Cl, 6; Br, 7; I, 8; P, 9. AD is the sum of the nearest atoms' values except the central phosphorus atom. For weight environment (WD), atom and bond environments are all taken into account. WD is the sum of BDXAD of the nearest atoms. The approach adopted in this paper is different from that used by Jurs. (12)

Among the eighty-two organophosphorus compounds examined, there are sixteen compounds discriminated as Class I and sixty-six as Class II, when the threshold value is 1000.

It is clear that the five major structure features predominating the extraction ability of uranium are: number of P-C bonds (+); atom environment (AD) (-); number of -CH - (non-ester) (+); number of P-O-C bonds (-); weight environment (WD) (-). In the parentheses the tendency of the feature which is necessary for compounds of Class I is given. Among the eleven types of organophosphorus compounds investigated, only oxygen or carbon atoms are bonded with phosphorus. The structural feature with the weight order 1, 2, 3 and 4 are closely related to the nature of the atoms bonded with phosphorus. In the meantime, the extraction ability of organophosphorus compounds are also evidently influeneed by the length of non-ester methylene linkage.

References

(1) D.S. Flett, Chem. & Ind., 1977, 941
(2) Yuan Chengye, Kexue Tongbao (Science) 22 465 (1977)
(3) Yuan Chengye, Proceedings ISEC'80 Paper NO. 80-81, Leige, Belgium.
(4) Yuan Chengye, Journal of Chinese Society of Rare Earths (to be published)
(5) Yuan Chengye, Ye Weizhen, Ma Enxin, Wu Fubing and Yan Xiaomin in "The rare Earths in Modern Science and Technology" (Ed. G.J. Mc Carthy) vol. 3 p. 499, Plenum Press, New York, 1982; Scientia Sinica (Series B) English Edition 25 1256 (1982)
(6) Yuan Chengye, Ye Weizhen, Ma Hengli, Wang Guoliang, Long Haiyan, Xie Jifa, Qin Xiuqing and Zhou Yongchang, Scientia Sinica (Series B) English Edition 25 7 (1982)
(7) Yuan Chengye, Liu Xiyan, Ma Hengli, Wang Guoliang, Xie Jifa, Acta Chimica Sinica 39 881 (1981)
(8) Ma Enxin, Yan Xiaomin, Wang Sanyi, Long Haiyan and Yuan Chengye Scientia Sinica English Edition 24 1237 (1981)
(9) Yuan Chengye, Li Shushen and Long Haiyan, Paper to be presented in ICPC'83 Nice, France
(10) Yuan Chengye, Zhou Chengming and Chen Kongchang Acta Chimica Sinica 39 699 (1981)
(11) Hui Yongzheng, Wang Qizhong and Yuan Chengye Kexue Tongbao (English Edition) 27 163 (1982)
(12) P.C. Jurs in "Computer Assisted Studies of Chemical Structure and Biological Function" (Ed. A.J. Stuper) John Wiley, New York 1979

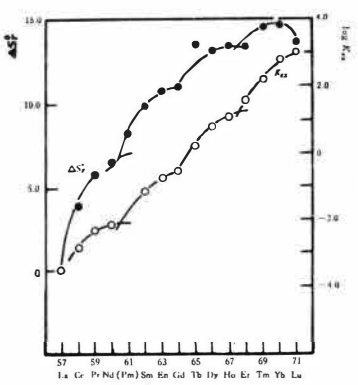

FIGURE 1

Tetrad Effect of K and ΔS in Extraction of Lanthanides by Isooctyl Isooctylphosphonate

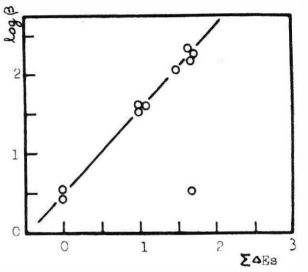

FIGURE 2

Plot of log β versus ΣΔEs in Extractive Separation of Nickel and Cobalt by mono-acidic Phosphorus Esters

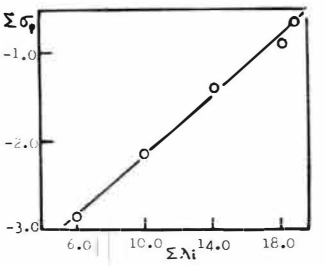

FIGURE 3

Correlation of Substituent Constants and Total π Energy of Neutral Phosphorus Esters

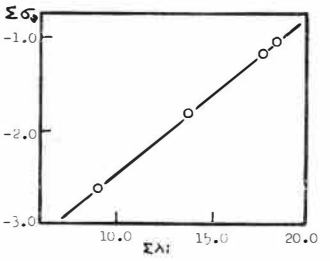

FIGURE 4

Correlation of Substituent Constants and Total π Energy of Acidic Phosphorus Esters

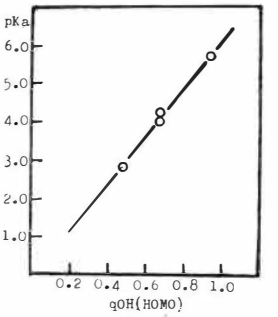

FIGURE 5

Dependance of Pka on qOH of Acidic Phosphorus Compounds

Table 4

Molecular Structure Descriptors Selected for KNN Classification of Organophosphorus Compounds

No.	Type of Features	Features	Weights	Order
A	Atom and bond descriptors	Total No. of C-atoms	7.3879×10^{-4}	12
B		Total No. of noncyclic C-atoms	7.8506×10^{-4}	13
C		Total No. of O-atoms	0.2172	6
D		No. of P—O—C bonds	0.2548	4
E		Ratio of length of C-chains (longest/shortest)	5.4241×10^{-4}	16
F		No. of P—C bonds	0.9883	1
G	Substructural descriptors	P—OH	0.1410	7
H		—C—	0.1147	9
I		—CH_2—(ester)	9.2476×10^{-4}	11
J		—CH_2—(non-ester)	0.2928	3
K			5.1771×10^{-4}	15
L		X—	6.8713×10^{-4}	14
M		Y—	5.3828×10^{-4}	17
N		>N—	0.1156	8
O	Environment descriptors	BD (bond environment)	0.1000	10
P		AD (atom environment)	0.7470	2
Q		WD (weight environment)	0.2848	5

DETERMINATION OF THE HEAT CHANGE IN SOLVENT EXTRACTION OF METALS—THE EXTRACTION OF ZINC(II) FROM HYDROCHLORIC ACID SOLUTIONS BY HIGH MOLECULAR WEIGHT AMINES IN VARIOUS ORGANIC SOLVENTS

Taichi Sato, Takato Nakamura and Masami Kuwahara

Department of Applied Chemistry
Faculty of Engineering, Shizuoka University
Hamamatsu, Japan

Although diluents play an important role in the solvent extraction of metals, their effect is not straightforward. Most of researchers have tried to explain the effect of diluent on the distribution coefficient using physico-chemical properties such as dielectric constant (1,2), dipole momemt (1) and solubility parameter (3-8).

We have also found that in the extraction of divalent manganese, cobalt, copper, zinc and cadmium by trioctylmethylammonium chloride (TOMAC, $R_3R'NCl$) in various organic solvents (9), the variation of distribution coefficient and change in enthalpy estimated by the use of van't Hoff equations follows the regular solution thoery. In relevance to the subject, calorimetry has been applied to measure the heat change directly associated with metal extraction (10). Results obtained by this method enable to discuss the distribution phenomena in more detail. Calorimetric investigations for metal extraction have been limited so far to the works by Marcus and Kertes (11-16). Therefore this paper extends the work to the extractions of zinc(II) by trioctylamine (TOA, R_3N) and TOMAC in various organic solvents from aqueous solutions of hydrochloric acid and/or lithium chloride.

EXPERIMENTAL

Reagents. TOA and TOMAC (Koei Chemical Co., Ltd.) were of high purity used without further purification and diluted with various organic solvents such as benzene, chlorobenzene, *o*-dichlorobenzene, toluene, *m*-xylene, nitrobenzene, carbon tetrachloride and 1,2-dichloroethane. Solutions of TOA were shaken with aqueous solution of a little excess hydrochloric acid to form R_3NHCl (TOAHCl) (17). A stock solution of zinc chloride was prepared by dissolving zinc chloride in hydrochloric acid in order to prevent its hydrolysis and diluted so as to get the aqueous solutions containing zinc chloride, hydrochloric acid and/or lithium chloride of the selected concentrations. Other chemicals were of analytical reagent grade.

Extraction and Analytical Procedures. Distribution coefficient of zinc(II) (the ratio of the equilibrium concentration of zinc in organic phase to that in aqueous phase, D) was obtained by the method described elsewhere (18).

$$\{(nV_e - V_c)/2.3\}(\delta_d^2/RT - 1/V_d) + \text{const}$$

where V and δ denote molar volume and solubility parameter, respectively, and subscripts c, e and d being the complex formed in the organic phase, extractant and diluent, respectively. Figure 1 showing the plots of log D *vs.* δ_d confirmed that equation (3) is satisfied in the extraction by TOMAC, while any relation between them is observed in that by TOAHCl.

In some papers on the extraction by tertiary amines, their hydrochloride adducts have been described like quaternary ammonium salts (23). In view of the effect of diluent on the extraction by TOAHCl and TOMAC stated above, the distribution phenomena are apparently of difference.

Heat Change Associated with Zinc(II) Extraction Using Benzene as Diluent. In Figure 2, the apparent molar heat change ($\Delta Q = \Delta q / [Zn]_{react}$), which comes from the complete extraction of zinc(II) from its aqueous solutions (2×10^{-4} mol) containing hydrochloric acid and/or lithium chloride with 0.05 M TOAHCl or 0.05 M TOMAC in benzene at 25 °C, is plotted as a function of initial concentration of total chloride in aqueous phase. It is seen that there is a striking similarity in the variation of the heat change between the extractions by TOAHCl and TOMAC. In the extraction from hydrochloric acid solutions, a maximal exotherm appears at 3 and 2 M HCl for TOAHCl and TOMAC, respectively. In the case of mixed solutions of lithium chloride in the presence of 0.01 M hydrochloric acid, the apparent molar heat change varies along with that for hydrochloric acid only up to the total aqueous chloride concentration below 2-3 M. It is thus evident that up to this concentration the heat change associated with zinc(II) extraction is controlled by chloride ion in aqueous phase.

At higher chloride concentration above 2-3 M, the apparent molar heat change for the extraction in the presence of lithium chloride continues to increase exothermally, contrary to that for hydrochloric acid only (Figure 2). This difference is related with the following fact: for the extraction from hydrochloric acid solutions, the molar ratios $[HCl]_{org} / [ACl]$ at 2, 3 and 5 M HCl are found to be 0.019, 0.032 and 0.12 for A = R_3NH, respectively, and 0.10, 0.28 and 0.69 for A = $R_3R'N$, respectively, suggesting the formation of the species such as $R_3NHCl \cdot HCl$ and $R_3R'NCl \cdot HCl$ correspondent to the earlier works (24,25); for that from lithium chloride solutions, only a slight increase in the amount of chloride extracted into organic phase is observed even if the concentration of lithium chloride is increased more than 2-3 M. This implies that in the extraction from aqueous solutions of higher concentration of hydrochloric acid by TOAHCl and TOMAC in benzene, the acid extracted into the organic phase by mixing the aqueous and organic phases in the sample reaction vessel may be released in part endothermally into aqueous phase accompanied by the extraction of zinc(II). This reaction contributes the decrease in the exotherm of the heat change observed.

Taking into account the facts as mentioned above, the theoretical heat change associated with zinc(II) extraction by TOAHCl and TOMAC in various diluents is written as

$$(4) \qquad \Delta Q_{theor} = -(1/n_t)\sum_{j=0}^{3}\Delta n_j \Delta h_j - Y$$

where Δn_j and n_t are initial concentration of the species $ZnCl_j^{(2-j)+}$ and total concentration of zinc in aqeuous phase, respectively, Δh_j refers to the change in enthalpies for the steps

$$(5) \qquad ZnCl_j^{(2-j)+}(a) + (4-j)Cl^-(a) \rightarrow ZnCl_4^{2-}(a),$$

and Y is the variable depending on the kind of diluent, because it is the sum of the change in enthalpies for some steps as seen in the reaction scheme described previously (26). Also, Y corresponds to the change in enthalpy estimated bt using van't Hoff equation.

Putting -3.4 kJ mol^{-1} obtained for the extraction of zinc(II) from aqueous solution of 0.05 M hydrochloric acid with 0.05 M TOMAC in benzene into Y, the change in enthalpy for the respective steps in the reactions (5) is estimated by linear least squares. This yields that the values of Δh_0, Δh_1, Δh_2 and Δh_3 are 6.67 ± 1.74, 4.26 ± 3.24, -37.2 ± 15.4 and -111.7 ± 26.1 kJ mol^{-1}, respectively, using the respective stability constants β_1, β_2, β_3 and β_4 as 3.7, 1.0, 0.27 and 0.13. The value of Y for TOAHCl in benzene is estimated to by -19.6 from mean difference between the apparent molar heat change for the extraction of zinc(II) by TOAHCl and TOMAC in benzene from the aqueous solutions containing 0.1 - 2 M hydrochloric acid. Utilizing this value, 7.61 ± 1.18, 2.14 ± 2.19, -15.3 ± 12.4 and -165.7 ± 17.7 kJ mol^{-1} are obtained for Δh_0, Δh_1, Δh_2 and Δh_3, respectively. Accordingly it is inferred that the change in the apparent molar heat change as a fucntion of hydrochloric acid concentration is mainly due to that in the distribution of the species $ZnCl_j^{(2-j)+}$ in aqueous phase.

Diluent Effect on Heat Change. The values of valuable Y obtained for other diluents used in this study, which are estimated using a set of Δh_j obtained for benzene, are compiled in Table 1. By assuming a regular solution, the change in enthalpy associated with the extraction of zinc(II) is expressed as

$$(6) \qquad Y = -2V_e\phi_e^2(\delta_d - \delta_e)^2 - V_c\phi'^2_d(\delta_d - \delta_c)^2 + \text{const},$$

where ϕ_d and ϕ'_d refer to the volume fractions of diluent. This provides the equation

$$(7) \qquad (Y - Y_s) / (\delta_d - \delta_s) = (V_c\phi'^2_d - 2V_e\phi_d^2)(\delta_d + \delta_s) + 2(2V_e\phi_d^2\delta_e - V_c\phi'^2_d\delta_c)$$

in which s stands for the diluent chosen as standard. Plots of $(Y - Y_s)/(\delta_d - \delta_s)$ *vs.* $(\delta_d + \delta_s)$ using nitrobenzene as standard give a straight line with a slope of -4.7 and an intercept of 75 in the extraction by TOMAC in various diluents except 1,2-dichloroethane, as illustrated in Figure 3. From this it is presumed that the extraction behaviour of zinc(II) by TOMAC follows the regular solution theory. In the extraction by TOAHCl, in contrast, it is seen that euation (7) is not satisfied, suggesting that non-random interactions between diluent and R_3NHCl and/or between diluent and the species $(R_3NH)_2ZnCl_4$ are present.

Moreover, a linear relationship between the apparent molar heat change and the heat of solution $\Delta Q_{s,TOMAC}$ for TOMAC is obtained except carbon tetrachloride: the plots of ΔQ at 1 M HCl *vs.* $\Delta Q_{s,TOMAC}$ give the straight line with a slope of 0.75. As the heat change arising from the reactions (5) is independent on the kind of diluent, the slope close to unitiy shows that the solvation of TOMAC into organic solvent is more important for the extraction of zinc(II) than that of the organic species $(R_3R'N)_2ZnCl_4$. These facts also indicate that the solutions of TOMAC in organic solvents are regarded as regular solutions. In the case of TOAHCl, the heat of solution does not correlate with the solubility parameter. No simple relation exists between the heat of solution and the dipole moment and dielectric constant of diluent which represent the polarities of molecule and solution, respectively.

CONCLUSION

From the distribution data of zinc(II) between hydrochloric acid solutions and solutions of TOAHCl or TOMAC in various diluents, it is found that in the extraction by TOMAC the distribution coefficient depends on the solubility parameter, while in the extraction by TOAHCl any clear-cut relation does not hold between the distribution behaviour and the physico-chemical properties of diluent. Calorimetry also supports these findings and proves that unsuccessful interpretation with the regular solution theory is ascribed to non-random interaction between diluent and TOAHCl.

ACKNOWLEDGEMENT

We are grateful to National Science Fundation, given by the Ministry of Eduction, Science and Culture, for support of this research through Grant-in-Aid for Scientific Research (No.554183).

REFERENCES

1. T.Sato, J.Inorg.Nucl.Chem.,27,1399(1965);30,1065(1968).
2. O.V.Singh and S.N.Tandon, J.Inorg.Nucl.Chem.,36,439(1974).
3. W.Smulek and S.Siekierski, J.Inorg.Nucl.Chem.,24,1651(1962); S.Siekierski and R.Olszer, J.Inorg.Nucl.Chem.,25,1351(1963).
4. V.M.Vdovenko, T.V.Kovaleva and M.A.Ryazanov, Radiokhimiya,7,133(1965).
5. H.A.Mottoland and H.Freiser, Talanta,13,55(1966);14,864(1967).
6. M.Leszko and W.Zaborska, Rocz.Chim.,51,1961(1977).
7. K.Akiba, M.Wada and T.Kanno, J.Inorg.Nucl.Chem.,43,1031(1981).
8. T.Kojima, T.Ukon and H.Fukutomi, Bull.Res.Lab.Nucl.React.,4,31(1979).
9. T.Sato, T.Nakamura and T.Fujimatsu, Bull.Chem.Soc.Jpn.,54,2656(1981).
10. T.Sato, T.Nakamura and M.Kuwahara, Chem.Lett.,731(1982); T.Sato, T.Nakamura and M.Kuwahara, "Proc. Symposium on Solvent Extraction of Metals, Hamamatsu, 1981", p.1(1981).
11. Y.Marcus and Z.Kolarik, J.Chem.Eng.Data,18,155(1973).
12. Y.Marcus and Z.Kolarik, Inorg.Nucl.Chem.Lett.,10,275(1974).
13. Y.Marcus and Z.Kolarik, J.Inorg.Nucl.Chem.,38,1069(1976).
14. A.S.Kertes and F.Grauer, J.Inorg.Nucl.Chem.,40,1781(1978).
15. F.Grauer and A.S.Kertes, J.Chem.Eng.Data,18,405(1973).
16. A.S.Kertes and E.F.Kassierer, Inorg.Chem.,11,2108(1972).
17. T.Sato, J.Appl.Chem.,15,10(1965).

18. T.Sato and H.Watanabe, Anal.Chim.Acta,49,463(1970).
19. T.Sato, K.Adachi, T.Kato and T.Nakamura, Sep.Sci.Technol.,17,1565(1982).
20. T.Sato and S.Murakami, Anal.Chim.Acta,82,217(1976).
21. T.Sato and T.Kato, J.Inorg.Nucl.Chem.,39,1205(1977).
22. G.Sibona, F.Orlandini and P.R.Danesi, J.Inorg.Nucl.Chem.,28,1318(1966).
23. E.g., H.M.N.H.Irving and A.D.Damodaran, Anal.Chim.Acta,48,267(1969).
24. T.Sato, H.Watanabe and S.Kikuchi, J.Appl.Chem.Biotechnol.,25,63(1975).
25. V.I.Goncharov, L.Kh.Genov, V.V.Sergievskii and G.A.Yagodin, Radiokhimiya,21, 563(1977).
26. T.Sato, T.Nakamura and M.Kuwahara, Solvent Extraction and Ion Exchange, (under the contribution).

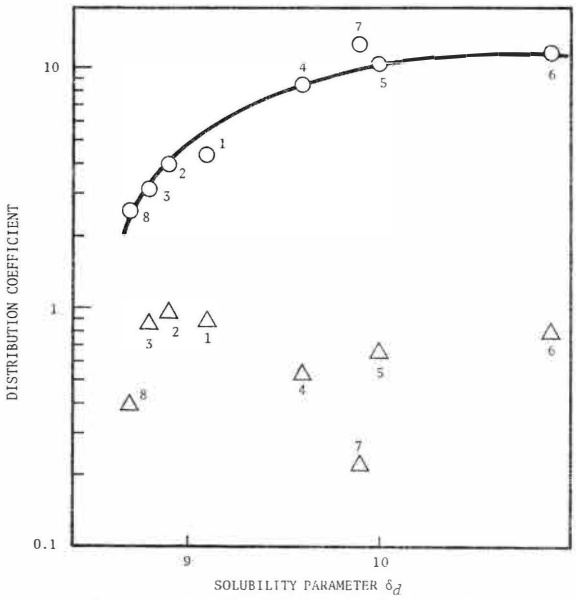

FIGURE 1. DEPENDENCE OF THE DISTRIBUTION COEFFICIENT ON THE SOLUBILITY PARAMETER OF DILUENT FOR THE EXTRACTIONS FROM 0.1 M HYDROCHLORIC ACID SOLUTION WITH 0.05 M TOAHCl (△) AND FROM 0.05 M HYDROCHLORIC ACID SOLUTION WITH 0.05 M TOMAC (○): 1) BENZENE, 2) TOLUENE, 3) *m*-XYLENE, 4) CHLOROBENZENE, 5) *o*-DICHLOROBENZENE, 6) NITROBENZENE, 7) *1,2*-DICHLOROETHANE, 8) CARBON TETRACHLORIDE

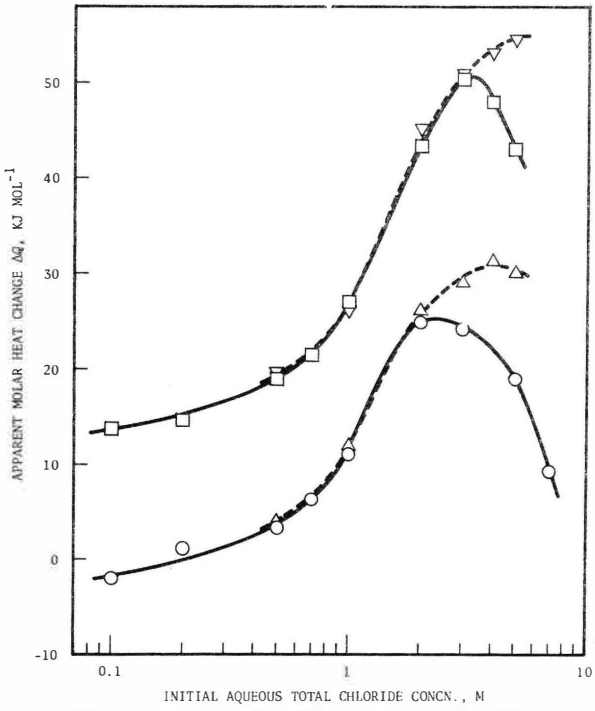

FIGURE 2. APPARENT MOLAR HEAT CHANGE IN THE EXTRACTION OF ZINC(II) FROM AQUEOUS SOLUTIONS CONTAINING HYDROCHLORIC ACID AND/OR LITHIUM CHLORIDE WITH 0.05 M TOAHCl (□,▽) OR 0.05 M TOMAC (○,△) IN BENZENE AT 25 °C AS A FUNCTION OF AQUEOUS CHLORIDE CONCENTRATION (□ AND ○ HCl ONLY: ▽ AND △ 0.01 M HCl + LiCl).

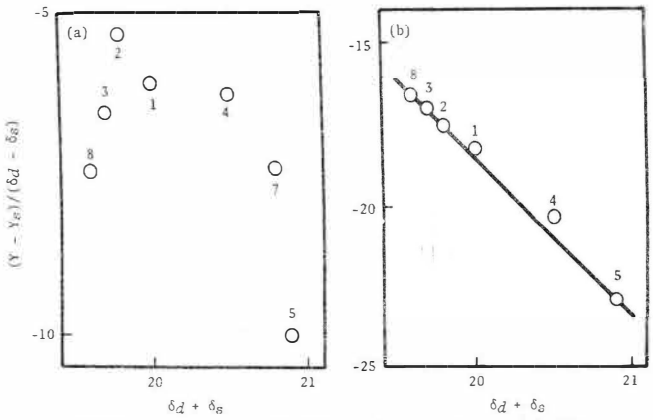

FIGURE 3. CORRELATION BETWEEN $(Y - Y_s)/(\delta_d - \delta_s)$ AND $(\delta_d + \delta_s)$ FOR THE EXTRACTION OF ZINC(II) FROM 1 M HYDROCHLORIC ACID SOLUTION WITH 0.05 M TOAHCl (a) AND 0.05 M TOMAC (b) IN VARIOUS DILUENTS: 1) BENZENE, 2) TOLUENE, 3) *m*-XYLENE, 4) CHLOROBENZENE, 5) *o*-DICHLOROBENZENE, 7) *1,2*-DICHLOROETHANE, 8) CARBON TETRACHLORIDE

TABLE 1. THE VALUES OF Y (KJ MOL^{-1}) OBTAINED FOR THE EXTRACTION OF ZINC(II) BY TOAHCl AND TOMAC IN VARIOUS DILUENTS

DILUENT	VARIABLE Y		SOLUBILITY PARAMETER δ_d
	TOAHCl	TOMAC	
C_6H_6	-19.6	-3.4	9.1
$C_6H_5CH_3$	-19.9	-1.26	8.9
m-$C_6H_4(CH_3)_2$	-16.8	-0.64	8.8
C_6H_5Cl	-22.4	-10.0	9.6
o-$C_6H_4Cl_2$	-21.5	-15.8	10.0
$C_6H_5NO_2$	-30.5	-36.4	10.9
$1,2$-$C_2H_4Cl_2$	-23.1	-41.1	9.9
CCl_4	-14.1	0.01	8.7

MONOLAYER STUDIES OF SOLVENT EXTRACTION REAGENTS

D. J. Chaiko and K. Osseo-Asare

Mineral Processing and Metallurgy Programs
The Pennsylvania State University
University Park, Pennsylvania 16802 USA

INTRODUCTION

A review of the solvent extraction literature reveals a distinct lack of systematic interfacial studies. Much of the data available to date deals with interfacial tension measurements and is either incomplete with regard to experimental conditions or the effects of impurities leave any interpretation questionable when commercial reagents and diluents have been used without purification.

In an effort to address this problem, a research program has been initiated involving a study of the interfacial chemistry of solvent extraction reagents using a variety of techniques and carefully purified reagents and diluents. This paper reports some initial results of interfacial pressure measurements using a film balance technique.

The film balance approach (Figure 1), based on the manipulation of spread monolayers, provides a convenient method of depositing molecules in an oriented manner as a monomolecular film at either the liquid/liquid or the liquid/gas interface. Through movement of the film barrier (Figure 1), the surface density of the monomolecular film can be controlled experimentally with a high degree of accuracy. An automated film balance allows the measurement of film pressure (π) during continuous film compression or expansion which can be recorded as a π-area isotherm. Other film characteristics which can be measured include interfacial viscosity and interfacial potential (1-2).

A few of the many areas of study which have employed monolayer techniques include the investigation of biological membrane structure and function (3-4), evaporation control (5), corrosion inhibition (6) and mineral flotation (7). However, until recently (8,9), the only published film balance study done specifically in the context of solvent extraction research was that due to Hunt (10) on the interaction of alkylphosphate monolayers with rare-earth metals.

EXPERIMENTAL

Reagents. Dinonylnaphthalene sulfonic acid (HDNNS), received from King Industries, was purified according to the method of Danesi et al (11). The anti-isomer of 5,8-diethyl-7-hydroxy-6-dodecanone oxime was isolated from the commercial reagent LIX63 (a product of Henkel) using the copper oximate technique described previously (12). The commercial reagent LIX65N (a product of Henkel), was purified by a method similar to that of Preston and Whewell (13) to give the anti-isomer of 2-hydroxy-5-nonylbenzophenone oxime. The anti-isomer of LIX65N was stored as the copper oximate until just prior to spreading when the oximate was stripped to generate the free oxime. Thin Layer chromatography indicated the presence of a small amount of syn-isomer although this amount was not quantified. Spreading samples were 10^{-3} kmol m^{-3} in spectrograde n-hexane. Monolayers were spread on an aqueous subphase containing 0.1 kmol m^{-3} KNO_3 at pH 2.5. KNO_3 was purum grade purchased from Fluka Chemical Co. Double distilled water was obtained from a Corning Model AG-11 glass still.

Apparatus and Methods. Pressure-area (π-A) isotherms were obtained with a Lauda film balance at 20.0±0.1°C and under a nitrogen atmosphere. Before spreading a monolayer, the aqueous subphase was prepared by sweeping the surface several times with teflon barriers. After a monolayer was spread, three minutes were allowed for evaporation of the spreading solvent before continuous film compression at a rate of 0.04 nm^2 $molecule^{-1}$ min^{-1}. The initial area per molecule of all spread monolayers was just over 1.9 nm^2.

RESULTS

The π-A isotherms obtained at the air/water interface for HDNNS, LIX63 and LIX65N are shown in Figure 2. As a reference, the structures of these molecules are shown in Figure 3. During compression, white streaks became visible on the aqueous surface at film pressures above 30 mN m^{-1} for HDNNS and 25 mN m^{-1} for the oximes. Compression of the HDNNS film above 19 mN m^{-1} resulted in a change of the miniscus shape from convex to concave at the compression barrier and continued compression eventually led to overflow at the trough edges.

The area per molecule that is obtained by extrapolating the linear part of the π-A curve back to π=0 for HDNNS is 1.21 nm^2. This limiting area is comparable with the value of 1.0 nm^2 obtained by Keeney and Osseo-Asare (8); however, it is considerably larger than the value of 0.27 nm^2 reported for 2-(n-tetradecyl) naphthalene sulfonate (13). It is likely that the presence of a mixture of structural isomers in our particular HDNNS sample prevents close packing of the naphthalene groups even at high film pressures. The limiting areas for LIX63 and LIX65N are 0.99 nm^2 and 0.81 nm^2 respectively. The π-A isotherms of HDNNS and LIX65N are of the liquid condensed type whereas the isotherm for LIX63 is liquid expanded. Collapse pressures for LIX65N and LIX63 were estimated at the point where ($-\gamma\pi/\gamma A$) began to decrease. The collapse pressure for LIX65N was about 17.2 mN m^{-1} and corresponds to a molecular area (A_c) of 0.62 nm^2. The collapse pressure for LIX63 was about 9.5 mN m^{-1} indicating that LIX63 monolayers are fairly unstable. The LIX63 film collapsed at an area (A_c) of 0.77 nm^2. The HDNNS isotherm did not exhibit a collapse point.

CONCLUSION

Contrary to a report at the 1977 International Solvent Extraction Conference (15) indicating that o-hydroxyoximes do not spread at the air/water interface, this study indicates that it is indeed possible to obtain oxime monolayers at the air/water interface. Based on the structural similarities between LIX65N and LIX70, SME529, and P50, it is likely that these o-hydroxyoximes will also form spread monolayers.

An area of 0.834 nm^2 has been reported by Flett (16) for LIX65N at the heptane/water interface and 1.14 nm^{-2} at the toluene/water interface. The limiting area (A_o) of 0.81 nm^2 for LIX65N in Figure 2 suggests that the orientations at the air/water and heptane/water interfaces are similar. There is also a close relationship between the interfacial area of LIX63 at the oil/water interface and the limiting area of 0.99 nm^2 obtained in Figure 2. Al-Diwan et al (17) have calculated an interfacial area of 1.01 nm^2 for LIX63 at the hexane/water interface and 1.76 nm^2 at the toluene/water interface.

It appears that LIX65N and LIX63 exhibit a similar orientation at the air/water and oil/water interfaces when the oil phase exhibits poor solvating properties toward the compound in question. This suggests that a study of extractant monolayers at the air/water interface is not totally unrelated to interfacial processes occurring during the liquid-liquid extraction of metals. Of course, great care must be exercised in extrapolating information from one interfacial system to another.

Working at the air/water interface avoids the experimental difficulties associated with monolayer studies at the liquid/liquid interface (18-20). However, in view of the fact that solvent extraction involves two liquid phases, it is hoped to eventually extend these studies to liquid/liquid systems using a Brooks film balance (18).

The Langmuir trough approach offers several advantages over interfacial tension measurements which include the ability to systematically alter the area per molecule and the measurement of surface potentials and surface viscosities. Furthermore, techniques have been developed which allow the interfacial crystallography and morphology to be studied (2). Reaction products between spread monolayers at the air/water interface and aqueous metal ions can be identified after transfer to an appropraite solid using the Blodgett method (2).

ACKNOWLEDGMENT

Support of this work by the U.S. National Science Foundation is gratefully acknowledged.

REFERENCES

1. J. T. Davies and E. K. Rideal, Interfacial Phenomena, Second Edition, Academic Press, New York (1963).
2. G. L. Gaines, Jr., Insoluble Monolayers at Liquid-Gas Interfaces, Interscience Publishers, New York (1966).
3. H. Davson and J. F. Danielli, Permeability of Natural Membranes, Cambridge University Press, Second Edition (1952).
4. B. A. Pethica, Structural and Functional Aspects of Lipoproteins in Living Systems, E. Tria and A. Scanu, Editors, Academic Press, New York, p. 37 (1969).
5. V. K. LaMer, Ed., Retardation of Evaporation by Monolayers: Transport Processes, Academic Press, New York (1962).
6. J. H. Schulman, R. B. Waterhouse and J. A. Spink, Kolloid. Z., 146, 77 (1956).
7. J. Leja, Proceedings of the Second International Congress of Surface Activity, Vol. III, Academic Press, New York, p. 273 (1957).
8. M. E. Keeney and K. Osseo-Asare, Polyhedron, 1, 541 (1982).
9. R. A. Uphaus, G. F. Vandegrift, and E. P. Horwitz, J. Colloid Interface. Sci., 90, 380 (1982).
10. E. C. Hunt, J. Colloid. Interface Sci., 29, 105 (1969).
11. P. R. Danesi, R. Chiarizia, and G. Scibona, J. Inorg. Nucl. Chem., 35, 3926 (1973).
12. K. Osseo-Asare and M. E. Keeney, Metal. Trans. B., 11B, 63 (1980).
13. J. S. Preston and R. J. Whewell, J. Inorg. Nucl. Chem., 39, 1675 (1977).
14. K. D. Dreher and P. S. Ossip, J. Colloid. Interfac. Sci., 46, 442 (1974).
15. M. Cox and D. S. Flett, Proceedings of the International Solvent Extraction Conference, Vol. I, Canad. Inst. Min. Metal., Toronto, p. 63 (1979).
16. D. S. Flett, Acc. Chem. Res., 10, 99 (1977).
17. T. A. B. Al-Diwan, M. A. Hughes and R. J. Whewell, J. Inorg. Nucl. Chem., 39, 1419 (1977).
18. J. H. Brooks and B. A. Pethica, Trans. Farad. Soc., 60, 1 (1963).
19. J. A. G. Taylor, J. Mingins, B. A. Pethica, B. Y. J. Tan, and C. M. Jackson, Biochem. Biophys. Acta., 323, 157 (1973).

20. J. Mingins, J. A. Grodon, B. A. Pethica, C. M. Jackson and B. Y. T. Yue, J. Chem. Soc. Farad. Trans., 78, 323 (1982).

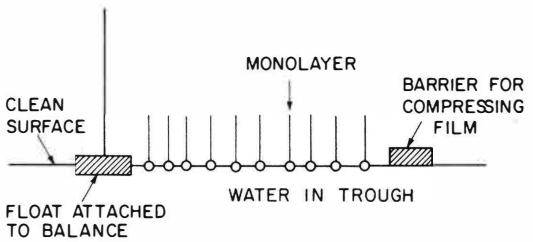

FIGURE 1. SCHEMATIC ILLUSTRATION OF THE LANGMUIR FILM BALANCE (2).

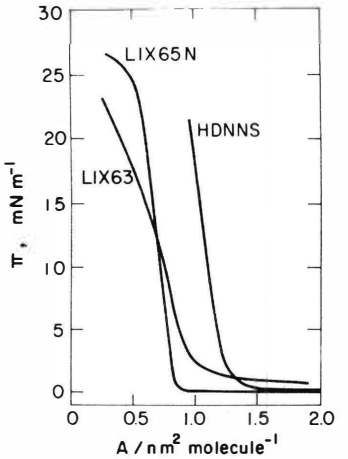

FIGURE 2. π-A ISOTHERMS FOR PURIFIED LIX63, LIX65N, AND HDNNS AT THE AIR/WATER INTERFACE. SUBPHASE: 0.1 kmol m^{-3} KNO_3, pH 2.5 AT 20°C.

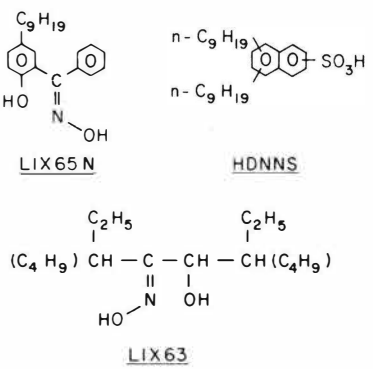

FIGURE 3. STRUCTURE OF LIX63, LIX65N, and HDNNS.

ELECTROPHORETIC MOBILITY STUDIES IN LIQUID-LIQUID EXTRACTION SYSTEMS

K. L. Lin and K. Osseo-Asare

Metallurgy Program
Department of Materials Science and Engineering
The Pennsylvania State University
University Park, Pennsylvania 16802 USA

INTRODUCTION

As a result of the low aqueous solubility of the commercial solvent extraction reagents, the encounter between the aqueous phase metal ions and organic extractants is likely to take place at the organic/aqueous interfacial region.

The interfacial activity of solvent extraction reagents is now widely recognized. However there has been a tendency to limit the experimental analysis of the interfacial characteristics of solvent extraction systems to interfacial tension measurements. In this paper, electrophoretic mobility results are presented which demonstrate that the ability of certain extractants to impart a charge to the organic/water interface may have significant effects on the observed metal extraction behavior.

EXPERIMENTAL

The diluents utilized were spectrograde hexane and toluene. Purified reagents were obtained from the commercial extractants by using the procedures of Tammi(1) for LIX63, Danesi et al. (2) for HDNNS, McDowell et al. (3) for HEDHP (di-(2-ethylhexyl) phosphoric acid) and Sato et al. (4) for Aliquat 336 (tricaprylmethyl ammonium chloride). All other chemicals were reagent grade and were used without further purification. The aqueous solutions were prepared with double-distilled water and contained 4×10^{-3} kmol m^{-3} KNO_3 for ionic strength control. The pH values were varied with KOH and HNO_3.

Electrophoretic mobility (EM) was measured with a Riddick Zeta Meter. The organic phase (0.35 ml. of hexane solution or 0.50 ml. of toluene solution) was dispersed in 500 ml. of aqueous solution by means of a 90 minute treatment with a wrist action shaker. The zeta potential (ζ), the potential at the plane of shear, was obtained from Equation (1), according to the Smoluchowski equation (5).

(1) ζ (mV) = 12.86 x EM (μm. sec. $^{-1}$/V cm^{-1})

RESULTS

Hexane and Toluene Systems. The EM of pure hexane and toluene droplets is shown in Figure 1. It is evident that the organic droplet surfaces are negatively charged in the pH range considered (i.e. pH > 3). The magnitude of EM increases with increasing pH value. At low pH, the toluene system has a higher EM than the hexane system.

Extractant - Hexane Systems. The EM results of various extractant-hexane systems are indicated in Figure 2. The hydroxyoxime reagent, LIX63, has very little effect on the EM of hexane. On the other hand, the extractants HDNNS and HDEHP impart a highly negative interfacial charge even at pH values as low as 3.

In the presence of the basic extractant, Aliquat 336, the charge at the organic/acqueous interface becomes less negative and even attains a positive value as the pH is decreased and the extractant concentration is increased. A mixture of HDNNS-Aliquat 336, (the respective concentrations being the same as those for which extraction antagonism was previously reported (6) i.e. 7×10^{-3} kmol m^{-3} Aliquat 336 and 1.4×10^{-4} kmol m^{-3} HDNNS, gives a positive charge to the hexane/water interface throughout the whole experimental pH range, (see Figure 2).

DISCUSSION

Hexane and toluene droplets are generally negatively charged. This negative surface charge results from the preferential adsorption of hydroxyl ions. The aromatic diluent, toluene, exhibits a more negatively charged interface compared with the aliphatic diluent, hexane. The aromatic double bond present in toluene has a higher affinity for hydroxyl ions and induces a greater surface charge. The adsorption of extractant molecules further modifies the interfacial charge. The surface charge induced by the adsorption of a surface active compound is strongly dependent on the degree of dissociation of the surfactant at the interface and on the type of end groups on the molecule. HDNNS and HDEHP are both acidic reagents and give highly negatively charged interfaces. However, the HDNNS systems is more negatively charged than that of HDEHP since HDNNS (pKa = 0.57 for naphthalenesulfonic acid (7)) is more acidic than HDEHP (pKa = 3.49 (8)). Increase in pH enhances the degreee of surface dissociation of these acidic surfactants. Nevertheless, due to the limit in the available surface area for occupation, a maximum amount of surface charge is expected to occur at a certain high pH value. Further increase in hydroxyl ion concentration would likely force the end groups at the interface back into the organic phase through electrostatic interaction. Aliquat 336, because of its basic character and its quaternary ammonium end group, gives a positive surface charge.

Electrostatic Interaction--Preliminary Step of Metal Extraction. The synergic extraction of nickel by LIX63-HDNNS mixtures at low pH (9,10) and the inhibition effect of Aliquat 336 on metal extraction by acidic reagents (6) can be further understood through the EM results. At pH3, the organic/aqueous interface is neutral for the LIX63-Hexane system, negatively charged for the HDNNS-hexane system and the LIX63-HDNNS-hexane systems; and positively charged for the Aliquat 336-hexane system. It seems reasonable therefore to suggest that in metal extraction by LIX63-HDNNS mixtures, the observed increase in extraction rate is related to the attraction of the positively charged metal ions to the negative interfacial charge. Thus the initial step of metal extraction by this system may be an electrostatic interaction between the metal ions and the negative interfacial charge, as shown in Figure 3. The antagonism in the presence of Aliquat 336 can then be attributed to a repulsion of the approaching cation by the positively charged organic/aqueous interface.

ACKNOWLEDGMENT

Support of this work by the U.S. National Science Fundation is gratefully acknowledged.

REFERENCES

1. T. T. Tammi, Hydrometallurgy, Vol. 2, pp. 371-380, 1976/1977.
2. P. R. Danesi, R. Chiarizia and G. Scibona, J. Inorg. Nucl. Chem., Vol. 35, pp. 3926-3928, 1973.
3. W. J. McDowell, P.T. Perdue and G. N. Case, J. Inorg, Nucl. Chem., Vol. 38, pp. 2127-2129, 1976.
4. T. Sato and H. Watanabe, Analytica Chimica Acta, Vol. 49, pp 463-471 1970.
5. D. C. Henry, Proc Roy, Soc., A133, pp. 106-129, 1931.
6. K. Osseo-Asare and M. E. Kenney, Proceedings ISEC '80, Liege, Belgium, Paper No. 80-121, 1980.
7. Handbook of Chemistry and Physics, p. D-150, 56th Ed., CRC press, Cleveland, Ohio.
8. G. F. Vandegrift and E. P. Horwitz, J. Inorg. Nucl. Chem., Vol. 42, pp. 119-125, 1980.
9. K. Osseo-Asare, H. S. Leaver and J. M. Laferty: pp. 195-207 in Process and Fundamental Considerations of Selected Hydrometallurgical Systems, M. C. Kuhn, ed.; SME-AIME, New York, 1981.
10. K. Osseo-Asare and M. E. Keeney, Metal. Trans. B, Vol. 11B, pp. 63-67 (1980).

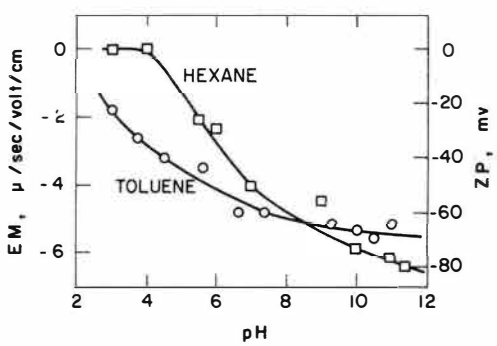

FIGURE 1. ELECTROPHORETIC MOBILITY OF HEXANE AND TOLUENE DROPLETS.

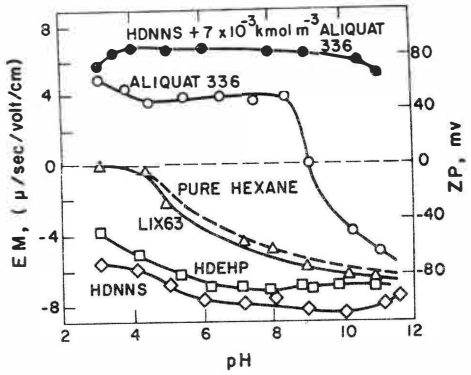

FIGURE 2. ELECTROPHORETIC MOBILITY OF SOLVENT EXTRACTION SYSTEMS. [HDNNS] = 1.4x10^{-4} kmol m^{-3}, [REAGENT] = 1.5x10^{-4} kmol m^{-3}.

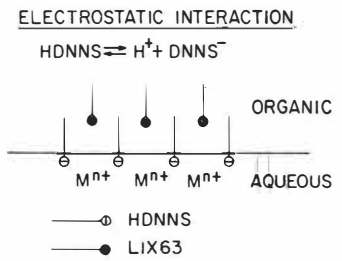

FIGURE 3. ELECTROSTATIC INTERACTION-PRELIMINARY STEP OF METAL EXTRACTION BY LIX63-HDNNS.

THE THEORETICAL AND EXPERIMENTAL INVESTIGATION OF THE SEPARATION OF RARE EARTH ELEMENTS BY ALKYLAMMONIUM SALTS

A. A. Kopyrin, V. V. Proyaev

Lensoviet Institute of Technology
Leningrad, USSR

Long chain tertiary amines and quaternary ammonium salts are perspective extractants for extraction and purifying of radioactive isotopes of rare earth elements (REE) (1). The high radiation stability of amines and good selection have to be taken into account. The metal extraction by amines is carried out from acid media. Therefore salts of ammonium inclined to self-association in non polar dissolvents because of strong depole-depole interactions take part in extraction.

The distribution in systems with association extractants has a number of peculiarities, connected with formation of a number of associates of extractant and extracting complexes in the organic phase (2). The association of the extractant is a cause of essential deflexions of organic phase from ideal and complicates the quantitative description of extraction equilibria.

The possible way of overcoming the arising difficulties is given in the work (3). The process of association in the organic phase is characterized by constants of association determined from independent data. Activity coefficients in organic phase ($\bar{\gamma}_A^n / \bar{\gamma}_{MA_n}$) are calculated theoretically. We used the method of "plurality of interactions in the organic phase" for working out the extraction model of REE by salts of alkylammonium (4).

The extraction of lanthanids by salts of alkylammonium is regarded as a totality of following reactions in organic phase:

$$\nu \bar{A}_1 + M \overset{K_\nu}{\rightleftharpoons} \overline{MA_\nu}$$

(1) $$\overline{MA_\nu} + A_1 \overset{\beta_{M_1}}{\rightleftharpoons} \overline{MA_{\nu+1}}$$

$$\overline{MA_{j-1}} + \bar{A}_1 \overset{\beta_{M_j}}{\rightleftharpoons} \overline{MA_j}$$

where A_1 is the monomer molecule of alkylammonium salt; M is the nitrate complex of REE answering for the distribution in the water phase.

As the first approach we consider that the constants of the additional solvation of metalcontaining complexes by free alkylammonium nitrate molekules for the first and the second coordination spheres (β_M) are not equal to the associative constants of the extractant (β). This difference is characterized by the parameter b:

(2) $$b = \beta_M / \beta,$$

beginning with the third solvate layer $b = 1$.

According to the given scheme the concentration of any complex of the distributing metal with extractant in the organic phase may be calculated by the equation:

(3) $$[\overline{MA_K}] = a_M [\overline{A_1}]^k \bar{\gamma}_{A_1}^k / \bar{\gamma}_{MA_K} \cdot K_\nu (b\beta)^{K-\nu}$$

Associative constants of alkylammonium salts were determined from independent cryoscopic measurements (1). The concentration of monomer molecules of alkylammonium salt was calculated according to the equation of material balance of extractant. In the case of extraction of microquantities of REE, the equilibrium concentration of alkylammonium salt is equal to outcoming and is determined by the equation:

(4) $$C_A = \Sigma_i [\overline{A_i}] = [\overline{A_1}] / (1 - \beta [\overline{A_1}])^2$$

Extraction constants K_ν and parameters b are calculated by the method of variation of parameters.

The associative constants of alkylammonium salts were determined by using different versions of the generalized theory of association equilibria (3). Activity coefficients of associates of the extractant and extracting complexes in the organic phase were calculated also on the base of the generalized theory of association equilibriums, according to the equation:

(5) $$\ln(\bar{\gamma}_{A_1}^k / \bar{\gamma}_{MA_K}) = k[\ln(m_S / \sum_D q_D m_D) + V_1(2-V_1)\omega_{12}/(RT)] - m_S / \sum_D q_D m_D - V_1(2-V_1)\omega_{12}/(RT) - R_M(z/2-1) \times \left\{ \ln[q_S \sum_D R_D m_D / (R_S \sum_D q_D m_D)] + V_1(2-V_1)\omega_{12}/(RT) \right\}$$

where m_D is the concentration of the component D (mol/1000g of the solvent); S is the index of solvent molecules; q_D is the parameter taking account of the form and the size of molecules of the component D; V_1 is part of contact sections of the type I from all particles in the solution; ω_{12} is the parameter of interchange; R_M, R_S are the quantity of places of quasi lattice of the solution occupied by the distributing complex of the metal and the molecule of the solvent accordingly.

Parameters of the interchange ω_{12} and assotiative constants β necessary for the calculation of the ratio of coefficients of activity in the organic phase were determined from independent crioscopic measurements. Obtained values ω_{12} and β are presented in table I.

Table I.

The associative constants β and parameters of enterchange ω_{12} of alkylammonium nitrates.

Alkylammonium salt	β, (mol/kg solvent)$^{-1}$	ω_{12} J/mol
Tri-n-octylammonium nitrate	19 ± 1	-(230 ± 20)
Methyl-di-n-octylammonium nitrate	50 ± 5	-(270 ± 30)
Tri laurilammonium nitrate	16 ± 1	-(120 ± 20)

Values of the extraction constante K_Y and parameters b calculated with the supposition $Y_{max}=3$, are given in table 2.

Table 2.

Extraction constants K_Y and parameters b describing the extraction nitrates of cerium (III) and europium by solutions of alkylammonium nitrates in p-xylene from 7,0 M solution of lithium nitrate

Parameter	Metall	$TON \cdot HNO_3$	$TLN \cdot HNO_3$	$MDONHNO_3$
K_1	Ce(III)	0.33 ± 0.08	1.14 ± 0.06	0.06 ± 0.01
	Eu	0.08 ± 0.02	0.50 ± 0.05	0.02 ± 0.01
K_2	Ce(III)	2.1 ± 0.1	0.8 ± 0.1	0.8 ± 0.1
	Eu	0.5 ± 0.1	0.4 ± 0.1	0.25 ± 0.10
K_3	Ce(III)	0.06 ± 0.01	0.40 ± 0.07	5.0 ± 0.4
	Eu	0.02 ± 0.01	0.20 ± 0.06	2.2 ± 0.2
b	Ce(III)	9.8 ± 0.3	6.8 ± 0.1	17.0 ± 0.5
	Eu	8.2 ± 0.1	6.0 ± 0.1	16.0 ± 0.8

High values of the parameters b testify to the considerable strengthening of the association around the metal-containing complexes. This is confirmed by the crioscopic measurements qualitatively. The saturation of the organic phase by the metal leads to the decrease of the temperature depression of the solution that is connected with the decrease of the quantity of particles in the system.

Data of the thin layer chromotogracher and IR-spectroscopy of saturate extracts can serve the confirmation of the additional solvatation of the extracting complexes .

The calculations of theoretical extraction isoterms show that it is necessary to take into account the possibility of formation of polynuclear complexes in the organic phase with increasing of the metal concentration. Our model of extraction was used for investigation of the influence of macroamounts of one lanthanide on the distribution of microamounts of another at the extraction by alkylammonium salts. It was established that the distribution of a microelement is determined in the main by two factors: the competition of metals for the extractant and the formation of polynuclear complexes in the organic phase. The effect "of common ion", playing a main role in chloride systems with phosphorus organic extractants, is displayed feebly.

The systematic study of the influence of the processes in the water phase on the extraction of REE by alkylammonium salts included the investigation of dependence of distribution coefficients and separation factors on the nature and concentration of salting-out agents, pH of water solution and the presence complexing additions. The most essential factor is the introduction of complexons. Separation factors of the pairs of REE are increased considerably. The maximum separation of the pairs of lanthanides of the cerium subgroup at the extraction by the solutions of nitrate tri-n-octyl ammonium has been achieved in the presence of diethylentriaminopentaacetic acid (DTPA) [5].

To determine conditions of the separation of REE in extraction systems with amines in the presence of complexones it is necessary to choose the area of pH of the optimum separation. The separation of indicator quantities of REE in the presence of DTRA is described by the equation:

$$\alpha'_{1,2} = \alpha_{1,2} \frac{1+(\beta_0''+\beta_1''[H]+\beta_2''[H]^2)C_L^0/A}{1+(\beta_0'+\beta_1'[H]+\beta_2'[H]^2)C_L^0/A} \quad (6)$$

$\alpha'_{1,2}, \alpha_{1,2}$ are separation factors of elements I and 2 in the presence and the absence of complexone; β_i are constants of stability of complexe of REE with complexone; A is the value, depending from pH of the equilibrium water phase; C_L^0 is the equilibrium concentration of complexone.

Values of stability constants of REE complexes with complexone in concentrate solutions of salting-out agents were determined by the extraction and potentiometric methods calculated and experimental values of separation factors of some pairs of REE and pH, corresponding optimum conditions of the separation, are presented in tables 3 and 4.

Table 3.

Separation factors of pair Ce-Pm at the extraction by 0.2 M solution of nitrate tri-n-octylammonium in -xylene from solutions of lithium nitrate in the presence of EDTA

C_{LiNO_3}, mol/l	$\alpha_{1,2}$	$\alpha'_{1,2\,exp}$	$\alpha'_{1,2\,calc.}$	pHexp	pHcalc.
5	3.2	26	31	3.0	3.0
6	3.0	26	28	2.5÷3.0	3.0
8	3.1	30	29	2.0÷2.3	2.3

Separation factors some pairs of REE at extraction by 0,2 M solution of nitrate tri-n-octylammonium from solutions of lithium nitrate in the presence of DTPA

Pair	$\alpha_{1,2}$	$\alpha'_{1,2\,exp}$	$\alpha'_{1,2\,calc.}$	pHexp	pHcalc.
Ce-Pm	3.0	28	24.7	2.4 ÷ 2.5	2.4 ÷ 2.5
Pm-Eu	1.4	6.3	6.2	2.0 ÷ 2.5	1.9 ÷ 2.5
Ce-Eu	5.8	140	152	2.3 ÷ 2.4	2.0 ÷ 2.5

It is clear that calculated and experimental data are in complete agreement. The study of influence of the temperature on the distribution and separation of REE by alkylammonium salts has showed, that in most systems the increasing of the temperature leads to the decreasing of coefficients of distribution and separation factors both in the absence and in the present of complexones.

The conducted investigations give us the possibility to make a number of practical recommendations about the rise of the efficiency of thin purifying of REE at the extraction by alkylammonium nitrates [5].

REFERENCES

1. Shmidt V.S. Extraction by amines. Moscow, Atomizdat (1980).
2. Kopyrin A.A., Komarov E.V., Proyaev V.V. The Theory of Extraction Processes. Leningrad, Lensoviet Institute of Technology (1979).
3. Komarov E.V., Komarov V.N. Uspechi Khimii, 43, No.4, 632 (1974).
4. Kopyrin A.A., Komarov E.V., Proyaev V.V., Afonin M.A. In: Sb. Lensoviet Institute of Technology, Leningrad, 39 (1980).
5. Kopyrin A.A., Murashov V.D. Proc. ISEC'80, 2-11-152.

SCALE-UP OF LIQUID MEMBRANE PERMEATION PLANTS

J. Draxler, R. Marr, A. Bouvier, A. Kriechbaumer, M. Prötsch

Institute of Chemical Engineering
Technical University Graz
Graz, Austria

Since Li's "(1)" discovery that the middle phase of a multiple emulsion acts as a liquid membrane, many possibilities of applications have been found. The most interesting application lays in hydrometallurgy, where Liquid-Membrane-Permeation (LMP) can be seen as an extension to solvent-extraction for extraction and stripping are materialized simultaneously in a single step. But LMP is not only a combination of extraction and stripping carried out one after another; the simultaneousness of these two steps enables by a special mechanism much better separations and enrichments of the metal ions. The carrier, which is the equivalent to the extractant in solvent-extraction, acts as a transport catalyst and LMP is therefore a kinetical controlled process. The state of equilibrium is given by the ratios of the ions to be separated to the stripping agents in both sides of the membrane "(2)"

$$(1) \qquad \left(\frac{C_{A,III}}{C_{A,I}}\right) = \left(\frac{C_{B,III}}{C_{B,I}}\right)^{\gamma}$$

Equation (1) is valid for the counter-transport system. Depending on the concentration of the stripping agent it is in most systems sufficient to reach the equilibrium once; therefore LMP can be seen as a single step process, where only the time to reach the equilibrium is relevant for the mass transport.
Because of the combination of extraction and stripping in one step LMP is a much more complex system than solvent-extraction and is influenced by much more parameters, and therefore an adequate mathematical discription is very difficult and only possible under certain simplified conditions. Several models were developed and most of them assume a diffusional mass transfer as the rate controlling step and use Fick's first "(3,4)" and second law "(2)" to describe the mass transfer. But also reaction models were developed "(5)", assuming that the reaction between the metal ions and the carrier at the outer interface is the rate controlling step. All these models describe the mass transfer in a special system very well, but equally are inadequate to comprise all parameters, which is absolutely necessary for the lay-out of large LMP-plants. For instance with the reaction model "(5)" the influence of the acid concentration in the inner water phase cannot be explained and is therefore not taken into consideration. But there is a great influence of the acid strength, as shown in Figure 1 for the permeation of copper.
For this reason a new attempt was made to describe the mass transfer in very simple terms, but which allow the scale-up of LMP-plants from base experiments. The mass transfer concept, which is widely used in liquid-liquid extraction, describes the mass transfer of the metalions from the outer water phase into the membrane phase. The transport through the membrane is not regarded, neither the enrichment in the inner water phase, which can be calculated by a mass balance.
The advantage of this concept is that it is independent of reaction or diffusion control, the disadvantage that the mass transfer coefficient k cannot be calculated theoretically because of the complexity of the system and must be measured experimentally.

$$(2) \qquad \frac{dC_{III}}{dt} = k.a.\Delta C$$

Formally it is analog to Fick's first law, but the particular terms have a different meaning. k comprises the reaction and diffusion terms as well as all other parameters influencing the mass transfer. a is the specific interface area and ΔC the concentration difference of the metal ions to be separated between the bulk and the interphase. The concentration of the uncomplexed metal ions at the interphase and in the membrane phase is negligible, so that ΔC is represented by the concentration in the bulk phase.

The product k.a is determined experimentally as shown in Figure 2. This value is only representative for this special system and cannot be transfered to other systems and other parameters. The influence of the various parameters can therefore be expressed by different values of k.a and equation (2) is extended to

$$(3) \qquad \frac{dC_{III}}{dt} = k'.a.\Psi_1^n.\Psi_2^m....C_{III}$$

If for instance the carrier concentration, the acid strength in the inner phase, the number of revolutions and the initial concentration are changed it was found that following equation is valid (for copper permeation with LIX 64N):

$$(4) \qquad \frac{dC_{III}}{dt} = k'.RPM^2.[Carrier]^1.[H_I^+]^{0,67}.C_{III,o}^{0}.C_{III}$$

The direct proportionality to the carrier concentration is valid in the range from 0 to 10 wt%, and the initial concentration of the metal ions is without influence on the transport rate. Integration of equation (2) or (4) yields the time to reach a certain degree of separation of the metal ions in the outer water phase.
So far the calculations for the discontinuous stirring vessel, which are similar to equations used in liquid-liquid extraction. For the calculation of continuous permeation plants there must be considered the differences between permeation and extraction.

As expressed by equation (1) Liquid-Membrane Permeation is mostly a single-step process. Therefore it would be inconvenient to use a mixer-settler battery or multistage columns. The repeated coalescence and redispersion expedites only the breakdown of the emulsion without having any influence on the mass transfer. Therefore columns like RDC or Kühni-extractors should not be used "(6)".

From this point of view only a single-step mixer-settler or special columns would be apt for LMP. Single-step mixer-settler cannot manage high throughputs, so we used counter-current columns with various stirring rods but without any internals. Two such columns were built, a smaller one with a throughput of 60 l/h and a large one with a throughpur of 1 m^3/h.

The calculations of the diameter of these columns could be made analog to the concepts used in liquid-liquid extraction, for the hydrodynamic behaviour of the two systems (permeation, extraction) is about the same. Slight differences are given by the use of emulsions as dispersed phase. Emulsion droplets show a smaller coalescence, so a higher holdup is possible, but also larger settlers are required.

The height of a column is given by the mass transfer. In liquid-liquid extraction it is determined by the height and number of transfer units and a certain efficiency. LMP is a single step process; therefore it may be regarded as a reaction system, independent of a possible diffusion control. The residence time to reach equilibrium is relevant for the mass transfer and for the height of the column and is equivalent to the reaction time in equation (2) and (4) resp.

Equation (2) may be used for columns only when all parameters are the same as in the discontinuous stirring vessel. There are no problems to transfer these parameters to columns but one. This is the specific surface area. In discontinuous stirring vessels the specific surface area, which is given by

$$(5) \qquad a = \frac{6x_d}{d_s}$$

is only a function of the number of revolutions because the holdup is constant.

In columns the holdup is not only a function of the stirring speed and droplet size distribution, but also of the throughput

of the continuous and dispersed phase. Thus there is one parameter more than in discontinuous stirring vessels, and the data obtained there must be transfered to columns at the same interfacial area.

Figure 3 shows the holdup vs. stirring speed at different throughputs of the dispersed phase. Together with a sauter mean diameter one can evaluate the specific surface area with equation (5) and calculate the residence time.

For the height of the column, given by equation (6), one needs the velocity of the continuous phase. This one can be calculated with a characteristic velocity, given by equation (7), together with equation (8), which yields the velocity of the dispersed phase and with the phase ratios.

$$H = v_k \cdot \tau_k \tag{6}$$

$$u = \frac{0{,}14\,(g \cdot \Delta\rho)^{0{,}73} \cdot d_s^{1{,}19}}{\rho_k^{0{,}27} \cdot \nu_k^{0{,}46}} \qquad \text{"(7)"}$$

$$\frac{v_d}{u} = \frac{0{,}474}{2 + \lambda} \qquad \text{for } \lambda \leqslant 1 \tag{8}$$

In consideration of the backmixing our two columns were calculated in this way for the separation of zinc out of an industrial waste water. In both columns (diameter: 80 and 150 mm; height: 1,4 and 7 m) the results of the batch experiments could be exactly reproduced.

Although both our columns work countercurrently, one should also consider a co-current column because of some characteristics of LMP. As shown in Figure 4 the transport rate is nearly independent of the metal concentration in the inner water phase as well as in the outer water phase. The driving force is therefore given only by the concentration difference of the auxiliary component (mostly protons) and this one is in counter-current and in co-current columns nearly the same. So the main advantage of counter-current columns is negligible and the advantages of co-current columns (higher throughputs, better control of residence time...) are effective.

CONCLUSIONS

Because of some characteristics of Liquid-Membrane Permeation one cannot use the same extractors as in liquid-liquid extraction.

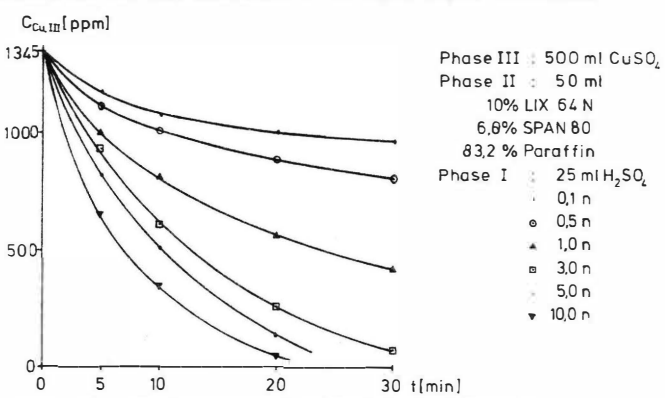

FIGURE 1. INFLUENCE OF ACID CONCENTRATION IN PHASE I

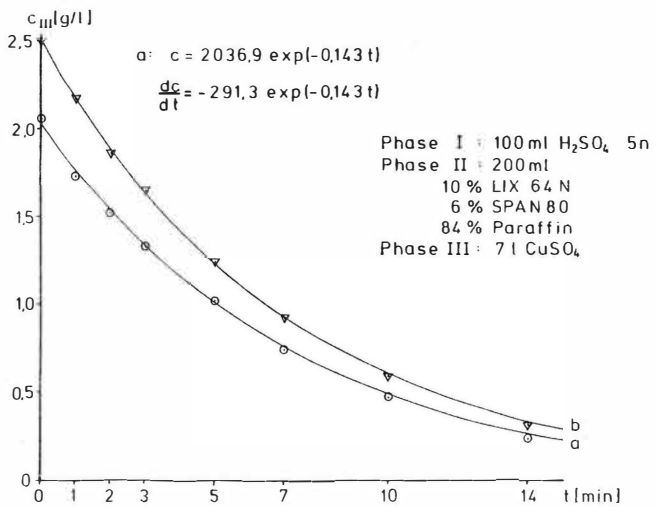

FIGURE 2. EXPERIMENTAL DETERMINATION OF k.a

For our purposes counter-current columns with special stirring rods and without any internals were considered best. Based on batch experiments it is shown how these columns were calculated.

NOMENCLATURE

- a.....specific interface area
- C.....concentration
- d_s.....sauter mean diameter
- g.....gravitation constant
- H.....height of column
- k.....mass transfer coefficient
- t.....time
- u.....characteristic velocity
- v.....velocity
- x_d.....holdup
- λ.....phase ratio
- ψ.....parameters influencing the mass transfer
- ρ.....density
- τ.....residence time

Indices

- A.....refers to ion to be separated
- B.....refers to stripping agent
- k,d....refers to continuous and dispersed phase
- o.....initial state
- ν.....stoichiometric coefficient
- I,III..inner and outer water phase

REFERENCES

1. Li N.N.,US Patent 3410794 (1968)
2. Kopp A., Thesis, TU Graz 1979
3. Hochhauser A.M., Cussler E.L., Sep.Purif.Methods 3 (1975),399
4. Völkel W., Halwachs W., Schügerl K., J.Membr.Sci. 6 (1980),19
5. Nakashio F. Kondo K., Sep.Sci.Techn., 15(4),(1980),1171
6. Prötsch M. Thesis, TU Graz (in edition)
7. Marr R., Husung G., Moser F., vt"verfahrenstechnik" 12 (1978), 3,139

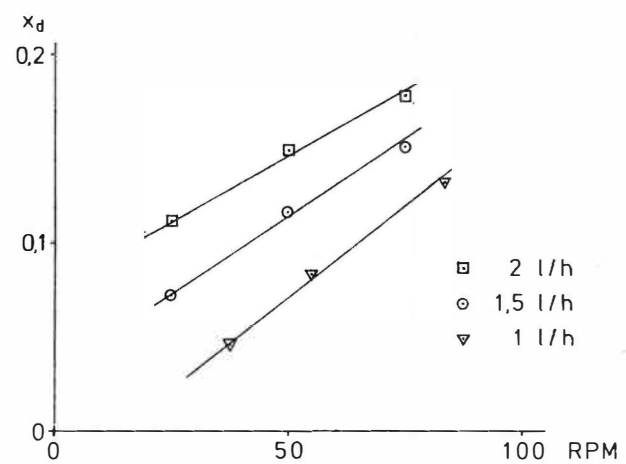

FIGURE 3. HOLDUP vs. STIRRING SPEED AT DIFFERENT THROUGHPUTS OF THE DISPERSED PHASE

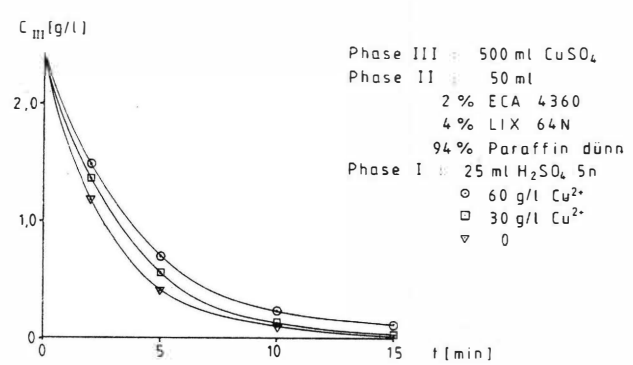

FIGURE 4. INFLUENCE OF METAL CONCENTRATION IN PHASE I

METAL EXTRACTION WITH 4-ACYLPYRAZOL-5-ONES: SYNERGISTIC EFFECTS WITH LIPOPHILIC AMMONIUM SALTS; APPLICATION TO LIQUID MEMBRANE TRANSPORT

J. P. Brunette, Z. Lakkis, M. Lakkis and M. J. F. Leroy

Université Louis Pasteur
Strasbourg, France

The liquid-liquid extraction of a metal cation from aqueous media with an acidic chelating extractant HL in an inert diluent is usually well-described by :

$$(1) \qquad M^{m+}_{aq.} + m\,\overline{HL} \xrightleftharpoons{K'_1} \overline{ML_m(H_2O)_n} + mH^+_{aq.}$$

The coordinated water limits the extraction efficiency. To substitute these molecules and therefore to enhance the extractions, a lipophilic donor ligand S is generally added in the organic phase (ex. S = TOPO), and the extracted species, ML_mS_n, are simple coordination coumpounds.
Another possibility, much less considered (1), is the substitution of H_2O by L^- anions to form anionic metal species like $ML^-_{(m+1)}$ which are coordination saturated and extractable as ion pairs associated with a lipophilic cation B^+.
This possibility of synergism is considered in the first part of the work with HL = 1-phenyl-3-methyl-4-benzoyl-pyrazol-5-one (HPMBP), as a representative example of the 4-acylpyrazol-5-ones, and B^+, the tertiary tri-n-octylammonium ($HTOA^+$) or the quaternary methyl-tri-n-octylammonium ($TOMA^+$) cations. The extracted metals are Cu^{2+}, Zn^{2+} and Cd^{2+}, in comparison with Co^{2+}, Ni^{2+} (2,3). The inorganic anions are ClO_4^-, NO_3^- and SO_4^{2-} (ionic strength = 1). Toluene is the usual diluent of the distribution experiments (log D vs pH at $[\overline{HL}]$ and $[B^+]$ constant) all performed in a thermostated vessel (25.0 ± 0.2°C) using a batch technique. Atomic absorption is the analytical procedure.

The second part of this work deals with kinetic aspects of Cu extraction with HPMBP in chloroform. A liquid membrane transport procedure using Lewis'type cells has been used.

SYNERGIC EXTRACTIONS WITH HPMBP + (B^+,X^-)* IN TOLUENE *(X^- = inorganic anion)

Three key equilibria are necessary to explain the experimental distribution curves :
First, the extraction equilibrium of M^{2+} with HBMBP alone (1), which is dependent on M^{2+} (Cu > Zn > Ni > Co > Cd) and X^- (ClO_4^- > NO_3^- > SO_4^{2-})
Second, the synergic equilibrium (2):

$$(2) \qquad \overline{ML_2(H_2O)_n} + \overline{(B^+,L^-)} \xrightleftharpoons{K'_2} \overline{(B^+,ML_3^-)}$$

which is dependent on M^{2+} (Ni ∿ Co > Cd > Zn >> Cu (K'_2 = 0)) and B^+ ($TOMA^+$ >> $HTOA^+$)
Third, the anionic exchange equilibrium (3):

$$(3) \qquad \overline{(B^+,X^-)} + \overline{HL} \xrightleftharpoons{K'_3} \overline{(B^+,L^-)} + H^+_{aq.} + X^-_{aq.}$$

that determines $[\overline{(B^+,L^-)}]$ and thus the magnitude of the synergic effect as a function of the inorganic anion nature. K'_3 follows the orders $SO_4^{2-}.HSO_4^-$ >> NO_3^- > ClO_4^- and $TOMA^+$ << $HTOA^+$. Under the experimental conditions, the formation of (B^+,L^-) is nearly quantitative for the sulphate medium and negligible for the perchlorate one. Consequently, the synergisms observed for these media can be respectively described by equilibria (2) and (4)

$$(4) \qquad \overline{ML_2(H_2O)_x} + \overline{HL} + \overline{(B^+,ClO_4^-)} \xrightleftharpoons{K'_4} \overline{(B^+,ML_3^-)} + H^+_{aq.} + ClO^-_{4aq.}$$

K'_1, K'_2 and K'_3 constants are given on table 1.
The total synergic effect results from equilibria (2) and (3). It follows that $(HTOA^+,X^-)$ is a better synergic agent than $(TOMA^+,X^-)$ towards the perchlorate medium (Δ log K'_4 ∿ 0.5) whereas $(TOMA^+,X^-)$ is better towards the sulphate medium (Δ log K'_2 ∿ 2).
The magnitude of the synergism follows the order Ni ∿ Co > Cd > Zn.
The Jahn-Teller effect hinders the CuL_3^- formation and thus, no synergism is observed for the Cu extraction.
Finally it must be noted that equilibrium (5) has to be also considered to explain the experimental data obtained with B^+ = $HTOA^+$

$$(5) \qquad \overline{HL} + \overline{TOA} \xrightleftharpoons{K'_5} \overline{(HTOA^+,L^-)} \qquad (\log K'_5 = 2.45)$$

(sulphate medium; other media at high pH) (2)

Diluent effect : If n-octanol is used as the diluent, the extractions with HPMBP alone are greatly enhanced in comparison with the one obtained in toluene : log K'_1 = -3.56 and -2.33 (X^- = ClO_4^-) -4.93 and -3.34 (X^- = SO_4^{2-}) for Cd and Zn respectively, which is due to the coordination of alcohol molecules on the extracted species (substitution of H_2O). With n-octanol, no synergism is observed if ammonium salts are added to the organic phase. On the contrary, antagonistic effects occur (SO_4^{2-} medium). They are due to the ammonium pyrazolonate formation (equilibrium 5) (2).

COUPLED TRANSPORT OF Cu THROUGH A HPMBP-$CHCl_3$ MEMBRANE

This preliminary work has been carried out in order to obtain useful information both on the liquid-liquid extraction mechanism of Cu and on the feasibility of its transport by using HPMBP as membrane carrier.

Experimental : A constant interfacial area stirred cell consisting of a cylinder rotating in a thermostated vessel (25 ± 0.2°C) was used (Typical experimental conditions : interfacial areas : S_I = 15 cm^2 and S_{II} = 30 cm^2 with respective aqueous volumes V_I = 50 cm^3 and V_{II} = 100 cm^3; V_{org} = 130 cm^3).
The chemical parameters were :
aqueous I : 10^{-3}M < $[Cu^{2+}]$ < 4 10^{-3}M; $[(H^+,Na^+)ClO_4^-]$ = 1M; 1.5 < pH < 2.
organic : $CHCl_3$; 0.005M < [HPMBP] < 0.04M.
aqueous II : $HClO_4$ 1M.
(Under these experimental conditions,the Cu extraction constant is log K'_1 = 0.37).

TABLE 1 : SYNERGIC EFFECTS WITH HPMBP + (B^+,X^-)

Extraction (1) and synergic (2) equilibria. Diluent = toluene							
Extractant	Constant	X^-	Cu	Zn	Cd	Co(2,3)	Ni(2,3)
HPMBP	log K'_1	ClO_4^-	0.94	-4.85	-8.13	-7.25	-6.71
		NO_3^-	a	-5.36	-8.63	a	a
		SO_4^{2-}	0.00	-6.22	-9.49	-7.78	c
HPMBP + $(HTOA^+,X^-)$	log K'_2	ClO_4^-	b	3.59	5.48	6.28	6.39
		NO_3^-	b	4.04	5.55	a	a
		SO_4^{2-}	b	3.91	5.50	6.10	c
HPMBP + $(TOMA^+,X^-)$	log K'_2	ClO_4^-	b	6.15	8.12	9.13	8.84
		NO_3^-	b	6.62	8.18	a	a
		SO_4^{2-}	b	6.01	8.18	8.07	c
Anionic exchange equilibria (3). Diluent = toluene							
(B^+,L^-)		X^-		log K'_3			
$(HTOA^+,L^-)$		ClO_4^-		-3.94			
		NO_3^-		-2.60			
		SO_4^{2-}		$[\overline{(HTOA^+,L^-)}]$ >> $[\overline{(HTOA^+,X^-)}]$			
$(TOMA^+,L^-)$		ClO_4^-		∿-7.0			
		NO_3^-		-4.22			
		SO_4^{2-}		$[\overline{(TOMA^+,L^-)}]$ >> $[\overline{(TOMA^+,X^-)}]$			

Experimental conditions : $[M^{2+}]_0$ ∿ 10^{-3}M, $[HL]_0$ = 0.02M and 0.0066M ≤ $[(B^+,X^-)]_0$ ≤ 0.1M. 25°C
a : not measured b : K'_2 ∿ 0 0.05 ≤ Δ log K'_i ≤ 0.10
c : slow extraction rate

* Granted from C.N.R.S. of Lebanon.

Aliquots of each aqueous phase were withdrawn to determine $[Cu]_{I \text{ or } II} = f(t)$. The curve $[Cu] = f(t)$ is obtained by mass balance calculations. Typical experimental curves are shown on fig. 1 and 2 (A : $[Cu]_I = f(t)$, B : $[Cu]_{II} = f(t)$, C : $[\overline{Cu}] = f(t)$.

Extraction rate : A plot of log J_{oI} vs log $[\overline{HL}]$ is shown on fig. 3 (J_{oI} = initial flux of Cu throughout the interfacial area I). The slope of the curve increases with increasing $[\overline{HL}]$, and thus, three regions, with slopes 2, 1 and 0, are defined. The 2 and 1 regions correspond to a mass transfer controlled by a diffusion through the organic layer and by chemical reactions respectively (4) whereas the 0 region may refer either to a mass transfer controlled by a diffusion through the aqueous layer or to an interfacial saturation effect. A variation of the stirring speed (65 to 200 rpm) in the 2 region has no effect on J_{oI} which confirms that a kinetical regime is obtained. In this region, variations of $[Cu]$, $[H^+]$ and $[\overline{HL}]$ show that experimental rate law is of first order towards these parameters.

$$J_{oI} = k\,[Cu^{2+}][\overline{HL}][H^+]^{-1}$$

with $k = (4.9 \pm 0.2)10^{-2}$ cm. mn^{-1}

Variations of the interfacial area have indicated that the reaction takes place at the interface. The rate law is similar to the one obtained with 2-hydroxy-5-tert-octylacetophenone oxime (5).

Transport rate : At higher HL concentrations the metal transport is partly governed by the limiting extraction reactions that take place at the first interface but the shape of the curves (fig. 1) shows clearly that at least a second rate limiting step occurs at the second interface (back extraction). At lower HL concentrations (fig. 2) the transport curves show that the transport is only controlled by diffusion in the organic layers and a pseudo-steady state is obtained after a few minutes. New experiments are needed to definitely conclude and to get a more quantitative approach.

REFERENCES

1) G. Duykaerts, J.F Desreux. CIM Special Volume 21, 73 (1977).

2) J.P. Brunette, M. Lakkis, G. Goetz-Grandmont, M.J.F. Leroy. Polyhedron 1, 461 (1982).

3) J.P. Brunette, G. Goetz-Grandmont, M. Lakkis, M. Taheri, M.J.F. Leroy. Proc. ICNAS 82, IV-1(P) (1982).

4) P.R. Danesi, E.P. Horwitz, G.F. Vandegrift, R. Chiarizia. Sep. Sci. Technol. 16, 201 (1981).

5) P.R. Danesi, R. Chiarizia, G.F. Vandegrift. J. Phys. Chem., 84, 3455 (1980).

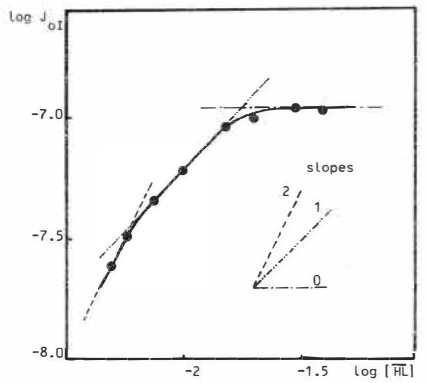

FIG. 3 : INITIAL COPPER FLUX THROUGH THE AQUEOUS I-ORGANIC INTERFACE pH 1.9; $[Cu]_o = 1.58\ 10^{-3}$

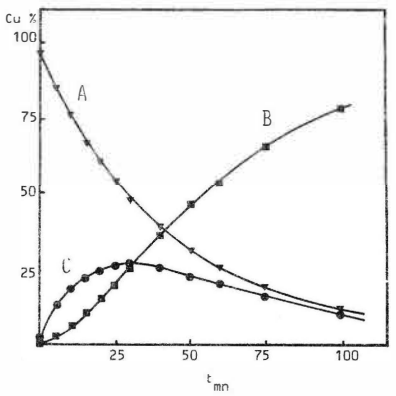

FIG.1 : COPPER TRANSPORT CURVES AT HIGH $[HL]$ (0.02M) pH 1.9; $[Cu]_o = 1.58\ 10^{-3}$

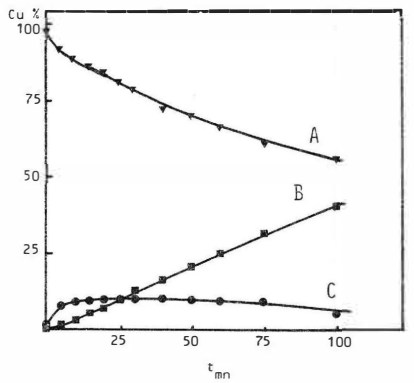

FIG. 2 : COPPER TRANSPORT CURVES AT LOW $[\overline{HL}]$ (0.005M) pH 1.9 $[Cu]_o = 1.58\ 10^{-3}$

EXTRACTION KINETICS OF COPPER WITH LIQUID SURFACTANT MEMBRANES CONTAINING HYDROXYOXIME IN A STIRRED TRANSFER CELL

Kazuo Kondo, Fumiyuki Nakashio* and Keisuke Funatsu

Kyushu University
Fukuoka, Japan

*F. Nakashio is a Member of AIChE.

With the commercial development of metal chelating agents such as LIX 65N and Kelex 100 reagents the practical application of the solvent extraction of metals has increased from the point of view of the recycling of industrial resources or energy conservation in the field of hydrometallurgical and waste-water treating processes(1,2). Using liquid surfactant membranes containing a mobile carrier, which has attracted special interest recently, testing of the practical application of selective separation and concentration of metallic ion in aqueous solution has been carried out(3-7). However, extraction mechanism of metal with liquid surfactant membranes has not necessarily been clarified completely.

In this work, the extraction of copper with liquid surfactant membranes containing anti-2-hydroxy-5-nonylbenzophenone oxime (henceforth referred to as HNBPO), which is the active component of LIX 65N, was carried out in a stirred transfer cell, along with the measurements of the extraction and the stripping rates of copper by the extractant. The experimental results were explained qualitatively by an interfacial reaction model proposed.

EXPERIMENTAL

Measurement of Extraction Rate of Copper The stirred transfer cell used was the same as that described in a previous paper(8). The aqueous and organic phases in the two compartments were stirred independently by two flat-blade stirrers in opposite directions at 150 rpm. The aqueous solution was prepared by dissolving commercial GR grade copper nitrate in deionized water. The pH of the aqueous solution was adjusted using 0.1 mol/dm^3 acetic acid - sodium acetate buffer solution. The organic solution was prepared by dissolving HNBPO in n-heptane. HNBPO separated and purified from commercial LIX 65N was used as the extractant. About ten small samples were taken at intervals from the organic phase. The copper concentration was determined by atomic absorption spectrochemical analysis.

Measurement of Stripping Rate of Copper Sulfuric acid solution with various concentrations was used as the aqueous solution. The organic solution was prepared by dissolving both Cu-HNBPO chelating complex and free HNBPO in n-heptane. The experimental procedure was the same as that of the above experiment.

Measurement of Extraction Rate of Copper with Liquid Surfactant Membranes The aqueous solution was the same as that used in the measurement of the extraction rate of copper mentioned above. The emulsion phase was made from both organic solution and internal aqueous solution by the same procedure shown in a previous paper(9). The organic solution was prepared by dissolving HNBPO as a mobile carrier and Span 80, a nonionic surfactant, in n-heptane and the internal aqueous solution was prepared by diluting sulfuric acid in deionized water. The experimental procedure was almost the same as that of the above experiment.

RESULTS

Extraction Rate of Copper The effect of pH on the initial extraction rate of copper is shown in Figure 1. The initial extraction rate is inversely proportional to the hydrogen-ion concentration in the low pH range, but in the high pH range is not affected by the hydrogen-ion concentration.

The effect of HNBPO concentration on the initial extraction rate is shown in Figure 2. It is found that the initial extraction rate is proportional to the HNBPO concentration in the low concentration range of HNBPO but that the rate is scarcely affected by the HNBPO concentration in the high concentration range.

The effect of copper concentration on the initial extraction rate is shown in Figure 3. It is evident that the initial extraction rate is proportional to the copper concentration in the low concentration range of copper but that the rate is scarcely affected by the copper concentration in the high concentration range.

Stripping Rate of Copper The effect of sulfuric acid concentration (activity) on the initial stripping rate of copper is shown in Figure 4. The initial stripping rate is proportional to the acid concentration in the low concentration range of sulfuric acid, but in the high acid concentration range is scarcely affected by the acid concentration.

The effect of free HNBPO concentration on the initial stripping rate is shown in Figure 5. The initial stripping rate is independent of the free HNBPO concentration in the low HNBPO concentration range, but in the high HNBPO concentration range varies inversely as the first power of the free HNBPO concentration.

The effect of Cu-HNBPO chelating complex concentration on the initial stripping rate is also shown in Figure 5. It is found that the stripping rate is proportional to the chelating complex concentration.

Extraction Rate of Copper with Liquid Surfactant Membranes The effect of pH in the external aqueous solution on the initial extraction rate of copper is also shown in Figure 1. The tendency of the pH dependency of the initial extraction rate is similar to that of the solvent extraction rate but the rates are significantly lowered. The effects of HNBPO concentration in the liquid surfactant membrane and copper concentration on the initial extraction rate of copper are also shown in Figures 2 and 3, respectively. These indicate that the extraction rate in liquid membrane system is lowered in comparison with that in solvent extraction system. This is considered to be caused by the surfactant used in liquid surfactant membrane system.

DISCUSSION

The experimental results mentioned above showed that the concentration dependency of the extraction and the stripping rates varied with the concentrations of hydrogen-ion, HNBPO and copper, etc. This indicates that the rates are affected by mass transfer rates of the species in the concentration range in which the reaction rate between copper and HNBPO is considerably high. The experimental results in region of reaction control will be discussed here.

Both HNBPO and Cu-HNBPO chelating complex are found to be interfacial active components from the measurement results of interfacial tension. To interpret our experimental results, the following interfacial reaction model accompanied with adsorption of Langmuir-Hinshelwood type is proposed.

$$(1)\quad HR_i + \theta_v = HR_{ad} \quad : K_{HR}$$

$$(2)\quad Cu_i^{2+} + HR_{ad} = CuR_{ad}^{+} + H_i^{+} \quad : K_1$$

$$(3)\quad CuR_{ad}^{+} + HR_i = CuR_{2ad} + H_i^{+} \quad : K_2$$

$$(4)\quad CuR_{2ad} = CuR_{2i} + \theta_v \quad : K_{CuR2}$$

where HR and CuR_2 denote HNBPO and Cu-HNBPO chelating complex, respectively. Subscripts ad and i indicate adsorbed species and species existing close to interface, respectively. Since total fractional coverage is one,

$$(5)\quad \theta_v + \theta_{HR} + \theta_{CuR} + \theta_{CuR2} = 1$$

Assuming that the rate-determining step is the reaction indicated by Equation (3), the reaction rate is expressed as follows.

$$(6)\quad r = k_f C_{CuRad} C_{HRi} - k_r C_{CuR2ad} C_{Hi}$$

From Equations (1), (2) and (4),

$$(7)\quad K_{HR} = \frac{\theta_{HR}}{C_{HRi}\theta_v S_{HR}}$$

$$(8)\quad K_1 = \frac{C_{Hi}\theta_{CuR} S_{HR}}{C_{Cui}\theta_{HR} S_{CuR}}$$

$$(9)\quad K_{CuR2} = \frac{\theta_{CuR2}}{C_{CuR2i}\theta_v S_{CuR2}}$$

The fractional coverage of each component can be obtained from using Equations (5), (7), (8) and (9). Substituting these into Equation (6), the final expression of the reaction rate becomes as follows.

$$(10)\quad r = \left(k_f K_1 K_{HR} \frac{C_{Cui} C_{HRi}^2}{C_{Hi}} - k_r K_{CuR2} C_{CuR2i} C_{Hi}\right)\theta_v$$

$$(11)\quad \theta_v = \left\{1 + \left(S_{HR} + \frac{K_1 S_{CuR} C_{Cui}}{C_{Hi}}\right) K_{HR} C_{HRi} + K_{CuR2} S_{CuR2} C_{CuR2i}\right\}^{-1}$$

r = reaction rate

C = concentration

θ_v = fraction of vacant site

k_f = forward reaction rate constant

k_r = reverse reaction rate constant

K_1 = equilibrium constant of intermediate complex formation

K_{HR}, K_{CuR2} = adsorption equilibrium constant of HR and CuR_2, respectively

S_{HR}, S_{CuR}, S_{CuR2} = interfacial area occupied by unit mole of HR, CuR and CuR_2, respectively

From analysis of the measurement results of interfacial tension of HNBPO, it was found that the values of K_{HR} and S_{HR} are 7.4×10^{-4} cm and 2.5×10^{9} cm^2/mol, respectively. By using these values, it can be assumed that $S_{HR} > K_1 S_{CuR} \times C_{Cui}/C_{Hi}$ and $S_{HR}K_{HR}C_{HRi} > 1$, $K_{CuR2}S_{CuR2}C_{CuR2i}$ Under these assumptions, Equations (10) and (11) are simplified as follows.

$$(12) \qquad r = \frac{k_f K_1}{S_{HR}} \frac{C_{Cui}C_{HRi}}{C_{Hi}} - \frac{k_r K_{CuR2}}{S_{HR}K_{HR}} \frac{C_{CuR2i}C_{Hi}}{C_{HRi}}$$

The experimental results of the extraction and the stripping rates of copper can be qualitatively explained by Equation (12).

Next, the experimental results of extraction rate of copper with liquid surfactant membranes are considered to be as follows. Span 80, nonionic surfactant, used as emulsifier strongly adsorbs at interface as well as HNBPO which is the extractant, and it is anticipated that θ_{HR} in liquid membrane system is lowered in comparison with that in solvent extraction system. Therefore, the extraction rate of copper with liquid surfactant membranes in region of reaction control is lowered compared with that of solvent extraction as seen in Figures 1, 2 and 3. In this case, θ_v expressed by Equation (11) must be modified considering adsorption of Span 80. Quantitative treatment with respect to this problem will be necessary to establish processes of liquid surfactant membranes.

CONCLUSION

The extraction of copper with liquid surfactant membranes containing anti-2-hydroxy-5-nonylbenzophenone oxime as mobile carrier was carried out in a stirred transfer cell, along with the measurements of the extraction and the stripping rates of copper by the extractant. The experimental results were explained qualitatively by the interfacial reaction model accompanied with adsorption of Langmuir-Hinshelwood type, which is proposed in this work. Further study of role of surfactant acting on the extraction rate of copper in liquid surfactant membrane system is necessary.

REFERENCES

1. D.S.Flett, D.N.Okuhara and D.R.Spink, J.Inorg.Nucl.Chem., 35, 2471 (1973)
2. C.Hanson, "Recent Advances in Liquid-Liquid Extraction", Pergamon Press, Oxford (1971)
3. A.M.Hochhauser and E.L.Cussler, AIChE Symp.Ser., 71, No.152, 136 (1975)
4. W.Völkel, W.Halwachs and K.Schügerl, J.Membr.Sci., 6, 19 (1980)
5. L.Boyadzhiev, T.Sapundzhiev and E.Bezenshek, Separ.Sci., 12, 541 (1977)
6. J.Strzelbicki and W.Charewicz, Separ.Sci.Technol., 13, 141 (1978)
7. F.Nakashio and K.Kondo, Separ.Sci.Technol., 15, 1171 (1980)
8. K.Kondo, K.Kita and F.Nakashio, J.Chem.Eng.Japan, 14, 20 (1981)
9. K.Kondo, K.Kita, I.Koida, J.Irie and F.Nakashio, J.Chem.Eng.Japan, 12, 203 (1979)

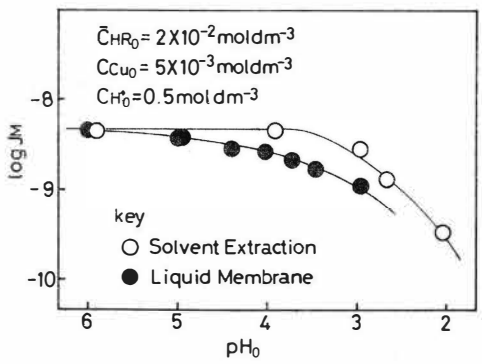

FIGURE 1. EFFECT OF HYDROGEN-ION CONCENTRATION ON EXTRACTION RATE

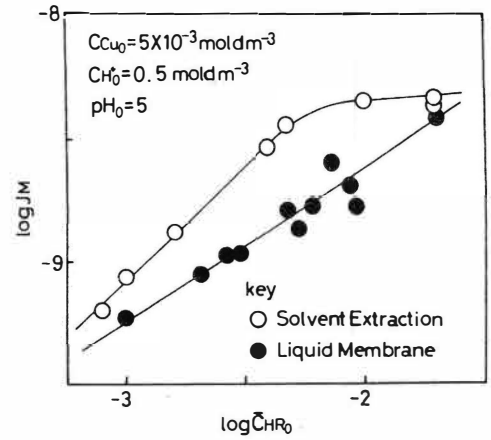

FIGURE 2. EFFECT OF EXTRACTANT CONCENTRATION ON EXTRACTION RATE

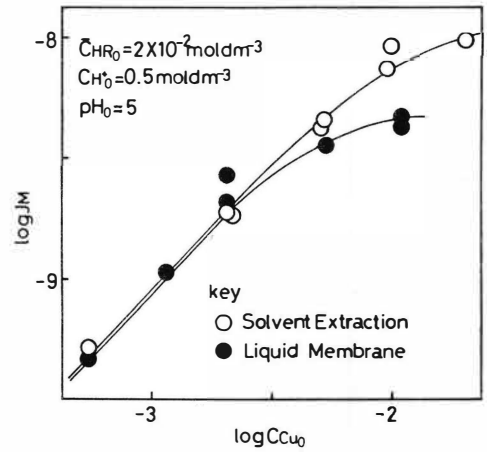

FIGURE 3. EFFECT OF COPPER CONCENTRATION ON EXTRACTION RATE

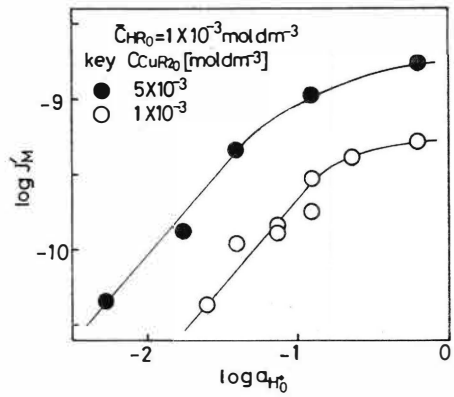

FIGURE 4. EFFECT OF ACID CONCENTRATION ON STRIPPING RATE

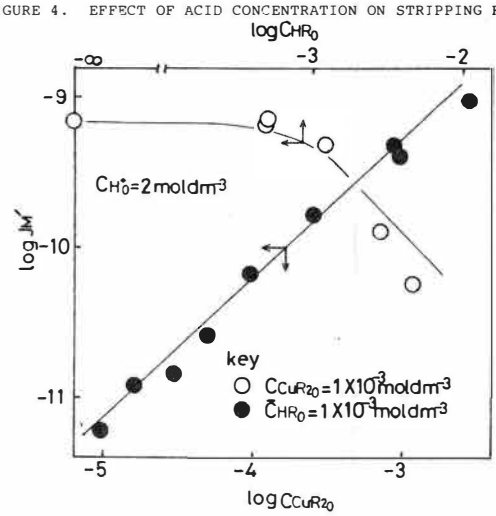

FIGURE 5. EFFECTS OF EXTRACTANT AND CHELATING COMPLEX CONCENTRATIONS ON STRIPPING RATE

ANALYTICAL AND EXPERIMENTAL STUDIES OF MASS TRANSPORT THROUGH LIQUID MEMBRANES

H. S. Park, J. H. Yoo, I. S. Suh, P. S. Han
Korea Advanced Energy Research Institute
Chung-Nam, Korea

W. K. Kang
Korea University
Seoul, Korea

M. Burgard and M. J. F. Leroy
E.N.S.C.
Strasbourg, France

A diffusion controlled mass transfer model for the permeation process within the emulsion drop is proposed. The model is based on the assumptions that the reaction interface advances into the emulsion drop as the diffused solute reacts instantaneously with the internal aqueous reagent and that pseudo-steady state approximation is valid.

The polydisperse character of the dispersed emulsion phase is also considered in order to avoid some errors caused by the assumption of uniform drop size. Computer simulations of the model equations are performed using the estimated value of the effective diffusivity, and the model calculations are compared with the experimental data. The experimental results obtained using a batch-type agitation vessel are also discussed on the various parameters.

DEVELOPMENT OF MODEL

The following assumptions, based on the extraction system, are made to analyze the extraction rate.

(a) There is no internal circulation in the emulsion drops because of the strong presence of surfactants in membrane phase.

(b) Since the interfacial tensions are very low due to the surfactants, there is no coalescence and redispersion of the emulsion drops in the continuous phase.

(c) The external phase mass transfer resistance is negligible when the emulsion phase is dispersed in the continuous phase under proper stirring.

(d) The radius of an emulsified aqueous droplet within the emulsion drop is so small that the contact area between the membrane phase and the internal aqueous phase is large enough to cause the solute to be distributed in local equilibrium.

(e) The effective diffusivity of solute within the emulsion drop is constant and independent on the concentration of solute.

(f) The reaction of solute with the internal reagent is instantaneous and the reaction products are membrane-insoluble. Hence there must exist a sharp moving boundary at which the reaction takes place.

Mathematical description. The following equations are derived to discribe the concentration of solute in drops and in the external water phase for a batch extraction,

(1)
$$\frac{\partial C}{\partial t} = \frac{D_e}{r^2}\frac{\partial}{\partial r}\left(r^2 \frac{\partial C}{\partial r}\right) \qquad \text{for } r_c \le r \le R$$
$$C = C_s \quad (r = R,\ t > 0)$$
$$C = 0 \quad (r = r_c,\ t > 0)$$
$$C = 0 \quad (0 \le r \le R,\ t = 0)$$

(2)
$$-\frac{dr_c}{dt} = \frac{bD_e}{\phi C_R}\frac{\partial C}{\partial r} \qquad (r = r_c,\ t > 0)$$
$$r_c = R \quad (t = 0)$$

(3)
$$-V_w \frac{dC_w}{dt} = 4\pi D_e \sum_i R_i^2 \left(\frac{\partial C}{\partial r}\right)_{r=R_i}$$

(4)
$$C_s = m C_w$$

where b is the stoichiometric coefficient of the internal reagent for 1 mol of solute, and n_i is number of drops of grade i, expressed by

(5)
$$n_i = \frac{V_d\, f(R_i)}{\frac{4}{3}\pi R_i^3}$$

Here we can show a certain region where the pseudo-steady state approximation is valid by analyzing the approximate solution for unsteady state, which can be derived by the same method as Bischoff[1] has used.

(6)
$$\frac{r_c}{R} = \frac{r_{co}}{R}\left[1 + \frac{bC_s\left(1 - \frac{r_{co}}{R}\right)}{6\phi C_R \left(\frac{r_{co}}{R}\right)^2} + \cdots\cdots\right]$$

Where r_{co} is the core radius for steady state. From Eq. (6), we can derive the ratio of mass permeated into the emulsion drop for steady state to that for unsteady state by neglecting the small quantity existed in membrane phase,

(7)
$$\frac{M_p}{M_o} = \frac{1}{1 - \dfrac{\psi\left(\frac{r_{co}}{R}\right)}{6\left\{1 + \frac{r_{co}}{R} + \left(\frac{r_{co}}{R}\right)^2\right\}}}$$

where
$$\psi = \frac{bC_s}{\phi C_R}$$

The plot of M_p/M_o vs. ψ is shown in Figure 2. As can be seen in the figure, there is very little error in the region of $\psi < 0.1$ which covers the most practical systems. Thus, the pseudo-steady state method can be applied to this mass transfer system with confidence.

For pseudo-steady state, Eq. (1) can be solved analytically to give

(8)
$$C^* = C_s^* \frac{r^* - r_c^*}{r^*(1 - r_c^*)}$$

where $r^* = \frac{r}{R}$ $\quad r_c^* = \frac{r_c}{R}$ $\quad C^* = \frac{C}{C_{so}}$ and $C_s^* = \frac{C_s}{C_{so}}$

For each grade i, the differential equations for r_c^* can be rearranged from Eqs. (2) and (8), and that for C_w from Eqs. (3), (5) and (8) as follows.

(9)
$$-\frac{dr_c^*}{dt} = \frac{bmD_e}{\phi C_R R_i^2}\frac{C_w}{r_c^*(1 - r_c^*)}$$

(10)
$$-\frac{dC_w}{dt} = 3mD_e C_w \frac{V_d}{V_w}\sum_i \frac{f(R_i)}{R_i^2}\frac{r_c^*}{1 - r_c^*}$$

Numerical solutions of Eqs. (9) and (10) can be obtained to give r_c^* and C_w vs. t for the system of nonuniform drops.

If we assume uniform drop size and use the Sauter mean diameter, the Eqs. (9) and (10) can be greatly simplified and solved analytically.

(11)
$$-\frac{dr_c^*}{dt} = \frac{bmD_e}{\phi C_R Rm}\frac{C_w}{r_c^*(1 - r_c^*)}$$

(12)
$$-\frac{dC_w}{dt} = \frac{3mD_e C_w}{Rm^2}\frac{V_d}{V_w}\frac{r_c^*}{1 - r_c^*}$$

Analytical solutions to the coupled Eqs. of (11) and (12) present the relation of r_c^* and C_w vs. t as follows.[2]

(13)
$$t = \frac{1}{3\alpha}\log\frac{\alpha r_c^{*3} - \beta}{\alpha - \beta} - \frac{1}{6\kappa\alpha}\left[\log\frac{\alpha r_c^{*3} - \beta}{(\kappa + r_c^*)^3} - \log\frac{\alpha - \beta}{(\kappa + 1)^3} + 2\sqrt{3}\left(\tan^{-1}\frac{2r_c^* - \kappa}{\sqrt{3}\kappa} - \tan^{-1}\frac{2 - \kappa}{\sqrt{3}\kappa}\right)\right]$$

where
$$\alpha = \frac{mD_e}{\kappa^2}\frac{V_d}{V_w} \qquad \beta = \frac{mD_e}{\kappa^2}\left(\frac{V_d}{V_w} - \frac{bC_{so}}{m\phi C_R}\right) \quad \text{and} \quad \kappa = -\sqrt[3]{\frac{\beta}{\alpha}}$$

(14)
$$C_w = \phi C_R \frac{V_d}{V_w}(r_c^{*3} - 1) + \frac{C_{so}}{m}$$

EXPERIMENTAL

W/O emulsions were prepared by adding an appropriate amount of aqueous HCl solution drop by drop to mineral oil (paraffinic oil with carbon number = 14 to 23) containing 1 - 5 wt % of SPAN 80 with agitating speed exceeding 1,000 rpm. A batch-type agitated vessel made of pyrex glass and a marine-type mixing impeller were used for the extraction equipment. The W/O emulsion, whose density is about 0.9, was mixed with the aqueous aniline solution in the extractor by agitating at 250 - 380 rpm. Four intermediate baffles were equipped between the wall and the center of the vessel to prevent the W/O emulsion phase from remaining at the surface as a layer.

The dispersion of the internal aqueous phase droplets in W/O emulsion was observed by means of a microscope, and the size of W/O emulsion drop was measured by a photographic method. The concentration of aniline in the outer aqueous phase was analyzed by an UV spectrophotometer.

RESULTS AND DISCUSSION

The stability of emulsion mixture. The quantity of HCl leaking out of the internal aqueous phase into the external water phase was measured after ten minutes' agitation at 340 rpm. The average breakup values of the emulsion mixture with the surfactant concentration of 1 wt %, 3 wt %, and 5 wt % were found to be 0.34 %, 0.2 %, and below 0.1 % respectively.

Distribution coefficient of aniline. The distribution coefficient m of aniline between water and oil was found to be m = 0.65 at 15 °C.

Size distribution of the internal aqueous phase droplets and W/O emulsion drops. The diameter of the aqueous HCl solution droplets, measured by a microscopic method, was found to be about 1 - 5 μm.
The W/O emulsion drops were about 0.5 - 1.5 mm in diameter.

Estimation of the effective diffusivity. When aniline dissolves in HCl solution, the equilibrium is given by[3]

(15)
$$K = \frac{[PhNH_2][H^+]}{[PhNH_3^+]} \quad \text{and} \quad PK = 4.6\ (25\ °C)$$

where K is the dissociation constant of anilinium ion.

Aniline can diffuse both in charged ion and neutral molecule like as $PhNH_3^+$ and $PhNH_2$ in the internal aqueous phase, that is, the concentration driving force is much higher than that in the membrane phase. In addition, the diffusivity D, of aniline in the internal aqueous phase is found to be considerably larger than D_m, the diffusivity in the membrane phase. As the result, the diffusional resistance in the internal aqueous phase may be greatly reduced. Therefore, the Keller's asymptotic equation,[4] in which the diffusivity in the internal phase is considered to be infinite, can be used to estimate the effective diffusivity D_e of aniline within the emulsion mixture.

$$(16) \qquad D_e = -\frac{1}{2}\pi D_m \left[\left(\frac{\pi}{6} - \phi\right) - \ldots \right]$$

The value of D_e was obtained to be 0.75×10^{-5} cm²/sec when the calculated value of D_m ($D_m = 1.27 \times 10^{-6}$ cm²/sec) using the Wilke-Chang correlation[5] was applied. The value of D, was also calculated to be 3.06×10^{-6} cm²/sec.

Comparison of the model calculations with experimental results. The computed results based on the estimated value of D_e are in fairly good agreement with the experimental results as shown in Figure 3, and the small differences are presumably due to coalescence and redispersion of the emulsion drops and the estimation itself of the effective diffusivity.

Effect of HCl concentration. The extraction rate is affected by the HCl concentration as shown in Figure 3. This result may be due to the differences in the location of the reaction interface. When the HCl concentration is decreased, it shrinks more rapidly and the mass transfer resistance to permeation through the membrane phase increases. Thus, with higher HCl concentration, the extraction rate is increased because there is a great diffusional resistance between drop surface and reaction interface.

Effect of volume fraction of internal aqueous phase in W/O emulsion phase. During the performance of a series of experiments, it was observed that the emulsion drop size became smaller as the volume fraction of internal aqueous phase, ϕ, was decreased. This is presumably due to the difference of interfacial tension between external aqueous phase and emulsion phase with ϕ.

As shown in Fig. 4, with smaller ϕ, the extraction rate was reduced even though the interfacial area for mass transfer was increased. This results also show us that there exists a great resistance in the membrane phase to aniline permeation.

CONCLUSION

(a) In the range of $\psi < 0.1$ for the extraction system, the pseudo-steady state approximation can give an adequate representation of the actual process.

(b) The present model can be used not only for uniform but also for non-uniform drop sizes.

(c) The model calculations based on the estimated value of the effective diffusivity have been in fairly good agreement with the experimental results.

(d) From the experimental results, it has been shown that the mass transfer resistance to aniline permeation exists mainly in the membrane phase.

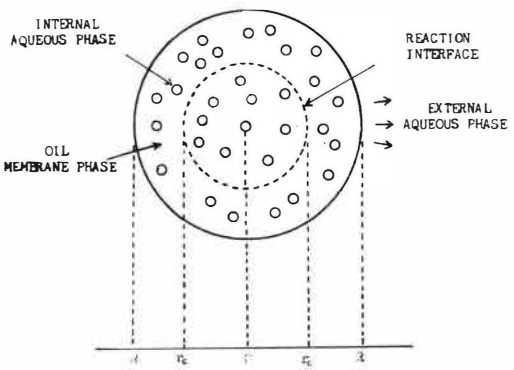

FIGURE 1. SCHEMATIC DIAGRAM OF W/O/W EMULSION SYSTEM

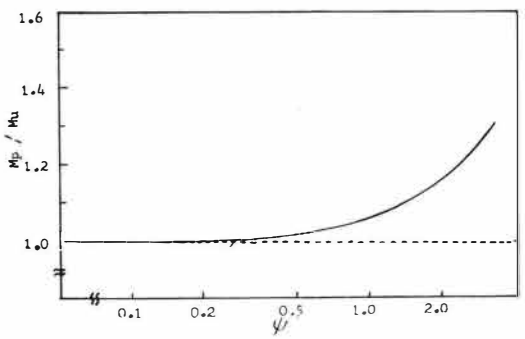

FIGURE 2. INITIAL RATIO OF MASS PERMEATED FOR PSEUDO-STEADY STATE, M_P, TO THAT FOR UNSTEADY STATE, M_U

NOTATION

C = solute concentration in membrane phase, M
C_R = initial concentration of reagent in the internal phase, M
C_s = solute concentration at drop surface, M
C_{so} = initial solute concentration at drop surface, M
C_w = solute concentration in external water phase, M
$f(R_i)$ = volume fraction of drops belonging to grade i
M_P = mass permeated for pseudo-steady state, g
M_U = mass permeated for unsteady state, g
r = radial coordinate, cm
r_c = inner core radius, cm
R = drop radius, cm
R_m = Sauter mean drop radius, cm
t = time, sec
V_d = volume of dispersed emulsion phase, cm³
V_w = volume of external water phase, cm³

REFERENCES

1. K.B.Bischoff, Chem. Eng. Sci., 18, 711 (1963)
2. W.S.Ho, T.A.Hatton, E.N.Lightfoot and N.N.Li, AIChE, 28 (4), 662 (1982)
3. J.A.Dean, Lange's Handbook of Chemistry, 11th ed. (1973)
4. J.Crank, The Mathematics of Diffusion, 2nd ed. (1975)
5. Reid, Prausnitz and Sherwood, The Properties of Gases and Liquids, 3rd ed. (1977)

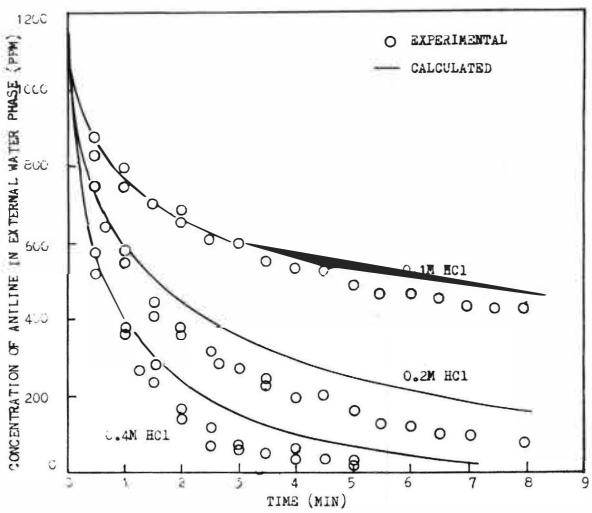

FIGURE 3. EFFECT OF HCl CONCENTRATION ON EXTRACTION RATE OF ANILINE : COMPUTED AND EXPERIMENTAL RESULTS

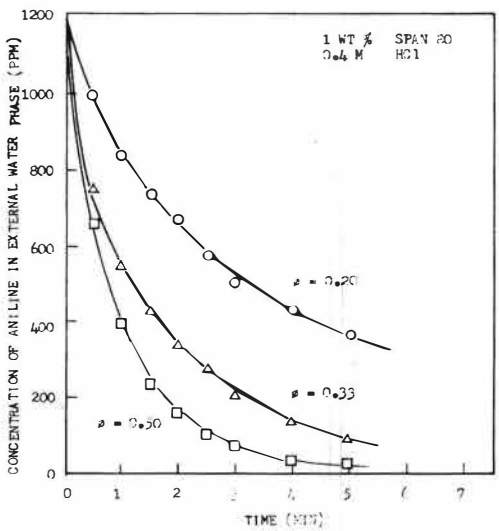

FIGURE 4. EFFECT OF THE VOLUME FRACTION OF INTERNAL AQUEOUS PHASE ON EXTRACTION RATE

THE USE OF NEW EXTRACTANTS IN LIQUID SURFACTANT MEMBRANES

Mamoun Muhammed and Manuel Valiente*

Department of Inorganic Chemistry
The Royal Institute of Technology
S-100 44 Stockholm, Sweden

*Permanent address: Universitad Autonoma de Barcelona, Dept. Quimica Analitica, Bellaterra, Barcelona, Spain

Complex formation in solution is governed by the donor-acceptor properties of metal ions and ligands and also by their particular sterical requirements. By suitable design of extraction reagents, one can exploite these differences in order to achieve highly specific extraction processes. Some of these reagents are described in another Abstract to this Conference (Högberg et al.). Their extraction properties and use in separations in acid sulphate solutions are described here.

Most of these reagents are highly soluble in organic diluents (mostly aromatics), however, the extracted complexes have a fairly low solubility (1 g/l) and the formation of a third phase complicates the practical utilization of these reagents.

One of the reagents (SER 48 = substituted, bisquinoline) has been extensively studied for the selective separation of copper and zinc from acidic sulphate solutions. Extraction data including extraction and stripping isotherms, kinetic data and data on the stability of the reagents are presented. The work has also included extraction of the metals using SER 48 and Span 80 dissolved in Shellsol 120 in a membrane phase using liquid surfactant membrane (LSM) technique.

The metals could be extracted and concentrated into the inner aquous (acid) solution. No indication of the precipitation of the metal-ligand complexes was noticed. Solutions with metal concentration of 5-10 g/l could be treated this way for the selective removal of the metals.

USE OF IMAGE INTENSIFICATION FOR SIMULTANEOUS MASS AND HEAT TRANSFER STUDIES IN LIQUID-LIQUID SYSTEMS

F. J. Aguirre, G. E. Klinzing, S. H. Chiang

Chemical and Petroleum Engineering Department
University of Pittsburgh
Pittsburgh, Pennsylvania 15261 USA

INTRODUCTION

In the study of mass transfer between partially miscible liquids, temperature perturbations have been found to have an important effect in the generation of interfacial activity, which in turn is considered responsible for the enhancement of mass transfer rates. In an effort to acquire a better understanding of the phenomena of instability in liquid-liquid systems, both temperature and concentration profiles have been measured upon contacting two partially miscible liquids. This paper presents the method developed for concentration measurements of an organic solute in an aqueous phase as a function of time and position. This experimental method is based in electro-optical image intensification of radiotracer compounds coupled with low light level photography. In general, it consists in homogeneously distributing a C-14 radioactively tagged species in the top liquid phase, which upon diffusion into the bottom liquid phase interacts with a scintillating material. The interaction between beta particles and a scintillating material produces photons, which are then transmitted through an image intensification system and photographed. The intensity of the light transmitted is a measure of the concentration of the tagged species, which can be quantitatively determined by proper calibration of the system with a reference material.

EXPERIMENTAL

The contacting of the liquid phases is performed in a cylindrical Teflon transfer cell as shown in Figure 1. The transfer cell is divided in two parts. The bottom section has one fluid well with a depth of 10 (mm) and a cross section of 90 (mm^2). This fluid well has a window on its side which consists in a fiber optic faceplate. A film coated with a very thin and homogeneous layer of the scintillating material ZnS:Cu,Al is placed on the inner surface of the fiber optic faceplate. The top section has two fluid wells, one of which has the same cross section as the one in the bottom section but with half its depth. This top fluid well has two openings in its top. A 1 (ml) hypodermic syringe is placed in one of them in order to introduce the lighter liquid which is radioactively tagged with C-14. Once the top and bottom fluid wells have been filled with the two partially miscible liquids, they can be contacted at a planar interface by smoothly rotating the upper section of the cell. Upon contact of the phases, some of the radioactive species will diffuse into the bottom phase generating photons by interaction with the scintillating material. These photons are transmitted through the fiber optic faceplate to the input of a RCA-4550 image intensifier tube, which amplifies the light signal 50000 times. The output signal from the image intensifier tube is recorded on photographic film at specified time intervals. A Pentax MX single lens reflex camera equipped with a 50 mm 1:1.2 standard lens and a Samigon M/C close up lens No. 4 was used. The data were recorded on Kodak Tri-X Pan film, obtaining an ASA exposure index of up to 3200 when developed in Diafine developer.

The use of this technique provides accurate concentration-position-time records of the radioactively tagged species in the bottom phase. Time exposures were required because the levels of light emitted at the output faceplate of the image intensifier tube were very low, and therefore photographic integration of the light signal was necessary.

The image developed on the photographic film was scanned using a microdensitometer to yield optical densities as a function of position at various times during the diffusional runs. Additional details concerning the experimental equipment and procedures are reported elsewhere (1).

OPERATING PARAMETERS

Several operating parameters such as specific activity of the tracer material, exposure time, time interval between measurements and others had to be determined prior to the experimental runs. All of these parameters are interrelated, so various tests were performed to find their optimum combination.

The intensity of the light signal obtained is directly related to the specific activity per unit volume of the tagged compound present in the bottom phase at any given time. As the specific activity of the solute increases, the exposure time required to record a given light signal on film decreases. The combination selected for these two variables was based on the volume requirement of tagged compounds. The specific activity of the pure organic compound in the top phase was of the order of 1 (uCi/µl), which required an exposure time of 2 minutes in order to detect a wide range of concentrations in the bottom phase. This exposure time is short enough such that for a mass transfer process it can be considered an instantaneous measurement. The only disadvantage of a 2 minute exposure is that the time interval between measurements had to be of the order of 30 minutes for a good signal to noise ratio. However, in one case the exposure time was decreased to 1 minute such that the time interval between measurements could be reduced to 15 minutes.

RESULTS AND DISCUSSION

Concentration measurements were performed with the partially miscible systems water/ethyl acetate and water/isobutanol. In both cases the organic compound was tagged with C-14, and its concentration in the aqueous phase was measured at various times. For most of the experimental runs the measurements consisted in a 2 minute photograph for times of 10, 30, 60, 90 and 120 minutes after the contacting of the two pure liquids had taken place.

The light signal generated by the interaction between beta particles and the scintillating material was recorded as a black spot on the photographic film, and the optical density at different positions in this spot is related to a concentration profile. A typical sequence of light signals for the water/ethyl acetate system is presented in Figure 2. In these photographs, the top boundary represents the edge of the fiber optic faceplate which is observing concentrations at a distance of 0.7 (mm) from the interface. The scanning of the film is done from top to bottom in the vertical direction, obtaining a concentration profile from a position close to the interface to the bulk of the aqueous phase.

The intensity of the white signal in these photographs represents the concentration of ethyl acetate in the aqueous phase. It is interesting to note from Figure 2 the growth of the boundary layer with time. For a time of 120 minutes, the light signal represents the region between 1 and 7 (mm) from the interface.

By calibrating the system with solutions of known specific activity, the optical densities could be related to actual concentrations. The experimental data were compared to the theoretical concentration profiles obtained from Fick's second law of diffusion (1). A plot of the average experimental data and theoretical profiles for the water/ethyl acetate system is presented in Figure 3. The solid lines represent the theoretical profiles due to pure diffusion, and they correspond to the same times as the experimental data with time increasing from left to right in the graph. Similar results were obtained for the water/isobutanol system.

There is an interesting characteristic of the experimental data which was noticed in all experimental runs. The experimental data for the water/ethyl acetate system showed an oscillatory behavior with time, having local maximums and minimums with a period of the order of 50 to 60 minutes. Figure 4 presents this behavior for four different positions in the bottom fluid well, in which the concentration of ethyl acetate in the aqueous phase is plotted as a function of time. This oscillatory behavior of the concentrations with a period of such magnitude suggests the existence of a very slow and intense convection process in the aqueous phase for up to 120 minutes after the contacting of the phases had taken place.

CONCLUSIONS

The use of electro-optical image intensification of the light emitted by radioactive tracers, coupled with low light level photography, proved to be an adequate method to measure concentration profiles close to a liquid interface as a function of time. In reference to the experimental results obtained for the two partially miscible systems studied, it was noticed that the experimental concentration profiles were consistently greater than those predicted by assuming pure diffusion. In addition, it can be observed from Figure 3 that at several positions the experimental concentrations of ethyl acetate in the aqueous phase are larger than the interfacial concentration or concentration at saturation conditions. This observation strongly suggests the presence of interfacial activity and convection which enhances the mass transfer rates, at least in the region close to the interface. Furthermore, the fact that some experimental concentrations are larger than the value at saturation conditions in the aqueous phase would lead to the conclusion that this interfacial activity is accompanied by the presence of some small droplets of the ethyl acetate-rich phase in the aqueous phase. The presence of just a few small droplets of the ethyl acetate-rich phase in the aqueous phase would greatly increase the value of the measured concentrations, since the specific activity per unit volume of the pure ethyl acetate is 12 times greater than that of the saturated aqueous phase. Similar conclusions were obtained for the water/isobutanol system.

As previously indicated, the oscillatory behavior of concentrations with time suggested the presence of a slow convection process in the aqueous phase. This convection process is probably accompanied by very large and rapid perturbations of the interface. However, since the measurements were made by using exposure times of 2 minutes, the results obtained are an average of the concentrations and possible perturbations during that period of time. In order to be able to evaluate all types of

convection patterns taking place in these systems it is necessary to make measurements with exposure times of just a few seconds, which can be achieved by increasing the specific activity of the radioactive tracers.

ACKNOWLEDGMENTS

The financial assistance o National Science Foundation is gratefully acknowledged.

REFERENCES

1. F. J. Aguirre, Ph.D. Thesis, University of Pittsburgh (1982).

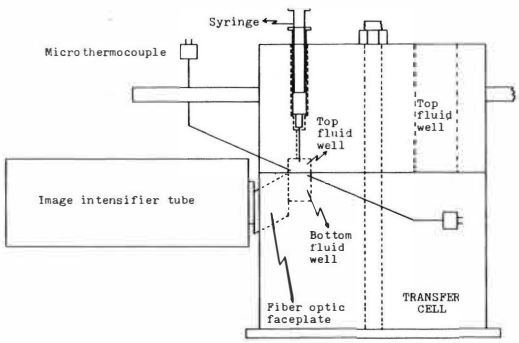

FIGURE 1: TRANSFER CELL FOR CONCENTRATION MEASUREMENTS

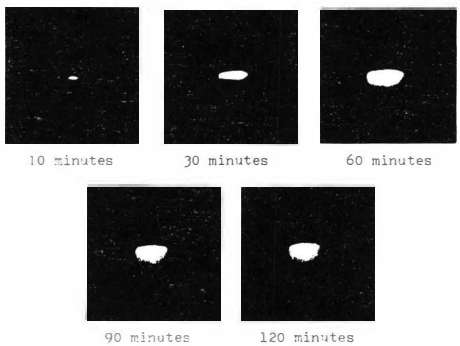

FIGURE 2: LIGHT SIGNAL REPRESENTING CONCENTRATION PROFILES AT VARIOUS TIMES FOR WATER/ETHYL ACETATE SYSTEM

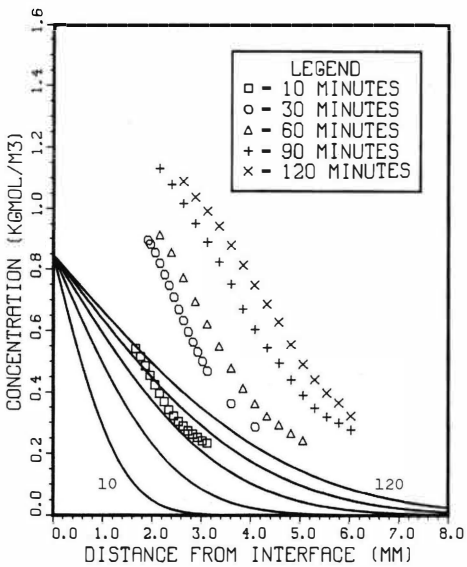

FIGURE 3: COMPARISON OF EXPERIMENTAL AND THEORETICAL CONCENTRATION PROFILES OF ETHYL ACETATE IN AQUEOUS PHASE

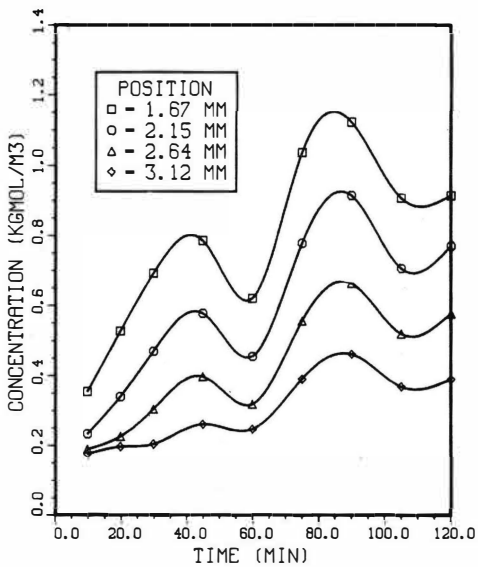

FIGURE 4: OSCILLATORY BEHAVIOR OF ETHYL ACETATE CONCENTRATION AS A FUNCTION OF TIME

A FLOW-THROUGH CONSTANT INTERFACE CELL TO STUDY THE KINETICS OF EXTRACTION IN THE Cu/LIX 64N SYSTEM

M. Bhaduri, C. Hanson, M. A. Hughes, R. J. Whewell*

Schools of Chemical Engineering
University of Bradford
Bradford, U.K.

*Current address: Department of Pure and Applied Chemistry, University of Strathclyde, Glasgow G1 1XL, Scotland.

The rate of extraction of copper by hydroxyoximes has so far been studied by several methods (1), (2), (3), (4). The relative importance of chemical reactions and diffusion processes (5), (6) in determining the overall rate of extraction is ascertained and estimates of rate more relevant to an industrial mixer settler should be obtained.

It is essential in any one technique either to account for hydrodynamics (4) or to stir the bulk and interface regions so that forced convection eliminates contributions from diffusion due to the mixing technique alone. In the Gauze cell described here, stirring actually takes place at the interface and it is possible to measure the interfacial area between the phases. The cell can be operated for times sufficiently long that equilibrium is nearly attained, so it is possible in principle to obtain rates near to equilibrium.

Three types of rate are illustrated in Figure 1.

(a) Rate 1 shows the rate appropriate to a mixer-settler operating under steady state conditions with perfect mixing of the phases at a degree of approach to equilibrium given by C_{ms}/C_{∞}.

(b) Rate 2 shows the "initial rates" previously under investigation in our laboratories (1), (5). A priori Rate 2 bears no relationship whatsoever to Rate 1, although data in this paper will be used to justify a link.

(c) A common industrial test is to express the ratio 100 C_T/C_{∞} as the "percentage kinetics", where T and t_{∞} are standard times of contact in a defined laboratory batch mixer. In a sense C_T gives a value of mean rate, but the rate is modified by dividing by C_{∞} and is thus a poor measure of extraction performance. Indeed, should the shape of a set of rate curves vary so that the curves intersect the ratios C_T/C_{∞} will be a misleading indicator of the values of Rate 1.

There is of course a serious analytical problem in determining the values of Rate 1 directly since the changes in copper concentration are only a tiny fraction of the total copper present. This problem is unavoidable in single drop experiments (1), but examination of trends in copper concentration in an assiduously sampled stirred cell gives a better estimate of the required rate.

THE GAUZE CELL

Apparatus. The apparatus (Figure 2) consists of a circular glass cell, diameter 80 mm, with a platinum gauze (100 mesh) sealed through the glass at a height of 20 mm above the base. Aqueous phase (presaturated with diluent) in the lower compartment is stirred with a magnetic follower and the interface with the organic phase lies at the platinum gauze. The area of the gauze is 29 cm^2 but the free surface of the gauze is some 40% of this area. A second stirrer bar rests on the gauze and stirs the 100 or 200 cm^3 portion of organic phase (presaturated with aqueous acid). Aqueous phase from a constant head tank flows through the lower compartment at a rate of about 10 $cm^3 min^{-1}$, and aqueous phase concentration thus remains sensibly constant throughout an experiment. The cell is immersed in a thermostat tank.

Analysis of the Organic Phase. Samples of 100 mm^3 (or 50 mm^3 at high copper concentrations) of organic phase are removed from the cell with a Lang-Levy self-zeroing micropipette and are diluted in the 1 cm spectrophotometric cell with 2 cm^3 AnalaR toluene. Absorbance is measured at 665 nm and the calibration graph (determined each day) is a straight line up to 0.15 g dm^{-3} copper in the toluene.

Effect of Interface Position on Rate. The position of the aqueous-organic interface with respect to the gauze is an important feature in determining the repeatability of the cell results. Careful alignment (± 1 mm) of the interface at varying heights was therefore carried out and the runs following checked for repeatability. Only the (linear) initial rate was studied, over a period of about 7 hours. The results are shown in Table 1.

TABLE 1

Effect of Interface Position on Initial Rate of Extraction from 3 g dm^{-3} Copper, 2 g dm^{-3} Sulphuric Acid with 20 vol % LIX64N in Escaid 100 at 28°C in the Gauze Cell (Stirrer Speed 115 rpm)

Mean Interface Position (mm below Gauze)	Initial Rate in g $m^{-2}s^{-1}$
0	0.0016
0	0.0016
3	0.0021
3	0.0020
5	0.0021
5	0.0025

Interfaces set at the gauze itself gave the most repeatable results, settings above the gauze gave meaningless results and those small missettings below the gauze resulted in appreciable but not catastrophic changes in the rates obtained.

Effect of Stirrer Speed on Rates. The effect of varying the stirrer speed (bars 25 mm in length) on the initial rates (<450 min) is shown in Table 2.

TABLE 2

Effect of Stirrer Speed on Initial Rate of Extraction

Stirrer speed (rpm)	Initial rate in g $m^{-2}s^{-1}$
40	0.0010
60	0.0013
80	0.0017
100	0.0015
115	0.0016
130	0.0017
160	0.0041

A 'plateau region' exists from 80 to 130 rpm, at which mass transfer is essentially independent of stirrer speed. Later experiments were carried out with 100 rpm stirring.

Rates of Forward Extraction. Full time-scale runs were undertaken at 28°C with a variety of aqueous phase and organic phase compositions. Instantaneous rates of mass transfer may be obtained by taking tangents, at the appropriate times, on the curves of organic copper concentration versus time.

Initial Rates. Values of the initial rates, taken as above, are compared in Table 3 with initial rates from rising drop experiment data (1) in Table 3.

TABLE 3

Initial Rates from Gauze Cell Experiments at 28°C

A. 20 volume % LIX64N in Escaid 100

Aqueous Concns Copper (g dm^{-3})	Aqueous Concns Acid (g dm^{-3})	Initial rates (g $m^{-2}s^{-1}$) Gauze Cell	Initial rates (g $m^{-2}s^{-1}$) Single Drop	Ratio	Equilibrium $[Cu]_{org}$ (g dm^{-3})
2	1	0.0027	0.0055	0.49	5.32
4	1	0.0038	0.0097	0.39	5.46
6	1	0.0050	0.0114	0.44	5.60
8	1	0.0061	0.0130	0.47	5.70
8	2	0.0052	0.0103	0.50	5.32
8	3	0.0048	0.0083	0.58	5.35
8	4	0.0038	0.0067	0.57	5.18
8	6	0.0020	0.0046	0.44	4.84
8	8	0.0017	0.0035	0.49	4.56

B. Aqueous concns for gauze cell 8 g dm^{-3} copper, 1 g dm^{-3} acid

Volume % LIX64N	Initial Rates (g $m^{-2}s^{-1}$) Gauze Cell	Initial Rates (g $m^{-2}s^{-1}$) Single Drop	Ratio	Oxime Monomer Concentration (mol dm^{-3})
5	0.0028	0.0013	2.15	0.04
10	0.0044	0.0022	2.00	0.05
20	0.0061	0.0035	1.74	0.07
30	0.0069	0.0043	1.60	0.08
40	0.0074	0.0051	1.45	0.09

Variation of Rate with Aqueous Phase Concentration. From Table 3A the ratio (gauze cell : single drop) of the initial rates lies generally between 0.47 and 0.58, with one value somewhat low. There is no systematic trend in the ratio with either copper or acid concentration and it is concluded that gauze cell initial rates are affected in the same way as single drop initial rates by aqueous phase concentrations.

Variation of Rate with LIX Concentration. In Table 3(B) the initial rates for the Gauze cell (aqueous phase 8 g dm^{-3} copper, 1 g dm^{-3} sulphuric acid) are compared with single drop initial rates (aqueous phase 2.64 g dm^{-3} copper, 1.76 g dm^{-3} sulphuric acid). There is a systematic trend in the ratio of initial rates with LIX64N concentration and the two types of experiment thus give divergent results when organic phase concentrations are varied (even though the results are directly related when only aqueous phase concentrations are changed). Table 3(B) also shows values of the oxime monomer concentration estimated (6) from interfacial tension measurements; the dependences of initial rate on the monomer concentration are approximately represented by:

$$\text{Rate} \propto [\text{monomer}]^{1.6} \quad \text{(single drop) and}$$

$$\text{Rate} \propto [\text{monomer}]^{1.1} \quad \text{(gauze cell).}$$

The former is in accordance with the expected order ≥ 1.5 (6).

Variation of rate with LIX64N concentration can also be investigated by relating rate to the unreacted oxime concentration as the extraction of copper proceeds. For 20% LIX64N and the aqueous phases shown in Table 3(A), the effect of the aqueous phase concentrations on the rate can be eliminated by dividing the rate of extraction at any time by the initial rate, and the unreacted oxime concentration can be calculated by subtracting twice the concentration of copper complex from the total oxime concentration (on the basis of 100 vol.% LIX64N = 0.90 mol dm^{-3}).

When the resulting rate ratio is plotted against the the unreacted oxime concentration, the graphs show that a single line represents all of the experiments on Table 3(A), but that there are deviations above 80% approach to equilibrium which are more apparent with the more highly acidic aqueous phases. Initial rate measurements are thus a good measure of the rate of extraction up to a point at which the rate of the reverse reaction becomes significant.

When the experiments at other total LIX64N concentrations (5 to 40 vol.%) are added, however, the dependence of rate on free oxime concentration is no longer a unique line and rates of extraction with low total LIX concentration are systematically higher than rates at high total LIX concentration, even though the free oxime concentration is the same. Two factors might cause this systematic trend:

(a) Chemical - it is conceivable that the copper-oxime complex forms an adduct with a free oxime molecule, thereby reducing the effective free LIX concentration for reaction. Since no worker in the field has produced evidence for this adduct in oxime systems (though there is evidence for other systems) it is unlikely that this explanation is real. Moreover were only this explanation correct, then the systematic trend in the ratio (Table 3B) of Gauze cell and single drop initial rates would be unexplained.

(b) Physical - the viscosity of LIX solutions increases with increasing total oxime concentration and is relatively unaffected by copper complexation of the oxime. The trend in viscosity matches the trends of the rate discrepancies, and the participation of organic phase diffusion processes in determining the rate of extraction is thus a possible explanation of these results.

Empirical Modelling - Logarithmic Plots. A number of empirical models relating organic copper concentration and time for individual experiments have been tried, and of these models a logarithmic plot proved reasonably successful. Plots of the type

$$(1) \qquad P = \frac{1}{At} \ln((C_o - C_\infty)/(C_t - C_\infty))$$

are suggested by the "penetration theory" (7), where P is the penetration constant, A is the interfacial area, and C_o, C_t and C_∞ are the organic copper concentrations at time zero, t and infinity respectively. Straight line graphs of log $(C_\infty - C_t)$ against time are obtained for these data; values of P are shown in Table 4 and are close in magnitude to those for salicylic acid transfer in the original reference (7).

TABLE 4

Values of P from Gradients, Data of Table 3

A. 20 volume % LIX64N			B. 8 g dm^{-3} copper, 1 g dm^{-3} acid	
Aqueous Concns Copper (g dm^{-3})	Acid	P in $cm^{-2}s^{-1}$	Volume % LIX64N	P in $cm^{-2}s^{-1}$
2	1	5.7×10^{-7}	5	19.8×10^{-7}
4	1	8.4×10^{-7}	10	16.1×10^{-7}
6	1	10.5×10^{-7}	20	13.6×10^{-7}
8	1	14.4×10^{-7}	30	9.6×10^{-7}
8	2	13.4×10^{-7}	40	7.6×10^{-7}
8	3	10.8×10^{-7}		
8	4	7.2×10^{-7}		
8	6	4.9×10^{-7}		

Since the model, Equation (1), differentiates to give

$$(2) \qquad \text{Rate (in g } dm^{-3}s^{-1}) = PA\,(C_\infty - C_t)$$

it would be expected that the value of P would be proportional to the initial rate with our solutions of very similar C_∞. Indeed the ratio of P ($cm^{-2}s^{-1}$) to initial rate (g $m^{-2}s^{-1}$) varies from 1.9×10^{-4} to 2.6×10^{-4} in accordance with calculations from equation (2). This model is thus internally consistent.

A feature of this otherwise satisfactory empirical model is that initial rate appears to be related directly to equilibrium copper loading, despite the evidence of Table 3(A); this may give rise to misunderstandings unless it is remembered that P as well as C_∞ is dependent on aqueous phase composition.

This empirical model underlies the plots of log (1 - E) presented in many of the reports to express kinetic results of batch stirred tank testwork (8), (9) although in batch tests the aqueous phase concentrations alter as the organic copper concentration increases.

Rates of Stripping. Pre-loaded solutions of 20 vol.% LIX64N in Escaid were stripped with varying concentrations of sulphuric acid (presaturated with Escaid) at 28°C in the Gauze cell. In earlier single drop experiments (1) on stripping, the expression

$$\text{Rate (in g } m^{-2}s^{-1}) = 8.2 \times 10^{-6} \; ([Cu]_{org} \text{ in g } dm^{-3}) \; ([H_2SO_4]_{aq} \text{ in g } dm^{-3})$$

was demonstrated up to values of the product ($[Cu]\,[H_2SO_4]$) = 500. The corresponding rate graphs for the Gauze cell result in the relation

$$\text{Rate (in g } m^{-2}s^{-1}) = 5.3 \times 10^{-6} \; ([Cu]_{org} \text{ in g } dm^{-3}) \; ([H_2SO_4]_{aq} \text{ in g } dm^{-3})$$

for values of the product up to 300. At higher values of the product, or in particular when the organic phase copper concentration exceeds 2 g dm^{-3}, divergence from the straight line relationship is noted and the rate of stripping is reduced from its straight line value. This reduction again arises from a change in organic phase properties rather than from a change in the dependence of rate on sulphuric acid concentration.

REFERENCES

1. R.J. Whewell, M.A. Hughes, C. Hanson, J. Inorg. Nucl. Chem. 37 2303 (1975).
2. C.A. Fleming, National Institute for Metallurgy, Johannesburg, South Africa, Report no. 1793 (1976).
3. V. Hancil, V. Rod, M. Rehakova, Chem. Eng. J. 16 51 (1978).
4. W.J. Albery, P.R. Fisk, Hydrometallurgy 81, Procs. of Society of Chemical Industry Symposium, Manchester, paper F5/4 (30 June 1981).
5. C. Hanson, M.A. Hughes, R.J. Whewell, J. Appl. Chem. Biotech. 28 426 (1978).
6. R.J. Whewell, M.A. Hughes, C. Hanson, ISEC'77, Toronto 185, Canadian Institute of Mining and Metallurgy (1979).
7. S. Sjöblin, Acta Physiol. Scand. 4 365 (1942).
8. A.D. Ryon, K.O. Johnson, U.S.A.E.C. Report ORNL-2213 (1956).
9. A.D. Ryon, F.L. Daley, R.S. Lowrie, U.S.A.E.C. Report ORNL-2951 (1960).

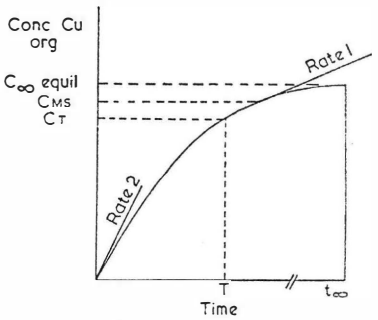

FIG 1. Position of instantaneous rates on the mass transfer versus time curve

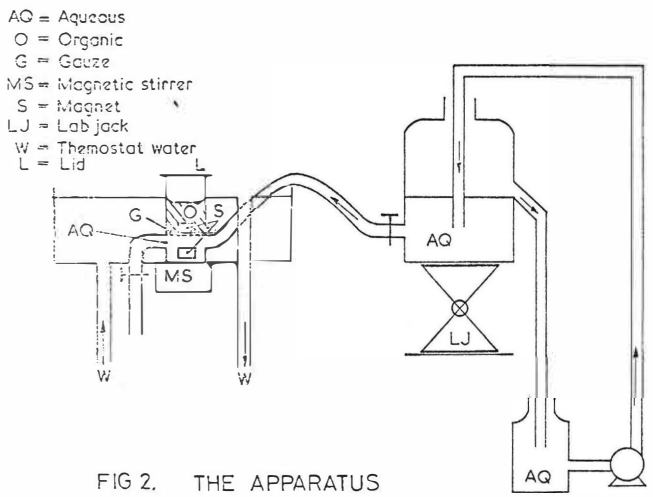

FIG 2. THE APPARATUS

THE INFLUENCE OF LIX63 ON COPPER EXTRACTION INTO LIX65N

E. Y. O. Paatero*
Laboratory of Industrial Chemistry
Abo Akademi
SF-20500 Abo, Finland

and

J. A. Golding
Department of Chemical Engineering
University of Ottawa
Ottawa, Ontario KIN 9B4, Canada

*Author to whom correspondence should be addressed.

The commercial extractant LIX64N is a mixture of LIX65N and a small amount of LIX63 which enhances the rate of extraction of copper(II) from acidic sulphate solutions. The active component in LIX65N is the *anti*-isomer of 2-hydroxy-5-alkylbenzophenone oxime and as the alkyl chain is predominantly a nonyl group, the compound is here abbreviated with *anti*-HNBPO. In LIX63 the active accelerating component is the *anti*-isomer of 5,8-diethyl-6-hydroxy-7-oximinododecane (*anti*-DEHOD). LIX64N, LIX65N and LIX63 are trade names of Henkel Co., USA.

EXPERIMENTAL

The modified Lewis cell was based on our previous works (1,2). The aqueous heavy phase was continuously pumped through the cell in order to keep the aqueous phase concentrations constant during the runs. The liquid-liquid interface was kept on a constant level by means of the arrangement shown in Figure 1. The pH of the aqueous feed was about 0.2 units higher than in the Lewis cell in order to compensate the hydrogen ion release taking place during the extraction.

The experiments in the dispersion cell were performed according to the method described earlier (1). The phase volume ratio was 1.0 and the total liquid volume was 300 cm^3. The rotation frequence of the stirrer was 11.9 s^{-1}.

The oximes were isolated from LIX65N and LIX63 according to the methods described in (3) for *anti*-HNBPO and in (4) for *anti*-DEHOD.

THEORY

The oxime extractants are weak acids with $pK_a > 10$ (5) which at low pH first attack the hydrated copper ion in molecular form and the deprotonation takes place after the chelation. The following cation exchange reactions can be written for the extraction of copper with a mixture of *anti*-HNBPO (=HR) and *anti*-DEHOD (=HB):

(1) $Cu^{2+} + HR \rightleftharpoons CuR^+ + H^+$

(2) $CuR^+ + HR \rightleftharpoons CuR_2 + H^+$

(3) $Cu^{2+} + HB \rightleftharpoons CuB^+ + H^+$

(4) $CuB^+ + HB \rightleftharpoons CuB_2 + H^+$

(5) $CuR^+ + HB \rightleftharpoons CuBR + H^+$

(6) $CuB^+ + HR \rightleftharpoons CuBR + H^+$

(7) $CuBR + HR \rightleftharpoons CuR_2 + HB$

It is generally agreed (6) that the addition of *anti*-DEHOD does not affect the extraction equilibrium. Complexes CuB_2 and CuBR are thus less stable than CuR_2. As has been pointed out by Laskorin (7) the stability of CuR_2 depends on the macrocyclic structure including two intermolecular hydrogen bonds between the ligands. Consequently CuBR is less stable than CuR_2 because there is in CuBR only one such intermolecular H-bond. CuB_2 is the least stable, because it is likely that no intermolecular H-bonds occur between the ligands. This conclusion is based on molecular models.

According to van der Zeeuw and Kok (8) and Preston (9) α-oximes (such as *anti*-DEHOD) and α-dioximes act as accelerators while β-oximes (such as *anti*-HNBPO) and β-dioximes do not have an accelerating effect. It was pointed out by van der Zeeuw and Kok that both the α-oximes and α-dioximes form five-membered rings with the copper ion while the β-oximes and β-dioximes form six-membered rings. Due to the molecular structure there seems to be also another difference. In *anti*-HNBPO there exists an intramolecular hydrogen bond between the phenolic hydrogen and the oxime nitrogen (7). In *anti*-DEHOD this type of H-bonding is unlikely as previously considered by Tammi (4). Reaction (1) can thus be thought to consist of two steps:

(8) HR (closed) $\rightleftharpoons$ HR (open)

(9) HR (open) + $Cu^{2+} \rightleftharpoons CuR^+ + H^+$

This means that the activity of the active "open" (= no intramolecular H-bond to the nitrogen) *anti*-HNBPO is lower than that of *anti*-DEHOD at equal concentrations. It is reflected also in the fact that *anti*-DEHOD is more easily protonated of the two oximes (5). The acceleration consequently depends on that $[CuB^+]$ is higher than $[CuR^+]$. The reaction route would thus include: Reaction (3) followed by Reaction (6) and finally the ligand exchange reaction (7) which takes place in the bulk of the organic phase.

RESULTS OF RATE STUDIES

The accelerating effect of LIX63 is believed to be influenced by several other factors in addition to the chemical reactions. The type of equipment and the purity of the reagents seem to be of importance, too.

Use of purified reagents. The addition of 4% *anti*-DEHOD (mole-% in respect to *anti* HNBPO) has been observed (1) to accelerate the initial rate of extraction about three fold in a Lewis cell. Additional *anti*-DEHOD neither accelerated nor retarded the extraction. In the dispersion cell (Figure 2) the initial rate continued to increase up to 9% *anti*-DEHOD. However, the lines in Figure 2 intersect each other which has as a practically important consequence that for instance 95% extraction can be achieved faster with 3% *anti*-DEHOD than with 9% *anti*-DEHOD.

Use of technical grade reagents. LIX64N contains except the *anti*-isomers of the oximes also the *syn*-isomers, nonylphenol and the original solvent. It is known (10) that *syn*-HNBPO and nonylphenol have a retarding effect on the rate of extraction. This retardation is prominent in mildly agitated equipment, such as the Lewis cell (3). According to Table 1 the rate of extraction with the purified *anti*-HNBPO alone is higher than that achieved with the addition of LIX63 to LIX65N. The concentration of LIX65N was adjusted so that the *anti*-HNBPO concentration was the same in each run. The drop in extraction rate at the highest LIX63 concentration is believed to depend on interfacial contamination by the impurities introduced to the system with LIX63.

TABLE 1: The initial extraction rate in a semistationary Lewis cell. Aqueous phase: 0.3 $kmol/m^3$ $CuSO_4$ at pH 2.25, stirrer Reynold's number Re_a = 3000. Organic phase: 0.02 $kmol/m^3$ *anti*-HNBPO in 2,2,4-trimethylpentane (LIX65N contained 1.00 $kmol/m^3$ *anti*-HNBPO), the amount of LIX63 is given as vol.-% in respect to *anti*-HNBPO, Re_o = 4400.

reagent	J_{Cu} ($\mu mol\ m^{-2}\ s^{-1}$) (*)
anti-HNBPO	98
LIX65N	41
LIX65N + 3.1% LIX63	52
LIX65N + 6.3% LIX63	71
LIX65N + 12.6% LIX63	61

(* The mean of 2-3 runs)

Acknowledgement: E.Y.O. Paatero acknowledges the award of a fellowship by Tekniikan edistämissäätiö for a research visit to the University of Ottawa 1981-82.

REFERENCES

1. L.Hummelstedt, E.Paatero, T.Nyberg and L.Rosenback, Proc. International Solvent Extraction Conference (ISEC'80), Vol. 2, paper 80-73, Association des Ingénieurs sortis de l'Université de Liége 1980.

2. J.A.Golding and V.N.Saleh, Proc. ISEC'80, Vol. 1, paper 80 194.

3. E.Y.O.Paatero, Hydrometallurgy (accepted).

4. T.T.Tammi, Hydrometallurgy 2 (1976/1977) 371.

5. J.S.Preston and R.J.Whewell, J.inorg.nucl.Chem. 39(1977) 1675.

6. D.R.Spink and D.N.Okuhara, Metallurgical Transactions 5(1974) 1935.

7. B.N.Laskorin, V.V.Yaksin and A.A.Mirokhin, Proc. ISEC'74, Vol. 2, p. 1775, Soc. Chem. Ind., London 1974.

8. A.J.van der Zeeuw and R.Kok, Proc. ISEC'77, Vol. 1, p. 17, Can. Inst. of Mining and Metallurgy, Montréal 1979.

9. J.S.Preston, J.inorg.nucl.Chem. 42(1980) 441.

10. R.J.Whewell, M.A.Hughes and C.Hanson, Proc. ISEC'77, Vol. 1, p. 185.

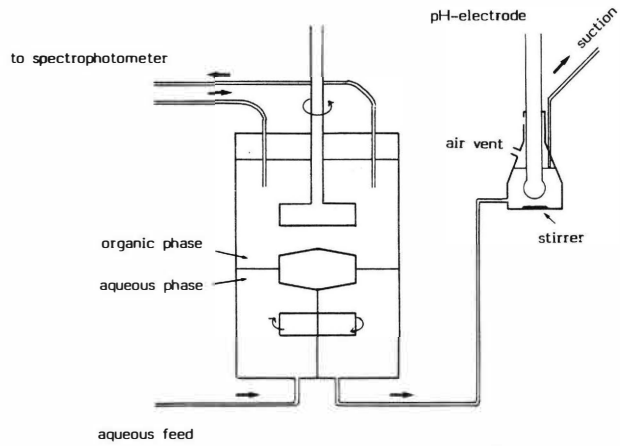

FIGURE 1: The semistationary modified Lewis cell. The internal diameter is 60 mm, the interfacial area is 23.2 cm^2 and the phase volume ratio in the cell is 1.0 (150 cm^3 of each phase).

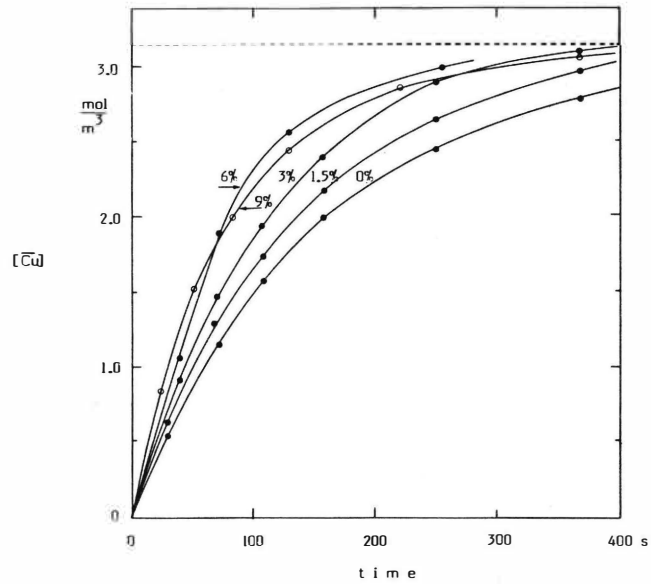

FIGURE 2. The change in the organic phase copper concentration with time in a dispersion cell. Organic phase: chloroform solution with 0.01 mol/dm^3 *anti*-HNBPO and varying amounts of *anti*-DEHOD. The percentage is calculated as 100·[*anti*-DEHOD] / [*anti*-HNBPO]. Aqueous phase: 0.05 kmol/m^3 $CuSO_4$ solution at pH 1.75. The dashed line corresponds to the extraction equilibrium where $[\overline{Cu}]$ = 3.08 ± 0.03 mol/m^3.

INTERFACIAL TENSION AND MASS TRANSFER RATE MEASUREMENTS FOR COPPER. EXTRACTION WITH A HYDROXYOXIME EXTRACTANT

Jorge M. R. de Carvalho and Michael J. Slater

Universidade Técnica de Lisboa, I.S.T.
Departamento de Tecnologia Quimica
Av. Rovisco Pais
1096 Lisboa Codex, Portugal

Schools of Chemical Engineering
University of Bradford
Bradford, West Yorkshire BD7 1DP, England

INTRODUCTION

The commercial application of solvent extraction to the recovery of metals has encouraged fundamental research on the equilibria and the kinetics of extraction reactions. O-Hydroxyaryloximes are finding wide acceptance as extractans for metals, particulary copper, from acid leach liquers. Fig. 1 below shows the general structure of the group of compounds, its dimeric forms and complexes.

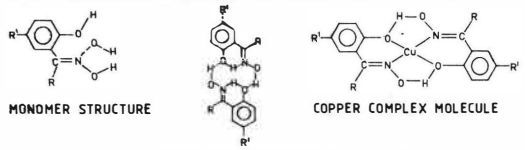

R' = C_9H_{19} (to decrease solubility of extractant in aqueous phase)

Substituent R	Commercial name	Registered Trademarks
H	P50	ACORGA Ltd
CH_3	SME 529	SHELL CHEMICALS Ltd
C_6H_5	LIX 65N	HENKEL Corp.

FIGURE 1. STRUCTURE OF O-HYDROXY ARYL OXIMES

Mass transfer, with reaction, between two "immiscible" liquid phases presents a dependence of rate on interfacial area. This dependence does not imply a truly interfacial mechanism for the reaction, since the volume of a finite homogeneous interphase zone will similarly be dependent on interfacial area. For the extraction of a metal by chelating reaction, a series of diffusion steps can be envisaged together with a chemical reaction in a certain zone. The rate of extraction might then be determined by these diffusional processes and/or by the chemical reaction steps in the reaction zone. The determination of the nature and site of the mechanistic step which controls the overall reaction kinetics (2-5), is relevant not only to the theory of solvent extraction chemistry but also to the design of improved commercial processes. For further developments of mass transfer models in liquid-liquid extraction, the knowledge of the surface activity of all the species involved together with the values of the diffusivities of the reactants in the aqueous and in the organic phases is necessary.

INTERFACIAL TENSION STUDIES IN SOLVENT EXTRACTION SYSTEMS

One of the ways of studying the interfacial activity of a reagent in a solvent extraction system is by measuring the interfacial tension. Previous studies dealt either with the prediction of coalescence rates (6, 7) or with the change of interfacial tension with concentration of surface active species and the corresponding area of interface occupied by simple molecules (8, 9, 10) to investigate mechanisms of solute transfer across interfaces. The interfacial concentrations of adsorbed species can be determined by means of the Gibb's adsorption isotherm (11, 12, 13) recently verified for oil-water interfaces (14). All the studies referred deal with static interfacial tensions and in a recent study of the drop weight method applied to systems containing surface active species, Flett and Singh (15, 16) found that equilibrium was reached if the drop was formed very slowly (3 minutes).

DYNAMIC INTERFACIAL TENSION STUDIES

Recently we reported (1) that some of the organic solvents used in solvent extraction exhibit a dynamic interfacial tension against the aqueous solutions generally used. Until now this problem and its implications have not been described for solvent extraction. We also found that the P50/aqueous system, when the solvent is nearly fully loaded presented a pronnounced dynamic effect.

DIFFUSIVITY. ANALYSIS USING DYNAMIC INTERFACIAL TENSION DATA

The dynamic interfacial tension is controlled in some cases by the diffusion of extractant molecules, under these conditions and using the variation with time of the concentration of those species, we can obtain a value for the diffusivity of the complex molecule at least for the P50 extractant. The variation of γ with time for a steady drop is assumed to be equivalent to the concentration of complex molecules at interface at each moment. To minimize the error, we choose conditions where the solvent is reasonably loaded, in order to increase the sensitivity of the process. The diffusivity of the complex molecule inside the organic phase out of the interface, which must be equal to the diffusion rate for the dimer travelling from the bulk into the interface, was determined using the Vermeulen approximation (17). This approach can be applied to concentrated and complex systems and not only to very dilute solutions. For dilute solutions the diffusivities can be calculated using the approach of Ward and Tordai (18). The fractional attainment of equilibrium as a function of time for a particle diffusion controlled isotopic exchange is represented by the equation

$$(1) \qquad U(t) \simeq 1 - \exp\left(-\frac{\bar{D}t\,\pi^2}{r_o^2}\right)^{1/2}$$

which can be used in the whole range $0 < U(t) < 1$ where,

$$(2) \qquad U(t) = \frac{\gamma_o - \gamma(t)}{\gamma_o - \gamma_f}$$

is equivalent to the fractional attainment of equilibrium, r_o is the drop radius (cm) assuming that its shape is spherical, t is time (s) upon formation of a fresh surface and $\bar{D}$ is the diffusivity in cm^2/s. Re-arranging

$$(3) \qquad 1 - \left(\frac{\gamma_o - \gamma(t)}{\gamma_o - \gamma_f}\right)^2 = \exp(-\alpha t) \qquad \alpha = \frac{\bar{D}\pi^2}{r_o^2}$$

EXPERIMENTAL

Reagents. The commercial reagents Escaid 100 (supplied by Esso in 1975), nonyphenol (ICI LTD., Ref. 1242) and Acorga P50 extractant were studied as delivered. The extractant as supplied contains 93.5 wt% of hydroxyoxime and 6.5 wt% of nonylphenol. The other reagents used were Analar grade.

Apparatus. A modified drop weight method (1) was used for all measurements of dynamic interfacial tension using an "Agla" micrometer syringe with an assembly (1) to form the organic drops.

Technique. The dynamic interfacial tension was analysed with the method and apparatus referred, which consists in forming organic phase drops of several volumes, corresponding to different γ values, having the same formation time. We wait for their release to record the time. A curve of γ interfacial (or surface) tension as a function of time was then drawn. To calculate interfacial tensions an average volume of not less than 4 drops was used in conjunction with the correction due to Harkins and Brown. The results are good to slightly better than 3.0% (1). Analysis for sulphuric acid in the presence of copper was by the method of Gran (1952). Copper analysis was carried out by atomic absorption spectrophotometer. For all the measurements of interfacial tension made in this work the two phases were mutually equilibrated by shaking for 24 hours in a shaker and next left one day to be separated completely.

RESULTS AND DISCUSSION

Several dynamic interfacial tension curves for systems at equilibrium conditions were drawn to study the effects of the amount of P50 and N.P. in the diluent, type of diluent, aqueous medium, level of copper in the solvent phase and the degradation of the solvent with the time. The curves are presented in Fig. 1 and details of the solvent and aqueous phases involved are presented in Table 1. Equation (3) was applied to some of the dynamic interfacial tension data presented in Fig. 1. In these studies the size of the drop through which diffusion is assumed to take place ranged between the maximum size and 12% lower. Example of calculations using equation (3) are presented elsewhere (1). Fig. 2 shows a very good fit with the Vermeulen equation and in Table 1 we present all the data involved in the calculations and the results. The diffusivities obtained with the exception of experiments 10 and 51 for loaded solvent respectively against distilled water, are much larger than those predicted by the Wilke and Chang correlation. The results depend on the ionic strength of the aqueous phase and so we must consider these values as apparent diffusion coefficients. With the approach proposed, the migration of the complex species in the organic phase is proportional to the apparent diffusion coefficient times the initial driving force ($\gamma_o - \gamma_f$). A large value of ($\gamma_o - \gamma_f$) also generates interfacial turbulence, increasing substantially the rate of mass transfer. Kinetic work carried out in a mixed tank with P50 copper sulphate systems identical to the ones presented in Table 1 and in Fig. 1, which are published elsewhere. This work shows that the apparent diffusion coefficient derived from interfacial tension measurements is too high to explain stirred tank rate data in terms of a pure mass transfer model. The results of the partial mass transfer coefficients assuming the proposed model (1), showed that there was a kinetic resistance in the overall process as well as diffusional resistance. However, sometimes static and dynamic interfacial effects can accelerate the diffusion process and compensate for chemical retardation, by improving coalescence or through interfacial turbulence. Sometimes the two effects may occur together and more or less cancel.

GENERAL CONCLUSIONS

1. The modified drop weight apparatus for solvent drops, described elsewhere (1), can be used successfully to follow interfacial tension changes with time with good accuracy.

2. Comparing the data in Figs. 1 - 2 we can conclude that when the solvent is loaded above 70.0% of its capacity two opposing effects may occur in the region of the interface; mainly a retardation of transfer due to a lower diffusivity value and an acceleration due to interfacial turbulence.

3. Apparent organic phase diffusivities can be derived from interfacial tension measurements and follow the pattern of the viscosities and the contributions to the diffusivity from other factors are less important.

4. The values of diffusivities calculated by the process described are the correct values to be used in theoretical expressions for the partial mass transfer coefficients in order to compare with experimental values for mechanism investigation.

NOMENCLATURE

$\bar{D}$ - diffusion coefficient of the solvent in the phase into which it is transferred, cm^2/s.

N.P. - nonylphenol.

r_o - radius of the spheric drop with the same volume than the one found at the assembly.

t - time coordinationate, min. or s.

U(t) - fractional attainment of equilibrium as a function of time for a particle diffusion controlled isotopic exchange, equation (3).

$\gamma(t)$ - dynamic surface or interfacial tension, as a function of the age (t) of a fresh surface. N/m, in general t is in minutes.

γ_f - dynamic surface or interfacial tension for a surface of age 25 min. or static value when a drop is formed very slowly using the drop weight method, N/m.

α - parameter, equal to $(\bar{D}\,\pi^2/r_o^2)$, s^{-1}.

REFERENCES

1. J.M.R. Carvalho, Ph. D. Dissertation, University of Bradford, U.K., (1982).
2. R.J. Whewell, M.A. Hughes and C. Hanson, J. Inorg. Nucl. Chem., 38, 2071 (1976).
3. R.L. Atwood, D.N. Thatcher and J.D. Miller, Met. Trans. A.I.M.E., 6B, 465 (1975).
4. D.S. Flett, D.N. Okuhara and D.R. Spink, J. Inorg. Nucl. Chem., 35, 2471 (1973).
5. C.A. Fleming, National Institute for Metallurgy Report No. 1793, Johannesburg, (1976).
6. A.R. Ferrin and R.R. Davison, AICHE Journal 17, No.5, 1021 (1971).
7. H. Groothius and F.J. Zuiderweg, Chem. Eng. Sci., 12, 288 (1960).
8. T.A.B. Al-Diwan, M.A. Hughes and R.J. Whewell, J. Inorg. Nucl. Chem., 39, 1419 (1977).
9. M. Pizzichini, R. Chiarizia and P.R. Danesi, J. Inorg. Nucl. Chem., 40, 669 (1978).
10. R. Chiarizia, P.R. Danesi, G. D'Alessandro and B. Scuppa, J. Inorg. Nucl. Chem., 38, 1367 (1976).
11. J.T. Davies and E.K. Rideal, Interfacial Phenomena, Ac. Press, N.Y. (1963).
12. R. Defay, I. Prigogine, A. Bellemans and D.H. Everett, "Surface Tension and Adsorption", Longmans (1966).
13. J.J. Bikerman, Physical Surfaces, Acad. Press, N.Y. (1970).
14. D.E. Graham, L. Chatergoon and M.C. Philips, J. Phys., 8, 696 (1975).
15. ... Cox and D.S. Flett, Proc. ISEC'77, 21,63.
16. L.R. Singh, P. Bahadur and S.N. Srivastava, Colloid. Polym. Sci., 253, 769 (1975).
17. T. Vermeulen and J. Crank, "The Mathematics of Diffusion", Oxford, University Press, N. York (1956).
18. A.F. Ward and L. Torday, Chem. Phys., 14, 453 (1946).

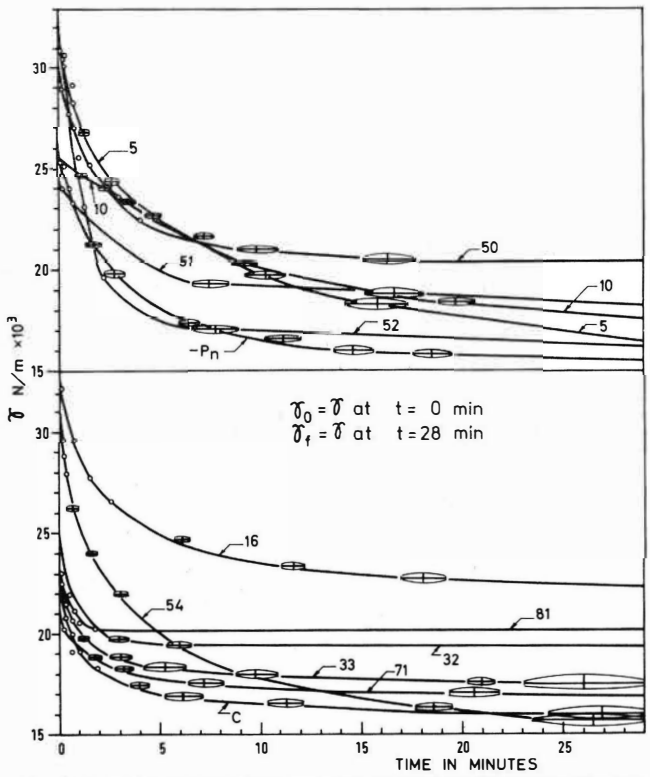

FIGURE 2. DYNAMIC INTERFACIAL TENSION OF SYSTEMS MUTUALLY SATURED. THE SOLVENT CONTAINS AN OXIME EXTRACTANT FOR COPPER (P50). SEVERAL AQUEOUS AND SOLVENT CONDITIONS WERE EXPERIENCED.

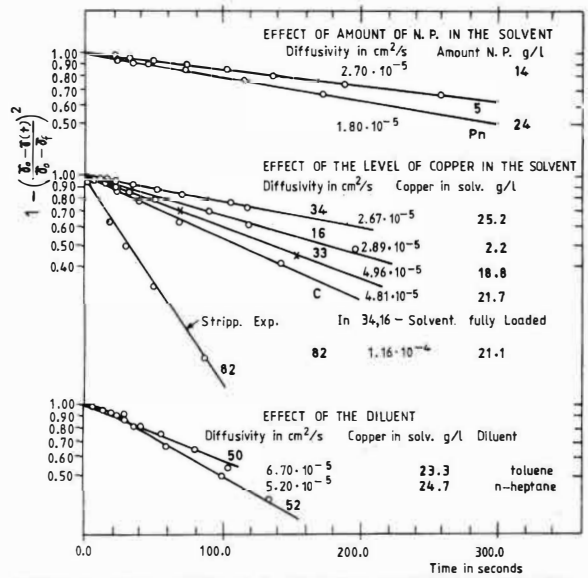

FIGURE 3. CALCULATION OF A DIFFUSION COEFFICIENT APPLYING THE VERMEULEN EQUATION IN AN ORGANIC DROP INTO AN AQUEOUS PHASE

Table 1

Calculation of a diffusion coefficient applying the Vermeulen equation

Exp. number in Fig. 1	Solvent Characteristics	Concentrations at equilibrium conditions* Copper in solvent g/ℓ	Aqueous characteristics g/ℓ	Range of Time** s	T °C	Diffusivity Coefficient x10⁵ cm²/s
5	200g/ℓ P50, 14g/ℓ N.P. or 14g/ℓ P50 as delivered in Escaid 100	24.5	14.10-Cu 14.2 -H_2SO_4	0.0-260.0	25	2.70
34		25.2	13.00-Cu 15.9 -H_2SO_4	0.0-120.0		2.67
C		21.7	3.30-Cu 30.9 -H_2SO_4	0.0-144.0		4.81
33		18.8	2.13-Cu 31.7 -H_2SO_4	0.0-158.0		4.96
Pn	200g/ℓ P50, 24g/ℓ N.P. in Escaid 100	24.7	11.90-Cu 18.0 -H_2SO_4	0.0-246.0		1.80
16	18.8g/ℓ P50, 1.31g/ℓ N.P.	2.2	11.0 -Cu 11.2 -H_2SO_4	0.0-198.0		2.89
50	200g/ℓ P50, 14g/ℓ N.P. in toluene	23.3	12.30-Cu	0.0-105.0	20	6.70
52	200g/ℓ P50, 14g/ℓ N.P. in n-heptane	24.7	12.10-Cu	0.0-135.0		5.20
71	It is 200g/ℓ P50, 14g/ℓN.P. in Escaid 100, was used for a year	16.1	1.13-Cu	0.0-196.0		2.30
81	becoming more concentrated in oxime (~ 255g/ℓ)	17.5	30.50-Cu	0.0- 80.0		11.10
82		21.1	40.50-Cu	0.0- 88.0		11.60
10	Loaded solvent (214g/ℓ P50 in Escaid 100) Dist. water	21.4	0.00-Cu	0.0-344.0		0.60
51	Unloaded solv. (214g/ℓ P50 in toluene) Dist. water	0.0	0.00-Cu	0.0-148.0		2.23

* The system was agitated for 24h in a shaker and next left 24h in a separator funnel

** Range of time considered in the dynamic interfacial data

INTERFACIAL PHENOMENA IN COPPER EXTRACTION

V. Tarasov, G. Yagodin, A. Pichugin, S. Ivakhno

Mendeleev Institute of Chemical Technology
A-47, Miusskaya sq., 9
Moscow, USSR

There are two possible ways of rate control in extraction processes. The first way consist in increasing mass transfer coefficient and effective value of the interfacial surface by introducing energy into the mixers. The second way consist in influence on the kinetics of processes accompaning extraction. The possibilities of the first way are limited by the increasing energy consumption. Now the second way became more importance, especially due to creation of centrifugal extraction apparatus. This way is more important for the processes with the rate limited by interfacial chemical reactions.

For example, copper extraction and its kinetics and mechanism recently have been the subject of intensive studies. At the same time the consistent model of this process which is known to be the basis of optimal control has not been developed so far. The essential question as to the localization of chemical reactions limiting the extraction rate remains unsettled. On this account the mechanism of catalytic influence is not clearly understood, since different means of their acceleration can be suggested depending on the localization of chemical reactions. Very often the authors prefer either reactions at interface, or reactions in volume, without any resons. Moreover, when reaction at interface takes place, authors suppose often the Langmeur's adsorption of the reagents. It is cannot be correct taking into account of the interfacial film formation.

The principal results of our study of oxyoximes copper extraction kinetics and catalysis are presented in this communication. The experimental study of copper extraction(stripping) kinetics was carried out by short-time phase contacting method (STCM). Interfacial tension mesurement was carried out by Wilhelmy plate method. The study has shown that regularities of kinetics and catalysis of copper extraction are due to following interfacial processes:

1. Extraction and stripping are limited by parallel chemical reactions both at interface(sub. index i) and in volume of aqueous phase layers adjacent to interface(sub. index v), their contributions Pi and Pv (Table 1) are comparable with and depend on concentration and for nonstationary processes on the time as well.

The values Pi and Pv are calculated by means of ourself worked out method (1). With the decrease of reagents concentration and time(in case of extraction) the reaction at the interface is dominating. It takes place with participation of adsorbed substances.

Thus, the kinetic scheme of extraction process is as follows:

$$Cu^{+2} + RH \rightleftharpoons CuR^{+} + H^{+} \quad - \text{ fast}$$
$$CuR^{+} + RH \rightleftharpoons CuR_2 + H^{+} \quad - \text{ slow}$$

The slow stage is an addition of second extractant molecule, occurs both at the interface and in the adjacent layers of the aqueous phase.

Kinetic scheme of stripping process is as follows:

$$CuR_2 + H^{+} \rightleftharpoons CuR^{+} + RH \quad - \text{ fast}$$
$$CuR^{+} \xrightarrow{H_2O} Cu^{+2} + R^{-} \quad - \text{ slow}$$
$$R^{-} + H^{+} \rightleftharpoons RH \quad - \text{ fast}$$

The limiting stage is the irreversible reaction of the complex destruction under water molecule action.

2. Ionic surfactant (IS) equally affect extraction and stripping rates, that indicates a nonspecific electrostatic catalysis due to the double electric layer field. Thus for example anionic IS (Na laurylsulphate, NaLS) gives an acceleration effect, while cationic IS (cytiltrimethylammonium bromide, CTAB) as a retardation one (Table 2). Specifically that IS change, in general, rate of reaction at interface (Table 2).

Substances extracting copper faster than oxyoximes (for instance ONP - orthonitrosophenol) also change equally the rate of direct and back reactions. These compounds change mainly the contribution of the reactions in adjacent layers of the aqueous phase (Table 2). The acceleration effects of these substances exeed those of IS by 2-3 times.

3. Oxyoximes adsorption at the interface is sutisfactorily described by Frumkin's equation. Adsorption isoterms (Figure 1) and attraction constant values (Table 3) indicate essential intermolecular interactions. These interactions are the reasons for formation of condensed interfacial films. The latter decrease considerably the rate of chemical reactions.

4. In a number of cases the dynamic interfacial tension is vary enough slowly particulary for oxyoximes with high molecular weight, it depends on the formation of interfacial films and their aging.

5. In the case of copper extraction in system with impregnaited and liquid membrane, containing Lix64N as a transfer agent, NaLS has considerable acceleration effect on extraction rate. Both "electrostatic" and "chemical" and "micellar" catalysis may also take place.

Table 1. Kinetics of copper extraction and stripping in system:

$CuSO_4 - H_2O -$ 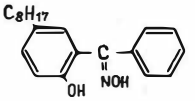 - Toluen

The values of contributions of RI (P_i) and of RV (P_v).

Extraction: pH_o=3.0; $C^{H_2O}_{Cu}$ = 0.021 kmol/m^3. Stripping: pH^o=2.4					
C^o_{ex} kmol/m^3	Pi	Pv	C^o_{Cu} kmol/m^3	Pi	Pv
0.22	0.31	0.69	0.031	0.37	0.63
0.11	0.31	0.69	0.018	0.39	0.61
0.08	0.41	0.59	0.010	0.38	0.62
0.06	0.74	0.26	0.008	0.40	0.60
0.028	0.86	0.14	0.003	0.42	0.58

C^o_{Cu} - copper concentration in organic phase

C^o_{ex} - extractant concentration

Table 3. Adsorption equilibrium parameters in system:

H_2O - toluen - 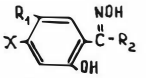

(t = 25°)

X	R_1	R_2	A	$\Gamma_\infty \cdot 10^9$ $\frac{kmol}{m^2}$	B $\frac{m^3}{kmol}$
CH_3O	H	C_6H_5	1.16	3.0	95
C_4H_9O	H	C_6H_5	1.27	3.7	75
$C_8H_{17}O$	H	C_6H_5	1.35	4.5	78
H	C_8H_{17}	C_6H_5	1.44	4.1	190
C_2H_5O	H	$C_{17}H_{35}$	1.70	6.5	6.0

Table 2. The catalysis in copper extraction and stripping in system: $CuSO_4$-H_2O-toluen- 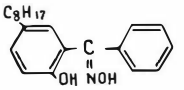

Catalyst	$C_{cat.}$ $\frac{kmol}{m^3}$	Extraction pH^o=3.0; C^o=0.11$\frac{kmol}{m^3}$			Stripping pH_o=2.4; C^o_{Cu}=0.031$\frac{kmol}{m^3}$		
		Fa	Pi	Pv	Fa	Pi	Pv
NaLS	10^{-5}	1.1	0.38	0.62	2.1	0.40	0.60
	$5 \cdot 10^{-5}$	1.5	0.45	0.55	3.6	0.43	0.57
	10^{-4}	2.5	0.63	0.37	4.5	0.58	0.42
	$5 \cdot 10^{-4}$	4.3	0.88	0.12	7.2	0.69	0.31
	10^{-3}	4.8	0.91	0.09	8.0	0.74	0.34
CTAB	10^{-5}	0.8	0.28	0.72	0.4	0.32	0.78
	$2 \cdot 10^{-5}$	0.63	0.21	0.79	0.3	0.30	0.70
	$5 \cdot 10^{-5}$	0.52	0.15	0.85	0.2	0.25	0.75
	$5 \cdot 10^{-4}$	0.13	0.10	0.90	0.05	0.20	0.80
	10^{-3}	0.11	0.07	0.93	0.04	0.17	0.83
ONP	10^{-4}	2.3	0.30	0.70	3.0	0.33	0.67
	$2 \cdot 10^{-4}$	4.8	0.25	0.75	3.5	0.21	0.79
	$8 \cdot 10^{-4}$	6.0	0.15	0.85	7.8	0.15	0.85
	$2 \cdot 10^{-3}$	10.0	0.09	0.91	12.0	0.17	0.83
	$5 \cdot 10^{-3}$	12.0	0.07	0.93	15.0	0.12	0.88

Fa - acceleration effect

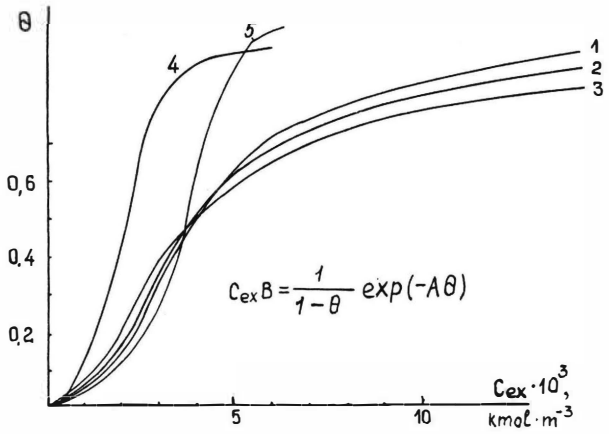

Figure 1. Adsorption isotherms in system:

H_2O - toluen - 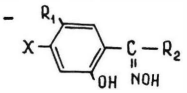 (t = 25°)

isotherm number	X	R_1	R_2
1.	CH_3O	H	C_6H_5
2.	C_4H_9O	H	C_6H_5
3.	$C_8H_{17}O$	H	C_6H_5
4.	H	C_8H_{17}	C_6H_5
5.	C_2H_5O	H	$C_{17}H_{35}$

REFERENCES.

1. G. Yagodin, V. Tarasov, A. Pichugin, Reaction in volume and reaction at interface. Calculation their contributions to overall extraction rate. Reports ISEC - 83.

EXTRACTION RATES OF COPPER WITH SME529

MECHANISM AND EFFECTS OF SURFACTANTS

Yoshikazu Miyake, Yoichiro Takenoshita and Masaaki Teramoto

Department of Industrial Chemistry
Faculty of Industrial Arts
Kyoto Institute of Technology
Matsugasaki, Kyoto 606, Japan

Introduction

It has been considered that the reaction between copper and industrial chelating agent such as LIX65N, which is poorly soluble in water and interfacially active, occurs at the interface(1,2). This means that the extraction rate is greatly influenced by interfacially active impurities in the extraction system.

In this study, the forward extraction rate of copper by anti 2-hydroxy-5-t-nonylacetophenone oxime, the active species of SME529, and the stripping rate were investigated. Furtheremore, the effect of addition of surfactants on the extraction rate was also examined.

Experimental

The interfacial area of a stirred transfer cell used for this study(3) was maintained constant at 12.6 cm^2 by a perforated plate fixed at the interface and the volumes of aqueous and organic phases were 200 cm^3 and 100 cm^3, respectively. The aqueous and organic phases were agitated at 25 l/s by a magnetic stirring bar and at 16.7 l/s by a two paddle agitator, respectively.

The forward extraction rate was obtained by the analysis of copper concentration in the sample removed from the organic phase at regular intervals. The stripping rate was also obtained by the similar procedures.

The chelating agents used were synthesized o-hydroxy acetophenone oxime (oHAPO) and anti 2-hydroxy-5-t-nonylacetophenone oxime (HNAPO) purified from SME529. Dispersol was used as a diluent and benzene for oHAPO. In the study of forward extraction rate, copper concentration was changed from 10^{-6} mol/cm^3 to 3×10^{-5} mol/cm^3 and the pH was adjusted in the range of 1.0 to 4.5 with the sulfuric acid or sodium hydroxide. In the study of the stripping rate, copper was stripped by H_2SO_4 (0.5-8mol/dm^3) or HCl (0.25-6 mol/dm^3) solutions from copper chelate in Dispersol. The nonionic, anionic and cationic surfactants with the same alkyl group ($-C_{12}H_{25}$) were used. All experiments were carried out at 298K.

Results and Discussion

Forward extraction rate; Figures 1 and 2 show that the forward extraction rate depends only on the ratio of copper and proton concentration. As the oHAPO is not interfacially active and is relatively soluble in water, it is presumed that the chelation occurs mainly in the aqueous stagnant layer. The reactions in the aqueous phase are assumed as follows.

$$(1)\quad \begin{array}{ccccc} HR & + Cu^{2+} & \underset{k_1}{\rightleftharpoons} & CuR^{+} & \xrightarrow{+(+HR)} CuR_2 \\ k_a \downarrow\uparrow k'_a & & & & \nearrow k_2 \\ R^- & + Cu^{2+} & & & \end{array} \qquad \text{(rapid, irreversible reaction)}$$

Since the concentrations of R^- and CuR^+ is negligibly small, a stationary state method can be applied to these species. Then the rate of CuR_2 formation can be described by Eq.(2).

$$(2)\quad r=\frac{d[CuR_2]}{dt}=\left(k_1[Cu^{2+}]+\frac{k_2k_a[Cu^{2+}]/[H^+]}{k'_a+k_2[Cu^{2+}]/[H^+]}\right)[HR]=k_{app}[HR]$$

The diffusion equations in the stagnant layer are given as follow

$$(3)\quad D\frac{d^2[HR]}{dx^2}=2r\ ,\qquad D\frac{d^2[CuR_2]}{dx^2}=-r$$

Boundary conditions; x=0 (at the interface)

$$(4)\quad [HR]=[HR]_i,\ [CuR_2]=[CuR_2]_i;\ J^a_{HR}=-D\frac{d[HR]}{dx}\ ,\ J^a_{CuR_2}=-D\frac{d[CuR_2]}{dx}$$

$x=x_L$ (at the edge of the stagnat layer)

$$(5)\quad [HR]=[CuR_2]=0$$

The additional conditions are necessary for the determination of the interfacial concentration.

$$(6)\quad k_o([\overline{HR}]_b-[\overline{HR}]_i)=J^a_{HR}+2r_s\ ,\ k_o[\overline{CuR_2}]_i+J^a_{CuR_2}=r_s$$

where k_o is the mass transfer coefficient in the organic phase and r_s is the formation rate of CuR_2 at the interface. From these equations, the extraction rate is derived as follows.

$$(7)\quad J_f=\frac{k_o[k_a(\beta-1)/2+r_s/[HR]_i]}{P_{HR}k_o+\beta k_a+2r_s/[HR]_i}[\overline{HR}]_b$$

$k_a=D/x_L$ (mass transfer coefficient in the aqueous phase)

$\beta=\gamma\coth\gamma \quad \gamma=(k_aPD)^{0.5}/k_a \quad P_{HR}=[\overline{HR}]_i/[HR]_i$

The solid line in Fig.1 was calculated from Eq.(7) by use of the observed and estimated values of parameters. The rate of copper extraction by oHAPO can be interpreted by the diffusion process with the reaction in the aqueous stagnant layer. On the other hand, the broken line in Fig.2 which was calculated from Eq.(7) for HNAPO is much lower than the observed data, suggesting that the interfacial reaction contributes greatly to the extraction rate. If the interfacial reaction is determined by the step of formation of CuR_2, the rate is expressed by Eq.(8) (1,2,3).

$$(8)\quad r_s=k_f\Gamma_{HR}P_{HR}[HR]_i[Cu^{2+}]/[H^+]$$

Then, the forward extraction rate, Eq.(7), can be rewritten as follows.

$$(9)\quad J=\frac{k_f\Gamma_{HR}[Cu^{2+}]/[H^+]}{1+2k_f\Gamma_{HR}[Cu^{2+}]/[H^+]/k_o}[\overline{HR}]_b$$

where the reaction in the aqueous phase was neglected and Γ_{HR} is shown by a Langmuir isotherm

$$(10)\quad \Gamma_{HR}=\Gamma^{\infty}_{HR}K_L[\overline{HR}]_i/(1+K_L[\overline{HR}]_i)$$

The solid line was calculated from Eq.(9) by use of $k_f=1.9\times10^4$ cm^3/(mol·s). This value is lower than $k_f\Gamma_{HR}=3\times10^{-4}$ cm/s (toluene), $k_f\Gamma_{HR}=5.2\times10^{-4}$ cm/s (n-heptane) for HNBPO (1) and $k_f\Gamma_{HR}=4\times10^{-4}$ cm/s (toluene) for HOAPO (2). This may be due to the differnce in the properties of the diluent and the aqueous acidic media.

Stripping rate: Since copper chelate of HNAPO is poorly soluble in water, it is presumed that the stripping reaction occurs mainly at the interface. As the mass transfer resistance in the aqueous phase is negligibly small in this study, the stripping rate is represented as follows.

$$(11)\quad J_r=k_r(a_H)_b([\overline{CuR_2}]_i-[\overline{CuR_2}]^*_i)=k_o([\overline{CuR_2}]_b-[\overline{CuR_2}]_i)$$

where $[\overline{CuR_2}]^*_i=K_{ex}[\overline{HR}]^2_i[Cu^{2+}]/(a_H)^2_b \ll [\overline{CuR_2}]_i$

Elimination of $[\overline{CuR_2}]_i$ gives the following equation.

$$(12)\quad J_r=\frac{k_r(a_H)_b[\overline{CuR_2}]_b}{1+k_r(a_H)_b/k_o}$$

Figure 3 shows the proton activity dependence of J_r, where a_H was calculated from the mean activity coefficient(4). With the increase in a_H, J_r approaches to a maximum value and the mass transfer coefficient, k_o, is calculated from this region as follows.

$$(13)\quad k_o=1.8\times10^{-4}\ \text{cm/s}$$

On the ther hand, the rate parameter, k_r, is calculated from the region where J_r is proportional to a_H as follows.

$$(14)\quad k_r=5\times10^{-2}\ \text{cm}^4/(\text{mol s})$$

Figure 4 shows the effect of the concentration of CuR_2 on J_r with $[\overline{CuR_2}]_b/(\overline{C}_{HR})_b$ kept constant. J_r is proportional to $[\overline{CuR_2}]_b$ at low $[\overline{CuR_2}]_b$ (region A) and the concentration dependence becomes smaller with the increase in $[\overline{CuR_2}]_b$ (region B). At higher $[\overline{CuR_2}]_b$, J_r is again proportional to $[\overline{CuR_2}]_b$ (region C) and the observed data in this region were reasonably simulated by Eqs.(12),(13) and (14) as shown by the solid lines in Fig.4. On the other hand, the broken line in Fig.4 shows the maximum value in Fig.3. Therefore, it is deduced that J_r in region (A) is determined by the diffusion process of CuR_2 in the organic phase. This means that the value of k_r decreases with the increase in the concentration of CuR_2 and/or HNAPO. Since the HNAPO is the stronger surface active species than the chelate CuR_2 and the stripping reaction mainly proceeds at the interface, it is considered that the apparent stripping rate constant decreases due to the adsorption of HNAPO. In region (C), the value of k_r becomes constant because the interface is saturated by the adsorbed layer of HNAPO. To confirm this deduction, a series of experiments was carried out in which HNAPO was added to the organic phase. Results are shown in Table 1. The stripping rate decreased from the value in region(B) to that in region (C) with the addition of HNAPO.

Effect of surfactant on extraction rate: Figures 5 and 6 show the effect of the addition of surface active agents on the forward extraction rate and stripping rate, respectively. Both rates were increased by the addition of an anionic surfactant but decreased by the addition of a cationic surfactant. It was also observed that J_f was decreased by the addition of a nonionic surfactant.

These results suggest that the forward and stripping rates were measurably affected by the properties at the interface. Although the detailed discussion is very difficult about these behavior the qualitative explanation is as follows. The adsorption of the surfactants lowers the rate due to the shielding effect, i.e., the decrease in the effective reaction field at the interface. On the other hand, the adsorption of the anionic surfactant gives the negative electrostatic potential at the interface. Then, the cupric and hydrogen ions are attracted to the interface by the electrostatic interaction. However, the divalent cupric ion is more concentrated at the interface than the univalent hydrogen ion. Then the concentration ratio $[Cu^{2+}]/[H^+]$ at the interface is higher than that in the bulk phase, resulting in the enhancement of the forward extraction rate expressed by Eq.(9). The stripping rate expressed by Eq.(12) is also enhanced by the concentration of the hydrogen ion at the interface. On the contrary, the adsorption of the cationic surfactant lowers the rate by rejecting the cupric and hydrogen ions from the interface.

Conclusion:

The forward extraction rate of copper by oHAPO was interpreted by the model that the reaction occurs in the aqueous stagnant layer. On the other hand, for the extraction by HNAPO the interfacial reaction contributes greatly to the extraction rate, because the solubility of HNAPO in water is much smaller than that of oHAPO. The stripping rate parameter decreases with the increase in the concentration of HNAPO. This behaviour was qualitatively explained by the decrease in the effective interfacial area due to the adsorption of the HNAPO. The effects of the addition of surfactants were also qualitatively explained by the shielding effect and the electrostatic interaction.

References;

(1) Komasawa,I, et al.;J.Chem.Eng. Japan,13,204(1980).
(2) Cox,M. et al.;ISEC80,80-118(1980).
(3) Miyake,Y. et al.;J.Chem.Eng. Japan,16, (1983).
(4) "Kagaku Benran Kisohen"p.1138,Maruzen,Tokyo(1974).

Acknowledgement;

We thank to Shell Chemical Co. of Japan, Ltd., for offering SME529 and Dispersol. We thank Mr. Y. Imanishi, A. Mistumoto and H. Okabe for performing the experiments.

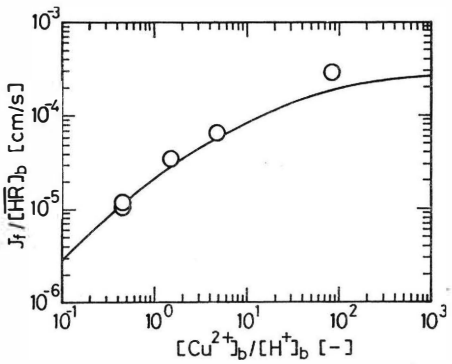

Figure 1 Forward extraction rate of copper by oHAPO ($[Cu^{2+}]_b = 10^{-6} - 3 \times 10^{-5}$ mol/cm^3, pH= 1.0 - 4.5 and $[\overline{HR}]_b = 0.9 \times 10^{-5}$ mol/cm^3)

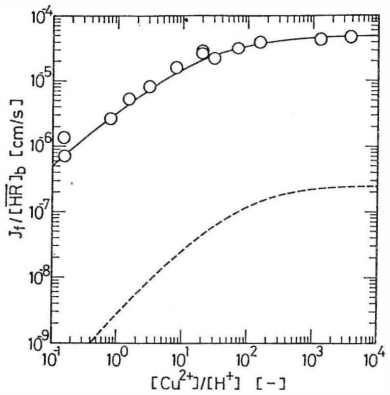

Figure 2 Forward extraction rate of copper by HNAPO ($[Cu^{2+}] = 10^{-6} - 3 \times 10^{-5}$ mol/cm^3, pH= 1.0 - 4.5 and $[\overline{HR}]_b = 0.9 \times 10^{-5}$ mol/cm^3)

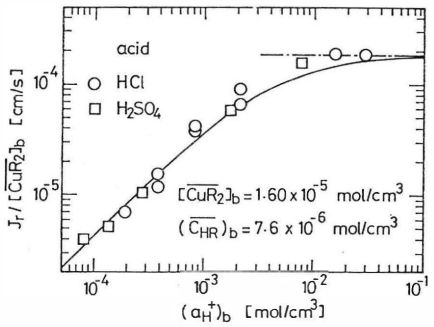

Figure 3 Effect of activity of proton on stripping rate.

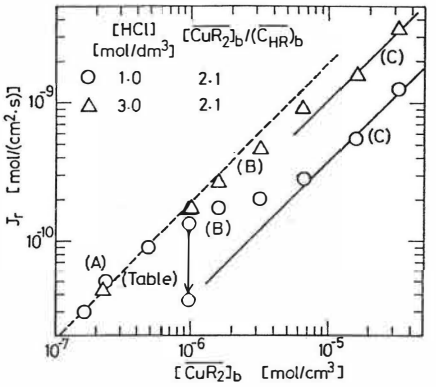

Figure 4 Effect of concentration of copper chelate on the stripping rate.

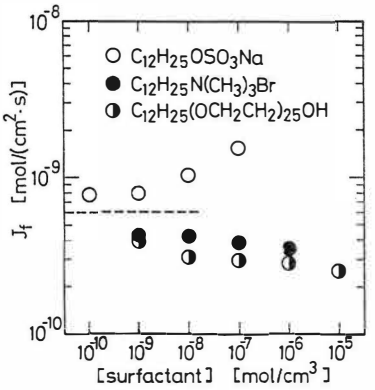

Figure 5 Effect of surfactants on the forward extraction rate. ($[Cu^{2+}] = 1.5 \times 10^{-5}$ mol/cm^3 and pH=3.0)

Table 1 Effect of added HNAPO on the stripping rate. ($[\overline{CuR_2}]_b = 9.1 \times 10^{-7}$ mol/cm^3)

$(\overline{C_{HR}})_b$ [mol/cm^3]	J_r [mol/(cm^{2}s)]	k_r [cm^4/(mol s)]
4.3×10^{-7}	1.2×10^{-10}	0.57
8.5×10^{-7}	7.0×10^{-11}	0.16
1.3×10^{-6}	5.2×10^{-11}	0.10
2.0×10^{-6}	4.3×10^{-11}	0.077
3.2×10^{-6}	3.8×10^{-11}	0.066
5.0×10^{-6}	3.5×10^{-11}	0.059
8.0×10^{-6}	3.3×10^{-11}	0.055
1.3×10^{-5}	3.5×10^{-11}	0.059

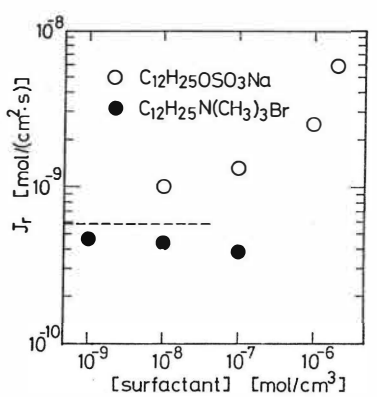

Figure 6 Effect of surfactants on the stripping rate. ($[HCl] = 1.0$ mol/dm^3 and $[\overline{CuR_2}]_b = 2.3 \times 10^{-5}$ mol/cm^3)

EXTRACTION KINETICS AND MECHANISM OF NICKEL WITH SME529

Katsutoshi Inoue, Hiroki Tsunomachi, Shin-ichi Tomita and Takeshi Maruuchi

Saga University
Saga, Japan

Extraction kinetics of nickel from aqueous ammonium nitrate - ammonia mixture with anti-2-hydroxy-5-nonylacetophenone oxime, the active species of SME 529, in MSB 210 diluent was studied as well as its fundamental extraction properties, distribution equilibrium of nickel, its aqueous solubility and interfacial adsorption equilibrium to infer the extraction mechanism.

INTRODUCTION

Hydroxyoxime extracting agents, which were originally developed as extractants for copper, have been also proposed to apply to hydrometallurgical processing of low grade oxide nickel ores such as laterites(1) or to that of manganese nodules(2) to separate copper from nickel.

Recently, a novel process to separate copper from nickel making use of the difference of extraction rates between these metals with a static mixer was proposed(3). It is necessary to obtain basic and detailed information about the extraction kinetics of these metals. Although numerous works(4,5,6,7,8) have been done about the extraction kinetics of copper with hydroxyoximes, those on that of nickel are very few.

The authors investigated the extraction kinetics of nickel from aqueous ammonium nitrate solution with anti-2-hydroxy-5-nonylacetophenone oxime, the active species of SME 529 and shortened to oxime hereinafter, in MSB 210 diluent to examine the concentration dependencies of nickel and hydrogen ion in the aqueous phase and of the oxime in the organic phase on the extraction rate to infer the extraction mechanism.

Prior to the study of extraction kinetics, we also investigated the distribution equilibrium of nickel and aqueous solubility and interfacial adsorption properties of the oxime, which are basic information for the analysis of the extraction kinetics.

EXPERIMENTAL

The oxime was purified from SME 529 donated by Shell according to the method proposed by Preston et al.(9) and was diluted to required concentration with MSB 210 diluent. 1M aqueous ammonium nitrate solution was used as an aqueous media to maintain the ionic strength constant and small amount of nitric acid or ammonia was added to adjust pH. All experiments were carried out at 30°C.

The measurement of the aqueous solubility of the oxime was carried out by converting all of the oxime in the aqueous phase into the copper-chelate adding excess amount of copper and by extracting the copper-chelate into MSB 210 to measure the absorbance at 348 nm.

Interfacial adsorption equilibrium of the oxime was studied by measuring the change of interfacial tension between the oxime solution and the aqueous phase by pH and by oxime concentration according to the drop-weight method. In addition, interfacial tension between the oxime solution completely loaded with copper or nickel and the aqueous phase was also measured to examine the interfacial adsorption equilibrium of the metal-oxime complexes.

Equilibrium concentration of nickel and hydrogen ion in the aqueous phase were measured after shaking the flask containing equal volumes of the aqueous and organic phases of known concentration for 24 hours to examine the distribution equilibrium. Nickel concentration in the aqueous phase was determined by titration with EDTA and murexide as an indicator and that of in the organic phase was calculated from the concentration in the aqueous phase by mass balance.

The extraction rate was measured in a stirred transfer cell of Lewis type, where the aqueous and organic phase were stirred independently by two flat-blade stirrers in opposite directions with equal speed of 150 rpm. After the initiation of stirring, small amount of samples were taken at intervals from the organic phase to measure the time-variation of the nickel content in the organic phase, determined by atomic absorption spectrochemical analysis after stripping the sample with 2N sulfuric acid.

RESULTS AND DISCUSSION

Aqueous Solubility Distribution of the oxime between the aqueous and organic phases is described as follows.

(1) $2HR_{org.} \rightleftharpoons H_2R_{2org.}$ K_m

(2) $HR_{org.} \rightleftharpoons HR_{aq.}$ K_1

(3) $HR_{aq.} \rightleftharpoons H^+_{aq.} + R^-_{aq.}$ K_2

Total concentrations in the organic (C_{B0}) and aqueous (C_{HR}) phases are expressed by equations (4) and (5), respectively.

(4) $C_{B0} = [\overline{HR}]+2[\overline{H_2R_2}] = [\overline{HR}]+2K_m[\overline{HR}]^2$

(5) $C_{HR} = [HR]+[R^-] = K_1[\overline{HR}](1+K_2/[H^+])$

Based on these equations and from the experimental results shown in Figure 1, K_m and K_1 were evaluated from the data in the lower pH region and K_2 was evaluated from those in the higher pH region as follows. $K_m = 3.1\times10^1[dm^3/mol]$, $K_1 = 2.2\times10^{-4}[-]$

Interfacial Adsorption Equilibrium Figure 2 shows the relation between the interfacial pressure of the oxime solution and the concentration of the undissociated monomeric oxime in the aqueous phase for various pH as a parameter. The results indicate that the monomeric oximes, not only undissociated species but also dissociated one, are highly interfacially active. Figure 3 shows relation between the interfacial pressure of the oxime solution completely loaded with copper or nickel and the concentration of the metal-oxime complexes in the organic phase, which indicates that these complexes also have interfacial activities.

Distribution Equilibrium of Nickel The stoichiometric relation in the extraction reaction of copper and nickel with aromatic β-hydroxyoximes is generally described as follows.

(6) $M^{2+} + 2HR_{org.} \rightleftharpoons MR_{2org.} + 2H^+_{aq.}$ K_e

From mass balance of the oxime in the organic phase, total oxime concentration (C_{B0}) is described as follows.

(7) $C_{B0} = [\overline{HR}]+2[\overline{H_2R_2}]+2[\overline{MR_2}]$

C_{B0} can be calculated from the metal concentration in the organic phase under the conditions of ultimate loading in the higher pH region ($C_{B0} = 2[\overline{MR_2}]$). The metal concentration in the organic phase is expressed by equation (8) in the lower pH region.

(8) $[\overline{MR_2}] = K_e([M^{2+}]/[H^+]^2)[\overline{HR}]^2$

where $[\overline{HR}]$ can be calculated from the mass balance equation of oxime in the organic phase, equation (4), and $[M^{2+}]$ is the concentration of free metal ion which is not coordinated by ammonia. Logarithm of equation (8) gives

(9) $log[\overline{MR_2}] = log([M^{2+}]/[H^+]^2) + a$

where

(10) $a = 2log[\overline{HR}] + logK_e$

Figure 4 shows log-log plot of $[\overline{NiR_2}]$ against $[Ni^{2+}]/[H^+]^2$ based on equation (9). From the values of the intercepts on the ordinate by the straight lines of slope 1 in this figure and those of $[\overline{HR}]$ corresponding to each C_{B0}, the extraction equilibrium constant, K_e, was evaluated as $K_e = 3.2\times10^{-5}[-]$ based on equation (10).

Extraction Kinetics Figure 5 shows a typical example of the experimental results of the extraction rate. Initial extraction rates were calculated from the slopes of the straight lines in these figures and the contact area between two phases and the volume of the organic phase in the cell.

Figures 6,7 and 8 show the concentration dependencies of monomeric oxime in the organic phase and nickel and hydrogen ion in the aqueous phase, respectively, on the initial extraction rate. These results indicate that the initial extraction rate is proportional to the concentration of nickel and monomeric oxime and inversely proportional to the hydrogen ion concentration in the regions of lower pH or lower concentration of nickel in case total oxime concentration is high enough and that it is independent of pH and nickel concentration and depends only on the total oxime concentration in the organic phase(C_{B0}) in the regions of higher pH or higher concentration of nickel, suggesting that dissusion of oxime in the organic phase is probable to be rate-determining in these regions.

EXTRACTION MECHANISM

Since the monomeric oxime is very insoluble in the aqueous phase and highly interfacially active as mentioned earlier, the complex-formation reaction is considered to take place at the interface between the aqueous and organic phases.

According to the interfacial reaction scheme proposed by Komasawa et al.(4) for the extraction reaction of copper with LIX 65N or by Cox(7) for that with anti-2-hydroxy-5-octylacetophenone oxime, which is composed of the elementary steps,

(11) $HR_{org.} \rightleftharpoons HR_{ad.}$

(12) $M^{2+}_{aq.} + HR_{ad.} \rightleftharpoons MR^+_{ad.} + H^+_{aq.}$

(13) $MR^+_{ad.} + HR_{org.}$ (or $HR_{aq.}$) $\rightleftharpoons MR_{2ad.} + H^+_{aq.}$

(14) $MR_{2ad.} \rightleftharpoons MR_{2org.}$

the initial extraction rate(N) is expressed as follows.

(15) $N = k[Ni^{2+}]\theta_{RH}[\overline{RH}]/[H^+]$

where the fractional coverage of the monomeric oxime at the interface, θ_{RH}, is considered to be nearly 1.0 under the present experimental conditions from the results shown in Figure 2.

Figure 9 shows log-log plot of the initial extraction rate against the value of $[Ni^{2+}][\overline{RH}]/[H^+]$ for all of the experimental

data obtained according to equation (15). In the region of lower value of $[Ni^{2+}][\overline{HR}]/[H^+]$, the plotted points cluster on a straight line of slope 1 as expected from equation (15) although they approach to constant values corresponding to each C_{B0} in its higher region. From the value of the intercept of the ordinate by the straight line of slope 1, the apparent reaction rate constant, k, was evaluated as $k = 1.1 \times 10^{-10}$ [cm/sec].

CONCLUSIONS

The extraction rate mechanism of nickel with anti-2-hydroxy-5-nonylacetophenone oxime can be fairly well explained by the reaction scheme that the extraction rate is determined by the second step in the formation of the metal-oxime complex at the interface (equation 13) in case of slow extraction rate and by diffusion process in the organic phase in case of rapid extraction rate.

REFERENCES

1. R.D.Eliasen and E.Edmunds Jr., CIM Bull., 67, No.742, 82(1974)
2. J.C.Agarwal, N.Beecher and G.L.Hubred, AIChE Symp.Ser., 76, No.192, 35(1980)
3. M.Zabelka, Sulzer Tech.Rev., 62, 111(1980)
4. I.Komasawa and T.Otake et al., J.Chem.Eng.Japan, 13, 204, 209(1980)
5. P.R.Danesi, R.Chiarizia and G.F.Vandegrift, J.Phys.Chem., 84, 3455(1980)
6. C.Hanson, M.A.Hughes and R.J.Whewell, J.Appl.Chem.Biotechnol., 28, 426(1978)
7. M.Cox, C.G.Hirons and D.S.Flett, Proceedings of ISEC'80, Paper 80-118(1980)
8. T.Kojima and T.Miyauchi, Ind.Eng.Chem.Fundam, 20, 14, 20(1981)
9. J.S.Preston and R.J.Whewell, J.Inorg.Nucl.Chem., 39, 1675(1977)

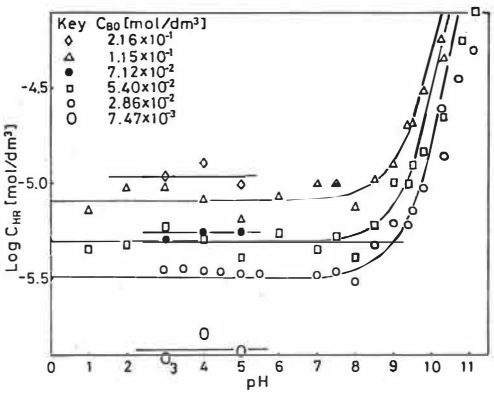

FIGURE 1. AQUEOUS SOLUBILITY OF ANTI-2-HYDROXY-5-NONYLACETOPHENONE OXIME

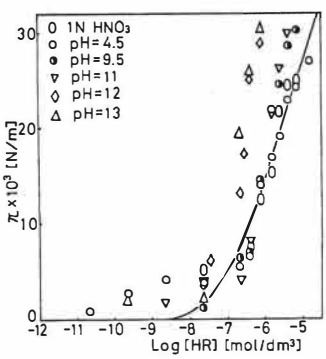

FIGURE 2. RELATIONSHIP BETWEEN INTERFACIAL PRESSURE AND OXIME CONCENTRATION IN THE AQUEOUS PHASE

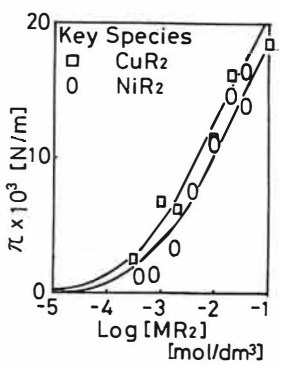

FIGURE 3. RELATIONSHIP BETWEEN INTERFACIAL PRESSURE AND CONCENTRATION OF METAL-OXIME COMPLEXES IN THE ORGANIC PHASE

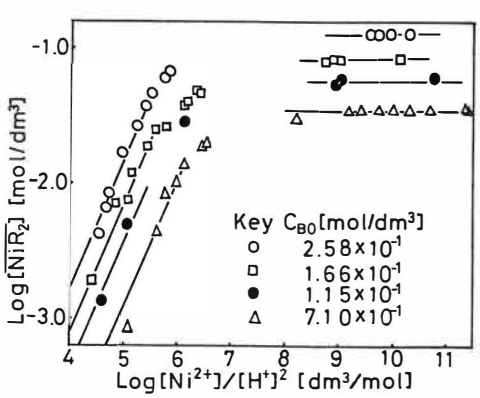

FIGURE 4. DISTRIBUTION EQUILIBRIUM OF NICKEL IN THE EXTRACTION WITH ANTI-2-HYDROXY-5-NONYLACETOPHENONE OXIME IN MSB 210 DILUENT

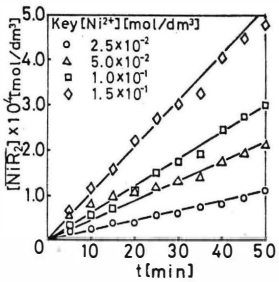

FIGURE 5. TIME-VARIATION OF THE NICKEL CONTENT IN THE ORGANIC PHASE (C_{B0} = 0.145 mol/dm³, pH = 6.5)

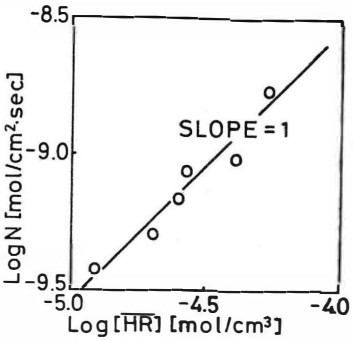

FIGURE 6. EFFECT OF MONOMERIC OXIME CONCENTRATION IN THE ORGANIC PHASE ON INITIAL EXTRACTION RATE ([Ni^{2+}]=0.05mol/dm³, pH=6.9)

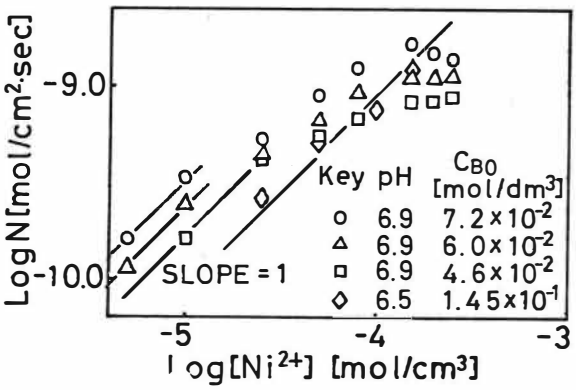

FIGURE 7. EFFECT OF NICKEL CONCENTRATION IN THE AQUEOUS PHASE ON INITIAL EXTRACTION RATE

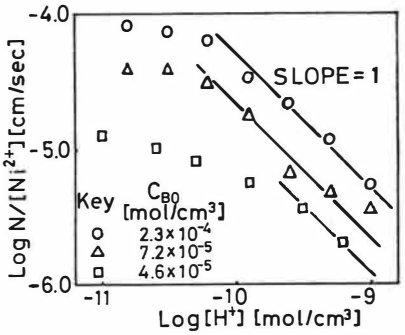

FIGURE 8. EFFECT OF HYDROGEN ION CONCENTRATION ON INITIAL EXTRACTION RATE

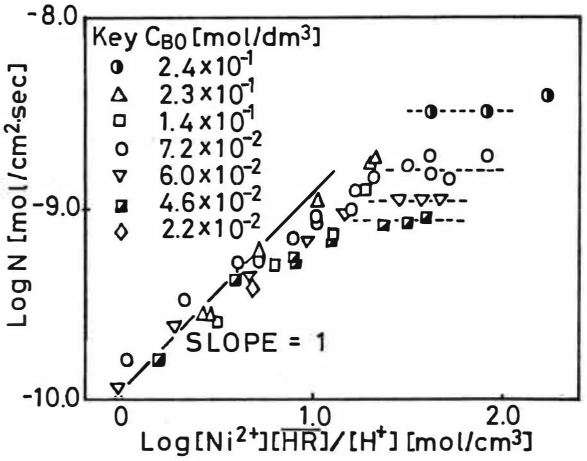

FIGURE 9. RELATION BETWEEN INITIAL EXTRACTION RATE AND $[Ni^{2+}][\overline{HR}]/[H^+]$ FOR VARIOUS C_{B0} AS A PARAMETER

THE KINETICS OF THE EXTRACTION OF V(IV) FROM ACID SULPHATE MEDIA BY DI-2-ETHYLHEXYLPHOSPHORIC ACID

M. A. Hughes and K. Ipinmoroti

Schools of Chemical Engineering
University of Bradford
Bradford, U.K.

Oak Ridge National Laboratory (1) established that di-(2-ethylhexyl) phosphoric acid (D2EHPA) would extract vanadium as the vanadyl (IV) ion, VO^{2+}, (or $V(OH)_2^{2+}$) from a reduced acid leach liquor. Other equilibria studies have been carried out (2,3,4,5). Islam and Biswas (6) have made a formal kinetic study of the system but their experimental technique involved shake-out flasks which has some obvious disadvantages and make their results of very limited practical use.

Kinetic results for the extraction of vanadium by D2EHPA in n-hexane using the single drop technique are reported. The interfacial area can be calculated. It simulates a sieve-plate column contactor; column contactors having been suggested by Ottertun and Strandell (7).

A model for mass transfer with chemical reaction involving an interfacial aqueous zone is proposed. The model accommodates the adsorption-desorption phenomenon for D2EHPA at the aqueous-organic interface. This must be important when extractants are as significantly surface active as D2EHPA (8).

EXPERIMENTAL

The single drop apparatus and technique have been described previously (9,10). The aqueous phase was maintained at 0.5 M with respect to sodium sulphate. Aqueous vanadium was restricted to the range: $0.05\ M \leqslant VO^{2+} \leqslant 0.15\ M$
The pH of the aqueous phase was adjusted within the range: $1.60 \leqslant pH \leqslant 3.00$

D2EHPA concentrations in n-hexane were varied within: $0.20\ M \leqslant D2EHPA \leqslant 1.00\ M$
The temperature was normally $28 \pm 0.5\ ^{o}C$.
Within the range $2.3 \leqslant pH \leqslant 2.8$, the rate, r_v, can be correlated by:

$$(1) \quad r_v = k\left[VO^{2+}\right]_{aq}\left[D2EHPA\right]_o^{0.30}\left[H^+\right]_{aq}^{-0.94}$$

where the "rate constant", k, has a value of $1.71 \times 10^{-4}\ s^{-1}$.
The activation energy of the extraction was found to be $38.8\ kJ\ mol^{-1}$.

A MODEL FOR MASS TRANSFER WITH CHEMICAL REACTION INVOLVING A SURFACE ACTIVE EXTRACTANT

Mass transfer with chemical reaction forms the basis for the model; see Figures 1 and 2. The minimum bulk organic concentration of D2EHPA required to saturate the n hexane/water interface has been calculated to be 0.025 M via the Gibb's adsorption isotherm (11).

The reaction product, MR_2, is reasonably assumed not to be surface active and builds up in the dispersed organic phase.

The Net Rate of Diffusion of HR to the Interface The net rate of diffusion of HR molecules is described by the processes 1 and 2 in Figure 2. Assuming that there is a thin stagnant film on the organic side of the interface, then for the net rate of adsorption,

$$(2) \quad \left[\frac{dn}{dt}\right]_{net} = \beta_1\left[HR\right]_{ob} - \beta_2\, n \exp\left[\frac{z\,\varepsilon\,\psi_o - W}{kT}\right]$$

where: n is the number of molecules at the interface

β_1 is a constant involving diffusion in the film and accommodating any fractional coverage of the interface

β_2 is an hydrodynamic constant, z is the valency of the long chain ion, and ε is electronic charge

ψ_o is the electrostatic potential in interface relative to the adjacent conducting phase

W is the constant total energy of desorption of the hydrocarbon chain at the oil/water interface

k is the Boltzmann constant, and T is the temperature.

But HR diffuses into the reaction zone by process (3) in Figure 2. This last rate is assumed to be proportional to the interfacial concentration, $\left[HR\right]_i$. Hence Equation (2) becomes:

$$(3) \quad \left[\frac{dn}{dt}\right]_{net} = \beta_1\left[HR\right]_{ob} - \beta_2\, n \exp\left[\frac{z\,\varepsilon\,\psi_o - W}{kT}\right] - \beta_3\left[HR\right]_i$$

where β_3 like β_1 and β_2 is a constant depending on the diffusional hydrodynamics in the aqueous film.

Taking $z = 1$, $\varepsilon = 4.77 \times 10^{-10}$ e.s.u. and ψ_o for a monolayer on the surface of an organic drop as 100 mV (11) and W to be 810 cal mol^{-1} per $-CH_2-$ unit in D2EHPA (11), the exponential part of Equation (3) is evaluated to be 1.15×10^{-8}.

Although β_1 and β_2 may alter separately, depending on the hydrodynamics of the system, their ratio has been shown to be a constant value of 1.2×10^{14} (11).

The surface concentration in a monolayer is calculated according to

$n = d \times \left[HR\right]_i \times \frac{N}{10^3}$ where: δ is thickness of the monolayer and N is Avogadro's number.

Also: $\frac{dn}{dt} = \frac{d}{dt}\left[HR\right]_i \times \frac{\delta . N}{10^3}$

Then if $\frac{10^3}{\delta . N} = C$, Equation (3) may be written as:

$$(4) \quad \frac{d}{dt}\left[HR\right]_i = C\beta_1\left(\left[HR\right]_{ob} - \frac{10^{-22}\left[HR\right]_i}{C}\right) - \beta_3\left[HR\right]_i$$

The Chemical Rate of Reaction in the Reaction Zone The rate of disappearance of HR in the reaction zone is given by Astarita's Equation (12) as:

$$(5) \quad -\frac{d}{dt}\left[HR\right]_z = \left(2D_{HR}\int_{\left[HR\right]_{ab}}^{\left[HR\right]_i} r_{HR}\, d\left[HR\right]\right)^{0.5}$$

where HR_z is the average concentration of HR in the reaction zone, and D_{HR} is the diffusivity of HR in the zone. Substituting $r_{HR} = \frac{k'\left[VO^{2+}\right]_{ab}\left[HR\right]_{ob}}{\left[H^+\right]_{ab}}$

and integrating, treating $\frac{\left[VO^{2+}\right]_{ab}}{\left[H^+\right]_{ab}}$ as a constant, we have:

$$(6) \quad -\frac{d}{dt}\left[HR\right]_z = \left(D_{HR}\, k' \frac{\left[VO^{2+}\right]}{\left[H^+\right]}\left(\left[HR\right]_i^2 - \left[HR\right]_{ab}^2\right)\right)^{0.5}$$

(Note: k' is the rate constant for the water replacement reaction on a vanadyl ion.)

The rate of change in $\left[HR\right]_z$ can be related to the organic bulk concentration:

$$(7) \quad -\frac{d}{dt}\left[HR\right]_{ob} = -\frac{1}{Q}\frac{d}{dt}\left[HR\right]_i$$

where Q is the ratio of the volume of a drop to that of the reaction zone. Therefore Equation (6) can be written as:

$$(8) \quad -\frac{d}{dt}\left[HR\right]_{ob} = \frac{1}{Q}\left(S\left[VO^{2+}\right]\left[H^+\right]^{-1}\left(\left[HR\right]_i^2 - \frac{\left[HR\right]_{ob}^2}{P^2}\right)\right)^{0.5}$$

where: $S = D_{HR}.k'$ and the partition coefficient, P, is given by: $P = \frac{\left[HR\right]_{ob}}{\left[HR\right]_{ab}}$

In order to interpret the model further, Equations (4) and (8) need to be solved simultaneously to yield values for the variation of $\left[HR\right]_{ob}$ with time as $\left[HR\right]_{ob}$ is gradually consumed during the formation of the metal complex. The computer program in basic language, BEDSOCS (Bradford Educational Simulation Language for Continuous Systems) (13), is used for this solution. When a solution of the differential equations is obtained, then the experimental data for the change of $\left[HR\right]_{ob}$ with time may be compared with the predicted values.

Fits of Experimental Data to the Model Examples of the fit of the model are demonstrated in Figures 3,4,5. The following constants are used.

$\left[HR\right]_i$ = 0.8308 M, the calculated saturation concentration of D2EHPA at the surface

β_1 = 10^{12} cm s^{-1}, estimated from reference (14)

β_3 = 10^{-2} cm s^{-1}, from a comparison with β_2, reference (14)

S = 1.57×10^{-3} cm^2 s^{-2}, calculated from $D_{HR} = 3.93 \times 10^{-6}$ cm^2 s^{-1}, reference (17) and $k' = 4 \times 10^2$ s^{-1}, reference (15).

C = 8.3×10^{-15} $mol^{-1}cm^{-1}$, calculated using d = 20 A°, reference (14)

Q = 40, estimated from volume of a drop of diameter 0.09 cm and thickness of zone = 8 - 10 µm, reference (17).

The $\left[VO^{2+}\right]_{ab}$, $\left[H^+\right]_{ab}$, and $\left[HR\right]_{ob}$ are varied as shown on the Figures. The figures 3, 4 and 5 show that the expected trends for changes in $\left[VO^{2+}\right]_{ab}$, $\left[H^+\right]_{ab}$ and $\left[HR\right]_{ob}$ are correctly predicted by the model.

REFERENCES

1. C.A. Blake, K.B. Brown, C.F. Coleman, U.S.A.E.C., Rep., ORNL-1903. May(1955).
2. C.A. Blake, C.F. Baes, K.B. Brown, C.F. Coleman, J.C. White, Proc. 2nd Conf. on Peaceful Uses of Atomic Energy,The United Nations, N.Y., 28, 289 (1958)
3. F. Islam, R.K. Biswas, J.I.N.C., 40, 421 (1978).
4. T. Sato, T. Kakeda, J.I.N.C., 32, 3387 (1970).
5. T. Rigg, J.O. Garner, J.I.N.C., 29, 2019 (1967).
6. F. Islam, R.K. Biswas, J.I.N.C., 42, 415 (1980).
7. H. Ottertun, E. Strandell, Proc. Int. Solv. Ext. Conf. - ISEC '77, C.I.M. Special Rep., 21, 501 (1979).
8. G.F. Vandergrift, E.P. Horwitz, J.I.N.C., 39, 1425 (1977).
9. F. Baumgartner, L. Finterwalder, J. Phys. Chem., 74, 108 (1970).
10. R.J. Whewell, M.A. Hughes, C. Hanson, J.I.N.C., 37, 2303 (1975).
11. "Interfacial Phenomena", by J.T. Davies and E.K. Rideal, publ. Acad. Press, 2nd Edn. (1963).
12. "Mass Transfer with Chemical Reaction", by G. Astarita, publ. Elsevier (1967).
13. "Computer Simulation of Continuous Systems", by R.J. Ord-Smith and J.S. Stephenson, publ. Cambridge University Press (1975). Also "BEDSOCS - Mk II", Bradford University, Computing Dept.
14. K.O. Ipinmoroti, Ph.D. Thesis, University of Bradford (1981).
15. K. Wuthrick, R.E. Connick, Inorg. Chem., 6, (3), 583 (1967).

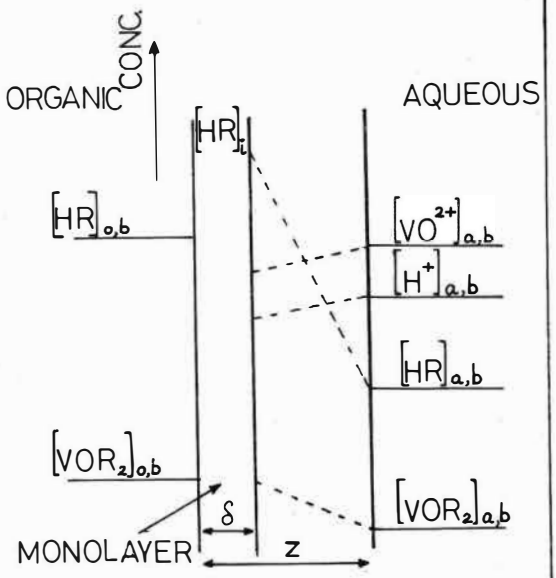

FIG. 1 CONCENTRATION PROFILES

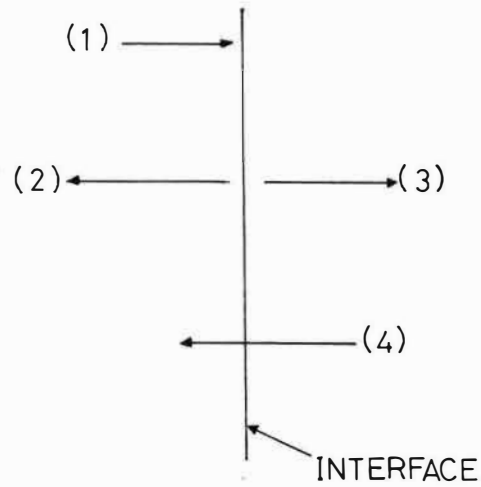

FIG. 2 TRANSFERS OF HR, (1),(2),(3), AND VOR_2 (4)

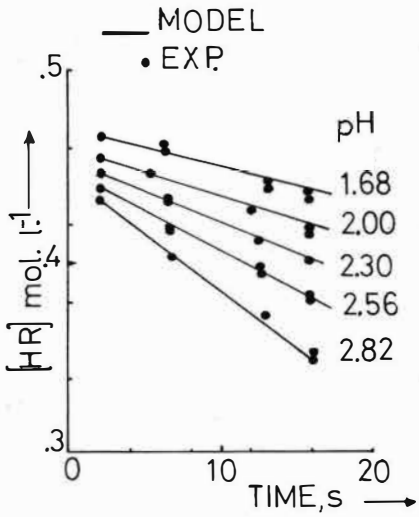

FIG. 3

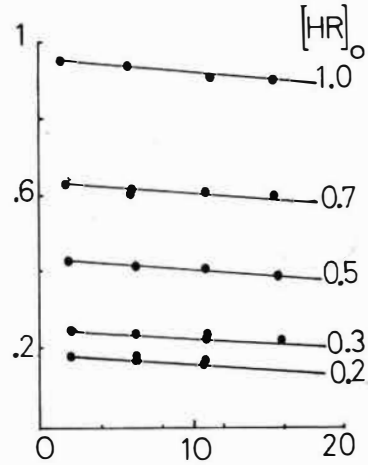

FIG. 4

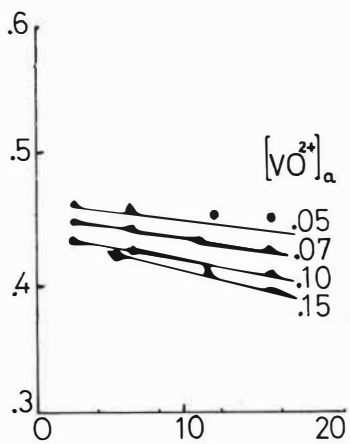

FIG. 5

EXTRACTION MECHANISM FROM THE KINETIC STUDY OF INTERFACIAL MASS TRANSFER OF TERBIUM IN DI(2-ETHYL HEXYL) PHOSPHORIC ACID IN CYCLOHEXANE-NITRIC ACID SYSTEM

S. Sarker, K. M. Ganguly and S. N. Bhattacharyya

Nuclear Chemistry Division
Saha Institute of Nuclear Physics
92, Acharya Prafulla Chandra Road
Calcutta-700009, West Bengal, India

Di (2-ethyl hexyl) phosphoric acid (HDEHP) has extensively been used as an effective extractant because of its large selectivity in separation of many metal ions. An attempt has been made to study the extraction mechanism of terbium (Tb-160) with HDEHP in cyclohexane - nitric acid system by means of kinetic analysis.

EXPERIMENTAL:

The kinetic experiments were performed in a specially designed glass apparatus (1). The rate experiments were carried out as a function of the concentrations of HDEHP and nitric acid at a constant stirring speed of 60 rpm. The temperature in all experiments was kept constant at 35 ± 0.1°C. Distribution ratios were measured separately using G.M. counter.

RATE DATA:

The mass transfer of a metal ion (in this case, terbium) from an aqueous phase to an organic phase can be represented as:

$$M_a \underset{k_{oa}}{\overset{k_{ao}}{\rightleftharpoons}} M_o \qquad (1)$$

where M represents the metal ion species, the suffixes a and o represent respectively the aqueous and the organic phases, k_{ao} and k_{oa} are the corresponding interfacial mass transfer coefficients. The rate equation (2) determining the mass transfer may be expressed as:

$$\ln\left(1-\frac{[M_o]}{[M_o^{\infty}]}\right) = \left\{-\frac{A}{V_o}\left(1+\frac{V_o}{V_a}\cdot D\right)k_{oa}\right\}.t \qquad (2)$$

where $[M_o]$ and $[M_o^{\infty}]$ are the metal ion concentrations in the organic phase at time t and at infinite time respectively, V_a and V_o are the volumes of the aqueous and organic phases respectively. A is the interfacial area and D is the distribution ratio. From the slope of the plots of left hand side of the above equation against t, and from the definition of D, the interfacial mass transfer coefficients, k_{ao} and k_{oa}, are computed.

RESULTS:

Variation of distribution ratio values with different nitric acid concentrations and also at different HDEHP concentrations have been shown in Figure-1. Acid dependent D-values have been determined at constant HDEHP concentration, e.g., 0.1F. At very low acid concentration, e.g., 0.01 to 0.001 M, the pH of the aqueous phase does not remain constant and this may arise from solubilization of HDEHP in the aqueous phase. The dotted line shows the D-values when the pH was controlled by using appropriate buffer. HDEHP dependent D-values are plotted at two different acid concentrations, e.g., 10^{-3} and 10^{-1} M. In the former the maintenance of constant pH was assured by using an appropriate buffer. In Figures 1b and 1c, HDEHP concentration above 0.01F is replaced by its activity computed from the equation referred to in Ref. (3). Figures 2 and 3 show the variation of interfacial mass transfer coefficients with different nitric acid and HDEHP concentrations.

DISCUSSION:

The reaction between the metal ion and the extractant like HDEHP occurs at the interface. Thus, it is expected that the products of the interfacial reaction would also be formed at the interface. The extent of reaction, however, will depend on the rate of dispension of these products from the reaction zone. Keeping this extraction model in view the overall mechanism can be conceived as constituting the following reactions:

$$M_a + NE_i \underset{k_{-1}}{\overset{k_1}{\rightleftharpoons}} (ME)_i + NH_i \qquad (3)$$

$$(ME)_i + RE_o \underset{k_2}{\overset{k_{-2}}{\rightleftharpoons}} (ME)_o + NE_i \qquad (4)$$

$$H_i \underset{k_3}{\overset{k_{-3}}{\rightleftharpoons}} H_a \qquad (5)$$

where M, as already stated, is the metal ion species, E represents HDEHP and H denotes H^+. The subscripts a, i and o refer to aqueous phase, interface and organic phase respectively. $(ME)_i$ and $(ME)_o$ represent the appropriate (metal-HDEHP) species at the interface and in the organic phase respectively.

The expressions for D, k_{oa} and k_{ao} can be computed undertaking appropriate mathematical manipulation (4)

$$D = \frac{k_{-2}\cdot k_1 [E_o]^R}{k_{-1}\cdot k_2 [H_i]^N} \qquad (6)$$

$$k_{oa} = \frac{k_{-1}\cdot k_2\cdot [H_i]^N [E_i]^N}{k_{-1}[H_i]^N + k_{-2}[E_o]^R} \qquad (7)$$

$$k_{ao} = \frac{k_{-2}\cdot k_1 [E_o]^R [E_i]^N}{k_{-1}[H_i]^N + k_{-2}[E_o]^R} \qquad (8)$$

These expressions for D, k_{oa} and k_{ao} are very useful to determine whether the extraction reaction is chemically controlled or not.

Distribution Ratio. From the equation 6, it is expected that the D-values should decrease with increase in acid concentration in the aqueous phase and the slope of this decrease will give the value of N. This is actually observed in the Figure-1a, but above the acid concentration of 0.01M. In this range it is clear that N=3. But at lower acid concentrations, the D-values remain more or less constant. This is due to the face that at low acid concentrations pH of the aqueous phase is not controlled because of solubilization of HDEHP. When the pH of the aqueous phase is controlled, then the course of D-values are shown by dotted lines in Figure 1a, but that was also not in accordance with equation 6. This is probably due to the fact that at low acid concentration rare earth metal ions form radiocolloidal hydrated species (5) which suppress the metal ions from being extracted. One may conceive that there are two equilibria in the system; one for the reaction of the metal ions with HDEHP and the other is for the hydration of the metal ions in the aqueous phase that may lead to hydrated colloidal species. As the concentration of the extractant increases, the ratio of the concentration of the metal complex to the total concentration of metal in solution has been reported to pass through a maximum (6). This explains why D-values when plotted against HDEHP concentration (Figure 1b) at constant pH 3 of the aqueous phase passes through a maximum. Again from the equation 6 it is expected that at constant acid concentration and in absence of other equilibria, the D-values should increase with increase in HDEHP concentration and the slope of this increase will give the value of R. This expectation holds good up to 0.1F HDEHP concentration above which discrepancy arises due to polymerization of HDEHP molecules (7). From the Figure 1c, the value of R was found to be equal to 3.

Interfacial Mass Transfer Coefficients. The course of interfacial mass transfer coefficients at different nitric acid and HDEHP concentrations can easily be explained with the help of equations 7 and 8 with the same suppositions that: i) at very low acid concentrations rare earth metal ions form colloidal hydrated species, and ii) at higher HDEHP concentrations polymerisation of HDEHP starts. The observed values of N and R also corroborate those that were derived in the course of distribution studies.

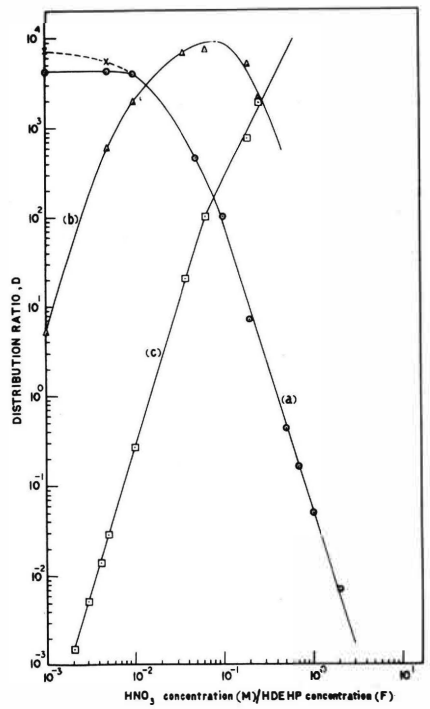

Fig. 1. Distribution ratio, D, a) against HNO_3 concentration, ●, [HDEHP] = 0.1 F, b) against HDEHP concentration, ▲, pH=3, c) against HDEHP concentration, □, $[HNO_3]$ = 0.1 M

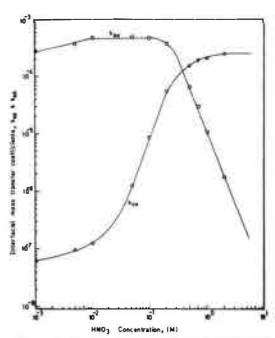

Fig. 2. Effect of HNO_3 concentration on interfacial mass transfer coefficients, k_{ao} & k_{oa}, [HDEHP] = 0.1 F, stirring rate = 60 rpm, temp. = 35° C.

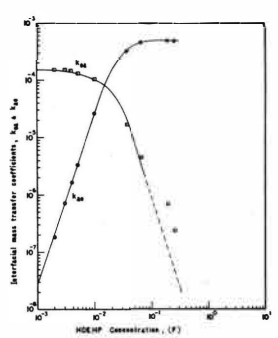

Fig. 3. Effect of HDEHP concentration on interfacial mass transfer coefficients, k_{ao} & k_{oa}, $[HNO_3]$ = 0.1 M, stirring rate = 60 rpm, temp. = 35° C.

CONCLUSION:

The diffusion of metal ions from the aqueous phase to the interface increases with increase in stirring speed. At the same stirring speed diffusion rate may thus be assumed to remain constant. Now, since the observed data can be explained with the help of equations 5-7, the characteristics of mass transfer rate may be thought of as being chemically controlled.

REFERENCES:

1. G.R. Dyrkacz, G.F. Vandegrift, M.W. Thomsen and E.P. Horwitz, J. Phys. Chem., 83, No. 6, 670 (1979)
2. H.P. Ting, G.L. Bertrand and D.F. Sears, Biophys. J., 6, 813 (1966)
3. P.R. Danesi and G.F. Vandegrift, Inorg. Nucl. Chem., Lett. 17, No. 3/4, 109 (1981)
4. G.F. Vandegrift and E.P. Horwitz, J. Inorg. Nucl. Chem., 39, 1425 (1977)
5. F. Kepák, Chem. Rev. 71, No. 4, 357 (1971)
6. K.B. Yatsimirskii and V.P. Vasil'ev, "Instability Constants of Complex Compounds," Pergamon Press, p. 9 (1960)
7. Z. Kolařik, Proc. ISEC '71, The Hague, 19-23 April, 1971, 753, Soc. Chem. Ind., London (1971)

EXTRACTION KINETICS OF POTASSIUM WITH CROWN ETHERS

Masaki Yoshio, Hideyuki Noguchi and Katsutoshi Inoue

Saga University
Saga, Japan

The extraction kinetics of potassium ion from alkaline solutions of Metanil Yellow (MY), picrate (PC), dipicrylaminate (DPA), and perchlorate (PCL) with 18-crown-6 (18C6) and dibenzo-18-crown-6 (DB18C6) into benzene have been studied at 30°C. The rates were increased linearly with increase in the concentration of potassium-18C6 complex. The extraction rates of PC- and DPA-18C6 have constant values at high K^+-18C6 complex concentration, at which the extraction rate could be controlled by the diffusion of PC or DPA in aqueous phase boundary layer. The extraction orders with respect to anion concentration were first order in PC-, DPA-, and PCL-18C6 system and MY-DB18C6 system. The order was decreased from 2 to 1 with increase in MY concentration. The extraction rate in MY-DB18C6 system depended linearly on the concentration of potassium ion and DB18C6. The extraction rate was constant at high DB18C6 concentration as same as PC- and DPA-18C6 system.

INTRODUCTION

Steric selective extraction of planar Pd(II)-PAR (4-(2-pyridylazo)-resorcinol anion complex with planar K^+-18C6 complex has been reported by the authors (1). Octahedral Cu(II), Ni(II), Zn(II), Fe(III) and Cd(II)-PAR complexes can not be extracted with planar K^+-18C6 complex, but partly extracted with semi-spherical protonated n-hexylamine-18C6 complex. The aim of this work is to get a detailed mechanism of steric selective extraction with crown ethers. Planar picrate and dipicrylaminate, spherical perchlorate and linear Metanil Yellow were chosen as counter anions. Extraction mechanisms will be discussed with relation to their shapes.

EXPERIMENTAL

18-Crown-6 and dibenzo-18-crown-6 were synthesized (2,3) and 18C6 was used as an aqueous solution and DB18C6 as a benzene solution. Potassium dipicrylaminate and Metanil Yellow were prepared from the reaction of acid form with KOH solution, and potassium picrate from the reaction between aqueous lithium picrate and potassium chloride solution. The others were all of analytical grade.

The concentration of picrate, dipicrylaminate, and Metanil Yellow in benzene were determined by spectrophotometrical method. The molar absorptivities of the complexes between K^+-18C6 and picrate, dipicrylaminate and Metanil Yellow in benzene were found to be 3.5×10^4 at 353 nm, 2.6×10^4 at 412 nm, and 1.9×10^4 at 400 nm, respectively. The concentration of perchlorate ion in organic phase was determined by Methylene Blue method (4) after back extraction with water.

Interfacial tension between the aqueous Metanil Yellow solution and benzene was measured at 30°C according to the drop-weight method.

150 ml of benzene was poured into 150 ml of aqueous solution containing 18C6, KCl, potassium picrate and KOH placed in the cylindrical vessel (contact area : 35.8 cm^2) at 30°C. The aqueous and organic phases were stirred independently by two flat-blade stirrers in opposite directions at the desired speed. Time dependency of potassium concentration in organic phase was measured and extraction rate was calculated.

RESULTS

Equilibrium study

Extracted 1:1:1 species of 18-crown-6, potassium ion, and anions (A^-) were confirmed by the slope analysis of distribution ratio of potassium (D_K) against aqueous crown ether concentration and anion concentration. Overall extraction constants (K_{ex}) obtained from figures 1 and 2 were same. Then, extraction equilibria were described by equations 1, 2, and 3.

$$(1)\qquad L \rightleftharpoons L_o \qquad K_{d.L} = [L]_o/[L]$$

$$(2)\qquad K^+ + L \rightleftharpoons KL^+ \qquad K_{KL} = [KL^+]/[K^+][L]$$

$$(3)\qquad K^+ + L + A^- \rightleftharpoons KLA_o \qquad K_{ex} = [KLA]_o/[K^+][L][A^-]$$

where L and A^- denote 18-crown-6 and anion and subscript "o" organic phase. The values of K_{ex} obtained and reported were listed up together with rate constants in table 1.

The interfacial tension between the aqueous Metanil Yellow solution and benzene was measured in the presence of 0.1 M-KCl and 4×10^{-4} M-KOH. The interfacial pressure was increased remarkably in the concentration of Metanil Yellow above 10^{-4} M, which suggested that Metanil Yellow was adsorbed at water-benzene interface.

Kinetic study

Initial extraction rate (V_o) was calculated from the initial slope of the curve as shown in figure 3. Constant V_o were obtained at the stirring speed in the range of 60 to 100 rpm for MY-18C6, 80 to 110 rpm for PC-18C6, 40 to 70 rpm for PCL-18C6, and 50 to 80 rpm for MY-DB18C6 system, respectively. The extraction rate in DPA-18C6 system was changed by the stirring speed as shown in figure 4.

The effect of K^+-18C6 concentration on extraction rate at the fixed stirring speed, where the rates did not depend on the stirring speed, was shown in figure 5. V_o was increased linearly with increase in K^+-18C6 concentration when MY and PCL were used as a counter anion. Linear relationships between V_o and K^+-18C6 concentration were obtained in a low K^+-18C6 or DB18C6 concentration solution in the case of PC-, and DPA-18C6 and MY-DB18C6 systems. V_o of them were constant in a high K^+-18C6 or DB18C6 concentration.

The dependency of anion concentration on the extraction rate were first order as shown in figure 6. The extraction rate obtained from MY-18C6 system, however, was decreased from second to first order with increase in MY concentration.

The extraction rate in MY-DB18C6 system depended linearly on the concentration of potassium ion.

DISCUSSION

The extraction mechanisms in the region controlled by the chemical reaction

Extraction rates of PC- and PCL-18C6 systems against the stirring speed were obtained in which constant V_o were shown in figure 4. In these stirring speed region, chemical reaction would be rate determing step because extraction rate was not affected by stirring speed (5). Extraction rates were linearly increased with increase in the concentrations of K^+-18C6 and anions. Then, the rates can be written as follows.

$$(4)\qquad KL^+ + A^- \underset{k_2}{\overset{k_1}{\rightleftharpoons}} KLA_o \qquad V_o = k_1[KL^+][A^-]$$

k_1 obtained from these results are shown in table 1.

The extraction rate at equilibrium state (V_e) is described as;

$$V_e = k_1[KL^+]_e[A^-]_e = k_2[KLA]_{oe}$$

where subscript "e" indicates equilibrium state. k_2 were calculated by equation (5) and shown in table 1.

$$(5)\qquad k_2 = k_1K_{KL}/K_{ex}$$

Extraction mechanisms of MY-18C6 and MY-DB18C6 are more complicated. A mediated transfer mechanism by adsorbed MY at the interface was proposed because MY could be adsorbed at the boundary as described before.

$$(6)\qquad MY^- \underset{}{\overset{K_6}{\rightleftharpoons}} MY^{-*}$$

$$(7)\qquad KL^+ + MY^- \rightleftharpoons KLMY \qquad K_7 = [KLMY]/[KL^+][MY^-]$$

$$(8)\qquad KLMY + MY^{-*} \underset{k_4}{\overset{k_3}{\rightleftharpoons}} KLMY^* + MY^-$$

$$(9)\qquad KLMY^* \underset{k_6}{\overset{k_5}{\rightleftharpoons}} KLMY_o$$

where subscript "*" denotes interface. The rate determing step is step (8) in a low MY concentration and step (9) in a high MY concentration. When surface coverage with MY is small, the initial extraction rate is described as follows.

$$(10)\qquad V_o = K_a[KL^+][MY^-]^2/(K_b + [MY^-])$$

where parameters K_a and K_b are $k_3k_5K_6K_7/k_4$ and k_5/k_4, respectively. K_a and K_b were found to be 1.5×10^{-5} l^2mol/cm^2sec and 1.5×10^{-4} mol/l by the curve fitting method, respectively. This mechanism is illustrated bellow. MY is expressed by a rod and hatched part is SO_3^-. Large circle is 18-crown-6 and small circle painted black is potassium ion.

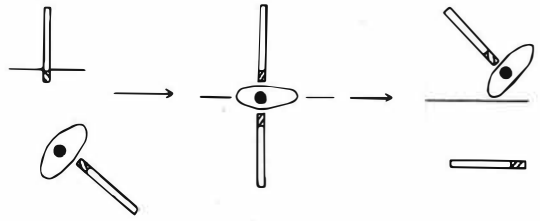

After ion-pair, KLMY, is formed near the interface, the association of KLMY with adsorbed MY occurs at the interface. Then, the exchange of MY occurs and KLMY enters into organic phase.

On the other hand, following extraction mechanism is proposed for the extraction of potassium Metanil Yellow with DB18C6 because DB18C6 could also be adsorbed under the presence of potassium ion (5) and DB18C6 would be adsorbed more strongly than MY.

(11) $L_o \overset{K_{11}}{\rightleftharpoons} L^*$

(12) $K^+ + MY^- + L^* \overset{K_{12}}{\rightleftharpoons} KLMY^*$

(13) $KLMY^* + L_o \xrightarrow{k_7} KLMY_o + L^*$

where L denotes DB18C6. Step (13) is the rate determing step. Then, the initial rate is described by

(14) $V_o = k_7 K_{11} K_{12} [K^+][L]_o^2 [MY^-]/(1 + K_{11}[L]_o)$

When the interface is fully occupied with DB18C6, $K_{11} \gg 1$. Equation (14) is approximated as follows,

(15) $V_o = k_7 K_{12} [K^+][L]_o [MY^-]$.

Extraction rate is controlled by the diffusion

When extraction rates were changed by the stirring speed, diffusion of anions at the phase boundary would be rate determing step because the rates were increased with increase in anion concentration, on the other hand, the rates were not changed by change in K^+-18C6 or DB18C6 concentration in the case of PC-, DPA-18C6 and MY-DB18C6 systems. Roughly calculated diffusion coefficients of PC, MY, and DPA by using Fick's law and extraction rates are 3×10^{-6}, 4×10^{-6} and 5×10^{-6} cm /sec, respectively, under the assumption that anion concentration at phase boundary is zero and that the thickness of diffusion layer is 0.01 cm at 100 rpm (6). These values are comparatible with that of acetate ion (1×10^{-5} cm^2/sec) (7).

Extractability and shapes of anions

K_{ex}, k_1 or K_a, and k_2 or k_6 obtained from our results were summerized in table 1. MY-18C6 system is rather complicated. So the value $k_1(=K_a)$ was obtained from the experiment at high MY concentration, in which the equation of the extraction rate resembles equation (4). Back extraction rate, $k_2(=k_6)$ was calculated from K_{ex} and K_a. The back extraction rate constants calculated are not changed largely by the change in anions. On the other hand, the extraction rate constants are changed remarkably. The planar picrate and dipicrylaminate have large k_1 values. Although Metanil Yellow is larger than picrate and dipicrylaminate, K_a of MY-18C6 is smaller than K_1 of PC- and DPA-18C6. Our results show larger extractability of planar anion is due to the larger k_1 value.

Table 1. K_{ex}, k_1 and k_2 values in various systems at 30°C

	PC	DPA	PCL	MY
K_{ex}	3.7×10^{4} (8)	3.5×10^{3}	2.5×10	2.5×10^{4}
k_1	1.1×10^{4}	7.1×10^{2}	9.0×10^{-8}	1.5×10^{5}
k_2	1.9×10^{7}	1.3×10^{8}	3.5×10^{-7}	6.0×10^{8}

REFERENCES

1. M.Yoshio, H.Noguchi, Anal. Lett., 15 1197 (1982)
2. G.W.Gokel, D.J.Cram, J. Org. Chem., 39 2445 (1974)
3. C.J.Pedersen, J. Amer. Chem. Soc., 89 7017 (1967)
4. I.Iwasaki, S.Utsumi, C.Hang, Bull. Chem. Soc. Jpn., 36 325 (1963)
5. P.R.Danesi, R.Chiarzia, A.Saltelli, J. Inorg. Nucl. Chem., 40 1119 (1979)
6. R.Chiarzia, P.R.Danesi, J. Inorg. Nucl. Chem., 39 525 (1977)
7. R.A.Robinson, R.H.Stokes, Electrolyte solutions, Butterworths (1959)
8. T.Iwachido, A.Sadakane, K.Toei, Bull. Chem. Soc. Jpn., 51 629 (1978)

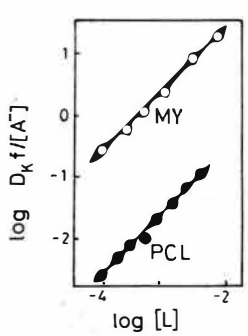

$f = 1 + K_{KI}[L]$

FIGURE 1. THE CURVES OF log $D_K f/[A^-]$ AGAINST log [L] at 30°C

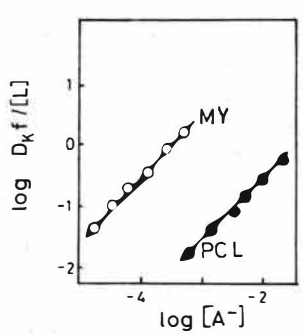

FIGURE 2. THE CURVES OF log $D_K f/[L]$ VS. log $[A^-]$

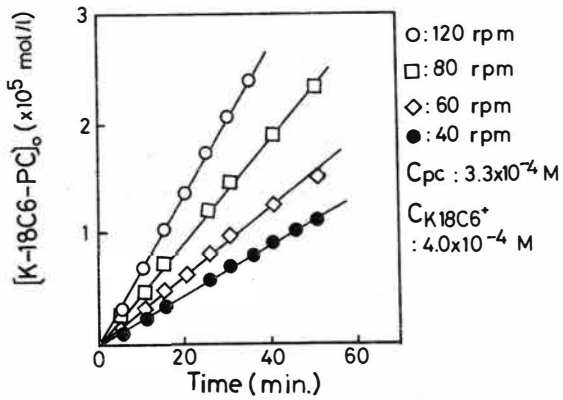

FIGURE 3. TIME DEPENDENCY OF EXTRACTED SPECIES, [K-18C6-PC], IN BENZENE AT 30°C.

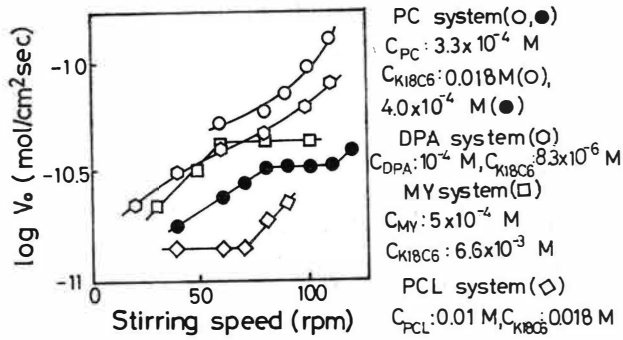

FIGURE 4. THE EFFECT OF STIRRING SPEED ON log V_o IN VARIOUS EXTRACTION SYSTEMS.

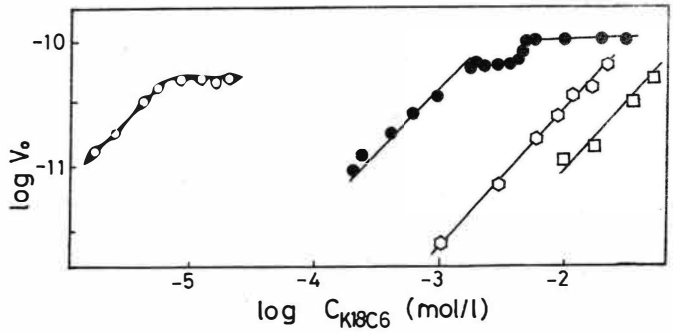

DPA : O , $C_{DPA} = 10^{-4}$ M, PC: ● , $C_{PC} = 3.3\times10^{-4}$ M, MY: O , $C_{MY} = 3.2\times10^{-4}$ M, PCL : □ , $C_{PCL} = 0.01$ M

FIGURE 5. log V_o VS. log C_{K18C6} CURVES IN VARIOUS EXTRACTION SYSTEMS

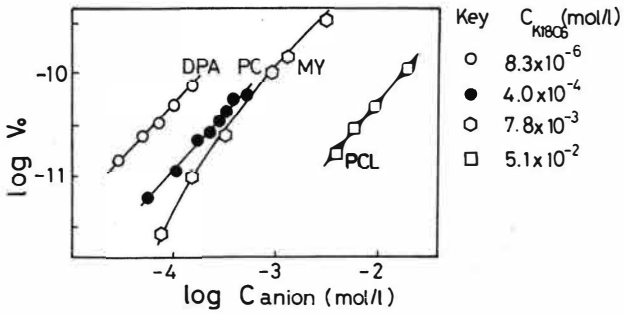

FIGURE 6. THE EFFECT OF ANION CONCENTRATION ON V_o

EXTRACTION RATES OF ACETIC ACID WITH LONG-CHAIN ALKYLAMINES IN HORIZONTAL RECTANGULAR CHANNEL

Yoshinobu Kawano, Kazuhito Kusano

Department of Industrial Chemistry
Miyazaki University
Miyazaki, Japan

Kazuo Kondo, Fumiyuki Nakashio

Department of Organic Syntheses
Kyūshū University
Fukuoka, Japan

Recently, solvent extraction with long-chain alkylamine have been studied to recover carboxylic acid from industrial waste water(1,2,3). In order to design the optimum process, it is important to obtain the information of the extraction kinetics beside the extraction equilibria of the systems. Our work was undertaken to examine the influence of a chemical reaction at the interface on mass transfer.

In this paper, the extraction equilibria of acetic acid with hexane solutions of amines, Amberlite LA-2 and tri-n-octylamine, were studied, and the species formed in the systems were estimated, and the equilibrium constants for these species were evaluated. Furthermore, the extraction kinetics of acetic acid with hexane solutions of these amines were studied in a horizontal reactangular channel. The experimental results were analyzed by the interfacial-reversible reaction model considered adsorption and desorption steps of the amine and products at the interface and suggest that rate determining step were desorption of the products.

1 EXPERIMENTAL PROCEDURES

1.1 Extraction equilibria

Equal volume of the aqueous acid and the organic amine solutions of known concentration were shaken in a flask in water bath maintaining 30 ± 0.1°C. After about 2 hours, the phases were separated and were analyzed for their acid contents.

1.2 Extraction kinetics in a horizontal rectangular channel

A horizontal rectangular channel (hereafter called call) shown in Fig.1 was used to measure the extraction rates of acetic acid with hexane solutions of amines, Amberlite LA-2(hereafter called LA-2) and tri-n-octylamine (hereafter called TOA) The aqueous acid and organic amine solutions are introduced separately into the cell settled in air bath maintaining 30±0.5 C by each inlet, and contact at the point of the separation plate. Both phases flow concurrently and are taken out separately by each outlet through level controller. The flow rates of these phases are equalized and are varied from 0.3 to 0.8 cm^3/s in which stable laminar flows are obtained.

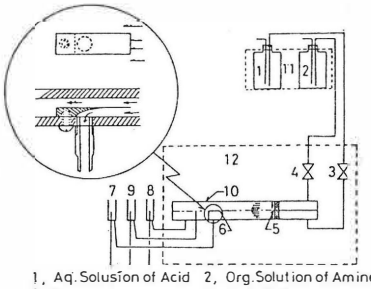

1, Aq.Solusion of Acid 2, Org.Solution of Amine
3, 4, Cock 5, Distributor
6, Aq.Sample Outlet 7, 8, 9, Level Controller
10, Extraction Section(Rectangular Channel)
11, Water Bath 12, Air Bath

Fig.1 Schematic diagram of experimental apparatus

2. EXPERIMENTAL RESULTS AND DISCUSSION

The experimental results of the extraction equilibria of acetic acid with hexane solutions of amines are shown in Fig.2 for LA-2 and TOA systems, respectively, in which the extent of the extraction equilibria, Z ($=\bar{C}_{AR}/\bar{C}_{BO}$) are plotted against the concentration of acid in aqueous phase, C_A, where $\bar{C}_{AR}$ is the concentration of acid reacted with amine in hexane. The value of Z independent of $\bar{C}_{BO}$ and increases to 4.0 with C_A. These experimental results indicate that acid (A) reacts consecutively with amine (B) to form A_nB species (n=1,2,3 and 4) by the following reactions,

(1) $A_{n-1}B_{org} + A_{org} \rightleftharpoons A_nB_{org}$; $K_{n1} = \bar{C}_{n1}/\bar{C}_{n-1,1}C_A$ (n=1,2,3,4)

where $\bar{C}_{n1}$ is the concentration of A_nB type species in hexane. Analyzing the experimental results with the method proposed in the previous paper(4), the equilibrium constants for Eq.(1), K_{n1} can be evaluated as shown in Table 1. In Fig.2, the solid lines calculaed by using the value of K_{n1} shown in Table 1 agree well with the experimental results. The fact indicates that the experimental results can be interpreted by the reaction model in which A_nB species are consecutively formed by the reactions shown in Eq.(1)

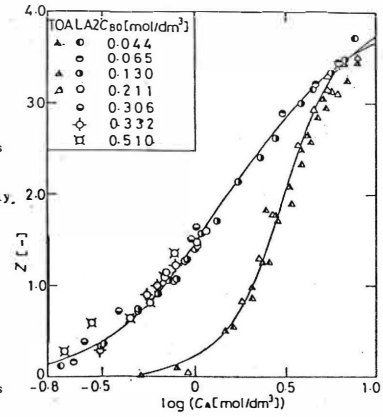

Fig. Experimental results for extraction equilibria for acetic acid with amines

The experimental results of the extraction rates of acetic acid with hexane solutions of amines are shown in Figs.3 and 4 in which dimensionless average extraction rate $\overline{Sh}$ ($=\Delta C_A\bar{u}_A h^2/C_{AO}D_A x_L$) are plotted against $\alpha\sqrt{\beta}$ ($=(C_{AO}/\bar{C}_{BO})\sqrt{D_A/D_B}$) for each inlet concentration of amine in hexane, $\bar{C}_{BO}$ at constant Greatz number, $Gz(=\bar{u}_A h^2/D_A x_L)=186$, for LA-2 and for TOA respectively. A dott-line in Figs.3 and 4 are the calculated results assuming that A_3B species form irreversibly and instantaneously at the interface. The solid lines and broken lines will be described later.

Amine and the products A_nB are insoluble in water and adsorb at the interface. Distribution of acetic acid in hexane is very small. Furthermore, the reaction rate between A and B is expected to be very rapid because of neutralization reaction. Under the condition, the reaction between A and B is could be expected to take place at the interface. It could be considered from the extraction equilibria of acetic acid with amines that in the range of $\alpha\sqrt{\beta}<10$, the concentration of A_4B species formed in the system is negligibly small compared with other products. Then, the reaction scheme can be assumed as that shown in Fig.5 (hereafter called interfacial reaction). The adsorption equilibrium constants shown in Table 2 were evaluated experimentally from dependence of the equilibrium concentrations on the interfacial tension at the equilibrium state.

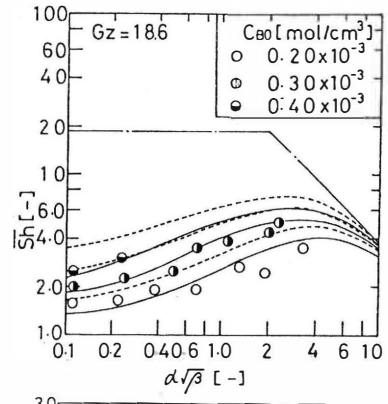

Fig.3 Experimental results for extraction rate of acetic acid with hexane solutions of Amberlite LA-2 at Gz=186

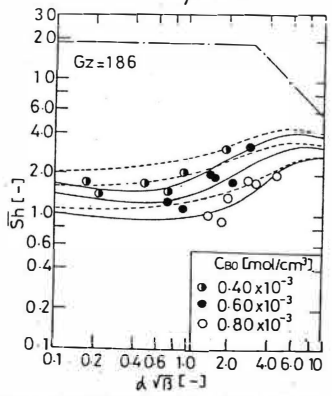

Fig.4 Experimental results for extraction rate of acetic acid with hexane solutions of TOA at Gz=186

When reaction proceed only at the interface, the fundamental equations are derived from the material balances of acid, amine and the products as follows;

(2) $u_B(\partial C_B/\partial x) = D_B(\partial^2 C_B/\partial y^2)$ (y>0)

(3) $u_B(\partial C_{n1}/\partial x) = D_{n1}(\partial^2 C_{n1}/\partial y^2)$ (n=1,2,..) (y>0)

(4) $u_A(\partial C_A/\partial x) = D_A(\partial^2 C_A/\partial y^2)$ (y<0)

where x is the horizontal distance from the point of contact between the two phases; y is the perpendicular distance from the interface; u_A and u_B are the linear velocities of the aqueous and the organic phase, respectively, and are function of y.

(5) $x \leq 0;\quad 0 \leq y \leq h;\quad C_B=C_{BO},\ C_{n1}=0\ (i=1,2,..)$

(6) $-h \leq y \leq 0;\quad C_A=C_{AO}$

(7) $x > 0;\quad y = 0;\quad D_B(\partial C_B/\partial y) = -R_A$

(8) $D_{n1}(\partial C_{n1}/\partial y) = -R_{n1}\ (n=1,2,..)$

(9) $D_A(\partial C_A/\partial y) = -R_B$

(10) $y = h;\ (\partial C_B/\partial y) = 0,\ (\partial C_{n1}/\partial y) = 0\ (n=1,2,..)$

(11) $y = -h;\ (\partial C_A/\partial y) = 0$

where D is diffusion coefficient and R's are reaction rate for each species. The following dimensionless terms can also be defined:

$a=C_A/C_{AO}$, $b=C_B/\bar{C}_{BO}$, $s_{n1}=C_{n1}/\bar{C}_{BO}$, $\xi=y/h$, $\eta=D_A x/u_A h^2$, $\alpha=C_{AO}/\bar{C}_{BO}$, $\beta=D_A/D_B$, $\beta_{n1}=D_{n1}/D_B$; $u_A^*=u_A/\bar{u}_A$, $u_B^*=u_B/\bar{u}_B$, $r=Rh/\bar{C}_{BO}D_B$

Substituting these dimensionless terms into the above fundamental equations and the boundary conditions, the following equations are obtained,

(12) $(\partial b/\partial \eta) = (1/u_B^*\beta)(\partial^2 b/\partial \xi^2)$

(13) $(\partial s_{n1}/\partial \eta) = (\beta_{n1}/u_B^*\beta)(\partial^2 s_{n1}/\partial \xi^2)\quad (n=1,2,...)$

(14) $(\partial a/\partial \eta) = (1/u_A^*)(\partial^2 a/\partial \xi^2)$

(15) $\eta \leq 0;\ 0 \leq \xi \leq 1.0;\quad b = 1.0,\ s_{n1} = 0\quad (n=1,2,..)$

(16) $-1 \leq \xi \leq 0;\quad a = 1.0$

(17) $\eta > 0;\quad \xi = 0;\quad (\partial b/\partial \xi) = -r_B,\ (\partial s_{n1}/\partial \xi) = -(1/\beta_{n1})r_{n1}$

(18) $;\quad (\partial a/\partial \xi) = -(1/\beta)r_A$

(19) $\xi = 1.0;\quad (\partial b/\partial \xi) = 0,\ (\partial s_{n1}/\partial \xi) = 0\quad (n=1,2,..)$

(20) $\xi = -1.0;\quad (\partial a/\partial \xi) = 0$

If the reaction rate equations are given, then the concentration distributions $a(\eta,\xi)$, $b(\eta,\xi)$ and $s_{n1}(\eta,\xi)$ will be given by the above equations, in term of α β and C_{BO}. But since u_A^* and u_B^* are function of ξ to the power 2, and also Eq.((17) and (18) are non-linear, an analytical solution of Eq.(12), (13) and (14) will be quite difficult, and the values of $a(\eta,\xi)$, $b(\eta,\xi)$ and $s_{n1}(\eta,\xi)$ will have to be found by numerical calculation. As a results of this, the mean extraction rate of acid across the interface can be determined in the following method.

(21) $\bar{N}_A = (1 - \bar{a}(\eta_L))C_{AO}hx_L/D_A$

$\bar{a}(\eta_L)$ is dimensionless mean concentration of acid in aqueous phase at $\eta=\eta_L$, and is defined as

(22) $\bar{a}(\eta_L) = \int_{-1}^{0} a(\eta_L,\xi)\, d\xi$

Since in the region of low extraction extent, the dimensionless extraction rate of $\bar{N}_A$ viz., $\bar{N}_A h/C_{AO}D_A$ will be Sherwood number, the dimensionless extraction rate hereafter are simbolized by $\overline{Sh}$. As point out above, the value of $\bar{a}(\eta_L)$ depend on α/β, $\bar{C}_{BO}$, Gz and interfacial reaction mechanism, then, the relations between $\overline{Sh}$ and α/β at constant Gz and $\bar{C}_{BO}$ depend on the interfacial reaction mechanism, as shown in bellow.

Assuming that all of steps in Fig.5 equilibrate at the interface, the relation between $\overline{Sh}$ and α/β are shown by the broken lines in Figs.3 and 4, respectively. The fact that most of experimental $\overline{Sh}$ values fall lower than the broken lines indicates that the extraction rates affected by the interfacial reaction rates. As the interfacial reaction mechanism, four cases which have following rate controlling steps are assumed, (1) adsorption of B at the interface (step 1), (2) reaction between B adsorbed and A in the aqueous phase (step 2), (3) both reaction steps of step 2 ,and between AB adsorbed and A in the aqueous phase (step 2 and 4), and (4) desorptions of A_nB formed at the interface into the organic phase (step 3,5 and 7). Solving the Eqs.(12) to (20) using rate equation of each case, the relation between $\overline{Sh}$ and α/β at constant Gz and $\bar{C}_{BO}$ are obtained.

To confirm the most suitable reaction mechanism, the mean deviation, $\bar{\sigma}$ of the difference of the experimental $\overline{Sh}$ value, $\overline{Sh}_i$ and the calculated $\overline{Sh}$ value, $\overline{Sh}_{cal,i}$ defined by

(23) $\bar{\sigma} = \sqrt{\sum_{i=1}^{N}((\overline{Sh}_i-\overline{Sh}_{cal,i})/\overline{Sh}_i)^2/(N-1)}$

are calculated for each case. The smallest values of $\bar{\sigma}$ in each amine were obtained from the case (4), and rate constants are shown in Table 3. In this case, the rate equations are written as follows;

(24) $R_{11} = k^o_{d11}C_{BO}^2\ ((\alpha a)b - s_{11}/(K_{11}C_{BO}))(1-\Theta)K_{11}K_{a11}$

(25) $R_{21} = k^o_{d21}C_{BO}^3\ ((\alpha a)^2 b - s_{21}/(K_{11}K_{21}C_{BO}^2))(1-\Theta)K_{11}K_{21}K_{a21}$

(26) $R_{31} = k^o_{d31}C_{BO}^4\ ((\alpha a)^3 b - s_{31}/(K_{11}K_{21}K_{31}C_{BO}^3)(1-\Theta)K_{11}K_{21}K_{31}K_{a31}$

where $(1-\Theta)$ is given as

$(1-\Theta)=1/(1+K_{a01}\bar{C}_{BO}b(1+K_{s11}\bar{C}_{BO}(\alpha a)+K_{s11}K_{s21}\bar{C}_{BO}^2(\alpha a)^2+K_{s11}K_{s21}K_{s31}\bar{C}_{BO}^3(\alpha a)^3))$

It is expected that the calculated results with the interfacial reaction model of case (4) most agree with the experimental results. The solid lines in Figs. 3 and 4 are the calculated results. At Gz=300, the experimental and calculated results are shown in Fig.6 for LA-2. The calculated results agree well with the experimental results for each Gz. Thus, above reaction model can be adopted as the most suitable model to express the experimental results.

3. CONCLUSION

The experiment of extraction equilibria of acetic acid with hexane solutions of long-chain alkylamines were carried out. The experimental results were interpreted by the reaction model of which A_nB (n-1,2,3 and 4) type species were formed in the systems. Furthermore, the extraction rates were measured in a horizontal rectangular channel. The extraction rates were interpreted by the interfacial reaction model in which the desorption steps are the rate determining steps.

Table 1 Extraction equilibrium constants

	K_{11}	K_{21}	K_{31}	K_{41}
	[m^3/mol]			
LA-2	0.38×10^{-3}	6.9×10^{-3}	0.05×10^{-3}	1.8×10^{-3}
TOA	0.14×10^{-3}	4.5×10^{-4}	0.28×10^{-3}	4.8×10^{-4}

Table 2 Desorption rate constants

	k^o_{d11}	k^o_{d21}	k^o_{d31}
	[mol/m^2.s]		
LA-2	2.2×10^{-5}	9.4×10^{-2}	-
TOA	5.0×10^{-5}	4.4×10^{-2}	2.4×10^{-2}

Table 2 Adsorption equilibrium constants

	K_{a01}	K_{a11}	K_{ap1}	S_{11}	S_{21}	S_{p1}
	[m]			[m^2/mol]		
LA-2	9.6×10^{-7}	2.8×10^{-2}	2.2×10^{-4}	4.1×10^{5}	2.5×10^{6}	1.1×10^{6}
TOA	2.8×10^{-6}	2.9×10^{-2}	3.3×10^{-4}	6.8×10^{5}	1.9×10^{6}	1.4×10^{6}

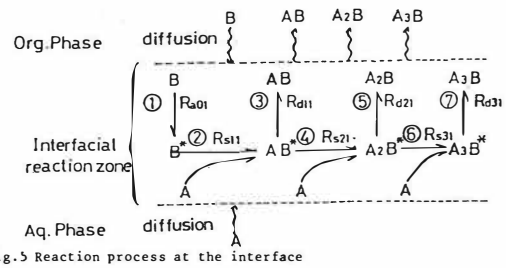

Fig.5 Reaction process at the interface

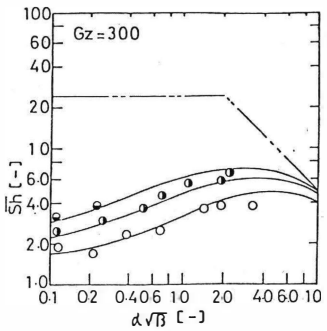

Fig.6 Exprimental results for extraction rate of acetic acid with hexane solutions of LA-2 at Gz=300

Nomenclature

C	: concentration	[mol/m^3]	R	: reaction rate	[mol/m^2s]
D	: diffusion coefficient	[m^2/s]	Sh	: Sherwood Number ($(\Delta C_A/C_{AO})Gz$)	[-]
Gz	: Greatz number ($\bar{u}_A h^2/D_A x_L$)	[-]	y	: distsnce from the interface	[m]
h	: depth of liquid phase	[m]	x	: distance of the contact point	[m]
K	: equilibrium constant	[mol/m^3]			
u	: linear velocity	[m/s]	Z	: extent of the extraction equilibria	[-]
$\bar{u}$	: average linear velocity	[m/s]			

Literature cited

(1) Hanson,C.: Chem. Eng., 86, 83 (1979)

(2) Ricker,N.L.: Ph.D.Dissertation of Chem. Eng. Univ. of California (1978)

(3) Ricker,N.L., J.N.Michaels and C.J.King: J.Sepr.Technol.,1,(1),23 (1979)

(4) Kusano,K. and Y.Kawano,: Chem. Eng. Thermodynamics, p.487 (1982)

MASS TRANSFER IN CATALYTIC SYSTEMS: MICELLES, LIQUID MEMBRANES AND SINGLE DROPS

K. Osseo-Asare, K. L. Lin
Metallurgy Program
The Pennsylvania State University
University Park, Pennsylvania 16802 USA

and

D. J. Chaiko
Mineral Processing Program
The Pennsylvania State University
University Park, Pennsylvania 16802 USA

INTRODUCTION

Surfactant micelles are known to be capable of increasing bulk phase reaction rates (1). Specific interactions between reactants and micelles can result in reactant concentrations at or near the micelle surface that are higher than the bulk concentration (1-4). The ability of mixtures of dinonylnaphthalenesulfonic acid (HDNNS) and the aliphatic α-hydroxyoxime extractant LIX63 (H_2Ox) to act synergistically in extracting nickel and cobalt from low pH solutions has been demonstrated by several investigators (5-7). According to recent work in this laboratory (8-11), this synergism can be attributed to: (a) the formation of mixed H_2Ox-HDNNS metal complexes, (b) the high concentration of HDNNS molecules at the organic/aqueous interface and (c) the presence of HDNNS micelles in the bulk organic phase.

This paper examines the roles of interfacial and bulk phase phenomena during metal extraction with LIX53-HDNNS mixtures. Both single drop and supported liquid membrane techniques are used to study cobalt and nickel extraction. The single drop method enables one to study the initial reaction kinetics of metal extraction under conditions where the interfacial area and the system hydrodynamics are well defined. This method has the added advantage of simulating droplet behavior during solvent extraction processes which use conventional mixer-settler technology. The use of supported liquid membranes allows one to work at high extractant concentrations where droplet instability may become a problem in the single drop technique due to a very low interfacial tension.

The interfacial properties which have been measured include the oil/water interfacial tension, the critical micelle concentration (CMC) of H_2Ox-HDNNS mixtures and the electrophoretic mobility of dispersed organic droplets. The bulk organic phase viscosity has also been determined.

An attempt is made to correlate the mass transfer behavior of cobalt and nickel with the interfacial and bulk organic phase properties. In addition, the use of micellar catalysis as a mechanism of increasing mass transfer in liquid membrane processes is examined.

EXPERIMENTAL

Dinonylnaphthalenesulfonic acid (HDNNS) was purified according to the method of Danesi et al. (12). The active extractant in LIX63, the anti-isomer of 5,8-diethyl-6-hydroxy-6-dodecanone oxime (H_2Ox) was isolated using the copper oximate technique described previously (8). All organic and inorganic chemicals were reagent grade except for the spectrograde n-hexane used in the electrophoretic mobility measurements.

Single drop experiments were carried out with a rising drop column (13) at 25°C. The continuous phase contained 5×10^{-3} kmol m^{-3} $Ni(NO_3)_2$ and 0.5 kmol m^{-3} KNO_3, at pH 2.5. The organic diluent was hexane. The membrane system used in this study consisted of a microporous polypropylene film (Celgard 2400) and dodecane as the diluent. The aqueous feed contained 0.03 kmol m^{-3} $CoSO_4$ and 0.08 kmol m^{-3} formic acid at pH 4.0. The strip solution was 1.0 kmol m^{-3} H_2SO_4.

Interfacial tensions were measured at 25 ± 0.1°C by the drop-weight method. Solution densities were measured with a Cahn microbalance. The electrophoretic mobilities of the organic droplets were measured with a Riddick Zeta meter. Samples were prepared by dispersing 3.5×10^{-4} L of the organic solution in 0.5 L of aqueous phase. The ionic strength of the aqueous phase was kept constant with 4.0×10^{-3} kmol m^{-3} KNO_3.

INTERFACIAL ADSORPTION OF HDNNS

The interfacial tension (γ) measurements in Figure 1 indicate that HDNNS is highly surface active and forms inverse micelles in organic solutions. In H_2Ox-HDNNS mixtures, the critical micelle concentration (CMC) is observed to be a function of the H_2Ox concentration. This dependence of the CMC on the H_2Ox concentration indicates that a specific interaction between H_2Ox and HDNNS occurs. Infrared spectra results have indicated that H_2Ox and HDNNS molecules interact through hydrogen bonding between the oxime and sulfonic acid functional groups (8).

The constant value of $\partial\gamma/\partial\log[HD]$ in Figure 1, regardless of the H_2Ox concentration, indicates that HDNNS is preferentially adsorbed at the oil/water interface.

ELECTROPHORETIC MOBILITY OF OIL DROPLETS

The results of the electrophoresis studies are presented in Figure 2. From this figure it is apparent that the presence of H_2Ox has little effect on the interfacial charge of hexane droplets whereas the presence of HDNNS leads to a highly negative interfacial charge. In H_2Ox-HDNNS mixtures, the HDNNS is the predominant specie which controls the zeta potential of oil droplets.

Ni EXTRACTION BY H_2Ox-HDNNS MIXTURES

The rate of nickel extraction by H_2Ox-HDNNS mixtures, measured by the rising drop technique, is presented in Figure 3. A linear relationship between Ni flux and HDNNS concentration is observed for the pure HDNNS system. However, in the presence of H_2Ox, a curve is obtained which approaches that of the HDNNS only system at sufficiently high HDNNS: H_2Ox ratios.

The Ni extraction results of Figure 3 are replotted in Figure 4. The linear dependence of Ni extraction with respect to $(\sqrt{t}/r)$ suggests that the interfacial transfer of Ni can be described by a radial diffusion model of the form:

$$(1) \quad C(t) = k\, C_o D^{1/2}\, t^{1/2}/r$$

where C(t) represents the nickel concentration in the organic drop at t > 0, D is the diffusion coefficient of the HDNNS micelle, r is the drop radius, C_o is the initial micelle concentration in the organic phase, and k is a constant.

ORGANIC PHASE VISCOSITY

The viscosities of the HDNNS-dodecane and the H_2Ox-HDNNS-dodecane systems are plotted in Figure 5. The two systems have very similar viscosities which indicates that the organic phase diffusivity is basically controlled by the HDNNS concentration. Up to 0.4 kmol m^{-3} HDNNS, there is very little change in the viscosity. However, the viscosity increases almost a hundred fold between 0.4 kmol m^{-3} and 1.0 kmol m^{-3} HDNNS.

Co EXTRACTION BY H_2Ox HDNNS MIXTURES

Cobalt flux across supported liquid membranes as a function of HDNNS concentration at several fixed H_2Ox concentrations is presented in Figure 6. In the HDNNS only system, three regions can be identified as the sulfonate concentration is increased: cobalt flux (i) first increases, (ii) reaches a plateau, and then (iii) decreases. It is believed that cobalt transport is controlled by organic phase diffusion in the low HDNNS region, by aqueous phase diffusion in the intermediate HDNNS region and again by organic phase diffusion in the highest HDNNS region. The decrease in flux in this latter region is most likely a result of the increase in the organic phase viscosity noted above. From the interfacial tension measurements in Figure 1, together with the extraction profiles of Figure 6, one can conclude that enhanced metal extraction occurs only in the presence of HDNNS micelles. At high HDNNS:H_2Ox ratios, the flux curves all converge to the single flux curve obtained for the HDNNS only system, an effect which is similar to that observed in the rising drop experiments in Figure 3. An examination of the Co flux curves in Figure 6 reveals that the decrease in metal transport occurs more sharply and at decreasing HDNNS concentrations as the oxime content of the organic phase is raised. In light of the viscosity measurements, which show little difference between the HDNNS and H_2Ox-HDNNS systems, the decrease in metal extraction rates in the mixed system at high HDNNS concentrations must be attributed to additional factors beyond the viscosity effect.

The Co flux profile for the 0.1 kmol m^{-3} H_2Ox-HDNNS extractant system in Figure 6 is characteristic of a micelle catalyzed reaction (14). The formation of micelles at the CMC results in a very rapid increase of reaction rate in the region of the CMC. The reaction inhibition observed at high HDNNS:H_2Ox ratios is attributed to the presence, in the organic phase, of a catalytic micelle of composition $(HDNNS)_m \cdot 3H_2Ox$ whose concentration goes through a maximum as the HDNNS concentration is increased. The catalytic micelle is shown with three H_2Ox molecules since previous work (10,11) suggests that the stoichiometry of the extracted Co and Ni complexes is $Me(H_2Ox)_3(DNNS)_2$.

CONCLUSIONS

In view of the above discussion, an extraction mechanism may be proposed which includes: (a) reaction between interfacially adsorbed HDNNS molecules and aqueous metal ions, (b) diffusion of the neutral HDNNS-metal complex into the bulk organic phase with subsequent interfacial replacement by HDNNS molecules, (c) diffusion of the catalytic micelle towards the oil/water interface, (d) reaction between the catalytic micelle and the HDNNS-metal complex within an organic film adjacent to the oil/water interface.

The experimental results reported in this paper indicate that both interfacial and bulk organic phase reactions can have significant effects on mass transfer rates during metal extraction.

ACKNOWLEDGMENT

Support of this work by the U.S. National Science Foundation is gratefully acknowledged.

REFERENCES

1. J. H. Fendler and E. J. Fendler: Catalysis in Micellar and Macromolecular Systems, Academic Press, New York, 1975.
2. J. Holzwarth, W. Knoche, and B. H. Robinson: Ber. Bunsenges. Phys. Chem., Vol. 82, pp. 1001-1005, 1978.
3. S. Diekman and J. Frahm: J. C. S. Farad. Trans., Vol. 75, pp. 2199-2210, 1979.
4. A. D. James and B. H. Robinson: J. C. S. Farad. Trans., Vol. 24, pp. 10-21, 1977.

5. S. O. Fekete, G. A. Meyer and G. R. Wicker: TMS-AIME preprint No. A77-95 (1977); U.S. Patent 4193969, March 18, 1980.

6. L. V. Gallacher: U.S. Patent 4,018,865 (1977).

7. K. Osseo-Asare, H. S. Leaver, and J. M. Laferty: pp. 195-207 in Process and Fundamental Considerations of Selected Hydrometallurgical Systems, M. C. Kuhn, ed.; SME-AIME, New York, 1981.

8. K. Osseo-Asare and M. E. Keeney: Metal. Trans. B, Vol. 11B, pp. 63-67 1980.

9. K. Osseo-Asare and M. E. Keeney: Proceedings ISEC '80, Liege, Belgium, paper No. 80-121, 1980.

10. K. Osseo-Asare, D. R. Renninger and J. D. Wagner: Solv. Extr. and Ion Exch. (in press).

11. K. Osseo-Asare and D. R. Renninger: Hydrometallurgy (submitted)

12. P. R. Danesi, R. Chiarizia and G. Scibona: J. Inorg. Nucl. Chem., Vol. 35, pp. 3926-3928, 1973.

13. P. R. Danesi, and R. Chiarizia: "The Kinetics of Metal Solvent Extraction," in CRC Critical Review in Analytical Chemistry, Vol. 10, pp. 1-126, 1980.

14. D. Piszkiewicz: J. Am. Chem. Soc., Vol. 98, pp. 3053-3055, 1976; Vol. 99, pp. 1550-1557, 1977; Vol. 99, pp. 7695-7697, 1968.

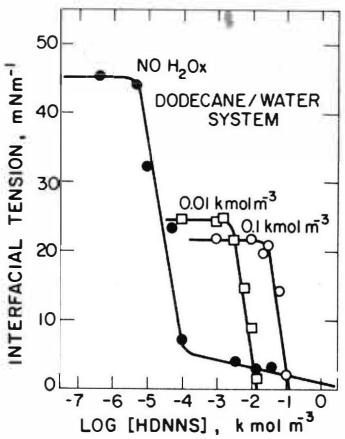

FIGURE 1. INTERFACIAL TENSION ISOTHERMS FOR HDNNS AND HDNNS-LIX63 MIXTURES. AQUEOUS PHASE: 0.03 kmol m^{-3} $CoSO_4$, 0.08 kmol m^{-3} FORMIC ACID, pH 4.0.

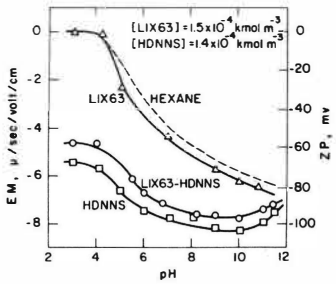

FIGURE 2. ELECTROPHORETIC MOBILITY OF HEXANE DROPLETS CONTAINING LIX63-HDNNS MIXTURES.

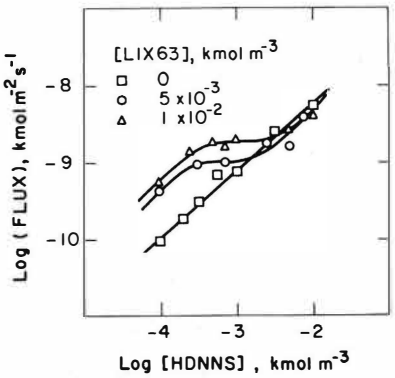

FIGURE 3. RATE OF NICKEL EXTRACTION BY LIX63-HDNNS MIXTURES USING THE RISING DROP TECHNIQUE 25°C.

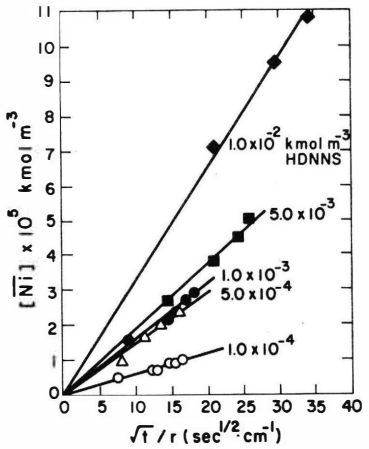

FIGURE 4. EXTRACTED NICKEL CONCENTRATION AS A FUNCTION OF $\sqrt{t}/r$. [LIX63] = 1.0x10^{-2} kmol m^{-3}, 25°C.

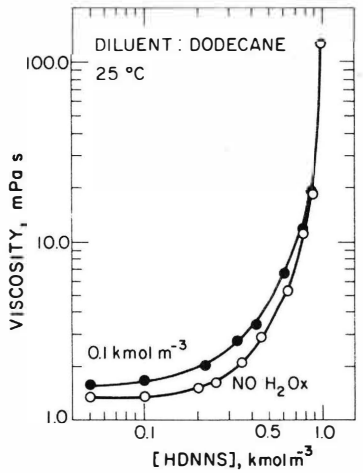

FIGURE 5. ORGANIC PHASE VISCOSITY.

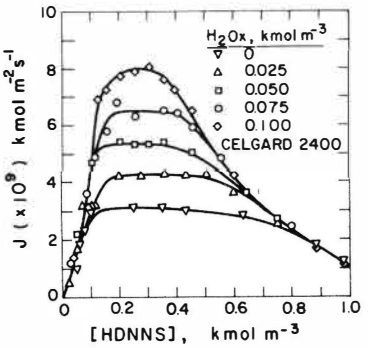

FIGURE 6. COBALT FLUX ACROSS SUPPORTED LIQUID MEMBRANES AS A FUNCTION OF HDNNS AND H_2Ox CONCENTRATIONS.

USE OF MICROEMULSIONS AS ORGANIC PHASE FOR FASTER KINETICS

D. Bauer and J. Komornicki

Ecole Supérieure de Physique et de Chimie
10, rue Vauquelin 75231
Paris, France

Microemulsions are optically transparent and thermodynamically stable oil-water dispersions. They are spontaneously formed when a surfactant and a cosurfactant, usually an alcohol, are added to a mixture of oil and water. Water-in-oil microemulsions are described as the dispersion in oil of droplets of water surrounded by a shell of the surfactant and cosurfactant molecules, and vice versa for oil-in-water microemulsions. The size of the droplets is comprised between 50 and 1000 Å. A microemulsion can exist as a single phase or may be found in equilibrium with an excess of water, an excess of oil or an excess of both oil and water (1).

Systems involving micelles have been used in L.L. extraction. Indeed, faster extraction rates have been obtained by use of surface active agents such as DNNS (2), long chain sulfonic acid (3), and so on.

Although the difference between microemulsions and micellar solutions is very narrow, because mainly due to the size of the droplets, the quantity of trapped water and the concentration of the surfactant, the word "microemulsion" is not mentioned in the literature dealing with surfactant enhanced extraction. Chin-Kwang et al. (4) have already reported the existence of a microemulsion in a L.L. extraction system but, in their case, the surfactant was the extractant itself and the microemulsion was subsequently destroyed as the metal was extracted. For the L.L. extraction of Ge(IV) by "Kelex 100" from the Bayer solutions of aluminate, one of us (8) has proved that a microemulsion is formed when "Versatic 10" (surfactant) and octanol (cosurfactant) are added to the system.

We have noticed that microemulsions and traditional L.L. extraction systems are suprisingly similar in their composition as underlined in Table I.

Microemulsion systems (Enhanced oil recovery)	L.L. extraction systems
Brine	salted aqueous phase
oil	diluant
cosurfactant (alcohol)	alcohol
surfactant (long chain sulfonic acid)	extractant and additives with tensioactive properties

Table I - Similarity between microemulsions and extraction systems

In the present paper, we investigate the kinetic effects due to the replacement of a traditional organic phase by a microemulsion. The extraction systems we describe are either two-phase or three-phase ones. The examples have been intentionally chosen among the couples metal-extractant which exhibit slow extraction rates in classical solvent systems.

Various types of microemulsions have been used depending on the acidity of the aqueous phase to be extracted. To check that the observed phenomena were not chemical but physical in nature, and to enlarge the validity of the process, the microemulsions were formed by using surface active reagents as chemically different as possible, and including both ionic or non-ionic surfactants.

EXTRACTION OF Ge(IV) BY "KELEX 100"

The extraction of Ge(IV) by "Kelex 100" (noted HK) has been studied in a classical system (5). In neutral media, Ge(IV) is slowly extracted as the complex $GeK_2(OH)_2$. About 15 hours are necessary to achieve the equilibrium, even in the presence of an alcohol. When a microemulsion replaces the traditional organic phase, the extraction is complete within 3 min (figure 1). In sulphuric acid media, the extracted species is $GeK_3^+ HSO_4^-$. The extraction is faster than in neutral media but still remains slow. In this case, the use of a microemulsion is also a good way to improve the kinetics of the system (figure 2). It must be noticed that the curve 4 in figure 2 corresponds to a three-phase system and that the rate is the overall one, that is to say the rate of the metal transfer from the aqueous solution into the organic one through the microemulsion layer.

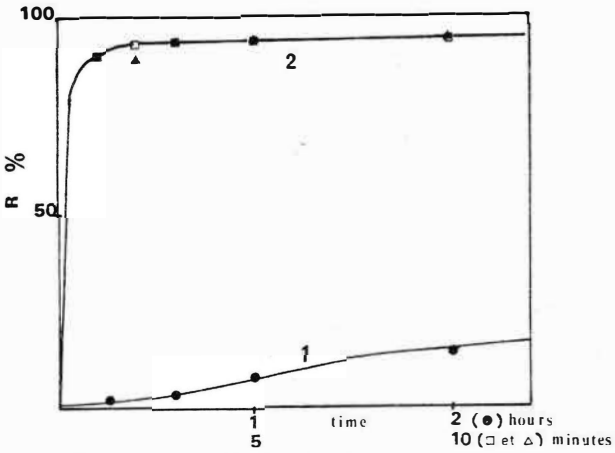

Fig.1 - Extraction rate of Ge(IV) at pH 4.
Aqueous phase : 10^{-2} M Ge(IV), 6.10^{-2} M Na_2SO_4 pH 4. O/W = 1
(1) Classical organic phase : Kerosene, 0.2 M "Kelex 100", 5 % octanol
(2) Microemulsion system : Kerosene, 0.2 M "Kelex 100", 16 % n-butanol, 2.5 % sodium dodecylbenzene sulfonate.

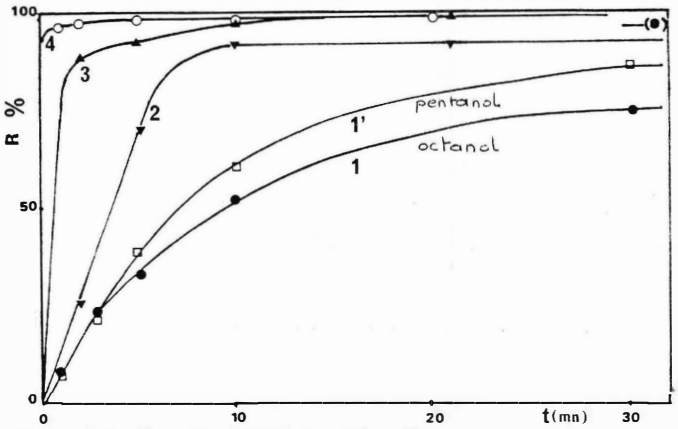

Fig.2 - Extraction rate of Ge(IV) in acidic media.
Aqueous phase : 10^{-2}M Ge(IV), 0.1 M H_2SO_4; O/W = 1
(1) Classical organic phase : Kerosene 0.2 M "Kelex 100", 10 % octanol.
(2) and (3) : two-phase system (water-microemulsion) (▼) 2.5 % sodium laurylsulfate, 10 % n-pentanol, (▲) 2.5 % nonylphenyl POE, NOE = 7, 14 % n-pentanol.
(4) Three-phase system (water-microemulsion-organic phase) (○) 2.5 % glucose decyl ether 6 % n-pentanol.

EXTRACTION OF Fe(III) BY "KELEX 100" IN ACIDIC MEDIA

The extraction of Fe(III) by "Kelex 100" is particularly slow (6). The results given in figure 3 show that the kinetics of the extraction can be dramatically accelerated by use of a microemulsion. With ionic surfactants, chemical interferences may occur. For instance, with sodium laurylsulphate the yield of the extraction significantly decreases and the UV-visible spectrum of the organic phase gives evidences of a modification of the structure of the extracted species.

With a microemulsion based on sodium dodecylbenzene sulfonate as the surfactant, Fe(III) is no more extracted. For non-ionic surfactants, the NOE is an important parameter.

EXTRACTION OF Fe(III) BY HDEHP

The extraction of Fe(III) by bis(ethyl-2 hexyl) hydrogenophosphate (HDEHP) is quantitative at pH > 2. The rate of its extraction decreases with pH (7). The kinetically limiting step is the formation of the complex

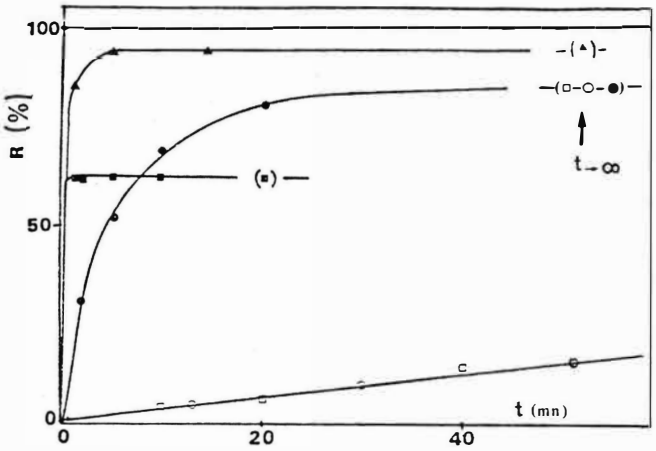

Fig.3 - Extraction rate of Fe(III) by "Kelex 100"
Aqueous phase : 10^{-3}M Fe(III), 10^{-1}M H_2SO_4, 6.10^{-2}M Na_2SO_4. O/W = 1.
Classical org. phase : (○) Kerosene, 5.10^{-2}M "Kelex 100" 10 % n-pentanol.
Water-microemulsion system with anionic surfactant : (■) 2.5 % sodium lauryl sulfate, 10 % n-pentanol.
Water-microémulsion system with non ionic surfactant (□) 2.5 % nonyl phenol POE, NOE = 5, 16 % n-hexanol; (▲) 4 % glucose decylether, 10 % n-hexanol.
Water-microemulsion-organic phase system (●) 2.5 % nonyl phenol POE, NOE = 7, 8 % n-pentanol.

$Fe(DEHP)_3$ at the interface (8). In the absence of any microemulsion, the achievement of the equilibrium requires about 30 min. Improvement of the kinetics is obtainable by using a two-phase water-microemulsion system. So, the highest extraction rate (equilibrium reached in less than 1 min) has been observed for a microemulsion formed with sodium lauryl sulphate (2.5 %) and n-pentanol (14 %) in kerosene and containing 0.2 M HDEHP. High extraction rates are also obtainable (less than 1 min) with non-ionic surfactants such as the nonyl phenol POE (NOE = 6) (2.5 % in the presence of 4 % n-pentanol . With glucose decylether as the surfactant, a three-phase system is formed. The overall phase transfer, i.e. from the aqueous phase into the organic one through the microemulsion layer, has also an acceptable kinetics (less than 2 min).

EXTRACTION OF Ni(II) BY "KELEX" at pH 4.5

Ni(II) is extractable from neutral aqueous solutions by "Kelex 100". The extracted complex is $NiK_2(HK)_2$. The extractions is slow (yield = 30 % after 30 min) and is only slightly accelerated by addition of 10^{-2} M of DNNS (9). On the other hand, the extraction rate is largely increased by use of microemulsions (two-phase or three-phase systems) based either on anionic or non-ionic surfactants. However, thermodynamic modifications also occur. For an aqueous solution containing 2.5 x 10^{-2} M Ni^{2+} + 0.1 M Na_2SO_4 + 0.1 M acetate buffer, and treated with an equal volume of 0.2 M HK in kerosene (two-phase system), the best results have been obtained with the two following surfactant-cosurfactant couples : (i) 2.5 % sodium lauryl sulphate/16 % n-pentanol and (ii) 2.5 % sodium dodecylbenzene sulfonate 13 % n-butanol.

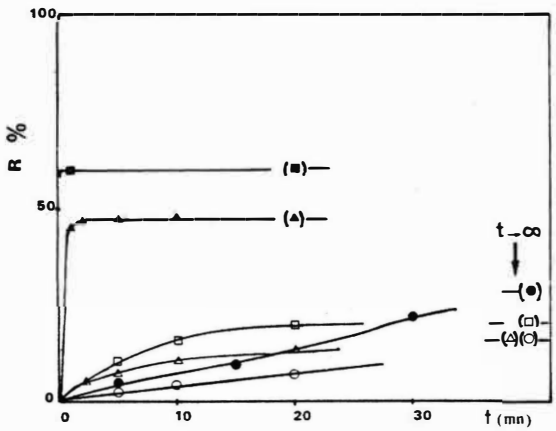

Fig.4 - Extraction rate of Ni(II) by LIX 70 + Versatic 911.
Aqueous phase 2.7 10^{-2}M Ni^{2+}, 0,1 M Na_2SO_4, 0.1 M acetate cuffer.
Classical organic phase (●) : Kerosene, 0.1 M LIX 70, 0.15 M Versatic 911, 8 % n-butanol. Water-microemulsion system with anionic surfactant: ■ 2.5 % sodium laurylsulfate, 18 % n-pentanol, (▲) 2.5 % sodium dodecylbenzene sulfonate, 8 % n-butanol or with non ionic surfactant (○) 2.5 % octyl phenyl POE (NOE=5), 15 % n-pentanol. Water-microemulsion-organic phase systems : (□) 2.5 % glucose decyl ether, 6 % n-hexanol, (△) 2.5 % nonyl phenol POE (NOE=8), 6 % n-pentanol.

With non-ionic surfactants, the kinetics is usually slower. For instance, 10 min are required to achieve the equilibrium with 2.5 % glucose ether, 16 % n-hexanol.

EXTRACTION OF Ni(II) WITH LIX 70 + VERSATIC 911

The addition of a carboxylic acid (e.g. Versatic 911) to a solution of α-hydroxyoxime (e.g. LIX 70) induces a favourable synergic effect on the yield of extraction of Ni(II), but the transfer rate becomes slow (2) . The presence of DNNS at low concentration improves the kinetics of the transfer (2).

The use of appropriate microemulsions allows to obtain both very fast kinetics and very favourable synergic effects (figure 4). The higher the laurylsulfate concentration, the more intense the synergic effect is.

EXTRACTION OF Al(III) WITH HDEHP IN ACIDIC MEDIA

The extracted species is the hexacoordinated $Al(DEHP)_6H_3$ complex (10), the formation rate of which decreases with pH. For extraction of Al(III) from an 0.1 M H_2SO_4 aqueous solution, the achievement of the half reaction requires 40 min. By using a two-phase or a three-phase microemulsion system based on an anionic surfactant the kinetics is considerably improved. The extraction of 10^{-2} M Al(III) from 0.1 M H_2SO_4 aqueous solutions with equal volume of 0.2 M HDEHP in kerosene has been investigated as an example. With the two following systems, (i) 2.5 % sodium dodecylbenzene sulfonate + 15 % n-butanol (two-phase system) and (ii) 2.5 % lauryl sulphate + 14 % n-pentanol (three-phase system), the Al(III) transfer has been found to be complete within less than 1 min. Moreover, the yield of extraction at the equilibrium is enhanced by the presence of dodecylbenzene sulfonate (80 % instead of 50 %). Conversely, Al(III) is not at all extracted by microemulsions based on non-ionic surfactants.

CONCLUSION

The use of microemulsions in solvent extraction is particularly attractive because it allows to obtain very fast phase transfers (achievement of the equilibrium within less than 1 min), even in the case of excessively slow L.L. extraction systems.

Synergic effects are observable in some cases. Consequently, great care must be taken in the selection of the tensio active reagents to obtain, if possible, positive synergic effects, and at least, to avoid any antisynergism.

REFERENCES

(1) as example : S. FRIBERG "Microemulsions, Theory and Practice" Academic Press, New-York 1977
(2) B.G. NYMAN et al., Proc. Int. Solv. Extr. Conf. 1974 SCI London 1974, 1, 669
(3) K. OSSEO-AZARE et al., Proc. Int. Solv. Extr. Conf., 1980 Paper 80-121
(4) W. CHIN-KWAN et al., Proc. Int. Solv. Extr. Conf., 1980 Paper 80-23
(5) B. MARCHON, G. COTE, D. BAUER, J. of Inorg. Nucl. Chem., 1979, 41, 1353
(6) P.S. NYHOLM et al., Proc. Int. Solv. Extr. Conf. 1974 Vol 1 p. 699
(7) C.F. BAES Jr., H.T. BAKER, J. Phys. Chem. 1960, 64, 89
(8) J.W. RODDY, C.F. COLEMAN, S. ARAI, J. of Inorg. Nucl. Chem. 1971, 33, 1099
(9) L. HUMMELSTEDT et al., Proc. Int. Solv. Extr. Conf. 1974, Vol 1, p. 829
(10) T. SATO, T. NAKAMURA, Anal. Chim. Acta 1975, 76, 407.

PREDICTION OF INTERFACIAL REACTIONS

Sümer M. Peker

Department of Chemical Engineering
Ege University
Bornova, Izmir, Turkey

Gibbs equation for surface excess states that there is a positive excess concentration at the interface if the change of interfacial tension with concentration is negative. As the surface tension of sulphuric acid first increases and then decreases with concentration, there should be an interfacial excess concentration of H_2SO_4 molecules existing at the surface, at concentrations of the acid greater than about 9 molar, corresponding to the maximum in the surface tension profile (1). If a similar trend is followed by the interfacial tension of sulphuric acid - toluene system, then an interfacial reaction has to exist in addition to a bulk phase reaction until the interfacial excess concentration is depleted. In fact Grosjean and Sawistowski (2) proposed the existence of an interfacial reaction in addition to the bulk phase reaction taking place almost totally in the acid phase as found by Cerfontain (3).

The verification of the proposal of an interfacial reaction in addition to a bulk phase reaction required the measurement of the interfacial tension of the reacting sulphuric acid - toluene system.

EXPERIMENTAL METHOD:

To follow the course of an interfacial reaction by measurement of an interfacial property, the reaction product has to cause a change in a physical property of the interface. Reeves and Harkaway (4) has shown that the surface activity of a sulphonic acid increases in direct proportion with the length of the hydrocarbon chain attached to the ring in para-position with respect to the sulpho group. As a consequence, toluene sulphonic acid is moderately surface - active.

An experimental set-up for the measurement of the interfacial tension of toluene/sulphuric acid system had to meet the following requirements:

1. Since toluene sulphonic acid is also soluble in the acid, the experimental set-up had to be free of external disturbances and bulk motion, to avoid the mixing of toluene sulphonic acid with the bulk phase by convection.
2. If there were a separate reaction at the interface, the interfacial concentration of toluene sulphonic acid would be greater than the bulk concentration. Therefore, measurement of interfacial tension had to be continuous without any break of the interface.

These requirements could be satisfied by the use of a modified Du Noüy technique in which the ring would be left at the interface at the maximum pull position and the interfacial tension be automatically recorded by an autobalance connected to the ring. Perkin - Elmer Autobalance AR 2 connected to a recorder was used for this end.

To correlate the interfacial excess concentrations found by the measurement of interfacial tensions with the rate of a possible interfacial reaction, bulk phase and total rate of reaction had to be estimated independently. As the bulk phase reaction is under mass transfer control at high concentrations of acid, the equation developed by Danckwerts (5) for a fast reaction was assumed to hold for this system and the rate of the bulk phase reaction N_{Tb}, was estimated by the equation

$$(1) \qquad N_{Tb} = K^o Ha\, C_{Ti} \cong K^o \beta\, C_{Ti} = (k_1 D_T)^{1/2} C_{Ti}$$

N_{Tb} : flux of toluene due to bulk phase reaction
Ha : Hatta number
K^o : mass transfer coefficient
C_{Ti} : interfacial concentration of toluene
k_1 : reaction rate constant
D_T : diffusivity of toluene in sulphuric acid

$$\beta = (k_1 D_T)^{1/2} / K^o$$

The total rate of reaction or the total flux of toluene was determined in a modified form of the stirred cell of Austin and Sawistowski (6), by measurement of the change of concentration of toluene sulphonic acid with respect to time.

RESULTS:

A typical interfacial tension profile obtained from the autobalance is given in Figure 1. Experiments coducted with various initial acid concentrations showed that the initial time rate of change of interfacial tension increased with the concentration of the acid, as given in Figure 2. In the same figure the variation of interfacial tension with initial acid concentration is also given, with time as the parameter. The trend in the variation of interfacial tension with sulphuric acid concentration is very similar to the trend of the variation of the surface tension of sulphuric acid: Below about 6 M concentration, the surface tension of sulphuric acid approaches that of water (72 dynes/cm), whereas the interfacial tension approaches that of water and toluene at mutual saturation (24 dynes/cm). Below about 12.8 M concentration no toluene sulphonic acid could be observed even after twelve hours of stirring of the phases in a reactor. Thus, the large variations in the interfacial tension profile between 7 - 13 M concentrations were attributed to a possible interaction of toluene molecules with the different proton hydrates and hydrated H_2SO_4 molecules existing in the acid phase in this concentration range.

In the concentration range of interest where a reaction takes place, the interfacial tension smoothly decreases with increasing acid concentration. The interfacial excess concentrations were calculated with the Gibbs equation (7):

$$(2) \qquad -d\sigma / d \ln a_{H_2SO_4} = RT\, \Gamma_{H_2SO_4} / (1 - (MC/\rho)_{H_2SO_4})$$

σ : interfacial tension
a : activity
R : universal gas constant
T : temperature
M : molecular weight
ρ : density
C : bulk concentration
Γ : interfacial excess concentration of sulphuric acid

The interfacial excess concentrations at the air/sulphuric acid and toluene/sulphuric acid interfaces calculated with this equation are given in Figure 3. These profiles cut the abscissa at 9 M and 13 M sulphuric acid concentrations, respectively. The latter value is in accordance with the π value of Guyot (8) for the termination of the reaction. If the intersection of the interfacial excess concentration profile with the abscissa denotes the termination of the reaction, the intersection of the two interfacial excess concentration profiles should denote the termination of the interfacial reaction with the same logic, the rate of the interfacial reaction being proportional to the difference between the interfacial excess concentrations.

To verify this proposal, the total rate of reaction, or equivalently, the transfer rate of toluene was determined in the stirred cell having a constant interfacial area, at 103 r.p.m. stirring rate for the initial sulphuric acid concentrations of 16.8 M, 17.6 M, and 18.4 M, where a bulk reaction in the "fast" regime was expected. The total rate of reaction, N_T, was determined by a mass balance over the sulphuric acid phase in the stirred cell. The total rate of reaction or the flux of toluene was in all cases greater than the flux of toluene required for the bulk phase reaction given by equation 1. The difference between these fluxes, R_{Ti},

(3) $$R_{Ti} = N_T - N_{Tb}$$

were attributed to an interfacial reaction. The ratio of R_{Ti} to the difference between the interfacial excess concentrations remained remarkably constant over the range of sulphuric acid concentrations investigated, suggesting a rate equation for the interfacial reaction as,

(4) $$R_{Ti} = 210.8\ (\Gamma_{int} - \Gamma_s)$$

for the toluene sulphuric acid system where Γ_{int} and Γ_s denote the interfacial and surface excess concentrations of sulphuric acid.

CONCLUSION:

The agreement between the interfacial excess concentrations determined by interfacial tension measurements and the rate of reaction determined in the stirred cell seems remarkable for the toluene-sulphuric acid system. However, this relation needs verification for other reacting systems.

REFERENCES:

1. E.W. Washburn,ed., International Critical Tables, 4, 464 (1928)
2. H. Sawistowski, P.R.L. Grosjean, Proceedings of ISEC '80, Liege.
3. H. Cerfontain, Mechanistic Aspects in Aromatic Sulphonation and Desulphonation, Interscience Publishers, London (1968)
4. R.L. Reeves, S.A. Harkawav, J. Coll. Interface Science., 64, 342 (1978)
5. P.V. Danckwerts, Gas - Liquid Reactions, Mc Graw Hill, New York (1970)
6. L.J. Austin, H. Sawistowski, I. Chem. E. Symp. Series, London, 26, 3 (1967)
7. A.W. Adamson, Physical Chemistry of Surfaces, Interscience Publishers, New York (1967)
8. Guyot, Chimie Industrie, 2, 879 (1919)

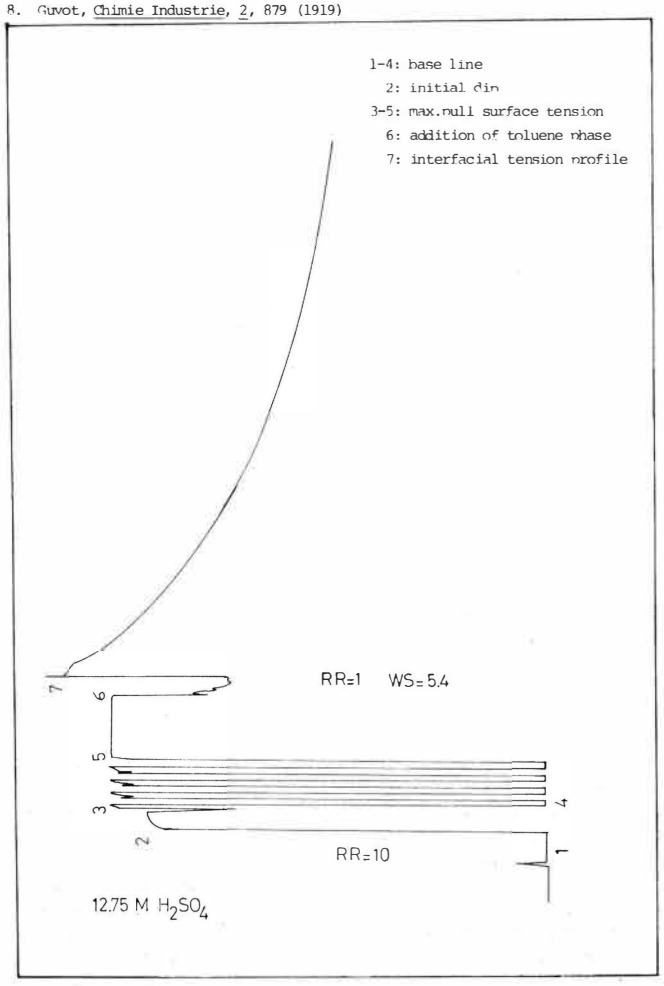

FIGURE 1: INTERFACIAL TENSION PROFILE OBTAINED FROM THE PERKIN - ELMER AUTOBALANCE AB - 2

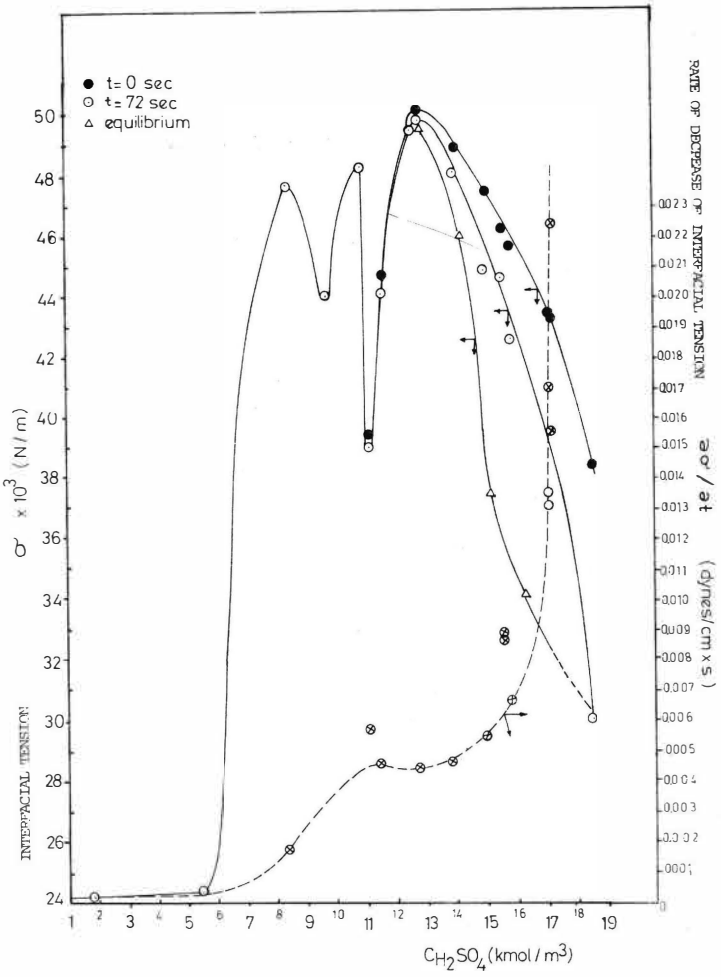

FIGURE 2: INTERFACIAL TENSION OF TOLUENE - SULPHURIC ACID SYSTEM

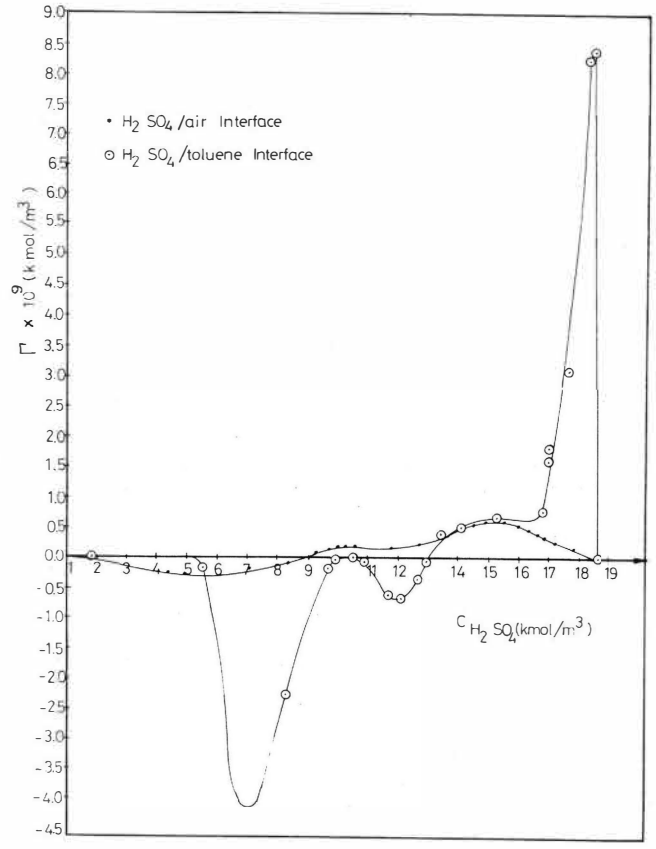

FIGURE 3: INTERFACIAL EXCESS CONCENTRATIONS

TOLUENE AND BENZENE SULPHONATION UNDER LAMINAR CONDITIONS

Morteza Sohrabi

Department of Chemical and Petrochemical Engineering
Tehran Polytechnic University
Tehran 15, Iran

The sulphonation of aromatic compounds is a unit process of considerable industrial importance. In technical scales, these reactions are either carried-out in gas-liquid system, with sulphur trioxide vapour as the sulphonating agent or, under liquid conditions using sulphuric acid solutions as the sulphonating entity. In both cases, the systems are heterogeneous and the overall rate may depend on both the chemical kinetics and the rate of diffusion of the reactants between the phases.

The present author (1,2) has demonstrated that in liquid-liquid systems, diffusional resistances are important only at high sulphuric acid concentration but that the overall rate can be correlated by a simple kinetic model at low acid concentration.

Considering the high sulphuric acid concentration systems of industrial importance, the present author (3) has used the approach of Danckwerts (4) and Astarita (5) to derive a rate model involving both chemical kinetic and diffusional resistances. This assumes all reaction to take place in the acid phase in a zone adjacent to the interface through which the aromatic hydrocarbon diffuses and leads to the relationship :

(1) $$R = A[ArH]_a^* \sqrt{Dk_2[H_2SO_4]_a}$$

R = rate of reaction per unit volume of the acid phase

A = interfacial area per unit volume of the acid phase

$[ArH]_a^*$ = saturation concentration of aromatic hydrocarbon in acid phase

D = diffusion coefficient for organic substrate in aqueous phase

k_2 = second order rate constant

$[H_2SO_4]_a$ = steady state concentration of sulphuric acid in aqueous phase

To examine the validity of this model, the system parameters should be known. Diffusion coefficients and solubilities of some aromatic hydrocarbons in concentrated sulphuric acid solutions have been measured (6,7,8,9), and second order rate constants have been determined (1,2,3). This, leaves 'A' as the only missing parameter.

There are some physical methods by which interfacial area in agitated vessels may be determined. However, these have been critically reviewed (10) and the conclusion has been reached that the data obtained by such methods are of doubtful accuracy. Also, the chemical methods described by Sharma *et al* (10,11) may not be applicable to aromatic sulphonation.

Steps were, therefore, taken to measure heterogeneous sulphonation rates using a laminar-jet apparatus, the technique of which is well known. One of the advantages of a laminar-jet is that the interfacial area can be measured accurately from its dimensions.

EXPERIMENTAL

Laminar-jet The experimental rig was similar to that used previously (3). It gave a laminar jet of sulphuric acid travelling through a static hydrocarbon phase.

The apparatus consisted of a cylindrical jet chamber made of 'Pyrex' glass 11.5cm long and 7.5cm internal diameter. Both the nozzle and receiver for the jet were made of 'Teflon' and were tapered to a knife edge to minimise disturbances of the surronding fluid. The interfacial area was measured from the diameter and length of the jet. The jet chamber assembly was placed in a thermostatic bath and the two feeds were introduced at the thermostat temperature. Any thermal effects due to chemical reaction would be very slight with the short contact time (maximum 5 seconds) and none were observed.

Materials and procedure The chemicals used in this study were all analytical grade.

During the start-up it was difficult to establish a stable jet without having any of the aqueous phase overflow the receiver and fall into the base of the main jet chamber. If concentrated sulphuric acid was in use, this reacted with the organic phase to an unknown extent. To overcome this difficulty, the jet was established with diluted sulphuric acid and this was switched to a feed of concentrated acid when stable conditions were reached. When the system had finally come to steady state, samples of the exit aqueous phase were removed and analysed for organic product.

Analysis Because of the short contact time between the two phases, only very low concentrations of sulphonic acid were present in the exit aqueous phase (the amount of aromatic substrate diffusing into the jet is much less than that corresponding to equilibrium distribution). Nevertheless, it was found possible to analyse the undiluted aqueous phase using a highly sensitive uv spectrophotometer at a wavelength of 262 nm for toluene sulphonic acid and 260 nm for benzene sulphonic acid.

RESULTS

Analysis of the exit aqueous phase gives the amount of sulphonic acid which is formed and remains in that phase. Back diffusion of sulphonic acid from aqueous into the organic phase did not occur, as no sulphonic acid were found to be present in the aromatic phase after a known period of time.

The change in concentration of aromatic hydrocarbon in the jet chamber during a run was extremely small and was neglected. Similarly, the concentration of sulphuric acid in the jet was assumed constant, since the change was far less than analytical error.

A comprehensive series of experiments was carried out using five sulphonating acid solutions stated in table 1 in conjunction with different jet lengths (1.5-3cm) and acid phase flow rates for toluene (7.5×10^{-4} - 26.1×10^{-4} $m^3.hr^{-1}$). Normally, eight conditions for each acid solution were considered. The mean rate was calculated for each acid and the results are included in table 1 together with the standard deviation. Rates corresponding to the five acid solutions were then estimated using equation (1) with measured values of k_2 and $[ArH]_a^*$ (1,2,6,7) and values of D from the literature (9) corrected for acidity. These estimated rates are compared with measured values in table 1.

Table 1 - Comparison of measured and predicted rates of toluene sulphonation under laminar conditions at 30°C.

Acid Series	Sulphuric acid concentration ($mol.l^{-1}$)	Sulphonation rate ($mol.m^{-3}.hr^{-1}$)		
		Measured mean	Standard deviation	Predicted using eqn.(1)
A	15.81	5.41×10^{3}	0.0209	5.25×10^{3}
B	16.10	7.24×10^{3}	0.0320	7.46×10^{3}
C	16.63	7.83×10^{3}	0.0311	7.68×10^{3}
D	17.36	8.76×10^{3}	0.0280	8.98×10^{3}
E	17.82	9.91×10^{3}	0.0261	9.66×10^{3}

One set of experiment was carried out in a similar way using benzene and 17.63 $mol.l^{-1}$ sulphuric acid. The mean rate found experimentally was 6.33×10^{3} $mol.m^{3}.hr^{-1}$ whilst the model predicted a value of 6.21×10^{3}.

It is clear that the model can only be expected to apply when the sulphuric acid concentration is sufficiently high for diffusional resistances to play a part in determining the overall rate. The chemical kinetics of sulphonation reactions are sensitive to sulphuric acid concentration and the present author (1,2,3) has previously outlined the conditions under which the two liquid phase sulphonation of certain aromatic hydrocarbons are likely to be kinetically controlled.

Considering acid solutions of such concentration that the assumption of mass transfer with simultaneous chemical reaction applies, an explanation can be found for the observed rates of competitive sulphonation. Some previous workers have used competitive sulphonation of an equimolar mixture of benzene and toluene in heterogeneous region as a criterion for detecting the presence of a diffusional resistance. Thus Chaudhry (12) found that the ratio of the apparent velocity constants (k_T/k_B) to be about 2.0. This may be compared with a value of about 60 for homogeneous sulphonation (2).

Taking the model as expressed by equation (1), the relative rates of formation of toluene and benzene sulphonic acids under two phase conditions from an organic phase with an equimolar ratio of toluene and benzene (assuming that this organic solution deviates only slightly from ideal behaviour(13)) will be:

(2) $$\frac{R_T}{R_B} = \frac{[C_6H_5\text{-}Me]_a^* \sqrt{D_T k_T}}{[C_6H_6]_a^* \sqrt{D_B k_B}}$$

Subscripts T and B are referred to toluene and benzene respectively. Substituting in this equation predicts R_T/R_B = 1.5-2.5, in excellent agreement with the value found experimentally (12).

On the other hand if the process is dependent only on chemical kinetics (1) :

(3) $$\frac{R_T}{R_B} = \frac{[C_6H_5\text{-}Me]_a^*}{[C_6H_6]_a^*} \cdot \frac{k_T}{k_B}$$

Substitution gives R_T/R_B = 50-55, very close to the value determined under homogeneous conditions (1).

CONCLUSIONS

Sulphonation in a lminar-jet has provided evidence that the rate of sulphonation of toluene and benzene under two liquid phase conditions with concentrated sulphuric acid solutions (higher than 15.5 $mole.l^{-1}$) can be described in terms of a fast reaction taking place in a zone in the aqueous phase adjacent to the interface.

The derived model, based on the above assumption, seems to predict rates which are in close agreement with those found experimentally.

A similar approach also provides an explanation of the observed results of the competitive sulphonation of toluene and benzene.

REFERENCES

1. M. Sohrabi, T. Kaghazchi, C. Hanson, J.appl.Chem.Biotechnol., 27,453 (1977)

2. M. Sohrabi and T. Kaghazchi, J.Chem.Tech.Biotechnol., 31,409 (1981)

3. M. Sohrabi, Paper presented at the 181st ACS Symposium, Atlanta (Spring 1981)

4. P.V. Danckwerts, Gas-Liquid Reactions, Mc.Graw-Hill Book Co., New York, (1970)

5. G. Astarita, Mass Transfer with Chemical Reaction, Elsevier Book Co., Amsterdam, (1967)

6. H. Cerfontain, Rec.Trav.Chim, 84,491 (1965)

7. H. Cerfontain and A. Telder, Rec.Trav.Chim, 84,545 (1965)

8. C. Hanson, M.W.T. Pratt, M. Sohrabi, ACS Advances in Industrial Nitration Chemistry, No.22, Chapter 15 (1976)

9. C. Hanson and A.M. Ismail, J.appl.Chem.Biotechnol., 26,111 (1976)

10. J.B. Fernandes and M.M. Sharma, Chem.Engng.Sci., 22,1267 (1967)

11. D.S. Sankholkar and M.M. Sharma, Chem.Engng.Sci, 28,2089 (1973)

12. M.S.K. Chaudhry, M.Sc. Thesis, University of Bradford, UK, (1970)

13. C. Hanson, M. Sohrabi, T. Kaghazchi, CHEMTECH, 7,700 (1977)

INTERFACIAL AND KINETIC STUDIES OF COPPER EXTRACTION BY β-DIKETONE EXTRACTANTS

Michael Cox and Michael Gray

The Hatfield Polytechnic
Hatfield, Herts, U.K.

Following the success of the hydroxyoxime reagents in the commercial liquid-liquid extraction of copper from weakly acidic solutions, several new reagents have appeared on the market. Some of these contain a β-diketone functional group and give improved performance in the extraction of copper from ammoniacal solutions. The aim of this work was to investigate the mechanism whereby copper is extracted by the β-diketones, LIX54*, XI51* and 1-phenyl-1,3-dodecanedione (PDD), with the added intention of clarifying the much discussed extraction of copper by hydroxyoximes.

THEORY

Kinetics. The kinetics of heterogenous reaction systems are intrinsically complex because a large number of rate processes and a choice of reaction sites may be involved. If the rate of extraction is determined by diffusion processes, the system is said to be in a "diffusion regime" (1). On the other hand, if diffusional processes are instantaneous in comparison to the chemical reactions, the system is said to be in a "kinetic regime". In fact, a significant amount of solvent extraction work appears to have been carried out in a "mixed regime" where the rates of diffusion and of chemical reaction cannot be neglected with respect to each other (1,2).

The overall equation for the extraction of copper by an acidic chelating extractant may be written:

$$(1) \qquad Cu^{++} + 2\overline{HA} \rightleftharpoons \overline{CuA_2} + 2\,H^+$$

where a bar denotes a species in the organic phase.
The forward rate equation for this reaction at a point far removed from equilibrium is of the form:

$$(2) \qquad \frac{-d[Cu]}{dt} = \frac{K[Cu]^l[\overline{HA}]^m}{[H]^n}$$

where l, m and n are the reaction orders, K is the forward rate constant and the charges have been omitted for clarity.
If the rate of extraction is first order with respect to the copper concentration and the pH and reagent concentration remain constant, then:

$$(3) \qquad \frac{-d[Cu]}{dt} = K'[Cu]$$

Integrating and rearranging:

$$(4) \qquad -\ln[Cu] = -\ln[Cu]_0 + K't$$

The gradient of a plot of this function will give K' which may be used to obtain the initial forward rate of extraction, $\vec{v}_0$:

$$(5) \qquad \vec{v}_0 = \left(\frac{-d[Cu]}{dt}\right)_0 = K'[Cu]_0$$

If the rate of extraction is proportional to the interfacial area, then a more meaningful parameter is the interfacial flux, $\vec{N}_0$, which is the number of moles of material transfered across unit area of the interface in unit time:

$$(6) \qquad \vec{N}_0 = \frac{\vec{v}_0}{a}$$

where a, the specific interfacial area, is the ratio of the interfacial area to the volume of the analysed phase.

Interfacial Adsorption. The boundary between two homogenous phases should not be regarded as a simple geometrical plane. Rather, it is a film of a definite thickness and so it is more properly termed an interphase (3). It is a region over which there is a gradation of properties merging into those of the bulk phases at its extremities. By considering the total internal energy of an interphase, Gibbs derived a general thermodynamic relationship for the excess number of molecules adsorbed at an interface:

$$(7) \qquad \partial\gamma)_T = -\sum_i \Gamma_i \partial\mu_i)_T$$

where Γ_i is the number of adsorbed molecules of species, i, per unit area of interface, μ_i is its chemical potential and γ is the interfacial tension.
From this may be derived an expression for the interfacial excess of a single, highly interfacially active solute. Assuming that the interfacial excesses of all other components are zero and that activity coefficients are unity:

$$(8) \qquad d\gamma = -\Gamma kT \ln c$$

where c is the concentration, k is the boltzmann constant, T is the absolute temperature and Γ, the interfacial excess of the solute, is defined as the algebraic excess of solute in unit cross section of the surface region over that which would be present in a bulk region containing the same number of moles of solvent (3). It can be seen that a plot of interfacial tension versus the logarithm of the extractant concentration should give a straight line the gradient of which determines the number of adsorbed molecules per unit area. Great care should be taken in the use of interfacial concentrations calculated from this equation because, in systems which do not conform to ideal behaviour, the proportionality constant is not equal to kT. However, a constant negative gradient of γ versus logc is still indicative of a constant (saturated) interfacial excess.

RESULTS AND DISCUSSION

Using a quiescent interface stirred cell similar to that described by Chin (4), it was found that the initial forward rate of extraction of copper by XI51 was directly proportional to the interfacial area. It was further found that the interfacial flux of copper produced by XI51 and by LIX54 was dependent on the aqueous phase stirring speed but independent of the organic phase stirring speed. Also, when the aqueous phase was not stirred, a copper depleted band was seen to extend into the aqueous phase from the interface. These results imply that the rate of extraction of copper by β-diketones, under the hydrodynamic conditions produced in this stirred cell, is controlled by the diffusion of copper from the bulk aqueous phase to the interface.

Further experiments to study the kinetics of solvent extraction of copper by XI51 were carried out using the stirred cell and a rising drop apparatus (5). The correlation between these results and the interfacial tension curve for XI51 are shown in figure 1. The most important point to note from this figure is the independence of the rate of extraction on the bulk phase extractant concentration when there is a constant interfacial excess of extractant. When the interface is not saturated, the rate of extraction is first order with respect to the extractant concentration in the rising drop apparatus. This implies that the rate of extraction of

* Henkel corporation

copper is first order with respect to the interfacial excess concentration of XI51 which in turn implies that the rate determining step is the reaction between copper ions and interfacially adsorbed extractant molecules or anions to form the 1:1 complex cation. The same conclusions are implied by figure 2 for LIX54 and PDD.

The copper/hydroxyoxime system is much more complex. There are added problems due to the existence of aggregation (6), a non-reactive isomer (7), additives and impurities. Consequently, there is a lot of scope for variation in experimental conditions and it is not surprising that a lot of varied and sometimes apparently conflicting results have been obtained by different workers.

Fleming et al (8) found that the extraction rate of copper by hydroxyoximes in a stirred cell was directly proportional to the interfacial area and dependent on the organic phase stirring but independent of the aqueous phase stirring. Whewell et al (6) further reported that, in a non-stirred system, a layer of copper complex was seen to build up on the organic side of the interface. These results imply a slow diffusion step of copper complex away from the reaction site.

On close scrutiny, the copper/hydroxyoxime kinetic results of many authors are compatible despite the differing conditions and equipment employed. Generally, there is a gradual change in reaction order and linearity is only observed over narrow concentration ranges of one order of magnitude or less. Below about 10^{-2} mol dm^{-3} of extractant there is a second order dependence and above that, when the interface is saturated and the total interphase concentration is no longer directly proportional to the bulk phase concentration, the order tends towards unity. This implies that, although the interface is saturated and there is a constant concentration of adsorbed extractant, the total interphase concentration still rises with, but proportionately slower than, the bulk phase concentration. Thus, the mechanism is probably one whereby copper (II) ions react first with hydroxyoxime molecules adsorbed at the aqueous phase/interphase boundary followed by the rate determining addition of the second extractant molecule within the interphase as implied by Hirons et al (9,10).

CONCLUSIONS

From the correlation between the curves of extraction rate and interfacial tension versus extractant concentration, the existence of two different interfacial species is indicated. One is an adsorbed species which forms an oriented monolayer at the interphase/aqueous phase boundary the concentration of which is constant above a certain bulk phase concentration. The second is a non-adsorbed species which exists within the interphase the concentration of which is directly related to the bulk phase concentration.

The rate of extraction of copper by acidic chelating extractants with high distribution coefficients is limited both by diffusion of species to or from the interface and by slow reaction steps at the interface. The relative importance of the reaction and diffusion processes depends on the hydrodynamics of the system but, in general, neither one of them may be ignored.

In general, it may be said that the extraction of copper by β-diketones is controlled by diffusion of copper ions to, and reaction with, extraction molecules or ions adsorbed at the aqueous phase/interphase boundary to form the 1:1 complex cation. The extraction of copper by hydroxyoximes is controlled by the addition of the second extractant molecule within the interphase and diffusion of the neutral complex into the bulk organic phase.

REFERENCES

1. P.R. Danesi and R. Chiarizia. CRC Critical Reviews in Analytical Chemistry, 10 (1) 1 (1980)

2. E.S. Perez de Ortiz. J.App.Chem.Biotechnol., 28 149 (1978)

3. M.J. Jaycock and G.D. Parfitt. "Chemistry of Interfaces" Ellis Horwood Ltd. (1981)

4. S.C. Chin. "A Novel Gradientless Contactor for Studying Mass Transfer with Reaction in Liquid-Liquid Systems" PhD Thesis, Univ. of New Brunswick (1975)

5. R.J. Whewell, M.A. Hughes and C. Hanson. J. Inorg & Nucl. Chem. 37 2303 (1975)

6. R.J. Whewell, M.A. Hughes and C. Hanson. Proceedings ISEC'77 CIM Special Volume 21 443 (1979)

7. A.W. Ashbrook. J. Chromatog. 105 141 (1975)

8. C.A. Fleming, M.J. Nicol, R.D. Hancock and N.P. Finkelstein. J. App. Chem. Biotechnol. 28 443 (1978)

9. C.G. Hirons. "Kinetic, Interfacial and Related Studies of the Copper-Hydroxyoxime Solvent Extraction System" PhD Thesis, Hatfield Polytechnic (1981)

10. M. Cox, C.G. Hirons and D.S. Flett. Proceedings ISEC'80 1 paper 80-118 (1980)

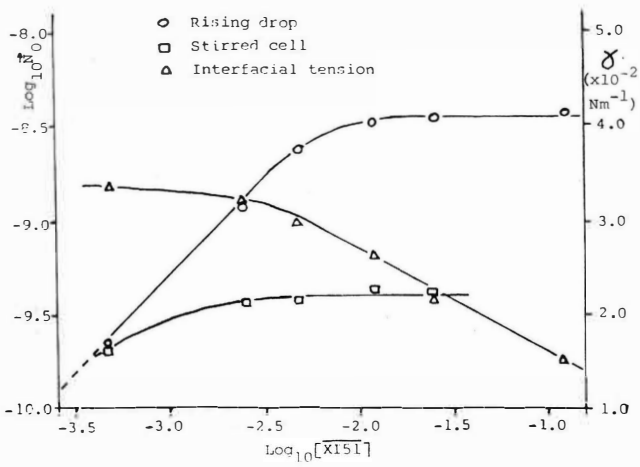

FIGURE 1. RATE AND INTERFACIAL TENSION VERSUS CONCENTRATION OF XI51

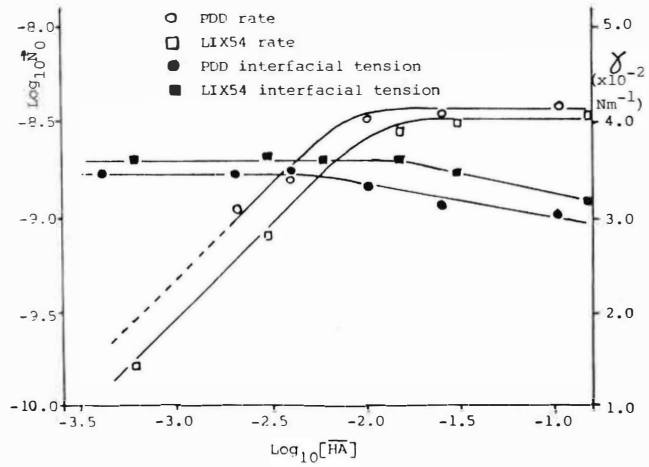

FIGURE 2. RATE AND INTERFACIAL TENSION VERSUS CONCENTRATION OF LIX54 AND PDD

DISPOSITION AND CONTROL OF IMPURITIES IN NICKEL AND COBALT SOLVENT EXTRACTION CIRCUITS IN THE PROCESSING OF LATERITE-DERIVED AMMONIACAL LEACH LIQUORS

D. N. Nilsen
Chemical Engineer
R. E. Siemens
Group Supervisor and Metallurgist
Albany Research Center
Bureau of Mines
U.S. Department of the Interior
P.O. Box 70
Albany, Oregon 97321 USA

The Bureau of Mines has devised a method (1-4) that allows near-specification-grade nickel and cobalt cathodes to be produced from low-grade domestic laterites. Laterite ore is subjected to selective reduction with carbon monoxide and then to an oxidation leach in an ammoniacal sulfate solution. The leach solubilizes the Ni, Co, and Cu as ammine complexes. The majority of the magnesium and manganese (>90 pct) that is also solubilized during the leach is precipitated by the addition of $NH_4H_2PO_4$, producing a fertilizer byproduct. Solvent extraction (SX) and electrowinning (EW) are then used to separate and recover Ni, Co, and Cu. Trace amounts of Zn, Ca, Mg, Mn, and NH_3 from the leach liquor, as well as several other impurities, must be contended with in the SX and EW circuits. The disposition of metal impurities was found, and control methods were devised and applied in a 230 kg/day (laterite) continuous circuit PRU (process research unit).

PRU SX-EW CIRCUITS

The continuous circuits shown in Figure 1 consisted of two sections: nickel-copper SX-EW, and cobalt SX-EW. Mixer-settler stages in the SX circuits were sized with 7.6-liter mixers (nickel-copper circuit and cobalt extraction stage) and 4.5-liter mixers (remaining cobalt circuit).

Nickel-Copper SX-EW. Nickel and copper were extracted from the ammonia-adjusted leach liquor with a LIX 64N[1/] solvent. Cobalt (III) is not extracted by LIX 64N; therefore, it remained in the raffinate. A crowd stage was used to minimize the extraction of zinc and ammonia by the solvent. Residual ammonia was scrubbed from the solvent with a pH-controlled $(NH_4)_2SO_4$ solution (equilibrium pH ~5.5). The scrub solution was recycled within the stage, and a bleed stream was used to control the $(NH_4)_2SO_4$ concentration in the range of 120 to 300 g/L. The scrub solution bleed stream was added to the leach liquor as a partial source of $(NH_4)_2SO_4$ makeup. Some $(NH_4)_2SO_4$ is lost with the tailings after leaching. Nickel was stripped from the solvent with a low-acid-level electrolyte (10 to 12 g/L H_2SO_4); copper was then stripped with a high acid level elecrolyte (~165 g/L H_2SO_4). Impurity problems in the nickel-copper circuit were generally considered to be minimal; the exception was some NH_3 transfer to the nickel electrolyte during periods of upset in the pH-controlled scrub stage. The level of cobalt in the recycled solvent remained essentially constant throughout the runs (0.01 to 0.03 g/L).

Resin column for impurity extraction. A column (15.2-cm I.D.) was packed with ~0.028 m^3 of dry ion-exchange resin (IRC-718). Prior to use, the resin was conditioned first by conversion to the hydrogen form with 100 g/L H_2SO_4 and then by washing with water. The resultant resin occupied a volume of ~0.020 m^3. Impurities from the nickel-copper raffinate were extracted with the conditioned resin in the following order: Ni, Mn >> Mg, Ca, and Zn with Co(III) not extracted. Profiles of the impurities in the resin column effluent are shown in Figure 2. As shown, the Co concentration remained constant throughout the run, Ni, and Mn remained at a very low level (0.001 g/L), and Cu remained at ~0.003 g/L. Zinc and calcium broke through after ~2,500 liters of nickel-copper raffinate had been processed (0.01 g/L was chosen as an arbitrary reference level for column breakthrough). Magnesium broke through after ~3,100 liters had been processed. The average impurity levels in the nickel-copper raffinate fed to the resin column were as follows: 0.043 g/L Ni, 0.003 g/L Cu, 0.018 g/L Zn, 0.023 g/L Ca, 0.012 g/L Mg, and 0.013 g/L Mn. The resin loading capacity for metal impurities at the time zinc and calcium broke through was estimated to be ~9.6 kg/m^3 of resin (as received, dry resin basis).

Cobalt SX-EW. The purified raffinate containing trivalent cobalt was treated in an air-excluded cobalt metal shot column to reduce the cobalt to the divalent state. The reduced cobalt was then extracted with LIX 51 solvent. The loaded solvent was first scrubbed for ammonia removal with a H_2O-$(NH_4)_2SO_4$ solution which removed ~70 pct of the ammonia without neutralization taking place. The ammonia was stripped from the scrub solution for recycle back to the process through heating (50° C) and air sparging. Residual ammonia was then scrubbed from the solvent with a pH-controlled $(NH_4)_2SO_4$ solution (equilibrium pH ~5.5). Finally, cobalt was stripped from the solvent with recycled electrolyte containing 50 g/L Co and 10 to 12 g/L H_2SO_4. The major impurity problems in the cobalt circuit were buildup of Ca in the recycled pH-controlled scrub solution and some buildup of Mg and NH_4 in the electrolyte.

Laboratory tests have shown that at least 10 g/L Mg and 14 g/L NH_4 can be tolerated in the cobalt electrolyte without detrimental effects on electrowinning. These levels can be maintained with a control bleed stream from the cobalt EW circuit back to the leaching circuit, and this would result in the recycle of <10 pct of the total cobalt flux into the cell. This was based on the transfer rates of magnesium and ammonia into the cobalt electrolyte averaged over a 92 hour continuous run.

Nickel and cobalt cathodes. Nickel cathodes produced from the circuit contained ~99.9 pct Ni and only 0.006 pct Cu and 0.01 pct Co (table 1). Of the impurities analyzed in the nickel cathode, only lead exceeded the ASTM Spec. B-39 levels (0.01 pct vs. spec. level of <0.005 pct). The current efficiency and energy consumption for nickel EW averaged about 64 pct and 5.34 kwhr/kg, respectively.

1/ Reference to specific equipment, trade names, or manufacturers does not imply endorsement by the Bureau of Mines.

TABLE 1. - Analyses of nickel cathode

Element	PRU run	ASTM Spec. B-39
Pct:		
Ni	99.9	99.8 (min)
Cu	.006	.02 (max)
Fe	.02	.02 (max)
Zn	NA	<.005
Pb	<.01	<.005
Mn	NA	<.005
Co	.01	.15 (max)
Ppm:		
H	12	NG
C	40	300
O	91	NG

NA Not analyzed.
NG Not given.

The cobalt cathode contained ~99.9 pct Co and only 0.02 pct Ni and 0.006 pct Cu. Comparison of this cathode with specifications obtained from a firm that purchases electrolytic cobalt (table 2) showed that only zinc and lead levels exceeded the specifications (0.01 pct vs. <0.008 pct specified and 0.007 pct vs. <0.001 pct specified, respectively). Cobalt EW current efficiency and energy consumption generally averaged about 65 pct and 3.85 kwhr/kg, respectively.

TABLE 2. - Analyses of cobalt cathode

Element	PRU run	Specs. from independent firm[1/]
Pct:		
Co	99.8, 99.9[2/]	99.5 (min)
Cu	.006	<.02
Fe	.02	<.15
Zn	.027, .010[2/]	<.008
Pb	.007	<.001
Mn	<.001	NG
Ni	.02	<.20
P	NA, .002[2/]	NG
Ppm:		
H	101, 3[2/]	NG
C	365, <10[2/]	NG
O	364, 38[2/]	NG
S	NA, <10[2/]	NG

NA Not analyzed.
NG Not given.
1/ UOP Inc., Mineral Sciences Division. New Procedure For Recovering Nickel and Cobalt From Western Laterites: Economic Feasibility contract J0285021). BuMines OFR 68-82, 1982, p. 35; NTIS PB 82-245945.
2/ Heat-treated cathode; atmosphere of 98 pct argon and 2 pct hydrogen at atmospheric pressure at 1,000° C for 2 hours.

To date, little effort has been made to tailor the EW or heat treatment (cathode degassing) conditions to minimize the level of lead in the cathodes. Therefore, since these levels are already reasonably close to specifications, it is felt that with more attention to the lead impurity, the specifications can probably be met through adjustment of the EW and/or heat treatment conditions. Preliminary data indicate that the zinc level in the cobalt cathode can be further reduced by somewhat altering the conditions during heat treatment.

ADDITIONAL TESTS (BENCH-SCALE)

Although the resin column reduced the transfer rate of calcium to the recycled pH-scrub solution (cobalt SX circuit) as compared to operation without the column, the buildup of calcium still presented a problem. To alleviate this problem, bench-scale continuous cobalt SX circuit tests were run using acidified water (~1.1 g/L H_2SO_4) in the pH-controlled scrub stage on a once-through basis. The concentration of impurities in the discharged scrub solution remained well below their solubility limits. The generated $(NH_4)_2SO_4$ concentration in the discharged solution ranged between 1.0 and 1.6 g/L.

A disadvantage of this method was a higher-than-normal organic entrainment level in the aqueous scrub solution (114 ppm vs 58 ppm). Therefore, the phase disengagement characteristics of the cobalt circuit, pH-controlled scrub stage were investigated in a laboratory-scale phase disengagement cell. Comparative tests were run with 124-g/L, 52-g/L, and 2-g/L $(NH_4)_2SO_4$ solutions (pH ~5.5) and with loaded LIX 51 solvent. The phase disengagement rates obtained with the three solutions were very similar (Figure 3). For example, a dispersion band thickness of ~10 cm corresponded to specific flow rates of 54 to 64 Lpm/m^2.

CONCLUSIONS

Near-specification-grade nickel and cobalt cathodes were produced from low-grade domestic laterites by the method shown diagrammatically in Figure 1.

The use of a resin column for impurity removal before reduction and extraction of cobalt (II) resulted in a cobalt cathode containing ~99.9 pct cobalt (cobalt-to-nickel ratio of ~5,000 to 1).

The use of acidified water on a once-through basis in the pH-controlled scrub stage (cobalt circuit) avoided the problem of calcium buildup and precipitation in that stage.

NOTATION LIST

kg/day	Kilograms per day
g/L	Grams per liter
pct	Percent
Lpm/m^2	Liters per minute per square meter
m	Meter
kwhr/kg	Kilowatt-hour per kilogram
ppm	Parts per million

REFERENCES

1. R. E. Mussler and R. E. Siemens. Electrowinning of Nickel and Cobalt From Domestic Laterite Processing. BuMines RI 8604, 1982, 20 pp.
2. D. N. Nilsen, R. E. Siemens, and S. C. Rhoads. Solvent Extraction of Cobalt From Laterite-Ammoniacal Leach Liquors. BuMines RI 8419, 1980, 23 pp.
3. D. N. Nilsen, R. E. Siemens, and S. C. Rhoads. Solvent Extraction of Nickel and Copper From Laterite-Ammoniacal Leach Liquors. BuMines RI 8605, 1982, 29 pp.
4. R. E. Siemens, P. C. Good, and W. A. Stickney. Recovery of Nickel and Cobalt From Low-Grade Domestic Laterites. BuMines RI 8027, 1975, 14 pp.

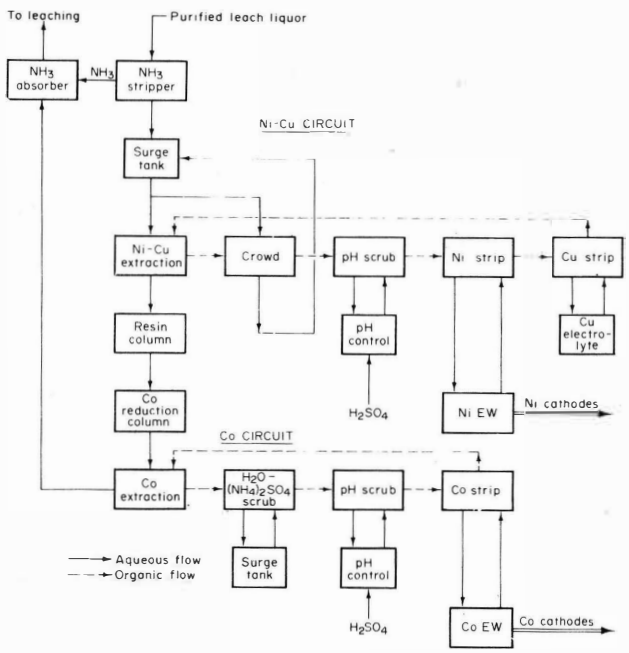

FIGURE 1. - CONTINUOUS SX-EW CIRCUITS FOR METAL RECOVERY.

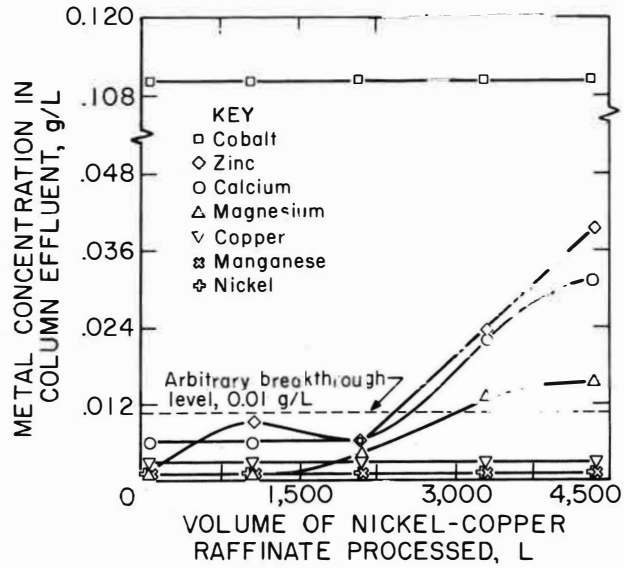

FIGURE 2. - PROFILES OF IMPURITIES IN RESIN COLUMN EFFLUENT.

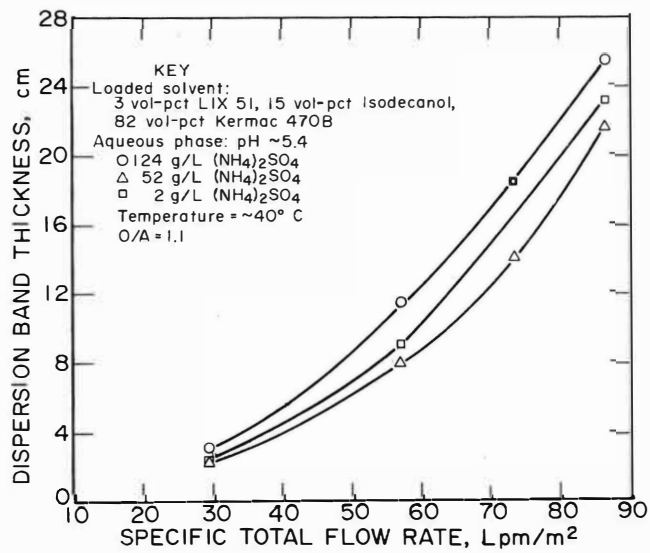

FIGURE 3. - EFFECT OF AMMONIUM SULFATE CONCENTRATION ON PHASE DISENGAGEMENT.

TEST OF AN AMINE PROCESS FOR REPROCESSING NATURAL URANIUM FUEL AT THE EUREX PILOT PLANT

G. R. Grant, D. G. Boase and D. R. McLean
Atomic Energy of Canada Limited
Whiteshell Nuclear Research Establishment
Pinawa, Manitoba, Canada R OE 1L O

F. Pozzi, A. Hall, V. Pagliai and G. Alonzo

Comitato Nazionale per L'Energia Nucleare e
L'Energia Alternative
Centro Di Saluggia
13040 Saluggia, Vercelli, Italy

INTRODUCTION

The reprocessing of irradiated, natural uranium fuel from CANDU reactors, where the plutonium only is to be recovered, appears to offer the potential for lower cost reprocessing plants that should be easier to operate (1). Long-chain tertiary amines have been considered previously for various applications in fuel-reprocessing operations (2-5), and they are particularly suitable for plutonium recovery. Extraction characteristics are such that plutonium could be extracted while uranium, which at normal exit burn-up from CANDU reactors is of little economic value, could be discarded with the fission-product wastes. The recovered plutonium could then be used for recycle with natural uranium fuel, or for other advanced fuel cycles employing thorium (6).

FLOWSHEET DEVELOPMENT

Using published distribution data for uranium and plutonium (7), and additional data obtained at WNRE (Whiteshell Nuclear Research Establishment), Morgan and Coady (8) devised an amine solvent-extraction process to recover plutonium from uranium-rich nitric-acid solutions. The solvent was Alamine-336[(a)] at 0.15 mol/L in a diluent of diethylbenzene. Use of the aromatic diluent prevented third-phase formation, a problem often encountered in amine extractions of actinides when using aliphatic diluents. The flowsheet was tested extensively in the laboratory and then actively in a small facility built in the WNRE Hot Cells. The latter facility used a single cycle of solvent extraction, followed by final plutonium-product purification by anion exchange. All aspects of the experiment appeared sufficiently promising that a test of the flowsheet at a larger scale was the next logical step.

The EUREX pilot plant in Saluggia, Italy, operated by ENEA (Comitato Nazionale per L'Energia Nucleare e L'Energia Alternative) had been built specifically for processing operations using amines, and it appeared to be the most suitable facility in which to extend the work.

By agreement between AECL (Atomic Energy of Canada Limited) and ENEA, 72 CANDU fuel bundles from the Pickering Generating Station were to be processed at the EUREX plant. However, since the plant had previously been used for recovery of enriched uranium from U-Al fuel, direct application of the WNRE single-cycle flowsheet for plutonium recovery was not possible without some compromise imposed by the existing plant. Plant facilities were used to advantage to perform two solvent-extraction cycles. The WNRE flowsheet was used for the first cycle, while the second cycle was the result of further development work performed at the Central Research Laboratories of ENEA (9). The combined flowsheets are shown in Figure 1.

The extractant is 7.5% (0.15 mol/L) Alamine-336 in mesitylene[(b)]. Extraction of plutonium takes place in the 1A contactor, leaving the bulk of the uranium and fission products in the aqueous phase. These exit the contactor in the 1AW stream. This combination of uranium with the high-level wastes has an impact on waste management operations and, therefore, requires further study. The extracted plutonium is scrubbed in the 1B contactor to increase decontamination from uranium and fission products. The plutonium is then stripped from the solvent in the 1C contactor using a mixture of dilute HNO_3 and H_2SO_4. The concentration of plutonium is increased by a factor of 20 in the first extraction cycle.

Following acid adjustment, the second extraction cycle is performed, but in this case, aqueous hydroxylamine nitrate (HAN) is used as the final plutonium-stripping agent.

PLANT OPERATIONS

Schedule. The fuel bundles were processed in five subcampaigns of about 15 bundles each over a period of about two and a half years (1980 to 83). Each subcampaign, consisting of chopping, dissolution, solvent extraction, solvent recovery and waste treatment, took about two months to complete. The burnup of most fuel bundles was normal, i.e. about 200 MWh/kg or more, but a few had burnups of about 100 MWh/kg. Average data for the fuel are shown in Table 1. Decay periods varied from about five to seven years.

TABLE 1

DATA FOR FUEL USED IN THE AECL-ENEA EXPERIMENT*

	Low Burn-Up Fuel	Normal Burn-Up Fuel
Avg. Burnup (MWh/kg)	~ 100	~ 220
^{235}U (g/kg U)	~ 3.9	~ 1.7
Total Pu (g/kg U)	~ 2.7	~ 4.2
^{144}Ce (GBq/kg U)	140	200
^{137}Cs (GBq/kg U)	460	960
^{125}Sb (GBq/kg U)	13	28
^{106}Ru (GBq/kg U)	120	270

* Data interpolated from AECL-4436/1 (10) for a cooling period of five years

(a) Product of General Mills, Inc., with the generic name of tricaprylyl amine (TCA), containing predominantly a mixture of octyl- and decyl-alkyl groups. The amine was purified by passing through an activated Al_2O_3 column before use.

(b) Mesitylene was supplied by ENI, San Donato M, Milan. Purity was > 99.5% 1-3-5-trimethylbenzene. It was given a wash with Na_2CO_3 at 1 mol/L before use.

Head-End Operation. Bundles were chopped individually into lengths of 2.5 cm, with the fuel and sheath segments dropping directly into the dissolver. The fuel was dissolved in 5.5 mol/L HNO_3 in batches of three bundles each. Off-gases were monitored for ^{85}Kr, ^{129}I and particulates during several batches (11). Following removal and rinsing of the hulls, the undissolved solids were removed in a continuous centrifuge operating at 1000 G. Solution clarity was monitored by visual inspection of samples.

To ensure essentially complete extraction of the plutonium, it must be in the (IV) valence state. To achieve this, the plutonium was first reduced to Pu(III) using ferrous sulfamate and then re-oxidized to Pu(IV) by passing NO_2 gas through the feed solution several hours before extraction operations were to begin.

Solvent Extraction. The feed solution was processed through the plant, one cycle at a time, using two 8-h shifts per day. The facility was shut down each night, with no deleterious effects being identified due to this mode of operation. About two weeks were required to process the feed solution for one subcampaign through the two cycles of solvent extraction and to flush the contactors afterwards.

Solvent Recovery. Two solvent circuits were used to keep the solvent for each extraction cycle separate. To minimize wastes generated in the solvent-recovery process, the aqueous streams used to wash the solvent were first contacted with the less contaminated solvent (i.e. 2CW) and then contacted with the first cycle solvent (1CW). Three wash streams were used; two were Na_2CO_3 solutions and the final wash was dilute HNO_3 solution.

EXPERIMENTAL DATA AND DISCUSSION

Steady-state data obtained for the two solvent extraction cycles over the five CANDU subcampaigns are presented in Table 2.

Plutonium losses to waste streams were low in most cases. However, they were somewhat higher than desired in the 1AW stream, amounting to about 0.6% of the plutonium in the feed. This may have been due to minor flow instabilities in the 1A contactor, or to traces of Pu(VI) in the feed solution, but was more likely due to the fact that fewer stages were available for extraction than in the earlier work in the WNRE Hot Cells, where losses to the 1AW stream were as low as 0.02%.

TABLE 2

DATA FROM TWO CYCLE AMINE PROCESS AT THE EUREX PILOT PLANT

	First Cycle	Second Cycle
Plutonium losses (%) to:	1AW - 0.6 1CW - < 0.01	2AW - 0.02 2CW - < 0.01
Fission Product DF* for:		
^{106}Ru	1.2×10^4	$> 10^2$
^{125}Sb	2.4×10^4	-
^{137}Cs	2.0×10^6	$> 5 \times 10^2$
Separation Factor (U from Pu)	$> 10^4$	$> 10^3$

$$^{*}\ DF = \text{Decontamination Factor} = \frac{\text{Activity/g(Pu) in 1AF}}{\text{Activity/g(Pu) in product}}$$

Both stripping agents, i.e. sulfuric acid in the first cycle, and HAN in the second cycle, performed very well at the flowsheet conditions, limiting losses of plutonium to the solvent streams to less than 0.01% in each cycle.

The steady-state separation factor (SF), which measures the degree of removal of uranium from the plutonium product, was also good. The overall SF for two cycles was greater than 1×10^7.

Because of the relatively long decay period before reprocessing, only limited data are available on the behaviour of fission products in the process. Table 2 indicates that overall decontamination factors (DF) are $> 1 \times 10^6$ for ^{106}Ru, $> 2.4 \times 10^4$ for ^{125}Sb, and $> 1 \times 10^8$ for ^{137}Cs. The earlier experiment at WNRE had DF values of 3×10^4 for ^{106}Ru, and 1×10^7 for both ^{125}Sb and ^{137}Cs for one extraction cycle. Although data for $^{95}Zr/Nb$ are not available from the EUREX experiments, DF values were $> 1 \times 10^5$ in the WNRE experiment.

Solvent Performance. Only trace quantities of plutonium remained in the solvent following washing operations, and the major fission-product activity remaining was ^{106}Ru with an equilibrium level of about 4×10^5 Bq/L.

Primary and secondary amines, which could be produced through acid or radiolytic degradation of the TCA, were essentially unchanged from the starting material, and amounted to a maximum of 0.009 mol/L in the solvent. This level of impurity did not have any measurable effect on solvent performance.

SUMMARY AND CONCLUSIONS

(1) The Amine flowsheet developed at WNRE has been successfully demonstrated in the first extraction cycle at the EUREX pilot plant.

(2) The ENEA modification of the flowsheet, principally the use of HAN to strip plutonium from the amine, has been successfully demonstrated in the second cycle at the plant.

(3) The two-cycle process is highly satisfactory for recovering plutonium from irradiated natural uranium fuels. However, further work needs to be done to determine the impact of the uranium/fission-product mixture in the high-level waste on waste management operations and waste disposal.

(4) This joint experiment has been useful and beneficial to the fuel recycle programs in both Italy and Canada.

REFERENCES

1. S.R. Hatcher and W.W. Morgan, AECL-6064 (1976).

2. A.S. Wilson, Second United Nations Conf. on Peaceful Uses of Atomic Energy 17, 48 (1958).

3. A. Chesne, G. Koehly and A. Bathellier, Nucl. Sci. and Eng. 17, 557 (1963).

4. W.W. Schulz, I and EC Process Design and Develop. 6, 115 (1967).

5. S. Cao, H. Dworschak and A. Hall, Proc. Int. Solv. Extr. Conf. 1974, Soc. of Chemical Industry, London, 1453 (1974).

6. G.R. Grant, W.W. Morgan, K.K. Mehta and F.P. Sargent, ACS Symposium Series, No. 117, 351 (1980).

7. F. Baroncelli, G. Scibona and M. Zifferero, Radiochimica Acta 1(2), 75 (1963).

8. W.W. Morgan and J.R. Coady, AECL Unpublished Information.

9. G. Grossi, in Proc. Solv. Extr. Conf., 1977, CIM Special Volume 21, 634 (1978)

10. L.J. Clegg and J.R. Coady, AECL-4436/1 (1977).

11. G.G. Alonzo, F.F. Castellani, G.G. Curzio, A.F. Gentili and L.F. Pieve, Proc. Int. Conf. on Radioactive Waste Management, CNS, 422 (1982).

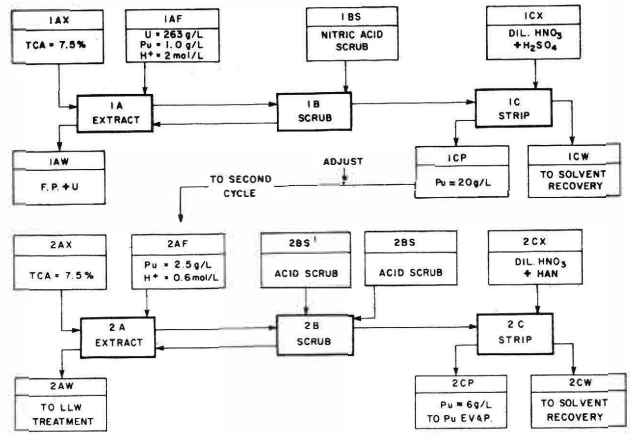

FIGURE 1. TWO CYCLE AMINE PROCESS USED AT EUREX PLANT

STUDIES ON REPROCESSING FBR FUEL

H.-J. Bleyl, K. H. Ebert, D. Ertel, W. Ochsenfeld

Kernforschungszentrum Karlsruhe
Federal Republic of Germany

Introduction

In Germany FBR fuel became available only recently. In 1978 the KNK II (Kompakte Natriumgekühlte Kernreaktoranlage) started full power operation. The former thermal reactor KNK I had received an unmoderated core: the inner test zone was equipped with UO_2/PuO_2 fuel elements, while the driver around it still contains UO_2 only.

Operating experience with the KNK II fuel has been extremely positive (1). According to the original design a maximum (peak)burnup of 60,000 MWd/t was to be achieved. Finally, a burnup of 100,000 MWd/t was attained before the reactor was shut down in 1982.

During operation two fuel element failures at 15,000 and 45,000 MWd/t, respectively, occured. Both defects were indicated very quickly by the reactor systems, based on delayed neutrons and cover gas activity. They were caused by failures at one pin only. No sweep-out of fuel into the coolant was observed.

After two years cooling time some fuel of the first defect element was shipped to the MILLI reprocessing facility (Purex process, 1 kg/day). Fuel of the core was mixed with fuel of blanket resulting in 11% plutonium related to all the heavy metals. The material was dissolved in 7 M nitric acid, the residue was treated with a 10 M HNO_3/0.1 M HF solution. HF was complexed by aluminum nitrate.

Extraction

For reprocessing the fuel three extraction cycles were applied:

- co-decontamination cycle
- uranium/plutonium separation cycle
- uranium final purification cycle

The flowsheet of the first cycle is given in the top part of Figure 1. Results can be noticed further down. Concentration profiles of the main constituents during the steady state condition have been plotted. The ordinate shows the concentrations of uranium and plutonium (g/l), the molarity of nitric acid and the concentrations of some fission products given in percentage of those in the feed solution. The abscissa represents the stage number according to the schematic drawing of the mixer-settlers shown above.

It is evident from Figure 1 that the losses of plutonium into the raffinate were $<$0,01%. In the product 0.4% Zr-95, 0.4% Ru-106, 4 x 10^{-3}% Cs-137 and 1.5 x 10^{-3}% Ce-144 were found, corresponding to decontamination factors of 250 for zirconium and ruthenium, 2.5 x 10^4 for cesium and 6 x 10^4 for cerium.

The constituent profiles in the extractors HA and HS are plotted again in Figure 2 (circles for the solvent phase, triangles for the aqueous phase). In addition, the results of mathematical process simulation by the program VISCO (2) are represented by lines. Except for the tails near the raffinate it seems very encouraging to model a Purex flowsheet by this program.

The uranium/plutonium separation cycle started with 2 M nitric acid. During extraction and scrubbing the decontamination factors for the fission products reached about 10^2. Losses of plutonium into the raffinate were $<$0.1%. This indicates that the conditions of the extractor HC concerning the following extractibility for plutonium were well suited.

To separate plutonium from uranium electrochemical reduction in the so called EMMA mixer-settler was applied. Details of the flowsheet as well as results are shown in Figure 3. The profiles indicate a steep slope(four orders of magnitude) of plutonium concentration from the feed point to the uranium product outflow. At the same time, the uranium is reduced by two orders of magnitude on the way to the plutonium product exit. One of the prerequisites of getting separation as high as that is an appropriate nitric acid profile (3).

Again modeling of the process was performed. The results are plotted in Figure 4. Concerning the reaction rates and activation energies, the same values were used as those given by Petrich and Schmieder in paper No. 10 n (4) of ISEC 83.

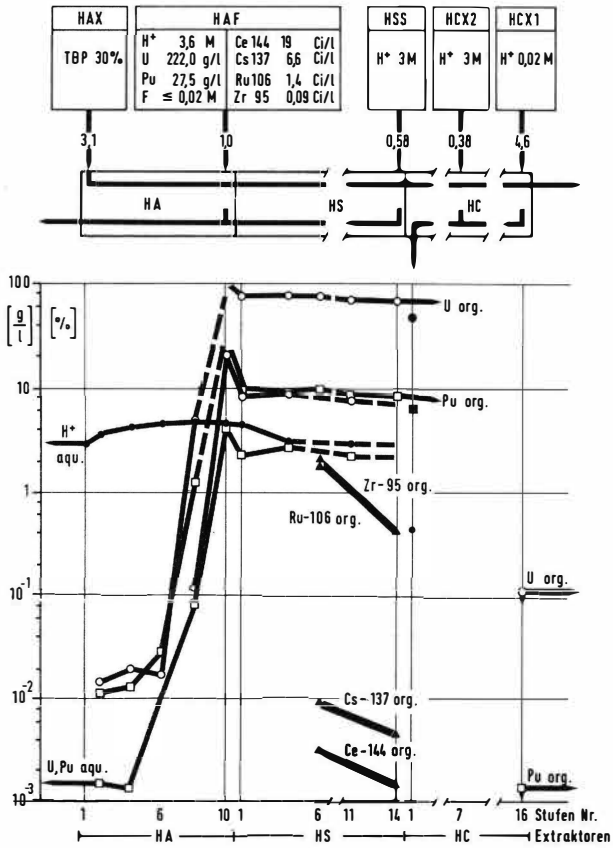

Figure 1: Co-decontamination cycle , flowsheet and experimental results

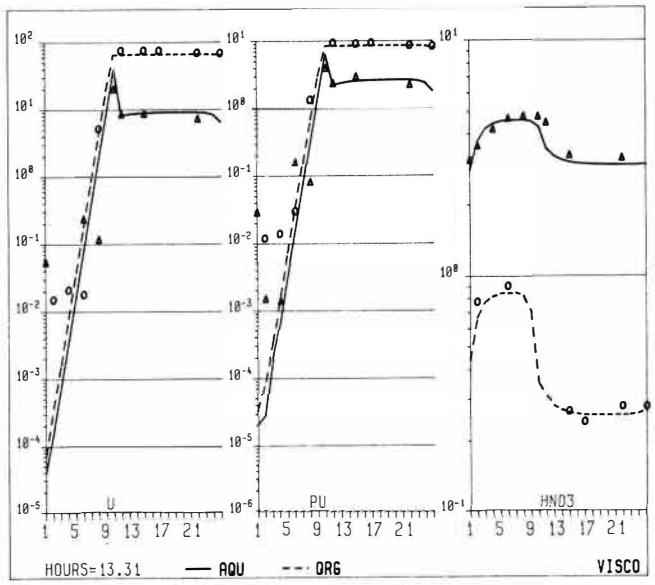

Figure 2: Co-decontamination cycle , HA and HS extractors, experimental and calculated results

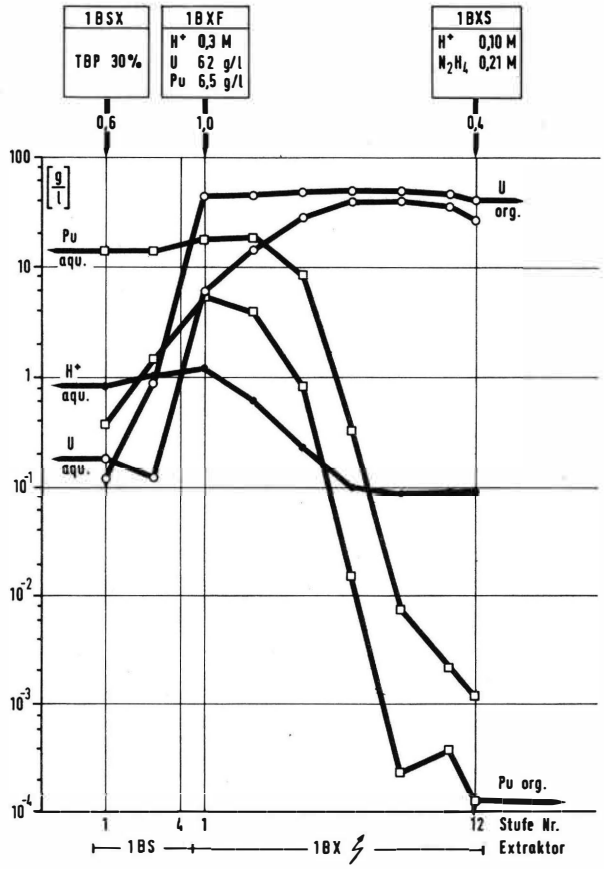

Figure 3: U/Pu separation cycle , 1 B extractor, flowsheet and experimental results

The plutonium product of the uranium/plutonium separation cycle already constituted the final product. Its composition after evaporation is listed in Table 1. In this table the separation factors related to the fuel solution are given as well.

COMPOSITION			DECONTAMINATION FACTOR
Pu	234	g/l	-
U	3,0	g/l	$6,3 \cdot 10^2$
HNO_3	6,2	M	-
Ru-106	100	µCi/l	$1,2 \cdot 10^5$
Zr-95	30	µCi/l	$2,6 \cdot 10^4$
Cs-137	20	µCi/l	$1 \cdot 10^6$
Sm, Eu, Gd, Dy	<1	ppm	
Nb, Mo, Ag, Sn	≥10	ppm	

Table 1: Composition of the Pu product solution and overall decontamination factors

To get the final uranium product an additional extraction cycle was applied. In this cycle, low amounts of plutonium and of fission products had to be removed. The flowsheet made use of a scrub containing uranium-IV. After backextraction of the uranium the product met the specifications. Table 2 gives the composition of the uranium product solution after evaporation; also the overall separation factors are listed.

COMPOSITION			DECONTAMINATION FACTOR
U	388	g/l	-
Pu	0,3	mg/l	$1,6 \cdot 10^5$
HNO_3	0,1	M	-
Cs-137	0,9	µCi/l	$10^6 - 10^7$
Ce-144	0,3	µCi/l	$10^7 - 10^8$
Fe	20	ppm	-
Co, Ni	<10	ppm	-

Table 2: Composition of the U product solution and overall decontamination factors

Subsequently, both products were used to refabricate nuclear fuel. The fuel is ready for reuse in KNK II. By this the closing of the fast reactor fuel cycle has been demonstrated for the first time in Germany.

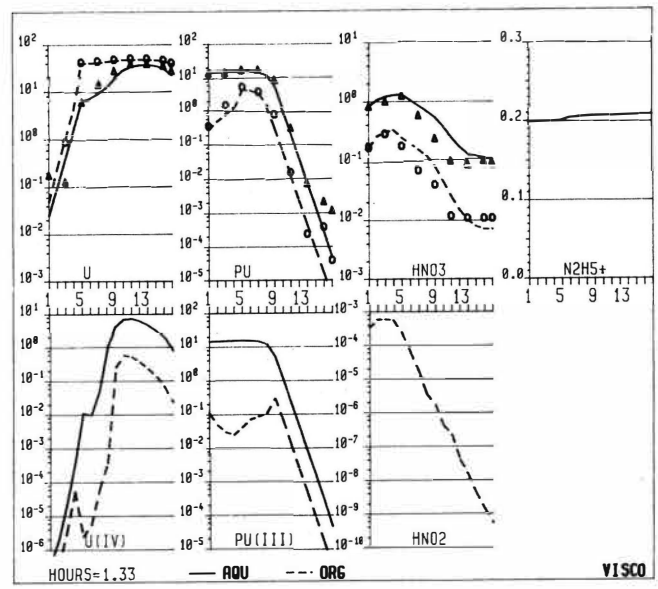

Figure 4: U/Pu separation cycle , 1 B extractor, experimental and calculated results

References

(1) W. Marth et.al., International ENS/ANS Conference, April 26-30, 1982, Brussels, Belgium

(2) G. Petrich in F. Baumgärtner (ed.), Nuclear Fuel Cycle, Volume 2, 317-332 (1983), Verlag Chemie, Weinheim, Fed. Rep. of Germany

(3) W. Ochsenfeld et.al., private communication, 1979

(4) G. Petrich and H. Schmieder, Paper No. 10 n, International Solvent Extraction Conference, August 26 - September 2, 1983, Denver, Colorado, USA

PLUTONIUM RE-EXTRACTION BY ELECTRO-REDUCTION IN A PULSED COLUMN

H. Goldacker, U. Galla, M. Kluth, R. Schlenker, H. Schmieder, H. Evers*

Kernforschungszentrum Karlsruhe
Institut fuer Heisse Chemie
D-7500 Karlsruhe, Federal Republic of Germany

*WAK Betriebsgesellschaft m.b.H., D-7514 Eggenstein-Leopoldshafen, Federal Republic of Germany

INTRODUCTION

The Pu reextraction by electro-reduction has been successfully demonstrated in mixer settlers of lab scale (1,2) and plant size, e.g. in the Karlsruhe Reprocessing Plant WAK (3). For future industrial applications the development of pulsed columns suited for in-situ reduction of Uranium and Plutonium has been started in the middle of the seventies (4,5). The first operational results achieved with such a column in a Pu extraction cycle are reported in the following paper.

THE PU CYCLE (PUTE)

The test facility is equipped with three pulsed columns: extraction, scrub, electro-reductive backextraction (ELKE). For reasons of technical representativity the columns are designed for a nominal throughput of 10 kg Pu/d. In cartrigde heights are 8 m. The Pu-(III) product solution from the electroreductive backextraction is oxidized at the anode of two electrooxidation cells (ROXI). This Pu(IV) product, which contains no more hydrazine, is recycled to the feed system of the extraction without evaporation.

The installation has additional auxiliary systems: a solvent wash, two in-line α-monitors in the AW and BW flow and a set of 4 neutron monitores, scanning permanently the Pu concentration profile in the electro column. The Pu inventory in the reported experiments amounted to 4 kg, enough to operate the facility at the design throughput. In order to limit waste volumes and Pu losses generated by the aqueous raffinate of the extraction (AW), the actual throughput had to be limited to a maximum of 5,5 kg Pu/d.

ELECTROREDUCTION COLUMN AND ELECTROOXIDATION CELLS

Generally, two design principles for an in-situ electroreduction column are possible and have been developed simultaneously. The development in the USA (Barnwell) uses a diaphragm for the separation of catholyte and anolyte (4), whereas in the FRG, diaphragms have been avoided from the very beginning.

The construction principles of ELKE are des ibed in (2,3,5) and shall only be mentioned briefly: The casing and sieve trays are made of titanium, serving as cathode. The anodical central rod is made of platinized tantalum. Highly sintered ceramic material is used for the insulators between anode and cathode. The generated electrode gas, partially H_2, is separated from the liquids by means of metal sheets in the top decanter and diluted by air to 2 Vol.% H_2, based on 100% current yield for H_2.

Two identical ROXI cells, made from titanium and from hafnium respectively, have been operated. Whereas the titanium cell has already proven its suitability (2,3), the neutron absorber hafnium was applied in the PUREX media for the first time. The construction principles are already published (2,3,5): The casing works as cathode and is made from titanium or hafnium. The anode is a compact structure of perforated platinized tantalum sheets. A controlled air flow is used for both purposes, dilution of H_2 and cooling the cell.

RESULTS OF ELKE

In the first extraction feed, the U/Pu ratio was adjusted to 0,8 and decreased after each recycling to values of 0.04. During each test run, the organic product concentrations (AP) were kept at a constant level. Corresponding to a throughput of 2,6 to 5,5 kg Pu/d the Pu concentrations varied stepwise between 6 to 10 g Pu/l over all runs.

In a compact form, fig.1 shows the essential results achieved with ELKE. Run 1 to 4 is characterized by decreasing U contents, causing a decrease of decontamination factors (DF_{Pu}) at nearly constant product concentrations (BP) and flow ratios for AP/BX (residence times of 4 h for the contineous aqueous phase).

In run 5 to 8, the column was operated at constant U concentrations and higher ratios AP/BX, resulting in a residence time of 5,5 to 8,4 h for the aqueous phase. The decontamination factors are decreasing again by a factor of 10 to 100.

Whereas in electroreductive U backextraction tests, a turnover of about 0.01 M $N_2H_5^+$/Ah was found, the $N_2H_5^+$ consumption in the Pu tests was 50% higher. Related to this figure, an average ammonia formation of 0.17 M NH_4^+/M $N_2H_5^+$ was measured.

96 to about 100% Pu(III) in the aqueous product exceeded the expected result. The calculated overall value of 25% formal current efficiency is based on the Pu throughput and does not take into account the Pu(III) oxidation at the anode and the possible reoxidation of U(IV) and Pu(III) in the organic phase.

DISCUSSION OF ELKE RESULTS

The Pu(III) production in electrochemical extractors can be described by the following equation, (2,6,7). The objective is to simulate multi- component extraction with simultaneous chemical and electrochemical reactions.

$$d[Pu(IV)]/dt=$$

(A) $$-\beta_{red}\Omega_{cath}[Pu(IV)] + \beta_{ox}\Omega_{anode}[Pu(III)]$$

(B) $$-k_1[Pu(IV)][N_2H_5^+]/([HNO_3]+k_2)$$

(C) $$-k_3[Pu(IV)][U(IV)]/([HNO_3]+k_4)([HNO_3]+k_5)$$

β = mass transfer coefficient for electrode reactions, cm/min.

Ω = specific electrode area, cm2/cm3 electrolyte

k = reaction rate coefficient

Part A covers direct Pu reduction or oxidation at the electrode. Part B considers the chemical Pu reduction by $N_2H_5^+$, resulting in ammonia and catalyzed by cathodic deposits of plutonium. Part C describes the indirect Pu reduction by electrochemically formed U(IV).

The decontamination factors (run 1 to 4), which are 10 times higher than for electrochemical mixersettlers (2,5), can be explained by the favorable value for Ω_{cath} and the comparatively low value for Ω_{anode}. Moreover, the rapid reoxidation of Pu(III) and U(IV) in the hydrazine free organic volume of settled organic phase in each settling compartment of a mixersettler contributes an essential part to the total reoxidation turnover. In ELKE, the aqueous hydrazine reacts momentarily with extracted nitrite at the pase boundary in the dispersion. Hence, a much lower reoxidation turnover can be assumed.

Obviously both effects also contribute to the surprisingly high reduction turnover (>96%). A low reoxidation rate in the organic phase for Pu(III) also restricts the ammonia formation, because a smaller total inventory of reoxidized Pu(IV) is available for the chemical reduction described by part B. The value of 0.17 M NH_4^+/M $N_2H_5^+$ is much less than expected by experience based on mixersettler runs. Ammonia formation mainly occurs in those parts of the column, where the chemical reduction by $N_2H_5^+$ competes with the direct but faster Pu reduction at the cathode. Here, the low U-concentration has practically no influence on the Pu(IV) turnover.

Compared to electroreductive U backextraction tests, the anode in the Pu tests was operated at higher current densities. The dependency of hydrazine turnover and anodic current, and the small ammonia formation which did not occur in the U tests, can explain the relatively high $N_2H_5^+$ consumption.

Part C of the equation normally controls the Pu reduction, for example in the U/Pu splitting step. Consequently, the main portion of the Pu reduction is shifted to part A and part B with decreasing residual U concentrations. This is the reason for the influences which decreasing U concentrations have on the decontamination factors. In addition, the strip rate of Pu-HDBP complexes in presence of low U concentrations is assumed to be slow and quantitatively not known.

Run 5 to 8 resulted in comparatively low DF's, due to increased flow ratios AP/BX. Calculations based on individual extractive mass transfer coefficients and estimated values for the specific mass transfer area in the dispersion show that the extractive mass transfer is not the limiting factor. With constant flow AP and decreasing flow BX, the column was operated under unfavorable hydraulic conditions, related to the flooding point (≈ 20 to 30%). The residence times of nearly 6 to more than 8 h for the aqueous phase caused severe axial backmixing

RESULTS OF ELECTRO OXIDATION IN ROXI

The alternating operation of both cells demonstrated the suitability of hafnium as cathode and casing material. $N_2H_5^+$ and Pu(III)) could be oxidized quantitatively. Anodic $N_2H_5^+$ oxidation and a sidereaction with cathodically formed NO_2^- resulted in current efficienies >100% related to anodic $N_2H_5^+$ oxidation. The ROXI feed has been acified to 1.5 to 2 M HNO_3 in order to suppress Pu(VI) formation, although 2 to 5% Pu(VI) could be detected in the product. This fact is in contradiction to laboratory results and is not yet explained.

FUTURE ASPECTS

Further experiments in ELKE should demonstrate the maximum achievable Pu product concentration (Pu refinery cycles), the possibility of a U/Pu splitting step in the absence of hydrazine. Finally, these tests should prove the applicability of the above mentioned modelling program.

Run No.	AP Pu [g/l]	AP U/Pu	Flow ratio AP BX	BP Pu [g/l]	BP U [g/l]	BP t_{BP} [h]	BP I_{ges} [A]	BW Pu [mg/l]	BW DF_{Pu}
1	8.67	0.86	2.12	18.8	0.80	4.2	80	< 0.05	> $1.7 \cdot 10^6$
2	9.09	0.81	2.01	18.1	1.28	4.3		0.01	$9.1 \cdot 10^5$
3	9.27	0.34	2.13	20.5	0.59	4.1		0.03	$3.1 \cdot 10^5$
4	9.82	0.06	1.99	19.9	0.41	4.1		0.24	$4.1 \cdot 10^4$
5	5.93	0.2	3.27	19.0	0.27	6.6	60	0.38	$1.6 \cdot 10^4$
6	5.84	0.16	3.90	24.5	0.47	8.4	50	3.11	$1.9 \cdot 10^3$
7	5.49	0.17	3.94	23.2	0.37	8.4	48	2.24	$2.5 \cdot 10^3$
8	4.98	0.18	4.26	19.5	0.31	5.5	75	1.49	$3.3 \cdot 10^3$

$[H^+]_{AP}$: 0.15 ÷ 0.35 M

$[H^+]_{BX}$: 0.1 ÷ 0.2 M

$[N_2H_4]_{BX}$: 0.22 ÷ 0.31 M

$[N_2H_4]_{BP}$: 0.08 ÷ 0.19 M

$[NH_4^+]_{BP}$: $2.4 \cdot 10^2$ M

ΔN_2H_4 : $15.3 \cdot 10^3$ M/Ah

$\frac{[\Delta N_2H_4]}{[Pu]}$: 1.7

$\frac{[NH_4^+]}{[\Delta N_2H_4]}$: 0.17

$\frac{[NH_4^+]}{[Pu]}$: 0.3

pulse: 60/min; 1.5 cm

i_{cath} : 1.6 ÷ 2.6 mA/cm²

$\frac{I_{th,Pu}}{I_{ges}}$: 0.25

ΔU : 2 ÷ 3 volts

T_{max} : 35°C

Fig. 1 Results of electroreductive Pu backextraction in ELKE

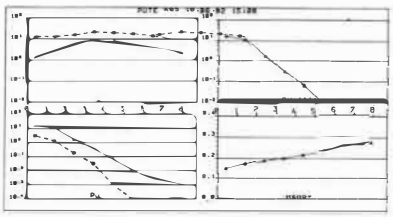

Fig. 2 Concentration profiles of ELKE run 2

ordinate: [Pu], [U] = g/l, $[N_2H_5^+]$ = M,
abscissa: cartridge heigth,
----- organic phase
——— aqueous phase

REFERENCES

1. F. Baumgärtner, H. Goldacker and H. Schmieder, ACS/CSJ Chemical Congress, Honolulu, Hawa i, April 1-6 (1979) Paper 163

2. H. Schmieder, H. Goldacker, M. Heilgeist and G. Petrich, Conf. on Fast Reactor Fuel Cycles, ICE, London (1981) Paper 47

3. H. Goldacker, H. Hausberger, H. Schmieder and H. Wiese, ANS Conf. Gatlinburg (1980)

4. A. Schneider and A.L. Ayers, U.S. Pat. 3616276

5. F. Baumgärtner and H. Schmieder in Radiochimica Acta 25, 191-210 (1978)

6. G. Petrich, 2. IASTED Davos, Int. Symposia, March 2-5 (1982), Davos, Switzerland.

7. G. Petrich and H. Schmieder, ISEC 83, August 26.-September 2, Denver, Colorado (1983), Paper 10 n.

ELECTRON SPIN RESONANCE SPECTROSCOPY. A TECHNIQUE ALLOWING DIRECT DETERMINATION OF SPECIATION OF METAL COMPLEXES FORMED BY COMMERCIAL SOLVENT EXTRACTION REAGENTS

P. O'Brien and J. R. Thornback

Department of Chemistry
Chelsea College
University of London
London, SW3 England

and

Department of Chemistry
Loughborough University of Technology
Loughborough, Leicestershire, U.K.

Electron spin resonance spectroscopy (ESR) is a technique which is widely employed in chemistry for the study of paramagnetic metal ions. The spectra obtained are dependent upon the co-ordination sphere around the metal ion. Copper(II) complexes have been widely studied and the factors affecting the spectral characteristics are well understood (1).

This technique focusses purely upon the metal complex and thus allows investigation of the species even in solvent mixtures such as those found in commercial solvent extraction reagents.

We report here our results with a range of aromatic and aliphatic hydroxy-oximes available commercially, which extract copper. Other extractants could be used and other metal ions are able to be studied by this technique.

Results

This work has concentrated upon answering three main problems found with the oxime extractants. Firstly the nature of the metal oxime complex with the aromatic (P50, SME529) oximes, secondly the interaction, if any, of these with ammonia and finally the nature of the copper: LIX63 complex (or complexes).

The ESR spectra were measured at 20°C (isotropic spectra) or as frozen glasses at 77 K (anisotropic spectra).

The isotropic spectra of the aromatic oxime copper complexes show five components due to nitrogen hyperfine on the high field line indicating that the oximes co-ordinate, as expected through the nitrogen atoms. The anisotropic spectra are typical of axial copper(II) species, i.e. a square co-planar complex is formed (figure 1). The parameters obtained are given in Table 1 (2).

If pyridine is added to the organic solution or the copper is extracted from ammoniacal solution the A and g parameters are shifted and a fine co-ordinated square pyramidal species is formed. The reaction is general for other nitrogeneous bases. Our results are the first positive identification of a 5-co-ordinate ammonia adduct being formed in hydrometallurgical processing. The reaction scheme is thus as shown in equations below:

$$Cu(H_2O)_6^{2+} + 2HR \rightleftharpoons CuR_2 + 2H^+ + 6H_2O$$

$$CuR_2 + N\text{-}R' \rightleftharpoons CuR_2 \cdot N\text{-}R'$$

The nature of the LIX63 copper complex has been greatly studied (3). ESR studies with both synthetic and commercial samples confirm that at low ligand to metal ratios a polymeric ESR silent species is formed in which there is strong coupling between the adjacent copper atoms. The complex is probably of the form shown in figure 2. The aliphatic oxime is capable of forming an extended two-dimensional system of five membered chelate rings which leads to strong copper-copper coupling. The aromatic oximes would lead to adjacent five and six membered rings if polymerisation took place. This system cannot be flat and the strong coupling is only possible between the copper centres for the aliphatic oxime and provides an extra driving force for polymerisation.

At ligand to metal ratios greater than 2 a similar complex to those obtained with the aromatic oximes is obtained. However at very high ligand to metal ratios with a commercial sample of LIX63 an impurity is present which forms a new species. We cannot identify the contaminant but it seems unlikely to be important in commercial processing except to remove last traces of copper from the organic phase. The ESR parameters are given in Table 2.

References

1. B.J. Hathaway and D.F. Billing, Co-ord.Chem.Res., 5, 1 (1970).
2. J.R. Wasson and C. Trapp, J.Phys.Chem., 73, 3763 (1969).
3. J.S. Preston, J.Inorg.Nucl.Chem., 37, 371 (1977).

SAMPLE	$g_{//}$	$A_{//}$	$g_{\perp}$	g_{av}	A_{avCu}	A_{avN}
$Cu(P50)_2$	2.187	211	2.05	2.095	97.8	18.5
$Cu(P50)_2.py$	2.261	188	2.07	2.130	77.6	14.9
$Cu(P50)_2.NH_3$	2.256	180	2.04	2.110	88.5	16.6
$Cu(SME\ 529)_2$	2.173	213	2.06	2.098	93	17
$Cu(SME\ 529)_2.py$	2.211	196	2.07	2.115	74	15

E.S.R. Parameters for P5000 series reagents and SME 529

b. $10^4 \times A_{//}/cm^{-1}$

TABLE 1

"Typical E.S.R. Parameters for LIX63 Copper(II) Complexes"

SAMPLE	g_{av}	A_{av} [a]	$g_{//}$	$A_{//}$ [a]	$g_{\perp}$
LIX63 (purified or as supplied) or pure oxime [b]	2.10 (±0.01)	118 (±3)	2.245 (±0.005)	178 (±5)	2.050 (±0.001)
Second Species [LIX63] : [Cu(II)]	–	–	2.285	160	–

a. 10 A cm⁻¹

b. maximum variation in $g_{//}$ and A values observed for the various sources of oxime.

TABLE 2

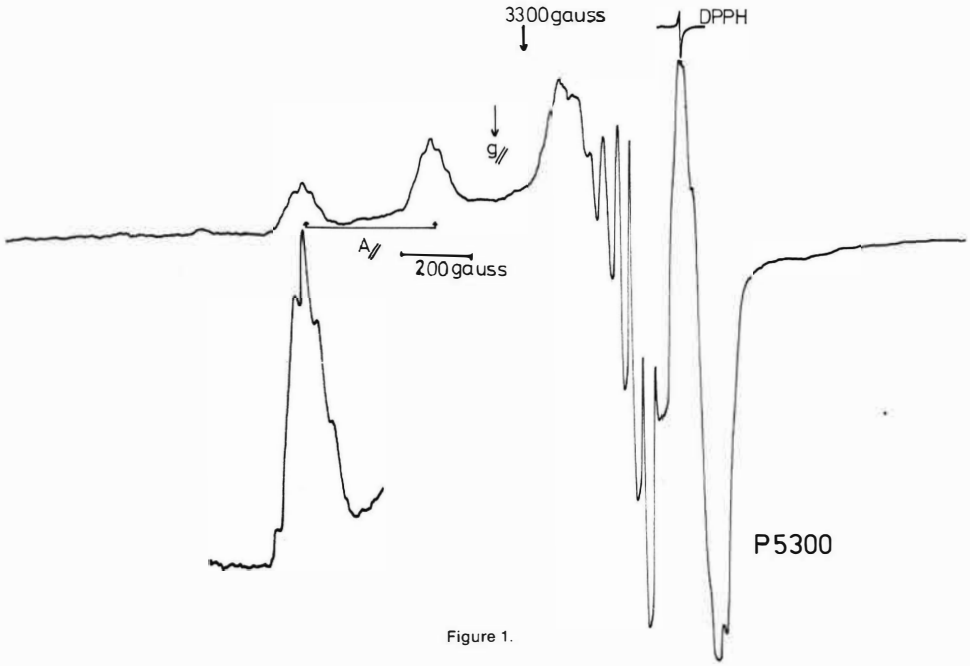

Figure 1.

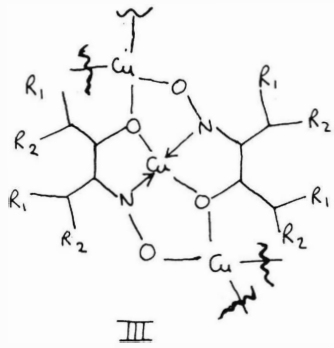

$R_1 = C_2H_5$ $R_2 = CH_3(CH_2)_3$

Figure 2.

EXTRACTION OF SULPHURIC ACID AND URANYL SULPHATE WITH BENZENE SOLUTION OF PRIMARY AMINE PRIMENE JM-T

Miroslav Mrnka, Prokop Nekovář, Vladislav Bízek, Daria Schrötterová

Prague Institute of Chemical Technology
Prague, Czechoslovakia

and

Alexander Mikhailovich Chekmarev, Alexander Vasilevich Ochkin, Svetlana Vladimirovna Chizevska

The Mendeleev Institute of Chemical Technology
Moscow, USSR

High-molekular amines are currently finding wide application in the hydrometallurgy of numerous rare metals. Since the first publication in the year 1948 devoted to amine extraction there have appeared in scientific literature a large number of papers dealing with practical as well as theoretical issues of extraction by means of high-molekular amines. However, the majority of papers is primarily concerned with tertiary and secondary amines and solely a few authors focus ·d their attention on the extraction via primary amines.

SULHURIC ACID EXTRACTION

It has been found in the extraction of sulphuric acid by means of benzene solutions PRIMENE JM-T that at the initial sulphuric acid concentration in the water phase $c^o_{H_2SO_4} < 1/2\ c'_A$ the sulphuric acid is being transfered quantitavely from the water phase to the organic phase where the normal amine sulphate is formed.

In IR spectra of the organic phase there appears the wide intensive peak on 1090 cm^{-1} corresponding to the valency vibrations ν_3 of the sulphate anion. Moreover, there is in the spectra a wide intesive peak on 1630 cm^{-1} corresponding to deformative vibration of the OH groups of the hydration water and finally there is a wide intensive peak on 3400 cm^{-1} corresponding to the valency vibration of the OH groups.

At a higher sulphuric acid concentration in the water phase $c^o_{H_2SO_4} > 1/2\ c'_A$ the normal amine sulphate is passing over to the hydrogen sulphate and in the IR spectra there appear three sharp peaks on 1170 cm^{-1}, 1090 and 875 cm^{-1}. The first two of them may be attributed to the anti-symmetrical and symmetrical valency vibrations of SO_3 groups whereas the third one is corresponding to the valency vibrations of the S-OH bonds.

The analytical determination of the water concentration in the organic phase has shown that also water together with sulphuric acid is passing over to the organic phase. Maximum water concentration in the organic phase was found to be at $c^o_{H_2SO_4} = 1/2\ c'_A$, that is to say at the sulphuric acid concentration, when all of the amine is being passed over to the normal sulphate. By comparing sulphuric acid extraction by means of tertiary amines /TOA, TLA/ with PRIMENE JM-T it was ascertained that normal sulphate of tertiary amines is being hydrated by 4 - 6 water molecules and PRIMENE JM-T sulphate by 10 water molecules. In addition to that was found that for the transfer of normal sulphate of tertiary amine in hydrogen sulphate there is essential a 3 - 4 times stechiometric surplus of sulphuric acid in the water phase while with PRIMENE JM-T there is necessary a 20 times stechiometric surplus.

URANYL SULPHATE EXTRACTION

On Figure 1 are quoted results gained by studying uranyl sulphate extraction in dependence on the initial sulphuric acid concentration in the water phase. The obtained results differ from literature data for tertiary and secondary amines. All these authors (1-8) being involved in uranyl sulphate extraction did find dependencies passing over the maximum. In the point of the maximum there is being assumed a maximum amine sulphate concentration in the organic phase. In the extraction of uranyl sulphate with PRIMENE JM-T solutions the uranium concentration in the organic phase is continuously decreasing with the growing sulphuric acid concentration in the water phase. Uranium extraction tends to be the highest provided sulphuric acid concentration is near zero, that is in the case, when almost all of the amine in the organic phase is in the form of a free base. This indicates that the extraction agent for uranium in the case of PRIMENE JMT is not only amine sulphate as such but also amine itself. In order to achieve a more thorough clarification of this phenomenon there have been investigated extraction isoterms at low initial sulphuric acid concentration / the applied uranyl sulphate and that is to say also its water solutions tend to contain a certain amount of sulphuric acid which is, in no case, however, sufficient enough to bring about the amine transfer to normal amine sulphate /. The obtained results are listed in Figures 2 and 3. It is evident from Figure 2 that the uranium concentration in the organic phase in dependence on the initial uranyl sulphate concentration is passing through the maximum, the position of which is being shifted with the growth of the amine concentration in the direction of a higher initial concentration. In the region prior to reaching maximum extraction tends to be a quantitative one. Analytical determination in the organic phase has proved that uranyl sulphate is being accompanied by the co-extraction of water / Figure 3 /. The dependence of water concentration in the organic phase on the initial uranyl sulphate concentration is passing through maxima the position of which is corresponding to maxima, being ascertained in the case of uranium extraction. Decrease in the maxima regions tends to be less steep than that in uranium extraction.

On the ground of the achieved results has been made up the following description of uranyl sulphate extraction via PRIMENE JM-T solutions:

The entire free sulphuric acid is passing over from the water phase to the organic phase while generating amine sulphate. The amine sulphate then, is extracting the corresponding share of uranyl sulphate according to the reaction

$$(1)\quad 2\ (RNH_3)_2SO_{4\ org} + UO_2SO_{4\ aq} \longrightarrow (RNH_3)_4UO_2(SO_4)_{3\ org}$$

In the organic phase there remains free amine reacting with uranyl sulphate according to the assumed equation:

$$(2)\quad 2\ RNH_{2\ org} + UO_2SO_{4\ aq} + 2\ H_2O \longrightarrow (RNH_3)_2UO_2(OH)_2SO_{4\ org}$$

The proposed mechanism according to equation (2) has been checked up by dissolving crystalline uranyl sulphate in amine. The results obtained are being quoted in Figure 4. It is obvious from Figure 4 that the uranium content in the organic phase is passing through the maximum. In order to verify both types of extracted complexes there have been performed investigations of IR spectra of the organic phase obtained while extracting uranyl sulphate from sulphuric acid environment and the organic phases obtained by dissolving crystalline uranyl sulphate in PRIMENE JM-T solution. In extract spectra being obtained according to equation (1) there appears a wide intensive peak on 1135 cm^{-1}, which may be attributed to the valency vibration of the amine group of amine sulphate the symmetry of which is being disturbed by the coordination on uranium. The sharp peak on 1020 cm^{-1} may be of the same origin like the preceeding one. The intensive peak on 955 cm^{-1} is obviously corresponding to anti-symmetrical valency vibration of the uranyl group.

In the organic phase being obtained according to reaction

(2) the wide intensive peak of the SO_4 groups is being shifted to 1120 cm^{-1}. The sharp peak on 1020 cm^{-1}, however, remains unchanged. The peak on the wave number 955 cm^{-1} does not turn up in the spectra - it is being replaced by the sharp peak on 895 cm^{-1}. The peak shift from wave number 955 cm^{-1} to 895 cm^{-1} thus tends to support the assumption about the formation of the complex $UO_2(OH)_2SO_4^{-2}$.

On the basis of the results obtained has been derived the mathematical model allowing to compute the composition of the organic phase while extracting uranyl sulphate from virtually neutral solutions. In Figure 5 is being quoted the composition of the organic phase being computed according to the proposed mathematical model.

REFERENCES

1. C.F.Coleman, K.B.Brown, J.G.Moore, D.J.Crouse, Ind.Eng.Chem. 50, 1756 (1958)
2. T.Sato, J.Inorg.Nucl.Chem. 30, 1065 (1968)
3. A.A.Lipovskij, M.G.Kuzina, Zh.neorg.chim. 10, 1360 (1965)
4. Ch.Boirie, Bull.Soc.Chim.France, 980 (1958)
5. W.E.Keder, A.S.Wilson, Nucl.Sci.Eng. 17, 287 (1963)
6. M.G.Kuzina, A.A.Lipovskij, Radiochimia 12, 393 (1970)
7. O.E.Zvjagincev, Ju.G.Frolov, V.V.Sergievskij, Chan Chun, Zh.neorg.chim. 11, 661 (1966)
8. K.A.Allen, J.Phys.Chem. 64, 667 (1960)

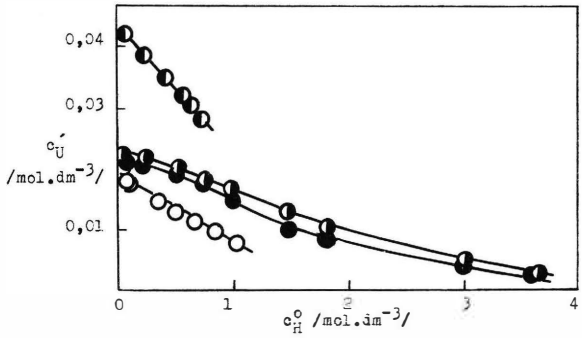

FIGURE 1.: THE DEPENDENCE OF URANYL SULPHATE EXTRACTION ON THE INITIAL SULPHURIC ACID CONCENTRATION c_i...mol.dm^{-3}

○ $c_A' = 0,096$ $c_U^o = 0,022$ ◐ $c_A' = 0,240$ $c_U^o = 0,044$
● $c_A' = 0,177$ $c_U^o = 0,021$ ◑ $c_A' = 0,263$ $c_U^o = 0,021$

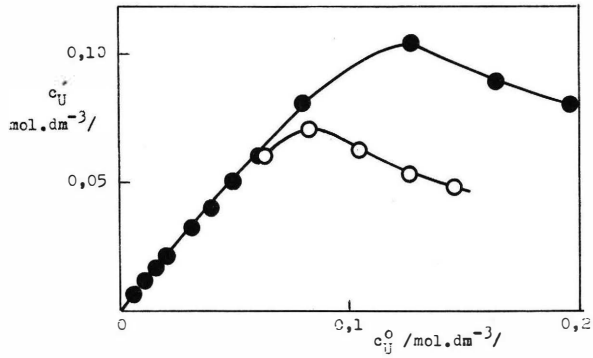

FIGURE 2.: ISOTHERM EXTRACTION OF UO_2SO_4 AT LOW INITIAL ACIDITY

○ $c_A' = 0,177$ mol.dm^{-3} ● $c_A' = 0,293$ mol.dm^{-3}

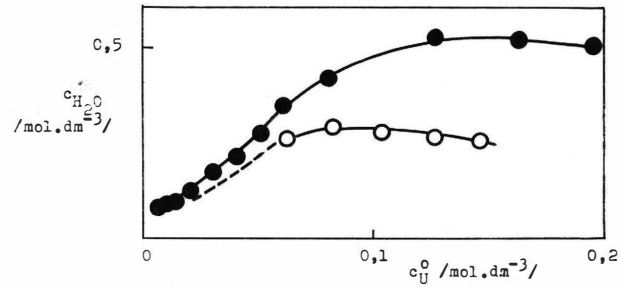

FIGURE 3.: CO-EXTRACTION OF WATER WHILE EXTRACTING UO_2SO_4 AT LOW INITIAL ACIDITY

○ $c_A' = 0,177$ mol.dm^{-3} ● $c_A' = 0,293$ mol.dm^{-3}

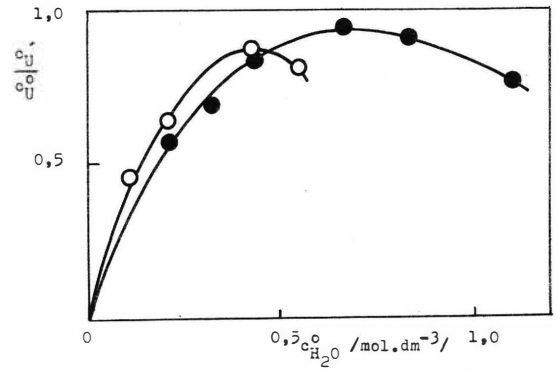

FIGURE 4.: DISSOLVING URANYL SULPHATE IN AMINE IN DEPENDENCE ON THE QUANTITY OF ADDED WATER

○ $c_A' = 0,140$ mol.dm^{-3} ● $c_A' = 0,264$ mol.dm^{-3}

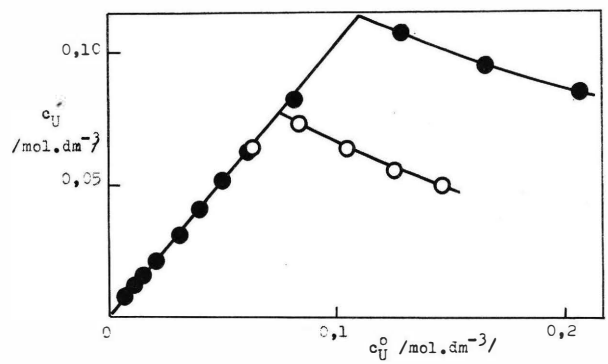

FIGURE 5.: THE COMPUTATION OF THE ORGANIC PHASE COMPOSITION FOR ISOTHERM EXTRACTION OF URANYL SULPHATE AT LOW INITIAL SULPHURIC ACID CONCENTRATION

○ $c_A' = 0,177$ mol.dm^{-3} ◐ $c_A' = 0,096$ mol.dm^{-3}
● $c_A' = 0,293$ mol.dm^{-3} ◑ $c_A' = 0,240$ mol.dm^{-3}

FTIR AND NMR STUDIES OF THE STRUCTURE OF ORGANIC PHASE OF SOME SAPONIFIED ACID EXTRACTANT-OCTYL ALCOHOL-KEROSINE MICROEMULSION SYSTEMS

Wu Jinguang, Gao Hongcheng, Shi Nai, Chen Dian
Jin Tianzhu, Xu Zhenhwa, Weng Shifu and Xu Guangxian

Department of Chemistry
Peking University
Beijing, China

INTRODUCTION

Through the investigation of several typical extractant systems commonly used in hydrometallurgy and nuclear industry, we suggested and proved that the saponification of extractants such as naphthenic acid, D2EHPA, etc.,is a process of the formation of a microemulsion of water in oil type(1). In the present investigation,we have studied the structure of the microemulsion by FT-IR and FT-NMR and obtained some new results.

EXPERIMENTAL

1. Instruments

Nicolet 7199-B Fourier Transform Infrared Spectrophotometer.

Varian XL-100-15 FT-NMR Spectometer.

2. Sample preparation:

The purified naphthenic acid was diluted with kerosine and then refluxed with Li, Na or K metals for about 6 hr. The alkali soap of naphthenic acid thus obtained is anhydrous.The anhydrous ammonium soap was prepared by passing anhydrous NH_3 gas into the naphthenic acid-kerosine solution, sec.octyl alcohol was then added to form a solution containing 22% naphthenic acid of sodium soap 18% ROH and 60% kerosine(Henceforth called Sample B).

Organophosphoric acid extractants: 50% 2-Ethyl-hexylphonic acid mono-2-ethyl-hexyl ester(HA) and 50% kerosine were refluxed with metallic sodium to form 86.1% NaA -20% sec.octyl-alcohol-kerosine(Henceforth called Sample A).

50% D2EHPA and 50% kero. were refluxed with Li,Na and K metals to form the alkali metal soap. The anhydrous ammonium soap was prepared by passing anhydrous NH_3 gas into the 50% D2EHPA-kerosine solution.

3. Experimental method:

(a) FT-IR: The spectra were recorded in the range 800-4000 cm^{-1}, using demountable BaF_2 cells. 1,5,10,20,30,50,100,200,300 and 500μl of deionized water were added to each aliquot of 1 ml of Sample A to form Samples Nos. A_1, A_2, A_3, A_4, A_5, A_6, A_7, A_8, A_9 and A_{10} respectively. All these samples were clear and transparent microemulsion. FT-IR spectra of these ten samples were determined together with their subtraction spectra using Sample A as reference substance and the CH_3- peak (1377 cm^{-1}) and $-(CH_2)_n$- peak (1460 cm^{-1}) as the basis for comparison and subtraction of the spectra.

Similarly 1,5,10,20,30,50,100,200 and 300μl of deionized water were added to each aliquot of 1 ml of Sample B to form Samples Nos. B_1, B_2, B_3, B_4, B_5, B_6, B_7, B_8 and B_9 respectively. All these samples were clear and transparent too. FT-IR spectra of these samples and their subtraction spectra were scanned using sample B as reference substance.

(b) NMR measurements: Different amounts of H_2O and D_2O (90%) were added to Sample B and C (1M D2EHPA-15% ROH-Kerosine,saponified with metallic sodium to form clear and transparent microemulsion), the proton chemical shift of which was measured using TMS as external standard.

Different amounts of H_2O were added to the anhydrous alkali and ammonium soaps of naphthenic acid and D2EHPA to form microemulsion,the proton chemical shift of which was measured.

RESULTS AND DISCUSSION

1. FT-IR spectra

Fig.1 shows the FT-IR spectra of samples. The following changes may be observed: The 979 Cm^{-1} peak which is attributed to P-O-H is diminished considerably during the saponification. The 1207 Cm^{-1}, peak of P=O stretching has changed to lower frequency 1195 Cm^{-1}. Hydration further lowers the freq. to 1159 Cm^{-1}, due to the formation of hydrogen bond as shown in structure (III).

Subtraction spectra: It may be seen from Fig.2 that, besides the water peak at 1650 Cm^{-1}, the intensities of P-O-C peak at 1045 Cm^{-1} and P=O peak at 1159 Cm^{-1} also increase with water content. The peak position of P-O-C does not change and is fixed at about 1045.5 cm^{-1}, while the intensity increases with water content, first rapidly at lower water content, then gradually becomes constant as water content > 20% (Fig. 3 Curve B). This may be explained as follows: At lower water content, there is a mixture of two structure.

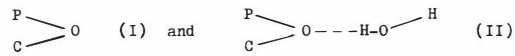

The molar extinction coefficient of (II) is greater than that of (I), because in the hydrogen bonded structure (II), the electronic cloud spreads wider and the dipole transition moment is larger than that of (I). When water content becomes 20%, only hydrogen bonded structure (II) predominates so that the optical density becomes constant.

P-O stretching band: In the subtraction spectra, we have observed two distinct peaks corresponding to the following two structures:

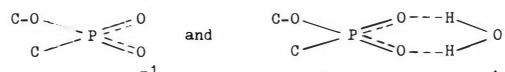

P=O: 1195 cm^{-1}. P=O H_2O: 1159 cm^{-1}.

In structure(II), the electronic cloud of P=O spreads over to the H atom of H_2O and hence weakens the P=O bond consequently lower the freq. by 36 cm^{-1}. As water content increases the relative concentration of (II) increases, while that of (I) decreases, so we have a positive band at 1159 cm^{-1} and a negative one at 1195 cm^{-1} (Fig. 2). From Fig. 3 Curve A, it may be seen that the optical density increases with water content and reaches a miximum value corresponding to the sitution that all molecules of structure (I) have converted to structure (II).

Naphthenic acid system:

Similar results were obtained in the saponified naphthenic system. Fig 4 shows the FT-IR spectra of sample S (Unsaponified), sample B and sample B_8. In sample S there is a strong peak at 1700 cm^{-1} attributed to the carbonyl group st. of the naphthenic acid dimer. The 1562 cm^{-1} and 1409 cm^{-1} peak in sample B were attributed to the asym. st. and sym. st. band of COO^- group respectively. In sample B_8 (water content 20%). There is a peak at 1647 cm^{-1} belonging to the H_2O band.

Fig. 5 shows the subtraction spectra of sample B_4, B_6 and B_8 versus sample B as reference substance.

It may be seen from Fig. 5 that beside the water peak at 1650 cm^{-1}, the intensities of asym, sym. COO^- st. and C=O peaks also increase, owing to the formation of hydration structures of COO^- and C=O groups.

2. NMR spectra

The proton chemical shift of liquid water is $\delta_{H_2O(L)}$=4.80 ppm and that of the water of hydration of metal ions usually observed differs only by ± 0.1 ppm from $H_2O(l)$, because the ratio of metal ions to H_2O molecules M^+/H_2O cannot exceed 0.36 even in very concentrated aqueous solutions. In the present investigation, we study the hydration of metal ions in microemulsion by adding different amounts of 90% D_2O and 10% H_2O to each aliquol of 1 ml. naphthenic acid saponified by metallic sodium, so that the $(Na^+)/(H_2O)$ may be as high as 170, a proton chemical shift δ=6.45 ppm, which differs from $H_2O(L)$ by as much as 2.65 ppm was observed (Fig. 6, 7). Similar results were observed for the D_2EHPA emulsion (Fig. 8, 9). Under such conditions, we have obtained the limits of $\delta_{H_2O(M)}$ for various cations as follows: 7.54 ppm (NH_4^+), 7.08(Li^+), 6.22(Na^+), 6.00(K^+), thus rendering NMR method an effective means to study the hydration of metal ions.

Conclusion

The saponification of extractants such as naphthenic acid, D_2EHPA, etc., is a process of the formation of a clear and transparent microemulsion of water in oil type. The water take-up in the organic phase may be as high as 20% (sodium soap) or 50% (ammonium soap). Evidences from FT-IR and FT-NMR studies show that there are strong hydration on both the cation and the extractant anion.

REFERENCE

(1) Wu Chin-kwang, et al., ISEC' 80 paper No. 80-23.

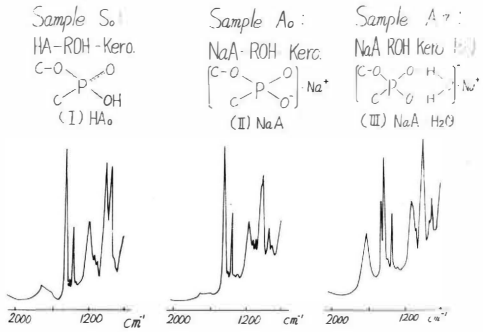

Fig. 1. FT-IR spectra of HA, Na A and Na A H_2O

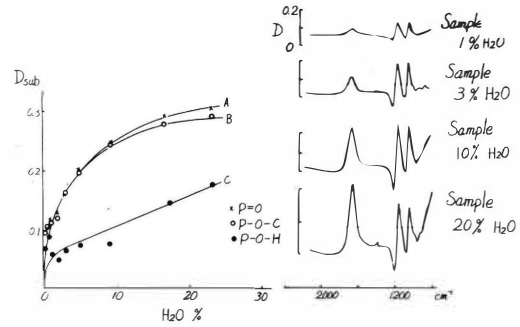

Fig. 3 Increments of Optical Density of P-O-C, P=O and P-OH vs water contents of Na'A---H_2O

Fig. 2. Subtraction spectra of NaA -H_2O containing different amounts of water vs NaA

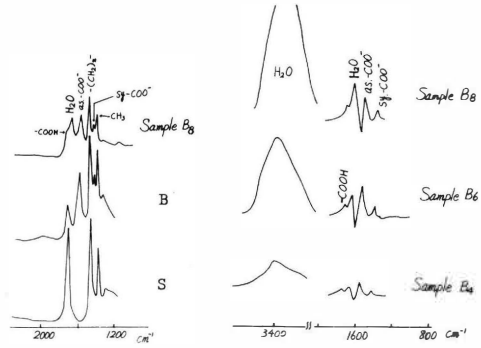

Fig. 4 FT-IR spectra of Sample S, Sample B and Sample B_8

Fig. 5 Subtraction spectra of B. containing different amount of water vs Sample B

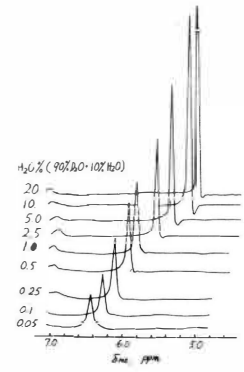

Fig 6. ^1H NMR spectra of Na Naphthenate-ROH-Kero. D_2O-H_2O Microemulsions

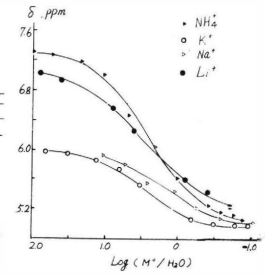

Fig. 7. Proton shifts vs log of molar ratio M^+/H_2O of alkali-naphthenate-ROH-H_2O microemulsion

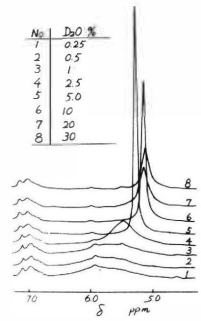

Fig. 8. ^1H NMR spectra of Na D_2EHPA-ROH-Kero-H_2O Microemulsions

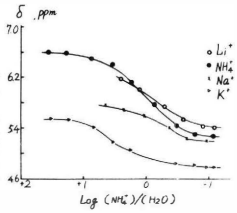

Fig.9. Proton shifts vs Alkali D_2EHPA-ROH-H_2O microemulsions

THE EFFECT OF SUBSTITUENTS ON THE STRENGTH OF O-HYDROXYARYLOXIME COPPER EXTRACTANTS

Raymond F. Dalton and Raymond Price

Imperial Chemical Industries P.L.C.
Organics Division, Hexagon House
Blackley, Manchester M9 3DA, England

In an earlier paper (1) an attempt was made to explain differences in strength between various o-hydroxyaryloxime copper extractants in terms of the inductive effect of substituents on the ease of ionisation of the phenolic hydroxyl group. Thus when 0.4 molar solutions of three different hydroxybenzaldoximes (I,III, and VI of Table 1) were equilibriated with equal volumes of an aqueous solution containing 10gpl of coper and 10 gpl sulphuric acid, it was shown when X = Br a much stronger extractant was obtained than when X = H whereas when X = tertiary pentyl a much weaker extractant was obtained.

TABLE 1

COPPER EXTRACTED BY VARIOUS SUBSTITUTED o-HYDROXYARYLOXIMES

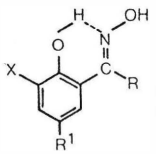

Compound Number	X	R	R^1	Copper transfer on single contact
(I)	Br	H	C_9H_{19}	99.6
(II)	CH_3	H	C_9H_{19}	93.7
(III)	H	H	C_9H_{19}	89.9
(IV)	H	C_6H_5	C_9H_{19}	56.2
(V)	H	CH_3	C_9H_{19}	51.6
(VI)	$^tC_5H_{11}$	H	$^tC_5H_{11}$	35.3

Close inspection of the data however shows a number of discrepancies, and the differences in strength can not be explained by inductive effects alone. For example, both compounds (I) and (II) are stronger than (III) even though Br is electron withdrawing and $-CH_3$ is electron donating. It is also difficult to rationalise the fact that the 2-hydroxybenzaldoxime (III) is so much stronger than either the benzophenone oxime (IV) or the acetophenone oxime (V). Also, there is little difference in strength between compounds (IV) and (V) even though $-CH_3$ is electron pushing and a phenyl group acts as an electron sink.

There have been numerous attempts to correlate stability constants of complexes with proton dissociation values (pK_A) of parent ligands (2, 3) but this seems neither reliable or appropriate. Most phenolic compounds, including o-hydroxyaryloximes are very weakly acidic, and with pK_A values of the order of 10 can be regarded as effectively unionised at the pHs at which copper is commonly extracted. When a phenolic hydroxyl group is co-ordinated to a metal however, its acidity is markedly increased as a result of donation of electrons from the oxygen atom to the metal and the consequent polarisation of the O-H bond. The effect is even greater when chelation and formation of stable ring structures is involved, and so the proton is readily lost and the apparent pK_A for compound (III) in Table 1 is reduced from about 10 to 0.8, i.e. by a factor $>10^9$.

It has been claimed that electrophilic and nucleophilic substituents can have a double effect on the stability of metal complexes (4, 5). Thus electron donating substituents ortho and para to the hydroxy group enhance the electron density, i.e. basicity of the donor oxygen atom favouring formation of a σ bond and giving the complex greater stability. The converse is true of electronegative substituents such as chlorine and bromine. Mesomeric, or resonance effects will also effect the electron density on the donor atom and here a, + R effect is obtained from alkyl and halogen substituents. Changing the electron density on the donor oxygen atom effects the π acceptor capability of the ligand by changing the strength of the donor π bond or back bonding from the metal, thus the effects of σ and π bond formation can work in opposite direction. The relative magnitude of these effects is also dependent on the position of substitution in the aromatic ring making predictions very difficult (5, 6)

Thus factors that affect the final complex stability are likely to be of greater significance than those that affect the acid dissociation constant (pK_A) in the absence of a metal.

We consider one factor of prime importance in the stability of complexes of o-hydroxyaryloximes to be steric effects, in particular the phenolic oxygen to oxime nitrogen interatomic distance in the ligand, how well the 'bite' of the ligand fits round the metal, and the maintenance of a planar hydrogen bonded arrangement of the ligands about the metal complex. X-ray crystallography has shown that the salicylaldoxime complex of copper is essentially planar (7) with a phenolic oxygen to oxime nitrogen distance of 2.63 Å and O-Cu-N bond angle of 91.6°, and we have recently obtained X-ray information confirming the planarity of both 4-methyl salicylaldoxime and 2-hydroxy-5-methyl benophenone oxime (8). The planarity and bond angles in these compounds means that the phenolic oxygen atom must be Sp^2 and not Sp^3 hybridised and therefore has a lone pair of electrons in the plane of the molecule at approximately 120° to the C-O bond.

Similarly, the hydroxyl group of phenols lies in the plane of the ring indicating Sp^2 hybridisation with one oxygen lone pair being delocalised in the benzene ring.

The finite volume and significant charge density of non-bonding electrons must not be overlooked in considering molecular interactions.

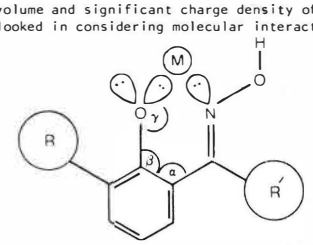

Applying this principle to substituted o-hydroxyaryloximes it can be seen that substituents R and R' can have a number of effects. As well as inductive effects, increasing the size of substituents R and R' pushes the phenolic oxygen and oxime nitrogen atoms closer together and when M is a hydrogen atom (as in the parent ligand) this causes an increase in the strength of hydrogen bonding between the phenolic proton and oxime nitrogen atoms. This is an example of the well known Thorpe-Ingoid, or Buttress Effect whereby strong hydrogen bonding provides a means of stabilising the close proximity of these atoms brought about by steric interference (9).

It is well known that strong hydrogen bonding does exist between the phenolic hydrogen atom and oxime nitrogen in these compounds (10). Useful means of determining the strength of this hydrogen bonding are by infrared and proton magnetic resonance spectroscopy (p.m.r.). We have therefore synthesised and studied the series of compounds shown below.

TABLE 2
INFRA-RED DATA

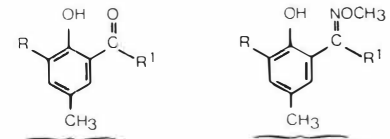

R	R^1	ν_{OH} cm^{-1}	$\nu_{C=O}$ cm^{-1}	ν_{OH} cm^{-1}	PMR δ H (ppm)
H	H	3200	1657	3250	9.56
CH_3	H	3150	1650	3210	9.67
C_4H_9	H	–	–	3160	9.95
H	C_6H_5	3050	1645	~3000	10.2
H	CH_3	3000	1640	~3000	10.8
CH_3	CH_3		1635	<3000	11.02

The -OMe substituted oximes were prepared to minimise effects due to intermolecular H-bonding that can also occur with these compounds. The decreasing frequency of both the OH and C=O vibrations when descending this series is strongly indicative of increasing strength of hydrogen bonding in both the parent carbonyl compounds and their O-methyl oximes. It will be noted that there is also a very good correlation with the chemical shift of the hydroxyl proton absorbance in the pmr spectra, again moving downfield and confirming increasing strength of hydrogen bonding as this series is descended. The effect is particularly pronounced for bulky substituents at R' and the data is indicative of strong hydrogen bonding in these compounds.

Inspection of the data in Table (1) on the strengths of hydroxyoxime extractants and of the spectroscopic data in Table (2) shows that there is a general correlation between strength of a particular ligand type and intramolecular hydrogen bonding. Thus the strongest extractants fall in to the class with the weakest intramolecular hydrogen bonding and hence lowest steric hindrance whereas the weaker extractants are those with strong steric interaction as indicated by strong intramolecular hydrogen bonding.

It should be noted that the optimum bond angles in the chelate ring are quite different for when M is a proton (O-H-N preferably linear), and a square planar copper ion for which the optimum O-Cu-N bond angle is 90°. Thus when M is H^+, reduction of the angles α, β, and γ will make the O-H---N angle more nearly linear and favour strong intramolecular hydrogen bonding. When M is Cu^{2+} however reducing the angles α, β and γ and opening up the O-Cu-N angle will make for a weaker chelate.

Alternatively, bulky substituents may tend to twist the oxygen Sp^2 lone pair of electrons or the oxime N-O-H out of plane. This would greatly reduce the opportunity for bonding with the Lewis acid (proton or metal ion), weaken the hydrogen bonding interactions in the complex, and destroy the electron delocalisation which requires planarity. It is quite apparent to us that hydrogen bonding in the final complex makes a major contribution to complex stability. This is clearly evidenced by the enormous differences between the hydroxyoximes and their $N-OCH_3$ derivatives e.g.

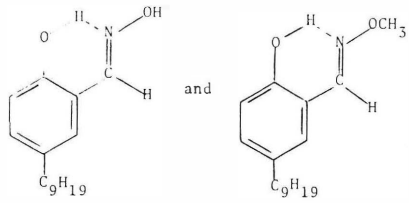

Whereas the oxime readily extracts copper at below pH 1, the N-OCH_3 derivative only satisfactorily extracts copper from ammoniacal solution. This can not be explained at all by electronic effects and the pK_As of the two compounds are very similar.

We consider that the differences are due to the inability of the N-OMe compounds to be able to form the planar annelated ring structure shown by the X-ray studies to exist in complexes of the hydroxyoximes. Such a structure where the metal atom is at the centre of a chelate system consisting of two five membered and two six membered rings is associated with particularly strong complex formation.

COMPUTER MODELLING OF STRUCTURES

In the absence of detailed X-ray crystallographic structural data on all these ligands we have relied on computer modelling of molecular structures applying standard molecular orbital calculations to derive predicted 'lowest energy state structures.' Data on the predicted structures of salicylaldoxime, 2-hydroxyacetophenone oxime and 2-hydroxybenzophenone oxime are presented below as calculated by the MINDO 3 computer programme.

FIGURE 2 MOLECULAR STRUCTURES CALCULATED BY MINDO 3

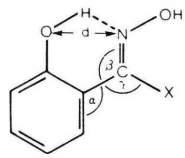

X =	H	CH_3	$C_6H_5^{\perp r}$
O↔N distance (d) Å	2.77	2.44	2.46
Bond angles (°) α	113.2	115.9	116.2
β	122.8	111.8	113.6
γ	112.5	122.4	125.4
Copper Complex d :	2.76Å		

The reliability of the MINDO 3 programme used is illustrated by comparison of the MINDO data for salicylaldoxime (X=H) with that obtained by X-ray crystallography which gives an O to N distance of 2.63 Å and a bond angle for β (Figure 2) of 121.9°. The data for 2-hydroxybenzophenone oxime was calculated assuming the lowest energy state to be with the the phenyl ring perpendicular to the plane of the phenolic ring. If the calculation is carried out assuming the whole molecule to be planar, then repulsion of the protons on the two phenyl rings would be expected to close the O N distance down to 2.1 Å and give an angle for β of only 100.6°. There is probably some rotation of the phenyl group about the C-C axis in the liquid state so the real situation probably lies somewhere between the two cases calculated, i.e. planar and perpendicular ($\perp^r$).

The closing down of the O to N distance for the ketoximes readily explains the increase in strength of the hydrogen bonding in these compounds as steric interaction opens up the phenolic to oxime O-H-N angle and the H-bonding stabilises the close proximity of the H and O atoms by overlapping their orbitals. On the other hand, it makes the O-Cu-N bond angle of 90° far more difficult to achieve, and closes down the O to N distance. The predicted O→N distance between 2.1 and 2.46 Å in the ligand should be contrasted with the O-N distance of ~ 2.75 Å in the copper complex of 2-hydroxybenzophenone oxime. In the case of salicylaldoxime the corresponding O→N distance is 2.63 Å in the free ligand and 2.76 Å in the copper complex (7) and indicates a much better fit.

It is also apparent that even a methyl group at R' can have a considerable steric interaction with the N-OH group as reflected by the strong hydrogen bonding in the ligand and the weakness of the complex relative to R'=H. MINDO 3 calculations predict an O-N distance of 2.4 Å for this compound again indicating that opening up of the 'bite' of the ligand and hence introduction of other strains and interactions in the molecule are necessary for it to chelate satisfactorily with copper.

The effect of alkyl substituents at R is of interest as it is apparent from Table 1 that the order of ligand strength for various groups R follows the order $-CH_3 > H \gg {}^tC_5H_{11}$.

The main electronic effect of an alkyl group is inductive, tending to increase electron density on the oxygen donor atom and hence ultimately complex stability. The inductive effect of a tertiary pentyl group is greater than for a methyl but this provides another good example of the overwhelming effect of steric interaction. It is apparent that the methyl group is small enough to interact only mildly with the oxygen lone pair electrons (e.g. ν_{OH} for R-CH_3 is 3206 cm^{-1} and ν CH for R=H is 3230 cm^{-1}) and overall the inductive effect enhances complex formation. When R=t-butyl or pentyl however steric interaction is clearly strong (ν OH = 3155 cm^{-1}) and the complexes very weak.

Some disturbance of the H-bonding and planarity of the complex could also be expected in this case but this can not be confirmed without an X-ray structure determination.

It has been proposed previously that the mechanism of complex formation between 2-hydroxy aryloximes and copper may be represented as substitution of the phenolic protons with a metal ion in a dimer of the extracting agent which serves as a matrix for complex formation (1, 10). This is still a contentious area and some have claimed that dimers are unlikely to be present at the interface owing to H-bonding association of the ligand with water. Whether the ligands approach the copper atom individually or in combination as a dimeric species is perhaps immaterial with regard to the stage where protons are lost to give the neutral L_2Cu complex. We believe that there is evidence to show that two ligands become associated with copper before proton loss and that hydrogen bonding in stabilisation of the intermediate complex is of paramount importance to final complex formation. The mechanism we propose therefore is not based on the consecutive reaction of charged copper species with 'non existent' oxime anions but on loss of protons from a charged chelate intermediate stabilised by hydrogen bonding. (Figure 3)

FIGURE 3

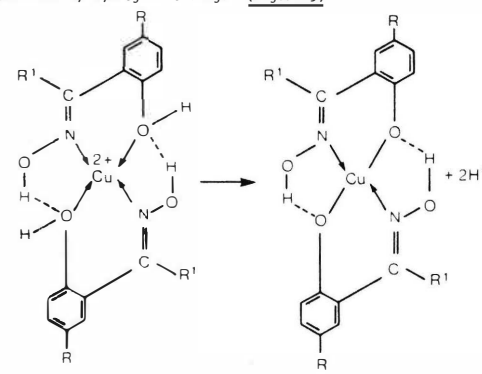

Such a mechanism is consistent with the unusual finding of other workers that for these ligands the stepwise stability constants are such that $K_1/K_2 \leqslant 1$ which is completely at variance with statistical probability. Berger et al in fact report that for salicylaldoxime $K_2 \gg K_1$ and they could only report the overall stability constant log β_2 values. They could find no evidence at all for the existence of a CuL^+ intermediate species (4). The mechanism we propose is also consistent with kinetic data in the literature which shows that if there is a stepwise complex formation

$$Cu^{++} + LH \xrightarrow{K_1} CuL^+$$

and

$$CuL^+ + LH \xrightarrow{K_2} CuL_2$$

then $K_2 > K_1$ (11)

If complex formation is by the mechanism we propose then again, formation and stability of the intermediate species will be very susceptible to strength of hydrogen bonding and steric interactions. The driving force for the intermediate complex formation will be the enormous entropy gain but in the intermediate, the sp^3 hybridisation of the phenolic oxygen atoms will mean that the H-bonded structure is non planar. There is therefore a considerable driving force to lose the protons and allow the complex molecule to take up the delocalised, hydrogen bonded planar structure. Conversely, if it is accepted that the reverse, or stripping reaction occurs by protonation of the phenolic oxygen as a prelude to opening up the complex, there is a high energy barrier to be overcome in destroying the highly stable planar configuration. Clearly, any bulky substituent groups that intoroduce strain into this structure or distort the planarity will give complexes that are readily stripped and thus far less stable.

CONCLUSIONS

In conclusion therefore, we believe that the major effects of substituents in o-hydroxyaryloximes are 1) electronic-including both inductive and mesomeric effects - and 2) steric, where steric interactions affect both the ease with which the ligand can react with the metal and the strength of the essential hydrogen bonding in the resulting complex. The magnitude of these effects depends on the substituent and its position in the molecule. These various effects may work in the same or opposite directions thus making predictions in this field very difficult.

REFERENCES

1. R.Price and J.A.Tumilty 'Hydrometallurgy'. Proceedings of Hydrometallurgy Symposium, UMIST, 1975. I.Chem.E.Symposium Series No 42.pp 18.1-18.7

2. J.G.Jones. J.B.Poole, J.C.Tomkinson and R.J.P.Williams. J.Chem.Soc. 1958, 2001.

3. "The Chemistry of The Metal Chelates" A.E.Martell and M.Calvin. Prentice Hall, New York, 1953.

4. K.Burger and I.Egyed. J.Inorg. Nucl. Chem. 1965, 27, 2361.

5. K.Burger, F.Ruff, I.Ruff and I.Egyed. Acta Chimica Hungaricae 1965, 46, 1.

6. J.R.Parrish. J.Sth. African Chem. Inst. 1970, 23, 129

7. M.A.Jarski and E.C.Lingafelter, Acta Cryst. 1964, 17 (9) 1109

8. P.Tasker and L.Drummond (North London Polytechnic) - Private Communication.

9. C.J.W.Brookes, G. Eglinton and J.F.Morman. J.Chem.Soc. 1961, 661.

10. B.N.Laskorin, V.V.Yaksin, V.S.Ul'yanov, and A.M. Mirokhin. Proceedings of International Solvent Extraction Conference 1974 pp 1775. The Society of Chemical Industry, London.

11. W.J. Albery and P. Fisk. Hydrometallurgy '81 Proceedings of Symposium at UMIST, 1981, Paper F5. The Society of Chemical Industry, London.

SOLVENT EXTRACTION OF TUNGSTEN AND MOLYBDENUM FROM HYDROCHLORIC ACID BY 1-PHENYL, 3-METHYL, 4-BENZOYLPRAZOLONE(5)

Gu Yidong, Song Yuan and Su Yaodang

Fudan University
Shanghai, China

Although it has been already more than twenty years since B.S.Jensen introduced acylpyrazolones as strong chelating agents in solvent extraction of metallic ions(1), and a large amount of research papers have appeared eversince, the studies on the extraction of molybdenum and tungsten by acylpyrazolones are rather scanty.

MOTIVE OF THIS STUDY

Yet the separation of molybdenum from tungsten by solvent extraction is at present an important field of study as reported in current literature. Chelating extraction agents do not seen to be popular in the connection. This is probably due to the prejudice that chelating agents are usually used only at low acidity, within PH range. Another hesitation may be due to the fact that both molybdenum and tungsten yield various types of aggreated ions under different conditions, with various degree of stability, reversibility, and also in different rates of transformation. Since acylpyrazolones are able to extract metallic ions at much higher acidity than the other chelating agents, the extraction of molybdenum and tungsten was tried here in high acidities, even of molarrity range. High acidity may favor conversion of negative ions of molybdenum and tungsten to the positive ions in certain cases. A series of extraction curves has thereby been obtained, and some interesting phenomena have been revealed. It is hoped that the accumulation of facts may eventually enable the design of extraction system for the separation of molybdenum and tungsten.

EXPERIMENTAL CONDITIONS

As a start for this series of study, the most popular acylpyrazolone, 1-phenyl,3-methyl,4-benzoyl pyrazolone(5), abbreviated as PMBP, represented hereafter in this paper as HA, is used. In aqueous phase, the hydrochloric acid concentration ranges from 0.2 to 6 molar. Solutions of Na_2MoO_4(I), Na_2WO_4(II) and sodium metatungstate, $Na_6H_2W_{12}O_{40}$(III) were used for comparison. Throughout the experiment, V_{org}: V_{aq} =1, t=20 $\pm$ 0.2 C, and the duration of mechanical shaking controlled at 5 min. throughout. The formation of polyacid ions from $MoO_4^{=}$ and $WO_4^{=}$, the decomposition of the metatungstate ion, as well as the formation of MO_2^{++} , can be revealed during the extration. But the determination of rate of change is not hereby studied.

SELECTION OF DILUENT

The nature of diluent in the system has significant effect on extraction. MIBK was first used. In Fig.1, Extraction~HCl concentration, curve a shows that the extractoon of molybdenum was virtually complete, due to intermediate MoO_2^{++} formation.

Before considering about the curves b and c, in Fig. 1, for tungsten, consider first Fig.2. Fig.2 represents the increase of extraction with increasing concentration of HCl. Only one curve is present. But it represents the extraction of metatungstic acid into MIBK, both with and without the presence of chelating agent PMBP. Evidently in that extraction system, the chelating effect of PMBP is nil or very slight. The solution effect is simply due to addition compound formation between metatungstic acid and MIBK, just like that between phosphotungstic acid and ethyl ether, one of the series of carboxo(2) compounds.

Now turn back to Fig. 1. Curve c represents extraction of tungsten from $WO_4^{=}$ with increasing HCl concentration into MIBK, without addition of PMBP. Curve b represents extraction with the addition of PMBP. We may then conclude that HCl can cause the formation of polytungstate from $WO_4^{=}$, and thus got partially extracted. (The nature of the polytungstate depends upon time and acidity). Curve b represents combined effect of carboxo addition and PMBP chelation.

At any rate, use of MIBK as solvent reveals something,But is confusing. Ethylene chloride was thus used as the inert solvent for the study of extraction.

In Fig.3, it is revealed that as compared with those curves in Fig.1 and Fig.2, when $C_2H_4Cl_2$ is used as solvent, the extraction of Mo is still high, but the extraction of $WO_4^{=}$ and $H_2(W_{12}O_{40})^{6-}$ derivative are less;yet they are not unextractable. The behavior of all the three extraction curves shows "Lazy S-Curve" form(3). That phenomenon is quite suggestive.

The extraction of Mo may be considered as due to preliminary formation of MoO_2^{++} within the whole HCl concentration interval. Similarly, the gradual rise of extraction of tungsten may be attributed to association, decomposition, with ultimate formation of WO_2^{++} intermediate.

Recalling the phenomenon of precipitation of yellow tungstic acid from homogeneous solution(4), and the dissolution of tungstic acid in 9 M HCl(5), in which $WO_4Cl_4^{=}$ formation may be assumed, we may suggest that the extraction of tungsten into $C_2H_4Cl_2$ layer may be partially due to $WO_2Cl_4^{=}$ intermediate, partially by polytungstate adduct. But the resistance of dissociation at high concentration of the formed chelate, both for Mo and W, can not be easily explained.

ISOLATION OF EXTRACTED MOLYBDENUM COMPOUND

Yet the capability of forming stable chelate at high acidity has been confirmed by the isolation of extracted species from the organic layer, for molybdenum. The corresponding compound for tungsten has not yet been isolated. The molybdenum complex was obtained by evaporation of the $C_2H_4Cl_2$ layer. Yellow needles first separated, with m.p. 91-92 ℃, and were found to be soluble in petroleum ether.On further evaporation, orange coloured crystals in cubic form were isolated, insoluble in petroleum ether, but soluble in $C_2H_4Cl_2$ and CCl_4. After washing with petroleum ether, m.p. 196 -198 ℃. Analysis for Mo,C,H and N suggested the isolated compound as MoO_2A_2.

IR spectra confirmed the β-ketone metal chelate with strong absorption bands at 1608,1555 and 1525 cm^{-1}. With pure PMBP, rather broad absorption bands appears at 1615 and 1560 cm^{-1}.

The same composition of molybdenum-PMBP complex can also be deduced by the method of stepwise extraction until organic medium composition becomes constant. Initial composition of organic layer was 0.005 M PMBP in $C_2H_4Cl_2$; composition of the successive aqueous solution to be extracted were 0.0005 M Na_2MoO_4 in 2.8 and 3.8 M HCl.

NONLINEARITY OF EXTRACTION CURVE

But it must be emphasized that isolation of Mo-PMBP complex does not mean that it is the only species present at various conditions. Returning to Fig.3, we can notice that although the extraction of Mo was quite high, but we prefer not to represent E~[HCl] plot as straight line. Lazy S-Curve was thus retained, in conformity with the two other W curves.

Another way of plotting is given in Fig.5. D_{Mo} was plotted against HCl concentration, with several fixed concentration of PMBP in $C_2H_4Cl_2$. The S shape then becomes very distinct. Maxima existed. The solid comlex compound, as mentioned above, was isolated at HCl concentration close to the maximum D_{Mo} in that Fig.5.

It is significant that in Fig.5 , those portion of curves to the left of maxima are quite close to linearity. That portion may be of value for estimation of "extraction constants".

EXTRACTION OF W

Corresponding curves, starting with $WO_4^{=}$, for D_W~HCl with several fixed concentration of PMBP in $C_2H_4Cl_2$, were also

studied. Within the range of HCl concentration studied, only concave curves were obtained. The rate of getting into equilibrium caused some difficulty.

Plotted curves, with %D or %E against C_{HA}, HCl concentration being kept fixed, are omitted in this report.

It deserves mentioning, that we have found 1-phenyl,3-methyl,4-trifluoroacetylpyrazolone(5), a stronger chelating agent (6) than PMBP, to be a better extraving agent for W, with metatungstate as starting solution. Its extraction is higher than $MoO_4^{=}$ at all concentrations of HCl, with $C_2H_4Cl_2$ as diluent. But separation of solids between two layers made the study complicated.

COMMENT

Finally, concerning the structure of acylpyrazolones, we must realize that they are not simple β-diketones. They contain in structure also a specific tertiary nitrogen atom at 2-position. Its joint function in effecting solvent extraction at high acidity may deserve special consideration.

REFERENCES

1. B.S.Jensen, Acta Chem. Scand., 13, 1668, 1890(1959).
2. S.Ahrland, J.O.Liljenzin and J.Rydberg, c/o Comprehensive Inorganic Chemistry, edited by J.C.Bailar, Jr., et al., (1973), Vol.5, p.557.
3. D.Peppard, Solvent Extraction Chemistry, edited by D.Dyrssen, J.O.Liljenzin and J.Rydberg (1967) pXIX
4. Y.T.Ku and S.T.Wang, J. of Chinese Chem. Soc., 17, p.291 (1950).
5. Y.T.Ku and K.Y.Hsieh, Acta Sc. Nat. Univ. Fudan, 104(1955).
6. Gu Yidong and Song Yuan, Chem. J. of Chinese Univ., 2, 139 (1981).

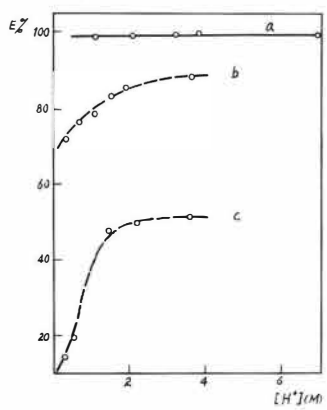

Fig.1.
E% against HCL concentration
MIBK as solvent
a. $MoO_4^{=}$ + PMBP
b. $WO_4^{=}$ + PMBP
c. metatungstate + PMBP

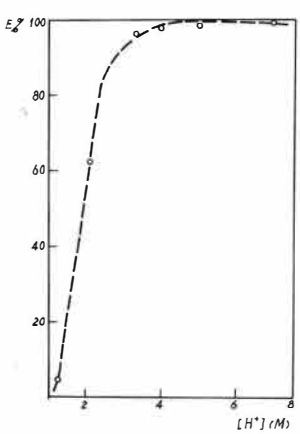

Fig.2.
E% against HCL concentration
MIBK as solvent
a. $WO_4^{=}$ + PMBP
b. metatungstate + PMBP

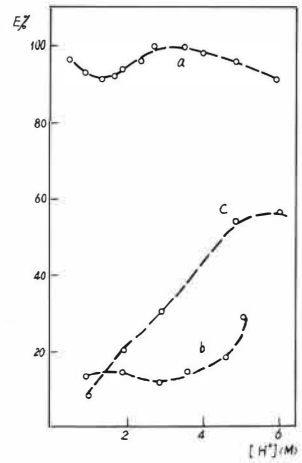

Fig.3.
E% against HCL concentration
$C_2H_4CL_2$ as solvent
a. $MoO_4^{=}$ + PMBP
b. $WO_4^{=}$ + PMBP
c. metatungstate + PMBP

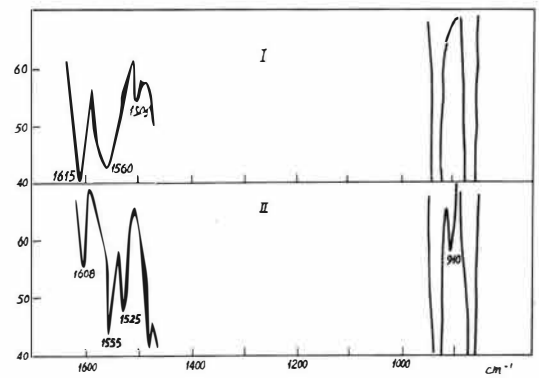

Fig. 4. IR spectra I. PMBP alone II. Mo-PMBP

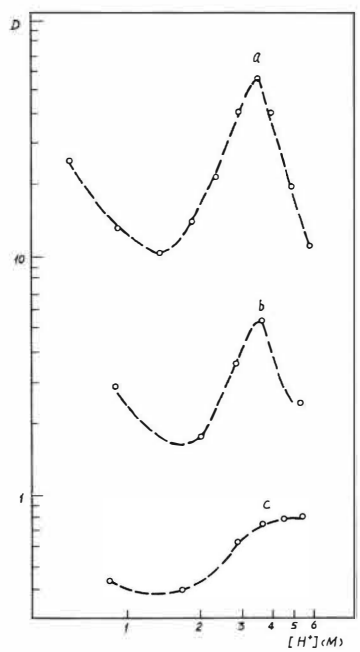

Fig. 5.
D against concentration HCl
[PMBP]:
a.0.05 b.o.o3 c.0.015 M

FAR INFRARED SPECTRA OF SOME RARE EARTH EXTRACTANTS AND EXTRACTED COMPLEXES

Wu Jinguang, Shi Nai, Jin Tianzhu, Chen Dian
Gao Hongcheng, Guo Hai, Weng Shifu and Xu Guangxian

Department of Chemistry
Peking University
Beijing, China

INTRODUCTION

The rare earth ions, M^{+++}, usually coordinate with the active donating atom X(e.g., O, N, S) of the extractants to form M-X bond. Since the atomic weights of the lanthanides are rather large, the M-X vibration bands are usually in the far infrared range. But studies on the far infrared spectra of the organic phase during the extraction of rare earths have seldom reported in the literature. In the present investigation, we have studied systematically the far infrared spectra of the rare earth complexes of the ammonium extractant N263 (like Aliquot 336), mono-(2-ethylhexyl)-2-ethylhexyl phosphonate, TTA and PZL(pyrazolone) and obtained some new results.

EXPERIMENTAL

1. Instrument: Nicolet 7199B Fourier Transform Infrared Spectrophotometer, using low density polyethylene windows and demountable cells for liquid samples and polyethylene powder or CsI tablet for solid samples. The spectral range studied is 100-400 cm^{-1}.

2. Preparation of samples:

(1) Prepare 30% mono-(2-ethylhexyl)-2-ethylhexyl phosphonate (EHPAEH) solution in kerosine, saponified to 40% by NH_4OH. Use the extractant solution thus prepared to extract the rare earth ions from the aqueous phase and record the far infrared spectra of the organic phase and also the solid compound formed.

(2) Dissolve methyl-trialkyl ammonium chloride (average molecular weight = 450, the alkyl groups contain 8-10 C atoms) in kerosine and secondary octyl alcohol, transform the chloride salt to thiocyanate or nitrate. Use the extractant solution thus prepared to extract rare earth ions from the aqueous solution and to take the far infrared spectra of the organic phase.

(3) TTA complexes of rare earths of the composition $M(TTA)_3 2H_2O$ were prepared from HTTA and rare earth chlorides.

(4) 1-Phenyl-3-methyl-4-benzoyl-pyrazolone-5 (PZL) complexes of rare earths of the composition $M(PZL)_3$ and $M(PZL)_3(HPZL)$ were prepared by adding rare earth nitrate solution to PZL solution.

RESULTS AND DISCUSSION

1. Far infrared spectra of the extracted complexes:

(1) Mono-(2-ethylhexyl)-2-ethylhexyl phosphonate system.

The pure extractant has no strong peak in the wave number range of 100-200 cm^{-1}. Upon extraction with rare earth ions, there appears a strong peak at 145-165 cm^{-1}, which was assigned to be due to the vibration of the rare earth-oxygen bond, M-O. A "tetrad effect" was observed for the variation of ν_{M-O} with the atomic number of the lanthanides, as shown in Fig.1.

(2) The quaternary ammonium salt system.

The pure extractant (either thiocyanate or nitrate) has no peak in the region 100-300 cm^{-1}. Upon extraction with rare earth ions, there appears a broad and strong peak at 190-260 cm^{-1}. In the nitrate system, the peak was assigned to ν_{M-O}. In thiocyanate system, the peak was assigned to ν_{M-N}. For the light and the heavy lanthanids, ν_{M-O} and ν_{M-N} are about the same, while for middle lanthanides, Sm, Eu, Gd, ν_{M-O} is larger than ν_{M-N} by about 20 cm^{-1}.

(3) Rare earth complexes of TTA and PZL.

There is a ring structure in HTTA molecule due to the hydrogen bond formed between the carbonyl group and the enol group, hence it has several bands in the far infrared spectra. When HTTA reacts with the rare earth ions, M^{+++}, to form $M(TTA)_3 2H_2O$, there are shifts in wave numbers of the original peaks, and several new peaks occur also. Similar changes were observed for the PZL complexes.

2. We have determined the crystal structure of $Ho(TTA)_3 2H_2O$, which belongs to C_2 point group. Owing to the coordination with water, the molecule is of low symmetry and the normally degenerate bands split. The crystal field effect also increases the complexity of the spectra. Fig.3A and 3B show the far infrared spectra of $Yb(PZL)_3 2H_2O$ and $Lu(TTA)_3 2H_2O$ respectively. Fig.4 and 5 show the variation of peak wave numbers with the atomic numbers of the central lanthanide ion. The absorption peaks near 450 cm^{-1} of $M(TTA)_3$ also show the "tetrad effect" as may be seen from Fig.5

CONCLUSIONS

1. Metal-ligand bands may be observed in the far infrared spectra of the rare earth complexes of quaternary ammonium nitrate or thiocyanate, acidic phosphorus extractant, TTA and PZL.

2. The variation of ν_{M-O} with the atomic number of the lanthanides is in a rather complex manner. The so-called "tetra effect" was observed only in the TTA complexes and the phophonic acid complexes.

3. Normal coordinate analysis of these complexes is under investigation in order to have clearer understanding of their vibrational modes.

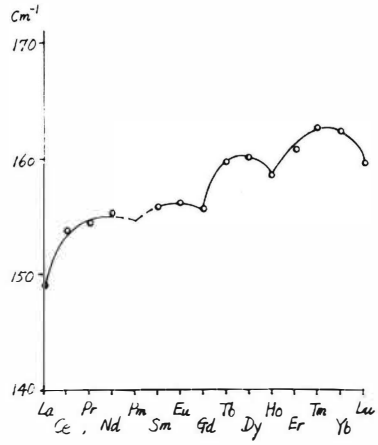

Fig.1 The tetrad effect of the variation of ν_{M-O} of the lanthanide complexes of EHPAEH with the atomic numbers of lanthanide.

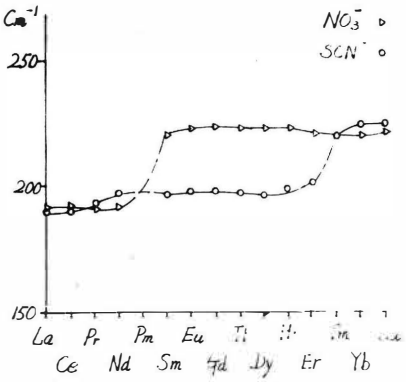

Fig. 2 The variation of ν_{M-O} and ν_{M-N} with the atomic numbers of lanthanide

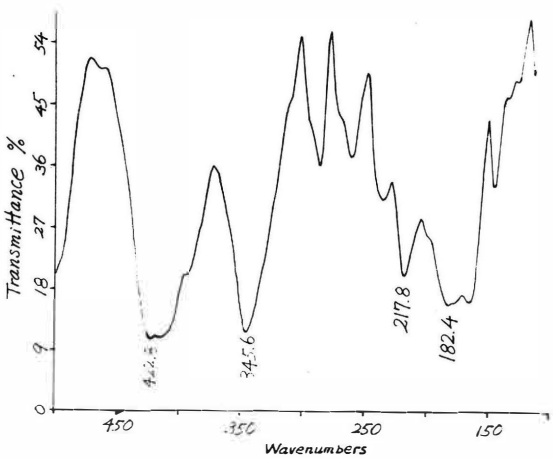

Fig. 3A The far infrared spectra of $Yb(PZL)_3 \cdot 2H_2O$

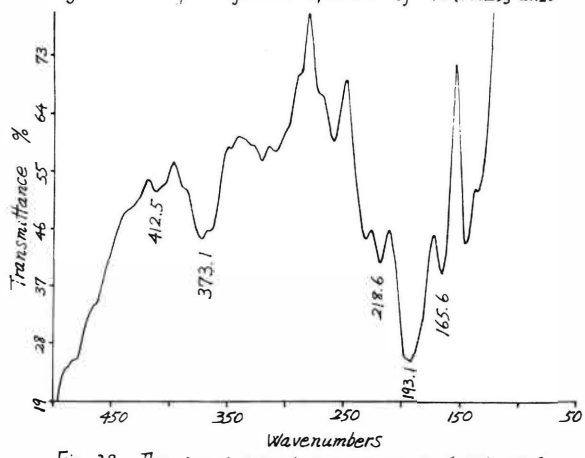

Fig. 3B The far infrared spectra of $Lu(TTA)_3 \cdot 2H_2O$

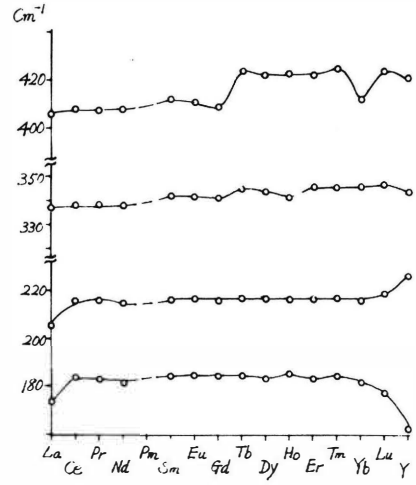

Fig. 4 Variation of ν_{M-O} of $M(PZL)_3 \cdot 2H_2O$ with the atomic numbers of M

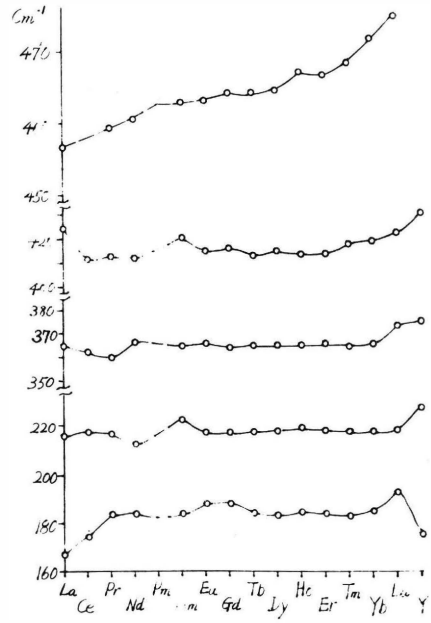

Fig. 5 The variation of ν_{M-O} near 455 cm⁻¹ of $M(TTA)_3$ with atomic numbers of M

EXTRACTION OF SALTS BY TBP CHARACTERIZATION OF THE EXTRACTED SPECIES

Jacques Ly, Claude M. Poitrenaud

Institut National des Sciences et
Techniques Nucléaires
Saclay, France

The general equilibrium for the extraction of a metallic salt by an organic solution of TBP in an inert diluent is :

$$(1) \qquad M^{n+} + pX^- + q\,\overline{TBP} + (r-t)\,H_2O \rightleftarrows \overline{M(OH)_r X_p\,(TBP)_q} + r\,H^+$$

where :

- M^{n+} is the hydrated cation of the metallic element in the aqueous phase
- X^- is the main hydrated anion present in the aqueous phase
- t is the number of H_2O molecules liberated in the aqueous phase by the species extracted by the organic phase
- species with bars refer to the organic phase

In these conditions the distribution coefficient of the metallic element between the two phases is :

$$(2) \qquad D = K^\circ \frac{(y_{\overline{TBP}})^q}{(y_{\overline{M}})} \frac{y_M\,(y_X)^p}{(y_H)^r} (a_{H_2O})^{r-t} \frac{[X^-]\,[\overline{TBP}]^q}{[H^+]^r}$$

where :

- K° is the thermodynamic constant of the equilibrium (1) which depends only on the temperature, the pressure and the reference states chosen for the activity coefficients y_M, y_X and y_H of the species M^{n+}, X^- and H^+ in the aqueous phase and $y_{\overline{TBP}}$ and $y_{\overline{M}}$ of the species TBP and $M(OH)_r X_p\,(TBP)_q$ in the organic phase
- (a_{H_2O}) is the water activity in the aqueous phase
- $[H^+]$, $[X^-]$ and $[\overline{TBP}]$ are the molar concentrations of these three species in their respective phases.

It is possible to characterize the extracted species (i.e.) to determinate q and r (or p, since r+p = n), by studying the variation of D with $[\overline{TBP}]$ and $[H^+]$ or $[X^-]$ in systems where the activity coefficients in both phases and the water activity are kept constant .

From the studies of Vdovenko and Ryazanov (1) the activity coefficient y_x of the species X in an aqueous solution may be represented by :

$$y_x = \frac{F\,(a_{H_2O})}{\Sigma\,\nu\,C}$$

where :

- $F\,(a_{H_2O})$ is a function of the water activity ; the parameters of this function depend only on the nature of the species
- $\Sigma\,\nu\,C$ is the total concentration of the species (except H_2O) present in the aqueous solution.

The activity coefficients in the organic phase depend on the composition of this phase in which the main species are : the TBP, the diluent and the extracted acide HX. These coefficients also depend on the water activity in the system.

In conclusion, to keep constant the activity coefficients in both phases one needs to keep constant the water activity, the total concentration of species in the aqueous phase and the composition of the organic phase.

Tables, giving the water activity (2, 3) in mixtures of alkaline salts AX and acids HX, enable to prepare aqueous phases with identic water activities (isotonic mixtures), identic concentrations of species and with different concentrations $[H^+]$ or $[X^-]$.

It is also possible to keep constant the composition of the organic phase by :

- introducing only very small quantities of acid HX in the system : in this case the organic phase is nearly a mixture of only two species, TBP and diluent, at known concentrations.
- using large quantities of acid HX ; in this case the concentration of the acid extracted by the organic phase depends only on the water activity in the system. Then the composition of the organic phase is unvarying if the water activity is kept constant.

This last result is proved in Figure 1 concerning the nitric acid. On this figure each curve represents the variation of the concentration $\overline{C}$ of the nitric acid extracted by the organic phase from a mixture of alkaline nitrates (at constant concentrations) with nitric acid (at varying concentration, increasing in the direction of the arrow on each curve). When the concentration of HNO_3 is high, the curve is identical with the limit-curve obtained when no salts are added to the acidic aqueous phase. Then the concentration $\overline{C}$ of the extracted HNO_3 only depend on the water activity in the system whatever may be the nature of the salts accompanying the acid in the aqueous phase.

In conclusion it is possible to keep constant the activity coefficients in both phases by appropriate choice of the compositions of these phases and using isotonic mixtures of acid with salts in the aqueous phase.

This method has been used to characterize the extracted species of UVI and PdII by TBP from aqueous nitrate solutions.

EXTRACTION OF THE URANYL(VI) NITRATE BY TBP

Figure 2 represents the variation of log D_u versus log $[\overline{TBP}]$ for various aqueous phases containing the diluted nitric acid (0.01 M) and an alkaline salt. The obtained curves are linear. Their slope is + 2. This indicates that the uranyl nitrate is extracted with two molecules of TBP as it has already been shown.

Figure 3 represents the variation of log D_u versus log $[H^+]$ for systems in which the aqueous phases are isotonic mixtures of nitric acid with sodium nitrate. It may be observed that D_u does not depend on $[H^+]$. Then the extracted species is $UO_2\,(NO_3)_2\,(TBP)_2$.

EXTRACTION OF THE PALLADIUM NITRATE BY TBP

The number q of TBP molecules accompanying the palladium nitrate in the organic phase has already been determined (4, 5) and is equal to 2. It has also been noticed that D_{Pd} depends on the acidity of the aqueous phase (4) and that PdII is highly hydrolysable (6). Then the extracted species of PdII might contain HO^- ions (r > 0).

Figure 4 represents the experimental variation of log D_{Pd} versus log $[H^+]$ for systems in which the aqueous phases are isotonic mixtures of nitric acid with unextractable nitrates. The obtained curve is linear. The slope is - 1. Then the extracted species is $Pd\,(OH)\,(NO_3)\,(TBP)_2$.

REFERENCES

1. V.M. Vdovenko and M.A. Ryazanov, Russ. J. Phys. Chem. 42, N° 8, 1018, (1968)
2. R.A. Robinson and R.H. Stokes, Electrolyte Solutions, 2nd Ed., Butterworths, London (1970)
3. W.J. Hamer and Y-C. Wu, J. Phys. Chem. Ref. Data, Vol. 1, N° 4, 1047 (1972)
4. K.P. Lunichkina, E.V. Renard and V.B. Shevchenko, Zh. Neorg. Khim. 19, 205 (1974)
5. B.N. Zaitsev and E.N. In'kova, Radiokhimiya 23, N° 6, 817 (1981)
6. B.I. Nabivanets and L.V. Kalabina, Russ. J. Inorg. Chem. 15, N° 6, 818 (1970)

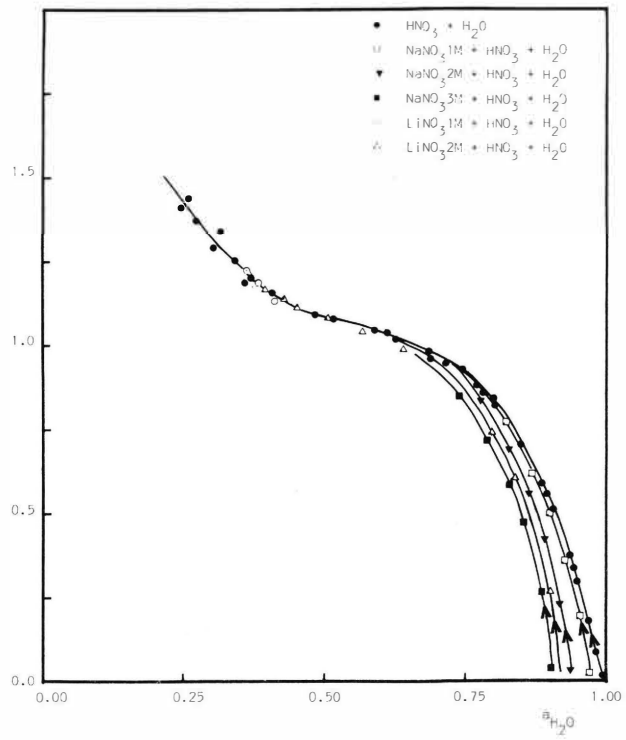

FIGURE 1. PARTITION OF NITRIC ACID BETWEEN AQUEOUS PHASES OF VARIOUS WATER ACTIVITIES AND AN ORGANIC PHASE (30 % TBP IN DODECANE). THE CONCENTRATION OF HNO_3 IS VARYING ON EACH CURVE AND INCREASING IN THE DIRECTION OF THE ARROW

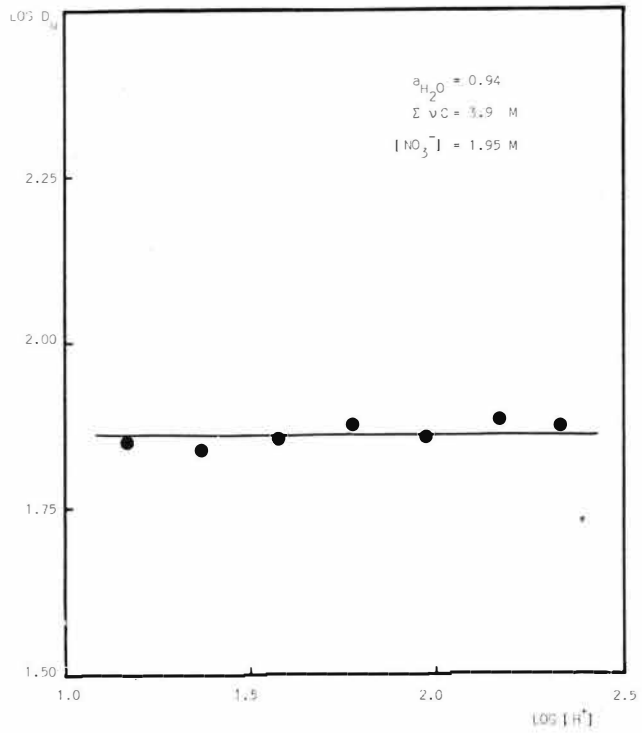

FIGURE 3. DISTRIBUTION OF TRACES OF URANYL NITRATE BETWEEN AN ORGANIC MIXTURE OF 30 % TBP WITH DODECANE AND AQUEOUS ISOTONIC MIXTURE OF NITRIC ACID (10^{-2} M) WITH SODIUM NITRATE 1.95 M

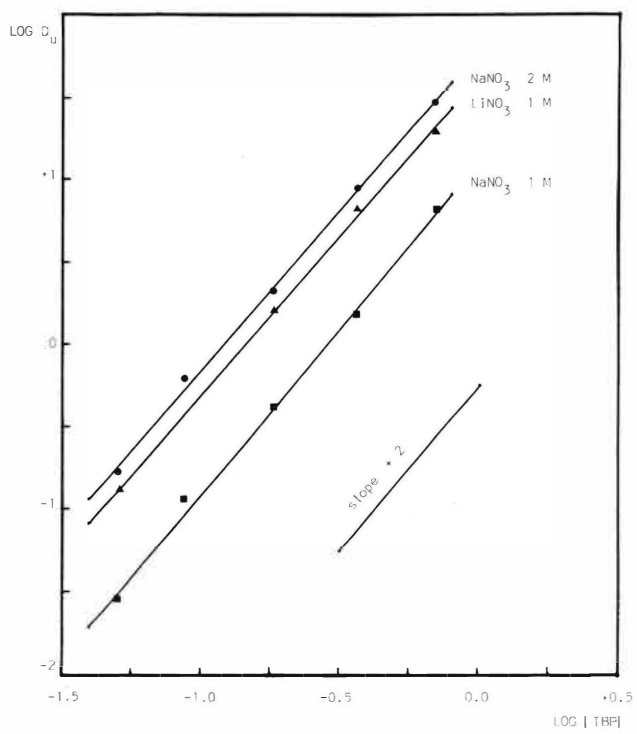

FIGURE 2. DISTRIBUTION OF TRACES OF URANYL NITRATE BETWEEN ORGANIC PHASES OF VARIOUS CONCENTRATION OF TBP AND AQUEOUS MIXTURES OF NITRATES WITH NITRIC ACID (10^{-2} M)

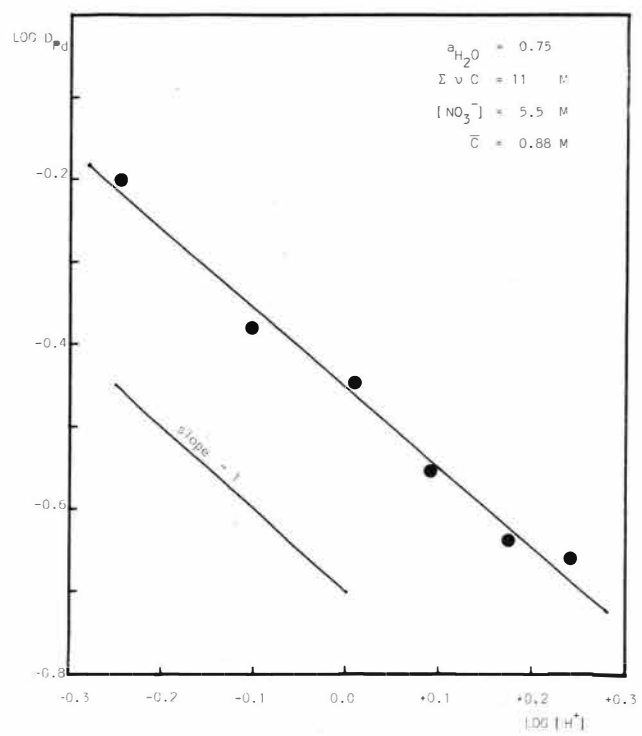

FIGURE 4. DISTRIBUTION OF TRACES OF PALLADIUM NITRATE BETWEEN AN ORGANIC MIXTURE AT 30 % TBP WITH DODECANE AND AQUEOUS ISOTONIC MIXTURES OF NITRIC ACID, LITHIUM NITRATE, SODIUM NITRATE AND CALCIUM NITRATE

CHARACTERIZATION AND REACTIVITY OF HYDROXY OXIME COMPLEXES OF COPPER AND NICKEL

M. E. Keeney and K. Osseo-Asare

Department of Materials Science and Engineering
The Pennsylvania State University
University Park, Pennsylvania 16802 USA

INTRODUCTION

The commercial success of the oxime-based extractants has prompted an enormous amount of research into the physicochemical behavior of hydroxyoximes in hydrometallurgical systems. Much of this work has been concerned with extraction kinetics and equilibrium metal distribution with little emphasis on the structure and reactivity of the extracted metal complexes.

In principle, the extraction of transition metals using hydroxyoximes can lead to the formation of several distinctly different complexes as a result of both the ambidentate coordination behavior of the hydroxyoxime ligands and the variabilty of the stereochemical arrangement of the ligands around the metal. The oxime may function as either a unidentate or a bidentate chelating ligand depending upon specific solution conditions or ligand structure. As an N O type chelating ligand, a variety of stereoisomers is possible for the transition metal complexes as a consequence of the oxidation state of the metal, ligand steric factors and inter- or intra-molecular hydrogen bonding.

In this paper direct analytical and spectroscopic techniques (e.g. elemental analysis; IR, magnetic, electronic, and HNMR spectra) are used to elucidate the structure and reactivity of Cu(II) and Ni(II) complexes of the hydroxyoxime reagents LIX63 and LIX65N.

EXPERIMENTAL

The anti-isomer of 5,8-diethyl-7-hydroxy-6-dodecanone oxime ([H_2Ox]) and the anti-isomer of 2-hydroxy-5-nonylbenzophenone oxime ([H_2BOx]) were prepared by purification of the commercial reagents LIX63 and LIX65N respectively (both products of Henkel Inc.)(1,2). The several complexes of these two compounds with Cu(II) and Ni(II) were synthesized and characterized as described in detail elsewhere (3,4).

RESULTS

Table 1 presents a summary of selected physical properties of the isolated metal hydroxyoxime complexes. It can be seen that Cu(II) and Ni(II) form analogous isomorphic complexes with [H_2Ox] and [H_2BOx]. However, despite previous reports (5,6) and repeated efforts, we have been unable to isolate the bis-[H_2Ox] complex with Cu(II), i.e. [$Cu(HOx)_2$].

The infrared spectra (Table 2) of the analogous Cu(II) and Ni(II) complexes are virtually identical suggesting similar structural symmetry. Generally, the phenolic or hydroxyl proton is lost upon coordination to the metal. Both hydroxyl protons are lost from $[Cu(Ox)]_n$ and $[Ni(Ox)]_n$ as a result of the polymerization of the complexes; however, neither of the hydroxyl protons is lost in [$Ni(H_2Ox)_3SO_4$] and [$Cu(H_2Ox)_3SO_4$] confirming that the hydroxoxime is coordinating to the metals as a neutral ligand.

The magnetic and electronic spectral properties of the complexes are presented in Tables 3 and 4 respectively. $[Cu(Ox)]_n$ and $[Ni(Ox)]_n$ exhibit anomalously low magnetic moments indicative of anti-ferromagnetic interaction as a result of their oligomeric behavior. The electronic absorption spectra suggest octahedral geometry. Octahedral geometry is also indicated for [$Ni(H_2Ox)_3SO_4$] by the presence of three principal bands of low intensity in the electronic absorption spectrum. The diamagnetism of the [$Ni(HOx)_2$]and [$Ni(HBOx)_2$] complexes indicates square-planar geometry. The electronic absorption spectra for both complexes are typical of square-planar Ni(II). The magnetic moments of [$Cu(HBOx)_2$] and [$Cu(H_2Ox)_3SO_4$] are typical for Cu(II) complexes. The value of 1.79 B.M. for [$Cu(HBOx)_2$] is characteristic of square-planar Cu(II). The electronic absorption spectrum of [$Cu(H_2Ox)_3SO_4$] exhibits a single broad band of weak intensity at 775 nm suggesting a tetragonally distorted octahedral geometry.

The proton magnetic resonance (PMR) data are also presented in Table 3. $[Cu(Ox)]_n$ and $[Ni(Ox)]_n$ show no hydroxyl protons in the PMR spectra confirming the loss of both the N-OH and C-OH protons. The PMR spectra of [$Cu(H_2Ox)_3SO_4$] and [$Ni(H_2Ox)_3SO_4$]clearly indicate that both the hydroxyl and oxime protons are retained upon coordination of the oxime to the metal. The PMR spectrum of [$Ni(HOx)_2$] has two sharp singlets at 12.50 and 17.40 ppm attributable to non-equivalent hydroxyl protons. The complex appears to have a square-planar structure in which the ligands are coordinated in a cis configuration.

As shown above, several of the Ni(II) and Cu(II) complexes are square-planar. As a result, many of these complexes would be expected to be capable of ligand addition reactions to achieve higher coordination numbers while others may undergo ligand exchange in order to form more stable species.

Orange [$Ni(HOx)_2$] is observed to slowly convert to a green liquid upon exposure of the neat complex to air for extended periods of time; the color change is more rapid if [$Ni(HOx)_2$] is contacted with H_2O. The green complex can be reconverted to orange [$Ni(HOx)_2$] by warming under high vacuum.

Infrared and electronic absorption spectral changes strongly suggest that [$Ni(HOx)_2$] is hydrating to form the hexacoordinated bis-aquo adduct [$Ni(HOx)_2(H_2O)_2$] with pseudo-octahedral symmetry. The addition of carboxylic acids to hexane solutions of [$Ni(HOx)_2$] also leads to dramatic orange to blue-green color changes. Figure 1 presents the electronic absorption spectral changes in the case of lauric acid addition. Figure 2 shows the result of contacting a hexane solution of [$Ni(HOx)_2$] with dilute H_2SO_4.

The electronic absorption spectral changes accompanying the titration of a [$Ni(HOx)_2$] solution with [H_2BOx] are shown in Figure 3. The final spectrum is identical to that of [$Ni(HBOx)_2$], indicating ready conversion from [$Ni(HOx)_2$]. On the other hand, reaction of [$Ni(HBOx)_2$] with [H_2Ox] occurs with difficulty, requiring approximately a five-fold excess of [H_2Ox] to completely displace [H_2BOx] from the metal. The final spectrum is similar to the spectrum of [$Ni(HOx)_2(H_2Ox)$] (obtained by the addition of excess [H_2Ox] to solutions of [$Ni(HOx)_2$]).

ACKNOWLEDGMENTS

This work was supported by the U.S. National Science Foundation.

REFERENCES

1. M. E. Keeney and K. Osseo-Asare, Hydrometallurgy, in press.
2. R. L. Atwood and J. D. Miller, Trans. SME, 254, 319 (1979).
3. M. E. Keeney and K. Osseo-Asare, Polyhedron, to be published.
4. M. E. Keeney, Ph.D. Thesis, The Pennsylvania State University, University Park, PA, U.S.A., 1981.
5. J. S. Fritz, D. R. Beuerman and J. J. Richard, Talanta, 18, 1095 (1971).
6. J. S. Preston, J. Inorg. Nucl. Chem., 37, 1235 (1975).

Table 1. Selected Physical Properties of Metal Oxime Complexes

Complex	Color	Form	MW[a]	mp(°C)	λ^e
$[Cu(Ox)]_n$	green	amorphous solid	2350[b] (333)	202	1.63
$[Ni(Ox)]_n$	olive	amorphous solid	1642[c] (329)		1.56
$[Ni(HOx)_2]$	orange	viscous liquid	606 (599)	-20	11.76
$[Cu(H_2Ox)_3SO_4]$	pale blue	amorphous solid	1009 (973)	110	9.21
$[Ni(H_2Ox)_3SO_4]$	pale blue	amorphous solid	1044[d] (969)	220 dec	
$[Cu(HBOx)_2]$	olive	crystalline solid	751 (740)	151	12.16
$[Ni(HBOx)_2]$	lt. green	crystalline solid	744 (735)	77	11.86

[a]VPO results in toluene. Calculated values (for monomers) in parentheses.
[b]n ∿ 7, [c] n ∿ 5, [d] Determined as 997 by Galbraith Laboratories, Inc.
[e]Molar conductance (λ; ohm^{-1} cm^2 mol^{-1}) as 1 x 10^{-3} M nitrobenzene solution at 25°C.

Table 2. Infrared Spectral Data[a] (cm^{-1})

Complex	ν_{NO-H}	ν_{CO-H}	$\nu_{C=N}$	ν_{N-O}	ν_{C-O}	δ_{O-H}
$[H_2Ox]$	3320 st br	3600 sp	1650 br	950 w	1105 s	1270 m
$[Cu(Ox)]_n$	---	---	1590 m	960 w	1110 s	---
$[Ni(Ox)]_n$	---	---	1580 m	950 w	1115 s	---
$[Ni(HOx)_2]$	---	---	1570 m	920 w	1115 s	1250 m
$[Cu(H_2Ox)_3SO_4]$	3000 st br	3600 sp	1645 br	910 w	1105 s	1250 m
$[Ni(H_2Ox)_3SO_4]$	2900 st br	3600 sp	1645 br	915 w	1105 s	1250 m
$[H_2BOx]$	3345 st br	3590 sp	1580 m	910 sp	1105 s	1260 sp
$[Cu(HBOx)_2]$	3000 st br	---	1545 m	915 w	1105 s	1255 sp
$[Ni(HBOx)_2]$	2950 st br	---	1545 m	915 w	1105 s	1255 sp

[a] Spectra in CCl_4 (4000-600 cm^{-1}); st = strong; m = medium; w = weak; sp = sharp; br = broad

Table 3. Magnetic Susceptibilities (X), Magnetic Moments (μ_{eff}) and PMR Spectral Data

Complex	N-O(H)	C-O(H)	X($\times 10^6$ cgs)	μ_{eff}(B.M.)
[H_2Ox]	b	6.1	---	---
[Cu(Ox)]$_n$	---	---	173	0.65
[Ni(Ox)]$_n$	---	---	1425	1.87
[Ni(HOx)$_2$]	17.50 s	12.50 s	diamagnetic	0
[Cu(H_2Ox)$_3$SO$_4$]	38 br	17 br	1835	2.10
[Ni(H_2Ox)$_3$SO$_4$]	38 t br	17 br	4360	3.24
[H_2BOx]	11.48 br	9.00 br	---	---
[Cu(HBOx)$_2$]	7.50 br	---	1318	1.78
[Ni(HBOx)$_2$]	10.84 s	---	diamagnetic	0

[a]Values given are in ppm measured in $CDCl_3$ solution. Samples are referenced to (CH_3) Si. s = singlet; t = triplet, br = broad. [b]Proton resonance unobserved.

Table 4. Electronic Absorption Spectral Data

Complex	λ_{max}(nm)	ε(l mole^{-1} cm^{-1})
[Cu(Ox)]$_n$	610, 425, 350	344, 3280, 1390
[Ni(Ox)]$_n$	595, 510 sh, 350	30, 46, 480
[Ni(HOx)$_2$]	530 sh, 455, 305 sh, 295	48, 143, 4080, 4620
[Cu(H_2Ox)$_3$SO$_4$]	775, 290 sh	65, 99
[Ni(H_2Ox)$_3$SO$_4$]	1050, 608, 360	8, 8, 25
[Cu(HBOx)$_2$]	665, 470 sh, 355, 273	142, 302, 8050
[Ni(HBOx)$_2$]	620, 460 sh, 395, 380 sh, 309	137, 230, 4530, 4160

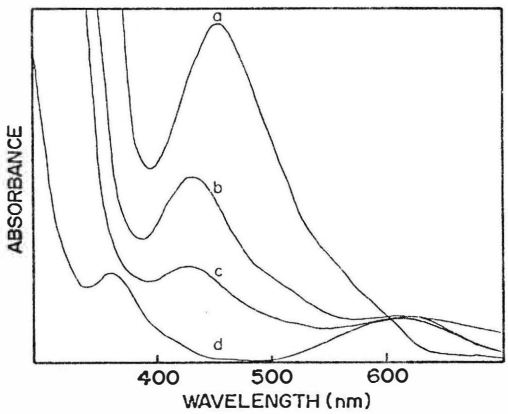

FIGURE 2. ELECTRONIC ABSORPTION SPECTRAL CHANGES OBTAINED FOR A HEXANE SOLUTION OF [Ni(HOx)$_2$] UPON CONTACTING A DILUTE H_2SO_4 SOLUTION. (A) INITIAL: (B) 5 SEC: (C) 10 SEC: (D) 15 SEC.

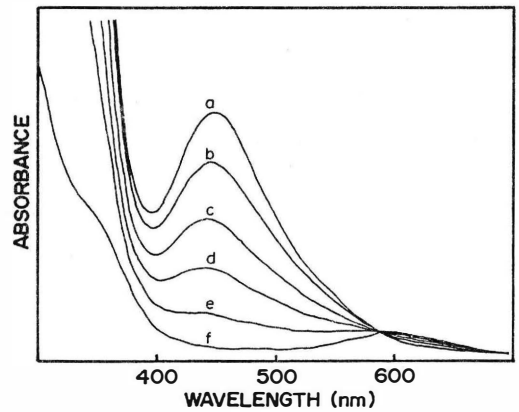

FIGURE 1. ELECTRONIC ABSORPTION SPECTRAL CHANGES OBTAINED DURING TITRATION OF A 4.90x10^{-3}kmol m^{-3} HEXANE SOLUTION OF [Ni(HOx)$_2$] WITH LAURIC ACID. LAURIC ACID CONCENTRATION (kmol m^{-3}): (A) 0; (B) 1.24x10^{-3}; (C) 3.16x10^{-3}; (D) 5.00x10^{-3}; (E) 7.00x10^{-3}; (F) 9.81x10^{-3}.

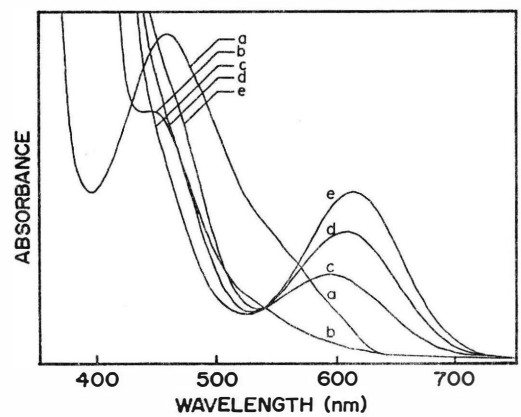

FIGURE 3. ELECTRONIC ABSORPTION SPECTRAL CHANGES OBTAINED DURING TITRATION OF A 6.64x10^{-3} kmol m^{-3} HEXANE SOLUTION OF [Ni(HOx)$_2$] WITH [H_2BOx]. [H_2BOx] CONCENTRATION (kmol m^{-3}): (A) 0, (B) 1.17x10^{-3}; (C) 6.53x10^{-3}; (D) 9.14x10^{-3}, (E) 1.34x10^{-2}.

SOLVENT EXTRACTION OF METAL PERCHLORATES WITH TRIOCTYLPHOSPHINE OXIDE

Satoshi Kusakabe and Tatsuya Sekine

Department of Chemistry
Science University of Tokyo
Shinjuku-ku, Tokyo, Japan

Several metal perchlorates are extractable from aqueous solutions with solvating type extractants. Since perchlorate ions scarcely form coordination bonds with metal ions, the nature of the extracted species should be different from that of such complexes as halide or thiocyanate; they are ion-pairs of solvated metal ions with the extractant and perchlorate ions. In the present study, the solvent extraction of several metal ions in aqueous perchlorate solutions with trioctylphosphine oxide(TOPO) in hexane is measured, the solvation number of the metal ions in the extracted species is estimated, and the extraction constants are calculated. On the basis of the results, the solvation of charged metal ions and of uncharged metal coordination complexes with extractants in liquid-liquid systems are compared and a discussion is made for the reason why the solvation number of perchlorates is larger than of coordination complexes of the same metal ion.

EXPERIMENTAL

The extraction experiments were carried out in a thermostated room at 298 K. The aqueous phase was always 1 mol dm^{-3} sodium perchlorate solution containing a small amount of the metal ions to be studied. The hydrogen-ion concentration was adjusted with perchloric acid when it was necessary. A portion of this aqueous solution and the same volume of hexane containing TOPO were placed in a stoppered glass tube, agitated vigorously, and centrifuged. The metal concentrations in the two phases were then measured by flame or atomic absorption spectrometry but those of uranium(VI) were determined by colorimetry. The contents of perchloric acid in the both phases were determined by titration with standard barium hydroxide solutions and those of ammonium ion were measured by potentiometry using an ammonia electrode.

STATISTICAL

The extraction constants are defined as:

$$(1) \qquad Kex_n = [M(ClO_4)_m E_{n'}]_{org}[M^{m+}]^{-1}[ClO_4^-]^{-m}[E]_{org}^{-n}$$

where E is TOPO. The subscript "org" denotes chemical species in the organic phase while lack of any subscript denotes those in the aqueous phase. By using these constants, the distribution ratio can be written as:

$$(2) \qquad D = [M(m)]_{org,total}[M^{m+}]^{-1} = \sum[M(ClO_4)_m E_{n'}]_{org}[M^{m+}]^{-1}$$

$$= \sum Kex_n[E]_{org}^{n}$$

Since the amount of TOPO in the aqueous phase is very small, the TOPO concentration at equilibrium, [E]org, can be calculated by the following equation:

$$(3) \qquad [E]_{org,total} = [E]_{org} + \sum n[M(ClO_4)_m E_{n'}]_{org}$$

$$+ 3[NaClO_4E_3]_{org} + 2[HClO_4E_2]_{org}$$

$$= [E]_{org} + \sum nKex_n[M^{m+}][ClO_4^-]^m[E]_{org}^{n}$$

$$+ 3K_{3Na}[Na^+][ClO_4^-][E]_{org}^{3} + 2K_{2H}[H^+][ClO_4^-][E]_{org}^{2}$$

where K_{3Na} is the extraction constant of sodium ion and K_{2H} is that of hydrogen ion in the aqueous phase (the values of these constants are given in Table 1). In Equation 3, the concentrations of metal ions in the both phases and of the hydrogen ion in the aqueous phase are experimentally measured and the concentration of TOPO at initial is known. The concentration of perchlorate ions in the aqueous phase is kept at 1 mol dm^{-3} and of sodium ions are also approximately 1 mol dm^{-3}. The extractions of all of the metal, sodium, and hydrogen ions are dependent on the TOPO concentration but the TOPO concentration decreases from the inital value by the extraction of them. Thus the value of [E]org at equilibrium and that of Kex_n are calculated simultaneously by a successive approximation method.

RESULTS AND DISCUSSION

When both of the TOPO and hydrogen-ion concentrations were high, the effect of the coextraction of perchloric acid and sodium perchlorate was not negligible. For example, when the total TOPO concentration is 0.1, 0.03, and 0.01 mol dm^{-3} and the hydrogen-ion concentration was 0.01 mol dm^{-3}, about 29%, 28%, and 18% of TOPO is calculated by Equation 3 to be combined with hydrogen or sodium ions and thus the concentration of effective TOPO, [E]org in Equation 3, became lower than the initial concentration. For this reason, corrections for this decrease in the TOPO concentration were indespensable under such conditions. The extraction of perchlorates should be essentially independent of the hydrogen ion except when hydrolysis occurs. However, the coextraction of the acid together with the metal perchlorate decreases the TOPO concentration and consequently also the metal extraction. This causes an apparent dependence of the extraction on the hydrogen ion.

When the extraction constant of metal ions was high and the initial TOPO concentration was low, a decrease in the effective concentration of TOPO occured in its lower concentration range because the amount of metal ions extracted with it was not very much smaller than that of TOPO. The correction for this effect was also made by Equation 3.

It was found in some cases that the slope of the log D vs log[E]org plot was not constant in all the TOPO concentration range studied. When the slope increases by an increase in the TOPO concentration it could be elucidated by an increase in the solvation number (for example, in the extractions of Rb^+ and Cs^+). However, when the slope decreases by an increase in that concentration, no explanation may be given on the basis of the law of mass action; it should be due to changes in the activity coefficients of the chemical species in the system and thus the data obtained in such a TOPO concentration range were not used for the calculation. Figure 1 gives extraction data of metal perchlorates. The extraction constants obtained are listed in Table 1 together with those reported previously by the present authors. As is seen from Table 1, the solvation number is four except univalent metal ions and ammonium ions. This solvation number, four, is larger than that in the extraction of usual metal coordination complexes containing anionic ligands such as halide or thiocyanate ions, for example, zinc(II) and lead(II) halides (1,2) are extracted with TOPO such a species as, $MX_2(TOPO)_2$. The solvation number, two, seems to be rather common when uncharged metal complxes with the neutral extractants are extracted. Since the nature of the interactions between the metal ion and the perchlorate ions in the extracted species should be electrostatic, the extracted species should be regarded as an ion-pair which can be given by $[M(TOPO)_n]^{m+}(ClO_4^-)_m$. For this reason, the higher solvation number of perchlorates than that of coordination complexes seems to be reasonable. In the latter, part of the coordination sites of the central metal ion are already occupied by the ligand ions. The uncharged nature and the partial occupation of the sites should reduce the hydration of the metal species in the aqueous phase. On the other hand, in the extraction of perchlorates, all of the coordination sites could be hydrated unless they are occupied by the extractant. The charge of the metal ion should cause stronger hydration than that in the uncharged

complexes. Thus the higher solvation should be necessary for an effective extraction of the perchlorates because then the interactions with water should be reduced. Furthermore, this higher solvation makes the volume of the molecule much larger and the whole species more hydrophobic.

The solvation number in the extraction of uranium(VI) perchlorate with TOPO in carbon tetrachloride was reported to be three and four (3) but it was always four in hexane in the present study. In Table 1, the values of the extraction constants of cobalt(II) and nickel(II) perchlorate with TOPO in hexane are a little different from those reported in previous papers from our laboratory or those can be obtained by calculation of these previous data (4). The present values have been obtained after recalculation of new experimental data on the basis of Equation 3.

The extraction constants of alkali and alkaline earth perchrlorates with TOPO are higher when the radius of the metal ions are smaller. This agrees with the general tendency of the complex formation of these metal ions; the smaller the size, the more stable the complexes. The relatively high extraction constant of ammonium ion was explained in terms of hydrogen bond formation between the ion and TOPO in the previous paper (5). The poor extraction of magnesium(II) was explained (6) in terms of a stronger hydration of the solvated species with TOPO.

The extraction behavior of the perchlorates of divalent transition metal ions and also of trivalent metal ions in Table 1 is complicated although the solvation number of TOPO is always four. The extraction of nickel(II) perchlorate is inferior to all of the divalent metal perchlorates in Table 1. This can also be explained in terms of strong hydration of the solvated species of this metal ion with TOPO in the solvent extraction systems. The extraction of copper(II) is inferior to that of manganese(II), cadmium(II) and lead(II) and this is somewhat different from the general tendency found among the extractions of these metal ions as coordination complexes; copper(II) usually forms more stable complexes and extracted much better than these metal ions. It is marked that the extraction constants of alkaline earth ions are nearly similar to those of the divalent transition metal ions in the table. This is different from the general tendency of the stability and extractability of complexes of these metal ions in aqueous solutions.

TABLE 1 EXTRACTION CONSTANTS OF METAL PERCHLORATES FROM AQUEOUS 1 MOL DM^{-3} $NaClO_4$ SOLUTIONS WITH TRIOCTYLPHOSPHINE OXIDE IN HEXANE

Cation	Solvation Number	Log Kex	Ref.	Cation	Solvation Number	Log Kex	Ref.
H^+	2	3.15	7	Mn^{2+}	4	6.14	*
Li^+	3	2.29	8	Fe^{2+}	4	5.5	*
Na^+	3	1.01	9	Co^{2+}	4	4.91	*
K^+	3	0.57	8	Ni^{2+}	4	4.54	*
Rb^+	3,4	0.06,0.99	8	Cu^{2+}	4	5.81	*
Cs^+	3,4	-0.17,0.95	8	Zn^{2+}	4	5.41	1
Tl^+	3	2.01	*	Cd^{2+}	4	6.35	10
NH_4^+	3	1.78	5	Pb^{2+}	4	6.92	11
Be^{2+}	4	8.01	6	UO_2^{2+}	4	10.1	*
Mg^{2+}	4	4.99	6	Fe^{3+}	4	11.86**	*
Ca^{2+}	4	6.39	6	Ga^{3+}	4	ca. 7	*
Sr^{2+}	4	5.13	6	In^{3+}	4	9.57	*
Ba^{2+}	4	4.92	6	La^{3+}	4	8.20	*

* present work.

** From aqueous 4 mol dm^{-3} $(Na,H)ClO_4$ solutions.

CONCLUSIONS

From the extraction data of metal ions in aqueous sodium perchlorate solutions with trioctylphosphine oxide(TOPO) in hexane, the following conclusions are drawn. (i) For an accurate estimation of the extraction, correction for the decrease in the TOPO concentration due to coextraction of sodium perchlorate and perchloric acid is necessary. (ii) The solvation number is larger than in extractions of metal coordination complexes. It is four with trivalent and divalent metal ions and three with univalent ions. This can be reasonablly explained from the stand point that the extracted species are ion-pairs of solvated metal ions with TOPO and perchlorate anion, $[M(TOPO)_n]^{m+}(ClO_4^-)_m$. (iii) The order of extraction of the metal perchlorates is somewhat different from that of coordination complexes of these metal ions.

REFERENCES

1. H. Moriya and T. Sekine, Bull. Chem. Soc. Jpn., 45, 1626 (1972).
2. S.Kusakabe and T. Sekine, Bull. Chem. Soc. Jpn., 55, 1965 (1982).
3. M. H. Konstantinova, Dokr. Borg. Akad. Nauk, 30, 1431 (1977).
4. T. Sekine, R. Murai, and M. Iguchi, Nippon Kagaku Zasshi, 92, 412 (1971); R. Murai, S. Iwahori, and T. Sekine, Bull. Chem. Soc. Jpn., 50, 1315 (1977).
5. S. Kusakabe, H. Hishikura, and T. Sekine, Bunseki Kagaku, 31, E157 (1982).
6. S. Kusakabe and T. Sekine, Bull. Chem. Soc. Jpn., 54, 2930 (1981).
7. M. Niitsu and T. Sekine, J. Inorg. Nucl. Chem., 37, 1054 (1975).
8. S. Kusakabe and T. Sekine, Bull. Chem. Soc. Jpn., 51, 2087 (1980).
9. S. Kusakabe and T. Sekine, Bull. Chem. Soc. Jpn., 51, 1759 (1980).
10. R. Murai and T. Sekine, Bunseki Kagaku, 31, E413 (1982).
11. S. Kusakabe and T. Sekine, Bull. Chem. Soc. Jpn., 54, 2533 (1981).
12. T. Sekine, H. Honda, and Y. Zeniya, J. Inorg. Nucl. Chem., 38, 1347 (1976).

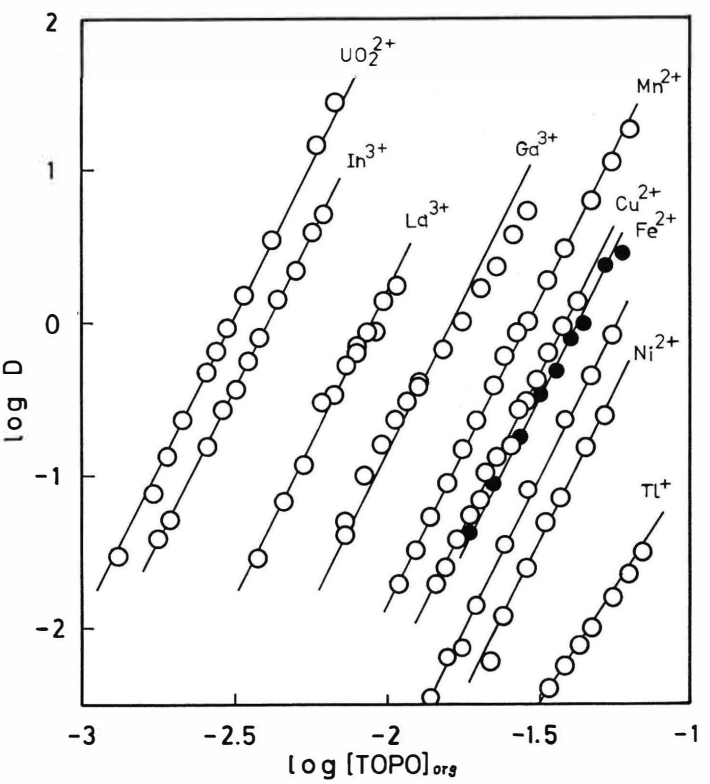

FIGURE 1 EXTRACTION OF METAL IONS WITH TRIOCTYLPHOSPHINE OXIDE IN HEXANE. AQUEOUS PHASE: 1 MOL DM^{-3} $NaClO_4$. THE CONCENTRATION OF TOPO AT EQUILIBRIUM IS CALCULATED BY EQUATION 3 BEING INTRODUCED THE EXTRACTION CONSTANT OF PERCHLORIC ACID AND SODIUM PERCHLORATE IN TABLE 1.

INFLUENCE OF ELECTRONIC STRUCTURE OF NEUTRAL NITROGEN-CARBONYL-CONTAINING COMPOUNDS ON THEIR REACTIVITY IN EXTRACTION PROCESSES

B. N. Lascorin, G. M. Chumakova, L. I. Rusin, V. S. Uljanov

All-Union Research Institute of Chemical Technology
State Committee on Utilization of Atomic Energy
Moscow, USSR

The aliphatic derivatives of nitrogencarbonyl-containing compounds such as amides of mono- and dicarboxylic acids or tetra-alcylurea find extensive application in various complex forming processes. Advantages of the compounds used in solvent extraction processes have been referred to (1 - 7). Therefor, a study on interrelation between the molecular structure of amides on the one hand and reactivity on the other hand appears to be important at the selection of an optimal extragent structure.

In order to reveal the influence of electronic and structural factors on the electrodonor ability of nitrogencarbonyl-containing compounds, extraction of nitric acid and uranyl nitrate has been investigated, the extraction being carried out by monoamides $RC(O)NR_2$, diamides $R_2NC(O)(CH_2)_nC(O)NR_2$ and urea $R_2NC(O)NR_2$ ($R = C_4H_9$).

The results of IR-spectra investigation, concerning amide extraction with nitric acid and uranyl nitrate, prove that the oxygen of the carbonyl group participates in the formation of a donor - acceptor bond.

The bilogarithmic dependence of distribution coefficients of nitric acid on the concentration of extragent as well as the analysis of the isotherms resulting from the extraction of nitric acid by 0.1M solutions of the compounds show that monoamides and tetrabutylurea extract HNO_3 as monosolvates. In case of diamide of amber and glutaric acids, complex formation of $(HNO_3)_2 \cdot B$-composition is possible in the organic phase besides the complex of $HNO_3 \cdot B$ -type (B is a molecule of the extragent).

By saturation and dilution methods it was established that disolvates were the extractable forms of uranium in case of monocaroxylic acid amides and tetrabutylurea, and mono- and disolvates in case of diamides.

According to the equations of nitric acid and uranium extraction by means of monocarboxylic acid amides and tetrabutylurea:

(1) $H^+_{aqua} + NO^-_{3\ aqua} + B_{org} \overset{\overline{K}}{\rightleftharpoons} (HNO_3 \cdot B)_{org}$

(2) $UO_{2\ aq} + 2NO^-_{3\ aq} + 2B_{org} \overset{\overline{K}}{\rightleftharpoons} [UO_2(NO_3)_2 \cdot 2B]_{org}$

and diamides of dicarboxylic acids:

(3) $H^+_{ac} + NO^-_{3\ aq} + B_{org} \overset{\overline{K}_1}{\rightleftharpoons} (HNO_3 \cdot B)_{org}$

(4) $2H^+_{aq} + 2NO^-_{3\ aq} + B_{org} \overset{\overline{K}_2}{\rightleftharpoons} [(HNO_3)_2 \cdot B]_{org}$

(5) $UO^{2+}_{2\ aq} + 2NO^-_{3\ aq} + B_{org} \overset{\overline{K}'}{\rightleftharpoons}{}^1 [UO_2(NO_3)_2 \cdot B]_{org}$

(6) $UO^{2+}_{2\ aq} + 2NO^-_{3\ aq} + 2B_{org} \overset{\overline{K}'_2}{\rightleftharpoons} [UO_2(NO_3)_2 \cdot 2B]_{org}$

effective extraction constants $\overline{K}$, $\overline{K}_1$, $\overline{K}_2$ and $\overline{K}'$, $\overline{K}'_1$, $\overline{K}'_2$ have been calculated (Table 1, 2).

Amides of monocarboxylic acids extract nitric acid and uranyl nitrate practically similarly ($\overline{K} \sim 0.05$, $\overline{K}' = 3.1 - 3.7$) (Table 1,2).

In case of dibutyl-aceto-amide the phenomena of hyper-conjugation of methyl and carbonyl groups take place, which explains the raised value of $\overline{K}$ equal 0.074 and $\overline{K}'$ equal 6.2.

At the values of $\overline{K}_1 = 0.059$ and $\overline{K}_2 = 0$ (Table 1) dibutyl amide of malonic ester can probably react with HNO_3 as a monodantate compound $RC(O)N(C_4H_9)_2$ in which radical $R = (C_4H_9)_2NC(O)CH_2$ influences the reactivity of carbonyl group of oxygen identically to the influence of $R \rightarrow C_4H_9$.

The longer the methylene bridge the more independent is each of C = O-groups, and a bicentral linkage of HNO_3 is possible.

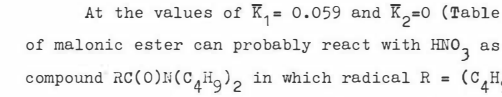

n=2.3

Due to independence of carbonyl groups, extraction ability of amber acid and glutaric acid diamides rises.

The comparison of the results presented in Table 2 shows that the presence of two carbonyl groups in amide molecule raises the extractive ability of the compounds in case of uranium. It is because the diamides in the complexes $UO_2(NO_3)_2$ are bidentate ligands. The monosolvate is likely to form the cycles:

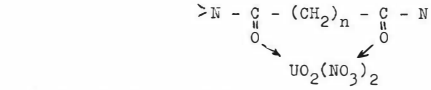

in the disolvate at least a molecule or two of diamide act as bidentate donors.

Presently it is accepted everywhere to regard reactivity of neutral extragents from the point of vew of thermod namic characteristics of the complexes with charge transfer, and in particular in studying intermolecular hydrogen bond (8).

For this purpose interactions of nitrogencarbonyl-containing compounds and phenol in tetrachloro-methane have been investigated using IR spectroscopy method.

The intermolecular hydrogen bond IR spectra in the range of 2000 - 4000cm^{-1} consist of a narrow frequency band ν_{free} that belongs to OH-group valent deviation of the "free" electronoacceptor and a broad frequency band ν_{ass} that corresponds to OH-group valent deviation associated with oxygen in carbonyl group of the electronodonor. As the ratio of the initial donor concentration and the initiel acceptor concentration rises, the optical dencity of the associated bond band increases and of the free bond band decreases, which proves the increased number of molecules in the complex and is characteristic of intermolecular hydrogen bond.

On the basis of the study of frequecy shift $\Delta\nu = \nu_{free} - \nu_{ass}$ and the change in the maximal intencity of absorption band, thermodynamic parameters for interaction of carbonyl-containing compound with phenol have been determined. The enthalpy values have been determined according to Jogansen's equation (9), the equilibrium constants for complex formation with the composition 1 : 1 -

according to the method of Benesi- Hildebrand (10) (Table 3).

For the compounds with one or two alkyl amide groups (Table 3, nos.5 - 14) values ΔG, ΔH, ΔS are practically constant and equal $-\Delta G = 2.6 \pm 0.1$, $-\Delta H = 5.7 \pm 0.1$, $-\Delta S = 10.3 \pm 0.5$. It follows that in the monocarbonyl-containing molecules participating in the formation of intermolecular hydrogen bond, one group NR_2 as substituent is sufficient for realization of electrodonor ability of fragment C = O displayed by values ΔG and ΔH. Be an alkyl or a second alkyl amide group present in $XC(O)NR_2$ structure, disregarding the length of hydrocarbon radical, it would have no influence on thermodynamic parameters of intermolecular hydrogen bond . If X is an alkoxy-radical (Table 3, no.2), there will be an evident acceptor influence on the electron dencity of carbonyl oxygen atom, which shows in decreasing ΔG and ΔH as compared with X = R or NR_2.

Approximation of the experimental results through linear functions proved that the reactions with monocarbonyl-containing compounds corresponded to the equation:

(7) $\Delta G = 0.63\Delta H + 0.98$ (r = 0.966, s = 0.15, n = 14)

and the reactions with dicarbon tetraalkyldiamide acids to:

(8) $\Delta G = 0.76\Delta H + 1.28$ (r = 1.0, s = 0, n = 3)

In accordance with corelation parameters, interrelations of compounds studed, together with a standard electronoacceptor such as phenol, have an isoequilibrium character.

An attempt to use thermodynamic characteristics of intermolecular hydrogen bond for a quantitative discription of solvent extraction type processes is logical because the energy parameters of complexes with charge transfer and reactions with intermolecular hydrogen bond formation are in agreement.

Dependence of ΔG values, at intermolecular hydrogen bond formation of extragents with phenol (Table 3), on the values of extraction constants of nitric acid and uranyl nitrate (Table 1 - 2) in tetrachloro-methane can be plotted as:

(9) $\lg K_{HNO_3} = -0.87\ G - 3.58$ (r = 0.962, s = 0.14, n = 9)

(10) $\lg K_{UO_2(NO_3)_2} = -2.02\ G - 4.88$ (r = 0.967, s = 0.12, n = 8),

where $K_{HNO_3} = \bar{K}, \bar{K}_1$, $K_{UO_2(NO_3)_2} = \bar{K}', \bar{K}'_2$.

The correlations of (9) - (10) type point, above all, to uniform character of complex formation mechanism, and thermodynamic characteristics of intermolecular hydrogen bond can be used for modelling and prediction of extraction ability in case of nitrogencarbonyl-containing compounds.

Table 1

VALUES OF EFFECTIVE CONSTANTS OF 0.1M NITRIC ACID EXTRACTION BY AMIDE SOLUTIONS IN CCl_4 AT ACIDITY OF AQUEOUS PHASE 1M-4M HNO_3

$XC(O)N(C_4H_9)_2$ where X is:	$(\bar{K} \pm \Delta\bar{K})\ 10^2$	$(\bar{K}_1 \pm \Delta\bar{K}_1)10^2$	$(\bar{K}_2 \pm \bar{K}_2)10^3$
CH_3	7.4± 2.0		
C_4H_9	5.8±0.3		
C_7H_{15}	5.5±0.4		
C_8H_{17}	5.5±0.5		
C_9H_{19}	5.8±0.3		
$(C_4H_9)_2$- (TBU)	4.9±0.9		
$(C_4H_9)_2NC(O)CH_2$ TBMA		5.9±0.3	0
$(C_4H_9)_2NC(O)(CH_2)_2$ TBAA		12.8±0.7	1.9±0.8
$(C_4H_9)NC(O)(CH_2)_3$ TBGA		17.4±3	5.9±5.2

Table 2

VALUES OF EFFECTIVE CONSTANTS OF URANYL NITRATE BY 0.1M AMIDE SOLUTIONS IN CCl_4 FROM 1M HNO_3

$XC(O)N(C_4H_9)_2$ where X is:	$\bar{K}' \pm \Delta\bar{K}'$	$\bar{K}'_1 \pm \Delta\bar{K}'_1$	$\bar{K}'_2 \pm \Delta\bar{K}'_2$
CH_3	6.2 ± 0.5		
C_4H_9	3.2 ± 0.7		
C_7H_{15}	3.3 ± 0.4		
C_8H_{17}	3.7 ± 0.5		
C_9H_{19}	3.6 ± 0.3		
TBU	2.5 ± 0.3		
TBMA		49 ± 19	-
TBAA		3.3 ± 1.0	34 ± 16
TBGA		5.1 ± 2	36 ± 13

Table 3

SPECTROSCOPIC PARAMETERS AND THERMODYNAMIC CHARACTERISTICS OF COMPLEX FORMATION OF CARBONYL-CONTAINING COMPOUNDS WITH PHENOL IN CCl_4

Electronodonor	K, M^{-1}	$-\Delta G$ (kilocal/mol)	$-\Delta S$ (kilocal/mol)	$-\Delta S$	$\Delta\nu$ cm^{-1}
1. $C_4H_9OC(O)C_4H_9$	5.35±0.73	0.99	3.6	8.8	158
2. $C_4H_9C(O)OC_4H_9$	13.6±0.4	1.54	3.8	7.6	171
3. $C_4H_9C(O)C_4H_9$	20.6±5.2	1.79	4.0	7.4	181
4. $C_4H_9C(O)CNC_4H_9$	36.6±1.9	2.13	5.2	10.4	287
5. TBU	94.9±2.8	2.69	5.9	10.7	352
6. $C_3H_7C(O)N(CH_3)_2$	61.2±8.9	2.43	5.5	10.7	330
7. $CH_3C(O)N(CH_3)_2$	85.6±3.2	2.63	5.9	11.1	355
8. $C_3H_7C(O)N(C_6H_{13})_2$	84.4±12	2.62	5.7	10.4	331
9. $CH_3C(O)N(C_4H_9)_2$	127±19	2.86	6.0	10.4	367
10. $C_3H_7C(O)N(C_4H_9)_2$	68.6±4.8	2.50	5.7	10.7	334
11. $C_4H_9C(O)N(C_4H_9)_2$	78.7±7.7	2.58	5.7	10.4	335
12. $C_7H_{15}C(O)N(C_4H_9)_2$	103±0.8	2.74	5.7	9.9	337
13. $C_8H_{17}C(O)N(C_4H_9)_2$	90.4±2.7	2.66	5.7	10.1	335
14. $C_9H_{19}C(O)N(C_4H_9)_2$	92.8±7.1	2.68	5.7	10.1	338
15. TBMA	112.3±13.0	2.79	5.4	8.8	305
16. TBAA	197±22.6	3.12	5.9	9.1	354
17. TBGA	221±19	3.19	5.8	9.1	347

REFERENCES

1. T.H. Siddall, J. Inorg. Nucl. Chem., 29. 1, 149, (1967)
2. T.H. Siddall, J. Phys. Chem., 64. 12, 1863, (1960)
3. T.H. Siddall, J. Inorg. Nucl. Chem., 25, 7, 833, (1963)
4. E.K. Dukes, T.H. Siddall, J. Inorg.Nucl.Chem.,28, 10,2307,(1966
5. V.S. Sokolov, Radiohimija, 11, 5, 535, (1969)
6. V.S. Shmidt, V.S. Sokolov, Radiohimija, 11, 5, 525, (1969)
7. G.M. Chumakova, V.V. Jakshin, E.A. Filippov, B.N. Laskorin, Radiohimija, 22, 2, 213, (1980)
8. V.V. Jakshin, B.N. Sharapov, B.N. Laskorin, Himija Urana, Nauka, M., p. 425, (1973)
9. A.V. Jogansen, B.V. Rassadin, J. Priklad. Spektroskopii, 11, 828, (1969)
10. H.A. Benesi, J.H. Hildebrand, J. Am. Chem. Soc., 71,2703,(1949)

ION-PAIR DISTRIBUTION OF ORGANIC COMPOUNDS IN SOLVENT EXTRACTION AND HIGH-PERFORMANCE LIQUID CHROMATOGRAPHY

Göran Schill

Department of Analytical Pharmaceutical Chemistry
University of Uppsala, Biomedical Center
P.O. Box 574
S-751 23 Uppsala, Sweden

In the traditional liquid-liquid extraction procedures, organic substances are distributed in uncharged form and the extraction degree is regulated by the properties of the organic solvent or, if the substances are protolytes, by pH of the aqueous phase. An important improvement of the flexibility and selectivity can be achieved if complex-forming agents participates in the distribution equilibrium. This approach, furthermore, is the only possibility when the compounds are charged or very hydrophilic.

Ion-pair extraction is a method for extraction of ionic compounds with the aid of a complexing agent of the opposite charge. The technique was used already in the 1940s for determination of amines using sulfonephtaleins (1). The approach was at that time empirical and systematic studies for the characterization of the systems by determination of distribution parameters were started only in the early 1960s (2-5). The increasing knowledge of the parameters that govern the ion-pair distribution equilibria has since then been a necessary background for the successful development of applications with this technique.

During the last decade the ion-pairing processes have found a widespread use in modern liquid chromatography, and they have proved to be very useful in improving the flexibility and selectivity of systems for separation of both anionic and cationic substances. Several reviews have been published on this topic (6-10).

ION-PAIR EXTRACTION

A charged solute HA^+ is distributed between a phase of high polarity (aqueous) and a phase of low polarity (organic) together with an ion of the opposite charge, a counter ion, X^-. The degree of ion-pair formation is usually high in the organic phase and the distribution equilibrium can then be illustrated by the process:

(1) $$HA^+_{aq} + X^-_{aq} \rightleftharpoons HAX_{org} \quad (\text{equil. constant: } K_{ex(HAX)})$$

The extraction constant expresses the combined effect of the phase transfer and the ion-pair formation.

The distribution ratio of HA^+, D_{HA}, depends, if no side reactions occur, on the magnitude of the extraction constant, $K_{ex(HAX)}$, and the concentration of the counter ion, X^-, in the aqueous phase.

(2) $$D_{HA} = \frac{[HAX]_{org}}{[HA^+]} = K_{ex(HAX)} \cdot [X^-]$$

EXTRACTION CONSTANTS

The value of the extraction constant changes with the properties of the counter ion and the organic phase (11). This gives almost unlimited possibilities to regulate the distribution ratio. An illustration of the width of variation is given in Table 1, which shows the influence of the counter ion on the extraction constant of a cationic compound, tetrabutylammonium, in a chloroform-water system.

Table 1

Extraction constants of tetrabutylammonium ion pairs

Organic phase: chloroform

Class	Anionic compound (X^-)	log $K_{ex(HAX)}$
Inorganic	Cl^-	-0.11
	Br^-	1.29
	NO_3^-	1.39
	I^-	3.01
	ClO_4^-	3.48
Carboxylate	acetate	-2.1
	phenylacetate	0.27
	3-hydroxybenzoate	-1.54
	benzoate	0.39
	salicylate	2.42
Phenolate	phenolate	0.05
	picrate	5.91
	2,4-dinitro-1-naphtholate	6.45
Sulfonate	toluene-4-sulfonate	2.33
	naphthalene-2-sulfonate	3.45
	anthracene-2-sulfonate	5.11
Sulfate	3-phenylpropyl sulfate	4.20
	2-naphthyl sulfate	4.90
"Acid dye"	methyl orange	5.47
	bromothymol blue	8.0
	hexanitrodiphenylamine	9.6

Ion-pair extraction has been studied systematically for almost two decades, but the number of systems that have been investigated in detail is fairly limited. Generalization of the observations is difficult due to the fact that the strength of the binding within the ion pair depends both on the structure of the ions and on the properties of the nonpolar phase (11). Prediction systems similar to those used for uncharged molecules have so far not been designed, and conclusions about the relationships between structures and constants must, in most cases, be kept on a qualitative level. Some examples are given below.

Within homologous series of anionic or cationic compounds, log K_{ex} increases by 0.5 - 0.6 units with the addition of one CH_2. The nature of the ionized group has a considerable influence on the distribution properties of the ion pair. The extraction constant of organic anions with the same content of alkyl or aryl carbons (and no other polar groups) increases in the order carboxylate < sulfonate < sulfate, while the extraction constant of ion pairs of alkylammonium ions with hydrogen-accepting anions usually increases in the order quaternary < primary < secondary < tertiary, when $CHCl_3$ or CH_2Cl_2 are used as extracting solvents. The order may change in hydrogen-accepting solvents as shown in Figure 1 (12) With ethyl acetate and methylisobutyl ketone there is a considerable decrease in K_{ex} for the tertiary and quaternary ammonium ions while the constant of the secondary ammonium ion remains almost unchanged owing to its higher ability to form hydrogen bonds with the hydrogen-accepting solvents. The non-hydrogen- bonding counter ion perchlorate in Figure 1 C gives a deviating extraction pattern.

Highly hydrophilic substituents, such as hydroxylic, carboxylic and amino groups, decrease the extraction constant by 1 - 2 log units when the organic phase is chloroform or a similar solvent. The decrease can be considerably smaller when the organic phase is strongly hydrogen-bonding, e.g. pentanol.

INFLUENCE OF ASSOCIATION AND DISSOCIATION PROCESSES

The extraction of ion pairs can be influenced by different kinds of secondary equilibria. Some of these processes, such as protolysis in the aqueous phase and complex formation in the organic phase can be regulated by an external agent. Other secondary equilibria such as association or dissociation in the organic phase, which only comprise the extracted compound, have an influence that changes with the concentration of the compound. Processes of this kind might limit the use of the extraction processes but disturbances can often be avoided by a proper choice of conditions.

When an ion pair extraction process is influenced by side-reactions it is convenient to express the equilibrium by a conditional equilibrium constant K^*_{ex}, defined by:

(3) $$K^*_{ex(HAX)} = \frac{C_{HAXorg}}{C_{HA^+} \cdot C_{X^-}} = K_{ex(HAX)} \cdot \frac{\alpha_{HAX}}{\alpha_{HA^+} \cdot \alpha_{X^-}}$$

The α-coefficients compensate for the additional equilibrium processes.

DISSOCIATION OF AN ION PAIR IN THE ORGANIC PHASE

The ion pair is an association complex and its stability depends on the nature of the binding forces between the ions and the dielectric properties of the solvent. The influence of the dissociation of HAX can be expressed by the dissociation constant:

(4) $$K_{diss(HAX)} = \frac{[HA^+]_{org} \cdot [X^-]_{org}}{[HAX]_{org}}$$

which combined with equation (3) gives:

(5) $$K^*_{ex(HAX)} = K_{ex(HAX)} \cdot \left(1 + \left(\frac{K_{diss(HAX)}}{K_{ex(HAX)} \cdot [HA^+] \cdot [X^-]}\right)^{\frac{1}{2}}\right)$$

The dissociation constants increase with increasing dielectric constant of the organic phase when the binding forces are mainly of electrostatic character. Some examples are given in Table 2.

Ion-pair dissociation in the organic phase can, as indicated by equation (5), be utilized for improvement of the extraction in the low concentration range (11,13). The extraction of the counter ion with other sample ions might, however, partly suppress the dissociation and limit the increase of the distribution ratio. An example is given in Figure 2 which shows the extraction of a hydrophobic quaternary ammonium compound (N-methylamitriptyline) as dihydrogenphosphate ion pair with 1-pentanol as extracting solvent. The suppressing effect increases with decreasing pH due to the higher extraction of phosphoric acid (14).

Measures must always be taken to stabilize the ion-pair dissociation in

Table 2

Dissociation constants of picrates in different organic solvents

Organic solvent	Dielectr. const.	Cation: Choline		Cation: Trimethylethylammonium	
		$\log K_{ex(HAX)}$	$-\log K_{diss(HAX)}$	$\log K_{ex(HAX)}$	$-\log K_{diss(HAX)}$
1-Pentanol	13.9	1.19	3.02	1.24	2.76
Methylisobutyl ketone	13.1	0.98	3.28	0.64	3.17
Ethyl acetate	6.0	0.69	5.68	0.45	5.27

ion-pair liquid chromatography where it is imperative that the distribution ratio of the analyte is independent of its concentration.

DIMERIZATION OF AN ION PAIR IN THE ORGANIC PHASE

Ion pairs might in the organic phase form higher aggregates (dimers, tetramers, etc.), which results in an increase of the conditional extraction constant. The dimerization constant

$$(6) \qquad K_{2(HAX)} = \frac{[H_2A_2X_2]_{org}}{[HAX]^2_{org}}$$

combined with equation (3) gives:

$$(7) \qquad K^*_{ex(HAX)} = K_{ex(HAX)}(1 + 2K_{2(HAX)} \cdot K_{ex(HAX)} \cdot [HA^+] \cdot [X^-])$$

Ion pairs of quaternary alkylammonium ions with halides, sulfonates or picrate have in chloroform dimerization constants of 10 to 10^2, while the ion pairs of these anions with primary and secondary ammonium ions have $K_{2(HAX)} = 10^3 - 10^4$ (11). The higher dimerization tendency of the latter kind of ion pairs might be due to their hydrogen-donating ability.

ION-PAIR FORMATION IN THE AQUEOUS PHASE

Ion-pair formation might also occur in the aqueous phase, but the tendency is, as a rule, rather low owing to the high dielectric constant of the medium.

Introduction of the ion-pair formation constant:

$$(8) \qquad K_{a(HAX)} = \frac{[HAX]}{[HA^+] \cdot [X^-]}$$

gives the following expression for the conditional constant:

$$(9) \qquad K^*_{ex(HAX)} = \frac{K_{ex(HAX)}}{(1 + K_{a(HAX)} \cdot [X^-]) \cdot (1 + K_{a(HAX)} \cdot [HA^+])}$$

Ion-pair formation studies presented in the literature have shown that small organic ions as a rule have $K_a < 10$, which means that ion-pair formation hardly has a significant effect on the distribution at an ion concentration lower than 0.01 M.

A considerably higher tendency to ion-pair formation in aqueous solution has been observed between certain hydrophobic components such as anions of bile acids and symmetrical quaternary alkylammonium ions. The ion-pair formation constant increases strongly with the alkyl content of the cation which indicates a significant hydrophobic interaction (15).

MECHANISM OF ION-PAIR EXTRACTION

Ion-pair extraction has so far been described by an equilibrium expression that only gives the starting material and the end product. The process includes, however, at least two steps: the transfer between the two liquid phases and the formation of the ion pair. Mechanistic features of the extraction process such as the site for the formation of ion pairs cannot be elucidated by constants for the ion-pair formation or dissociation since they will illustrate prevailing equilibria in the system only. A better understanding of the ion-pair extraction can be achieved by measurements of the transfer rate for the ion-pair components between the phases.

It has been observed that the transfer rates from the aqueous into the organic phase can be at least about 100 times higher when the degree of ion pair formation is low than when it is high. The fact that a low degree of ion-pair formation increases the transfer rate indicates that the extraction process comprises a fast transfer of the ions to the organic phase and a slower ion-pair formation in that phase. The process can be described by the model given in Figure 3 (16,17).

The studies behind this model have been made with a quaternary ammonium compound and bromide as ion pair components using methylene chloride as organic phase. The validity of the model for other kinds of ions and organic phases has so far not been tested.

COMPLEX FORMATION IN THE ORGANIC PHASE

A systematic change of the distribution ratio can be achieved by combining the partition process with a complexation to a hydrophobic agent in the organic phase.

When a cationic compound, HA^+, is extracted with a counter ion, X^-, in the aqueous phase and an uncharged complexing agent, S, in the organic phase, ion-pair complexes are formed in the organic phase as illustrated by:

$$(10) \qquad HAX_{org} + nS_{org} = HAX.S_{n,org} \qquad (\text{equil. const.: } K_n)$$

If $HAX.S_n$ dominates in the organic phase, the distribution ratio of HA^+ is given by:

$$(11) \qquad D_{HA} = K_{ex(HAX)} \cdot K_n \cdot [X^-] \cdot [S]^n_{org}$$

D_{HA} can then be regulated by the nature and concentration of both S and X^-.

The influence of complexation on ion-pair extractions has been studied in numerous cases, mainly with lipophilic alcohols as complexing agents (cf. (11, 18,19)).

A high extraction selectivity can be obtained by use of structure-specific adduct-forming agents such as cyclic polyethers (crown ethers). Dibenzo-18-crown-6 gives highly stable 1:1-complexes with ion pairs containing primary ammonium ions, while ammonium ions with a higher degree of substitution have rather small complex constants. The effect is illustrated in Figure 4. Two cations, octylammonium and trimethylnonylammonium, are extracted into chloroform as ion pairs with salicylate. Addition of the crown ether gives a large increase of the distribution ratio of the primary ammonium ion pair while the distribution of the quaternary ammonium ion pair is affected to a much smaller extent (20).

EXTRACTION OF HYDROPHILIC IONS

Hydrophilic organic ions are difficult to extract into an organic phase of low polarity, and highly hydrophobic counter ions have to be used to get an extraction constant of sufficient magnitude. However, the possibilities of increasing the degree of extraction by use of highly hydrophobic counter ions are limited since the available concentration of the counter ion in the aqueous phase decreases when its hydrophobic character increases, owing to decreasing solubility. A highly hydrophobic counter ion is also prone to be extracted as ion pair with other hydrophilic components in the aqueous phase (e.g. buffer ions).

A more efficient way of increasing the extraction of a hydrophilic ion is to use protolytic, hydrophobic agents that can act both as counter ions and complex-forming agents. The principle is demonstrated in the following example where HA^+ represents the hydrophilic ion and HX the hydrophobic extracting agent.

$$(12) \qquad HA^+_{aq} + nHX_{org} = HAX.(HX)_{n-1,org} + H^+_{aq}$$

If this ion-pair complex dominates in the organic phase, the distribution ratio is given by:

$$(13) \qquad D_{HA} = \frac{K_{ex(HAX)} \cdot K_{n-1} \cdot [HX]^n_{org} \cdot K'_{HX}}{K_{D(HX)} \cdot a_{H^+}}$$

$K_{D(HX)}$ is the distribution constant of HX, K'_{HX} its acid dissociation constant, while K_{n-1} is the formation constant of the complex between the ion pair and the extracting agent in uncharged form (21-23).

Alkylphosphoric acids, such as bis-(2-ethylhexyl) phosphoric acid (HDEHP), are typical examples of powerful, protolytic extractants which can be used for the extraction of aminoalcohols and aminophenols of low molecular weight. In the optimum pH-range, and with a HDEHP concentration of 0.1 M, ion-pair complexes containing one anion and two uncharged molecules of HDEHP are extracted. This means that groups containing in all 48 alkyl carbons are coupled to the cation and this permits a quantitative extraction into chloroform of such hydrophilic compounds as adrenaline, synephrine and isoproterenol (24,25).

ION-PAIR EXTRACTION AS MEANS FOR PHOTOMETRIC OR FLUORIMETRIC QUANTITATION

Organic ions without inherent light-absorbing or fluorescent properties can be quantified by fluorimetry or photometry after extraction as ion pairs with counter ions with suitable optical properties. The method, which can be applied to anionic as well as cation compounds, requires a thorough knowledge of the distribution properties of the ion-pair components.

The determination of an alkylammonium ion, HA^+, as ion pair with a UV-absorbing, aprotic counter ion, Y^-, can be used as an illustration. The extraction ratio of HA^+ as ion pair with Y^-, D_{HAY}, is given by:

$$(14) \qquad D_{HAY} = K_{ex(HAY)} \cdot \frac{a_{H^+}}{a_{H^+} + K'_{HA} \cdot (1 + K_{D(A)})} \cdot [Y^-]$$

$D_{HAY} \geq 100$ is required for a quantitative determination when the phase volumes are equal. The yield will decrease with increasing pH when $a_{H^+} \leq 100 \cdot K'_{HA} \cdot (1 + K_{D(A)})$ but this can be compensated for by using a more hydrophobic counter ion or a higher counter ion concentration.

Reagents suitable for determination of organic cations are presented in Table 3 (26-28). A pure reagent is a pre-requisite for good results: the reagents are used in high excess and even a low degree of impurity can give serious errors.

Table 3

Reagents for quantitation of cations by ion-pair extraction

Organic phase: chloroform or methylene chloride

Reagent	Quantitation technique	pH	Minimum alkyl-ammonium ion	Sensitivity (mol/L)
Dipicrylamine	photometry	11-14	4	$8 \cdot 10^{-6}$
Bromothymol blue	"	7.5-11	8	$5 \cdot 10^{-6}$
Picric acid	"	6.5-12	11	$1.5 \cdot 10^{-5}$
Methylorange	"	2-13	14	$2 \cdot 10^{-5}$
Dimethoxyanthacene-2-sulfonic acid	fluorimetry photometry	2-13	14	$2 \cdot 10^{-8}$ $2 \cdot 10^{-6}$
Anthracene-2-sulfonic acid	fluorimetry photometry	1-13	15	$3 \cdot 10^{-8}$ $2 \cdot 10^{-6}$
Naphthalene-2-sulfonic acid	photometry	1-13	18	$2 \cdot 10^{-5}$

ION-PAIR CHROMATOGRAPHY

The ion-pair distribution technique is applicable to both liquid-liquid and liquid-solid chromatography. The distribution of the charged analyte between the mobile and the stationary phase, which decides its retention, is in principle governed by the same means as in liquid-liquid extraction, but different approaches must be used when the solid phase acts as adsorbent and as support for a liquid stationary phase (29-33).

Ion-pair chromatography is normally performed in the high-performance mode with a solid phase of porous particles with a low mean diameter (5 or 10 µm). The particles are usually made from silica, which is a strong adsorbent for hydrophilic compounds. Hydrophobic solid phases are obtained by reacting the silica with alkyl or aryl silanes. A liquid stationary phase can usually be applied by injecting small amounts until the support is saturated, i.e. the pores are filled.

LIQUID-LIQUID SYSTEMS

The design of typical liquid-liquid systems and the methods for control of the capacity ratio is outlined in Table 4. Changes of the distribution ratio can be made both by the counter ion and by the polar solvent component in the organic phase, which gives an almost unlimited number of possibilities to regulation of the capacity ratio. It must be emphasized that the systems can be used both in the straight phase mode, i.e. with an aqueous stationary phase, and in the reversed phase mode with an organic solvent as the stationary phase. In the straight phase systems, the sample ion migrates as an ion pair, in the reversed phase systems it is retained as an ion pair.

Table 4

Liquid-liquid ion-pair chromatography: regulation of capacity ratio (k')

Analyte: HA^+

$$k'_{HA} = \frac{V_{stat}}{V_{mob}} \cdot \frac{(C_{HA})_{stat}}{(C_{HA})_{mob}}$$

Phase	Composition	Binding to organic phase is increased by
Organic	polar agent (S) in nonpolar solvent (L)	increasing content and polarity of S
Aqueous	counter ion (X^-) in buffer	increasing content and hydrophobicity of X^-

L and S slightly soluble in water

In reversed phase systems, the organic stationary phase is coated on a hydrophobic adsorbent. The demands for long-term stability makes the choice of organic liquid rather limited, but hydrogen-bonding solvents such as higher alcohols and nitriles have shown suitable properties (34,35). Highly hydrophilic samples will in 1-pentanol-water systems get a rather low retention even in the presence of a counter ion of high hydrophobicity. The strongly hydrogen-bonding tributylphosphate is often suitable as liquid stationary phase in such cases and gives stable systems with high selectivity for e.g. catecholamines (36).

In straight phase systems, the stationary phase is aqueous, coated on a hydrophilic adsorbent. The choice of organic phase is very free and mainly limited by the fact that it should have a low solubility in the aqueous phase. The retention can often be regulated by a change of the content of a polar component in the eluent as demonstrated in Figure 5 (37). The solutes are amines with different degrees of substitution, which migrate with the mobile organic phase as ion pairs with the counter ion, naphthalene-2-sulfonate, applied in the stationary aqueous phase. The mobile phase is a mixture of chloroform and 1-pentanol and the retention decreases with increasing content of the polar component, 1-pentanol. The relation between log k' and log of the pentanol concentration is linear, and the slope of the line increases with increasing degree of substitution at the amino group, which means that the separation selectivity changes with the pentanol content.

A further improvement of the separation selectivity might be possible in systems where the samples can migrate both as ion pairs and in uncharged form. When a weak acid, HX, migrates in a system with an organic liquid as stationary phase and a buffered solution of a quaternary ammonium ion, Q^+, as the mobile phase, its capacity ratio, k'_{HX}, is given by:

$$(15) \quad k'_{HX} = \frac{V_s}{V_m} \cdot \frac{[HX]_{org}+[QX]_{org}}{[HX] + [X^-]} = \frac{V_s}{V_m} \cdot \frac{(K_{D(HX)} \cdot a_{H^+})+(K_{ex(QX)} \cdot [Q^+] \cdot K'_{HX})}{(K'_{HX} + a_{H^+})}$$

K'_{HX} and $K_{D(HX)}$ are the acid dissociation constant and the distribution ratio of the acid. The change of k' with pH is highly specific for each acid since it depends on properties that are related to the structure (38).

LIQUID-SOLID [illegible]

Liquid-solid ion-pair chromatography is so far mainly performed with solid phases of surface-modified silica carrying alkyl or aryl groups that act as hydrophobic adsorbents.

One of the major differences between a liquid-liquid and a liquid-solid system concerns the capacity of the retaining phase. In a liquid-liquid system it can usually be assumed that the capacity of the stationary liquid phase is unlimited and no change of its properties will occur during a normal chromatographic run. The adsorbing stationary phase in a liquid-solid system has, on the other hand, a limited capacity and this will have influence both on the separating efficiency of the system and on the methods for regulation of the retention.

The liquid-solid systems with hydrophobic solid phase and aqueous eluent are highly suitable for separation of charged compounds by ion-pair distribution technique. Models for the retention can be based on the following principles.

1. When solute ions are transferred to the solid phase, electroneutrality is maintained by a simultaneous transfer of a counter ion or displacement of an ion of the same charge.

2. Ionic solutes and ionic components in the eluent compete for the limited number of binding sites on the adsorbing surface.

The principles are summarized in the following expression for the capacity ratio of a solute, HA^+. The ionic components in the eluent are X^- and Q^+, and the solute occupies a very small fraction of the binding capacity.

$$(16) \quad \log k'_{HA} = \log K^o \cdot q + \log K_{HAX} \cdot [X^-] - \log (1 + K_{QX} \cdot [Q^+] \cdot [X^-])$$

This simplified expression is based on the assumption that the adsorbent has a homogenous surface. K_{HAX} and K_{QX} are the extraction constants of HA^+ and Q^+ as ion pairs with X^-, defined in analogy with equation (1). q is the phase volume ratio: g of adsorbent /mL of mobile phase in the column. The influence of uncharged compounds is omitted to simplify the equation. K^o is the capacity of the adsorbent (moles/g).

The capacity ratio increases with increasing extraction constant of the solute and increasing counter ion concentration, in agreement with the general principles for ion-pair chromatography. The adsorption of the solute is counteracted by the adsorption of ionic eluent components with the same charge, in the present case represented by $[Q^+]$. Uncharged components in the eluent can have an analogous influence. The consequence of this relationship is illustrated in Figure 6 which shows the effect of a change of the counter ion concentration. The solutes are anions of carboxylic acids and the competing component in the mobile phase is dihydrogenphosphate ion. Increase of the concentration of the counter ion, tetrabutylammonium, influences the adsorption of both sample and competing ion, which results in a curved relationship.

The liquid-solid systems are also suitable for separation of polyvalent, organic ions and efficient separations can be performed of substances of widely varying charge. An example is given in Figure 7 which shows a separation of a series of oligonucleotides with charges of -1 to -4 with tetramethylammonium as counter ion (39).

EFFECTS OF COMPETING IONS IN LIQUID-SOLID SYSTEMS

The means commonly used for regulation of the retention are summarized in Table 5. One of the parameters for regulation of k' is of particular importance: the competing ion $[Q^+]$ which has an effect that is specific for the liquid solid systems.

Table 5

Liquid-solid ion-pair chromatography: regulation of k'

Sample: HA^+

Adsorbent	Mobile phase	k' is increased by
Nonpolar	counter ion (X^-) and competing ion (Q^+) in aqueous buffer containing a polar organic solvent (S)	1. increasing content and hydrophobicity of X^- 2. decreasing content and hydrophobicity of Q^+ 3. decreasing content of S 4. increasing hydrophobicity of adsorbent

The competing effect can be utilized not only for regulation of the retention but also for change of the separation selectivity when the sample components are affected to a different extent by the competing agent. Of even higher importance is, however, its use for improvement of the separation efficiency as demonstrated in Figure 8. Hydrophobic ions do not show good chromatographic behaviour in simple ion pair system with hydrophobic solid phase and aqueous mobile phase. The retention is very high and the peaks tail strongly. This indicates an overloading of the system, i.e. the amount of adsorbed ion pair is too large compared with the capacity of the adsorbent,

which gives rise to changes of k' with the concentration of the sample. The problem can be solved by adding a strongly competing ion, dimethyloctylammonium, to the mobile phase. It decreases the binding of the sample ion pair to the adsorbent, and good peak symmetry is achieved.

AMPLIFICATION OF DETECTION

One of the advantages of ion-pair chromatography is the considerable increase of the detector response that can be obtained by a proper choice of counter ion. The method has so far mainly been applied to photometric detectors where the ion-pair chromatographic technique offers possibilities to a high detector response even for non-UV-absorbing compounds by using a counter ion of high molar absorptivity at the measuring wavelength.

When the method is used in straight phase systems, an aqueous solution of the detectable counter ion is applied as stationary phase on a hydrophilic support. A sample ion migrates with the organic mobile phase as an ion pair and detector response is obtained owing to the detectable properties of the counter ion. Amines, amino acids and dipeptides have been determined by this technique in amounts down to 0.1 nmoles with naphthalene-2-sulfonate as counter ion and silica as support (37,40).

For detection of non UV-absorbing anions it is advantageous to use a quaternary ammonium compound as counter ion, since its charge is independent of pH. Silica is unsuitable as support for the stationary aqueous phase due to its strong interaction with quaternary ammonium ions, but a system with good properties can be obtained if a surface-modified silica carrying alkanediol chains is used as support. With the highly UV-absorbing N,N-dimethylprotriptyline as counter ion it is possible to detect down to 0.03 nmoles of different kinds of anions such as halogenides, alkylsulfonates, alkylsulfates and carboxylates (41).

Reversed-phase systems that enable detection and quantification of nanogram amounts of non-UV-absorbing charged and uncharged compounds by UV detection have also been developed (42-45). The mobile phase is a buffered solution of a highly UV-absorbing or fluorescent ion, while hydrophobized microparticulate silica is used as stationary phase. Injection of samples in the system gives rise to two kinds of migrating zones: one zone for each of the sample components and one zone that is charateristic for the chromatographic system.

Solutes give rise to positive or negative peaks depending on their charge and retention relative to the detectable ion. The response is independent of the nature and concentration of other sample components. Quantifications can be based on height or area of the peaks independent of their direction. The highest sensitivity is obtained when the solute and the detectable ion have approximately equal retention. Systems have been developed that enable detection of compounds of widely different hydrophobicity, uncharged substances as well as organic and inorganic ions. It is possible to quantify down to 20 nmoles of charged compounds while the response for uncharged substances seems to be somewhat lower.

SEPARATION OF ENANTIOMERIC IONS

Enantiomers can be resolved by distribution as ion pairs in liquid-liquid systems with an optically active complexing agent in the mobile phase. Cram and co-workers have developed excellent methods for primary amines and esters of amino acids with crown compounds as complexing agents (46-49), while Prelog et al. (50) have used esters of tartaric acid as complexing agent for separation of α-aminoalcohols.

The resolution of enantiomeric ions can also be based on chromatographic separation of diastereomeric ion pairs formed with a chiral counter ion (51,52). The counter ion is dissolved in an organic mobile phase of low polarity and the diastereomeric ion pairs are separated using a conventional (non-chiral) adsorbing phase.

Chiral amines have been used for the separation of enantiomers of acids. With (-)-quinine as counter ions it is possible to separate enantiomers of carboxylic acids such as 2-phenoxyacetic acid and tropic acid with separation factors of 1.3 - 1.6. Enantiomeric aminoalcohols can be resolved with (+)-10-camphorsulfonic acid as chiral counter ion. By use of a detectable counter ion, it is possible to follow the separation process for compounds without inherent detectable properties. An example is given in Figure 9.

REFERENCES

1. C.W. Ballard, J. Isaacs and P.G.W. Scott, J. Pharm. Pharmacol. 6, 971 (1964).
2. G.J. Divatia and J.A. Biles, J. Pharm. Sci. 50, 916 (1961).
3. G. Schill and M. Marsh, Svensk Farm. Tidskr. 67, 385 (1963).
4. R.L. Hall and J.A. Biles, J. Pharm.Sci. 53, 869 (1964).
5. G. Schill, Acta Pharm. Suecica 2, 13 (1965).
6. G. Schill, in Methodological Surveys in Biochemestry, Vol.7, E. Reid, ed., Ellis Horwood Ltd., Chichester, 195 (1978).
7. G. Schill and K.-G. Wahlund, in Proceedings of the 9th Materials Research Symposium, National Bureau of Standards Special Publication 519, 509 (1979).
8. M.T.W. Hearn, in Advances in Chromatography, Vol. 18, J.C. Giddings, E. Grushka, J. Cazes and P.R. Brown, eds., Marcel Dekker, New York, Chap. 2, 59 (1980).
9. B.A. Bidlingmeyer, J. Chrom. Sci. 18, 525 (1980).
10. G. Schill, Acta Pharm. Fenn. 90, 43 (1981).
11. G. Schill, Ion Exchange and Solvent Extraction, Vol. 6, J.A. Marinsky and Y. Marcus, eds., Marcel Dekker, New York, 1 (1974).
12. R. Modin and G. Schill, Talanta 22, 1017 (1975).
13. S. Eksborg and B.A. Persson, Acta Pharm. Suecica 8, 605 (1971).
14. A.K. Kolstad, Acta Pharm. Suecica 20, (1983), in press.
15. B. Fransson and G. Schill, Acta Pharm. Suecica 12, 417 (1975).
16. T. Nordgren and E.K. Sjödén, Acta Pharm. Suecica 15, 241 (1978).
17. T. Nordgren and A.K. Kolstad, Proceedings of the International Solvent Extraction Conference, ISEC 80, Liège, Chap. 15, 80 (1980).
18. B.A. Persson, Acta Pharm. Suecica 5, 343 (1968).
19. K.O. Borg, M. Gabrielsson and T.E. Jönsson, Acta Pharm. Suecica 11, 313 (1974).
20. M. Schröder-Nielsen, Acta Pharm. Suecica 11, 541 (1974).
21. R. Modin, Acta Pharm. Suecica 8, 509 (1971).
22. M. Schröder-Nielsen, Acta Pharm. Suecica 13, 133 (1976).
23. H.W. Stuurman, K.-G. Wahlund and G. Schill. J. Chromatogr. 204, 43 (1981).
24. R. Modin and M. Johansson, Acta Pharm. Suecica 8, 561 (1971).
25. G. Hoogewijs and D.L. Massart, Anal. Chim. Acta 106, 271 (1979).
26. R. Modin and G. Schill, Acta Pharm. Suecica 4, 301, (1967).
27. A.M. Wahbi, H. Abdine, M.A. Korany and M.H. Abdel-Hay, Analyst 103, 876 (1978).
28. D. Westerlund and K.H. Karset, Anal. Chim. Acta 67, 99 (1973).
29. S. Eksborg and G. Schill, Anal. Chem. 45, 2092 (1973).
30. S. Eksborg, P.O. Lagerström, R. Modin and G. Schill. J. Chromatogr. 83, 99 (1973).
31. B.A. Persson and B. Karger, J. Chromatogr. Sci. 12, 521 (1974).
32. K.-G. Wahlund, J. Chromatogr. 115, 411 (1975).
33. A. Tilly-Melin, Y. Askemark, K.-G. Wahlund and G. Schill, Anal. Chem. 51, 976 (1979).
34. I.M. Johansson, K.-G. Wahlund and G. Schill, J. Chromatogr. 149, 281 (1978).
35. I.M. Johansson, J. Liquid Chrom. 4(8), 1435 (1981).
36. H.J.L. Janssen, U.R. Tjaden, H.J. de Jong and K.-G. Wahlund, J. Chromatogr. 202, 223 (1980).
37. J. Crommen, Acta Pharm. Suecica 16, 111 (1979).
38. I.M. Johansson and K.-G. Wahlund, Acta Pharm. Suecica 14, 459 (1977).
39. W. Jost, K. Unger and G. Schill, Anal. Biochem. 119, 214 (1982).
40. J. Crommen, B. Fransson and G. Schill, J. Chromatogr. 142, 283 (1977).
41. L. Hackzell, M. Denkert and G. Schill, Acta Pharm. Suecica 18, 271 (1981).
42. N.A. Parris, J. Liquid Chromatogr. 3, 1743 (1980).
43. M. Denkert, L. Hackzell, G. Schill and E. Sjögren, J. Chromatogr. 218, 31 (1981).
44. T. Gnanasambandan and H. Freiser, Anal. Chem. 53, 909 (1981).
45. L. Hackzell and G. Schill, Chromatographia 15, 437 (1982).
46. D. Cram, R. Helgeson, L. Sousa, J. Timko, M. Newcomb, P. Moreau, F. DeJond, G. Gokel, D. Hoffman, L. Domeier, S. Peacock, K. Madan and L. Kaplan, Pure Appl. Chem. 43, 327 (1975).
47. L. Sousa, G.D. Sogah, D. Hoffman and D. Cram, J. Am. Chem. Soc. 100, 4569 (1978).
48. M. Newcomb, J.L. Toner, R. Helgeson and D.Cram, J. Am. Chem. Soc. 101, 4941 (1979).
49. Y. Chao, G. Weisman, G. Sogah and D. Cram, J. Am. Chem. Soc. 101, 4948 (1979).
50. V. Prelog, Z. Stojanac and K. Kovacevic, Helv. Chim. Acta 38, 377 (1982).
51. C. Pettersson and G. Schill, J. Chromatogr. 204, 179 (1981).
52. C. Pettersson and G. Schill, Chromatographia 16, 192 (1982).

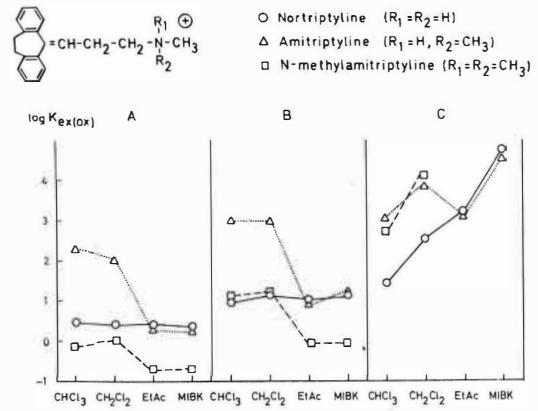

FIGURE 1. ION-PAIR EXTRACTION OF AMINES WITH DIFFERENT DEGREES OF N-METHYLATION COUNTER IONS: A: Cl^- B: Br^- C: ClO_4^-
MIBK = METHYLISOBUTYL KETONE, EtAC = ETHYLACETATE

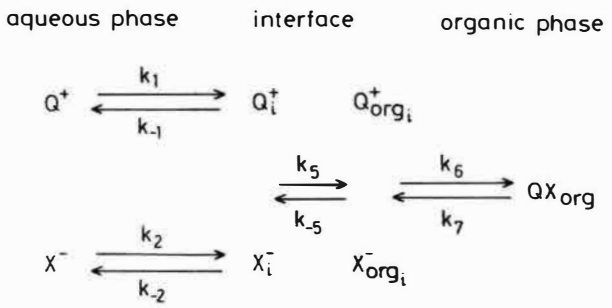

FIGURE 3. MODEL FOR THE ION-PAIR EXTRACTION PROCESS

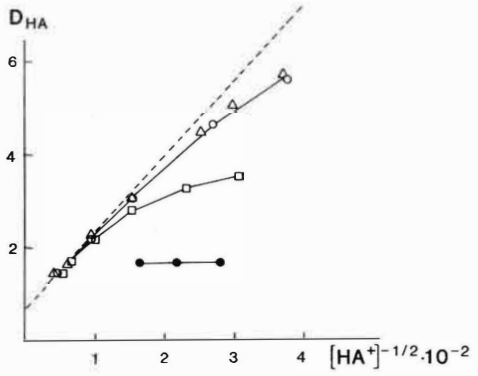

FIGURE 2. DISTRIBUTION OF N-METHYLAMITRIPTYLINE BETWEEN 1-PENTANOL AND PHOSPHATE BUFFER.
($[H_2PO_4^-]$ = 0.10) pH: ● 1.0; □ 2.0; ○ 3.0; △ 4.0

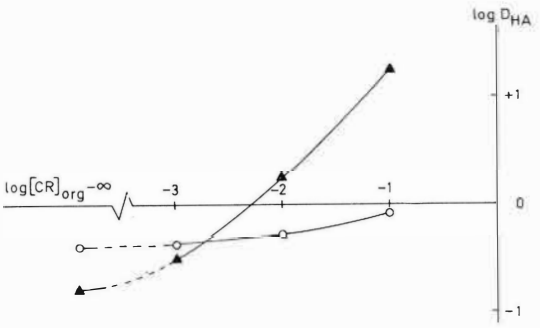

FIGURE 4. DISTRIBUTION OF OCTYLAMMONIUM ▲ AND TRIMETHYLNONYLAMMONIUM ○ AS SALICYLATE ION PAIRS BETWEEN DIBENZO-18-CROWN-6 (CR) + $CHCl_3$ AND AQUEOUS BUFFER

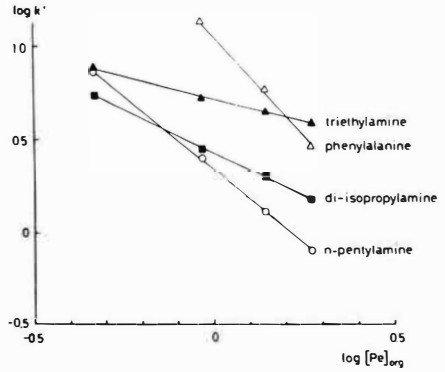

FIGURE 5. RETENTION OF ION PAIRS IN LIQUID-LIQUID CHROMATOGRAPHY
MOBILE PHASE: CHLOROFORM + 1-PENTANOL (Pe)
STATIONARY PHASE: NAPHTHALENE-2-SULFONATE 0.1 M, pH 2.1

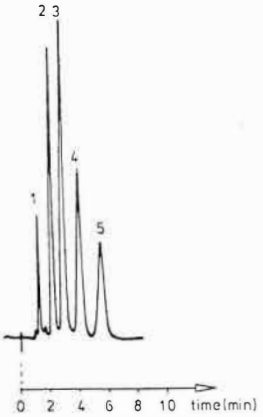

FIGURE 7.
SEPARATION OF OLIGOURIDYLIC ACIDS
MOBILE PHASE:
TETRAMETYLAMMONIUM CHLORIDE
0.1 M, pH 7.0
1. URIDINE 2. UpU^{-1}
3. $(Up)_2U^{-2}$ 4. $(Up)_3U^{-3}$
5. $(Up)_4U^{-4}$

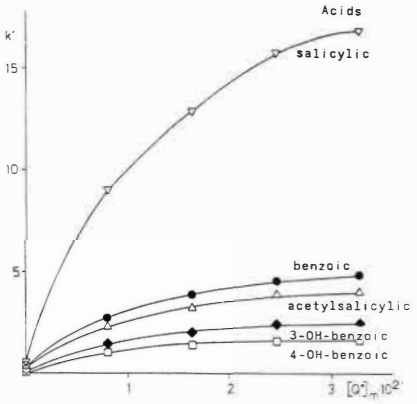

FIGURE 6. RETENTION OF ION PAIRS IN LIQUID-SOLID CHROMATOGRAPHY
MOBILE PHASE: TETRABUTYLAMMONIUM (Q^+) IN ACETONITRILE + PHOSPHATE BUFFER pH 6

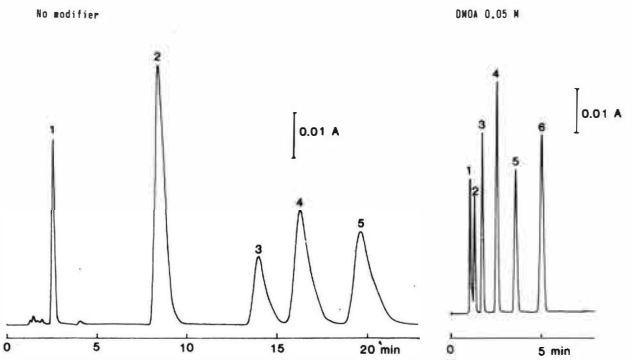

FIGURE 8. INFLUENCE OF IONIC MODIFIER (DIMETHYLOCTYLAMINE) ON RETENTION OF ION PAIRS IN LIQUID SOLID CHROMATOGRAPHY

MOBILE PHASE: PHOSPHATE BUFFER pH 2.2 WITH MODIFIER (DMOA)

SAMPLE: 1-PHENOXY-2-ISOPROPYLAMINO-2-PROPANOL DERIVATIVES

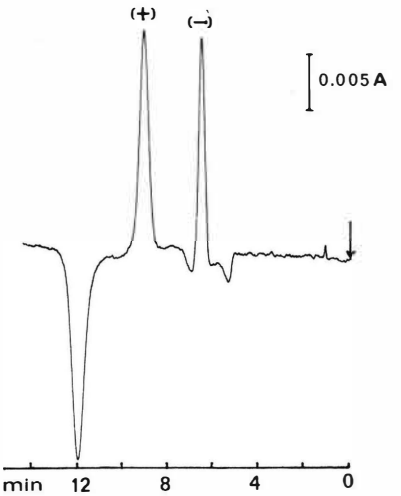

FIGURE 9. SEPARATION OF ENANTIOMERS OF 10-CAMPHORSULFONIC ACID

MOBILE PHASE: (-)-QUININE SALT IN METHYLENE CHLORIDE

STATIONARY PHASE: HYDROPHILIC, SURFACE-MODIFIED SILICA

NON-CHELATING OXIMES IN THE SOLVENT EXTRACTION OF BASE METALS

John S. Preston

Council for Mineral Technology
Randburg, Transvaal
Tranvaal, South Africa

The commercial use of chelating oximes, such as aliphatic or aromatic hydroxyoximes, in the solvent extraction of metals such as copper, nickel and cobalt is now well established. A considerable amount of research, both of practical and fundamental nature, has been carried out with such extractants. In contrast, simple oximes containing no other functional group (non-chelating oximes) do not appear to have received consideration as potential extractants for base metals.

In a recent study of the solvent extraction of cobalt and nickel by organo-phosphorus acids (1), we noted certain differences in the nature of the extracted complexes that suggested that interesting synergistic effects might occur in the presence of nitrogen-donor additives such as non-chelating oximes. We found that the normal selectivity of organophosphoric acids such as D2EHPA for cobalt over nickel was reversed in the presence of simple aldoximes (e.g., octanal oxime), thereby presenting the possibility of developing a new type of nickel-selective extraction system. We have now extended our work to the investigation of the use of non-chelating oximes in conjunction with acidic extractants of various types for the separation of base metals.

ORGANOPHOSPHORUS ACID SYSTEMS

The $pH_{0.5}$ values for extraction of nickel and cobalt by some organo-phosphorus acids and by their mixtures with non-chelating aldoximes are shown in Table 1. The synergistic effects obtained are greater for nickel than for cobalt in all cases. With the exception of the phosphinic acid extractant (which shows a high selectivity for cobalt in the absence of oxime), the mixed extractant systems display selectivity for nickel over cobalt, although the selectivities are not great enough to be of practical use for the separation of these metals.

The data for the extraction of various base metals by mixtures of D2EHPA and 2-ethylhexanal oxime (EHO), shown in Table 2, reveal that marked synergistic effects are found for divalent (but not for trivalent) transition metals. Whereas the order of extraction of the divalent metals by D2EHPA alone:

Zn > Cr > Cu, Mn > Fe > Co > V, Ni

clearly reflects the ease with which the metal ions adopt a tetrahedral configuration, the magnitude of the synergistic effect produced by the addition of EHO:

Zn < Cr < Mn < Fe < Co < Cu < V < Ni

represents (with the exception of Cr^{2+}) the order of increasing ligand-field stabilization of the octahedral complexes over the corresponding tetrahedral species. The complexes of copper, cobalt and nickel extracted by mixtures of organophosphoric acids (H_2A_2) and non-chelating oximes (B) have the compositions $Cu(HA_2)_2B_2$, $Co(HA_2)_2B_2$ and $NiA(HA_2)B_3$, respectively (3).

The absence of synergistic effects with ions such as Ca^{2+}, Mg^{2+} and NH_4^+ can be made use of to minimize the problems caused by the co-extraction of these ions when D2EHPA alone is used for the recovery of nickel, for example. Figure 1 shows the extraction curves for these species using D2EHPA in the absence and in the presence of EHO. Use of the mixed reagent permits extraction of nickel in a pH region in which co-extraction of calcium, magnesium and ammonium ions is minimal (4).

CARBOXYLIC ACID SYSTEMS

Carboxylic acids, in contrast to organophosphorus acids, show some selectivity for nickel over cobalt (up to about 0.2 pH units). Figure 2 shows that in the presence of non-chelating aldoximes much improved selectivities are obtained. Variation of the nature of the carboxylic acid component permits metal extraction under a wide range of conditions (5), and useful practical separations of nickel from cobalt can be effected (6).

Data for the extraction of various base metals by the aliphatic carboxylic acid, versatic 10, and by its mixtures with octanal oxime (CAO) and with 2-ethylhexanal oxime (EHO) are shown in Table 3. The large synergistic effects obtained for nickel and cobalt, in contrast to the much smaller effects for metals such as manganese and zinc, reflect the relative contributions of the ligand-field stabilization energies for the octahedral complexes of the different metals. The nickel and cobalt complexes extracted by mixtures of carboxylic acids (H_2A_2) and non-chelating aldoximes (B) have the compositions NiA_2B_4 and CoA_2B_4, respectively (5). The anomalously small synergistic effects observed for copper probably result from the characteristic dimeric structure of the copper carboxylate complex (7), which is not broken down in the presence of moderate amounts of oxime. Limited synergism can arise by replacement of the two axially coordinated water (or other solvent) molecules of the dimer.

It is interesting to note that the mixed-extractant systems described here do not suffer from the disadvantage of slow rates of extraction of nickel observed with previously reported systems based on mixtures of carboxylic acids and commercial chelating hydroxyoximes (8,9). Further, the formation of intractable cobalt(III) complexes that is characteristic of mixtures containing chelating oximes (9) does not occur when the latter are replaced by non-chelating oximes.

In addition to the selectivity of these mixtures for nickel over cobalt noted above, the selectivity for nickel and cobalt over manganese (Table 3) may be of interest. However, although the mixed extractants bring about a reversal of the normal selectivity of the carboxylic acids for zinc over cadmium, we were unable to obtain selectivities of greater than 0.34 pH units under the various conditions examined (Table 4).

SULPHONIC ACID SYSTEMS

Sulphonic acids, such as dinonylnaphthalene sulphonic acid (DNNS), extract nickel and cobalt under strongly acidic conditions, but no separation of the metals can be obtained. In the presence of non-chelating aldoximes, small selectivities for nickel over cobalt are observed (0.15 to 0.35 pH units), and slight depressions of extraction relative to the sulphonic acid alone are obtained (Figure 3). This depression of extraction is undoubtedly due to a strong interaction between the components of the extraction mixture, which is only partly counteracted by the interaction between the oxime and the metal sulphonate. This is confirmed by the observation that the addition of non-chelating oximes of the ketoxime type, which coordinate only weakly to metal ions on account of steric constraints (3, 5) but which nevertheless can interact strongly with the free sulphonic acid, causes very marked depressions of metal extraction (Figure 3)

Interestingly, the addition of non-chelating oximes to sulphonic acid reagents considerably improves the phase-separation characteristics of the system, solutions containing sulphonic acids alone show a marked tendency toward formation of emulsions. Similar beneficial effects were found with those carboxylic acids that tend to give poor phase separations (5), and with those organophosphoric acids that tend to give rise to third-phase formation (3).

OTHER EXTRACTANT SYSTEMS

Under certain conditions, non-chelating oximes are able to extract metals such as nickel and copper in the absence of any auxiliary extractant. Thus, at pH values close to those which cause the precipitation of the metal hydroxides (pH 3.5 to 4.0 for copper, and pH 6.5 to 7.5 for nickel) these metals can be extracted from nitrate media by, for example, solutions of isodecanal oxime (IDO) in xylene. Nickel is extracted as a dark blue complex, which gradually assumes a purple colour on standing. Copper is extracted as an emerald green complex, which forms very slowly under conditions close to equilibrium. The addition of phenolic compounds produces a synergistic effect, the magnitude of which increases with increasing acidity of the phenol (Figure 4).

In the presence of chloride ions, copper can be extracted by non-chelating aldoximes - even from quite acidic solutions - as a bright blue complex, for which slope analysis data suggest the formulation $CuCl_2B_4$.

Extraction of this type of complex is rapid and is not pH-dependent. Stripping can be effected by contact with aqueous phases low in chloride (Figure 5).

REFERENCES

1. R.J. Whewell and C. Hanson, Ion Exchange and Solvent Extraction 8, 1 (1981).
2. J.S. Preston, Hydrometallurgy 9, 115 (1982).
3. J.S. Preston, Hydrometallurgy 10, 000 (1983).
4. J.S. Preston and C.A. Fleming, 3rd International Symposium on Hydrometallurgy, Atlanta, 1983.
5. J.S. Preston, Hydrometallurgy, In press.
6. J.S. Preston, J. S. Afr. Inst. Min. Metall., In press.
7. D.P. Graddon, J. Inorg. Nucl. Chem. 17, 222 (1961).
8. D.S. Flett and D.W. West, Proc. Inst. Solvent Extr. Conf. ISEC 71, 214 (1971).
9. B.G. Nyman and L. Hummelstedt, Proc. Inst. Solvent Extr. Conf. ISEC 74, 669 (1974).

Table 1. Extraction of nickel and cobalt by mixtures of organophosphorus acids (0.5M) and EHO (0.5M) in xylene at 20°C

Organophosphorus acid	$pH_{0.5}$			$\Delta pH_{0.5}$ [a]	
	Ni	Co	Co-Ni	Ni	Co
Phosphoric acids					
Di(2-ethylhexyl)	1.58	1.99	0.41	2.53	1.69
Di(4-octylphenyl)	0.42	0.79	0.37	2.21	1.74
Mono(2-ethylhexyl) [b]	1.05	1.50	0.45		
Phosphonic acids					
2-Ethylhexyl 2-ethylhexylphosphonate	3.06	3.25	0.19	2.06	0.65
Phosphinic acids					
Dicyclohexyl	4.58	4.22	-0.36	0.62	0.00

Initial aqueous phases contained 0.1M metal nitrate in 1.0M NH_4NO_3

[a] $\Delta pH_{0.5} = pH_{0.5}$ (acid plus oxime) - $pH_{0.5}$ (acid alone)

[b] Extraction of 0.02M metal nitrates in 0.5M $NaNO_3$ by 0.1M organophosphorus acid plus 0.2M isodecanal oxime

Table 2. Extraction of base metals by D2EHPA (0.5M) and by mixtures of D2EHPA (0.5M) and EHO (0.5M) in xylene at 20°C

Metal ion	D2EHPA $pH_{0.5}$	D2EHPA plus EHO $pH_{0.5}$	$\Delta pH_{0.5}$
Cu^{2+}	2.90	1.05	1.85
Ni^{2+}	4.12	1.60	2.52
Co^{2+}	3.70	2.00	1.70
Fe^{2+}	3.56	2.10	1.46
Mn^{2+}	2.82	2.02	0.80
Cr^{2+}	2.15	1.47	0.68
V^{2+}	4.15	2.25	1.90
Mg^{2+}	3.81	3.69	0.12
Ca^{2+}	2.85	2.97	-0.12
Zn^{2+}	1.42	1.58	-0.16
Fe^{3+}	-0.32	-0.40	0.08
Cr^{3+}	3.12	2.98	0.14
Al^{3+}	1.53	1.51	0.02

Initial aqueous phases contained 0.1M metal nitrate in 1.0M NH_4NO_3, except for Cr^{2+} and V^{2+}, which were present as 0.1M sulphates in 0.33M Na_2SO_4

Table 3. Extraction of base metals by versatic acid (0.5M) and by mixtures of versatic acid (0.5M) with non-chelating aldoximes (0.5M) in xylene at 20°C

Metal ion	Versatic $pH_{0.5}$	Versatic plus CAO $pH_{0.5}$	$\Delta pH_{0.5}$	Versatic plus EHO $pH_{0.5}$	$\Delta pH_{0.5}$
Ni^{2+}	6.34	4.07	2.27	4.45	1.89
Co^{2+}	6.55	5.02	1.53	5.30	1.25
Cu^{2+}	4.01	3.27	0.74	3.34	0.67
Mn^{2+}	6.79	6.39	0.40	6.52	0.27
Zn^{2+}	5.45	4.81	0.64	5.00	0.45
Cd^{2+}	6.06	4.51	1.55	4.90	1.16
Fe^{3+}	1.84	1.72	0.12		

Initial aqueous phases contained 0.05M metal nitrate in 1.0M $NaNO_3$

Table 4. Extraction of cadmium and zinc by mixtures of carboxylic acids (0.5M) and non-chelating oximes (0.5M) in xylene at 20°C

Carboxylic acid	Oxime[a]	Aqueous phase	$pH_{0.5}$ Cd	Zn	Zn-Cd
Versatic 10	None	1.0M $NaNO_3$	6.06	5.45	-0.61
	None	1.0M Na_2SO_4	6.57	5.96	-0.61
	EHO	1.0M $NaNO_3$	4.90	5.00	0.10
	CAO	1.0M $NaNO_3$	4.51	4.81	0.30
Naphthenic	None	1.0M $NaNO_3$	5.48	5.47	-0.01
	None	0.3M Na_2SO_4	5.91	5.91	0.00
	None	1.0M Na_2SO_4	6.02	5.98	-0.04
	IDO	0.3M Na_2SO_4	4.99	5.27	0.28
Decanoic	CAO	1.0M $NaNO_3$	4.43	4.77	0.34

[a]EHO = 2-ethylhexanal oxime; CAO = octanal oxime; IDO = isodecanal oxime

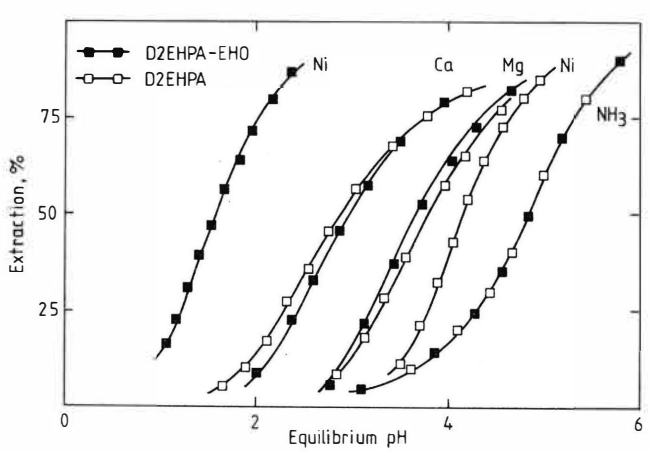

Figure 1. Extraction of nickel, calcium, magnesium and ammonia from 1.0M NH_4NO_3 by 0.5M D2EHPA and its mixture with 0.5M 2-ethylhexanal oxime (EHO)

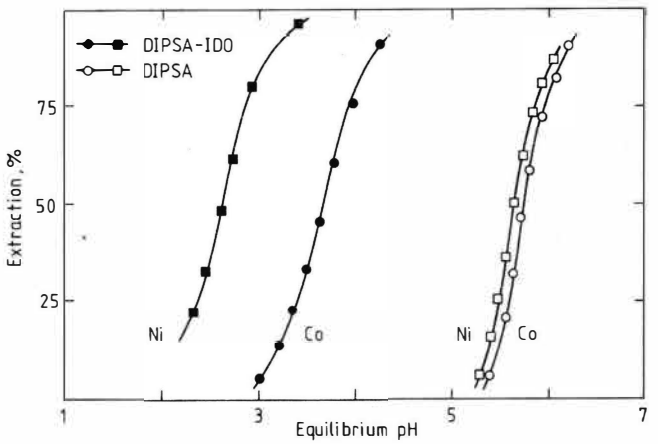

Figure 2. Extraction of nickel and cobalt from 0.3M $(NH_4)_2SO_4$ by 0.5M diisopropylsalicylic acid (DIPSA) and its mixture with 1.0M isodecanal oxime (IDO)

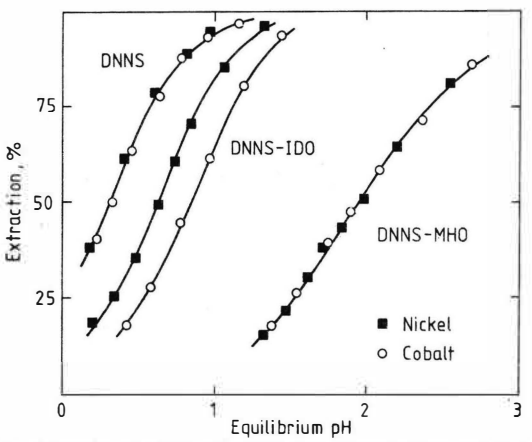

Figure 3. Extraction of nickel and cobalt from HNO_3 solutions by 0.2M DNNS and its mixtures with 0.2 M isodecanal oxime (IDO) and octan-2-one oxime (MHO)

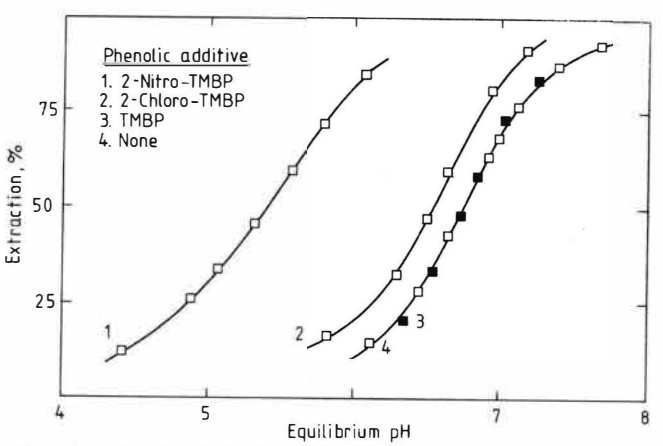

Figure 4. Extraction of nickel from 0.9 $NaNO_3$/0.1M NH_4NO_3 by 0.5M isodecanal oxime (IDO) and its mixtures with 4-octylphenol (TMBP) derivatives (0.5M)

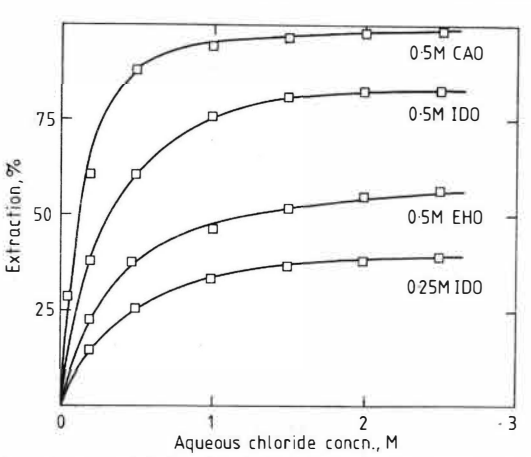

Figure 5. Extraction of copper from 0.01M HNO_3/4.0M $Na(Cl,NO_3)$ by octanal oxime (CAO), isodecanal oxime (IDO) and 2-ethylhexanal oxime (EHO)

THE DETERIORATION OF NICKEL EXTRACTANT LIX64N AND ITS REGENERATION

Mitsuo Takahashi, Takashi Ogata, Hiroshi Okino and Yoshibumi Abe

Technical Research Center
Nippon Mining Co.
Saitama, Japan

I. INTRODUCTION

The Nippon Mining Co. has been producing high quality nickel and cobalt metals from a mixture of nickel sulfide and cobalt sulfide in the Hitachi Smelter and Refinery since 1975. In this hydrometallurgical process treatment, the following three solvent extraction processes are employed, (A) the elimination of zinc using di-2-ethyl-1-hexyl phosphoric acid(D2EHPA), (B) separating cobalt from nickel using 2-ethyl-1-hexyl phosphonic acid mono-2-ethyl-1-hexyl ester(M2EHPA) and (C) nickel extraction with LIX64N(1). The extractant used in the nickel and cobalt separation was changed from D2EHPA to M2EHPA in 1978, because the cobalt-nickel separation factor of M2EHPA is about 200 times greater than that of D2EHPA(2).

When D2EHPA was used in the nickel and cobalt separation process, the raffinate from the process contained 100-500 mg/l of cobalt because of the small cobalt-nickel separation factor of D2EHPA. Thus, the pH of the raffinate from the cobalt-nickel separation process was adjusted to 9 - 9.5 with ammonia water for the feed solution to the nickel extraction. The divalent cobalt extracted with LIX64N is usually oxidized to trivalent cobalt in the organic phase with air, and cannot be stripped out of the organic phase(3). On the other hand, trivalent cobalt is not extracted with LIX64N(4).

A part of the cobalt remaining in the aqueous feed, which was extracted with LIX64N accumulated during the nickel extraction. At the same time, the nickel loading capacity of LIX64N decreased gradually. Furthermore, the decreasing rate of the loading capacity was more rapid than the accumulating rate of cobalt in LIX64N.

The solvent for the nickel extraction was initially composed of 25 % by volume of LIX64N and 75 % by volume of n-paraffine as diluent. The nickel loading capacity of the solvent was 6.2 g/l at pH 9. Soon after operating the nickel extraction process, the nickel loading capacity of the solvent began to decrease. The fresh LIX64N was added constantly in order to maintain the nickel loading capacity of the solvent. Despite the volume ratio of LIX64N had risen to 42.3 %, the nickel loading capacity of the solvent was only 4.6 g/l. The concentration of cobalt in the solvent was 1.5 g/l. This means that about 35 % of the total LIX64N charged lost the ability to extract nickel.

The investigation reported here was carried out to determine the cause of the decreasing of the nickel loading capacity of the solvent and the regeneration of LIX64N.

II. ANALYSIS OF THE SOLVENT IN THE NICKEL EXTRACTION PROCESS

1. SEPARATION OF THE COMPONENTS IN THE SOLVENT AND THEIR CONSTITUENTS

The deteriorated solvent in the nickel extraction process of the Hitachi plant was separated into each component by means of a silicagel column chromatography technique using benzene, ethyl acetate and methanol as eluents. Each component was analyzed by Infrared Spectroscopy(IR), combined Gas Chromatography/Mass Spectrometry(GC-MS) and ^{13}C-Nuclear Magnetic Resonance Spectroscopy(^{13}C-NMR). The results are shown in Fig. 1.

Component A, the fraction eluted with benzene, and component B, the fraction eluted with ethyl acetate, were identified as 2-hydroxy-nonyl-benzophenone and 2-hydroxy-5-nonylbenzophenone oxime, respectively. The fraction eluted with methanol, component C, was estimated to be

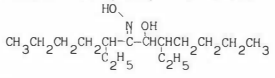

(LIX63)

and/or some oxidized products.

LIX64N is a mixture of 2-hydroxy-5-nonylbenzophenone oxime and 7-hydroxy-5,8-diethyl-6-dodecanone oxime(5). Thus, benzophenone(component A) is supposed to be a product derived from benzophenone oxime. It is assumed that the decrease of the nickel loading capacity is caused by the chemical change of the oxime into ketone as shown in the reaction (1).

(1)

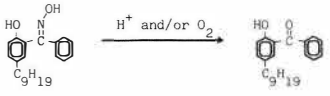

2. SEMI-QUANTITATIVE MEASUREMENT OF BENZOPHENONE OXIME AND BENZOPHENONE IN THE ORGANIC PHASE OF THE NICKEL EXTRACTION

To evaluate the degree of deterioration of LIX64N, measurement of benzophenone oxime and benzophenone was carried out. It was found that rod thin layer chromatography(rod TLC) with flame ionization detector(FID) using a sintered silicagel rod was simple and effective. Quantitative analysis of the rod TLC is based on the FID technique, that is, electric resistance of the hydrogen flame decreases in proportion to the quantity of the organic compounds developed on the rod.

The analysis procedure is as follows;

(i) first development: the sample spotted on the TLC rod is developed with n-hexane in order to elute only the diluent(n-paraffine) to the front of the rod keeping other components at the origin(the spotting point).

(ii) elimination of the diluent: the developed diluent is burned away in the hydrogen flame.

(iii) second development: benzophenone oxime and benzophenone are developed with benzene to separate each other on the rod.

(iv) quantitative analysis: each component is analyzed by a Thinchrograph®.

The result, that is, the Thinchrograph chart, is shown in Fig 2.

The analyses were performed on the solvents sampled periodically from 1976 to 1977 from the nickel extraction process at the Hitachi plant by the method mentioned above. The nickel loading capacity of the solvent was decreasing during this period. The results are shown in Fig. 3.

It is clear that the relative concentration of benzophenone oxime decreases while that of benzophenone increases in the course of the operation. The decreasing rate of the nickel loading capacity correlates well with the results shown in Fig. 3.

III. CAUSE OF THE DETERIORATION

The chemical reaction mechanisms of the deterioration of LIX64N are supposed to be (a) hydrolysis caused by the contact with sulfuric acid during stripping or (b) oxidation, caused by air, catalyzed with LIX64N-metal complex. The former reaction mechanism, hydrolysis, was denied because the nickel loading capacity of the solvent scarcely decreased after contacting with sulfuric acid solution (40 g-H_2SO_4/l).

In order to check the latter, accelerative oxidation experiments were carried out. The solvent loaded with or without metal ion(nickel, cobalt or copper) were kept in reactors of 120 ml volume at 7.2 kg/cm^{2}G oxygen pressure at 100 °C. The results are shown in Fig. 4. In the absence of metal ions, LIX64N suffered little decomposition, while LIX64N-metal complex showed strong catalytic activity to oxidize the benzophenone oxime in LIX64N to benzophenone. The catalytic activity order among the metal ions tested is as follows;

Co > Cu > Ni

Based on these data, it was concluded that the catalytic oxidation reaction was the major cause of the deterioration of LIX64N.

IV. REGENERATION OF DETERIORATED LIX64N

Ketones react with hydroxylamine salts in alkaline solution to yield oximes. As benzophenone turned out to be the major component of deteriorated LIX64N, it is expected that the benzophenone would be converted to its oxime by reacting it with hydroxylamine salts in alkaline solution. The conversion into its oxime was investigated. The reaction would take place according to the following equation (2).

(2)

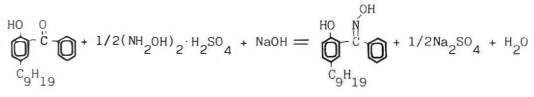

From the results of the basic investigation, the optimum reaction condition was determined. Its condition was confirmed in a batch scale experiment under the following procedures:

(i) 19.8 l of the deteriorated solvent are mixed with 2.8 l of 40 % sodium hydroxide aqueous solution.

(ii) 4 l of hydroxylamine solution(180 g/l) are added to the mixed solution.

(iii) The reaction is continued for four hours while stirring the mixture.

The degree of regeneration was checked both by the nickel loading capacity measurement and the nitrogen content analysis of the regenerated solvents sampled during the regeneration reaction. The only organic nitrogen compound in the solvent is oxime. As the regeneration reaction proceeds, the nitrogen content of the solvent is expected to increase. The results are shown in Fig. 5. and Fig. 6.

In accordance with the degree of regeneration, the nickel loading capacity recovered markedly as high as the degree of the fresh extractant. These results proved that the deterioration of the solvent and the decrease of nickel loading capacity were caused by the chemical change of extractant benzophenone oxime to benzophenone.

V. CONCLUSIONS

The deterioration of LIX64N, or the decrease of the nickel loading capacity of LIX64N is caused by the oxidation of benzophenone oxime in LIX64N to benzophenone. The oxidation reaction is catalytically promoted by cobalt-oxime complex. It is necessary to keep the cobalt content in the aqueous feed to the nickel extraction process as low as possible in order to avoid the deterioration of LIX64N.

Deteriorated LIX64N that contained benzophenone can be regenerated by the reaction with hydroxylamine sulfuric acid salt in sodium hydroxide solution. The nickel loading capacity can be recovered with the increasing of the relative ratio of benzophenone oxime to benzophenone by the regeneration reaction. By this reaction, benzophenone can be changed to benzophenone oxime at the yield of more than 90 %.

As mentioned in the introduction, the extractant for separating cobalt from nickel was changed from D2EHPA to M2EHPA in 1978. The cobalt concentration in the raffinate decreased from about 500 mg/l to less than 5 mg/l by changing the extractant. As this raffinate from the cobalt-nickel separation process is fed to the nickel extraction process, the deterioration of LIX64N at the Hitachi plant has been free from troubles.

REFERENCES

(1) Nishimura, S.; Ext. Metall. '81, IMM, pp 404 - 412 (1981)

(2) Kasai, T., Nakayama, H., Motoba. K. and Itoh, E.; "New N.M.C. Process for Winning Nickel and Cobalt from Sulfate Solution", Paper presented at Fourth Joint Meeting MMIJ-AIME, Tokyo, Nov., (1980).

(3) Merigold, C. R., and Sudderth, R. B.; Int. Symp. on Hydrometall., AIME, Chapt. 21, pp 562 - 563 (1973)

(4) Merigold, C. R., and Sudderth, R. B.; Int. Symp. on Hydrometall., AIME, Chapt. 21, p 559 (1973)

(5) Atwood, R. L., Thatcher, D. N., and Miller, J. D.; Metall. Trans. B, 6B, p465 (1975)

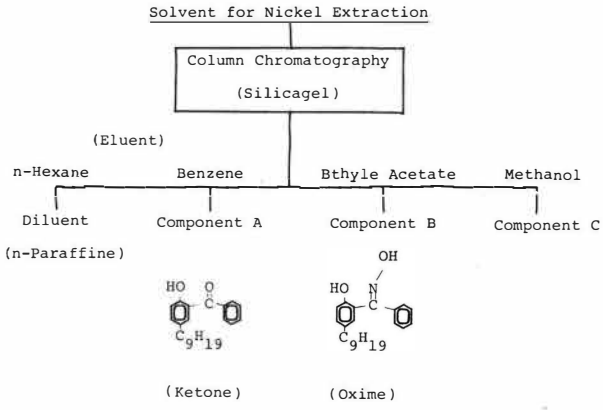

Fig. 1. Separation of the Constituents

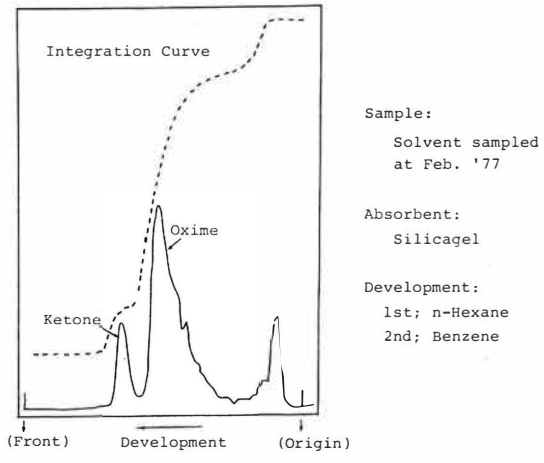

Fig. 2. Thinchrograph chart of the deteriorated solvent

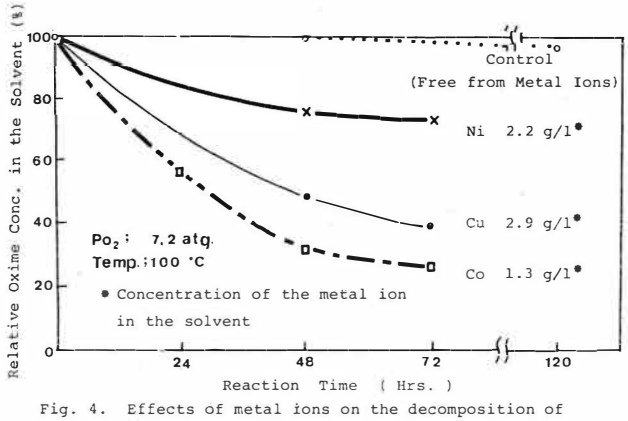

Fig. 4. Effects of metal ions on the decomposition of benzophenone oxime in the solvent

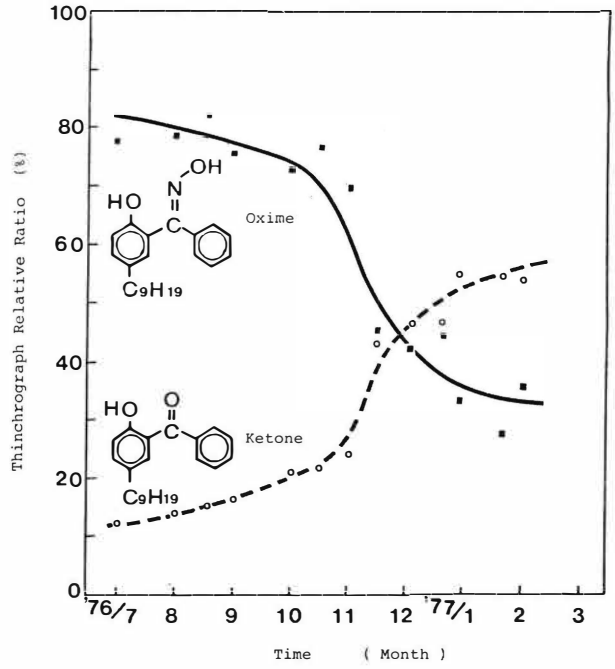

Fig. 3. Change of the relative ratio of Ketone and Oxime in the solvent during the operation

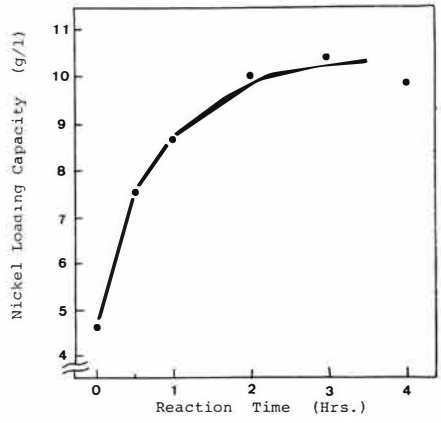

Fig. 5. Change of the nickel loading capacity with the regeneration reaction time

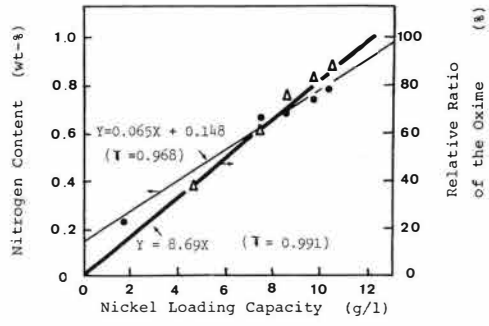

Fig. 6. Relationship between the nitrogen content, the relative ratio of the oxime concentration and the nickel loading capacity of the solvent

REMOVAL OF COPPER AND IRON FROM NICKEL AND COBALT SULFATE SOLUTION CONTAINING CHLORIDE ION BY EXTRACTION WITH QUATERNARY AMMONIUM CHLORIDE

Xue-xi Zhou, Quan ling Suo, Tun Zhu and Shu-lan Huang

Institute of Chemical Metallurgy
Academia Sinica
Beijing, China

When quarternary ammonium chloride was used to remove copper and iron from chloride containing cobalt and nickel sulfate solution, it was found that the extraction of copper and iron was not decreased by the competive reaction of the two ions. Even more, the extent of extraction of these two ions was higher than that are present separately. Ioffe and his coworkers[1] found the similar phenomena when they used tertiary amine to separate copper from iron in chloride solution.

It is possible, in certain condition, to remove ferrous ions with quaternary ammonium salt directly, without oxidation of them frist to ferric ions following by precipitation or solvent extraction . With 3-4 stages of extraction, iron content of several gram per liter(g/l) in the solution initially could be decreased to less than 0.003 g/l. Using of this process and in connection with separation of cobalt from nickel with quaternary ammonium thiocyanate,[2] an improved process to purify nickel electroly or to treat leaching solution of matte or other cobalt containing materials can be developted.

Recently, Ivanov and coworkers[3] developted new process to purify nickel sulfate solution with trialkylbenzylammonium chloride as solvent.

ABSORPTION SPECTRUM OF LOADED ORGANIC PHASE

Figure 1 shows the visible-violet absorption of the loaded organic phase, which was obtained contacting quaternary ammonium chloride solvent with $FeCl_3$, $FeCl_2$, $CuCl_2$ and CuCl solution respectively. CuCl was extracted from 3 mole/dm^3 hydro-chloric acid solution and others were from 3 mole/dm^3 sodium chloride solution. It can be seen from this figure that the organic phase loaded with Fe(III) has an absorption peak at 364 nm, Fe(II) has very weak absorption around this wave length region, organic phase with Cu(II) has a peak at 410 nm and with Cu(I) has practically no absorption in whole visible-violet region because of the full d- electron orbits. However, the loaded organic phase obtained by contacting with the aqueous phase containing both Cu(II) and Fe(II) being loaded both copper and iron has spectrum which is the same as the one contains only Fe(III)——having an only peak at 364nm. It indicates that copper and iron in the loaded organic phase are Cu(I) and Fe(III), and redox reaction took plase during the extraction process.

As usually known, the following eqilibrium occurs in aqueous solution,

(1) $Cu^{2+} + Fe^{2+} = Cu^{+} + Fe^{3+}$

In the chloride medium Cu(I) and Fe(III) are easier to be extracted into the organic phase containing quaternary ammonium salt because of chloride complex anions of Cu(I) and Fe(III) are more stable than those of Cu(II) and Fe(II), respectively.

The reaction (1) is shifted to the right side during extraction as shown in next equation

(2) $Cu^{2+} + Fe^{2+} + (m-n)Cl^{-} + n\overline{R_4NCl} = (\overline{(R_4N)_aCuCl_p} + (\overline{(R_4N)_bFeCl_q}$

(Superscript bar represents those species in the organic phase.)

Remarkable change in the absorption spectrum was observed when reductant such as $NH_2OH \cdot HCl$ was added to the cupric chloride solution during extraction with quaternary ammonium chloride solvent. The characteristic peak of Cu(II) at 410nm became weak and disappeared gradually. By adding oxidant to the ferrous chloride solution frist, the organic phase obtained by extraction with quaternary ammonium chloride has a spectrum very similar to the spectrum of organic phase loaded with Fe(III). It indicates that the asumption of redox reaction occurred during extraction is resonable.

COMPOSITION OF THE EXTRACTED COMPLEXES

Analysis of the saturated loaded organic phase The concentration of quaternary ammonium chloride in stock solvent was determined by analysing its chloride content.

Table 1

contents / extracts	Fe	Cu	Cl	R_4NCl
Cu(I)		0.50	1.01	0.54
Fe(III)	0.49		1.92	0.54

Table 1 is the compositions of the Cu(I) and Fe(III) extracted complexes. And the amount of metals and total chloride ion in the loaded organic phase were determined after stripping them by dilute sulfuric acid. The ratios of the components of the Cu(I) Fe(III) extracted complex are as follows:

Cu(I) : Cl : R_4N = 1.00 : 2.02 : 1.08 ≈ 1 : 2 : 1

Fe(III) : Cl : R_4N = 1.00 : 3.92 : 1.10 ≈ 1 : 2 : 4

The formular of the extracted complex should be R_4NCuCl_2 and R_4NFeCl_4 respectively and are the same as those reported by Good, Srivstava and Holland[4] and later Irving and Nabilsi[5].

Slope method From Equation (2) it can be obtained that

(3) $$K = \frac{[(\overline{R_4N})_a\overline{CuCl_p}][(\overline{R_4N})_b\overline{FeCl_q}]}{[Cu(II)][Fe(II)][Cl]^{m-n}[\overline{R_4NCl}]^n}$$

Substituting the distribution coefficient of copper and iron D_{Cu}, D_{Fe} into Equation (3), then Equation (4) is obtained

(4) $$K = \frac{D_{Cu} \cdot D_{Fe}}{[Cl]^{m-n}[\overline{R_4NCl}]^b}$$

Equation (5) will be obtained by taking logrithm.

(5) $$\log(D_{Cu} \cdot D_{Fe}) = \log K + (m-n)\log[Cl] + n\log[\overline{R_4NCl}]$$

In this experiment 0.1 mole/dm^3 quaternary ammonium chloride was used throughout and when its concentration is much more than the concentration of metals in the aqueous solution following equation can be obtained,

(6) $$\log(D_{Cu} \cdot D_{Fe}) = \log K_1 + (m-n)\log[Cl]$$

K_1 is a constant including the concentration of $\overline{R_4NCl}$.

When Cl^- concentration in the feed solution is constant and much higher than these of iron and copper, Equation (5) can be converted into,

(7) $$\log(D_{Cu} \cdot D_{Fe}) = \log K_2 + n\log[\overline{R_4NCl}]$$

K_2 is another constant including the chloride concentration. Regression of data according to Equation (6) and (7) results in m-n = 4.3 and n = 1.6. Approximately, a =1, b = 1, p = 2 and q = 4 were obtained from these results and came to the conclusion as described earlier that the extracted complexes could be presented as R_4NCuCl_2 and R_4NFeCl_4

EXTRACTION OF COPPER AND IRON FROM SULFATE SOLUTIONS CONTAINING SOME CHLORIDE ION

The effect of chloride ion concentration Figure 2 shows that the extraction of coppe and iron versus the concentration of chloride. The extraction of Fe(III) increases steeply with increase of Cl^- concentration when it is low and becomes quite slow after the chloride concentration reaching 50 g/l. Unlikely, the extraction of Cu(II) increases quickly when the Cl^- concentration is higher than 50 g/l, and the extraction of ferrous ions is very low and only shows minor trend with Cl^- concentration. Nevertheless, when Cu(II) and Fe(II) are coextraction from chloride medium, the extraction of both ions are higher than that when they are present separately, especially when the Cl^- concentration is higher than 50 g/l (Fig.3)

When Cu(II) and Fe(III) are coextracted, the extraction of both ions is decreased because of the competing extraction and while Cu(II), Fe(II) and Fe(III) are contained in the solution, the amount extracted is in between those obtained with the two cases just described.

The effect of the concentration of R_4NCl and metals The extraction behaviors of cupric and ferrous ions depend on their relative concentrations. Keeping initial Fe(II) concentration in the feed solution constant the extraction of iron increases with the increase of Cu(II) concentration, however, the extraction of copper decreases with the increasing of its own concentration in the feed slotion, and vice versa. At the same time, the extraction amount is also a function of the concentrations of both quaternary ammonium chloride and chloride ions.

The effect of nickel and cobalt in solution on the extraction and separation of copper and iron It has been found experimentally that the concentration of $NiSO_4$ and $CoSO_4$ in the feed solution have not much influence on the extraction and separation of copper and iron. Nickel is not taken into the organic phase at all and the extraction of cobalt is very low with Cl^- concentration about 50 g/l. The separation factor between iron and cobalt $\beta_{Fe/Co}$ and that between copper and cobalt $\beta_{Cu/Co}$ are about 300 and 90 respectively so the separation of iron and copper from cobalt and nickel is possible with Cl^- concentration 50 g/l. Figure 4 is the results for a feed solution containing Fe 2.0 g/l, Cu 4.24 g/l, Ni 60.7g/l, and Co 16.28 g/l.

The isothermal of coextraction of Cu(II) and Fe(II) Figure 5 shows the isothermal of Cu(II) and Fe(II) coexisting in both phases with Cl^- of 51.2 g/l. It can be concluded from McCabe-Thiele diagram that the iron concentration in the aqueous solution can be reduced to less than 0.01 g/l, with about 1 g/l Cu still remained in the

solution. A number of stages are required to reduce copper content to the limit set up by the widely adopted nickel electrolysis practise.

The further removal of copper Reducing Cu(II) to Cu(I) the distribution coefficient of copper can be greatly improved. Adding 0.2-0.4 g/l sodium sulfite to the synthetic aqueous solution the distribution coefficient of copper D_{Cu} can be increased to more than ten times, but with real leaching solution to which some oxidant had been added to remove iron, the amount of Na_2SO_3 needed to increase the D_{Cu} to the same extent as obtained with synthetic solution was 2-3 g/l.

STRIPPING AND REGENERATION OF THE ORGANIC SOLVENT

It is quite easy to strip the loaded organic phase such as by using water. But copper can not be striped thoroughly by water or by dilute acid solution. It was reported that 0.3% H_2O_2 solution could striped 70-99% of copper from organic solution of secondary and tertiary amine, and it was not very efficient with quaternary ammonium salt solution. In our experiments using 0.3% H_2O_2 to strip copper loaded quaternary ammonium salt solution approximatly the same results reported for the secondary and tertiary amine have been obtained. To prevent iron hydrolysis and to give better stripping efficiency some acid has been added to the stripping solution. From the view of price cheaper $Fe_2(SO_4)_3$, which gives similar results as shown in Table 2, is a better oxidant in comparison with H_2O_2. Copper in ferric sulfate stripping solution could recovered by cementation with iron scrap.

Part of the chloride ions in the organic phase is removed with the stripping of copper and iron, meanwhile, part is exchanged with bisulfate ion according to the following equation

$$(8) \qquad \overline{R_4NCl} + HSO_4^- = \overline{R_4NHSO_4} + Cl^-$$

To make up the loss of chloride ion, the organic phase is contacted with 150 g/l NaCl solution and the equilibrium of the reaction as shown in Equation (8) would move to the left side. Then the organic solution became clear and can be recycled to the extraction stage. After neutralizing, the NaCl solution can be used again.

FLOWSHEET RECOMMENDED

The flowsheet presented in Figure 6 includes two parts, fristly copper and iron are removed with quaternary ammonium chloride solution then the cobalt is separated from nickel with quaternary ammonium thiocynate solution. This process can be applied to the cobalt and nickel sulfate solution containing Cu(II) and Fe(II) as impurities and also 45-55 g/l Cl^-, such as the hydrochloric-sulfuric acid leaching solution of cobalt removal cake from nickel elecrolysis process or solution of leaching cobalt-nickel matte. It is not necessry to remove iron from the solution by any pretreatment procedure or to oxiding ferrous to ferric in beforehand.

MINIPLANT SCALE EXPERIMENT

Counter current extraction has been carried out with a series of mixer-settlers to treat leaching solution of cobalt removal cake from nickel electrolysis process with the feed solution of 62.72 g/l Ni, 10.31 g/l Co, 3.9 g/l Cu, 1.70 g/l Fe, and 51.2 g/l Cl and pH 2. with three stages of primary removal of copper and iron (phase ratio A/O = 1) and with additional three stages for further removal of copper (O/A = 0.5), both copper and iron contents in the raffinate were less than 0.005 g/l. the separation factor β_{Fe} was 72, while β_{Co} was 230. The concentration of cobalt in the organic phase was 0.2 g/l. With four stages for stripping using a solution containing 4 g/l $Fe_2(SO_4)_3$ and 10 g/l H_2SO_4 could practically all the copper and iron and the contents of both iron and copper in barren organic phase were less than 0.002 g/l.

CONCLUSION

1. When Cu(II) and Fe(II) are coextracted from low chloride concentration solutions with solution of quaternary ammonium chloride, the redox reaction occurred between Cu(II) and Fe(II) has been elucidated by the experiments as indicated by the following equation:

$$Cu^{2+} + Fe^{2+} + 4Cl^- + 2R_4NCl = \overline{R_4NCuCl_2} + \overline{R_4NFeCl_4}$$

2. A process to remove copper and iron impurities from cobalt and nickel sulfate solutions with solution of quaternary ammonium chloride, followed by separating of cobalt from nickel with that of quaternary ammonium thiocynate has been developed and recommended for treatment of different nickel and cobalt containing solution.

Table 2

stripping solution	results of stripping			
	Cu g/l	Cu %	Fe g/l	Fe %
$Fe_2(SO_4)_3$ 5.38g/l	5.20	99.8	7.20	
$Fe_2(SO_4)_3$ 5.38; Cl^- 15g/l	4.60	88.3	6.00	
$Fe_2(SO_4)_3$ 5.38; Cl^- 37.6	3.33	63.9	3.24	
H_2SO_4 5g/l	3.80	73.0	2.03	99.0

Loaded organic phase containing Cu 5.21, Fe 2.05 g/l

ACKNOWLEDGEMENT

The authors wish to thank Professor CHEN Jiayong for his support to this work and our colleagues in Institute of Chemical Metallurgy for analyses and pilotplant work.

REFERENCES

1. E. I.Ioffe, et al, Nonferrous Metals (USSR), No.8, 33(1969).
2. I. F.Ivanov, et al, Hydrometallurgy, 4 377(1979).
3. ZHU Tun, HUANG Shu-lan and JIAO Da-ming, Chem.Metall.(China) No.1, 53(1982).
4. M. L. Good, J. C. Srivstava and F.F.Holland, Anal.Chim.Acta 31, 534(1964).
5. H. H. N. H. Irving and A. H. Nabilsi, Anal. Chim. Acta, 82 217(1968).

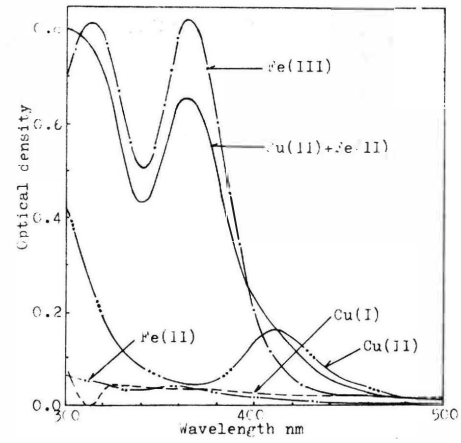

Figure 1 Absorption spectrum of loaded organic phase
Diluent : Xylene

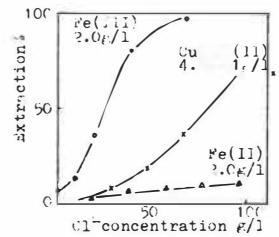

Figure 2 Effect of Cl^- concentration on the metals extraction

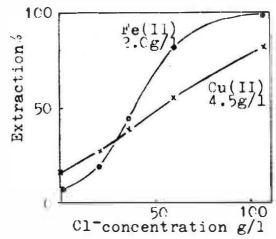

Figure 3 Effect of Cl^- concentration on the coextraction of Cu(II) and Fe(II)

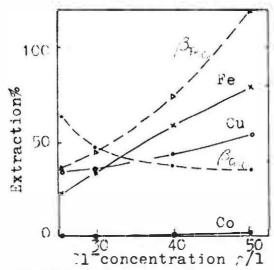

Figure 4 Relation between extraction and separation of metals in different Cl^- concentration

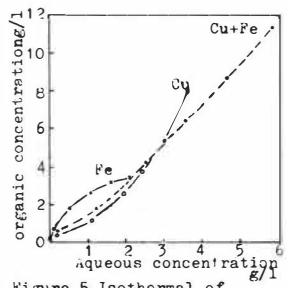

Figure 5 Isothermal of coextraction of Cu(II) and Fe(II)

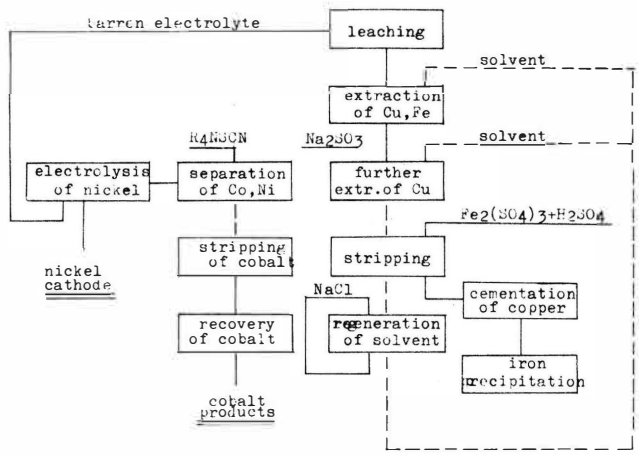

Figure 6 Schematic flowsheet

X-RAY DIFFRACTION STUDIES OF THE STRUCTURES OF ORGANIC-PHASE SOLVENT-EXTRACTION COMPLEXES

John H. Burns

Chemistry Division
Oak Ridge National Laboratory
Oak Ridge, Tennessee 37830 USA

INTRODUCTION

The molecular structure of the extraction complexes to be described here are being studied to add to the understanding of the mechanisms by which some solvent-extraction systems operate. Although there is a long history of the study of kinetic and equilibrium behavior of the transfer of metal ions from an aqueous to an organic phase, little has been done toward establishing the structures of the extraction complexes involved. From extraction equilibria and slope analysis the stoichiometry of many complexes has been deduced, but the nature of their molecular connectivities has been mainly a matter of speculation, occasionally supported by i.r. or Raman spectroscopic evidence.

The present work is focused on determination of the structures of complexes which form when the uranyl ion is extracted from nitric acid solutions with some organophosphorus reagents, individually and in synergistic combinations. These extractants are proven to be effective and of practical importance, and their equilibrium behavior has been the subject of much inquiry (1). But, rather than attempt to study the complexes in solution directly, the approach has been to prepare them in solid form, to determine the structures by crystallographic methods, and then to ascertain by X-ray scattering from solutions whether the solid-state molecular structures are maintained after dissolution of the complex.

EXPERIMENTAL METHODS

Those complexes which could be crystallized were analyzed by single-crystal X-ray and neutron diffraction methods, while liquids and solutions were studied by large-angle X-ray scattering techniques. The organophosphorus extractants used included di-2-ethylhexyl phosphoric acid (HDEHP) and di-n-butyl phosphoric acid (HDBP) as well as the neutral compounds tri-i-butyl phosphate (TiBP) and tri-n-butyl phosphine oxide (TBPO).

Crystals suitable for X-ray diffraction were obtained by melting together the pure ligand and $UO_2(NO_3)_2 \cdot 6H_2O$, followed by removal of the water released and cooling to induce crystallization. The complexes whose structures were determined included $UO_2(TBPO)_2(NO_3)_2$, $UO_2(TiBP)_2(NO_3)_2$ (2), $UO_2(DBP)_2$, and $UO_2(DBP)(TBPO)NO_3$. X-ray and neutron diffraction data were obtained from single crystals by use of computer-controlled four-circle diffractometers. The structures were determined by use of heavy-atom methods and their parameters refined by the method of least squares.

A 0.5 M solution of $UO_2(DBP)(TBPO)NO_3$ in toluene, pure $UO_2(DEHP)_2$, and a 1.3 M solution of $UO_2(DEHP)_2$ in toluene were studied by X-ray scattering. The liquid samples were contained in a thin quartz cylinder and the intensity of a beam of MoK_α X-rays scattered from about 3 cm^2 of the liquid's surface was measured at angles ranging from 2° to 130°. The techniques and method of data reduction are detailed elsewhere (3).

RESULTS AND DISCUSSION

The crystal structures of $UO_2(TBPO)_2(NO_3)_2$ and $UO_2(TiBP)_2(NO_3)_2$ contain individual molecules having the 1:2:2 stoichiometry (Figure 1b,1c). The equatorial plane perpendicular to each linear $[O{=}U{=}O]^{2+}$ ion is occupied by six O atoms; these are provided by two bidentate nitrate ions and by two monodentate neutral ligands. Indeed, this configuration has been found to exist in so many cases that such an arrangement is virtually assured in any $UO_2(NO_3)L_2$ complex in which L is a good electron donor. Other known neutral organophosphorus ligands which form complexes having this structure include $(CH_3O)_3PO$ (4), $(C_2H_5O)_3PO$ (5), and $(C_6H_5)_3PO$ (6). When water is the neutral ligand, as in $UO_2(NO_3)_2 \cdot 2H_2O$ (7), $UO_2(NO_3)_2 \cdot 3H_2O$ (8), or $UO_2(NO_3)_2 \cdot 6H_2O$ (9) (Figure 1a), it occupies the same site as L in the above compounds. From the bond lengths between the O atom of water and the U atom (2.40-2.45 Å) it is inferred that the attraction is somewhat weaker than that between the phosphoryl O atom and the U atom (2.36 Å).

Therefore, when these neutral ligands are employed for extraction, it is reasonable that the mechanism involve the displacement of water from the UO_2^{2+} coordination by phosphoryl groups at the organic-aqueous interface, followed by attachment of nitrate ions and movement of the complex into the organic phase. The existence in solution of complexes of this type with the same stoichiometry has been deduced by other methods (10).

Extraction of the uranyl ion with a substituted phosphoric acid produces a quite different kind of complex. Some idea of the nature of this complex can be gained from the crystal structure of $UO_2(DBP)_2$. It contains polymeric chains in which the uranyl ions are doubly bridged by phosphate groups as shown in Figure 2. The existence of polymers in this compound was predicted earlier (11), although the sixfold coordination of the U atom and the details of the bridging were not correctly anticipated. This prediction was based on another model which had been used to explain the behavior of U(VI)-HDEHP interactions in organic solutions (12). That model proposed that the polymer exists in solution when the U:HDEHP ratio is about 1:2, but that at lower concentrations, the chains are shorter and ultimately form a 1:4 monomeric complex. As yet, this monomer has not been isolated.

Perhaps the best known synergistic combination for extraction of U(VI) is HDEHP and tri-n-octylphosphine oxide (TOPO). The product extracted from nitrate solution using this mixture is a liquid, but a solid complex can be prepared from an analogous system whose components are HDBP and TBPO. This solid was analyzed and its crystal structure shown to contain dimeric molecules of $[UO_2(DBP)(TBPO)NO_3]_2$, Figure 3. Examination of this molecule may provide some clues as to the role of structure in synergism. For example, there is the double bridge of phosphate groups linking uranyl ions as in the $UO_2(DBP)_2$ polymer; but instead of continuing, the chain is terminated by a TBPO molecule and a nitrate ion. This suggests that the neutral molecule helps fill the coordination requirements of the U atom, interferes with polymerization, and thereby produces a more extractable species.

As a result of all these crystal studies we know considerably more details concerning these molecules in the solid state, but it is yet to be determined if they retain the same structure or even the same stoichiometry in solution. Toward this objective we have begun the study of some solutions of these complexes by large-angle X-ray scattering (13). If the known molecular structures persist in solution it may be possible to identify them by this method. Some preliminary results are shown in Figure 4. The radial distribution function g(r), a measure of the number and kind of atomic interactions at a separation r, was obtained for a 0.5 M solution of $UO_2(DBP)(TBPO)NO_3$ in toluene. Another such distribution, labelled "difference," was obtained by subtracting the contribution of the solvent. In this curve some of the peaks are tentatively identified as follows: C-C (1.45 Å), U=O (1.85 Å), U···O (2.33 Å), and U···P (3.69 Å). (Peaks below 1.2 Å are an artifact from data termination at finite angles). While these results alone do not establish the structure in solution, the fact that there are some recognizable features is promising; and the full potential of using this technique is yet to be established.

Acknowledgement. This research was sponsored by the Division of Chemical Sciences of the U.S. Department of Energy under Contract W-7405-eng-26 with the Union Carbide Corporation.

REFERENCES

1. C. A. Blake, C. F. Baes, Jr., and K. B. Brown, Ind. Eng. Chem. 50, 1763 (1958).
2. Neutron diffraction by G. M. Brown, ORNL (1982).
3. A. H. Narten and H. A. Levy in "Water, A Comprehensive Treatise," V. 1, F. Franks, Ed., Plenum Press, N.Y. (1979) p. 311.
4. G. Agostini, G. Giacometti, D. A. Clemente, and M. Vicentini, Inorg. Chim. Acta 62, 237 (1982).
5. J. E. Fleming and H. Lynton, Chem. and Ind. 1415 (1960).
6. N. W. Alcock, M. M. Roberts, and D. Brown, J.C.S. Dalton 25 (1982).
7. N. K. Dalley, M. H. Mueller, and S. H. Simonsen, Inorg. Chem. 10, 323 (1971).
8. V. M. Udovenko, E. V. Stroganov, and A. P. Sokolov, Soviet Radiochem. 5, 83 (1963).
9. J. C. Taylor and M. H. Mueller, Acta Cryst. 19, 536 (1965).
10. L. L. Burger, J. Phys. Chem. 62, 590 (1958); T. V. Healy and H. A. C. McKay, Recueil, 75, 730 (1956).
11. T. V. Healy and J. Kennedy, J. Inorg. Nucl. Chem. 10, 128 (1959).
12. C. F. Baes, Jr., R. A. Zingaro, and C. F. Coleman, J. Phys. Chem. 62, 129 (1958).
13. J. H. Burns and A. H. Narten, 1983.

ORNL-DWG 83-9933

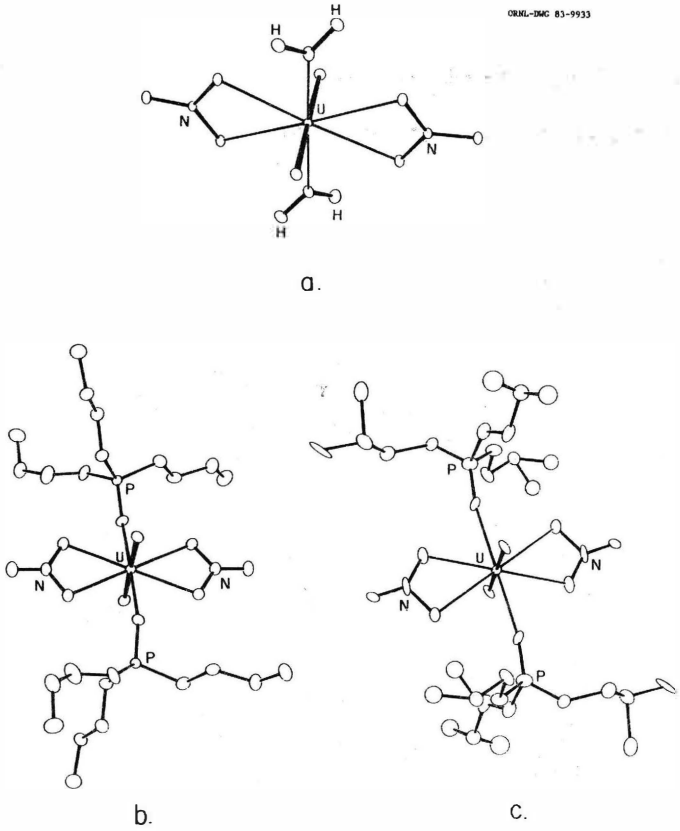

FIGURE 1. (a) URANYL NITRATE HEXAHYDRATE (b) $UO_2(NO_3)_2(TBPO)_2$ (c) $UO_2(NO_3)_2(TiBP)_2$

ORNL-DWG 83-9934

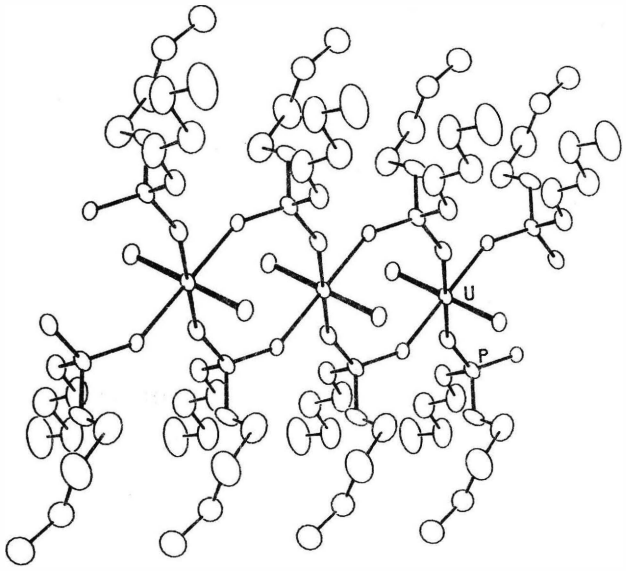

FIGURE 2. A POLYMERIC CHAIN IN THE STRUCTURE OF $UO_2(DBP)_2$

ORNL-DWG 83-9932

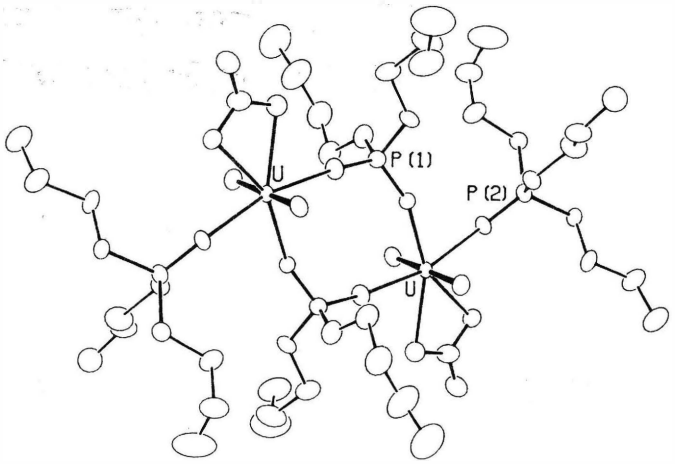

FIGURE 3. THE DIMERIC MOLECULE OF $UO_2(DBP)(TBPO)NO_3$

ORNL-DWG 83-9728

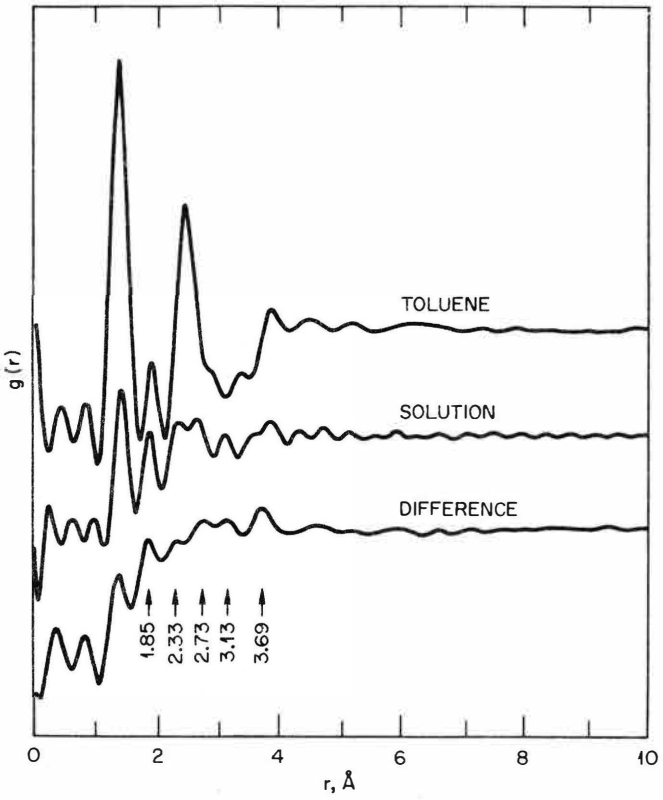

FIGURE 4. RADIAL DISTRIBUTION FUNCTION FOR TOLUENE, A 0.5 M SOLUTION OF $UO_2(DBP)(TBPO)NO_3$ IN TOLUENE, AND A DIFFERENCE FUNCTION

COEXTRACTION OF URANIUM AND TECHNETIUM IN TBP-SYSTEMS

T. N. Jassim, J. O. Liljenzin, R. Lundqvist, G. Persson

Department of Nuclear Chemistry
Chalmers University of Technology
S-412 96 Göteborg, Sweden

INTRODUCTION

The distribution ratio of technetium between tri-n-butyl phosphate (TBP) solutions and nitric acid is affected by the presence and extraction of uranyl nitrate (1,2), generally yielding higher distribution ratios below 0.2-0.5 M HNO_3 and above 2-3 M HNO_3, than expected from the behavior in absence of uranium. MASACEK and KABRABOVA studied the phenomenon at low acidities and 30% TBP (3,4). Previous studies at other laboratories (1,2) have been limited to 30% TBP and $\leq$ 4 M HNO_3.

The present trends in the development of the PUREX process, towards higher acidities and higher uranium loading, makes a model for technetium coextraction with uranium desirable. The increasing concern for the final storage of radioactive wastes, for which Tc plays an important role (5), further emphasizes the importance of its fate in the PUREX process. In a previous paper by us (6), the coextraction of Tc with uranium was studied in a larger nitric acid interval (0.05-9 M HNO_3) at 30% TBP and for 6 M HNO_3 at varying TBP concentrations. An equation was derived for calculation of the contribution from the coextraction with uranyl nitrate to the distribution ratio of Tc at 6 M HNO_3 and room temperature.

The PUREX process normally operates at elevated temperatures in some sections, in order to obtain improved decontamination or better stripping conditions. The variation of the distribution ratio of Tc with temperature is therefore important in calculations of its behavior in the PUREX process. The aim of the present work is to extend the knowledge of technetium extraction in the presence of uranyl nitrate towards higher temperatures and to derive an equation for the coextraction of Tc with uranyl nitrate that is valid in an extended interval of acidities and temperatures for different TBP concentrations.

EXPERIMENTAL

Tri-n-butyl phosphate was obtained, purified, and diluted with an odourless kerosene diluent as previously described (6). All other chemicals were of analytical grade and were used as obtained.

^{99m}Tc was eluted from a ^{99}Mo-^{99m}Tc generator and was obtained in a saline solution. It was therefore purified by extraction with cyclohexanone as described by SCHULZ (7).

All experiments have been made using ARUFVE equipment (8). ^{99m}Tc was measured on-line using γ-scintillation counting (2" x 2" NaI(Tl)) and detector cells with variable volume to allow subtraction of the activity from ^{99m}Tc adsorbed on the cell walls. The uranium content in the solutions affects the γ-measurements in two ways, by the γ-activity emitted from uranium and its daughters, adding to the true value, and by the absorption of the γ-activity from ^{99m}Tc, subtracting from the true value. To account for this, separate calibration experiments were made, one with only uranium present in varying concentrations, determining the measured γ-activity from uranium, one with a known amount of ^{99m}Tc present, measuring the activity as function of the uranium added. In the latter case, the ^{99m}Tc-activity was assumed to decrease with time with a half-life of 6.02 h.

Uranium was measured on-line by the transmission of the 60 keV γ-line from a mechanically chopped ^{241}Am source through fixed volume detector cells. Background effects from varying concentrations of TBP and nitric acid and varying temperature were determined in separate calibration runs and the measurements were corrected accordingly.

The nitric acid concentration in each phase was determined by titration with sodium hydroxide at room temperature on samples withdrawn during the experiment and stored in stoppered vials. For samples containing uranium, titrations were carried out after addition of KF to resolve the equivalence points (6,9).

RESULTS AND DISCUSSION

The distribution of Tc and HNO_3 were measured in the absence of uranium at a series of temperatures from 20 to 60°C for nitric acid concentrations from 1 to 6 M and 5, 10, 20, 30 and 40% TBP. The extraction constant for nitric acid at different temperatures was calculated from the data obtained. It was found that the extraction constant was independent of temperature and TBP concentration within experimental errors. The extraction constant was then calculated as a mean of all data at each nitric acid concentration. These data were then interpolated to obtain the value of the extraction constant at any acidity within the range studied. The distribution of Tc was found to agree better with the data given by LIESER et.al. (2) than those given by PRUETT (10).

The extraction of technetium, nitric acid and uranium was measured at 5 M aqueous nitric acid concentration in the aqueous phase, aqueous uranium concentrations from about 10 to about 100 g/l, temperatures from 20 to 60°C and 10, 20 and 30% TBP. It was observed that the distribution of uranium decreases with temperature but that the distribution of nitric acid increases with temperature, see Figure 1. This can be interpreted as due to the different number of molecules involved in extraction of nitric acid and uranyl nitrate. A decreasing uranium extraction then increases the concentration of "free" TBP which leads to an increased extraction of nitric acid. The behavior of technetium is more complex. To remove the effect of a varying aqueous uranium concentration the data for each temperature were interpolated to a series of constant aqueous uranium concentrations. It can be seen from Figure 2 that the temperature effect on the behavior of technetium gradually shifts with the uranium concentration. This can be interpreted as due to formation, in the aqueous phase, of one (or more) extractable complex containing both uranium and technetium.

The distribution data for technetium, uranium and nitric acid (164 sets of values) were used for fitting of the empirical equation used in our earlier paper (6).

$$(1) \qquad \log D_{Tc} = A + B \log(H)_{aq} + C \log(TBP)_{free}$$

The "free" TBP concentration was calculated from the measured distribution of nitric acid using the extraction constant determined in the first series of experiments. Data from different temperatures gave slightly different values for A, B, and C, see Figure 3. By fitting the equation to all data with the assumption that A, B, and C were linear functions of temperature, it was found that A was independent of temperature within experimental errors, and that the assumption that B and C changed linearly with temperature fitted well to the data. The following values were obtained from this fit, where T stands for temperature in degrees centigrade.

$$A = 2.219 \pm 0.043$$
$$B = 0.816 \pm 0.021 + (0.00528 \pm 0.00053)\,T$$
$$C = 1.451 \pm 0.022 + (0.00484 \pm 0.00036)\,T$$

These constants agrees well with our previous values for 6 M nitric acid and room temperature. To illustrate the fit obtained, eqn. 1 was transformed to

$$(2) \qquad (H)_{aq} = \sqrt[B]{\frac{D_{Tc}}{10^{A}\,(TBP)^{C}_{free}}}$$

The aqueous uranium concentrations were then calculated backwards from eqs. 2 for all data, using measured D-values for Tc and nitric acid, the total TBP concentration and the extraction constant for nitric acid. The result was plotted against measured values on $(U)_{org}$, see Figure 4.

The experiments are still in progress and more data will be given in the final paper.

REFERENCES

1. C.H. Sidall III, Report DP-966 (1963).
2. K.H. Lieser, A. Krüger, R.N. Singh, Radiochim. Acta, 28, 97 (1981).
3. F. Masacek, Radiochem. Radioanal. Letters, 22, 175 (1975).
4. F. Masacek, J. Kadrabova, J. Radioanal. Chem., 51, 97 (1979).
5. M.D. Hill, Report HRPD-P86 (1979).
6. T.N. Jassim, J.O. Liljenzin, G. Persson, Radiochim. Acta, in press.
7. W.W. Schulz, Proc. Solvent Extraction Conf. 1980 (ISEC-80), Liege, Belgium, Paper 80-108 (1980).
8. J. Rydberg, H. Reinhardt, J.O. Liljenzin, Ion Exchange and Solvent Extraction, Vol. 3, (J.A. Marinsky, Y. Marcus, Eds.) Marcel Dekker, New York 1973, p. 111.
9. H.H.Ph. Moeken, W.A.H. Van Neste, Eurochemic Technical Report ETR-202 (1967).
10. D.J. Pruett, Radiochim. Acta, 28, 153 (1981).

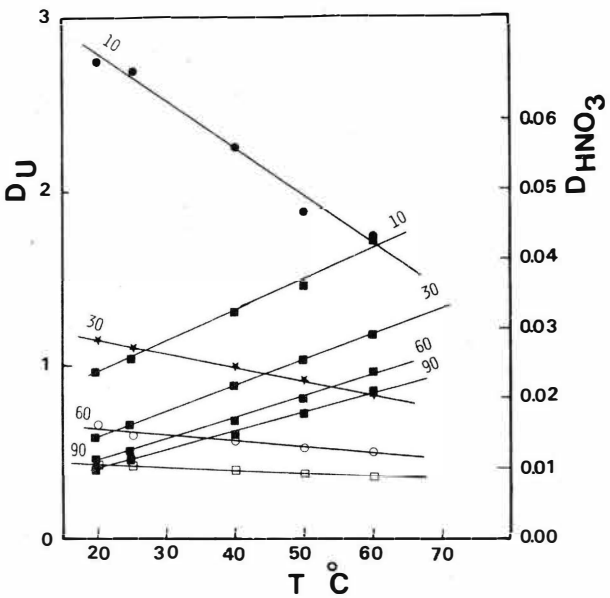

FIGURE 2. DISTRIBUTION RATIOS OF U AND HNO_3 AS FUNCTION OF TEMPERATURE AT CONSTANT URANIUM CONCENTRATION IN THE AQUEOUS PHASE, 6 M HNO_3, AND 30 % TBP. NUMBERS ON THE CURVES ARE AQUEOUS URANIUM CONCENTRATIONS IN G/L. ■ HNO_3; ● ✱ ○ □ U.

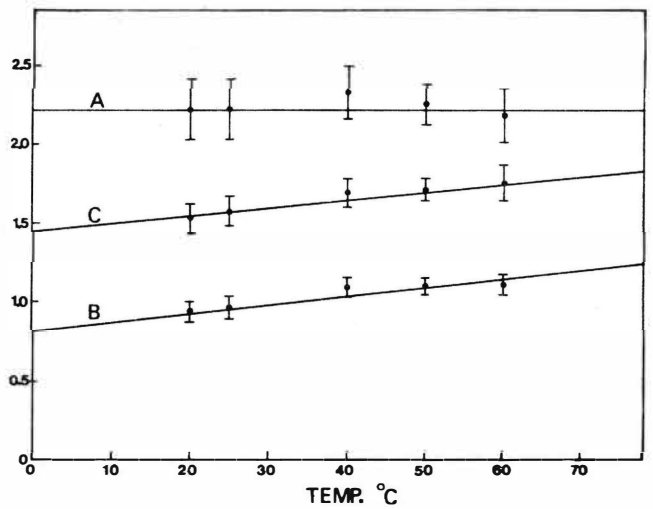

FIGURE 3. CONSTANTS A, B, AND C, CALCULATED FROM MEASUREMENTS AT DIFFERENT TEMPERATURES.

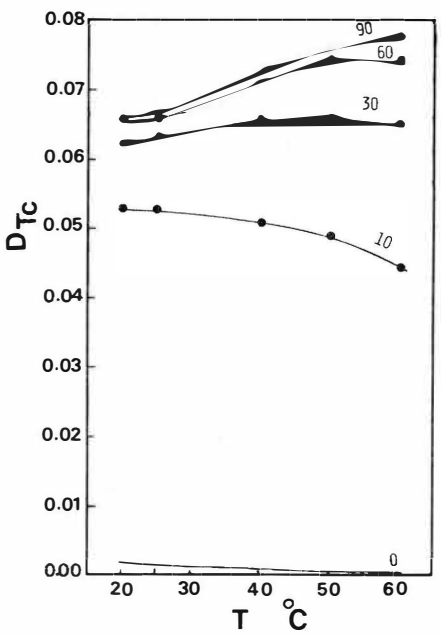

FIGURE 4. [illegible] AS FUNCTION OF TEMPERATURE AT CONSTANT URANIUM CONCENTRATION IN THE AQUEOUS PHASE, 6 M HNO_3, AND 30 % TBP. NUMBERS ON THE CURVES ARE AQUEOUS URANIUM CONCENTRATIONS IN G/L.

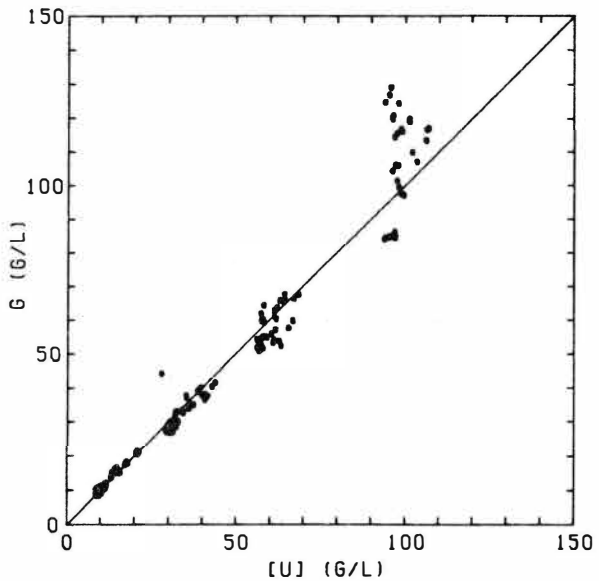

FIGURE 4. CORRELATION BETWEEN CALCULATED, G, AND MEASURED URANIUM CONCENTRATIONS.

SYNERGISM IN THE EXTRACTION OF ZINC(II) AND CADMIUM(II) WITH LOWER FATTY ACIDS IN THE PRESENCE OF NITROGEN CONTAINING ORGANIC BASES

S. K. Gogia, D. Singh, O. V. Singh and S. N. Tandon

Department of Chemistry
University of Roorkee
Roorkee 247667 (U.P.), India

The last decade has seen a growing interest in the study of synergism in the extraction of metal carboxylates. Relatively very little work has been reported on synergism in the extraction with lower fatty acids. Pyatnitskii et.al. (1-3) investigated the extraction of Cu (II), Co (II), Ni (II), and Fe (III) with lower aliphatic monocarboxylic acids and observed that the extractions are synergistically enhanced in the presence of amines. In the absence of any such data on Zn (II) and Cd (II), it was planned to systematically investigate the extraction of these metal ions with a series of lower fatty acids in the presence of various aliphatic and heterocyclic amines.

The present communication reports the extraction of Zn (II) and Cd (II) with chloroform solution of propionic, butyric and valeric acids using aliphatic amines viz. n-butylamine, dibutylamine and tributylamine and heterocyclic amines viz. B-picoline, pyridine and quinoline as synergists. The effect of pH of the aqueous phase and concentration of the metal ion, acid and amine on extraction has been investigated. The probable compositions of the extracting species have been proposed by the method of slope analysis. On the basis of extraction data the extraction constants (K_{ex}) have been calculated and the relative effectiveness of the amines as synergists compared.

EXPERIMENTAL

The partition of the acids and amines between aqueous and chloroform phases was determined by the usual volumetric methods. The partition coefficient (P_B) of amine in the presence of acids was determined by titrating the organic phase with perchloric acid in glacial acetic acid using methyl violet in chlorobenzene as indicator (4). To study the distribution of Zn (II) and Cd (II) between water and chloroform solution of acid and amine equal aliquots (10 ml) were shaken at room temperature, 30 $\pm$ 2°C, for about five minutes to complete equilibration. The equilibration pH of the aqueous phase was recorded after each extraction by expanded scale pH meter (ECIL, India). After clear separations of the two phases the activity of suitable aliquots was measured; for ^{65}Zn a well type NaI (Tl) scintillation counter was used and B-activity of ^{115m}Cd was counted using a G.M. counter. Each experiment was run in duplicate and the average values have been used. The values of percent extraction show a precision within $\pm 2\%$ at about 65% extraction.

EQUILIBRIUM TREATMENT

The extraction equilibrium may be written as

$$(1)\quad M^{n+}_{aq} + p(B.HA)_{org} + \frac{n-p+x}{2}(H_2A_2)_{org} \rightleftharpoons (M.B_p.A_n.xHA)_{org} + nH^+_{aq}$$

where

M^{n+} = metal ion

n = valency of metal ion

p = number of amine molecules coordinated

B = amine

HA = monomeric acid molecule

x = number of solvating acid molecules

$(H_2A_2)_{org}$ = dimeric acid molecule in organic phase

Hence, equilibrium constant

$$K_{ex} = \frac{[M.B_p.A_n.xHA]_{org}.[H^+]^n_{aq}}{[M^{n+}]_{aq}.[B.HA]^p_{org}.[H_2A_2]^{(n-p+x)/2}_{org}}$$

or

$$(2)\quad \log D = \log K_{ex} + npH + \frac{n-p+x}{2}\log[H_2A_2]_{org} + p\log(B.HA)_{org}$$

where

distribution coefficient $D = \frac{[M.B_p.A_n.xHA]_{org}}{[M^{n+}]_{aq}}$, assuming that the metal does not form any other complex with the excess of acid.

From equation (2) by differentiation with respect to pH

$$\left[\frac{\delta \log D}{\delta pH}\right]_{(H_2A_2)_{org}} = n$$

Thus the slope of log D versus pH plot at constant acid concentration in the organic phase will give the number of protons liberated due to the consumption of acid molecules in the complex formation.

The total concentration of acid in both phases

$$(3)\quad [HA]_{total} = 2[H_2A_2]_{org} + [HA]_{org} + [HA]_{aq} + [A^-]_{aq}$$

similarly total concentration of amine

$$(4)\quad [B]_{total} = [B]_{org} + [B]_{aq} + [BH^+]_{org}$$

Therefore, the equilibrium concentration of amine in the aqueous phase can be found from the equation,

$$(5)\quad [B]_{aq} = \frac{[B]_{total}.K_b}{P_B.K_b + K_b + [H]^+}$$

where

[B] = amine concentration

P_B = partition coefficient of amine

K_b = protonation constant of amine

similarly

$$[HA]_{aq} = \frac{[HA]_{total}.K_a}{P_{HA}.K_a + K_a + [H^+]}$$

where

K_a = protonation constant of acid

P_{HA} = partition coefficient of acid.

RESULTS AND DISCUSSION

Distribution ratio of propionic, butyric and valeric acids between chloroform and water increases with the increase in initial acid concentration. This may be ascribed to the dimerization of the acid molecules in the chloroform. For dimeric molecules in the organic phase,

$$(6)\quad D = \frac{C_{org}}{C_{aq}} = P_{HA} + 2K_D P^2_{HA}[HA]_{aq}$$

K_D = dimerization constant of acid.

or

$$\frac{C_{org}}{C^2_{aq}} = \frac{P_{HA}}{C_{aq}} + 2K_D P^2_{HA}$$

when dimerization is more or less complete

(7) $\log C_{org} = \log 2K_D p_{HA}^2 + \log C_{aq}$

The plots of log C_{org} versus log C_{aq} for all acids gave straight lines with slopes around 2, thus confirming the assumption of dimerization of acids in chloroform. The average values of partition coefficient for propionic, butyric and valeric acids between chloroform and water are 0.26, 1.4. and 16.5 respectively.

Partition coefficients of amines between chloroform and water in the presence of acids show higher values, suggesting the formation of amine salts in chloroform. This is confirmed by the comparison of the nmr spectra of the acids with and without the presence of amines. The shift in the signal of -COOH group towards the weaker field as compared with the corresponding signal of acid in the absence of amines indicates the intermolecular interaction of the acid with the amine through hydrogen bonds.

It has been observed that Zn (II) and Cd (II) show very poor extractions into chloroform solution of propionic, butyric and valeric acids. If, however, amine is added to the system extractions are synergistically enhanced to $\gg$ 90%. The enhancement is probably due to the fact that organic bases are effective in replacing the water molecules from the coordination sphere of the metal, thus rendering the species less hydrophilic. The incorporation of the amine molecule in the extracting species is indicated by the uv spectra of the organic extract.

EFFECT OF pH OF THE AQUEOUS PHASE

The extraction increases with increase in pH and reaches a maximum near the hydrolysis pH of the metal ion except in the case of n-butylamine where the pH range of maximum extraction is extended to 10.5. Therefore, all subsequent studies were carried out at constant pH 6.5 except with n-butylamine where pH was 10.5. The results of plot of log D versus pH at constant metal ion (1×10^{-4}M), acid (0.50 or 1.0M) and amine (0.50 or 1.0M) concentrations indicate straight lines with slope near 2. This suggests the release of 2 protons by the utilization of 2 acid molecules per metal atom to neutralize che charge on the metal ions.

EFFECT OF METAL ION CONCENTRATION

The effect of metal ion concentration (10^{-6} - 10^{-3}M) on extraction has been found to be practically insignificant ($\pm$3%). This rules out the possibility of extraction of any polymeric species in the above mentioned concentration range. A concentration of 1.0×10^{-4}M of the metal has been chosen for the present investigations.

EFFECT OF ACID CONCENTRATION

The concentration of acids were varied at constant pH and amine concentration and it was found that with the increase in the concentration of the acid the extraction increases. It was also observed that with increase in the number of carbon atoms (C_3 - C_5) in the acid the extraction efficiency increases and shows the following order:

valeric $\rangle$ butyric $\rangle$ propionic

From the slope of the plots of log D versus log $[H_2A_2]_{org}$ at constant amine concentration the number of acid molecules solvated with the extracted species have been calculated and found to be 3 and 2 in the case of aliphatic and heterocyclic amines, respectively. Some typical plots are given in figure 1.

EFFECT OF AMINE CONCENTRATION

Figure 2 shows a typical plot of log D versus log [amine] at constant pH and acid concentration. Straight lines with slope near 1 and 2 were obtained suggesting the incorporation of 1 and 2 molecules of aliphatic and heterocyclic amines, respectively in the extracted species. On the basis of above results the compositions of the extracted species for Zn(II) and Cd(II) may be represented as $ZnA_2 \cdot 3HA \cdot B$ and $CdA_2 \cdot 3HA.B$ and $ZnA_2 \cdot 2HA.2B$ and $CdA_2 \cdot 2HA.2B$ in the case of aliphatic amines and heterocyclic amines, respectively.

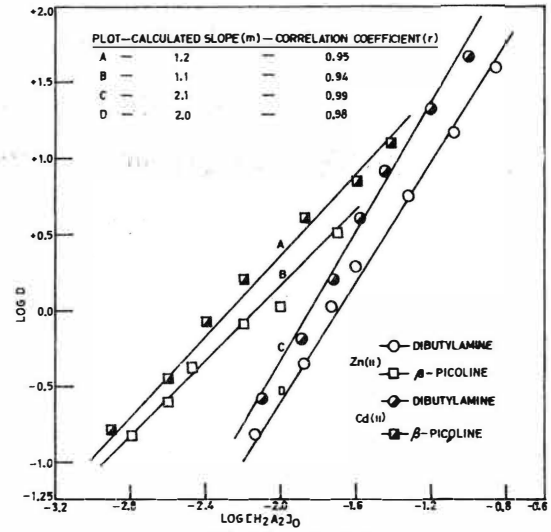

FIGURE 1. VARIATION OF DISTRIBUTION RATIO FOR Zn(II) & Cd(II) AS A FUNCTION OF DIMERIC BUTYRIC ACID CONCENTRATION AT CONSTANT pH (6.5) AND AMINE CONCENTRATION (0.50M).

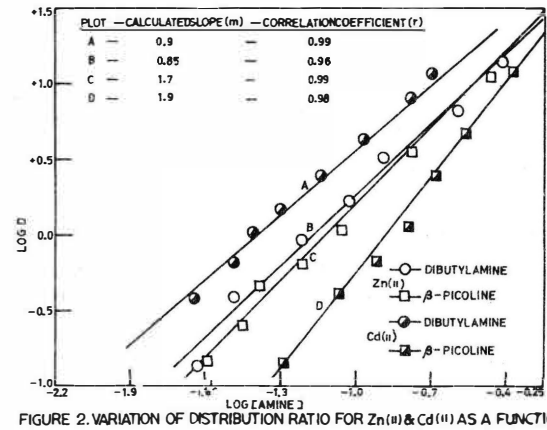

FIGURE 2. VARIATION OF DISTRIBUTION RATIO FOR Zn(II) & Cd(II) AS A FUNCTION OF AMINE CONCENTRATION AT CONSTANT pH (6.5) AND BUTYRIC ACID CONCENTRATION (0.50M).

CALCULATION OF EXTRACTION CONSTANTS (K_{ex})

The equation (2) has been used for the calculation of extraction constants for Zn (II) and Cd (II) with different acids in the presence of various aliphatic and heterocyclic amines. Based on extraction constant values it is apparent that heterocyclic amines are better synergists than the aliphatic counterparts. The relative order of their effectiveness as synergists in the two series is

(i) dibutylamine $\rangle$ tributylamine $\rangle$ n-butylamine

(ii) pyridine $\approx$ B-picoline $\rangle$ quinoline

REFERENCES

1. I.V. Pyatnitskii, Aie Omode, V.V. Sukhan, V.A. Frankovskii, Zh. Anal. Khim., 28, 50 (1973).
2. V.V. Sukhan, I.V. Pyatnitskii, A.G. Sakhno, Zh. Anal. Khim., 28, 541 (1973).
3. I.V. Oyatnitskii, Aie Omode, V.V. Sukhan, Zh. Anal. Khim., 28, 2317 (1973).
4. J.S. Fritz, Anal Chem., 22, 1028 (1950).

SOLVENT EXTRACTION OF METAL IONS BY IONIZABLE CROWN ETHERS

Richard A. Bartsch, Witold A. Charewicz*, and Sang Ihn Kang

Department of Chemistry
Texas Tech University
Lubbock, Texas 79409 USA

*Visiting Research Professor from the Institute of Inorganic Chemistry and Metallurgy of Rare Elements, Technical University of Wroclaw, 50-370 Wroclaw, Poland.

INTRODUCTION

The preparation of novel organic complexing agents often results in the development of new separation systems for aqueous ions. Thus, the synthesis and study of highly lipophilic hydroxy oximes led to the current utilization of these compounds as commercial extractants for the hydrometallurgy of non-ferrous metals (1).

The potential of crown ethers (macrocyclic polyethers) as the next generation of specific extracting agents for metal ions (2-4) has been markedly enhanced by the introduction of crown ethers which bear a pendant carboxylic acid group (5). In such molecules, novel bifunctional complexing agents are created by the combination of an ionizable group with an ion-binding cavity having fixed dimensions. These ionizable crown ethers possess a distinct advantage over neutral crown ether compounds in that extraction of a metal cation from an aqueous phase into an organic medium does not require the concomitant transfer of the aqueous phase anion (6).

In earlier studies (6-10), we examined the solvent extraction of alkali and alkaline earth cations from water into chloroform by several dibenzo crown ether carboxylic acids. These complexing agents exhibited extraction efficiencies and selectivites which surpassed those of a closely-related, non-ionizable dibenzo crown ether and of lipophilic carboxylic acids (6,7,9). By attachment of lipophilic groups, loss of the crown ether carboxylic acid from the organic medium into the aqueous phase could be prevented (8,10).

We now report results for the solvent extraction of alkali and alkaline earth cations from water into chloroform by highly lipophilic ionizable crown ethers 1-8 in which the lipophilic group attachment site, crown ether cavity size, and ionizable group are systematically varied.

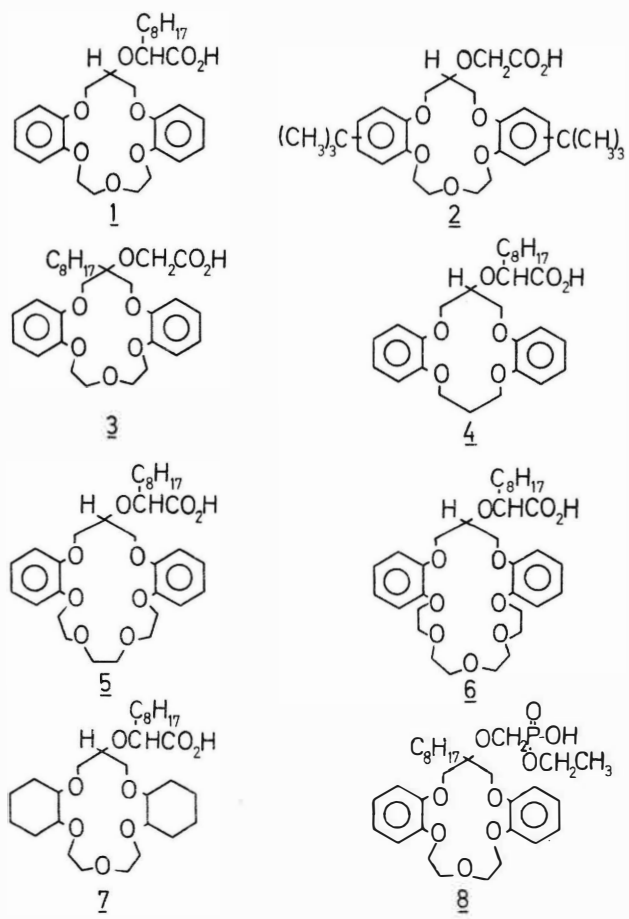

EXPERIMENTAL

Procedures for extraction of aqueous alkali metal chloride solutions (0.25 N in each of LiCl, NaCl, KCl, RbCl, and CsCl) or aqueous alkaline earth chloride solutions [0.25 N (2 equivalents per mole) in each of $MgCl_2$, $CaCl_2$, $SrCl_2$, and $BaCl_2$] with 0.050 N solutions of the ionizable crown ether in chloroform were the same as previously described (6-8).

RESULTS AND DISCUSSION

Typical data for the concentrations of metals in the chloroform phase vs. the equilibrium pH of the aqueous phase in competitive extractions of alkali metal cations by a crown ether carboxylic acid are shown in Figure 1. The observed pH dependence verifies that significant extraction occurs only when the carboxylic acid group is ionized.

Table 1 presents a compilation of extraction selectiviety and efficiency (organic phase loading of metals) information for extraction of alkali metal and alkaline earth cations by ionizable crown ethers 1-8.

Dibenzo crown ether carboxylic acids 1-3 are structural isomers which differ only in the site(s) of lipophilic group attachment. All three exhibit similar selectivities for Na^+ in competitive extractions of alkali metal cations. However for 3 the efficiency (maximal metal loading of the organic phase) is appreciably higher than with either 1 or 2.

Table 1. Selectivity and Efficiency of Metal Ion Extraction from Water into Chloroform by Ionizable Crown Ethers.

Compound	Extraction Selectivity and Selectivity Coefficients[a,b]	Maximal Metal Loading of the Organic Phase[c]
1	Na^+ > K^+ > Li^+ > Rb^+ > Cs^+ (5, 17, 36, 83)	68%
	Ba^{2+} > Ca^{2+} > Sr^{2+} > Mg^{2+} (2, 6, 7)	96%
2	Na^+ > K^+ > Rb^+ > Cs^+ > Li^+ (7, 20, 34, ND[d])	58%
3	Na^+ > K^+ > Li^+, Rb^+, Cs^+ (7, ND[d])	98%
	Ba^{2+} > Ca^{2+} > Sr^{2+} > Mg^{2+} (2, 4, 22)	80%
4	Na^+ > Li^+ > K^+ > Rb^+ > Cs^+ (2.5, 5, 19, 60)	100%
	Ba^{2+} > Sr^{2+} > Ca^{2+} > Mg^{2+} (2, 3, 15)	90%
5	K^+ > Na^+ > Rb^+ > Cs^+ > Li^+ (4, 7, 11, 28)	100%
	Sr^{2+} > Ba^{2+} ~ Ca^{2+} > Mg^{2+} (6, 6, 60)	100%
6	K^+ > Rb^+ > Li^+ > Cs^+ > Na^+ (1.5, 1.9, 2.8, 3.0)	100%
	Ba^{2+} > Ca^{2+} > Sr^{2+} > Mg^{2+} (14, 33, 89)	100%
7	Na^+ > Li^+ > K^+ > Rb^+ > Cs^+ (4, 8, 24, 45)	48%
8	Na^+ > K^+ > Li^+, Rb^+, Cs^+ (15, ND[d])	100%
	Mg^{2+} > Ca^{2+} > Ba^{2+} > Sr^{2+} (1.2, 9, [illegible])	97%

[a]Selectivity coefficients are listed below the cation chemical symbol and express the ratio between the chloroform phase concentrations of the best extracted cation and the indicated cation. [b]Data are for an equilibrium pH = 10 for alkali metal cations and pH = 8 for alkaline earth cations. [c]For alkaline earth cations, a loading of 100% signifies complete formation of a ML_2 complex. [d]Not detected.

Compounds 4, 1, 5, and 6 form a series of lipophilic dibenzo crown ether carboxylic acids in which the polyether rings contain 14-, 16-, 19-, and 22-members, respectively. Estimated polyether cavity diameters for these compounds as well as literature values (11) for the diameters of the alkali metal and alkaline earth cations are presented in Table 2. Strongest complexation of monovalent and divalent metal cations by neutral crown ethers is observed when the ratio of the cation diameter to the polyether cavity diameter is 0.9 (12). Therefore in competitive extractions of alkali metal cations by compounds 4, 1, 5 and 6, selectivity for Li^+, Na^+, K^+ or Rb^+, and Cs^+, respectively, might be expected. The extraction selectivity data in Table 1 reveal that only with 1 and 5 are the predicted selectivities observed. Thus, factors other than the polyether cavity size must also be important in determining extraction selectivity. The same conclusion may be drawn from the observed selectivities in alkaline earth cation extractions.

Table 2. Polyether Cavity and Metal Ion Diameters (in angstroms).

Compound	Estimated Diameter	Alkali Metal Cation	Diameter	Alkaline Earth Cation	Diameter
4	1.2-1.5	Li^+	1.36	Mg^{2+}	1.56
1	2.0-2.4	Na^+	1.96	Ca^{2+}	2.12
5	3.0-3.5	K^+	2.66	Sr^{2+}	2.54
6	4.2-5.0	Rb^+	2.98	Ba^{2+}	2.83
		Cs^+	3.30		

Compounds 1 and 7 are identical except for replacement of the unsaturated benzo rings of 1 by saturated cyclohexano rings in 7. Compared with 1, compound 7 should be a stronger cation complexing agent since it contains only the more basic dialkyl ether oxygens in the polyether ring. Although both compounds show extraction selectivity for Na^+, the second best extracted ion is K^+ for 1 but is Li^+ for 7. The lower efficiency of 7 appears to arise from an extraction complex stoichiometry of ML•HL for this complexing agent.

The effect of varying the ionizable group is probed with compounds 3 and 8 which are identical except that 3 is a carboxylic acid and 8 is the mono ethyl ester of a phosphonic acid. Due to the greater acidity of the latter, extraction of alkali metal and alkaline earth cations from acidic aqueous solutions into chloroform is possible. In competitive alkali metal cation extractions by either 3 or 8, good selectivity for Na^+ and high efficiency are noted. The Na^+/K^+ extraction ratio is somewhat greater for the phosphonic acid derivative In view of these similarities in alkali metal cation extraction, the differences for alkaline earth cation extractions are striking. With 3 there is extraction selectivity for Ba^{2+} whereas with 8 Mg^{2+} and Ca^{2+} are the dominant cations in the chloroform phase. These results suggest that for alkaline earth cation complexation as the ionizable group becomes more acidic (less basic) the fit of the cation within the polyether cavity becomes more important in determining selectivity.

Further studies of metal ion extraction by ionizable crown ethers are in progress.

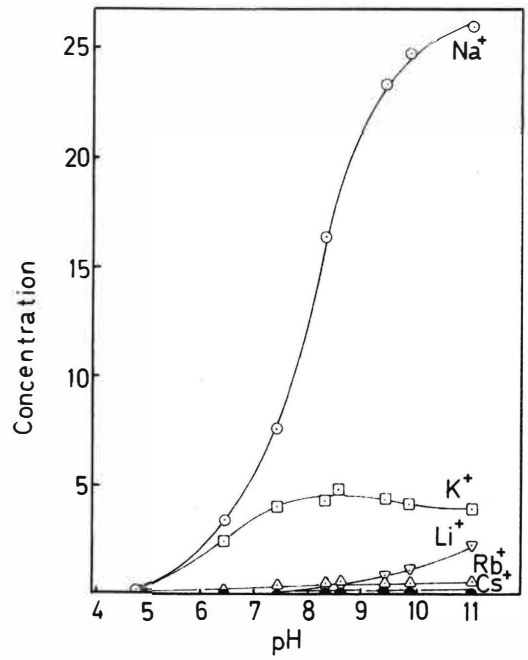

FIGURE 1. CONCENTRATIONS OF METALS (X 10^3) IN THE CHLOROFORM PHASE VS. THE EQUILIBRIUM PH OF THE AQUEOUS PHASE FOR COMPETITIVE EXTRACTIONS OF 0.25 N ALKALI METAL CATIONS BY 0.050 N 1

REFERENCES

1. D.S. Flett, J. Chem. Technol. Biotechnol. 29, 258 (1979).
2. Y. Marcus and L.E. Asher, J. Phys. Chem. 82, 1246 (1978).
3. I.H. Gerow and M.W. Davis, Sep. Sci. Technol. 14, 395 (1979).
4. I.H. Gerow, J.E. Smith, and M.W. Davis, Sep. Sci. Technol 16, 519 (1981).
5. R.A. Bartsch, G.S. Heo, S.I. Kang, Y. Liu, and J. Strzelbicki, J. Org. Chem. 47, 457 (1982).
6. J. Strzelbicki and R.A. Bartsch, Anal. Chem. 53, 1894 (1981).
7. J. Strzelbicki and R.A. Bartsch, Anal. Chem. 53, 2247 (1981).
8. J. Strzelbicki and R.A. Bartsch, Anal. Chem. 53, 2251 (1981).
9. J. Strzelbicki, G.S. Heo, and R.A. Bartsch, Sep. Sci. Technol. 17, 635 (1982).
10. W.A. Charewicz, G.S. Heo, and R.A. Bartsch, Anal. Chem. 54, 2094 (1982).
11. W.E. Moore, D. Amman, R. Bissig, E. Pretsch, and W. Simon in "Progress in Macrocyclic Chemistry," R.M. Izatt and J. J. Christensen (Eds.), Wiley-Interscience, New York, 1979, Vol. 1, p. 9.
12. J.J. Christensen, D.J. Eatough, and R.M. Izatt, Chem. Rev. 74, 351 (1974).

ACKNOWLEDGEMENT

This research was supported by the Office of Basic Energy Sciences of the Department of Energy (Contract DE-AS05-80ER-10604) and the Texas Tech University Center of Energy Research.

THE APPLICATION OF LANTHANIDE INDUCED SHIFTS IN SOLUTION NMR STUDIES OF COORDINATED EXTRACTANTS

Dale G. Kalina and E. P. Horwitz

Chemistry Division
Argonne National Laboratory
Argonne, Illinois 60439 USA

Over the past several years there has been a renewed interest in the examination of compounds which have the potential of behaving as bidentate, or chelating, extractants (1-3). In particular extractants containing the carbamoylmethylphosphoryl (CMP) moiety (A) have been the subject of numerous investigations. Because of the rather unique ability of these compounds to efficiently extract trivalent lanthanide and actinide ions from highly acidic solutions, these species have been under consideration for applications in fuel reprocessing schemes.

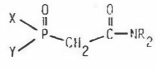

A

Although these extractants have been studied extensively by a number of research groups, there still remains some confusion as to the exact nature of the metal complex which is extracted by the CMP molecules. It had been assumed for many years that the CMP extractants behaved as bidentate extractants (B) based on the high distribution ratios of metal ions at high acidity, however no solid evidence backing this assumption had been presented. Research in our laboratories has indicated that this assumption is valid only under certain circumstances. Our results indicated that in solution, the complexes formed between metal nitrates and CMP compounds contained monodentate, phosphoryl bound extractant molecules (C) (2). On the other hand, data obtained for the extraction of metal thiocyanate complexes by these same extractants indicated that the CMP compounds were behaving as bidentate extractants in this system (3).

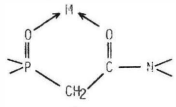

B

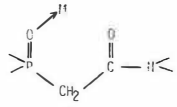

C

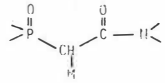

D

Recent structural studies (4) have shown that in addition to neutral mono- and bidentate coordination, the CMP compounds can also behave as anionic ligands (D) in solid compounds isolated from the reaction of metal nitrates with CMP's.

As a result of this obvious variety of coordination modes exhibited by the CMP extractants, we felt that it would be extremely useful to obtain information regarding the coordination of these extractants under conditions that would as closely as possible duplicate those encountered in liquid-liquid extraction processes. As one means to this end we have initiated a nuclear magnetic resonance (NMR) study of these and other extractants and their metal complexes employing paramagnetic lanthanide ions as a method of probing the solution structure of the extracted species.

LANTHANIDE SHIFT REAGENTS

Lanthanide ions have been used as solution structural probes for a number of years (5,6). Typically, a lanthanide tris(beta-diketonate) complex is used as the lanthanide shift reagent which, when complexed to an organic molecule containing a basic coordination site, induces a dipolar shift in the NMR spectrum of the organic compound which can be related to the solution structure of the molecule through the use of the equation:

$$\Delta_n = K \frac{3\cos^2\theta_n - 1}{r_n^3} \qquad (1)$$

where Δ_n is the induced shift in the resonance of a nucleus n due to complexation, r_n is the (through space) distance of that nucleus from the lanthanide ion, θ_n is the angle between the lanthanide-nucleus vector and the principle magnetic axis of the complex (E), and K is a constant which is dependent on the lanthanide under study. In the case of rotationally averaged positions of the complexed molecule, the principle magnetic axis can usually be taken to be the metal-coordination site bond (5). This fairly simple representation has proved to be quite useful in the elucidation of the solution structure of many organic species.

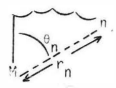

E

Because we were interested in studying the conformation of extractant molecules which had been extracted from aqueous solutions, rather than using beta-diketonate complexes of the lanthanides as shift reagents, we have used the lanthanide ions and their counter-ions (nitrate or thiocyanate in this case) complexed to the extractant molecules in an organic diluent as our shift system. This has given us an extractant-metal complex whose geometrical configuration should correlate directly with actual species involved in the solvent extraction reaction.

MONOFUNCTIONAL EXTRACTANTS

Although our main interest in this study has been to evaluate the conformation of the CMP extractants about lanthanide ions, it was also important to examine the better understood, monofunctional analogs of these compounds so that the validity of this approach could be tested and so that comparisons could be made between the bonding for these two types of extractant molecules. Therefore, a series of monofunctional phosphoryl extractants - tributylphosphate, dibutylbutylphosphonate and butyldibutylphosphinate - was studied using three different lanthanide nitrates - Pr(III), Eu(III), and Yb(III) - to determine if the induced shifts in similar nuclei in these related extractant molecules would reflect similar coordination geometries for these extractants throughout the lanthanide series. As an example the induced shifts for the lanthanide nitrate complexes of dibutylbutylphosphonate are shown in Table 1. One of the criteria for isomorphus complexes and the applicablity of equation (1) is that the ratios of the lanthanide induced shifts for the different lanthanides be constant. It is apparent from the data in Table 1 that the shift ratios for the Pr and Eu complexes are in quite good agreement, while the values for Yb have greater deviations. Since there is other evidence to suggest that the earlier members of the lanthanide group may form complexes of slightly different structures than do the later, smaller members (4b), this small deviation was not entirely unexpected.

As an additional check on the consistency of the shift ratios in a related series of extractant complexes, we have examined the complexes of a given lanthanide ion with a homologous series of extractants, as shown in Table 2 for the Pr complexes of TBP, DB[BP], and B[DBP]. Again, the agreement between equivalent protons in the three extractants is very good.

The results in Table 1 and Table 2 also show quite clearly the effect of increasing the separation of a nucleus from the lanthanide ion. In the absence of large deviations in the value of θ, it would be expected that the magnitude of the induced shift should decrease in a fairly regular manner as the metal-nucleus distance is increased by increasing the number of intervening bonds (i.e., if $3\cos^2\theta-1$ remains approximately constant, then $\Delta \propto r^{-3}$) (5b). The data in Tables 1 and 2 are in agreement with this simplification of equation (1) and provide a first-order approximation to the relative values of r.

Table 1. Induced Shifts in the ^{1}H NMR Spectra of the Lanthanide Nitrate Complexes of Dibutylbutylphosphonate[a]

$$(\underset{d}{CH_3}-\underset{c}{CH_2}-\underset{b}{CH_2}-\underset{a}{CH_2}O)_2-\overset{O}{\overset{\|}{P}}\underset{e}{CH_2}-\underset{f}{CH_2}\underset{g}{CH_2}-\underset{h}{CH_3}$$

Resonance	ΔPr	ΔEu	ΔYb
a	1.00	1.00	1.00
b	.35	.37	.38
c	.21	.16	.26
d	.04	.04	.15
e	1.66	1.36	1.21
f	.82	.85	.63
g	.32	.35	.53
h	.14	.15	.26

[a]Data obtained in $CDCl_3$ solution, normalized to shift a = 1.00.

Table 2. Induced Shifts in the ^{1}H NMR Spectra of the Praseodymium Nitrate Complexes of TBP, DB[BP], and B[DBP][a]

$$(\underset{d}{CH_3}-\underset{c}{CH_2}-\underset{b}{CH_2}-\underset{a}{CH_2}O)_x-\overset{O}{\overset{\|}{P}}(\underset{e}{CH_2}-\underset{f}{CH_2}-\underset{g}{CH_2}-\underset{h}{CH_3})_{3-x}$$

Resonance	ΔTRP(x=3)	ΔDB[BP](x=2)	ΔB[DBP](x=1)
a	1.00	1.00	1.00
b	.37	.35	.36
c	.24	.21	.20
d	.05	.04	.04
e	-	1.66	1.47
f	-	.82	.81
g	-	.32	.28
h	-	.14	.10

[a]Data obtained in $CDCl_3$ solution, normalized to shift a = 1.00.

BIFUNCTIONAL EXTRACTANTS

With these encouraging results for the monofunctional extractant complexes we felt confident that the use of this technique was justified and thus undertook the study of CMP complexes. The primary focus of our attention has been directed toward the study of DHDECMP (X = Y = $CH_6H_{13}O$, R = C_2H_5 in A), the most widely studied member of this class of extractant. Data for the lanthanide induced shifts in the complexes of Pr^{3+} extracted from 4 M $LiNO_3$ (which our previous solvent extraction work (2) indicated should result in a

Table 3. Induced Shifts in the ^{1}H NMR Spectra of the Praseodymium Nitrate Complexes of DECMP Extracted from Aqueous Solution[a]

$$(CH_3\text{-}CH_2\text{-}CH_2CH_2\text{-}CH_2\text{-}CH_2\text{-}O)_2\text{-}P(=O)CH_2\text{-}C(=O)\text{-}N(CH_2\text{-}CH_3)_2$$

f e d b a g h i j,k

Resonance	$\Delta Pr(NO_3)_3$[b]	$\Delta Pr(SCN)_3$[c]
a	1.00	1.00 & .68
b	.40	.33
c	.32	.32
d	.05	.07
g	2.45	2.90
h	.08	.00
i	-.90	-2.33
j	.15	.18
k	-.78	-1.85

[a]Data obtained in C_7D_8 solution, normalized to shift a = 1.00.
[b]Extracted from 4.0 M $LiNO_3$/0.01 M HNO_3.
[c]Extracted from 3.0 M NH_4SCN/0.01 M HCl.

monodentate complex) and from 3 M NH_4 SCN (which we postulated to form a bidentate complex (3)) are compiled in Table 3. It can be clearly seen that the shifts of the phosphoryl substituents are much the same as those observed previously for the monofunctional analogs. The most surprising difference in these data is the nature of the shifts observed for the substituents on the amide portion of the molecule, where small positive and substantial negative values are seen.

Although the simple $\Delta\alpha r^{-3}$ relationship invoked earlier obviously cannot explain such behavior, these shifts can be readily rationalized in terms of equation (1). The numerator of this expression contains the angular function $3\cos^2\theta_n-1$ which is positive for $\theta < 54.7°$. For angles greater than this value, this term becomes negative, changing the sign of the induced shift. If one considers the metal-to-phosphoryl oxygen bond to be the reference for calculating θ, then any interaction between the amide group and the metal ion (as in a bidentate bonding mode or even a weaker "semi-bidentate", electrostatic interaction) would result in drawing the amide portion of the molecule into the region where the sign of the induced shift would be negative or only slightly positive. The magnitude of the negative shifts in the thiocyanate system seems to imply a larger value of θ coupled with (perhaps) a smaller value of r. The combination of these two effects, which suggests a substantial amide-metal (i.e., bidentate) interaction, would result in substantial negative shifts, whereas the less negative shifts observed in the nitrate system could be interpreted in terms of smaller values of θ or larger values of r - implying less of a metal-amide interaction.

Further studies and analyses of the data will be presented to more completely identify the bonding characteristics of these extractants.

Acknowledgment. The authors wish to thank Art Kostka for technical assistance in obtaining the NMR spectra. This work was performed under the auspices of the Office of Basic Energy Sciences, Division of Chemical Sciences, U. S. Department of Energy under Contract W-31-109-Eng-38.

REFERENCES

1. W. W. Schultz and J. D. Navratil, in Recent Developments in Separation Science, Vol. VII, N. N. Li, Ed., CRC Press, Boca Raton, Florida, 1981.

2. a) E. P. Horwitz, A. C. Muscatello, D. G. Kalina, and L. Kaplan, Sep. Sci. Technol., 16, 417 (1981); b) E. P. Horwitz, D. G. Kalina, L. Kaplan, G. W. Mason, and H. Diamond, ibid. 17, 1261 (1982).

3. A. C. Muscatello, E. P. Horwitz, L. Kaplan, and D. G. Kalina, ibid. 17, 859 (1982).

4. a) S. M. Bowen, E. N. Duesler, and R. T. Paine, Inorg. Chem., 22, 286 (1983); b) S. M. Bowen, E. N. Duesler, and R. T. Paine, Inorg. Chim. Acta, 61, 155 (1982); c) S. M. Bowen, E. HN. Duesler, R. T. Paine, and C. F. Campana, ibid. 59, 53 (1982).

5. a) F. Imagaki and T. Miyazawa, Prog. NMR Spectroscopy, 14, 67 (1981); b) C. N. Reilley, B. W. Good, and R. D. Allendoerfer, Anal. Chem., 48, 1446 (1976).

6. W. E. Stewart and T. H. Siddall, Ion Exchange Solvent Extraction, Vol. 3, p. 83, 1973.

URANIUM RECOVERY WITH COUPLED-TRANSPORT MEMBRANES

Walter C. Babcock, Donald J. Kelly, Dwayne T. Friesen

Bend Research Inc.
64550 Research Road
Bend, Oregon 97701-8599 USA

In recent years, hydrometallurgical processing of ores has become increasingly important, replacing the more polluting and energy-intensive pyrometallurgical techniques. Hydrometallurgical leach solutions contain low concentrations of the desired metal ion as well as impurity metal ions. Present methods for product recovery from these solutions include solvent extraction, ion exchange, and precipitation.

Since 1975, Bend Research has been developing an alternative recovery process that utilizes coupled-transport membranes. These are liquid membranes consisting of a water-immiscible, liquid complexing agent held by capillary forces within the pores of a thin, microporous polymeric support. When the membranes are placed between a hydrometallurgical leach solution and another aqueous solution, metal ions from the leach solution are extracted into the membrane and diffuse across it as a neutral organic complex. Under suitable conditions, diffusion can occur "uphill," i.e., against the metal-ion concentration gradient of the aqueous solutions. The energy for concentrating metal ions is provided by the coupled diffusion of a second ionic species. By using conventional solvent extraction agents in the membranes, it is possible to combine the high selectivity and ability to concentrate ions of solvent extraction with large throughputs and continuous processing capability of modern membrane technology. A major advantage of the process over solvent extraction is that problems associated with phase separation and solvent entrainment are eliminated.

The process is illustrated in Figure 1 for the coupled transport of uranyl sulfate anions by a tertiary amine. Here, "feed solution" refers to the leach solution and "product solution" is the concentrate from which yellow cake would be precipitated. On the feed side of the membrane, the uranyl sulfate anions plus two hydrogen ions are extracted into the membrane via the reaction

$$2H^+_{(aq)} + UO_2(SO_4)_2^{--}{}_{(aq)} + 2R_3N_{(org)} \rightleftarrows (R_3NH)_2UO_2(SO_4)_{2(org)}, \qquad (1)$$

where (org) and (aq) refer to species soluble only in the organic membrane phase or aqueous phase, respectively. The uranium-amine complex diffuses across the membrane to the product side, where the reverse reaction in Equation (1) occurs (due to the low H^+ concentration on the product side), releasing the uranyl sulfate anion and two hydrogen ions to the aqueous phase. The free amine then diffuses back across the membrane and the process is repeated. Thus, uranyl sulfate anions are transported from left to right (in Figure 1), and electrical neutrality is maintained by the coupled transport of hydrogen ions in the same direction. In this way, uranyl sulfate anion can be chemically pumped up its concentration gradient as hydrogen ion diffuses down its concentration gradient in the same direction.

During this past year a field test was conducted at a uranium mine in Wyoming. The test unit contained 400 ft^2 of membrane area in the form of four 100-ft^2 hollow-fiber modules. A photograph of the test unit is shown as Figure 2. The unit operated for about 50 days on a leach solution containing 125 ppm uranium. Typically the uranium concentration in the raffinate was reduced to less than 5 ppm and the uranium concentration in the product solution (150-g/L Na_2CO_3) was about 1 wt%. Under these conditions, the unit recovered about 2 lb of uranium/day, i.e., the transmembrane flux of uranium was approximately 2 lb/ft^2-year. For two weeks of the test the unit was operated on partially clarified leach solution. Although no fouling problems due to suspended solids were experienced, organic flocculents in the solution did cause membrane fouling.

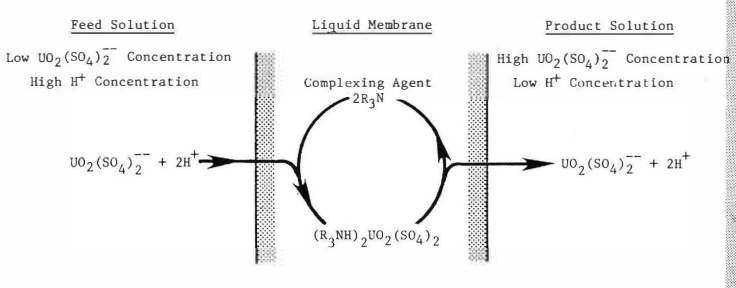

Figure 1. Coupled Transport of Uranium Across a Liquid Membrane

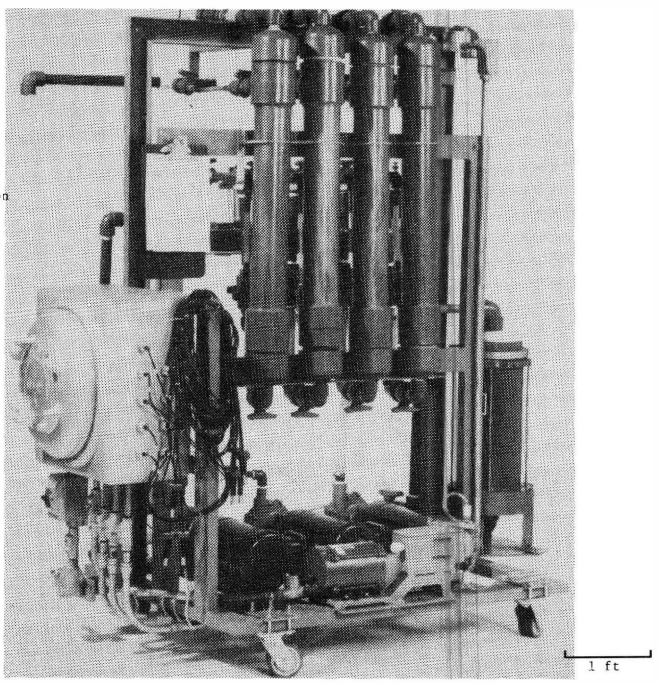

Figure 2. Coupled-Transport Unit for Recovery of Uranium from a Hydrometallurgical Leach Solution

MODELING OF FACILITATED TRANSPORT IN HOLLOW FIBER TUBES

Richard D. Noble

National Bureau of Standards
Center for Chemical Engineering, 773.1
Boulder, Colorado 80303 USA

INTRODUCTION

Facilitated transport is a separation process by which an active chemical carrier will selectively bind with a permeate, transport the permeate across a liquid film, and release the permeate at the other boundary. It has high potential for obtaining high selectivity while achieving high enough flux rates to be commercially feasible. There are several review articles which describe this process in detail [1-9].

The most common mechanism postulated is

$$\uparrow A + B \underset{k_2}{\overset{k_1}{\rightleftarrows}} AB \qquad (1)$$

where A: component being transported across the membrane
B: active chemical carrier
AB: active carrier complex

The arrow next to A indicates that it is the component being transported.

There have been various models developed to describe the steady-state one-dimensional flux of a permeate. Olander [10] described simultaneous mass transfer combined with an equilibrium chemical reaction. He showed the effect of reaction on the total mass transfer rate. Four different cases were analyzed analyzed. Friedlander and Keller [11] used a linearized form of the reaction rate expression to describe the flux of permeate with reversible chemical reaction to the simple diffusional flux. Their assumptions were based on the reacting system being near reaction equilibrium. Ward [12] derived analytical solutions for the steady-state transport of NO through ferrous chloride solution under two limiting conditions, reaction-limited ("frozen" condition) and diffusion-limited (reaction equilibrium). He found that this system was not operating at a limiting condition but somewhere in between. He used a numerical method to solve for the flux. Kreuzer and Hoofd [13] used the concept of a reaction boundary layer to explain the physical problems with assuming instantaneous reaction equilibrium at the membrane boundary. Their results showed that an equilibrium core existed through the main portion of the membrane with reaction boundary layers at each boundary. Goddard et al. [14] and Smith et al. [15] also demonstrated this result.

Yung and Probstein [16] used a similarity transform method to develop a single equation which described the concentration profiles for all components. The equation describes steady-state conditions in flat plate geometry. The equation could be evaluated by numerical methods to obtain the facilitated flux over the entire range of operating conditions. The solution is iterative and could cause some convergence problems. They also present some simplifications under limiting conditions.

Smith and Quinn [17] developed an analytical solution for the facilitation factor for flat-plate membranes under steady-state conditions. They obtained this result by assuming that there is a large excess of carrier. This allows them to linearize the reaction rate expression. They show that their result has the correct limiting behavior for both reaction-limited and diffusion-limited cases. Their model shows good agreement with previously published results. Their model becomes less accurate as you approach reaction equilibrium (diffusion limited).

Hoofd and Kreuzer [18] developed an analytical solution to steady-state one-dimensional facilitated transport. They approximate the permeate concentration as having two components. One component is based on the assumption of chemical reaction equilibrium and is a function of carrier concentration. The second term accounts for departures from chemical equilibrium and is function of position only. By solving for these two components, one obtains an analytical solution. Their result is consistent with Smith and Quinn's for this case.

There has been some previous work done on one-dimensional facilitated transport in cylindrical geometry. Stroeve and Eagle [19] developed equations for the facilitation factor in reactive slabs, cylinders, and spheres. They studied dispersed phase shapes in a continuous phase and provide a graph which shows the effect of geometry when subjected to a uni-directional flux of the diffusing species. Hoofd and Kreuzer [20] solve the problem of oxygen uptake in a cylindrical muscle. They use the same mathematical approach as they had earlier used in planar geometry [18]. Their calculations compared very well with previous calculations. Noble [21] developed analytical expressions for shape factors under both limiting conditions of being either diffusion-limited or reaction-limited. These expressions allowed one to determine facilitated flux for cylindrical or spherical geometries if one knows the flux for a flat-plate geometry. He found that a flat-plate geometry yielded the highest flux under identical operating conditions.

The objective of this study is to develop a mathematical model for the steady-state two-dimensional transport of a permeate in a cylindrical geometry. The permeate is advected axially through the hollow interior portion of the cylinder and transported radially through the cylinder walls by facilitated transport. The cylindrical geometry represents a hollow fiber tube which has great potential for industrial application due to its mechanical strength and high surface area to volume ratio. The pores of the hollow fiber are impregnated with a liquid containing the carrier compound. The radial transport takes place through the pores filled with liquid.

THEORY

The hollow fiber is shown in figure 1. The mixture containing the permeate is transported axially through the tube and the permeate is transported radially through the tube walls by facilitated transport. It can be assumed that there is no axial transport in the tube walls due to the pore structure.

A steady-state macroscopic mass balance on the permeate in the tube (see the control volume in figure 1) yields

$$\langle v_x \rangle \frac{dC_A}{dx} = -\frac{A}{V} N_{A_T} \qquad (2)$$

$\langle v_x \rangle$ = average velocity in axial direction (assumed constant)
C_A = bulk (cup-mixing) concentration of permeate in the interior (hollow) region of tube

$\frac{A}{V}$ = effective surface area to volume ratio

N_{A_T} = flux of permeate into tube wall

Equation (2) neglects radial diffusion in the hollow portion of the hollow fiber tube. The permeate flux through the tube walls can be written as

$$N_{A_T} = \left(\frac{2\pi r_o L}{2\pi r_i L}\right)(S)(F)\frac{D_A}{t}\left(C_A^{\,1} - C_{A_o}^{\,1}\right) \qquad (3)$$

if equation (1) describes the reversible reaction taking place in the pores of the tube wall.

D_A = permeate diffusion coefficient in liquid film

$C_A^{\,1}$ = permeate concentration in liquid film at $r = r_i$.

$C_{A_o}^{\,1}$ = permeate concentration in liquid film at $r = r_o$.

S is the shape factor defined by Noble [21]. It relates the facilitated flux in a cylindrical geometry to the facilitated flux in a planar geometry. S is based cylindrical geometry to the facilitated flux in a planar geometry. S is based on the outside surface area. That is why the surface area ratio is included in equation 3. F is the facilitation factor in a planar geometry. This is the ratio of the total facilitated flux in planar geometry to the simple diffusion flux in planar geometry. Analytical expressions are available for both S and F.

$$S = \frac{\frac{t}{r_2}}{\ln\left[\frac{1}{(1-\frac{t}{r_2})}\right]} \qquad (4)$$

Equation (4) is the equation described by Noble [21] for the case where the system is diffusion-limited (reaction equilibrium). This equation will hold for a wide range in reaction conditions.

$$F = \frac{1 + A}{1 + \frac{A}{\Phi}\tanh\Phi} \qquad (5)$$

where

$$A = \frac{D_{AB}K_{eq}C_B}{D_A} \qquad (6)$$

$$\Phi = \frac{1}{2}\sqrt{\frac{k_1 C_B t^2}{D_A}\left(\frac{1+A}{A}\right)} \qquad (7)$$

D_{AB} = diffusion coefficient of carrier-permeate complex in liquid film

$K_{eq} = {}^{k_1}/_{k_2}$

C_B = carrier concentration in liquid film (assumed constant)

Equation (5) was derived by Hoofd and Kreuzer [18] by approximately the permeate concentration as having two components. One component is based on the assumption of chemical reaction equilibrium and is a function of carrier concentration. The second term accounts for departures from reaction equilibrium and is a function of position only. By solving for these two components, one obtains an analytical solution. Smith and Quinn [17] derived the same result by assuming that there is a large excess of carrier concentration.

Substituting equation (3) into equation (2), one obtains

$$\frac{dC_A}{dx} = -\Lambda\left(C_A - C_{A_o}\right) \qquad (8)$$

where

$$\Lambda = -\frac{2}{r_i}\left(\frac{r_o}{r_i}\right)\frac{(S)(F)D_A}{\langle v_x \rangle t H} \qquad (9)$$

$H = {}^{C_A}/_{C_A^{\,1}}$ = partition coefficient

Note that Λ is a constant and independent of permeate concentration. Equation (8) can be made dimensionless by defining the following dimensionless variables

$$C_A^{\,*} = \frac{C_A}{C_{A_i}} \qquad (10)$$

C_{A_i} = inlet permeate concentration

$$\mathcal{X} = \frac{X}{L} \tag{11}$$

Equation (8) then becomes

$$\frac{dC_A^*}{d\mathcal{X}} = -\Lambda L\,(C_A^* - C_{A_o}^*) \tag{12}$$

Equation (12) can be solved with the following boundary condition

$$\mathcal{X} = 0 \qquad C_A^* = 1 \tag{13}$$

The solution is

$$\frac{C_A^* - C_{A_o}^*}{1 - C_{A_o}^*} = e^{-\Lambda L \mathcal{X}} \tag{14}$$

Equation (14) can be substituted into equation (3) to obtain the permeate flux at any position $\mathcal{X}$.

$$N_{A_T} = \left(\frac{r_o}{r_i}\right)(S)(F)\,\frac{D_A C_{A_i}}{Ht}\,(1-C_{A_o}^*)e^{-\Lambda L \mathcal{X}} \tag{15}$$

Equation (15) can be integrated along the axial length of the tube to obtain the total permeate flux through the tube walls.

$$\int_0^1 N_{A_T}\, d\mathcal{X} = \eta = \left(\frac{r_o}{r_i}\right)\frac{D_A C_{A_i}}{Ht}\,\frac{(S)(F)}{\Lambda L}\,(1-C_{A_o}^*)\left[1-e^{-\Lambda L}\right] \tag{16}$$

Equation (16) can be rearranged to yield the ratio of the permeate flowrate through the tube walls to the inlet permeate flow rate.

$$\Omega = \frac{\eta}{\langle v_x \rangle C_{A_i}}\left(\frac{2L}{r_i}\right) = (1-C_{A_o}^*)\left[1-e^{-\Lambda L}\right] \tag{17}$$

Ω is the fraction of permeate removed. To test the validity of equation (17), the model was compared to experimental data presented by Hughes, Mahoney, and Steigelman [22]. Their data for ethylene permeation through hollow fiber walls containing 6.0 M $AgNO_3$ is shown in Table 1. Substituting their experimental values in equation (17), one obtains Ω = 0.325. This is in excellent agreement with their value of 0.338.

Examination of equation (17) shows the proper functional relationship between the variables and Ω. As C_{A_o} increases, the gradient across the tube wall decreases and Ω decreases. As L increases, Ω increases since more surface area becomes available for radial transport. As Λ increases, Ω increases. An examination of the factors contained in Λ indicate that this makes sense physically.

CONCLUSIONS

A mathematical model has been developed to describe the steady-state dimensional permeate transport in hollow fibers. The permeate is advected axially and transported radially through the hollow fiber walls by facilitated transport. Comparison with experimental data is very good. This model can be very useful in sizing hollow fiber modules for separations using facilitated transport.

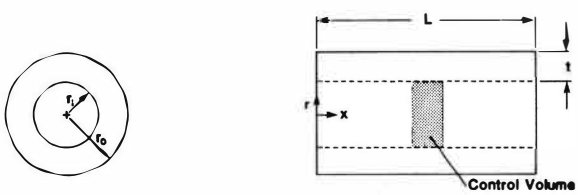

FIGURE 1: HOLLOW FIBER TUBE

$r_i = 1.07 \times 10^{-2}$ cm, $r_o = 1.15 \times 10^{-2}$ cm } effective dimensions for radial transport

$r_i = 4.05 \times 10^{-3}$ cm } based on cross-sectional area available for flow

L = 1.78 cm } effective axial length based on effective surface area

$D_A = 1.85 \times 10^{-5}\ cm^2/s$

$$H = 0.879\ \frac{(g\text{-moles}/cm^3)\ gas}{(g\text{-moles}/cm^3)\ liquid}$$

F = 34.3 } calculated from data in their Table IV for 6.0 M $AgNO_3$

$\langle v_x \rangle = 5.31 \times 10^2\ \frac{cm}{s}$ } calculated from permeation rate data in their Table VII

$C_{A_i} = 2.27 \times 10^{-4}\ \frac{g\text{-moles}}{cm^3}$, $C_{A_o} = 6.03 \times 10^{-5}\ \frac{g\text{-moles}}{cm^3}$ } calculated from data in their Table VII

Ω = 0.338

Table 1. Experimental data of Hughes, Mahoney, and Steigelman for ethylene permeation through hollow fiber tubes containing 6.0 M $AgNO_3$.

References

1. Schultz, J. S., Goddard, J. D., and Suchdeo, S. R., AIChE Jour., 20, 3, 417 (1974).
2. Goddard, J. D., Schultz, J. S., and Suchdeo, S. R., AIChE Jour., 20, 4, 625 (1974).
3. Smith, D. R., Lander, R. J., and Quinn, J. A., Recent Dev. in Sep. Sci., 3, 225 (1977).
4. Goddard, J. D., Chem. Eng. Sci., 32, 795 (1977).
5. Kimura, S. G., Matson, S. L., and Ward, W. J. III, Rev. Dev. Sep. Sci., 5, 11 (1979).
6. Halwachs, W. and Schugerl, K., Intl. Chem. Eng., 20, 4, 519 (1980).
7. Way, J. D., Noble, R. D., Flynn, T. M., and Sloan, E. D., Jour. Mem. Sci., 12, 1, 239 (1982).
8. Kreuzer, F. and Hoofd, L., "Facilitated Diffusion of O_2 and CO_2", Handbook of Physiology, at press.
9. Meldon, J. H., Stroeve, P., and Gregoire, C. K., "Carbon Dioxide Transport in Aqueous Solutions: A Review", Chem. Eng. Comm., at press.
10. Olander, D. R., AIChE Jour., 6, 2, 233 (1960).
11. Friedlander, S. K. and Keller, K. H., Chem. Eng. Sci., 20, 121 (1965).
12. Ward, W. J. III, AIChE Jour., 16, 3, 405 (1970).
13. Kreuzer, F. and Hoofd, L., Respir. Phys., 8, 280 (1970).
14. Goddard, J. D., Schultz, J. S., and Bassett, R. J., Chem. Eng. Sci., 25, 665 (1970).
15. Smith, K. A., Meldon, J. H., and Colton, C. K., AIChE Jour., 19, 1, 102 (1973).
16. Yung, D., and Probstein, R. L., Jour. Phys. Chem., 77, 18, 2201 (1973).
17. Smith, D. R. and Quinn, J. A., AIChE Jour., 25, 1, 197 (1979).
18. Hoofd, L. and Kreuzer, F., J. Math. Biology, 8, 1 (1979).
19. Stroeve P. and Eagle, K., Chem. Eng. Comm., 3, 189 (1979).
20. Hoofd, L., and Kreuzer, K., AIChE Symposium Series, 77, 202, 123 (1981).
21. Noble, R. D., I EC Fund., 22, 1, 139 (1983).
22. Hughes, R. D., Mahoney, J. A., and Steigelman, "Olefin Separation by Facilitated Transport Membranes", presented at AIChE mtg., Houston, TX, April, 1981.

ENRICHMENT AND SEPARATION OF METALS BY LIQUID MEMBRANE WITH TRI-n-OCTYLAMINE

Makoto Harada (Speaker), Fumio Yamazaki
Motonari Adachi and Wataru Eguchi

Institute of Atomic Energy
Kyoto University
Kyoto, Japan

The functions of the liquid membrane are summarized as follows:1)enrichment of solutes by up-hill transport and 2)Separation of particular species from the mixture of more than two solute species. In this work,we discuss the characteristics of the liquid membrane with tri-n-octylamine(TOA)-HCl complex,forcussing on these functions.

EXPERIMENTAL

In this work, the permeation of Fe(III) and/or Zn(II) through the liquid membrane with TOA-HCl was treated. The aqueous phases consisted of the solution of hydrochloric acid,which gave potential to the up-hill transport of metals. Benzene or n-decane was used for the diluent of the carrier. The liquid membrane apparatus used is shown in Fig.1. A teflon membrane filter(50μm thick,void fraction 0.75) was used for supporting the liquid membrane. Temperatures were 25°C.

EQUILIBRIUM AND PERMEATION RATES OF METALS

The equilibrium relationships of Fe(III) and Zn(II) can be described as follows for TOA-HCl in benzene-hydrchloric acid aqueous solution system(1):

$$(1)\quad m\,M^{z+} + mz\,Cl^- + \ell\,\overline{TOAHCl} \rightleftarrows \overline{(TOAHCl)_\ell (MCl_z)_m}\ ;\ K_{M\ell m}$$

$$(2)\quad \begin{aligned} \overline{C}_M &= \sum_\ell \sum_m m K_{M\ell m}[\overline{TH}]^\ell (\phi_M C_M)^m \\ \overline{C}_N &= \sum_M \sum_\ell \sum_m \ell K_{M\ell m}[\overline{TH}]^\ell (\phi_M C_M)^m + 2K_{20}[\overline{TH}]^2 + [\overline{TH}],\ M=Fe \text{ or } Zn \end{aligned}$$

Here, $\overline{C}_M$=total concentration of metal M in the organic phase, $\overline{C}_N$=total concentration of amine in the organic phase, $[\overline{TH}]$=TOA-HCl monomer concentration and C_M=total concentration of metal M in the aqueous phase. ϕ_M is the "catch-all" coeffecient which is introduced to evaluate the effect of activity coefficients of metal and chloride ion, and of the chloride ion concentration in the aqueous phase. These $K_{M\ell m}$ and ϕ_M values are shown in Table 1. The $\overline{C}_M$ value is given from eqs.(1) and (2) to be a function of $\phi_M C_M$,if $\overline{C}_N$ is constant:

$$(3)\quad \overline{C}_M = f_M(\phi_F C_F,\ \phi_Z C_Z)\ ,\ \text{subscript F:Fe,Z:Zn}$$

The rate of metal permeation through the membrane is described as (2)

$$(4)\quad J_M = (1/R_M)[C_M^I - P_M^{II} C_M^{II}/P_M^I],\ R_M = 1/k_w^I + 1/k_{Mr}^I + 1/k_{Mm}^I P_M^I + P_M^{II}/P_M^I k_{Mr}^{II} + P_M^{II}/P_M^I k_w^{II}$$

Here,P_M=distribution ratio of metal M, k_w=mass transfer coefficient in aqueous phase, $1/k_{Mm}$=mass transfer resistance in membrane and the superscript j(j=I or II) represents the aqueous j-phase in the membrane operation. The $1/k_{Mr}$ is the interfacial resistance due to the interfacial reaction between the metal in the aqueous phase and the TH adsorbed on the interface and is described as(2)

$$(5)\quad k_{Mr}^j = k_M \phi_M^j [\overline{TH}]^j/(1+K_{TH}[\overline{TH}]^j),\ K_{TH}=1.4\times10\ dm^3/mol$$

$[\overline{TH}]^j$ is the TOA-HCl monomer concentration at the interface between the aqueous j and the membrane phases. For Fe(III), k_F=2830 cm^4/mol.s. and for Zn(II) the interfacial resistance can be neglected. Fig.2 shows the contribution of each resistance to the total ones for Fe-transfer. From this,we can find the conditions that the rate determining step is in the diffusional step in the aqueous phase I.

ENRICHMENT OF METALS BY TOA MEMBRANE

In the membrane operation, the agent which gives driving force to up-hill transport of metal will permeate through the membrane. Thus, a phase trajectory concerned with the concentrations of metal and the agent describes the feature of the enrichment of metal. Fig.3 shows this trajectory for Fe-enrichment. The trajectories start from the initial points i_1 and i_2 and approach the closed circles which were evaluated from eq.(3) and $\overline{C}_F^I = \overline{C}_F^{II}$ by assuming immobility of HCl:

$$(6)\quad C_F^{II}/C_F^I = \phi_F^I/\phi_F^{II},\ \sum_j C_F^j V^j = \sum_j C_{F0}^j V^j,\ V^j\text{=volume of j-phase,subscript 0=initial}$$

From this result, it is concluded that the amine liquid membrane acts as impermeable membrane for HCl and that the spontaneous enrichment of metal can be realized without controlling the acid concentrations in both aqueous phases.

Table 1 Formation constants and ϕ_M values vs.acid conc.,C_H

	K_{M41} $10^6 M^{-4}$	K_{M42} $10^7 M^{-5}$	K_{M43} $10^6 M^{-6}$	K_{M44} $10^2 M^{-7}$	K_{M21} $10^4 M^{-2}$	K_{20} M^{-1}
M:Fe	1.2	9.0	1.4	4.6	-	-
M:Zn	-	-	-	-	2.6	-
HCl	-	-	-	-	-	35.5

C_H,M	0.05	0.1	0.5	1.0	2.0	3.0
ϕ_F	0.018	0.045	1.0	5.2	36	410
ϕ_Z	0.020	0.060	1.0	5.4	-	-

SELECTIVE SEPARATION OF METAL

Figure 4 shows the phase trajectories of Zn-separation from Zn-Fe binary solution which were obtained at the conditions given in the figure. In this experiment,the acid permeation through the membrane was negligibly small as in the preceding experiment for Fe-enrichment. The trajectories started from the initial point i and Zn in the aqueous phase I was preferentially pumped up to the aqueous phase II . During Zn-transfer, Fe-transport was very weak at $\overline{C}_N$=0.01 mol/dm^3 and efficient separation of Zn was performed. This trajectory is estimated to change along the solid curve which was calculated from rate equation,eq.(4), and metal balance equation. After preferential transport of Zn, Fe started to permeate slowly through the membrane and the trajectory approached quasi-equilibrium points f_1 and f_2. The preferential transport of Zn is attributed to the difference in the permeation rates between Zn and Fe. Figure 5 shows initial permeation rates of Zn and Fe. As is clear in Fig.5, the Zn-rate is about 100 times larger than the Fe-rate at $\overline{C}_N$=0.01 mol/dm^3. At $\overline{C}_N$=0.3 mol/dm^3,the separation of Zn is less efficient than at $\overline{C}_N$=0.01 mol/dm^3, reflecting rather small difference in the Zn and Fe permeation rates.

The maximum separation of Zn is, in the above case,performed at J_Z/J_F=infinite. The corresponding trajectory becomes a horizontal line through the initial point i. More efficient separation than the above horizontal trajectory,i.e.,the trajectory with negative slope,can be performed with the use of the membrane with mixed carriers. This is demonstarted in the following section.

SEPARATION FUNCTION OF THE MEMBRANE WITH MIXED CARRIERS

Consider two kinds of carriers. The one is the amine which extracts metals according to eq.(1). When the acid concentration in the aqueous phase increases, the distribution of metals to the organic phase increases. A chelating agent or acidic organophosphorus compound is used as another carrier:

$$(7)\quad M^{z+} + z\,\overline{RH} \rightleftarrows \overline{R_zM} + z\,H^+$$

The distribution of metals to the organic phase,in this case, decreases,when C_H increases. If a liquid membrane containing these two kinds of carriers is used, the particular species of the metals which are pumped up from the aqueous phase I to II by the amine carrier can be back-transported with the help of the function of the second carrier. The corresponding separation trajectory as shown in Fig.4 has negative slope and thus Zn and Fe permeate through the membrane in countercurrent. To check this idea, TOA-HCl and di(2-ethylhexyl)phosphoric acid (D2EHP) in n-decane were used as the carriers.

Figure 6 shows typical examples of the Zn separation from the Zn-Fe mixture. The trajectory A is almost horizontal line through the initial point i and the amine carrier plays significant role in the metal transfer in this experimental condition(TOA-conc.,$\overline{C}_N$=0.05 and D2EHP conc.,$\overline{C}_R$=0.13 mol/dm^3). The amine-free membrane permeates Fe preferentially as shown by the trajectory B($\overline{C}_R$=0.13 mol/dm^3). The trajectory C ($\overline{C}_N$=0.02,$\overline{C}_R$=0.13 mol/dm^3) displays countercurrent permeation of Fe and Zn in the membrane and efficient separation of Zn and Fe is realized.

It is interesting to examine the phase trajectory at the condition that the aqueous phase I alone contains metals and the phase II contains no metal. The trajectories at this condition are shown in Fig.7. The triangle keys represent the experimental result for the membrane with TOA-HCl carrier in benzene. As $\overline{C}_N$=0.01 mol/dm^3, initial rate of Zn permeation is 100 times larger than the ones for Fe. However, the Fe-permeation into the aqueous phase II is significant. The circle keys are the experimental result for the membrane with mixed carriers($\overline{C}_N$=0.05, $\overline{C}_R$=0.13 mol/dm^3). In this case, Fe-permeation into the aqueous phase II is very weak compared with the case of amine membrane.

We must mention the interference effect between the amine and phosphoric acid. The extraction ability of D2EHP strongly decreases by the presence of the amine. This interference effect should be analyzed for evaluating the detailed feature of metal separation by the liquid membrane with mixed carriers. This is left to future works.

REFERENCES

1. M.Harada,M.Araki,A.H.Bokhari,W.Eguchi and Y.Yamada,Chem.Eng.J.,in press
2. M.Harada,F.Yamazaki and M.Adachi,to be submitted.

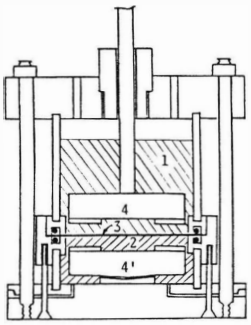

1,2 : Aqueous phases, 3: Membrane
4,4': Stirrers
Fig.1 Experimental set up

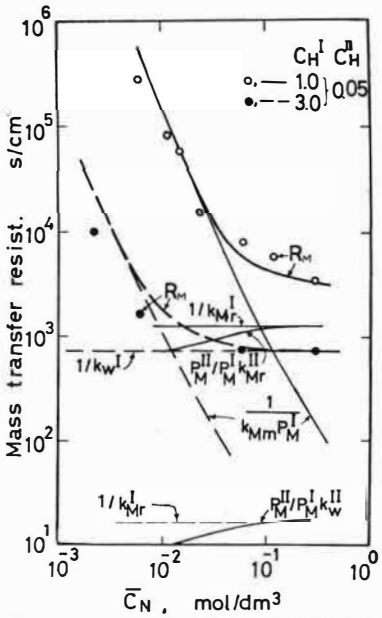

Fig.2 Contributions of each mass transfer resistance to overall resistance for Fe permeation. ($C_F^I=C_F^{II}=10^{-3}$ mol/dm³). $P_M^{II}/P_M^I k_{Mr}$ and $P_M^{II}/P_M^I k_w$ are less than 10 s/cm for C_H^I=3.0 mol/dm.

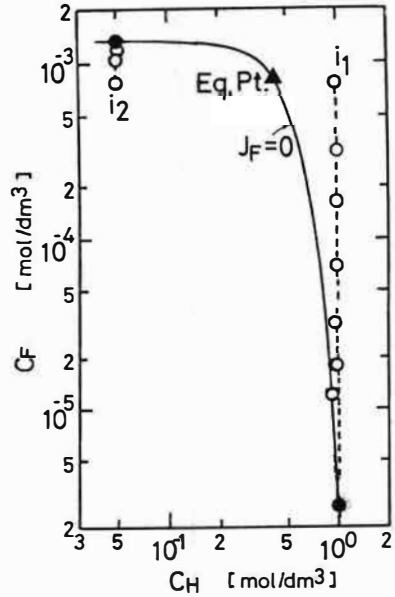

Fig.3 Phase trajectory of Fe-enrichment. o :Experimental, ---:Calc. from eqs. (4) and (5), ——: J_F=0. ($\bar{C}_N$=0.3 mol/dm³) Diluent: Benzene.

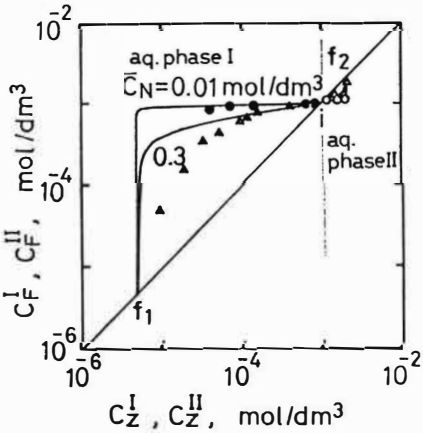

Fig.4 Phase trajectories for Zn separation from Zn-Fe binary metal mixture (C_H^I=1.0, C_H^{II}=0.05, $C_{ZO}^I=C_{ZO}^{II}=C_{FO}^I=C_{FO}^{II}$=1.0x10⁻³ mol/dm³). o,●,Δ,▲: experimental, —— :calc. Diluent: Benzene.

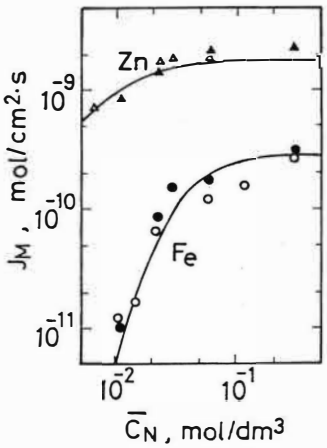

Fig.5 Permeation rate of metals. C_H^I=1.0, C_H^{II}=0.05, o: $C_F^I=C_F^{II}$=1x10⁻³, ●: $C_F^I=C_F^{II}=C_Z^I=C_Z^{II}$=1x10⁻³, Δ: $C_Z^I=C_Z^{II}$=1x10⁻³, ▲: $C_F^I=C_Z^I=C_F^{II}=C_Z^{II}$=1x10⁻³, in mol/dm³. —:Calc. from eq.(4) and (5) for permeation of single metal. Diluent: Benzene.

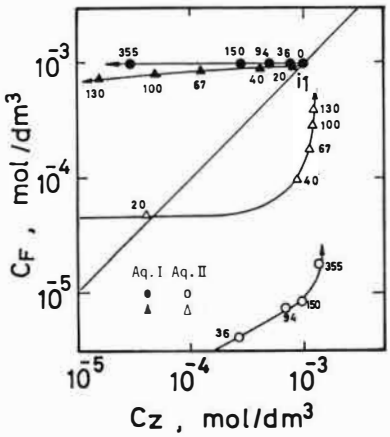

Fig.7 Trajectories of Zn-separation. ●,o :mixed carriers, C_H^I=1.0, C_H^{II}=0.1, $\bar{C}_R$=0.13, $\bar{C}_N$=0.05, $C_F^I=C_Z^I$=1x10⁻³, $C_F^{II}=C_Z^{II}$=0, Diluent: n-decane. ▲,Δ: C_H^I=1.0, C_H^{II}=0.05, $\bar{C}_N$=0.01, $\bar{C}_R$=0, $C_F^I=C_Z^I$=1x10⁻³, $C_F^{II}=C_Z^{II}$=0, Diluent: Benzene. The numerical values attached to the keys are time, min.

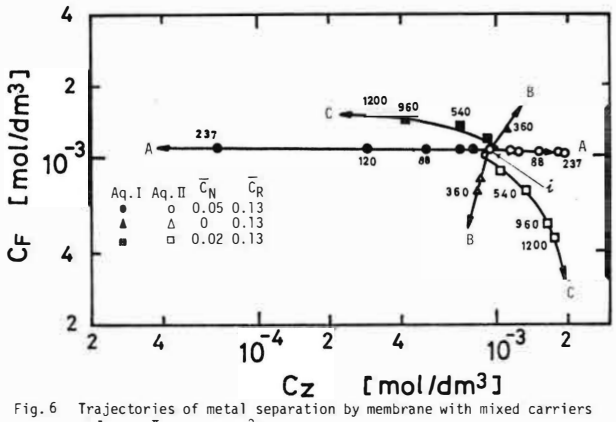

Fig. 6 Trajectories of metal separation by membrane with mixed carriers (C_H^I=1.0, C_H^{II}=0.1 mol/dm³). Numerical values attached to the keys are time, min. Diluent: n-decane.

PERMEATION RATE OF METAL SPECIES THROUGH SUPPORTED LIQUID MEMBRANES: DIFFUSIONAL AND CHEMICAL RESISTANCES WITH CATIONIC AND ANIONIC CARRIERS

P. R. Danesi, E. P. Horwitz, and P. G. Rickert

Chemistry Division
Argonne National Laboratory
Argonne, Illinois 60439 USA

INTRODUCTION

Facilitated transport through supported liquid membranes, SLM, was recently proposed as a new technology for the selective separation, concentration, and recovery of metal ions. In this type of transport metal ions can be transported across the membrane "uphill", i.e., against their concentration gradient. A mobile carrier, dissolved in a water immiscible organic diluent and adsorbed on a thin microporous polymeric film, which forms a membrane soluble metal complex with the aqueous metal ions, is responsible for the facilitated membrane permeation process. The carrier is generally selected according to its metal extracting properties. Many solvent extraction reagents can be used in facilitated transport studies. Therefore the membrane carriers can be classified in the same way as the solvent extraction reagents. One possible and useful classification is the one based on the fact that metal species can extract into the SLM as cationic, neutral, or anionic species. Membrane cationic carriers are acidic extractants which react with aqueous metal cations according to the simplified scheme:

(1) $$M^{+z} + z(\overline{BH}) \rightleftharpoons \overline{MB}_z + zH^+$$

BH is the cationic carrier and the bar indicates membrane phase species. Similarly, membrane anionic carriers are represented by basic or neutral extractants which extract metal cations together with the aqueous anions which are required by charge neutralization. The simplified extraction schemes can be written as

(2a) $$MX_z^0 + \overline{A} \rightleftharpoons \overline{AMX_z}$$

(2b) $$MX_n^- + \overline{AH^+...Y^-} \rightleftharpoons \overline{AH^+...MX_n^-} + Y^-$$

(2c) $$M^{+z} + zX^- + \overline{A} \rightleftharpoons \overline{AMX_z}$$

X^- is an aqueous soluble complexing agent and A is the anionic membrane carrier. No distinction is here made between the case where (a,b) the aqueous metal complex actually bears a negative or zero charge, or (c) the complex between M^{+z} and X^- is apparently formed only during the extraction reaction. Examples of cationic carriers are: alkylphosphoric acids (HDEHP), β-hydroxy oximes (LIX), long chain carboxylic acids (versatic acid). Examples of anionic carriers are: long chain aliphatic amines (TLA), neutral monofunctional phosphorous extractants (TBP, TOPO), neutral bifunctional phosphorous extractants (O⊕D[IB]CMPO).

The main feature which distinguishes cationic from anionic membrane carriers with respect to SLM permeability resistance is that, in most cases, cationic carriers extract metal cations into the SLM as unhydrated species. Anionic carriers extract instead metal species which already contain ligands, other than water. It follows that with cationic carriers appreciable chemical resistance to the membrane permeation can develop whenever metal cations characterized by low values of the rate constant of water substitution are transported. On the contrary negligible chemical resistance has to be expected with most anionic carriers (exceptions do however exist).

PERMEABILITY EQUATION

A permeability coefficient equation for the facilitated transport of metal species through SLM was previously derived (1) and successfully tested (2-4) by us. This equation takes into account (a) aqueous diffusional resistances through stagnant layers on the aqueous sides of the membrane, (b) membrane diffusional resistances, (c) chemical resistances arising from possible slow interfacial chemical reactions between the permeating metal species and the membrane carrier. Figure 1 schematically describes the processes which are contributing to the overall membrane flux, J. The permeability coefficient, P, at the steady state is described by the equations:

(3) $$P = \frac{k_1}{k_1\Delta_a + k_{-1}\Delta_o + 1}$$

(4) $$P = J/C = -\frac{dC}{Cdt}\frac{V}{Q}$$

(5) $$\ln(C/C_o) = -\frac{Q}{V}Pt$$

where J = membrane flux, C = feed metal concentration at time t, C_o = feed metal concentration at time zero, V = volume of feed solution, Q = membrane area, $\Delta_a = d_a/D_a$, $\Delta_o = d_o/D_o$, d_a = aqueous diffusion film thickness, d_o = membrane thickness, D_a = aqueous diffusion coefficient of metal species, D_o = membrane diffusion coefficient of the complex formed between the metal species and the carrier. k_1 and k_{-1} are the pseudo first order rate constants of the interfacial reactions occurring between the metal species and the membrane carrier. k_1 and k_{-1} depend on the concentration of the carrier and on any other chemical species participating in the interfacial reaction, except the metal containing species. The specific type of dependence is a function of the specific rate law which describes reactions (1) or (2). k_1 and k_{-1} are time independent only when the concentration variation of the metal species does not affect the concentration of the carrier and of the other reacting chemical species. This condition holds at tracer level metal concentrations. k_1 and k_{-1} are correlated through

(6) $$k_1/k_{-1} = K_d$$

with K_d = distribution ratio of the metal between the membrane phase and the adjacent aqueous phase.

MEMBRANE RESISTANCES

From equation (3) and considering that the overall membrane resistance, R, is equal to the inverse of the membrane permeability coefficient, R = 1/P, it follows that

(7) $$R = R_a + R_o + R_c$$

where

(8) $$R_a = \Delta_a \text{ (aqueous diffusion film resistance)}$$

(9) $$R_o = \Delta_o/K_d \text{ (membrane diffusion resistance)}$$

(10) $$R_c = 1/k_1 \text{ (chemical resistance)}$$

With most anionic carriers $R_c \ll R_a + R_o$ and the overall resistance is only determined by the aqueous film diffusion and membrane diffusion resistance.

The relative contribution of R_a and R_o to R is a function of the concentration of the various species through K_d. R_a and R_o depend on the aqueous phase stirring (or linear flow velocity) and the membrane thickness through d_a and d_o, respectively.

CATIONIC CARRIERS

For the reasons briefly discussed in the introduction, when the metal ions which cross the SLM are characterized by low values of the rate constants of water exchange (Cr^{3+}, Fe^{3+}, Al^{3+}, etc.) or, more generally, the rate of the interfacial ligand exchange reaction is expected to be low (e.g., Fe^{3+}, Cu^{2+} with aromatic β-hydroxy oximes), R_c can be comparable with R_a and R_o. The different contribution of R_a, R_o, and R_c to R can be numerically evaluated with equations (3), (7)-(10). As an example the facilitated transport of Cu^{2+} and Fe^{3+} ions through a SLM consisting of a 0.1 M solution in toluene of 2-hydroxy-5-tert-octylacetophenone oxime, HOx, adsorbed on a Celgard™ 2500 polypropylene film, will be shortly discussed. The feed and strip aqueous phases are assumed to be stirred in such a way to minimize aqueous polarization effects and to have the following composition: Feed: $[Cl^-]$ = 2 M, $[H^+]$ = variable, $[Cu^{2+}]$ or $[Fe^{3+}]$ = tracer concentrations; Strip: $[Cl^-]$ = 2 M, $[H^+]$ = 1 M. With these conditions the following values of the diffusional parameters can be assumed for both Fe(III) and Cu(II) (3): $\Delta_a = 2.4 \times 10^2$ sec cm^{-1}, $\Delta_o = 1.1 \times 10^3$ sec cm^{-1}.

The equations describing the reactions of Cu(II) and Fe(III) with the carrier which are responsible for facilitated transport are the following (5,6):

Cu(II)

(11) $$Cu^{2+} + 2(\overline{HOx}) \rightleftharpoons \overline{CuOx_2} + 2H^+$$

(12) $$K_d = 0.55\ [\overline{HOx}]^2/[H^+]^2$$

(13) $$k_1 = 2.9 \times 10^{-4}\ (cm.sec^{-1})[\overline{HOx}]/[H^+]$$

(14) $$k_{-1} = 5.1 \times 10^{-4}\ (cm.sec^{-1})[H^+]/[\overline{HOx}]$$

Fe(III):

(15) $$Fe^{3+} + 3(\overline{HOx}) \rightleftharpoons \overline{FeOx_3} + 3H^+$$

(16) $$K_d = 5.5 \times 10^{-4}\ [\overline{HOx}]^3/[H^+]^3$$

(17) $$k_1 = 1.94 \times 10^{-5}(cm.sec^{-1})[\overline{HOx}]/[H^+] + 9.2 \times 10^{-4}(cm.sec^{-1}.M^{-1})[\overline{HOx}]$$

(18) $$k_{-1} = 3.5 \times 10^{-2}(cm.sec^{-1})[H^+]^2/[\overline{HOx}]^2 + 1.7(cm.sec^{-1}.M^{-1})[H^+]^3/[\overline{HOx}]^2$$

Equations (11) to (18) have been used to evaluate the distribution ratios K_d and the chemical resistances. The result of the calculations are shown in Table I. The figures indicate that for both metals at pH = 2 the chemical resistance accounts for more than 50% of the total membrane resistance. Nevertheless the contribution of the chemical resistance rapidly drops in the Cu(II) case when the pH of the aqueous feed solution is increased or decreased. As the equations for the pseudo first order rate constants show (cf. eq. (13),(14),(17),(18)), different trends have to be expected when different carrier concentrations are used. However the results of Table I have to be

*Work performed under the auspices of the Office of Basic Energy Sciences, Division of Chemical Sciences, U. S. Department of Energy under Contract W-31-109-ENG-38

considered only as indicative since effects produced by aggregation processes in the membrane phase, not negligible aqueous metal concentrations, and concentration dependent diffusion coefficients, which show up in practical permeation processes, have been here neglected.

ANIONIC CARRIERS

With anionic membrane carriers the interfacial chemical reactions are generally fast and the contribution of R_c to R can be neglected. In this case only aqueous film diffusion and membrane diffusion resistances control the membrane permeability coefficient. The different contributions of R_a and R_o to R, at constant aqueous stirring and membrane thickness, depend on the concentration of the membrane carrier, the pH and concentration of the various aqueous ions present in the feed, and the concentration of the permeating metal species. The equation which describes the permeability coefficient is now simply given by:

$$P = \frac{K_d}{K_d\Delta_a + \Delta_o} \tag{19}$$

When the permeating metal species are initially present in the feed solution at low concentration levels K_d and P are time independent. Then, if the hydrodynamic conditions are kept constant, the permeability coefficient goes from a region where it is entirely membrane diffusion controlled to a region where it is entirely aqueous diffusion film controlled, as long as K_d increases. The maximum value reached by P is equal to $1/\Delta_a$, i.e., independent of membrane diffusional parameters. Figure 2 shows a typical P vs carrier concentration curve for the transport of Am^{3+} through a SLM containing a neutral bifunctional extractant as carrier. In this case Am^{3+} crosses the membrane together with three NO_3^- anions. The chemical reaction which is responsible for the facilitated transport is:

$$Am^{3+} + 3NO_3^- + 3\,\overline{CMPO} \rightarrow \overline{Am(NO_3)_3(CMPO)_3} \tag{20}$$

CMPO represents the bifunctional extractant OϕD[IB]CMPO. In the region where the permeability is controlled by membrane diffusion P varies with the concentration parameters in the same way as K_d. This explains the +3 slope of the initial part of the log P vs log carrier concentration plot.

The influence of the inital metal concentration on the type of diffusional resistance which controls the permeability coefficient is shown in Figure 3B. In this case the permeability coefficient is proportional to the slope of the curve log (C/C_o) vs time (cf. eq. (5)). The data of Figure 3B were obtained using an initial Sm^{3+} concentration in the feed of 10^{-2} M, in addition to ^{241}Am present at tracer levels. Since Sm^{3+} and Am^{3+} behave in the same way with respect to extraction by Oϕ[IB]CMPO, the data are representative of the total decrease of metal concentration in the aqueous feed. It can be observed that as long as time increases the permeability coefficient increases reaching a limiting value equal to the one obtained with only Am^{3+} at tracer levels (cf. Figure 3A). This limiting value is obtained when the membrane permeation process is only controlled by aqueous film diffusion. At the other extreme of the curve a low permeability coefficient is observed. This low value is caused by the large membrane diffusional resistance which dominates the overall resistance. The first part of curve 3B ($0 < t < 20 \times 10^3$ sec) is in fact quantitatively explained by the equation:

$$P = \frac{[\overline{E}]}{3C\Delta} \tag{21}$$

where $[\overline{E}]$ is the total extractant concentration and C is the total aqueous feed metal concentration at time t. The above example indicates that in practical membrane separation processes performed under hydrodynamically efficient conditions, the nature of the rate determining resistances is expected to change as long as the permeation process proceeds. The quantitative description of the time variations of the permeability coefficient, or the corresponding flux, on the basis of the equations reported above, is then extremely important for the correct design of industrial size membrane separation modules and for predicting their performance.

REFERENCES

1. P. R. Danesi, E. P. Horwitz, G. F. Vandegrift, and R. Chiarizia, Sep. Sci. Technol. 16, 201 (1981).
2. P. R. Danesi, E. P. Horwitz, and P. Rickert, Sep. Sci. Technol. 17, 1183 (1982).
3. R. Chiarizia, A. Castagnola, P. R. Danesi, and E. P. Horwitz, J. Membr. Sci., in press.
4. P. R. Danesi, R. Chiarizia, and A. Castagnola, J. Membr. Sc., in press.
5. R. Chiarizia and P. R. Danesi, Sep. Sci. Technol. 16, 1181 (1981).
6. P. R. Danesi, R. Chiarizia, and G. Vandegrift, J. Phys. Chem. 84, 3455 (1980).

TABLE I

COPPER (II) PERMEATION

$[H^+]$, M	P(cm · sec^{-1})	K_d	% R_c	% R_a	% R_o
10^{-3}	3.64×10^{-3}	5.5×10^{3}	12.55	87.37	0.07
10^{-2}	1.65×10^{-3}	5.5×10	57.05	39.70	3.25
1	4.32×10^{-6}	5.5×10^{-3}	14.91	0.10	84.99

IRON (III) PERMEATION

10^{-3}	1.36×10^{-3}	5.5×10^{2}	67.00	32.70	0.27
10^{-2}	1.75×10^{-4}	5.5×10^{-1}	61.00	4.19	34.78
1	5.00×10^{-10}	5.5×10^{-7}	0	0	100.00

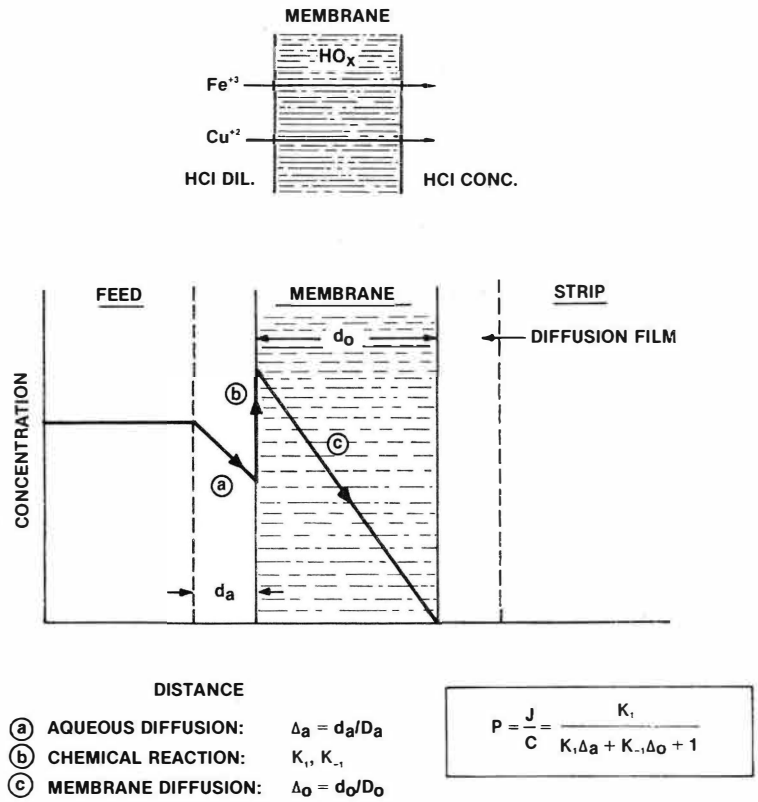

FIGURE 1. SCHEMATIC REPRESENTATION OF THE PROCESSES CONTROLLING MEMBRANE PERMEABILITY.

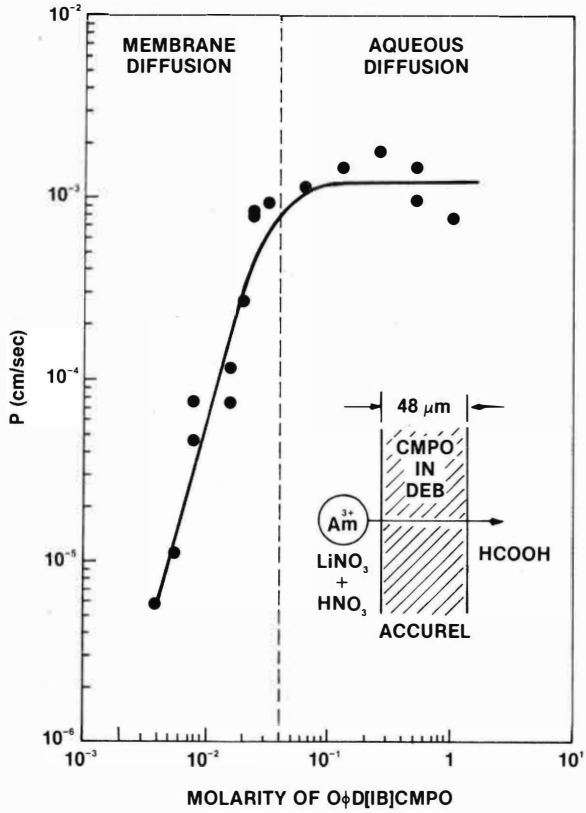

FIGURE 2. INITIAL PERMEABILITY COEFFICIENT OF Am^{+3}, P, VS MOLAR CONCENTRATION OF OϕD[IB]CMPO. FEED: [$LiNO_3$] = 2 M, pH = 2. STRIP: [HCOOH] = 0.5 M.

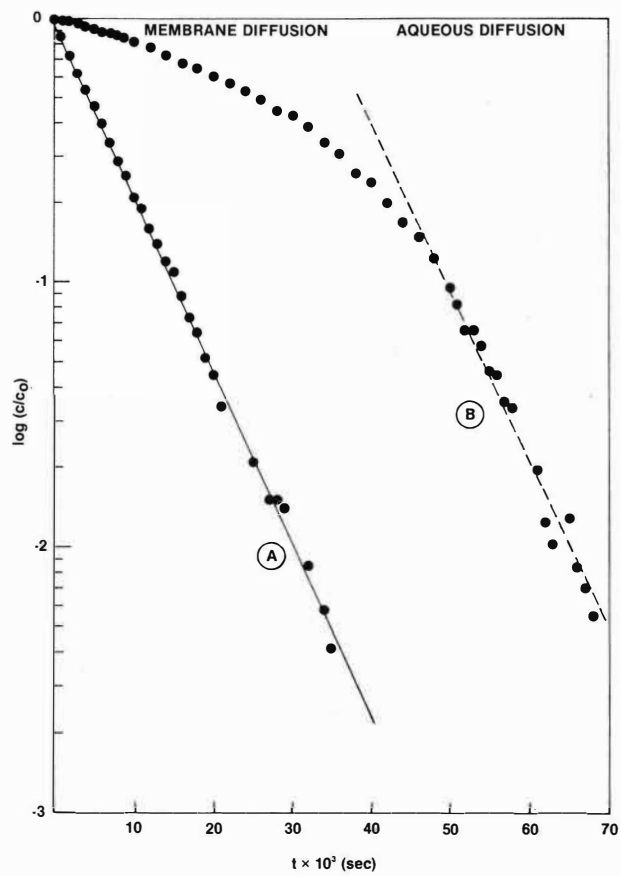

FIGURE 3. LOG (C/C_0) VS TIME PLOT FOR Am^{+3} TRANSPORT THROUGH A 0.1 M OϕD[IB]CMPO IN DEB SUPPORTED LIQUID MEMBRANE. Ⓐ ^{241}Am TRACER. Ⓑ ^{241}Am TRACER + [Sm^{+3}] = 0.01 M. FEED: [$LiNO_3$] = 2 M, pH = 2.0. STRIP: [HCOOH] = 0.5 M.

USING GELS AS SIZE-SELECTIVE EXTRACTION SOLVENTS

E. L. Cussler and Marcus Stokar

University of Minnesota
Minneapolis, Minnesota USA

Gels as Size Selective Extraction Solvents

Introduction

The research in this paper aims at the use of gels as extraction solvents to separate biological materials like proteins and amino acids. The basic way in which the gels function is shown schematically in Figure 1. Small gels spheres are added to a dilute solution. The spheres swell, absorbing the low molecular weight solvents but excluding high molecular weight solutes. The raffinate, now concentrated in the high molecular weight solutes, can then be separated from the swollen gel by filtration.

The swollen gel must now be regenerated. We use gels whose swelling is a function of pH, so adding acid collapses the gel and releases most of the absorbed solvents. The collapsed gel s separated from the released solvents by filtration and added to a small amount of base. The gel can then be added to fresh solutions, where it will swell again.

The value of this separation depends on two characteristics of the gel which make it different from the other extraction solvents. First, it absorbs according to molecular size. For example, if the gel interacts equally with water and with a protein solute, it will still absorb only the water because the protein is too large to diffuse between the gel's crosslinks. As a result, gels are like extraction solvents whose selectivity depends on differences in diffusion. They are like absorbants whose capacity is over ten times their mass.

The second interesting characteristics of these gels is the ease of which they can be regenerated. The gels used can undergo phase transitions. As a result, their swelling can be a violent function of temperature, pH, solvent character, and electric field. Such violent changes make the gel regeneration straightforward.

Experimental

The gel emphasized in our experiments is made by hydrolyzing cross-linked polyacrylamide beads produced commercially as packing for gel permeation chromatography (Bio-Rad Laboratories, Richmond, California). The gel emphasized, sold as Bio-Gel-6 (50-100 mesh), has a particle size in water of 150-300 x 10^{-6} meters. It was hydrolyzed for 24 hours at 60°C in 0.5 molar sodium bicarbonate. This hydrolysis makes the gel increasingly ionic, so that its volume becomes a stronger function of pH. Small solutes were reagent grade and were used as received. Proteins were purified by dialysis and recrystallized. Polystyrene latex was obtained from the Dow Chemical Company.

The basic apparatus consists of a centrifuge tube containing two compartments, separated by a filter. The gel and the appropriate solution were mixed in the top compartment until the gel had swollen to its equilibrium extent. This usually is complete within a few minutes. The gel and raffinate are rapidly separated by centrifugation. The raffinate concentration is then measured by spectophotometery, refractive index, or electron microscopy.

Results and Discussion

Three types of measurements were made in this research. The first shows that gel absorption can be selective: the gels absorb low molecular weight solvents, but reject high molecular weight solutes. The second shows how the gel volume changes with variations in pH. The third type of measurement shows that the gels are sufficiently strong to be used repeatedly. These measurements are discussed sequentially.

That the gel can function as a size selective extraction solvent is shown by the experiment reported in Table I. The first three columns of the table give the solutes to be concentrated and their properties. Columns four and five give the initial and final concentrations of the solution; in other words, they give the increases in concentration achieved with a small amount of gel. Finally the last column in

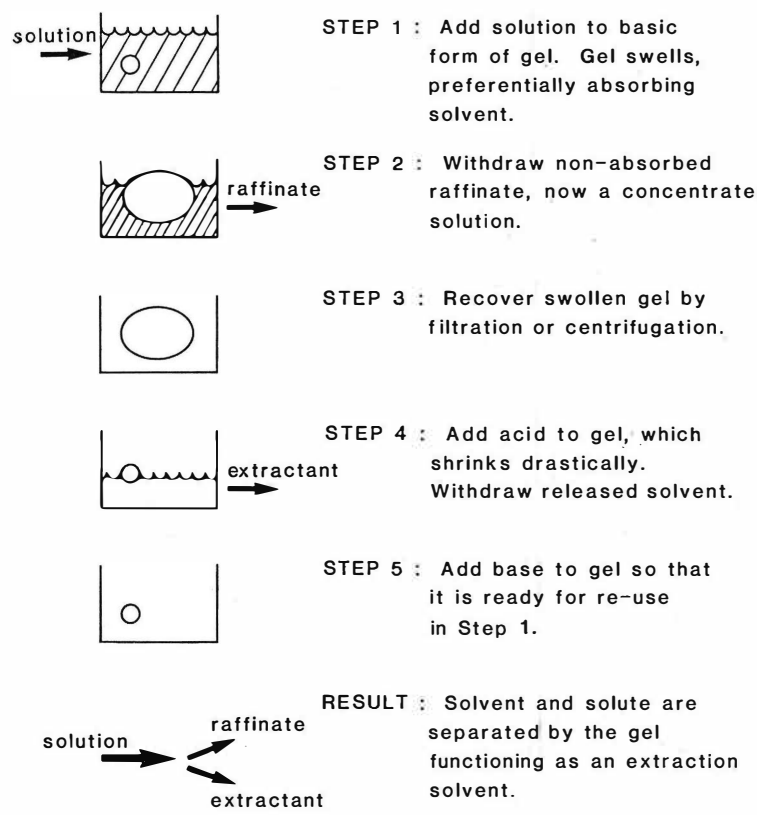

Figure I Gels as Extraction Solvents

Gels can absorb solvent from solutions, leaving behind a concentrated solution of high molecular weight solutes. The gels can then be regenerated by manipulating the pH.

Table I. Concentration of Dilute Aqueous Solutions Using Hydrolyzed Polyacrylamide Gels

Solute	Molecular Weight	Solute Size, Å	Feed Concentration[a]	Raffinate Concentration[a]	Percent Efficiency[b]
Polystyrene Latex	--	9900[c]	0.21	0.35	85
Polystyrene Latex	--	346[c]	0.91 0.50[f]	1.40 1.23[f]	82 93[f]
Silica	--	50[c]	1.82	3.03	80
Bovine Serum Albumin	66,000	72[d]	$.08_2$	$.18_3$	93
Hemoglobin	64,500	62[d]	0.73	1.26	91
Polyethylene Glycol	3000-3700	38[e]	0.56	1.09	91
Sucrose	342	8.4[d]	1.00	1.09	6
Urea	60	5.3[d]	3.00	3.00	0

(a) As weight percent.

(b) Defined as (measured increase in concentration) x (raffinate volume)/(initial solution volume).

(c) Measured by electron microscopy.

(d) Estimated from the diffusion coefficient in water using the Stokes-Einstein equation. (Cussler, 1983).

(e) Reported by the manufacturer from light scattering.

(f) Obtained with a dextran gel (Sephadex C-50).

Table I gives the efficiency of extraction expressed as the measured concentration change compared to that expected from the altered volume.

The results in Table I show that solutes which are greater than 30 Å in diameter can be concentrated with an efficiency of at least 80%. This efficiency is compromised by weak solutes adsorption on the surface of the gel. This adsorbed material can usually be removed by washing increasing the efficiency to better than 95%.

For these separations to be commercially significant the gels must also be regenerated. This regeneration depends on large changes of gel volume with small changes of process conditions like pH. At low pH, the gel used here has a constant volume. At pH 5-6, the gel volume increases 5 to 10 times. At higher pH, it goes through a soft maximum. These volume changes are the results of gel ionization, counter ion bonding, Donnan equilibrium and non Gaussian polymer chains. We believe that gel ionization is the most important factor involved. On this basis, we have developed a theory which predicts that the (-2/3) power of the gel volume should vary linearly with the reciprocal of the total amount of base added to the gel. That this is observed is shown by the data in Figure 2. However, we expect that in the future, more accurate experiments will discover cases where other factors are significant.

Finally, to test the repeated use of these gels, we prepared a dilute suspension of 346 Å polystryrene latex. We removed a fraction of the water in this suspension using a small amount of gel, and we then measured the raffinate concentration. We repeated this procedure over 40 times and found that increasing concentrations show that the gel removes constant amounts of water in each cycle. As a result, the gel is remaining chemically intact for at least 40 cycles. We do not believe that gel stability will be a major problem in these separations.

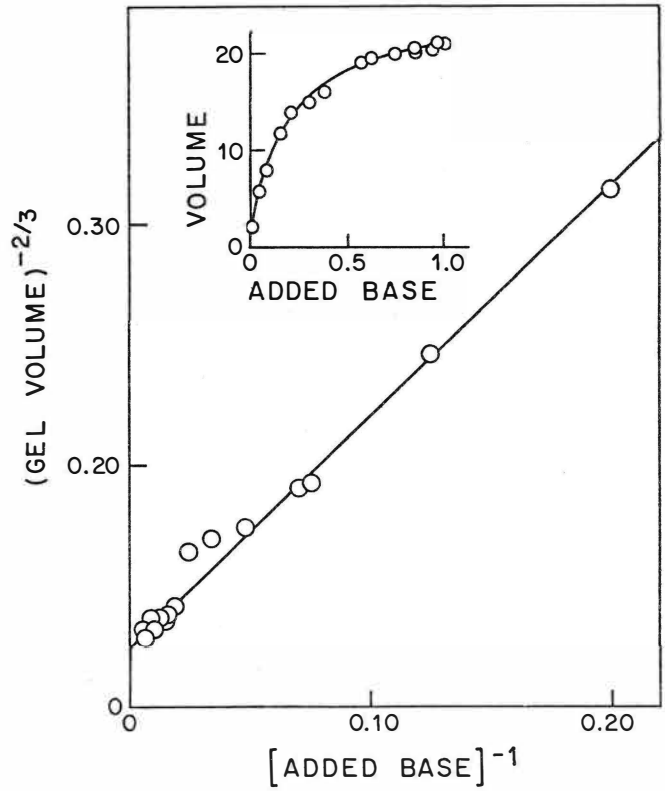

Figure 2 Gel Volume vs. Added Base

The gel volume varies strongly with added base, as shown in the inset. If this variation is due to altered ionization of the gel, then the (-2/3) power of gel volume will be proportional to the reciprocal of added base.

Conclusion

We have successfully used polyelectrolyte gels to concentrate macromolecular solutions by as much as forty times. This concentration is selective for solutes greater than 30 Å in diameter but not for solutes less than 10 Å in diameter. Solutes concentrated include polystryrene latex, polyethylene glycol, and hemoglobin. The gel used is hydrolyzed, cross-linked polyacrylamide, which can reach its equilibrium swelling in a minute, so that separation is potentially fast. The separation depends on gel swelling changing very sharply as a function of pH; this variation is consistent with the assumption that gel ionization is the dominant factor in gel swelling. These separations have particular potential for biological solutes like proteins produced by genetically engineered fermentation.

THE EFFECT OF AQUEOUS ORGANIC ALCOHOL/AMINE SOLVENTS IN THE DELIGNIFICATION OF WOODY BIOMASS

Ramkrishna G. Nayak, Gary C. April, John K. McGee, Perry L. Daley, Jamal Meraab

The University of Alabama
Chemical & Metallurgical Engineering Deparmtent
Tuscaloosa, Alabama USA

The selective delignification of woody biomass has become a necessity, either in the manufacture of pulp or in the efficient enzymatic conversion to alcohols. Presently known commercial processes suffer from the severe degradation of the carbohydrates and water and air pollution problems. However with many organic solvents and even with mixed aqueous organic solvent systems, the lignin monomers or dimers frequently are soluble, primarily because of the organophilic nature of the lignin. Among the various organosolv lignin extractions, alcohols and amines are the likely candidates for the commercial realization of the process. Recently an interesting organosolv pulping has been discovered. Coded, Omega Sigma I as a result of possible patent consideration of the idea, this system truly consists of aqueous organic solvents and is free of pollution oriented inorganic additives.

PROGRESS OF ALCOHOL AND AMINES IN ORGANIC SOLVENT DELIGNIFICATION

The use of ethanol in organic solvent extraction of lignin was first studied by Kleinert (1). Aronovsky (2) used butanol in the place of ethanol. Recently Diabold et al. (3) claimed a U.S. patent based on plurality of extraction of lignin from the wood using ethanol. Katzen (4) estimated the operating cost of such a system.

The pioneering work of ethanol delignification in the presence of acid catalyst was carried out by Sarkanen's laboratory (5). Several acid catalysts like $AlCl_3$, $FeSO_4$, oxalic acid were used but were found to be effective only in the delignification of hardwoods. Further research in ethanol pulping by the same research group resulted in ethanol-sulfide pulping. Ammonium sulfide in the presence of aqueous ethanol was found to delignify softwoods to a low level of lignin content without affecting the degradation of carbohydrates. In order to avoid the inherent pollution problem associated with sulfides, aqueous ethanol delignification was also attempted in the presence of alkali and in the absence of sulfides, independently by Marton et al. (6) and April et al. (7).

The growth of amine pulping took place very much in parallel to the advance of alcohol pulping. Peterson and Wise (8) patented a process using ethanol amine as delignifying agent. The use of ethylenediamine in combination with alkali pulping was attempted by two groups, Julien et al. in the United States (9) and Kubes et al. in Canada (10). Delignification of red spruce in the presence of sodium and ammonium sulfide was successfully attempted by Nayak et al. (11).

FLEXIBILITY OF ORGANOSOLV DELIGNIFICATION PROCESSES TO VARIOUS LIGNOCELLULOSIC MATERIALS

The catalysed or uncatalysed alcohol delignification processes are very much limited to hardwoods except for the ethanol-sulfide and ethanol-alkali pulping systems. Similarly in the case of amine pulping, amines alone do not fiberize the softwoods, however they do so in the presence of alkali or sulfides.

Table 1 summarizes the delignification potential of various organic solvents. As can be seen from the table, the desired level of delignification (4-5% lignin content in pulp) can only be attained when these solvents are combined with one of the inorganic components of the kraft pulping liquor (i.e. alkali or sodium sulfide). It is also observed that softwoods require severe organosolv pulping conditions as opposed to the relatively mild conditions for the hardwoods.

PROCESS CONDITIONS

The process conditions employed for the organosolv delignification vary with the type of organic solvents, species and catalyst used. Alcohols generally demand higher pulping temperature compared to amines. Because of the lower vapor pressure, the digester pressure during ethylenediamine pulping would be only 80-90 psig, while it would reach 400-500 psig during ethanol pulping. The pulping conditions for various pulping processes are summarized in Table 1.

SELECTIVITY IN DELIGNIFICATION

Figure 1 illustrates the selectivity of various organosolv pulping processes. The relative increase in percent residual pulp yields are plotted at different kappa numbers (kappa number is an index for measuring the lignin content in pulp) for different organosolv pulping processes.

Ethanol and ethylenediamine, when used in combination with sodium hydroxide actually gave lower yield compared to kraft pulp, indicating the severe degradation of the carbohydrates. On the other hand, ethanol in combination with ammonium sulfide gave a significant increase in yield, while with sodium sulfide increase was only marginal. The loss of pulp yield with sodium sulfide in contrast to ammonium sulfide could be due to the higher hydroxyl ion concentration promoting the carbohydrate peeling reactions. The selectivity of ethylenediamine pulping in combination with the sulfides falls in between ethanol-ammonium sulfide and ethanol-sodium sulfide pulping systems; the former giving a higher yield compared to the latter.

Among all the presently known pulping systems, ethanol-ammonium sulfide seems to be the most selective one. However, the Omega Sigma I (this code name is given as a result of possible patent consideration of the idea) system, a new organosolv pulping system identified by the authors (12), was found to even surpass the selectivity of ethanol-ammonium sulfide system. Additionally, softwoods can be delignified to as low as 20 kappa number.

PULP COMPOSITION

Pulp composition analysis indicates what kind of polysaccharides survived the organic solvent extraction of the wood. The results are summarized in Table 2. As can be seen from Table 2, xylans and mannans are very much resistent to ethanol-ammonium sulfide pulping. On the other hand, much of the xylan is lost to the extracting solvent in ethylenediamine-sulfide pulping, while mannans have survived the extraction. The retention of xylans in the pulp produced from Omega Sigma I organic-solvent extraction is as good as the corresponding kraft pulp and mannans and glucans are practically completely retained in the former pulping process as opposed to the severe degradation observed in kraft pulping.

CONCLUDING REMARKS

Among the organosolv pulpings presently known, ethanol-ammonium sulfide and ethylenediamine-ammonium sulfide seem to be very selective in delignification. Degradation of xylan is observed with ethylenediamine-sulfide pulping, while both mannans and xylans are retained in ethanol-ammonium sulfide pulping.

In order to avoid the pollution problem associated with the sulfides there is a need to develop alternative chemical additives in organosolv pulping. Recently experiments with an organosolv lignin extraction system (Omega Sigma I) provides such an alternative. This is not only the most selective among the presently known systems, but is also flexible to various lignocellulosic materials. A very high recovery of the chemicals coupled with the ease of delignification of wood to a very low level lignin content are the added features of the system. A U.S. patent application has been filed and further work is in progress.

REFERENCES

1. T. N. Kleinert, Tappi 57 (8), 99 (1974).
2. S. J. Aronovsky and R. A. Gortner, I&EC 28 (11), 1270 (1936).
3. V. B. Diebold, W. F. Cowan & J. K. Walsh, U.S. Patent 4,100,016, July 11 (1978).
4. R. Katzen, CEP (2) 62 (1980).
5. K. V. Sarkanen, S. Assiz and V. Chang, Paper presented at the 89th AIChE meeting, Portland, Oregon (1980).
6. R. Marton and S. Granzow, Tappi 65 (6), 103 (1982).
7. G. C. April and J. McGee, Interim report, NSF Contract No. CPE 80-15591, October 1982.
8. F. C. Peterson and L. K. Wise, U.S. Patent 2,218,479, (1940).
9. L. M. Julien and B. C. H. Sun, Tappi 62 (8), 63 (1979).
10. G. J. Kubes and H. I. Bolkes, Tappi Alkaline Pulping Conference (Washington, D.C.), Papers 297-310.
11. R. G. Nayak and J. L. Wolfhagen, Paper presented at the Ninth Cellulose Conference, Syracuse, New York (1982).
12. R. G. Nayak and G. C. April, Unpublished experimental results.
13. X. N. Nguyen, V. Venkatesh, D. B. Marsland and I. S. Goldstein, Paper presented at the Eighty-Ninth National AIChE Meeting, Portland, Oregon, August (1980).
14. K. V. Sarkanen and V. L. Chang, Private communication with S. Assiz (1982).

Table 1. Summary of Recent Organosolv Pulping Studies

	Aqueous Ethanol						Ethylenediamine			
	1	2	3	4	5	6	7	8	9	10
Ligiwood ratio	10:1	10:1	10:1	10:1	10:1	6:1	-	10:1	6:1	4:1
Cooking Temp.°C	210	170	170	200	180	180	170	170	170	176
Cooking Time,min.	240	60	60	40	240	240	120	120	120	100
Ethanol/EDA Concentration V/V%	50	50	50	50	50	30	30[a]	50	26	100
NaOH % on wood	-	-	-	20.0	-	-	-	-	14.0	-
Sulfide Concentration										
i) sodium moles/L	-	-	-	-	0.25	-	-	-	-	-
ii) ammonium moles/L	-	-	-	-	-	0.3	-	-	-	9.0[b]
Acid catalysts % on wood										
a) $AlCl_3$	-	1.34	-	-	-	-	-	-	-	
b) Alum	-	-	-	-	-	-	-	-	-	
c) $Fe_2(SO_4)_3$	-	-	2.73	-	-	-	-	-	-	
Species	So.Y.P.	S.Gum	S.Gum	So.Y.P.	W.Hem.	W.Hem.	Aspen	So.Y.P.	So.Y.P.	Red Sp.
Kappa number	87.0	-	-	32.0	32.5	45	20	Not Fib.	42.5	28.8
% Lignin in pulp	13.5	3.2	5.6	5.0	-	-	-	-	-	-
Residual pulp yield % on wood	48.6	37.5	43.2	42.3	47.3	64.8	61.0	-	51.0	54.3
Reference	April(7)	Ngyen(13)	Ngyen(13)	April(7)	Sarkenen (14)	Sarkenen (14)	Julien(9)	Julien(9)	Julien(9)	Nayak(11)

[a] 3.0 g EDA/g. wood.

[b] 9.0 % on wood.

Table 2. Percentage Carbohydrates Retained in Organosolv Pulps

Species	Western Hemlock		Red Spruce			Southern Yellow Pine	
	Ethanol-$(NH_2)_4S$	Kraft	EDA-Na_2S	EDA$(NH_4)_2S$	Kraft	Omega Sigma I	Kraft
Xylans	68.0	29.0	26.0	20.1	34.4	40.5	49.6
Mannans	78.0	24.0	57.0	74.0	25.3	91.4	35.5
Glucans	90.0	86.0	90.0	93.5	77.1	95.2	80.7
Reference	Sarkanen et al.(1982)		Nayak et al. (1982)			Nayak et al. (1983)	

Figure 1. Relative Effectiveness of Organosolv Systems Based on Improvement in Yield

Curve	Solvent System	Wood Type	Investigator
a	Omega Sigma I	Sou. Yellow Pine	April et al
b	EDA-Amm. Sulfide	Spruce	Nayak
c	EtOH-Amm. Sulfide	West. Hemlock	Sarkanen
d	EDA-Sodium Sulfide	Spruce	Nayak
e	EtOH-Sodium Sulfide	West. Hemlock	Sarkanen
f	EDA-Sodium Hydroxide	Sou. Yellow Pine	Kubes
g	EtOH-Sod. Hydroxide	Sou. Yellow Pine	April et al.

x-axis label: Kappa Number

y-axis label: Relative Increase in Percent Yield

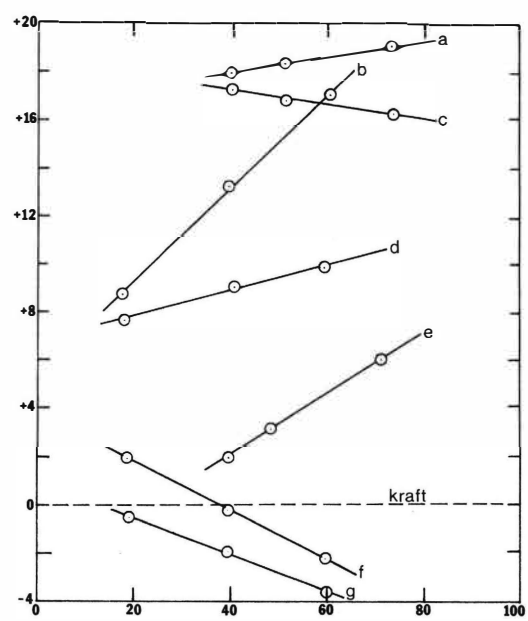

EXTRACTION OF CHOLESTEROL FROM BLOOD USING LIQUID MEMBRANES

G. Yagodin, Yu Lopukhin, E. Yurtov, T. Guseva, V. Sergienko

Mendeleev Institute of Chemical Technology
A-47, Miusskaya sq., 9
Moscow, USSR

At present the body detoxifying and homeostasis correction are useful and effective medical measures. The application of a sorption technology employing activated carbons and ion exchange resins.are under intensive development. Recently the solvent extraction was used for these purposes (1,2).

Extraction of toxines from biological fluids can be employed in two methods: by the common techique und using liquid membranes. The latter is often preferable because the substances which react with toxines in an aqueous receptor phase are separated from blood by liquid membranes. This makes possible to use many different substances and to achieve better compatibility of the extractant with blood.

We deal with extraction of cholesterol from blood using liquid membranes. If would be useful to remove the excess of cholesterol from blood as on of the medical measures for atherosclerosis. The liquid membrane formulation is selected to be a water-soluble substances barrier so that many other blood om components such as proteins, ions, glucose, calcium, inorganic phosphorus and the blood cells cannot diffuse through out the membrane phase. We used paraffin oil as a liquid membrane. The dispersed phase was a water suspension of saponin. Surfactant was sorbitan oleate being 2% of the membrane volume. Encapsulated phase: membrane volume ratio = 3 : 1. The emulsion used to form the liquid membrane capsules were formed by conventional methods of drop-wise additions of the active phase into the continuous phase with intense agitation by a propeller turning. Saponins are surfactants therefore the smaller part of them sorbs on the interface of the emulsion. That is the cause of hemolysis when blood is brought into contact with the emulsion (Figure 1). That is why the fresh emulsion must be pre-equilibrated with the isotonic buffer solution before the extraction from blood.

Table 1 shows the change in blood hemolysis for different numbers of the pre-equilibrations when digitonin is washed partly out of the emulsion. As a model of blood in hemolysis study we used 2% emulsion of erythrocytes in phosphate buffer (pH = 7.4). Phase volume ratio 1 : 1. Table 1 shows that there is an acceptable number of the pre-equilibrations after ahich hemolysis doesn't inerease. It is important that the loses of the emulsion digitonin after these pre-equilibrations are not significant. After the acceptable pre-equilibration digitonin cannot be washed away and the emulsion can be employes for the extraction from blood.

For our situation there is a considerable incentive to a great stability of the emulsion. Any of encapsulated digitonin mustnot be in blood. That is why the emulsion stability was very high owing to the viscous membrane phase. Actually, there was no visible change in the emulsion surface all day long.

When the separatory funnels are used and the mixing was gentle, the most of cholesterol was extracted by the emulsion during 1,5-2 howes, that is similar to the extraction of cholesterol is fast and leads to the formation of sediment, so the overall rate of process is affected by mass-transfer from blood to membrane and the diffusion through the membrane, viscosity of which is high. Saponins react selectively with the free cholesterol, so the saponin emulsions extract the most of the free cholesterol and the smaller part of cholesterol esters, probably, because of its certain solubility in the emulsion and the sorption at the interface of the emulsion.

Table 2 shows the recovery factor of total and free cholesterol for different cholesterol concentrations in blood when the digitonin concentration in the emulsion increases the recovery factor rises up to 80-85% of the recovery factor of free cholesterol and then further increase in the digitonin concentration in the emulsion doesn't change the recovery factor of cholesterol (Table 2, Figure 2).

The initial point in the Figure 2 corresponds to the extraction by the emulsion without digitonin.

The scheme of extraction by digitonin emulsion is shown in Figure 4. For comparison the extraction scheme of cholesterol by tri-n-octyl-amine(TOA) which was reported before (2), is demonstrated. Appraising the emulsion extraction scheme in comparison with the TOA one we ought to say the following:

1. TOA damages erythrocytes, so the blood cells must be separated from plasma before extraction from blood. Emulsion can extract cholesterol from blood without hemolysis.

2. Therefore it is nessesary to extract TOA impurities from plasma after the extraction of cholesterol. After the extraction by the emulsion it is not essential.

3. The recovery factor is higher for the amine extraction, so the digitonin emulsion extracts on the whole the free cholesterol and TOA extracts total cholesterol.

Finelly we should like to make a conclusion that the choice of extraction scheme depends on many factors and, probably, cannot be the same in all cases but the extraction by the emulsion is more attractive due to its smaller danger to human.

REFERENCES.

1. G. Yagodin and al. Extraction from biological fluids, Proc. of ISEC'80, 80-157.
2. W. Halwachs and al. Removal of toxines from plasma and blood with liquid surfactant membranes, Proc. of ISEC'80, 80-88.

DIGITONIN CONCENTRATION, mM				DECREASE IN HEMOLYSIS AFTER PRE-EQUILIBRATION, ΔHl %			
ENCAPSULATED PHASE	BUFFER ISOTONIC SOLUTION AFTER PRE-EQUILIBRATION WITH EMULSION						
	1	2	3	ΔHl_1	ΔHl_2	ΔHl_3	ΔHl_4
0.0	0.00	0.00	0.00	0.0	0.0	0.0	0.0
1.6	0.02	0.00	0.00	1.0	0.5	0.0	0.0
5.0	0.15	0.04	0.01	7.5	1.5	0.5	0.0
10.6	0.49	0.09	0.03	22.0	13.0	4.0	0.0

TABLE 1. HEMOLYSIS AFTER PRE-EQUILIBRATION WITH THE ISOTONIC BUFFER SOLUTION

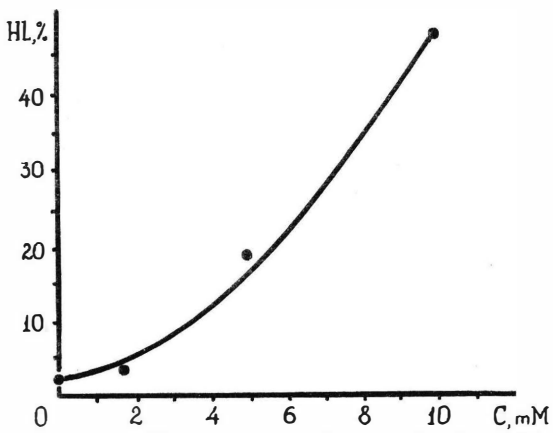

FIGURE 1. HEMOLYSIS VS THE DIGITONIN CONCENTRATION IN THE ENCAPSULATED PHASE

CHOLESTEROL CONCENTRATION, mM				RECOVERY FACTOR, R %	
TOTAL		FREE			
INITIAL	EQUILIBR.	INITIAL	EQUILIBR.	TOTAL	FREE
4.92	3.27	1.56	0.26	33.5	83.5
3.48	2.80	0.78	0.13	19.5	83.5
12.20	9.36	4.15	1.30	23.5	68.6
5.95	4.86	1.42	0.57	18.3	60.0
3.11	2.33	1.17	0.52	25.1	55.5

TABLE 2. EXTRACTION OF FREE AND TOTAL CHOLESTEROL BY THE DIGITONIN EMULSION

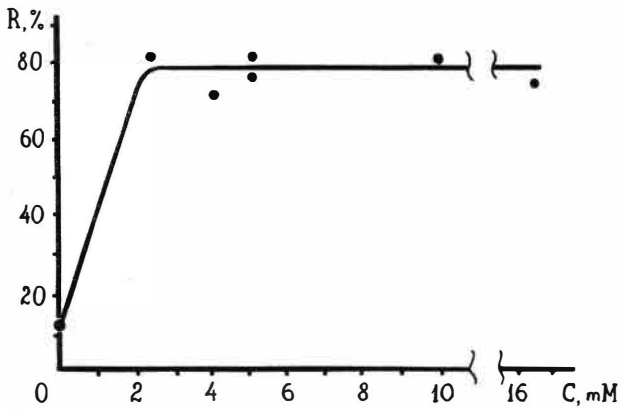

FIGURE 2. RECOVERY FACTOR OF THE CHOLESTEROL VS THE DIGITONIN CONCENTRATION IN THE ENCAPSULATED PHASE

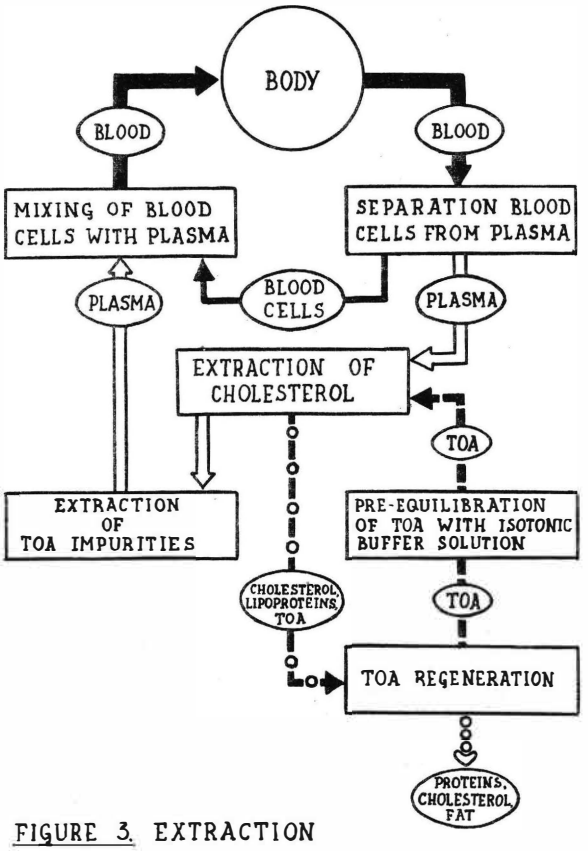

FIGURE 3. EXTRACTION OF CHOLESTEROL FROM BLOOD BY TRI-N-OCTYLAMINE (TOA)

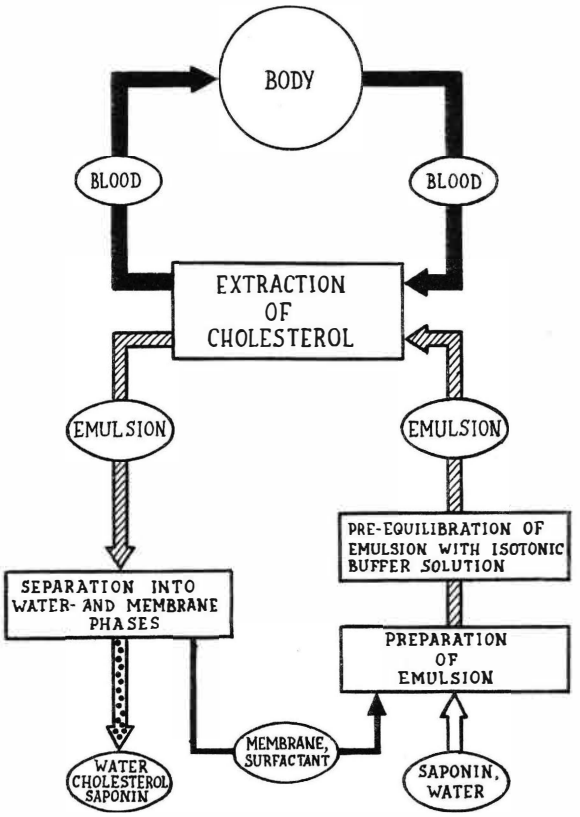

FIGURE 4. EXTRACTION OF CHOLESTEROL FROM BLOOD BY THE SAPONIN EMULSION

HIGHER YIELDS IN FURFURAL PRODUCTION BY USING SOLVENT EXTRACTION

G. Aly, R. Wennersten and G. Zacchi

Lund Institute of Technology
Dept. of Chemical Engineering
Box 740
S-220 07 Lund, Sweden

INTRODUCTION

Furfural and its derivatives comprise an industrially significant class of heterocyclic compounds known as furans, with furfural being the most important member. Furfural is produced commercially from pentosan-containing agricultural sources, such as cereal grasses, bagasse, wood, and wood products. The raw material is treated with strong inorganic acid where the pentosans are hydrolyzed to pentoses and the pentoses subsequently cyclo-dehydrated to furfural. Formation of furfural is also accompanied by side reactions such as resinification of the furfural produced and condensation of furfural with an intermediate compound between furfural and xylose. The overall reaction takes place as follows:

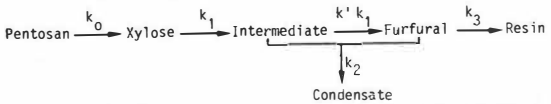

k' is much larger than k_1 and consequently k_1 is rate determining. Schonemann (1,2) obtained the different reaction velocity constants from measurements of xylose degradation and furfural resinification at 140-160°C in 1% HCl using dilute xylose solution. It was concluded that furfural formation is enhanced by high temperatures, low furfural concentrations and high $[H^+]$. To supress the undesirable side reactions, furfural formed in the reaction should be moved as soon as formed to prevent its resinification and condensation. In all industrial processes for furfural production, this is achieved by blowing high pressure steam through the mass and, after attaining operating temperature and pressure, furfural is steam distilled. The condensed reactor vapors are fed to a distillation unit comprising of two columns since the water-furfural system forms a heterogeneous azeotrope. High consumption of steam in this process is a major drawback and solvent extraction seems to have a good potential in reducing energy requirements.

In a solvent extraction process for furfural production, 3 steps will be necessary:

- Hydrolysis of pentosans to pentoses,
- Dehydration of pentoses to furfural with simultaneous extraction so that the furfural produced is transferred as quickly as possible to the solvent in order to prevent its degradation,
- Separation and purification by distillation.

Knight (3) extracted furfural with toluene in a packed column. Distribution coefficient values (K_D defined as weight fraction of solute in the extract phase divided by that in the raffinate phase) in the range of 6-29 were measured. Conway and Philips (4) investigated the ternary system furfural-MIBK-water and obtained K_D-values in the range of 7-13. Tare et al. (5) used benzene and ethyl acetate as solvents and obtained results which indicated that benzene was likely to be a better choice in comparison to other solvents such as toluene, MIBK and ethyl acetate. They did not however base their conclusions on any economical calculations. Trimble and Durlop (6) proposed a process for the extraction of furfural from aqueous solutions using ethyl acetate as solvent. They calculated the total steam consumption for the extraction-distillation process to approx. 5 kg steam/kg anhydrous furfural, and for the distillation process to 6.5 kg steam/kg anhydrous furfural. The feed concentration was rather high (7 wt.%) and 99.9% recovery was achieved. A phase ratio of 1:1 was used in the extractor and a reflux ratio of 2.0 was used in the stripper. Both ratios seem rather high. Rigamonti and Marchetti (7) measured a K_D-value of 2.9 for the system furfural-caprylic acid-water and vapor-liquid equilibria for the binary system furfural- caprylic acid at 3 and 13 kPa. Kikic et al. (8) presented experimental LLE data for 3 furfural-solvent-water systems where the solvents were chlorobenzene, butylchloride and tetrachloroethylene. Butylchloride was chosen as an optimal solvent based upon unclear reasons. A flow sheet for a distillation-extraction process was also proposed. Neither energy requirements nor process analysis was given. Wennersten et. al. (9) examined 6 different solvents in combined extraction-distillatin processes for the recovery of furfural from 1.0 wt-% aqueous solutions. The most important criterion for solvent selection for this specific system were outlined.

Most of literature data discussed above were determined at room temperature. One of the main objectives of this work was to determine data for the distribution coefficients in solvent-furfural-water systems at 150-200°C. For this purpose, an equilibration cell was designed and used for LLE data at pressures up to 20 bar. Furthermore, reaction-extraction runs were performed using the optimum solvent and a xylose solution obtained by hydrolyzing straw. Finally minimum energy requirements were computed and compared to these of the conventional distillation process.

EXPERIMENTAL

An equilibration cell, made of stainless steel, was constructed for pressures up to 20 bar. The cell, shown in Figure 1, consists of a cylindrical mantle provided with two view windows opposite to each other and an oil-heated element placed in the centre of the cell. The cell is sealed by a flange which is removed on charging the chemicals. Mixing is achieved by an eccentric device connected to an electric motor and a speed variator. Temperature and pressure are measured and recorded.

An equilibration experiment is conducted by charging the cell equal amounts of the aqueous and organic phases, preheating to a prescribed temperature and mixing under a certain reaction time. After equilibration, the motor is stopped and the mixture is allowed to separate under a period of 15-60 min. depending on the system. Before discharging the contents of the cell, nitrogen gas is introduced to the cell to supress boiling during the sampling. If any flashing would occur, a water cooler completely condenses the vapors.

Analyses of the raffinate and extract phase were made by manually injecting samples by syringe into a Varian Model 200 gas chromatograph equipped with a flame-ionization detector and a Porapak Q-S column, 0.32 cm in diameter, 2.0 m long and with 80/100 mesh. Calibration was done with sucessively diluted standards and a reproducibility within 5 % could be attained.

SOLVENT SCREENING

During the preliminary solvent screening, caprylic acid, tetralin (high-boiling solvents) as well as ethyl acetate, toluene and methyl isobutyl ketone (low-boiling solvents) were tested. Both of the high-boiling solvents were discarded because of poor separation properties at high temperatures. Ethyl acetate was decomposed to ethanol and acetic acid and was also discarded at an earlier stage.

The equilibrium distribution coefficient for extraction of furfural from water into toluene and MIBK was determined at 5 different initial furfural concentrations. K_D is expressed in this work as y/x where y and x are the weight fractions of furfural in the extract and raffinate phases, respectively, at equilibrium. The results are tabulated in Table 1. As can be seen, K_D for toluene shows a linear dependence on the furfural concentration in the aqueous phase. A mean K_D-value was calculated to 3.54 ± 0.18. The K_D for MIBK is a non-linear function of furfural concentration and is comparatively higher within the investigated concentration interval. For this reason, together with favourable separation properties and thermal stability at high temperatures, MIBK was chosen for further study. It was found that the experimentally measured distribution coefficients were independent of temperature within the interval 150-200°C.

REACTION WITH SIMULTANEOUS EXTRACTION

Runs were performed to investigate the dependence of furfural yield on reaction temperature and time. For this purpose, straw material was hydrolyzed using concentrated H_2SO_4. This resulted in a 2.2 wt-% xylose solution (pH = 1.5) which was then dehydrated in presence of MIBK as the organic solvent. Table 2 displays some results for these runs. As can be seen, the experiments were performed at two temperature levels and under three different reaction times. Parallel dehydration runs without simultaneous extraction were carried out for the sake of comparison. Thus, the furfural yield at 150°C was increased from 47% without extraction to 79% with a reaction time of 3.5 hrs. At the higher temperature of 175°C, the yield was increased from 56% to 92% with a reaction time of 2.5 hrs. The results clearly reveal that the increase in the furfural yield at the higher temperature level was 64% compared to 49% at the lower temperature level, both for a reaction time of 2.5 hrs.

It is noteworthy to mention that the reaction mixture had to be separated into two liquid phases, while still in the equilibration cell, before sampling could take place. This means that the dehydration reaction could proceed in the aqueous phase, after the prescribed reaction time, with no or negligible furfural transfer across the phase boundary. This could give rise to erroneous furfural concentration specially in the aqueous phase. It is thus recommended that the numerical values for the furfural yield in Table 2 should be interpreted with caution.

MINIMUM ENERGY REQUIREMENTS

In the furfural manufacturing process, the aqueous furfural stream is fed to a distillation unit usually comprising two columns. A stripper may be connected to the furfural recovery column according to the multi-effect principle in order to save live steam.

A typical configuration for a recovery process using a lower-boiling solvent such as MIBK is shown in Figure 2. In this case high K_D-values and that the solvent does not form a homogeneous azeotrope with furfural are two major design factors, affecting both the overall process configuration and energy consumption.

A computer program PRIMCALC was used to estimate the minimum energy requirements for the above mentioned 3 cases. PRIMCALC is a group of computer programs specially designed in order to simplify the calculations of energy requirements in combined extraction-distillation processes for the recovery of organic chemicals from diluted aqueous solutions. On executing the program on the furfural system, the following assumptions were made:

- Solvent extraction. Having specified the degree of solute recovery, a phase ratio of 1.5 times $(V/L)_{min}$ is used. A constant K_D-value is assumed, and chosen as the lowest value in the concentration range considered. The solute does not affect the mutual solubility between solvent and water.

- Solvent regeneration: The solvent recovery column in Figure 2 is assumed to produce pure components, i.e. pure furfural as bottoms and pure MIBK as distillate. A minimum reflux ratio is used in that column, as well as in the solvent stripping column to reach azeotropic concentration in the distillate. In this latter column, the lowest steam consumption, which can be tolerated for practical reasons, is taken as 1% of its feed.

A feed concentration of 0.27 mole-% furfural, corresponding to 2.2 wt-% xylose, was used in the simulations. The following minimum energy requirements, expressed in ton live steam/ton furfural produced, were obtained:

Simulation case	Minimum energy requirements
Conventional dist.	17.7
Conv. dist. + stripper	13.5
Extraction	6.0

As can be seen, only 34% of the minimum energy requirements in the conventional distillation recovery process will be consumed by using MIBK simultaneous extraction.

CONCLUSIONS

Equilibrium distribution coefficients were experimentally measured, in the temperature interval 150°-200°C, for extraction of furfural from water into toluene and methyl isobutyl ketone. MIBK gave higher K_D-values and was selected for simultaneous extraction of furfural formed by dehydrating a 2.2 wt-% xylose solution at two temperature levels. The results revealed that the furfural yield can be increased by 49% if the reaction is performed at 150°C, and by 64 % if it is performed at 175°C. Minimum energy requirements were computed for a recovery process based on extraction by MIBK. It was found that only 1/3 of the minimum energy requirements in the conventional distillation recovery process will be used.

REFERENCES

1. K. Schonemann, Chem. Ing. Tech., 29, 665 (1957).
2. K. Schonemann, Chemical Reaction Engineering, Pergamon Press (1957).
3. O.S. Knight, Trans Am Inst Chem Eng, 39, 439 (1943).
4. J.B. Conway and J.B. Philips, Ind Eng Chem, 45, 1083 (1953).
5. J.P. Tare, S.A. Puranik and M.G. Kher, Indian Chem Eng, XVII, 8 (1975) and XVIII, 27 (1976).
6. F. Trimble and A.P. Dunlop, Ind Eng Chem, Anal Ed, 12, 72 (1940).
7. R. Rigamonti and S. Marchetti, La Chimica E L'industria, XXXVII, 1039 (1955).
8. I. Kikic, P. Alessi and A. Cividini, Can J Chem Eng, 58, 119 (1980).
9. R. Wennersten, G. Zacchi and G. Aly, Presented at CHISA'81 Conf., Prague (1981).

Table 1: Experimentally measured equilibrium distribution coefficients for extraction of furfural from water into toluene and MIBK

Feed conc., wt-% furfural	K_D from water into	
	Toluene	MIBK
5.4	3.59	5.20
4.1	3.49	5.59
2.7	3.55	6.06
2.0	3.72	6.89
1.4	3.36	7.24

Table 2: Furfural yield as function of reaction time and temperature

Components	Phase Ratio (aq/org)	Temperature (°C)	Time (h)	Furfural conc., wt-% Aq. phase	Furfural conc., wt-% Org. phase	Furfural Yield, %
xylose only	-	150	1.5	0.67	-	47
	-	175	2.5	0.80	-	56
xylose + MIBK	1:1	150	1.5	0.37	0.45	52
			2.5	0.30	0.87	70
			3.5	0.30	0.90	79
	0.6:1	150	1.5	0.40	0.32	59
	1:1	175	2.5	0.19	1.40	92

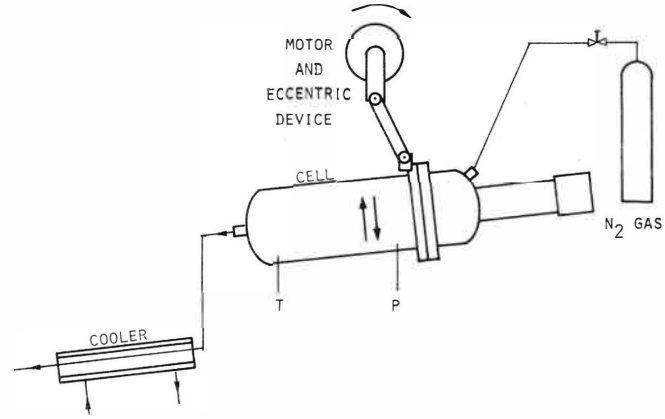

FIGURE 1: THE EQUILIBRATION CELL

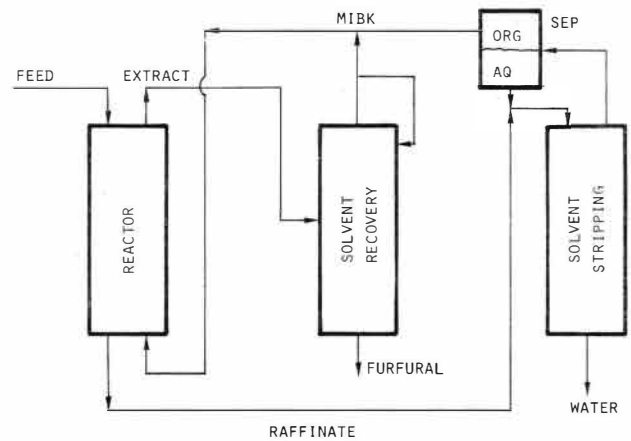

FIGURE 2: EXTRACTION OF FURFURAL WITH MIBK

PREPARATION OF L-AMINO ACIDS BY MEANS OF CONTINUOUS ENZYME-CATALYZED D,L-AMINO ACID ESTER HYDROLYSIS INSIDE LIQUID SURFACTANT MEMBRANES

T. Scheper, W. Halwachs, K. Schügerl

Institut für Technische Chemie
der Universität Hannover
Hannover, Federal Republic of Germany

During recent years the demand for L-amino acids has permanently increased (1). There are only few methods for a continuous preparation of L-isomers from a racemic mixture of amino acids. Biotechnology commonly utilizes enzymatic or crystallization techniques to split a racemic mixture, usually in batch operation (2). A new continuous working process was found by immobilizing α-chymotrypsin in a liquid surfactant membrane.

THE IMMOBILIZED ENZYME

α-chymotrypsin hydrolyses D,L-phenylalanine methyl ester into L-phenylalanine and D-ester. The aqueous enzyme solution was immobilized in an applicable membrane phase. Stable emulsions can be obtained by kerosene or cyclohexane with 5 % Span 80 in the organic phase (Table 1).

The influence of the membrane phase on the enzyme activity was tested. The loss of activity with different amounts of emulsifier is shown in Figure 1. The optimal working conditions are 25 °C and pH 6, whereby the activity decrease amounts to about 70 %, and the loss of the encapsulated enzyme into the outer phase is beyond 1 % per hour.

TRANSPORT MECHANISM

The major fraction of the substrate in the outer phase is protonated at a pH-value of 6. Only the small amount of unprotonated ester permeates the membrane due to its physical solubility and reacts with the enzyme in the inner phase. In this way the substrate is removed from the equilibrium and has to be deprotonated in the external phase in order to enter the inner phase. These protons can be titrated. Thus the conversion as well as the reaction rate can be determined. The produced L-phenylalanine has a zwitterionic character in the inner phase. Consequently a liquid quaternary ammonium salt (Adogen 464) is needed as an anion exchanger to transport the amino acid in its anionic form from the inner enzyme phase through the organic membrane phase. The carrier countertransports hydroxide and chloride ions (Figure 2).

KINETIC MODEL AND CHARACTERIZATION OF THE ENZYME EMULSION

The hydrolysis of the D,L-ester by α-chymotripsin can be described by an extended Michaelis-Menten model. When the ester concentration is increased, the measured K_M-values increase proportionally (v_{max} decreases correspondingly). A Michaelis-Menten kinetics with competitive inhibition, accompanied by a small fraction of noncompetitive inhibition explains this behavior. In equation (1) the inhibitive effect of the D-ester is included.

$$-R = \frac{\frac{v^o_{max}}{1+C_{DE}/K_N} \cdot C_{LE}}{C_{LE} + K_M\left(1 + \frac{C_{DE}}{K_I}\right)}$$

Some simplifications yield equation (2).

$$-R = \frac{v_{max} \cdot C_{LE}}{C_{LE}+K_S}$$

This equation (2) seems to be identical with the reaction rate of the simple Michaelis-Menten model, but the parameters refer to a different mechanistic model.

In continuous runs conversions can be calculated by this two-parameter model (using v_{max} and K_S):

$$\frac{dc}{dt} = \frac{F_V}{V_R}(c^o - c) - \frac{v_{max} \cdot c}{c+K_S}$$

(c: L-ester concentration; F_V: flow rate; V_R: volume of reactor)

v_{max} and K_S were determined by linear regression analysis from data obtained in batch tests (3). The results of these tests indicate an interchange between reaction and mass transfer. With higher enzyme concentrations the reaction rate increases, therefore, the reaction occurs with lower concentrations in the disperse phase, thus diminishing the enzyme's catalyst efficiency: v_{max} increases slower than the enzyme protein concentration.

CONTINUOUS TESTS

The continuous tests were performed in an apparatus shown in Figure 3. The CSTR was fed with a solution of the D,L-ester, the working pH was kept at 6; the product and the nonconverted substrate were continuously drawn off. The pH-control was seperated from the reactor by using a membrane filter to avoid the sticking of the emulsion to the electrode.

In Figure 4, the results of two hours of continuous runs with different residence times of the ester solution in the reactor are shown. The encapsulated amount of enzyme was kept constant during these tests. In this figure the measured and the calculated data are compared. In other tests residence time and amount of encapsulated enzyme were verified. The aim of the kinetic studies was to gain information about the influence of engineering parameters on the conversion and not to attain conversions close to 100 %. For this purpose conversions up to 80 % are more appropriate.

When comparing measured and calculated data, the latter are always slightly higher. This effect can be explained by the model applied. It cannot explain the complex mechanism of transport and reaction in the emulsion. However, this model yields a sufficient explanation of the experimental results.

The enzymatic hydrolysis must be followed by an isolation of the L-amino acid from the reaction mixture. The D-ester can be racemizated and be fed again into the reaction cycle.

REFERENCES

1. M.S. Sadovinka, V.M. Belikov, Russ. Chem. Rev. 47 199 (1978)
2. Y. Izumi, J. Chibata, T. Itoh, Angew. Chem. 90 187-194 (1978)
3. W. Halwachs, Biotechnol. Bioeng. 20 281-285 (1978)

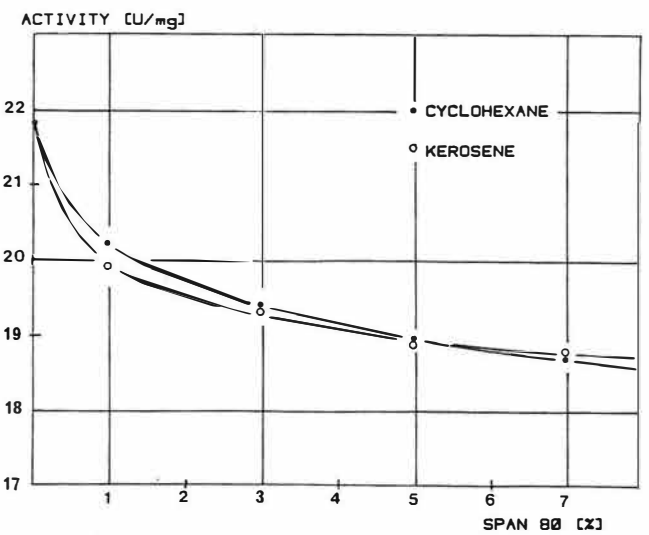

FIGURE 1. ENZYME ACTIVITY AT VARIOUS CONCENTRATIONS OF SPAN 80 IN THE ORGANIC PHASE

MEMBRANE PHASE	TENSID	ENZYMESOL.	EMULSION-PHASE-RATIO W/O	STABILITY
PARAFFIN THICK/ PARAFFIN THIN 3: 2	5%LECITHIN 5%DODECANOL	YES	9: 5	INSTABLE
PARAFFIN THICK PARAFFIN THIN 3: 2	5%LECITHIN 5%DODECANOL	NO	9: 5	STABLE
PARAFFIN THICK/ PARAFFIN THIN 3: 2	5%SPAN 80	YES	9: 5	CREAMING AFTER 1 H
PARAFFIN THIN	5%SPAN 80	YES	9: 5	CREAMING AFTER 1 H
CYCLOHEXAN	1%SPAN 80	YES	9: 5	CREAMING AFTER 1 H
CYCLOHEXAN	5%SPAN 80	YES	9: 5	STABLE
KEROSIN	5%SPAN 80	YES	9: 5	STABLE

TABLE 1. SUITABILITY OF DIFFERENT MEMBRANE COMPOSITIONS FOR THE ENCAPSULATION

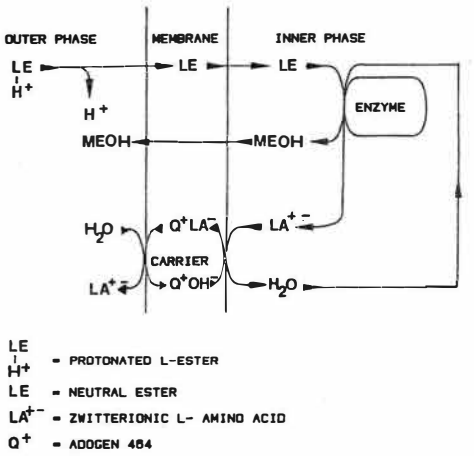

FIGURE 2. MODEL OF TRANSPORT MECHANISM IN THE ENZYME EMULSION

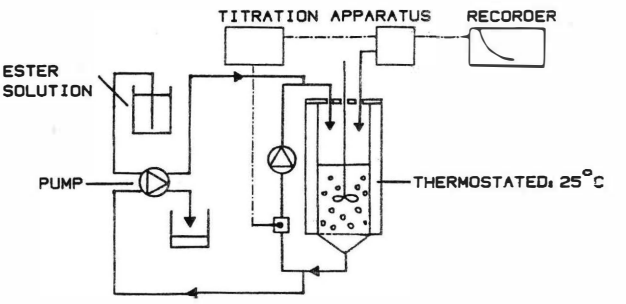

FIGURE 3. EXPERIMENTAL SETUP FOR CONTINUOUS RUNS

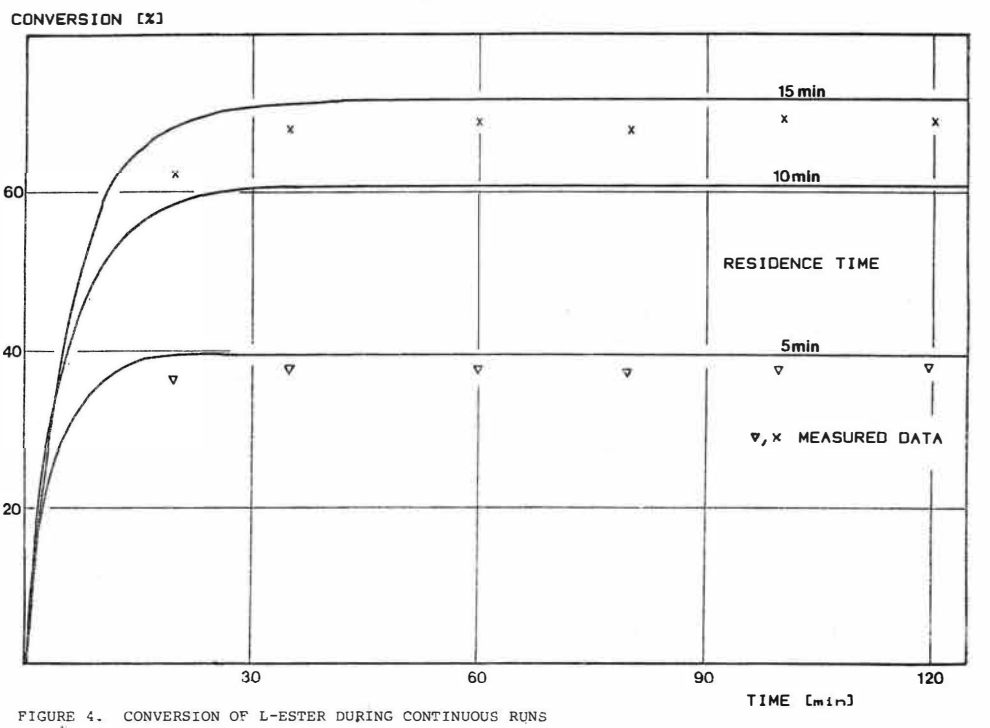

FIGURE 4. CONVERSION OF L-ESTER DURING CONTINUOUS RUNS

MASS TRANSFER IN THREE-LIQUID-PHASE SYSTEMS

L. Boyadzhiev, Z. Lazarova, E. Bezenshek

Central Laboratory of Chemical Engineering
Bulgarian Academy of Sciences
1040 Sofia, Bulgaria

INTRODUCTION

A new separational operation, based on solute transfer in three- liquid- phase systems became in the last years an object of intensive studies. This operation, known under various names as pertraction, liquid membrane separation, carrier mediated extraction, coupled transport is merely an integration in time and space of two commonly applied in separational practice operations - extraction and reextraction or solvent stripping (1-4).

The principal advantage such integration schematicaly shown in Figure 1a fallows from the fact that two almost freely chosen phase equillibria could provide complete removal of any specie in a simple one-step contact. Furthermore, since the insoluble "membrane" acts as a short time intermediator its capacity is not a vital characteristic as in the classical liquid-liquid extraction. This renders possible the introduction of various untypical solvents, oils or diluted solutions of tailor made selective solid "carriers" in neutral, water insoluble liquids.

TRANSFER MECHANISMS

The four transfer schemes, shown in Figure 1 represent almost all possible pertraction cases (5). The simple physical transfer - Figure 1a, irspite of the initial interest and various studied oil-water-oil systems is not acceptable from economical point of view and nowadays has a didactical meaning only. By the second scheme (b), a large number of solutes like ammonia, phenol, some organic bases and acids, forming with the added agent B oil insoluble products AB, can be extracted quantitatively. The third scheme (c) represents promoted or facilitated transfer since a selective "carrier" X is added into the intermediate phase S. By means of this agent desired components are transported and accumulated in the phase R, due to the different stability of AX-complexes on the first and second interfaces. Co-transportations of water and other molecules are common phenomena in this case. The last scheme (d) is an ion exchange process: the transfer of A is accompanied with equivalent counter transfer of C. Usually metal cations or anions are replaced by protons or hydroxilic groups respectively.

The last two schemes and their more complicated versions (4) are the most prospective pertraction schemes, regardless what technique is applied.

PROCESS MODELLING

There are two approaches for mathematical modelling of liquid pertraction. In the more popular differential or membrane permeation approach one takes into account steady or unsteady state diffusion across the membrane phase only (6-9). Some attempts were made to include chemical reaction kinetics at the interfaces. The principal drawback of this approach is that one does not take into account the phenomena and changes in the other two phases. Since the volumes of all liquids are finite, the solute transfer causes changes of their concentrations, pH-values and other properties, which in turn modify equillibrium conditions and hence, the rate of transfer. In some pertraction techniques side phenomena like osmosis, phase intermixing etc, cause more drastic deviations from the ideal membrane model.

The alternative approach (10-12) is based on mass balances of all components in the multiphase system. The principal concept is that the liquid pertraction is considered as an integration of two liquid-liquid extraction processes. Therefore time concentration changes and mass transfer resistences in all phases are taken into account.

TECHNIQUES FOR PRACTICAL REALIZATION.

The integration of extraction and reextraction steps in a single three-liquid-phase operation is without doubt an old idea. However, the difficulties to create a stable large scale system of three liquids, using small amount of intermediate phase, providing enormous relative areas and high mass transfer coefficients and preventing in the same time any direct contact between phases F and R, explane the retardation in the industrial applications. At least ten various techniques and their modifications were proposed and tested in laboratory scale after 1970. Three of them, double emulsion method (DEM), soaked porous solid membranes (SPSM) and creeping film method (CFM) will be discussed and compared here.

The DE technique, proposed by N.Li (13) seems to be one of the most widely studied. The method is a three-step procedure: Preparation of R in S microemulsion, using a proper emulsifier (1,14), reatement of feed F with this microemulsion and destruction of enriched emulsion to remove the product and reuse the intermediate phase S. In the second, SPSM method solutions F and R are separated by thin porous usualy polymer membrane impregnated with the intermediate phase S (15-16). The main advantage of this solid-liquid membrane over the conventional solid membranes is based on the large difference of diffusivity coefficients in solids and stagnant liquids. In the CF method (17) all three liquids are in continuous movement: F and R flow as thin creeping films along parallel hydrophylic supports. The space between these films is occupied by the "membrane" phase S, flowing also as a thicker film in co- or coutercurrent. Flowrate ratio Q_F/Q_R can be controlled in very wide range, keeping both interfacial areas F/S and S/R constant.(see Figure 3).

EXPERIMENTAL RESULTS

The three abovementioned techniques were studied and compared with model systems: (I) Removal of phenol from phenolic water, with initial concentration x_{Fo} = 100 mg/l, pH_o= 5, using normal parafines (C_{11} - C_{13}) as intermediate phase and 0.5 percent aqueous solution of NaOH as receiving phase; (II) Extraction of Cu (2+) from sulfate solution with initial content 250 mg/l, pH = 3,5, using a 2 percent solution of salicylaldoxime ACORGA-5300 (Acorga Ltd) in normal parafines (C_{11} - C_{13}) and 3n aqueous solution of sulfuric acid as receiving phase. In studies by DEM 5 percent emulsifier SPAN 80 (Atlas Co) was added to the oil phase. All experiments were carried out at 20°C.

Results obtained by DE method. The microemulsions were prepared using a high speed centrifugal pump, recirculating phases S and R for 10 min. 0.5 liter (or 1 l. in case of phenol) of freshly prepared emulsion (volumic phase ratio V_S/V_R = 1) was poured into a 20 l baffled agitator equiped with turbine impeller and containing 10 l feed phase. Dispersion was stirred genly producing emulsion globules about 1 mm in diameter. Durring each run small samples of F-phase were analysed (photocollorimetricaly in the case of phenol and A.A.spectrophotometricaly in case of copper) and pH values measured. The rate of emulsion break-up was obtained by means of "blank" runs, measuring in situ pH values continuously. Swelling of F-phase into emulsion was measured after each run. Selected typical results are shown in Figure 4. The superposition of diffusional transfer and emulsion break-up results in a typical for this method maximum in each efficiency curve. The mean measured values of mass transfer coefficient K_F and external relative area $a_{F/S}$ are 4 - 8.10^{-4}cm/s and 1 - 6 cm^{-1}. The amount of swelled water was about 1/20 of F-phase for the case of phenol, and about 1/15 for the case of copper extraction in the moment of maximum efficiency.

Results obtained by SPSM method. By this method extraction of copper cations was studied only. A polyethylene membrane, 20

microns thick with uniform pore diameter of 0.6 microns and 15 percent porosity, impregnated with phase S was clamped between two compartments containing F and R phases respectively. Each 180 cm^3 compartment, with 78 cm^2 exposed membrane area, was equiped with stirrer. The speed of rotations , over 300 rpm was chosen in a way to eliminate the contributions of mass transfer resistances in both aqueous phases. The curve shown in Figure 5 demonstrates a transfer controlled by the molecular diffusion of copper complex across the organic liquid in the pores. Mass transfer coefficient measured was 9.10^{-5} cm/s. When continuous flows of both water solutions through the compartments was applied, a membrane leakage was observed after 48 hours operation.

Results obtained by CF method. A CF, laboratory scale pertractor of 600 cm^3 total volume, including 280 cm^3 organic phase was used. Exposed vertical creeping film areas were 340 cm^2. Flowrates of receiving liquors were kept constant at 5 cm^3 per hour without noticeable effect on pertraction efficiency. Flowrates of feed phase were varied in the range of 30 to 600 cm^3 per hour. Circulation velocity of organic phase was a parameter affecting strongly removal efficiency. Figure 6 presents the rates of pertraction of phenol and copper versus mean residence time of treated F-phase in the apparatus, with and without forced circulation of intetmediate organic phase. The maximum mass transfer coefficients obtained are close to the coefficients achieved using DE method for the same purpose, if the flowrate ratios $Q_F/Q_R < 30$. If a high concentrated product is demanded, the overall mass transfer coefficients in CF method are relatively higher.

CONCLUSIONS

Liquid pertraction is an efficient separational process, very promising for removal and concentration of various valuable species from natural or industrial diluted solutions. All three techniques compared are suitable for this purpose and they have their advantages and shortcommings. The principal mass transfer characteristics: effective contact area and mass transfer coefficients, with respect to the treated phase F and for phase ratios $V_F/V_R \sim 50$, can be arranged as fallows:

$$a_{SPSM} > a_{CF} > a_{DE} \quad \text{and} \quad K_{CF} > K_{DE} > K_{SPSM}$$

Emulsion break-up and feed phase swelling are important shortcommings of DE method. The other methods avoid the multioperational mode and the use of surfactants. CF method uses more complicated designs, but avoid the risks of membrane leakage even after 2000 hours continuous round'o'clock operation.

REFERENCES

1. N. Li, A. Shrier, in: Recent Dev. in Sep. Sci., 1, 163 (1972)
2. C. Reush, E. Cussler, AICHE Journal, 19, 736 (1973)
3. L. Boyadzhiev, G, Kyuchoukov, J. Membr. Sci., 6, 107 (1980)
4. R. Marr, A. Kopp, Chem.-Ing.-Tech., 52, 399 (1980)
5. L. Boyadzhiev, Proceed. Int. Congr. CHISA, Prague (1978)
6. G. Goddard, J. Schulz. S. Suhdec, AICHE Journal, 20, (1974)
7. A. Hochhauser, E. Cussler. AICHE Journal, S.Ser. 71,136(1975)
8. E. Matulevichus, N. Li, Sep.& Purif. Methods, 4, 73 (1975)
9. P. Danesi et al., Sep. Sci.& Technology, 16, 201 (1981)
10. L. Boyadzhiev, T. Sapoundjiev, E. Besenshek, Sep.Sci., 12, 541 (1977)
11. K. Kondo et al., J. Chem. Eng. Jap., 12 203 (1979)
12. V. Kremesec, Sep.& Purif. Methods, 10, 117 (1981)
13. N. Li, AICHE Journal, 17, 459 (1971)
14. G. Casamatta et al. Chem. Eng. Sci., 29, 2005 (1974)
15. R. Baker et al, J. Membr. Sci., 2, 213 (1977)
16. E. Cussler, D. Evans, Sep.& Purif. Methods, 3, 399 (1974)
17. L. Boyadzhiev et al, Sep. Sci.& Technology (in press)

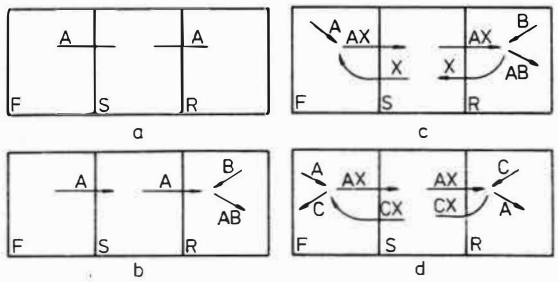

FIGURE 1. PRINCIPAL SCHEMES OF SOLUTE TRANSPORT

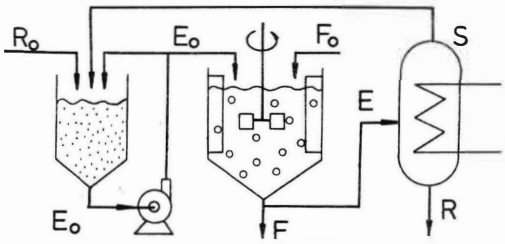

FIGURE 2. FLOW DIAGRAM IN DOUBLE EMULSION METHOD (DEM)

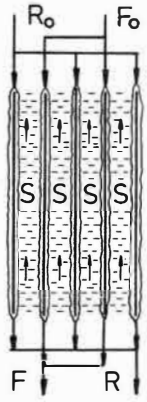

FIGURE 3. SCHEME OF CREEPING FILM PERTRACTOR (CFP)

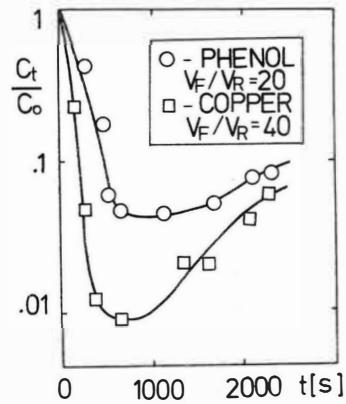

FIGURE 4. EXTRACTION OF PHENOL AND COPPER VS. TIME BY DOUBLE EMULSION METHOD

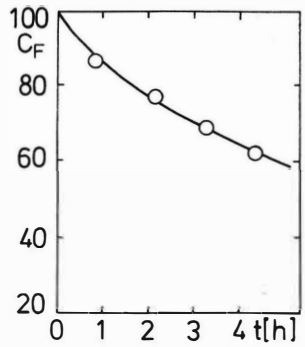

FIGURE 5. EXTRACTION OF COPPER VS. TIME BY SPSM METHOD

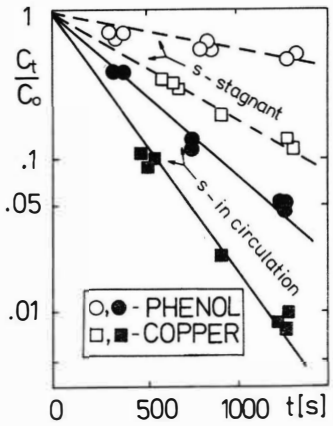

FIGURE 6. EXTRACTION OF PHENOL AND COPPER VS. TIME BY CF METHOD

MASS TRANSFER RATE THROUGH SOLID SUPPORTED LIQUID MEMBRANES. USE OF A TERTIARY AMINE SALT AS CARRIER OF METAL SPECIES FROM CHLORIDE MEDIA (1)

R. Chiarizia, A. Castagnola

Laboratorio Chimica Applicata
TIB-CHI, CRE Casaccia, ENEA
Rome, Italy

In this work some results obtained studying the transport of cadmium and zinc chloride species through a solid supported liquid membrane containing as carrier a tertiary amine salt are reported. The possibility to perform cadmium/zinc separations by this technique is also examined.

EXPERIMENTAL

The supported liquid membrane consisted of a Celgard 2500 (Celanese) microporous polypropylene film on which a solution of tridodecylammonium chloride (TLAHCl) in triethylbenzene was absorbed.

The pH of the Cd and/or Zn containing aqueous chloride feed solution was generally kept constant at 1 ($[HCl]$ = 0.1 M) while the strip solution was buffered at pH 7 by CH_3COONH_4.

The apparatus used to follow the Cd and/or Zn transfer from the feed to the strip solution was made of two cells separated by 18 cm^2 of membrane. The volume of each aqueous solution was 150 cm^3.

The concentration variations of both cations in the aqueous solutions were followed by oscillopolarography. From the slope of the plots ln C/C_o (where C is the feed metal concentration at time t and C_o is the feed metal concentration at zero time) vs t, the permeability coefficient P (cm s^{-1}) was evaluated for each transport experiment by means of the equations

$$(1) \qquad P = J/C = -\frac{dC}{C\,dt} \cdot \frac{V}{Q}$$

$$(2) \qquad \ln \frac{C}{C_o} = -\frac{Q}{V} P t$$

where J = membrane flux, V = volume of feed solution, Q = membrane area.

After an initial induction time the experimental ln C/C_o vs t data always fell on a straight line.

The stirring speed was kept constant at 680 rpm in both the feed and strip solutions since preliminary experiments allowed us to state that beyond this stirring speed value the permeability becomes independent of it.

REACTION STOICHIOMETRY

For both cadmium and zinc in the Cl^- concentration range experimentally explored ($[Cl^-]$ = 0.1 ÷ 2 M) and for low metal concentrations the extraction stoichiometry can be represented as follows:

$$(3) \qquad MCl_2 + 2\,\overline{TLAHCl} \overset{K_e}{\rightleftharpoons} \overline{(TLAHCl)_2MCl_2}$$

where M = Cd or Zn and the bar indicates organic species.

The K_e value for cadmium has been calculated from distribution experiments ($K_e = 2.9\ 10^4\ M^{-2}$), the K_e value for zinc has been taken from the literature(2) ($K_e = 3.3\ 10^4\ M^{-2}$).

It follows for the metal partition coefficient

$$(4) \qquad K_d = K_e\,[\overline{TLAHCl}]^2\,\alpha_2$$

with α_2, degree of formation of MCl_2, given by

$$(5) \qquad \alpha_2 = \frac{\beta_2\ a^2}{1 + \sum_i \beta_i\ a^i}$$

where β_i = overall formation constant of the M-Cl complexes taken from reference (3) and a = effective ligand activity.

CO-TRANSPORT MECHANISM

At the feed-membrane interface, where the pH is low enough to prevent the hydrolysis of the carrier, reaction (3) takes place between the carrier and the metal species which has reached the interface, diffusing through the aqueous boundary layer.

The metal-carrier complex diffuses then through the membrane and reaches the strip-membrane interface where the reaction

$$(6) \qquad \overline{(TLAHCl)_2MCl_2} \rightleftharpoons 2\,\overline{TLA} + 2\,H^+ + M^{+2} + 4\,Cl^-$$

occurs. The CH_3COONH_4 buffer in the strip solution causes the hydrolysis of the carrier and the complexation of the released metal cation.

The TLA diffuses back to the feed side where it is converted again into TLAHCl. At each cycle both M and HCl are in this way co-transported from the feed to the strip solution.

PERMEABILITY EQUATION

In previous papers (4-6) it was shown that when the partition coefficient of the metal species at the feed-membrane interface is much larger than at strip-membrane interface, for low aqueous metal concentrations and fast interfacial reactions, the following equation describes the steady state permeability process:

$$(7) \qquad P = \frac{K_d}{\frac{d_a}{D_a} K_d + \frac{d_o}{D_o}}$$

where d_a = aqueous diffusion film thickness

d_o = membrane thickness

D_a = aqueous metal species diffusion coefficient

D_o = organic (membrane) metal species diffusion coefficient

By inserting equation (4) in equation (7) the following permeability equation is obtained:

$$(8) \qquad P = \frac{K_e \alpha_2 [\overline{TLAHCl}]^2}{K_e \alpha_2 [\overline{TLAHCl}]^2 \frac{d_a}{D_a} + \frac{d_o}{D_o}}$$

Equation (8) represents well the experimental data, obtained for the cadmium transport rate as function of the carrier and Cl^- concentrations, reported in Figures 1 and 2 . The solid curves of both Figures have been in fact calculated by means of equation (8) with the following diffusion parameters:

$d_a/D_a = 2.9\ 10^2\ cm^{-1}s$ and $d_o/D_o = 7.8\ 10^2\ cm^{-1}s$

(the K_e value reported above and α_2 values calculated by means of equation (5) have been also used).

CADMIUM-ZINC SEPARATION

The data of Figure 2 show that with $[\overline{TLAHCl}]$ = 0.3 M, in the Cl^- concentration range 0.1 ÷ 2 M, the cadmium permeability is nearly independent of the chloride ion concentration.

On the contrary the Cl^- concentration has a pronounced effect on the zinc permeability coefficient as shown in Figure 3, where the permeability coefficient of cadmium and zinc are plotted in logarithmic scale as function of the aqueous feed chloride concentration for $[\overline{TLAHCl}]$ = 0.03 M.

The different behaviour of cadmium and zinc can be mainly ascribed to the lower tendency of Zn^{+2}, as compared to Cd^{+2}, to undergo complexation by Cl^- ions. This reflects in different α_2 values which in the given chemical conditions are much lower for zinc.

A consequence of the different α_2 values for cadmium and zinc is that different mechanisms control the permeation rate. In the case of cadmium infact the high value of α_2 makes the second term of the sum in the denominator of equation (8) negligible. It follows:

$$(9) \qquad P_{Cd} \simeq D_a/d_a$$

that is the permeability is essentially aqueous diffusion controlled.

In the case of zinc, on the contrary, the situation is reversed and the permeability equation becomes:

$$(10) \qquad P_{Zn} \simeq K_e \alpha_2 [\overline{TLAHCl}]^2 \frac{D_o}{d_o}$$

that is the permeability is essentially membrane diffusion controlled.

At $[Cl^-]$ = 0.1 M and $[\overline{TLAHCl}]$ = 0.03 M the cadmium and zinc permeabilities differ 63 times. In these conditions a good separation of the metal species can be obtained. This is shown in Figure 4 where the metal concentrations in the strip solution are plotted as function of the time (the initial feed concentration is 1 millimolar for both metals). It can be observed that after about 200 minutes 75% of the cadmium is recovered at practically 100% purity.

REFERENCES

1. A FULL VERSION OF THIS WORK IS GOING TO BE PUBLISHED ON THE JOURNAL OF MEMBRANE SCIENCE
2. D.Dyrssen and M.De Jesus Tavares, Acta Chem.Scand., 20, 2050(1966)
3. R.M.Smith and A.E.Martell, Critical Stability Constants, vol.4, Plenum Press, New York-London, 1976
4. P.R.Danesi, E.P.Horwitz, G.F.Vandegrift and R.Chiarizia, Sep.Sci.Tech., 16, 201 (1981)
5. P.R.Danesi, E.P.Horwitz and P.Rickert, Sep.Sci.Tech., 17, 1183(1982)
6. R.Chiarizia, A.Castagnola, P.R.Danesi and E.P.Horwitz, J.Membrane Sci., in press

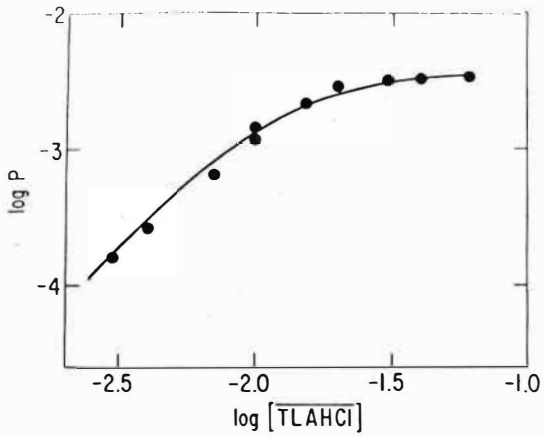

FIGURE 1 : log P (cm s^{-1}) vs log [$\overline{TLAHCl}$] (M) .
Feed: [HCl] = 0.1 M, [NaCl] = 0.9 M, [Cd^{+2}] = 5 10^{-4} M.
Strip: [CH_3COONH_4] = 0.2 M, [NaCl] = 0.8 M.
The solid curve was calculated by equation (8)

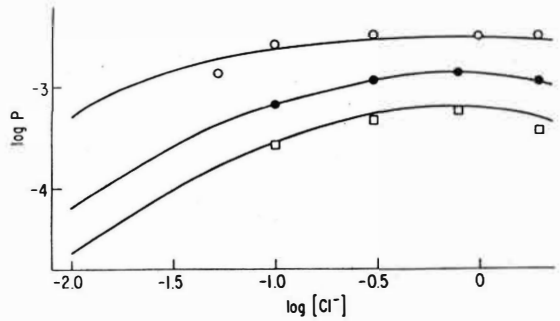

FIGURE 2 : log P (cm s^{-1}) vs log [Cl^-] (M) in the feed solution.
Feed: [HCl] = 0.1M, [NaCl] = X M, [Cl^-] = (0.1 + X) M,
[Cd^{+2}] = 5 10^{-4}M
Strip: [CH_3COONH_4] = 0.1 M, [NaCl] = X M
Membrane: [$\overline{TLAHCl}$] = 0.03 M (o),0.01 M (•),0.006 M (□) in triethylbenzene
The solid curves were calculated by equation (8)

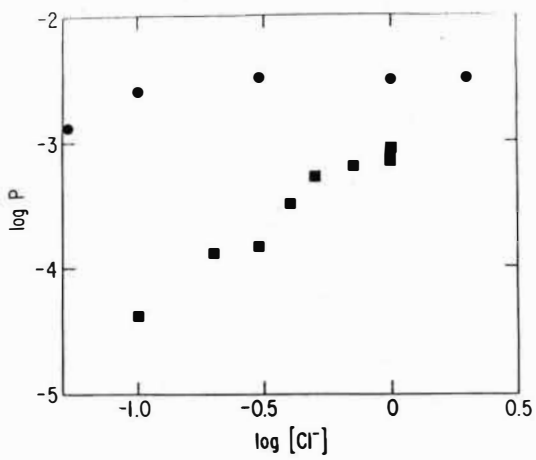

FIGURE 3 : log P_{Cd} (●) and log P_{Zn} (■) (cm s^{-1}) vs log [Cl^-] (M) in the feed solution.
Feed and strip solutions as in Figure 2. Membrane: [$\overline{TLAHCl}$] = 0.03 M in triethylbenzene

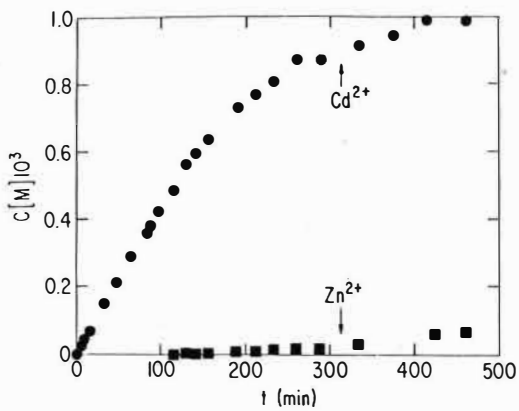

FIGURE 4 : molar concentrations of Cd and Zn in the strip solution (C) vs time (t). Initial concentrations of Cd and Zn in the feed solution = 1 10^{-3} M.
Feed : [HCl] = 0.1 M . Strip = [CH_3COONH_4] = 0.1 M .
Membrane : [$\overline{TLAHCl}$] = 0.03 M in triethylbenzene

THE RECOVERY OF PLUTONIUM BY MEANS OF SOLID SUPPORTED LIQUID MEMBRANES

Giulio M. Gasparini, Giuseppe Grossi, Maurizio Casarci and Armando D'Andrea

E.N.E.A. - C.R.E. Casaccia
Rome, Italy

Supported liquid membrane separations present attractive possibilities of applications in many hy-drometallurgical leach solutions containing low concentrations of one or more metals.

This new technology has not yet reached the sufficiently elevated reliability degree to be employed in industrial applications.

The future development of this kind of membranes needs more extended basic studies to increase the knowledge of the interaction between the membrane, the carrier and the diluent.

One of the conditioning steps for the future diffusion of this new method is the possibility to ensure sufficiently prolonged lifetimes of the charged membranes.

At the moment these researches are conditioned upon the lack of membranes of different materials with controlled characteristics.

Despite these numerous points of incertitude, the potential possibilities of the supported liquid membranes stimulate many researchers to propose original applications.

We describe there our researches aimed to evaluate the possibility to utilize as a carrier in a supported liquid membrane a neo alkyl hydroxamic acid.

In our previous researches (1) (2) we have studied the behavior of the neo alkyl hydroxamic acids with this structure:

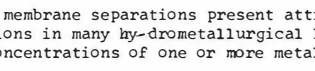

with regard to some actinides, and fission products in liquid - liquid extraction.

These compounds are strong extractants of Pu, Zr, Nb, Mo, Fe, V from acidic media (1 - 5 M HNO_3, H_2SO_4, HCl, $HClO_4$).

Other complexing agents (Phosphoric esters, phosphinoxides, carbamoyl phosphonates) have similar properties with a more wide selectivity. But all these compounds are ineffecting in alkaline media for their poor extracting power or their elevated solubility in basic media. On the contrary, neo alkyl hydroxamic acids with a suitable molecular weight, can be employed directly (without any previous acidification) in an alkaline solution; this is a peculiar characteristics of these extractants.

We have employed, for these preliminary investigations, several commercial membranes with given characteristics:
- Celgard 2500 and Celgard 4510 produced by Celanese Co
- Accurel PP produced by Armak Co.
- PTFE T 30 of Schleichleir and Scull

The experimental apparatus employed for the discontinuous tests has a very simple glass apparatus illustred in Fig. 1.

An hollow fiber propilene module is now under investigation for continuous tests.

The aqueous feed solutions utilized have been 1M Na_2CO_3, 1M $NaHCO_3$ 0,1 - 1M HNO_3 solutions have been also tested.

The product (or strip) solution has been, 0,5 oxalic acid buffered at pH 2,25 with ammonia.

For the preliminary investigations on the effect of the different variables Fe59 has been used as Pu simulant, since the stability constants of the Fe^{+3} - hy-droxamic acid complex are very similar to that of Pu^{+4}.

Pu^{239} has been employed in the final tests. We have chosen as carrier the tributyl aceto hydroxamic acid (TBAH), because this compound has been widely studied in our previous investigations in liquid - liquid procedures. With this acid, a mixture of diethyl benzene 5% 2-octanol has been employed as diluent.

The membranes have been prepared by dipping them into a solution containing the carrier during a night; after extraction and a little shake, the membrane has been placed into the apparatus between two PTFE O ring. Procedures proposed by other researchers did not give a better reproducibility.

Each experience has been carried out as follows:
5 ml. of the feed solution has been introduced into the upper tube and 50 ml. of the product solution into the lower tube.

The apparatus has been thermostatated and the agitation turned on. 0.1 ml. of a standard Fe 59 or Pu^{239} solution of known activity, has been introduced into the feed, and samples of the product solution have been taken for the counting. The activity of the feed solution has been controlled only at the end of the experience.

The pH of both the solutions were controlled continuously.

The research can be divided into 3 steps:

1) Study of the feasibility of the system and choice of the principal variables (diluent, carrier concentration, metal concentration, temperature etc.) with Fe^{59} as Pu simulant.

2) Verification of the Pu behavior in some discontinuous tests.

3) Continuous tests with hollow fiber modules.

RESULTS

In the following Figures we have illustrated the more interesting results of our research in discontinuous apparatus (FIG.2 - 5)

Their aim is to verify the influence of the more important variables on the transfert rate and the possibility to utilize this supported membrane for the Pu separation.

Now we are carring out some runs with a continuous hollow fiber model.

REFERENCES

1) G.M. GASPARINI : The trialkyl aceto hydroxamic acids as selective extractants in the reprocessing of irradiated nuclear fuels. Proc. of the Intern. Solvent Extraction Conf. ISEC 77 - Toronto, 9- 16, Sept. 77.
2) G.M. GASPARINI - Gazz. Chim. Ital. 109 357 (1979)

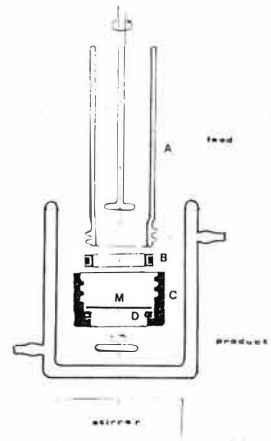

FIG 1 EXPERIMENTAL APPARATUS

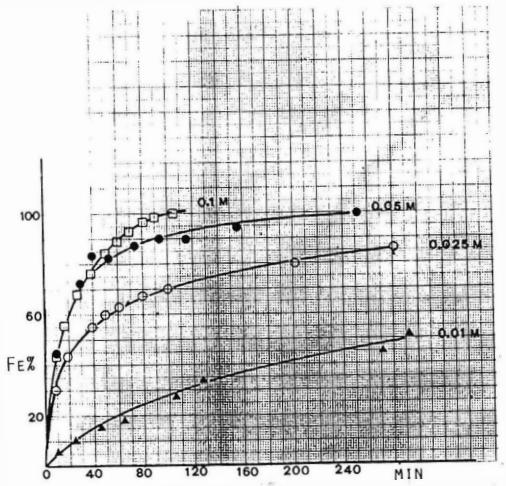

FIG 2 THE BEHAVIOR OF DIFFERENT MEMBRANES
•FEED:1M Na_2CO_3+Fe^{59};STRIP:0.5M$(COOH)_2$

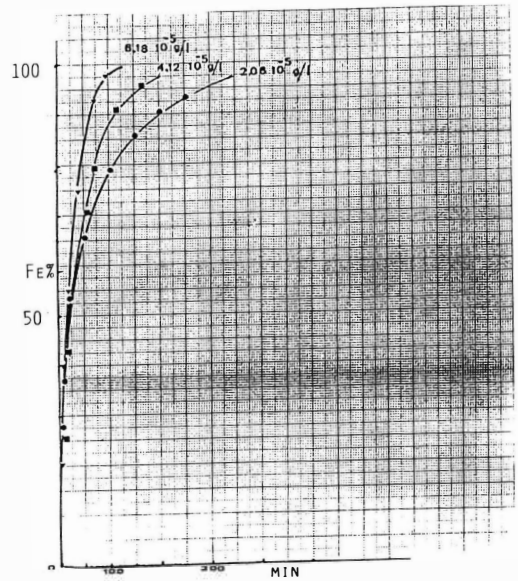

FIG 3 INFLUENCE OF THE Fe CONC ON THE TRANSERT RATE
FEED:0.1M Na_2CO_3+Fe^{59}; STRIP: 0.5M $(COOH)_2$
CELGARD 2500 +0.1 TBAH IN DEB

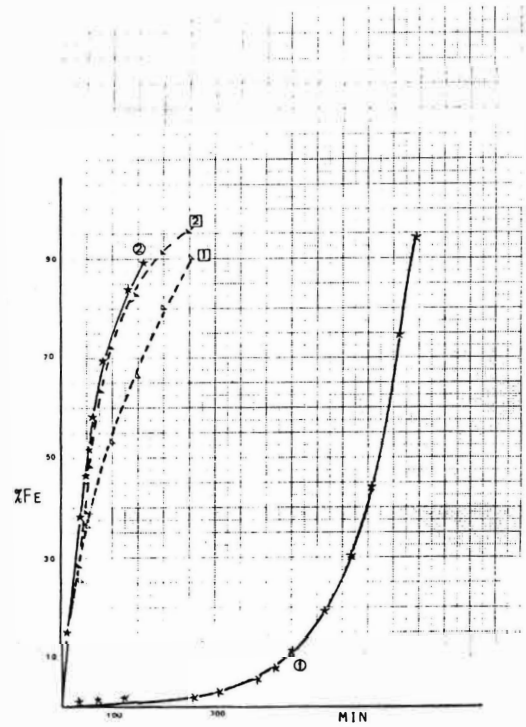

FIG 4 INFLUENCE OF THE FEED NATURE-INDUCTION TIME
DOTTED LINE:FEED K BIPHTALATE pH 4.5 ;STRIP:$(COOH)_2$
FULL LINE :FEED Na_2CO_3 1M pH11.8 ; " "
MEMBRANE:CELGARD 2500
1=FIRST TEST:
2=TEST REPEATED WITH THE SAME MEMBRANE

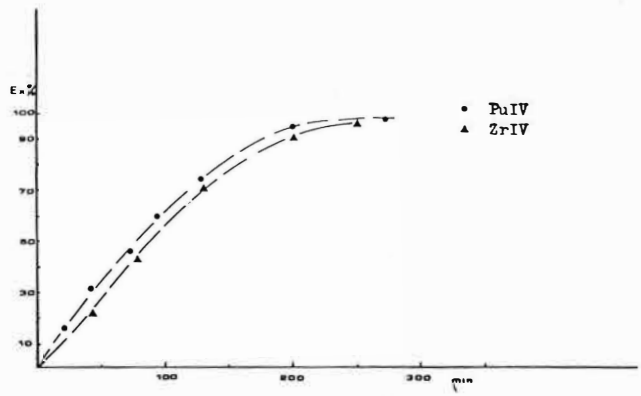

FIG 5 THE Pu^{IV} AND Zr^{IV} TRANSFERT
FEED:1M 1M Na_2CO_3,0.6M $NaNO_3$;STRIP: 0.5M$(COOH)_2$
MEMBRANE:CELGARD 2500

COUPLED TRANSPORT IN URANIUM EXTRACTION

T. J. Hardwick

Gulf Research & Development Company
P.O. Drawer 2038
Pittsburgh, Pennsylvania 15230 USA

In coupled transport, the porous walls of hollow plastic fibers are filled with an extracting solvent; in the case for uranium, 30% Alamine 336 in kerosene was used. Uranium-loaded feed circulates through the center of these fibers (0.07 mm in diameter) while strip solution passes around the outside. The concentration gradient across the wall (0.06 mm thick) effects a transport of uranium from loaded feed to the strip solution.

Early work on this system used flat membranes dividing two halves of a cell; one side was filled with feed, the other with strip solution. (1,2,3) Several conclusions were reached, both from experimental results and from a theoretical analysis of the system:

1. The rate of transport of uranium (flux) increases with the uranium concentration, but there is a maximum value.
2. The flux is proportional to the concentration profile of the uranium across the membrane.
3. An agglomeration of the uranium-amine complex occurs. This can be sufficient to hinder free flow of constituents across the membrane.
4. Maximum flux occurs when the amine is present as a 30% solution in kerosene in the solvent-filled pores.

The present experiments were undertaken to evaluate the mechanism in dynamic systems typical of commercial operation, and to quantify the effect of variables for scaleup.

EXPERIMENTAL

Bend Research, Inc. supplied four units, each unit consisting of a bundle of approximately 1240 fibers, each 50 cm long, and potted in parallel inside a clear plastic pipe. The fibers were impregnated with 30% Alamine in Kermac solvent 470B. Provision was made for acid feed to flow upward through the hollow fiber core, while strip solution (sodium carbonate solution) circulated about the outside of the fiber walls.

The features of coupled transport were studied in a dynamic steady state mode, using equipment assembled as shown in figure 1. Feed enters as stream A, recycles as stream BCD and exits as the raffinate E. If the prefixes relating to flow and concentration are F and C respectively, then it can be shown that in a single transit of the column

(1) $$CB = (FAxCA)+(FB-FA)xCE\ /FB$$

The concentration loss is CB-CE, and the fraction of material lost is CE/CB (=P). The rate of transport is (CB-CE)xFB.

Experimentally, feed entered the recycling system at a pressure of 5 psi. The flow rate was controlled by a variable peristaltic pump on the raffinate and the recycle rate by a valve between the centrifugal recycling pump and the column. The strip solution was recycled around the fibers. A steady but slow feed of strong sodium carbonate solution entered the strip circuit; the overflow was collected as product. The pH of the strip solution was maintained by addition of sodium hydroxide solution, added by pH-controlled demand.

Typical runs lasted four hours, with samples of streams taken and total flows or flowrates measured every half hour. Steady state operation was assumed if the last three samples had the same value. The experimental program tested individually the following variables: acid, uranium and sulfate concentrations in the feed, carbonate concentration and pH in the strip solution, and the operating variables of flow and recycle rate. The range of variables was limited to those expected in industrial practice.

It should be noted that the concentrations discussed are those entering the column at steady state. It was thus difficult to fix all variables, but in the range normally used, the effect of minor deviations was very small.

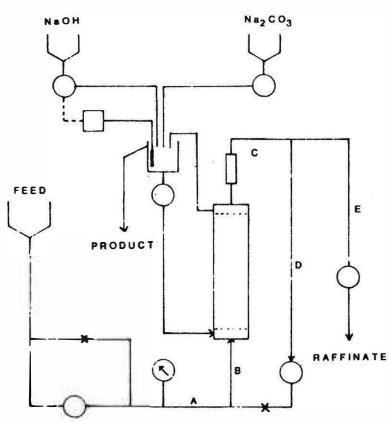

FIGURE 1 EXPERIMENTAL SYSTEM FOR A COUPLED TRANSPORT UNIT

RESULTS

EXPERIMENTS WITH ACID ONLY

Dilute sulfuric acid was used as feed. The alkali content and pH of the strip solution made no difference, provided the pH was at least 8. Above an acid concentration of 70 mN, the rate of transfer of acid was zero order - 20.3 meq/min; at lower acid values the rate decreased, and below 25 mN, the rate was first order. This is shown in figure 2; also shown are the rate expressions for each regime.

EXPERIMENTS WITH PURE ACID URANIUM SULFATE

A. Effect of uranium concentration on its rate of transport. With the acid concentration entering the column being maintained at 0.1 - 0.2N, the rate of uranium transport was proportional to its concentration; the fraction of uranium not removed from solution on passing through the column was constant. Figure 3 shows a plot of P versus CB (U). At low concentrations P = 0.73. Above CB = 2.5mM/l (600 ppm U) there is a decrease in P.

B. Effect of uranium concentration on the rate of acid transport. With acid solutions entering the column between 0.1 and 0.2N, the uranium concentration was varied while the rate of acid transport was measured. The results (figure 4) show that the rate of acid transport decreases steadily to a value of 10.3 meq/min, and remains constant at higher uranium concentrations. If the acid concentration is below 70mN, then the expected de- crease due to low acid is prorated with the uranium data.

C. Effect of sulfate ion concentration in the feed. Sulfate ion is usually present in mill feeds in concentrations from 0.2 - 0.5M/l. In this range there is a small effect of the sulfate ion concentration; P = 0.698 + 0.049x(SO4).

D. Effect of pH of the strip solution. There is a linear relation between the maintained pH of the solution and the value of P. P = 1.136 - (0.0397 x pH)

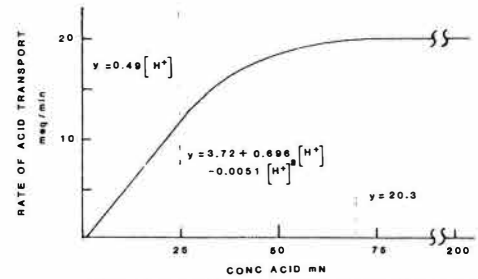

FIGURE 2 EFFECT OF ACID CONCENTRATION ON ITS RATE OF TRANSPORT

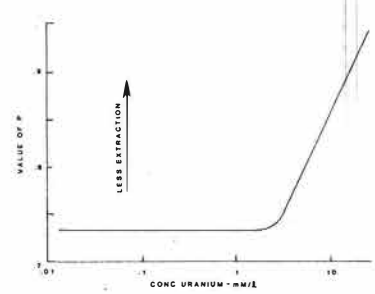

FIGURE 3 EFFECT OF URANIUM CONCENTRATION ON ITS RATE OF TRANSPORT

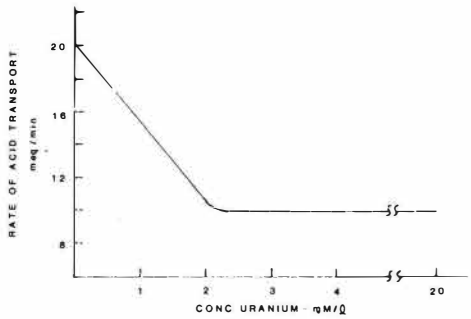

FIGURE 4 EFFECT OF URANIUM CONCENTRATION ON THE RATE OF ACID TRANSPORT

E. Effect of carbonate ion concentration in the recycling strip solution. A plot of the log of the divalent carbonate ion concentration ($CO_3^=$) not (HCO_3^-) versus the value of P gives a straight line. It is important that the true carbonate ion concentration be used, as opposed to the sum of $CO_3^=$ and HCO_3^- Corrections for dilution must also be made. $P = 0.689 - \ln(CO_3^=)$.

F. Effect of feed rate into the system. Feed rates of 20 -1200 ml/min have been used with a fixed acid recycle rate of 2000 ml/min. With normalization for the effects as per equation (1), the results agreed with those already established.

G. Effect of recycle rate. Recycle rates were varied from 500- 3500 ml/min. Above 1200ml/min the results were as predicted, but below this value, an erratic decrease in uranium extraction occurred, but no corresponding decrease in the rate of acid transfer. In this system a recycle rate of 2000 ml/min corresponds to a linear flow of 5 cm/sec in the hollow fibers.

MATERIAL BALANCE

The material balance of acid loss from the feed has always agreed well with the alkali loss in the strip system. Uranium balance was reasonably satisfactory, considering the many measurements of flow rate and uranium analyses which contribute. Sulfate balance has been measured occasionally and is reasonable.

MODELING

We have been able to quantify these variables into a mathematical model which predicts the effluent concentrations of uranium and acid from inputs of a) feed rate, b) recycle rate, c) acid, uranium and sulfate in the feed, d) flow rates and concentration of sodium hydroxide and sodium carbonate, e) pH of the strip solution.

DISCUSSION

It is difficult to develop a mechanism which will explain quantitatively the effects of the variables as we observed them. That which is most satisfactory is the concept of recessed interfaces; a suggested portrayal is given in figure 5. In any filling of the pores with solvent, it is unlikely that all will be filled flush with the irregular surface of the fiber. Those which are initially flush may lose some material to the scouring action of the turbulently flowing feed. The net result is a very small element of volume, having contact with the interface, but stagnant to the point that diffusion laws govern the migration of the species present. A similar argument can be made for the strip side of the fiber.

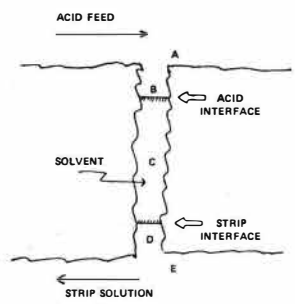

FIGURE 5 CONCEPT OF RECESSED INTERFACES

MECHANISM

Protonation. This occurs at the interface, where the amine reacts efficiently with either H_3O^+ or HSO_4^-. Above 70 mN acid the rate is controlled by the rate of diffusion of the amine to the interface, as there is sufficient acid within the recess. At lower acid concentrations the rate is controlled by the migration of acid to the interface; below 25 mN the rate of protonation is the rate of acid migration into the recess, and this is dependent on the acid concentration in the bulk of the feed. The rate of acid transport thus changes from zero to first order between 70 and 25 mN acid concentration.

Complex Formation. The protonated amine reacts with either sulfate ion or the uranyl sulfate anion to form a neutral complex. Uranium complex formation is favoured; little change is found in the rate of uranium transport from 0.1 to 0.7M $SO_4^=$.

Over a wide range (0.005 - 2 mM/l) the rate of uranium transport is first order with respect to uranium concentration. This suggests that the rate governing step is the rate of diffuion of the uranyl sulfate anion into the recess, and this in turn is dependent on the uranium concentration in the bulk feed. The diffusion rate of the uranyl sulfate anion is much smaller than that of the sulfate ion; there will be sufficient protonated amine available to combine with any uranyl sulfate anion reach- ing the interface.

Above 2mM/l, the rate of diffusion of this complex from the feed solution into the recess, although increasing, is insufficient to maintain first order kinetics with respect to its concentration in the bulk feed. Accordingly, the value of P increases at the higher uranium concentrations.

Hindered Diffusion. The presence of uranium in the feed, even at low concentrations, results in a decrease in the rate of acid transport. We consider this due to the formation of agglomerates of the amine-uranium complex in the solvent. Such behaviour has been recognized in amine-uranium systems (4), and applied to this system by previous workers. (2,3)

With further agglomeration the increasing size of the diffusant retards its migration to the strip interface. Unless the pore is blocked, the rate of travel of free amine in the reverse direction will not be affected, and there will be an accumulation of the uranium-amine complex in the pore. The net effect is to reduce the amount of free amine in the organic phase and hence the extent of its diffusion to the acid interface. The rate of protonation will decrease, and this will be observed as a decrease in the rate of transport of hydrogen ion.

Above 2mM/l uranium in the feed, the rate of acid transport is constant at half its maximum value. We assume that one-half the amine is tied up as the uranium complex. This upper limit of uranium concentration is about that where the rate of diffusion of uranium into the recess becomes rate-controlling.

Effect of pH. The pH of the strip solution affects the rate of uranium transfer, but not the rate of acid transfer provided the strip solution is alkaline. Amine-sulfate complex migrating to the strip interface will always find sufficient alkalinity to release sulfate ion to the aqueous solution; the rate of acid transfer will be unaffected. If, on the other hand, the release of uranium specifically requires reaction with the divalent carbonate ion, a lower pH value will decrease the concentration of that ion, and the rate of discharge of uranium across the strip interface will decrease. Similarly, if less sodium carbonate is added to the system, there will be a lower rate of uranium transfer across the strip interface. In a manner analogous to the recess mechanism on the acid side, local depletion of carbonate ion may occur at high rates of transport.

Critical to the acceptance of this mechanism is the understanding that the bulk concentrations in feed and strip solution are not those at the reacting interface. It should also be noted that data are specific to this particular unit. This has been deliberate as an aid to clarity in the discussion. All data can be converted to absolute units, (e.g. probability of uranium transport per unit time per unit area of fiber surface).

REFERENCES

1. R.W.Baker, M.E.Tuttle, D.J.Kelly and H.K.Lonsdale, J. Membrane Sci., 2, 213 (1977)

2. W.C.Babcock, R.W.Baker, E.D.LaChapelle and K.L.Smith, J. Membrane Sci., 7, 71 (1980)

3. ibid. 7, 89 (1980)

4. D.F.C.Morris, J. Colloid Interface Sci., 51, 52 (1975)

LIQUID MEMBRANE STUDIES: TRANSPORT AGAINST THE CONCENTRATION GRADIENT OF $AuCl_4^-$

M. Burgard, P. Elisoamiadana and M. J. F. Leroy

E.N.S.C.
Université Louis Pasteur
Strasbourg, France

and

H. S. Park

Dae Duk Engineering Center of K.A.E.R.I.
Dae Duk Danji, Korea

Application of the Liquid Membrane Technique for the recovery of metal ionic species has recently aroused a great deal of interest. The principle of the process is based on the ability for a desired ion A to diffuse against its concentration gradient ("uphill transport"), the energy being supplied by the concentration gradient of another ion B which diffuses across the membrane as well. In this process, an important role is played by the mobile carrier contained in the membrane which "reacts" with A and B and transports them. Many examples of such transports have been given in the literature; in most of them, B is the proton (pH pump).
If A is a cation, the carrier is a cation exchanger, H^+ and A diffusing in opposite directions (Counter transport); if A is an anion (e.g. an anionic metallocomplex), the carrier is a base, H^+ and A diffusing in the same direction (co-transport).
Thus, transport has been described for a great number of metallic species including alkali, alkaline earths, Uranium, rare earths, transition metals (1).
Studies on the development of Liquid Membrane Technique for the recovery of precious metals have been undertaken in our laboratory; in this presentation we summarize some preliminary results on the transport of $AuCl_4^-$.

EXPERIMENTAL SECTION

The transport experiments were performed using the set-up shown in the Figure 1. The carrier solution was located at the bottom of a thermostated cell (T = 25 ± 1°C). A glass bell cylinder suspended above the bottom of the cell separated the inner aqueous phase (aqueous phase I) and the outer aqueous phase (aqueous phase II). A synchronous motor (Heidolph RZR 2000) was attached to the cylinder to provide constant turning of the cylinder and stirring of the phases (200 rpm). An immobile glass obstacle immersed in both the organic phase and the aqueous phase I ensured a rapid homogenization of concentration in the phases. Samples in the inner aqueous phase were taken by stopping momentaneously the rotation and by introducing a seringe or pipet through the window of the cylinder (see Figure I). Analyses were carried out using an IL 453 atomic absorption spectrophotometer. The poly(oxyehtylene) derivative (compound L) was supplied by the Société Nationale des Poudres et Explosifs.

CO-TRANSPORT K^+ or H^+ - $AuCl_4^-$

"Uphill" transport of $AuCl_4^-$ can be achieved by means of co-transport with M^+ or H^+, the mobile carrier being a neutral complexing agent or solvating agent for M^+ or H^+. The energy for the transport is supplied by the concentration gradient of M^+ or H^+ (scheme).
The carriers considered are :
. a poly(oxyethylene) derivative (compound L) complexing K^+(see scheme)
. Butex (Dibutylcarbitol) which solvates H^+.

CO-TRANSPORT K^+ - $AuCl_4^-$ WITH A POLY(OXYETHYLENE) DERIVATIVE AS CARRIER

Previous work has confirmed the binding properties of this type of carrier towards alkali ions as well as their ability to extract alkali salts (2). K^+ - $AuCl_4^-$ coupled transport using compound A as carrier is illustrated in Figure I and Figure III.
Comparison of K^+ and gold concentrations in the receiving phase shows a negligible transport of Cl^- with respect to $AuCl_4^-$. Otherwise diluent effects seem important : A quantitative recovery of gold in the receiving phase is achieved when choloroform is used as diluent, whereas it is observed that the membrane tends to saturate when dichloroethane is the diluent. This phenomenon is related to the corresponding liquid-liquid extractions constants which have been found to be higher for dichloroethane than for chloroform (chloroform : Ke # 3.10^2 M^{-2} l^{-2}; dichloroethane : Ke # $1,5.10^3$ M^{-2} l^{-2}).
Figure III illustrates the effect of the KCl concentration in aqueous phase I on the transport.
The deduced initial transport rate

$$V_o = \left(\frac{dc_{Au}}{dt}\right)_{t=0}$$

can be interpreted assuming a diffusion-limiting mechanism for the co-transport (3).
The transport rate V_o can be written :

$$V_o = A \frac{K_e L_o y_+|K^+| y_-|AuCl_4^-|}{1 + K_e y_+|K^+| y_-|AuCl_4^-|} \qquad \text{(equation I)}$$

where K_e is the extraction constant of the equilibrium

$$K^+ + AuCl_4^- + \overline{L} \rightleftharpoons \overline{KLAuCl_4}$$

L_o is the total concentration of carrier in the membrane, $y_+|K^+|$ and $y_-|AuCl_4^-|$ the potassium and $AuCl_4^-$ activity in the aqueous phase I; A is a constant (3).
The rate law expressed by equation I can be verified by assuming that y_+y_- is approximately equal to the square of the mean activity coefficient of KCl in the aqueous phase I :

$$y_+y_- = y_{\pm(KCl)}^2$$

The following expression for log V_o is then deduced :

$$\log V_o = cte + \log \frac{y_\pm^2 |K^+|}{1 + y_\pm^2 K_e |K^+||AuCl_4^-|}$$

$$= cte + \log X$$

A log V_o = f(log X) plot should give a line of slope 1.
Figure IV shows the results using the experimental value for K_e :
Ke = 3.10^2 M^{-2} l^{-2}. Satisfactory agreement is observed which confirms the diffusion limiting mechanism.

CO-TRANSPORT H^+ - $AuCl_4^-$ WITH BUTEX

Butex (Dibutylcarbitol) has been used for the extraction of precious metals from aqua regia (4). Because of difficult back extraction (stripping), pure Butex cannot be used as a carrier for gold. However, chloroformic solutions of Butex have been found to be good liquid membranes for the co-transport H^+ - $AuCl_4^-$ (Figure IV).

CONCLUSIONS AND FURTHER STUDIES

Transport against the concentration gradient for $AuCl_4^-$ is achieved by means of a co-transport with M^+ or H^+ using a neutral carrier which complexes or solvates M^+ or H^+.
Chemical factors (extraction constant, diluent effects) determine the performance of the process.
Further studies are in progress in order to evaluate the selectivity of the transport with respect to other chlorometallates (e.g. $PtCl_6^=$, $PdCl_4^=$ etc...).

REFERENCES

1) a- J.D. WAY, R.D. NOBLE, T.M. FLYNN and E.D. SLOAN, J. Membr. Sc. 12, 239, (1982) and references therein.
b- P.R. DANESI, E.P. HORWITZ and P. RICKERT, Sep. Sc. and Techn., 17, 1183, (1982).
2) a- M. BURGARD, A. ROLLAT, M.J.F. LEROY, H.S. PARK, J.C. GAUTIER and S. LECOLLIER, Proceedings of "ISEC 80" paper n° 80-125.
b- H.S. PARK, Diplôme de Docteur-Ingénieur, E.N.S.C. Strasbourg 1981.
c- M. BOURDONNEAU, Diplôme de Docteur-Ingénieur, E.N.S.C. Strasbourg 1982.
3) E.L. CUSSLER, "Multicomponent Diffusion" Elsevier (1976).
4) B.F. RIMMER, Chem. Ind., 19, 63, (1974).

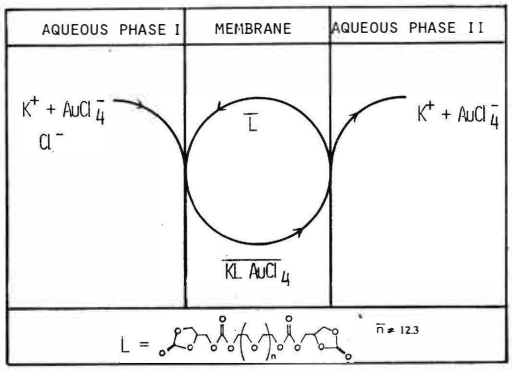

SCHEME: CO-TRANSPORT K^+-$AuCl_4^-$ FACILITATED BY A A NEUTRAL CARRIER.

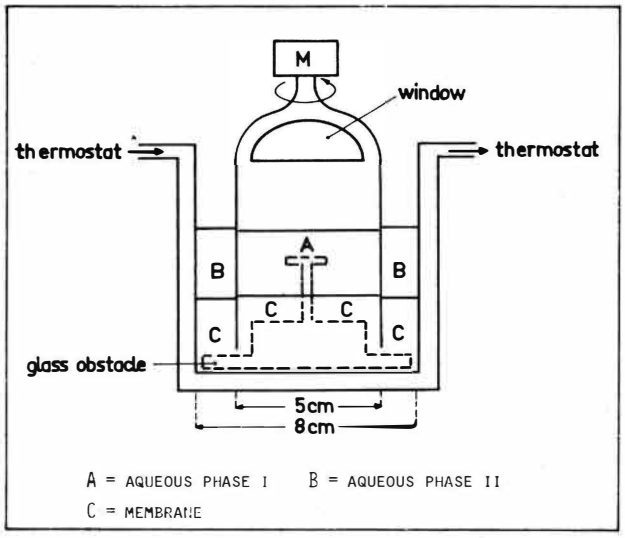

FIGURE I: EXPERIMENTAL SET UP USED FOR THE TRANSPORT MEASUREMENTS.

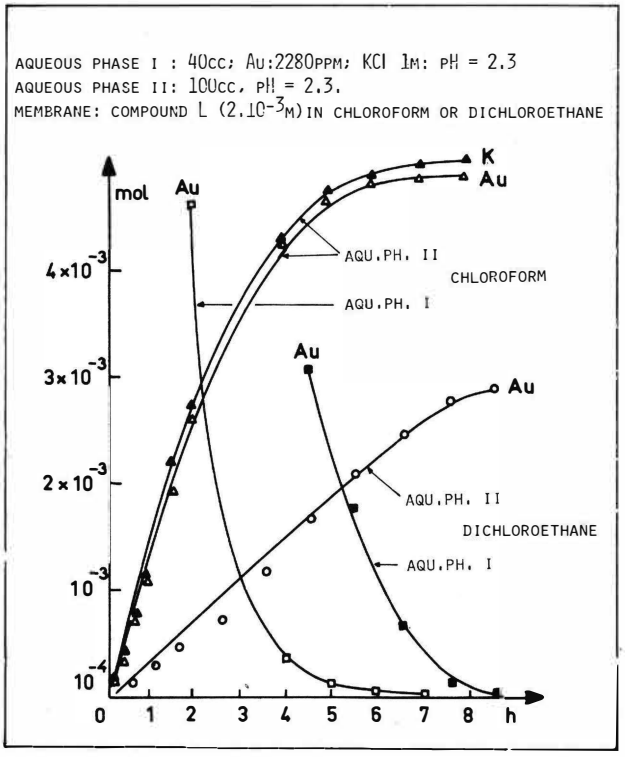

FIGURE II: TRANSPORT OF GOLD AND POTASSIUM WITH CARRIER L

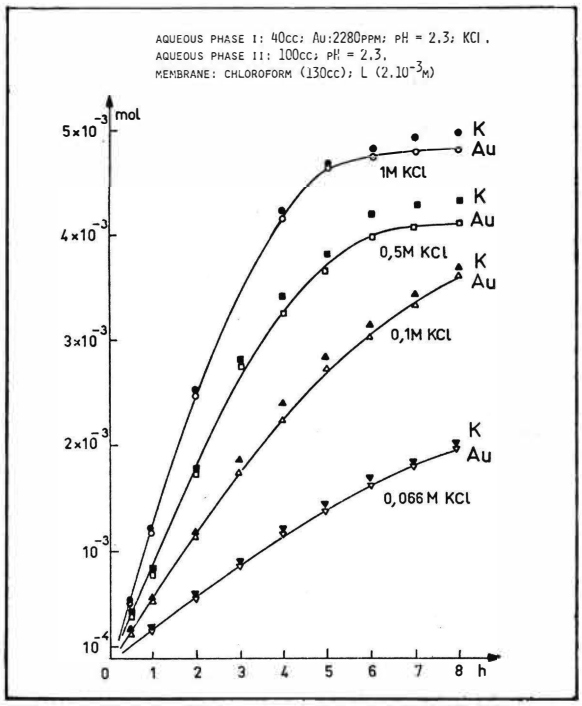

FIGURE III: EFFECT OF THE KCl CONCENTRATION IN AQU.PH.I. METAL CONCENTRATIONS IN AQU.PH.II/TIME.

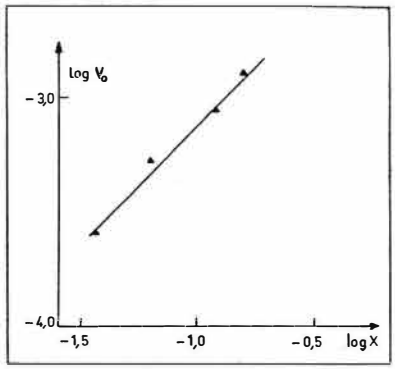

FIGURE IV: ANALYSIS OF THE INITIAL TRANSPORT RATE. **log V_0 = f(log X); (see Text).**

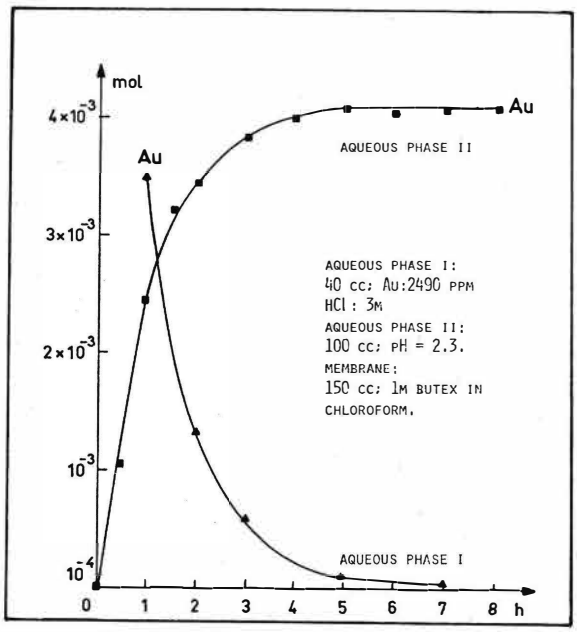

FIGURE V: GOLD TRANSPORT BY MEANS OF A CO-TRANSPORT H^+-$AuCl_4^-$. CARRIER: BUTEX IN CHLOROFORM

THE EXTRACTION OF IRON (III) FROM ALUMINIUM NITRATE SOLUTIONS WITH VERSATIC ACID

M. I. Stefanakis and A. J. Monhemius

Department of Metallurgy and Materials Science
Royal School of Mines, Imperial College
London SW7 2BP, U.K.

INTRODUCTION

There has been much research and development work in recent years into methods of extracting alumina from non-bauxitic alumino-silicate raw materials such as clays, coal ashes, colliery wastes, etc. If acid leaching is used to extract aluminium from these raw materials, one of the major problems in the subsequent processing of the crude leach liquors is the removal of iron, which is dissolved during acid leaching. Solvent extraction can be used for iron removal and the work described in this paper was initiated to investigate the use of a carboxylic acid, Versatic 10, for the removal of iron from concentrated aluminium nitrate solutions, arising from the leaching of coal ashes with nitric acid. Extraction by carboxylic acids, rather than the more usual alkyl phosphoric acids, was selected so that iron could subsequently be removed from the organic phase as hematite by hydrolytic stripping (1), as opposed to conventional mineral acid stripping. The iron-containing aqueous strip liquors produced by the latter method would give rise to considerable disposal problems in view of the quantities involved in a large-scale alumina production process. This paper is concerned with the detailed analysis of distribution data for Fe(III) extraction by Versatic 10 to determine equilibrium constants for the extraction reactions. These equilibrium constants were used to develop a chemical model of the extraction system with the objective of using computer simulation studies for the design and optimisation of the counter-current extraction of iron from aluminium nitrate solutions.

EXPERIMENTAL

Versatic 10 (15% w/w) in Escaid 110 was used to extract Fe(III) from concentrated solutions of $Al(NO_3)_3$. Extraction data were obtained using an AKUFVE 110 system combined with a Metrohm pH-stat apparatus for pH control. Iron concentrations in each phase were determined by off-line analysis. Dichromate titrations were used to analyse aqueous phase samples and UV-visible spectrophotometric analysis for organic phase samples. It was found that there was negligible extraction of aluminium into the organic phase under the conditions studied.

RESULTS

Preliminary experiments based on 2-level factorial designs were used to investigate the general behaviour of the extraction system. The following points were established: -

i) As the ionic strength of the aqueous phase is increased by increasing the aluminium nitrate concentration, iron can be extracted from increasingly acidic solutions e.g. under comparable conditions, the pH_{50} for iron extraction was found to increase from about pH=1.0 for solutions containing 32g/l Al (I = 7.1M) to about pH=0.1 at 64g/l Al (I = 14.2M). It is therefore beneficial to carry out iron extraction from as highly concentrated $Al(NO_3)_3$ solutions as possible.

ii) Increases in total Fe(III) concentration cause increased iron extraction indicating that polymerisation of the metal species occurs in the organic phase.

iii) Increasing temperature increases iron extraction at ionic strengths below about 9M and has the reverse effect at higher ionic strengths. This is attributed to changes in water activity and ionic activity coefficients with ionic strength.

A series of distribution isotherms was obtained for Fe(III) extraction with 15% Versatic 10 (0.8M) from aluminium nitrate solutions containing 64g/l Al (2.37M) at 30°C. The isotherms were determined at a series of constant pH's ranging from 0.01 to 0.88, and are shown in Figure 1. Organic iron concentrations of up to 16g/l Fe (0.29M) were obtained. The following observations were made: -

i) Extraction of Fe(III) occurs under very acidic conditions, due to the high ionic strength of the aqueous phase, as previously noted.

ii) Except at high pH (>0.6), the isotherms are S-shaped, indicating polymerisation occurs in the organic phase.

iii) Iron extraction is favoured by increasing pH up to about pH = 0.67. Above this value, there is little change in the position of the isotherms and phase separation becomes difficult. This behaviour is attributed to the formation of colloidal ferric hydroxide in the aqueous phase.

DATA ANALYSIS

A generalised equilibrium equation for the extraction of Fe(III) by Versatic acid (HV) may be written as follows:

$$(1) \qquad Fe_{(aq)} + (n+s)/2.(HV)_{2(org)} = 1/x(FeV_n.sHV)_{x(org)} + nH^+_{(aq)}$$

where n = association number, s = solvation number, x = polymerisation number. $Fe_{(aq)}$ represents all possible aqueous iron complexes. HV is assumed to be mainly dimeric in the organic phase. The association number n may be less than 3, the valency of iron, with electroneutrality in the organic phase maintained by incorporation of $(3-n)OH^-$ in the organic complex.

For conditions where activity coefficients in each phase remain constant, the equilibrium constant K for reaction (1) may be expressed as: -

$$(2) \qquad \log K = \log D - (x-1)/x.\log [Fe]_{org} - (1/x)\log x - npH$$
$$-(n+s)/2.\log([HV]_i/2-(n+s)/2.[Fe]_{org})$$

Equation (2) was used to analyse the distribution data represented by the isotherms in Figure 1 to determine the most probable iron complexes in the organic phase, using the statistical technique introduced by Van der Zeeuw (2). Apart from the parameters n, s and x, Equation (2) contains only known or measurable concentrations. Thus values of logK can be calculated for various combinations of the unknown parameters, which are each allowed to take values 1,2 or 3. A constant value for logK over a range of extraction conditions indicates that the organic complex corresponding to that particular combination of n, s and x is the most probable iron species in the organic phase. This will occur only if the activity coefficients in each phase remain constant or approximately so over the range of conditions studied. Because of the large variations in the composition of the organic phase as iron was loaded in, it was found necessary to divide the distribution data into several sub-ranges of organic concentration in order to fulfil the requirement of approximately constant organic activity coefficients. Aqueous phase activity coefficients were assumed constant because of the very high and constant ionic strength (14.2M) due to the aluminium nitrate in solution. A computer programme was written to carry out the data analysis in which all possible permutations of the parameters, n, s and x were evaluated and the derived log K values were statistically tested to determine the combinations of parameters which gave the most constant values for log K. It was found that in each sub-range of organic iron concentration there were several complexes with high statistical probabilities. The most probable complex existing in each organic iron concentration sub-range is listed in Table 1 together with the corresponding log K value.

Table 1 Most Probable Organic Phase Complexes

Aq. Phase: $Al(NO_3)_3$ = 2.34M; pH range = 0 - 0.88; initial Fe conc. = 0 - 18g/l; Temp = 30°C.
Organic Phase: 15% w/w (0.8M) Versatic 10 in Escaid 110.

$[Fe]_{org}$		Complex	log K
g/l	M		
0 - 3·4	0 - 0·06	$(FeOHV_2.1{\cdot}75HV)_2$	1·471
3·4 - 4·5	0·06 - 0·08	$(FeOHV_2.2{\cdot}75HV)_2$	2·100
4·5 - 8·6	0·08 - 0·15	$(FeOHV_2.1{\cdot}25HV)_2$	1·620
8·6 -11·1	0·15 - 0·20	$(Fe(OH)_{1{\cdot}12}V_{1{\cdot}88}0{\cdot}75HV)_3$	1·526
11·1 -13·7	0·20 - 0·25	$(Fe(OH)_{1{\cdot}14}V_{1{\cdot}86}0{\cdot}5HV)_2$	1·099
13·7 -15·7	0·25 - 0·28	$(Fe(OH)_2V\ 0{\cdot}75HV)_2$	1·127

Although the organic iron complexes listed in Table 1 are those which were found to be the most acceptable by statistical analysis. It must be emphasised that in each concentration sub-range it was found that there were at least two other complexes which also showed high statistical probabilities. The composition of the organic phase is thus extremely complex. The following general conclusions were drawn from the statistical analysis.

i) The association number (n) can be estimated with more confidence than the solvation (s) and polymerisation numbers (x)

ii) The highest statistical probabilities for the formation of some complexes are obtained by the assignment of non-integer values to the parameters (n) and (s). The resultant species are considered to be a mixture of complexes in equilibrium.

iii) Complexes with an association number of 2 predominate i.e. $FeOHV_2$, except at high iron loadings in the organic phase, where $Fe(OH)_2V$ type complexes become evident.

iv) In general, the solvation number (s) decreases with increasing iron concentration in the organic phase.

v) Monomeric, dimeric and trimeric complexes appear to exist under all conditions, although dimers and trimers predominate.

CHEMICAL MODELLING OF COUNTER-CURRENT EXTRACTION

The log K values listed in Table 1 were incorporated in a chemically-based computer model which simulated the behaviour of a counter-current extraction system. The programme, called MIXSET 1, was an adaptation of a programme published by Forrest (3). Modifications of Forrest's programme were made in order to incorporate the equilibrium constants for metal distribution calculations, instead of the empirical regression equations of distribution data used in the original. Empirical expressions were required in MIXSET 1, however, in order to relate the pH change in the aqueous phase to the amount of iron extracted. These empirical pH relationships were established by batch shake-out tests and the experimental correlations were incorporated in the programme.

The output of MIXSET 1 was tested against results obtained from counter-current simulation experiments. These simulation experiments were carried out by the batch shake-out procedure detailed by Treybal (4). A number of experimental simulations were made of a 4-stage countercurrent cascade in which aluminium nitrate solutions (64g/l Al) containing various initial concentrations of Fe(III) were extracted with 15% Versatic acid solutions at different A/O ratios. In all cases, agreement between the experimental results and those predicted by MIXSET 1 was better than ± 15%. An example set of experimental and predicted results is given in Figure 2

FIGURE 1 EXTRACTION ISOTHERMS FOR Fe(III)

Aq. phase: 2·37M $Al(NO_3)_3$ (64g/l Al)
Org. phase: 15% HV in Escaid 110

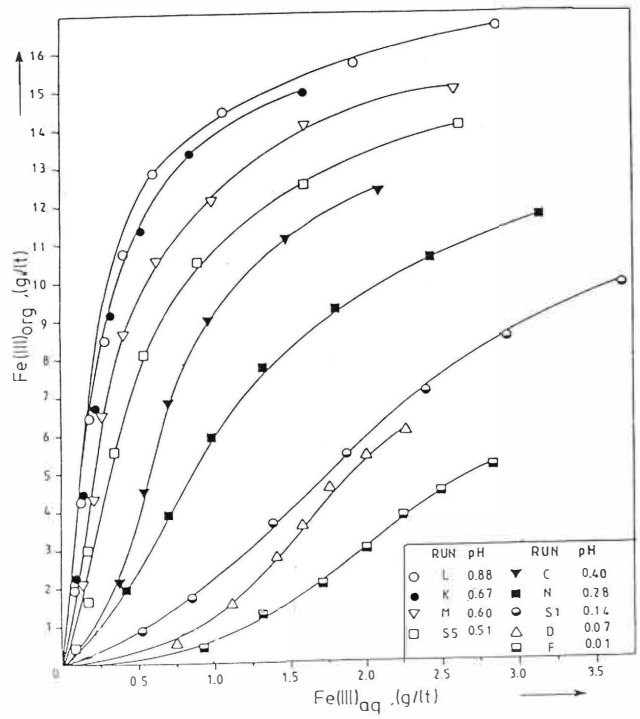

FIGURE 2 COMPARISON BETWEEN EXPERIMENTAL AND COMPUTER-PREDICTED RESULTS FOR 4 STAGE COUNTER-CURRENT EXTRACTION.

Conditions: A/O flow ratio = 2/1
Aqueous feed: 64 g/l Al; 2·02 g/l Fe; pH = 0·63
Organic feed: 15% HV; 0 g/l Fe

Concentrations are in g/l Fe for both phases and experimental results are bracketed.

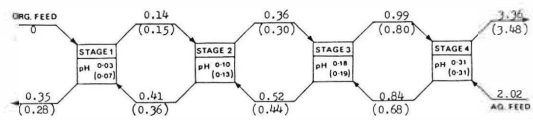

REFERENCES

1. A.J. Monhemius and G. Thorsen. Proc ISEC 80 Vol 3, Paper 80-91
2. A.J. Van der Zeeuw. Hydrometallurgy 4, 21 (1979)
3. C. Forrest. PhD Thesis. University of Bradford U.K. (1977)
4. R.E. Treybal. Liquid-liquid extraction. McGraw-Hill (1963)

SOLVENT EXTRACTION SEPARATION STUDY OF Fe(III) AND Zn(II) FROM AQUEOUS SOLUTION WITH D2EHPA AND D2EHPA MIXED WITH TBP IN HYDROCARBON DILUENTS

Ying-Chu Hoh, Jin-Pang Wang and Tieh Ma

Institute of Nuclear Energy Research CAEC
P.O. Box 3-7, Lung-Tan
Taiwan, China

INTRODUCTION

Investigations on the extraction of iron from acidic aluminum-containing solutions have been reported by George and Stone (1), Feller (2), Flood (3), and George (4). The extraction of titanium(IV), iron(III) and iron(II) by D2EHPA in benzene has been studied by Islam et al. (7). Maximum extraction was shown at 323°K (50°C) for Ti(IV) and Fe(II) and 313°K (40°C) for Fe(III). Sato and Nakamura (5) also studied the partition of iron(III) between sulfuric or hydrochloric acid and solutions of D2EHPA in benezene by varying the concentration of acid, solvent and aqueous iron at different temperatures.

The object of the present work is to investigate the extraction of iron(III) and zinc(II) and their separation by D2EHPA in Kermac 470B as a function of diluent, aqueous pH, contact time, phase ratio, temperature and the concentration of the stripping solution. In addition, the synergistic extraction and separation of iron(III) and zinc(II) are also presented.

EXPERIMENTAL

Material. Aqueous solutions of ferric sulfate, zinc sulfate were prepared by dissolving reagent grade ferric sulfate and zinc sulfate in distilled water and adjusting the pH to 0.25 - 2.2 with ammonium hydroxide or sulfuric acid. Di-2-ethylhexyl phosphoric acid (D2EHPA) with a purity of 98% supplied by Union Carbide, was used as the organic solvent. Toluene, xylene, n-octane and Kermac 470B were used as the hydrocarbon diluent. Kermac 470B was supplied by Kerr-McGee and all other diluents were reagent grade.

Experiments. Shake-out test which was described by Hoh et al. (6) was used in the laboratory evaluation on the separation of iron(III) from zinc with regard to the following variables: (1) the diluent effect, toluene, xylene, n-octance and Kermac 470B were used as the diluents, (2) the pH dependency, varied from 0.25 to 2.2, (3) the phase ratio (A/o), varied from 1/2 to 10, (4) the rate of extraction and stripping, varied from 1 to 60 minutes, (5) the temperature dependency, varied from 291° to 326°K, and (6) the hydrochloric acid concentration on stripping, varied from 1 to 7 mol dm^{-3}.

In addition, equilibrium data on extraction and stripping as well as synergistic extraction by D2EHPA mixed with TBP in Kermac 470B were also studied by shake-out test.

Analysis. Aqueous phases were analyzed for zinc and iron by a Perkin-Elmer model 603 atomic absorption spectrophotometer. Organic metal concentrations were obtained by difference from the initial metal concentrations and were checked from time to time by stripping a sample of organic phase with 7 mol dm^{-3} hydrochloric acid solution and analyzing it in the same way as for aqueous samples.

RESULTS AND DISCUSSION

Diluent Effect. Table 1 shows the diluent effect on the system Fe^{3+}-Zn^{2+}-H_2SO_4-20% D2EHPA-diluent. It indicates that the pure aliphatic diluent (n-octane) gives the highest separation factor α_{Zn-Fe}. It is also noted that a decrease in the separation factor of the two metals with an increase in the polarity (n-octane). Based on the above results, Kermac 470B containing 34 vol % of paraffines, 49 vol % of naphthalenes and 17 vol % of aromatics, was then selected as the diluent in the subsequent studies due to its high extractability of iron(III).

pH Dependency. It is well known that the extraction of metal by D2EHPA is a function of the acid content of the aqueous phase. Then the extraction mechanism can be represented by Equation 1.

$$Fe^{3+}_{A} + 3\,(HG)_{2\,o} \;====\; Fe\,(HG_2)_{3\,o} + 3\,H^{+}_{A} \qquad (1)$$

where G is the anion $(C_8H_{17}O)_2PO_2^-$ and $(HG)_2$ the dimeric solvent. Figure 1 shows the pH dependency of the percentage extraction of iron and zinc for equal volumes of organic and aqueous phases. The percentage extraction increases with increasing aqueous pH and levels off at a pH range from 1 to 2.2. It also presents that the extractability of iron(III) by D2EHPA is much better than that of zinc. In the rest of the studies, all aqueous pH's are adjusted to 1.5 and the mole ratio of zinc to iron was in the order of 5. Figure 2 indicates that at an aqueous pH greater than 1.5 one obtains a very good separation efficiency, α_{Zn-Fe}, defined as

$$\alpha_{Zn-Fe} = \frac{D_{Zn}}{D_{Fe}} \qquad (2)$$

where D_{Zn} and D_{Fe} denote the distribution coefficients for zinc and iron, respectively. Although at lower aqueous pH, for example pH = 0.5, the separation factor, α_{Zn-Fe}, looks very good, the extractability of iron is relatively poor compared with higher aqueous pH (pH = 1.5). Therefore it is preferable to adjust the initial aqueous pH to 1.5 in order to achieve a higher extraction of iron and a better separation efficiency between iron(III) and zinc.

Effect of Hydrochloric Acid Concentrations on Iron(III) Stripping. Preliminary results indicate that very poor stripping efficiency was obtained when sulfuric acid was used as the stripping reagent. Therefore, it is impractical to employ sulfuric acid as the stripping reagent. Results from contacting equal volumes of iron-loaded organic extractant with different level of hydrochloric acid solutions indicate that the stripping efficiency increases with increasing hydrochloric acid concentration. The percentage stripping reaches to 91.53% while the stripping reagent concentration reaches to 7 mol dm^{-3}.

Effect of Temperature. The effect of temperature on the separation of iron from zinc was studied in a Dubnoff Metabolic Shaking Incubator with a temperature range from 292 to 323°K. The frequency of the incubator was 160 rev. min^{-1} and the amplitude was 4 cm. Equal volumes of organic and aqueous solutions were carefully transferred at the operation temperature into an extraction bottle and then equilibrated in the incubator for 30 min. Table 2 shows the temperature effect on the separation of iron from zinc. It indicates that the extractabilities of the metals and their separation efficiency decrease with rising temperature from 292° to 323°K. The heat of reaction (change in enthalpy) in Equation 1 was estimated to be 99.76 kJ $mole^{-1}$ for iron(III) and 17.42 kJ $mole^{-1}$ for zinc. Such dramatic increases in the distribution coefficients, D_{Fe} and D_{Zn}, are not common. Similar results were obtained by Islam et al. (7). However, Sato and Nakamura (5) reported on the extraction of iron(III) from aqueous solutions containing ferric sulfate or chloride in sulfuric or hydrochloric acid with 0.05 or 0.1M D2EHPA in kerosene at temperature between 293° to 323°K. A completely reversed temperature effect, the distribution coefficient decreasing with rising temperature was noted by them. The contrast is quite interesting. However, it is difficult to infer the results except that the diluent used by Islam et al. (7), Sato and Nakamura (5) and this work was different. The results on the stripping of iron(III) from its loaded organic phase by 3 or 4 mol dm^{-3} hydrochloric acid indicated that the stripping efficiency increases with rising temperature from 291° to 326°K. The heat of reaction, ΔH, in Equation 1 was estimated to be 36.38 kJ $mole^{-1}$ for iron(III) and 32.74 kJ $mole^{-1}$ for zinc.

Rate of Extraction and Stripping. Shake-out tests were used to study the rate of extraction on the system Fe^{3+}-Zn^{2+}-H_2SO_4-D2EHPA-Kermac 470B. Results from contacting equal volumes of organic and aqueous phases indicated that at the experimental conditions 30 minutes are required to reach extraction equilibrium for iron(III) and 10 minutes for zinc(II). Sato and Nakamura (1971) reported that it took 90 minutes to reach extraction equilibrium in the system Fe^{3+}-H_2SO_4-D2EHPA-Kerosene. Therefore, it can be inferred that the diluent used in this work significantly improves the extraction kinetics. At equilibrium, the separation factor α_{Zn-Fe} obtained, 0.889×10^{-3}, indicates that an excellant separation efficiency between iron(III) and zinc is achieved.

Results from the study of the rate of stripping of iron(III) from its loaded organic extractant by 3 and 6 mol dm^{-3} hydrochloric acid indicated that only 1 minute is required to reach stripping equilibrium.

Effect of Phase Ratio on the Extraction, Stripping and Separation. Results from the study of the effect of phase ratio, i.e. A/o ratio; on the co-extraction of iron(III) and zinc from sulfate solution by 20 vol % of D2EHPA diluted with Kermac 470B indicated that the extractability of iron and zinc in the system studied decrease with increasing A/o ratio. Figure 3 shows the effect of A/o ratio on the separation factor, $_{Zn-Fe}$. It implies that the best separation efficiency between iron(III) and zinc can be obtained at an A/o ratio of 1. At an aqueous pH of 1.5 and an A/o ratio of 1, the distribution coefficient for iron (III) is 174 and 0.128 for zinc. Therefore, it gives a separation factor α_{Zn-Fe} of 7.35×10^{-4} which indicates a very good separation efficiency.

Synergic Extraction. Synergistic system D2EHPA-TBP was used to study the solvent extraction separation of iron(III) and zinc(II) from sulfate solution. Different volume percentages of organic mixture diluted with Kermac 470B were used as the organic phase. Sulfate solution with a Zn(II) to Fe(III) mole ratio of 5 and a pH of 1.5 was used as the aqueous phase. Results from contacting equal volumes of organic and aqueous phases at 285°K are presented in Figure 4. The diagonal dotted line in Figure 4 represents the predicted line for neither synergism nor antagonism. From the separation point of view, an excellent result is noted from this figure. Numerically, the predicted percentage extraction for iron(III) and zinc(II) by the organic extractant consisting of 15 vol% TBP, 5 vol% D2EHPA and 80 vol% Kermac 470B should be equal to 25% for iron(III) and 3% for zinc. However, the experimental results indicate that the percentage extraction for iron(III) and zinc(II) is equal to 44.5% and 0.3%, respectively. It indicates an apparent improvement on iron(III) extraction and a depressed effect on zinc(II) extraction. In other words, a synergism with respect to iron(III) and an antagonism with respect to zinc are obtained. This result is quite interesting and uncommon to the other synergistic extraction systems. However, it is a good encouragement to study this system in a greater detail.

CONCLUSIONS

The percentage extraction of Fe(III) and Zn(II) from sulfate solution by the organic extractant containing 20 vol% D2EHPA in Kermac 470B increases with increasing pH and levels off at a pH ranged from 1 to 2.2. For the sake of extractability and separation efficiency of iron(III) and zinc(II), the optimum aqueous pH is at 1.5.

Raising the temperature causes an increase in the extractabilities of iron (III) and zinc(II). The same results are obtained in the stripping operation. From the extraction and the separation points of view, the optimum phase ratio is one.

An apparent synergism on iron extraction and antoganism on zinc extraction is noted with the system D2EHPA-TBP-Fe^{3+}-Zn^{2+}-Kermac 470B. It is a good encouragement to further study of this synergistic extraction system in greater detail.

ACKNOWLEDGEMENT

The authors wish to thank the Institute of Nuclear Energy Research, CAEC for the necessary information provided and assistance for the publication of this paper.

REFERENCES

1. J.H.B. George and E.W. Stone, US Patent 3,211,521 (1965).
2. H.I. Feller, US Patent 3,320,032 (1967).
3. H.W. Flood, US Patent 3,586,477 (1971).

4. D.R. George, US Patent 3,545,920 (1970).
5. T. Sato and T. Nakamura, Proc., ISEC, vol. 1, p. 238 (1971).
6. Y. C. Hoh, B.D. Lee and T. Ma, Hydrometallurgy 8, pp.83-94 (1982).
7. F. Islam, H. Rahman, M. Ali, J. Inorg. Nucl. Chem., 41, p. 217 (1971).

Table 1. Diluent effect on the extraction of Fe(III) and Zn(II) by D2EHPA*

Organic Solvent	Diluent	$(Fe)_A$ (mol dm^{-3})	$(Fe)_o$ (mol dm^{-3})	$(Zn)_A$ (mol dm^{-3})	$(Zn)_o$ (mol dm^{-3})	D_{Fe}	D_{Zn}	α_{Zn-Fe} (x10^{-2})
20 vol.% D2EHPA	Xylene	0.0085	0.0349	0.195	0.017	4.106	0.0872	21.237
	Toluene	0.0103	0.0331	0.200	0.012	3.214	0.0600	18.668
	n-Octane	0.0090	0.0344	0.180	0.032	3.822	0.1778	46.520
	Kermac 470B	0.0040	0.0394	0.185	0.027	9.850	0.1459	14.812

*$(Fe)_A^F$ = 0.0434 mol dm^{-3}, $(Zn)_A^F$ = 0.212 mol dm^{-3}, Phase Ratio (A/o) = 1, Temp. = 297°K, Shaking Time = 5 min.

Table 2. Effect of temperature on the extraction of Fe(III) and Zn(II)*

Temp. (°K)	$(Fe)_A$ (mol dm^{-3})	$(Fe)_o$ (mol dm^{-3})	$(Zn)_A$ (mol dm^{-3})	$(Zn)_o$ (mol dm^{-3})	D_{Fe}	D_{Zn}	α_{Zn-Fe} (x 10^{-3})
292	0.005909	0.054091	0.202	0.018	9.15	0.0891	9.738
303	0.001705	0.058295	0.194	0.026	34.19	0.1340	3.919
313	0.000465	0.059535	0.190	0.030	128.03	0.1579	1.233
323	0.000143	0.059857	0.187	0.033	418.58	0.1765	0.422

*$(Fe)_A^F$ = 0.06 mol dm^{-3}, $(Zn)_A^F$ = 0.22 mol dm^{-3}. Org. = 20 v/o D2EHPA in Kermac 470B
$(pH)^F$ = 1.5, Phase Ratio (A/o) = 1

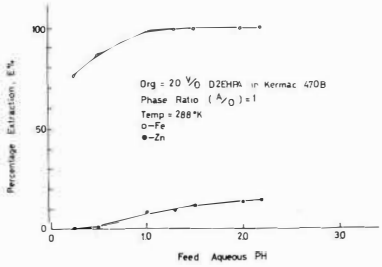

Fig. 1. Effect of aqueous pH on iron(III) and zinc(II) extraction

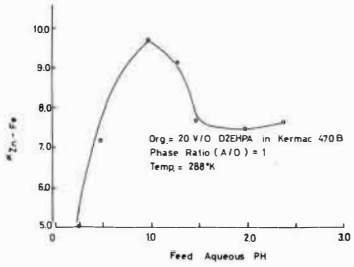

Fig. 2. Effect of aqueous pH on the separation of iron(III) and zinc(II)

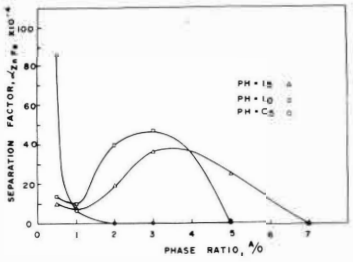

Fig. 3. Effect of phase ratio A/o on Fe(III) and Zn(II) separation

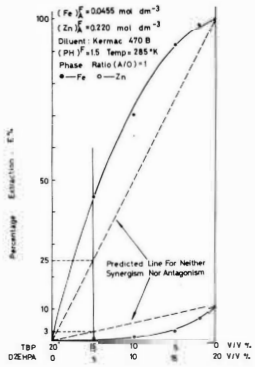

Fig. 4. Synergistic effect on the extraction of Fe(III) and Zn(II) by D2EHPA + TBP + Kermac 470B

PROCESS DEVELOPMENT FOR THE COMPREHENSIVE UTILIZATION OF LUDWIGITE

Yu Da-Yue, Yang Xiao-Dong and Zhu Pin-Hua

East China Institute of Chemical Technology
Shanghai, China

The largest boron deposit available in the north-east part of China occurs as ludwigite.

$$(Mg,Fe^{2+})_2Fe^{3+}(O_2/BO_3)$$

It has not been successfully processed and utilized as a source of either boron or iron.

A typical sample of ludwigite ore was analyzed and has a composition as shown in Table 1, in which the theoretical composition calculated according to the formula of the mineral is also given for comparison.

Table 1 Composition of ludwigite, %

Component	B_2O_3	Fe_2O_3	MgO	CaO	Al_2O_3	SiO_2	ignition loss
ludwigite (theoretical)	18.1	40.5	41.4				
poor iron sample	12.9	17.0	43.4	2.2	0.6	9.1	14.5

The present paper is to report the result of the development work done for the purpose of making good use of its components.

HYDROCHLORIC ACID USED FOR THE DECOMPOSITION OF LUDWIGITE

The progress in the following three aspects encouraged the authors to try using hydrochloric acid as decomposing agent:

Firstly, the success was gained in laboratory in processing ascharite by decomposing the mineral and extracting the boron value by 2-ethylhexanol from low acid aqueous medium (1) Secondly, the investigations of using the acid residue as raw material of certain glass products and of using the raffinate from extraction as packing or building material were promising (2)(3). Thirdly, the preliminary result of pilot plant study confirms the feasibility of the proposed process (1).

Preliminary tests with hydrochloric acid showed a good result and the reaction conditions to obtain high percentage of decomposition were studied in detail. By compromising some of conflicting factors, the following conditions are suggested:

(A) The ore to be pulverized to pass 60 mesh

(B) Concentration of hydrochloric acid used being $\geqslant$ 6N with about 20% excess over the necessary amount to neutralize all metallic oxides.

(C) Solid (in kg) to liquid (in litre) ratio being about 1 to 5-6

(D) Temperature of digestion being 100-105°C.

Under these conditions, > 95% decomposition can be achieved in 60 minutes and the composition of the solution obtained is shown in Table 2.

Table 2 composition of filtered liquor

Component	H_3BO_3	$MgCl_2 + CaCl_2$*	$FeCl_3$	HCl
g/l	31.8	277	51.3	0.95N

* Using part of raffinate in making digesting liquor to raise the concentration to about 280 g/l.

This solution was used as feed in extraction experiments. Referring to the previous work (1), the solvent 2-ethylhexanol extracts both boric acid and $FeCl_3$. Although the separation factor is fairly large, it would be preferable if any solvent extracts only one of them but not the other.

SELECTION OF SOLVENT

As discussed above, such a solvent could be found to extract $FeCl_3$ only but not H_3BO_3. Literature (4) disclosed many potential extractants which extract Fe(III) preferentially, but most of them are expensive reagents and only good for analytic use. Commercial extractants such as D2EHPA and TBP extract Fe(III) only from HCl solutions of high acidity. As acidity drops the extractibility fall very rapidly. In addition, the stripping of Fe(III) is difficult.

Many authors reported (5) that dialkylsulfoxides is good extractants for metals and acids due to their S=O bond which resembles P=O bond of neutral organophosphorus compounds. Furthermore, dialkylsulfoxide and petroleum sulfoxide have been used in this laboratory for sometime hence selected by the present authors in this investigation.

R_2SO AS EXTRACTANT FOR Fe(III)

Dibutylsulfoxide (DBSO) is partly miscible with water. This will result in large volume changes of phases during extraction. Besides, the high solubility of DBSO in water necessitates additional steps for the recovery of the extractant in raffinate and stripping solution and means increasing processing cost. Therefore, dioctylsulfoxide (DOSO) was used to test its ability of extracting Fe(III) and boric acid. The preliminary result indicates that DOSO dissolved in a proper diluent can extract Fe(III) but not boric acid at low acidity.

Diluent Since the melting point of DOSO is 71°C., it is necessary to use a diluent to keep it in liquid state at ambient temperature. Subsequent experiment showed that mixed xylene is one of the best diluents with respect to the solubility, distribution coefficient and other properties, such as volatility and flash point.

Fig.1 shows the extraction isotherms of different concentrations of DOSO in mixed xylene at 50°C. when filtered leaching liquor was used without further adjustment of acidity. It seems there is a stoichiometric relation between $FeCl_3$ and the extractant. Using 0.4 M DOSO, the loading of $FeCl_3$ can be as high as 27 g/l (about 0.17M). But due to the limited solubility of extractant in xylene the temperature is maintained at 50°C in order to avoid the separation of DOSO.

Time of equilibration Times required to attain equilibrium and subsequent phase separation are very short when DOSO in xylene is mixed with the aqueous feed. The interface is usually clean and sharp. At 20°C., only one minute is sufficient to reach equilibrium. In all the subsequent experiments either 5 or 10 minutes were used for equilibration.

Temperature of extraction The distribution coefficient D is strongly dependent upon temperature. When 0.1M DOSO in xylene is used, the change of D with temperature is shown in Fig.2. The heat effect of extraction may be roughly estimated from the experimental data.

Effect of acidity As discussed earlier, 2EHPA and TBP are good extractants for $FeCl_3$ at high acidity. DOSO behaves quite similarly (Fig.3), e.g. D rises exponentially as the acidity increases from 1.5N, yet at low acidity the value of D is still appreciable and good for $FeCl_3$ removal.

Presence of other solutes From Table 2 there are magnesium and calcium chlorides and boric acid existing in the aqueous solution from decomposition of ludwigite. Experiments were carried out to study whether DOSO co-extracts other components. The results may be concluded as follows:

(A) When the acidity is between 1.0 to 3.0 N HCl, the amounts of Ca^{2+} and Mg^{2+} extracted into 0.1 M DOSO in xylene were not detected. This confirms the result obtained by D.C. Kennedy and J.S.Fritz (5).

(B) When the acidity changes from 0.5 to 3.0 N $MgCl_2$ or $CaCl_2$ changes from about 90 to 300 g/l, the extraction of H_3BO_3 by 0.1 M DOSO in xylene is nil.

Therefore, from academic point of view the solvent used is ideal for the separation of $FeCl_3$ from other ingredients present in the acid solution of ludwigite.

Effect of $MgCl_2$, $CaCl_2$ and H_3BO_3 on D of $FeCl_3$ At low concentrations, e.g. $\leqslant$ 100 g/l $MgCl_2$ or $CaCl_2$, the extraction ability of 0.1 M DOSO is very low ($D < 0.01$), but increases very rapidly at high concentrations of the chloride due to salting-out effect. Therefore, the recycle of a part of raffinate containing alkaline earth chlorides to enhance the salt concentration in leach solution plays an important role in the success of the removal of Fe from the solution. The effect of $MgCl_2$ and $CaCl_2$ on D is shown in Fig.4.

Besides, the presence of H_3BO_3 also promotes the extraction of $FeCl_3$ in a much small extent (see Fig.5).

STRIPPING OF $FeCl_3$

In contrary to the stripping of $FeCl_3$ from loaded D2EHPA, DOSO shows its merit that water acidulated to pH = 1-2 will strip more than 60% of $FeCl_3$ at aqueous to organic ratio of 1/5 (see Fig.6). At this low pH value, $FeCl_3$ can be kept in solution without hydrolysis hence causes no trouble in operation.

Percentage of Fe(III) stripped increases slowly with rising temperature. As shown in Fig.7, an increment of only about 5% is observed when temperature changes from 30° to 90°.

McMABE-THIELE DIAGRAMS FOR EXTRACTION AND STRIPPING

Fig.8 and 9 show the extraction and stripping diagrams. The shape of both extraction and stripping isotherms are very favorable and only limited number of theoretical stages are required to achieve very high extraction and stripping efficiencies. Therefore, the removal of iron from boric acid solution may be quite complete and stripped iron is also pure.

PROPOSED FLOW SHEET

Due to the raffinate from $FeCl_3$ extraction almost consisting of boric acid and magnesiam and calcium chlorides only, it resembles the solution obtained from decomposition of ascharite and can be further processed similarly. Therefore, the following flow sheet is proposed:

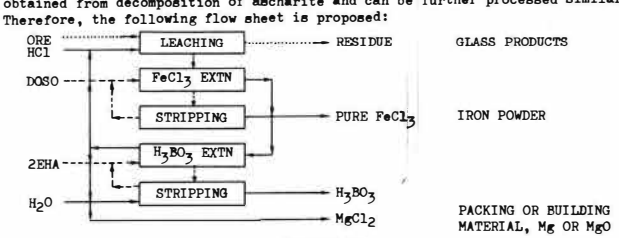

REFERENCES

1. Y. F. Su, D. Y. Yu and S. D. Chen, Proceedings ISEC'80, v.2, S7, Paper 57.

2. B. N. Zhu and L. F. Yu, Chemical World (Shanghai) 152, 1983 (Chinese).

3. H. Z. Zhou, Chemical World (Shanghai) 248, 1982 (Chinese).

4. A. K. De, S. M. Khopkar and R. A. Chalmers, "Solvent Extraction of Metals" VNR Company, London, 1970.

5. Remendra Shanker and K. V. Venkateswarler, J.I.N.C. 3, 2369 (1970)
D. C. Kennedy and G. S. Fritz, Talanta, 823 (1970).
W. J. McDowell and H. D. Harmon, J.I.N.C. 33, 3107 (1971).
A. Sambasiva Reddy and Y. Seshe Sayi, J.I.N.C. 40, 1125 (1978).

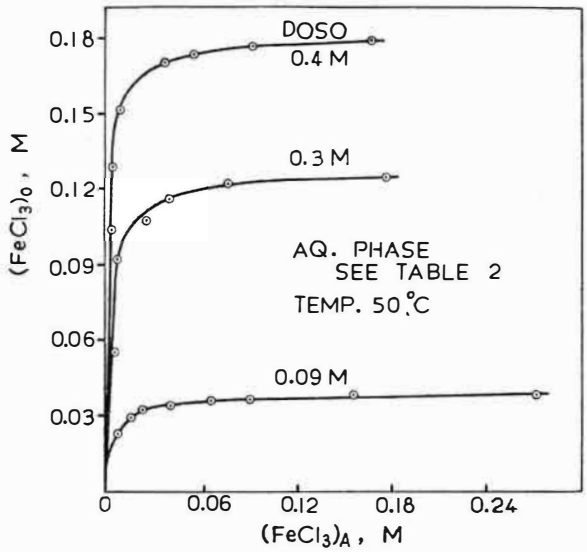

FIG.1 EXTRACTION ISOTHERMS

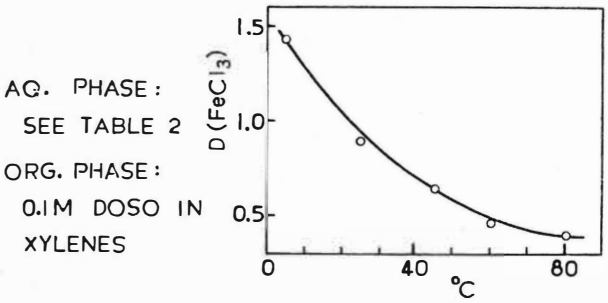

FIG. 2 EFFECT OF TEMPERATURE

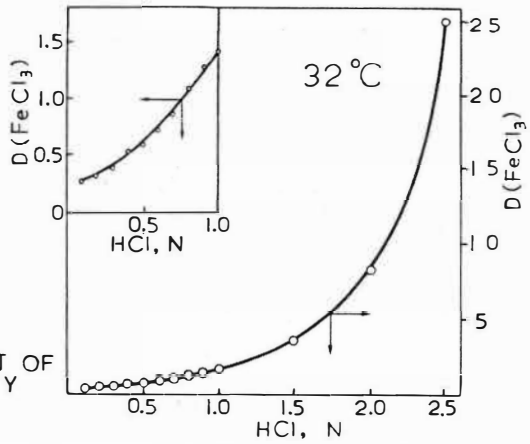

FIG. 3
EFFECT OF
ACIDITY

AQ. PHASE: $FeCl_3$ 4.86 g/l
$MgCl_2$ 180 g/l
HCl ~2.5 N
ORG. PHASE: 0.1 M DOSO IN XYLENES

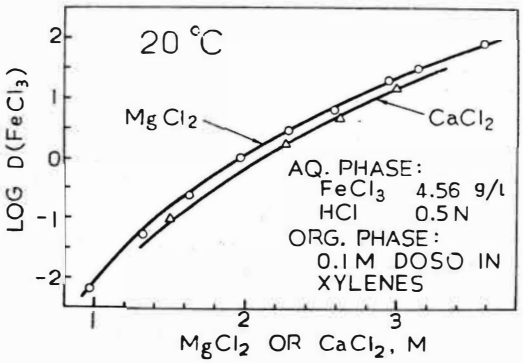

FIG. 4 EFFECT OF $MgCl_2$ AND $CaCl_2$

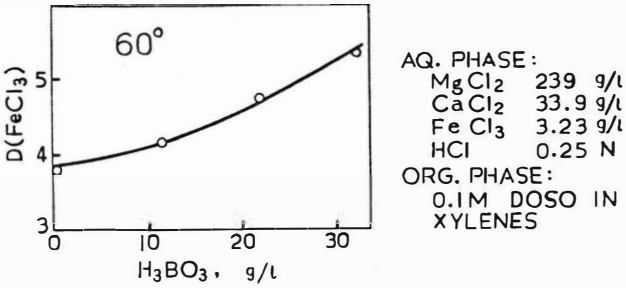

FIG. 5 EFFECT OF H_3BO_3

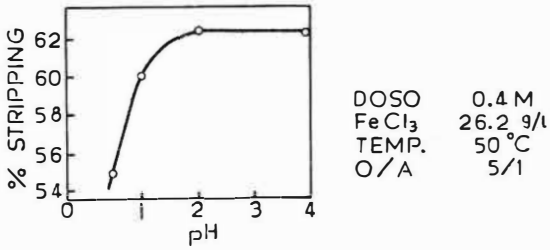

FIG. 6 EFFECT OF pH

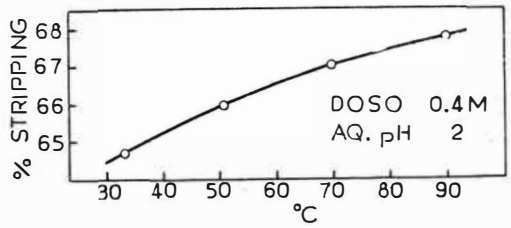

FIG. 7 EFFECT OF TEMPERATURE

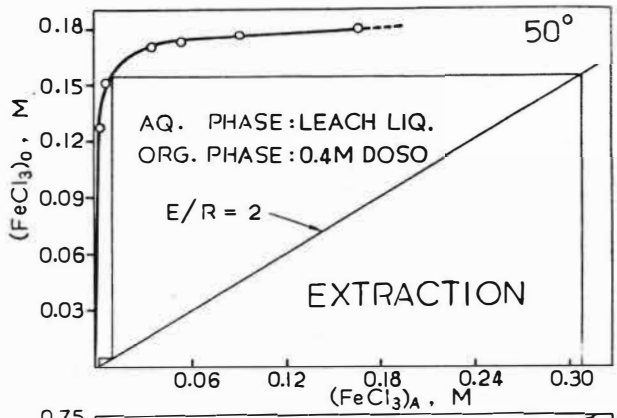

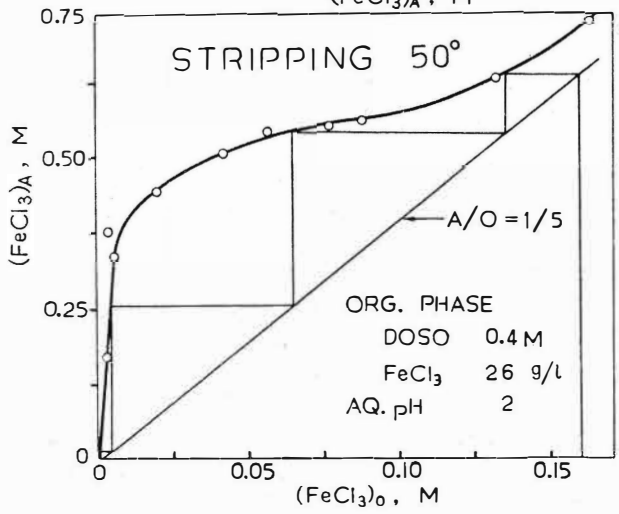

FIGS. 8 and 9 McCabe–Thiele Diagrams

STUDY OF SOLVENT-EXTRACTION OF PHOSPHORIC ACID WITH DBSO

Zhou Jian-Zhong, Jian Yu-Ming and Li Dao-Chun

East China Institute of Chemical Technology
Shanghai, China

I. Introduction. The study of liquid-liquid equilibrium of the tenary system containing phosphoric acid, water and an organic solvent is of importance in the solvent extraction process of phosphoric acid from an aqueous solution obtained from the wet process of treating rock phosphate with sulfuric acid, hydrochloric acid or nitric acid.

Gilbert et.al. (1) and others (2) have reported the use of the organic solvent dibutyl sulfoxide in the above-mentioned extraction process, but liquid-liquid equilibrium data have not been given so far for this system. In this investigation, the authors studied the equilibrium of the tenary system, dibutyl sulfoxide-phosphoric acid-water at 40°C.

II. EXPERIMENTAL 1. Liquid-liquid equilibrium of the DBSO-H_3PO_4-H_2O system.

Chemicals 1. Dibutyl Sulfoxide (DBSO): The crude product of dibutyl sulfoxide (3) was redissolved in benzene, and recrystallized several times, and was recovered under partial vacuum distillation. After purification (4), the final product of DBSO is odorless, white, transparent crystals and kept in desiccator for use. In Table I the physical properties of DBSO are compared with those in the literature.

Table I. Physical Properties of DBSO

Normal Melting Point °C		Refractive Index at 40°C		Density at 40°C	
Exptl.	Lit.	Exptl.	Lit.	Exptl.	Lit.
32.8	32.6 (5)	1.4603	1.4606 (6)	0.9228	0.9216 (6)

2. Phosphoric acid: High purity grade phosphoric acid from Shanghai Hong Wei Insecticide Factory, containing more than 85% by weight of H_3PO_4.

3. Water: Redistilled water was used.

The binodal curve data was determined at 40°C for this system by the turbidity method, and plotted in Fig. 1. The binodal curve of this system was compared with that of n-butyl alcohol-phosphoric acid-water system (7) (dotted line in Fig. 2).

The tie line (8,9). The tie line data was obtained by the analysis of the aqueous and organic phases for the H_3PO_4 content (10,11) and shown in Fig. 1.

The plait point was determined by different empirical treatment of the tie line data (12). In this paper, two formulas were used (13).

(1) Hand method (14):

$$\lg (Y_A/Y_S) = A \lg (X_A/X_W) + B$$

(2) Othmer-Tobias method (15):

$$\lg \frac{100-Y_S}{Y_S} = C \lg \frac{100-X_W}{X_W} + D$$

The results were plotted in Fig. 3 and the composition of the plait point is listed in Table II.

Table II. Composition of the plait point (Data in weight %)

	Hand Method	Othmer-Tobias Method
H_3PO_4	51.78	52.17
DBSO	19.85	18.80
H_2O	28.37	29.03

The distribution of phosphoric acid between DBSO and H_2O, and the selectivity of the system. Fig. 4 and 5 were the distribution of phosphoric acid between DBSO and water and the selectivity for this system. They were compared with that of a n-butyl alcohol-phosphoric acid-water system. The conclusion is that DBSO has higher distribution coefficient and selectivity than n-butyl alcohol, and is a good solvent for the extraction of phosphoric acid.

Correlation of equilibrium data. According to Rod's model (16) the equilibrium data of DBSO-H_3PO_4-H_2O ternary liquid-liquid system can be correlated as follows:

$$\ln m_1 = 3.320(y_1 - 0.5217) + 12.97(y_1 - 0.5217)^2 + 13.33 (y_1 - 0.5217)^3$$

$$\ln m_2 = -27.15(y_1 - 0.5217) - 84.67(y_1 - 0.5217)^2 - 80.38 (y_1 - 0.5217)^3$$

$$\ln m_3 = 9.828(y_1 - 0.5217) + 25.00(y_1 - 0.5217)^2 + 20.02 (y_1 - 0.5217)^3$$

where y_1 is the amount of H_3PO_4 in organic phase.

m_1, m_2 and m_3 are the distribution coefficient of H_3PO_4, DBSO and water respectively.

Equilibrium data of DBSO-H_3PO_4-H_2O ternary liquid-liquid system can be calculated by the above three equations. Fig. 6 gives the comparison of calculated binodal curve with experimental data for the DBSO-H_3PO_4-H_2O system.

2. Multi-stage countercurrent extraction test.

Table III Operating Conditions

Temp. °C.	Feed (wet process acid):	Raffinate	Loaded extractant	Extractant	Initial phase ratio (O/A)
40°C.	H_3PO_4 50.3, H_2SO_4 2.18, wt.%	H_3PO_4 6.0 wt.%	H_3PO_4 31 wt.%	DBSO (saturated w/H_2O)	1.2 by wt.

Total flow rate, liter/hr.	Velocity of agitation, rpm	Type of mixer-settler	Volume of mixer, liter	Volume of settler, liter	Number of stages
6	350-450	box	1	3	6

The number of theoretical stages for the process by graphical method from ternary phase diagram was equal to 4.9.* Using wet process acid as feed liquor in the simulation test, 5 stages were obtained. The two phase equilibrium data of pure phosphoric acid and wet process acid are shown in Fig. 8. The experimental measurements at steady state acid concentrations achieved in the multi-stage countercurrent quite agreed with the graphical method from ternary phase diagram (Fig. 9,10). There are some deviations noted in each of three figures in the range of low concentrations. *See Fig. 7.

3. Proposed flow sheet (17). A process based upon solvent extraction has been developed for the recovery of phosphoric acid from a leaching liquor obtained by decomposition of phosphate rock with sulfuric acid.

Using di-n-butyl sulfoxide as extractant and multi-stage countercurrent extraction and stripping, pure phosphoric acid, potassium dihyrdrogen phosphate or sodium triphosphate can be produced on one hand, and precipitated calcium phosphate (secondary calcium phosphate) on the other. The proportion of both products may be economically adjusted in accordance with varying demands. This process will leave an effluent which is less polluting than any existing process. (Fig. 11)

Many large scale corporations have adopted this process, such as "TOYO Soda" Company in Japan (17). Secondary calcium phosphate ($CaHPO_4 \cdot 2H_2O$) is white crystal, if fluorine content is less than 0.2-0.3%, and it can be used to feed the animals. On account of using extraction method, there was no air pollution. But the fluorine content of the waste water leaving the digester exceeds the data listed in "Industrial Waste Water Codes, China," and is less polluting than any existing process in phosphate fertilizer industry. Waste water from this test is transparent with suspension less than 50mg/liter, pH = 6.3-7, F = 63 mg/liter, and COD of 3144 ppm (18). The purity of KH_2PO_4 produced by this process was tested by x-ray diffraction and chemical analysis. The content of KH_2PO_4 is more than 99.50% with MgO = 0.017%, Fe_2O_3 = 0.07%, F = 0.18% (18).

III. Results and Discussion. The ternary system of dibutyl sulfoxide-phosphoric acid-water has been studied at 40°C, and DBSO is the extractant for phosphoric acid. Its phase diagram was completed and the tie line data with the plait point were determined experimentally. The number of theoretical stages can be obtained from this phase diagram. It is probably the pioneering work ever done in this field and should be useful in designing work.

High grade potassium dihydrogen phosphate (a complex fertilizer (19)) can be produced by wet process phosphoric acid, if it is purified by DBSO. The quality of this product is almost the same as that from thermal process acid. Davister et. al.(20) reported the thermal phosphoric acid production consuming about 3.4 times more calories and about 13.4 times more kWh than the wet process.

NOMENCLATURE

X_A -- phosphoric acid in aq. phase, wt. %; X_W -- water in aq. phase, wt.%
Y_A -- H_3PO_4 in organic phase, wt. %; Y_W -- H_2O in organic phase, wt. %
Y_S -- DBSO in organic phase, wt. %; Z_A -- H_3PO_4 in binodal curve, wt. %
Z_W -- H_2O in binodal curve, wt. %; Z_S -- DBSO in binodal curve, wt. %

REFERENCES

(1) Gilbert, et.al., U.S.P. 3,438,746
(2) Hukuniuk, to. E., u gp. "Yenenu Xuwise" 12, emp, 2233 (1976)
(3) Jiang Yuming, Li Daochun, Su Yuanfu: Fertilizer Industry, (China) No. 2., (1982)
(4) National Standards of Chemical Reagents, China.
(5) Robert, C.W., Handbook of Chemistry & Physics, 58th ed.
(6) Jerry F.C., et. al.; J. Chem. Engg. data, 14,198 (1974)
(7) Muralimohan, S., Rao, P.B., J. Chem. Engg. data 12,494 (1967)
(8) Alders, "Solvent Extraction" (Translated into Chinese) 44, (1959)
(9) Treybal, R.E., "Liquid Extraction" 2nd ed., pp.30-37, McGraw-Hill, New York, 1963.
(10) Francis, A.W., Liquid-liquid Equilibriums, 45. 1963
(11) Bassett, et. al. Vogel's "Textbook of Quantitative Inorganic Analysis" 4th ed., p. 308
(12) Treybal, R.E., Ind. Eng. Chem., 38. 817 (1946)
(13). Carniti, Paolo, et. al., "Fluid Phase Equilib.", 2, pp. 39-47,1978

(14) Hand, B., J. Phys. Chem. 34. 1961 (1930)
(15) Othmer, D.F., Tobias, P.B., Ind. Eng. Chem., 34,693 (1942)
(16) Rod, V., Chem. Eng. J., 11,105 (1976)
(17) Yamamoto, et. al., "Sulfuric Acid and Industry", 27 (7), Japan, 1974
(18) Jiang Yuming, Li Daochun, Su Yuanfu; Journal of Chemical Industry and Engineering (China) 4, 310 (1982)
(19) Phosphate Fertilizer, Shanghai Research Institute of Chemical Technology, 1964
(20) Davister, A., et. al., Chem. Eng. Prog., March 35 (1982

ACKNOWLEDGMENT: It is a pleasure to acknowledge the helpful suggestions received from our colleagues, especially from Prof. Su Yuan-fu.

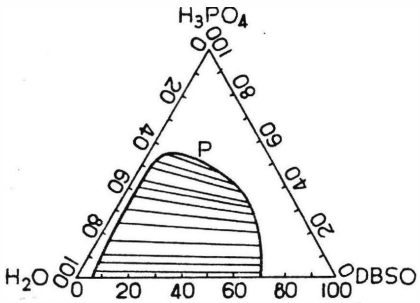

FIG. 1 DBSO-H_3PO_4-H_2O SYSTEM TERNARY PHASE DIAGRAM

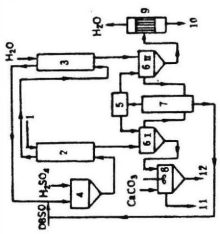

FIG. 11 PROPOSED FLOW SHEET
1 WET PROCESS ACID
2 EXTRACTION
3 RE-EXTRACTION
4 pH ADJUSTED
5 C_6H_6 TANK
6 RECOVERY I, II
7 DISTILLATION
8 DIGESTER
9 EVAPORATION
10 PURE H_3PO_4
11 WASTE WATER
12 $CaHPO_4 \cdot 2H_2O$

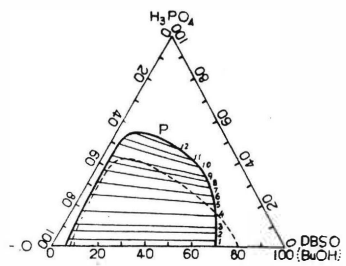

FIG. 2 COMPARISON OF DBSO-H_3PO_4-H_2O WITH Bu OH-H_3PO_4-H_2O (IN DOTTED LINE)

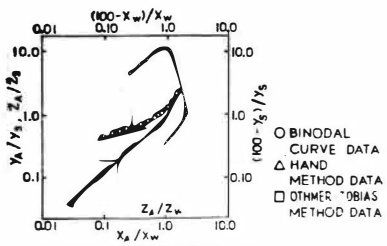

FIG. 3 TIE LINE CORRELATION AND PLAIT PT. DETERMINATION

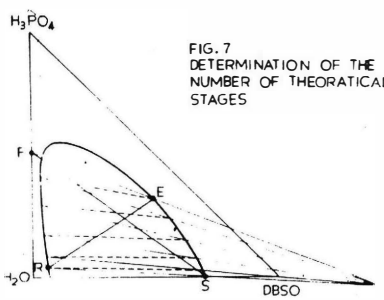

FIG. 7 DETERMINATION OF THE NUMBER OF THEORATICAL STAGES

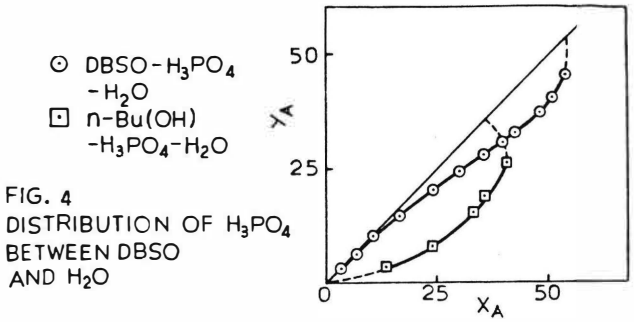

FIG. 4 DISTRIBUTION OF H_3PO_4 BETWEEN DBSO AND H_2O

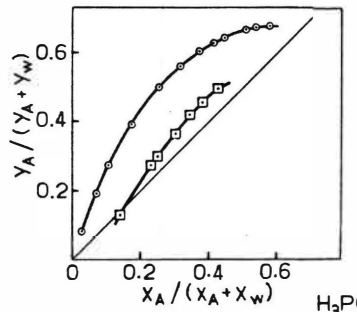

⊙ DBSO-H_3PO_4-H_2O
⊡ n-Bu(OH)-H_3PO_4-H_2O

FIG. 5 SELECTIVITY OF DBSO H_3PO_4 H_2O SYSTEM

O EXPERIMENTAL DATA
— MODEL CALCULATED VALUE

FIG. 6 COMPARISON OF V.ROD'S MODEL CALCULATED BINODAL CURVE WITH EXPERIMENTAL DATA

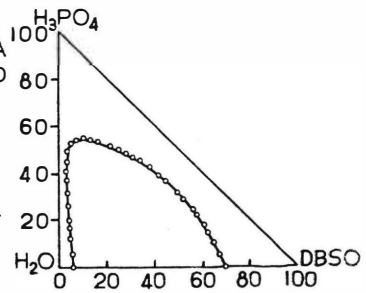

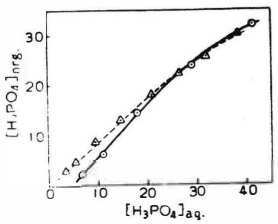

FIG. 8 EQUILIBRIUM DATA OF H_3PO_4

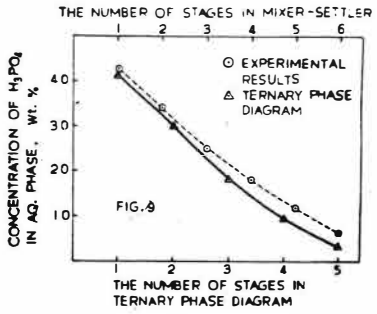

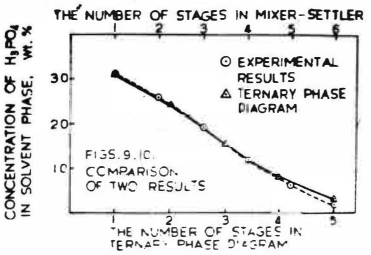

MECHANISM OF SYNERGISTIC EXTRACTION OF RHENIUM(VII) BY PRIMARY AMINE & NEUTRAL PHOSPHORUS ESTER

Shu-chiou Yu and Chia-yung Chen

Institute of Chemical Metallurgy
Academia Sinica
Beijing, China

ABSTRACT It has been found that Re(VII) can be quantitatively separated from Mo(VI) in alkaline solution by synergistic extraction with a mixture of primary amine and neutral phosphorus esters. The separation factor can be as high as in the order of 10^5. This new extraction system for Re(VII) is very effective and much better in comparison with widely studied quaternary ammonium salts with respect to extraction and stripping. The mechanism of synergistic extraction was studied. The composition of the extraction species is $(RNH_2).(HReO_4)_2.(R_3P{=}O)_2$ formed through hydrogen bonds.

SELECTION OF EXTRACTANTS FOR Re(VII) To find an effective extractant for separation of Re(VII) from Mo(VI) in alkaline solution, a number of extraction systems have been investigated. The typical experimental results are shown in Table 1 and 2. Although all the extractants shown in Table 1 contain active hydrogen atoms, their ability to extract Re(VII) is quite different. The hydrogen atoms attached to nitrogen in an unconjugated system has acceptor property to certain extent. In combination with reagents containing donor atoms, these extractants can extract rhenium(VII) veryeffectively through hydrogen bonding. However, the amount of Re extracted is very low with the active hydrogen atom containing extractant such as primary amine alone. With only one hydrogen atom attached to nitrogen of secondary amine, its acceptor property is much weaker in comparison with that of primary amine and thus secondary amine is a poor extractant for synergistic extraction of Re(VII).

With reagents such as dodecanoic acidamide, O-phenylene diamine and diphenyl amine, the lone pair electron of nitrogen is in conjugation with carboxyl group and benzene ring respectively and the acceptor property of active hydrogen attached to nitrogen is very strong. These reagents are solid at room temperature due to association through hydrogen. They are insoluble in inert diluents and soluble only in solvents capable of forming hydrogen bonds such as alcohols. The strong hydrogen bonds are formed between alcohol and acidamide and Re(VII) can't be extracted by them as no free active hydrogen atoms available for solvation with rhenium. The active hydrogen atoms of methylene group of β-diketones do not act as acceptor, however, they are synergistic donor extractant with primary amines (Table 2).

Table 1 Extraction of Re(VII) with TBP and reagents containing active hydrogen atoms.

Aq. : PH=9.0; ionic strength = 0.33 (Na_2SO_4)
Org.: Conc. of reagents with active hydrogen 0.05 M, diluent: kerosene or isooctanol.
Extraction time 10 min; 15°C, org./aq.= 1.

Org. phase Reagents	TBP M	Aq. Re(VII) g/l	Distr. ratio α	Synerg. factor D
Pri.amine 7101	1.0	1.86	0.333	11.4
" " " "	0	"	0.0193	
Pri.amine N1923	1.0	2.79	0.302	12.7
Pri.amine N1923	0	"	0.0138	
$C_{12}H_{25}CONH_2$	1.0	1.86	~0	
diphenyl amine	1.0	"	0.011	
" "	0	"	"	
acetylacetone	1.0	"	0.010	
"	0	"	0.006	
sec.amine 7206	1.0	"	0.064	4.2
" " "	0	"	0.0054	

Table 2 Extraction of Re(VII) with primary amine and reagents containg donor atoms.

Org.: diluent, kerosene
Extraction time 10 min, 15°C, O/A = 1.

Org. phase Donor reag. M	pri. amine M	Aq. Re g/l	PH	Distr. ratio α	Synerg. factor D
TBP 1.0	0.05	1.86	9.0	0.333	12.7
X* 1.0	"	"	"	36.2	1034
MIBK 1.0	"	"	"	0.110	5.2
TBP 1.8	0.1	0.217	"	144	906
" 0.5	0.05	0.100	8.5	99	503
X* 1.0	0	1.86	9.0	0.016	
MIBK 1.0	0	1.86	9.0	0.0018	
TBP 1.0	0	1.86	9.0	0.010	
TBP 1.8	0	0.217	9.0	0.10	
TBP 0.5	0	0.100	8.5	0.0929	
0	0.05	1.86	9.0	0.019	
0	0.1	0.217	9.0	0.059	
0	0.05	0.100	8.5	0.104	

X* cyclohexyl phosphonic di-(isoamyl) ester.

It can be found from Table 2 that reagents with different donor groups have different degree of enhancement of extraction of Re(VII) by primary amines. Their synergistic effect is in consistent with their donor properties as:

neutral phosphates
or phosphonates > β-diketones > ketones > esters > ethers
increasing donor property
enhancement of synergistic effect

The synergistic effect of neutral phosphates increases with the increase of the number of alkyl groups directly connected to phosphorus. Therefore, TOPO has been found to give highest synergistic effect to primary amines.

STUDIES ON THE SYNERGISTIC EXTRACTION OF Re (VII)

Fig. 1 shows the results of extraction of Re(VII) from alkaline solutions by a mixture of primary amine and neutral phosphorus esters. It can be seen that aqueous PH increases with the increase of amount of rhenium extracted. The rhenium loaded organic phase contains no potassium atoms as determined by atomic absorption spectropy. It can be assumed rhenium is extracted into the organic phase in the form of perrhenic acid $HReO_4$ with the release of hydroxyl groups into the aqueous phase to increase the solution PH during extraction:

$$ReO_4^- + H_2O \rightleftharpoons HReO_4 + OH^-$$

The effect of contact time on Re(VII) extraction is shown in Fig. 2. Both the contact time and the rate of agitation have great effect on the extent of extraction through solvation mechanism. However, with anion exchange mechanism of extraction, the extraction equilibrium will be approached in a few seconds. The kinetic characteristics of slow rate of synergistic extraction of Re(VII) probably depends on the rate of formation of $HReO_4$ by hydrolysis and the rate of dissociation of associated primary amines by hydrogen bonding. High rate of agitation is also required to break associated primary amine to free the active hydrogen atoms for synergistic extraction.

STUDIES ON THE COMPOSITION OF EXTRACTION COMPLEXES

The composition of synergistic extraction species of Re(VII) with primary amine and TBP was studied with slope method, method of continuous variation and method of saturation capacity respectively as shown in Fig. 3-5 and Table 3. Results indicate from these studies that the mol ratio of primary amine, rhenium and neutral phosphorus ester is 1:2:2 in the extraction species.

Table 3. Saturation capacity of extraction of Re(VII) by primary amine and neutral phosphorus ester.

Aq. : PH=7.0; 0.010 and 0.0179 M Re(VII) resp.
Org.: $RR'CHNH_2$+ 0.25 M cyclohexyl-di(isoamyl) phosphonic ester in n-octane.

Primary amine conc. $M_1 \times 10^3$	Re in loaded organic $M_2 \times 10^3$	Mole ratio M_1/M_2
4.5	8.6	0.52
2.25	4.13	0.54
0.90	1.72	0.52

DISCUSSION OF RESULTS

It can be considered from the experimental results that the synergistic extraction of Re(VII) by a mixture of primary amine and neutral phosphorus esters from alkaline solution is by solvation. $HReO_4$ is extracted into the organic phase by formation of hydrogen bonds with active hydrogen atoms of primary amine and with phosphryl oxygen of neutral phosphorus ester. The extraction reaction can be represented by:

$$2\ ReO_4^- + RNH_2 + 2\ PO(R)_3 + 2\ H_2O \rightleftharpoons RNH_2.2(HReO_4).2PORR_3 + 2\ OH^-$$

The structure of extraction species can be expressed as shown in Fig. 6.

Synergistic extraction as an effective method of separation or solvent extraction has been studied rather thoroughly. Its mechanism has also been investigated. For synergistic extraction with chelating agent and neutral extractant, the enhancement of extraction is considered due to the replacement of chelating agent or water molecule in extraction species by hydrophobic neutral extractant and thus more stable mixed complex is formed during extraction(1,2). For synergistic extraction with two neutral extractants, the enhancement factor of extraction is rather low and the mechanism of extraction is rather complicated.

In discussion of synergistic extraction of Cs^+ with a mixture of carboxylic acid and phenol, it has been proposed (3) that hydrogen bonds are formed between these two extractants in the extraction species. A number of studies have indicated that a mixture of two ketones or two alcohols does not show any synerism toward extraction. However, synerism can be observed in the extraction with a mixture of alcohol and ketone. In the synergistic extraction of pertechnetic acid with a mixture of alcohol and ketone, it was considered that the associated alcohol is dessociated by the addition of ketone and the activity of alcohol is increased (4). In regard to the synergistic extraction with amine and alkyl phosphoric acid, the cationic amine salt was proposed to be present in the extraction complex. For extraction of uranyl sulfate from sulfuric acid solution, the reaction can be written as (5) :

$$UO_2SO_4 + (H_2MBP)_n + R_3NH^+ \rightleftharpoons (UO_2SO_4 \cdot HMBP \cdot (H_2MBP)_{n-1} \cdot R_3NH^+)$$

A mixture of primary amine and neutral donor extractants is an effective extraction system for Re(VII) and also for separation of Mo(VI) from Re(VII) in alkaline solution. Results indicate that the role of primary amine in this synergistic extraction system is different from those reported before as far as we know. The experimental results also show the synerism of amines is decreased in the order of primary, secondary and tertiary amines. The chemical bond formed between perrhenate and amine salt has been studied by infrared spectra. It indicates that inner hydrogen bond as R-N-H⁺..O is formed and the strength of H-bond is decreased in the order of tertiary, secondary and primary amines and has no relation with the structure or size of alkyl groups whatsoever (6). The tertiary amine has highest tendency to form salt in comparison with primary and secondary amines and also has highest power of extraction by ion exchange mechanism. Two active hydrogen atoms attached to the nitrogen atom of primary amine must be involved in the present studied synergistic extraction system. The absorption of infrared by the stretching vibrations of $-NH_2$ in primary amine has been broadened after forming hydrogen bonds with perrhenic acid during synergistic extraction as indicated in Fig.7. The rate of extraction is different with different extraction mechanism. In extraction with amine salt by anion exchange in acid solution, the extraction can be completed instantaneously. The extraction equilibrium constant with anion exchange mechanism is about 10^3 times as that of the present synergistic extraction reaction.

From either the synergistic extraction system or the mechanism of extraction, the present system of synergistic extraction of Re(VII) with primary amine and neutral donor extractant is different from the ordinary discussed four or six kinds of synergistic extraction systems. The present results indicate that a mixture of acceptor type reagent with neutral donor atom extractant can extract synergistically the oxyacids of transition metals effectively from alkaline solutions through the formation of hydrogen bonds.

The laboratory and bench scale extraction experiments have been carried out with synthetic solution and also with the solution from high pressure alkaline leaching of molybdenite. By crystallization once, potassium perrhenate $KReO_4$ of purity over 99% has been obtained from the leaching solution by synergistic extraction with primary amine and TBP.

CONCLUSIONS

A new synergistic extraction system has been found for the extraction of Re(VII) from the alkaline solutions. Mechanism of synergism has been studied. The hydrogen bonds are formed between primary amine and perrhenic acid and also between the acid and neutral donor extractant during synergistic extraction. The composition of extraction species has been determined. It can be considered that the present extraction system can be extended to the extraction of oxyacids of some other transition metals.

REFERENCES

1. Rao, V.P.K. et al: J. Inorg. Nuclear Chem. 1974, 36, 415.
2. Genov, L. et al: Monatsh Chem. 1973, 104, 750
3. Kertes, A.S. and Marcus, Y., Editors: Solvent Extraction Research (1969)
4. Boyd, G.E. et al: J. Phys. Chem. 1960, 64, 988
5. Deptula, C.:J. Inorg. Nuclear Chem. 1970, 32, 277
6. Petrow, K. Y., y dr.:Zh. Neorg. Khim. 1969, 14(12), 3230

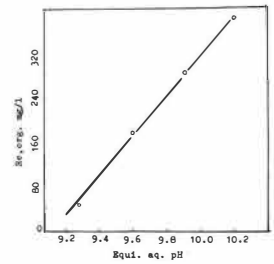

FIGURE 1. RELATIONSHIP BETWEEN AQUEOUS pH AT EQUILIBRIUM WITH AMOUNT OF Re EXTRACTED.

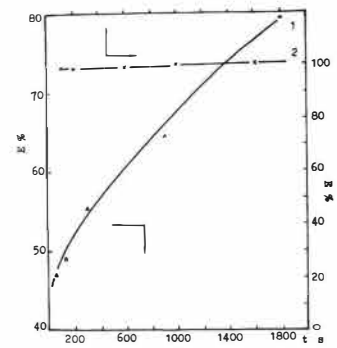

FIGURE 2. RATE OF EXTRACTION OF Re WITH DIFFERENT MECHANISMS.
1. Solvation extraction 790 rpm., aq. Re 1 g/l, pH 8.6; org. 4 % N1923-50 % TBP-kerosene.
2. Anion exchange extraction 210 rpm, pH 2.0, org. 4 % N1923-kerosene (acidified first).

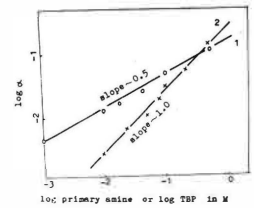

FIGURE 3. EFFECT OF CONCENTRATION OF PRIMARY AMINE AND TBP ON DISTRIBUTION RATIO α OF Re(VII).
1. TBP 1.0 M, different conc. of primary amine.
2. primary amine 0.05 M, different conc. TBP.

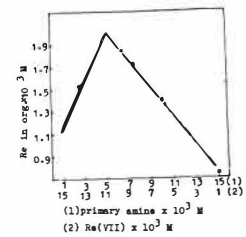

FIGURE 4. METHOD OF CONTINUOUS VARIATION TO DETERMINE COMPOSITION OF EXTRACTION SPECIES (CONSTANT TBP CONC.).

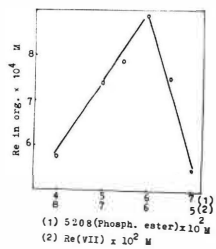

FIGURE 5. METHOD OF CONTINUOUS VARIATION TO DETERMINE COMPOSITION OF EXTRACTION SPECIES (CONSTANT PRIMARY AMINE CONC.).

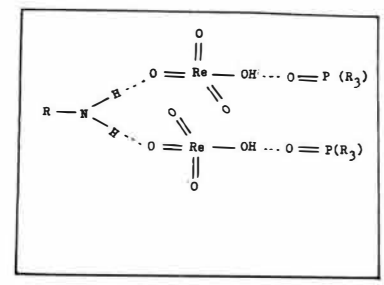

FIGURE 6. SCHEMATIC REPRESENTATION OF SYNERGISTIC EXTRACTION SPECIES OF Re(VII) BY PRIMARY AMINE AND NEUTRAL PHOSPHORUS ESTERS.

R -- alkyl or alkyloxy group.
.... hydrogen bond.

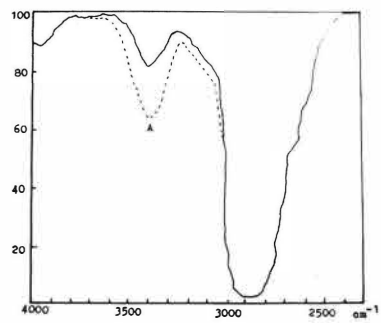

FIGURE 7. INFRARED SPECTRA OF SYNERGISTIC EXTRACTION OF Re(VII) WITH PRIMARY AMINE AND NEUTRAL PHOSPHORUS ESTERS.

solid line solvent, 0.025 M primary amine 7101 + 0.5 M cyclohexyl di(isoamyl)-phosphonic ester + cyclohexane.

dotted line solvent as above loaded with Re(VII) 0.0123 M.

RECOVERY OF ACIDS AND REACTIONS IN CONCENTRATED AQUEOUS SOLUTIONS MEDIATED BY ACID-BASE SOLVENTS

Aharon M. Eyal, Klara Hajdu, Charles Appelbaum, Avraham M. Baniel

Casali Institute of Applied Chemistry
School of Applied Science and Technology
The Hebrew University of Jerusalem
91904 Jerusalem, Israel

THE ACID-BASE EXTRACTANTS

A new family of extractants was described (1,2) for the separation of strong mineral acids from other species present in aqueous solutions. The extractants consist of a strong organic acid and an amine dissolved in a carrier solvent. Both the organic acid and the amine are water insoluble in free and in salt form. The extracted mineral acid can be recovered by backwashing of the extractant phase with water at concentrations approaching those in the original solutions. Even higher concentration may be obtained by using common ion effects or temperature effects.

The equilibrium involved in reversible extractions of a mineral acid HA by an extractant prepared by mixing an organic base b and an organic acid Ha in a carrier solvent is represented by:

(1) $HA\ (aq) + bHA\ (solv) \rightleftarrows bHA\ (solv) + Ha\ (solv)$

(aq - aqueous, solv - solvent). The driving force for transfer is determined by hydrogen ion activity. The largest energies involved are those of acid-base reaction. Secondary energies are those deriving from steric factors, hydration and other molecular interactions.

FITTING EXTRACTANTS TO PROCESSES

Careful composing of the extractant-base strength, acid strength, structural features of acid and base for steric effects, base to acid proportions, carrier solvent composition and concentration - may be used to achieve desired results: high loadings, stripping efficiencies, minimizing number of transfer stages. Distribution of HCl between H_2O and extractants composed of various bases and acids is shown in Figure 1. It illustrates the variety of behaviours obtainable by suitably composed extractants. The effect of temperature is also demonstrated.

The ability to extract selectively and reversibly strong mineral acids from aqueous phase at practically any concentration level make these extractants applicable for various industrial processes, several of which are briefly described:

RECOVERY OF H_2SO_4 FROM A WASTE STREAM OF TiO_2 MANUFACTURE

In the manufacture of TiO_2, ores are attacked by H_2SO_4 and the product is hydrolyzed. A waste liquor is obtained consisting of an aqueous solution of H_2SO_4 and $FeSO_4$ as main constituents. This liquor presents serious disposal problems. Separation of H_2SO_4 from $FeSO_4$ could simplify disposal and enable the concentration of H_2SO_4 and its recycle to the main process.

A process based on acid-base extractant is shown in Figure 2. In L.L.C.1 the H_2SO_4 is selectively extracted (with practically no Fe^{II}). In L.L.C.2 the acid is simply backwashed from the extractant by water.

The concentration at which H_2SO_4 is recovered is of great significance since it determines the load on subsequent evaporation. Backwashing H_2SO_4 at a concentration even higher than in the waste liquor is obtainable with a suitably composed extractant due to temperature effects and common ion effects.

PURIFICATION OF PHOSPHORIC ACID

The phosphoric acid obtained by attack of phosphate rock by H_2SO_4 (wet process acid) is usually concentrated to 50-54% P_2O_5. The main impurities in the resulting acid are: H_2SO_4 1-6%, F 0.2-1.2% (most of it in the form of H_2SiF_6), Fe 0.6-1.2%, Al 0.3-0.8%, Mg 0.1-0.4%, smaller amounts of Ca, K, Na, Si and traces of many other cations (3).

Figure 3 shows a process for separation of part of the H_3PO_4 content as purified phosphoric acid with very small concentrations of impurities. This process takes advantage of the selectivity and reversibility of extraction with the acid-base extractant: The regenerated extractant is loaded with H_2SO_4 and H_2SiF_6 to a level which is in equilibrium with the aqueous feed to L.L.C.1. Thus, only H_3PO_4 is extracted in L.L.C.1 - H_2SO_4, H_2SiF_6 and the cations remain in the raffinate. The loaded extractant is back-extracted with water in L.L.C.2. As the order of selectivity for the acid-base extractant is $H_2SO_4 > H_2SiF_6 > H_3PO_4$ (2,4), partial wash will result in the regenerated extractant and purified H_3PO_4 at a concentration approaching feed concentration.

SULFURIC ACID FROM CALCIUM SULFATE

About 60% of all H_2SO_4 is used for production of H_3PO_4 in the wet process:

(2) $Ca_5(PO_4)_3F + 5H_2SO_4 \rightleftarrows 5CaSO_4 + 3H_3PO_4 + HF.$

A process for the recovery of H_2SO_4 from waste gypsum by means of heat and of CO_2 is equivalent to the replacement of sulfur by fuel (5). Such a process is shown in Figure 4. The recovered acid is concentrated and recycled to phosphate rock attack. The calcium of $CaSO_4$ is obtained as $CaCO_3$ which, as a waste, is far more environmentally acceptable than $CaSO_4$.

The overall transformation is:

(3) $CaSO_4 + CO_2 \xrightarrow{H_2O,\ energy} CaCO_3 + H_2SO_4$

It is achieved by a sequence of three reactions:

(4) $CaSO_4\ (s) + CO_2\ (g) + 2NH_3\ (g) \xrightarrow{H_2O} CaCO_3\ (s) + (NH_4)_2SO_4\ (aq)$

(5) $2(NH_4)_2SO_4\ (s) \xrightarrow{heat} 2NH_4HSO_4\ (l) + 2NH_3\ (g)$

(6) $2NH_4HSO_4 \xrightarrow{brine,solvent} (NH_4)_2SO_4\ (s) + H_2SO_4\ (solv).$

The acid-base extractant is used to shift the equilibrium in equation (6) to the right by extraction of H_2SO_4. An extractant composed of quaternary amine and sulfonic acid in aromatics-free white spirit is suitable for this process: satisfactory high loadings are obtained in contact with an aqueous solution in the selected area of the H_2O-H_2SO_4-$(NH_4)_2SO_4$ phase diagram; the backwash of the loaded extractant with water is efficient.

K_2SO_4 MANUFACTURE

The ability to shift equilibrium by selective extraction of a by-product acid could be used in the manufacture of K_2SO_4. Amines extract HCl preferably to H_2SO_4. Acid-base extractants retain the selectivities of the amines (2). Thus a suitably composed acid-base extractant should shift the reaction

(7) $2KCl + H_2SO_4 \rightleftarrows K_2SO_4 + 2HCl$

to the right by extraction of HCl. Backwash of loaded extractant should result in a regenerated extractant and a by-product HCl solution.

ACKNOWLEDGEMENT

We gratefully acknowledge the assistance of Miss Y. Afrati in much of the experimental work.

REFERENCES

1. A. Baniel. U.S. Patent 4,291,007.
2. A. Eyal, A. Baniel. Ind. Eng. Chem. Process Des. Dev., 21, 337 (1982).
3. Phosphoric Acid ed. by A.V. Slack p. 646, Marcel Dekker, Inc. N.Y. (1968).
4. A. Baniel, A. Eyal. Israel Patent Application 63097 (1981).
5. A. Baniel, A. Eyal. Israel Patent Application 64712 (1982).

ABBREVIATIONS

L.L.C.	-	Liquid Liquid Contact
TLA	-	trilauryl amine (Alamine 304, General Mills)
ABL	-	α-bromolauric acid (prepared by bromination of lauric acid)
NTCA	-	methyl tricaprylyl amine (Aliquat 336, General Mills)
DN	-	dinonylnaphthalene sulfonic acid (Synex DN-052, King Industries)

The carrier solvent was aromatics free white spirit.

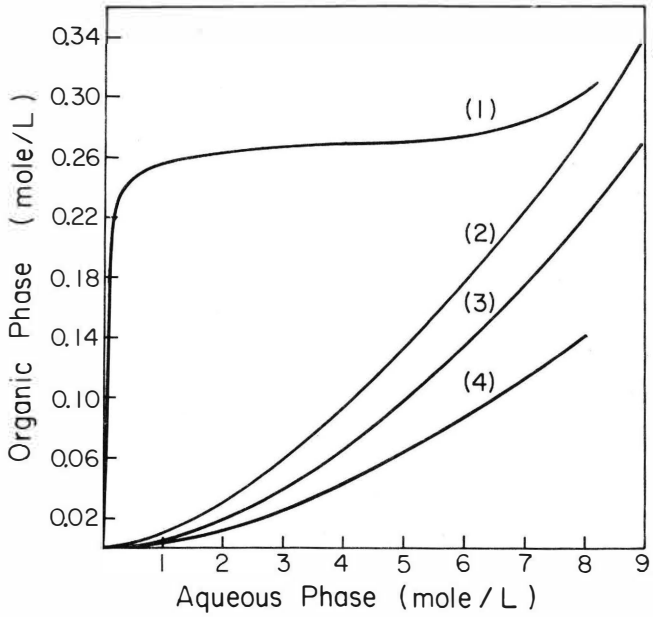

FIGURE 1: DISTRIBUTION OF HCl BETWEEN H_2O AND VARIOUS EXTRACTANT
(1) TIA + ABL at 20°C (3) MTCA + DN at 80°C
(2) MTCA + DN at 20°C (4) TIA + DN at 20°C

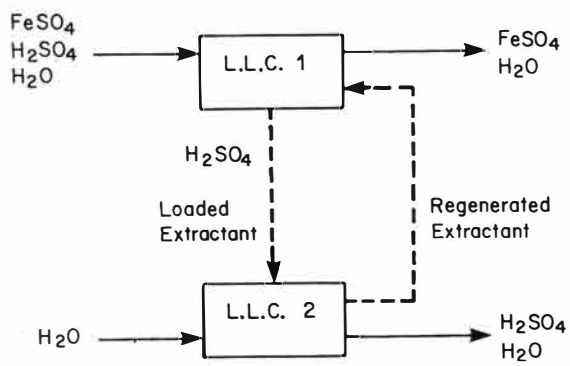

FIGURE 2: RECOVERY OF H_2SO_4 FROM WASTE STREAM OF TiO_2 MANUFACTURE.
---- Extractant stream —— Aqueous stream
L.L.C - Liquid Liquid Contact

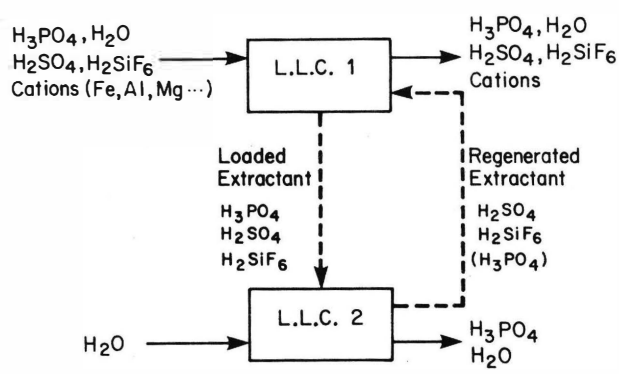

FIGURE 3: EXTRACTION OF H_3PO_4 FROM WET PROCESS PHOSPHORIC ACID.
---- Extractant stream —— Aqueous stream
L.L.C - Liquid Liquid Contact

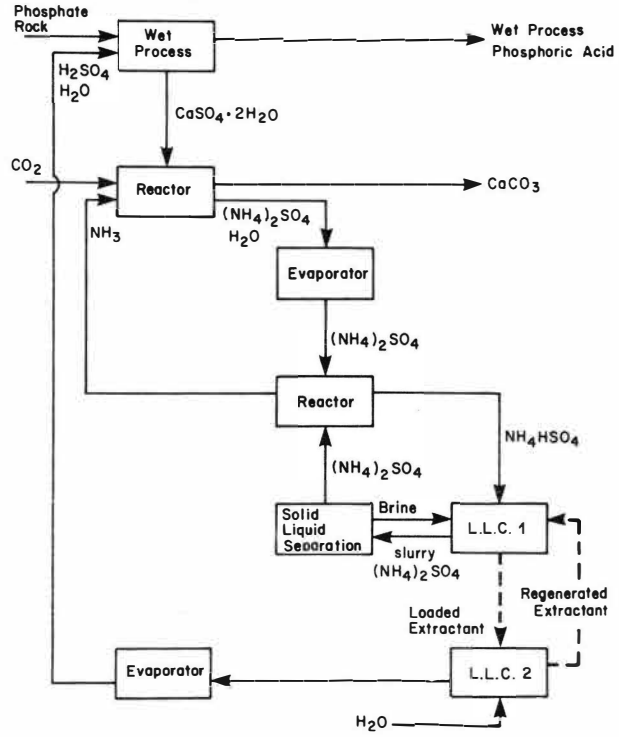

FIGURE 4: SULFURIC ACID FROM CALCIUM SULFATE
---- Extractant stream —— Aqueous stream
L.L.C - Liquid Liquid Contact

USE OF CONCENTRATED BRINE TO IMPROVE PHOSPHORIC ACID EXTRACTION

E. Ben-Yoseph, D. Kellerman, D. Meyer, S. Wahrmann

IMI(TAMI) Institute for Research and Development
P.O. Box 313
Haifa 31002, Israel

INTRODUCTION.

In the purification of wet process phosphoric acid by solvent extraction with aliphatic alcohols is usually difficult to achieve recoveries of better than 70 percent, because of the fact that the distribution coefficient (solvent/aqueous) drops off rapidly with the concentration of the acid (figure 1). This is not too much of a disadvantage if the residual acid containing most of the impurities can be utilised, e.g. in the production of fertilisers. However where this is not the case, it limits the applicability of solvent extraction processes.

To obtain a higher recovery one of the possibilities is to add a strong electrolyte to the aqueous solution; this increases the distribution coefficient of the phosphoric acid (figure 1). The added electrolyte is either extracted only to a minor extent and is readily in a purification step (e.g. $CaCl_2$) or is volatile and is separated during concentration (e.g. HCl).

A process using a recycle solution of $CaCl_2$, with intermediate reconcentration, was developed by IMI.(1)

A further implementation of this principle, incorporating some new ideas, is presented here.

PROCESS PRINCIPLES.

Inevitably the process of purification leads to a loss of concentration; because of the high costs of energy special emphasis is laid on keeping this to a minimum.

At the Dead Sea Works Plant at Sdom a concentrated waste brine of mainly magnesium chloride (for composition see Materials) is discarded in very large quantities. The process uses this brine on a once through basis thus avoiding the need for reconcentrating the recycle brine, as in the normal purification process

Role of HCl.

Addition of HCl at the raffinate end of the extraction battery has several advantages: it acts as a strong electrolyte and also provides hydrogen ions which act specifically to increase the distribution coefficient of phosphoric acid; it also provides acidity to prevent the precipitation of salts as a result of hydrolysis. When it appears at the extract end however it has two important disadvantages: it is extracted into the solvent together with considerable quantities of water, which at the stage of backwashing the phosphoric acid leads to dilution and consequent thermal loads on the evaporation section; it also increases the conversion of impurity cations to anionic complexes(e.g. $FeCl_4^-$), which are extracted into the solvent and complicate purification.
The addition of HCl was therefore held to a minimum and confined to the raffinate end as much as possible.

Addition of brine.

The addition of a chloride brine to phosphoric acid has the effect of adding HCl; for the reasons given above this should be avoided at the extract end. Since the distribution coefficient for high concentrations of phosphoric acid is reasonable (figure 1), the brine is injected at the point where the distribution coefficient decreases appreciably. The amount added (about 1:1 vol/vol) is such as to give a concentration of about 120 g/l Ca equivalent, which ensures an adequate extraction without excessive dilution.

Purification.

The degree of purification obtained is a function of the amount of washing recycle used and entails a penalty of loss of concentration and of product recycle. On the basis of past experience it was decided to limit this loss to 20 percent.

Figure 2 presents the basic flowsheet, including indicative compositions based on the results of this work.

MATERIALS.

The acid was produced from Zin phosphate rock and its composition after sulphate removal was:

P_2O_5	52.7 %	Cr	120 ppm	
F	0.1 "	Ni	70 "	
Ca	0.29 "	Cu	26 "	
Fe	0.17 "	Co	30 "	s.g. 1.57
Organics (as C)	0.5 "	Mo	23 "	
		Cl	190 "	
		SO_4	440 "	

The brine was Dead Sea Works End Brine of the following composition:

Ca	33.0 g/l			
Mg	84.5 "	Cl	316.4 g/l	s.g. 1.32
Mg+Ca (as Ca)	172.1 "			

(In the following Ca expresses the equivalent concentration of Ca+Mg.)

The alcohol was technical iso-amyl alcohol (2/3 n-pentanol; 6% H_2O).

EXPERIMENTAL.

Three types of experiments were carried out.

1. Equilibrium constants were determined for synthetic mixtures by contacting at high phase ratios (40:1) with solvent.

2. On the basis of the these and previous data, cross extraction experiments were performed on the actual acid.

3. The basic process concepts were tested on a continuous bench scale mixer- settler unit of 15 stages to reveal cumulative effects. Since the whole process could not be tested simultaneously, this was done by sections with critical stages being incorporated in several configurations.

RESULTS AND DISCUSSION.

Some typical illustrative results are shown in tables 1-5.
In the first two tables partial profiles of the two sections of the extraction battery are presented,which were obtained using simulated feed inputs. The behaviour of the P_2O_5 is as expected. Of interest is the profile of the HCl; it tends to build up towards high stationary concentrations in the middle of the battery. In the A section these high concentrations are due to the large change in volume in the aqueous phase because of the massive transfer of P_2O_5, which in turn lead to small distribution coefficients for HCl. The net effect is that about half of the HCl in the solvent is turned back.

Table 1: Profile of section A of Extraction Battery.

		To stage	s.g.	P_2O_5(g/l)	HCl(g/l)	H_2O(g/l)
Feeds:	Solvent	5	0.90	28.0	26.0	81.1
	Aqueous	1	1.57	800	1.1	

Weight Ratio (solvent:aqueous) 2:1

Stage	Concentration (in g/l) Organic P_2O_5	Organic HCl	Organic H_2O	Aqueous P_2O_5	Aqueous HCl
1	178.0	14.6	90	603.5	16.1
2	84.5	20.4		376.3	57.5
3	57.5	26.3		312.0	110.0
4	41.2	28.5		234.0	120.7
5	34.1	29.2	80	176.2	140.0

In the B section one sees very high distribution coefficients for HCl, and these facts confirm the thesis that the presence of HCl is of doubtful benefit and should be confined to the minimum necessary to provide acid conditions at the raffinate-stripping end of the battery.

Table 2: Profile of section B of Extraction Battery.

		To stage	s.g.	P_2O_5(g/l)	HCl(g/l)	H_2O(g/l)	Ca equ.(g/l)
Feeds:	Solvent	5	0.81	6.0	30.0	72.0	
	Aqueous	1	1.4	74.6	62.0		110.0

Weight Ratio (solvent:aqueous) 1.74:1

Stage	Concentration (in g/l) Organic P_2O_5	Organic HCl	Organic H_2O	Aqueous P_2O_5	Aqueous HCl	Aqueous Ca equ
1	25.4	41.2	91	53.2	22.6	119.5
2	18.3	32.0		32.0	12.8	120.5
3	10.3	28.8	65	26.6	10.0	126.0
4	9.2	26.6	75	26.5	13.7	117.5
5	8.5	28.8	77	21.3	14.7	108.5

when a combined extraction battery was simulated using production acid precipitates were formed in the A section. These were found to be mainly magnesium and calcium phosphates. Various ways to overcome the problem were tested and the solution finally adopted was to wash the solvent leaving section B with a small amount of water; the resultant solution can either be returned to section B or to the purification. Table 3 shows a partial profile of this implementation.

Table 3: Profile of Extraction Battery with Ca/Mg removal.

		To stage	s.g.	P2O5(g/l)	HCl(g/l)	H2O(g/l)	Ca equ.(g/l)
Feeds:	Solvent	11	0.84	1.4	30.0	84.2	
	Acid	1	1.57	830	1.1		3.5
	End Brine	6	1.31				165

Weight Ratio (solvent:acid:end brine) 2.2:1:1.03
Weight Ratio (water for Ca/Mg removal:solvent) 1:25

Stage	Concentration (in g/l) Organic P2O5	HCl	H2O	Aqueous P2O5	HCl	Ca equ
1	169.3	14.6	86	790.5	ND	ND
3	53.0	21.3	70	332.8	ND	ND
5	18.8	30.5	66	162.2	ND	ND
	Ca/Mg removal on solvent					
6	11.6	29.0	65	46.5	37.0	93
7	8.0	35.2	60	22.5	30.0	95
9	2.9	32.4	63	5.8	26.0	100
11	1.3	30.4	67	3.2	16.5	109

Table 4 shows a profile of a 7 stage purification battery using water as the washing stream. It is interesting to note the low ratio of Fe/P2O5 in the feed as compared with the wet process acid (see Materials), due to the low chloride concentrations. Although there is a considerable removal of impurities making the acid obtained suitable for many applications, a further proprietary cleaning step has to be applied in order to obtain highest quality acid.

Table 5 shows a profile of washing an unpurified extract in 10 stages showing that a concentration of over 500 g/l is attainable.

A flowsheet is presented in figure 2: it is not optimal, but it serves to illustrate the conception.

Ideas for process improvements include further reduction in HCl addition and improving the purification both to obtain a better product and to avoid dilution of the extract.

Table 4: Profile of Purification Battery.(7 stages)

- phase ratio solvent/water (w/w) = 15:1 -

Stage	feed	1		3		5		6		7	
Comp.	org	org	aqu	org	aqu	org	aqu	org	aqu	org	aqu
P2O5 g/l	166	172	575	186	536	183	520	201	494	134	428
HCl	12	12		13		15	13	16	17	15	20
Ca ppm	139	103	2950	33	981	6	170	3	58	0.2	22
Mg	490		10625							0.5	
Fe	485		11550							13.4	
Cu	8.6		90							1.8	
Cd	11		3.7							9.6	
V	80		1260							3.5	
Mo	17		88							5.0	
F	225		3400							125	
SiO2			64							107	
Ni	5.8									0.0	
Zn	185		58							166	
Cr	9		50							0.1	

Table 5: Profile of the Washing Battery.(10 stages)

Stage	Aqueous Phase (in g/l): P2O5	HCl	Organic Phase (in g/l): P2O5	HCl	H2O
1	508	13.9	172	14.3	146
3	438	25.9	139	14.6	144
4	374	39.8	114	18.2	130
5	292	49.3	91.6	20.8	
7	104	43.1	30.5	14.6	
9	14.4	7.6	4.2	2.3	
10	2.1	0.6	0.6	0.2	78

REFERENCE.

1. A.Banier, R.Blumberg: Solvent Extraction: Chloride Extraction and Temperature cycling (pp 709-19) in Phosphoric Acid, A.V.Slack (Ed) Vol.I,Part II Marcel Decker Inc. 1968

FIGURE 1 DISTRIBUTION COEFFICIENT (SOLVENT/AQUEOUS)

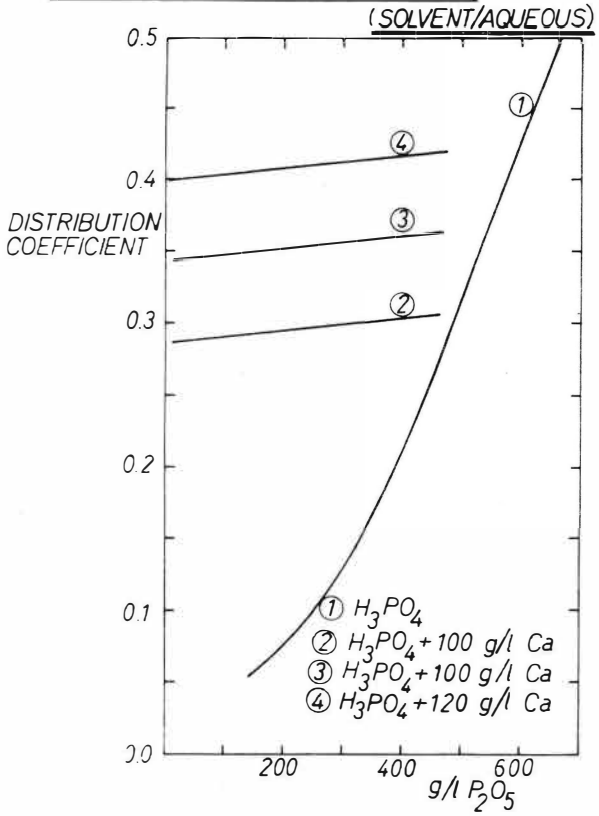

FIGURE 2 BASIC FLOWSHEET

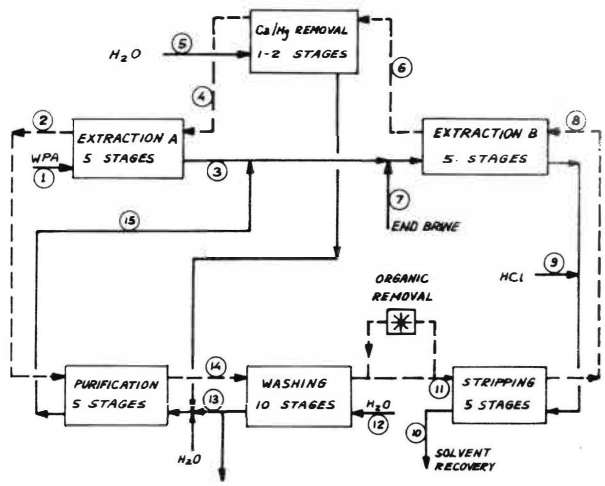

WEIGHT FLOWS AND COMPOSITIONS

STREAM	1	2	3	4	5	6	7	8	9	10	11	12	13	14	15
FLOW	100				16		110		25		400	110	30		
P_2O_5 g/l	830	176	238	21.5		23.0		3.9		5.2	0.6		364	134	575
HCl g/l		13	26	19.5		23.7		24.1	220	4.6	0.2		22	15	0.5
Ca equ g/l	4.3	0.14	16	0.9		4.7	172	2.2		102					9.2
DENSITY	1.57						1.32		1.19		0.83				

THE LINEAR RULE OF INDIVIDUAL RARE EARTHS EXTRACTION

Li Han

Changchun Institute of Applied Chemistry
Academia Sinica
Changchun, China

Since mono(2-ethyl-hexyl)2-ethyl-hexyl phosphonate (HEH(EHP)) has been an effective extractant and applied in industry for the separation of light and heavy rare earths, the study of it is of more significance.

LINEAR RULE

Experiments for the extraction of fifteen individual rare earths La-Lu and Y with HEH(EHP) (1.0M)-kerosene-HCl at a phase ratio 1/1 were carried out.

The shape of equilibrium curves of all rare earths are the same as shown in figure 1. If the general method for the correlation of equilibrium rare earth concentration in organic phase (C_o) and in aqueous phase (C_a) is used, the results will be very complicated. It was found that, relations between inverse distribution ratio (1/D) and C_a form a group of excellent straight lines at various initial acidity as shown in figure 2. Hence, the correlation was simplified as

(1) $$1/D = a + bC_a$$

Coefficients a and b are functions of initial acidity (H) and their values were calculated by least square method. The mean relative errors of D calculated by equation (1) are less than 5% as compared with the experimental data.

Since the initial concentration of rare earth (C_i) is

(2) $$C_i = C_o + C_a$$

then from equation (1) there is

(3) $$C_i = \frac{C_a}{a + bC_a} + C_a$$

For given H and C_i, equilibrium parameters can be calculated easily from equation (3).

From equation (1), as C_a is increased, C_o turns to 1/b. Then at a certain acidity 1/b can be considered as the maxium concentration of rare earth in organic phase. When C_i is decreased, 1/D turnsto a.

Further, all of the a and b for the fifteen rare earths can be correlated with H

(4) $$1/D_{La} = 0.6949e^{41.16H} + (0.01757-0.1581H)^{-1}C_a$$

(5) $$1/D_{Ce} = (1.1717-10.713H)^{-1} + (0.03735-0.2213H)^{-1}C_a$$

(6) $$1/D_{Pr} = 0.3838e^{18.648H} + 24.562e^{11.179H}C_a$$

(7) $$1/D_{Nd} = -7.3556+99.22H+102.04H^2+(-52.71+1061.3H-971.84H^2)C_a$$

(8) $$1/D_{Sm} = 0.1377e^{9.753H} + 15.55e^{2.955H}C_a$$

(9) $$1/D_{Eu} = 0.0718e^{10.942H} + (13.641+42.793H)C_a$$

(10) $$1/D_{Gd} = 0.07187-1.7061H+20.11H^2+12.308e^{1.8669H}C_a$$

(11) $$1/D_{Tb} = 0.0571e^{5.5708H} + 9.4776e^{1.6618H}C_a$$

(12) $$1/D_{Dy} = 0.284-2.3066H+5.5563H^2+8.9846e^{0.8332H}C_a$$

(13) $$1/D_{Ho} = 0.2925-1.9996H+3.9147H^2+(6.7244+13.799H)C_a$$

(14) $$1/D_{Er} = 1.1571H^{1.4926} + (0.1301-0.05465H)^{-1}C_a$$

(15) $$1/D_{Tm} = -0.1176+0.1336H+0.69543H^2+(0.13524-0.02891H)^{-1}C_a$$

(16) $$1/D_{Yb} = 0.3065H^{1.905} + (0.157-0.03226H)^{-1}C_a$$

(17) $$1/D_{Lu} = 0.19566H^{2.0053} + (0.15337-0.028165H)^{-1}C_a$$

(18) $$1/D_Y = 0.1184-0.421H+1.7846H^2+(0.13487-0.05347H)^{-1}C_a$$

$H_{La}=1\times10^{-4}-0.04N$, $H_{Ce}=0.01-0.07N$, $H_{Pr}=0.01-0.10N$, $H_{Nd}=0.10-0.50N$, $H_{Sm}=0.10-0.30N$, $H_{Eu}=0.01-0.30N$, $H_{Gd}=0.10-0.70N$, $H_{Tb}=0.10-0.70N$, $H_{Dy}=0.10-1.0N$, $H_{Ho}=0.10-1.25N$, $H_{Er}=0.10-2.0N$, $H_{Tm}=0.50-2.50N$, $H_{Yb}=0.50-3.0N$, $H_{Lu}=0.50-3.0N$, $H_Y=0.10-2.0N$.

Rare earth concentrations are 0.05-0.30M.

Mean relative errors of D calculated by equation (4)-(18) are less than 5% as compared with the experimental data.

For other systems, such as the extraction of rare earths with HEH(EHP)-HNO_3 and naphthenic acid, the linear rule is also valid (1-3).

CHANGE OF PHASE RATIO

For HEH(EHP) (1.0M)-kerosene-HNO_3 (0.10-0.50N)-$Gd(NO_3)_3$(0.05-0.30M) system, when the phase ratio (P) changed from 1/2-5/1, D and P were correleated as

(19) $$D = aP^b$$

For given C_i, a and b are functions of initial acidity. Thus

(20) $$D = 1.651e^{-4.356H}\,P^{-0.1019-0.3954H} \qquad C_i=0.10M$$

(21) $$D = 0.6664e^{-2.953H}\,P^{-0.282} \qquad C_i=0.20M$$

(22) $$D = 0.4305e^{-2.197H}\,P^{-0.3641} \qquad C_i=0.30M$$

Mean relative errors of D calculated by equation (19)-(22) are less than 5% as compared with the experimental data.

CHANGE OF CONCENTRATION OF EXTRACTANT

For the system described above there is a simple relation at P=1/1 and extractant concentration (HA)=0.5-1.6M, there is

(23) $$D = a(HA)^b$$

For given C_i, a and b are functions of initial acidity. Thus

(24) $$D = e^{2.2003-11.769H+9.2613H^2}\,(HA)^{2.2444+0.6H-2.8889H^2} \qquad C_i=0.05M$$

(25) $$D = e^{0.7612-6.7541H+4.1957H^2}\,(HA)^{1.5367+2.2444H-4.0889H^2} \qquad C_i=0.10M$$

(26) $$D = e^{-0.4474-2.8506H}\,(HA)^{1.3462+1.3846H-2.1923H^2} \qquad C_i=0.20M$$

(27) $D = e^{-0.8943-2.2132H}(HA)^{1.2838+0.2386H}$

$C_i = 0.30M$

mean relative errors of D calculated by equation (23)-(27) are less than 5% as compared with the expermental data.

Generally, the mechanism of extraction is determined by the value of n in equation (28)

(28) $$\lg D = \lg K + n\lg(HA) - n\lg(H)_e$$

K-equilibrium constant, $(H)_e$-hydrogen ion concentration in equilibrium aqueous phase.

When C_i turns to zero, K becomes constant and (HA) turns to the initial concentration of extractant. For different C_i, the values of lgD and $\lg(H)_e$ of the fifteen rare earths La-Lu and Y extracted with HEH(EHP)-kerosene-HCl and HNO_3 were treated by least square method and values of n_i for different C_i were obtained. It was found that all of the values of n_i turn to three by extrapolating n_i to the limiting value of C_i on the C_i versus n_i plot. So that, at usual acidity, the mechanism of individual rare earths extracted with HEH(EHP)-HCl and HNO_3 may be considered as (cf. Figure 3)

$$Ln^{+3} + 3(HA)_2 = Ln(HA_2)_3 + 3H^+$$

As compared with reference (3) for the system of HEH(EHP)-HNO_3 it was found that all of the values of D for the fifteen rare earths in HCl system are smaller than those in the HNO_3 system, especially for heavy rare earths, which may be only one half of those in HNO_3 system. But the difference in separation factors(ß) for neighbouring elements in HCl and HNO_3 systems are not evident.

CONCLUSIONS

A linear rule for the extraction of individual rare earths with HEH(EHP)-HCl was proposed, which has the characters of easy calculation, more accuracy and fit for many other systems.

The variations of D for the change of phase ratio and concentration of extractant were studied and correlations were obtained.

The mechanism of individual rare earths extracted with HEH(EHP) HNO_3 and HCl at usual acidity were determined by the use of extrapolation method.

The values of D and ß for HCl and HNO_3 system were compared, all the values of D in HCl are smaller than those in HNO_3.

Acknowledgement- The author thanks Meng Shulan for some experimental work.

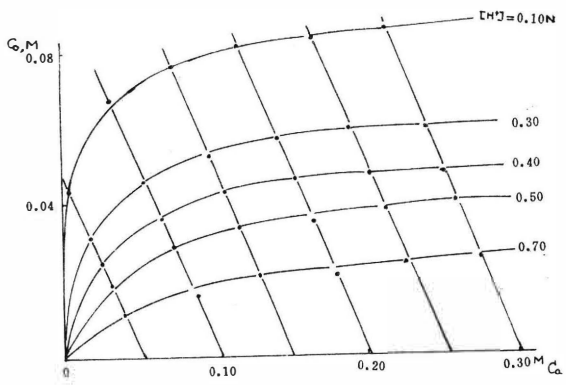

FIGURE 1. EQUILIBRIUM CURVE OF HEH(EHP)-KEROSENE-HCl-$TbCl_3$ SYSTEM

REFERENCES

1. Li Han, Wan Xiong and Dai Zhenrong. Collected Papers of the Changchun Institute of Applied Chemistry, Academia Sinica, 18, 94 (1982).
2. Mu Guangjie, Li Han, Wan Xiong and Zhao Yanju. Rare Metals, 2, 84, (1982)
3. Li Han, Wan Xiong, Lin Suxian Meng Shulan and Kan Xianglan. to be published

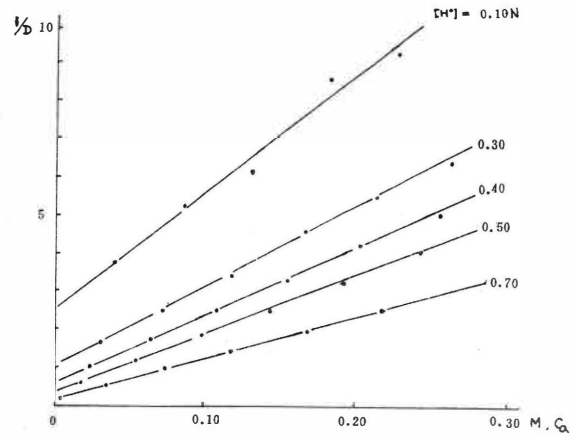

FIGURE 2. 1/D VERSUS C_a OF HEH(EHP)-KEROSENE-HCl-$TbCl_3$ SYSTEM

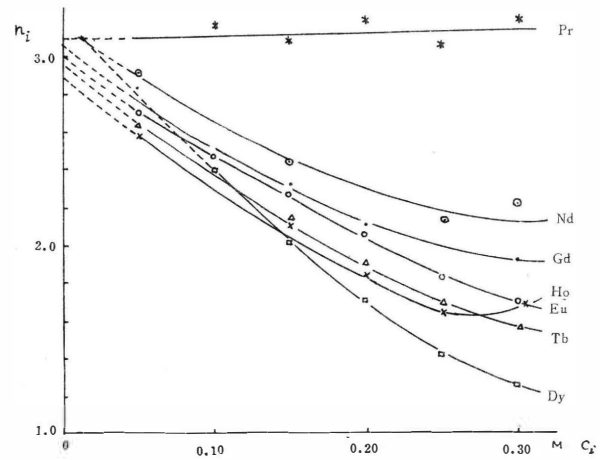

FIGURE 3. n_i VERSUS C_i FOR THE EXTRACTION OF INDIVIDUAL RARE EARTHS

MATHEMATICAL SIMULATION OF MIXED RARE EARTHS EXTRACTED WITH HEH (EHP)

Li Han, Wan Xiong, Lin Suxian, and Meng Shulan

Changchun Institute of Applied Chemistry
Academia Sinica
Changchun, China

Owing to the interference between rare earths, their distributions on extraction are different from those of the individual rare earths (1),(2). Authors attempt to estabilish the empirical formula for extraction of mixed rare earths. The separation of them by counter current extraction were studied.

EMPIRICAL FORMULA

The extraction of mixed (Sm,Gd), (Gd,Tb), (Ho,Er), (Tm,Yb) by HEH(EHP) (1.0M)-kerosene-HNO_3 and (Pr,Nd), (Yb,Lu) by HEH(EHP) (1.0M)-kerosene-HCl was carried out with the definite total rare earth concentration (C_t) and phase ratio (1/1). The equilibrium curves are shown in Figure 1,2. All the systems are the same. C_a is the equilibrium rare earth concentration in aqueous phase and C_o is the concentration in organic phase. It was found that if $\lg C_a$ and the logarithm of initial mole fraction of rare earth ($\lg Y$) were selected for correlating parameters, the results of all above systems will be simplfied as

(1) $$C_a = aX^b$$

Coefficients a and b are functions of initial acidity (H) and were calculated by least square method. The mean relative errors of C_a calculated by equation (1) are less than 5% as compared with the experimental data.

If C_i is the initial rare earth concentration of one component, then from equation (1) the distribution ratio (D) and separation factor (β) can be easily obtained by

(2) $$D = \frac{C_i - aX^b}{aX^b}$$

(3) $$\beta = \frac{(C_{i,A} - a_A X^{b_A}) a_B X^{b_B}}{(C_{i,B} - a_B X^{b_B}) a_A X^{b_A}}$$

For given C_i, X and H, Dand β can be calculated easily.

Coefficients a and b can be correlated with H, thus

(4) $$C_{a,Sm} = (0.1814+0.02757\lg H)\ X_{Sm}^{(0.9721-7.539\times10^{-4}H^{-1})}$$

$$C_{a,Gd} = (0.1143+0.1535H)\ X_{Gd}^{(0.8218+0.3995H)^{-1}}$$

$$C_t=0.2M,\ H=0.01-0.60N$$

(5) $$C_{a,Gd} = (0.185e^{0.4928H})\ X_{Gd}^{0.8626e^{0.3211H}}$$

$$C_{a,Tb} = (0.1482e^{0.6347H})\ X_{Tb}^{0.1401e^{0.5744H}}$$

$$C_t=0.25M,\ H=0.10-0.40N$$

(6) $$C_{a,Ho} = (0.0783+0.05085H)\ X_{Ho}^{0.7653+0.08893H}$$

$$C_{a,Er} = (0.06247+0.04912H)\ X_{Er}^{1.1005-0.05891H}$$

$$C_t=0.175M,\ H=0.25-1.50N$$

(7) $$C_{a,Tm} = (0.0866e^{0.2626H})\ X_{Tm}^{0.6997e^{0.1426H}}$$

$$C_{a,Yb} = (0.1757H^{0.2356}-0.09)\ X_{Yb}^{1.1642H^{-0.3492}}$$

$$C_t=0.25M,\ H=0.75-2.0N$$

(8) $$C_{a,Pr} = e^{-1.2611+0.7253H}\ X_{Pr}^{0.9503+0.2213H}$$

$$C_{a,Nd} = e^{-1.3430+0.7589H}\ X_{Nd}^{1.0013}$$

$$C_t=0.30M,\ H=0.01-0.10N$$

(9) $$C_{a,Yb} = (0.1532+0.04055H)\ X_{Yb}^{0.9489}$$

$$C_{a,Lu} = (0.1443+0.03865H)\ X_{Lu}^{1.02}$$

$$C_t=0.30M,\ H=0.10-2.50N$$

Mean relative errors of C_a calculated by equation (4)-(9) are less than 5% as compared with the experimental data.

For other systems, such as HEH(EHP)-HNO_3-(Er,Tm)$(NO_3)_3$ and naphthenic acid-HCl-(Nd,Sm)Cl_3, equation (1)is also valid (3),(4).

CHANGE OF PHASE RATIO AND TOTAL RARE EARTH CONCENTRATION

Experiments of (Sm,Gd) extracted with HEH(EHP)-kerosene-HNO_3 at phase ratio 2 1 and 4/1 were carried out. It was found that the form of correlations are remained the same as equation (1)

(10) $$C_{a,Sm}^{2/1} = (0.1306+0.0855H)\ X_{Sm}^{(0.0145+0.98H)^{-1}H}$$

$$C_{a,Gd}^{2/1} = (0.09473+0.1078H)\ X_{Gd}^{(0.9604-0.13821gH)}$$

(11) $$C_{a,Sm}^{4/1} = (0.1828+0.06823\lg H)\ X_{Sm}^{(0.9061+0.1826H^2)}$$

$$C_{a,Gd}^{4/1} = (0.07773+0.1012H)\ X_{Gd}^{(0.8816-0.30911gH)}$$

$$C_t=0.2M,\ H=0.01-0.60N$$

Mean relative errors of C_a calculated by equation (10),(11) are less than 5% as compared with the experimental data.

There are simple relations for C_a at phase ratio 1/1 ($C_a^{1/1}$), 2/1 ($C_a^{2/1}$) and 4/1 ($C_a^{4/1}$)

(12) $$C_{a,Sm}^{2/1} = b_{Sm} C_{a,Sm}^{1/1}$$

$$C_{a,Sm}^{4/1} = b_{Sm}^2 C_{a,Sm}^{1/1}$$

$$C_{a,Gd}^{2/1} = b_{Gd} C_{a,Gd}^{1/1}$$

$$C_{a,Gd}^{4/1} = b_{Gd}^2 C_{a,Gd}^{1/1}$$

$b_{Sm} = 0.9333$, $b_{Gd} = 0.8218$.

Mean relative errors of C_a calculated by the above equations are less than 5% for Gd and 6% for Sm as compared with experimental data.

If the total rare earth concentration is changed, the forms are remained the same as equation (1)

(13) $$C_{a,Sm}^{2/1} = (1.2153+8.7525H)^{-1}\ X_{Sm}^{(0.0145+0.98H)^{-1}H}$$

$$C_{a,Gd}^{2/1} = (0.1005+0.07961gH)\ X_{Gd}^{0.9604-0.13821gH}$$

$$C_t=0.1M$$

When H is substituted by the hydrogen ion concentration in

equilibrium aqueous phase $(H)_e$, the forms are also the same as equation (1).

COUNTER CURRENT EXTRACTION

Experiments of counter current extraction for the separation of (Sm,Gd) and (Ho,Er) were carried out. For (Sm,Gd) system, at 0.2M feed concentration (Sm/Gd = 2/1, P^H = 2), 1.0M HEH(EHP), 0.73N HNO_3 strip solution and the volume ratio of solvent (S), feed (F) and strip solution (W) is 4/1/1. Through 8 extraction stages and 8 strip stages, purities of Gd > 99% and Sm > 96.7% are obtained. For (Ho,Er) system, at 0.175M feed concentration (Ho/Er = 1/1, 0.20N HNO_3), 1.0M solvent (HEH(EHP)), 1.15N HNO_3 strip solution and the volume ratio of S/F/W = 3/2/1. Through 12 extraction stages and 8 strip stages, purities of Ho > 99.8% and Er > 95.8% are obtained.

Values of C_a calculated by equation (10)-(13) are satisified as compared with the experimental data.

VALUES OF D AND β FOR INDIVIDUAL AND MIXED RARE EARTHS

Because of the interference between rare earths, at the same initial concentration of a certain rare earth, the values of D in mixed system are all less than those in the corresponding individual systems. Especially for the diffcult-extractive component, the values of D may decreased several foldes. For example, 1.0M HEH(EHP)-kerosene-0.5N HCl-$YbCl_3$(0.15M) system, $LuCl_3$(0.15M) system (1) and mixed (Yb(0.15M), Lu(0.15M))Cl_3 system, the values of D are 2.406 and 3.087 for individual Yb and Lu and 0.5947 and 0.8586 for mixed Yb and Lu.

Although the values of D are quite different, the separation factor (β) for the above systems are nearly the same, as $\beta_{Lu/Yb}$ is 1.283 and 1.437 for individual and mixed systems respectively. There are the similiar results for other systems.

CONCLUSIONS

The empirical formula for the mixed two rare earths extracted with HEH(EHP) was obtained, which has the characters of easy calculation, more accuracy and fit for many systems.

The effect of phase ratio and total rare earth concentration on extraction are discussed.

Counter current extraction for the separation of (Sm,Gd) and (Ho,Er) with HEH(EHP) were carried out and satisfactory results were given.

The differences of D and β for individual and mixed rare earths are discussed.

Acknoledgement- The authors thank Lin Jingxiang, He Chunfu and Chen Zhichuan for their work.

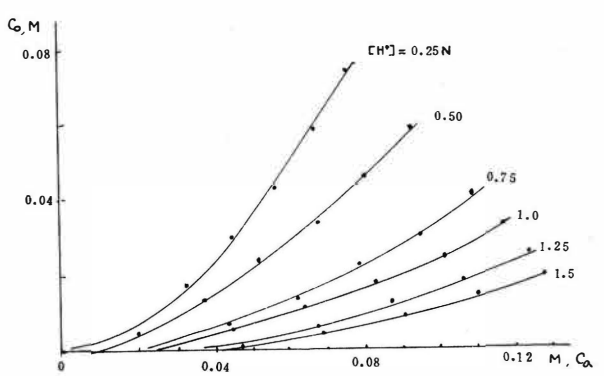

FIGURE 1. EQUILIBRIUM CURVE OF Ho FOR HEH(EHP)-KEROSENE-HNO_3-(Ho,Er) $(NO_3)_3$ SYSTEM

REFERENCES

1. This proceeding Paper No. 31h
2. Li Han, Wan Xiong, Lin Suxian, Men Shulan and Kan Xianglan. to be published.
3. Mu Guangjie, Li Han, Wan Xiong and Zhao Yanju. Rare Metals, 2, 24, (1982).
4. Li Han, Wan Xiong and Dai Zhengrong. Collected Papers of the Changchun Institute of Applied Chemistry, Academia Sinica, 18, 94 (1982).

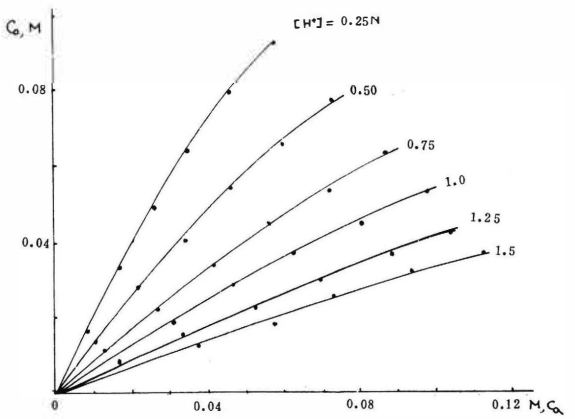

FIGURE 2. EQUILIBRIUM CURVE OF Er FOR HEH(EHP)-KEROSENE-HNO_3-(Ho,Er)$(NO_3)_3$ SYSTEM

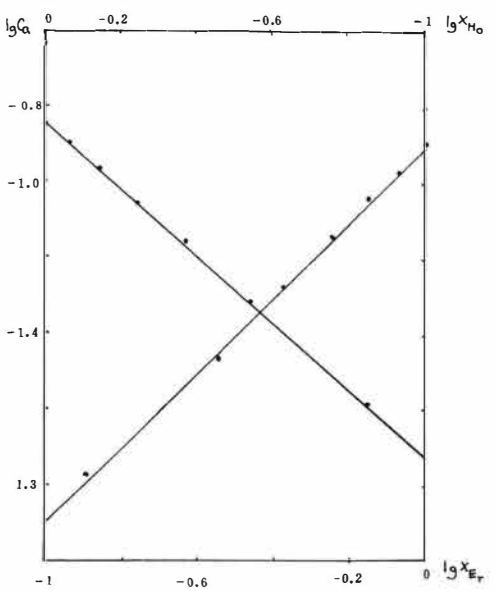

FIGURE 3. lgC_a VERSUS lgX OF HEH(EHP)-KEROSENE-HNO_3-(Ho,Er)$(NO_3)_3$ SYSTEM

SEPARATION AND PREPARATION OF GADOLIUM OF HIGH PURITY (99.99%) BY SYNERGIC EXTRACTION WITH QUARTERNARY AMMONIUM SALT AND TBP OR DI(1-METHYL-HEPTYL)METHYL PHOSPHONATE MIXED EXTRACTANTS

Chen Dian, Li Sengchung and Zhang Roufei

Department of Chemistry
Peking University
Beijing, China

Валько[1] reported, that there existed a synergistic effect when rare earth elements were extracted with quarternary ammonium salt (N_{263}) and TBP mixed extractants. Our present work further shows that the synergistic effect obviously increases the separation factor $S_{Eu/Gd}$ when N263 and TBP mixed extractants are used. The impurity Eu in Gd can be removed to less than 6 ppm by using the above mixed extractants. A synergistic effect can also be observed when N263 mixed with other neutral phosphonate ester such as di(1-methyl-heptyl)methyl phosphonate.

In the present paper the separation of Eu and Gd by means of two pairs of synergistic extractants N263-TBP-toluene and N263-di(1-methyl-heptyl)methyl phosphonate-toluene (P350) were studied.

Experimental

Trialkyl-methyl-ammonium nitrate $R_3CH_3N^+NO_3^-$ where R denotes an alkyl group containing 8-10 carbon atoms and has an average molecular weight of 450.

The experiments were carried out in a separation funnel. Equilibrations were reached within 20 min. by mechanical shaking under constant temperature 20± 0.5 °C.

The total rare earth concentration was determined by EDTA titration, while Eu was analyzed by polarographic method.

Results and discussion

1. The synergistic effect of N263-P350-toluene system

The distribution ratio (D) of Eu or Gd obviously increases by using the N263 and P350 mixed extractants. The total D is much greater than the sum of their individual D, indication a synergistic effect in above system.

2. Dependence of D and $S_{Eu/Gd}$ on pH

The effect of pH on D and $S_{Eu/Gd}$ for the N263-TBP-toluene and N263-P350-toluene system was investigated. The result is shown in Fig. 1-3. It can be seen that D increases with the pH value incresing from 1 to 2 and becomes constant from pH value 2 to 5 then increases rapidly when pH>5.

The separation factor of the two system decreases some few with increasing pH.

3. Dependence of D and $S_{Eu/Gd}$ on the concentration of TBP and P350.

The effects of the concentration of TBP and P350 on D and $S_{Eu/Gd}$ are shown in Fig. 4 and 5. It may be seen that D and $S_{Eu/Gd}$ increases with incresing concentration of TBP. The D increases also with increasing concentration of P350, while $S_{Eu/Gd}$ remains constant with incresing concentration of P350. The result shows that the synergistic effect obviously increases the $S_{Eu/Gd}$.

4. The effect of content of Eu in Gd on the $S_{Eu/Gd}$

The result is given in table 1. It shows that the $S_{Eu/Gd}$ keeps contant with the increasing concentration of Eu in Gd.

Table 1. Dependence of Content of Eu in Gd on the $S_{Eu/Gd}$

$Gd(NO_3)_3$ M	0.01923	0.01923	0.01923	0.01923
$Eu(NO_3)_3$ M	0.00399	0.00200	0.00123	0.000998
pH	2.11	2.11	2.10	2.09
D_{Eu}	0.900	0.893	0.900	0.907
D_{Gd}	0.443	0.455	0.457	0.458
$S_{Eu/Gd}$	2.03	1.97	1.97	2.01

Aqueous phase: NH_4NO_3 2.5 M

Organic phase: N_{263} 0.75 F P_{350} 0.75 M toluene as diluent

5. The effect of octanol in the organic phase on D and $S_{Eu/Gd}$

In some cases the physical property of organic phase may be improved by adding octanol to it. In order to observe the effect of octanol on D and $S_{Eu/Gd}$ value, the extraction system

Eu 5.58×10^{3} M NH_4NO_3 2M N_{263} 0.75 F in toluene
Gd 6.93×10^{3} M pH 2.2

was investigated. The result is shown in Fig. 6. It can be seen that with increasing concentration of octanol the D and $S_{Eu/Gd}$ decrease rapidly, when the concentration of octanol reaches 22% , the $S_{Eu/Gd}$ approching 1. So the addition of octanol to the organic phase is very harmful to the separtion and extraction of Eu and Gd.

6. Variation of D and $S_{Eu/Gd}$ with atomic number Z

Fig. 7 shows the variation of D with atomic number Z. It may be noted that in the N_{263}-TBP system D decreases with increases Z and Y situates between Tm and Yb. In the N_{263}-P_{350} system there appears a Pr peak, Y situates between Er and Tm.

Fig. 8 shows the separation factor S as a function of the rare earth pair. It may be seen that $S_{Eu/Gd}$ is the largest one in all of the rare earth pairs.

Based on the above experiments we took the mixed rare earth oxide as raw meterial in a counter-current extraction system using the N_{263}-TBP-kerosine system, the impurity Eu in Gd could be decreased to less than 6 ppm then by using the HDEHP as extractant to remove the trace amount of heavy rare earth, a product Gd_2O_3 of 99.99% purity were obtained.

7. Mechanism of extraction of Eu and Gd by N_{263}-TBP-toluene system

Kwang-Hsien Hsu[3] reported that the N263 existed in the form of dimer in toluene. We assume the extraction reaction to be

$$RE^{+++} + 3\,NO_3^- + n(N_{263})_{2(o)} + m\,TBP_{(o)} = RE(NO_3)_3\cdot mTBP_{(o)}$$

$$K = \frac{RE(NO_3)_3\cdot 2n(N_{263})\cdot mTBP_{(o)}}{(RE)(NO_3)^3((N_{263})_2)^n(TBP)^m_{(o)}}$$

$$\log D(\text{synergism}) = \log K + 3\log(NO_3) + n\log(N_{263})_{2(o)} + m\log(TBP)_{(o)}$$

$$= \log K + 3\log(NO_3)_3 + n\log\left(\frac{C_S - 2n(RE)}{2}\right) + m\log(TBP)_{(o)}$$

$$= \log K\ 3\log(NO_3)_3 - n\log 2 + n\log(C_S - 2n(RE)) + m\log(TBP)_{(o)}$$

where the subcript (O) stands for the organic phase, C_S is the formal concentration of the extractant N_{263}, RE^{+++} represents the rare earth ion, (RE) is the molar concentration of the extracted compound.

The experimental data obtained for the extraction of Eu and Gd by N_{263}-TBP mixture are given in Fig 9 and Fig 10. The plots of log(synergism) vs log(TBP) and logD vs log(N_{263}) were determined

The dependences are liner of slops 1 for n and 1 for m. Where D(synergism) = D(total) - D(N_{263})- D(TBP). Consequently, the extraction of Eu and Gd can be described by the following reactions:

$$RE^{+++} + 3\,NO_3^- + (N_{263})_{2(o)} + TBP_{(o)} = RE(NO_3)_3\cdot 2N_{263}\cdot TBP_{(o)}$$

8 Mechanism of extraction of Eu and Gd by N263-P350-toluene system

We assume the extraction reaction to be

$$RE^{+++} + 3\,NO_3^- + n(N_{263})_{2(o)} + mP_{350(o)} = RE(NO_3)_3 2n\,N_{263}\cdot P_{350(o)}$$

The results are shown in Fig. 11 and 12. It may be seen that n=0.5 and m=1. So the extraction of Eu and Gd by N_{263}-P_{350} system can be represented by the reaction:

$$RE^{+3} + 3\,NO_3^- + 0.5(N_{263})_{2(o)} + 2P_{350(o)} = RE(NO_3)_3 2P_{350(o)}$$

Comparing the two systems N_{263}-TBP and N_{263}-P_{350}, it may be concluded that their extraction behavior are similar but the composition of the extractable species are different. The extractable species is found to be $RE(NO_3)_3 \cdot 3N_{263}$ using N_{263} alone as extractant. When TBP or P_{350} is added to the organic phase, the TBP or P_{350} replaces a part of N_{263} from the extractable complex. The complex ability of P_{350} is large than TBP, it replaces two N_{263} and formes the extractable complex with the composition $RE(NO_3)_3 2P_{350}$, but TBP only replaces one N_{263} and forms the extractable complex with the composition $RE(NO_3)_3 \cdot 2N_{263} \cdot TBP$.

Reference

1. Вальков А. В., Известия высших учебных заведений, химия и химическая, технология, Том 21 , 542 ,1978.
2. Hsu Kwang-Hsien, et al., 1980 ISEC Held in Liege, BELGIUM Paper No. 80-82.

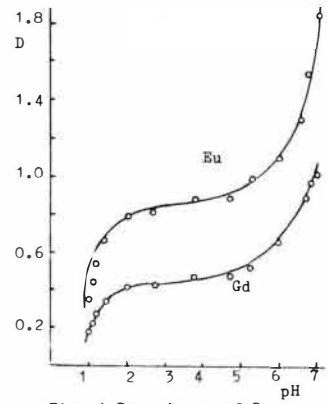

Fig. 1 Dependence of D on pH NH_4NO_3 2 M N_{263} 0.75 F TBP 0.75 M Toluene as diluent

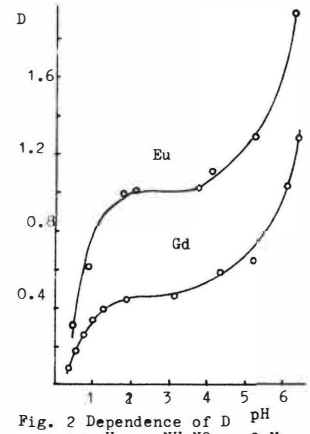

Fig. 2 Dependence of D on pH NH_4NO_3 2 M N_{263} 0.75 F P_{350} 0.40 M Toluene as diluent

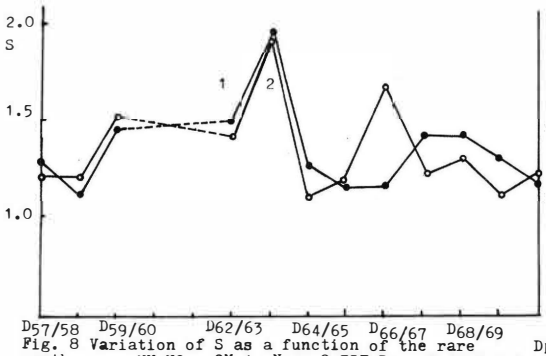

Fig. 8 Variation of S as a function of the rare earth NH_4NO_3 2M 1. N_{263} 0.75F-P_{350} 0.40 M-toluene 2. N_{263} 0.75F-TBP 0.75M-toluend

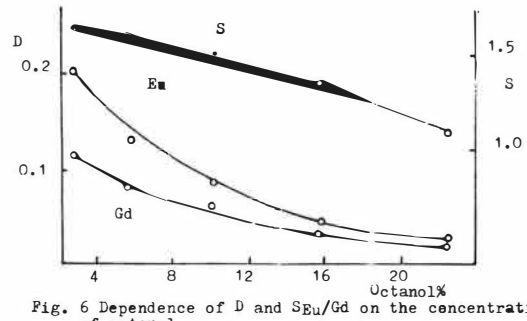

Fig. 6 Dependence of D and $S_{Eu/Gd}$ on the concentration of octanol NH_4NO_3 2 M pH 2.1 N_{263} 0.75 F Toluene as diluene

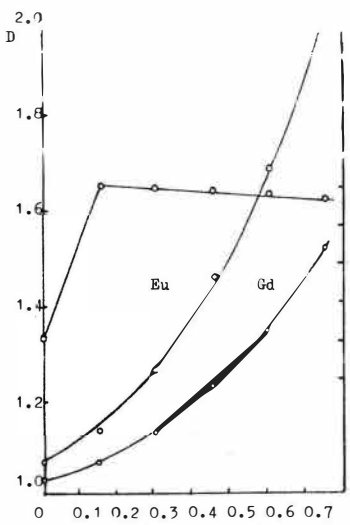

Fig. 5 Dependence of D and $S_{Eu/Gd}$ on the concentration of P_{350} NH_4NO_3 2M pH 2.5 N_{263} 0.75F Toluene as diluent

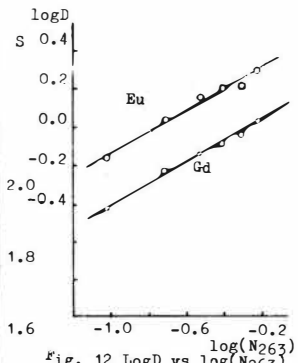

Fig. 12 LogD vs $\log(N_{263})$ NH_4NO_3 2.5 M pH 2.6 P_{350} 0.75 M Toluene as diluent

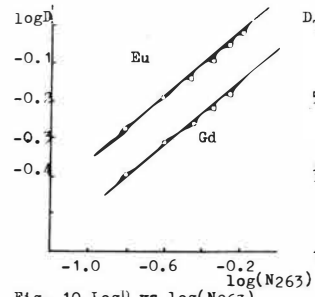

Fig. 10 LogD vs $\log(N_{263})$ NH_4NO_3 2.0 M pH 2.5 TBP 0.75 M Toluene asdiluent

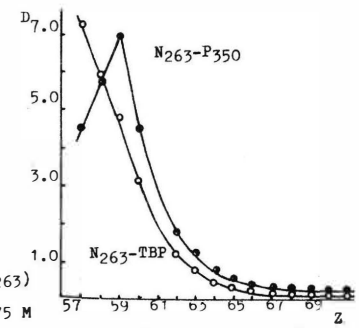

Fig. 7 Dependence of D with atomic number Z NH_4NO_3 2M pH 3.0 N_{263} 0.75 F P_{350} 0.40 M Toluene as diluent

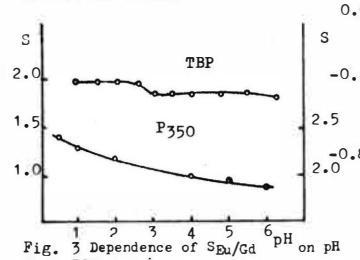

Fig. 3 Dependence of $S_{Eu/Gd}$ on pH N_{263}-TBP-toluene N_{263}-TBP-toluene

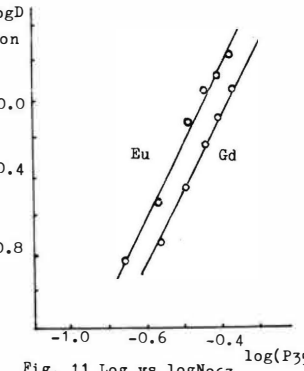

Fig. 11 Log vs $\log N_{263}$ NH_4NO_3 P_{350} 0.75 M Toluene

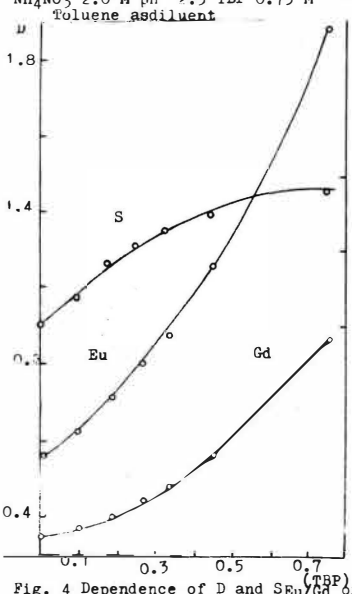

Fig. 4 Dependence of D and $S_{Eu/Gd}$ on the concentration of (TBP) NH_4NO_3 2M N_{263} 0.75F Toluene as diluent

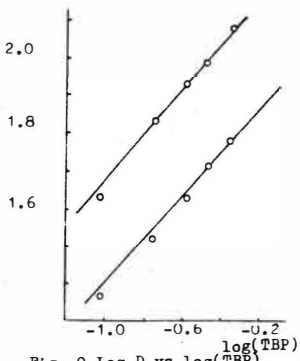

Fig. 9 Log D vs log(TBP) NH_4NO_3 2 M N_{263} 0.75 F Toluene as diluent

A PROCESS FOR THE DEPHOSPHORIZATION OF IRON ORES

I. Grenthe, M. Muhammed and Y. Zhang*

Department of Inorganic Chemistry
The Royal Institute of Technology
S-100 44 Stockholm, Sweden

*Permanent address: Department of Chemical Engineering Wuhan Chemical Engineering Institute, Wuhan, People's Republic of China.

Some Swedish iron ores have a high phosporous content, 0.1% or more. The phosphorous is present as apatite grains or seams in the ore and can be removed by flotation of the crushed and ground material. This is then converted into pellets.

Phosphorous can also be removed by chemical leaching of the crushed ore (sinterfine). The process outlined below has been developed and tested in laboratory scale, some optimization and cost-analyses have also been performed.

The ore is leached with HNO_3 in order to dissolve apatite. After washing and neutralization, a material containing less than 0.05% P is obtained. The alkali content decreases with approximately 50% during the leaching procedure. The product has excellent sintering properties.

In order to improve the process economy, it is necessary to regenerate the HNO_3 and to recover the phosphorous as products of high value (phosphoric acid or ammonium phosphate). H_3PO_4 and excess HNO_3 can be recovered from the leach solution through extraction processes. Three different extractants, butanol, isoamyl alcohol and TBP have been studied extensively, both in batch and continuous (mixer-settler) tests. The acids are selectively extracted into the organic phase, leaving most of the salts in the raffinate. After a scrubbing to remove salts, the organic phase is stripped with water. The aqueous phase contains H_3PO_4 and some extractant which may be separated by distillation or by using a second extraction system. Two such systems methyl-isobutyl ketone and butyl acetate have been tested.

The raffinate from the first extraction containing mainly HNO_3, nitrates and a small amount of H_3PO_4 is treated with H_2SO_4 in order to regenerate the leaching acid. The gypsum formed is filtered and washed prior to disposal. The regenerated acid is concentrated by distillation and is then recycled to the leaching step.

PILOT-PLANT INVESTIGATION ON H_2SO_4 EXTRACTION BY ALCOHOLS FROM SPENT ELECTROLYTES

Dante Buttinelli, Carlo Giavarini, Andrea Mercanti

Department of Chemical Engineering and Metallurgy
University of Rome
Rome, Italy

Generally, industrial waste acidic solutions such as spent electrolytes contain sulphuric acid in high concentrations, up to 250 g/l or more, and various amounts of metallic ions. It seems reasonable to forecast that future hydrometallurgical processing may recover such metals by selective solvent extraction (1-3).The use of many extractants, such as DEHPA and low-cost carboxylic acids, gives rise to some problems owing to the necessity of partially neutralizing the solutions before metal extraction, with consequent higher costs, sludge formation and metal losses. In any case, the acidic waste liquor is to be neutralized before it is discharged.

In the present work the possibility was taken into account of extracting the acid before the metals. Considering the relatively low cost of H_2SO_4 , its recovery would probably not be of interest unless we consider the above-mentioned problems of neutralization and the possibility of employing, after acid extraction, low-cost solvents capable of recovering metals in the medium pH range ($\geq$ 5).

The problem of acids extraction has been considered both in the nuclear industry (extraction of nitric acid with TBP)and in the chemical industry, where many processes have been proposed for extraction and purification of phosphoric acid with solvents (4). A few data are known concerning H_2SO_4 : besides amines and alcohols, TBP also seems suitable for extraction, but only from extremely concentrated solutions.

BATCH TESTS

Initial extraction data were obtained from batch shake-out tests by using equal portions of organic and aqueous solution. An industrial electrolyte was used with the following composition (g/l):

232 H_2SO_4; 14.5 Zn ; 17.3 Mg ; 1.4 Mn and

minor amounts of Fe, Cu, Cd, Ni, As, Sb. The stripping solution was distilled water. Following a first series of tests during which many solvents were experimented, analytical grade isobutyl-alcohol (IBA) and isoamyl alcohol (IAA) were selected to continue the experimental work, thanks to their relatively good extraction capacity, low cost, easy regenerability and recovery.

Figure 1 shows, for the industrial electrolyte, the dependence of the distribution coefficient, $D_{H_2SO_4}$, on the initial concentration of the acid in the aqueous phase. From these data we can reasonably forecast that in an industrial operation the recovery of the acid will not be complete. The negative effect of the temperature on the equilibrium was negligible in the 15-35°C range, but became appreciable at higher temperatures.

The mixing times necessary to achieve equilibrium were in the 2-3 minute range for both alcohols; the phase disengagement times were 1-2 minutes at room temperature. Acid stripping by water was possible also by employing organic/aqueous (O/A) ratios higher than during the extraction, in order to obtain more concentrated solutions. The selectivity of the solvent was quite good: in the stripped acidic solution only a few mg/l of Zn, Mg and Mn were detected.

PILOT-PLANT CONTINUOUS TESTS

Further investigations were then carried out at room temperature on a small-scale continuous pilot-plant which consisted of a battery of sixteen mixer-settlers mod. ERIES AT-1, eight for the extraction steps and eight for the stripping steps (Figure 2). The flow-rate of the two phases was 3-4 litres/hour. The electrolyte was the same as in the batch tests; the alcohols (commercial grade IBA and IAA furnished by C. ERBA) were saturated with H_2O before use in order to avoid strong volume variations of the phases, due to mutual solubility.

The pilot plant worked continuously for about six months, four with IBA and two with IAA. During some preliminary runs the O/A ratio (referred to inlet phase volumes) was periodically changed to achieve good extraction yields and a satisfactory H_2SO_4 loading charge of the alcoholic phase. The results of a series of short runs performed with 6-8 extraction steps by using IBA are reported in table 1; it is evident that it is more convenient to work with high O/A ratios during extraction.

A considerable change in phase volumes was observed : during extraction the organic-phase volume was reduced by 7-10% and the electrolyte volume increased to over 15% due to the losses of alcohol by solubility in aqueous phase and to the H_2SO_4 solvent effect. These volume variations entailed some difficulties in O/A ratio control and in step-to-step material balance calculations.

TABLE 1

O/A ratio (inlet phases)	3.5	6	8.5	10.5
H_2SO_4 in raffinate (g/l)	97.5	63.9	40.2	33.1
H_2SO_4 in solvent (g/l)	39.3	31.3	21.4	17.7
H_2SO_4 extr. yields (%)	59	73	83	86

Figure 3 shows the pseudo-equilibrium curves of long-term runs in pilot-plant ; together with table 1 it indicates that H_2SO_4 can be extracted leaving a minimum residual content in the electrolyte of 15-20 g/l, by using a high O/A ratio; however, the corresponding acid concentration in the solvent is quite low.

If H_2SO_4 extraction is considered as a part of a process for metals recovery from electrolytes (i.e. Zn and Mn in this case) a choice must be made between the opposite necessities of leaving a low H_2SO_4 content in the extracted electrolyte or of obtaining a sufficient acid concentration (~ 3N) in the aqueous solution from stripping. This is shown in the test runs reported as an example in Figure 4. It is evident that IAA needs more extraction steps and less stripping steps than IBA.

ACID PURITY

As confirmed in previous bach tests, alcohols should not, in practice, extract metallic ions from electrolytes; however, appreciable amounts of Zn and Mg (100-150 ppm) and of Mn (up to 20 ppm) were found in the H_2SO_4- solution, probably due to transport phenomena.

If this solution is then used for stripping the zinc recovered in a successive extraction stage, no purification is necessary. When an higher purity is required, it can be obtained by a water-scrubbing step before the solvent stripping ; after this scrubbing step Zn and Mg content drops to 15-10 ppm and Mn to 1-2 ppm, as it was experimentally observed.

SOLVENT LOSSES

IAA and, especially, IBA show a high solubility in water which decreases in salt solutions. Alcohol losses due to the solubility in the aqueous raffinate and in H_2SO_4 stripped solution, determined by gas chromatography, are reported in Table 2.

TABLE 2

	Alcohol conc. (g/100 g) in :	
	Aq. raffinate	H_2SO_4 solution
I.B.A.	2.9 - 4.1	5.5 - 6.5
I.A.A.	1.2 - 1.4	1.9 - 2.1

Considering these values, a recovery of both alcohols is necessary; this can be effected by distillation as in H_3PO_4- Phorex process (5). In our case alcohol recovery was provided for only in H_2SO_4 solution. The recovery from aqueous raffinate is probably not necessary if a subsequent neutralization step is to be provided. In fact, it was observed that during neutralization of the raffinate 50-60% of dissolved solvent was recovered, owing to the decreased solubility of the alcohol. Total solvent losses were extimated to be in the range 1.0 - 1.5% for IBA and less than 1.0 for IAA.

CONCLUSIONS

The possibility has been confirmed of extracting H_2SO_4 with isobutyl and isoamyl alcohol from spent electrolytes. To obtain good extraction yields (i.e. 85%) a high O/A ratio and a sufficient number of stages (6-8) is necessary.

The acid recovery is of interest if we consider, in a second step, the solvent extraction of the metals contained in the electrolyte; in this case we can use low-cost solvents for metals recovery, thus avoiding many neutralization problems.

The most effective of the two alcohols for acid extraction is IBA, which is also the cheapest.

Solubility losses are lower for IAA; however, a recovery by distillation must be provided also for IAA. Therefore, we can conclude from our experimental work that IBA is the preferable extractant for H_2SO_4.

REFERENCES

1- A.W. FLETCHER, D.S. FLETT in " Solvent Extraction Chemistry of Metals", H.A.C. Mc.Kay, T.V. HEALY, T.L. JENKINS, A. NAYLOR, MAC. MILLAN, London 1965, p. 359.

2- G. THORSEN, A. GRISLINGAS, J. OF METALS, 1, 24 (1981)

3- D. BUTTINELLI, C. GIAVARINI, Chem. Ind., London, 6, 395 (1981)

4- R. BLUMBERG in " Solvent Extraction Reviews", Y. MARCUS Vol. 1 DEKKER, New York 1971, p. 93.

5- J. BERGDORF, R. FISCHER, CEP 74, 11, 41 (1978)

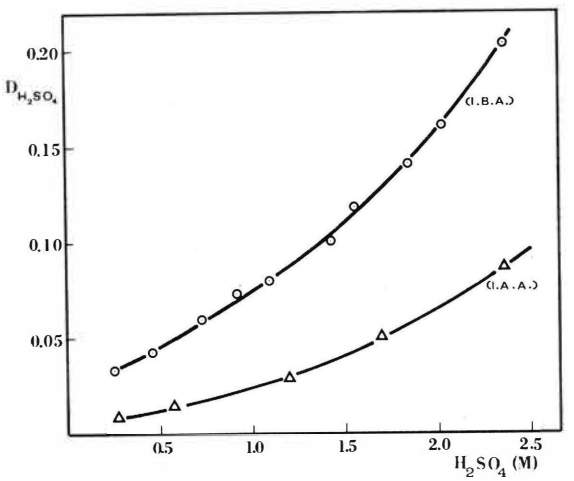

FIG. 1 - EFFECT OF ACID CONCENTRATION ON H_2SO_4 DISTRIBUTION COEFFICIENT AT 20°C (BATCH TESTS).

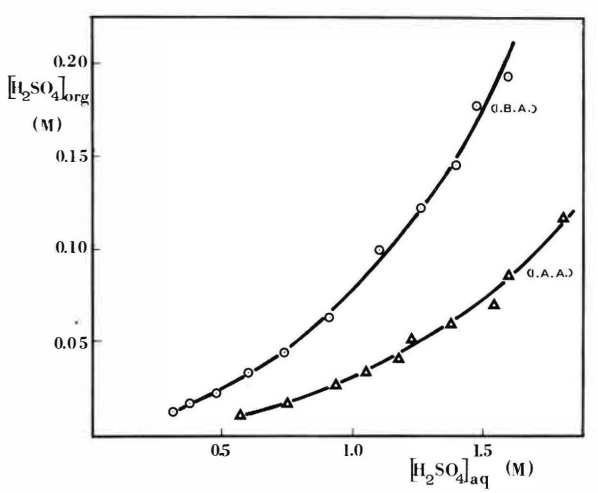

FIG. 3 - EQUILIBRIUM DISTRIBUTION OF H_2SO_4 AS DETERMINED IN PILOT -PLANT TESTS.

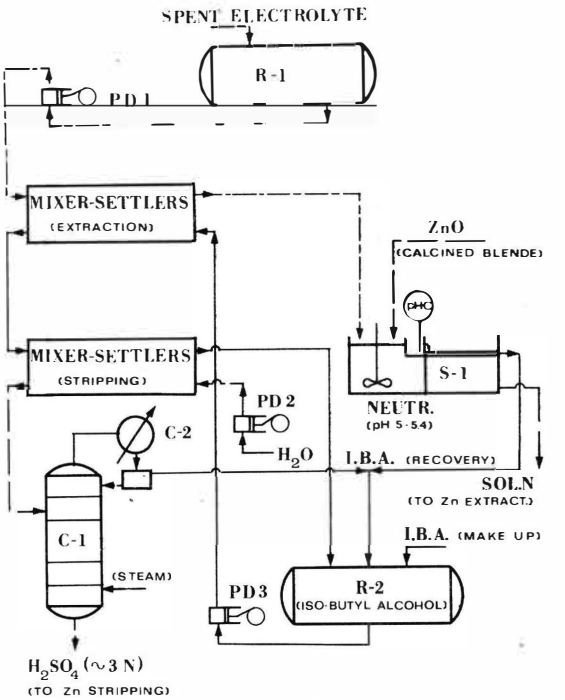

FIG. 2 - FLOW-SHEET OF THE H_2SO_4 EXTRACTION PILOT - PLANT PD-1/2/3: FEED PUMPS; C-1 ALCOHOL DISTILLATION COLUMN; C-2 CONDENSER; R-1/2 TANKS WITH LEVEL INDICATORS; S-1 : SETTLING TANK.

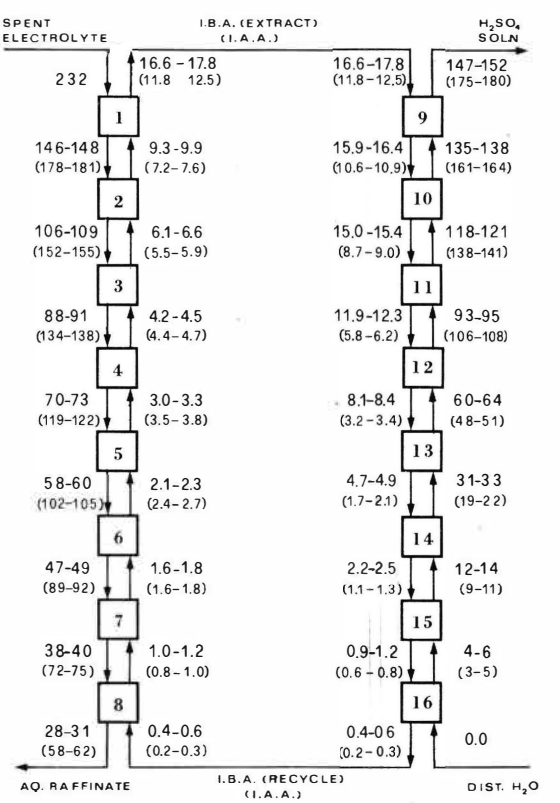

FIG. 4- ACID CONCENTRATION (g/1) PROFILE OF AN INDICATIVE PILOT-PLANT RUN WITH IBA AND IAA (IN BRAKETS).

1-PHENYL-3-METHYL-4-ACYLOXIMEPYRAZOL-5-ONES AS CHELATING EXTRACTANTS

Amrit N. Patel

Department of Chemistry
University of Nigeria
Nsukka, Anambra State, Nigeria

INTRODUCTION

The separation study of divalent nickel, cobalt, copper and manganese by the solvent extraction methods using various extractants (1-4) including β-diketones (4-7) and O-hydroxy aryl oximes (8-13) is receiving greater attention from several researchers in view of the industrial importance of these metals. In continuation of solvent extraction studies of these metals with 1-phenyl-3-methyl-4-benzoylpyrazol-5-one (PMBP.OH) (14-15), this paper reports the solvent extraction behaviour of these metals with the oximes PMBP.OH, namely 1-phenyl-3-methyl-4-benzoyloximepyrazol-5-one (PMB.NOH.P.OH) and 1-phenyl-3-methyl-4-acetyloximepyrazol-5-one (PMA.NOH.P.OH) dissolved in carbon tetrachloride from the aqueous chloride, sulphate and nitrate systems in the range of acid concentration from 0.1M to 4.0M. The isomeric structures of the oxime derivatives and the composition of the extracted complex species have been discussed.

EXPERIMENTAL

All chemicals used in this study were of standard reagent quality. The extractants, PMB.NOH.P.OH and PMA.NOH.P.OH were prepared by the methods described in the literature (16,17,24).

0.02M solutions of the oximes in carbon tetrachloride served as the organic phase. The stock solutions of 0.01M metal ions concentration of nickel(II), cobalt(II) and manganese(II) were prepared by dissolving appropriate salts in aqueous acid solutions of required molarity.

Two equal volumes (25 ml.) of the organic and aqueous phases were shaken for about 30 minutes at 25°C. The metal ions concentrations in the aqueous phases were determined by the complexometric titration with EDTA (18) and those in the organic phases were checked by a method where a known volume (20 ml.) of the organic phase was evaporated to dryness, followed by addition of concentrated hydrochloric acid (5 ml.) and evaporation to dryness again. The residue was dissolved in dilute hydrochloric acid and made up to 25 ml. The metal ion concentration was determined as in the case of the aqueous phase.

The solid metal complexes were isolated by evaporating the organic phases under reduced pressure and by addition of a small quantity of ether. The metal complexes were analysed for metal and nitrogen contents. The analysis indicated the stoichiometric ratio of 1:2 for M:OPB.NOH.MP (M = Ni(II), Co(II), Mn(II) and PMB.NOH.P.O, an anion).

The infrared spectra of the extractants and the complexes were recorded using the Nujol mull technique on a Perkin Elmer infrared model 257 spectrophotometer.

RESULTS AND DISCUSSION

The oxime derivatives, PMB.NOH.P.OH and PMA.NOH.P.OH are likely to exist predominately in the two isomeric forms as shown in Figure 1, although other possible isomeric forms could not be ruled out. The intramolecular hydrogen bonding, the nature of the acyl group, R-CO-, the conjugative effect and the spectroscopic data favoured these two isomeric forms of the oximes. If R is a phenyl group, the hydrogen bonding effect between the hydrogen of the =NOH group and the π electrons of the phenyl group (19) will help to stabilise the enolic structure (II) in Figure 1, thereby leading a better condition for complex formation with metal ions. The structure (II), and α- form of the monoxime, allows co-ordination of the metal ions via oxygen of the C=C-OH group and nitrogen of the =NOH group. Thus a six membered ring complexes will be formed.

The syngeric effect (20,21) of the inert diluents has been reported to increase in the order of cyclohexane > hexane > carbon tetrachloride > benzene > chloroform. Among these diluents, carbon tetrachloride being in the middle of the order and having a large density differnece with water, was selected as a solvent in order to enhance the separation of the aqueous phase from the organic phase.

Since nonpolar solvents usualy extract monpolar or neutral species from polar media, the extraction of metal chelates from highly polar aqueous media with carbon tetrachloride postulates the formation of a neutral complex. The extraction reaction of PMB.NOH.P.OH dissolved in carbon tetrachloride for the divalent metal ions may be represented as

$$M^{2+}_{aq} + [\overline{M}PB.NOH.P.OH]_{org} \rightleftharpoons [\overline{M}(PMB.NOH.P.O)_2]_{org} + 2H^+_{aq} \quad (1)$$

where, M = Ni (II), Co (II) and Mn (II).

The distribution ratio, D, expressed as:

$$D = \frac{[\overline{M}(PMB.NOH.P.O)_2]_{org}}{[M^{2+}]_{aq}} \quad (2)$$

is related to the per cent extraction, E:

$$D = \frac{E}{100 - E} \quad (3)$$

The results of the extraction studies for the three metal ions with PMB.NOH.P.OH dissolved in carbon tetrachloride are summarised in Table 1.

Table 1. Per cent extraction of metal ions

Metal ions concentrations in the aqueous phase, 0.01M, PMB.NOH.P.OH concentration in the organic phase, 0.02M.

A HCl, M Initial	Per cent extraction Ni (II)	Co (II)	Mn (II)
0.5	61.60	38.50	10.50
1.0	62.50	36.30	10.65
1.5	62.90	36.40	10.85
2.0	63.50	36.20	10.10
3.0	66.60	36.10	7.90
4.0	65.30	36.00	7.80

B H_2SO_4,M Initial	Per cent extraction Ni (II)	Co (II)	Mn (II)
0.5	63.00	26.50	8.00
1.0	70.20	24.00	5.90
1.5	73.50	19.50	4.80
2.0	68.90	15.75	4.00
3.0	65.90	13.65	3.50
4.0	65.00	11.90	3.00

C HNO_3,M Initial	Per cent extraction Ni (II)	Co (II)	Mn (II)
0.5	55.85	27.90	12.50
1.0	56.50	27.20	12.00
1.5	56.80	24.90	13.80
2.0	54.30	21.00	13.70
3.0	54.00	20.40	13.50
4.0	53.60	18.70	11.00

The per centage extraction values for nickel (II) ions with PMB.NOH.P.OH are found to be high compare to those of cobalt (II) and manganese (II) ions. The per centage extraction values for these metal ions with PMA.NOH.P.OH were found to be lower than 35.00, 18.00 and 10.00 for nickel (II), cobalt (II) and manganese (II) respectively. This can easily be explained by a fact that PMA.NOH.P.OH is likely to exist in the β-form in the absence of hydrogen bonding effect between the hydrogen atom of the =N.OH group and the CH_3- group. It is also known that the β-form of monoximes does not form complexes with metal ions very easily. The β-form of PMA.NOH.P.OH is likely to be stabilised by the hydrogen bonding effect due the hydroxyl groups of the C=C-OH and =N.OH groups present in the molecule.

The infra-red spectra of the reagent PMB.NOH.P.OH and its complexes with the metal ions are quite complex, due to the presence of a number of functional groups, viz: C=O, C=C, C=N, =N-N=, C=N-OH, C=C-OH and $-C_6H_5$ as well as their conjugative effects. The infra-red band around 3380-3200 cm^{-1} indicated the presence of hydrogen bonded hydroxyl group in PMB.NOH.P.OH. however, this band disappeared in the IR spectra of the complexes, thereby indicating the removal of hydrogen of the hydroxyl group, C=C-OH during the complex formation. Also the IR band near 1635 cm^{-1} in the parent ketone for the carbonyl group is absent in the IR spectrum of the oxime, thereby supporting the enolic structure (II) for the extractant. The IR bands about 1580 and 1535 cm^{-1} in the spectrum of the reagent were assigned to the C=N linkage of the oxime group and the pyrazolone ring respectively. The frequency of the IR band at 1550cm^{-1} for the C=N-OH group was observed to shift about 1535cm^{-1} on complex formation. The IR band near 1020cm^{-1} observed in the IR spectra of the reagent and metal complexes may be assigned to the N-O linkage. The new IR band at 910 cm^{-1} in the IR spectra of the metal complexes may be assigned to the -M-O- bond (22,23,24).

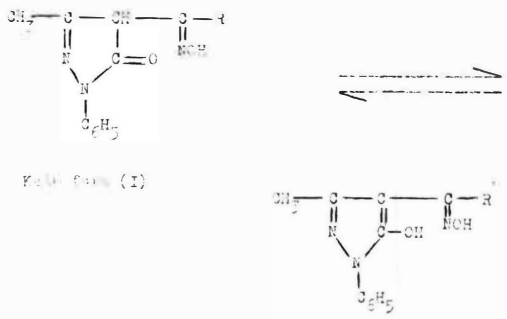

Figure 1. Keto-enol forms of 1-phenyl-3-methyl-4-acyl oximepyrazol-5-one.

REFERENCES

1. A.K.De, and A.K. Sen, Separation Sciences, 1(5), 641(1966).
2. D.S. Flelt and D.R. Spink, Hydrometallurgy, 1, 207(1976).
3. D.S. Flelt, Chemistry and Industry, September, 706(1977).
4. J.B. Barnes, J.H. Setchifield and J.O. Williams, J. Inorg. Nucl. Chem. 38, 1065(1976)
5. T. Sekine, S. Iwahori and R. Murai, J. Inorg. Nucl. Chem., 38,363(1977)
6. K. Akaiwa and H. Kawamoto, J. Inorg. Nucl. Chem., 81, 1141(1969).
7. R. Murai, K. Kurakane and T. Sekine, Bull Chem. Soci. Japan, 49, 335(1976)
8. S. Dobson and A.J. Van der Zeeuw, Chemistry and Industry, 175 (1975).
9. M.A. Hughes, Chemistry and Industry, 1042(1975).
10. R.F. Dalton, F. Houxwell and J.A. Tumilty, Chemistry and Industry, 181(1976).
11. A.J. Van der Zeeuw and R. Kok, Proceedings, ISEC '77, CIM Special vol. 21, 17(1979).
12. R.F. Dalton, Proceedings, ISEC '77, CIM special vol. 21,40(1979).
13. C.A. Fleming et al., Proceedings, ISEC'77, CIM special vol.21, 193(1979).
14. A.N. Patel, Z. Naturforsch, 34B, 44 (1979).
15. A.M. Patel, Proceedings, ISEC'80, vol.3, 80-190(1980).
16. B.S. Jensen, Acta. Chem. Scand., 13, 1668(1959).
17. A.I. Vogel, A. Text Book Practical Organic Chemistry, Longman (London), 1978.
18. A.I. Vogel, A. Text Book Quantitative Inorganic Analysis, 4th Ed., Longman (London), 1978.
19. B. Sen and D. MaCone, J. Inorg. Nucl. Chem., 34, 3509(1972).
20. G. Duyckaerts and J.P. Desreux, Proceedings, ISEC'77, CIM special vol. 21, 73 (1977).
21. K. Akiba, J. Inorg. Nucl. Chem., 35, 2525, 3323 (1973).
22. G.N. Rao and H.C. Arora, J. Inorg. Nucl. Chem., 39, 2057(1979).
23. B. Tamhina and M.J. Herak, J. Inorg. Nucl. Chem., 39, 391(1979).
24. A.K. Rana and J.R. Shah, Indian J. Chem., 20A, 142 (1981).

SOLVENT EXTRACTION OF METALS WITH SOME SCHIFF BASE LIGANDS

G. N. Rao and A. Varadarajulu

Indian Institute of Technology Delhi
New Delhi, India

Solvent extraction of metals with schiff base ligands has not been exhaustively studied so far. Some of the analytical applications of schiff base ligands have been reviewed (1). Extraction of copper (II) by some quadridentate schiff base ligands has been investigated by Aggett and Richardson (2,3). Though salicylidene aminothiophenol and salicylidene aminophenol have been used in some spectrophotometric and colorimetric determinations no systematic study of metals with tridentate schiff base ligands has been published so far. In this paper the results of our studies on the extraction of copper (II), cobalt (II) and nickel (II) with several tridentate schiff base ligands are reported.

EXPERIMENTAL

Tridentateschiff base ligands salicylidene aminothiophenol (H_2A), naphthalidene aminothiophenol (H_2B), naphthalidene aminophenol (H_2C) and salicylidene aminopyridine(HD) were synthesized using standard methods adopted in the preparation of schiff base ligands. Melting points of the ligands are 135°C, 142°C, 256°C and 52°C respectively for H_2A, H_2B, H_2C and HD. Melting points are uncorrected and the estimated error is ± 2°C Their purity was established from analytical data (carbon, hydrogen and nitrogen) and infrared spectrophotometry. Salicylaldehyde, 2-hydroxy-1-naphthaldehyde, O-aminophenol, O-aminothiophenol and 2-aminopyridine were procured from B.D.H. England and Adrich Co. U.S.A. and were purified before use by distillation and recrystallization. Benzene, chloroform, methanol were purified employing standard techniques. Buffer solutions were prepared from sodium acetate, acetic acid, ammonia and ammonium chloride depending on the pH range required in the experiments. For spectrophotometric measurements Bausch-Lomb spectrophotometer was used and the pH measurements were carried out using an Elico pH meter. Ten milliliters of the aqueous phase containing the metal ion and the buffer was mixed with equal volume of the organic phase containing the requisite amount of the tridentate schiff base ligand. Stoppered bottles containing the two phases were shaken in a mechanical shaker for one to three hours at 30 ± 2°C. In each system equilibration time was determined from preliminary experiments. In all the experiments the ionic strength was maintained at 0.10 M in the aqueous phase. After separating the two phases the concentration of the metal ion was determined using sodium diethyl dithiocarbamate method for copper(II), sodium nitroso-R-salt method for cobalt (II) and dimethyl glyoximate method for nickel(II). Some of the results were checked afterwards by determining the metal ion concentration with pye unicam SP 191 atomic absorption spectrophotometer. Distribution ratio D_o was calculated as the ratio of the total metal(II) concentration in the organic phase to that in the aqueous phase.

RESULTS AND DISCUSSION

To find out the nature of the species extracted and also to determine the equilibrium constants for the extraction equilibria two sets of experiments were performed- (1) variation of the ligand concentration keeping the pH constant, (2) variation of the pH keeping the ligand concentration constant. Slope of the plot of the concentration of ligand at equilibrium versus log D_o from set (1) gives the number of ligand molecules attached to the metal atom in the extract speces. Similarly slope of the plot of log D_o versus pH from set (2) gives the number of hydrogen ions released in the extraction process. This is the standard approach adopted by many workers and the approximations inherent in this approach have been summarized by Marcus and Kertes in their book (4). From such investigations the mechanism of the extraction process could be represented in the systems where the slope of the plots in sets (1) and (2) is two $M^{2+}(aq) + 2\,HL\,(org) \xleftrightarrow{Kex} M(L)_2\,(org) + 2H^+(aq)$ where M^{2+} represents the metal ion and HL the ligand. It can be easily shown that log Kex is related to D_o, $[HL]$ and pH in such cases by the equation.

$$\log D_o = \log K_{ex} + 2 \log [HL]_{org} + 2\,pH$$

Values of K_{ex} obtained in the systems studied are listed in table 1.

Though several factors such as solubility and stability of the ligand in aqueous and organic phases etc. have to be considered for a full comparison, it is possible to compare the effectiveness of two ligands for the extraction of a particular metal if K_{ex} data is available under identical or near identical conditions of extraction (i.e. solvent, temperature, etc.) A perusal of the data shows that K_{ex} values with the two ligands containing sulphur as donor atom are of the same order as that observed with thenoyl trifluoroacetone(4).

The schiff base ligands may be broadly classified in the following order on the basis of K_{ex} values.

Salicylidene aminothiophenol > naphthalidene aminothiophenol > Naphthalidene aminophenol > salicylidene aminopyridine

The order with respect to metal ions is broadly Cu(II) > Ni(II) > Co(II).

However one of the disadvantages of the tridentate schiff base ligands is the relatively low solubility of the ligands and metal complexes formed by them in noncoordinating solvents like benzene and carbontetrachloride. By using coordinating solvents like isoamylalcohol and methyl isobutyl ketone considerable amount of improvement in this direction resulted. Addition of synergistic ligands such as heterocyclic-N-bases, phosphorus esters and substituted sulphoxides also helps and the extraction of metals is considerably enhanced. Zolotov and coworkers[5] employed a mixture

of chloroform and iso-amylalcohol to overcome the same difficulty in their extraction studies with 1-phenyl 3-methyl 4-benzoyl 5-pyrazolone. However, benzene (or chloroform) was used as solvent here since the literature data with other ligands is available in benzene medium mainly.

Attempts made to extract copper(II), cobalt(III), nickel(II) and zinc(II) with salicylidene aminophenol into benzene as solvent met with little success, though extraction was observed in presence of pyridine. Several other schiff base ligands were also prepared initially by condensing O-aminophenol or O-aminothiophenol with acetyl acetone, benzil, benzoin and acetophenone. But they did not offer any advantage over the ligands finally chosen for this work. It appears that the tridentate schiff base ligands would be particularly valuable in other analytical applications like spectrofluorometric determination of elements like aluminium.

It has been observed that stability constants of palladium(II) platinum(II), gold(III), copper(I), silver (I) and mercury(II) complexes with sulphur ligands are very high. Being typical(b) class metals they can form $d\pi - d\pi$ bonds by donating electron pairs to the ligands while forming strong bonds with soft ligands. All schiff base ligands with sulphur donor atoms, contain nitrogen donor atoms also due to the inevitable presence of C = N bond in such compounds. Nitrogen atoms tend to lower the solubility of complexes in non coordinating solvents. In solvent extraction, this low solubility is not advantageous and schiff base ligands would be of advantage in special cases rather than as general reagents like β-diketones.

A systematic study of the extraction of several metal ions with salicylidene aminothiophenol was carried out and the main results could be summarised as follows(6):

(6) A. Varadarajulu Ph.D. thesis, Analytical applications of schiff base ligands and studies in synergistic extraction, I.I.T. Delhi, (1977).

TABLE (1)

Extraction data with tridentate schiff base ligands (30°C, μ=0.1)

Name of the schiff base	Extraction constant			Solvent
	Cu(II)	Co(II)	Ni(II)	
1. Salicylidene aminothiophenol	-	-5.70	-5.20	benzene
2. Salicylidene aminopyridine	-5.6	-12.5	-12.2	benzene
3. Naphthalidene aminophenol	-9.70	-10.5	- 4.9[a]	chloroform
4. Naphthalidene aminothiophenol	-	- 3.25[a]	- 3.2[a]	chloroform

[a] Extracted species of ML type where L is the anion of the ligand.

(a) Metal ions which could be quantitatively extracted under certain pH ranges-lead(II) (8.0 to 8.5), cadmium(II) (7.0 to 10.0), mercury(II) (3.5 to 8.5), vanadium(V) (1.0 to 4.5), cerium(IV) (2.0 to 4.0), cobalt(II) (5.5 to 7.3), and nickel (II) (6.5 to 8.5)

(b) Metal ions with a percentage extraction in the range 50 to 90 calcium(II), lanthanum(III), aluminium(III), thorium(IV), Zinc(II), zirconium(IV), uranium(VI), molybdenum(VI) and tungsten(VI).

(c) Metal ions with a percentage extraction less than 50 - iron(II), iron(III), manganese(II), beryllium(II), chromium(III) and silver(II).

CONCLUSIONS

Tridentate schiff base ligands show promise as reagents for solvent extraction. Selectivity is good with ligands containing sulfur as a donor atom. Solubility of these ligands in nonpolar solvents is low but it could be increased by using coordinating solvents. These ligands are also useful as spectrophotometric and fluorimetric reagents for the estimation of some metals.

REFERENCES

(1) E.Jungreis and S. Thabet in "Chelates in analytical Chemistry, Volume 2" edited by H.A. Flaschka and A.J. Barnard Jr. Marcel Dekker, New York, (1966).

(2) J. Aggett and R.A. Richardson, Anal. Chim. Acta, 50, 269, (1970).

(3) J. Aggett and R.A. Richardson, Anal. Chim. Acta 51, 528 (1970).

(4) Y. Marcus and A. S. Kertes, Ion exchange and solvent extraction of metal complexes P, 509 Wiley, New York(1969).

(5) Yu.A. Zolotov, Extraction of chelate compounds P-228, Ann Arbor-Humphrey Science Publishers, London(1970).

ON THE MECHANISM OF THE MUTUAL INFLUENCE OF METALS IN THEIR EXTRACTION WITH GAS NITRATES

Yu A. Zolotov, V. V. Bagreev and S. O. Popov

V. I. Vernadsky Institute of Geochemistry
and Analytical Chemistry, Academy of Sciences
Moscow, USSR

When the simultaneous extraction of the micro- and macro-amounts of elements with long-chain amines and quarternary ammonium salts (QAS) is took place, a decrease in the microelement extraction (i.e. suppression of the microelement extraction) has been shown to occur (1). To explain the mechanism of this phenomenon it is necessary to know the state of simple and metal-containing QAS in extracts. The dissociation of ion-pairs in an organic diluent and their molecular aggregation to dimers and other multimers frequently greatly affects the metal extraction suppression.

In the present work the thorium or iron concentration dependence of the distribution quotient of the microelements has been investigated for rare earths at their concentrations about 10^{-5} M which distributing between lithium nitrate and trioctylalkylammonium nitrate (with alkyl radicals C_1- C_8) solutions using benzene, toluene, nitrobenzene and nitromethane as organic diluents. The most probable mechanism of the extraction suppression in the investigated system is considered.

THEORETICAL EXPRESSIONS

The extraction of rare earths as their nitrates by QAS nitrates may be represented by the following equations (2)

$$n\,R_4NNO_{3(org)} + Ln(NO_3)_{3(aq)} \xrightarrow{K_{ex}} (R_4N)_nLn(NO_3)_{3+n}$$

$$n\,R_4NNO_3 + (R_4N)_nLn(NO_3)_{3+n} \xrightarrow{K_{sol}} (R_4N)_nLn(NO_3)_{3+n}R_4NNO_3$$

.....

$$R_4NNO_3 + (R_4N)_n\,Ln(NO_3)_{3+n}(R_4NNO_3)_{L-1} \xrightarrow{K_{sol}} (R_4N)_nLn(NO_3)_{3+n}(R_4NNO_3)_L$$

.....

(where K_{ex} is the extraction constant and K_{sol} is the constant of the additional solvation of the metal-containing alkylammonium salt by free extractant). It is supposed as a first approach that the constants of the additional solvation, K_{sol}, are to be equal numerically to the aggregation constants of the simple QAS molecules, K_{agg}. Although these equilibriums are too simple to account adequately for all the complications occuring in the extraction by QAS, they are a good starting point as they emphasize the role of aggregation process These purely organic phase equilibriums are known to be a function of the nature of the QAS and its concentration and the nature of the organic diluent employed. The extraction of rare earths by QAS is strongly decreased in macrocomponent presence. Let us introduce the extent of the suppression of the microelement extraction, S, i.e. the ratio of the extraction coefficient in the absence of macrocomponent (D_1) to the corresponding value received in its presence (D_2). Considering that the macroamounts of thorium or iron are present in the organic phase as the complexes with the molar ratio of QAS to the metal as 2:1 and that they should bind the extraction reagent thus diminising its free concentration, neglecting ionization of the species in the organic phase, we assume that the formation of dimers and higher aggregates follows the mass action law and we obtain the following equation for the extent of the extraction suppression, S,

$$(1)\quad S = \frac{D_1}{D_2} = \frac{[R_4N]_1^n\,(1 + K_{sol}[R_4N]_1 + \dots + K_{sol}^L\,[R_4N]_1^L + \dots)}{[R_4N]_2^n\,(1 + K_{sol}[R_4N]_2 + \dots + K_{sol}^L\,[R_4N]_2^L + \dots)}$$

where $[R_4N]$ denotes the free extractant concentration, n is the quantity of the QAS particles in the inner coordination sphere of the metal-containing anion and L is the quantity of the QAS particles in the outer coordination sphere. If $K_{sol}[R_4N]$ is greater or equal to unit, it is necessary that the rows ($1 + K_{sol}[R_4N] + \dots$) were restricted with the term $K_{sol}^L\,R_4N^L$. If $K_{sol}[R_4N]$ is less that unit then the equation (1) can be transformed in a more simple form:

$$(2)\quad S = \frac{D_1}{D_2} = \frac{R_4N_1^n\,(1 - K_{sol}[R_4N]_2)}{R_4N_2^n\,(1 - K_{sol}[R_4N]_1)}$$

The aggregation constants of the extractants were calculated by means of two theoretical models of solutions, for non-polar solvents (model 1) and high-polar solvents (model 2). The generalized variant of the associative equilibriums theory was applied for elaborating the first model (3). In the case of nitrobenzene and nitromethane when it is impossible to neglect the influence of the extractable species dissociation in the organic phase on the behavior of a microcomponent in the presence of a macrocomponent, the aggregation constants, K_{agg}, were computed by means of model 2 taking into account that the QAS can dissociate partially as follows from the conductance theory of Onsager-Fuoss (4) using cryoscopic, conductivity and viscosity measurements of the various QAS extracts. The specially prepared computer programs were used for the calculations.

EXTRACTION RESULTS

The experimental results for the variation in the extraction of rare earths in the presence of iron from lithium nitrate solutions with trioctylmethylammonium (TOMA) nitrate solutions in benzene are given as an example in Fig.1. The acidity of the lithium nitrate solutions was close to 0.01 M nitric acid and adjusted so that the pH at the extraction equilibrium was 2.0 ∓ 0.2. The repression of the extraction of rare earths leads to a 100-fold decrease in D at the macroelement concentration over 0.01 M. It should be noted that for all metals studied the nature of the microelements does not change the shape of the log S versus log C_{Macro} plots.

It can be seen that in all extraction systems the presence of thorium or iron in the organic phase causes the increase of the log S values but the increases corresponding to the same C_{Macro} vary in magnitude with different extractants (Fig.2). Increasing chain length in the molecules of trioctylalkylammonium nitrate unfavours the effect of the extraction suppression.

The dependences of log D versus the macrocomponent concentration at a constant free extractant concentration are shown in Fig.3. These experimental curves may be used to obtain the information concerning the mechanism of the mutual influence. The extraction of rare earths does not depend on the thorium or iron concentration in the range investigated. All curves are practically parallel to the absciss axis. Hence, we can conclude that the shortage of the extractant in the organic phase, another words, the decrease of the free extractant concentration in the presence of the macroelement should be the main reason determining the mutual influence of metals in the systems under consideration. For a given alkylammonium cation in the QAS molecules, the suppression of the rare earths extraction increases in the order of the diluents: toluene benzene nitrobenzene nitromethane. S changes by more then 10 times in the extraction from en toluene to nitromethane used as diluents. In general, the higher is the dielectric constant of the solvent, the stronger is the suppression of the microelements extraction.

CALCULATED RESULTS

The aggregation and dissociation constants of the simple and metal-containing TOMA salts in different solvents were calculated by means of the above-mentioned theoretical models. Some

quantitative data concerning the state of the $TOMANO_3$ and its Ln-containing salt are summarized in the following Table.

The aggregation (K_{agg}) and the dissociation constants (K_{diss}) and the interchange parameters (W_{ns}) of the TOMA salts in different solvents

Diluent	Extractable species	K_{agg} l/mol	K_{diss} l/mol	W_{ns} kcal/mol
Nitrobenzene	$TOMANO_3$	1.02	$3.2\ 10^{-2}$	-351.5
	$(TOMA)_2Ln(NO_3)_5$	3.04	$9.6\ 10^{-2}$	-326.4
Benzene	$TOMANO_3$	39.9	$5.9\ 10^{-5}$	-26.4
	$(TOMA)_2Ln(NO_3)_5$	40.3	$7.3\ 10^{-4}$	-8.2
Toluene	$TOMANO_3$	41.4	$6.4\ 10^{-5}$	-15.5

The K_{agg} and K_{diss} values are found to be substantially higher in the case of the metal-containing TOMA salts than for $TOMANO_3$ itself. It should be noted that the reduction of the aggregation constants values in the order of diluents: toluene benzene nitrobenzene nitromethane is took place. The interchange parameters are changed in the same sequence.

The experimental values of the extraction suppression of rare earths in the presence of iron and thorium were compared with the theoretical values which were calculated by using equations (1) and (2). To calculate log S it is necessary to set the values of the n and L parameter and to know the free extractant aggregation constants in the organic phase. Using n and L as the variable parameters we plotted a family of curves of the dependence of log S versus log C_{Macro} which were compared with the plots of the experimental points, as shown in Fig.1 and 2. Only those curves, the sum of the parameters n and L of which was equal to four in the case of benzene and toluene and equal to two in the case of the high-polar diluents, shown quite good agreement with the extraction data.

The NMR H^1 measurements were conducted to define more precisely the composition and the structure of the extractable complexes. As an example, the structure of di(trioctylmethylammonium)erbiumpentanitrate in nitrobenzene is shown in Fig.4. The paramagnetic shifts data allowed to calculate the cation-to--anion distance (R) and the angle between the principal magnetic axis and the $N-CH_3$ direction in this ion-pair. It was impossible in the geometrical sense that more than two TOMA cations were situated in the inner coordination sphere of the anion.

From this one can deduce that the microamounts of the rare earths are extracted in the form $(R_4NNO_3)(R_4N)_2Ln(NO_3)_5$ in the extraction systems with benzene and toluene and in the form $(R_4N)_2Ln(NO_3)_5$ with nitrobenzene and nitromethane.

Decreasing the extent of the microelements extraction suppression in the presence of the macroelements with the alkyl radical length growth in the molecules of the alkylammonium nitrates we can connect easily with diminishing the aggregation constants of the substituted QAS salts.

CONCLUSION

The effect was discovered of extraction suppression of the rare earth microamounts in the presence of iron or thorium at their simultaneous extraction by QAS nitrates.

The value of the extent of the extraction suppression in the given systems is determined by the shortage of the free extractant in the organic phase and by stoichiometry of the extractable species.

The method was suggested of the calculation of the degree of the microelement extraction suppression.

REFERENCES

1. V.V.Bagreev, C.Fischer, L.M.Yudushkina, Yu.A.Zolotov. J.Inorgan.Nucl.Chem., 40, 553 (1978).
2. S.O.Popov, V.V.Bagreev, Yu.A.Zolotov. Z.Neorgan.Khim., 27, No. 10, 2628(1982).
3. J.A.Barker, F.Smith. J.Chem.Phys., 22, No.3, 375 (1954).
4. Y.Marcus, A.S.Kertes. Ion Exchange and Solvent Extraction of Metal Complexes. Wiley-Interscience, Bristol, GB, 1969.

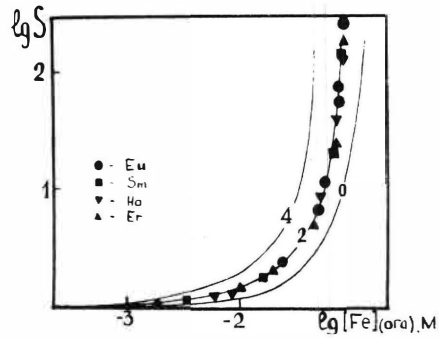

FIGURE 1. EXTRACTION OF RARE EARTHS BY 0.2 M $TOMANO_3$ IN BENZENE. THE NUMBERS IN OF THE CURVES ARE THE VALUES OF THE PARAMETER L IN Eq.(1) (AT n=2 L=2).

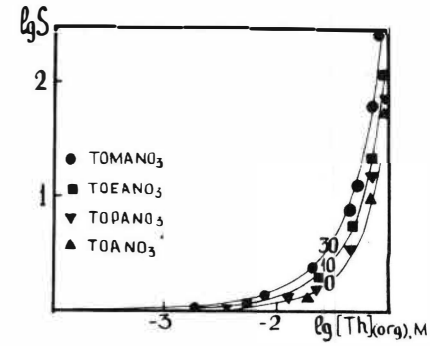

FIGURE 2. EXTRACTION OF EUROPIUM BY 0.2 M QAS IN TOLUENE. $TOMANO_3$ = trioctylmethylammonium nitrate, $TOPANO_3$ = trioctylpropylammoniun nitrate, $TOEANO_3$ = trioctylethylammonium nitrate, $TOANO_3$ = tetraoctylammonium-nitrate. THE NUMBERS IN OF THE CURVES ARE THE VALUES OF THE AGGREGATION CONSTANTS (n=2)

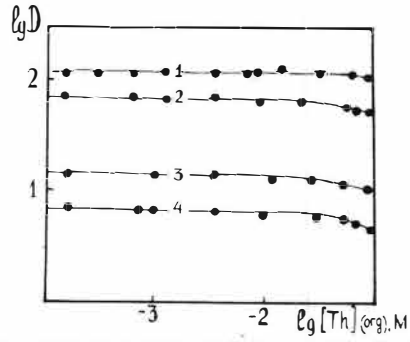

FIGURE 3. EXTRACTION OF THORIUM BY 0.15 M $TOMANO_3$ IN NITROMETHANE (1), NITROBENZENE (2), BENZENE (3), TOLUENE (4) AT A CONSTANT CONCENTRATION OF FREE EXTRACTANT.

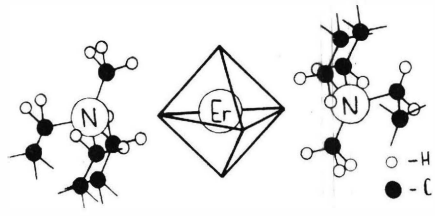

FIGURE 4. STRUCTURE OF DI(TRIOCTYLMETHYLAMMONIUM)ERBIUMPENTA-NITRATE IN NITROBENZENE (R = 8.2 A, φ =62°).

1-(2'-THIAZOLYLAZO)-2-NAPHTHOL AS EXTRACTIVE SPECTROPHOTOMETRIC REAGENT FOR SOME TRANSITION ELEMENTS

M. C. Eshwar, U. G. Gaokar and J. Krishnamacharyulu

Department of Chemistry
Indian Insitute of Technology
Powai, Bombay 400 076, India

Pyridylazo and thiazolylazo dyes find considerable application (1,2) in analytical chemistry. 1-(2'-Pyridylazo)-2-naphthol (PAN) has been employed as extractive spectrophotometric reagent for determination of trace amounts of trivalent yttrium (3,4), ferrous iron (5), ferric iron (3) and tetravalent vanadium (6). It is considered worthwhile to study the utility of 1-(2'-thiazolylazo)-2-naphthol (TAN), thiazolylazo analogue of PAN, for determination of these ions.

APPARATUS

Absorbance was measured on a Spektromom 204 spectrophotometer and pH on a Cambridge pH meter. Absorption spectra was recorded on a Varian Superscan 3 UV-Visible spectrophotometer.

REAGENTS

Stock solutions of yttrium nitrate, ammonium ferrous sulphate, ferric nitrate and vanadyl sulphate were prepared from pure samples and the solutions kept slightly acidic with appropriate acid. Standardisation of vanadium (IV) and iron (II) solutions was carried out by redox titrations, while complexometry was used for standardisation of iron(III) and yttrium(III) solutions. 0.1% TAN was prepared by dissolving 0.1 g of 1-(2'-thiazolylazo)-2-naphthol (Fluka A.G., purum) in 100 ml of methanol. All other reagents employed were of AnalaR grade (BDH).

PROCEDURE

Aliquots of yttrium(III) iron(II), iron(III) and vanadium (IV) containing $\leq$ 12, 30, 16 and 50 µg respectively were adjusted to pH or treated with buffer of appropriate pH. One ml of 0.1% TAN was added to Y(III), Fe(II) and V(IV). In case of Fe(III), 2 ml of 20% KSCN and 0.25 ml of 0.1% TAN were added. The contents were diluted 10 ml, wherever necessary, thoroughly shaken and equilibrated with 10 ml of appropriate solvent. The layers were allowed to separate, a crystal of anhydrous sodium sulphate was added to Fe(II) and Fe(III) extracts, and absorbance measured at 580 nm for Y(III), 575 nm for Fe(II), 535 nm for Fe(III) and 605 nm for V(IV) against reagent blank prepared under identical conditions.

RESULTS AND DISCUSSION

1-(2'-Thiazolylazo)-2-naphthol reacts with yttrium(III), iron(II), iron(III) in presence of thiocyanate, and vanadium(IV) to yield sparingly soluble chelates. A critical study of various parameters affecting complexation and subsequent determination has been carried out, which is summarised in Table 1.

pH : The effect of pH on complexation for different metal ions is presented in Fig.1.

Reagent concentration : When volume of 0.1% TAN added was varied from 0.05 to 2.0 ml, maximum absorbance was observed on addition of $\geq$ 0.9 ml of reagent for Y(III), Fe(II) and V(IV). In case of Fe(III), absorbance increased gradually on addition of upto 0.25 ml reagent, but decreased on further addition.

Solvent : Among various solvents employed for extraction, benzene, isobutylmethyl ketone and chloroform were found to quantitatively extract the chelates of Fe(II), Fe(III) and V(IV). Eventhough Y(III) - TAN complex was quantitatively extracted into benzene, the extracted complex was not stable and started decomposing soon after extraction. However, the complex was found to be stabilised in presence of even very small amounts of acetone in benzene. Hence, the complex was extracted into 10 ml of 1% acetone in benzene.

Spectral characteristics : Absorption spectra of Y(III)-TAN and V(IV)-TAN complexes along with those of their reagent blanks are presented in Fig.2, while the spectra of Fe(II)-TAN and Fe(III)-SCN-TAN complexes along with those of their reagent blanks are given in Fig.3, which also contains the absorption spectrum of Fe(III)-SCN. The wavelengths corresponding to maximum absorbance in each case were chosen for determinations.

Composition : Job's continuous variation and mole ratio methods were employed for determining composition of Y(III), Fe(II) and V(IV) complexes. Absorbance was found to increase continuously in case of Fe(III), evidently due to the presence of excess of thiocyanate. Since the above methods were thus not useful, slope ratio method was employed for determining composition of Fe(III) complex.

Formation constant : Log K was calculated from mole ratio method (7).

Extracted species : The nature of extracted species in each case was ascertained from a plot of log D vs log [TAN] at constant pH.

Diverse ions : Interference of various ions usually associated with each of the elements in various materials has been studied setting the tolerance limit to cause an error of $\pm$ 2.0% in the recovery. A summary of effect of diverse ions is returned in Table 2.

Application : The methods have been employed for duplicate determination of each of the elements in alloy steel samples, and details are given in Table 3.

REFERENCES

1. R.G. Anderson and G. Nickless, Analyst., 92,207 (1967).
2. Havard R. Hovind, ibid., 100, 769 (1975).
3. Shozo Shibata, Anal.Chim.Acta., 25, 348 (1961).
4. Shozo Shibata, Nagoya Kogyo Gijutsu Shikensho Hokoku., 10, 712, 609 (1961)., c.f. Chem.Abstr.,61,8893b,11309c(1964)
5. Shozo Shibata, K. Goto and R Nakashima, Anal.Chim. Acta., 46, 146 (1969).
6. U. Dubravka and M. Legin, Narta, Zagr., 23, 203 (1972) c.f. Anal.Abstr., 25, 1661 (1973).
7. A.E. Harvey and D.L. Manning, J.Am.Chem.Soc., 72, 4489 (1950).

Table 1 - Summary of various parameters

Parameter	Y(III)	Fe(II)	Fe(III)	V(IV)
Colour	Orange-red	Red	Orange-red	Reddish brown
pH chosen	8.7	3.0	3.0	4.1
Volume of buffer	10 ml borate	5 ml acetate	5 ml acetate	-
Amount of reagent	1.0 ml	1.0 ml	0.25 ml	1.0 ml
Solvent chosen	1% acetone in benzene	Benzene	IBMK	Chloroform
Stability	2.5 h	> 24 h	24 h	45 m
λ_{max}(nm)	580	575	535	605
Composition	1:3	1:3	1:1:1	1:1
Log K	14.9	4.64	-	3.5
Extracted species	$Y(TAN)_3$	$H[Fe(TAN)_3]$	$[Fe(SCN)(TAN)]^+NO_3^-$	$[VO(TAN)]^+HSO_4^-$
Beer's law range(µg/ml)	0.05-1.2	0.1-3.0	0.1-1.6	0.25-5.0
Molar absorptivity	7.07×10^4	1.40×10^4	2.03×10^4	0.41×10^4
Sandell sensitivity	0.0013	0.004	0.0028	0.013
Rel.std.devn. ($\pm$ %)*	0.17	0.18	0.10	0.56
Rel.mean error($\pm$%)*	0.54	0.48	0.86	0.75

* Calculated from ten repeat determinations

Table 2 - Effect of diverse ions

Ion determined	No. of ions studied	Typical interferences from	Significant separations from
Y(III)	56	$EDTA^{4-}$, Ti, Zr, Hf, Mn	Sc, La, Ce
Fe(II)	55	Co, Ni, Cu, Mo, W	Fe(III), Ti, V, Cr, Mn
Fe(III)	57	Cu, Zr, Ru, Pd	Fe(II), Ti, Cr, Mo, W
V(IV)	45	Co, Ni, Cu, Pd	V(V), Cr, Mn, Fe

Table 3 - Analysis of alloy steels

Ion determined	Amount found(%) 1	2	Amount present (%)	Other constituents
Y(III)	0.75	0.74	0.76	C, Si, P, S, Cr, Mn, Ni, Mo and Fe
Fe(II)	0.60	0.59	0.61	Mg, Ti, V, Cr, Mn, Ni, Cu, Zn, Ga, Sn and Pb
Fe(III)	0.60	0.60	0.61	Same as above
V(IV)	0.96	0.93	1.00	Cr, W and Fe

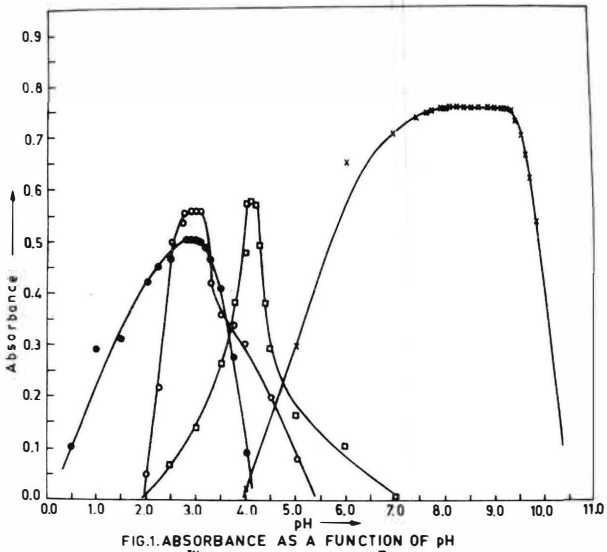

FIG.1. ABSORBANCE AS A FUNCTION OF pH
-o- V^{IV} -TAN COMPLEX; -•- Fe^{II} -TAN COMPLEX;
-•- Fe^{III} -SCN-TAN COMPLEX; -•- Y^{III} -TAN COMPLEX

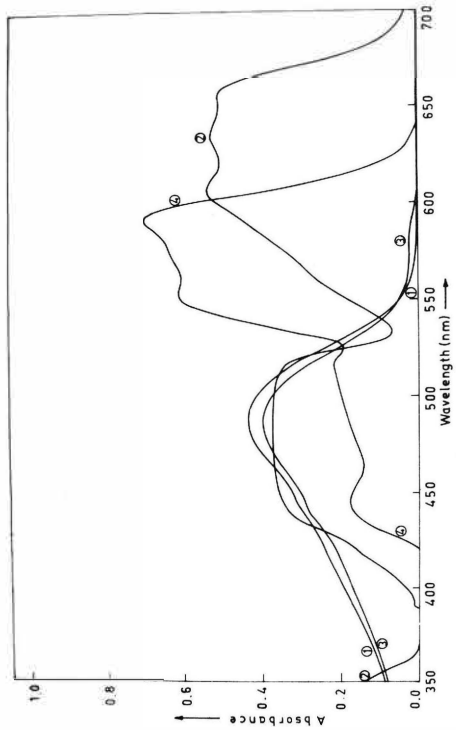

FIG.2 ABSORPTION SPECTRA
① REAGENT BLANK Vs SOLVENT (V^{IV}-TAN)
② V^{IV}-TAN COMPLEX Vs REAGENT BLANK
[V(IV)]=1.178 x 10^{-4} M [TAN]=2.686 x 10^{-5} M, c.l. CURVE 1
③ REAGENT BLANK Vs SOLVENT (Y^{III}-TAN)
④ Y^{III}-TAN COMPLEX Vs REAGENT BLANK
[Y(III)]= 1.12 x 10^{-5} M; [TAN]= 2.14 x 10^{-5} M, c.l. CURVE 3

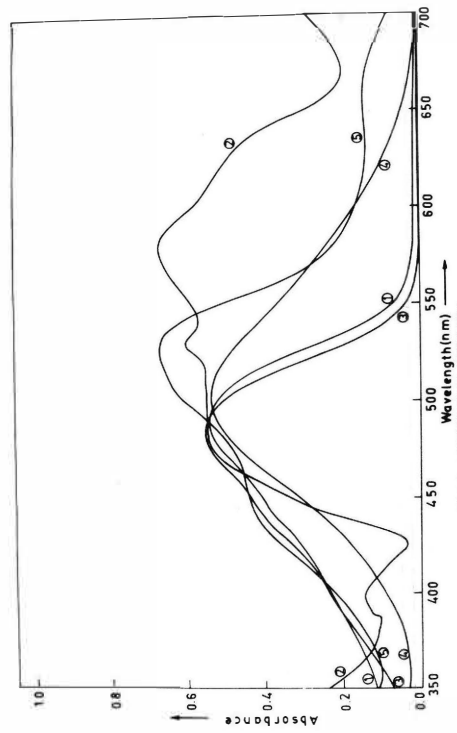

FIG.3. ABSORPTION SPECTRA
① REAGENT BLANK Vs SOLVENT (Fe^{II}-TAN)
② Fe(II)-TAN COMPLEX Vs REAGENT BLANK
[Fe(II)]= 4.476 x 10^{-5} M; [TAN]= 2.019 x 10^{-5} M, c.l. CURVE 1
③ REAGENT BLANK Vs SOLVENT (Fe^{III}-SCN-TAN)
④ Fe(III)-SCN COMPLEX Vs SOLVENT
⑤ Fe(III)-SCN-TAN COMPLEX Vs REAGENT BLANK
[Fe(III)]= 2.686 x 10^{-5} M; [SCN]=0.4116M; [TAN]=2.686 x 10^{-5} M, c.l. CURVE 3

SOLVENT EXTRACTION AT NEAR-NEUTRAL pH

Nandani Rajapakse and Harmon L. Finston

Department of Chemistry
City University of New York, Brooklyn College
Brooklyn, New York 11210 USA

Preliminary studies indicate that it is possible to perform solvent extractions at near neutral pH by the following expedient. A ligand is added which forms a charged complex with the cation, the pH is adjusted to near neutral, and the cation is then extracted into a non-polar solvent by equilibrium with another complexing agent which forms a neutral complex. These conditions at near neutral pH favor the enolate form of chelating extractants and the anionic form of the various monodentate complexing agents. It is anticipated that pH dependence will be much less significant under these conditions and that group extractions will be favored.

We have also found that combining this technique with the technique of homogeneous liquid-liquid solvent extraction affords more rapid equilibrium under all conditions and greater extraction efficiencies under optimum conditions. Propylene carbonate, which has the unusual property of being completely miscible with aqueous solutions above 71°C and becomes immiscible again upon cooling (13,14), has proved a versatile solvent for a variety of both chelating and monodentate complexing agents and makes the homogeneous technique possible.

Methods of separation and determination based on this combination of techniques for applications in hydrometallurgy and chemical analysis are being developed.

Almost without exception, solvent extraction procedures are performed under very acid conditions, i.e., pH = 3.5, which is a necessary condition ordinarily to prevent precipitation of the hydrated oxides of the metal cations. For example, at pH = 3, solubility of Fe(III) is only of the order of 5 ng/ml.

Calculation of the solubility of Fe(III) based only on the simple one-step reaction

$$Fe(OH)_3 = Fe^{3+} + 3OH^- \qquad K_{sp} = 10^{-38.7}$$

shows the marked change in solubility as a function of pH.

Table I. Solubility of Fe(III)

pH	Fe(III) Concentration
1	112 mg/l
2	112 ug/l
3	112 ng/l
4	112 pg/l
5	112 fg/l

This shows an increase in pH by 1 unit corresponds to a thousand-fold decrease in Fe(III) solubility.

Thus, under relatively acid conditions, it is possible to lose significant amounts of analyte, even when present at only trace concentration. However, acid conditions are not favorable for the formation of extractable (i.e., neutral) metal cation complexes with all the usual complexing agents. For example, the competing associations of H^+ with CN^-, SCN^-, the carboxylates, and the beta-diketones such as thenoyltrifluoroacetone, acetylacetone, etc. to form the very weak undissociated acids which are themselves extracted into the organic solvents, are favored at low pH.

It is proposed that the expedient of adding an auxiliary ligand to form a water-soluble charged complex with the cation sould enable the extraction of a neutral complex at higher pH. For example, ammonia is already used as such an auxiliary ligand in the extraction of nickel following separation of copper on the commercial scale. The copper is extracted at pH below 2, after which the nickel is extracted at pH 4.5 to 5 (15). Under these conditions, the nickel(II) exists in the aqueous phase as the ammine complex:

$$Ni^{2+} + 4NH_3 = Ni(NH_3)_4^{2}$$

and is extracted into the organic phase as a chelate complex. A beta-diketone, under these conditions, would exist in the aqueous phase as the enolate ion (En^-) and can readily react to form the neutral chelate complex:

$$Ni(NH_3)_4^{2+}{}_{(aq)} + 2En^-{}_{(aq)} = Ni(En)_{2(aq)} + 4NH_{3(aq)}, \text{ and}$$

$$Ni(En)_{2(aq)} = Ni(En)_{2(org)}$$

The criterion for an ideal auxiliary ligand is that it should form a stable charged complex soluble at near neutral pH (5-8) and yet not hinder the formation of an uncharged complex with the extracting chelate. This necessary balancing of two competing equilibria suggests the use of malonate and succinate rather than oxalate for iron(III). Ammonia is an appropriate ligand for use with copper, nickel, cobalt, cadmium, and silver.

The systems under intial study are UO_2^{2+}-carbonate-chelate, copper(II)-ammine-chelate, nickel(II)-ammine-chelate, iron(III)-succinate-chelate, and iron(III)-malonate-chelate extracted into propylene carbonate. The special properties of propylene carbonate permit a direct comparison of analyte concentration in each phase with standard. Propylene carbonate/aqueous/ethanol in the ratio 2/2/1 yields a single homogeneous phase. Thus, propylene carbonate and ethanol are added to the aqueous phase (and standard) and aqueous plus ethanol are added to the propylene carbonate phase enabling direct comparison and material balance.

The possibility of a preliminary extraction of UO_2^{2+}-nitrate into propylene carbonate (homogeneous liquid-liquid extraction) suggests application also to processing spent fuel elements. The final separation and purification could

be accomplished by UO_2^{2+}-carbonate-chelate extraction into propylene carbonate from a medium much reduced in radioactivity. The advantages of propylene carbonate over ether are lower volatility, higher flash point, and no possible formation of explosive peroxides, all of which result in much greater safety, at comparable cost and rapid equilibration by heating to above 70°C and cooling to room temperature.

Solvent extraction procedures for hydrometallurgy of copper are still of great current interest as evidenced by the large number of papers on copper ore processing at the International Solvent Extraction Congress, Liege, 1980. Copper and nickel both form highly colored ammine complexes which are readily determined at low concentrations by spectrophotometry, and they are less stable (i.e., formation constants are lower) than the chelates.

The iron(III)-chelate complexes are similarly strong complexes with large absorption coefficients so they too can be determined by absorption spectrophotometry. Iron is of particular interest in hydrometallurgical processing since it is both ubiquitous and frequently an interference.

Alternative methods of analyses of these cations are readily available for determination of extraction coefficients, e.g., proton induced x-ray fluorescence (PIXE), AAS, and tracer techniques. The PIXE technique is particularly advantageous because it gives simultaneous multielement analysis. Thus, it provides an instantaneous measure of both specificity and efficiency of the extraction.

Although we have pointed out that the ammine complexes, for example, have lower formation constants than the chelates, this may not be a necessary condition. Even under unfavorable ratios of constants, the extraction of the cation into the organic phase will shift the equilibrium to favor formation of the neutral complex. Therefore, regardless of the relative magnitudes of the respective formation constants, investigation should be directed toward achieving optimum conditions.

The beta-diketones are a class of chelating agents of particular interest for study because they readily form strong complexes with a wide variety of cations. Furthermore, a number of homolgues into which various substituents have been introduced have been widely studied.

The expedient herein proposed to add an auxiliary ligand and to perform extractions at higher pH favors formation of the enolate ion, thus eliminating the slow step in chelate extraction. Thus, under these conditions, even the simple and inexpensive acetylacetone should afford rapid and quantitative extraction.

RESULTS TO DATE

Only preliminary experiments have been performed so far with the following results.

Copper was extracted into toluene from copper ammine solution adjusted to pH 7.0, 7.5, and 8.0 respectively as the TTA complex. Equilibrium was reached very rapidly. The maximum extraction--75% to 80%--was attained within 10 minutes.

The extraction from copper ammine solution into TTA-propylene carbonate at pH 6, 7, and 8 respectively gave 100% extraction in all cases in 25 minutes. Equilibrium was attained somewhat more rapidly at pH 6.

Nickel has been extracted into TTA-toluene from Ni-ethylene diammine solution at pH 5, 6, and 7 respectively. Equilibrium was attained rapidly, less than 10 minutes in all cases. The percent extracted was 34% at pH 7, 51% at pH 6, and 32% at pH 5.

Uranium has been extracted from ammonium nitrate solution into propylene carbonate and, subsequently, stripped into aqueous carbonate solution. The various phases were analyzed colorimetrically with dibenzoylmethane reagent (17) (yields intense yellow color) indicating extraction and recovery. The uranyl ion was completely extracted from the carbonate solution by a solution of dibenzoylmethane in propylene carbonate.

REFERENCES

1. Finston, H. L., and Inoue, Y., J. Inorg. Nucl. Chem. 29, 199 (1967).
2. Ibid, 29, 2431 (1967).
3. Rahaman, Md. Syedur and Finston, H. L., Anal. Chem. 40, 1709 (1968).
4. Rate Effectived Synergic Solvent Extraction. H. L. Finston and Elisheva Gnizi. Plenary Symposium Lecture, 11th Intl. Conf. on Coordination Chemistry, Jerusalem, Israel, Sept. 1968. Published in "Solvent Extraction Research. Proceedings of the Fifth Intl. Conf. on Solvent Extraction Chemistry." Edited by A. S. Kerstes and I. Marcus, Wiley Intersci., 1970.
5. Rahaman, M. S., and Finston, H. L., Anal. Chem. 41, 2023 (1969).
6. Fischman, A. J., Finston, H. L., and Goldberg, D. E., J. Inorg. Nucl. Chem. 35, 2497 (1972).
7. Raphael, D. M., Finston, H. L., and Fischman, A. J., Ibid. 35, 2507 (1972).
8. Hong, Chia-Swee, "Homogeneous Liquid-Liquid Extraction of Metal Thenoyltrifluoroacetonates," Master's Thesis, Brooklyn College, C.U.N.Y.
9. Hong, Chia-Swee, Finston, H. L., Williams, E. T., and Kertes, A. S., J. Inorg. Nucl. Chem. 41, 420 (1979).
10. Hong, Chia-Swee, "Homogeneous Liquid-Liquid Extraction," Ph.D. Thesis, City University of New York, Brooklyn College.
11. "Homogeneous Liquid-Liquid Extraction," Chia-Swee Hong, Evan T. Williams, and Harmon L. Finston, Presented and published in the Proceedings of the Intl. Solvent Extraction Conf., Liege, Belgium, Sept. 1980.
12. Habashi, Fathi, "Hydrometallurg," A Special Report, Chem. & Eng. News, 46-58, Feb. 8, 1982.
13. "Propylene Carbonate," Tech. Bull., Jefferson Chemical Co, Inc., Houston, Texas, 1960.
14. Hong, C. S., Wakslak, R., Finston, H. L., and Fried, V., J. Chem. Eng. Data, 27, 146 (1982).
15. "The Chemistry of Metals Recovery Using LiX Reagents," Tech. Bull., Henkel Corp., Tucson, AR, 1978.
16. Taft, R. W., Jr. and Cook, E. H., J. Am. Chem. Soc. 81, 46 (1959).
17. Yoe, John H., Will, Fritz, and Black, Robert A., Anal. Chem. 25, 1200 (1953).

EXTRACTION AND BACK-EXTRACTION OF METALS WITH ORGANIC REAGENTS IN CHELATE EXTRACTION AND THE ION-ASSOCIATION EXTRACTION SYSTEMS

Honjo Takaharu

Kanazawa University
Department of Chemistry
Ishikawa 920, Japan

INTRODUCTION

The behavior of trace amount of metals in extraction and back-extraction has been examined in order to ascertain the basic conditions for the mutual separation of various metals as their metal complexes. The results have been applied to the separation of metals by means of back-extraction and extraction chromatography. In extraction chromatography, the extraction and back-extraction may recur many times throughout the chromatographic process, the separation of the difficultly-separable compounds can be achieved (1). The relation between the extraction chromatography and the liquid-liquid extraction in batches has also been considered. These results may also be useful for the preconcentration and separation of metals by Donnan dialysis (2). In Donnan dialysis, the extraction and back-extraction may proceed through organic liquid membranes between two aqueous phases, and it will be called "Extraction Dialysis". This article is the summary of the papers reported previously (3-10).

EXPERIMENTAL

The experimental procedures were almost the same as have previously been described (3-10). Organic reagents used were Ox (oxine), Dz (dithizone), DDTC (diethylammonium diethyldithiocarbamate), AA (acetylacetone), TTA (thenoyltrifluoroacetone), STTA (monothiothenoyltrifluoroacetone), SDBM (monothiodibenzoylmethane), BPhen (batho phenanthroline), TBP (tributyl phosphate), TOA (trioctylamine), and TCA (trichloroacetic acid).

RESULTS

1) Metal-0.01-0.1M Ox-$CHCl_3$ System (3). The difference in $pH_{1/2}$ (the pH of the half extraction) in extraction and back-extraction gives larger in the order of Fe(III), Sc(III), Zn(II) < Cd(II), Eu(III) < Bi(III) < In(III) < Hg(II) < Ce(III) < Ag(I) < Pb(II) < Mn(II) < Co(II). The disagreement of the $pH_{1/2}$ values appearing in the liquid-liquid extraction of the chelates indicates that the extraction equilibrium is not strictly reached within 30 min. The fact that the extraction and the back-extraction curves of cobalt oxinate are quite different, i.e., the nonequilibrium nature of the process caused by the transformation of $Co(Ox)_2^+$ into a certain inert complex such as $Co(Ox)_3$, was useful for the back-extraction separation of cobalt(II) and iron(III).

2) Metal-10^{-5}-10^{-4} M Dz-CCl_4 System (4). The difference in $pH_{1/2}$ in extraction and back-extraction after a few hours' shaking gives larger in the order of Ag(I), Cu(II) < Zn(II) < Bi(III), Hg(II) < Co(II). The valence of cobalt changes from 2 to 3 to form $Co(Dz)_3$ chelate.

The behavior of secondary copper dithizonate in carbon tetrachloride, chloroform, 1,2-dichloroethane, benzene, monochlorobenzene, o-dichlorobenzene, and nitrobenzene has been investigated by a kinetic study of the back-extraction of the copper ion in order to clarify the extraction mechanism and to ascertain the chemical form of this chelate. It is concluded that the extraction equilibrium between the secondary copper dithizonate and the primary dithizonate is reversible and that the secondary copper dithizonate is of the Cu(II)Dz type.

3) Metal-5X 10^{-3} M DDTC-CCl_4 System (5). The extraction and back-extraction behavior of metal diethyldithiocarbamates in carbon tetrachloride can be classified into the following extraction processes: Reversible extraction process — Cu(II), Zn(II), As(III), Se(IV), Cd(II), Sb(III), Hg(II), Tl(I), Pb(II), and Bi(III); irreversible process caused by the change of the valence of metals — Cr(VI), Mn(II), Fe(II), Co(II), Tl(III), As(V), Se(VI), and Sb(V); irreversible process caused by the slow rate of chelate formation — Fe(III) and Ni(II); irreversible process caused by the change of the composition of metal complexes — Au(III).

4) Metal-50% AA-$CHCl_3$ and 0.2M TTA-MIBK Systems (6). The extraction and back-extraction behavior of the Al(III) and Cr(III)-AA-$CHCl_3$ system and of the Mg(II), Pb(II), Mn(II), Co(II), Ni(II), and Cu(II)-TTA-MIBK (isobutyl methyl ketone) system have been studied. The difference in $pH_{1/2}$ gives larger in the order of Mg(II), Mn(II), Co(II), Ni(II), Cu(II), Al(III) < Pb(II) < Cr(III). The results have been applied to the separation of these metals as their AA and TTA-complexes by extraction chromatography. Synergism in the liquid-liquid extraction and extraction chromatography of Mn(II), Co(II), and Zn(II) in the TTA-TOPO (trioctylphosphine oxide)-cyclohexane extraction system has also been studied.

5) Metal-10^{-3} M STTA-Cyclohexane System (7). The $pH_{1/2}$ values decrease in the order of Cd(II)-In(III)-Zn(II)-Fe(III)-Ni(II)-Ag(I)-Bi(III)-Co(II)-Pb(II)-Cu(II)-Hg(II). This order was found to hold also in the back-extraction, except for cobalt, which was not back-extracted even with 1-12M HCl. The extraction equilibrium of Zn seemed to be rapid, that of Ni showed its rate-determining step to be the formation of $Ni(STTA)^+$, and that of Co seemed to be accompanied by a transformation of $Co(STTA)_2$ to $Co(STTA)_3$. The results have been applied to the separation of Hg(II), Co(II), Ni(II), and Zn(II) as their STTA complexes by back-extraction and extraction chromatography.

6) Metal-10^{-3} M SDBM-CCl_4 System (8). The overall stability constants of Ni(II), Cu(II), and Zn(II) chelates with SDBM in aqueous solution have been determined by means of the extraction and the back-extraction methods. The extraction equilibrium of Zn(II) was achieved within 30 min, while that of Cu(II) required about 2 h. The extraction equilibrium of Ni(II) was irreversible within 2 h. The rate constants of the back-extraction of $Cu(SDBM)_2$ chelate in carbon tetrachloride with an uncomplexed SDBM were -4.77 M min^{-1}. The rate constant of the back-extraction increased about 10 times by addition of chloride ion. The back-extraction of $Cu(SDBM)_2$ may proceed through the following steps, that is, hydrogen ion assisted in the dissociation of $Cu(SDBM)_2$ followed by reaction of chloride ion.

7) Metal-10^{-3} M BPhen-1,2-Dichloroethane-0.1M $NaClO_4$ System. The extraction behavior of ion pair complexes of Mn(II), Fe(II), Co(II), Ni(II), Cu(II), Zn(II), and Cd(II)-batho phenanthroline cations with perchlorate ions in 1,2-dichloroethane has been investigated. The rate of the extraction of Fe(II), Co(II), and Ni(II) was very slow; the effect of which was dependent on the structure of chelating agents, the nature of organic solvents, and pH. The extraction equilibrium of Co(II) showed its rate-determining step to be the complex formation between hydrated Co(II) with BPhen in an aqueous solution.

8) Metal-100% TBP- HCl System. The difference in $HCl_{1/2}$ in extraction and back-extraction gives larger in the order of Sn(IV), Fe(III) < Au(III), Hg(II), Re(VII), Tl(III).

The results have been applied to the separation of the six metals as their TBP complexes by extraction chromatography.

9) Metal-20% TOA-CCl_4-System (9). The behavior of milligram amounts of Ag(I), Bi(III), Cd(II), and Zn(II) in extraction and back-extraction has been studied with 20% TOA in carbon tetrachloride. The difference in $HCl_{1/2}$ gives larger in the order of Ag(I)-Bi(III)-Zn(II)-Cd(II). The results have also been applied to the separation of the four metals as their TOA complexes by extraction chromatography.

10) Metal-Isopentyl alcohol-2M TCA System (10). Many metal ions, such as Th(IV), Bi(III), Tm(III), Fe(III), Cr(III), Al(III), Hg(II), Co(II), Mn(II), Ba(II), Ca(II), and Cs(I), could be extracted from trichloroacetate buffer solutions into polar solvents involving a donor oxygen atom like isopentyl alcohol, but not into inert solvents.

Chromium(III) is extracted with TOPO into cyclohexane as an ion association complex like $Cr(H_2O)_6^{3+}(TCA^-)_3 \cdot 3TOPO$, and the extraction constant is $10^{7.68}$.

The extractability of Cr(III) depends most effectively on the concentration of HTCA-free TOPO in the organic phase.

REFERENCES

1. T. Honjo, Kagaku, 37, 203 (1982).

2. J. E. Dinunzio, R. L. Wilson and F. P. Gatchell, Talanta, 30, 57 (1983).

3. T. Honjo, K. Ameno, M. Horiuchi and T. Kiba, Bull. Chem. Soc. Jpn., 47, 1799 (1974).

4. T. Honjo, T. Unemoto and T. Kiba, Bull. Chem. Soc. Jpn., 48, 1651 (1975).

5. T. Honjo and H. Imura, Bull. Chem. Soc. Jpn., 53, 1753 (1980).; T. Honjo, S. Abe and T. Kiba, Bull. Chem. Soc. Jpn., 51, 1239 (1978).

6. T. Honjo, Y. Honda, T. Matsumoto, R. Honda and T. Kiba, Bull. Chem. Soc. Jpn., 50, 3051 (1977). ; T. Honjo, M. Horiuchi and T. Kiba, Bull. Chem. Soc. Jpn., 47, 1176 (1974).

7. T. Honjo, S. Yashima and T. Kiba, Bull. Chem. Soc. Jpn., 46, 3772 (1973). ; T. Honjo and T. Kiba, Bull. Chem. Soc. Jpn., 46, 1694 (1973). ; T. Honjo, T. Unemoto and T. Kiba, Bunseki Kagaku, 23, 203 (1974).

8. T. Honjo and H. Freiser, Anal. Chem., 53, 1258 (1981).

9. T. Honjo, S. Ushijima and T. Kiba, Bull. Chem. Soc. Jpn., 46, 3764 (1973).

10. T. Kiba, H. Imura and T. Honjo, Chem. Lett., 1977, 805. ; H. Imura, T. Kiba and T. Honjo, Bull. Chem. Soc. Jpn., 52, 2563 (1979).

EXTRACTION CHROMATOGRAPHIC SEPARATION OF VANADIUM, MOLYBDENUM, GOLD AND GERMANIUM WITH TRIBUTYL PHOSPHATE

S. N. Bhosale and S. M. Khopkar

Indian Institute of Technology
Bombay 400 076, India

Although several methods for the solvent extraction separation of vanadium, molybdenum, gold and germanium are known, extraction chromatographic techniques involving organophosphrus compounds are limited. Vanadium(IV) was studied on fluoroplast-4 support with tributylphosphate and benzohydroxamic acid as the extractant (1). The extraction chromatographic separation of molybdenum from mineral acid media with TBP as the stationary phase were carried out (2-4) on silica gel column. But it did not permit separation from common elements. Gold was separated by extraction chromatography with TBP as extractant on polyurethane foam (5), silica (6), but in all cases it was necessary to use high concentration of nitric acid as the mobile phase. Germanium was separated from associated elements with trioctylamine as an extractant on corvic support (7). However systematic investigations on extraction chromatographic separation of these elements with TBP as stationary phase are lacking. Hence such studies are reported in this paper.

EXPERIMENTAL

Apparatus and reagents. The column used was 8 mm bore pyrex tubes fitted with glass wool plug at the bottom. Tributylphosphate b.p. 142-143°C at 5 mm Hg.

A stock solution of vanadium, molybdenum, gold and germanium was prepared by dissolving 3.66 g of sodium metavanadate, 1.823 g of molybdic acid, 0.5 g of gold chloride and 1.27 g of germanium oxide in 500 ml of distilled water containing acid. On standardisation (8) the solutions were found to contain 4.87 mg/ml vanadium, 2.7 mg/ml molybdenum, 0.47 mg/ml of gold and 3.57 mg/ml of germanium. The diluted solutions were prepared by appropriate silution. Silica gel was made hydrophobic by exposure to dimethyldichlorosilane followed by its coating with TBP in benzene on rotary vacuum evaporator.

General procedure. An aliquot of solution containing 309 µg of vanadium in 6 N hydrochloric acid; or 108 µg of molybdenum in 3 N hydrochloric acid; or 125 µg of gold in 0.01 N hydrochloric acid or 64 µg of germanium in 6 N hydrochloric acid was passed on the column at a flow rate of 0.5 ml/min. The concerned element from the column was stripped with various mineral acids or salts as eluants and were determined (9) spectrophotometrically as vanadium 4-(2 pyridylazo) resorcinol at 546 nm; molybdenum [thiocynate at 470 nm]; gold [Rhodamine B at 570 nm] and germanium (phenylfluorone at 510 nm]. The amount of metal in the stripped solution was computed from the calibration curve.

RESULTS AND DISCUSSION

Elution studies. The studies as shown in Table 1 indicated that vanadium, molybdenum, gold or germanium were stripped well with mineral acids. The salts were efficient for elution of vanadium and molybdenum. In case of gold 0.5 N hydrochloric acid containing 70% acetone was best eluant. Germanium was best eluted with 3 N hydrochloric acid.

Separation from binary mixtures. These four elements were separated from alkali, alkaline earths, scandium, yttrium, cobalt, nickel, copper, zinc, lead, aluminium and many other elements in binary mixtures by exploiting the difference in acidity at which these elements are extracted by TBP. Since vanadium was extracted from 6 N hydrochloric acid, it was separated from all other elements not extracting at this acidity. Similarly metals not extractable at 3 N acidity with TBP were separated from molybdenum. In case of gold, most of the elements were unextracted at 0.01 N hydrochloric acid and were thus separated; finally germanium was separated at 6 N acidity (Table 2) from interfering elements.

Separation from multicomponent mixtures. Vanadium was separated from multicomponent mixtures by exploiting the differences in acidity of hydrochloric acid at which metals were extractable with TBP. After extraction of elements vanadium was separated from titanium, chromium, manganese, molybdenum, iron, copper etc (Table 3) by using various concentrations of hydrochloric acids as stripping agent. Vanadium was eluted with 3 N hydrochloric acid while other elements were eluted at various acid concentration.

The separation of molybdenum from thorium, chromium, vanadium, cobalt, uranium, copper and iron was accomplished by selective elution with hydrochloric acid. After extraction of quaternary of multicomponent mixtures on the column, they were sequentially stripped with different concentrations of hydrochloric acid as shown in Table 3.

The separation of gold in multicomponent mixtures from aluminium, vanadium, iron, chromium, copper, molybdenum, nickel, germanium etc were done by stripping gold with 0.5 N hydrochloric acid containing 70% acetone. The interfering ions were first eluted with 6-0.001 N hydrochloric acid (Table 4).

The separations of germanium from iron, chromium, nickel, cobalt, aluminium etc in quaternary mixtures was effected by eluting various elements with hydrochloric acid. Germanium was generally eluted with 3 N hydrochloric acid (Table 4).

The most interesting feature of this work was the separation of vanadium (IV) from vanadium (V), wherein after extraction, vanadium (IV) was eluted with 6 N hydrochloric acid while vanadium (V) was eluted with 0.001 N hydrochloric acid (10). Such method permitted separation of vanadium (IV) from vanadium (V) in any ratio.

These methods were extended for the analysis of vanadium in steel, molybdenum from soil, gold in alloys and germanium in semiconductor materials. The methods were simple, rapid and reproducible.

REFERENCES

1. I.A. Tsarkovnitskaya and V.A. Luginin. Fiz. Khim. 162, 1964. Chem. Abstr. 71 119214 (1969).
2. W. D'ollesslager, M. D'hont. Meded Kon Vlaam Acad Wetensch. Chem. Abstr. 75 13830 (1971).
3. W. D'ollesslager and M. D'hont. J. Nucl. Mat. 44 185 (1972)
4. J. Mincewski and C. Ruzyckii. Chemia Anal (Warsaw) 10 965 (1965).
5. T. Braun and A.B. Farag. Anal Chim. Acta 65 115 (1975).
6. I. Fidelis, R. Gowsids and S. Siekierski. Nucleonika 8 327 (1969).
7. G. Pohlandt and T.W. Steele. Talanta 19, 839 (1972).
8. A.I. Vogel. The text book of quantitative inorganic analysis, Longmans Green (1964).
9. E.B. Sandell. Colorimetric determination of traces of metals, Van Nostrand Reinhold Co. (1970).
10. A.K. De, S.M. Khopkar, R.A. Chalmers. Solvent extraction of metals, Van Nostrand Reinhold (1970).

Table 1 : Elution Studies of Various Elements

Eluant (M)		% Recovery of Elements			
		V	Mo	Ge	Au
HCl	0.5	101.8	100.2	100.2	100 with 70% acetone
	1.0	99.2	100.0	100.0	0
	2.0	101.4	-	100.0	0
	3.0	100.8	-	99.4	0
HNO_3	0.5	100.2	100.2	99.9	0
	1.0	100.8	101.4	99.6	0
	1.5	101.2	101.4	100.2	0
	2.0	98.6	100.4	100.2	0
H_2SO_4	0.5	98.2	100.6	99.8	0
	1.0	101.6	102.0	100.2	0
	1.5	102.1	100.1	101.2	0
	2.0	101.2	101.2	100.2	0
NH_4Cl	0.5	101.6	99.6	-	0
	1.0	100.0	101.2	-	0
	1.5	100.0	100.8	100.1	0
LiCl	0.2	101.1	-	100.2	0
	1.0	98.8	-	100.3	0
NaCl	1.0	100.8	100.5	-	0
	2.0	101.2	101.5	-	0

Table 2 : Separation of Elements from Binary Mixtures

Element	% recovery			
	V	Mo	Au	Ge
Li	100.0	100.0	98.9	100.0
Rb	100.6	101.5	100.4	99.7
Mg	99.7	101.8	98.3	99.4
Sr	101.0	98.8	99.4	100.0
Ba	100.0	100.9	101.1	100.0
Sc	100.0	100.9	100.2	-
Y	102.3	100.0	100.5	99.7
Zr	99.7	98.6	100.8	99.7
Th	99.0	100.1	99.8	100.0
V(IV)	100.0	99.5	100.5	99.4
Cr(III)	101.0	100.0	100.0	99.4
Mn(II)	102.3	100.4	99.7	100.0
Co	98.7	99.2	100.8	100.0
Co	102.3	100.2	98.4	99.4
Ni	100.0	100.0	100.2	100.0
Cu	101.6	100.0	101.4	100.0
Zn	-	-	98.9	99.7
Al	101.6	100.0	99.9	99.7
Pb	98.4	100.9	100.0	100.0
Bi	102.0	100.0	99.2	99.4

Table 3 : Separation of Vanadium and Molybdenum from Mixtures

S.N.	Vanadium			Molybdenum		
	Element	Amt. taken µg	Eluant HCl(M)	Element	Amt. taken µg	Eluant HCl (M)
1	Ti(V)	247.5	6.0	Th/Mn	250.6	2
	V(V)	309.0	3.0	Mo(VI)	216.0	0.5
	Cr(VI)	300.8	0.001	Cr(VI)	300.8	0.001
2	Mn(II)	260.2	6.0	Co/Ni	310.0	2
	V(V)	309.0	3.0	Mo(VI)	108.0	1.5
	Mo(VI)	245.8	0.001	Fe(III)	208.6	0.001
3	Cu(II)	200.8	6.0	Cr(III)	160.4	6
	V(V)	309.0	3.0	V(V)	240.8	2
	Fe(III)	310.0	0.001	Mo(VI)	216.0	0.001
4	Mn/Ni	290.2	6.0	Co(II)	206.4	5
	V(V)	309.0	3.0	U(VI)	110.8	2
	Mo(VI)	122.9	1.0	Mo(VI)	216.0	0.001
	Tl(III)	130.0	0.1+4% thiourea	-	-	-
5	Mn(II)	260.2	6.0	Cu(II)	160.8	6
	V(V)	309.0	3.0	V(V)	240.8	2
	Fe(III)	155.3	1.0	Mo(VI)	108.0	1.5
	Tl(III)	130.2	0.1+4% Tu	Fe(III)	208.6	0.001
6	Ni/Mn	260.2	6.0	Th(IV)	120.4	6
	V(V)	309.0	3.0	U(VI)	110.8	2
	Mo(VI)	122.9	1.5	Mo(VI)	108.0	1.5
	Fe(III)	310.0	0.5	Fe(III)	208.6	0.5
	Cr(VI)	300.8	0.001	Cr(VI)	300.6	0.001

Table 4 : Separation of Gold and Germanium from Mixtures

S.N.	Gold			Germanium		
	Element	Amt. taken	Eluant HCl(M)	Element	Amt. taken	Eluant HCl (M)
1	Al	142.5	6	Ge(IV)	64.3	3
	V(V)	154.5	3	Fe(III)	100.1	1
	Fe(III)	155.3	0.5	Cr(VI)	200.3	0.001
	Cr(VI)	150.4	0.001	-		
	Au	125.3	0.5+70% acetone	-		
2	Ni	164.2	8	Ni/Bi	300.8	6
	Sc	126.2	6	Ge(IV)	128.7	1
	Ge	128.4	2	Cr(VI)	400.6	0.001
	Fe(III)	210.6	0.01	-		
	Au	125.3	0.5+70% acetone	-		
3	Cu(II)	200.8	6	Co/Cr(III)	200.3	6
	V(V)	154.5	3	Ge(IV)	128.7	3
	Mo(VI)	122.9	1.5	Fe(III)	510.3	0.5
	Fe(III)	310.6	0.5	-		
	Cr(VI)	300.8	0.001	-		
	Au	125.3	0.5+70% acetone	-		
4	Ti(V)	147.5	8	Al	70.3	6
	Sc	126.2	6	Ge(IV)	64.3	3
	V(IV)/U(VI)	154.5	2.5	Fe(III)	100.1	1
	Mo(VI)	122.9	1.5	Cr(VI)	200.3	0.001
	Fe(III)	210.6	0.5	-		
	Cr(VI)	300.8	0.01	-		
	Au	125.3	0.5+70% acetone	-		

EXTRACTION SPECTROPHOTOMETRIC DETERMINATION OF PALLADIUM AS RESACETOPHENONEOXIMATE

G. R. Reddy and K. Saraswathi and S. Brahmaji Rao

Chemical Laboratories
S. V. University College
Tirupati 517 502, India

Chemical Laboratories
S. K. University
Anantapur 515 003, India

Oxime reagents give highly selective extraction methods for the determination of palladium[1]. Resacetophenone Oxime (RPO) has been widely employed in our laboratories for the determination of many metal ions by various methods[2-6]. The reaction between palladium and reagent forms a water-insoluble chelate which is extractable into methyl isobutyl ketone(MIBK). The high tolerance limit of nickel makes the method useful for the determination of palladium in nickel ores.

EXPERIMENTAL :

The oxime reagent was prepared by usual method from resacetophenone. The stock solution of the reagent (0.05M) was prepared in 25% aqueous alcohol.

Palladium chloride (BDH, India) was dissolved in concentrated hydrochloric acid and the solution diluted with water. The final acid concentration was adjusted to 0.2M. The solution was standardized for palladium content by the dimethylglyoximate method[7]. All other chemicals are of AR quality.

Absorbance measurements were made using UV spectrophotometer (ECIL, India).

RESULTS AND DISCUSSION :

The extraction of the water-insoluble light yellow chelate into methyl isobutyl ketone was very facile and there was no change in the absorbance for several hours. Quantitative extraction, as evidenced by the absence of polarographic wave for palladium in the aqueous phase, could be achieved in one single extraction and within five minutes of shaking. The complex showed an absorption maximum at 368nm (Fig. 1). Neither the reagent nor the metal ion has any absorbance in the range of study.

Effect of acidity. The chelate showed maximum absorbance of the same magnitude in the region of 0.1-0.25M HCl. An acidity of 0.2M was selected in order to eliminate the interference of some more metal ions.

Effect of reagent concentration. Atleast a ten-fold excess of the reagent (RPO) is necessary for consistency in absorbance.

General procedure. 10ml. of aqueous solution containing the metal ion, RPO, 0.2M HCl and 0.1M $MgSO_4$ were shaken with 10ml. of MIBK for a couple of minutes. Magnesium sulphate was added to maintain sufficient ionic strength to hasten the separation of phases. The organic phase was separated, dried over anhydrous Na_2SO_4 and measured the absorbance at 368 nm. The extraction procedure was repeated with aqueous solution devoid of the metal ion and the organic phase thus obtained was used as the blank.

Applicability of Beer's law. The linear plot (Fig.2) obtained between the amount of the metal ion and absorbance showed that the quantitative determination of palladium can be made in the range 2µg - 25µg of Pd per 10ml. of the organic layer. The molar absorptivity of the complex and Sandell sensitivity were found to be 3.2×10^3 l $mol.^{-1}$ $cm.^{-1}$ and 0.0343 µg/$cm.^2$ respectively.

Composition and stability of the complex. Job's method (Fig. 3) and slope ratio method (Fig. 4) were employed to obtain the composition of the complex according to which the ratio of the metal to ligand is 1:2. The stability constant as calculated from Asmus method[8] (Fig. 5) is 5.35×10^6.

Effect of foreign ions

Palladium : 2×10^{-4}M.
Acidity : 0.2M HCl.

Tolerance limit (molar)	Ions present
2×10^{-2}	Ni(II), Co(II), Cu(II), Cd(II), Zn(II), Mn(II).
1×10^{-2}	Pb(II), Hg(II), Fe(III), Sb(III), Bi(III), La(III), Cr(III), Au(III), V(III), V(IV), Pt(IV), Ce(IV), Th(IV), Zr(IV), Ti(IV), Mo(VI), U(VI), fluoride, phosphate, tartrate, oxalate.

The slight interference from Fe^{3+}, Sb^{3+}, Bi^{3+} and V^{3+} is eliminated by tartaric acid and Ti^{4+} by oxalic acid. V^{5+} interfered seriously.

Palladium is often found in nickel ores besides base metals such as copper and noble metals such as platinum. Hence, the determination of palladium in the presence of large excess of nickel and small amounts of platinum can be successfully achieved by this method.

REFERENCES

1. Marczenko, Z., Spectrophotometric determination of elements 1st Ed., John Wiley and Sons, Inc., New York, 247 (1976).
2. Raja Reddy, G., Curr. Sci., 36, 665 (1967).
3. Mangeswara Rao, P. and Brahmaji Rao, S., Ind. J. Chem., 9, 1014 (1971).
4. ——— and ———, Z.Anal.Chem., 272, 128 (1974).
5. Krishna Reddy, Y. et.al., Talanta, 22, 545 (1975).
6. Prabhakar Reddy, S. et.al., Z.Anal.Chem. 272, 207 (1974).
7. Vogel, A.I., A Text Book of Quantitative Inorganic Analysis, Longmans, Green and Co. Ltd., 3rd Ed., 309 (1961).
8. Asmus, E., Z. Anal.Chem., 178, 104 (1960).

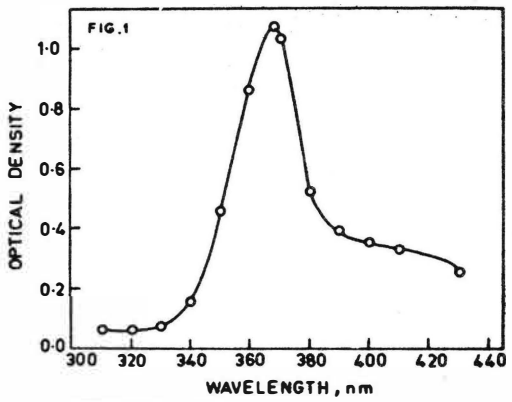
FIG.1
OPTICAL DENSITY
WAVELENGTH, nm

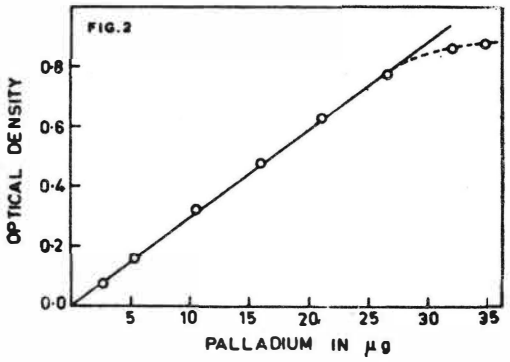
FIG.2
OPTICAL DENSITY
PALLADIUM IN μg

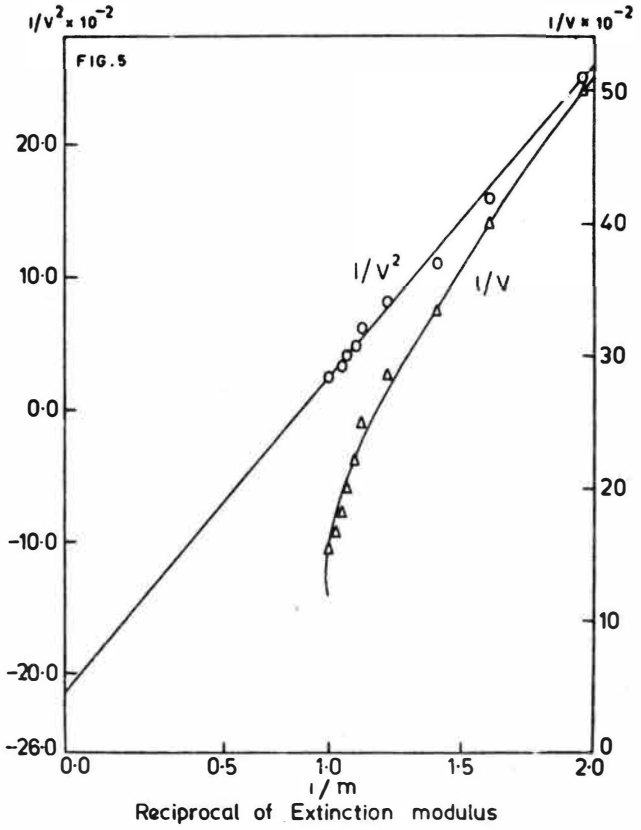
FIG.5
1/V² x 10⁻²
1/V x 10⁻²
1/V²
1/V
1/m
Reciprocal of Extinction modulus

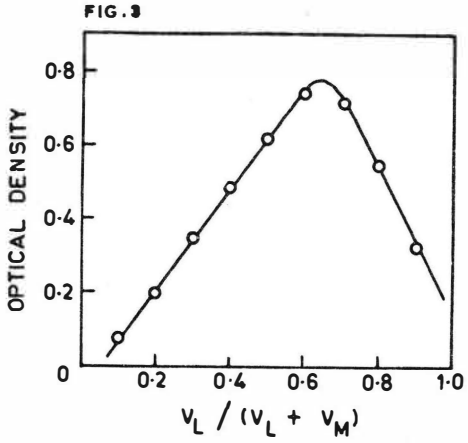
FIG.3
OPTICAL DENSITY
VL / (VL + VM)

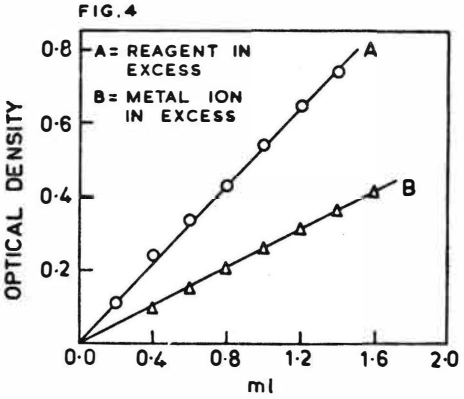
FIG.4
A= REAGENT IN EXCESS
B= METAL ION IN EXCESS
A
B
OPTICAL DENSITY
ml

SYNTHESIS OF SULFOXIDES AND THEIR STRUCTURE - REACTIVITY STUDIES ON THE LANTHANIDE EXTRACTION

Yuan Chengye, Long Haiyan, Ma Enxin
Chen Wuhua and Yan Xiamin

Shanghai Institute of Organic Chemistry
Academia Sinica, Shanghai, China

INTRODUCTION

Sulfoxides owing to the presence of sulfenyl oxygen with higher charge density possess stronger coordination ability towarding metal ions. The extraction behaviours of dialkyl sulfoxides both synthetic products and those derived from petroleum origin for rare earths have been reported eleswhere.(1-4) However, no data was available concerning the dependence of chemical structure of sulfoxides on their extraction properties of lanthanides. The present paper describes the synthesis of various types of sulfoxides and their structure-reactivity studies on the lanthanide extraction.

The sulfoxides studies in this paper may be represented by the formulas:

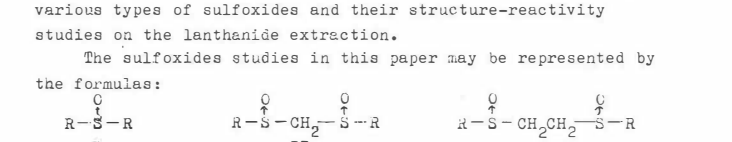

I II III

R = n-C_8H_{17}-, (a); $C_4H_9CH(C_2H_5)CH_2$-, (b); $C_6H_{13}CH(CH_3)$-, (c).

Dialkylsulfoxides(I) as extractants for metal ions including rare earths are wellrestablisked. However, there is lacking in data relating their structure-reactivity studies. As shown by our early reports the selectivity and lipophilicity of an extractant could be improved by introducing branched alkyl groups. In the present paper, the influence of steric hindrance on the extraction behaviours of dialkylsulfoxides with three isomeric octyl groups (Ia, Ib and Ic) for lanthanide was investigated.

Bis(alkylsulfenyl)alkanes (II and III) may be regarded as ligands with two sulfoxide groups being separated by various number of carbon atoms. It is interesting to study the structural effect of ligands on the extraction properties of sulfenyl oxygen, particularly in respects on their ring formation with metal ions. Though the separation of rare earths by bis (octylsulfenyl)methane (BOSM) (IIa) and bis(octylsulfenyl) ethane (BOSE) (IIIa) on reversed phase chromatography has been described(5) but no data on extraction are available. The coordination compound of diethylsulfoxide with rare earth perchlorate has been reported.(6) The methods for the synthesis of compounds II and III with high purity were reported in this paper. Most of them were first published as compound except Ia, Ic, IIa and IIIa.

RESULTS AND DISCUSSIONS

1. Synthesis of Sulfoxides

Dialkylsulfide may be oxidized to corresponding sulfoxide by calculated amount of hydrogen peroxide. The structure and purity of dialkylsulfites strongly influenced the quality of their oxidation products. Under analogous conditions sulfoxides with straight alkyl chains (IIa and IIIa) always contaminated with sulfones as impurity showing SO_2 at 1125cm^{-1} in the infrared region while the IR spectra of sulfoxides with branched alkyl chains (Ib,c; IIb,c and IIIb,c) show only S O at 1020-1030cm^{-1}. It would be rationalized that the presence of branch chain obstrusts the further oxidation process due to steric hindrance. In order to get pure sulfoxide, excess oxidizing agent is avoided and the parent alkylsulfides should be purified carefully.

Most of the synthesized sulfoxide and their intermediates alkylsulfides were unknown as compound. The purity of these compounds was checked by elemental analysis. The data of IR, NMR and Mass spectra were summarized.

2. Chemical Structure and Extraction Behaviours of Sulfoxides

Regularities in extraction of rare earth by sulfoxide from nitrate media

The distribution ratio of rare earth was determined in extraction with various structure of sulfoxide, using 0.5M extractant in xylene as organic phase pre-equilibrated with acid solution of $LiNO_3$. The aqueous solution was composed of 0.05M rare earth nitrate, 6M $LiNO_3$ and 0.28M HNO_3. The acidity of the equilibrated aqueous phase is considerable stable, laying on 0.28±0.05M as a result of using pre-equilibrated organic solvent. The plots of estimated distribution ratio (D) versus atomic number of lanthanides are shown in Figure 1. The D values of $Eu(NO_3)_3$ in extraction by bis(octylsulfenyl) alkanes in chloroform were also estimated.

Influence of types of sulfoxides on their extraction behaviour of rare earth As indicated by Table 1 and Figure 1, under similar extraction conditions, the types of sulfoxide possess significant influences either on their extracting capacity or on the regularities in lanthanide extraction. Mono-sulfoxides, i.e. dioctylsulfoxides, offer lowest D value while di-sulfoxide in which sulfenyl groups were being separated by ethylene linkage, i.e. bis(octylsulfenyl)ethane gives highest D value in lanthanide extraction. Bis(octylsulfenyl)methane, i.e. two sulfenyl groups being separated by methylene unit, locates on medium position in extraction. However, the extracted complex of BOSE with rare earth gives only poor solubility in organic diluents. Similar to the extraction behaviour of neutral alkylphosphate or phosphonate, dioctyl sulfoxides provide apparent tetrad effect in lanthanide extraction. Tetrad effect was also observed in lanthanide extraction by sulfoxide of type II though the beaviour of light rare earths is more or less abnormal in such extraction system. The tetrad effect is not obviously in extraction with sulfoxide of type III due to the sudden increase in D value of Tb, Dy, Ho, Er and Tm, Yb.

Dioctylsulfoxides possess higher separation factor in extraction of light rare earths. For the medium and heavy rare earths, disulfoxide (II and III) show better separation properties. The apparent difference in extraction behaviours amony sulfoxides may be regarded as a result of entropy effect arised from ring formation or formation of polymeric species in which participate two sulfenyl group of disulfoxides in their extraction reaction.

The D value of Y is closely to that of Nd and Yb in extraction by dioctylsulfoxides. For extraction with IIb, IIc and IIIc, the D value of Y is lower than other rare earths except Yb and Lu.

Influence of structure of alkyl group in sulfoxide on their extraction behaviour for rare earths The degree of branch of alkyl group in sulfoxide molecule influences not only on the solubility of the sulfur-containing ligand but also on the behaviour of these compounds in extraction of rare earths. As the incriare of the branch chain near the sulfur atom the extraction ability of either mono-sulfoxide (I) or disulfoxide (II, III) decreased evidently with the seguenc order: n-octyl iso-octyl sec-octyl. The observed structural effect is very similar to that of neutral organophosphonates. For the separation of light rare earths the Pr/La value are closely related to the structure of alkyl group in the mono-sulfoxide (I) with the order: Ib Ic Ia. The compound with iso-octyl radical gives highest separation factor. Analogous situation has been formed for dialkylisopropyl phosphonates and allied extractants. (7, 8)

Influence of diluents on the extraction behaviour of sulfoxides As shown by the data from our experiments the better per-

formance was given by extraction with sulfoxide in xylene rather than in chloroform. The difference in their D values for lathanids laies in two orders of magnitute. This is attributted to the effect of hydrogen bonding resulted from interaction of chloroform with sulfenyl oxygen.

Extraction of nitric acid and water by sulfoxides The distribution ratio of nitric acid in extraction by sulfoxide from agueous 6M $LiNO_3$ solution was determined. A significant difference between the behaviours of nitric acid and rare earths in sulfoxide-extraction was observed. The D value of HNO_3 was decreased in order of dioctylsulfoxide BOSE BOSM. The extraction of nitric acid was inhibited apparently by the higher degree of branch chain in the identical type of sulfoxide. The fact that disulfoxides possess no advantage over monosulfoxides in nitric acid extraction may be associated with the mechansium of extraction. It may be regarded that nitric acid was extracted by sulfoxide via simple solvation mechansium, which is strongly dependent on the charge density of the sulfenyl oxygen. In the molecule of disulfoxides, the Lewis basicity of the coordinating oxygen was reduced by the presence of another neighboring sulfenyl group due to field effect.

By the Karl-Fisher method, the water contents in loaded organic phase in lanthanide extraction by Ia, Ib, Ic and IIb, IIc were estimated. A tendency, though no regularity, towarding the nature of rare earth of the degree of water content in extraction was found. The average water contents in lanthanide extraction by sulfoxides are given: Ia(0.103M) Ib(0.0977M) Ic (0.0740M); IIb(0.39[illegible]M) IIc(0.132M). These data indicate that the water content in organic phase is proportional to the amount of rare earth extracted. The water molecule in organic phase may be associated either with sulfenyl oxygen or with metal ion as hydrated species.

3. The Composition and Physico-Chemical Properties of Coordination Compounds of Disulfoxide with Lanthanium and Proseodymium Nitrate

Method of contimeous variation Results show that either mono-sulfoxide (Ia, Ib) or di-sulfoxide (IIIc) have maxium extraction capacity at L / La =3.0 or 2.0 in both phasess. It may thus be considered that the composition of extracted species will be $La(NO_3)_3$ 3L and $La(NO_3)_3$ 2L.

There is no illegible maximum in continuous variation study for extraction systems of IIb and IIc. Maximum extraction was achieved between 2 and 3 in L to M ratio.

Elemental Analysis, IR and Thermoanalysis of Coordination Compound of Sulfoxide and Rare Earth Nitrate Elemental analytical data for solid complex prepared from IIIb, IIc with lanthanum or neodymium nitrate coincide the calculated value (in parenthesis) for L/M=2. On the other hand, Ia coordinates neodymium nitrate with the formation of $Nd(NO_3)_3$ 3Ia which is confirmed by the method of continuous variation.

The IR spectra of the complex and parent IIIb are given on Figure 3. By comparing the IR spectra of praseodymium complex with the parent ligand IIIb, some obvious differences were observed. With the disceppearance of the original S O sharp absorption ($1020cm^{-1}$) in the ligand, a new band at $980cm^{-1}$ characteristic for associated sulfenyl group was produced.

It is clear that the sulfenyl oxygen participates in coordination. The IR spectra of complex show absorption at 1280 and $1460cm^{-1}$ designating as bidentate feature of C_2V symmetric NO_3 group.

The absorption band at $3400cm^{-1}$ for water molecule in the parent ligand was enhanced and a new broad band at $2300-2600cm^{-1}$ was obsered. So it may be concluded that there is a coordinated water molecule in the prepared complex. Analogous results give IR spectra of complex of IIIb and IIIc with lanthanum nitrate.

The differential thermo-gravimetric analysis of $Ln(NO_3)_3$· IIIc (Fig 4) indicates that decomposition and weight loss on heatint occurs at 207°C and terminated at about 500°C. Residual weight is 32.7% corresponding to calculated wt. value (31.7%) for $La(NO_3)_3$ based on L/M=2.0 in complex composition. The residue thus obtained was further decomposed by heating. The final residue obtained at 745°C weights 14% which is approximately to the calculated value (15.7%) for La_2O_3. Based on the differential thermal analytical data as well as data from method of continuous variation and elemental analysis we may predict that disulfoxide consisting two sulfenyl groups forms coordination compound with lanthanum nitrate possessing composition of L/M=2, As shown by IR spectra, both of two sulfenyl groups participate in coordination and the nitro group acts as bidentate. So the coordination number of lanthanum will be as high as 10. It is resonable to postulate that the two sulfenyl group either form ring compound or bridged as polymeric species with lanthanum ion. For the elucidation of the fine structure of these coordiation compounds, further investigation seems necessary.

References

(1) Mikhailichenko, A. I. Proceedings of International Solvent Extraction Conference 1974 Vol.2, p.16.

(2) Никитин, Д.Е. Успехи Химии 12(1976) 2233.

(3) Дяскорин, В.Н. ДАН СССР сер.Хим. 241 (1978) 107.

(4) Ramakrishna, V. V. J. Radiochem. Chem. 47 (1978) 57.

(5) Konnedy, D. C. USAEC IS-T-293 (1969); Talanta 17 (1970)

(6) Lakatos Osorio, V. K. de Oliveira, A. and Giesbrecht, E. J. Inorg. Nucl. Chem., 42 (1980) 930.

(7) Yuan Chengye, Ye Weizhen, Ma Enxin, Wu Fubing and Yan Xiaomin, "The Rare Earths in Modern Science and Technology Vol.3 Proceedings of 15th Rare Earth Research Conference" Ed. by G. J. McCarthy, Plenum Publishing Co. New York, N. Y. 1982 pp 499-503.

(8) Yuan Chengye, Ye Weizhen, Ma Enxin, Wu Fubing and Yan Xiaomin, Scientia Sinica (Series B) 1982, 597; English Edition, 25 (1257) 1982.

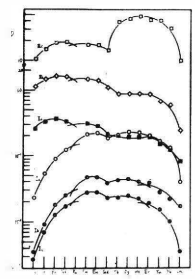

FIGURE 1
Lanthanide Extraction by Sulfoxides (25°C) O-Ia, ●-Ib, ◐-Ic, ◇-IIb, ◆-IIc, ◑-IIc [Extractant] 0.5M in xylene. $[Ln(NO_3)_3]$0.05M, $[HNO_3]$ 0.280M, $[LiNO_3]$6M

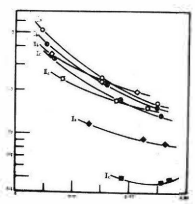

FIGURE 2
Extraction of Nitric Acid by Sulfoxides [Extractant]0.5M in xylene, $[HNO_3]$0.280M, $[LiNO_3]$6M

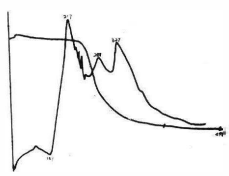

FIGURE 4
TG and DTA Diagram of Complex of Bis(1-methylheptylsulfenyl) ethane (IIIc) with Lanthanum Nitrate

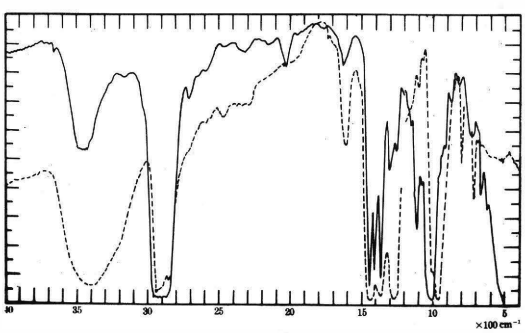

FIGURE 3
IR Spectra of Bis(2-ethylhexylsulfenyl)ethane (solide line) and its Complex with Praseodymun Nitrate (dasned line)

EXTRACTION OF U(VI) FROM NITRIC ACID BY DI(2-ETHYLHEXYL) SULFOXIDE, A PROMISING NEW BRANCHED-CHAIN EXTRACTANT*

Bruce Moyer, W. J. McDowell and G. N. Case

Chemical Technology Division
Oak Ridge National Laboratory
Oak Ridge, Tennessee 37830 USA

*Research sponsored by the Division of Chemical Sciences, U.S. Department of Energy under contract W-7405-eng-26 with the Union Carbide Corporation.

Dialkyl sulfoxides have for many years been considered attractive potential extractants for use in nuclear applications (1-4). Their advantages include good thermal stability, low toxicity, potentially abundant and economical supply, noncorrosivity, nonvolatility, and good coordination ability. However, the chief appeal of sulfoxide extractants lies in the inherently weak extractive power of their possible radiolytic degradation products such as sulfides and sulfones. Hence, the ability of the sulfoxide extraction system to reject fission products is not expected to deteriorate greatly with increasing radiation dose. Such an advantage would represent a significant improvement over extraction systems based on tributyl phosphate (TBP), which gives rise to troublesome degradation products. Although further investigations into the effects of radiolysis are required, the limited data available indicate that the selectivity characteristics of dialkyl sulfoxides do indeed hold up well under high radiation conditions in comparison with TBP (5-6).

Despite widespread interest in sulfoxide extractants, practical application of dialkyl sulfoxides in nuclear separations has been severely impeded by the impractically low solubility of dialkyl sulfoxides in nonaromatic hydrocarbon diluents. Following encouraging results from an earlier study of unsymmetrical sulfoxides (7), we were led to study di(2-ethylhexyl) sulfoxide (DEHSO), which is, in fact, completely miscible with dodecane. In this paper, we wish to report our results on the extraction of uranyl nitrate from nitric acid by DEHSO in dodecane.

EXPERIMENTAL SECTION

DEHSO was obtained commercially (Fairfield Chemical Co.), purified by molecular distillation, and analyzed by IR spectrophotometry, thin layer chromatography, liquid chromatography, and elemental analysis. Samples estimated to be 97 and 99.5% pure were used with no apparent difference in extraction behavior. Except as noted, solutions of DEHSO in dodecane were pre-equilibrated with uranium-free nitric acid solutions before contact with the respective uranium-containing solutions to ensure that the aqueous nitric acid concentration would remain unchanged during uranium extraction experiments. Equilibrations were carried out at 25°C with slow stirring for at least 10 h. Natural uranium at relatively low aqueous concentrations (less than 0.01 M) was augmented with U-233 tracer for analysis by alpha liquid scintillation counting.

NITRIC ACID EXTRACTION

In general, dialkyl sulfoxide extractants similar to DEHSO have little tendency to aggregate in dilute solution, but they do extract mineral acids, especially nitric acid, to a significant degree (1-6,8-11). To aid in the interpretation of the uranium extraction data, nonaqueous titrimetry was employed to determine the nitric acid extraction isotherm at 25°C using 0.1 M DEHSO in dodecane. It was observed that at aqueous nitric acid concentrations greater than 0.5 M, appreciable concentrations of nitric acid exist in the solvent (i.e., $[HNO_3]_{org} > 0.005$ M). Over the aqueous concentration range 0.1 to 8 M HNO_3, the mole ratio of extracted nitric acid to total sulfoxide increased to a plateau value of 1.0, suggesting the stoichiometric formation of the nitric acid complex DEHSO·HNO_3. At higher aqueous nitric acid concentrations, excess nitric acid was extracted, but this was associated with the formation of a third phase and was not characterized further. At the lower nitric acid concentrations, the leveling off of the isotherm at the 1:1 stoichiometric ratio suggests the equilibrium

$$(1) \qquad H^+ + NO_3^- + \underline{\text{DEHSO}} \rightleftharpoons \underline{\text{DEHSO}\cdot HNO_3}$$

where dotted underlining denotes organic phase species. Following previous workers (5,6,8-11), we have analyzed the equilibrium in terms of the equilibrium expression

$$(2) \qquad K_h' = \frac{[\text{DEHSO}\cdot HNO_3]}{a_{HNO_3}[\text{DEHSO}]} = \frac{[HNO_3]_{org}}{a_{HNO_3}\,([\text{DEHSO}]_o - [HNO_3]_{org})}$$

where a_{HNO_3} is the aqueous nitric acid activity (12), $[HNO_3]_{org}$ is the organic nitric acid molarity, and $[\text{DEHSO}]_o$ is the initial concentration of DEHSO (0.1 M). The pseudo equilibrium constant K_h' is related to the thermodynamic equilibrium constant K_h through the expression $K_h' = K_h(\gamma/\gamma_h)$ where K is multiplied by the ratio of activity coefficients of sulfoxide to sulfoxide-nitric acid complex. As was also done for the case of uranium extraction, the ratio of activity coefficients of organic species was assumed practically constant. A plot of $\log([HNO_3]_{org}/([\text{DEHSO}]_o - [HNO_3]_{org}))$ vs $\log a_{HNO_3}$ gave a slope of 0.88, indicating predominant formation of the 1:1 complex, DEHSO·HNO_3. The small discrepancy in the experimental slope compared to the theoretical value of 1 suggests that more highly solvated nitric acid species such as $(\text{DEHSO})_2\cdot HNO_3$ may also be involved to some degree.

Using least squares curve fitting procedures, the mathematically predicted isotherm is, in fact, a significantly better fit to the data when both DEHSO·HNO_3 and $(\text{DEHSO})_2\cdot HNO_3$ are assumed to be present than when the chemical model includes only DEHSO·HNO_3. To determine the species present and their respective equilibrium constants with high confidence, we are currently measuring HNO_3 extraction isotherms as a function of DEHSO concentration. However, for equilibrium aqueous nitric acid concentrations greater than 0.5 M, Eqs. 1 and 2 approximate the isotherm to within 10% using the value $K_h' = 0.45$, which is in line with other known values (5,6,8-11). Hence, for correction to the free DEHSO concentration, we are employing the approximation

$$(3) \qquad [\text{DEHSO}] = [\text{DEHSO}]_o - [HNO_3]_{org} = [\text{DEHSO}]_o\left(\frac{1}{1 + K_h' a_{HNO_3}}\right)$$

U(VI) EXTRACTION

Like TBP and related neutral complexing extractants, dialkyl sulfoxides extract U(VI) chiefly via a disolvated complex in which the extractant functions as an oxygen-donor ligand (1-6,11,13-16). The relevant equilibrium and associated pseudo equilibrium constant are given in Eqs. 4 and 5:

$$(4) \qquad UO_2^{2+} + 2NO_3^- + \underline{2\text{DEHSO}} \rightleftharpoons \underline{(\text{DEHSO})_2UO_2(NO_3)_2}$$

$$(5) \qquad K_u = \frac{[(\text{DEHSO})_2UO_2(NO_3)_2]}{[UO_2^{2+}][NO_3^-]^2\gamma_\pm^3[\text{DEHSO}]^2}$$

where $\gamma_\pm$ is the aqueous uranyl nitrate activity coefficient. To confirm the validity of this model, we employed slope analysis of the results of U(VI) distribution experiments as a function of the concentrations of sulfoxide, aqueous U(VI), and aqueous nitrate. It was assumed throughout the analysis that the effect of the low organic concentration of U(VI) on the effective concentration of DEHSO was negligible. However, three potentially significant effects complicate the overall picture. First, nitric acid extraction, approximated by Eq. 3, decreases the effective concentration of sulfoxide available for the U(VI) extraction. Second, uranyl ion undergoes complexation with nitrate ion in the aqueous phase according to the equilibrium

$$(6) \qquad UO_2^{2+} + NO_3^- \rightleftharpoons UO_2(NO_3)^+$$

$$(7) \qquad \beta = \frac{[UO_2(NO_3)^+]}{[UO_2^{2+}][NO_3^-]}$$

The extent of this complexation may be estimated from the pseudo equilibrium constant β (defined in Eq. 7), having values in the range 0.2 to 0.5 (17-19). Assuming that the uranyl ion and its nitrate complex together comprise the total aqueous uranium concentration $[U]_{aq}$, Eq. 7 becomes

$$(8) \qquad [UO_2^{2+}] = [U]_{aq}\left(\frac{1}{1 + \beta[NO_3^-]}\right)$$

The third effect involves the tendency of nitric acid to become associated in aqueous nitric acid solutions more concentrated than approximately 1 M (12). Under such conditions, it is necessary to correct the free nitrate concentration for partial association, but under the conditions that we employed in the slope analysis, the aqueous nitric acid was low enough that this effect may be safely considered negligible.

The combined effect of nitric acid extraction and aqueous nitrate-uranium complexation on the overall extraction equilibrium may be obtained by substitution of Eqs. 3 and 8 into Eq. 5. Defining the U(VI) distribution coefficient as $D = [U]_{org}/[U]_{aq} = [(\text{DEHSO})_2UO_2(NO_3)_2]/[U]_{aq}$ where $[U]_{org}$ is the total organic uranium concentration, we have approximately

$$(9) \qquad D = K_u\left(\frac{1}{1 + \beta[NO_3^-]}\right)[NO_3^-]^2\gamma_\pm^3[\text{DEHSO}]_o^2\left(\frac{1}{1 + K_h' a_{HNO_3}}\right)^2$$

With suitable choice of conditions, Eq. 9 readily yields to slope analysis to confirm the stoichiometric coefficients of the model extraction equilibrium (Eq. 4).

Over the U(VI) concentration range 0.0004 to 0.01 M in 1 M HNO_3, the U(VI) distribution coefficient using 0.1 M DEHSO remained constant (0.34 ± 0.01) as expected on the basis of Eq. 9 since all the variables are essentially constant. In the general sense, the constancy of the distribution coefficient implies the mononuclear nature of the extracted U(VI) species. The solvation number was confirmed by measuring D as a function of the sulfoxide concentration with the aqueous nitric acid concentration fixed at 1 M. Simplification of Eq. 9 leads to $\log D = 2\log[\text{DEHSO}]_o$ + constant, predicting a linear plot of slope = 2. As shown in Figure 1, over the interval 0.003 to 0.4 M DEHSO, a linear plot of log D vs $\log[\text{DEHSO}]_o$ with slope = 2.1 was obtained, in close agreement with the prediction based on formation of a disolvated complex.

As implied by Eq. 9, the U(VI) distribution coefficient varies in a complicated fashion with aqueous nitrate ion concentration due to nitric acid extraction, partial nitric acid dissociation, and aqueous complexation phenomena. However, if the acidity and nitrate concentration are relatively low, these effects become negligible. Distribution coefficients were therefore measured at a constant acid concentration of 0.02 M HNO_3, adjusting the total nitrate concentration with 0 to 0.2 M $NaNO_3$. Uranyl nitrate activity coefficients were estimated from Debye-Huckel considerations. Under these conditions, Eq. 9 reduces to

$$(10) \qquad \log(D/\gamma_\pm^3) = 2\log[NO_3^-] + \log(K_u[\text{DEHSO}]_o^2)$$

In agreement with this expression, we obtained a linear plot of $\log(D/\gamma_\pm^3)$ vs $\log[NO_3^-]$ with slope = 2.05. The value for the pseudo equilibrium constant K_u was found to be 5.0 (±0.2) x 10^2, well within the rather wide range of known values for dialkyl sulfoxides (1-6,11,13-16). However, since DEHSO is the first sulfoxide to be so characterized in an alkane diluent, it is difficult to make any judgment concerning

its effectiveness in comparison with the other sulfoxides, which by necessity have been studied in other solvents.

COMPARISON WITH TBP

Since much of the research concerning nuclear fuel cycle separations has focused on TBP chemistry, a direct comparison of U(VI) extraction behavior by TBP and DEHSO (both 0.4 M in dodecane) was obtained as a function of nitric acid concentration (see Figure 2). Both extractants form disolvated uranyl nitrate complexes according to the stoichiometry of Eq. 4, and the curves therefore exhibit similar behavior, rising with slope near 2 and then falling off at moderately high nitric acid concentrations. The downturn is widely ascribed to the competing effect of nitric acid extraction. As a result of the generally stronger electron donor properties of dialkyl sulfoxides compared to trialkyl phosphates (1-4), DEHSO extracts U(VI) more strongly than TBP over much of the nitric acid concentration range. However, the greater tendency of the more basic sulfoxide to extract nitric acid causes the DEHSO curve to start falling off at lower nitric acid concentration than does the TBP curve.

The comparison shows that DEHSO is a suitably strong extractant for U(VI). Obviously, a complete assessment of its potential in nuclear applications must include many factors such as ease of stripping, radiation stability, and especially selectivity over fission products. In the complete analysis, the stronger extraction capabilities of sulfoxides may or may not prove to be a real advantage. With regard to selectivity, sulfoxides are expected to behave much like TBP (1-4) with the notable exception of certain metals like palladium which may apparently be extracted by sulfoxides by sulfur bonding. Not nearly enough work has been done to evaluate sulfoxide performance.

CONCLUSIONS

A promising new branched-chain sulfoxide extractant, di(2-ethylhexyl) sulfoxide, has been introduced for possible application in nuclear fuel cycle separations. Its primary advantages include complete miscibility with dodecane, good U(VI) extraction characteristics, and likely resistance to degraded performance under high radiation conditions. Slope analysis applied to U(VI) distribution experiments from nitric acid solutions indicated predominant formation of the disolvated organic phase complex $(DEHSO)_2UO_2(NO_3)_2$. The pseudo equilibrium constant for U(VI) extraction was found to be 5.0 (±0.2) x 10^2. At aqueous nitric acid concentrations greater than approximately 0.5 M, nitric acid extraction competes with uranium extraction by the predominant formation of the species $DEHSO{\cdot}HNO_3$. Uranium distribution coefficients for DEHSO are significantly higher than those for TBP at nitric acid concentrations below 2 M and are roughly comparable in the range 2 to 7 M HNO_3 where nitric acid extraction strongly interferes.

ACKNOWLEDGMENTS

This work was supported by the Division of Chemical Sciences, U.S. Department of Energy under Contract W-7405-eng-26 with the Union Carbide Corporation. We would also like to thank R. R. Shoun for liquid chromatographic analyses and C. F. Coleman for valuable advice and guidance.

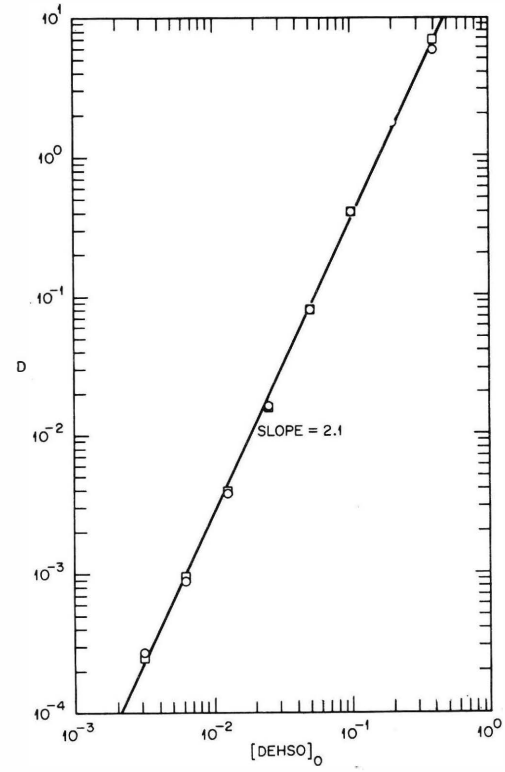

Figure 1. VARIATION OF U(VI) DISTRIBUTION WITH DEHSO CONCENTRATION. Two sets of data are shown, representing two different distillation fractions of DEHSO (O - 97% and □ - 99.5% pure). Conditions: 1 M HNO_3, 25°C.

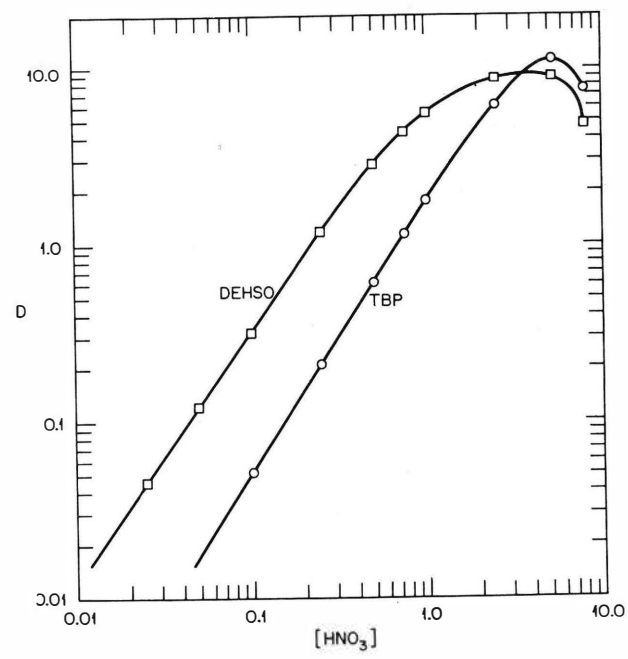

Figure 2. COMPARISON OF U(VI) EXTRACTION BY TBP AND DEHSO. Conditions: 0.4 M DEHSO or TBP in dodecane (not pre-equilibrated with nitric acid), 25°C.

REFERENCES

1. M. T. Chaleb and G. Laurence, Energ. Nucl. 13, 106 (1971).
2. A. M. Rozen, Y. I. Murinov, Y. E. Nikitin, and V. S. Pilyugin, Radiokhimiya 16, 118 (1974).
3. V. A. Mikhailov, V. G. Torgov, E. N. Gilbert, L. N. Mazalov, and A. V. Nikolaev, Proceedings of the International Solvent Extraction Conference, The Hague, 1971, vol. II, Society of Chemical Industry, London, 1971, pp. 1112-19.
4. V. A. Mikhailov, Proceedings of the International Solvent Extraction Conference, Toronto, 1977, vol.1, The Canadian Institute of Mining and Metallurgy, 1979, pp. 52-60.
5. J. P. Shukla, S. A. Pai, and M. S. Subramanian, Sep. Sci. Technol. 14, 883 (1979).
6. S. A. Pai, J. P. Shukla, P. K. Khopkar, and M. S. Subramanian, J. Radioanal. Chem. 42, 323 (1978).
7. W. J. McDowell and H. D. Harmon, J. Inorg. Nucl. Chem. 33, 3107 (1971).
8. W. Korpak, Nukleonika 8, 747 (1963).
9. M. T. Chaleb and G. Laurence, Bull. Chim. Soc. Fr., 1233 (1972).
10. A. M. Rozen, Y. I. Murinov, Y. E. Nikitin, and N. Z. Mineeva, Radiokhimiya 14, 750 (1972).
11. D. M. Petkovic and G. J. Laurence, Bull. Chim. Soc. Fr., 949 (1975).
12. W. Davis, Jr., and H. J. de Bruin, J. Inorg. Nucl. Chem. 26, 1069 (1964).
13. V. G. Torgov, A. V. Nikolaev, V. A. Mikhailov, L. G. Stadnikova, and I. L. Kotlyarevskii, Rus. J. Inorg. Chem. 13, 119 (1968).
14. A. M. Rozen, Y. I. Murinov, and Y. E. Nikitin, Radiokhimiya 12, 355 (1970).
15. R. P. Fedoezzhina, E. P. Buchikhin, A. I. Zarubin, and E. A. Kanevskii, Radiokhimiya 16, 638 (1974).
16. G. Laurence, J. Inorg. Nucl. Chem. 32, 3065 (1970).
17. R. H. Betts and R. K. Michels, J. Chem. Soc., S286 (1949).
18. S. Ahrland, Acta Chem. Scand. 5, 1271 (1951).
19. R. A. Day, Jr., and R. M. Powers, J. Chem. Soc., 3895 (1954).

N-NITROSO-N-CYCLOHEXYLHYDROXYLAMINE AS A REAGENT FOR THE GROUP SOLVENT METAL EXTRACTION

O. Petruchin and N. Kolycheva

D. I. Mendeleev Institute of Chemical Technology
Moscow, USSR

N-Nitroso-N-phenylhydroxylamine (NPHA) which ammonium salt is known as cupferron, is one of the highly efficient reagents used for the metal group solvent extraction. Cupferron is particularly suitable to extract readily hydrolyzable metal ions since it allows one to extract them from acidic solutions. A low stability to oxidation, especially at elevated temperatures, is a serious limitation for cupferron and its analogues when used as extracting reagents. The more stable analogue of cupferron, N-nitroso-N-cyclohexylhydroxylamine (NCHA), was proposed for the first time by Buscarons et. al.(1) as a reagent for the precipitation of a large number of metals. We studied the properties of NCHA and the possibilities to use it for a metal group solvent extraction.

NCHA and its sodium and ammonium salts were synthesized as described in (2,3) from chlorohexane and nitrosyl chloride. It was shown on the basis of spectral studies that two tautomeric structures, namely, nitroso-N-hydroxylamine (I) and N-hydroxydiimide-N-oxide (II), are inherent for NCHA as well as for other derivatives of N-nitroso-N-hydroxylamines:

|1|

Tautomers ratio in a series of analogous reagents varies with electrophilic properties of a hydrocarbon fragment R. The oxidative destruction of a reagent, accompanied by the nitrogen-nitrogen bond breaking, follows the equilibrium shift in favour of tautomer I. The less extent of this shift for NCHA, as compared with that of cupferron, is namely the reason for its higher stability in oxidation reaction. The kinetics and mechanism of NCHA destruction in various media was studied. We have shown the possibility to use NCHA for solvent metal extraction even from strongly acidic aqueous media and at elevated temperatures. The NCHA sodium salt is the most stable form of the reagent. Practically it is not decomposed when stored under convenient conditions for more than four years.

The constants, characterizing NCHA as extracting reagent, were also determined. NCHA is of a more basic nature than its aromatic analogue, NPHA. In aqueous $NaClO_4$ solution (μ=0.1) at 20±1°C NCHA yields the following ionization constants: $pK_{H_2A^+}$=0.42, pK_{HA} =5.58±0.04 (P=0.95, m=7). The dissociation constants for NCHA were also determined in water-dioxan $NaClO_4$ solutions (μ=0.1) at 25±1°C. The pK_{HA} values (with different volume content of dioxan being shown in brackets) are as follows: 6.82±0.04 (40%), 7.60 ±0.03 (62.5%), 7.81±0.03 (70%), 8.01±0.03 (75%). The distribution of NCHA between aqueous $NaClO_4$ solutions (μ=0.1) and organic solvents: chloroform, hexane and decane-was studied. Here are the corresponding partition constants (lgP_{HA}): 1.98±0.03; 0.9±0.1 and 0.6±0.1 (m=5 ÷ 7, P=0.95).

The complex formation by some metal ions with NCHA in aqueous solution is characterized by stability constants listed in Table 1. These were obtained when studying the water-chloroform partition of metals.

Table 1

Overall ($lg\beta_n$) and stepwise (lgK_n) stoichiometric stability constants for NCHA chelates in aqueous solution (μ=0.1, $NaClO_4$) at 20°C±1 (m=8÷13, P=0.95)

M	lg K_1	lg K_2	lg β_2	lg K_3	lg β_3
Cu(II)	7.7±0.6	7.2±0.6	14.9±0.3	-	-
La(III)	3.5±0.5	2.6±0.5	6.1±0.5	2.4±0.3	8.5±0.5
Eu(III)	5.6±0.6	3.9±0.6	9.5±0.5	4.6±0.5	14.1±0.4
Lu(III)	4.6±0.3	4.6±0.3	9.2±0.3	3.4±0.3	12.6±0.9

The stability constants ($lg\beta_n$) in water-dioxan (70 vol.% of dioxan) solution (μ=0.1, $NaClO_4$) are listed below for chelates of copper (CuA_2), REE (LnA_3, for Ln = La, Nd, Sm, Eu, Gd, Tb, Er, Lu) and thorium (ThA_4), respectively, obtained by potentiometry at 25°C: 13.3±0.6; 18.1±0.1; 18.0±0.7; 18.8±0.4; 19.0±0.9; 17.3±0.2; 18.2±0.7; 18.8±0.5; 17.6±0.7 and 30.0±0.5. Linear correlations of the chelate stability constants with parameters that measure both the electrostatic and covalent bond forming ability of metal ions have been obtained. Such correlations suggest two different models for complex formation, namely, ionic and covalent, for different (class "a" and "b", or "hard" and "soft") metal ions. At the same time, the spectrometric data indicated the change of ligand electronic structure in chelates (ligand tautomerism like |1|) with the nature of central atom. It is the ligand tautomerism that explains the group chelating and hence the extraction properties of NCHA.

The possibility of extraction of 26 metals by NCHA was estimated through the extraction paper chromatography. The distribution of some metal chelates between aqueous solutions of different acidity and chloroform was studied too. NCHA, like cupferron, extracts from mineral acid solutions the following metal ions: Mo(VI), V(V), Ti(IV), Zr(IV), Hf(IV), Th(IV), Fe(III), Bi(III), Al(III), Cu(II). Thus titanum is best extracted in the acidity range from 2.6N H_2SO_4 up to pH 7.5 . For iron the pH interval ranges from 1.5 to 6.0 . The maximal values for the aluminium distribution coefficient (lg D~3.5) are obtained in the pH range 4÷8. However, aluminium is well extracted from slightly acidic solutions (pH 1) too. The data presented below characterize some extraction systems involving NCHA and cupferron. The part of the data was obtained by ourselves, the other (for copper and lantan cupferronate systems) is cited from (4-7). The solvent, unless otherwise stated, is chloroform (μ=0.1, $NaClO_4$).

Table 2

M	pH^{I}_{50}	lg K_{ex}	$lg(\beta_N \cdot P_{MA_N})$	$lg\beta_N$	lgP_{MA_N}	Reagent	Ref.
Cu(II)	-0.65	1.35	17.9	14.9	3.0	NCHA	
	-1.4	2.66	15.3			NPHA	(4,5)
La(III)	4.2	-11.4	10.3	8.5	1.8	NCHA	
	2.1	-6.22	12.7			NPHA	(5)
	1.9		12.7			NPHA	(6)
	1.5*		13.7*	12.9	0.75*	NPHA	(7)
Eu(III)	2.2	-7.6	16.2	14.1	2.1	NCHA	
	1.3				0.9	NPHA	
Lu(III)	2.4	-6.3	15.2	12.6	2.6	NCHA	

*) Solvent - methyl isobutyl ketone.

The low extent of REE cupferronates extraction was attributed by Dyrssen (7) to their high hydration. Chelates with a more basic NCHA are hydrated to a less extent. The extraction of these chelates declines in a series $LaA_3 < LuA_3$ in step with the decrease in their stability constants.

The composition of chelates of some REE with NCHA is determined by elemental and thermogravimetric analyses, confirmed by extraction data, and corresponds to the following formula: $LnA_3 \cdot nH_2O$, where n=1 for Ln=La,Eu, and n=0 for Ln=Er,Lu. Water is removed from lanthanum and europium chelates in the temperature range of 117 - 137°C and 102 - 122°C, respectively. This evidences in favour of a low degree of hydration of REE N-nitroso-N-cyclohexylhydroxylaminates. The hydration of chelates decreases in a series $LaA_3 > LuA_3$.

The effect of donor-active compounds, triphenyl- (TPPO) and tri-n-octylphosphinoxide (TOPO), on the extraction of some REE chelates with NCHA and cupferron, was studied. When interacting with TPPO the acceptor ability of chelates with NCHA varied in a series $LaA_3 > LuA_3$. These data were substantiated by the PMR studies on the formation equilibria of mixed complexes MA_nB_m, where B is the TPPO molecule, in the deuterochloroform solution. Thus the formation of two lanthanum adducts, LaA_3B and LaA_3B_2, and just one, much less stable, lutecium adduct, LuA_3B, was established. The addition of a more basic donor, TOPO, into the europium (III)/NCHA extraction system caused antagonistic effect. Changing TOPO for TPPO required the concentrations of the latter high enough for the europium synergetic extraction (Fig.1). At the same time the addition of even 0.1M TPPO solution in chloroform into the cupferron-containing system resulted in the appreciable synergetic effect (Fig.2). This fact is accounted for by the less acceptor ability of europium-NCHA chelate as compared with that of corresponding cupferronate. The formation energy of adducts of europium N-nitroso-N-cyclohexylhydroxylaminates with TOPO and TPPO is comparable with that of H-bonding of NCHA with phosphinoxides.

Extraction of lanthanum and lutecium by NCHA into molten benzophenon at 60°C was studied. The conditions were established for the extraction enrichment of REE, yttrium and scandium followed by the X-ray fluorescent determination of elements in the solid benzophenon matrix. TPPO or stearic acid was added to the system to ensure the quantittative element extraction in a single process (especially at higher volume ratio of aqueous and organic phases). TPPO is the most effective additive when extracting the microelements. The extraction - X-ray - fluorescent method was developed for the determination of REE, yttrium and scandium, over a wide range of their concentrations. The method is characterized by the high rates of a process, fair precision ($S_r \leqslant 0.05$) and low detection limits (of 10^{-7} g/ml order of magnitude).

CONCLUSIONS

1. N-Nitroso-N-cyclohexylhydroxylamine (NCHA) is the analogue of cupferron, which is more stable to the thermal oxidation destruction. It can be used for effective group extraction of a large number of metals from acidic and neutral solutions.

2. NCHA is preferable to cupferron when used to extract the metal ions with high and variable coordination number, e.g. REE, due to the formation of less hydrated chelates.

3. The acceptor ability of Ln(III)-NCHA chelates declines in a series of central atoms from lanthanum to lutecium.

4. The method is developed for the extraction - X-ray - fluorescent determination of REE, yttrium and scandium over a wide range of element concentrations. The method is characterized by the fair precision and low detection limits.

REFERENCES

1. Buscarons F., Canela J., Anal. Chim. Acta, 67, 349 (1973)
2. Muller E., Metzger H., Ber., 89, 396 (1956)
3. Pape M., Raff P., F.R.G. Patent 1,543,376 , Int. Cl.: C 07c, 111/00; C 07c, 83/00
4. Equilibrium constants of liquid-liquid distribution reactions. Part IV. Chelating extractants.(Prepared for publication by J. Stary and H. Frieser,-Oxford-N.Y., Pergamon Press, 1978
5. Stary J., Smizanska J., Anal. Chim. Acta, 29, 545 (1963)
6. Dyrssen D., Dahlberg V., Acta Chem. Scand., 7, 1186 (1953)
7. Dyrssen D., Svensk. Kem. Tidskr., 66, 234 (1954)

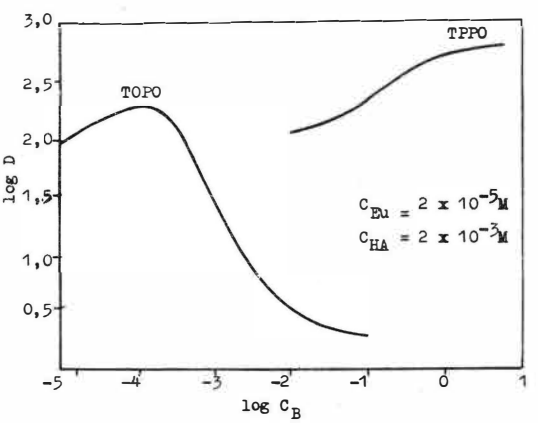

FIG.1. EXTRACTION OF EUROPIUM (III) BY NCHA AND NEUTRAL EXTRACTANTS (C_B) (TPPO or TOPO) IN CHLOROFORM. AQUEOUS PHASE: 0.1 M $NaClO_4$, 10^{-3}-10^{-4} M ACETATE; pH 7.6±0.2

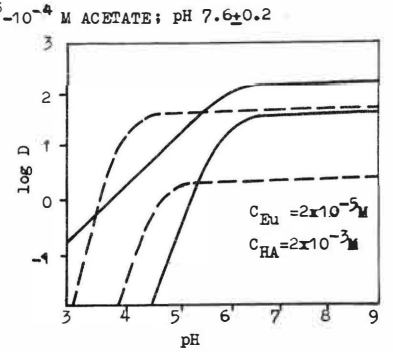

FIG.2. EXTRACTION OF EUROPIUM (III) BY NCHA or CUPFERRON (NPHA) AND THEIR MIXTURES WITH TPPO IN CHLOROFORM: 1 - NCHA; 2 - NCHA+TPPO; 3 - NPHA; 4 - NPHA+TPPO. AQUEOUS PHASE: 0.1 M $NaClO_4$, 10^{-3}-10^{-4}M ACETATE

NN' DIALKYL ALIPHATIC AMIDES AS ALTERNATIVE EXTRACTANTS FOR ACTINIDES: FURTHER STUDIES ON THE INFLUENCE OF THE CHEMICAL STRUCTURE ON THE EXTRACTIVE BEHAVIOR

Giuseppe Grossi, Giulio M. Gasparini, Maurizio Casarci

E.N.E.A.-C.R.E. Casaccia
Rome, Italy

INTRODUCTION

N N' Dialkyl aliphatic amides:

$$R - \underset{\underset{O}{\|}}{C} - N\begin{matrix} R' \\ R' \end{matrix} \qquad R = C_n H_{2n+1} \ (n = 1\text{-}8)$$

$$R' = C_{n'} H_{2n'+1} \ (n' = 1.6)$$

are good extractants of U^{VI}, Pu^{IV} and Np^{IV} and at same time, they do not extract fission products. During the past years we have studied extensively the extracting behavior of some of these compounds and we have proposed some applications of those extractants expecially regarding the separation of uranium from thorium. The work carried out until now, in laboratory mini pilot and pilot plant scale have been reported elsewhere (1) (2).
However, the most interesting application of these compounds is as alternative extractants of TBP for the separation of U and Pu from the fission products. Amides, in fact, present some evident advantages with regard to the TBP as summarized in Table 1 : in particular, the U stripping is much easier, and the degradation products are much less dangerous.
Moreover the behavior of the distribution curves for U and Pu, for some amides of particular structure, show the possibility to separate these two actinides without any Plutonium reduction. On the other side, the most evident disadvantage of amides with respect to TBP is a more elevated tendency to give third phases.
Both these aformentioned properties are strongly influenced by the aliphatic chains structure.
In order to better clarifly the influence of the aliphatic chain structure on the extractive behavior of N,N dialkyl alkyl amides, a systematic study has been carried out.
The study is still continuing, and this paper shows the most interesting results until now obtained concerning the following items:

- preparation and characterization of new amides of different structure;
- their behavior with respect to third phase formation during uranium extraction;
- the extractive behavior of some of the most representative amides prepared with respect to two typical separations problems: the separation of trivalent actinides from rare earths (this problem is related to the elimination of alpha actinides from liquid radioactive wastes), and the separation of plutonium from uranium without adding any reducing or complexing agent (this problem is relatel to the partition cycle aqueous reprocessing of spent nuclear fuels)

PREPARATION AND CHARACTERIZATION OF NEW AMIDES

Starting from the N N'di - n - butyl n octanamide, chosen as reference compound with completely straight-chain structure, and extensively studied previously (1-2), about 20 new amides have been prepared, where the aliphatic chain bound to the carbonyl group and or to the nitrogen atom are more or less branched.
Apart from the availability of the starting carboxylic acid or secondary amine, the following general criteria have been followed:total carbon atoms higher than 12; side chain lenght less then 9 carbon atoms.
In such a way, the solubility of the prepared compounds in organic diluents and the insolubility in aqueous phase is assured, and the easy washing of their possible degradation products (carboxylic acids, secondary amines) is always guaranteed.
The radiation stability of the prepared amides in the presence of aqueous HNO_3 has been tested
For this purpose a Co-60 irradiator (0,2 Megarad/hour dose rate) has been employed. The results show that the general behavior of almost all the amides tested is very similar to that of TBP under the same conditions (1).

THIRD PHASE FORMATION

All the amides prepared have been compared for their tendence to give third phases when contacted (dissolved in an hydrocarbon -type diluent) with aqueous HNO_3 and aqueous uranyl nitrate solutions.
From the results it appears evident that the straight chain amides give the widest utilization range and the more the chain is branched, the more this range is limited.
If one considers that the separation factor between tetravalent and hexavalent actinides is enhanced by the branching of the side chain bound to the carbonyl or to the nitrogen (1), the N N' di-n-butyl, 3,3 di methyl butiramide (branching in the carbonyl side chain) and the N N' di-sec-butyl pentanamide (branching on the nitrogen side chain) show the most promising performance from this point of wiew.
Anyway, as expected, the branching of the aliphatic chain determines in almost all the cases the formation of third phases with lower uranium concentration with respect to the corresponding straight chain compounds.

SEPARATION PERFORMANCE

The results permit to choose some promising amides to investigate on the influence of the structure on the separation behavior of these compounds.
Until now we have investigated the behavior of these three amides, chosen ad reference compounds for each type of structure:

- N N' di-n-hexyl octanamide (long-straight chain) (DHOA)
- N N' di-n-butyl 2 ethyl hexanamide (α branching of the carbonyl chain) (DB2EHA)
- N N' di-n-butyl 3,3 dimethyl butirramide (β branching of the carbonyl chain) (DBMB)
- N N' di-sec-butyl hexanamide (branching of the nitrogen) (or pentanamide) chain) (DSBH)

As mentioned, before, two typical separation problems have been studied: the trivalent actinides-rare earths separation, and the plutonium uranium separation.
In Fig. 1: the distribution coefficient of Am (III) and Eu (III) (chosen as reference for actinides and rare earths), as a function of increasing HNO_3 concentration, are shown for the four amides under investigation.
Even if the values of the distribution coefficients are very low thus increasing the range of their uncertainty, the influence of the structure on the americium and europium extraction may be still seen. In particular, the amide DSBH branched to nitrogen side chain shows the best performance. Unfortunately, the low value of the distribution coefficient does not permit to suggest any practical application.
The possibility of performing the U-Pu separation without adding any reducing or complex ing agent in the aqueous phase has been also studied for the amides under investigation.
From the results until now obtained, shown in the Fig. 2 and Fig. 3 ,some interesting considerations can be deduced:

- The best separation behavior for the U-Pu couple is shown by the amide DSBH branched on the carbonyl side chain. It is useful to remember here that this amide has also shown the best performance of all branched amides with respect to the tendence to third phase formation.
- the separation of Pu from can be performed with amides(DBOA and DSBH) only by changing the aqueous HNO_3 concentration, from 3 - 4 M HNO_3 to 0.7-1 M HNO_3 . At this HNO_3 concentrations any risk of Pu (IV) polimerization does not exist. This possibility represents a consistent advantage with respect to TBP;
- with amides DBOA and DSBH, but with amide DHOA too, it is possible to realize the recovery of plutonium together with a fixed amount of uranium (coprocessing);
- the better behavior of branched-type amides with respect to staight chain ones in the separation of hexavalent from tetravalent actinides has been confirmed by these results.
  In particular, for this application the branching to the carbonyl side chain is preferred to that of nitrogen, contrarly to the application discussed before (Am - Eu separation).

REFERENCES

1)G.M.GASPARINI,G.GROSSI- Sep.Sci. and Techn.15(4) 825 (1980)

2) G.GROSSI,G.M.GASPARINI,W.DEMBINSKI-Proc.of Int.Extr.Conf. Liegi 1980

	AMIDE 30% IN MESITYLENE	TBP 30% IN KEROSENE
U^{VI} EXTRACTION FROM 3M HNO_3	$D_U = 8 - 14$	$D_U = 20 - 30$
Pu^{IV} EXTRACTION FROM 3M HNO_3	$D_{PU} = 30$ (STRAIGHT CHAINS) $D_{PU} = 2$ (BRANCHED CHAINS)	$D_{PU} = 8-14$
HNO_3 EXTRACTION	$D_{HNO_3} = 2\ 10^{-1}$	$D_{HNO_3} = 2-3\ 10^{-1}$
THIRD PHASE FORMATION	MAX 80 gU/L IN ORG.PH. WITH 3M HNO_3	MAX 100 gU/L IN ORG PH. WITH 3M HNO_3
SOLUBILITY LIMITS	NO DATA FOR Pu	MAX 46gPu/L IN ORG. PH. WITH 3M HNO_3
STRIPPING FROM 0.1M HNO_3	$D_U = 10^{-2}$	$D_U = 0.35-0.5$
FD DECONTAMINATION FROM 3M HNO_3	$D_{ZR} = 10^{-1}-10^{-2}$ $D_{RU} = 10^{-3}$ $D_{EU} = 10^{-3}$	$D_{ZR} = 0.35$ $D_{RU} = 10^{-3}$ $D_{EU} = 10^{-3}$
RADIATION STABILITY	ABOUT THE SAME	
AVAILABILITY AND COST	AMIDES ARE EASIER TO BE PREPARED BUT AT THE MOMENT ARE MORE EXPENSIVE	
TOXICITY	UNDER INVESTIGATION	MAY IRRITATE THE MUCOSE MEMBRANE
DANGEROUS DEGRADATION PRODUCTS	NONE	DBP AND MBP
WASHING OF DEGRADATION PRODUCTS	VERY EASILY WASHED	PARTIALLY WASHED
SOLUBILITY IN AQUEOUS PHASE	10^{-2} g/L	0.4 g/L
SOLUBILITY IN ORG.PH.	COMPLETE	COMPLETE
PHASE DISENGAGEMENT	WITH AMIDES IS QUICKER THAN WITH TBP	

TAB. 1 A COMPARISON BETWEEN AN AMIDE AND TBP

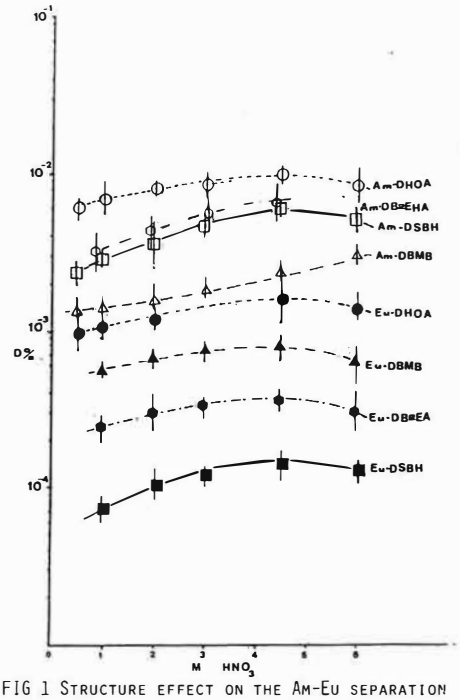

FIG 1 STRUCTURE EFFECT ON THE AM-EU SEPARATION

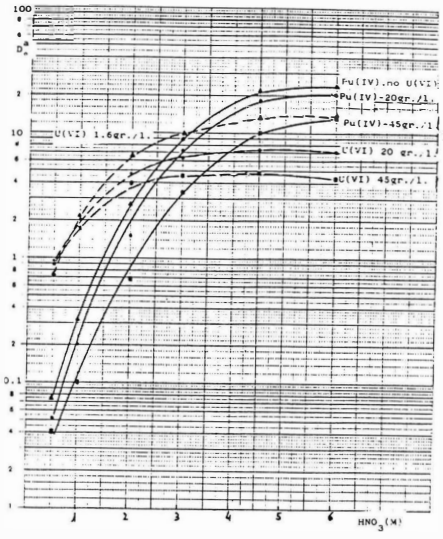

FIG 2 1M DI SEC BUTYL HEXAMIDE IN MESITYLENE

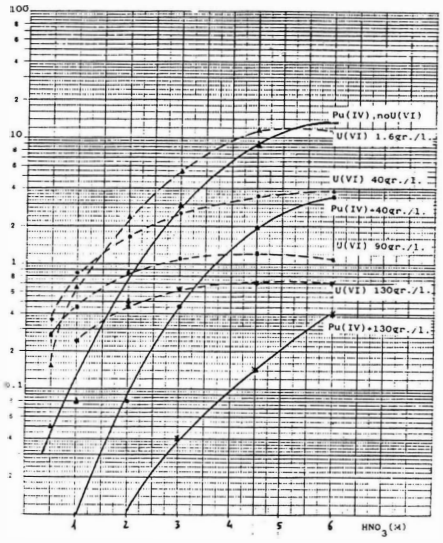

FIG 3 0.1M DIBUTYL33DIMETHYLBUTIRRAMIDE-MESITYLENE

DOAA—AN EXCELLENT NOVEL EXTRACTANT

Yuan Chengye, Tu Tongyan, Ma Enxin and Li Shusen

Shanghai Institute of Organic Chemistry
Academia Sinica
Shanghai, China

INTRODUCTION

N,N-Dialkylacylamides have been studied extensively as extractants for metals from nitrate media by Siddall (1) and Blake et al (2). The characteristic structural feature of the substituted amides indicates that the charge density of carbonyl oxygen is evidently increased by the $p\pi$-conjugation resulted from the interaction of lone pair electrons of the nitrogen atom and π electron of the carbonyl group. Together with carbonyl oxygen, the amido-nitrogen atom can also be served as coordinating centre, depending on the acidty of the species to be extracted (3).

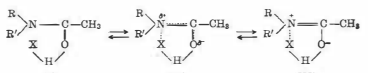

(I) (II) (III)

R'—H or R

However, there was no commercial extractant of substituted amide group available until the development of A101, N,N-dialkylacetamide with mixed straight chain composed of C_8-C_{10} in alkyl radical (4). On the basis of structure-reactivity studies we found that the spatial configuration of the N-alkyl group of N,N-disubstituted acetamide gives some advantages over the corresponding straight chain derivatives in higher selestivity in extraction, lower solubility in water, better solubilization in aliphatic diluents and good performance in stripping process. N,N-Di(1-methylheptyl)acetamide (abbreviated as DOAA, commercial name N503) was thus introduced as an effective extractant by us (5).

PREPARATION AND PROPERTIES

DOAA was prepared by acetylation of di(1-methylheptyl)amine, which was synthesized either by amination of 2-chloro-octane or by direct aminolysis of octanol-2 in the presence of a nickel catalyst with satisfactory yield (6). DOAA is a pale yellow viscous liquid, b.p. 157-160°C/9mm. 142-144°C/7mm.; d_4^{25} 0.8648-0.8684; n_D^{25} 1.4550-1.4560; η^{25} 18.5+1.0. IR νC=O 1640cm^{-1}. ^{1}H NMR(CCl_4,HMDS) : 0.79-0.84(6H,m,2XCH_3), 0.84-1.1(6H,m,2X$(CH_2)_5CH_3$), 1.1-1.3(20H,s,2X$(CH_2)_5$), 1.87(3H,s,CH_3CO-). DOAA has surface tension $\gamma_{25°}$ 29.3 dynes/cm; freezing point -54°C; flash point 190°C; solubility in water $\leqslant$ 10mg/liter and LD_{50} 8.2gm/kg mice. (6,7)

EXTRACTION OF URANIUM AND RELATED ELEMENTS

As neutral oxygen-containing extractant, DOAA extracts uranium and related metal nitrates with notable superiorities over TBP, which is commonly used for the separation of nuclear fuels from their fusion products as shown in Table 1.

TABLE 1 EXTRACTIVE SEPARATION OF U, Pu, Zr-Nb AND Ru BY DOAA

EXTRACTANT	U		Pu		Zr-Nb		Ru	
	D	E%	D	E%	D	βU/ZrNb	D	βU/Ru
$(C_4H_9)_3PO$	2.26	87.1	1.37	80.6	2.1×10^{-2}	1.08×10^{2}	4.7×10^{-2}	48.1
$CH_3CON(C_8H_{17}i)_2$	1.76	84.1	9.21	96.5	5.9×10^{-3}	2.98×10^{2}	2.5×10^{-2}	70.4
$CH_3CON(C_8H_{17}s)_2$	3.97	92.3	0.86	71.5	1.0×10^{-3}	3.99×10^{3}	1.8×10^{-2}	2.7×10^{2}

[Extractant] 1M in kerosene, [HNO_3] 1N, [U] 240g/l, O/A = 3/1

[Pu] 500-2500 pulse/min. 0.1ml., Zr^{95}-Nb^{95} in trace amount,

[Zr] as carrier 2.5×10^{-4}M, [Ru] 1×10^{-4} M.

The straight chain derivative, N,N-di-n-octylacetamide, is not suitable for this purpose owing to the low solublity of its nitrate and extracted coordinated compound in kerosene.

EXTRACTION OF ANIONIC HALIDE METAL COMPLEXES

Being a Lewis base, DOAA forms oxonium salt in acid mediun, which is capable of extracting anionic halide metal complexes by ion-pair mechanism. It is clear that metals forming halide metal complex would be separated from other metals which is unable to give anionic species by extraction with DOAA.

DOAA possesses excellent properties for the separation of gold from other precious metals and base metals from hydrochloric acid. (Fig.1)

As shown in Figure 1 the extraction capability of DOAA for Au is apparently greater than base metals such as Cu, Ni even Fe and other precious metals including Pt, Pd, Ir and Rh. The prospective application of DOAA in the separation of gold from chloride system is encouragable.

Removal of iron from leach liquor is one of the essential problems in hydrometallurgy. Ferric ions in form of $HFeCl_4$ could be extracted by DOAA almost quantitatively. The loading capacity of DOAA(30%) for iron is 30.9g. per liter from 3N HCl containing 11.8g.Fe/l. In order to prevent formation of third phase during extraction, addition of alkanol with high molecular weight is necessary. (Figure 2) It was well demonstrated by the fine extraction performance of DOAA in separating iron from rare earths. A quantitative removal of iron was achieved where only less than 1% of RE was being coextracted.

It is necessary to emphasized that in comparison with TBP, DOAA has no detectable swelling effect to PVC, a widely used structural material for mix-and-settle extractor. As illustrated by the Photo 1, TBP has serious swelling effect to PVC since evident damage was found after 3 days standing and the whole mass turned to paste upon 2 years storage. There is no significant change for PVC in keeping with DOAA for two years.

The fundamental chemistry of extraction of iron by DOAA has been studied in our Laboratory. By the method of distribution equilibria, the composition of extracted species was deduced as Fe·3DOAA. On the other hand, the cooridination compound prepared by saturation method has the formula of Fe·2DOAA based on elemental analyses and spectroscopic studies. In the IR spectra of Fe 2DOAA, it is evidently shown that the characteristic frequency of νCO at 1640cm^{-1} of the parent ligand was disappeared and substituted by a strong band at 1578cm^{-1} designating as coordinated CO band with $\Delta\nu$CO of 62cm^{-1}. As indicated by magnetic measurements, pure Fe 2DOAA and with dilution by two or three volumes of DOAA gave effective magnetic moment 6.04, 5.93 and 5.87 respectively. These data coincide the calculated value of 5.92 μ_B for Fe^{3+} in high spin of $3d^5$ orbital. It may thus be considered that Fe·2DOAA is a Fe^{3+} containing coordination compound with outer orbit octahedron configuration.

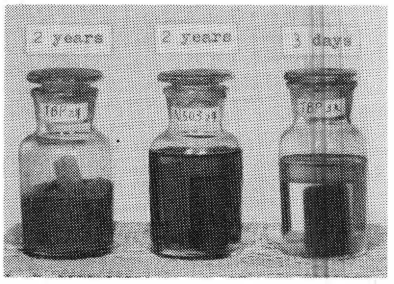

Photo 1

Comparison of DOAA with TBP in Swelling Effect on PVC.

Both Niobium and Tantalum are capable to form anionic halide complex, we have succeeded in separating them from HF-H_2SO_4 by DOAA extraction. This extraction system is distinguished for higher extraction capacity, better separation factor and particularly for the absence of harmful impurities like phosphorus in the final product which is usually occured in TBP extraction. (Figure 3,4)

By means of the distribution method and the method of continuous variation, as well as IR spectral and chemical analyses of the loaded organic phases, the composition of the extracted species was shown to be $HMF_6 \cdot nS$, probably together with some of $H_2MF_7 \cdot nS$, where M = Nb or Ta, S = DOAA and n = 1, 2. The sulfuric acid acts mainly as a salting-out agent in the process of extraction. After extraction of HF, the νCO of DOAA was shifted to 1590 versus 1660cm^{-1} in the ligand, indicative of the donation of the electrons by the carbonyl oxygen atom of the extractant (I). (Figure 5) As the acidity of the extracted acid complexes enhanced, the loaded organic phase shows a

new band at 1710cm^{-1} commonly attributed to C=N stretching frequency. Thus a "bidentate" mechanism (III) was deduced.(3) As DOAA is unable to form III, due to steric hindrance, an intermediate mechanism (II) was proposed, which is well substantiated by the data in distribution equilibria and the IR spectra of the coordination compound in the related organic phases.

EXTRACTION OF ORGANIC ACIDS

The basicity of carbonyl oxygen of DOAA is strong enough to extract a series of organic acids including phenol and its derivatives. Table 2 shows the excellent behaviours of DOAA in extracting phenol.

TABLE 2 DISTRIBUTION RATIO OF PHENOL IN EXTRACTION BY VARIOUS ORGANIC SOLVENTS

Solvent	Alkanes	Aromatics	Ethers	Alkanols	Esters	Ketones	DOAA
D Value	0.1-0.6	1.2-2.0	1-30	8-25	27-50	10-500	500

The influence of spatial configuration of alkyl group in substituted amide on phenol extraction is illustrated on Table 3.

TABLE 3 INFLUENCE OF STRUCTURE OF N-ALKYL GROUP IN ACETAMIDE ON THEIR EXTRACTION CAPABILITY TO PHENOL

Extractant	$CH_3CON(C_8H_{17}n)_2$	$CH_3CON(C_8H_{17}i)_2$	$CH_3CON(C_8H_{17}s)_2$
E%	90.1	88.3	85.6

The data show the steric hindrance of ligand in extracting phenol. However, DOAA provides higher loading capacity, fine performance in alkali-stripping good stability against acid, alkali even under higher temperature, very low solubility in water and almost non-toxicity. DOAA is therefore being used as an effective extractant not only for the recovery of phenol from various manufacturing processes but also for the dephenolization from industrial effluents of different sources.

The mechanism of extraction of phenol by DOAA has been studied by us. (7) The isotherms of the extraction equilibrium have been given and the constant in the equation $Y = aX^b$ thereby calculated (X and Y denote the concentration of phenol in aqueous and organic phase respectively). The distribution ratio of phenol is shown to be as high as 500 in the extraction by pure DOAA. With the aid of Clausius-Clapeyron equation the enthalpy of the extraction reaction has been estimated as $\Delta H = -4.0$ Kcal/mole. By means of the slope method and the method of continuous variation, the composition of the extracted species is deduced to be $C_6H_5OH \cdot DOAA$.(Figure 6,7) A marked carbonyl shift was observed in the IR spectra of the loaded organic phases. It is a consequence of the coordination effect during the process of extraction. As indicated by the NMR spectrum the value of the chemical shift of the hydroxyl proton in phenol was increased significantly in the extracted complex resulting from the effect of the intermolecular hydrogen bonding. The structure of the extracted species may thus be elucidated as $C_6H_5O\text{-}H\cdots O{=}C(CH_3)N(C_8H_{17}sec)_2$. (Figure 8)

REFERENCES

(1) T.H.Siddall III, J.Phys.Chem. 64 1863 (1960)
(2) C.A.Blake, J.M.Schmitt, W.E.Oxendine ORNL - 3496 (1963) p.70
(3) Li Shusen, Yuan Chengye Acta Chemica Sinica 33 11 (1975)
(4) The Solvent Extraction Group , Changsha Research Institute of Mining & Metallurgy "The Amide Type Extractant A101 and Its Application" (Material distributed in ISEC'80 Liege-Belgium)
(5) Yuan Chengye Huaxue Tongbao (Chemistry) 1977,86
(6) Tu Tongyuan, Wang Caoqing, Sheng Zhichu and Yuan Chengye Youji Huaxue (Organic Chemistry) 1982, 185
(7) Department of Extraction Acta Chemica Sinica 38 167 (1980)

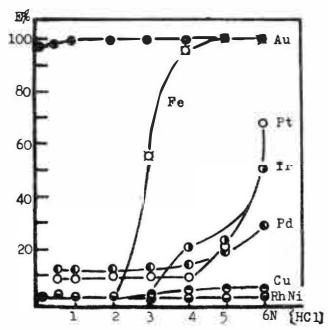

Figure 1

Extractive Separation of Gold From Other Precious and Base Metals By DOAA(.M) in Kerosene

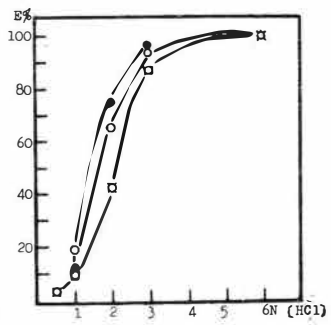

Figure 2

Extraction of Iron By 30% DOAA in Kerosene(●) in Addition With 10%Alkanol(O) or 20%Alkanol(□)

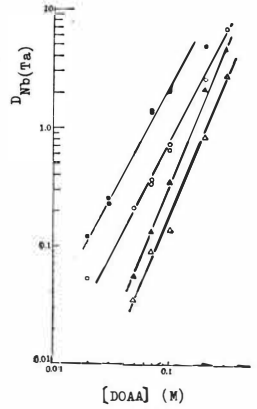

Figure 3

Plot of log $D_{Nb(Ta)}$ vs. [DOAA]
O-DOAA.Nb(1.94), ●-DOAA.Ta(1.98)

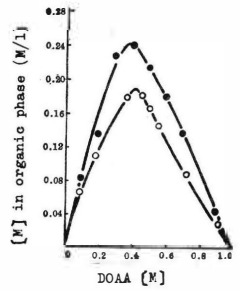

Figure 4

Method of Continuous Variation in Extraotion of Nb,Ta by DOAA [DOAA+Nb]0.611M[DOAA+Ta]0.800M

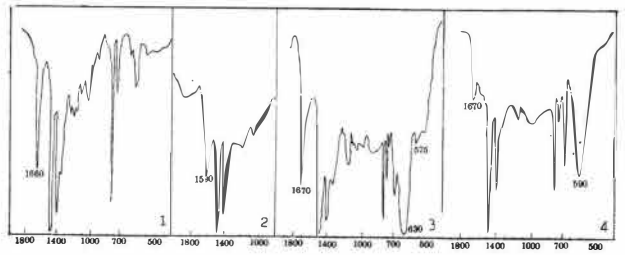

Figure 5

IR Spectra of DOAA(1),DOAA-HF(2),DOAA-Nb(3),DOAA-Ta(4).

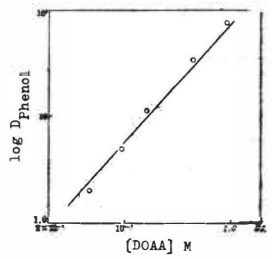

Figure 6

Plot of log D_{Phenol} vs. [DOAA]

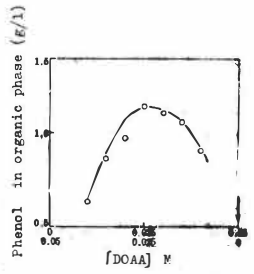

Figure 7

Method of Continuous Variation in Extraction Phenol with DOAA [DOAA+Phenol] 0.05M

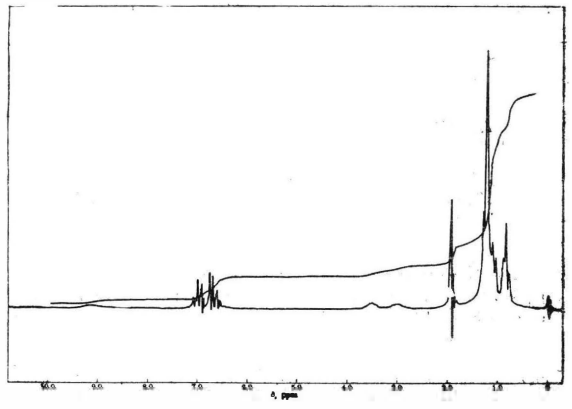

Figure 8

'H NMR of Coordination compound of DOAA with Phenol

NEW BIDENTATE EXTRACTANTS FOR ACTINIDES(III) AND LANTHANIDES(III) SEPARATIONS FROM CONCENTRATED NITRIC ACID

C. Musikas, H. Hubert

Centre d'Etudes Nucléaires de
Fontenay-Aux-Roses B.P. n° 6 - 92260
FONTENAY-AUX-ROSES, France

I. INTRODUCTION

Highly radioactive nuclear wastes contain α and β emitters whose half life are very different. The α emitters, actinides, are the minor component and will be radioactive for thousands of years whereas the fission products, β emitters will be inactive after one or two centuries. Thus, the separation of the two kinds of radionuclides before storage is suitable. The main difficulty for this separation is the extraction of the trivalent actinides from the concentrated nitric acid waste solutions. This difficulty is due to the general weak extractibility of f series trivalent ions from acidic media and to the presence in the waste solutions of numerous highly hydrolysable ions which will precipitate when pH will be increased.

Polydentates extractants containing P = O donor group have been proposed (1) (2) as extractants of trivalent actinide and lanthanide from nitric acid solutions. Although the replacement of monodentate HDEHP, or TBP by tetraalkylcarbamoylmethylene phosphonates was a serious improvment, several problems (dialkylphosphoric acids and phosphoric acid as degradation products..) are still troublesome and drive us, to investigate tetraalkylmethylenediamides ability to extract trivalent actinide and lanthanide from concentrated nitric acid. Negative results were reported by Siddall in 1963 (3) for tetrabutylmalonamide or tetrabutyl succinamide as lanthanide extractant.

However, amides extractant properties might depend of the aliphatic substituent lenght more drastically than organophosphorus compounds because of the amide molecular rigidity and it seemed interesting to undertake systematic investigations of trivalent actinide and lanthanide extraction. Progress in this field will be reported in this communication, especially the influence of the diluent, the alkyl chains lenght and the aqueous acidity.

II. Am(III) and Eu(III) EXTRACTION FROM HNO_3 SOLUTIONS BY VARIOUS TETRAALKYLMALONAMIDES.

In order to select an extractant we synthetized (4) several malonamides whose formula and abbreviation are given Table 1 with the Am(III) maximum extraction ratios when aqueous HNO_3 concentrations are varied.

Table 1. Influence of the substituents* R_1, R_2 upon the Am(III) distribution ratios** (malonamide 0.5 M in benzene).

Extractant	R_1	R_2	$D_{Am(III)}$
DCHDEMA	C_2H_5	C_6H_{11}	0.11
TBMA	C_4H_9	C_4H_9	0.18
DODMPA	C_3H_7	C_8H_{17}	0.45
DBMMA	CH_3	C_4H_9	0.55
DODMMA	CH_3	C_8H_{17}	1.06

* Malonamides general formula

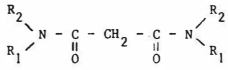

** $D_{Am(III)}$ are the maximum on the curves $(D_{Am(III)} = f(HNO_3))$. This maximum lies between 2N and 5N HNO_3.

At first glance two factors seemed to play a role in Am(III) distribution coefficients : the presence of methyl groups and the total number of carbon atoms. The first factor is probably associated with the steric hidrance near the C = O donor groups, whereas the second is correlated with the lipophilic character of the metallic complexes. As a consequence DODMMA is the best extractant and TBMA one of the poorest. DBMMA is a better extractant than TBMA despite of its lower lipophilic character.

Am(III) and Eu(III) distribution ratios between 1 M DODMMA into t-butylbenzene and nitric acid solutions were measured as a function of acidity (figure 1).

It can been seen that, DODMMA behaves like a typical basic neutral extractant. From 0.01 to 3M HNO_3 there is an increase of the trivalent ions distributions ratios whereas for higher HNO_3 concentrations, the competition between the metal and HNO_3 for the diamide coordination sites stems the decreasing part of the curves.

Malonamides-nitric acid adducts, solubility into non polar diluents, especially hydrocarbons, is limited. We found that, t-butylbenzene is a convenient diluent only for DODMMA. For acidities between 0 and 10 N no third phase formation was observed, contrary to DBMMA.

However limited proportions of dodecane can be added to aromatic diluents and higher distribution coefficients are then obtained. The influence of diluent over Am(III) and Eu(III) distribution ratios is shown table II.

Table II. Diluent effect upon Am(III) and Eu(III) distribution ratios between 0.5 M DODMMA and aqueous solutions (1N HNO_3, 4M $NaNO_3$).

DILUENT	$D_{Am\ (III)}$	$D_{Eu\ (III)}$
Benzene	0.75	0.6
Xylene	1.05	0.8
Mesitylene	1.1	0.8
t-butylbenzene	1.6	1.1
Dodecane 80 % Decanol 20 %	2.7	2.05
Dodecane 80 % Xylene 20 %	7.5	5.8

III. Am(III) and Eu (III) EXTRACTION MECHANISMS

Am(III) and Eu(III) distribution ratios logarithm vary linearly with DODMMA concentrations logarithm, with a slope of 4.

The variation as a function of aqueous nitrate is 3 and indicate that the extraction mechanism is :

$$M^{3+} + 3NO_3^- + 4\ DODMMA \longrightarrow M(NO_3)_3(DODMMA)_4$$

The higher number of ligands around the metallic ion suggest that some of them are in the second coordination sphere. Raman spectroscopy indicate that NO_3^- are bidentate and in the first coordination sphere. These results confirm that in the complexes some diamides molecules are in the second coordination sphere. When it is bonded to M^{3+} ions, the DODMMA, C = O stretching bands are modified and C = N bands remain inchanged, showing that the f trivalent ions are linked to oxygen amide rather to nitrogen.

IV. EXTRACTION OF THE HIGHER OXIDATION STATE ACTINIDES IONS.

U(VI) and Pu(IV) distribution coefficients as a function of HNO_3 concentrations are given figure 2. NpO_2^+ ions are poorly extracted.

V. CONCLUSIONS

From the data presented in this communication it can be seen that diamides are rather good extractants for tri, tetra et hexavalent actinide ions, contained in acidic nitrate solutions and further investigations will tell if they present a real advantage over the carbamoylmethylene phosphonates. Changes in aliphatic radicals is more important for their extracting power than such changes in organophosphorus extractants but a complete knowledge of the effects of the chains nature need much more fundamental investigations.

References.

1 - T. H. SIDDAL, III, Method for Extracting Lanthanides and Actinides, US Patent 3243 254 (1966)

2 - W. SCHULZ, J. D. NAVRATIL, Solvent extraction with neutral bidentate organophosphorus reagents. Recent Developments in Separation Science Vo. VII - Chapt. 2, p. 31, N.N. Li (Ed), CRC Press - (1982)

3 - T. H. SIDDAL, III J. Inorg. Nucl. Chem. 25, 883 (1963)

4 - All the alonamides were synthetized and purified by G. THIOLLET (IRCHA-Vert-le-Petit).

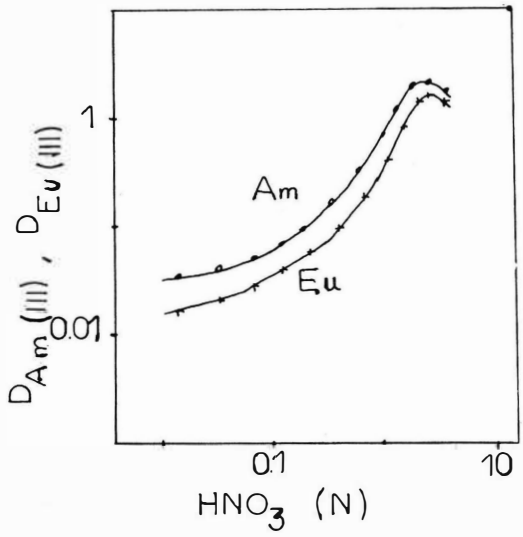

FIG.1. Am(III), Eu(III) DISTRIBUTION

(DODMA 1 M - t BUTYLBENZENE)

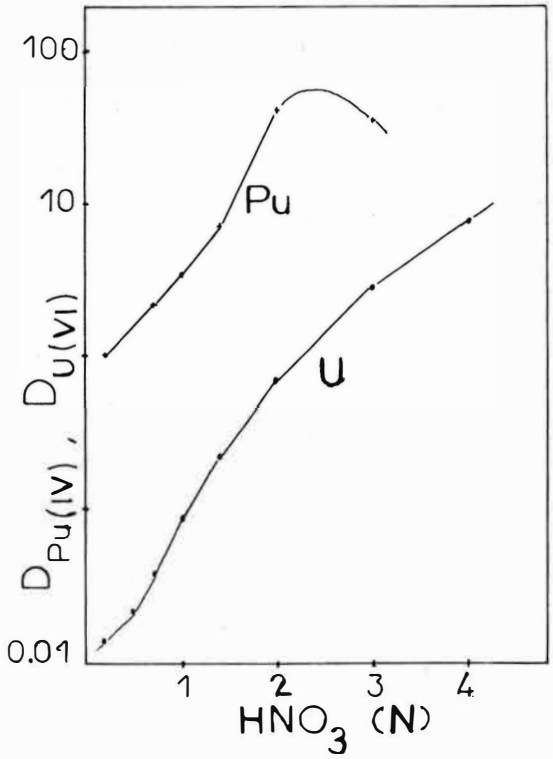

FIG.2. Pu (IV), U (VI) DISTRIBUTION

(DODMA 0.1 M - t-BUTYLBENZENE)

OCTYL(PHENYL)-N,N-DIISOBUTYLCARBAMOYLMETHYLPHOSPHINE OXIDE AS AN EXTRACTANT FOR ACTINIDES FROM NITRIC ACID WASTE

E. P. Horwitz, H. Diamond, D. G. Kalina
L. Kaplan and G. W. Mason

Chemistry Division
Argonne National Laboratory
Argonne, Illinois 60439 USA

INTRODUCTION

The ability of neutral bifunctional organophosphorus compounds to extract trivalent actinides, specifically Am(III), from nitric acid solution has stimulated investigations into the processing of PUREX high level liquid waste (1-5). The authors' work in this area has focused primarily on derivatives of carbamoylmethylphosphine oxide (CMPO) (6). We have found that the best extractant of this type is octyl(phenyl)-N,N-diisobutylmethylphosphine oxide (abbrev. OϕD[IB]CMPO). This extractant has a unique combination of substituent groups which impart to the resulting molecule substantially improved ability to extract actinides from acidic nitrate media and to withstand hydrolytic and radiolytic degradation. At the same time good selectivity of Am(III) actinides over fission products and favorable solubility properties on actinide loading are maintained (7,8).

This paper describes the application of OϕD[IB]CMPO to the extraction of transuranium elements (Np, Pu, and Am) and fission product rare earths (F.P.R.E.) from evaporated highly acidic (5 M HNO_3) PUREX waste. Additional information on the influence of phenyl substitution in CMPO's and mixed CMPO-TBP extractant solutions on D_{Am} is also presented.

EXPERIMENTAL PROCEDURE

Synthetic high level liquid waste (HLLW) used for flowsheet testing was prepared from synthetic LWR-HLLW (8) by diluting to one-third, increasing the acidity to 5 M HNO_3 and making the final solution 0.7 M in aluminum nitrate and 0.3 M in HF. This mixture simulates approximately the PUREX waste produced at Hanford. Flowsheet testing was performed by batch counter-current extraction using thermostated separatory funnels.

RESULTS AND DISCUSSION

Effect of Phenyl Substituents on CMPO Moiety. Earlier studies by the authors (7) showed both the advantages and disadvantages of replacing a hexyl group in dihexyl-N,N-diethylCMPO (DHDECMPO) with one phenyl group. The major advantages of the resultant hexyl(phenyl)-N,N-diethylCMPO (HϕDECMPO) were the increase in D_{Am} at high acidity (>1 M HNO_3), the decrease in D_{Am} at low acidity (<0.5 M HNO_3) and the improved selectivity of Am(III) over Fe(III). The major disadvantage was the very poor solubility of actinide-HϕDECMPO complexes [using Nd(III) as a stand-in for Am(III)] in common aromatic diluents. We found that the solubility problem could be significantly improved by replacing the ethyl groups in the amide moiety with isobutyl groups. Additional studies have been performed on N,N-diisobutylcarbamoylmethylphosphine oxide (D[IB]CMPO) extractants to determine if the diphenyl derivative (DϕD[IB]CMPO) shows significant advantages over the OϕD[IB]CMPO compound as an actinide extractant.

Figure 1 shows the expected improvement in D_{Am} at high acidity for DϕD[IB]CMPO. Because of the low solubility of DϕD[IB]CMPO in diethylbenzene (DEB) at 25°C the comparison of the three D[IB]CMPO derivatives was performed at 0.1 M extractant concentration. However, the significant superiority of OϕD[IB]CMPO over DHDECMPO at high acidity is not very evident at 0.1 M extractant concentration because of the higher extractant dependency of the octyl-(phenyl) derivative. Although the DϕD[IB]CMPO compound does show some advantages over the OϕD[IB]CMPO as an extractant for Am(III) from high nitric acid, its low solubility in high boiling aromatic diluents, even lower solubility in aliphatic diluents, and the very poor solubility of metal-DϕD[IB]CMPO complexes negates its practical application. Chmutova et al. (9) have recently described the actinide(III) extraction behavior of diphenyl-N,N-di-n-butyl CMPO but only compared this compound to dihexyl-N,N-diethylcarbamoylmethylphosphonate.

Mixed OϕD[IB]CMPO-TBP as an Am(III) Extractant. To improve further the phase compatibility properties of OϕD[IB]CMPO we studied CMPO-TBP mixtures as Am(III) extractants. A continuous variation study of TBP-OϕD[IB]CMPO mixtures in DEB at total extractant concentration of 0.5 M showed no evidence of mixed complexes of the type $Am(NO_3)_3\cdot(TBP\text{-}CMPO)_n$ or synergistic effects, which is at variance with results reported by Navratil and Martells (10). However, a significant improvement in the solubility of the OϕD[IB]CMPO extractant in non-aromatic diluents may be achieved by addition of TBP. For example, mixing TBP with OϕD[IB]CMPO enables one to replace DEB with decalin and avoid the formation of a second organic phase when equilibrated with high concentrations of HNO_3 or Nd(III). Since distribution ratios are higher in alicyclic diluents than in aromatic diluents, one may achieve a given D_{Am} value using less OϕD[IB]CMPO. This effect is shown in Figure 2. D_{Am} is very similar for the two extractant solutions at 5-6 M HNO_3, which is the concentration range of HNO_3 of interest. It is interesting to note that TBP generally suppresses the influence of acidity on D_{Am} for OϕD[IB]CMPO. This effect may be explained by the acid buffering effect caused by the large concentration of basic P=O groups. An intramolecular buffering effect was postulated to explain the resistance of the CMPO extractants to high concentrations of acids (6,7). The following equation describes the extraction of Am(III) by OϕD[IB]CMPO from highly acid (>1 M HNO_3) solutions:

$$Am^{3+} + 3NO_3^- + \overline{3E\cdot(HNO_3)_n} - \overline{Am(NO_3)_3\cdot E_3\cdot(HNO_3)_m} + (3n - m)HNO_3$$

where E = OϕD[IB]CMPO, $E\cdot HNO_3$ represents HNO_3 hydrogen bonded to CMPO, and the bar denotes species in the organic phase. When 0.5 M OϕD[IB]CMPO in DEB is loaded with Nd from 6 M aqueous HNO_3, n = 2 and m = 2. We believe that the HNO_3 associated with the Am-CMPO complex is hydrogen bonded to amide moiety.

FLOW SHEET

A flowsheet for the extraction of uranium and all transuranium elements (Np, Pu, Am) together with fission product rare earths (F.P.R.E.) from evaporated PUREX high level waste is shown in Figure 3. The flowsheet is based on the use of a mixture of OϕD[IB]CMPO and TBP in decalin. This system minimizes the quantity of CMPO required in the process, has rapid phase disengagement behavior, and eliminates the possibility of a second organic phase forming if the extractant were inadvertently saturated with F.P.R.E.'s. Distribution ratios for selected fission products, Cr, Fe, and Ni, and actinides are given in Tables I and II. All distribution ratio measurements and flowsheet testing were performed at 50°C because of the anticipated radiolytic heating produced from fission products. This temperature may be somewhat high and since D's usually decrease with an increase in temperature, estimated Am(III) decontamination factors based on 50°C values are probably conservative.

One of the major features of the flowsheet shown in Figure 3 is that the initial actinide extraction is performed from a moderately high nitric acid concentration. One of the advantages of operating at this acidity, as opposed to the more conventional PUREX waste acidity of 2-3 M HNO_3, using carbamoylmethylphosphoryl (CMP) type of extractants, is that Tc, Ru, and Pd have much lower D's and thus report largely to the raffinate and are more readily scrubbed from the organic phase. On the other hand Fe(III), Zr(IV), and Mo(VI) are readily extracted by CMPO extractants from 5 M HNO_3, although the Fe(III) extraction is slow and D_{Fe} varies with equilibration time. Removing Fe, Zr, and Mo from the raffinate could be beneficial if additional processing of this stream for Ru, Rh, and Pd and/or ^{90}Sr and ^{137}Cs is planned. Zr, Mo, Fe are readily stripped from the organic phase using a mixture of HNO_3 and oxalic acid. However this waste stream must be contacted with a small quantity of fresh extractant to ensure high decontamination from Am(III). TRU stripping is readily performed using formic acid with hydroxylammonium nitrate (HAN). Under these conditions the TRU's are concentrated approximately threefold relative to the feed. The uranium will remain largely in the organic phase and is subsequently removed with Na_2CO_3 during the solvent wash step.

The calculated removal of Am(III) from the raffinate using an extraction factor (D × Phase Ratio) of 2 for the extraction stages and 8 for the scrub stages and using nine extraction stages and four scrub stages is 99.9%. If the temperature of the waste solution were 40°C, then D_{Am} = 6.3 and the percent removal would be >99.99 for the same number of extraction and scrub stages. Since Np(V) is not very stable in 5 M HNO_3 and Pu is extractable in the III, IV, and VI oxidation states, the removal of either element from the waste does not present any problem. Furthermore, the fraction of ^{237}Np and ^{239}Pu which must be removed from the waste is much less than ^{241}Am to achieve 100 nanocurie/gram of solid.

Acknowledgment. The authors would like to thank Mr. Edmund Huff of the Chemical Technology Division, ANL, for performing the inductively coupled plasma atomic emission spectrographic analysis.

Table I. Distribution Ratios of Selected Elements in Synthetic PUREX-HLLW 50°C

	Feed (HLLW) O/A = 0.5	1.5 M HNO_3 - 0.075 M $H_2C_2O_4$ O/A = 2
Sr	<0.01	
Y	1.7	1.1
Zr	15	<0.01
Mo	10	<0.1
Tc	0.30	
Ru	0.05	
Rh	<0.02	
Pd	<0.02	
Ag	<0.1	
Cd	<0.01	
Ba	<0.01	
Cr	<0.05	
Fe	5	<0.01
Ni	<0.1	

*Work performed under the auspices of the Office of Basic Energy Sciences, Division of Chemical Sciences, U. S. Department of Energy under Contract W-31-109-Eng-38.

Table II. Distribution Ratios of Selected Elements in Synthetic PUREX-HLLW 50°C

	Feed (HLLW) O/A = 0.5	1.5 M HNO_3 - 0.075 M $H_2C_2O_4$ O/A = 2
La	0.72	2.2
Ce	1.4	3.4
Pr	1.9	3.8
Nd	2.4	3.9
Sm	3.1	3.9
Eu	3.4	3.7
Gd	2	-
U	$>10^2$	$>10^2$
Np	62	13
Pu	$>10^3$	39
Am	3.9	6.6

REFERENCES

1. W. W. Schulz and J. D. Navratil, in Recent Developments in Separation Science, Vol. VII, N. N. Li, Ed., CRC Press, Inc., Boca Raton, Florida, 1981, p. 31.
2. R. R. Shown, W. J. McDowell, and B. Weaver, in Proceedings of the International Solvent Extraction Conference, Toronto, Canada, September 9-16, 1977, Vol. 1, p. 101, Canadian Institute of Mining and Metallurgy, Montreal, Quebec, 1979.
3. W. W. Schulz and L. D. McIsaac, in Proceedings of the International Solvent Extraction Conference, Toronto, Canada, September 9-16, Vol. 2, p. 619, Canadian Institute of Mining and Metallurgy, Montreal, Quebec, 1979.
4. L. D. McIsaac, J. D. Baker, J. F. Krupa, R. E. LaPointe, D. H. Meikrantz, and N. C. Schroeder, Study of Bidentate Compounds for the Separation of Actinides from Commercial LWR Reprocessing Waste, Allied Chemical Idaho Chemical Programs Report ICP-1180, Idaho Falls, Idaho, February 1979.
5. M. K. Chmutova and N. E. Kochetkova, and B. F. Myasoedov, J. Inorg. Nucl. Chem., 42, 897 (1980).
6. D. G. Kalina, E. P. Horwitz, L. Kaplan, and A. C. Muscatello, Sep. Sci. Technol., 16, 1127 (1981).
7. E. P. Horwitz, D. G. Kalina, L. Kaplan, G. W. Mason, and H. Diamond, Sep. Sci. Technol., 17, 1261 (1982).
8. E. P. Horwitz, H. Diamond, and D. K. Kalina, in Plutonium Chemistry, ACS Symposium Series, Vol. 216, Chapter 27, 1983.
9. M. K. Chmutova, N. P. Nesterova, N. E. Kochethova, V. E, Koiro, and E. F. Myasoedov, Radiokhimiya, 24, 31 (1982).
10. J. D. Navratil and L. L. Martella, Sep. Sci. Technol., 16, 1147 (1981).

FIGURE 1. COMPARISON OF D_{Am} VS HNO_3 FOR 0.1 M SOLUTIONS OF DIHEXYL-, OCTYL(PHENYL)-, AND DIPHENYL-N,N-DIISOBUTYLCMPO IN DEB. TEMP. 25°C.

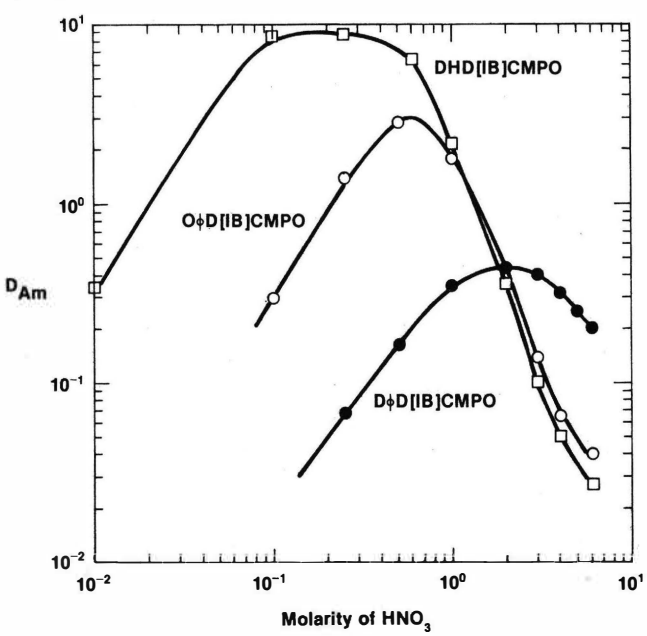

FIGURE 2. COMPARISON OF D_{Am} VS HNO_3 FOR 0.5 M OϕD[IB]CMPO IN DEB AND FOR 0.25 M OϕD[IB]CMPO - 0.75 M TBP IN DECALIN. TEMP. 50°C.

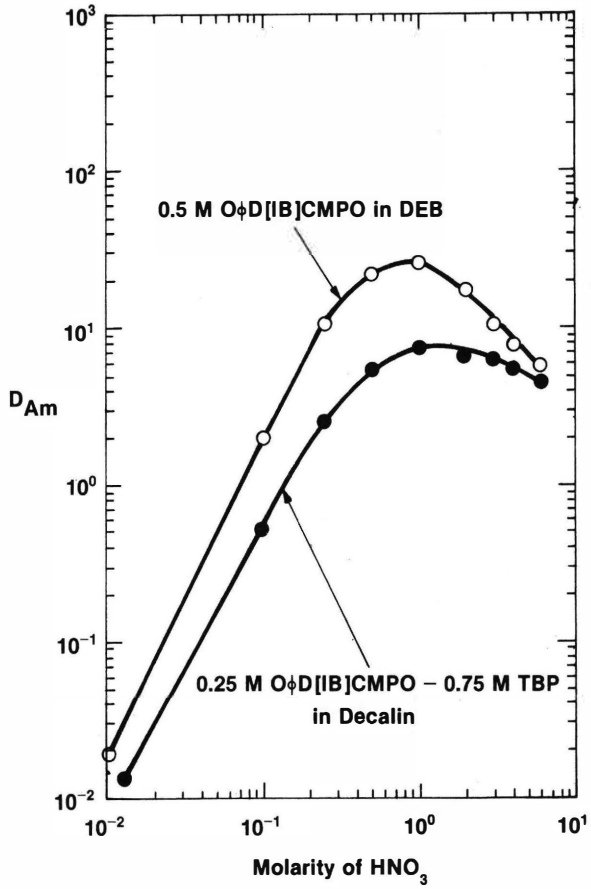

FIGURE 3. FLOWSHEET FOR THE RECOVERY OF TRU'S (Np, Pu, Am) AND FISSION PRODUCT R.E.'S FROM PUREX HIGH-LEVEL WASTE

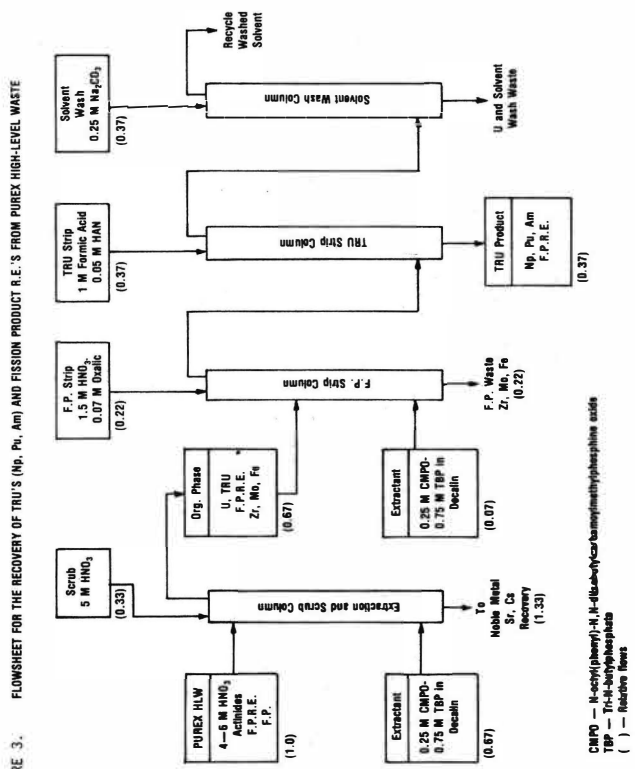

CHEMISTRY OF CROWNETHER COMPLEXES OF ACTINIDES: INVESTIGATION ON THE EXTRACTION OF U(IV) AND U(VI) WITH CYCLOPOLYETHERS

Zhu Lin, Chen Shaojin, Feng Yijuin
Liu Zongquin, Chen Wenjuin

Sichuan University
Chengdu, China

The extraction behaviour of crownetyers for alkali, alkali-earth metals have reported in a great deal of papers. There are some research on that of actinides as well (1-4). Yakshin (1) investigated the extractionof U, Np and Pu nitrates with several crownethers in 1,2-dichloroethane. The extraction efficiency of uranium was reported quite low.

The authors found that a series of crownethers form complexes of variable stability with U(IV) and U(VI) chlorides (5), and that under appropriate condition they can be extracted into an organic solvent effectively (6,7). This paper reports the results of extraction of U(IV) and U(VI) with several crownethers of different hole size and derivatization, the composition of extractable complexes and their conditional extraction constants.

The extraction was performed in the following system

$$U^{4+} \text{ or } UO_2^{2+} \ / \ HCl,\ LiCl \ / \ \text{crownethers-}CH_3NO_2$$

The crownethers, dicyclohexyl-18-crown-6 (DC18C6), benzo-18-crown-6 (B18C6), benzo-15-crown-5 (B15C5), dibenzo-18-crown-6 (DB18C6), dibenzo-24-crown-8 (DB24C8) and dibenzo-30-crown-10 (DB30C10) in nitromethane are investigated. The foregone research (6,7) showed the extractable complex is of the character of ion-pair complex, and by using the polar solvent CH_3NO_2 the distribution ratio of both U(IV) and U(VI) complexes can be enhanced remarkably. UO_2Cl_2 stock solution was prepared in the usual way, whereas UCl_4 was obtained by reducing UO_2Cl_2 with power silver (99.9%), standardized by coulombmetric titrametry and preserved under purified N_2 atmosphere. Concentration of U(IV) and U(VI) were analyzed spectrometrically with Arsenazo III.

I. The extraction of U(VI)

The extraction distribution ratio of U(VI) is strikingly effected by the concentration of LiCl. The D value is rather low at C_{LiCl} less than 3M, but it raises steeply after that. D is independent upon U concentration in the range of C_U of $1\cdot10^{-4}$ - $1\cdot10^{-3}$M, denoting the formation of mononucclear complex. The extraction equations are assumed as

$$(1)\qquad UO_2^{2+} + (p+2)\,Cl^- + p\,H^+ + q\,L_{(o)} \rightleftharpoons H_pUO_2Cl_{(p+2)}\cdot qL_{(o)}$$

$$(2)\qquad K = \frac{(H_pUO_2Cl_{(p+2)}qL)_o}{(UO_2)\,(Cl)^{p+2}(H)^p(L)_o^q}$$

By introducing a function D', defined as

$$D' = \frac{DY}{(Cl)^2}$$

where Y stands for the complexation degree for U(VI), that is $\sum \beta_i(Cl)^i$, the following relation can be established:

$$(3)\qquad \lg D' = \lg K + p\lg[(H)(Cl)] + q\lg(L)_o$$

Then p, q were determined graphically from the slops of the corresponding lg-lg plots, (Fig 1,2). Table (1) summerized those results. They are consistent with the following extraction equilibrium

$$(4)\qquad UO_2^{2+} + H^+ + 3Cl^- + L_{(o)} \rightleftharpoons HUO_2Cl_3\cdot L_{(o)}$$

for the crownethers studied except DC18C6. In the latter case, it seems like formation of a mixture of $HUO_2Cl_3\cdot L$ and $HUO_2Cl_3\cdot 2L$. The conditional extraction constants for eq. (4) were listed in Tab.1 as well.

A sequence of extraction ability of crown ethers studied for UO_2Cl_2

DC18C6 > B15C5 > DB30C10 > DB24C8 > DB18C6

is obtained according to the result mentioned above, even though the difference among the last four is comparatively small. This sequence is resonable considering the attractive effect of phenyl group and the exclusive effect of cyclohexyl group on the bonding ability of co-ordination atoms, oxygen. A decreasingly sequence among three dibenzo- crownethers expectantly reflects the attractive effect of phenyl group weakens along the enlargement of the ring of crownether.

Tab.1

crownether	q	p	$(C_{LiCl}=4M)$
B15C5	1.03	0.99	12.0±1.0
DB18C6	0.99	0.95	3.8±0.2
DB24C8	0.97	0.97	5.7±0.5
DB30C10	0.98	1.03	8.5±0.3
DC18C6	1.51	0.81	

II. The extraction of U(IV)

The extraction of U(IV) differs from that of U(VI) by the needness of much higher concentration of salting agent (greater than 7M LiCl). The investigative method is just similar to that for U(VI). D' now is defined as

$$D' = \frac{DY}{(Cl)^4}$$

Results are summerized in Table 2. The extractive equilibrium is found as (Fig. 3,4)

$$(5)\qquad U^{4+} + 2H^+ + 6Cl^- + L_{(o)} \rightleftharpoons H_2UCl_6\cdot L_{(o)}$$

for crownethers studied except DC18C6.

The sequence of extraction ability of crownethers for UCl_4 is not identical with that for UO_2Cl_2.

DC18C6 > DB24C8 > B18C6 > DB18C6

The abnormal extractionability of DB24C8 probably reflects its flexible structure may fit U(IV) better than the rigid plane structure of 18-member ring.

Tab.2

crownether	q	p	K (est.)* (C_{LiCl}=7.5M)
B18C6	1.0	2.1	0.20
DB24C8	1.0	2.1	0.68
DB18C6	0.9	2.0	0.056
DC18C6	1.7	2.0	

*Deviation caused by the uncertainty of Y estimates.

REFERENCES

1. В. В. Якшин и.т.д., ДАН СССР, том. 241, 159 (1978).
2. W. J. McDowell et al, CONF-770907-4(Report),(1977).
3. Chang Wenqin et al, Journal of Science and Tecnology of Atomic Energy, 4, 433 (1982). (China)
4. Wang Wenji et al, Journal of Nuclear and Radiochemistry, 3, 139 (1982). (China)
5. Zhu Lin et al, J. of Sichuan Univ.(Nat. Sci. Ed.), 1,(1980).
6. Zhu Lin et al, ibid, 13 (1980). (China)
7. Chen Wen-jun et al, ibid, 25 (1980).

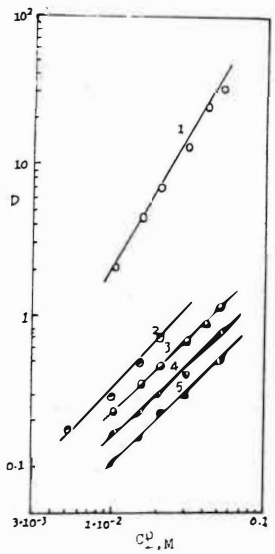

Fig.1 lgD - lgC_L^o

(C_{LiCl}=4M, C^o_{HCl}=0.25M, $C^o_{UO_2}$=5·10^{-4}M)

1. DC18C6 2. B15C5
3. DB30C10 4. DB24C8
5. DB18C6

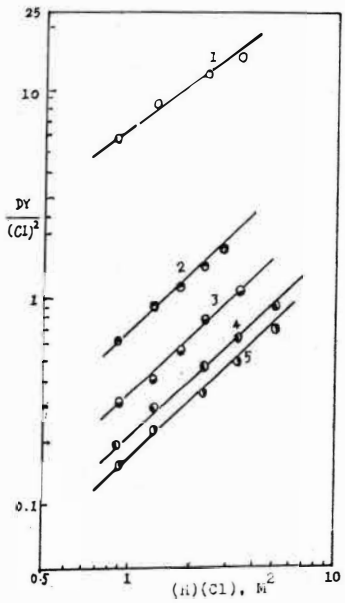

Fig.2 lgD'-lg(H)(Cl)

(C_{LiCl}=4M, C^o_L=2·10^{-2}M, $C^o_{UO_2}$=5·10^{-4}M)

1.DC18C6 2.B15C5
3.DB30C10 4.DB24C8
5.DB18C6

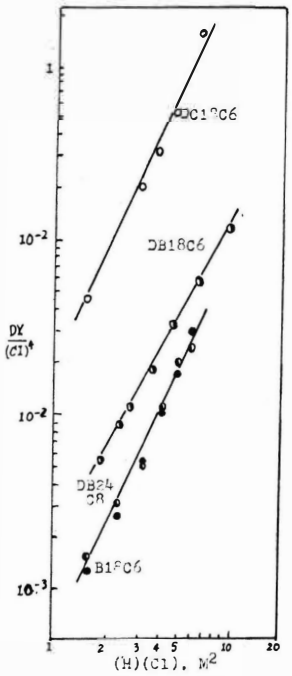

Fig.4 lgD'-lg(H)(Cl)

(C^o_U: 2 10^{-4}M)

DC18C6: C^o_L 2 10^{-2}M, C_{LiCl} 7.5M
DB18C6: 2 10^{-2}M, 8.5M
DB24C8: 1 10^{-2}M, 7.5M
B18C6: 2 10^{-2}M, 7.5M

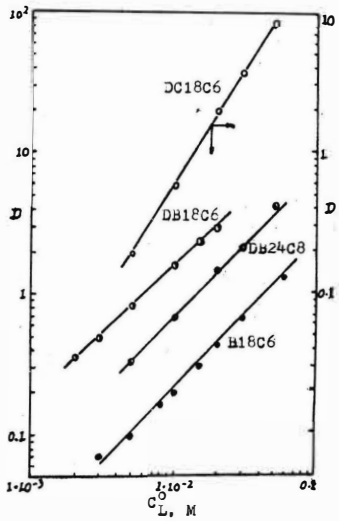

Fig.3 lgD-lgC_L^o

(C^o_{HCl}:0.2M, C^o_U:2 10^{-4}M)

C_{LiCl}:7.0M(DC18C6);
8.5M(DB18C6);
7.5M(DB24C8 & B18C6)

FURTHER STUDIES OF MACROCYCLIC COMPOUNDS AS SIZE-SELECTIVE SYNERGISTS IN SOLVENT EXTRACTION SYSTEMS*

W. J. McDowell, G. N. Case, D. W. Aldrup

Chemical Technology Division
Oak Ridge National Laboratory
Oak Ridge, Tennessee 37830 USA

*Research sponsored by the Division of Chemical Sciences, U.S. Department of Energy under contract W-7405-eng-26 with the Union Carbide Corporation.

SIZE-SELECTIVE SYNERGISM

In previous publications (1-3) we reported that macrocyclic ethers, which are known to complex certain alkali and alkaline earth metal ions, are poor extractants for the mineral acid salts of these ions because of the difficulty of solubilizing the hydrophilic anion in an organic phase of low polarity. We also reported that combining an organic-phase-soluble acid in solution with the macrocycle improves extraction, with large synergistic enhancement of the extraction by the organic-phase acid in many cases. Since the degree of synergism appears to be related to the correspondence between the ion diameter and the crown ether cavity size, we call this phenomenon "size-selective synergism."

ORGANIC/AQUEOUS-PHASE DISTRIBUTION OF REAGENTS

Since an objective is to find reagents having potential for process applications, both good solubility in organic solvents (diluents) of low polarity and low distribution to aqueous phases from such solutions are necessary prerequisities. In our tests for size-selective synergism, the cation exchangers (organic-soluble acids) bis(2-ethylhexyl)phosphoric acid (HDEHP), (branched) didodecylnaphthalenesulfonic acid (HDDNS), and an alpha-carbon-branched or "neo" carboxylic acid of mw ≃ 258 (V-Acid) were found to meet these requirements. Table 1 summarizes data on the solubility in toluene and the distribution to water from 0.1 M solutions in toluene of the macrocyclic compounds tested. Both 12-crown-4 and cyclohexo-15-crown-5 are too highly distributed to the aqueous phase to be useful process extractants or even desirable compounds to study. Other compounds, as indicated in the table, are not sufficiently soluble in toluene (our test equivalent of a process diluent) to be useful.

EFFECTIVE SIZE RANGE

The compounds that we selected to cover the ion-size range from 1.2 to 5.6 Å are designated by asterisks in Table 1. In the cavity-size range 1.7 to 4.3 Å, excellent size-selective synergism is observed for the extraction of alkali metals sodium through rubidium when either HDDNS or HDEHP is used as the cation exchanger. For the cavity size of 12-crown-4 and 14-crown-4, however, very poor synergism is observed for lithium, and a diminished and less selective effect is observed with 21-crown-7 and 24-crown-8 as extractants for cesium (1,2).

ALKALINE EARTH EXTRACTION

The carboxylic acid, V-acid, was used as the cation exchanger for the alkaline earths. Excellent synergistic effects were obtained for strontium (Figure 1) and barium (Figure 2) with macrocycles having 18-crown-6 and 21-crown-7 nuclei; 24-crown-8 and 15-crown-5 were less effective. Calcium extraction was synergized only slightly by TBC15C5 and DC24C8.

TRANSITION ELEMENT EXTRACTION

Of the first-row elements, chromium through zinc, the extractions of Mn^{2+}, Co^{2+}, and Zn^{2+} were synergized by TBC15C5 when the cation exchanger was HDDNS. Trivalent chromium and iron extractions were not synergized with macrocycles that should fit either the bare trivalent ion or the hydrated ion.

STOICHIOMETRY AND BONDING

Continuous-variation and reagent-dependence studies suggest that the preferred organic-phase species consists of enough acid groups to satisfy the valence charge on the ion plus one macrocycle. At present, the reason for strong size-selective synergism in some cases and a lack of synergism and even antagonism in others is not apparent; indeed, there may be more than one reason. For alkali metal and alkaline earth ions, the existence of very strong hydration bonds may prevent bonding to the macrocycle. In the transition elements, the existence of directional bonds may make bonding to the nearly planar coordination sites of the macrocycle unfavorable. The importance of three-dimensional positional conformation is suggested by the strong synergistic effect of DTBDC18C6 or strontium extraction by V-acid and the very much weaker effect of DTBDB18C6, although the latter effect could, at least partially, be attribited to the weaker electron donating abilities resulting from the presence of adjacent electron-withdrawing benzene rings. The synergistic factor is 1560 in the first case, with alicyclic side rings, and 20 in the second, with aromatic (planar) side rings.

CHELATE AND MACROCYCLE EFFECTS AND PREPOSITIONED BONDING SITES

The fact that bonding sites in a prepositioned arrangement in a single molecule can enhance complex formation is familiar to us (e.g., in chelates), and this effect was dramatically demonstrated here by comparing the synergistic effect of a crown ether with that of a monodentate ether and a phosphine oxide. Even though the phosphine oxide is a much stronger electron donor, the synergistic factor obtained for strontium extraction by V-acid is much smaller than that observed with the crown ether. The synergistic factor, $D_{Sr}(\text{mixture})/[D_{Sr}(\text{V-acid}) + D_{Sr}(\text{donor})]$, with 0.1 M V-acid + 0.05 M DC18C6 is 2000, while that with 0.1 M V-acid + 0.3 M TOPO is only 3.6. Hexyl ether at the same coordinator-site concentration gives a synergistic factor of 2.9.

It is clear that entropic effects are important here, and the results suggest that three-dimensional positioning of coordinating sites may contribute strongly to the effectiveness of the multidentate coordinator's bonding strength. Much more systematic and detailed fundamental investigations need to be done to understand these systems and their potential usefulness.

REFERENCES

1. W. F. Kinard and W. J. McDowell, J. Inorg. Nucl. Chem., 43, 2947 (1981).
2. W. F. Kinard, W. J. McDowell, and R. R. Shoun, Sep. Sci. Technol., 15, 1013 (1980).
3. W. J. McDowell and R. R. Shoun, Proceedings of ISEC '77, pp. 95-99 (1977).

TABLE 1.

Organic-Phase Solubilities and Aqueous-Phase Distributions of Some Macrocyclic Compounds

Compound	Acronym	Solubility in Toluene (M)	Dist. to Water (%)	Cavity Size (Å)
12-Crown-4	12C4	Infinite	90	1.2 - 1.5
*Benzo-14-Crown-4	B14C4	>0.1	<2	1.2 - 1.5
*Octamethylperhydrocyclotetrafurfurylene	OMPCTF	0.123	<0.1	1.2 - 1.5
Cyclohexo-14-Crown-4	C14C4	Infinite	50	1.2 - 1.5
Cyclohexo-15-Crown-5	C15C5	Infinite	30	1.7 - 2.2
**tert*-Butylcyclohexo-15-Crown-5	TBC15C5	Infinite	<1	1.7 - 2.2
Dibenzo-18-Crown-6	DB18C6	<0.01	—	2.6 - 3.2
Diformyldibenzo-18-Crown-6	DFDB18C6	<0.01	—	2.6 - 3.2
Dibutyryldibenzo-18-Crown-6	DBDB18C6	<0.01	—	2.6 - 3.2
*Di-*tert*-butyldibenzo-18-Crown-6	DTBDB18C6	>0.2	<0.1	2.6 - 3.2
*Dicyclohexo-18-Crown-6	DC18C6	>0.5	7	2.6 - 3.2
*Di-*tert*-butyldecyclohexo-18-Crown-6	DTBDC18C6	>0.2	<0.1	2.6 - 3.2
*Dicyclohexo-21-Crown-7	DC21C7	Infinite	0.2	3.4 - 4.3
*Dicyclohexo-24-Crown-8	DC24C8	Infinite	0.2	4.5 - 5.6
Tetramethyltetraazacyclotetradecane	TMTACTD	>0.1	—	—
meso-Tetraphenylporphine	MTPP	0.008	0.1	—

ORNL-DWG 82-19823R

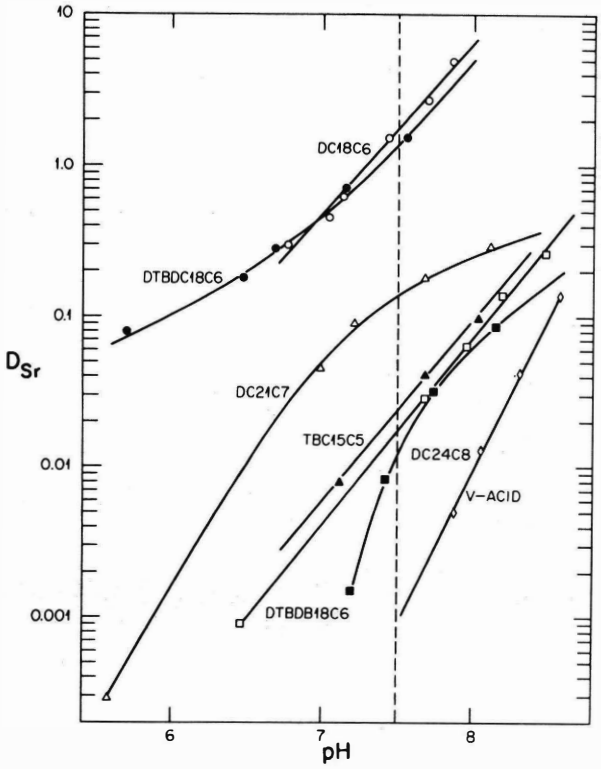

FIGURE 1. SYNERGISTIC ENHANCEMENT OF STRONTIUM EXTRACTION WITH VERSATIC ACID BY VARIOUS CROWN ETHERS.

ORNL-DWG 83-8169

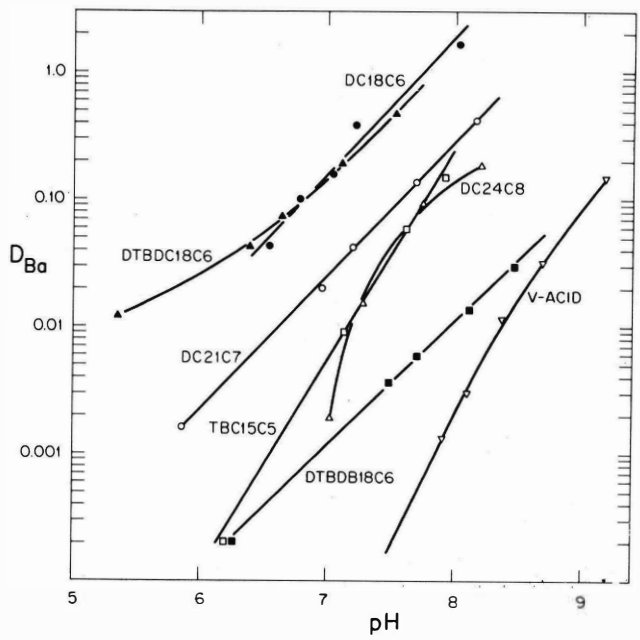

FIGURE 2. SYNERGISTIC ENHANCEMENT OF BARIUM EXTRACTION WITH VERSATIC ACID BY VARIOUS CROWN ETHERS.

SEPARATION OF URANIUM ON POLYURETHANE FOAM IMPREGNATED WITH TRI-OCTYLPHOSPHINE OXIDE

J. Korkisch and I. Steffan

Institute of Analytical Chemistry
University of Vienna
Vienna, Austria

A method is described for the quantitative separation of uranium from practically all other elements in 1M hydrochloric acid solution containing ascorbic acid. From such a solution uranium is retained selectively by a column containing open-cell polyurethane foam impregnated with tri-n-octylphosphine oxide (TOPO). The uranium together with TOPO is eluted with ethanol and then it is adsorbed on a column of Dowex 1 anion exchange resin from a hydrochloric acid - organic solvent system. After elution with 1M hydrochloric acid, uranium is determined fluorimetrically. The method was applied successfully to determine uranium in reference samples and manganese nodules.

WORKING PROCEDURE:

To 10 ml of 1M hydrochloric acid solution (= sample solution containing the uranium and the elements to be separated from it) 0.1 g of ascorbic acid was added to reduce the iron to the non-extractable divalent state and the resulting mixture was passed through a 4 g column of TOPO-impreganated polyurethane foam using a flow-rate which corresponded to the back-pressure of the column. Subsequently the column was washed first with 30 ml of 1M hydrochloric acid containing 0.3 g of ascorbic acid and then with 10 ml of 1M hydrochloric acid. Afterwards uranium and TOPO were eluted with 100 ml of ethanol and the volume of the eluate was reduced to 50 ml by evaporation. These 50 ml were mixed with 40 ml methyl glycol and 10 ml of 6M hydrochloric acid and the mixture (= organic solvent-sorption solution) was passed through a 2 g column of Dowex 1 (pretreated with 50 ml of a mixture consisting of 50% tetrahydrofuran, 40% methyl glycol and 10% 6M hydrochloric acid) using a flow-rate which corresponded to the back-pressure of the resin column. TOPO passed into the effluent while uranium was strongly retained by the resin which was then washed with 50 ml of the same tetrahydrofuran-methyl glycol-6M hydrochloric acid mixture followed by 50 ml of 6M hydrochloric acid. Finally uranium was eluted with 50 ml of 1M hydrochloric acid and its quantitative determination was performed fluorimetrically (1).

APPLICATION:

This technique has been applied to the analysis of reference samples and manganese nodules giving the results shown in Tables 1 and 2, from which it is seen that uranium was isolated quantitatively in all cases. Therefore, this method is very well suited for the analysis of natural uraniferrous materials of both high and very low uranium contents.

Table 1. Results of uranium determinations in IAEA reference samples and manganese nodules

Reference sample No.	Uranium found (% U_3O_8)	Recommended value (% U_3O_8)
S 1	0.469	0.471
S 2	0.313	0.313
S 3	0.418	0.418
S 4	0.374	0.375
S 12	0.0139	0.014
S 13	0.039	0.039
Manganese nodule No.	**Uranium found (ppm)**	
	This method	**Previous method(2)**
1	1.46	1.46
	1.47	1.48
2	2.79	2.77
	2.77	2.76

Table 2. Results of uranium determinations in South African Reference Materials for the uranium industry

Sample	Uranium found (ppm U_3O_8)	Certified value (ppm U_3O_8)	Limits[x] at 95% confidence level
Urem 1	35	34	33-35
Urem 2	507	505	502-513
Urem 3	447	439	430-447
Urem 4	103	100	100-101
Urem 5	775	775	756-792
Urem 6	1871	1887	1867-1925
Urem 7	52	51	50-53
Urem 8	127	130	125-133
Urem 9	260	258	256-261
Urem 10	1244	1241	1222-1252

[x] in ppm U_3O_8

REFERENCES

1. J. Korkisch and F. Hecht, Handbook of the Analytical Chemistry of Uranium, Third Part; Quantitative Analysis, Vo.VI., b; B, Springer-Verlag, Berlin-Heidelberg (1972).

2. J. Korkisch, I. Steffan, G. Arrhenius, M. Fisk and J. Frazer, Anal. Chim. Acta, 90, 151 (1977).

LIQUID ANION EXCHANGE EXTRACTION AND SEPARATION OF LANTHANIDES

V. M. Shinde

Shivaji University
Kolhapur 416004, India

Elements such as Y(III), Nd(III), Sm(III) and Gd(III) find commercial applications. For instance, Y(III) and Sm(III) promises to have an interesting future in the field of nuclear technology due to the low cross section for neutron capture and high temperature stability. Sm(III) and Nd(III) finds application in ceramic industry for coloring glasses and as glazers. Gadolinium is useful in nuclear technology, as a refractory material and in ceramic industries. In view of these applications the purification of Y,Nd,Sm and Gd is desired and this demand is fulfilled most effectively by ion exchange and solvent extraction techniques.

In this work high relative molecular mass amines such as tri-n-octylamine (TOA) and tricaprylmethyl ammonium salt (aliquat 336) have been used for the anion-exchange extraction of Y,Nd,Sm and Gd from succinate solution. The metal ions in the organic phase are stripped and determined spectrophotometrically (1-4).

EXPERIMENTAL

Reagents

The stock solutions of Y(III) and Sm(III) were prepared by dissolving yttrium nitrate (1.65g) and samarium nitrate (1.75g) in 10 ml of HNO_3 and diluting the resultant solution to 100 ml with distilled water. The Nd(III) and Gd(III) solutions were prepared by dissolving Nd_2O_3 (0.7g) and Gd_2O_3 (1.2g) in perchloric acid or nitric acid (10 ml) respectively and diluting to 100 ml with distilled water. The stock solutions were standardized and diluted as required for each working solution.

Extracting Solution

A 5% solution (w/v) of TOA or aliquat 336 (Koch light, England) in benzene, equilibrated for 30 min with equal volumes of 2M sodium succinate, were used for extracting purpose.

0.1% aqueous solution of arsenazo I was used for photometric estimation of Y, Sm and Gd (1-3) whereas 0.1% PAR was used for Nd estimation (4).

Procedure for Extraction of Y(III), Nd(III), Sm(III) and Gd(III) with TOA :

Place an aliquot of solution containing Y(10-75µg), Nd(10-100µg), Sm(25-100µg) or Gd(25-100µg) in a beaker; add enough sodium succinate to give a concentration of 0.06 M (for Y and Nd) or 0.01 M (for Sm) or 0.05 M (for Gd) in a total volume of 25 ml. Adjust the pH of the aqueous solution to 6.5-7.5 (for Y and Nd with dilute HNO_3 and NaOH or $HClO_4$ and NaOH respectively), or 7-8 (for Sm with dilute HNO_3 and NaOH) or 10.5-11.0 (for Gd with dilute HNO_3 and NaOH) and transfer the solution into a 100 ml separating funnel. Extract the solution for 5 min with two 5-ml portions of 5% TOA dissolved in benzene. Collect the organic phase and strip the metal ions with three 5 ml-portions of 0.1 M $HClO_4$. Equilibrate the combined aqueous phase with 5 ml of benzene to remove traces of dissolved TOA and estimate the metal ions photometrically by the recommended procedure (1-4).

Procedure for Extraction of Y(III) and Nd(III) with Aliquat 336:

Place an aliquot of a solution containing 25 to 75 µg of Y(III) or Nd(III) in a beaker, add enough sodium succinate to give a concentration of 0.025 M (for Y) or 0.1 M (for Nd) in a total volume of 25 ml. Adjust the pH of the aqueous solution to 10.5-11.5(for Y with dilute HNO_3 and NaOH solution) or 7-8 (for Nd with dilute $HClO_4$ and NaOH solution) and transfer the solution into a 100-ml separating funnel. Extract the solution for 5 min with 5 ml of 5% aliquat 336 solution, collect the organic phase and strip the metal ion from organic phase with two 5-ml portions of 0.1 M $HClO_4$. Equilibrate the combined aqueous phase with 5 ml of benzene to remove traces of dissolved aliquat and estimate the metal ion photometrically by the recommended procedure.

RESULTS AND DISCUSSION

Extraction Conditions :

The extractions of Y(III), Nd(III), Sm(III) and Gd(III) were studied at various pH values (Fig.1 & 2), sodium succinate concentrations and extractant concentrations. The optimum extraction conditions are given in Table 1. The variation in amine concentration using benzene as diluent showed that a 5% solution of TOA or aliquat is necessary for quantitative extraction of metal ions. Stripping of the metal ions were tried with mineral acids such as HNO_3, HCl, H_2SO_4, $HClO_4$ and NaOH solutions. However, the most effective stripping agent is perchloric acid (0.1 M)which causes complete removal of the metal ions from amine phase. The percentage extraction of the metal ions were calculated by measuring the absorbance of the coloured complexes and referring to calibration graphs. The distribution ratios were calculated as usual (5).

Nature of the Extracted Species and Probable Mechanism of Extraction

The log-log graphs of distribution ratio versus succinate concentration(at fixed pH and amine conc.)or versus amine concentration (at fixed pH and succinate conc.) indicate a molar ratio of 1:1 with respect to extractant and 1:2 with respect to succinate. The amine-succinate salt (in benzene) acts as a liquid anion exchanger and causes the extraction of Y(III), Nd(III), Sm(III) or Gd (III) ions by exchanging the metal-succinate from aqueous phase. The probable extraction mechanism could be written as -

$$(1)\quad \underset{\text{amine succinate salt}}{[2R_3NH^+, C_4H_4O_4^{2-}]_o} + \underset{\text{metal succinate}}{2M(C_4H_4O_4)^-_{2aq}} \rightleftharpoons \underset{\text{Extraction}}{2[R_3NH^+, M(C_4H_4O_4)^-_2]_o} + C_4H_4O_4^{2-}$$

$$(2)\quad \underset{\text{amine succinate salt}}{[2R_4N^+, C_4H_4O_4^{2-}]_o} + \underset{\text{metal succinate}}{2M(C_4H_4O_4)^-_{2aq}} \rightleftharpoons \underset{\text{Extraction}}{2[R_4N^+, M(C_4H_4O_4)^-_2]_o} + C_4H_4O_4^{2-}$$

Effect of diverse ions

Varying amounts of foreign ions were added to a fixed amount of Y(III),Nd(III),Sm(III) and Gd(III) and the recommended procedure for the extraction and spectrophotometric determination was followed. Table 2 show the ions tolerated and notable interference. The tolerance limit was set at the amount required to cause less than 1% error in the recovery of Y, Nd, Sm and Gd.

Separation of Y(III),Nd(III) and Sm(III) from La(III), Dy(III), Hf(IV) and U(VI)

Extraction of Y, Nd and Sm into TOA by the recommended procedure facilitates their separation from La,Dy,Hf and U(VI) which do not extract and remain quantitatively in the aqueous phase. Similarly La(III) do not extract into aliquat along with Y or Nd. In the aqueous phase La(III) is determined with arsenazo I (6), U and Dy are determined with PAR (7,4) and Hf is determined with arsenazo III (8). Y,Nd or Sm from the amine phase are subsequently stripped and estimated as described in the extraction procedure. U(VI) and Dy(III) coextract in the aliquat extraction of Y & Nd; they are however separated by selective scrubbing with water which do not back strip either Y or Nd. The recoveries of all were $\geq$99.0%, for mixtures of 25 µg of Y and 50-100 µg of Nd and 100 µg of Sm with $\leq$ 100 µg La,Dy; $\leq$ 1.0 mg Hf; $\leq$ 2.0 mg U(VI) etc.

Separation of Y(III) & Nd(III)from Sc(III),Th(IV),Ce(IV) & Zr(IV)

Sc,Th,Ce and Zr coextract with Y and Nd into TOA. Their separation is achieved by selective stripping technique. From

amine phase, Th is first stripped with 0.5 M HNO_3 (2x5 ml) and then Y or Nd are stripped with 0.1 M $HClO_4$. Stripping of Y or Nd with 0.1 M $HClO_4$ also facilitates their separation from Sc, Zr(IV) and Ce(IV) which remains in organic phase and subsequently removed by stripping with either 1 M HCl (for Sc & Zr) or with 6.5 M H_2SO_4 (for Ce). Th(IV) and Ce(IV) also coextract with Y and Nd in aliquat extraction. Their separation is done by stripping Th with 0.1 M HNO_3(2x5 ml) and subsequent stripping of Y or Nd with 0.1 M $HClO_4$ or stripping of Ce(IV) with 6 M H_2SO_4 (2x5 ml) and subsequent stripping of Y or Nd with 0.1 M $HClO_4$. Thorium is estimated complexometrically (9); Zr & Sc are determined with arsenazo (8,10) and cerium is determined titrimetrically (11). The recoveries of all metal ions were $\geq$99.0% for mixtures of 25 µg of Y and 50-100 µg of Nd with $\leq$100 µg each of Sc & Zr and $\leq$2.5 mg each of Th & Ce(IV).

Separation of Sm(III) from Y(III) and Nd(III)

Extraction of Y and Nd into 5% TOA from 0.06 M sodium succinate solution of pH 6.5-7.5 permits their separation from Sm which remains in the aqueous phase and determined with arsenazo I. Y or Nd are removed from the organic phase and determined as described earlier. Th recoveries of all were $\geq$99.0% for mixtures of 100 µg of Sm with $\leq$50 µg of Y(III) & Nd(III).

Separation of Nd(III) from Sc(III)

Scandium coextract with Nd when extracted with aliquat from 0.1 M succinate solution of pH 7. Sc(III) is however separated from Nd by stripping with 1 M HCl (10 ml). Nd is then stripped with 0.1 M $HClO_4$ and determined as described. Separation of Sc and Y is however not possible by the proposed method. The recoveries of both Sc & Y are greater than 99.0%. The separation of Sc (III) & Y(III) and that of Y(III) & Nd(III) is however not feasible by the proposed method.

Separation of Gd(III) from Dy(III) and U(VI)

Dy(III) and U(VI) coextract with Gd when extracted with 5% TOA from 0.05 M sodium succinate solution. They are however removed from amine phase by scrubbing with water and in the combined aqueous phase uranium and dysprosium are estimated with PAR whereas Gd from amine phase is stripped and determined as described earlier. The recoveries of Gd, Dy & U(VI) are $\geq$99.0%.

Accuracy and Precision

The proposed method has good precision and the reproducibility of results was satisfactory (Table 3).

REFERENCES

1. S.P.Pande and K.N.Munshi, Curr.Sci 41,330 (1972).
2. K.Okamoto and T.Takehiko, Japan Analyst 20,870 (1971)
3. A.Kosturiak and D.Kalavska, Acta Fac.Rerum 27,47 (1979).
4. K.N.Munshi and A.K.Dey, Anal.Chem. 36, 2003 (1964).
5. S.B.Gawali and V.M.Shinde, Anal Chem 48, 63 (1976).
6. S.Shibata, F.Takevchi and T.Matsumae, Anal.Chim.Acta 21, 177 (1959).
7. A.I.Busev and V.M.Ivanov, Ser.Khim 52, 3 (1960).
8. W.A.Dupraw, Talanta 19, 807 (1972).
9. J.S.Fritz and J.J.Ford, Anal.Chem.25, 1640 (1953).
10. T.Shimizo, Anal.Chim.Acta 37, 75 (1967)
11. A.I.Vogel, 'A Text book of Quantitative Inorganic Analysis' Longmans, London, 1978, P 369.

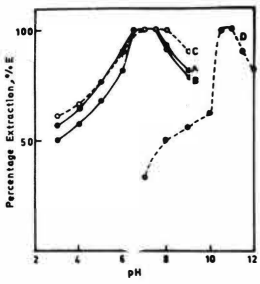

Fig.1 – Extraction behaviour of Y(A), Nd(B), Sm(C) and Gd(D) as a function of pH with 5% TOA as an extractant.

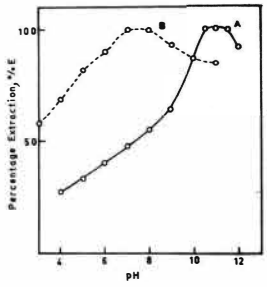

Fig.2 – Extraction behaviour of Y(A) and Nd(B) as a function of pH with 5 % aliquat as an extractant.

Table 1 - Optimum Extraction Conditions of Y(III), Nd(III), Sm(III) and Gd(III).

	With 5% Trioctylamine		With 5% aliquat 336	
	Succinate conc/M	pH	Succinate conc/M	pH
Y (III), 10 - 75 µg	0.06	6.5 - 7.5	0.025	10.5 - 11.5
Nd (III), 10 - 100 µg	0.06	6.5 - 7.5	0.1	7 - 8
Sm (III), 25 - 100 µg	0.01	7 - 8	-	-
Gd (III), 25 - 100 µg	0.05	10.5 -11.0	-	-

Table 2 - Effect of Diverse Ions

Metal ion	Ions tolerated, µg	
	in TOA extraction	in aliquat extraction
Y(III), 25 µg	2500 µg each of Cd,Co(II), Pb,Pd,Ca,Ba,Fe(III), Bi(III),Cl^-,Br^-,SO_4^{2-}, NO_3^-,SCN^-,PO_4^{3-}, tart, ascorb, thiourea. 2000 µg each of Ni, Mn, La(III),U(VI),Mo(VI), Cr(VI) 1000 µg each of Zn,Hg, Zr(IV),V(V),Nb(V),Ta(V). Interference:Sc(III),Th(IV), Pt(IV),Ce(IV),Cit,Oxalate and EDTA.	1000 µg each of Pr(III), PO_4^{3-}, NO_3^-. 500 µg each of La,Th,Nd, Ce(IV),Mo(VI),V(V),Cu, Os(VIII) and F^-. 200 µg each of Sm(III), Ti(IV),Cr(VI),Pd and Ru(III). 100 µg each of Gd,Dy,Zn and Ni Interference: Sc,Fe(III), tart and EDTA.
Nd(III), 50 µg	2500 µg each of Hg,Mn, Sm(III),Co(II),Pb,Ce,Ba, Th(IV),Pt(IV),Mo(VI),W(VI), Cr(VI),Cl^-,Br^-,F^-,SO_4^{2-},NO_3^-, SCN^-,tart,ascorb and thiourea. 2000 µg each of Ni,Fe(III), La(III),Ce(IV),V(V) and U(VI). 1500 µg each of Zn,In(III), 1000 µg each of Pd,Nb & Ta. Interference: Cd,Sn(IV) and EDTA.	1000 µg each of Sm(III), Gd(III),Y(III),Pr(III), Ce(IV),Pt(IV),Ir(III), cit,tart,oxalate, thiourea & ascorbate. 500 µg each of La,Mo(VI), Sc,Th(IV),Co(II),Cd, NO_3^-, Cl^- and F^-. 250 µg each of Ti(IV),Zr. and U(VI). 100 µg each of Ni,Dy(III), Ta and Rh(II) Interference: Fe(III), NO_3^-, and EDTA.
Sm(III), 50 µg	2500 µg each of Cd,Hg,Mn,Pb,Sn(II), Ca,Ba,Fe(III),La(III),Bi(III), Ce(IV),Cl^-,$Br^-$$SO_4^{2-}$, NO_3^-, SCN^-, tart, ascorb and PO_4^{3-}. 2000 µg each of Ce(IV),U(VI) and Cr(VI). 1000 µg each of Zn,Pd,In,Tl(III), Sc(III),Zr(IV),Pt(IV),V(V),Nb, Ta,Mo(VI) and W(VI). Interference: Th(IV),cit,oxalate, EDTA.	
Gd(III), 50 µg	2500 µg each of Cl^-,SO_4^{2-},NO_3^-,CO_3^{2-}. 1000 µg each of Cu,As,Au,Cd,Os(VIII), Cr(VI), V(V),Mo(VI),Pb,Bi, tart, SCN^- and thiourea. 500 µg each of Dy,U(VI),Zn,Ni,Co(II), Ti(IV), PO_4^{3-} and F^-. 250 µg each of Pd,Pt(IV) and Mn. Interference : Fe(III), Ir(III).	

Table 3 - Precision Data

Metal	conc,µg	Absorbance (Mean of 6 determinations)	Standard deviation	Coefficient of variation, %
Y (III)	25	0.21	0.004	2.1
	50	0.42	0.005	1.4
Nd(III)	50	0.30	0.005	1.9
	100	0.60	0.005	0.9
Sm(III)	50	0.20	0.005	2.6
	100	0.40	0.004	1.2
Gd(III)	50	0.30	0.002	5.1
	100	0.61	0.007	1.2

SULFOXIDES AS POTENTIAL EXTRACTANTS FOR ACTINIDES

J. P. Shukla, M. S. Nagar and M. S. Subramanian

Radiochemistry Division
Bhabha Atomic Research Centre
Trombay, Bombay 400085, India

Long-chain sulfoxides (R_2SO) extracting inorganic compounds in the solvate form, are promising novel extractants and superior to tri-n-butyl-phosphate (TBP) in their extractive power (1). Sulfoxides are pyramidal molecules with both the sulphur and the oxygen atoms containing lone electron pairs capable of donation. The stability of solvates depends upon the basicity of the corresponding sulfoxide. Generally, aliphatic sulfoxides possess higher basicity than aromatic ones. Aliphatic or cycloaliphatic derivatives or their mixtures (petroleum sulfoxides) obtained as by-products from petroleum refining (2-4) are being extensively employed as highly selective extractants for many radioactive, rare, trace as well as some inorganic and organic acids (5-12). Potential applications in hydrometallurgy and non-ferrous metallurgy of sulfoxides as extractants and floatation agents have also been suggested (4). Furthermore, sulfoxides are known to possess adequate chemical and radiation stability (9, 10, 13, 14).

As a part of our continuing programme concerning the extraction of actinides and associated long-lived fission product contaminants (encountered during Pu reprocessing) with different sulfoxides, we have reported data on their extraction with sulfoxides (9-12). Additional data on their extraction with several new sulfoxides, viz. di-isoamyl-(DISO), dibutyl-(DBuSO), diphenyl-(DPSO), benzyl methyl-(BMSO), allyl-phenyl-(APSO), benzyl phenyl(BPSO) sulfoxides are presented here. An attempt has been made to summarise the results obtained so far by our group employing these as extracting agents. Solvesso-100, mainly consisting of a mixture of isomeric trimethylbenzenes, was selected as the diluent. Attempts have been made to understand the nature of the metal ion species extracted into the sulfoxide diluent phase. Effect of temperature, acidity and other variables on extraction has also been examined. The influence of several water-miscible additives on the extraction behaviour of the actinides has also been studied.

EXPERIMENTAL

DBuSO $[(C_4H_9)_2SO]$ and DISO $[(C_5H_{11})_2SO]$ were synthesised according to a two-step process (10). DPSO $[(C_6H_5)_2SO)]$, BMSO $[C_6H_5\ SO\ CH_3]$, BPSO $[C_6H_5\ SO\ C_6H_5CH_2]$ and APSO $[C_3H_5\ SO\ C_6H_5]$ procured from K&K Labs. were used without further purification. Commercial grade Solvesso-100 was washed with dil. NaOH, dil. HNO_3 and water and finally distilled. The middle fraction (boiling range: 158-160°C) was used as the diluent. ^{241}Am, ^{239}Pu, $^{237,239}Np$, ^{233}U, $^{85,89}Sr$, ^{95}Zr, $^{103,106}Ru$, ^{141}Ce and $^{152,154}Eu$ tracers were used to study their extraction.

^{239}Pu was purified by anion exchange and double peroxide precipitation and adjusted to the tetravalent state by addition of sodium nitrite (~0.03M). All other tracers were obtained from Isotope Division, Bhabha Atomic Research Centre.

^{239}Pu and ^{233}U were assayed by $4\pi\alpha$-liquid scintillation counting. All other γ-emitters were counted in a well-type 3" x 3" NaI(Tl) gamma-scintillation detector coupled with a single channel analyser.

Distribution Experiments. Equal volumes (2 ml) of the aqueous and pre-equilibrated organic phases containing the required tracer were stirred mechanically for 10-15 min. After equilibration, suitable aliquots from both the phases were pipetted out for radioassay. The distribution ratio, D_M, was taken as the ratio of the activity in the organic phase to that present in the aqueous phase. All measurements were done in duplicate and the agreement in the D_M values obtained was within ± 2% with good material balance (> 95%). There was good agreement in the forward and reverse D_M values when both the phases used were pre-equilibrated with the corresponding opposite phases.

In studying the effect of various organic additives such as alcohols, dioxane, acetone and acetonitrile etc. on the metal ion extractability, the procedure adopted was essentially the same except that the aqueous phase contained the appropriate organic solvent.

RESULTS AND DISCUSSION

Extraction of actinides by sulfoxides has been reported to be fast, attaining equilibrium within a few minutes (7,9-11). Preliminary experiments carried out on the extraction of UO_2^{2+}, Np^{4+}, Am^{3+} and various fission products from aqueous nitric acid solutions with different alkyl sulfoxides including DISO and DBuSO confirmed this. The distribution ratios, observed to be virtually independent of the initial metal ion concentration employed (~10^{-4} to 10^{-6} M), indicated the absence of polynuclear species in the extraction system. Sulfoxides, in general, are monomeric in solutions of organic solvents(15). Values of D_M obtained by taking different metal ion activity initially in either phase remained unaltered, thereby confirming the reversibility of the extraction process (16).

Extraction of HNO_3 by sulfoxides. By plotting $\log [H^+]_{org} - 2 \log [H^+]_{aq}$. against $\log [\text{extractant}]_{org}$ drawn with a unit slope, the species extracted has been established to be $HNO_3.R_2SO$(10,11). The values of K_H for the various sulfoxides has been computed from the equation:

$$\log [\text{acid}]_{org} - \log a_{\pm}\ HNO_3(aq) = n \log [R_2SO]_{org} + \log K$$

where K_H = K/(dissociation constant of HNO_3, i.e. 23.5). Values of K_H for three sulfoxides reported here are higher than that for TBP as seen from the data given below:

Extractant	$H^+_{aq} + NO_3^-_{aq} + (\text{extractant})_{org} \xrightarrow{K_H} (HNO_3.\text{extractant})_{org}$
TBP	0.16
DISO	0.21
DHSO	0.37
DOSO	0.42

The order of basicity is: DOSO > DHSO > DISO > TBP; values of K_H for other sulfoxides viz. DPSO, BMSO, APSO, BPSO and DDSO were not determined since their extractive power for actinides was generally poor.

Effect of HNO_3 Concentration on Actinide Extraction. Data on the extraction of various actinides and associated fission products from different aqueous nitric acid media with sulfoxides/solvesso-100 are summarised in Table 1. With an increase in aqueous acidity, extraction of all the actinides first increases, passes through a maximum at around 2 to 5 M and then decreases. Against this, D_M of Zr increases while of Ru decreases with increasing acid concentration. No detectable extraction of Eu, Ce or Sr was observed at any acidity. The decrease in the D_M values at higher molarities may be attributed to the formation of less extractable acid nitrato complexes (17) and also to the competition of nitric acid for the sulfoxides at higher concentrations. The pattern of acid dependence of extraction encountered here is similar to that observed in many other systems (18,19).

A comparison of the extraction of actinides with sulfoxides under identical conditions, shows that they are extracted in the order: Pu(IV) > U(VI) > Np(IV). In the acid range between 2-8 M HNO_3, extraction of fission products like Zr, Ru, Eu, Ce and Sr is almost negligible and thus their decontamination should pose no problem during spent fuel reprocessing. Extraction of metal ions with 0.2 M solutions of DPSO, APSO and BPSO was extremely poor (< 5%) at all acidities. Very poor extraction of Am(III) even from concentrated acid solutions (upto 8M HNO_3) necessitated the use of salting out agents (12). Extractability of Am increased with increasing amounts of all the salting

TABLE 1. EXTRACTION OF METAL IONS WITH SULFOXIDES AS A FUNCTION OF NITRIC ACID CONCENTRATION

HNO_3 (M)	Sulfoxide (0.2M)	Distribution Ratio, D_M: Pu	Np	U	Zr($\times 10^{-2}$)	Ru($\times 10^{-2}$)	Eu	Ce	Sr
0.5	DOSO	2.58	0.13	1.67	0.33	Neg.	Neg.	Neg.	Neg.
	DHSO	-	0.22	-	-	-	Neg.	Neg.	Neg.
	DISO	0.06	0.06	-			Neg.	Neg.	Neg.
1.0	DOSO	3.18	0.35	3.15	0.45	8.40			
	DHSO	2.25	0.61	2.41	4.12	2.56			
	DISO	0.40	0.21	1.22					
	DBuSO	0.54	-	0.92					
	BMSO	Neg.		Neg.					
2.0	DOSO	5.13	1.06	4.93	1.25	5.05	Neg.	Neg.	Neg.
	DHSO	4.02	1.04	3.43	4.43	1.96			
	DISO	1.07	0.47	2.05					
	DBuSO	1.50		1.96					
	BMSO	0.01		0.02					
4.0	DOSO	8.13	1.17	4.11	4.01	1.35	-	-	-
	DHSO	4.59	1.16	3.33	6.52	0.54			
	DISO	1.91	0.73	2.18					
	DBuSO	2.83		2.61					
	BMSO	0.04		0.07					
7.0	DOSO	6.56	1.32	2.52	11.57	0.42	Neg.	Neg.	Neg.
	DHSO	4.90	1.40	2.35	13.86	0.66			
	DISO	1.26	1.02	1.47					
	DBuSO	2.42		1.98					
	BMSO	0.15		0.17					
10.0	DOSO	3.28	0.68	0.55	21.77	0.23	Neg.	Neg.	Neg.
	DHSO	1.98	0.93	0.78	83.49	0.46			
	DISO	1.06	0.57	0.61					
	DBuSO	1.94		0.82					
	BMSO	0.10		-					

Neg. = Negligible extraction

out agents studied and their effect followed the sequence: $Al^{3+} > Mg^{2+} > Ca^{2+} > Li^{+} > NH^{4+}$; this is also the relative dehydrating effect of the cations.

Dependence on Extractant Concentration. The dependence of extractant concentration on the metal ion extraction was investigated at 2M HNO_3 with respect to DISO (0.1 - 1 M), DBuSO (0.1 - 1 M), DPSO (0.1 - 0.5 M) and BMSO (0.1 - 0.5 M) employing Solvesso-100 as the diluent. Similar experiments could not be conducted with APSO as well as BPSO due to their limited solubility. Slopes of ~2 were obtained for UO_2^{2+} and Pu^{4+} which indicated the species extracted to be the disolvates. A comparison of the distribution ratios of an actinide, obtained under identical conditions into the above sulfoxides shows the extraction order to be: DOSO ~ DHSO > DISO > DBuSO ≫ DBSO > BMSO as expected from their basicity order. A 0.5 M solution of DOSO, DISO or DBuSO extracts more than 90% of U(VI) or Pu(IV) in a single step.

A similar study was not possible with the fission products due to their very poor extractability. The absorption spectra of U(VI) and Pu(IV) complexes extracted with various sulfoxides are strikingly similar to those extracted by TBP indicating the similarity of the species involved. However, a bathochronic shift of the peaks in the spectra of Pu(IV) and U(VI) complexes is observed both with sulfoxides and TBP as compared to the spectrum in aqueous acidic solutions.

Dependence of D_M on Organic Additive Concentration. Preliminary experiments revealed that extraction of uranium and plutonium with sulfoxides increased with increasing amounts of the organic additives. Table 2 summarises representative data on the extraction of Pu(IV) and U(VI) with DISO and DBuSO from 2M HNO_3 media in presence of varying amounts of methanol, ethanol, propanol, dioxane, acetone and acetonitrile in the aqueous phase.

In general, the effect of water-miscible additives on actinide extraction was found to increase in the order: dioxane < alcohols < acetone ~ acetonitrile. This enhancement can be explained by the fact that dissociation of electrolytes diminishes in the presence of organic solvents with lower dielectric constants. The less polar the additive, the higher is the tendency to form neutral metal complexes which ultimately brings about an increase in the extraction. At low additive concentration the dehydration effect (20) due to the presence of additives, which provides a better chance for interaction with the nitrate ion to form the extractable nitrate complexes, should lead to an increase in the metal ion extraction.

With the subsequent increase of additive concentration, the extraction of nitric acid increases leading to a drop in metal extraction. Generally, the substitution of water by organic solvents increases the acid activity and hence decreases or increases the D_M depending upon the extractive behaviour of the element. Partition of polar organic component between aqueous and organic phases is one of the most important features in these systems. Mason et.al.(21) and Nedden et.al.(22) have also reported a synergic effect of alcohol on di-acidic organophosphorous acid extractants. Contrary to this, higher aliphatic alcohols were found to decrease actinide extraction when added to the aqueous phase. Addition of acetone or acetonitrile into the aqueous phase is, therefore, advisable for the recovery of these actinides from moderate acid solutions.

Temperature Dependence of Extraction. The extraction of different actinides from 2M HNO_3 aqueous medium with several sulfoxides was investigated at fixed temperatures in the range 25-50°C to optimise the conditions for maximum extraction. The results indicate that the extraction of UO_2^{2+}, Np^{4+} and Pu^{4+} decreased with increasing temperature, suggesting that the reaction is exothermic. The temperature coefficient of extraction is known to be generally negative for

TABLE 2. EFFECT OF ORGANIC ADDITIVES ON THE EXTRACTION OF Pu(IV) AND U(VI) WITH 0.2M SULFOXIDES FROM 2M HNO_3

Organic Additive		$D_{Pu(IV)}$		$D_{U(VI)}$	
		DISO	DBuSO	DISO	DBuSO
Nil		0.83	1.50	2.05	1.96
Acetone	: 20%	2.65	2.05	2.11	2.19
	30%	3.66	2.71	2.15	2.39
	40%	4.48	3.10	2.19	2.39
	50%	3.46	3.37	2.25	2.51
Acetonitrile	: 20%	2.68	2.40	2.15	2.66
	30%	3.61	2.93	2.30	2.75
	40%	4.22	3.19	2.32	2.87
	50%	3.14	4.28	2.20	2.85
Dioxane	: 20%	1.45	1.09	1.71	1.75
	30%	1.59	0.98	1.58	1.36
	40%	1.57	1.10	-	-
	50%	0.94	0.88	1.36	1.24
Methanol	: 20%	2.07	1.46	1.67	1.18
	30%	2.52	1.53	1.45	0.97
	40%	2.55	1.12	1.28	0.68
	50%	0.63	0.85	0.96	0.45
Ethanol	: 20%	2.02	1.92	1.46	1.46
	30%	3.15	1.54	1.41	1.03
	40%	3.05	1.26	1.34	0.76
	50%	0.96	0.78	1.04	0.54
n-Propanol	: 10%	0.68	0.65	1.52	1.20
	30%	0.50	0.40	0.82	0.49
	50%	0.31	0.32	0.40	0.37

weak solvate complexes(23).

Extraction of Macro Amounts of Actinides and Their Stripping. Macro amounts of actinides like uranium, neptunium and plutonium are present during reprocessing of spent fuel and hence their extraction characteristics with a sulfoxide was investigated at such concentration levels. In all these studies acidity was maintained at around 2M HNO_3.

More than 80% (~10 mg/ml) of uranium could be extracted with 0.5M DISO in single contact which could be successfully stripped with an aqueous solution of pH 2. Likewise, extraction of neptunium (~3 mg/ml) under similar conditions was greater than 85%. Since the distribution ratio of Np(IV) into sulfoxides is fairly high even from dilute nitric acid solutions, the stripping of neptunium from the sulfoxide phase by reducing the aqueous HNO_3 concentration is not practicable. Extraction of plutonium (~3 mg/ml) from 2M HNO_3 with 0.5M DISO/Solvesso-100 was in excess of 90% in a single step. About 10 mg/ml of Pu(IV) was loaded into the organic phase without encountering the formation of a third phase. Plutonium could be back-extracted to the extent of 80% with ~0.4M HNO_3. The use of some complexing/reducing agents such as acetic and formic acids (1-5M) is preferable for process applications when used for the back-extraction of Np(IV) as well as Pu(IV). Similar behaviour has been encountered with other sulfoxides.

Effect of Radiation on Extraction. Experiments were conducted to study the effect of gamma radiation on the extraction properties of sulfoxides. The extraction, scrubbing and stripping behaviour of uranium, plutonium and some long-lived fission products, e.g. ^{95}Zr, $^{103,106}Ru$, $^{152,154}Eu$ etc. with gamma irradiated sulfoxides and TBP was studied. This was done by irradiating a pre-equilibrated extractant solution for different lengths of time upto a dose of 170 Mrads. All irradiations were carried out in the presence of air at room temperature with a ^{60}Co source (~2000 Ci) at a dose rate of 1.256×10^{17} eV g^{-1} min^{-1} (0.1176 Mrad/hr.)

Unlike TBP, extraction of U(VI) and Pu(IV) with sulfoxides gradually decreased with irradiated dose throughout. Overall plutonium losses have been found to be negligible at all doses. Decontamination factor (DF) of U and Pu with respect to both Ru and Zr-Nb are many times higher with irradiated sulfoxides as compared to TBP at all doses. Stripping percentage of uranium with TBP decreases sharply with dose reaching a negligible value above 100 Mrad, whereas with sulfoxide it increases with dose reaching almost a quantitative value at this dose. This can be explained due to the formation of synergistic complexes of uranium with TBP and its radiolytic degradation products unlike in the case of sulfoxides where the degradation products are reported to be inert(13). With irradiation, the decrease of DF with TBP is much more rapid as compared to those with sulfoxides.

The effect of gamma irradiation on some physical properties of the sulfoxides vis-a-vis TBP such as density and viscosity was investigated. The density and viscosity increased with dose for both sulfoxides and TBP. However, TBP showed the highest increase in viscosity (29%) as compared with 20% for DHSO and 8.4% for DOSO at the highest dose studied. Increase in viscosity is not desirable in solvent extraction as it enhances emulsion formation and phase separation time.

Based on this work, it can be concluded that aromatic as well as unsymmetrical sulfoxides containing aliphatic and aromatic groups are poor extractants for actinides. However, long-chain aliphatic sulfoxides have been found to be good extractants with potential use in the reprocessing of spent fuels involving high radiation fields.

REFERENCES

1. D.C. Kennedy, Ph.D. Thesis, Iowa State University, Ames, Iowa, p.25, 1969.
2. Y.E. Nikitin, Y.I. Morinov and A.M. Rozen, Russ. Chem. Rev. 45, 1155 (1976).
3. V.A. Mikhailov, Proc. Intern. Solvent Extraction Conf., Toronto, p.52(1977).
4. N.K. Lyapina, Russ. Chem. Rev. 51, 189 (1982).
5. V.A. Mikhailov, U.G. Torgov, E.N. Gilbert, L.N. Mazalov and A.V. Nikolaev, Proc. Intern. Solvent. Extraction Conf. Vol. 2, Hague, London, p.1112(1971).
6. G.T. Laurence, M.T. Chaieb and J. Talbot, ibid, p.1150.
7. S.R. Mohanty and A.S. Reddy, J. Inorg. Nucl. Chem. 37, 1791, 1977 (1975).
8. Y.E. Nikitin, Y.I. Murinov and A.M. Rozen, Proc. Intern. Solvent Extraction Conf. Toronto, p.38 (1977).
9. S.A. Pai, J.P. Shukla, P.K. Khopkar and M.S. Subramanian, J. Radioanal. Chem. 42, 323 (1978).
10. J.P. Shukla, S.A. Pai and M.S. Subramanian, Sept. Sci. & Tech. 14, 885 (1979).
11. J.P. Shukla, S.A. Pai and M.S. Subramanian, J. Radioanal. Chem. 56, 53 (1980).
12. J.P. Shukla, M.S. Nagar and M.S. Subramanian, ibid 62, 61 (1981).
13. Ref. 5, p. D-75.
14. S.A. Pai, J.P. Shukla and M.S. Subramanian, Radiochem. Radioanal. Lett. 53, 5 (1982).
15. W. Korpak, Nukleonika, 8, 747 (1963).
16. J.C. Sullivan and J.C. Hindman, J. Am. Chem. Soc. 76, 5931 (1954).
17. F. Baroncelli, G. Scibona and M. Ziffereo, J. Inorg. Nucl. Chem. 24, 541 (1962).
18. W. Korpak, Nucleonika 9, 1 (1964).
19. T. Sato, J. Appl. Chem. 15, 489 (1965); 16, 53 (1966).
20. Y. Yoshino and Y. Kurimura, Bull. Chem. Soc. Japan 30, 563 (1957).
21. G.W. Mason, S. McCarty and D.F. Peppard, J. Inorg. Nucl. Chem. 24, 967 (1962).
22. P.J. Zur Nedden, M. Janil and G. Duyckaerts, Proc. Intern. Solvent Extraction Conf. ISEC-1971, The Hague, p. 993.
23. J.M. Fletcher and C.J. Hardy, Nucl. Sci. Eng. 16, 421 (1963).

EXTRACTION OF CHROMIUM(III) AND CHROMIUM(VI) INTO ORGANOPHOSPHORUS COMPOUNDS AND AMINE SYSTEMS

V. M. Rao and M. N. Sastri

Department of Chemistry
Andhra University
Waltair 530 003, India

The separation and determination of chromium at trace levels is receiving considerable attention in view of its recognised role in biosystems. For ease of manipulation and routine operation solvent extraction procedures are prefered for the separation step. This paper describes our studies on the extraction of Cr(III) and Cr(VI) in to organophosphorus systems (TBP, TOPO) and into amine systems, (TOA, TLA and Aliquat-336). These studies mainly deal with our investigations on:

1. Photometric and titrimetric methods for the determination of chromium using these systems and
2. The nature of the extracted species from various mineral acid media and the effect of the diluent on the extraction.

EXTRACTIVE PHOTOMETRIC AND TITRIMETRIC METHODS FOR THE DETERMINATION OF CHROMIUM:

The highly unstable blue peroxychromic acid formed by the addition of H_2O_2 to an acidified solution of potassium dichromate is optically stable for about 48 hours when extracted into TBP. An extractive photometric method for the quantitative determination of Cr(VI) at 575nm is developed on this basis for concentrations of Cr(VI) upto 100mg/ml. Similar methods (2,3,4) for determination of chromium as blue peroxychromic acid are also developed employing ion-association systems such as tertiary amines, tri-n-octylamine, tri-isooctylamine, trilauryl amine and the quatermary ammonium compound Aliquat-336. The extracts are however optically stable for about 40 minutes. As in the previous case Cr(VI) can be determined at 575nm when present in concentrations upto 100mg/ml. The volumetric determination of chromium after back extraction which is also feasible in the case of tertiary amines as extractants is not satisfactory with Aliquat-336 since the back extraction is not quantitative.

THE NATURE OF THE EXTRACTED SPECIES:

The extraction of Cr(VI): The extraction of Cr(VI) (at Conc. $\leq$ 0.052mg/ml) from hydrochloric sulphiric, nitric, perchloric, acetic and orthophosphoric acid solutions in to trilauryl amine (TLA) is studied using ^{51}Cr radiotracer. The extraction from hydrochloric, sulphuric, acetic and orthophosphoric acid solutions is quantitative while it is partial from the nitric acid medium. On the other hand, the extraction from perchloric acid is negligible. The dissimilar extraction trends from various acid systems point to the possibility of association of the anion of the acid with the extracted Cr (VI) species. This has been tested by carrying out distribution studies using ^{36}Cl, ^{35}S and ^{32}P in respective acid media as a function of aqueous Cr(VI) concentration. The results indicate that the mole ratio of Cr(VI) to the anion of the acid in the extracted species is 1 : 0 in the case of sulphuric and orthophosphonic acid systems. This observation confirms that the extracted Cr(VI) species from sulphuric and orthophosphoric acid solutions are not associated with sulphate or phosphate ions. On the other hand, similar studies from hydrochloric acid solutions using ^{36}Cl indicate that the mole ratio of Cr(VI) to Cl in the extracted Cr(VI) species is 1:0.72, the ratio being constant even after saturation of the organic phase with Cr(VI). This indicates that from hydrochloric acid solutions, the Cr(VI) is extracted in the form of more than one species, the predominant species being CrO_3Cl^- This is further confirmed by the U.V. and visible spectral data (5-7). On the basis of these observations a mechanism of extraction of Cr(VI) by amine systems is suggested. These studies are confined to lower acid systems (< 0.1M) only in view of the preferential extraction of the acid at higher acidities.

The extractions of Cr(VI) aqueous mineral acid systems by organophosphorus compounds such as tri-n-butyl phosphate (TBP) and tri-n-octyl-phosphine oxide (TOPO) are quantitative even at higher acidities (> 1M). In the hydrochloric and orthophosphoric acid solutions (8), Cr(VI) is extracted as a mixture of species predominantly $HCrO_3Cl$, and $H_2Cr_2O_7$ and/or H_2CrO_4 from hydrochloric acid solutions and predominantly H_3CrPO_7 and $H_2Cr_2O_7$ and / or H_2CrO_4 from orthophosphoric acid solutions. From other acid media the extracted species is exclusively $Cr_2O_7^{2-}$. As in the case of amine systems the extraction from nitric acid is partial while from perchloric acid it is negligible.

The blue peroxychromic acid formed by the addition of H_2O_2 to an acidified solution of potassium dichromate is highly unstable. The blue species is however readily extracted (4) into TBP, TOA and Aliquat-336 The influence of variables such as H_2O_2 concentration, concentration of hexavalent chromium, extractant and the diluent is investigated (7). It is found that extraction of blue peroxychromic acid into ion-association systems occurs through the formation of anionic haloperoxychromate (VI), $CrO(O_2)_2X^-$ (X = Cl, Br). The anionic species is isolated as solid and characterised by I.R. and thermal methods (9).

The extraction of Chromium(III): Fewer studies have been reported on the extraction of Cr(III). An investigation on the extraction behaviour of carboxylate complexes of Cr(III) has been taken up. The extraction of tris (oxalato) chromate (III) from various mineral acid media by TLA and Aliquat-336 is carried out. The composition of the extracted species, the effect of acid and the effect of diluent have been studied (7,10). The data on the effect of diluent (11) is correlated with the solubility parameter of the organic solvent employed as diluent by the application of the theory of regular solutions.

The extraction of Cr(III)-EDTA complex with Aliquat-336 in the pH range 2-6 was earlier studied (12).

Maximum extraction was observed at pH 5.8 and the extracted species was identified as $CrY(H_2O)^-$ (H_4Y=EDTA). The blue complex, $Cr(OH)Y^{2-}$ formed at higher pH (pH 7.0) is not extractable. The diluent has a marked effect on the extraction with nitrobenzene giving maximum extraction (80%). Irving and Aljarrah also reported (13) the extraction of Cr(III)-EDTA complex into tetra-n-hexylammonium chloride in dichloromethane.

REFERENCES

1. D.S. Sundar and M.N. Sastri., Z.anal.Chem. 185 343 (1963).
2. D.S. Sundar and M.N. Sastri,, Anal.Chim.Acta 30 340 (1965).
3. T.S.R. Prasada Rao, D.S. Sundar and M.N. Sastri., Curr.Sci. 35(12) 307 (1966).
4. D.S. Sundar, Studies on the extraction of blue peroxychromic acid Ph.D. Thesis, Andhra University Waltair, India (1964).
5. V.M. Rao and M.N. Sastri, J. Indian Chem.Soc.53 1006 (1976).
6. V.M. Rao and M.N. Sastri, Indian J.Chem. 14 635 (1976).
7. V.M. Rao, Studies on the Solvent Extraction of Chromium, Ph.D. Thesis, Andhra University, Waltair, India (1977).
8. M.V.N. Murthy, V.M. Rao and M.N. Sastri, J.Indian Chem.Soc.57 688 (1980).
9. M.N. Sastri and T.S.R. Prasada Rao, J. Inorg.Nucl.Chem. 10 1727 (1968).
10. V.M. Rao and M.N. Sastri J. Indian Chem.Soc. 55 657 (1978).
11. M.V.N. Murty, V.M. Rao and M.N. Sastri, Acta Ciencia Indica 7(3) 142 (1981).
12. V.K. Rao, Some aspects of complexation of Chromium by EDTA Ph.D. Thesis, Andhra University, Waltair, India (1967).
13. H.M.N.H. Irving and R.H. Aljarrah, Anal.Chim.Acta 55 135 (1971).

EXTRACTION OF Sr AND Ba BY THE NITROBENZENE SOLUTION OF COBALT DICARBOLIDE IN THE PRESENCE OF ETHYLENOXIDE COMPOUNDS

E. Makrlík, P. Selucký, P. Vaňura
J. Rais, M. Kyrš and I. Podzimek

Nuclear Research Institute
Řež 250 68, Czechoslovakia

The aim of this paper was to determine the composition of compounds formed in the organic phase in the solvent extraction of Sr^{2+} and Ba^{2+} (M^{2+}) into nitrobenzene in the presence of $HCo(C_2B_{11}H_9)_2$ (1) (HB, dicarbolide acid) and glymes (L, $CH_3O-(CH_2-CH_2-O)_n-CH_3$) and to investigate the potential usefulness of similar systems for analytical purposes (2).

COMPOSITION OF COMPLEXES

In systems (1,2), where microamounts of Ba and Sr were extracted in the presence of PEGs 200, 300, 400 and HB the following equilibria were observed: $L \rightleftharpoons \bar{L}$ (K_D) (A); $\bar{H}^+ + L \rightleftharpoons \overline{HL}^+$ ($K_{ex}(HL^+)$ (B);
$M^{2+} + 2\bar{H}^{2+} \rightleftharpoons \bar{M}^{2+} + 2H^+$($K_{ex}(M^{2+})$)(C); $M^{2+} + L + 2\bar{H}^+ \rightleftharpoons \overline{ML}^{2+} + 2H^+$ ($K_{ex}(ML^{2+})$)(D); Here symbols with bars refer to the organic phase. In the present systems three additional equilibria were considered: $\bar{H}^+ + 2L \rightleftharpoons \overline{HL_2^+}$ ($K_{ex}(HL_2^+)$(E). $M^{2+} + 2L + \overline{2H^+} \rightleftharpoons \overline{ML_2}^{2+} + 2H^+$($K_{ex}(ML^{2+})$) (F) and $M^{2+} + L \rightleftharpoons ML_2^{2+}$(G). The equilibrium $M^{2+} + L \rightleftharpoons ML^{2+}$ is shifted to the left as found elsewhere.
The experiments included the determination of distribution ratios of Ba and Sr in dependence on the concentration of L, HB and aqueous acidity ($HClO_4$). The comparison of experimental $D_{M^{2+}}$ curves with theoretical ones based on the different assumptions of equilibria involved allowed the assessment of the participating equilibria. The K_d values 0.22 (monoglyme,n=1), 0.25 (n=2), 0.30 (n=3) and 0.45 (n=4) were determined using the method of concentration dependent distribution. The $K_{ex}(Sr^2)$ and $K_{ex}(Ba^{2+})$ found in this paper are reasonably independent of the value n and close to those found previously (5,0 for Sr; 7,0 for Ba).

The calculated values of equilibrium constants for different assumptions and the degree of coincidence of theoretical and experimental curves are summarized in Table 1. The extraction of M^{2+} in the presence of diglyme and that of Ba^{2+} with monoglyme corresponds the theory based on reactions (A)-(D) only. The reactions (E) and (F) are manifested with triglyme and tetraglyme but even then the reactions (A)-(D) dominate. The participation of reaction (G) could not be observed in any case. The rather surprising increase in the number of ligands with the value n can probably be ascribed to the higher affinity of ligands with more oxoethylene groups in this range of n values. Comparing the behaviour of the tetraglyme with that of PEG 200 (close n values), which exhibits higher stability constants (1.5 order for protonization in organic phase, 3.5 for $K(ML^{2+})$) seems to indicate higher affinity of ions toward -OH than $O-CH_3$ groups. The higher hydrophobicity of the glyme (K_d = 0.45 compared to K_d (PEG 200) = 1.6×10^{-3}) cannot counterbalance higher stability of the complexes of PEG in organic phase so that Sr and Ba are extracted by the glyme about hundred times less efficiently. Also separation factors $\alpha_{Ba/Sr}$ with glymes are lower than those observed for PEG 200 (log α for the diglyme is 0.9; 1.3 for tri-, and 1.7 for tetraglyme).

ANALYTICAL APPLICATIONS

Due to the high stability constants of Ba^{2+} and Pb^{2+} ions with polyethyleneglycols in nitrobenzene the analytical methods of the determination of the three above components can be conceived. The main interest in this work was in the determination of PEGs content by radiometric extraction titration method as this method permits in comparison with known and used procedures, as are molybdophosphoric acid method and tetraiodobismuthate method, to reach much higher sensitivity. Critical review of the used methods for the determination of PEGs was given recently by Nuysing and Koopal (3).

In the present method the excess of the hydrophobic anion was used (mainly 1.10^{-3}M $H^+(C_2B_9H_8Cl_3)_2Co^-$ (4)), the concentrations of the PEG to be determined are to be in the range 4.10^{-7}M to cca 2.10^{-4}M and the concentration of Ba^{2+} (Pb^{2+}) ions varied within the limits 10^{-7}M - 10^{-3}M. Typical titrations curves for PEG 400 are given in Figure 1. Also the curve where no PEG was present is given. The PEGs used were of Koch-Light provenience.

Several conclusions can be driven from the Figure 1. First, it is seen that the determination of the inflexion point is rather accurate even for the lowest concentration of PEG used. Secondly, it is seen that the titration curves are not generally symmetrical. The shape of the curves is determined in the region of high Ba^{2+} concentrations by the extraction of bare Ba^{2+} ion, whereas at low Ba^{2+} concentrations Ba : PEG 400 (1:1) complex is extracted. This conclusion may be proved if the curves from Figure 1 are plotted as extraction izotherms. No saturation is observed at high Ba^{2+}/PEG 400 ratios. The extraction of Ba^{2+} is also seen from the curve 0 in Figure 1. The shape and position of the titration curves can be well fitted with theoretical calculations on the basis of a program comprising the extraction of the macroamounts of H^+, $HPEG^+$, Ba^{2+}, and $BaPEG^{2+}$ (to be published elsewhere). Next conclusion issuing from Figure 1 is the fact that, whereas at $C_{PEG\ 400} > 6.10^{-5}$M the stoichiometry reaches expected 1:1 composition, at lower PEG concentrations the inflexion point occurs at relatively lower titrant consumptions. As this effect is rather regular, the correction factor can be easily deduced from Figure 1. The sensitivity of the proposed method lies around 4.10^{-7}mol/l of PEG 400 or ~0.2 mg/l. This means at least 50 fold enhancement of the sensitivity over the classical spectrophotometric methods since the latter are in the reported 10 mg/l limit handicaped by the concomitant error (±100 %) when measuring the absorbances as low as 0.05 or less (3).

The extraction of Ba^{2+} and Pb^{2+} in the presence of the PEGs of varying ethylene oxide chain length was studied. The classical titration curves were obtained for all PEGs with m.w. >300 (PEG 200 differs markedly from all other higher PEGs also when spectrophotometric methods are used (3)). The results were quantified by the following method. The relative number of EOU of the respective PEG was calculated from its m.w. divided by the number of EOU of PEG 400. The quotient log $[(n_{EOU})_x/(n_{EOU})_{400}]$ is denoted as n_r (teor) in the following table. This is conpared with an experimentally determined quotient $n_r(exp)$=log $[(I)_x/(I)_{400}]$ where I is the titrant consumption for respective PEG or PEG 400, the two being in the same molar concentrations (10^{-5} or 10^{-6} M).

PEG 400	1,000	1,500	4,000	6,000	20,000
$n_r(teor)^a$ 1	0.41	0.59	1.02	1.16	1.72
$n_r(exp)^b$ 1	0.34	0.55	0.95	1.08	1.72
a/b 1	1.21	1.07	1.07	1.07	1.00

It is seen that by the proposed method the total number of ethylene oxide units is determined in principle. For lower PEGs there is a marked tendency to obtain experimentally lower EOU contents than calculated (e.g. for PEG 600 a/b ~1.5). However, it should be recognized that the differences reflected in a/b ratio can be given in part by differences of the real and stated m.w. of the respective PEGs or by the polydispersity of the samples. The check on homogenous samples of PEGs is clearly desired. There is no mathematical treatment available of the extraction of Ba^{2+} in the presence of multifunctional PEGs for which the

presence of the particles nBa PEG^{2n+} is to be expected.

The curves from Figure 1 may be used as calibration curves for the determination of unknown Ba^{2+} or Pb^{2+} content in the sample. As said above, bare Ba^{2+} is extracted at high Ba^{2+} contents, so that substechiometric method of determination is not applicable (see also (5)). As there is apparently no difference between the behaviour of Ba^{2+} and Pb^{2+} the sum of both can be only determined. This method of determination seems to be limited to the special cases, sensitive methods for Pb^{2+} determination are known (stripping voltametry).

REFERENCES

1. P. Vaňura, J. Rais, P. Selucký and M. Kyrš, Coll. Czech. Chem. Commun. 44, 157 (1979).
2. P. Vaňura, E. Makrlík, J. Rais and M. Kyrš, Coll. Czech. Chem. Commun. 47, 1444 (1982).
3. J. Nuysink and L.K. Koopal, Talanta 29, 495 (1982).
4. M. Benešová, L. Kuča, M. Kyrš, H. Petržílová and J. Rais, International Symposium on the Management of Alpha-Contaminated Wastes, Vienna, Austria, Proceedings IAEA-SM-246/72 p. 563.
5. M. Štefek, M. Kyrš and J. Rais, Zh. Anal. Khim. 31, 1364 (1976).

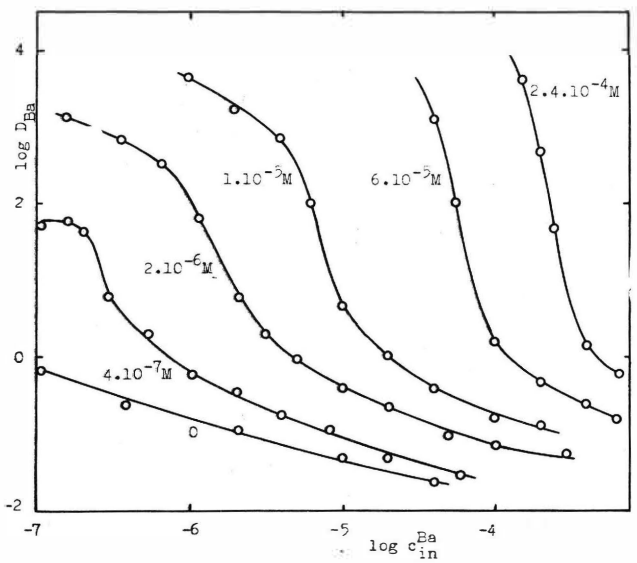

FIGURE 1. TITRATION CURVES OF PEG 400 WITH Ba^{2+} IONS. 1.10^{-3} M $H^+(C_2B_9H_8Cl_3)_2Co^-$ IN NITROBENZENE AND 0.01 M HNO_3 IN WATER, $v_a = v_o$.

Table I

Equilibrium constant values of the dominant reactions of Sr and Ba in the extraction by glymes and dicarbolide with nitrobenzene.

Model	log K_{ex}	U	i
	Ba-monoglyme		
*Ba^{2+}, BaL^{2+}, HL^+	0.94±0.03[b], 2.64±0.11, 1.05±0.07	0.07046	60
Ba^{2+}, BaL^{2+}, BaL_2^{2+}, HL^+, HL_2^+	0.94, 2.63±0.12, <2.65, 1.03±0.10, 0.52(0.82)	0.07017	60
	Ba-diglyme		
*Ba^{2+}, BaL^{2+}, HL^+	0.93±0.07, 3.69±0.10, 1.45±0.07	0.2089	60
Ba^{2+}, BaL^{2+}, BaL_2^{2+}, HL^+, HL_2^+	0.93, 3.89(4.33), 5.43±0.05, 1.82(2.38), 2.38(2.86)	0.1850	60
	Ba-triglyme		
Ba^{2+}, BaL^{2+}, HL^+	0.85, 5.50±0.16, 2.00±0.12	3.222	82
*Ba^{2+}, BaL^{2+}, BaL_2^{2+}, HL^+, HL_2^+	0.85, 5.88(6.16), 8.20(8.66), 2.60(2.91), 3.53 (3.84)	2.466	82
	Ba-tetraglyme		
Ba^{2+}, BaL^{2+}, HL^+	0.85, 6.72±0.06, 2.60±0.05	0.2111	60
*Ba^{2+}, BaL^{2+}, BaL_2^{2+}, HL^+, HL_2^+	0.85, 6.79±0.11, 7.66(8.25), 2.67±0.12, 2.92 (3.52)	0.1805	60
	Sr-diglyme		
*Sr^{2+}, SrL^{2+}, HL^+	0.51±0.05, 2.96±0.12, 1.61±0.07	0.1361	60
Sr^{2+}, SrL^{2+}, SrL_2^{2+}, HL^+, HL_2^+	0.51, 3.08±0.15 3.68(4.16), 1.74±0.16 1.71(2.16)	0.1258	
	Sr-triglyme		
Sr^{2+}, SrL^{2+}, HL^+	0.41±0.12, 4.23±0.08, 1.97±0.06	0.3904	75
*Sr^{2+}, SrL^{2+}, SrL_2^{2+}, HL^+, HL_2^+	0.41, 4.36±0.03 6.26±0.04, 2.23±0.06, 3.28(3.57)	0.1799	
	Sr-tetraglyme		
Sr^{2+}, SrL^{2+}, HL^+	0.58±0.22, 5.14±0.16, 2.73±0.10	0.8306	73
*Sr^{2+}, SrL^{2+}, SrL_2^{2+}, HL^+, HL_2^+	0.58, 5.91±0.23 8.19(8.52), 3.52(0.23), 4.33(4.56)	0.3229	

U- criterion of the discrepancy of theoretical and experimental distribution functions, i - number of experimental points (2). The same intervals of reliability are used as recommended by L.G. Sillén and B. Warnqvist (1969). No intervals are indicated if the value is predetermined from (1) or from a simpler model. The asterisk refers to the model preferred.

CORRELATION OF PHASE EQUILIBRIA IN THE WET-PROCESS PHOSPHORIC ACID/SULFURIC ACID/ISOBUTANOL SYSTEM

Steven J. Dougherty

International Minerals and Chemical Corporation
Terre Haute, Indiana USA

Solvent extraction of wet-process phosphoric acid to obtain a purified phosphoric acid suitable for industrial, detergent, and food uses is practiced by a number of European companies, and by companies in Africa and Japan. Some of the solvents used include methyl ethyl ketone, isopropyl ether (1), and isobutanol (2).

One of the problems in the development and implementation of the various solvent extraction processes is the inability to characterize the phase equilibria, which in turn complicates scaleup, startup, and process control. A correlational method is proposed based on a modified Renon equation. Starting with a wet-process-acid model comprised of phosphoric acid, sulfuric acid, magnesium sulfate, isobutanol, and water, results are reported for the ternary and quaternary combinations of the subsystem comprised of phosphoric acid, sulfuric acid, isobutanol, and water.

MODEL BASIS

For two liquid phases at thermodynamic equilibrium, the reference fugacities in both phases are the same so that:

(1) $$\gamma_i' x_i' = \gamma_i'' x_i''$$

where ' and " denote the two phases, γ_i is the activity coefficient of component i, and x_i is the mole fraction of component i. β_i is defined as the distribution of component i between the two phases:

(2) $$\beta_i = \frac{x_i'}{x_i''}$$

From equations (1) and (2):

(3) $$\beta_i = \frac{\gamma_i''}{\gamma_i'}$$

With a suitable model for γ_i, where:

(3) $$\gamma_i = f(x_i, x_j \ldots, T, A, B, \ldots)$$

the parameters A, B... can be determined from phase equilibria data.

The activity coefficient model chosen for this study is based on the Renon equation (3) with empirical modifications to deal with the electrolytes. For a multicomponent system, the Renon equation yields:

(4) $$\ln \gamma_i = \frac{\sum_{j=1}^{m} \tau_{ji} G_{ji} x_j}{\sum_{\ell=1}^{m} G_{\ell i} x_\ell} + \sum_{j=1}^{m} \frac{x_j G_{ij}}{\sum_{\ell=1}^{m} G_{\ell j} x_\ell} \left[\tau_{ij} - \frac{\sum_{r=1}^{m} x_r \tau_{rj} G_r}{\sum_{\ell=1}^{m} G_{\ell j} x_\ell} \right]$$

where:

$$\tau_{ij} = \frac{(g_{ij} - g_{jj})}{RT}$$

$$G_{ij} = \exp(-\alpha_{ij} \tau_{ij})$$

$$\alpha_{ij} = \alpha_{ji}$$

$$\alpha_{ij} = 0$$

$$g_{ij} = g_{ji}$$

The empirical modification, as suggested by Funk (4), ignores the dissociation of the electrolytes and corrects for the long range effects not accounted for in the Renon equation by adjusting the activity coefficient of a given electrolyte in the mixture in terms of correction terms added to the activity coefficient which is otherwise given by the Renon equation. The correction for electrolyte j in the presence of other electrolytes, k, is given by:

(5) $$\ln \gamma_j = \ln \gamma_j^\circ + \sum \Delta_{jk} x_k$$

where γ_j° is the activity coefficient of electrolyte j as calculated by the Renon equation with all electrolyte interaction parameters set to 0.

DATA

Data for the phosphoric acid, water, isobutanol ternary were obtained from the literature (5). Data for the sulfuric acid, water, isobutanol system, and for the four-component system, were collected in this laboratory by isothermal shakeouts at 25°C. These are shown in Tables I and II.

RESULTS

The data for the two ternary combinations of phosphoric acid, water, isobutanol and sulfuric acid, water, isobutanol were simultaneously regressed by varying all applicable parameters, except for $\alpha_{H_2O\text{-}iBuOH}$, using a simplex optimization. A value of 0.2 was arbitrarily used for $\alpha_{H_2O\text{-}iBuOH}$. With the set of parameters shown in Table III, the average absolute deviation between the experimental and theoretical distributions for each of the four components is:

	|Average|	Mean of Residuals
Phosphoric Acid	7.1%	0.3
Sulfuric Acid	11.3%	-3.1
Water	4.7%	3.5
Isobutanol	7.3%	-3.7

The expected deviation based on experimental error is about 5%. Thus, there is some scatter which the model cannot explain. However, for engineering calculations, the fit is satisfactory.

The binary parameters shown in Table III for water (i)-isobutanol(j) compare with the parameters determined from binary data as shown:

	Ternary Data	Binary Data(6)
α_{ij}	0.2 (fixed)	0.2 (fixed)
τ_{ij}	3110.61	2833.43
τ_{ij}	-554.403	-483.715

The agreement between the two methods for determining the binary parameters is excellent; the parameters determined from binary data alone would provide a satisfactory fit.

With the parameters from Table III, data for the quaternary system of phosphoric acid, sulfuric acid, water, and isobutanol were regressed using equation (5). The two fitted Δ parameters are:

H_3PO_4 - H_2SO_4: 16.6565
H_2SO_4 - H_3PO_4: -11.7657

The average absolute deviation between experimental and theoretical distributions for each of the four components is:

	|Average|	Mean of Residuals
Phosphoric Acid	6.8	0.2
Sulfuric Acid	9.2	-4.6
Water	5.7	5.7
Isobutanol	6.4	6.3

Although the results show a slight deterioration over those for the two ternary systems, the regression is suprisingly good.

The analysis to date has demonstrated the acceptability of equations (4) and (5) for correlating liquid-liquid equilibria in the four-component system phosphoric acid, sulfuric acid, water, and isobutanol. However, quaternary data are required. Further work will include the magnesium sulfate component and will determine if the data basis can be limited to four-component systems.

REFERENCES

1. A. Davister and G. Martin, AIChE Annual Meeting, New Orleans, No. 26b (1981).
2. J. Bergdorf and R. Fischer, CEP, 41 (November, 1978).
3. H. Renon and J. M. Prausnitz, AIChE Journal 14 No. 1, 135 (1968).
4. E. W. Funk, in Thermodynamics of Aqueous Systems with Industrial Applications (S. A. Newman, ed.), ACS Symposium Series No. 133, 717 (1980).
5. S. Moroto and A. Watanabe, Nagoya Gijutsu Shikensho Hokoku. 18 No. 6, 103 (1968).
6. J. M. Sorensen and W. Arlt, Liquid-Liquid Equilibrium Data Collection V Part 1, Schön and Wetzel, Frankfurt, 244 (1979).

TABLE 1

Liquid-Liquid Equilibria Data for the Three-Component System of Sulfuric Acid, Water, and Isobutanol at 25°C

Aqueous Phase Mole Fractions			Organic Phase Mole Fractions		
H_2SO_4	H_2O	i-Butanol	H_2SO_4	H_2O	i-Butanol
.0397	.9439	.0164	.0176	.4508	.5316
.0399	.9436	.0164	.019	.4546	.5264
.0069	.9768	.0163	.0068	.4113	.5819
.0248	.9588	.0164	.008	.4026	.5894
.0489	.9347	.0164	.0289	.4521	.519
.048	.935	.0169	.0276	.4551	.5173
.0466	.9372	.0162	.027	.4346	.5384
.0459	.9366	.0174	.0299	.4682	.5019
.0626	.9197	.0177	.0479	.5152	.437
.0158	.9692	.015	.0073	.4078	.5848
.033	.951	.016	.0185	.4306	.5509
.0563	.9262	.0175	.0416	.4926	.4658
.0755	.904	.0204	.0662	.5992	.3346
.08	.8968	.0232	.0746	.6460	.2795
.088	.8817	.0303	.0823	.7015	.2162
.0737	.9073	.019	.0616	.5877	.3507
.0769	.9018	.0213	.0676	.6182	.3141
.0881	.8822	.0297	.0805	.6856	.2339
.0936	.8611	.0453	.0922	.7356	.1722
.0693	.9123	.0184	.0546	.5482	.3972
.0771	.9023	.0206	.0648	.6111	.3241
.0837	.8921	.0242	.0748	.6468	.2784
.0905	.8772	.0324	.0844	.7088	.2068
.00305	.9764	.0200	.00056	.437	.5624
.0318	.9513	.0169	.0121	.4352	.5527
.0525	.9312	.0163	.0333	.4934	.4733

TABLE II

Liquid-Liquid Equilibria Data for the Four-Component System of Phosphoric Acid, Sulfuric Acid, Water, and Isobutanol at 25°C.

Mole Fractions (Aqueous Phase/Organic Phase)			
H_3PO_4	H_2SO_4	H_2O	i-Butanol
.016	.0267	.9407	.0166
.0095	.0162	.4513	.5230
.0175	.0473	.9178	.0174
.0131	.0332	.5033	.4504
.0138	.0632	.9041	.019
.0146	.0541	.578	.3532
.0125	.0765	.8822	.0288
.0151	.0718	.6783	.2348
.0367	.0182	.9261	.0189
.0181	.0075	.4331	.5414
.0331	.0363	.912	0.185
.0238	.0213	.4721	.4828
.0322	.0521	.8962	.0195
.029	.041	.5425	.3874
.029	.0685	.8804	.0221
.0309	.0611	.6487	.2592
.0752	.0186	.8868	.0194
.0563	.0127	.4883	.4428
.068	.0346	.8757	.0217
.0648	.0312	.5719	.3322
.0664	.0543	.8435	.0357
.0655	.0493	.6802	.205
.1176	.0184	.8360	.028
.1124	.0175	.6107	.2595

TABLE III

Parameters for the Ternary Combinations of Phosphoric Acid or Sulfuric Acid with Water and Isobutanol

Binary Combination (i,j)	$\alpha_{i,j}$	$g_{ij}-g_{jj}$
H_3PO_4 - H_2SO_4	-	-
H_3PO_4 - H_2O	0.0	-1703.74
H_3PO_4 - iBuOH	0.337916	956.913
H_2SO_4 - H_3PO_4	-	-
H_2SO_4 - H_2O	0.0	-138.816
H_2SO_4 - iBuOH	0.487295	684.211
H_2O - H_3PO_4	0.0	6425.70
H_2O - H_2SO_4	0.0	553.900
H_2O - iBuOH	0.2	3110.61
iBuOH - H_3PO_4	0.337916	2583.10
iBuOH - H_2SO_4	0.487295	833.981
iBuOH - H_2O	0.2	-554.403

LIQUID-LIQUID EQUILIBRIUM DATA FOR SYSTEMS CONTAINING HEAVY SOLVENTS

P. O. Ferreira, A. G. Medina

Contro de Engenharia Quimica
Faculdade de Engenharia
Rua dos Bragas
4099 Porto Codex, Portugal

INTRODUCTION

Solvent extraction is widely used in the petrochemical industry for the separation of aromatics and non aromatics. N-methylpyrrolidone is a common solvent in several plants currently in operation. However the experimental information available in the open literature for systems with NMP,aromatics and non aromatics is very limited. In a recent survey published by Sørensen and Arlt (1) only the binary system NMP/heptane and the ternary system NMP/bezene/heptane,studied by Fabries et al. (2),are reported. More recently Nagpal et al. (3) published experimental results for mixtures of NMP/toluene/heptane.

No interaction parameters allowing the use of group contribution methods for the prediction of equilibrium data for systems including NMP are available (4).

In the present work,experimental results obtained for the binary system NMP/ /heptane in the temperature range 15-50°C and for the ternary system NMP/toluene/ /heptane at 15°C,25°C and 40°C are presented. This experimental program was in progress when the work published by Nagpal et al.(3) became available.

Due to the disagreement between the two sets of experimentalresults, which became apparent from a comparison of results obtained at 40°C,it was decided to complete the planned experimental program.

The experimental information is used together with previous results (2),(5) as a data base for the determination of UNIFAC interaction parameters between a new group NMP and the groups alkane,water and aromatics (ACH,$ACCH_2$).

EXPERIMENTAL

Materials: Heptane and toluene (Carlo Erba) were dried over 5Å molecular sieves. N-methylpyrrolidone (BDH) was distilled under vacuum (2cm H_g) in a high efficiency column.

Procedure: The experimental work was carried out using a thermostatted glass cell similar to that described by Soares (6). Temperature was controlled within an accuracy of 0.1°C by means of a precision thermometer. For each temperature different tie-lines,covering the two phases region,were determined. An experimental procedure previously described was followed (7). Phase compositions were determined by means of a gas-liquid chromatograph (Perkin Elmer Sigma 3) equipped with a thermal conductivity detector and connected to an integration unit (Perkin Elmer Sigma 10B). A 10ft x 1/8" stainless steel column packed with Carbowax 20M + 2% KOH on Chromosorb WAW DMCS 80/100 and operating at 170°C was used; the flow rate of carrier gas, helium, was kept constant at $20cm^3\ min^{-1}$. Mass fraction measurements were reproducible to within ±0.002.

RESULTS AND DISCUSSION

The experimental results obtained for the partially miscible binary system NMP/heptane at different temperatures in the range 15-50°C are represented in Figure 1 together with those obtained by Fabries et al. (2) for the same system. The disagreement between light phase compositions is due to the presence of water traces in NMP (2).

The results obtained for the ternary system at three different temperatures 15,25 and 40°C are represented in Figures 2a,b,c.

A possible explanation for the difference between the new results and those published by Nagpal et al. (3) is the presence of impurities, namely water. It is known that water traces increase the two phases region (2).

ESTIMATION OF UNIFAC PARAMETERS

In this work UNIFAC interaction parameters between a new group "NMP" and the main groups "CH_2","ACH","$ACCH_2$" and "H_2O" were estimated. Table 1 summarises the experimental liquid-liquid equilibrium information available. A computer program developed by Magnussen (8) was used for the calculations. The same computer program allowed the back calculation of the binodal curves.

The new UNIFAC interaction parameters, a_{mn}, are presented in Table 2. The differences between experimental and calculated results were quantified in terms of the residual function defined by eqn (1)

$$(1) \quad F = \sqrt{\sum_k \min \sum_i \sum_j (x_{ijk} - \hat{x}_{ijk})^2 / 6M} \times 100$$

where min denotes minimum values, M is the number of experimental points, x the experimental composition (mole fraction), $\hat{x}$ the calculated composition (mole fraction), i denotes component i (i=1,2,3), j denotes phase j (j=1,2) and k is the tie-line k (k=1...M).

TABLE 1

Liquid-liquid equilibrium data used for the estimation of new UNIFAC parameters

System	Reference	Temperature (°C)
NMP/benzene/heptane	(2)	25
NMP/toluene/heptane	this work	15,25,40
Water/NMP/naphthalene,1-methyl	(5)	20,40,60
Water/NMP/tridecane	(5)	20,40,60

TABLE 2

New UNIFAC interaction parameters, a_{mn}*

$a_{CH_2,NMP}$	a_{NMP,CH_2}	$a_{ACH,NMP}$	$a_{NMP,ACH}$	$a_{ACCH_2,NMP}$	$a_{NMP,ACCH_2}$	$a_{H_2O,NMP}$	a_{NMP,H_2O}
236.15	9.44	- 66.31	58.29	- 9.96	62.21	1022.96	-464.96

*$a_{mn} = (u_{mn} - u_{nn}) / R\ (k)$

Residual values are presented in Table 3. The mean absolute deviation between experimental and predicted equilibrium compositions is 2.46 mole per cent. For seventeen test systems Magnussen et al. (9) obtained an average deviation of 1.85 mole per cent.

TABLE 3

Comparison between experimental results and predicted values based on new UNIFAC parameters

System	Temperature (°C)	Nº of data points	F
NMP/benzene/heptane	25	5	0.71
NMP/toluene/heptane	15	9	2.3
NMP/toluene/heptane	25	10	0.62
NMP/toluene/heptane	40	4	3.9
Water/NMP/naphthalene,1-methyl	20	4	2.2
Water/NMP/naphthalene,1-methyl	40	4	1.7
Water/NMP/naphthalene,1-methyl	60	7	2.7
Water/NMP/tridecane	20	4	1.8
Water/NMP/tridecane	40	7	2.7
Water/NMP/tridecane	60	6	6.0

CONCLUSIONS

Experimental equilibrium compositions were determined for the binary system NMP/heptane in the temperature range 15-50°C and for the ternary system NMP/toluene/heptane at 15,25 and 40°C. The new results disagree with previous ones obtained by Fabries et al. (2) and Nagpal et al. (3). The equilibrium compositions for these systems, which contain a highly hygroscopy component NMP, are strongly affected by traces of water. It is believed that differences between the present results and those previously published are a consequence of that phenomena.

Using a limited data base, with ten data sets, UNIFAC parameters between a new NMP group and four other groups were determined. The back calculation of equilibrium compositions originates a mean deviation of 2.46 mole per cent.

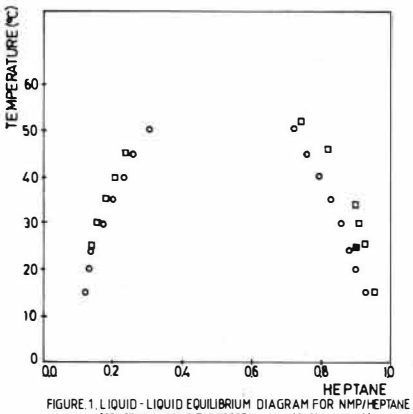

FIGURE.1. LIQUID - LIQUID EQUILIBRIUM DIAGRAM FOR NMP/HEPTANE (CONCENTRATIONS EXPRESSED AS MASS FRACTIONS).
○ THIS WORK
□ FABRIES ET AL.(2) OBTAINED BY CLOUD POINT METHOD
■ FABRIES ET A.L.(2) OBTAINED BY CHOMATOGRAPHIC ANALYSIS

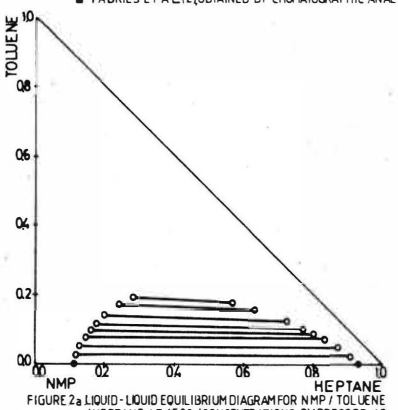

FIGURE.2a LIQUID - LIQUID EQUILIBRIUM DIAGRAM FOR NMP / TOLUENE /HEPTANE AT 15°C (CONCENTRATIONS EXPRESSED AS MASS FRACTIONS).

REFERENCES

1. J.M. Sørensen and W. Arlt. Liquid-liquid Equilibrium Data Collection, DECHEMA, Frankfurt.(1979).

2. J.F. Fabries,J.L. Gustin and H. Renon. J. Chem. Eng. Data 22. 303 (1977)

3. J.M. Nagpal and B.S. Rawat. J. Chem. Tech. Biotechnol. 31. 146 (1981)

4. T. Magnussen,P. Rasmussen and Aa. Fredenslund. Ind. Eng. Chem. Proc. Des. Dev. 20. 331 (1981)

5. A.Z. Bikkulov et al. Nefteklim Protsessy Prod.,Bashkir editor. 52 (1976)

6. L. Soares. Ph.D. Thesis, University of Birmingham,Birmingham,Gt. Britain. (1972)

7. M.E. Soares,A.G. Medina and P.J. Bailes. Fluid Phase Equilibria 9. 177 (1982)

8. T. Magnussen. Ph.D. Thesis, Technical University of Denmark,Lyngby, Denmark.(1980)

9. T. Magnussen,J.M. Sørensen ,P. Rasmussen and Aa. Frendenslund. Fluid Phase Equilibria 4. 151 (1980)

Note: Detailed experimental results and correlation parameters can be obtained from the authors.

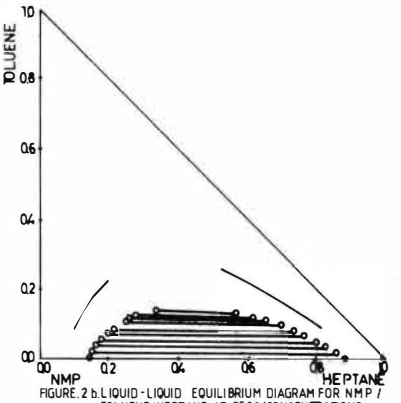

FIGURE.2 b. LIQUID - LIQUID EQUILIBRIUM DIAGRAM FOR NMP / TOLUENE/HEPTANE AT 25°C (CONCENTRATIONS EXPRESSED AS MASS FRACTIONS).
—— NAGPAL ET AL. (3).

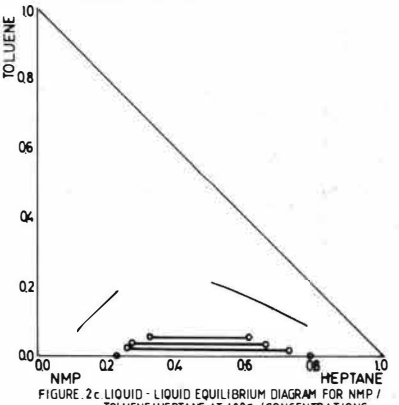

FIGURE.2c LIQUID - LIQUID EQUILIBRIUM DIAGRAM FOR NMP / TOLUENE/HEPTANE AT 40°C (CONCENTRATIONS EXPRESSED AS MASS FRACTIONS).
—— NAGPAL ET AL. (3).

THE EXTRACTION OF IRON(III) FROM 6M HCl BY LONG CHAIN AMINES DISSOLVED IN CHLOROFORM

Robert W. Cattrall and Mirna Z. Ilic

La Trobe University
Melbourne, Australia

The extraction of iron(III) from aqueous chloride solutions by high molecular weight amines, mainly tertiary amines, in low dielectric constant diluents has been widely studied (1-6). The equilibrium data on iron(III) extraction is generally inconsistent with spectral observations. The amine to metal ratio in the organic phase varies between one and two depending on the amine and the diluent whereas the absorption spectra of the organic extracts correspond to extraction of the species $FeCl_4^-$ which requires a value of unity for the amine to metal ratio.

There is a strong tendency in these systems, particularly in low dielectric constant diluents, for the formation of mixed dimers as we have shown for the extraction by tri-n-octylammonium chloride in chloroform (7).

In this paper we present further observations on the extraction of iron(III) from HCl solutions by a series of secondary amines, di-isooctylamine, di-n-octylamine, di(3,5,5-trimethylhexyl)amine, and di-n-nonylamine, an additional tertiary amine, tri-isooctylamine, and a primary amine, n-dodecylamine all dissolved in chloroform.

We have previously reported the aggregation behaviour of the amine hydrochlorides in chloroform (8) and have shown that the secondary amine salts generally dimerize, whereas the tertiary amine salts are monomeric and the primary amine salt is possibly tetrameric or higher.

THE DEPENDENCE OF THE EXTRACTION ON THE HCl CONCENTRATION

Figure 1 shows the increase in extraction with increase in acid concentration which is consistent with increasing amounts of the extractable species $FeCl_4^-$. In this system the extraction curves do not have a maximum but do show a tapering off at high acid concentrations particularly for the secondary and tertiary amines. Two reasons are generally accepted for this, the protonation of the $FeCl_4^-$ species, and the extraction of acid by the amine salt which competes with the extraction of Fe(III).

Figure 1 shows an increase in extraction efficiency from primary to secondary to tertiary amines and the behaviour correlates well with the trends in aggregation of the salts in chloroform. The extractants with the lowest tendency towards aggregation (e.g. the tertiary amine salts) exhibit the highest extraction efficiency, whereas the most highly aggregated salt, n-dodecylammonium chloride, is the least effective extractant. Amongst the secondary amine salts the straight chain ones DOA.HCl and DNA.HCl, and the branched chain DTHA.HCl, which have high dimerisation constants, are less effective extractants than DIA.HCl which shows a lower tendency to dimerise.

Since the lower extraction efficiency correlates well with an increased tendency to aggregate, it is reasonable to assume that the monomer of the amine salt is the most important extractant species relative to the dimer and higher oligomers.

TWO-PHASE TITRATION STUDIES

These were carried out using 6M HCl solutions where the extraction of excess acid is negligible. The general expression for the equilibrium reaction is

$$(1)\quad q\ BHCl_{org} + p\ FeCl_{3\,aqu} \overset{k_{pq}}{\rightleftharpoons} (BHCl)_q(FeCl_3)_{p\,org}$$

The equilibrium data is obtained in the form of Z (total iron(III) concentration in the organic phase/total reagent concentration) plotted against $\log[FeCl_3]_{aqu}$. Representative plots are shown in figure 2. Initially, a graphical procedure according to Sillén (9) and described in detail by Högfeldt and Fredlund (10) is used to obtain the averages $\bar{p}$ and $\bar{q}$, which are the average numbers of BHCl and $FeCl_3$ moities respectively per complex.

Once the average compositions of the complexes have been evaluated guesses are made as to the major extracted complexes. The extraction equilibrium constants (equation (2)) can be estimated graphically using normalised curves (11) for those systems where there is no aggregation of the reagent. Alternatively, a computer program is used to search for the equilibrium constants and for possible minor species by minimizing the error square sum $UZ = \Sigma(Z_{obs} - Z_{calc})^2$.

$$(2)\quad k_{pq} = \frac{[(BHCl)_q(FeCl_3)_p]_{org}}{[BHCl]^q_{org}[FeCl_3]^p_{aqu}}$$

EXTRACTION RESULTS

Secondary amine salts. A large number of stoichiometries were tested for the secondary amine salts after inclusion of the dimerisation constants (8) in the treatment and the combinations giving the lowest UZ values are listed in table 1. Composition graphs (figure 3) for the organic phase show that the sets of equilibrium constants yield a predominance of heterogeneous aggregates such as (1,2), (1,3) and (1,4).

NDA.HCl. The aggregation of the primary amine salt is more extensive than for the secondary amine salts (8) and it is not possible to obtain data for the aggregation constants. Thus, the extraction data was only treated by neglecting aggregation. The $\bar{p}$ and $\bar{q}$ values for this reagent suggest a predominance of (1,1) and (1,2) complexes. Table 1 shows that inclusion of larger heterogeneous aggregates improves the fit to the experimental data, however, composition curves suggest that the (1,1) and (1,2) complexes are the predominant ones (figure 3).

TIA.HCl. In contrast to the primary and secondary amine salts, tertiary amine salts are monomeric in chloroform (8) which facilitates the equilibrium data treatment. The $\bar{p}$ and $\bar{q}$ values for TIA.HCl are similar to those reported previously for TOA.HCl (7) and suggest the important complexes are (1,2) and (2,4). As with TOA.HCl an improved fit was obtained by including a (1,1) complex in the treatment. The extraction equilibrium constants for TIA.HCl are shown in table 1 and are very similar to those obtained for TOA.HCl, and, as with TOA.HCl, yield composition curves (figure 3) showing a predominance of the (1,2) mixed dimer. However, the (2,4) complex is present in larger amounts in the TIA.HCl system than for TOA.HCl.

CONCLUSIONS

The results for the three classes of amine salts studied demonstrate a strong tendency to form heterogeneous aggregates in the extraction of iron(III) from hydrochloric acid solutions. The results also suggest that the reagent monomer is the important species in the extraction and that the initial reaction involves the formation of a (1,1) complex which then reacts with additional monomer to form the heterogeneous aggregates. This agrees with a kinetic study of these systems (12) where the rate data can be understood in terms of a first order rate determining step involving the formation of a (1,1) complex.

For TIA.HCl the predominant species is the (1,2) complex and its structure in chloroform is probably very similar to that suggested by Work and McDonald (13) in the analogous system involving tri-n-octylamine in benzene. The preferred structure consists of two cations hydrogen bonded to one chloride ion with this ion triplet further associated with $FeCl_4^-$.

For the secondary and primary amine salts, hydrogen bonding interactions are expected to be more pronounced and it is not surprising to find higher heterogeneous aggregates in these systems.

REFERENCES

1. M.L. Good and S.E. Bryan, J. Amer. Chem. Soc., 82, 5636 (1969).
2. M.L. Good and S.C. Srivastava, J. Inorg. Nucl. Chem., 27, 2429 (1965).
3. A.D. Nelson, J.L. Fasching and R.L. McDonald, J. Inorg. Nucl. Chem, 27, 439 (1965).
4. J.M. White, P. Kelly and N.C. Li, J. Inorg. Nucl. Chem., 16, 337 (1961).
5. L. Kuča and E. Högfeldt, Acta Chem. Scand., 22, 183 (1968).
6. O. Levy, G. Markovits and A.S. Kertes, J. Inorg. Nucl. Chem., 33, 551 (1971).
7. R.W. Cattrall and M.Z. Ilic, J. Inorg. Nucl. Chem., 40, 1446 (1978).
8. R.W. Cattrall and M.Z. Ilic, J. Inorg. Nucl. Chem., 43, 2855 (1981).
9. L.G. Sillén, Acta Chem. Scand., 15, 1981 (1961).
10. E. Högfeldt and F. Fredlund, Trans. Royal Inst. Technol., No. 226 (1964).
11. M. Muhammed, J. Szabon, and E. Hogfeldt, Chemica Scripta, 6, 61 (1974).
12. M.Z. Ilic, Ph.D. Thesis, La Trobe University (1981).
13. R.A. Work and R.L. McDonald, J. Inorg. Nucl. Chem., 34, 3123 (1972).

TABLE 1

Extraction equilibrium constants for $(BHCl)_q(FeCl_3)_p$ Complexes

Reagent	log k_{pq}								UZ x10³	log β_2*
	(1,1)	(1,2)	(1,3)	(1,4)	(2,2)	(2,4)	(3,3)	(4,4)		
DOA.HCl	1.42	4.95		10.62		12.90		15.33	0.90	3.77
DNA.HCl	1.58	5.03		10.25	6.79	12.50			0.65	3.51
DIA.HCl	2.31	5.05	6.77		7.24	11.60			0.33	2.70
DTHA.HCl	1.69	5.09		9.57		12.06	10.87		0.75	3.23
NDA.HCl	0.89	2.06							0.39	
	0.93	1.90	2.60						0.31	
	0.91	2.00		3.40					0.28	
	0.92	1.94	3.22	2.28					0.31	
TIA.HCl	2.43	4.81							18	
	2.63	4.42				10.46			2.6	
TOA.HCl**	2.29	4.54				9.10				

*ref. (8)
**ref. (7)

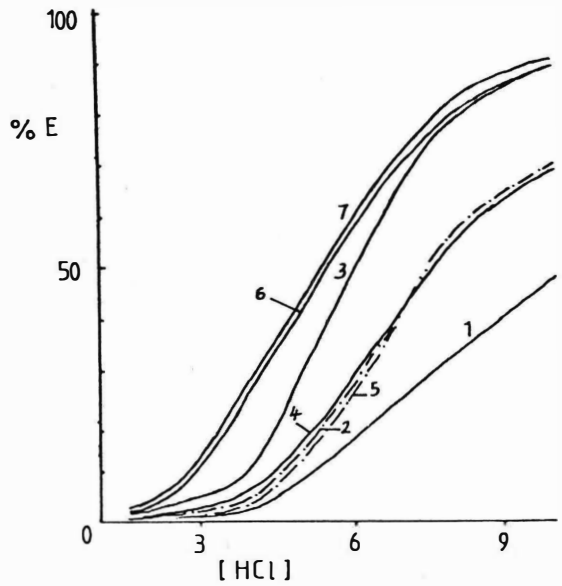

FIGURE 1. Extraction efficiency as a function of HCl Concentration.

1. NDA.HCl, 2. DOA.HCl, 3. DIA.HCl, 4. DNA.HCl, 5. DTHA.HCl, 6. TOA.HCl, 7. TIA.HCl.

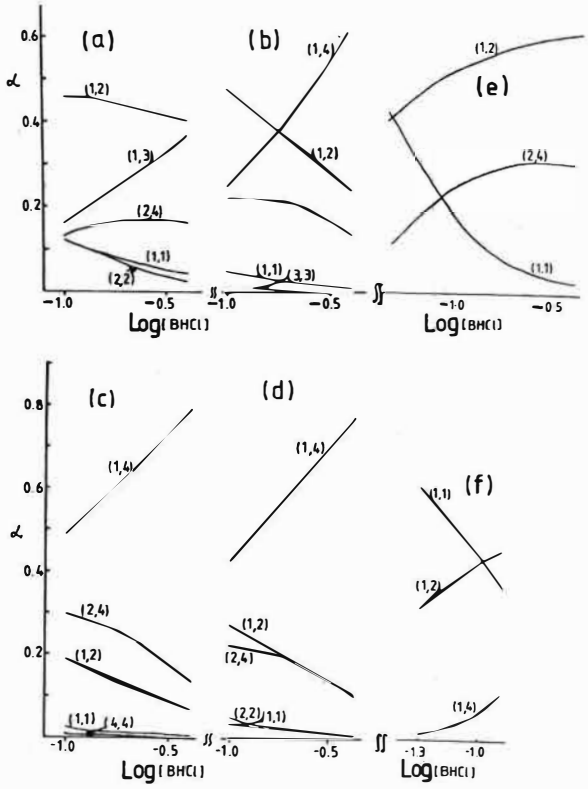

FIGURE 3. Mole fraction of each complex

(a) DIA.HCl, (b) DTHA.HCl, (c) DOA.HCl, (d) DNA.HCl, (e) TIA.HCl, (f) NDA.HCl

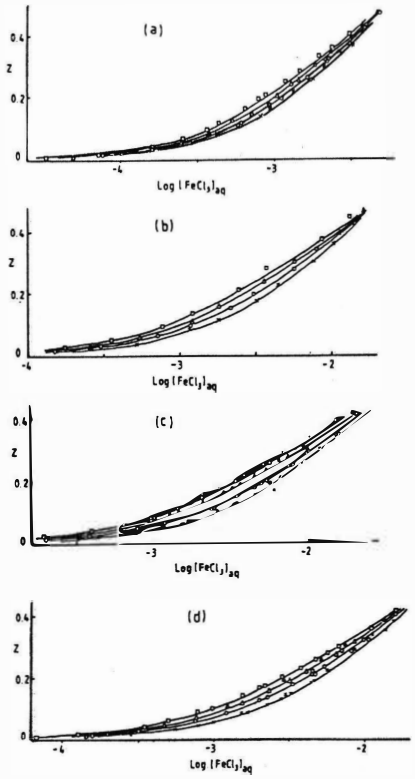

FIGURE 2. Equilibrium Data

(a) DIA.HCl, (b) DTHA.HCl, (c) DOA.HCl, (d) DNA.HCl.
(Solid lines calculated using the constants in Table 1).

THE EFFECT OF DILUENT FOR THE SEPARATION OF Zn(II) AND Pb(II) HALIDE COMPLEXES IN AMINE EXTRACTION SYSTEMS

Carlo Abbruzzese

CNR, Institute of Mineral Processing
Roma, Italy

Current research has set up that diluent plays an active role in solvent extraction by affecting the kinetics and the efficiency of the operation. Therefore diluent is not merely considered as a carrier but as a partecipant in the extraction process.

The diluent influence on the liquid-liquid extraction of single divalent metal ion from chloride solution by amines has been studied in the past (1)(2). In addition the zinc-lead selective separation in the $HCl-R_3N$ system was investigated (3). In the range 4-8N HCl zinc is preferentially transferred into kerosene with high separation factors by means of tertiary amines.

In this paper diluent effect on the selective extraction of Zn over Pb in HCl solutions by tertiary amines is examined in respect to physical and chemical parameters of the solvent.

EXTRACTION ISOTHERMS

Acid aqueous (4N HCl)solutions of 0.02M Zn^{2+} and Pb^{2+} were equilibrated at 20.0°C with an equal volume of organic phase containing 0.1M tri-n-octylamine (TOA) dissolved in various diluents.

The extraction reactions can be expressed as:

$$\overline{2(R_3NH)Cl} + ZnCl_4^{2-} = \overline{(R_3NH)_2ZnCl_4} + 2Cl^-$$

$$\overline{(R_3NH)Cl} + PbCl_3^- = \overline{(R_3NH)PbCl_3} + Cl^-$$

According to the Principle of Hard-Soft Acids and Bases (4),lead is extracted by TOA to a lesser extent than zinc because the less hard $PbCl_3^-$ is more stable (β_3=1.91) in the aqueous phase than $ZnCl_4^{2-}$ (β_4=0.2): the latter will form ion pair with the hard alkylammonium cation. At acidities higher than 4N HCl, the acidic cation HCl_2^- competes strongly with the metal halocomplexes for the extraction into the organic phase (5).

The diluent efficiency for zinc and lead extraction, depicted in Figure 1, decreases in the following order: hexane,cyclohexane,toluene,nitrobenzene,trichloroethylene,chloroform. Similar sequence has been found for the extraction of other halocomplexes (1)(6).

PHYSICAL PROPERTIES OF DILUENT

No satisfactory theory has been developed to explain the role of diluent in ion pair extraction. However, bulk diluent properties (dielectric constant,dipole moment) are often utilised to explicate solvent behaviour since they can strongly influence the dissolving power of diluent. This generalisation has been modified later on by introducing the electrostatic factor which takes into account the effect of both parameters on the electrostatic solvation of solutes (7).

The comparison between physical properties of diluent and their effect on metal distribution indicates that no straight correlation exists for the extraction with TOA (Table 1). High separation factors are shown by hydrocarbons ($\varepsilon \leq 2.5$) as well as dipolar aprotic solvents ($\varepsilon \geq 17$).

Hydrogen bonding diluents exhibit low values of distribution ratio D for both zinc and lead halocomplexes.

TABLE 1. THE DISTRIBUTION OF Zn(II)-Pb(II) AND THE PHYSICAL PROPERTIES OF DILUENTS

Diluent	Dielectric Constant ε	Dipole Moment μ	Electrostatic Factor	D_{Zn}	D_{Pb}	Separ. Factor Zn/Pb
Hexane	1.89	0.08	0.15	202	1.27	159
Cyclohexane	2.02	0.00	0.00	188	1.33	141
Toluene	2.38	0.36	0.86	146	1.21	118
Chloroform	4.81	1.01	4.85	0.26	0.05	5
Trichloroethylene	3.42	1.71	5.85	0.44	0.02	22
Nitrobenzene	34.82	4.22	146.9	166	0.17	977

Bulk diluent properties toghether with specific solute-solvent interactions represent now the current approach to explain the solution behaviour. In fact molecules, moving through a solvent towards their reaction partner, need to have an unsolvated site for collision. Therefore the nature of various ion pairs formed (contact,solvent shared,solvent separated) will influence the reaction. Hydrogen bonded liquids, which exhibit both acidic and basic sites, will effectively solvate the cation and the anion of the alkylammonium salt avoiding the metal extraction process.

EMPIRICAL PARAMETERS OF SOLVENT POLARITY

The simple application of diluent dielectric constant often fails to represent electrostatic solute-solvent interactions when ion pairs are involved. As an alternative empirical measure of these interactions, spectral shifts due to solvent effect on some dyes have been proposed(8). To date, the most comprehensive solvent polarity scale, developed via the determination of the transition energies of adsorption bands, is given by the E_T values (9). These empirical parameters have been determined for a lot of diluents. In Figure 2 the relation between the E_T values and zinc-lead extractability with TOA into organic phase is shown.

The extraction behaviour of zinc and lead into apolar hydrocarbons seems not to be influenced by increasing the value of E_T. Halogenated hydrocarbons behave differently lying on a second curve.

REGULAR SOLUTIONS APPROACH

Hildebrand (10) has introduced the solubility parameter δ_o which correlates some molecular properties of diluent when regular solution is concerned. This approach has been utilised to explain the solvent effect of the extraction of metal chelates and neutral halide complexes.

The δ_o values were plotted against the extraction data already noted in Table 1. An increase of δ_o seems not to affect zinc and lead extraction into apolar diluents, as shown in Figure 3. The anomalous results for halogenated hydrocarbons are attributable to the hydrogen bonding contribution δ_h to the solubility parameter value, according to Hansen's approach (11). As a matter of fact metal extractability into diluents having $\delta_h \geq 2.0$ appears on a different curve. The lower values for D when halogen-containing solvents are employed can be explained by the intensive interaction between ion pair and electron donor solvent.

CONCLUSIONS

In the case of extraction systems investigated, a change of diluent was shown to affect the metal distribution coefficient into organic phase. From the experimental data an empirical order of diluent efficiency was established. However no correlation between the distribution ratio of metal halocomplexes and the physical properties of diluent was found out.

Ion association extraction implies more or less aggregated bulky ions with mutual dipole interactions. The simple theory of regular solutions (10) fails for the system concerned because one of the basic assumption (ideal entropy of mixing) is not envisaged with ion pairs. In fact, since ion pairing is not merely electrostatic, a short-range chemical interactions between ion pair and diluent were supposed (12).

The various attempts at an explanation of diluent effect on the amine salts extraction are based on qualitative consideration only. Two types of solvation can be assumed to occur: an electrostatic one related to the dielectric constant and dipole moment of diluent; and a chemical one related to specific solute-solvent interactions.

Hydrocarbons show higher extraction than other diluents because of the absence of short-range chemical interactions with the solute. Slightly acidic diluents will interact with the extractant so decreasing the metal distribution coefficient. High distribution ratio for zinc with nitrobenzene is attributable to the stabilization of the alkylammonium cation via the interaction with π-electrons of aromatic ring.

Finally it is quite evident that the best separation factors occur when hydrocarbons are employed to dilute the extractant. The extraction of both zinc and lead is suppressed by halogenated hydrocarbon solutions of tertiary amines. Nitrobenzene exhibits the highest value of the separation factor, although the distribution coefficient for zinc in this system seems lower than it is when hydrocarbons are employed as diluents.

REFERENCES

1. T.Sato. ISEC 80 Proceedings,3,183,Liege(1980).
2. J.F.Desreux. ISEC 71 Proceedings,2,1328,The Hague (1971).
3. C.Abbruzzese. Int.J.Min.Proc.,4,4,307(1977).
4. R.G.Pearson. J.Am.Chem.Soc.,85,22,3533 (1963).
5. B.Chu and R.M.Diamond. J.Phys.Chem.,63,2021 (1959).
6. W.Muller and R.M.Diamond. J.Phys.Chem.,70,3469 (1965).
7. M.Szwarc. Ions and Ion Pair in Organic Reactions. Wiley,New York (1972).
8. L.G.S.Brooker,G.H.Keyes,D.W.Heseltine. J.Am.Chem.Soc.,73,5350, (1951).
9. K.Dimroth,C.Reichardt,T.Siepmann,F.Bohlmann. Liebigs Ann.Chem., 1,661 (1963).
10. J.H.Hildebrand and R.L.Scott. Regular Solutions. Prentice Hall, Englewood Cliffs,NJ (1962).
11. C.M.Hansen. J.Paint.Tech.,39,104 (1967).
12. R.M.Diamond. Solvent Extraction Chemistry. North Holland, Amsterdam (1967),pp 349-361.

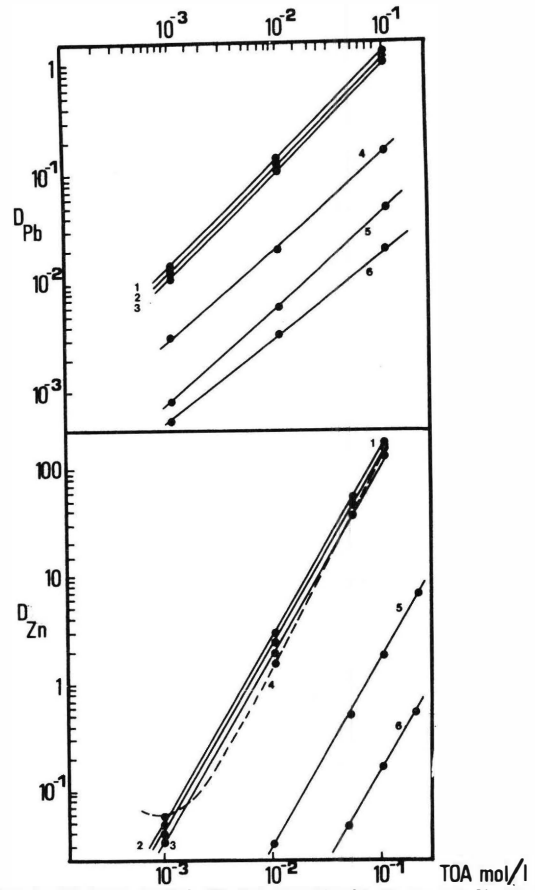

FIGURE 1. DILUENT EFFECT ON THE EXTRACTION OF Zn AND Pb BY TOA (1:hexane; 2:cyclohexane;3:toluene; 4:nitrobenzene; 5:trichloroethylene; 6: chloroform)

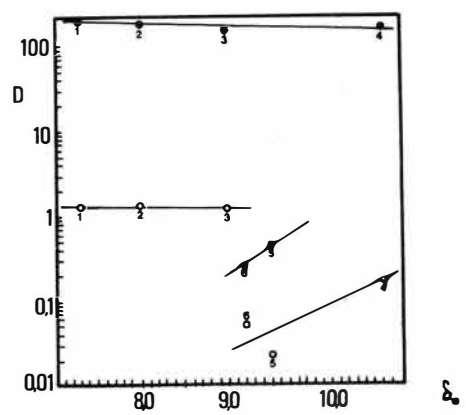

FIGURE 2. RELATIONSHIP BETWEEN THE DISTRIBUTION OF Zn(•) AND Pb(o) AND THE SOLUBILITY PARAMETER OF DILUENT

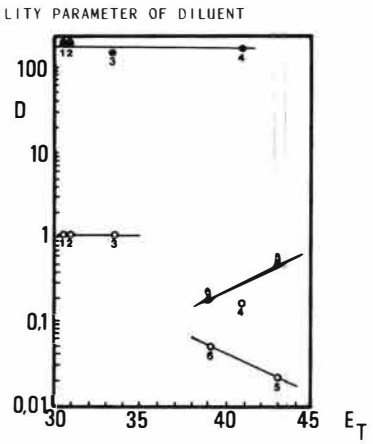

FIGURE 3. RELATIONSHIP BETWEEN THE DISTRIBUTION COEFFICIENTS OF Zn(•) AND Pb(o) AND THE EMPIRICAL PARAMETER OF DILUENT E_T

THE PECULIARITIES OF ZIRCONIUM SULPHATE EXTRACTION BY PRIMARY AMINES

G. Yagodin, M. Mrnka, A. Chekmarev

Prague Institute of Chemical Technology
Mendeleev Institute of Chemical Technology
A-47, Miusskaya sq., 9
Moscow, USSR

In our work, we used 0.25m solutions of primary amines normal sulphates (p - dodecylaniline - DDA - and Primene - JMT) as extractants, and benzene as a diluent. The amines sulphates were prepared as in (1).

For plotting the isotherm of nonhydrolized zirconium sulphate (solution of $Zr(SO_4)_2$ in 1M H_2SO_4) concentration of metal in extracts was determined by means of metal hydroxide precipitation by NH_4OH directly from organic phase.

After phases contacting (O : W = 1 : 1) for 30 min. and settling for 2-3 hrs the aliquot of organic phase was taken, diluted by acetone (1 : 10) and mixed with water solution oh NH_3.

After filtration and washing with acetone the hydroxide was calcined to ZrO_2. The above method of determination enabled us to obtain the isotherm of an ordinary type; saturation was reached using the solutions with initial concentration 0,4 M Zr; the DDA : Zr ratio was equal to (6÷8) : 1. Concentration of Zr in extract sligatly increases with the increase of initial concentration of Zr in water phase. But for initial concentration of $(Zr)_{aq} > 0,6M$ the settling at the interphase has been observed. It is known that in case of the third phase formation in the extracting sistem (the second organic phase) the concentration of metal in it is usually high.

To verify the hypothesis about the third phase formation and transition of a significant amount of Zr into it (naturally, it can not be established by the direct analysis of organic phase) one might determine the content of Zr in the extract from the difference of its content in initial and equilibrium water phase. It is also possible to raise solubility of the solvate formed under high Zr concentration by adding octanol to the organic phase.

The isotherms of extraction obtained by the two methods: direct analysis of organic phase (curves 1 : 3) and determination of the difference of Zr content in water phase (curves 2 : 4) are given in Figure 1. Different amounts of octanol were introduced in the organic phase.

In the region of high Zirconium concentration there is a significant difference (Δ) in data of the two methods of determination. Δ decreases with increasing of octanol concentration. In Figure 2 the values of Δ against octanol concentration are given. It is clear that only 30% addition of octanol provides the complete solution of formed solvate (under high Zr concentration).

The obtained data confirm the assumption about the third phase formation without octanol and the transition of a significant amount of Zr into it.

Thus, the actual view of the isotherm is the curve with intermediate saturation. Such appearance of the isotherm can be explained by the formation in the extraction system of at least two extracting compounds (solvates): under low Zr concentration intermediate solvate (amine: Zr = (6 ÷ 8) : 1) and normal solvate (amine: Zr = 4 : 1). Increasing of Zr water phase concentration leads to the rupture of intermediate solvate; additional saturation of organic phase takes place, it being obviously accompanied by the formation of a compound characteristic for the extraction of nonhydrolized sulphate Zr complexes by tertiary amines (2). Solubility of the normal solvate in benzene, in this case, is low and leads to the third phase formation.

Evidently, in the field of the normal solvate formation the extraction mechanism wich is similar to the mechanism of nonhydrolized Zr sulphate complexes extraction by tri-n-octylamine is realized.

Discussion of the possible mechanism of extraction in the field of intermediate solvate existance seems to be of interest.

It has been noticed that variation in amine concentration leads to changing of amine: Zr ratio in intermediate solvate (intermediate plateu). Thus, lower concentration than 0,1 mol/dm^3 DDA make this ratio almost equal to 6; increasing the amine condentration to 0,2 M leads to changing the ratio to 8. In Figure 3 the dependence of H_2O concentration in organic phase upon the Zr concentration in water phase is given. It should be pointed out that intermediate solvate formation leads to a sharp fall of water concentration in extract, which subsequently increases (as far as the additional saturation takes place) and tends to the concentration which is characteristic for the nonhydrolized sulphate extraction by tertiary amines (amine : H_2O = 1 : 1). In the field of intermediate solvate existence the ratio of amine: H_2O is nearly 2 : 1. As it is indicated in (3,4) micellar mechanism of extraction is possible in case of highly associated salts of primary and tertiary amines . We have determined the degree of association of DDA sulphate in benzene by cryoscopy as 6-8 moles of amine per one particle. It may be supposed that in organic phase the primary amine salt associate exists in the form of inverse micelle - hydrate water molecules are inside micelle and hydrophobic parts of amine salt molecules are directed the implantation of a metal salt into micelle (without its being destroyed) results in foreing out the water molecules. In case such a me-

chanism is realized, the view of the isotherm of extraction should depend on the temperature of the process.

In Figure 4 the isotherms obtained at different temperatures are given. It is clear that the rise in temperature promotes displacement of the beginning of intermediate solvate destoying process (transition to ordinary extraction mechanism) to the region of lower Zr concentrations. Such dependence on temperature of the process does not argue the assumptions concerning the mechanism of reaction wich have already been made.

REFERENCES.

1. Yu. Frolov, V. Sergievsky. Proceedings of Moscow Mendeleev Institute of Chemical Technology, N 49, 1965, p. 190.
2. G. Yagodin, A. Chekmarev, L. Vladimirova, J. Inorg. Chem. (Russ.), v.14, N 6, 1969, p. 1603.
3. Gourisse D. "Solvent extraction Chemistry". Proceedings of Intern. Conf. Gothenburg, Sweden, 1966.
4. Shmidt V. "Amine extraction", Moscow, Atomisdat, 1980, p. 27.

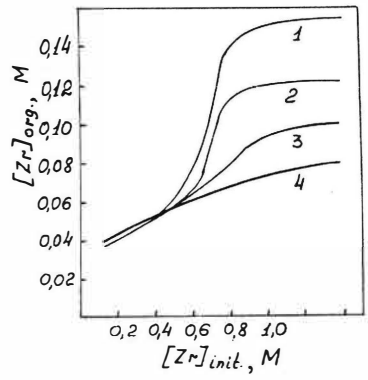

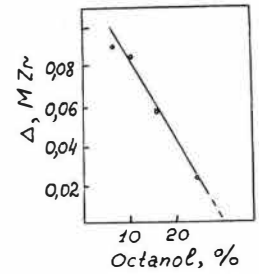

Fig. 2. Difference in data of the two methods of (Zr)org. determination against octanol concentration.

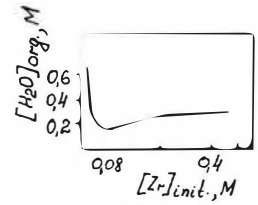

Fig. 3. Variation of water concentration in extracts against (Zr)org.

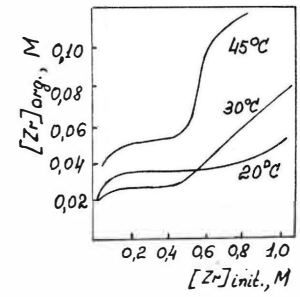

Fig. 1. The extraction isotherms, obtained by the two methods by analysis of organic phase (3;4) and by analysisof water phase on difference of Zr concentration (1;2). Octanol concentration: 7% - curves 1;4; 25% - curves 2;3.

Fig. 4. The extraction isotherms for different temperatures.

THE CAUSE OF ZIRCONIUM (HAFNIUM) EFFECT ON HDEDHP EXTRALIABILITY

A. Afanasiev, O. Sinegribova, G. Yagodin

Mendeleev Institute of Chemical Technology
A-47, Miusskaya sq., 9
Moscow, USSR

The phenomenon of amplification of extractability of some elements into organophosphoric acids(OPA) in presence of zirconium (hafnium)(1), discovered by B.Weaver, was primarily studied by authors with the example of extraction of europium nitrate. It was found out that the reason for extraction enhancement was the formation of the compound $H_2Zr(Hf)A_6$ in organic phase(where "A" is organophosphoric acid anion) which had a better ability for extraction in comparison with individual OPA due to a higher degree of dissociation of coordinated OPA mulecules to $Zr(Hf)A_4$(2).

But still there is a question why some elements and solutions do not extract well into OPA in the presence of Zr(Hf). That is why the additional number of elements (Eu, Ca, Fe(III)) and conditions of extraction (HNO_3 and HCl) were studied.

It was stated that zirconium(hafnium) enhances the extraction in HDEHP: of europium from nitrate solutions, of calcium from nitrate as well as from hydrochloric solutions, of iron(III) from hydrochloric solutions. At the same time zirconium decreases extraction of europium from hydrochloric solutions and iron(III) from nitrate solutions(see Figures 1-3).

The definition of the composition of the extracting compounds showed that in case of a better extraction in presence of zirconium(hafnium) the ions $Eu(NO_3)^{2+}$, Ca^{2+} and $FeCl^{2+}$ transfer into organic phase. The ions Eu^{3+} and Fe^{3+} are extracted worse (Table 1).

Table 1. The ratio M:Cl in organic phase. Europium(A), calcium(B) and iron(C) extraction from HCl into HDEHP(HA) containing zirconium. Diluent - octane. Zirconium concentration in (B) and (C) corresponds to extremal points of dependencies $D_{Me} = f(C^o_{Zr})$.

	Extractant	$C^{initial}_{metal}$, M	$C^{initial}_{HCl}$	Metal : Cl
	0,167 M H_2ZrA_6	$13,9 \times 10^{-2}$	0,01	30:1
A	0,167 M H_2ZrA_6	1.31×10^{-2}	0.52	25:1
B	0.1M HA+0.015M Zr	1.25×10^{-2}	0.003	20:1
	0.1 M HA + + 0,0055 M Zr	13.0×10^{-2}	0.50	3:1
C	0.3 M HA + + 0,023 M Zr	2.86×10^{-2}	2.0	1.2:1
	1.0 M HA + + 0,167 M Zr	15×10^{-2}	5.0	1:1.4

D_{Me} = distribution coefficients of metalls

C_{Zr} = concentration of zirconium in organic phase

$C^{init.}_{met.}$ = initial concentration of metalls in aqueous phase

$C^{init.}_{HCl}$ = initial concentration of HCl in aqueous phase

When bicharged cations(K) are extracted the stable polynuclear compounds are formed in organic phase. Their fragment is:

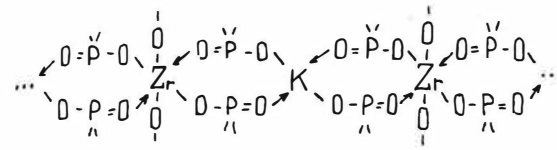

The ability of this element to form that sort of a compound defines a possibility to carry out the process of extraction by acidic zirconium dialkylphosphate.

When extracted the ions with the charge more than 2 and there is the interaction with more than 2 HDEHP molecules the compound $H_2Zr(Hf)A_6$ is destroyed. In this case only individual HDEHP molecules take part in the reaction of formation of the extracted compound and the increasing of Zr(Hf)-con centration in organic phase results in decreasing of the extraction of other elements.

In case of iron(III) extraction from HNO_3 the picture is more complicated because of simultaneous extraction by both mechanisms. The ions Fe^{3+} and $Fe(NO_3)^{2+}$ are extracted.

Kinetic data showed that mixed complexes containing both zirconium and another element to be extracted form the structural mechanic barrier(SMB) at the interface. This SMB greatly decreases the mass transfer from aqueous phase especially under the conditions of not renovated or little renovated interface (Figure 4, curves 1,2). With great renovation of interface interfacial films of this type are easily destroyed and the mass transfer greatly increases (Figure 4, curves 3,4).

If the mixed complexes are not formed(for instance, europium extraction from hydrochloric solution into HDEHP containing Zr) noticeable film formation at the interface is not seen.

REFERENCES

1. B.Weaver. J.Inorg.Nucl.Chem., 30, 2233 (1968).
2. N.A.Plesskaya, O.A.Sinegribova, G.A.Yagodin. Z.Neorg.Chem., 22, 1640 (1977).

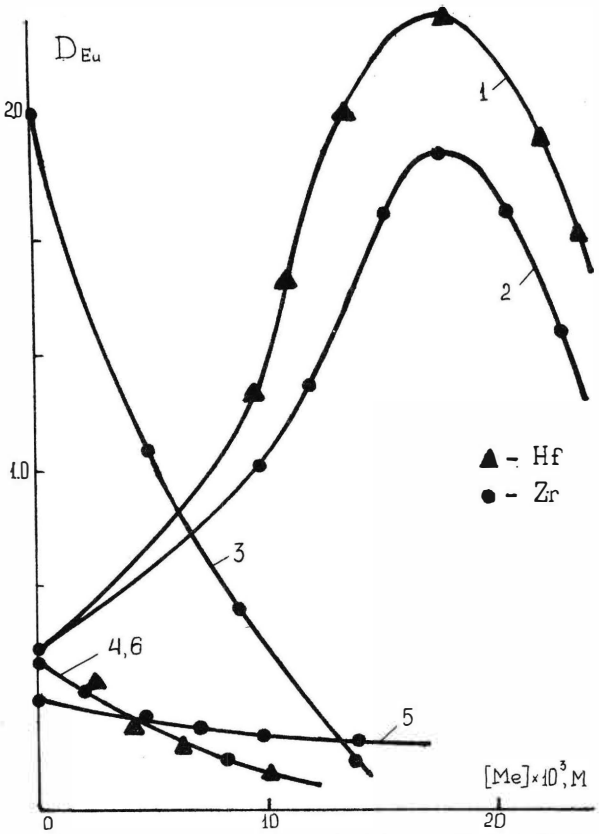

Figure 1. Dependence of europium distribution coefficients on Zr(Hf) content in HDEHP(HA). (1,2) - 0,1M HA; 0,39M HNO_3; (3) - 0,1M HA; 0,10M HCL; (4,6) - 0,1M HA; 0,30M HCl; (5) - 0,5M HA; 1,0M HCl

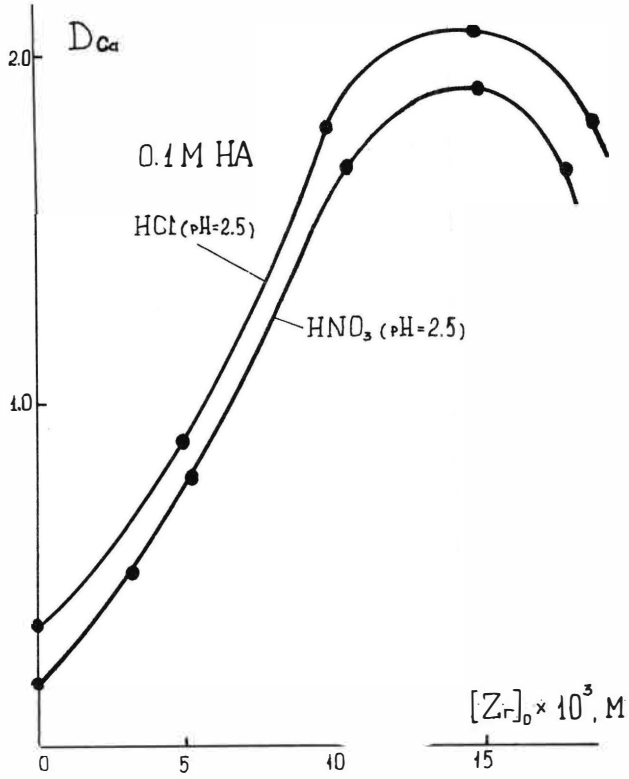

Figure 3. Dependence of calcium distribution coefficients on Zr content in HDEHP(HA)

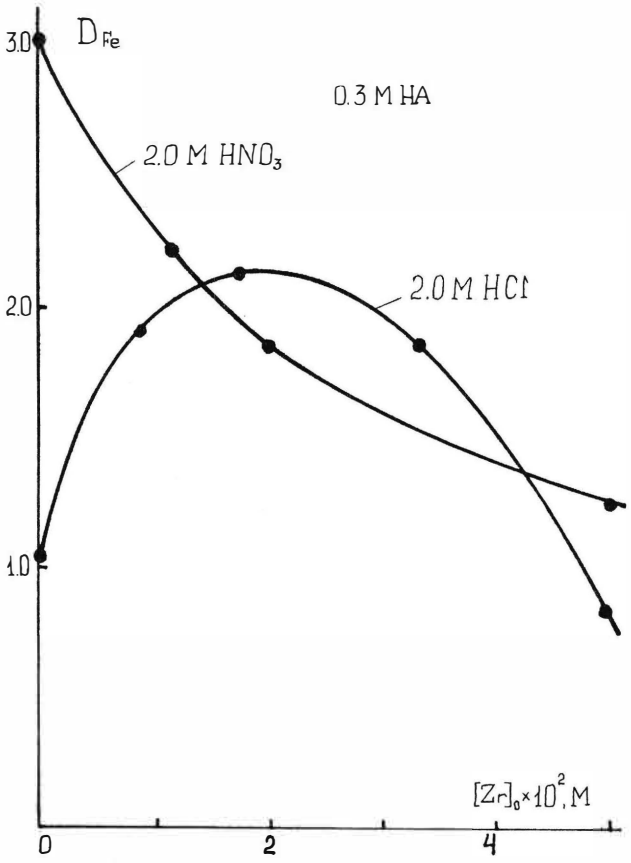

Figure 2. Dependence of IRON(III) distribution coefficients on Zr content in HDEHP(HA)

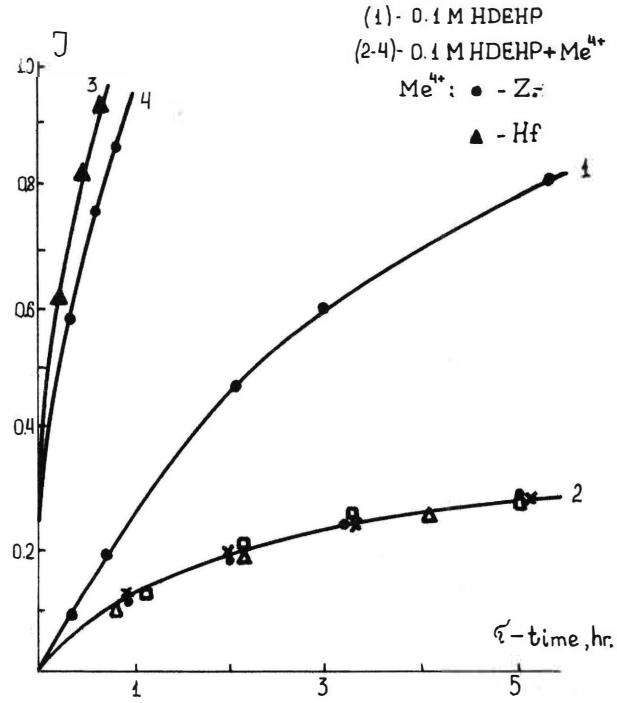

Figure 4. The effect of Zr(Hf) on europium extraction rate by HDEHP out from HNO_3.
(1,2) - little renovated interface
(3,4) - great renovated interface

PERIODIC VARIATIONS OF LANTHANIDES SYNERGIC EXTRACTION BY THENOYLTRIFLUOROACETONE AND TRIPHENYLPHOSPHINE OXIDE MIXTURE

H. F. Aly, S. M. Khalifa and Nadia Zakareia

Atomic Energy Establishment
Cairo, Egypt

It has been found that the periodicity of certain property of the lanthanide elements, in many cases, can be divided into, four sibgroups (1-5). When the property of the lanthanides is plotted against the atomic number Z, the four subgroups obtained are the tetrad-effect(2), or the double-double effect (3). If the property of the lanthanides is related to the total angular momentum of the trivalent ion, four linear segments usually are produced and the obtained relationship is known as the "Inclined-W" relationship (4). In a preliminary study (5), we found that the lanthanides are synergitically extracted by TPPO-HTTA mixture in benzene and under comparable conditions, the separation factors as well as the synergic factors followed the aforementioned variations. The present study is a detailed investigations of the extraction of the whole lanthanide series, except Pm and Lu, with HTTA and TPPO mixture in benzene. The aim is to find the type of the main adduct extracted, examine and evaluate the periodic variations of the stability of the different species formed through the series and compare the extraction equilibrium with analogous systems.

Experimental :

Thenoyltrifluoroacetone (HTTA) and triphenylphosphine oxide (TPPO) were of A.R. grade and obtained from Eastman, U.S.A. The diluent benzene used was A.R. label from B.D.H., England. The radiotracers used were ^{140}La, ^{144}Ce, ^{142}Pr, ^{142}Nd, ^{153}Sm, $^{152+154}Eu$, ^{153}Gd, ^{160}Tb, ^{165}Dy, ^{166}Ho, ^{171}Er, ^{169}Yb and ^{170}Tm of high radiochemical purity. The extraction procedure used is identical to that previously reported (5). Duplicate samples of radioactivity from both phases were assayed to a counting error of 3%. In all cases, the aqueous phase has a constant ionic strength of 0.2 (H^+, $NaClO_4$) and all the experiments were performed at constant temperature, 22±2°C.

Results and Discussion

Slope analysis of the different parameters affecting the extraction as function of the distribution ratio of the different lanthanides indicated that the main lanthanide species in the organic phase are of the types $Ln(TTA)_3$ and $Ln(TTA)_3$ 2TPPO in the absence and presence of TPPO, respectively. Therefore, the main extraction equilibria involved in the systems are :

$$Ln^{3+} + \overline{3\ HTTA} \rightleftharpoons \overline{Ln(TTA)_3} + 3\ H^+, \qquad K_{3,0}$$

and

$$Ln^{3+} + \overline{3\ HTTA} + \overline{2\ TPPO} \rightleftharpoons \overline{Ln(TTA)_3\ 2TPPO} + 3\ H^+, \qquad K_{3,2}$$

and

$$\overline{Ln(TTA)_3} + \overline{2\ TPPO} \rightleftharpoons \overline{Ln(TTA)_3}\ 2\ TPPO, \qquad \beta_{3,2}$$

and

$$\beta_{3,2} = \frac{K_{3,2}}{K_{3,0}}$$

The values of $K_{3,0}$, $K_{3,2}$ and $B_{3,2}$ obtained are given in Table (1). In Figure (1), the variations of log $K_{3,0}$ and log $\beta_{3,2}$ with the atomic number showed four groups with downward and upward concavities in the case of log $K_{3,0}$ or log $\beta_{3,2}$, respectively. When log $K_{3,0}$ and log $\beta_{3,2}$ are plotted against the total angular momentum of the ground state of the different trivalent lanthanides, the Inclined-W relationship is realized, Figure (2). It is suggested that these regularities are related to the following, i- the quantum mechanical interelectronic repulsion of the n-electrons in the $4f^4$ electron configuration, ii- Spin-orbit coupling, iii- crystal field stabilization energy, and iv- the change in the coordination number of the lanthanide ions along the series.

Based on theoretical calculations, Jørgensen (6) and Nugent (7) attributed the tetrade grouping to be mainly a result of the first factor. They also concluded that the spin-orbit coupling and the crystal field stabilization energy may contribute to this grouping, yet their contribution is not significant compared to the interelectronic repulsion within the lanthanide series. Based on thermodynamic data, Fidelis (8) suggested that the regularities in the properties of the lanthanides lie in the internal feature of the free f electrons, and not in their immediate environment, however the immediate environment may influence the magnitude of this effect. The Inclined-W relationship introduced by Sinha (4) lack theoretical justification, since there cannot be a linear relation between the property of a substance and any quantum number of the atoms. Nevertheless, indirect relationships can exist through the L-S coupling.

The change of the coordination number through the lanthanide series is very important factor that can disturb any expected periodicity. This is mainly, due to the fact that the coordination number affects the aforementioned factors responsible for the observed regularities. In the studied systems, the lanthanide chelates, $Ln(TTA)_3$, gave an adduct of a general formula, $Ln(TTA)_3$ 2TPPO, allover the whole series. No information are available concerning the coordination of water molecules to the chelate or the adduct. Therefore, the formation of the adduct is achieved either by substitution of TPPO for coordinated water in the metal chelate or by addition with the increase in the coordination of the central ion or by both mechanisms. If the mechanism of adduct formation is the same allover the lanthanide series, one should expect that the variation between log $K_{3,0}$ and log $\beta_{3,2}$ should be linear through the series. This was partially realized in Figure (3), where two parallel linear relationships were obtained. The first line starts with Yb and ends with Sm, and the second starts with Pr and ends with La. Nd lies in the middle between the two lines. This suggests that the change in the coordination by adduct formation for the Yb-Sm group is different than that of the Pr-La group. In many cases, it was suggested that the lighter members of lanthanides La-Nd have 9-coordination numbers whereby the Gd-Lu have a coordination number of 8 in solutions (9).

Alstad et al. (10-11) observed the tetrad-effect between log $\beta_{3,2}$-Z relation for the systems $Ln(TTA)_3.2X$, where x stands for TBP or DBuSO. For comparison, the ratio $B_n = \beta_{3,2(x)} / \beta_{3,2(TPPO)}$ was for the different lanthanides were calculated. For both system a positive values are obtained indicating the high basicities of TBP and DBuSO over TPPO. Further, the B_n values where almost constant (log $B_{n(TBP)}$ = 3.5±0.2 and B_n(DBuSO) = 3.0±0.2) for the lanthanides laying between Ce and Tm. For La and Yb, B_n are much lower, a behaviour which can be related to steric differences between the synergistic ligands.

References

1. B.F.Dzhurinskii, Russian J. Inorg. Chem., English edition, 25, 41 (1980).
2. D.F.Peppard, G.W.Mason and S.Lewey, J. Inorg. Nucl. Chem., 32, 339 (1970).
3. S.Siekerski and I.Fidelis, J. Inorg. Nucl. Chem., 33, 3191 (1971).
4. S.P.Sinha, Helv. Chem. Acta, 58, 1978 (1975).
5. H.F.Aly, S.M.Khalifa, N.Zakareia and A.A.Abdel-Rassoul, Radiochem. Radioanal. Letters, 48(1), 31 (1981).
6. C.K.Jørgensen, J. Inorg. Nucl. Chem., 32, 3128 (1970).
7. L.J.Nugent, J. Inorg. Nucl. Chem., 32, 3485 (1970).
8. I.Fidelis, Bull. Acad. Pol. Sci. Ser. Sci. Chem., 18, 681 (1970).
9. F.A.Cotton and G.Wilkinson, Advanced Inorganic Chemistry, Third edition, Interscience Publishers, N.Y. (1972).
10. L.Farbu, J. Alstad and J.H.Augusteon, J. Inorg. Nucl. Chem., 36, 2091 (1974).
11. J.H.Augusteon, L. Farbu and J.Alstad, J. Inorg. Nucl. Chem., 37, 1243 (1975).

Table 1 : Extraction equilibrium constants $K_{3,0}$ for $Ln(TTA)_3$ chelate and $K_{3,2}$ for $Ln(TTA)_3$ 2TPPO and formation Constants : $\beta_{3,2}$ for $Ln(TTA)_3$ with 2TPPO in benzene*

$$K_{3,0} = [Ln(TTA)_3][H^+]^3 [Ln^{3+}]^{-1} [HTTA]^{-3}$$

$$K_{3,2} = [Ln(TTA)_3\ 2TPPO][H^+]^3 [Ln^{3+}]^{-1} [HTTA]^{-3} [TPPO]^{-2}.$$

$$B_{3,2} = [Ln(TTA)_3\ 2TPPO][Ln(TTA)_3]^{-1} [TPPO]^{-2}.$$

Metal	log $K_{3,0}$	log $K_{3,2}$	log $\beta_{3,2}$
La	-10.25	3.34	6.90
Ce	- 9.04	3.14	5.91
Pr	- 8.41	2.99	5.42
Nd	- 8.23	2.93	5.39
Pm	-	-	-
Sm	- 7.93	2.72	5.26
Eu	- 7.79	2.65	5.14
Gd	- 7.70	2.60	5.10
Tb	- 7.21	2.73	4.66
Dy	- 6.98	2.49	4.48
Ho	- 6.88	2.47	4.41
Er	- 6.69	2.41	4.28
Tm	- 6.55	2.39	4.15
Yb	- 6.45	2.66	4.06
Lu	-	-	-

* In all cases, the aqueous phase has ionic strength of 0.2 (Na^+, $HClO_4$) and the extraction temp. is 22±2°C. The limits of the error in the different constants does not exceeds ± 3%.

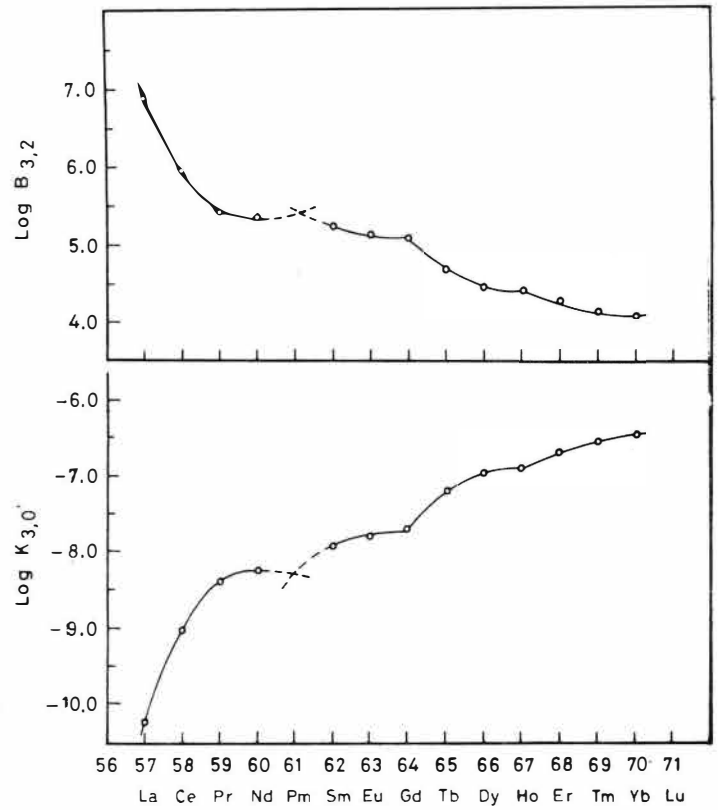

Fig.(1)

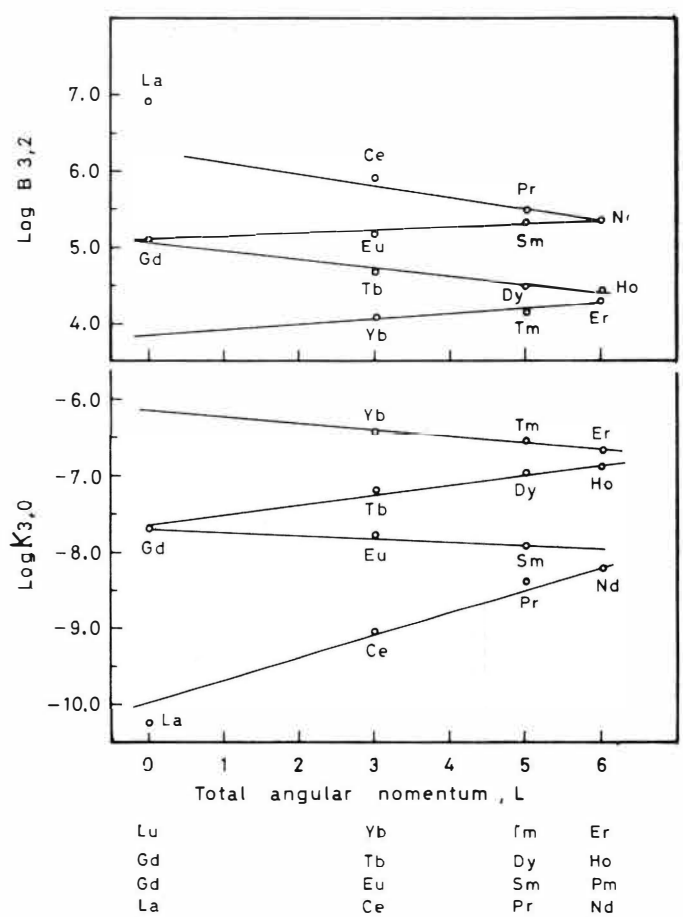

Fig.(2)

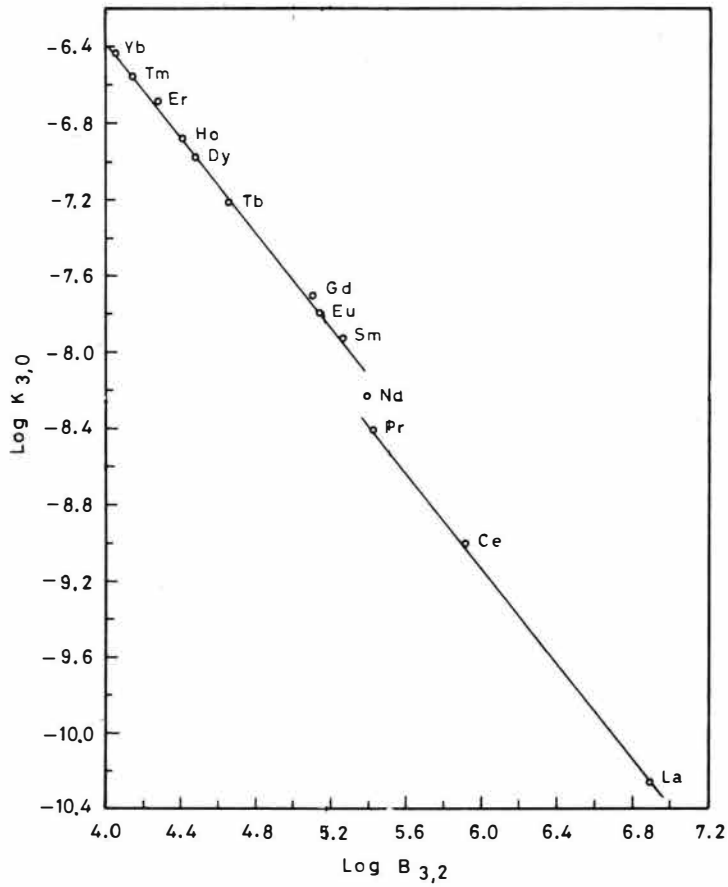
Yb
Tm
Er
Ho
Dy
Tb
Gd
Eu
Sm
Nd
Pr
Ce
La
-6.4
-6.8
-7.2
-7.6
-8.0
-8.4
-8.8
-9.2
-9.6
-10.0
-10.4
Log K 3,0
4.0
4.4
4.8
5.2
5.6
6.0
6.4
6.8
7.2
Log B 3,2

Fig.(3)

THE DETERMINATION OF THE ACTIVITY COEFFICIENTS OF TBP AND EXTRACTION COMPLEX $UO_2(NO_3)_2 2TBP$ IN VARIOUS SOLVENTS

Gao Hong-Cheng, Pen Qi-Ziu, Pen Li-E
Wang Wen-Qing and Hsu Kwang-Hsien

Department of Technical Physics
Peking University
Beijing, China

The activity coefficients of various components in the organic phase during the extraction process are very important in order to obtain the true thermodynamic equilibrium constants, but have not been much investigated owing to the difficulties and tediousness encountered in their determinations. In the present investigation, the activity coefficients of TBP and $UO_2(NO_3)_2 \cdot 2TBP$ in various solvents have been determined by the ^{32}P-labeled TBP distribution method and the vapor-isopiestic method respetively.

Principle of the ^{32}P-labeled TBP distribution method

So far as the authors aware, this method has not been used before. It is simpler, more rapid, and the concentration range of TBP is broader than other physico-chemical methods for the determination of the activity of TBP. The principle underlying this method is as follows:

When the equilibrium of distribution of TBP between the water and solvent is attained, the thermodynamic equilibrium constant of $TB^{32}P$ is equal to the ratio of the activities in both phases:

$$\lambda^{\circ} = \frac{a_{(o)}}{a} = \frac{N_2 f_2}{k A_2}$$

where N_2 and f_2 are mole fraction of TBP in the organic phase and the correspoding activity coefficient respectively; $A_2 = I/I_o$, I_o and I are radioactivities of $TB^{32}P$ in the aqueous phase equilibrated with pure TBP and TBP-solution respectively; k is a constant. As the solubility of TBP in water is very low, the activity coefficient of TBP in water may be assumed to be equal to unity. If pure TBP is chosen as the standard state, then we have

$$\lim_{\substack{N_2 \to 1 \\ f_2 \to 1}} (N_2/A_2) = 1$$

thus

$$f_2 = 1/(N_2/A_2)$$

Experimental results

A_2 values correspoding to different N_2 for solvents were given in Fig.1, f_2 may then be calculated by the above equation and were given in Fig.2.

In a given concentration range of TBP, these activity coefficients may be expressed by the following equations:

$$\text{Log } f_2 = a N_1^2 \quad \text{and} \quad \text{Log } f_2 = A/(1+By)^2$$

where $y = N_2/N_1$, N_1 and N_2 are molfractions of solvent and TBP respectively, and constants a, A and B were obtained by graphical method(see Fig. 3), for example:

In TBP-C_6H_6 system:

$$\text{Log } f_2 = 0.47 N_1^2 , (N_1 = 0 \text{ to } 1)$$

$$\text{Log } f_2 = 0.39/(1 + 0.63 y)^2 , (N_2 = 0 \text{ to } 0.8)$$

In TBP-C_8H_{18} system:

$$\text{Log } f_2 = 0.70 N_1^2 , (N_1 = 0 \text{ to } 0.9)$$

$$\text{Log } f_2 = 0.83/(1 + 1.18 y)^2 , (N_2 = 0 \text{ to } 0.7)$$

As an alternate approach, we chose an infinitely dilute solution of TBP in various solvents as the reference state, i.e., at infinitely dilute solution, activity coefficients f_2' were taken to be unity. The standard state is the hypothetical state in which TBP would exist if it followed Henry's Law up to a mole fraction N_2 equal to one. From f_2', activity coefficients γ (based on molality) and y(based on molarity) were obtained by the following equation:

$$\gamma = \frac{f_2'}{1 + 0.001Mm} , \quad y = \frac{md_o}{c} \cdot \gamma$$

where d_o is the density of the pure solvent.

Discussion

It has been shown from Fig.2 that the values of f_2 are quite different in various solvents, due to different conditions of intermolecular interactions:

(1) In solvents,such as $CHCl_3$ and n-octyl alcohol which form hydrogen bond with TBP, f_2's are much smaller than one. this indicates that the interation between TBP and the solvent molecule is much stronger than the Van der waals' interaction among the TBP molecules themselves.

(2) In solvents,such as C_6H_6, CCl_4, n-amyl acetate, f_2's are slightly greater than one. This indicates that the Van der waals' interactions between the solvent and TBP molecules are slightly weaker than those among TBP molecules themselves.

(3) In solvents,such as C_6H_{14},C_8H_{18}, f_2's are much greater than one. This indicates that the interactions between TBP and the solvent molecule are much weaker than those among TBP molecules or solvent molecules themselves.

The activity coefficients of $UO_2(NO_3)_2 \cdot 2TBP$

The activity coefficients of $UO_2(NO_3)_2 \cdot 2TBP$ in C_6H_6, CCl_4 and $CHCl_3$ have been determined by vapor-isopiestic method.

The reference solution TBP-solvent(C_6H_6,CCl_4 or $CHCl_3$) , and the sample solution $UO_2(NO_3)_2 \cdot 2TBP$-solvent(C_6H_6,CCl_4 or $CHCl_3$), were placed in an evacuated container until equilibrium was attined thus the activities of the solvent are the same in both the solutions.

Since the activity coefficient of solute f_2' in the reference solution TBP-solvent has been determined, the activity coefficient of the solvent f_1 may be calculated by Gibbs-Duhem equation:

$$N_1 \, dLn \, f_1 + N_2 \, dLn \, f_2' = 0$$

or

$$Ln \, f_1 = - \int_0^{N_2} \frac{N_2}{N_1} d \, Ln \, f_2'$$

through graphical integration. This f_1 is also equal to the activity coefficient of solvent in the sample solution $UO_2(NO_3)_2 \cdot 2TBP$-solvent, which has the same vapor pressure as the reference solution. The activity coefficient of the solute $UO_2(NO_3)_2 \cdot 2TBP$, $f_2'(UO_2(NO_3)_2 \cdot 2TBP)$, can then be calculared by using Gibbs-Duhem equation:

$$Ln \, f_2' = - \int_0^{N_1} \frac{N_1}{N_2} d \, Ln \, f_1$$

The mole fractions N_1 and N_2 for the reference as well as the sample solutions at equilibrium were determined by gravimetric mehtod.

The expremental results showed that at low concentration of $UO_2(NO_3)_2 \cdot 2TBP$, its activity coefficient was approximately equal to that of TBP (i.e., $f'_{TBP} = f'_{UO_2(NO_3)_2 \cdot 2TBP}$). From $f'_{UO_2(NO_3)_2 \cdot 2TBP}$ γ and y were calculated, m and γ ,c and y may be related by the expressions:

$$Log \, \gamma = \frac{m}{A + Bm}$$

$$Log \, y = ac + bc^2$$

For C_6H_6 system:

$$Log \, \gamma = m/(4.2 + 5.0 \, m)$$

$$Log \, y = 0.28 \, c^2$$

For CCl_4 system:

$$Log \, \gamma = m/(11 + 0.2 \, m)$$

$$Log \, y = 0.2 \, c + 0.09 \, c^2$$

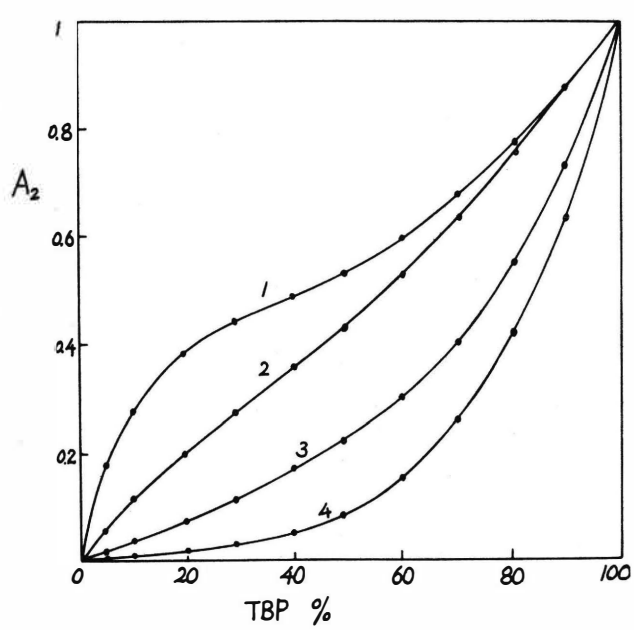

Fig 1 (a).

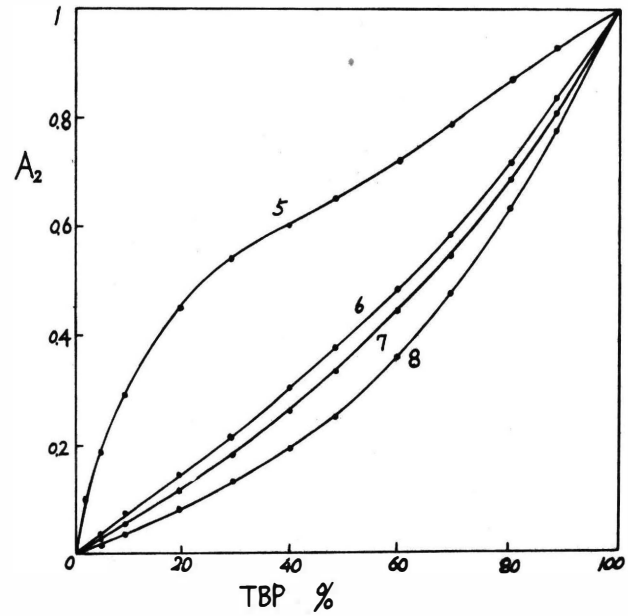

Fig. 1 (b).

1. C_6H_{14} 2. C_6H_6 3. CCl_4
4. $CHCl_3$ 5. n-C_8H_{18}
6. methyl cyclohexanone($CH_3C_6H_9O$)
7. n-amyl acetate(AmAc)
8. n-$C_8H_{17}OH$

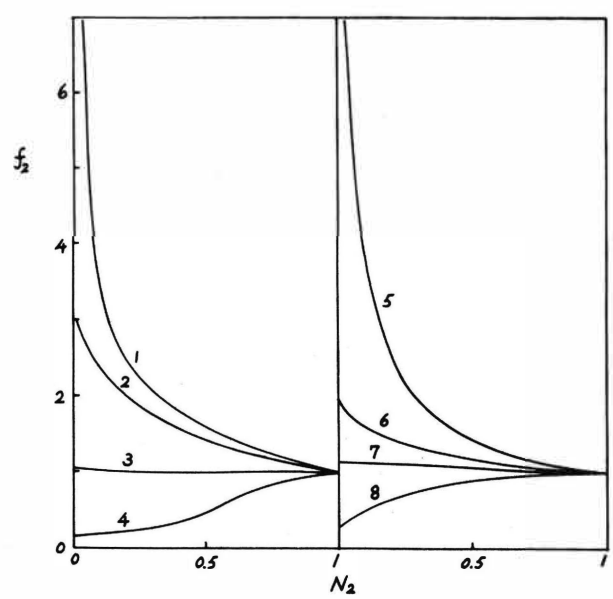

Fig 2.

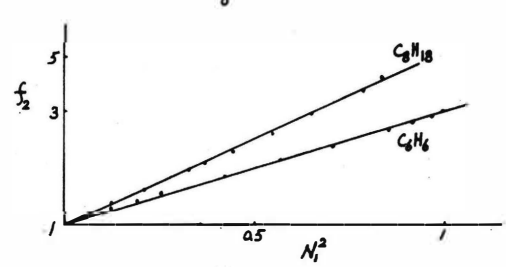

Fig 3.

SYNERGISTIC EXTRACTION OF ABB AND ABC TYPES EXTRACTION MECHANISM OF URANIUM(VI) WITH TERNARY SYSTEM PMBP = TBP + ϕ_2SO AND PMBP + TBP + ϕ_4AsCl

Wang Wenqing, Yi Min, Chen Dinfong, Mou Xiru

Peking University
Beijing, China

The phenomenon of synergistic extraction has been broadly applied since Blake[1] discovered it. For the purpose of finding and proving the regularity of synergistic extraction, we have studied the synergic extraction of Uranium(VI) by the binary system of AB species composed of HDEHP + ϕ_2SO[2] and HDEHP +DBBP[3], the synergic extraction of uranium thiocyanate by AC species composed of PMBP + ϕ_4AsCl[4] and the synergic extraction of uranium nitrate by BB species composed of TBP +ϕ_2SO[5].

The results of the study of two ternary systems is discussed. The first system focused on the synergic extraction of uranyl nitrate with the binary system of I-phenyl-3methyl-4-benzoyl pyrazolone-5(PMBP) and tributylphosphate(TBP) or diphenyl sulfoxide(ϕ_2SO) and the ternary system of the ABB type consisting of PMBP+TBP+ϕ_2SO. The binary synergic equilibrium constants were determined to be log β_{I2}= 3.58 (PMBP+TBP system) and log β_{I3}= 3.61 (PMBP+ϕ_2SO system) respectively as shown by the following equilibria:

$$UO_2^{2+} + 2HA + TBP \xrightleftharpoons{\beta_{I2}} UO_2A_2 \cdot TBP + 2H^+$$

$$\beta_{I2} = \frac{D_{I2}\ Y\ (H^+)^2}{(HA)_o^2\ (TBP)_o}$$

$$\log \beta_{I2} = \log D_{I2} + \log Y + 2\log(H^+) - 2\log(HA)_o - \log(TBP)_o$$

$$UO_2^{2+} + 2\ HA + \phi_2SO \xrightleftharpoons{\beta_{I3}} UO_2A_2 \cdot \phi_2SO + 2\ H^+$$

$$\beta_{I3} = \frac{D_{I3}\ Y\ (H^+)^2}{(HA)_o^2\ (\phi_2SO)_o}$$

Here Y is the complex formality of uranium (VI) with nitrate ion.

As the coordination number of uranium (VI) is equal to eight, we assume that a coordinate water molecule is contained in the structural formula of $UO_2A_2 \cdot TBP$ and $UO_2A_2 \cdot \phi_2SO$ and it can be replaced by a neutral extractant to decrease the hydrophilic ability producing a ternary synergic effect of the ABB species. The views mentioned above were proved by the fact that the ternary synergic effect occurred during the extraction of uranium (VI) with the benzene solution of PMBP + TBP + ϕ_2SO. The formation of a ternary extracted complex $UO_2A_2 \cdot \phi_2SO \cdot TBP$ was confirmed by the slope method.

A new method is proposed in this work for the calculation of the equilibrium constant which was evaluated to be log β_{I23}= 5.58 as shown by the following reaction

$$UO_2^{2+} + 2HA_{(o)} + TBP + \phi_2SO_{(o)} \xrightleftharpoons{\beta_{I23}} UO_2A_2 \cdot TBP \cdot \phi_2SO + 2H^+$$

$$\beta_{I23} = \frac{D_{I23}\ Y\ (H^+)^2}{(HA)_o^2\ (TBP)_o (\phi_2SO)_o}$$

$$D_{I23} = D_{total} - D_I - D_{I2} - D_{I3}$$

Here D_I is the distribution ratio of U (VI) by PMBP.

D_{I2} is the distribution ratio of binary synergic extraction by (PMBP + TBP) system.

D_{I3} is the distribution ratio of binary synergic extraction by (PMBP +ϕ_2SO) system.

D_{I23} is the distribution ratio of ternary synergic extraction by (PMBP + TBP +ϕ_2SO) system.

Secondly, we have studied the other ternary system of the ABC type consisting of PMBP + TBP +ϕ_4AsCl. The binary synergistic equilibrium constants were determined to be log β'_{I2}=4.25 (PMBP+TBP system). logβ'_{I3}=5.49 (PMBP+ϕ_4AsCl system) and log β'_{23}=4.94 (TBP+ϕ_4AsCl system) respectively. The purpose of this work was to investigate the ternary synergic extracting mechanism of chelate extracting system, ion association system and neutral complex extracting system. Owing to the unsaturated coordination number of uranyl ion in the binary synergistic complex, we presume a ternary synergic effect of ABC species may have existed. It was found that synergic effect occurred during the extraction of uranyl thiocyanate with chloroform solution of PMBP+TBP+ϕ_4AsCl. The formation of a ternary extracted complex $\phi_4AsUO_2(NCS)A_2 \cdot TBP$ was confirmed by the usual slope method. The following reaction was found to describe the system.

$$UO_2^{2+} + NCS^- + x\ HA + y\ TBP + z\phi_4As^+ \xrightleftharpoons{\beta_{I23}} z\phi_4AsUO_2(NCS)A_x \cdot yTBP + x\ H^+$$

$$\beta_{I23} = \frac{D_{I23}\ Y\ (H^+)^x}{(NCS^-)(HA)_o^x (TBP)_o^y (\phi_4As^+)^z}$$

$$D_{I23} = \frac{\left[z\phi_4AsUO_2(NCS)A_x yTBP\right]_o (H^+)^x}{(UO_2^{2+})\ Y}$$

$$= D_{total} - D_{I2} - D_{I3} - D_{23}$$

We have obtained the following values: x=2, y=I, z=I. Using the same method, the equilibrium constant was evaluted to be log β_{I23}= 7.23.

REFERENCES

I. C.A.Blake et. al., Proceedings of 2nd International Conference on the Peaceful Uses of Atomic Energy 28, P/I550, 289 (I958).

2 Yi Min et. al., Science and Technology 3. I2 (I98I).

3. Wang Wenqing et. al., Chinese Journal of Nuclear Science and Engineering 2 (2), I65 (I982).

4. Wang Wenqing et. al., Acta Scientiarm Naturalium Universitatis Pekinenis I. 47 (I982).

5. Yi Min et. al., Journal of Nuclear and Radiochemistry 4 (2), 73 (I982).

EFFECT OF NONELECTROLYTES ON THE SOLVENT EXTRACTION OF URANYL AND NITRIC ACID BY TBP

J. Ortega and J. A. Suárez

Junta de Energia Nuclear
Madrid, Spain

This study has been realized as a result of the use of tartaric acid in uranium-plutonium partition, in the TBP-uranyl nitrate-plutonium (IV) nitrate-nitric acid-water system. The presence of the tartaric acid in aqueous phase increases the distribution coefficient of the nitric acid and uranyl nitrate, Figure 1. In other respects the tartaric acid has a low distribution coefficient, which decreases in the presence of nitric acid and uranyl nitrate, Figure 2.

The effect of the tartaric acid on the distribution coefficient of the nitric acid may be adequately interpreted in the same manner as the hydration of electrolytes in relation to the salting-out effect. The hydration of the tartaric acid decreases the number of moles of "free" water molecules and therefore increases the nitric acid activity in the aqueous phase.

A definite activity of nitric acid in the aqueous phase corresponds to a definite activity of nitric acid in the organic phase, so that

$$(1) \qquad \frac{[NO_3H]_o}{[NO_3H]_w} = \text{constant}$$

If we introduce a "hydratable" nonelectrolyte in the aqueous phase, the "apparent" nitric acid concentration in this phase must decrease in order that the nitric acid concentration in the organic phase, N_o, remains constant. For a constant nitric acid concentration in the organic phase, the nitric acid activity in the aqueous phase, in the presence and in the absence of the nonelectrolyte, must be the same. If we express the nitric acid activity in terms of molality, we obtain the following equation.

$$(2) \qquad \frac{N_N^o}{d_o - 0.001\, N_N\, M_N} = \frac{N_N}{d - 0{,}001\left[N_N M_N + N_s M_s + n_h N_s M_w\right]}$$

N_s = nonelectrolyte concentration in aqueous phase, moles in one litre of solution.

N_N^o = nitric acid concentration in aqueous phase, moles in one litre of solution, in equilibrium with an organic, which contains N_o mol/l of nitric acid. In the absence of nonelectrolyte.

N_N = nitric acid concentration in aqueous phase, moles in one litre of soluction, in equilibrium with an organic phase which contains N_o mol/l of nitric acid. In the presence of nonelectrolyte.

N_N and N_N^o are each one in equilibrium with the identical nitric acid concentration in the organic phase, N_o.

d_o = density of the solution which contains N_N^o mol/l of nitric acid.

d = density of the solution which contain N_N mol/l of nitric acid and N_s mol/l of nonelectrolyte.

M_s = molecular weight of the nonelectrolyte in grams

M_N = molecular weight of nitric acid in grams

M_w = molecular weight of the water in grams

n_h = hydration number, molecular number of water which solvates one molecule of nonelectrolyte.

According to the equation (2), the hydration number for a nonelectrolyte can be given in the form

$$(3) \qquad n_h = \frac{55{,}55 - N_N\,(3.5 + \alpha)}{N_s} - \frac{M_s}{18}$$

α represents the relation between the moles of water and nitric acid contained in one litre of solution, in absence of a nonelectrolyte.

If we express the nitric acid activity in molarity, instead of molality, we obtain the following equation,

$$(4) \qquad N_N^o = \frac{N_N}{1 - 0{,}001\left[N_s V_s + n_h N_s V_w\right]}$$

V_s and V_w are molar volumes of the nonelectrolyte and water respectively in the hydrated compound. Both volumes are given in c.c.

From the equation (4) we can deduce the hydration number in the form

$$(5) \qquad n_h = \frac{1000\left[1 - \frac{N_N}{N_N^o}\right]}{N_s\, V_w} - \frac{V_s}{V_w}$$

According to the equation (5) the hydration number may be obtained if we know the values of V_s and V_w. We have adopted the value of 18 c.c. for V_w and the molar volume of the pure nonelectrolyte for V_s(1), as a working hypothesis.

4.- RESULTS DISCUSSION

The experimental data indicate tartaric acid molecules have no direct interaction with nitric acid and uranyl nitrate, neither in the organic phase nor in the aqueous phase. If tartaric acid would form in the organic phase some additional compound with uranyl nitrate or nitric acid, the presence of these substances would increase the tartaric acid solubility in this phase. Results obtained, Fig. 2, show an opposite effect, the tartaric acid solubility decreases in the presence of uranyl nitrate and nitric acid. Otherwise, if the tartaric acid would form some compound with these products in the aqueous phase, its presence in this phase would decrease their distribution coefficients. Fig. 1 shows on the contrary that the presence of tartaric acid in the aqueous phase increases the distribution coefficients of both products.

In the organic phase nitric acid and uranyl nitrate are solvated by TBP and therefore the number of moles of "free" TBP molecules decreases and in consequence also decreases the tartaric acid solubility. In the aqueous phase the effects of tartaric acid can be interpreted by a similar way: the tartaric acid is solvated by water and therefore the number of moles of "free" water molecules decreases and in consequence increases the distribution coefficients of nitric acid and uranyl nitrate.

We have prefered to use in our study the TBP-nitric acid-water system, because the TBP-uranyl nitrate-water system is very much more complicated. In the absence of nitric acid uranyl nitrate may be hydrolized, tartaric acid dissociated and the tartrate and bitartrate ions associated with uranyl ions. In the nitric acid medium there is practically no dissociation of tartaric acid and the tartaric acid-water interaction can be interpreted as the hydration of a nonelectrolyte.

In order to determine the influence of the alcohol and caboxilic groups in the nonelectrolyte hydration, we have studied two acids with different numbers of carboxilic groups and two sugars with different number of alcohol groups.

From results obtained for citric acid, tartaric acid, sucrose and glucose it can be observed:

(1) Five levels of nitric acid concentrations have been used, between 0,1 and 0,5 M in the organic phase. Seven different concentrations of nitric acid and nonelectrolyte in equilibrium with each level of nitric acid concentration in the organic phase, have been used in aqueous phase. The nonelectrolyte concentrations ranges from zero to 2,5 M, except in the case of the sucrose whose solubility presents problems in the presence of nitric acid. At nitric acid concentrations in the organic phase higher than 0,5 M, the nitric acid concentration in the aqueous phase is superior to 5 M and the hydration numbers are insignificant. It is possible that, at this high nitric acid concentration, the nonelectrolyte may be slighty hydrated and it would have some type of interaction with nitric or its ions.

(2) The hydration number obtained, using both equations, (3) and (5), are in good agreement between themselves. This agreement shows that the "working hypothesis" was correct: in aqueous solution these molecules have the same volume as in the pure state and the water molecules bonded to the nonelectrolyte have the same volume as the "free" water molecules.

(3) The hydration number, at constant concentration of nitric acid and nonelectrolyte decreases in the order: citric acid, tartaric acid, sucrose, glucose. In Fig. 3 we present the hydration numbers of four nonelectrolytes as a function of the nitric acid concentration in the aqueous phase, for a nonelectrolyte concentration of 1,5 M. When the nitric acid concentration increases the hydration number of the four nonelectrolytes decreases. At nitric acid concentration higher than 1.5 M, the variation of the hydration numbers of the four nonelectrolytes shows a certain paralle-

lism. However, at lower concentrations of nitric acid, the hydration number of tartaric and citric acid increases more rapidly than that of sucrose and glucose.

Miller and Co. (2), by adiabatic compressibility method, showed that the number of water molecules hydrated to the sugars increased with an increasing number of OH^- groups. These results are in good agreement with the hydration number obtained for us. In the same work Miller showed that succinic acid has, for infinite dilution, a positive value for the partial molar adiabatic compressibility, while sugars have negative values. Negative values indicate that the molecules are highy hydrated.

The results obtained in the nitric acid extraction by TBP show that in the presence and in the absence of succinic acid, this nonelectrolyte has no influence on the distribution coefficient of nitric acid. Therefore succinic acid in a nitric acid medium is slightly hydrated. The low hydration of succinic acid may be the reason why its distribution coefficient is ten times superior to the corresponding ones of citric and tartaric acid.

Fig. 4 shows the density of aqueous nitric acid solutions as a function of the citric acid concentration. The slope of these lines is a constant, and is in accord with the theoretical equation for nonelectrolyte solutions:

$$d = d_N + \left[1 - \frac{0,997}{d_s}\right] \frac{M_s N_s}{1000} \qquad (6)$$

d_N = density of solutions which contain only nitric acid

d_s = density of pure nonelectrolyte

Tartaric acid, glucose and sucrose densities present similar effects as citric acid, but each one with its corresponding slope. Densities obtained from experimental slopes, d_p, have been compared with values collected from handbook, d_s (1). There is a good agreement between d_p for and d_s for sucrose, glucose, tartaric acid and citric acid.

The value of dp sucrose is slightly higher than d_s, while for another three nonelectrolytes dp is slightly lower than d_s. These data are on good terms with the values of n_h obtained from equations (3) and (5).

REFERENCES

1. Handbook of Chemistry and Physic, Ed. The Rubber Co., 61st Edition, 1980-81.

2. A. Lo Surdo, C. Shin and F.S. Millero; J. Chem. and Eng. Data 23 (3), 197 (1978).

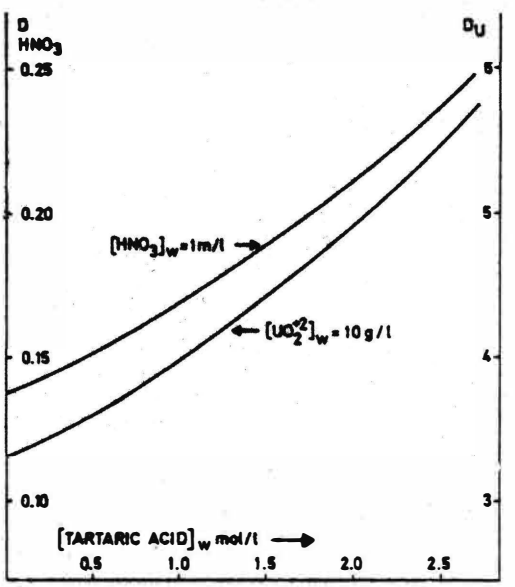

Fig.1- Nitric acid and uranyl nitrate distribution; coefficients between 20 % TBP in kerosene and nitric acid 1.0 M, as a function of the tartaric acid concentration.

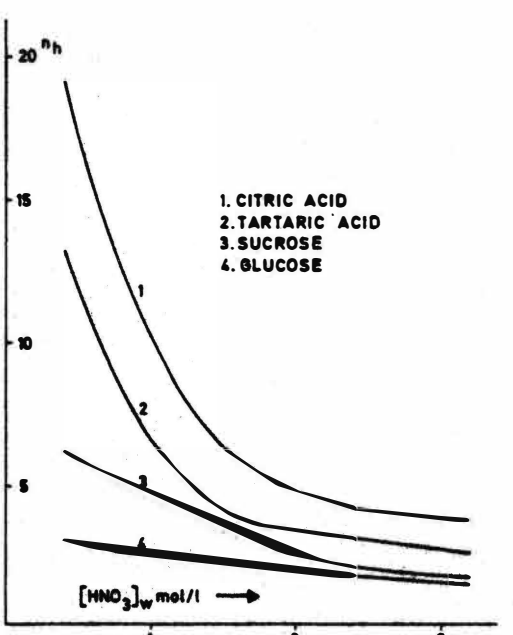

Fig. 3- Variation of the hydration number, n_h, as a function of the nitric acid concentration in the aqueous phase. Nonelectrolyte concentration of 1.5 M.

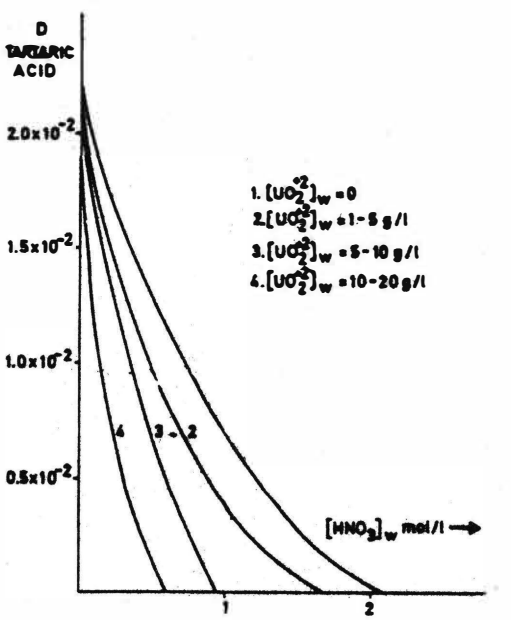

Fig.2- Tartaric acid distribution coefficient between 20 % TBP in kerosene and aqueous solutions of 1 M nitric acid and uranyl nitrate.

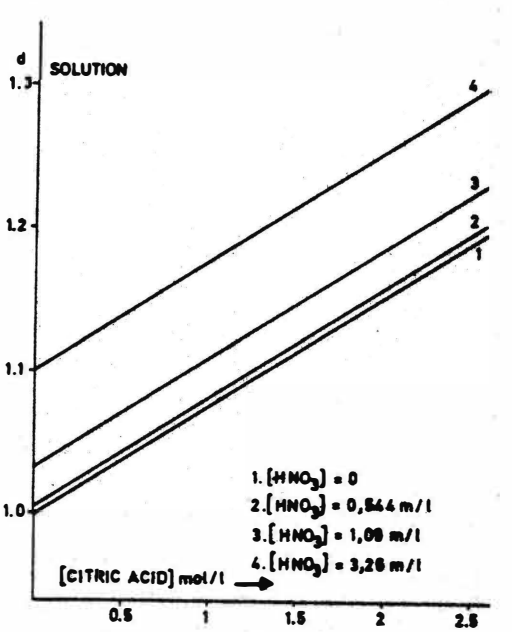

Fig.4- Densities of nitric acid and citric acid solutions.

DISTRIBUTION OF U(IV), U(VI), Pu(III), Pu(IV), AND NITRIC ACID BETWEEN TRIBUTYL PHOSPHATE (TBP) IN DODECANE AND AQUEOUS NITRATE SOLUTIONS

S. Tachimori and Z. Kolarik

Institute of Hot Chemistry
Nuclear Research Centre
Karlsruhe, Federal Republic of Germany

Knowledge of distribution ratios of acitinides and nitric acid in the extraction with TBP is of great importance for the modelling of extraction operations in the reprocessing of nuclear fuel. Rather little is known about distribution equilibria under the conditions of a reductive separation of uranium from plutonium, especially about the extraction behaviour of U(IV) and Pu(III) and their influence on the distribution of U(VI) and nitric acid. Neither the effect of temperature on the distribution of U(IV) and Pu(IV) has been studied in detail. In this work we studied the distribution of the title components between a 30 vol.% solution of TBP in dodecane and aqueous solutions containing one or more actinide nitrates, nitric acid and, except in the presence of Pu(IV), hydrazine nitrate. The number of distribution ratios measured at 25°C was 394 for U(IV), 194 for U(VI), 22 for Pu(III), and 196 for nitric acid. 54 distribution ratios of each U(IV) and nitric acid and 105 distribution ratios of Pu(IV), 55 of them at ≤0.37M U(VI), were measured at 15 - 70°C. Equilibrium concentrations in the aqueous phase varied in the ranges 0 - 0.64M U(IV), 0 - 0.76M U(VI), 0 - 0.15M Pu(III), 0.04 - 5.8M nitric acid and 6×10^{-4} - 2.1M hydrazine nitrate. At 25°C, the distribution ratios of U(IV), U(VI) and nitric acid were measured as functions of the concentrations of all above components except Pu(IV), while the concentration of hydrazine nitrate was negligibly changed in the measurement of the distribution ratio of Pu(III). Since measurements at only one concentration varied would have been time consuming (due to the necessary preequilibration of the organic phase), we varied in a series of measurements the concentration of one component in a broad range and allowed the concentrations of other components to vary in narrow ranges. To assess the influence of single variables on the distribution ratios, we smoothed the data in using empirical equations analogous to those given in (1).

Each component can influence the distribution of itself and of other components in two counteracting ways:

- self-salting-out or salting-out, which increases the distribution ratios (henceforth salting action), and
- bonding a fraction of TBP in the organic phase, which lowers the free TBP concentration and, consequently, suppresses the distribution ratios (henceforth replacement action).

To evaluate the salting action, we extended the empirical equations for terms expressing the apparent number of nitrate ions, n_N, contributed by actinide or hydrazine nitrates to the total analytical concentration of nitrate ions and related to arbitrarilly one nitrate ion contributed by nitric acid. The terms are based on a conventional application of Harned coefficients, which are treated as empirical functions of the ionic strength. The n_N values can be understood as apparent thermodynamic activities of actinide or hydrazine nitrates related to the thermodynamic activity of nitric acid.

Examples of dependences of distribution ratios on the concentrations of some components are given in Figures 1 and 2. They illustrate the strong salting action of U(IV) nitrate and its rather weak replacement action. Contrary to U(IV) and U(VI), nitric acid is weakly salted-out by U(IV) nitrate. Figure 3 demonstrates the apparent number of nitrate ions contributed by U(IV) nitrate to the total nitrate ion concentration in the extraction of U(IV) and U(VI).

The replacement action of hydrazine nitrate is expectedly negligible and the salting action of the mononitrate $N_2H_5NO_3$ is similar to that of nitric acid. The dinitrate $N_2H_6(NO_3)_2$, formed in the aqueous phase to a significant degree at >1M nitric acid, exhibits stronger salting-out properties. At high concentrations of hydrazine nitrate, the dependence of the distribution ratio of U(IV) on the nitric acid concentration has an unusual form with a minimum (Figure 4). The distribution ratio of Pu(III) ranges from 0.01 to 0.03 at ≤0.024M U(IV), ≤0.12M U(VI) and 1 - 2M nitric acid in the equilibrium aqueous phase.

The extractability of U(IV) tends to decrease with increasing temperature. At a low concentration of U(IV) and in the absence of U(VI), the plot of the logarithm of the distribution ratio of U(IV) vs. 1/T is linear, but its slope decreases from 1200 at 0.1M nitric acid to zero at 3.0M nitric acid in the aqueous phase. Pu(IV) becomes generally more extractable with increasing temperature. The dependence of the logarithm of the distribution ratio of Pu(IV) on 1/T is again linear and its slope ranges from -8 at 0.8M nitric acid to -500 at 2.6M nitric acid. The dependence retains its linear form, and its slope remains acid dependent at higher Pu(IV) concentrations (Figure 5). As in the case of U(IV), the variability of the slope can be ascribed to heat effects connected with the extraction of nitric acid and to a change of the temperature dependence of activity coefficients with the concentration of nitric acid. In the presence of U(VI) the plot of the logarithm of the distribution ratio of Pu(IV) vs. 1/T is curved, due to a weakening of the replacement action of U(VI) with increasing temperature.

REFERENCE

1. Z. Kolarik and G. Petrich, Ber. Bundesges. Phys. Chem. 83, 1110 (1979).

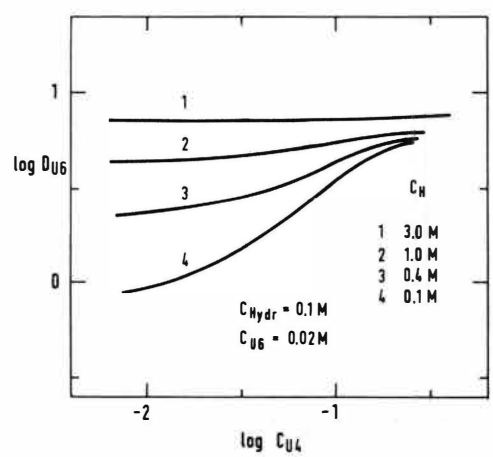

FIGURE 1. SMOOTHED LOGARITHMIC DEPENDENCE OF THE DISTRIBUTION RATIO OF U(VI) ON THE U(IV) CONCENTRATION AT DIFFERENT CONCENTRATIONS OF NITRIC ACID AND CONSTANT CONCENTRATIONS OF HYDRAZINE NITRATE AND U(VI) IN THE EQUILIBRIUM AQUEOUS PHASE AT 25°C

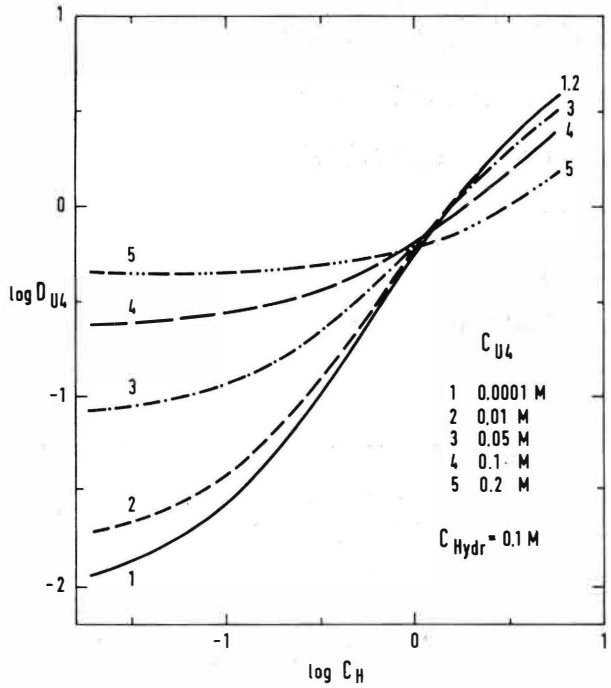

FIGURE 2. SMOOTHED LOGARITHMIC DEPENDENCE OF THE DISTRIBUTION RATIO OF U(IV) ON THE CONCENTRATION OF NITRIC ACID AT DIFFERENT U(IV) CONCENTRATIONS AND A CONSTANT CONCENTRATION OF HYDRAZINE NITRATE IN THE EQUILIBRIUM AQUEOUS PHASE AT 25°C

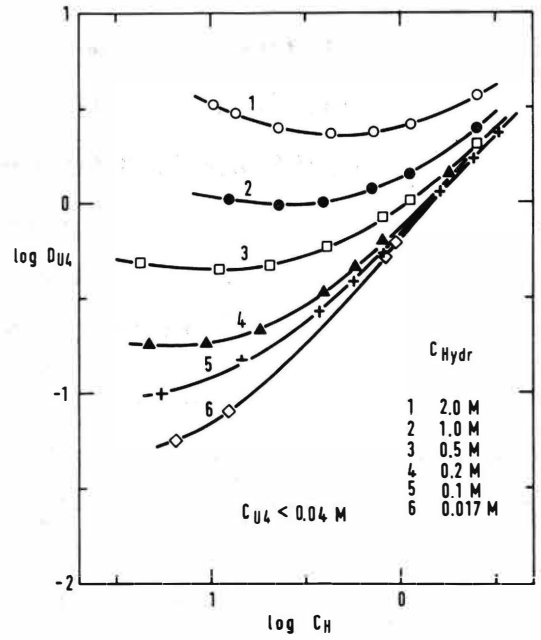

FIGURE 4. LOGARITHMIC DEPENDENCE OF THE DISTRIBUTION RATIO OF U(IV) ON THE CONCENTRATION OF NITRIC ACID AT DIFFERENT CONCENTRATIONS OF HYDRAZINE NITRATE AND A LOW CONCENTRATION OF U(IV) IN THE EQUILIBRIUM AQUEOUS PHASE AT 25°C

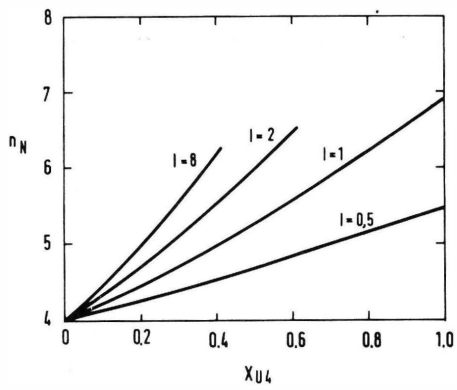

FIGURE 3. THE APPARENT NUMBER OF NITRATE IONS CONTRIBUTED BY A MOLECULE OF U(IV) NITRATE TO THE TOTAL CONCENTRATION OF NITRATE IONS, PLOTTED VS. THE FRACTION OF THE IONIC STRENGTH FORMED BY U(IV) NITRATE, AT DIFFERENT IONIC STRENGTHS AND 25°C

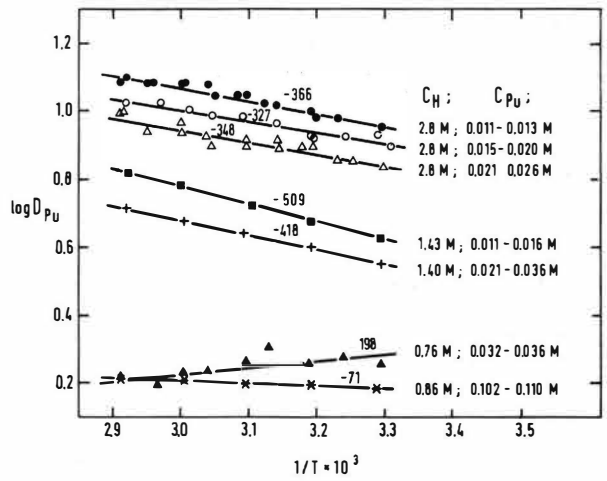

FIGURE 5. THE LOGARITHM OF THE DISTRIBUTION RATIO OF Pu(IV) AS A FUNCTION OF THE REVERSED ABSOLUTE TEMPERATURE AT DIFFERENT CONCENTRATIONS OF NITRIC ACID AND Pu(IV) IN THE EQUILIBRIUM AQUEOUS PHASE; NUMERALS ON THE LINES ARE THE SLOPES

EXTRACTION OF CHROMIUM (VI) BY TRI-n-DODECILAMONIUM CHLORIDE AND TRI-n-DODECILAMONIUM HYDROGENSULPHATE DISSOLVED IN BENZENE

A. Sastre, N. Miralles, M. Aguilar and M. Elizalde

Cátedra de Química I, E.T.S.E.I.B.
Universitat Politecnica de Barcelona
Diagonal 647, Barcelona, 28 Spain

Departamento de Química Analítica
Universidad del País Vasco
Bilbao, Spain

It is known that chromium (VI) anions may be extracted fro... acidic aqueous phase with basic extractants like amines.

The extraction of chromium (VI) by various amines has been studied by different authors (1-4).

Deptuła (3, 4) found CrO_3Cl^- in organic phase when extracting chromium (VI) with TOA from concentrated hydrochloric acid and $Cr_2O_7^{2-}$ from other mineral acids.

Rao and Sastri (1, 2) suggested a mixture of CrO_3Cl^- and $Cr_2O_7^{2-}$ or $HCrO_4^-$ when extracting chromium (VI) from hydrochloric acid by TLA in chloroform and only $Cr_2O_7^{2-}$ from sulphuric or phosphoric acid.

In the present work the extraction of chromium (VI) with TLAHX ($X^- = Cl^-, HSO_4^-$) has been studied following the distributio ratio of the metal as a function of pH and TLAHX concentration at two different ionic media.

The experimental data, treated both graphically and numerically by means of the program LETAGROP-DISTRB (5) have been interpreted in terms of stoichiometry of the extracted species and their extraction constants (Table 1).

EXPERIMENTAL

The distribution equilibria studies were carried out at 25 °C, equilibrating equal volumes (15 ml) of the organic phase and the aqueous phase. The composition of the organic phase was C mol dm^{-3} of TLAHX in benzene. The composition of the aqueous phase was B mol dm^{-3} of chromium (VI) and NaCl and Na_2SO_4 were used as ionic medium.

Chromium (VI) concentration was measured spectrophotometrically at 540 nm using 1,5-diphenilcarbazide. Chromium (VI) in organic phase was determined by stripping the metal with NaOH (3).

RESULTS

The extraction of chromium (VI) by TLAHX can be written:

$$(1)\quad q\,CrO_4^{2-} + p\,H^+ + r\,TLAHX_{(org)} + (n-r)\,X^- \rightleftharpoons (CrO_4)_qH_p(TLAH)_rX_n\,(org)$$

and β_{pqrn} is the stoichiometric equilibrium constant

$$(2)\quad \beta_{pqrn} = \frac{|(CrO_4)_qH_p(TLAHX)_rX_n|_{(org)}}{|CrO_4^{2-}|^q\,|H^+|^p\,|TLAHX|_{(org)}\,|X^-|^{n-r}}$$

Since the total chromium (VI) concentration is lower than 1.0 mol dm^{-3} no polynuclear complexes are assumed to be formed in organic phase and q = 1 in equation (1).

Considering the distribution coeficient for chromium

$$(3)\quad D = \frac{|Cr(VI)|_{(org)}}{|Cr(VI)|_{(aq)}}$$

and substituting equation (2) in (3)

$$(4)\quad D = \frac{\sum_{prn}\sum \beta_{prln}\,|H^+|^{p-1}\,|TLAHX|^r_{(org)}\,|X^-|^{n-r}\,|CrO_4^{2-}|}{|Cr(VI)|_{(aq)}}$$

For each ionic medium, two type of data were taken, $\log D = f(pH)_{TLAH^+,\,Cr(VI)}$ and $\log D = f(TLAH^+)_{pH,\,Cr(VI)}$ for each chromium (VI) concentration.

a) Sulphate medium. Assuming that only one specie is extracted into the organic phase, equation (4) can be written:

$$(5)\quad \log D = \log \beta_{plrn} + r \log |TLAH_2SO_4|_{(org)} - \log \alpha + (n-r) \log |HSO_4^-| - (p-1)\,pH$$

where α includes the concentration of chromium (VI) species present in aqueous phase.

Experimental data plotted as log D vs. pH and log D + pH vs. $\log |TLAH_2SO_4|_{(org)}$ are represented in Figure 1 and Figure 2. From these plots, values of p = 2 and r = 2 were determined. Since the extracted species must be neutral (6), n = 2 hence, the extracted specie may have stoichiometry $CrO_4H_2(TLAH_2SO_4)_2$.

b) Chloride medium. A preliminar graphical treatment sho... that two species of type $CrO_4H_2TLAHCl$ and $CrO_4H_2(TLAHCl)_2$ were formed in organic phase.

In order to determine their extraction constants, the data plotted as $\log D + pH - \log |TLAHCl|_{(org)}$ vs $\log |TLAHCl|_{(org)}$ were compared with the theoretical function $\log Y = \log (1 + u)$ Figure 3.

Refinement of this model was done by computer treatment. The results are shown in Table 1

TABLE 1. Equilibrium constants calculated by differen methods for the Cr(VI) - TLAHX system.

Method of calculation	$\log \beta_{2111}$	$\log \beta_{2122}$
Extraction with TLAHCl		
GRAPHICAL	11.64	14.48
LETAGROP-DISTRB	11.94 ± 0.30	14.53 ± 0.15
Extraction with $TLAH_2SO_4$		
GRAPHICAL		15.29
LETAGROP-DISTRB		16.47 ± 0.10

REFERENCES

1. Rao, V.M., Sastri, M.N., Indian J. Chem., 14, 635 (1976)
2. Rao, V.M., Sastri, M.N., J. Indian Chem. Soc., 53, 1006 (1976)
3. Deptuła, C., J. Inorg. nucl. Chem., 30, 1309 (1968)
4. Deptuła, C., Rocz. chem., 41, 3 (1967)
5. Liem, D.H., Acta Chem. Scand., 25, 1521 (1971)
6. Morrison, G.H., Freiser, H., Solvent Extraction in Comprehensive Analytical Series, Vol I, Elsevier Publishing Company, London, 1959.

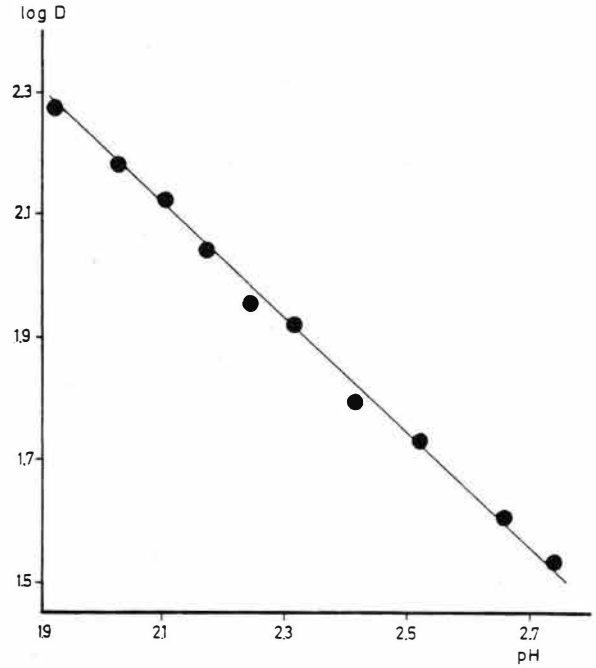

FIGURE 1. Log D as a function of pH in sulphate medium

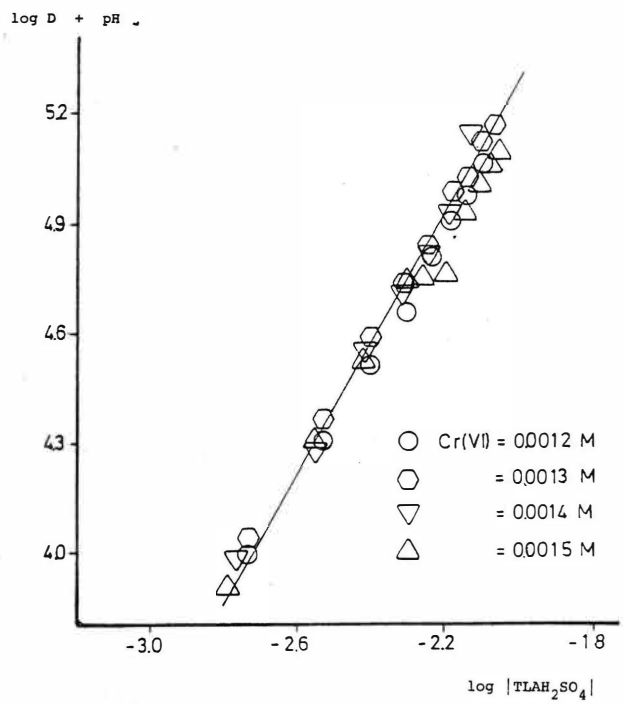

FIGURE 2. Plot of log D + pH as a function of the free concentration of $TLAH_2SO_4$

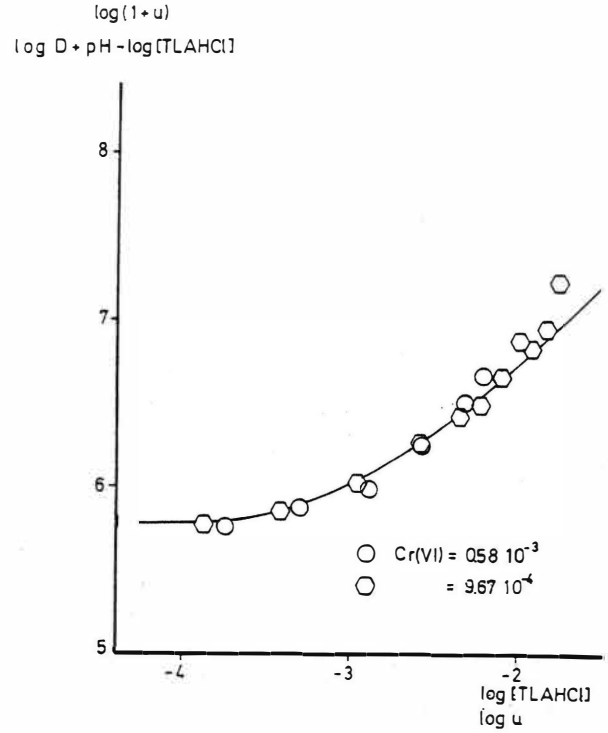

FIGURE 3. Plot of the experimental data in the extraction of Cr(VI) with TLAHCl. The full-drawn line has been calculated using the theoretical function log Y = log (1 + u)

ON THE AGGREGATION OF 5,8-DIETHYL-7-HYDROXYDODECAN-6-OXIME IN TOLUENE

M. Aguilar and M. P. Elizalde and J. M. Castresana

Cátedra de Química I, ETSIIB
Universidad Politécnica de Barcelona
Barcelona, Spain

Departamento de Química
Universidad del País Vasco
Bilbao, Spain

The study of the aggregation equilibria in organic solvents is essential in order to ascertain the stoichiometry of the extracted metallic species and their corresponding distribution constants in systems involving hydroxyoximes. It has been pointed out (1,2) the importance of the determination of the oxime monomer concentration in the organic phase to explain the disagreements on the extraction rate among different studies on extraction kinetics. In spite of that, the majority of the works on aggregation of hydroxyoximes in organic solvents only reports data of mean aggregation numbers from which rough values of monomer concentration have been estimated.

In the present work the aggregation equilibria of the anti-isomer of the 5,8-diethyl-7-hydroxydodecan-6-oxime (DEHO), the active component of the commercial LIX 63, in toluene have been studied by Vapour Pressure Osmometry at 301 and 323 K.

EXPERIMENTAL

The 5,8-diethyl-7-hydroxydodecan-6-oxime was synthesized following the method of Swanson (3) as an oily yellow liquid. The anti-isomer was isolated by the preparation of its copper complex and the pure anti-isomer regenerated stripping the copper with acid and removing the solvent to yield a white waxy solid. The composition and functional groups of the anti-isomer obtained were confirmed by IR and NMR spectroscopy and elemental analysis.

Benzil Merck p.a. was twice recrystallized from dried methanol and used as standard. All the other chemicals and solvents were of analytical reagent grade and used without further purification. The osmometric measurements were carried out using a Knauer model 1974 Vapour Pressure Osmometer.

RESULTS

In Figure 1 the differences of resistence ΔR for both DEHO and the standard have been plotted against the total concentration, B, at the two temperatures. The results show clearly a deviation from the monomeric behaviour for DEHO solutions which demonstrates the aggregation in the organic phase.

The aggregation processes can be represented as follows:

$$n\ \mathrm{DEHO} \rightleftharpoons (\mathrm{DEHO})_n \tag{1}$$

with the corresponding formation constants:

$$\beta_n = |(\mathrm{DEHO})_n|\ |\mathrm{DEHO}|^{-n} = |(\mathrm{DEHO})_n|\ b^{-n} \tag{2}$$

The mass balance for DEHO reagent will be:

$$C_{\mathrm{DEHO}} = B = b + \sum_n n\,\beta_n\, b^n \tag{3}$$

On the other hand, defining S as the sum of the concentrations for all solute species,

$$S = b + \sum_n \beta_n\, b^n \tag{4}$$

From the experimental data (ΔR,B) and taking into account the respective calibration constants for each temperature, the average aggregation number, $\bar{n}$, can be obtained:

$$\bar{n} = \frac{\sum_n n\,\beta_n\, b^n}{\sum_n \beta_n\, b^n} = \frac{B}{S} \tag{5}$$

Differentiating and rearranging equation (4) and taking into account equation (5) the following expression can be obtained:

$$\log b - \log b_o = \int_{S_o}^{S} \frac{1}{\bar{n}}\, d \log S \tag{6}$$

b values were determined by graphical integration of the curve $1/\bar{n}$ against log S, being S_o so low a value that $b_o = S_o$, i.e. association can be neglected.

The stoichiometry of the species responsible of the aggregation of DEHO in toluene as well as their formation constants were evaluated from the data (B,b) and (ΔR,B) using graphical and numerical methods respectively.

TREATMENT OF THE DATA

Both linear and curve fitting analysis of the data were done for different models involving monomer-multimers equilibria. The results showed that the experimental data could be explained by the formation of dimer and trimer species in variable proportion depending on the temperature. The contribution of higher aggregates turned to be negligible in the range of concentration and temperatures studied.

If the monomer-dimer-trimer model is responsible for the aggregation of DEHO in toluene, equation (3) can be rearranged to:

$$\frac{B - b}{b^2}\ \frac{1}{2\,\beta_2} = 1 + \frac{3\,\beta_3}{2\,\beta_2}\, b \tag{7}$$

Let us define the normalized variables:

$$Y = \frac{B - b}{b^2}\ \frac{1}{2\,\beta_2} \quad \text{and} \quad X = \frac{3\,\beta_3}{2\,\beta_2}\, b \tag{8}$$

The plot of the experimental data log $(B-b)b^{-2}$ as a function of log b will have the same shape that the theoretical curve log Y = f (log X) if the proposed model is valid. From the translations in both axes a position of fit was found and values of log β_2 and log β_3 were determined. The limits of error in both constants may be estimated by the permisible displacements from the position of best fit, taking into account the experimental uncertainty.

From the superimposition of the functions for both temperatures showed in Figure 2 can be inferred that the contribution of the trimer is important at 301 K but only dimer species are responsible for the aggregation of DEHO at 323 K.

Finally, the data (ΔR,B) were numerically treated by means of the program LETAGROP-SUMPA (4) leading to the same results as far as the stoichiometry of the aggregates is concerned.

Table 1 summarizes the results of graphical and numerical treatments for the aggregation of DEHO in toluene at the two temperatures.

In Figure 3 the distribution diagrams for DEHO species in the organic solution have been represented as mole fraction vs C_{DEHO} at 301 and 323 K, using the aggregation constant values obtained by the LETAGROP-SUMPA program.

TABLE 1. VALUES OF DEHO AGGREGATION CONSTANTS OBTAINED BY THE GRAPHICAL AND NUMERICAL TREATMENTS.

T (K)		$\log \beta_2$	$\log \beta_3$
301	Graphical	0.38	1.38
	LETAGROP-SUMPA	0.45 ± 0.19	1.31 ± 0.05
323	Graphical	0.91	-
	LETAGROP-SUMPA	0.89 ± 0.05	-

REFERENCES

1. L. Hummelstedt, Proc. Int. Conf. Solvent Extraction Chem. (ISEC), p. 86, Toronto (1977).

2. R. J. Whewell, M. A. Hughes and C. Hanson, Proc. Int. Conf. Solvent Extraction Chem. (ISEC), p. 185, Toronto (1977).

3. R. R. Swanson, U.S. Patent 3.224.873 (1965).

4. B. Warnqvist, Chemica Scripta, 1, 49 (1971).

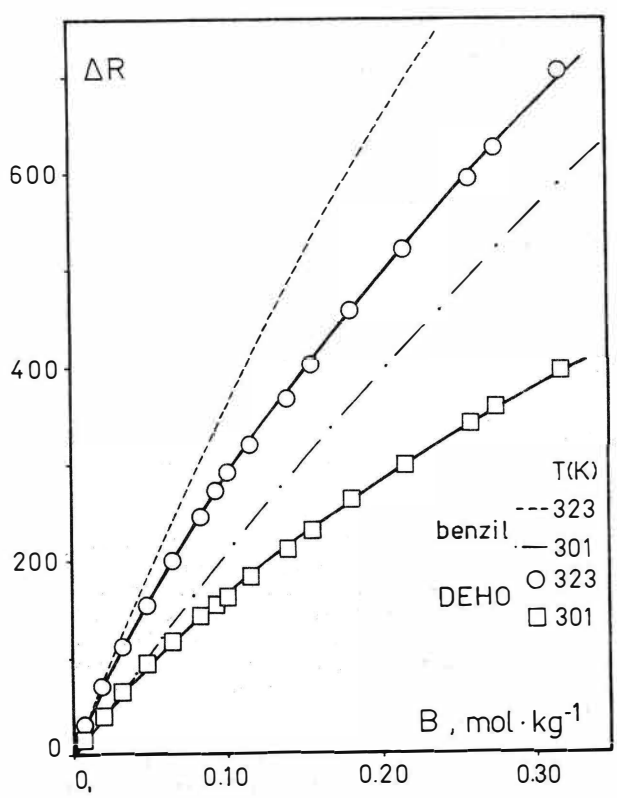

FIGURE 1. OSMOMETRIC RESULTS FOR THE STANDARD AND DEHO IN TOLUENE. CONTINUOUS LINES HAVE BEEN DRAWN USING THE PROPOSED AGGREGATION CONSTANTS FOR DEHO.

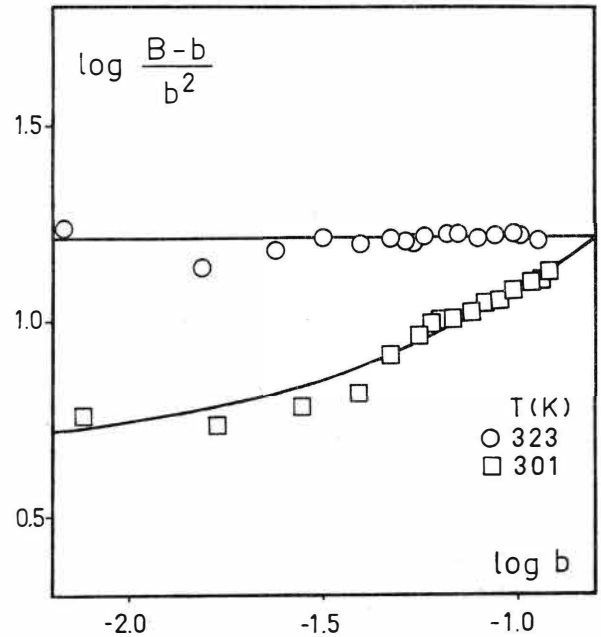

FIGURE 2. SUPERIMPOSITION OF THE EXPERIMENTAL FUNCTIONS AND THE THEORETICAL ONES (CONTINUOUS LINES) FOR THE MONOMER-DIMER-TRIMER EQUILIBRIA AT THE TWO TEMPERATURES STUDIED.

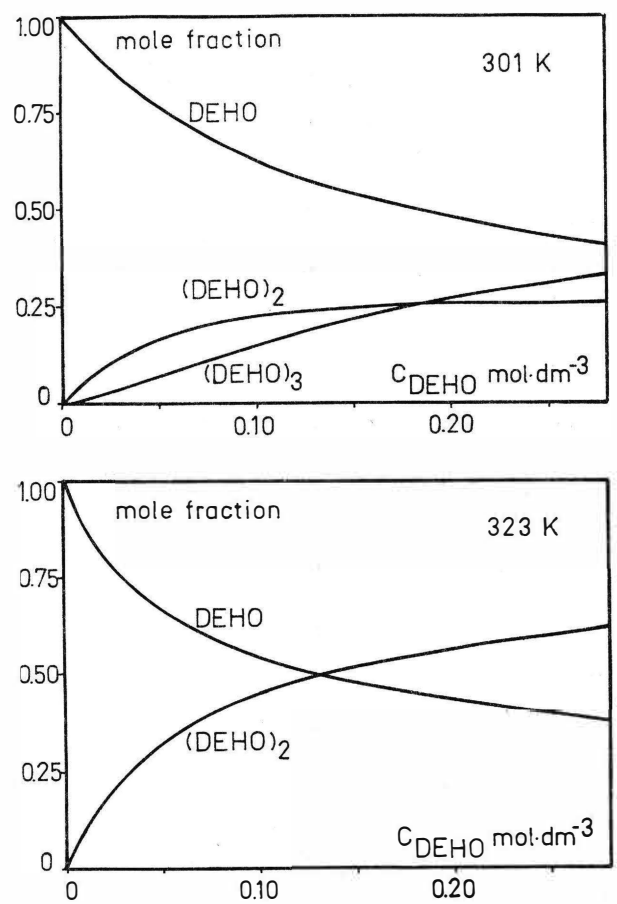

FIGURE 3. DISTRIBUTION DIAGRAMS FOR DEHO SPECIES IN TOLUENE.

EXTRACTION OF Ni(II) BY 5,8-DIETHYL-7-HYDROXYDODECAN-6-OXIME IN MIXTURES WITH OTHER EXTRACTANTS AND TOLUENE

M. Aguilar and M. P. Elizalde and J. M. Castresana

Cátedra de Química I, ETSIIB
Universidad Politecnica de Barcelona
Barcelona, Spain

Departamento de Química
Universidad del País Vasco
Bilbao, Spain

In a previous work (1) the extraction equilibria of Ni(II) by 5,8-diethyl-7-hydroxydodecan-6-oxime (DEHO), di-(2-ethylhexyl) phosphoric acid (DEHPA) and di-n-octyl phosphinic acid (DOPA) dissolved in toluene have been studied. A great synergic effect in the extraction of Ni(II) has been observed when different mixtures of DEHO, DEHPA and DOPA were used as extractants. Table 1 shows the pH values for 50% extraction ($pH_{0.5}$) for the different systems and their mixtures, as well as the synergic coefficients (S.C.) (2) obtained. The observed synergic effect has been interpreted in terms of mixed species formation in the organic phase. Extraction constants for the different species are given.

EXPERIMENTAL

The distribution equilibria studies were carried out by equilibrating equal volumes (10 cm^3) of the organic phases (C_{HL} $mol.dm^{-3}$ DEHO and C_{HR} $mol.dm^{-3}$ DOPA or DEHPA in toluene) and the aqueous phases (0.5 $mmol.dm^{-3}$ Ni(II) in 1.0 $mol.dm^{-3}$ $NaNO_3$) for at least ten hours. Nickel concentration in both phases was measured by Atomic Absorption Spectroscopy. Nickel in the organic phase was determined by stripping the metal with acidified aqueous solutions.

RESULTS

The extraction of Ni(II) by mixtures of DEHO and DOPA or DEHPA can be described by the following general equation:

$$(1) \qquad j\,Ni^{2+} + p\,HL_{org} + n\,NO_3^- + \frac{q}{2}(HR)_{2\,org} \rightleftharpoons Ni_jL_p(NO_3)_nH_rR_{q\,org} + (p+q-r)\,H^+$$

where HL represents the extractant DEHO and HR the organophosphorous acids which behave as dimers in organic solutions (3,4).

Being k_{jpnrq} the stoichiometric equilibrium constant for this reaction the distribution coefficient for nickel can be expressed as follows:

$$(2) \qquad D = \frac{\sum_j \sum_p \sum_n \sum_r \sum_q j\, k_{jpnrq}\, |HL|^p_{org}\, |NO_3^-|^n\, |(HR)_2|^{q/2}_{org}}{|Ni^{2+}|^{1-j}\, \alpha_{Ni}\, |H^+|^{p+q-r}}$$

where α_{Ni} represents the side reaction coefficient taking into account the nitrato-complexes of Ni(II) in the aqueous phase (5).

Equation (4) has been taken as starting point for the different graphical analysis made in order to determine the stoichiometric coefficients and k_{jpnrq} values.

Ni(II)-NO_3^- / DEHO-DOPA-TOLUENE SYSTEM

The extraction of Ni(II) by mixtures of DEHO and DOPA has been studied following the distribution of the metal as a function of the pH of the aqueous phase. Two series of data have been collected from which functions of the type log D = f (log $|HL|)_{C_{HR}}$ and log D = f (log $|(HR)_2|)_{C_{HL}}$ were constructed.

Experimental data have been represented in Figures 1 and 2. As it can be seen, the plot of log D against pH at several DOPA concentrations and constant C_{HL} shows a slope equal to 2.0 (Figure 1) but this function at constant C_{HR} and variable C_{HR} shows two different slope values: 2.0 at high C_{HL} values and 1.5 approximately at lower C_{HL} (Figure 2)

The different graphical analysis used as well as the numerical treatment by means of the program LETAGROP-DISTR (6) lead to the formation in the organic phase of two metallic species according to:

$$Ni^{2+} + 2\,HL_{org} + \frac{1}{2}(HR)_{2\,org} \rightleftharpoons NiL_2HR_{org} + 2\,H^+$$

$$2Ni^{2+} + 2HL_{org} + 2NO_3^- + \frac{1}{2}(HR)_{2\,org} \rightleftharpoons Ni_2L_2(NO_3)_2HR_{org} + 2\,H^+$$

with $\log k_{12011} = 1.46 \pm 0.03$ and $\log k_{22211} = 4.21 \pm 0.14$

Ni(II)-NO_3^- / DEHO-DEHPA-TOLUENE SYSTEM

Experimental data have been represented in Figure 3 as log D vs pH at several DEHPA concentrations and constant C_{HL}. Further experiments confirmed that DEHO reagent extracts nitric acid from very acidic (pH < 0.5) aqueous solutions. Graphical curve fitting analysis and numerical treatment by the LETAGROP-DISTR program showed that the experimental results could be explained by the following extraction reactions and equilibrium constants:

$$Ni^{2+} + 2\,HL_{org} + \frac{1}{2}(HR)_{2\,org} \rightleftharpoons NiL_2HR_{org} + 2\,H^+$$

$$Ni^{2+} + HL_{org} + NO_3^- + \frac{1}{2}(HR)_{2\,org} \rightleftharpoons NiL(NO_3)HR_{org} + H^+$$

with $\log k_{12011} = 2.81 \pm 0.10$ and $\log k_{11111} = 2.41 \pm 0.12$

In Figure 4 the distribution diagrams of Ni(II) as mole fraction vs C_{HR} at C_{HL} constant have been plotted for both systems.

TABLE 1. VALUES OF $pH_{0.5}$ AND S.C. FOR THE EXTRACTION OF Ni(II) IN THE DIFFERENT SYSTEMS.

EXTRACTANT 0.050 $mol.dm^{-3}$	$pH_{0.5}$	EXTRACTANT MIXTURE $C_{HL}=C_{HR}=0.050$ $mol.dm^{-3}$	$pH_{0.5}$	S.C.
DEHO	4.78			
DOPA	6.08	DEHO + DOPA	1.13	7.30
DEHPA	5.11	DEHO + DEHPA	0.20	9.16

REFERENCES

1. M. P. Elizalde, Ph.D. Thesis, University of Basque Country, Bilbao, Spain (1982).

2. M. Taube and S. Siekierski, Nukleonika, 6, 489 (1961).

3. D. H. Liem, Acta Chem. Scand., 26, 191 (1972).

4. D. F. Peppard, G. W. Mason and S. Lewey, J. Inorg. Nucl. Chem., 27, 2065 (1965).

5. V. A. Fedorov, I. I. Shmyd'ko, A. M. Robov, L. S. Simaeva, V. A. Kukhtina and V. E. Mironov, Russ. J. Inorg. Chem., 18, 673 (1973).

6. D. H. Liem, Acta Chem. Scand., 25, 1521 (1971).

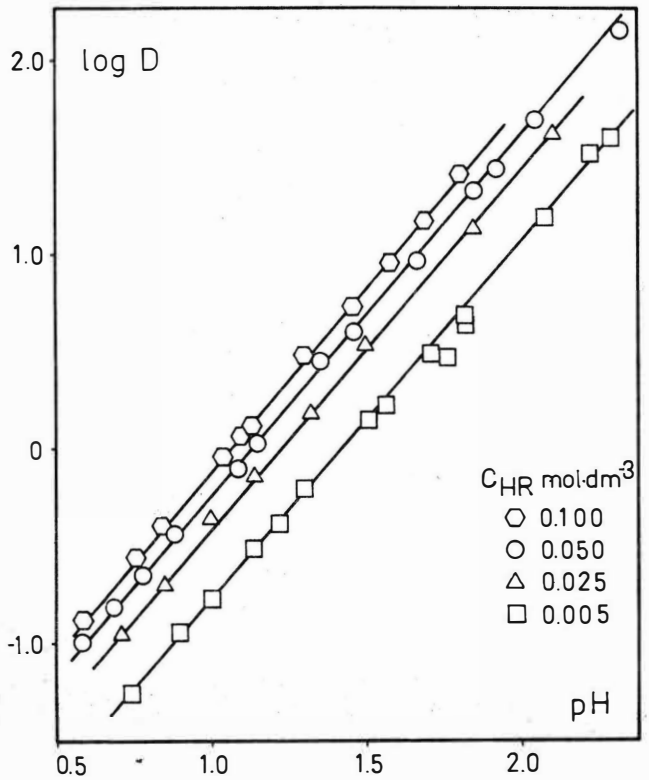

FIGURE 1. NICKEL DISTRIBUTION COEFFICIENT AS A FUNCTION OF pH AT CONSTANT DEHO CONCENTRATION AND SEVERAL DOPA CONCENTRATIONS. CONTINUOUS LINES HAVE BEEN DRAWN USING THE PROPOSED NICKEL EXTRACTION CONSTANTS. (C_{HL} = 0.050 mol.dm^{-3}).

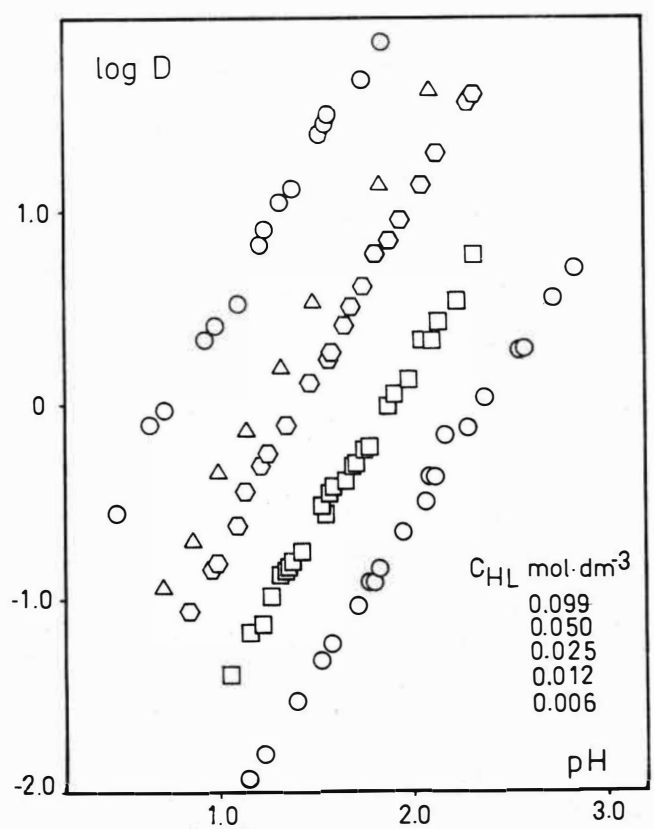

FIGURE 2. log D = f(pH) FOR THE EXTRACTION OF Ni(II) AT CONSTANT DOPA CONCENTRATION AND SEVERAL DEHO CONCENTRATIONS.

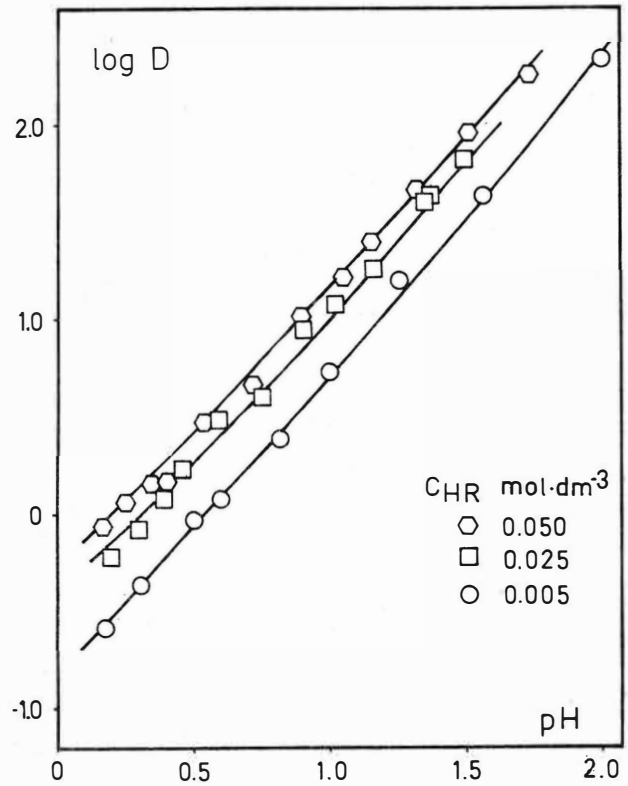

FIGURE 3. NICKEL DISTRIBUTION COEFFICIENT AS A FUNCTION OF pH AT CONSTANT DEHO CONCENTRATION (0.050 mol.dm^{-3}) AND SEVERAL DEHPA CONCENTRATIONS. CONTINUOUS LINES HAVE BEEN DRAWN USING THE PROPOSED NICKEL EXTRACTION CONSTANTS.

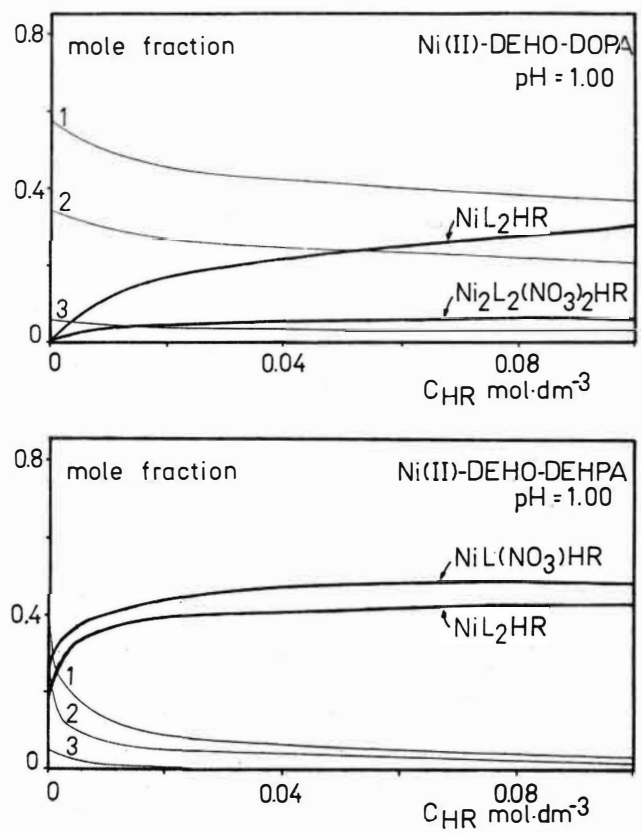

FIGURE 4. NICKEL DISTRIBUTION DIAGRAMS IN BOTH SYSTEMS AT pH=1.00 AND C_{HL}=0.050 mol.dm^{-3}. (1: Ni^{2+}, 2: $NiNO_3^+$ and 3: $Ni(NO_3)_2$).

EXTRACTION OF Co(II) - AND Zn(II) - THIOCYANATE COMPLEXES BY TRILAURILAMMONIUM NITRATE DISSOLVED IN BENZENE

J. M. Madariaga, R. M. Jiménez and M. D. Ruiz and M. Aguilar

Departamento de Química
Universidad del País Vasco
Aptdo. 644
Bilbao, Spain

Cátedra de Química I, ETSIIB
Diagonal 647
Barcelona 28, Spain

The ions Co^{2+} and Zn^{2+} form metal thiocyanate complexes which are readily extracted with organic solutions of long-chain amines. In nitrate medium the extraction of both metals with trilaurylamine (TLA) seems to proceed via the formation of species of the type $(TLAHSCN)_p(M^{2+})_q(SCN^-)_n$. In order to ascertain the composition of the species and their formation constants, experimental data in the form $\log D = f(|TLAH^+|_{tot})$ have been treated both graphically and numerically by means of the program LETAGROP-DISTR (1) The results of this calculation (Table I) indicate that polymerization equilibria of the TLAHSCN must be taken into account to fit the data.

EXPERIMENTAL

The extraction equilibria of Co(II) and Zn(II) at trace levels in the presence of SCN^- by the trilaurylammonium nitrate dissolved in benzene from an aqueous $(H^+,Na^+)NO_3^-$ solution of constant strength have been followed by measuring the distribution coefficient between two solutions S_1 and S_2 of general composition:

S_1 : $|Metal|_{tot} = B$ mol.dm^{-3}
$|HNO_3|_{tot} = 0.010$ mol.dm^{-3}
$|NaSCN|_{tot} = L$ mol.dm^{-3}
$|NaNO_3|_{tot} = A$ mol.dm^{-3}

$I = A+B+L+0.010$ mol.dm^{-3}

S_2 : $|TLAHNO_3|_{tot} = C$ mol.dm^{-3}

for Co(II), L= 0.050 mol.dm^{-3} and for Zn(II), L= 0.015 mol.dm^{-3}

Equal volume (10 cm^{-3}) of both phases were mixed and allowed to come to equilibrium (5 minutes). After centrifugation, aliquots from both phases were taken for metal concentration analysis. The metal in the organic phase was determined after stripping with H_2SO_4 2.0 mol.dm^{-3} (2). The Co(II) was analysed using UV spectrophotometry and the Zn(II) by atomic absortion spectrometry.

Preliminary experiments done in order to determine the influence of pH in the extration process indicate that the total amount of metal extracted is independent of the aqueous acidity in the range 1.1<pH<3.5, so that a pH around 2 was selected.

Log D was determined as a function of the total ammonium salt concentration keeping constant the aqueous acidity and the total concentration of metal, thiocyanate and nitrate ions. For each metal level, three ionic strengths 0.1, 1.0 and 3.0 mol.dm^{-3} were investigated. Experimental data are show in figures 1 and 2.

DATA TREATMENT

First of all, the competition between nitrate and thiocyanate for the trilaurylammonium cation must be taken into account. From the formation constants of the amine with nitric (3) and thiocyanic acid (4), the following reaction can be written:

(1) $TLAHNO_{3\,org} + SCN^- \rightleftharpoons TLAHSCN_{\,org} + NO_3^-$ log = 1.17

The extraction of both metals can be expressed by

(2) $q\,M^{2+} + p\,TLAHSCN_{\,org} + n\,SCN^- \rightleftharpoons (TLAHSCN)_p(M^{2+})_q(SCN^-)_{n\,org}$

As the ionic strength is constant in the aqueous phase and the maximum concentration of ammonium salt in the organic phase is 25 mmol.dm^{-3} (5), concentrations can be used instead of activities, so that the equilibrium constant for Equation (2) is

(3) $k_{pqn} = |(TLAHSCN)_p(M^{2+})_q(SCN^-)_n|\,|M^{2+}|^{-q}\,|SCN^-|^{-n}\,|TLAHSCN|^{-p}$

From the experimental results (see Figures 1 and 2) no polynuclear species containing metal in the organic phase can be concluded, so that q = 1. With this value and taken into account the electroneutrality condition for the extracted species (2q=n), the stoichiometry index n = 2 is obtained.

Using the mass balance equations for the metal in both phases

(4) $|M|_{org} = \Sigma\, k_{p12}|M^{2+}|\,|SCN^-|^2\,|TLAHSCN|^p$

(5) $|M|_{aq} = |M^{2+}| + \Sigma\beta_j|M^{2+}|\,|SCN^-|^j$

where β_j is the formation constant for the reaction

(6) $M^{2+} + j\,SCN^- \rightleftharpoons M(SCN)_j^{2-j}$

the distribution coefficient takes the form

(7) $$D = \frac{|M|_{org}}{|M|_{aq}} = \frac{\Sigma\, k_{p12}|SCN^-|^2\,|TLAHSCN|^p}{1 + \Sigma\beta_j|SCN^-|^j}$$

For each point a conditional distribution coefficient D' can be calculated so that

(8) $D' = \Sigma\, k_{p12}\, c^p$

where $c \equiv |TLAHSCN|$ and $D' = D|SCN^-|^2(1 + \Sigma\,\beta_j|SCN^-|^j)$

From Equation (8) a graphical treatment was done in which two-species model functions, constructed on the assumption of two-species containing metal in the organic phase, were compared with the experimental data. The results of this treatment seems to indicate the existence of a fixed species for which the ratio amine/metal is 2 and a second species for which the index p=4 (with I=3.0 mol.dm^{-3}) or 5 (with I=0.1 and 1.0 mol.dm^{-3}).

In a secons step LETAGROP-DISTR treatment was performed. Models with one, two and three species were tried. In the models with three species, always one of them was sistematically rejected (log k_{pqn} was set equal to zero). The numerical treatment confirmed the stoichiometries (2,1,2) and (5,1,2) for the I=0.1 and 1.0 mol.dm^{-3} data and the stoichiometries (2,1,2) and (4,1,2) for the I=3.0 mol.dm^{-3} ones. The residuals in log D are shown in Figure 3. As seen, no sistematic deviations can be observed.

The second species can be formulated as follows $(TLAHSCN)_2(M^{2+})(SCN^-)_2.|TLAHSCN|_{p-2}$. The difference in the number of TLAHSCN molecules solvated to the ion pair (2,1,2) as the ionic strength increases can be correlated with the decreasing in the formation of TLAHSCN (see Figure 4).

In Table I the values of the formation constants obtained with the LETAGROP-DISTR program are summarized.

REFERENCES

1. D.H. Liem, Acta Chem. Scand., 25, 152 (1971)

2. J.M. Madariaga, M. Aurrekoetxea and I. Katime, Chem. Scripta, in press.

3. M. Aguilar, Chem. Scripta, 9, 58 (1976)

4. J.A. Marco, H. Iturriaga and M. Aguilar, to be published

5. E. Högfeldt, Solvent Extraction Research (ed. A.S. Kertes and Y. Marcus), p.157, Willey, New York, (1969).

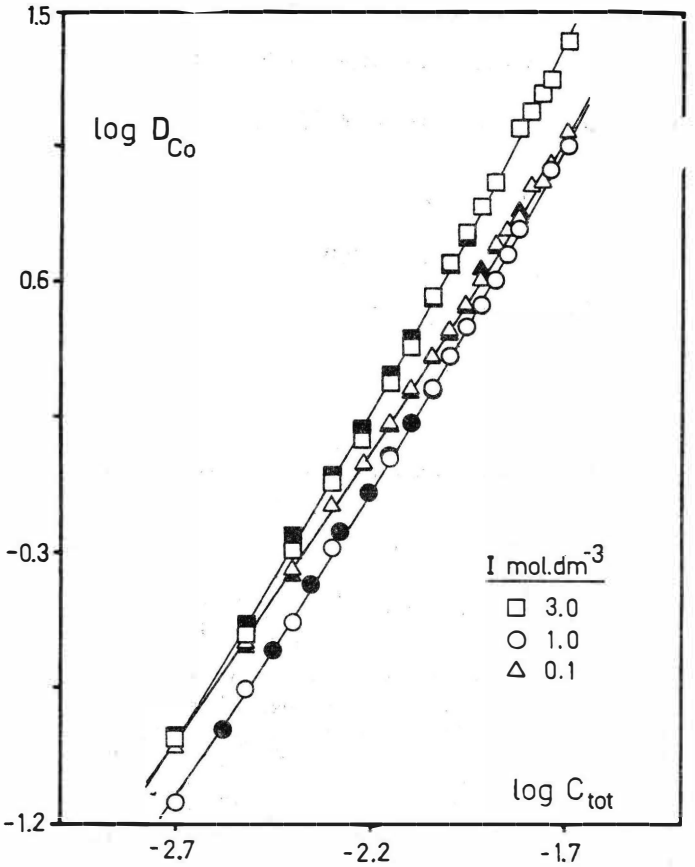

FIGURE 1 . Distribution coefficient for Co(II) as a function of the total ammonium salt concentration. The lines have been calculated using the constants given in TABLE I.

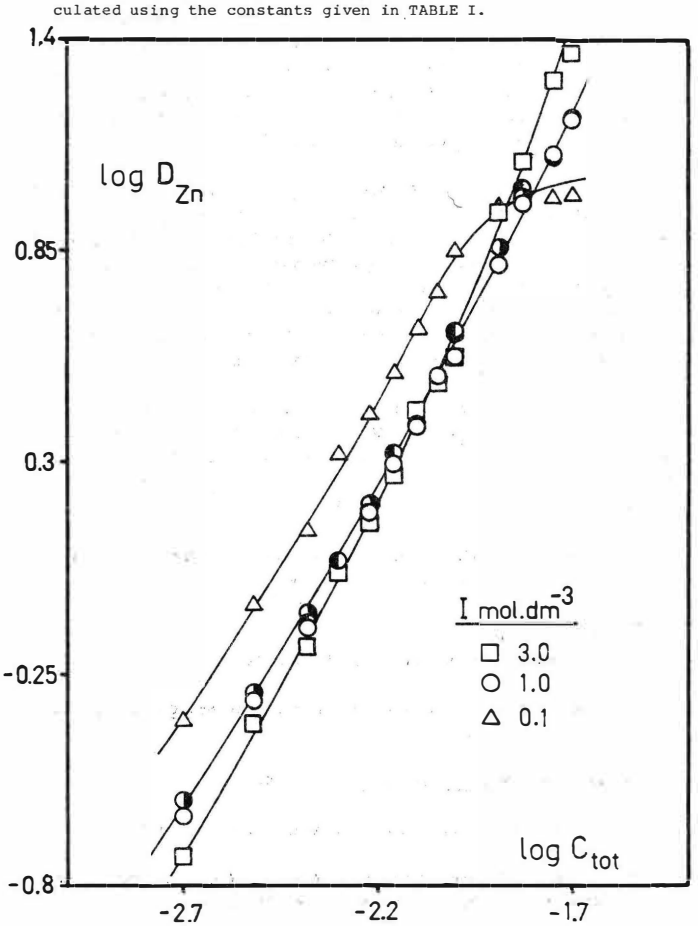

FIGURE 2 . Distribution coefficient for Zn(II) as a function of the total ammonium salt concentration. The lines have been calculated using the constants given in TABLE I.

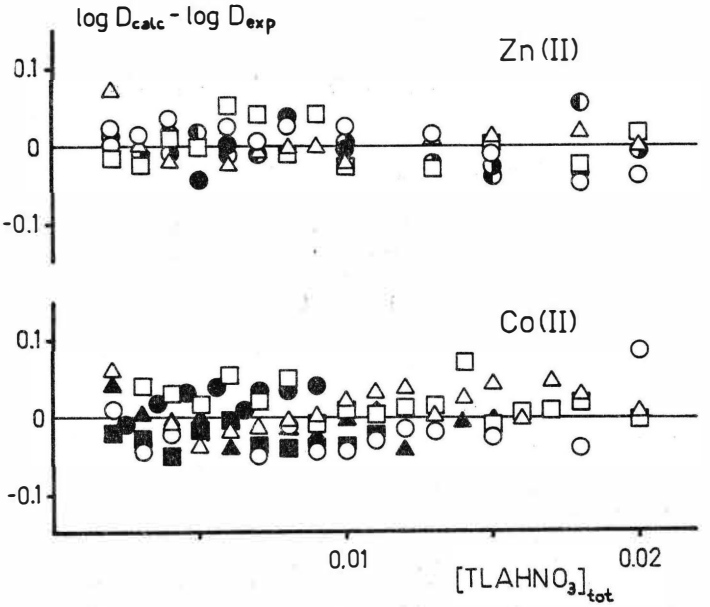

FIGURE 3 . The residuals in log D as a function of the total ammonium salt concentration.

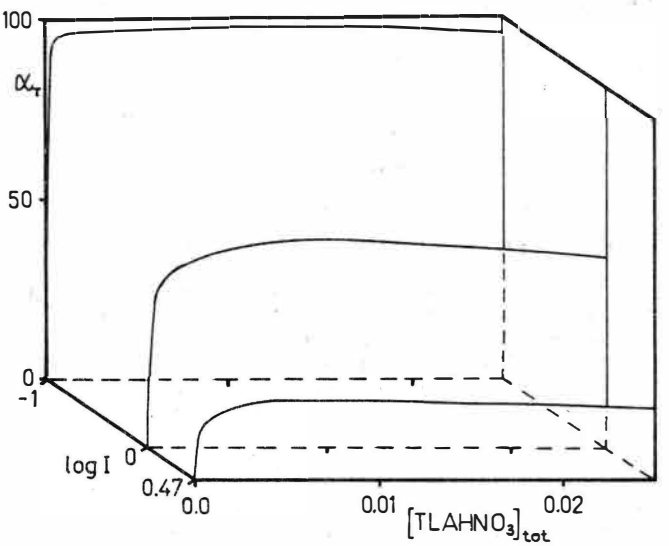

FIGURE 4.- $\alpha_T = (|TLAHSCN| + 2|(TLAHSCN)_2|)/|TLAHNO_3|_{tot}$ as a function of $|TLAHNO_3|_{tot}$ at different ionic strengths.

TABLE I. log k_{pqn} for metal-containing species in organic phase.

(p,q,n)	I = 0.1	I = 1.0	I = 3.0	metal
(2,1,2)	10.23 ± 0.06	10.46 ± 0.08	11.11 ± 0.11	
(4,1,2)	-	-	20.20 ± 0.05	Co(II)
(5,1,2)	21.16 ± 0.03	22.82 ± 0.08	-	
(2,1,2)	12.08 ± 0.19	12.97 ± 0.25	13.62max13.96	
(4,1,2)	-	-	24.80 ± 0.06	Zn(II)
(5,1,2)	25.19 ± 0.08	25.84max26.14	-	

EXTRACTION OF CADIUM(II) - CHLORIDE BY TRI-n-DODECYLAMMONIUM CHLORIDE DISSOLVED IN BENZENE

J. de Pablo and M. Aguilar and M. Valiente

Cátedra de Química I, E.T.S.E.I.B
Universitat Politecnica de Barcelona
Diagonal 647
Barcelona 28, Spain

Departamento de Química Analítica
Universitat Autonoma de Barcelona
Bellaterra, Spain

Introduction

The extraction of Cd(II)-chloride by tri-n-dodecylammonium chloride dissolved in benzene has been studied at different ionic strength following the distribution of the metal as a function of the total TLAHCl concentration.

The results treated both graphically by means of model functions as well by LETAGROP-DISTR. program, have been interpreted assuming the formation of different metal species in the organic phase.

In table 1 composition of the different complexes and their extraction constants are given.

The values of the extraction constants obtained at the different ionic strength have been correlated by using the specific ionic interaction theory. This treatment allows the determination of interaction coefficient of aqueous ions from extraction data. The results have been discussed.

Experimental

Distribution coefficient defined by $D = \frac{|Cd(II)|_{org}}{|Cd(II)|_{aq}}$ has been calculated after shaking equal volumes (15 cm^3) of the organic phase (20 to 100 10^{-3} mol dm^{-3} of TLAHCl dissolved in benzene) and the aqueous phase (Cl^- = 0.1,1.0,3.0 mol dm^{-3}; Cd(II) = 0.007 to 0.012 mol dm^{-3}).

When equilibrium was attained Cd(II) concentration in both phases was determined by EDTA titration using NET as indicator. Experiments were carried out at pH=2, which remained constant during the extraction process.

Results

The extraction equilibrium of Cd(II) can be described by:

$$(1) \quad q\,Cd^{+2} + 2q\,Cl^- + p\,TLAHCl \rightleftarrows (CdCl_2)q(TLAHCL)_p$$

Experiments at different Cd(II) concentration indicate the absence of polinuclear complexes in the organic phase, it means q=1.

Hence, at each ionic strength the equilibrium constant can be represented by:

$$(2) \quad K_{p1} = \frac{|CdCl_2(TLAHCl)_p|}{|Cd^{+2}|\,|Cl^-|^2\,|TLAHCl|^p}$$

Taking into account the mass balance equation in both phases and the aqueous cadmium chloride complexesthe following distribution coefficient can be written:

$$(3) \quad D = \Sigma\, K'_{p1}\, |TLAHCl|^p$$

Where K'_{p1} is the conditional extraction constant at each ionic strength.

On the other hand, the TLAHCl equilibrium concentration can be calculated by using the equation:

$$(4) \quad |TLAHCl|_{Tot} = |TLAHCl| + |(TLAHCl)_2| + p|Cd(II)|_{Tot,org}$$

As, equation (3) indicate, p was determined comparing experimental log D = f(TLAHCl)$_{Cl^-}$ with model functions of the type log D = f(u). From the graphical analysis p = 2 and 3, log K'_{p1} were determined. (See fig 1).

LETAGROP-DISTR. program confirm these results which are collected in table 1.

TABLE 1

Ionic strength	Complex	log K_{31}	log K_{21}
0.1 mol dm^{-3}	$CdCl_2(TLAHCl)_3$	10.84±0.08	
	$CdCl_2(TLAHCl)_2$		8.05 max 8.34
1.0 mol dm^{-3}	$CdCl_2(TLAHCl)_3$	11.28±0.17	
	$CdCl_2(TLAHCl)_2$		9.41±0.08
3.0 mol dm^{-3}	$CdCl_2(TLAHCl)_3$	11.59±0.24	
	$CdCl_2(TLAHCl)_2$		10.09±0.08

Correlation of the conditional extraction constants

The values given in table 1 for the different ionic strength have been correlated by using the specific ionic interaction theory. Two different extraction reactions have been considered in the treatment described below.

1.- The following expression is used to correlate the values of the constant K_{p1} at the different ionic strength.

$$(5) \quad \log K^0_{p1} = \log K^I_{p1} + \frac{6\,A\sqrt{I}}{1+1.5\sqrt{I}} + bI$$

where A=0.5109, I is the ionic strength in mol Kg^{-1} and b stands for the ionic interaction among the different ions in solution(1).

In our case:

$$(6) \quad b = \varepsilon_{Cd^{+2},Cl^-} + 2\,\varepsilon_{Na^+,Cl^-}$$

where ε is the ionic interaction coefficient.

Only Na^+ and Cl^- molality are considered against the other ions.

From log K^I_{p1} + 6R vs. I plot, b value for p = 2 and 3 have been obtained. Using expression (6) the interaction coefficient $\varepsilon_{Cd^{+2},Cl^-}$ has been determined. The ε_{Na^+,Cl^-} value has been taken from refence (3). The values obtained are collected in table 2. log K^0_{p1} at zero ionic strength are also given.

2.- Taking into account that long chain tertiary alkylammonium chlorides are anionic extractants. Equation (1) can be rewritten as follows:

$$(7) \quad CdCl_4^{-2} + 3\,TLAHCl \rightleftarrows CdCl_4(TLAH)_2TLAHCl + 2\,Cl^-$$

$$(8) \quad CdCl_4^{-2} + 2\,TLAHCl \rightleftarrows CdCl_4(TLAH)_2 + 2\,Cl^-$$

taking into account the aqueous cadmium chloro complexe constants ref. (2) and the activity coefficient of Cl^- and $CdCl_4^{-2}$the following expression can be considered:

$$(9) \quad \log K^0_{ep1} = \log K^I_{p1} - \log \beta_4 + 2\,R + bI$$

in this case:

$$(10) \quad b = \varepsilon_{CdCl_4^{-2},Na^+} - 2\,\varepsilon_{Cl^-,Na^+}$$

Figure 2 shows log K^I_{p1} - log β_4 + 6R vs I plot. Using expression (10) the interaction coefficient $\varepsilon_{CdCl_4^{-2},Na^+}$ has been determined, this value and the log K^0_{ep1} are collected in table 3.

Discussion

As it is reported in the literature for systems of the same ionic charge a correlation between the ionic radius and the ε values is obtained. A comparation of the values for different sys

tems included Cd^{+2},Cl^{-} has been made, the value reported here differ considerably.

On the other hand the interaction coefficient between $CdCl_4^{-2}$ and Na^+ calculated seems to be more consistent related to the above mentioned ionic radius.

Those considerations lead to a conclusion the known behaviour of TLAHCl as anionic extractant which involves the extraction reaction considered in equation (7) and (8).

A similar extraction reaction is given by other authors(4,5) who explain the extraction of Cu(II) from chloride media by long chain tertiary alkylammonium chloride in the same way.

TABLE 2

Ionic strength	$\log K_{31}^{I} + 6R$	$\log K_{31}^{0}$	b	$\varepsilon_{Cd^{2+}Cl^{-}}$
0.10054 mol Kg^{-1}	11.80			
1.0319 mol Kg^{-1}	12.51	11.78	0.55	0.49
3.3508 mol Kg^{-1}	13.70			

Ionic strength	$\log K_{21}^{I} + 6R$	$\log K_{21}^{0}$	b	$\varepsilon_{Cd^{+2}Cl^{-}}$
0.10054 mol Kg^{-1}	9.88			
1.0319 mol Kg^{-1}	10.63	9.80	0.55	0.49
3.3508 mol Kg^{-1}	11.94			

TABLE 3

Ionic strength	$\log K_{31}^{I} - \log \beta_4 + 2R$	$\log K_{e31}^{0}$	b
0.10054 mol Kg^{-1}	8.36		
1.0319 mol Kg^{-1}	9.32	8.30	0.59
3.3508 mol Kg^{-1}	10.18		

$$\varepsilon_{CdCl_4^{-2},Na^+} = 0.65$$

TABLE 3

Ionic strength	$\log K_{21}^{I} - \log \beta_4 + 2R$	$\log K_{e21}^{0}$	b
0.10054 mol Kg^{-1}	5.86		
1.0319 mol Kg^{-1}	7.08	5.79	0.59
3.3508 mol Kg^{-1}	8.45		

$$\varepsilon_{CdCl_4^{-2},Na^+} = 0.65$$

References

1. G. Scatchard, "Equilibrium in solution.Surface and Colloid Chemistry",Harvard University Press,Cambridge,Massachusetts (1976)
2. G. Biedermann,J. Lagrange & Ph. Lagrange, Chemica Scripta 5, 153 (1974)
3. L. Ciavatta, Annali di Chimica, Società Chimica Italiana, 550 (1980)
4. S. Lindenbaum & G.E. Boyd, J. Phys. Chem. 67, 1238 (1963)
5. T. Sato & K Adachi, J. Inorg. nucl. Chem. 31, 1395 (1969)

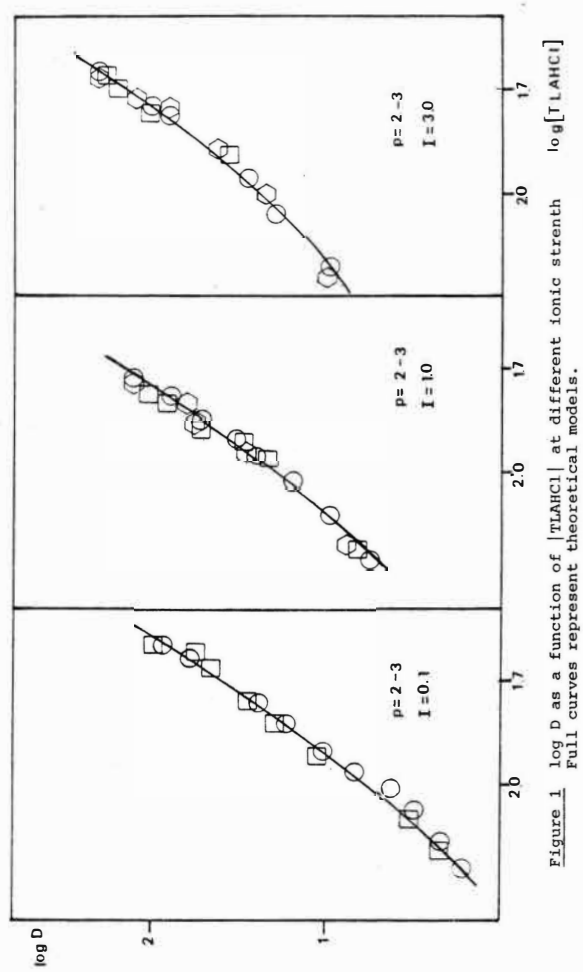

Figure 1 log D as a function of |TLAHCl| at different ionic strenth Full curves represent theoretical models.

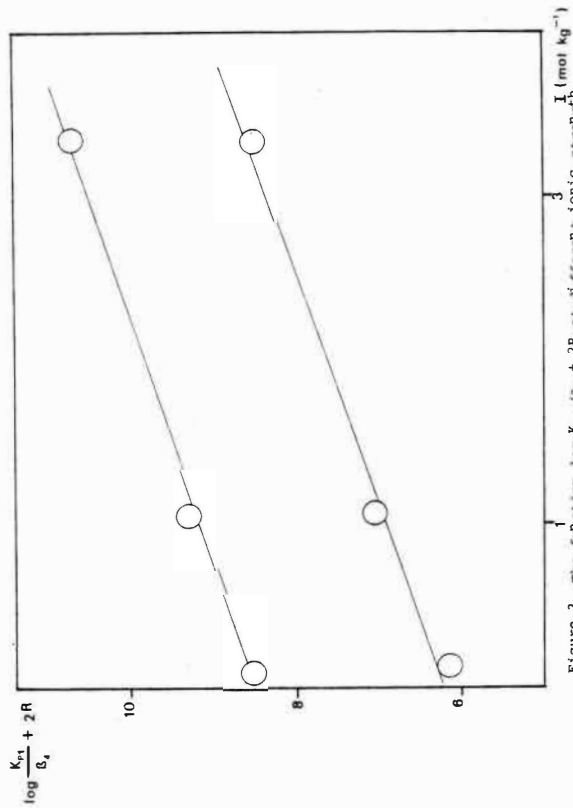

Figure 2 The function log K_{p1}/β_4 + 2R at different ionic strength

CONCISE QUANTITATIVE DESCRIPTION AND PREDICTION OF LARGE FILES OF ANION-EXCHANGE EXTRACTION CONSTANTS FOR VARIOUS ANIONS BY MEANS OF LINEAR FREE ENERGY EQUATIONS

V. S. Shmidt, E. A. Mezhov, K. A. Rybakov

Large files of anion-exchange extraction constants, K_x^y, are described by means of equations $\lg K_x^y = \varkappa(\Delta G_x^* - \Delta G_y^*)$, where ΔG^* - hydration parameters of exchanging anions, and $\varkappa$ is constant for each series of systems in which only the nature of exchanging anions is varying. ΔG^* - parameters are calculated on the basis of treating large files of anion-exchange extraction constants for various systems. The summary of ΔG^*-parameters is presented in table 1. The coefficient $\varkappa = 0.055$ when extractants are quaternary ammonium salts, and when diluent is a compound not posessing a strong ability for specific solvation of an extractant ("BP"-parameter $\geqslant -0.6$). In case of diluent anions posessing a strong ability for specific solvation of anions $\varkappa$ diminishes and is near to zero when alcohols are used as diluents.

Table 1

Hydration Parameters, ΔG^*, Calculated from the Extraction Data

Anion	$\frac{KDj}{g\text{-ion}}$	Anion	$\frac{KDj}{g\text{-ion}}$
1	2	1	2
OH^-	-377	BrO_3^-	-314
F^-	-364	4-OH-bensenesulphonate	-314
CH_3COO^-	-356	benzoate	-310
$C_2H_5COO^-$	-347	$C_6H_{13}COO^-$	-305
$HCOO^-$	-347	Br^-	-301
HCO_3^-	-347	$C_7H_{15}COO^-$	-297
$C_3H_7COO^-$	-339	$C_8H_{17}COO^-$	-289
IO_3^-	-335	NO_3^-	-289
Cl^-	-331	3-nitrobenzoate	-285
$C_4H_9COO^-$	-331	naphtoate	-285
HSO_4^-	-320	ClO_3^-	-285
$C_5H_{11}COO^-$	-318	benzenesulphonate	-280
4-nitrobenzoate	-280	goldanate	-247
p-C_3H_7O-benzoate	-280	$HgCl_3^-$	-247
$C_9H_{19}COO^-$	-272	naphtalenesulphonate	-243
p-C_4H_9O-benzoate	-272	ClO_4^-	-243
methylred-anion	-272	erdmannate	-239
2-OH-benzoate	-268	p-$C_7H_{15}O$-benzoate	-239
I^-	-268	$BiCl_4^-$	-239
3-nitrophenolate	-264	ReO_4^-	-239
SCN^-	-260	p-$C_8H_{17}O$-benzoate	-230
p-$C_5H_{11}O$-benzoate	-260	methylorange-anion	-230
4-nitrophenolate	-255	dinitrophenolate	-226
octanesulphate	-252	butylorange-anion	-226
4-(2-PAR)*	-251	$BiBr_4^-$	-205
TcO_4^-	-251	$HgBr_3^-$	-201
p-$C_6H_{13}O$-benzoate	-247	picrate	-188
3-nitrobenzenesulphonate	-247	HgI_3^-	-134
4-nitrobenzenesulphonate	-247	$AuCl_4^-$	-130
		$AuBr_4^-$	-100

*Anion of 4-(2-pyridyl-azo) rezorcinole.

PREDICTION OF DILUENT NATURE INFLUENCE ON PHYSICAL PARTITION BY MEANS OF BP*-PARAMETERS

V. S. Shmidt, K. A. Rybakov

It is shown that it is possible to describe partition constants, P_o, of extracted compounds on varying the solvent nature, by means of equations of the type $\lg P_o = \alpha + \beta BP^*$ (1), where α and β - are constant coefficients within each extraction series of systems, varying only by the solvent nature, BP* - are parameters (abreviated Russian "Влияние разбавителя" - diluent influence), characteristic for each solvent. BP*-scale is developed on the basis of treatment of large files of experimentally measured partition constants for varions systems. The summary of BP*-parameters is presented in table 1. Table 2 tabulates the coefficients α and β of equation (1) for the partition of various compounds which are used as extractants: phosphynoxides, sulphoxides, amine oxides, dialkylphosphoric acids, β-diketones and some chelates, along whith correlation coefficients, r, and average deviations, s.

Table 1

BP*-Parameters for Various Diluents

Diluent	BP*	Diluent	BP*
1	2	1	2
n-hexadecane	-1.1	butylbenzene	1.3
n-dodecane	-1.0	isobutylbenzene	1.4
n-decane	-1.0	trimethylbenzene	1.45
n-octane	-0.9	diethylbenzene	1.6
n-heptane	-0.6	p-xylene	1.7
n-hexane	-0.4	m-xylene	1.8
1	2	1	2
cyclohexane	0.5	ethylbenzene	1.8
dibutyl ether	0.8	o-xylene	1.9
trisethylbenzene	0.95	benzene	2.3
tetrachloroethylene	1.1	chlorobenzene	2.4
dodecane+6% octanol	2.3	bromoform	4.0
Iodbenzene	2.5	methylenechloride	4.0
bromobenzene	2.5	nitrotoluene	4.1
methylisobutylketone	2.5	nitrobenzene	4.3
1.2-dibromomethane	2.6	2-nitropropane	4.3
bromoethyl	2.7	chloroform	4.5
o-dichlorobensene	2.8		
1,2,4-trichlorobenzene	2.8	toluene	1.8
anisole	2.9	tetrachloromethane	1.4
octane+1% octanol	2.9		
1,2-dichloroethane	3.5		

Table 2

Coefficients of Equations of Type (1), Describing Partition of Various Compounds

Compound	α	β	r	s
1	2	3	4	5
tris-isoamylphosphine oxide	1.11	0.70	>0.99	0.05
tris-isooctylphosphine oxide	2.19	0.73	>0.99	0.12
triphenylphosphine oxide	0.66	0.75	>0.99	0.08
tributylphosphine oxide	-0.99	0.87	>0.99	0.11
diphenylsulphoxide	1.11	0.55	>0.99	0.06
diamylsulphoxide	0.82	0.60	0.99	0.14
dihexylsulphoxide	2.22	0.58	>0.99	0.09
2-nonylpyridine oxide	2.18	0.58	>0.99	0.09
trioctylamine oxide	3.34	0.45	>0.99	0.09
2-hexylchinoline oxide	2.21	0.52	>0.99	0.02
dibutylphosphoric acid	-1.73	0.49	0.99	0.16
1	2	3	4	5
diamylphosphoric acid	-0.17	0.42	>0.99	0.07
dihexylphosphoric acid	-0.90	0.45	0.95	0.24
dioctylphosphoric acid	4.18	0.28	0.93	0.17
acetylacetone	0.12	0.27	>0.99	0.04
benzoyl acetone	2.11	0.30	0.99	0.06
uranyl acetylacetonate	-1.06	0.61	>0.99	0.12
Zinc acetylacetonate	-1.13	0.49	>0.99	0.07
Copper acetylacetonate	-0.34	0.64	>0.99	0.08
beryllium acetylacetonate	0.80	0.61	0.99	0.13

THE THERMODYNAMICS OF THE EXTRACTION OF Eu(III) AND Am(III) WITH SYNERGISTIC MIXTURES OF THENOYLTRIFLUOROACETONE AND A LINEAR POLYETHER*

D. D. Ensor and A. H. Shah

Tennessee Technological University
Chemistry Department
Cookeville, Tennessee 38505 USA

and

Transuranium Research Laboratory
Oak Ridge National Laboratory
Oak Ridge, Tennessee 37830 USA

*Research sponsored by the Division of Chemical Sciences, Office of Basic Energy Sciences, U.S. Department of Energy, under contracts DE-AS05-79-ER10489 with TTU and W-7405-eng-26 with Union Carbide Corp.

The extractions of trivalent lanthanides and actinides by synergistic mixtures of thenoyltrifluoroacetone (HTTA) and a variety of neutral oxygen donors are well documented (1). The large increase in the extent of extraction of the metal ion into the organic phase is believed to occur by one of three possible mechanisms (2). The first involves the direct replacement of residual waters of hydration on the metal by the neutral donor. In the second proposed mechanism, the residual waters remain attached to the metal and the neutral oxygen donor hydrogen bond to the complex through the waters. The final mechanism assumes the complex is not hydrated and the addition of the neutral donor requires the metal to increase its coordination number. A recent review (3) of the synergistic effect showed that the proper interpretation of the mechanism requires the measurement of ΔH and ΔS for the reaction.

The synergistic capabilities of a linear polyether, 1,13-bis-[8-quinolyl]-1,4,7,10,13-pentaoxotridecane (K-5), in conbination with HTTA to extract Am(III) and Eu(III) have been recently reported (4). The presence of the K-5 in the organic phase not only increased the extraction of the trivalent metals, but also showed a preference for Am(III) over Eu(III). This result was surprising since most neutral donors do not alter the selectivity of HTTA. In an effort to better understand the synergistic mechanism of the K-5/HTTA system, the thermodynamic parameters have been measured by a temperature variation method.

EXPERIMENTAL

All reagents used in the study were analytical reagent grade. The K-5 (Krytofix 5) was supplied by PCR Research Chemicals Inc. and used without further purification. The HTTA was recrystalized from cyclohexane (mp 43°C) and stored away from light under vacuum. All organic solutions were prepared by dissolving weighted quantities of K-5 and HTTA in chloroform. The aqueous phase contained 0.5 M $NaNO_3$ and 0.01 M acetate buffer. The pH was defined as -log [H^+] using a 1.00 X 10^{-3} M HCl + 0.5 M $NaNO_3$ (pH = 3.00) solution as a standard.

The radioisotopes used were 241-Am(III) and 152-Eu(III). These isotopes were supplied by Oak Ridge National Laboratory and their radioactive purity was checked by alpha or gamma spectrometry. The isotopes were assayed using an automated NaI(Tl) well counter.

The distribution, D, of the metal ion was measured by placing equal volumes of aqueous and organic phases in a culture tube, spiking with the desired isotope, and mixing on a rotating paddle for 8-10 hours in a constant temperature bath (10°-35°C). After equilibration the phases were separated, the pH of the aqueous phase measured, and the D_{EXP} calculated by determining the ratio of the metal activity in the organic phase to the metal activity in the aqueous phase. The distribution values were reproducible to <2%.

DATA TREATMENT

The extraction system can be represented by the following equations:

(1) $$M^{+3}aq + X\ HTTA\ org \xrightleftharpoons{K_{TTA}} M(TTA)_x\ org + X\ H^+aq$$

(2) $$M^{+3}aq + X\ HTTA\ org + K\text{-}5\ org \xrightleftharpoons{K_{SYN}} M(TTA)_x{\cdot}K\text{-}5 + X\ H^+aq$$

(3) $$M(TTA)_x\ org + K\text{-}5\ org \xrightleftharpoons{\beta_{ORG}} M(TTA)_x{\cdot}K\text{-}5$$

The experimentally measured distribution of the metal ion was corrected for the presence of metal acetate complexes in the aqueous phase using equation (4).

(4) $$D = \frac{[M\ org]}{[M(III)aq]} = D_{EXP}\ (1 + \beta_{acetate}\ [CH_3CO^-])$$

The stability constants used were taken from reference (5).

The concentration quotients for K_{TTA} and K_{SYN} were defined by the following equations:

(5) $$K_{TTA} = \frac{[M(TTA)_x\ org][H^+aq]^x}{[M(III)aq][HTTA\ org]^x}$$

(6) $$K_{SYN} = \frac{[M(TTA)_x{\cdot}K\text{-}5\ org][H^+aq]^x}{[M(III)aq][HTTA\ org]^x[K\text{-}5\ org]}$$

The organic phase stability quotient, β_{K-5} was expressed as:

(7) $$\beta_{K-5} = \frac{[M(TTA)_x{\cdot}K\text{-}5\ org]}{[M(TTA)_x org][K\text{-}5\ org]}$$

This treatment is consistent with the analysis of synergistic equilibrium by Sekine and Hasagowa (1).

RESULTS AND DISCUSSION

Previous studies of K-5 have shown it to have no extraction capabilities under the present experimental conditions; therefore, the synergistic factor for the HTTA/K-5 system is equal to Log D_{SYN}/D_{TTA}. Figure 1 shows the effect of the addition of K-5 to the organic phase. The magnitude of the effect is much greater for Am(III) than for Eu(III).

The concentration quotients for the equations 1, 2, and 3 can be obtained by graphical evaluation of D_{SYN} as a function of [K-5]. Table I contains the results for both Am(III) and Eu(III). The magnitude of Log β_{K-5} is greater for Am(III) which accounts for the greater synergistic effect.

The temperature variation over the range 10-35°C for reaction 2 has been measured. The ΔH and ΔS for each of the reactions have been calculated using plots of log K and log β_{K-5} vs. 1/T. Figure 2 shows the temperature variation data for equation (3). Table 2 contains the thermodynamic parameters for equations (1) and (3). Values for the identical reactions with the neutral donor tributylphosphate (TBP) are included for comparison purposes.

The values for the formation of the $Eu(TTA)_3$ chelate are in good agreement with previous data (6) considering the differences in ionic strength and organic solvent. The large negative ΔH observed for the formation of $M(TTA)_3{\cdot}K\text{-}5$ is also comparable to the values observed for formation of similar complexes of TBP and TOPO. This supports the mechanism for synergism in which the coordination number of the metal is increased. A negative entropy change such as observed for Eu is consistent with this interpretation. The data for Am(III) shows a negative ΔH but a positive ΔS. This observation is not unexpected based on earlier data on complexation reactions of lanthanides and actinides (5) in aqueous solution with the magnitude of ΔS possibly explained by additional dehydration of the actinide metal ion.

TABLE I. Concentration Quotients at 25°C

	Log K_{TTA}	Log K_{SYN}	Log β_{K-5}
Eu(III)	-7.63 ± .02	-4.01	3.62 ± .01
Am(III)	-8.00 ± .02	-3.88	4.10 ± .01

TABLE 2. Thermodynamic Parameters at 25°C

	ΔG($kJ{\cdot}m^{-1}$)	ΔH($kJ{\cdot}m^{-1}$)	ΔS($J{\cdot}m^{-1}{\cdot}K^{-1}$)	Reference
	$M^{+3}aq + 3\ HTTA\ org \rightleftharpoons M(TTA)_3\ org + 3\ H^+aq$			
Eu(III)	43.5 ± 0.1	+37 ± 3	-20 ± 3	Present work
	41.47	+40.3	-4	6
Am(III)	45.6 ± 0.1	+24 ± 2	-72 ± 10	Present work
	$M(TTA)_3\ org + S\ org \rightleftharpoons M(TTA){\cdot}S\ org$			
		S=K5		
Eu(III)	-20.6 ± 0.1	-40 ± 4	-65 ± 10	Present work
Am(III)	-23.4 ± 0.1	-17 ± 2	+20 ± 5	Present work
		S=TBP		
Eu(III)	-24.7	-24	+3	7

ACKNOWLEDGEMENTS

Research sponsored by the Division of Chemical Sciences, Office of Basic Energy Sciences, U. S. Department of Energy, under contracts DE-AS05-79ER10489 with TTU and W-7405-eng-26 with Union Carbide Corp.

REFERENCES

1. T. Sekine and Y. Hasegawa, "Solvent Extraction Chemistry", Marcel Dekker Inc., New York, 1977, p. 411.

2. Y. Marcus and A. S. Kertes, "Ion Exchange and Solvent Extraction of Metal Complexes", Wiley-Interscience, New York, 1969, p. 818.

3. G. R. Choppin, Sep. Sci. and Tech., 16, 1113 (1981).

4. D. D. Ensor and A. H. Shah, Solvent Extraction and Ion Exchange, to be published.

5. G. R. Choppin and J. K. Schneider, J. Inorg. Nucl. Chem., 32, 3283 (1970).

6. A. T. Kandil and K. Farah, J. Inorg. Nucl. Chem., 42, 1491 (1980).

7. J. N. Mathur, S. A. Pai, P. K. Khopkar and M. S. Subramanian, J. Inorg. Nucl. Chem., 39, 653 (1977).

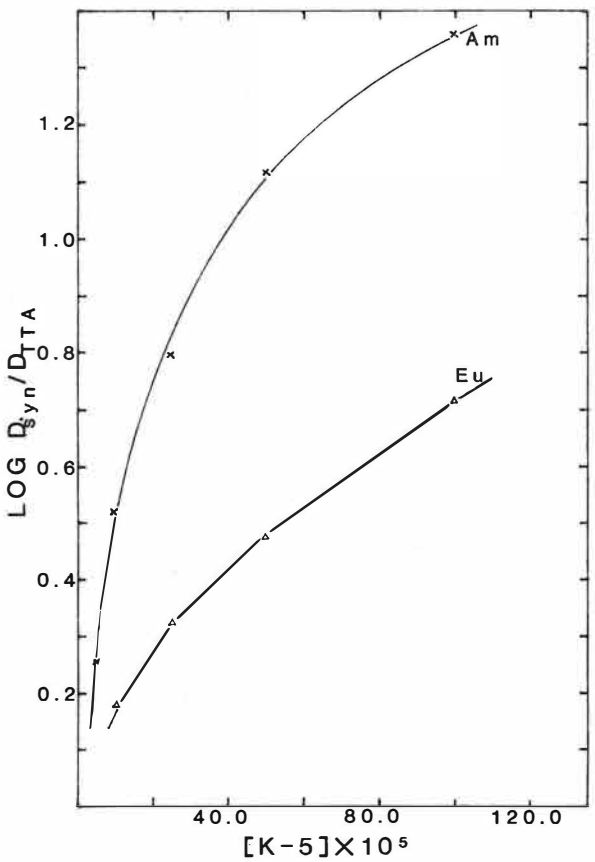

Figure 1. The variation of the synergestic factor as a function of [K-5]

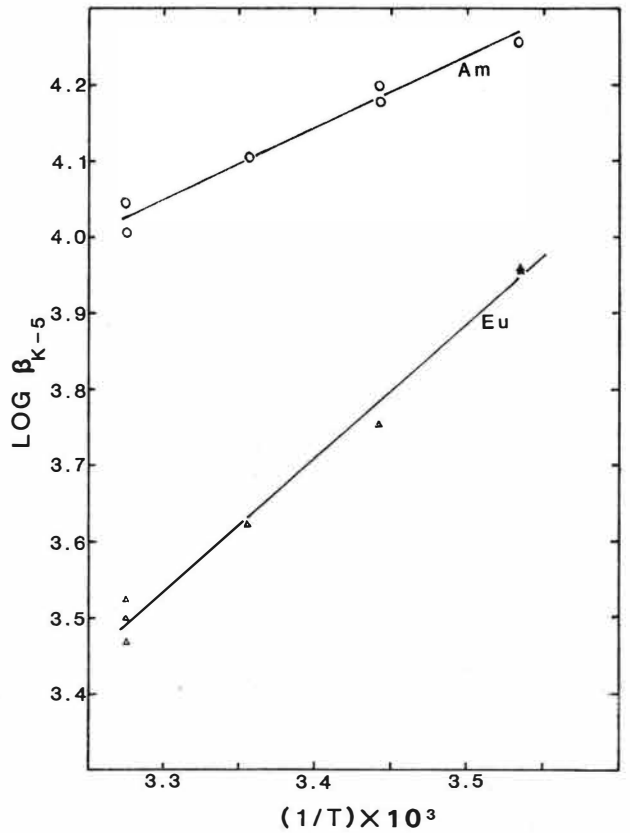

Figure 2. Temperature variation of log β_{K-5}

QUANTITATIVE TREATMENTS OF DISTRIBUTION EQUILIBRIA IN EXTRACTION METAL SALTS BY ALCOHOL

G. Yagodin, B. Sergievsky, O. Kunelskaya

Mendeleev Insitute of Chemical Technology
A-47, Miusskaya sq., 9
Moscow, USSR

The alcohols are used in extraction of inorganic salts from aqueous salutions. As a rule the extracted substances pass to the organic phase in the form of undissociated hydrated complexes. The distribution of the salts can be described by the equation:

$$(1)\quad K_{1,\nu} = \frac{\bar{m}\bar{\gamma}}{Q\, m^{\nu}\gamma_{\pm}^{\nu}} = \tilde{K}_{1,\nu}\bar{\gamma}$$

where $\bar{m}$ and m are the molal concentration of the salt in organic and aqueous phases, $Q = \nu_+^{\nu_+}\nu_-^{\nu_-}$, $\nu = \nu_+ + \nu_-$ is the mole number of ions in one mole of electrolyte, $K_{1,\nu}$ and $\tilde{K}_{1,\nu}$ are the thermodynamic and effective partition constants, $\gamma_{\pm}$ is the mean activity coefficient and $\bar{\gamma}$ is the activity coefficient of undissociated salt in the extract. Functional dependences of $\bar{\gamma}$ on the salt concentration are not known and this fact complicates the calculation of $K_{1,\nu}$ values. That is why we shall use the following equation for the calculation of the activity coefficients of salts in the alcohol-water mixtures (1,2):

$$(2)\quad \bar{\gamma} = \bar{\gamma}_0 \exp[h_{1,\nu}(1-a_w)]$$

where $\bar{\gamma}_0$ are the activity coefficients of salt in dry alcohol which are considered to be equal to one, $h_{1,\nu}$ is the degree of salt hydration at $a_w = 1$, and a_w is the water activity.

By introducing (2) in (1) we have

$$(3)\quad K_{1,\nu} = \tilde{K}_{1,\nu} \exp[h_{1,\nu}(1-a_w)]$$

Therefore the scope of $\ln \tilde{K}_{1,\nu}$ plots as function of a_w-1 are $h_{1,\nu}$. This kind of functions is realized when one describes the available data (3-8) for the metal nitrates extraction by alcohols. The parameters of the equation (3) and the correlation coefficients (r) for the systems of water-metal and nitrate-alcohol are obtained by the least-square technique and they are presented in Table I. The adequancy of $h_{1,\nu}$ values obtained by the equation (3) to the composition of organic phase is verified with help of the unequality:

$$(4)\quad \bar{m}_w > h_{1,\nu} a_w \bar{m}$$

where $\bar{m}_w$ is water solubility in the organic phase. The unequality (4) is realized in all cases for the systems under consideration. Thus, during the extraction of examined metal nitrates the undissociated nonstoichiometric hydratosolvates are formed. The $h_{1,\nu}$ values increase when molecular mass of the alcohole reduce, that corresponds with the data of water distribution. The partition constants increase when the degree of salt hydration grows and the radius of cation reduces. They linearly correlate with water solubilities in pure alcohols.

If the salt is partially dissociated in the extract the equation for the distribution isotherm is:

$$(5)\quad \bar{m} = \sum_1^{\bar{\nu}} \bar{m}_{\bar{\nu}} = \sum_1^{\bar{\nu}} \left\{ Q\,\bar{Q}^{-1} K_{\bar{\nu},\nu}\, m^{\nu}\gamma_{\pm}^{\nu} \exp[\bar{\nu}\, h_{\bar{\nu},\nu}(a_w-1)] \right\}^{1/\bar{\nu}}$$

where $\bar{Q} = \bar{\nu}_+^{\bar{\nu}_+}\bar{\nu}_-^{\bar{\nu}_-}$, $\bar{\nu} = \bar{\nu}_+ + \bar{\nu}_-$ is the mole number of ions in one mole of dissociated electrolyte in the organic phase (it is suppoused that in the absence of dissociation $\bar{\nu} = 1$), $K_{\bar{\nu},\nu}$ is the thermodynamic partition constant, $h_{\bar{\nu},\nu}$ is the hydration degree of ions, $\bar{m}_{\bar{\nu}}$ is the concentration of salt dissociated into $\bar{\nu}$ ions.

According to equation (5) the plots of $\ln \tilde{K}_{\bar{\nu},\nu}$ as a function of a_w-I are nonlinear. The estimation of the parameters of equation (5) is realized by the computer taking into consideration the equations of material balance and the unequality:

$$(6)\quad \bar{m}_w > \sum_1^{\bar{\nu}} h_{\bar{\nu},\nu} a_w \bar{m}_{\bar{\nu}}$$

The analysis of equation (5) and the resulte of mathematical modelling show that the distribution isotherms may have different forms. In particular under high values of $h_{\bar{\nu},\nu}$ and alterations of the water activity extremes may be found on the distribution isotherms (Figure I). Almost all types of the computed distribution isotherms have been obtained experimentally (9) for the sodium chlorid-aliphatic alcohol extraction systems (Figure 2).

The curves of $\ln \tilde{K}_{1,2} = f(a_w)$ for these systems are similar (Figure 3) irrespective of the form of distribution isotherms. An adequate description of the equilibrium is obtained by using of the parameters of equation (5) given in Table 2. Therefore the "anomalous" forms of the distribution isotherms may be explained by the salt hydration decreasing due to the water activity reducing and the ion association growth.

Let us compare the data for the hydration of salts obtained by various methods: the hydration numbers of some electrolyte in iso-amyl alcohol (h), determined by Yates method (10,11), the hydration numbers of same electrolyte in aqueous solution (n_w) and the degree of hydration according to the equations (3,5). The values of h are smaller than of n_w (Table 3). It is concluded from these data (10), that during the extraction of lithium salts the substitution of 4-5 molecules of water in the hydrate shell by the same quantity of alcohol molecules takes place. In our opinion the values $h_{1,\nu}$ better reflect the salt hydration in the extracts than h. The values $h_{1,\nu}$ are close to n_w and one may conclude that the salts of alkaline and alkaline-earth metals are extracted by isoamyl alcohol together with the hydrate shell and solvated by the alcohol molecules only in the secondary shell. The water molecules are replaced by the alcohol molecules on the decrease of the water activity. Thus the nonideality of the organic phases during the extraction by alcohol is explained mainly by the nonstoichiometric hydration and the ion association.

REFRENCES.

1. A. Chekmarev, A. Ochkin, V. Sergievsky, V. Tarasov, G. Yagodin. Proc. Int. Solv. Extr. Conf., v.2, Paper 80-158 (1980)
2. G. Yagodin et al. Osnovy zhidkostoy ekstrakcii, Moscow, Khimiya (1981)
3. C. Templeton, L. Daly. J. Amer. Chem. Soc., 73 3983 (1951)
4. C. Templeton. J. Phys. Colloid Chem. 54 1255 (1950)
5. W. McManamey. J. Appl. Chem. II 44 (1961)
6. W. McManamey. J. Phys. Chem. 65 1033 (1961)
7. C. Templeton, L. Daly. J. Phys. Chem. 56 215 (1952)
8. V. Sergievsky. Radiokhimiya 19 302 (1977)
9. R. De Santis, L. Marrelli, P. Muscetta. Chem. Eng. II 207 (1976)
10. A. Rozen, A. Mikhailichenko. Zh. Neorg. Khim. 12 729 (1967)
11. T. Kazas, K. Krasnov. Zh. Neorg. Khim. 19 1375 (1974)
12. R.S. Robinson, R.A. Stokes. Electrolyte Solutions. London, Butterworth (1965)

TABLE 1

PARAMETERS OBTAINED FROM EQUATION (3) FOR THE METAL NITRATE - ALCOHOL SYSTEMS

SALT	$-\ln K_{1,\nu}$	$h_{1,\nu}$	r
	n.butyl alcohol		
$Cu(NO_3)_2$	0,62	16,4	0,994
$Co(NO_3)_2$	0,48	20,2	0,994
$Zn(NO_3)_2$	0,71	20,1	0,990
	amyl alcohol		
$Cu(NO_3)_2$	3,06	12,8	0,999
$Co(NO_3)_2$	3,90	13,0	0,998
$Zn(NO_3)_2$	3,61	15,4	0,994
	n.hexyl alcohol		
$Mg(NO_3)_2$	4,49	15,3	0,952
$Ca(NO_3)_2$	6,97	4,1	0,891
$Zn(NO_3)_2$	4,78	13,4	0,997
$Co(NO_3)_2$	4,17	13,8	0,998
$Al(NO_3)_2$	-0,43	25,0	0,998
	n.octyl alcohol		
$Ca(NO_3)_2$	7,23	0	-
$Co(NO_3)_2$	5,36	11,7	0,999
$Zn(NO_3)_2$	6,97	3,3	0,994

TABLE 2

PARAMETERS OBTAINED FROM EQUATION (5) FOR THE NaCl - ALCOHOL SYSTEMS

ALCOHOL	$\ln K_{2,2}$	$h_{2,2}$	$-\ln K_{1,2}$	$h_{1,1}$	Average relative deviation %
n.propanol	1,76	27,2	2,90	10,2	3,5
isopropanol	11,75	55,4	0,41	17,6	3,6
n. butanol	-6,47	26,5	3,82	13,9	2,7
isobutanol	-7,72	27,4	3,69	15,8	3,6
secbutanol	-4,13	42,3	3,31	18,7	2,0
tertbutanol	3,14	50,5	2,00	20,1	2,7

TABLE 3

HYDRATION OF SOME SALTS IN ISOAMYL ALCOHOL AND WATER

SALT	h	$h_{1,\nu}$	n_w
LiCl	1 (10)	7,2	6,5
LiBr	2 (10)	8,3	7,1
LiI	5 (10)	10,5	10,0
$CaCl_2$	5 (11)	14,9	12,0
$CaBr_2$	6 (11)	14,8	14,6
CaI_2	16 (11)	21,2	17,0

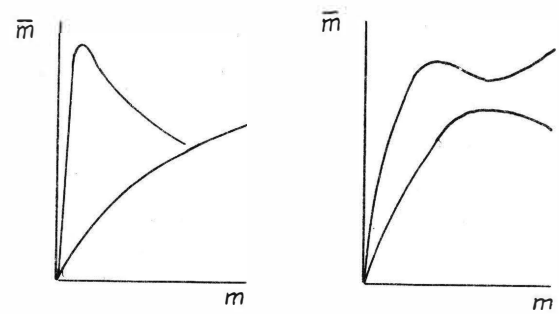

Figure 1. DISTRIBUTION ISOTHERMS OF SALTS CALCULATED BY EQUATION (5)

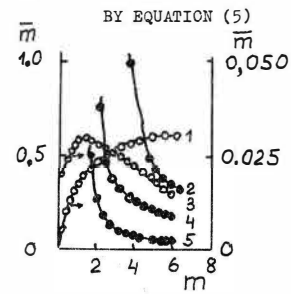

Figure 2.

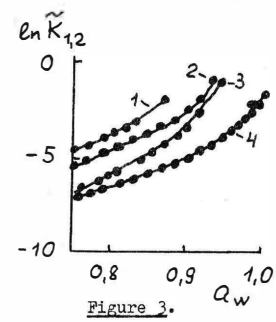

Figure 3.

Figure 2. DISTRIBUTION ISOTHERMS OF NaCl IN n.BUTYL-(1), ISOPROPYL-(2), SEC.-BUTYL-(3), n-PROPYL-(4) AND TERT.-BUTYL-(5) ALCOHOL FROM REFERENCE (9)

Figure 3. PLOTS OF LN $K_{1,2}$ AS A FUNCTION OF a_w - I IN THE EXTRACTION OF NaCl BY ISOPROPYL-(1), n-PROPYL-(2), TERT-BUTYL-(3) AND n-BUTYL-(4) ALCOHOLS

EXTRACTIVE BIOCONVERSIONS

Hydrolysis of starch in an aqueous two phase system

Ronald Wennersten — Dept. of Chemical Engineering

Folke Tjerneld — Department of Biochemistry

Mats Larsson and Bo Mattiasson — Dept. of Pure & Appl. Biochemistry

Chemical Center, University of Lund
P.O. Box 740
S-220 07 Lund, Sweden

ENZYMATIC HYDROLYSIS OF STARCH TO GLUCOSE.

The hydrolysis of starch-containing material to fermentable sugars traditionally includes a cooking step at 130 - 150°C. In this highly energy intensive step the starch is gelatinized (dissolved) and partly hydrolyzed by α-amylase. The α-amylase is not stable at this temperature and therefore the solution is cooled to 80-90°C and more α-amylase is added. Holding time in this step is 15-30 min. The result of this treatment is a mixture of dissolved dextrins, which are oligosaccharides composed of glucose monomeres. In order to make a glucose syrup from the dextrins the solution is cooled to 55°C and a second enzyme, glucoamylase, is added to break down the dextrins completely to glucose. In this conventional process the enzymes are not reused.

In the conversion studied here we used starch from waxy maize (5). It is also possible to use starch from wheat. The enzymes used for hydrolysis were Termamyl and SAN 150, both generous gifts from NOVO A/S, Bagsvaerd, Denmark. Termamyl is a heat stable α-amylase produced by a strain of Bacillus licheniformis. SAN 150 is a glucoamylase prepared by cultivation of Aspergillus niger. As can be seen in Figure 2 a mixture of the two enzymes is more efficient for converting starch polymers into glucose than either of the two enzymes separately.
The bioconversion chosen for these experiments is one of the established enzyme reactions run on a large scale industrially; enzymatic conversion of starch to glucose.

AQUEOUS TWO-PHASE SYSTEMS

Aqueous two-phase systems are obtained when mixing aqueous solutions of two different polymers (e.g. poly(ethylene glycol) and dextran). The two phases both have a high water content and are compatible with particles and macromolecules of biological origin. Aqueous two-phase systems are characterized by an extremely low interfacial tension. The partition of particles and macromolecules in aqueous two-phase systems can be strongly influenced by the pH, the ionic composition, the choice of polymers and the polymer concentrations (2). Water-soluble low-molecular weight compounds are usually distributed more or less evenly between the two phases whereas macromolecules and particles are normally mainly partitioned to one or the other of the two phases and in some cases to the interface between them.

Aqueous two-phase systems can be constructed so that particles and macromolecules are partitioned to the bottom phase. In this way it is possible to combine biological conversion of a substrate by enzymes or microorganisms in the bottom phase with the removal of the product to the top phase. Because of low interfacial tension very little agitation is needed to create a fine emulsion which facilitates mass transfer. On the other hand separation times will be longer.

We have used the phase system consisting of crude dextran (a generous gift from Sorigona AB, Staffanstorp, Sweden) and poly(ethylene glycol) (PEG) with average mol. wt. of 15000 - 20000 from Union Carbide, N.Y. USA. The experimental binodial and tie lines of this system are shown in Figure 1.

Biotechnological processes are in general run at low concentrations of reactants as compared to what is normal in, for example, organic synthesis. This gives diluted product streams. Lack of efficient and cheap ways to increase product concentration is one of the main problems in biotechnology today. It would be advantageous to enrich the products from dilute product stream in a solvent extraction step and thus the need for extractive processes is great.
Furthermore, most biocatalysts are characterized by being sensitive to product inhibition. The reaction may stop when only a small fraction of the substrate has been converted into product. In such cases there is a strong need for continuous extractive procedures. The integration of bioconversion and extraction is called extractive bioconversion.

In biotechnology, extraction with organic solvents is useful only in a few specific cases because in most situations such a treatment is detrimental to the biomolecules. When biological macromolecules are present they require very gentle extraction systems so that their native conformation are not destroyed. The large differences in surface tension and dielectric constants between water and organic solvents inevitably cause biomolecules to unfold when they are exposed to the interface between the two solvents. Thus, extraction systems for biotechnological applications must be much gentler. Aqueous two-phase systems seem to fulfill most of the basic requirements (1).
A semi-continuous test was carried out in which starch was hydrolyzed according to the experimental set-up shown in Figure 3. The phase system used consisted of 5% crude dextran, 3% poly(ethylene glycol) and 0.02% azide (to prevent microbial growth) in 50mM acetate buffer pH 5.0 containing 50 mg $CaCl_2 \cdot 2H_2O$ per liter. In this phase system the starch particles are completely partitioned to the dextran-rich bottom phase. The enzymes, which are adsorbed to the starch particles(i.e. the substrate), are thus also partitioned to the bottom phase. Glucose produced was partitioned equally between the PEG-rich top phase and the dextran-rich bottom phase. The top phase was continuously removed and replaced with fresh top phase. In this system the enzymes can be used again and again in contrast to the conventional method where the enzymes can only be used once. Starch (not gelatinized) was added discontinuously to the bottom phase in a separate vessel which was held at 50°C. The bottom phase was then fed using a peristaltic pump to a mixer-settler unit with a hold-up volume of 15 liters. The total volume of the system was 22 liters. In the mixer the bottom phase was mixed with top phase using a flat blade turbine. The emulsion separated in the settler, which had an inclined bottom to avoid starch accumulation. From the settler both phases were recirculated to the mixer via external vessels. The ratio between the volumes of the two phases was 1:1. The flow of the top phase out of the system was 0.24 L/h and the flow rate of each recirculated phase in the system was 2.1 L/h. The temperature in the mixer-settler was held at 37°C. The initial intention was to add starch through a screw feeder which was controlled by a spectrophotometer equipped with a flow-cell measuring the O.D. at 600 nm. However, the screw had a tendency to plug because of evaporation from the vessel where the starch was added.
Twenty grams of each of the enzyme preparations and 3,0 kg of starch were added at the beginning of the experiment.
The sugar concentration was allowed to increase in the top phase to approximately 150g/liter. Then the top phase was continuously withdrawn and replaced with fresh top phase (5% PEG 20.000, 0.2% crude dextran and 0,05% azide in a 50 mM acetate buffer pH 5.0) using a peristaltic pump. Starch was added and the concentration of reduced sugars was measured (using the DNS -method with glucose as a standard (3) (Fig. 4)

RESULTS AND DISCUSSION

The experiments discussed here clearly demonstrate that enzymatic degradation can efficiently be run on ungelatinized starch even at the moderate temperature of 37°C. The continuous extraction of the formed glucose by the top phase, which was removed from the system, gives a net transfer of glucose from the site of production in the bottom phase. Furthermore, by recirculating the bottom phase it was also possible to recirculate the enzymes efficiently, and only minor decreases in the activity were observed over the 80 hrs the experiment was run (Fig. 4). The starch conversion was approximately 90 % when the experiment was terminated.

The concentration of glucose in the top phase was kept at a high level during the experiment and is sufficient for most purposes such as fermentation to alcohols. Furthermore, at concentrations above 150-200 g/L it may be difficult to keep microorganisms actively growing.

A problem that has often been discussed but tested very little experimentally is that of separation of the product in the top phase from the phase constituents. In this case it can be done, either by fermenting it *in situ* followed by separation of the fermentation products, or with ultrafiltration using a membrane capable of retaining the high molecular weight PEG-molecules but allowing the small glucose molecules to pass trough. Work on this line is in progress.
If the product is charged, an ion exchange chromatographic step could be sufficient for isolation. Several methods to precipitate the polymer are also at hand.
It should be pointed out that these phase systems are rather cheap. The phase constituent have been selected for technical applications in large scale and are thus not of the highest qualities. PEG costs less than $2 per kg and crude dextran approximately $6/kg.
The price per liter of the phase system is then only 0.36$.
Aqueous two-phase systems have earlier been applied in biotechnological processes (4,5) but only at a very small scale.

ACKNOWLEDGEMENTS

This project was supported by the National Swedish Board for Technical Development.

References

1. B. Mattiasson, Trends in Biotechnology, in press
2. P.-Å. Albertsson, Partition of Cell Particles and Macromolecules, Wiley, New York, 1971.
3. G.L. Miller, Anal. Chem. 31, 426 (1959)
4. B. Mattiasson and B. Hahn-Hägerdal in "Immobilized Cells and Organelles" ed. B. Mattiasson. CRC-Press. Boca Raton FL, USA. in press.
5. B. Mattiasson, M. Larsson, B, Svensson, B. Hahn-Hägerdal, Conversion of Starch in an Aqueous Two-phase System (submitted).

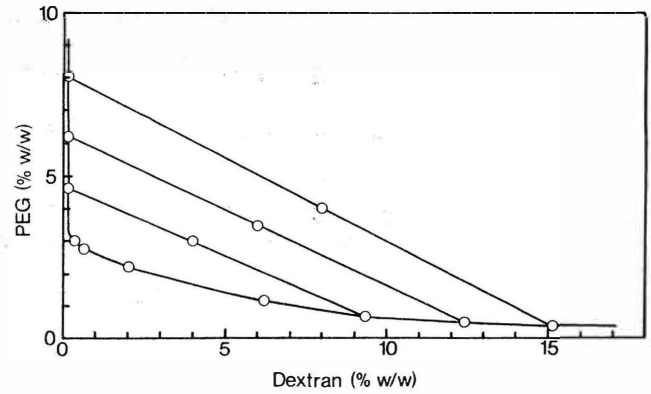

Fig. 1.
Phase diagram of the system crude dextran - poly(ethylene glycol) (PEG 20.000) - water at 20°C. Experimental binodial and tie lines (2).

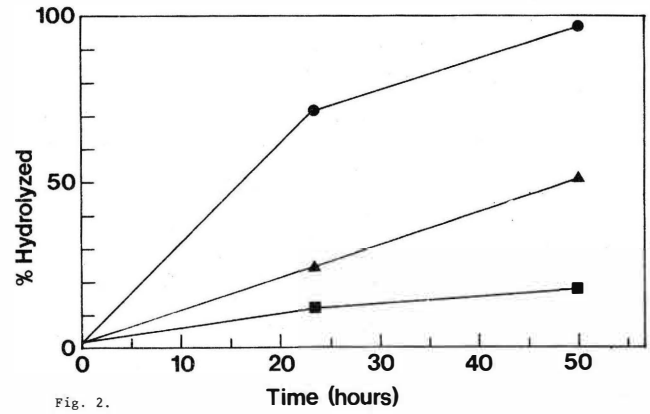

Fig. 2.
Hydrolysis of starch in an aqueous two phase system consisting of 4% crude dextran, 4% PEG 20.000 and 17% starch (Waxy maize) at 37°C and pH 4,8 (5). Enzymes added:
■ 0.17% Termamyl ▲ 0.17% SAN 150 ● 0.17% Termamyl + 0.17% SAN 150

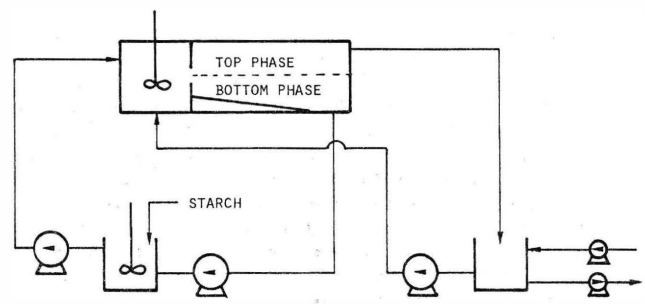

Fig. 3. Apparatus for continuous hydrolysis of starch.

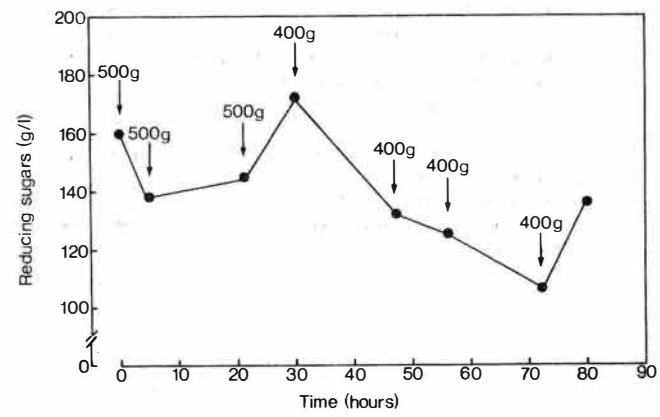

Fig 4.
Reducing sugars (expressed as glucose) in the removed top phase versus time. Additions of starch are indicated by arrows.

INVESTIGATION OF ETHANOL EXTRACTION FROM FERMENTATION LIQUORS

G. Zacchi, G. Aly and R. Wennersten

Lund Institute of Technology
Department of Chemical Engineering
P.O. Box 740
S-220 07 Lund, Sweden

INTRODUCTION

The increased interest in fermentation ethanol as a liquid fuel extender has accelerated research activities in this field. The most energy intensive step in the ethanol fermentation process is the separation of ethanol from water. Improved distillation schemes, adsorbent drying, use of cation exchange resins, solvent extraction and membrane methods are a variety of possible separation methods. Another problem deals with the ethanol productivity. The conventional batch or continuous flow systems yield at maximum a fermentation ethanol concentration of 10-12 wt-%. The alcohol decreases the viability of the cells and inhibits its own production. The cell viability begins to decrease at very low ethanol concentrations. However, the supression of ethanol production is not complete until the surrounding ethanol concentration reaches 10-12 wt-%. At these high concentrations the viability of the cells start to decrease rapidly.

Several continuous fermentation processes have been suggested in order to avoid high ethanol concentrations and to recirculate non-fermented substrate. To achieve high productivity (expressed as g produced ethanol / g solution), the process must fulfill the following basic requirements:

- High cell concentration in the fermentor,
- The ethanol concentration should be kept as low as possible (< 60 g/L),
- The substrate concentration should be kept at a certain level.

The last two requirements are needed to maintain a high viability of the cells. High cell concentration (without loss of substrate needed for cell growth) and low ethanol concentration can be achieved by continuous withdrawal of ethanol and by recycling both the cell mass and the mash residue. Recycling of the cell mass can be achieved by centrifugation while ethanol withdrawal can be achieved by either vacuum or extractive fermentation.

The vacuum fermentation approach (1-2) is based on the high volatility of ethanol and its removal by distillation during fermentation. Minier and Goma (3) used a plug flow reactor and solvent extraction (dodecanol as solvent) to achieve continuously the extractive fermentation of ethanol. Both methods have to overcome many problems to effectuate an industrial breakthrough. For instance, extractive fermentation has two major drawbacks; phase separation will be difficult to achieve and the hold-up of the organic phase in the fermentor will be so high that it may counterbalance the high ethanol productivity in the aqueous phase.

One of the main objectives of this work was to investigate the possibility of using solvent extraction for the recovery of ethanol from aqueous fermentation liquors. The equilibrium distribution coefficients in solvent-ethanol-water systems were experimentally measured. Computer simulations were performed to determine steam consumption as function of inlet ethanol concentration for the conventional distillation process and for two different solvent extraction process configurations; extraction with low-boiling solvents and extraction with high-boiling solvents. It must be emphasized that whatever separation method may be chosen, it must end up with comparing the energy requirements in conventional distillation and the selected separation method (capital costs are assumed to be nearly the same).

DISTRIBUTION COEFFICIENTS

The equilibrium distribution coefficient for extraction of ethanol from water into different solvents was determined at a constant temperature of 25°C. Distribution coefficients are expressed in this work in terms of weight fractions as $K_D = y/x$ where y and x are the weight fractions of ethanol in the extract and raffinate phases, respectively, at equilibrium as well as in terms of mole fractions, K_D^*.

A 25-mL solution containing 5 wt-% ethanol was added to 25-mL of solvent in a separatory funnel. The funnel was agitated for enough time to ensure equilibrium and was then allowed to settle before sampling. Analyses of the raffinate phase were made by manually injecting samples by syringe into a Varian Model 200 gas chromatograph equipped with a flame-ionization detector and a Porapak Q-S column, 0.32 cm in diameter, 2.0 m long and packed with 80/100 mesh chromosorb 101. Calibration was done with successively diluted standard (i-propanol) and a reproducibility within 5 % could be attained.

Low-boiling solvents such as triethylamine, Di-iso-propyl ether and ethyl acetate and high-boiling solvents such as hexanol, octanol, Tributyl phosphate (TBP), methyl isobutyl ketone (MIBK) and Versatic 10 were used in the experiments. The results are tabulated in Table 1. Equilibrium distribution coefficients were experimentally measured for more solvents and are reported in (4).

SOLVENT EXTRACTION

The first and most crucial step in the development of a solvent extraction process is to select an optimal solvent. The major factors affecting the selection of solvents are outlined elsewhere (5) and will not be mentioned here.

Extraction with low-boiling solvents

Figure 1 shows a typical configuration for a recovery process using low-boiling solvents. The flowsheet includes the usual three major steps: solvent extraction, solvent recovery from the extract phase and solvent stripping from the aqueous raffinate phase. The necessity of the last column depends on the toxicity of the solvent with respect to the yeast cells since most of the water stream, obtained as bottoms, is usually recycled to the fermentor. In an industrial process, both steps for solvent regeneration would contribute to most of the capital investment cost and nearly all of the energy requirements. The low-boiling solvents have some advantages. The solvent is taken overhead. The water content of the extract phase is also taken overhead since, in most cases, water and solvent form a minimum-boiling heterogeneous azeotrope. Both distillation columns operate at relatively low temperatures, so boiler energy can be supplied by low-pressure steam or possibly by waste heat.

Some criteria must be fulfilled in this class of solvents. High K_D-values and that the solvent does not form an azeotrope with ethanol are two major design factors, affecting both the overall process configuration and energy requirements. Other criteria are high relative volatility of the solvent to ethanol and high stripping factor in the solvent stripping column.

A rough estimate of minimum energy requirements for the configuration shown in Figure 1 can be made assuming constant molar heats of vaporization. Thus

$$S_{min} = 0.39/(x_F \cdot K_D^*) \quad \text{kg steam/kg ethanol}$$

where S_{min} is the minimum steam consumption, x_F is the ethanol inlet concentration (mole fraction) and K_D^* is the equilibrium distribution coefficient expressed in terms of mole fractions.

The above relationship was used to calculate K_D^*-values which give the same energy consumption as in the conventional distillation process. For an inlet ethanol concentration of 4 and 8 wt% (1.6 and 3.3 mole % resp.), the conventional distillation process requires 3.24 and 1.99 kg steam/kg ethanol respectively. This would require solvents with K_D^*-values exceeding 7.5 and 5.9 respectively. Neither the solvents investigated in this work nor literature results on other low-boiling solvents can attain such high K_D^*-values.

Extraction with high-boiling solvents

Two of the most important criteria for this class of solvents are good selectivity and that the solvent should not negatively affect the relative volatility of ethanol to water in the organic phase. The second criterium can be explained by considering an aqueous solution containing, for instance, 45 wt-% ethanol. The relative volatility α for this binary mixture is 3.6. After extraction with either octanol or dodecanol, the α-value in the organic phase will decrease to 0.52 or 0.40 respectively. These values were calculated using the UNIFAC-model and assuming that the organic phase is saturated with water. Decreasing the α-value to such level will greatly affect the energy needed in the ethanol separation column. Other criteria are: a K_D-value around 1.0 and that the solvent does not form an azeotrope with ethanol.

A computer program PRIMCALC was used to estimate the minimum energy requirements for this class of solvents. The process configuration shown in Figure 2A was used for these simulations. PRIMCALC is a group of computer programs specially designed in order to simplify the calculations of energy requirements in combined extraction-distillation processes for the recovery of organic chemicals from diluted aqueous solutions. On executing the program on the ethanol system, the following assumptions were made:

- Solvent extraction: Having specified the degree of solute recovery, a phase ratio of 1.5 times $(V/L)_{min}$ is used. A constant K_D-value is assumed, and chosen as the lowest value in the concentration range considered. The solute does not affect the mutual solubility between solvent and water.
- Solvent regeneration: The system in the solvent recovery column was assumed to be binary and consisting of water and solvent. Data for the heterogeneous azeotrope between water and solvent was used for the solvent stripping column.
- Ethanol separation column: The feed is concentrated to a distillate containing 93.5 wt-% ethanol and bottoms consisting of pure water. The energy requirements for this column were calculated according to the method discussed below.

The simulation results are displayed in Figure 3 where minimum steam consumption is plotted as function of inlet ethanol concentration for hexanol, octanol and methyl isobutyl ketone (MIBK). Steam consumption in the recovery process using distillation only is also plotted for comparison. The latter curve was computed using another computer program called DESTLA (6). This program is based on a modular general distillation plant and uses so-called unit cells together with a description of the plant flow sheet as a connection matrix. The following assumptions were made:

- constant molar heats of vaporisation
- feed at its boiling point
- 30 theoretical plates
- ethanol conc. in distillate = 93.5 wt-%
- ethanol losses in bottoms = 0.2 % of inlet amount
- negligible pressure drop in the column

DESTLA was also executed to investigate the reliability of the assumptions made for PRIMCALC runs. For this purpose, the process configuration shown in Figure 2B was considered. The simulation was based on an inlet ethanol concentration of 8 wt-% and octanol as the solvent. Furthermore, the above assumptions were used. Selectivity and K_D data give an extract phase containing 4 wt-% of both ethanol and water. VLE-data were computed using the Wilson equation for calculating the activity coefficients. Necessary parameters were obtained from literature (7) for the ethanol-water binary, applying the UNIFAC method for the octanol-water binary, while ideal behaviour was assumed for the ethanol-octanol binary.

Feed plate and reflux ratio were varied until a distillate containing 93.5 wt-% ethanol was obtained. This resulted in a reflux ratio (in the total condenser) of 7.5/1 and the optimal feed plate would be the 12th from the top.

According to the rigorous calculations (DESTLA), 4.10 kg steam/kg ethanol will be needed while the preliminary calculations (PRIMCALC) resulted in 3.86 kg steam/kg ethanol. This would suggest that the assumptions made in executing PRIMCALC are acceptable regarding the large savings in computer time associated with that program.

The high-boiling solvents were not able to generate favourable values for energy requirements compared to the conventional distillation process. Improved distillation schemes for ethanol recovery by distillation only were investigated by Zacchi (8). It was found that multi-effect distillation would save 40% while mechanical vapor recompression of the overheads would save as high as 70% of the energy requirements.

CONCLUSIONS

Equilibrium distribution coefficients were experimentally measured for extraction of ethanol from water into both low-boiling and high-boiling solvents. The more common solvents give K_D-values less than 1.0. Minimum steam consumption for two process configurations based on solvent extraction were computed and compared to steam consumption in the conventional distillation process. For both classes of solvent, it was found that ethanol recovery by solvent extraction would consume more steam and thus economically unfeasible assuming that both alternatives have nearly the same capital cost.

REFERENCES

1. A. Ramalingham and R.K. Finn, Biotechnol. Bioeng., 19, 583 (1977).
2. G.R. Gysewski and C.R. Wilke, Biotechnol. Bioeng., 19, 1125 (1977).
3. M. Minier and G. Goma, Biotechnology Letters, 3, 405 (1981).
4. E. Janbris and B. Neigart, Report LUTKDH/(TKKA-5015)/1-18/(1981), Dept. of Chem. Eng., Lund Inst. of Technol. (1981).
5. R. Wennersten, G. Zacchi and G. Aly, Presented at CHISA'81 Conf., Prague (1981).
6. G. Zacchi and Å. Jernqvist, Report LUTKDH/(TKKA-3001)/1-40/(1978), Dept. of Chem. Eng., Lund Inst. of Technol. (1978).
7. J. Gmehling and U. Onken, DECHEMA Chem. Eng. Data Series, Vol I/1 (1977).
8. G. Zacchi, Unpublished data.

TABLE 1: EXPERIMENTALLY MEASURED EQUILIBRIUM DISTRIBUTION COEFFICIENTS FOR EXTRACTION OF ETHANOL FROM WATER INTO DIFFERENT SOLVENTS (25°C)

SOLVENT	FEED CONC., WT-% ETHANOL	DISTRIBUTION COEFFICIENTS	
		K_D	K_D^*
TRIETHYL AMINE	0.59	0.93	4.0
DI-ISOPROPYL ETHER	0.88	0.22	1.2
ETHYL ACETATE	0.69	0.54	2.2
HEXANOL	0.39	0.63	
OCTANOL	4.10	0.54	
TBP	5.50	0.47	
MIBK	0.76	0.41	
VERSATIC 10	0.87	0.21	

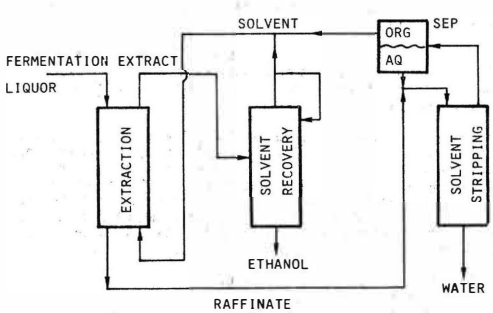

FIGURE 1: EXTRACTION OF ETHANOL WITH LOW-BOILING SOLVENTS

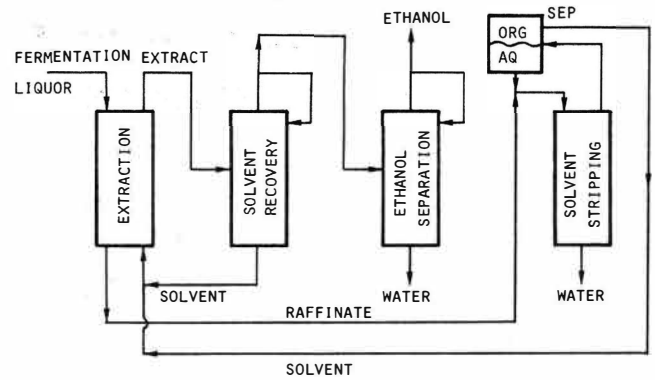

FIGURE 2A: EXTRACTION OF ETHANOL WITH HIGH-BOILING SOLVENTS

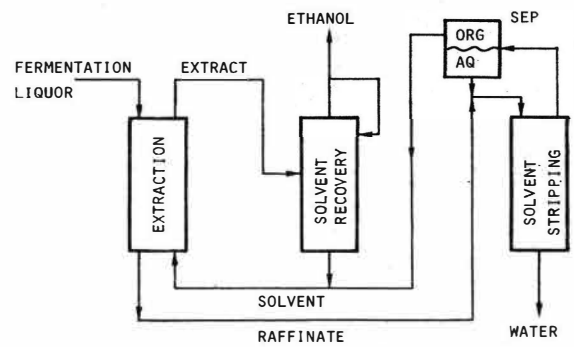

FIGURE 2B: EXTRACTION OF ETHANOL WITH HIGH-BOILING SOLVENTS

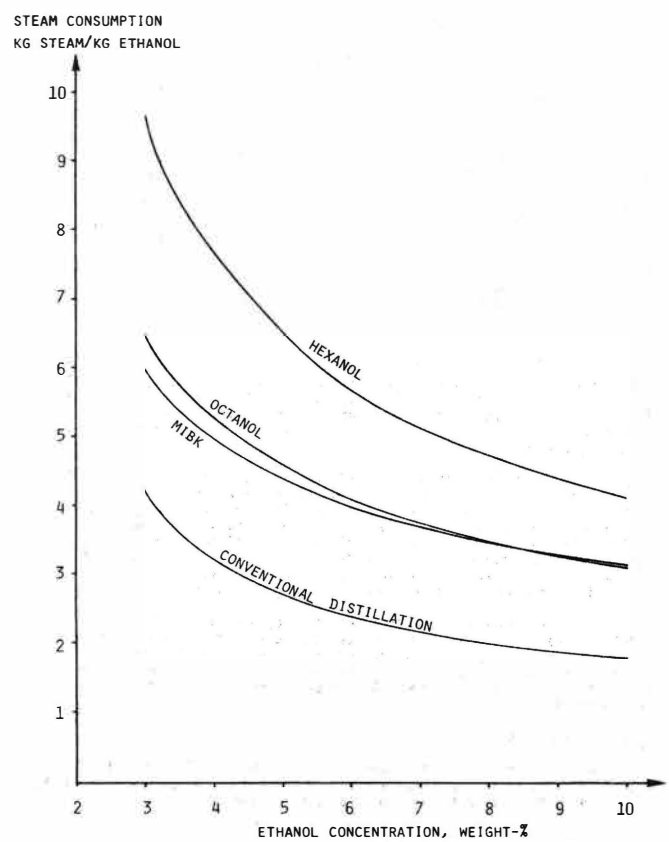

FIGURE 3: STEAM CONSUMPTION AS FUNCTION OF ETHANOL CONCENTRATION IN THE FERMENTATION LIQUOR

FACTORS INFLUENCING SOLVENT SELECTION FOR EXTRACTION OF ETHANOL FROM AQUEOUS SOLUTION

Curtis L. Munson and C. Judson King

Department of Chemical Engineering
University of California
Berkeley, California 94720 USA

Results are presented for measurements of equilibrium distribution coefficients (K_D, expressed on a weight-fraction basis) and separation factors (α, selectivity with respect to extraction of water) for extraction of ethanol from dilute aqueous solution by a number of different solvents and solvent mixtures. Results for solvent mixtures are shown in Figures 1 and 2, which show that certain mixtures of ketones and carboxylic acids are synergistic for K_D. For any class of solvents, there is a trade-off between K_D and α. This is displayed in Figure 3, which also shows that Lewis acids have more favorable combinations of K_D and α than do Lewis bases. For alcohol and carboxylic acid solvents, branching increases α substantially for a given solvent molecular weight (Figure 4). The cone angle γ, defined in Figure 5, serves to rationalize the effect of branching in increasing α (Figure 6).

Requirements for solvent selectivity can be ameliorated by the use of an extractive-distillation dewatering step, which receives the extract as feed and utilizes the properties of the solvent for enhancing the relative volatility of water to ethanol (Figure 7). Other important solvent properties are its volatility in a distillative solvent-recovery step and the ease with which residual solvent may be removed from water by stripping or other means.

References

Roddy, J. W., Ind. Eng. Chem. Proc. Des. & Dev., 1981, 20, 104.

Souissi, A.; Thyrion, F.C., Proc. 2nd World Congress of Chem. Eng., 1981, 4, 443.

---

* - The full text of this paper is to be published, under the same title, in Industrial & Engineering Chemistry Process Design and Development, an American Chemical Society publication.

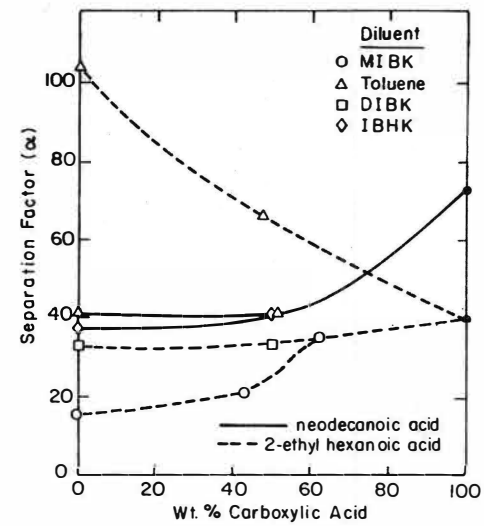

Figure 2. Separation Factors with Solvent Mixtures

Figure 1. Distribution Coefficients for Extraction of Ethanol from Water by Solvent Mixtures.

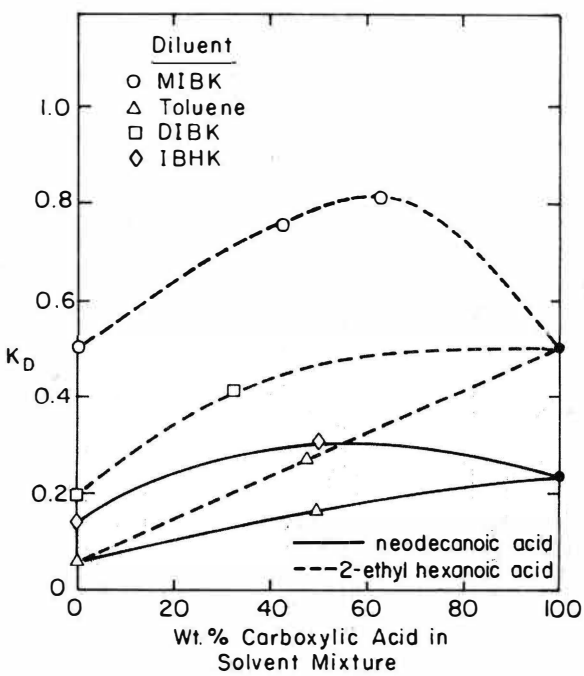

Figure 3. Equilibrium Distribution Coefficients and Separation Factors for Extraction of Ethanol from Water. Data of Roddy (1981), Souissi et al. (1981) and the present work for temperatures between 20°C and 30°C.

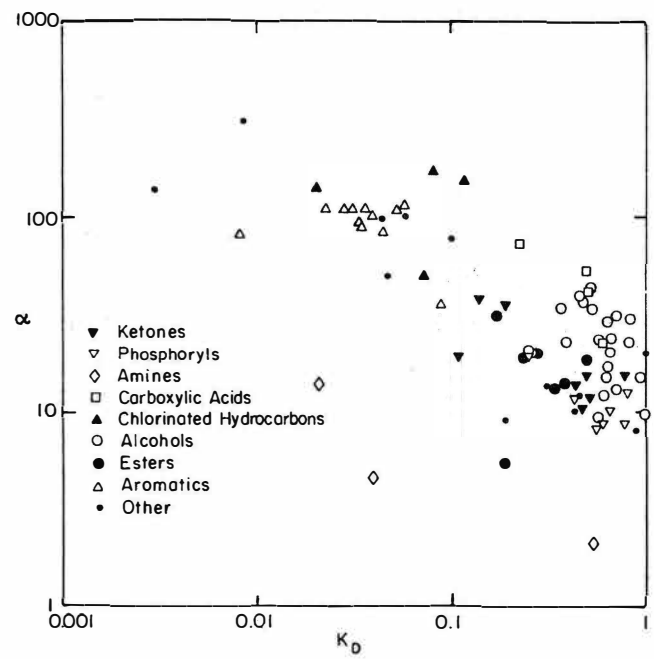

Figure 4. Equilibrium Distribution Coefficients and Separation Factors for Extraction of Ethanol from Water into Alcohols and Carboxylic Acids.

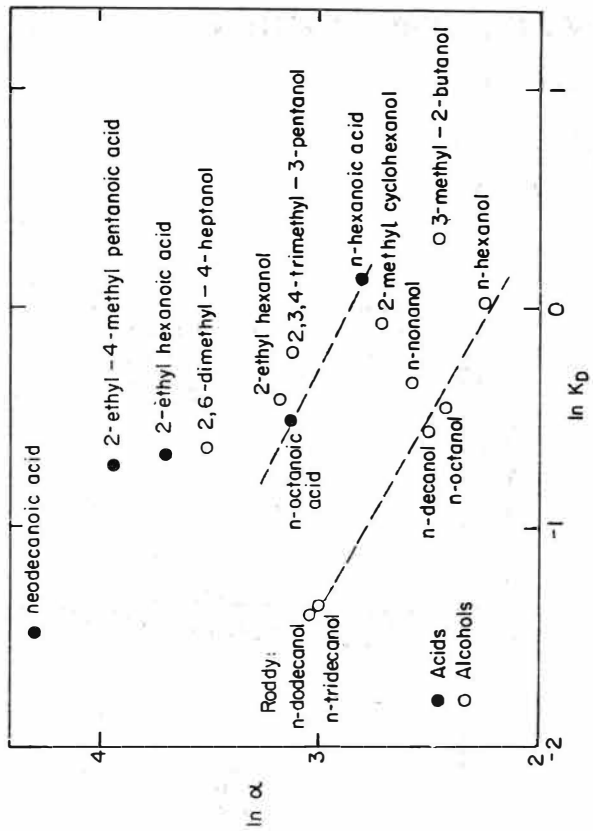

Figure 5. Equivalent Cone Angles of a Hydrogen Atom and of a Methyl Group Bonded to a Carbon Atom.

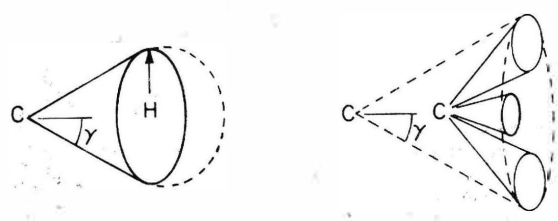

Figure 6. Separation Factors for Alcohols as a Function of Steric Cone Angle.

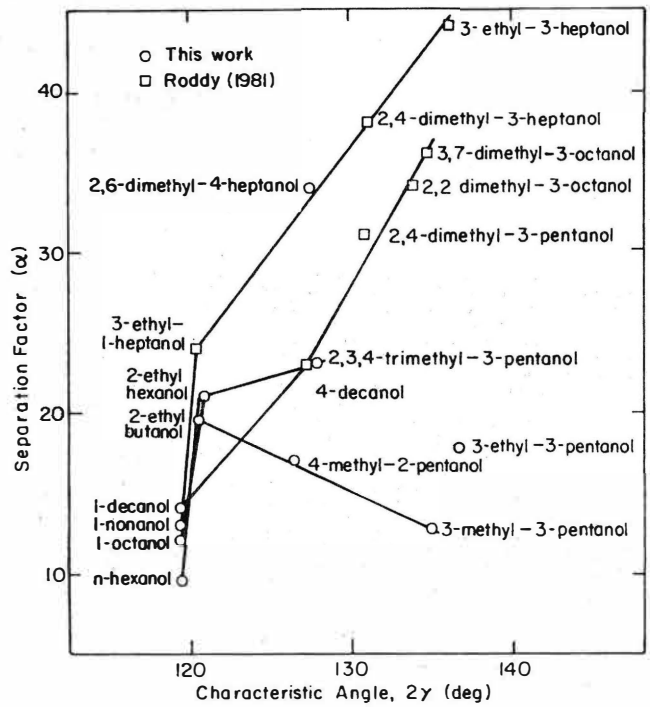

Figure 7. Use of a Solvent to Volatilize Water in a Subsequent Extractive Distillation, Thereby Lessening Requirements for Solvent Selectivity in Extraction. Heat Exchangers are not shown.

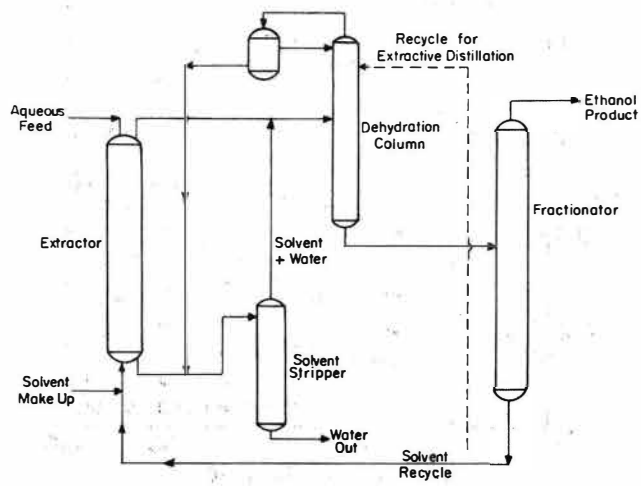

EXTRACTION OF ETHANOL FROM WATER WITH LIQUID PROPYLENE

John G. Victor

Institute of Gas Technology
Chicago, Illinois USA

THERMODYNAMIC BEHAVIOR OF ETHANOL AND WATER MIXTURES

If ethanol and water formed an ideal mixture (such as that formed by pouring water into water), the enthalpy change upon mixing would be zero and the Gibbs free energy change would be:

$$\Delta G = RT \Sigma X_i \ln(X_i)$$

X_1 = mole fraction of ethanol
X_2 = mole fraction of water
R = gas constant
T = absolute temperature

Table 1 shows that the actual change in free energy when ethanol is mixed with water decreases less with increasing temperature than would occur with an ideal mixture.

Table 1: Ideal, Excess, and Actual Gibbs Free Energy Change from Mixing Ethanol and Water to 0.05 Mole Fraction Ethanol at Various Temperatures (1)

Temperature, K	Gibbs Free Energy Change, Joules/G-Mole Solution		
	ΔG (Ideal)	ΔG (Excess)	ΔG (Actual)
303	-500.5	167.3	-333.2
323	-533.5	200.4	-333.1
343	-567.1	225.5	-341.6
363	-599.6	243.9	-355.7

To separate ethanol from water by distillation requires 40 to 50 times this minimum Gibbs free energy of mixing, at least in conventional distillation units. Also, ethanol forms an azeotrope with water, limiting the ability of distillation to concentrate ethanol much beyond 92 wt % ethanol. These considerations have prompted researchers to investigate solvent extraction as an alternative separation technique. This extended summary describes the use of liquid propylene as solvent.

DISTRIBUTION COEFFICIENT OF ETHANOL BETWEEN WATER AND SEVERAL SOLVENTS

Hydrocarbon solvents of ethanol experience a temperature dependence of the free energy change of mixing with ethanol more nearly like that of an ideal mixture. Because the amount of ethanol which can transfer from water to hydrocarbon solvents is a function of the minimum Gibbs free energy the system can attain, more ethanol should transfer to these solvents at higher temperatures; i.e., the distribution coefficient of ethanol should increase. Table 2 shows experimental measurements (2) of the distribution coefficients of ethanol between several hydrocarbon solvents and water at 20°C and 40°C, which all bear out this contention.

Table 2: Values of Ethanol Distribution Coefficient (D_{EtOH})[a] for 0.1M Ethanol in Several Solvents at 20°C and 40°C (2)

Solvent	Temperature, °C	
	20	40
Cyclohexane	4.7×10^{-3}	1.4×10^{-2}
Benzene	3.9×10^{-2}	7.1×10^{-2}
Toluene	3.2×10^{-2}	5.7×10^{-2}
Xylene	2.5×10^{-2}	4.7×10^{-2}
Diethylbenzene	2.0×10^{-2}	3.6×10^{-2}

[a] $D_{EtOH} = [EtOH]_{solvent}/[EtOH]_{aq}$, where [EtOH] is concentration, molarity.

PREDICTED DISTRIBUTION COEFFICIENT OF ETHANOL BETWEEN LIQUID PROPYLENE AND WATER

The vapor pressure of liquid propylene at 25°C is about 11 atm, absolute. The solubility of propylene in water at temperatures and pressures where propylene is liquid is about 1×10^{-3} (mole fraction), a relatively small value. Ethanol is miscible in all proportions with liquid propylene, as it is with water. Liquid propylene thus satisfies the minimum requirements to be considered as a solvent to separate ethanol from water. The UNIFAC "contribution-of-functional groups" model (3) predicts excess Gibbs free energy of mixing propylene and ethanol sufficiently negative as to result in a calculated distribution coefficient $D_{EtOH} = 0.13$ (weight fraction basis) at 25°C for a weak aqueous ethanol concentration. However, the UNIFAC model is only theoretically valid to pressures of 4-5 atm, and extrapolating excess Gibbs free energy of mixing beyond this range may lead to calculating spurious values for D_{EtOH}.

MEASURED VALUES OF THE DISTRIBUTION COEFFICIENT

An elevated pressure liquid-liquid contacting apparatus was used to determine the mutual solubility phase boundary of the system ethanol-propylene-water with results shown in Figure 1. If tie lines were shown on the figure, they would have slopes equal to D_{EtOH}. Because practical difficulties arose in obtaining upper layer (propylene-rich) liquid samples for analysis, a formula derived from component mass balances was used to calculate D_{EtOH} from values of the weight fraction ethanol in the water layer, the weight fraction ethanol initially introduced, and the weight fraction of water in the water layer and that initially introduced. The formula is:

$$D_{EtOH} = \frac{Z_e}{X_e}\left(\frac{\dfrac{(Z_e \times X_w)-(Z_w \times X_e)}{X_e - Z_e} + (X_w \times D_{HOH})}{\dfrac{(Z_e \times X_w)-(Z_w \times X_e)}{X_e - Z_e} + Z_w}\right)$$

X_e = weight fraction EtOH in lower layer
X_w = weight fraction H_2O in lower layer
Z_e = weight fraction EtOH initially present
Z_w = weight fraction water initially present

(D_{HOH} is the distribution coefficient of water, assumed small)

Most values of D_{EtOH} found, shown in Table 3, were derived by the formula; however, for the last point, a representative sample of the propylene-rich upper layer was obtained and analyzed. Its ethanol content divided by the aqueous layer's is the "measured" D_{EtOH}.

The formula method to calculate D_{EtOH} did not give consistent results when the initial compositon of propylene was less than 0.4 (weight fraction), possibly due to a failure to achieve equilibrium. The other results tend to support the UNIFAC model's prediction of D_{EtOH}, despite its application for a system at 11 atm.

The separation factor ($S = D_{EtOH}/D_{HOH}$), although not measured, appears to be high for the ethanol-propylene-water system, because of the closeness of the mutual solubility phase boundary to the propylene-ethanol axis.

Table 3: Distribution Coefficient Determined from Liquid Layer Composition Measurements for Propylene, Ethanol, and Water at 75°F, 200 psig.

Weight Fraction Initially Present			D_{EtOH}[a] Found	
Propylene	Ethanol	Water	Formula	Measured
0.400	0.200	0.400	0.14	
0.300	0.200	0.500	0.065	
0.499	0.200	0.301	0.16	
0.373	0.275	0.372	-0.03	
0.300	0.200	0.500	-0.03	
0.500	0.200	0.300	0.12	
0.401	0.200	0.399	0.25	
0.400	0.100	0.500	0.12	0.19

[a] D_{EtOH} = wt fraction EtOH in upper layer/EtOH in lower layer.

PROCESS APPLICATION

Figure 2 is a process flow schematic for the solvent extraction of ethanol from water with propylene. Aqueous ethanol, 7.1 wt %, such as is produced from fermentation, is heated to 60°C, pumped to about 26 atm absolute, and sent to the top of a liquid extraction column. The column is filled with plastic rings to promote good liquid-liquid contact. The heavier aqueous ethanol descends through the column and is extracted of nearly all the ethanol by liquid propylene entering at the bottom and rising through the column. Assuming D_{EtOH} at 60°C is 0.2, about 10 times (volume basis) as much propylene circulates through the column as aqueous ethanol feedstock. The weight fraction of near-absolute (assumed) ethanol in the propylene leaving the top of the column is about 0.012.

Real aqueous ethanol feedstocks to distilleries contain significant concentrations of "fusel oil," mostly longer-chain alcohols and aldehydes. These would likely also be extracted by liquid propylene, and are assumed part of the ethanol product.

The ethanol-rich propylene stream issuing from the top of the extraction column flows to a series of membrane separators. The first is a hydrophobic (e.g., polypropylene) membrane, assumed capable of purifying (reducing the ethanol content by a factor of over 200) most of the propylene solvent for returning to storage and makeup. The ethanol concentrates to about 10% by weight, and is pumped to a hydrophilic (e.g., cellulose acetate) membrane capable of concentrating the ethanol to about 60% by weight. This concentrated ethanol flows to a small distillation column, assumed capable of achieving nearly total propylene removal from the ethanol product.

Water leaving the extraction tower has small amounts of ethanol and propylene, and is sent to a flash vaporizer to recover the solvent propylene. Ethanol leaving the vaporizer with the propylene is condensed and returned to the ethanol feed tank. Propylene is compressed and sent to the distillation tower.

Propylene is lost mainly in the spent water. Propylene solubility in warm water is less than 100 ppm, and solvent makeup for a large (45,000 gallons EtOH per day) plant would be about 50 gallons/day. Estimated actual energy requirements for a process plant, including combustion inefficiencies for process heating and electric power production for liquid pumping, amounts

to about 31 times the minimum Gibbs free energy of separation, with most of the energy going to heat the ethanol feed to 60°C. While this seems a modest improvement over conventional distillation's previously mentioned separation energy requirement, a preliminary cost estimate indicates a coincidental decrease in installed plant cost for separating ethanol from water using liquid propylene, instead of conventional distillation. Few advanced ethanol-water separation techniques offer both reduced energy requirements and reduced plant cost compared with conventional distillation.

REFERENCES

1. R. C. Pemberton and C. J. Mash, "Thermodynamic Properties of Aqueous Non-electrolyte Mixtures. II. Vapour Pressures and Excess Gibbs Energies for Water + Ethanol at 303.15 to 363.15K Determined by an Accurate Static Method," J. Chem. Thermodynamics 10, 1978, 867-888.

2. James W. Roddy, "Distribution of Ethanol-Water Mixtures to Organic Liquids," Ind. Eng. Chem. Process Des. Dev. 20, 104-108 (1981).

3. Aage Fredenslund, Jurgen Gmehling, and Peter Rassmussen, Vapor-Liquid Equilibria Using UNIFAC. Amsterdam: Elsevier Scientific Publishing Company (1977).

154/PAP/ext-eth

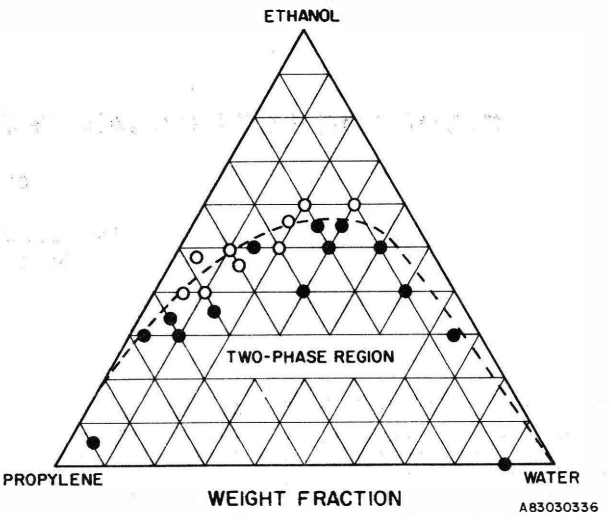

Figure 1. MUTUAL SOLUBILITY PHASE BOUNDARY: PROPYLENE, ETHANOL, AND WATER AT 75°F, 200 psig (Open circles, single layer observed; closed circles, two layers observed)

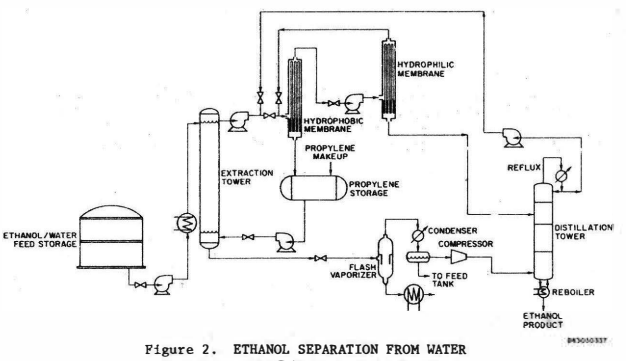

Figure 2. ETHANOL SEPARATION FROM WATER USING SOLVENT EXTRACTION WITH PROPYLENE

LIQUID-LIQUID EXTRACTION: A PROCESS FOR RECOVERY OF ORGANONITROGEN COMPOUNDS AND POLLUTION CONTROL

Teh C. Lo

Hoffmann-La Roche Inc.
Nutley, New Jersey USA

INTRODUCTION

An organonitrogen compound was originally recovered from a process stream via a multi-stage crosscurrent batch extraction process. Aqueous raffinate from the last stage was directly sewered. Product loss in the raffinate was significant economically and the loss also created a wastewater pollution problem.

In order to minimize pollution and to achieve maximum recovery, a continuous countercurrent extraction process was developed to reduce the organonitrogen compound concentration in the raffinate to less than 10 mg./l. In the development of the process, distribution coefficients for the organonitrogen compound were measured. Pilot studies were carried out in a 3" x 36-stage Scheibel column. Performance data from the 3" Scheibel column were used for scale-up and design of a 28" diameter x 46-stage Scheibel column. Final design includes two stages of evaporation for solvent recovery and a raffinate solvent stripper.

EXPERIMENTAL

Distribution Coefficients. Liquid-liquid equilibrium data were measured for the organonitrogen compound using a one-liter, jacketed and baffled separatory funnel provided with a glass teflon stirrer. The actual plant feed samples were extracted several times with fresh methylene chloride (MCl) to obtain measurement over a wide range of concentrations. Analyses were done by an external standard gas chromatographic method. Effects of salt concentration and pH on the distribution coefficients were also determined.

It was observed that the plant column will operate within a concentration range (1 g./100 ml.) in which the distribution coefficient is nearly constant at a value of

$$D = 3.75 \frac{\text{wt./vol. of solute in MCl phase}}{\text{wt./vol. of solute in aqueous phase}}$$

$$D = 3.35 \frac{\text{wt./wt. of solute in MCl}}{\text{wt./wt. of solute in aqueous phase}}$$

PILOT STUDIES IN A 3" SCHEIBEL COLUMN

A 3" x 36-stage Scheibel column (1) (glass shell, stainless steel internals, 1" stage height) was used to develop the process for the continuous extraction of the organonitrogen compound. Methylene chloride was used as an extracting solvent. A water backwash section was installed below the feed point to remove salt from the methylene chloride phase. A summary of the process conditions and performance data is given in Table 1.

The data indicate that both throughput and agitation speed had a significant effect on the extraction efficiency. Runs 1A, 1B, and 3C (cf. Table 1) indicated that product concentrations below 10 mg./l. in the raffinate could be achieved in a 3" column with throughputs as high as 150 gph/ft.^{2}. At 200 gph/ft.^{2} (run 2B), the dispersion was noticeably poor, and the product concentration in the raffinate was found to be 990 ppm. Runs 3A, B, and C indicated that the product concentrations in the raffinate steadily decreased with an increase in agitation. At 280 rpm, the concentration was 1,350 mg./l., whereas, at 430 rpm, the value fell below 10 mg./l. The column flooded at an agitation of 475 rpm.

SCALE-UP AND DESIGN

The process conditions for an optimized run (No. 3C) are given in Table 2. An extraction efficiency of 99.97%, which is equivalent to a product concentration of <10 mg./l. in the aqueous raffinate, was achieved by using a solvent/feed (S/F) ratio of 1.23 w/w in the 3" x 36-stage column. There were 26 stages in the extraction section and 10 stages in the wash section. The column was operated at a specific throughput of 150 gph/ft.^{2} with the interface at bottom. Data from the 3"-diameter column were used to scale up to a 28"-diameter Scheibel column (1-3). Scale-up data for the Scheibel column are summarized in Table 2.

PERFORMANCE OF A COMMERCIAL EXTRACTION PLANT

A schematic flow diagram for the recovery of the organonitrogen compound using a continuous countercurrent extraction process is shown in Figure 1 and performance data are summarized in Table 2. The aqueous process solution containing 4.7 g./100 ml. of organonitrogen compound is fed into the 28" x 37-stage Scheibel column. Methylene chloride and city water are introduced at the top and bottom of the column, respectively.

Solvent is recovered via two stages of evaporation. It is necessary to reduce the product concentration in the methylene chloride overhead to less than 5 mg./l. since this recovered solvent is fed into the extractor in which the raffinate from the column is designed to contain less than 10 mg./l. VLE data show that some degree of fractionation is required to strip the product from the vapor of the first-stage evaporator. The aqueous raffinate, which contains .2% methylene chloride, is steam-stripped to recover the solvent prior to discharge into the sewer. The stripped raffinate contains 20 mg./l., which is acceptable to the waste treatment plant.

CONCLUSIONS

The continuous countercurrent extraction process was successfully started up in 1979 and has been running smoothly ever since.

Following are conclusions and comments:

- A content as low as 5 mg. of organonitrogen compound per liter of raffinates has been achieved. This is equivalent to a recovery of 99.97%. Thus, contaminants of the organonitrogen compound in the wastewater have been eliminated. Also, additional product is recovered.
- The solvent in the raffinate is steam-stripped to less than 20 ppm prior to discharge into the sewer.
- The investment for the extraction plant was approximately one million dollars. The value of the additional product recovered by this continuous extraction process is approximately $250,000/yr. The discounted rate of return on investment is 20%.
- The solvent extraction process described herein has the greatest potential applicability where the organic solute has a low solubility in water, partitions easily into a solvent of low water solubility and is valuable. It seems likely that solvent extraction may find wider future application in the treatment of water effluents (4, 5) containing toxic organic compounds such as phenols and halogenated hydrocarbons, organonitrogen and organosulfur compounds, or valuable compounds for recovery.

ACKNOWLEDGEMENTS

The author is grateful to Hoffmann-La Roche Inc. for permission to publish this work. Thanks also to Messrs. F. Alechny and A. Quiam for their assistance in performing experiments and on correlation of the data, and to Mr. P. Wong for his assistance in preparing the manuscript.

REFERENCES

1. E. G. Scheibel, A.I.Ch.E. Journal, 2, 74 (1956)
2. T. C. Lo, Section on Commerical Liquid-Liquid Extraction Equipment in "Handbook of Separation Techniques for Chemical Engineers", P. Schweitzer (ed.), McGraw-Hill Book Co., New York (1979)
3. E. G. Scheibel, "Scheibel Extraction Columns" in the "Handbook of Solvent Extraction", T. C. Lo, M. Baird, and C. Hanson (ed.), Wiley-Interscience, New York (1983)
4. D. Mackay and M. Medir, "Industrial Effluent Treatment" Chapter 23, in the "Handbook of Solvent Extraction", T. C. Lo, M. Baird, and C. Hanson, (ed.), Wiley-Interscience, New York (1983)
5. L. A. Robbin, Chem. Eng. Prog., 58, (1980)

Table 1

Summary of the Organonitrogen Compound Extraction Runs in a 3" Scheibel Column[1,2]

Run No.	Flow Rate, ml./min. Feed	MeCl[2]	Wash Water	Specific Throughput, GPH/Ft.[2]	Agitation Speed, RPM	Organonitrogen Compound, GC Assay Feed, gm./100 ml.	Aqueous Raff., ml./l.	% Recovery
1 (A)	75.7	84.5	14.0	56	530	4.4	<10	99.97+
1 (B)	135.2	151	25	100	450	4.4	<10	99.97+
2 (A)	270.4	302	50	200	210	4.4	3,080	91.9
2 (B)	270.4	302	50	200	280	4.4	990	97.4
3 (A)	202.8	226.5	37.5	150	280	4.4	1,350	96.5
3 (B)	202.8	226.5	37.5	150	360	4.4	88	99.77
3 (C)	202.8	226.5	37.5	150	430	4.4	<10	99.97+
9	202.8	226.5	37.5	150	380	5.5	10	99.98
10 (A)	202.8	226.5	37.5	150	380	4.2	138	99.55
10 (B)	202.8	226.5	37.5	150	400	4.2	102	99.67

1. Aqueous phase is the continuous phase in all runs.

2. Column consists of 36 actual stages: 25 stages above feed; 10 stages below feed.

Table 2

Summary of Data on Scale-up and Performance of a 28"-Diameter Scheibel Extractor

	Pilot Scale	Plant Performance
Column Diameter	3"	28"
Column Overall Height	48 1/2"	27'-6"
Total Throughput, GPH/ft^2	150	213
Extraction Section		
No. of Actual Stages	26	36
Height Per Stage	1"	5"
Total Height Extraction Section	25"	14'-5"
Solvent Ratio (H/L, v/v)	0.94	0.88
Stage Efficiency	24%	20%
HETS	4.2"	25.4"
No. of Theoretical Stages	6.2	6.9
Product Lost in Raffinate	<10 ppm	<10 ppm
Recovery Efficiency, %	99.97	99.98
Wash Section		
No. of Actual Stages	10	11
Height Per Stage	1"	4.8"
Total Height of Wash Section	10"	4'-5"
Stage Efficiency, %	10	20
HETS	-	24"
No. of Theoretical Stages	-	2.2
Drive, HP	1/4	3
Total Throughput, GPH	7.4	912
Volumetric Efficiency, Hr.$^{-1}$ (Extraction Section)	57	13.5

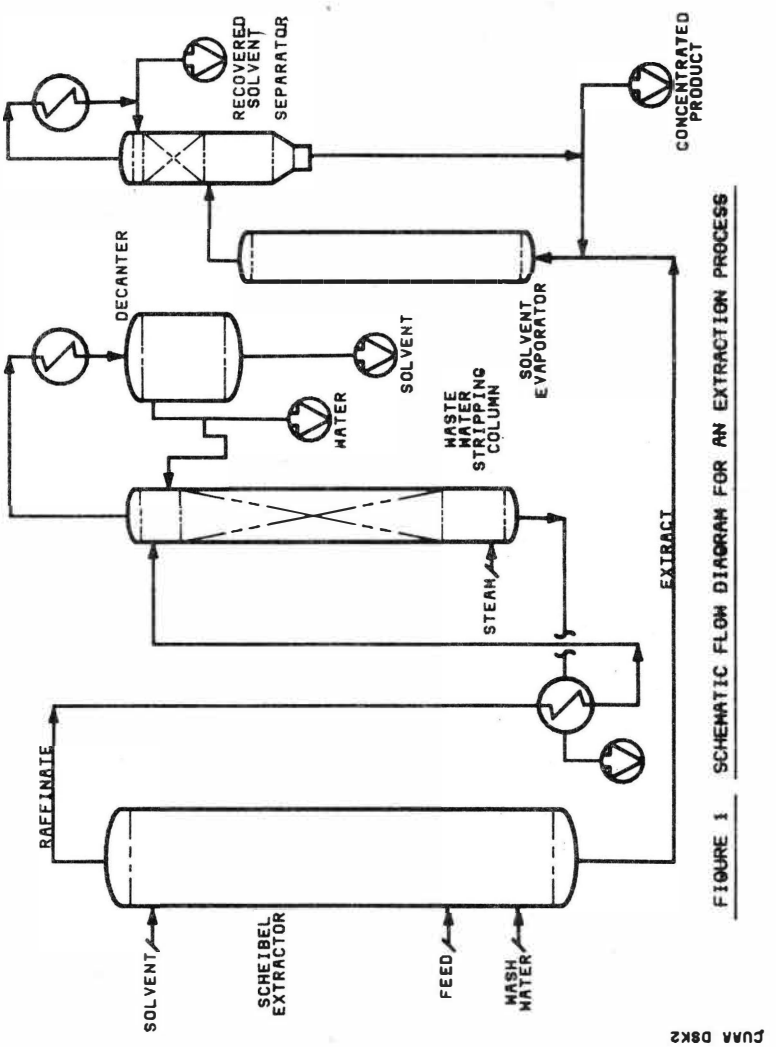

FIGURE 1 SCHEMATIC FLOW DIAGRAM FOR AN EXTRACTION PROCESS

FUMA DSK2

THE APPLICATION OF DUAL-SOLVENT EXTRACTION TO THE REFINING OF A COMPLEX NATURAL SYSTEM

J. J. Warner and I. J. Harris

C.S.I.R.O., Division of Textile Industry
Belmont, Victoria, Australia

Department of Chemical Engineering
University of Melbourne
Parkville, Victoria, Australia

ORIGINS

The processing of raw wool for use as a textile includes washing in hot detergent solution (scouring) to remove wool-grease, other metabolic by-products and mineral dirt.

The grease is a mixture of numerous high molecular weight esters together with small amounts of polar material such as steroidal free alcohols, fatty acids and oxidized material which influences the colour.

It is usual to recover a fraction of the grease, including some of the scouring detergent, by centrifuging the heated scouring solution. The main use of the recovered grease is for the production of pharmaceutical grade lanolin which is of specified quality (1).

In recent years more stringent environmental protection legislation has provided incentive for increased recovery of the raw grease from the aqueous scour effluent to reduce the cost of treatment before discharge. A less desirable consequence of increased grease recovery is that a greater proportion of undesirable polar material and detergent is present in the recovered grease. These must be separated to produce lanolin of acceptable quality.

Preliminary batch extractions and subsequent counter-current extraction in a Rotating-disc-contactor showed it was possible to remove the unwanted polar components from a solution of wool-grease in hexane by extraction with 60% V/v isopropanol in water (IPA) (2). However two problems hindered further development: (i) the lack of equilibrium data accounting for known component interactions; and (ii) the lack of a multi-component design procedure for Dual-Solvent Extraction (DSE).

Solutions to both problems are presented here. These were tested by comparing the predicted separations of characteristic wool-grease components with those determined experimentally using a mixer-settler pilot plant.

EQUILIBRIUM SPECIFICATION

Specification of the equilibrium distribution of wool-grease components was complicated by: (i) the large number of esters formed from more than 180 different alcohols and 75 different acids; and (ii) the high degree of component interaction found in the hexane/IPA system.

In this appraoch wool-grease was separated into a series of fractions by counter-current solvent extraction. The principal components of the fractions were identified by a range of qualitative analytical methods for lipids. Characteristic pure components were selected to create a managable multi-component model. As well as representing the distribution characteristics of the fractions, the model components must be amenable to accurate quantitative analysis in both the hexane-rich and IPA-rich phrases. Components satisfying these requirements were: (i) cholesteryl stearate; (ii) cholesterol; (iii) stearic acid; and (iv) a refined detergent. High-performance-liquid-chromatography (HPLC) methods were developed for their analysis.

The scouring detergents commonly recovered with wool-grease are condensation products of nonyl-phenol and ethylene oxide, containing a broad distribution of ethoxy chainlengths. Distribution between the solvents and the interaction effect of the detergent were found to depend on chainlength. Because it was impossible to buy or synthesize a sufficient amount of representative single chainlength detergent, a refined detergent of narrow chainlength distribution was produced by multi-stage extraction of a commercial product.

The equilibrium distribution of the model components between pre-equilibrated hexane and IPA was investigated over a range of concentrations correspondingto those likely to be encountered in solvent-extraction refining. Factorial experiments indicated an empirical equation containing terms to account for binary interactions was satisfactory. Coefficients were fitted to the experimentally determined phase-compositions by multi-variable least-squares regression (3).

DESIGN OF MULTI-COMPONENT D.S.E. SYSTEMS

The design procedure comprises two parts shown in Figure 1:

(i) The region of permissible solvent flowrates, for which the design separation can be achieved with a finite number of extraction stages, is determined by an adaptation of Prochazka and Jiricnys' two solute approach (4).

(ii) The number of stages required to achieve the design separation at a suitable set of solvent flowrates selected from within the permissible region is determined by systematically solving specified operating problems to converge on a configuration which satisfies the requirements.

The operating problem solution uses an iterative matrix method which simultaneously solves the mass balance and equilibrium relationships describing the extraction system. The method is based on that of Napthali and Sandholm (5) for distillation systems.

TESTING OF METHOD

A hexane solution of the model components was counter-currently extracted with aqueous IPA in a 12-stage mixer-settler pilot-plant. Hexane-rich solvent (L_O) entered at stage 1, IPA-rich solvent (V) entered at stage 12 and the feed solution (L_F) entered at stage 5.

Two model grease compositions were used as feed. One had an excess of cholestrol, stearic acid and detergent compared to typical wool grease, to test the system with high distribution interactions (Runs 1, 2, 3). Runs 4 and 5 used a feed with component concentrations simulating a typical grease. For all runs $L_O/L_F = 0.5$.

Once steady-state operation was achieved samples of both raffinate (hexane-rich) and extract (IPA-rich) were withdrawn from each settler and analysed by HPLC methods to determine the concentrations of the four model components. Solute flowrates were then calculated and material balances performed.

COMPARISON OF PREDICTED AND EXPERIMENTAL RESULTS

For all five runs the iterative matrix method converged rapidly and predicted flowrates of the model wool-grease components that generally agreed well with experimental values. Figure 2 shows the solute flowrates in the raffinate and extract leaving each extraction stage for a run with the feed containing the high proportions of polar components at the ratio $V/L_F = 1.5$. Despite interactions for this feed being much higher than those typical of wool-grease, the only significant discrepancy was for cholesteryl stearate in the raffinate. The problem was traced to the HPLC analysis. Because of the large size and non-polar nature of the cholesteryl stearate molecule, it was separated by the HPLC column more on the basis of size than selective adsorption. Consequently its retention time on the chromatographic column was almost as short as the elution solvent. At high concentrations of cholesteryl stearate the response peak due to cholesteryl stearate overlapped that of the solvent and was difficult to accurately measure. There was little overlap for the extract samples which were of lower cholesteryl stearate concentration.

The overall extraction performance may be summarized by calculating the fraction of the input of each component in the feed removed by either the extract leaving stage 1 or the raffinate leaving stage 12. Table 1 compares the predicted removals with those obtained experimentally.

The mass balance closures for cholestrol and detergent were generally good, while that for stearic acid was poor. The main discrepancies occurred between predicted and experimental removals of the acid in the extract phase. Run 4 in particular showed a large unaccounted acid loss.

Since less than 1% of the input of cholesteryl stearate was in the extract, concentration in the raffinate could be reliably calculated by mass balance. This was used in preference to direct analysis.

Overall the results of the five runs showed that:

(i) detergent was almost completely removed from the raffinate leaving stage 12 for both feeds was at the lowest extraction ratio ($V/L_F = 1.5$);

(ii) at similar extraction ratios less stearic acid was extracted for runs using the "high interaction" feed;

(iii) cholesterol was not preferentially extracted even at the high extraction ratio ($V/L_F = 5$);

(iv) cholestryl stearate was recovered almost completely in the raffinate leaving stage 12. (viz. undesirable losses of valuable ester components are negligible).

Subsequent extractions of real wool-greases of varying characteristics have confirmed the applicability of the above to the natural grease. The combination of the equilibrium specification and multi-component design procedure should provide a valuable tool for the design of extraction systems to refine wool-grease.

APPLICATION TO SYSTEMS OTHER THAN WOOL-GREASE

Although the equilibrium specification was developed specifically for wool-grease and the matrix method tested on the model wool-grease, the procedure developed have a wider applicability. Complex natural systems can be simulated by model components and meaningful extraction data collected. The mathematical form of the equilibrium specification should be tailored to suit the interactions observed for the selected model components. The only modifications to the DSE design procedure will be to the subrountines used by the matrix method to evaluate the derivatives of the distribution coefficient.

REFERENCES

1. "U.S. Pharmacopoeia", 19th Revision, Mack Publishing Co., Easton, P.A.

2. J.J. Warner and G.F. Wood, Proc. 6th Int. Wool Textile Research Conf., Pretoria, South Africa, p. 173 (1980).

3. J.J. Warner and I.J. Harris, J. AOCS, 59, 386 (1982).

4. J. Prochazka and V. Jiricny, C.E.S., 31, 179 (1976).

5. L.M. Napthali and D.P. Sandholm, J. A.I.Ch.E., 17, 148 (1971).

TABLE 1 Comparison of Predicted (P) and Experimentally measured (E) component removal.

COMPONENT	% Removal of Component								Solvent Ratio	
	1		2		3		4			
	P	E	P	E	P	E	P	E	$\frac{V}{L_F}$	$\frac{L_o}{L_F}$
Run 1									5.05	0.545
EXTRACT	0.1	0.6	0	1.8	20.5	0.5	100	103.6		
RAFFINATE	99.9	-	100	99.2	79.5	89.0	0	0		
Run 2									2.10	0.480
EXTRACT	0	0.2	0	0.1	4.5	1.6	100	110		
RAFFINATE	100	-	100	133	95.5	113	0	1.4		
Run 3									1.45	0.467
EXTRACT	0	0.2	0	0.5	2	0.7	100	97.2		
RAFFINATE	100	-	100	107	98	98.9	0	0.7		
Run 4									5.78	0.439
EXTRACT	0.8	0	0.1	25.1	74.4	10.3	100	110		
RAFFINATE	99.2	-	99.9	66.1	25.6	35.2	0	0		
Run 5									2.43	0.450
EXTRACT	0	0	0	0	16.0	0	100	116		
RAFFINATE	100	-	100	88.1	83.9	88.7	0	0		

NOTE 1.

COMPONENTS: 1 - CHOLESTERYL STEARATE
2 - CHOLESTEROL
3 - STEARIC ACID
4 - DETERGENT

NOTE 2.

Direct determination of cholesteryl stearate in the raffinate phase was not feasible due to solvent interference.

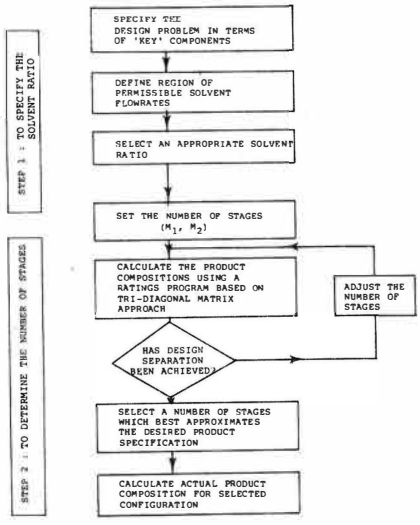

FIGURE 1. FLOW DIAGRAM FOR DESIGN PROCEDURE

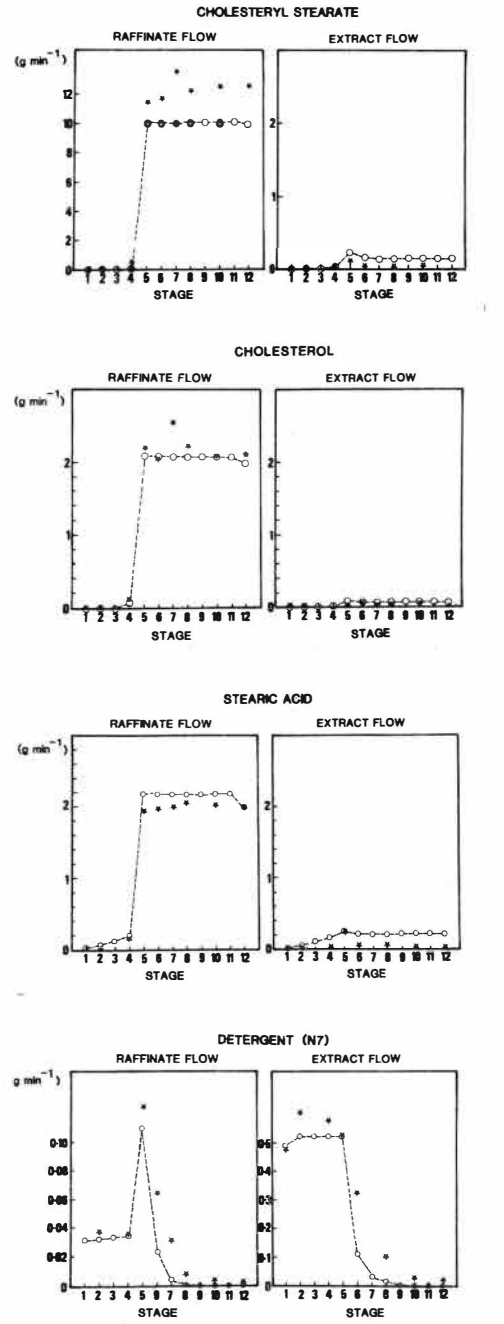

FIGURE 2. SOLUTE FLOWRATES IN THE EXTRACT AND RAFFINATE.
Basis : 1 l/min of feed to stage 5

✱ experimentally determined
○ predicted
● determined by material balance

STUDY ON EXTRACTION OF CITIRC ACID

Jian Yu-Ming, Li Dao-Chen and Su Yuan-Fu

East China Institute of Chemical Technology
Shanghai, China

Citric acid (2-hydroxy-1,2,3,-propanetricarboxylic acid) is now produced commercially by fermentation method. The fermentation broth is first filtered. The acid is then precipitated as calcium salt and is again liberated by adding sulfuric acid as fairly pure compound which is further purified by ion exchange and decolorized by active carbon. The final product is obtained after evaporation and crystallization.

The repeated precipitations, filtrations and washings with hot water and the disposal of unsaleable calcium sulfate become main disadvantages of the conventional process. As an alternative means of its recovery, liquid-liquid extraction has been tried by many workers. Several patents disclosed the use of amines and amide as solvents (1) (2). Renald Wennersten (3) reported a number of solvents and their distribution coefficients and proposed to use different temperatures for extraction and stripping. But he failed in overcoming the emulsion problem when the fermentation broth was used in stead of pure citric acid solution. It was announced that a citric acid plant by solvent extraction would be erected (4), but the product is not to be used in food and pharmacentical industries.

The present paper pays special attention to the key problems for the successful use of solvent extraction to obtain citric acid for edible purpose from fermentation broth.

SELECTION OF EXTRACTANT

The filtered solution from fermentation broth contains about 100 g/l citric acid. A number of potential solvents were tested and the preliminary results were shown in Table 1.

Table 1 Distribution coefficients D(O/A) of citric acid
Temperature 25°C, aqueous feed 100 g/l,
phase ratio 1:1

Extractant	i-amyl alcohol	C=O bond			amines	
		Cyclohexanone	MIBK	N503[a]	N235[b]	Trioctylamine
D(O/A)	0.13	0.37	0.20	0.36	50.0	15.4
Extratant		P=O bond			S=O bond	
		TBP	R_3PO[c]	P277[d]	$(C_4H_9)_2SO$	Petrol sulfoxide[e]
D(O/A)		1.49	7.61	0.82	3.24	1.02

(a) Dibinaryoctyl ethylamide (b) Tertiary amine (C_8-C_{10})
(c) Trialkyl phosphine oxide (average mol. wt. 312)
(d) Dialkyl phosphonate (e) average mol. wt. 176

From Table 1, it is apparent that iso-amyl alcohol and those solvents with C=O bond give distribution coefficients much less than other solvents and are considered ineffective. The amines have the highest distribution coefficients. But there are three drawbacks, firstly, the very high coefficient which is desirable in extraction means very difficult for the acid to be stripped with pure water; secondly, the unknown toxicity of amines will prevent their use in the recovery of the acid for edible purpose; and thirdly, a stable emulsion is formed and causes great trouble in extraction.

Dibutylsulfoxide (DBSO) and petroleum sulfoxide have moderate distribution coefficients and behave similar to TBP and R_3PO. In comparison with neutral organophosphorus compounds, the solubility of DBSO in water is fairly large and a means of its recovery from raffinate and stripping solution must be taken into account.

The solvents having P=O bond all show promising extraction abilities which follow the order: TRPO > TBP > $R(RO)_2PO$. TRPO and TBP were then selected for further study.

EXTRACTED COMPLEX

The complex formation reaction between citric acid (H_3A) and organophosphorus compound (S) may be expressed as follows:

(1) $$H_3A + pS + rH_2O = H_3A \cdot pS \cdot rH_2O$$

In ideal case,

(2) $$K_{ex} = \frac{(H_3A \cdot pS \cdot rH_2O)_o}{(H_3A)_a\,(S)_o^p}$$

(3) $$D = K_{ex}(S)_o^p$$

The composition of TBP complex was reported (5) to be $C_6H_8O_7 \cdot 3TBP \cdot 2H_2O$. In the present study the following methods were used to identify the complexes formed by interaction between extractants and citric acid.

(A) Double logarithm plots Eq. 3 may be written in logarithmic form:

(4) $$\log D = \log K_{ex} + p \log (S)$$

From the distribution coefficients D obtained by varying concentrat ons of TBP and TRPO respectively the values of p have been found from the slopes of the straight lines on log-log plot. The equations for TBP and TRPO are

(5) $$\log D_1 = 2.58 \log (TBP)_o - 0.48$$

$$\log D_2 = 1.81 \log (TRPO)_o$$

(B) Continued variate method To maintain the sum of concentrations of the extractant in organic phase and citric acid in aqueous phase constant and equal to 3 M (O/A = 1), the ratio of H_3A to S in organic phase at equilibrium changes continuously as shown in Fig. 1. The maxima of the curves give the molecular ratio (TBP)/(H_3A) = 3 and (TRPO)/(H_3A) = 2 respectively.

(C) Water moleculaes in the complex By using "Moisture Meter", the combined water in the complexes was determined (Table 2).

Table 2 Data obtained from "Moisture Meter"

Complex model	H_3A, g/l	H_3A, mol/l	H_2O, %	H_2O, mol/l
$H_3A \cdot 3TBP \cdot 2H_2O$	80.6	0.445	1.64	0.845
$H_3A \cdot 2TRPO \cdot H_2O$	110	0.606	1.15	0.576

(D) Elementary analysis To verify the composition of the complex, C and H were analyzed. The values obtained agree well with those calculated.

(E) IR and NMR studies In Figs. 2 and 3 the IR spectra of the extractants and their complexes are shown. It is found that $\bar{\nu}_{P=O}$ of TRPO moves towards low frequency from $\bar{\nu}_{P=O}$ = 1150 cm^{-1} to 1125 cm^{-1}, i.e. $\Delta\bar{\nu}_{P=O}$ = 25 cm^{-1} (Fig. 3). Similary, in Fig. 4 $\bar{\nu}_{P=O}$ of TBP moves from 1269 cm^{-1} to 1240 cm^{-1}, i.e. $\Delta\bar{\nu}_{P=O}$ = 29 cm^{-1} and that of $\bar{\nu}_{P-O-C}$ moves from 1040 cm^{-1} to 1015 cm^{-1} with $\Delta\bar{\nu}_{P-O-C}$ = 25 cm^{-1}.

The proton NMR was also studied and the results are shown in Figs. 4 and 5. The difference of chemical shift of $-CH_2-$ of TRPO is $\Delta\sigma$ = 0.35 ppm (from δ = 3.20 ppm of pure TRPO to 2.85 ppm of the complex). Whereas the difference of chemical shift of $-CH_2-O-$ of TBP is $\Delta\sigma$ = 0.13 ppm (from δ = 3.90 ppm of TBP to 4.03 ppm of extracted complex.

The difference in the sign and magnitude of chemical shifts of the two extractants indicates that TRPO exerts stronger coordination force hence possesses higher extracting power than TBP.

DILUENT

In order to improve the physical properties and to facilitate phase separation, diluent and modifier are usually added to the extractant. In addition, the use of diluent to adjust the distribution coefficient to meet the requirements of both extraction from aqueous broth and stripping into pure water is important in the present case. A mixed solvent considerad the most suitable.

TEMPERATURE EFFECTS

According to the thermodynamic relationship, the enthalpy change of the extraction process may be written as follows:

(6) $$K = K_o \exp(-\Delta H/RT)$$

Because the distribution coefficient D is proportional to equilibrium constant K, then

(7) $$\ln D = \ln D_o + (-\Delta H/R)T^{-1}$$

In the temperature range between 15° and 80°, D values were determined for two mixed solvents and the data have been plotted in Fig. 6. It follows that

For 30% TRPO + 70% kerosene,

$$\log D = 0.083 \times 10^4 T^{-1} - 16, \quad \Delta H = -3.8 \text{ Kcal/mol}$$

For 80% TBP + 20% kerosene,

$$\log D = 0.116 \times 10^4 T^{-1} + 3.78, \quad \Delta H = -5.1 \text{ Kcal/mol}$$

Both extraction processes are exothermic, so the extractions are favarably carried out at lower and strippings at higher temperatures.

Provided that a proper value of distribution coefficient is adjusted by adding inert diluent and extraction is carried out at 20°-30° and stripping at 80°-90°C, the theoretical stages required to attain high percentage recovery

may be kept at reasonable numbers.

COMPOSITION OF BROTH

Preliminary test shows that both the magnitude of distribution coefficient and the form of the extraction isotherm are affected by the presence of impurities in the broth. However, the most serious problem encountered during the extraction is the formation of a stable emulsion when two phases are mixed. The ingredients are liable to cause emulsification and impurities may be coextracted have been examined and shown in Table 3.

Table 3 Composition and extraction behavior

Substance	Citric acid g/l	Reducing sugar %	Protein %	Ca ppm	Mg ppm	Fe ppm
Composition	108.4	0.80	0.40	8	14	15
D(TRPO)		0.063		0.125	0.043	0.93
$\beta(H_3A/imp)$		94.0		47.4	138	6.57

PROBLEM OF EMULSIFICATION

Protein in solution lowers the interficial tension appreciably (see Fig. 6) and is adsorbed on the surface of dispersed phase droplets to form stable emulsion which may stand for months without phase separation. The O/W type emulsion formed in the present case is shown as Fig. 7. When amine of long chain is used as an extractant, emulsion will form even with pure citric acid solution, since the long chain aliphatic amine itself is a good surfactant. Using HLB (Hydrophilic and Lipophiloc Balance) method, emulsion type may be identified by computation, e.g. the HLB value of N235 is between 2.25 to 5. The emulsion should be W/O type which is confirmed by microscopic photograph (Fig. 8). A high alcohol, which is a stronger surfactant and tend to take the position occupied by amine but does not form stable surface film, may be added so that the droplets may coalesce on collision.

REMOVAL OF THE PROTEIN

Its removal may be effected by adsorbing it on active carbon or by any chemical means. The adsorption of protein on carbon follows Freundlich isotherm (65°C):

(8) $$x/m = kC^{0.592}$$

were x - amount adsorbed, arbitrary unit
m - amount of carbon used
C - amount adsorbed at equilibrium in aqueous phase

The removal of protein is considered as key step to the success of extraction operation.

TOCICITY

As the present investigation is to produce the citric acid for edible purpose, the first consideration is to avoid the use of extractant of high toxicity. The literature (6) has revealed that amine which has no replaced bond is poisonous. The LD50 values of amines are much smaller that those of neutral organophosphorus extractants, e.g. LD50 value of N235 is 442 mg/kg, whereas those of TBP and TRPO are 3000 and 3370 mg/kg respectively.

Although sulfoxides are considered harmless, the toxicity and unpleasant odour of alkylsulfides which may be present in sulfoxide as impurities are the reasons not being selected in this investigation.

The citric acid produced in kilograms by using TRPO as extractant had been proved to accord with the demands of British Pharmaceutical Codex (1977) and passes "AMES" test. It is also proved there is no organic phosphorus residue left in the crystals.

PROPOSED RECOVERY PROCESS

Fig. 9 is a proposed flow diagram for the recovery of citric acid from fermentation broth. In comparison with the conventional Ca-salt process, the solvent extraction replaces two precipitations and two filtrations; the proposed process does not need to use any chemicals hence no problem of disposal of calcium sulfate sludge. Besides, the only change is to treat the broth with active carbon before extraction in stead of aftertreatment.

REFERENCES

(1) A.M. Baniel, R. Blumberg and K. Hajdu, British. Pat. 1,426,018 (1973).
(2) J.E. Alter and R. Blumberg, U.S. Pat. 4,251, 671 (1981).
(3) Ronald Wennersten, Proceedings ISEC'80, vol. 2, 80-63.
(4) The News, Fermentation and Industry (Japan) 39(3) (1981).
(5) A.M. Loking (editor), Extraction handbook (USSR), ATE Company, Moscow (1976).
(6) Bolikutsehaku, "Pollution and Toxicity" (Japan) MBC Press, Tokyo (1978).

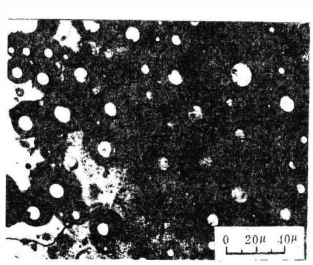

FIG. 7
EMULSION FORMED WITH PROTEIN, O/W TYPE

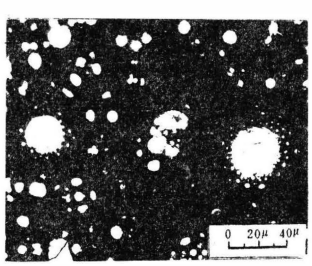

FIG. 8
EMULSION FORMED WITH AMINE, W/O TYPE

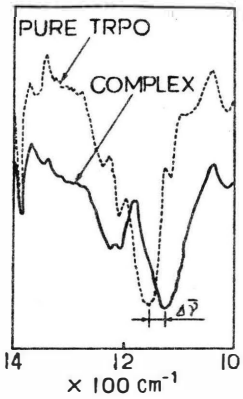

FIG. 2
IR SPECTRA

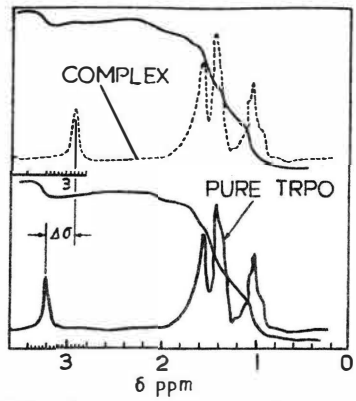

FIG. 4
PROTON NMR SPECTRA

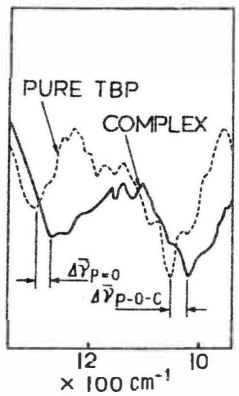

FIG. 3
IR SPECTPA

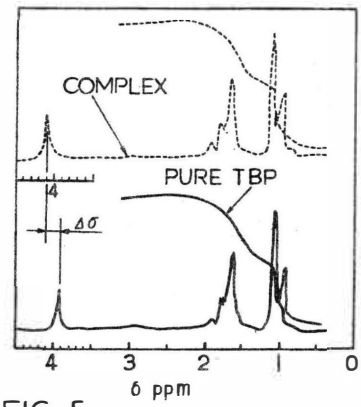

FIG. 5
PROTON NMR SPECTRA

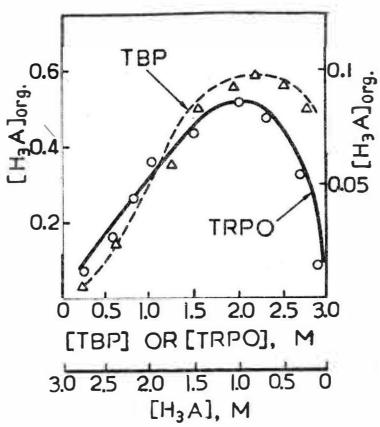

FIG.1 CONTINUED VARIATE METHOD

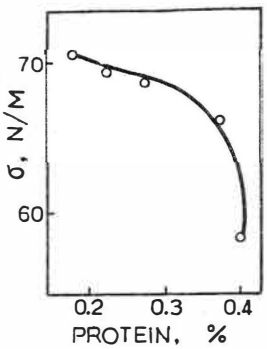

FIG.6 EFFECT OF PROTEIN CONTENT ON INTERFACIAL TENSION

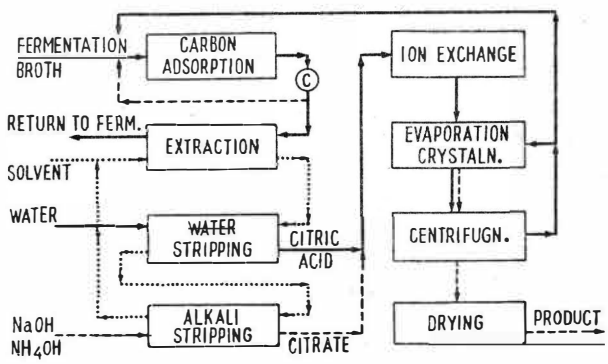

FIG. 9 PROPOSED RECOVERY PROCESS

PLANTS AND PROCESS ENGINEERING FOR HIGH-PRESSURE EXTRACTION OF NATURAL PRODUCTS

E. Lack, G. Bunzenberger, R. Marr

Institut of Chemical Engineering
Technical University Graz
Graz, Austria

INTRODUCTION

The number of research activities in extraction of natural substances with the high-pressure technology using gases in it's liquified or supercritical state still increased in the last few years (1,2,3). In difference to the conventional extraction processes this technology uses solvents which are gaseous under normal conditions. Therefore high pressures are applied to give these gases a density and solvent power which are simmilar to usual solvents. For extraction of natural substances which often are sensitive to heat or oxidation (4), carbon dioxide is a propper solvent in the extraction process. Out of a great number of small scale laboratory experiments, energetic optimation has to be done and the best operation conditions for industrial scale have to be found. In accordance to the experiences obtained in conventional leaching processes, these experiences have to be checked wether they can be applied to the new high-pressure extraction technology. As a final result it should be possible to reduce the great number of pilot experiments for plant optimization,

DESCRIPTION OF THE PROCESS

Up to now all known industrial applications of HPE are batch processed (Fig.1). First the raw material is filled into the extraction vessel (or in a cascade of extraction vessels). Compressed and preheated carbon dioxide flows through the extractor and the leaching process starts and is continued until the demanded degree of extraction (yield) is reached. The charged solvent normally is stripped by pressure reduction or by change of temperature (isobar). In the case of pressure reduction, the cicle CO_2 is completely evaporated to minimize the solubility and to insure that now extract phase is carried back with the solvent. The settled extract can easily be drained of the separation vessel through a valve. The extract-free gaseous CO_2 is condensed and flows back into the storage vessel. The cycle of the solvent CO_2 is:

- priming
- compressing
- solving of the substance
- changing of pressure
- separation of solutes and solvent
- priming

PLANT AND PROCESS ENGINEERING

Because of the numerous different natural substances which can be isolated with HPE (5) each material demands it's own conceptions and the design parameters must be evaluated separately. Some basic data have to be known

- proposed quantity of extract
- concentration of the desired substance in the raw material
- the preparation of the material before the extraction process (drying, milling, grinding, pelletizing etc.)
- spezific volume of the prepared raw material
- operating mode (continous, batch-processed)

For the evaluation of the process parameters, laboratory scale and pilot plant experiments are necessary. For plant design, thermodynamic and energetic studies and the optimization of the mass-transfer must be combined.

The experimental work starts with the determination of the thermodynamic conditions (6,7) given by pressure and temperature, where the highest solubility of the value agent is in the extraction step, the lowest solubility in the separation step. Temperatures are often limited by the thermal instability of natural compounds. Pressures are strongly influenced by investment costs. In most cases where CO_2 is applied the extraction pressures are between 50 and 300 bar. The temperatures vary from 5^oC to 50^oC.

The third parameter which influences the values of pressure and temperature is the minimization of energy costs for the CO_2 cycle. After pressures and temperatures are estimated, the next step is the measurement and the optimization of mass-transfer itself. First of all, mass transfer is a function of the diffusion-coefficients, the particle size and the velocity with which the solvent (CO_2) passes the particles. The mass transfer velocity is strongly influenced by the diffusion of the CO_2 through the cell membrane (the permeability of the cell membrane for CO_2) but can hardly be improved. To keep the boundary layer on the particle surface as thin as possible and to avoid the formation of "solvent channels" through the extraction vessel, slight agitation of the contents (raw-material) can be applied. The CO_2-throughput resulting from these considerations determines the extraction time.

DESCRIPTION OF THE HPE-PROCESS IN THE TS-DIAGRAM

Concluding, two examples should show how the HPE technology can be applied for two different kinds of raw material. The first one (Fig. 2) has useful ingredients which could be extracted easily at very low extraction pressures because the solubility in the CO_2 is very high. The second raw material (Fig. 3) shows increasing solubility with increasing extraction pressure and at relative high temperatures. In the separation step there is no need to throttle into the two phase region of CO_2 because there is only a very little solubility at the estimated separation pressure which still is a little bit over the critical pressure of CO_2.

REFERENCES

/1/ D.F. Williams, Chem.Ing.Sci.36(11) 1769 (1981)

/2/ G.Brunner and S.Peter, Chem.Ing.Techn.,53(7), 529 (1981)

/3/ T.R. Bott, Chem.Ind.(London), 228 (March 15, 1980)

/4/ E.Stahl and E.Schütz, Planta Med., 40,12 (1980)

/5/ R.Eggers and R.Tschiersch, Chem.Ing.Tech.,50(11),842 (1978)

/6/ D.Peng and D.Robinson, Ind.Eng.Chem.,Fundam.,15(1),59 ; (1976)

/7/ J.Chrastil, J.Phys.Chem.,86, 3016 (1982)

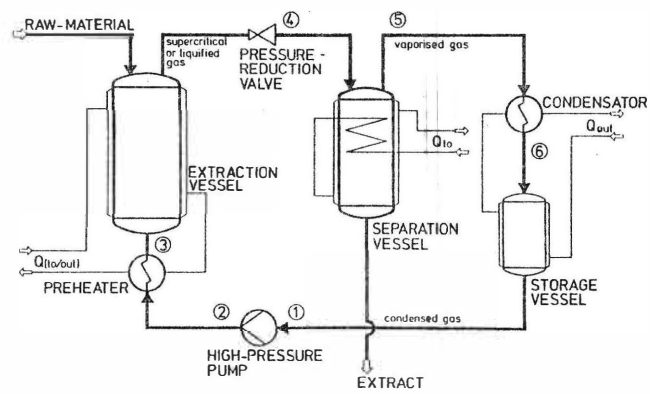

Fig.1: Flow sheet

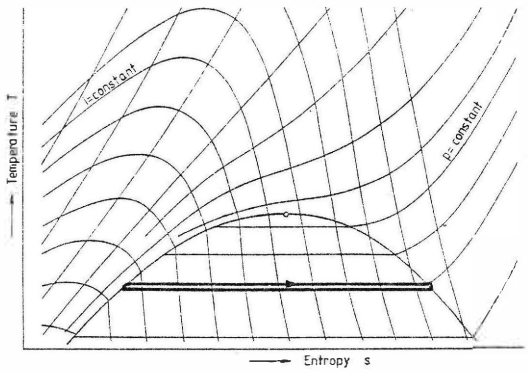

Fig.2: Extraction of a light soluble value agent under subcritical extraction conditions with total evaporation in the separation step.
e.g.: etherical oils such as anethol, carvon.....

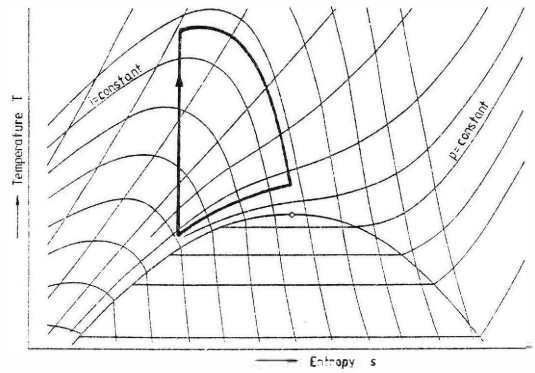

Fig.3: Extraction of a value agent with satisfactory solubility under high pressure and supercritical extraction conditions and with supercritical separation.
e.g.: vegetable oils

MASS TRANSFER FROM SOLID MATERIAL IN GAS EXTRACTION

G. Brunner

Technical University of Hamburg-Harburg
West Germany

Extraction of substances from solid substrates by supercritical dense gases can be divided in two steps:

1. transport of the substances to be extracted within the solid material to the interface solid-gas
2. transition of the extracted substances into the gas and transportation with the bulk of the extracting gas.

The first step can be modelled by unsteady depletion of the solid substrate of the extracted substances. Essential parameters are diffusion coefficients and length of the diffusion path for the extractants. In extraction processes from solids, solvents enhance the diffusion coefficients. Compressed gases which are dissolved in the condensed phases of the solid material act similarily since they diminish density and viscosity of those phases.

During the second step of the extraction, the substances cross the interface and are taken away by the bulk of the gas. The solubility of the extracted substances in the supercritical gas is a physical limit for the capacity of the gas, which in real processes is never reached. For mass transport from the solid to the gas diffusion coefficients of the substances in the gas and throughput of the gas are decisive.

A quantitative evaluation of these process steps should result in a fairly accurate value for the time needed for the extraction process.
In this work the unsteady diffusion within the solid material is calculated approximately by using the first term of the general solution of the problem, obtained by Fourier analysis. Thus extraction time is a function of the ratio between mass transfer coefficient to the gas and diffusion coefficient in the solid material and of the amount of extracted substances.

$$t = \frac{L^2}{4 \cdot E\,(Bi) \cdot D_S} \cdot \ln \frac{C_q\,(Bi)}{1 - m/m_C}$$

Bi - Biot number : $Bi = \frac{\beta \cdot L}{D_S}$

β - mass transfer coefficient

L - characteristic length

D_S - diffusion coefficient in the solid material of substance (s) to be extracted

E,Cq - numerical values of the approximate solution

m - amount of extracted substance(s) at time t

m_C - amount of substance(s) to be extracted

The mass transfer coefficient can probably be calculated from correlations obtained for mass transfer at low gas velocities in fixed beds. In this work calculation of the mass transfer coefficient is achieved by making use of the principle of analogy to heat transfer, applying the following correlation:

$$\frac{\alpha}{\beta} = \frac{\lambda}{D} \cdot Le^{-1/3} = \frac{\lambda}{D} \left(\frac{D}{\lambda} \cdot \rho \cdot c_p\right)^{1/3}$$

This equation should be valid for laminar flow which is neither thermally nor hydrodynamically developed

λ - thermal conductivity of the gas

D - diffusion coefficient of the extracted substances in the gas

Le - Lewis number

ρ - density

c_p - specific heat at constant pressure

Heat transfer coefficients are calculated for cross flow on single particles - and adjusted to a fixed bed of particles by an empirical function dependent on mean bulk porosity

$$Nu_b = \phi(\psi) \cdot Nu$$

Nu=Nusselt number $\alpha \cdot L/\lambda$

ϕ - empirical function

ψ - mean bulk porosity

By this procedure a function for β can be obtained, which reads:

$$\beta = 0{,}664 \cdot \phi\,(\psi; Pe) \cdot \psi^{-1/2} \cdot \left(\frac{\dot{V}}{A_t}\right)^{1/2} \cdot L^{-1/2} \cdot D^{2/3} \cdot \nu^{-1/6}$$

with:

Pe _ Peclet number

$\dot{V}$ - throughput of gas

A_t - area of cross section of the extraction vessel

ν - viscosity

Results of evaluating extraction time by this procedure are compared with experimental results of gas extraction processes.

RESIDUUM OIL/PROPANE-PHASE EQUILIBRIUM UNDER SUPERCRITICAL CONDITIONS

H. H. Oelert, U. Lutz

Technical University of Clausthal
West Germany

In the past decades, several processes of supercritical extraction-including petroleum residues- have been developed. The objective of this paper is -proceeding of principial known extraction systems- to investigate the influence of entrainers. This components should improve the quality and yield of the upgraded product (SCF-extract).

An apparatus for measuring phase equilibria -up to 300 bar and 300°C- was developed. Samples from the gas and liquid phase can be taken out of the 1l autoclave.The phase equilibrium is not disturbed by this operation. While the gas-content of the samples is measured by a gas burette, the liquid portion is determind gravimetrically.

In the first part of this investigatins, quasi-binary equilibria were measured in a range from 50-300 °C and a maximumm operation pressure of 250 bar (see pictures 1). As feedstock a long residue and a short residue were used, the supercritical component in this case was propane.

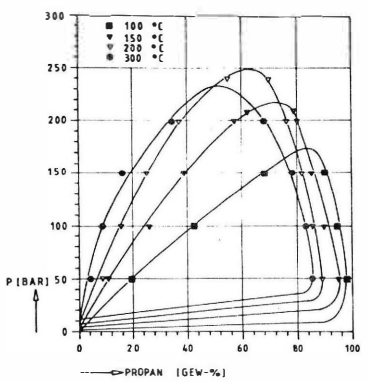

The extract was analyzed and characterized by ^{1}H-NMR, IR, mass spectroscopy, elementary analysis and average molecular weight. From this experiments the following results were obtained:

- increasing pressure at constant temperature delivers products with a lower H/C ratio, that means the content of aromatics increases.
- the average molecular weight increases with increasing pressure (T = const.).
- with increasing temperature at constant pressure the average molecular weight decreases.

In the second part of the investigations a third component, which acts as an entrainer, was added in the range of 10 - 20 wt% to the residue/propane-system. Applied have been e.g. benzene, i-propanol, cyclohexane etc. The fractions, which were obtained by this operations, were analyzed by the same methods as in part 1. Some of the results are listed below:

- benzene, cyclohexane for example, increase extract-quantity.
- toluene, chlorbenzene and ethyl-methyl-keton decrease the extract quantity.
- in case of higher extract-quantity, the average molecular weight increases, the H/C ratio tends toward 1, that means the content of aromatic increases. This result is confirmed by ^{1}H-NMR spectroscopy.

SELECTIVE SOLUBILIZATION IN AQUEOUS MICELLAR SOLUTIONS

E. Ruckenstein and R. Nagarajan

Department of Chemical Engineering
SUNY at Buffalo
Amherst, New York 14260 USA

Department of Chemical Engineering
The Pennsylvania State University
University Park, Pennsylvania 16802 USA

ABSTRACT

Experimental data are presented demonstrating that aqueous micellar solutions can selectively solubilize organic molecules depending on their molecular volume and polarity. The origin of this selectivity has been interpreted in terms of the competitive energetic changes accompanying solubilization. It is proposed that aqueous micellar solutions may be used as extractants in extraction or purification processes involving polar organic molecules.

INTRODUCTION

Surfactant molecules self-assemble in aqueous solutions to form molecular clusters known as micelles (1). The micelles have an hydrocarbon like interior made up of the surfactant tails and a polar exterior made up of the dipolar or ionic surfactant head groups. Organic molecules which are sparingly soluble in water find a more compatible environment in the oil like interior of the micelles. Consequently, the solubility of such organic molecules is enhanced very significantly in aqueous micellar solutions (2, 3).

The enhancement of solubility in micellar solutions is found to depend upon the characteristics of the molecule being solubilized. In this paper, experimental data on the extent of solubilization are reported for a number of organic molecules. Data are also presented on the selectivity ratio for one component over another when binary organic mixtures are solubilized by the aqueous micellar solutions. Experimental results show that aqueous micellar solutions selectively solubilize organic molecules of smaller molecular volume and some polarity compared to highly nonpolar and larger organic molecules. These results are interpreted in terms of the energetic changes associated with solubilization, using a thermodynamic approach developed by us earlier (4, 5).

EXPERIMENTAL METHOD

Determination of Molar Solubilization Ratio. The extent of solubilization of a number of organic molecules have been measured in 0.1 M cetyl pyridinium chloride (CPC) micellar solution at 25°C. The method involves contacting equal volumes of aqueous CPC solution and the solubilizate phase over a period of 24 hr to achieve equilibration. The total amount of solubilizate extracted into the aqueous micellar solution is determined by a direct gas chromatographic analysis using a flame ionization detector. The extent of solubilization is quantitatively represented in terms of the molar solubilization ratio, defined as the number of solubilizate molecules per surfactant molecule in a micelle.

$$\text{(1)}\quad \text{Molar Solubilization Ratio} = \frac{\text{Moles of Total Solubilizate in Micellar Solution} - \text{Moles of Singly Dispersed Solubilizate in Micellar Solution}}{\text{Moles of Total Surfactant in Micellar Solution} - \text{Moles of Singly Dispersed Surfactant in Micellar Solution}}$$

The concentration of singly dispersed surfactant corresponds to its critical micelle concentration. The concentration of singly dispersed solubilizate corresponds to its solubility in pure water. Experimental molar solubilization ratios have been determined in a number of surfactant solutions other than CPC as well, and the detailed results will be presented elsewhere (6).

Determination of Selectivity Ratio. When binary organic mixtures, say of components A and B are solubilized, the molar solubilization ratios as defined above are determined for each of the solubilizates. Of course, the moles of singly dispersed solubilizates A and B in this case are influenced by the composition of the organic mixture. Using the experimental molar solubilization ratios for both components, one can calculate the selectivity ratio for component A over B as

$$\text{(2)}\quad \text{Selectivity Ratio for A} = \frac{(X_A/X_B)\text{ in micelles}}{(X_A/X_B)\text{ in organic phase}}.$$

Here, X_A and X_B refer to the mole fractions of components A and B. The selectivity ratios for benzene over hexane have been determined as a function of the organic phase composition, in 0.1 M CPC, 0.1 M sodium dodecyl sulfate (SDS) and 0.1 M dodecyl trimethyl ammonium chloride (DTAC) surfactant solutions. The selectivity ratios for a few other binary mixtures have also been measured and the results will be presented elsewhere (6).

RESULTS AND DISCUSSION

Solubilization of Single Components. The molar solubilization ratios of a number of organic molecules in 0.1 M CPC solutions are shown in Figure 1 as a function of the molecular volume v of the solubilizates. The data are also plotted as a function of $(\sigma v^{2/3}/kT)$ which accounts for the combined influence of the molecular volume v of the solubilizate and its polarity as measured by the solubilizate-water interfacial tension σ.

The data show that a qualitative correlation exists between the molar solubilization ratio and the molecular volume of the solubilizates, the smaller molecules generally exhibiting larger molar solubilization ratios. However, this correlation is not sufficiently satisfactory as can be seen from a comparison of the data for cyclohexane and toluene. Whereas both these molecules have comparable molecular volumes, toluene exhibits a significantly higher molar solubilization ratio compared to cyclohexane.

When the molar solubilization ratios are plotted against $(\sigma v^{2/3}/kT)$ of the solubilizate molecules, a significantly improved correlation is observed. The correlation shows that solubilizates of smaller molecular volume and some polarity exhibit higher molar solubilization ratios compared to highly nonpolar and larger solubilizate molecules. The larger molar solubilization ratio of toluene compared to cyclohexane is thus a consequence of the polarity of toluene arising from its aromaticity.

Solubilization of Binary Organic Mixtures. The molar solubilization ratios of benzene and hexane have been measured in different surfactant solutions by contacting them with binary mixtures of benzene and hexane. The experimental data are plotted in Figure 2 in terms of the selectivity ratio for benzene over hexane. The selectivity ratio is shown as a function of the composition of the binary organic phase, in 0.1 M CPC, 0.1 M SDS and 0.1 M DTAC micellar solutions. In all the cases, the data show that benzene is selectively solubilized compared to hexane. The selectivity of micellar solutions for benzene is large especially when the organic phase is poorer in benzene, the ratio being as high as 8 in DTAC solutions. One may note that the molar solubilization ratio of benzene as a pure component is significantly larger than that of hexane as a pure component.

When binary mixtures of cyclohexane and hexane are solubilized, there is still selectivity exhibited by micellar solutions for cyclohexane compared to hexane (6). However, the selectivity ratio for cyclohexane over hexane is smaller than that for benzene over hexane. It may be noted that the difference in the molar solubilization ratios of cyclohexane and hexane as single components is not as large as that between benzene and hexane.

Thermodynamic Interpretation of Solubilization Data. The larger molar solubilization ratios obtained for polar molecules of small molecular volume can be anticipated from a consideration of the energetic changes associated with solubilization. Both micellization and solubilization processes are driven by the need for hydrophobic (surfactant tail and the solubilizate) molecules to decrease their contact with water. In this process, an hydrophobic micellar core-water interface gets generated. Also, the polar head groups of the surfactant are brought in close proximity of one another at the micellar surface. Consequently, the positive free energy change associated with the creation of the micelle core-water interface and the steric and electrostatic repulsions among the polar head groups at the micellar surface determine the nature of micellization and solubilization.

When solubilizate molecules are incorporated into micelles the surface area per amphiphile of the micelle increases. This increase in area causes an increase in the repulsive (positive) interfacial free energy of the micelle core-water interface. On the other hand, it decreases the steric and electrostatic repulsions between surfactant head groups at the micelle surface. The extent of solubilization is thus principally determined by a balance between these two competing effects. An additional factor favoring solubilization is the increased entropy of mixing of the surfactant and solubilizate in the micelle. For a given increase in surface area per amphiphile, one can introduce a smaller number of large solubilizate molecules or a larger number of small solubilizate molecules into micelles. This explains why a correlation exists between the molecular volume of the solubilizates and their molar solubilization ratios.

However, the interfacial free energy of the micelle core-water interface is determined not only by the area of that interface but also by the interfacial tension at that interface. When highly nonpolar molecules are solubilized, their interfacial tension is similar to the interfacial tension of the surfactant tails and hence the micelle core-water interfacial tension remains large (say 50 dyne/cm for saturated aliphatic molecules). In contrast, when polar aromatic molecules like benzene or toluene are solubilized, they are partially located at the interface (7) causing the interfacial tension to decrease somewhat (to values below 50 dyne/cm). As a result, the increase in the repulsive interfacial free energy associated with solubilization is smaller for polar solubilizates compared to highly nonpolar solubilizates. This explains why solubilization is selective for polar molecules. Also, the origin of the better correlation demonstrated by $(\sigma v^{2/3}/kT)$ which accounts for both molecular volume and the polarity of the solubilizate is thus elucidated.

CONCLUSIONS

Experimental results are presented demonstrating that polar organic molecules of small molecular volume are selectively solubilized in aqueous micellar solutions. When binary organic mixtures are solubilized, the selectivity ratio for one component over another is large if the two pure components have widely differing molar solubilization ratios. Further, the selectivity ratio for the preferred component is large, especially when the organic phase has a low concentration of this preferred component. This selectivity is shown to arise from the competition between an increase in repulsive interfacial energy of the micelle core-water interface and a decrease in the repulsive head group interactions at micelle surface, both caused by the increasing surface area of the micelle triggered by solubilization. Since solubilization is quite selective, especially when the preferred component is present in small quantities in the organic phase, it may be possible to use aqueous micellar solutions for extraction processes. Further, the method will be advantageous if the preferred component could be used in its solubilized form for end applications.

REFERENCES

1. C. Tanford, "The Hydrophobic Effect," Wiley, New York, 1973.
2. M. E. L. McBain and E. Hutchinson, "Solubilization and Related Phenomenon," Academic Press, New York, 1955.
3. P. H. Elworthy, A. T. Florence and C. B. McFarlane, "Solubilization by Surface Active Agents," Chapman and Hall, London, 1968.
4. R. Nagarajan and E. Ruckenstein, Sep. Sci. Technol., 16, 1429 (1981).
5. R. Nagarajan and E. Ruckenstein, in "Surfactants in Solution," Ed. K. L. Mittal, Plenum Press, New York (in press).
6. R. Nagarajan, Mark A. Chaiko and E. Ruckenstein, J. Colloid Interface Sci. (submitted).
7. P. Mukerjee, in "Solution Chemistry of Surfactants," Ed. K. L. Mittal, Plenum Press, New York, 1979.

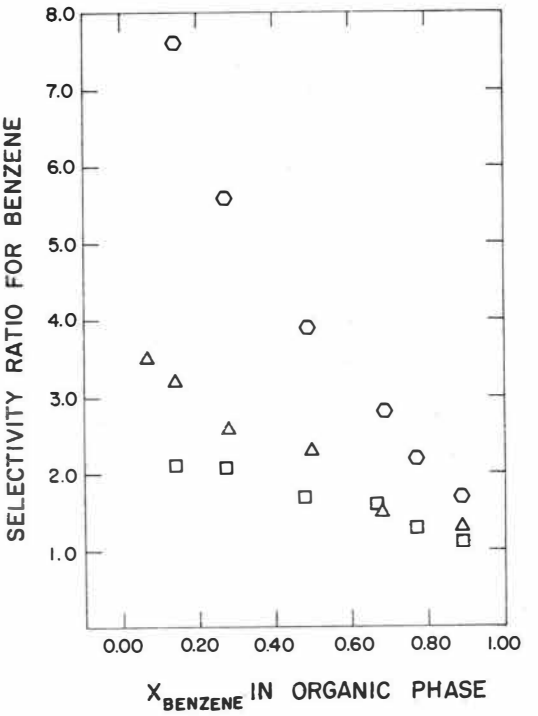

FIGURE 2. SELECTIVITY RATIO FOR BENZENE IN MICELLAR SOLUTIONS AS A FUNCTION OF THE MOLE FRACTION OF BENZENE IN BULK SOLUBILIZATE PHASE. HEXAGONS: 0.1 M DTAC; TRIANGLES: 0.1 M CPC: SQUARES: 0.1 M SDS.

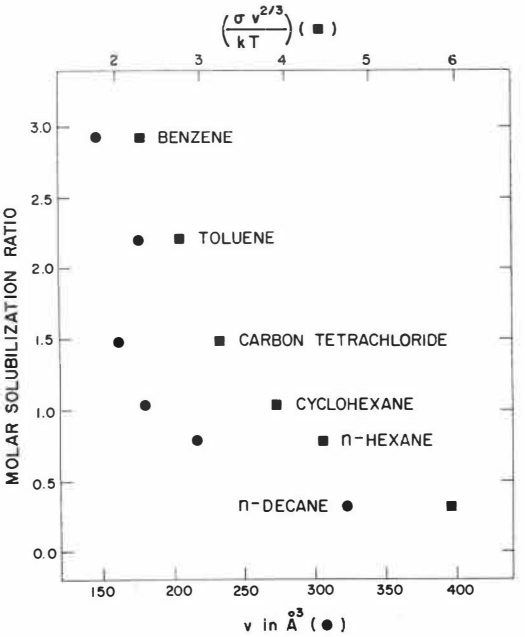

FIGURE 1. MOLAR SOLUBILIZATION RATIO OF ORGANIC MOLECULES IN 0.1 M CETYL PYRIDINIUM CHLORIDE (CPC) MICELLAR SOLUTION.

SIMULTANEOUS STRIPPING AND EXTRACTION FOR RECOVERY OF AMMONIA FROM SOUR WATER

Patricia D. Mackenzie and C. Judson King

Department of Chemical Engineering and
Lawrence Berkeley Laboratory
University of California
Berkeley, California 94720 USA

In many industrial applications, volatile weak acids, such as CO_2 and H_2S, and weak bases, such as NH_3, are present in significant quantities in wastewaters. Condensate waters from coal-conversion processes contain all three of these components at a pH around 8.5 to 9. Refinery sour waters typically contain NH_3 and H_2S at pH about 7.5. Energy requirements for removing these contaminants by ordinary steam stripping can be large, requiring a boil-up of 10 to 20% of the feed water (1). Isolating individual components in order to sell the ammonia and/or to send the H_2S to a Claus plant is even more energy intensive. For example, the Phosam-W and the all-distillation processes require a boil-up of about 25 to 30% of the feed water (2). These high steam requirements result from the interaction between the acidic and basic components, suppressing the volatilities. At the pH of these wastewaters, NH_3, CO_2 and H_2S are largely ionized. Only the unionized form is volatile, so the presence of the base serves to decrease the volatility of the acid and vice versa.

Cahn et al.(3) have proposed combining two separation processes to remove ammonia and acid gases from wastewaters more effectively. They suggest using liquid-membrane extraction to remove ammonia and simultaneous steam stripping to remove the acid gases--a combined process which they call extripping. This combination overcomes the self-limiting factors of either process alone. Stripping the acid gases from solution raises the pH, increasing the permeability of the ammonia through the liquid membrane. Removing the NH_3 by permeation lowers the pH, increasing the volatility of the acid gases. These combined effects can lower steam requirements. In addition, both this process and the one suggested below have the advantage of isolating the NH_3 from the acid gases. However, if a strong acid is used as the inner phase in liquid-membrane extraction of NH_3, there is no easy way to convert the salt back to NH_3.

In the present work, the possibility of combining solvent extraction with simultaneous steam stripping is investigated. A primary goal is to define a suitable solvent for the process that [1] has a high capacity and selectivity for either the basic or the acidic components, [2] results in low solvent losses to the aqueous phase through solubility losses and/or incomplete phase separation, [3] is easily regenerable by stripping or distillation at a temperature above that of the original extraction, [4] has a reasonable viscosity and density, and [5] is inexpensive and readily available.

SOLVENT SELECTION

No common solvents were found to be effective for extraction of either CO_2 or H_2S (4). Attempts to remove ammonia from an aqueous ammonium bicarbonate solution with neodecanoic acid (Exxon Chemical Co.), 2-ethylhexanoic acid, octanol, 50% decanol in toluene, toluene or methyl isobutyl ketone (MIBK) also met with failure.

These results reveal the need to extract the ionic form of the desired species, rather than relying on the physical solubilities of the gases in an organic solvent. Therefore, liquid cation exchangers were tested as possible extractants for ammonia. These compounds exchange their hydrogen ions for ammonium ions at the aqueous/organic interface. The equilibrium becomes more favorable at higher pH, up until the point where competition from another ion used to raise the pH becomes important. The liquid cation exchangers tested -- dinonylnaphthalene sulfonic acid (DNNSA), octylphenyl phosphoric acid (OPAP), and di-2-ethylhexyl phosphoric acid (D2EHPA) -- all readily extract ammonia, typically exhibiting an equilibrium distribution coefficient (weight-fraction basis) for NH_3 substantially greater than unity(4). OPAP, a stronger acid than D2EHPA, was found to be more water soluble than D2EHPA. DNNSA, also a stronger acid than D2EHPA and therefore a stronger extractant, could not be regenerated by stripping at elevated temperatures. No ammonia was stripped from the loaded solvent at temperatures less than 150°C, and above about that temperature a solid precipitated out of the solvent. Analysis of the solid showed that it contained nitrogen in addition to carbon, hydrogen, oxygen and sulfur. This indicated that ammonia was incorporated into the thermal degradation product of DNNSA. In light of these results, D2EHPA was the extractant chosen for further analysis.

D2EHPA, commonly used in the hydrometallurgical industry, is a viscous liquid with a density of 0.973 g/ml. Therefore, to achieve desirable physical properties, it is necessary to mix D2EHPA with a less viscous, lower-density diluent. In addition, several other difficulties can arise in the use of liquid ion exchangers such as D2EHPA. Since they are ionic, they tend to be surface active and significantly soluble in the aqueous phase, particularly in the salt form. This can result in poor phase separation and excessive extractant losses. The choice of organic diluent can greatly influence these properties, as well as the capacity of the extractant for ammonia and its regenerability.

CAPACITY FOR AMMONIA AND EXTRACTANT LOSSES

Capacity for ammonia and extractant losses were quantified as follows: A solution of 0.2M D2EHPA in a given diluent was contacted with an aqueous ammonium bicarbonate solution containing 0.58M ammonia in a single batch-equilibrium contacting at an aqueous-to-organic phase ratio of 0.185. The pH of the feed aqueous solution was about 8. The ammonia concentrations in the feed and the raffinate were measured with a specific-ion electrode (Orion Corp., Model 951000). The concentration of phosphorus-containing compounds in the raffinate was measured by a standard decomposition and preciptation method(5). All D2EHPA used was first purified by the copper-salt-precipitation method (6).

A diluent which associates preferentially with D2EHPA on a molecular level will lower the activity of D2EHPA and thus decrease its ability to extract ammonia. However, if the diluent interacts more strongly with the ammonia-D2EHPA complex than with the D2EHPA itself, a higher percent extraction of ammonia results. Lowering the activity of either D2EHPA or its ammonium salt can also lead to lower extractant losses through aqueous solubility.

The degree of ammonia extraction by D2EHPA is greater in the presence of an inert diluent, such as an aliphatic hydrocarbon, than in the presence of an aromatic, such as toluene. This is probably due to the interaction of the π electrons of the aromatic with D2EHPA, which reduces the availability of D2EHPA for extraction of ammonia. Under identical conditions, using Norpar 12 (C_{11} to C_{13} paraffins, King Industries) as diluent, 96% of the ammonia is extracted from an aqueous solution, while only 94% is extracted when the diluent is toluene. Likewise, replacing an aliphatic diluent with an aromatic reduces extractant losses by about 50%, because the aromatic can solvate the D2EHPA and its ammonium salt better than the aliphatic can.

Using a mixed diluent of toluene plus a modifier with D2EHPA takes advantage of the chemical nature of a modifier which might be too viscous to be used alone. Several Lewis acids and bases added as modifiers to toluene in a mixed diluent were examined for their effects on the capacity of D2EHPA for ammonia and on extractant losses to the aqueous phase. Figures 1 and 2 summarize the data.

The bases tested, in order of decreasing ability to donate electrons, were Amberlite LA-2 (secondary amine, Rohm and Haas), Adogen 364 (tertiary amine, Sherex Div. Ashland Chemicals), TOPO (trioctylphosphine oxide, American Cyanamid Corp.), isobutyl heptyl ketone (IBHK), and n-hexyl ether. The strongest bases appear to interact to the greatest extent with D2EHPA and dramatically decrease both the degree of ammonia extraction and the aqueous extractant loss (Figure 1). These effects lessen as base strength decreases. In fact, the two weakest bases tested have little effect on ammonia extractability and actually increase extractant losses. 1,1,2,2-Tetrachloroethane, a Lewis acid, increases aqueous extractant losses to a still greater extent. On the other hand, the use of carboxylic acids, especially straight-chain ones such as 1-decanoic acid, as modifiers with D2EHPA and toluene greatly enhances the extraction of ammonia (Figure 2), although these acids themselves do not have a high capacity ammonia. Extractant losses are significantly decreased by the addition of these acids. Sterically unhindered alcohols, such as n-decanol and n-octanol, and phenols, such as 2,4-dimethyl phenol and nonyl phenol, behave similarly. More hindered compounds, such as neodecanoic acid, 2-ethyl-1-hexanol and 4-sec-butyl-2(α-methylbenzyl) phenol, do not exhibit this same degree of enhancement. Apparently, only compounds with available -OH groups can solvate both D2EHPA and its ammonium salt to the extent necessary to reduce extractant losses yet maintain reasonable D2EHPA capacity for ammonia.

To simulate extractant losses in an aqueous stream leaving a stripper, raffinates from a batch extraction were extracted a second time with fresh organic. For a 50% decanol-in-toluene (v/v) diluent, aqueous D2EHPA1 losses were reduced to 84 ppm by the second extraction. At a D2EHPA cost of \$5.95 per kg., this loss corresponds to \$0.50 (U.S.) per m^3 of water treated. For a 6.5% decanol-in-toluene (v/v) solution as diluent, losses after the second extraction were 116 ppm, corresponding to \$0.69 (U.S.) per m^3 of water treated.

PHASE SEPARATION

Poor phase separation in these systems manifests itself as a white emulsion at the interface. In order to improve the phase separation, attempts were made to reduce the surfactant nature of the system. The ammonium salt of D2EHPA is highly surface active, and so it was found that operating under conditions such that there was low conversion of the D2EHPA to the salt form improved the phase separation. Modifiers that interact with the ammonium salt of D2EHPA can decrease its interfacial activity and thereby improve phase separation. Hence, the sterically unhindered carboxylic acids, alcohols and phenols added as modifiers to toluene greatly improve phase separation, particularly at high modifier concentrations. Likewise the modifiers IBHK and n-hexyl ether, which do not interact strongly with the ammonia-D2EHPA complex, have poor separation properties. Other factors which appear to result in poor phase separation are certain combinations of low raffinate concentrations, high initial concentrations of D2EHPA in the organic phase, and low solvent-to-water ratios, which indicate a tendency to form oil-in-water emulsions.

REGENERATION

The above results lead to the choice of 50% decanol in either an aromatic or aliphatic as a suitable diluent for D2EHPA. Attempts to regenerate a solution containing 0.2M D2EHPA in a diluent composed of 50% isodecanol in Chevron Solvent No. 25 (mixed alkylbenzenes, Chevron Chemical Co.), loaded to 0.1M NH_3, by stripping at 165°C for four hours, led to significant decomposition of the D2EHPA (4). Regeneration of a similar solvent at 110°C for seven hours yielded no signs of thermal decomposition of the solvent. Decomposition of the solvent was qualitatively monitored through color change of the solvent and through a comparison of D2EHPA aqueous extractant losses from the regenerated solvent and from fresh solvent in two successive batch extractions, as described above.

Quantitative data for the partial pressure of ammonia above an organic solvent that is 0.48M D2EHPA in 50% isodecanol/Norpar 12, originally loaded to 0.47M NH_3, indicate that NH_3 has less than one-tenth the volatility needed for convenient regeneration by stripping at atmospheric pressure and 100°C. Further regeneration studies are needed, either at higher temperatures (but probably less than 165°C), or with an inhibitor that is effective against D2EHPA decomposition, or with a diluent that has a lower extraction efficiency for ammonia, corresponding to the ammonia being not as tightly held and therefore more readily liberated from the solvent. A trade-off may exist here between costs for extractant losses, through either aqueous solubility or thermal decomposition, and steam requirements for regeneration.

STRIPPING VS. EXTRIPPING

Figure 3 compares results for batch stripping and batch extripping processes. In both experiments, 50 mL of an aqueous solution containing 0.6M CO_2 and 0.56M NH_3 were stripped with nitrogen at room temperature. In the extripping experiment an organic solvent containing 0.2M D2EHPA in Norpar 12 was also present, at a solvent-to-water ratio of 5. A comparison of the two experiments shows that the CO_2 volatility is greatly increased in the extripping case, as indicated by its much more rapid removal from solution. Further, in the extripping case 93% of the ammonia was extracted into the organic phase, while less than 0.5% of it was stripped from solution. These are precisely the characteristics desired - an enhancement in CO_2 volatility and an isolation of the NH_3 from the CO_2.

CONCLUSIONS

1. Liquid cation exchangers extract ammonia effectively from aqueous ammonium bicarbonate solutions.
2. D2EHPA is an effective extractant for ammonia.
3. Compounds with available - OH groups are desirable modifiers to add to the diluent for D2EHPA, subject to the need for sustaining sufficient NH_3 volatility for regeneration.
4. Simultaneous stripping and selective solvent extraction of an aqueous solution of NH_3 and CO_2 does produce the desired results of enhanced CO_2 volatility and isolation of NH_3 from CO_2.

ACKNOWLEDGEMENT

This work was supported by the Assistant Secretary for the Environment, Office of Environmental Compliance and Overview, Division of Environmental and Safety Engineering, Environment Control Technology Branch, Division of the U.S. Department of Energy under Contract No. DE-AC03-76SF00098. Subsequent support came through the Morgantown Energy Technology Center.

REFERENCES

1. R.C. Darton, P.F. van Grinsven and M.M. Simon, The Chemical Engineer, 924 (December, 1978).
2. Water Purification Associates, "Water Conservation and Pollution Control in Coal Conversion Processes", U.S. Environmental Protection Agency Report No. EPA-600/7-77-065 (June, 1977).
3. R.P. Cahn, N.N., L. and R.M. Minday, Environmental Science and Technology, 12(9), 1051 (1978).
4. P.D. Mackenzie, Ph.D. Dissertation, Department of Chemical Engineering, University of California, Berkeley.
5. F. Pregl and J. Giant, Quantitative Organic Microanalysis, The Blakiston Company, Phila, PA, p. 140-146 (1951).
6. W.J. McDowell, P.T. Perdue and G.N. Case, J. Inorg. Nucl. Chem. 38, 2127 (1976).

Figure 3. COMPARISON OF RATE OF REMOVAL OF CO_2 BY STRIPPING WITH THAT BY EXTRIPPING.

(Stripping: Aqueous Feed = 50 ml of 0.6 M CO_2, 0.56 M NH_3. Extripping: Aqueous Feed = same; Organic Phase = 0.2 M D2EHPA in Norpar 12; Organic/Aqueous Phase Ratio = 5/1, v/v).

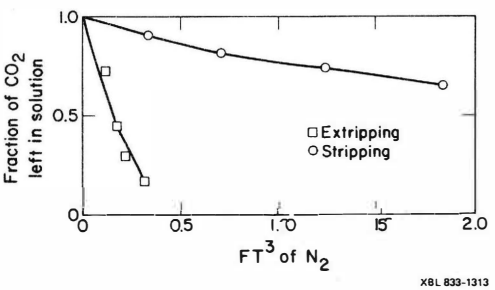

Figure 1. EFFECTS OF VARIOUS LEWIS ACIDS AND BASES AS MODIFIERS MIXED WITH TOLUENE AS DILUENTS FOR D2EHPA.

(Aqueous Feed = 0.58 M NH_4HCO_3; 0.2 M D2EHPA in Organic Phase; Organic/Aqueous Phase Ratio = 5/1, v/v. Modifiers: TOPO = Tri-octylphosphine oxide; TCE = 1,1,2,2-Tetrachloroethane; HE = n-hexyl ether; IBHK = isobutyl heptyl ketone; nC_{10}-OH = n-decanol; LA2 = Amberlite LA2; A364 = Adogen 364).

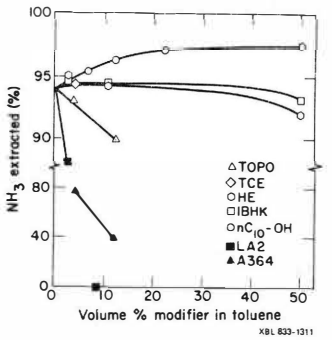

a. Effects of Modifiers on Extraction of Ammonia.

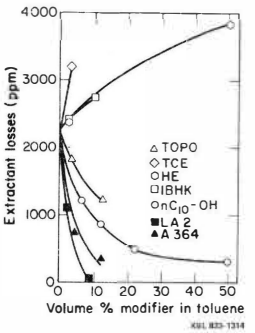

b. Effects of Modifiers on Phosphorus Content of Aqueous Phase, expressed as ppm D2EHPA.

Figure 2. EFFECTS OF VARIOUS ALCOHOLS, ACIDS AND PHENOLS AS MODIFIERS MIXED WITH TOLUENE AS DILUENTS FOR D2EHPA.

(Aqueous Feed = 0.58 M NH_4HCO_3; 0.2 M D2EHPA in Organic Phase; Organic/Aqueous Phase Ratio = 5/1 v/v. Modifiers: neo-DA = neodecanoic acid; EHOH = 2-ethyl-1-hexanol; n-DA = n-decanoic acid; NP = nonyl phenol; DMP = 2,4-dimethyl phenol; nC_{10}-OH = n-decanol; nC_8-OH = n-octanol; BAMBP = 4-sec-butyl-2-(α-methyl benzyl)phenol).

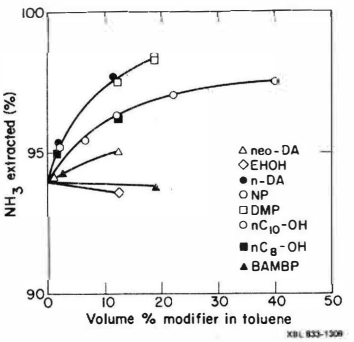

a. Effects of Modifiers on Extraction of Ammonia.

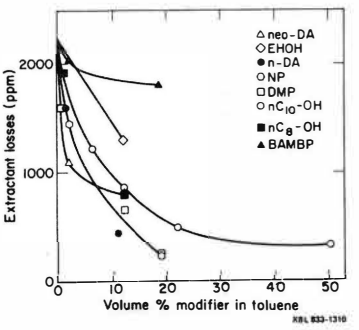

b. Effects of Modifiers on Phosphorus Content of Aqueous Phase, expressed as ppm D2EHPA.

INVESTIGATION OF PARAMETERS AFFECTING ATMOSPHERIC EXTRACTION YIELDS AND EXTRACT QUALITIES OF TWO TURKISH LIGNITES

Türker Gürkan and Sedat Gürer

Department of Chemical Engineering
Middle East Technical University
Ankara, Turkey

Various aspects of coal extraction have been studied for the production of chemicals (1), and also for a better understanding of the nature and structure of coal (2). These studies have shown that upon atmospheric extraction, peat and low grade coals such as lignites and brown coals dissolve to a significant extent in various organic solvents. The bitumen extracted from such coals with certain common solvents are generally termed as montan wax and contain various proportions of waxes, resins and asphaltic matter. Atmospheric extraction of two of the Turkish lignitic coals, Mengen and Elbistan, were studied in this work. Four sets of extractions of the two Turkish lignites have been performed in soxhlet type extractors varying the time of extraction, particle size of the lignite, its moisture, and the solvent.

EFFECT OF PARTICLE SIZE ON THE YIELDS:

Different size fractions of the coals were extracted with benzene in small soxhlet extractors (capacity 90 grams of coal). Moisture content of the coals were adjusted to about 10-12 percent by drying and humidification as necessary. Based on the results of some preliminary experiments Mengen lignite was extracted for 30 hours and Elbistan lignite for 24 hours. Benzene was separated from the extracts by simple distillation and the last traces were removed by heating over a bath. Table 1 shows the yields obtained. Basing on these results, particles in the size range 20-60 Tyler mesh for Mengen and 10-60 Tyler mesh for Elbistan lignites were used in most of the subsequent experiments. The decrease in yield as the particle size is reduced below 60 mesh is attributed to particle swelling resulting in difficulties in the penetration of the solvent into the tightly packed coal mass.

EFFECT OF EXTRACTION TIME ON THE YIELDS:

Air dried samples (10-12 percent moisture) of both lignites in the size range 20-60 Tyler mesh were extracted in soxhlet apparatus which has a capacity of 1-1.5 kg coal, for periods up to 72 hours. Figure 1 shows the yields obtained.

The change in yield becomes minor after 30 hours of extraction of Mengen lignite. In the first five hours 68 percent of the total extractable matter is recovered from the Mengen lignite and 98 percent is recovered from the Elbistan lignite. Basing on these results, extraction times of 30 hours and 24 hours have been chosen for the Mengen and Elbistan lignites respectively, for subsequent extractions. The more porous structure of the Elbistan lignite shortenes the time necessary to extract all soluble matter. Figure 1 reveals the fact that resistance in the solid phase controls the rate of mass transfer.

Extraction periods were kept as short as possible to minimize the extent of reaction between the coal material and the solvent. Material balance computations indicate that such reactions do not take place to any significant extent (3).

EFFECT OF MOISTURE CONTENT OF THE LIGNITES ON THE YIELDS:

Lignites with moisture contents of 0-30 percent were extracted with benzene in the small sized soxhlet extractors. Particle size ranges were 20-60 Tyler mesh for Mengen and 10-60 Tyler mesh for Elbistan lignites. Mengen lignite was extracted for 30 hours and Elbistan lignite for 24 hours. Figure 2 illustrates the variation of the yield with respect to the moisture content of the lignites. Low yields obtained with dried lignites might be explained in terms of the formation of some insoluble molecules through a polymerization process during drying (4), or in terms of the effect of water on the colloidal properties of the particles (5).

EXTRACT YIELDS WITH VARIOUS SOLVENTS:

Extractions with various solvents were carried out in the larger soxhlet extractors. Mengen lignite with 10-12 percent moisture and 20-60 Tyler mesh size was extracted with the selected solvents for 30 hours. Elbistan lignite with 20 percent moisture and 10-60 Tyler mesh size was extracted with the same solvents for 24 hours. Measured temperatures in the extraction cylinder were generally 15-25 K lower than the boiling points of the solvents. Yields obtained are shown in Table 2.

High yields obtained with benzene-alcohol mixtures are in agreement with the suggestion that mixtures of one polar and one nonpolar solvent affect the yields in a positive manner. High yields obtained with tetrahydrofuran and dimethylformamide are in agreement with the bituminous coal extraction model suggested by Marzec et al. (6) and quantitatively expressed in terms of DN and AN numbers.

PROPERTIES OF EXTRACTS:

Crude wax obtained from both lignites are hard and brittle. Extracts of Mengen lignite differ from those of Elbistan lignite in that they are darker in color and are sensed to be more sticky on touch.

Crude wax samples were subjected to various tests. Melting point, acid, saponification and ester values, ash content, resin, asphaltic matter and pure wax fractions were determined by standard procedures (1). Resin is the part of the crude wax which is soluble in hexane at 273-278 K. Asphaltic matter is the part which is insoluble in hot isopropyl alcohol.

Infrared spectra of four of the extracts were taken in a Perkin-Elmer model 137B Infracord Spectrometer.

Melting points of Elbistan lignite extracts are between 338-359 K. Extracts of Mengen lignite obtained by using different solvents have melting points varying considerably from one another. Benzene extract of Mengen lignite melts at 329 K while tetrahydrofuran extract is still hard at 433 K. Melting characteristics of the extracts are also different in that the extracts of benzene-alcohol mixtures melt in a wider temperature interval than the benzene extracts. This means that when benzene-alcohol mixtures are used in place of benzene as the solvent more compounds in number are extracted from the lignite and the complexity of the extract increases. For both lignites melting points of the extracts can only be determined as a range rather than by a single point, since crude montan wax is a complex mixture of a number of large hydrocarbon molecules. The main difference observed relating to the melting points of Mengen and Elbistan lignite extracts is that the latter has sharper melting points. This shows that Elbistan lignite extracts are more uniform in chemical structure. Higher melting points of Mengen lignite extracts are probably due to high percentages of asphaltic matter in these extracts. An interesting correlation is observed between the melting points of Mengen lignite extracts and their resin and asphaltic matter contents: In general, as the resin content decreases and as the asphaltic matter content increases, melting point of the extract increases. This is in accordance with the information given in the literature (7).

As can be seen in Table 3 montan waxes obtained from Mengen and Elbistan lignites are found to be richer in free acids and esters compared with commercial montan waxes. Waxes obtained from other Turkish lignites show similar characteristics (8-10).

Infrared spectra results indicate a majority of aliphatic molecules and minor quantities of alcoholic or phenolic compounds. Acidic functional groups are clearly in abundance.

Mengen lignite may be a promising raw material for industrial scale montan wax production. Yields varying between 10-14 percent on dry basis have been obtained from Mengen lignite with benzene-ethanol and benzene-methanol mixtures. Table 4 shows the yields of some well-known montan waxes for comparison. Mengen lignite is comparable in yield with other commercial wax sources. It yields about the same amount of extract as German lignites which are used for the production of Riebeck montan wax. However asphaltic matter content of Mengen lignite extracts are generally high and some purification of the wax seems to be necessary.

REFERENCES

1. H.Bennett. Industrial Waxes, two volumes. Chem.Publ.Co., New York (1963).
2. I.Wender, L.A.Heredy, M.B.Neuworth and I.G.C.Dryden. In: M.A.Elliott (Editor). Chemistry of Coal Utilization, Second Supplementary Volume. Wiley, New York, 479 (1981).
3. S.Gürer. MS Thesis. METU, Ankara, Turkey (1981).
4. A.J.Howard and D.Hamer. J.Am.Oil Chem.Soc., 37. 478 (1960).
5. R.J.Camier and S.R.Siemon. Fuel, 57. 85 (1978).
6. A.Marzec, M.Juzwa, K.Betlej and M.Sobkoviak. Fuel Processing Technology, 2.35 (1979).
7. E.M. Kampouris, C.Constantinoglou, N.Prounias and T.Sideropoulos. Fuel, 52. 47 (1973).
8. M.Seval. MS Thesis. İstanbul Technical Univ., İstanbul, Turkey (1977).
9. F.Varlık. MS Thesis. İstanbul Technical Univ., İstanbul, Turkey (1976).
10. S.H.Doğan. MS Thesis. METU, Ankara, Turkey (1977).

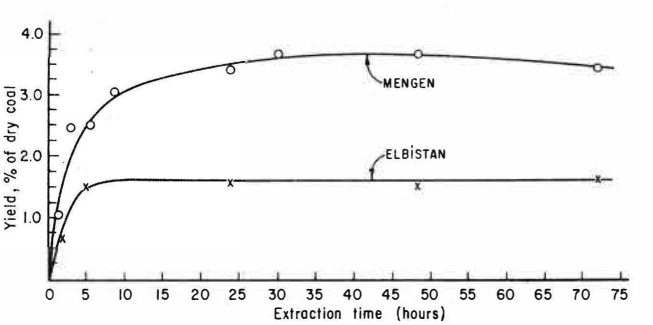

Figure 1. Yield vs. Extraction Time Curves for Mengen and Elbistan Lignites

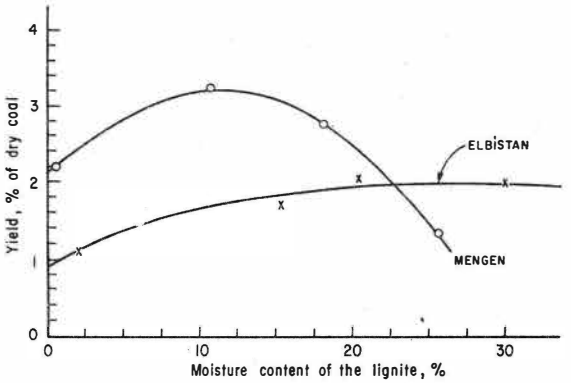

Figure 2. Variation of the Extract Yields with the Moisture Content of Lignites

Table 1. The Effect of Particle Size of the Lignite on the Extraction Yields

Particle size range (Tyler mesh)	Yield, % of dry coal	
	Mengen	Elbistan
3-5	-	0.6
5-7	-	0.9
7-10	-	1.3
10-20	2.0	1.9
20-32	3.2	1.7
32-48	3.2	1.6
48-60	2.7	1.5
60-80	2.5	1.4
80-100	2.7	1.6
>100	2.5	1.5

Table 3. Comparison with the Properties of Commercial Waxes

Wax	Acid value	Saponification value	Ester value
Riebeck crude montan wax	27	95	68
Alpco waxes	46-56	112-141	66-85
Czechoslovakian montan wax	36	89	53
American montan wax	38	105	67
Montan wax from Mengen lignite*	56	152	95
Montan wax from Elbistan lignite*	65	163	98

*The values are for benzene extracts of these lignites.

Table 4. Extraction Yields of Commercial Montan Waxes

Wax or lignite	Solvent	Crude wax yield, % of dry lignite
Arkansas, Hot Spring, air-dried	Benzene	9.5-11.1
	Benzene-Ethanol (50v/50v)	14.9-16.4
California, Amador, air-dried	Benzene	6.6-14.2
	Benzene-Ethanol (50v/50v)	9.5-21.2
Devon, English lignite	Benzene	4.5
Czechoslovakian lignite	Benzene	1-2.5
Riebeck crude montan wax	Benzene	9-16

Table 2. Extraction Yields of Mengen and Elbistan Lignites with Several Solvents

Solvent	Yield, % of dry coal	
	Mengen	Elbistan
Benzene	3.7	1.6
Benzene-Ethanol, 75v/25v	12.2	3.4
Benzene-Ethanol, 50v/50v	14.3	*
Benzene-Ethanol, 25v/75v	12.6	*
Benzene-Methanol,75v/25v	10.1	2.2
Benzene-Methanol,50v/50v	14.2	*
Benzene-Methanol,25v/75v	9.8	*
Tetrahydrofuran	12.5	3.5
Methylethylketone	10.3	2.5
Dimethylformamide	9.3	2.1
Toluene	5.1	2.4
Chloroform	5.9	1.9
Ethanol	0.9	1.3
Methanol	0.6	0.6

*Because of the low yields obtained with benzene-alcohol (75v/25v) mixtures, other compositions of these solvents were not tested with Elbistan lignite.

ALTERNATIVE METHOD FOR POLYAMINE SALTS SYNTHESIS

K. Y. Lee

Los Alamos National Laboratory
Los Alamos, New Mexico

INTRODUCTION

A few years ago we investigated methods to prepare the ammonium salt of 3,5-dinitro-1,2,4-triazole (ADNT). A patent was issued in 1980 for the process of producing ADNT by solvent extraction with liquid anion exchangers (1). Because of the versatility of the process, we studied the possibility for preparing other salts by the same method and found that many amine salts can be prepared by use of high-molecular-weight, water-insoluble amines, for example Alamine 304 (Trilauryl amine).

DESCRIPTION OF REACTION MECHANISM AND BASIC PROCEDURE

The synthesis of amine salts is based mainly on two reactions. The first involves the extraction of acid anion (H^+X^-) from aqueous solution by the base extractant (R_3N) in organic diluent to form the water-insoluble amine salts as shown in Eq. 1.

$$(1)\quad (H^+X^-)_{aq} + (R_3N)_{org} \rightleftharpoons (R_3NH^+X^-)_{org}$$

The production of the required amine salt is then completed by regeneration of the extractant to its free-base form with a basic stripping agent, Eq. 2.

$$(2)\quad (R_3NH^+x^-)_{org} + \text{Base} \longrightarrow BHX\downarrow + R_3N$$

A 20 vol% solution of liquid anion exchanger (such as trilauryl amine) in a suitable organic diluent is prepared. The concentration of the acid anion in the reaction mixture is determined. The two solutions are mixed with a 1:1 mole ratio in a separatory funnel and shaken well to ensure complete equilibration of the two phases. After the mixture is allowed to stand for 10 min, the organic phase, which contains the amine salt, is separated from the aqueous phase and is dried with anhydrous magnesium sulfate. After filtering, the stirred solution is cooled in an ice bath (optional) and the appropriate amount of base is added. The solids thus precipitated are collected by filtration and are washed with the solvent to remove excess extractant. The regenerated amine is washed with water and dried with a dehydrating agent for future use.

PREPARATION OF THE AMMONIUM SALT OF 5-NITROTETRAZOLE (ANT) AND THE ETHYLENEDIAMINE SALT OF 5-NITROTETRAZOLE (ENT)

The organic acid, 5-nitrotetrazole (NT), is prepared by diazotization of 5-aminotetrazole with nitrous acid in the presence of sodium nitrite and copper sulfate (2). If the base is anhydrous ammonia (NH_3^-), the product is ANT, Eq. 3.

(3)

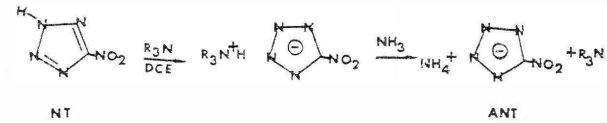

If the base is ethylenediamine (EDN), the product is ENT, Eq. 4.

(4)

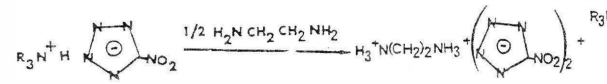

The solvent in both cases is dichloroethane (DCE).

PREPARATION OF AMMONIUM AZIDE (NH_4N_3)

A solution of sodium azide (NaN_3) is acidified with the appropriate amount of acid to give hydrazoic acid ($H^+N_3^-$) as shown in Eq. 5. The base is anhydrous ammonia (NH_3).

$$(5)\quad H^+N_3^- \underset{\text{Toluene}}{\overset{R_3N}{\rightleftharpoons}} R_3N^+HN_3^- \xrightarrow{NH_3} NH_4N_3\downarrow + R_3N$$

PREPARATION OF POLYAMINE SALTS

The acid anion is nitrate ($H^+NO_3^-$) and the stripping base has the general formula: $H_2N(CH_2CH_2NH)_xH$.

For X = 1, the base is ethylenediamine and the corresponding product is ethylenediamine dinitrate (EDD).

For X = 2, the base is diethylenetriamine and the corresponding salt is diethylenetriaminetrinitrate (DETN)

For X = 3, the base is triethylenetetramine and the corresponding salt is triethylenetetramine tetranitrate (TETN).

CONCLUSIONS

We have demonstrated that many amine salts can be prepared in a more efficient, economical, and safe manner by using liquid anion exchangers than through other procedures.

In addition to those compounds outlined, other compounds, such as tetramethyl ethylenediamine dinitrate and the amine salts of 2,4,6-trinitro immidazole and trinitro methyl tetrazole can also be prepared.

REFERENCES

1. K. Y. Lee and D. G. Ott, U.S. Patent 4,236,014 (1980).
2. K. Y. Lee and M. D. Coburn, J. of Energetic Materials. In press.

THE SOLVENT EXTRACTION OF GOLD FROM AUROCYANIDE SOLUTIONS

Michael B. Mooiman, Jan D. Miller and Maribel M. Mena

Department of Metallurgy and Metallurgical Engineering
University of Utah
Salt Lake City, Utah 84112 USA

INTRODUCTION

The solvent extraction of gold from cyanide solutions has importance from several different perspectives. First, from an analytical viewpoint, quaternary amines have long been used to concentrate $Au(CN)_2^-$ from dilute solutions (1,2). However, quaternary amines are not very selective and will extract most other anions from aqueous solution as well. Second, from a refining viewpoint, the lack of a selective extractant for $Au(CN)_2^-$ from basic solution precludes the use of cyanidation as a processing alternative in refining operations. Finally, from a resource viewpoint, solvent extraction could provide an interesting alternative in the processing and recovery of gold from cyanide leach liquors or from plating shop solutions. An economic assessment of the potential of solvent extraction for gold recovery from cyanide solution will be discussed in a paper to be presented at the SME Fall Meeting in Salt Lake City, October 1983 (3).

The solvent extraction of gold was reviewed in both 1976 (2) and 1980 (4). From these reviews it is apparent that, of the amines, only the tertiary and quaternary amines have received some study. Russian researchers showed that gold is extracted as $HAu(CN)_2$ at low pH values by ethers, alcohols, ketones, and aldehydes (5). But, other than the quaternary amines, all the extractants require pH values of 8 or less. This is not desirable for solutions containing free cyanide ion.

The development of an extractant that could selectively extract gold from cyanide solutions at a pH value compatible with free cyanide would be welcomed by both the analytical chemist and metallurgist. In this regard, research is in progress to investigate the details of gold solvent extraction from alkali cyanide solution. Results presented in this paper are limited to the analysis of the equilibrium distribution of $Au(CN)_2^-$ between aqueous solutions and organic solutions of various amines, TBP, and combinations thereof. The most significant aspect of these results has been the ability to control amine basicity so that amine extraction of gold need not be limited to pH values less than 8. The general significance of this finding will be discussed in the paper "Control of Amine Basicity in Anionic Solvent Extraction Systems" to be presented at the SME Fall Meeting, Salt Lake City, October 1983 (6).

EXPERIMENTAL

The equilibrium distribution of $Au(CN)_2^-$ between the organic and aqueous phases was determined by contacting the two phases by rapid stirring. The pH was adjusted by small additions of concentrated H_2SO_4 or NaOH and was continually monitored by a combination pH electrode. After phase disengagement, samples (2 ml) of the aqueous solution were removed for analysis by atomic absorption. Equal amounts of the organic phase were also removed to maintain a fixed phase ratio.

The composition of all the aqueous solutions was, unless otherwise stated, 1.0 gl^{-1} $NaAu(CN)_2$ ($5x10^{-3}$ M) in 0.5 M Na_2SO_4. The sodium sulphate was added to maintain a constant ionic strength during the extraction. In all cases, the organic to aqueous phase ratio was 1:1.

RESULTS AND DISCUSSION

The amines are the best known and most useful anion extractants and, therefore, were the first reagents tested. Next, extraction by solvating extractants and especially TBP is described. In the final section results are presented which demonstrate the the basicity of amines can be controlled to facilitate gold extraction at pH values exceeding pH 8.

Amine Extractants. Percent extraction of $Au(CN)_2^-$ is shown in Figure 1 as a function of pH for typical primary, secondary, and tertiary amines. The order of increasing pH_{50}: tertiary < primary < secondary follows the order of increasing basicity of alkyl amines in water (7). However in aprotic organic diluents the order of increasing basicity is primary < secondary < tertiary (8). These results will be discussed in detail in a later contribution, but, suffice it to say at this time, the amine basicity demonstrates a sensitivity to the type of anion present in the system. Variations in the nature of the amine alkyl chains, in terms of branching and/or length, does not have a marked effect on the relative position of the curves for each type of amine. This is demonstrated by the pH_{50} values for different amines presented in Table 1.

The value of the pH_{50} is largely dictated by the nature of the amine, whether primary, secondary, or tertiary. The secondary amines appeared to be the most attractive for further study as they extracted gold at the highest pH values. Therefore, many subsequent tests were performed with the secondary amines.

The effect of diluent type on the pH_{50} values for amine extraction of gold was found to be insignificant in the case of the primary amines. The aliphatic diluent, hexane, reduced the pH_{50} values for secondary and tertiary amines by 0.5 pH unit compared to the aromatic diluent, xylene.

For both aliphatic and aromatic diluents, the pH_{50} value of the secondary amine, Adogen 283, increases as the amine concentration increases; i.e., better loading at higher pH values is obtained as the extractant concentration increases. This, as expected, is due to the mass action effect, shifting the extraction equilibrium to the right:

$$\overline{R_2NH} + H^+ + Au(CN)_2^- = \overline{R_2NH_2Au(CN)_2}$$

Table 1. pH_{50} Values for Gold Extraction from Aurocyanide Solutions (1.0 gl^{-1}) by Various Amine Extractants (0.05 M in Xylene)

AMINE	SUPPLIER	STRUCTURE		pH_{50}
Primary				
Primene 81-R	Rohm & Haas	$R-NH_2$	$R=C_{12-14}$	6.55
Primene JM-T	"		$R=C_{18-22}$	6.05
Secondary				
Adogen 283	Sherex	R_2NH	$R=C_{13}$	7.15
LA-2	Rohm & Haas	"	$R=C_{10-12}$	7.15
Alamine 204	Henkel	"	$R=C_{12}$	7.15
Alamine 226	"	"	$R=C_{16-18}$	7.06
Tertiary				
Adogen 364	Sherex	R_3N	$R=C_{8-10}$	5.55
Adogen 364	"	"	$R=C_{13}$	5.35
Alamine 308	Henkel	"	R=iso-C_8	5.45
Alamine 310	"	"	R=iso-C_{10}	5.35
Alamine 336	"	"	$R=C_{8-10}$	5.66

The effect of the background electrolyte, namely Na_2SO_4, was investigated by performing percent extraction versus pH experiments with and without 0.5M Na_2SO_4. There was little or no effect due to the inert electrolyte and it was concluded that ionic strength was not a significant parameter in determining the extent of gold extraction.

Solvating Extractants. Several solvating extractants were evaluated, and the percent extraction versus pH behavior appears in Table 2.

Table 2. Percent Extraction of $Au(CN)_2^-$ (1.0 gl^{-1}) versus pH for Selected Solvating Extractants. No Diluent Addition.

pH	% Extraction by TBP	% Extraction by MIBK	% Extraction by DBC
1	100	54.35	42.21
4	100	16.85	22.37
7	100	18.15	19.48
10	99.99	19.16	19.84
13	99.01	15.52	16.23

TBP -- Tributyl Phosphate, MIBK -- Methyl Isobutyl Ketone,
DBC -- Dibutyl Diethylene Glycol

The extraction behavior of MIBK and DBC, i.e., good extraction at low pHs, is due to the formation of the neutral $HAu(CN)_2$. This is in accord with the results obtained previously for gold extraction by alcohols, ketones etc (5). However, the excellent extraction by TBP over the whole pH range has not been reported, and these results were investigated in further detail.

The extent of gold extraction by TBP is presented in Figure 2 as a function of pH for various concentrations of TBP.

The first and most important trend to notice is that the percent extraction over the whole pH range increases as the fraction of TBP in the diluent increases. Complete, or almost complete, extraction of gold over the whole pH range is only obtained for 100% TBP. For the lower TBP concentrations, the percent extraction increases at pH values close to one. Again, this must be due to the formation of aurocyanic acid, $HAu(CN)_2$. The TBP concentration effect indicates that the extraction is not due to the formation of a stoichiometric $Au(CN)_2^-$/TBP complex because even at 10% TBP (0.3 M), the TBP concentration far exceeds the $Au(CN)_2^-$ concentration ($5x10^{-3}$M).

The mechanism of extraction might then be of the ion pairing type, i.e.,

$$Na^+(aq) + Au(CN)_2^-(aq) = \overline{NaAu(CN)_2}$$

In this regard, the effect of ionic strength on the extraction by 100% TBP was investigated. Ionic strength had a marked effect on the extraction of gold and ionic strengths exceeding 0.5 M were required to obtain 90% extraction. However, even when only $NaAu(CN)_2$ is present in solution (no indifferent electrolyte), 30% extraction can be obtained. This is indicative of a relatively high ion association constant for the aurocyanide/cation ion pair. The effect of cation and anion type has also been investigated and the results indicate no marked effect of either anion or cation type.

To summarize our findings on gold extraction from cyanide solutions: TBP extraction requires extensive ionic strength adjustment, and amine extraction is limited to pH values less than pH 8. For amine extraction of gold at high pH values (pH 9-11), of interest from a processing standpoint, it became apparent that another approach would have to be found to alter the basicity of the amines since the alkyl chain length and structure have only a small effect on the basicity. In this regard, a significant, and previously unreported, effect that can be used to control amine basicity in solvent extraction systems was discovered. This control of amine basicity which is based on solvation considerations involves the synergistic action of amines and tributyl phosphate and is described in the following section.

Controlled Basicity of Amines. The base strength of amines is far greater in water than in aprotic organic diluents. For example, secondary amines have pKa values in water of about 11 (9), while in toluene the pKa values are in the range 5-7 (8). Further, weak base resins containing alkyl amine functional groups are strong bases as evidenced by their extraction of gold in the 9 to 11 pH range (10). Increase in base strength would seem to be related to the ability of water to solvate the amine and/or amine salt. Thus one should be able to increase the basicity of the amine by increasing the water content, and thus solvation of the amine, in the organic phase. Tributyl phosphate is known to extract water into the organic phase. In fact, undiluted TBP will extract water almost in a 1:1 TBP:water mole ratio (11). Following this thinking, TBP was added as a modifier to the amine extractants, and some of the results are presented in Figure 4 and Table 3. No Na_2SO_4 was added to adjust the ionic strength owing to the previously discussed extraction of gold by TBP at high ionic strengths.

Table 3. The effect of TBP on the Extraction of Gold ($1.0\ gl^{-1}$) by Amines (0.05 M)

Amine	pH_{50} no TBP addition	pH_{50} 50% TBP in xylene
Primene JM-T	6.05	9.85
Adogen 283	7.15	10.05
Alamine 336	5.66	8.05

There is a marked positive effect on the extracting ability of the amines by addition of TBP, as indicated by the dramatic shift of the extraction curves to the high pH range. The ability to extract $Au(CN)_2^-$ at higher pH values is indicative of an increase in base strength. However, at this stage, it cannot be unequivocally stated that the effect of TBP is due to increased water content (and thus amine solvation) in the organic phase or whether TBP itself is solvating the amine. TBP and its derivatives are unique in this respect. Other well-established modifiers such as isodecanol and MIBK actually reduce the amine basicity. The effect of the fraction of TBP in the xylene diluent is shown in Figure 4 for the three types of amine at 0.05 M. The increase in pH_{50} is plotted against percent TBP in the diluent, xylene.

It is interesting to observe that the TBP has an increasing effect in the order tertiary secondary primary amine. This appears to be in accord with the water-solvation/amine-basicity concept. It is thought that the primary amines have three waters of solvation, secondary two, and tertiary one. Thus the solvating effect and the increase in basicity should be greater for primary amines than for secondary than for tertiary (12). This is exactly what is observed in our experiments. However, as mentioned previously, it could, in fact, be TBP which is solvating the amine.

At the present time the selectivity of this extraction system is being investigated. In addition, our studies have been extended to the extraction of other metal anions as well as the use of other phosphorus derivatives to control the basicity of amines. The mechanism of the effect is being studied in detail using spectroscopic techniques and will be reported on at a later date.

CONCLUSIONS

The extraction of gold from aqueous aurocyanide solutions by the primary, secondary, and tertiary amines as well as by tributyl phosphate has been reported. The alkyl amines are shown to be good extractants at pH values less than pH 7. Previously unreported, it has been shown that TBP acts as an excellent extractant for gold over the whole pH range, at ionic strengths exceeding 0.5 M. Most significantly, it has been shown that gold can be extracted by amines at pH values as high as 10.5 by control of amine basicity. The base strength of the amine is controlled with TBP additions and can be increased by as much as four orders of magnitude. The results have been explained by increased water solvation of the amine in the organic phase. The higher basicity allows for gold extraction from alkaline solutions containing free cyanide.

ACKNOWLEDGEMENT

MBM wishes to thank the Council for Mineral Technology, South Africa, for sponsorship of his graduate studies. Partial support for this research activity was provided by University of Utah Research Committee.

REFERENCES

1. Andersen, T. N., Parr, J. C., Stone, L. C., and Metcalf, D., AIME Annual Meeting, Chicago, Preprint 81-78, (Feb., 1981).
2. Das, N. R. and Bhattacharyya, S. N., Talanta, 23, 535 (1976).
3. Hendriksz, A. R., Hiskey, J. B., Miller, J. D., and Mooiman, M. B., to be presented at Heap Leaching Symposium, SME Fall Meeting, Salt Lake City, Utah, October (1983).
4. Ritcey, G. M. and Ashbrook, W. A., "Solvent Extraction--Part II," Elsevier, Amsterdam (1979).
5. Zuyagintsev, O. E. and Zakharov-Nartsissov, O. L., Russ. J. Inorg. Chem., 5, 59 (1960).
6. Mooiman, M. B. and Miller, J. D., "Control of Amine Basicity in Solvent Extraction Systems," U.S.A. Patent Pending.
7. Hall, H. K., JACS, 79, 5541 (1957).
8. Grinstead, R. R., ISEC, Amsterdam, Holland, 426 (1967).
9. "The Chemistry of the Amine Group," ed. Patai, S., Interscience, London, 176 (1968).
10. Fleming, C. A. and Nicol, M. J., Proc. Hydromet. 81, Manchester, England (1981).
11. Marcus, Y. and Kertes, A. S., "Ion Exchange and Solvent Extraction of Metal Complexes," Wiley-Interscience, London, 660 (1969).
12. Ibid., 743.

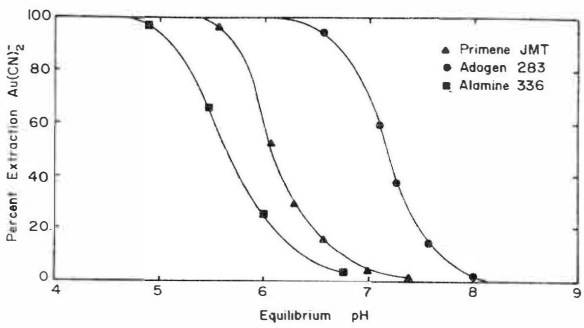

Figure 1 Percent Extraction of $Au(CN)_2^-$ ($1.0gl^{-1}$ in 0.5M Na_2SO_4) versus pH for Primary, Secondary and Tertiary Amines (0.05M in Xylene)

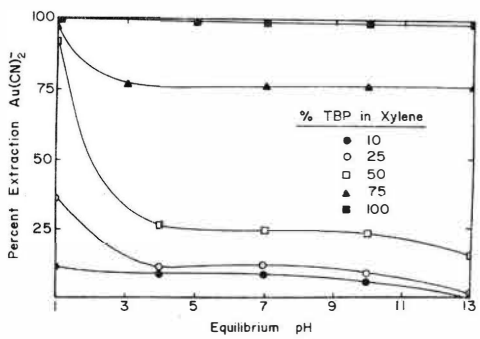

Figure 2 Percent Extraction of $Au(CN)_2^-$ ($1.0gl^{-1}$ in 0.5M Na_2SO_4) versus pH for Varying Concentrations of TBP in Xylene

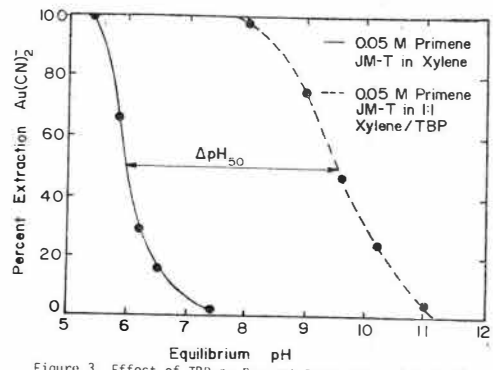

Figure 3 Effect of TBP on Percent Extraction of $Au(CN)_2^-$ ($1.0gl^{-1}$) by a Primary Amine (0.05M)

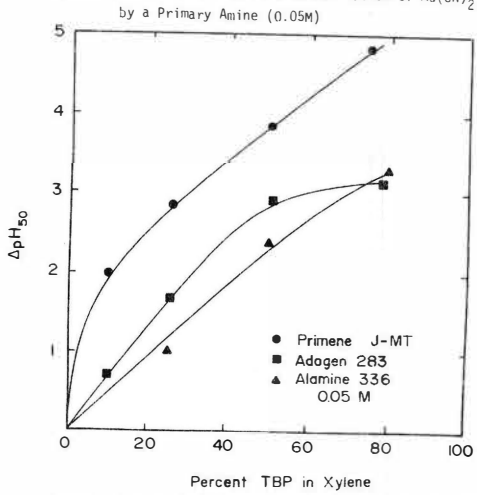

Figure 4 Effect of TBP concentration on the pH_{50} for $Au(CN)_2^-$ ($1.0gl^{-1}$) Extraction for Primary, Secondary, and Tertiary Amines (0.05M)

RECUPERATION AND SEPARATION OF COPPER AND ZINC FROM CYANIDE ELECTROPLATING EFFLUENTS BY SOLVENT EXTRACTION

P. Van Acker, M. Verhaege, A. Van Peteghem, L. Gyselinck

Laboratory of Non-Ferrous Metals
University of Gent
Gent, Belgium

INTRODUCTION.

Last decade, continuously growing research efforts are made looking for new techniques to eliminate toxic and polluating substances from industrial effluents at reasonable cost. Special attention should be paid to processes which combine elimination with recuperation and recycle into one of the process streams. Solvent extraction has already been proposed to treat metal finishing effluents "(1)". Some aspects of the chemistry of the extraction of metalcyanidecomplexes with liquid anionexchangers was studied by Irving and co. "(2)". Moore and co. described the elimination and recuperation of zinccyanide from galvanic effluents "(3)". In this paper the recuperation and separation of copper and zinc from cyanide plating effluents has been investigated.

CHEMISTRY OF THE PROCESS.

Copper and zinc are simultaneously extracted from the effluent with a quaternary ammoniumchloride extractant solved in kerosene. Stripping of the zinc from the loaded solvent is done by contacting the extract with a sodiumhydroxyde solution. In this way, zinccyanide complexes are converted to zinchydroxycompounds which show less affinity to the extractant than free cyanide. Coppercyanide complexes are not removed from the extractant by contact with this hydroxyde solution, but can be stripped from the solvent with a concentrated acqueous CN^- solution.

The chemical equilibria which have to be considered are :

$Zn^{2+} + xCN^- \leftrightarrow Zn(CN)^{2-x}$ with $\beta_2 = 11,07$ $\beta_3 = 16,05$ $\beta_4 = 19,62$

$Zn^{2+} + xOH^- \leftrightarrow Zn(OH)^{2-x}$ with $\beta_2 = 11,19$ $\beta_3 = 16,31$ $\beta_4 = 17,70$

$Cu^{+} + xCN^- \leftrightarrow Cu(CN)^{1-x}$ with $\beta_2 = 24$ $\beta_3 = 28,6$ $\beta_4 = 30,3$

($\beta_n = \log K_n$)

Figure 1 shows the proportion of the different zinccyanide- and hydroxy-complexes as a function of pH and figure 2 those of the copper-cyanide complexes as a function of increasing CN^- concentration.

The extraction reaction can be written as follows :

$$\{Me^{n+}(CN)_x^{-(x-n)}\}_a + (x-n)\{R_4NCN\}_o \leftrightarrow \{(R_4N)_{x-n}.Me(CN)_x\}_o + (x-n)\{CN\}_a$$

For copper x = 2,3,4 ; for zinc x = 3,4

a denotes species in the aqueous phase and o species in the organic one.

The strip reaction of zinc with NaOH is formulated as :

$$\{(R_4N)_{x-n}Zn(CN)_x\}_o + x\{(OH^-)\}_a \leftrightarrow (x-n)\{R_4NCN\}_o + \{Zn(OH)_x^{-(x-2)}\}_a$$

The stripreaction of copper with CN^- can be written as :

$$\{(R_4N)_{x-n}Cu(CN)_x\}_o + (x-n)\{CN^-\}_a \leftrightarrow (x-n)\{R_4NCN\}_o + \{Cu(CN)_x^{-(x+1)}\}_a$$

CHEMICALS.

The extractant used was ADOGEN ® 464 from Ashland, solved in kerosene (BP). 1-Decanol (Merck) was added to the solvent as modifier (2,5 vol.%). The separate extraction of both metals was studied in a series of batch experiments. Appropriate amounts of salts were solved in destilled water. The feed in the continuous operated unit was an actual industrial effluent.

EQUILIBRIUM TESTS.

1) Extraction of zinc from cyanide solutions :

The solvent which contained 20 g/l of extractant (R_4NCl) and 2,5 vol.% 1-decanol was contacted 10 times at a volume ratio of 1:1 with a fresh aqueous solution containing 51,5 mg/l Zn, 100 mg/l CN^- and 0,05 M NaOH. The results are shown in table I. From these results it can be seen that subsequent contact of the solvent with cyanide bearing solutions increases the extraction of the zinc complex.

TABLE I

Number of contacts	mg/l Zn aq.phase	mg/l Zn org.phase	log D	% E
1	0,145	51,4	2,55	99,7
2	0,08	102,8	3,11	99,9
3	<0,03	154	>5	100
4 → 10	-	515		100

This can be explained by the fact that the extraction order of anions for this extractant is : $CN^- >> Cl^- > HCO_3^- > OH^- > CO_3^{2-}$ and the originally quaternary ammoniumchloride is converted to the cyanide salt, which shows to have greater affinity to the zinccyanide complexes than the chloride form.

2) Determination of the loading capacity of the solvent with copper and zinc.

In this experiment 30 ml of solvent (46,8 mM quaternary ammoniumsalt in kerosene) was contacted five subsequent times with 300 ml of aqueous solution. The composition of the aqueous solution was 100 mg/l of metal (copper or zinc) and 118 m M CN^-, 0,01 M NaOH and 0,5 M NaCl.

Table II shows the results.

TABLE II

Number of contacts	(Zn) mg/l		(Cu) mg/l	
	in a.ph.	in o.ph.	in a.ph.	in o.ph.
1	0,15	998,5	0,11	998,4
2	47,5	1525	87	1128
3 → 5	100	1525	100	1128

From the table it can be calculated that at the maximal loading the ratio of R_4N^+ to Zn is 2 and for copper 2,64. The ratio of R_4N^+ to Cu is depending on the concentration of free cyanide in the aqueous phase and balances between 2 and 3.

3) Stripping of zinc with NaOH and of copper with NaCN solution.

Figure 3 shows the strip-equilibrium of zinc for three different aqueous NaOH solutions : 2M, 5M and 7M. From figure 3 it is obvious that strip efficiency increases with increasing NaOH concentration and decreasing organic zinc concentration.

Copper cannot be stripped by sodiumhydroxyde solutions. Among several possible stripsolutions a sodiumcyanide solution was chosen "(5)". Table III shows the stripefficiences obtained with this reagent.(vol.ratio : 1:1).

TABLE III

Aqueous NaCN concentration	Loaded solvent (0,04 M Q.A.S. 2,5% decanol) 840 mg/l Cu
1 M	78,9 %
2 M	99,2 %
5 M	99,4 %

CONTINUOUS EXTRACTION OF COPPER AND ZINC.

The industrial effluent treated, contained : 85 mg/l copper, 4 mg/l zinc and 150 mg/l cyanide. The organic phase was a 0,04 M solution of ADOGEN 464 with 2,5 vol.% decanol in kerosene. The contact device used was a 5 stage Croda mixer-settler unit as described elsewhere "(6)". The flowrate of the aqueous and organic feed was 2,5 l/h and 0,25 l/h respectively. One mixer-settler unit was sufficient to extract all the copper and zinc from the effluent . Removal of remaining free cyanide and entrained organic material was done by passing the raffinate through an absorption column filled with "active

carbon". C.O.D. and CN^- concentration in this effluent was lower than 50 mg/l and 0,1 mg/l respectively.

CONTINUOUS STRIPPING OF ZINC WITH NaOH SOLUTION.

The extract containing 40 ppm zinc and 840 ppm copper was fed into the next mixer-settler unit operating at a 1:1 volume ratio of both phases. The strip solution was a 5 molair NaOH solution. Stripping of zinc was complete in one unit.

CONTINUOUS STRIPPING OF COPPER WITH NaOH SOLUTION.

Stripping of copper was done using two stages of the mixer-settler unit. The stripsolution contained 2 M NaCN and 0,75 M NaOH. These salt concentrations are often encountered in copper cyanide electroplating balts. The volume ratio between the organic phase and the stripsolution was 3. The strip efficiency of the unit was higher when the solvent was dispersed into the aqueous stripsolution. To produce an aqueous continuous dispersion, it was necessary to recycle part of the aqueous phase (1,7 l/h). Table IV shows some typical analysis of this stripsection.

TABLE IV.

	(Cu^+) mg/l	
	org. phase	aq. phase
org. feed	840	
stage 2	75	2470
stage 1	19	170
aq. feed		0

CONCLUSIONS.

Copper- and zinccyanides can be eliminated from an industrial cyanide plating effluent by solvent extraction. Both metals are removed from this effluent in a single extraction stage. Zinc is removed from the extract in one stripping stage, fed with a 5 M sodiumhydroxyde solution.
The back extraction of copper is possible in a two stage unit using a stripsolution containing 2 M NaCN and 0,75 M NaOH. A flowsheet of the proposed process is shown in figure 4. The concentrated stripsolution containing copper or zinc can be recirculated to copper and zinc plating solutions. Plating baths containing recycled solutions have been tested without any difficulty.

REFERENCES.

1. Mc.Donald C. and Bafiva R.
   Separation science, 12(4), 1977, 435-445
2. Irving H and Damodcran A.
   Analytica chim. acta, 53, 1971, 267-275
3. Moore F. and W.S.Groewien
   Plating and surface finishing , aug. 1976, p.26-29
4. O'Neill C.F., Ettel V.A. and Olivier A.J.
   CIM bulletin, october 1976
5. Van Acker P., Verhaege M. and Van Peteghem A.
   2nd symp. on materials and energy from refuse, Antwerp, Belgium, 20-22 oct., 1981
6. Solvent extraction, part II.
   G.M.Retchey and A.W.Ashbrook
   Elsevier scientific publishing company, 1979, p.31

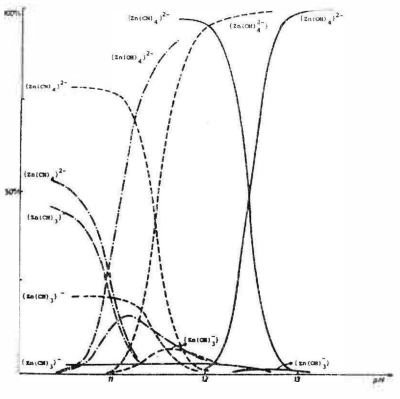

Fig. 1 Proportion of the different zinccyanide- and hydroxy-complexes as a function of pH .

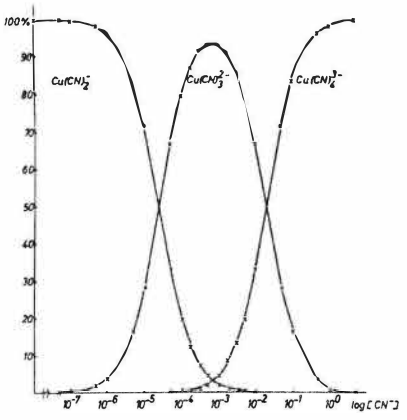

Fig. 2 : Proportion of the different coppercyanide-complexes as a function of $(CN)^-$

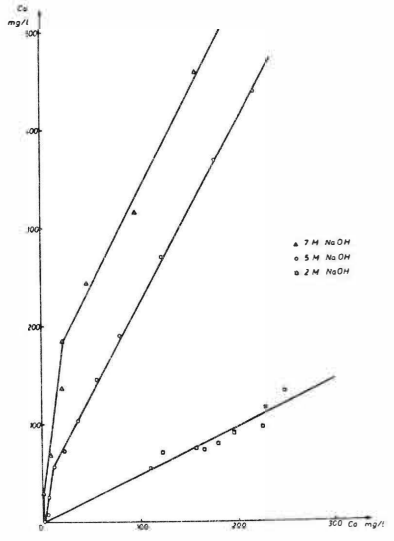

Fig. 3 : Stripequilibria of zinc for various NaOH concentrations

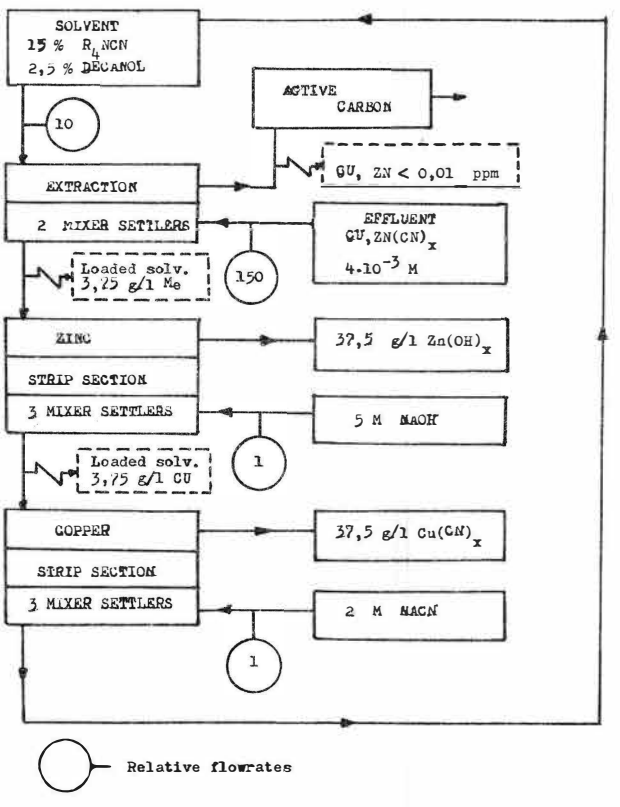

Fig. 4 Proposed flowsheet for the process

PROCESS FOR RECOVERY OF COPPER FROM AMMONIACAL ETCH LIQUOR USING A MIXED EXTRACTANT

G. M. Ritcey and E. W. Wong

CANMET
Energy, Mines and Resources Canada
555 Booth Street
Ottawa, Ontario, Canada K1A OG1

INTRODUCTION

For the processing of ammoniacal copper etch solutions the present techniques of solvent extraction employs the use of an extracting reagent, beta-diketone (trade name LIX 54 of Henkel Inc.) (1,2). In the patented process, the copper is reduced from a level of about 150 g Cu/L in the leach etch liquor, down to about 100 g Cu/L after solvent extraction. That is, 2/3 of the copper is recycled to the leach circuit in the alkaline NH_4Cl medium. The H_2SO_4 strip liquor goes on to electrowinning.

There is an obvious drawback to such a process, in that the copper level is only reduced to 100 g/L in the extraction. This means that the leaching and solvent extraction circuits are going to be larger, and more expensive, than if the leach liquor could be reduced to a much lower copper level, so that the recycled etch solution is more favourable for the subsequent leach of the circuit boards upon recycle to the leaching stage.

This paper describes the bench work and the continuous testing in mixer settlers leading to the development of an improved process for the treatment of copper etch solutions. Based on evaluating several selected extractants, a mixed extractant, to provide for synergism, was chosen.

BENCH SCALE RESULTS

EXTRACTION

Screening of Selected Extractants

Based on previous processes (1-10) on the extraction of copper from ammoniacal solutions, selected extractants were evaluated by contacting with the feed liquor for 5 minutes in separatory funnels. The results of these screening tests indicated that all the extractants, by themself, are capable of reducing the feed copper concentration from 146 g/L to about 100 g/L. The Acorga P5100 and Versatic 911 gave the best performance of the extractants evaluated. The 25% Acorga appeared to provide for the lowest raffinate while the 40% Versatic gave the highest loading of copper. Because of such results it was considered that a mixture of the two extractants might provide for a synergistic extraction system.

Examination of Loading Properties of Solvents and Solvent Mixtures for NH_3

Tests were performed on the components of the solvent mixture, and compared with the mixture, to determine whether NH_3 was loading preferentially on one of the components. The results, indicated that the carboxylic acid, Versatic 911, is extracting more NH_3 than is the Acorga P5100. (Therefore it might be considered to decrease the Versatic 911 component.) The synthetic feed solution contained 134.7 g Cu/L and 154 g NH_3/L.

Additional screening tests to determine the relative extraction of Cu and NH_3 were performed on several solvents. The data in Table 1 indicates again that the Acorga P5100 has the greatest discrimination of Cu/NH_3 of those solvents evaluated. The synthetic feed solution contained 120 g Cu/L, 120 g NH_3/L and the tests were performed at A/O ratio of 1.

Table 1 - Comparison of Solvents for Co-Extraction of Cu and NH_3

Solvent Composition	Loaded Solvent (g/L)		Cu/NH_3 Ratio
	Cu	NH_3	
40% Versatic + 10% Acorga P5100	38.3	19.0	2.01
40% Versatic + 10% Acorga P5300	39.0	18.0	2.17
40% Versatic 911	36.6	16.0	2.29
25% Acorga P5100	17.8	4.0	4.45
25% Acorga P5300	11.4	5.0	2.28

Kinetics and Extraction of Cu and NH_3

A series of tests was conducted over a contact time period of 5 seconds to 300 seconds to determine whether a significant difference in extraction of either Cu or NH_3 occurred with time. The results showed a constant extraction of Cu (representing saturation loading of about 40 g/L Cu) and NH_3 over the time period investigated. The phase ratio was 1 in all tests. That is, the extraction is rapid and constant for both Cu and NH_3.

SCRUBBING OF NH_3

Screening of Scrubbing Agents for NH_3 Removal

The continuous tests in the mixer settler circuit indicated that considerable ammonia (up to 20%) could be extracted with the copper. If not scrubbed and recovered before copper stripping the ammonia would be lost to the strip electrolyte. Therefore it would be preferable to selectively scrub and recover the ammonia without stripping the copper at the same time. The results of scrubbing tests indicated that of the solutions tested, a copper chloride solution at pH 0.5 resulted in the removal of 6.59 g NH_3/L after one stage at A/O 1/1. The contact time was for 3 minutes at room temperature and the loaded solvent contained 32 g Cu/L.

Scrubbing with $CuCl_2$

A loaded solvent containing 26.7 g Cu/L was scrubbed 5 successive times, A/O 1/1, with a $CuCl_2$ solution at pH 0.70 containing 8.53 g Cu/L. The data in Table 2 indicates that ammonia, together with some copper, are removed by scrubbing. One to two scrub stages should be sufficient.

Table 2 - Successive Scrubbing for NH_3 Removal - 8.53 g Cu/L as $CuCl_2$ at pH 0.7

Contact	Scrub Aqueous (g/L)	
	Cu	NH_3
1	3.78	5.90
2	12.4	1.68
3	13.9	0.78
4	15.0	0.31
5	15.3	0.09

Effect of H_2SO_4 Concentration on Stripping of 40% Versatic + 10% Acorga

Stripping tests were performed at varying concentrations of H_2SO_4 to determine whether any selectivity over ammonia or chloride occurred. The data in Table 3 are for a loaded solvent (but not scrubbed) containing 30 g Cu/L contacted in a single stage at an O/A of 3/1. The results indicate that as the strip acid concentration is increased from 135 to 180 g H_2SO_4/L, the copper concentration is increased from 27 to 60 g/L in the strip, while the NH_3 decreases slightly from 28.8 to 23.5 g/L. Chloride is stripped with increasing acidity. Also at the higher strip acidity, there is less interface emulsion.

Table 3 - Effect of H_2SO_4 Concentration on Stripping

Strip Feed g H_2SO_4/L	O/A Ratio	Equil. pH	Strip Solution (g/L)			Remarks
			Cu	NH_3	Cl	
135	3/1	3.42	27.3	28.8	0.16	interface emulsion
150	3/1	3.20	39.7	27.9		some emulsion. Aqueous phase cloudy
180	3/1	2.85	59.7	23.5	2.51	small emulsion. Some white crystals

SCRUBBING OF SOLVENT FOR $SO_4^=$ REMOVAL

In the design of the circuit, following stripping of copper with H_2SO_4, the stripped solvent would be returned to the extraction circuit. Because of the possible presence of $SO_4^=$ anion on the solvent due to stripping, the $SO_4^=$ would require removal before contact with the ammonium chloride solution containing copper. Otherwise a build-up of $SO_4^=$ would occur in the etch solution. Scrub tests using water (A/O 1/1) and 5% NH_4Cl (A/O 3/1) at pH 7.5 were performed on the solvent, using an A/O ratio of 1. The results, in Table 4, of five successive contacts indicate the $SO_4^=$ is removed by scrubbing, and that NH_4Cl is the most effective scrub.

Table 4 - Water Scrubbing for $SO_4^=$ Removal

Contact	Scrub Solution (g SO_4/L)	
	Water	5% NH_4Cl at pH 7.5
1	0.23	3.08
2	0.21	0.54
3	0.17	0.23
4	0.20	0.077
5	0.20	0.011

CONTINUOUS TESTING

Mixer Settler Data

Based on the early bench data (before scrubbing and stripping were optimized) a continuous circuit was evaluated on a Bell Engineering mixer settler unit. The object was to test the possible flowsheet whereby 5 stages of extraction (O/A 4/1), 3 stages of stripping (O/A 1.3/1) with 150 g H_2SO_4/L and 2 stages of water scrubbing (to remove $SO_4^=$) would be evaluated. The solvent mixture consisted of 40% Versatic 911 + 10% Acorga P5100 diluted in Shell 140 kerosene. The synthetic aqueous feed contained 115 g Cu/L, 135 g NH_3/L and 151.6 g Cl^-/L. The run operated extremely well with no obvious chemical problems nor phase disengagement problems. An extraction of 99.99% Cu was achieved and the stripping was 99.91% effective.

Degradation Tests on Recycled Solvent

After recycling the solvent mixture through extraction, stripping and scrubbing, the equilibrium isotherms as compared to fresh solvent indicated very little change occurred, as a result of recycling.

Electrowinning of Copper Strip Solution

A quantity of strip liquor from the continuous run was subjected to electrowinning. The feed solution contained 35 g Cu/L, 2.21 g NH_3/L and 2.27 g Cl^-/L. Before electrowinning the strip solution was passed through a bed of activated carbon to remove any organic present. These preliminary electrowinning tests at about 20 amp/ft^2 produced smooth, compact deposits and reduced the concentration to 15 g Cu/L. No additive was necessary.

CONCEPTUAL FLOWSHEET

The conceptual flowsheet is shown in Figure 1.

CONCLUSIONS

This paper has described a flowsheet for the treatment of copper etch solutions that would result from the NH_4Cl leaching of printed circuit boards. The process, has the following features:

1. Use of a mixed extractant system to provide for synergistic extraction and increased kinetics, to improve the extraction capabilities and provide for a low 1 g Cu/L raffinate.

2. Use of a scrub stage before stripping to improve the product quality if necessary.

3. Smaller size circuit because of increased extraction effectiveness and therefore a reduction in costs.

4. Possibility to recycle leachant.

5. No apparant degradation of the solvent with recycle.

6. Appears to produce good copper cathode.

The tests to data have been conducted on bench scale and on a continuous scale in a mini pilot plant. Additional continuous testing would be required to optimize the operating parameters.

REFERENCES

1. U.S. Patent 4,083,758.

2. Private communication to G.M. Ritcey.

3. C.P. Birch, Proceedings of International Solvent Extraction Conference, Lyons, Pub. Soc. Chem. Ind., London, 1974, Vol. 3, p. 2837.

4. C.R. Merigold and R.B. Sudderth, in International Symposium on Hydrometallurgy, Chicago, 1973, AIME, Pub. Port City Press, Inc., Baltimore, U.S.A., pp. 552-588.

5. C.R. Merigold and W.H. Jensen, in Proceedings of International Solvent Extraction Conference, Lyons, 1974, Pub. Soc. Chem. Industry, London, pp. 1231-1262.

6. G.M. Ritcey and B.H. Lucas, Trans. CIMM, Vol. LXXV, pp. 82-86, 1972, also U.S. Patent 3,761,249 (1973).

7. G.M. Ritcey and B.H. Lucas, "Extraction and Separation of Copper, Nickel, Zinc and Cobalt from Ammoniacal Solution Using Kelex 100", presented at Annual Meeting AIME, Dalls, Feb. 1974; CIM Bull. February 1975.

8. M.C. Kuhn, N. Arbiter and H. Kling, CIMM Bulletin, Feb. 1974, pp. 62-79.

9. A.J. Van der Zeeuw, in Extractive Metallurgy of Copper - Hydrometallurgy and Electrowinning, Vol. 2, proceedings of International Symposium, 1976, AIME, Pub. Port City Press, Baltimore, U.S.A., pp. 1039-1055.

10. A.W. Ashbrook, G.M. Ritcey and E.G. Joe, Journal of Metals, AIME, 18, No. 1, pp. 18-21 (1966), also U.S. Patent 3,455,680 (1969).

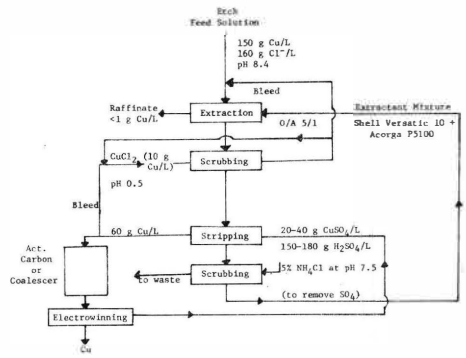

Figure 1 - Schematic for Treating Etch Solution for Copper Recovery.

EXTRACTION OF CUPRIC CHLORIDE FROM IRON CHLORIDE LEACH LIQUORS

T. Danielssen, G. H. Bøe, P. M. Finne

Elkem a/s, Norway

B. Townson

ICI, England

INTRODUCTION

Ferric/cupric chloride leaching of complex sulfide concentrates, as well as leaching of chalcopyrite concentrates, give a resulting pregnant leach solution with a wide variety of elements dissolved as chlorides. To arrive at a high-purity copper product by electrowinning copper directly from the leach solution has not been possible, and selective extractants for copper chloride has up till now not been available.

The new extractant DS 5443 /1/, developed by Imperial Chemical Industries, has been tested out on real ferric chloride leach solutions obtained by leaching a complex zinc/copper/lead/silver concentrate.

This extractant opens up the route to high-quality copper without having to go via anode quality copper refining. The extractant is also discriminating against silver, and allows separation of copper and silver in two separate products.

Tests with DS 5443 have been performed in Elkem's hydrometallurgical pilot plant, Kristiansand. The main objectives for the tests have been to:

- Verify that DS 5443 offers the possibility of producing high-quality copper from a leach liquor obtained by leaching of a complex sulfide concentrate.
- Demonstrate that the Elkem complex ore process /2/, /3/ (ELCO process), can be modified to suit the particular demands of the extractant DS 5443.
- Give an overall feeling for the economics in a modified ELCO process with the extractant DS 5443.

PROCESS

The chemistry and theoretical aspects of the new extractant DS 5443 is dealt with in another paper at this conference /4/. The extractant functions by a chemical principle which is novel in the field of solvent extraction, viz.:

$$2\ L(org) + Cu^{2+}(aq) + 2\ Cl^{-}(aq) = L_2CuCl_2(org)$$ Neutral species of defined stoichiometry.

The equilibrium is controlled by chloride ion concentration in the aquous phase, the extraction process taking place at high chloride ion concentrations, and the stripping at lower chloride ion concentrations.

The basic operations for hydrometallurgical treatment or complex sulfides may be broadly described by the circuit shown in Figure 1.

Option No. 1 on Figure 1, shows the direct electrowinning of an impure copper product from the leach solution.

Option No. 2 comprises solvent extraction with DS 5443 followed by electrowinning of high-quality copper from the strip solution. The No. 2 option offers distinct advantages compared with the first option. The use of DS 5443 for solvent extraction at stage 3 in the process has demonstrated very effectively its high selectivity for copper and its ability to produce an advanced electrolyte suitable for direct electrowinning. The produced copper is of high (wirebar) quality.

The other steps shown in Figure 1 ($PbCl_2$ crystallization, Zn Solvent Extraction and Leach Regeneration) have been described in detail earlier /5/. A brief description is as follows:

- $PbCl_2$ crystallization by cooling of pregnant leach liquor
- Zinc solvent extraction by extraction of $ZnCl_2$ by TBP and electrowinning of zinc and Cl_2. /6/
- Leach liquor regeneration and iron precipitation with air at elevated temperatures/pressures.

This paper will focus on the special leaching conditions the use of DS 5443 demands /7/, the impact on copper product quality, and the economic advantages it offers compared to direct electrowinning of copper from pregnant leach solution.

Literature:

/1/ R.Price, P.M.Quan and B.Townson: "Novel Solvent Extractants for Copper from Chloride Media. Their Application in the Processing of Complex Base Metal Concentrates", EEC/Canada Conference on Complex Sulfides, Ottawa 1982.

/2/ C.Haakonsen and T.Thomassen: Norw.Pat.Appl.80.2986 (Oct. 7, 1980), US Pat.Appl. 254,955 (April 16, 1981).

/3/ A.Bjune, G.H.Bøe, T.Danielssen: Norw.Pat.Appl. 79.1261 (April 17, 1979), US Pat.Appl. 137,569 (April 7, 1980).

/4/ R.F.Dalton, R.Price, P.M.Quan: "Novel Solvent Extractants for Chloride Leach Systems", ISEC conference, 1983.

/5/ G.H.Bøe et al: "Production of Base Metals from a Complex Sulfide Concentrate by the Ferric Chloride Route in a Small Continuous Pilot Plant", I.M.M., Rome 1980.

/6/ T.Danielssen: "Adaption of a Zinc Solvent Extraction Process to Norwegian Copper Concentrates with a Low Zinc Content", Oslo Symposium on Ion Exchange and Solvent Extraction, Oslo 1982.

/7/ G.H.Bøe and E.Andersen: Patent Pending.

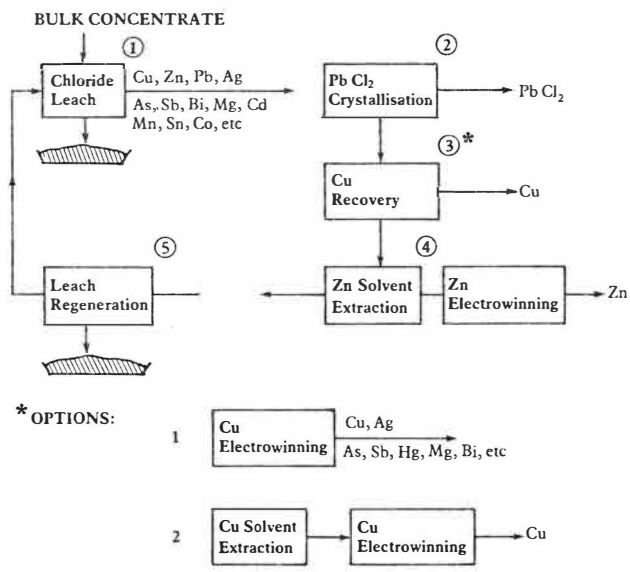

PHASE EQUILIBRIA IN MULTICOMPONENT SOLVENT EXTRACTION SYSTEMS

J. E. Alter and R. Blumberg

Miles Laboratories, Inc.
Elkhart, Indiana USA

A necessary criterion for equilibrium in multicomponent liquid-liquid systems is that the activity a_i for each component must be the same in the two phases i.e. $a^1 i = a^{11} i$ i - 1, 2--n components. In cases where one of the liquid phases is an aqueous phase, it is expedient to use this phase as the reference phase at equilibrium since there are various accepted modes of measuring activities in aqueous solution.

In a liquid-liquid system where components distribute between the two phases, the distribution coefficient is the accepted manner of describing the relative concentrations of a component at equal activity. This distribution coefficient is the resultant of all the equilibrium constants which apply. In different systems, different equilibrium constants may be the limiting ones which determine the ultimate distribution. Thus e.g. solubility product in presence of a solid phase, or ionization constant i.e. pK will be determining for acid or base systems, or dissociation, or hydrolysis constant, etc. in relevant cases.

The concept of the "half titration pH" as a measure of acid or base strength of essentially water insoluble acids or bases is fully accepted in liquid-liquid extraction.(1) Similarly, for separating cations by ion pair formation or ion exchanges with particular acids, a pH scale has been accepted as defining the system at equilibrium.(2)

$$MA + \overline{HR} \rightleftarrows HA + \overline{MR}$$

We have extended this approach to the separation of acids from a solvent phase by controlled neutralization as a function of pKs of the acids and using an ion exchange model, also for recovery of weak bases or acids from aqueous medium.

The important point is that by this approach the required data base of distributions is greatly reduced since behavior can be predicted from a few limiting measurements which define the system.

ACID SEPARATION

Several simple examples that have recently been encountered may illustrate this approach. Suppose there are two acids that require separation, HA and HB. Each has an ionization constant,

$$HA \rightleftarrows H^+ + A^- \qquad K_A$$

$$HB \rightleftarrows H^+ + B^- \qquad K_B$$

and a distribution constant to an organic phase used for separation,

$$HA + \overline{S} \rightleftarrows \overline{HA.S} \qquad K_{A.S}$$

$$HB + \overline{S} \rightleftarrows \overline{HB.S} \qquad K_{B.S}$$

It is not uncommon in this situation to mix HA and HB together and determine their distributions to the solvent phase under various ratios, concentrations, and pHs. If different solvents are also included, this can become a very large analytical and experimental task.

The above case can be greatly simplified, however, with the realization that the distributions to the solvent phases are limiting and that under high solvent loading the case is really one of an anion exchange reaction

$$HA + \overline{HB.S} \rightleftarrows HB + \overline{HA.S}$$

{HA} and {HB} given at any pH by K_A and K_B. Thus, a few measurements will define the system well enough so that a decision can be made whether further experimental work is warranted. With these two acids it was found that at high acidity and because the materials were at widely differing concentrations, separation by normal extraction, stripping and recycle, were impossible within reasonable economic constraints. The recourse to a higher pH changed the situation and allowed adequate separation on the back extraction from the solvent phases. The number of stages was at first experimentally determined, but this was a tedious job involving a week's experimental time on each set because of the interactive nature of the system. Once it was realized that the system was a simple ion exchange with total hydrogen ion controlling, the system was easy to model and, as important, control in actual production.

CATION EXCHANGE

Another case in cation exchange also shows a similar circumstance. A fermentation broth had a very low concentration of an organic cation that it was desired to separate from the other normal fermentation impurities, each at much higher concentration. Ion exchange had been used previously, and it was thought that solvent extraction might be given a try. The analysis for the desired product was long and involved, and so minimum experimental work was necessary to demonstrate separation before a large program was started. Again, one approach would be to try separating the cation from the impurities over different conditions of pH, impurity level, and so on. This indeed was attempted, but it was soon realized that the approach was impractical because of time limits. The appropriate equilibria can be used to define the experiments needed for feasibility. The organic cation's conjugate acid has an ionization constant, a distribution to the solvent phase and the cationic impurities have distributions as well. In addition, the cation exchange solvent ionizes. Thus

$$ORG\text{-}H^+ \rightleftarrows H^+ + ORG \qquad K_{ORG}$$

$$\overline{RH} \rightleftarrows \overline{R^-} + H^+ \qquad K_{RH}$$

$$RH + ORG\ H^+ \rightleftarrows H^+ + \overline{R^-ORG^+} \qquad K_D$$

Cationic Impurities

$$A^+_{1--n} + \overline{RH} \rightleftarrows \overline{R^-A}_{1--n} + H^+$$

Most other impurities were not cations, and therefore their distributions would be expected to be quite low.

Some of the A^+_{1--n} were known, i.e. K^+, but most were not. However, this knowledge is not necessary since their only affect, collectively, is to control the pH by exchanging with solvent. They may be grouped together as if only one material. With this knowledge, two pieces of experimental information are required:

1. The total amount of cation present. This may be easily determined by titrating the material to be purified with the solvent of choice. The total acid released is the total cation present. The half titration pH may be also obtained.

2. The distribution of the wanted $ORG\text{-}H^+$ to the solvent phase in the absence of impurities at several concentrations.

The above data can be used to calculate whether the separation was feasible. Experiments later confirmed this.

One of the great advantages of liquid-liquid extraction is the fact that the solvent may be varied at will to produce a separation media of slightly or strongly varying properties. On the other hand resins, membranes, along with other techniques of separation, are extremely difficult to vary in any systematic fashion without a great deal of effort. Given this fact, an important part of a liquid extraction study is solvent screening. The two examples show this task may be much simplified given a basic understanding and a simple modeling of the system. This is very often done after the experiments are finished, rather than before the experiments begin. This is not necessary, as even with a small amount of information and a model, the real needed experiments for project definitions may be very limited. This situation also would apply to other techniques such as ion exchange.

REFERENCES

1. R. Blumberg, J. E. Gai, K. Hajdu, Proceedings International Solvent Extraction Conference 1974, Vol 3, 2789.

2. C. Hanson, Recent Advances in Liquid-Liquid Extraction, Pergamon Press (1971).

PHASE EQUILIBRIA IN SOLVENT EXTRACTION - THERMODYNAMIC DESCRIPTION

Alexander Apelblat

Department of Chemical Engineering
Ben Gurion University of the Negev
Beer Sheva, Israel

INTRODUCTION

A quantitative description of extraction equilibria is complicated because the aqueous and organic phases deviate considerably from ideal behaviour. However, there are many processes where substances to be separated are in micro quantities and they are to be separated from one solute which is present in both phases in macro quantities. It is evident, in this case, that distribution of micro components is to a great extent influenced by the presence of this solute and therefore a detailed investigation of the fundamental ternary system which includes the solute, water and extractant (solvent) is of considerable importance.

In this paper a procedure is described which gives us the possibility to characterize the extraction equilibria in the fundamental ternary system in terms of thermodynamic parameters. The proposed procedure has been already applied to quite different systems which included neutral organophosphates and alcohols as solvents and strong mineral acids and several nitrates as solutes (1-6). The data of interest can be obtained by simple means without elaborate physical measurements. Only the composition of the aqueous and organic phases and their densities (in order to express the concentrations in molal units) are needed.

Frequently, extractants are mixed with a suitable diluent, in order to reduce the price of solvent or prevent its losses in the process by reducing the solubility of it in the aqueous phase. In spite of the fact that diluents are important from a practical point of view, their role in the extraction process is only secondary. The diluent effect is usually described in terms of physical solubility rather than specific interactions or complexing reactions and therefore is omitted here.

The basic assumption used in the proposed approach is that the extraction equilibrium, expressed by the extraction isotherm, can be considered as a complex formation reaction, i.e., tha mass action law can be applied to the ternary system. Over a whole concentration range, several complexes may be formed, but it is supposed that only one principal complex exists at infinite dilution in the organic phase. Evidently in this description, a simultaneous formation of the complexes at finite concentrations influences the activity of components and more explicitly the value of activity coefficients.

EXTRACTION EQUILIBRIUM IN TERNARY SYSTEMS

If an electrolyte A is distributed between the aqueous solution of A and the solvent S and the complex $B=A(H_2O)_hS_q$ is formed , then:

$$(1)\quad A + q\bar{S} + hH_2O \overset{K}{\rightleftharpoons} \bar{B}$$

where q and h are the solvation and hydration numbers of the complex B and the quantities in the organic phase are denoted with a bar. In principle, the complex may not only be hydrated but also dissociated in the organic phase. Introducing activities of all species, the thermodynamic equilibrium constant of the complex formation reaction is

$$(2)\quad K = \frac{\bar{a}_B}{a_A(a_W)^h\,(\bar{a}_S)^q}$$

In definition of chemical potentials, the unsymmetrical reference system is applied to the solute A in both phases and the symmetrical reference system for the solvent S.

The procedure for evaluation of the activities in (2), the equilibrium constant K and the stoichiometric parameters of the complex B, q and h, from composition and densities of both phases(which permits conversion from molar to molal units) is presented below.

DETERMINATION OF THE ACTIVITIES a_A AND a_W.

Since in the extraction systems the solvent S is practically unsoluble in the aqueous phase, it can be considered that the aqueous phase is a binary system. In this case, for most of electrolytes the values of osmotic coefficients ϕ and activity coefficients $\gamma_\pm$ are known in the literature (7). The activity of water, a_W, is given by:

$$(3)\quad a_W = \exp(-\nu m_A\phi/55.51)$$

where $\nu = \nu_1 + \nu_2$ is the total number of ions (ν_1- cations and ν_2 -anions) coming from the dissociation of the solute A and m_A denotes its molality in the aqueous phase. The activity of the solute A is

$$(4)\quad a_A = (\nu_1)^{\nu_1}(\nu_2)^{\nu_2}(m_A\gamma_\pm)^{\nu}$$

It is generally accepted, that the error caused by neglection of the solubility of S in the aqueous phase is very small.

DETERMINATION OF THE SOLVENT ACTIVITY $\bar{a}_S$.

From the Gibbs-Duhem equation used for the organic phase and taking into account the equality of chemical potentials of components in both phases(the aqueous phase once again is supposed to be a binary system) one has:

$$(5)\quad \ln(\bar{a}_S/\bar{a}_S^W) = \frac{M_S}{1000}\int_0^{a_A}\left(\frac{\bar{m}_W m_A}{55.51} - \bar{m}_A\right)d\ln a_A$$

where M_S is the molecular weight of solvent. The integral (5) includes only measurable quantities m_A, $\bar{m}_A$ and $\bar{m}_W$, where the functional dependence $a_A=f(m_A)$ has already been discussed. $\bar{a}_S^W$ is the activity of solvent saturated with water and its value is evaluated from the correlation between the activity and solubility of water in solvent $\bar{m}_W = f(a_W)$. The variation of the water activity with water molality in the solvent is usually expressed by the Setchenov type equation:

$$(6)\quad \ln(a_W/\bar{m}_W) = \lambda_0 + \lambda_1\bar{m}_W + \lambda_2(\bar{m}_W)^2$$

where determination of the constants λ_0, λ_1 and λ_2 is described in (8). The value of $\bar{a}_S^W$ is given by:

$$(7)\quad \ln\bar{a}_S^W = -\frac{1000}{M_S}\bar{m}_W\left(1 + \frac{\lambda_1}{2}\bar{m}_W + \frac{2}{3}\lambda_2\bar{m}_W^2\right)$$

where $\bar{m}_W$ is evaluated from (6) for $a_W = 1$.

EVALUATION OF THE SOLVATION q AND HYDRATION h NUMBERS.

The solvation number q is determined usually by so-called slope analysis ($D \sim [S]^q$ where $D = \bar{m}_A/m_A$) in such way that $m_A \gg \bar{m}_A$. The total concentration of solvent [S] is changed by mixing it with a suitable diluent, assuming that the ratio of activity coefficients $\bar{\gamma}_B/(\bar{\gamma}_S)^q$ remains constant over a wide range of dilutions. However, often noninteger values of q are observed as a result of several overlapping equilibria or of nonequivalent distribution of water. The water-diluent interactions are usually stronger then the solute-diluent interactions and therefore in order to reduce the water-diluent effect it is recommended not to use an "inert" diluent but rather such diluent which has some structure elements similar to those of the solvent S.

The total amount of water in the organic phase $\bar{m}_W$ is the sum of the water bonded to the complex B and dissolved in S. If it is assumed that these processes are independent, the hydration number is the limit of

$$(8)\quad h = \lim_{\bar{m}_A \to 0} \frac{d[\bar{m}_W - \bar{m}_W^*]}{d\bar{m}_A}$$

where values of $\bar{m}_W^* = f(a_W)$ are given in (6) for corresponding values of $m_A = g(\bar{m}_A)$ through (3)

EVALUATION OF THE COMPLEX ACTIVITY $\bar{a}_B$ AND THE EQUILIBRIUM CONSTANT K.

For the undissociated complex B in the organic phase, the equilibrium constant K is obtained from the extrapolation:

$$(9)\quad K = \lim_{\bar{m}_A \to 0} \frac{\bar{m}_A}{a_A(a_W)^h(\bar{a}_S)^q}$$

then from (2)

$$(10)\quad \bar{a}_B = \bar{m}_A\bar{\gamma}_A = Ka_A(a_W)^h(\bar{a}_S)^q$$

If in the extrapolation to zero as a function of $\bar{m}_A$, the right-hand side of equation (9) has a hyperbolic form, the complex B is partially dissociated, then in this case:

$$(11)\quad K = \lim_{\bar{m}_A \to 0} \frac{(\bar{m}_A)^2}{a_A(a_W)^h(\bar{a}_S)^q}$$

and

$$(12)\quad \bar{a}_B = \bar{m}_A^2(\gamma_{B\pm})^2 = Ka_A(a_W)^h(\bar{a}_S)^q$$

A weak concentration dependence of activity coefficients $\bar{\gamma}_B$ or $\bar{\gamma}_{B\pm}$ over a wide concentration range can give an indication about the correct choice of the principal complex(i.e., values of q and h), taking also in consideration that the activities differ considerably from concentrations and they are more sensitive to experimental errors.

REFERENCES

1. A. Apelblat, J. Chem.Soc.,(A), 1271,(1970)
2. A. Apelblat, J. Chem. Soc.,(A), 3459, (1971)
3. A. Apelblat, J. Chem.Soc., Dalton Trans.,1198, (1973)
4. A. Apelblat and R. Levin, J. Chem.Soc.,Dalton Trans.,1476,(1974)
5. A. Apelblat, J. Chem.Soc.,Faraday Trans I.,70, 769,(1974)
6. A. Apelblat, J.Chem.Soc.,Faraday Trans I.,70, 2033,(1974)
7. R.A. Robinson and R.H. Stokes, Electrolyte Solutions,Butterworths,(1970)
8. A. Apelblat, Ber. Bunsenges. Phys. Chem.,in press

REVIEW OF THE THERMODYNAMICS OF SYNERGISM

Gregory R. Choppin

Department of Chemistry
Florida State University
Tallahassee, Florida 32306 USA

INTRODUCTION

Synergism in solvent extraction relates to the enhancement in metal extraction when two extractants are present compared to the sum of the extraction by the individual extractants (1). Such synergism is observed for many extractant combinations and is also dependent on the organic solvent. Particularly large synergistic extractions are obtained with β-diketonates and neutral adducts (e.g. organophosphorous compounds) in organic solvents of low water solubility. The synergic coefficient, s.c., has been defined (2) as:

$$\text{s.c.} = \log \frac{D_{(1+2)}}{D_1 + D_2}$$

where D_n represents the distribution ratios of extractants 1,2 and 1 + 2. Many factors have been shown to affect the s.c. values such as the basicities of the β-diketonate anions and of the neutral adducts, the coordination number of the metal, the solvation of the extractants and the interaction between the two extractants. However, the primary cause of synergism is attributed generally to an increase in the hydrophobic character of the extracted metal species upon addition of the adduct.

The chelate rings of the β-diketonate ligands may not coordinately saturate the metal. In this case, the extracted species may retain hydrate molecules which are replaced by the adduct. Alternately the extracted species in such a coordinately unsaturated case may be anhydrous and addition of adduct molecules results in expansion of the coordination sphere. It has been proposed that in cases of saturation of the metal coordination by the β-diketonate chelate rings, addition of adduct occurs via ring openings. Usually the synergic reaction is defined by the equation:

$$(1) \quad MX_n + {}_mS = MX_nS_m; \; \beta_{nm} = [MX_nS_m][MX_n][S]^m$$

where X = β-diketonate, S = neutral adduct. From values of $\beta_{n,m}$ (or $\Delta G_{n,m}$) it would be difficult to define with confidence which of these mechanisms is operating in any particular system of M/X/S/solvent. Entropy, $\Delta S_{n,m}$ values, however, could be much more informative. Similarly, questions of solvent interaction, extractant basicities, etc. might be answered by $\Delta H_{n,m}$ data. Therefore, measurement of the thermodynamic parameters of synergism would be helpful in better understanding the factors involved (3).

DILUENT EFFECTS

The term diluent effects is to be interpreted as including solvation effects, particularly of the extractants, ligand-adduct interaction and hydration effects. Any or all of these effects may be influencing the extraction in any particular system, complicating any interpretation of the synergistic reaction (Eq. 1) from extraction data. Attempts to obtain ΔH and ΔS data for Eq. 1 from the temperature coefficient of the extraction coefficients would also be of doubtful value in most systems.

β-Diketones can exist in keto, enol and ketohydrate forms in wet organic solvants. The enol form reacts with the metal as well as with the neutral adducts. Jacobs (4) reported a value of 40 ± 10 for the equilibrium constant in benzene for the reaction of the enol form of HTTA with TOPO. The same reaction involving TBP has a value of 3 in benzene and 0.2 in CCl_4 (5). Moreover, water interferes to form the ketohydrate with HTTA and the TBP·H_2O hydrate. Extractant solvation is also poorly studied but values of 0.2, 0.9 and 6.1 are reported for the interaction of TBP with C_6H_6, CCl_4 and $CHCl_3$ (5).

Table 1 lists the thermodynamic parameters for synergistic reaction of Nd^{+3} and Th^{+4} in different solvents. The data are consistent with the order of TBP-solvent interaction effects since the greater extent of TBP solvation in $CHCl_3$ would make the ΔH and ΔS terms more positive than in C_6H_6. Using the solvent association constants given above, we can calculate values corrected for TBP solvation listed as $-\Delta G^c_{n,m}$ in Table 1. The agreement would indicate that other "diluent effects" are less important in the M/HTTA/TBP systems. This is unlikely to be the situation generally and much more data is needed to more fully evaluate these diluent effects in a variety of systems.

LIGAND-ADDUCT EFFECTS

Some of the available thermodynamic data for the synergistic reactions forming MX_nS_m are listed in Table 2 (from ref. 3 unless noted otherwise).

The large ΔS value for $Ca(TTA)_2(TBP)_2$ has been ascribed to the reaction:

$$H(H_2O)_4^+Ca(TTA)_3^-{}_{(o)} + 2TBP_{(o)} = Ca(TTA)_2(TBP)_{2(o)} + H^+_{(aq)} + 4H_2O_{(aq)}$$

No expansion in coordination sphere for Ca^{+2} is involved. However, the negative ΔS for the formation of $Zn(TTA)_2$·TBP is understood as reflecting an increase in the coordination number of Zn^{+2} from 4 to 5. The uranyl data is consistent also with addition of the adduct by expansion of the coordination number for the UO_2^{+2} from 4 to 5.

The lanthanide data is interpreted as being due to the reaction

$$Ln(TTA)_3(H_2O) + S = Ln(TTA)_3 \cdot S + 2H_2O$$

Addition of a second adduct molecule would result in more negative values of ΔH and ΔS, as observed for 2,2-dipyridyl and TBP. Apparently, the greater hydration of TOPO as well as its larger effect on the keto = enol equilibrium of HTTA results in a reversal of the expected trends in ΔH and ΔS.

The $Th(TTA)_4$·TBP reaction should increase the coordination number for Th^{+4} from 8 to 9 ($Th(TTA)_4$ is not hydrated). The negative values of ΔH and ΔS are consistent with such a reaction.

CONCLUSIONS

Calorimetric measurements of organic phase synergistic reactions in wet and in dry systems would be very helpful in providing a more complete understanding of the various diluent effects and of the mechanism (C.N. expansion vs. hydrate replacement) of adduct addition. Such experiments are underway at present.

This research was supported by a contract with the U.S.D.O.E. Office of Basic Energy Sciences.

Table 1

Thermodynamic Values for the Reaction
$M(TTA)_n + S = M(TTA)_n \cdot S$

Species	Solvent	$-\Delta G^{\dagger}_{3,1}$	$-\Delta H^{\dagger}_{3,1}$	$\Delta S^{*}_{3,1}$	$-\Delta G^{c\dagger}_{n,m}$	Ref.
$Nd(TTA)_3$(dipy)	$CHCl_3$	20.6	33.1	42	25.1	6a
$Nd(TTA)_3$(dipy)	C_6H_6	31.8	41.9	34	27.8	6b
$Th(TTA)_4$(TBP)	C_6H_{12}	34.7	47.6	-43.5	-	7
$Th(TTA)_4$(TBP)	C_6H_6	26.5	43.7	-58.2	22.5	7
$Th(TTA)_4$(TBP)	$CHCl_3$	18.5	29.5	-37.2	23.0	7

† $kJ \cdot m^{-1}$

* $J \cdot m^{-1} \cdot K^{-1}$

Table 2

Thermodynamic Values for the Reactions
a) $M(TTA)_n + S = M(TTA)_n \cdot S$
b) $M(TTA)_n \cdot S + S = M(TTA)_n \cdot S_2$

System	$-\Delta G^{\dagger}$	$-\Delta H^{\dagger}$	ΔS^{*}
Ca/HTTA/2TBP	39.13	9.58	162
Zn/HTTA/TBP	20.46	28.2	-26
Eu/HTTA/TBP	24.73	24.0	3
Eu/HTTA/2TBP	16.49	36.0	-65
Eu/HTTA/TOPO	37.8	28.8	29
Eu/HTTA/2TOPO(a)	30.8	11.2	66
Nd/HTTA/2,2dipy(b)	31.8	41.9	-34
Nd/HTTA/2(2,2dipy)(c)	8.8	28.5	-67
UO_2/HTTA/TBP(c)	10.34	21.8	-38
UO_2/HTTA/TOPO(c)	27.6	15.8	40

† $kJ \cdot m^{-1}$

* $J \cdot m^{-1} \cdot K^{-1}$

(a) ref. 8; (b) ref. 6b; (c) ref. 9

REFERENCES

1. C.A. Black, C.F. Baes, K.B. Brown, C.F. Coleman, and J.C. White, Proc. Intern. Conf. on Peaceful Uses of At. Ener., Vol. 28, IAEA, Vienna, 1959, p. 289.

2. M. Taube and S. Siekierski, Nukleonika, (1961), 6, 489.

3. G.R. Choppin, Sep. Sci. Tech., (1981) 16, 1113.

4. E.B. Jacobs, At. Ener. Australia, (1975), 18, 15.

5. S.K. Patil and V.V. Ramakrishna, BARC-1090, Bhabha At. Res. Centre, Bombay, India, 1980.

6. a. A.S. Kertes and E.F. Kassierer, Inorg. Chem., (1972), 11, 2108;
   b. J. Inorg. Nucl. Chem., (1972), 34, 3221.

7. S.K. Patil, V.V. Ramakrishna and M.S. Sajun, Thermochim. Acta., (1980), 42, 281.

8. A.T. Kandil and K. Farah, J. Inorg. Nucl. Chem., (1980), 42, 1491.

9. M.S. Subramanian and S.A. Pai, J. Inorg. Nucl. Chem., (1970), 32, 3677.

THERMODYNAMICS OF THE EXTRACTION OF Hf(IV) WITH ACETYLACETONE

Robert F. D. Lundqvist

Department of Nuclear Chemistry
Chalmers University of Technology
S-412 96 Göteborg, Sweden

The extraction mechanisms for some bivalent metalyl ions i.e. UO_2^{2+}, PaO^{2+}, HfO^{2+} and VO^{2+} with β-diketones have previously been described (1). It was concluded that the extraction mechanism and type of metal complexes depend on both the metal and the ligand. Hf(IV) is, for example, extracted by benzoylacetone (HBA) and thenoyltrifluoroacetone (HTTA) as $Hf(BA)_4$ and $Hf(TTA)_4$ while a different mechanism was indicated with acetylacetone (HAA). Hence, in analogy with Pa(IV) it seemed that Hf(IV) was extracted as $MO(AA)_2$ contrary to the composition in solid state in which both $Hf(AA)_4$ and $Hf(AA)CL_3$ have been prepared. The aim of this work is to verify the extraction mechanism of Hf(IV) with HAA and to study it under various conditions like different solvents, ionic media and temperature.

Earlier (2), partial processes for the partition of the neutral metal acetylacetonates have been proposed from thermodynamic data for Be, Cu, Zn, Ce, Hf, Th, U and Np. This work includes also the metal complexation of Hf.

CHARACTERIZATION OF THE EXTRACTION MECHANISM

The distribution of Hf(IV) between dilute solutions of HAA in benzene and 1 M $NaClO_4$ was studied. The distribution ratios $D = [Hf(org)]/[Hf(aq)]$ were determined by radiochemical measurements using $^{175,181}Hf$ at tracer level concentrations of Hf. D-values were obtained at different constant HAA concentrations as a function of pH yielding a relation log D = f(pAA) shown in Figure 1.

According to the general theory (3,4) for evaluation of the composite metal complex $M_m(AA)_n(OH)_pHAA)_r(org)_s(H_2O)_t$ in a liquid-liquid distribution system we conclude from the obtained relationship between log D and pAA that the only possible type of Hf(IV)-HAA complex is $HfO(AA)_2$ since the limiting slope $\delta \log D/\delta pAA = -2$ and since all data coincide into one single curve. Hence, the distribution of Hf(IV) can be described by equation (1)

$$\log D = \frac{\lambda_2 \beta_2 [AA^-]^2}{I + \beta_I [AA^-] + \beta_2 [AA^-]^2} \quad (1)$$

where λ_2 = the distribution constant for $HfO(AA)_2$ and β_n are the formation constants. $pAA = -\log [AA^-]$ was calculated as follows (equal phase volumes):

$$pAA = pK_a - pH + \log(K_d + 1 + K_a[H^+]^{-1}) - \log[HAA]^{init}_{org} \quad (2)$$

where K_a is the dissociation constant for HAA and K_d its distribution constant $[HAA]_{org}/[HAA]$. The values of these constants were determined for every studied system (various solvents, temperatures and ionic strengths). Following the equation (1) one finds that the only Hf complexes needed to describe the distribution system between pH 1 and pH 8 are HfO^{2+}, $HfOAA^+$ and $HfO(AA)_2$ of which the latter distribute between the two phases. At pH above 8 a decrease in the distribution is observed which indicates hydrolysis of HfO^{2+} and/or formation of $HfO(AA)_3^-$. Any hydrolysis before pH 8 in our system is completely depressed by the stronger complexation with HAA. Experiments were also performed with 1 M $HClO_4$ and the relationship between log D and log $[HAA]^{init}_{org}$ was determined. Even at such high acidity it seems that most of the Hf(IV) is extracted in the form of $HfO(AA)_2$, but a possible coextraction of $Hf(AA)_4$ cannot be excluded.

INFLUENCE OF SYSTEM PARAMETERS

Organic solvent. The effect of the solvent on the distribution curves log D = f(pH) at constant total acetylacetone concentration was determined. Figure 2 shows the elevation of the distribution curve with a substitution of the solvent in the following series n-hexane < n-heptane < toluene < carbon tetrachloride < benzene < chloroform. This behaviour can be analyzed (5,6) with the theory of regular solutions and the following relation was found to fit our data:

$$\log \lambda_{2,solvent} = n \log K_{d,solvent} + const. \quad (3)$$

The value of n was determined to be $n \approx 2.5$ (1 M $NaClO_4$, seven solvents). Further, a decrease in the λ_2 values were observed upon increasing the HAA concentration from 1 M to 8 M in benzene, while the K_d was near constant (1 M $NaClO_4$).

Ionic strength. The influence of an increase in the ionic strength from 0 to 1 M on the relationship log D = f(pH) was slight for 5°C, 25°C and 45°C which is also indicated by the small variation in the β_n and λ_2 values listed in Table 1. At higher ionic strength an increase in the distribution was observed. The distribution values of $HfO(AA)_2$ was studied at 0-6 M $NaClO_4$ and $LiClO_4$ and with n-hexane, benzene and chloroform. The simultaneous behaviour of K_d was opposite to that of λ_2.

Temperature. The distribution of Hf(IV) increases appreciably even upon a 5 degrees increase in temperature. Figure 3 shows the distribution curves log D = f(pH) at 5°C, 13.8°C, 25°C and 45°C. ΔH_λ and ΔS_λ for the partition of the neutral $HfO(AA)_2$ complex between benzene and 0, 0.1 and 1 M $NaClO_4$ were derived, Table 1. ΔH_λ and ΔS_λ decrease a little (about 10%) when we increase the ionic strength from 0 to 1 M $NaClO_4$. This pattern was also found (2) for other bivalent metal acetylacetonates $Be(AA)_2$, $Cu(AA)_2$, and $Zn(AA)_2$. The higher numerical values of ΔH_λ and ΔS_λ for $HfO(AA)_2$ than for the other metal acetylacetonates indicate a stronger hydration of $HfO(AA)_2$. Because of the covariance with the thermodynamics of the dissociation and partition of HAA itself we will discuss ΔH and ΔS for β_1 and β_2 elsewhere together with a presentation of the behaviour of HAA.

Stability constants. The constants β_n and λ_2 have been calculated using a modified specially designed least squares program for solvent extraction data (7) and the values for 0, 0.1, 1 and 4 M $NaClO_4$ at 5°C, 25°C and 45°C are collected in Table 1.

CONCLUSIONS

The thermodynamics of the distribution of Hf(IV) between aqueous $NaClO_4$ and organic solutions containing acetylacetone (>0.1 M HAA) proves that

- HfO^{2+} is the dominating Hf(IV) species in 1 M $NaClO_4$ (pH 1-3).
- $HfO(AA)_2$ is the only extractable Hf(IV) complex, pH 1-9.
- $HfO(AA)_2$ thermodynamically belongs to the class of bivalent metal acetylacetonates, like $Be(AA)_2$, $Cu(AA)_2$, $Zr(AA)_2$ and $PaO(AA)_2$.

REFERENCES

1. R. Lundqvist, Proc. International Solvent Extraction Conference ISEC'80, Liège, Belgium, Sept. 6-12, 1980, Vol. 1, Session 16, paper 80-51, and references therein.
2. B. Allard, S. Johnson, J. Narbutt, R. Lundqvist, Proc. International Solvent Extraction Conference ISEC'77, Toronto, Sept. 9-16, 1977, Canadian Institute of Mining and Metallurgy, CIM Special Vol. 21, 150 (1979).
3. J. Rydberg, Rec. Trav. Chim. Pays-Bas 75, 737 (1956).
4. R. Lundqvist and J. Rydberg, Acta. Chem. Scand. A28, 399 (1974).
5. T. Wakahayashi, S. Oki, T. Omori and N. Suzuki, J. Inorg. Nucl. Chem. 26, 2555 (1964).
6. T. Omori, T. Wakahayashi, S. Oki and N. Suzuki, J. Inorg. Nucl. Chem. 26, 2565 (1964).
7. J.C. Sullivan, J. Rydberg and W.F. Miller, Acta. Chem. Scand. 13, 2023 (1959).

TABLE 1. Stability and thermodynamic constants for the Hf(IV)-HAA(benzene)/ $NaClO_4$ system.

Ionic strength μ	t^oC	$\log \beta_1$	$\log \beta_2$	$\log \lambda_2$	ΔH_λ $kJmol^{-1}$	ΔS_λ $Jmol^{-1}\ deg^{-1}$
0 M $NaClO_4$	5	8.06±0.25	15.24±0.18	0.39±0.02		
0 " "	25	7.77±0.09	14.20±0.08	1.33±0.04	64±7	239±23
0 " "	45	7.74±0.13	13.80±0.11	1.89±0.03		
0.1 " "	5	8.04±0.12	14.94±0.09	0.44±0.02		
0.1 " "	25	7.52±0.38	14.15±0.30	1.34±0.06	64±5	241±16
0.1 " "	45	7.65±0.13	13.82±0.15	1.96±0.08		
1 " "	5	8.09±0.12	14.88±0.10	0.76±0.02		
1 " "	25	7.84±0.08	14.31±0.10	1.43±0.02	58±3	221±9
1 " "	45	7.73±0.09	13.62±0.08	2.12±0.02		
4 " "	5	9.11±0.20	16.20±0.18	1.45±0.10		

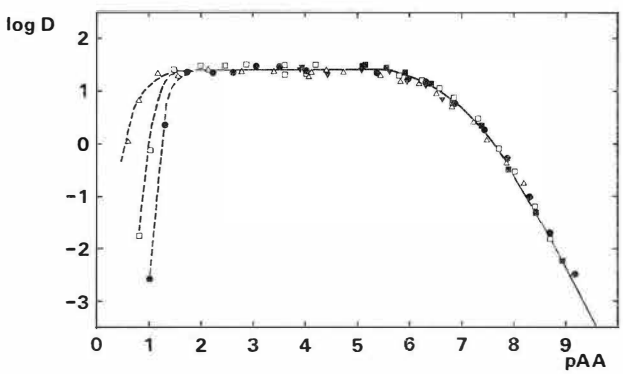

FIGURE 1. The distribution D of Hf(IV) between acetylacetone (HAA) in benzene and 1 M $NaClO_4$ as a function of the ligand concentration (pAA = -log[AA^-]), 25°C. The pH was varied between 1.2 and 9.6. Initial concentrations of HAA are denoted as follows (△) = 0.152 M; (●) = 0.330 M; (□) = 0.769 M; (▼) = 2.00 M and (△) = 2.50 M.

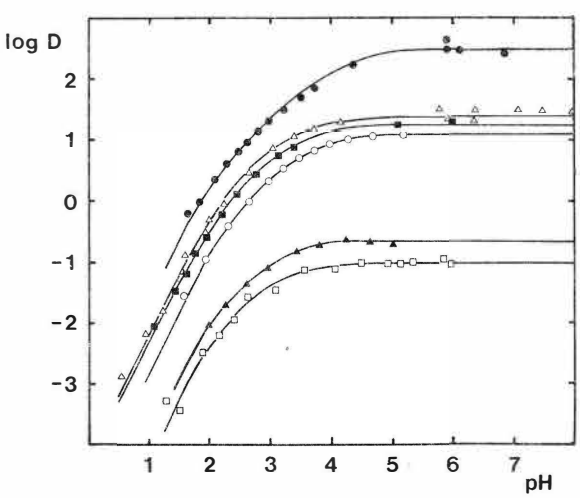

FIGURE 2. The effect of different solvents on the distribution of Hf(IV) between acetylacetone (HAA) containing organic phases and 1 M $NaClO_4$ as a function of pH at 25°C. The initial HAA concentration in the organic phase was 0.769 M. (●) = chloroform, (△) = benzene, (■) = carbon tetrachloride, (○) = toluene, (▲) = cyklohexane, (□) = n-hexane.

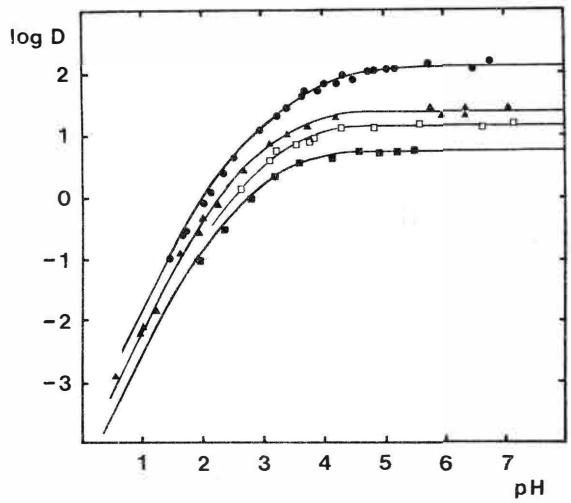

FIGURE 3. The influence of temperature on the relation $\log D_{Hf} = f(pH)$. Aqueous phase: 1 M $NaClO_4$, Organic phase: 0.769 M HAA (initial) in benzene. (■) = 5°C, (□) = 13.8°C, (▲) = 25°C and (●) = 45°C.

PREDICTION OF TERNARY LIQUID-LIQUID EQUILIBRIA

Ireneo Kikic, Paolo Alessi, Romano Lapasin, Maurizio Fermeglia

Istituto di Chimica Applicata e Industriale
Università di Trieste
Trieste, Italy

For a rational design of a liquid-liquid extraction process, equilibrium thermodynamic data relative to the components involved are important and essential even if these information are not sufficient:fluodynamic and mass transfer problems are normally encountered in the apparatus design.Since the correct design will utilize all these information, it is desirable to solve the "equilibrium" problem with the minimum experimental effort.For this reason accurate predictive methods of the liquid-liquid equilibrium conditions should be very useful expecially in the preliminary steps of the development of the process.It is obvious that in the practical realization of the plant no one should reliably base the project only on predicted data: experimental equilibrium data are needed in this case.

From all these reasons it is worthwhile to note that the development and the test of predictive methods for the liquid-liquid equilibrium will lie within well defined limits; these methods have a meaning only in the step of the choice of the solvent and of the anti-solvent, but not in the step of the project expecially if one does not know perfectly the limits of the method used.

The results reported in this work derive from a research program having the following scopes:

- to define methods for the prediction of liquid-liquid equilibrium data;
- to look,in particular, for "mixed" predictive methods,i.e. methods which use some minimum experimental information (however lower than the complete experimental determination of the equilibrium data);
- to establish well defined limits of the reliability of these methods in order to help the possible user in their application;
- to give some guidelines in the search of the essential thermodynamic data.

PREDICTIVE METHODS

Predictive methods of liquid-liquid equilibria can be classified as follows:
- completely predictive methods: they don't need any experimental data;
- mixed predictive methods.

To the first class of methods,we can refer to solubility parameter theory(1) and to the methods based on group contribution concept (2).

The solubility parameter theory,namely the regular solution theory,has been extensively used for solvent extraction systems.The principal defect of regular solution theory is the assumption that the entropy of mixing is ideal;this approximation leads to significant errors for many extraction systems.The original theory has been further developed to take into account associated and hydrogen bonded systems but still the method is not even qualitatively reliable for hydrogen bonded systems with a very high value of the infinite dilution activity coefficient.For example the regular solution theory shows that n-decane is immiscible with both diethylene glycol and 1-butanol while it is experimentally evident that the binary system n-decane-1-butanol is perfectly miscible.Figure 1 shows how the ternary system diethylene glycol-1-butanol-n-decane can be predicted by the regular solution theory and the significant error that one obtains in applying this theory.

The group contribution methods are a very useful tool fot the prediction of the equilibrium and for the solvent screening.Ad hoc liquid-liquid equilibrium (LLE) parameters have been published for one of the most used method,namely the UNIFAC (3).These parameters are calculated from a rather big amount of LLE ternary data collected in a LLE data bank (4).The main limit of the UNIFAC method is in the number of groups characterized;on the other hand the method is extremely powerful and gives very good prediction, certainly better that that obtained with the regular solution theory,as it is shown in Figure 1.

The mixed predictive methods are called in this way because they use a small amount of experimental information for the prediction of the equilibrium.In particular in this work we have considered as possible information the following:

- infinite dilution activity coefficients for both the components of binary systems;
- mutual solubilities relative to partially miscible binary systems.

In order to give a detached evaluation of this prediction method, a complete analysis on artificial systems was made and a comparison with the results obtained on real systems was performed.

ANALYSIS ON ARTIFICIAL SYSTEMS

From a theoretical point of view the analysis carried out on artificial systems leads to results which are more reliable than those obtained from an analysis of a high number of real systems. Moreover according to the procedure based on artificial systems, eventual and casual coincidences due to the concomitance of the choice of the thermodynamic model and of the particular system are left out of consideration.

The technique employed in the generation of the artificial system is the following (Figure 2) :

- Generation of a series of equilibrium data (or tie lines) opportunately spaced, through a calculation of a liquid-liquid flash by using a thermodynamic model (NRTL equation (5)) and the numerical values of the parameters relative to the three constituting binary systems. This set of perfect data is practically a number of tie lines as high as 50-100 for each ternary system.
- Perturbation of the data sets. These perfect values of composition are perturbated by adding errors randomly picked from a set of infinite errors with a Gaussian distribution with mean zero and standard deviation σ_x = .005 mole fraction. The data sets satisfy the maximum likelihood criterium and the criteria for the application of least squares since the errors are small, independent and normally distributed. The model is able to fit these new composition values.
- Comparison of the results obtained from the complete data set and subsets casually chosen, of the same data. This comparison is justified by the fact that, in the literature, 6-7 tie lines are normally reported for the ternary system investigated. From this comparison a standard deviation can be obtained and the average value of the root mean square will be the quantity used for evaluating the goodness of the prediction.

Infinite dilution activity coefficients, which will be employed for the prediction, are generated starting from NRTL parameters. To these numerical values errors are added in a casual way; practically the errors introduced correspond to the average values of errors obtainable with the different experimental techniques used in infinite dilution activity coefficient determination.

It is important to point out that the same model and the same interaction parameters have been used for the generation of the artificial liquid-liquid equilibrium and infinite dilution data.This statement is thermodynamically true: the reality is only one and all the different properties should be predicted by the same model.Unfortunately no one of the available thermodynamic models is perfect and their flexibility is generally not good enough for the prediction of properties and conditions far from the experimental data fitted.

Calculated or extrapolated infinite dilution activity coefficients are sometime far off the experimental values. For this reason an higher value for the standard deviation of the infinite dilution activity coefficient has been introduced. An analysis on several different artificial systems shows that the standard deviation on the parameters obtained from vapor-liquid equilibrium data and infinite dilution data is of the same order of magnitude even if the parameters might be very different (6).

Once the artificial and consistent system is generated it is possible to evaluate the goodness of the prediction starting with the different information. The model used in the prediction is the same model already used for the generation of the artificial systems, namely the NRTL equation.

Since six parameters are needed (two per binary) the following cases for the prediction of a Type 1 ternary system (component 3 is the solvent) are considered:

a) knowledge of six infinite dilution activity coefficients and the mutual solubilities of the binary 1-3 (x_{13} and x_{31});
b) knowledge of six infinite dilution activity coefficients;
c) knowledge of the mutual solubilities of the binary 1-3 (x_{13} and x_{31}) and four infinite dilution activity coefficients (for the systems 1-2 and 2-3).

For the prediction of a Type 2 ternary system (component 3 is the solvent), the following cases are considered:

a) knowledge of six infinite dilution activity coefficients and four mutual solubilities (x_{23} and x_{32} for the system 2-3, x_{13} and x_{31} for the system 1-3);
b) knowledge of four activity coefficients at infinite dilution (for the binary systems 1-2 and the activity coefficients of component 1 and 2 in the solvent 3) and four mutual solubilities ;
c) knowledge of four activity coefficients (as point b) and two mutual solubilities (x_{13} and x_{23});
d) knowledge of six infinite dilution activity coefficients ;
e) knowledge of two activity coefficients at infinite dilution (for the system 1-2) and four mutual solubilities (x_{23} and x_{32} for the system 2-3 and x_{13} and x_{31} for the system 1-3).

In all the cases considered information about the system 1-2 can also be obtained from vapour-liquid equilibrium data (6).

The analysis on artificial systems described above has been applied on many different ternary systems : binodal curves with different size and shape , and different tie line distributions have been considered as well as different values for the binary solubilities.Results are reported for both Type 1 and Type 2 ternary systems.

REAL SYSTEMS

As mentioned above, values of infinite dilution activity coefficients and of mutual solubilities are the experimental information needed for the "mixed" predictive methods considered. One can generally assume that infinite dilution data for the system 1-2 (referring to a typical ternary liquid-liquid extraction system ,where component 3 is the solvent and may be immiscible with one or both the other components) are available or can be calculated from vapor-liquid equilibrium data relative to the same system.

The problem is the availability of data for the systems 1-3 and 2-3. If the vapor pressure of one component (a) is much bigger than the vapor pressure of the other (b), infinite dilution activity coefficients of component a in component b are generally available (7) or may be experimentally determined by gas-liquid chromatographic method. Unfortunately for the same system activity coefficients of component b infitely diluted in component a are not available. Experimental data for systems with approximately the same pure component vapor pressure are rather difficult to find in the open literature but they can be determined by ebulliometric method: various authors (8-10) have lately measured infinite dilution activity coefficients with this method and the availability of such experimental data is increasing.

When experimental information on infinite dilution activity coefficients are missing one can use the already mentioned UNIFAC method to predict them. The prediction capability of the UNIFAC method is therefore tested on systems where the experimental data are available. A comparison is presented also with the results obtained by utilizing experimental gaschromatographic infinite dilution activity coefficient values for the generation of UNIFAC parameters.

Finally some examples of prediction of ternary liquid-liquid equilibrium data are reported; special attention is given to the separation of paraffinic - aromatic hydrocarbons with polar solvents.

ACKNOWLEDGEMENT

This work was carried out with the support of M.P.I. (Rome).

REFERENCES

1. J.G.Helpinstill and M.Van Winkle, Ind.Eng.Chem.Proc.Des.Dev.,7 ,213,(1968).
2. R.C.Reid,J.M.Prausnitz,T.K.Sherwood,"The Properties of Gases and Liquids", Mc Graw-Hill,N.Y.,(1977).
3. T.Magnussen,P.H.D.Thesis,University of Lyngby,DK (1980).
4. J.M.Sorensen and W.Arlt,"Liquid Liquid Equilibrium Data Collection",Chemistry Data Series,Dechema-Frankfurt (1979).
5. H.Renon,L.Asselieneau,G.Cohen,C.Rainbault,"Calcul sur ordinateur des equilibres liquide-vapeur et liquide-liquide",Inst.Franc.du Petrol,Paris,(1971).
6. I.Kikic,P.Alessi,M.Fermeglia,Proc 3rd Conf. Fluid Properties & Phase Equilibria for Chemical Process Design,Georgia,(1983).
7. A.Alessandrini,P.Alessi,M.Fermeglia,I.Kikic,Proc. 3rd Chem. Eng.Conference, Graz,pag 230,(1982).
8. E.R.Thomas,B.A.Newman,G.L.Nicolaides,C.Eckert, J.Chem.Eng.Data,27,233,(1982).
9. G.M.Loblen and J.M.Prausnitz, Ind.Eng.Chem.Fundam.,21,109,(1982).
10. K.Tochigi,K.Kojima, J.Chem.Eng.Japan,9,267,(1976).

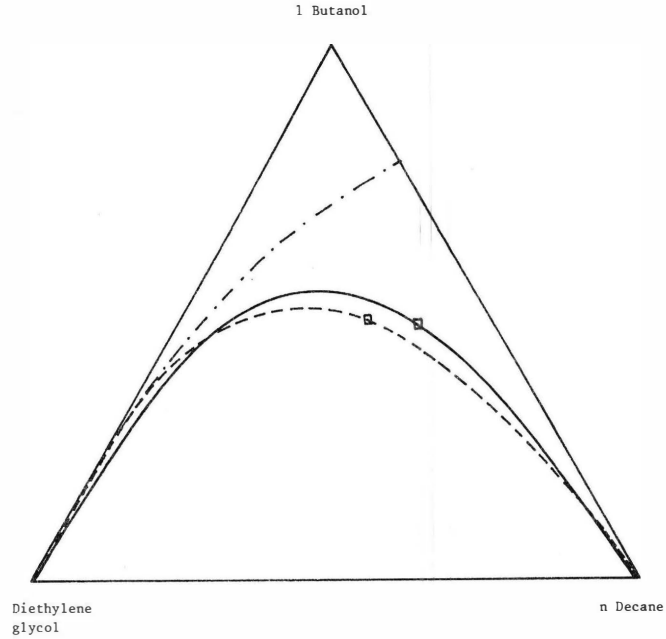

Figure 1: Binodal curve for the system Diethylene glycol - 1 Butanol - n decane at T= 303.15 K (- - - exp(4);—— UNIFAC; -·-·- sol.parameter).

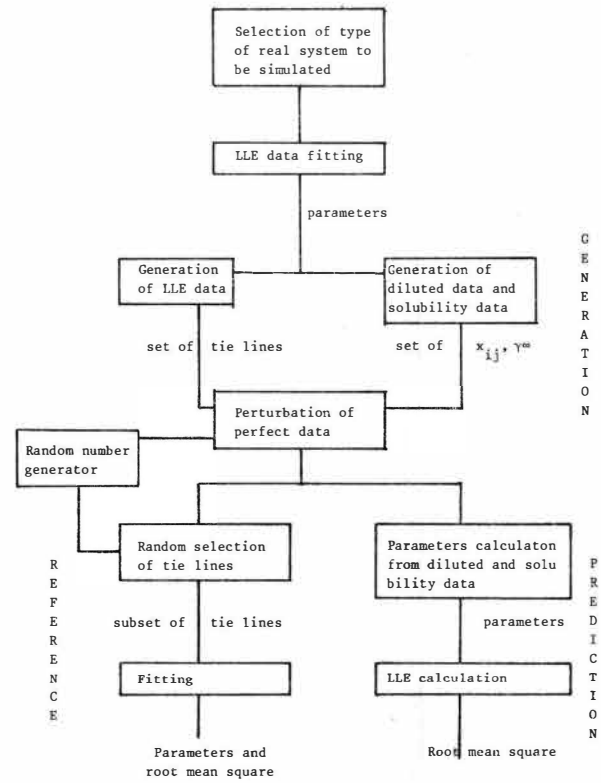

Figure 2 : Artificial systems analysis procedure.

PREDICTION OF TWO-PHASE EQUILIBRIUM DATA AND DETERMINATION OF ACTIVITY COEFFICIENTS IN SOLVENT EXTRACTION OF METALS BY AN IMPROVED SCATCHARD-HILDEBRAND MODEL

Teng Teng, Li Yi-gui, Han Jin-wen, Ding Hong-bing

Tsinghua University
Beijing, China

INTRODUCTION

In the early thirties Scatchard[1] and Hildebrand[2] used the molecular radial-distribution function and inter-molecular dispersion energy function to calculate the total cohesion energy of a system. With some assumptions they deduced the following equations to calculate the excess Gibbs energy of a mixing process and activity coefficients for a binary liquid mixture:

$$\Delta G^E = (n_1 V_1 + n_2 V_2)(E_{11} + E_{22} - 2E_{12})\phi_1\phi_2 \quad (1)$$
$$= (n_1 V_1 + n_2 V_2)(\delta_1 - \delta_2)^2 \phi_1\phi_2 \quad (2)$$

$$\ln f_1 = V_1\phi_2^2(\delta_1 - \delta_2)^2/RT \quad (3)$$
$$\ln f_2 = V_2\phi_1^2(\delta_1 - \delta_2)^2/RT \quad (4)$$

where ΔG^E is the excess Gibbs energy of mixing process for a binary system, n_1, n_2 are moles for components 1 and 2 respectively in a system, V_1, V_2 are volume fractions of components 1 and 2,

$$\phi_1 = n_1 V_1/(n_1 V_1 + n_2 V_2)$$
$$\phi_2 = n_2 V_2/(n_1 V_1 + n_2 V_2)$$

δ_1, δ_2 are solubility parameters of components 1 and 2,

$$\delta = (\Delta E^v/V)^{1/2}$$

ΔE^v is the heat of vaporization of pure liquid component, f_1, f_2 are activity coefficients of components 1 and 2 in liquid phase, using pure liquid component as reference state, E_{12} are the interaction energy between molecules 1 and 2, T is the absolute temperture and R is the gas constant. Their assumptions are:

(1) The interaction energy between two molecules is only dependent on their distance and their orientation, and is independent of the properties of the surrounding molecules.

(2) The molecules are distributed randomly. Their distribution is independent of the position or orientation or other properties of the molecules.

(3) $\Delta V^E = 0$

(4) $\Delta S^E = 0$

(5) The interaction energy between different molecules was assumed to be the geometric mean of two interaction energies between the same molecules, i.e.,

$$E_{12} = (E_{11} E_{22})^{1/2} \quad (5)$$

Based on the fifth assumption, $(\delta_1 - \delta_2)^2$ are always positive and

$$f_1 \geqslant 1, \quad f_2 \geqslant 1,$$

it means that the system is always of positive deviation.

Many investigators such as T. Wakahayashi,[3-6] Z. Kolarik,[7-8] B.M. Vdovenko,[9] T. Sato[10] and H.M.N.H.Irving[11] use this model to correlate the physical and chemical extraction processes with some success. They find it is applicable to estimate the distribution coefficient for some organic and metal-solvent systems. But all their applications are restricted to the (1) binary systems, (2) solutes which are of micro-components and (3) solutions with positive deviation. It is obvious that the early Scatchard-Hildebrand model can only be used to estimate the extraction distribution data approximately for different diluents in binary systems (binary organic phase) and it cannot be used to calculate or predict the equilibrium data accurately for multi-component chemical extraction system (such as the solvent-metal system with macro-component metal-complex solutes and with strong polarity both in aqueous and organic phases).

THEORETICAL CONSIDERATION

The fifth assumption of Scatchard-Hildebrand model is correct only when there is dispersion force between molecules. This restricts the wide application of this model, because besides the dispersion force, in polar mixtures there are dipole force, induced dipole force and hydrogen-bond force between molecules. So we suppose that the following relationship is reasonable:

$$E_{12} = (E_{11} E_{22})^{1/2}(1 - l_{12}) \quad (6)$$

where l_{12} is a revised coefficient with regard to the polar intermolecular energy. It is also a binary parameter and its value may be positive or negative. Substituting Eq.(6) into Eq.(1), we get the following revised equation:

$$\ln f_1 = V_1\phi_2^2((\delta_1 - \delta_2)^2 + 2l_{12}\delta_1\delta_2)/RT = V_1\phi_2^2 A_{12}/RT \quad (7)$$
$$\ln f_2 = V_2\phi_1^2((\delta_1 - \delta_2)^2 + 2l_{12}\delta_1\delta_2)/RT = V_2\phi_1^2 A_{12}/RT$$

where $A_{12} = (\delta_1 - \delta_2)^2 + 2l_{12}\delta_1\delta_2$, A_{12} is the terminal constant of revised Scatchard-Hildebrand's model with regard to the intermolecular force between components 1 and 2. Thus A_{12} may be positive (for non-ideal solution with positive deviation ($f > 1$)) or negative (for that with negative deviation ($f < 1$)).

For ternary system, the mathematical expressions of this revised model are:

$$\ln f_1 = V_1(\phi_2^2 A_{12} + \phi_3^2 A_{13} + \phi_2\phi_3(A_{12} + A_{13} - A_{23}))/RT$$
$$\ln f_2 = V_2(\phi_1^2 A_{12} + \phi_3^2 A_{23} + \phi_1\phi_3(A_{12} + A_{23} - A_{13}))/RT \quad (8)$$
$$\ln f_3 = V_3(\phi_1^2 A_{13} + \phi_2^2 A_{23} + \phi_1\phi_2(A_{13} + A_{23} - A_{12}))/RT$$

For quaternary system, their expressions are:

$$\ln f_1 = V_1(A_{12}\phi_2^2 + A_{13}\phi_3^2 + A_{14}\phi_4^2 + (A_{12} + A_{13} - A_{23})\phi_2\phi_3 + (A_{12} + A_{14} - A_{24})\phi_2\phi_4 + (A_{13} + A_{14} - A_{34})\phi_3\phi_4)/RT \quad (9)$$

The calculating equations of $\ln f_2$, $\ln f_3$ and $\ln f_4$ are analogous to Eq.(9).

We tried to use the above revised Scatchard-Hildebrand model to treat the binary, ternary and quaternary systems for metal-solvent extraction process.

EXAMINATION OF VARIOUS SYSTEMS

(1) The binary system

The extractant TBP (tributyl phosphate) with a series of hydrocarbon as diluent was tested. The activity coefficients of diluents at 25°c were determined by gas-chromatography. Our experimental data indicate that the revised Scatchard-Hildebrand model fits these binary systems quite well. The terminal parameters A_{12} and the revised coefficients l_{12} were also determined (see Table 1).

TABLE 1 A_{12} and l_{12} in TBP-n-C_nH_{2n+2} binary solutions

n	system	A_{12}(ex)	l_{12}(ex)
6	TBP-nC_6H_{14}	15.20	-0.0827
7	TBP-nC_7H_{16}	17.06	-0.0953
8	TBP-nC_8H_{18}	17.22	-0.0981
12	TBP-n$C_{12}H_{26}$	19.99	-0.122

(2) The ternary system

The metal-solvent extraction system without diluent (TBP-UO_2Cl_2, TBP-$UO_2(NO_3)_2$) were tested. The organic phases in these systems are composed of three components: (1) water, (2) extractant, (3) metallic complex. The method for calculating the activity coefficients of all components has been discussed in detail in our earlier paper.[23] The revised Scatchard-Hildebrand model fits these ternary systems very well within the whole metal concentration in organic phase (from very dilute to saturated metallic complex in organic solutions). The experimental regressed terminal parameters for these two systems are shown in Table 2. It can be seen from Table 2 that A_{12} and A_{13} are positive while A_{23} is negative. This means that the revised Scatchard-Hildebrand model may be applied to non-ideal solutions where both the positive and negative deviations exist and can fit the non-ideal solutions with negative deviations as well as to those with positive deviations.

TABLE 2 The regressed terminal parameters A_{ij} of revised Scatchard-Hildebrand model in ternary systems
1. H_2O, 2. TBP, 3. UO_2Cl_2.2TBP or $UO_2(NO_3)_2$.2TBP

system	A_{12}	A_{23}	A_{13}
TBP-UO_2Cl_2	112.1	-3.81	59.13
TBP-$UO_2(NO_3)_2$	114.7	-4.34	174.7

(3) The quaternary system

The metal-solvent extraction system with diluent (including neutral system: TBP-UO_2Cl_2,[12] $(C_6H_5)_2SO$-$UO_2(NO_3)_2$,[13] acidic system: D2EHPA (di-2-ethyl hexyl phosphoric acid)-$CuCl_2$,[14] chelate system: LIX64N (α-hydroxy-oxime)-$CuCl_2$) were tested. All of these systems can be fitted by the revised Scatchard-Hildebrand model. The components in organic phase in these extraction systems are: (1) water, (2) diluent (o-$C_6H_4(CH_3)_2$, n-C_6H_{14}, n-C_7H_{16} or $CH_2ClCHCl_2$), (3) extractant and (4) metallic complex, the concentrations of which are all macro-components. The activity of each component can be determined or calculated by the following thermodynamic method:

1. The activity of water in organic phase is in equilibrium with the aqueous phase and can be calculated by Eq.(11):

$$\ln a_1 = \ln x_1 f_1 = -0.018\phi'(\Sigma \nu_k m_k) \quad (11)$$

where subscript k denotes various electrolytes in aqueous solution, ν is the number of ions dissociated by an electrolyte in water, ϕ' is the practical osmotic coefficient, which can be calculated by using Pitzer's mixed electrolyte solution theory.[16-18]

2. The activity of diluents (a_2) is determined directly by gas-chromatography.

3. The activity of extractants (a_3) can be calculated directly by a set of equilibrium data with the same original extractant concentration using Eq.(12), while in our earlier papers[23] a complicated cross-integration must be used with 3-5 set of different original extractant concentrations. For LIX64N-$CuCl_2$ system, the calcalating equation is:

$$\ln a_3 = \ln x_3 f_3 = \ln a_{3(o)} - \int (x_1/(x_3+2x_4))\, d\ln a_1 - \int (x_2/(x_3+2x_4))\, d\ln a_2 + \int (x_4/(x_3+2x_4))\, d\ln (a_{H^+}/a_{Cu^{2+}}) \quad (12)$$

where $a_{3(o)}$ denotes the activity of extractant in organic phase without copper. The organic phase saturated with water but without Cu-complex is taken as the lower limit of integration.

4. The activity of metallic-complex (a_4) can be calculated by Gibbs-Duhem equation:

$$\ln f_4 = \ln (a_4/x_4) = -\int (x_1/x_4)\, d\ln f_1 - \int (x_2/x_4)\, d\ln f_2 - \int (x_3/x_4)\, d\ln f_3 \quad (13)$$

Table 3 gives the comparison of calculated and experimental values of activity coefficients for one series of data with revised Scatchard-Hildebrand model in chelate extractant organic phase. The mean relative deviation for calculated and experimental f_i are less than 4%.

TABLE 3 Comparison of calculated and experimental values of activity coefficients for the H_2O-n-C_7H_{16}-LIX64N-Cu(LIX64N) quaternary system with revised Scatchard-Hildebrand model (the original conc. of LIX64N in organic phase is 0.5N) at 25°c
1.H_2O, 2.n-C_7H_{16}, 3.LIX64N, 4.Cu(LIX64N)

x_1	f_1(ex)	f_1(cal)	x_3	f_3(ex)	f_3(cal)	x_4	f_4(ex)	f_4(cal)
0.0161	61.98	57.77	0.0693	1.522	1.482	0.0046	0.1123	0.1147
0.0153	65.07	67.94	0.0616	1.636	1.698	0.0086	0.1185	0.1146
0.0141	70.51	74.20	0.0577	1.938	1.908	0.0106	0.1247	0.1221
0.0126	78.78	80.28	0.0537	2.193	2.190	0.0128	0.1322	0.1337
0.0118	84.00	84.78	0.0512	2.335	2.364	0.0141	0.1401	0.1399
0.0110	89.98	88.76	0.0487	2.545	2.557	0.0155	0.1475	0.1466
0.0098	100.74	96.97	0.0445	2.912	2.884	0.0177	0.1521	0.1568

PREDICTION OF THE COMPOSITION IN THE EQUILIBRATED ORGANIC PHASE

During the extraction process design and development, the composition of organic phase usually needs to be estimated from the known composition of equilibrated aqueous phase. For chelate extractant system, the extraction reaction is as follows:

$$2\ HR + Cu^{2+} = CuR_2 + 2H^+$$

where HR represents the extractant LIX64N. After reaching the extraction equilibrium, four independent equations can be formulated:

$$Ka = x_4 f_4 m_{H^+}^2 r_{H^+}^2 / x_3^2 f_3^2 m_{Cu^{2+}} r_{Cu^{2+}} \quad (14)$$

$$\ln x_i f_i = -0.018\phi (\sum_n v_{in} m_n) \quad (15)$$

$$(x_3+2X_4)/x_2 = \text{const.} \quad (16)$$

$$x_1 + x_2 + x_3 + x_4 = 1 \quad (17)$$

All the f_i in these equations can be calculated by revised Scatchard-Hildebrand model. When the composition of the equilibrated aqueous phase (m_{H^+}, $m_{Cu^{2+}}$) is given, we can solve the set of simultaneous non-linear equations for x_1, x_2, x_3, and x_4 with a non-linear least-squares algorithm on a computer.

This mathematical model has been verified with our own experimental data for all the ternary and quaternary extraction systems mentioned above. During the calculation, certain experimental point were used to regress the terminal parameters in the Scatchard-Hildebrand model and the remaining points were used to check the results so calculated. It has been found that either interpolated or extrapolated data can be well predicted. As an illustration, the compositions predicted for the n-C_7H_{16}-0.7N LIX64N-$CuCl_2$-HCl-H_2O system are compared with the experimental organic compositions in Table 4. The mean relative deviation for concentrations of components x_i (expressed as mole fraction) are less than 5%.

TABLE 4 Comparison of predicted and experimental composition in organic phase for 0.7N LIX64N -nC_7H_{16}-$CuCl_2$-HCl-H_2O system (at 25°c)

aqueous phase		equilibrated organic phase						
$m_{Cu^{2+}}$	m_{H^+}	x_1(ex)	x_1(cal)	x_2(ex)	x_2(cal)	x_3(ex)	x_3(cal)	
0.0368	0.0002	0.0251	0.0261	0.1079	0.1079	0.0030	0.0029	**
0.0585	0.0014	0.0246	0.0249	0.1046	0.1047	0.0048	0.0047	
0.1212	0.0117	0.0222	0.0223	0.0961	0.0961	0.0093	0.0093	
0.1467	0.0199	0.0209	0.0209	0.0915	0.0917	0.0119	0.0119	*
0.1755	0.0355	0.0194	0.0198	0.0870	0.0876	0.0143	0.0141	
0.1951	0.0503	0.0184	0.0190	0.0836	0.0846	0.0161	0.0157	*
0.2141	0.0669	0.0176	0.0182	0.0805	0.0815	0.0178	0.0174	
0.2444	0.1022	0.0170	0.0169	0.0757	0.0760	0.0204	0.0204	

Note: * represents interpolated value and ** is extrapolated value.

CONCLUSIONS

(1) Using the relationship $E_{12}=(E_{11}E_{22})(1-l_{12})$ instead of $E_{12}=(E_{11}E_{22})$, our revised Schatchard-Hildebrand model can be applied not only to non-ideal solution with positive deviation, but also to that with negative deviation.

(2) Our experimental results show that the revised Scatchard-Hildebrand model can be used to binary, ternary and quaternary systems with polar components. It seems reliable and flexible to calculate component activity coefficients and to predict the composition in equilibrated organic phase in the neutral, acidic and chelate solvent-metal extraction systems.

(3) Because the revised Scatchard-Hildebrand model is of a linear equation for its terminal parameters, it is easy to solve by using a linear least-square algorithm on a computer. For different extraction systems, it is convinient to use only by changing a set of A_{ij} and V_i with the same mathematical model.

(4) Although the simultaneous equations for predicting the equilibrated organic compositions are non-linear, an iterative solution converges also quickly and easily with a non-linear least-square algorithm. A new way has been found for calculating the metal-solvent extraction equilibrium data by applying the achievement in solution theory and thermodynamic method instead of the empirical formulas.

REFERENCES

1. G.Scatchard. Chem. Reviews, 8,321 (1931).
2. J.H.Hildebrand, R.L.Scott, Regular Solution, (1962).
3. T.Wakahayashi, Bull. Chem. Soc., Japan, 40,2836 (1967).
4. T.Wakahayashi, S.Old, T.Omori, N.Suzuld, J. Inorg. Nucl. Chem., 26, 2255, (1964).
5. N.Suzuki, K.Akiba, T.Kanno, T.Wakahayashi, J. Inorg. Nucl. Chem., 30, 2521, (1968).
6. T.Omori, T.Wakahayashi, S.Old, N.Suzuki, J. Inorg. Nucl. Chem., 26, 2265, (1964).
7. Z.Kolarik, J.Hejna, H.Pankova, J. Inorg. Nucl. Chem., 30, 253, (1968).
8. Z.Kolarik, J.Hejna, H.Pankova, J. Inorg. Nucl. Chem., 30, 2795, (1968).
9. V.M.Vdovenko, T.V.Kovaleva, M.A.Raazanov, Radiokhim., 7, 132, 1965).
10. T.Sato, T.Shimomura, T.Nakamura, T.Fujimatsu, ISEC-80, Vol.3, Session 16A, 80-183, (1980).
11. H.M.N.H.Irving, Ion Exchange and Solvent Extraction, Vol.6, edited by J.A.Marinsky, Y.Marcus, p.140, (1974).
12. Teng Teng, Yi-gui Li, Liang-ping Zhang, Hydrometallurgy, 8, 261, (1982).
13. Yi-gui Li, Teng Teng, Zhen-hua Cheng, Liang-ping Zhang, Hydrometallurgy, 8, 273, (1982).
14. Liang-ping Zhang, Teng Teng, Yi-gui Li, Zhen-hua Cheng, Hydrometallurgy, 8, 289, (1982).
15. Teng Teng, Yi-gui Li, Zong-cheng Li, Tie-zhu Bao, CIESC/AIChE Proceedings, Vol.1, Joint Meeting of Chem. Eng., (1982).
16. K.S.Pitzer, J. Phy. Chem., 77, 268, (1973).
17. K.S.Pitzer, G.Mayorga, J. Phy. Chem., 77, 2300, (1973).
18. K.S.Pitzer, J.J.Kim, J. Amer. Chem. Soc., 96, 5701, (1974).

EXTRACTION OF TRIVALENT ACTINIDES WITH 1-PHENYL-3-METHYL-4-(3:5-DINITROBENZOYL) PYRAZOLONE-5 AND ITS SYNERGISTIC MIXTURES WITH NEUTRAL DONORS

P. K. Khopkar and J. N. Mathur

Radiochemistry Division
Bhabha Atomic Research Centre
Trombay, Bombay-400085, India

The enhancement in the extraction of trivalent actinide and lanthanide metal chelates by the addition of a neutral donor has been used in the analytical determinations as well as in the separation of these metal ions. Thenoyltrifluoroacetone (HTTA) has been frequently used as the chelating agent (1-6). Recently, another chelating agent 1-phenyl-3-methyl-4-benzoyl pyrazolone-5 (HPMBP) and its various derivatives have been found to be of great use in estimation(7) or separation(8) of trivalent actinides. HPMBP with a pKa of 4.11 has been found to extract metal ions from more acidic solutions as compared to HTTA (pKa 6.23). Another chelating agent of the HPMBP group, namely, 1-phenyl-3-methyl-4(3:5-dinitrobenzoyl) pyrazolone-5 (HDMPP) with a pKa value nearly 2 units smaller than HPMBP, should extract metal ions in a much better way as compared to HPMBP or HTTA. In the present study the synergistic extraction of trivalent Am, Cm, Bk and Cf has been carried out with a mixture of HDMPP and tri-n-octyl phosphine oxide (TOPO) in $CHCl_3$. Also the extraction of Am(III) and Eu(III) by mixtures of one of the β-diketones HPMBP, HDMPP, HTTA or benzoyl trifluoroacetone (HBTFA) and TOPO in $CHCl_3$ has been studied.

EXPERIMENTAL

The radioactive tracer solutions were prepared and assayed as described earlier(6). HPMBP (m.p. 92°C) and HDMPP (m.p. 225.5°C) were prepared in this laboratory. HTTA (Merck), HBTFA (Peninsular Chemresearch Inc.) and TOPO (Eastman Kodak) were used as such. $CHCl_3$ (B.D.H. Analar) was used as a diluent throughout this work. All other chemicals used were of A.R. grade. The details of the experimental procedure used for liquid-liquid extraction were as given in Ref.(5,6). For the absorption spectral studies of Fe(III) with different β-diketones the procedure recommended by Khopkar and De(9) has been used.

CALCULATION OF THE EQUILIBRIUM CONSTANTS

The equilibrium constant values (β_1, β_2 and K_2) for the organic phase addition reactions of MA_3 with TOPO, where A is the anion of HTTA, HBTFA and HDMPP, may be represented by

$$(1)\quad M(A)_3 + TOPO \xrightleftharpoons{\beta_1} M(A)_3.TOPO$$

$$(2)\quad M(A)_3 + 2\ TOPO \xrightleftharpoons{\beta_2} M(A)_3.2\ TOPO$$

$$(3)\quad M(A)_3.TOPO + TOPO \xrightleftharpoons{K_2} M(A)_3.2\ TOPO$$

whereas the same with HPMBP as the chelating agent (where the chelate is extracted as a self-adduct $M(PMBP)_3.HPMBP$) may be represented as:

$$(4)\quad M(PMBP)_3.HPMBP + TOPO \xrightleftharpoons{\beta_1} M(PMBP)_3.TOPO + HPMBP$$

$$(5)\quad M(PMBP)_3.HPMBP + 2\ TOPO \xrightleftharpoons{\beta_2} M(PMBP)_3.2\ TOPO + HPMBP$$

$$(6)\quad M(PMBP)_3.TOPO + TOPO \xrightleftharpoons{K_2} M(PMBP)_3.2\ TOPO$$

The details of the calculation of the equilibrium constants of these organic phase reactions have been given in Ref.(10,11). In the calculation of these equilibrium constants, which refer only to the concentration quotients, it has been assumed that the activity coefficients of the species involved do not change significantly under the experimental conditions employed.

RESULTS AND DISCUSSION

The stoichiometry of the metal chelates and the synergistic species extracted into the organic phase have been arrived at by the slope analysis method where the distribution coefficient values, D are plotted against the relevant experimental variables. In the case of trivalent actinides Am, Cm, Bk and Cf extracted by HDMPP alone in $CHCl_3$, the chelate species extracted was observed to be $M(DMPP)_3$, as against the self-adduct species $M(PMBP)_3.HPMBP$ extracted with HPMBP in $CHCl_3$ as well as in xylene(11). The formation of a self-adduct with HPMBP and not with HDMPP may probably be explained on the basis of the pKa values of these two β-diketones. HDMPP with lower pKa value (~ 2 log units) is more ionized under the experimental conditions and hence the availability of unionized HDMPP is less resulting in the formation of only the chelate species $M(DMPP)_3$ and not the self-adduct. However, it should be remembered that the concentrations of these chelating agents used in the present extraction studies were quite different (HDMPP 0.01 to 0.015M; HPMBP 0.08 to 0.16M). The synergistic species extracted in the systems trivalent actinides/HDMPP/TOPO are $M(DMPP)_3.n$ TOPO (where n = 1, or 2). The equilibrium constants for the formation of these species in the organic phase are given in Table 1. It can be seen that there is no particular order in the β_1 or β_2 values of these trivalent actinides, which is in agreement with the observations reported earlier for these trivalent actinides in HTTA(5,6) and in HPMBP(11) systems. However, Chmutova et.al(12) have reported that the synergistic coefficient increases in the order Cf(III)< Bk(III)< Cm(III)< Am(III) for the HPMBP/TOPO systems.

The equilibrium constant values of these trivalent actinides/HDMPP/TOPO/$CHCl_3$ systems cannot be compared with our earlier data of these actinides/HPMBP/TOPO systems, since the diluent used earlier was xylene(11). The only data available in the $CHCl_3$ medium is log β_1 (0.9) and log β_2 (7.6) for Am/HPMBP/TOPO system reported by Bacher and Keller(13). These values are quite different than the present values (Table 2) of Am/HDMPP/TOPO system and even of the Am/HPMBP/TOPO system in the same diluent $CHCl_3$. These authors(13) have not reported the formation of any self-adduct and, also, their high β_2 value leads to the conclusion that $K_2 \gg K_1$ which is quite unlikely in the normal conditions. Comparing the β_1 and β_2 values of Am/HPMBP/TOPO in $CHCl_3$ (present work) and that in xylene(11) it is quite clear that the values in xylene are 2 to 4 log units higher than those in $CHCl_3$. This follows the general observation(14) that extraction and synergistic extraction of trivalent metal ions are higher in benzene (or xylene) than that in $CHCl_3$.

TABLE 1. EQUILIBRIUM CONSTANTS FOR THE ORGANIC PHASE SYNERGISTIC REACTIONS OF TRIVALENT ACTINIDES - HDMPP CHELATE WITH TOPO IN $CHCl_3$

M(III)	log β_1	log β_2	log K_2	log K_{HA}
Am	4.56	6.69	2.13	-2.81
Cm	4.03	5.99	1.96	-2.20
Bk	4.02	5.60	1.58	-1.82
Cf	5.14	6.56	1.42	-2.70

TABLE 2. EQUILIBRIUM CONSTANTS FOR THE ORGANIC PHASE SYNERGISTIC REACTIONS OF Am(III) AND Eu(III) BY MIXTURES OF β-DIKETONES AND TOPO IN $CHCl_3$

M(III)	log β_1	log β_2	log K_2	log K_{HA}
		HPMBP + TOPO		
Am	2.72	4.42	1.70	-3.67
Eu	2.85	4.17	1.32	-3.37
		HDMPP + TOPO		
Am	4.56	6.69	2.13	-2.81
Eu	4.46	-	-	-2.01
		HTTA + TOPO		
Am	4.91	7.37	2.46	-8.72
Eu	5.11	-	-	-8.25
		HBTFA + TOPO		
Am	5.08	-	-	-9.65
Eu	4.77	-	-	-8.55

In the extraction of Am(III) and Eu(III) by HPMBP and TOPO the first step (eqn. 4) is the replacement of one HPMBP molecule by TOPO from the self-adduct species $M(PMBP)_3.HPMBP$, but the second step, i.e. the attachment of one TOPO molecule to the $M(PMBP)_3.TOPO$ species (eqn. 6) is an addition reaction. In case of all the other β-diketones, irrespective of the number of TOPO molecules attached (1 or 2), it is an addition reaction (eqns. 1-3). Considering the synergistic extraction of Am(III) with HPMBP or HDMPP and TOPO, naturally the formation of the first synergistic species is not comparable, but in the second step (addition in both cases) it is observed that K_2 (HDMPP) > K_2(HPMBP). This may be explained on the basis that HPMBP having higher pKa value will give metal chelates of higher stability, which results in the lower stability of the synergistic adduct as compared to that with HDMPP. The equilibrium constant values of Am(III) with TOPO using HTTA or HBTFA as chelating agents are very much comparable to those with HDMPP and are about 2 log units higher than these values when HPMBP was used as the chelating agent. Further, it has been observed that in all these systems the synergistic equilibrium constant values of Eu(III) are very much comparable to those obtained for Am(III) under identical experimental conditions.

It can be further seen from Table 1 that the β_1 and β_2 values for Bk(III)/HDMPP/TOPO system are lowest as compared to that with other trivalent actinides, a result similar to that reported earlier with HTTA(5,6) and HPMBP(11) systems using these trivalent actinides. It was suggested(11) that Bk(III) (III - IV redox potential - 1.54 V) could conceivably interact with β-diketones by a charge-transfer type mechanism. An examination of the spectra of Bk(III) extracted by the β-diketones would be the direct proof, but due to lack of availability of Bk in large enough quantities, the same could not be studied. Since the charge-transfer interaction between Fe(III) and β-diketones is well-known, the spectra of Fe(III) extracted by four β-diketones (HTTA, HBTFA, HPMBP and HDMPP) in $CHCl_3$ as well as in xylene (only the first three β-diketones) was examined. The separation factor is indicative of the special effect observed in the extraction of Bk(III) by these β-diketones as compared to that of other trivalent actinides. The variation of extinction coefficient (ε) values with the separation factors of Bk and Cf (D_{Bk}/D_{Cf}) in these systems is shown in Figure 1. An increasing trend in the ε values with increasing separation factor (Bk, Cf) in xylene medium is clearly observed. This could probably be taken as an indirect proof of the charge-transfer type interaction between Bk(III) and the β-diketones. A similar trend has also been observed when $CHCl_3$ was used as a diluent (Table 3). This brings out the importance of the effect of structural changes of the β-diketones on the extraction of these trivalent actinides.

TABLE 3. SEPARATION FACTORS (D_{Bk}/D_{Cf}) AND THE MOLAR EXTINCTION COEFFICIENTS OF Fe(III) (at 460 nm) IN XYLENE AND $CHCl_3$ WITH DIFFERENT β-DIKETONES

β - Diketone	Xylene		$CHCl_3$	
	S.F. (D_{Bk}/D_{Cf})	ε, Fe(III)	S.F. (D_{Bk}/D_{Cf})	ε, Fe(III)
HTTA	14.7	3788	0.55	3159
HBTFA	92.5	3996	1.6	2787
HDMPP	-	-	7.5	6924
HPMBP	772	4790	48	4508

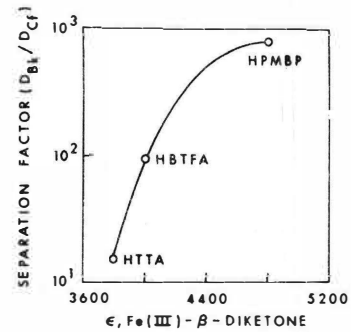

FIGURE 1. VARIATION OF SEPARATION FACTOR (D_{Bk}/D_{Cf}) vs. ϵ OF Fe(III) - β - DIKETONE (AT 460 nm) IN XYLENE.

REFERENCES

1. H. Irving, Solvent Extraction Chemistry, North Holland, Amsterdam, 91 (1967).
2. T.V. Healy, Solvent Extraction Research, Wiley, New York, 257 (1969).
3. G. Duyckaerts and J.F. Desreux, International Solvent Extraction Conference, Toronto, 73 (1977).
4. J.N. Mathur, Solvent Extraction and Ion Exchange (In Press).
5. P.K. Khopkar and J.N. Mathur, J. Radioanal. Chem. 60, No. 1, 131 (1980).
6. P.K. Khopkar and J.N. Mathur, Sepn. Sci. Technol. 16, 957 (1981).
7. J.N. Mathur and P.K. Khopkar, Solvent Extraction and Ion Exchange (In Press).
8. B.F. Myasoedov, M.K. Chmutova and I.A. Lebedev, Proc. Inter. Solv. Extr. Conf., The Hague, Netherland, 815 (1981).
9. S.M. Khopkar and A.K. De, Anal. Chim. Acta 22, 223 (1960).
10. J.N. Mathur, S.A. Pai, P.K. Khopkar and M.S. Subramanian, J. Inorg. Nucl. Chem. 39, 653 (1977).
11. J.N. Mathur and P.K. Khopkar, Sepn. Sci. Technol. 17, 985 (1982).
12. M.K. Chmutova, B.F. Myasoedov, N.E. Kochetkova, B.Y. Spivakov and Y.A. Zolotov, Chemistry of Transuranium Elements (V.I. Spitzyn and J.J. Katz, eds.), Pergamon, 157 (1976).
13. W. Bacher and C. Keller, J. Inorg. Nucl. Chem. 35, 2945 (1973).
14. T.V. Healy, J. Inorg. Nucl. Chem. 19, 328 (1961).

COLUMN EXTRACTION CHROMATOGRAPHY: A USEFUL TOOL FOR THE SEPARATION AND DETERMINATION OF RADIONUCLIDES IN ENVIRONMENTAL AND BIOLOGICAL SAMPLES

Corrado Testa

ENEA-CRE Casaccia
00060 Rome. Italy

In the field of Radiation Protection it often occurs that some radionuclides, especially alpha and beta emitters, must be separated and determined in biological and environmental samples, such as water, fall-out, sediments, foods, urines, feces, animal organs, etc. The separation method adopted depends on the type of sample and on the chemical behaviour of the radionuclide. Several chemical steps such as wet ashing, dry ashing, coprecipitation, filtration, solvent extraction, ion exchange, etc., are generally used to isolate the radionuclide of interest. Sometimes these methods are complicated and timeconsuming and usually they do not permit to reach the final result before one or two days.

Reversed-phase Partition Chromatography (Extraction Chromatography) was applied to this purpose because it shows some real advantages compared to other techniques, as far as the simplicity, selectivity and sensitivity of the procedure is concerned.

Extraction Chromatography is a type of chromatography in which the stationary phase consists of a non-polar extractant adsorbed on an inert support and the eluant is a polar aqueous solution (1). Two different methods, column and batch extraction, have been used to isolate the radionuclide from the samples. The choice of either method depends on: a) the sample volume to be analyzed; b) the desired decontamination factors; c) the possibility to separate and to determine more than one radionuclide in the same sample; d) the desired recovery; e) the time spent on the analysis.

INERT SUPPORTS

Several synthetic polymeric materials have been tested as inert supports on the basis of their ability to adsorb the stationary phase.

Low density Kel-F(polytrifluorochloroethylene 100 - 170 mesh) showed very good properties ofsupporting irreversibly a volume of the stationary phase up to a ratio 1:1 (v/w), but, because of its high cost, it was replaced by Microthene (microporous polyethylene), which is supplied at very low cost. The 50 - 100 mesh powder of this polymer can support about the same volume as the Kel-F, although a ratio 5/4 (w/v) is preferred. In Table 1 Kel-F is indicated as K and Microthene as M.

STATIONARY PHASES

The stationary phases have been chosen in order to obtain a selective isolation of the radionuclides from the samples after the preliminary chemical treatment. To this purpose the existing analytical and extracting properties of some organic compounds were taken into account (2). The used stationary phases were the following:
Tri-n-octylamine (TNOA) for plutonium in urine (3); Tri-n-butylphosphate (TBP) for uranium in urine (4); Di(2-ethylhexyl)phosphoric acid (HDEHP) for strontium-90 (yttrium-90) in urine (5), for iron-55 in air filters (6) and for americium-241 in urine (7), feces (8 and marine samples (9); Tri-n-octylphosphine oxide (TOPO) for natural thorium (10), enriched uranium (11), plutonium (12) and neptunium-237 (13) in urine and for plutonium in sea water, sediments, marine organisms and animal organs (14); Neo tridecano hydroxamic acid (HX-70) for plutonium and neptunium in urine (15).

Other high molecular weight hydroxamic acids (tri-butylacetohydroxamic acid; 2-ethyl, 2-butyl, nonyl hydroxamic acid, etc.) were recently prepared (16,17) and supported on Microthene to obtain interesting metal ion separations and preconcentrations (18).

All these compounds were dissolved in organic solvents (cyclohexane, toluene, etc.); their concentration ranged from 0.1 to 1.5M and was selected in order to obtain a sufficiently good extraction of the radionuclide and a prompt and selective elution from the column.

PREPARATION OF THE SLURRY

The preparation of the slurry to be used for Extraction Chromatography is very simple. The stationary phase is added, drop by drop and under a gentle stirring, to the inert support in the wanted ratio: the slurry is then stirred for about one hour with a sufficient volume of the conditioning solution in order to obtain a homogeneous product and to discard floating particles. Generally 2 - 5 g of the support impregnated of 2 - 5 ml of the stationary phase are sufficient both for the batch extraction (B.E.) and the chromatographic column procedure (C.C.). The diametre of the beds ranges from 8 to 25 mm and the height from 30 to 150 mm; the flow-rate ranges between 0.5 and 5 ml/min.

CHEMICAL PRETREATMENT

The samples to be analyzed are generally subjected to a simple wet ashing treatment (W.M.) with nitric acid. In some particular cases a dry mineralization (D.M.) is necessary.

The final concentration of nitric acid must then be adjusted to an optimum value to obtain the quantitative extraction of the radionuclide.

COLUMN EXTRACTION CHROMATOGRAPHY (C.C.)

This technique is usually preferred when samples having a final volume of 10 ÷ 200 ml have to be analyzed. The feeding solution is passed through the column; after a washing with a minimum volume of the same solution, the radionuclide is eluted by means of a suitable eluting agent. In the case of human urine the large volumes to be analyzed (250 - 1000 ml) must be concentrated or the radionuclide coprecipitated with Ca or Mg phosphate (P.P.). This procedure is time-consuming and complicated and therefore it has been generally substituted with batch extraction which appears to be simpler and faster.

BATCH EXTRACTION PROCESS (B.E.)

The nitric acid solution is adjusted at the desired concentration and stirred together with the slurry, which is then trasferred to a 10 mm diameter chromatographic column for following washing and elution. This procedure is generally fast, but the extraction efficiency of a radionuclide depends on several parameters such as: a) concentration of the extractant in the stationary phase; b) stirring time; c) granulometry of the inert support; d) HNO_3 concentration of the aqueous solution; e) presence of complexing agents in the aqueous solution.

Generally the solvent extraction data in the literature (2) give the first information about the possibility of an almost quantitative extraction of radionuclides. This information is necessary as the procedure is not advisable when the extraction coefficients (E_a^o) are too small. Since in batch extraction the element is not on the top of the column, but it is homogeneously distributed, a fraction could be lost from the lower part of the bed if the distribution coefficient is not so high. Sometimes the extraction conditions must be verified, in order to obtain a rapid extraction and a successive elution elution of the radionuclide with a small volume of solution (<100 ml).

TABLE 1

DETERMINATION OF RADIONUCLIDES BY EXTRACTION CHROMATOGRAPHY

RADIONUCLIDE	SAMPLE	PRETREATMENT	MOLARITY HNO_3	INERT SUPPORT	STATIONARY PHASE	CHROMATOGR. PROCEDURE	ELUTING AGENT	FINAL RECOVERY, %	SENSITIVITY LIMIT
^{89}Sr	FALL-OUT	D. M.	7.5	M	1.5M HDEHP	C. C.	6M HCl	~ 96	—
	AIR FILTERS	D. M.	7.5	M	1.5M HDEHP	C. C.	6M HCl	~ 94	—
^{90}Y (FOR ^{90}Sr)	URINE	W. M.	0.3	M	1.5M HDEHP	B. E.	6M HCl	91.7	5 pCi/l
Th (NATURAL)	URINE	W. M.	4.0	K	0.1M TOPO	C. C.	0.5M HCl	97.5	1 μg/l
	URINE	W. M.	4.0	M	0.5M TOPO	B. E.	0.3M H_2SO_4	98.2	0.2 μg/l
U (ENRICHED)	URINE	W. M.	7.5	K	CONC. TBP	C. C.	WATER	91.1	2 dpm/l
	URINE	W. M.	4.0	M	0.5M TOPO	B. E.	1M HF	70.0	1 dpm/l
Pu	SEA WATER	D. M.	4.0	M	0.3M TOPO	B. E.	6M HCl-0.02M HI	62.6	3 fCi/100l
	SEDIMENTS	D. M.	4.0	M	0.3M TOPO	B. E.	6M HCl-0.02M HI	45.4	5 fCi/100g
	MARINE ORGANISMS	D. M.	4.0	M	0.3M TOPO	B. E.	6M HCl-0.02M HI	81.7	2 fCi/100g
	URINE	P. P.	2.0	K	0.1M TNOA	C. C.	CONC. H_2SO_4	90.5	0.04 pCi/l
	URINE	W. M.	4.0	M	0.3M TOPO	B. E.	6M HCl-0.01M HI	70.5	0.07 pCi/l
	ANIM. URINE	W. M.	6.0	M	0.3M TOPO	C. C.	1M HF	87.6	0.1 pCi/day
	ANIM. FECES	D. M.	6.0	M	0.3M TOPO	C. C.	1M HF	86.0	0.4 pCi/day
	URINE	W. M.	2.0	M	0.3M TOPO	B. E.	6M HCl-0.1M HI	76.5	0.10 pCi/l
	URINE	P. P.	2.0	M	0.3M HX-70	C. C.	2M HNO_3-0.15% hydroquinone	73.5	0.08 pCi/l
	FECES	D. M.	4.0	M	0.3M TOPO	B. E.	6M HCl-0.01M HI	63.8	0.04 pCi/day
^{237}Np	URINE	W. M.	6.0	M	0.1M TOPO	B. E.	6M HCl-Cl_2	83.2	0.05 pCi/l
	URINE	P. P.	2.0	M	0.3M HX-70	C. C.	0.1M oxalic acid	82.3	0.04 pCi/l
^{241}Am	URINE	W. M.	0.001	M	1.5M HDEHP	B. E.	3M HNO_3	85.9	0.05 pCi/l
	FECES	D. M.	0.001	M	1.5M HDEHP	B. E.	3M HNO_3	65.4	0.05 pCi/day

ELUTION

The elution of a radionuclide from the column is obtained by an accurate choice of the eluant solution (Table 1). Sometimes a change of the HNO_3 concentration is sufficient, following the liquid-liquid solvent extraction curves. In some cases a complexing agent is necessary. When possible, a redox reagent can be used to change the valence of the radionuclide: for instance plutonium is eluted by reduction to Pu(III) and neptunium by oxidation to Np(V).

Sometimes the kinetics of the redox reaction is slow and must be accelerated by improving the temperature and granulometry conditions (13).

DECONTAMINATION FACTORS

These methods give generally good decontamination factors (Table 2); this is due to the peculiar features of Extraction Chromatography which offers the following possibilities: a) to support an organic extractant suitable for a quantitative and selective isolation of an ion; b) to change the quantity and the concentration of the organic extractant in order to obtain the best conditions of extraction and elution; c) to select the eluant solution in order to improve the isolation of the radionuclide.

TABLE 2

Decontamination factors of Pu, Np and Am from some actinide elements by Extraction Chromatography

Radionuclide	Supported extractant	Th	Pa	U	Np	Pu	Am
Plutonium	TOPO	100	2000	600	300	-	4000
Plutonium	HX-70	1000	-	1000	500	-	200
Neptunium	TOPO	-	-	30	-	100	10000
Neptunium	HX-70	1000	-	1000	-	20	200
Americium	HDEHP	70	60	80	100	100	-

FINAL RECOVERY AND SENSITIVITY

The final percent recoveries of the various methods range between 45 and about 100 %, as Table 1 shows. A low value of the final recovery can be accepted if the method assures a good reproducibility; the extraction chromatography shows such a feature, as the standard deviations from the mean values of the final recovery are of the order of 5 %. When a low recovery and reproducibility are met a radioactive internal standard is added and an alpha spectrometry is performed (9, 14).

The sensitivity limit of a single radionuclide depends on the adopted radiochemical method. Sometimes it is necessary to reach a very low sensitivity limit especially when some alpha emitters, such as plutonium or transplutonium elements, have to be detected in biological or environmental samples. In these cases very pure chemical reagents, electroplating procedures, and low-background alpha detectors must be used together with the chromatographic isolation technique in order to obtain such low sensitivity limits (femtocuries order).

COLUMN REDOX EXTRACTION CHROMATOGRAPHY

Redox Extraction Chromatography has been described as a technique for the separation of some actinide elements (19).

The application of such a technique was suggested in the literature which described the possibility to carry out some redox reactions on columns supporting solid hydroquinones and to reduce selectively plutonium to Pu(III) in organic solutions containing simultaneously HDEHP and a di-tert-alkyl-hydroquinone (20).

A single cyclohexane solution of an extractant (TOPO) and of a reducing compounds was used as the stationary phase and it was supported on Microthene-710. 2,5-di-tert-pentylhydroquinone (DPHQ) showed the best features as far as its stability on the column is concerned. Such a column was efficient especially with respect to neptunium and plutonium which have several valence states in acid solution. As a matter of fact it was not possible to separate quantitatively plutonium with a TOPO column because of the simultaneous presence of different valence states (Pu(III), Pu(IV), Pu(VI), Np(IV), Np(V), Np(VI) of both elements in 6M HCl. However, a complete separation was obtained with a TOPO - DPHQ column which reduces all plutonium to Pu(III) and all neptunium to Np(IV); Pu(III) is not retained on the column and it is found in the eluate whilst Np(IV) remains on the column and it is subsequently eluted with 1M HF.

CONCLUSIONS

From the experimental results the following conclusions can be drown. Extraction Chromatography can be usefully employed for the isolation of radionuclides in biological and environmental samples, especially when quick and simple analyses have to be carried out. The recoveries, the standard deviations, the sensitivity limits and the decontamination factors are sufficiently good.

The advantages of this kind of isolation procedure over the liquid-liquid extraction are the following: a) the possibility of using a greater volumes ratio: aqueous phase/organic phase; b) the elimination of the foams which form often when biological samples are shaken with an organic solution; c) the possibility of transforming the liquid-liqui extraction into a column chromatography and of separating two or three radionuclides by using suitable eluting solution.

The advantages of the Extraction Chromatography over the ion exchange resins are the following: a) the possibility of faster exchange rates; b) the possibility of supporting many different organic extractants having the suitable extraction features for a quantitative and selective isolation of an ion; c) the possibility of changing the quantity and the concentration of the organic extractant in order to obtain the best condition of extraction and elution;d) the possibility of supporting a suitable redox organic compound together with the extractant in order to fix a wanted valence state of the radionuclide.

REFERENCES

1. T. Braun, G. Ghersini, Extraction Chromatography, Elsevier, Amsterdam (1975).
2. Y. Marcus, A.S. Kertes, Ion Exchange and Solvent Extraction of Metal Complexes, Wiley Ed. Interscience, London (1969).
3. C. Testa, Giornale Fis. Sanit., 10, 202 (1966).
4. C. Testa, G. Masi, Minerva Nucleare, 9, 22 (1965).
5. C. Testa, G. Santori, Energia Nucleare, 17, 320 (1970).
6. G. Bagliano et al., Proc. XVI Italian Congress on Health Physics, vol. II, p. 489, (1964).
7. A. Delle Site, G. Santori, C. Testa, Rapp. CNEN, RT/PROT(81)6 (1981).
8. A. Delle Site, G. Santori, C. Testa, Rapp. CNEN, RT/PROT(76)6 (1976).
9. A. Delle Site, V. Marchionni, Proc. Techniques for identifying transuranic speciation in aquatic environments, IAEA, Vienna (1981).
10. C. Testa, Proc. Radiological Health and Safety in Mining and Milling of Nuclear Materials, IAEA, Vol. II, p. 489 (1964).
11. C. Testa, D. De Rosa, A. Salvatori, Rapp. CNEN, RT/PROT(68)6 (1968).
12. C. Testa, G. Santori, Giornale di Fisica Sanitaria, 16, 1 (1972).
13. G. Santori, C. Testa, J. Radioanal. Chem., 14, 37 (1973).
14. A. Delle Site et Coll., Analytica Chimica Acta, 117, 217 (1980.
15. A. Delle Site, J. Radioanal. Chem., 14, 45 (1973).
16. G.M. Gasparini, E. Polidori, J. of Chem. and Eng. Data, 21, 504 (1976).
17. G.M. Gasparini, A. Brignocchi, Rapp. CNEN, RT/CHI(78)4 (1978).
18. C. Testa et Coll., Studi Urbinati, Fac. Farmacia, 55, 7 (1982).
19. A. Delle Site, C. Testa, Anal. Chim. Acta, 72, 155 (1974).
20. C. Coleman, B.S. Weaver, U.S. Patent 3, 580, 705 (1971).

EXTRACTION AND COMPLEX FORMATION OF PLUTONIUM (IV) WITH 1-PHENYL-2-METHYL-3-HYDROXY-4-PYRIDONE (PMHP)

M. J. Herak and Z. Kolarik

Laboratory of Analytical Chemistry
Faculty of Science
University of Zagreb
Zagreb, Yugoslavia

and

Institute of Hot Chemistry
Nuclear Research Centre
Karlsruhe, Federal Republic of Germany

Among derivatives of 4-pyridone, the title compound (PMHP) forms with metal ions stable chelate complexes extractable by chloroform (1,2). It was of interest to obtain information about the extractability of plutonium(IV), which in its tetravalent state plays an important role in the nuclear chemistry. We studied the extraction of plutonium(IV) by PMHP from the weakly complexing nitrate, perchlorate and chloride media.

EXPERIMENTAL

All experiments were performed at ~23°C (room temperature) with chloroform as diluent. A mixture of plutonium isotopes ($^{239,240,241}Pu$) was purified from the ^{241}Am daughter and from nonextractable forms of Pu(IV) and used at a trace concentration (10^{-6}M). The distribution ratio of plutonium(IV), D_{Pu}, was determined by alpha scintillation counting in both phases, and concentrations of other components were calculated from the known initial concentrations and from equilibrium constants of side reactions determined in this work. There was a good consistency between reasults obtained at shaking times of 5 to 60 min. The ionic strength was 1.0, adjusted in each system by the sodium salt of the respective mineral acid.

RESULTS AND DISCUSSION

The distribution of the extractant. At acid concentrations higher than 0.001M, the extractant (initially present in the organic phase) is partially or predominantly transferred into the aqueous phase (Figure 1). The stoichiometry of reactions responsible for the distribution behaviour of PMHP, as well as the corresponding equilibrium constants, were determined from the dependency of the distribution ratio of PMHP on the concentration of hydrogen ions. The dependency (Figure 1) was measured at two different PMHP concentrations and the distribution reactions of PMHP can be characterized as follows (a bar above a formula denotes species present in the organic phase):

$$HX \rightleftharpoons \overline{HX} \qquad K_p = 62$$

$$\overline{HX} + H^+ \rightleftharpoons H_2X^+ \qquad K_b = 1730$$

$$H_2X^+ + NO_3^- \rightleftharpoons \overline{HX.HNO_3} \qquad K_{ex} = 0.030$$

The extractant exhibits no tendency toward dimerization in the organic phase at concentrations of ≤0.01M. The equilibrium concentration of hydrogen ions in the aqueous phase and of the undissociated extractant species HX in the organic phase can then be calculated by successive iterations from initial concentrations of the extractant and a mineral acid, $\overline{C}_{X,init}$ and $C_{H,init}$ respectively. The equations used, as derived from the material balance, are

$$(1) \quad [\overline{HX}] = C_{X,init}(1 + K_p^{-1} + K_bK_p^{-1}(1+K_{ex})[H^+])^{-1}$$

$$(2) \quad [H^+] = C_{H,init}(1 + K_bK_p^{-1}[\overline{HX}])^{-1}.$$

The species $HX.HNO_3$, little contributing to the material balance in the nitrate system, was neglected in the systems involving perchlorates and chlorides.

The distribution of plutonium(IV). There is a strong dependency of the distribution ratio of plutonium(IV), D_{Pu}, on the concentration of hydrogen ions: the variation of the D_{Pu} value with the $[H^+]$ value ranges from the fourth power to the sixth power in the extraction from the nitrate and perchlorate media respectively. This is due to a decrease of the concentration of the extractant species HX in the organic phase with increasing acid concentration in the aqueous phase. To evaluate the log D_{Pu} = f(log $[H^+]$) dependency at a constant concentration of the extractant in the organic phase, we preliminary determined the slope of the dependency of the log D_{Pu} value on the logarithm of the initial extractant concentration at a constant initial acid concentration in the aqueous phase. Under such conditions the fraction of the extractant in the organic phase is independent of its initial concentration. The log D_{Pu} = f(log $C_{X,init}$) dependencies had the slopes n = 2, 2.5 and 3 in the extraction of Pu(IV) from the nitrate, chloride and perchlorate media respectively. Then we plotted log D_{Pu} - n log $[\overline{HX}]$ vs. log $[H^+]$ and obtained straight lines with essentially the same slopes from the three different aqueous media (Figure 2). This indicates that the extractant is bound to the plutonium(IV) ion as the anion X^- only and not as the undissociated species HX. The dependency log D_{Pu} = f(log $C_{X,init}$) could not be measured at a strictly constant concentration of hydrogen ions, due to the formation of the species H_2X^+ in the aqueous phase. Thus we refined the dependency by plotting log D_{Pu} + n log $[H^+]$ vs. log $[\overline{HX}]$ and obtained straight lines (Figure 3) confirming the slopes given above.

As seen, anions of the extractant only partially compensate the charge of the plutonium(IV) ion in the organic phase. It can be accepted that anions of the aqueous medium take part in the formation of the extracted complexes. Such conclusion is strongly supported by the significant influence of the aqueous medium on the extractability of plutonium(IV) by PMHP, which decreases in the sequence nitrate > perchlorate > chloride (Figure 3). The extraction reactions can be written, and their equilibrium constants will be denoted as follows:

$$Pu^{4+} + 2\overline{HX} + 2NO_3^- \rightleftharpoons \overline{PuX_2(NO_3)_2} + 2H^+ \qquad ({}^nK_{2,2})$$

$$Pu^{4+} + 2\overline{HX} + 2Cl^- \rightleftharpoons \overline{PuX_2Cl_2} + 2H^+ \qquad ({}^cK_{2,2})$$

$$Pu^{4+} + 3\overline{HX} + Cl^- \rightleftharpoons \overline{PuX_3Cl} + 3H^+ \qquad ({}^cK_{3,1})$$

$$Pu^{4+} + 3\overline{HX} + ClO_4^- \rightleftharpoons \overline{PuX_3(ClO_4)} + 3H^+ \qquad ({}^pK_{3,1})$$

The dependencies of the logarithm of the distribution ratio of plutonium(IV), as presented in Figures 2 and 3, should be curved in the extraction from the chloride media, where two complexes coexist in the organic phase. However, the curvature is very slight in the concentration ranges studied and the experimental points can well be fitted both to straight lines with intermediate slopes and to nonlinear theoretical curves. The latter fit was not done graphically in Figures 2 and 3, but was done numerically for the calculation of the corresponding equilibrium constants.

The equilibrium constants of the extraction reactions are:

log ${}^nK_{2,2}$ = 5.57 ± 0.05 log ${}^cK_{2,2}$ = 2.1 ± 0.1

log ${}^pK_{3,1}$ = 7.1 ± 0.2 log ${}^cK_{3,1}$ = 3.6 ± 0.1

If extracted by 0.01M PMHP in chloroform from an aqueous solution containing 0.1M nitric acid and 0.9M sodium nitrate, plutonium(IV) can be separated from americium(III) with a separation factor of approximately 3 x10^5 (D_{Pu} ~240).

REFERENCES

1. M. J. Herak, I. Prpić and B. Tamhina, Proc. Int. Solvent Extraction Conf. ISEC'77, CIM Spec. Vol. 21, p. 462. Canadian Inst. Mining Metallurgy, Montreal (1979).

2. B. Tamhina and M. J. Herak, J. Inorg. Nucl. Chem. 38, 1505 (1976).

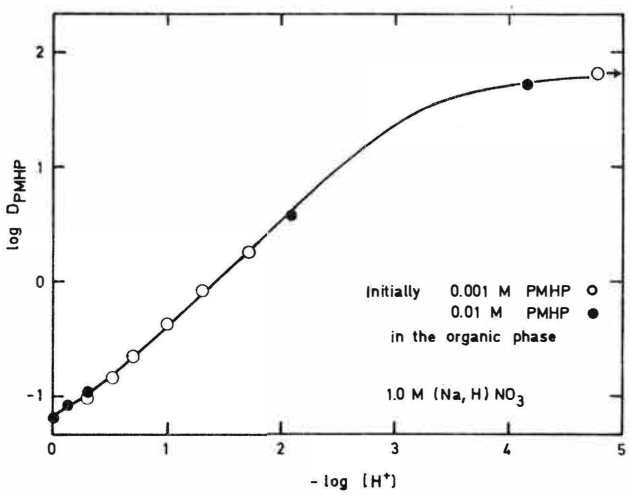

FIGURE 1. LOGARITHMIC DEPENDENCY OF THE DISTRIBUTION RATIO OF PMHP ON THE EQUILIBRIUM CONCENTRATION OF HYDROGEN IONS IN THE AQUEOUS PHASE

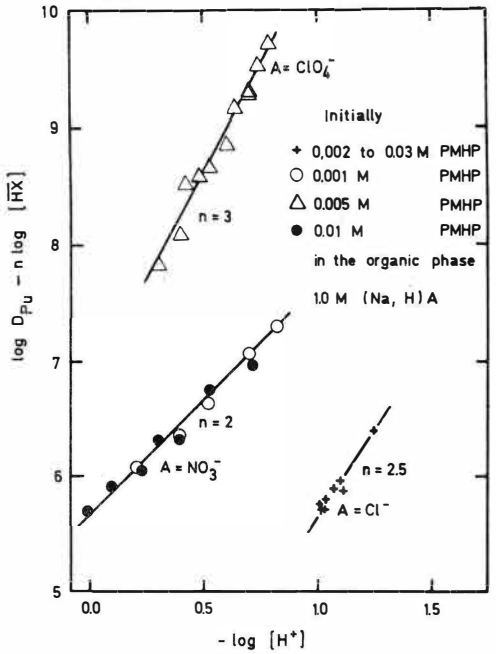

FIGURE 2. LOGARITHMIC DEPENDENCY OF THE DISTRIBUTION RATIO OF Pu(IV), CORRECTED FOR VARIATIONS OF THE EXTRACTANT CONCENTRATION, ON THE EQUILIBRIUM CONCENTRATION OF HYDROGEN IN THE AQUEOUS PHASE

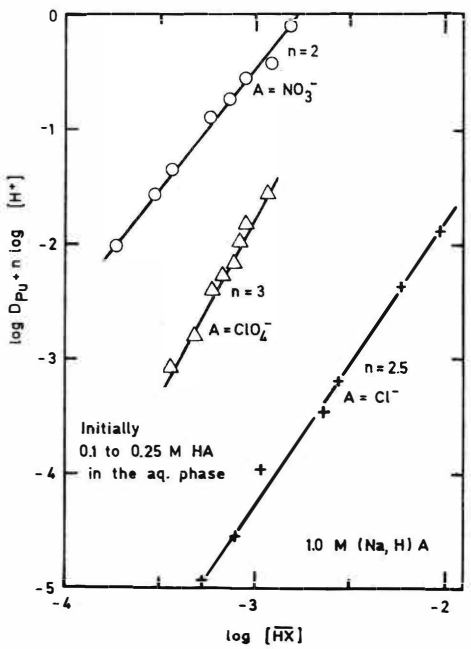

FIGURE 3. LOGARITHMIC DEPENDENCY OF THE DISTRIBUTION RATIO OF Pu(IV), CORRECTED FOR VARIATIONS OF THE HYDROGEN ION CONCENTRATION, ON THE EQUILIBRIUM CONCENTRATION OF THE EXTRACTANT IN THE ORGANIC PHASE

EXTRACTION COLORIMETRIC AND FLUORIMETRIC DETERMINATION OF ALKALI AND ALKALINE EARTH METAL IONS USING CROWN ETHER-BASED ORGANIC REAGENTS

Makoto Takagi, Hiroshi Nakamura and Keihei Ueno

Department of Organic Synthesis
Faculty of Engineering
Kyushu University, Hakozaki, Higashi-ku
Fukuoka, 812 Japan

We have studied previously the extraction of alkali and alkaline earth metal ions by chromogenic crown ethers, 1(a,b,c) and 2 and reported that they are useful to the extraction photometric determination of calcium and some of the alkali metal ions (1,2). They have phenolic side arms on the crown ether skeleton and the phenolate oxygen can make chelate-like interaction with the metal bound in the crown ether moiety. In the present work, other types of phenolic chromogenic groups, alizarine and 4-methylumbelliferone were introduced to monoaza- and diaza-crown ethers via methylene linkage by Mannich reaction, to give 3 and 4 and 5. Alizaline, well-known reddish dye, has two phenolic groups, both of which may or may not be used for interaction with metals in the crown ether 3. On the other hand, umbelliferone is a mono-phenolic dye which gives strong blue fluorescence on exposure to ultraviolet light, and there is a chance that 4 and 5 can serve as fluorimetric reagents for alkali and alkaline earth metal determination.

SYNTHESIS OF REAGENTS

Reagent 3 was readily synthesized from alizarine, formaldehyde and monoaza-15-crown-5 by Mannich reaction. Fluorescent reagents 4a and 4b were similarly synthesized by commercially-available 4-methylumbelliferone. the structures were fully supported by elemental, ir, and ^{1}H nmr analyses.

EXTRACTION OF ALKALI AND ALKALINE EARTH METAL IONS

The extraction of alakli and alkaline earth metal ions was carried out as follows. A ten-ml aqueous solution containing 1 - 1 x 10^{-3} M (M = mol dm^{-3}) alkali or alkaline earth metal salt was buffered at various pH by 0.02 M tetramethyl ammonium salt of boric acid, Tricine, MES, or tartaric acid. The solution was shaken with a 10-ml 1,2-dichloroethane solution of 3, 4a, 4b or 5, and centrifuged. Absorption or emission spectra of the organic phase was measured.

RESULTS AND DISCUSSION

Figure 1 shows the spectra of organic phase when Li^+ was extracted with reagent 3 and 4a. The absorption maximum of 3 shifted from 440 nm to 550 nm and that of 4a shifted from 326 nm to 373 nm as the complexes were formed. Figure 2 shows typical emission spectra of organic phase when Li^+ ion was extracted with reagent 4a. The maximum of exitation spectrum for the intense fluorescence at 440 nm shifted from 326 nm to 380 nm in accord with the Li^+ complex formation. The extraction constants were evaluated from these spectrometric data.

The extraction reactions and extraction constants are formulated in equation (1) and (2) for alkali metal ions, and in equation (3) and (4) for alkaline earth metal ions.

$$(HL)_o + (M^+)_a \rightleftharpoons (ML)_o + (H^+)_a \qquad (1)$$

$$K_{ex}^{1} = [(ML)_o][(H^+)_a]/[(HL)_o][(M^+)_a] \qquad (2)$$

$$(H_2L)_o + (M^{2+})_a \rightleftharpoons (ML)_o + 2(H^+)_a \qquad (3)$$

$$K_{ex}^{2} = [(ML)_o][(H^+)_a]^2/[(H_2L)_o][(M^{2+})_a] \qquad (4)$$

Subscripts o and a denote organic and aqueous phases, respectively. Since the crown ether reagents and their complexes always remained in the organic phase, the extraction constants defined in equation (2) and (4) could be determined spectrophotometrically in a standard manner reported previously(1,2). Tables 1 and 2 summarize the extraction constants of 3, 4a and 4b for alkali metals, and of 5 for alkaline earth metals.

The 15-crown-5 type reagents 3 and 4a both extract Li^+ most effectively, and the ease of extraction of alkali metal ions is in the order, $Li^+ > Na^+ > K^+ > Rb^+, Cs^+$. This order is the same as that of 2 previously reported (2). A rather strong interaction between Li^+ and the pendant phenolate ion seems to be contributing to the preferred extraction of Li^+ over Na^+. The 18-crown-6 type reagent 4b extracts K^+ most effectively. The extractability of alkali metal ions was in the order, $K^+ > Na^+ > Li^+$. This order is quite usual for 18-crown-6 type complexes (2,3).

In comparison with the corresponding absorptionphotometric reagent 2, the extraction constants of the umbelliferone type reagents 4a and 4b are lowered by 1 log unit. On the other hand, the extraction constants of alizarine type reagent 3 turn to be higher by 1 log unit. Since the extraction constants defined in equation (2) and (4) implicitly contain the proton dissociation constants of the reagents in aqueous phase, this might be attributed to the lower and higher proton dissociation constants of 4 and 3,respectively than 2.

Bifunctional fluorescent reagent 5 extracts alkaline earth metals, but scarcely alkali metals. The order of extractability is $Ca^{2+} > Sr^{2+} > Ba^{2+} >> Mg^{2+}$. This order is the same as that of the corresponding p-substituted phenolic homologues compound 1 (1). however, the values are lower by 2 log unit than 1b. This difference may be rationalized by recalling the difference between 2 and 4a mentioned above, noting that this time reagent 5 has two 4-methylumbelliferone parts.

With regard to the extraction of alkaline earth metals with bifunctional reagents 3 (H_2L), the spectral data indicated that barium was extracted by forming a Ba·L type complex. Calcium on the other hand, was extracted in the form of Ca·HL·X (X= NO_3^-, ClO_4^-) only in the presence of added lipophilic anion such as NO_3^- and ClO_4^-. An exact comparison of the extractability among the metals can not be straightforward because of such difference in the mode of extraction, but if follows approximately the order, $Ba^{2+} > Mg^{2+} > Sr^{2+} > Ca^{2+}$.

Reagent 4a, 4b and 5 are useful as fluorimetric reagents. They have an excitation maximum around 326 nm in a free reagent form, and around 380 nm in the complexed form with alkali and alkaline earth metals. The emission maxima are about 440 nm in both forms (Figure 2). If the excitation wave length is fixed at 380 nm, only the complex fluoresces, and the intensity is proportional to the amount of the complex extracted.

Figure 3 shows the pH dependence of fluorescence intensity when alkali metals were extracted with reagent 4a. The results paralleled the absorbance change which was observed in the same extraction experiment. Similar results were also obtained with reagent 4b and 5. By using 2.5x10^{-4} M 1,2-dichloroethane solution of reagent 4a and 5, straight calibration lines were obtained for lithium and calcium, respectively. About 10 ppm of lithium and 1 ppm of calcium could be determined by this method.

CONCLUSION

The crown ether-based fluorimetric reagents 4a and 5 have been introduced for determination of ppm-level lithium and calcium, respectively. However, rather basic conditions required pose some inconvenience in its application to general purposes. Extraction constants have to be improved by increasing the acid dissociation constants of the reagents; basic nitrogens have to be better eliminated from the crown ether skeleton (4). The unique metal extraction property of 3 urges further exploration of such alizarine-type crown ether reagents.

REFERENCES

1. H. Nishida, M. Tazaki, M. Takagi and K. Ueno, Mikrochim. Acta, I, 281 (1981).
2. H. Nakamura, H. Sakka, M. Takagi and K. Ueno, Chem. Lett., 1305 (1981).
3. H. Nakamura, M, Takagi and K. Ueno, Anal. Chem., 52, 1668 (1980).
4. H. Nakamura, H, Nishida, M. Takagi and K. Ueno, Anal. Chim. Acta, 139, 219 (1982).

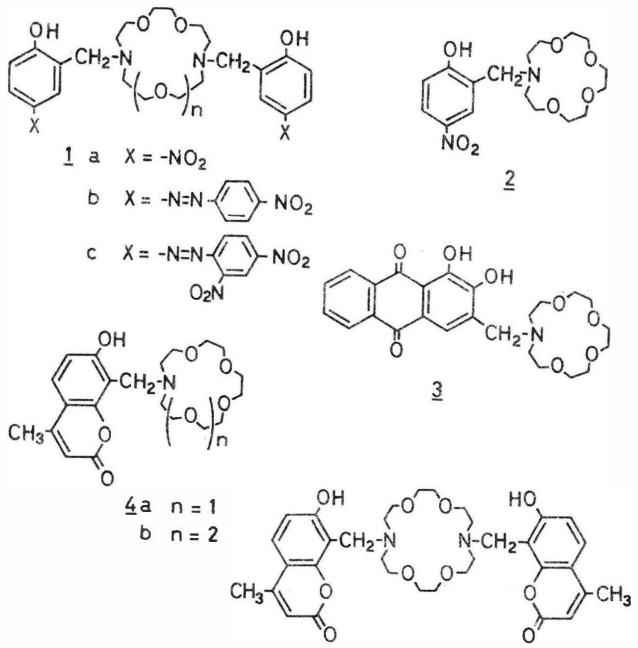

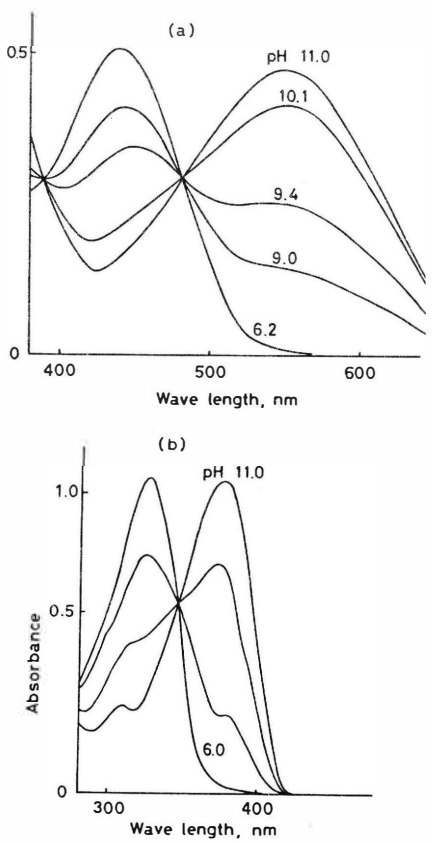

Fig. 1 Absorption spectra of reagent 3 (a) and 4a (b) in 1,2-dichloroethane equilibrated with aqueous lithium chloride. [3],[4a] = 1.0 x10^{-4} M, [LiCl] = 1.0 M.

Table 1 Extraction Constants of Alkali Metal Ions

Metal	3		4a		4b	
	pK_{ex}^{1}	λ_{max}, nm	pK_{ex}^{1}	λ_{max}, nm	pK_{ex}^{1}	λ_{max}, nm
H^+		440		326		326
Li^+	8.3	550	9.70	373	10.30	373
Na^+	8.7	555	10.30	380	10.25	380
K^+	9.6	558	11.50	380	10.00	380

Water - 1,2-dichloroethane, 25°C.

Table 2. Extraction Constants of Alkaline Earth Metal Ions

Metal	5	
	pK_{ex}^{2}	λ_{max}, nm
H^+		330
Mg^{2+}	>17.8	373
Ca^{2+}	14.72	375
Sr^{2+}	16.11	375
Ba^{2+}	17.10	373

Water - 1,2-dichloroethane, 25°C.

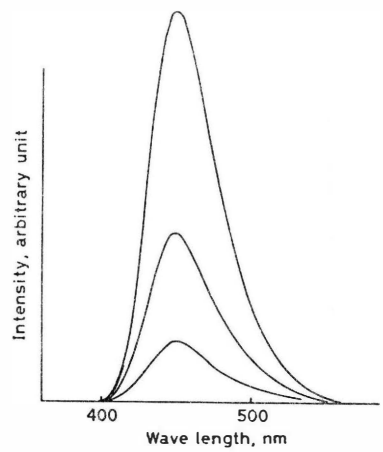

Fig. 2 Emission spectra of 4a in 1,2-dichloroethane equilibrated with aqueous lithium chloride. [4a] = 1.0 x 10^{-4} M, [LiCl] = 1.0 M

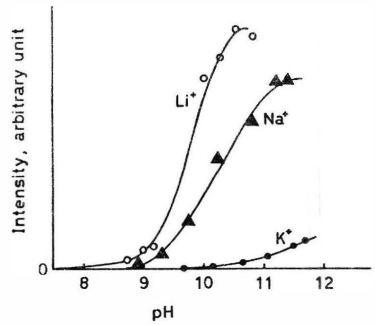

Fig. 3 Dependence of fluoresecence intensity on pH in the extration of alkali metal ions with 4a. [4a] = 1.0 x 10^{-4} M, [K^+] = 0.4 M, [Na^+] = 1.0 M, [Li^+] = 1.0 M

SOME EXTRACTIONS AND SEPARATIONS WITH CARBON DIOXIDE AT NEAR-CRITICAL CONDITIONS

T. R. Bott, M. B. King and D. M. Kassim

University of Birmingham
P.O. Box 363
Birmingham B15 2TT, UK

Iraq Petroleum Company
Baghdad, Iraq

INTRODUCTION

In recent years, there has been considerable industrial interest in the use of compressed CO_2 as a solvent (1). It is not hard to find the reasons for the interest. CO_2 has a number of advantages (2,3) including:-

1. Low cost
2. Non flammable properties
3. Generally non toxic properties (at least in low concentrations likely to be encountered in the vicinity of process plant but of course, gross exposure in high concentration can result in asphyxiation).
4. Low viscosity
5. High diffusivity
6. Many properties are well documented.

In addition, it has advantages when applied to industrial separations (2):-

7. High boiling components can be gasified at relatively low temperatures and separations achieved which are not possible by other techniques.
8. Recovery of the solute and solvent is relatively easy from solutions at near critical conditions.
9. Heat sensitive materials may be safely processed.

Extraction has been found effective around the critical point of CO_2 and Brogle (3) has indicated the regions on the pressure/temperature diagram where extraction and separation are likely to be productive. A simplified version of the diagram is reproduced as Figure 1. Large scale plant has been described by Eggers (4).

REPORTED EXTRACTIONS AND SEPARATIONS

The applications of CO_2 for extraction and separation have largely been concerned with relatively high value products which can generally be classified as natural products such as essences, flavours or perfumes. Decaffeination of coffee and the extraction of hops represents the present large scale commercial application of CO_2 treatment. There are other applications, but it would appear that these are not so far, of such great commercial interest. An extremely valuable source of data and processes contained in the review paper (containing 172 references) by Randall (5).

Coffee Extraction (Decaffeination). The extraction of green beans is accomplished on a commercial scale using carbon dioxide in the presence of water, which appears to enhance the separation. Attempts at extraction of roasted beans has not been successful due to the loss of aroma. Little quantitative information is available, however, it is reported that extractors of 40 m^3 are used in the process (6).

Hop Extraction There has been considerable interest in the brewing industry in a process using compressed CO_2 for extracting the bitter taste of hops attributed to the so called α acids and aroma (6,7,8). Liquid rather than supercritical CO_2 has been the preferred technique, but supercritical conditions have been applied (6). Grimmett (6) reports that the extraction product is entirely satisfactory. Gardner (8) reports that 95% of the available α acids may be extracted with liquid CO_2.

Tobacco Extraction (Nicotine and Tar Removal) Hubert and Vitzthum (1) report some data on CO_2 extraction of tobacco. The object is to remove nicotine and some of the condensable material thereby rendering the tobacco less harmful to health. As with the extraction of coffee, it would appear that the presence of moisture is required (up to 25% - the normal moisture content being 10-13%) to achieve meaningful extraction. However, it has to be emphasised that different tobaccos from different growing areas have different extraction properties. King and Bott (10) also noted different extraction results using different feed stocks.

Other Extractions A wide range of applications for CO_2 extraction has been discussed by de Filippi (11) including fats and oils and the extraction of organics from aqueous solution. An extremely interesting possibility for the process is the removal of contaminants from transformer oils demonstrating how the process can be adapted for speciality applications. Other papers discuss applications in the flavour and perfumery industries (12), even for the extraction of wine (13).

Separations Attention has been paid to the separation of glycerides in a "distillation" column (14,15) and Peter and Brunner (14) have attempted to asign costs to the process. There is considerable scope for the development of similar separations at near critical conditions.

THEORETICAL AND DATA REQUIREMENTS

Although there are a number of published papers dealing with the theory and provision of data on the use of CO_2 at elevated pressure, for example Schneider (16), there is a great need to augment the data. In a number of applications, it would appear that the presence of a third component (or entrainer) is important, but its function requires an improved fundamental understanding.

WORK AT BIRMINGHAM

Interest at Birmingham in extraction operations carried out with compressed or liquefied gases was stimulated by Professor S.R.M. Ellis about twenty years ago, and a number of papers describing the progress of this work have been published in the intervening years (15,17,18,19,20,21). In recent work, compressed carbon dioxide has increasingly been used as solvent. Mass transfer characteristics have been discussed in a recent paper (20) and another paper, (19) describes some vapour/liquid and vapour/solid equilibrium measurements which are of relevance for the development of extraction operations with near-critical solvents. Advantages and disadvantages in the use of carbon dioxide as solvent are discussed in this paper. Equilibrium data for the systems carbon dioxide/n-butanol/n-octane (19) and carbon dioxide/n-hexadecane/diphenylmethane (10,19) have been measured at 40 and 110°C and successfully correlated using the Redlich-Kwong equation of state. This equation was also successful in correlating data for the solubilities of oleic acid, mono-olein, naphthalene and n-dotriacontane in carbon dioxide. Although it would appear that this equation may be of use for equilibrium data correlation for some of the simpler systems of interest in critical fluid extraction work, this would certainly not be true of the complex "natural product" types of system described earlier and below.

In addition to the work on clearly defined systems, the solubilities in compressed carbon dioxide of the components in commercial mixtures of glycerides and also tobacco leaves, rape seed, pinex wood chips and crude palm oil have been investigated.

As part of the work on glycerides, a complex granular mixture of glycerides was contacted with compressed recirculating carbon dioxide at 35°C and pressures up to 165 bar (these conditions fall between regions 2 and 3 on Figure 1). A vapour loading of about 0.3 weight % was obtained at 160 bar. Samples of the equilibrium vapour phase were isolated both at medium pressures (130 to 155 bar) and "high pressure" (155 to 165 bar) and the amounts of the acid groups present in the extracts and feed material were determined by "FAME" analysis. The acid groups predominantly present in the feed sample were palmitic (C_{16}:0) and stearic (C_{18}:0), though small amounts of lower molecular weight groups down to C_{12} (lauric) were also present. Traces of oleic (C_{18}:1), linoleic (C_{18}:2) nonadecanioc (C_{19}:0), archidic (C_{20}:0) and behenic (C_{22}:0) acid groups were detected in the feed mixture. Traces of the oleic and linoleic acid groups were also detected in the extracts, though there was no evidence of the extraction of groups higher than C_{18}.

The results obtained (20) showed clear evidence of selective absorption and were consistent with the extraction of palmitic acid groups (C_{16}) and groups of lower molecular weight at the expense of the stearic acid groups (C_{18}). The result of raising the pressure was to increase slightly the proportion of high molecular weight groups in the extract, i.e. to reduce the selectivity. This is in accord with the general principles outlined by Brogle, namely that the result of increase of pressure is normally to increase loading and reduce selectivity (see Figure 1). The loadings obtained in the work on the glyceride mixture are shown as a function of pressure in Figure 3a.

Figures 3b and 3c show the gas loadings obtained when crude palm oil and wood chips respectively were contacted with recirculating carbon dioxide at 35 and 60°C and pressures up to about 200 bar. It is seen that in the case of the crude palm oil the result of increasing the temperature was to decrease the amount of material dissolved in the gas phase over this pressure range, though this effect becomes less pronounced as the pressure increases. In the case of the wood chips, solubility decreased with increase in temperature at pressures up to about 190 bar : above this pressure, the result of increasing the temperature was to increase the solubility. Similar inversions in the effect of temperature on solubility have been noted by other workers on other systems (11,22).

The equipment used for the above equilibrium loading determinations has been described in detail in reference 19: a schematic diagram is shown in Figure 2. A is a stainless steel cylinder, the bottom part of which contains either a bed of solid material to be extracted or (when a liquid is to be extracted) a fluid contactor. CO_2 at the required pressure is pumped round the closed circuit from the equilibrium cell to the sample bomb and back until equilibrium has been sufficiently closely achieved. The sample bomb is then sealed off and the contents analysed. Having carried out the analysis, the sample bomb is recharged with fresh carbon dioxide before opening up to the equilibrium cell and proceeding with the next test. The analysis is carried out by allowing the contents of the sample bomb to expand very gently via a set of glass receivers (placed directly beneath the sampling outlet) and thence into a previously evacuated expansion vessel of known volume and temperature. The amount of carbon dioxide in the sample is calculated from the pressure rise in this vessel. The amount of material of low volatility in the sample is found by washing the condensate from the sample bomb and connecting tubing into the glass receiver using a suitable volatile solvent from the burette. The solvent is then evaporated off and the amount of heavy material is determined by weighing, prior to subsequent analysis. The simple procedure outlined above suffers from the disadvantage that comparatively volatile components (including water) are lost from the extract: also, when used to study the extraction of liquids, it is inconvenient that continuous analysis of the liquid phase is not possible. Procedures appropriate for more volatile extracts and equipment in which both gas and liquid phases may be recirculated and analysed are given with results for a number of binary and ternary systems in ref.19.

The work on wood chips was carried out in conjunction with Hercules Inc., who analysed the extract and residue samples. These tests have not yet been repeated, and this work is regarded as preliminary only. The initial free moisture content of the chips was 33.2% and the resin acid content was 13.3%. During the equilibrium tests (Figure 3) CO_2 was recirculated through the chips at a rate of 1.8 dm^3/hr for 2 hours prior to each sampling. Extract deposited during expansion of the cell contents was washed into the glass receivers with benzene (though acetone was also used in a few of the tests at 35°C). The benzene was then evaporated off in a vacuum oven at 30°C and a pressure of 20 torr a process which usually took about 3 hours.

Having carried out these tests, stagnant liquid CO_2 at 19.5°C and 70 bar was contacted with the chips for 24 hours: a very slow stream of liquid CO_2 at the same conditions was then allowed to enter the equilibrium cell and thence to pass to atmosphere through the sample bomb. After a few minutes, the sample bomb was valved off and the contents analysed as above. The loading at 19.5°C & 70 bar was found to be 0.17 wt.%. This procedure was adopted to obtain as close an approximation as possible to equilibrium conditions without using the recirculation pump. It was inconvenient to use at temperatures below about 35°C because of solid deposition on reducing the pressure.

Finally, about 9kg of liquid CO_2 at 21°C and a pressure a little above the vapour pressure was passed through the chips without recirculation and thence via the sample bomb and the glass receivers (where extract was collected continuously) to atmosphere. The extract collected in all three types of test was dark brown in colour and resembled pitch in consistency; 90% of the extract was collected during the final continuous extraction test. The samples were stored under nitrogen to prevent oxidation and analysed. The residue was also analysed. It was found that a reduction of 26% had occurred in the weight of the chips. The resin acid content had fallen from 13.3 to 6.5% and, apparently, the "free moisture" content had fallen from 33.2% to 6.5%. There appears to be some inconsistency in these data since the drop in "free moisture" content (12.9g) exceeds the drop in weight (11.9g) of the chips. It is possible that some of the free moisture might have become chemically bound due to a hydrolysis reaction, though it appears more likely that experimental difficulties in measuring "free moisture" in a non-homogenous natural product account for the discrepancy. (A more typical initial moisture content is about 23 wt.%). Despite this ambiguity, it is clear that substantial drying of the residue took place. This was also observed in some extraction tests on rape seed and is not surprising, since it is known that liquid CO_2 equilibrated with water at 22.6°C contains 0.1 wt.% water. If equilibrium was approached in the contactor during the continuous extraction test, about 9g of water would have been removed. The three extracts (at 35, 60 and 21°C) were similar in having dehydroabietic and isopimaric acids as the major resin acids present. Abietic and neoabietic acids were present in smaller amounts. Typically, wood resin contains only about 10% dehydroabietic acid and the presence of substantial amounts of dehydroabietic and isopimaric acids suggests that some degree of isomerisation and aromatization may have occurred. This conclusion should be viewed with caution, however, since other workers have reported no such changes (25). The 35°C extract was also analysed for terpenes, and the main component found was paracymene. The terpene content was quite low, probably because these more volatile components were lost when the benzene was stripped from the sample. In conclusion, it is evident from these few examples and much other work that has appeared in the literature that quite a wide range of naturally occurring products may be extracted with near-critical CO_2. In particular, it has been claimed (25) that the extraction of wood chips in this way should be competitive with other methods. Before such processes can be adequately costed, however, more information on rates of mass transfer is required (10,20).

REFERENCES

1. T.R. Bott, Chem.Ind. (London), 228 (1980).
2. T.R. Bott, Chem.Ind. (London), 394 (1982).
3. H. Brogle, Chem.Ind. (London), 385 (1982).
4. R. Eggers, Angew.Chem.Int.Ed.Engl., 17, 751 (1978).
5. L.G. Randall, Sep.Sci.Tech., 17, 1 (1982).
6. C. Grimmett, Chem.Ind. (London), 359 (1981).
7. R. Vollbrecht, Chem.Ind. (London), 397 (1982).
8. D.S. Gardner, Chem.Ind. (London), 402, (1982).
9. P. Hubert and O.G. Vitzthum, Angew.Chem.Int.Ed.Engl., 17, 710 (1978).
10. M.B. King and T.R. Bott, Sep.Sci.Tech., 17, 119 (1982).
11. R.P. de Filippi, Chem.Ind. (London), 390 (1982).
12. J.P. Calame and R. Steiner, Chem.Ind. (London), 399 (1982).
13. D.R.P. Jolly, Proc.Biochem., 16, 5, 36 (1981).
14. S. Peter and G. Brunner, Angew.Chem.Int.Ed.Engl., 17, 746 (1978).
15. F. Panzner, S.R.M. Ellis and T.R. Bott, J.Chem.E. (London), Symposium Series No.54, 165 (1978).
16. G.M. Schneider, Angew.Chem.Int.Ed.Engl., 17, 716, 1978.
17. S.R.M. Ellis and R.L. Valteris, Chem.Ind. (London), 442 (1966).
18. M.B. King, Birmingham Univ.Chem.Engr., 26 (2-3), 35 (1975).
19. M.B. King, D.A. Alderson, F.H. Fallaha, D.M. Kassim, K.M. Kassim, J.R. Sheldon and R.S. Mahmud, to be published as Chapter in book "Chemical Engineering at Supercritical Conditions", J. Penninger (Ed.), Ann Arbor (1983). (Paper 31b, delivered at Symposium on Chemical Engineering at Supercritical Conditions held during annual meeting of the AIChE at New Orleans in November 1981).
20. M.B. King, K.M. Kassim and T.R. Bott, to be published in Fluid Phase Equil., (1983).
21. F. Panzner, S.R.M. Ellis and T.R. Bott, Proc.International Solvent Extraction Conference, ISEC '77, 685 (1975).
22. K.W. Quirin, Fette Seifen Arotrichmittel, 84, 460 (1982).
23. D.M. Kassim, Ph.D. Thesis, University of Birmingham (1981).
24. G. Brunner, Ph.D. Dissertation, University of Erlangen (1978).
25. E. McDonald, J. Howard and B. Bennett, to be published in Fluid Phase Equil.

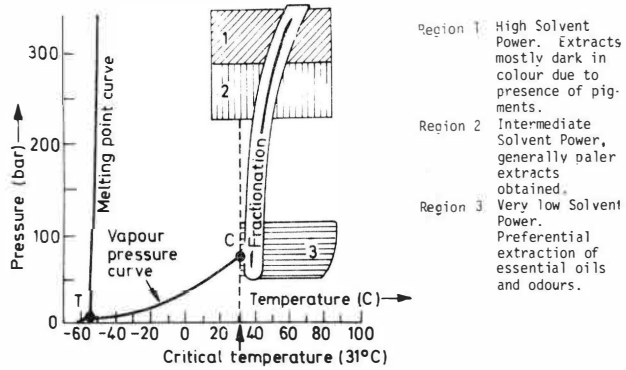

Figure 1 Influence of Extraction Conditions on Solvent Power of Carbon Dioxide

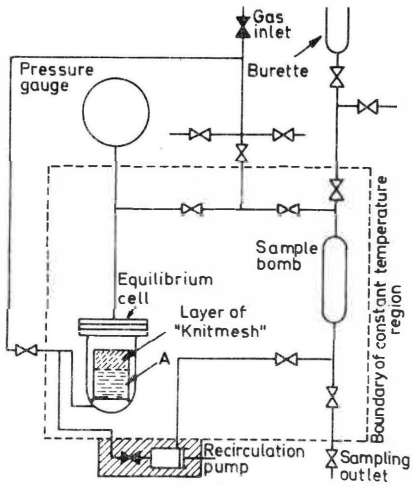

Figure 2 Schematic Diagram of apparatus used for measuring equilibrium loadings.

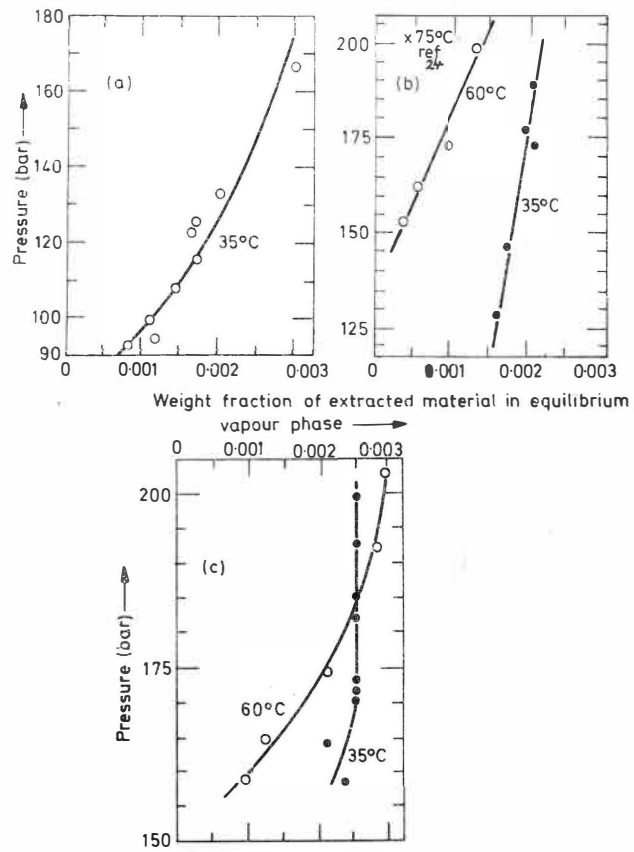

Figure 3 Equilibrium Vapour Phase Loadings obtained when
(a) a granular mixture of glycerides (b) crude palm oil
(c) pinex wood chips were contacted with recirculating CO_2

SELECTION OF SOLVENTS FOR SUPERCRITICAL EXTRACTION

Gerd Brunner

Technical University Hamburg-Harburg
Hamburg, West Germany

and

Siegfried Peter

University of Erlangen-Nuernberg
Erlangen, West Germany

For Supercritical extraction the main characteristic feature is that the extracting solvent is supercritical. Since in most cases supercritical extraction has been investigated for applications in a temperature range from ambient temperature to about 100° C the choice of the supercritical extractant has been limited to relatively few gases (Fig.1). By far the most investigated compound has been carbon dioxide because of its favourable properties of handling. In the following it is tried to accumulate rules for the selection of the supercritical solvent, depending on the properties of the mixture to be separated.

The self evident goal is that the intended separation can be achieved in a favourable way compared to more conventional methods. The points in favour for gas extraction may evolve from
- easier regeneration of the solvent
- lower operating temperatures
- improved yield
- improved product properties
- combination of several process steps.

In general a more costly equipment operating at often unfamiliar conditions has to be outweighed by these advantages.

From the mixture to be separated the following properties should be known prior to selection of a supercritcal solvent:

- state of the feed
- temperature limits
- melting point (if applicable)
- chemical nature of the components
- accompanying substances
- general information on the chemical properties and the behaviour of the components.

The state of the feed homogeneous or heterogeneous and the degree of dispersion in a liquid or solid substrate - is important since it may determine the mode of operation. So far no continuously operated feeding system for solids into a pressurized system has been proven technically feasible at a pressure level necessary for gas extraction. The highest temperature to which the mixture can be exposed limits the choice of the supercritical solvent to a critical temperature well below the maximum operating temperature. The melting point of a mixture may be of interest, since in its neighbourhood with respect to temperature a complicated phase behaviour in combination with the supercritical solvent may occur which can cause operation of the equipment to be difficult. The chemical nature of the component to be extracted is important since it determines the interactions between solvent and extractant. Like in liquid solvent extraction or in extractive distillation similar compounds are more soluble and therefore e. g. polar gases dissolve polar substances more readily. Information on accompanying substances in the mixture are important since these substances may accumulate during the process, initiate or hinder deterioration of the extracted material.
Since no discussion can be accomplished on individual mixtures, subsequently mixtures will be treated according to the volatility of their substances, or more precisely the solubility of their substances in the supercritical solvent.

We can distinguish three cases:

I. The substances to be extracted are the only ones soluble in all likely solvents.

II. Between the soluble components exist essential differences in solubility.

III. The substances to be separated are similar soluble in all likely solvents at the operating conditions for supercritical extraction.

In case I solubility is solely determining the choice of solvent and operating conditions. The solvent can be chosen according to the maximum solubility, provided availability, toxicity, security considerations or other limiting factors do not oppose it. As appropriate examples the decaffeination of coffee, the extraction of oil from seeds and separation of finely dispersed mineral matter may be considered.

An entrainer can considerably enhance solubility.
In case II again solubility is the determining parameter. Yet operating conditions cannot be chosen arbitrarily since according to phase behaviour and selectivity there are more or less favourable conditions possible which can be discussed using the example of deacidifying natural oils.
In case III selectivity is more decisive than solubility for effectively being able to achieve the goal of the process. An example may be the separation of mono and diglycerides, but mixtures of sterols or of model components having the same vapour pressure are more suitable for representing this case which so far has been least taken into consideration for practical applications. In this case an entrainer, both to enhance selectivity and solubility, may be effectful.

Having such gathered information on the mixture to be separated, one can choose the solvent from a relatively limited list of substances, the most favoured of which are: ethylene (9.9° C), carbon dioxide (31° C), ethane (32.2° C), nitrous oxide (36.5° C), propane (96.8° C) and the higher alcanes up to hexane (234.2° C), methanol (240° C), benzene (288.9° C), toluene (320.8° C) and water (374.1° C). With the higher critical temperatures, esp. with water the limit of pure physical solubility is crossed and during solubilization cracking of the material simultaneously takes place.

The solubility in the supercritical solvent so far has been found to be decisive for the process. Information on this can be gathered from phase equilibria, especially from binary phase equilibria of supercritical components with substances to be extracted. On such binary phase equilibria vast information has been compiled in recent years.
Knowing the behaviour of the binary systems in most cases reliable conclusions can be drawn on the behaviour of ternary and more complex systems.
Solubility of low volatile substances in supercritical components mainley depends on density. Since at moderate pressures the density of the gas is highest in the neighbourhood of the critical temperature and can be changed easily by pressure or temperature variation the solvent is chosen to have a reduced temperature of Tr = 1.05 to 1.3 at the operating temperature.
If the difference between operating temperature and critical temperature of the solvent is significantly greater, solubility is essentially lower. But even gases with about the same critical temperature dissolve substances in different amounts. Natural and mineral oils are for better dissolved by ethane than by carbon dioxide.
For a certain gas and at constant temperature solubility increases with pressure. If volatilities of the components to be separated at least differ essentially it may be useful to apply a pressure which is high enough so that one binary system is supercritical and the low volatile component of this binary can be dissolved in nearly all quantities. In general this is possible if supercritical solvent and nonvolatile substance are chemical similar as e. g. is the case for ethane-hexadecane. The other extreme case mostly occours with water as one of the subcritical components. Nonpolar and slightly polar gases at temperatures up to about 150° C dissolve water only in small amounts and nearly independently of pressure. Therefore if water is present in the mixture, its gas phase concentration is determined mainly by temperature.

A certain gas dissolves substances which are chemically similar according to the molecular weight. This is also valid for chemically dissimilar substances if differences in molecular weight are considerable. Substances of equal volatility but different functional groups, are dissolved (at given conditions of temperature and pressure) in different amounts by gases having the same critical temperature.
As a general rule selectivity decreases with increasing solubility. Selecting a gas with a high solvent power results in a low separation factor.
Economy is mainly determined by the ratio of product quantity to circulated gas. For a given mixture to be separated this ratio is directly proportional to the concentration of nonvolatile substances in the gas, provided the concentration in the feed gas stream is the same. The capacity of the gas can be enhanced by enhancing solubility, that is by higher pressure or by a lower concentration of extracted substances in the recirculated feed, which may be achieved by a greater pressure drop or a greater temperature change between extraction and regeneration. Since these measures raise investment and operating cast, application of an entrainer may be favourable.

An entrainer is a substance of medium volatility. Its critical temperature is well above the operating temperature of gas extraction. In most cases normal organic solvents may be taken into consideration for an entrainer, preferably substances which are present in the mixture.

The modifying effect of an entrainer can be summarized:

- enhancing solubility,
- enhancing temperature and pressure dependence of solubility
- enhancing of the separation factor.

Rules for applying entrainers:
The critical temperature of the entrainer must be higher than the process temperature. To make properly use of the enhanced solubility, the behaviour of the binary entrainer - supercritical gas is decisive. Operating pressure and temperature should be chosen in such a way that the binary system entrainer - supercritical gas is just supercritical. It should have a two phase region which does extend to very high pressures. The entrainer can be chosen in the same way as an ordinary liquid solvent.
An example may illustrate this.
For processing heavy oil residues by gas extraction propane can be used as supercritical component. The residue may have a lower boiling end point of 350° C. Propane has a critical temperature of 96.8° C. A first choice for an operating temperature may be 100 to 200° C. As entrainer any hydrocarbon compound or a mixture thereof can be used, if its boiling temperature is from 50 to 300° C, preferably from 80 to 150° C, e. g. heptane. As a first guess for the operating pressure the two - to threefold of the critical pressure of most hydrocarbons (40-50 bar), i. e. 100 - 150 bar can be chosen. This pressure is high enough to ensure that the binary system entrainer-gas is supercritical, provided the temperature is not too high. At 150° C (and 150 bar) the solubility increases continuously with concentration of the entrainer. At 200° C and low concentrations of the entrainer the solubility decreases with increasing amount of entrainer. At higher concentration of the entrainer solubility again increases with increasing amount of entrainer.
Therefore 150° C will be an appropriate operating temperature. In systems with hydrocarbon compounds the operating temperature should be in the neighbourhood of the critical temperature of the gas, possibly not higher than about T_R = 1.2.